2016

ANNUAL PROGRESS REPORT

DOE Hydrogen and Fuel Cells Program

U.S. DEPARTMENT OF ENERGY

DOE/GO-102017-4891
February 2017

U.S. Department of Energy
1000 Independence Avenue, S.W.
Washington, D.C. 20585-0121

FY 2016
PROGRESS REPORT FOR THE DOE HYDROGEN AND FUEL CELLS PROGRAM

February 2017
DOE/GO-102017-4891

Approved by Sunita Satyapal, Director, Hydrogen and Fuel Cells Program

NOTICE

This report was prepared as an account of work sponsored by an agency of the United States government. Neither the United States government nor any agency thereof, nor any of their employees, makes any warranty, express or implied, or assumes any legal liability or responsibility for the accuracy, completeness, or usefulness of any information, apparatus, product, or process disclosed, or represents that its use would not infringe privately owned rights. Reference herein to any specific commercial product, process, or service by trade name, trademark, manufacturer, or otherwise does not necessarily constitute or imply its endorsement, recommendation, or favoring by the United States government or any agency thereof. The views and opinions of authors expressed herein do not necessarily state or reflect those of the United States government or any agency thereof.

Available electronically at SciTech Connect http:/www.osti.gov/scitech

Available for a processing fee to U.S. Department of Energy
and its contractors, in paper, from:

U.S. Department of Energy
Office of Scientific and Technical Information
P.O. Box 62
Oak Ridge, TN 37831-0062
OSTI http://www.osti.gov
Phone: 865.576.8401
Fax: 865.576.5728
Email: reports@osti.gov

Available for sale to the public, in paper, from:

U.S. Department of Commerce
National Technical Information Service
5301 Shawnee Road
Alexandria, VA 22312
NTIS http://www.ntis.gov
Phone: 800.553.6847 or 703.605.6000
Fax: 703.605.6900
Email: orders@ntis.gov

Printed on paper containing at least 50% wastepaper, including 20% postconsumer waste

Outline

I. Introduction

II. Hydrogen Production

- II.0 Hydrogen Production Program Overview
- II.A Hydrogen Production Analysis
  - II.A.1 Strategic Analysis, Inc.: Hydrogen Pathways Analysis for H2 Production via a Monolithic Piston Reforming Reactor and Reformer-Electrolyzer-Purifier Technology
- II.B Electrolysis
  - II.B.1 National Renewable Energy Laboratory: Renewable Electrolysis Integrated System Development and Testing
  - II.B.2 Giner, Inc.: High-Performance, Long-Lifetime Catalysts for Proton Exchange Membrane Electrolysis
  - II.B.3 Proton OnSite: High Performance Platinum Group Metal Free Membrane Electrode Assemblies through Control of Interfacial Processes
  - II.B.4 Giner, Inc.: High Temperature, High Pressure Electrolysis
  - II.B.5 FuelCell Energy: Solid Oxide Based Electrolysis and Stack Technology with Ultra-High Electrolysis Current Density (>3A/cm^2) and Efficiency
  - II.B.6 Proton OnSite: Economical Production of Hydrogen Through Development of Novel, High Efficiency Electrocatalysts for Alkaline Membrane Electrolysis
  - II.B.7 Tetramer Technologies, LLC: New Approaches to Improved PEM Electrolyzer Ion Exchange Membranes
- II.C High-Temperature Thermochemical
  - II.C.1 Sandia National Laboratories: High Efficiency Solar Thermochemical Reactor for Hydrogen Production
  - II.C.2 University of Colorado Boulder: Flowing Particle Bed Solarthermal RedOx Process to Split Water
  - II.C.3 Savannah River National Laboratory: Electrolyzer Component Development for the HyS Thermochemical Cycle
  - II.C.4 University of Colorado Boulder: NSF/DOE Solar Hydrogen Fuel: Accelerated Discovery of Advanced RedOx Materials for Solar Thermal Water Splitting to Produce Renewable Hydrogen
- II.D Photoelectrochemical
  - II.D.1 National Renewable Energy Laboratory: High-Efficiency Tandem Absorbers for Economical Solar Hydrogen Production
  - II.D.2 University of Hawaii: Wide Bandgap Chalcopyrite Photoelectrodes for Direct Solar Water Splitting
  - II.D.3 University of California, Irvine: Tandem Particle-Slurry Batch Reactors for Solar Water Splitting
- II.E Biological
  - II.E.1 National Renewable Energy Laboratory: Biomass to Hydrogen
  - II.E.2 Virginia Polytechnic Institute and State University: Sweet Hydrogen: High-Yield Production of Hydrogen from Biomass Sugars Catalyzed by in vitro Synthetic Biosystems
  - II.E.3 Oregon State University: Novel Hybrid Microbial Electrochemical System for Efficient Hydrogen Generation from Biomass
- II.F Separations
  - II.F.1 Pacific Northwest National Laboratory: Monolithic Piston-Type Reactor for Hydrogen Production through Rapid Swing of Reforming/Combustion Reactions
  - II.F.2 FuelCell Energy, Inc.: Reformer-Electrolyzer-Purifier (REP) for Production of Hydrogen [CO_2 Pump]

III. Hydrogen Delivery

- III.0 Hydrogen Delivery Program Overview
- III.1 Argonne National Laboratory: Hydrogen Delivery Infrastructure Analysis
- III.2 Sandia National Laboratories: Fatigue Performance of High-Strength Pipeline Steels and Their Welds in Hydrogen Gas Service

III. Hydrogen Delivery (Continued)

- III.3 Oak Ridge National Laboratory: Vessel Design and Fabrication Technology for Stationary High-Pressure Hydrogen Storage
- III.4 Southwest Research Institute: Hydrogen Compression Application of the Linear Motor Reciprocating Compressor (LMRC)
- III.5 Oak Ridge National Laboratory: Steel Concrete Composite Vessel for 875 bar Stationary Hydrogen Storage
- III.6 Wiretough Cylinders: Low Cost Hydrogen Storage at 875 Bar Using Steel Liner and Steel Wire Wrap
- III.7 Gas Technology Institute: Compressor-Less Hydrogen Refueling Station Using Thermal Compression
- III.8 GVD Corporation: Advanced Barrier Coatings for Harsh Environments
- III.9 National Renewable Energy Laboratory: Improved Hydrogen Liquefaction through Heisenberg Vortex Separation of Para and Ortho-hydrogen
- III.10 Pacific Northwest National Laboratory: Magnetocaloric Hydrogen Liquefaction
- III.11 National Renewable Energy Laboratory: 700 bar Hydrogen Dispenser Hose Reliability Improvement
- III.12 NanoSonic, Inc.: Cryogenically Flexible, Low Permeability H_2 Delivery Hose
- III.13 Argonne National Laboratory: Hydrogen Fueling Station Precooling Analysis
- III.14 National Renewable Energy Laboratory: H2FIRST—Consolidation
- III.15 Lawrence Livermore National Laboratory: Cryo-Compressed Pathway Analysis (2016)

IV. Hydrogen Storage

- IV.0 Hydrogen Storage Program Overview
- IV.A Analysis
  - IV.A.1 Argonne National Laboratory: System Analysis of Physical and Materials-Based Hydrogen Storage
  - IV.A.2 Strategic Analysis, Inc.: Hydrogen Storage Cost Analysis
- IV.B System Engineering
  - IV.B.1 Savannah River National Laboratory: Hydrogen Storage Engineering Center of Excellence
  - IV.B.2 National Renewable Energy Laboratory: Hydrogen Storage System Modeling: Public Access, Maintenance, and Enhancements
  - IV.B.3 Savannah River National Laboratory: Investigation of Metal and Chemical Hydrides for Hydrogen Storage in Novel Fuel Cell Systems
- IV.C Advanced Materials
  - IV.C.1 Sandia National Laboratories: HyMARC: A Consortium for Advancing Solid-State Hydrogen Storage Materials
  - IV.C.2 Sandia National Laboratories: Hydrogen Storage Materials Advanced Research Consortium: Sandia Effort
  - IV.C.3 Lawrence Livermore National Laboratory: HyMARC: Hydrogen Storage Materials Advanced Research Consortium (LLNL Effort)
  - IV.C.4 Lawrence Berkeley National Laboratory: HyMARC: A Consortium for Advancing Solid-State Hydrogen Storage Materials
  - IV.C.5 Lawrence Livermore National Laboratory: Improving the Kinetics and Thermodynamics of Mg(BH4)2 for Hydrogen Storage
  - IV.C.6 Ames Laboratory: High-capacity Hydrogen Storage Systems via Mechanochemistry
  - IV.C.7 National Renewable Energy Laboratory: H_2 Storage Characterization and Optimization Research Efforts
  - IV.C.8 California Institute of Technology: Design and Synthesis of Materials with High Capacities for Hydrogen Physisorption
  - IV.C.9 Texas A&M University: High-Capacity and Low-Cost Hydrogen-Storage Sorbents for Automotive Applications
  - IV.C.10 University of Michigan: Hydrogen Adsorbents with High Volumetric Density: New Materials and System Projections
  - IV.C.11 Savannah River National Laboratory: Electrochemical Reversible Formation of Alane

IV. Hydrogen Storage (Continued)

IV.C Advanced Materials (Continued)

IV.C.12 Ardica Technologies, Inc.: Low-Cost α-Alane for Hydrogen Storage

IV.D Advanced Tanks

IV.D.1 Pacific Northwest National Laboratory: Enhanced Materials and Design Parameters for Reducing the Cost of Hydrogen Storage Tanks

IV.D.2 Lawrence Livermore National Laboratory: Thermomechanical Cycling of Thin Liner High Fiber Fraction Cryogenic Pressure Vessels Rapidly Refueled by Liquid Hydrogen Pump to 700 Bar

IV.D.3 Center for Transportation and the Environment: Conformable Hydrogen Storage Pressure Vessel Project

IV.D.4 Materia, Inc.: Next Generation Hydrogen Storage Vessels Enabled by Carbon Fiber Infusion with a Low Viscosity, High Toughness System

IV.D.5 Composite Technology Development, Inc.: Optimizing the Cost and Performance of Composite Cylinders for H_2 Storage using a Graded Construction

IV.D.6 PPG Industries: Achieving Hydrogen Storage Goals through High-Strength Fiber Glass

IV.D.7 Oak Ridge National Laboratory: Melt Processable PAN Precursor for High Strength, Low-Cost Carbon Fibers (Phase II)

IV.D.8 Sandia National Laboratories: Innovative Development, Selection and Testing to Reduce Cost and Weight of Materials for BOP Components

V. Fuel Cells

V.0 Fuel Cells Program Overview

V.A Catalysts & Electrodes

V.A.1 Los Alamos National Laboratory: Non-Precious Metal Fuel Cell Cathodes: Catalyst Development and Electrode Structure Design

V.A.2 University of New Mexico: Development of PGM-free Catalysts for Hydrogen Oxidation Reaction in Alkaline Media

V.A.3 Northeastern University: Innovative Non-PGM Catalysts for High-Temperature PEMFCs

V.A.4 Argonne National Laboratory: Tailored High Performance Low-PGM Alloy Cathode Catalysts

V.A.5 Brookhaven National Laboratory: Platinum Monolayer Electrocatalysts

V.A.6 National Renewable Energy Laboratory: Extended Surface Electrocatalyst Development

V.A.7 3M Company: Highly Active, Durable, and Ultra-low PGM NSTF Thin Film ORR Catalysts and Supports

V.A.8 General Motors Company: Highly-Accessible Catalysts for Durable High-Power Performance

V.A.9 Illinois Institute of Technology: Corrosion-Resistant Non-Carbon Electrocatalyst Supports for PEFCs

V.B Fuel Cell Performance & Durability

V.B.1 Los Alamos National Laboratory: Fuel Cell-Performance and Durability (FC-PAD) Consortium Overview

V.B.2 Argonne National Laboratory: FC-PAD Fuel Cell – Performance and Durability Electrocatalysts and Supports

V.B.3 National Renewable Energy Laboratory: FC-PAD: Electrode Layer Integration

V.B.4 Lawrence Berkeley National Laboratory: FC-PAD: Ionomer, GDLs, Interfaces

V.B.5 Los Alamos National Laboratory: FC-PAD: Modeling, Evaluation, Characterization

V.B.6 Lawrence Berkeley National Laboratory: Multiscale Modeling of Fuel Cell Membranes

V.B.7 Hawaii Natural Energy Institute: The Effect of Airborne Contaminants on Fuel Cell Performance and Durability

V.C Membranes/Electrolytes

V.C.1 3M Company: New Fuel Cell Membranes with Improved Durability and Performance

V.C.2 Colorado School of Mines: Advanced Hybrid Membranes for Next Generation PEMFC Automotive Applications

V.C.3 FuelCell Energy, Inc.: Smart Matrix Development for Direct Carbonate Fuel Cell

V. Fuel Cells (Continued)

V.C Membranes/Electrolytes (Continued)

V.C.4 Giner, Inc.: Ionomer Dispersion Impact on Fuel Cell and Electrolyzer Performance and Durability (SBIR)

V.C.5 University of Delaware: Highly Stable Anion-Exchange Membranes for High-Voltage Redox-Flow Batteries

V.C.6 Los Alamos National Laboratory: Advanced Materials for Fully-Integrated MEAs in AEMFCs

V.C.7 National Renewable Energy Laboratory: Advanced Ionomers and MEAs for Alkaline Membrane Fuel Cells

V.C.8 Giner, Inc.: Dimensionally Stable High Performance Membranes (SBIR)

V.C.9 Amsen Technologies LLC: Low-Cost Proton Conducting Membranes for PEM Fuel Cells (SBIR)

V.C.10 NanoSonic Inc.: Novel Hydrocarbon Ionomers for Durable Proton Exchange Membranes (SBIR)

V.C.11 NEI Corporation: Novel Nanocomposite Polymer Electrolyte Membranes for Fuel Cells (SBIR)

V.D MEAs, Cells, and Other Stack Components

V.D.1 3M Company: High Performance, Durable, Low Cost Membrane Electrode Assemblies for Transportation Applications

V.D.2 TreadStone Technologies, Inc.: Novel Structured Metal Bipolar Plates for Low Cost Manufacturing (SBIR)

V.D.3 Argonne National Laboratory: Rationally Designed Catalyst Layers for PEMFC Performance Optimization

V.D.4 Redox Power Systems, Inc.: Affordable, High Performance, Intermediate Temperature Solid Oxide Fuel Cells

V.D.5 Advent Technologies, Inc.: Facilitated Direct Liquid Fuel Cells with High Temperature Membrane Electrode Assemblies

V.D.6 Giner, Inc.: Advanced Catalysts and Membrane Electrode Assemblies (MEAs) for Reversible Alkaline Membrane Fuel Cells

V.E Fuel Cell System

V.E.1 pH Matter, LLC: Regenerative Fuel Cell System

V.F Testing and Technical Assessment

V.F.1 Oak Ridge National Laboratory: New Fuel Cell Materials: Characterization and Method Development

V.F.2 National Institute of Standards and Technology: Neutron Imaging Study of the Water Transport in Operating Fuel Cells

V.F.3 Los Alamos National Laboratory: Technical Assistance to Developers

V.F.4 National Renewable Energy Laboratory: Fuel Cell Technology Status: Degradation

V.F.5 Argonne National Laboratory: Performance and Durability of Advanced Automotive Fuel Cell Stacks and Systems with Nanostructured Thin Film Catalyst Based Membrane Electrode Assemblies

V.F.6 Strategic Analysis, Inc.: Fuel Cell Vehicle and Bus Cost Analysis

V.F.7 Battelle: Stationary and Emerging Market Fuel Cell System Cost Analysis--Primary Power and Combined Heat and Power Applications

V.F.8 Lawrence Berkeley National Laboratory: A Total Cost of Ownership Model for Design and Manufacturing Optimization of Fuel Cells in Stationary and Emerging Market Applications

V.G Basic Energy Sciences

V.G.1 Brookhaven National Laboratory: Structure and Function in Electrocatalysis of Reactions for Direct Energy Conversion

V.G.2 Brookhaven National Laboratory: Catalysis and Electrocatalysis for Advanced Fuel Synthesis: Hydrogen Production and the Water-Gas Shift

V.G.3 John Hopkins University: Control of Reactivity in Nanoporous Metal/Ionic Liquid Composite Catalysts

V.G.4 Pacific Northwest National Laboratory: Multifunctional Catalysis to Synthesize and Utilize Energy Carriers

V.G.5 Texas A&M University: Modeling Catalyzed Growth of Single Walled Carbon Nanotubes

V. Fuel Cells (Continued)

V.G Basic Energy Sciences (Continued)

V.G.6 University of Connecticut: Room Temperature Electrochemical Upgrading of Methane to Oxygenate Fuels

V.G.7 Wayne State University: Nanostructured, Targeted Layered Metal Oxides as Active and Selective Heterogeneous Electrocatalysts for Oxygen Evolution

V.G.8 University of Michigan: Analysis of the Mechanisms of Electrochemical Oxygen Reduction and Development of Ag-alloy and Pt-alloy Electrocatalysis for Low Temperature Fuel Cells

V.G.9 University of Massachusetts Amherst: Computational Design of Graphene-Nanoparticle Catalysts

V.G.10 University of Wisconsin: Atomic-Scale Design of Metal and Alloy Catalysts: A Combined Theoretical and Experimental Approach

V.G.11 University of Houston: Dual Site Requirements for Hydrodeoxygenation of Model Biomass Compounds

V.G.12 Oak Ridge National Laboratory: Fundamentals of Catalysis and Chemical Transformations

V.G.13 University of New Mexico: Sub Nanometer Sized Clusters for Heterogeneous Catalysis

V.G.14 Central Michigan University: Element Specific Atomic Arrangement of Binary and Ternary Alloy Nanosized Catalysts in As-Prepared and Active State

V.G.15 University of Utah: Thermodynamic, Kinetic and Electrochemical Studies on Mixed Proton, Oxygen Ion and Electron (Hole) Conductors

V.G.16 University of Chicago: Computer Simulation of Proton Transport in Fuel Cell Membranes

V.G.17 National Renewable Energy Laboratory: Hydroxide Conductors for Energy Conversion Devices

VI. Manufacturing R&D

VI.0 Manufacturing R&D Program Overview

VI.1 National Renewable Energy Laboratory: Fuel Cell Membrane Electrode Assembly Manufacturing R&D

VI.2 Ohio Fuel Cell Coalition: Clean Energy Supply Chain and Manufacturing Competitiveness Analysis for Hydrogen and Fuel Cell Technologies

VI.3 Virginia Clean Cities at James Madison University: Fuel Cell and Hydrogen Opportunity Center, www.hfcnexus.com

VI.4 GLWN – Westside Industrial Retention & Expansion Network: U.S. Clean Energy Hydrogen and Fuel Cell Technologies: A Competiveness Analysis

VI.5 Automated Dynamics: Continuous Fiber Composite Electrofusion Coupler

VI.6 Mainstream Engineering: In-line Quality Control of PEM Materials

VI.7 National Renewable Energy Laboratory: Manufacturing Competitiveness Analysis for Hydrogen Refueling Stations

VII. Technology Validation

VII.0 Technology Validation Program Overview

VII.A Vehicles

VII.A.1 National Renewable Energy Laboratory: Fuel Cell Electric Vehicle Evaluation

VII.A.2 National Renewable Energy Laboratory: Technology Validation: Fuel Cell Bus Evaluations

VII.A.3 Argonne National Laboratory: Fuel Cell Electric Truck (FCET) Component Sizing

VII.A.4 Center for Transportation and the Environment: Fuel Cell Hybrid Electric Delivery Van Project

VII.B Hydrogen Fueling Stations

VII.B.1 National Renewable Energy Laboratory: Hydrogen Station Data Collection and Analysis

VII.B.2 Gas Technology Institute: Performance Evaluation of Delivered Hydrogen Fueling Stations

VII.B.3 Proton OnSite: Validation of an Advanced High Pressure PEM Electrolyzer and Composite Hydrogen Storage, with Data Reporting, for SunHydro Stations

VII.B.4 California State University, Los Angeles: CSULA Hydrogen Refueling Facility Performance Evaluation and Optimization

VII.B.5 National Renewable Energy Laboratory: Brentwood Case Study

VII. Technology Validation (Continued)

VII.C Hydrogen Infrastructure Support

VII.C.1 National Renewable Energy Laboratory: Hydrogen Component Validation

VII.C.2 Sandia National Laboratories: Development of the Hydrogen Station Equipment Performance (HyStEP) Device

VII.C.3 Air Products and Chemicals, Inc.: Advanced Hydrogen Fueling Station Supply: Tube Trailers

VII.C.4 Lawrence Livermore National Laboratory: Performance and Durability Testing of Volumetrically Efficient Cryogenic Vessels and High Pressure Liquid Hydrogen Pump

VII.C.5 National Renewable Energy Laboratory: Hydrogen Meter Benchmark Testing

VII.C.6 California Fuel Cell Partnership: Station Operational Status System (SOSS) 3.0 Implementation, SOSS 3.1 Upgrade, and Station Map Upgrade Project

VII.D Hydrogen Energy Storage/Grid Integration

VII.D.1 National Renewable Energy Laboratory: Stationary Fuel Cell Evaluation

VII.D.2 National Renewable Energy Laboratory: Material Handling Equipment Data Collection and Analysis

VII.D.3 Idaho National Laboratory: Dynamic Modeling and Validation of Electrolyzers in Real Time Grid Simulation

VIII. Safety, Codes and Standards

VIII.0 Safety, Codes & Standards Program Overview

VIII.1 National Renewable Energy Laboratory: National Codes and Standards Deployment and Outreach

VIII.2 Sandia National Laboratories: R&D for Safety, Codes and Standards: Materials and Components Compatibility

VIII.3 Los Alamos National Laboratory: Hydrogen Fuel Quality

VIII.4 Sandia National Laboratories: R&D for Safety, Codes and Standards: Hydrogen Behavior

VIII.5 Sandia National Laboratories: Hydrogen Quantitative Risk Assessment

VIII.6 Pacific Northwest National Laboratory: Hydrogen Safety Panel, Safety Knowledge Tools and First Responder Training Resources

VIII.7 National Renewable Energy Laboratory: NREL Hydrogen Sensor Testing Laboratory

VIII.8 Fuel Cell & Hydrogen Energy Association: Fuel Cell & Hydrogen Energy Association Codes and Standards Support

VIII.9 Pacific Northwest National Laboratory: Compatibility of Polymeric Materials Used in the Hydrogen Infrastructure

VIII.10 Sandia National Laboratories: Enabling Hydrogen Infrastructure Through Science-based Codes and Standards

IX. Systems Analysis

IX.0 Systems Analysis Program Overview

IX.1 Argonne National Laboratory: Employment Impacts of Hydrogen and Fuel Cell Technologies

IX.2 Argonne National Laboratory: Life-Cycle Analysis of Water Consumption for Hydrogen Production

IX.3 Argonne National Laboratory: Impact of Fuel Cell and H_2 Storage Improvements on FCEVs

IX.4 Sandia National Laboratories: Hydrogen Analysis with the Sandia ParaChoice Model

IX.5 Argonne National Laboratory: Life Cycle Analysis of Emerging Hydrogen Production Technologies

IX.6 University of Tennessee: Policies to Promote Alternative Fuel Vehicles

IX.7 National Renewable Energy Laboratory: Sustainability Analysis of Hydrogen Supply and Stationary Fuel Cell Systems Using the Hydrogen Regional Sustainability (HyReS) Framework

IX.8 National Renewable Energy Laboratory: Evaluation of Technology Status Compared to Program Targets

IX.9 National Renewable Energy Laboratory: Expanded Capabilities for the Hydrogen Financial Analysis Scenario Tool

IX.10 University of Chicago: The Business Case for Hydrogen-powered Passenger Cars: Competition and Solving the Infrastructure Puzzle

IX.11 National Renewable Energy Laboratory: National FCEV and Hydrogen Fueling Station Scenarios

X. Market Transformation
- X.0 Market Transformation Program Overview
- X.1 Hawaii Natural Energy Institute: Hydrogen Energy Systems as a Grid Management Tool
- X.2 Plug Power: Ground Support Equipment Demonstration
- X.3 Sandia National Laboratories: Maritime Fuel Cell Generator Project
- X.4 Pacific Northwest National Laboratory: Demonstration of Fuel Cell Auxiliary Power Units (APUs) to Power Truck Refrigeration Units (TRUs) in Refrigerated Trucks
- X.5 Federal Express Corporation: FedEx Express Hydrogen Fuel Cell Extended–Range Battery Electric Vehicles

XI. Small Business Innovation Research (SBIR) Fuel Cell Technologies Office New Projects Awarded in FY 2016
- XI.0 Small Business Innovation Research (SBIR) Fuel Cell Technologies Office New Projects Awarded in FY 2016

Phase I Projects
- XI.1 General Engineering & Research, LLC: Development of Low Cost Magnetocaloric Nanomaterials for Sub 80 K Refrigeration Applications
- XI.2 Nanohmics, Inc.: Development of Next-Generation Magnetocaloric Materials
- XI.3 Giner, Inc.: High Charge Density Hydrocarbon-Based PEMs
- XI.4 NanoSonic, Inc.: Novel Hydrocarbon Ionomers for Durable Proton Exchange Membranes
- XI.5 NEI Corporation: Novel Nanocomposite Polymer Electrolyte Membranes for Fuel Cells
- XI.6 Amsen Technologies LLC: Low-Cost Proton Conducting Membranes for PEM Fuel Cells

Phase II Projects
- XI.7 Mainstream Engineering Corporation: Cross-Polarized Near-UV/Vis Detector for In-line Quality Control of PEM Materials
- XI.8 Sustainable Innovations, LLC: Hydrogen Contamination Detection
- XI.9 PH Matter, LLC: Regenerative Fuel Cell System
- XI.10 Proton Energy Systems: Economical Production of Hydrogen Through Development of Novel, High Efficiency Electrocatalysts for Alkaline Membrane Electrolysis
- XI.11 Southwest Sciences, Inc.: Diode Laser Sensor for Contaminants in Hydrogen Fuel

XII. Acronyms, Abbreviations, and Definitions

XIII. Primary Contacts Index

XIV. Hydrogen and Fuel Cells Program Contacts

XV. Project Listings by State

XVI. Project Listings by Organization

I.0 Introduction

The U.S. Department of Energy's Hydrogen and Fuel Cells Program (the Program) includes a comprehensive range of research, development, and demonstration (RD&D) activities that enable the widespread commercialization of hydrogen and fuel cell technologies across diverse applications. The Program is coordinated across the U.S. Department of Energy (DOE or the Department), incorporating activities in the offices of Energy Efficiency and Renewable Energy (EERE)—led through the Fuel Cell Technologies Office (FCTO)—Science (SC), Nuclear Energy, and Fossil Energy (FE). Every year, the Program publishes an Annual Progress Report documenting progress, accomplishments, and technology status with respect to performance metrics.

In Fiscal Year (FY) 2016, Congress appropriated approximately $119 million for the DOE Hydrogen and Fuel Cells Program in addition to $30 million for solid oxide fuel cell related activities. More detailed discussions of Program activities and plans can be found in the Hydrogen and Fuel Cells Program Plan, as well as in the plans of the program offices—FCTO's Multi-Year RD&D Plan; FE's Hydrogen from Coal RD&D Plan; and SC's Basic Research Needs for the Hydrogen Economy.[1]

Just last year, Hyundai and Toyota both introduced their fuel cell electric vehicles (FCEVs) for commercial sale, and several auto manufacturers, including Honda, GM, Daimler, and BMW, are working toward commercial production of FCEVs in the near term. In California, hydrogen is a fueling option at 25 retail gas stations (and counting) and there are plans for several fueling stations to be opened soon in the Northeast United States. The industry also celebrated the second annual National Hydrogen and Fuel Cell Day with a week of events, activities, and media announcements across the country.

In 2016, the Program enabled a new hydrogen refueling advanced technology demonstration station as well as the first-ever government FCEV fleet in Washington, D.C. The Program launched the H2@Scale national lab big idea concept, enabling the value of hydrogen across transportation, stationary, and industrial sectors. There are more than 580 patents and more than 30 commercial technologies in the market due to Program funding. Another 65 technologies may be commercialized within the next three to five years.

PROGRESS AND ACCOMPLISHMENTS BY KEY ACTIVITY

This report includes more than 1,000 pages of accomplishments achieved by DOE-funded projects in the last year. The following summaries include only a few examples. More details can be found in the individual program introductions, subsequent project reports, and in the corresponding 2016 Annual Merit Review and Peer Evaluation Report.[2]

Fuel Cells

The Fuel Cells program supports RD&D of fuel cell technologies for transportation applications, as well as enabling stationary and early market applications, with a primary focus on reducing cost and improving durability.

Cost

One of the most important metrics used to guide the program's R&D efforts is the projected high-volume manufacturing cost for automotive fuel cells, which is tracked on an annual basis. The program is targeting a cost reduction to $40/kW by 2020. Long-term competitiveness with alternative powertrains is expected to require further cost reduction to $30/kW, which represents the program's ultimate cost target. This year, the preliminary cost projection for an 80-kWnet automotive polymer electrolyte membrane (PEM) fuel cell system based on next-generation laboratory technology and operating on direct hydrogen is $53/kWnet when manufactured at a volume of 500,000 units/year, and $59/kWnet when manufactured at 100,000 units/year. For comparison, the expected cost of automotive PEM fuel cell systems that are based on current technology and planned for commercialization in the 2016 time frame is approximately $230/kWnet when manufactured at a volume of 1,000 units/year.[3]

[1] https://www.hydrogen.energy.gov/roadmaps_vision.html
[2] https://www.hydrogen.energy.gov/annual_review16_report.html
[3] https://energy.gov/eere/fuelcells/downloads/mass-production-cost-estimation-direct-h2-pem-fuel-cell-systems-0

To enable vehicle commercialization, fuel cell systems must also meet the program's durability targets. These targets vary by application; for automotive systems, DOE has set a 2020 target of 5,000 hours (Figure 1) and in 2016 increased its ultimate durability target to 8,000 hours. This increase serves to more accurately represent the durability requirement in terms of miles driven (150,000 miles) for a larger range of drivers (e.g., specifically capturing requirements for people who drive at a lower average speed). As of late 2016, the current average lab-tested durability status is approximately 3,900 hours.

FC-PAD Consortia

To simultaneously address performance and durability challenges, the program continues to build upon its Fuel Cell Performance and Durability (FC-PAD) Consortium, which was launched in FY 2015. The consortium coordinates work under the thrust areas defined in Figure 2 and has been highlighted as a comprehensive, cohesive, and valuable new asset to the program and its stakeholders across industry, academia, and national labs.

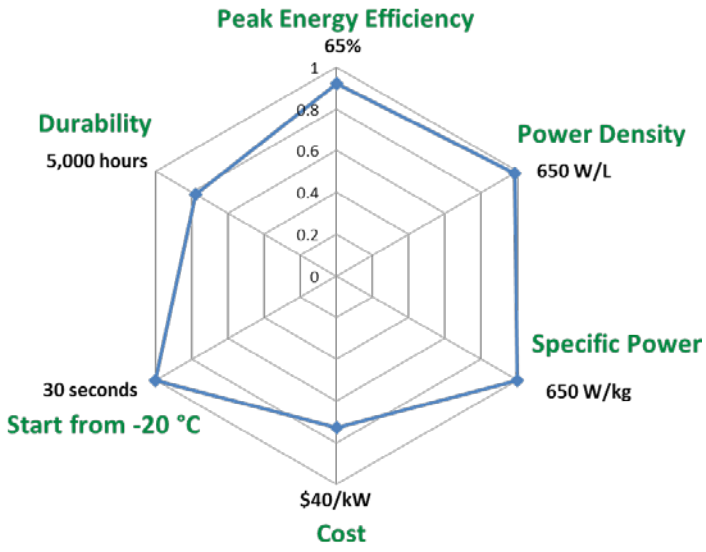

FIGURE 1. Fuel cell 2020 targets versus status (blue) for light-duty vehicle applications (the status is indicated as a fraction of the targets)

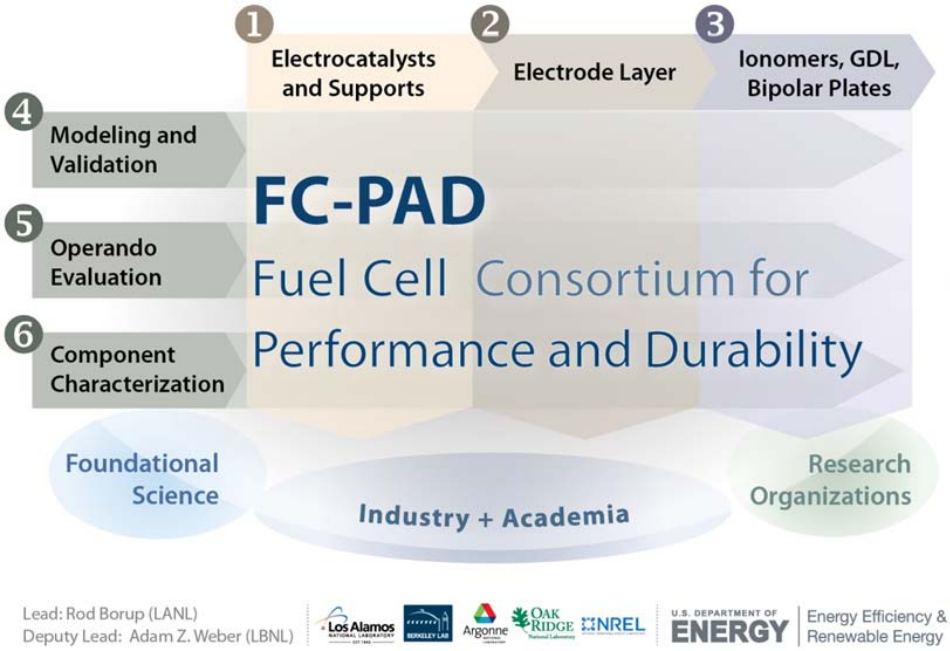

GDL – gas diffusion layer; LANL – Los Alamos National Laboratory; LBNL – Lawrence Berkeley National Laboratory

FIGURE 2. FC-PAD is structured across six components and cross-cutting thrusts

ElectroCat

Launched in FY 2016, the Electrocatalysis Consortium (ElectroCat) is an initiative to accelerate the development of catalysts made without platinum group metals for use in automotive fuel cell applications. ElectroCat's activities are primarily focused in the areas of (1) high-throughput capability development, (2) multi-scale modeling, and (3) catalyst synthesis and characterization methods. The first two activity areas will enable researchers to test potential catalyst materials at an unprecedented pace and do so in an informed manner. The third activity area will play a foundational role in developing the consortium toolset, aiding consortium partners in catalyst and electrode development, and maximizing the benefit of the consortium overall. ElectroCat is co-led by Argonne National Laboratory (ANL) and Los Alamos National Laboratory (LANL).

Characterization and Analysis

In FY 2016, microstructural and microchemical studies continued to provide insight into materials comprising membrane electrode assemblies, offering valuable information into the stability and durability of specific components during operation. Studies were primarily focused on three-dimensional electron tomography of electrocatalysts, supports, and fully intact catalyst layers.

System material-derived contamination of the fuel cell has also been studied and has led to a public dataset of materials providing leaching indices, identities and quantities of contaminants, and recommended testing procedures to assess contamination. These materials include structural plastics, hoses, lubricants, adhesives, and seals. Researchers correlated a high "leaching index" to membrane electrode assemblies degradation and lower material cost (see Figure 3). Based on these findings, the project identified a cleaner polyphthalamide (PPA) structural material that resulted in no significant increase in material cost yet afforded higher performance (see Figure 4). The publicly available balance-of-plant material screening data tool and extensive database have had approximately 1,400 site visits since May 2013 (see http://www.nrel.gov/hydrogen/system_contaminants_data/).

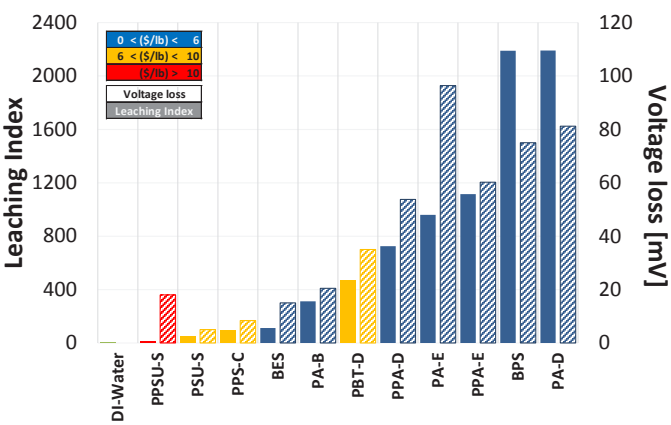

FIGURE 3. Leaching index for various materials increased with decreasing material cost (see the acronym list in Section XII for the full material names)

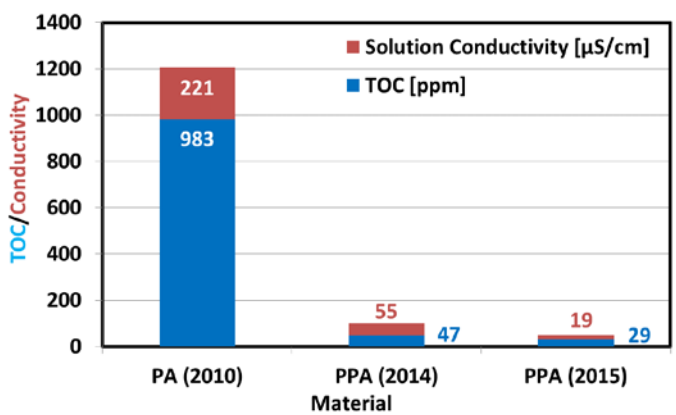

FIGURE 4. 25x improvement in combined total organic carbon (TOC) and solution conductivity for a cleaner PPA (2015) material

Hydrogen Production

In FY 2016, the Hydrogen Production program continued efforts to develop technologies that will enable the long-term viability of hydrogen as an energy carrier for a range of applications, with a focus on hydrogen from low-carbon and renewable sources. Progress continued in several key areas, including electrolysis, photoelectrochemical, biological, and solar-thermochemical hydrogen production. A world-record efficiency of greater than 16% was demonstrated for III-V semiconductor photoelectrochemical tandem devices in FY 2016. This was enabled through the use of an inverted metamorphic multijunction, which dramatically reduced voltage loses at

interfaces. This result represents an important step forward in demonstrating solar-to-hydrogen conversion efficiencies of >20% using photoelectrochemical devices.

Following a widely attended workshop on advanced water splitting in 2016, the program launched the HydroGEN advanced water splitting materials consortium as part of DOE's Energy Materials Network to accelerate materials discovery and development critical to advanced water splitting technologies for renewable hydrogen production. HydroGEN identified technical and analytical resources available at the national laboratories to support state-of-the-art renewable hydrogen production research. HydroGEN also developed a website to provide public information on its available expertise and capabilities.[4]

Launched in 2014, the two-year, $1 million H2 Refuel H-Prize competition challenges America's engineers and entrepreneurs to develop affordable systems for small-scale, non-commercial hydrogen fueling. One team, SimpleFuel, was selected by an independent panel of judges and safety experts to reach the finalist stage. To win the $1 million prize, they need to show that their system can meet a challenging set of targets, including requirements for cost, availability, safety, and hydrogen purity. Testing began in September 2016, and the outcome is expected to be announced in early 2017. This effort will complement the current focus by states and industry to deploy retail hydrogen fueling stations and will incentivize opportunities for small-scale hydrogen generation.

Hydrogen Delivery

The goal of the Hydrogen Delivery program is to reduce the costs associated with delivering hydrogen to a point at which its use as an energy carrier in fuel cell applications is competitive with alternative transportation and power generation technologies. In FY 2016, significant progress was made by the Hydrogen Delivery program on several important fronts.

Station technologies, in particular compression and onsite storage, are a key area of focus for the program. Efforts in this area aim to improve the reliability and reduce the cost of the technologies. In FY 2016, the program worked with the California Air Resources Board (CARB) to successfully deploy the Hydrogen Station Equipment Performance (HyStEP) testing device in California, including execution of a contract between Sandia National Laboratories (SNL) and CARB for the loan of the device to collect the data needed to validate California stations as part of the Hydrogen Fueling Infrastructure Research and Station Technology (H2FIRST) project. Additionally, all relevant designs and control software for the duplication of the device have been made publically available through the H2Tools website.

Also in FY 2016, an 875 bar stationary pressure vessel design was approved by the American Society of Mechanical Engineers. Initial results from hydrogen assisted fatigue crack growth data (under compressive loading) indicate that compressive loading has a comparable effect on hydrogen-assisted fatigue crack growth as low load ratios in tension.

Liquefaction represents more than 50% of the cost of hydrogen delivered via the liquid pathway and requires significant energy consumption. In FY 2016, the liquefaction of propane from room temperature using magnetocaloric materials was demonstrated at a laboratory scale. Additionally, the implementation of a bypass loop in an eight-layer magnetocaloric system increased the system cooling by 25%.

Hydrogen Storage

The Hydrogen Storage program's objective is to develop technologies that provide sufficient onboard hydrogen storage to allow fuel cell devices to provide the performance and run-time demanded for the applications. In the near term, automotive companies plan to commercialize FCEVs that use 700 bar compressed hydrogen storage systems onboard, with system cost being one of the most important challenges to commercialization.

In FY 2016 the program's materials-based storage portfolio launched a major new effort: the Hydrogen Materials–Advanced Research Consortium (HyMARC). Comprised of a core team of three national laboratories (SNL—lead, Lawrence Livermore National Laboratory, and Lawrence Berkeley National Laboratory [LBNL]), the HyMARC team is addressing the scientific gaps impeding the advancement of solid-state storage materials for storage of hydrogen onboard vehicles. Better

[4] https://www.h2awsm.org/

onboard hydrogen storage could lead to more reliable and economic hydrogen fuel cell vehicles. Launched as part of DOE's Energy Materials Network, HyMARC research activities will focus on the thermodynamic and kinetic limitations of storage materials, including mass transport, surface chemistry, and processes at solid–solid interfaces.

Five new projects were selected in 2016 to collaborate with the HyMARC national laboratory core team to develop specific hydrogen storage materials with potential to meet the performance requirements for onboard FCEV hydrogen storage. These projects will be led by University of Missouri–St. Louis, University of Hawai'i at Mānoa, The Pennsylvania State University, Liox Power Inc., and ANL.

The Hydrogen Storage program continued efforts to develop and improve hydrogen storage materials in FY 2016 with potential to meet the 2020 onboard storage targets. For the first time, teams validated the adsorption of two hydrogen molecules bound to a single open metal site in a sorbent material, as confirmed by neutron powder diffraction. The program also initiated a multi-laboratory, round-robin study on volumetric uptake in sorbents, which includes national laboratories, universities, industry, and international participants, to identify sources of error in volumetric uptake measurements, the results of which will be disseminated to the adsorption community to improve data reliability.

FY 2016 marked the last year of the Hydrogen Storage Engineering Center of Excellence (HSECoE), which covered the program's materials engineering efforts. This year the HSECoE completed the evaluation of the HexCell and the Modular Adsorption Tank Insert, two sorbent prototype systems designed to achieve higher hydrogen adsorption densities, and finalized the validation of the framework models for the metal hydride, chemical hydrogen, and sorbent systems. Other models that were finalized through the HSECoE include the metal hydride acceptability envelope and finite element models and the tank volume/cost estimator model. A major milestone achieved during FY 2016 was making these models and resources accessible through the HSECoE.org website for use by the materials-based hydrogen storage R&D community. A subset of the HSECoE partners (National Renewable Energy Laboratory [NREL], Pacific Northwest National Laboratory, and Savannah River National Laboratory) made improvements to the performance of the modelling package and incorporated an improved graphical user interface that is better suited for end users.

Manufacturing R&D

The Manufacturing R&D program supports activities needed to reduce the cost of manufacturing hydrogen and fuel cell systems and components. Advances in the enhancement of domestic hydrogen and fuel cell supply chains as well as in the quality control of fuel cell materials in FY 2016 include the following.

- Four regional Technical Exchange Centers were established, located at the National Fuel Cell Center at the University of California, Irvine; NREL; Connecticut Center for Advanced Technology; and Ohio Fuel Cell Coalition. The regional Technical Exchange Centers will collect and categorize regional hydrogen and fuel cell information that will be included in a national web-based database to facilitate purchases of hydrogen and fuel cell components and systems.
- Virginia Clean Cities at James Madison University set up a nationwide online database known as HFC NEXUS: The U.S. Hydrogen and Fuel Cell Directory.[5] HFC Nexus is a business-to-business directory that helps suppliers connect with buyers. The website includes information on a number of different company types, such as automakers, integrators, and suppliers; users can also search for products such as catalysts, electrodes, and hydrogen pump/ejectors (see Figure 5). Recently, Virginia Clean Cities added a feature called MatchMaker that lists organizations that are seeking or offering products, goods, services, etc., in hydrogen and fuel cell markets. Its goal is to help organizations connect with each other in the supply chain to improve communications and speed up development of these critical technologies.
- In 2015, Mainstream Engineering began a Tech Transfer Opportunity project through the Small Business Innovation Research (SBIR) and Small Business Technology Transfer (STTR) programs. Mainstream Engineering proposed to develop a low-cost optical detector for continuous analysis of membranes for PEM fuel cell membrane electrode assemblies based on a licensing agreement with NREL. In 2016, Mainstream demonstrated an optical system that detected 40 out of 40 100-µm pinhole defects in real time on NREL's continuous roll-to-roll web line running a Nafion 211 membrane at speeds of up to 30 ft/min. With post processing, all defects were successfully identified at web line speeds up to 100 ft/min.

[5] http://hfcnexus.com/

FIGURE 5. HFC Nexus is a business-to-business directory that helps suppliers connect with buyers

Basic Research

The Basic Energy Sciences (BES) program in the DOE Office of Science supports a number of fundamental scientific research projects addressing critical challenges related to hydrogen storage, hydrogen production, and fuel cells. These basic research efforts complement the applied R&D projects supported by the other offices in the Program. Progress in any one area of basic science is likely to spill over to other areas and bring advances on more than one front.

The subjects of basic research most relevant to the Program's key technologies are:

- Hydrogen Production: approaches such as photobiological and direct photochemical production of hydrogen.
- Hydrogen Storage: nanostructured materials; theory, modeling, and simulation to predict behavior and design new materials; and novel analytical and characterization tools.
- Fuel Cells: nanostructured catalysts and materials; integrated nanoscale architecture; novel fuel cell membranes; innovative synthetic techniques; theory, modeling, and simulation of catalytic pathways, membranes, and fuel cells; and novel characterization techniques.

By maintaining close coordination between basic science research and applied R&D, the Program ensures that discoveries and related conceptual breakthroughs achieved in basic research programs will provide a foundation for the innovative design of materials and processes that will improve the performance, cost, and reliability of fuel cell

technologies and technologies for hydrogen production and storage. This coordination is accomplished at the program level through bi-monthly coordination meetings between the participating offices within DOE, and at the researcher level through joint meetings of principal investigators who are funded by the participating offices.

In June 2016, the Program included a number of presentations and posters from BES-funded researchers on fundamental-science-related topics at the Annual Merit Review and Peer Evaluation Meeting in conjunction with presentations by EERE- and Advanced Research Projects Agency-Energy-funded researchers.

Technology Validation

The Technology Validation program demonstrates, tests, and validates hydrogen and fuel cell technologies and uses the results to provide feedback to R&D activities. In addition to validating FCEV and hydrogen infrastructure technologies, continuing efforts include the real-world evaluation of fuel cell bus technologies at various transit authorities and monitoring performance of fuel cells in stationary power, backup power, and material handling equipment (MHE) applications.

Fuel Cell Electric Vehicles

- Over the last 10 years, NREL has completed analysis of more than 220 on-road FCEVs that have accumulated almost 6.4 million miles.
- Fuel cell durability has steadily and significantly improved over the last decade, to over 4,100 hours (and counting).
- The maximum vehicle odometer reading achieved to date is 190,300 miles (approximately 10% of vehicles have passed 100,000 miles).
- The maximum fuel cell operation hours achieved to date is 5,605.

Fuel Cell Electric Buses

- Eleven fuel cell power plants achieved operation time in excess of 12,000 hours—one of these systems logged more than 22,600 hours in service (surpassing the 2016 target of 18,000 hours), and three additional systems surpassed 16,000 hours.
- Reliability has shown a marked increase over time, reaching the ultimate targets for both bus miles between road calls and fuel cell system miles between road calls, and fuel-cell-related issues made up only 15% of the road calls during the period.

Hydrogen Stations

- The HyStEP (Hydrogen Station Equipment Performance) device was developed to accelerate commercial hydrogen station acceptance and commissioning by measuring hydrogen dispenser performance against SAE J2601 protocols. The device has been used at three stations and has provided consistent, reliable performance tests for over 45 fills, including leak checks, sensor and instrument checks, Infrared Data Association communications checks, and original equipment manufacturer test fills.
- Station Operational Status System (SOSS) is a client app for use on a cell phone or vehicle dashboard that mitigates the early-stage problem of customers arriving at a station that is unavailable for fueling. In FY 2016, another 20 open retail stations were added to the existing seven for a total of 27 stations that are currently participating in SOSS.
- In the hydrogen station data collection and analysis project, data from state-of-the-art hydrogen fueling facilities were collected and analyzed by NREL. Based on this data, fills greater than 1 kg with pre-cooling at -40°C had an average fueling rate of 0.87 kg/min, and time to fill was 3.7 min.

Market Transformation

To ensure that the benefits of the Program's efforts are realized in the marketplace, the Market Transformation program continues to facilitate the growth of early markets for fuel cells used in stationary, specialty vehicle, and truck fleet applications. Program activities are helping to reduce the cost of fuel cells by enabling economies of scale through early market deployments; these early deployments also help to overcome a number of barriers, including the lack of operating performance data, the need for applicable codes and standards, and the need for user acceptance. The

program also partners with other federal agencies and stakeholders to deploy fuel cell systems in applications such as marine cargo transport operations.

One of the key accomplishments of the Market Transformation program in FY 2016 was deploying the world's first zero emissions electric generator for on- and off-board ship auxiliary power. This project, being conducted in collaboration with the U.S. Maritime Administration, is demonstrating the value proposition of using fuel cell power for specialty marine needs, particularly auxiliary power, where variable loads make fuel cells more energy-efficient than conventional generators such as diesel engines. This year the marine power system was tested in real operating conditions at a port facility to power refrigerated shipping containers that need continuous power both on- and off-board ocean-going vessels. The system being demonstrated is two to three times more efficient than incumbent internal-combustion-engine-powered units, particularly at lower power loads.

Education

Although the Program relies on prior-year resources for the Education program's activities, leveraging other resources for education and outreach continues to be important for hydrogen and fuel cell technology. With the advent of commercial systems, industry has taken the lead on education, but stakeholders still rely on DOE for providing technically accurate and objective information to key target audiences that are directly and indirectly involved in the use of hydrogen and fuel cells. In FY 2016, the Program published more than 130 success stories through news articles, blogs, press releases, and media announcements and conducted 13 webinars, averaging more than 150 attendees per webinar. The FCTO monthly newsletter reached more than 15,000 subscribers.

Safety, Codes and Standards

The Safety, Codes and Standards program identifies needs and performs high-priority R&D to provide an experimentally validated, fundamental understanding of the relevant physics, critical data, and safety information needed to define the requirements for technically sound and defensible hydrogen and fuel cell codes and standards. During the past year, the program continued to identify and evaluate safety and risk management measures that can be used to define the requirements and close the gaps in codes and standards in a timely manner.

- In FY 2016, the Hydrogen Risk Assessment Model (HyRAM) version 1.0 was released for public use and is available to download online.[6]
- To advance infrastructure deployment, experimental efforts were initiated to help inform separation distances for liquid hydrogen. H2Tools.org, which was launched in June of 2015, received over 80,000 page views in its first year. Of those site visits, just over 50% are from outside the United States, including visits from the United Kingdom, Canada, India, Japan, and Germany.
- Through in-person and online training and resources, we have reached more than 36,000 code officials and first responders to date.
- Additional information was added to the community resource tool H2Tools.com, including codes and standards resources and permitting guides, landing pages for the H2FIRST project and the HyStEP device, and Vehicle Emergency Response Guides.

Source: H2Tools.org

Systems Analysis

The Systems Analysis program focuses on examining the economics, benefits, opportunities, and impacts of hydrogen and fuel cells through a consistent, comprehensive, analytical framework. The team made several significant contributions to the Program during FY 2016.

On June 1, the United States Driving Research and Innovation for Vehicle efficiency and Energy sustainability (U.S. DRIVE) Cradle-to-Grave Working Group published a report entitled "Cradle-to-Grave Lifecycle Analysis of U.S. Light-Duty Vehicle-Fuel Pathways: A Greenhouse Gas Emissions and Economic Assessment of Current (2015) and Future (2025–2030) Technologies."[7] The study provides a comprehensive cradle-to-grave analysis of the cost, greenhouse gas (GHG) emissions, levelized cost of driving, cost of avoided greenhouse gas emissions, and technology

[6] http://energy.sandia.gov/transportation-energy/hydrogen/quantitative-risk-assessment/hydrogen-risk-assessment-model-hyram/
[7] https://greet.es.anl.gov/publication-c2g-2016-report

readiness level of key fuel and vehicle technology pathways. Co-authors are from ANL; DOE's Vehicle Technologies, Fuel Cell Technologies, and Bioenergy Technologies Offices; NREL; the Electric Power Research Institute; Fiat Chrysler Automobiles; General Motors; Chevron; and Ford Motor Company.

Lifecycle Analysis Record

In FY 2016, the Greenhouse gases, Regulated Emissions, and Energy use in Transportation (GREET) model was used to compare the GHG emissions associated with current gasoline, hybrid electric, battery electric, and fuel cell vehicles versus future versions of gasoline and alternative fuel vehicles based on expected technology advancements. As shown in Figure 6, the lifecycle GHG emissions of the current alternative vehicles are 20%–50% less than those of the current gasoline internal combustion engine vehicle. The GHG emissions of the future versions of these vehicles are 20%–50% lower than those of the current versions.

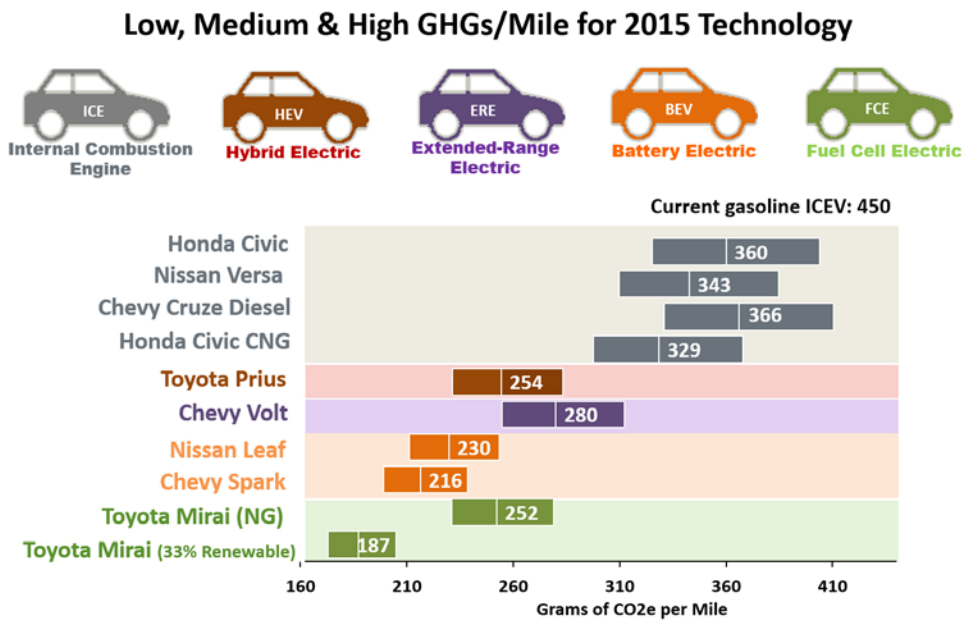

CNG – compressed natural gas; NG – natural gas

FIGURE 6. Well-to-wheels GHG emissions of hydrogen FCEV pathways compared to gasoline internal combustion engine vehicle pathways

Analysis of Current Hydrogen Cost and Targets

The current delivered cost of hydrogen was assessed relative to the early market cost target, which was developed to guide and prioritize R&D for the Program. Figure 7 shows the current delivered cost of hydrogen is \$13/gge–\$16/gge compared to the early market hydrogen cost target of \$7/gge, untaxed and dispensed at the pump, and the ultimate target of <\$4/gge. This current hydrogen cost was documented in DOE Hydrogen Program Record #15012, which was peer-reviewed by a panel that included industrial gas suppliers.[8]

Program Benefits

The implementation of fuel cell technology R&D has resulted in a cumulative GHG emissions reduction of over one million metric tons of CO_2. Figure 8 shows that the largest GHG reduction has resulted from the stationary fuel cell penetration in the power market. Fuel cell applications in the transportation sector have produced lower GHG reductions due to their lower market penetration to date. The ANL GREET model was used to perform this analysis.

[8] https://www.hydrogen.energy.gov/pdfs/15012_hydrogen_early_market_cost_target_2015_update.pdf

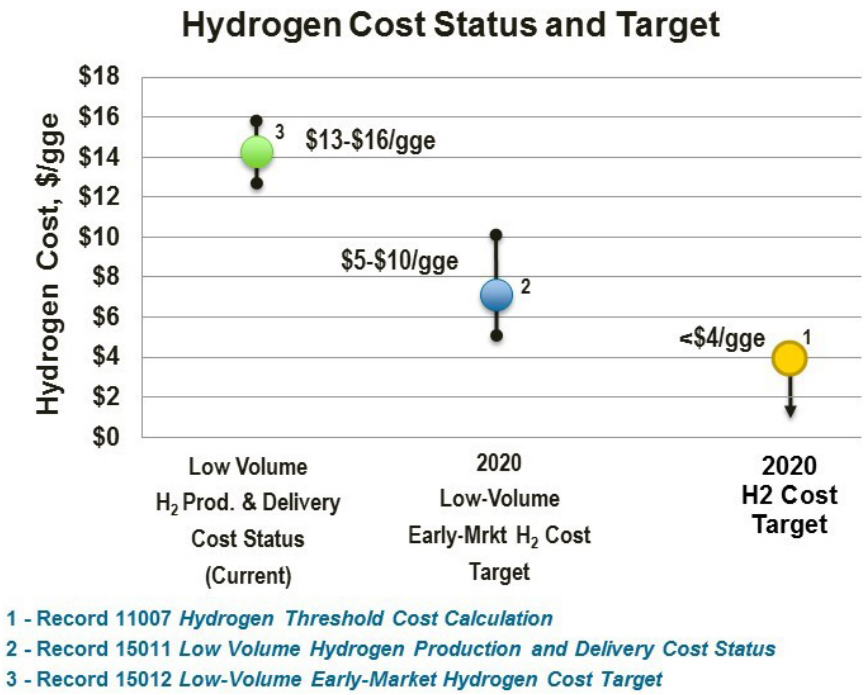

FIGURE 7. Hydrogen cost status and targets

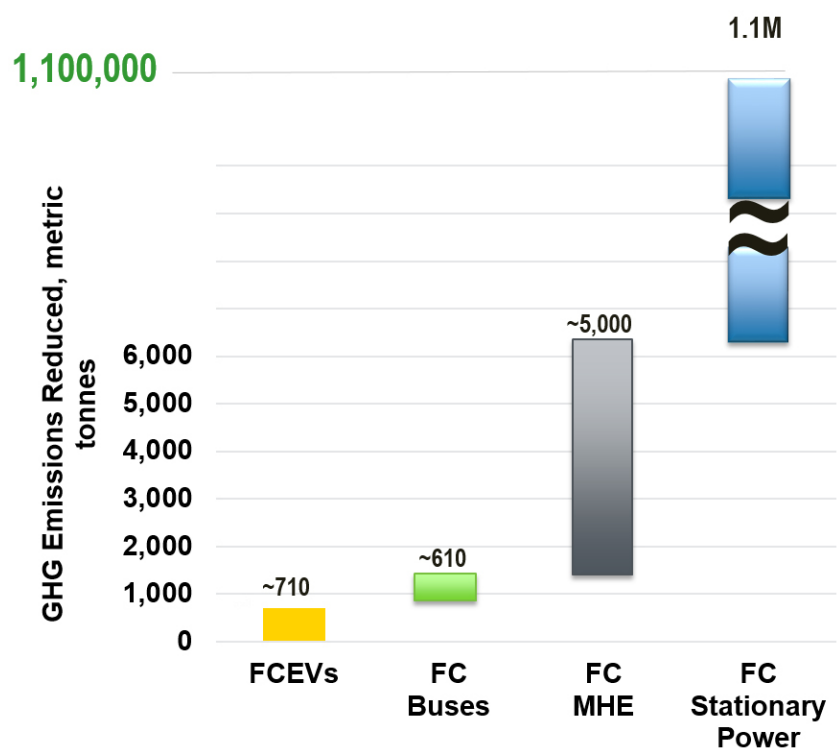

FIGURE 8. Cumulative GHG emissions reductions from fuel cell (FC) deployments

OTHER PROGRAM ACTIVITIES AND HIGHLIGHTS FROM FY 2016

Tracking Commercialization

Key indicators of the robustness and innovative vitality of an RD&D program are the number of patents granted and the number of technologies commercialized. The Program continued to assess the commercial benefits of funding by tracking the commercial products and technologies developed with the support of FCTO. As shown in Figure 9, R&D efforts funded by FCTO have resulted in more than 580 patents, more than 30 commercial technologies that cumulatively entered the market, and 65 technologies that are projected to be commercialized within three to five years (as of October 2014).[9]

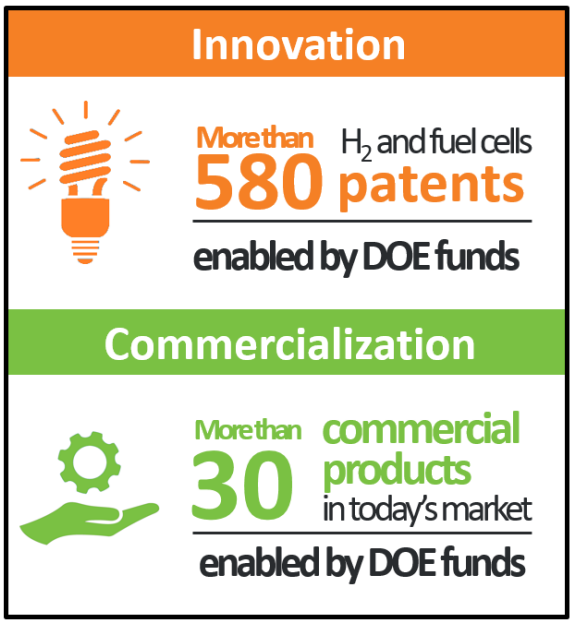

FIGURE 9. R&D efforts funded by FCTO have resulted in more than 580 patents, more than 30 commercial technologies in the market, and 65 technologies that are projected to be commercialized within three to five years (as of October 2014)

Awards & Distinctions

During the last year, a number of researchers within the Program were recognized through various awards. For example:

- ANL's nanofibrous catalyst for fuel cells project was among four ANL entries named as finalists for the 2016 R&D 100 Awards.
- Jesse Adams of FCTO was recognized with a USCAR Research Partner Award at its 16th Annual USCAR Recognition Event by the United States Council for Automotive Research LLC (USCAR), the collaborative automotive technology company of General Motors, FCA US LLC, and Ford Motor Company.
- Adam Weber of LBNL was awarded the International Association of Hydrogen Energy's Sir William Grove Award for Leadership in Electrochemical Area.
- Robert Kolasinski of SNL has been selected as one of only 49 scientists to receive significant funding for research as part of DOE's Early Career Research Program.
- Siti Khatum Kamarudin, Deputy Director of the Fuel Cell Institute at Universiti Kebangsaan in Malaysia, has been included in the 2015 edition of "Highly Cited Researchers" by THOMSON Reuters.
- FCTO researcher Piotr Zelenay of LANL was one of four researchers selected as 2015 Laboratory Fellows.
- For a second consecutive year, NREL has been selected as the Outstanding Co-Op Employer by the University of South Carolina Career Center.
- Andrew Baker, a Ph.D. candidate at LANL, received the 2nd place 2015 Bernard Baker Student Award during the Fuel Cell Seminar and Energy Exposition in Los Angeles, California, on November 19, 2015.
- Peter Dudenas, a student researcher at LBNL, won first place at the PEFC (Polymer Electrolyte Fuel Cells) 15 Student Poster Competition at the Electrochemical Society Meeting in October 2015 for his excellent scientific contributions in the field of polymer electrolyte fuel cell research.
- Katrina Groth and Ethan Hecht of SNL were recognized in October 2015 at the IA-HySafe International Conference on Hydrogen Safety with the inaugural Robert Schefer Best Paper award.
- Dr. Thomas A. Zawodzinski was selected as a fellow of the American Chemical Society POLY division and awarded a Royal Academy of Engineering Distinguished Visiting Fellowship to spend one month in England, hosted by Imperial College.

[9] Pathways to Commercial Success, http://www.energy.gov/eere/fuelcells/market-analysis-reports#mkt_pathways

Key Reports and Publications

Every year, the Program commissions a number of key reports, providing vital information to industry and the research community. Some of these are released on an annual basis—such as the Market Report (2015 Fuel Cell Technologies Market Report), the commercialization report (2015 Pathways to Commercial Success: Technologies and Products Supported by the Fuel Cell Technologies Office), and the State of the States: Fuel Cells in America 2016 report—while others are published when studies are complete, projects have ended, or key milestones have been reached. Key examples include the following.

- The ***2015 Fuel Cell Technologies Market Report*** finds that hydrogen and fuel cells continue to grow at an unprecedented rate, with more than 60,000 fuel cells, totaling roughly 300 megawatts, shipped worldwide in 2015. The number of megawatts shipped grew by more than 65% compared to 2014.[10]
- ***State of the States: Fuel Cells in America 2016***, the seventh annual report on state activities, details fuel cell and hydrogen activities and policies in the 50 states and the District of Columbia.[11]
- ***Pathways to Commercial Success: Technologies and Products Supported by the Fuel Cell Technologies Office***, the Program's annual commercialization report, indicates that FCTO efforts have successfully generated more than 580 patents, more than 30 commercial technologies, and 65 technologies that are expected to reach commercial scale within the next three to five years.[12]
- ***The Business Case for Fuel Cells*** illustrates how top American companies are using fuel cells in their business operations to advance their sustainability goals, save millions of dollars in electricity costs, and reduce carbon emissions by hundreds of thousands of metric tons per year.[13]
- The ***Cradle-to-Grave Lifecycle Analysis of U.S. Light-Duty Vehicle-Fuel Pathways: A Greenhouse Gas Emissions and Economic Assessment of Current (2015) and Future (2025–2030) Technologies*** was published by the U.S. DRIVE Cradle-to-Grave Working Group on June 1. The study provides a comprehensive cradle-to-grave analysis of the cost, greenhouse gas emissions, levelized cost of driving, cost of avoided greenhouse gas emissions, and technology readiness level of key fuel and vehicle technology pathways.[14]

Workshops and Events

In FY 2016, the Program organized a number of workshops and events valuable to both stakeholders and DOE, including those listed below.

- On April 1, 2016, FCTO, NREL, and LANL hosted the ***Alkaline Membrane Fuel Cell Workshop*** in Phoenix, Arizona, to bring together experts to share information and identify the current status and R&D needs for alkaline membrane fuel cell technology.[15]
- On April 14–15, 2016, FCTO, LBNL, and Stanford University held the ***Advanced Water Splitting Materials Workshop*** in Stanford, California, to gather stakeholder input that was foundational in establishing DOE's Energy Materials Network HydroGEN consortium, which will accelerate the RD&D of advanced water splitting technologies for renewable hydrogen production.[16]
- On June 10, 2016, FCTO hosted a ***Cross-Cutting Hydrogen Station Infrastructure Review*** to evaluate FCTO's activities related to hydrogen station infrastructure, discuss the critical technical barriers to expanding hydrogen infrastructure and the strategies to overcome them, and gather feedback to better inform strategies to address RD&D needs for hydrogen infrastructure.[17]
- On July 11–12, 2016, EERE hosted the first **Sustainable Transportation Summit** in Washington, D.C. The summit brought together transportation and mobility leaders to discuss the technology, policy, and market

[10] http://energy.gov/eere/fuelcells/downloads/2015-fuel-cell-technologies-market-report
[11] State of the States: Fuel Cells in America 2016, https://energy.gov/eere/fuelcells/downloads/state-states-fuel-cells-america-2016
[12] Pathways to Commercial Success: Technologies and Products Supported by the Fuel Cell Technologies Office, https://energy.gov/eere/fuelcells/market-analysis-reports#mkt_pathways
[13] The Business Case for Fuel Cells, https://energy.gov/eere/fuelcells/market-analysis-reports#mkt_business
[14] Cradle-to-Grave Lifecycle Analysis of U.S. Light-Duty Vehicle-Fuel Pathways: A Greenhouse Gas Emissions and Economic Assessment of Current (2015) and Future (2025–2030) Technologies, https://greet.es.anl.gov/publication-c2g-2016-report
[15] http://energy.gov/eere/fuelcells/downloads/2016-alkaline-membrane-fuel-cell-workshop
[16] http://energy.gov/eere/fuelcells/downloads/advanced-water-splitting-materials-workshop
[17] http://energy.gov/eere/fuelcells/downloads/cross-cutting-hydrogen-station-infrastructure-review

innovations that hold the potential to shape the transportation system of the future. The **H2USA Breakout Session** on July 12 featured three panels discussing H2USA and H2@Scale.[18] The first panel provided an overview of H2USA, a public-private collaboration among DOE, industry, state agencies, and other key stakeholders to address key challenges in deploying hydrogen infrastructure. The second panel covered stakeholder perspectives on hydrogen infrastructure. The third panel introduced a new DOE multi-lab initiative called H2@Scale, which offers the potential for renewable hydrogen as a flexible, clean energy carrier that can accelerate market penetration of renewables while also deeply decarbonizing our energy system.

- On August 24, 2016, FCTO hosted the ***Identifying Potential Pathways for Lower-Cost 700 bar Storage Vessels Workshop*** at USCAR in Southfield, Michigan, to identify and prioritize R&D strategies that have high potential to lower the costs of composite overwrapped pressure vessels for 700 bar hydrogen storage.[19]
- On September 27, 2016, FCTO held a ***Hydrogen and Fuel Cell Supply Chain Development Session*** as part of the 2016 Ohio Fuel Cell Symposium, in North Canton, Ohio, to enable a robust, high-quality, and low-cost domestic supply chain for the hydrogen and fuel cell industry across multiple applications.[20]
- On October 5, 2016, FCTO hosted a ***National Press Club*** briefing celebrating the week of National Hydrogen and Fuel Cell Day, in Washington, D.C. DOE Office of Energy Efficiency and Renewable Energy representatives spoke about the history and future plans of DOE's hydrogen and fuel cell program, beginning forty years ago with the national laboratories. Senator Byron Dorgan (ret.) also provided opening remarks. With the world's first commercial fuel cell cars now available, automakers and hydrogen infrastructure providers discussed their latest plans and progress.[21]
- On October 29, 2015, FCTO and Pacific Northwest National Laboratory hosted the ***Advanced Composite Materials for Cold and Cryogenic Hydrogen Storage Applications in Fuel Cell Electric Vehicles Workshop*** in Dallas, Texas, to gather input and discuss the state of knowledge on composite materials and processing for use at sub-ambient temperatures and to identify research needs and recommended development pathways for use of composite materials in sub-ambient-temperature, high-pressure applications.[22]

New Funding Opportunity Announcements (FOAs) and Awards

The Program conducted FOAs and selected new projects consistent with the overall portfolio and congressional budget justification language and appropriations.

- **$14 million** in funding was awarded for the advancement of hydrogen fuel technologies. Specifically, these selections included advanced high-temperature water splitting, advanced compression, and thermal insulation technologies. Selected projects are located in Utah, Connecticut, Massachusetts, South Carolina, California, and Virginia.
- **$13 million** was awarded to advance fuel cell performance and durability and hydrogen storage technologies. Projects awarded under the FC-PAD consortium are located in Minnesota, Connecticut, Michigan, and Tennessee. Selected projects awarded under the HyMARC consortium are located in Illinois, Pennsylvania, Hawaii, and Missouri.
- **$4.75 million** was awarded to two projects for analysis and to support the Climate Action Champion's development of education and outreach programs to increase the deployment of FCEVs and hydrogen infrastructure. The city of San Francisco has been selected as the first Climate Action Champion to pursue hydrogen and fuel cell technologies for local transportation, and Strategic Analysis, Inc. was awarded new analysis projects.

The Program also participated in a number of SBIR/STTR FOAs and awards.

- The **2017 SBIR/STTR Phase I Release 1** FOA included two subtopics focused on hydrogen and fuel cell technologies. The fuel cell subtopic included novel, durable supports for low-platinum-group-metal catalysts for PEM fuel cells. The hydrogen delivery subtopic focused on metal hydride materials for compression.

[18] http://energy.gov/eere/fuelcells/downloads/2016-sustainable-transportation-summit-h2usa-breakout-session
[19] https://energy.gov/eere/fuelcells/downloads/doe-physical-based-hydrogen-storage-workshop-identifying-potential-pathways
[20] http://energy.gov/eere/fuelcells/downloads/2016-ohio-fuel-cell-symposium
[21] http://energy.gov/eere/fuelcells/downloads/lab-road-forty-years-fuel-cells-doe-national-press-club-briefing
[22] http://energy.gov/eere/fuelcells/downloads/advanced-composite-materials-cold-and-cryogenic-hydrogen-storage

- **2016 SBIR/STTR Phase II Release 1** award winners included three projects focused on catalysis for fuel cell and hydrogen production as well as hydrogen fuel contaminants detection. These projects were awarded through the Office of Basic Energy Sciences and are located in New Mexico, Ohio, and Connecticut.
- **2016 SBIR/STTR Phase I Release 1** award winners included four projects focused on durable and inexpensive polymer electrolyte membranes for transportation and stationary fuel cell applications. These projects were awarded through the Office of Basic Energy Sciences and are located in New Jersey, Virginia, Arizona, and Massachusetts.
- **2016 SBIR/STTR Phase I Release 2** topics included magnetocaloric materials development for hydrogen delivery and two technology transfer opportunities (TTOs). The first TTO is focused on developing a durable, high-activity electrocatalyst with low platinum content and low cost for PEM fuel cell applications. The second TTO is focused on safety sensors for hydrogen infrastructure applications.

Requests for Information (RFIs)

The Program uses RFIs to solicit feedback from the stakeholder community in an open and transparent process that informs the Program's current activities and future plans. Key examples in FY 2016 included collecting feedback on:

- H2@Scale: determining RD&D necessary for clean hydrogen production to enable multi-sectoral deep decarbonization (November 2016)
- Hydrogen infrastructure RD&D: identifying project priorities to address deployment barriers (August 2016)
- Hydrogen technology showcase and training facility (July 2016)
- Medium- and heavy-duty fuel cell electric truck targets (July 2016)
- Cost reduction and performance improvements of overwrapped pressure vessel systems for compressed hydrogen for onboard vehicle applications (June 2016)
- Research, development, and business strategy needs for hydrogen and automotive PEM fuel cells (April 2016)
- Advanced thermal insulation and composite material compatibility for cold/cryogenic compressed gas fuel storage for onboard vehicle applications (November 2015)

Webinars

The Program held a number of webinars throughout the year, providing valuable information to the entire stakeholder community. The complete list of FY 2016 webinars is shown below; all are archived on the Program's website.[23]

Date	Title	Summary
August 30, 2016	International Hydrogen Infrastructure Update	Discussed the status of international hydrogen infrastructure deployment. The webinar introduced the current status of the technology in several countries, including Japan and Germany. Several perspectives on global hydrogen refueling infrastructure initiatives were also provided.
July 28, 2016	H2@Scale – A Potential Opportunity	Focused on the role of hydrogen at the grid scale and the efforts of a large, national laboratory team assembled to evaluate the potential of hydrogen to play a critical role in our energy future. Facts about hydrogen were shared, as was the vision of how it will fit into our future energy system. The R&D needs to enable this future were also discussed.
May 26, 2016	Hydrogen Fuel Cells for Small Unmanned Air Vehicles	Highlighted the Naval Research Laboratory's (NRL's) incorporation of fuel cells into its small unmanned air vehicles, and the resulting fuel and energy saving benefits. NRL has contributed to fundamental and applied fuel cell technology research for well over a decade and has collaborated with FCTO through interagency working groups.
April 26, 2016	Overview of HyRAM (Hydrogen Risk Assessment Models) Software for Science-based Safety, Codes and Standards	Provided an introduction to the new HyRAM research software developed by SNL and supported by FCTO. The HyRAM toolkit was designed to address key barriers to hydrogen infrastructure deployment, including limited access to safety data, lack of models describing hydrogen behavior, and challenges using technical data to revise standards.

[23] http://energy.gov/eere/fuelcells/2016-webinar-archives

Date	Title	Summary
March 14, 2016	Detectape – A Localized Visual Detector for Hydrogen Leaks	Discussed DetecTape, a color-changing, self-fusing silicone tape designed to detect hydrogen gas leaks in fuel cells, transmission, storage, and generation facilities. Hydrogen equipment operators can use the tape to quickly identify precise leak locations and initiate maintenance protocols, expediting the restoration of equipment while maintaining a safe workplace.
February 25, 2016	Update to the 700 bar Compressed Hydrogen Storage System Cost Projection	Strategic Analysis (SA) presented results of its cost analysis of onboard compressed hydrogen storage systems (updating its 2013 analysis, which serves as the baseline). The hydrogen storage systems analyzed are 700 bar pressure vessels made of a carbon fiber composite wrapped polymer liner (Type IV). The webinar familiarized participants with SA's Design for Manufacturing and Assembly approach, explained what processes and materials are used to manufacture composite storage vessels, and discussed the improvements in hydrogen storage systems that have led to cost reductions.
January 21, 2016	Potential Strategies for Integrating Solar Hydrogen Production and Concentrating Solar Power: A Systems Analysis	Discussed an analysis conducted by SNL exploring potential synergies that could be realized by integrating solar hydrogen production and concentrating solar power (CSP) technologies. The webinar presented the results of the analysis, including a discussion of the conditions that may favor the integration of hydrogen production and CSP.
January 12, 2016	Assessing Steel Pipeline and Weld Susceptibility to Hydrogen Embrittlement	Understanding the impact of hydrogen on structural steel (commonly referred to as "hydrogen embrittlement") is critical to the design of equipment used in hydrogen service, such as compressors, storage vessels, and pipelines. This webinar discussed the breadth of testing performed at SNL and the effects of hydrogen gas on steel pipelines and welds. The webinar also demonstrated how measured fatigue crack growth laws can be applied to calculate minimum wall thickness needed for steel hydrogen pipelines.
January 7, 2016	FCTO Consortia Overview (HyMARC and FC-PAD)	Provided an overview of the Fuel Cell Consortium for Performance and Durability (FC-PAD) and the Hydrogen Materials—Advanced Research Consortium (HyMARC), including a summary of the organization of these consortia, their planned scientific activities, and the role of individual projects selected to work with these consortia through the FY 2016 FOA.
December 10, 2015	Hydrogen Equipment Certification Guide	Introduced the Hydrogen Equipment Certification Guide, a document intended to aid in equipment approval until listed equipment are available for the entirety of equipment and components. The webinar also started a public comment phase of the document for soliciting stakeholder feedback in preparation for a September 2016 release.
December 1, 2015	Northeast States' Hydrogen Economy	Focused on state efforts to support the regional development of hydrogen infrastructure for the deployment of FCEVs in the Northeast United States. The presentation identified strategies, methods, and policies being employed in the Northeast states, from Maine to Maryland, to coordinate stakeholders, manage information, reduce potential barriers, and create new market opportunities for logical deployment of high-efficiency FCEVs.
October 13, 2015	Reference Designs for Hydrogen Fueling Stations	The goal of the H2FIRST Reference Station Design Task is to accelerate acceptance of near-term hydrogen infrastructure build-out by exploring the advantages and disadvantages of various station designs. This webinar discussed the process and findings of the work, recommended future R&D topics, and outlined planned next steps for the Reference Station Design Task.

The Program published multiple blogs focused on hydrogen and fuel cell activities.

Date	Title	Summary
October 12, 2016	ON THE VERGE OF A HYDROGEN TIPPING POINT?	Across the country this past week, scientists and engineers have been celebrating National Hydrogen and Fuel Cell Day. Aptly chosen to represent the atomic weight of hydrogen (1.008), National Hydrogen and Fuel Cell Day was celebrated for the first time on October 8, 2015, and this year we're keeping the momentum going.
October 6, 2016	3 QUESTIONS WITH A 'FOUNDING FATHER' OF HYDROGEN AND FUEL CELLS: BYRON MCCORMICK	In honor of National Hydrogen and Fuel Cell Day on October 8, we sit down with Byron McCormick, one of the "founding fathers" of hydrogen and fuel cells, to talk about his experiences during his more than 50 year career. Byron began his career in 1974 at Los Alamos National Laboratory, where he first explored the possibility of using fuel cells in vehicles.
July 19, 2016	5 THINGS TO KNOW WHEN FILLING UP YOUR FUEL CELL ELECTRIC VEHICLE	Filling up your fuel cell electric vehicle is just as easy as filling up a gasoline-powered car. The Energy Department's Office of Energy Efficiency and Renewable Energy offers five tips to follow when filling up at a hydrogen fuel station for the first time.

Date	Title	Summary
July 11, 2016	D.C. SHOWCASES CUTTING-EDGE HYDROGEN FUELING STATION DEMO	The Department of Energy and the Department of Interior's National Park Service have officially opened a new technology demonstration hydrogen refueling station in Washington, D.C. This hydrogen station should help grow and advance the benefits of hydrogen power as a fuel, and highlight the benefits of fuel cell electric vehicles firsthand throughout the region.
June 30, 2016	FIRST-EVER SUSTAINABLE TRANSPORTATION SUMMIT TO TALK FUTURE OF TRANSPORTATION, ENERGY, AND MOBILITY	The inaugural 2016 Sustainable Transportation Summit will serve as a forum to share ideas and perspectives on opportunities to accelerate the commercialization and deployment of advanced transportation technologies and smart mobility systems over the next decade.
June 8, 2016	A CLOSER LOOK AT HYDROGEN REFUELING	What's the difference between a hydrogen refueling dispenser and a traditional gasoline dispenser that you see at your local gas station? Not that much, actually...
June 6, 2016	10 QUESTIONS WITH HYDROGEN AND FUEL CELL EXPERT GLENN RAMBACH	Glenn Rambach is a world-renowned expert in the hydrogen and fuel cell industry. He talks about the history of fuel cells, what he's seen in his 45-year career, and what he thinks the future has in store for fuel cell electric vehicles.
June 3, 2016	ANNUAL MERIT REVIEW EVALUATES IMPACT OF SUSTAINABLE TRANSPORTATION PROJECTS	Nearly 400 Energy Department activities and projects will be judged by reviewers from a variety of scientific backgrounds at the Vehicle Technologies Office and Hydrogen and Fuel Cells Program Annual Merit Review and Peer Evaluation Meeting in Washington, D.C., which is free of charge and open to the public.
May 23, 2016	FUEL CELL ELECTRIC VEHICLES GETTING A BOOST IN SAN FRANCISCO	Last week, the city of San Francisco was named the first Climate Action Champion to be focused on hydrogen and fuel cells in the United States by the Energy Department's Fuel Cell Technologies Office.
May 9, 2016	FUEL CELL COMPANIES COMMIT TO HIRING VETERANS THROUGH JOINING FORCES INITIATIVE	In April 2015, the First Lady participated in an event celebrating how far we have come and announcing new private-sector commitments to train or hire 90,000 veterans and military spouses. At the event, two Fuel Cell Technologies Office-supported companies were acknowledged for their commitment to these efforts.
February 2, 2016	Energy Secretary Moniz at the 2016 Washington Auto Show	This video of Energy Secretary Moniz at the 2016 Washington Auto Show describes how the Energy Department played a role in the resurgence of the auto industry by supporting advanced vehicle technologies that boost fuel efficiency and grow America's clean energy economy.
January 27, 2016	PHOTO GALLERY: 2016 WASHINGTON AUTO SHOW	Scroll through the photos to see some of the Energy Department-supported technologies that are lowering carbon pollution and moving America's economy forward.
January 22, 2016	THE YEAR OF THE FUEL CELL: LOOKING BACK TO GET AHEAD	As EERE hits the ground running in 2016, let's take a minute to celebrate our hard work in 2015 that advanced hydrogen and fuel cells to where they are today. From research and development, to real-world deployment, 2015 was a landmark year for the hydrogen and fuel cell industry.
January 13, 2016	Fuel Cell Technologies Office: 2015 Recap and the Year Ahead	At the beginning of 2016, Sunita Satyapal, Director of the Fuel Cell Technologies Office, reflects on the Program's 2015 accomplishments and highlights some of the plans for 2016.
December 3, 2015	COLORADO JOINS THE HYDROGEN AND FUEL CELLS RACE	When one thinks of clean energy, they often think of California, which is committing up to $100 million over five years to build 100 hydrogen stations across the state, as the biggest mover and shaker. But Colorado is quickly gaining ground when it comes to hydrogen and fuel cells.
October 23, 2015	TAKE A TEST DRIVE IN THE WORLD'S FIRST COMMERCIAL FUEL CELL SUV	The Department of Energy hosted an exciting and unique visitor last week: the world's first commercially available, zero emissions fuel cell electric sport utility vehicle (SUV). The first-of-its-kind vehicle was brought to Washington, D.C., by Hyundai executives from South Korea who were in the United States as part of South Korean President Park Guen-hye's delegation visiting the president of the United States.
October 8, 2015	STACKED FOR SUCCESS: CELEBRATING NATIONAL HYDROGEN AND FUEL CELL DAY	Do you know the atomic weight of hydrogen? It's 1.008, which makes today, October 8, a great day to celebrate National Hydrogen and Fuel Cell Day! But at the Department of Energy, we're not just celebrating the confluence of the calendar and the periodic table. We're starting to see a hydrogen future to our roads today.

INTERNATIONAL ACTIVITIES

International Partnership for Hydrogen and Fuel Cells in the Economy

The International Partnership for Hydrogen and Fuel Cells in the Economy (IPHE) includes 18 member countries (Australia, Austria, Brazil, Canada, China, France, Germany, Iceland, India, Italy, Japan, the Netherlands, Norway, the Republic of Korea, the Russian Federation, South Africa, the United Kingdom, and the United States) and the European Commission. The IPHE is a forum for governments to work together to advance worldwide progress in hydrogen and fuel cell technologies. IPHE also offers a mechanism for international R&D managers, researchers, and policymakers to share program strategies. IPHE members embarked upon a second 10-year term in November 2013. An independent secretariat was established in 2015, and the current Chair of IPHE is from France. The United States continues its strong role as Vice Chair. In FY 2016, the IPHE Steering Committee met in Grenoble, France (December 2015), and in Berkeley, California (May 2016), to share progress and plans related to hydrogen and fuel cells.

International Energy Agency

The United States is also involved in international collaboration on hydrogen and fuel cell R&D through the International Energy Agency's Technology Collaboration Programs (TCPs), and is a member of both the Advanced Fuel Cells TCP and the Hydrogen TCP. The TCPs provide a mechanism for member countries to share the results of R&D and analysis activities. The DOE Hydrogen and Fuel Cells Program is a strong contributor to numerous International Energy Agency tasks and activities in the Advanced Fuel Cells and Hydrogen TCPs.

In May 2016, Wiley published a book, Fuel Cells Data, Facts, and Figures, edited by Detlef Stolten, R. Can Samsun, and Nancy L. Garland of the Systems Analysis Annex of the Advanced Fuel Cells TCP. [24] The short chapters, some written by DOE staff and researchers, provide economic data for cost considerations and a full overview of demonstration data, and cover topics such as fuel cells for transportation, fuel provision, and codes and standards.

EXTERNAL COORDINATION, INPUT, AND ASSESSMENTS

H2USA Partnership

To help address the challenge of hydrogen infrastructure, in 2013 DOE co-launched H2USA, a public-private collaboration focused on the widespread commercial adoption of FCEVs. H2USA currently consists of more than 50 participants, including the state of California, as well as developers, car companies, and hydrogen providers.

In FY 2016, the Hydrogen Fueling Infrastructure Research and Station Technology (H2FIRST) project, in support of H2USA, launched the Hydrogen Station Equipment Performance device, or HyStEP, to reduce the time to commission new stations from months to just one week. HyStEP acts as a surrogate for vehicles, eliminating the need for each automotive manufacturer to test separately. HyStEP is equipped with modular tanks and all of the instrumentation that automotive manufacturers would use in performing their own tests. HyStEP initially will be used to accelerate commissioning of refueling stations in California. Eventually, it could be used in other states as they develop hydrogen refueling networks.

HyStEP will help California meet its ambitious goal of commissioning up to 35 new refueling stations by the end of 2016, which translates to one new station every one to two weeks. The target is a hydrogen refueling network of more than 50 retail stations in this timeframe, primarily in the Los Angeles metro area, Orange County, and the Bay Area.

Hydrogen and Fuel Cells Technical Advisory Committee (HTAC)

As required by the Energy Policy Act of 2005, HTAC was created in 2006 to advise the Secretary of Energy on issues related to the development of hydrogen and fuel cell technologies (including associated safety, economic, and environmental issues), and to provide recommendations regarding DOE's programs, plans, and activities. HTAC members include representatives of domestic industry, academia, professional societies, government agencies, financial organizations, and environmental groups, as well as experts in the area of hydrogen safety. HTAC met twice in FY 2016. In August 2016, HTAC released its eighth annual report, which summarizes progress in hydrogen and fuel

[24] https://www.amazon.com/Fuel-Cells-Data-Facts-Figures/dp/3527332405

cell technologies, domestic and international RD&D, and commercialization activities, and offers recommendations on the Department's hydrogen-related programmatic and policy initiatives.

The Committee established four new subcommittees in FY 2016. The Safety and Event Response Plan Subcommittee's goal is to enable a comprehensive, consistent, and coordinated response to hydrogen safety-related events, and the subcommittee will prepare a report identifying existing resources and resource gaps for responding to safety-related events at retail hydrogen stations, as well as recommended actions to address current and projected needs. The Near-Term Hydrogen Fueling Options Subcommittee will address fuel availability from the hydrogen fueling infrastructure perspective and provide an assessment of whether or not there are one or more paths to resolve this dilemma using existing or near-term technology and business approaches. The Hydrogen Enabling Resiliency, Renewables and Security Subcommittee was reengaged to provide feedback on a multi-lab idea currently under development. The proposed effort is on H2@Scale to enable renewables as well as to provide hydrogen as a fuel (or other value-added applications) or for ancillary services. Finally, the HTAC Oversight Framework Subcommittee will develop a framework from which to govern HTAC activities that provides clear linkage to Committee responsibilities as defined by Congress; grounding and context for HTAC discussion and deliberation; a foundation from which to identify areas for HTAC focus and structure Committee debates; consistency and continuity from year to year as membership and leadership changes; and organization for HTAC reviews, recommendations, and reporting.

Federal Inter-Agency Coordination

The Hydrogen and Fuel Cell Interagency Task Force, mandated by the Energy Policy Act of 2005, includes senior representatives from federal agencies supporting hydrogen and fuel cell activities, with DOE/EERE serving as the chair. The Hydrogen and Fuel Cell Interagency Working Group (IWG), also chaired by DOE, supports the initiatives and actions passed down by the Interagency Task Force. The IWG meets monthly to share expertise and information, coordinate activities of federal entities involved in hydrogen and fuel cell RD&D, and ensure efficient use of taxpayer resources. One example of interagency collaboration was the development a federal fleet strategy for early adoption of FCEVs to drive initial demand, meet Executive Order GHG reduction goals, and lead by example. Four separate federal agencies—Veterans Affairs, Department of Defense, DOE, and National Aeronautics and Space Administration—each expressed interest in leasing FCEVs in California to make use of and help grow the nascent hydrogen infrastructure there.

Another example involves DOE and the U.S. Postal Service (USPS). The USPS has recently expressed interest in fuel-cell-powered material handling equipment for their Network Distribution Centers. The IWG held a webinar on the results of previous fuel cell forklift deployments within the Department of Defense and DOE, which led the USPS to move forward on its first deployment at their Capitol Heights (Maryland) Network Distribution Center. A third example is the opening of a hydrogen refueling station in the Washington, D.C., area. DOE and National Park Service worked together to establish the station at the National Park Service Maintenance Facility in the Brentwood neighborhood of Washington, D.C. Several IWG members attended the opening event representing their agencies, and events continue to be added to a ride-and-drive calendar that will provide education and outreach of this zero-emission technology to citizens and stakeholders throughout the National Capitol Region.

FY 2016 Annual Merit Review and Peer Evaluation (AMR)

The Program's AMR took place June 6–10, 2016, in Washington, D.C., and provided an opportunity for the Program to obtain expert peer reviews of the projects it supports and to report its accomplishments and progress. Acting Assistant Secretary David Friedman kicked the meeting off, and Senator Byron Dorgan (ret.) gave the keynote plenary presentation. For the eighth time, this meeting was held in conjunction with the annual review of DOE's Vehicle Technologies Office. During the AMR, reviewers evaluate the Program's projects and make recommendations; DOE uses these evaluations, along with other review processes, to make project funding decisions for the upcoming fiscal year. The review also provides a forum for promoting collaborations, the exchange of ideas, and technology transfer. This year, approximately 1,800 participants attended, and more than 340 experts peer-reviewed 130 of the Program's projects. The report summarizing the results and comments from these reviews is available on DOE's website.[25] The 2017 Annual Merit Review and Peer Evaluation Meeting will be held June 5–9, 2017, in Washington, D.C.

[25] https://www.hydrogen.energy.gov/annual_review16_report.html

Funds Saved through Active Project Management

The AMR is a key part of the Program's comprehensive approach toward active management of its projects. Termination of underperforming projects—identified through the AMR as well as through other go/no-go decisions (with criteria defined in the project scope of work)—helped the Program redirect $2.4 million in funding in FY 2016, $0.6 million in funding in FY 2015, $3.0 million in funding in FY 2014, and over $39 million since FY 2010. In addition, the Program implements EERE's robust Active Project Management policy to identify and resolve issues early and to mitigate risks in impactful ways, helping underperforming projects get back on track.

DOE Cross-Cutting Activities

Hydrogen Energy Storage/Grid Integration: Hydrogen energy storage may provide a broad range of energy services and typically involves the production of hydrogen from electricity via electrolyzers. Increasing capacity for variable renewable energy technologies (e.g., wind and solar) on the grid is going to be a major challenge facing future deployment as these technologies make up a larger portion of the power generation mix. FCTO's project portfolio includes a joint project between NREL and Idaho National Laboratory, which involves demonstrating electrolyzer-based energy storage to support the grid through ancillary services and demand response, in addition to hydrogen production for retail sale to transportation technologies. FCTO is also supporting four projects within the Grid Modernization cross-cutting effort (involving various offices within EERE and the Office of Electricity), with an objective to help set the nation on a cost-effective path to an integrated, secure, and reliable grid. Two of these projects are foundational: LBNL is developing a siting and optimization tool for distributed energy resources, while Idaho National Laboratory is implementing smart technology solutions to enhance the reliability of the Idaho Falls Power distribution network. The other two projects relate more specifically to FCTO: LBNL is developing a tool to quantify and optimize interactions between hydrogen stations, vehicles, and the grid; NREL is developing optimal dispatch and control strategies to improve the management of fuel cell-integrated building systems.

Wide Bandgap (WBG) Semiconductors for Clean Energy Initiative: WBG semiconductor materials allow power electronic components to be smaller, faster, more reliable, and more efficient than their silicon-based counterparts. These capabilities make it possible to reduce weight, volume, and life-cycle costs in a wide range of power applications, including fuel cells and hydrogen production technologies. EERE's technology offices, through the Advanced Manufacturing Office, are working together to harness these capabilities to lead to dramatic energy savings in industrial processing and consumer appliances. The flagship of this cross-cutting effort is the "Power America" Institute, DOE's National Network for Manufacturing Innovation focused on accelerated development of next-generation WBG semiconductor products. In FY 2015 and FY 2016, FCTO identified numerous applications of hydrogen and fuel cell technologies that could benefit from the development of next-generation WBG power electronics, including fuel-cell-powered material handling equipment and FCEVs in the transportation sector and large-scale grid integration of fuel cells and electrolyzers in the stationary power sector. FCTO is working with Power America and with leading innovators in the WBG electronics industry to organize a workshop (being held in December 2016) to further explore opportunities for product development responsive to the market pull of these hydrogen and fuel cell technology applications.

Energy Materials Network (EMN): In FY 2014, FCTO initiated an effort to explore the use of high-throughput computational and experimental methods toward the accelerated discovery and development of critical materials for hydrogen and fuel cell technologies. This approach leverages the scientific methodologies of the President's Materials Genome Initiative launched in 2011. In FY 2015, several DOE offices identified complementary Materials Genome Initiative-related research interests in several key material domains, with plans to align their materials research through the establishment of broad research consortia supporting teams of industry, academic, and national lab partners and conducting focused research within these domains. Together, these consortia form the EMN, a resource network with capabilities in materials design, synthesis, characterization, manufacturing, and digital data management and informatics. In late FY 2016, FCTO established three EMN consortia: ElectroCat for the development of platinum-group-metal-free fuel cell catalysts, HyMARC for the development of viable materials-based hydrogen storage materials, and HydroGEN for the development of advanced water splitting materials for renewable hydrogen production. All three leverage the world-class research facilities and expertise at participating national laboratories, addressing challenges in theory, computation, synthesis, and characterization for accelerating RD&D in these three high-impact fields. In each EMN consortium, the extensive network of research capabilities is expected to support competitively selected collaborative research among industry, academia, and the national laboratories for accelerating progress toward commercialization.

IN CLOSING ...

After the first oil embargo back in the mid-1970s, a group of national laboratory researchers met with leaders from the private sector and federal government at Los Alamos National Laboratory in New Mexico. They came together to brainstorm ideas, like hydrogen and fuel cells, that would ultimately revolutionize the transportation sector as we know it. Based on these ideas, General Motors temporarily relocated their fuel cell division to Los Alamos. Over time, national lab scientists helped teach industry scientists how to make optimized electrodes—the heart of the fuel cell—and eventually these partnerships led to major advancements. Forty years later we have commercial FCEVs on the road!

It's been a great year for fuel cells! Over the past year, Hyundai and Toyota both introduced their FCEVs, and Honda has plans to introduce this year. Several other companies also plan to release FCEVs very soon, including General Motors, Daimler, Honda, and BMW. In California, hydrogen is a fueling option at more than 25 retail gas stations, and there are plans for several fueling stations to be opened soon in the Northeast United States.

The Program's latest Fuel Cell Technologies Market Report[26] shows the fuel cell industry continuing to grow at an unprecedented rate, with more than 60,000 fuel cells, totaling roughly 300 megawatts, shipped worldwide in 2015. The number of megawatts shipped grew by more than 65% compared to 2014. This continues to uphold the consistent 30% annual market growth rate since 2010. EERE-funded R&D has resulted in more than 580 patents, more than 30 commercial technologies, and 65 technologies that are projected to be commercialized within three to five years.[27]

With so much FCTO-supported activity in the last year, only a few accomplishments are highlighted in the summary that follows.

DOE and the U.S. Department of Interior's National Park Service officially opened a new hydrogen fueling demonstration station in Washington, D.C., on July 11, 2016. Acting Assistant Secretary David Friedman attended the official opening of the station, along with a range of dignitaries and partners from industry, including several key automakers. Though not a public station, advances demonstrated through this project will enable public retail stations of the future.

The July 11 event celebrated not only the opening of the hydrogen fueling demonstration station, but also the delivery of two of the world's first commercially available FCEVs to DOE and U.S. Department of Interior fleets—a Hyundai Tucson Fuel Cell and a Toyota Mirai. As part of DOE's technology validation efforts, the technology advances embodied in these vehicles are demonstrated under real-world conditions, and data is collected to further advance research and development. This collaboration between DOE and the Department of Interior will showcase cutting-edge hydrogen generation technology and provide an opportunity to demonstrate FCEVs at federal agencies and the surrounding region.

Also on July 11, sustainable transportation stakeholders came together to hear from distinguished transportation and mobility thought leaders, including the Secretary of Energy, as they shared their expertise and insights on Day 1 of the Energy Department's inaugural 2016 Sustainable Transportation Summit. Through a series of engaging keynotes and interactive plenary sessions, speakers focused on critical sustainable transportation topics, including deep decarbonization for U.S. transportation systems, consumer adoption of new vehicle technology, net-zero carbon fuels, and the future of mobility. Day 2 featured a panel on H2USA and another on H2@Scale.

In August 2011, the president of the United States challenged the private sector to hire 100,000 veterans and military spouses. The Joining Forces Initiative was created, a nationwide initiative calling all Americans to rally around service members, veterans, and their families. In April 2015, an event celebrated how far we have come and announced new private-sector commitments to train or hire 90,000 veterans and military spouses. At the event, two FCTO-supported companies were acknowledged for their commitment to these efforts: Air Liquide committed to making veterans 10% of their annual hires, and PDC Machines committed to making veterans or military spouses 8–10% of their workforce by 2020.

Across the country in October, scientists and engineers celebrated National Hydrogen and Fuel Cell Day. Aptly chosen to represent the atomic weight of hydrogen (1.008), National Hydrogen and Fuel Cell Day was celebrated for the first time on October 8, 2015, and this year EERE worked hard to keep the momentum going. Leading up to the big day, EERE celebrated with a number of events, including ride-and-drives, hydrogen station tours, informational presentations, and even a networking coffee hour at DOE. The week was also peppered with social media posts

[26] Fuel Cell Technologies Market Report, http://energy.gov/eere/fuelcells/downloads/2015-fuel-cell-technologies-market-report
[27] Pathways to Commercial Success, http://energy.gov/eere/fuelcells/market-analysis-reports#mkt_pathways

ranging from Tweets and Facebook posts to blogs and videos. In total, the hydrogen and fuel cell message was viewed over social media almost half a million times.

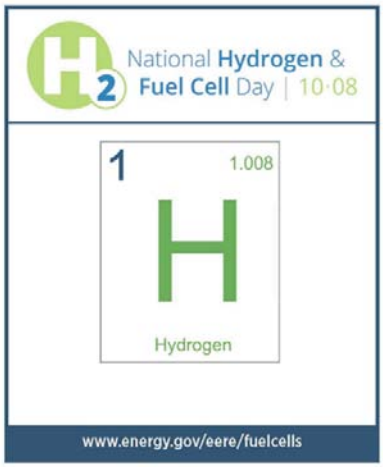

On September 12, 2016, FCTO released an RFI seeking feedback on the H2@Scale concept. Formed as part of an EERE Big Idea, H2@Scale is a concept that describes the potential of wide-scale renewable hydrogen production to enable the value of hydrogen across multiple sectors of the U.S. economy and dramatically reduce U.S. greenhouse gas emissions. Hydrogen is currently a feedstock for numerous industrial applications: petroleum refining, fertilizer production, biofuels production, and others (e.g., plastics, cosmetics, and food industries). Ten million metric tons of hydrogen are currently produced in the United States every year (95% of which is via centralized reforming of natural gas). Widespread use of technologies that are clean and/or renewable to produce hydrogen would be a paradigm shift that deeply decarbonizes current industries, along with emerging value-added applications, such as synthetic natural gas production or use of hydrogen in metals refining.

The Program also hosted an H2@Scale workshop on November 16–17, 2016, in Golden, Colorado, to identify the current barriers and research needs related to the H2@Scale concept. This workshop was meant to guide the development of a DOE roadmap on RD&D activities that can enable hydrogen as an energy carrier at a national scale. Proceedings from that workshop are now available.[28]

This is a critical time for fuel cells and hydrogen. The DOE Hydrogen and Fuel Cells Program will continue to work in close collaboration with key stakeholders and will continue its strong commitment to effective stewardship of taxpayer dollars in support of its mission to enable the energy, environmental, and economic security of the Nation. In support of these efforts, the following nearly 1,000 pages document the results and impacts of the Program in the last year.

Sunita Satyapal
Director
Fuel Cell Technologies Office
U.S. Department of Energy

[28] http://energy.gov/eere/fuelcells/downloads/h2-scale-workshop

II.0 Hydrogen Production Program Overview

INTRODUCTION

The Hydrogen Production program supports research and development (R&D) of technologies that will enable the long-term viability of hydrogen as an energy carrier for a diverse range of end-use applications including transportation (e.g., specialty vehicles, cars, trucks, and buses), stationary power (e.g., backup power and combined heat and power systems), and portable power (e.g., auxiliary power units). A portfolio of hydrogen production technology pathways utilizing a variety of renewable energy sources and renewable feedstocks is being developed under this program.

Multiple DOE offices are engaged in R&D relevant to hydrogen production:

- The Fuel Cell Technologies Office (FCTO), within the Office of Energy Efficiency and Renewable Energy (EERE), is developing technologies that include conversion of biomass-derived feedstocks, advanced water splitting (including high temperature/pressure operations and novel catalysts/membranes), direct solar water splitting (including thermochemical and photoelectrochemical processes), and biological processes.
- The Office of Science's Basic Energy Sciences (BES) program conducts research to expand the fundamental understanding of processes and mechanisms relevant to hydrogen production through photoelectrochemical water splitting, catalysis, membranes for gas separation, and biological and biomimetic processes.
- The Office of Nuclear Energy (NE) is currently collaborating with EERE on a study of nuclear–renewable hybrid energy systems, called Hydrogen at Scale (H2@Scale). Consistent with the vision of H2@Scale, many of the systems being evaluated by this study use hydrogen production as a form of energy storage or as an input to industrial processes.
- The Office of Fossil Energy (FE) is advancing the technologies needed to produce hydrogen from fossil fuel resources, including co-production of hydrogen and electricity and steam methane reformation. FE also continues to develop technologies for carbon capture, utilization, and storage, which could ultimately enable reduced emissions pathways for hydrogen production from fossil resources.

GOAL

The goal of this program is to develop low-cost, highly efficient hydrogen production technologies that utilize diverse domestic sources of energy, including renewable resources (EERE), nuclear power (NE), and fossil resources with carbon sequestration (FE).

OBJECTIVES

The objective of the Hydrogen Production program is to reduce the cost of renewable hydrogen dispensed at the pump to a cost that is competitive on a cents-per-mile basis with competing vehicle technologies. Based on current analysis, this translates to a hydrogen cost target of <$4/kg H_2 (produced, delivered, and dispensed, but untaxed) by 2020[1], with <$2/kg apportioned for production only[2]. Technologies are being developed to achieve this goal in timeframes appropriate to their current stages of development.

FISCAL YEAR (FY) 2016 TECHNOLOGY STATUS AND PROGRESS

Recent and current status for the high-volume projected costs of hydrogen production for several of the near- to mid-term production pathways are shown in Figure 1 below. The figure highlights the reduction in costs in recent years resulting from continued R&D. Natural gas reforming (without carbon capture) already meets the FCTO cost target of <$2/kg, but ongoing R&D is needed to accelerate development and reduce cost in all the renewable hydrogen production technology pathways for large-scale production in the mid to long terms.

[1] DOE Hydrogen and Fuel Cells Program Record #11007, Hydrogen Threshold Cost Calculation, 2012, http://www.hydrogen.energy.gov/pdfs/11007_h2_threshold_costs.pdf
[2] DOE Hydrogen and Fuel Cells Program Record #12001, Hydrogen Production and Delivery Cost Apportionment, 2012, http://hydrogen.energy.gov/pdfs/12001_h2_pd_cost_apportionment.pdf

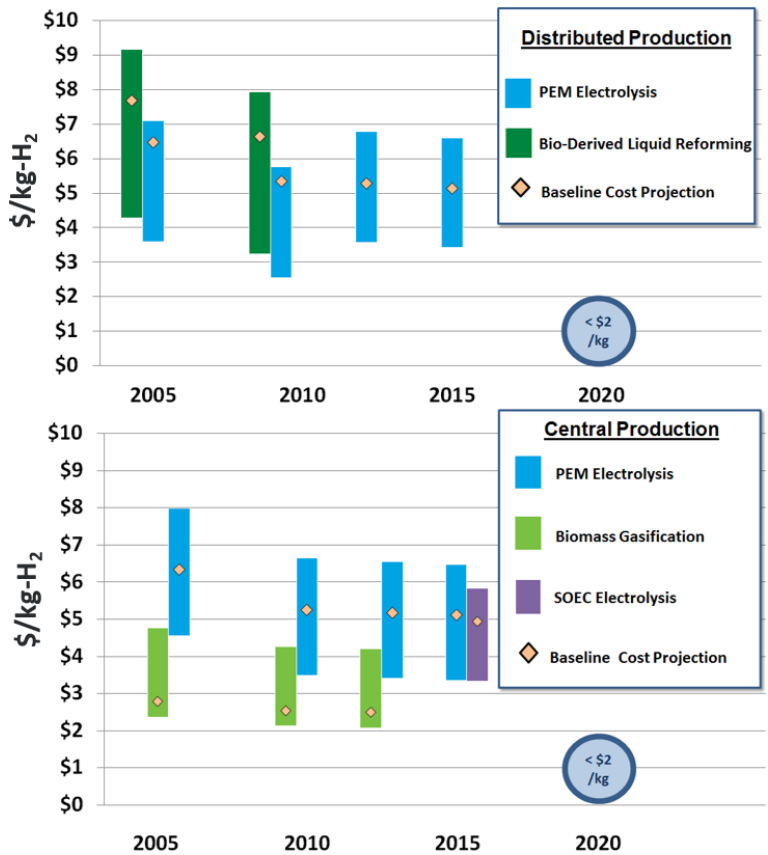

PEM – polymer electrolyte membrane; SOEC – solid oxide electrolysis cell

Figure 1. Range of hydrogen production costs, untaxed, for near- to mid-term distributed and centralized pathways. The high end of each bar represents a pathway-specific high feedstock cost as well as an escalation of capital cost, while the low end reflects a low end on feedstock cost and no capital escalation. Bars for different years in the same pathway represent improvements in the costs of the specific pathway based on specific reference data for the appropriate year and pathway. Detailed information is included in the DOE Hydrogen and Fuel Cells Program Records #14005[3] and #16014[4].

Program-Level Accomplishments

In FY 2016, significant progress was made by the Hydrogen Production program on several important fronts.

- A workshop was held in April 2016 to engage stakeholders in advanced water splitting materials and share information on electrochemical, photoelectrochemical (PEC), and solar thermochemical pathways for producing hydrogen using renewable energy sources. A workshop web page was launched, including the workshop presentation materials.
- The HydroGEN advanced water splitting materials consortium was launched as part of DOE's Energy Materials Network to accelerate materials discovery and development of critical to advanced water splitting technologies for renewable hydrogen production. HydroGEN has begun work to identify technical and analytical resources available at the national laboratories to support state-of-the-art renewable hydrogen production research. HydroGEN is also developing a website to provide public information on the expertise and capabilities that will be available through collaboration with the HydroGEN consortium.

[3] DOE Hydrogen and Fuel Cells Program Record #14005, Hydrogen Production Status 2006-2013, 2014, https://www.hydrogen.energy.gov/pdfs/14005_hydrogen_production_status_2006-2013.pdf
[4] DOE Hydrogen and Fuel Cells Program Record #16014, Hydrogen Production Cost from Solid Oxide Electrolysis , 2016, https://www.hydrogen.energy.gov/pdfs/16014_h2_production_cost_solid_oxide_electrolysis.pdf

- Several FCTO-funded projects made significant achievements, including advances in low-carbon hydrogen production from bio-feedstocks; progress in advanced electrolysis technologies for alkaline exchange membrane and solid oxide-based electrolyzers; and progress on PEC and solar-thermochemical hydrogen (STCH) production goals as well as innovative materials research to advance PEC and STCH pathways (all described in further detail below).

Project-Level Accomplishments

During FY 2016, progress was made by existing projects in several key areas.

New Project Selections

In FY 2016, FCTO released one Funding Opportunity Announcement (FOA) to support R&D efforts to address critical challenges and barriers to hydrogen production and delivery technology development and, specifically, the long-term goal of hydrogen production at <$2/kg H_2. Innovative materials, processes, and systems are needed to establish the technical and cost feasibility for renewable and low-carbon hydrogen production and delivery. Specifically, the FOA sought research on materials improvements for increased durability and efficiency in high temperature electrolysis.

Three electrolysis projects were selected in FY 2016 under the Production portfolio and will begin work in early FY 2017:

- Giner Inc., Newton, Massachusetts, will work to develop high-temperature molten hydroxide alkaline water electrolyzers with improved electrical efficiency at a reduced cost.
- Ceramatec Inc., Salt Lake City, Utah, will aim to improve the performance of durable materials for high-temperature water splitting by developing a novel stack technology.
- FuelCell Energy, Inc., Danbury, Connecticut, will demonstrate a highly efficient solid oxide electrolysis cell (SOEC) system with a goal of producing hydrogen at a cost of $2/kg.

Additionally, one analysis project was awarded in FY 2016 and will begin work in FY 2017:

- Strategic Analysis Inc., Arlington, Virginia, will perform detailed cost analyses for hydrogen production and delivery technologies to assess the potential of each pathway to meet the DOE hydrogen cost goal of <$4/kg H_2 by 2020 and identify critical barriers for the given technologies.

Hydrogen Production Pathway Analysis

Case studies of hydrogen production costs for both a monolithic piston-type bio-oil reformation reactor and a reformer–electrolyzer–purifier system are nearing completion using the H2A v3 tool, and selected results from these studies will be made publically available. In these studies, industrial-scale systems were modeled based on input from the key researchers involved in the projects developing these technologies. The technoeconomic case study process included soliciting relevant, detailed information from research institutions followed by synthesizing and amalgamating the data into base cases with sensitivity analysis using baseline parameters and sensitivity limits that were vetted by the industry collaborators. (Strategic Analysis, Inc., National Renewable Energy Laboratory [NREL], Argonne National Laboratory).

Electrolytic Hydrogen Production

The major emphases of the electrolysis projects were on cost and greenhouse gas emission reduction by improving cell and stack efficiency and durability. Technical progress included the following:

- Developed a new solid oxide electrolysis cell and stack capable of ultra-high-current operation. Demonstrated an SOEC short stack operating at a current density of 3 A/cm^2 at less than 1.6 V and developed the preliminary ultra-high-current-density SOEC system conceptual design. (Versa Power Systems)
- Operated an alkaline exchange membrane (AEM)-based electrolysis cell with precious-group-metal-free anode and cathode at less than 2 V at 500 mA/cm^2. This is one of the first known demonstrations of an AEM electrolyzer membrane electrode assembly operating with no precious group metal content. (Proton Onsite)

Photoelectrochemical Hydrogen Production

The main focus of projects in this area was on using state-of-the-art theory, synthesis, and characterization tools to develop viable PEC material systems and prototypes with improved efficiency and durability. Technical progress included the following:

- A world-record efficiency of greater than 16% was demonstrated for III-V semiconductor PEC tandem devices. This was enabled through the use of an inverted metamorphic multijunction, which dramatically reduced voltage losses at interfaces. This result represents an important step forward toward demonstration of solar-to-hydrogen conversion efficiencies >20% using PEC devices. (NREL)
- Photoactive $CuInGaS_2$ with controlled composition and tunable bandgap in the 1.5–2.4 eV range was successfully fabricated. Photocurrents of over 10 mA/cm^2 were achieved, and new protective coatings were applied to increase durability. (University of Hawaii)
- A model developed for particle-based, tandem PEC reactors showed that a 1% solar-to-hydrogen efficiency is possible for over 200 days without mechanical agitation. This accomplishment, combined with technoeconomic analysis, provides an important foundation for experimental work on particle-based PEC devices. (University of California, Irvine)

Thermochemical Bio-Feedstock Conversion Production

The technical focus of projects in this area was on using thermochemical methods to produce hydrogen from biomass-derived and other feedstocks. Technical progress included the following:

- Using commercial molten carbonate fuel cell components in electrolyzer mode, reformer–electrolyzer–purifier technology was successfully demonstrated at the 100 kg H_2/d scale using natural gas as the representative feedstock. Cell performance with greater than 30% increase in hydrogen production and greater than 20% increase in hydrogen purity was achieved through implementation of the electrolysis step (compared to the base process without the electrolysis step). (FuelCell Energy, Inc.)
- An active and novel catalyst system for the steam reforming of bio-oil with periodic regeneration by combustion was demonstrated, and a new flow distributor design that successfully distributes bio-oil evenly into the monolith catalyst channels under reaction conditions was developed. (Pacific Northwest National Laboratory)

Biological Hydrogen Production

The focus of the projects in the biological hydrogen production portfolio was on biological methods to produce hydrogen from biomass resources and addressing key barriers such as low hydrogen production rates and yields as well as feedstock utilization using molecular biology and genetic engineering techniques along with improved systems engineering. Technical progress included the following:

- Successfully deleted two metabolic pathways that compete with hydrogen production, resulting in a higher specific rate of hydrogen production. (NREL)
- Doubled the volumetric productivity of in vitro enzymatic hydrogen production from starch to a peak rate of 320 mmol H_2/L/h. (Virginia Polytechnic Institute and State University)
- Identified fermentative bacterial cultures capable of producing hydrogen from major sugars in lignocellulosic biomass hydrolysate at a hydrogen yield reaching 40% of the theoretical maximum, and an exoelectrogenic bacterial culture capable of utilizing all liquid fermentation products and generating a current density up to 15 A/m^2 of anode surface area. (Ohio State University)

Solar-Thermochemical Hydrogen Production

Efforts in these projects were directed toward performance characterization of water splitting by novel, non-volatile metal-oxide based reaction materials and development of new reactor concepts to optimize efficiency of the reaction cycles as well as advancing the electrolytic step of the hybrid sulfur thermochemical cycle. Technical progress included the following:

- A prototype 3 kW cascading pressure reactor/receiver was designed, and the approach to materials discovery and engineering of thermochemical properties was extended such that greater than 50 new compounds have been synthesized and characterized. (Sandia National Laboratories)
- Successful collaboration between the National Science Foundation (NSF) and DOE accelerated materials discovery and characterization with 955 binary spinal structures and 1,343 binary perovskite materials screened for solarthermal water splitting potential. Eight materials have been synthesized for experimental validation. (University of Colorado Boulder)
- Trade-off studies were completed that resulted in a baseline design that permits continuous hydrogen production at high thermal efficiency and demonstrates potential to meet DOE hydrogen cost goals. Detailed flowsheets were designed and modeled in Aspen Plus™ for both 2015 and 2020 plant design cases. (Savannah River National Laboratory)

BUDGET

The FY 2016 appropriation for the Hydrogen Production and Delivery programs was $25.4 million. Funding was distributed approximately evenly between Production and Delivery, with Production allocated $13.6 million and Delivery allocated $11.9 million. This split reflects the priority to maintain a balanced R&D portfolio focused both on near- and longer-term technology options. The request for Production and Delivery in FY 2017 is $28.1 million, with $17.1 million slated for Production projects. The estimated budget breakdown for Production funding in FY 2016 and FY 2017 is shown in Figure 2.

With the near-term emphasis on forecourt stations and infrastructure in the Delivery portfolio, and with natural gas reforming a viable option for supplying near-term hydrogen demands, the Production R&D portfolio has increasingly focused on mid- to longer-term, renewable pathways such as advanced conversion of bio-derived feedstocks, advanced electrolysis, and direct water-splitting through PEC and STCH processes. Previous projects

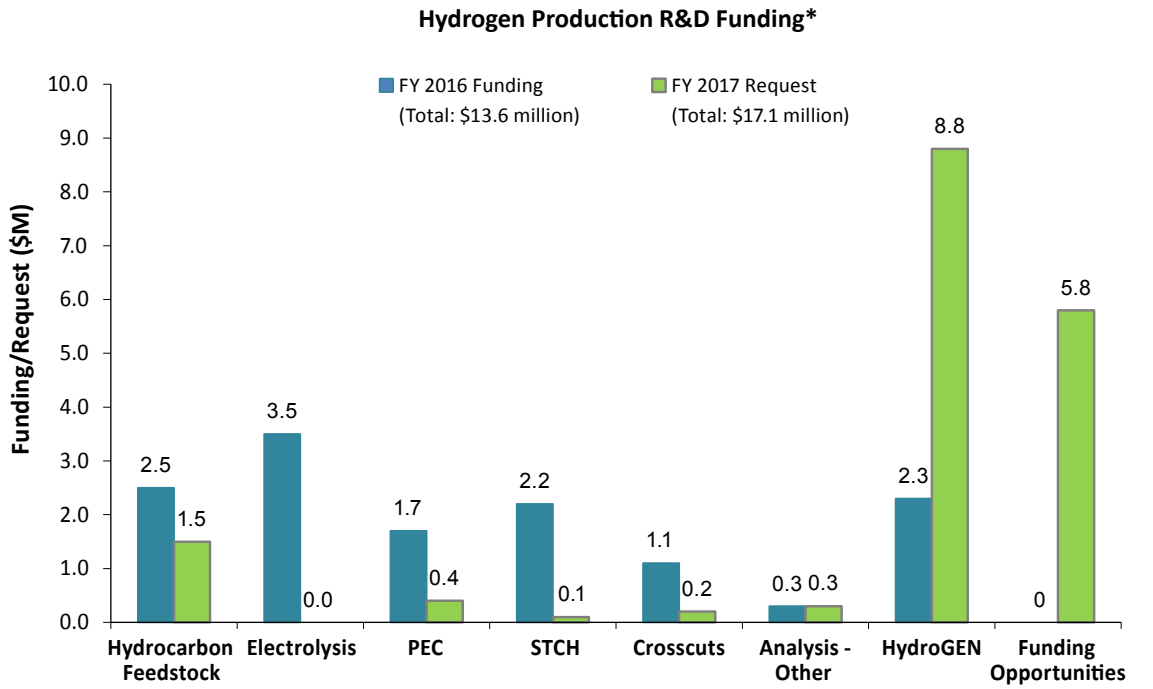

Subject to appropriations, project go/no-go decisions, and competitive selections. Exact amounts will be determined based on research and development progress in each area.

FIGURE 2. Budget breakdown for FY 2016 through FY 2017

scheduled for completion within the next two years include FY 2014 FOA projects in areas of bio-derived feedstock conversion and PEC and STCH water splitting, four joint NSF/FCTO projects in solar water splitting, and five incubator projects in topics including advanced electrolysis and reversible fuel cells. Moving forward into FY 2017, the Production and Delivery emphasis on renewable technologies is expected to ramp up with the establishment of the HydroGEN consortium, part of the DOE Energy Materials Network, to accelerate the discovery and development of innovative materials for enabling commercial-scale renewable hydrogen production through electrochemical, photoelectrochemical, and thermochemical water-splitting processes.

FY 2017 PLANS

General Hydrogen Production program plans for FY 2017 include the following:

- Initiate projects selected in the FY 2016 FOA.
- Continue to demonstrate substantial progress in the six Production projects selected in the FY 2014 FOA, the five projects selected under the 2015 Incubator FOA, and the four advanced water-splitting projects selected under the FY 2014 NSF/FCTO joint solicitation.
- Continue emphasis on materials durability, production efficiency, and process optimization for all pathways, and develop and refine materials characterization protocols and performance metrics for early development technologies.
- Assess the sustainability of incumbent hydrogen production technologies (e.g., steam methane reforming and carbon sequestration), as well as renewable alternatives. Baselines will be developed through collaboration with industry and reviews of existing literature, including H2A case studies and life-cycle analyses.
- Continue collaboration with the NSF, the DOE Office of Science's BES program, and the DOE Advanced Research Projects Agency-Energy.
- Ramp up research efforts centered on the HydroGEN consortium on advanced water-splitting technologies, including enhancement of core capabilities in materials–device and system-level development for advancing the technology readiness level in technologies including advanced low-temperature electrolysis, advanced high-temperature electrolysis, as well as direct PEC and STCH water splitting.

Important pathway-specific milestones planned for FY 2017 in the Hydrogen Production program projects include the following:

- Demonstrate >500 h of hydrogen production from bio-derived liquids with in situ CO_2 capture and >90% pure H_2.
- Design a megawatt-scale STCH production plant for 100,000 kg/d, and show, through modeled performance analysis, the capability to meet the $2/kg cost target.
- Develop photovoltaic-grade, wide-bandgap, thin-film absorbers with PEC solar photocurrent densities ≥13 mA/cm^2 to enable >16% solar-to-hydrogen conversion efficiency.

Eric Miller
Hydrogen Production & Delivery Program Manager
Fuel Cell Technologies Office
Office of Energy Efficiency and Renewable Energy
U.S. Department of Energy
1000 Independence Ave., SW
Washington, DC 20585-0121
Phone: (202) 287-5829
Email: Eric.Miller@ee.doe.gov

II.A.1 Hydrogen Pathways Analysis for H_2 Production via a Monolithic Piston Reforming Reactor and Reformer-Electrolyzer-Purifier Technology

Brian D. James (Primary Contact),
Daniel A. DeSantis, Jennie M. Moton,
Cassidy Houchins
Strategic Analysis, Inc. (SA)
4075 Wilson Blvd., Suite 200
Arlington, VA 22203
Phone: (703) 778-7114
Email: bjames@sainc.com

DOE Manager: Katie Randolph
Phone: (720) 356-1759
Email: Katie.Randolph@ee.doe.gov

Contract Number: DE-EE0006231

Project Start Date: March 15, 2013
Project End Date: September 30, 2016

Overall Objectives

The objectives of this project are to:

- Analyze hydrogen production and delivery (P&D) pathways to determine the most economical, environmentally-benign, and societally-feasible paths for the P&D of hydrogen fuel for fuel cell vehicles.
- Identify key technical and economic barriers to the success of these pathways, primary cost drivers, and remaining research and development challenges.
- Assess technical progress, benefits and limitations, levelized hydrogen costs, and potential to meet U.S. Department of Energy (DOE) P&D cost goals of <$4 per gasoline gallon equivalent (gge) (dispensed, untaxed) by 2020.
- Provide analyses that assist DOE in setting research priorities.
- Apply the H2A Production Model as the primary analysis tool for projection of levelized hydrogen costs (U.S. dollars per kilogram of H_2 [$/kg H_2]) and cost sensitivities.

Fiscal Year (FY) 2016 Objectives

In 2015–2016, these overall project objectives were applied to:

- Complete documentation for high temperature solid oxide electrolysis cell and dark fermentation of bio feedstocks.
- Develop hydrogen pathway case studies for hydrogen generation via:
  - Pacific Northwest National Laboratory's (PNNL's) Monolithic Piston-Type Reactor for hydrogen production.
  - Fuel Cell Energy Inc.'s (FCE) Reformer-Electrolyzer-Purifier (REP) electrolyzer technology.

Technical Barriers

This project addresses the following technical barriers from the Hydrogen Production section of the Fuel Cell Technologies Office Multi-Year Research, Development, and Demonstration Plan.

Hydrogen Generation by Water Electrolysis

(F) Capital Cost

(G) System Efficiency and Electricity Cost

(K) Manufacturing

Reformer-Electrolyzer-Purifier

(F) Capital Cost

(G) System Efficiency and Electricity Cost

(K) Manufacturing

Fermentative Hydrogen Production

(AX) Hydrogen Molar Yield

(AY) Feedstock Costs

(AZ) Systems Engineering

Monolithic Piston Reforming of Bio-oil to Hydrogen

(AX) Hydrogen Molar Yield

(AY) Feedstock Costs

(AZ) Systems Engineering

Technical Targets

This project conducts cost modeling to attain realistic cost estimates for the production and delivery of hydrogen fuel for fuel cell vehicles. These values can help inform future technical targets.

- DOE P&D cost goals < $4/gge of H_2 (dispensed, untaxed) by 2020

FY 2016 Accomplishments

- A no-cost extension was granted to SA by DOE.
- Finalized documentation for hydrogen production via dark fermentation of corn stover.
  - H2A cases and DOE record are to be published upon final approval of DOE.
- Finalized documentation for hydrogen production via high temperature solid oxide electrolysis cell.
  - H2A cases and DOE record were published online after receiving approval from DOE.
- Initiated case studies for hydrogen production via the Monolithic Piston-Type Reactor.
  - Initial design completed using generic bio-oil feedstock.
  - Defined reactors and estimated cost using Design for Manufacturing and Assembly methodology commonly used by Strategic Analysis Inc.
  - Completed ASPEN Hysys® simulations to verify all stream properties and production capacity.
    - Several system components are sized according to the production capacity, including heat exchangers and pumps.
  - Pyrolysis oil is selected as the preferred feedstock based on PNNL recommendation.
    - Pyrolysis oil is modeled on a synthesis of H2A default values and data from recent National Renewable Energy Laboratory (NREL) reports.
    - Models are to be updated as information is provided by NREL.
  - Created a future case H2A model for the process.
    - The project is assessed at a low technology readiness level (TRL), and a current case analysis is not appropriate at this time.
    - Conducted a sensitivity analysis.
    - Preliminary cost estimate is \$3.69/kg for H_2 production from pyrolysis oil.
- Initiated case studies for H_2 production via FCE's REP technology.
  - Received process data from FCE.
    - Utilized FCE inputs as a comparison point. All FCE inputs (capital cost, fuel usage, electrical inputs, and water usage) were put into H2A with SA's "standard" indirect and replacement costs.
    - Examined both an Integrated Configuration (FCE plus REP) and Standalone Configuration (REP alone).
  - Completed ASPEN Hysys® simulations of REP to identify reactant and product stream thermodynamic properties which were used to appropriately size system components and provide input values for the H2A cases.
  - Preliminary results suggest \$1.77/kg H_2 and \$2.51/kg H_2 for the integrated and standalone REP systems, respectively. Results are similar to past FCE published costs.

✧ ✧ ✧ ✧ ✧

INTRODUCTION

This report reflects work conducted in the third year of a three-year project to analyze innovative hydrogen production and delivery pathways and their potential to meet the DOE hydrogen P&D cost goal of <\$4/gge by 2020. Work in the first year of the project concentrated on hydrogen production from proton exchange membrane electrolysis. Work in the second year focused on solid oxide electrolysis cell technology and dark fermentation. Work in the third year has focused on hydrogen production from the monolithic piston-type project being researched by PNNL and the Reformer-Electrolyzer-Purification work developed by Fuel Cell Energy, Inc. The analysis methodology utilizes DOE's H2A distributed and central hydrogen production models.[1] Those models provide a transparent modeling framework and apply standard mass, energy, and economic analysis methods agreed upon by DOE's hydrogen and fuel cell technology teams.

APPROACH

The following steps summarize the analysis methodology applied to each of the hydrogen production pathways examined in the project.

- Conduct literature review.
- Develop, circulate, and analyze results from an industry survey covering the targeted technology.
- Define generalized cases for systems of different sizes and TRLs.
- Run H2A models with general case input data to calculate the levelized cost of hydrogen (\$/kg H_2).
- Perform sensitivity analyses (including tornado and waterfall charts) to identify key cost drivers.
- Document case study results.
- Vet case study results with DOE, industry, and team partners.
- Repeat these steps until agreement attained among project partners.

[1] http://www.hydrogen.energy.gov/h2a_analysis.html

Specific Approach to Monolithic Piston System

Initial system designs were developed from the published 2015 U.S. Department of Energy Hydrogen and Fuel Cells Program Annual Merit Review (AMR) documentation delivered by the PNNL principle investigator [2]. All system designs were based on a forecourt model with a target production of 1,500 kg H_2/d. The monolithic piston plant was considered at only a future technological development time horizon due to its assessed low TRL (as determined by SA and NREL). The future case represents a 2025 technology year with system manufacturing and design maturity.

System designs were simulated in both Excel and ASPEN Hysys®. The system is primarily a two-bed, cyclic reactor which toggles between steam-oil reforming and catalyst regeneration mode. Figure 1 shows a partial schematic of the system, with one reactor operating in reformer mode and the other in regeneration mode. The chemical reforming process consists of the oil feedstock and steam being supplied at approximately 300°C and 24 bar to a reactor which contains a TiO_2 monolith that is coated with a non-precious metal catalyst. The steam-oil reaction that occurs produces H_2, CO_2, and a coking compound. The reactor monolith also contains a composite sorbent primarily made of dolomite that captures the CO_2 upon production. It is assumed that approximately 90% of the CO_2 is captured in the process. The coke produced deposits on the reactor internals. The reactor exhaust is a relatively pure stream (~97%) of H_2 with some CO_2, unreacted oil, and steam. The exhaust gas stream passes through several heat exchangers and a condensation tank in which the unreacted oil and steam condense and can be recovered and recycled. The gas is passed onto a pressure swing adsorption column for further purification.

After 10 minutes of reforming, the flow of oil and steam is stopped. Air is then passed through the reactor, burning the deposited coke, regenerating the reactor. The heat produced during this regeneration process provides heat to the reactor and the reactor internals. At the end of the regeneration reaction, the reactor internals are expected to be at 700°C. After 10 minutes of regeneration, air flow is stopped and the reactor returns to reforming mode. When the next reforming reaction occurs in the recently regenerated reactor, the reactor has an internal temperature of 700°C, which provides sufficient heat to complete the 10 minute cycle of reforming. To minimize downtime and maintain flow of H_2 out of the system, two reactors are proposed operating out of sync is proposed, so that one reactor is reforming while the other is regenerating.

Data from the reforming and regeneration simulations were used to size the equipment. Quotes were solicited for equipment and the reactor prices were generated by Design for Manufacturing and Assemblymethods. The capital costs were incorporated into an H2A analysis. H2A results were further supplemented with a sensitivity analysis in order to identify the primary cost identifiers.

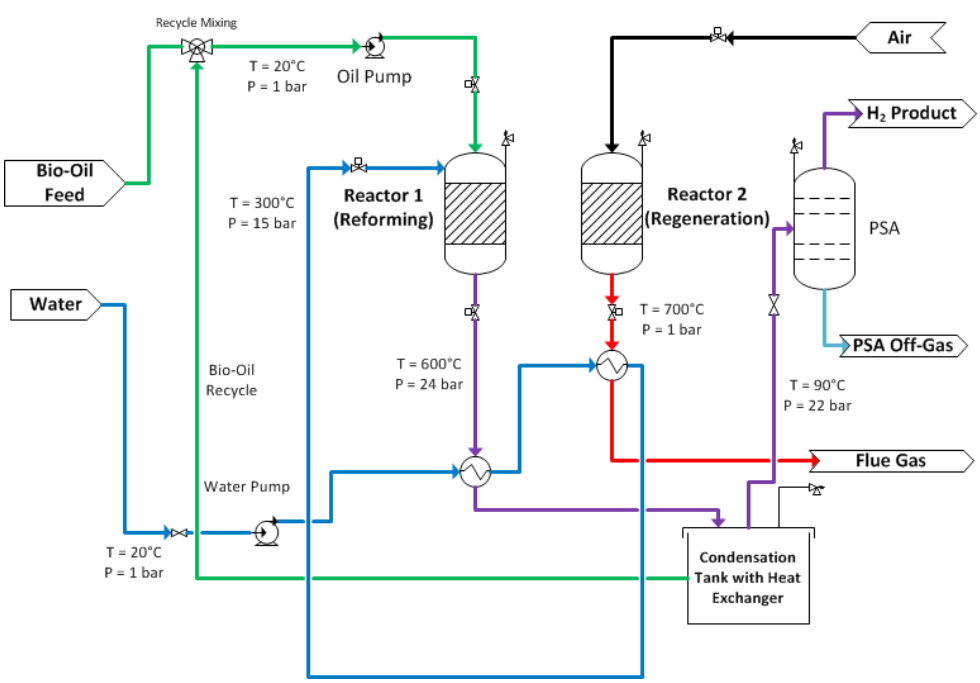

FIGURE 1. Partial system diagram for monolithic piston-type reforming project. Process flow diagram shows Reactor 1 in reforming mode and Reactor 2 in regeneration mode. For simplicity and clarity of operation, not all system connections are shown.

Specific Approach to Reformer-Electrolyzer-Purifier

Initial system designs were developed from the published 2015 AMR documentation [1] and additional input from FCE. All system designs were based on a forecourt model with a target production of 1,500 kg H_2/d. SA assesses the TRL of this project as very high because the technology in question is essentially the same as Fuel Cell Energy's molten carbonate fuel cell which is already in production. Further, FCE has demonstrated pilot scale systems operating in REP mode. As such, a current case analysis has been conducted for forecourt operation. Two system designs were analyzed:

- Standalone Configuration: Natural gas is fed to a reformer in two streams. One stream is fed to a combustion system which provides heating for the system. The other stream is mixed with water and heated by the combustion chamber, converting some of the methane into H_2 and CO_2. The pre-reformed gas enters the REP unit, which further reforms the gas. The CO_2 in the gas then reacts with steam at the anode to form CO_3 that is transported across the molten carbonate electrolyte leaving a purified stream of H_2 on the anode. This process is the same operation as a standard molten carbonate fuel cell, but run in electrolyzer mode and therefore requires an electrical input as opposed to producing electricity. The H_2 is then sent to a pressure swing adsorption unit for further purification to reach fuel cell vehicle requirements.
- Integrated Configuration: This system utilizes existing Fuel Cell Energy's molten carbonate direct fuel cell (DFC). A surplus of natural gas is fed to a commercial DFC. The surplus fuel (approximately 15% of the feed) is reformed within the reforming section of the DFC but is pulled from the system before reaching the fuel cell anode. The removed fuel is heated, passed through an external reformer to further convert any remaining natural gas into H_2 and CO_2, and fed to an REP unit. The REP unit then finishes any reforming of the natural gas and purifies the gas by removing CO_2 from the stream. Electrical energy for the REP unit can be supplied from the DFC. The purified H_2 is sent to a pressure swing adsorption unit to create an ultra-pure H_2 stream suitable for alternative fuel vehicles.

RESULTS

Monolithic Piston System Cost Results: Current H2A analysis is still ongoing, but preliminary results indicate hydrogen production costs from a pyrolysis oil feedstock are approximately \$3.69/kg H_2. Figure 2 details the cost breakdown. Cost drivers are, predictably, the feedstock and capital cost. Figure 3 identifies the sensitivity of the cost drivers, providing a potential range of prices from \$3.21–\$4.17/kg H_2.

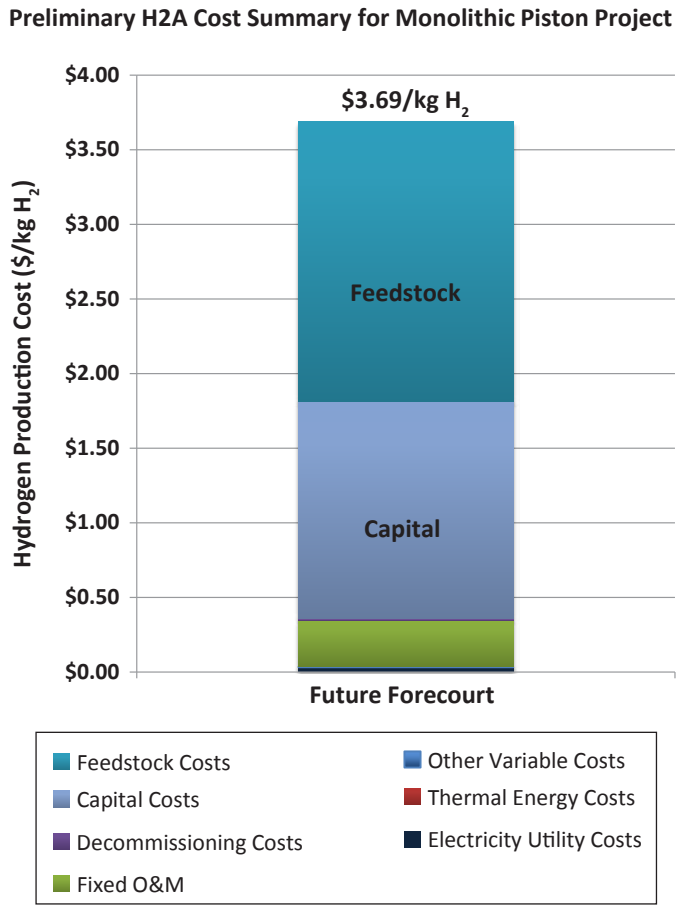

O&M – Operating and maintenance

FIGURE 2. Preliminary H2A cost summary for piston-type reforming reactor with pyrolysis oil feedstock

While pyrolysis oil is the targeted and experimentally demonstrated fuel, a side analysis was conducted using soybean oil as the feedstock to assess the hydrogen cost from a currently available commodity bio-oil with high specific energy. Comparatively, the specific energy of soybean oil (~37 MJ/kg) [3] is approximately double the specific energy of pyrolysis oil (~17 MJ/kg) [4] but costs a factor of 2.5 more (\$0.66/kg oil[2] compared to \$0.245/kg oil [4] for pyrolysis oil). The estimated hydrogen cost from soybean oil is \$4.07/kg H_2 using the monolithic oil reforming process described above.

REP System Cost Results: A preliminary current forecourt H2A analysis of the REP systems was conducted based on inputs from FCE for fuel feedstock, energy usage, water usage, and maintenance costs. To the extent possible, SA independently validated these values and augmented then with standard H2A analysis assumptions to estimate hydrogen cost. Preliminary hydrogen production for the integrated REP system and standalone REP

[2] Price reflects soybean commodities price index between January and February of 2016.

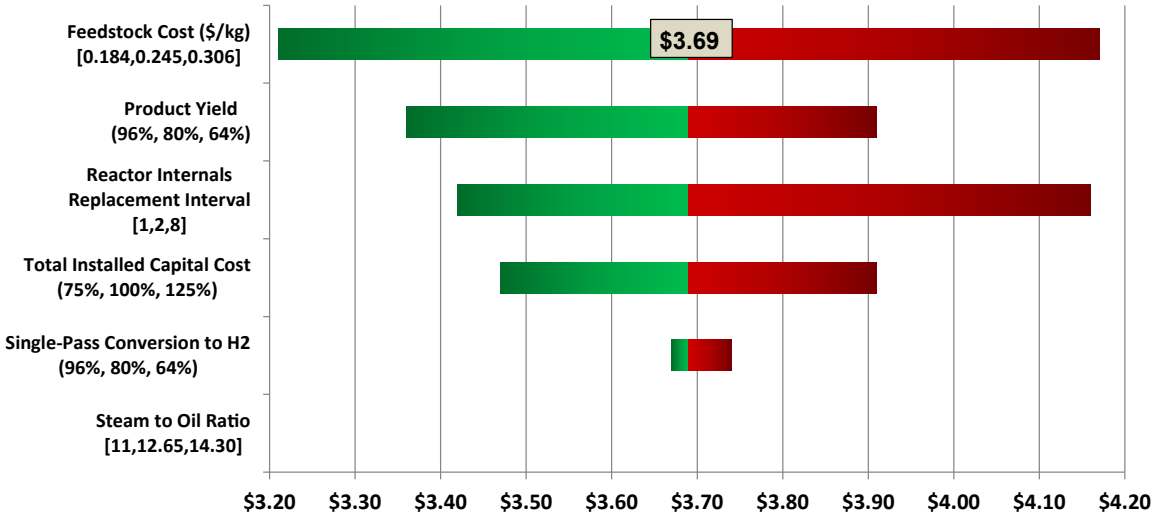

FIGURE 3. Tornado chart for hydrogen production via piston-type reforming reactor with pyrolysis oil feedstock. Replacement of reactor internals encompasses replacement of the monolith, catalyst, and sorbent in the reactor.

system are $1.77/kg ($3.92/kg delivered) and $2.51/kg ($4.58/kg delivered), respectively. These results are in general alignment with published cost results released by FCE. Additionally analysis is planned to further vet assumptions and finalize the cost projections.

CONCLUSIONS AND FUTURE DIRECTIONS

In its third year, this project made key observations and important achievements.

- Representative pathway analysis cases were completed for H_2 generation via the Monolithic Piston System and FCE's REP technology.
- Costs were estimated for the Monolith Piston System with a feedstock of pyrolysis oil.

FY 2016 PUBLICATIONS/PRESENTATIONS

Presentations

1. Cassidy Houchins, Brian James, and Daniel DeSantis. "Techno-Economic Analysis: Assessing Progress of Emerging Technologies towards Meeting Cost and Performance Targets." 2016. Presentation. 3/7/2016, Solar Fuels Workshop, University of Delaware.

2. Brian James, Cassidy Houchins, and Daniel DeSantis. "Techno-Economic Analysis: Water Splitting Technologies and Metrics." 2016, Presentation. 4/14/2016, Water Splitting Workshop, Stanford University.

3. Brian James, Cassidy Houchins, Genevieve Saur, Jennie M. Huya-Kouadio, and Daniel DeSantis. "Analysis of Advanced H2 Production Pathways." 2016. Presentation. 6/8/2016, AMR, Washington, D.C.

REFERENCES

1. Jahnke, F. "Reformer-Electrolyzer-Purifier (REP) for production of Hydrogen." in *AMR* (2015).

2. Liu, W., "Monolithic Piston-Type Reactor for Hydrogen Production through Rapid Swing of Reforming/Combustion Reactions." in *AMR* (2015).

3. Patzek, T.W., "A First Law Thermodynamic Analysis of Biodiesel Production From Soybean." *Bull. Sci. Technol. Soc.* **29,** 194–204 (2009).

4. Ringer, M., Putsche, V. & Scahill, J., "Large-Scale Pyrolysis Oil Production: A Technology Assessment and Economic Analysis." *NREL/Tp-510-37779* 1–93 (2006). doi:10.2172/894989

II.B.1 Renewable Electrolysis Integrated Systems Development and Testing

Mike Peters (Primary Contact), Kevin Harrison, Huyen Dinh
National Renewable Energy Laboratory (NREL)
15013 Denver West Parkway
Golden, CO 80401-3305
Phone: (303) 524-0864
Email: Michael.Peters@nrel.gov

DOE Manager: Dave Peterson
Phone: (720) 356-1747
Email: david.peterson@ee.doe.gov

Subcontractor:
Spectrum Automation Controls, Arvada, CO

Project Start Date: October 1, 2003
Project End Date: Project continuation and direction determined annually by DOE

Overall Objectives

- Collaborate with industry to research, develop, and demonstrate improved integration opportunities for renewable electrolysis systems for energy storage, vehicle refueling, grid support and industrial gas end uses.
- Design, develop, and test advanced experimental and analytical methods to validate electrolyzer stack and system efficiency; including contributions of sub-system losses (e.g., power conversion, drying, electrochemical compression, water pumps) of advanced electrolysis systems.

Fiscal Year (FY) 2016 Objectives

- Test NREL's variable flow drying technique on large active area polymer electrolyte membrane (PEM) stacks.
- Continue long-duration testing on the three 10 kW PEM stacks from Proton OnSite, comparing decay rates of variable operation versus constant powered operation.
- Create a design package for an electrolyzer that is operated entirely on direct current (DC) enabling easy coupling with renewable electricity sources.

Technical Barriers

This project addresses the following technical barriers from the Hydrogen Production section (3.1.5) of the Fuel Cell Technologies Office Multi-Year Research, Development and Demonstration Plan.

(G) System Efficiency and Electricity Cost

(J) Renewable Electricity Generation Integration (for central production)

(M) Control and Safety

Technical Targets

This project is conducting applied research, development, and demonstration to reduce the cost of hydrogen production via renewable electrolysis for both distributed and central production pathways to help meet the following DOE hydrogen production and delivery targets found in the Fuel Cell Technologies Office Multi-Year Research, Development and Demonstration Plan.

Technical Targets: Central Water Electrolysis using Green Electricity (Table 3.1.5)

- Stack efficiency:
  - 44 kWh/kg H_2 (76% LHV, lower heating value) by 2015
    - NREL validated Giner PEM stack efficiency in 2013 to be 73.6% (LHV) at 15,00 mA/cm^2, 80°C, 390 psig
  - 43 kWh/kg H_2 (78% LHV) by 2020
- System efficiency:
  - 46 kWh/kg H_2 (73% LHV) by 2015
  - 44.7 kWh/kg H_2 (75% LHV) by 2020
- By 2015 reduce the cost of central production of hydrogen from water electrolysis using renewable power to $3.00/gge at plant gate. By 2020, reduce the cost of central production of hydrogen from water electrolysis using renewable power to ≤$2.00/gge at plant gate.

FY 2016 Accomplishments

- NREL demonstrated 2.5% hydrogen savings using their variable drying technique compared to typical fixed orifice drying.
- Stack failure led NREL to prematurely finalize long-duration testing of three 10 kW PEM stacks inside a Proton H-Series Electrolyzer.

- NREL identified balance of plant differences in a typical electrolyzer versus an electrolyzer that runs entirely on DC power.
- NREL continued to report on system and stack failures.

✧ ✧ ✧ ✧ ✧

INTRODUCTION

The capital cost of commercially available water electrolyzer systems, along with the high cost of electricity in many regions, limits widespread adoption of electrolysis technology to deliver low cost hydrogen. PEM electrolyzer manufacturers have scaled up their systems into the megawatt range to improve system energy efficiency and capital cost. Along with capital cost reductions and efficiency improvements, low temperature electrolyzers are beginning to be deployed at utility-scale and are capable of advanced grid integration functionality as well as integrated into networks containing high penetration of renewable electricity sources. An integrated system with advanced sensing and communications will enable grid operators to take advantage of the controllable nature and fast response of distributed and central water electrolysis systems to maintain grid stability. Electrolytic production of hydrogen, where fossil fuels are the primary electricity source, will not lead to significant carbon emission reduction without carbon sequestration technologies.

Renewable electrolysis is inherently distributed, but large-scale wind and solar installations are being planned to take advantage of economies of scale and achieve system-level energy efficiencies less than 60 kWh per kilogram. Renewable electricity sources, such as wind and solar, can be closely, and in some cases directly, coupled to the hydrogen-producing stacks of electrolyzers to reduce energy conversion losses and capital costs investment of this near-zero-carbon pathway.

APPROACH

Results and insights gained from this research, development, and demonstration project aim to benefit the hydrogen-based industry and relevant stakeholders as the market for this hydrogen production equipment expands. Results from the project have demonstrated opportunities to improve efficiency and capital cost of an integrated renewably coupled electrolysis system.

The research now being conducted at NREL's Energy Systems Integration Facility is advancing the integration of renewable electricity sources with state-of-the-art electrolyzer technology. Real-world data from daily operations are demonstrating opportunities for improved system design and novel hardware configurations to advance the commercialization of this technology. Lessons learned and data-driven results provide feedback to industry and to the analytical components of this project. Finally, this project provides independent testing and verification of the technical readiness of advanced electrolyzer systems by operating them from the grid and renewable electricity sources.

RESULTS

Long-Duration Testing

NREL completed side-by-side testing and comparison of stack voltage decay rates between constant and variable power operation on PEM stacks. Six 10 kW 34-cell stacks were tested from November 2010 to October 2015. The stacks operated three at a time inside an H-Series PEM electrolyzer from Proton OnSite. During the five years of testing, the electrolyzer was operated for over 17,000 h resulting in 39% utilization over that time period.

Through the duration of testing, four of the stacks operated with a variable (e.g., renewable) profile and two of the stacks operated with a constant profile (control). The variable profile used ramps the stack current randomly up and down but maintains an average stack current of 80% of full rated current (full rated current 150 A, 80% of full rated current 120 A). To maintain a fair comparison, NREL sets the constant stack current to a constant value of 80% of full current. The stacks are operated in steady-state full-current mode (150 A) for a period of time (typically 100–200 h) to obtain a stack decay rate (μV/cell-h) comparison. Figure 1 shows the three different types of stack operation throughout the five years of testing.

Decay rate was determined using NREL's technology validation program tool that was developed to find decay rate of fuel cell stacks in material handling equipment and fuel cell electric vehicles. The tool tracks current and voltage performance over the duration of testing and uses curve fitting techniques to determine decay rates at certain points in time. The tool allows for all of the data sets over the

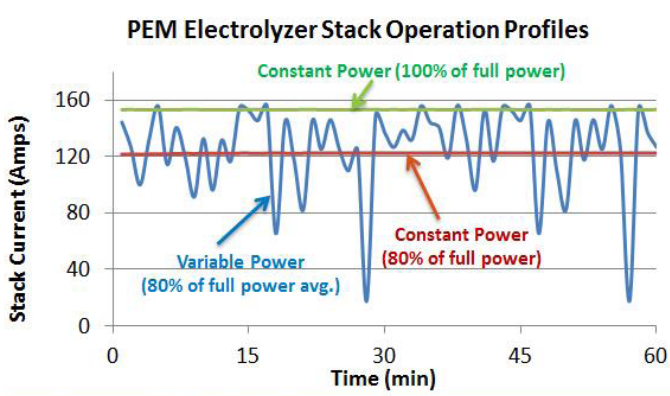

FIGURE 1. Stack operation for long-duration testing

17,000 h of testing to be analyzed at once using MATLAB as the software platform. Table 1 shows the decay rate results from the five years of testing.

TABLE 1. Decay Rate on Six 10 kW PEM Stacks

Profile Type	Total Hours	Decay Rate (μV/cell-h)
Variable	7,257	13.3
	10,112	1.0
	10,014	0.1
	4,330	-10.1
Constant	7,257	30.2
	12,069	2.1

The decay rate comparison showed no significant difference between variable and constant power operation. The research also demonstrated the importance of maintaining the electrolyzer balance of plant as premature failure of the electrolyzer stacks became a limiting factor for this testing. NREL worked with Proton to evaluate a stack to understand why it was exhibiting higher than expected voltage – a second stack performing properly was sent along as the control. Proton found both stacks to be within the factory acceptance levels using multiple tests at their facility. However, they also found a high concentration of silica in residual water shipped in the stacks. NREL inspected the electrolyzer balance of plant and found that dirt and dust from a passive open vent may have entered the electrolyzer generator compartment and contaminated the water. Further analysis performed by NREL on the system data, found that multiple unexpected facility power interruptions may also have contributed to the abnormal stack voltages that led to abrupt electrolyzer shutdowns. In this case, electrolyzer balance of plant issues seems to be the main driver of stack decay rate, regardless of variable or constant operation.

Variable Flow Drying

NREL completed baseline characterization and testing of a hydrogen drying approach that aims to reduce hydrogen drying losses under variable stack power (e.g., renewable) electrolyzer power profiles. The new drying approach aims to improve electrolyzer system efficiency to help achieve the DOE goal of 44 kWh/kg by 2020. NREL's variable hydrogen drying flow approach was implemented on a pressure swing adsorption (PSA) dryer attached to the output of the NREL designed and built electrolyzer stack test bed located in the Energy Systems Integration Laboratory in Golden, CO. The electrolyzer stack test bed operated under five different variable profiles with a 120 kW PEM electrolyzer stack from Proton OnSite. Performance of the PSA dryer system was monitored with multiple dew point sensors to track the parts per million by volume (ppmv) of water vapor in the hydrogen; a water content of less than 5 ppmv is required by SAE J2719 standard, which defines the Hydrogen Fuel Quality for Fuel Cell Vehicles.

Data was collected on multiple variable stack power profiles (e.g., photovoltaic, wind) with the PSA drying system set to lose 3.5% of rated hydrogen output for desiccant regeneration. This technique, referenced as fixed orifice, was the control variable for this testing. NREL's variable flow approach aims to maintain drying losses at 3.5% of actual hydrogen output flow, instead of a constant 3.5% of rated hydrogen flow. In the NREL system, the rated hydrogen flow is 2.16 kg/h and 3.5% of the rated flow equates to a loss of 0.076 kg/h or 1.8 kg in a 24-hour period. If the system is losing 3.5% of rated hydrogen flow (fixed orifice technique) the hydrogen lost is always 0.076 kg/h regardless of the hydrogen production flowrate. On the other hand, 3.5% of hydrogen output flow refers to the system maintaining a 3.5% loss based on the actual hydrogen flow from the stack. If the stack is being operated under variable power, the drying system would adjust and only lose 3.5% of the hydrogen output flow, saving hydrogen in the process (variable hydrogen drying flow technique). This testing provides a comparison of the two techniques in a PSA drying system.

The test results show that there was no measurable difference in hydrogen quality from the fixed orifice operation compared to the variable flow technique. Furthermore, NREL's variable drying approach saved between 2–10% of the produced hydrogen versus the typical fixed orifice approach. The large range of savings is a function of the type of variable power profiles that the stack was operated at during the testing. If the stack power profile calls for a majority of time at lower power levels, then the hydrogen savings increases significantly. The total hydrogen savings between the two approaches, based on the stack power profiles used through this testing, were equivalent to saving 1 kg of hydrogen for every 40 kg of hydrogen produced or 2.5% hydrogen savings.

DC System Design

NREL is creating a design package for an electrolyzer that operates solely on DC. The electrolyzer is being designed for off-grid operation that would be directly coupled with renewable electricity sources. NREL leveraged the bill of materials that was created for the electrolyzer stack test bed as the base for the DC electrolyzer design. Reviews of the design have been on-going between team members and significant progress has been made on the uniqueness of this system compared to other systems. Replacing typical alternating current balance-of-plant components with DC components allows for a comparison of cost and efficiency between the two types of equipment. NREL plans on completing the design of the system by the end of FY 2016.

CONCLUSIONS AND FUTURE DIRECTIONS

- Finalize the design for the DC balance of plant standalone renewable electricity electrolyzer system.
- Monitor and analyze in situ performance of cell voltages of a 50- and 100-cell stack under variable conditions.
- Continue developing and testing hydrogen drying techniques and materials to improve system efficiency.

FY 2016 PUBLICATIONS/PRESENTATIONS

1. Harrison, K. "Large Active Area Electrolyzer Stack Test Bed – Design, Data, and Development," 228th Electrochemical Society Meeting. Phoenix, Arizona. October 2015. (presentation)

2. Harrison, K. "Lifetime Prediction of PEM Water Electrolysis Stacks Coupled with RES." 2nd International Workshop, Durability, and Degradation Issues in PEM Electrolysis Cells and its Components. Freiburg, Germany. February 2016. (presentation)

3. Harrison, K. "Renewable Electrolysis – Systems Integration and Optimization." Solar Fuel Generation – PV and Electrolysis Workshop. Institute of Energy Conversion, University of Delaware Energy Institute. February 2016.

1. Peters, M.; Harrison, K; Dinh, H.; Terlip, D.; Kurtz, J.; Martin, J. "Renewable Electrolysis Integrated System Development & Testing." DOE Annual Merit Review and Peer Evaluation Meeting. June 2016. (presentation)

II.B.2 High-Performance, Long-Lifetime Catalysts for Proton Exchange Membrane Electrolysis

Hui Xu (Primary Contact), Brian Rasimick, Robert Stone, Shuai Zhao, and Litao Yan
Giner, Inc.
89 Rumford Ave.
Newton, MA 02466
Phone: (781) 529-0573
Email: hxu@ginerinc.com

DOE Manager: David Peterson
Phone: (720) 356-1747
Email: David.Peterson@ee.doe.gov

Contract Number: DE-SC0007471

Subcontractor:
National Renewable Energy Laboratory (NREL)
Golden, CO

Vendor
3M Company, Minneapolis, MN

Project Start Date: April 21, 2015
Project End Date: April 20, 2017

Overall Objectives

- Scale up catalyst synthesis to short production (>20 g/batch).
- Extend electrolyzer catalyst durability tests using accelerated stress test (AST) and steady-state operation up to 5,000 h.
- Transfer the selected catalysts to membrane electrode assembly (MEA) in a large-scale fabrication platform.
- Build a sub-megawatt electrolyzer using selected catalysts with low-platinum group metal (PGM) loading.
- Demonstrate sub-megawatt electrolyzer performance and durability.
- Perform economic analysis of the cost savings provided by the new catalysts at the megawatt scale.

Fiscal Year (FY) 2016 Objectives

- Scale up catalyst synthesis to short production (>20 g/batch).
- Extend catalyst durability tests to 5,000-h testing in a short electrolyzer stack.
- Establish an AST protocol to study the degradation of oxygen evolution reaction (OER) catalyst and MEA.

Technical Barriers

This project addresses the cost barriers of the Hydrogen Production section of the Multi-Year Research, Development, and Demonstration (MYRDD) Plan.

(F) Capital Cost

- By 2020, reduce the cost of distributed production of hydrogen from water electrolysis to <$2.30/gge (≤$4.00 delivered and dispensed)
- By 2020, reduce the cost of central production of hydrogen from water electrolysis using renewable power to ≤$2.00/gge at plant gate

Technical Targets

The target of this project is to develop high-performance and long-lifetime OER catalysts that may help meet the technical targets of DOE distributed forecourt water electrolysis as shown in Table 1. Included in this table is Giner's status as of 2013.

TABLE 1. Technical Targets: Distributed Forecourt Water Electrolysis [1]

Characteristics		Units	2015	2020	Giner Status (2013)
Hydrogen Levelized Cost[2]		$/kg-$H_2$	3.90	<2.30	3.64[3] (5.11)[4]
Electrolyzer Cap. Cost		$/kg-$H_2$	0.50	0.50	1.30 (0.74)[5]
Efficiency	System	%LHV (kWh/kg)	72 (46)	75 (44)	65 (51)
	Stack	%LHV (kWh/kg)	76 (44)	77 (43)	74 (45)

[1] 2012 MYRDD Plan. [2]Production Only. [3]Utilizing H2A Ver.2. [4]Utilizing H2A Ver.3 (Electric costs increased to $0.057/kW from 0.039$/kW) . [5] Stack Only

LHV – lower heating value

FY 2016 Accomplishments

- 3M has realized roll-to roll production of Ir-supported nanostructured thin film (NSTF) (anode) and Pt-NSTF (cathode) and delivered a variety of catalyst decals and catalyst-coated membranes (CCMs) to Giner.
- Giner built six-cell short stacks using 3M NSTF anode catalyst and successfully completed a 2,000-h durability on one stack with minimal performance loss.
- Larger production of $Ir/W_xTi_{1-x}O_2$ catalyst was conducted at Giner. The catalyst-based anode demonstrated comparable performance to the standard anode but with one order of magnitude lower Ir loading.
- AST was performed to establish "Catalyst Durability Test" protocol for water electrolysis. The microstructures of aged MEAs under different AST conditions and stages were characterized and their correlation to performance analyzed.

✧ ✧ ✧ ✧ ✧

INTRODUCTION

Hydrogen production for mobility and energy storage from polymer electrolyte membrane (PEM) water electrolysis is attractive due to its efficiency, ability to quickly cycle up and down, and delivery of hydrogen with high and differential pressure. However, capital costs are high due to expensive materials, especially the membrane and catalyst. Though membrane costs are predicted to decrease, precious metal catalysts costs will come to control capital costs as this technology matures. Decreasing the precious metal requirement for PEM electrolysis is therefore vital for the widespread use of this technology. The overall objective of the Phase IIB project is to commercialize the low precious metal loading, high-performance catalysts for PEM water electrolysis that we have successfully developed in our Phase II project, which may significantly lower the capital cost of water electrolyzers. Both Giner's $Ir/W_xTi_{1-x}O_2$ and 3M's Ir-NSTF catalysts developed under this project have been successfully scaled up for commercialization and are currently being tested for durability and performance.

APPROACH

In the Phase IIB project, Giner aims to transition this game-changing, innovative catalyst technology to successful commercialization. The Phase IIB catalyst commercialization plan is illustrated in Figure 1. First, we will scale up the catalyst synthesis process to make small production runs (30 g). Second, we will develop an effective MEA fabrication process to make reproducible, full-sized MEAs. Small pieces cut from full MEAs will be subjected to extensive durability tests via accelerated stress and electrolyzer durability tests. These MEAs will be subsequently integrated into Giner's low-PGM loading sub-megawatt electrolyzers to test their performance and durability. The degradation study for MEAs after ASTs and electrolyzer tests will be aided by scanning electron microscopy–energy-dispersive X-ray spectroscopy mapping and transmission electron microscopy. Finally, detailed economic analysis of catalyst production costs and the impact of the catalysts on electrolyzer operations will be performed..

RESULTS

First, Giner's $Ir/W_xTi_{1-x}O_2$ catalyst (Ir; 45 wt%) has been scaled up and built into a short stack, as shown in Figure 2a. There were three groups of cells in the short stack: Group 1

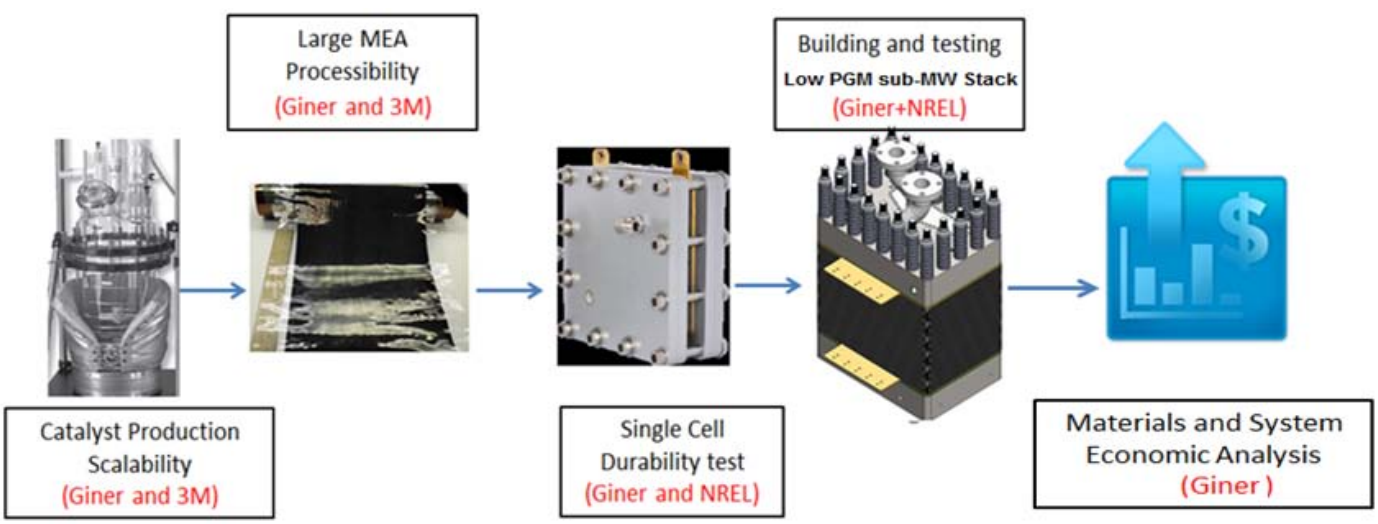

FIGURE 1. Catalyst development and commercialization approach

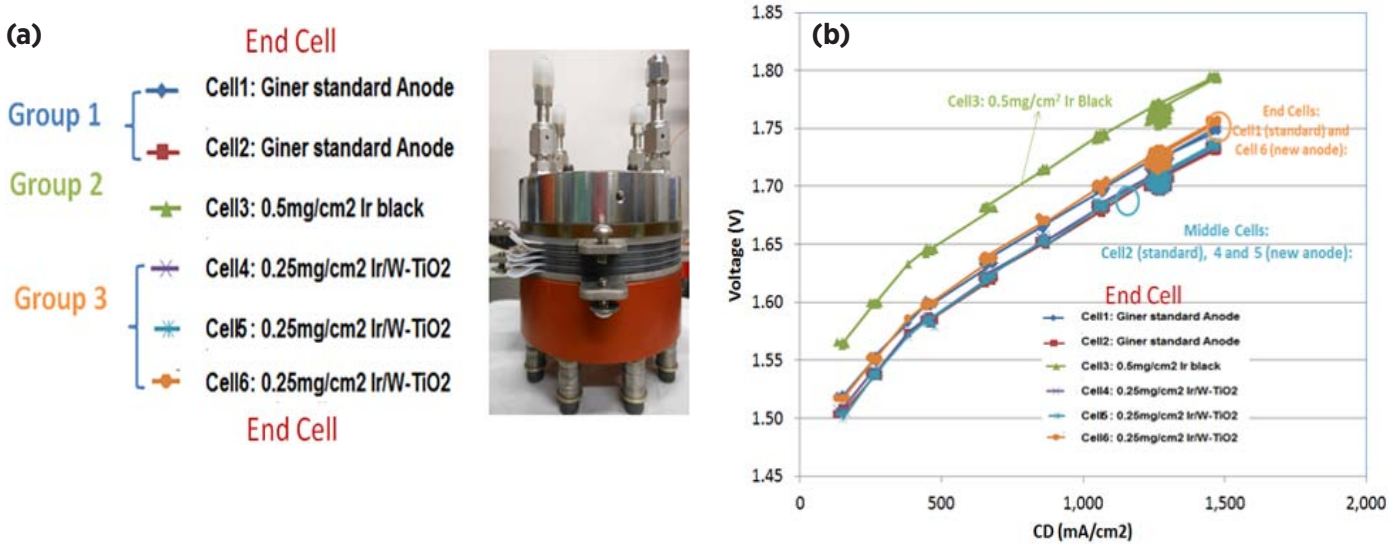

FIGURE 2. Short electrolyzer stack (a) and cell performance at 80°C (b) for $Ir/W_xTi_{1-x}O_2$ catalyst developed at Giner Inc. Membrane: Nafion 115; cathode: 0.4 mg/cm^2 Pt from Tanaka Pt/C; anode of standard MEA: 3 mg/cm^2 PGM.

contained two standard cells with an anode PGM loading of 3 mg/cm^2; Group 2 had one cell using commercial (Johnson Matthey) Ir catalyst at low loading, 0.5 mg/cm^2; and Group 3 contained three cells using $Ir/W_xTi_{1-x}O_2$ catalyst at extremely low loading, 0.25 mg/cm^2. The membrane is Nafion 115 and the active area is 50 cm^2. The performance of these cells operated at 80°C is shown in Figure 2b. First, the cells with low Ir loadings from the $Ir/W_xTi_{1-x}O_2$ catalyst performed significantly better than that with the commercial iridium black as the former has a 50 mV lower overpotential. Second, the cell performance of the $Ir/W_xTi_{1-x}O_2$ anode approached the performance of the Giner standard anode even the former anode had one order of magnitude lower Ir loading. The significantly higher activity of the $Ir/W_xTi_{1-x}O_2$ has been demonstrated. The durability of the short stack has also been tested, but the data is not shown because the malfunction of test station caused the fast decay of the cell performance.

3M has delivered a few batches of NSTF decals and CCMs to Giner for short stack testing. The most successful CCM is NSTF (cathode: 0.25 mg/cm^2 Pt from Tanaka Pt/C; anode: 0.5 mg/cm^2 Ir from Ir-NSTF) deposited on 3M 100 µm 800 equivalent weight membrane. This CCM was built into a short stack compared to standard cells using Nafion 115 and anode PGM loading of 3 mg/cm^2. The performance of these cells operated at 80°C is shown in Figure 3a. It can be seen that NSTF cells demonstrated much better performance than standard cells, as the former had 150 mV lower overpotential at 5,000 mA/cm^2. The superior performance of the NSTF cells is due to their high catalyst activity and thinner membrane with low equivalent weight resulting in less ohmic loss. The durability of this short stack was shown in Figure 3b. The durability test has passed 2,000 h and NSTF cells demonstrate significant durability without any performance loss.

In this project, we have also made great efforts to establish an AST protocol for the OER catalysts and elucidate the cause of performance decay after ASTs. As shown in Figure 4a and 4b, NREL evaluated the stability of a series of commercially available catalysts under rotating disk electrode conditions, which includes Johnson Matthey Ir black and Umicore Ir supported on TiO_2. It clearly shows that most catalysts lost their activity after the hold at 1.6 V for 13.6 h. Giner performed voltage cycling from 1.4–2.0 V using an MEA containing 0.1 mA/cm^2 Ir black. It can be seen from Figure 4c that as the cycle number increases, the overpotential of the tested cell continuously goes up, indicating decreasing MEA performance. The decreased MEA performance can be due to catalyst agglomeration and more pronouncedly, Ir migration. The latter is clearly displayed in Figure 4d, where a number of Ir particles are seen in the membrane, leading to the loss of the catalyst from the anode.

CONCLUSIONS AND FUTURE DIRECTIONS

Several conclusions can be drawn:

- Giner's $Ir/IrO_2/W_xTi_{1-x}O_2$, $Ir/W_xTi_{1-x}O_2$, and 3M's Ir-NSTF anode catalysts have been scaled up and tested in short stacks (5–6 cells, 50 cm^2).
- Giner's $Ir/W_xTi_{1-x}O_2$-based anode demonstrated superior performance to standard anode in short-term testing.
- 3M's Ir-NSTF on 100 µM low equivalent weight membrane demonstrates great performance and durability after 2,000 h of testing.
- Catalyst durability AST protocol developed through a cohesive collaboration between NREL and Giner and a variety of OER catalysts have been characterized.

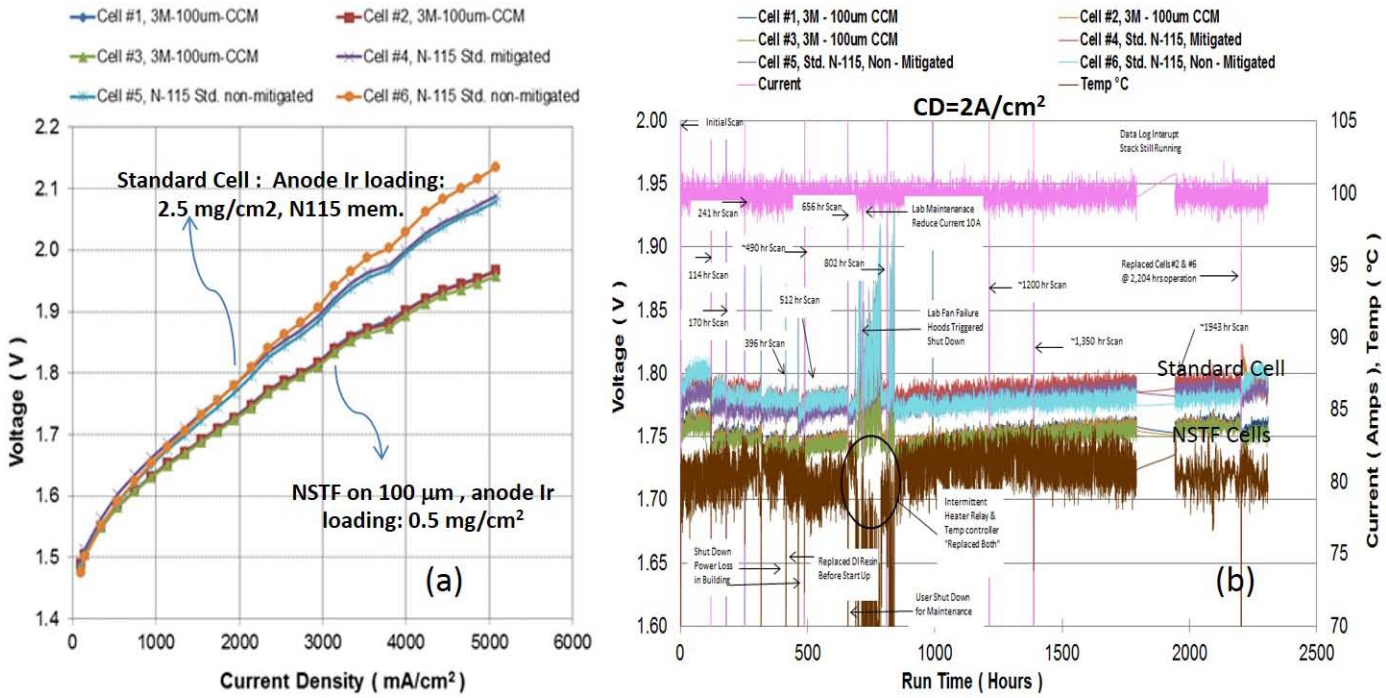

FIGURE 3. The comparison of 3M's NSTF MEAs with standard MEAs at 80°C. Standard MEA (anode: 3 mg/cm^2 PGM; membrane: Nafion 115; cathode: 0.4 mg/cm^2 Pt from Tanaka Pt/C), NSTF MEA (anode: 0.5 mg/cm^2 Ir from Ir/NSTF; membrane: 3M 100 µm 800 equivalent weight membrane; cathode: 0.4 mg/cm^2 Pt from Tanaka Pt/C).

Future work includes:

- Complete AST durability test protocols and correlate with real performance test.
- Complete 5,000-h stack durability of selected Giner and 3M catalysts.
- Select catalysts for Giner sub-megawatt electrolyzer stack construction.

SPECIAL RECOGNITIONS & AWARDS/ PATENTS ISSUED

1. Xu, H., C. Mittelsteadt, B. Rasimick, and A. Stocks, "Anode Catalyst Suitable for Use in an Electrolyzer," US 2015/0368817A1.

FY 2016 PUBLICATIONS/PRESENTATIONS

1. Invited talk: "Advanced Oxygen Evolution Catalysts for Water Electrolysis," presented at the 250th ACS Meeting, Division of Energy and Fuels, Boston, MA, August 18, 2015.

2. "Studies of MEA Durability in Proton Exchange Membrane Water Electrolysis," Abstract #1516, presented at the 228th ECS Meeting, Phoenix, AZ, October 11–15, 2015.

3. Invited Talk: "Water Electrolysis: from Components to Systems," presented in TechConnect World Innovation Conference, Washington, D.C., May 22–25, 2016.

4. "High-Performance, Long-Lifetime Catalysts for Proton Exchange Membrane Electrolysis," presented at the DOE Hydrogen and Fuel Cells Program Annual Merit Review Meeting, Washington, D.C., June 4–8, 2016.

5. Shaun M. Alia, Brian Rasimick, Chilan Ngo, K.C. Neyerlin, Shyam S. Kocha, Svitlana Pylypenko, Hui Xu, and Bryan S. Pivovar, "Activity and Durability of Iridium Nanoparticles in the Oxygen Evolution Reaction," J. Electrochem. Soc. 2016 163(11): F3105-F3112; doi:10.1149/2.0151611jes.

6. Shaun M. Alia, Katherine E. Hurst, Shyam S. Kocha, and Bryan S. Pivovar, "Mercury Underpotential Deposition to Determine Iridium and Iridium Oxide Electrochemical Surface Areas," J. Electrochem. Soc. 2016 163(11): F3051-F3056; doi:10.1149/2.0071611jes.

REFERENCES

1. Hamden, M., "PEM Electrolyzer Incorporating an Advanced Low Cost Membrane." Presentation in DOE 2012 Hydrogen and Fuel Cells Annual Merit Review meeting, http://www.hydrogen.energy.gov/pdfs/review12/pd030_hamdan_2012_o.pdf (2012).

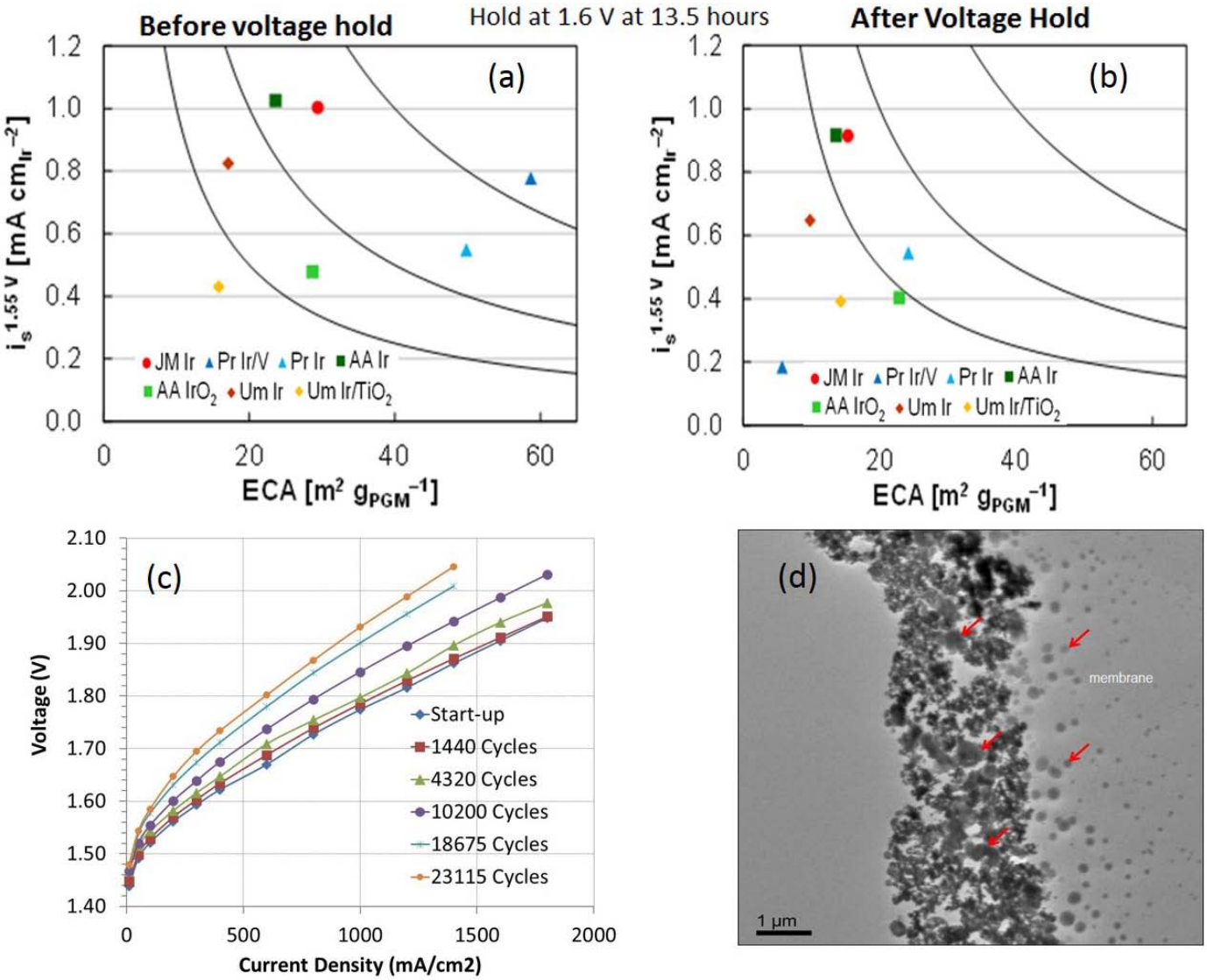

FIGURE 4. AST for catalyst degradation studies and structure characterization. (a) and (b): hold at 1.6 V for 13.5 h; (c) voltage cycling from 1.4 V to 2.0 V with 0.1 mg/cm^2 Ir black at the anode; (d) structure of anode and adjacent membrane after voltage cycling from (c), transmission electron micrograph taken by Dr. Karren More at Oak Ridge National Laboratory.

II.B.3 High Performance Platinum Group Metal Free Membrane Electrode Assemblies through Control of Interfacial Processes

Katherine Ayers (Primary Contact), Chris Capuano, Nem Danilovic
Proton OnSite
10 Technology Drive
Wallingford, CT 06492
Phone: (203) 678-2190
Email: KAyers@protononsite.com

DOE Manager: David Peterson
Phone: (240) 562-1747
Email: David.Peterson@ee.doe.gov

Contract Number: DE-EE0006958

Subcontractors:
- Pennsylvania State University, College Park, PA
- University of New Mexico, Albuquerque, NM
- Northeastern University, Boston, MA

Project Start Date: May 1, 2015
Project End Date: April 30, 2017

Overall Objectives

- Evaluate non-platinum group metal (PGM) catalysts in gas diffusion electrodes (GDEs) in half cells.
- Evaluate most promising non-PGM GDEs in full-cell anion exchange membrane (AEM) water electrolysis configuration against PGM counter electrode.
- Further the fundamental understanding of non-PGM active sites and reaction mechanisms using synchrotron based in situ spectroscopy.
- Demonstrate translation from solution testing to solid electrolyte interface.
- Conduct assessment of ex situ and in situ stability comparisons to connect ex situ lab evaluation and in situ device results.
- Improve membrane and ionomer durability vs. current commercial options.
- Optimize water management through improved flow field and gas diffusion layer (GDL) design.
- Fabricate full-scale membranes and ionomer solution for electrolyzer testing.
- Identify most promising non-PGM GDEs for full-cell operation and test PGM-free membrane electrode assembly (MEA) for durability (continuous operation at 500 mA/cm^2 for up to 500 h).

Fiscal Year (FY) 2016 Objectives

- Evaluate most promising non-PGM GDEs in full-cell AEM water electrolysis configuration against PGM counter electrode.
- Further the fundamental understanding of non-PGM active sites and reaction mechanisms using synchrotron based in situ spectroscopy.
- Demonstrate translation from solution testing to solid electrolyte interface.
- Conduct assessment of ex situ and in situ stability comparisons to connect ex situ lab evaluation and in situ device results.

Technical Barriers

This project addresses the following technical barriers from the Hydrogen Production section of the Fuel Cell Technologies Office Multi-Year Research, Development, and Demonstration Plan:

(F) Capital Cost

Technical Targets

This project is working to establish a new cost curve for water electrolysis through elimination of the highest cost materials in the cell stack, such as PGMs and valve metals such as titanium. While electrolysis still has significant needs in manufacturing in order to reach 2020 targets and beyond, the end cost will be largely dependent on raw material costs. In the long-term, non-PGM catalysts for the hydrogen and oxygen evolution reactions (HER and OER) are needed. The current program aims at meeting the following targets:

- PGM content: none
- Cell voltage: <2 V
- Cell current: 500 mA/cm^2
- Durability: 500 h of stable operation

FY 2016 Accomplishments

- Synthesized HER and OER catalysts with desired compositions (Ni-metal oxide materials) with similar physical properties (surface area, conductivity) to standard PGM catalysts.
- Achieved HER overvoltage of less than 200 mV at 20 mA/cm^2.
- Achieved OER performance of <1.55 V vs. RHE at 20 mA/cm^2.

- Operated an electrolysis cell with non-PGM metals at less than 2V at 500 mA/cm^2.
- Designed and built a membrane fixture for measuring water transport through membranes and gas diffusion layers with pressure.
- Developed a test system for operation in anode or cathode water feed mode.

✧ ✧ ✧ ✧ ✧

INTRODUCTION

Completely carbon-neutral fuel cell vehicles will require a renewable source of hydrogen fuel, such as water electrolysis powered by wind or solar. The DOE cost goals for the production of renewable hydrogen are aggressively set to compete with existing fossil fuel-based infrastructure. Fuel cells and electrolyzers based on proton exchange membranes (PEMs) are well-known and continue to realize reductions in cost and improvements in performance. To meet DOE goals for renewable hydrogen production, and for growing energy markets, reductions in capital and operating costs are needed in order to justify electrolysis as a solution, particularly without incentives for zero carbon emissions.

To date, the only pathway with promise to achieve PGM-free electrode formulations in membrane-based electrolysis cells is utilization of AEMs. The basic local environment of the membrane allows a range of stable transition metals and metal oxides to be utilized at high potential for catalysis. AEMs also enable the use of much less expensive flow field materials other than the titanium often used in PEM systems. At the same time, the solid state electrolyte eliminates the need for corrosive liquid electrolytes such as concentrated potassium hydroxide and allows leveraging of high-performance MEA technology. Proton and team members Northeastern University and Penn State University have been exploring this technology since 2010 through an Advanced Research Projects Agency-Energy project in the Grid-Scale Rampable Intermittent Dispatchable Storage program and have made significant progress in understanding the limitations and potential of this AEM chemistry.

APPROACH

In the first year, project focus will be on catalyst synthesis and activity screening. HER catalysts will be based on Ni–Mo nanoparticles and other mixed oxides, while OER catalysts will focus on ternary catalysts based on Ni, Fe, Co, and Mo. A sacrificial support method (SSM) will be used to synthesize novel catalyst materials in high surface area format. Electrochemical characterization will be used to downselect materials with appropriate physical parameters for in cell testing. In parallel, polymers based on polyphenylene oxide will be synthesized for use in ionomer solutions and membrane materials to look for higher membrane and ionomer stability than incumbent polymer materials. GDL materials and flow field designs will be optimized for AEM electrolysis performance and incorporated into the cell stack. Materials selection as well as application methods for coatings will be examined for controlling the hydrophobicity and hydrophilicity of the GDL materials.

In Year 2, results from the first year will be leveraged to optimize the GDE interface, including treatments for improved water management. Additional characterization methods will be used to study the structure–activity relationships of the non-PGM catalysts, to understand catalyst–ionomer interactions. The best performing catalysts based on the SSM approach will be scaled up to 10–25 g batches. On the membrane task, cation spacer polymers will be explored based on 5–10 times greater hydroxide stability vs. the side chain benzyl-linked cation materials. System architectures will be determined for optimum performance, and a test system will be built with capability for anode water feed, cathode water feed, or both. A water transport cell will also be fabricated to help understand flow characteristics as a function of membrane type, GDL, and operating conditions. Focus in cell testing will be on longer term durability testing, once initial performance targets have been met.

RESULTS

Initial catalyst synthesis was performed to demonstrate control over the process and composition. Mixed metal oxides were confirmed to have the desired composition and microstructure via scanning electron microscope and X-ray diffraction. In parallel, nickel oxide materials were synthesized via SSM to demonstrate the ability to reach the desired physical parameters such as surface area, conductivity, and onset potential in comparison to typical PGM catalysts for PEM electrodes. Surface areas of 20 m^2/g and other metrics met targets as the synthesis was tuned (Table 1). The technique was then successfully translated to the mixed metal oxides. Rotating disk electrodes (RDEs) were then used to characterize catalyst activity. While our experience in the AEM environment is that good RDE results in strongly basic electrolyte do not always translate over to the ionomer-based environment, RDE can still act as a tool for screening out poor catalysts. Several candidates for

TABLE 1. Table of OER Catalyst Parameters for SSM vs. Baseline

OER Catalyst	Conductivity [S/cm]	Onset Potential [V] vs RHE
NiO	0.00200	1.53
I-22 NiO SSM	0.00308	1.52
I-28 $NiCoO_3$ SSM	0.389	1.54
NiMoCu-II	4.47	1.51
IrOx reference	0.0102	1.43

RHE – reversible hydrogen electrode

both OER and HER were tested which met the performance targets (Figure 1).

The best performing catalysts were then integrated into full cells and tested individually against PGM counter electrodes. Once stable short-term performance was achieved that was close to the full cell targets, a fully non-PGM cell was built and tested. The combined performance met the initial targets (Figure 2). This cell hardware is intended for screening and therefore is not qualified for unattended operation, but the stability of the cell over the first several hours was very encouraging.

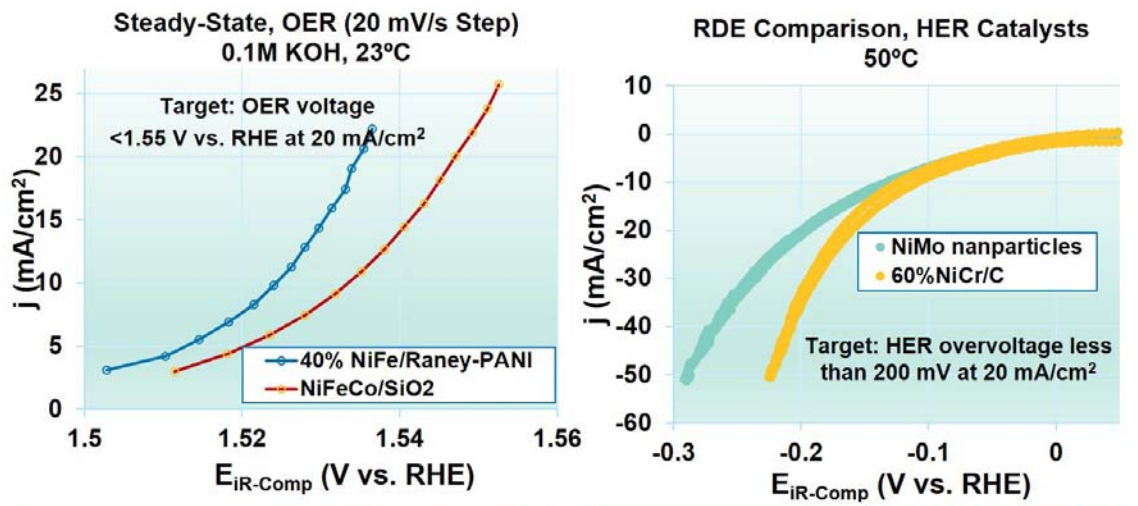

OER Catalyst	Overvoltage at 20mA/cm²
Ni-Fe-Co/SiO_2	1.546 V
40%Ni-Fe/Raney-PANI*	1.534 V
40%Ni-Fe-Co/Raney-PANI	1.547 V

HER Catalyst	Overvoltage at 20mA/cm²
Ni-Mo	193.9 mV
60% Ni-Cr/Ketjen 600*	160.2 mV
20% Ni/50% Vox/C	199.8 mV

PANI – polyaniline

FIGURE 1. RDE data and overpotentials for OER and HER catalysts meeting targets

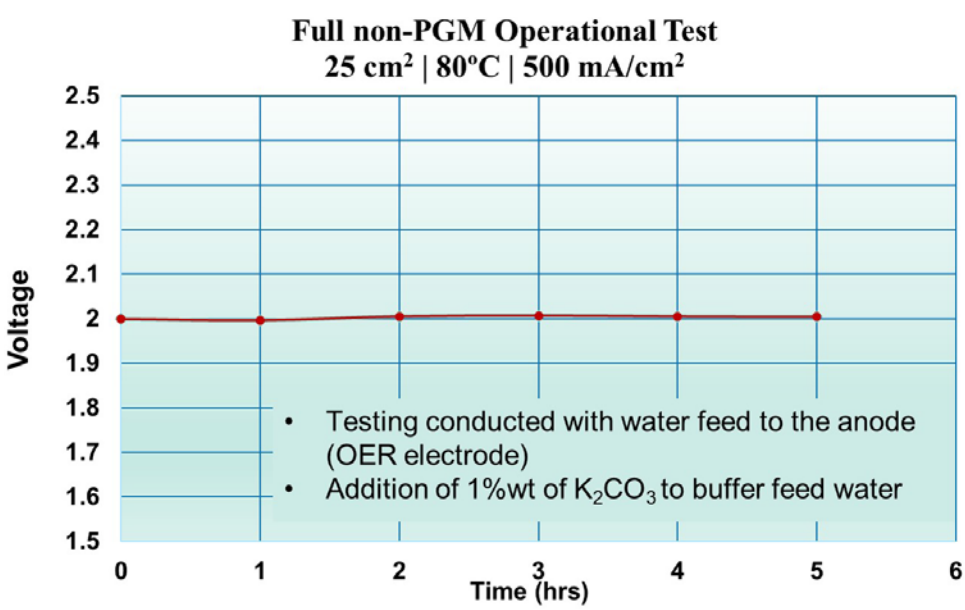

FIGURE 2. Fully non-PGM AEM electrolysis cell performance

In parallel to the catalyst work, membranes were synthesized with spacers between the polymer backbone and the ion exchange sites in order to minimize electron withdrawing effects in the main chain and add hydroxide stability. Ionomers were fabricated into inks and deposited on the membrane samples. Initial electrodes were highly unstable, with poor mechanical integrity. Step by step exposure of the membranes to components of the ink revealed that the membrane surface was melting in contact with the solvents, and was unstable. New samples have incorporated cross-linking to further stabilize the backbone, and improved stability has been achieved over short term tests.

Finally, design and assembly work has been initiated on the dual water feed test stand and water transport fixture. Components for the water transport fixture are being procured, and the test stand has passed initial design reviews and has been assembled. Currently, the system is undergoing final safety checks in preparation for operation (Figure 3).

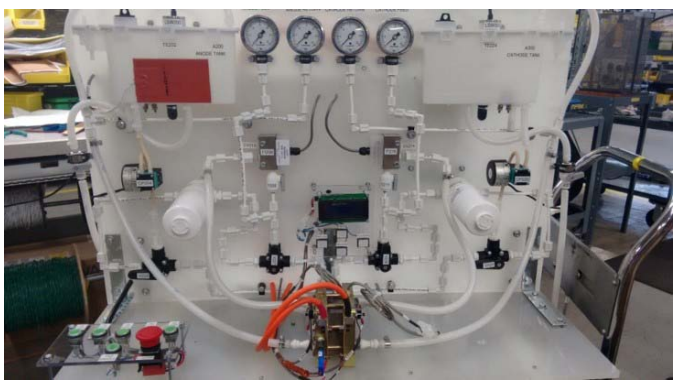

FIGURE 3. Proton test stand for dual water feed operation

CONCLUSIONS AND FUTURE DIRECTIONS

The Year 1 quarterly milestone was achieved, as demonstrated in discrete operation of the HER and OER electrodes in a liquid cell and in a full solid polymer membrane operational test. The full operational test not only represents the first full non-PGM MEA operated in AEM water electrolysis, but also demonstrated performance that was stable enough to operate for several hours at the overall program current density targets of 500 mA/cm^2. Next steps include further optimization with the high surface area catalyst synthesis methods, and work on longer durability membranes, as well as testing in dual operational modes (anode or cathode water feed).

FY 2016 PUBLICATIONS/PRESENTATIONS

Presentations:

1. Fuel Cell Seminar, November 2015, "R&D Advances in AEM Electrolysis."

2. Power Sources Conference (Poster), June 2016, "Research Advances in Anion Exchange Membrane Electrolysis to Enable Low-Cost Hydrogen Energy Storage."

II.B.4 High Temperature, High Pressure Electrolysis

Cortney Mittelsteadt (Primary Contact),
Jason Willey
Giner, Inc.
89 Rumford Avenue
Newton, MA 02466
Phone: (781) 529-0529
E-mail: cmittelsteadt@ginerinc.com

DOE Manager: David Peterson
Phone: (240) 562-1747
Email: David.Peterson@ee.doe.gov

Contract Number: DE-SC0011310

Subcontractor:
Prof. Judy Riffle, Virginia Polytechnic Institute and State University (Virginia Tech), Blacksburg, VA

Project Start Date: November 18, 2014
Project End Date: November 17, 2016

Overall Objectives

- Develop a polymer electrolyte membrane (PEM) with a high ratio of conductivity to permeability, which leads to an increase in efficiency.
- Optimize lifetime of developed PEM using various methods.
- Demonstrate improved lifetime and efficiency under high pressure (350 bar) operation.

Fiscal Year (FY) 2016 Objectives

- Optimize formulation of non-perfluorinated membranes for conductivity/permeability ratio and lifetime.
- Demonstrate increased lifetime with medium pressure (70 bar) operation.
- Demonstrate high lifetime and efficiency at 350 bar operation.

Technical Barriers

This project addresses the following technical barriers from the Hydrogen Production section of the Fuel Cell Technologies Office Multi-Year Research, Development, and Demonstration Plan.

(F) Capital Cost

(G) System Efficiency and Electricity Cost

(L) Operations and Maintenance

Technical Targets

Progress has been made in achieving the DOE targets listed in the Multi-Year Research, Development and Demonstration Plan. Table 1 lists the DOE's technical targets and where our research and development efforts stand to date.

TABLE 1. DOE Technical Targets and Giner, Inc. Status

Characteristic	Unit	2015 Target	2020 Target	Giner, Inc. Status
Electrolyzer System Capital Cost	$/kg $/kW	0.50 300	0.50 300	0.57 1,000
System Energy Efficiency	% (LHV) kWh/kg	72 46	75 44	67 50
Stack Energy Efficiency	% (LHV) kWh/kg	76 44	77 43	75 44.5

LHV – lower heating value

The goal of this project is to increase the efficiency of the PEM electrolyzer stack and to improve durability of the membrane electrode assemblies (MEAs), while providing hydrogen at a pressure of 350 bar. These goals would contribute significantly to reaching the 2020 DOE hydrogen production targets of:

- Hydrogen Levelized Cost: $4/kWh (dispensed)
- Stack Energy Efficiency: 43 kWh/kg H_2
- Electrolyzer System Capital Cost: $300/kW

FY 2016 Accomplishments

- Optimized crossover mitigation with the Virginia Tech non-perfluorinated membranes.
- Evaluated 15 different membrane variations at 70 bar and 95°C (when possible) for membrane degradation and performance.
- Manufactured hardware and MEA for 350 bar testing.

✧ ✧ ✧ ✧ ✧

INTRODUCTION

Electrolysis of water is an important tool for energy storage in wind and solar applications. The DOE has identified a need for electrolyzer efficiencies to reach 77% LHV by 2020. High-pressure direct electrolysis is a desirable method for hydrogen generation and energy storage due to the reduced need for high-pressure pumps and compressors.

Direct electrolysis at elevated pressure permits hydrogen and/or oxygen tanks to be refilled directly, and reduces the overall mass, complexity, and cost of the electrolysis system. Efficiency can be increased by operation at a higher temperature, which increases both conductivity and oxygen evolution kinetics. However, this comes at the expense of higher permeability. Gas crossover (permeability) plays an increasingly significant role in performance as pressure rises, decreasing efficiency and accelerating membrane degradation while leading to potentially dangerous levels of hydrogen in oxygen and vice-versa. Increasing membrane thickness or lowering cell operating temperature can decrease crossover, but also decreases efficiency. Given the permeability and conductivity at a given temperature, it is straightforward to optimize membrane thickness for efficiency. The key to making efficiency gains then is to increase the ratio of conductivity/permeability (C/P) and operate at as high a temperature as possible without compromising the membrane. The overall objective for this DOE Small Business Innovation Research program is the development of a PEM with maximum conductivity/permeability ratio while simultaneously greatly reducing membrane degradation rates (2x and 10x improvement over Nafion®, respectively). Perfluorinated sulfonic acid- (PFSA) and hydrocarbon-based membranes generated with various additives, ionomer compositions and support structures were prepared and evaluated for conductivity and permeability as a function of temperature and water activity. The initial goal was to produce membranes with conductivity/permeability ratios greater than 2 with reference to Nafion, and this goal has been achieved. These membranes were then tested for degradation and performance at 70 bar.

APPROACH

The general approach for this project is to test the C/P ratio for both commercial and experimental membranes. Those membranes showing conductivity/permeability ratios more than twice that of Nafion are tested for durability. The durability is then tested with unadulterated membrane, and with membrane to which additives have been added to increase durability and to decrease gas crossover. The best performing of these membranes will be scaled up into a short stack build which will then be tested at high pressure and high temperature for performance and durability.

The initial stage of the project has been completed with several non-PFSA membranes showing promise. Testing is now focused on medium pressure testing for durability and performance.

RESULTS

The initial goal in Phase I of this project was to fabricate, test and select membranes that possess C/P ratios higher than that of Nafion, to achieve the DOE goal of 76% LHV electrolyzer efficiency. A secondary goal was to ready a test station for testing membranes early in Phase II. Both of these goals were realized.

In total, 15 different ionomers were procured or fabricated and tested for conductivity and hydrogen permeability in Phase I. Excluding unmodified Nafion, six were PFSA ionomers – three modified N1100 membranes and three low equivalent weight membranes. The remaining eight were hydrocarbon-based membranes made by Virginia Tech, our Phase I partner and Rensselaer Polytechnic Institute. Figure 1 shows the results of testing for the 15 membranes.

As can be seen in the figure, three hydrocarbon membranes exceed the Phase I goal of a ratio of 2. Only one of these membranes was included in the Phase II testing – HQS-22 – due to the difficulty in consistently fabricating the other two ionomers. One PFSA membrane tested close to the goal – the Solvay Aquivion 790 equivalent weight membrane with a C/P of 1.7. In the interests of keeping a PFSA membrane in the study the Solvay ionomer was included in the durability testing.

Durability and performance testing is almost complete for all the membranes configurations in the matrix. The main marker for chemical degradation of PFSA ionomers is fluoride release rate. Giner measures fluoride in the cell exit water as a measure of membrane degradation. Figure 2 shows the typical durability test. Fluoride numbers for the test shown in the figure were below the detectable limit (~20 ppb) for the entire test, and voltage was stable at the various temperatures. This suggests that chemical degradation was not an issue for this membrane with the degradation modification. Table 2 shows the results of the degradation testing for all the membranes in the matrix.

Notable is the large jump in estimated lifetimes for PFSA with degradation mitigation. The Solvay ionomer shows improvement in estimated lifetime with degradation mitigation, but this improvement is not nearly as large as for

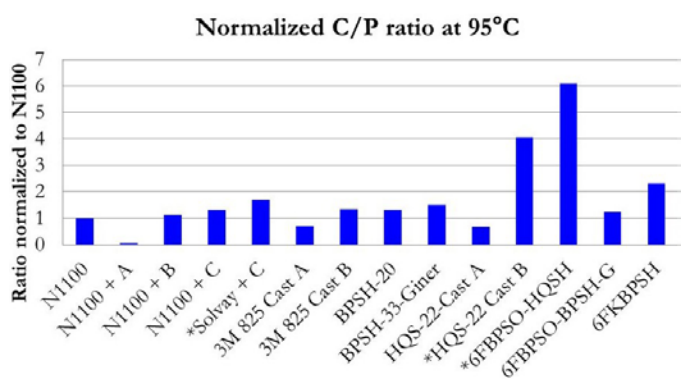

FIGURE 1. Conductivity, permeability and the C/P ratio for the membranes tested under the Phase I program. The go/no-go ration is 2, and membranes above this ratio were moved on to the durability stage.

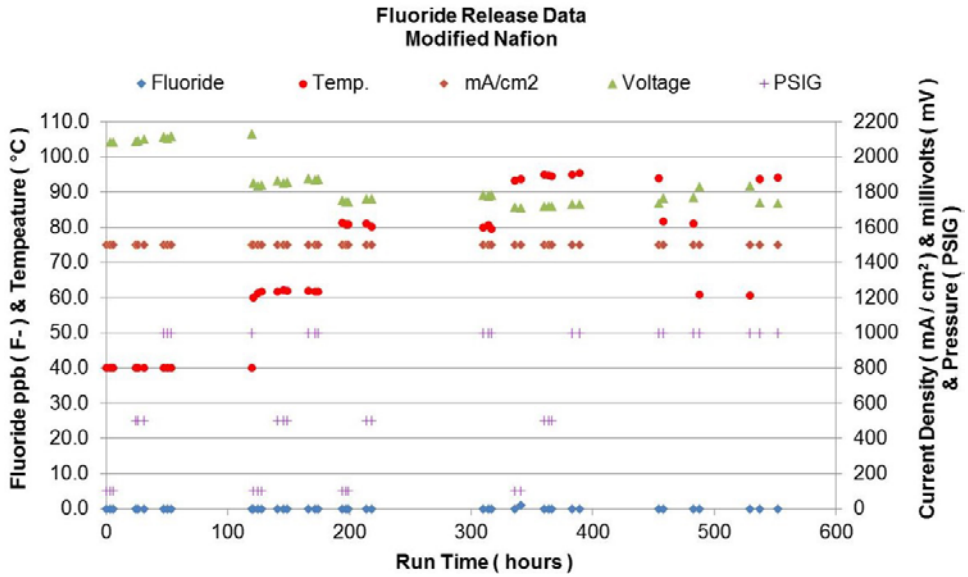

FIGURE 2. Various parameters measured during the durability test of a Nafion membrane treated with a degradation mitigant

TABLE 2. Results for Degradation Testing (40–95°C, 7–70 bar)

Test #	Membrane	Type	XM*	DM (%)**	Test length (h)	Failure	Est. Life (h)†
1	N115	PFSA	yes	0	518	no	7,000
2	N115	PFSA	yes	0.25	456	no	>100,000
3	N115	PFSA	yes	0.5	411	no	>100,000
4	N115	PFSA	yes	1	552	no	>100,000
5	N115	PFSA	yes	2.5	1017	no	>100,000
6	Solvay E79	PFSA	yes	0	697	no	4,000
7	Solvay E79	PFSA/DSM	yes	0.5	488	no	15,000
8	Solvay E79	PFSA	yes	0.5	356	yes	-
9	HQS-22	HC/DSM	no	0	25	no	-
10	HQS-22	HC/DSM	yes	0	41	yes	-
12	HQS-22	HC	yes	0	74	yes	-
13	HQS-22	HC/DSM	yes	0.5	20	yes	-
14	HQS-22	HC/DSM	yes	0.5	2	yes	-

* XM – Crossover mitigation added. ** DM – Degradation mitigation level as multiple of baseline amount.
† Estimated lifetimes are for MEAs operated at 95°C and 70 bar.
DSM - Dimensionally Stable Membrane; HC - Hydrocarbon

Nafion. Unfortunately, the HQS-22 MEAs degraded very quickly under test conditions in all configurations. Virginia Tech has just provided the project with two direct-fluorinated hydrocarbon membranes that show promise, but have not been tested at the time of this publication. Giner will also test one more PFSA under the degradation test protocol. This will be a 3M ionomer of low equivalent weight.

Testing at 350 bar is ready to commence at Giner, and will begin after the last degradation test is competed. This test will be biased to hydrogen pressure, with the cathode operating at 350 bar and the anode at <5 bar. The first MEA on test will be a Solvay E79 incorporated with Giner's DSM technology, which strengthens the membrane via a polymer matrix. Figure 3 shows an image of the 350 bar hardware.

FIGURE 3. Fuel cell stack hardware designed to withstand 350 bar operational pressure

CONCLUSIONS AND FUTURE DIRECTIONS

Conclusions at this time:

- Giner's degradation mitigation can improve expected lifetimes of PFSA ionomers significantly, affecting capital cost.
- This degradation mitigation transfers well to other PFSA ionomers.

Future work includes:

- High pressure (350 bar) testing of membranes for performance and degradation.
- Testing short-stack configuration of the best MEAs under high-pressure conditions.

FY 2016 PUBLICATIONS/PRESENTATIONS

1. C. Mittelsteadt. "The Next Generation of PEM Electrolysis" (paper presented at BIT's 6th Annual New Energy Forum 2016, Goyang City, South Korea, June 30 – July 2, 2016).

II.B.5 Solid Oxide Based Electrolysis and Stack Technology with Ultra-High Electrolysis Current Density (>3A/cm^2) and Efficiency

Randy Petri (Primary Contact), Eric Tang, Tony Wood, Casey Brown, Micah Casteel, Michael Pastula, Mark Richards
FuelCell Energy
3 Great Pasture Rd
Danbury, CT 06810
Phone: (303) 226-0762
Email: rpetri@fce.com

DOE Manager: David Peterson
Phone: (240) 562-1747
Email: David.Peterson@ee.doe.gov

Contract Number: DE-EE0006961

Subcontractor:
Versa Power Systems, Ltd., Calgary, Alberta, Canada

Project Start Date: May 1, 2015
Project End Date: June 30, 2017

Overall Objectives

Develop solid oxide electrolysis cell (SOEC) technology capable of:

- Operating at ultra-high current density (>3 A/cm^2).
- Operating with a cell voltage upper limit of 1.6 V, equivalent to 77% efficiency, lower heating value (LHV).

Technical Barriers

This project addresses the following technical barriers from the Hydrogen Production section of the Fuel Cell Technologies Office Multi-Year Research, Development, and Demonstration Plan.

(F) Capital Cost

(G) System Efficiency and Electricity Cost

(J) Renewable Electricity Generation Integration

Technical Targets

- Develop a solid oxide electrolysis cell platform capable of operating with current density up to 4 A/cm^2 at or below a voltage of 1.6 V (2020 Stack Energy Efficiency Target: 77% LHV).
- Demonstrate stable SOEC operation with high current density of 3 A/cm^2 for 1,000 h.
- Design a solid oxide electrolysis stack platform capable of operating with the high current density (>3 A/cm^2) cell technology at an upper voltage limit of 1.6 V/cell (2020 Stack Energy Efficiency Target: 77% LHV).
- Demonstrate stable solid oxide electrolysis stack operation with high current density of more than 2 A/cm^2 for 1,000 h.
- Complete a solid oxide electrolyzer process and system design that accommodates the ultra-high operating current density platform, all to meet the Department of Energy (DOE) 2020 target for advanced electrolysis technologies (2020 System Energy Efficiency Target: 75% LHV).

Fiscal Year (FY) 2016 Accomplishments

- Developed and demonstrated a high power density (HiPoD) solid oxide cell platform in electrolysis mode capable of operating with current density more than 4 A/cm^2 at a voltage of 1.6 V at 750°C, meeting the DOE 2020 stack energy efficiency target of 77% LHV. In particular, two HiPoD cells were further tested to a current density of 6 A/cm^2 at 800°C.
- Demonstrated stable SOEC operation with high current density of 3 A/cm^2 for 1,000 h with a degradation rate of 1.81% per 1,000 h.
- Demonstrated a solid oxide electrolysis stack platform capable of operating with the high current density of 3 A/cm^2, at an average cell voltage of only 1.493 V/cell. This corresponds to a demonstrated stack efficiency of 83% LHV, which exceeds the DOE 2020 Stack Energy Efficiency Target of 77% LHV.
- Demonstrated stable solid oxide electrolysis stack operation with high current density of 2 A/cm^2 for 1,000 h with a degradation rate of 1.2% per 1,000 h.

✧ ✧ ✧ ✧ ✧

INTRODUCTION

Hydrogen, a valuable commodity gas, is increasingly recognized as an important fuel and energy storage pathway of the future. Demand for hydrogen as a fuel for fuel cells, in both transport and stationary applications, will continue to grow alongside hydrogen for energy storage (including power-to-gas and power-to-liquids pathways). The renewed interest in developing electrolysis systems is driven, in part, by burgeoning solar and wind industries and the need for

an energy conversion and storage technology that can serve as the vehicle for converting intermittent solar and wind energy into the production of hydrogen. Although current electrolysis systems have the potential to integrate with wind and solar energy sources, the key challenges are low system efficiency and high capital costs. This project aims to address these barriers with an innovative solid oxide fuel cell (SOFC)-based electrolysis cell and stack technology with ultra-high steam electrolysis current (>3 A/cm^2) for potentially ultra-low-cost, highly efficient hydrogen production from diverse renewable sources.

APPROACH

FuelCell Energy (previously Versa Power Systems) has a strong solid oxide cell and stack development history through its previous Office of Energy Efficiency and Renewable Energy sponsored project and through over 15 years of cell and stack advancements from previous efforts (DOE, Solid State Energy Conversion Alliance, and Defense Advanced Research Projects Agency projects). Leveraging this experience, the project objectives will be met by executing the following scope:

- Addressing high current density electrolysis cell performance limitations by conducting multiple materials development and cell design-of-experiments, integrating them with cell production technology development.
- Developing SOEC stack engineering modeling and process fabrication designs to address high current density operating requirements and identifying key operating parameters for the design of an integrated, SOEC-based energy conversion and storage system for renewable energy sources (wind and solar).
- Down-selecting cell technology developments and demonstrating high current density SOEC operation via single cell and stack tests.
- Investigating a high current density solid oxide electrolyzer system, including the option of integration with renewable energy sources, to meet DOE 2020 Advance Electrolysis Technologies targets.

RESULTS

In this project, solid oxide based HiPod cells have been developed such that, when run in electrolysis mode, they are capable of operating at ultra-high electrolysis current density. Those *cathode-supported cells* have been developed using conventional SOFC materials comprising a nickel oxide and yttria stabilized zirconia cathode and 8 mol% yttria-stabilized zirconia electrolyte. (Note: electrolysis electrochemical nomenclature is used here. In fuel cell mode, these same cells are called *anode supported;* in electrolysis mode they are technically accurate to be referred to as *cathode supported*.) The cell utilizes an all-ceramic anode with no noble metals. Electrochemical testing (current-voltage response) of the cells was performed up to 6 A/cm^2 in electrolysis mode as shown in Figure 1. The steam and air are supplied in the horizontal plane, perpendicular to one another, in what is termed a cross-flow geometry. The test housing (and current collection) is made from low-cost ferritic stainless steel and the current collection and seal materials used are the same as those used in SOFC stacks. The cell voltage includes all interfaces and the stainless steel current collection jigs; and, as such, is believed to be representative of the unit cell of an electrolysis stack. The cell platform dimensions are 5 cm x 5 cm x 0.03 cm with an active electrode area of 16 cm^2. This area requires a current input of 96 A to reach a current density of 6 A/cm^2 during electrolysis testing. Gas flows and compositions are as annotated in the figures and consistent across all temperatures tested. Figure 1 shows cell voltage plotted against current density for four different temperatures up to 6 A/cm^2 in electrolysis mode. A remarkable cell voltage of 1.67 V at 6 A/cm^2 was achieved at 800°C. Even at 750°C, the cell exceeded the project performance target of 4 A/cm^2 at 1.6 V. Recently, a HiPoD cell has been operating for more than 1,000 h at 3 A/cm^2 current density with a low degradation rate of 1.8% per 1,000 h.

A 20-cell electrolysis stack was built using HiPoD cells and an ultra-compact, low-cost stack design platform. A photograph of the stack installed in a test stand with thermocouple and voltage lead instrumentation attached can also be seen in Figure 2.

This stack was used to explore the boundaries of high current density electrolysis operation and achieved a very high stack current density of 3 A/cm^2 (67 A) with an average cell voltage of only 1.493 V. Figure 2 shows the load-up, tuning, and operation at this current density over a five-hour

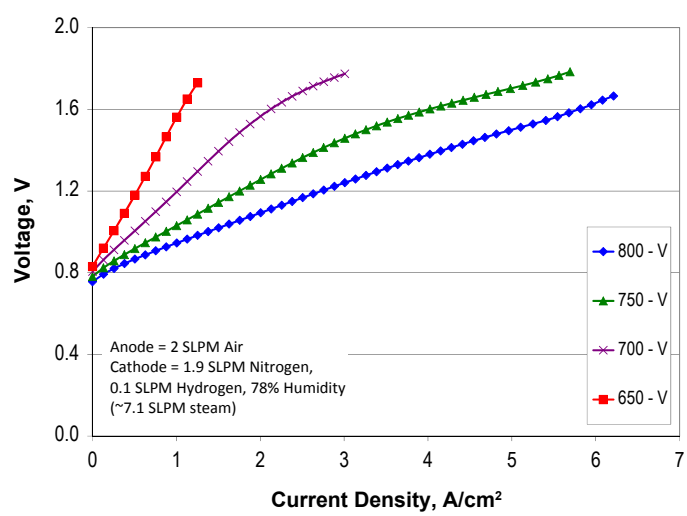

FIGURE 1. Voltage–current density curves for HiPoD cell electrolysis operation 650–800°C

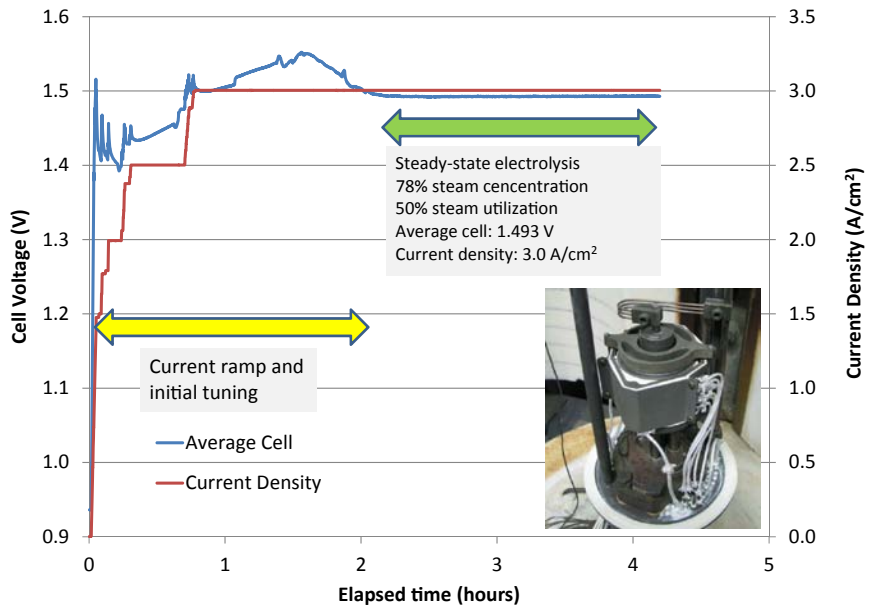

FIGURE 2. Load-up, tuning, and high current density operation of a 20-cell SOEC stack

period. The cathode composition is 78% water and 22% hydrogen (20.11 slpm water, calculated, 5.672 slpm hydrogen, steam utilization is 50.0%). After load-up and tuning, stack voltage is 29.856 V (1.493 V/cell) and stack current is 67 A (3.004 A/cm^2). At this test condition, the stack is producing 50.3 g/h hydrogen with a stack volume of only 200 cm^3 using 2 kW input. This equates to 2.5 kg H_2 per day for a 225-cell stack of this platform design. The stack was further operated in steady-state electrolysis at 2 A/cm^2 for more than 1,000 h. Early in the testing there were three unplanned and uncontrolled test interruptions which resulted in full thermal cycles. The degradation appears to have increased for a period after the first interruption, but the overall degradation for the test period was relatively low at 7.2 mV per 1,000 h per cell or 0.57% per 1,000 h.

A preliminary system design was developed by integrating the inputs from electrochemistry, cell/stack performance data, and system level implications of configuration and operational parameters. Several variations were hypothesized and modeled and the most promising were iterated several times in order to determine the best-case baseline system. The resulting system design is yet to be fully optimized; however, it provides excellent insights to the potential of a high current density, high temperature water splitting system.

CONCLUSIONS AND FUTURE DIRECTIONS

The project team will continue on the current development path. This includes:

- Complete 10 kW rated SOEC stack design freeze incorporating final design changes suggested by stack test results and any further modeling effort as well as final design elements that permit stacking into a 10 kW stack package.
- Complete in-depth SOEC hot module configuration design.
- Demonstrate stable operation of an SOEC stack with a hydrogen production rate of 250 g/hr at a current density of more than 2 A/cm^2.
- Complete a comprehensive techno-economic study of an ultra-high current density SOEC system integrated with renewable energy sources.

FY 2016 PUBLICATIONS/PRESENTATIONS

1. Oral presentation at the 2016 DOE Hydrogen and Fuel Cells Program and Vehicle Technologies Office Annual Merit Review and Peer Evaluation Meeting in June 2016.

2. "Solid Oxide Electrolysis Development at Versa Power Systems," Tony Wood, Hongpeng He, Tahir Joia, Mark Krivy, Dale Steedman, Eric Tang, Casey Brown, Khun Luc; 12th European SOFC & SOE Forum 2016.

3. "Performance Evaluation of Solid Oxide Electrolysis Cells at Versa Power Systems," H. He, A. Wood, T. Joia, M. Krivy, and D. Steedman; 229th ECS Meeting, San Diego, 2016.

4. J. Electrochem. Soc. 2016 Volume 163, Issue 5, F327-F329, Communication—"Electrolysis at High Efficiency with Remarkable Hydrogen Production Rates," Anthony Wood, Hongpeng He, Tahir Joia, Mark Krivy, and Dale Steedman.

II.B.6 Economical Production of Hydrogen Through Development of Novel, High Efficiency Electrocatalysts for Alkaline Membrane Electrolysis

Katherine Ayers (Primary Contact), Chris Capuano, Nem Danilovic
Proton OnSite
10 Technology Drive
Wallingford, CT 06492
Phone: (203) 678-2190
Email: KAyers@protononsite.com

DOE Manager: David Peterson
Phone: (240) 562-1747
Email: David.Peterson@ee.doe.gov

Contract Number: DE-SC0007574

Subcontractors:
- Washington University, St. Louis, MO
- Georgia Technology Institute, Atlanta, GA
- Pajarito Powder, Albuquerque, NM

Project Start Date: April 11, 2016
Project End Date: April 10, 2018

Overall Objectives

- Refine the pyrochlore synthesis technique for electrocatalysis of oxygen evolution.
- Replicate catalyst synthesis in the manufacturing environment and scale up.
- Compare commercial and optimized ionomers and refine formulations based on results.
- Scale up downselected ionomers for demonstration in electrolyzers.
- Integrate optimized catalyst, membrane and ionomer materials into the cell stack and verify performance through durability testing.
- Develop and implement accelerated stress tests for the anionic chemistry.
- Verify a 12–14-cell stack configuration for laboratory scale hydrogen generation.
- Complete the design and build of a 12–14-cell prototype system.

Fiscal Year (FY) 2016 Objectives

- Select oxygen evolution catalysts from synthesis optimization.
- Complete cell testing for selected catalysts.

Technical Barriers

This project addresses the following technical barriers from the Hydrogen Production section of the Fuel Cell Technologies Office Multi-Year Research, Development, and Demonstration Plan:

(F) Capital Cost

Technical Targets

The only metrics for hydrogen production are $/kW and $/kg at the system level. Because of the infancy of the manufacturing processes for electrolyzer technology, these high level metrics cause difficulties in highlighting even major changes at the component level. However, the end cost will be largely dependent on raw material costs. Reducing platinum group metal content and eliminating valve metals such as titanium is therefore critical to meeting the end targets. Developing and scaling stable alkaline membrane technology is also important in establishing feasibility of the technology. The current program aims at meeting the following targets:

- Scale up of catalyst synthesis to 50 g batches and show pathway to kilogram scale
- Verify cell stack scale up to 12–14 cells
- Durability: 500 h of stable operation

FY 2016 Accomplishments

- Synthesized higher surface area pyrochlor catalysts and downselected candidates for cell testing. (milestone)
- Initiated product requirements document for laboratory scale hydrogen generator product.

✧ ✧ ✧ ✧ ✧

INTRODUCTION

As the need for renewable energy capture grows, the balance between electricity feedstock cost and capital cost shifts, due to the ability to obtain low cost electrons but at

lower capacity factors. Since the electrolyzer is on for a lower percentage of the time, the capital cost has a larger impact on the overall lifecycle cost. Anion exchange membrane (AEM)-based electrolyzers offer a pathway to significantly reduce the cost of the cell stack, by enabling low cost oxygen flow fields such as nickel or stainless steel, as well as reduction or elimination of platinum group metals in the catalyst layer. The team has demonstrated the exceptional activity and stability of lead ruthenate pyrochlore electrocatalysts for the oxygen evolution reaction. While these catalysts still contain some noble metal, eliminating the titanium from the cell has a greater impact on cost and provides an initial stepping stone for product cost reduction.

In theory, AEM-based electrodes should represent a drop in replacement to Proton's existing cell stack designs. However, the supply chain for AEMs is still developing, and membrane formats are smaller than the typical Nafion® rolls produced for fuel cell and electrolyzer applications. Introduction of new materials into the cell stack that are unproven in the field also represents a large capital risk at megawatt scale. Proton's laboratory product provides an opportunity to introduce these materials to market at a lower risk entry point and gain field experience on the pathway to eventually applying AEM technology for larger energy related applications.

APPROACH

Proton will continue to work with the Ramani group at Washington University to scale up catalyst synthesis and transition to a commercial company such as Pajarito Powder. Proton will also continue to incorporate the most promising membrane and ionomer combinations in order to optimize performance and stability. While the baseline Tokuyama materials are available commercially and may provide acceptable performance with buffered electrolyte and lower temperature operation, there are better options which may be selected if a commercial pathway to the polymer fabrication is determined to be feasible. As one option, Proton will compare the Tokuyama materials with ionomers developed in Paul Kohl's group at Georgia Tech, which have been used in systems at Acta.

In parallel, Proton will work to scale the stack to an appropriate capacity for the laboratory product portfolio. The planned capacity will supplement existing options rather than supplanting an existing product, to provide more value for the same investment. This work also leverages work done for the U.S. Air Force on a higher capacity hydrogen generator with similar footprint to our lab line (Figure 1). Approaches for electrolyte management (pure water or supporting electrolyte) will be finalized and the resulting system design completed.

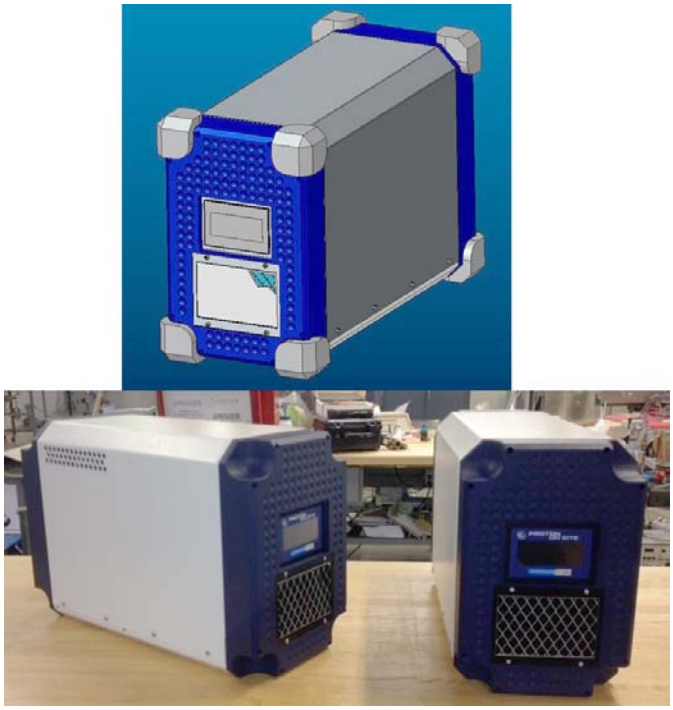

FIGURE 1. System schematic and prototype from Air Force program

FUTURE DIRECTIONS

Next steps include evaluation of advanced materials, and work to define the eventual system design, as follows:

- Characterize potential degradation mechanisms for Georgia Tech ionomers based on post-operational analysis.
- Reproduce pyrochlore synthesis at commercial supplier and perform manufacturing study for volume manufacturing.
- Define system parameters including thermal management and dryer sizing.
- Integrate and test multi-cell stack with integrated AEMs and catalysts.

II.B.7 New Approaches to Improved PEM Electrolyzer Ion Exchange Membranes

Earl H. Wagener (Primary Contact), Brad P. Morgan
Tetramer Technologies, LLC
657 S. Mechanic St.
Pendleton, SC 29679
Phone: (864) 646-6282
Email: earl.wagener@tetramer.com

DOE Manager: David Peterson
Phone: (240) 562-1747
Email: David.Peterson@ee.doe.gov

Contract Number: DE-SC0011305

Subcontractor:
Proton OnSite, Wallingford, CT

Project Start Date: April 6, 2015
Project End Date: April 5, 2017

Overall Objectives

- Optimize electrolyzer membrane performance.
- Refine polymer/membrane and cell architecture to maximize durability.
- Down select materials for optimization of membrane composite configuration.
- Scale-up of polymers and confirm cost estimates.
- Build prototype.

Fiscal Year (FY) 2016 Objectives

- Optimize membrane polarization loss.
- Reduce hydrogen permeation and crossover.

Technical Barriers

This project addresses the following technical barriers from the Hydrogen Production section of the Fuel Cell Technologies Office Multi-Year Research, Development, and Demonstration Plan.

(F) Capital Cost

(G) System Efficiency and Electricity Cost

(K) Manufacturing

(L) Operations and Maintenance

Technical Targets

- Membrane polarization loss after 500 h (200 mA/cm^2, 400 psi, 50°C) <10 mV
- Maintain high performance from Phase I
- Crossover loss at 50°C and 400 psi <1 mA

FY 2016 Accomplishments

- Significant reduction (~$0.60/kg H_2) in energy requirements for hydrogen production
- A 4X increase in output at 70% efficiency
- A 400 mV improvement in performance at 2 A/cm^2
- A 71% lower heating value (LHV) – exceeding the target of 68%
- A reduction in hydrogen crossover – exceeding the target by a factor of 2
- Membrane polarization loss of 9 mV after 500 h (200 mA/cm^2, 400 psi, 50°C)
- Crossover loss at 50°C and 200 psi 4 mA

✧ ✧ ✧ ✧ ✧

INTRODUCTION

The performance needs for improved ion exchange electrolyzer membranes having the properties described under subtopic 13a Membranes and Materials for Energy Efficiency: "Membranes for Electrochemical Systems" [1] were stated as:

(a) "Electrolyzers based on ion exchange membranes are typically operated at high differential pressures, leveraging the low additional overpotential required to electrochemically compress the hydrogen to eliminate stages of mechanical compression. These membranes must therefore withstand significantly higher mechanical loads than fuel cells in order to maintain stack sealing."

(b) "The high differential pressure increases back diffusion of hydrogen, requiring additional design features to mitigate buildup of hydrogen in the oxygen stream, and resulting in efficiency losses."

(c) "Thick membranes are often used to overcome both issues leading to higher ionic resistance and therefore efficiency losses in the cell stack. Thinner membranes and higher temperatures will assist in reducing this

overpotential, but also increase polymer creep and gas permeation."

(d) "New membrane approaches are needed to enable very high efficiencies at moderate hydrogen generation pressures (e.g., 55 bar and below), and acceptable efficiencies at high hydrogen pressures (e.g., 350 bar and above)."

(e) "Membrane chemistries and reinforcement approaches are solicited that reduce hydrogen gas permeation while achieving improved LHV stack efficiencies to reach the goal of over 76% LHV stack efficiency by 2015."

Overall, the target metrics should demonstrate hydrogen permeation below that of commercial membranes while achieving improved ionic conductivity, stability up to 80°C and improved baseline efficiency, including the development of accelerated tests for electrolysis cells to prove long term durability.

APPROACH

The design of unique polymer architectures at Tetramer has been shown to be a vital part of many membrane applications. This unique approach to membrane chemistry has been employed herein to generate a membrane that meets the need for electrolyzer applications. This approach has led to a wide range of modifications to the structure of the membrane that have been explored. These modifications have been the focus of this research and have led to many advancements in technologies that have the potential to dramatically influence the current electrolyzer markets.

RESULTS

This project is well on target and no significant foreseeable problems or changes to the direction of the research have been identified. The Phase II targets shown in Figures 1 and 2 represent very aggressive goals that no commercial material has satisfied. These targets were set to dramatically influence current markets and we have chosen to compare ourselves with relevant commercial samples to ensure viability of the technology. Benefits will be seen downstream in all the technical barriers listed above. As seen by the highlighted accomplishments above, there has been a significant amount of work done to date and our progress has been very encouraging. Currently we have made a large amount of progress in the area of molecular architecture design through the use of a variety of backbone architectures that have resulted in polymers with a range of ion exchange capacities. Membranes have been designed with polymers that vary in molecular weight, contain additives, were cast from various solvents and differ in thickness to determine the effects on performance and durability. This has lead to a much more refined system being studied where the ion exchange capacities are being fine-tuned, molecular weights are being held consistent and any other potential changes are being addressed systematically since initial results have already been collected. The membrane configuration has been defined based on the testing of over 37 membranes. Many of these membranes have shown promising electrolyzer performance as seen by Figure 1, which shows preliminary electrochemical evaluations of some selected membranes. These membranes performed comparably with 2 mil Nafion® electrochemically, but with the advantage of significantly lower hydrogen crossover, which is discussed later.

Electrolyzer membrane thickness has a large influence on performance, durability and hydrogen permeation. The thinner membranes for electrolyzers are highly desired, yet still have many limitations including an increase in hydrogen crossover. This will cause the lower explosion limit to increase and is not desired. Current membranes within this project have been found to have as little as one-third the permeation of Nafion (Figure 2) for similarly thick membranes. Great progress has been made towards reaching the set target and continued research will be tailored to continue to minimize this permeation.

Increased durability has been pursued actively as well and has resulted in many modifications that have been

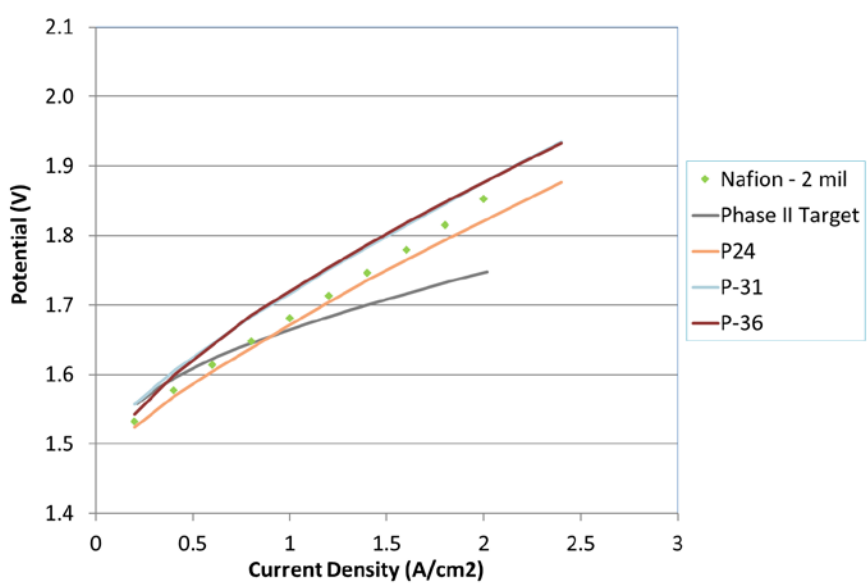

FIGURE 1. Preliminary electrochemical evaluation of several membranes with promising permeation results

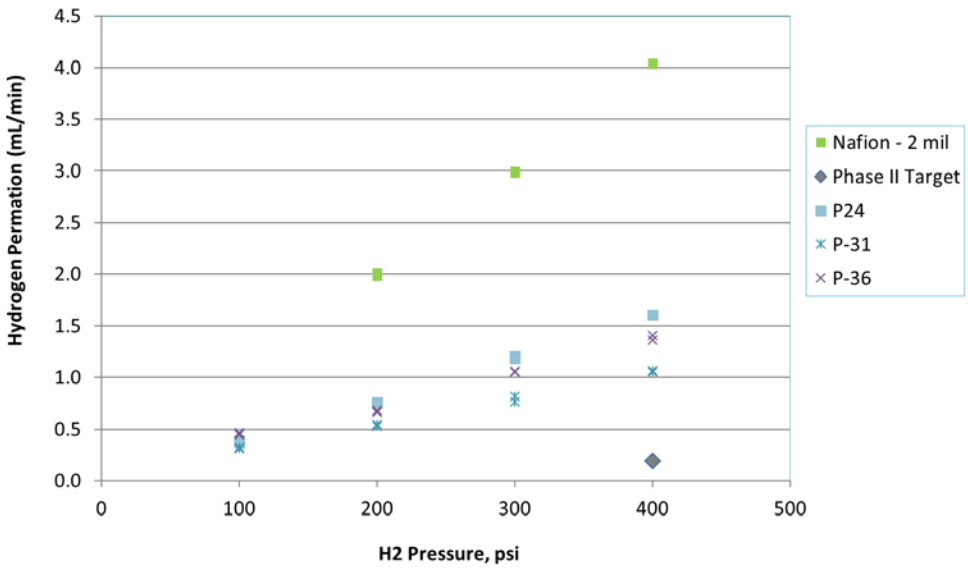

FIGURE 2. Hydrogen permeation through membranes measured electrochemically in situ on 28 cm^2 active area electrolysis cells

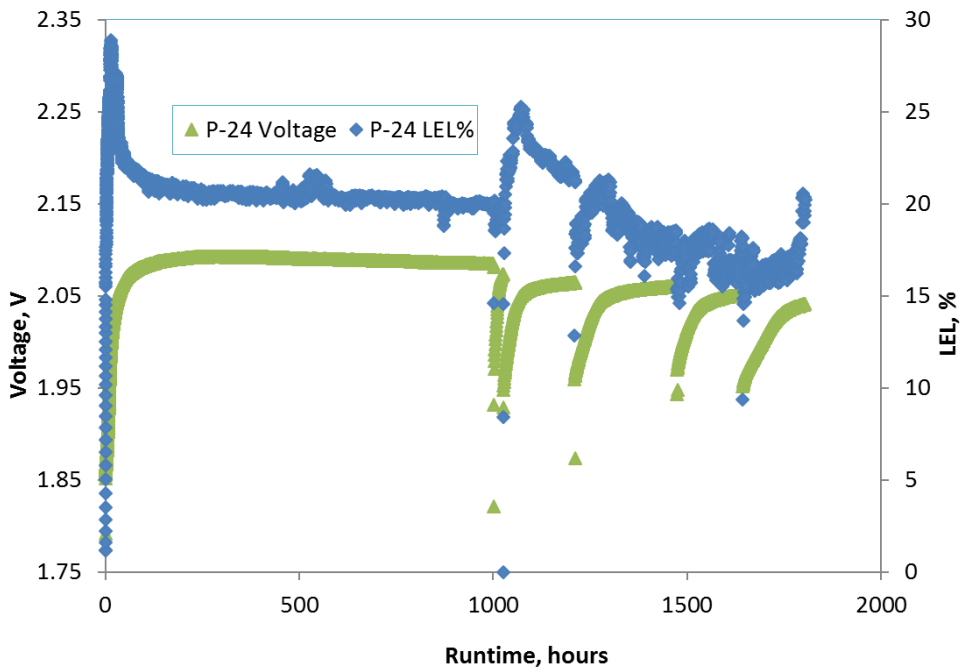

FIGURE 3. Long-term durability test on P-24 showing stable operation and acceptable percent lower explosion limit operated at 50°C, 1.8 A/cm^2 and 200 psi differential hydrogen pressure (gaps in data indicate non-stack related restarts)

explored and have shown a promise to mitigate current degradation mechanisms. This task is currently in the early stages but has already shown over 1,000 h of durability (Figure 3) and will continue to be explored.

CONCLUSIONS AND FUTURE DIRECTIONS

The current technology has currently shown to be a viable way to improve current electrolyzer membranes and will continue to be explored in the future. The need for further long-term durability measurements will be

the primary focus for the following year. The current performance improvements are very promising and if durability can be improved the material will be a dramatic improvement to current membrane materials.

REFERENCES

1. U.S. Department of Energy Topics for 2014 SBIR STTR Phase I Release I DE-FOA-0000969 Topic 13a "Membranes for Electrochemical Systems" http://science.energy.gov/~/media/sbir/pdf/docs/FY14_PIR1_Topics_07-24-13_Final_Ver_5.pdf

II.C.1 High Efficiency Solar Thermochemical Reactor for Hydrogen Production

Anthony McDaniel
Sandia National Laboratories
MS9052
P.O. Box 969
Livermore, CA 94550
Phone: (925) 294-1440
Email: amcdani@sandia.gov

DOE Manager: Katie Randolph
Phone: (240) 562-1759
Email: Katie.Randolph@ee.doe.gov

Subcontractors:
- Prof. Ellen Stechel and Prof. Nathan Johnson, Arizona State University, Tempe, AZ
- Prof. Nathan Siegel, Bucknell University, Lewisburg, PA
- Prof. Ryan O'Hayre and Dr. Michael Sanders, Colorado School of Mines, Golden, CO
- Prof. Christopher Wolverton, Northwestern University Evanston, IL
- Prof. William Chueh, Stanford University, Stanford, CA

Project Start Date: October 1, 2014
Project End Date: December 31, 2016

Overall Objectives

- Verify the potential for solar thermochemical cycles for hydrogen production to be competitive in the long term and by 2020, develop this technology to produce hydrogen with a projected cost of $3.00/gge at the plant gate.
- Develop a high-efficiency particle bed reactor for producing hydrogen via a thermochemical water-splitting (WS) cycle, and demonstrate eight continuous hours of operation on a solar simulator producing greater than 3 L of H_2.

Fiscal Year (FY) 2016 Objectives

- Discover and characterize suitable materials for two-step, non-volatile metal oxide thermochemical water-splitting cycles. (Barrier S and T)
- Construct and demonstrate a particle receiver-reactor capable of continuous operation at 3 kW thermal input. (Barrier T)
- Conduct full techno-economic, sensitivity, and trade-off analysis of large-scale hydrogen production facility using a plant-specific predictor model coupled to H2A. (Barrier X)

Technical Barriers

This project addresses the following technical barriers from the Hydrogen Production section of the Fuel Cell Technologies Office Multi-Year Research, Development, and Demonstration Plan.

(S) High-Temperature Robust Materials

(T) Coupling Concentrated Solar Energy and Thermochemical Cycles

(X) Chemical Reactor Development and Capital Costs

Technical Targets

This project is conducting fundamental studies on materials for use in concentrated solar power applications and designing reactor concepts that, when combined, will produce hydrogen from thermochemical WS cycles. Insights gained from these studies will be applied toward the design and optimization of a large scale solar receiver and reactor that meets the following ultimate DOE hydrogen production targets.

- Hydrogen cost: <$2/kg H_2
- Material of reaction cost: ≤$11,000/yr TPD H_2
- Solar-to-hydrogen (STH) conversion ratio: ≥26%
- One-sun hydrogen production rate: ≥2.1 x 10^{-6} kg/s m^2

FY 2016 Accomplishments

- Extended approach to material discovery and engineering of thermochemical properties by demonstrating an entropy engineering concept using Sr–CeO_2, and by applying density functional theory (DFT) to guide synthesis and characterization of binary ABO_3 perovskites.
- Identified key trends in material properties under thermal reduction, from approximately 200 compound formulations, that informed a heuristic approach to assessing material viability.
- Completed design of Sandia's cascading pressure receiver–reactor (CPR^2) moving particle bed reactor and in process of fabrication. Design choices were validated using modeling, simulation, and lab tests in order to increase the likelihood of meeting overall project objectives.
- Finalized a component-level model of Sandia's reactor concept to enable more advanced techno-economic analysis that will increase the fidelity and accuracy of

H2A cost analysis and allow for detailed sensitivity and cost performance tradeoff analysis.

✧ ✧ ✧ ✧ ✧

INTRODUCTION

This research and development project is focused on the advancement of a technology that produces hydrogen at a cost that is competitive with fossil-based fuels for transportation. A two-step, solar-driven WS thermochemical cycle is theoretically capable of achieving an STH conversion ratio that exceeds the DOE target of 26% at a scale large enough to support an industrialized economy [1]. The challenge is to transition this technology from the laboratory to the marketplace and produce hydrogen at a cost that meets or exceeds the DOE target of <$2/kg H_2.

Conceptually, heat derived from concentrated solar energy can be used to reduce a metal oxide at high temperature producing oxygen (Step 1). The reduced metal oxide is then taken "off sun" and re-oxidized at lower temperature by exposure to water, thus producing hydrogen (Step 2) and completing the cycle. Commercial success of solar thermochemical hydrogen production is contingent upon developing suitable redox active materials and incorporating them into an efficient reactor. There are numerous material chemistries that have attributes suitable for inclusion in a thermochemical hydrogen production system [2-4]. The challenge is to identify an optimally performing material. In addition, the development of redox material and reactor are not mutually exclusive, but must be conducted in parallel [5]. To maximize the probability of success, this project also addresses the reactor- and system-level challenges related to the design of an efficient particle-based reactor concept [6].

APPROACH

Thermochemical WS reactors are heat engines that convert concentrated solar energy (heat) to chemical work. Our approach is to discover materials to accomplish the WS chemistry and pair these with a novel cascading pressure receiver–reactor (CPR^2) that, when combined, can achieve an unprecedented STH conversion ratio. The material discovery work involves expanding our understanding of the underlying thermodynamics and kinetics in order to make performance improvements and/or formulate new, more redox active compositions. Sandia's patented CPR^2 technology is based on a moving bed of packed particles that embodies key design attributes essential for achieving high efficiency operation: (1) sensible heat recovery; (2) spatial separation of pressure, temperature, and reaction products; (3) continuous on-sun operation; and (4) direct absorption of solar radiation by the redox active material. Research efforts are focused on demonstrating this technology in a 3 kW-scale prototype.

RESULTS

Materials Research and Development Thrust. Over the course of this project, Sandia and collaborators have synthesized and screened a select group of compounds for redox and WS activity from perovskite, lanthanum molybdenum oxide, fluorite, and zircon-type crystal structures derived from 15 elements (Al, Ba, Ca, Ce, Fe, La, Mn, Mo, Nb, O, Sn, Sr, Ti, V, and Zr). Through this effort, guided by experience gained from investigating oxides for two-step thermochemical WS cycles and DFT, the $Ce^{3+/4+}$, $Fe^{2+/3+}$, $Mn^{2+/3+/4+}$, $Mo^{3+/4+}$, $Sn^{2+/4+}$, $Ti^{2+/4+}$, and $V^{4+/5+}$ redox couples were explored. More than 200 compounds were synthesized and screened using various thermogravimetric analysis (TGA) protocols, the most efficient of which measured oxygen evolution behavior during a single heat cycle and then inferred WS candidacy from two figures of merit: (1) a redox capacity that exceeds CeO_2 (0.01 mol O/mol sample), and (2) an onset temperature for oxygen release (T_{OR}) where the extent of oxygen non-stoichiometry (δ) exceeds 0.005. Viable WS candidates have a T_{OR} between $Sr_{0.6}La_{0.4}Mn_{0.6}Al_{0.4}O_3$ (SLMA6464) (850°C) and CeO_2 (1,350°C). Approximately 50 compounds with high figures of merit were further characterized in Sandia's stagnation flow reactor.

Shown in Figure 1 is a summary of the most relevant results from this project's material research and development thrust. The filled circles represent specific oxide formulations, for example CeO_2 or SLMA6464, plotted as a function of the maximum δ observed by mass loss measured using TGA (T_{RED} = 1,350°C and $pO_2 < 10^{-8}$ atm) versus the temperature at which δ exceeds 0.005. Compound formulations known to split water upon re-oxidation with steam are found in the yellow and green shaded areas. Two key trends in material redox behavior are evident in Figure 1. First, materials that exhibit a large δ (>0.25) generally do not split water under practically accessible oxidation conditions even though the crystal structure may support a large oxygen deficiency. Second, many WS-active compounds were identified, and achieved a larger δ than CeO_2 at lower temperatures. However, moving from right to left along the solid green line in Figure 1, the amount of steam required to re-oxidize the material relative to the amount of H_2 produced increases dramatically. Going from a 1:1 H_2O:H_2 ratio at the far right (characteristic of CeO_2) to a value greater than 10,000:1 on the left. This means that the thermodynamic driving force to move oxygen back into the solid becomes less favorable for compounds that reduce at relatively low temperatures and support larger δs. It is unclear yet if these trends comprise a universal truth for nonstoichiometric oxides, but these results may bound the discovery space and could be leveraged in a high-throughput screening study.

During this project year, we also extended our approach to engineering of thermochemical properties and material discovery by: (1) demonstrating an entropy engineering

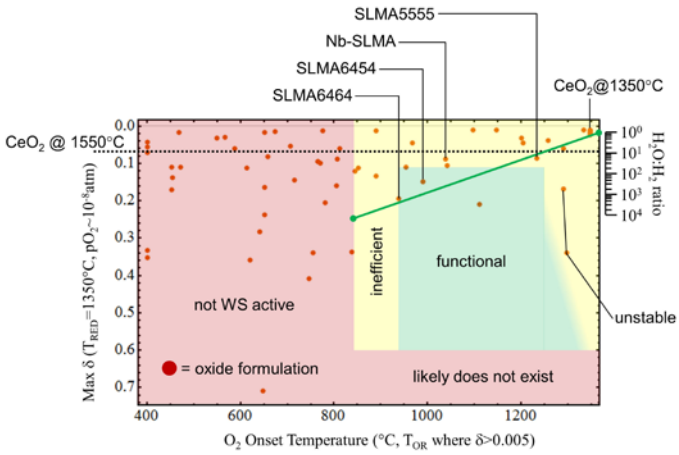

FIGURE 1. Graphic summarizing pertinent results from this project's materials discovery effort. Each filled circle represents a specific compound formulation that was synthesized and tested for redox activity and WS efficacy using TGA and stagnation flow reactor techniques. The ordinate is the maximum oxygen nonstoichiometry (δ) inferred by mass loss measured under reduction at 1,350°C and pO_2~10^{-8} atm using TGA. The abscissa is the temperature at which δ exceeds a value of 0.005. The horizontal black, dashed line is the maximum δ for CeO_2 at 1,550°C, which we believe is a practical operating limit for concentrated solar powered reactors. New materials have potential if their maximum δ is below the black, dashed line. The green solid line is a trend in the H_2O:H_2 ratio that fixes the gas-phase oxygen chemical potential required to achieve full re-oxidation at temperatures between 800–1,000°C. Values closer to unity are considered more commercially viable.

concept, using Sr-doped CeO_2 as a model compound to effectively increase hydrogen production by 10% relative to undoped CeO_2 through lattice softening induced by aliovalent substitution, and (2) by applying a high-throughput DFT approach to screen 5,329 cubic and distorted binary ABO_3 perovskite formulations for WS activity. Using DFT, we identified 139 materials as potential candidates for WS, and tested 10 of them. No *new* commercially viable WS oxides were discovered.

CPR² Fabrication and Demonstration Thrust. By the conclusion of this project, this team will demonstrate continuous operation of a 3 kW prototype thermochemical WS reactor capable of producing >0.3 L/min H_2. The salient components of the CPR² are shown in Figure 2. Starting from top to bottom in the numbered schematic (particles flow by a combination of gravity and "slip-stick" action): 1-particle supply chamber that stores enough redox active material for 10 h of operation, holding high vacuum at ~800°C; 2-solar simulator module comprised of multiple lamps each producing a peak flux of ~1,000 kW/m² (Figure 3 shows the design and measured irradiance of the simulator modules in greater detail); 3-solar receive/reactor (TR chamber) where particles are brought to temperatures in excess of 1,500°C by exposure to simulated solar radiation, and reduced in high vacuum; 4-heat rejection chamber where the particle temperature is lowered to <1,000°C under high vacuum; 5-pressure separation segment capable of withstanding a 200x pressure differential between the TR and WS without fluidizing the packed particle bed; 6-WS chamber where particles are re-oxidized by steam at near ambient pressure and 800°C; and 7-particle reservoir chamber where fully oxidized material accumulates for return to the supply chamber. The schematic in Figure 2 shows a single TR configuration. A second TR chamber and simulator will be added at the conclusion of this project.

During the last 12 months, our project team progressed from notional concepts of the CPR² to fabrication and assembly. Innumerable design choices were considered for each critical component and system operation, ultimately vetted using detailed modeling and experiments on suitable proxies for subcomponents to ensure feasibility, robustness, and high-efficiency operation at this scale. The entire system is a blend of steel, ceramic, and glass that meets the following key design criteria: (1) direct irradiation of redox material without particle shading, (2) precise control of particle flow rate and residence time in the TR chambers, (3) pressure separation without internal mechanical components like valves, (4) counter-flow mass exchange between steam and particles in WS chamber (i.e., no mixing or fluidization during re-oxidation), and (5) eight hours of continuous operation producing at least three liters of hydrogen. Thus far we have incorporated our extensive understanding of this process into the design of a 3 kW-scale reactor. The CPR² is a one-of-a-kind instrument that will be used to evaluate all reactor functions, inclusive of hydrogen production and material durability. Data collected from this instrument will be used to further refine reactor designs, and analytically up-scale Sandia's technology to a multi-megawatt centralized tower system.

Technoeconomic Analysis Thrust. We have finalized a design of a baseline model for a single centralized tower receiver (~29 MW) that, when combined with ~82 others, will constitute a 100 mt H_2/day solar thermochemical water splitting plant. The tower receiver model, shown in Figure 4a, is comprised of 14 major components that represent mass and energy flows between solar field, solar receivers, TR, WS, heat exchangers, recuperators, condensers, and pumps. The complexity and interdependency of this system is evident from the colored lines that crisscross the figure connecting one component to another. Accurately capturing system behavior is necessary to better inform H2A, as well as conduct time and DNI-dependent analysis. Engineering Equation Solver™ is used to exercise the one-dimensional steady state quasi-equilibrium model, which is capable of calculating system cost and STH efficiency, as well as perform sensitivity and tradeoff analysis. The latter is done through changing the system design configuration, component-level parameters, and state point values to affect system-level metrics.

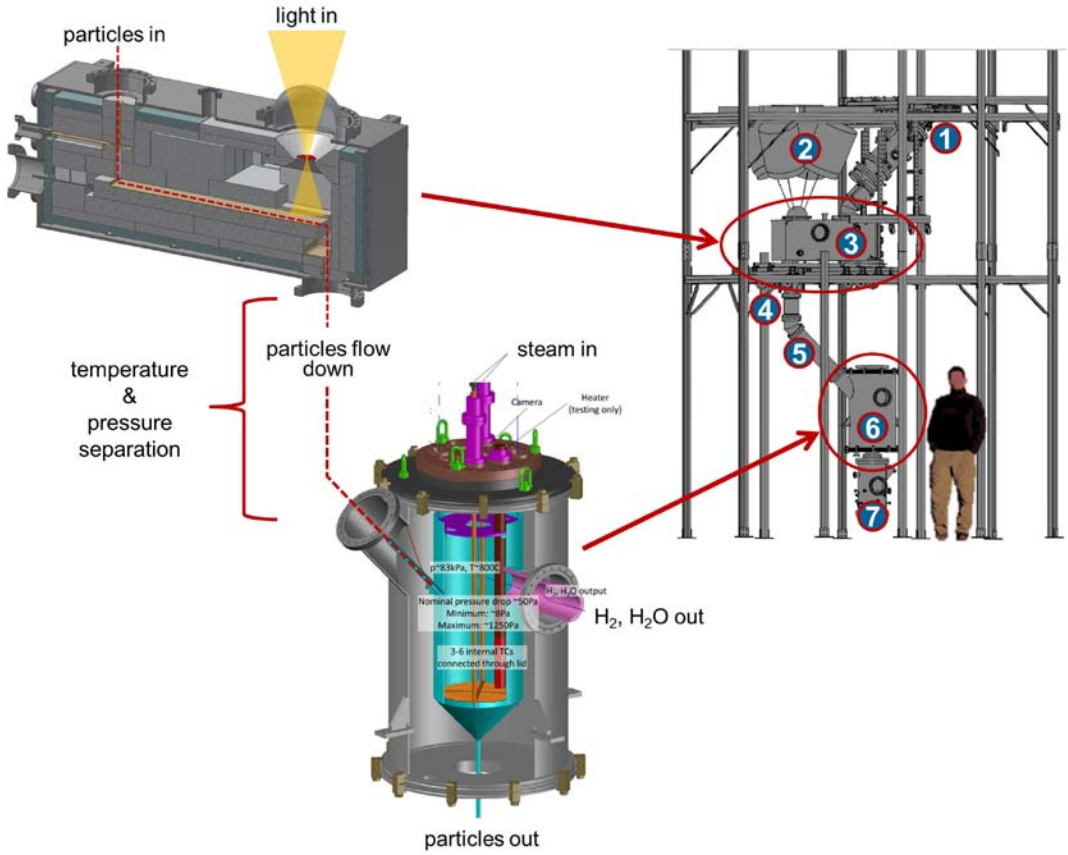

FIGURE 2. Detailed CPR^2 schematics for TR and WS chambers, as well as a numbered list of major system components (see text for discussion). In one year our team went from notional concepts of component design to fabrication and assembly of the CPR^2. Particles flow through system by a combination of gravity in vertical components, and "slip-stick" action along horizontal plates in the TR chambers. This design enables precise control of the particle flow rate and residence time under irradiance. The system will demonstrate Sandia's patented technology (i.e., pressure separation via moving particle bed and pressure cascade for high efficiency) and will be capable of producing >0.3 L/min H_2 continuously.

A representative example of component interdependency, and hence system complexity, is illustrated using the G-S recuperator. Two variables of interest are the steam flow rate entering G-S (16) and recuperator surface area (Hx Area). The particle flow rate (7) is dependent on the instantaneous solar flux (1), and we want the recuperator exit temperature of both streams (8, 17) to be as close as possible. The data in Figure 4b shows that Hx Area will grow unrealistically large if we attempt to bring the exit temperatures of steam and particle to the same value, and therefore the existing steam flow (16) is not sufficient to cool the particles to the desired WS temperature. Simply increasing steam flow into G-S is not an option because of other upstream interdependencies. As such, we must consider inserting another heat exchanger between G-S and WS, or expect suboptimal STH efficiency because particles entering the WS chamber are too hot. Herein lies the crux of tradeoff analysis, taking the lesser cost penalty between increased investment and lower operational efficiency. Upon completion of this project, we will combine our analysis with H2A to produce a roadmap from 2015 to the "Ultimate" case identifying system and material requirements needed to meet DOE cost targets for hydrogen production.

FUTURE DIRECTIONS

- Produce ~150 kg of pelletized CeO_2 redox material for full scale CPR^2 tests.
- Produce at least three standard liters of hydrogen in eight continuous hours of operation of CPR^2.
- Complete techno-economic and cost-performance tradeoff analysis for a 100 mt H_2/day solar-thermochemical production plant.
- Disseminate project results through publications in peer-reviewed journals.

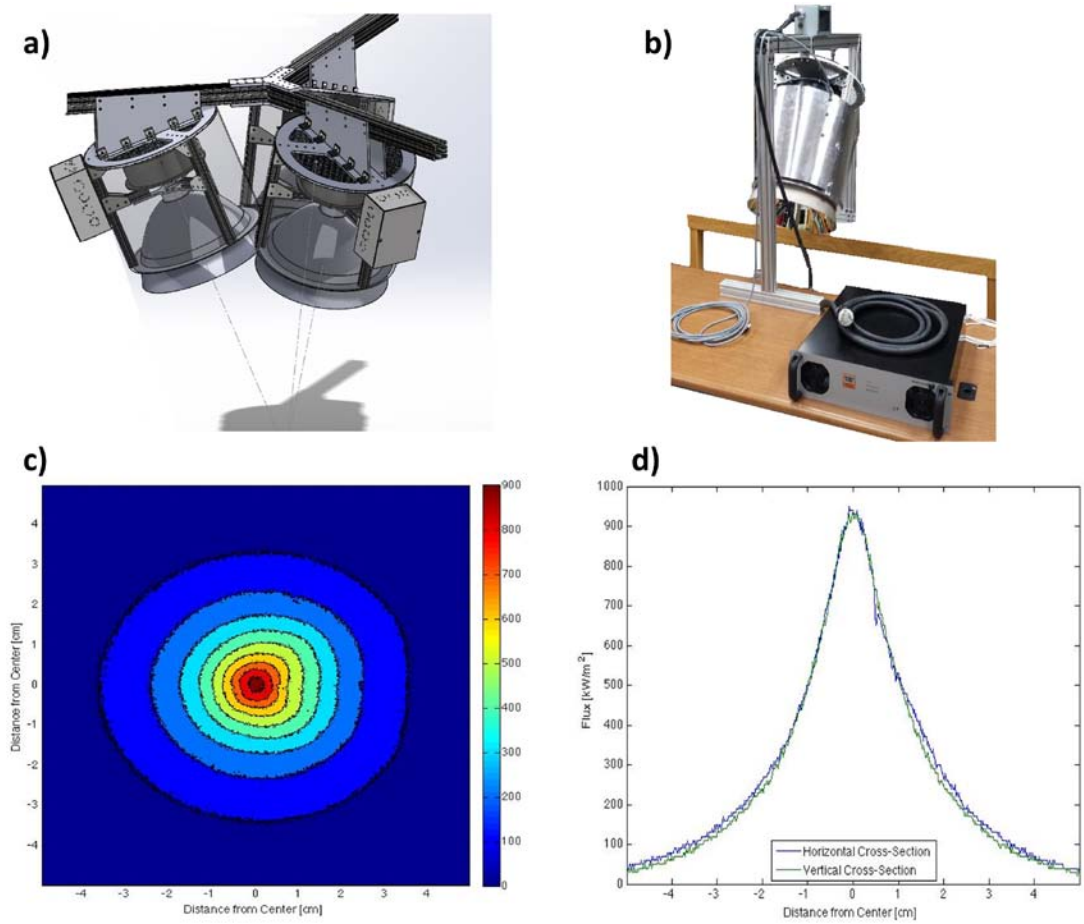

FIGURE 3. (a) Solid model of Bucknell's three-lamp simulator module that will be used to power one of the TR chambers in the CPR[2]. A four-lamp module will also be used, for a total of 7 kW of radiant energy delivered to two separate TR chambers. (b) A photograph of a single lamp module and ballast controller. (c) Flux map for a single lamp module. (d) Plot of radiative flux as a function of distance along horizontal and vertical centerlines taken from the flux map in (c). These flux maps were imported into ray-tracing models and used to design the lamp layout and predict the performance of the multi-lamp arrays, as well as explore the expected thermal behavior of the radiant cavity housed within each TR chamber (e.g., locate potential hot spots).

FY 2016 SELECTED PUBLICATIONS/ PRESENTATIONS

1. I. Ermanoski, J. Grobbel, A. Singh, J. Lapp, S. Brendelberger, M. Roeb, C. Sattler, J. Whaley, A. McDaniel, N.P. Siegel, "Design and Construction of a Cascading Pressure Reactor Prototype for Solar-Thermochemical Hydrogen Production." In *AIP Conference Proceedings*; Cape Town, South Africa, 2016; Vol. 1734, p 120001.

2. W.C. Chueh, "Electrochemical Redox of Late Transition Metal Perovskite Oxides," American Chemical Society National Meeting. Mar. 15, 2016. San Diego, CA USA (Invited).

3. A.M. Deml, R. O'Hayre, C. Wolverton, V. Stevanovic, "Predicting DFT total energies and enthalpies of formation of metal-nonmetal compounds by linear regression," Phys. Rev. B. 93, 085142, (2016).

4. A.M. Deml, A.M. Holder, R.P. O'Hayre, C.B. Musgrave, and V. Stevanović, "Intrinsic Material Properties Dictating Oxygen Vacancy Formation Energetics in Metal Oxides," J. Phys. Chem. Lett., 6, 1948–1953 (2015).

5. A. McDaniel, D. Barcellos, M. Sanders, J. Tong, R. O'Hayre, N. Ahlborg, C.B. Gopal, W. Chueh, A. Emery, C. Wolverton, J. Miller, "Solar Thermochemical Water Splitting: Advances in Materials and Methods," Invited Talk, 6th ECI Conference on Nonstochiometric Compounds, Santa Fe, NM, USA, September 5–9, 2016.

6. R. O'Hayre, "Materials for Solar Thermochemical Hydrogen Production: Can We Beat Ceria?" Presentation to the Board of The Edward Orton Junior Foundation, Columbus, Ohio. June 17, 2016.

7. R. O'Hayre, "Materials for Electrochemical Energy Conversion," Materials Science and Engineering Departmental Seminar, The Ohio State University, Columbus, OH. June 16, 2016.

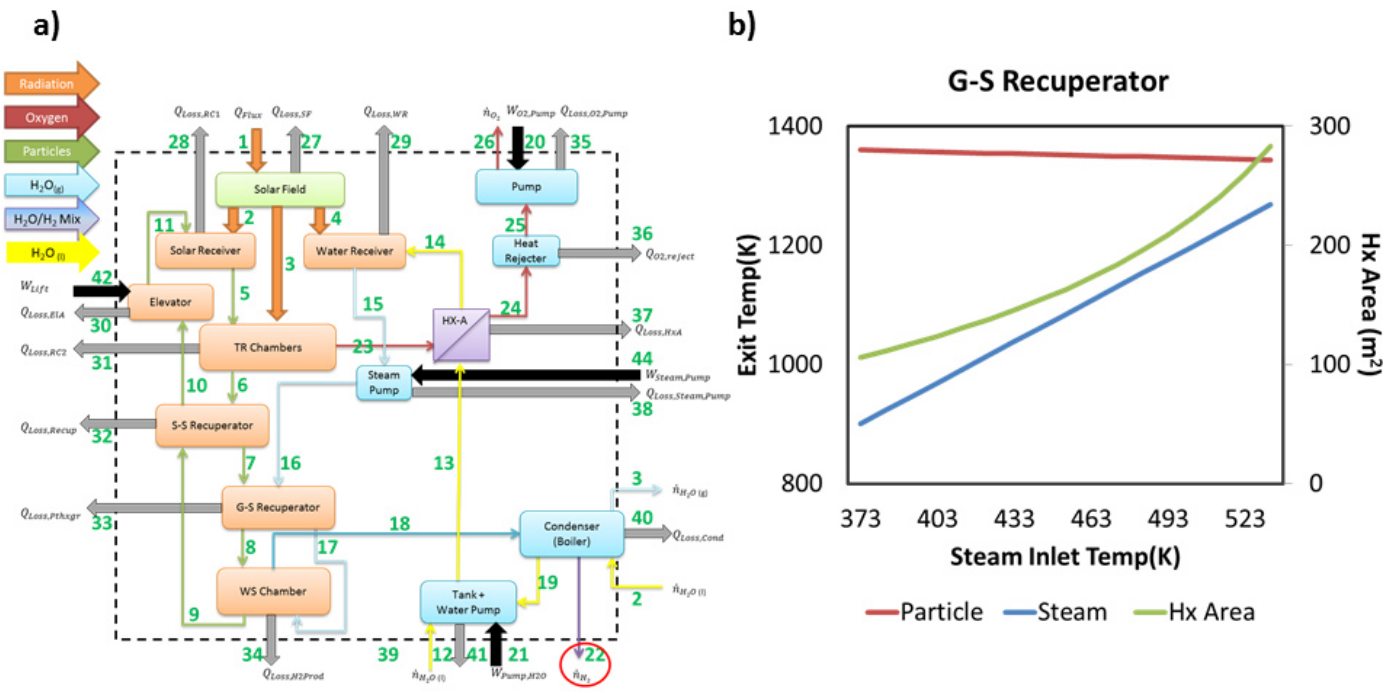

FIGURE 4. (a) Component diagram for a single tower, multiple receiver (Solar Receiver + TR Chambers), concentrated solar powered thermochemical WS system using a non-volatile metal oxide in a two-step process. This diagram represents the minimum number of unit operations needed to implement our thermochemistry. We envision this tower running at 29 MW, and that approximately 82 such towers will be needed to produce 100 mt H_2/day. (b) Model predictions showing how the heat exchanger surface area scales with process parameters for the G-S recuperator. While desirable to have particle and steam temperature as close to each other as possible, the recuperator surface area becomes too large, thus requiring a decision between operational efficiency and capital cost (see text).

8. A. Deml, A. Holder, V. Stevanovic, and R. O'Hayre, "Incorporating Finite Temperature Effects into Materials by Design: Complex Functional Oxides," Invited Talk, 2nd International Conference on Functional Oxide Thin Films for Advanced Energy and Information Technology, Cancun, Mexico, March 5–8, 2016.

9. R. O'Hayre, C. Duan, M. Sanders, D. Clark, M. Shang, D. Diercks, B. Gorman, S. Ricote, and J. Tong, "Materials for Electrochemical Energy Conversion," Invited Seminar, Korea Institute of Materials Science, South Korea, August 10, 2015.

10. R. O'Hayre, C. Duan, M. Sanders, D. Clark, M. Shang, D. Diercks, B. Gorman, S. Ricote, and J. Tong, "Materials for Electrochemical Energy Conversion," Invited Seminar, Korea Tech, South Korea, August 6, 2015.

REFERENCES

1. N.P. Siegel, J.E. Miller, I. Ermanoski, R.B. Diver, and E.B. Stechel, *Ind. Eng. Chem. Res.*, **52**, 3276–3286 (2013).

2. W.C. Chueh and S.M. Haile, *Philos. Trans. R. Soc. Math. Phys. Eng. Sci.*, **368**, 3269–3294 (2010).

3. R.B. Diver, J.E. Miller, M.D. Allendorf, N.P. Siegel, and R.E. Hogan, *J. Sol. Energy Eng.*, **130**, 041001(1)-041001(8) (2008).

4. A.H. McDaniel, E.C. Miller, D. Arifin, A. Ambrosini, E.N. Coker, R. O'Hayre, W.C. Chueh, and J. Tong, *Energy Environ. Sci.*, **6**, 2424–2428 (2013).

5. J.E. Miller, A.H. McDaniel, and M.D. Allendorf, *Adv. Energy Mater.*, **4**, 1300469 (2014).

6. I. Ermanoski, N.P. Siegel, and E.B. Stechel, *J. Sol. Energy Eng.*, **135**, 31002 (2013).

Sandia National Laboratories is a multi-mission laboratory managed and operated by Sandia Corporation, a wholly owned subsidiary of Lockheed Martin Corporation, for the U.S. Department of Energy's National Nuclear Security Administration under contract DE-AC04-94AL85000.

II.C.2 Flowing Particle Bed Solarthermal Redox Process to Split Water

Alan W. Weimer (Primary Contact),
Charles Musgrave, Brian Ehrhart,
Ibraheam Al-Shankiti, Amanda Hoskins,
Samantha Miller, Scott Rowe, Caitlin Majlinger
University of Colorado Boulder
Campus Box 596
Boulder, CO 80309-0596
Phone: (303) 492-3759
Email: alan.weimer@colorado.edu

DOE Manager: Katie Randolph
Phone: (240) 562-1759
Email: Katie.Randolph@ee.doe.gov

Contract Number: DE-EE0006671

Subcontractor:
National Renewable Energy Laboratory, Golden, CO

Project Start Date: September 1, 2014
Project End Date: August 31, 2017

Overall Objectives

The University of Colorado's overall objective is to design and test individual components of a novel flowing particle solarthermal water splitting (STWS) system by optimizing active redox materials, reactor containment materials, and reactor design, with the ultimate goal of demonstrating our technology by producing three standard liters of hydrogen in eight hours on-sun in a prototype fluidized particle reactor.

Fiscal Year (FY) 2016 Objectives

- Develop and test reactive materials with high productivity and stable reactivity.
- Synthesize and characterize high temperature containment materials.
- Test containment materials for steam resistance.
- Build test system for reactor containment materials evaluation.
- Collaborate closely with joint National Science Foundation (NSF) and the Department of Energy's (DOE) materials discovery "sister" project to screen improved active materials.
- Work with the National Renewable Energy Laboratory to ready reactor for on-sun testing.
- Update process model and H2A to reflect experimental progress toward DOE goals.

Technical Barriers

This project addresses the following technical barriers from the Hydrogen Production section of the Fuel Cell Technologies Office Multi-Year Research, Development, and Demonstration Plan:

(S) High-Temperature Robust Materials

(W) Materials and Catalysts Development

(X) Chemical Reactor Development and Capital Costs

Technical Targets

The project's performance towards DOE's technical targets were projected using experimental results from our materials testing and thermodynamic modeling, a process model of a 50,000 kg H_2/d industrial-scale production plant, a detailed solar field model, and DOE's H2A techno-economic (TEA) analysis program and are outlined in Table 1.

TABLE 1. Progress toward meeting technical targets for solar-driven high-temperature thermochemical hydrogen production.

Characteristics	Units	2015 Target	2020 Target	CU 2016 Status
Solar-Driven High-Temperature Thermochemical Cycle H_2 Cost	$/kg	14.80	3.70	14.67
Active Material Cost per Year	$/yr-TPD H_2	1.47M	89K	62.7K*
STH Energy Conversion Ratio	%	10	20	9.3**
1-Sun Hydrogen Production Rate	kg/s per m^2	8.1×10^{-7}	1.6×10^{-6}	7.5×10^{-7}

CU – University of Colorado; STH – Solar-to-hydrogen ratio
*Assuming reaction material replacement lifetime of 1 yr
**Analysis uses hercynite as the active material

FY 2016 Accomplishments

- Manufactured and characterized large, spherical, highly active hercynite materials via spray drying and dynamic mixing techniques. Measurements show active materials can produce >150 µmol H_2/g active material.
- Acquired electrically heated high-temperature oxygen transport membrane and testing is underway.
- Integrated particle flow test system with transport membrane to study kinetics and mass transfer properties of test particles.
- Updated laboratory test systems used to determine production and long-term stability of active materials.
- Altered scaled-up process model to more realistically reflect reactor concept, thermodynamic efficiencies and test material characteristics.
- Collaborated with DOE/NSF sister project to screen 955 binary spinel structures and 1,343 binary perovskite materials for STWS potential. Eight materials have been synthesized for experimental validation.

✧ ✧ ✧ ✧ ✧

INTRODUCTION

In order to meet DOE targets for economical and efficient solarthermal hydrogen production at the commercial scale, advances in active redox materials and reactor fabrication materials are needed. Ideal STWS materials have high hydrogen production capacity, relatively low thermal reduction temperatures (closer to 1,200°C than 1,500°C), fast reaction kinetics, reduction enthalpies on the order of the water splitting enthalpy, are solid in both oxidized and reduced forms, operate with a small ΔT between reduction and oxidation and are highly stable over hundreds of thousands of cycles. We will develop new materials which possess these properties in conjunction with project collaborators. Initial materials development has focused on the doped-hercynite cycle (Red: $Co_{0.4}Fe_{0.6}Al_2O_4 \rightarrow Co_{0.4}Fe_{0.6}Al_2O_{4-\delta} + \delta/2\ O_2$) and perovskite structure (Red: $ABO_3 \rightarrow ABO_{3-\delta} + \delta/2\ O_2$) materials, which have both shown promise in reaching the materials targets. Efficient flowing particle reactors need active materials that are robust, attrition resistant and not limited by slow heat or mass transfer properties. Therefore, we are developing particle fabrication procedures using spray drying technology so that the particles are flowable, reactive, and robust. Additionally, we are evaluating reactor containment materials to ensure stability at the high temperatures at which water splitting occurs. In the end, we will produce reactor ready materials with demonstrated hydrogen productivities to drive the field closer to meeting DOE's technical targets, as determined from our process model and TEA.

APPROACH

A highly efficient STWS reactor must have a scalable and mechanically sound design that maximizes heat flux to the reactive materials and optimizes mass transfer. We are designing a novel reactor which maximizes heat flux, and minimizes heat and mass transfer limitations by fluidizing the active particles. The particles move through the reduction zone by gravity and are entrained in steam flow through the oxidation zone. Since such high-temperatures are required, the absence of moving parts greatly reduces the risk of critical reactor failure. The near-isothermal nature (ΔT < ~150°C) of the reactor design minimizes the need to reheat materials between oxidation and reduction, which leads to low efficiencies in other STWS designs. The reduction step will be carried out using inert sweep gas to achieve the low oxygen partial pressures necessary for the reduction reaction.

In this project we are examining the individual components of the reactor system to determine their feasibility and efficiency. These include kinetic and thermodynamic behavior of spray dried redox materials in a fluidized system, performance of coated reactor containment materials, effect of vacuum pumping vs. inert gas flow for oxygen removal following reduction, and solar concentration modeling. Using this information we are constructing and operating a solar-powered system that can produce at least three liters of hydrogen in eight hours on-sun. By the end of the project, we will have an Aspen model that integrates the individual portions of the reactor system. This will be used in a TEA showing that we are capable of meeting the < \$2/kg H_2 at 50,000 kg H_2/d ultimate project goals.

RESULTS

Significant progress has been made over the past year in preparing active solid spherical reactive particles via spray drying. One technique that showed very promising results for improving the morphology of spray dried particles was pH tuning, whereby the pH of suspensions is altered to match the isoelectric point of the solids. This increases particle flocculation, leading to particles that are larger, more solid, and more spherical. The use of an ultrasonic nebulizer in our spray drier has increased morphology further still. This nozzle tip uses vibration, rather than a compressed gas stream, to aerosolize the suspension. This creates larger droplets, which turn into larger particles when dried. Images of these particles in Figure 1 show a clear improvement in particle size and morphology.

A new reactor system was constructed for determining the long-term hydrogen production of spray dried particles. Testing is underway and we are on track to meet our go/no-

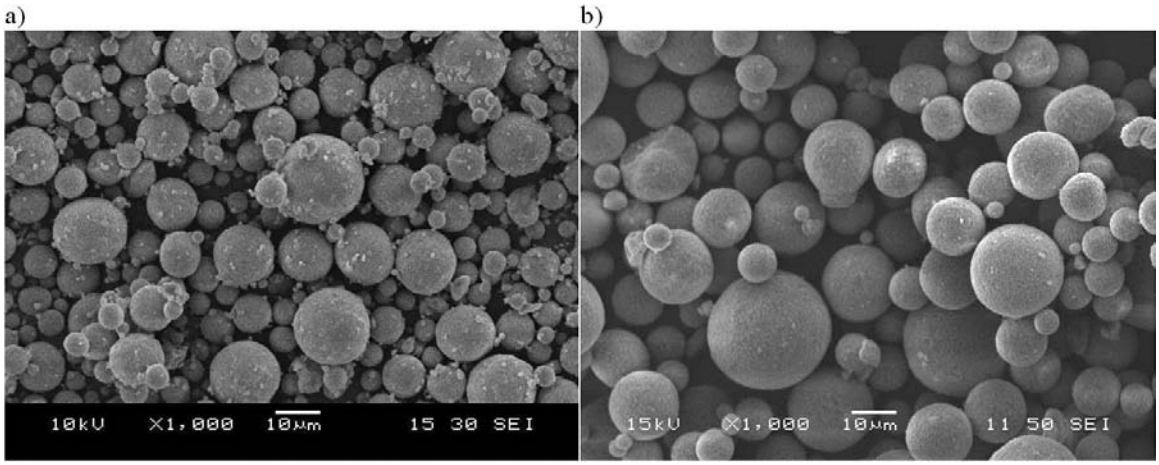

FIGURE 1. Scanning electron microscopy images of calcined hercynite spray dried particles with 20 wt% solids and no organic, made with an iron oxide nanopowder suspension and boehmite suspension in water and the solution was modified to a pH of 7.4 and sprayed using an (a) two-fluid compressed air nozzle and (b) ultrasonic nebulizer.

go target to produce at least 150 µmol H_2/g, while not losing more than 10% reactivity between cycles 100 and 200. All of the spray dried materials tested thus far have generated more than 150 µmol H_2/g, exceeding our go/no-go target as shown in Figure 2. Even materials that had not been optimized via pH tuning and ultrasonic spraying exceeded the required production.

Work to identify new candidate active materials with our DOE/NSF STWS material "sister" project is ongoing. The STWS behavior of 955 binary normal spinel materials was screened based on the oxygen vacancy formation energy determined through a fundamental material descriptor model. Investigations into the effect of spinel inversion, metal oxide structure, and magnetic ordering on density functional theory calculations indicate that all three factors are critical in accurately predicting the STWS behavior of candidate materials.

Progress on the development of stable containment materials has been focused on the growth of atomic layer deposition (ALD) films with desirable properties. During the past year we have deposited alumina and silica films on SiC and developed a method for generating mullite (3 Al_2O_3 : 2 SiO_2) ALD films. Coated particles have been thoroughly characterized to determine the quality, dispersity, and conformity of the deposited films. The transmission electron microscopy images in Figure 3 show the deposited films are conformal and cover the entire particle surface. Inductively coupled plasma analysis has confirmed we are producing the desired stoichiometry. Energy-dispersive X-ray spectroscopy has confirmed the films are uniformly dispersed and there is no preferential deposition of either alumina or silica.

The oxidation resistance of coated SiC has been analyzed via thermogravimetric analysis. We have exposed coated and uncoated SiC particles to steam at 1,000°C for 20 h

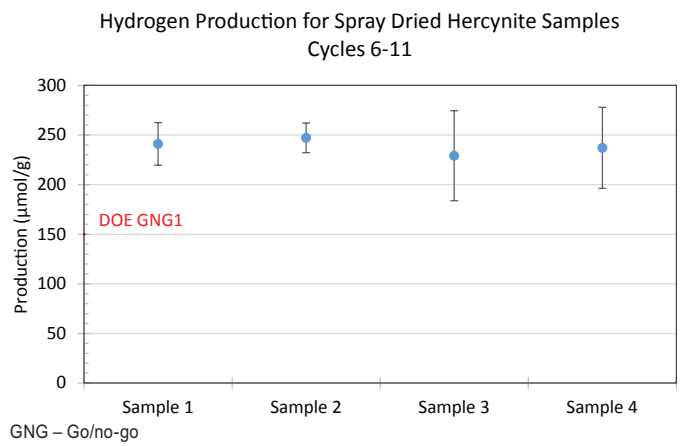

FIGURE 2. Average hydrogen production for four spray dried doped hercynite samples for cycles 6–11 with 95% confidence intervals on the mean.

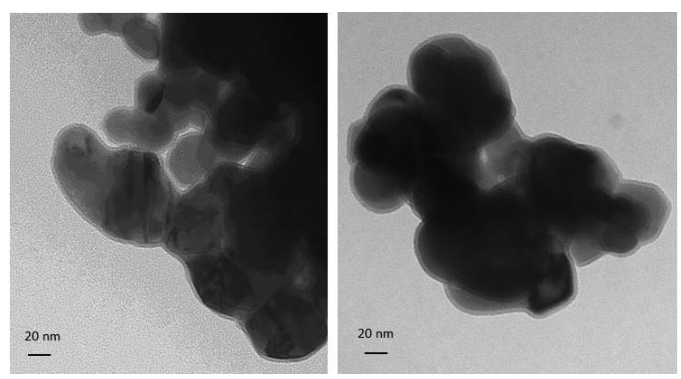

FIGURE 3. Transmission electron microscopy images of zirconia particles coated with 50 cycles mullite ALD.

and recorded the percent mass gain. The results show that alumina films of equal thickness outperform initial mullite films. The best performing sample shows a 10% improvement over uncoated SiC. Since we expect boron nitride films to outperform Al_2O_3 films significantly, we believe to be on track for meeting our go/no-go target of 25% improvement by the end of September 2016.

Over the past year, a fluidization test system has been built to study kinetic and thermodynamic behavior of our redox materials. This system operates using an inert gas sweep to achieve low oxygen partial pressures. Coupled with this system is a selective, high-temperature oxygen transport membrane used to remove oxygen after reduction. In a scaled-up system the inert gas could be recycled, greatly reducing operating costs. Initial testing of the membrane shows promising results. The oxygen content of an O_2/He mixture was reduced from 1.03 mass% O_2 to 15 ppm at 1 SLPM with 21% efficiency.

Computational modeling of our proposed reactor system is ongoing. A method to couple ray tracing (RT) and finite volume (FV) radiation models at an arbitrary surface via spatial as well as angular discretization was developed. The interfacing method was validated by comparing its results with full RT simulations of a compound parabolic concentrator as well as a large-scale solar-thermal reactor, as shown in Figure 4. The validated model was used to investigate the effects of SiC tube radius on the efficiency of ceria reduction. Decreasing the reactor tube radius from 25–5 cm reduced the total ceria production rate but increased the extent of conversion when the particle bed velocity was maintained.

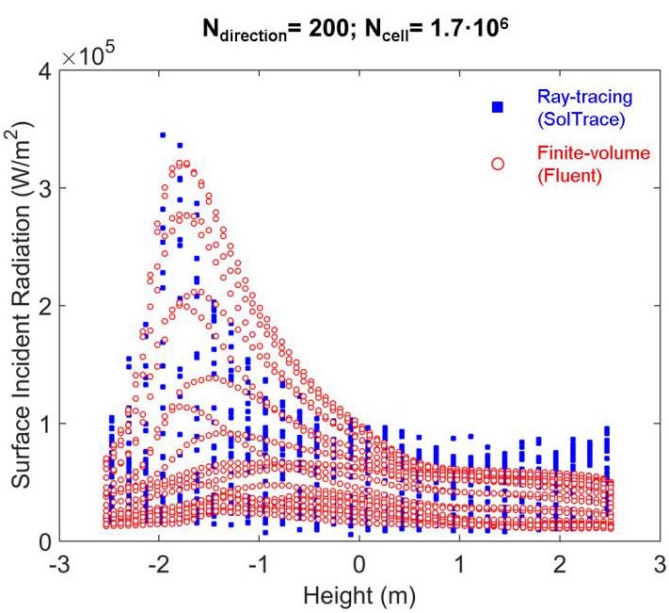

FIGURE 4. Comparison of RT and FV radiation model predicted surface incident radiation profiles along a single reactor tube. Radiation was simulated in the complete reactor geometry by both models. RT and FV predicted total radiative power on the reactor tube are 4.73·105 and 4.69·105 W, respectively. RT predicted peak flux of 3.45·105 W/m^2 (uncertainty ±5%) is ~7% higher than that from the FV simulations (3.21·105 W/m^2).

Our H2A has been updated to reflect advances in the project. Rather than using vacuum pumping to achieve low O_2 partial pressures, an inert gas sweep was used. This was coupled with an oxygen transport membrane, using experimentally-determined efficiencies. Aspen's fluidized bed model was used to determine the size of reactors. Sensitivity analysis identified heliostat cost, material replacement frequency, and SiC cost as the biggest cost drivers. Although last year's analysis identified heat exchanger effectiveness as the biggest driver, the changes made to the model give a higher overall STH efficiency, which reduced the dependency on heat exchanger effectiveness. Overall, the TEA predicts an a hydrogen cost of $2/kg in 2025.

CONCLUSIONS AND FUTURE DIRECTIONS

After the completion of the second year of the project, several conclusions can be drawn:

- Spray dried particles are able to produce well above the go/no-go goal.
- Ultrasonic nebulizer and pH tuning of the spray dry suspension led to the largest and most solid spherical particles in spray drying.
- Mullite ALD has been shown to produce conformal films with the desired stoichiometry.
- Thermogravimetric analysis of ALD-coated SiC shows a 10% improvement in oxidation resistance in a high temperature steam environment.
- Experimental efficiencies of oxygen transport membrane are likely to be sufficient to meet the DOE cost target of $2/kg H_2.
- Modeling demonstrates reactor tube diameter is positively correlated with hydrogen production and negatively correlated with extent of conversion.
- TEA shows capability of process to produce hydrogen for $2/kg using 2025 DOE targets.

Future work will include:

- Pursuing further experimental validation of high-performance STWS materials predicted by density functional theory.
- Demonstrating long-term stability of active particles that lose no more than 10% of reactivity between 100th and 200th redox cycle.
- Developing containment materials that provide a 25% increase to the stability of SiC under redox conditions.

- Updating TEA based on results of theoretical and experimental studies.
- Studying the kinetic behavior of hercynite for both reduction and oxidation.
- Producing three standard liters of hydrogen during eight hours on-sun at the National Renewable Energy Laboratory's high-flux solar furnace using a lab-scale reactor and fabricated particles.

FY 2016 PUBLICATIONS/PRESENTATIONS

Publications:

1. Muhich, C.L., B. Ehrhart, V. Witte, S.L. Miller, E. Coker, C.B. Musgrave, A.W. Weimer, "Predicting the Solar Thermochemical Water Splitting Ability and Reaction Mechanism of Metal Oxides: a Case Study of the Hercynite Family of Water Splitting Cycles," *Energy and Environmental Science*, 8, 3687–3699 (2015). DOI: 10.1039/C5EE01979F

2. Muhich, C.L., V. Poole-Aston, R.M. Trottier, A.W. Weimer and C.B. Musgrave, "A First Principles Analysis of Cation Diffusion in Mixed Metal Ferrite Spinels," *Chemistry of Materials*, 28 (1), 214–226, (2016). DOI: 10.1021/acs.chemmater.5b03911

3. Muhich, C.L., Erhardt, I. Al Shankiti, B.J. Ward, C.B. Musgrave and A. W. Weimer, "A Review And Perspective of Efficient Hydrogen Generation Via Solar Thermal Water Splitting," *WIREs Energy and Environment*, 5 (3), 261–287 (2016). DOI: 10.1002/wene.174

Presentations:

1. Muhich, C., B. Ehrhart, S. Miller, V. Witte, B. Ward, C. Musgrave, A. Weimer "Active and Flowable Doped-Hercynite Materials for Solarthermal Redox Processing to Split Water," American Institute of Chemical Engineers Annual Meeting, Salt Lake City, November 2015.

2. Trottier, R., S. Miller, C. Muhich, C. Musgrave and A. Weimer "Rapid Computational Screening of Metal Oxides for Water Splitting: Kinetics of H2 Production," American Institute of Chemical Engineers Annual Meeting, Salt Lake City, November 2015.

3. Miller, S., R. Trottier, C. Muhich, C. Musgrave and A. Weimer "Screening of Metal Oxide Materials for Solar Thermochemical Water Splitting," American Institute of Chemical Engineers Annual Meeting, Salt Lake City, November 2015.

4. Witte, V., B. Ehrhart, B.J. Ward, A. Weimer "Hydrogen Fuel Production Using Reactive Metal Oxides in a Solar Thermal Water Splitting (STWS) Cycle," American Institute of Chemical Engineers Annual Meeting, Salt Lake City, November 2015.

5. Groehn, A., A. Weimer "Efficiency and Design of High-Temperature Solar-Thermal Reactors," American Institute of Chemical Engineers Annual Meeting, Salt Lake City, November 2015.

6. Ehrhart, B., I. Al-Shankiti, A. Weimer "Impact of Reduction of Flowing Particles on System Efficiency for Solar Thermochemical Hydrogen Production," American Institute of Chemical Engineers Annual Meeting, Salt Lake City, November 2015.

7. Ehrhart, B., I. Al-Shankiti, A. Weimer "Reduction of Flowing Particles for Efficient Solar Thermochemical Hydrogen Production," American Institute of Chemical Engineers Annual Meeting, Salt Lake City, November 2015.

II.C.3 Electrolyzer Component Development for the HyS Thermochemical Cycle

William A. Summers (Primary Contact),
Héctor Colón-Mercado, Maximilian Gorensek,
Claudio Corgnale, Mark Elvington
Savannah River National Laboratory (SRNL)
SRS, Building 999-2W
Aiken, SC 29808
Phone: (803) 617-8590
Email: bill.summers@src.energy

DOE Manager: Eric Miller
Phone: (202) 287-5829
Email: Eric.Miller@ee.doe.gov

Subcontractor:
Savannah River Consulting LLC, Aiken, SC

Project Start Date: June 1, 2013
Project End Date: September 30, 2016

Overall Objectives

- Develop highly efficient process designs for coupling the Hybrid Sulfur (HyS) thermochemical process with a concentrated solar energy system capable of achieving a hydrogen cost at the plant gate of <$2 per kilogram of H_2.
- Demonstrate SO_2-depolarized electrolysis (SDE) using improved electrocatalysts and high temperature proton exchange membranes (PEMs) that permit high efficiency hydrogen production.

Fiscal Year (FY) 2016 Objectives

- Analyze and select a baseline plant design that utilizes high-temperature solar heating, energy storage and permits 24-hour hydrogen production.
- Develop Aspen Plus™ process flowsheet models, calculate plant performance and efficiency.
- Estimate capital and operating and maintenance (O&M) costs for a commercial plant and utilize the H2A analysis tool to determine projected hydrogen production costs for 2015 and 2020 design concepts.
- Utilize the Pressurized Button Cell Test Facility (PBCTF) to test candidate high-temperature PEMs and demonstrate SDE performance improvements of 80 mV over performance with the baseline Nafion® PEM.

Technical Barriers

This project addresses the following technical barriers from the Hydrogen Production section of the Fuel Cell Technologies Office Multi-Year Research, Development, and Demonstration Plan.

(S) High-Temperature Robust Material

(T) Coupling Concentrated Solar Energy and Thermochemical Cycles

(U) Concentrated Solar Energy Capital Cost

(W) Materials and Catalysts Development

(AC) Solar Receiver and Reactor Interface Development

Technical Targets

This project is conducting system design studies and electrolyzer development and testing in order to improve the performance and lower the capital and operating costs for the HyS thermochemical cycle. Detailed flowsheet analysis and mass and energy balances are used to estimate potential overall system efficiency. Capital cost estimates used in the H2A analysis for hydrogen production costs are based on previous work funded by the DOE Office of Nuclear Energy combined with solar system cost estimates based on goals for the Office of Energy Efficiency and Renewable Energy's (EERE) Solar Program. Electrolyzer performance projections represent current estimates of performance based on extrapolations to cell operation at 130°C. Heliostat capital cost and solar-to-electric conversion efficiency are consistent with the current viewpoint of the EERE Solar Program.

TABLE 1. Progress towards Meeting Technical Targets for Solar-Driven High-Temperature Thermochemical Hydrogen Production

Characteristic	Units	2015 Target	SRNL 2015 Projections	2020 Targets	SRNL 2020 Projections
Solar-Driven Hydrogen Cost	$/kg	14.80	7.58	3.70	3.52
Solar-to-Hydrogen (STH) Energy Conversion Ratio	%	10	15.6	20	19.1
Heliostat Capital Cost	$/m^2	140	140	75	75
Solar-to-Electric Efficiency	%	---	20.6	---	25

FY 2016 Accomplishments

- Conducted flowsheet analyses and tradeoff studies to identify preferred solar-driven HyS system design configurations and selected a baseline solar HyS plant design.
- Completed full Aspen Plus flowsheet and overall process efficiency determination including pinch point analysis and design of heat exchange network.
- Utilized DOE H2A analysis tool to estimate hydrogen production cost for solar-driven HyS process for current status (2015) and projected Calendar Year (CY) 2020 conditions.
- Identified several high temperature PEMs and characterized them in the PBCTF.
- Achieved FY 2015 go/no-go criteria of >50 mV improvement in SDE voltage versus baseline Nafion membranes.

✧ ✧ ✧ ✧ ✧

INTRODUCTION

Thermochemical water splitting processes produce hydrogen by using heat to drive a series of linked chemical reactions that result in water being split into separate hydrogen and oxygen streams with all the intermediate chemicals being recycled. Hybrid thermochemical cycles have an electrochemical step in the process, and therefore require some electricity input in addition to the thermal input. The HyS process is one of the most advanced of the thermochemical water-splitting cycles; each of the major reaction steps has been experimentally validated and detailed system designs have been created. However, much of the previous development work was based on the idea that the heat would be provided from a high temperature nuclear reactor operating continuously. Therefore, new designs are necessary to accommodate the use of solar energy, which requires either intermittent operation or a means of energy storage. HyS is the only practical two-step thermochemical cycle with all fluid reactants. In the first step, sulfuric acid is thermally decomposed at high temperature (>800°C) to produce sulfur dioxide (SO_2) and oxygen. In the second step the SO_2 is used to depolarize the anode of a water electrolyzer, resulting in the production of hydrogen at the cathode and sulfuric acid (which is sent to the decomposer) at the anode. The overall reaction is the splitting of water into H_2 and O_2. The electrolyzer, known as the SDE, requires only about one-third as much electricity as a conventional water electrolyzer.

APPROACH

The project is divided into two main tasks: (1) system design and analysis and (2) electrolyzer development and testing. The goals of Task 1 are to utilize modelling and flowsheet analyses to develop efficient and cost effective HyS plant designs based on the use of concentrated solar power. Task 2 involves experimental work relating to the development of the SDE, the key reaction step in the process. The focus of the research is to improve performance by developing better electrocatalysts and PEMs while increasing the cell's operating temperature from the 70–90°C range to 120–130°C. A new PBCTF was built in 2015 to permit the higher temperature testing and to facilitate rapid characterization of membrane candidates.

RESULTS

Several alternative configurations for the solar HyS flowsheet were studied. These included the following options:

- Gaseous-fed or liquid-fed electrolyzer
- Continuous or diurnal operation
- Thermal versus chemical energy storage
- Direct or indirect heating of the acid decomposer
- Integrated or separate operation of process sections (electrolysis and acid decomposition)

In addition, three different design options where evaluated for the solar receiver, as follows:

- Falling particle receiver (FPR) (uses heated "sand" for thermal energy storage)
- Cavity receiver to heat helium (requires chemical energy storage)
- Direct solar-heated acid vaporizer and decomposer (requires chemical energy storage)

Tradeoff studies resulted in the selection of a baseline conceptual design consisting of a liquid-fed electrolyzer, an indirectly heated acid decomposition reactor, thermal energy storage, and a solar receiver based on the FPR concept being developed by Sandia National Laboratories. The use of heated sand to provide high temperature thermal energy storage permits continuous, 24-hour operation of the complete HyS plant. A diagram of the FPR is shown in Figure 1.

Aspen Plus flowsheets were completed and mass and energy balances were calculated in order to determine the process efficiency. The performance of the solar portion of the plant was based on assumptions from the EERE Solar Program. The overall solar-to-hydrogen (STH) conversion ratio for the CY 2020 design was estimated to be 19.1%.

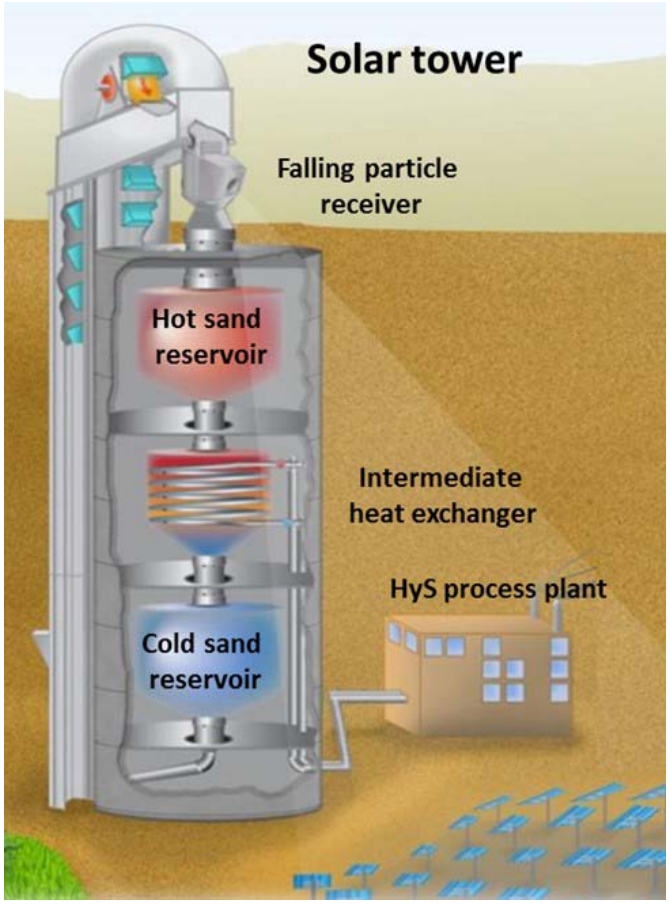

FIGURE 1. Diagram of the falling particle receivier

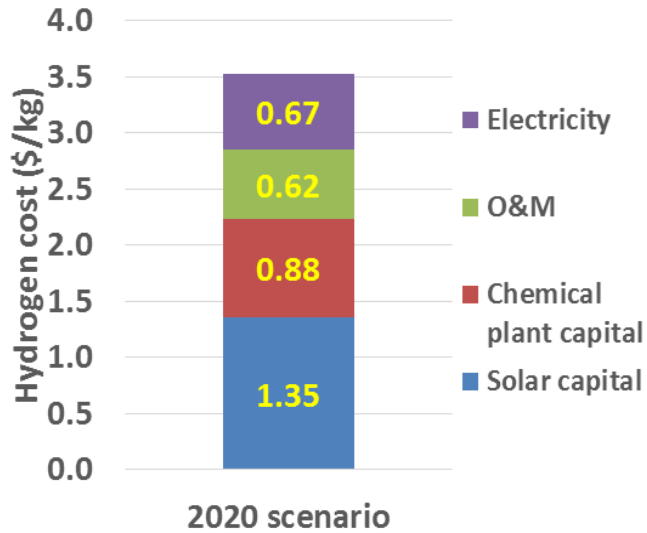

FIGURE 2. Cost breakdown for the 2020 solar HyS plant

Hydrogen production cost estimates using the DOE H2A program resulted in a projected cost for CY 2020 of $3.52/kg, exceeding DOE goals. A breakdown of the production cost estimate is shown in Figure 2. Electricity costs assumed solar-generated electricity at 6¢/kWhr.

Electrolyzer development included the fabrication and testing of membrane electrode assemblies (MEAs) in the PBCTF. MEAs consisting of a Nafion 115 PEM, with Tanaka Kikinzoku Kogyo platinized carbon electrocatalyst for both the anode and cathode, were used to determine the baseline SDE performance. Tests were performed at temperatures between 60ºC and 90ºC in water and in 30 wt% sulfuric acid. As expected, it was observed that the performance improves as a function of temperature, primarily as a result of increased reaction rate and a corresponding reduction in the kinetic overpotential at the anode. This result is paramount in utilizing advanced high temperature membranes, since operating at elevated temperature necessitates the use of non-Nafion based PEMs. Several alternative high temperature membranes were selected for potential application in the HyS electrolyzer. These membranes are required to have a combination of good chemical stability (resistant to H_2SO_4 corrosion), high ionic conductivity at high temperature (>120°C), and low SO_2 flux. Tests were conducted using a sulfonated-diels-alder-poly-phenylene membrane from Sandia National Laboratories. Testing at 91°C showed a 50 mV improvement over the baseline Nafion MEA, which met the project's FY 2015 go/no-go criteria. Deconvolution of the data indicated the potential for >150 mV improvement at 130°C. High temperature testing to verify this result is ongoing. The goal is to demonstrate stable SDE performance of 600 mV at a current density of 500 mA/cm^2.

CONCLUSIONS AND FUTURE DIRECTIONS

Work this year has resulted in the following conclusions:

- A solar HyS design, based on detailed modeling and equipment sizing and costing, has the potential to meet DOE's goals for hydrogen production cost and STH conversion ratio.
- The baseline system design consists of the FPR, thermal energy storage, an indirectly heated acid decomposer, a liquid-fed SDE and continuous (24/7) hydrogen production.
- SDE performance improves with increasing temperature; new high temperature PEMs are necessary for tests above 90°C; operation at ≥130°C is projected to meet SDE performance targets.

Future work (not currently funded) should include the following:

- Updating the process design and H2A analysis for an ultimate plant design meeting the DOE hydrogen production cost goal of <$2/kg H_2.
- Modelling and testing of the "bayonet" acid decomposition reactor.

- Fabrication of MEAs with high temperature membranes and various electrocatalyst compositions and testing in the PBCTF at >130°C for up to 1,000 hr.
- Construction and testing of an integrated HyS process at laboratory scale.
- Integrated testing of the acid decomposition system with a FPR.

FY 2016 PUBLICATIONS/PRESENTATIONS

1. William A. Summers, Maximilian Gorensek, Hector Colon-Mercado, Claudio Corgnale and Mark Elvington, "Electrolyzer Component Development for the HyS Thermochemical Cycle, Project PD096," DOE EERE Fuel Cell Technologies Office, 2016 Annual Merit Review and Peer Evaluation, Washington, D.C., June 8, 2016.

II.C.4 NSF/DOE Solar Hydrogen Fuel: Accelerated Discovery of Advanced RedOx Materials for Solar Thermal Water Splitting to Produce Renewable Hydrogen

Christopher Muhich, Samantha Miller,
Ryan Trottier, Alan Weimer, and Charles Musgrave
(Primary Contact)
University of Colorado Boulder
Campus Box 596
Boulder, CO 80309-0596
Phone: (303) 735-0411
Email: charles.musgrave@colorado.edu

DOE Manager: Katie Randolph
Phone: (240) 562-1759
Email: Katie.Randolph@ee.doe.gov

Contract Number: NSF Grant No. 1433521

Project Start Date: October 1, 2014
Project End Date: September 30, 2017

Overall Objectives

- Develop a computationally accelerated and experimentally validated materials-by-design approach to design materials with optimum thermodynamic, mass transport, and kinetic properties for solar thermal water splitting (STWS) that can be tailored for materials discovery for other technologies.
- Use our accelerated materials discovery approach to screen doped perovskite and spinel metal oxide materials for STWS and provide a rank-ordered list of promising redox active materials.
- Address fundamental and broad materials chemistry questions in accomplishing the two overall objectives above.
- In conjunction with DOE sister project (DE-EE0006671), test promising redox materials identified by our rapid screening process using a stagnation flow reactor to validate screening methods.

Fiscal Year (FY) 2016 Objectives

- Apply a descriptor model [1] to predict the oxygen vacancy formation energy of binary spinels.
- Investigate spinel inversion as a method for identifying new materials.
- Validate computational methods for predicting hydrogen production capacities in binary perovskites.
- Determine reaction barriers on hercynite and doped hercynite surfaces.
- Determine transport barriers for hercynite and doped hercynite materials.

Technical Barriers

This project addresses the following technical barriers from the Hydrogen Production section of the Fuel Cell Technologies Office Multi-Year Research, Development, and Demonstration Plan.

(W) Materials and Catalyst Development

Technical Targets

This project involves conducting fundamental studies of novel perovskite and spinel redox active materials to identify those with high hydrogen production capacities (>200 μmol $H_2/g_{material}$/cycle), low thermal reduction temperatures (<1,400°C), fast kinetics, low cost, and enthalpies of reduction high enough to drive the water splitting reaction, but not so high as to be thermodynamically inefficient. Insights gained from these studies will be applied towards the design of a flowing particle solar water splitting system that meets the following DOE ultimate hydrogen production targets:

- Solar-Driven High-Temperature Thermochemical Cycle Hydrogen Cost: $2.00/kg
- Annual Reaction Material Cost: $11,000/yr.-TPD H_2
- Solar to Hydrogen Energy Conversion Ratio: 26%

FY 2016 Accomplishments

- Developed a robust approach for predicting STWS ability of materials.
- Screened 1,041 binary normal spinels for thermodynamic viability. 52% of materials were found to have an O-vacancy formation energy potentially capable of driving STWS.
- Incorporated inversion into screening of spinels to identify additional promising materials.
- Evaluated the effect of structure and spin on the predicted STWS behavior for 1,343 perovskites.
- Determined the bulk transport barriers in hercynite and doped hercynite.

- Worked to identify descriptors for reaction kinetics in spinels.
- Determined reaction barriers for water dissociation reactions on hercynite and doped hercynite.

✧ ✧ ✧ ✧ ✧

INTRODUCTION

Two-step thermochemical redox processes based on metal oxide cycles are a promising route to efficiently capture and store solar energy because they have the potential to operate at high thermal efficiencies, are chemically simple, and require less land and water to operate than competing biomass, artificial photosynthesis, and photovoltaic-driven electrolysis. In two-step metal oxide based STWS, a metal oxide is heated using concentrated solar thermal energy to a temperature at which it reduces, generating O_2. Subsequently, H_2O is introduced to the system as steam to re-oxidize the material to its initial state and generate H_2. Materials which operate via an oxygen vacancy based mechanism, as shown in Equations 1 and 2, are of particular interest due to their thermal stability owing to the formation of oxygen vacancies within the lattice rather than complete phase change of the material.

Equation 1. MO_x à $MO_{x-\delta} + \delta/2\ O_2$

Equation 2. $MO_{x-\delta} + \delta\ H_2O$ à $MO_x + \delta\ H_2$

The ideal material for efficiently driving STWS has not yet been identified, although a large number of materials have been examined. To be a STWS material, a candidate material must undergo both reduction and water oxidation; to be a practical STWS material, it must reduce at temperatures which are achievable using concentrated sunlight and at which reactor containment materials do not degrade (<~1,700°C). The assessment of STWS materials and cycles has generally been undertaken by one of two approaches, (1) evaluating a set of previously proposed water splitting cycles for their practical viability or (2) identifying novel materials from a broad set of candidates by predicting their ability to drive STWS. Because an optimal STWS material or cycle has not yet been identified, our focus is on the latter of these two approaches, which we call "STWS materials screening."

APPROACH

Our STWS materials screening approach to discover materials for an efficient cost effective hydrogen production process involves (1) using computational materials modeling based primarily on density functional theory quantum mechanical simulations to (2) rapidly predict basic materials properties, which we use as descriptors within a model we will develop for predicting the redox properties of candidate materials. The computational screening will be used to (3) guide an experimental effort to synthesize and validate promising redox materials identified by our rapid screening process.

Although in principle an ab initio approach could predict the redox properties of candidate metals oxides directly, the large number of possible materials (e.g., over 1.3 million possibilities just for earth abundant, non-radioactive, non-toxic, quaternary perovskites with the formula $A^1_{0.75}A^2_{0.25}B^1_{0.75}B^2_{0.25}O_3$), the properties of which are unknown *a priori*, makes this approach intractable. Thus, we are developing a computationally accelerated STWS material discovery and development method where density functional theory is used only to predict materials stability relative to melting and phase segregation and to predict basic materials properties. We are developing an advanced descriptor model informed by density functional theory calculated band gaps, materials heats of formation, and other fundamental properties to predict a material's redox thermodynamics and will apply this descriptor model to screen materials for STWS performance. Materials predicted to possess favorable thermodynamic properties for STWS will be analyzed for their kinetic properties for STWS using a novel descriptor method to quickly predict the kinetics of the rate-limiting step. At each stage of the screening process, the rigor and the associated computational costs of the methods is being increased, and materials not meeting material performance criteria, i.e., possessing a high likelihood of poor STWS performance, are eliminated. Throughout this process, experiments are being carried out in conjunction with our DOE sister project led by Prof. Alan Weimer to validate the computational models, analyze stability and water spitting behavior, and inform the choice of performance criteria for material down-selection. This stage of computational "prototyping" will identify materials that are likely to have high H_2 production capacity (>200 µmol H_2/g/cycle), low thermal reduction temperature (<1,400°C, chosen to be high enough to enable fast kinetics and high extents of reduction, but still significantly below the 1,700°C temperature at which the reactor materials degrade), an enthalpy of reduction sufficiently high to drive the reactions at reasonable rates but not so high as to be thermodynamically inefficient (near the enthalpy of splitting water, 280 kJ/mol), and short reduction and oxidation times (<15 min).

RESULTS

During this fiscal year, active redox material development has focused on understanding computationally complex factors impacting predicted thermodynamic behavior of spinels (AB_2O_4) and perovskites (ABO_3), and performing kinetic studies of surface and bulk processes in spinels.

We previously established that the viability of candidate STWS materials can be assessed using the criteria that

the reduction enthalpy of a material must be greater than 286 kJ/mol to drive water splitting [1]. However, if this reduction enthalpy is too high, the material will have sufficient energy to split water, but the extent of reduction, and thus the associated H_2 production capacity, will likely be too low to meet the \$2/kg H_2 production target. 500 kJ/mol has been initially chosen as the threshold to develop this screening approach. Using this screening criteria in conjunction with a predictive O-vacancy formation energy (E_v) model [2], we screened 1,041 out of a possible 1,089 binary normal spinel materials for STWS thermodynamic capability. As shown in Figure 1, we found that 52% of the materials screened have an E_v potentially capable of driving STWS.

In normal spinels, like those used for the high-throughput screening, each oxygen atom is bound to three B cation and one A cation; however, these structures may have cation disorder leading to oxygen atoms having different local cation environments in the lattice. To study the effect of this on our calculations, for six spinel materials, we calculated the E_v for oxygen vacancies in four different cation environments, ranging from 1 A to 4 A cation nearest neighbor. Each of the materials shows decreasing E_v with increasing number of A cation nearest neighbors, as shown in Figure 2a. Two materials, shown in light blue and dark blue, are found to have lower oxygen formation energies at 4 A-atom nearest neighbors than the experimentally tested material, shown in green, while maintaining the minimum required enthalpy. This indicates that they are predicted to have a higher extent of reduction at a given temperature. In

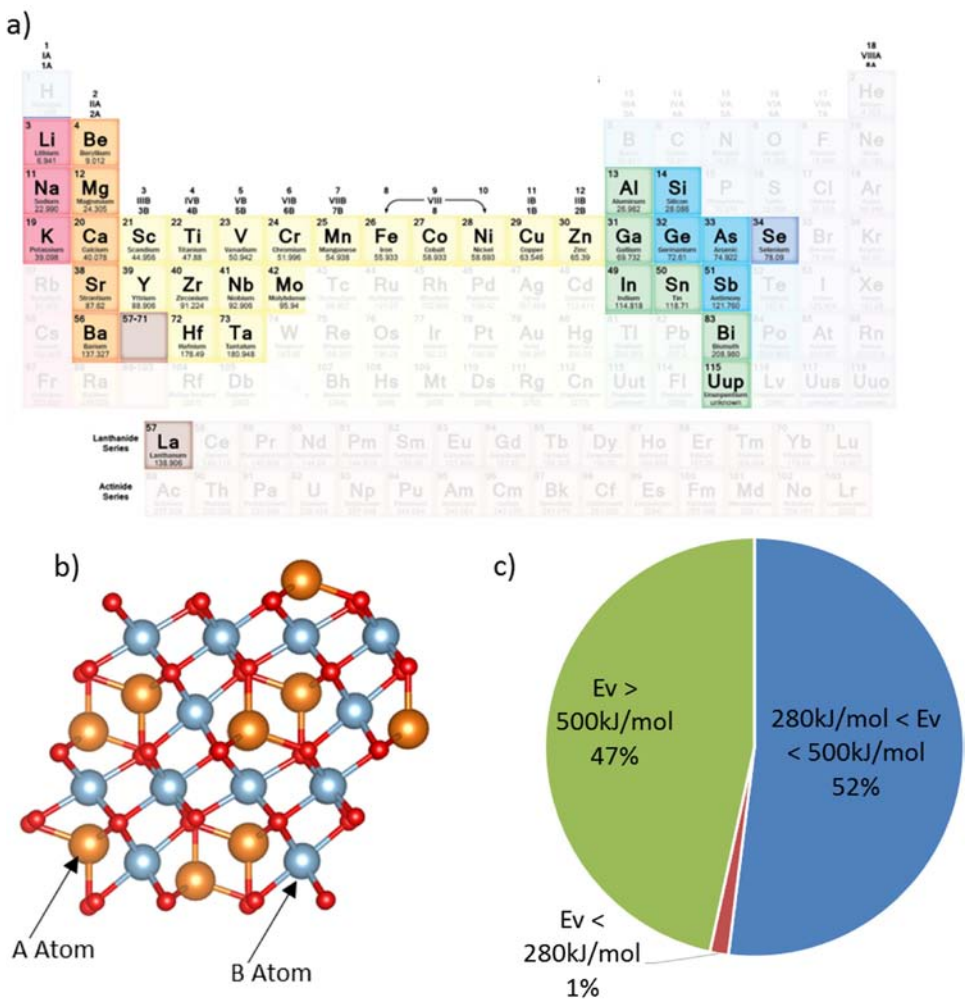

FIGURE 1. (a) All earth abundant, non-radioactive, and non-toxic elements under consideration for spinel computational screening. (b) Representative spinel structure used for high-throughput computational screening. The normal spinel structure consists of A cations which are octahedrally coordinated (orange spheres), B cations which are tetrahedrally coordinated (blue spheres), and oxygen anions (red spheres) which are bound to three A atoms and one B atom. (c) Screening results of 1,041 binary spinels.

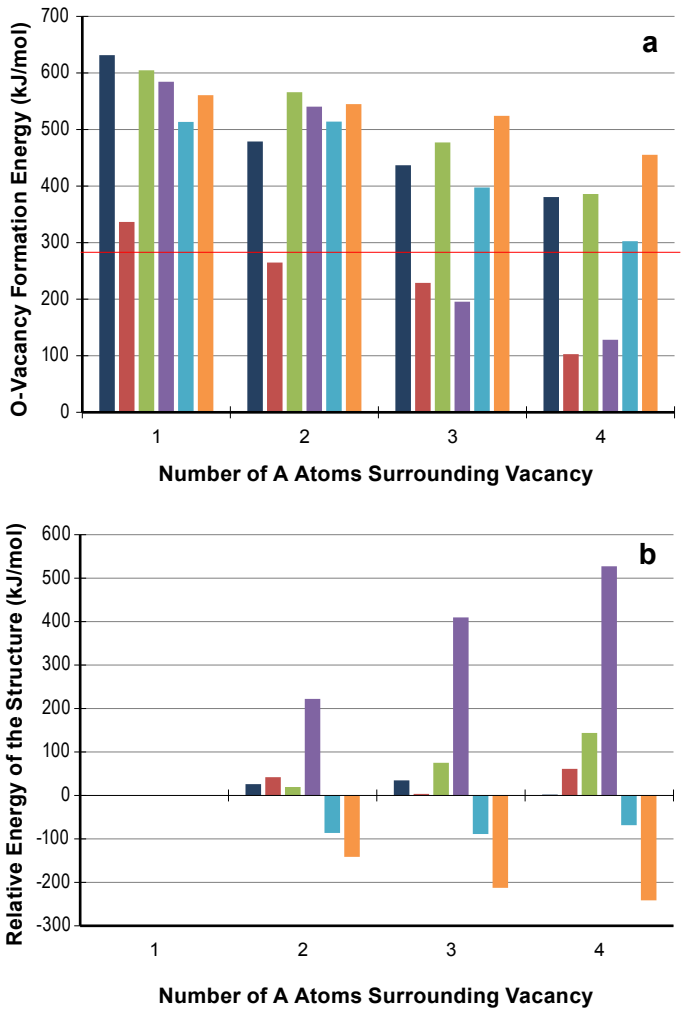

FIGURE 2. (a) Calculated O-vacancy formation energies at sites with varying numbers of A cation nearest neighbors for six spinel materials. The red line indicates the minimum required reduction enthalpy to split water. (b) The relative energies of exchanging cations to produce O sites with multiple A cation nearest-neighbors. A negative value indicates that the inverse structure is more favorable than the normal structure.

addition, as shown in Figure 2b, those two materials have negative or near zero relative structure energy at 4 A-atom nearest neighbors which indicates that these structures are more favorable than the inverse structure of the experimental material, and thus will have more active sites present. Since these materials have both a lower reduction enthalpy and more favorable inverse structures than the experimental material, they are promising materials for STWS as either dopants in the known water splitting material or as binary spinels.

For our study of perovskites, we focused on understanding the effect of structure and magnetic order on the computed STWS capability of the materials. Of particular interest, is understanding how elevated temperatures impact these factors. This work is ongoing, but completion of this study will allow us to correctly model new perovskite materials for STWS.

To examine the kinetic properties of these materials for STWS we have been studying dopants that can be substituted into hercynite in order to improve the reaction rate. Our previous work showed that the lowest barrier to reaction occurs with what we will refer to as a hydride intermediate, a negatively charged hydrogen atom (H^-) adsorbed atop a surface metal. This can be seen in Figure 3. Our work this year has focused on the effects of doping the hercynite lattice on the sites specified in Figure 3. The most important steps for this pathway are the initial dissociation of water, and the formation of hydrogen. On undoped hercynite, dissociation is rate limiting: occurring with a significantly higher barrier (50 kcal/mol) than hydrogen formation (20 kcal/mol). Doping on nearest neighbor, and subsurface sites does not qualitatively change this picture, regardless of the dopant. The small quantitative effects can be seen for the dissociation reaction in Figure 4. Only active site doping has an appreciable effect on the reaction barrier. This year we have focused on the rate limiting step on undoped hercynite, water dissociation. A strong trend for this reaction can be seen just by visual inspection of Figure 4. Earlier transition elements have high barriers, and later transition elements have lower barriers. A simple linear fit of the periodic column to activation barrier has an r^2 value of 0.821. A few other

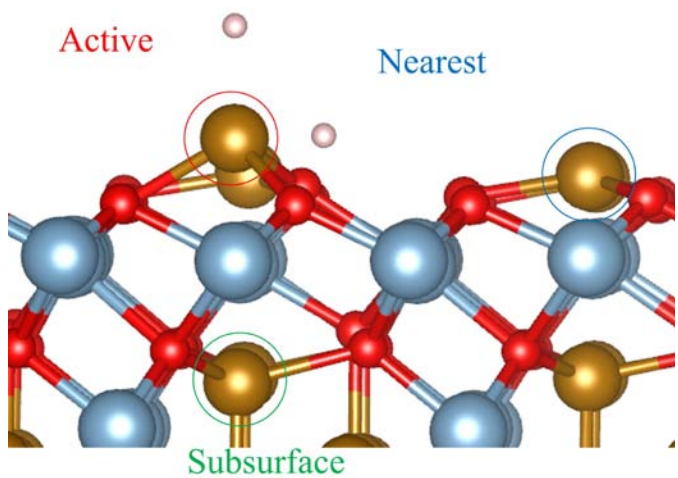

FIGURE 3. Products of water dissociation along the most active pathway, forming a surface hydride adsorbed to Fe, and a proton adsorbed to O. Also marked are the various dopant sites considered, and how they are labeled. The active site, denoted in red, participates in bonding during the reaction. The nearest site, blue, does not participate directly in reaction but neighbors the active site on the surface. The subsurface site, green, also does not participate directly in the reaction. It is the nearest Fe-dopant site to the active site

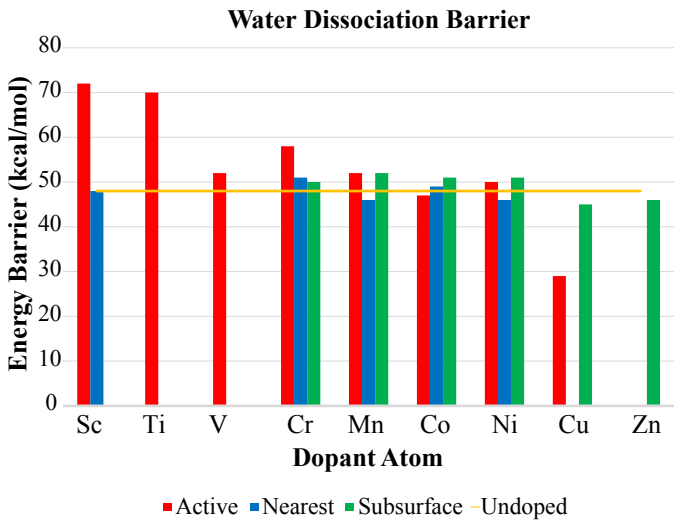

FIGURE 4. Kinetic pathways for hydrogen formation on hercynite. The surface without oxygen vacancies is show in blue, while the hydroxide and hydroxyl oxygen vacancy pathways are in black and green respectively. Dashed lines connect stable states for which the transition state has not been identified. Geometries for the oxygen vacancy pathways are depicted, and color coded to match the lines. Note that the first two states, H_2O in Vacuum and Adsorbed H_2O are identical and only shown once.

descriptors, d-band center, reaction energy, and adsorption energy, were tried but did not have as strong a fit.

The limitation of our current focus, is that we are assuming identical rate limiting steps, regardless of the dopant introduced. This coming year we will need to address this assumption because we have already encountered evidence to the contrary. Earlier transition metals appear to favor a different pathway entirely. Many of the attempted transition state calculations favored relaxing towards a new pathway, which is unstable for pure hercynite. Preliminary calculations also show that later transition metals have a significant increase in the hydrogen formation reaction, causing it to be rate limiting. However, the barrier for hydrogen formation appears to be closely tied to the reverse reaction of the process. Time permitting, we would like to test this hypothesis, but it has provided an initial justification for focusing on the hydrogen dissociation reaction.

We have also begun work characterizing the relevant bulk reactions in hercynite, notably oxygen vacancy migration. So far, only a limited number of calculations have been done, but we have a found a few important trends. Due to the symmetry of the spinel lattice of hercynite there are only three possible oxygen vacancy migration pathways. Of these three, one has a significantly lower barrier than the other two. This holds even when Cu, Co, or Mn are added into the lattice. This barrier is of similar order to the surface reaction, and which reaction is most important for describing hydrogen production would be dependent on the pre-exponential factors, and the size of the reactant particle.

CONCLUSIONS AND FUTURE DIRECTION

- Used O-vacancy formation descriptor model to screen 1,041 binary spinels for STWS capabilities.
- Identified two potential water splitting spinel materials based on screening of inverse structures.
- Evaluated the effect of structure and magnetic ordering on STWS capability of perovskites.
- Water dissociation on hercynite shows a strong periodic trend.
- Determined nearest neighbor dopants do not have a strong influence on transition state properties of reactions.
- Will apply computational approach for predicting water splitting abilities to doped perovskites and additional binary spinels.
- Will utilize knowledge gained in study of perovskites to accurately screen new materials.
- Will modify screening methods to compute the O-vacancy formation energy of inverse spinels in a high-throughput manner.
- Will begin screening doped perovskite and spinel metal oxides for STWS capability.
- Will continue to model bulk reactions for all first row transition elements.
- Will look at other potential rate limiting steps for the surface hydrogen evolution reaction.
- Will study kinetics of promising thermodynamic candidates.

FY 2016 PUBLICATIONS/PRESENTATIONS

1. Muhich, C.L. et al., "Predicting the solar thermochemical water splitting ability and reaction mechanism of metal oxides: a case study of the hercynite family of water splitting cycles." *Energy Environ. Sci.* **8**, 3687–3699, doi:10.1039/c5ee01979f (2015).

2. Muhich, C.L., V. Poole-Aston, R.M. Trottier, A.W. Weimer and C.B. Musgrave, "A First Principles Analysis of Cation Diffusion in Mixed Metal Ferrite Spinels," *Chemistry of Materials*, **28** (1), 214–226, (2016). DOI: 10.1021/acs.chemmater.5b03911

3. Muhich, C.L., Erhardt, I. Al Shankiti, B.J. Ward, C.B. Musgrave and A.W. Weimer, "A Review And Perspective of Efficient Hydrogen Generation Via Solar Thermal Water Splitting," *WIREs Energy and Environment*, **5** (3), 261–287 (2016). DOI: 10.1002/wene.174.

4. S. Miller, C. Muhich, R. Trottier, B. Ehrhart, C. Musgrave, and A. Weimer, "Screening of Metal Oxide Materials for Solar

Thermochemical Water Splitting." Presented at the annual meeting for the American Institute of Chemical Engineers, November 2015 (Salt Lake City, UT).

5. S. Miller, R. Trottier, K. Sun, A. Weimer, and C. Musgrave, "Evaluating the Effect of Modeling Variables and Experimental Conditions on Material Development for Solar Thermochemical Water Splitting." To be presented at the annual meeting for the American Institute of Chemical Engineers, November 2016 (San Francisco, CA).

6. R. Trottier, S. Miller, and C. Musgrave. "Kinetic Evaluation of Doped Hercynite for Two Step Solar Thermochemcial Water-Splitting," To be presented at the 2016 Theory and Applications of Computational Chemistry Conference, August 2016 (Seattle, WA).

REFERENCES

1. Muhich, C.L. et al., "Predicting the solar thermochemical water splitting ability and reaction mechanism of metal oxides: a case study of the hercynite family of water splitting cycles." *Energy Environ. Sci.* **8**, 3687–3699, doi:10.1039/c5ee01979f (2015).

2. Deml, A.M., Holder, A.M., O'Hayre, R.P., Musgrave, C.B. & Stevanovic, V. "Intrinsic Material Properties Dictating Oxygen Vacancy Formation Energetics in Metal Oxides." *J Phys Chem Lett* **6**, 1948–1953, doi:10.1021/acs.jpclett.5b00710 (2015).

II.D.1 High-Efficiency Tandem Absorbers for Economical Solar Hydrogen Production

Todd G. Deutsch (Primary Contact), John A. Turner, James L. Young, Henning Döscher, Ellis Klein, Anthony Abel
National Renewable Energy Laboratory
15013 Denver West Parkway
Golden, CO 80401
Phone: (303)275-3727
Email: Todd.Deutsch@nrel.gov

DOE Manager: David Peterson
Phone: (240) 562-1747
Email: David.Peterson@ee.doe.gov

Subcontractors:
- University of Nevada, Las Vegas, Las Vegas, NV (XGB-2-11673-01)
- University of Hawaii, Honolulu, HI (XGJ-5-52227-01)

Project Start Date: October 2014
Project End Date: September 30, 2017

Overall Objectives

- Develop a semiconductor-based, solar-driven, water-splitting photoelectrochemical (PEC) device with greater than 20% solar-to-hydrogen (STH) efficiency and several thousand hours of stability under normal operating conditions.
- Incorporate components that can be fabricated cost-effectively and are straightforward to scale up such that a plant scaled to 50,000 kg H_2/d can achieve an estimated production cost of \$1–\$2/kg hydrogen using only sunlight and water as feedstocks.
- Demonstrate a prototype photoreactor that produces 3 L of standard hydrogen within an 8-hour period under moderate solar concentration (~10X).

Fiscal Year (FY) 2016 Objectives

- Perform techno-economic analysis on higher-concentration (100X) systems and use H2A hydrogen analysis tool to generate a tornado plot that shows the sensitivity of a Type 4 reactor to optical concentration.
- Using a surface-modified semiconductor device capable of over 15% STH efficiency, show less than a 20% loss in efficiency after 875 h of continuous operation at short-circuit.
- Fabricate a photoreactor for use on a tracker.

Technical Barriers

This project addresses the following technical barriers from the Hydrogen Production (3.1) section of the Fuel Cell Technologies Office Multi-Year Research, Development, and Demonstration Plan.

(AE) Materials Efficiency – Bulk and Interface

(AF) Materials Durability – Bulk and Interface

(AG) Integrated Device Configurations

(AI) Auxiliary Materials

Technical Targets

This project is a materials discovery investigation to identify a single semiconductor material that meets the technical targets for efficiency and stability. The 2015 technical targets from the Multi-Year Research, Development, and Demonstration Plan PEC hydrogen production goals in Table 3.1.8.A are the following:

- 15% solar-to-hydrogen (STH) conversion efficiency
- 900-hour replacement lifetime (1/2 yr at 20% capacity factor)
- \$300/m^2 PEC electrode cost

FY 2016 Accomplishments

- We discovered and quantified systematic errors in efficiency measurements that consistently lead to over-reporting by our lab and others. We published a manuscript on the topic in *Energy & Environmental Science*.
- Using actual, direct solar illumination that is collimated and precisely characterized, we measured over 16% STH efficiency, which is a new world record, on an inverted metamorphic multijunction (IMM) cell.
- We used H2A to model the effect that varying solar concentration (10X, 50X, 100X) for a Type 4 PEC reactor system has on the levelized cost of hydrogen.
- We used COMSOL Multiphysics® to model a PEC reactor under solar concentration and calculated that the ohmic potential drop in solution under 10X is less than 300 mV, but calculated that a pressure of 147 atm is required to keep the hydrogen in solution and prevent bubbles from scattering incident light.
- We discovered that GaAs has a high intrinsic stability as a photocathode, which we hypothesized is due to the in situ formation of a protective metallic As layer. We

published a manuscript on our results in the *Journal of Materials Chemistry A* special issue on water splitting and photocatalysis.

- We used scanning transmission electron microscopy (STEM) to image the original champion $GaInP_2$ sample that had nitrogen ion bombardment and unintentional PtRu applied to its surface and confirmed the University of Nevada, Las Vegas observation that recent attempts to replicate the champion sample have much higher PtRu loadings.
- We characterized $CuGaSe_2$ from the University of Hawaii and determined that it has an ideal bandgap and sufficient below-bandgap transmission to serve as the top electrode in a dual-absorber water-splitting system.
- We designed and fabricated a photoreactor for outdoor testing and procured a solar tracker to dedicate to this effort.
- We filed a non-provisional patent application on IMM cells for high-efficiency water splitting.

✧ ✧ ✧ ✧ ✧

INTRODUCTION

Photoelectrolysis cells combine a light-harvesting system and a water-splitting system into a single, monolithic device. The catalyzed surface of a semiconductor is the light-harvesting component, as well as one part of the water-splitting system, with the balance consisting of a spatially separated counter electrode. Discovering a semiconductor system that can efficiently and sustainably collect solar energy and direct it toward the water-splitting reaction could provide renewable and economically competitive fuel for the hydrogen economy.

The goal of this work is to develop a semiconductor material set or device configuration that:

- Splits water into hydrogen and oxygen spontaneously upon illumination without an external bias.
- Has a solar-to-hydrogen efficiency of at least 15%, with a clear pathway to exceed 20%.
- Can ultimately be synthesized via high-volume manufacturing techniques with a final hydrogen production cost below $2/kg.

APPROACH

All proven zero-bias PEC devices with STH over 1% rely on two series-connected semiconductor junctions (tandem cell) to increase the majority-carrier potential at the counter electrode [1-4], providing sufficient potential difference (photovoltage) for water splitting. Tandem devices also overcome the band-alignment challenge common to PEC materials.

For maximum efficiency, the subcell currents in series-connected devices must be equal, creating the requirement of current matching. The maximum theoretical current generated by a semiconductor can be calculated by assuming unity quantum yield for every above-bandgap photon in the solar spectrum. Using the accepted lower heating value efficiency equation [5], 20% STH corresponds to a short-circuit current density of 16.26 mA/cm^2 under AM1.5G (1-sun). The largest bottom-cell bandgap that can be used and still achieve 20% STH is 1.41 eV. However, quantum yields are never 100% and semiconductors are not true step-function devices. Therefore, to realistically achieve STH values in excess of 20%, we must use lower top-cell and bottom-cell bandgap combinations, which guides our selection of candidate semiconductors.

An additional variable that can be used to match the currents is the thickness of the top cell—a thinner cell will allow more photons through to the bottom cell. This gives us some additional flexibility in the bandgaps that may be used. The lower limit of useable bandgaps is ~0.8 eV [6], dictated by the short penetration depth of lower-energy photons through water.

We will focus on III-V semiconductors, which exhibit the highest conversion efficiencies among all photoabsorber materials, and design tandem junctions to maximize the spectrally split device current, while achieving sufficient voltage to drive the maximum current through the device. We plan to initially focus on devices grown by conventional III-V metal-organic vapor-phase epitaxy to demonstrate maximum possible efficiencies. We will then port successful device structures to emerging synthesis techniques—such as spalling, epitaxial lift-off, or hydride vapor-phase epitaxy—that have the potential to meet low-cost absorber targets. We plan to improve the stability of III-V semiconductor water-splitting electrodes by a variety of surface-protecting modifications that include nitridation and sputtering, atomic layer deposition of oxides or nitrides, and thin coatings of MoS_2.

RESULTS

Surface Stability

In an effort to better understand the PtRu surface microstructure of the "champion" durability sample, we obtained STEM images of the last-remaining untested piece of it. This champion sample was from our original discovery of nitridation and PtRu sputtering and had the highest durability yield of any surface modification we have ever observed, with every electrode exhibiting remarkable stability (several 10s of hours), even after durability testing, electrode deconstruction, reconstruction, and retesting.

One of these electrodes even survived a cumulative 115 h of testing [7].

The imaging mode used was high-angle annular dark-field (HAADF) STEM under which heavier elements, such as Pt and Ru, appear as a lighter contrast against a darker background. Comparison of HAADF-STEM of the champion and an attempt to replicate it (Figure 1) suggest a much higher PtRu loading on the replicate. The HAADF-STEM images corroborate our University of Nevada, Las Vegas collaborators' discovery, based on X-ray photoelectron spectroscopic analysis, that the replication attempts have significantly higher amounts of PtRu than the champion. Our goal is to adjust the surface-modification treatment parameters to achieve surfaces that are more similar to the champion surface, with the hope of observing similar remarkable durability.

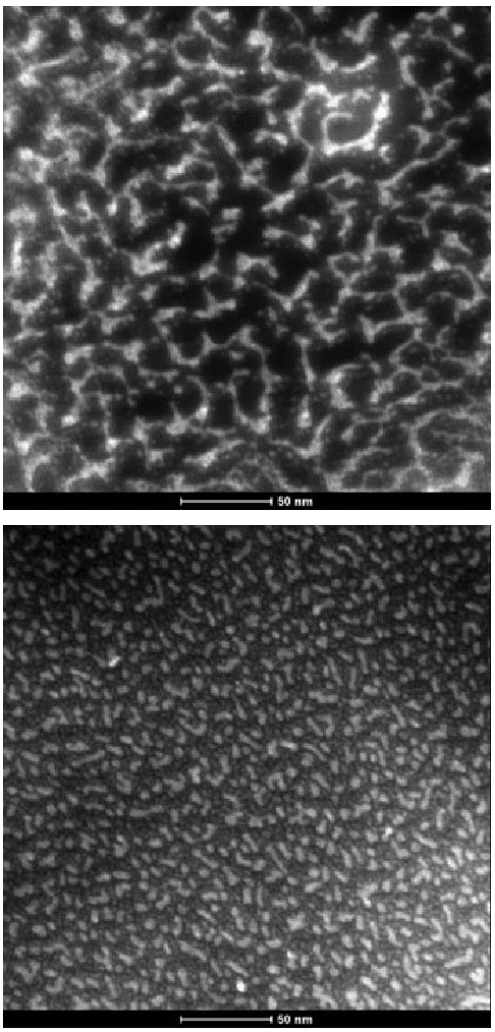

FIGURE 1. HAADF-STEM of the champion durability sample (top) and a recent attempt to replicate its surface (bottom). The heavier elements, such as Pt and Ru, are the lighter contrast against the dark background. Although the particles are nominally similar sizes in the two surfaces, the replicate clearly has a much higher level of PtRu loading. (Images by Andrew Norman, National Renewable Energy Laboratory).

We also discovered that GaAs has unexpected stability during operation as a photocathode in acidic electrolytes, which we attribute to the in situ formation of a metallic As layer. The details can be found in Publication 1. The discovery that arsenides have a greater intrinsic stability than phosphides is significant because it makes accessible several possible new III-V material compositions that had previously been considered too unstable for PEC applications.

Techno-Economic Modeling

This year we used the H2A Future Central Hydrogen Production from the Photoelectrochemical Type 4 version 3.0 case study [8] to evaluate the sensitivity of hydrogen production costs to optical concentration. All values were calculated assuming a 1,000 kg/d (1 tonne per day or TPD) plant scaled to 2,000 kg/d with 98% operating capacity factor. A 25% solar capacity factor was used and a hydrogen production rate of 1.702×10^{-6} kg/m^2-s is assumed for a 20% STH device. Using these inputs, the solar capture area required for 1 TPD at 20% STH is 20,400 m^2, 25% STH is 16,320 m^2, and 15% is 27,199 m^2. Because H2A requires inputs to be in 2005 dollars, the component costs have to be adjusted in the following ways. The lens array was assumed to be \$75/m^2 in 2010 dollars and Plexiglas was \$124/m^2 in 2007 dollars, giving \$67.17 and \$116.8 in 2005 dollars, respectively. To calculate capital (and replacement) costs, the lens cost was multiplied by the capture area whereas the Plexiglas cost was multiplied by three times the absorber area. The lens cost was assumed to be independent of concentration factor. The PEC absorber area required was calculated by dividing the capture area by the concentration factor. Lenses and Plexiglas reactor parts were replaced every 10 years. Within the range of the inputs used, hydrogen levelized costs are most sensitive to PEC absorber costs, followed by concentration factor (Figure 2a). Using current PEC absorber costs of \$10,000/m^2, concentration is by far the most effective route to reducing hydrogen levelized cost (Figure 2b). If PEC absorber costs are able to achieve the \$200/m^2 "ultimate" target, then hydrogen levelized cost becomes more sensitive to efficiency as balance-of-system costs dominate (Figure 2c).

Although concentration up to 100X may demonstrate a route to economic plausibility, technological feasibility is limited by physical processes occurring in actual photoreactor cells. We used COMSOL Multiphysics® modeling to calculate physical parameters of our photoreactor cell to estimate losses under operating conditions. Our COMSOL Multiphysics® modeling calculated minimal (<300 mV) ohmic losses at 10X concentration, but losses can exceed several volts at 100X using our current reactor geometry. Much higher concentrations are reasonable with redesigned reactor geometry, specifically ones that more

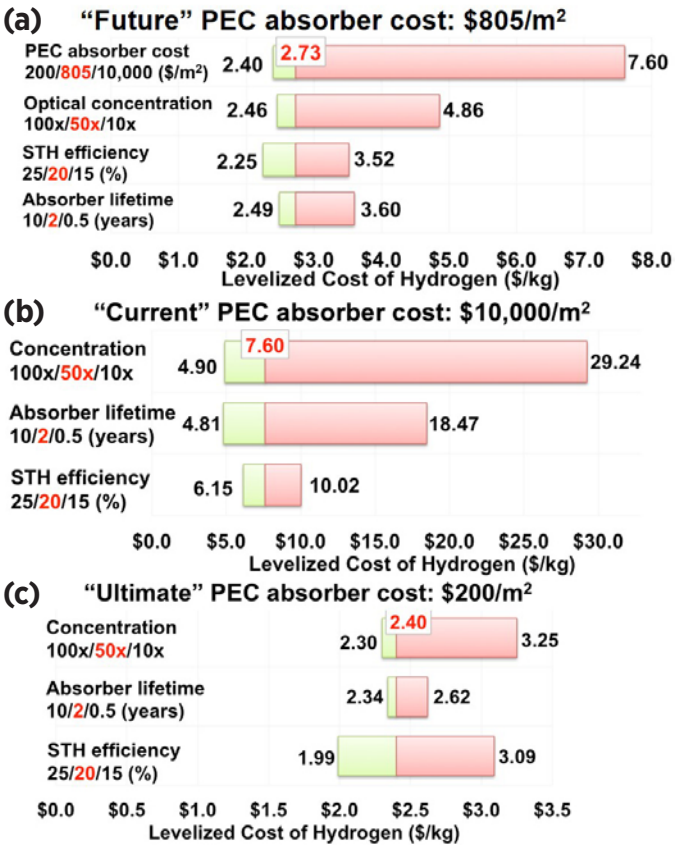

FIGURE 2. Sensitivity analysis showing influence of absorber costs, concentration factor, STH efficiency, and absorber lifetime on hydrogen costs. Hydrogen costs from a Type 4 concentrator PEC reactor using (a) future, (b) current, and (c) ultimate absorber costs for baseline projections.

closely approximate electrolyzers where current densities can reach several A/cm^2. The use of buried-junction devices allows the flexibility to make these geometries attainable. We also used COMSOL Multiphysics® to calculate the pressure—specifically, 147 atm—required to keep hydrogen in solution, which could prevent bubbles from scattering incident light. Operating at this pressure is not practical, so other engineering measures must be considered in designing a reactor that minimizes the light attenuation due to hydrogen gas evolution from the illuminated photocathode surface.

Solar-to-Hydrogen Efficiency Benchmarking

We discovered several potential sources of experimental error while performing efficiency measurements on our IMM cells. Almost all of these errors lead to artificially higher photocurrents and overrate the measured efficiency. The errors are a consequence of common experimental techniques, so we published a manuscript to raise awareness of this issue and proposed specific remedies that we hope will be adopted by the PEC community.

The errors are due to two main categories of uncertainty: absorber area and illumination. We discovered that the Hysol Loctite 9462 epoxy we use, although nominally opaque, actually transmits a significant fraction of incident illumination (20–60%) at thicknesses up to 1.2 mm. We (and many others) typically use this epoxy to define the active area of the electrode and had assumed only the exposed area was responsible for collecting light. We found that photons absorbed by the semiconductor under the area masked by epoxy can inflate photocurrent density measurements by 20% or more, depending on the ratio of total semiconductor area to the area exposed. We have moved to a more transparent epoxy and settled on a more conservative definition of active area that includes the total area of the semiconductor chip, including the portion covered by epoxy.

The other main sources of error are due to spectral mismatch between the simulated light source and the reference light spectrum, as well as light piping and concentration effects of photoreactor cells. The spectral mismatch is especially important in multi-junction absorbers, where one junction is typically current-limiting. Over-illuminating the current-limiting junction can lead to measured device photocurrent densities that exceed what is possible under real solar illumination. Additionally, exposing an entire photoreactor to diffuse (scattered) light—as is present in the "global" spectrum—can cause coupling of photons to the sample via light piping that would otherwise not be available to it. We propose making efficiency measurements under "direct" solar illumination with a collimating tube and a well-defined electrode area to minimize the above sources of error. The current density measured under these conditions should be validated by integrating the incident photon-to-current efficiency response over the AM1.5D reference spectrum to check for self-consistency. Publication 2 discusses these issues in much greater detail. We used these advanced benchmarking protocols to confirm over 16% STH efficiency on an IMM III-V device and have submitted a manuscript to a peer-reviewed journal describing the study.

CONCLUSIONS AND FUTURE DIRECTIONS

- Using higher optical concentration in solar-hydrogen photoreactors is one way to offset the disproportionately large contribution of the current cost of III-V semiconductor absorbers to achieve reasonably priced hydrogen in the short term. Managing the elevated current densities achieved under higher optical concentration requires re-engineering of the photoreactor to minimize electrode distances to achieve an acceptable ohmic (internal resistance) potential loss due to ion transport.
- Our new higher-efficiency devices have a buried *p-n* junction at the surface closest to the electrolyte. Using

a buried *p-n* junction allows incorporation of more robust encapsulation schemes because current can be collected through a conduit and does not require the passivating layer to be conductive. Transparent, insulating encapsulants that have known stability, such as poly(methyl methacrylate) and silicone, can now be considered. We plan to leverage these encapsulating strategies to achieve several hundred hours of stability at a high solar-to-hydrogen efficiency.

FY 2016 PUBLICATIONS/PRESENTATIONS

1. "Remarkable Stability of Unmodified GaAs Photocathodes during Hydrogen Evolution in Acidic Electrolyte," James L. Young, K. Xerxes Steirer, Michael J. Dzara, John A. Turner, and Todd G. Deutsch, *J. Mater. Chem. A*, **4**, 2831–2836 (2016).

2. "Solar to Hydrogen Efficiency: Shining Light on Photoelectrochemical Device Performance," H. Döscher, J.L. Young, J.F. Geisz, J.A. Turner, and T.G. Deutsch, *Energy Environ. Sci.,* **9**, 74–80 (2016).

3. "Reversible $GaInP_2$ Surface Passivation by Water Adsorption: A Model System for Ambient-Dependent Photoluminescence," James L. Young, Henning Döscher, John A. Turner, and Todd G. Deutsch, *J. Phys. Chem. C*, **120**, 4418−4422 (2016).

4. "Molybdenum Disulfide as a Protection Layer and Catalyst for Gallium Indium Phosphide Solar Water Splitting Photocathodes," Reuben J. Britto, Jesse D. Benck, James L. Young, Christopher Hahn, Todd G. Deutsch, Thomas F. Jaramillo, *J. Phys. Chem. Lett.,* **7**, 2044–2049 (2016).

5. "III-V Semiconductor Systems as the Only Viable Candidates for Commercial PEC H_2 Production Devices," Solar Fuels Network: Moving from Materials to Devices, London, England. July 7, 2015. (Turner) *invited*

6. "Photoelectrochemical Water Splitting, from Fundamentals to Devices," Modern Topics in Energy and Power Technical Meeting, Army Research Lab, Adelphi, MD. July 14, 2015. (Turner) *invited*

7. "Inverted Metamorphic Tandem Devices for Efficient Photoelectrochemical Water Splitting" 20th American Conference on Crystal Growth and Epitaxy, Big Sky, MT. August 4, 2015. (Döscher)

8. "Semiconductor Systems and Catalysts for Photoelectrochemical Water Splitting," ALS User's Meeting, LBNL, Berkeley CA. October 5, 2015. (Turner) *invited*

9. "Improving Onset Potential for Higher Efficiency Water Splitting with III-V Tandems," American Vacuum Society 62nd Meeting, San Jose, CA. October 20, 2015. (Young)

10. "Inverted Metamorphic Multijunction Semiconductors for Exceptionally High Photoelectrolysis Efficiencies: Materials Development and Measurement Challenges," Physics Department seminar, Denmark Technical University, Copenhagen, Denmark. November 18, 2015. (Deutsch) *invited*

11. "Tandem Device Design for Photoelectrochemical Water Splitting: The Impact of Sunlight Absorption in Aqueous Electrolytes and the Role of Inverted Metamorphic III-V Epitaxy," Institut für Solarenergieforschung Hameln (ISFH), Kolloquium, Hameln, Germany. November 24, 2015. (Döscher)

12. "Solar Energy to Hydrogen Fuel via Highly Efficient III-V Semiconductors," Postdoctoral Researcher Candidate Seminar, NREL, Golden, CO. January 21, 2016. (Young)

13. "The Hydrogen Economy and Photoelectrochemical Water Splitting," REMRSEC graduate student seminar, Colorado School of Mines, Golden, CO. February 9, 2016. (Turner) *invited*

14. "Frontiers, Opportunities and Challenges for a Hydrogen Economy," IGERT graduate student seminar, Arizona State University, Glendale, AZ. February 12, 2016. (Turner) *invited*

15. "Maximizing Photocurrent Onset Potential of III-V Photoelectrochemical Junctions," Materials Research Society Spring Meeting, Phoenix, AZ. March 31, 2016. (Young)

REFERENCES

1. Abdi, Fatwa F., Lihao Han, Arno H. M. Smets, Miro Zeman, Bernard Dam, and Roel van de Krol. 2013. "Efficient Solar Water Splitting by Enhanced Charge Separation in a Bismuth Vanadate-Silicon Tandem Photoelectrode." *Nature Communications* **4** (January). Nature Publishing Group: 2195. doi:10.1038/ncomms3195.

2. Brillet, Jeremie, Jun-Ho Yum, Maurin Cornuz, Takashi Hisatomi, Renata Solarska, Jan Augustynski, Michael Graetzel, and Kevin Sivula. 2012. "Highly Efficient Water Splitting by a Dual-Absorber Tandem Cell." *Nature Photonics* **6** (12). Nature Publishing Group: 824–28. doi:10.1038/nphoton.2012.265.

3. Kainthla, R.C., B. Zelenay, and J. O'M. Bockris. 1987. "Significant Efficiency Increase in Self-Driven Photoelectrochemical Cell for Water Photoelectrolysis." *Journal of The Electrochemical Society* **134** (4): 841. doi:10.1149/1.2100583.

4. Khaselev, O., and J. A. Turner. 1998. "A Monolithic Photovoltaic-Photoelectrochemical Device for Hydrogen Production via Water Splitting." *Science (New York, N.Y.)* **280** (5362): 425–27. http://www.ncbi.nlm.nih.gov/pubmed/9545218.

5. Chen, Zhebo, Thomas F. Jaramillo, Todd G. Deutsch, Alan Kleiman-shwarsctein, Arnold J. Forman, Nicolas Gaillard, Roxanne Garland, et al. 2010. "Accelerating Materials Development for Photoelectrochemical Hydrogen Production: Standards for Methods, Definitions, and Reporting Protocols." *Journal of Materials Research* **25** (1): 3–16. doi:10.1557/jmr.2010.0020.

6. Döscher, H., J.F. Geisz, T.G. Deutsch, and J.A. Turner. 2014. "Sunlight Absorption in Water – Efficiency and Design Implications for Photoelectrochemical Devices." *Energy & Environmental Science* **7** (9): 2951. doi:10.1039/C4EE01753F.

7. https://www.hydrogen.energy.gov/pdfs/review12/pd035_turner_2012_o.pdf

8. https://www.hydrogen.energy.gov/h2a_prod_studies.html

II.D.2 Wide Bandgap Chalcopyrite Photoelectrodes for Direct Water Splitting

Nicolas Gaillard
Hawaii Natural Energy Institute
University of Hawaii
2440 Campus Road, Box 368
Honolulu, HI 96822
Phone: (808) 956-2342
Email: ngaillar@hawaii.edu

DOE Manager: David Peterson
Phone: (240) 562-1747
Email: David.Peterson@ee.doe.gov

Contract Number: DE-EE0006670

Subcontractors:
- University of Nevada, Las Vegas, Las Vegas, NV
- Stanford University, Stanford, CA
- Lawrence Livermore National Laboratory, Livermore, CA
- National Renewable Energy Laboratory, Golden, CO

Project Start Date: October 1, 2014
Project End Date: September 30, 2017

Overall Objectives

In line with the Fuel Cell Technologies Office Multi-Year Research, Development, and Demonstration Plan, our project aims to identify suitable semiconducting materials for efficient and durable photoelectrochemical (PEC) hydrogen production at a cost of $2/kg or less. Specifically, our project aims to

- Develop efficient copper chalcopyrite ($Cu(In,Ga)(S,Se)_2$)-based materials with ideal optoelectronic properties for PEC water splitting.
- Identify appropriate surface treatments to prevent photocorrosion, improve surface energetics, and enhance the hydrogen evolution reaction.
- Demonstrate 3 L of hydrogen produced in 8 hours using a copper chalcopyrite-based standalone PEC device.

Fiscal Year (FY) 2016 Objectives

- Demonstrate copper chalcopyrite photoelectrode material with bandgap >1.7 eV that generates at least 10 mA/cm^2.
- Improve chalcopyrite stability in aqueous electrolytes using MoS_2 as protection layers, with a durability goal of 750 h continuous operation at 8 mA/cm^2.
- Demonstrate $CuInGaS_2$ solar cells with a photoconversion efficiency >6%.

Technical Barriers

This project addresses the following technical barriers from the Hydrogen Production section of the Fuel Cell Technologies Office Multi-Year Research, Development, and Demonstration Plan.

(AE) Materials Efficiency

(AF) Materials Durability

(AG) Integrated Device Configurations

(AJ) Synthesis and Manufacturing

Technical Targets

This project aims to develop efficient and durable PEC devices using low-cost semiconducting materials. Specifically, our project aims to modify the optoelectronic properties of the photovoltaic (PV)-grade copper chalcopyrite material class for PEC water splitting. Alongside, we are engineering new surface treatments to improve chalcopyrites' surface energetics, their catalysis toward the hydrogen evolution reaction, as well as their resistance against photo-corrosion. The status of this project's technical targets is documented in Table 1.

TABLE 1. Progress towards This Project's Technical Targets for FY 2016

FY 2016 Milestones	Due date	Status
$Cu(In,Ga)S_2$ solar cells with a photoconversion efficiency >6%	12/2015	Complete
Photocurrent density relevant to 15–16% STH with chalcopyrite 12–13 mA/cm^2	03/2016	90%
Durability >750 hrs at mA/cm^2, with a stretch goal of 1,000 hrs	06/2016	30%
Fabricate $Cu(In,Ga)S_2$ cells with V_{OC} >750 mV	09/2016	95%

STH – solar-to-hydrogen; V_{OC} – open circuit voltage

FY 2016 Accomplishments

Accomplishments during the current project period include:

- Over 10 mA/cm^2 achieved with $CuGa(S,Se)_2$, $CuGa_3Se_5$, and $CuInGaS_2$ chalcopyrite materials (go/no-go criteria for Year 1).
- Modeling of optical bandgap and electronic defects in $CuGa(S,Se)_2$.

- Validation of in situ studies of chalcopyrites/electrolyte interface.
- Improvement of $CuGaSe_2$ photoelectrode durability using TiO_2 and MoS_2 as a protective coating.

✧ ✧ ✧ ✧ ✧

INTRODUCTION

The goals of this project are to demonstrate PEC hydrogen production with a dual absorber system capable of generating at least 3 L of hydrogen in 8 hours as well as to develop a standalone system with a STH conversion efficiency of 15% and operational life up to 2,000 hours.

APPROACH

The chalcopyrite material class, typically identified by its most popular *PV-grade* alloy $CuInGaSe_2$, provides exceptionally good candidates for PEC water splitting. A key asset of this bandgap tunable, direct absorber, thin film semiconductor material is the outstanding photon-to-electron conversion efficiency, as demonstrated with $CuInGaSe_2$ (CIGSe)-based PV cells. A STH efficiency of 4% was achieved by our team in 2012 using a 1.6 eV bandgap $CuGaSe_2$ (CGSe)- photocathode connected in series with three a-Si PV drivers (side-by-side architecture). The use of such coplanar architecture was dictated by the bandgap of $CuGaSe_2$, which was too narrow for a "stacked" multi-junction integration. With wide bandgap chalcopyrites, we will be able to stack the PEC device over the PV driver and increase the STH efficiency.

RESULTS

PV-grade wide bandgap absorbers: theoretical modeling. To better inform the experimental synthesis of desirable alloys, we have focused on assessing the bandgap and thermodynamic stability of absorber alloys as a function of composition and have also begun calculations to characterize how point defects may influence the resulting properties of the alloys. We have focused on the $CuGa(S,Se)_2$ (CGSSe) alloys that have received the most attention from our experimental efforts and summarize the calculated bandgap and stability as a function of S content in Figure 1. We find that these alloys are readily mixed to form solid solutions and are stable against phase separation at modest processing temperatures. Additionally, CGSSe alloys exhibit bandgaps within the target range of ~1.8–2 eV for Ga-contents ranging from ~20–40%, with a nearly linear dependence on composition. Additional calculations on $Cu(In,Ga)S_2$ alloys identify that the bandgaps of these alloys display slightly more nonlinear behavior with composition than those of the CGSSe alloys. This is evident in our calculated bandgap bowing parameter of 0.05 eV, as seen in Figure 1a, compared to the 0.2 eV calculated for $Cu(In,Ga)S_2$ alloys. We also continue to evaluate the solubilities and electronic character of native and extrinsic defects in pure CGSe and $CuGaS_2$ (CGS). We are currently assessing the stability of defects with deep states like the Ga_{Cu} deep donors that have previously been suggested to play a role in limiting the performance of high-Ga CIGSe photovoltaics. In Figure 1c we include the deep levels associated with this defect in both CGSe and CGS and find that they are deeper in the CGS bandgap by ~0.5 eV relative to CGSe and may also be problematic for pinning the Fermi level if their concentrations are high enough.

PV-grade wide bandgap absorbers: synthesis. During this reporting period, development of new wide bandgap chalcopyrites with great potential for PEC water splitting continued. Theoretically, wide bandgap chalcopyrites may be obtained by replacing some of the selenium with sulfur in $CuGaSe_2$, creating the alloy $CuGa(S,Se)_2$. We were able to experimentally verify this by synthesizing CGSSe alloys with

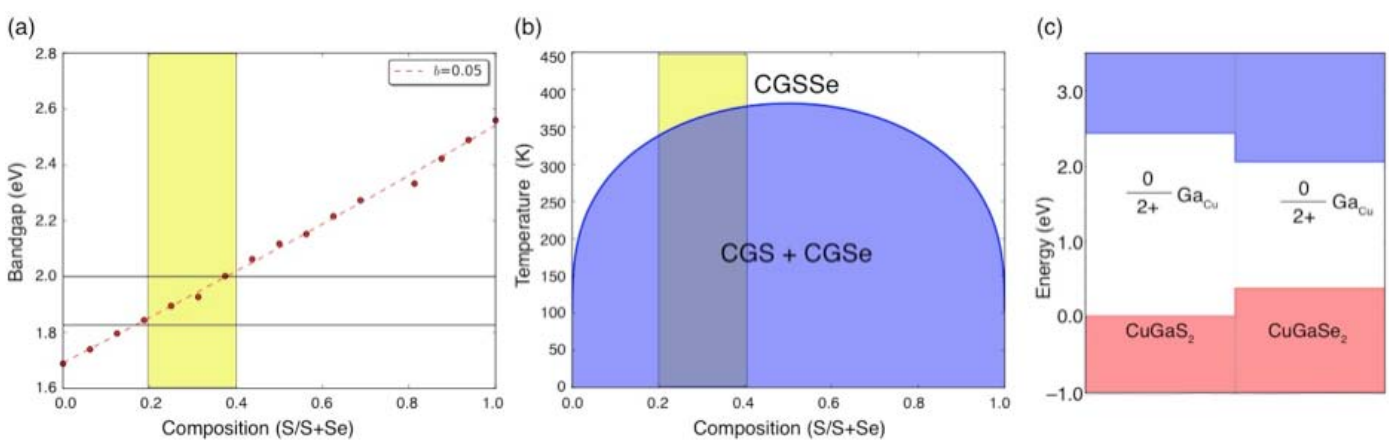

FIGURE 1. (a) Calculated bandgap, (b) thermodynamic stability, and (c) defect levels associated with Ga_{Cu} antisite of $CuGa(S,Se)_2$ alloys as a function of composition

a bandgap between approximately 1.7 eV and 2.4 eV, which is shown in Figure 2. CGSSe films were fabricated with a two-step process first involving the co-evaporation of a selenide-based precursor and then a sulfurization step. By controlling the amount of sulfur present during the sulfurization process, we were able to synthesize films anywhere within the aforementioned bandgap range. With this material class, our team has demonstrated a current density of approximately 11.0 mA/cm^2 with a 1.72 eV bandgap CGSSe. Also during this reporting period, ordered defect chalcopyrite $CuGa_3Se_5$ electrodes were grown in an ultrahigh vacuum cluster tool system. A photocurrent density of 11 mA/cm^2 was achieved with a 1.84 eV $CuGa_3Se_5$. Both CGSSe and $CuGa_3Se_5$, along with $CuInGaS_2$, satisfied the go/no-go criteria for Year 1.

Sub-surface energetics improvement: advanced characterization. This project year, the world-wide first S $L_{2,3}$ X-ray emission spectroscopy (XES) measurements of a solid–liquid interface of a PEC material were collected at the Advanced Light Source, Lawrence Berkeley National Laboratory. Such measurements allow for the characterization of the solid–electrolyte interface between custom-deposited $CuInGaS_2$ thin films on Au-coated, C-based membranes and a highly acidic, sulfur-free electrolyte. The S $L_{2,3}$ XES spectra of the first two solid–liquid interface experiments, along with corresponding reference samples, are shown in Figure 3. Furthermore, we have continued our ion treatment regime for surface and bulk compositional analysis of two CGSe-based absorbers: one "bare absorber" composed of CGSe and one sulfurized absorber ($CuGaSSe_2$, CGSSe). Ion treatments at variable ion energies allowed us to determine whether certain elements (carbon, oxygen, and sodium in particular) are only present as surface adsorbates, or integrated into the surface and/or bulk of the respective films. X-ray photoelectron spectroscopy survey spectra of the CGSSe absorber surface before and after low-energy ion treatments revealed a small reduction of C, O, and Na surface adsorbates ("ion-treated") and a complete removal of C and Na (but not of O) after sputtering. Next project steps include additional sputter treatments to further identify the presence or absence of oxygen in the bulk of the films, a detailed analysis of the S $L_{2,3}$ and the Se $M_{2,3}$ XES measurements recently completed at the Advanced Light Source, as well as an analysis of a new sample series specifically designed to allow for a full band alignment determination of the CdS–Cu(In,Ga)S_2 interface.

Surface catalysis and corrosion resistance. During the second year of our project we worked to develop conformal MoS_2 coatings to protect CGSe electrodes from corrosion in sulfuric acid electrolyte during photoelectrochemical hydrogen evolution. In Year 1, we showed that physical vapor deposition methods, which have been effective in protecting silicon photoelectrodes from corrosion in the past, were effective in protecting CGSe for only short periods of time. Physical vapor deposition is a directional deposition method and was unable to conformally coat the CGSe electrodes.

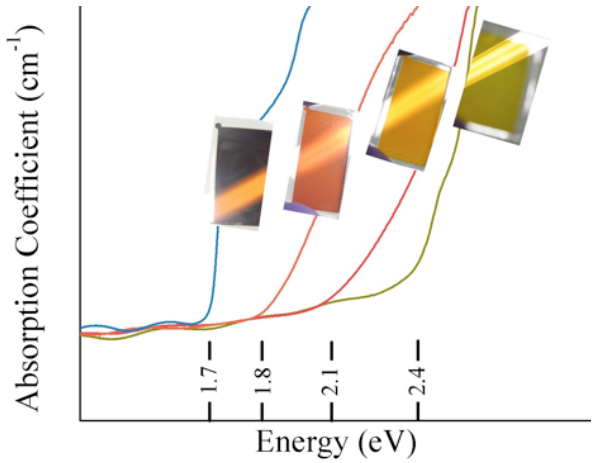

FIGURE 2. Optical absorption of samples of CGSSe with varying ratios of sulfur to selenium, confirming the feasibility of tailoring the bandgap of the alloy

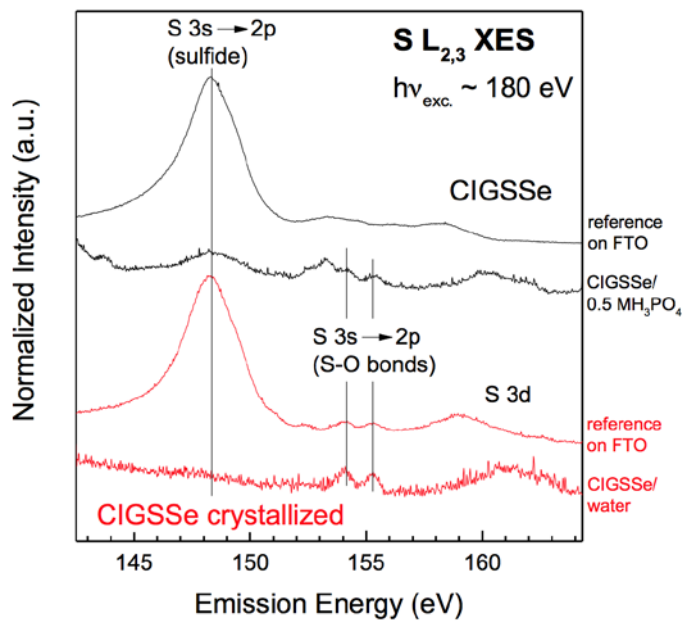

FIGURE 3. S $L_{2,3}$ soft XES of CIGSSe samples. Top (black): Sulfurized "CIGSSe" sample, both as a reference on a fluorine-doped tin oxide (FTO) substrate, and as a solid–liquid interface with a 0.5 M H_3PO_4 electrolyte solution. Bottom (red): Sulfurized and crystallized CIGSe sample ("CIGSSe crystallized"), measured as a reference on FTO and at the solid–liquid interface with water.

Instead, atomic layer deposition (ALD), a gas-phase self-limiting method, was used to deposit conformal films. We developed an oxygen plasma assisted method to deposit molybdenum oxide (MoO_x) by ALD and then converted the MoO_x to molybdenum sulfide (MoS_2), a material known for its high durability in acid electrolyte, using a 10% H_2S–90% H_2 sulfiding gas. Unfortunately, the oxygen plasma damages the surface of the CGSe electrode, leading to high resistivity

and low hydrogen evolution activity. We determined that it was necessary to add a barrier layer of TiO_2 deposited by thermal ALD to protect the CGSe samples from oxygen plasma damage during MoO_x deposition. The TiO_2 also has the added benefit of enhancing durability. Figure 4 shows the results of our surface protection schemes and includes durability measurements for bare CGSe electrodes, CGSe electrodes with 15 nm of TiO_2 deposited by ALD and 1 nm Pt as a catalyst, and CGSe electrodes with 7 nm of ALD-deposited TiO_2 and 4 nm of ALD-deposited MoO_x that has been converted to MoS_2. All samples were tested by measuring the potential required to obtain a constant current density of -8 mA cm^{-2}. Both the TiO_2-coated samples significantly outlast the uncoated CGSe electrode. The Pt-catalyzed CGSe electrode catastrophically fails after about 250 h of continuous operation, while the MoS_2-containing sample has operated approximately 270 h as of this writing without failure. Likely there is some additive effect to durability by employing both MoS_2 and TiO_2 films, both of which are known to resist electrochemical corrosion.

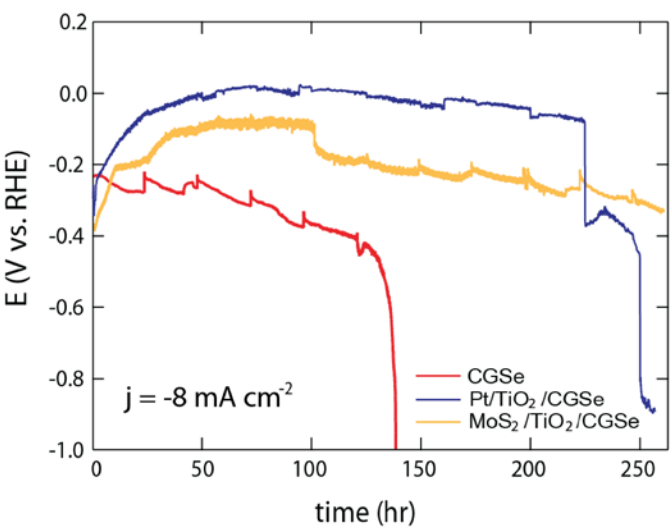

RHE – reversible hydrogen electrode

FIGURE 4. Chronopotentiometry plot of CGSe electrodes with different catalytic and protecting schemes. This plot was generated by holding the electrodes at -8 mA/cm^2 continuously with one linear sweep voltammogram every 24 h. The electrode pairing TiO_2 with MoS_2 has shown our highest durability to date.

CONCLUSIONS AND FUTURE DIRECTIONS

- Over 10 mA/cm^2 achieved with 1.73 eV $CuGa(S,Se)_2$, 1.84 eV $CuGa_3Se_5$, and 1.75 eV $CuInGaS_2$ chalcopyrite materials (go/no-go criteria for Year 1). Materials development will continue to increase the photocurrent output of newly formed chalcopyrites.
- Over 250-h durability demonstrated with MoS_2- and TiO_2-coated chalcopyrites. Coating methods will be adjusted to improve material coverage and enhance photoelectrode durability.
- Over 700 mV V_{oc} demonstrated with wide bandgap chalcopyrite materials. New buffers and surface treatments will be evaluated to meet Year 2 go/no-go criteria (750 mV V_{oc}).
- Complete PEC structures made of wide bandgap-based photoelectrodes and narrow bandgap PV drivers will be fabricated and tested.

FY 2016 PUBLICATIONS/PRESENTATIONS

1. *Identifying Optimal Chalcopyrite Alloys for Photoelectrochemical Hydrogen Production through First-Principles,* J.B. Varley, F. Zhou, V. Lordi, T. Ogitsu, N. Gaillard, Materials Research Society Spring Meeting, Symposium EE2-Advancements in Solar Fuels Generation: Materials, Devices and Systems, EE2.4.01, Phoenix, AZ (2016).

2. *Wide-Bandgap Tuneable CuGaSSe Photocathodes For PEC Water Splitting,* A.D. Deangelis, N. Gaillard, Materials Research Society Spring Meeting, Symposium EE2-Advancements in Solar Fuels Generation: Materials, Devices and Systems, EE2.4.02, Phoenix, AZ (2016).

3. *Wide Bandgap Copper Indium Gallium Disulfide Thin Film Materials for Photoelectrochemical Hydrogen Production,* N. Gaillard, A. Deangelis, M. Chong and D. Prasher, 228th Electrochemical Society Meeting, Symposium L06 Photocatalysts, Photoelectrochemical Cells, and Solar Fuels 6, 1702, Phoenix, AZ, 2015.

4. *Efficient Solar-to-Hydrogen Production Materials and Devices,* H. Wang, J. Ager III, N. Gaillard, E. Miller, 228th Electrochemical Society Meeting, Symposium L06 Photocatalysts, Photoelectrochemical Cells, and Solar Fuels 6, 1683, Phoenix, AZ, 2015.

II.D.3 Tandem Particle-Slurry Batch Reactors for Solar Water Splitting

Shane Ardo (Primary Contact),
Houman Yaghoubi, William Gaieck, Kevin Tkacz,
Christopher D. Sanborn
University of California, Irvine
1102 Natural Sciences II
Irvine, CA 92697
Phone: (949) 824-3796
Email: ardo@uci.edu

DOE Manager: David Peterson
Phone: (240) 562-1747
Email: David.Peterson@ee.doe.gov

Contract Number: DE-EE0006963

Subcontractors:
- Adam Z. Weber and Rohini Bala Chandran, Lawrence Berkeley National Laboratory (LBNL), Berkeley, CA
- Chengxiang Xiang, California Institute of Technology (Caltech), Pasadena, CA

Project Start Date: August 1, 2015
Project End Date: July 31, 2017

Overall Objectives

- Experimentally validate a benchtop-scale tandem particle-slurry batch reactor as a scalable technology for solar hydrogen production at a projected cost of ≤$20.00 per gallon of gasoline equivalent.
- Demonstrate a ~12-inch by ~12-inch model reactor that generates H_2 at a rate of >3 L per 8 hours of solar illumination.

Fiscal Year (FY) 2016 Objectives

- Using numerical simulations, demonstrate the feasibility of a reactor that exhibits a 1% solar-to-hydrogen (STH) conversion efficiency while using at least 80% less pipes and energy required to pump and circulate the electrolyte than modeled for similar reactors analyzed in the 2009 techno-economic analysis.

Technical Barriers

This project addresses the following technical barriers from the Hydrogen Production section of the Fuel Cell Technologies Office Multi-Year Research, Development, and Demonstration Plan.

(AG) Integrated Device Configurations

(AH) Reactor Designs

(AI) Auxiliary Materials

(AJ) Synthesis and Manufacturing

Technical Targets

This project entails combined numerical modeling, simulations, and experimental studies related to a new tandem particle-slurry batch reactor design for solar water splitting using photocatalyst semiconductor particle suspensions and consisting of two stacked compartments. Insights gained from these studies will be applied toward the design of plant-scale reactors to meet the following DOE hydrogen production targets for dual bed photocatalyst systems.

- Cost: ≤$20.00/kg H_2
- STH Energy Conversion Ratio: ≥1% and >3 L H_2 per 8 hours of solar illumination

FY 2016 Accomplishments

- Demonstrated in silico that a 1% STH efficient dual bed reactor can satisfy the go/no-go decision and the 2015 DOE Multi-Year Research, Development, and Demonstration Plan STH efficiency target.
- Demonstrated that a combination of two particle electrodes can attain the voltage required to split water.
- Developed several small-scale reactors of varying sizes in order to assess the validity of the numerical models and to serve as benchtop-scale prototypes.

✧ ✧ ✧ ✧ ✧

INTRODUCTION

Economically, particle-slurry reactors are projected to be one of the most promising technologies for clean solar photoelectrochemical hydrogen production via water splitting, according to a 2009 techno-economic analysis commissioned by the U.S. Department of Energy and performed by Directed Technologies, Inc. [1,2]. This techno-economic analysis compared four plausible reactor designs: two panel-based reactors, which resembled typical wafer-based solar cells immersed in a liquid electrolyte, and two particle-slurry reactors. On an energy basis, the hydrogen produced from the particle-slurry reactors was projected

to be by far the most cost-competitive with fossil fuels, further supporting the viability of the hydrogen economy. This project describes a new design for a particle-slurry reactor, where the main innovation is the use of a stacked-compartment arrangement, instead of the typical design where the compartments are arranged side-by-side. By stacking the compartments, which results in much shorter mass transport distances and provides efficiency advantages due to the tandem light absorbers, it is projected that over five times less pipes and pumping energy are required to circulate the electrolyte, which results in a lower plant cost than that of the least expensive proposed particle-slurry reactors to date.

As part of the proposed work plan, the device physics of the reactor designs were numerically modeled and simulated, and it was determined that in the absence of piping and pumps, a 1% STH efficient reactor with specific particle concentrations and redox shuttles could continuously operate for over one year and therefore, essentially operate indefinitely. This is significant because it satisfies our go/no-go decision and suggests that the 2015 DOE Multi-Year Research, Development, and Demonstration Plan targets can be met with this significantly less expensive design. We have also begun fabricating and testing small-scale experimental prototypes to aid in numerical model validation and to isolate the effects of underlying physical phenomena on the overall reactor performance. Eventually, we will leverage the numerical model and small-scale prototypes to fabricate a benchtop-scale (12-inch by 12-inch) reactor prototype that will be evaluated experimentally. Toward this, we have synthesized several state-of-the-art semiconductor particle materials, and, using electrodes cast from state-of-the-art Rh-modified $SrTiO_3$ nanoparticles and $BiVO_4$ nanoparticles, we have demonstrated that together they can generate the photovoltage required to split water. We have also demonstrated bipolar electrodeposition of electrocatalysts on model spherical carbon particles, hundreds of microns in size, and measured a photovoltage response from one-to-few TiO_2 nanoparticles covalently attached to a single nanopore in a poly(ethylene terephthalate) thin film when wetted on both sides by electrolyte, indicative of interfacial electronic charging and photovoltaic behavior. These contactless techniques for depositing materials and measuring performance of nanoparticles afford in situ and in operando fabrication and characterization abilities.

APPROACH

The overarching approach to achieving the objectives of the project was to combine theoretical and numerical modeling efforts with experimental measurements to design and optimize reactor performance. Simulation results were used to evaluate optimal semiconductor particle concentrations, redox shuttle concentrations, and reactor heights to attain desired reactor performance.

The numerical model is transient, two-dimensional, and implemented in COMSOL multiphysics simulation software. The modeling domain is shown in Figure 1. The model included the following relevant physics:

- Gaussian diurnal illumination cycles to mimic solar illumination.
- Optical absorption that follows the Beer–Bouger–Lambert law.
- Competitive light absorption by the redox shuttle.
- A photodiode as the power supply driven by the input sunlight.
- Butler–Volmer reaction kinetics for state-of-the-art oxygen-evolving electrocatalysts and hydrogen-evolving electrocatalysts, but with equal charge-transfer coefficients to expedite implementation.
- Volumetric reaction rates, instead of areal current densities, to represent solution redox chemistries.
- Species transport due to diffusive and migratory fluxes.
- Effects of the separator porosity on species diffusivities
- Optional daily recirculation of the electrolyte between the compartments.

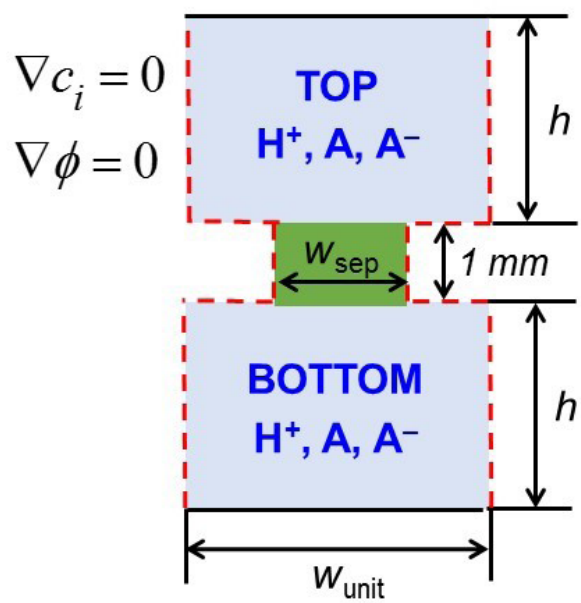

FIGURE 1. Numerical device physics modeling domain under periodic boundary conditions for a tandem stacked-compartment particle-slurry reactor, where each reactor is of height, h, and contains regularly spaced and sized separators of width, w_{sep}, per width of the reactor, w_{unit}. The aqueous electrolyte solutions in each reactor include protons (H^+), oxidized and reduced versions of the redox shuttle (A/A^-), and counterions.

- Counterions for the redox shuttle, other than protons.
- Dissolved gas transport to optimize the size of the porous separator.

In order to validate the computational approach, small-scale experimental prototypes were also developed. For example, the use of Fickian diffusion to model solution species transport behavior was validated experimentally using a rectangular electrochemical cell filled with an aqueous solution of electrolyte redox shuttle. The absorbance was monitored spectroscopically at a fixed position from an electrode biased to drive solution redox chemistry to evaluate transient concentration profiles. The numerical and experimental data sets were in good agreement, therefore validating the physics. Discrepancies between theory and experiments were used to fine-tune both via feedback loops. This process afforded checks and balances to the work in order to minimize time spent on a specific task or aspect of the project that was unlikely to succeed.

RESULTS

The numerical model was used to optimize the reactor size and semiconductor particle and redox shuttle concentrations to achieve at least 1% STH efficiency, consistent with the go/no-go decision. We focus here on presenting the case using 10-cm-tall compartments, which are consistent with the heights modeled in prior techno-economic analyses of similar reactor designs.

From the standpoint of designing a reactor to operate sustainably with only passive diffusion facilitating mass transport, the main factors we considered were the diffusivity and aqueous solubility of the redox shuttle, and the tradeoffs in increasing the redox shuttle concentration on competitive light absorption. Based on reported data in the literature, iodine-based and iron-based redox shuttles (I_3^-/I^- and Fe^{3+}/Fe^{2+}) have been used in the most efficient tandem particle suspensions. However, at the estimated minimum species concentrations needed to sustain indefinite reactor operation, i.e., 1–2.5 M, these redox shuttles substantially absorb visible light, therefore greatly attenuating absorption by the particles. Model results indicated that for 10-cm-tall compartments, concentrations less than 1 mM were required in order to generate rates of hydrogen evolution consistent with a 1% STH efficiency.

Therefore, we considered organic redox shuttles, such as quinones, as alternatives in order to reduce the extent of light absorption and to utilize the added benefit of proton-coupled electron transfer that can enable sustained reactor operation at near-neutral pH, i.e., pH ≈ 7 (~10^{-7} M H^+). By coupling electron transfer and proton transfer reactions, concomitant with H_2 evolution or O_2 evolution reactions, no net protons are liberated or consumed and, therefore, small concentrations of protons, e.g., 10^{-7} M, can be maintained during operation. Model results for the average concentration profiles of the redox shuttle, initially present as 1 M *para*-benzoquinone (Q), 1 M hydroquinone (QH_2), and 10^{-3} M protons (H^+), are shown in Figure 2a. These simulations assumed 10-cm-tall compartments with particle concentrations of 0.0013 g/L $BiVO_4$ in the top compartment and 1.7 g/L Rh-modified $SrTiO_3$ in the bottom compartment. The reactor attained approximate steady-periodic operating conditions after 200 days, at which time each compartment operated at a projected current density of ~0.85 mA/cm^2, a rate consistent with a 1% STH efficiency. Even though the Q/QH_2 redox shuttle has an aqueous solubility less than 0.6 M, higher solubilities exist when Q/QH_2 is modified with sulfonate groups [3]. Therefore, we have demonstrated that the proposed design can operate safely and sustainably with only diffusive mass transport in the absence of any pumps or piping infrastructure. Figure 2b depicts the time

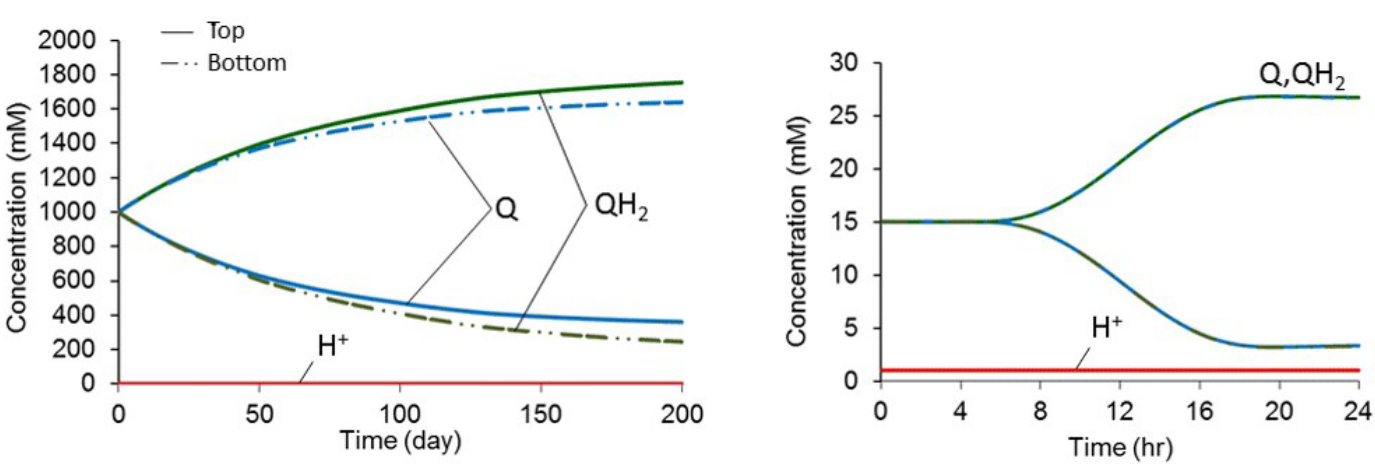

FIGURE 2. Species concentration profiles of *para*-benzoquinone (Q), hydroquinone (QH_2), and protons (H^+) for compartments each 10-cm tall containing 0.0013 g/L $BiVO_4$ in the top compartment and 1.7 g/L $SrTiO_3$:Rh in the bottom compartment with initial pH of 3 and Q/QH_2 concentrations of (a) 1 M and (b) 15 mM

evolution of species concentration for reactor operation over one day, suggesting that even at 15 mM Q/QH_2, the reactor can operate at a 1% STH efficiency. Based on our calculations, operating the pumps for one hour every night, and decreasing the amount of pipes by ~90%, provides convective recirculation and stirring sufficient to homogenize the reactor contents. This process is expected to consume less than 0.03 kW, which is an 85% reduction from the pumping power estimated in prior techno-economic analyses of similar reactor designs. Modeling results therefore suggest a reasonable potential toward sustainably operating a 1% STH efficient prototype tandem particle-slurry batch reactor for close to one year in 10-cm-tall reactor compartments, consistent with meeting the go/no-go decision. These results are important to achieving the DOE Multi-Year Research, Development, and Demonstration Plan targets because they demonstrate the validity of the reactor design for a 1% STH efficient system.

Figure 3 shows experiment results from photoelectrochemical measurements with electrodes made from Rh-modified $SrTiO_3$ and $BiVO_4$. These data indicate that together these two materials can generate the voltage required to split water, a process that requires at least 1.23 V of potential at standard state. While the electrolytes used were at different pH values, these data suggest that these materials, or closely related materials, are likely the best combination to drive overall solar water splitting. These results are important to achieving DOE targets because they demonstrate that a two-particle tandem particle-slurry reactor could split water using sunlight.

Figure 4 shows the open-circuit photovoltage over time that resulted from illumination of a single nanopore in

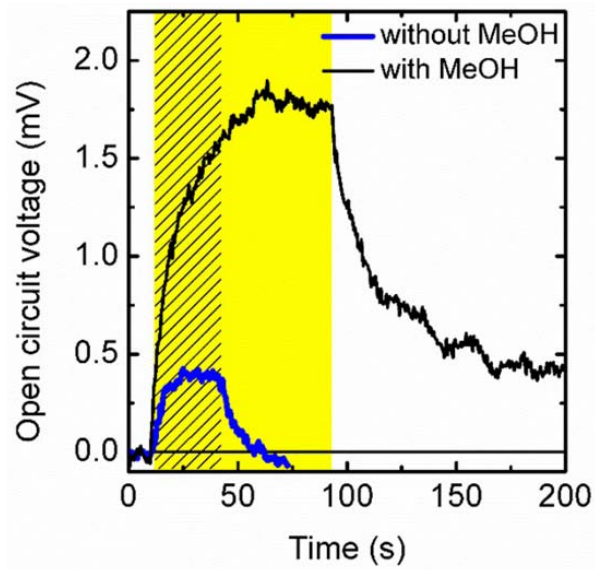

FIGURE 4. Open-circuit photovoltage over time for one-to-few TiO_2 nanoparticles covalently attached to a single nanopore in a poly(ethylene terephthalate) thin film when wetted on both sides by aqueous electrolyte that did or did not contain methanol. Illumination times are indicated by the hashed or yellow highlights.

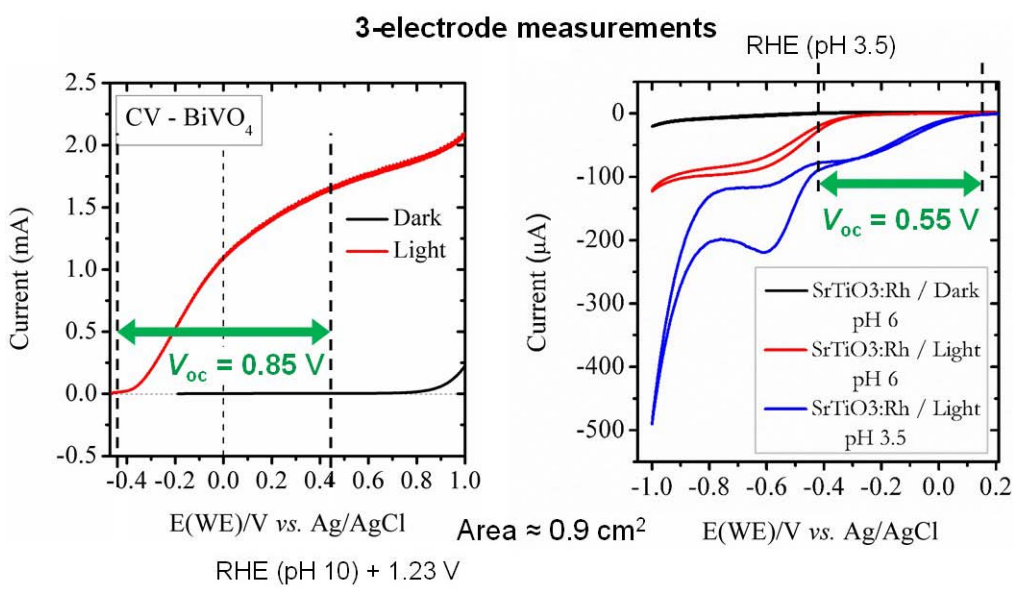

RHE – Reversible hydrogen electrode

FIGURE 3. Three-electrode current–potential behavior for photoelectrodes immersed in aqueous electrolyte, illuminated with simulated 1 Sun irradiance, and consisting of particles of (a) $BiVO_4$ and (b) Rh-modified $SrTiO_3$

poly(ethylene terephthalate) containing covalently-linked TiO_2 nanoparticle(s). This response is due to electrostatic charging of the interface and is interesting because for the first time, a photovoltage response was measured from one-to-several nanoparticles completely wetted by electrolyte. These results are important to achieving DOE targets because they demonstrate that the photoelectrochemical properties of one-to-few nanoparticle(s) can be measured under relevant conditions.

CONCLUSIONS AND FUTURE DIRECTIONS

Numerical models and simulations suggest that a dual bed reactor consisting of stacked compartments and no convection can achieve at least a 1% STH efficiency. Next, we will assess this concept experimentally using benchtop-scale prototypes, and we expect that a ~12-inch by ~12-inch model reactor of this design will be capable of generating >3 L of H_2 per 8 hours of solar illumination.

FY 2016 PUBLICATIONS/PRESENTATIONS

1. C. Xiang, A.Z. Weber, S. Ardo, A. Berger, Y. Chen, R. Coridan, K. Fountaine, S. Haussener, S. Hu, R. Liu, M.A. Modestino, M. Shaner, M. Singh, J. Stevens, K. Sun, and K. Walczak, *Angew. Chem. Int. Ed.*, **2016**, *accepted*, *Modeling, Simulation, and Implementation of Solar-Driven Water-Splitting Devices*.

2. S. Ardo, *U.S. DOE EERE FCTO Annual Merit Review,* **June 2016**, Washington, D.C., *Tandem particle-slurry batch reactors for solar water splitting.*

3. D.M. Fabian, S. Hu, N. Singh, F.A. Houle, T. Hisatomi, K. Domen, F.E. Osterloh, and S. Ardo, *Energy Environ. Sci.*, **2015**, *8*, 2825–2850, *Particle Suspension Reactors and Materials for Solar-Driven Water Splitting.*

4. H. Yaghoubi, W. Gaieck, K. Tkacz, A.S. Fathabadi, and S. Ardo, *229th Electrochemical Society Meeting*, **2016**, San Diego, CA, *Evaluation of State-of-the-Art Visible-Light-Absorbing Photocatalysts for Use in New Particle Slurry Reactors for Solar Water Splitting.*

5. R. Bala Chandran, S. Breen, Y. Shao, S. Ardo, and A.Z. Weber, *229th Electrochemical Society Meeting*, **2016**, San Diego, CA, *(Invited) Numerical Modeling of a Particle-Suspension Reactor for Solar Water Splitting.*

REFERENCES

1. Directed Technologies, Inc., *DOE Project Report*, **December 2009**, Contract Number: GS-10F-009J, *Technoeconomic Analysis of Photoelectrochemical (PEC) Hydrogen Production*.

2. B.A. Pinaud, J.D. Benck, L.C. Seitz, A.J. Forman, Z. Chen, T.G. Deutsch, B.D. James, K.N. Baum, G.N. Baum, S. Ardo, H. Wang, E. Miller, and T.F. Jaramillo, *Energy Environ. Sci.*, **2013**, *6(7)*, 1983–2000, *Technical and economic feasibility of centralized facilities for solar hydrogen production via photocatalysis and photoelectrochemistry.*

3. B. Yang, L. Hoober–Burkhardt, F. Wang, G.K. Surya Prakash, and S.R. Narayanan, *J. Electrochem. Soc.*, **2014**, *161(9)*, A1371–A1380, *An Inexpensive Aqueous Flow Battery for Large-Scale Electrical Energy Storage Based on Water-Soluble Organic Redox Couples*.

II.E.1 Biomass to Hydrogen

Pin-Ching Maness (Primary Contact),
Katherine Chou, and Lauren Magnusson
National Renewable Energy Laboratory (NREL)
15013 Denver West Parkway
Golden, CO 80401
Phone: (303) 384-6114
Email: pinching.maness@nrel.gov

DOE Manager: Katie Randolph
Phone: (720) 356-1759
Email: Katie.Randolph@ee.doe.gov

Collaborators:
- Steve Singer, Lawrence Berkeley National Laboratory
  Berkeley, CA
- Ken Sale, Sandia National Laboratories
  Albuquerque, NM

Subcontractor:
Bruce Logan, Pennsylvania State University
University Park, PA

Start Date: July 2015
Projected End Date: Project continuation and direction determined annually by DOE

Overall Objectives

- Optimize rates and yields of hydrogen production in a sequencing fed-batch bioreactor by varying hydraulic retention time and reactor volume replacement.
- Demonstrate hydrogen production by *Clostridium thermocellum* from biomass pretreated either with ionic-liquid or alkaline de-acetylation aimed at lowering feedstock cost.
- Optimize genetic tools to transform *C. thermocellum* and obtain mutants lacking the targeted competing pathway to improve hydrogen molar yield.
- Demonstrate hydrogen production from the NREL fermentation effluent to improve overall energy efficiency in hydrogen production from cellulosic biomass using a microbial electrolysis cell (MEC) reactor.

Fiscal Year (FY) 2016 Objectives

- Optimize sequencing fed-batch parameters and ferment corn stover lignocellulose to hydrogen and replace or reduce medium components aimed to lower hydrogen cost.
- Demonstrate growth of *C. thermocellum* in the presence of up to 10% of cholinium-based ionic liquids; determine most appropriate ionic liquid for future experiments based on *C. thermocellum* tolerance.
- Determine the highest saccharification efficiency for corn stover pretreated with several cholinium-based ionic liquids and correlate with hydrogen production by *C. thermocellum*.
- Identify the most important hydrogenase in *C. thermocellum* for over-expression aimed to increase hydrogen molar yield via fermentation.
- Use the genetic tools developed at NREL tailored for *C. thermocellum* and delete both the formate and lactate competing pathways; aimed to improve hydrogen molar yield via fermentation.
- Design MEC cathodes with reduced volume to increase maximum hydrogen production rate to 1.2 $L/L_{reactor}/d$ based on overall reactor volume reduction using Pt/C cathodes.
- Examine alternative materials and catalysts for the cathode and achieve hydrogen production rate to 1.2 $L/L_{reactor}/d$ without platinum catalyst.

Technical Barriers

This project supports research and development on DOE Technical Task 6, subtasks "Molecular and Systems Engineering for Dark Fermentative Hydrogen Production" and "Molecular and Systems Engineering for MEC," and it addresses barriers AX, AY, and AZ in the Hydrogen Production section of the Fuel Cell Technologies Office Multi-Year Research, Development, and Demonstration Plan.

(AX) Hydrogen Molar Yield

(AY) Feedstock Cost

(AZ) System Engineering

Technical Targets

See Table 1.

FY 2016 Accomplishments

- Identified, reduced, or eliminated three nutrient components (resazurin, cysteine, and a buffer reagent) in the *C. thermocellum* growth media with no impact on cell fitness or hydrogen production. The outcome reduced relative cost of the medium by up to 66% when the costly buffer chemical was replaced with KOH in a bioreactor with pH control.

TABLE 1. Progress toward Meeting DOE Technical Targets in Dark Fermentation

Characteristics	Units	Current Status	2015 Target	2020 Target
Yield of H_2 from glucose	Mole H_2/mole glucose	2–3.2	6*	--
Feedstock cost	Cents/lb glucose	13.5	10	8
Duration of continuous production (fermentation)	Time	17 days	3 months	--
MEC cost of electrodes	$/m^2	$2,400	$300	$50
MEC production rate	L-H_2/L-reactor-d	1	1	---

*Yield of H_2 from glucose: DOE has a 2015 target of an H_2 molar yield of 6 (4 from fermentation and 2 from MEC) from each mole of glucose as the feedstock, derived from cellulose.
Feedstock cost: The DOE Bioenergy Technologies Office is conducting research to meet its 2015 target of 10 cents/lb biomass-derived glucose. NREL's approach is to use cellulolytic microbes to ferment cellulose and hemicellulose directly, which will result in lower feedstock costs.

- Initial experiments showed that growth of *C. thermocellum* was inhibited at ≤3% of the cholinium-based ionic liquids. Adaptation experiments identified cholinium glutamate ([Ch][Glu]) as the most promising ionic liquid for tolerance experiments. Cultures of *C. thermocellum* were adapted to be tolerant to up to 9% [Ch][Glu].
- Pretreatment and saccharification with cholinium-based ionic liquids ([Ch][Glu], cholinium succinate, cholinium malate) demonstrated that corn stover pretreated with [Ch][Clu] yielded the highest amount of glucose. The saccharification results correlated with hydrogen production results, which indicated that [Ch][Glu]-pretreated biomass was a good substrate for release of hydrogen by *C. thermocellum*.
- A *C. thermocellum* mutant was generated which lacks both the pyruvate-to-formate and pyruvate-to-lactate electron-competing pathways. An increase in specific rate of hydrogen production was detected, yet with a concomitant increase in ethanol production, highlighting the importance of deleting the latter competing pathway.
- Hydrogen production in the MEC was increased to 1.4±0.2 L-H_2/L-reactor/d using hydraulic flow control past the electrode, in a reduced cathode chamber volume to improve performance. It was determined that increased pH did not adversely impact current generation.

✧ ✧ ✧ ✧ ✧

INTRODUCTION

Biomass-derived glucose feedstock is a major operating cost driver for economic hydrogen production via fermentation. DOE's FCTO is taking advantage of the DOE's Bioenergy Technology Office's investment in developing less expensive glucose from biomass to meet its cost target of 10 ¢/lb by 2015. One alternative and viable approach to addressing the glucose feedstock technical barrier (Technical Barrier AZ) is to use certain cellulose-degrading microbes that can ferment biomass-derived cellulose directly for hydrogen production. One such model microbe is the cellulose-degrading bacterium *Clostridium thermocellum*, which was reported to exhibit one of the highest growth rates using crystalline cellulose [1].

Another technical barrier to fermentation is the relatively low molar yield of hydrogen from glucose (mol H_2/mol sugar; Technical Barrier AX) using existing metabolic pathways in the cells. Biological pathways maximally yield 4 mol hydrogen per 1 mol glucose (the biological maximum) [2]. However, most laboratories have reported a molar yield of 2 or less [3,4]. Molecular engineering to block competing pathways is a viable option toward improving hydrogen molar yield. This strategy has resulted in improved hydrogen molar yield in *Enterobacter aerogenes* [5].

A promising parallel approach to move past the biological fermentation limit has been developed by a team of scientists led by Bruce Logan at Pennsylvania State University. In the absence of O_2, and by adding a slight amount of negative potential (-250 mV) to the circuit, Logan's group has produced hydrogen from acetate (a fermentation byproduct) at a molar yield of 2.9–3.8 (versus a theoretical maximum of 4) in a modified microbial fuel cell (MFC) called an microbial electrolysis cell (MEC) [6]. It demonstrated for the first time a potential route for producing up to eight moles of hydrogen per mole of acetate or potentially up to 12 moles of hydrogen per mole of glucose when coupled to a dark fermentation process. Indeed, in FY 2009 the team reported a combined molar yield of 9.95 when fermentation was coupled to an MEC in an integrated system [7]. Combining fermentation with MECs could therefore address Technical Barrier AX and improve the techno-economic feasibility of hydrogen production via fermentation.

APPROACH

NREL's approach to addressing high feedstock cost is to optimize the performance of the cellulose-degrading bacterium *C. thermocellum* using corn stover lignocellulose as the feedstock. To achieve this goal, we are optimizing

the various parameters in a sequencing fed-batch reactor to improve longevity, yield, and rate of hydrogen production. Two types of biomass pretreatment technologies were tested, one via alkaline de-acetylation at NREL, and a second approach using ionic liquid, conducted at Lawrence Berkeley National Laboratory and Sandia National Laboratories. To improve hydrogen molar yield, we are selectively blocking competing metabolic pathways in this organism via genetic methods. Through a subcontract, Pennsylvania State University is testing the performance of an MEC using both a synthetic effluent and the real waste stream from lignocellulosic fermentation generated at NREL.

RESULTS

Lower Medium Cost for Lignocellulose Fermentation

C. thermocellum is normally cultured in a growth medium containing buffer, mineral salts, and vitamins. The top three most expensive components per liter medium are: 3-morpholinoproprane-1-sulfonic acid (MOPS) buffer ($10.92), resazurin ($1.57), and cysteine ($1.31). Resazurin is used as a redox or O_2 indicator to ensure anaerobicity of the growth medium. Cysteine is normally added to poise lower redox potential and also scavenges O_2. The removal of either resazurin or cysteine from growth medium has no impact on cell growth (data not shown), or hydrogen production (Figure 1A). MOPS is added to maintain pH at 7.0, optimal for *C. thermocellum* cell growth. With no external pH control, feeding MOPS at 50% level has little impact on either growth or hydrogen production, yet its complete removal severely impacted both parameters (Figure 1A), suggesting the importance of proper pH maintenance. To circumvent pH effect, we carried out hydrogen production in bioreactor with pH control (maintaining at pH 7 throughout) by adding the less costly KOH. Under this condition a complete removal of MOPS has no impact on hydrogen production (Figure 1B), lowering the medium cost from $0.55/mM H_2 to $0.18/mM. The outcomes identified the cost saving components with their removal or replacement lowering medium cost without compromising final hydrogen productivity.

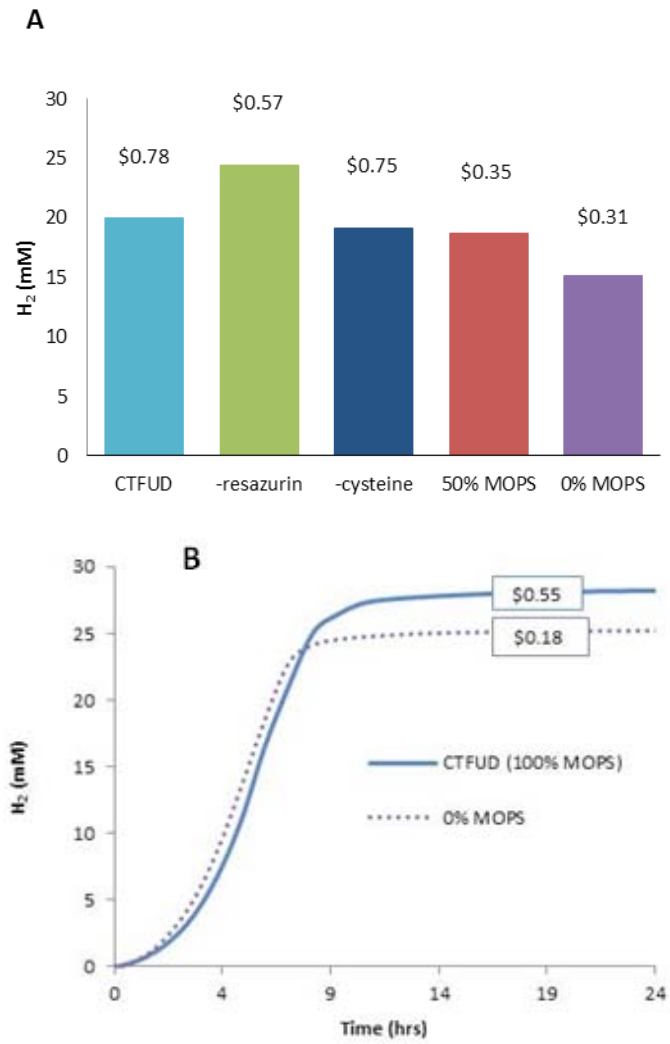

FIGURE 1. (A) Hydrogen production on CTFUD medium with removal of a single ingredient. Values above each bar represent $ per mmoles H_2 and are based on the costs of each medium after removal of the corresponding ingredient; (B) hydrogen production in pH-controlled bioreactor with and without MOPS buffer. When MOPS was removed from the medium, the cost of hydrogen decreased from $0.31/mM H_2 (1A) to $0.18/mM H_2 (1B) due to more hydrogen being produced in the latter. The nutrient cost was calculated based on catalog price of Sigma Chemical Co. It is anticipated the nutrient cost will be greatly reduced when purchase in bulk in scale-up applications.

Fermentation of Pretreated Biomass using Ionic Liquid (Lawrence Berkeley National Laboratory and Sandia National Laboratories)

The goal of this work is to integrate a novel pretreatment process, ionic liquid pretreatment, into the production of hydrogen from biomass using *C. thermocellum*. Ionic liquids are a remarkably effective pretreatment for biomass, and biologically derived cholinium-based ionic liquids offer the possibility of performing biomass pretreatment and saccharification in the same bioreactor, reducing the cost of the process [9]. To establish whether a combined pretreatment/saccharification process is feasible, the ability of *C. thermocellum* to produce hydrogen from [CH][Glu]-pretreated corn stover at 75% of the comparable production from cellobiose was demonstrated (Table 2). Preliminary cultivations of cellobiose-grown *C. thermocellum* demonstrated that growth was inhibited at ~3% [Ch][Glu] and at lower levels of [Ch][Mal] and [Ch][Suc]. Adaptation of *C. thermocellum* to grow on up to 9% [Ch][Glu] was demonstrated and hydrogen production from cellobiose at 7% [Ch][Glu] was observed that was ~74% that of the control. The growth of the cellobiose culture containing 7% [Ch][Glu]

was 50% of the control, suggesting that inhibiting growth may contribute to decreased total hydrogen production. Efforts to obtain a stable culture growing at 10% [Ch][Glu] are currently being pursued.

TABLE 2. Tolerance and Hydrogen Production in Ionic Liquids

Ionic liquid	Hydrogen production from pretreated corn stover (mL)[1]	Maximum tolerance of *C. thermocellum* (w/v)[2]
[Ch][Glu]	24 ± 2	9%
[Ch][Suc]	11 ± 1	3%
[Ch][Mal]	ND	1%

[1]Based on production in cultures containing 0.5% pretreated corn stover incubated at 55°C for 60 h
[2]Percentage of ionic liquid at which *C. thermocellum* can achieve >50% growth relative to an unamended control. Hydrogen production in 0.5% cellobiose (without ionic liquid) was 31±4 mL.

Metabolic Engineering

The goal of this approach is to use genetic tools to inactivate genes encoding competing metabolic pathways, thus redirecting more cellular flux (i.e., electrons) to improve hydrogen molar yield. We have designed a plasmid suited for genetic transformation in *C. thermocellum* strain DSM 1313 as the model cellulose-degrader. Following the protocols developed by Argyros et al. [10], we have created mutants lacking the pyruvate-to-lactate pathway encoded by lactate dehydrogenase (LDH) either in the wild type background or in a host lacking also the pyruvate-to-formate pathway catalyzed by pyruvate formate lyase (PFL), as verified by PCR (Figure 2). The double mutant indeed exhibited higher specific rate of hydrogen production based on cell dry weight. To further increase hydrogen production, an effort is ongoing to delete the competing ethanol pathway in the double mutant to conserve more electrons for hydrogen production.

Cathode Chamber Design

The cathode chamber electrolyte was recirculated past the cathode to improve operation and allow a reduction in volume (76 mL→28 mL) using a chamber width of 0.7 cm. The anode chamber was operated using synthetic fermentation effluent (1.2 g COD/L, HRT=8 h) comprised of acetate, BSA, dextrose, ethanol, and lactate in 50 mM phosphate buffer solution (PBS), and a catholyte with 50 mM PBS. Theoretical calculations suggested that the pH increase that would result from this operation would impair performance, but no impact was found relative to an increase in pH even with the buffered solution. Due to the smaller

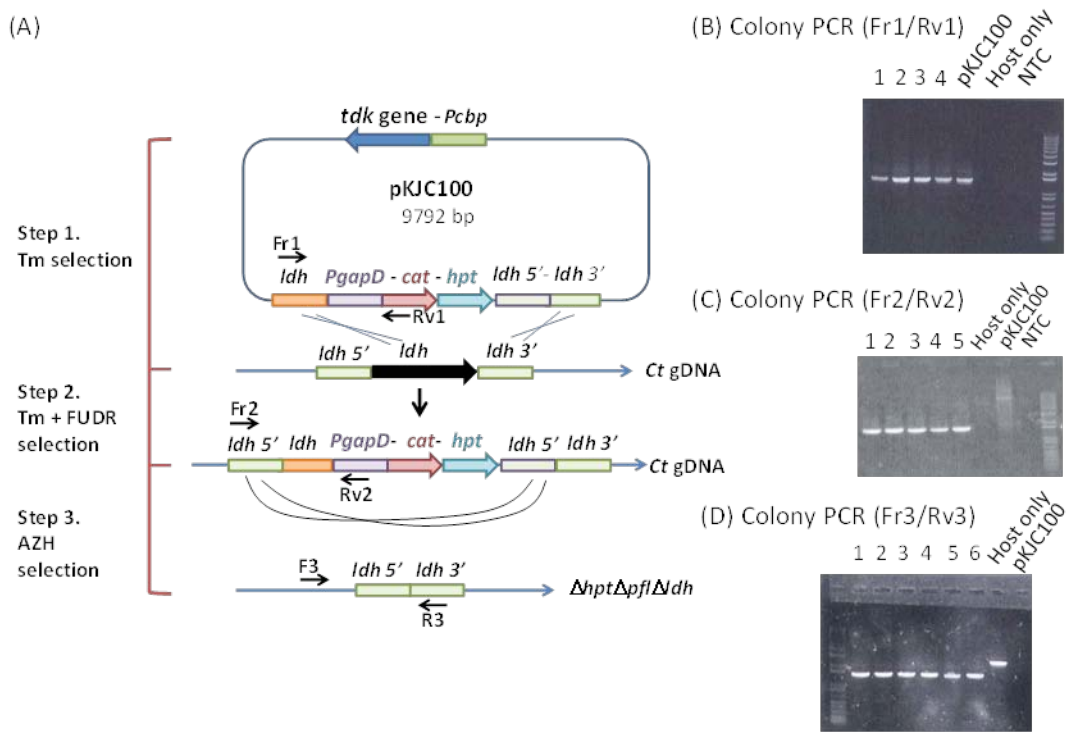

FIGURE 2. Creating the LDH pathway mutant in the Δ*hpt*Δ*pfl* strain yielding Δ*hpt*Δ*pfl*Δ*ldh*. (A) Schematic illustration of the three steps to generate the knockout; (B to D) colony PCR data validating each of the three steps and the final step yielding Δ*hpt*Δ*ldh*.

reactor volume, current density was greater than that of the previous MEC 76 mL cathode chamber, as well as a pervious MREC (microbial reverse electrodialysis electrolysis cell) that had a 163 mL cathode chamber (Figure 3). The improved (reduced volume) MEC produced 1.4±0.2 L-H_2/L-reactor/d over more than three anode HRT cycles, meeting the milestone for this part of the project. An MEC with a reduced volume cathode chamber was further tested using both 50 mM phosphate buffer (PBS, 5.6 mS/cm, initial pH 7) and 200 mM PBS (17.5 mS/cm, initial pH 7) as the catholyte. Hydrogen production using 200 mM PBS was not significantly different than gas production with the 50 mM buffer.

Alternative Cathode Materials

The cathode chamber was redesigned (63 mL) to position the electrode more centrally in the cathode chamber, in order to improve flow across the cathode surface. Three different cathode materials (stainless steel mesh, SSM; SS fiber felt, SSFF; SS wool, SSW) were tested as alternative cathode materials to platinum and a Pt/C (0.5 mg/cm^2) cathode was also tested as a control. Chronopotentiometry results at recirculation rates of 40 mL/min showed that for the alternative cathode materials, the better performances were obtained in order of SSW>SSFF>SSM, with the Pt/C cathode performing better than all three (Figure 4). The SSW cathode is a 3-dimensional material which has a high specific surface area, and this might be the reason for showing higher performance than SSM and SSFF cathodes.

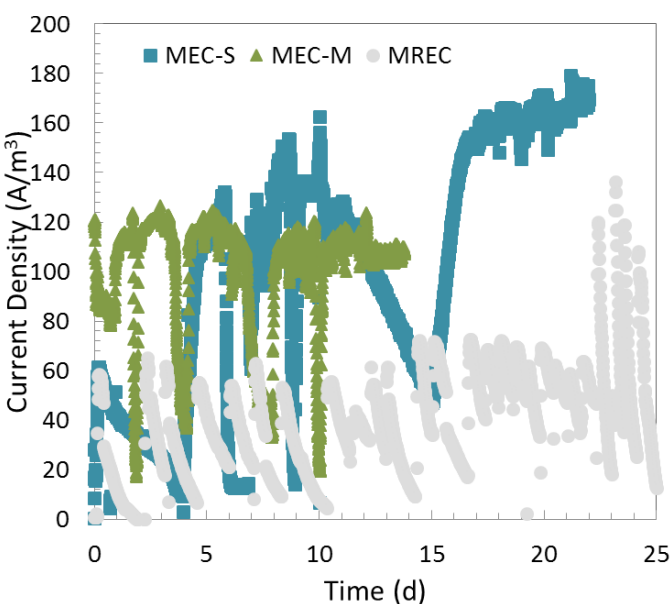

FIGURE 3. Current density of the MEC with a modular, continuous flow cathode chamber (MEC-S: 28 mL, 5.6 min HRT, 50 mM phosphate buffer; MEC-M: 76 mL, 3–15 min HRT, 50 mM phosphate buffer) compared to the previous MREC study (MREC: 163 mL, 8 min HRT, 1 M sodium bicarbonate buffer).

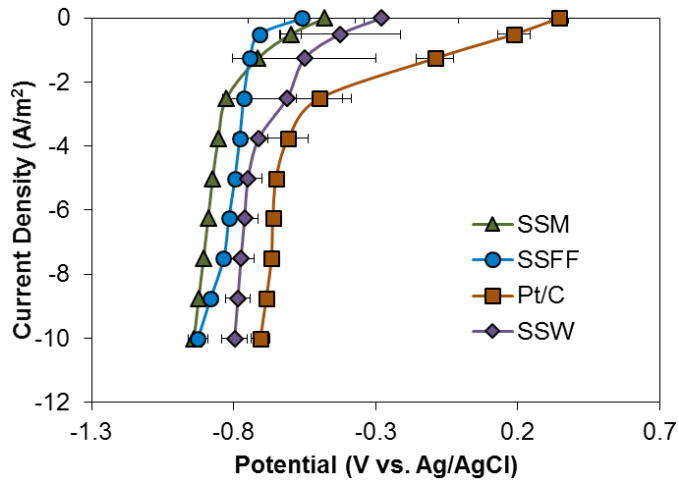

FIGURE 4. Chronopotentiometry tests with different cathode materials (SSM, SSFF, SSW, and Pt/C, recirculation rate: 20 mL/min) in the cathode chamber (set current 20 min/step, 40 cm^2 projected surface area).

CONCLUSIONS AND FUTURE DIRECTIONS

- We determined that resazurin and cysteine can be completely eliminated from growth medium for culturing *C. thermocellum* and hydrogen production. Moreover the costly MOPS can be replaced by KOH for pH maintenance, hence lowering the cost of the medium from \$0.55/mM H_2 to \$0.18/mM H_2, lowering the cost of hydrogen production from biomass.
- Following published protocols and using the NREL proprietary plasmid, we deleted both the pyruvate-to-formate pathway and the pyruvate-to-lactate pathway in a double mutant. The mutant indeed displayed higher specific rate of hydrogen production but with an increased level of ethanol production, suggesting deleting the latter is a priority for future research to increase hydrogen molar yield.
- Stable cultures of *C. thermocellum* growing on high levels of [Ch][Glu] that produce hydrogen have been established and will be tested in combined pretreatment/hydrogen production scenarios with the data applied toward a techno-economic analysis.
- Saccharification and hydrogen production experiments have demonstrated that [Ch]Glu] pretreatment of corn stover is a promising pretreatment for hydrogen production. Optimization of pretreatment and integration with *C. thermocellum* growth experiments will be continued.

- Hydrogen production in the MEC was increased to 1.4±0.2 L-H_2/L-reactor/d, and a higher catholyte pH did not adversely impact performance.

In the future, we will operate the sequencing fed-batch bioreactor fermenting DMR-pretreated corn stover lignocellulose generated from either a de-acetylated process or via ionic liquid pretreatment. We will increase solid loading to achieve higher rates of hydrogen production. We will further replace the commercial yeast extract with brewery yeast waste to decrease medium cost aimed at lowering hydrogen selling price. Deleting the ethanol-competing pathway is deemed essential to redirect more electrons toward hydrogen production and will continue to be a part of this effort. Past efforts had led to unstable isolates likely due to redox imbalance. To circumvent, we will delete the ethanol pathway in a host with higher levels of hydrogen production, hence using proton reduction as the new sink. This new host strain will be generated via replacing the native promoter with a stronger promoter to drive hydrogenase overexpression. The team will continue to adapt *C. thermocellum* to tolerate higher levels of ionic liquid (10% [Chl][Glu]) so that pretreatment and fermentation can occur in the same reactor to save reactor cost. hydrogen production and substrate utilization will be profiled to measure fermentation efficiency. The data will be input into a techno-economic model to determine the rate-limiting steps and cost drivers to guide future research direction. We will further investigate high surface area cathode materials by designing and constructing macroporous stainless steel material (brushes and fiber felt) for cathodes using the newly re-designed cathode chamber. We will also examine alternative materials and catalysts for the cathode with improved gas diffusion properties to improve reactor operation aimed at increasing hydrogen production and lowering MEC cost.

FY 2016 PUBLICATIONS/PRESENTATIONS

1. Maness, P.C., and Logan, B. 2016. DOE Fuel Cell Technologies Office Annual Merit Review, June 7, 2016, Washington, D.C. Presentation PD038.

REFERENCES

1. Zhang, Y.P.; Lynd, L.R. (2005). "Cellulose utilization by *Clostridium thermocellum*: bioenergetics and hydrolysis product assimilation." *Proc. Natl. Acad. Sci. USA* **102**, 7321–7325.

2. Hawkes, F.R.; Dinsdale, R.; Hawkes, D.L.; Hussy, I. (2002). "Sustainable fermentative hydrogen production: Challenges for process optimisation." *Intl. J. Hydrogen Energy* **27**, 1339–1347.

3. Logan, B.E.; Oh, S.E.; Kim, I.S.; Van Ginkel, S. (2002). "Biological hydrogen production measured in batch anaerobic respirometers." *Environ. Sci. Technol*. **36**, 2530–2535.

4. Van Ginkel, S.; Sung, S. (2001). "Biohydrogen production as a function of pH and substrate concentration." *Environ. Sci. Technol.* **35**, 4726–4730.

5. Rachman, M.A.; Furutani, Y.; Nakashimada, Y.; Kakizono, T.; Nishio, N. (1997). "Enhanced hydrogen production in altered mixed acid fermentation of glucose by *Enterobacter aerogenes*." *J. Ferm. Eng.* **83**, 358–363.

6. Cheng, S.; Logan, B.E. (2007). "Sustainable and efficient biohydrogen production via electrogenesis." *Proc. Natl. Acad. Sci. USA*. **104**, 18871–18873.

7. Lalaurette, E.; Thammannagowda, S.; Mohagheghi, A.; Maness, P.C.; Logan, B.E. (2009). "Hydrogen production from cellulose in a two-stage process combining fermentation and electrohydrogenesis." *Intl. J. Hydrogen Energy* **34**, 6201–6210.

8. Guss, A.; Olson, D.G.; Caiazza, N.C.; Lynd, L.R. (2012). "Dcm methylation is detrimental to plasmid transformation in *Clostridium thermocellum*." *Biotechnol. Biofuels* **5**, 30–41.

9. Liszka, M., Kang, A., Konda, S., Tran, K., Gladden, J., Singh, S., Keasling, J.D., Scown, C.D., Lee, T.S., Simmons, B., Sale, K.L. 2016. "Switchable Ionic Liquids Based on Di-Carboxylic Acids for One-Pot Conversion of Biomass to an Advanced Biofuel." *Green Chemistry*, DOI: 10.1039/C6GC00657D.

10. Argyros, D.; Tripathi, S.A.; Barrett, T.F.; Rogers, S.R.; Feinberg, L.F.; Olson, D.G.; Foden, J.M.; Miller, B.B.; Lynd, L.R.; Hogsett, D.A.; Caiazza, N.C. (2011). "High ethanol titers from cellulose by using metabolically engineered thermophilic anaerobic microbes." *Appl. Environ. Microbiol.* **77**, 8288–8294.

II.E.2 Sweet Hydrogen: High-Yield Production of Hydrogen from Biomass Sugars Catalyzed by in vitro Synthetic Biosystems

Y-H Percival Zhang (Primary Contact)
Virginia Polytechnic Institute and State University
304 Seitz Hall, Campus Mail 0303
Blacksburg, VA 24061
Phone: (540) 808-8985
Email: ypzhang@vt.edu

DOE Manager: Katie Randolph
Phone: (240) 562-1759
Email: Katie.Randolph@ee.doe.gov

Contract Number: DE-EE0006968

Subcontractor:
Mike Adams, Biochemistry and Molecular Biology Department, University of Georgia, Athens, GA

Project Start Date: June 15, 2015
Project End Date: June 30, 2016 (Phase I), June 30, 2017 (Phase II)

Overall Objectives

- Decrease the production costs 1,000-fold from ~$10,000/kg (current estimated level) to ~$10/kg of hydrogen as estimated by using the H2A model by the end of the project.
- Increase the volumetric productivity five-fold from current levels of ~150 mmol H_2/L/h to 750 mmol H_2/L/h.
- Scale up in vitro enzymatic hydrogen production 1,000-fold from 1-mL to 1-L bioreactor.

Fiscal Year (FY) 2016 Objectives

- Decrease hydrogen production costs by co-expression of multi-enzyme in one host, discovery of novel enzymes, and coenzyme engineering.
- Increase hydrogen production rates two-fold (i.e., 300 mmol H_2/L/h).
- Scale up hydrogen production volume by 10-fold (i.e., 10 mL bioreactor).
- Demonstrate 10-fold volume scale-up with two-fold increase in hydrogen peak production rate (i.e., 300 mmol H_2/L/h) on starch.

Technical Barriers

This project addresses the following technical barriers of biological hydrogen production from the Hydrogen Production section of the Fuel Cell Technologies Office Multi-Year Research, Development, and Demonstration Plan pertaining to dark fermentation.

(AX) Hydrogen Molar Yield

(AY) Feedstock Cost

(AZ) Systems Engineering

Technical Targets

Progress of in vitro enzymatic hydrogen production has been made in achieving the project targets. Table 1 lists the project technical targets (i.e., production cost, productivity, and reactor volume) and where our research and development efforts stand to date. The overall goals of this project are to decrease enzymatic hydrogen production cost, increase its production rate, and scale up its production volume. Our goals would clear up doubts pertaining to enzymatic hydrogen production cost, rate, and scalability for future distributed hydrogen production from renewable liquid sugar solution.

FY 2016 Accomplishments

- Achieved one of the highest biological H_2 generation peak rates – 320 mmole of H_2/L/h (i.e., ~164 L H_2/L/day).

TABLE 1. Virginia Tech and University of Georgia Status

Targets	Units	June 2016 Project Target	June 2017 Project Target	Year 2020 Plant Gate
Production Cost	$/kg H_2	1,000 (estimated)	10	10 (2020 DOE goal for advanced biological generation technologies)
Productivity	mmol H_2/L/h	320 (achieved)	750	2,000 (our goal)
Reactor Volume	L of reactor	0.01 (achieved)	1	2,777* (our goal)

*200 kg H_2 per day

- Scaled up recombinant enzyme production 1,000-fold from several milligrams to tens of grams and recombinant hydrogenase production 50-fold from ten milligrams to 500 milligrams.
- Designed and validated biomimetic electron transport chains for accelerating hydrogen peak generation rates five-fold from ~60 mmol to ~300 mmol of H_2/L/h.
- Validated the feasibility of engineering dehydrogenases to work on a low-cost and more stable biomimetic coenzyme, nicotinamide riboside (NR).
- Found out ways to precisely control expression level of each enzyme in multiple-gene coexpression.

✧ ✧ ✧ ✧ ✧

INTRODUCTION

Water splitting for hydrogen production is critical for sustainable, renewable hydrogen production. Water electrolysis suffers from high production costs and low electrolysis efficiencies. Water splitting at high temperature requires high temperature thermal energy sources and raises serious material challenges. Water splitting at low or even ambient temperature is highly desired when considering material challenges, availability of high-temperature thermal energy sources, and distributed hydrogen production systems. A few methods conducted at low temperatures are under investigation, including photocatalytic water splitting, photo-electrochemical water splitting, photobiological water splitting, and microbial electrolysis cells. However, they suffer from low hydrogen generation rates and/or low energy conversion efficiencies.

Renewable hydrogen production via water splitting energized by chemical energy stored in biomass is extremely attractive because biomass sugars are the most abundant renewable chemical energy [1]. However, microbial anaerobic fermentation (dark fermentation) suffers from low hydrogen yields, where the theoretical yield is 4 H_2 per glucose molecule according to the reaction: $C_6H_{12}O_6 + 2\ H_2O = 4\ H_2 + 2\ CH_3COOH$ (acetate) $+ 2\ CO_2$. Although microbial electrolysis cells enable the utilization of acetate or other organic matter supplemented with an electrical input to split water to generate more hydrogen, this two-step conversion requires two reactors, has decreased energy efficiency compared to the theoretical hydrogen yield (i.e., 12 H_2 per glucose molecule and water) due to electricity consumption, slow hydrogen generation rates, and requires high capital investment of microbial water electrolysis. Recently, we demonstrated in vitro synthetic enzymatic biosystems to generate theoretical yields of hydrogen energized by numerous carbohydrates, such as, starch, cellodextrins, glucose, xylose, and xylooligosaccharides [2]. But some serious barriers to industrial scale-up potential remain, including (1) enzyme production cost, (2) enzyme stability, (3) coenzyme cost and stability, (4) (slow) reaction rates, and (5) scale-up feasibility [3]. In this project, we propose to address the above issues at the laboratory scale.

APPROACH

The general approach for this project is to apply biochemistry and protein engineering, microbiology, molecular biology, chemistry, and engineer design principles to address technical barriers pertaining to industrial needs of enzymatic hydrogen production (i.e., production costs, reaction rate, and scalability). We have multiple subtasks aiming to achieve each objective. To decrease hydrogen production costs, we co-expressed multiple enzymes in one *E. coli* host and found out the best strategy to precisely control protein expression levels; discovered new hyperthermophilic enzymes; and engineered coenzyme preference of dehydrogenases to biomimetic coenzymes. To increase hydrogen generation rates, we developed kinetic model and identified the rate-limiting steps; constructed novel biomimetic electron transport chains; and built enzyme complexes featuring substrate channeling. To scale up hydrogen production, we scaled up recombinant protein production in *E. coli* and recombinant hydrogenase production, as well as demonstrated hydrogen productions in large bioreactors.

RESULTS

The overall goal of the first phase of this project was to demonstrate 10-fold volume scale-up with two-fold increase in hydrogen peak production rate (i.e., 300 mmol H_2/L/h) on starch. Figure 1A shows the profile of hydrogen evolution from the starch/water solution catalyzed by the synthetic enzymatic biosystem, which was conducted in a 10-mL bioreactor (Figure 1B). The peak hydrogen generation rate demonstrated was 320 mmol H_2/L/h (meeting the Phase 1 go/no-go criteria), which is one of the highest biological hydrogen production rates reported, compared to dark fermentation, photobiological means, and microbial electrolysis cells.

To decrease hydrogen production costs, we have three subtasks: (1) decrease enzyme production costs, (2) discover better enzymes, and (3) engineer the coenzyme preference of dehydrogenases.

Decrease Enzyme Production Costs

To decrease enzyme production costs and the number of *E. coli* hosts for protein production, we co-expressed four enzymes in one host at its maximum recombinant protein production capacity and hoped to precisely control each enzyme expression level for nearly equal enzyme activities, where individual apparent activity is equal to specific

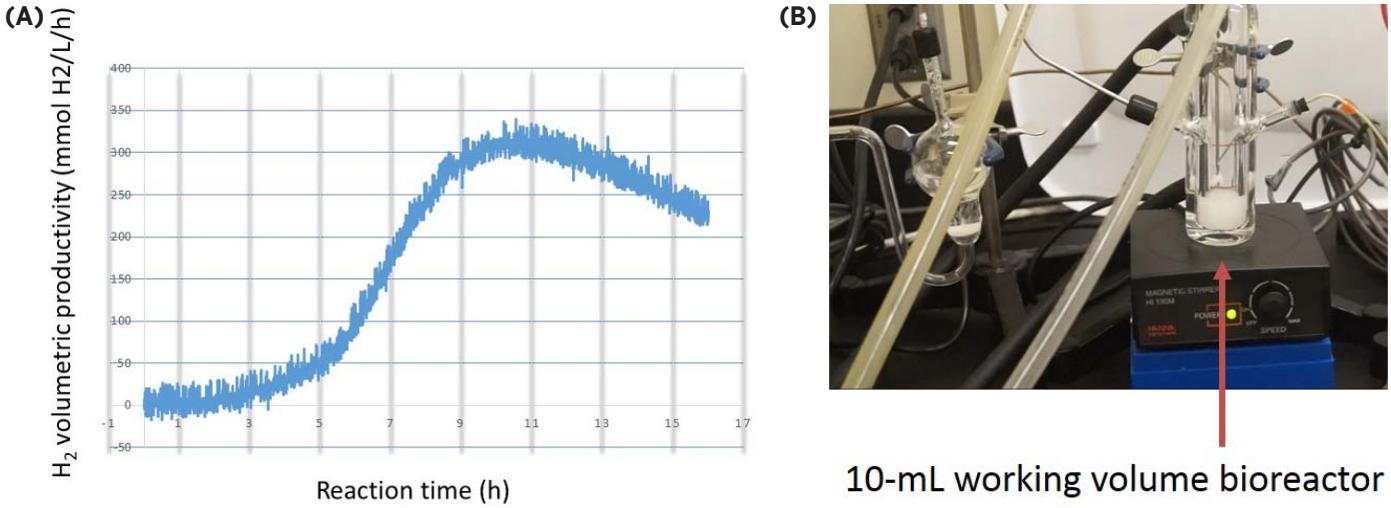

FIGURE 1. The profile of the hydrogen evolution from isoamylase-treated corn starch (A) and photo of 10-mL bioreactor for enzymatic hydrogen production based on starch (B).

activity of individual enzyme multiplied by individual enzyme percentage in the cell lysate. We tested four different strategies, testing one vector (Cases 9, 10, and 11) versus two vectors (Case 8), and different deoxyribonucleic acid transcription regulation mechanisms, whether to put the T7 terminator behind each gene (Cases 8 and 11) or only after the last gene (Cases 9 and 10) and/or T7 promoter before the each gene (Cases 8, 10, and 11) or only before the first gene (Case 9) to control protein expression levels (Table 2). The best strategy for our four enzymes is Case 8 with two vectors, each of which encodes two genes and each gene has its own promoter and terminator (Table 2). Consequently, the calculated apparent activity for each of the enzymes in Case 8, based on the enzyme proportion results from the sodium dodecyl sulfate polyacrylamide gel electrophoresis (SDS-PAGE) and the previously tested specific activity for each enzyme, wherein specific activities of αGP, precious group metal (PGM), glucose 6-phosphate dehydrogenase (G6PDH), and 6-phosphogluconate dehydrogenase (6PGDH) are 20, 350, 35, and 16 U/mg, respectively [2], is similar for all enzymes in the cell lysate being ~1.6 U/mL of cell culture (Table 2). This suggests that none of the enzymes were over-expressed relative to the others.

Discover Better Enzymes

To decrease the enzyme costs through the use of enzymes with more stability (i.e., longer lifetime) and higher specific activities (i.e., less protein use in terms of mass), we have cloned nine new hyperthermophilc enzymes to replace previous modestly thermophilic enzymes. Also, all of the enzymes used in this project can be easily purified by heat precipitation, where ~80°C heat treatment can deactivate all of the *E. coli* proteins. In the future, enzymatic hydrogen can be produced by a mixture of the heat-treated cell lysates without costly enzyme purification steps.

Engineer the Coenzyme Preference of Dehydrogenases

To decrease coenzyme costs of in vitro biosystems, we did coenzyme engineering, changing the coenzyme

TABLE 2. Comparison of Four-Enzyme Co-Expression Cases in *E. Coli*. The apparent activities of the individual enzyme in the cell lysates and the total activities of the four-enzyme cell lysates based on xylitol formation.

Case Name[a]	Expression ratio (%)					Apparent activity (U/mL)[b]				Total activity (mM)[c]
	αGP	PGM	G6PDH	6PGDH	Sum	αGP	PGM	G6PDH	6PGDH	
Case 8	17	0.75	28	20	66	1.6	1.9	1.9	1.3	24.58
Case 9	30	6.2	4.2	1.6	42	2.8	16	0.29	0.10	15.48
Case 10	28	6.9	3.9	1.3	40	2.6	18	0.27	0.083	15.27
Case 11	16	5.4	3.6	17	42	1.5	14	0.25	1.1	16.67

[a] Case 8, two vectors, each of vector encodes two enzyme genes and each gene has its own T7 promoter and T7 terminator; Case 9, 10 and 10, one vector encoding four enzymes. Case 9, one gene-cluster containing *6pgdh, g6pdh, agp,* and *pgm* (one T7 promoter and one T7 terminator); Case 10, the four T7 promoters for the four genes and one T7 terminator in the end of the four-gene cluster; Case 11, one T7 promoter and one T7 terminator for each gene.
[b] apparent activity = specific activity of individual enzyme ´ individual enzyme percentage in the cell lysate.
[c] total activity of the four-enzyme cell lysate was measured based on the formation of xylitol from xylose.

preference of two dehydrogenases (i.e., G6PDH and 6PGDH) from nicotinamide adenine dinucleotide phosphate (NADP) to small-size, low-cost and high-stability nicotinamide riboside (NR). The general strategy for coenzyme engineering is based on a combination of rational design and directed evolution. Rational design is a tool of protein engineering based on protein structure, catalytic mechanism, and site-directed mutagenesis; while directed evolution mimics the process of natural selection to evolve enzymes toward a user-defined goal, involving site-saturation or random mutagenesis and screening. To significantly increase 6PGDH activity on NR, we propose to increase its activities from NADP to nicotinamide adenine dinucleotide (NAD) to NR, where NAD is a coenzyme as a bridging compound for coenzyme engineering (Figure 2A). First, we used rational design to identify key amino acids responsible for binding the phosphate group of the NADP via amino acid sequence comparison of wild-type Tm6PGDH to other NADP-preferred 6PGDHs and two NAD-preferred 6PGDH mutants (Figure 2B) and homology structure modeling of Tm6PGDH and NADP (Figure 2C). Second, we generated the deoxyribonucleic acid mutant libraries for covering the key amino acids of dehydrogenases and then screened mutants with enhanced activities on NAD on the plate (Figure 2D). We developed novel high-throughput screening methods for rapid identification of mutants by using a redox dye (revised manuscript submitted to Scientific Reports for publication). Third, the mutants' enzymes, purified via heat precipitation (70°C for 30 min), were characterized for their activities on NADP, NAD, and nicotinamide adenine. The mutagenesis and screening steps can be conducted repetitively. The best mutant, Tm6PGDH (N31E/R32I/T33I), had a reversal of coenzyme preference from NADP to NAD. Also, this mutant has a great increase of its activities on NR, being 0.197 + 0.034 U/mg on NR at 80°C. Similarly, the other G6PDH enzyme mutant also worked on NR. The above results suggest that we have achieved the milestone of coenzyme engineering specific activities of dehydrogenases on NR of more than 0.1 U/mg. In Phase II, we will continue improving the activities of two dehydrogenases on NR.

To increase volumetric productivity of hydrogen, we built a kinetic model for experimental data accommodation

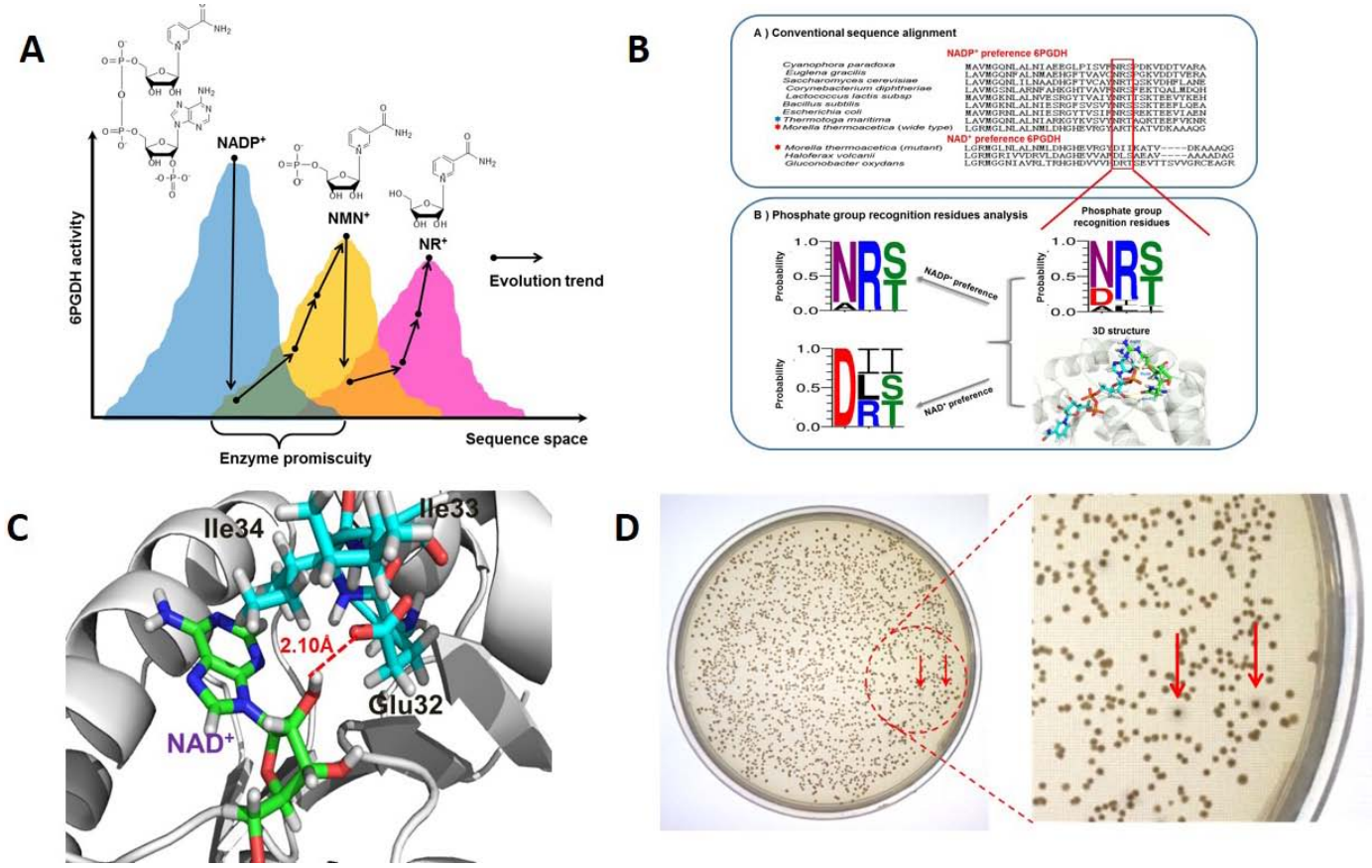

FIGURE 2. Strategy of coenzyme engineering ofTm6PGDH. (A) Concept of G6PDH coenzyme engineering from its natural coenzyme NADP to NAD to NR with the structures of coenzymes; (B) amino acid sequence analysis for coenzyme-binding motifs of various G6PDH enzymes with different coenzyme preferences for the identification of key amino acids; (C) molecular homology model of the NAD-G6PDH complex; and (D) photo of the petri-dish-based screening for the identification of positive G6PDH mutants with enhanced activities on NAD, where positive mutants were indicated by arrows.

and confirmed that the rate-limiting step of the whole biosystem is hydrogen generation from NADPH catalyzed by hydrogenase SH1. Inspired by the natural electron mediator ferredoxin protein for high-speed biohydrogen production bacteria, we investigated the use of small-size non-protein electron mediators such as, benzyl viologen (BV), methyl viologen, and neutral red. We discovered that the best electron mediator was BV for NADPH. The biomimetic electron transport chain was from NADPH (generated from the pentose phosphate pathway) to BV catalyzed by NADPH rubredoxin oxidoreductase (NROR), to hydrogen catalyzed by SH1 (Figure 3A). Starting from substrate G6P via the biomimetic enzymatic pathway, the peak hydrogen generation rate was 310 mmol H_2/L/h at 80°C (Figure 3B). We also constructed six G6PDH-6PGDH-SH1 enzyme complexes, which may facilitate electron transfer among adjacent enzymes. Our preliminary data indicates the feasibility of further reaction rate enhancements.

To scale up enzymatic hydrogen production, we conducted high-cell density fermentation in 6-L fermenter and accomplished the cell density of ~50 g dry cell weight per liter. Compared to 1-L flask, we were able to increase enzyme production capability by more than 1,000-fold. Such information suggests that bulk enzyme production costs could be as low as $50/kg [4]. By changing the promoter and enzyme purification tag of SH1, we increased SH1 production capability by 50-fold. Consequently, we scaled up our hydrogen production in 10-mL reactor.

CONCLUSIONS AND FUTURE DIRECTIONS

Although sweet hydrogen production is still in its early stage. Several conclusions can be made:

- The high biological H_2 generation rates achieved suggests that these in vitro hydrogen generation rates are fast enough to produce hydrogen at stationary hydrogen bioreactors.
- Engineered dehydrogenases were able to work on biomimetic coenzymes and novel high-throughput screening methods for biomimetic coenzyme engineering were established.

Future work includes:

- Further increase hydrogen production rate.
- Enhance activities of dehydrogenase mutants working on biomimetic coenzymes.
- Scale up enzymatic hydrogen production to 1 L.
- Conduct detailed economic analysis of enzymatic hydrogen production by using H2A model.

FY 2016 PUBLICATIONS/PRESENTATIONS

1. Moustafa, Hanan M.A., Taha I. Zaghloul, and Y.H. Percival Zhang. "A Simple Assay for Determining Activities of Phosphopentomutase from a Hyperthermophilic Bacterium *Thermotoga Maritima*." *Analytical Biochemistry* 501 (2016): 75–81.

2. Moustafa, H.M.W., E-J. Kim, Z.G. Zhu, C-H. Wu, T.I. Zaghloul, M.W.W. Adams, and Y-HP. Zhang. "Water Splitting for High-Yield Hydrogen Production Energized by Biomass Xylooligosaccharides Catalyzed by an Enzyme Cocktail." *ChemCatChem* (2016): DOI: 10.1002/cctc.201600772, in press.

3. Kim, J-E., R. Huang, H. Chen, C. You, and Y-H.P. Zhang. "Facile Insertion of a Large-Size Random Gene Mutagenesis Library into *Escherichia Coli* Plasmid without Restriction Enzymes." *Biotechnology Journal* (2016): DOI: 10.1002/biot.201600121.

4. Huang R., Chen H., Zhong C., Kim J-E., Zhang Y-H.P. "High-throughput screening of coenzyme preference change of thermophilic 6-phosphogluconate dehydrogenase from $NADP^+$ to NAD^+." *Scientific Reports* (2016), accepted.

5. Invited keynote talk. "Biomanufacturing 4.0: in vitro synthetic enzymatic biosystems beyond the cells' constraints." International Metabolic Science Conference. Shanghai Jiao-Tong University. Shanghai, China (12/15/2016).

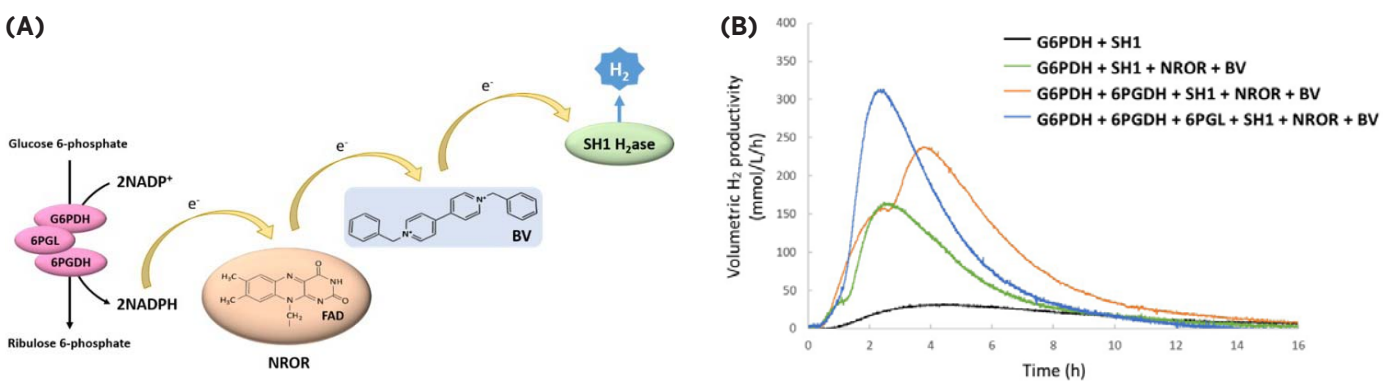

FIGURE 3. Scheme of the biomimetic electron transport chain from G6P to NADPH to H_2 via BV, where the enzymatic cocktail contains G6PDH, 6PGDH, 6PGL, DI, and SH1 (A) and the high-speed H_2 evolution profile by using the enzyme cocktail: G6PDH, 6PGDH, 6PGL, deionized water and SH1, plus BV, on glucose 6-phosphate (B).

6. Invited talk. "Biomanufacturing 4.0: in vitro synthetic enzymatic biosystems beyond the cells' constraints." Tianjin University Sino-USA Synthetic Biology Conference. Tianjin, China. (12/04/2015)

7. Invited keynote talk. "In vitro metabolic engineering would solve key problems of to the food-energy-water nexus." Metabolic Engineering Summit 2015, Beijing, China (12/02/2015).

8. Invited plenary talk. "Beyond cell's constraints: in vitro synthetic enzymatic biosystems for next generation biomanufacturing." Division 15A speaker for lenary symposium of the AIChE National Conference 2015. Salt Lake City, UT, USA. (11/08/2015)

9. Invited keynote talk. "Biomanufacturing 4.0: in vitro Synthetic Enzymatic Biosystems." The 8th Sino-US Joint Conference on Chemical Engineering. Shanghai, China. (10/23/2015).

REFERENCES

1. Zhang, Y-H.P. "Next Generation Biorefineries Will Solve the Food, Biofuels, and Environmental Trilemma in the Energy-Food-Water Nexus." Energy Sci. Eng. 1 (2013): 27–1.

2. Rollin, J.A., J.C. Martin, S. Myung, F. Sun, C. You, A. Bakovic, R. Castro, et al. "High-Yield Hydrogen Production from Biomass by in Vitro Metabolic Engineering: Mixed Sugars Co-utilization and Kinetic Modeling." Proc. Nat. Acad. Sci. USA 112 (2015): 4964–4969.

3. Zhang, Y-H.P. "Production of Biofuels and Biochemicals by in Vitro Synthetic Biosystems: Opportunities and Challenges." Biotechnol. Adv. 33 (2015): 1467–1483.

4. Demain, A.L., and G. Vaishnav. "Production of Recombinant Proteins by Microbes and Higher Organisms." Biotechnol. Adv. 27 (2009): 297–306.

II.E.3 Novel Hybrid Microbial Electrochemical System for Efficient Hydrogen Generation from Biomass

Hong Liu (Primary Contact), Yuyan Shao, Vilayanur Viswanathan, Murthy Ganti
Oregon State University/Pacific Northwest National Laboratory
116 Gilmore Hall
Oregon State University
Corvallis, OR 97331
Phone: (541) 737-6309
Email: liuh@engr.orst.edu

DOE Manager: Katie Randolph
Phone: (240) 562-1759
Email: Katie.Randolph@ee.doe.gov

Project Start Date: February 1, 2016
Project End Date: January 31, 2019

Overall Objectives

- Design and fabricate a low-cost, robust, and highly efficient fermentation and microbial electrochemical system.
- Determine the techno-economic feasibility of the system using biomass hydrolysates and wastewater.

Fiscal Year (FY) 2016 Objectives

- Identify a bacterial culture capable of producing hydrogen from all major sugars in biomass hydrolysate.
- Investigate hydrogen producing capability of lab culture from various liquid fermentation products in microbial electrolysis cell (MEC).
- Develop efficient and low-cost cathode materials.

Technical Barriers

This project addresses the following technical barriers from the Hydrogen Production section of the Fuel Cell Technologies Office Multi-Year Research, Development, and Demonstration Plan:

(AX) Hydrogen Molar Yield

(AAA) Electrode Cost

(AAB) Solution Density (Production Rate)

Technical Targets

Progress has been made in achieving the DOE targets listed in the Multi-Year Research, Development, and Demonstration Plan. Table 1 lists DOE's technical targets and where our research and development efforts stand to date.

TABLE 1. Progress towards Meeting Technical Targets for Dark Fermentative Hydrogen Production and Microbial Electrolysis Cells (MECs)

Characteristic	Units	DOE 2015 Targets	DOE 2020 Targets	Project Status
Yield of H_2 production from glucose by integrated MEC – fermentation	mol H_2 /mol glucose	6	9	7.6
MEC cost of electrodes	$\$/m^2$	300	50	150

The overall goal of this project is to develop and scale-up our novel hybrid fermentation and MEC system that can be integrated with well-developed lignocellulose pretreatment/hydrolysis or wastewater treatment processes for efficient hydrogen production at a cost less than \$2/kg H_2. This project was initiated in February 2016 and is still in the early stages.

FY 2016 Accomplishments

- Identified fermentative bacterial cultures capable of producing hydrogen from major sugars in lignocellulosic biomass hydrolysate. The hydrogen yield reached 40% of theoretical yield, which is defined as the maximum for known metabolic pathways.
- Identified an exoelectrogenic bacterial culture capable of utilizing all liquid fermentation products and generating a current density up to 15 A/m^2 of anode surface area.
- Discovered that fermentative hydrogen production is a much faster process compared to the MEC process in a hybrid system and determined that further optimization should focus on the MEC process.
- Synthesized nonprecious metal catalyst with an intrinsic activity very close to Pt/C electrocatalyst. Synthesized nitrogen doped porous carbon (N-C) with surface area tunable between 1,000–2,500 m^2/g, which will be integrated with the synthesized metal catalyst for MEC cathode fabrication.

✧ ✧ ✧ ✧ ✧

INTRODUCTION

The global interest in hydrogen production has been stimulated by the promise of the clean operation and high efficiencies of hydrogen fuel cells. Currently, almost all the hydrogen produced is from non-renewable fossil sources. Hydrogen can be produced from renewable biomass by biological dark fermentation. Unfortunately, the hydrogen yields using current fermentation techniques are low. Hydrogen can also be produced by MEC, which can overcome the fermentation barrier and achieve higher hydrogen yield. However, the key challenges for realizing the practical applications of MECs include (1) difficulty in utilizing biomass directly and in utilizing certain biomass components, such as sugars; (2) low hydrogen production rate or high energy input due to inefficient reactor designs, high cathode over potential, and high solution resistance; and (3) high capital cost due to high electrode and membrane or separator costs. In this project, we will develop a hybrid system that integrates the dark fermentation and MEC processes and overcomes the challenges identified above.

APPROACH

The overall approach of this project is to develop an efficient fermentation and microbial electrolysis cell (F-MEC) for hydrogen generation from lignocellulosic biomass hydrolysates and sugar-rich wastewater through maximizing the hydrogen production rate and yield of both processes. Since MEC cathode material is a key factor affecting both capital and operational costs of the system, robust and low-cost cathode materials with low over-potentials will also be developed. A cost-performance model will be used to supplement the H2A analysis tool throughout the project to prioritize the critical factors and demonstrate potential to meet DOE cost goals.

For the first phase of this project, we have been focusing on identifying suitable fermentative and exoelectrogenic bacterial cultures for the hybrid system and determining the optimal operational conditions using small lab hybrid reactors. Non-precious metal catalyst and nitrogen doped porous carbon were also synthesized and are being integrated for fabricating low-cost MEC cathode materials.

RESULTS

H_2-producing capability of bacterial cultures from major sugars in lignocellulosic biomass hydrolysates. We investigated the capability of three mixed bacterial cultures in generating H_2 from major sugars in hydrolysates, including glucose, xylose, mannose, and galactose, and a mixture of the sugars using serum bottle reactors operated in batch mode. Our results demonstrate that all three tested cultures are capable of producing hydrogen from all tested sugars. The lab culture enriched from wastewater with glucose as carbon source demonstrated the highest hydrogen yield (Figure 1).

Direct H_2 production from mixed sugars in F-MECs. We also investigated direct mixed sugar fermentation by our lab exoelectrogenic culture enriched from acetate in microbial fuel cells (MFCs). Figure 2A demonstrates that the lab culture is capable of fermenting all tested sugars without the addition of a fermentative bacterial inoculum. Figure 2B illustrates the liquid fermentation products distribution and

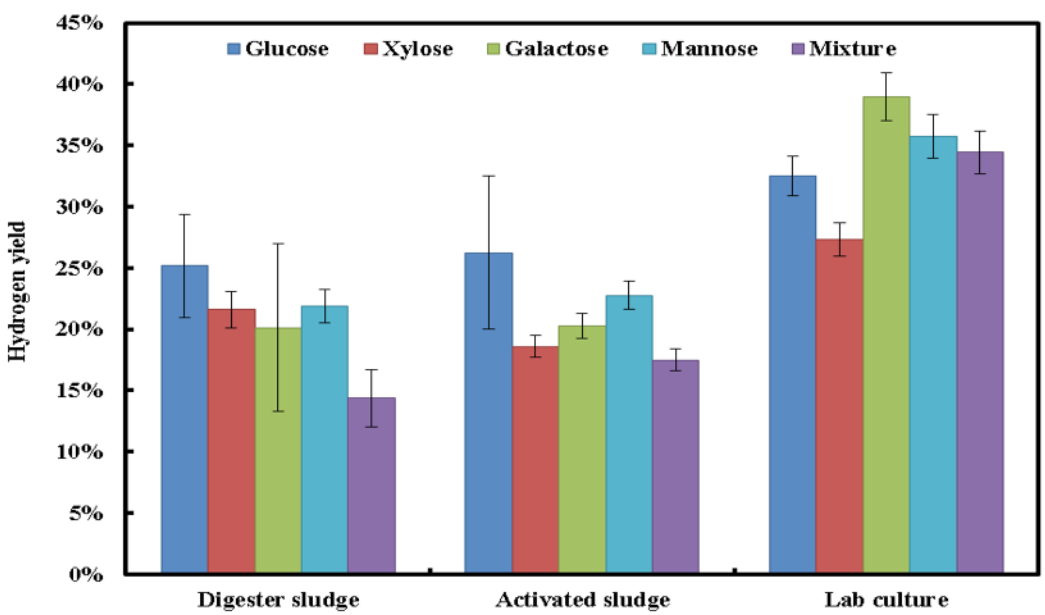

FIGURE 1. Hydrogen yields (defined as the maximum for known metabolic pathways) of three tested bacterial cultures (n = 3, error bars represent standard deviation)

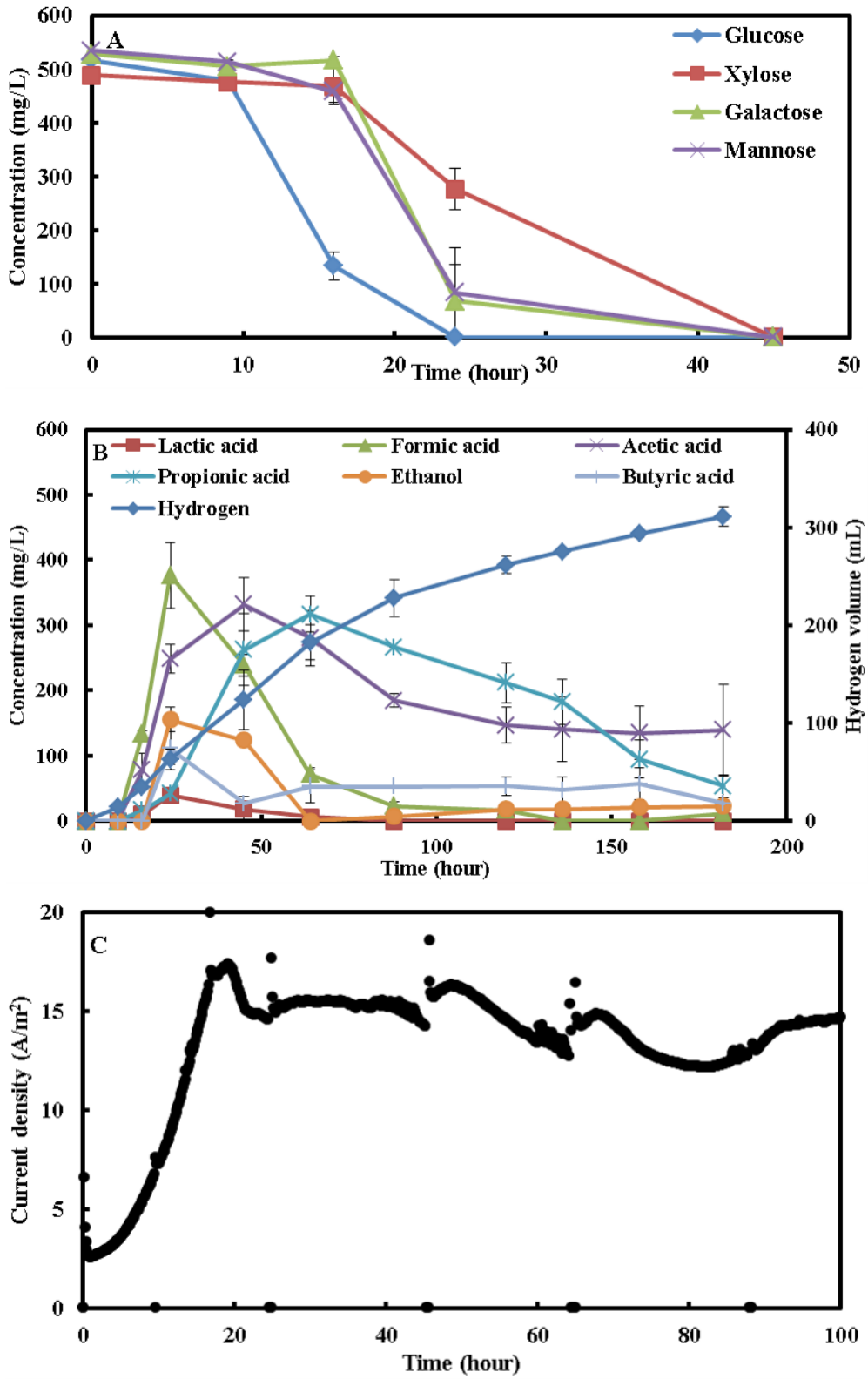

FIGURE 2. (A) Sugar utilization by the lab exoelectrogenic culture enriched with acetate in F-MECs; (B) liquid fermentation products distribution and hydrogen production in F-MECs; (C) current generation in MEC process (n = 3, error bars represent standard deviation in Figures 2A and 2B)

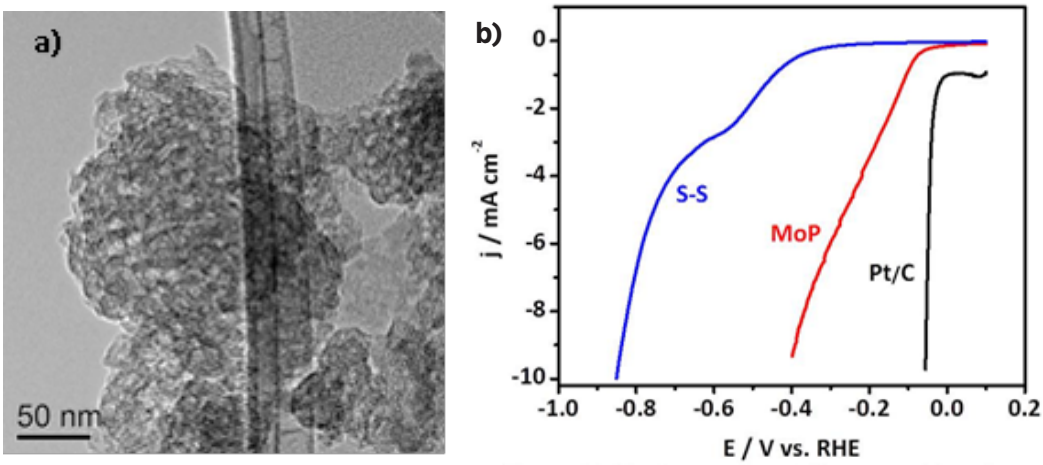

RHE – Reference hydrogen electrode

FIGURE 3. (a) TEM image of nitrogen-doped high surface area carbon; (b) Hydrogen evolution reaction linear sweep voltammongrams on different electrodes (0.1 M PBS, 10 mV/s)

hydrogen production in the F-MECs and Figure 2C shows current generation from the liquid fermentation products in the MEC process. The relatively long operational time for fully utilizing the fermentation liquid products suggests that the MEC process in the tested batch reactor is much slower than the fermentation process. Further optimization will focus on MEC process.

MEC cathode development. We have synthesized nitrogen doped high surface area carbon (N-C) using sucrose as a precursor (Figure 3a). The surface area of N-C is tunable between 1,000-2,500 m^2/g using various activation protocols. We have also synthesized and tested nonprecious metal catalysts. Figure 3b shows the hydrogen evolution reaction (HER) linear sweep voltammograms on different electrocatalysts (0.1 M PBS, 10 mV/s). Stainless steel (S-S) is the most commonly used electrode in today's MECs. Our electrocatalyst MoP shows much higher activity than S-S, with an onset HER potential close to Pt/C electrocatalyst, indicating its intrinsic activity is close to Pt/C. But the current density at higher overpotentials is still lower than Pt/C, probably due to the less active sites. Through optimization of the structure and composition of the nonprecious metal electrocatalysts and integration with nitrogen doped porous carbon, we expect to increase the active sites and the overall catalytic activity significantly.

CONCLUSIONS AND FUTURE DIRECTIONS

Although the project is still in early stages several conclusions can be drawn:

- Mixed bacterial cultures enriched from digester sludge, active sludge, and wastewater are capable of producing hydrogen from all major sugars in lignocellulosic biomass hydrolysate.
- Our lab's exoelectrogenic bacterial culture is capable of fermenting all major sugars and generating current from fermentation products in the MEC.
- MoP, a nonprecious metal catalyst, has demonstrated an intrinsic activity close to Pt/C electrocatalyst for hydrogen evolution in solution chemistry of the MEC.

Future work includes:

- Further MEC development through integrating the newly developed cathode materials.
- Optimization of fermentative and MEC processes in continuous-flow reactors.
- Hybrid system design, fabrication, and evaluation
- Cost performance modeling.

FY 2016 PUBLICATIONS/PRESENTATIONS

1. Luguang Wang, Ningshengjie Gao, Cameron Platner, Cheng Li and Hong Liu. *Hybrid Microbial Electrochemical System for Efficient Hydrogen Generation from Lignocellulosic Hydrolysate*, 2016 NA ISMET Meeting. Accepted.

II.F.1 Monolithic Piston-Type Reactor for Hydrogen Production through Rapid Swing of Reforming/Combustion Reactions

Kenneth G. Rappé (Primary Contact), Shari Li, Erica Cutsforth, Richard Zheng, Chaitanya Sampara, Wei Liu (former employee)
Pacific Northwest National Laboratory (PNNL)
P.O. Box 999
Richland, WA 99354
Phone: (509) 372-4413
Email: ken.rappe@pnnl.gov

DOE Manager: Katie Randolph
Phone: (240) 562-1759
Email: Katie.Randolph@ee.doe.gov

Subcontractors:
- Dr. Bang Xu, Dason Technology, Richland, WA
- Prof. Yong Wang, Washington State University (WSU), Pullman, WA

Project Start Date: November 1, 2014
Project End Date: October 31, 2017

Overall Objectives

- Develop a compact reactor unit for the production of hydrogen from biomass-derived liquids at a high enough efficiency and low enough capital cost to be economically attractive for distributed application, while resulting in lower net greenhouse gas emissions compared to natural gas reforming.
- Develop low-temperature steam reforming (SR) nano-composite catalysts and rapid regeneration methods to address catalyst deactivation challenges.
- Integrate the in situ capture of CO_2 formed during SR to produce a hydrogen-rich stream in one step, and couple catalyst and sorbent in monolithic reactor form.
- Demonstrate the sorption-enhanced hydrogen production (SEHP) swing-reactor concept at 2 kg/day scale.

Fiscal Year (FY) 2016 Objectives

- Optimize the metal oxide composite catalyst and monolith compositions to improve hydrogen selectivity and productivity for bio-oil reforming.
- Understand the impacts of monolith catalyst structures and reaction conditions on bio-oil reforming performance.
- Routinely prepare sets of monolith catalysts for Dason for bio-oil reformation testing.
- With WSU, develop a fundamental understanding of the impact of the TiO_2 monolith support on SR reaction performance, and an assessment of the impact of sorbents with different promotors on bio-oil reforming (and vice versa).
- Effectively scale up CO_2 sorbent preparation to hundreds of grams scale.

Technical Barriers

This project addresses the following technical barriers from the Hydrogen Production (from Renewable Liquid Feedstocks) section of the Fuel Cell Technologies Office Multi-Year Research, Development, and Demonstration Plan:

(A) Reformer Capital Costs and Efficiency

(B) Operations and Maintenance (O&M)

Technical Targets

This project is focused on developing: (1) a nano-composite SR catalyst, (2) a dolomite-based CO_2 sorbent, and (3) a method of integrating in monolithic reactor form, for effective coupled operation in SEHP fashion employing PNNL's novel swing reactor operation concept. The advancements made in this development effort will allow for economic and durable reforming of biomass-derived liquids in the forecourt that achieve the following DOE distributed hydrogen production 2020 targets as they relate to biomass-derived renewable liquids:

- Hydrogen Production Cost: \$2.30/gge (kg H_2)
- Production Equipment Total Capital Investment: \$1.2 million
- Production Energy Efficiency: 75%
- Production Equipment Availability: 97%

FY 2016 Accomplishments

- The K-NiCu-Ce(D)-Al-O [D = Mg or La] metal oxide nano-composite catalyst has been demonstrated as an active and novel catalyst system for the SR of bio-oil with periodic regeneration by combustion.
- TiO_2 monoliths (supplied by CormeTech) loaded with the composite catalyst show exceptionally higher SR activity after certain activation, which is believed to result from the interaction with TiO_2 and the formation of highly active catalytic structures/phases inside the monolith channel walls.

- The integrated reactor testing unit constructed by Dason Technology has been commissioned and allows bio-oil reforming reaction tests at oil feed rates 10–100 times higher the bench-scale testing units at PNNL and WSU; Dason's new flow distributor design has been successfully demonstrated to distribute bio-oil evenly into the monolith catalyst channels under reaction conditions.
- Bio-oil reforming tests of the monolith catalyst modules at both PNNL and Dason Technology confirm that the monolith channels are not fouled during bio-oil reforming reactions.

✧ ✧ ✧ ✧ ✧

INTRODUCTION

Biomass is a renewable resource that is produced over a wide range of territory in the United States. The conversion of bio-mass thermally or thermo-catalytically to bio-oil in centralized fashion presents an attractive potential energy carrier for distributed hydrogen production to support many facets of the economy, but most importantly transportation. However, the unstable nature and chemical characteristics of neat bio-oil presents some unique challenges for hydrogen production from bio-oil relative to conventional hydrocarbon SR processes.

A significant fraction of bio-oil is nonvolatile, and bio-oil is also highly reactive. This combination results in coking and charring as major obstacles to the effective reforming of bio-oil. Additionally, bio-oil contains higher amounts of oxygen and lower amounts of hydrogen than conventional hydrocarbon resources. This dictates that reforming strategies will need to be highly energy efficient in order to be economically viable.

APPROACH

Catalyst deactivation challenges (associated with coking and charring) along with heat transfer challenges are addressed by using a multi-bed reactor system with rapid switching between endothermic SR and exothermic regeneration operation. A monolith reactor provides the basis for multi-scale engineering of a catalyst bed of different functions, including reforming catalyst and CO_2 sorbent, forming a SEHP system. During endothermic SR, CO_2 produced by the reaction is captured by a metal oxide sorbent via an exothermic carbonation reaction that supplies heat to the endothermic SR process. During regeneration, air in introduced to burn off coke and char in exothermic fashion which subsequently provides energy to the carbonate decomposition sorbent regeneration process.

Bio-oil SR is conducted at intermediate temperatures (<700°C) to benefit the long-term stability of the catalyst and sorbent. The metal oxide nano-composite catalyst is a promising catalyst system for the low-temperature SR process, and consists of, amongst other additions, transition metal oxides, alkaline earth metal and cerium oxide, and aluminum oxide.

RESULTS

Efforts were undertaken to begin to develop an understanding of the micro-structure characteristics of the composite CO_2 sorbents. Scanning electron microscopy imaging indicates that the sorbents have a porous structure with grains or dense crystals less than 1.0 µm. Furthermore, elemental mapping of Mg, Ca, Na and K conducted in concert with scanning electron microscopy (shown in Figure 1 for a spent sorbent, which reflects what is observed in the fresh sorbent) shows uniform distribution of all four elements. The crystal phases of the composite sorbent were also measured by X-ray diffraction; Figure 2 shows X-ray diffration peaks for the fresh (no CO_2, top) and activated (with CO_2, bottom) sorbents. The major crystal phases are $Ca(OH)_2$, MgO, $CaCO_2$, and CaO. The MgO phase remains predominantly unchanged, indicating that its role is as a structural stabilizer under the present set of testing conditions, whereas CaO is predominantly the active phase for CO_2 sorption as indicated by its disappearance and emergence of $CaCO_3$ in the activated sorbent. These results indicate that uniform elemental distribution, relative particle size, and crystal phases can be used as tools for evaluating sorbent relative activity and potential degradation mechanisms.

Efforts are also underway to increase the production scale of the composite sorbent, and subsequently load the active sorbent into the TiO_2 monolith. Initial trials of sorbent manufacture at increased scale have identified challenges associated with segregation of the Na and K components of the eutectic phase of the sorbent; to form an active eutectic phase, Li, Na and K carbonates need to coexist in durable fashion. These efforts will continue to identify an active and durable eutectic phase of the composite sorbent. A method has been developed for loading CO_2 sorbent into the TiO_2 monolith channels. Reproducibility was demonstrated with nine monolith samples prepared using this technique.

Efforts were also undertaken to develop a consistent method for preparing the reforming catalyst in monolith form. An impregnation method has been developed that shows durable formation of active catalyst in monolith form, and is shown to be superior and more durable than coating with slurry. The monolith catalyst stability was assessed by conducting repeated reforming and regeneration cycles under constant flow conditions. The monolith catalyst prepared showed excellent stability as illustrated by hydrogen productivity performance exceeding the project target value of 0.6 g H_2/h/g cat over 11 cycles. This represents

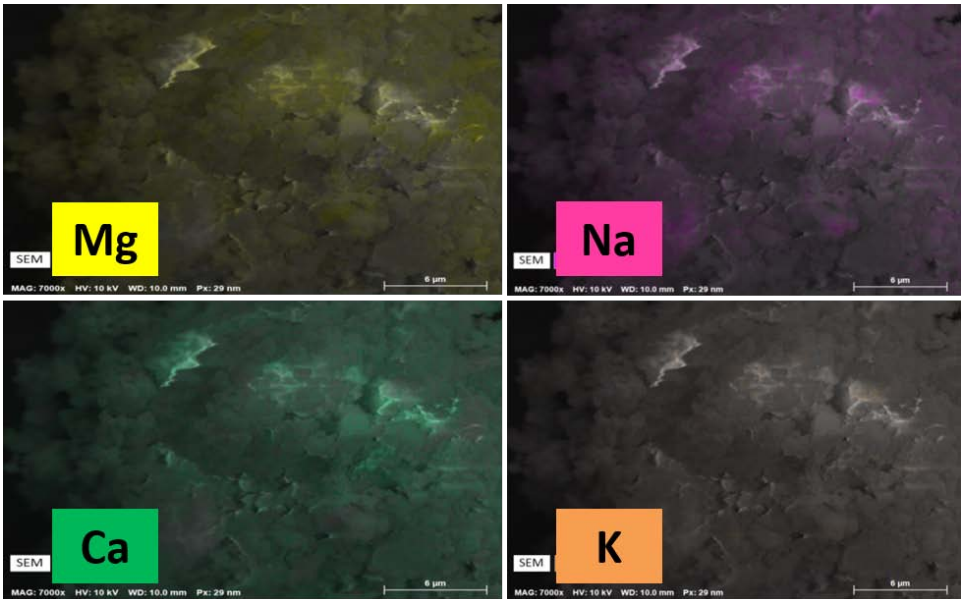

FIGURE 1. Scanning electron microscopy elemental mapping of spent sorbent

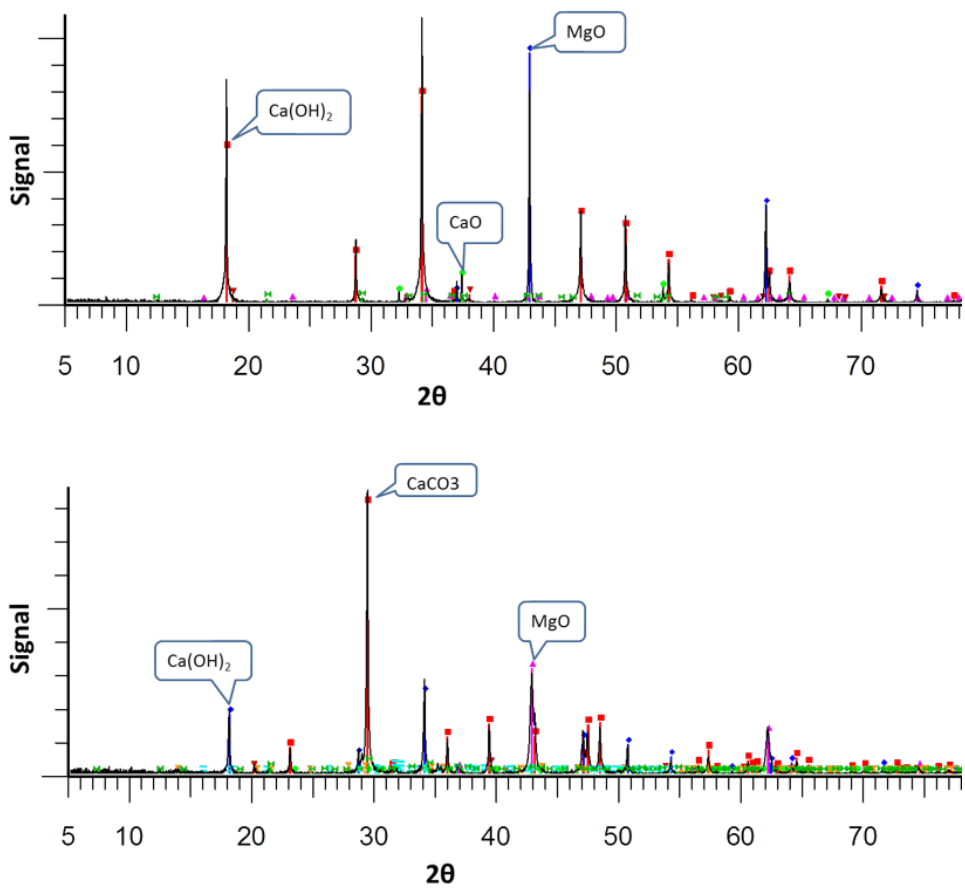

FIGURE 2. X-ray diffraction patterns of dolomite composite sorbent containing 5 wt% eutectic LiNaK-carbonate with (bottom) and without (top) CO_2

advancement in the state-of-the-art with regards to hydrogen productivity from bio-oil SR. It has been discovered that the monolith catalyst activity can be enhanced by conditioning treatment in situ. Figure 3 shows that hydrogen productivity increased by ~10X following activation which was accompanied by significantly improved selectivity. This mechanism will be investigated further in the project. And finally, catalyst performance sensitivity to different feed stream and oil rates were investigated and is shown in Figure 4. The sensitivity of productivity to space velocity is high, indicative of high overall conversion; if conversion is small, the productivity would be close to the rate constant of the reaction and minimally affected by space velocity. Additionally, the SR reaction on the catalyst tested shows excellent versatility over a wide range of steam to oil ratios, as indicated by Figure 4.

CONCLUSIONS AND FUTURE DIRECTIONS

Efforts will continue to identify an active and durable eutectic phase of the composite sorbent. Preliminary studies have identified negative synergy between CO_2 capture and reforming functionalities. A path forward for integrating CO_2 capture and reforming in concerted fashion will be developed and reduced to practice with the help of Dason Technology. Preliminary improved fundamental understanding of SR catalyst functionality and structure–activity relationship will be developed with the assistance of WSU to inform the path

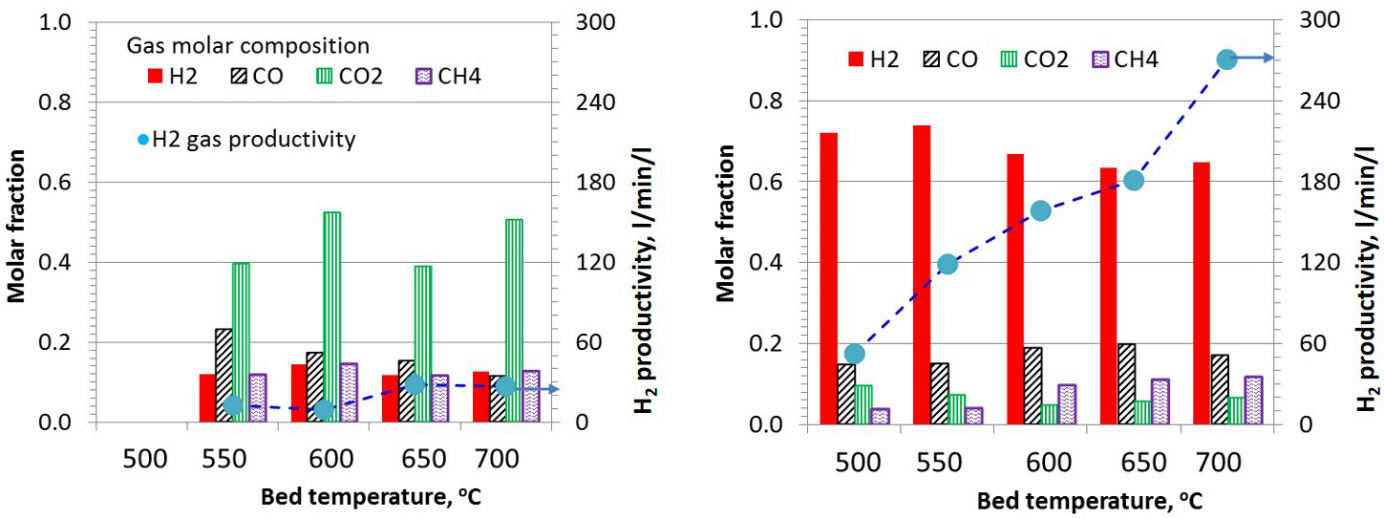

FIGURE 3. Performance of the same K-NiCu-Ce(Mg)-Al-O/TiO_2 monolith catalyst before (left) and after (right) activation

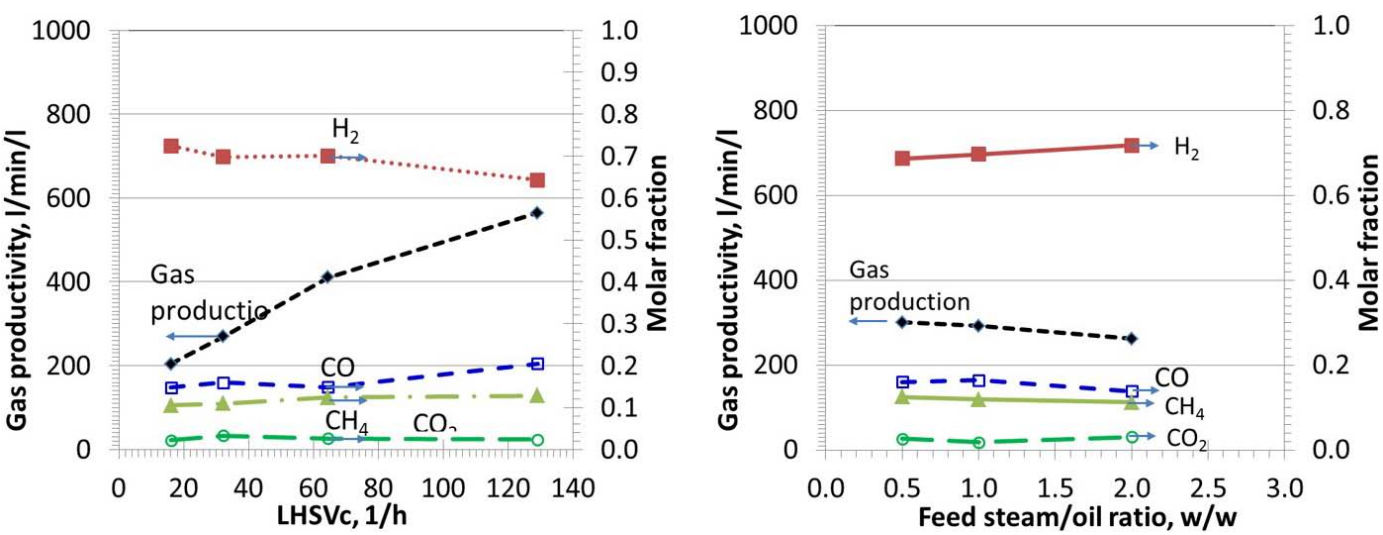

LHSV – Liquid hourly space velocity

FIGURE 4. Impact of feed stream flow and conditions on K-NiCu-Ce(Mg)-Al-O/TiO_2 monolith catalyst performance

forward for final engineering of an active, highly selective, and durable reforming catalyst.

The final phase of the project will be focused on extended demonstration of the integrated monolith reactor system at 2 kg-H_2/d production capacity, 0.10 kg-H_2/kg-bio-oil yield, and 80% overall energy efficiency. The intent is to move the technology to a technology readiness level of 4 or above (i.e., TRL $\geq$ 4).

SPECIAL RECOGNITIONS & AWARDS/ PATENTS ISSUED

1. W. Liu, S. Li "A Reactor, CO2 Sorbent System, and Process of Making H2 with Simultaneous CO2 Sorption," U.S. Patent application #15012791 filed on February 1, 2016.

FY 2016 PUBLICATIONS/PRESENTATIONS

1. Wei Liu, Shari Li, Richard Zheng, Paul Armatis, Erika Cutsforth. "Integrating CO_2 Capture with Steam-Reforming Reactions," Presentation at the AIChE Annual Meeting, Salt Lake City, UT, November 8, 2015.

2. Wei Liu "Reversible Carbonate & CO_2 Reaction System for High-Temperature Thermo-Chemical Energy Storage," Presentation at the AIChE Annual Meeting, Salt Lake City, UT, November 12, 2015.

3. Wei Liu, Shari Li, Feng Zheng "Enhancing stability and productivity of solid sorbents for CO_2 capture from hot humid gas," cleared for Ind. Eng. Chem. Res.

II.F.2 Reformer-Electrolyzer-Purifier (REP) for Production of Hydrogen [CO_2 Pump]

Fred Jahnke (Primary Contact), Matt Lambrech, Pinakin Patel
FuelCell Energy, Inc.
3 Great Pasture Rd.
Danbury, CT 06810
Phone: (203) 825-6108
Email: FJahnke@FCE.com

DOE Manager: David Peterson
Phone: (240) 562-1747
Email: David.Peterson@ee.doe.gov

Contract Number: DE-EE 0006669

Subcontractor:
University of California, Irvine, Irvine, CA

Project Start Date: September 30, 2014
Project End Date: September 30, 2016

Overall Objectives

FuelCell Energy's overall objectives are based on the Fuel Cell Technologies Office Multi-Year Research, Development, and Demonstration (MYRDD) Plan of 2015 to reduce the cost of hydrogen production to <$2.00/gge (<$4.00/gge delivered and dispensed). In addition, the technology used should minimize CO_2 emissions. To achieve this, FuelCell Energy has the following key objectives, all of which were successfully completed:

- Build and test the performance of a large scale REP stack (reformer-electrolyzer-purifier) using commercial cell components from our production line.
- Optimize parameters based on single cell testing and parametric studies.
- Test single cell long-term to establish expected life.
- Optimize process configuration and economics.
- Analyze the economics and cost of hydrogen using performance data from the tests.
- Support consultant (SAI) who is working to confirm the economics.

Technical Barriers

This project addresses the following technical barriers from the Hydrogen Production section (3.1) of the Fuel Cell Technologies Office MYRDD Plan (from 2007 plan).

(A) Reformer Capital Costs

(B) Reformer Manufacturing

(C) Operation and Maintenance

(D) Feedstock Issues

(E) Greenhouse Gas Emissions

(F) Control and Safety

Technical Targets

The REP combines reforming and electrolysis into one unit. Therefore, the technical targets for hydrogen production from natural gas and from water electrolysis are both addressed by this program.

As shown in Tables 3.1.2 and 3.1.4 of the MYRDD Plan (Table 1 and 2 below), where the expected REP performance has been added to MYRDD targets below, the efficiency of the system is substantially higher than the target efficiencies. These higher efficiencies reduce operating costs sufficiently to offset the higher capital so that the total hydrogen cost target of $2.00/kg is still achieved. The higher efficiencies also have the advantage of reducing CO_2 and other emissions associated with typical hydrogen production from natural gas and electrolysis.

TABLE 1. Technical Targets for Natural Gas (2007 MYRDD Plan)

Table 3.1.2. Technical Targets: Distributed Production of Hydrogen from Natural Gas			
Characteristics	Units	2015 Target	REP Technology
Production Unit Energy Efficiency	% (LHV)	75.0%	96.2%* (up to 130% eff with waste heat)
Production Unit Capital Cost (Uninstalled)	$ (1,500 kg/d unit)	580K	947K
Total Hydrogen Cost	$/gge H_2	2.00	1.66

* efficiency for 80% of hydrogen generated from natural gas
LHV – Lower heating value

TABLE 2. Technical Targets for Electrolysis (2007 MYRDD Plan)

Table 3.1.4. Technical Targets: Distributed Water Electrolysis Hydrogen Production a, b, c			
Characteristics	Units	2017 Target	REP Technology
Hydrogen Cost	$/gge	<3.00	1.66
Electrolyzer Capital Cost	$/gge $/kW	0.30 125	Included above
Electrolyzer Energy Efficiency	% (LHV)	74%	83.4%**

** efficiency for 20% of hydrogen generated from steam electrolysis

FY 2016 Accomplishments

Accomplishments during FY 2016 include:

- Constructed 30-cell test stack using full scale cells from FuelCell Energy's commercial manufacturing facility.
- Tested 30-cell stack and met all performance targets including:
  - Greater than 100 kg per day of hydrogen production
  - Greater than 95% hydrogen purity (97% to 98% achieved)
  - Less than 8 kWh/kg of hydrogen power consumption
  - Excellent thermal profile across stack, even during load changes
- Confirmed REP hydrogen after methanation can be used without further purification to power a polymer electrolyte membrane fuel cell and/or be used as feed to an electrochemical hydrogen compressor. The electrochemical hydrogen compressor produces high purity, high pressure hydrogen suitable for fuel cell vehicles in one step.
- Developed accurate performance model and completed configuration analysis.

✧ ✧ ✧ ✧ ✧

INTRODUCTION

The current conventional technology for production of hydrogen from natural gas suffers from excess CO_2 production due to incomplete conversion of methane and CO to hydrogen. The proposed technology would incorporate a high temperature electrochemical purification system to remove CO_2 from the reformed gas during the reforming process and drive the conversion of methane to H_2 and CO_2 to near completion, producing hydrogen from natural gas in a manner which approaches the theoretical minimum of CO_2 emissions.

The REP system (Figure 1) incorporates components developed for FuelCell Energy's commercial molten carbonate direct fuel cell (DFC®) technology. When this technology is operated in purification mode as an electrolyzer, it will pump out almost all of the carbon from the feed gas as $CO_3^=$ leaving pure hydrogen from the reformed methane. In addition, the system efficiently produces additional hydrogen by dissociation of steam (electrolysis) in the formation of $CO_3^=$ during the pumping step. Thus natural gas would provide about 80% of the hydrogen produced with the other 20% provided by the electrolysis reaction. The system appears to be highly attractive economically based on H2A modeling, and testing the system confirmed the performance is as expected when using full scale components from our commercial DFC® production line. When operated without cathode sweep gas, byproduct CO_2/O_2 (67%/33%) can also be produced with only a minor (~10%) power penalty.

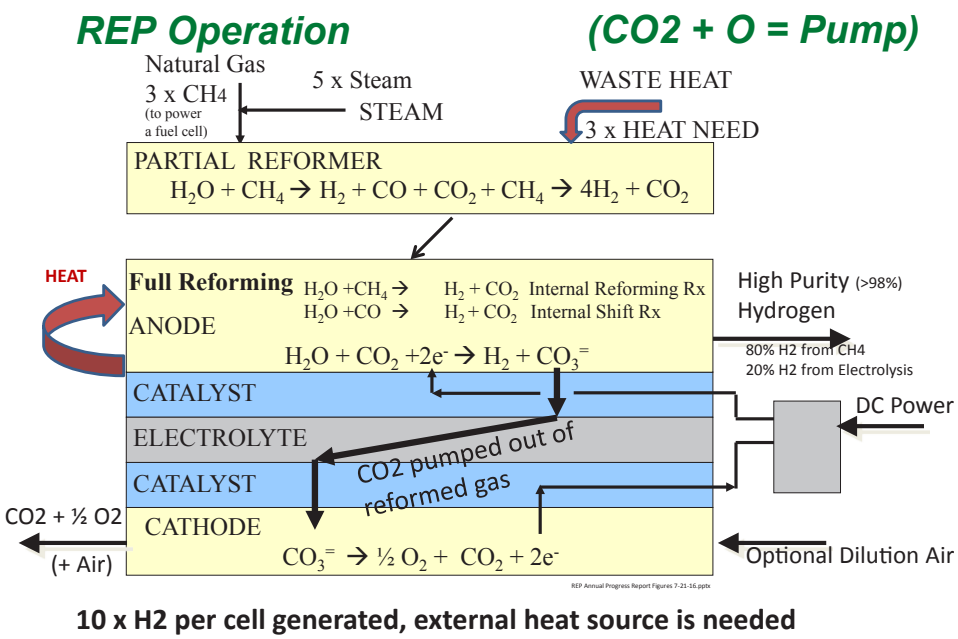

Rx - Reaction; DC - Direct current

FIGURE 1. Operation of Reforming-Electrolyzer-Purifier (REP)

APPROACH

Because the system will be based on our commercial DFC® add registered trademark symbol fuel-cell components, the emphasis of our work was to make sure that the system works as expected. Based on FuelCell Energy's long history of research and development, initial testing was done on a single 300 cm² cell. Experience has shown that this size cell provides a good reflection of the performance of our larger commercial scale cells. Testing of the large cells was done in Phase 2 of the program and confirmed there are no unexpected results from the flow distribution or the thermal distribution within the cells. The large cell testing was done on a short stack of approximately 30 cells which we have found accurately reflects the performance and temperature profile of a commercial unit. We tested a single cell under various operating conditions to determine their impact on the cell performance. The same performance was shown by the large-scale test.

Long-term single cell tests, including microscopic scanning electron microscopy examination of the cell during posttest analysis, indicated that a commercial stack should have a good operating life and a reasonable performance degradation (2–5 years life). See Figure 2.

Based on the results of the testing, detailed system configurations and performances have been simulated using ChemCAD. The results of the simulation were then used in the H2A model to confirm the economic attractiveness of the system as shown in Table 4. After the brief successful short stack testing, we now would like to follow that with a longer test of the 30-cell stack (~6 mo), but that test was not included in the current program.

RESULTS

The results were excellent and the performance of the REP system is slightly better than the performance estimated in the initial proposal (Table 3). Using the data from the single cell and large scale tests, a detailed model was developed which allows us to accurately predict the

TABLE 3. Successful Test Results from Stack Using Commercial Cells

	Target	Design	Test Results	
Amps		1040	950	
Volts/cell	<1.35	1.21	1.22	Meets Target
H2 Purity	>95%	97.4	97.5	Meets Target
Kwh/kg	<8	7.4	7.6	Meets Target
Kg/day	~100	123	110	Meets Target
CO2,g/gge	~5,500	4,900	4,700	Meets Target

Large Scale REP stack proven to be capable of 97%+ pure H2 production with low power input

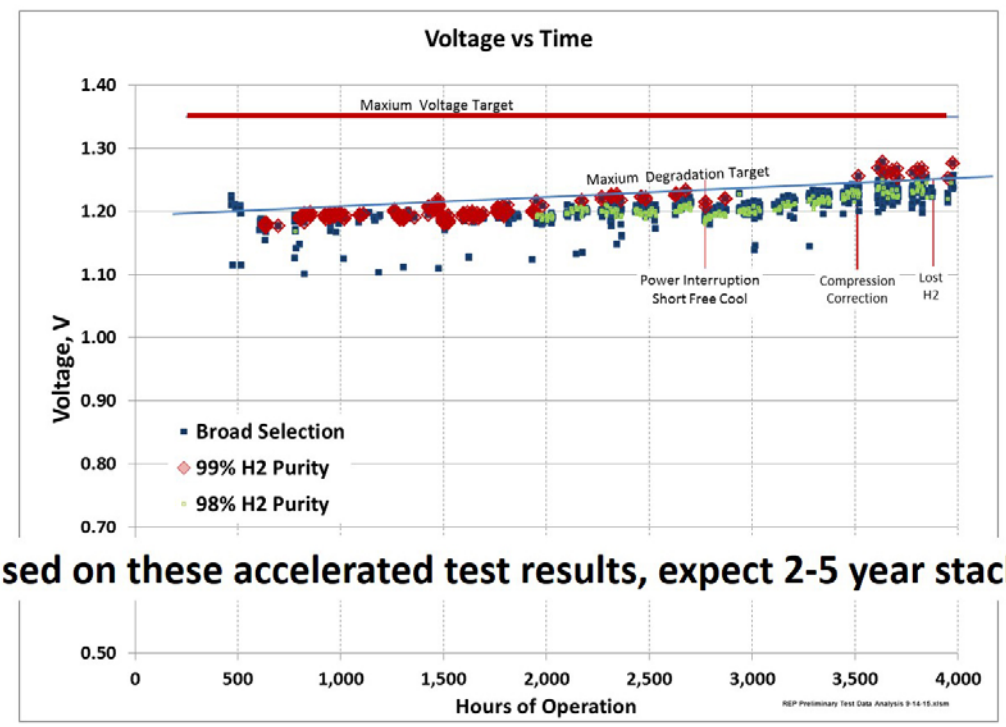

Based on these accelerated test results, expect 2-5 year stack life.

FIGURE 2. Single cell tests indicate stable operation and good cell life

TABLE 4. Configuration Analysis Based on Heat and Meaterial Balances and H2A Model

Case	mmbtu NG /kg	REP Power, kwh/kg	Operating Costs, $/kg(1)	CO2, g/gge(2)	Prod Rate, kg/d (8)	Capital Cost, $/(kg/d)	H2A Total H2 Cost, $/kg(9)
1. Base Case - Integrated with DFC®	0.069	7.915	0.925	4,529	1,622	$610	$1.47
2. Standalone - Grid Power, NG heat	0.114	7.216	1.188	6,619	1,622	$1,076	$2.07
Est Standalone - CO2 Capture	0.114	7.817	1.223	0(7)	1,622	$1,076	$2.11
3. Standalone - External LP Steam	0.095	7.211	1.058	5,590	1,622	$871	$1.78
4. Standalone - Self Powered	0.138	0.000	0.936	8,082	582	$2,112	$2.71
5. Standalone - ADG Feed	0.104	10.277	1.296	0(6)	1,192	$1,135	$2.11
6. Standalone - Renewable Syngas	0.066	12.181	1.529	0(6)	985	$1,294	$2.25
7. DFC® AE feed for Power Storage	0.010	29.518	1.886	0(4)	437	$2,012	$3.60
8. SOFC AE feed, Power Storage	0.000	23.768	1.529	0(4,5)	561	$1,352	$2.63

(1) Assumes $6.77/mmbtu NG (LHV), $0.057/kwh power.
(2) Does not include CO2 from power used, ~3,200 g/gge @ 7.5 kwh/kg
(3) All water needed is already in SOFC anode exhaust
(4) No additional CO2 emitted other than CO2 from power production
(5) Potential CO2 capture for zero CO2 power from NG as well as H2
(6) Renewable Hydrocarbon Feed
(7) Assumes CO2 Capture
(8) Production rate based on one DFC® stack
(9) 98+% H2 purity

NG – Natural gas; SOFC – Solid oxide fuel cell; LP – Low pressure; AE – Anode exhaust; ADG – Anaerobic digester gas; gge – Gasoline gallon equivalent

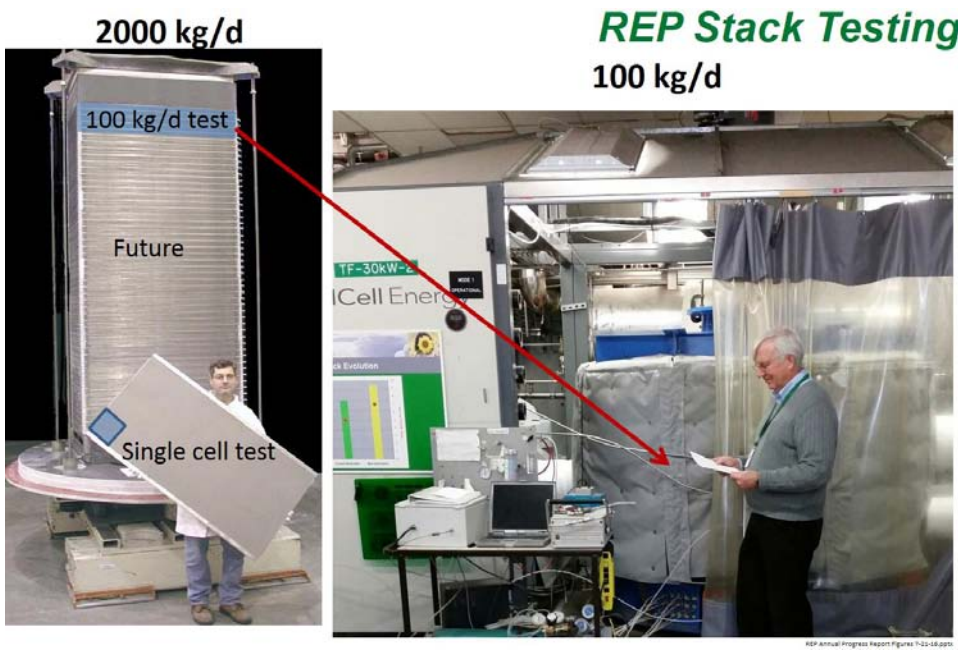

FIGURE 3. Testing of commercial cells in short stack

REP performance for various configurations and feedstocks. Based on this model and detailed process flow diagrams, heat and material balances were performed, and equipment costs were estimated. The results were then analyzed using the DOE H2A model. As can be seen in Table 4, the cost of hydrogen meets the DOE target of $2/kg for two cases and is close to the target for most of the cases.

In addition to the performance of the system, we were also concerned about the life of the cell. To address this concern, a long-term test of a single cell was performed. As shown in Figure 2, 4,000 hr of operation have been achieved with the voltage remaining well below the maximum target voltage. We are currently testing a second single cell operating to produce both H_2 and CO_2/O_2. By eliminating the

optional air sweep of the cathode, a slight power increase is incurred (~10%), but the cell now generates a second valuable CO_2/O_2 (67%/33%) stream. This stream can be used for CO_2 capture, low-cost oxygen, and other applications. We are also looking at additional cases, including cases involving CO_2 capture as well as power storage.

The system can use waste heat at various temperature levels to reduce fuel consumption and cost as can be seen in Case 3 which assumes low pressure steam at no cost is available to the process. Approximately 40% of the heat required by the system is for the production of low pressure steam.

CONCLUSIONS AND FUTURE DIRECTIONS

Conclusions derived from the work are:

- The REP system performs well in a stack of commercial cells as well as in a single test cell.
- The economics of the REP system are highly attractive based on detailed configurations and material balances for distributed hydrogen and could provide competitive distributed hydrogen for many applications in the near-term.
- Testing of commercial cells showed excellent performance and temperature profiles within the stack.
- Not only does the REP system provide low-cost hydrogen but it has the potential to be a good technology for excess electricity storage and CO_2 capture. These alternate uses should be explored further.

Future work required to commercialize the process will comprise:

- Longer testing (minimum 3–6 mo) of the 30 commercial cell short stack (not included in current program).
- Integration with larger scale pre-reformer.

SPECIAL RECOGNITIONS & AWARDS/ PATENTS ISSUED

1. A patent application for the process, including multiple configuration arrangements, was filed January 31, 2015, prior to start of program.

FY 2016 PUBLICATIONS/PRESENTATIONS

1. "Reformer-Electrolyzer-Purifier (REP) for Production of Hydrogen," 2016 AMR (Annual Merit Review), Washington D.C., Fred Jahnke, FuelCell Energy, Inc. June 8, 2016, Project ID #:PD112.

2. "Reformer-Electrolyzer-Purifier (REP) for Production of Low Cost Hydrogen," 2015 Fuel Cell Seminar, Los Angeles, CA, Fred Jahnke, FuelCell Energy, Inc. November 19, 2015.

3. Zhao L., Brouwer J., Jahnke F., Lambrech M., and Patel P., "A Novel Hybrid Reformer-Electrolyzer-Purifier (REP) for Distributed Production of Low-Cost, Low Greenhouse Gas Hydrogen," The Electrochemical Society, 2015 Fuel Cell Seminar & Energy Expo proceedings.

4. 2015 Annual Progress Report, "II.F.2 Reformer-Electrolyzer-Purifier (REP) for Production of Hydrogen," https://hydrogendoedev.nrel.gov/pdfs/progress15/ii_f_2_jahnke_2015.pdf.

III.0 Hydrogen Delivery Program Overview

INTRODUCTION

The Hydrogen Delivery program addresses all hydrogen transmission and distribution activities from the point of production to the point of dispensing. Research and development (R&D) activities address challenges to the widespread commercialization of hydrogen technologies in the near-term through development of tube trailer and liquid tanker technologies as well as station compressors, dispensers, and bulk storage; and in the mid- to long-term through development of pipeline and advanced delivery technologies. Technoeconomic analysis is used by the program to identify cost, performance, and market barriers to commercial deployment of hydrogen technologies, and to inform program planning and portfolio development.

GOAL

The goal of this program is to reduce the costs associated with delivering hydrogen to a point at which its use as an energy carrier in fuel cell applications is competitive with alternative transportation and power generation technologies.

OBJECTIVES

The objective of the Hydrogen Delivery program is to reduce the cost of hydrogen dispensed at the pump to a cost that is competitive on a cents-per-mile basis with competing vehicle technologies. Based on current analysis, this translates to a low-volume hydrogen threshold cost of <$7 per gallon gasoline equivalent (gge) (produced, delivered and dispensed, but untaxed) by 2020.[1] To achieve this near-term objective, delivery pathways that can meet a low-volume cost of <$5/gge are needed. To be cost-competitive in the long-term, an ultimate target of <$4/gge (produced, delivered and dispensed, but untaxed) must be met via renewable pathways.[2] This cost target has been apportioned to be <$2/gge for the renewable production and <$2/gge for the delivery and dispensing.[3] The program plans to meet these objectives by developing low-cost, efficient, and safe technologies to deliver hydrogen from the point of production to the point of use in both stationary fuel cells and fuel cell electric vehicles (FCEVs). This objective applies to all of the possible delivery pathways. Key objectives for specific delivery components include:

- **Station Technologies:**
  - Compression: Develop lower-cost, higher-reliability hydrogen compression technology for terminal and station applications.
  - Storage: Develop lower-capital-cost off-board bulk storage technology.
  - Dispensers: Improve the cost, reliability, and accuracy of 700 bar dispensers.
- **Pipeline Technology:** Develop mitigation strategies for combined material fatigue and hydrogen embrittlement in steel pipelines; advance the development and acceptance of alternative composite pipe materials that can reduce installed pipeline costs; and develop lower-cost, higher-reliability compression technology for hydrogen transmission by pipeline.
- **Liquid Hydrogen Technology:** Reduce the capital and operating costs of hydrogen liquefaction facilities.
- **Analysis:** Conduct comprehensive analyses on near- and longer-term hydrogen delivery options to identify the advantages of each and areas for potential improvement.

[1] DOE Hydrogen and Fuel Cells Program Record #15012, Hydrogen Early Market Cost Target, 2015, https://www.hydrogen.energy.gov/pdfs/15012_hydrogen_early_market_cost_target_2015_update.pdf
[2] DOE Hydrogen and Fuel Cells Program Record #11007, Hydrogen Threshold Cost Calculation, 2011, https://www.hydrogen.energy.gov/pdfs/11007_h2_threshold_costs.pdf
[3] DOE Hydrogen and Fuel Cells Program Record #12001, Hydrogen Production and Delivery Cost Apportionment, 2012, https://www.hydrogen.energy.gov/pdfs/12001_h2_pd_cost_apportionment.pdf

FISCAL YEAR (FY) 2016 TECHNOLOGY STATUS AND ACCOMPLISHMENTS

In FY 2016, the Hydrogen Delivery program kicked off nine new projects, competed one Funding Opportunity Announcement (FOA), participated in one workshop, and saw significant progress in research, development, and demonstration (RD&D) activities of existing projects.

Program Level Accomplishments

In FY 2016, significant progress was made by the Hydrogen Delivery program on several important fronts. Several highlights include:

- The Hydrogen Delivery Cost Projection Record was updated. The publicly available record now provides details to support the modeled cost of delivering hydrogen from a centralized production facility and dispensing to FCEVs. These modeled costs cover a range of gaseous and liquid hydrogen delivery options using current (2015) technologies projected at economies of scale.
- The Hydrogen Delivery Scenario Analysis Model (HDSAM) 3.0 was released. This release includes updated assumptions of the costs of key delivery equipment, allows users to simulate the impact of technology maturity on hydrogen cost, and allows users to simulate the effects of varying station utilization rates over a 30-year analysis period.
- A solicitation for research on advanced compression technologies was released as part of the Fuel Cell Technologies Office's 2016 office-wide FOA.
- Through the Hydrogen Fueling and Infrastructure Research and Station Technology (H2FIRST) project, DOE and several original equipment manufacturers have developed, tested, and validated the Hydrogen Station Equipment Performance Device (HyStEP). Since December 2015, the device has already been used to commission multiple stations in California.
- The H-Prize competition (H2 Refuel) finalist (SimpleFuel) was announced. The team has begun working on their on-site refueling solution. This $1 million competition challenges America's innovators to deploy an onsite hydrogen generation system to fuel hydrogen-powered vehicles. The system may use electricity or natural gas and can be sited in homes, community centers, small businesses, or similar locations.

Project Level Accomplishments

During FY 2016, progress was made by existing projects in several key areas, including:

Station Technologies

Station technologies, in particular compression, onsite storage, and dispensing, are a key area of focus for the program. Efforts in this area aim to improve the reliability and reduce the cost of the technologies.

- The automated dispensing hose testing apparatus at the National Renewable Energy Laboratory (NREL) completed more than 3,100 test cycles of commercial dispensing hoses. The test cycles simulated various fills of hydrogen at 700 bar and -40°C, per the the SAE J2601 fueling protocol. The apparatus and fueling station at NREL were upgraded in April with additional compression and storage capacity. The apparatus is now capable of up to 1,500 autonomous cycles per week.
- A project to create a U.S. supplier for metal-free 700-bar hydrogen dispensing hoses made significant progress in FY 2016. The small business, NanoSonic, has developed a polymer matrix resin with ultra-low hydrogen permeance before and after being subected to the harsh 180-degree triple fold, cold flex test, conducted at -50°C. In FY 2016, NanoSonic demonstrated effective use of a ceramer to prevent the hose from pulling out of fittings at high pressures, and developed a novel proprietary fiber reinforcement expected to enhance burst strength. (NanoSonic)
- Fuel station precooling analysis identified major drivers for precooling capacity/cost and performance. The analysis also acquired performance data at different ambient temperatures for a typical hydrogen refueling station precooling system and developed an algorithm to optimize the size of precooling equipment and heat exchanger for lowest precooling cost. (Argonne National Laboratory)

- The HyStEP testing device was successfully deployed in California with the California Air Resources Board (CARB), including execution of a contract between Sandia National Laboratories (SNL) and CARB for the loan of the device to collect the data needed to validate stations in California as part of the H2FIRST project. Additionally, all relevant designs and control software for the duplication of the device have been made publically available through the H2Tools website. (SNL, NREL)
- An 875-bar stationary pressure vessel design has been approved by the American Society of Mechanical Engineers (ASME). The vessel is manufactured by autofrettaging commercially available steel liners and then wrapping them with high-strength wire. The vessel design is expected to cost 50% less than vessels currently on the market. (Wiretough)

Pipeline Technologies

Pipelines are an attractive delivery pathway for mature market scenarios. Advances in both pipeline compression and fiber-reinforced polymer pipelines continue to improve the economics of the scenario, while work on hydrogen embrittlement of steel continues to improve the understanding of the performance of traditional pipeline materials for the hydrogen pipeline transmission and distribution network.

- Fatigue analysis showed that X100A base metal exhibited comparable hydrogen-accelerated fatigue crack growth rates to lower-strength base metals. Future experimentation will identify high-strength steel microstructures with acceptable hydrogen-accelerated fatigue crack growth performance. (SNL)

Liquid Hydrogen Technologies

Liquefaction represents over 50% of the cost of hydrogen delivered via the liquid pathway, due largely to energy consumption.

- As part of the new project to improve liquefaction efficiency using vortex tubes, the first helium-hydrogen-neon liquid phase density measurements for refrigerant mixtures have been completed. (NREL)
- As part of a project to use magnetocaloric materials to liquefy hydrogen, a world record was set in achieving a 100-K temperature span with magnetocaloric materials. These materials were then used to liquefy propane gas from room temperature. Further work increased the system cooling power through the implementation of a bypass loop in an eight-layer magnetocaloric system. (Pacific Northwest National Laboratory)

Workshops

The *Fourth International Workshop on Hydrogen Infrastructure and Transportation*, organized by the New Energy and Industrial Technology Development Organization (NEDO) of Japan, the National Organisation Hydrogen and Fuel Cell Technology (NOW) of Germany, and the DOE and hosted by the European Commission's Joint Research Center, was held in May of 2016 in the Netherlands. The workshop included members of industry, academia, and government from Japan, Germany, the European Union, Scandinavian countries, and the United States. This year representatives from China and Korea were also able to attend. Key takeaways from the workshop are summarized in Table 1 below.

TABLE 1. Key Issues Discussed at 4th International Infrastructure Workshop

Fueling	Germany, Japan, and the United States all have devices in place to collect data for validation of stations against refueling requirements.
Hydrogen Quality	The technical, cost, and time requirements of hydrogen quality monitoring remain common concerns. Several devices are under development to perform inline monitoring for key contaminants.
Metering	Japan has implemented interim meter accuracy targets similar to those adopted in California. Germany has not yet made a decision to adopt such targets. Dispensing error continues to be measured at 4–8% in the field depending on the volume of hydrogen dispensed.
Hardware	Both the reliability and availability of stations continues to be a concern for all participants. While compressor failures are decreasing, the maintenance interval remains a concern. Additionally, dispenser improvements are necessary to improve the user experience.

Publications

In FY 2016, the Delivery program published a program record that provides details to support modeled costs of delivering hydrogen from a centralized production facility and dispensing to FCEVs. The modeled costs range from $3.00/gge to $5.00/gge for 700 bar dispensing, and $2.70/gge to $3.70/gge for 350 bar dispensing. These modeled costs cover a range of gaseous and liquid hydrogen delivery options using current (2015) technologies projected at economies of scale. Prior-year cost estimates were calculated using the H2A Hydrogen Delivery Scenario Analysis Model (HDSAM) V2.3 along with assumptions of the commercial readiness of delivery/dispensing technologies in the respective years. In 2015, HDSAM was updated to Version 3.0 to reflect the then-current status of delivery technologies. Before its release, the model was vetted through comparisons of its projections with the real-world cost estimates provided by station developers in funding applications to the California Energy Commission. The 2015 cost estimates and 2020 projections in this record were made using HDSAM 3.0 along with assumptions about the readiness levels of each technology in the delivery pathway for commercialization.

FY 2016 Funding

The Fuel Cell Technologies Office announced one delivery-focused FOA topic in FY 2016 to fund projects in the area of advanced compression and one Small Business Innovation Research (SBIR) FOA on magnetocaloric materials discovery.

Three *advanced compression* projects were awarded in FY 2016 in the Delivery portfolio and will begin work in FY 2017. The three advanced compression projects are as follows:

- Giner, Inc., Newton, Massachusetts, will demonstrate a cost-effective method for compressing hydrogen while eliminating the need for mechanical compressors, which typically have significant reliability issues.
- Greenway Energy, LLC, Aiken, South Carolina, will combine two novel technologies, Electrochemical Hydrogen Compression and Metal Hydride Compression, into a new hybrid solid state hydrogen compressor, to overcome the reliability issues of mechanical compression and the efficiency challenges of solid state compression technologies.
- Sandia National Laboratories, Livermore, California, will work to investigate and demonstrate a laboratory-scale two-stage metal-hydride-based hydrogen gas compressor.

Two *magnetocaloric materials* SBIR projects were awarded in FY 2016 in the Delivery portfolio. The two SBIR projects are as follows:

- Nanohmics, Inc, Austin, Texas, will design next-generation technologies to cool hydrogen from room temperature by leveraging both the magnetocaloric and magnetoelastic effects in known magnetocaloric materials. The team will leverage their capabilities in nanofabrication to develop and demonstrate materials with geometries that maximize these effects.
- General Engineering & Research, LLC, San Diego, California, aims to develop a low-cost magnetocaloric material for sub-80-K refrigeration applications. Most magnetocaloric materials in use today are high in cost because they use rare earth metals, such as gadolinium. This project will synthesize and characterize novel materials that avoid rare earth metals and have demonstrated potential in previous research.

Additionally, one award was made from the FY 2015 FOA for advanced dispensing technologies.

- Ivys, Inc., Waltham, Massachusetts, will develop a 700 bar hydrogen dispenser that achieves 2% accuracy and durable operation through the use of wireless dedicated short range communication and advanced Coriolis metering technologies.

Three new projects were also initiated in FY 2016 through a lab call released in FY 2015.

- Pacific Northwest National Laboratory, Richland, Washington, will demonstrate a laboratory-scale hydrogen liquefier with a figure of merit increase from 0.3 up to 0.5 using magnetocaloric materials.
- National Renewable Energy Laboratory, Golden, Colorado, will develop a proof-of-concept small modular hydrogen liquefaction system that utilizes kinetic parahydrogen–orthohydrogen separation and conversion via vortex tubes to provide a pathway to achieving a figure of merit of 0.5.

- Sandia National Laboratories, Livermore, California, will work with National Institute of Standards and Technology and Oak Ridge National Laboratory to identify pathways for developing high-strength pipeline steels by establishing the relationship between microstructure constituents and hydrogen-accelerated fatigue crack growth.

BUDGET

The FY 2016 appropriation provided $25.4 million for the Hydrogen Production and Delivery program, with approximately $11.9 million provided for Delivery RD&D. The estimated budget breakdown for Delivery in FY 2016 and FY 2017 is shown in Figure 1. The request for Hydrogen Production and Delivery in FY 2017 is $28.1 million, with $11.0 million planned for Delivery RD&D, with an emphasis on improving reliability and reducing costs of near-term technologies, such as dispensers and storage at the station, and developing technologies for longer-term pathways, such as liquefaction.

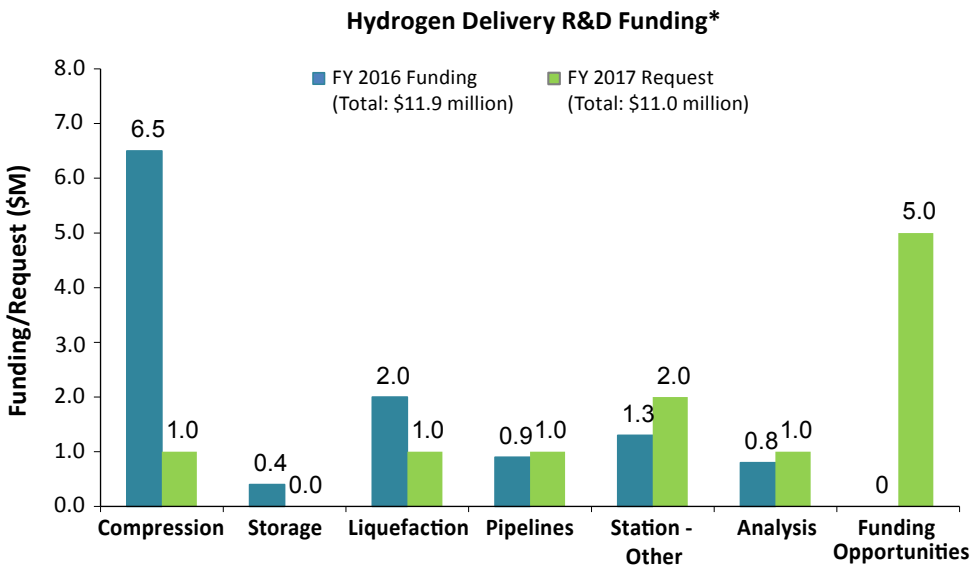

FIGURE 1. Hydrogen delivery budget. Budget amounts for FY 2016 and projected amounts for FY 2017, contingent upon appropriations, are shown broken down by the different delivery pathways. Exact distribution of funds in FY 2017 will not be defined until funds have been appropriated and new projects selected.

FY 2017 PLANS

In FY 2017, the Hydrogen Delivery program will focus on several key efforts, including the following:

- Review the current state of the art in carrier technology and publish the results.
- Focus on improving compressor reliability through new projects focused on advanced compression technologies. (SNL, Giner, and Greenway)
- Continue to address near-term hydrogen station R&D needs through the H2FIRST project, including work on reducing station footprint for urban sites and research to improve dispensing reliability. (NREL and SNL)

Neha Rustagi
Hydrogen Production and Delivery Team
Technology Development Manager
Fuel Cell Technologies Office
Office of Energy Efficiency and Renewable Energy
U.S. Department of Energy
1000 Independence Ave., SW
Washington, DC 20585-0121
Phone: (202) 586-8424
Email: Neha.Rustagi@ee.doe.gov

III.1 Hydrogen Delivery Infrastructure Analysis

Amgad Elgowainy (Primary Contact), and Krishna Reddi
Argonne National Laboratory
9700 South Cass Avenue
Argonne, IL 60439
Phone: (630) 252-3074
Email: aelgowainy@anl.gov

DOE Manager: Erika Gupta
Phone: (202) 586-3152
Email: Erika.Gupta@ee.doe.gov

Project Start Date: October 2007
Project End Date: Project continuation and direction determined annually by DOE

Overall Objectives

Evaluate hydrogen delivery and refueling concepts that can reduce hydrogen delivery cost towards meeting the delivery cost targets.

Fiscal Year (FY) 2016 Objectives

- Update and publish Hydrogen Delivery Scenario Analysis Model (HDSAM) with station configurations, market data, and cost information of delivery components for near-term and long-term markets.
- Enable estimation of delivery cost for early markets with varying station utilization over the life of the project or analysis period.

Technical Barriers

This project directly addresses Technical Barriers A, B, C, and E in the Hydrogen Delivery section of the Fuel Cell Technologies Office Multi-Year Research, Development, and Demonstration Plan. These barriers are:

(A) Lack of Hydrogen/Carrier and Infrastructure Options Analysis

(B) Reliability and Costs of Gaseous Hydrogen Compression

(C) Reliability and Costs of Liquid Hydrogen Pumping

(E) Gaseous Hydrogen Storage and Tube Trailer Delivery Costs

Technical Targets

Update the HDSAM model with market data, component cost data for near-term and long-term markets (with varying market penetration), station configuration options, and utilization scenarios.

Contribution to Achievement of DOE Hydrogen Delivery Milestones

This project contributes to the following DOE milestone from the Hydrogen Delivery section of the Fuel Cell Technologies Office Multi-Year Research, Development, and Demonstration Plan.

- Task 1.5: Coordinating with the H_2 Production and Storage sub-programs, identify optimized delivery pathways that meet a H_2 delivery and dispensing cost of <$2/gge for use in consumer vehicles. (4Q, 2020)
- Task 6.1: Define potential RD&D activities for other long-term market fueling/terminal needs. (4Q, 2015).
- Task 6.3: By 2020, reduce the cost of hydrogen delivery from the point of production to the point of use in consumer vehicles to <$2/gge of hydrogen for the gaseous delivery pathway. (4Q, 2020).

Accomplishments

- Updated the HDSAM model and publicly released the updated Version 3.0.
- The new version includes updates of market data, cost indexes, alternate liquid delivery station configurations, and quantified the cost reduction potential with higher market penetrations.
- Studied the impact of various parameters including station design capacity, utilization rate, and station configuration on the hydrogen delivery cost.

✧ ✧ ✧ ✧ ✧

INTRODUCTION

HDSAM is an Excel-based tool that uses a design calculation approach to estimate the contribution of individual components of delivery infrastructure to hydrogen cost, energy use, and greenhouse gas emissions. The model links individual components in a systematic market setting to develop capacity and flow parameters for a complete hydrogen delivery infrastructure. Using that systems level perspective, HDSAM calculates the full, levelized cost (summed over all components) of hydrogen delivery, accounting for losses and tradeoffs among the various component costs. Users of HDSAM can specify their own inputs to the model or select default inputs, which are based on quotes from vendors of specific delivery components or

from stakeholder inputs, data from the literature, or derived from basic engineering design calculations. The quality of the data and the direction of the analysis are vetted in formal interaction with partners from other national laboratories and independent consultants, and also via presentations to the Hydrogen Delivery Technical Team.

APPROACH

The HDSAM model has been updated with recent market data including key statistics of urban population, vehicle ownership rate, annual vehicle miles travelled, and average vehicle fuel economy for calculating market demand with vehicle penetration scenarios for all U.S. cities with population greater than 50,000. Cost formulas for all delivery components that are consistent with the latest cost data acquired for today's technologies, scale and production volumes have been updated. The model was also updated to include cost reduction factors for all delivery components for three hydrogen station market penetration scenarios to reflect the impact of learning, technology advancement and economies of scale, as shown in Table 1. The model was also updated to include an option to define a utilization scenario for hydrogen refueling stations over the station lifetime. The greenhouse gas (GHG) emissions data of all the delivery pathways have been updated consistent with the GREET® model 2015.

With increase in market penetration of the fuel cell vehicles, the number of hydrogen refueling stations are expected to increase. For this analysis we have considered three market scenarios: (i) "low," with 200 stations worldwide representing the current status of low volume production of refueling components; (ii) "high," with 10,000 stations worldwide representing a future mature market when refueling components are produced at high volume; and (iii) "mid," with about 5,000 station worldwide representing a midpoint between the first two.

In consultation with industry experts, all the delivery components have been divided into three technology baskets characterized by the current status of technology and scope for possible cost reduction through innovation and economies of scale. The three technology baskets and the cost reduction potential are summarized in Table 1.

RESULTS

Hydrogen Delivery Cost Reduction with Station Size and Production Economies of Scale

The Figures 1, 2 and 3 show the delivery cost contribution of each component of the tube-trailer, liquid tanker and pipeline delivery pathways respectively for a 16 metric ton (MT) per day market demand and 80% refueling station capacity utilization. All the three pathways enable a $4/kg delivery cost in a mature market (with 82 MT/d demand) taking advantage of the station economies of scale with large stations and cost reduction of components with increase in production volume.

For tube-trailer delivery pathways the hydrogen refueling station contributes (Figure 1) to about half the delivery cost for all market scenarios and that contribution decreases at larger station capacities. The contribution of the hydrogen refueling station and tube-trailer together is expected to reduce with market penetration of fuel cell vehicles from about $14/kg for 100 kg/d station at today's costs to about $2.5/kg for 1,000 kg/d station in a mature market. For the liquid delivery pathway the station contribution (Figure 2) is higher for smaller stations mainly due to the limitation

TABLE 1. Cost Reduction Factors for Different Technology Baskets for Different Market Penetrations

Cost Reduction Factors			
	Market (Production Volume)		
Technology baskets and definitions	Near-Term (low volume)	Mid-Term	Long-Term (high volume)
#1 Mature (low potential for cost reduction, 5% with each production volume doubling) Ex: *Low-Pressure Storage, Cryogenic Storage, H_2 Pipeline Cost Premium*	1	0.79	0.75
#2 Established (moderate potential for cost reduction, 10% with each production volume doubling) Ex: *Station Cascade Storage, Station Refrigeration, Tube-Trailer Vessel, LH_2 Truck Vessel*	1	0.61	0.55
#3 Developing (high potential for cost reduction, 15% with each production volume doubling) Ex: *Dispensers, Compressors, Cryogenic Pump, Station Controls/Safety Equip*	1	0.47	0.40

LH_2 - Liquid hydrogen

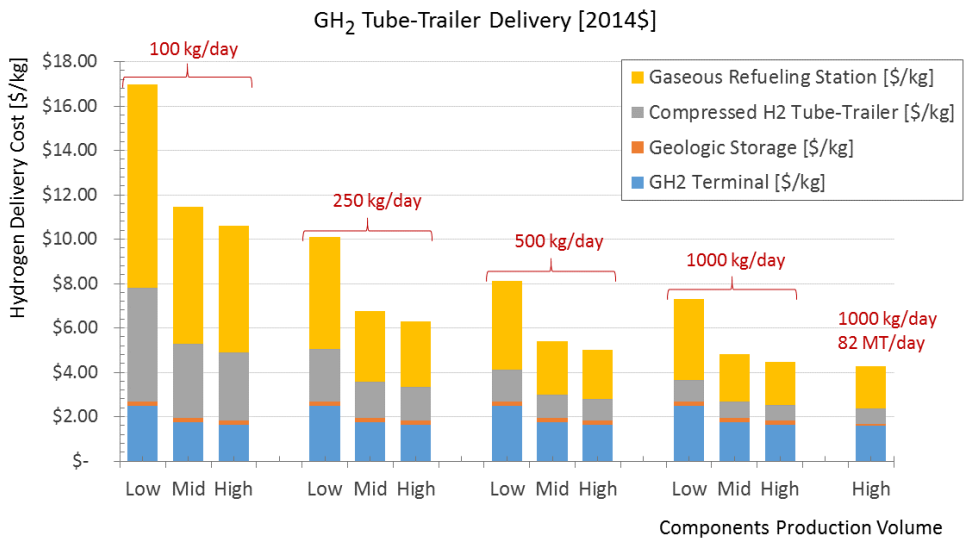

GH2 – Gaseous hydrogen

FIGURE 1. Delivery cost estimates for tube-trailer delivery pathway for different station capacities and production volumes

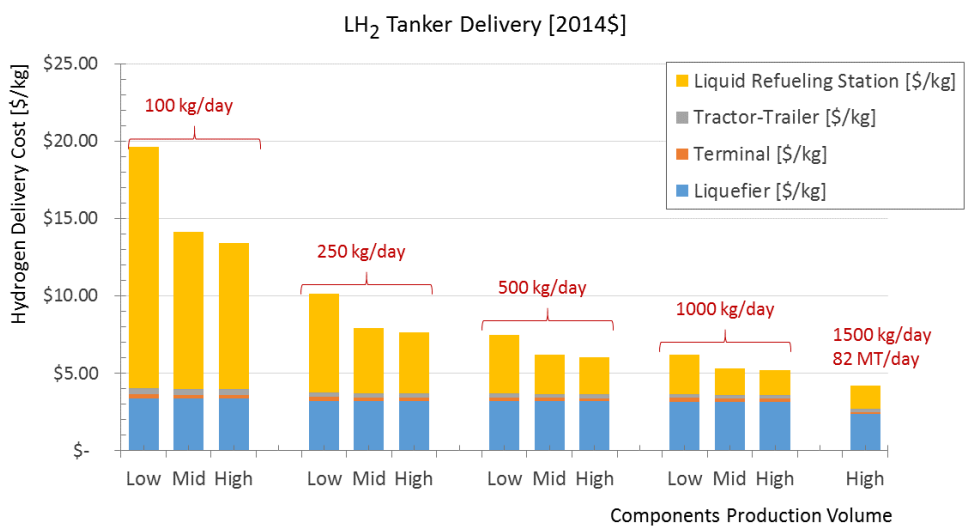

FIGURE 2. Delivery cost estimates for liquid tanker delivery pathway for different station capacities and production volumes

of available options for low boil-off pumps. In the current version of HDSAM a single version of low boil-off pumps have been incorporated, which has a capacity of about 120 kg/d costing about $700,000 (2014$). Due to the high capacity and cost of the pump, the liquid pumping option appears not suitable for stations with capacities lower than about 500 kg/d, making the liquid delivery pathway less attractive for smaller stations. The pipeline delivery pathway requires high capital investment and becomes economically viable at larger market demands with larger station capacities. For smaller markets and smaller stations, a larger distribution pipeline network is required, and contributes to about half (Figure 3) of the total delivery cost of hydrogen.

GHG Emissions Reduction with Cleaner U.S. Electric Grid

As shown in Figure 4, the GHG emissions are lower by about 40% when comparing the 2015 U.S. grid mix to the 2005 grid mix in previous version of HDSAM model. Updating the electricity supply to the 2015 U.S. grid mix resulted in lower GHG emissions for the liquid and tube-trailer delivery pathways compared to these estimated by the previous version of HDSAM.

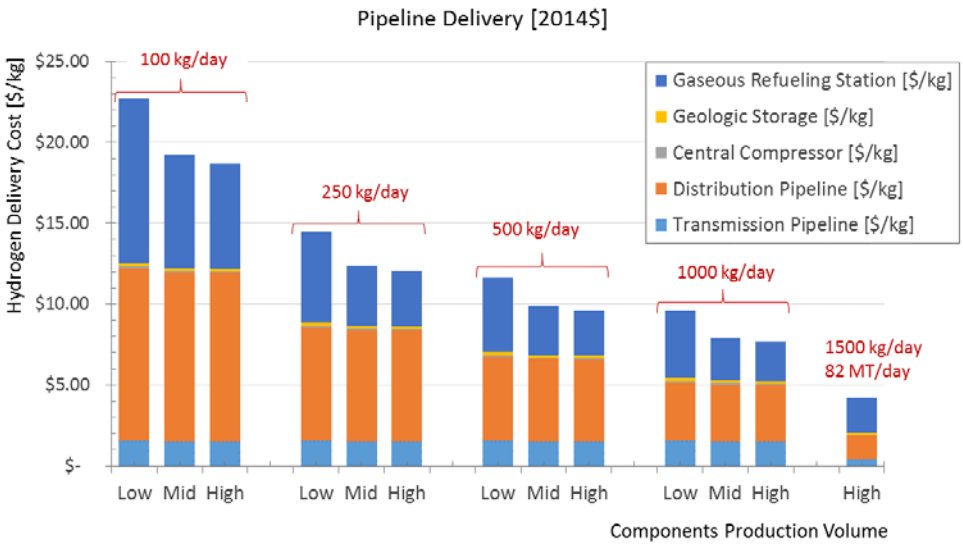

FIGURE 3. Delivery cost estimates for pipeline delivery pathway for different station capacities and production volumes

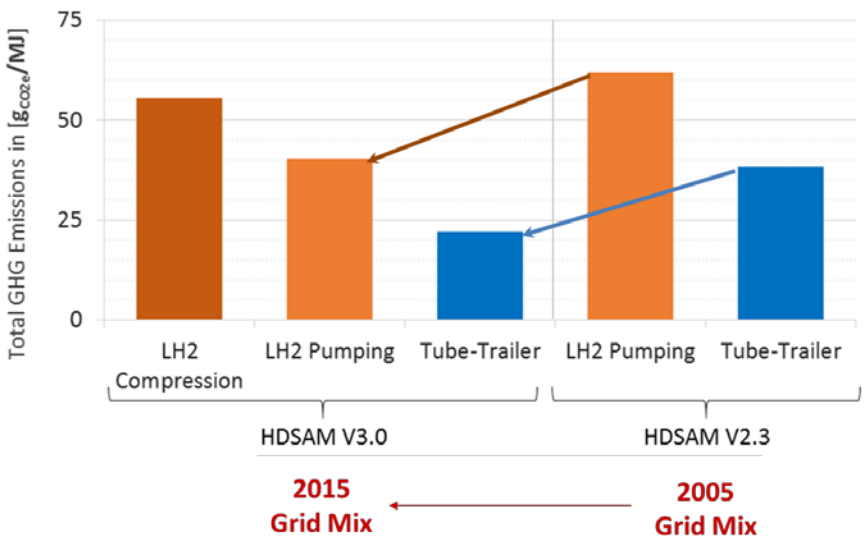

FIGURE 4. The GHG estimates from the current (V3.0) compared to the previous version (V2.3) of HDSAM model for liquid tanker and tube-trailer delivery pathways

CONCLUSIONS AND FUTURE DIRECTIONS

The tube-trailer delivery pathway appears as the most economical for early markets and smaller stations. The liquid delivery pathway is economical for moderate to large station sizes due to the limited options available for cryo-pumps in the current marketplace. The pipeline delivery pathway is economically viable only for supplying large stations in a mature market with large demands. Though each of the delivery pathways has its limitations, all the delivery pathways enable a delivery cost of $4/kg of hydrogen with larger station capacities and high market demand (i.e., high penetration of fuel cell vehicles). For the remainder of FY 2016, efforts will be directed toward updating, documenting, and publishing a newer version of HDSAM.

In the future, HDSAM will be updated with available cost data, emerging technologies and new pathways to evaluate new concepts and identify cost reduction potential towards meeting hydrogen delivery performance and cost targets.

PUBLICATIONS

1. Reddi, K., Elgowainy, A., Wang, M. 2016, "Special Section: Energy - Fuel Cells for Mobile Applications," July edition, CEP Magazine by AIChe.

2. Reddi, K., Mintz, M., Elgowainy, A., Sutherland, E. 2016, "Building a hydrogen infrastructure in the United States," in Compendium of Hydrogen Energy. Volume 4: Hydrogen Use, Safety and the Hydrogen Economy, eds. M. Ball, A. Basile, T. Nejat Veziroglu, Woodhead Publishing, pp. 293.

III.2 Fatigue Performance of High-Strength Pipeline Steels and Their Welds in Hydrogen Gas Service

Joseph Ronevich (Primary Contact),
Zhili Feng (ORNL), Andrew Slifka (NIST),
Elizabeth Drexler (NIST),
RobertAmaro (Colorado School of Mines)
Sandia National Laboratories (SNL)
7011 East Avenue
Livermore, CA 94550
Phone: (925) 294-3115
Email: jaronev@sandia.gov

DOE Manager: Erika Gupta
Phone: (202) 586-3152
Email: Erika.Gupta@ee.doe.gov

Project Start Date: October 1, 2015
Project End Date: September 30, 2018

Overall Objectives

- Enable significant cost savings through implementation of high strength steels as compared to lower strength pipes.
  - Demonstrate that girth welds in high strength steel pipe exhibit fatigue performance similar to lower strength steels in high-pressure hydrogen gas.
  - Identify pathways for developing high strength pipeline steels by establishing the relationship between microstructure constituents and hydrogen-accelerated fatigue crack growth (HA-FCG).

Fiscal Year (FY) 2016 Objectives

- Complete triplicate HA-FCG measurements for each material region (base metal, weld fusion zone, and heat-affected zone [HAZ]) in current practice arc weld at hydrogen pressure, load cycle frequency (1 Hz), & load ratio (R = 0.5). (SNL)
- Complete HA-FCG tests at constant ΔK to identify most susceptible locations in the fusion zone and HAZ of current-practice arc weld. (SNL)
- Develop controlled microstructures using Gleeble™. (Oak Ridge National Laboratory [ORNL])
- Fabricate a high strength steel girth weld using an alternative consumable. (ORNL)

Technical Barriers

This project addresses the following technical barriers from the Hydrogen Delivery section of the Fuel Cell Technologies Office Multi-Year Research, Development, and Demonstration Plan.

(D) High As-Installed Cost of Pipelines

(K) Safety, Codes and Standards, Permitting

Technical Targets

This project impacts the following technical targets for hydrogen delivery components (Table 3.2.4 of the Fuel Cell Technologies Office Multi-Year Research, Development, and Demonstration Plan) related to pipelines for gaseous hydrogen delivery.

- Total capital investment: $695,000/mile (FY 2020)
- Transmission pressure: 100 bar (FY 2020)
- Lifetime: 50 years (FY 2020)

Design codes such as the America Society of Mechanical Engineers (ASME) B31.12 [1] contain structural integrity models which enable safety assessment of low strength steel pipelines subjected to pressure cycling. Currently there are prescribed safety factors specifically for hydrogen service (i.e., materials performance factors) to accommodate the potential for hydrogen embrittlement. These materials performance factors are a function of the specified minimum yield strength (SMYS) for the steel. While, allowable stresses are significantly more restricted for high strength steel pipe compared to low strength, recent testing performed at both SNL and National Institute of Standards and Technology (NIST) [2-4] have shown similar fatigue performance of steel pipelines over a large range of SMYS. The conservative allowable stress restrictions in the current code nullify any cost savings that would be afforded by high strength steels. Direct reductions in capital costs would be realized if higher strength steels with thinner wall pipe thicknesses were permitted.

FY 2016 Accomplishments

- Paper accepted to *Materials Performance and Characterization*. The paper documents fatigue behavior of lower strength welded steel pipelines tested in a previous project.
- Performed triplicate fatigue crack growth rate tests on X100 base metal at 21 MPa and a single test at 5.5 MPa, at load ratio of R = 0.5, and loading frequency of 1 Hz.

- Developed a detailed procedure to generate controlled-microstructure gradients in the laboratory using Gleeble™ on low alloy carbon steel specimens.

✧ ✧ ✧ ✧ ✧

INTRODUCTION

Steel pipelines represent an economical means of transporting gaseous hydrogen over long distances; however, it is well known that these carbon-manganese steels are susceptible to hydrogen degradation. Current steel pipelines codes (e.g., ASME B31.12 [1]) place limitations on allowable stresses based on the SMYS of the material. These material performance factors reflect the general trend that hydrogen embrittlement can be more severe in high-strength steels. However, recent testing [2–4] of pipeline steels with a range of SMYS from 358 MPa to 689 MPa have not exhibited this trend and suggest that hydrogen assisted fatigue crack growth may not increase with strength. The conservative allowable stresses currently permitted in the code inhibit cost savings that could be realized if higher strength steel pipelines were permitted with reduced material performance factors. When material performance factors are not accounted for, increasing the strength of steel reduces the requisite wall thickness in a pipeline for a given operating pressure; higher strength steels could therefore reduce material and installation costs if their material performance factors were reduced [5].

This project focuses on developing a pathway to enable the use of high-strength steel in pipelines. One means to accomplishing this goal is to assess the fatigue performance of high-strength steel pipelines in high pressure hydrogen gas. The fatigue crack growth rate (da/dN) versus stress-intensity factory range (ΔK) relationship is a necessary input to structural integrity models applied to steel hydrogen pipelines. One specific assessment methodology for steel hydrogen pipelines is published in the ASME B31.12 code [1], and requires testing of the base metal, weld, and heat-affected zones of the pipe. A gap in the current understanding of steel pipelines is the fatigue performance of high strength steel welds; it is unknown whether welds will have the same behavior as base metal exhibited in the SMYS range of interest. An additional void in the research to date is the existence of physics-based relationships that correlate fatigue crack growth rates and microstructure. Physics-based relationships would greatly enhance the reliability of structural integrity models, and drastically reduce the burden of testing required to qualify materials for hydrogen use. The relationships between the microstructures of high-strength steels and welds, and hydrogen-assisted fatigue crack growth rates are evaluated in this study.

APPROACH

The objectives for this project are to (1) characterize the fatigue performance of girth welds of high-strength steel pipe in high-pressure hydrogen gas and (2) identify pathways for development of high-strength pipeline steels by establishing the relationship between microstructure constituents and HA-FCG. Based on these project objectives, the technical tasks are designed to furnish innovative high-strength steel products for evaluation, and to measure performance metrics for these high-strength steel products (i.e., fatigue crack growth rates in hydrogen gas) with high reliability. Completion of these tasks will assist in reaching the goal of this work: the deployment of steel pipe with reduced wall thickness, which can lower costs for hydrogen pipeline installation.

RESULTS

One objective in FY 2016 was to measure the hydrogen-assisted fatigue crack growth behavior of a high-strength pipeline girth weld. To accomplish this task, an X100 gas metal arc girth welded pipe, designated X100A, was supplied by NIST to Sandia in the first quarter of FY 2016. Figure 1

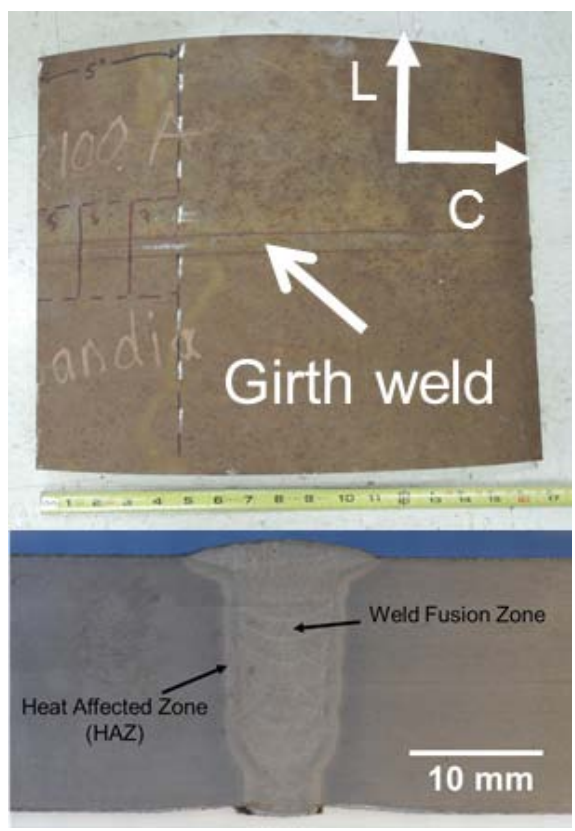

FIGURE 1. Section of X100 steel pipe containing girth weld. Macrograph of the girth weld showing the weld fusion zone and heat-affected zone

shows the supplied pipe section. A cross-section of the weld was polished and etched to reveal the microstructure of the weld as shown in Figure 1. The weld fusion zone and heat-affected zones are clearly identifiable in the macro-image of the weld. This welded pipe represents a fusion weld fabricated according to current practices. The base metal pipe has a nominal thickness of 19 mm and longitudinal yield strength of 731 MPa. Compact tension and eccentrically loaded single edge notched specimens were extracted from the base metal and weld fusion zone according to ASTM E647-11 [6] in the C-L and L-R orientations, respectively. The C-L terminology implies that the load is applied in the circumferential (C) direction and the crack growth is in the longitudinal (L) direction. Similarly the L-R orientation indicates load applied in longitudinal (L) direction and crack growth in radial (R) direction.

Fatigue crack growth rate versus stress-intensity factor range relationships were measured of the base metal at 21 MPa, load ratio of R = 0.5, and frequency of 1 Hz as shown in Figure 2. A single test was also completed at 5.5 MPa, although triplicates are planned. For comparison, a test was performed in air at a frequency of 10 Hz. All tests in hydrogen exhibited HA-FCG. The triplicate tests at 21 MPa showed good repeatability throughout the da/dN vs. ΔK curves. The test at 5.5 MPa exhibited HA-FCG; however, the onset of HA-FCG was shifted to the right (e.g., higher ΔK). Overall the fatigue crack growth rates appear to be lower in 5.5 MPa compared to in 21 MPa. This pressure dependence of HA-FCG is consistent with previous results reported by NIST [2,7]. Overall the HA-FCG behavior at 21 MPa in the X100A base metal was similar to other lower strength pipes tested in high pressure hydrogen [2-4]. Testing is planned for the weld fusion zone and heat affected zone using the eccentrically loaded single edge notched specimens in 21 MPa hydrogen gas.

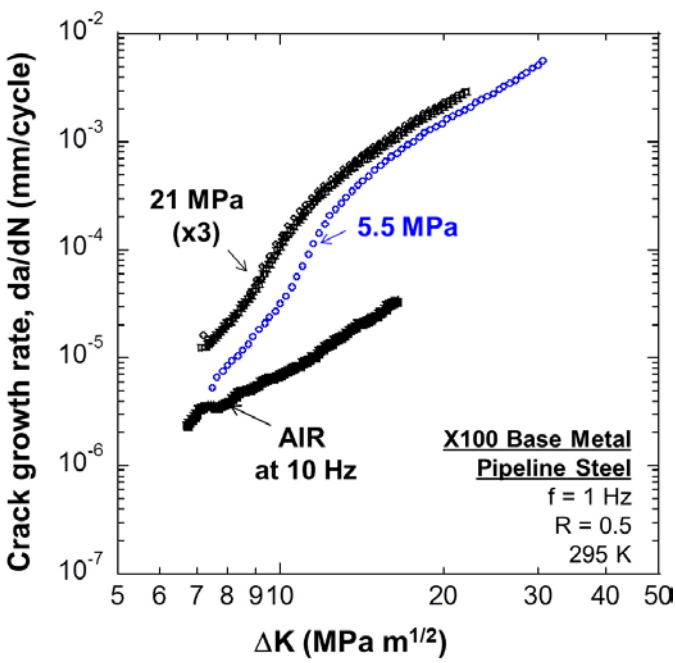

FIGURE 2. Fatigue crack growth curves (da/dN vs. ΔK) for X100A base metal tested at 5.5 MPa and 21 MPa hydrogen gas at R = 0.5 and frequency of 1 Hz

One of the complexities associated with welds and heat affected zones is the possibility of varied microstructure and strength across the weld due to the non-uniform thermal history generated by the welding process. As a result, certain microstructural regions of the weld might be more susceptible to HA-FCG than others. Constant stress intensity factor range tests are planned to assess the possibility that fatigue crack growth rates may be higher for particular locations in the HAZ and weld fusion zone. Constant-ΔK tests serve as a means to survey the microstructure and identify the most susceptible regions of the weld or HAZ. In this test, a crack will propagate through the weld and HAZ at a constant applied ΔK while measurements of crack growth rate are recorded. Microstructural regions identified as having higher crack growth rates will be the focus of subsequent tests to measure the full da/dN vs. ΔK behavior. Initial testing proved to be a challenge as crack extension was impeded or was non-uniform. The cause is likely due to residual stress. Measurements of residual stress are planned to help determine a path forward for constant ΔK testing.

NIST developed a phenomenological model that can predict HA-FCG in pipeline steels as a function of hydrogen pressure and mechanical loading parameters [7]. The model in its published form must be calibrated for each material of interest and does not take into account microstructure [7]. One reason for this shortcoming of the model is a gap in fundamental understanding of the relationship between microstructure constituents and HA-FCG. Development of a physics-based model to describe HA-FCG as a function of microstructure is one of the goals of this project. Current efforts of the model are focused on laying the groundwork for the physics-based implementation of microstructure specific phenomena such as hydrogen transport, plasticity, decohesion laws, and orientation specific mechanical properties at the grain level. The model is in its infant stages but has been shown to accurately predict some experimental results in the literature.

In order to enable a detailed study of the relationship between microstructure and hydrogen-assisted fatigue crack growth, a novel approach was developed to produce laboratory controlled microstructures using a Gleeble™ at ORNL. Low-carbon steel samples were subjected to non-uniform heating by placing the sample in between two internally cooled copper jaws. Samples were fixed with thermocouples and the sample was heated followed by rapid cooling with the predominant heat transfer in the longitudinal direction. The goal was to generate a microstructure gradient that encompasses microstructures typical of high-

strength steels, welds, and heat affected zones. Compact tension specimens can then be extracted from the Gleeble™ samples and constant ΔK tests can be performed in high pressure hydrogen gas to determine the relationship between microstructure and HA-FCG. Due to heat transfer characteristics of the specimen, the microstructure gradient is expected to exist only in the direction of crack propagation of the specimen. The optimized specimen geometry is shown in Figure 3 along with the peak temperature distribution in the direction of crack propagation as experimentally measured on the surface.

CONCLUSIONS AND FUTURE DIRECTIONS

- Repeatable fatigue crack growth curves were measured for X100A base metal in 21 MPa gas and 5.5 MPa. Results were comparable with lower strength pipeline data, tested previously, exhibiting some pressure dependence.
- (Future) Perform fatigue crack growth testing on X100 weld and heat affected zoned at 21 MPa and compare behavior to lower strength steel welds.
- Developed procedure to generate laboratory-controlled microstructures using Gleeble™.
- (Future) Fatigue test specimens will be extracted from Gleeble™ samples with imposed microstructure gradients to measure relationship between microstructure and HA-FCG.

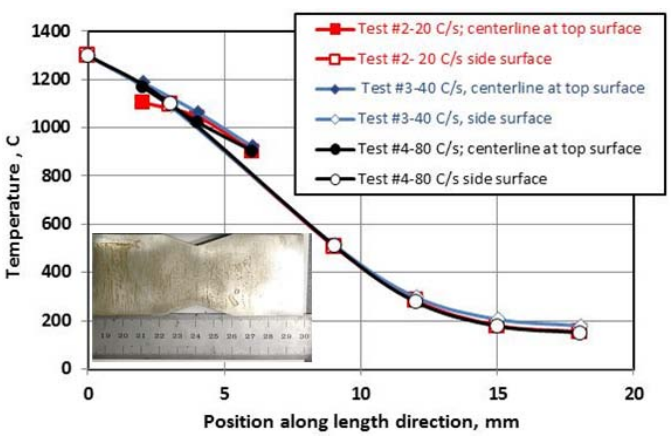

FIGURE 3. Optimized specimen geometry for producing graded microstructure using Gleeble™, and the temperature profile measured on the specimen as function of distance from center

FY 2016 PUBLICATIONS/PRESENTATIONS

1. J. Ronevich, "Fatigue Performance of High-Strength Pipeline Steels and Their Welds in Hydrogen Gas Service," SAND2016-3003 PE, Hydrogen Delivery Tech Team meeting, Livermore, CA, April 5, 2016.

2. J.A. Ronevich, B.P. Somerday, "Assessing Gaseous Hydrogen Assisted Fatigue Crack Growth Susceptibility of Pipeline Steel Weld Fusion Zones and Heat Affected Zones," Materials Performance and Characterization, *accepted April 2016.*

3. J. Ronevich, B. Somerday, "Accelerated Fatigue Crack Growth in Pipeline Steels and Their Welds in High Pressure Hydrogen Gas," NACE Corrosion conference, Vancouver, Canada, March 9, 2016.

4. J. Ronevich, B. Somerday, "Assessing Steel Pipeline and Weld Susceptibility to Hydrogen Embrittlement," Fuel Cell Technologies Office webinar, January 12, 2016.

REFERENCES

1. ASME, "B31.12 Hydrogen Piping and Pipelines," ed. New York, NY: ASME, 2011.

2. A.J. Slifka *et al*., "Fatigue crack growth of two pipeline steels in a pressurized hydrogen environment," *Corrosion Science*, vol. 78, 2014, pp. 313–321.

3. J.A. Ronevich, B.P. Somerday, C.W. San Marchi, "Effects of microstructure banding on hydrogen assisted fatigue crack growth in X65 pipline steels," *Int. J. of Fatigue,* Vol. 82, 2016, pp. 497–504.

4. C. San Marchi, B.P. Somerday, K.A. Nibur, D.G. Stalheim, T. Boggess, S. Jansto, "Fracture resistance and fatigue crack growth of x80 pipeline steel in gaseous hydrogen," in ASME Pressure Vessles & Piping Division, Baltimore, Maryland, USA, 2011.

5. J.R. Fekete, J.W. Sowards, and R.L. Amaro, "Economic impact of applying high strength steels in hydrogen gas pipelines," *International Journal of Hydrogen Energy,* vol. 40, pp. 10547–10558, 2015.

6. ASTM International, "E647-11 Standard test method for measurement of fatigue crack growth rates," ed. West Conshohocken, PA, 2011.

7. R.L. Amaro, E.S. Drexler, and A.J. Slifka, "Fatigue crack growth modeling of pipeline steels in high pressure gaseous hydrogen," *International Journal of Fatigue*, vol. 62, pp. 249–257, 2014.

III.3 Vessel Design and Fabrication Technology for Stationary High-Pressure Hydrogen Storage

Zhili Feng (Primary Contact), Yanli Wang, Yong Chae Lim, Jian Chen and Lawrence Anovitz
Oak Ridge National Laboratory
1 Bethel Valley Rd.
P.O. Box 2008, MS 6095
Oak Ridge, TN 37831
Phone: (865) 576-3797
Email: fengz@ornl.gov

DOE Manager: Neha Rustagi
Phone: (202) 586-8424
Email: Neha.Rustagi@ee.doe.gov

Subcontractors:
- Global Engineering and Technology LLC, Camas, WA
- Ben C. Gerwick, Inc., Oakland, CA
- MegaStir Technologies LLC, Provo, UT
- Kobe Steel, LTD., Japan
- Hanson Pressure Pipe, Grand Prairie, TX
- Harris Thermal Transfer Products, Newberg, OR
- Temple University, Philadelphia, PA

Project Start Date: October 1, 2010
Project End Date: Project continuation and direction determined annually by DOE

Overall Objectives

- Address the significant safety and cost challenges in high-pressure stationary hydrogen storage technology.
- Develop and demonstrate a novel steel/concrete composite vessel (SCCV) design and fabrication technology for stationary hydrogen storage systems.

Fiscal Year (FY) 2016 Objectives

- Establish the experimental procedure and instrumentation for long-term hydrogen cyclic testing of the SCCV prototype.
- Initiate and perform the long-term testing of the SCCV prototype under cyclic, high-pressure hydrogen loading, simulative of hydrogen charging and discharging cycles at hydrogen refueling stations (one to two cycles per day from 100–430 bar).

Technical Barriers

This project addresses the following technical barrier from the Hydrogen Delivery section (3.2) of the Fuel Cell Technologies Office Multi-Year Research, Development, and Demonstration Plan.

(E) Gaseous Hydrogen Storage and Tube Trailer Delivery Cost

Technical Targets

This project aims to develop and demonstrate SCCVs as a low-cost, safe means of stationary storage for gaseous hydrogen. SCCVs are scalable to different pressures and capacities, and can therefore satisfy a variety of applications at hydrogen fueling stations, renewable energy hydrogen production sites, and other non-transport storage sites. As shown in Table 1, the current generation composite vessel made using existing design and manufacturing technologies exceeds the DOE cost targets in place when the project began [1].

TABLE 1. Progress towards Meeting Technical Targets for Stationary Gaseous H_2 Storage Tanks (For Fueling Sites, Terminals, or Other Non-Transport Storage Needs)

Pressure	DOE 2015 Status*	Current SCCV	DOE 2020 Target*
Low Pressure (160 bar) Purchased Capital Cost ($/kg of H_2 stored)	$850	$681	$700
Moderate Pressure (430 bar) Purchased Capital Cost ($/kg of H_2 stored)	$900	$713	$750
High Pressure (860 bar) Purchased Capital Cost ($/kg of H_2 stored)	$1,200	$957	$1,000

*Per 2012 version of Multi-Year Research, Development, and Demonstration Plan in place when project began

FY 2016 Accomplishments

- Completed the modification and upgrade of the testing site capabilities to meet the requirements for the long term hydrogen cyclic testing of the demonstration SCCV.
- Automated data acquisition from strain gauges, and pressure and temperature sensors that monitor the vessel performance during cyclic loading.
- Completed the pre-test (including nitrogen purge and hydrogen purge), refined the operating procedure for long term hydrogen cyclic testing, and initiated hydrogen cyclic testing.
- Completed hydrogen impurity analysis of the supplied hydrogen gas and confirmed acceptable hydrogen purity level in the vessel after high purity hydrogen purge.

INTRODUCTION

Low-cost infrastructure, such as off-board bulk stationary hydrogen storage, is critical to successful market penetration of hydrogen-based transportation technologies. Stationary storage is needed in many locations ranging from hydrogen production plants to refueling stations. The design capacity and pressure of the stationary storage vessel are expected to vary considerably depending on the intended usage, the location, and other economic and logistic considerations. For example, storage vessels at a hydrogen refueling station may have higher pressures but smaller storage capacity when compared to those at a renewable energy hydrogen production site. Therefore, it is important to develop vessel designs that are scalable to different pressures and capacities. Moreover, since storage vessels provide the surge capacity to handle hourly, daily, and seasonal demand variations, they endure repeated charging and discharging cycles. Thus, the hydrogen embrittlement in structural materials, especially the accelerated crack growth due to fatigue cycling, needs to be mitigated to ensure the vessel safety. Safety and economics are two prevailing drivers behind the composite hydrogen storage technology.

In this project, Oak Ridge National Laboratory leads a diverse multidisciplinary team consisting of industry and academia to develop and demonstrate an integrated design and fabrication technology for cost-effective high-pressure steel/concrete composite storage vessel that can meet different stationary hydrogen storage needs.

APPROACH

A novel SCCV has been specifically designed and engineered for stationary high-pressure gaseous hydrogen storage applications. SCCV has several inherent features aimed at solving the two critical limitations and challenges of today's high-pressure hydrogen storage vessels—the high capital cost and the safety concerns of hydrogen embrittlement of high-strength steel vessels.

The SCCV technology comprises four major innovations: (1) flexible modular design that can be scaled to meet different pressure and capacity needs, as well as different manufacturing scenarios; (2) composite design that combines an inner steel vessel with a pre-stressed outer concrete reinforcement; (3) layered steel vessel wall and vent holes to solve the hydrogen embrittlement problem *by design*; and (4) integrated sensor system to monitor the structural integrity and operation status of the storage system. Together, these innovations make the SCCV cost-competitive and inherently safe for stationary high-pressure hydrogen storage services. The inner steel vessel is composed of multiple layers with strategically placed vent holes to prevent the intake and accumulation of hydrogen in all steel layers except the innermost layer. Since the innermost layer is the only one to face significant volumes of hydrogen, it is the only layer made of stainless steel. This layered design thereby minimizes steel vessel cost while ensuring resistance to hydrogen embrittlement. Furthermore, the novel steel/concrete composite vessel design allows for the stresses or the structural load from the high-pressure hydrogen to be shared between the inner steel vessel and the pre-stressed outer concrete reinforcement, thereby offering the flexibility to optimize the use of low-cost commodity materials (such as structural steels and concretes) and industry-accepted fabrication technologies for cost reduction. For example, the layered steel vessel technology is proven and accepted in industry standards and codes (e.g., American Society of Mechanical Engineers [ASME] Boiler and Pressure Vessel Code). Moreover, the layered steel vessel has potential for further cost reduction through advanced fabrication technologies, such as friction stir welding.

The prototype SCCV was subjected to two types of tests designed to validate the SCCV technology for high pressure hydrogen storage. First, the SCCV was subjected to hydrostatic testing at 8,950 psi (or 615 bar, 1.43 times of the 430 bar design pressure), to validate the constructability of the SCCV per ASME Boiler and Pressure Vessel Code requirement. In FY 2015, hydro-static test of the demonstration SCCV was successfully completed and both the constructability and performance of the SCCV were validated. Second, a long-term high hydrogen pressure cyclic testing was designed to confirm the suitability of the vessel under expected high pressure hydrogen charging and discharging operation condition, especially the effects of hydrogen embrittlement on structural steels in long-term operation with high pressure hydrogen. This second test is the primary focus in FY 2016.

RESULTS

The primary focus in FY 2016 was to evaluate the performance of the demonstration SCCV under high pressure hydrogen cyclic testing condition that could simulate a typical service condition of a stationary hydrogen storage vessel. The target is to have the vessel subject to cyclic hydrogen pressure loading from 2,000–6,000 psi (i.e., up to 96% of the maximum allowable operation pressure) for a total of 250 cycles to validate its performance for high-pressure gaseous hydrogen storage. It is expected that one to two pressure loading cycles will be carried out per day.

The existing testing facility was modified and upgraded for the high-pressure hydrogen cyclic testing. The demonstration SCCV was placed in a controlled access area restricted to personnel that have been trained in the testing procedure. The test area is readily accessible to the local fire department. The testing setup and the area meet related

standards such as National Fire Protection Agency (NFPA) 55, ISA-12.12.01-2007, National Electrical Code NFPA 70 and ASME Boiler and Pressure Vessel Code Section VIII, Division 2 code. The fire marshal has visited the testing site and approved the hydrogen testing arrangement. Figure 1 shows arrangement of the hydrogen cyclic testing site. Multiple strain gauges, pressure sensors, and temperature sensors were placed on the vessel at various locations to provide the much needed experimental data for monitoring the integrity of the vessel under service condition. The test control and data acquisition were automated.

For safety reasons, the demonstration SCCV was filled with glass beads to reduce the hydrogen net volume for the cyclic testing. This reduced the effective volume to about 30% (i.e., 26.7 kg H_2 at 430 bar). The control system allows the hydrogen gas to be recycled to reduce testing cost and safety risk of discharging hydrogen to environment.

A detailed testing procedure was developed for testing of the SCCV. A leak test was performed to check the SCCV and associated piping utilizing nitrogen at pressure of 2,500 psi. After completion of the leak test, the vessel was subjected to a vacuum cycle and multiple step purges using nitrogen, low purity hydrogen and high purity hydrogen to ensure testing of the vessel using hydrogen gas that meets SAE J2719 requirements. Gas samples from the vessel and supplied hydrogen gas were collected and analyzed before and after the final purge steps. Unexpected high level of impurities was detected after the final purge step. After extensive chemical composition analysis and inspection of the testing system, the source of the impurities was later determined to be primarily from out-of-specification high purity hydrogen gas supply. The impurity issue of the supply gas has been addressed. Furthermore, analysis of the hydrogen gas in the demonstration vessel suggested there are minimum releases of oxygen and other impurities from the glass beads in the vessel, validating the appropriateness of using glass beads in lieu of hydrogen.

FIGURE 1. Arrangement of the testing site for hydrogen cyclic testing of the demonstration SCCV

After completion of the purging process and verification of the control and data acquisition system, the hydrogen cycle testing was initiated. However, unexpected leakages were detected while pumping hydrogen into the vessel. It was found that the vessel could not be pressurized above 2,200 psi. A leakage in the sealing gasket in the manway was identified to be the cause. It should be noted that the vessel was successfully pressurized to 9,000 psi during the hydrostatic testing before the hydrogen cyclic pressure test. The leakage is under investigation, and a key question is to determine whether or not it is a hydrogen specific issue or gasket installation issue. A detailed plan has been developed in order to identify and isolate the cause of the leak. The high-pressure hydrogen cyclic testing will resume as soon as this leakage issue is addressed.

CONCLUSIONS AND FUTURE DIRECTIONS

The project so far has achieved the following.

- Completed the test setup for the long term hydrogen cyclic testing of the demonstration SCCV.
- Established the procedures for hydrogen impurity analysis and for hydrogen cyclic testing of the demonstration SCCV.
- Initiated hydrogen cycle testing.

Future planned activities include:

- Determining the cause of the leakage and formulate a plan to resolve the issue accordingly.
- Completing the long-term testing of the demonstration SCCV performance under cyclic hydrogen pressure loading, simulative of expected hydrogen charging and discharging cycles of hydrogen refueling stations (1–2 cycles per day from 100–430 bar).
- Continuing with the lessons learned in this project to further optimize all aspects of SCCV technology for additional major cost reduction in a follow-up project (Generation II SCCV).
- Technology commercialization.

FY 2016 PUBLICATIONS/PRESENTATIONS

1. Zhili Feng, "Vessel Design and Fabrication Technology for Stationary High-Pressure Hydrogen Storage," 2016 DOE Hydrogen and Fuel Cells AMR, Washington, D.C., June 2016.

2. Yanli Wang, Maan Jawad, Fei Ren, Jian Chen, Yong Chae Lim, and Zhili Feng, "Steel-Concrete Composite Vessel for Stationary High-Pressure Hydrogen Storage." Proc. ASME 2016 Pressure

Vessels and Piping Conference, July 17–21, 2016, Vancouver, British Columbia, Canada, Paper No PVP2016-63371.

3. Yanli Wang, Fei Ren, Yong Chae Lim, Jian Chen, Maan Jawad and Zhili Feng, "Design and Testing of Steel-Concrete Composite Vessel for Stationary High-Pressure Hydrogen Storage." 2016 International Hydrogen Conference–Material Performance in Hydrogen Environments, Jackson Hole, WY, September 11–14, 2016.

REFERENCES

1. W. Zhang, F. Ren, Z. Feng, and J. Wang, "Manufacturing Cost Analysis of Novel Steel/Concrete Composite Vessel for Stationary Storage of High-Pressure Hydrogen," Oak Ridge National Laboratory Report, ORNL/TM-2013/113, Oak Ridge National Laboratory, Oak Ridge, TN, March 2013.

III.4 Hydrogen Compression Application of the Linear Motor Reciprocating Compressor (LMRC)

Eugene L. Broerman (Primary Contact),
Norm Shade (ACI Services), Klaus Brun,
Jeffrey Bennett, Nathan Poerner, Diana Strickland,
Jerome Helffrich, Shane Coogan, Aaron Rimpel,
Pablo Bueno
Southwest Research Institute® (SwRI®)
6220 Culebra Rd.
San Antonio, TX 78238
Phone: (210) 522-2555
Email: EBroerman@swri.org

DOE Manager: Erika Gupta
Phone: (202) 586-3152
Email: Erika.Gupta@ee.doe.gov

Contract Number: DE-EE0006666

Subcontractor:
Norm Shade, ACI Services, Cambridge, OH

Project Start Date: September 5, 2014
Project End Date: October 4, 2017

Overall Objectives

- Demonstrate the Linear Motor Reciprocating Compressor (LMRC) by integrating individually-developed Technology Readiness Level 4 or higher components.
- Demonstrate that the compressor portion of the LMRC has improved compression efficiency and a reduced capital and maintenance cost compared to conventional reciprocating compression technology.
  - Improve isentropic efficiency above 73% by minimizing aerodynamic losses and using low-friction bearings (goal is above 95%).
  - Reduce capital costs to half those of conventional reciprocating compressors by minimizing part count.
  - Reduce required maintenance by simplifying the compressor design to eliminate common wear items.
- Meet the flow and pressure requirements: compress hydrogen from 290 psia (20 bara) to 12,690 psia (875 bara) with flow rates greater than 22 lbm/hr (10 kg/hr).

Fiscal Year (FY) 2016 Objectives

The overall objective for FY 2016 is fabrication and testing of the LMRC.

- Perform detailed mechanical design.
- Estimate cost projection for full-scale version of LMRC compressor.
- Develop test matrix for bench-scale testing, design compressor test stand for low pressure (LP) stage; develop plans for commissioning, safety, and operation of test stand.
- Fabricate and assemble LP stage compressor parts.
- Construct the test stand and integrate the compressor.
- Commission and start-up the demonstration model.
- Test the bench scale system.
- Analyze the single stage test results.

Technical Barriers

This project addresses the following technical barriers from the Hydrogen Delivery section of the Fuel Cell Technologies Office Multi-Year Research, Development, and Demonstration (MYRDD) Plan.

(B) Reliability and Costs of Gaseous Hydrogen Compression

Technical Targets

During the proposal phase and kick-off of the project, the DOE technical targets were based on the 2012 MYRDD Plan. A 2015 MYRDD Plan was updated in August of 2015. Table 1 compares the predicted characteristics of the LMRC design with 2020 targets from both MYRDD reports.

FY 2016 Accomplishments

- Finalized the detailed mechanical design of the compressor.
- Calculated and estimated the cost to manufacture a full-scale version of the LMRC.
- Developed a test matrix for bench-scale testing.
- Designed the compressor test stand for the LP stage.
- Developed plans for commissioning, safety, and operation of the test stand.

TABLE 1. Progress towards Meeting Technical Targets for Hydrogen Delivery with Small Compressors: Fueling Sites (~100 kg H_2/h peak flow)

Characteristic	Units	2012 MYRDD Target for 2020	2015 MYRDD Target for 2020	LMRC 2020 Status (Predictions)
Reliability		High	NA	High
Availability	%	NA	≥85	TBD
Compressor Efficiency	Isentropic %	80%	NA	80% - all 3 stages
Compressor Specific Energy	kWh/kg	100 bar inlet: NA 500 bar inlet: NA	100 bar inlet: 1.6 500 bar inlet: 1.4	20 bar to 875 bar: 1.8 (Compressor Only) 9.2 (LMRC) 100-bar Inlet Pressure: 1.45 (Optimized LMRC)
Losses of H_2 Throughput	% of flow	<0.5%	0.5%	<0.4%
Uninstalled Capital Cost (Based on 1,000 kg/d Station, [~100 kg H_2/h Peak Compressor Flow])	$	$240,000 (1 Compressor, No Backup)	NA (1 Compressor, No Backup)	20 bar to 875 bar: $284,000 (1 Compressor, No Backup)
Uninstalled Capital Cost (Based on 750 kg/d Station, [~100 kg H_2/h Peak Compressor flow])	$	100-bar inlet: NA 500-bar inlet: NA (1 Compressor, No Backup)	100-bar inlet: 275,000 500-bar inlet: 90,000 (1 Compressor, No Backup)	100 bar to 875 bar: $195,000 500-bar inlet: $105,000 (1 Compressor, No Backup)
Annual Maintenance Cost	% of Installed Capital Cost	2.0%	4%	1.2% of Uninstalled Capital Cost
Outlet Pressure Capability	bar	860	950	875
Compression Power	kW	240 (20 bar at Inlet)	NA	170 (20 bar at Inlet) (Compressor Required Power)

NA – Not applicable; TBD – To be determined; 100-bar inlet – Pipeline delivery of gas to the compressor; 500-bar inlet – Tube trailer delivery of gas to the compressor

- Fabricated and assembled many of the LP stage compressor parts.
- Construction of the test stand is underway.

✧ ✧ ✧ ✧ ✧

INTRODUCTION

SwRI® and ACI Services, Inc. are developing a LMRC to meet the DOE goal of increasing the efficiency and reducing the cost of forecourt hydrogen compression. The proposed advanced compression system utilizes a novel and patented concept of driving a permanent magnet piston inside a hermetically-sealed compressor cylinder through electromagnetic windings. The LMRC is an improvement over conventional reciprocating compressors as it minimizes the mechanical part count, reduces leakage paths, and is easily modularized for simple field installation (U.S. Patent 8,534,058) [1].

APPROACH

The LMRC is a novel concept compared to conventional reciprocating compression technology. The compression system replaces the functions of an electric motor drive and reciprocating compressor with an integrated, linear, electrically-actuated piston. It will have a magnetic piston within a cylinder and a gas compression chamber at each end of the piston. The compressor cylinder is comprised of an electromagnetic coil that is operable with the piston to convert an input of electrical power to a reciprocating movement of the piston. This uses the same technology seen in magnetic bearings in turbomachinery and does not require oil for lubrication. Since the driver and compressor are integrated into the same hermetically-sealed component, there is a significant reduction in the number of parts and materials needed to construct this device. In addition, the simplicity of the design reduces required maintenance, minimizes seal leakages and wear, and allows for oil-free operation.

The LMRC system minimizes parasitic losses by using reduced piston speeds, low-pressure-drop contoured valves, and inter-stage cooling manifolds. Working at low reciprocating speeds of approximately 300 cycles per minute (5 Hz), the LMRC prototype is expected to meet an isentropic efficiency goal of greater than 95% per stage [2]. That efficiency can be compared with current state-of-the-art technology that typically has an efficiency of closer to 73%. The improved isentropic efficiency and reduced mechanical losses result in an increase in overall efficiency for the LMRC system.

RESULTS

The detailed mechanical design, including all detailed manufacturing drawings, assembly drawings, and bills of material (material lists), were completed for the first-stage LMRC. The first-stage LMRC assembly drawing is shown in Figure 1. Detailed mechanical design efforts included design of the skid to support the LMRC during testing. That skid was designed to meet the American Petroleum Institute 618 [3] requirements for reciprocating compressors. The separation margin requirement was verified with a modal analysis, and the steady-state response requirements were verified with a forced-response analysis of the system. Figure 2 shows a computer assisted design model of the skid design, constructed of structural steel beams.

Cost of a full-scale version of the LMRC compressor based on supplier quotes for the bench-scale version was estimated to be $284,000 when designed to compressor gas from 20 bar to 875 bar. Strategies were identified to meet the capital and operating and maintenance targets in the MYRDD Plan for 2020 of $240,000 per compressor with an operating and maintenance cost of less than $4,800 per year in high-volume production. Full-scale was defined by DOE during the project proposal phase as a compressor that can produce a flow rate of 100 kg/h of hydrogen while achieving the goal of compressing the gas from 20 bar to 875 bar. Another MYRDD target is to deliver the required pressures and flow rates with an isentropic efficiency of greater than 73%. Summaries of the cost and capabilities of the LMRC as compared with the 2020 targets are listed in Table 1.

The LMRC test loop was designed, and plans were developed for testing and safety. A schematic showing the approximate location of the LMRC test loop in relation to the existing building can be seen in Figure 3.

In order to complete the LMRC parts fabrication, all components were ordered and entered into production. Machining of the pressure containing components—central casing, cylinders, heads, and manifold—commenced and are complete. Component machining photos can be seen in Figure 4. Also depicted in Figure 4 are pistons and bushing seals deliveries from third parties that were received.

Significant progress has been made for the LMRC test stand construction. The concrete foundation has been poured,

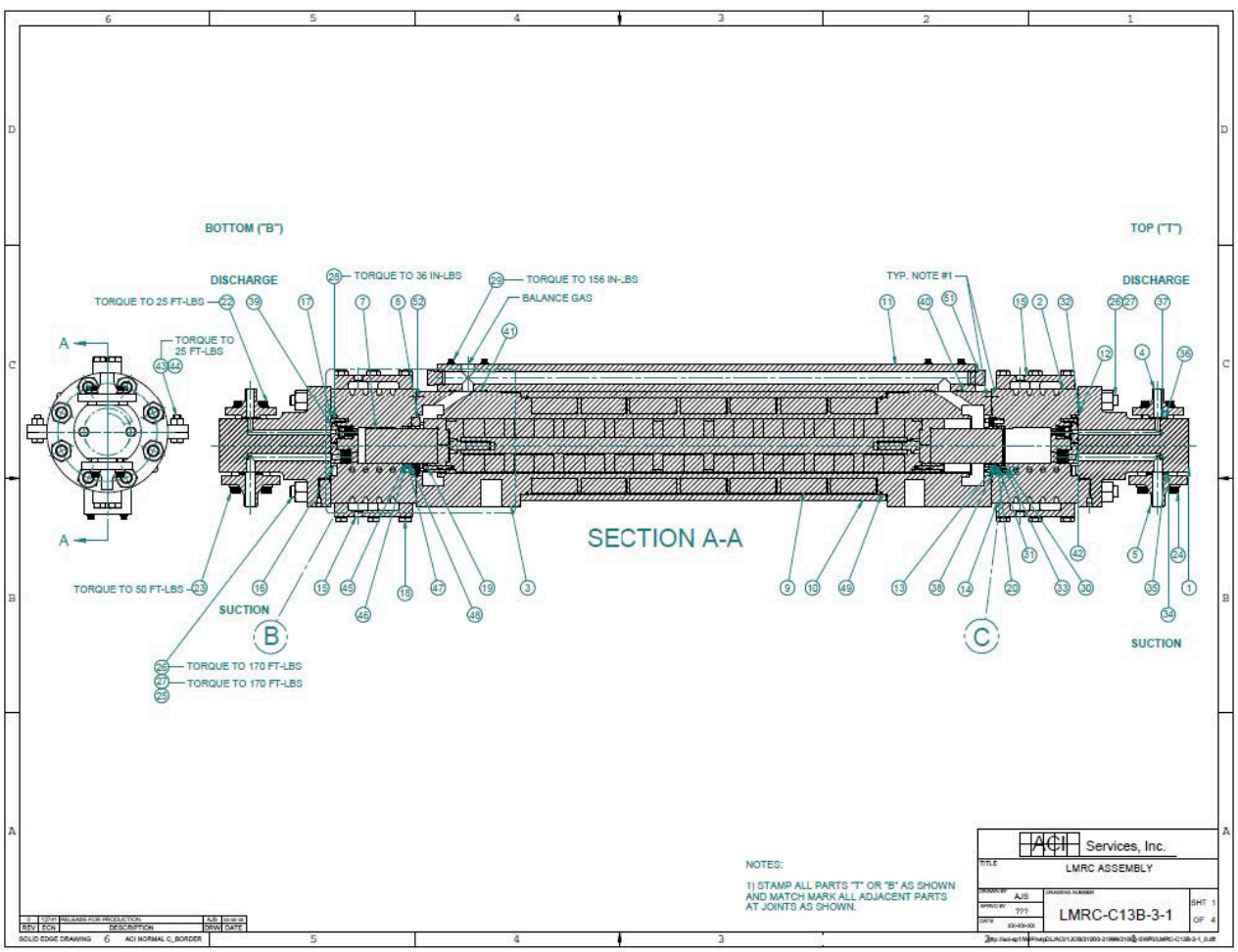

FIGURE 1. First-stage LMRC assembly drawing

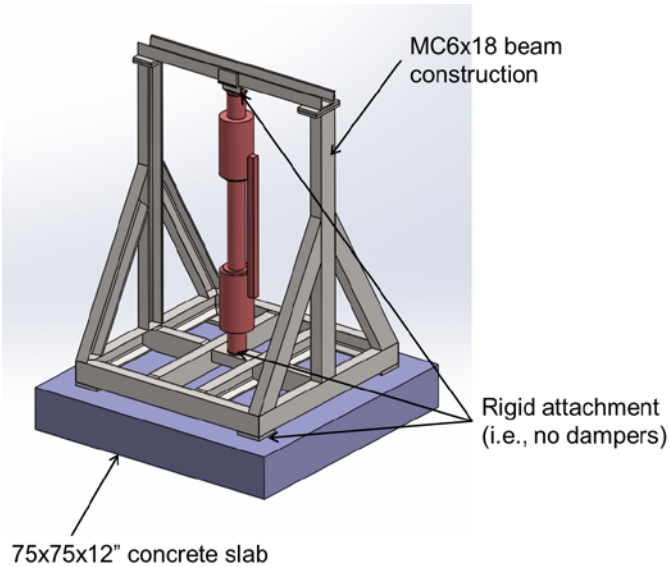

FIGURE 2. Computer assisted design model of the LMRC skid design

and the compressor test frame and connecting brackets have been delivered. The two chillers, electrical panel and filter, water tank, and gas cylinders rack have been moved into position. Additionally, electrical wiring has been laid underground and run to the necessary locations. While the compressor manufacturing is being finished by ACI Services, SwRI is focused on preparing all systems to support the testing.

CONCLUSIONS AND FUTURE DIRECTIONS

Conclusions derived from the work conducted in FY 2016 are:

- Hydrogen embrittlement and powerful magnetic forces add a significant degree of difficulty to the design of a compressor system.
  - The potential for hydrogen embrittlement was considered for all of the LMRC parts that will come in contact with hydrogen, and material selection was limited for some parts due to the application.
  - Lower cost, high strength magnetic materials cannot be used for the central case for the LMRC, where high strength is required.
  - Special tools were designed to safely assemble the magnets on the central shaft without damaging the magnets or other parts.
- The cost of $284,000 to manufacture the full-scale LMRC is higher than the 2012 MYRDD goal for 2020 when the LMRC is designed for a pressure range of 20 bar to 875 bar. However, when using a higher compressor inlet pressure (100 bar or 500 bar), a stage or two of compression is removed and the cost of the LMRC is significantly reduced to approximately $200,000 or less.
- Updated predictions still indicate that highly efficient hydrogen compression is possible with an LMRC used for the compression process.

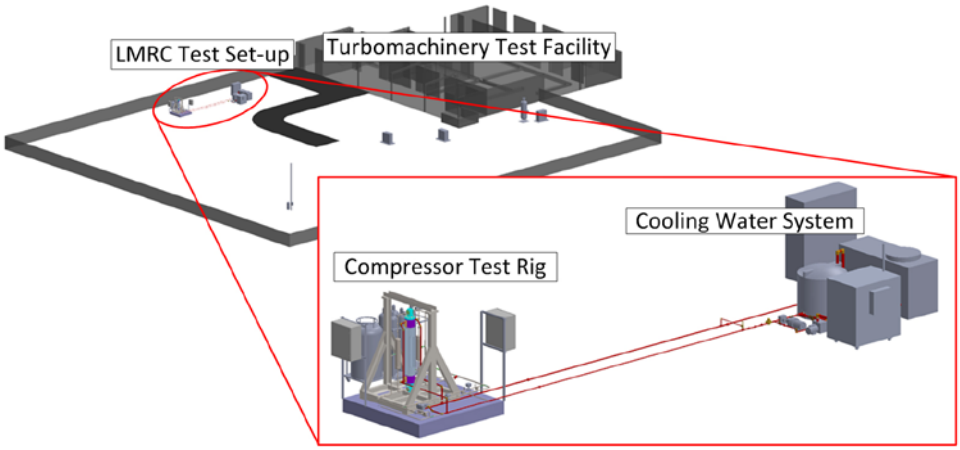

FIGURE 3. Location of the LMRC test loop in relation to the existing building

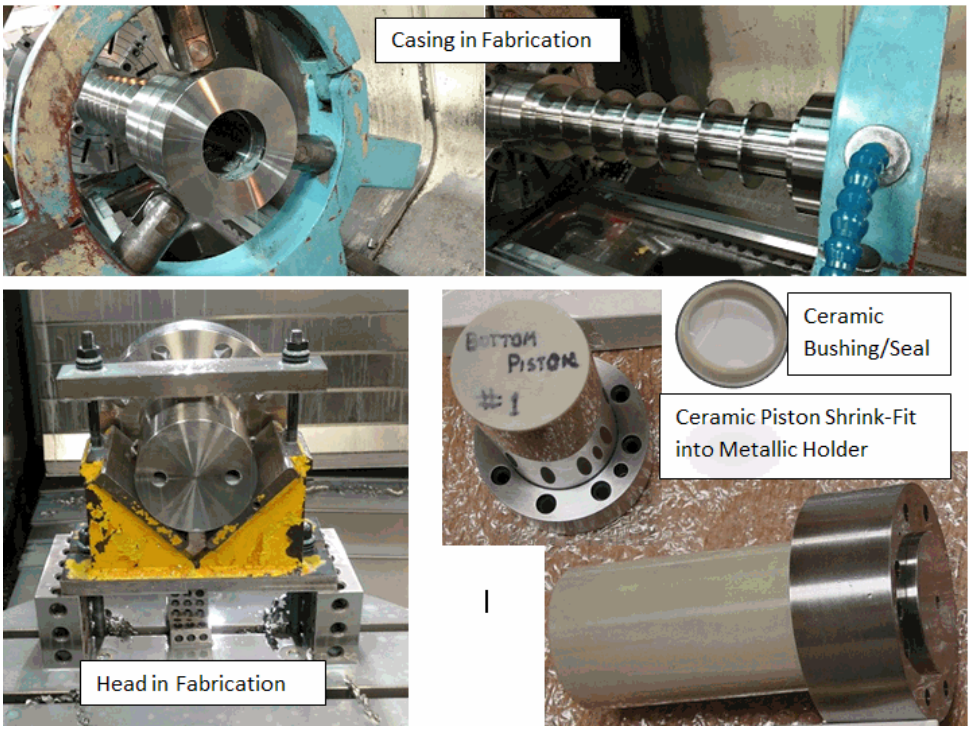

FIGURE 4. Major component photos: items delivered and items being machined or assemble

Future work in Project Year 3 (FY 2017) will include:

- Develop and check fabrication and manufacturing drawings for compression stages two and three. Identify vendors and obtain quotes for the fabrication of the various components.
- Develop a test matrix for the full three-stages system testing. Design test fixtures and select instrumentation needed to test the compressor and measure the system performance.
- Fabricate and assemble the other two compressors and the associated supporting components.
- Select and purchase hardware and fabricate the extended test stand.
- Commission the test bench using an inert gas and following the plan previously defined.
- Complete testing of the LMRC system according to the defined test matrix with hydrogen.
- Analyze the results from the full system testing (20 bar to 875 bar pressure range).

FY 2016 PUBLICATIONS/PRESENTATIONS

1. Broerman, E.L., J. Bennett, K. Brun, N. Shade, L. Chordia, "Designing a Linear Motor Recip Compressor to Achieve 12,700 psia (875.6 bara) Outlet Pressure." COMPRESSORtech[2], July 2016.

REFERENCES

1. U.S. Patent 8,534,058. Issued Sept. 17, 2013. "Energy Storage and Production Systems, Apparatus and Methods of Use Thereof," Patented in United States of America.

2. Deffenbaugh, D., et al., "Advanced Reciprocating Compression Technology," DOE Award No. DE-FC26-04NT42269, SwRI Contract No. 18.11052, December 2005.

3. American Petroleum Institute 618, 2007, "Reciprocating Compressors for Petroleum, Chemical, and Gas Industry Services," Fifth Edition, American Petroleum Institute, Washington, D.C.

III.5 Steel Concrete Composite Vessel for 875 bar Stationary Hydrogen Storage

Zhili Feng (Primary Contact), Yanli Wang, Yong Chae Lim, Jian Chen, and Brian Gibson
Oak Ridge National Laboratory
1 Bethel Valley Rd.
P.O. Box 2008, MS 6095
Oak Ridge, TN 37831
Phone: (865) 576-3797
Email: fengz@ornl.gov

DOE Manager: Neha Rustagi
Phone: (202) 586-8424
Email: Neha.Rustagi@ee.doe.gov

Subcontractors:
- Air Liquide, Houston, TX
- AccerlorMittal, East Chicago, IN
- Adaptive Intelligent Systems LLC, Lexington, KY
- Bevilacqua Knight Inc., Sacramento, CA
- Global Engineering and Technology LLC, Camas, WA
- Forterra Water Pipe, Grand Prairie, TX
- LightSail, Berkeley, CA
- MegaStir Technologies LLC, Provo, UT
- POSCO, South Korea
- SustainX, Seabrook, NH
- Temple University, Philadelphia, PA
- WireTough Cylinders, Bristol, VA

Project Start Date: October 1, 2014
Project End Date: September 30, 2017

Overall Objectives

- Address the significant safety and cost challenges in high-pressure stationary hydrogen storage system.
- Develop and demonstrate the second generation (GEN II) steel/concrete composite vessel (SCCV) design and fabrication technology for stationary high pressure hydrogen storage at 875 bar.
- Reduce the purchased capital cost of GEN II SCCV for forecourt hydrogen refueling station to \$800/kg H_2 at 875 bar in 2017, and meet all other DOE funding opportunity announcement (FOA) requirements including material compatibility with hydrogen, projected service life of at least 30 years, scalability to 1,000 kg of storage, and versatility in meeting the footprint requirement of different forecourt hydrogen fueling stations including underground storage.

Fiscal Year (FY) 2016 Objectives

- Perform holistic design and engineering optimization toward achieving the project cost target of \$800/kg H_2 stored at 875 bar. Provide a detailed cost analysis report that validates the \$800/kg H_2 cost target, using a detailed bottom-up, high-fidelity cost analysis methodology.
- Complete the design and engineering of 875 bar storage demonstration vessel with all major features of GEN II SCCV technology optimized for cost reduction.

Technical Barriers

This project addresses the following technical barrier from the Hydrogen Delivery section of the Fuel Cell Technologies Office Multi-Year Research, Development, and Demonstration Plan.

(E) Gaseous Hydrogen Storage and Tube Trailer Delivery Costs

Technical Targets

This project aims at developing GEN II SCCV that will be more cost-effective for forecourt hydrogen fueling station applications. Specific technical targets are:

- Meet or exceed the cost targets (<\$1,000/kg H_2) stored at pressures of 875 bar or greater as specified in DOE DE-FOA-0000821 under which this project was awarded.
- Demonstrate compatibility of design materials with hydrogen, and durability under pressure.
- Meet all performance requirements included in the DOE FOA 821 over a 30-year service life.
- Demonstrate scalability and footprint of the storage system for versatility in application.
- Construct and test a prototype demonstration vessel of sufficient size to adequately validate the technical concept, manufacturability and cost-effectiveness of the technology for forecourt high-pressure hydrogen storage scalable to >1,000 kg H_2.

FY 2016 Accomplishments

- Finalized the design features for the GEN II vessels and identified major areas of cost reduction for GEN II SCCV to meet the cost target of \$800/kg H_2.
- Completed baseline reference design for four different hydrogen storage capacities: 100 kg, 200 kg, 500 kg, and

1,000 kg. The team performed design and engineering optimization to develop the technical basis towards cost reduction below \$800/kg H_2 at 875 bar.

- High-fidelity bottom-up cost analysis showed that the final GEN II reference designs with capacity from 100–1,000 kg H_2 at 875 bar could be produced for a cost in the range of \$550–700/kg H_2 for a number of design, manufacturing, and capacity options using today's relevant American Society of Mechanical Engineers (ASME) Boiler and Pressure Cessel (BPV) code, high-strength steels that are currently accepted by ASME BPV code, and today's pressure vessel manufacturing practices.

✧ ✧ ✧ ✧ ✧

INTRODUCTION

In a previous DOE Fuel Cell Technologies Office project, a novel SCCV technology referred to as first generation (GEN I) SCCV in this report, has been specifically developed and demonstrated for stationary high-pressure gaseous hydrogen storage applications. The newly developed SCCV technology, GEN II SCCV, comprises four major innovations: (1) flexible and scalable modular design for different storage pressure and capacity needs, for cost optimization, and for system reliability and safety; (2) composite storage vessel design and construction with a pre-stressed inner steel vessel encased in an outer reinforcement; (3) the use of a hydrogen permeation barrier in a layered vessel structure and vent holes to solve the hydrogen embrittlement (HE) problem *by design*; and (4) integrated sensor system to monitor the structural integrity and operation status of the storage system. Together, these innovations form an integrated approach to make the SCCV cost competitive and inherently safe for stationary high-pressure hydrogen storage services. The SCCV solved the two critical limitations and challenges of today's high-pressure hydrogen storage vessels: high capital cost, and the safety risk posed by HE in high-strength steels. The SCCV can be designed and constructed using mature and proven fabrication technologies acceptable by pertinent industrial codes and standards. Therefore, while the concept of SCCV is new, SCCV technology as a whole is relatively mature. The SCCV technology is expected to be commercialized for hydrogen fueling station applications in near future.

During the GEN I research, a number of design, materials and manufacturing options were identified that, upon further research and development, could lead to substantial cost reduction over the reference GEN I design. The GEN II project aimed to build upon the success of GEN I SCCV, and to optimize major aspects of the SCCV technology for further significant cost reduction for forecourt hydrogen fueling station applications.

APPROACH

A systematic approach is employed in this project to refine and optimize all major aspects of SCCV technology (design, engineering, materials, and fabrication) to achieve the DOE FOA cost target. The R&D in this project will effectively utilize the knowledge obtained in developing the GEN I SCCV, including the evaluation of the following of R&D areas for potential further cost reductions.

- Cost reduction by materials. High-pressure hydrogen vessels have in the past avoided the use of high-strength steels due to HE concerns. Our innovative approach to eliminate HE by design minimizes vessel exposure to hydrogen, thereby eliminating the potential HE issue[1]. High-strength steels can therefore be used for vessel construction without penalties in design allowable stress (static and fatigue) typically assumed with their use. Increase in the strength of steel used reduces the necessary vessel wall thickness and the associated fabrication cost. The GEN II design targeted a 35–60% increase in steel strength over GEN I; GEN 1 was composed of 50–75 ksi (SA-765 Grade IV and SA-724 Grade B) steel, while Gen II steel was 100–120 ksi yield strength. This allowed the design allowable stresses in the vessel to reach ~50 ksi in GEN II vs. 33 ksi in the GEN I design, per the ASME BPV code.
- Cost reduction by vessel design optimization. We applied the cost analysis methodology developed previously to further optimize the SCCV design for cost reduction. Options investigated included (a) optimizing the shape and dimension of the SCCV, (b) replacing the stainless steel inner liner with a lower cost hydrogen permeation barrier, and (c) optimizing the pre-stress level of the vessel. The design optimization considered the limits and constraints of today's manufacturing technologies and availability of materials; the manufacturing technologies chosen in the design optimization are available for such vessel fabrication per appropriate code requirements.
- Fabrication and sensor technologies. The following options were investigated: (a) remote non-contact vessel inspection and remote repair welding technologies, (b) application of friction stir welding, and (c) new wire wrapping technologies for pre-stressing.

RESULTS

The GEN II design has improved upon the success of GEN I SCCV. It not only kept the unique features of GEN I

[1] The SCCV comprises an inner liner surrounded by multiple layers of steel that each have mm-sized vent holes engraved within them. These vent holes allow any hydrogen that escapes the liner to escape the vessel. It is expected that these vent holes will therefore ensure that hydrogen is never in contact with the outer layers of steel (composed of high-strength steel alloys) long enough to cause embrittlement.

SCCV to mitigate the hydrogen embrittlement risk by design, but also incorporated a number of new design and manufacturing innovations developed in this project for cost reduction. These technology innovations formed the basis for cost optimization. A bottom-up, high-fidelity cost analysis methodology was used to determine the project cost of GEN II reference designs.

In order to investigate the scalability of the GEN II vessel technology, a set of *reference designs* has been selected for design optimization. These reference designs were studied for the following aspects:

- For cost optimization
- For detailed fabrication-construction engineering
- For high-volume manufacturing engineering
- For validation of technology scalability

Four initial reference designs were chosen: 100 kg, 200 kg, 500 kg, and 1,000 kg H_2 at 875 bar. In later stages of the design optimization, some intermittent capacities were also identified as they provided better material utilization and reduced manufacturing cost.

These reference designs were designed and analyzed in detail to ensure that they could be provided to vessel manufacturers for off-the-shelf production and order for refueling stations. These reference designs can be combined to meet a wide variety of capacity requirement of fueling stations.

The cost optimization of GEN II designs was systematically carried out in three different stages. Each stage served a different purpose during the course of the design iterations toward optimization. The designed details and cost analysis were progressed from simple to more comprehensive. The results from the early stage analysis served as the basis for more comprehensive design optimization for the later stage analysis. Stage I primarily focused on the effect of the vessel geometry (i.e., length vs. diameter of the vessel) on the cost. Stage II added the effects of different materials for the head, cylinder and the permeation barrier. Based on the findings from Stage I and Stage II, candidate reference designs for different hydrogen storage capacities were identified. In Stage III, a high fidelity, bottom-up cost analysis determined the projected costs of the reference designs from step-by-step cost analysis of vessel fabrication using fabrication flows recommended by U.S. domestic vessel manufacturers.

The final reference designs in Stage III cost analysis are summarized in Table 1. ASME BPV code accepted high strength steel SA-517 was used in cost analysis. SA-517 represented a middle point of steel prices surveyed in this project. The inner diameter of the vessel was set at nominal 30 inches based on the consideration of available material and manufacturing options. The scalability of the GEN II design was investigated with different vessel length for H_2 storage capacity ranging from 100 kg to 1,000 kg. Whereas the GEN II design was readily scalable to 1,000 kg or more of H_2 (for one vessel), 320 kg was regarded as a practical upper limit for most fueling station applications, due to weight limitations for the transportation of fabricated vessels to fueling station sites (80,000 lb including truck and freight would be the upper limit for trucking without significant cost penalty.)

For the final reference designs in Table 1, four different manufacturing options with a total of 24 design cases are analyzed in detail for the cost. These four options are extruded shell with overlaid head liner (ESOL), formed shell with overlaid head liner (FSOL), extruded shell with loose head liner (ESLL), and formed shell with loose head liner (FSLL). The projected costs are summarized in Figure 1, using the high-fidelity, bottom-up cost analysis methodology. For all design options, the unit costs of the vessel decrease as the storage capacity increases for storage capacity between 100 kg and 320 kg. The unit cost for the 500 kg storage capacities are high due to the cost penalty for transportation. Among the 24 design cases, 22 have a unit cost less than the \$800/kg H_2 target, and two were at \$810/kg H_2 and \$805/kg H_2, slightly over the cost target. More importantly, six cases had projected costs less than \$600/kg H_2 stored. The six cases with the lowest costs are those with capacities between 200 kg and 320 kg H_2.

The design and engineering for GEN II SCCV followed the design rules in ASME BPV code, Section VIII Division 2. The final reference designs in Table 1 also

TABLE 1. Design Parameters of Six GEN II SCCV using SA517-E High Strength Steel

Capacity (kg H_2)	100	167	200	270	320	500
Head/Shell Thickness (in)	2.125					
Inner Diameter (in)	30					
Layer of Wrap	5					
Outer Diameter* (in)	38.5					
Total Length (ft)	17	28	32.9	44	52.5	78.7
Total Weight* (lb)	20,400	33,500	40,000	53,750	63,700	98,700

* Including wire wrapping (~1 in thick) and protective (~1 in thick) layers

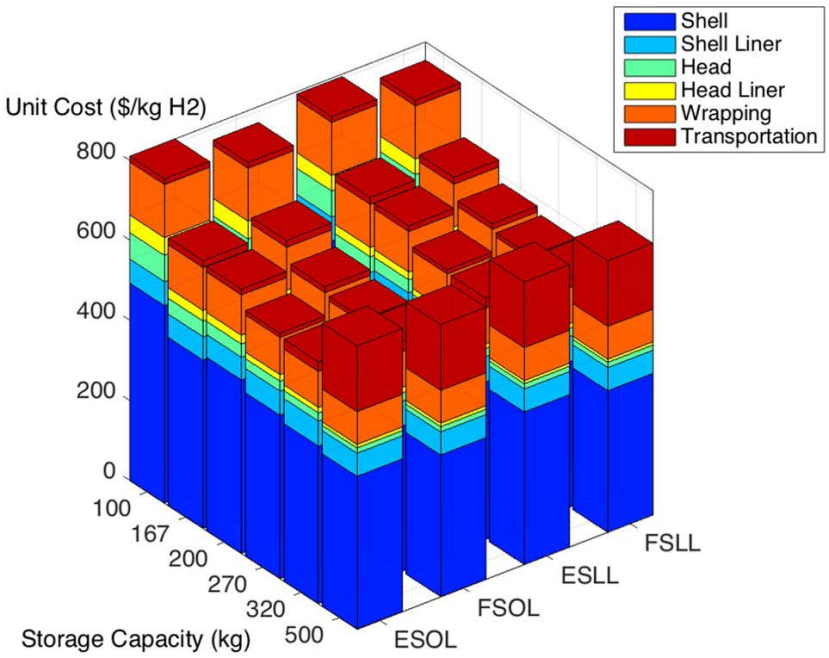

FIGURE 1. Unit storage costs ($/kg H2) of all GEN II SCCVs analyzed in the Stage III analysis

meet or exceed the 11,000 pressure cycles for the 30-year design life, which corresponds to the anticipated high-usage scenario: the vessel will be re-charged each day. The fatigue assessment was performed in accordance with Annex 3-F of Section VIII Division 2, using in-air fatigue design data and assuming maximum possible pressure changes in the vessel from 50 bar to the max design pressure of 875 bar in a cycle. The use of Division 2 design rules avoided uncertainties in assuming or specifying manufacturing related issues, such as the minimum manufacturing flaw size assumption required in Division 3 for more precise fatigue life prediction. The Division 2 analysis resulted in fatigue design lives of 78,877 cycles for the vessel head, 22,041 cycles for the vessel cylinder, and 12,681 cycles for the weld region. Detailed finite element model analysis of the final reference designs also identified that the nozzle region was problematic. Due to high stress concentrations at the inside corner of the original nozzle configuration, the design life was only 3,324 cycles. This necessitated nozzle design modification, to reduce the stress concentration. The modified nozzle design resulted in a design life of 50,230 cycles. The hydrogen permeation barrier liner was upgraded to stainless steel to ensure a high design life of 29,997 cycles.

CONCLUSIONS AND FUTURE DIRECTIONS

Through substantial engineering design work and economic analyses, project accomplishments in FY 2016 have included:

- Completed baseline reference design of GEN II SCCV for different hydrogen storage capabilities ranging from 100 kg to 1,000 kg.
- Performed holistic design and engineering optimization and achieved the $800/kg H_2 cost target using a bottom-up, high-fidelity cost analysis methodology.

Future Planned Activities for FY 2017:

- Complete the design and engineering of a GEN II SCCV mockup at 875 bar, and publish report detailing design and cost.

FY 2016 PUBLICATIONS/PRESENTATIONS

1. Zhili Feng, "Steel Concrete Composite Vessel for 875 bar Stationary Hydrogen Storage," 2016 DOE Hydrogen and Fuel Cells AMR, Washington, D.C., June 2016.

2. Y. Wang, Z. Feng, Y.C. Lim, J. Chen, F. Ren, M. Jawad, and M. Kelly, "Cost Analysis of Hydrogen Storage Vessel at 875 bar," ORNL/TM-2016/94, ORNL technical report, 2016.

III.6 Low Cost Hydrogen Storage at 875 bar Using Steel Liner and Steel Wire Wrap

Amit Prakash (Primary Contact) and Ashok Saxena
Wiretough Cylinders, LLC
14570 Industrial Park Rd., Suite C
Bristol, VA 24202
Phone: (276) 644-9120
Email: aprakash@wiretough.com; asaxena@uark.edu

DOE Manager: Neha Rustagi
Phone: (202) 586-8424
Email: Neha.Rustagi@ee.doe.gov

Contract Number: DE-EE0006668

Subcontractors:
- Oak Ridge National Laboratory, Oak Ridge, TN
- N & R Engineering, Parma Heights, OH
- CP Industries, McKeesport, PA
- Ashok Saxena, Consultant, Fayetteville, AR
- Structural Integrity Associates, Inc., San Jose, CA
- Hy-Performance Materials Testing, LLC, Bend, OR

Project Start Date: September 15, 2014
Project End Date: June 14, 2017

Overall Objectives

The goal of this project is to develop a pressure vessel to safely store hydrogen at 875 bar with a safety factor of 3 or higher that also meets the DOE storage tank cost target of <$1,000/kg hydrogen. The objectives are:

- To wire wrap a standard American Society of Mechanical Engineers (ASME) approved, 406 mm diameter and 9.14 m long cylinder with a capacity of 765 L rated at a pressure of 460 bar to boost its pressure capacity to 875 bar and meets the ASME Pressure Vessels and Piping (PVP) Section VIII-Division 3, KD-10 requirements for storing hydrogen.
- To keep the cost of producing the storage tanks to less than $1,000/kg of stored hydrogen, maintain a design life of 30 yr, and deliver hydrogen that meets the SAE J2719 hydrogen purity requirements.

Fiscal Year (FY) 2016 Objectives

- Perform a detailed elastic–plastic stress analysis to assist in the fine tuning the design of the pressure vessel.
- Explore the possibility of reliably detecting initial flaw sizes that are larger than 2% of the liner wall thickness.
- Commence testing of steel wrapping wires in hydrogen environment.
- Conduct testing to explore the effects of negative load ratios on fatigue crack growth rate behavior of the liner material.
- Develop full length cylinder wire wrap machine capable of wrapping 9.1 m to 12.2 m long cylinders.
- Obtain ASME certifications for use of wire wrapped cylinders for high pressure hydrogen storage.

Technical Barriers

This project addresses the following technical barrier from the Hydrogen Delivery section of the Fuel Cell Technologies Office Multi-Year Research, Development, and Demonstration Plan.

(E) Gaseous Hydrogen Storage and Tube Trailer Delivery Costs

Technical Targets

This project's goals are to meet the 2020 targets for high-pressure hydrogen storage in the 2012 version of the Fuel Cell Technologies Office Multi-Year Research, Development, and Demonstration Plan, as shown in Table 1.

TABLE 1. Wiretough's Progress toward Meeting Technical Targets for High Pressure Hydrogen Ground Storage Systems (Fuel Cell Technologies Office 2012 Multi-Year Research, Development, and Demonstration Plan)

Characteristics	2020 Target	Wiretough
High Pressure (860 bar) Purchased Capital Cost ($/kg of H_2 stored)	$1,000	On target to meet in 2017

FY 2016 Accomplishments

- Elastic–plastic finite element analysis was conducted to simulate the autofrettage process and subsequent service pressure cycle conditions to estimate maximum, minimum and cyclic stresses in the critical regions of the cylinder.
- Finite element model was used to identify approaches to reduce stresses in transition region between the wire wrap and the dome of the liner.
- Fatigue crack growth tests in hydrogen at negative load ratios were performed and the study was completed.

- Fatigue testing in hydrogen was performed on high strength wire at Oak Ridge National Laboratory.
- Alternate methods of nondestructive evaluation were explored to reliably detect flaw sizes greater than 2% of the wall thickness, which is a significant improvement over the current industry standard of greater than 3% of the wall thickness.
- Specifications were developed for wire wrapping machine for 9.1 m to 12 m long cylinders, and an order was placed. Installation of the machine is scheduled to begin in July of 2016 with a completion date of end of August of 2016.
- After a review of the stress analysis, manufacturing process, and inspection standards conducted by an ASME team, an ASME U3 Stamp was granted on March 9, 2016. The approval is for the following design:
  - Approval was granted under ASME's Boiler and Pressure Vessel Code Section VIII- Division 3.
  - Liner outer diameter of 406 mm (16 in), length ranging from 7.7 m (25 ft) to 9.2 m (30 ft) with a capacity of 700+ L.
  - Round and flat wires using SA905, Class 1 minimum ultimate tensile strength = 2.04 GPa (296 ksi), minimum yield = 1.8 GPa (260 ksi), wires with the specified pre tension.
  - Allowable maximum pressures in the range of 69 MPa (10,000 psi) to 103.4 MPa (15,000 psi).
  - Certification applies to pressure vessels for ground storage of gases such as compressed natural gas, hydrogen, air etc. For storage of hydrogen, an additional step of self-certification of compliance with ASME KD-10 requirements is necessary.

✧ ✧ ✧ ✧ ✧

INTRODUCTION

The Fuel Cell Technologies Office within the Office of Energy Efficiency and Renewable Energy is supporting research and development activities leading to the development of low cost, high pressure hydrogen storage systems for use in hydrogen refueling stations (forecourt). The goal of this project is to develop a pressure vessel to safely store 750 L of gaseous hydrogen at 875 bar that meets the ASME PVP Section VIII- Division 3 design requirements and also meets the DOE storage tank cost target of <$1,000/kg H_2 stored.

APPROACH

Type I metal cylinders (406 mm outer diameter) have been used for compressed natural gas and hydrogen storage for several decades but are limited to pressures of 55 MPa for various technical reasons. Wiretough has a patented process to wrap these commercially available cylinders with ultra-high strength steel wires (2 GPa in strength) to approximately double the pressure capability of the cylinders with a proven record of safely storing hydrogen. These wire-wrapped cylinders are further subjected to an autofrettage process in which they are subjected to pressures high enough to plastically deform the inner liner, but the wire jacket remains elastic. Upon release of the autofrettage pressure, the inner liner is left with high residual compressive hoop stresses. This process decreases the maximum tensile hoop stress in the liner under the operating pressure and can thus enhance the fatigue life of the vessel very significantly. In this project, this concept was first demonstrated using short, 1.9 m long cylinders and is now being extended to 9.14 m long cylinders.

RESULTS

Design Analysis and Optimization: Finite element analysis was performed to conduct sensitivity analyses in support of fine tuning of the design as described below:

- Effect of varying orthotropic properties of the wrap on liner stresses was systematically explored using the finite element model. Analyses were conducted assuming elastic properties of the wrap in the radial and axial directions to be 5%, 10%, and 20% of the properties in the circumferential directions. The maximum difference in maximum stress values observed was less than 2%. Thus, determining the orthotropic elastic properties of the wrap was only of marginal value.
- The effects of varying wire pre tension load from 17.8–35.6 N (4–8 lb) on the maximum stress in the liner wall was investigated using the finite element model. It was shown that increasing the wire pretension load did not significantly affect the maximum wall stress on the inside surface of the liner.
- The effect of extending the wrap further toward the dome region of the liner was explored. In the baseline analysis, the wire wrap is assumed to begin at approximately 25.4 mm (1 in) from the start of the dome region. Extending the wrap to the transition point leads to a stress reduction of approximately 11%. Moving the wrap from the baseline case to a point on the head provides a stress reduction of approximately 20%. It is therefore beneficial to extend the steel wrap as far as possible in the direction of the dome. Further reductions in maximum stress are possible by reinforcing a portion of the dome with carbon fiber composite.
- The effect of varying yield strength of the liner material on the peak stresses in critical locations of the cylinder was explored. It was shown that reducing yield strength of the liner material was the most effective means of reducing the stress in the critical region. Liner material with a

lower yield strength allows for a lowering the autofrettage pressure. The peak stress was shown to be reduced by 45%. The stresses in the dome region are not affected because the dome does not have a wrap around it.

Effect of Hydrogen on the Fatigue Crack Growth Rate Behavior in the Liner Material: Sandia National Laboratory data on the effect of hydrogen on the fatigue crack growth rate (FCGR) behavior of ASME SA372 Grade J Class 70 steels used in the liner shows a significant acceleration of the crack growth rates relative to the rates in benign environment [1-3]. However, this data is only for load ratios, R, between 0.1 and 0.5. Wiretough's wire-wrapped and autofrettaged cylinder design places the liner wall into compression when there is no pressure. Thus, service loading conditions consist of negative load ratios and fatigue crack growth rate data are needed for negative load ratios. Wiretough designed and verified a single-edge-notch-tension geometry specimen to obtain this data. The hydrogen pressure during these tests was approximately 10 MPa and the tests were performed at room temperature in accordance with the latest version of American Society for Testing and Materials (ASTM) Standard E647: Standard Method for Fatigue Crack Growth Testing. The FCGR behavior for $-1.0 \leq R \leq 0.2$ is shown in Figure 1. The constants in the regression fits, Equation 1, for the various trends are also given in Figure 1.

$$\frac{da}{dN} = C(\Delta K)^m \qquad \text{Equation 1.}$$

Where, C and m are constants that are derived from regression of the da/dN versus ΔK data in the hydrogen environment. The ΔK for the negative load ratios of -1 and -0.5 are based only on the positive K portion of the loading cycle since K is defined only for crack opening conditions. Values of C in Equation 1 are listed for the mean trend and the upper bound of the 95% confidence interval. For comparison, the values of C and m are also listed for air environment from ASME Section VIII Division 3 Article KD-4 [4].

Tests were performed under constant ΔK conditions to explore the effects of cyclic frequencies between 0.001 Hz and 6 Hz on the FCGR behavior in hydrogen. There appear to be no systematic effects of frequency, and the tests at 1 Hz appear to provide representative conditions for assessing crack growth behavior of the liner materials at all frequencies. Similarly, the differences between the FCGR behavior in hydrogen pressures of 10 MPa and 100 MPa were addressed using literature data at R values of 0.1 and 0.2 and the behavior was found to be comparable. This is consistent with the observations in the literature in that no significant trends related to loading frequency and hydrogen pressure are found for several high strength low alloy steels [2] especially

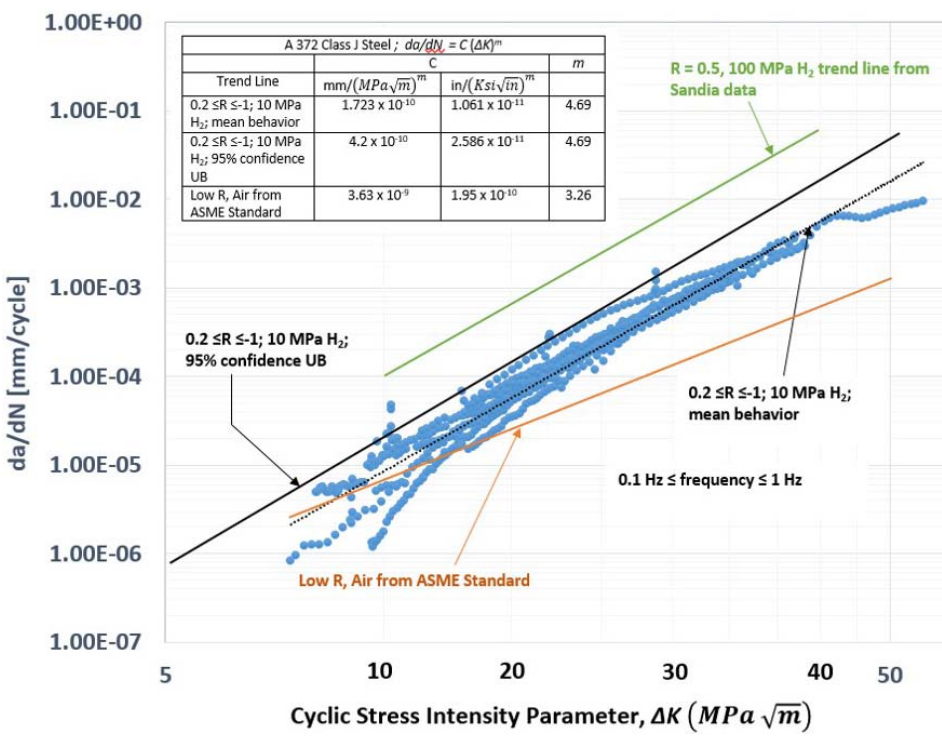

FIGURE 1. Fatigue crack growth rate data in hydrogen at a pressure of 10 MPa for load ratios between -1.0 and 0.2. The trend line labeled Sandia data was taken from Somerday et al. [2]. The air trend line from ASME KD-4 [4].

at low R values and in the ΔK range of 8–25 MPa(m)$^{1/2}$. In fact, the behavior in hydrogen and in air seems to converge near ΔK values of 10 MPa(m)$^{1/2}$ and lower.

Design Life Estimation: The above data were used in a crack growth calculation to estimate design lives of wire wrapped hydrogen storage cylinders containing SA 372 Grade J steel liners that were 406 mm (16 in) outside diameter with a wall thickness of 31.75 mm (1.25 in). The method of calculation followed the procedure outlined in ASME Section VIII, Division 3 article KD-10 [5]. The initial flaw sizes assumed for the calculations were (i) based on the currently used nondestructive testing capability that is said to reliably detect flaws that have a depth of 3% of the wall thickness or greater and (ii) based on recent work performed by Wiretough Cylinders in collaboration with its suppliers of liners that showed that cracks that are 2% of the wall thickness or greater can also be reliably detected. The initial flaw length on the surface (2c) is taken as three times the depth, a. The final crack size is assumed to be 0.25 of the wall thickness because of the high toughness of the steel used in the liners. The K-expressions for these calculations were from Newman and Raju [6,7]. For a stress level of 310 MPa (45 ksi), design lives of 30,000 and 21,000 cycles were estimated for initial flaw sizes of 0.03 and 0.02 of the wall thickness, respectively. These cycles are sufficient for the design life of 30 yr at 2 cycles/d.

Reinforcement of the Cylinder to Dome Transition Region Using Carbon Fiber Composite: The process development for wrapping the cylinder to dome transition region of the cylinder with carbon fiber composite was completed. The liners were first wrapped with 48 layers of wire starting 25.4 mm from the transition zone between the cylinder and hemisphere. Six layers of wire were each stepped back from the transition zone by 3 mm per step. Each step of wire consisted of six layers for total a total of 48 layers of wire. Next, approximately 6.25 mm wide carbon fiber ribbons were wrapped on two of the ends to approximately 16 mm thickness. Each layer of the carbon wrap was started at the beginning of the transition region and extended to 38 mm beyond the hemisphere boundary for the first six passes. This was done at 13.35 N (3 lb) tension for the first six layers. To prevent the carbon tape from slipping, a very light spray of "77" adhesive was used on the bare cylinder and on consecutive six pass layers. Each six layer assembly was stepped toward the transition zone 1 mm and wrapped at only 4.45 N (1 lb) tension in order to reduce slippage of the layers underneath. Figure 2 shows a successful carbon fiber wrapped cylinder.

ASME Certification of the Wiretough Pressure Vessel Design: Structural Integrity Associates conducted an analysis of a 406 mm (16 in) outside diameter cylinder with a wall thickness of 8.8 mm (0.346 in) and a length of approximately 1,981 mm (78 in). The wire wrap consisted of a flat wire currently approved by ASTM with a tension of about 20 N (4.5 lb). These results were incorporated by Structural Integrity Associates in the code case application. After a review of the stress analysis of the structure, manufacturing process, and inspection standards conducted by an ASME Team, ASME U3 Stamp was granted on March 9, 2016. Approval was gained under ASME's Boiler and Pressure Vessel Code Section VIII- Division 3 for a liner outer diameter of 406 mm (16 in) and liner length ranging from 7.7 m to 9.2 m (25 ft to 30 ft) with a capacity of 700+ L. Both round and flat wires using SA905, Class 1 minimum ultimate tensile strength = 2.04 GPa (296 ksi), minimum yield = 1.8 GPa (260 ksi) wires with specified pretension are admissible, and the allowable maximum pressures are in the range of 69.9 MPa to 103.4 MPa (10,000 psi to 15,000 psi). The certification applies to pressure vessels for ground storage of gases such as compressed natural gas, hydrogen, air etc. This authorization opens the door for self-certifications of future designs based on rules specified by ASME Section VIII-Division 3 Article KD-10.

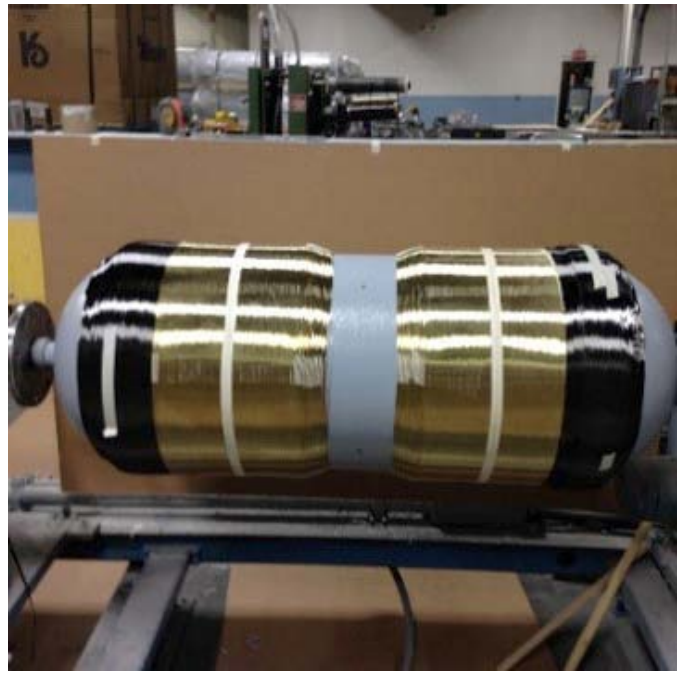

FIGURE 2. Carbon fiber wrap over transition areas of the cylinder

CONCLUSIONS AND FUTURE DIRECTIONS

- The results produced during FY 2016 on this project appear promising for meeting the targets set by DOE as scheduled. All major milestones for Budget Period 2 are on target.
- Finite element model analysis to optimize transition region design will be further fine-tuned.
- Complete FCGR testing in hydrogen environment and document the results in the form of a report.

- ASME KD-3 and KD-10 analysis of the 9.5 m long cylinder will be completed in support of the self-certification of Wiretough's design.
- Explore yield strength and ultimate tensile strength reduction of liner material for reducing autofrettage pressures and peak stresses.
- Complete the development of nondestructive evaluation criteria for liners based on initial crack sizes to be 2% of the wall thickness.
- Testing of wires in hydrogen environment to be completed by Oak Ridge National Laboratory.
- 9.5 m long (750 L) cylinders will be produced and wire wound to demonstrate the manufacturing processes and cost estimates.

SPECIAL RECOGNITIONS & AWARDS/ PATENTS ISSUED

1. A. Prakash, G.R. Sharp, B.T. Deeken, W.J. Head, W.H. Thomson, "Steel Wrapped Pressure Vessel," U.S. Patent 9,266,642B2, Issue date February 23, 2016.

FY 2015 PUBLICATIONS/PRESENTATIONS

1. A. Prakash and A. Saxena, "Low Cost Hydrogen Storage at 875 Bar Using Steel Liner and Steel Wire Wrap," DOE Hydrogen and Fuel Cells Program Annual Merit Review, Washington, D.C., June 6–10, 2016.

2. A. Saxena, A. Prakash, K.A. Nibur, I. Miller, "Considerations of the Effects of H_2 in Design of Type II Storage Vessels Built for Fatigue Resistance," Paper accepted for presentation at the 2016 International Hydrogen Conference, Jackson Hole, WY, September 11–14, 2016.

REFERENCES

1. B.P. Somerday, K.A. Nibur, C. San Marchi, "Measurement of Fatigue Crack Growth Rates for Steels in Hydrogen Containment Components," Unpublished data reproduced with permission.

2. B.P. Somerday, C. San Marchi, Kevin Nibur, "Measurement of Fatigue Crack Growth Rates for SA372-Gr J Steel in 100 MPa Hydrogen Gas Following Article KD-10," Proceedings of the ASME 2013 Pressure Vessels and Piping Conference, PVP 2013, July 14–18, 2013, Paris, France. Reproduced with permission.

3. K.A. Nibur, B.P. Somerday, C. San Marchi, J.W. Foulk, M. Dadafarnia, P. Sofronis, Met Trans., Vol. 44A, 2013, pp. 248–269; reproduced with permission.

4. ASME Section VIII Division 3, Article KD-4, PVP Code, Fracture Mechanics Evaluation, ASME, 2013.

5. Rana, M.D., Rawls, G.B., Sims, J.R., Upitis, E., "Technical Basis and Application of New Rules on Fracture Control of High Pressure Hydrogen Vessel in ASME Section VIII Division 3, PVP 2007–2603, 2007, ASME PVP Conference, July 22–26, San Antonio, TX.

6. Newman, J.C. and Raju, I.S., "Stress-Intensity Factors for Internal Surface Cracks in Cylindrical Pressure Vessels," Transactions of the ASME, Vol. 102, 1980, pp 342–346.

7. Raju, I.S. and. Newman, J.C., "Stress-Intensity Factors for Internal and External Surface Cracks in Cylindrical Vessels," Journal of Pressure Vessel Technology, Vol. 104, 1982, pp 293–298.

III.7 Compressor-Less Hydrogen Refueling Station Using Thermal Compression

Kenneth Kriha (GTI) (Primary Contact), Guillaume Petitpas (Lawrence Livermore National Laboratory), Zhili Feng (Oak Ridge National Laboratory), Yanli Wang (Oak Ridge National Laboratory), Herie Soto (Shell)

Gas Technology Institute (GTI)
1700 S Mt Prospect Rd.
DesPlaines, IL 60018
Phone: (847) 768-0871
Email: kenneth.kriha@gastechnology.org

DOE Manager: Erika Gupta
Phone: (202) 586-3152
Email: Erika.Gupta@ee.doe.gov

Contract Number: DE-EE0006966

Project Start Date: August 3, 2015
Project End Date: August 3, 2017

Overall Objectives

- Demonstrate the technical and economic feasibility of the thermal compression concept for compressor-less hydrogen refueling stations.
- Quantify the total station costs, both capital and operating, to determine if a thermal compression station can achieve a hydrogen levelized cost reduction of 15% when compared to a conventional liquid hydrogen (LH2) refueling station.

Fiscal Year (FY) 2016 Objectives

- Develop a transient simulation model to capture the thermodynamics of the thermal compression station.
- Optimize a preliminary full scale station design using outputs from the transient simulation model.
- Research and determine the most cost-effective high pressure cryogenic vessel (HPCV) design suitable for use in the thermal compression station.

Technical Barriers

This project addresses the following technical barriers from the Hydrogen Delivery section of the Fuel Cell Technologies Office Multi-Year Research, Development, and Demonstration Plan.

(A) Lack of Hydrogen/Carrier and Infrastructure Options Analysis

(B) Reliability and Costs of Gaseous Hydrogen Compression

Technical Targets

This project is a feasibility study which will identify the potential advantages of a thermal compression station versus a conventional LH2 refueling station. Because this station will not use a hydrogen compressor, this project addresses all of the DOE targets for small compressors specifically:

- Availability: >90%
- Uninstalled Capital Costs: $170,000
- Annual Maintenance: 2%

The thermal compression station will not require refrigeration equipment upstream of the gas dispenser, so this project will also address refrigeration equipment target:

- Uninstalled Capital Cost: $70,000

FY 2016 Accomplishments

- Completed a transient thermodynamic model capturing the physics of the thermal compression fueling station.
- Showed how the model could be used to optimize the size and quantity of HPCVs required for a 400 kg/d station.
- Showed how the model could be used to analyze the effects of eleven physical and operational station variables to study their impact on the amount of hydrogen boil-off losses that occur during the process.
- Developed a process flow diagram showing the major equipment needed for a 400 kg/d thermal compression station.
- Initiated research into the type of materials and designs of HPCVs suitable for the thermal compression cycles.

✧ ✧ ✧ ✧ ✧

INTRODUCTION

The thermal compression refueling station concept utilizes the thermomechanical exergy of LH2 to create the

pressure necessary for 700 bar dispensing. In this station, LH2 delivered to onsite LH2 dewars will be used to fill custom designed HPCVs. The liquid hydrogen will then be heated at constant volume allowing the pressure to build within the HPCV to the necessary 800–900 bar dispensing pressure. A thermal compression refueling station utilizing a series of HPCVs will be designed and optimized to satisfy the hydrogen fueling demand of a mid-sized refueling station (400 kg/d).

The goal of this project is to assess the technical and economic feasibility of thermal compression for cost effective high-pressure (700 bar) hydrogen refueling stations. This concept has the potential to reduce fueling station costs by eliminating expensive and maintenance-prone compressors. The target station size for this project is 400 kg/d, and with this size station, 15% reductions in capital and operational costs (hydrogen levelized) when compared to traditional LH2 refueling stations are to be demonstrated.

APPROACH

The approach that will be used to demonstrate this conceptual station consists of two major steps. The first step is to optimize the design of the station in terms of equipment and utilization of the LH2 delivered to the station. This step is achieved by developing a rigorous transient thermodynamic model of the station that allows multiple physical and operational variables to be investigated for their impact on station design. The model will be used to optimize the size and quantity of HPCVs and identify station parameters that will minimize the hydrogen boil-off that occurs during the process. The second step of the approach is to evaluate the design options for the HPCVs. A study is being conducted of existing pressure vessel designs as well as some innovative alternatives. This study will conclude with a list of potential HPCV designs which will be evaluated for economic impact on the station.

The thermodynamic modeling and the HPCV evaluation will define the major equipment needed for a thermal compression station. This station design will be compared to a traditional LH2 refueling station using Argonne National Laboratory's Hydrogen Delivery Scenario Analysis Model assumptions and economic analysis. If the thermal compression station shows a 15% reduction in hydrogen levelized cost, the project can move forward to the next phase. The second phase of the project will be to build a small scale test loop to demonstrate key aspects of the thermal compression process, such as pressurization and dispensing rates.

RESULTS

In May of 2016 the thermodynamic simulation modeling of the thermal compression station was completed. Two Fortran subroutines were written. The first subroutine modeled the operation of the fueling station in order to determine how many HPCVs are needed to satisfy station demand. Inputs to the subroutine include variables such as vehicle fueling profile, vehicle capacity, number of dispenser hoses in use, and HPCV volume. The charts in Figure 1 show how the model can be used to investigate the influence of station variables on the required number of HPCVs. The results shown in Figure 1 are for a Type III vessel with an aluminum liner and carbon fiber wrapping. Note that this analysis will be repeated and refined later in the project when a better understanding of the HPCV design is achieved. A material cost can be applied to each cylinder volume. Chart A of Figure 1 shows a relationship between the overall cost of HPCV materials for the station versus the HPCV volume. This type of analysis lead to the conclusion that a larger quantity of smaller HPCVs would be more cost effective that fewer larger HPCVs.

The second thermodynamic simulation subroutine focused on quantifying the amount of hydrogen boil-off that occurs during the thermal compression process. The thermal compression process involves the transfer of LH2 to the HPCVs and recycling of gaseous hydrogen from the HPCVs back to the LH2 dewar. The boil-off subroutine was used to investigate eleven key station variables to determine how these variables influence the amount of hydrogen that is stranded during the hydrogen transfers. Thousands of model runs were conducted in order to try to identify which variables have the largest impact on the amount of hydrogen vented. The results of the modeling were quite scattered and machine learning techniques such as Sobol indices were used to help understand sensitivities.

This second subroutine was also used to investigate the overall process flow, especially the recycling of hydrogen back to the LH2 dewar from the HPCVs. The model was run to determine the differences between returning the hydrogen to the top or bottom of the dewar. Figure 2 shows that bottom return is the preferred location because top return results in excessively high LH2 dewar pressures. The subroutine was then used to analyze the thermal flows in the process. As a result, the thermal compression process steps were re-evaluated and two new flow strategies were conceived to minimize the amount of hydrogen losses. The first strategy, "topping off," uses warm stranded gas in one of the HPCV vessels to pressure equalize with a vessel that has just been filled with LH2. The second strategy, "pre-cooling," utilizes the cold gas that is a product of flashing LH2 during the HPCV filling process to pre-cool the next vessel in line to be filled with LH2. The boil-off subroutine was modified to incorporate bottom return and these two new process steps and the impact on the reduction in boil-off was significantly improved as can be seen in Table 1.

A mid-sized, 400 kg/d, station capacity was targeted for a detailed design. Other station parameters such as

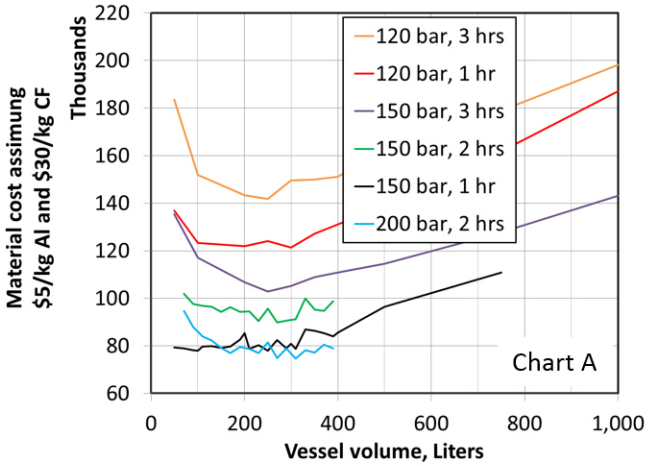

- "**Smaller & more vessels**" designs reduce material cost, by enabling more refilling/emptying cycles per vessel
- Optimal : ~200-400 Liters, ~20-40 vessels

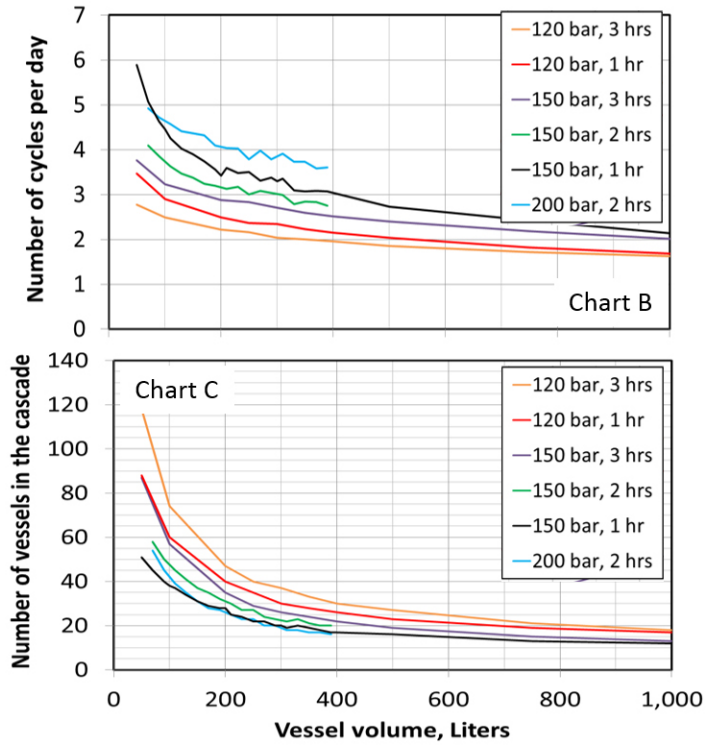

FIGURE 1. Influence of switch pressure, time off-line and vessel volume on overall material cost, number of cycles per vessel and number of vessels in the cascade, assuming a Type III pressure vessel design

Top return:
- Very important pressure rise
- BUT lowest liquid temperature (20 K) , thus higher density, thus colder vessel in filling step, thus virtually no boil-off during filling of HPCVs
- Recycle step sensitive

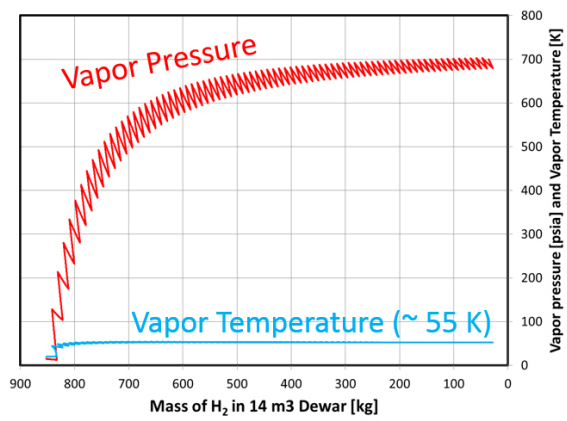

Bottom return:
- Moderate pressure rise (<100 psi), low pressure at low mass in Dewar
- BUT higher liquid temperature, thus more boil-off during HPCV filling
- HPCV filling step sensitive

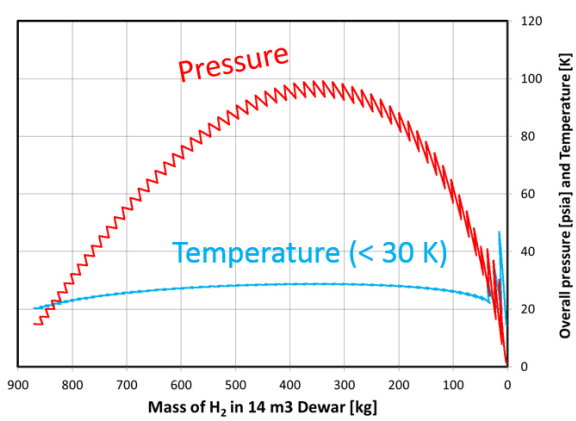

FIGURE 2. Pressures and temperature in LH2 dewar for top versus bottom return

TABLE 1. Impact of Pre-Cooling and Topping-Off on Total Hydrogen Boil-Off, Assuming LH2 Initially at 20.3 K in the Dewar and 110 bar Switch Pressure

Case #	Initial LH2 in Dewar (kg)	Dewar Volume (m^3)	Topping-Off	Pre-Cooling	Extra Cooling During Filling	Max Dewar Pressure (psia)	Boil-Off Total (% of kg delivered)
1	900	14	No	No	No	100	77
2	900	14	Yes	No	No	87	44
3	900	14	Yes	Yes	No	100	20
4	900	14	Yes	Yes	Yes	105	11
5	900	20	Yes	Yes	Yes	85	9
6	900	25	Yes	Yes	Yes	75	8.5
7	600	14	Yes	Yes	Yes	85	9
8	400	14	Yes	Yes	Yes	67	7.5

fueling profile, number of dispenser hoses, and the amount of hydrogen delivered to each vehicle were also locked in as station constants. Using these inputs and some known properties of Type III vessels, the model determined that 20–30 HPCVs with a volume of 200–300 L would likely be a near-optimum station design. The final station design is dependent on the HPCV design study, so these results will be refined at the completion of that study. A preliminary process flow diagram has been created assuming a station size of 30 HPCV of 250 L internal volume. A snapshot of this drawing is shown in Figure 3. The equipment identified in this drawing will be accounted for in the economic analysis of the thermal compression station.

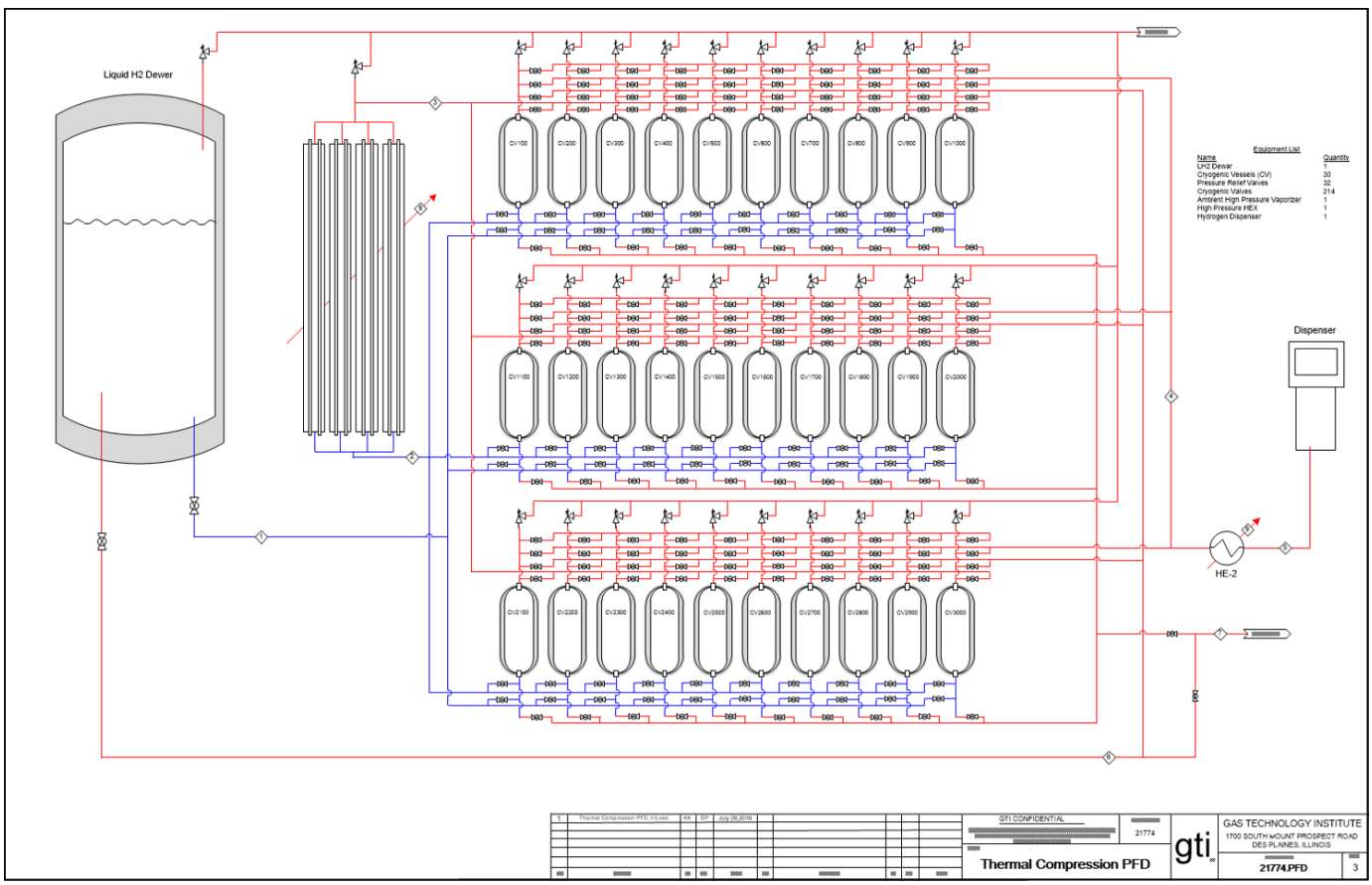

FIGURE 3. Preliminary process flow diagram of the thermal compression fueling station concept

The evaluation of HPCVs is due to be completed in early November of 2016. The HPCV must be able to withstand the following cycle conditions:

1 bar @ 20 K → 900 bar @ 160 K (3–5 cycles per day)

To date most of the research has been focused on Type I, all metal, pressure vessels. Type I vessels can be designed and fabricated according to the American Society of Mechanical Engineers code rules. While there is cryogenic data and hydrogen compatibility data available for some common metals, such as stainless steel 316, data is very limited for less popular metals that may have a cost advantage over stainless steel. Lower cost metals as well as other pressure vessel types will continue to be evaluated with the understanding that additional testing will be required to collect necessary data on the performance of these materials at the thermal compression cycle conditions.

CONCLUSIONS AND FUTURE DIRECTIONS

Based on the work conducted throughout the year several conclusions can be drawn.

- The thermodynamic simulation modeling of the thermal compression station has proven to be a useful tool both in providing input for station design as well as identifying processes steps that required improvements in order to make this concept viable.
- Modeling work shows that a larger number of smaller vessels has economic advantages over a smaller number of larger cylinders.
- The larger number of cylinders and the need for pre-cooling and top-off steps has increased the complexity of the station. The station's valve count has increased which will have a greater impact on the overall station cost than originally expected.
- The availability of HPCVs suitable for the extreme temperature and pressure is very limited.

Future Work includes:

- Completion of HPCV evaluation.
- Economic comparison between thermal compression station and conventional LH2 station.
- Small scale demonstration if a 15% cost reduction for thermal compression station over conventional station can be shown.

SPECIAL RECOGNITIONS & AWARDS/ PATENTS ISSUED

1. Copyright for Thermal Compression Station Simulation (TCSS). Version 1.0 issued 04/20/2014, limited distribution, OCEC-16-064, LLNL-CODE-689637.

III.8 Advanced Barrier Coatings for Harsh Environments

W. Shannan O'Shaughnessy (Primary Contact), Scott Morrison
GVD Corporation
45 Spinelli Place
Cambridge, MA 02138
Phone: (617) 661-0060
Email: soshaughnessy@gvdcorp.com

DOE Manager: Erika Gupta
Phone: (202) 586-3152
Email: Erika.Gupta@ee.doe.gov

Contract Number: DE0SC0011339

Project Start Date: April 4, 2015
Project End Date: April 5, 2017

Overall Objectives

- Optimize polymeric and inorganic layers using initiated chemical vapor deposition (iCVD) and plasma enhanced chemical vapor deposition (PECVD) processes.
- Demonstrate a 10-fold reduction in hydrogen permeation through coated elastomeric substrates.
- Develop a low-friction top coat of polytetrafluoroethylene (PTFE) for friction wear reduction of plastic piston-head seals.
- Demonstrate improved seal life in field testing by a hydrogen compressor end user.
- Develop a coating system to provide conformal seal coatings at reasonable cost.

Fiscal Year (FY) 2016 Objectives

- Optimize polymeric and inorganic layers using iCVD and PECVD processes.
- Select lubricious coating parameters to maximize dynamic seal wear reduction.
- Demonstrate a 10-fold reduction in hydrogen permeation through coated elastomeric substrates.
- Initiate field testing of GVD coatings in hydrogen compression systems.

Technical Barriers

This project addresses the following technical barriers from the Hydrogen Delivery section of the Fuel Cell Technologies Office Multi-Year Research, Development, and Demonstration Plan.

(B) Reliability and Costs of Gaseous Hydrogen Compression

Technical Targets

This project is conducting fundamental studies of coatings to improve seal life for hydrogen compressor systems. Insights gained from these studies will be applied toward the design and manufacture of coatings applied to seals used in hydrogen delivery systems to help meet the following FY 2020 DOE targets.

- Annual Maintenance: 4% of installed capital cost
- Losses: 0.5% of H_2 throughput
- Small Compressor Lifetime: 10 years

FY 2016 Accomplishments

- Designed and optimized a barrier coating deposition system for scalability to enable high throughput and reduced cost of coating application in commercial production.
- Validated optimal barrier coating properties through chemical analysis, adhesion testing and acetone soak testing.
- Initiated head-to-head compressor seal trials using a PTFE coated and uncoated seal, periodically evaluating wear via seal mass and effective compressor operation, to compare seal life improvement in a real-use environment.

✧ ✧ ✧ ✧ ✧

INTRODUCTION

A key cost driver in hydrogen compression systems is the frequent maintenance required to replace seals that fail in operation. Seals fail under a variety of conditions, but primary factors are hydrogen ingress and wear in the high pressure, high temperature dynamic operating environment. Seal failure is a major contributor to process downtime and is the largest cause of unscheduled maintenance, the cause of >25% of hydrogen leaks, and redundant compression is often specified to alleviate the issue.

GVD Corporation specializes in thin-film coatings applied using a low-temperature vapor deposition process. One of these films, a polysiloxane material branded Exilis which is currently used by GVD to provide corrosion protection and electrical insulation to circuit boards, was modified in a publication by GVD's founding laboratory at the Massachusetts Institute of Technology to act as a

vapor barrier. GVD identified a clear opportunity to use our expertise with Exilis and commercializing coating technology to pursue a solution to problems plaguing the hydrogen processing industry. This project has resulted in the commercial scale up and manufacture of a production system to deposit this effective barrier coating, previously only evaluated in an academic setting. In partnering with compressor manufacturers and seal designers, GVD will have real-operation data demonstrating improved seal-life which will reduce the annual maintenance costs for hydrogen compressor systems. The project targets an improvement in seal life from the current <1,500 hr to >8,000 hr (a 5X reduction in maintenance frequency) and enables reduced cost for hydrogen operation and delivery.

APPROACH

GVD's approach to improving seal life and reducing maintenance for hydrogen compression systems uses two types of coatings: a vapor barrier and a low friction coating. Initial evaluations validate and optimize these two coatings to provide the most effective solution for improving seal life. The barrier coating is optimized to reduce permeability of hydrogen into the elastomer seal; hydrogen ingress accelerates seal degradation and wear. The low friction coating is optimized to reduce the amount of wear seen in dynamic seal operation, extending the seal life.

Partnership with national laboratories, compressor manufacturers and seal manufacturers allow the development work performed by GVD to be tested in laboratory environments that closely mimic the real world as well as field testing in systems used for production, resulting in meaningful data that demonstrates improved seal life. Hydrogen permeation tests are performed comparing a barrier coated elastomer and an uncoated elastomer made of seal materials typically used in hydrogen compression systems. The best performing barrier coatings are optimized in a scaled coating system developed during this project. Seal wear testing of the low friction coating was initially evaluated using tribometry to identify a coating with optimal lubricious properties. The best performing low friction coating is then tested in a production environment against an uncoated seal, using dynamic seal mass loss as an indicator of reduced wear in operation.

RESULTS

The first phase of this project was to optimize the polymeric and inorganic layers of the barrier coating by changing from an alternating deposition process between iCVD and PECVD to have both layers deposited via plasma-iCVD for increased throughput and processing simplification. GVD developed an alternative plasma-based process for depositing the Exilis polymeric layers. This development was carried out in GVD's iMax system, using a purpose-built radio frequency electrode assembly. Prior plasma deposition was performed using the same hot-filament arrangement used for iCVD of Exilis. Using a hot-filament arrangement is not ideal, since the generated plasma tends to be non-uniform and on both sides of the assembly, resulting in excessive deposition elsewhere in the chamber.

Initial development work focused on choosing the optimal deposition pressure and flow rates for the film precursors as well as radio frequency input power. GVD identified an organic layer deposited by plasma-iCVD with nearly identical chemical structure to the organic layer deposited by iCVD. Optimization of the plasma-iCVD organic layer resulted in:

- Improved coating uniformity, +/-10% over a 10 in by 10 in area.
- Faster growth rates, 25 nm/min, a 4–5X increase over iCVD
- Reduced precursor use, 18 times less compared to iCVD

These improvements will aid in throughput and cost reduction for commercial production. Optimized plasma-iCVD coatings were evaluated for adhesion (Figure 1) and flexibility, with the best performing coating used for vapor permeation testing.

GVD is testing hydrogen permeation with Oak Ridge National Laboratory. Testing methods resulted in damage to the coating on the elastomer material; data showed a permeability of 1.33×10^{-11} mol-m/(m^2-s-Pa) which resulted in only a 5% reduction in hydrogen permeability at 3 µm of coating thickness versus an uncoated substrate. This contrasted starkly with the helium permeability GVD measured on undamaged samples of 5.23×10^{-13} mol-m/(m^2-s-Pa), which would have resulted in a 70–90% reduction at 3 µm of coating thickness. GVD is working with Oak Ridge National Laboratory to optimize

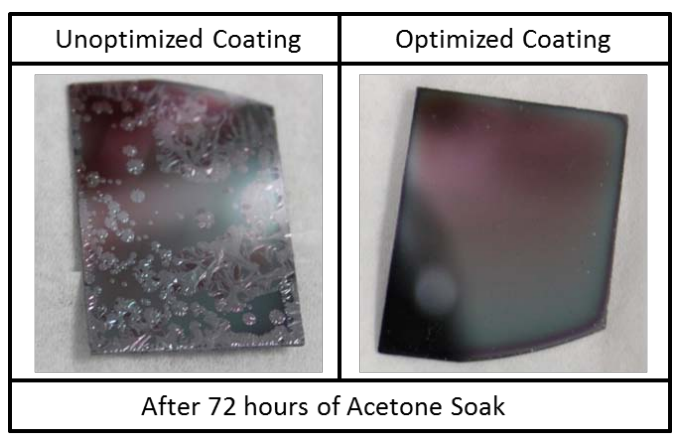

FIGURE 1. Comparison of plasma-iCVD coatings before and after optimization

the testing method to reduce damage to the coating prior to testing and further optimize the barrier coating for rugged use.

GVD has developed a lubricious PTFE coating that is undergoing field testing with a PowerTech, an industrial user of Hydro-Pac's hydrogen compression systems. The PTFE coating was selected after yielding satisfactory results during tribological testing. The lifetime of the seals will be compared to uncoated seals installed simultaneously in a double-ended single stage hydrogen compressor with an inlet pressure of 5,000 psi and hydrogen compression pressure of 13,500 psi. Mass measurements are periodically taken to demonstrate wear between 50 hr and 200 hr of use, at 500 hr, then after failure. Approximately 100 hr of use has been achieved thus far; testing is in too early a stage to expect any meaningful difference between coated and uncoated seals.

GVD has completed the construction of a low-volume scaled system for plasma-iCVD. This system is adapted from an existing system which had been used as a high-vacuum oven. Figure 2 shows the system after removing the high-vacuum components (diffusion pump, ion gauge, etc.). The chamber is a cylinder, and has a deposition zone of approximately 35 in by 18 in. This new deposition chamber has been dubbed Omega.

FIGURE 2. Original system

The system's gas distribution was designed using fluid flow simulation in SolidWorks. A simple inlet tube without any diffusion would result in vortices and regions of stagnation, particularly near the door of the chamber (Figure 3). Several different types of gas distributors were designed in SolidWorks and then tested in simulation. A gas distributor was finally settled on as a solution that is easier to manufacture while still resulting in good laminar flow in the chamber (Figure 4).

CONCLUSIONS AND FUTURE DIRECTIONS

GVD has demonstrated the scalability of the technology by:

- Transitioning from a two-system deposition process to a single-system deposition process, including validation of coatings.
- Designing, building and validating a production coating system.

GVD has demonstrated the efficacy of the coating to improve seal life by:

- Optimizing low friction coatings for use in high temperature high pressure hydrogen compressor use environments.

Future work includes:

- Characterize hydrogen permeability of the barrier coating with a revised test method at Oak Ridge National Laboratory.
- Continue to generate wear and seal-life data with the low-friction coating.
- Design a plasma tumble-coating process for the production system.

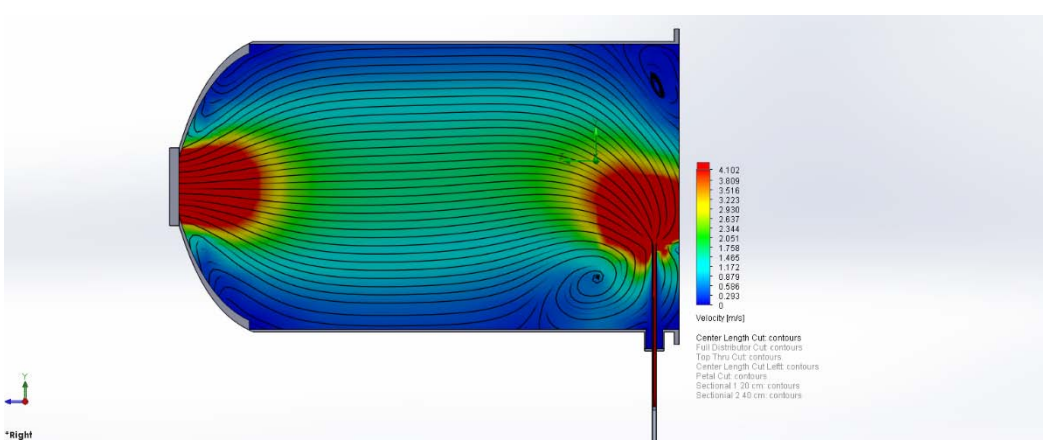

FIGURE 3. Gas flow simulation in Omega system, no gas distribution

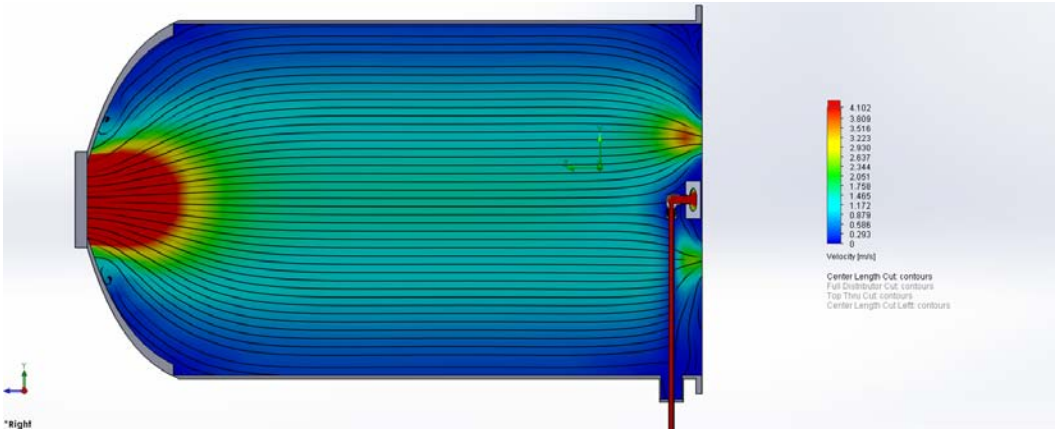

FIGURE 4. Gas flow simulation in Omega system with selected gas distributor

FY 2016 PUBLICATIONS/PRESENTATIONS

1. W. O'Shaughnessy, "Advanced Barrier Coatings for Harsh Environments," 2016 Hydrogen and Fuel Cells Program Annual Merit Review. Presentation.

III.9 Improved Hydrogen Liquefaction through Heisenberg Vortex Separation of Para- and Orthohydrogen

Chris Ainscough (NREL) (Primary Contact),
Jake Leachman (WSU)
National Renewable Energy Laboratory (NREL)
15013 Denver West Parkway
Golden, CO 80401-3305
Phone: (720)-431-7296
Email: Chris.Ainscough@nrel.gov

DOE Manager: Neha Rustagi
Phone: (202) 586-8424
Email: Neha.Rustagi@ee.doe.gov

Technical Advisor: Joe Schwartz
Email: Joe.Schwartz@praxair.com

Subcontractor:
Washington State University (WSU), Pullman, WA.

Project Start Date: November 11, 2015
Project End Date: September 30, 2018

Overall Objectives

- Increase liquefaction cycle efficiency from figure of merit (FOM) 0.35 to > 0.5.
- Lower liquefier installed capital cost (~$2.5M/metric tonne per day [MTPD])/unit capacity (30 MTPD).
- Lower cost of liquid hydrogen delivery toward the DOE target of $2/gge.

Fiscal Year (FY) 2016 Objectives

- Complete the first house of quality in a quality function deployment analysis of the vortex tube and the liquefaction cycle which will contain it. Identify three critical-to-quality metrics.
- Determine pressure–volume–temperature–x measurements of cryogenic helium–hydrogen–neon mixtures focusing on gas dissolved in liquid and at high pressure (<200 bar). Prepare a review of available measurements and needs for cycle design.
- Analysis of vortex performance through experiments and numerical (first order and computational fluid dynamics [CFD]) analysis. Develop device and cycle design house of quality matrices.
- Go/No-Go: While flowing <500 gm/h of hydrogen to a vortex tube, obtain thermal conductivity measurements and calculations showing endothermic para/ortho conversion of 5% of a stream.
- Complete technoeconomic and thermodynamic analysis based on models and data developed in the project to date of a 5,000–30,000 kg/d liquefier. Compare to DOE goals of FOM 0.5, 12 kWh/kg H_2, and incumbent technologies.

Technical Barriers

This project addresses the following technical barriers from the Hydrogen Delivery section of the Fuel Cell Technologies Office Multi-Year Research, Development, and Demonstration Plan:

(H) High-Cost and Low Energy Efficiency of Hydrogen Liquefaction

Technical Targets

TABLE 1. DOE Targets for Small Scale (30 MTPD) Liquefaction

Characteristic	Units	DOE 2020 Targets	Project Status
Installed Capital Cost	$MM	70	TBD
Figure of Merit	Unitless	0.5	Modeling shows 0.5 is achievable

TBD – To be determined

FY 2016 Accomplishments

- Completed first house of quality, determining critical to quality metrics.
- Developed predictive first order and CFD models of vortex tubes at cryogenic temperatures with hydrogen.
- Completed first helium–hydrogen–neon liquid phase density measurements for refrigerant mixtures.
- Developed a steady state model of cycle performance and conducted energy analysis.

✧ ✧ ✧ ✧ ✧

INTRODUCTION

This project has dual aims: (1) improve the efficiency of hydrogen liquefaction to show a path to an FOM of 0.5, (2) enable the scale-down of liquefaction plants to capacities that can be optimally located to both utilize low cost hydrogen sources and minimize liquid delivery costs

to customers. The team will achieve this by addressing a fundamental reality of liquefaction—the ortho-para conversion of hydrogen spin isomers.

Efficient small-modular hydrogen liquefiers have not been developed due to the difficulty of refrigerating below 77 K. Below 77 K the largest entropy change of any material is orthohydrogen-parahydrogen conversion which is an exothermic reaction that significantly hinders liquefaction efficiencies. In this work we will develop a proof of concept small-modular hydrogen liquefaction system that uses vortex tubes to enable kinetic parahydrogen-orthohydrogen separation and conversion via vortex tubes. This approach allows for an endothermic parahydrogen-orthohydrogen reactions to be catalyzed, such that bulk cooling occurs before the orthohydrogen is separated and recycled in a liquid nitrogen bath. This scalable approach is anticipated to significantly increase the efficiency of small-modular hydrogen liquefiers, enabling their use with electrolysis and enabling low-cost liquid hydrogen to supply backup power and hydrogen fueling stations.

APPROACH

The team will develop and optimize the concept of vortex tube separation for para- and orthohydrogen. The vortex tube will not only separate the two allotropes of hydrogen, but will use para to ortho conversion within the device to drive bulk cooling.

First, WSU will optimize and then, at the bench scale, verify the operation of the vortex tube. Then, NREL and WSU will up-scale the device and build a proof-of-concept system around it. NREL will additionally develop both technoeconomic and liquefaction plant models to further optimize the system design and placement.

RESULTS

The team successfully measured and characterized the thermodynamic state of ternary helium, neon, hydrogen mixtures, and will develop the necessary equations of state. These equations of state will ultimately be implemented in the National Institute of Standards and Technology's Reference Fluid Thermodynamic and Transport Properties Database. See Table 1, which shows sample measurements of a binary system of neon and helium.

The team successfully completed development of first order models of vortex tube performance, using all available literature worldwide. The models show that vortex tubes should be able to perform better than Joule-Thompson throttles under nearly all operating conditions. See Figure 1.

The team successfully completed the first house of quality, identifying the para/ortho conversion rates and refrigerant mixture as critical to quality metrics. The team evaluated a number of vortex tube geometric parameters, which will be more fully explored using detailed CFD studies. See Figure 2.

The team created a steady-state thermodynamic model showing that the goal of FOM = 0.5 is achievable. See Figure 3. This model found an optimal design point at pressure ratio of 2.

TABLE 1. Sample Refrigerant Mixture Properties

PURE NEON				
Temperature	Pressure	Density	Ref. Density	
[K]	[PSI]	[kg/m^3]	[kg/m^3]	
31.2	50.4	1133.0	1130.4	
34.0	174.6	1076	1076.3	
38.0	238.8	976.4	975.92	
42.0	281.3	809.2	807.97	
Neon-Helium Mixtures				
Temperature	Pressure	Density	Neon	Helium
[K]	[PSI]	[kg/m^3]	(% Mole)	(% Mole)
32.0	69.1	1112	98.4	1.6
36.0	134.5	1012	97.8	2.2
33.0	285.0	1095	98.7	1.3
38.0	298.3	939.9	98.2	1.8

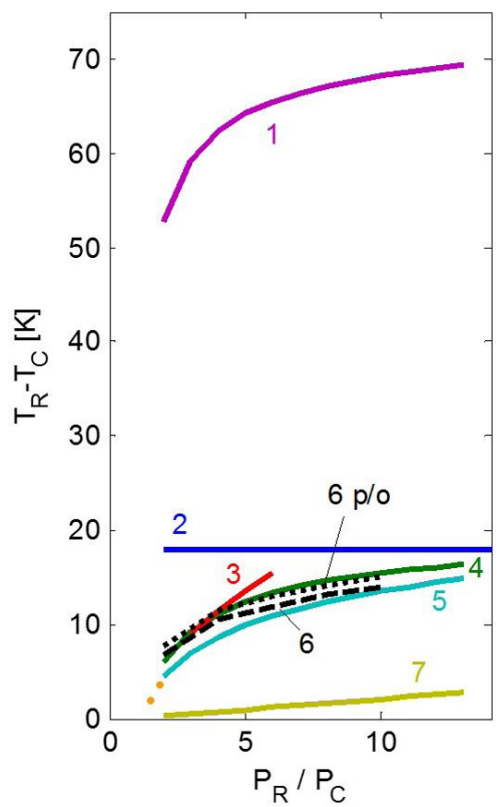

FIGURE 1. First order vortex tube model performance prediction

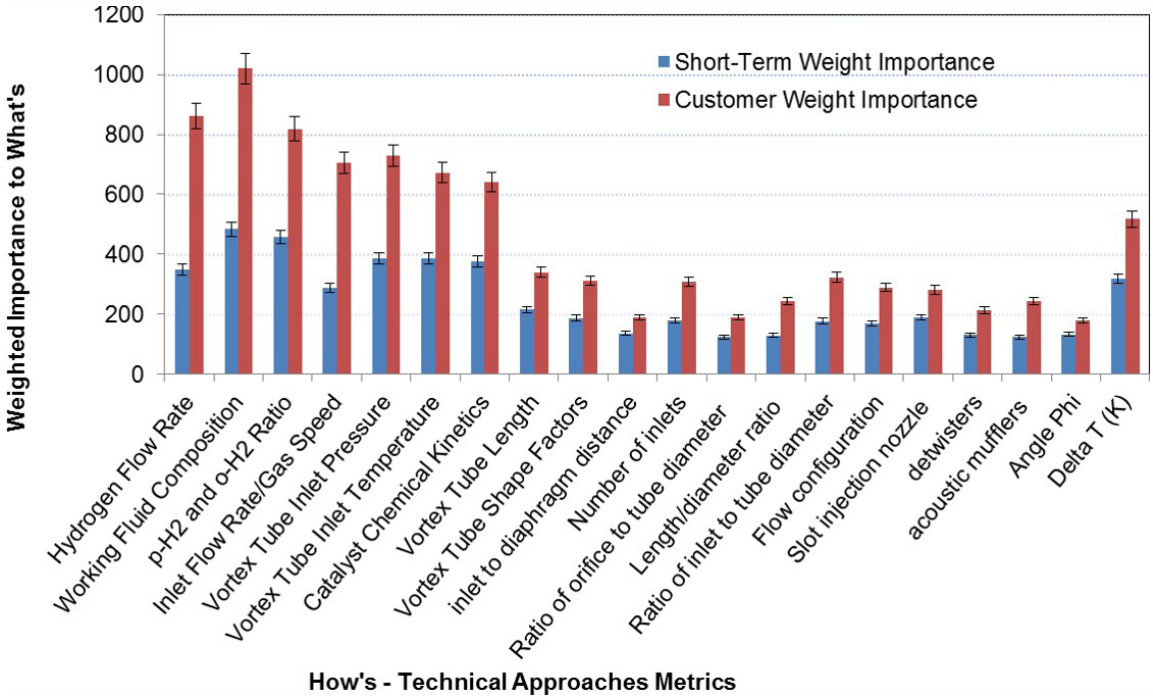

p-H2 – parahydrogen; o-H2 – orthohydrogen

FIGURE 2. First house of quality identifying critical to quality metrics

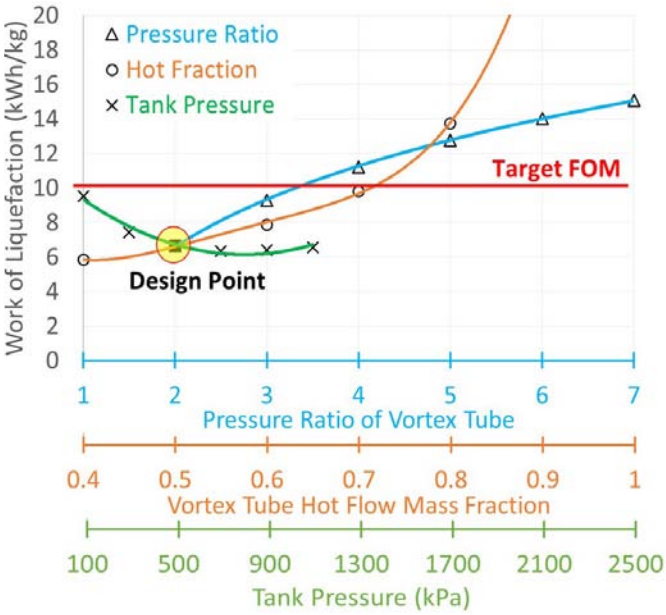

FIGURE 3. Thermodynamic model showing the feasibility of FOM = 0.5

CONCLUSIONS AND FUTURE DIRECTIONS

The team has the following go/no-go milestone to complete by September 30, 2016: while flowing <500 gm/h of hydrogen to a vortex tube, obtain thermal conductivity measurements and calculations showing endothermic para/ortho conversion of 5% of a stream. The team will also complete the first round of technoecoomic analysis by that time.

FY 2016 PUBLICATIONS/PRESENTATIONS

1. Ainscough, C., Leachman, J., *Improved Hydrogen Liquefaction through Heisenberg Vortex Separation of para and ortho-hydrogen,* Washington, DC: U.S. Department of Energy, 2016.

III.10 Magnetocaloric Hydrogen Liquefaction

Jamie Holladay (Primary Contact),
Kerry Meinhardt, Evgueni Polikarpov, and
Ed Thomsen, John Barclay, Jun Cui (PNNL/Ames Laboratory), Iver Anderson (Ames).
Pacific Northwest National Laboratory (PNNL)
P.O. Box 999, MS: K1-90
Richland, WA 99352
Phone: (509) 371-6692
Email: Jamie.Holladay@pnnl.gov

DOE Manager: Neha Rustagi
Phone: (202) 586-8424
Email: Neha.Rustagi@ee.doe.gov

Subcontractor:
Emerald Energy NW LLC, Redmond, WA

Project Start Date: October 1, 2015
Project End Date: September 30, 2018

Overall Objectives

- Quantify and incorporate novel configurations to achieve simpler, more efficient liquefier designs.
- Identify, characterize, and fabricate magnetic materials in shapes suitable for high-performance active magnetic regenerators (AMRs) from 280 K to 20 K.
- Fabricate and characterize improved multi-layer magnetocaloric regenerator performance.
- Design, fabricate, test, and demonstrate a lab-scale magnetocaloric hydrogen liquefier (MCHL) system.
- Demonstrate a lab-scale hydrogen liquefier with a figure of merit (FOM) increase from 0.3 up to 0.5.
- Perform techno-economic analysis on a proposed full-scale (30 tons per day) system.

Fiscal Year (FY) 2016 Objectives

- Complete characterization of first generation (GEN I) system for impact of bypass flow of heat transfer gas on improved engineering liquefier designs in second and third generations (GEN II and GEN III).
- Complete characterization of dual, multi-layer magnetic regenerators.
- Demonstrate gas liquefaction.
- Prepare and characterize candidate magnetocaloric materials for use in GEN II and GEN III system. This physical and thermomagnetic characterization is required to complete the system designs.
- Produce magnetocaloric spherical particles using the rotating disk atomizer. This requires upgrading the apparatus to be able to operate with rare earth materials.
- Finalize GEN II design and order parts.
- Refine the capital equipment cost estimates of a modular scale MCHL system.

Technical Barriers

This project addresses the following technical delivery barrier from the Hydrogen Delivery section (3.2) of the Fuel Cell Technologies Office Multi-Year Research, Development, and Demonstration Plan.

(H) High-Cost and Low Efficiency of Hydrogen Liquefaction

Technical Targets

Conventional hydrogen liquefiers at any scale have a maximum FOM of ~0.35 due primarily to the intrinsic difficulty of rapid, efficient compression of either hydrogen or helium working gases (depending on the liquefier design). The novel approach of this MCHL project uses solid magnetic working refrigerants cycled in and out of high magnetic fields to execute an efficient active magnetic regenerative liquefaction cycle that avoids the use of gas compressors. Numerical simulation modeling of high performance MCHL designs indicates certain achievable designs have promise to simultaneously lower installed capital costs per unit capacity and to increase thermodynamic efficiency from an FOM of ~0.35 toward 0.5–0.6. Results from experimental prototypes should support the design and deployment of hydrogen liquefier plants that meet the DOE hydrogen production and delivery targets.

- $70 million capital cost for a turnkey plant with a capacity of 30,000 kg H_2/d
- Operational efficiency of a complete liquefier plant of 75% as defined by DOE and commensurate with a liquefier FOM of approximately 0.5–0.6

FY 2016 Accomplishments

- Set a world record by demonstrating propane liquefaction. To our knowledge this is the first time a magnetocaloric system was used to liquefy a gas from room temperature.
- Demonstrated 25% increase in cooling power using bypass configuration with a layered regenerator.

- Reduced requirement for magnetocaloric materials in liquefaction system by up to 88% through the implementation of a bypass configuration that completely precools the process stream.
- Completed preliminary GEN II designs with rotating belt, rotating wheel, and reciprocating cylinder configurations.
- Projected cost of MCHL system to be $1.5M/t H_2/d. This is 36% less than current Claude cycle based systems and the DOE targets.
- Upgraded the rotating disk atomizer and demonstrated spherical particle production.
- Characterize magnetization vs. temperature for eight materials to be used in the GEN II system.

INTRODUCTION

MCHL technology promises cost effective and efficient hydrogen liquefaction because it eliminates gas compressors, the largest source of inefficiency in the traditional Claude cycle liquefiers, and the use of liquid nitrogen to precool the hydrogen. The Claude cycle liquefier is the current industrial choice for hydrogen liquefaction and uses a variety of configurations with processes where helium, hydrogen, or gas mixtures are coolants. In the case of hydrogen as the refrigerant gas and the process gas, the hydrogen feed to the process is first cooled by liquid nitrogen, and then further cooled in counter flow heat exchangers where the cooling power is provided by turbo expansion of a portion of the pre-cooled hydrogen stream. Liquefaction of the pre-cooled, high-pressure hydrogen stream is finally accomplished by throttling in a Joule-Thomson valve into a phase-separator collection vessel. Conventional liquefier technology for hydrogen is limited to an FOM of ~0.35 for a large facility, and of typically less than 0.3 for a smaller facility.

The MCHL initial design (GEN I) is an AMR system which uses regions of high or low magnetic field and reciprocating magnetocaloric materials to transfer heat between hot and cold thermal reservoirs. In one step of the AMR cycle the magnetic material in a high performance regenerator is adiabatically placed in a high magnetic field. The conservation of total entropy in this adiabatic process requires the magnetic refrigerants in the regenerators to increase in temperature to compensate for the increased magnetic order (lower entropy) among the material's magnetic moments. The increased thermal energy is transferred to a heat sink by the cold-to-hot flow of heat transfer fluid. After the cold-to-hot heat transfer fluid flow is completed, the magnetic material is adiabatically removed from the high magnetic field resulting in an increase in entropy among the magnetic moments of the refrigerant in the regenerators so to maintain constant total entropy; the temperature of the magnetic refrigerants decreases in this step. During the subsequent hot-to-cold flow of the heat transfer fluid at constant low magnetic field, the colder magnetic regenerator cools the heat transfer fluid before it exits the regenerator and accepts heat from the thermal load (i.e., the hydrogen process stream). At the end of this flow, the active magnetic regenerative cycle is repeated again at the operating frequency. The principle of operation is shown in Figure 1. The AMR cycle can be highly efficient because the magnetization–demagnetization temperature changes are only a fraction of the adiabatic temperature changes of a gas compression process and the magnetic regenerators can be designed to have much higher effectiveness than a gas-to-gas counter flow heat exchanger, The MCHL project is developing liquefier designs that use magnetocaloric refrigeration to achieve an efficient thermodynamic liquefaction cycle. Detailed modeling of the MCHL technology coupled with experimental validation

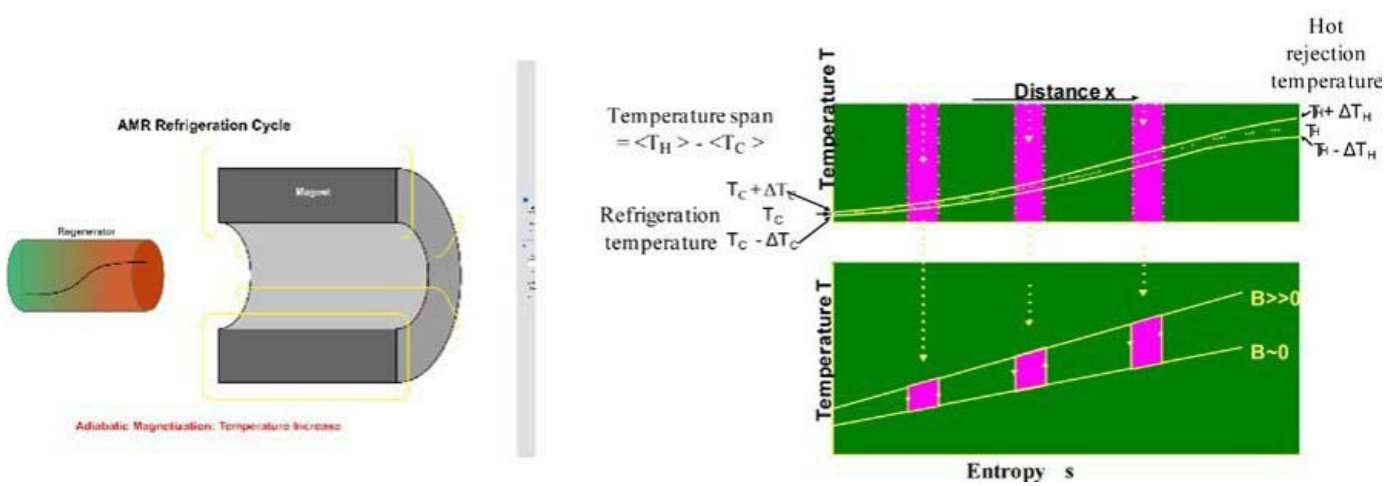

FIGURE 1. Active magnetic regenerative liquefier principle of operation

in prototypes indicate this technology has the potential to simultaneously lower liquefier installed capital costs per unit capacity, delivery cost, and to increase thermodynamic efficiency from an FOM of ~0.3 toward 0.5–0.6.

APPROACH

This project builds upon work first pioneered by Dr. John Barclay (partner). We utilized reciprocating dual regenerator design (GEN I) to evaluate magnetic materials, and better understand the temperature distribution in the regenerators. A simplified process flow diagram of the GEN I unit is shown in Figure 2. The operation and experimental results from FY 2015 are located in the results section of this report. Based upon the results of GEN I, a GEN II MCHL design is being developed. The GEN II initial choice was a rotary regenerator design, which promises to intrinsically balance the magnetic forces upon the magnetic refrigerants going into and out of the high magnetic field region for maximum work recovery. Its continuous magnetic material rotation enables constant magnetic flux, which reduces induced flux jumps that occur in a persistent mode magnet during reciprocating motion of dual magnetic regenerators. The rotary MCHL is an advanced concept that has not been successfully implemented previously. In consideration of the likelihood of encountering unforeseeable technical challenges within limited resources and time, the development of a rotary MCHL will be divided into two phases. In Phase 1, a fully independent prototype (GEN II) will be designed, constructed, and evaluated. GEN II will have only one superconducting (S/C) magnet subsystem, 4 K cryocooler, cold box, heat transfer gas circulator, data acquisition, integrated structures, and drive motors; but, it will incorporate the new novel configuration and have the capability to test several different magnetic wheels that are designed to operate over selected temperature ranges between 280 K and 20 K. For example, the regenerative wheel will be designed for 280–120 K which is the first stage of a multistage MCHL designed specifically to take advantage of the novel configuration. A complete liquefaction system will contain multiple stages, each with a wheel designed to operate over a specific temperature range. Depending on the effectiveness of the new configuration innovations to be done in Phase I, a total of three to four stages may be required rather than six or more without the innovation. This approach will develop the necessary technical knowhow for the rotary system, including an arc shaped superconductor magnet, multilayered refrigerant wheels, fabrication of suitable refrigerant materials, and micro-channel heat exchangers. Phase II focuses on a multi-wheels system (GEN III) capable of liquefying gaseous H_2 (GH_2) from 280 K. The key for a successful Phase II lies in the seamless integration of multiple wheels, magnets, and heat exchange subsystems, as well as successful preparation of refrigerant materials, which will require complete metallurgical understanding of 10–14 different rare earth metals and alloys. All lessons from GEN II will be incorporated into the design of GEN III, which will need multiple magnet subsystems, additional process and heat exchangers, and interconnections among the multiple refrigerant wheels to directly convert gaseous feedstock H_2 to LH_2. The GEN III prototype will be designed, constructed, commissioned, and evaluated. The results will provide a validated, realistic technical and economic assessment of the MCHL technology in general.

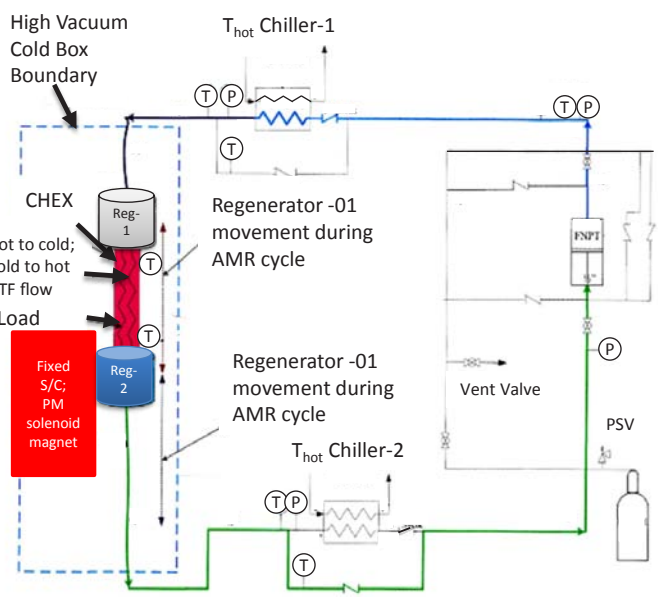

PM – Permanent magnet; PSV – Pressure safety valve

FIGURE 2. Process flow diagram of GEN I with bypass

RESULTS

The magnetocaloric materials we are using have a second-order phase transition[1] as they are cooled or heated through a characteristic ordering temperature in external magnetic fields. Magnetic refrigerants with this type of magnetic order are also characterized by a lower total heat capacity in higher magnetic fields compared to that in lower magnetic fields below the ordering temperature (Curie temperature). This is a unique feature of an AMR cycle that we've learned how to exploit. Our design uses dual active magnetic regenerators thermally connected by heat transfer fluid (Figure 3). In this design the heat transfer fluid flows through AMR 1 after AMR 1 is adiabatically removed from a magnetic field to cool it. In this AMR, the heat transfer fluid (HTF) is cooled and then flows to a heat exchanger to cool the process stream. Upon leaving the heat exchanger, the HTF flows to AMR 2 which is magnetized by a high magnetic field (i.e., it is "hotter" than the demagnetized regenerator). The HTF flows from cold to hot and cools hotter AMR 2 and then dumps the excess heat to the environment

[1] Second-order magnetic transitions do not have a latent heat associated with them.

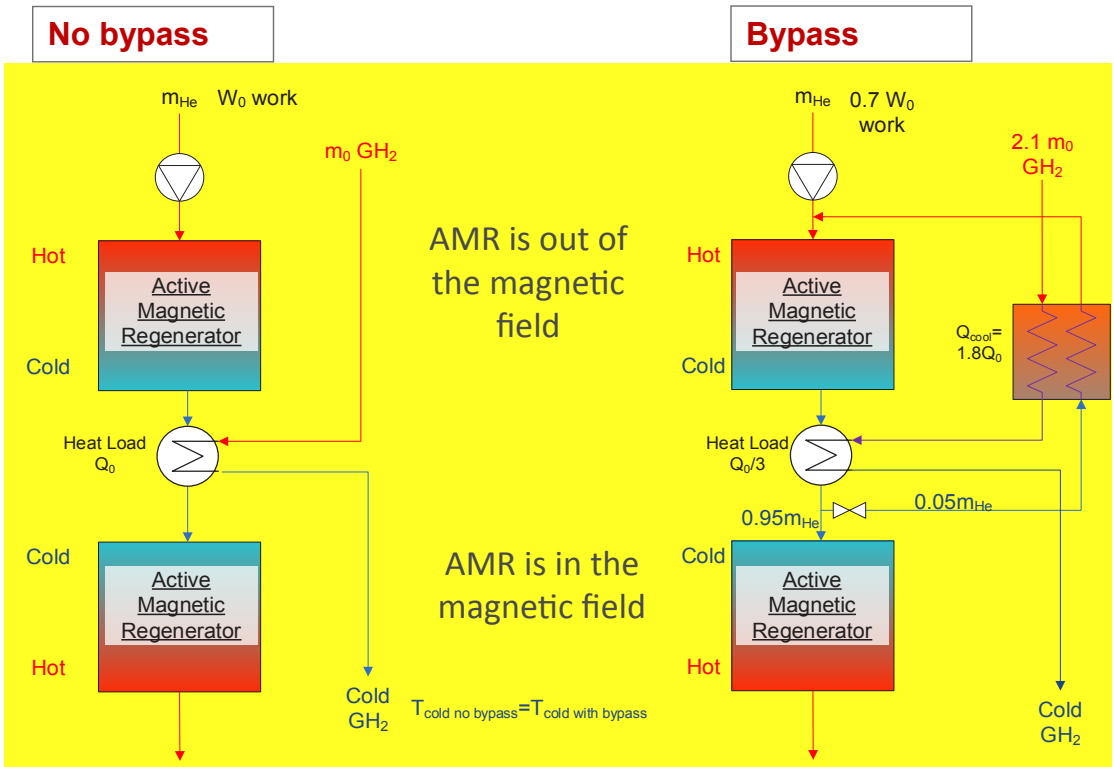

FIGURE 3. Bypass mode operation compared to regular operation with no bypass

in another heat exchanger. Once this heat flow is complete, the AMRs are moved so that AMR 2 is demagnetized which cools it down and AMR 1 is magnetized which heats it up. The HTF flow is reversed and the cooling–heating cycle continued. Because the total heat capacity of the magnetic material subjected to the magnetic field is lower than the magnetic material not subjected to the magnetic field, less HTF is needed to cool the hotter magnetic material in the magnetic field, than to transfer heat in the colder magnetic material outside of the magnetic field. To create the most efficient AMR cycle, a small slip stream of HTF should be removed from the cold heat exchanger (CHEX) prior to the HTF flowing into the hotter AMR. This slip stream can be used to pre-cool the process stream which increases the total cooling power for the same work input. While this theory has been known, it has never been demonstrated nor has the significant impact on improvement of FOM been appreciated. Our GEN II and GEN III designs incorporated the ability to operate in "bypass" mode (Figures 2 and 3). We tested this operation mode and were able to show a 25% increase (Figure 4) in cooling power in our conditions (3.3 to 0.6 Tesla field change). This was extremely promising. We then projected the impact of using bypass configuration to completely pre-cool the process stream at a larger magnetic field change. As shown in Table 1, this design choice resulted in a decrease in magnetic material requirement for the same liquefaction capacity by up to 88%.

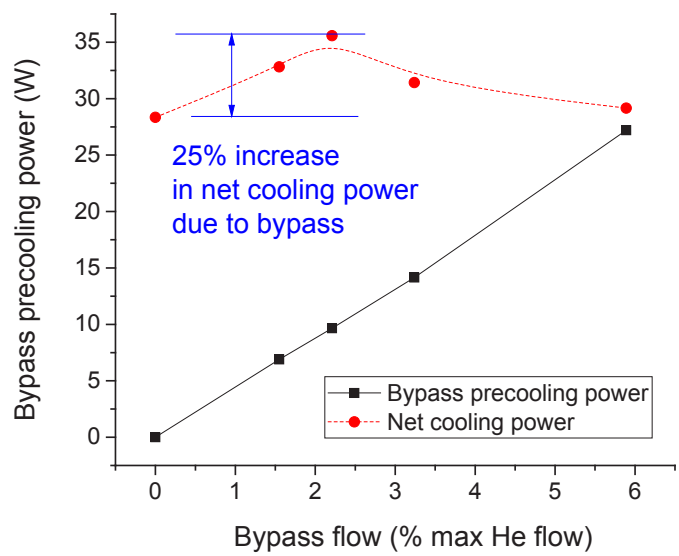

FIGURE 4. 25% increase in cooling power operating in bypass mode. Conditions include 215 g Gd regenerator, 215 g Gd/$Gd_{0.74}Tb_{0.26}$ regenerator, 3.3–0.6 Tesla field, 200 psia He gas HTF, 4 s AMR cycle.

The ultimate purpose of this work is to efficiently liquefy hydrogen. To demonstrate this potential, we demonstrated the liquefaction of propane gas from room temperature. We built and integrated a simple heat exchanger/condenser into

TABLE 1. Projected Impact of Bypass*

	No Bypass	6% Bypass	% Improvement
Thermal Load	4.3 kW	2.9 kW	32% reduction
HTF Flow	31 L He/sec	~4 L He/sec	87% reduction
Magnetic Material Required	184 kg	22.3 kg	**88% reduction**
FOM	0.4	>0.7	**87% increase**

***assumes the system is scaled by increasing the magnetic field to 7Tesla and increasing the HTF size.**

the CHEX of GEN I for this experiment. The design and operation details are in journal article under preparation. We successfully fed propane from an external tank to the CHEX of GEN I, where it was condensed and collected in a small storage vessel as a liquid. To our knowledge, this is the first time a magnetocaloric system has been used to liquefy a gas from room temperature.

Based upon the experimental results from the GEN I system, we selected a rotary system which used regenerator cartridges mounted on belts for GEN II. The figure of merit of the design is predicted to be 0.6 or higher. It could incorporate layered materials and bypass of the HTF. The primary R&D challenges for GEN II were the performance of the seals between the moving regenerator-belt assembly and the fixed housing, belt drive stresses and the fact that it has not been demonstrated previously for cryogenic temperatures. We developed novel labyrinth face seals which allow the cartridges to move while still retaining a seal. The initial seals still leaked too much, and their spring loading was therefore increased. The increased spring loading reduced the leakage to acceptably small amounts but the friction between the sliding face seals and the rotating belt was too large to be acceptable. This exploratory effort was stopped because of lack of funding for an experimental study of acceptable seals.

We did a preliminary cost analysis of various GEN II and GEN III designs and projected the installed capital cost to be ~\$1.5M/t H_2/d. Figure 5 has the breakdown for a 10 t H_2/d system. This cost is a 36% cost reduction compared to the DOE target of \$70M for a 30,000 t/d system (which equates to ~\$2.33M/t H_2/d). An interesting alternative which was also examined was co-locating the hydrogen liquefier with a compressed natural gas (CNG) plant. In this instance, we can use the cooling from the conversion of liquefied natural gas (LNG) to CNG to precool the hydrogen. By co-locating the projected installed cost decreases substantially to ~\$0.7M/t H_2/d.

In addition to the system work, Ames has led an effort for materials analysis and production. We have identified eight materials required for the GEN II system, which is designed to operate from room temperature to about 125 K (sufficient to liquefy methane). Ames has been using their unique capabilities to evaluate the magnetization of materials as a function of temperature, in the range of 320 K to 10 K.

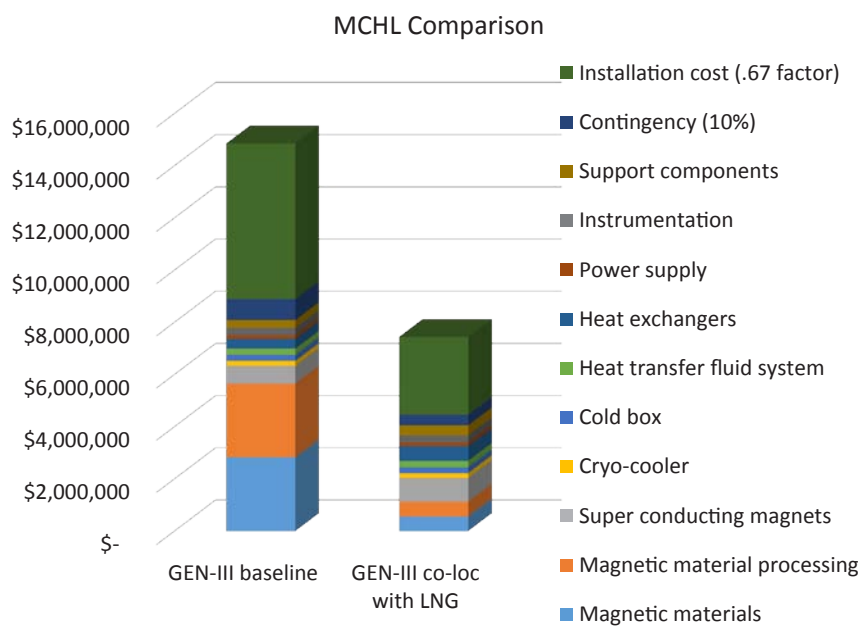

FIGURE 5. 10 t H_2/da installed capital cost for a standalone system and a system co-located with LNG/CNG

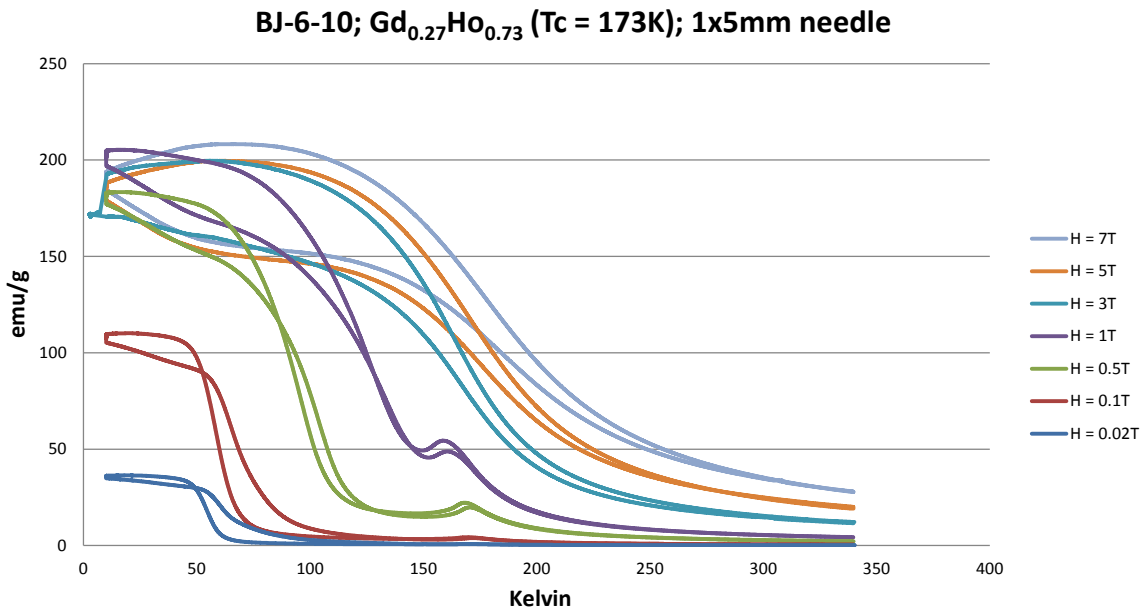

FIGURE 6. Magnetization vs. temperature

The materials evaluated have Curie temperatures ranging from ~293 K to ~150 K. An example of the magnetization vs temperature curves is shown in Figure 6 for $Gd_{0.27}Ho_{0.73}$ (Tc = 173 K). At higher magnetic fields, the magnetization curves indicate that this material has a significant magnetic moment per rare earth atom and a well-defined Curie temperature of ~173 K. The adiabatic temperature changes as a function of magnetic field for materials like this alloy are 1–2 K/Tesla of applied magnetic induction at the Curie temperature. This type of magnetic material also will exhibit the difference in heat capacity at high and low magnetic fields, a requirement for use of bypass flow of the HTF. These initial M (H, T) data support that it is one very promising magnetic refrigerant of the eight used in GEN II.

Our cost projection estimated that materials and processing cost accounted for ~20% of the installed cost of the MHCL. Therefore, in order to reduce capital cost we are looking at lowering the materials processing costs. Ames has a unique rotating disk atomizer system that produces spherical rare earth particles with a low operating cost, and can be up-scaled to relatively high volume. This system was originally designed for low-density calcium production so significant changes were required for use with the rare earth materials used in this project. In the system a crucible melts the metal and, when properly superheated, a stopper rod lifts and drains the molten metal as a stream through an orifice onto the spinning disk. Molten droplets are spun off the periphery of the disk into a co-rotating oil bath. If the disk is rotating at the appropriate speed, perfectly spherical particles with a very narrow size distribution, centered on 180–200 µm are produced. The oil bath quenches the droplets so they solidify and retain a spherical shape. A published empirical correlation has been used to determine the correct disk spinning speed (rpm), based on the surface tension and viscosity of molten Gd. Most of the system upgrades were completed and Gd spheres with ~180 µm diameter have been produced. The rest of the upgrades should be completed by the end of FY 2016. We project that the rotating disk atomizer can reduce manufacturing cost by 10–30% compared to the cost of commercial plasma rotating electrode process (PREP) atomization, while improving quality by adding a thin surface passivation surface film. The chief additional cost for PREP processing is the cost of casting each alloy into a chill mold and for careful machining of the ingot into a precise cylinder. Also, PREP requires an un-atomized cylindrical stub that is constantly necessary for the rotation drive and bearings. Moreover, the ingot used in PREP is constrained to specific size ranges, which is not the case for the rotating disk atomizer. The selected rotating disk method allows a higher yield of the alloy feed stock because the entire charge is melted prior to being poured onto the spinning disk. It works with a wide range of alloys and also with intermetallic compounds. Any shape of charge material that fits into the melting crucible can be melted, which allows scrap and off-size powder to be recycled. Although it has not been measured yet, the effective yield of spheres of the optimum diameter from the spin melting technique may be approximately 30% higher than PREP atomization technique. It is excellent to have both options available. Further advances in regenerator design may also enable higher thermal effectiveness from thin sheets or other high specific area starting materials for the magnetic regenerators.

CONCLUSIONS AND FUTURE DIRECTIONS

We have successfully demonstrated:

- 25% increase in cooling power by using bypass operation.
- Up to 88% reduction in material requirements using bypass operation
- Propane liquefaction, which to our knowledge, is the first gas liquefaction from room temperature using a magnetocaloric system.
- Projected installed system cost of ~$1.5M/t H_2/d which is 36% lower than the DOE targets.
- Magnetization vs. temperature characterization of seven materials for use in GEN II.
- New particle manufacturing process capable of producing high grade, consistent diameter spheres with the potential to reduce materials production cost by 10–30%.

Future directions:

- GEN II system
  - 8-layered system design completed.
  - Components have been ordered and are being received.
  - Upgrades to the vacuum cold box are underway; this should allow for >6 T operation.
  - System will be tested in FY 2017.
- Materials
  - Characterization underway for the key materials.
  - Spinning disk atomizer upgrades will be completed and materials for GEN II and GEN III will be provided by Ames.

SPECIAL RECOGNITIONS & AWARDS/ PATENTS ISSUED

1. Three provisional patent applications have been submitted.

FY 2016 PUBLICATIONS/PRESENTATIONS

Presentations

1. Holladay J.D., J.A. Barclay, J. Cui, K.D. Meinhardt, E. Polikarpov, E.C. Thomsen, and I.E. Anderson. "Advancements in Magnetocaloric Gas Liquefaction at PNNL." Presented at taking the temperature of phase transitions in cool materials, Royal Society, London, United Kingdom. February 8, 2016, PNNL-SA-114806.

2. Holladay J.D., J.A. Barclay, J. Cui, K.D. Meinhardt, E. Polikarpov, E.C. Thomsen, and I. Anderson. 2015. "Advancements in Magnetocaloric Gas Liquefaction." MRS Spring Meeting March 2016. PNNL-SA-113858.

Papers in preparation

1. Holladay J.D., J.A. Barclay, J. Cui, K.D. Meinhardt, E. Polikarpov, E.C. Thomsen, and I. Anderson. 2015. "Advancements in Magnetocaloric Gas Liquefaction." MRS Spring Meeting.

2. Paper on liquefaction under development.

III.11 700 bar Hydrogen Dispenser Hose Reliability Improvement

Kevin Harrison (Primary Contact), Owen Smith
National Renewable Energy Laboratory (NREL)
15013 Denver West Parkway
Golden, CO 80401-3305
Phone: (303) 384-7091
Email: Kevin.Harrison@nrel.gov

DOE Manager: Erika Gupta
Phone: (202) 586-3152
Email: Erika.Gupta@ee.doe.gov

Subcontractor:
Marc Mann, Spectrum Automation Controls, Inc., Arvada, CO

Project Start Date: July 2013
Project End Date: Project continuation and direction determined annually by DOE

Overall Objectives

- Working closely with original equipment manufacturers (OEMs) Spir Star, Yokohama Rubber, and other groups developing advanced high-pressure hydrogen hoses, NREL's hose reliability project aims to characterize and improve the reliability of 700-bar hydrogen refueling hose assemblies, and ultimately reduce the cost of dispensing hydrogen into fuel cell electric vehicles by identifying points of failure.
- The project will operate a fully automated test system that unifies the four stresses of pressure, temperature, time, and bending. The test apparatus will reveal the compounding impacts of high-volume 700-bar fuel cell electric vehicle refueling that has yet to be experienced in today's low-volume market. Testing includes pre- and post-cycling chemical and physical analysis of the inner hose liner to determine any relative changes in bulk properties and degradation mechanisms due to the stress of repeated fueling events.

Fiscal Year (FY) 2016 Objectives

- Continue hose cycling towards 25,000 cycles or until failure using the test apparatus that unifies the stresses to which the hose is subjected during high-volume back-to-back fueling events, following profiles as close to technical specification SAE J2601 fueling protocol as possible with the exception of total mass dispensed per cycle.
- Gather and analyze data on hydrogen leakage rates, timing, and sources through the use of a vacuum sampling pump system with combustible gas detectors and the deployment of chemochromic leak indication tape.

Technical Barriers

This project is conducting applied research, development, and demonstration to reduce the cost of hydrogen delivery systems. This project addresses the following technical barriers from the Hydrogen Delivery section of the Fuel Cell Technologies Office Multi-Year Research, Development, and Demonstration Plan:

(I) Other Fueling Site/Terminal Operations

(J) Hydrogen Leakage and Sensors

Technical Targets

This project aims to generate data that will help OEMs and hose developers improve reliability and replacement intervals for high-pressure gaseous hydrogen dispenser hoses. This data provided by this project will ultimately reduce the cost of hydrogen delivery from the point of production to the point of use in consumer vehicles by providing robust dispenser operation with lower maintenance costs and improved customer satisfaction.

- Target Hose Replacement Interval: 25,000 cycles
- Target Cost of Hydrogen Delivery: <$2.00/gge by 2020

FY 2016 Accomplishments

- Completed 3,500 cycles on Hose Assembly #1 from Spir Star with 700-bar hydrogen precooled to -40°C (H70-T40) using various SAE J2601 fueling protocol cases with good accuracy on pressure controls.
  - Average mass of 57 grams consumed per cycle after precooling completed.
  - Station upgrades and automation implemented to increase high-pressure hydrogen capacity and recovery and to enable unattended hose testing to increase future cycle rate.
- Detected and investigated a leak pattern from dispenser end of Hose Assembly #1.
  - Vacuum sampling pump system detected several small leaks from the crimp fitting on the dispenser end. The leak pattern was not consistently reproducible between sets.
  - Data gathered shows leak seems to occur mainly on depressurization, only after several cold cycles—no clear pattern identified yet.

– Multiple safety features were implemented as part of experiment design, allowing the hose to be run throughout leaks without risk.

✧ ✧ ✧ ✧ ✧

INTRODUCTION

NREL operates and maintains a unique user facility known as the Energy Systems Integration Facility (ESIF). The ESIF houses a broad array of capabilities and laboratories focused on energy integration research, where fast and flexible swapping of research test articles is a hallmark of the hydrogen infrastructure testing. NREL partners with DOE, as well as hydrogen industry and market stakeholders, in order to provide critical testing and validation all along the product research and development process. NREL's approach to integrated systems testing simplifies the interfaces between hydrogen production, compression, storage, delivery, and end use systems. The hose reliability test stand is housed in the ESIF's High Pressure Test Bay (HPTB), which offers a safe and controlled environment to test components under high pressure to failure while minimizing dangers to personnel or equipment.

Operation and maintenance costs of dispensing are a large part of the cost of hydrogen stations. NREL has found that about 17% of maintenance hours for hydrogen fueling infrastructure are associated with dispensers, with a significant amount attributed to hydrogen leaks or failed parts. This data can be found in NREL's infrastructure composite data products (CDPs) CDP-INFR-21 and CDP-INFR-24 [1]. These CDPs provide an early look at maintenance and reliability issues of the prospective 700-bar vehicle refueling stations. Station operators have reported that they are replacing the high-pressure hoses earlier than expected in intervals of a few months. Although high-pressure hoses are not a high capital cost item compared to the nozzle and breakaway, the frequency of replacement could result in the high-pressure hoses becoming a significant lifetime cost over 10 years. By accelerating the cycle rate, monitoring the leakage patterns, and continuing past the point of typical replacement, valuable data on post-cycled specimens can be supplied to OEMs to improve reliability through this project.

APPROACH

This project aims to perform long-duration accelerated life testing using high-pressure, low-temperature hydrogen with commercial or prototype hose assemblies. This work is unique and goes beyond standard OEM and certification standards agency acceptance testing in that it simultaneously stresses the hose assembly with realistic precooled fueling conditions closely following the technical specification SAE J2601-2014 fueling protocol for H70-T40 fills. In addition, the project applies mechanical bending and twisting stress to the hose and nozzle assembly to simulate people refueling vehicles. Finally, the short time in between back-to-back fills, of a yet-to-be-realized high-volume hydrogen refueling market, will simulate a busy station where the dispensing equipment is kept cold most of the time and subjected to frequent decompression and thermal cycles. The main difference between the test plan and a high-volume station is that the mass dispensed per fill will be less than the 3–5 kilograms (kg) of a typical vehicle fill. To prevent overtaxing the production and compression capabilities of the ESIF's hydrogen system, the target mass dispensed per fill is 100 to 200 grams. Back-to-back filling will maintain hose temperatures under the Cold Dispenser cases of SAE J2601. The performance of the hose will be monitored over time using a hydrogen sampling system attached to an outer protective sleeve near each flared crimp fitting to identify leaks as they occur. In FY 2016, chemochromic leak indication tape was also wrapped over the hose end assemblies to further identify exact methods of leakage.

The project also includes analysis of the physical and chemical property changes of the inner hose liner due to long-duration hydrogen cycling. Chemical tests previously identified and performed on pre-cycled specimens in fiscal years 2014 and 2015 include scanning electron microscopy to ultimately identify blistering due to hydrogen permeation and characterization testing, such as Fourier transform infrared spectroscopy, thermogravimetric analysis, differential scanning calorimetry, X-ray spectroscopy, and dynamic mechanical analysis methods, to identify material degradation and compositional changes.

RESULTS

Automated Hose Reliability Test Stand

A hose reliability test stand was developed to support full 700-bar fueling simulation capabilities. The test stand uses a six-axis robot using pre-programmed motion paths to capture realistic stresses resulting from human interaction with the hose assembly while maintaining a compact footprint to safely operate in the 100-ft^2 blast-rated HPTB. The test stand closely mirrors an actual dispenser in its design and pressure ramping capabilities. A tankless control algorithm was successfully developed using the interaction of an air-loaded pressure regulator on the dispenser side of the test apparatus and flow control valves on the vehicle side. The pressure ramp is controlled using a proportional, integral and derivative (PID) method set to SAE J2601 average pressure ramp rates (APRRs) and target pressures, similar to commercially available dispensers. The temperature is controlled using an air operated valve for faster precooling flow to reach the target gas temperature (-33°C to -40°C) within 30 seconds per SAE J2601 protocols. After this target

temperature is attained, the air operated valve closes, but flow continues through a bypass motorized needle valve at a rate just enough to maintain the temperature inside the hose. Good automated control of both pressure and temperature was obtained using a minimum of dispensed mass using hydrogen at full pressure scales, shown in Figure 1. This example set, after precooling, had an average mass dispensed of 57 grams, an average hose temperature of -30.5°C, and a cycle time of 4 minutes 2 seconds with 46 seconds of non-fueling time. The current design takes about two to four cycles of increased flow for components to reach full operating temperature, then uses less than 100 grams per cycle and is able to maintain temperature. The software control program allows for a variety of cases to be manually input from SAE J2601 tables.

Hose Fitting Detected Leak Characteristics

The hose reliability test stand features a leak detector system consisting of open-area combustible gas detectors and two active vacuum pump sampling systems (Figure 2). The Venturi vacuum pump aspirates air from two sampling chambers installed around both crimp fittings at the hose ends. The aspirated air passes through a cell attached to a combustible gas detector and a flowmeter set at 400 mL/min. The sampling chambers are not airtight; thus, a constant suction flow is created instead of a stable vacuum. The system has been measured to have a delayed response of 1.5 seconds on the dispenser-side hose end and a delayed response of 9.5 seconds on the nozzle-side hose end due to the pickup tubing and flow rate. The hydrogen levels detected are accurate as measured by calibration gasses at 25% and 50% lower flammable limit (LFL).

The detector system on the dispenser-side hose end first started to register leaks at Cycle 1856, while the nozzle-side hose end did not start to register the first leaks until Cycle 3033. The amount was relatively small, with about 1 milligram of hydrogen that was captured by the detectors per leak incident. This hose might not be considered failed in a field deployment, although it is possible users may hear the leak. The leaks were inconsistent from day to day but exhibited some patterns. Specifically, the leaks would only occur after several chilled cycles had already been completed, and the highest frequencies of leaks happened during the depressurization and motion back to the dispenser.

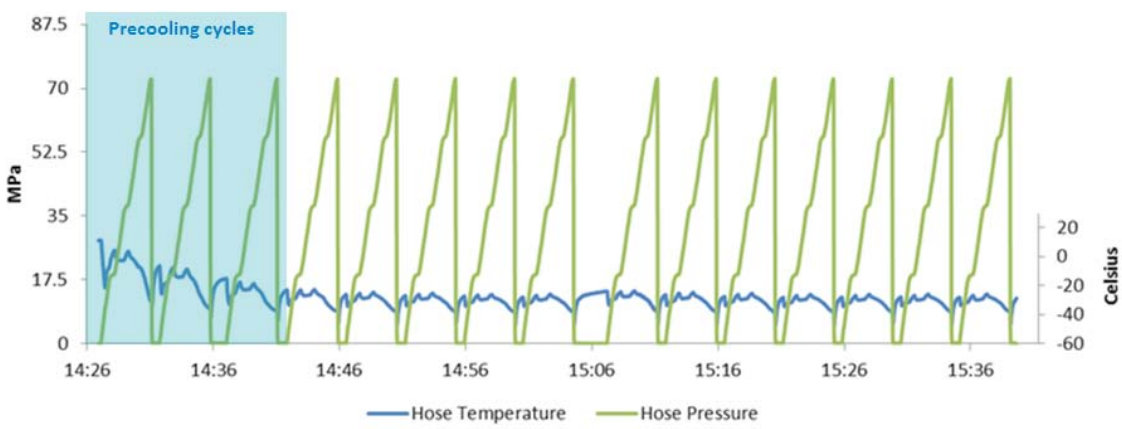

FIGURE 1. Example set of a cycle showing precooling phase and back-to-back fueling

FIGURE 2. Leak detection system with fixed-area detector and two vacuum pump active sampling detectors

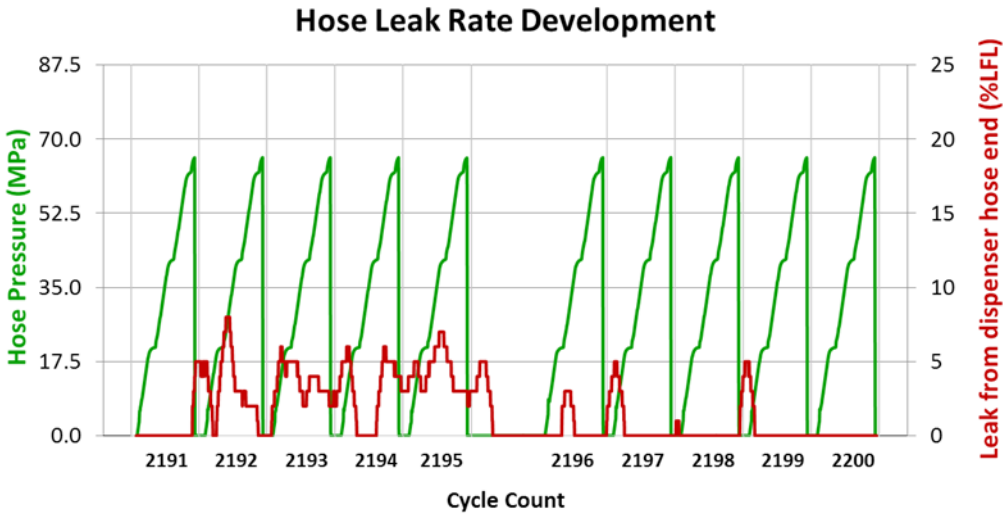

FIGURE 3. Example pattern of hose leak rate development as measured by sampling detector

This could possibly indicate leakage from the plastic-to-metal seal during venting or cracking of the inner liner during motion. The leaks tended to occur over several cycles and often did not reoccur after extended non-fueling periods. An example can be seen in Figure 3.

Leaks were confirmed from the vicinity of the hose end with a handheld detector, but the exact leak site was unable to be identified. After the leaks were detected and recorded, researchers partnered with Element One, Inc., a manufacturer of chemochromic leak indication tape, to deploy their tape to test it on extremely cold surfaces. The tape has been wrapped around the crimp fitting as shown in Figure 4, and around other potential background leak sources such as valves. The permeable chemochromic tape will darken when hydrogen passes through it, and photographs may help identify if the leak is from the metal fitting, the crimp fitting, or if it is leaking from the inner liner through the permeable outer jacket. This will also help identify specific areas to study with post-cycle testing.

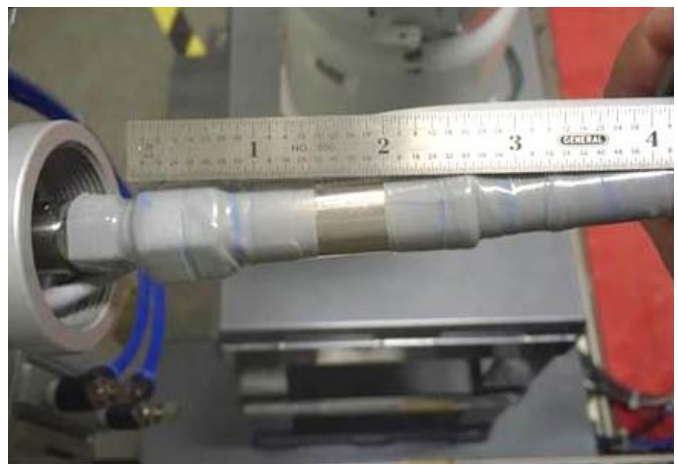

FIGURE 4. Deployment of chemochromic leak indication tape on nozzle-side hose end

CONCLUSIONS AND FUTURE DIRECTIONS

- **Conclusion:** Operated 700-bar hydrogen hose reliability test stand using a low-volume (i.e., tankless) SAE J2601 filling algorithm to achieve over 3,300 realistic H70-T40 cooled fills while mechanically stressing the hose and monitoring likely leak points of the hose assembly.
  - **Future:** Upgrading hydrogen station automation, compression, and storage capacities will allow for increased cycling rate, a wider range of cases with higher target pressures, and unattended operation of the hose test apparatus to be accomplished in FY 2016.
- **Conclusion:** Hydrogen leaks first detected at Cycle 1856 from hose near the breakaway end suggest possible patterns related to decompression or motion of hose after hose has been cooled for several cycles. Hydrogen leaks were first detected at the nozzle end of the hose at Cycle 3033. The amount of hydrogen leaking from these events is in the range of 1 mg as captured by the sampling system.
  - **Future:** Develop test plan with variations to characterize leak development and use chemochromic leak indication tape to pinpoint leak sources and identify specific hose sections for further post-cycling studies.
  - **Future:** Collaborate with industry partners like NanoSonic, SpirStar, and Yokohama Rubber. In the case of NanoSonic, there may be a potential

opportunity to test prototype hoses from their Small Business Innovation Research Phase II project, "Cryogenically Flexible, Low Permeability Thoraeus Rubber™ Hydrogen Dispenser Hose."

FY 2016 PUBLICATIONS/PRESENTATIONS

1. International Hydrogen Energy Development Forum 2016
International Symposium of Hydrogen Polymers Team, HYDROGENIUS & I2CNER Joint Research Symposium, Kyushu University, Fukuoka, Japan – February 2016.

REFERENCES

1. Sprik, Sam, Jennifer Kurtz, Chris Ainscough, Genevieve Saur, Michael Peters, and Matthew Jeffers. "Next Generation Hydrogen Station Composite Data Products - Data through Quarter 4 of 2015." Hydrogen Fueling Infrastructure Analysis. May 2016. http://www.nrel.gov/docs/fy16osti/66580.pdf.

III.12 Cryogenically Flexible, Low Permeability H_2 Delivery Hose

Jennifer Lalli (Primary Contact), William Harrison, Keith Hill, Tod Distler, Vince Baranauskas, and Richard Claus
NanoSonic, Inc.
158 Wheatland Drive
Pembroke, VA 24136
Phone: (540) 626-6266
Email: jhlalli@nanosonic.com

DOE Manager: Erika Gupta
Phone: (202) 586-3152
Email: Erika.Gupta@ee.doe.gov

Contract Number: DE-SC0010162

Subcontractors:
- National Renewable Energy Laboratory, Golden, CO
- Swagelok, Solon, OH
- New England Wire Technologies, Inc., Lisbon, NH

Project Start Date: July 28, 2014
Project End Date: August 27, 2016

Overall Objectives

NanoSonic's overall objectives for hydrogen dispenser technologies mirror those of the Office of Energy Efficiency and Renewable Energy (EERE) Fuel Cell Technologies Office for hydrogen delivery to enable the widespread commercialization of hydrogen and fuel cell technologies. Outcomes of this project will include:

- A highly durable hose that can reliably perform at 875 bar (for H70 service, 70 MPa delivery) and over a temperature range of -50°C to +90°C
- A new Class D hydrogen dispensing hose, for use on station side applications, that is chemically engineered to survive 51,240 fills (70 fills/d, 2 yr) and meets the requirements outlined in American National Standards Institute (ANSI)/Canadian Standards Association (CSA) Hydrogen Gas Vehicle (HGV) 4.2-2013, with a dispenser compliant with SAE Technology Information Report J2601 and National Institute of Standards and Technology Handbook 44
- A state-of-the-art, metal-free hose based on a unique fiber reinforced, high performance, cryogenically flexible polymer to resist hydrogen embrittlement, that can survive the Joule-Thompson effect thermal cycles, perform consistently at pressures greater than 875 bar, and endure mechanical wear and fatigue at the pump
- The first U.S. supplier of hydrogen dispenser hoses qualified for H70 service

Fiscal Year (FY) 2016 Objectives

- Quantify the burst strength of the new hydrogen hose.
- Down-select a metal-free, fiber reinforced hose.
- Optimize the durability via pressure cycle testing.
- Demonstrate environmental durability and delivery of fuel cell grade hydrogen with total impurities <100,000 ppb.

Technical Barriers

This project addresses the following technical barriers from the Hydrogen Delivery section (3.2.5) of the Fuel Cell Technologies Office Multi-Year Research, Development, and Demonstration Plan:

(I) Other Fueling Site/Termination Operations

Technical Targets

The goals of this project mirror those of EERE to advance hydrogen delivery system technologies toward the DOE hydrogen delivery 2017 delivery targets [1]. NanoSonic has reduced the cryogenic flexibility of our hydrogen delivery hose by decreasing the glass transition temperature (T_g) to -100°C, and increasing upper thermal stability to 350°C (5% weight loss via thermogravimetric analysis [TGA]). This will enable a significantly wider service use temperature range than the competitor's hose with a service temperature range of -40°C to +65°C. Burst strength has been increased from 2,000 psi to 9,000 psi during first quarter testing by crimping hose fittings in-house. The burst strength will be increased in 2015 to 51,000 psi, four times the maximum allowing working pressure of 12,690 psi by a modification of the fiber–polymer interface design, and through the use of a fitting rated for >5,000 psi. Compression strength has been increased from 10 kN to >50 kN (>11,200 lb) through the use of a novel ceramer enhancement. Solvent and abrasion resistance are being tested per the targets outlined in ANSI/CSA HGV 4.2-2013; and evolved gas analysis and quality are being tested per the targets outlined in SAE J-2719 and International Organization for Standardization PDTS 14687-2. Current cost projections based on materials for 300 m of hose are two times less than the current technology. Cost savings based on durability; normalized for lifetime, predict a 4x savings. NanoSonic's planned scale-up method predicts an 8x cost savings normalized for lifetime and 600 m hose, per targets given in Table 1.

TABLE 1. Progress towards Meeting Technical Targets for Durable Hydrogen Hose for Fuel Cell Vehicles

Characteristic	Units	2017 Targets	NanoSonic
Tg for Cryogenic Service Temperature	°C	-50	meets
TGA 5% Weight Loss for Upper Service Temperature	°C	90	meets
Burst Strength	psi	51,000	>16,500
Cycle Pressure Test	cycles	50,000 cycles at MAWP at -40 °C and 50,000 cycles at 85 °C	in progress
Compression Strength	psi	12,690	>11,200
Hose Cost	$/m	< 200	<60

MAWP - maximum allowable working pressure

FY 2016 Accomplishments

- Developed low T_g (-100°C) hose with 5% weight loss at 350°C with ultra-low hydrogen permeance after 180° bending, three times in a -50°C chamber.
- Kevlar and carbon fiber reinforced hoses approached burst pressure of metal wrap.
- Innovative ceramer coupling agent enhances crimp survivability.
- Ceramer coupling agent developed for enhanced crimp survivability and increased compression strength, which exhibits compression strength >11,200 psi.
- Reduced cost to $300/m via scale-up.
- Collaborating with gas distribution original equipment manufacturers, fittings manufacturers, national laboratories, and safety standards groups to qualify the hose for H70 service.

✧ ✧ ✧ ✧ ✧

INTRODUCTION

NanoSonic is developing and manufacturing a cost effective new hose to offer reliable delivery of hydrogen for fuel cell vehicles as a safe, reliable, and cost competitive replacement for gasoline per EERE Fuel Cell Technologies Office for hydrogen delivery goals. This American made hose will meet EERE technical targets to enable the hydrogen economy through enhanced safety and durability. There is a need for a highly durable hose that can reliably perform at 875 bar (for H70 service, 70 MPa delivery) and over a temperature range of -50°C to +90°C.

NanoSonic has worked during this DOE Small Business Innovative Research program to produce a new Class D hydrogen dispensing hose, for use on station side applications. NanoSonic's hose was systematically and chemically engineered to survive 51,240 fills, or 70 fills/d for a period of at least two years. Our state-of-the-art hose is based on a unique fiber reinforced high performance, cryogenically flexible polymer to resist hydrogen embrittlement, survive the Joule-Thompson effect thermal cycles, perform consistently at pressures greater than 875 bar, and endure mechanical wear and fatigue at the pump. Currently, there is only one hydrogen dispenser hose that qualified for H70 service. This non-U.S., German made hose from Spir Star, is rated for a working pressure of 875 bar, though it does not meet the service requirement of 25,550 fills/yr, nor does its price allow for a cost of $2–4 gallon of gas equivalent.

APPROACH

The new hydrogen hose involves an all polymer material approach in contrast to the currently qualified hose that utilizes steel as its reinforcing agent. The unique polymer fiber reinforcement design shall meet the current burst strength requirements, and surpass the durability of steel based hoses which are susceptible to weakening and catastrophic failure via hydrogen embrittlement. NanoSonic's state-of-the-art hose is based on a unique fiber reinforced high performance, cryogenically flexible polymer to resist hydrogen embrittlement, survive the Joule-Thompson effect thermal cycles, perform consistently at pressures greater than 875 bar (for H70 service, or 700 bar with a safety overpressure), and endure mechanical wear and fatigue at the pump. The polymer core is based on an ultra-low T_g backbone for cryogenic flexibility and modified for adhesion to the fiber reinforcing agents and ceramer inclusions for enhanced compression strength.

NanoSonic's manufacturing approach towards cost savings and enhanced durability is three-fold. First, a unique three-dimensional mold allows for tailored designs from the inner high pressure stable core to the fiber reinforced placement, and the outermost abrasion and solvent resistant jacket. Second, NanoSonic has two large scale reactors that allow for the cost effective production of 55-gal and 200-gal drum batches of our nanocomposite resins. Finally, NanoSonic has invested in a crimper to integrate the end connection fittings directly onto our hoses. This allows for enhanced adhesion and mechanical fit between the fitting and the hose. Crimping in-house also yields a product with complete fit and finish for qualification and distribution.

RESULTS

NanoSonic's major focus during FY 2016 is on unique fiber reinforcement designs and fittings to our hoses for hydrostatic strength and pressure cycle testing. The 2016 hoses are shown in Figure 1. Previously, NanoSonic delivered hoses to Swagelok for crimping. The low modulus hoses pulled out of the fitting during hydrostatic strength tests at CSA Group per Clause 2.4 in the hydraulic burst chamber, per the set up shown in Figure 2. The pressurization rate was set for 14,500 psi per minute. Failure pressure ranged between 200 psig to 2,100 psig, whereas the target value is four times (51,000 psi) the maximum allowable working pressure of 12,700 psi (875 bar) for H70 (70 MPa) service. Our Phase II fittings partner at Swagelok recommended that NanoSonic consider doing the fittings installation in house due to time constraints on their end. NanoSonic purchased a crimping machine from the recommended supplier. The crimper allows for installation of various dies for diameters down to 4 mm. NanoSonic owns crimping dies #12, 14, and 16 for an outer diameter (OD) crimping range of 12 mm to >19 mm.

NanoSonic produced hoses fitted with end connectors that were 15 in in length, as determined by the bend radii or as specified by the evaluating experiment scheduled at CSA laboratory. CSA was contracted to perform the two rounds of pressure evaluations on NanoSonic's high pressure hoses. The scheduled tests were (a) hydrostatic strength and (b) pressure cycle test. The description of each test is described below.

a. Hydrostatic Strength (Section 2.4) of ANSI/CSA HGV 4.2-2013 standard for hoses for compressed hydrogen fuel stations, dispensers and vehicle fuel systems. Requires a 1 min hold without burst or visible loss of fluid at a hydrostatic pressure of four times the manufacturers specified MAWP. Up to a 10,000 psi MAWP hose assembly. Two production assembly samples of each model at 12-in length are required.

b. Pressure Cycle Test (Section 2.17) of ANSI/CSA HGV 4.2-2013 standard for hoses for compressed hydrogen fuel stations, dispensers, and vehicle fuel systems. Requires 50,000 cycles with maximum allowable working pressure (assuming 10,000 psi) at -40°C and 50,000 cycles with MAWP (assuming 10,000 psi) at 85°C followed by compliance testing to Leakage (Section 2.2a) and Electrical Conductivity (Section 2.5). Two production assembly samples of each model hose length of "π(minimum bend radius) + 2(hose OD)" are required.

FIGURE 2. NanoSonic hose in hydrostatic burst strength test configuration

CSA Group evaluated a new series of hoses given in Table 2 for hydrostatic burst strength, as a function of fitting as shown in Figure 3. The hydrostatic burst results here demonstrate that the ceramer is a beneficial additive in all cases as a coupling agent between the fittings and hoses (both NanoSonic and Spir Star), and with each type of fitting, as shown in Figure 4. The Swagelok fitting survived >50,000 psi with the Spir Star hose, though the DHH fitting did not. In future deliverables, NanoSonic shall continue with

FIGURE 1. NanoSonic's hydrogen delivery hoses demonstrating cryogenic flexibility

TABLE 2. CSA Group Hydrostatic Burst Pressure Data

Test ID	Hose Material	Length (inch)	Fitting Manufacturer	Fitting O.D. (mm)	Ceramer in Hose	Ceramer at Fitting	Burst Pressure (psi)
WH208-8A	NanoSonic	17	Swagelok	15.9	NO	YES	7,081
WH208-8B	NanoSonic	17	DHH	15.9	NO	YES	8,306
WH208-8C	NanoSonic	17	Swagelok	15.9	YES	NO	6,446
WH208-8D	NanoSonic	17	DHH	15.9	YES	NO	4,304
WH208-8E	NanoSonic	17	Swagelok	15.9	YES	YES	8,334
WH208-8F	NanoSonic	17	DHH	15.9	YES	YES	7,016
WH208-9A	Spir Star	17	Swagelok	15.9	NA	NO	52,959
WH208-9B	Spir Star	17	DHH	15.9	NA	NO	9,635
WH208-9C	Spir Star	17	Swagelok	15.9	NA	YES	58,449
WH208-9D	Spir Star	17	DHH	15.9	NA	YES	26,136

FIGURE 3. NanoSonic hydrogen hoses with varied fittings

the Swagelok fittings. Additionally, the ceramer fill within the entire hose did not enhance the compression strength, but rather weakened the polymer matrix due as potentially anticipated. Finally, the hose formulation was developed to survive extreme cold. Thus, the elastomeric matrix has a very low T_g, of ~ -100°C. This will need to be increased in the next deliverable set as the material does not exhibit the toughness required to survive >50,000 psi.

NanoSonic revised our metal-free hose design to include a series of materials with unique fibers. While the specific designs are proprietary, the data is given in Table 3. It was found that our weaves exhibits double the burst strength relative to wraps, and that our X layer system yields 80% burst strength of metal wrap having eight layers. Additionally, two of our weaves at X mm thick yields ~50% strength of metal wrap with a 1.25 mm thickness.

FIGURE 4. NanoSonic hydrogen hose with ceramer technology

CONCLUSIONS AND FUTURE DIRECTIONS

Conclusions derived from the work in FY 2016 are:

- NanoSonic is currently testing our hose with fittings against the Spir Star hose for hydrostatic burst strength and pressure cycling.
- We will also be testing our hose against emerging potential commercial competitors, such as Yokohama Rubber and Iwatani Industrial Gases, ContiTech, and Togawa Rubber. Yokohama's hose is rated for 70 MPa

TABLE 3. CSA Group Hydrostatic Burst Pressure Data

Sample	Failure Pressure (psig)	Comments
Nano4A	16700	Hose Rupture
Nano5A	1510	Hose assembly pulled out of end connections
Nano2B	9100	Hose assembly pulled out of end connections
Nano4B	11030	Hose Burst
SpirStar	21200	Hose assembly pulled out of end connections

and the Togawa hose is rated for 35 MPa. There are few details given for ContiTech products.

- Environmental robustness and fuel quality is being established through testing with CSA and National Renewable Energy Laboratory.

FY 2016 PUBLICATIONS/PRESENTATIONS

1. Jennifer Lalli, "Cryogenically Flexible, Low Permeability H_2 Delivery Hose," *DOE Hydrogen and Fuel Cells Program and Vehicle Technologies Office Annual Merit Review and Peer Evaluation Meeting, 2016.*

III.13 Hydrogen Fueling Station Precooling Analysis

Amgad Elgowainy (Primary Contact) and Krishna Reddi
Argonne National Laboratory
9700 South Cass Avenue
Argonne, IL 60439
Phone: (630) 252-3074
Email: aelgowainy@anl.gov

DOE Manager: Erika Gupta
Phone: (202) 586-3152
Email: Erika.Gupta@ee.doe.gov

Project Start Date: October 2014
Project End Date: Project continuation and direction determined annually by DOE

Overall Objectives

Evaluate the cost and energy consumption of precooling system at hydrogen refueling stations, and identify system design strategies for minimizing the precooling cost and energy.

Fiscal Year (FY) 2016 Objectives

- Evaluate the available design strategies used for precooling at a hydrogen refueling station (HRS).
- Analyze tradeoff between different design concepts.
- Identify the impact of various refueling station parameters including back-to-back (B2B) fills, Joule–Thomson (J-T) expansion temperature rise, and hydrogen flow rate on precooling equipment and heat exchanger (HX) design and cost.

Technical Barriers

This project directly addresses Technical Barriers A and I in the Hydrogen Delivery section of the Fuel Cell Technologies Office Multi-Year Research, Development, and Demonstration Plan. These barriers are:

(A) Lack of Hydrogen/Carrier and Infrastructure Options Analysis

(I) Other Fueling Site/Terminal Operations

Technical Targets

This project investigates the major drivers for precooling cost and energy consumption, including the impact of frequency of fills, number of B2B fills, J-T temperature rise, and the hydrogen fill rate.

Contribution to Achievement of DOE Hydrogen Delivery Milestones

This project contributes to the following DOE milestone from the Hydrogen Delivery section of the Fuel Cell Technologies Office Multi-Year Research, Development, and Demonstration Plan:

- Task 6.3: By 2020 reduce the cost of hydrogen delivery from the point of production to the point of use in consumer vehicles to <$2/gge of hydrogen for the gaseous deliver pathway. (4Q, 2020)

FY 2016 Accomplishments

- Acquired performance data at different ambient temperatures for a typical HRS precooling system.
- Developed an algorithm to optimize size of precooling equipment and HX for lowest precooling cost.
  - Evaluated the tradeoff between on-demand cooling vs. large thermal mass HX.
- Evaluated the impact of temperature increase due to J-T expansion and B2B fills.
- Evaluated energy consumption for precooling.

✧ ✧ ✧ ✧ ✧

INTRODUCTION

The cost of the precooling system per single dispensing position is currently in the range of $150,000–$200,000, representing approximately 10% of the total station capital cost. The SAE J2601 fueling protocol requires the HRS to achieve -40°C within 30 s from the start of fueling, which has led to oversized refrigeration capacity and/or HX thermal mass. Different precooling design concepts highlight the tradeoff between cost and other design constraints such as the physical size of equipment and the station's B2B fill capability. Reports from operating hydrogen refueling stations indicates that precooling electrical energy consumption is between 0.5–50 $kWh_e/kg\ H_2$. The different precooling design concepts and the wide range of reported electric consumption warrants a detailed modeling of precooling systems to understand the parameters that impact cost and energy consumption of precooling at HRS.

While the refueling station compression and storage requirements depend on the fueling pressure and demand profile, the cooling requirement depends on the hydrogen supply temperature and desired dispensing temperature, fill rate, fueling frequency or B2B fills, and performance requirements in the fueling protocol. There are several

precooling system designs and configurations employed by various companies at HRS around the world. The variation of implementation of precooling systems at HRS is mainly in the way energy from hydrogen is removed before dispensing, (1) through a large HX mass (cooling block) maintained at low temperature (below -40°C) by a refrigeration unit with relatively low cooling capacity or (2) through a small HX mass supported by a refrigeration unit with relatively high cooling capacity. This project evaluates the sizing of these components or combinations of these components through a cost optimization algorithm and using basic laws of thermodynamics and heat transfer. A comparison between two HX design concepts is presented in Table 1.

RESULTS

Basic laws of thermodynamics were used to calculate the cooling energy requirement for -40°C dispensing. The corresponding electrical energy consumption and cooling capacity were estimated based on reported performance of a typical refrigeration unit at different ambient temperatures. Figure 1 shows the impact of ambient temperature on the

TABLE 1. Comparison between the Considered HX Options

	Large thermal mass HX (or cooling block) 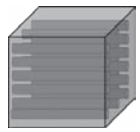	Compact thermal mass HX with high UA*
Physical size	Large mass and volume (typical block: about 1 ton, 27 ft^3)	Very small mass and volume (very high heat transfer area to volume ratio)
Cooling power requirement	Relatively small	Relatively large
Impact of ambient temperature on system cooling capacity	Less sensitive	More sensitive
Overhead cooling energy	Large (large thermal mass)	Small (very small thermal mass)
B2B fill capability	HX size increases with the number of B2B fills	Virtually infinite
Packaging/footprint	Large	Small (can fit inside dispenser cabinet)
Purchase cost	Low	High
Shipping and installation cost	High	Low

*UA – (U: overall heat transfer coefficient) x (A: heat exchange area)

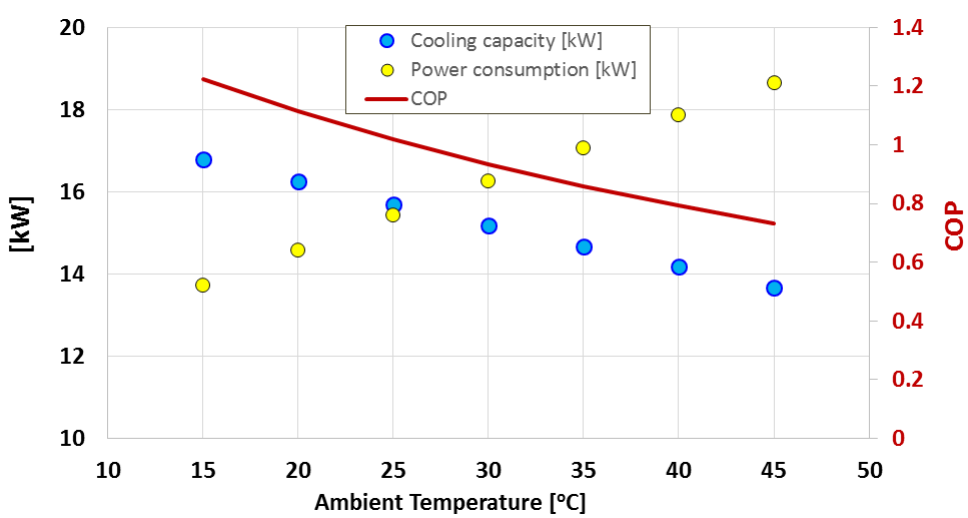

COP – Coefficient of performance

FIGURE 1. Performance of a typical precooling unit at an HRS at different ambient temperatures

performance a typical refrigeration unit at the HRS. With the increase of ambient temperature, the cooling capacity of the unit decreases while the power consumed increases. Figure 2 shows the total cost, condensing unit cost and HX cost of a precooling system required to support four B2B fills at an ambient temperature of 25°C while limiting the temperature rise of the HX unit to 2°C throughout the sequence of fills. An HX with large cooling block acts as a cooling buffer so that a low capacity condensing unit is required, while a small mass HX requires a high capacity condensing unit and large HX surface area. Considering the cost of the condensing unit and HX, an optimum combination of these two systems can be estimated for minimum cost, while meeting the design constraints of interest such as HX temperature rise, number of B2B fills and design point for ambient temperature. Figure 3 shows a typical HRS setup with a variable area control device (VACD) which controls the flow hydrogen between the high-pressure buffer storage and the HX of the precooling unit. During the refueling event, the pressure differential across the VACD valve results in a temperature rise due to J-T expansion across the VACD. Figure 3 also shows the temperature of hydrogen at the outlet of the VACD and inlet of the HX, indicating that hydrogen may reach the HX at a higher temperature compared to the ambient, which represents an added load on the precooling system. Figure 4 shows the electric energy consumption of a typical precooling unit measured at a refueling station with the daily ambient temperature varying between a low of 10°C and a high of 18°C. The figure shows a daily overhead electric energy consumption (to keep the HX cold) of approximately 10 kWh at these ambient temperatures. Such daily electric energy should be amortized over the entire daily dispensed amount, and then added to the electricity consumption for cooling the hydrogen (approximately 0.3 kWh/kg H_2) to estimate the total precooling electric energy consumption per kilogram of dispensed hydrogen.

CONCLUSIONS

When sizing the precooling unit components (condensing unit and HX) to satisfy a specific performance target (e.g., -40°C and number of B2B fills), there is an optimum combination of the precooling system components for a minimum total cost. The temperature rise due to J-T effects across the VACD is significant and should be taken into account while designing the station layout. It may be favorable to cool the hydrogen using an ambient HX upstream of the precooling system.

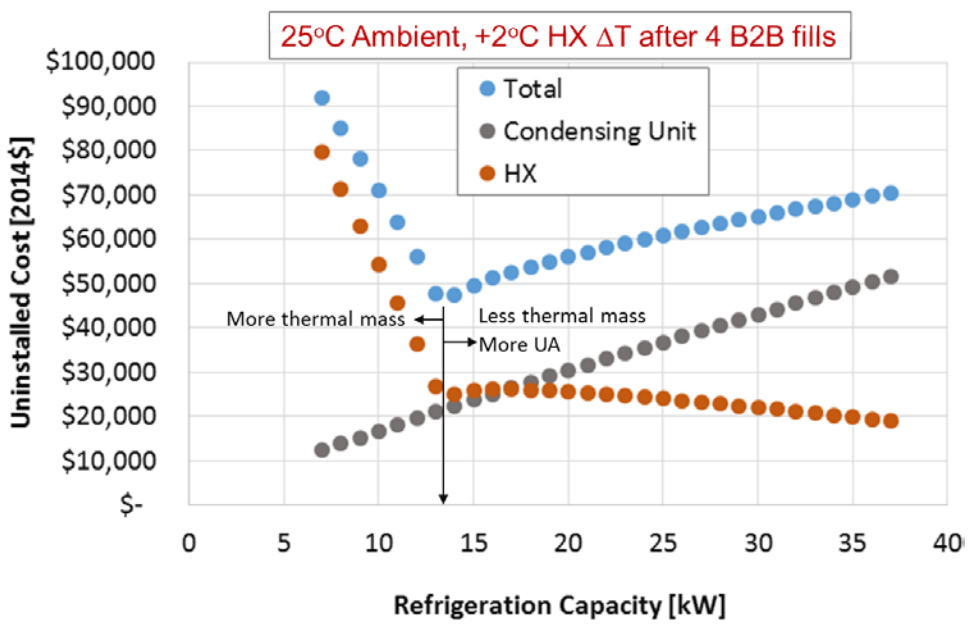

ΔT – Change in temperature

FIGURE 2. Cost of various precooling system design concepts (four B2B fills at an ambient temperature of 25°C with HX temperature rise limited to 2°C)

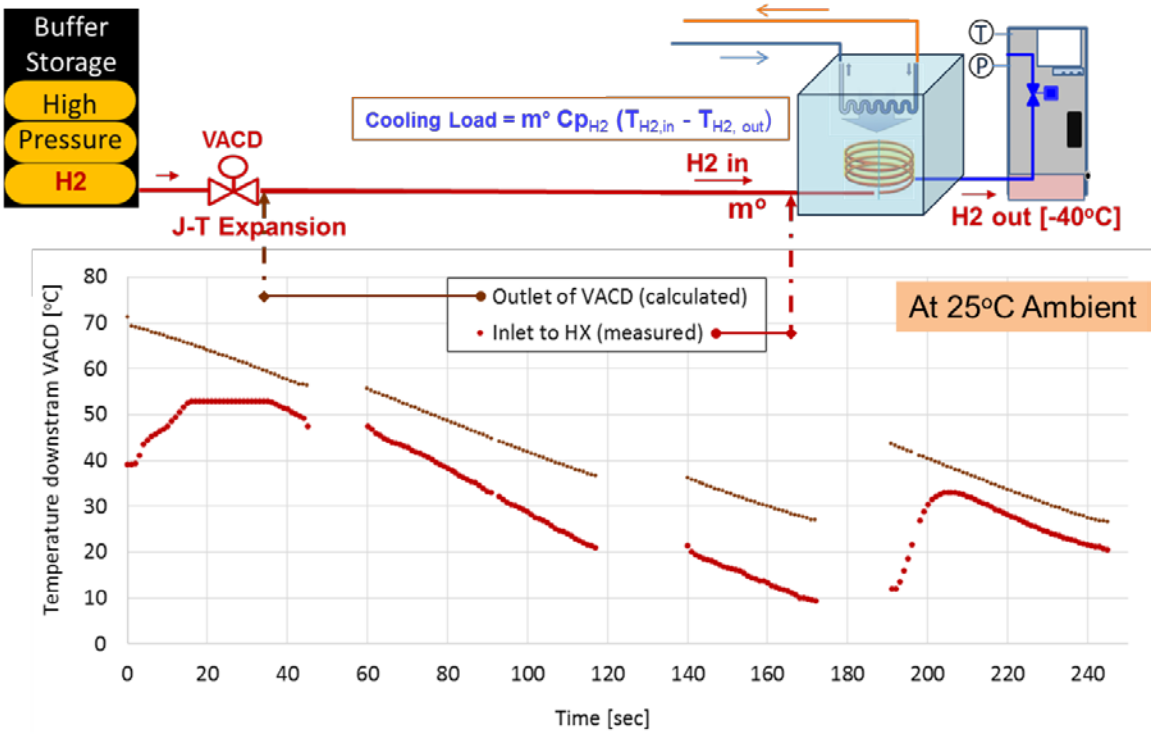

FIGURE 3. Hydrogen temperature variation downstream of the VACD during a typical refueling event

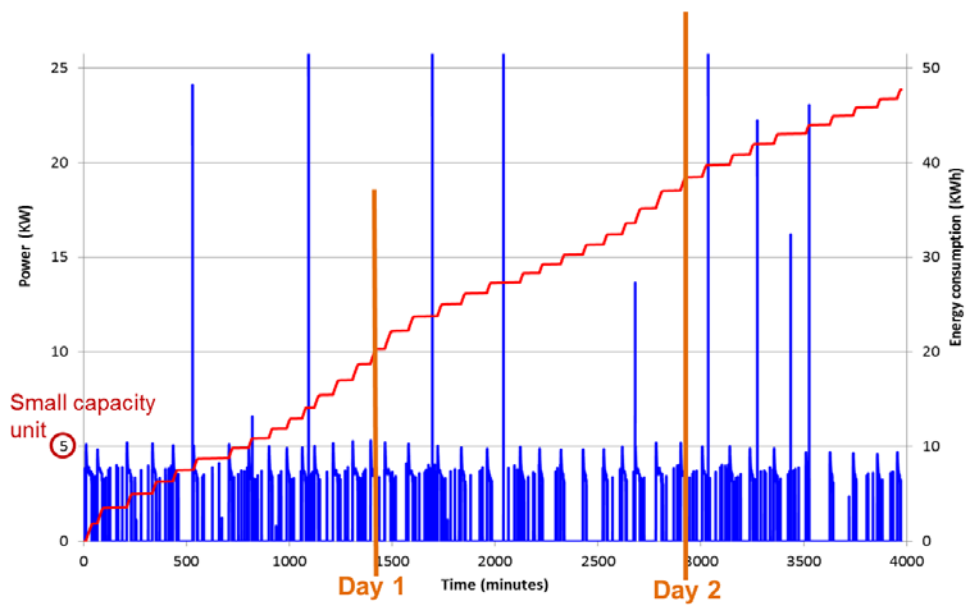

FIGURE 4. Electric energy consumption by precooling system during a typical station daily operation (daily ambient temperature varying between a low of 10°C and a high of 18°C)

III.14 H2FIRST—Consolidation

Chris Ainscough (NREL, Primary Contact)
Danny Terlip (NREL), Amgad Elgowainy (ANL),
Kareem Afzal (PDC), Krishna Reddi (ANL),
Josh Martin (NREL),
National Renewable Energy Laboratory (NREL)
15013 Denver West Parkway
Golden, CO 80401-3305
Phone: (720) 431-7296
Email: Chris.Ainscough@nrel.gov

DOE Manager: Erika Gupta
Phone: (202) 586-3152
Email: Erika.Gupta@ee.doe.gov

Subcontractor:
PDC Machines, Warminster, PA

Project Start Date: October 1, 2015
Project End Date: September 30, 2017

Overall Objectives

- Decrease the cost contribution of station capital to the cost per kilogram of hydrogen at fueling stations.
- Reduce the compression contribution to hydrogen cost (in terms of $\$/kg_{H2}$) by approximately 50% (current compressors for large stations ~500 kg/d can cost ~$1,000,000).
- Maximize station performance in terms of back-to-back fills.

Fiscal Year (FY) 2016 Objectives

- Design and build vehicle simulator capable of simulating five back-to-back fills at H70-T40 conditions.
- Evaluate the system design, ensure it is deemed both effective (capable of storing 200 kg of hydrogen at 240 bar, 40 kg at 900 bar, and of completing five back-to-back fills of 4.5–5 kg in an hour).
- Evaluate safety via a process hazards analysis (relative to National Fire Protection Agency 2, NREL Environmental Health and Safety requirements, and other relevant standards) by industry and internal stakeholders reviewing the design.
- Procure long lead items such as ground storage and vehicle tanks.
- Design controls strategy.
- Perform operation simulations and optimization with actual performance specifications.

Technical Barriers

This project addresses the following technical barriers from the Technology Validation and Hydrogen Delivery sections of the Fuel Cell Technologies Office Multi-Year Research, Development, and Demonstration Plan.

Technology Validation

(D) Lack of Hydrogen Refueling Infrastructure Performance and Availability Data

Delivery

(E) Gaseous Hydrogen Storage and Tube Trailer Delivery Costs

Technical Targets

TABLE 1. Relevant DOE Cost Targets for Uninstalled Hydrogen Compression

Characteristic	Units	DOE 2020 Targets	Project Status
Uninstalled Capital Cost ($)	$ (Based on 750 kg/d Station [~100 kg/hr peak Compression Flow])	90,000	TBD, Too Early in Project to Evaluate

TBD – To be determined

FY 2016 Accomplishments

Hydrogen Infrastructure Test and Research Facility Buildout

- Low pressure storage 200 bar, 189 kg
- Medium pressure storage 400 bar, 103 kg
- High pressure storage 875 bar, 62 kg
- Precooling 16 hp, triple block R404a refrigerant (H70, T40 capability)
- Dual hose dispenser 350/700 bar SAE J2601

Vehicle Simulator

- 875 bar, 1.45 kg each times 15 tanks, Type IV
- Infrared Data Association communications for SAE J2799 and Canadian Standards Association Hydrogen Gaseous Vehicle 4.3 tests
- Back-to-back fill capability three tanks per fill line, simultaneous fill and vent
- Class I, Division II, Group B

✧ ✧ ✧ ✧ ✧

INTRODUCTION

The project aims to decrease the cost contribution of hydrogen station capital to the cost per kilogram of hydrogen at fueling stations. The project also aims to maximize station performance in terms of back-to-back fills. These aims will be accomplished through demonstration of Argonne National Laboratory's (ANL's) tube-trailer consolidation concept and its potential to provide significant compression cost reduction at a 700 bar hydrogen refueling station. The project will demonstrate the operation and improve the optimization of refueling station design by utilizing various tube-trailer consolidation schemes. The project will instrument and collect operational data to validate ANL's model predictions, identify control issues, and verify the consequent economic benefits.

The proposed concept is projected to reduce the compression contribution to hydrogen cost (in terms of $\$/kg_{H2}$) by approximately 50% (current compressors for large stations ~500 kg/d can cost ~$1,000,000). Deploying 700 bar hydrogen stations capable of multiple back-to-back T40 vehicle refueling involves high capital investment. Low utilization and reliability of installed station equipment in early fuel cell electric vehicle markets escalates the station's contribution to the cost of hydrogen even further. The compression component alone comprises about half of the refueling station installed capital cost across various refueling station capacities. ANL has developed a novel tube-trailer consolidation concept and estimated that it can operate the compressor at approximately 10 times its rated throughput (in terms of kg/hr at supply pressure of 20 bar), and thus can reduce the compressor size dramatically. This enables efficient utilization of the tube-trailer payload and compressor operation, which ultimately will result in reduce capital expenditure on stations based on this concept.

APPROACH

The project takes place in three phases:

Phase I: Demonstration Setup

Phase II: Demonstration Preparation

Phase III: Demonstration Testing

Phase I was just completed as of July 2016. The general approach is as follows. In order to validate the consolidation concept, the project team will upgrade the existing Hydrogen Infrastructure Testing and Research Facility station at NREL in order accomplish full-scale operation of the consolidation concept. As the refueling components at NREL were not sized for optimum performance and cost, but rather research flexibility. Demonstrating the benefits of the consolidation concept using NREL's existing station requires careful sizing of required supplemental components and proper design of experiment. Such sizing and design must be done with the constraints of the already existing equipment at NREL (e.g., single dispenser) and the available PDC Machines compressor models, while also minimizing the overall cost of the project. ANL ran a matrix of simulations to determine the size requirement of high-pressure vessels required for buffer storage, as well as vessels that will mimic the tube-trailer. The simulations also determined the optimum number of banks, and number of tubes in each bank, for the buffer storage and tube-trailer systems.

Prior to beginning this project, the station capacity at NREL was limited to 20 kg/d with no back-to-back fast fill capability. As noted above, the promise of the consolidation concept lies in its ability to improve the number of back-to-back fast fills, and to satisfy large station daily demands by enhancing the compressor throughput during peak demand periods. ANL sized the tube-trailer vessels to satisfy 100 kg/d demand, and also adjusted the demand profile to simulate the number back-to-back fills (during peak hours) for a 300 kg/d station.

Once the sizing and configuration of the refueling components were established, and the operation of the different operation strategies (i.e., with and without consolidation) understood by the project team, NREL and PDC developed a process flow diagram, piping and instrumentation diagram, control strategy flow chart, and detailed bill of material.

RESULTS

In order to quantify the improvements possible from the consolidation concept, a detailed simulation was completed. The results can be seen in Figure 1. This simulation shows the performance of a consolidation-enabled station compared to a station without such capability. As can be seen in the figure, the consolidation station is able to maintain a 4–5X increase in number of fills until the final state of charge of the vehicle drops below an unacceptable 90%.

The performance of the two stages of the PDC compressor has been validated as being sufficient for the overall concept validation. See Figures 2 and 3. The machine is capable of discharging 999 bar hydrogen with an inlet pressure of 52 bar. The first stage discharge is 200 bar, consistent with the storage pressure of a tube trailer.

For the process hazards analysis, five nodes were defined. The new PDC compressor was broken in to two separate systems, medium pressure compression and high pressure compression. See Figure 4. The five nodes include:

- Low pressure system
- Gas management panel to PDC compressor second stage inlet
- Medium pressure to low pressure cross over
- High pressure system

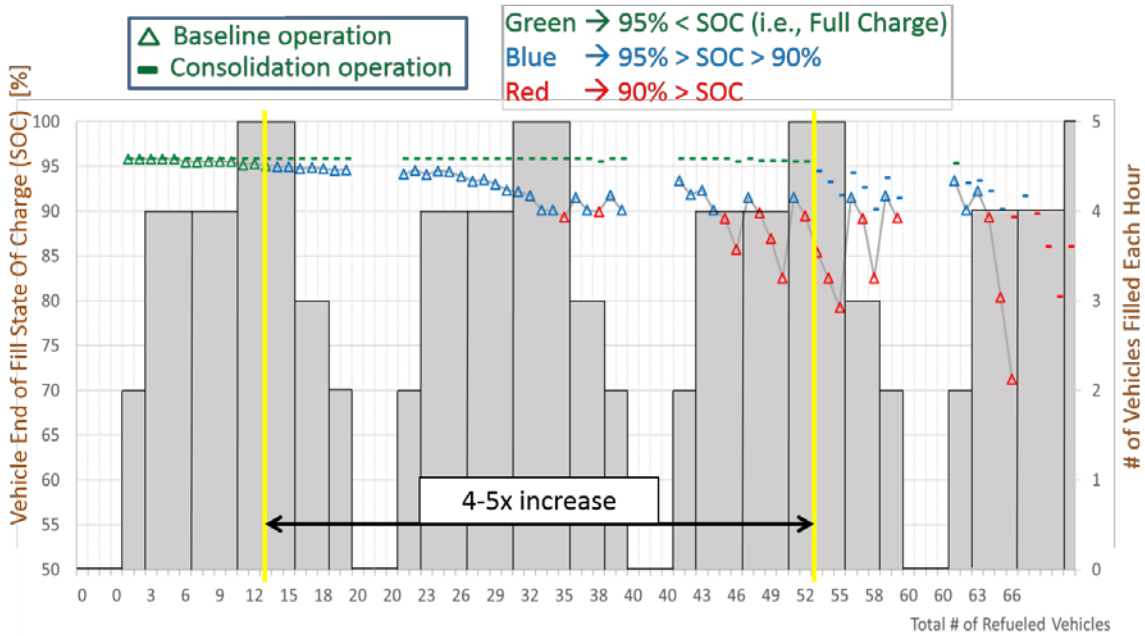

FIGURE 1. Simulated station performance shows 4–5X increase in vehicle fills, fill operation with 3.7 kg fills and two-bank buffer storage (one hose)

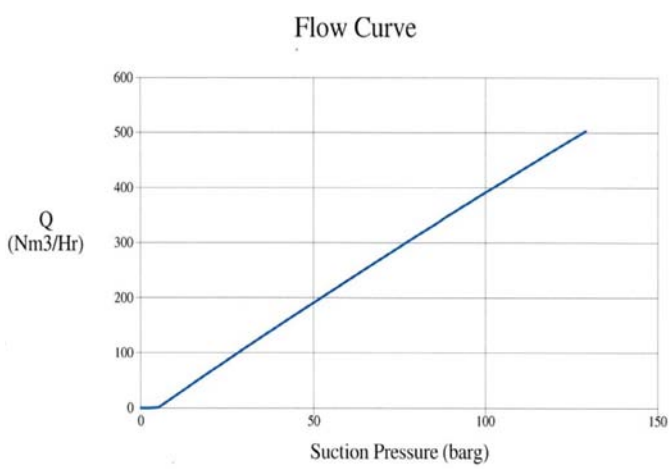

FIGURE 2. Flow curves satisfactory for algorithm validation: Stage 1 inlet 52 bar, discharge 200 bar, flow 198 Nm^3/hr

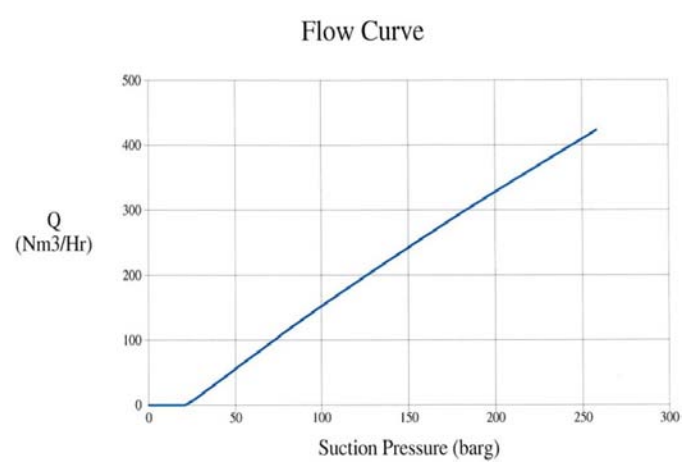

FIGURE 3. Stage 2 Flow curves satisfactory for algorithm validation: inlet 200 bar, discharge 999 bar, flow: 328 Nm^3/hr

- PDC compressor first stage discharge to gas management panel

CONCLUSIONS AND FUTURE DIRECTIONS

The process hazards analysis generated 12 recommendations for the system. Those recommendations will be implemented prior to operation. Two long lead items remain to be received, the triple block chiller and the compressor. The next year's plan will involve finishing the controls implementation and placing all the equipment. Validation testing will begin in January 2017.

FY 2016 PUBLICATIONS/PRESENTATIONS

1. Terlip, D., et al., *Consolidation,* Washington, D.C.: U.S. Department of Energy, 2016.

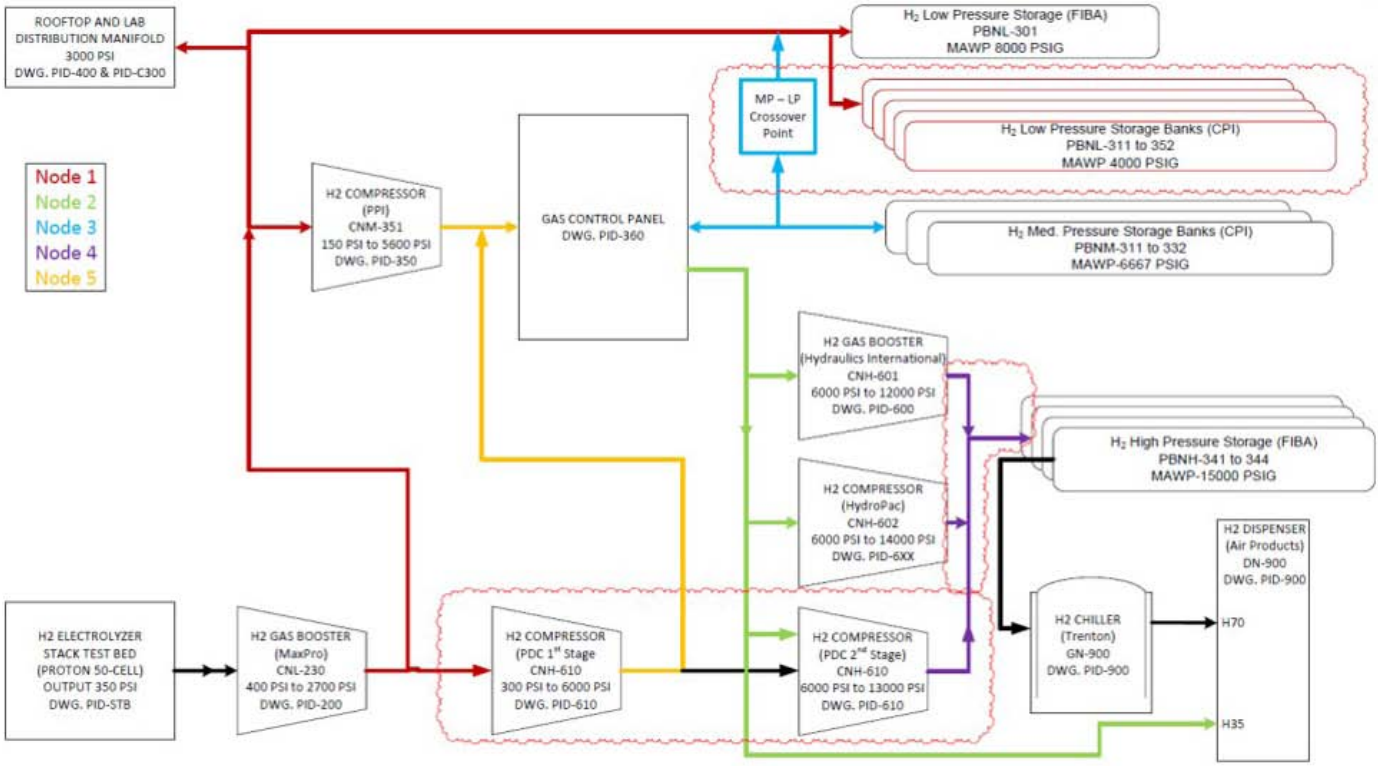

MAWP – Maximum allowable working pressure

FIGURE 4. Process Hazard Analysis nodes

III.15 Cryo-Compressed Pathway Analysis (2016)

A.J. Simon
Lawrence Livermore National Laboratory (LLNL)
7000 East Avenue
Livermore, CA 94550
Phone: (925) 422-9862
Email: simon19@llnl.gov

DOE Manager: Erika Gupta
Phone: (202) 586-3152
Email: Erika.Gupta@ee.doe.gov

Project Start Date: October 1, 2015
Project End Date: Project continuation and direction determined annually by DOE

Overall Objectives

- Quantify the techno-economic performance of cryo-compressed hydrogen (CcH2) pathways.

Fiscal Year (FY) 2016 Objectives

- Develop well-to-wheels cost estimates for CcH2 pathways.
- Develop well-to-wheels emissions estimates for CcH2 pathways.

Technical Barriers

This project addresses the following technical barriers from the Hydrogen Delivery and Systems Analysis sections of the Fuel Cell Technologies Office Multi-Year Research, Development, and Demonstration Plan.

Hydrogen Delivery

(C) Lack of Hydrogen/Carrier and Infrastructure Options Analysis

(G) Reliability and Costs of Liquid Hydrogen Pumping

Systems Analysis

(A) Future Market Behavior

Technical Targets

This project is conducting systems analyses of the CcH2 delivery pathway. Insights gained from these analyses will be applied to inform hydrogen delivery technology development toward meeting the DOE hydrogen delivery targets.

- Delivery costs associated with centralized hydrogen production: $2/gge
- Liquid hydrogen pumps uninstalled capital costs: $650,000
- Liquid hydrogen pumps specific energy: 0.5 kWh/kg

FY 2016 Accomplishments

- Incorporated physics-based estimates of boil-off losses into the liquid hydrogen delivery chain which are applicable to both the CcH2 pathway as well as the liquid–compressed–gas pathway.
- Identified and remediated hydrogen loss mechanisms from delivery to LLNL's cryo-compressed testing facility.
- Estimated well-to-wheels costs of hydrogen to be $7.85/kg, and costs of driving to be $0.44/mi under well-defined assumptions.
- Estimated well-to-wheels CO_2 emissions of hydrogen to be 280 g CO_2/mi under similar assumptions.

✧ ✧ ✧ ✧ ✧

INTRODUCTION

Several different pathways for delivering hydrogen to vehicles are under development at DOE and beyond. The cost, environmental impact, and safety of hydrogen are all affected by how hydrogen is transported from its production site and delivered to vehicle platforms. Tradeoffs between different delivery pathways can be analyzed using techno-economic models of hydrogen delivery. The results of these analyses inform researchers, policymakers and other stakeholders of the potential benefits of improved hydrogen delivery technology.

Cryo-compressed hydrogen is defined as cold liquid hydrogen (20–40 K), delivered to the vehicle at high pressures (300–900 bar). Potential advantages of CcH2 include very high volumetric and gravimetric energy density, and innate compatibility with efficient liquid hydrogen delivery to filling stations. Potential tradeoffs include the energy consumed in liquefaction and compression, and the possibility of hydrogen losses to the atmosphere through boil-off of liquid hydrogen in storage, transport or transfer. The objective of this project is to generate estimates of the costs and environmental impacts of the CcH2 fueling pathway, informed by a fundamental understanding of the behavior of cryogenic and cryo-compressed systems, and by recent experience with such systems at LLNL's cryo-compressed test facility.

APPROACH

The Hydrogen Delivery Systems Analysis Model (HDSAM), an Excel-based calculation tool developed by Argonne National Laboratory, is the platform on which this analysis was performed. Two major pieces of analysis were integrated with HDSAM to achieve results: physics-based estimates of hydrogen boil-off and other losses throughout the delivery chain and parameterized well-to-wheels calculations of costs and emissions for the entire enterprise.

Hydrogen can be lost from the delivery pathway through several mechanisms: (1) leak-related losses at the liquefier and terminal, (2) boil-off from the transportation trailer from heat infiltration in transit, (3) venting of the vapor-space in low pressure cryogenic vessels at filling stations, (4) venting from the trailer during de-pressurization after unloading at a filling station, (5) boil-off from steady-state heat infiltration into the cryogenic components of a filling station (tank, lines, pump, etc.), and (6) boil-off from the heat deposited by running the pump during dispensing. In this project, HDSAM was extended to estimate most of these losses from known or measurable quantities in operating prototype systems.

Also integrated with HDSAM are estimates of the non-delivery components of a hydrogen enterprise that contribute to the total lifecycle cost and environmental impact of CcH2 delivery. Such components include vehicle cost, hydrogen production cost, greenhouse gas (GHG) emissions from hydrogen production, etc. Standardized calculations were used to integrate the delivery-specific costs and emissions (based on the above physics-based refinements) with parameterized estimates of non-delivery factors to estimate top-line results such as the cost and GHG emissions per mile driven on CcH2.

RESULTS

The objective of this project was to generate analyses of the total cost and GHG of driving a fuel cell electric vehicle fueled through a CcH2 delivery chain. That objective was realized by extending and exercising the HDSAM model over a range of assumptions relevant to CcH2 delivery.

Figure 1 depicts *potential* hydrogen losses from boil-off through the delivery chain. The large fraction of hydrogen lost to boil-off in this specific scenario is representative of early market conditions and low technology levels. This scenario is used for illustrative purposes because each loss mechanism is clearly visible; it is not representative of a realistic large-scale deployment of CcH2 technology.

Engineering estimates of steady-state heat transfer ($Q = kA\Delta T/L$) into the various vessels and piping were used to calculate individual boil-off rates ($m = Q/h_{fg}$) that would occur if those vessels were held at constant temperature and pressure. Calculated losses include venting during trailer transport (assuming typical trailer dewar configurations), venting due to onsite storage at service stations, and venting due to heat infiltration into the pump-vessel and associated piping at service stations.

Losses associated with pumping, and losses avoided by pumping were also estimated through basic thermodynamic analysis. It was assumed that a certain fraction of the mechanical energy used by the pump would end up in the hydrogen (due to the mechanical inefficiency of the

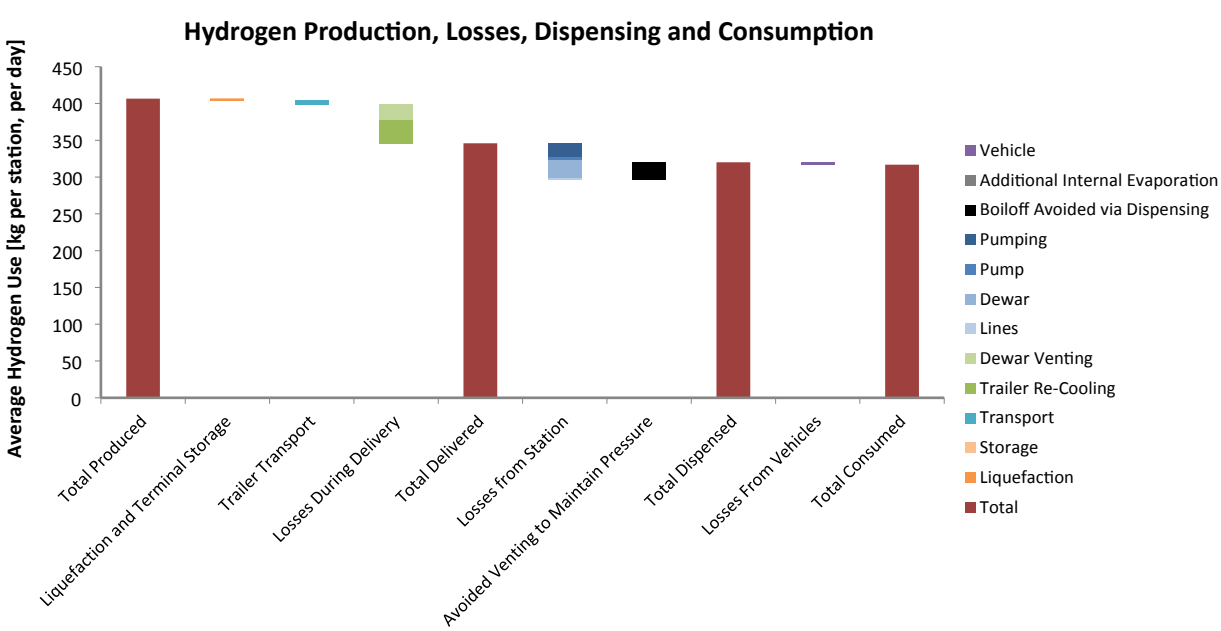

FIGURE 1. Waterfall chart depicting all potential loss (venting and boil-off) mechanisms along the CcH2 delivery pathway

pump) and that some fraction of that energy would heat the low-pressure fluid in which the pump is immersed. This deposited energy would evaporate some of the stored liquid hydrogen. On the other hand, hydrogen dispensed during pump operation is removed from the system; and some of the remaining liquid hydrogen must be evaporated to maintain constant volume (again, assuming constant temperature and pressure operation). The black bar labeled "Avoided Venting to Maintain Pressure" reflects the logic that hydrogen may be vented if vaporization exceeds dispensing demand, and that no venting would occur (and heat would be admitted to maintain pressure) when dispensing demand exceeds heat infiltration.

Losses during liquefaction were estimated to be 0.5% of hydrogen liquefied based on industry experience. This estimate may be refined in future analyses. Losses from CcH2 tanks on vehicles were estimated to be 1% fleetwide. This crude estimate may also be refined in the future, as it depends on wide variations in drive cycles (a regularly driven vehicle will vent no hydrogen from a CcH2 tank, while a long-dormant vehicle could vent a significant fraction of its tank capacity in certain, rare circumstances).

Losses during delivery were estimated under both best-case and worst-case scenarios. LLNL has taken several deliveries of liquid hydrogen to the (relatively small – 800 kg) dewar associated with its onsite CcH2 test facility. LLNL personnel have observed significant venting of hydrogen associated with two phases of the delivery process in this premarket setting: (1) venting from the dewar during transfer of hydrogen from the trailer to the dewar, and (2) venting of hydrogen from the trailer after the transfer is complete and before the trailer leaves the site.

In a best-case scenario, no hydrogen would be vented during delivery because cold hydrogen from the trailer "collapses" the warm hydrogen vapor that builds up at the top of the dewar, and adequate management of heat transfer and mixing within the trailer can be used to control pressure excursions. In a worst-case scenario (which has been observed), the dewar is filled from the bottom, displacing (and venting) the cool, dense hydrogen vapor at the top of the dewar. Additionally, the trailer is brought to full thermodynamic equilibrium during transfer (effectively warming the liquid hydrogen to pressurize it), and then is vented and well mixed to bring the entire volume back to a cold "over-the-road" low pressure. Such a procedure can cause over 10% of delivered hydrogen to be lost, as depicted by the green bars in Figure 1.

After performing this analysis, LLNL personnel worked with our hydrogen supplier to minimize delivery losses by top-filling the dewar and minimally heating the trailer for pressurization. This was an unexpected benefit of the analysis and is a positive outcome for both DOE and LLNL.

Figure 2 depicts an analysis of delivery costs. The costs depicted do include the loss of hydrogen throughout the delivery chain, but do not include the production cost of the hydrogen that is dispensed. The early market scenario depicted assumes a relatively small station (with a design capacity of 400 kg/d and an average dispensing rate of 320 kg/d). The modified HDSAM analysis shows that the largest fraction of CcH2 delivery costs are associated with liquefaction; and the terminal and trucking costs are a small fraction of the overall delivery cost. Station capital and labor are also major contributors to delivery costs, while station energy consumption (some of which is associated with cryo-compression) is not.

Not explicitly depicted is the capital cost of the cryopump itself; that cost is part of the station capital cost. In this specific scenario, the estimated capital cost of $225,000 per pump, installed, represents ~27% of the capital cost of the station, or $0.29/kg of hydrogen dispensed (6% of

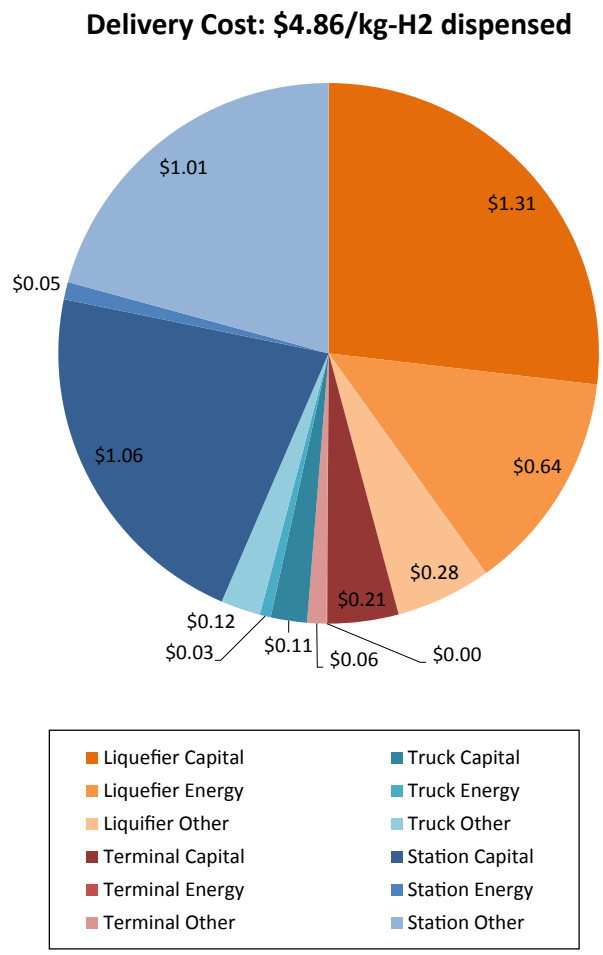

FIGURE 2. Contributions to the total cost of delivery by the major components of the delivery pathway for CcH2. The scenario depicted here is for small, early market stations (designed to dispense up to 400 kg/d) and mature delivery and dispensing technology.

the delivery cost). This cost is a major factor, and should be compared to equipment in other delivery pathways (compressors and chillers in the liquid–compressed–gas pathway, and storage cascades in the compressed gas pathway).

The total GHG emissions of the CcH2 pathway are shown in Figure 3. Production (assumed to be central station steam methane reforming) and liquefaction (assumed to be central and co-located with the terminal) dominate the pathway's total GHG emissions per mile of driving. Diesel-fueled liquid hydrogen trucking, and electricity-driven station operation, are small contributors. In fact, in scenarios where there is significant boil-off or hydrogen venting, eliminating the GHG emissions associated with the production and liquefaction of lost hydrogen can fully offset the GHG emissions from trucking and dispensing.

Multiple sensitivities to pathway parameters were investigated. Figure 4 depicts the sensitivity of hydrogen venting losses (using our observed "worst-case scenario" delivery practices) to station size. In this study, larger stations result in fewer losses because each delivery causes hydrogen venting in proportion to the residual hydrogen in the trailer, and because larger stations have lower surface area-to-volume ratios. Several other sensitivity studies were conducted to investigate the effects of pump cost, pump efficiency and heat transfer coefficients. The modified HDSAM tool is capable of analyzing the effects of almost any cost or performance parameter on hydrogen losses, delivery costs, costs of driving, and GHG emissions.

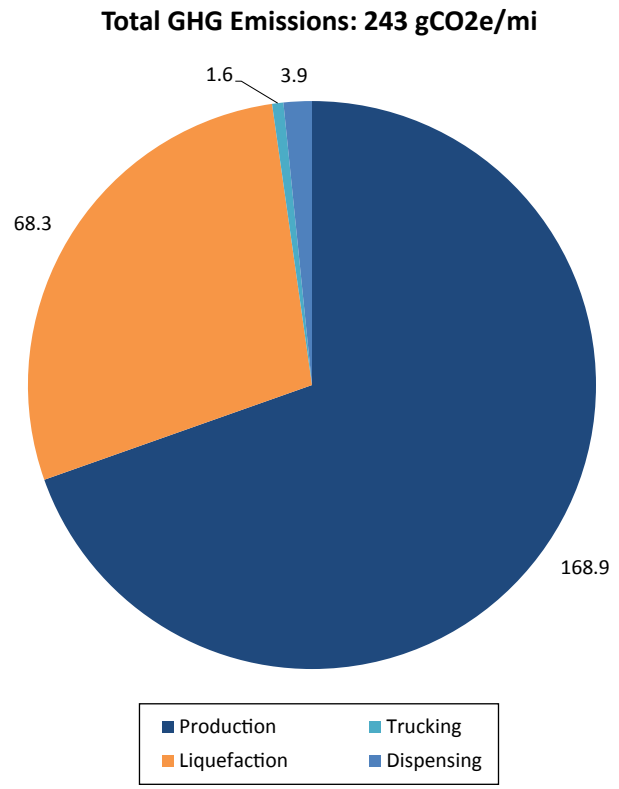

FIGURE 3. Contributions to the total GHG emissions from a light-duty vehicle fueled with CcH2. These results reflect the same scenario as depicted in Figure 3.

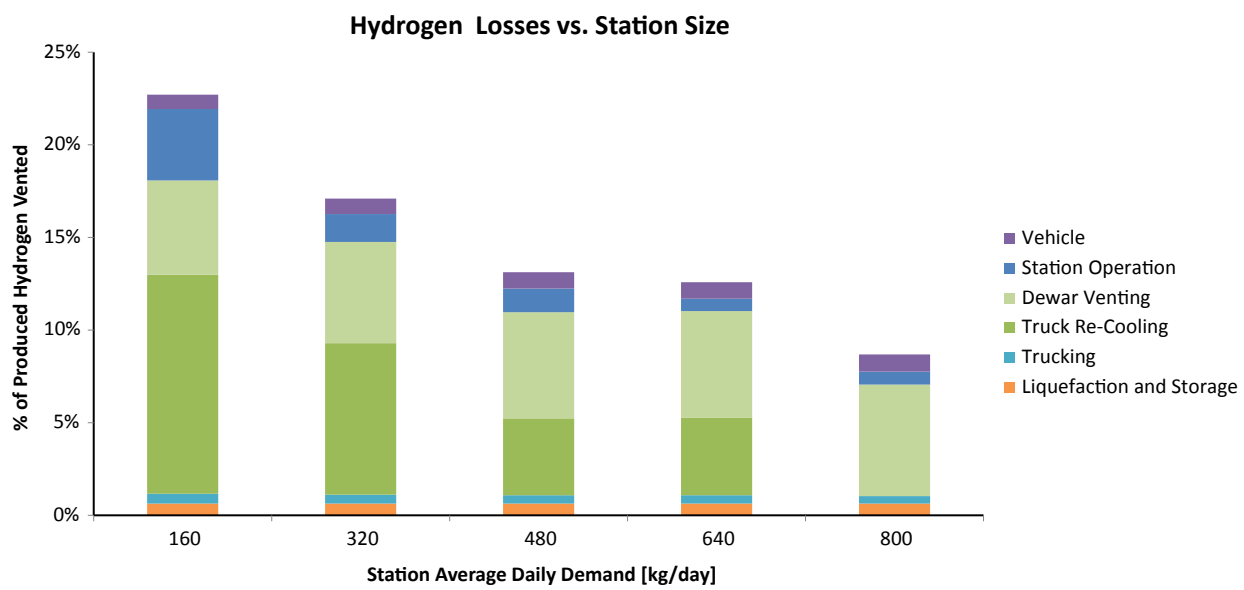

FIGURE 4. Sensitivity of hydrogen boil-off to station size. All parameters except the average station size were held fixed at a low technology level (large heat transfer rates, inefficient delivery practices) to illustrate the potentially compounding effects of observed losses on early markets.

CONCLUSIONS AND FUTURE DIRECTIONS

Top-line estimates of \$5.75/kg H_2 (total cost of hydrogen to the consumer), \$0.41/mi (cost of driving), and 240 g CO_2/mi were generated as representations of a mature CcH2 market, and the sensitivity of these figures to changes in technology cost and performance were thoroughly investigated.

In future years, the thermodynamic analysis of hydrogen transfers will be extended to include best practices of non-equilibrium pressurization of the trailer and dewar. System models will be benchmarked against performance measured at LLNL's CcH2 test facility. The CcH2-specific and generally relevant liquid hydrogen analyses will be formally included in a future version of HDSAM.

IV.0 Hydrogen Storage Program Overview

INTRODUCTION

The Hydrogen Storage program supports research and development (R&D) of materials and technologies for compact, lightweight, and inexpensive storage of hydrogen for automotive, portable, and material handling equipment (MHE) applications. The Hydrogen Storage program has developed a dual strategy, with a near-term focus on improving performance and lowering the cost of high-pressure compressed hydrogen storage systems and a long-term focus on developing advanced cold/cryo-compressed and materials-based hydrogen storage system technologies.

In Fiscal Year (FY) 2016, the program initiated efforts on conformable high-pressure storage tank design and continued to focus on the development of lower-cost precursors for high-strength carbon fiber and alternative fiber and resins to lower the cost of composites used in high-pressure compressed hydrogen systems for ambient and sub-ambient conditions. The program also continued advanced material R&D efforts for metal hydrides and sorbents and launched the Hydrogen Materials-Advanced Research Consortium (HyMARC), a collaborative, comprehensive, materials-based hydrogen storage R&D effort.

GOAL

The program's goal is to develop and demonstrate advanced hydrogen storage technologies to enable widespread commercialization of fuel cells in transportation applications as well as enable early markets such as portable power and material handling equipment applications.

OBJECTIVES

The Hydrogen Storage program's objective is to develop technologies that provide sufficient onboard hydrogen storage to allow fuel cell devices to meet the performance and run-time demanded for the applications. For light-duty vehicles this means providing a driving range of more than 300 miles (500 km) while meeting packaging, cost, safety, and performance requirements competitive with current vehicles. Although some fuel cell electric vehicles (FCEVs) have been demonstrated to travel more than 300 miles on a single fill using high-pressure tanks, this driving range must be achievable across the full range of vehicle models without compromising space, performance, or cost. The Hydrogen Storage program has developed comprehensive sets of hydrogen storage performance targets for onboard automotive, portable power, and MHE applications. The targets can be found in the Hydrogen Storage section of the *Multi-Year Research Development and Demonstration Plan* (MYRDD Plan).

By 2020, the program aims to develop and verify onboard automotive hydrogen storage systems achieving the following targets that will allow some hydrogen-fueled vehicle platforms to meet customer performance expectations:

- 1.8 kWh/kg system (5.5 wt%)
- 1.3 kWh/L system (0.040 kg hydrogen/L)
- $10/kWh ($333/kg stored hydrogen capacity)

To achieve widespread commercialization of hydrogen FCEVs across the full range of light-duty vehicle platforms, the program has established the following Ultimate Full Fleet onboard hydrogen storage targets to meet the needs for full fleet adoption:

- 2.5 kWh/kg system (7.5 wt%)
- 2.3 kWh/L system (0.070 kg hydrogen/L)
- $8/kWh ($266/kg stored hydrogen capacity)

Tables that include the complete sets of nearer-term and longer-term targets for onboard automotive, portable power, and MHE applications can be found in the MYRDD Plan. Targets are currently under revision based on recent progress and will be updated in FY 2017.

FY 2016 TECHNOLOGY STATUS AND ACCOMPLISHMENTS

Given that hydrogen storage system cost remains a key barrier in the commercialization of FCEVs, the program continued to focus on analysis to understand the costs associated with high-pressure hydrogen storage systems. The projected cost status for 700 bar compressed hydrogen storage systems remained at $15/kWh, which reflects technology advancements supported by the Hydrogen Storage program to reduce the cost of carbon fiber precursor and resin, balance of plant components integration, as well as changes in tank design to better reflect commercially manufactured pressure vessels. Figure 1 shows the 2013 and the 2015 breakdown of projected costs at high volume for 700 bar compressed hydrogen storage systems for light-duty vehicles.

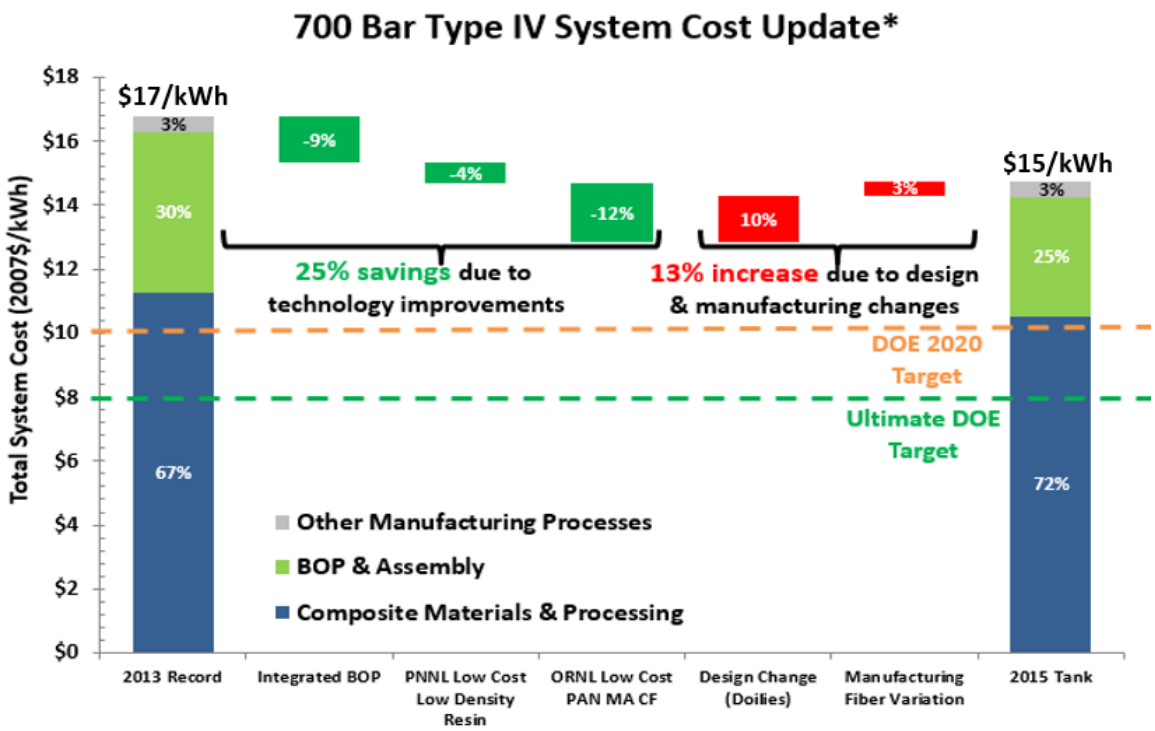

*At 500k units/yr. Based on Program Record 15013

PNNL – Pacific Northwest National Laboratory; ORNL – Oak Ridge National Laboratory; PAN – polyacrylonitrile; MA – methyl acrylate; CF – carbon fiber; BOP – balance of plant

FIGURE 1. Revised projected costs for 700 bar compressed hydrogen storage systems for light-duty vehicles at 500,000 systems per year, comparing analyses between 2013 and 2015

The Hydrogen Storage program's near-term strategy focused on high-pressure compressed hydrogen storage systems and remained consistent with FCEV industry trends in 2016. Automotive companies are now in their second year of commercializing FCEVs that use 700 bar compressed hydrogen storage systems onboard, and system cost remains one of the most important challenges to widespread commercialization. Currently, there are two FCEV models that are available for lease or commercial sale in California, and both are equipped with 700 bar compressed hydrogen systems onboard.

In FY 2016, projects spanning the program's physical storage portfolio made progress in the areas of low-cost, high-strength carbon fiber precursors; alternative fiber and resin; cold-temperature operation; and conformable tank designs. For example, ORNL and partners have identified plasticizers effective in reducing the melt temperature of PAN/MA blends to the range of 145–175°C, significantly below the cross-linking temperature, to allow melt processing. Materia has demonstrated improved and optimized vacuum processing for the resin impregnation of dry fiber wound tanks and demonstrated equivalent burst strength to baseline conventional tanks. Additionally, work by Composite Technology Development Inc. (CTD) and partners on conformable tank design moved the project a step

closer to the development of conformable 700 bar hydrogen storage systems by selecting the resin for the prototype vessel permeability testing. In terms of cold-temperature operation, the program initiated a new project in FY 2016, led by Vencore Services and Solutions, focusing on thermal insulation for cold and cryogenic automotive tank applications.

In addition to system cost and as shown in Figure 2, current projected energy densities for compressed hydrogen storage systems are unable to meet the program's 2020 targets. Given these limitations and as a longer-term strategy, the Hydrogen Storage program continues to pursue less mature materials-based hydrogen storage technologies that have the potential to satisfy all onboard hydrogen storage targets, including those related to energy density. These technologies include cold compressed (sub-ambient temperatures as low as ~150–200 K) and cryo–compressed (temperatures <150 K) hydrogen and materials-based storage technologies. In FY 2016, Lawrence Livermore National Laboratory (LLNL) constructed and commissioned their cryogenic hydrogen test facility allowing for the safe testing of full-size cold/cryogenic hydrogen storage vessels using a hydrogen cryo-pump supplying high-pressure supercritical hydrogen.

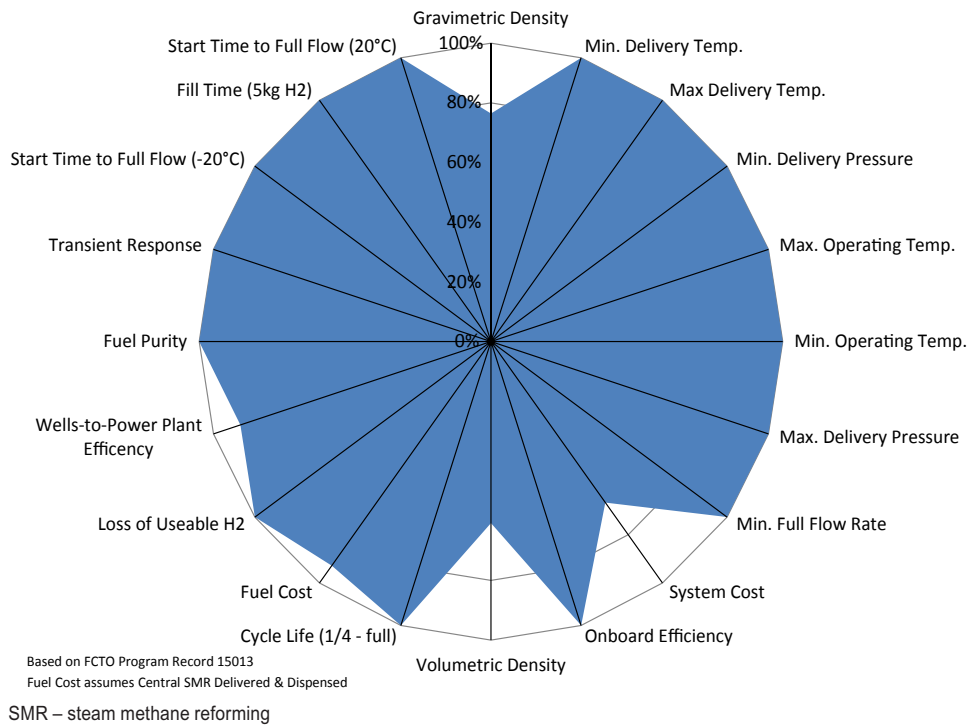

FIGURE 2. Current projected performance of a state-of-the-art 700 bar compressed hydrogen storage system with 5.6 kg usable hydrogen storage with the 2020 onboard automotive targets

In FY 2016, the materials-based storage efforts were focused to a greater extent on advanced hydrogen storage materials development and to a lesser extent on total systems engineering. A significant materials-based scientific breakthrough in the area of hydrogen adsorption within metal organic frameworks (MOFs) was achieved. A collaborative effort between University of California, Berkeley, Lawrence Berkeley National Laboratory (LBNL), and National Institute of Standards and Technology (NIST) demonstrated, for the first time, the binding of two hydrogen gas molecules to a single open metal site within an MOF, paving the way for a synthetic path to identifying materials with higher densities of adsorbed hydrogen and with the potential to meet the program's 2020 and ultimate density targets. Figure 3 shows a portion of the synthesized organic structure with multiple hydrogen molecules adsorbed at a single metal site.

A major FY 2016 effort initiated in the program's materials-based storage portfolio was the launch of HyMARC. Comprised of a core team of three national laboratories (Sandia National Laboratories [SNL]-lead, LLNL, and LBNL), the HyMARC team is addressing the scientific gaps impeding the advancement of solid-state storage materials. HyMARC's scientific activities will provide the foundational understanding of the interaction of hydrogen with

materials, such as the thermodynamic and kinetic properties of storage materials, including mass transport, surface chemistry, and processes at solid-solid interfaces, information which is critical in achieving all of the program's 2020 and ultimate targets. Five new individual projects were selected in 2016 to collaborate with the HyMARC national laboratory core team to develop specific hydrogen storage materials with the potential to meet the demanding performance requirements for onboard FCEV hydrogen storage. These projects will be led by University of Missouri–St. Louis, University of Hawaii–Manoa, The Pennsylvania State University, Liox Power Inc., and Argonne National Laboratory (ANL).

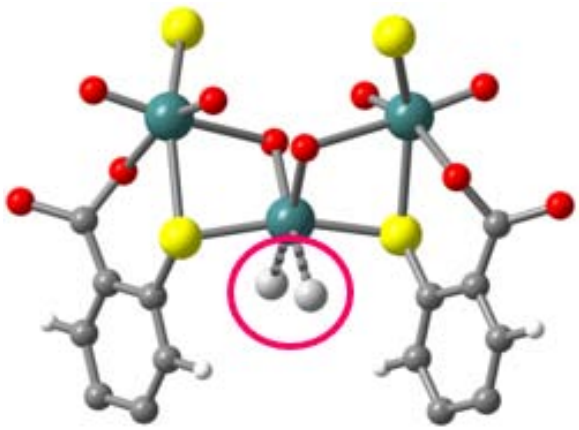

FIGURE 3. Crystal structure of Mn2(dsbdc) with two hydrogen molecules (gray spheres, circled) bound at the open metal site (Mn atoms shaded in green, S atoms in yellow, O atoms in red, and C atoms in gray) [Tomče Runčevski, et al., Chem. Commun., 2016, 52, 8251-8254, DOI: 10.1039/C6CC02494G]

In FY 2016, the program consolidated the core characterization and validation activities into the Hydrogen Storage Characterization Optimization Research Effort (HySCORE). The HySCORE team is led by researchers at National Renewable Energy Laboratory (NREL) and includes LBNL, PNNL, and NIST's Center for Neutron Research. This team provides a wide range of capabilities to support the program's materials-based storage development project portfolio, including HyMARC. These capabilities cover the validation of hydrogen capacity measurements, thermal conductivity measurements, infrared (IR) and nuclear magnetic resonance (NMR) spectroscopy, advanced microscopy, neutron scattering, and diffraction measurements, among others. The expertise and resources of the HyMARC national laboratory core team and the HySCORE team are available to support the individual projects in the program's materials-based hydrogen storage portfolio to accelerate progress.

FY 2016 marked the last year of the Hydrogen Storage Engineering Center of Excellence (HSECoE), which covered the program's materials engineering efforts. The HSECoE completed the evaluation of the HexCell and the Modular Adsorption Tank Insert (MATI), two sorbent prototype systems designed to achieve higher hydrogen adsorption densities, and finalized the validation of the framework models for the metal hydride, chemical hydrogen, and sorbent systems. Other models that were finalized through the HSECoE include the metal hydride acceptability envelope and finite element models and the tank volume/cost estimator model. A major milestone achieved during FY 2016 was making these models and resources accessible through the HSECoE.org website for use by the materials-based hydrogen storage R&D community. In FY 2016, a subset of the HSECoE partners (NREL, PNNL, and Savannah River National Laboratory [SRNL]) made improvements to the performance of the modeling package and incorporated an improved graphical user interface that is better suited for the end users.

Testing and Analysis

In FY 2016, the Hydrogen Storage program continued carrying out technoeconomic assessments of hydrogen storage technologies. Technical analysis and cost modeling of Type IV pressure vessel systems remained a critical focus during FY 2016. Analyses were performed to investigate strategies to improving carbon fiber utilization as a means of reducing cost. Analyses were also conducted for the hydrogen storage tanks deployed on the Toyota Mirai.

Additionally, initial reverse engineering analyses were performed to map the desired material physical, transport, thermodynamic, and kinetic properties needed for the hybrid high-pressure metal hydride tank system to approach the near-term system performance targets.

Specific accomplishments include:

- **Impact of winding speed:** Analyzed faster carbon fiber winding speeds (enabled by use of pre-preg or dry fiber winding) showing potential system cost reductions up to 3% markup versus lower manufacturing variations and faster winding speed tradeoffs for carbon fiber pre-impregnated with resin (pre-preg). (Strategic Analysis, Inc. [SA])
- **Alternate design:** Analyzed winding pattern improvements and tank boss redesign (as published by Toyota) showing system cost reductions of $0.50/kWh. (SA)

- **Balance of plant:** Evaluated impact of changing integrated valve from 316 stainless steel to aluminum, which results in a cost reduction of $0.16/kWh. (SA)
- **Vehicle tank analysis:** Studied the Toyota Mirai tank design and conducted ABAQUS simulations and determined the amount of carbon fiber required for 700 bar Type IV tanks that have similar design features as the Toyota Mirai tanks. The analysis predicted the design features could reduce the amount of carbon fiber composite by 4 to 7 weight percent for tanks with length-to-diameter ratios of 2.8–3.0. The carbon fiber composite weight reduction can be as high as ~20% if the tank is wound with the higher-strength T720 carbon fiber. (ANL)
- **Hybrid system modeling:** Evaluated a hybrid system concept of incorporating hydrogen storage materials into a 350 bar high-pressure tank and identified key material characteristics required for the hybrid system to match or exceed the performance of a 700 bar compressed hydrogen storage system. Initial analyses indicate the need for a material with an enthalpy and corresponding entropy of absorption of -21 kJ/mol and -104 J/mol·K, respectively, or less with a gravimetric capacity of at least 5.8 wt%. (ANL)

Advanced Physical Storage

In FY 2016 the program continued to investigate varying approaches to reduce the cost of compressed hydrogen gas storage tanks, with efforts focused on low-cost, high-strength carbon fiber precursors, alternative fiber and resin, cold-temperature operation, and conformable tank designs. Lightweight compressed gas storage vessels requiring a composite overwrap to contain hydrogen gas are considered the most likely near-term hydrogen storage solution for the initial commercialization of FCEVs, as well as for other early market applications. The carbon fiber composite used as overwraps can contribute as much as 75% or more to the overall cost of advanced Type IV tanks. The Hydrogen Storage program supported efforts at ORNL to reduce the cost of PAN-based fibers used as precursors to produce high-strength carbon fibers. The ORNL efforts focused on advanced precursor materials and processing since precursors have been shown to contribute approximately 50% of the total cost of high-strength carbon fibers. The team continued to investigate the development of melt-spinnable PAN precursors and processing techniques to replace the current spinning methods, which tend to be a more costly solution. Additionally, a team led by PNNL focused on reducing the cost of a Type IV tank system by developing enhanced operating conditions that demonstrated routes to increase carbon fiber usage efficiency.

Specific accomplishments include:

- **Cold gas tank testing:** Completed cold gas burst tests, with average burst pressure for tanks precooled to 200 K at 714 bar exceeding the target room temperature burst of ~625 bar. (PNNL)
- **Melt-spun PAN development:** Selected processing conditions and water–plasticizer formulations and demonstrated melt spinning of PAN-MA precursor fiber with >100 filament tows and >10 m in length. (ORNL)
- **Alternative manufacturing processes:** Demonstrated improved vacuum infused composite tank processing with reduced fabrication time from 2 h to 0.5 h for high-quality 7.5 L prototype vessels. Also achieved equivalent burst strength (26,586 psi) in static testing of small prototype vessels (Type III, 7.5 L). (Materia)
- **Alternative material qualification:** Quantified fatigue performance for low-Ni austenitic stainless steel (21Cr-6Ni-9Mn) with nominally the same fatigue performance as the tested strain-hardened 316L, allowing potential cost saving for balance of plant components. (SNL)
- **High-strength glass development:** Successfully demonstrated a high-throughput, high-temperature melting unit run to make high-strength fiber glass cullet. (PPG Industries Inc.)
- **Conformable tank development:** Completed initial testing with baseline compressed natural gas vessels and proved test system workability. Also measured baseline permeability performance for a storage vessel resin with permeability value at about half of the expected value. (Center for Transportation and the Environment)
- **Alternative design:** Evaluated both coupons and prototype tanks fabricated with a graded construction (i.e., replacing outer layers of higher-strength carbon fiber with a lower-strength carbon fiber) to demonstrate it as a viable option for lower-cost tanks. (CTD)
- **Cryo-compressed:** Constructed and commissioned a cryogenic hydrogen test facility allowing for the safe testing of full-size cold/cryogenic hydrogen storage vessels using a hydrogen cryo-pump to supply high-pressure supercritical hydrogen. (LLNL)

Advanced Materials Development

In FY 2016 the program continued efforts in developing and improving hydrogen storage materials with potential to meet the 2020 onboard storage targets. Both the HyMARC and HySCORE teams were initiated, and the first round of individual projects was selected. Overall efforts on metal hydrides continued to emphasize material discovery coupled with reducing desorption temperatures and improving kinetics. For hydrogen sorbents, efforts were focused on increasing the isosteric heat of adsorption through inclusion of open metal centers or metal atom doping of carbons to increase the adsorbed capacity at higher temperatures, and improving standard measurement practices for hydrogen capacity.

Five new awards were selected in FY 2016 as the initial individual projects within HyMARC:

- **Argonne National Laboratory** will develop novel graphene-encapsulated complex hydride (hydride@graphene) composite materials which display high gravimetric capacities with improved thermodynamics, kinetics, and reversibility compared to the bulk metal hydrides.
- **The Pennsylvania State University** will synthesize boron-doped polymers containing high surface areas and exposed acidic binding sites for enhanced hydrogen adsorption enthalpies.
- **University of Hawaii** will develop new magnesium boride etherate compounds in an effort to find improved kinetic and thermodynamic pathways for the reversible hydrogenation of magnesium boride to magnesium borohydride.
- **University of Missouri-St. Louis** will develop functionalized porous carbons doped with nitrogen heteroatoms to kinetically stabilize alane and improve its reversibility.
- **Liox Power, Inc.** will investigate the inclusion of a thin solvent layer to improve sorption kinetics of hydrogen storage materials at moderate temperature and pressure conditions.

Specific accomplishments include:

- **Multiple H_2 adsorption:** Validated, for the first time, the adsorption of two hydrogen molecules bound to a single open metal site in a sorbent material, as confirmed by neutron powder diffraction. (LBNL, NIST)
- **Round-robin testing:** Initiated a multi-laboratory, round-robin study on volumetric uptake in sorbents, which includes national laboratories, universities, industry, and international participants, to identify sources of error in volumetric uptake measurements—the results of which will be disseminated to the adsorption community to improve data reliability. (NREL)
- **Characterization method development:** Developed new advanced NMR techniques which allowed the measurement of solid-state ^{1}H NMR spectra for hydrogen physisorbed to an open metal site in a MOF to gain insight into binding energies. (PNNL)
- **Computational method development:** Made significant progress using several types of computational techniques to move towards multiscale simulations that investigate thermodynamics and kinetics at interfaces and surfaces of storage materials. (LLNL)
- **Sample handling development:** Developed and implemented clean, air-free techniques for sample transfer for X-ray studies, and established X-ray adsorption spectroscopy as a tool for probing metal hydrides, including separate bulk- and surface-sensitive approaches. (SNL)
- **High-throughput computational screening:** Utilized computational screening of structure databases to discover MOFs that display improved hydrogen capacities over the baseline MOF-5 material, with IRMOF-20 experimentally demonstrated to have 27% higher usable gravimetric capacity at 100 bar. (University of Michigan)

Engineering

FY 2016 was the final year of the HSECoE. The effort for the year was focused in two areas: completing the evaluation of the two hydrogen sorbent prototypes and validating and posting the various models developed through the HSECoE. SRNL led the testing and evaluation of the sorbent prototypes, one with flow-through cooling using an aluminum honeycomb cell core heat exchanger (HexCell) and a second with a liquid N_2 cooled microchannel MATI heat exchanger. NREL will lead a continuing effort to maintain and improve the various models developed through

the HSECoE and available to the research community through a website. SRNL and PNNL will collaborate with NREL in this effort. SRNL also leveraged the system models and system engineering expertise from the HSECoE to design a materials-based storage system for use on a U.S. Navy unmanned underwater vehicle (UUV) and provided a bench-scale prototype for evaluation. Preliminary analyses indicate a fuel cell system with alane hydrogen storage can provide two to three times the energy storage of battery systems.

Specific accomplishments include:

- **Prototype testing:** Completed evaluation of the HexCell and MATI prototype hydrogen adsorbent systems and validation of the HexCell and MATI vehicle-level system models. (SRNL)
- **System models development:** Updated and integrated several HSECoE storage system models within the vehicle modeling framework and posted them on HSECoE's website portal. These included a 700 bar physical storage model, a metal hydride model, two cold hydrogen models, and two adsorbent system models. (NREL, SRNL, PNNL)
- **Model dissemination:** Completed documentation website updates for the posted models (including website text and downloadable user manual). (NREL, SRNL, PNNL)
- **System development:** Completed an engineering analysis to screen for the most attractive solid-state hydrogen storage material to meet Navy requirements for UUV application, performed testing to demonstrate alane storage and delivery performance against steady-state and transient operations, and prepared and delivered a bench-scale prototype system to the Naval Underwater Warfare Center for evaluation. (SRNL)

BUDGET

The FY 2017 budget request allocates $15.6 million to the Hydrogen Storage program. This is consistent with the FY 2016 congressional appropriation of $15.6 million. In FY 2017, the Hydrogen Storage program will continue to focus on nearer-term R&D to lower the cost of high-pressure storage systems through low-cost carbon fiber precursors, demonstrate alternative fibers and resins, and identify innovative approaches to tank design. Longer-term advanced materials R&D work will be coordinated through the newly established HyMARC and HySCORE efforts to ensure impact is maximized and resources are utilized effectively. The program will also continue to complete systems analyses. The program plans to initiate new activities in these areas for onboard automotive applications.

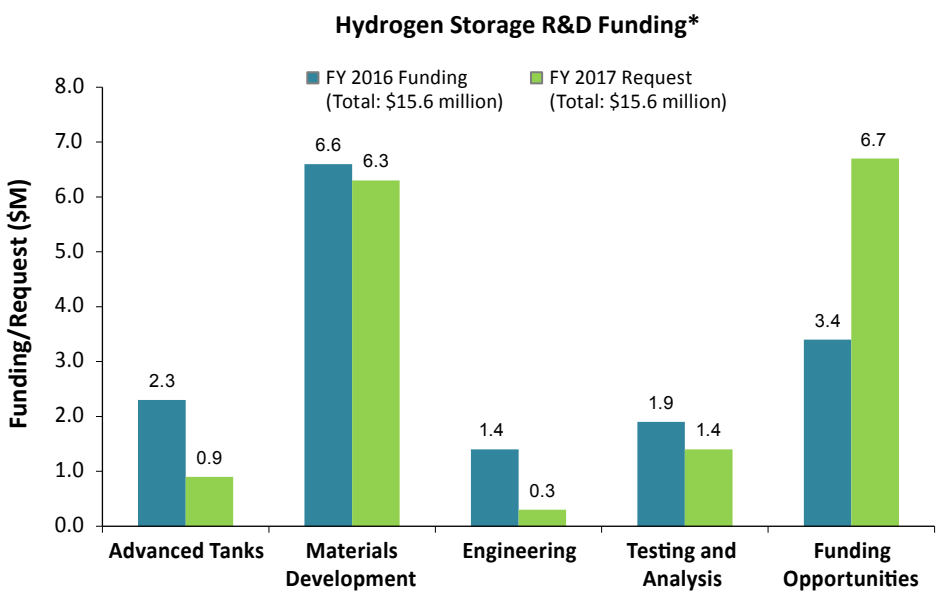

*Subject to appropriations, project go/no-go decisions, and competitive selections. Exact amounts will be determined based on research and development progress in each area.

FIGURE 4. FY 2016 budget appropriations and FY 2017 budget request for the Hydrogen Storage program, indicating funds allocations per technology area

FY 2017 PLANS

The technology portfolio for the Hydrogen Storage program emphasizes materials R&D to meet system targets for onboard automotive and non-automotive applications. The emphasis on developing lower-cost physical storage technologies will continue and will be coordinated with related activities through the Vehicle Technologies Office and Advanced Manufacturing Office (AMO) within the Office of Energy Efficiency and Renewable Energy. Specifically, the program will continue to coordinate with and leverage efforts through the AMO-led Institute for Advanced Composite Manufacturing Innovation to develop approaches to low-cost compressed gas storage systems manufacturing. System analysis will continue through efforts at ANL and SA. With the newly established HyMARC and the consolidation of the characterization and validation efforts, the existing and future materials-based hydrogen storage R&D efforts and individual projects will be coordinated to maximize the use of capabilities and ensure collaboration across groups to enable results that are both impactful and relevant to the Hydrogen Storage program's 2020 and ultimate goals.

Ned Stetson
Hydrogen Storage Program Manager
Fuel Cell Technologies Office
Office of Energy Efficiency and Renewable Energy
U.S. Department of Energy
1000 Independence Ave., SW
Washington, DC 20585-0121
Phone: (202) 586-9995
Email: Ned.Stetson@ee.doe.gov

IV.A.1 System Analysis of Physical and Materials-Based Hydrogen Storage

Rajesh K. Ahluwalia (Primary Contact), T.Q. Hua, J-K Peng, and Hee Seok Roh
Argonne National Laboratory
9700 South Cass Avenue
Argonne, IL 60439
Phone: (630) 252-5979
Email: walia@anl.gov

DOE Manager: Grace Ordaz
Phone: (202) 586-8350
Email: Grace.Ordaz@ee.doe.gov

Start Date: October 1, 2004
Projected End Date: Project continuation and direction determined annually by DOE

Overall Objectives

- Model various developmental hydrogen storage systems.
- Provide results to DOE for assessment of performance targets and goals.
- Develop models to "reverse-engineer" particular approaches.
- Identify interface issues, opportunities, and data needs for technology development.

Fiscal Year (FY) 2016 Objectives

- Perform ABAQUS analysis of Type-IV tanks that incorporate the design features similar to the Toyota Mirai compressed hydrogen storage tanks.
- Determine the potential and attributes of high pressure metal hydrides that can improve the performance of high-pressure hydrogen storage tanks. Analyze the performance metrics for a 350 bar hybrid tank storage system.

Technical Barriers

This project addresses the following technical barriers from the Hydrogen Storage section of the Fuel Cell Technologies Office Multi-Year Research, Development and Demonstration Plan.

(A) System Weight and Volume

(B) System Cost

(C) Efficiency

(E) Charging/Discharging Rates

(J) Thermal Management

(K) System Life Cycle Assessments

Technical Targets

This project is conducting system level analyses to address the DOE 2017 technical targets for on-board hydrogen storage systems.

- System gravimetric capacity: 1.8 kWh/kg
- System volumetric capacity: 1.3 kWh/L
- Minimum hydrogen delivery pressure: 5 bar
- Refueling rate: 1.5 kg/min
- Minimum full flow rate of hydrogen: 0.02 g/s/kW

FY 2016 Accomplishments

- Conducted ABAQUS simulations to determine the amount of carbon fiber (CF) for 700 bar Type-IV tanks that have similar design features as the Toyota Mirai storage tanks. The analysis predicts that these design features could reduce the amount of CF by 4–7% for tanks with length-to-diameter (L/D) ratio of 2.8–3.0, but there is no impact for tanks with L/D ~1.7. The CF composite weight reduction is ~20% if the tank is wound with the higher strength T720 carbon fiber.
- Established new 2015 status performance metrics for 700 bar compressed hydrogen storage tanks: 1.40 kWh/kg gravimetric capacity, 0.81 kWh/L volumetric capacity, 97 kg T700 CF composite.
- Conducted reverse engineering analysis to map the desired material physical, transport, thermodynamic, and kinetic properties needed for the hybrid high-pressure metal hydride tank system to approach the near-term system performance targets. The analysis shows that a hybrid hydrogen storage system with a 350 bar Type-IV tank has the same volumetric and gravimetric capacities as a compressed hydrogen (cH_2) storage system with a 700 bar Type-IV tank. The required amount of carbon fiber in such a hybrid system is 51 kg compared to 97 kg in a 700 bar Type-IV cH_2 tank, and 62 kg in a 350 bar Type-IV cH_2 tank.

✧ ✧ ✧ ✧ ✧

INTRODUCTION

Several different approaches are being pursued to develop on-board hydrogen storage systems with the goal of meeting the DOE targets for light-duty vehicle applications. Each approach has unique characteristics, such as pressure and temperature, the thermal energy and temperature of charge and discharge, kinetics of the physical and chemical process steps involved. The approaches take into account the requirements for the materials and energy interfaces between the storage system, the fuel supply system, and the fuel user. Other storage system design and operating parameters influence the projected system costs as well. Models are being developed to understand the characteristics of storage systems based on the various approaches, and to evaluate their potential to meet the DOE targets for on-board applications, including the off-board targets for energy efficiency.

APPROACH

The approach is to develop thermodynamic, kinetic, and engineering models of the various hydrogen storage systems being developed under DOE sponsorship. These models are then used to identify significant component and performance issues, and to assist DOE and its contractors in evaluating alternative system configurations and design and operating parameters. Performance criteria are established that may be used, for example, in developing storage system cost models. Data is refined and validated as the models become available from the various developers. The team works with the Hydrogen Storage Systems Analysis Working Group to coordinate research activities with other analysis projects to assure consistency and to avoid duplication. An important aspect of this work is to develop overall systems models that include the interfaces between hydrogen production and delivery, hydrogen storage, and the fuel cell.

RESULTS

Physical Storage

The team conducted ABAQUS analysis of the hydrogen storage tanks deployed on the Toyota Mirai. The Toyota Mirai storage tanks have three distinct features [1] that differ from conventional tanks: (1) the liner has a sharp transition from the dome to the cylinder, (2) hoop winding is concentrated in the inner portion of the overwrap with high angle helical winding eliminated, and (3) the boss has a smaller opening diameter and longer flange. The general winding sequence [2] consists of one helical layer over the entire liner, followed by concentrated hoop winding over the cylinder and finally helical/hoop winding over the tank as typically encountered in conventional tanks. Furthermore, the team considers an alternative winding scheme in which glass fiber is used for the first helical layer to take advantage of its high failure strain (3.5% compared to <2% for carbon fiber).

The team analyzed two tanks that have the same volume (~60 L) and length-to-diameter ratio (L/D = 2.8) as the Mirai front tank. The first tank is a conventional tank and the second incorporates the Mirai tank design features. Both tanks are wrapped with T700 carbon fiber. The conventional tank requires 43.0 kg carbon fiber composite (CF), while the tank with the Mirai design features requires 39.9 kg, a 7.2% reduction. The 3.1 kg reduction in CF comprises of 1.9 kg reduction in the cylinder section and 1.2 kg in the domes.

The team also analyzed two tanks that have the same volume (~62 L) as the Mirai rear tank, which has an L/D ratio of 1.7. The results show practically no difference (~0.3 kg) in the required amount of CF between a conventional tank and one that incorporates the Mirai design features. The reduction in the amount of CF wrapped over the domes (1.94 kg) is offset by a larger increase in the amount of CF wrapped through the cylinder section (2.24 kg). In terms of hoop/helical windings, there is a small reduction in hoop windings, which is offset by a small increase in helical windings. The distribution of CF in the cylinder section and the domes are shown in Table 1 for the front and rear tanks.

The team applied the Mirai design features and fiber winding scheme in constructing a finite element analysis (FEA) model for a full-sized tank that has a L/D ratio of 3.0 and holds 5.6 kg of usable hydrogen. The team considered four choices of composite materials: (1) T700 CF with epoxy, (2) T700 CF with vinyl ester low cost resin, (3) T700 CF with low cost resin and alternate sizing, and (4) T720 CF with epoxy. For each of the T700 CF composites, two tanks were analyzed, one with the conventional design and another that incorporates the Mirai design features. First, two tanks differing only in the boss configuration were analyzed to determine the impact of the boss on the amount of helical

TABLE 1. ABAQUS Results for 2.3-kg H_2 Front (L/D = 2.8) and Rear (L/D = 1.7) Tanks

	Front Tank (60 L), L/D = 2.8			Rear Tank (62 L), L/D = 1.7		
	Conventional	Mirai Design	Difference	Conventional	Mirai Design	Difference
Cylinder	34.6	32.7	-1.9	29.5	31.8	2.3
Dome	8.4	7.2	-1.2	15.3	13.4	-1.9
Total	43	39.9	-3.1	44.9	45.2	0.3

winding: one approximated the Mirai boss and another used a more typical boss that has a larger opening diameter and shorter flange. The results in stress distributions and amount of helical winding are practically unchanged. It should be noted that the Mirai boss simulated in the FEA model is derived from the drawing published in Reference 1. Details of the boss configuration and dimensions are not available.

The analysis results, presented in Figure 1, show that the T700 CF composite weight in the tanks that incorporated the Mirai design is 4.1–6.3% lower than that for comparable conventional tanks. In reference to the 2015 baseline tank which requires 97 kg carbon fiber composite [3], changing the liner design and winding method reduced the amount of composite to 92.3 kg (4.8% reduction). If glass fiber is used for the first helical layer, the amount of carbon fiber composite is further reduced to 90.8 kg, but 2.7 kg glass fiber is added to the tank. The tank wound with T720 CF composite weighs substantially less, because T720 CF has higher tensile strength, therefore less material is needed for reinforcement. The effect of L/D is illustrated in Figure 2. It compares the percentage reduction in CF composite weight relative to a conventional tank for tanks that hold 2.3 kg H_2 and 5.6 kg H_2. The tanks are reinforced with T700 CF/epoxy or T700 CF with low cost resin and alternate sizing. The integration of the Mirai tank design features could reduce the CF composite weight by 5–7% for tanks with L/D ~2.8–3.0, but has little or no impact for tanks with L/D ~1.7 due to geometric effect given constant volume.

Hydrogen Storage in High Pressure Metal Hydrides

The team developed a model for high pressure metal hydrides (HPMH) and used it to determine a map of desirable material properties to augment the performance of cH_2 systems. For the purpose of this study, HPMH is defined as a metal hydride that is unstable at room temperature and pressure, but can be formed at elevated hydrogen pressures. As a first application, a hybrid concept is considered in which hydrogen is stored as compressed gas at 350 bar in a Type-IV tank, which also contains HPMH to improve its overall volumetric capacity. The following is a list of some desirable material properties that HPMH should have for this hybrid storage concept.

- The equilibrium pressure at 80°C should be less than 200 bar so that the tank can be refueled at 350 bar (P_c) without exposing the liner to temperatures above the allowable limit for HDPE used in Type-IV tanks. The team has included a $\Delta P = P_c - P_{eq}(80°C)$ of 150 bar to accommodate for reasonable charge kinetics.
- The equilibrium pressure should be above the minimum delivery pressure (P_d = 5 bar) at all allowable operating and ambient temperatures. The requirement that the fuel cell is able to start at -40°C requires that $P_{eq}(-40°C)$ should be higher than 5 bar. Without this requirement, a buffer tank would be needed to supply hydrogen to the fuel cell until the tank pressure reaches 5 bar.
- The hybrid storage system has 100% on-board efficiency (i.e., all the stored hydrogen is available to the fuel cell) if HPMH can be discharged using the stack coolant as the heat source. In the fuel cell systems of current interest, the steady-state coolant temperatures may vary between 60°C and 90°C. The team requires that the HPMH should discharge at the lowest coolant temperature and, for reasonable discharge kinetics, $\Delta P = P_{eq}(60°C) - P_d$ be higher than 50 bar.

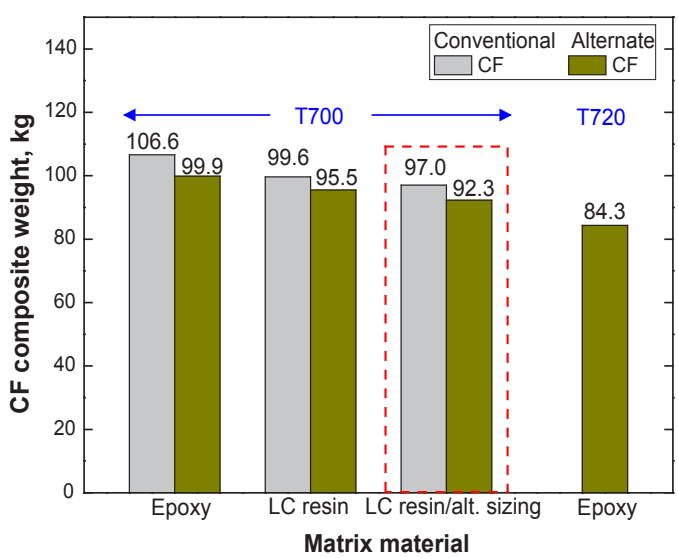

FIGURE 1. Composite weight in conventional tanks and tanks with Toyota Mirai design features

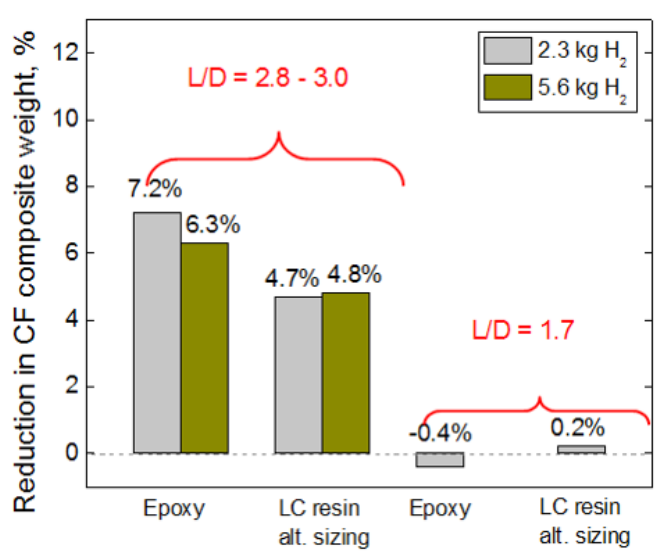

FIGURE 2. Effect of length-to-diameter ratio on carbon fiber savings

Figure 3 presents a ΔH vs. ΔS thermodynamic acceptability map of HPMH materials that meet the above requirements and for which the van't Hoff equation for plateau pressure is applicable. The boundary AB in Figure 1 is determined from the third requirement to discharge HPMH using the stack coolant at 60°C as heat source. The boundary BC is determined from the second requirement to maintain the tank pressure above 5 atm at all operating temperatures including -40°C. The boundary CD is determined from the first requirement to maintain reasonable ΔP while refueling the tank to 350 atm at 80°C

The team developed a dynamic model for refueling of a hybrid tank containing HPMH and incorporated the dynamic refueling model in the system analysis code. The combined code was used to conduct an initial study to determine HPMH properties, such that a hybrid hydrogen storage system with a 350 bar Type-IV tank (see Figure 4) has the same volumetric and gravimetric capacities as a cH_2 storage system with a 700 bar Type-IV tank, while also satisfying all other system targets. As shown in Table 2, the required amount of CF in such a hybrid system is much smaller than the CF needed in a 700 bar Type-IV cH_2 tank and is even smaller than the CF needed in a 350 bar Type-IV cH_2 tank.

Table 3 summarizes the initial results for HPMH material properties needed to satisfy the listed constraints. The results indicate that the material needs to have 6.9 wt% intrinsic hydrogen capacity with 10% minimum and 93% maximum state-of-charge (SOC) for the system to reach 4.3 wt% gravimetric capacity. The HPMH needs to be compacted to 292 kg/m^3 bulk density for 24.6 g/L volumetric capacity. The model includes an allowance of 10 wt% expanded natural graphite (ENG) for the medium to reach

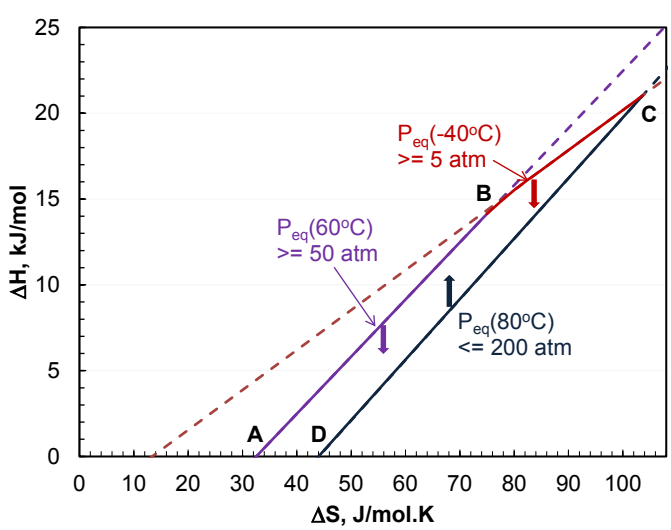

FIGURE 3. Thermodynamic acceptability map of high pressure metal hydrides. Boundary AB is determined from HPMH discharge temperature, BC from minimum operating pressure, and CD from refueling kinetics.

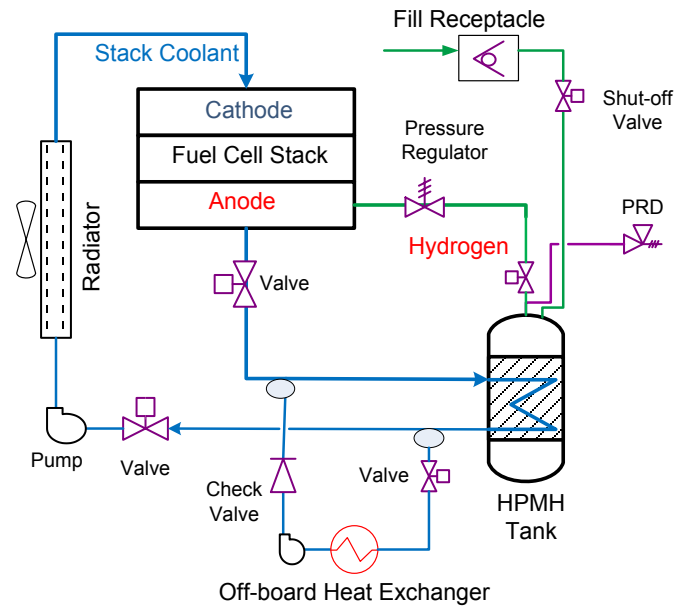

FIGURE 4. Hybrid system with 350-bar Type-IV tank filled with high pressure metal hydrides

TABLE 2. Performance of Hybrid Storage Concept Relative to Compressed Hydrogen Systems, All Systems with 5.6 kg Recoverable Hydrogen Capacity

Storage System	Compressed H_2		Hybrid
Storage Pressure	700 bar	350 bar	350 bar
Volumetric Capacity	24.4 g/L	17.7 g/L	24.6 g/L
Gravimetric Capacity	4.2 wt%	5.4 wt%	4.3 wt%
Carbon Fiber	97 kg	62 kg	51 kg

5 W/m.K bed conductivity. The hybrid system can satisfy the 1.6 g/s full flow target even at the minimum SOC, if the HPMH discharge kinetics is such that SOC decreases isothermally in 6.2 min (τ_d) from 93% to 10% at 5 bar backpressure and 60°C. Similarly, the hybrid system can satisfy the 1.5 kg/min refueling rate target if the HPMH charge kinetics is such that SOC increases isothermally in 3.7 min (τ_c) from 10% to 93% at 350 bar backpressure and 60°C.

Only 45% of the 5.6 kg recoverable hydrogen in the hybrid system is stored in HPMH; the remaining 55% is stored in the voids and pores as compressed gas. According to our model, the charge kinetics is fast enough to reach 90% SOC during the refueling time, but hydrogen absorption continues even after the coolant flow is stopped. Future studies will evaluate the possibility of taking credit for the continuing hydrogen absorption after the refueling event.

TABLE 3. Desired HPMH Physical, Transport, and Kinetic Properties

Variables	Related Variables	Reference Values	Constraints
HPMH Intrinsic Capacity		5.8% H capacity	4.3 wt% gravimetric
Fill Ratio	Bulk Density Thermal Conductivity	80.6% bed porosity 292 kg/m^3 HPMH bulk density 5 W/m.K bed conductivity	24.6 g/L volumetric
Desorption Kinetics	X_{min} = 10%	τ_d = 6.2 min	1.6 g/s min full flow
Sorption Kinetics	X_{max} = 93%	τ_c = 6.7 min	X_{min} to X_{max} in 3.7 min
HX Tube Spacing	Number of Tubes	r_2/r_1 = 4.5, 58 U tubes	1.5 kg/min refueling
Refueling Pressure	Storage Pressure	410 atm	350 bar pressure 25% overpressure limit
Mass of HPMH	Mass of Expanded Natural Graphite	46.5 kg HPMH 4.7 kg ENG ΔH = 14.8 kJ/mol DS = 77.2 J/mol.K E_A = 45 kJ/mol	5.6 kg usable H_2 3.4 kg as cH_2 2.5 kg H_2 in HPMH

CONCLUSIONS AND FUTURE DIRECTIONS

- The team estimates 4–7% (varying with tank capacity) reduction in the amount of T700 composite for a tank that incorporates the Mirai tank design features and with L/D ~2.8–3.0, but no reduction for L/D ~1.7. Replacing carbon fiber with glass fiber for the first helical layer could further reduce the carbon fiber amount by an additional 2–5%. The team estimates ~20% reduction in composite weight for a full-sized tank (5.6 kg H_2), with Mirai tank features, the majority of the reduction is due to switching to higher strength T720.
- The ABAQUS FEA results show practically no difference in the required amount of helical winding for using a boss with smaller diameter opening and longer flange.
- The team estimates that a hybrid system that stores hydrogen as compressed gas at 350 bar and also contains HPMH matches the gravimetric and volumetric capacities of a 700 bar cH_2 system. The required amount of CF in such a hybrid system is 47% less than the CF needed in a 700 bar Type-IV cH_2 tank and is even smaller than the CF needed in a 350 bar Type-IV cH_2 tank.
- The team estimates that 45% of the 5.6 kg recoverable hydrogen in the hybrid system is stored is in HPMH; the remaining 55% is in the voids and pores as compressed gas. According to the model, the charge kinetics is fast enough to reach 90% SOC during the refueling time, but hydrogen absorption continues even after the coolant flow is stopped.
- In FY 2017, the team will conduct ABAQUS simulations to determine potential CF savings in alternate tank concepts, such as an elliptical tank and assess the manufacturability of alternate concepts. The team will investigate the feasibility of packaging alternate tank configurations onboard light-duty vehicles to achieve optimal volumetric capacity.
- In FY 2017, the team will conduct fatigue and autofrettage analysis to determine the fatigue life of liner in Type-III tanks storing hydrogen at ambient and cryogenic temperatures. Additionally, the team will conduct MultiMech analysis to investigate the effect of void content in resin on the degradation of composite performance in pressure vessels.
- In FY 2017, the team will analyze the cryocompressed hydrogen storage option for captured fleets (e.g. busses, waste trucks) where dormancy is less of an issue. The team will utilize recent Lawrence Livermore National Laboratory data for cryotanks and the Linde liquid hydrogen pump in the system model.
- In FY 2017, the team will update the sorption model to analyze the performance of the best-of-class metal organic frameworks (e.g., M_2(m-dobdc), M = Mg, Mn, Fe, Co, Ni series of frameworks), developed at Lawrence Berkeley National Laboratory, in a representative on-board storage system under realistic operating conditions.

FY 2016 PUBLICATIONS/PRESENTATIONS

1. R.K. Ahluwalia, J.K. Peng, and T.Q. Hua, "Sorbent Material Properties for On-board Hydrogen Storage for Automotive Fuel Cell Systems," International Journal of Hydrogen Energy. 40 (2015) 6373–6390.

2. R.K. Ahluwalia and T.Q. Hua, "Pressurized Systems," Chapter 15 in Data, Facts and Figures on Fuel Cells, Detlef Stolten and Remzi and Nancy Garland (Editors), Wiley-VCH, 2016, 143–148.

3. R.K. Ahluwalia and T.Q. Hua, "Onboard Safety," Chapter 18 in Fuel Cells Data, Facts and Figures, Detlef Stolten and Remzi Samsun and Nancy Garland (Editors), Wiley-VCH, 2016, 177–182.

4. R.K. Ahluwalia, J.K. Peng, and T.Q. Hua, "Implementing Hydrogen Storage Based on Metal Hydrides," Chapter 32 in Hydrogen Science and Engineering, Materials, Processes, Systems and Technology, Vol 2, Detlef Stolten and Bernd Emonts (Editors), Wiley-VCH, 2016, 791–808.

5. H.S. Roh, T.Q. Hua, and R.K. Ahluwalia "Modeling of Type IV Hydrogen Storage Tanks and the Toyota Mirai Storage Tank Design," Storage System Analysis Working Group Meeting, November 16, 2015.

6. R.K. Ahluwalia, T.Q. Hua, J.K. Peng, and H.S. Roh, "System Level Analysis of Hydrogen Storage Options," Hydrogen Storage Tech Team Meeting, Southfield, MI, March 17, 2016.

REFERENCES

1. Yamashita, A., Kondo, M., Goto, S., and Ogami, N., "Development of High-Pressure Hydrogen Storage System for the Toyota "Mirai"," SAE Technical Paper 2015-01-1169, 2015, doi:10.4271/2015-01-1169.

2. Hirokazu Otsubo and Shiro Nishibu, U.S. Patent US20130299505A1, November 2013.

3. DOE Hydrogen and Fuel Cells Program Record, Record # 15013, September 30, 2015.

IV.A.2 Hydrogen Storage Cost Analysis

Brian D. James (Primary Contact),
Cassidy Houchins, Jennie M. Moton,
Daniel D. DeSantis
Strategic Analysis, Inc.
4075 Wilson Blvd., Suite 200
Arlington, VA 22203
Phone: (703) 778-7114
Email: bjames@sainc.com

DOE Manager: Grace Ordaz
Phone: (202) 586-8350
Email: Grace.Ordaz@ee.doe.gov

Contract Number: DE-EE0005253

Project Start Date: September 30, 2012
Project End Date: September 29, 2016

Overall Objectives

- Identify and/or update the configuration and performance of a variety of hydrogen storage systems for both vehicular and stationary applications.
- Conduct rigorous cost estimates of multiple hydrogen storage systems to reflect optimized components for the specific application and manufacturing processes at various rates of production.
- Explore cost parameter sensitivity to gain understanding of system cost drivers and pathways to lowering system cost.

Fiscal Year (FY) 2016 Objectives

- Update and expand the cost analysis of onboard hydrogen storage in pressurized carbon composite (fiber and resin) pressure vessels.
- Incorporate reduced cost, integrated balance of plant (BOP) components into cost model.
- Assess cost and performance impact of Pacific Northwest National Laboratory (PNNL) enhanced materials and design concepts for pressurized hydrogen storage
- Identify cost drivers and pathways to lowering cost.
- Document all analysis results and assumptions.

Technical Barriers

This project addresses the following technical barriers from the Hydrogen Storage section of the Fuel Cell Technologies Office (FCTO) Multi-Year Research, Development, and Demonstration Plan.

(B) System Cost

(H) Balance of Plant (BOP) Components

(K) System Life-Cycle Assessments

Technical Targets

This project conducts cost modeling to attain realistic, process-based system costs for a variety of H_2 storage systems. These values can inform future technical targets for System Storage Cost.

- System Storage Cost: <$12/kWh net (2017 target)

FY 2016Accomplishments

- Updated Type IV 700 bar storage system cost status.
- Investigated cost impact of manufacturing and fiber variations.
- Estimated uncertainty in gravimetric and volumetric capacity.
- Investigated strategies to improving carbon fiber utilization as a means of reducing cost.
  - Vacuum infiltration to reduce resin void fraction
  - Analyzed markup versus lower manufacturing variations and faster winding speed tradeoffs for carbon fiber pre-impregnated with resin (pre-preg)
  - Winding pattern improvements and tank boss redesign (as demonstrated by Toyota)
- Evaluated impact of changing integrated valve from 316SS to aluminum.

✧ ✧ ✧ ✧ ✧

INTRODUCTION

The FCTO has identified hydrogen storage as a key enabling technology for advancing hydrogen and fuel cell technologies and has established goals of developing and demonstrating viable hydrogen storage technologies for transportation and stationary applications. The cost assessment described in this report supports the overall FCTO goals by identifying the impact of components, performance levels, and manufacturing and assembly techniques on storage system cost at a variety of annual manufacturing rates. The results of this analysis enable the

DOE to compare the cost impact of new components, etc., to the overall 2017 and Ultimate DOE cost targets. The cost breakdown of the system components and manufacturing steps can then be used to guide future R&D decisions.

Since the last Annual Progress Report, Strategic Analysis and FCTO issued a joint update to the status of 700 bar type IV hydrogen storage system cost [1] based on advances made in materials and BOP components and included an explicit accounting of manufacturing and fiber variations which result in additional carbon fiber composite used to meet statutory requirements. In addition to the model updates described in Ordaz, et al. [1], a preliminary estimate of the uncertainty in capacity (gravimetric and volumetric) was also analyzed using test results from PNNL and Hexagon Lincoln. Using the status reported in Ordaz, et al. as a baseline for comparison, processs, and design strategies were investigated to explore potential cost savings by decreasing the total amount of carbon fiber composite used.

APPROACH

A Design for Manufacturing and Assembly style cost analysis methodology was used to assess the materials and manufacturing cost of hydrogen storage systems and components. Key system design parameters and engineering system diagrams describing system functionality and postulated manufacturing process flows were obtained from a combination of industry partners, Argonne National Laboratory (ANL), and internal analysis. This data was used to develop a mechanical design of each component, including materials, scaling, and dimensions. Based on this design, the manufacturing process train was modeled to project the cost to manufacture each part. Cost was based on the capital cost of the manufacturing equipment, machine rate of the equipment, equipment tooling amortization, material costs, and other financial assumptions. Once the cost model was complete for the system design, sensitivity data for the modeled technology was obtained by varying key parameters. Results were shared with ANL, the National Renewable Energy Laboratory, and industry partners to obtain feedback and further refine the model.

The analysis explicitly includes fixed factory expenses such as equipment depreciation, tooling amortization, utilities, and maintenance as well as variable direct costs such as materials and labor. However, because this analysis is intended to model manufacturing costs, a number of components that usually contribute to the original equipment manufacturer price are explicitly not included in the modeling. These costs are excluded in this analysis: profit and markup, one-time costs such as non-recurring research, design, engineering, and general expenses such as general and administrative costs, warranties, advertising, and sales taxes.

RESULTS

Updated Type IV 700 bar storage system cost status were based on reductions due to balance of plant component integration, lower cost and lower density resin, and carbon fiber cost reductions from low-cost precursor fiber. Major cost increases in the updated status were due to composite mass increase due to replacing the previously used carbon fiber dome reinforcements with additional helical windings, and increasing the total composite to account for manufacturing and fiber variations per current industrial practice. The baseline system cost is projected to be $14.8/kWh with a 90% confidence interval of [-$0.8/kWh, +1.7/kWh] estimated using Monte Carlo error analysis.

In addition to updating the cost status, uncertainty in capacity (gravimetric and volumetric) was estimated and reported for the first time this year. Data provided by PNNL was used to assess the uncertainty in gravimetric and volumetric capacity for the tank while a 10% mass contingency was assumed for the BOP. Based on the PNNL data, the coefficient of variation in tank masses was found to typically be between 1% and 1.5%. Tank-to-tank manufacturing variation in the carbon fiber (CF) mass within a single tank manufacturer is expected to be very small due to tight manufacturing tolerances. On the other hand, the resin mass may vary measurably given its low-viscosity and the likelihood that resin will drip and be squeezed out from the fibers due to tension and compression during the wet-winding process. BOP mass uncertainty data are not available; consequently a ±10% BOP mass uncertainty was assumed as a reasonable approximation. Uncertainty in the volumetric capacities was calculated using the mass variations described above and the density of the respective materials. The resulting uncertainty (±0.04 kWh/kg and ±0.01 kWh/L) represents the best available estimate given the data available, but may understate the uncertainty.

High volume manufacturing of composite pressure vessels with an extended service life requires some level of overdesign to ensure safety and statutory requirements. Consequently, vessels are designed with enhanced wall thickness and burst pressure to account for both fiber strength and manufacturing process variations in high volume manufacturing. Current design practice is based on a 3σ[1] overdesign which is consistent with burst testing of every 200th tank. Based on conversations with tank manufacturers, typical coefficients of variation (COV) for manufacturing and fiber variation are around 3% each. In previous analyses, ANL included a 10% increase in composite mass to account for variations in fiber strength: this is approximately equivalent to a 3σ overdesign and a fiber COV of 3.3%. In order to explicitly account for manufacturing variability and to be consistent with current manufacturing practices, a manufacturing COV of 3.3% was assumed. This results in a

[1] $\sigma = \text{standard deviation} = \sqrt{(COV_{manufacturing}^2 + COV_{fiber}^2)}$

combined fiber and manufacturing overdesign of 14% in the baseline design.

Strategies to reduce cost by improving carbon fiber utilization and increasing winding speed were investigated. Tank winding is a time-consuming step, projected to take as long as five hours per tank in the current model using an average winding speed of 26 meters of carbon fiber per minute. Figure 1 shows the manufacturing cost (the amortized cost of the winding machinery, electricity, and labor cost) of winding a single 5.6 L 700 bar pressure vessel as a function of winding speed. At the baseline 26 m/min, the total winding manufacturing cost is $0.80/kWh or a little more than 5% of the total system cost. The current cost model assumes a winding speed of 40 m/min for carbon fiber pre-impregnated with resin (pre-preg); however, some have suggested pre-preg winding speeds of 90 m/min may be possible which is projected to reduce the winding manufacturing cost to around $0.20/kWh or ~1% of the total system cost.

In addition to investigating potential cost reductions from increasing the winding speed, tradeoffs between faster winding time and manufacturer's markup on pre-preg were investigated. Compared to wet-winding, and in addition to faster winding speeds, pre-preg is expected to achieve lower resin wastage and may achieve a lower manufacturing coefficient of variation ($COV_{manufacturing}$) resulting in lighter tanks. To understand these tradeoffs, we parametrically analyzed the cost of materials and manufacturing for pre-preg and compared them at multiple markup rates against the cost of wet winding. Figure 2 shows a parametric examination of the total material (carbon fiber and resin) and manufacturing cost of pre-preg as a function of winding speed and manufacturer's markup (a percentage multiplier). The red line marks the cost of wet winding materials and manufacturing (at 26 m/min). Where the grey dashed lines cross the red line is where the cost of pre-preg is expected to be at cost parity with wet winding for a given markup. This analysis suggests that pre-preg would be an economical choice for markups below around 9% assuming winding speeds are faster than wet winding. For instance, the average winding speed would need to be around 50 m/min to reach cost parity with wet winding for an 8% markup. Pre-preg is not used by most tank vendors, presumably due to the current high cost of pre-preg (>9% markup) which may result from low production volume.

Toyota has reported Type IV tank designs that result in lower carbon fiber usage by using alternate liner geometry to eliminate high-angle helical winding, an alternate winding scheme, a smaller diameter boss with a longer flange, and high strength T-720 carbon fiber. In the Toyota two-tank configuration, the front tank has an aspect ratio (length/diameter) of 2.8 while the rear tank has an aspect ratio of 1.7. ANL finite element analysis model results predict a 4.8% CF mass reduction for the high aspect ratio (2.8) tank using T-700 carbon fiber and the PNNL lower cost, low density resin; however, no CF mass reductions is predicted for the low aspect ratio (1.7) tank. Additional mass savings are possible by switching to higher strength T-720 CF but there is insufficient data on T-720 price to project accurate system cost results. When the Toyota CF reductions are applied to the Strategic Analysis single and two-tank configurations, cost is reduced around $0.50/kWh as shown in Table 1.

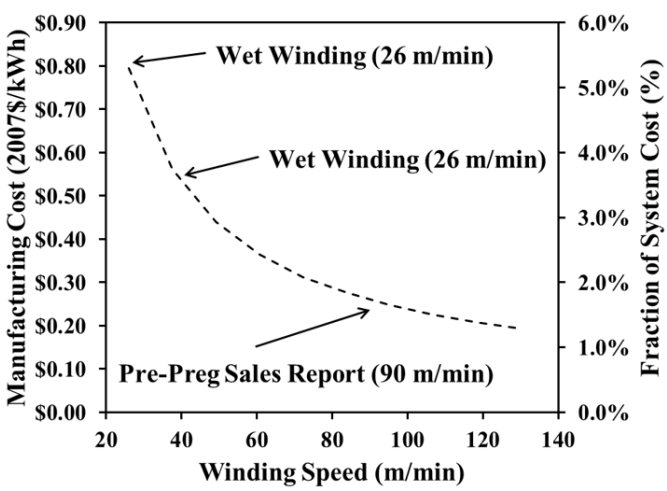

FIGURE 1. Manufacturing cost of pressure vessel winding as a function of winding speed

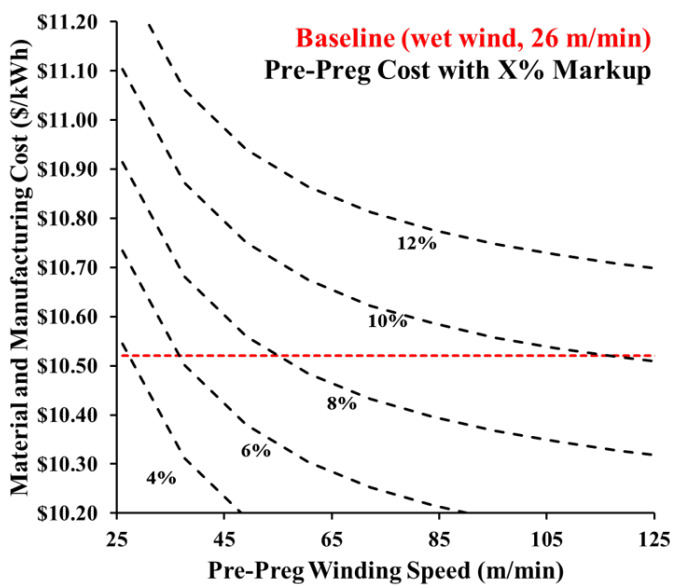

FIGURE 2. Comparison of material and manufacturing costs as a function of winding speed for pre-preg at multiple markups. Dashed black lines represent cost curves for pre-preg at the indicated markup (e.g., the upper curve has a 12% markup applied; the next curve has a 10% markup). The red dashed line marks the cost for wet winding at 26 m/min. The analysis is based on a 1.6% $COV_{manufacturing}$ for pre-preg and 3.3% $COV_{manufacturing}$ for wet winding.

A final avenue of investigation into reducing cost by decreasing carbon fiber usage is vacuum resin infusion being investigated by Materia [3]. To understand the cost impact of the Materia process, the cost of the composite (materials and manufacturing) was analyzed as a sensitivity study against a case with no composite reduction. Figure 3 presents a summary tornado chart of these results. If there is no composite mass reduction for the Materia process, the cost of the composite material, winding, and resin application at 500,000 systems/year would be $12.03/kWh compared to $10.52/kWh for the baseline storage vessel. The higher cost is due largely to the higher resin cost: $13.5/kg for dicyclopentadiene with Grubb's catalyst compared to $4.52/kg for vinyl ester used in the baseline tank. The additional processing cost associated with the vacuum infiltration process itself also contributes an additional $0.51/kWh. In order to offset these additional costs and reach cost parity with wet winding, a 14% composite mass reduction would need to be realized. If Materia meets the 30% composite mass reduction project objective, these results project a system cost savings of $1.79/kWh.

CONCLUSIONS AND FUTURE DIRECTIONS

Based on work completed this year the major conclusions are:

- System cost for the single tank 700 bar pressure vessel system has come down by 12% over the 2013 baseline system (at 500,000 systems per year).
- Addition improvements have been analyzed.

TABLE 1. Projected system cost savings for single and two tank configurations using the Toyota winding patterns compared with current winding patterns. System costs are modeled assuming aluminum valve and regulator bodies, assuming a 3.3% COV_{Fiber} for the Oak Ridge National Laboratory polyacrylonitrile with methyl acrylate fiber, and PNNL lower cost, low density resin.

	Available H_2 (kg)	L/D	CF Reduction (%)	System Cost Reduction ($/kWh)
Baseline (single tank)	5.6	3	--	--
Single tank w/Toyota winding pattern	5.6	3	-4.8%	0.50
Two-Tank Configuration	5.6	3	--	--
Two-Tank w/Toyota winding pattern	5.6	3	-4.8%	0.49

L - Length; D - Diameter

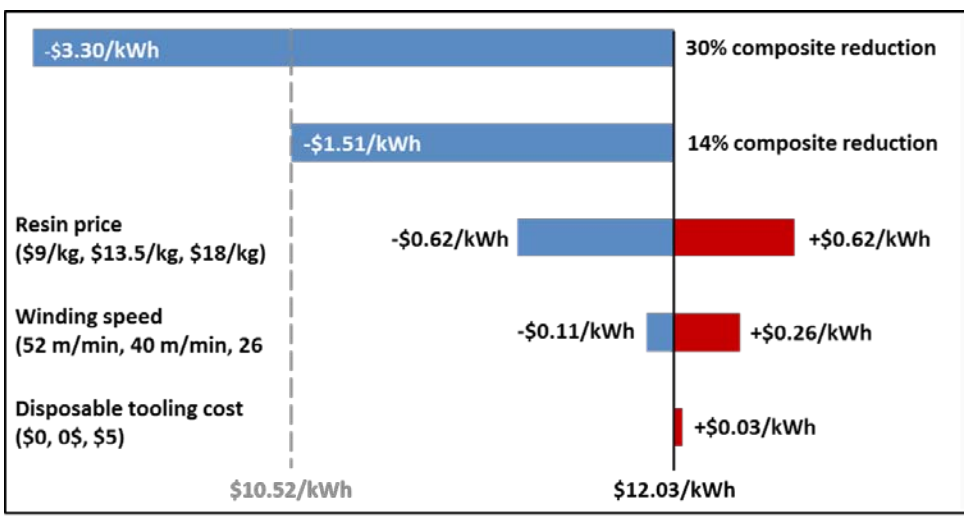

FIGURE 3. Single variable sensitivity analysis of the Materia vacuum infiltration process for a single 147 L tank with 5.6 kg usable H_2 produced at 500,000 systems per year. The black line ($12.03/kWh) shows the modeled tank cost using the Materia process with no carbon fiber reduction. The grey dashed line ($10.52/kWh) is the baseline tank cost.

  - Replacing stainless steel BOP components result in a reduction of $0.16/kWh.
  - Tank design and winding patterns demonstrated by Toyota suggest additional savings of around 3%.

Based on results from this year, Strategic Analysis plans to:

- Further investigate and validate the Toyota tank design.
- Track and model improvements from current DOE funded projects looking at lower cost materials, sorbents, and strategies to reduce carbon fiber usage as appropriate.
- Re-evaluate commercially available BOP components to validate current BOP costs and to investigate further price reductions.

FY 2016 PUBLICATIONS/PRESENTATIONS

1. Ordaz, Grace, Cassidy Houchins, and Thanh Hua. "Onboard Type IV Compressed Hydrogen Storage Systems-Cost and Performance Status 2015." U.S. Department of Energy, 2015.

2. Brian D. James, Cassidy Houchins, Daniel DeSantis, Jennie Huya-Kouadio, "Cost of On-Board Hydrogen Storage Systems: Status and Technical Challenges" Hydrogen Storage Technical Team Meeting, USCAR, Southfield, MI, March 17, 2016.

3. Brian D. James, "Hydrogen Storage Cost Analysis" 2015 DOE Hydrogen and Fuel Cells Program Review, Arlington, VA, June 8, 2016.

REFERENCES

1. Grace Ordaz, Cassidy Houchins, and Thanh Hua. "Onboard Type IV Compressed Hydrogen Storage Systems-Cost and Performance Status 2015." U.S. Department of Energy, 2015.

2. Scott McWhorter and Grace Ordaz, "Onboard Type IV Compressed Hydrogen Storage Systems-Current Performance and Cost." U.S. Department of Energy, 2013.

3. Brian Edgecombe, "Next Generation Hydrogen Storage Vessels Enabled by Carbon Fiber Infusion with a Low-Viscosity, High-Toughness Resin System." 2016 DOE Hydrogen and Fuel Cells Program Review, Washington DC, June 9, 2016.

IV.B.1 Hydrogen Storage Engineering Center of Excellence

Donald L. Anton (Primary Contact), Bruce J. Hardy, David A. Tamburello, Claudio Corgnale, and Martin Sulic
Savannah River National Laboratory
Bldg. 999-2W
Aiken, SC 29808
Phone: (803) 507-8551
Email: Donald.Anton@srnl.doe.gov

DOE Manager: Ned Stetson
Phone: (202) 586-9995
Email: Ned.Stetson@ee.doe.gov

Technical Advisor: Robert Bowman
Phone: (818) 354-7941
Email: rcbjr1967@gmail.com

Subcontractors:
- Pacific Northwest National Laboratory, Richland, WA
- United Technologies Research Center, East Hartford, CT
- General Motors, Warren, MI
- Ford Motor Company, Dearborn, MI
- National Renewable Energy Laboratory, Golden, CO
- Los Alamos National Laboratory, Los Almaos, NM
- Jet Propulsion Laboratory, Pasadena, CA
- University of Michigan, Ann Arbor, MI
- California Institute of Technology, Pasadena, CA
- Oregon State University, Corvallis, OR
- Hexagon Lincoln LLC, Lincoln, NE
- Université du Québec a Trios-Rivieres, Trois-Rivieres, QC, Canada

Project Start Date: February 1, 2009
Project End Date: December 31, 2016

Overall Objectives

- Develop system models that will lend insight into overall fuel cycle efficiency.
- Compile all relevant materials data for candidate storage media and define future data requirements.
- Develop engineering and design models to further the understanding of onboard storage energy management requirements.
- Develop innovative onboard system concepts for metal hydride, chemical hydrogen storage materials, and adsorbent materials-based storage technologies.
- Design components and experimental test fixtures to evaluate the innovative storage devices and subsystem design concepts, validate model predictions, and improve both component design and predictive capability.
- Design, fabricate, test, and decommission the subscale prototype components and systems of each materials-based technology (adsorbents, metal hydrides, and chemical hydrogen storage materials).

Fiscal Year (FY) 2016 Objectives

- Coordination and facilitation of partner's activities.
- Complete evaluation of a 2-L adsorbent subscale prototype utilizing a HexCell heat exchange system.
- Complete evaluation a 2-L adsorbent subscale prototype utilizing a Modular Adsorbent Tank Insert (MATI) heat exchange system.
- Validated thermo-physical models of the mass and heat flow for a flow through adsorbent subscale prototype system.

Technical Barriers

This project addresses the following technical barriers from the Hydrogen Storage section of the Fuel Cell Technologies Office Multi-Year Research, Development, and Demonstration Plan.

(A) System Weight and Volume

(B) System Cost

(C) Efficiency

(D) Durability/Operability

(E) Charging/Discharging Rates

(G) Materials of Construction

(H) Balance of Plant Components

(J) Thermal Management

(K) System Life Cycle Assessments

(L) High Pressure Conformality

(P) Lack of Understanding of Hydrogen Physisorption and Chemisorption

(S) By-Product/Spent Material Removal

Technical Targets

The projected scaled performance of the two adsorption systems, HexCell and MATI, being evaluated are given in Table 1 in comparison to the technical targets.

FY 2016 Accomplishments

- Completed characterization experiments of metal organic framework (MOF)-5 on the flow through subscale prototype system and model validation.

TABLE 1. System Status vs. Technical Targets for the Cryo-Adsorbent System

Target	Units	2020 DOE Goal (System)	Ultimate DOE Goal (System)	Projected Scaled HexCell (System)	Projected Scaled MATI (System)
Gravametric Capacity	kg H_2/kg system	0.055	0.075	0.0321	0.315
Volumetric Capacity	kg H_2/L system	0.04	0.07	0.019	0.021
System Cost	$/kg H_2 stored	333	266	486	516
Fuel Cost	$/gge at pump	2-4	2-4	6	6
Min. Operating Temp	°C	-40	-40	-40	-40
Max. Operating Temp	°C	60	60	60	60
Min. Delivery Temp	°C	-40	-40	-40	-40
Max. Delivery Temp	°C	85	85	85	85
Cycle Life	Cycles	1500	1500	1500	1500
Min. Delivery Pressure	bar	5	3	5	5
Max. Delivery Pressure	bar	12	12	12	12
Onboard Efficiency	%	90%	90%	90%	97%
Well to Power Plant Efficiency	%	60%	60%	40%	40%
System Fill Time	min.	3.3	2.5	3.3	3.3
Min. Full Flow Rate	(g/s/kW)	0.02	0.02	0.02	0.02
Start Time to Full Flow (20°C)	sec.	5	5	5	5
Start Time to Full Flow (-20°C)	sec.	15	15	15	15
Transient Response	sec.	0.75	0.75	0.75	0.75
Fuel Purity	%H_2	99.97	99.97	99.99	99.99
Permeation, Toxicity, Safety	-	Meets or Exceeds Standards	Meets or Exceeds Standards	Meets or Exceeds Standards	Meets or Exceeds Standards
Loss of Useable Hydrogen	(g/h)/kg H2 stored	0.05	0.05	0.81	0.69

gge – Gasoline gallon equivalent

- Completed characterization experiments of MOF-5 on the MATI subscale prototype system.
- Completed validation of the HexCell and MATI vehicle-level system models.

✧ ✧ ✧ ✧ ✧

INTRODUCTION

The Hydrogen Storage Engineering Center of Excellence brought together all of the materials and hydrogen storage technology efforts to address onboard hydrogen storage in light-duty vehicle applications. The effort began with a heavy emphasis on modeling and data gathering to determine the state-of-the-art in hydrogen storage systems. This effort spanned the design space of vehicle requirements, power plant and balance of plant requirements, storage system components, and materials engineering efforts. These data and models were then used to design components and subscale prototypes of hydrogen storage systems which were evaluated and tested to determine the status of potential system against the DOE 2020 and ultimate technical targets for hydrogen storage systems for light-duty vehicles.

APPROACH

A team of leading North American national laboratories, universities, and industrial laboratories, each with a high degree of hydrogen storage engineering expertise cultivated through prior DOE, international, and/or privately sponsored programs was assembled to study and analyze the engineering aspects of condensed phase hydrogen storage as applied to automotive applications. The technical activities of the center were divided into three system architectures: adsorbent, chemical hydrogen storage, and metal hydride matrixed with six technologies areas: Performance Analysis, Integrated Power Plant/Storage System Analysis, Materials Operating Requirements, Transport Phenomena, Enabling Technologies and Subscale Prototype Construction, and Testing and Evaluation. The program was divided into three phases: Phase 1 – System Requirements and Novel Concepts, Phase 2 – Novel Concept Modeling Design and Evaluation, and Phase 3 – Subscale System Design, Testing, and Evaluation.

RESULTS

HexCell Prototype

The experimental measurements on the 2-L HexCell prototype using tap density MOF-5 adsorbent at a density of 0.19 g/cc system were completed. Model validation utilizing the experimental results have been carried out for the flow-through system at Savannah River National Laboratory. Table 2 lists the experimental work completed on the HexCell system with data model validation noted.

Figure 1 illustrates the model and experimental data for the HexCell prototype. For each thermocouple measurement, the numerical values closely parallel the experimental data to within 10°C for charging and to within 15°C for discharging. All changes in temperature were fully captured by the models and thus all relevant physical phenomena are taken into consideration. Existing temperature differences are most likely due to thermocouple placement error, and non-uniform packing of the adsorbent media.

In addition to static charging and discharging, dynamic full system cycling was performed to evaluate material capacity over several cycles. A total of 24 consecutive cycles over a pressure range of 5–60 bar were performed with no observed degradation in storage capacity via total standard liters of hydrogen required to reach maximum operational pressure as shown in Figure 2.

TABLE 2. Experimental Work Completed on the HexCell System

	Test	H_2 flow (SLPM)	P_{max} (bar)	Min H_2 Temp (K)	Max Bed Temp (K)
Adsorption	Static charge	200	40, 80	110	
	Flow-through cooling	100*, 500 , 1000	17, 40*, 80*	110	
Desorption	Without heat	11, 25	40, 80		160
	With heat	11*, 25, 50, 100	40*, 80*		160

* HexCell systems with data model validation

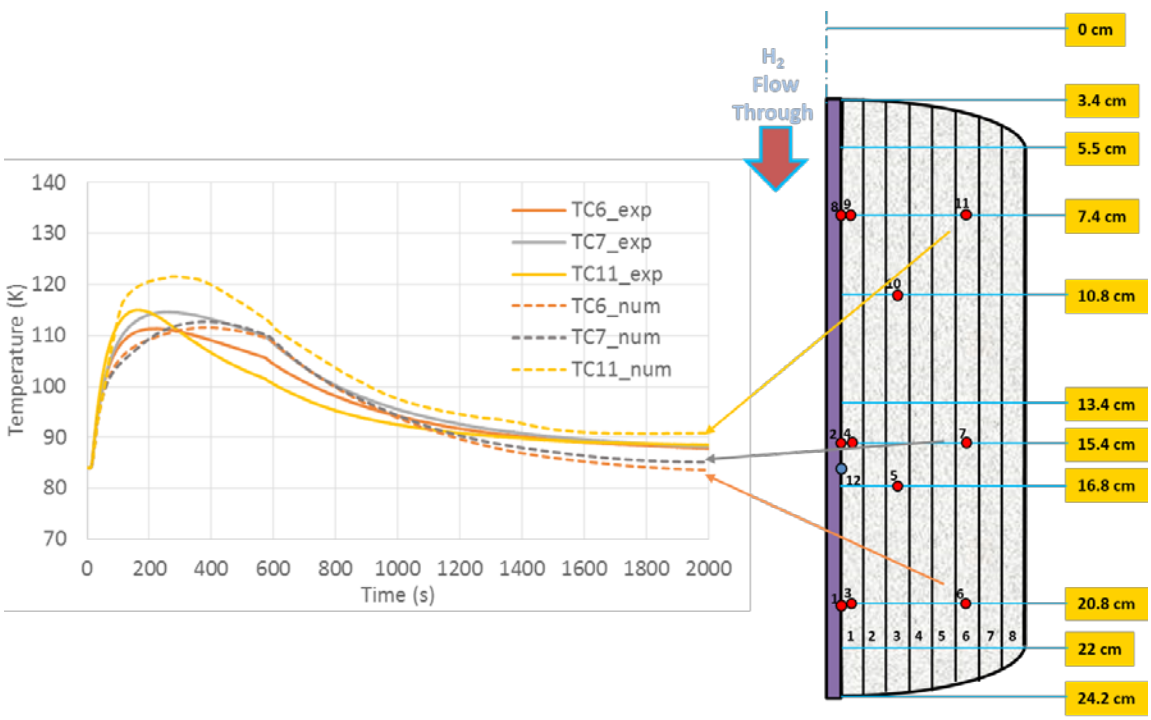

FIGURE 1. Charging of MOF-5 powder in the HexCell flow-through storage system, experimental and numerical data compared

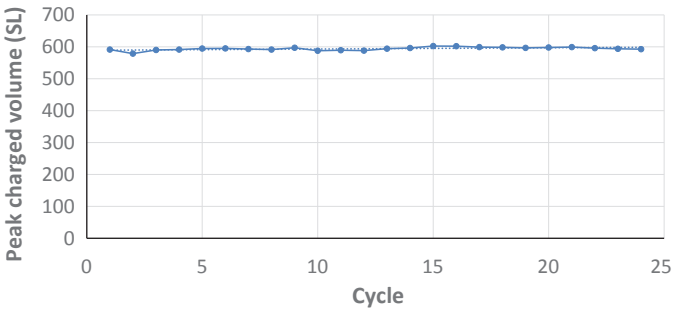

FIGURE 2. Consecutive cycling of the flow-through HexCell MOF-5 hydrogen storage system

MATI Prototype

Final experimental tests were performed on the 2-L MATI prototype system utilizing compacted MOF-5 pucks having a volumetric density twice that of the tap density powder used in the HexCell system at 0.40 g/cc. Table 3 lists the set of half-cycles (charging and discharging) experimental work performed on the MATI prototype system.

In total, over 100 different measurements were performed on the MATI prototype system. In addition, consecutive cycling testing was also conducted, as outlined in Table 4. A representative set of adsorption half cycle data is shown if Figure 3 for hydrogen flows of 150 slpm and 300 slpm. The charging time of technical target of 3 min was achieved at a flow of 300 slpm.

Unlike the HexCell system, the 2-L MATI prototype system could only be run through 9–10 consecutive cycles due to gas volume restrictions within the laboratory. However, the MATI prototype system was cycled not only in the range of 5–60 bar, but also 5–100 bar (100 bar cycling limited the number of consecutive cycles even less). Results for both 60 bar and 100 bar cycling showed similar results. Figure 4 illustrates the cycling capacities for both charging and discharging over eight cycles. No apparent change in capacities was observed through the cycles tested.

Adsorbent System Comparison

Using the experimental and modeling data presented above, the adsorbent storage systems were compared within the vehicle framework. Table 5 shows the subscale prototype experimental results and projected full-scale 5.6 kg hydrogen systems based on the validated models. Note that only the adsorbent and heat exchanger portions of the model were validated using the 2-L prototypes, while the tank sizing tool and the balance of plant estimates were validated/updated based on the latest information from other Hydrogen Storage Engineering Center of Excellence sources.

The adsorbent storage system comparisons are listed in Table 5, which includes columns for the 0.19 g/cc powder MOF-5 HexCell heat exchanger storage system design, and the 0.4 g/cc compacted MOF-5 MATI heat exchanger storage system design. The rows shown in Table 5 correspond to the experimental measurements of 2-L prototype-level adsorbent + heat exchanger values, the projected full-scale adsorbent + heat exchanger values, and the projected full-scale full storage system estimates. The adsorbent storage system models were able to estimate the 2-L prototype experiments within 10% of the recorded values.

TABLE 3. List of the Half Cycle (Charging and Discharging) Experiments Performed on the 2-L MATI Prototype System

Test	P_{min} (bar)	$P_{max(c)}$ (bar)	$P_{max(v)}$ (bar)	H_2 flow (SLPM)	N_2 Flow (SLPM)
Adsorption	1, 5	60, 80, 100	60, 100	0, 50, 100, 150, 200, 300	0, 50, 100, 150, 200
Desorption	1, 5	60, 80, 100		0, 50, 100, 150	0, 50, 100, 150, 200

TABLE 4. List of the Cycling Experiments Performed on the 2-L MATI Prototype System

Test	Consecutive Cycles	Total Cycles	H_2 flow (SLPM)	N_2 Flow (SLPM)
5 to 60 bar cycling	9-10	20	300	150
5 to 100 bar cycling	3	6	130	150

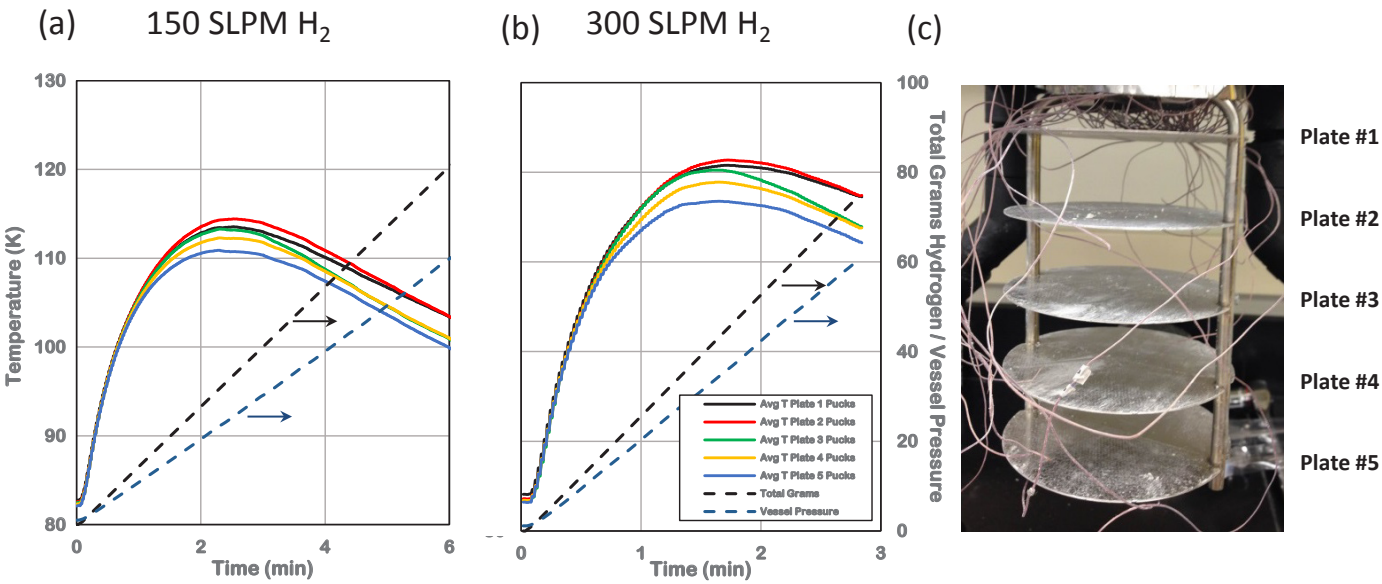

FIGURE 3. Temperature profiles for 2-L MATI prototype charging experiments at hydrogen flows of (a) 150 slpm, (b) 300 slpm, and (c) plate geometry

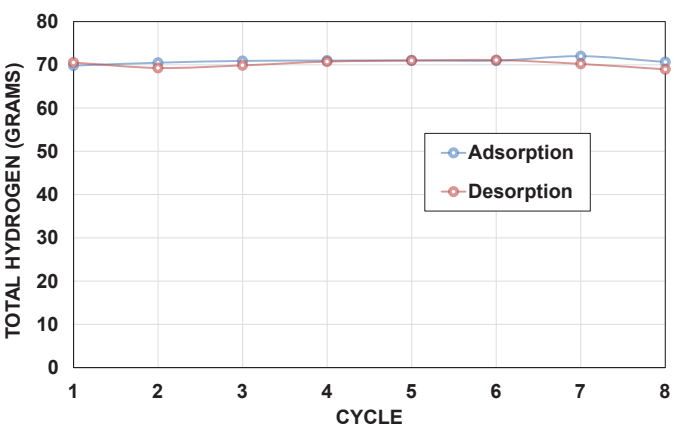

FIGURE 4. Total capacity of hydrogen (in during adsorption or out during desorption) during the 2-L MATI prototype cycling experiments between 5 bar and 60 bar

TABLE 5. HexCell and MATI Adsorbent Storage System Comparisons

	Powder MOF-5 HexCell HX	Compact MOF-5 MATI HX
Measured 2-liter Prototype (material + $HX_{internal}$)	(90 K, 80 bar) ➔ (85 K, 1.7 bar)	(84.5 K, 100 bar) ➔ (83.7 K, 1.1 bar)
Gravimetric Capacity	0.112 g/g	0.092 g/g
Volumetric Capacity	23.6 g/l	37.2 g/l
Full-scale 5.6 kg System model (material + $HX_{internal}$)	(80 K, 100 bar) ➔ (160 K, 5.0 bar)	(80 K, 100 bar) ➔ (160 K, 5.0 bar)
Gravimetric Capacity	0.125 g/g	0.100 g/g
Volumetric Capacity	32.9 g/l	44.4 g/l
Full-scale 5.6 kg System model (full system)	(80 K, 100 bar) ➔ (160 K, 5.0 bar)	(80 K, 100 bar) ➔ (160 K, 5.0 bar)
Gravimetric Capacity	0.0321 g/g	0.0315 g/g
Volumetric Capacity	18.9 g/l	21.0 g/l

HX – Heat exchanger

CONCLUSIONS AND FUTURE DIRECTIONS

The prototype experiments, including the cycling experiments described above, have been completed for both the 2-L HexCell and 2-L MATI prototype systems. The systems performed repeatable and within design specification. The detailed heat and mass transfer computational models for the HexCell system have been validated against experimental data and found to capture all relevant physical phenomena to within 15°C. In addition, the vehicle-level system models for both the HexCell and MATI systems have been used to predict full-scale 5.6 kg H_2 automotive systems. These projections have shown the high density compacted MOF-5 adsorbent utilizing a MATI heat exchanger would surpass a 700 bar Type 4 compressed gas tank in volumetric capacity, and the low density MOF-5 adsorbent system utilizing the HexCell heat exchanger would beat it in cost.

Future technical work will include:

- Characterize the fluid-flow inequality between the five plates of the MATI internal heat exchanger.
- Create and validate detailed models of the MATI prototype system based on the prototype experimental results described above.
- Update the Simulink cryo-adsorbent system models so new materials can be tested within it to predict their full-scale system performance.

IV.B.2 Hydrogen Storage System Modeling: Public Access, Maintenance, and Enhancements

Matthew Thornton (Primary Contact)[1], David Tamburello[2], Kriston Brooks[3], Jeff Gonder[1], and Sam Sprik[1]

[1]National Renewable Energy Laboratory (NREL)
15013 Denver West Parkway
Golden, CO 80401
Phone: (303) 275-4273
Email: Matthew.Thornton@nrel.gov

[2]Savannah River National Laboratory (SRNL)
Savannah River Site, Bldg 999-2W
Aiken, SC 29808
Phone (803) 507-4449
Email: david.tamburello@srnl.doe.gov

[3]Pacific Northwest National Laboratory (PNNL)
P.O. Box 999
Richland, WA 99352
Phone (509) 372-4343
Email: kriston.brooks@pnnl.gov

DOE Manager: Ned Stetson
Phone: (202) 586-9995
Email: Ned.Stetson@ee.doe.gov

Project Start Date: October 1, 2015
Project End Date: September 30, 2018

Overall Objectives

- Coordinate the public access of select models developed under the Hydrogen Storage Engineering Center of Excellence (HSECoE) activity, including web posting documentation and tracking downloads and web activity.
- Maintain performance of existing storage system models and update and validate as new experimental data becomes available.
- Enhance and expand existing models to improve simulation speed and application to other uses. This will focus on expanding the parameterization of the models and their flexibility in evaluating new hydrogen storage material candidates. This will also include the development of pre-processor sizing routines for both the adsorbent and chemical hydrogen storage systems.

Fiscal Year (FY) 2016 Objectives

- Coordinate the public access of selected HSECoE models, including web posting documentation and tracking downloads and web activity.
- Update storage system model documentation.
- Update all adsorbent and chemical hydrogen (CH) storage HSECoE models based on experimental results.
- Develop storage system sizing pre-processor (CH storage system).
- Develop a stand-alone isotherm data fitting routine to convert raw excess adsorption H_2 data into its Dubinin-Astakhov parameters.

Technical Barriers

This project addresses the following technical barriers from the Hydrogen Storage section of the Fuel Cell Technologies Program's Multi-Year Research, Development, and Demonstration Plan.

(A) System Weight and Volume

(B) System Cost

(C) Efficiency

(E) Charging/Discharging Rates

(I) Dispensing Technology

(K) Systems Life-Cycle Assessments

Technical Targets

This project is conducting simulation and modeling studies of advanced onboard materials-based hydrogen storage technologies. Insights gleaned from these studies are being applied toward the design and synthesis of hydrogen storage vessels that meet the following DOE 2020 hydrogen storage for light-duty vehicle targets.

- Cost: to be determined
- Specific energy: 0.055 kg H_2/kg system
- Energy density: 0.040 kg H_2/L system
- Charging/discharging rates: 3–5 min
- Well to power plant efficiency: 60%

FY 2016 Accomplishments

- Updated and integrated several HSECoE storage system models within the vehicle modeling framework and posted them on the website portal. These included a 700 bar physical storage model, a metal hydride model, two CH models, and two adsorbent system models.

- Update all adsorbent and CH HSECoE models based on experimental results. Validated adsorbent models based on 2-L prototype experimental results.
- Develop storage system sizing pre-processor (CH storage system).
- Completed documentation updates for the posted models (including website text and downloadable user manual).
- Adjusted CH tank size to ensure 5.6 kg of usable hydrogen.
- Troubleshooting of compiler and software versions.
- Tracking and monitoring web activity and downloads.

✧ ✧ ✧ ✧ ✧

INTRODUCTION

Overcoming challenges associated with onboard hydrogen storage is critical to the widespread adoption of fuel cell electric vehicles. The overarching challenge is identifying a means to store enough hydrogen onboard to enable a driving range greater than 300 miles within vehicle-related packaging, cost, safety, and performance constraints. As new hydrogen storage materials are discovered and created, material developers must predict their full-scale vehicle performance and compare their performance with pure hydrogen storage (700 bar, cryo-compressed, and liquid H_2 storage). The goal of this work is to provide material developers with the modeling tools necessary to make these predictions based on the work done by the HSECoE.

APPROACH

The approach for FY 2016 is to update, document, and perform validation, enhancement, troubleshooting, and debugging of these framework and other models developed by HSECoE so that they can be made accessible to and useful for other research within the hydrogen storage community. During subsequent years, these models will be updated with alternative storage system formulations, such as different isotherm models for adsorbents and alternative chemical reaction kinetic expressions for CHs. In addition, stand-alone system estimators that do not require special software will be developed to serve as a scoping tool for the new hydrogen storage materials.

RESULTS

The following will provide results from work completed this year with a focus on the coordination of the public access of select HSECoE models, including web posting documentation and tracking downloads and web activity. The multi-lab team worked on the validation, refinement, graphical user interface (GUI) improvements, troubleshooting, improving simulation run time, updating model documentation for selected web postings, and monitoring or tracking web activity and model downloads. To date, there have been 120 downloads of the tank volume and cost model, 85 down loads of the framework model, 53 down loads of the metal hydride (MH) finite element model, and 36 down loads of the MH acceptability envelop.

Model validation work on the HSECoE adsorbent and CH framework models, based on experimental data from the center, have been compete. Documentation and users guides for all of these HSECoE models have also been updated this year and all are currently available via the HSECoE web site (www.hsecoe.org). Figure 1 shows a screen caption of the current HSECoE home page as well as the models page, which has direct links to the documentation, user guides, and download area for all available models. All of the select HSECoE models that are available on the website are listed in Table 1.

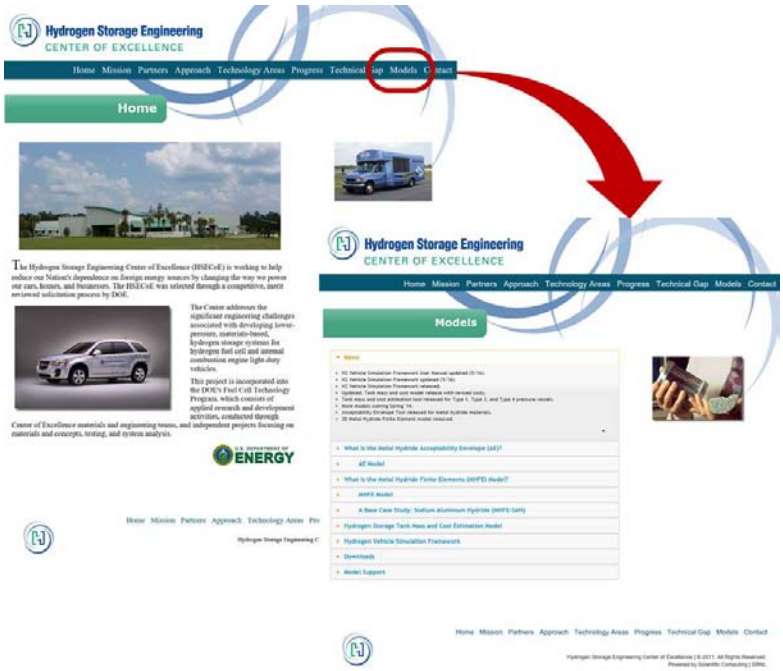

FIGURE 1. HSECoE web home page and web models documentation and download page

TABLE 1. HSECoE Models Available on Web Portal and Model Posting Status

Model Name	HSECoE Lead	Status
MH Acceptability Envelop	SRNL	Complete
MH Finite Element Model	SRNL	Complete
AD Finite Element Model	SRNL	Complete
Tank Volume/Cost Model	PNNL	Complete
MH Framework Model	UTRC/NREL	Complete
CH Framework Model	PNNL/UTRC/NREL	Complete
AD Framework Model	SRNL/UTRC/NREL	Complete

AD – Adsorption; UTRC – United Technologies Research Center

One purpose of the framework is to provide a model that can be used by material developers to evaluate newly identified materials in terms of system sizing and drive cycle performance. The current chemical hydrogen storage module within the framework requires that these material developers not only determine kinetic and thermodynamic properties of the material, but also estimate the dimensions of the system components and the control parameters. Estimating system sizing and control parameters would be challenging to those not familiar with the model. To allow greater use of the framework by the hydrogen storage community, PNNL developed a pre-processor that uses the kinetic and thermodynamic information for a new material that would normally be measured experimentally (i.e., fraction of hydrogen, reaction enthalpy, activation energy) to estimate the system sizing and control parameters. Such design parameters as the mass of chemical hydrogen storage material required, the length of the radiators and reactors, and the volume of the ballast tank are estimated and can then be used in the model. Additionally, control parameters such as the initial reaction and maximum temperatures are estimated. Currently the pre-processor is a stand-alone model, but it will be implemented into the framework next fiscal year to allow seamless operations between the initial size estimation and the framework.

The preliminary pre-processor was tested using material properties for ammonia borane (AB) and alane. While the values produced by the pre-processor are different than those assumed during the system storage model development, the framework models using the predicted system sizing both AB and alane run successfully. The model result with the US06 aggressive cycle run are compared for the two inputs shown in Table 2. The pre-processor estimates for reactor length and ballast tank volume are less than the values originally included in the model resulting in a reduced storage system mass and volume. The onboard efficiency and raw distance traveled are similar between the original and preprocessor values.

TABLE 2. Framework Results for Chemical Hydrogen Storage Materials with US06 Drive Cycle Comparing Originally Estimated Model Inputs and the Pre-processor Inputs

Framework Input Parameter	Ammonia Borane		Alane	
	Original Values	Pre-processor	Original Values	Pre-processor
Reactor Length (m)	1.2	0.96	2.0	1.45
Ballast Tank Volume (m^3)	0.02	0.007	0.03	0.017
Mass CH (kg)	86	82	140	155
Length Gas HX (m)	1.25	1.39	1	1.45
Length Liquid HX (m)	1.33	0.9	1	1.08
Framework Output Parameters				
Useable H_2 (kg)	5.7	5.5	5.41	5.48
Storage System Mass (kg)	138	131	186	199
Storage System Volume (L)	146	128	164	162
On-Board Efficiency	97.8%	97.8%	84.2%	85.1%
Maximum Temperature (°C)	301	333	329	315
Raw Distance (miles)	333	320	314	317

HX – Heat exchanger

Using experimental data (and finite element model results in the case of the HexCell storage system), the adsorbent storage system model was validated prior to being updated within the vehicle framework. Table 3 shows the experimental measurements and the projected resulting full-scale vehicle models based on the validated models. Note that the adsorbent and heat exchanger portions of the model were validated using the 2-L prototypes, while the tank sizing tool (based on the Tank Volume/Cost Model) and the balance of plant estimates were validated and updated based on the latest information from other HSECoE sources.

The adsorbent storage system validation (as listed in Table 3) includes columns for the powder metal organic framework (MOF)-5 HexCell heat exchanger storage system design, 0.4 g/cc compacted metal organic framework MOF-5 modular adsorbent tank insert (MATI) heat exchanger storage system design, and images corresponding to the validation and projection rows. The rows shown in Table 1 correspond to the experimental measurements of 2-L prototype-level adsorbent + heat exchanger values; the projected full-scale adsorbent + heat exchanger values; and the projected full-scale full storage system estimates. The adsorbent storage system models were able to estimate the 2-L prototype experiments within 10% of the recorded values.

The current version of the adsorbent storage system model has the capability of sizing the adsorbent system for a wide range of operating conditions and target usable hydrogen. However, as of the writing of this document, the user is limited to analyzing only powder and compacted MOF-5. No other adsorbents, nor the capability to add

another adsorbent, are currently available. During the next set of GUI updates, this will change and the capability to add new adsorbents (via their physical and adsorptions properties) will be included. In addition, a stand-alone fitting routine is being developed (estimated availability is 9/30/2016) to allow material developers to fit their raw excess adsorption hydrogen storage data into its Dubinin-Astakhov isotherm parameters so that it can be directly implemented within the adsorbent storage models.

In FY 2015 UTRC, NREL, and other HSECoE partners teamed on the GUI improvement effort. The updated version of the GUI framework is shown in Figure 2, which highlights the model selection pulldown menu showing the hydrogen storage models available to the user at this time. Specific storage system diagrams for each of the storage models have also been added to the GUI (not shown). In the coming months, the GUI updates will continue and include increased user controls as well as additional results options for the storage systems. Some of the planned updates include the ability to run sizing pre-processors and modify material properties for each of the storage systems.

Now that several HSECoE models are available to a wider research audience via the HSECoE web page, the final task for this year has been to continue tracking and documenting website activity and model down loads. Figure 3 shows the latest web site activity over the last three months. The site has received over 1,100 visitors during this

TABLE 3. Adsorbent Storage System Validation Information

	Powder MOF-5 HexCell HX	Compact MOF-5 MATI HX
Measured 2-liter Prototype (material + $HX_{internal}$)	(90 K, 80 bar) ➔ (85 K, 1.7 bar)	(84.5 K, 100 bar) ➔ (83.7 K, 1.1 bar)
Gravimetric Capacity	0.112 g/g	0.092 g/g
Volumetric Capacity	23.6 g/l	37.2 g/l
Full-scale 5.6 kg System model (material + $HX_{internal}$)	(80 K, 100 bar) ➔ (160 K, 5.0 bar)	(80 K, 100 bar) ➔ (160 K, 5.0 bar)
Gravimetric Capacity	0.125 g/g	0.100 g/g
Volumetric Capacity	32.9 g/l	44.4 g/l
Full-scale 5.6 kg System model (full system)	(80 K, 100 bar) ➔ (160 K, 5.0 bar)	(80 K, 100 bar) ➔ (160 K, 5.0 bar)
Gravimetric Capacity	0.0321 g/g	0.0315 g/g
Volumetric Capacity	18.9 g/l	21.0 g/l

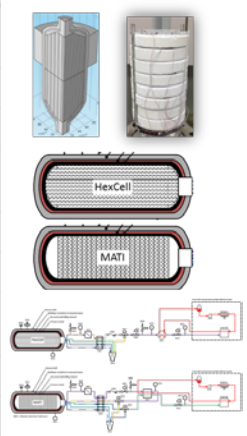

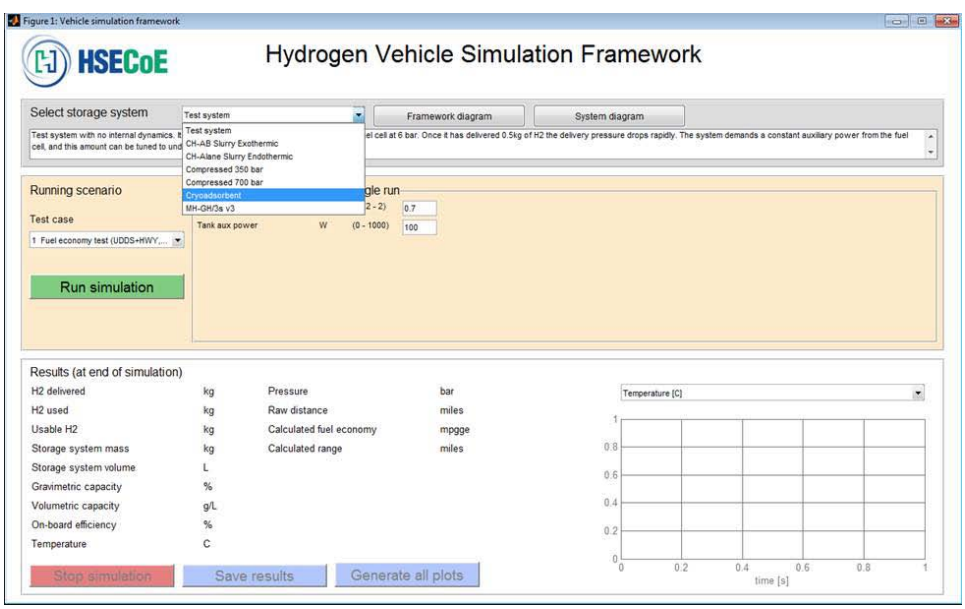

FIGURE 2. HSECoE framework model GUI

time, with roughly 83% of those being new visitors. The bounce rate, which indicates sessions under 10 s, is 85%, indicating that 15% of the visitors stay longer than 10 s and have an average stay of approximately 48 s. Figures 4 and 5 provide the user flows for the site and user origin countries, respectively.

FUTURE DIRECTION

- Work with center partners to continue to update and improve center developed models available and accessible to the broader research and academic community through a controlled web-based access portal and track downloads and website activity.
- Create stand-alone executable versions of the center developed material storage models to provide first-order storage system estimates based on material property information.
- Update the hydrogen storage equations with additional, alternative theoretical storage system formulations to allow users to choose the most appropriate system for their material.

FIGURE 3. HSECoE web analytics: three-month site activity metrics

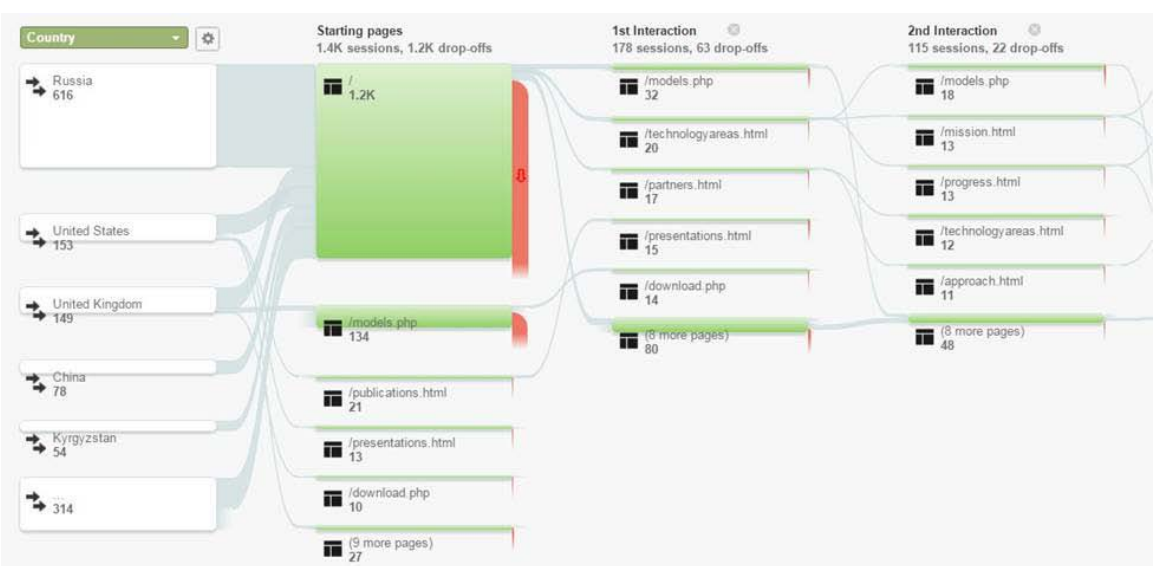

FIGURE 4. HSECoE web analytics: user flows

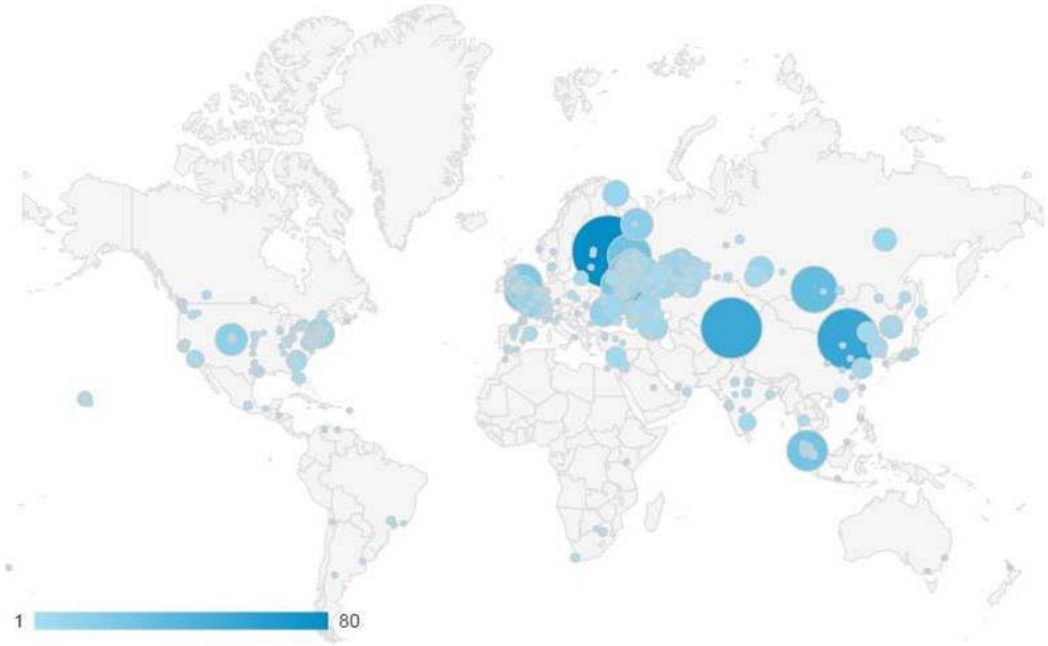

FIGURE 5. HSECoE web analytics: user origin countries

FY 2016 PUBLICATIONS/PRESENTATIONS

1. Thornton, M., D. Tamburello, K. Brooks, J. Gonder, S. Sprik, "Hydrogen Storage System Modeling: Public Access, Maintenance, and Enhancements," U.S. Department of Energy Hydrogen and Fuel Cells Program Annual Merit Review and Peer Evaluation Meeting, June 9, 2016.

2. Thornton, M., D. Tamburello, K. Brooks, J. Gonder, S. Sprik, "HSECoE Models on the WEB," Hydrogen Storage Technical Team Review, February 18, 2016.

IV.B.3 Investigation of Metal and Chemical Hydrides for Hydrogen Storage in Novel Fuel Cell Systems

Bruce Hardy, Theodore Motyka (Primary Contact), Joseph Teprovich, and Claudio Corgnale
Savannah River National Laboratory (SRNL)
Bldg. 999-2W
Aiken, SC 29808
Phone: (803) 645-7819 or (803) 295-3393
Email: bruce.hardy@srnl.doe.gov or ted.motyka@srnl.doe.gov

DOE Manager: Ned Stetson
Phone: (202) 586-9995
Email: Ned.Stetson@ee.doe.gov

Subcontractor:
Savannah River Consulting, Aiken, SC

Project Start Date: March 1, 2015
Project End Date: Project continuation and direction determined annually by DOE

Overall Objectives

- Develop a methodology that incorporates engineering modeling and analysis tools to screen and down-select storage materials and material systems against cost and performance targets (initially developed and applied by SRNL to light-duty vehicle in the Hydrogen Storage Engineering Center of Excellence (HSECoE).
- Apply this methodology to an initial system design for an Unmanned Underwater Vehicle (UUV) application for the Navy to reduce design time and lead to a more cost effective and better performing final product.
- Maintain hydrogen storage system capabilities and expertise at DOE and SRNL to support a variety of hydrogen and energy initiatives.
- Extends the long-term partnership between DOE and the Department of Defense in hydrogen and renewable energy systems.

Fiscal Year (FY) 2016 Objectives

DOE Funded Activities

- Use engineering analyses to screen hydrogen storage systems against DOD targets & requirements (FY 2015).
- Identify suitable hydrogen storage materials and suitable vehicle demonstration platforms.
- Develop a preliminary design of an integrated UUV design with a solid hydrogen storage system.
- Complete detailed design of a hydrogen storage system.
- Complete integrated system design.

Navy Funded Activities

- Design and build a small bench-scale, alane-based, hydrogen storage vessel.
- Perform preliminary testing on the bench-scale, storage system.
- Package and ship bench-scale vessel and alane material to the Navy.
- Provide technical support to Navy's Naval Underwater Warfare Center (NUWC) for further testing and evaluation.

Technical Barriers

This project addresses the following technical barriers from the Hydrogen Storage section of the Fuel Cell Technologies Office Multi-Year Research, Development, and Demonstration Plan.

(A) System Weight and Volume

(B) System Cost

(C) Efficiency

(D) Durability/Operability

(E) Charging/Discharging Rates

(G) Materials of Construction

(H) Balance of Plant (BOP) Components

(J) Thermal Management

(K) System Life-Cycle Assessment

Technical Targets

SRNL has worked with the Navy to modify the DOE hydrogen storage targets [1] developed for light-duty vehicles to Navy UUV requirements. The proposed hydrogen storage and performance targets for Navy UUV systems include both near-term (Generation 1) and longer-term (Generation 2) requirements. The main difference between near and long-term UUV targets are higher hydrogen storage densities and capacities and higher associated fuel cell average and peak power requirements. While many of the proposed Navy UUV targets are similar to DOE hydrogen storage targets some areas where they differ substantially are in initial material

cost and material durability since most DOD applications can withstand higher costs and shorter operating lifetimes than consumer passenger vehicles.

FY 2016 Accomplishments

- Completed an engineering analysis to screen the most attractive solid-state hydrogen storage materials for UUV applications.
- Alane was selected as the most attractive candidate.
- Testing was performed to demonstrate alane hydrogen storage and delivery performance including steady-state and transient operations.
- Delivered alane material and test module to NUWC for further testing by the Navy.
- Ongoing systems and detailed modeling for UUV platforms are in progress.
- Preliminary analyses indicate two to three times the energy storage compared to battery systems.
- End of year objective is to develop a preliminary prototype alane-based UUV system design and system model for potential Navy applications.
- Long-term path forward is to work with the Navy to develop a final design, fabrication and testing of a prototype UUV system.

✧ ✧ ✧ ✧ ✧

INTRODUCTION

This project builds upon the core capabilities of DOE and SRNL and leverages their collective experiences to new roles in other hydrogen applications, which includes the rapidly growing fuel cell areas for portable power and material handling equipment. This project can provide the basis for additional collaborations between DOE and DOD in fuel cell technology. Advances today in small and portable electronic devices offer consumers more and more options but require more and more power to operate. Today's, and even tomorrow's, batteries are not expected to be able to meet this growing power and capacity demand. This demand is perhaps even more evident in military power systems for soldier as well as unmanned aerial vehicle and UUV applications.

One solution that is actively being evaluated is to use fuel cells. Fuel cells offer efficient and high quality power but require safe, efficient, and cost-effective hydrogen storage systems to make them practical. An attractive means for storing hydrogen is the use of solid-state materials that have demonstrated the ability to increase the density of hydrogen by a factor of more than twice that of liquid hydrogen and more than five times that of compressed gas at 70 MPa [2]. A number of materials exist that appear to be suitable for hydrogen storage for DOD UUV applications. However, the viability of storage systems based on these materials has not been fully established for UUV operating conditions.

APPROACH

The overall approach of this research is to develop a methodology that incorporates engineering modeling and analyses to efficiently screen, design, and select storage materials and material systems against cost and performance targets leading to an initial system design for a UUV application. This methodology, which was initially developed by SRNL and applied to light-duty vehicle in HSECoE, requires updates and modifications for it to be useful for other hydrogen and fuel cell applications. More specifically in this research, this methodology will be applied to UUVs to reduce design time and lead to a more cost effective and better performing final product. The modeling analysis, applied to this project, integrates various hydrogen storage system options with other system components, including fuel cell and balance of plant models to evaluate and compare the overall performance of the onboard hydrogen storage system.

RESULTS

Initial engineering screening analyses on a variety of metal and chemical hydride candidate materials were performed using a modified version of the acceptability envelope tool [3] developed for light-duty vehicles in the HSECoE. The acceptability envelope tool was used to apply the Navy's UUV targets and requirements to several standard hydrogen storage system designs and configurations. Based on the results from the study and discussions with Navy personnel, aluminum hydride or alane (AlH_3) was selected as the leading candidate material. Figures 1a and 1b shows the results from a sensitivity analysis depicting the expected storage performance of an alane-based system against the Navy UUV gravimetric and volumetric hydrogen requirements and a variety of key storage parameters. From Figures 1a and 1b, it can be seen that an alane system can meet or exceed most the longer-term (Generation 2), higher capacity and density UUV targets requested by the Navy.

Following selection of alane as the preliminary candidate hydrogen storage material for this project, a demonstration reactor was designed and fabricated utilizing commercially available parts and connectors. The purpose of the reactor was to provide the Navy with a simple system to evaluate the characteristics of an alane storage system to better understand its operation and performance under a variety of temperature conditions. Since alane is a chemical hydride and not rechargeable with hydrogen pressure, it's performance needs to be further evaluated by the Navy. The test reactor consists of an alane containing vessel that fits inside of a larger annular vessel that contains a heat transfer

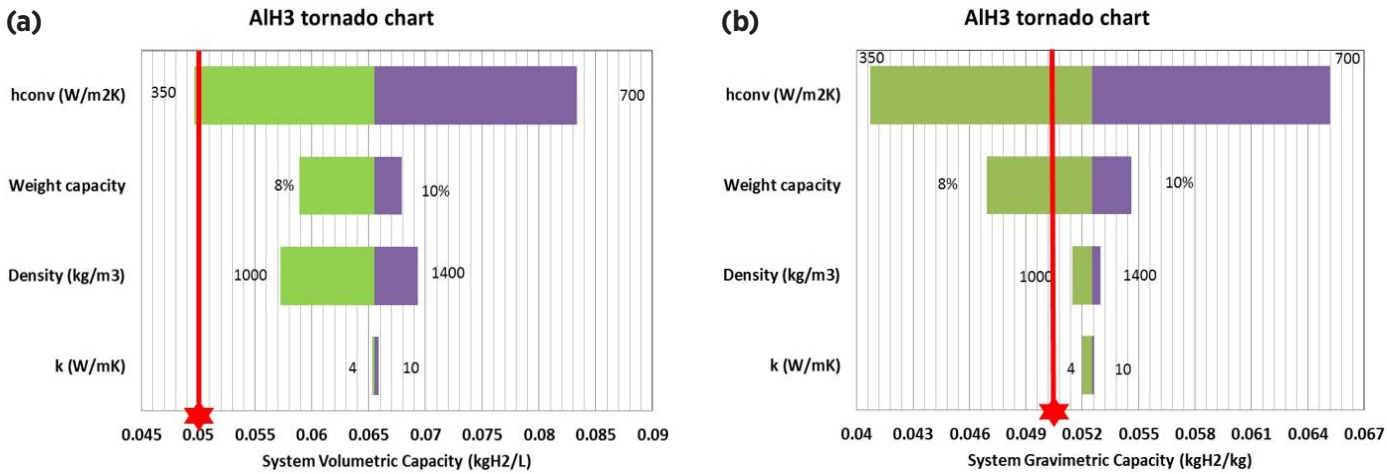

FIGURE 1. Sensitivity analysis results for an alane storage system versus system volumetric density (1a) and gravimetric density (1b)

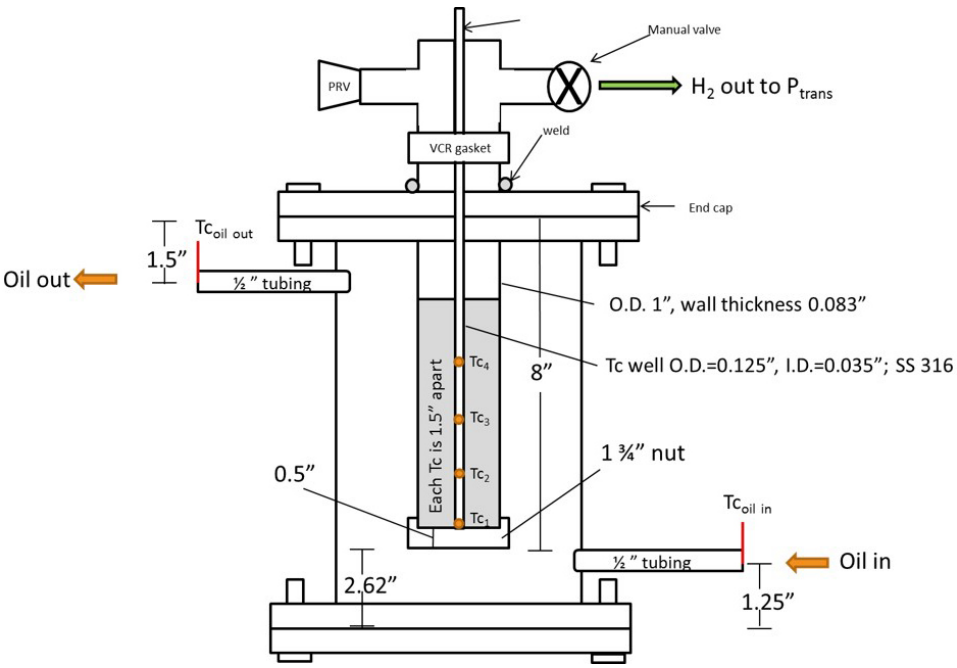

O.D. – Outside diameter; I.D. - Inside diameter; PRV - Pressure reducing valve

FIGURE 2. Alane test reactor design

fluid (Figure 2). The heat transfer fluid is circulated by two circulator baths. One bath is designated as the hot loop, which is set at a temperature high enough to facilitate hydrogen release from the alane (typically 130–145°C). The other is designated as the cold loop and is set to 20°C. The hot or cold loop is manually directed into the reactor to either initiate the release of hydrogen from alane or to stop the release of hydrogen, respectively. Two large gas collection cylinders (35 L volume) were attached to the test rig for the collection of gas along with a pressure transducer to monitor the rate of hydrogen release from the material. Preliminary test results of the demonstration reactor are shown in Figure 3. The results show the ability to control hydrogen desorption from alane in the system by cooling and heating the reactor. This is a key requirement for the UUV system and further testing of the prototype reactor under various temperature and flow conditions will be carried out by the NUWC.

Models for the UUV alane based hydrogen storage system were developed using Comsol™ Multiphysics software. The models are general and are readily applicable to a wide range of conceptual designs. The model solves the governing equations for mass, momentum, and energy conservation that are coupled to expressions for chemical

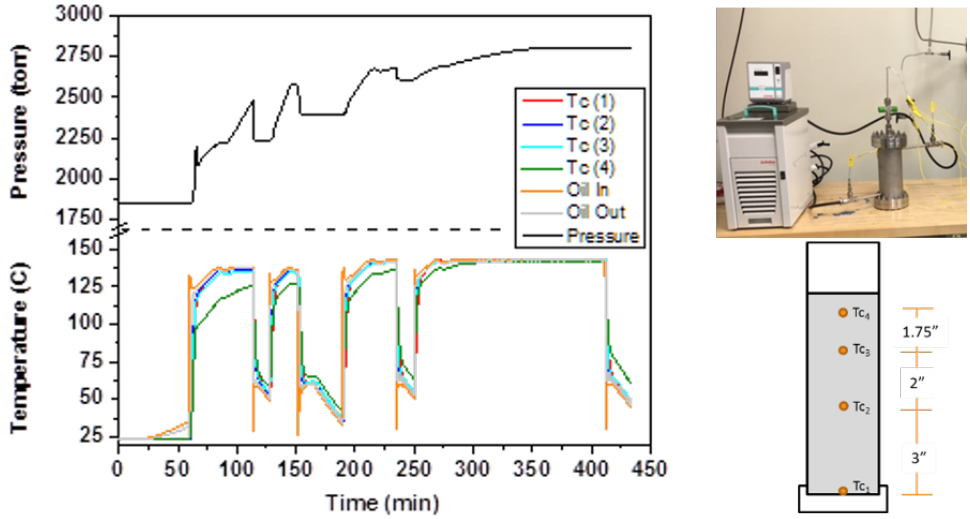

FIGURE 3. Heating and cooling experimental results of test reactor with alane. Inserts shows test reactor connected to oil heating and cooling bath and position of thermocouples during testing.

kinetics and thermodynamics. In this study, the models were applied to the bench-scale demonstration unit.

The test article was modeled in half-symmetry to improve computational speed. The model approximated the alane volume as a cylinder with a radius of 1.06×10^{-5} m and a height of 3.1×10^{-1} m. The mass and volume of alane are 0.06 kg and 6.81×10^{-5} m^3, respectively. The oil flowrate at the inlet was constant at 0.5 m/s. The volume of oil contained in the bath is 1.75×10^{-3} m^3. Surrogate alane kinetics and heat of reaction included in the model provided a hydrogen source and a heat sink due to the endothermic nature of the decomposition reaction.

A heating and cooling cycle was modeled as a test calculation to demonstrate the ability to start and stop the release of hydrogen. In this application the system was at an initial temperature of 293.15 K and alane pressure of 1 atm. The oil inlet flowrate was fixed at 0.5 m/s and raised from 293.15 K to 450 K over the first 4 s of the transient, then held at 450 K until 780 s, then reduced to 293.15 K over the next 10 s and held at 293.15 K for the remainder of the calculation. The resulting temperature profiles are shown in Figure 4.

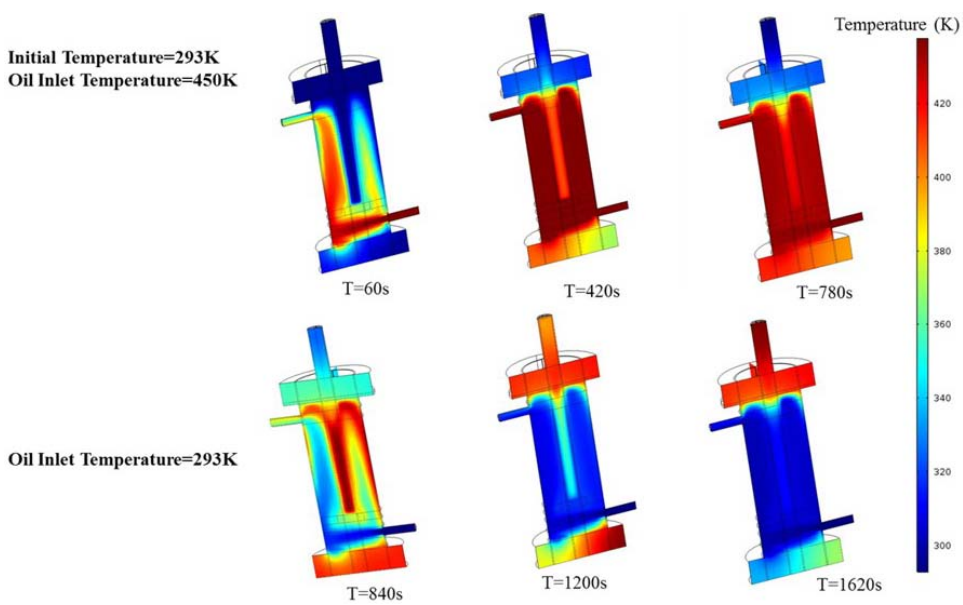

FIGURE 4. Heating and cooling modeling results for test article shipped to Navy

CONCLUSIONS AND FUTURE DIRECTIONS

An engineering analysis was completed to screen the most attractive solid-state hydrogen storage materials for UUV applications. Alane was selected as the most promising candidate material that has the best potential to meet and to exceed many of the Navy UUV targets and requirements. Testing was performed to demonstrate an alane-based hydrogen storage system delivery and performance including steady-state and transient operations. The demonstration reactor was delivered along with a supply of alane material for further testing by the Navy.

Ongoing systems and detailed modeling for UUV platforms are currently underway. Preliminary analyses indicate two to three times the energy storage compared to battery systems. Future objectives include the development of an actual, prototype alane-based UUV system design and system model for potential Navy applications.

2016 PUBLICATIONS/PRESENTATIONS

1. Motyka T. et al., "ONR Undersea Power and Energy Program Review," National Harbor, Maryland, April 20–22, 2016.

REFERENCES

1. U.S. Department of Energy Targets for Onboard Hydrogen Storage Systems for Light-Duty Vehicles; http://www1.eere.energy.gov/hydrogenandfuelcells/storage/pdfs/targets_onboard_hydro_storage.pdf.

2. Klebanoff, L.; Keller, J., "5-Year Review of Metal Hydride Center of Excellence," Int. J. Hydrogen Energy 38 (2013) 4533–4576. In Proceedings of the 2010 U.S. Department of Energy Hydrogen Program Annual Merit Review, Washington, D.C., USA, 7–11 June 2010; Available online: http://www.hydrogen.energy.gov/pdfs/review10/st029_klebanoff_ 2010_o_web.pdf.

3. Corgnale C., Hardy, B.J., Tamburello, D.A., Garrison, S.L., Anton, D.L., "Acceptability envelope for metal hydride-based hydrogen storage systems." Int J Hydrogen Energy 2012;37:2812e24 http://dx.doi.org/10.1016/j.ijhydene.2011.07.037.

IV.C.1 HyMARC: A Consortium for Advancing Solid-State Hydrogen Storage Materials

Mark D. Allendorf
Sandia National Laboratories (SNL)
7011 East Avenue, MS 9161
Livermore, CA 94551-0969
Phone: (925) 294-2895
Email: mdallen@sandia.gov

DOE Manager: Ned Stetson
Phone: (202) 586-9995
Email: Ned.Stetson@ee.doe.gov

Project Start Date: September 17, 2015
Project End Date: September 30, 2018

Overall Objectives

- Accelerate discovery of breakthrough storage materials by developing foundational understanding of phenomena governing the thermodynamics and kinetics limiting the development of solid-state hydrogen storage materials.
- Develop community tools and capabilities to enable materials discovery, including computational models and databases, new characterization tools and methods, and tailorable synthetic platforms.

Fiscal Year (FY) 2016 Technical Milestones

- Prepare a library of bulk-phase model storage systems. (first quarter, FY 2016)
- Demonstrate a size control method for one prototype complex hydride nanostructure. (second quarter, FY 2016)
- Demonstrate in situ soft X-ray ambient pressure X-ray photoelectron spectroscopy, X-ray absorption spectroscopy, and X-ray emission spectroscopy tools, with sample heating. (third quarter, FY 2016)
- Identify hydride mobile species and diffusion pathways. (fourth quarter, FY 2016)
- Synthesize a library of nanoparticles (1–5 nm, 5–10 nm, >10 nm) for one prototype metal hydride. (fourth quarter, FY 2016)

Technical Barriers

This project addresses the following technical barriers from the Hydrogen Storage section of the Fuel Cell Technologies Office Multi-Year Research, Development, and Demonstration Plan.

(A) System Weight and Volume

(E) Charging/Discharging Rates

(O) Lack of Understanding of Hydrogen Physisorption and Chemisorption

Technical Targets

This project will develop foundational understanding and new capabilities that will enable accelerated discovery of breakthrough materials in all classes of storage materials, in particular metal hydrides and sorbents. Specific targets include: (1) validated models of hydrogen uptake and release by storage materials, accounting for all relevant length scales (atomic/molecular to macroscale morphology); (2) databases of thermodynamic and kinetic properties that can be used in materials discovery; and (3) synthetic routes to nanoscale storage materials and a suite of characterization tools for understanding their behavior. It is anticipated that the insights gained from this research, coupled with new synthetic, characterization, modeling, and database tools that will be made available to the hydrogen storage research community, will lead to materials that meet DOE system targets, such as gravimetric and volumetric capacity, system fill time, delivery temperature, and cost.

FY 2016 Accomplishments

- Project teams were established for each of the five tasks (Thermodynamics, Mass Transport, Surface Chemistry, Internal Interfaces, and Additives).
- Four new postdoctoral appointees were hired since the onset of the project.
- User proposals were submitted and approved that permit access by HyMARC staff to the Molecular Foundry, Advanced Light Source, and Spallation Neutron Source.
- A webinar and several invited presentations by HyMARC leadership informed the hydrogen storage community of the new project and its objectives.
- Collaborations with the Hydrogen Storage Characterization and Optimization Research Effort were initiated in the areas of complex metal hydride kinetics, synthesis at ultrahigh pressures (≥700 bar), and vibrational spectroscopy at elevated hydrogen pressure.

- The first journal articles describing HyMARC research were published.

✧ ✧ ✧ ✧ ✧

INTRODUCTION

Storage of hydrogen onboard vehicles is one of the critical enabling technologies for creating hydrogen-fueled transportation systems that can reduce oil dependency and mitigate the long-term effects of fossil fuels use on climate change. Stakeholders in developing hydrogen infrastructure (e.g., state governments, automotive original equipment manufacturers, station providers, and industrial gas suppliers) are currently focused on high-pressure storage at 350 bar and 700 bar, in part because no viable solid-phase storage material has emerged. Nevertheless, solid-state materials, including novel sorbents and high-density hydrides, remain of interest because of their unique potential to meet all DOE targets and deliver hydrogen at lower pressures and higher onboard densities. A successful solution would significantly reduce costs and ensure the economic viability of a United States hydrogen infrastructure.

DOE-supported individual projects and the Centers of Excellence collectively synthesized and characterized hundreds of candidate materials documented in the DOE Hydrogen Storage Materials Database. Although materials meeting some of the key targets were identified, progress continues to be hindered by a lack of understanding of the kinetics and thermodynamics underlying the physical properties of interest. For sorbents, the biggest limitation is volumetric capacity within the target operating temperatures, whereas hydrides are limited by insufficient gravimetric capacity and/or reaction kinetics to meet the fill time target. At a recent (January 2015) Office of Energy Efficiency and Renewable Energy Material-Based Hydrogen Storage Summit, principal investigators (PIs) identified the following high-priority needs for accelerating development of viable solid-state storage materials:

- Validated multi-scale models for determining metal hydride structure-property correlations.
- Computational tools to guide design of nanoporous sorbent pore size distributions.
- Synthetic strategies to increase the strength of hydrogen interactions with sorbent adsorption sites.
- Rates and mechanisms of kinetic processes that limit metal hydride reversibility.
- Design rules for nanostructuring that improve metal hydride kinetics and thermodynamics.
- Models describing the structure, chemistry, and mass transport on surfaces and at interfaces.

APPROACH

The HyMARC consortium seeks to address these needs by leveraging recent advances in predictive multiscale modeling, high-resolution in situ characterization, and material synthesis that were unavailable to the Centers of Excellence. Combined with materials informatics, this strategy embodies the approach highlighted within the Materials Genome Initiative Strategic Plan for accelerated materials development. By focusing on the underlying thermodynamic and kinetic limitations of storage materials, HyMARC will generate foundational understanding that will accelerate the discovery and development of all types of advanced storage materials, including sorbents, metal hydrides, and liquid carriers. Thus, DOE investments will be fully leveraged for future external materials-focused projects.

RESULTS

Organizational aspects: HyMARC was launched in September 2015, with a kickoff meeting held in October. The full team is comprised of approximately 30 individuals, including research staff and postdoctoral appointees, representing the three consortium national laboratories (SNL in Livermore, CA; Lawrence Livermore National Laboratory [LLNL]; and Lawrence Berkeley National Laboratory [LBL]). The leadership structure (Figure 1) includes the consortium director, lead PIs at all three laboratories, and PIs for each of the consortium tasks. The team also includes points of contact at two DOE–Basic Energy Sciences user facilities: the Molecular Foundry and the Advanced Light Source (ALS). Key activities at the full consortium level this year included assembling the full research teams, hiring several new postdoctoral appointees, familiarizing team members with the full set of capabilities represented by the consortium via on-site meetings and lab tours, and establishing a regular series of task meetings for exchange of information. A web data repository was brought on line for internal use; development of an external web site is underway. Finally, HyMARC leadership provided informational briefings about the formation of HyMARC to the national and international hydrogen storage research communities, via a webinar in January 2016 and several presentations at major international conferences.

HyMARC capabilities: Achieving the HyMARC goal of developing a suite of modeling tools that span all length and time scales relevant to hydrogen storage requires a combination of facile, controllable synthetic approaches, high-performance computing hardware, and state-of-the-art characterization tools that can be used to test and validate these models. The scope of the HyMARC modeling initiative is illustrated in Figure 2, which indicates that phenomena from the atomic to the macroscale must be addressed. Access to high-performance computing capabilities at the three consortium laboratories was in

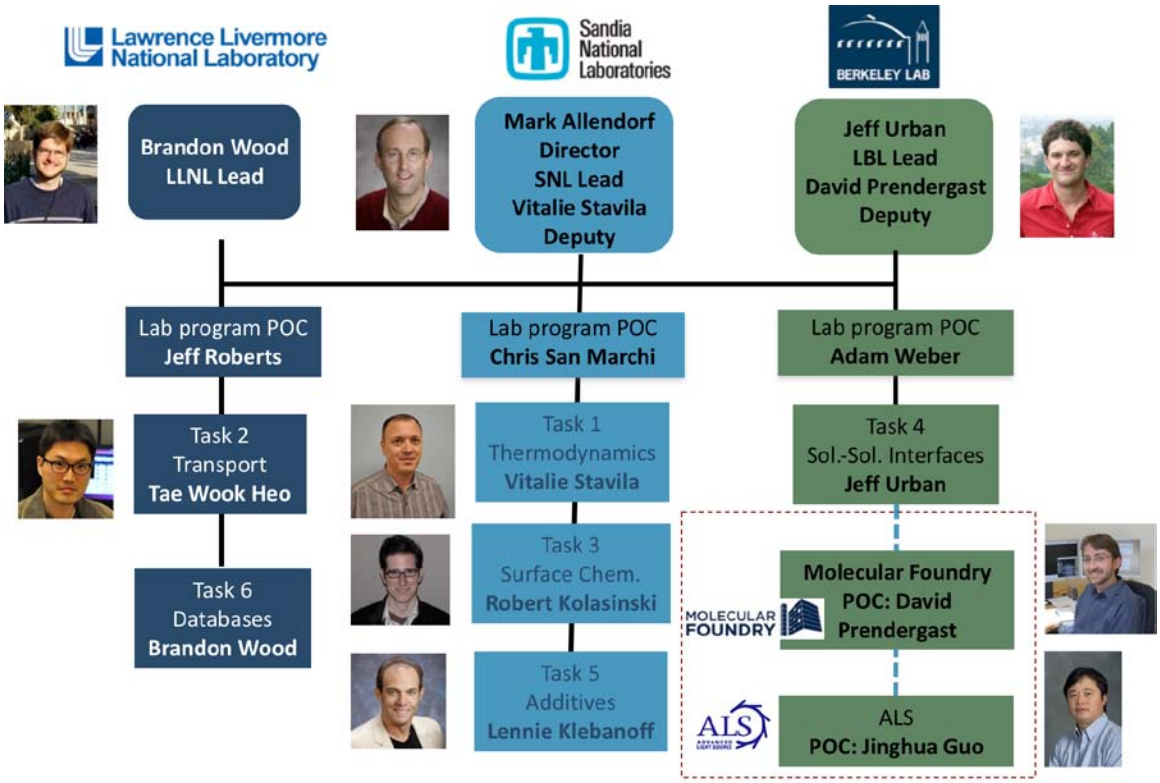

POC – Point of contact

FIGURE 1. HyMARC organizational structure and key points of contact

place at from the outset of HyMARC, as were a number of unique diagnostic and synthetic capabilities. However, some of the most powerful characterization tools available today are located at DOE–Basic Energy Sciences user facilities, which require approval of submitted research proposals to obtain time on the instrument. To this end, the HyMARC team submitted user proposals to the Molecular Foundry, ALS, and Spallation Neutron Source, all of which were approved. At the Molecular Foundry, access was approved to use the first-principles computational spectroscopy models for interpreting data obtained at the ALS, and to the electron microscopy, atomic force microscopy, and X-ray photoelectron spectroscopy available in the Imaging and Manipulation of Nanostructures Facility. At the ALS, an "Approved Program" proposal was granted that allocates a block of dedicated time for three years on two beam lines. The first of these provides access to soft X-ray spectroscopies (e.g. X-ray absorption and emission), which will be used to probe composition and coordination environment. This tool can also distinguish the bulk chemical environment from that of the near-surface region. The second beam line will be used for scanning transmission X-ray microscopy measurements, which enable composition, phase, and microstructure to be probed with 30-nm resolution. At the Spallation Neutron Source, a user proposal was approved that provides access to the VISION vibrational spectrometer, which provides information about molecular structure, chemical bonding, and intermolecular interactions. Experiments at all three user facilities have already been conducted or are scheduled as of the writing of this report.

Collaborations: The geographical colocation of the three partner laboratories strongly enhances the ability of the HyMARC team to collaborate in a fluid and responsive way. This was readily apparent this year, as efforts to employ the unique consortium tools at all three laboratories were initiated. Task meetings routinely involved in-person participation by representatives of all three laboratories. A number of joint investigations were initiated, in which staff from one partner laboratory went on site to a partner laboratory to be trained on relevant equipment and conduct experiments. Use of precious beam time at the ALS was also greatly facilitated by the proximity of SNL and LLNL to LBL. The ability to plan experiments by in-person meetings with various beam-line scientists and transport equipment and samples easily from one site to another greatly simplified logistics for staff involved in experiments running around the clock.

In addition, several collaborations with the Hydrogen Storage Characterization and Optimization Research Effort were initiated, with the twin objectives of facilitating information exchange and to assemble powerful interdisciplinary teams combining the unique capabilities of each team to address the most challenging problems. The first

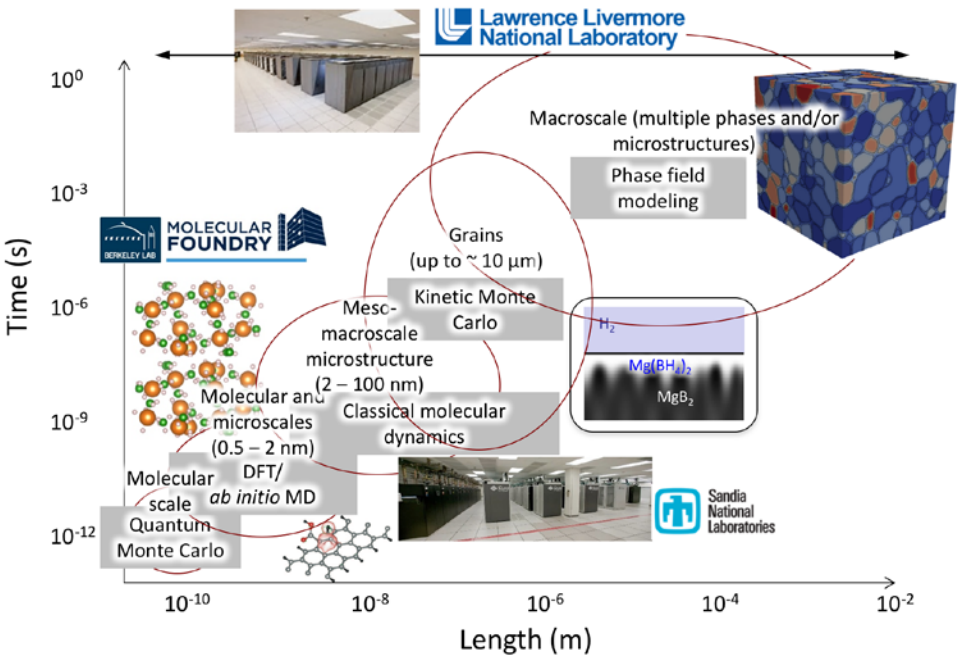

FIGURE 2. Length and time scales relevant to hydrogen storage material properties and corresponding modeling tools employed by HyMARC to address these. Supercomputing facilities at all three consortium laboratories are being employed to develop a suite of modeling tools spanning the atomic/molecular to macroscale/multiphase materials.

of these is a joint effort to understand the complex kinetics of hydrogen desorption and uptake by magnesium borohydride ($Mg(BH_4)_2$). HyMARC investigators are focusing on hydrogen uptake kinetics, while the Hydrogen Storage Characterization and Optimization Research Effort team is developing mechanisms of hydrogen desorption. Sample exchanges and jointly planned experiments are underway.

Technical progress: Details of the progress toward FY 2016 milestones (listed above) are provided in the individual annual reports for the three consortium laboratories. Briefly, however, as of the writing of this report, Milestones 1 and 2 are complete and Milestones 3, 4, and 5 are in progress. Noteworthy, the first two journal publications resulting from HyMARC research appeared in the literature, one describing a new molecular dynamics approach to computing hydrogen diffusion constants through materials, the other an exciting new method for synthesizing metal hydride nanoparticles.

FY 2016 PUBLICATIONS/PRESENTATIONS

Publications

1. X.W. Zhou, F. El Gabaly, V. Stavila, M.D. Allendorf "Molecular Dynamics Simulations of Hydrogen Diffusion in Aluminum," *J. Phys. Chem. C* 2016, *v. 120*, p. 7500.

2. E.S. Cho, A.M. Ruminski, S. Aloni, Y.-S. Liu, J. Guo, J.J. Urban "Graphene Oxice/Metal Nanocrystal Multilaminates as the Atomic Limit for Safe and Selective Hydrogen Storage," *Nature Comm.* 2016, *vol. 7*, p. 10804.

Presentations

1. M.D. Allendorf "Hydrogen Materials Advanced Research Consortium," FCTO Overview Webinar, January 7, 2016.

2. M.D. Allendorf, B.C. Wood, j. J. Urban, J. Guo, T. W. Heo, L.E. Klebanoff, R. Kolasinski, V. Stavila "HyMARC: A Consortium for Advancing Solid-State Hydrogen Storage Materials," *Int. Symp. Hydrogen & Energy*, Febuary 22–26, 2016, Sendai, Japan.

3. M.D. Allendorf "HyMARC: A Consortium for Advancing Solid-State Hydrogen Storage Materials," Toyota Central R&D Laboratories, Febuary 26, 2016, Nagoya, Japan.

IV.C.2 Hydrogen Storage Materials Advanced Research Consortium: Sandia Effort

Mark D. Allendorf (Primary Contact),
Vitalie Stavila, Lennie Klebanoff, Rob Kolasinski,
Farid El Gabaly, Xiaowang Zhao, James White
Sandia National Laboratories
7011 East Avenue
Livermore, CA 94551
Phone: (925) 294-3059
Email: mdallen@sandia.gov

DOE Manager: Ned Stetson
Phone: (202) 586-9995
Email: Ned.Stetson@ee.doe.gov

Project Start Date: September 17, 2015
Project End Date: September 30, 2018

Overall Objectives

- Provide technical leadership to HyMARC via leadership of Task 1 (Thermodynamics), Task 3 (Gas Surface Interactions) and Task 5 (Additives).
- Provide gas sorption and other property data required to develop and validate thermodynamic models of sorbents and metal hydrides, including the effects of high hydrogen pressure.
- Identify the structure, composition, and reactivity of gas–surface and solid–solid hydride surfaces contributing to rate-limiting desorption and uptake.
- Synthesize metal hydrides and sorbents in a variety of formats (e.g. bulk powders, thin films, nanostructures) and develop in situ techniques for their characterization.
- Apply Sandia multiscale codes to discover new materials and new mechanisms of storing hydrogen, provide input for database development.
- Elucidate the role of additives in improving hydrogen storage adsorption and desorption reactions.

Fiscal Year (FY) 2016 Objectives

- Synthesize library of bulk-phase model storage systems.
- Size control method for one prototype complex hydride nanostructure.
- Demonstrate in situ soft X-ray ambient pressure X-ray photoelectron spectroscopy (XPS), X-ray absorption spectroscopy (XAS), X-ray emission spectroscopy tools, with sample heating.
- Identify hydride mobile species and diffusion pathways.
- Synthesize and characterize library of nanoparticles for one hydride: 1–5 nm, 5–10 nm, >10 nm.
- Assess bulk additives (TiF_3, $TiCl_3$) for their reactivity towards hydrogen.
- Assess low-energy ion scattering (LEIS) as a tool for measuring H atom surface diffusion on a thermally sensitive surface.

Technical Barriers

This project addresses the following technical barriers from the Hydrogen Storage section of the Fuel Cell Technologies Office Multi-Year Research, Development, and Demonstration Plan.

(A) System Weight and Volume

(B) System Cost

(C) Efficiency

(D) Durability/Operability

(E) Charging/Discharging Rates

(O) Lack of Understanding of Hydrogen Physisorption and Chemisorption

Technical Targets

The goal of this project is to develop foundational understanding of phenomena governing thermodynamics and kinetics of hydrogen release and uptake in all classes of hydrogen storage materials. Insights gained from these studies will be applied toward the design and synthesis of hydrogen storage materials that meet the following DOE 2020 hydrogen storage targets.

- Cost: $10/kWh net
- Specific energy: 1.8 kWh/kg
- Energy density: 1.3 kWh/L

FY 2016 Accomplishments

- A molecular dynamics modeling framework was established to accurately predict the diffusion kinetic barriers; proof-of-concept demonstrated for H-diffusion in Pd and Al.

- The Sandia high-pressure (up to 1,000 bar) system was upgraded to provide improved temperature control and enable the simultaneous use of multiple reaction cells.
- Synthesized and characterized a suite of metal-organic frameworks (MOFs) to validate quantum Monte Carlo and grand canonical Monte Carlo models of the interaction potentials and predict hydrogen isotherms.
- Established X-ray absorption spectroscopy as a tool for probing metal hydrides, including separate bulk- and surface-sensitive approaches. Used titanium-doped $NaAlH_4$ as a model system.
- Elucidated the extent to which the bulk additives $TiCl_3$ and TiF_3 by themselves (no hydride present) are reactive towards hydrogen gas using a combination of X-ray emission spectroscopy, XAS, Fourier transform infrared spectroscopy, and Sieverts hydrogen uptake measurements.
- Developed synthetic protocols for synthesizing ≤10 nm particles of $LiNH_2$/2LiH in nanoporous carbons and MOFs.
- Demonstrated that LEIS can be used to measure H atom surface diffusion on the thermally sensitive Mg(0001) surface.
- Developed clean, air-free techniques for sample transfer for XPS, Auger, XAS, and LEIS in situ studies.

✧ ✧ ✧ ✧ ✧

INTRODUCTION

Storage of hydrogen on board vehicles is one of the critical enabling technologies for creating hydrogen-fueled transportation systems that can reduce oil dependency and mitigate the long-term effects of fossil fuels on climate change. Stakeholders in developing hydrogen infrastructure (e.g., state governments, automotive original equipment manufacturers, station providers, and industrial gas suppliers) are currently focused on high-pressure storage at 350 bar and 700 bar, in part because no viable solid-phase storage material has emerged. Nevertheless, solid-state materials, including novel sorbents and high-density hydrides, remain of interest because of their unique potential to meet all DOE Fuel Cell Technologies Office targets and deliver hydrogen with lower storage pressures and higher on-board densities. However, the existing materials suffer from thermodynamic and kinetic limitations, which prevent their application as practical hydrogen storage media.

Sandia's objectives/responsibilities within HyMARC are to: (1) provide technical leadership to the consortium at the director level, as well as through leadership of Task 1 (Thermodynamics), Task 3 (Gas-Surface Interactions), and Task 5 (Additives); (2) provide gas sorption and other property data required to develop and validate thermodynamic models of sorbents and metal hydride storage materials, including the effects of 350 bar and 700 bar hydrogen delivery pressures, serving as a resource for the consortium; (3) identify the structure, composition, and reactivity of gas–surface and solid–solid hydride surfaces contributing to rate-limiting desorption and uptake; (4) provide metal hydrides and MOFs in a variety of formats tailored for specific consortium tasks; (5) develop sample preparation methods and experimental protocols to enable facile use of the new characterization probes employed by the consortium; (6) apply Sandia multiscale codes to discover diffusion pathways and mechanisms of storage materials; (7) elucidate the role of additives in promoting hydrogen storage reactions; and (8) determine if LEIS can be used as a unique tool to measure H atom diffusion on thermally sensitive materials.

APPROACH

HyMARC seeks to address critical gaps in the science of hydrogen storage by leveraging recent advances in predictive multiscale modeling, high-resolution in situ characterization, and novel material synthesis techniques. By focusing on the underlying thermodynamic and kinetic limitations of storage materials, we will generate foundational understanding that will accelerate the development of all types of advanced storage materials, including sorbents, metal hydrides, and liquid carriers.

RESULTS

Substantial progress was made on each of the five tasks being performed at Sandia, with all of the quarterly goals met on time. Sandia principal investigators led the organization of task groups, helping to guide the science in collaboration with our partners, and scheduling and coordinating task team meetings involving all three HyMARC laboratory partners. Technical results include the following:

Task 1: Thermodynamics. A suite of porous carbons, including B- and N-doped materials, were prepared or obtained from other institutions and were characterized to determine pore size distributions and surface areas; these will be used to validate new modeling capabilities. Several MOFs are also included in this test set and were synthesized and characterized by X-ray diffraction (Figure 1) and porosimetry. In collaboration with Task 5 (Additives), pressure–composition–temperature studies on titanium-doped $NaAlH_4$ show that the adsorption-desorption thermodynamics change as the $TiCl_3$ dopant concentration increases, indicating that its effect is not purely catalytic (Figure 2), but also thermodynamic. X-ray diffraction shows that a crystalline intermetallic, TiAl, forms when $TiCl_3$-doped $NaAlH_4$ is dehydrogenated.

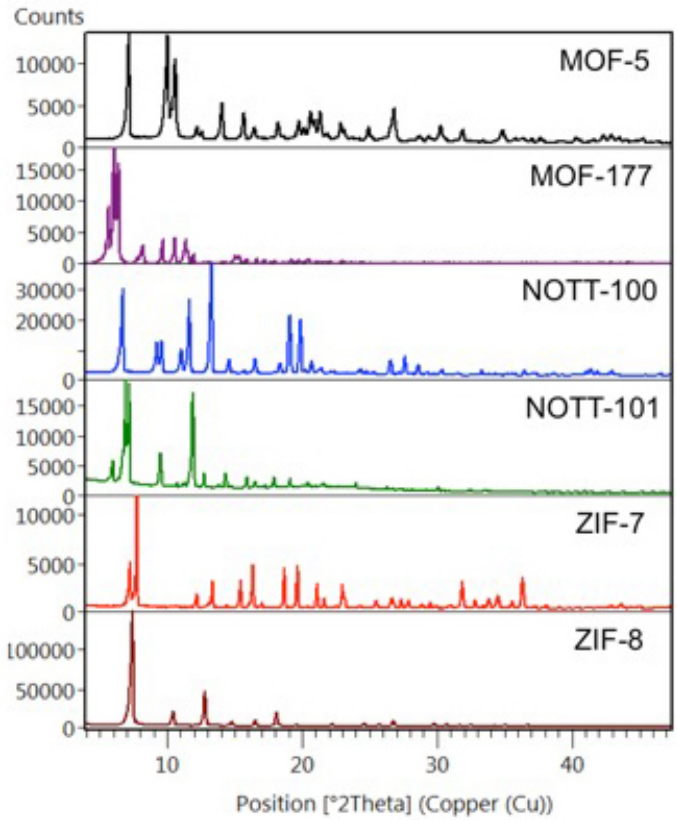

FIGURE 1. X-ray diffraction patterns confirming phase-purity of MOF-5, MOF-177, NOTT-100(101), ZIF-7(8)

Task 2: Kinetics of Mass Transport. A new molecular dynamics-based modeling capability was developed to simulate hydrogen diffusion through solids. Hydrogen diffusion through aluminum and hydrogenated palladium (PdH_x) were modeled as test systems (Figure 3), employing thousands of simulations to determine appropriate values of the numerous independent parameters in such calculations. The calculated energy barrier for H transport in Al, determined from the Arrhenius plot of diffusion constants obtained at several temperatures, was found to be ~0.4 eV, matching experimental results. Hydrogen diffusion in PdH_x is found to be independent of composition below x = 0.7, with an activation energy of 0.15 eV. However, above that threshold, at least two diffusion pathways are active. This new tool allows hydrogen transport in an evolving material to be modeled, such as a metal hydride undergoing dehydrogenation.

Task 3: Surface Science. Several new surface analytical techniques were deployed, both at Sandia and at the Advanced Light Source. New "clean transfer" sample holders that prevent exposure to air and moisture were designed and fabricated for both the Auger electron spectroscopy/LEIS and XPS systems at Sandia, and for ambient-pressure XPS at the Advanced Light Source. Data from a model system, $TiCl_3$-doped $NaAlH_4$, provide new insight into the chemistry

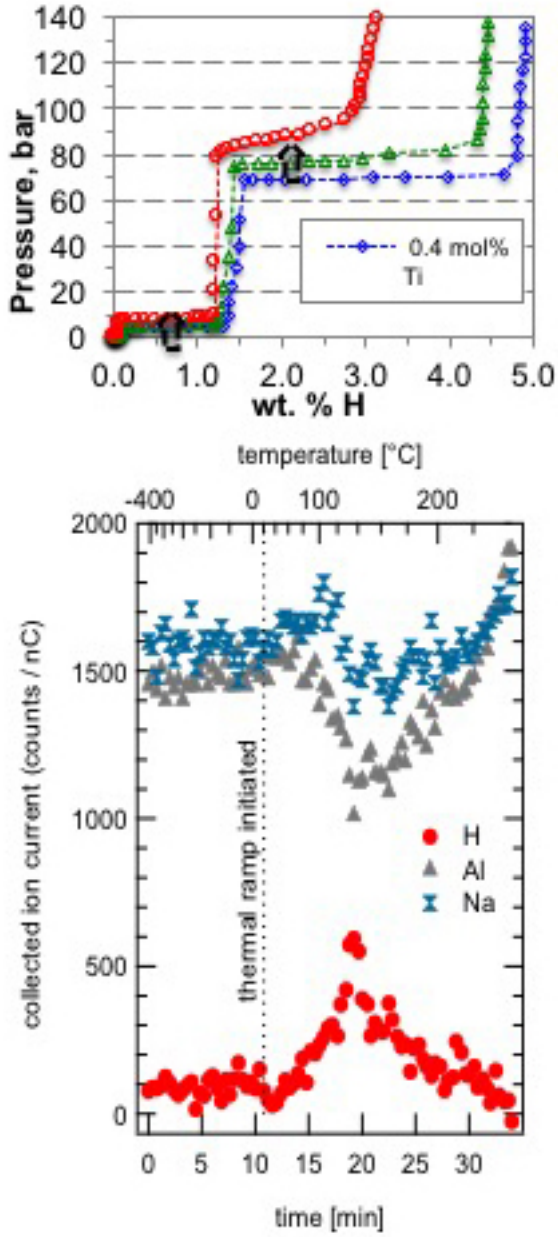

FIGURE 2. Top: Pressure–composition–temperature isotherms of $NaAlH_4$ doped with differing amounts of $TiCl_3$, showing increases in plateau pressures with higher loadings. Bottom: LEIS measurements of 2 mol% $TiCl_3$-doped $NaAlH_4$ during sample heating.

of hydrogen desorption. After ball-milling, Ti is undetectable by XPS or Auger electron spectroscopy, indicating that it is present only in the bulk. Both in situ and ex situ studies show that surface Al-H decreases upon heating to 150°C and metallic Al increases as dehydrogenation proceeds. LEIS, which can detect hydrogen at the gas-surface interface, indicates that surface H increases during hydrogen release from the decomposing sample (Figure 2). The surface also becomes sodium-rich and surface Al (in all forms) is

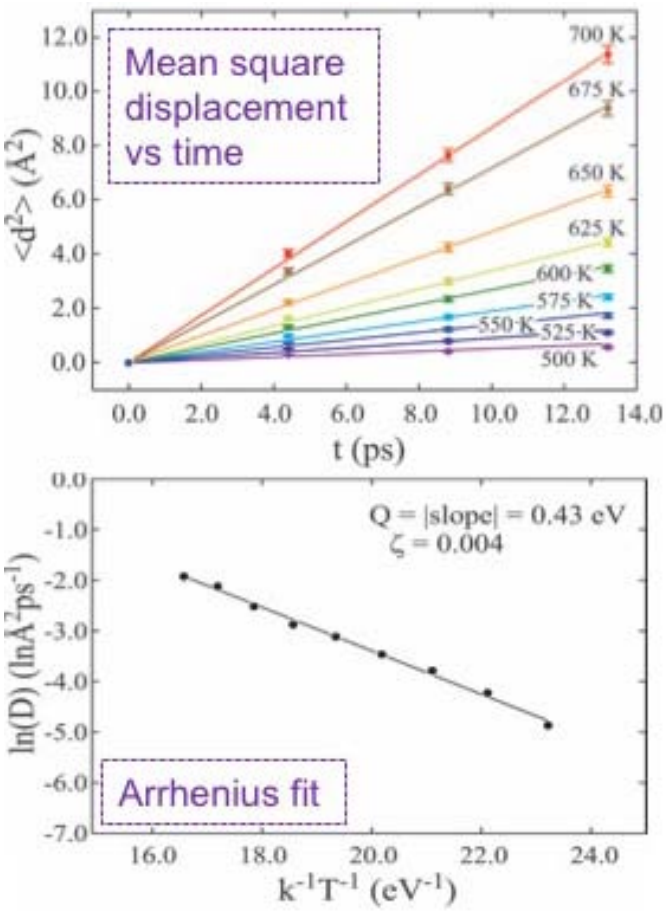

FIGURE 3. Molecular dynamics calculations of mean-square displacements and the corresponding Arrhenius plots of hydrogen diffusion in aluminum at various temperatures

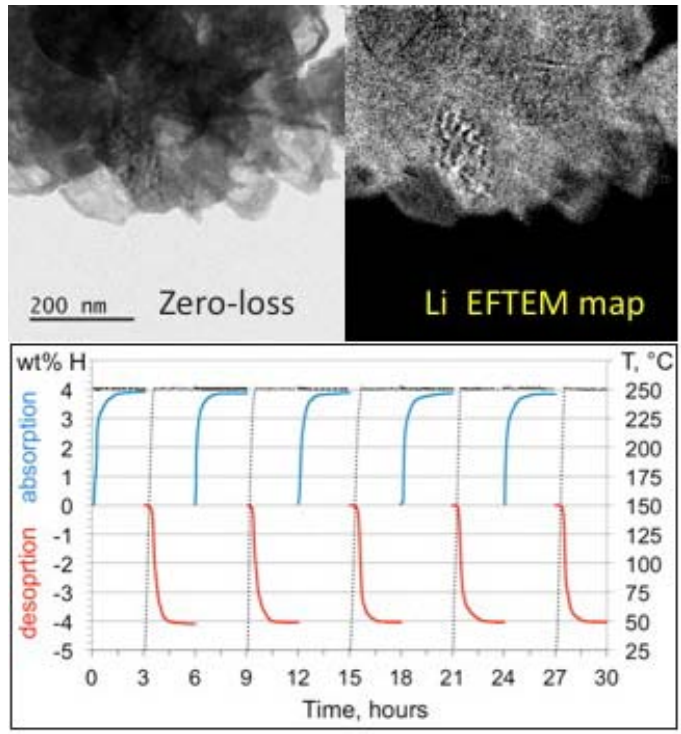

FIGURE 4. Top: Zero-loss transmission electron microscopy and energy filtered transmission electron microscopy (EFTEM) Li elemental maps in nano-confined Li_3N@3.2nm-carbon. Bottom: Sieverts data showing 4 wt% reversible hydrogen uptake and release in Li_3N@3.2nm-carbon.

depleted. LEIS was also employed to probe the diffusion of hydrogen on surfaces, using the Mg(0001) surface for demonstration purposes. This newly developed capability involves dosing the surface with hydrogen, followed by creating a well-defined H-free surface region using the low-energy ion beam. Hydrogen is then detected by LEIS as the cleared region is repopulated. LEIS can now be applied to other materials and will be used in conjunction with theory being developed to determine rates of two-dimensional hydrogen transport.

Task 4: Solid-Solid Interfaces. A novel ammonia solution-based method was developed that allows $LiNH_2$ and Li_3N to be incorporated into porous carbons with average pore sizes from 3–12 nm. The presence of Li-containing species confined within the pores was confirmed by EELS mapping (Figure 4). The hydrogenation and dehydrogenation of this nano-confined Li_3N is found to be a single-step process, unlike the two-step mechanism in bulk Li_3N. Moreover, complete cycling occurs 180°C lower than the bulk, allowing up to 4 wt% H incorporation (Figure 4). Theoretical predictions in collaboration with LLNL indicate nanoscaling Li_3N particles effectively eliminates the metastable Li_2NH intermediate due to its high interfacial energy.

Task 5: Additives. The additives TiF_3 and $TiCl_3$, which are known to be catalytic for the cycling of $NaAlH_4$, were studied in pure form to determine their hydrogenation reactivity. XAS, which can detect $TiCl_3$ in concentrations at least as low as 0.4 mol%, was employed to monitor the Ti chemistry. $TiCl_3$ and TiF_3 exposed to 120 bar hydrogen at both room temperature and 200°C for 17 h exhibit negligible hydrogen uptake. The XAS spectra show no changes in the local electronic structure at Ti or F for TiF_3 upon H_2 exposure, and the Ti local electronic structure remained unmodified. Vibrational spectroscopy indicates no change in the chemical properties of the bulk additives upon exposure to H_2 under the same conditions.

CONCLUSIONS AND FUTURE DIRECTIONS

In the first year of HyMARC the SNL team developed new synthetic, modeling, and diagnostic tools that provide new insights into seemingly well-understood storage materials such as Ti-doped $NaAlH_4$, magnesium, and titanium hydrides. These tools are now available, through

collaborations with the HyMARC team, to accelerate development of new storage materials. Future work will extend these to more complex, less understood, storage materials that can meet DOE targets, such as $Mg(BH_4)_2$. Highly accurate quantum Monte Carlo calculations are expected to provide new understanding of H_2 binding to open metal sites in MOFs and other sorbents. In addition, a database development task will commence, with the objective of creating web-based tools to allow the hydrogen storage community to access HyMARC results.

SPECIAL RECOGNITIONS & AWARDS/ PATENTS ISSUED

1. V. Stavila, L. Klebanoff. "*Nanostructured metal amides and nitrides for hydrogen storag,*" U.S. Patent Application 62/235,930, November, 2015.

FY 2016 PUBLICATIONS/PRESENTATIONS

Publication

1. X.W. Zhou, F. El Gabaly, V. Stavila, M.D. Allendorf, "Molecular Dynamics Simulations of Hydrogen Diffusion in Aluminum," *J. Phys. Chem. C*, 2016, *v. 120*, p. 7500.

Presentations

1. V. Stavila, B. Wood, L. Klebanoff, T.W. Heo, et al. "Nanoscale effects in complex metal hydrides," Pacifichem-2015, Honolulu, HI, December 2015.

2. V. Stavila, L. Klebanoff, E. Majzoub, J. Vajo. "Phase minimization as a promising strategy to improve hydrogen storage properties of complex metal hydrides," MRS Spring Meeting, Phoenix, AZ, April 2016.

IV.C.3 HyMARC: Hydrogen Storage Materials Advanced Research Consortium (LLNL Effort)

Brandon Wood (Primary Contact), Tae Wook Heo, Keith Ray, Jonathan Lee, ShinYoung Kang, Stanimir Bonev, Miguel Morales, Roman Nazarov, Patrick Shea, Theodore Baumann, Patrick Campbell
Lawrence Livermore National Laboratory (LLNL)
7000 East Ave., L-413
Livermore, CA 94550
Phone: (925) 422-8391
Email: brandonwood@llnl.gov

DOE Manager: Ned Stetson
Phone: (202) 586-9995
Email: Ned.Stetson@ee.doe.gov

Project Start Date: September 17, 2015
Project End Date: September 30, 2018 (Phase I End)

Overall Objectives

- Provide community tools and foundational understanding of phenomena governing thermodynamics and kinetics to enable development of solid-phase hydrogen storage materials.

Fiscal Year (FY) 2016 Objectives

- Establish protocols for more accurate first-principles computations of hydride and sorbent thermodynamics.
- Adapt methods to account for non-ideal factors (e.g., defects and interfaces) in hydride simulations.
- Devise initial multiscale framework for simulating hydride kinetics, including mass transport and phase evolution, and compare against experiments on a model system.
- Establish protocols for synthesis of tailored carbon sorbents and soft X-ray characterization of hydride materials and catalysts.

Technical Barriers

This project addresses the following technical barriers from the Hydrogen Storage section of the Fuel Cell Technologies Office Multi-Year Research, Development, and Demonstration Plan.

(O) Lack of Understanding of Hydrogen Physisorption and Chemisorption

(A) System Weight and Volume

(E) Charging/Discharging Rates

Technical Targets

This project will develop foundational understanding and new capabilities that will enable accelerated discovery of breakthrough materials in all classes of storage materials, in particular metal hydrides and sorbents. It is anticipated that the insights gained from this research, coupled with new synthetic, characterization, modeling, and database tools that will be made available to the hydrogen storage research community, will lead to materials that meet DOE system targets such as gravimetric and volumetric capacity, system fill time, delivery temperature, and cost.

FY 2016 Accomplishments

- Demonstrated approaches for computing accurate physisorption energetics of hydrogen on metal organic framework (MOF) metal sites (including hydrogen loadings beyond the dilute limit), and for simulating charge and field effects in carbon sorbents.
- Established protocols for more accurate density functional theory (DFT) computations of hydride thermodynamics accounting for finite temperature contributions, microstructure, and phase morphology.
- Improved thermodynamic phase fraction predictions of Li-N-H system as a function of pressure, temperature, and size within multi-phase framework.
- Developed non-equilibrium statistical approach to quantify effects of non-ideal interfaces and additives on reaction pathways.
- Demonstrated large-scale ab initio molecular dynamics (AIMD) for elucidating possible transport and reaction pathways and enable finite temperature calculations of thermodynamic and spectroscopic quantities.
- Applied coupled atomistic and mesoscale framework combining thermodynamics, mechanical stress, and phase nucleation and growth to model solid phase transition kinetics in an interstitial hydride system (PdH_x).
- Used X-ray absorption spectroscopy for probing catalyst chemistry and surface versus bulk hydrogenation effects on catalysts within doped hydrides.

✧ ✧ ✧ ✧ ✧

INTRODUCTION

Storage of hydrogen onboard vehicles is one of the critical enabling technologies for creating hydrogen-fueled transportation systems that can reduce oil dependency and mitigate the long-term effects of fossil fuels on climate change [1-2]. Stakeholders in developing hydrogen infrastructure (e.g., state governments, automotive original equipment manufacturers, station providers, and industrial gas suppliers) are currently focused on high-pressure storage at 350 bar and 700 bar, in part because no viable solid-phase storage material has emerged. Nevertheless, solid-state materials, including novel sorbents and high-density hydrides, remain of interest because of their unique potential to meet all DOE Fuel Cell Technologies Office targets and deliver hydrogen with lower storage pressures and higher onboard densities. However, the existing materials suffer from thermodynamic and kinetic limitations that are often poorly understood, which prevent their application as practical hydrogen storage media.

APPROACH

HyMARC seeks to address these gaps by leveraging recent advances in predictive multiscale modeling, high-resolution in situ characterization, and novel material synthesis techniques. By focusing on the underlying thermodynamic and kinetic limitations of storage materials, we will generate foundational understanding that will accelerate the development of all types of advanced storage materials, including sorbents, metal hydrides, and liquid carriers. LLNL objectives and responsibilities within HyMARC include (1) providing technical leadership for Tasks 2 (Mass Transport) and Task 6 (Materials Informatics and Databases) and for the theory efforts; (2) providing computational methods for more accurate prediction of sorbent and hydride thermodynamics; (3) developing tools for multiscale modeling of hydride kinetics, including mass transport, chemical kinetics, and phase kinetics; (4) synthesizing carbon frameworks and sorbents with tailored porosity and chemistry; and (5) supporting HyMARC characterization efforts surrounding soft X-ray spectroscopy.

RESULTS

Sorbent thermodynamics (Task 1A): On the sorbent side, our key computational goal is to improve predictions of sorbent-H_2 interaction energetics and provide understanding of beyond-van der Waals (vdW) interactions in sorbents. Three general types of interactions are being considered: metal site coordination (e.g., open metal sites in MOFs), second-neighbor and cooperative interactions (e.g., polarization effects), and charge transfer or electrostatic effects (e.g., Lewis acids, electronic and chemical doping, and electric field effects). Our strategy relies on more computationally intensive methods that can be used as "gold standards" for energy computations (e.g., quantum Monte Carlo [QMC]), which can benchmark cheaper methods (e.g., vdW-corrected DFT) that can be readily run on many different sorbent systems. Future activities will focus on direct prediction of isotherms (validated against well-characterized MOFs) to provide guidance for MOF design.

MOF-505 was selected as a test sorbent material, with the geometry taken from the CoRE Database [3] and relaxed using DFT. Dilute-limit H_2 physisorption energies were calculated using QMC, which carries significant computational expense but promises chemical accuracy while including the full extended geometry of the substrate [4]. These results were used to evaluate which flavors of vdW-corrected DFT gave reliable binding energies for each possible binding site (Figure 1). Sites were identified by performing AIMD; future efforts will focus on MOFs with sites predetermined via neutron diffraction. Binding geometries amongst different DFT flavors were very consistent, although energies differed by wide margins that were site dependent (up to 500 meV; see Figure 1a). A similar approach will be used to benchmark DFT molecular coordination chemistry calculations and quantify the role of the extended MOF framework in determining binding energetics; indeed, our early calculations suggest extended effects alter bond lengths by as much as 4% with respect to finite clusters. The physisorption energy for higher hydrogen loading on MOF-505 was also computed, taking into account the full interactions between H_2 and the lattice. The results, shown in Figure 1b, demonstrate that the binding energy depends non-trivially on the hydrogen concentration (note that the expected behavior for a weakly interacting system would be flat or monotonic). We conclude that explicit calculations at higher loadings will be necessary for accurate isotherm prediction. The changes in bond lengths with loading should also result in different vibrational modes, which are currently being computed for comparison with infrared spectroscopy performed by partners on the Characterization and Validation team.

Our theoretical investigations on carbon sorbents have centered on the use of electrostatic interactions (charge, field, and polarization effects) to enhance binding of hydrogen, using graphene as a model system to tune the surface charge. These calculations, based on the Effective Screening Medium Method of Otani, et al. [5], show how the application of a strong electric field from positively charged graphene ($> +0.025e$ per carbon atom) is able to introduce enough polarization to bring hydrogen physisorption into the required range. A similarly large change was found in the binding energy and surface diffusion barrier for atomic H, which has possible implications for graphene-induced hydrogen dissociation processes. Efforts towards experimental verification are underway.

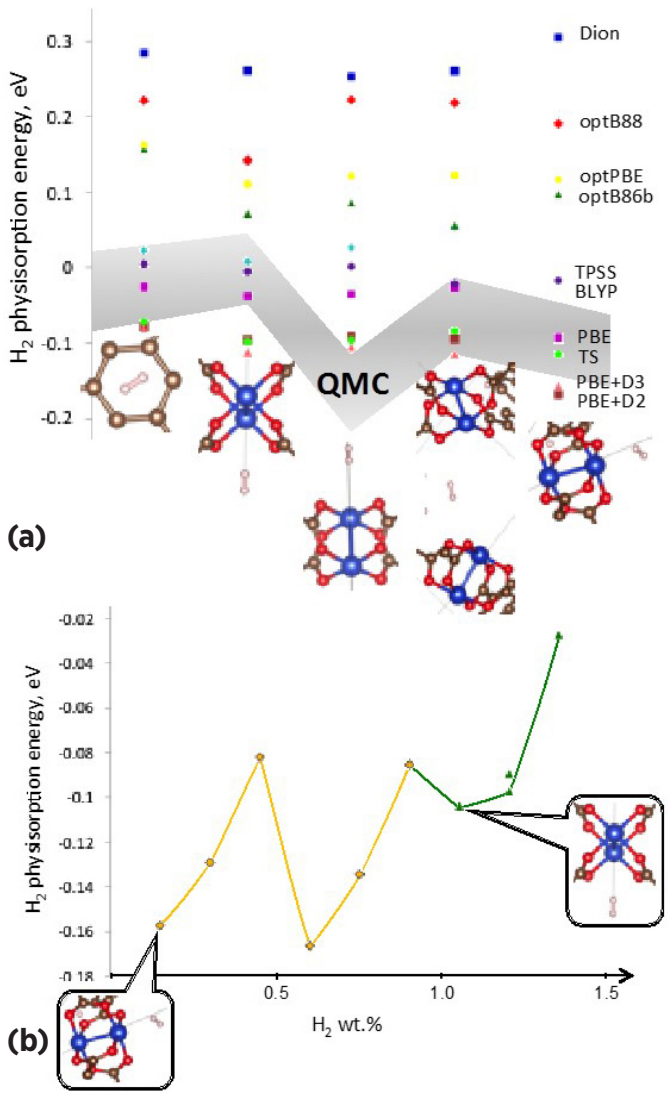

FIGURE 1. Computed physisorption energies for (a) binding of an H_2 molecule in MOF-505 with geometries shown below each data set (the gray region bounds the high-confidence statistical uncertainty for the QMC results, and the colored symbols are the results for different vdW-corrected DFT functionals); and (b) higher-pressure loading with multiple H_2 adsorption sites (the color change indicates a shift in the preferred site with loading).

On the synthesis end, we have been working to establish reproducible synthesis pathways for three-dimensional graphene macro-assemblies with tailored porosity and chemistry based on previous successes with heat treatment and mechanical compression [6-8]. Graphene oxide-derived aerogels were synthesized with varying crystallinity and pore size, which was achieved by subjecting the aerogels to process temperatures ranging from 1,050°C to 2,500°C. The materials were delivered to HyMARC and Characterization and Validation partners for analysis and use as nano-confinement media.

Beyond-ideal hydride thermodynamics (Task 1B): Our computational strategy on the thermodynamics of metal hydrides have centered on more realistic and accurate assessment of thermodynamics using DFT. Three primary factors are being considered, (1) explicit finite-temperature contributions to the free energy, including anharmonicity and thermal distortions; (2) microstructural effects, including interfaces; and (3) morphological considerations, such as amorphous, defect-rich, or solid solution phases. Alongside experimental validation and characterization partners, HyMARC will quantify these factors to determine which may be relevant for accurate prediction of realistic phase pathways.

One focus area has been the inclusion of anharmonic contributions to the free energy, which are typically associated with molecular modes in complex hydrides. We have devised a model for more accurate computation of these contributions using AIMD, based on separation of diffusive and non-diffusive contributions to the vibrational power spectrum [9]. This formalism has the added advantage of spatially decomposing the entropy density, which can be used to independently assess surface contributions. Successful application to the Mg-B-H system shows that anharmonicity can contribute >12 kJ/mol to stability of certain phases, reflecting the soft anion modes that are connected to the mass transport and phase transformation mechanisms. Significantly greater anharmonic contributions can appear at surfaces due to surface-induced disordering and undercoordination. We conclude that accurate free energy computations of complex hydrides should consider vibrations beyond the ideal harmonic limit.

To study the effects of microstructure, we have used the Li-N-H system as our test case. This system is attractive for isolating phase kinetics and thermodynamics, since Li_3N and $LiNH_2$ are known superionic Li conductors and are therefore unlikely to be diffusion limited, and the reaction pathway is well established. Using several model core-shell-derived microstructures based on a careful analysis of previous studies, we computed the predicted thermodynamic phase fractions as a function of pressure, temperature, and particle size (Figure 2). To do so, we developed an extension to the Grand Canonical Linear Programming method [10] by incorporating the effects of interfaces and microstructure in the free energy formulation. Solid interface effects were estimated based on an established semi-empirical procedure for grain boundaries [11], in which the interface energy g_{ij} is calculated as $g_{ij} = p_{ij} (s_i + s_j)$. Here s_i is the surface energy, which we computed within DFT and averaged over possible exposed facets within the Wulff construction to represent a randomly oriented phase boundary (Figure 2a). Furthermore, to explore the effects of the varying interfacial energies due to the heterogeneity of structural characteristics present in real interphase boundaries (e.g., interfacial coherency, chemical bonding characteristics, contents of additives), we devised a novel approach for analyzing the phase fractions statistically by independently varying the prefactor p_{ij} and gathering statistics for all sampled configurations of p_{ij} at

the given hydrogen pressures. For small particles (<20 nm), the interface penalties become sufficiently severe that the ordinarily stable Li_2NH intermediate is suppressed in favor a single-stage reaction pathway between Li_3N and $LiNH_2$+2LiH for both hydrogenation (at P = 100 bar) and dehydrogenation (at P = 1 bar) processes (Figure 2b shows one case for p_{ij} = 0.5). This prediction agrees with measurements performed by HyMARC partners at Sandia, establishing the importance of microstructure and internal interfaces within the particle. Notably, this introduces a new paradigm for progressing towards ultimate hydrogen storage targets by engineering internal microstructure [12]. We are currently working to generalize our phase-fraction prediction code to consider multiple model microstructures.

Modeling interfaces and defects (Tasks 1 & 4): Within our kinetic phase transformation modeling framework (see sections below), one of the most important yet challenging ingredients for predicting accurate kinetics is the computation of reliable solid interface energies and compositions. Semi-empirical approaches based on surface energy calculations benefit from simplicity but lack much of the physics of the complex models and may therefore be limited in their predictive capability. Within HyMARC, we are pursuing several additional strategies for computing interfacial energies and benchmarking against kinetics experiments using model materials. In this way, we hope to select a practical solution that balances accuracy with reasonable computational cost and can be applied to a wide variety of materials.

For interstitial hydrides, free energies of interfaces can be computed explicitly with full finite-temperature effects using large-scale molecular dynamics, which captures the full interface complexity (an example based on Pd-H is discussed in further detail below [13]). For somewhat more complicated hydrides where charge transfer is relevant and large-scale molecular dynamics may be impractical, we are exploring methods based on zero-temperature DFT. Here, our model system is the Mg-H system, with interface kinetics characterization supplied from HyMARC partners at Lawrence Berkeley National Laboratory. For simple hydrides (e.g., Mg-H), the interface enthalpy can in principle be calculated within DFT using large supercells; however, accurately accounting for the possibility space of interface orientations, thicknesses, and structural defects is extremely costly, motivating development of an improved heuristic model. Mechanical strain contributions (E_{mech}) are relatively straightforward to include by computing the elastic strain energy from the strain tensor and the elastic stiffness tensors. For the remaining chemical contributions (E_{chem}) associated with bond breaking and atomic rearrangement, we treat the immediate interface region as a mixed phase and investigate the mixing enthalpy (Figure 3). Considering the distinct atomic arrangements of host Mg ions in *hcp* Mg and MgH_2, H insertion and extraction were considered in both lattice frameworks. This approach is currently being evaluated

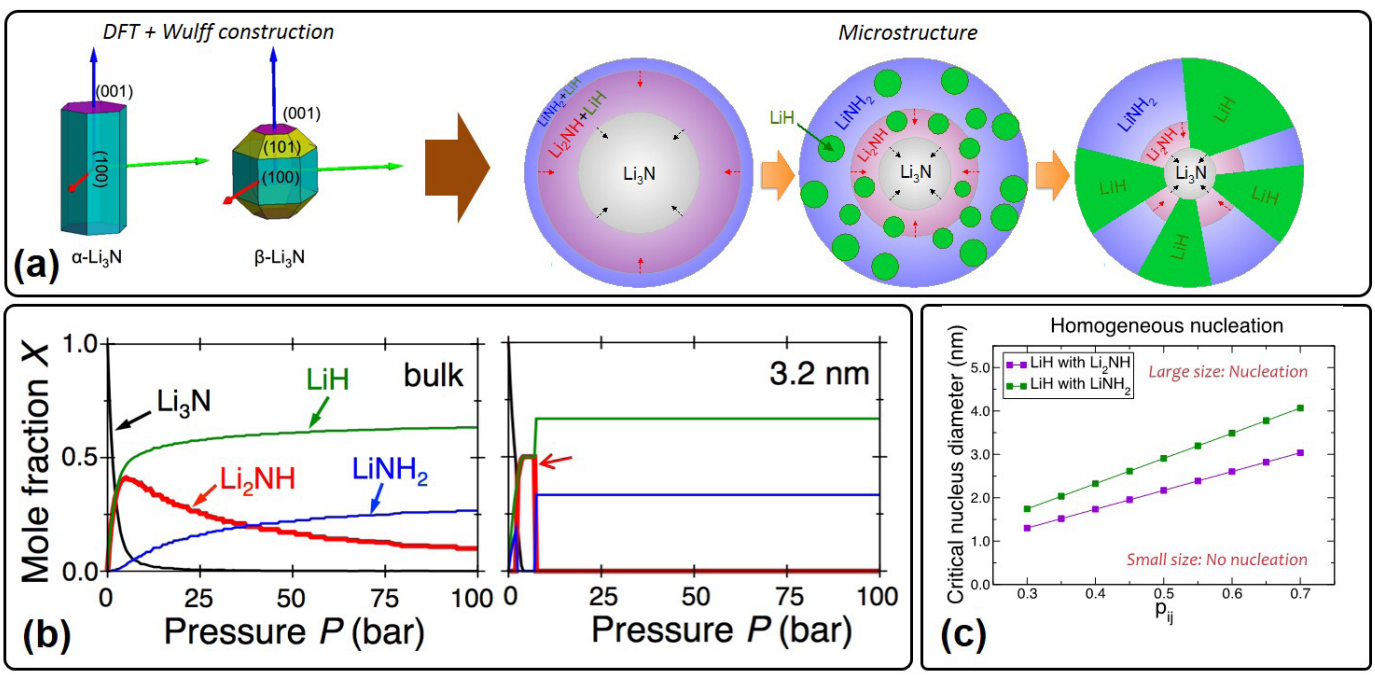

FIGURE 2. (a) Illustration of the phase fraction calculation procedure that combines DFT-derived interfacial energies with model microstructures for the Li-N-H system; (b) computed mole fractions of relevant phases as a function of H_2 upon isothermal hydrogenation of the bulk material (left) and d = 3.2 nm (right), showing size-induced suppression of Li_2NH; and (c) estimated critical nucleus diameter of a LiH crystallite within $LiNH_2$ or Li_2NH for different values of p_{ij} representing different interface energy approximations.

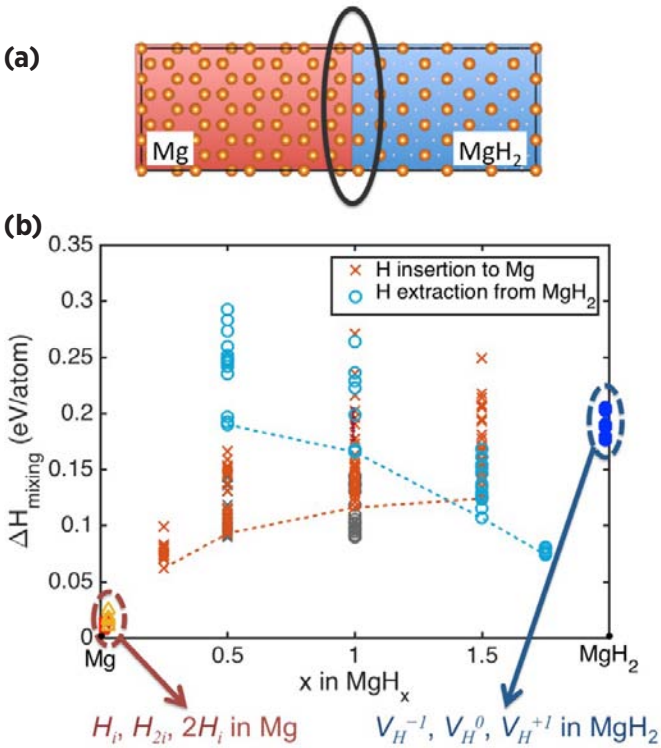

FIGURE 3. (a) Schematic of the atomistic Mg/MgH_2 interface; and (b) calculated composition-dependent mixing enthalpy of Mg-H in the *hcp* Mg lattice framework (orange cross: lattice parameter fixed to pristine Mg) and in the pyrite MgH_2 lattice framework (blue circle: lattice parameter fixed to pristine MgH_2), based on testing multiple atomic configurations. The dotted lines connect the lowest-energy configurations, and the grey circles show values with a fully relaxed lattice parameter. The defect formation energies of hydrogen interstitials (H_i) and vacancies (V_H) in Mg and MgH_2, respectively, are also shown.

against full interface energy computations for Mg/MgH_2 for select interface orientations.

Complex hydrides, which have more realistic potential to achieve ultimate targets, introduce additional complexities that require an entirely new approach. Here, various reactions between constituents must be considered and interface alignments are generally ill defined due to phase incommensurability. Accordingly, we are developing a new model based on a diffuse interface that combines mass transport near the interface boundaries with chemical reactivity and solution thermodynamics in the interface interior. This formalism, being developed in collaboration with the Characterization and Validation team and tested on the Mg-B-H system, is currently based on chemical kinetics computed with DFT, although high-temperature AIMD simulations are also being pursued as an avenue to extract possible chemical pathways. Further development and validation of this complex hydride interface model will be a key future direction for HyMARC.

Chemical pathways and diffusion (Tasks 2 & 3): Understanding the kinetics of mass transport is a critical ingredient for developing a more comprehensive mechanistic model of hydrogen storage in metal hydrides. Our theory efforts in this regard have centered on two activities. The first is the computation of defect formation energies and mobilities using zero-temperature approximations to identify which hydrogen-bearing species can diffuse effectively in the bulk materials. The defect formation energies are computed as function of electronic and atomic chemical potentials, which allow varying defect concentrations to be integrated directly within our mesoscale models that consider changes in chemical potential at interfaces and surfaces. Our second activity involves the use of AIMD to investigate transport pathways at surfaces and interfaces. A Python-based framework has been developed to automate setup and execution of the AIMD simulations, which will facilitate rapid application to other materials.

Both the defect-based and AIMD-based approaches have been applied to investigate the Mg-B-H system, focusing on MgH_2, $Mg(BH_4)_2$, and several potential B_xH_y-containing intermediates. The results point to the possibility of low-barrier interfacial and surface hydrogen structural diffusion pathways that are accessible to the picosecond timescales of AIMD. In certain cases, for instance, in β-$Mg(BH_4)_2$, these facile pathways emerge even though bulk diffusion is inhibited [14]. The different bulk, surface, and interface mobilities can be combined into an effective polycrystalline diffusivity, which we will integrate into our mesoscale models. Notably, the diffusion kinetics can also be matched to direct analysis of experimental uptake curves in regimes where diffusion limitations are expected; indeed, more closely connecting the theoretical and experimental kinetics analysis will be a key future focus.

Another activity, which is being pursued in close collaboration with HyMARC partners at Sandia performing low-energy ion scattering (LEIS) experiments, involves coupling atomistic surface diffusion models to concentration-driven continuum Fickian diffusion. This multiscale approach carries a twofold purpose. First, it is intended to improve the quantitative interpretation of LEIS data in terms of self-diffusion coefficients. Second, it will improve understanding of mass transport under the non-equilibrium conditions of (de)hydrogenation, in contrast to conventional DFT-based nudged elastic band or AIMD mobility calculations that can only probe diffusion under equilibrium conditions. As an initial test, we are investigating hydrogen migration on Al, Mg, and graphene, since the carefully controlled and well-defined nature of these surfaces allows for better experimental validation of models. However, the framework should be generalizable to any surface. A more complete analysis comparing the theoretical predictions with the experimental results on these materials is forthcoming.

Hydride phase transformation kinetics (Task 4): To understand the phase transformation kinetics and associated microstructural features of metal hydrides, it is important to analyze the relevant phase transition mechanisms for products and intermediates, which often occur through nucleation and growth. Using the DFT-derived thermodynamics and statistically sampled interfacial energies created upon nucleation (see discussion above), we evaluated the critical nuclei sizes and corresponding nucleation barriers employing classical nucleation theory. Applying this framework to predict the critical nuclei size of LiH crystallites showed that crystalline LiH is unlikely to nucleate in small particles until very late in the reaction (see Figure 2c), offering more accurate picture of microstructure evolution in the nanoscale Li-N-H model storage system [12].

Furthermore, we established an integrated atomistic and mesoscale framework for modeling interface kinetics and internal phase microstructure evolution within metal hydrides. The approach combines the atomistically derived materials thermodynamic and kinetic parameters with the phase-field modeling approach as illustrated in Figure 4a. We have applied this integrated approach to a Pd-H system as the simplest model interstitial hydride for which the phase transformation is governed exclusively by diffusional processes without any crystallographic structural change. The phase-field model was fully parameterized using temerature- and composition-dependent Gibbs free energies, elastic moduli, lattice parameters, interfacial energies, and diffusion coefficients derived (by HyMARC partners at Sandia) from classical molecular dynamics simulations using an embedded-atom potential [15]. Isothermal phase-

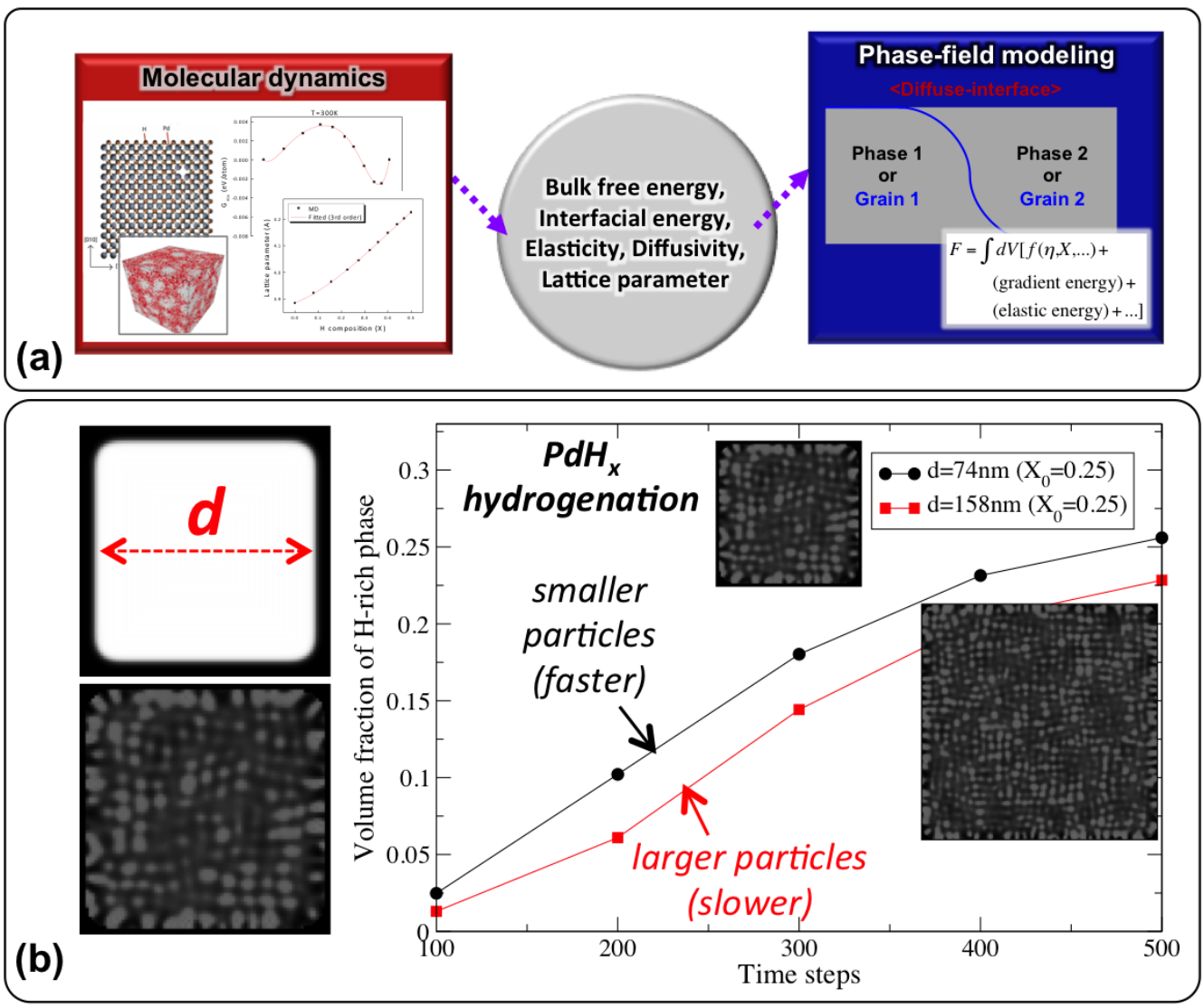

FIGURE 4. (a) Illustration of the integrated atomistic and mesoscale modeling framework, and (b) examples of simulated phase transformation kinetics for a Pd-H system.

field simulations for two different particle sizes successfully captured experimentally measured differences in phase evolution kinetics as shown in Figure 4b [13]. Encouraged by this successful demonstration, we are now extending this same formalism to the other systems that involve both diffusional and crystallographic structural transformations.

Additives (Task 5): To better understand the role of additives in metal hydrides, LLNL has been working closely with the other HyMARC partners to measure and interpret X-ray absorption and emission spectroscopy of $TiCl_3$-doped $NaAlH_4$. Because the system has been studied extensively with other techniques, we can leverage the wealth of published information to validate and further inform our interpretations. Synchrotron X-ray absorption spectroscopy experiments performed by the LLNL team at the Advanced Light Source to probe the Ti L_2 and L_3 edges of $TiCl_3$-doped $NaAlH_4$ show that hydrogen-induced chemical changes to the Ti environment are signaled by a change in signal strength that increases dramatically at higher additive concentrations. This indicates a likely change in the surface concentration of Ti upon exposure to hydrogen. Further analysis is underway, including accompanying theoretical modeling and comparison to proposed mechanisms in the literature [16].

CONCLUSIONS AND FUTURE DIRECTIONS

- Accurate binding energy calculations on MOF-505 suggest H_2 interactions carry a significant dependence on H_2 loading, leading to likely deviations from model isotherms.
- Internal interfaces can modify the reaction pathway for nanoscale Li_3N, suggesting microstructure and morphology engineering as a new strategy for improving hydrides.
- Multiscale integration of atomistic and continuum approaches can reproduce size-dependent phase kinetics of model interstitial hydride systems.
- *Future direction*: Use benchmark calculations to select a computational strategy for sorbent thermodynamics that balances accuracy and computational efficiency.
- *Future direction*: Apply improved hydride thermodynamic calculation protocols to other model hydride systems for quantitative evaluation.
- *Future direction*: Demonstrate multiscale surface transport simulation for validation and interpretation of LEIS results.
- *Future direction*: Evaluate different approaches for interface modeling and apply phase kinetics framework to a complex metal hydride.
- *Future direction*: Work with HyMARC partners to develop interpretation of soft X-ray spectra on catalyzed hydride materials.

FY 2016 PUBLICATIONS/PRESENTATIONS

1. Wood, B.C. et al., "Nanointerface-driven reversible hydrogen storage in the nanoconfined Li-N-H system," *Materials Research Society Spring Meeting*, Phoenix, AZ, April 2016.

2. Wood, B.C., V. Stavila, N. Poonyayant, T.-W. Heo, K. Ray, L.E. Klebanoff, T.J. Udovic, J. Lee, N. Angboonpong, J.D. Sugar, and P. Pakawatpanurut. "Nanointerface-driven reversible hydrogen storage in the nanoconfined Li-N-H system." *Submitted* (2016).

REFERENCES

1. Klebanoff, L.E., and J.O. Keller. "5 Years of hydrogen storage research in the US DOE Metal Hydride Center of Excellence (MHCoE)." *Int. J. Hydr. Energy* 38 (2013): 4533–4576.

2. Pasini, J.M., C. Corgnale, B.A. van Hassel, T. Motyka, S. Kumar, and K.L. Simmons. "Metal hydride material requirements for automotive hydrogen storage systems." *Int. J. Hydr. Energy* 38 (2013): 9755–9765.

3. Y.G. Chung, et al. "Computation-ready, experimental metal-organic frameworks: A tool to enable high-throughput screening of nanoporous crystals." *Chem. Mater.* 26 (2014): 6185.

4. Dubecký, M.S., P. Jurečka, R. Derian, P. Hobza, M. Otyepka, and L. Mitas. "Quantum Monte Carlo methods describe noncovalent interactions with subchemical accuracy." *J. Chem. Theory Comput.* 9 (2013): 4287.

5. Otani, M. and O. Sugino. "First-principles calculations of charged surfaces and interfaces: A plane-wave nonrepeated slab approach." *Phys. Rev. B* 73 (2006): 115407.

6. Worsley, M. A., P.J. Pauzauskie, T.Y. Olson, J. Biener, J.H. Satcher, Jr., and T.F. Baumann. "Synthesis of graphene aerogel with high electrical conductivity." *J. Am. Chem. Soc.* 132 (2010): 14067–14069.

7. Worsley, M.A. et al. "High surface area, sp^2-cross-linked three dimensional graphene monoliths." *J. Phys. Chem. Lett.* 2 (2011): 921–925.

8. Worsley, M.A. et al. "Synthesis and characterization of highly crystalline graphene aerogels." *ACS Nano* 8 (2014): 11013–11022.

9. Teweldeberhan, A.M. and S.A. Bonev. "Structural and thermodynamic properties of liquid Na-Li and Ca-Li alloys at high pressure." *Phys. Rev. B* 83 (2011): 134120.

10. Akbarzadeh, A.R., V. Ozoliņš, and C. Wolverton. "First-Principles Determination of Multicomponent Hydride Phase Diagrams: Application to the Li-Mg-N-H System." *Adv. Mater.* 19 (2007): 3233–3239.

11. Porter, D.A., and K.E. Easterling, *Phase Transformations in Metals and Alloys.* 2nd ed.; Chapman & Hall: London, UK (1992).

12. Wood, B.C., V. Stavila, N. Poonyayant, T.-W. Heo, K. Ray, L.E. Klebanoff, T.J. Udovic, J. Lee, N. Angboonpong, J.D. Sugar,

and P. Pakawatpanurut, "Nanointerface-driven reversible hydrogen storage in the nanoconfined Li-N-H system." *Submitted* (2016).

13. Zhou, X.W., T.W. Heo, B.C. Wood, V. Stavila, and M.D. Allendorf. "Molecular dynamics analysis of thermodynamic and kinetic parameters controlling hydriding/dehydriding of palladium hydrides." *Manuscript in preparation* (2016).

14. Wolverton, C., et al. *U.S. DOE Hydrogen and Fuel Cells Program Annual Report* (2013).

15. Zhou, X.W., J.A. Zimmerman, B.M. Wong, and J.J. Hoyt. "An embedded-atom method interatomic potential for Pd-H alloys." *J. Mater. Res.* 23 (2008): 704–718.

16. Frankcombe, T.J. "Proposed mechanisms for the catalytic activity of Ti in $NaAlH_4$." *Chem. Rev.* 112 (2012): 2164–2178.

IV.C.4 HyMARC: A Consortium for Advancing Solid-State Hydrogen Storage Materials

Jeffrey J. Urban (Primary Contact),
David Prendergast, Jinghua Guo, Brandon Wood (Lawrence Livermore National Laboratory),
Felix Fischer, Gabor Somorjai, Vitalie Stavila (Sandia National Laboratories), and
Maciej Haranczyk.
Lawrence Berkeley National Laboratory (LBNL)
1 Cyclotron Road Mail Stop 67R4110
Berkeley, CA 94720
Phone: (510) 486-4526
Email: jjurban@lbl.gov

DOE Manager: Ned Stetson
Phone: (202) 586-9995
Email: Ned.Stetson@ee.doe.gov

Project Start Date: September 17, 2015
Phase I End Date: September 30, 2018

Overall Objectives

- Focus on light materials and synthesis strategies with fine control of nanoscale dimensions to meet weight and volume requirements via encapsulation and confinement.
- Design interfaces with chemical specificity for thermodynamic and kinetic control of hydrogen storage and sorption and selective transport.
- Explore novel storage concepts and/or obtain a fundamental understanding of established processes via known or idealized systems and materials.
- Develop in situ and in operando soft X-ray characterization capabilities in combination with first-principles simulations to extract atomic and molecular details of functional materials and interfaces.

Fiscal Year (FY) 2016 Objectives

- Develop graphene-encapsulated, metal-nanocrystal composites to produce environmentally-stable, high performance hydrogen storage materials.
- Optimize each material building block in the composite to derive the best performance possible by finely tuning the structure of encapsulating layers (graphene derivatives) and tailoring the elements and size of metal nanocrystals.
- Conduct X-ray spectroscopy characterization of model systems for solid-state metal hydrides.
- Produce mesostructured cellular foam (MCF)-17 with varying amounts of grafted Al, and assess population of acid sites, generate hydrogen adsorption isotherms, and study the impact of mesopore size and shape.
- Develop a predictive approach to simulate the X-ray absorption spectra of hydrogen storage materials under working conditions and begin studies of interfacial systems related to encapsulation of hydrogen storage media.

Technical Barriers

This project addresses the following technical barriers from the Hydrogen Storage section of the Fuel Cell Technologies Office Multi-Year Research, Development, and Demonstration Plan.

(O) Lack of Understanding of Hydrogen Physisorption and Chemisorption

(A) System Weight and Volume

(E) Charge/Discharge Rate

Technical Targets

This project will develop foundational understanding and new capabilities that will enable accelerated discovery of breakthrough materials in all classes of storage materials, in particular metal hydrides and sorbents. It is anticipated that the insights gained from this research, coupled with new synthetic, characterization, modeling, and database tools that will be made available to the hydrogen storage research community, will lead to materials that meet DOE targets such as system gravimetric and volumetric capacity, system fill time, and delivery temperature.

FY 2016 Accomplishments

- Designed a graphene encapsulation for metal nanocrystals with a solution-based synthetic approach. This is based upon prior work in the Urban group integrating polymers with metal hydrides, but represents a big step forward in using functional materials.
- Prepared 3 nm-sized Mg nanocrystals encapsulated by reduced graphine oxide (rGO) layers and achieved 6.5 wt% hydrogen capacity in terms of the total material weight with an excellent cyclability (detail in Figure 1).

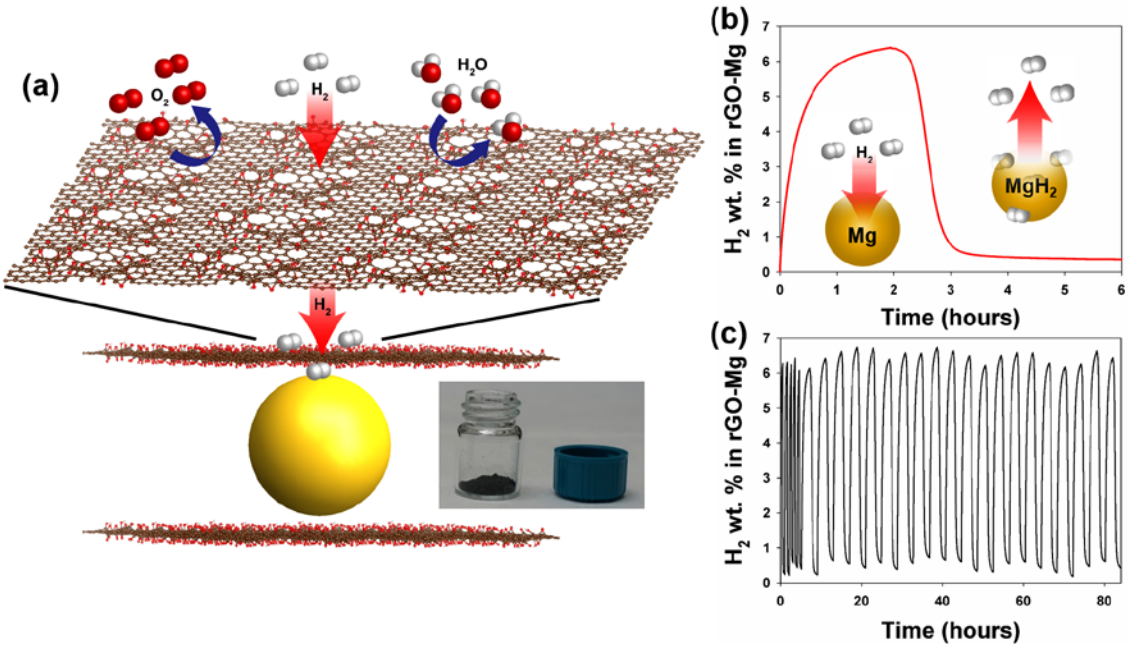

FIGURE 1. (a) Illustrations depicting the structure of the rGO-Mg composites where rGO layers prevent O_2 and H_2O from penetrating, while allowing the diffusion of H_2 (photograph of rGO-Mg in air). (b) Hydrogen absorption/desorption (at 200ºC and 15 bar H_2/300ºC and 0 bar) for the prepared rGO-M. (c) Hydrogen absorption/desorption cycling of rGO-Mg that were first exposed to air overnight. The first five cycles were performed at 250ºC and 15 bar H_2/350ºC and 0 bar, and the additional 20 cycles at 200ºC and 15 bar H_2/300ºC and 0 bar. As mentioned in the report we aim to translate these controls and insights into more complex metal hydrides moving forward.

- Exploited different kinds of graphene nanoribbons (GNRs) to encapsulate Mg crystals, accomplishing 7.1 wt% hydrogen capacity based on the total composite. Investigated the effect of different edge-functional groups of GNRs on the hydrogen adsorption (some examples in Figure 2; key point is that functional group differences can be linked to large [>30 kJ/mol] changes in enthalpy and corresponding rate enhancements).
- Synthesized 3d-transition metal doped rGO-Mg composite to enhance the hydrogen sorption thermodynamics and kinetics of Mg and studied their influence on hydrogen storage property of the composite. Collaboration with Lawrence Livermore National Laboratory on atomistic modeling of the dopant distribution was essential.
- Characterized structure and function in a series of candidate samples using in situ X-ray spectroscopic methods at the Advanced Light Source (ALS): Al_2O_3, $LiAlH_4$, $NaAlH_4$, and Ti-doped $NaAlH_4$, NaOH, $NaHCO_3$, $NaNH_2$, NaH, $NaBH_4$, $NaAlH_4$ and Ti doped $NaAlH_4$ as the model systems.
- Identified an initial set of representative metal organic framework (MOF) structures with open metal sites to be characterized by the project team to obtain reliable experimental data to validate the corresponding computational efforts.
- Successfully produced mesoporous silica doped with varying amounts of aluminum by grafting method, permitting control of the density of acid sites (of the Lewis and Brønsted types) per unit internal surface area, characterized using a developed in situ cell for temperature-dependent Fourier transform infrared spectroscopy based on pyridine adsorption. Hydrogen adsorption isotherms were measured at low partial pressure and low temperature (below 1 atm and 77 K), indicating that condensation of hydrogen is insensitive to the size and shape of mesopores in our silica samples.
- Established first-principles simulations of X-ray absorption near-edge structure spectra of various standard hydrogen storage materials for comparison with existing literature and in tandem with ongoing measurements at ALS by J. Guo (LBNL) and began to explore the details of electronic interactions between magnesium surfaces and reduced graphene oxide and their ability to modulate hydrogen adsorption rates.

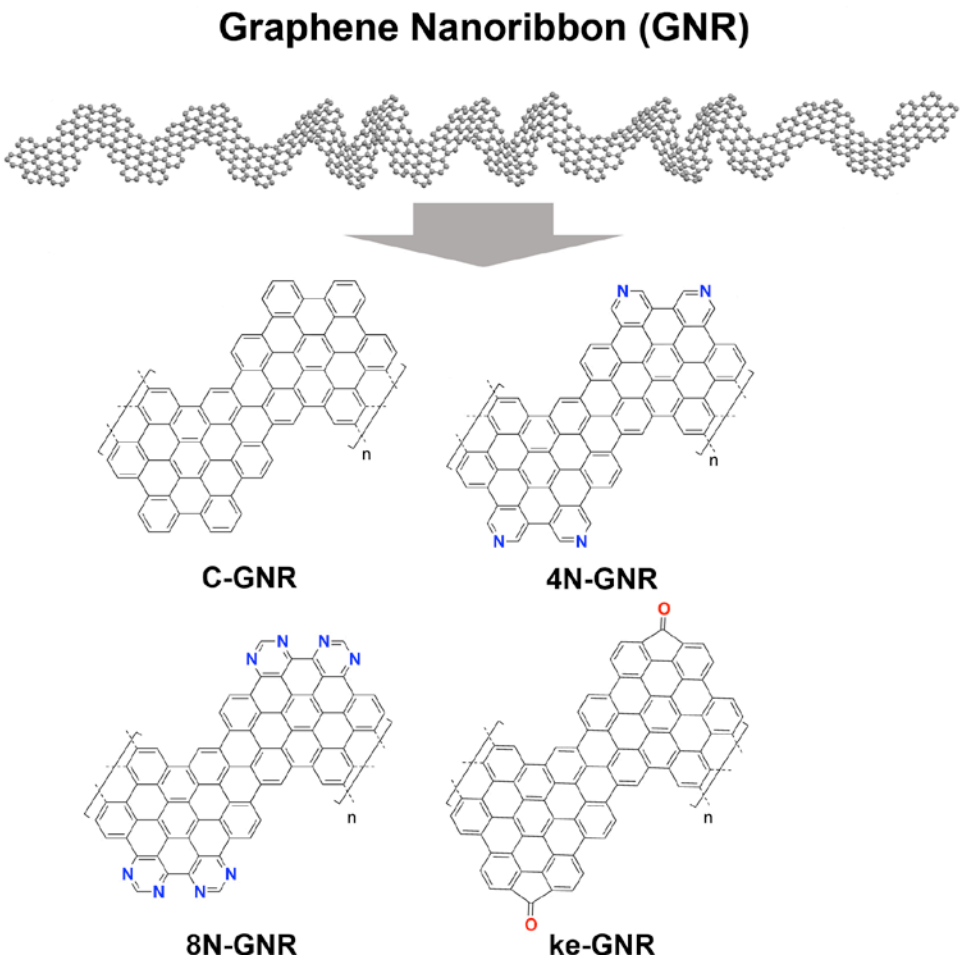

FIGURE 2. The chemical structures of GNRs with different edge-functional groups. As mentioned in the report, the intent is to use these chemical functionalities as a complementary extrinsic doping strategy to enhance the thermodynamics of metal hydrides.

INTRODUCTION

Storage of hydrogen onboard vehicles is one of the critical enabling technologies for creating hydrogen fueled transportation systems that can reduce oil dependency and mitigate the long-term effects of fossil fuels on climate change. Stakeholders in developing hydrogen infrastructure (e.g., state governments, automotive original equipment manufacturers, station providers, and industrial gas suppliers) are currently focused on high-pressure storage at 350 bar and 700 bar, in part because no viable solid-phase storage material has emerged. Nevertheless, solid-state materials, including novel sorbents and high-density hydrides, remain of interest because of their unique potential to meet all Fuel Cell Technologies Office targets and deliver hydrogen at lower pressures and higher onboard densities. A successful solution would significantly reduce costs and ensure the economic viability of a U.S. hydrogen infrastructure.

DOE-supported individual projects and the centers of excellence collectively synthesized and characterized hundreds of candidates documented in the DOE Hydrogen Storage Materials Database. Although materials meeting some of the key targets were identified, progress continues to be hindered by a lack of fundamental understanding of the kinetics and thermodynamics underlying the physical properties of interest. For sorbents, the biggest limitation is volumetric capacity within the target operating temperatures, whereas hydrides are limited by insufficient gravimetric capacity and/or reaction kinetics to meet the fill time target. At the recent Office of Energy Efficiency and Renewable Energy Material-Based Hydrogen Storage Summit, principal investigators prioritized the following major scientific challenges for the development of viable solid-state storage materials.

- Multi-scale model validation for developing metal hydride structure-property correlations.

- Computational tools to guide design of nanoporous sorbent pore size distributions.
- Synthetic strategies to increase the strength of H_2 interactions with sorbent adsorption sites.
- Rates and mechanisms of kinetic processes that limit metal hydride reversibility.
- Design rules for nanostructuring that improves metal hydride kinetics and thermodynamics.
- Models describing the structure, chemistry, and mass transport on surfaces and at interfaces.

APPROACH

The HyMARC consortium seeks to address these gaps by leveraging recent advances in predictive multiscale modeling, high-resolution in situ characterization, and material synthesis that were unavailable to the centers of excellence. Combined with materials informatics, this strategy embodies the approach highlighted within the recent Materials Genome Initiative Strategic Plan for accelerated materials development. By focusing on the underlying thermodynamic and kinetic limitations of storage materials, we will generate fundamental understanding that will accelerate the development of all types of advanced storage materials, including sorbents, metal hydrides, and liquid carriers. Thus, DOE investments will be fully leveraged for future external materials-focused projects. Clearly, Office of Energy Efficiency and Renewable Energy funding is essential, since the fundamental goals are too high risk for industry; such funding will allow establishment of the consortium as a Fuel Cell Technologies Office core capability.

Thermodynamics: Conceptually, the limitations of sorbents and hydrides can be thought of in terms of effective thermal energy required to release H_2, $\Delta E(T)$, and the corresponding gravimetric and volumetric capacities for a given material. $\Delta E(T)$ is comprised of thermodynamic and kinetic terms: $\Delta E(T) = \Delta H°(T) + E_a$, in which $\Delta H°(T)$ is the standard enthalpy of desorption at temperature T, and E_a is the activation energy for desorption. There are no materials today that meet the DOE requirements for $\Delta H°(T)$ in large part because the targeted thermodynamics are in a mesoscale energy region where there are few examples, other than interstitial hydrides, which do not meet capacity targets. For sorbents, the targeted $\Delta H°(T)$ (15–20 kJ/mol H_2) is stronger than van der Waals forces, but much weaker than covalent or ionic bonds. In contrast, $\Delta H°(T)$ of high-capacity reversible metal hydrides is above the ≤27 kJ/mol H_2 target set by the engineering center of excellence. A major challenge, therefore, is to address the thermodynamic barriers to designing materials. The LBNL arm of the consortium is addressing this via new synthetic approaches to hybrid metal hydride sorbents, guided by theory and modeling, which use an "inside-out" approach to doping: complementary internal additives (e.g., Ni, Co) with externally grafted graphene nanoribbons with targeted functional groups to lower transition state energies. Details of the atomic origins of these energetic changes and how to optimize these remain. Similarly, LBNL arm (Haranczyk) plans to use computational high-throughput screening to identify porous sorbents with strong H_2 binding sites such as MOFs with open metal sites. To enable such screening, an approach to introduce accurate description of hydrogen-binding site interaction needs to be implemented into molecular simulations of adsorption, an effort undertaken in collaboration with Lawrence Livermore National Laboratory team (Wood).

Kinetics: Kinetics also play a crucial role in determining H_2 uptake and release. Ideally E_a would be small for fast desorption and sorption; this is typically the case for sorbent materials, where $\Delta E(T) \approx \Delta H°(T)$. However, E_a can be large (>50 kJ/mol) for many metal hydrides, causing materials that should be reversible thermodynamically to become unviable. The specific processes governing the slow kinetics may include bulk surface and interface mass transport processes, gas-surface reactions, and processes at solid-solid interfaces, including phase nucleation and growth. These phenomena are intrinsically interrelated, yet operate across broad ranges of length and time scales that make them difficult to characterize and model. Moreover, each is affected by chemistry, atomic structure, and microstructure in ways that are poorly understood. For example, certain additives can improve kinetics, but the lack of mechanistic understanding inhibits rational design. Dramatic improvements can also be obtained by reducing the critical hydride dimensions to the nanoscale. However, bulk approaches, such as ball milling, yield unacceptable heterogeneity in particle size, shape, and microstructure, whereas templating strategies using microporous hosts are unlikely to be practical due to the associated capacity loss. Properly leveraging these and other strategies for improving kinetics requires greatly increased fundamental understanding, but will require material platforms and characterization tools that enable individual processes and their interactions to be modeled and probed. Consequently, a second major challenge is to understand and prevent the kinetics of hydrogen desorption and uptake from making thermodynamically acceptable materials unusable. In addition to the work above, LBNL has established first-principles simulations of X-ray absorption near-edge structure spectra of various standard hydrogen storage materials for comparison with existing literature and in tandem with ongoing measurements at ALS and begun to explore the details of electronic interactions between magnesium surfaces and reduced graphene oxide and their ability to modulate hydrogen adsorption rates. This complements new in situ work being done on modified samples of this type.

Experimental Sample Handling: Our study showed that rGO-Mg composites have a self-protection layer which keep

the Mg nanoparticles (NPs) stable for a reasonable period of time. However, when performing experimental X-ray measurements at ALS for the $NaAlH_4$, and Ti-doped $NaAlH_4$ from Lawrence Livermore National Laboratory, sample preparation and transfer into the experimental system was critical. We have used glove box and vacuum suitcase to eliminate the possible exposure of the samples to air (water and O_2). The surface sensitive detection (total electron yield) and bulk sensitive detection (total fluorescence yield) were applied at the same time. Thus, the variation of surface and bulk chemical and structure properties can be utilized in the comparison with the first-principles simulations obtained by D. Prendergast [1]. Further in situ X-ray characterizations are carried out as the instrumentation is developed.

RESULTS

Theoretical Modeling of X-ray Spectroscopy Studies: Using our previously developed first-principles approach to model X-ray absorption spectra (XAS) of materials (based on density functional theory [1]), we have explored a number of hydrogen storage materials to establish a predictive capability for XAS simulation to provide interpretation of measurements to be made at ALS by J. Guo (LBNL) and others. In summary, we have found reasonable agreement at the sodium K-edge for a range of materials, including $NaAlH_4$. We see less favorable agreement at the Al K-edge and we are currently exploring the reasons for this. We have had previous success in interpreting the spectra of molecular Al-organic crystals [2]. One possibility is that the very light H atoms require some accounting of their nuclear quantum distribution rather than a classical approximation that would afford them a much smaller spatial distribution about their average high symmetry positions at finite temperature. We see little effect on either absorption edge associated with Ti-dopants, as yet, apart from any phase separation into metallic (Al) or intermetallic (AlTi) phases, which clearly appear as intensity below the absorption edge of the hydrides.

We have also worked towards understanding the means by which selective and environmentally insensitive hydrogen adsorption occurs in Mg nanoparticles encapsulated in rGO, as demonstrated by Urban. We model the rGO in an initial ideal case as porous graphene (Figure 3a) and explore the pore size dependence of the activation energy for passage of

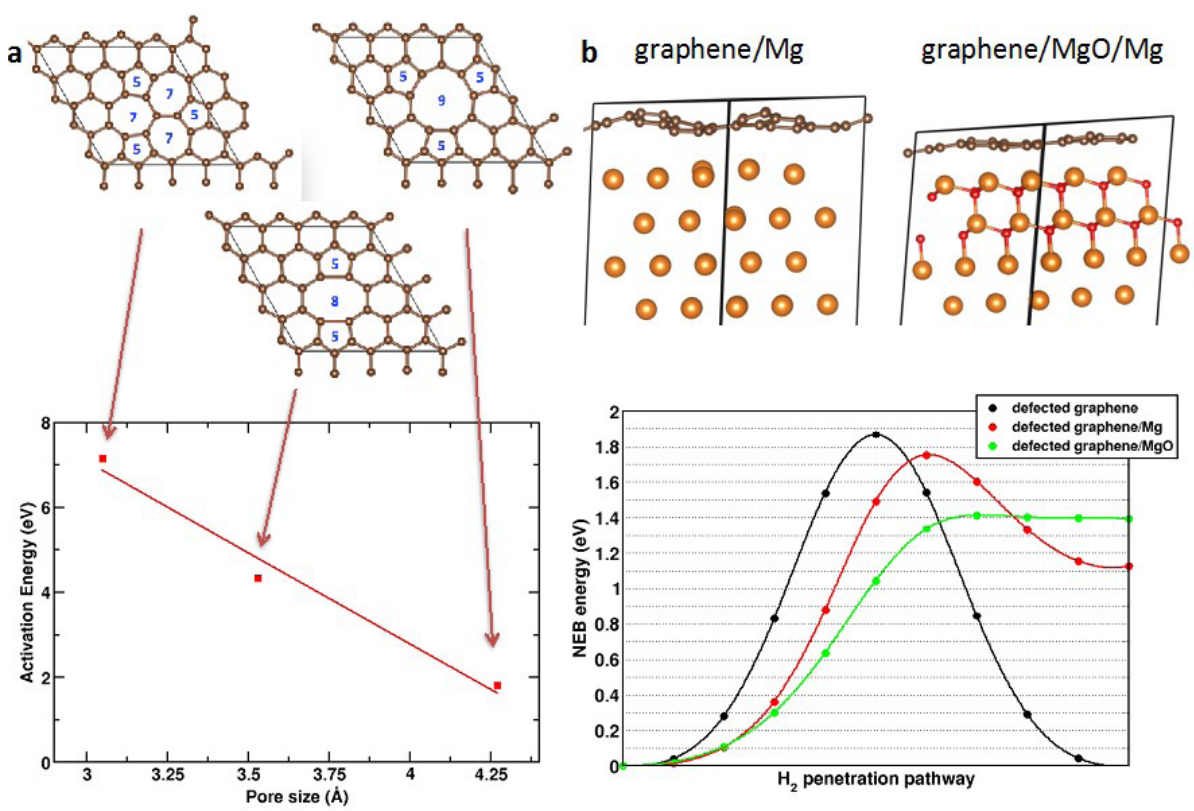

FIGURE 3. (a) Top: Various simple defects that result in pores in graphene: the 555-777 divacancy, the 5-8-5 divacancy, and the 555-9 tetravacancy. Bottom: The dependence of activation barrier in eV for dihydrogen to pass through various defects as a function of their pore size. (b) Top: The structure of 555-9 defective graphene on top of the (0001) surface of hexagonal close-packing Mg and a suboxide layer at the Mg surface. Bottom: Variation in the nudged-elastic-band energy profile (eV) for passage of dihydrogen through the 555-9 defect for just graphene (black), graphene on Mg (red), and graphene on an oxidized Mg surface (green).

a dihydrogen molecule across this atomically thin membrane. We find that the activation energy is inversely proportional to the minimum pore dimension (Figure 3b). In addition, for the largest pore dimension considered (the so-called Y-tetravacancy [3]) we note that contact with the [0001] Mg surface (for the bulk hexagonal close-packing phase) slightly reduces the activation barrier for the passage of dihydrogen through the pore. In addition, the presence of a few suboxide layers (introduced as interstitial defects in the Mg surface) greatly enhances the adhesion of graphene to the Mg surface and also further reduces the barrier to insertion of dihydrogen (Figure 3d). We will seek validation of this idealized picture through further XAS measurements to determine if any suboxide is present in the synthesized samples, possibly as part of the graphine oxide reduction process.

We have developed and synthesized a series of lightweight nanostructured materials derived from graphene and evaluated these structures as a stabilizing matrix for highly reactive (pyrophoric) metal (Mg, Al) nanoparticles used in hydrogen storage. The role of these atomically defined GNRs (Figure 2) in composite materials for hydrogen storage extends beyond a common support material but integrates the ability to rationally tune performance parameters such as selective gas permeability, high thermal conductivity, and the potential to incorporate molecularly defined catalysts that can promote the dissociation and association of dihydrogen during the loading and unloading processes. Our results show that Mg NPs embedded in a GNR matrix (<5 wt%) are stable to moisture and air (unprotected bare Mg NPs are pyrophoric) while fully retaining the high storage capacity inherent to the Mg/MgH_2 system. We further demonstrated that the selective introduction of functional groups along the edges of GNRs directly affects the adsorption and desorption kinetics. This experimental result supports a mechanism in which the immediate chemical environment created by the functionalized GNRs stabilizes the rate determining transition state in the hydrogen uptake in Mg nanoparticles. Furthermore, we have embarked on the design and synthesis of GNRs featuring multidentate ligands for molecular-defined catalysts that promote the dissociation of dihydrogen in the immediate proximity of the metal NPs.

Spectroscopy and Characterization: Ti doped $NaAlH_4$ samples synthesized by V. Stavila (Sandia National Laboratories) were found to have dramatic changes in kinetics even with very low doping concentration. The experimental XAS characterization on Al and Na K-edge was performed at ALS. The results have been analyzed and compared with theoretical simulation as described above. The effect of Ti doping is also investigated by the Ti L-edge XAS shown in Figure 4. The precursor $TiCl_3$ used in the synthesis is displayed as the reference comparison. The XAS spectral shape of the hydrogenated and dehydrogenated forms of 10 mol% Ti doped $NaAlH_4$ sample suggests an amorphous phase around the Ti local structure, which is in line with the expectation of V. Stavila. However, the neighboring coordination of Ti remains further study. Also the 10 mol% Ti doped $NaAlH_4$ sample shows a small portion of $TiCl_3$ preserved in the dehydrogenated form.

Sorbents (Theory): Our goal for the first year was to establish necessary references and benchmarks for the development of ab initio H_2 adsorption isotherm calculations for MOFs with open metal sites. This effort included selection of representative MOFs with open metal sites, and gathering reliable experimental data as well as a set of verified and curated crystal structures necessary to conduct simulations. The resulting material set includes CuBTC, PCN-14, NOTT-100–NOTT-103 series, and the MOF-74 analogue series with various metal types. Furthermore, we conducted a literature search to identify available models and classical potentials for prediction of H_2 adsorption within MOFs, and set up a

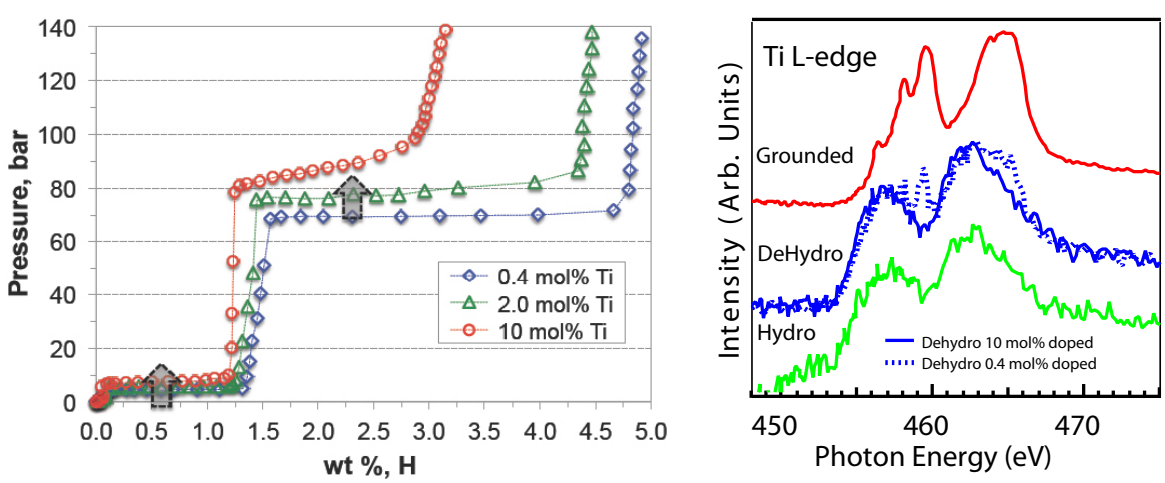

FIGURE 4. (Left) Increasing the concentration of $TiCl_3$ in $NaAlH_4$ leads to increased plateau pressures. (Right) X-ray absorption spectroscopy spectra of $TiCl_3$ grounded mixing and Ti doped $NaAlH_4$.

grand-canonical Monte Carlo simulation code, RASPA, to execute those. We also investigated available approaches to include polarizable electrostatic interactions between the H_2 quadrupole moment and MOF atoms. For each MOF in our experimental test set, we obtained H_2 adsorption isotherms at 77 K and 298 K using the available approaches, and identified errors with respect to experimental results. This effort has set benchmarks for the following effort to introduce ab initio isotherm calculations for the selected systems.

Sorbents (Experiment): We developed a technique to dope silica with aluminum as a means to introduce acid sites (Lewis and Brønsted acids) in mesoporous structures. We were able to dose these sites using infrared spectroscopy and pyridine adsorption (Figure 5, Table 1, Table 2). These samples are currently under investigation to determine if the acid sites influence the hydrogen adsorption properties (wt% adsorbed, kinetics, and thermodynamics).

CONCLUSIONS AND FUTURE DIRECTIONS

Theory of X-ray spectroscopy: Thus far in our simulation efforts, we have shown that we can accurately predict Na K-edge X-ray absorption near-edge spectroscopy but that we have some issues in predicting those at the Al K-edge. We will explore issues related to sample handling, self-absorption in the X-ray absorption near-edge spectroscopy measurement and fundamental issues related to the broader quantum nuclear distribution of hydrogen atoms in hydrides, which to date have been approximated at classical particles. We also see a strong dependence on pore size and interfacial

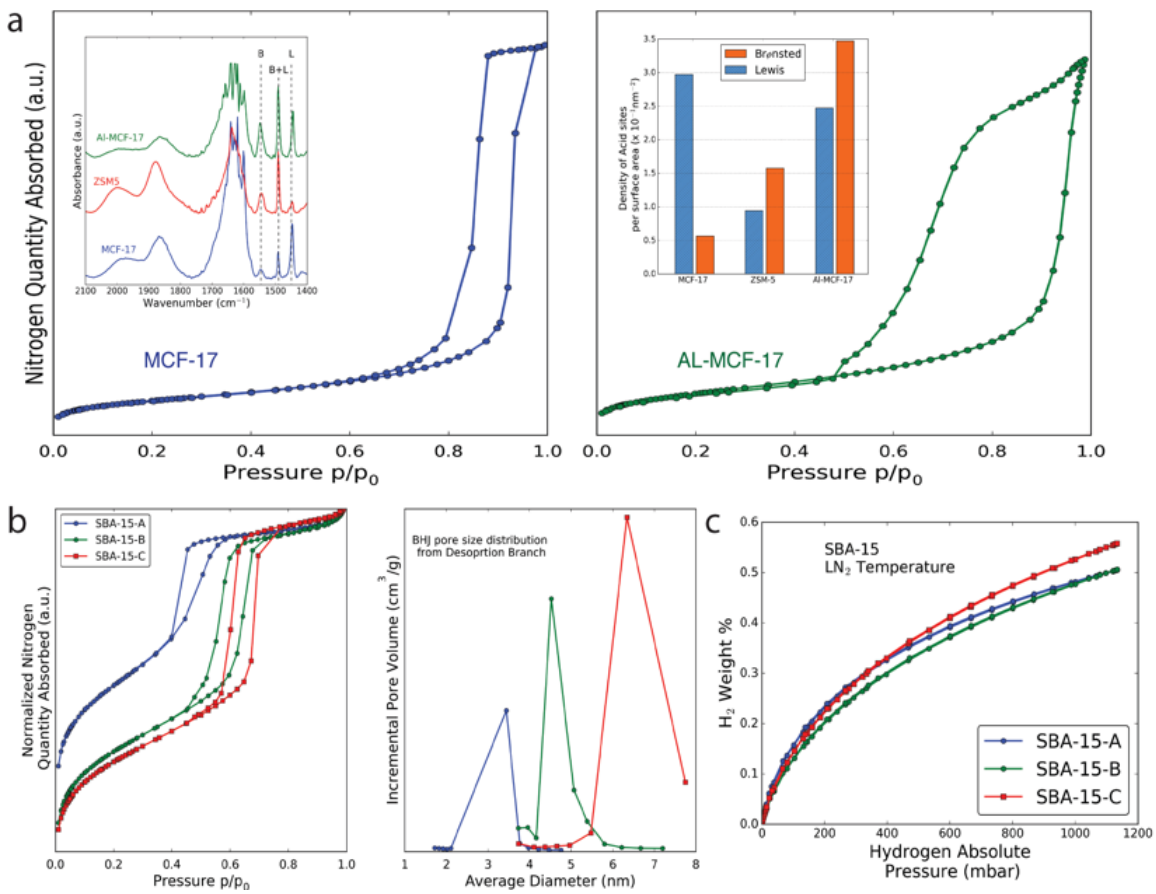

a.u. – Arbitrary units

FIGURE 5. (a) Nitrogen adsorption isotherms for, (left) MCF-17 and (right) Al-MCF-17. For both measurements, the nitrogen adsorption was done at liquid nitrogen temperature prior to which water was evacuated by degassing the samples at 450°C under vacuum. (left) Evaluation of MCF-17 and Al-MCF-17 acid sites using pyridine adsorption and infrared spectroscopy (transmission mode). (right) Density of sites per surface area of samples. (b) Physisorption experiments on Santa Barbara Amorphous (SBA)-15: (left) normalized nitrogen adsorption isotherms for sample A, B, and C; (right) the pore size distribution according to the Barrett-Joyner-Halenda model in terms of incremental pore volume. Measurements at liquid nitrogen temperature after the samples have been degassed at 450°C under vacuum for 5 h (remove water). (c) Hydrogen adsorption isotherms on the SBA-15 samples. Experiments were run at liquid nitrogen temperature and samples were degassed at 450°C under vacuum prior to testing.

The surface area was extrapolated using the Brunauer-Emmett-Teller (BET) theory model. The average mesoporous diameter and volume were obtained from the desorption branch of the isotherm using the Barrett-Joyner-Halenda model. The micropores volume was derived from the isotherms using the t-plot methodology (Table 1, Figure 5).

TABLE 1. Summary of the Data Obtained by Nitrogen Physisorption Measurements (see Figure 5)

Samples	Surface Area (m^2/g)	Average Porous Diameter (nm)	Mesopores Volume (cm^3/g)	Micropores Volume (cm^3/g)
MCF-17	672	23.6	3.18	0.0016
Al-MCF-17	473	25.0	1.71	0.0010

The surface area was extrapolated using the BET model. The average mesoporous diameter and volume were obtained from the desorption branch of the isotherm using the Barrett-Joyner-Halenda model. The micropores volume was derived from the isotherms using the t-plot methodology (Table 2, Figure 5).

TABLE 2. Summary of the Data Obtained by Nitrogen Physisorption Measurements (see Figure 5).

Samples	BET (m^2/g)	Average Porous Diameter (nm)	Mesopores Volume (cm^3/g)	Micropores Volume (cm^3/g)
SBA-15-A	525	3.3	0.25	0.091
SBA-15-B	760	5.0	0.55	0.093
SBA-15-C	810	6.2	0.65	0.099

interactions in the activation energy for the passage of dihydrogen molecules through defective graphene, which we propose as a model for the rGO encapsulated magnesium nanoparticles. We will continue to add more realistic detail to this model of the system synthesized by Urban and try to explain the success of this nanoscale composite in terms of chemical stability to atmospheric impurities, such as oxygen, water, and carbon dioxide. We will also pursue validation of this model through X-ray based characterization at ALS.

Spectroscopy at ALS: The experimental characterization at ALS will continue on the modeled systems. We learned from our measurement that the existing literature does not have a reliable XAS spectrum even for the standard $NaAlH_4$. Thus, we need to perform the study of aging effect for the sensitive samples, and possibly synthesize new samples using different precursors and/or different protocols.

Mg Nanocrystals Encapsulated by Graphene Derivatives at Urban Group: The Urban group has synthesized Mg nanocrystals wrapped by different kinds of graphene derivatives, including graphene oxide layers. Transition metal dopants, particularly Ni, have been added to this system for the purpose of improving hydrogen sorption kinetics. In our material system, both high capacity and kinetics have been achieved, along with good air stability and cyclability. We learned that doping on metal hydrides can be managed with different material elements which ultimately tweak the hydrogen sorption properties of the composite material. In the future study, we will pursue the graphene wrapping system with different kinds of metal and complex hydride materials such as $Mg(BH_4)_2$; and, different kinds of doping will be attempted to optimize the hydrogen sorption properties of the materials

We intend to expand the scope of GNR composite nanomaterials by developing structures that are competent at stabilizing Al NPs featuring a higher theoretical hydrogen storage capacity. We will further explore the unusual mechanism by which GNR supports modulate the H_2 absorption and desorption kinetics ant the surface of Mg NPs. This very fundamental exploration will heavily rely on new characterization tools developed through HyMARC such as a hydrogen gas flow cell compatible with in situ X-ray spectroscopy.

Sorbents: Measurement of adsorption isotherms at pressures up to 100 bar on inorganic samples are complex, and we are currently developing a method, in collaboration with Quantachrome, to succeed in this field. Our plan for the next fiscal year is to acquire a high pressure system allowing for testing of our sample under high pressure and various temperature (from cryogenic to room temperature) to obtain thermodynamics and kinetics information. We plan on investigating the structural effect of inorganic support such as the meso- and micropores at high pressure. In parallel, acid samples and metal loaded samples will be investigated to figure if these additives can serve as catalytic add-ons to improve molecular hydrogen adsorption.

SPECIAL RECOGNITIONS & AWARDS/ PATENTS ISSUED

1. Jeffrey J. Urban, Eun Seon Cho, Anne M. Ruminski, Shaul Aloni, Yi-Sheng Liu, Jinghua Guo, "Graphene Oxide/Metal Nanocrystal Laminates: the Atomic Limit for Safe, Selective Gas Storage," US patent application serial no. 62/203, 198, filed on August 10, 2015.

2. Felix R. Fischer, Jeffrey J. Urban, Eun Seon Cho, Anne M. Ruminski, Ryan Cloke, Tomas Marangoni, Cameron Rogers, "Nanostructured Composites for Gas Separations and Storage," US patent application serial no. 62/157, 952, filed on May 6, 2015

FY 2016 PUBLICATIONS/PRESENTATIONS

Publications

1. Eun Seon Cho, Anne M. Ruminski, Shaul Aloni, Yi-Sheng Liu, Jinghua Guo, Jeffrey J. Urban, "Graphene Oxide/Metal Nanocrystal Multilaminates as the Atomic Limit for Safe and Selective Hydrogen Storage," *Nature Communications*, 7 (2016), 10804.

Presentations

Jeffrey J. Urban

1. July 2016—Department of Chemical Engineering, EPFL Sion, Switzerland (Invited).

2. July 2016—Department of Materials Engineering, ETH Zurich, Switzerland (Invited).

3**.** May 2016—Presentation to International Panel of Hydrogen and Fuel Cells for the Economy, Berkeley, CA (Invited).

4. April 2016—Department of Chemical Engineering, Stanford University, Palo Alto, CA (Invited).

5. April 2016—Presentation to Technical Team of Hydrogen Fuel Cell Manufacturers, Berkeley, CA (Invited).

6. April 2016—Department of Applied Physics, Eindhoven University, Netherlands (Invited).

Felix R. Fischer

1. Department of Chemistry Seminar Swiss Federal Institute of Technology, Zurich, Switzerland, November 16, 2015.

2. Department of Chemistry Seminar Columbia University, New York, NY, U.S.A., January 28, 2016.

3. Department of Chemistry Seminar Boston College, Boston, MA, U.S.A., February 2, 2016.

4. Department of Chemistry Seminar Massachusetts Institute of Technology, Boston, U.S.A., February 3, 2016.

5. Department of Chemistry Seminar Stanford University, Stanford, CT, U.S.A., February 10, 2016.

6. Department of Chemistry Seminar Northwestern University, Evanston, IL, U.S.A., February 26, 2016.

7. Dozententagung, German Chemical Society, Heidelberg, Germany, March 21–23, 2016.

8. Department of Chemistry Seminar University of California San Diego, San Diego, CA U.S.A., April 11, 2016.

9. Department of Chemistry Seminar California Institute of Technology, Pasadena, CA, U.S.A., April 13, 2016.

10. Department of Chemistry Seminar Cornell University, Ithaca, NY, U.S.A., May 1, 2016.

11. Max-Planck Institute for Carbon Research, Muelheim, Germany, May 18, 2016.

12. Department of Chemistry Seminar Technical University of Dresden, Dresden, Germany, May 25, 2016.

13. Department of Chemistry Seminar Technical University of Braunschweig, Braunschweig, Germany, May 27, 2016.

Jinghua Guo

1. "In-Situ/Operando and High Pressure Soft X-Ray Spectroscopy of Chemical Reactions," The 1st Workshop on Synchrotron Radiation Research and Energy Science between FUNSOM-ALS, Soochow University, Suzhou, China (October 28–29, 2015).

2. "In-Situ/Operando Soft X-Ray Spectroscopy of Catalytic and Electrochemical Reactions," The 9th International Conference on Inelastic X-ray Scattering (IXS2015), NSRRC, Hsinchu, Taiwan (November 22–26, 2015).

3. "Probing the Optical Property and Electronic Structure of Nanostructured TiO_2," MRS2016 Spring Meeting, Symposium EE14 - Titanium Oxides: From Fundamental Understanding to Applications, Phoenix, AZ (March 28–April 1, 2016).

4. "Insights of Catalytic and Electrochemical Reactions from the In-Situ/Operando Soft X-Ray Spectroscopy," Department of Chemistry, Boston College, MA (April 4, 2016).

5. "Perspectives of In-Situ/Operando Soft X-Ray Spectroscopy in Energy Science," X-Ray & Electron Spectroscopies, Uppsala, Sweden (15–17 June 2016).

REFERENCES

1. Prendergast, D.; Galli, G. "X-ray adsorption spectra of water from first principles calculations." *Phys. Rev. Lett.* 96, 215502 (2006).

2. Altman, A. B. et al, "Theory and X-ray Absorption Spectroscopy for Aluminum Coordination Complexes – Al K-Edge Studies of Charge and Bonding in (BDI)Al, (BDI)AlR_2, and (BDI)AlX_2 Complexes." *J. Am. Chem. Soc.* 137, 10304 (2015).

3. Robertson, A. W. et al, "Stability and Dynamics of the Tetravacancy in Graphene." *Nano Lett.* 14, 1634 (2014).

IV.C.5 Improving the Kinetics and Thermodynamics of $Mg(BH_4)_2$ for Hydrogen Storage

Brandon Wood (Primary Contact),
Lennie Klebanoff, Vitalie Stavila, Tae Wook Heo,
Keith Ray, Jonathan Lee, ShinYoung Kang,
Hui-Chia Yu, Katsuyo Thornton
Lawrence Livermore National Laboratory
7000 East Ave., L-413
Livermore, CA 94550
Phone: (925) 422-8391
Email: brandonwood@llnl.gov

DOE Manager: Jesse Adams
Phone: (720) 356-1421
Email: Jesse.Adams@ee.doe.gov

Subcontractors:
- Sandia National Laboratories, Livermore, CA
- University of Michigan, Ann Arbor, MI

Project Start Date: August 1, 2014
Project End Date: August 31, 2017

Overall Objectives

- Combine theory, synthesis, and characterization across multiple scales to understand the intrinsic kinetic and thermodynamic limitations in $MgB_2/Mg(BH_4)_2$.
- Construct and apply a flexible, validated, multiscale theoretical framework for modeling (de)hydrogenation kinetics of the Mg-B-H system and related metal hydrides.
- Devise strategies for improving kinetics and thermodynamics through nanostructuring and doping.

Fiscal Year (FY) 2016 Objectives

- Synthesize high-purity MgB_2 nanoparticles with size selectivity.
- Use theory-characterization feedback loop to understand chemical kinetic processes governing hydrogenation of MgB_2.
- Establish soft X-ray spectroscopic reference library to aid in identification of Mg-B-H intermediate phases.

Technical Barriers

This project addresses the following technical barriers from the Hydrogen Storage section of the Fuel Cell Technologies Office Multi-Year Research, Development, and Demonstration Plan.

(O) Lack of Understanding of Hydrogen Physisorption and Chemisorption

(A) System Weight and Volume

(E) Charging/Discharging Rates

Technical Targets

This project is conducting fundamental studies of hydrogenation and dehydrogenation of nanoscale $Mg(BH_4)_2$-based materials using a combined theory and experiment approach. Insights will be applied toward the design and synthesis of hydrogen storage materials that meet the following DOE hydrogen storage targets.

- Specific energy: 1.8 kWh/kg
- Energy density: 1.3 kWh/L
- Minimum delivery pressure: 5 bar
- Minimum delivery temperature: 85°C
- System fill time: 1.5 kg H_2/min

FY 2016 Accomplishments

- Demonstrated size-selective synthesis of MgB_2 nanoparticles with diameter <10 nm.
- Completed joint experiment-theory X-ray absorption spectroscopy (XAS) and X-ray emission spectroscopy (XES) studies of bulk material; computed library of spectra for intermediate identification with <1 eV agreement with measured references (completed go/no-go).
- Showed that high-pressure hydrogenation of MgB_2 can lead to direct conversion to $Mg(BH_4)_2$ with intermediates suppressed.
- Compared spectroscopic data with ab initio computations and kinetic analysis to show that hydrogenation of MgB_2 likely initiates at interfaces and defect sites.
- Completed bulk free energy and surface energy calculations for $Mg(BH_4)_2$ polymorphs, MgB_2, and commonly observed dehydrogenation intermediates for parameterization of kinetic models.

✧ ✧ ✧ ✧ ✧

INTRODUCTION

$Mg(BH_4)_2$ is one of very few metal hydride candidates that lie close to the "viability window" of capacity (14.9 wt% H) and desorption enthalpy (ΔH_{des}) required to satisfy the 2020 and ultimate DOE hydrogen storage targets [1-2]. However, $Mg(BH_4)_2$ suffers from extremely poor kinetics whose origin is not well understood. If the kinetic limitations could be removed and the effective ΔH_{des} slightly improved, then facile hydrogen uptake and release could be attained, and a complex metal hydride-based system could achieve long-term targets. Prior work points to particle size reduction and doping with additives as viable and cost-effective improvement strategies [3]. However, it is difficult to fully leverage these without comprehending how, why, and under what conditions these improvements are observed. This project applies multiscale theoretical and experimental tools to develop a fundamental understanding of kinetic and thermodynamic limitations in the Mg-B-H hydrogen storage system, and to devise specific strategies for optimizing its performance under cycling conditions.

APPROACH

This project aims to establish a closely coupled theory/characterization/synthesis approach to understand the roles of nanostructuring and doping in the Mg-B-H system, and apply it to devise possible strategies for improving kinetics and thermodynamics. We focus on three objectives: (1) identifying chemical, phase nucleation, or transport processes and determining which are rate limiting; (2) understanding the origin of the kinetic and thermodynamic changes upon nanosizing and doping; and (3) devising and implementing rational modifications for improvement of H_2 storage properties. Our modeling effort relies on the application of a multiscale framework that combines atomistic density functional theory (DFT) for predictive chemistry and thermodynamics with continuum phase-field modeling for describing phase nucleation and growth and non-equilibrium transport kinetics. The predictions are informed and validated by controlled synthesis of size-selected nanoparticles free from binders and nanoscaffolds that may otherwise burden the system with unacceptably high gravimetric penalties. To better understand the kinetic pathways and processes, we apply gravimetric and thermochemical analysis, and utilize in situ and ex situ microscopy and spectroscopy aided by computational interpretations to derive chemical and phase compositions. Particular emphasis is placed on understanding kinetic factors governing the rehydrogenation of MgB_2, which is generally less well understood than dehydrogenation.

RESULTS

Improved thermodynamic predictions: A key goal of the project is the computation of more accurate thermodynamics of reactants, products, and intermediates in the Mg-B-H system, motivated by the need to reconcile discrepancies between experiments and theoretical predictions from DFT for the stability of reaction intermediates and pathways. We have been evaluating the possible relevance of three factors that are often neglected in DFT-computed reaction enthalpies: (1) explicit finite-temperature contributions to the free energy, including anharmonicity arising from B_xH_y molecular modes; (2) microstructural effects, including surface and interface contributions to the free energy; and (3) possible non-crystalline phases, including solid solutions, amorphous, and polycrystalline morphologies.

To address finite-temperature free energy contributions, we have applied a theoretical method being developed under HyMARC that separates contributions from the vibrational density of states within long ab initio molecular dynamics simulations [4]. This allows more accurate computation of entropic contributions rather than extrapolating from zero-temperature results. An added advantage is the ability to spatially decompose the entropy density to examine surface free energy contributions independently to predict size-dependent nanoparticle stability. Our calculations confirm that explicit calculations of the entropy can differ significantly from zero-temperature approximations (e.g., by 12 kJ/mol for β-$Mg(BH_4)_2$ at 600 K), with effects augmented at surfaces where molecular reorientations are minimally constrained.

Surface energies were also computed for several of the known phases (see examples in Table 1). These surface energies were then averaged according to the Wulff construction to better represent the variety of likely crystallite domain geometries, and were computed at the limits of low and high chemical potentials of Mg. These energies are currently being used as the basis for initial estimates of interfacial energies for inclusion within the HyMARC phase fraction prediction code. They are also being used to compute nucleation barriers and critical nucleus sizes for each of the phases, which gives a way to connect size-dependent thermodynamics directly to phase kinetics. For instance, high MgB_2 surface energy implies high interface energies and nucleation barriers, which may help to explain the difficulty in fully dehydrogenating $Mg(BH_4)_2$. These computations will be a key focus as validation data on MgB_2 nanoparticles becomes available.

Measured and computed X-ray spectroscopy for intermediate identification: XAS and X-ray emission spectroscopy (XES) can provide information about local electronic structure, which can be used alongside nuclear magnetic resonance and vibrational spectroscopy to identify intermediates and understand phase evolution. XAS and XES

TABLE 1. Calculated Surface Energies for Select Mg-B-H Compounds

Phase	Surface Orientation	σ (J/m²)	Phase	Surface Orientation	σ (J/m²)
γ-$Mg(BH_4)_2$	{111}	0.22	MgB_2	{1-100}	4.04
	{110}	0.22		{0001} Mg line	1.82
β-$Mg(BH_4)_2$	{010} term 1	0.57		{0001} Mg diamond	1.82
	{010} term 2	3.43		{0001} B line	5.18
$MgB_{12}H_{12}$	{100}	0.13		{0001} B diamond	7.77
	{010}	0.01		{0001} B zigzag	2.18
	{001} Mg line	0.15		{11-20}	2.40
	{001} Mg para	0.12		{1-101}	1.80
	{001} BH line	0.65	MgH_2	{100}	0.94
	{001} BH zigzag	0.26		{001}	0.84
				{101}	3.12

are particularly useful for probing MgB_2, since it features delocalized electronic states that differ qualitatively from insulating $Mg(BH_4)_2$ and the ionic salts proposed as reaction intermediates. Using methods described in Prendergast, et al. [5], we simulated XAS and XES spectra of $Mg(BH_4)_2$, MgB_2, and intermediates predicted near the convex hull in the calculations of Zhang et al. [6]. Averages over ab initio molecular dynamics simulations were used to account for thermal effects. In collaboration with HyMARC, these were compared with measured spectra on select single-phase samples to establish the validity of the combined experiment-theory spectroscopy approach and build a library of reference spectra for interpreting intermediates. Once proper protocols for controlling oxidation during sample handling were established, we found <1 eV agreement between the measured and computed reference spectra, fulfilling our go/no-go requirement (see Figure 1). The predictive capability of the computational approach ensures it can confidently be applied to phases and configurations that cannot be experimentally isolated in pure form. Discernible differences

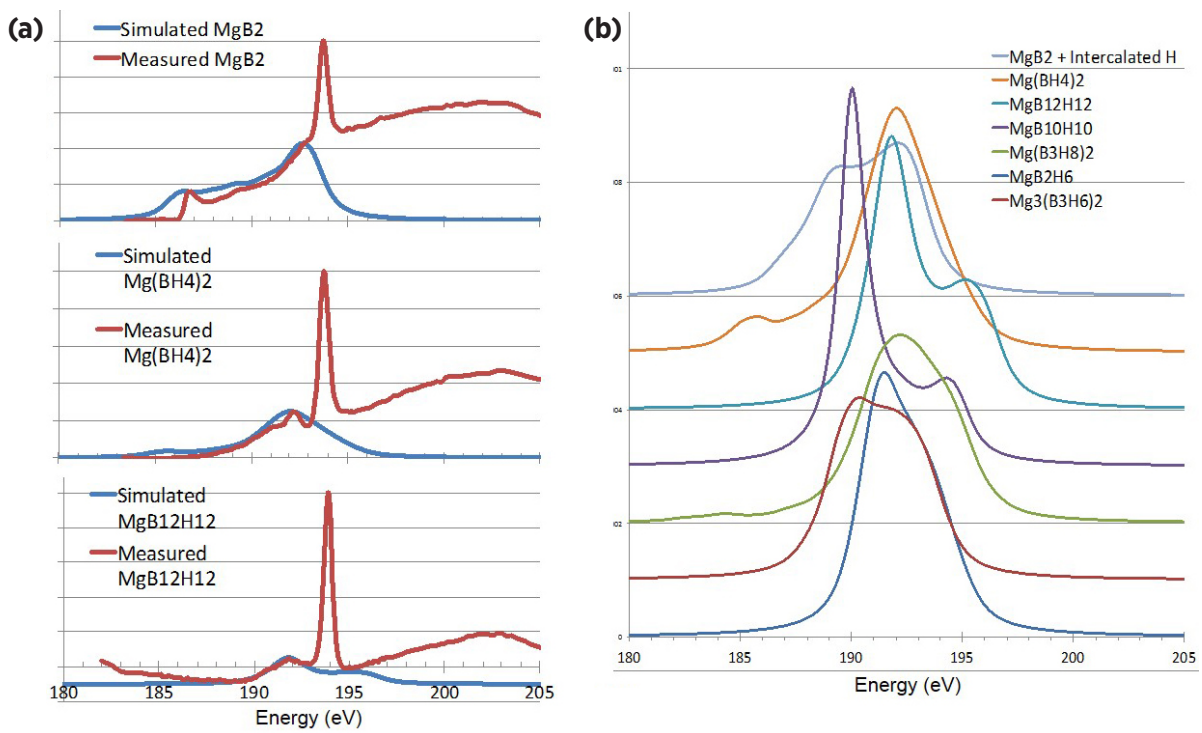

FIGURE 1. (a) Comparison between simulated (blue) and measured (red) XAS spectra at the boron K-edge, showing similar resonances to within ~1 eV (the sharp peak below 194 eV in the experimental spectrum is oxide-derived); (b) Calculated boron K-edge XAS spectra for intermediate phases at 300 K.

between the XAS and XES spectra also confirm the technique's usefulness for identifying intermediate species.

Understanding chemical kinetic processes in (de) hydrogenation: Our kinetics studies have been broadly aligned along two aspects: first, understanding chemical changes with hydrogen composition within single phases; and second, understanding structural phase transitions between different phases. The first is based on combining ab initio chemical modeling and spectroscopy, and the second combines phase-field kinetic modeling with experimental phase discrimination. Whereas the structural phase transitions were a key focus of the previous year, this year's primary focus has been on understanding chemical changes in single-phase regimes. Particular emphasis has been placed on elucidating kinetic processes and mechanisms during the initial hydrogenation of MgB_2, which remain poorly understood.

We applied a more detailed kinetic analysis to MgB_2 hydrogen uptake curves measured within a Sieverts apparatus at P = 145 bar H_2 (T = 364°C, 378°C, and 391°C; total uptake ~0.85 wt% H) by using Arrhenius fitting to extract separate barriers *for each level of hydrogenation* (Figure 2).

The quality of the Arrhenius fits were also recorded as a measure of the heterogeneity of the process, since non-Arrhenius behavior is typical of processes with a variety of barriers. The initial uptake region (< 0.25 wt% H) is non-Arrhenius, leading us to suspect that it represents the initial dissociation of H_2 at heterogeneous surface sites. The corresponding barrier is also quite similar to the dissociation barrier of 0.89 eV computed by Wang et al. [7]. From 0.2 wt% H to 0.7 wt% H, the behavior is more regular, and likely indicates a diffusive and/or reactive regime. This analysis confirms the presence of multiple governing processes in initial hydrogenation.

To understand these processes in more detail, we applied synchrotron soft X-ray spectroscopy, Fourier transform infrared spectroscopy, and nuclear magnetic resonance to the initially hydrogenated (0.85 wt% H) MgB_2 samples (Figure 3). Comparison with reference XAS spectra showed that there is a signature in the boron K-edge XAS spectrum that is unique to MgB_2, whose disappearance can be tracked to indicate transitions to other chemical environments (marked with * in Figure 3b). This spectral signature is only weakly affected by the introduction of hydrogen, which suggests very few boron atoms exist in an altered chemical environment. This implies concentration of hydrogen at a small number of sites where boron is highly hydrogenated. To illustrate this point, consider that conversion to lower hydrogenation states in the form of $MgB_{12}H_{12}$ or homogeneously dispersed B-H bonds should theoretically result in a ~20% reduction in intensity of the key spectral signature (*). In addition, comparison with our single-phase reference spectra showed no signatures specific to

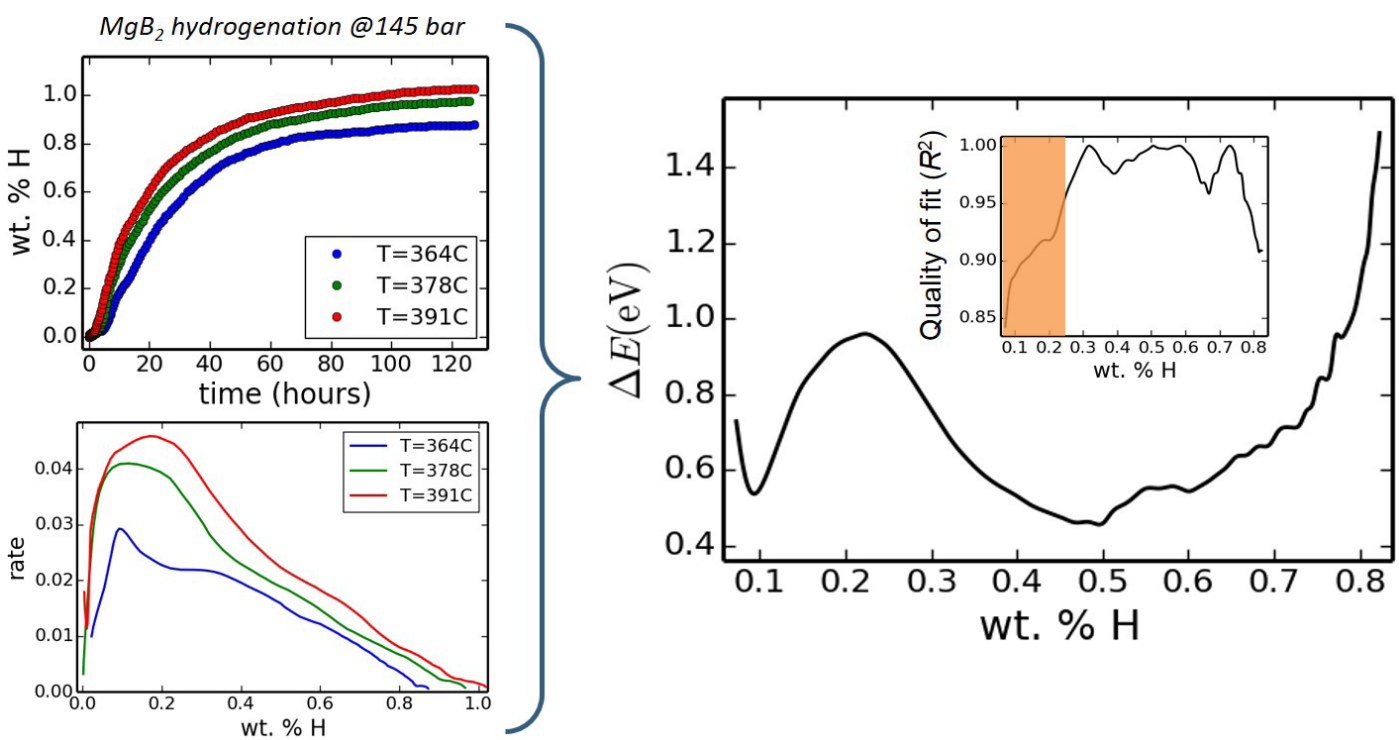

FIGURE 2. Arrhenius kinetic analysis of the isotherm uptake curves and corresponding rates for MgB_2 at 145 bar (left panels). The inset of the right-hand figure shows the quality of the Arrhenius fits, from which it is clear that early reaction stages (< 0.25 wt%H) are dominated by non-Arrhenius processes indicative of significant heterogeneity.

intermediates (e.g., $MgB_{12}H_{12}$). At the same time, the Fourier transform infrared spectrum for the initially hydrogenated sample (Figure 3c) shows features consistent with a linear mixture of MgB_2- and $Mg(BH_4)_2$-like spectra. Again, no features corresponding to $B_{12}H_{12}$ or dispersed B-H bonds are detected. We conclude that initial MgB_2 hydrogenation manifests as direct conversion to a BH_4-like coordination environment.

To better interpret the microscopic details of the MgB_2 hydrogenation process and understand the underlying spectral features, we performed a series of first-principles calculations of the energetics, electronic structure, and XAS and XES spectra of possible model interaction geometries. By directly comparing the computed and measured spectra, we were able to judge which of the models are compatible with our experimental samples. A comparison between the computed XAS spectrum for MgB_2 and the electronic density

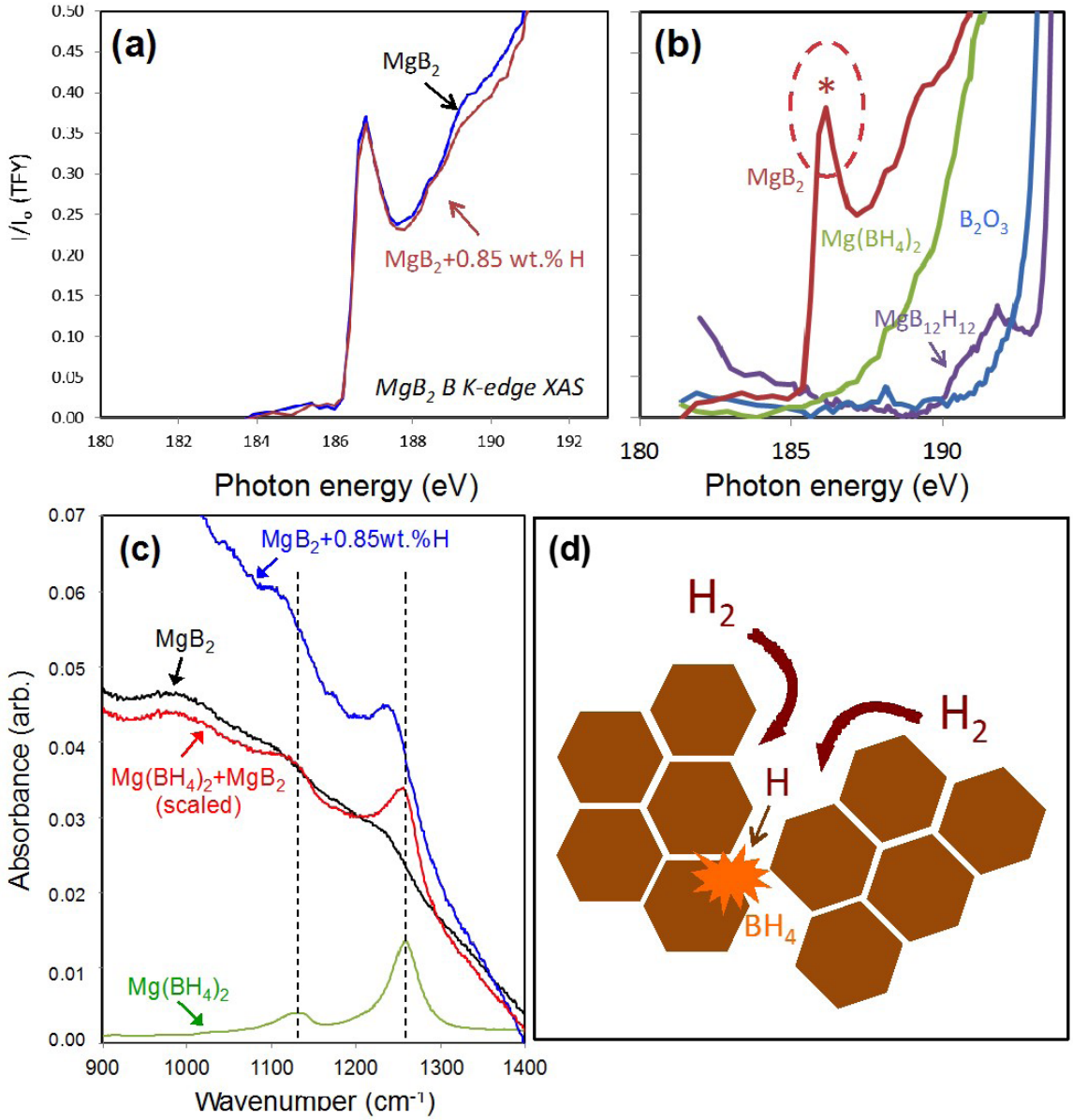

FIGURE 3. (a) XAS spectra at the boron K-edge for pure and partially hydrogenated MgB_2 (0.85 wt% H); (b) XAS spectrum for MgB_2 compared to reference spectra for B_2O_3, $MgB_{12}H_{12}$, and $Mg(BH_4)_2$, showing the signature boron p_{xy} spectral feature (*) unique to MgB_2; (c) Fourier transform infrared spectrum of partially hydrogenated MgB_2 (0.85 wt% H; blue), compared to reference $Mg(BH_4)_2$ (green), MgB_2 (black) spectra, and a linear $Mg(BH_4)_2/MgB_2$ mixture with the expected stoichiometric ratio (red); (d) Proposed mechanism of initial hydrogenation of MgB_2, in which hydrogen dissociates and diffuses rapidly along interfaces and grain boundaries to collect at high-energy bonds and directly form highly coordinated BH_4-like molecular complexes.

of states showed that the (*) feature in Figure 3b is actually a signature of the boron p_{xy} state, which disappears if this state is disrupted by hydrogen bonding. Using this understanding as a guide, we set about computationally testing specific sites for hydrogen incorporation and comparing their spectra to the measured ones. The most intuitive structure involved atomic hydrogen incorporation into the bulk material. The most stable bulk site involves intercalation of H between Mg and B planes; however, this was very energetically unfavorable with respect to H_2 (+1.3 eV/H), meaning there is no thermodynamic basis for H incorporation into the ideal structure. Computing the XAS spectrum further allowed us to confirm that H incorporation into bulk MgB_2 is incommensurate with the experimental data, since even small amounts of hydrogen significantly impact the boron p_{xy} feature as hydrogen donates electrons into the boron sheets.

Since bulk intercalation of atomic hydrogen does not fit the data, we instead computed energetics of hydrogen insertion at edges and surfaces, which we used as simple models for solid-state interfaces. We find that these sites are significantly more favorable (about -0.8 eV per H for edges and -0.5 eV per H for surfaces). We conclude that high-energy B-B bonds at interfaces are the likely targets for initial hydrogenation, and that these bonds act as magnets for subsequent hydrogen atoms to form highly coordinated BH_4 complexes. Morevoer, these sites already have highly strained and irregular electronic orbitals, which explains why hydrogenation initially has little impact on the boron p_{xy} states in this case. These interfaces and grain boundaries were also predicted in our calculations to be the preferred diffusion pathways for atomic hydrogen, which rationalizes our uptake results with prior computational studies suggesting bulk diffusion should be nearly impossible under these conditions [8]. The combined experiment and theory investigation therefore points to the scenario shown in Figure 3d, with hydrogenation initiating at grain boundaries or interfaces and "etching" the boron from these edges inward [9]. Notably, this mechanism is fundamentally different from the dehydrogenation process, and suggests that $Mg(BH_4)_2$ can be directly upon hydrogenation of MgB_2 without significant intermediates. It also suggests higher relative surface and interface volume (e.g., in nanoparticles) should improve MgB_2 uptake kinetics. Our spectral interpretation remainined consistent for samples hydrogenated up to 7 wt% H at higher pressure (700 bar).

We have also been running ab initio quantum molecular dynamics to obtain direct insights into the chemistry and transport processes active during the initial dehydrogenation of β-$Mg(BH_4)_2$. These computations are intensive, but can be extremely informative and account directly for finite-temperature kinetic effects inaccessible to more conventional calculations. The example in Figure 4 shows B-H bond activation at a (001) surface of β-$Mg(BH_4)_2$. This process is difficult in the bulk material owing to the rigidity of the Mg^{2+} coordination environment, but becomes feasible at surfaces and interfaces due to spontaneous surface disordering. Because BH_4 rotational disorder and B-H bond activation are necessary ingredients for structural diffusion, their manifestation in the finite-temperature simulation implies a facile surface–interfacial hydrogen transport pathway. This contrasts with the >2 eV barrier predicted by Wolverton and Ozolinš for vacancy-driven transport in an ideal bulk crystal of $Mg(BH_4)_2$ [8], and is instead more consistent with isotope exchange measurements [10].

Modeling multiphase kinetics: Our phase kinetics modeling efforts have proceeded along three fronts:

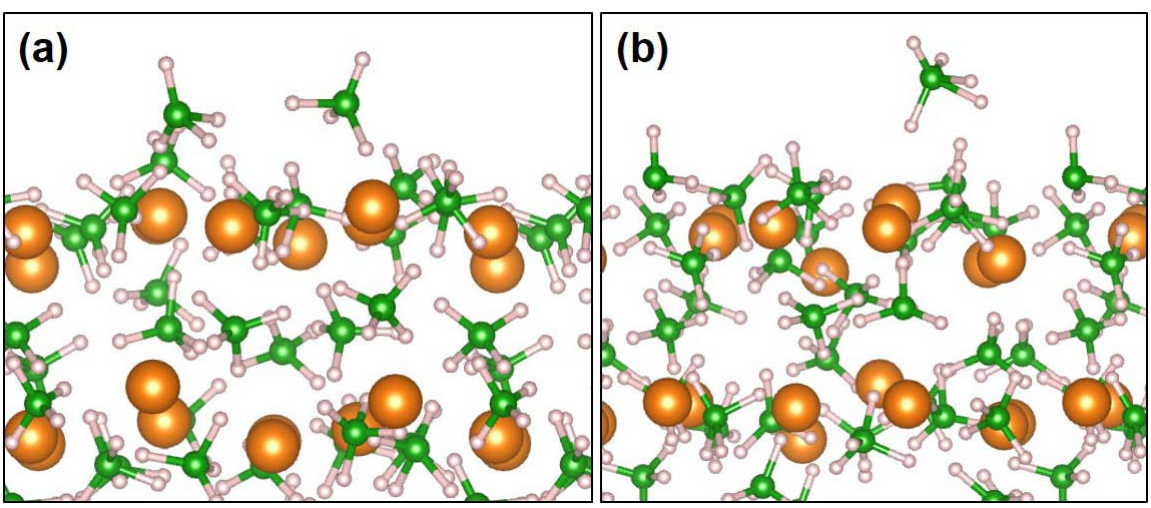

FIGURE 4. Signature of structural diffusion of hydrogen at a surface of β-$Mg(BH_4)_2$ taken from ab initio molecular dynamics of a (001) surface at 800 K. Surface disordering facilitates interaction between the two BH_4^- polyhedra in the left panel, leading to B-H bond activation and hydride transfer. In this instance, the process is accompanied by Mg^{2+} reduction (not shown).

nucleation modeling, stability analysis based on microstructure, and phase-field modeling of full reaction kinetics. First, we have used the DFT-computed surface energies s_i to estimate interfacial energies g_{ij} using a semi-empirical approximation derived from grain boundary models [11], in which $g_{ij} = p\,(s_i + s_j)$. Instead of fitting the constant *p*, our approach tests a range of values (e.g., from 0.3 to 0.7) to extract reasonable ranges of possible interfacial energies. These interfacial energies were used within classical nucleation theory to estimate ranges of homogeneous and heterogeneous nucleation barriers for the various phases in Mg- or B-rich conditions. The smallest stress-free homogenous nucleation barrier was found for $MgB_{12}H_{12}$ (below 1 meV) and the largest for MgB_2 (up to 600 meV), which may explain the difficulty in forming the latter phase upon dehydrogenation. However, stress factors, which are neglected in the current model, are likely to significantly penalize nucleation of the lower-density intermediate phases such as $MgB_{12}H_{12}$ due to the accompanying volume expansion, which along with diffusion limitations may favor observation in amorphous or solid solution forms.

Second, in collaboration with HyMARC, we have developed an extension to the Grand Canonical Linear Programming method [12] that takes into account the microstructure and interfacial energies associated with multiphase coexistence. These corrections are expected to play an increasingly important role in nanoparticle systems, which will be studied in detail in the next project phase. We have applied this formalism to model reactions and microstructures in the Mg-B-H as proof of concept, but will return to this effort as our characterization reveals further evidence of the relevant phases and microstructures that need to be considered during operating conditions.

Third, again in collaboration with HyMARC, we have been developing a phase-field model for reaction kinetics based on previously demonstrated methods. The Mg-MgH_2 portion of the phase diagram is being modeled with an interstitial hydride model [13], whereas all other relevant reactions are considered by adapting a multiphase conversion model previously developed for battery materials [14]. Although early feasibility tests are promising, this model requires parameterization of the free energy surface for the single-phase and multi-phase regions of the phase diagram, which rely on further parameterization from the additional experiments and computations being performed as part of the project. Demonstration of this integrated model will meet our final project milestone.

Size-selective MgB_2 nanoparticle synthesis: Our progress in understanding the bulk material has set the stage for the next phase of the project focusing on nanoscale materials. To this end, we have also been working to synthesize phase-pure MgB_2 nanoparticles with narrow size distributions. Specifically, we developed a new approach for the synthesis of MgB_2 nanoparticles using surfactant-assisted ball-milling. The method consists of milling MgB_2 powder in the presence of oleic acid and oleylamine in a hydrocarbon such as hexane or heptane. The powders were milled using a SPEX-8000 high-energy mill. We optimized the milling conditions to allow the synthesis of sub-50 nm nanoparticles, which can be easily separated from the reaction mixture. Scanning transmission electron microscopy imaging confirmed agglomerates of small particles, with the size histogram indicating most of the particles are 10–20 nm in diameter. The particles can be purified by washing and centrifugation steps in the presence of ethanol. We plan to explore surfactant removal techniques to control the surface chemistry of the MgB_2 nanoparticles for subsequent hydrogenation tests.

CONCLUSIONS AND FUTURE DIRECTIONS

- High-pressure hydrogenation of MgB_2 can lead to direct conversion to $Mg(BH_4)_2$ with intermediates suppressed, suggesting different phase pathways for hydrogenation and dehydrogenation.
- Feedback loop between theory and experimental characterization was used to show that MgB_2 hydrogenation likely initiates at interfaces and defect sites, suggesting morphological and microstructural engineering could improve kinetics.
- *Future direction*: Refine nanoparticle synthetic procedures for higher phase purity and repeat spectroscopic characterization of nanoparticles for comparison to predictions.
- *Future direction:* Complete quantitative assessment of the importance of "beyond-ideal" contributions to the computed thermodynamics of reactants, products, and intermediates, including anharmonicity, morphology, and microstructural considerations in bulk and nanoscale materials.
- *Future direction:* Perform high-temperature ab initio molecular dynamics of phase mixtures to identify additional possible chemical pathways.
- *Future direction:* Complete and validate reactive-diffuse interface model for inclusion in phase-field framework.

FY 2016 PUBLICATIONS/PRESENTATIONS

1. Wood, B.C. et al. "Improving the kinetics and thermodynamics of $Mg(BH_4)_2$ for hydrogen storage." *U.S. DOE Hydrogen and Fuel Cells Program Annual Merit Review*, Washington, D.C., June 2016.

2. Stavila, V. et al., "Understanding and controlling hydrogen release and uptake in complex metal hydrides," *Pacifichem*, Honolulu, HI, December 2015.

3. Wood, B.C. et al., "Nanointerface-driven reversible hydrogen storage in the nanoconfined Li-N-H system," *Materials Research Society Spring Meeting*, Phoenix, AZ, April 2016.

4. Wood, B.C., V. Stavila, N. Poonyayant, T.-W. Heo, K. Ray, L.E. Klebanoff, T.J. Udovic, J. Lee, N. Angboonpong, J.D. Sugar, and P. Pakawatpanurut. "Nanointerface-driven reversible hydrogen storage in the nanoconfined Li-N-H system." *Submitted* (2016).

REFERENCES

1. Klebanoff, L.E., and J.O. Keller. "5 Years of hydrogen storage research in the US DOE Metal Hydride Center of Excellence (MHCoE)." *Int. J. Hydr. Energy* 38 (2013): 4533–4576.

2. Pasini, J.M., C. Corgnale, B.A. van Hassel, T. Motyka, S. Kumar, and K.L. Simmons. "Metal hydride material requirements for automotive hydrogen storage systems." *Int. J. Hydr. Energy* 38 (2013): 9755–9765.

3. Fichtner, M., Z. Zhao-Karger, J. Hu, A. Roth, and P. Weidler. "The kinetic properties of $Mg(BH_4)_2$ infiltrated in activated carbon." *Nanotechnology* 20 (2009): 204029.

4. Teweldeberhan, A.M. and S.A. Bonev. "Structural and thermodynamic properties of liquid Na-Li and Ca-Li alloys at high pressure." *Phys. Rev. B* 83 (2011): 134120.

5. Prendergast, D., and G. Galli. "X-ray absorption spectra of water from first principles calculations." *Phys. Rev. Lett.* 96 (2006): 215502.

6. Zhang, Y., E. Majzoub, V. Ozoliņš, and C. Wolverton. "Theoretical Prediction of Metastable Intermediates in the Decomposition of $Mg(BH_4)_2$." *J. Phys. Chem. C* 116 (2012): 10522–10528.

7. Wang, Y., K. Michel, Y. Zhang, and C. Wolverton. "Thermodynamic stability of transition metals on the Mg-terminated MgB2 (0001) surface and their effects on hydrogen dissociation and diffusion." *Phys. Rev. B* 91 (2015): 155431.

8. Wolverton, C., et al. *U.S. DOE Hydrogen and Fuel Cells Program Annual Report* (2013).

9. Ray, K.G., J.R.I. Lee, L.E. Klebanoff, V.N. Stavila, T.W. Heo, S. Kang, and B.C. Wood. "Key mechanisms in the initial hydrogenation of MgB_2." *Manuscript in preparation* (2016).

10. Hagemann, H., V. D'Anna, J.-P. Rapin, and K. Yvon. "Deuterium-hydrogen exchange in solid $Mg(BH_4)_2$." *J. Phys. Chem. C* 114 (2010): 10045–10047.

11. Porter, D.A., and K.E. Easterling, *Phase Transformations in Metals and Alloys.* 2nd ed.; Chapman & Hall: London, UK (1992).

12. Akbarzadeh, A.R., V. Ozoliņš, and C. Wolverton. "First-Principles Determination of Multicomponent Hydride Phase Diagrams: Application to the Li-Mg-N-H System." *Adv. Mater.* 19 (2007): 3233–3239.

13. Voskuilen, T.G., and T.L. Pourpoint. "Phase field modeling of hydrogen transport and reaction in metal hydrides." *Int. J. Hydrogen Energy* 38 (2013): 7363–7375.

14. Yu, H.-C., F. Wang, G.G. Amatucci, and K. Thornton. "A phase-field model and simulation of kinetically asymmetric ternary conversion-reconversion transformation in battery electrodes." *J. Phase Equil. Diff.* 37 (2016): 86–89.

IV.C.6 High-Capacity Hydrogen Storage Systems via Mechanochemistry

Vitalij K. Pecharsky (Primary Contact),
Duane D. Johnson, Marek Pruski, Shalabh Gupta
Ames Laboratory
Iowa State University
253 Spedding Hall
Ames, IA 50011-3020
Phone: (515) 294-8220
Email: vitkp@ameslab.gov

DOE Manager: Ned Stetson
Phone: (202) 586-9995
Email: Ned.Stetson@ee.doe.gov

Subcontractor:
Eric Majzoub, University of Missouri, St. Louis, MO

Project Start Date: August 1, 2015
Project End Date: July 30, 2018

Overall Objectives

The overarching goal of the project is to discover and develop hydrogen storage materials that are constituted largely from earth abundant and low cost elements, such as silicon and boron. The specific objectives of this project are:

- Identify computationally and synthesize hitherto unknown high H-capacity Si-based borohydrides (Si-BHs) with useable gravimetric density of over 10 wt% H_2, and decomposition enthalpies of 25–35 kJ/mol-H_2, such that H_2 desorption occurs at the operating temperature (~80–100°C) of the proton exchange membrane (PEM) fuel cells.
- Develop simple and scalable strategies to form two-dimensional graphene/hydride composites that will directly address the (re)-dehydrogenation kinetics issues plaguing the performance of high capacity borohydrides and other known complex metal hydrides.
- The successful completion of this project would afford a H-storage material with kinetic and thermodynamic properties tailored appropriately to supply high-purity hydrogen to PEM fuel cells, satisfying one of the most important goals of the DOE and the Fuel Cell Technologies Office and the Hydrogen Storage program.

Fiscal Year (FY) 2016 Objectives

- Use prototype electrostatic ground states (PEGS) [1] and multi-gas canonical linear programming (MGCLP) [2] tools to screen for stable hypersalts of Si-based borohydrides of the type $(A/AE)_xSi_y(BH_4)_z$, in which A and AE are light alkali and alkaline earth metals, respectively. Identify candidates that provide finite-temperature enthalpies within 27 ± 10 kJ/mol-H_2. The new Si-BHs are expected to have H-contents of at least 10 wt% and volumetric capacity in excess of 130 g H_2/L.
- Synthesize the most promising Si-BHs identified computationally using mechanochemical processes involving metathesis (exchange) reactions, and characterize the newly synthesized borohydrides by X-ray diffraction (XRD), solid state nuclear magnetic resonance (SSNMR), and gas volumetric pressure-composition-temperature techniques.

Technical Barriers

This project addresses the following technical barriers from the Hydrogen Storage section (3.3) of the Fuel Cell Technologies Office Multi-Year Research, Development, and Demonstration Plan.

(A) System Weight and Volume

(B) System Cost

(D) Durability/Operability

(O) Lack of Understanding of Hydrogen Physisorption and Chemisorption

Technical Targets

The project addresses lack of suitable materials impeding implementation of materials-based onboard hydrogen storage systems. Successful completion would lead to hydrogen storage materials with high gravimetric and volumetric capacity, and kinetics and thermodynamics suitable to supply high-purity H_2 to a PEM fuel cell. The new materials identified and synthesized as an outcome of this project will achieve or exceed the DOE targets listed in Table 1.

TABLE 1. H-Storage Parameters of Si-Based Borohydrides in Comparison with the DOE Targets

Storage parameters	DOE Technical Targets*	Our Targets**
Gravimetric capacity (kg H_2/kg)	0.075	>0.100
Volumetric capacity (kg H_2/L)	0.070	>0.130

*Ultimate (2020) system level targets, **material basis

FY 2016 Accomplishments

- More than 10,000 structures were examined by PEGS and density functional theory (DFT), and the most thermodynamically stable candidates were considered for synthesis; silicon, when present in an environment coordinated by $[BH_4]^-$ tetrahedra, prefers a 2+ state. The bi-alkali hypersalts are more stable than the mono-alkali hypersalts.
- Nearly 20 exchange or metathesis reaction systems were studied mechanochemically. There are clear indications that Si-BHs can be stabilized mechanochemically.
- The presence of halogen or sulfur in the structure stabilizes silicon borohydrides.
- Decomposition temperatures and amount of H_2 released from hypersalts meet the DOE targets; high purity H_2 was obtained from the mixed Si-BHs with no diborane release.

✧ ✧ ✧ ✧ ✧

INTRODUCTION

A safe and efficient hydrogen storage method suitable for powering hydrogen fuel cell cars and supporting other H-based technologies remains an outstanding technological and scientific challenge. Because of the practical barriers associated with the H-storage in liquid and gaseous forms, hydrogen storage in solid materials continues to be the most promising alternative and an emerging technology. The target materials should store a large amount of hydrogen in a light, compact form and be amenable to rapid recharging, safe, and affordable. Despite the discovery and synthesis of a large number of hydrogen rich compounds, their utility for H-storage and delivery remains limited by unfavorable thermodynamics or/and poor kinetics of H_2 release and uptake [3]. The U.S. Department of Energy (DOE), in collaboration with the automotive industry defined the criteria for onboard H-system, which requires 1–10 bar H_2 equilibrium pressure at the working temperature of a PEM fuel cell. Only a few known hydrides can satisfy these conditions and have a useful gravimetric density with enthalpies of dehydrogenation in the range of -25 kJ/mol-H_2 to -30 kJ/mol-H_2.

Guided by robust and validated computational tools, this project seeks to (1) discover a hitherto unknown silicon (Si)-based borohydrides and optimize processes for their low cost synthesis in high purity powder form, and (2) develop mechanochemical processes to formulate nano-composites based on graphene-derived, two-dimensional carbon allotropes. Both classes of materials will be experimentally accessed via a versatile and sustainable, green, and energy-efficient mechanochemical process, offering a cost effective solution for large scale production.

APPROACH

A combination of computational screening and shortlisting followed by synthesis of the most promising candidates is adopted to cover a wide range of compositional landscape available for multi-cation Si-BH hypersalts. The computational search is performed using PEGS followed by structure relaxation using DFT. Thermodynamic properties of selected decomposition pathways are determined using MGCLP. Promising reaction systems are tested mechanochemically by utilizing double-exchange or metathesis reactions. Comprehensive structure and phase characterization is performed using powder XRD and SSNMR and the hydrogen de-absorption and absorption properties are evaluated using volumetric methods.

RESULTS

<u>Screening candidate Si^{n+} hypersalt compounds using PEGS:</u> Silicon borohydride, $Si(BH_4)_n$, $n = \{1,2,3,4\}$, candidate structures with Si oxidation states from +1 to +4 were generated using the PEGS algorithm and relaxed using DFT and conjugate gradient method. The calculated Born effective charge for Si (Z^{eff}_{Si}) in each structure, irrespective of its coordination, indicates that Si prefers a nominal 2+ state when surrounded by the $[BH_4]^-$ tetrahedra. Free energy minimization at T = 300 K via the MGCLP method showed that $Si(BH_4)_2$ is relatively more stable than the others towards decomposition to elements.

Alkali (A) and alkaline earth (AE) metal based hypersalts of Si-BHs were examined next for stability against decomposition into the elements in their standard states, and into the associated A, AH, AE, or AEH_2. The calculated total energy (static + dynamic) and Helmholtz free energy changes for the decomposition reactions indicate that mono-A hypersalts are less stable than the bi-A hypersalts. In particular, $LiKSi(BH_4)_4$ and $NaKSi(BH_4)_4$ were found to be the most stable compositions and good candidates for experimental screening.

<u>Screening, synthesis, and characterization of novel Si-BHs via hypersalt stabilization:</u> Targeted synthesis of multi-cation borohydrides in multiple systems is based on mechanochemical exchange reactions, some examples are listed in Table 2. A few systems, such as $LiBH_4$-$AlHal_3$-$SiHal_4$ and ABH_4-SiS_2, etc. (where Hal = Cl or Br) have shown potential for the hypersalt stabilization and promising hydrogen desorption and absorption properties, and are discussed in details. A few other systems that will continue to have attention are also presented in Table 2.

<u>$LiBH_4$-$AlCl_3$-$SiCl_4$ system</u>: In an attempt to prepare aluminum stabilized Si-BHs, $LiBH_4$, $AlCl_3$ and $SiCl_4$ were mechanochemically reacted in varying proportions. The reference reactions carried without $SiCl_4$ yielded potentially new phases for 13:3 and 3:1 molar ratio of $LiBH_4$ and $AlCl_3$

TABLE 2. Systems Currently under Investigation to Synthesize Si-Based Borohydride Hypersalts

Target compound	H_2, wt%*	Reactions examined
$LiSi(BH_4)_5$	18.4	$4LiBH_4+TBABH_4+SiCl_4$; b)+$Li[Al\{OC(CF_3)_3\}_4$
		SiS_2 + $nABH_4$ (n = 2-8; A = Li, Na)
		$Si(CH_3COO)_4$ + $5LiBH_4$
$K_2Si(BH_4)_6$	12.4	$K_2SiF_6+6ABH_4$ (A = Li, Na)
$(NH_4)Si(BH_4)_5$	20.0/16.7	$NH_4Cl+5LiBH_4+SiCl_4$
$MgSi(BH_4)_6$	17.1	$MgSiF_6+6ABH_4$ (A = Li, Na)
		$Mg(BH_4)_2+4NaBH_4+SiBr_4$
$CaSi(BH_4)_6$	15.4	$CaCl_2+6LiBH_4+SiCl_4$
$AlSi(BH_4)_7$	17.8	$AlHal_3+nABH_4+SiCl_4$ (n=3, 7; Hal = Cl, Br; A = Li, Na)
$LiSi(BH_4)_3$	15.0	Li + $3ABH_4$ + $SiCl_4$ (A = Li, Na)
$CaSi(BH_4)_4$	12.5	Ca + $4ABH_4$ + $SiCl_4$ (A = Li, Na)

* Total gravimetric capacity of the pure compound as written; for the ammonium salt, second number is H-content excluding NH_4.

and full phase analysis and structure determination is in progress. Excess $SiCl_4$ during these reactions yields only LiCl and a known compound, $Al_3Li_4(BH_4)_{13}$ [4] in the 13:3 reaction. $SiCl_4$ has a more pronounced effect on the 3:1 reaction. Apart from LiCl, a new compound with yet unidentified structure appears. Based on XRD and hydrogen desorption analysis the product is expected to have a composition close to "$LiAlSiCl_5(BH_4)_3$", see Equation1 below:

$$3LiBH_4 + AlCl_3 + SiCl_4 \rightarrow 2LiCl(s) + LiAlSiCl_5(BH_4)_3 \quad (1)$$

Consistent with Equation 1, the product yields 3.2 wt% of pure H_2 with onset at ~57°C (Figure 1).

Based on XRD, the isostructural Br analogue $LiAlSiBr_5(BH_4)_3$ forms with $SiBr_4$. These isostructural compounds are orthorhombic with *Ccca* space group. The presence of BH_4 group has been confirmed by ^{11}B SSNMR measurements. ^{27}Al SSNMR shows 5-coordinated Al in both compounds, which is not present in the starting materials. Consistent with PEGS, ^{28}Si Direct Polarization Magic Angle Spinning NMR showed signal attributed to $SiCl_4$ in the structure. PEGS points to stable structures with Si^{4+} in $AlSiCl_n(BH_4)_3$ and $AlSiLiCl_n(BH_4)_3$ n = {1,2,3,4} composition spaces (Figure 2). Stable structures in both systems feature layers of $SiCl_4$ tetrahedra with planar and non-planar $Al(BH_4)_3$ units in $AlSiCl_4(BH_4)_3$ and $AlSiLiCl_5(BH_4)_3$, respectively.

<u>$LiBH_4$-SiS_2 system:</u> The mechanochemical reaction of $LiBH_4$ and SiS_2 in 2:1 molar ratio shows formation of an amorphous product that is currently under investigation. Thermodynamic calculations based on MGCLP have identified possible existence of a sulfur-stabilized hypersalt with the composition $Li_2SiS_2(BH_4)_2$. Nearly 5.1 wt% of H_2 is released from the products, which is close to the theoretical

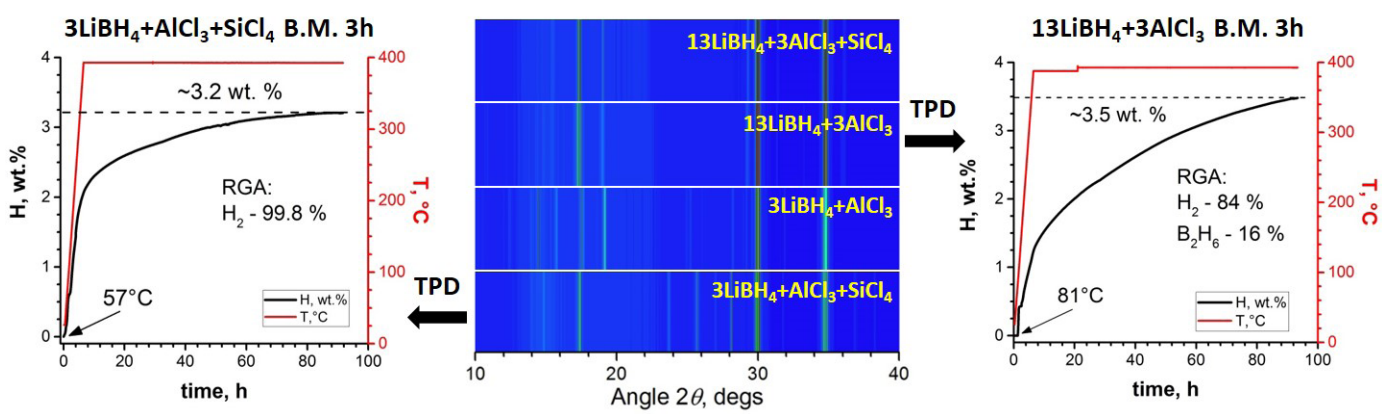

TPD – Temperature programmed desorption; RGA – Residual gas analysis

FIGURE 1. The XRD patterns and temperature programmed decomposition plots of the $LiBH_4$ - $AlCl_3$ mixtures in the presence and absence of $SiCl_4$, ball milled for 3 h

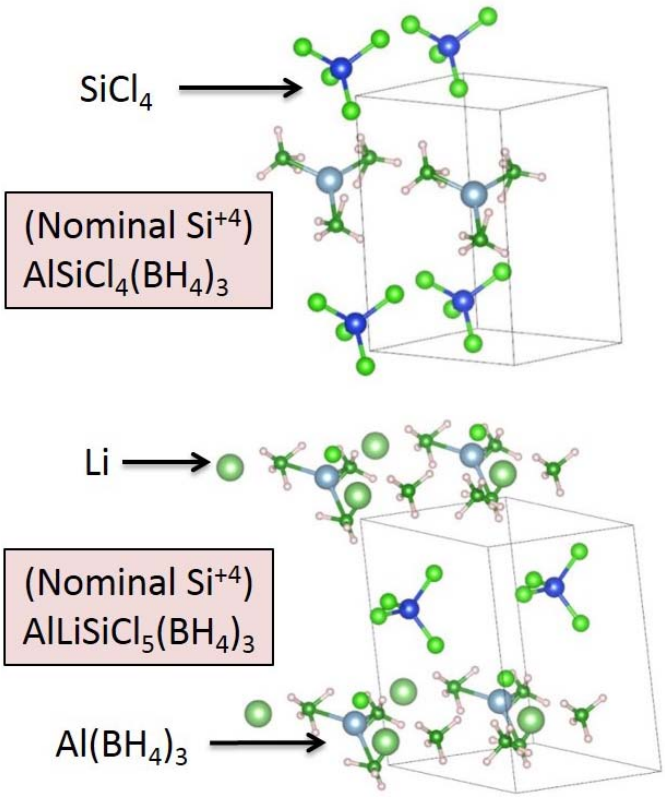

FIGURE 2. DFT-relaxed PEGS prototypes of $AlSiCl_4(BH_4)_3$ and $AlSiLiCl_5(BH_4)_3$ structures

value of 5.9 wt% for $2LiBH_4+SiS_2$. Further, $6LiBH_4$-SiS_2 composition releases the highest amount of hydrogen (~8.2 wt%) on heating to 385°C with 92°C onset (Figure 3). Based on pressure-composition-temperature and XRD data, the possible reaction can be described as follows in Equation 2:

$$6LiBH_4 + SiS_2 \rightarrow 2Li_2S + \text{“}Li_2SiB_6H_4\text{”}_{(amorph.)} + 10H_2 \qquad (2)$$

Additional SSNMR, hydrogen de/absorption experiments of fully and partially (de)hydrogenated samples are in progress to determine the local structures of the amorphous product.

CONCLUSIONS AND FUTURE DIRECTIONS

Analysis of numerous multi-cation systems using available computational and experimental tools shows that Si-BH hypersalts can be stabilized, and synthesized mechanochemically. Although most Si-BH hypersalts have borderline stability, evidence suggests that they can be stabilized by sulfur or halogen ions in the structure. These new materials have low desorption onset temperatures and release uncontaminated hydrogen. There is a strong likelihood of formation of sulfur stabilized Si-BHs in the $LiBH_4$-SiS_2 system. We will continue to focus on this and

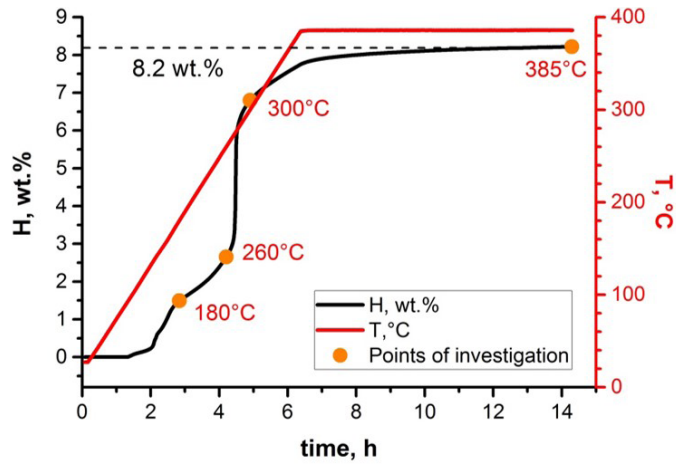

FIGURE 3. The temperature-programmed decomposition of the $6LiBH_4$-SiS_2 mixture and points of investigations at different temperatures

other sulfur-based systems using precursors like Al_2S_3 and B_2S_3. The high pressure milling is expected to be recommissioned and fully functional by the end of August, at which point most mechanochemical reactions shown in Table 1 and other will be performed under ~350 bar H_2 pressure. Milling at cryogenic temperatures will also remain in focus.

Preliminary experiments on graphene-hydride composites have shown significant reduction in desorption onset temperature of $LiBH_4$, along with considerable improvement in kinetics. Future work will aim at optimizing milling parameters, characterizing the composites and introduction of other borohydrides. Computational studies will be initiated to evaluate relative stabilities of Si-borohydrides and their hypersalts on graphene surface.

FY 2016 PUBLICATIONS/PRESENTATIONS

1. T. Kobayashi, O. Dolotko, S. Gupta, M. Pruski, E. Majzoub, V.K. Pecharsky “Insights into the role of composition for purity of released hydrogen from the $LiBH_4$-$AlCl_3$ system” *manuscript in preparation*.

2. O. Dolotko, T. Kobayashi, S. Gupta, M. Pruski, E. Majzoub, V.K. Pecharsky “Hydrogen generation from the $LiBH_4$-SiS_2 system.” *manuscript in preparation*.

3. O. Dolotko, S. Gupta, T. Kobayashi, M. Pruski, V.K. Pecharsky “Improved method of hydrogen generation from borohydrides by introducing sulfide materials” *IPDR in preparation*.

REFERENCES

1. E.H. Majzoub, V. Ozolins Phys. Rev. B. 2008, 77, 104115

2. N. Poonyayant, V. Stavila, E.H. Majzoub, L.E. Klebanoff, R. Behrens, N. Angboonpong, M. Ulutagay-Kartin, P. Pakawatpanurut, E.S. Hecht, J.S. Breit J. Phys. Chem. C., 2014, 118, 14759.

3. L.E. Klebanoff, J.O. Keller, Int. J. Hydrogen Energy 2013, 38, 4533.

4. Lindemann, R.D. Ferrer, L. Dunsch, Y. Filinchuk, R. Cerny, H. Hagemann, V. D'Anna, L.M.L. Daku, L. Schultz, and O. Gutfleisch, Chem. Eur. J. 2010, 16, 8707.

IV.C.7 H_2 Storage Characterization and Optimization Research Efforts

Thomas Gennett[1](Primary Contact), Jeffrey Long[2], Tom Autrey[3], Craig Brown[4], Phillip Parilla[1], Martin Head-Gordon[2], Mark Bowden[3], Terrence Udovic[4], Michele Olsen[1], Katherine Hurst[1], Arrelaine Dameron[1], Jeff Blackburn[1], Jacob Tarver[1,4], Mirjana Dimitrievska[1,4], Yeh-Yung Lin[2], Tomče Runčevski [2], Günther Thiele[2], Abhi Karkamkar[3], Bojana Ginovska[3], Herman Cho[3], Marina Chong[3], Adrian Houghton[3], Gary Edvenson[3], Graduate students: Henry Jiang[2], Matthew Kapelewski[2], Dana Levine[2], Mercedes Taylor[2], David Zee[2]

[1]National Renewable Energy Laboratory (NREL)
15313 Denver West Parkway
Golden, CO 80401
Phone: (303)-384-6628
Email: thomas.gennett@nrel.gov

[2]Lawrence Berkeley National Laboratory (LBNL)
1 Cyclotron Rd.
Berkeley, CA 94720

[3]Pacific Northwest National Laboratory (PNNL)
902 Battelle Blvd.
Richland, WA 99354

[4]National Institute of Standards and Technology (NIST)
100 Bureau Drive
Gaithersburg, MD 20899

DOE Manager: Jesse Adams
Phone: (720) 356-1421
Email: jesse.adams@ee.doe.gov

Subcontractor:
Prof Craig Jensen, University of Hawaii at Manoa (with PNNL), Honolulu, HI

Project Start Date: October 1, 2015
Project End Date: Project continuation and direction determined annually by DOE

Overall Objectives

- Develop a series of advanced characterization tools that allows for rapid advancement and in-depth understanding of next-generation hydrogen storage materials.
- Develop a hydrogen storage material with a total materials-based capacity of >45 g/L above 150 K, that is possible with hydrogen overpressures <100 bar and reversible for multiple cycles.
- Optimize thermal management in hydrogen storage systems by the incorporation of unique phase-change materials.
- Demonstrate the importance of computational methods in developing and understanding of next generation hydrogen storage materials.

Fiscal Year (FY) 2016 Objectives

- Develop new characterization tools (specifically thermal conductivity, nuclear magnetic resonance [NMR], Fourier transform infrared).
- Demonstrate the ability to bind two H_2 molecules to one metal center in a metal-organic framework, porous aromatic framework, or carbon-based material.
- Demonstrate the ability to increase the binding energy in high surface area carbon-based sorbents.
- Demonstrate the ability to control binding energies in sorbent materials.
- Develop computational methodologies for predicting hydrogen storage properties in sorbents with unsaturated metal centers.

Technical Barriers

This project addresses the following technical barriers from the Hydrogen Storage section of the Fuel Cell Technologies Office Multi-Year Research, Development, and Demonstration Plan.

General

(A) System Weight and Volume

(B) System Cost

(C) Efficiency (Refueling Time)

Reversible Solid-State Material

(O) Lack of Understanding of Hydrogen Physisorption and Chemisorption(P) Reproducibility of Performance

Technical Targets

Hydrogen Storage Materials:

This project is conducting validation studies of various framework materials, sorbents, hydrides, and model compounds. Concurrently, the team also is developing new characterization tools for the rapid enhancement of materials development. Insights gained from these studies will be applied toward the design and synthesis of hydrogen

storage materials that meet the following DOE onboard 2020 automotive hydrogen storage targets.

- 1.8 kWh/kg system (5.5 wt% hydrogen)
- 1.3 kWh/L system (0.040 kg hydrogen/L)
- Cost of $10/kWh ($333/kg H_2 stored).
- An onboard efficiency of 90% and minimum delivery pressure of 3 bar
- Total refuel time of 5 min

FY 2016 Accomplishments

- Observed and verified the binding of two hydrogen molecules to an unsaturated metal center within a metal organic framework material.
  - Established through neutron diffraction and inelastic scattering spectroscopy.
  - Developed NMR methods to validate 2 H_2/metal site in an amorphous material.
- Established control of desorption temperatures with the molecular hydrogen in model oxocarbon species by changing the metal centers for a final range from 80 K to 300 K.
- Established the ability to modify carbon sorbents with the introduction of unsaturated metal sites with overall increasing desorption temperature from 80 K to 110 K.
- Enhanced the kinetics of hydrogen interaction with borohydride materials.
  - Validated key additives to increase the rate of H_2 uptake and release in $BH_4/B_{10}H_{10}$ cycle.
  - Demonstrated the regeneration of borohydride from closo-decaborane.
- Developed a one-of-a-kind thermal conductivity apparatus that can operate from 50–380 K with gas overpressures up to 100 bar.
- Developed advanced porous aromatic framework materials with >1,000 m^2/gram surface area.
- Designed and ordered a state-of-the-art in situ infrared spectrometer for measuring spectra in H_2-dosed materials.
- Established the capacities of multiple external laboratory materials under investigation for DOE.
- Established a consensus with DOE, tech team, and international partners as to protocols for reporting volumetric capacity of sorbent materials.
- Established multiple experimental and modeling partnerships and collaborations with the HyMARC team.

✧ ✧ ✧ ✧ ✧

INTRODUCTION

The Hydrogen Storage program supports research and development of technologies to lower the cost of near-term physical storage options and longer-term material-based hydrogen storage approaches. The program conducts R&D of low-pressure, materials-based technologies and innovative approaches to increase storage potential and broaden the range of commercial applications for hydrogen. These advanced materials activities focus on development of core capabilities designed to enable the development of novel materials with the potential to store hydrogen near room temperature, at low-to-moderate pressures, and at energy densities greater than either liquid or compressed hydrogen on a systems basis. Key activities include improving the energetics, temperature, and rates of hydrogen release. Advanced concepts include high-capacity metal hydrides, chemical hydrogen storage materials, and hydrogen sorbent materials, as well as novel material synthesis processes. The overarching goal of the Fuel Cell Technologies Office Hydrogen Storage program is to develop and demonstrate viable hydrogen storage technologies for transportation, stationary, portable power, and specialty vehicle applications (e.g., material handling equipment, airport ground support equipment), with a key goal of enabling >300-mile driving range across all light-duty vehicle platforms, without reducing vehicle performance or passenger cargo space.

APPROACH

This national laboratory collaboration between NREL, PNNL and LBNL, and NIST brought together internationally recognized leaders in hydrogen storage materials characterization and development. This collaboration is predicated on a synergistic approach to further validate hydrogen storage concepts and develop the key core-capabilities necessary for accurate evaluation of hydrogen storage materials capacity, kinetics, and sorption and desorption physio-chemical processes. The overall approach involves collaborative experimental and modeling efforts. We are validating concepts and utilizing core capabilities to rapidly define, model, synthesize, and characterize the appropriate materials necessary for achieving the 2020 Hydrogen Storage goals set forth by DOE. The approach is multifaceted to mitigate risk and ensure success as we bridge the gap between physisorption and chemisorption to provide the basis for a new generation of hydrogen storage materials technologies.

Our work in FY 2016 included efforts to develop state-of-the-art characterization techniques for hydrogen storage in thermal conductivity, infrared spectroscopy and NMR spectroscopy. Through a theoretical and experimental interaction, we focused on the validation of recently provocative concepts in hydrogen storage including the possibility of multiple hydrogen molecules being adsorbed on

an unsaturated metal center within a sorbent. Is it possible to enhance the kinetics of hydride formation with additives, and how can one alter or increase the hydrogen binding energies for physisorption in non-crystalline and crystalline sorbents?

RESULTS

Concept Validation

The goal of FY 2016 was our primary go/no-go decision: determine if more than one hydrogen molecule can adsorb to an unsaturated metal center in a sorbent material (Figure 1). The most notable result was the discovery of a material that can bind two hydrogen molecules to a single metal center. This material, Mn_2(dsbdc) (dsbdc^{4-} = 2,5-disulfido-benzene-1,4-dicarboxylate), features a similar structure to the well known Mn_2(dobdc) analog, yet exhibits structural differences that result in the ability of this material to bind two H_2 molecules to a single metal center. In particular, the ligand contains sulfido groups rather than oxido groups, leading to a different geometry around the metal centers. Thus, rather than having five-coordinate metal centers with the sixth coordination site occupied by a solvent molecule, Mn_2(dsbdc) exhibits alternating four- and six-coordinate Mn^{2+} centers down the *c* axis. Two solvent molecules can be removed from the four-coordinate Mn^{2+} center, resulting in two open metal centers. Gratifyingly, D_2-dosed powder neutron diffraction studies determined that two D_2 molecules bind to this single Mn^{2+} center, as expected (Figure 2). This is the first example of two H_2 (D_2) molecules binding to a single metal center in a metal organic framework (MOF).

In our attempts to control the desorption temperature of the hydrogen from sorbents we investigated a series of oxo-carbon species with different metal centers. Since the modeling had predicted the trends for hydrogen binding energies, we investigated specifically a series of metal croconate ($C_5O_5^{2-}$) and metal-oxalate ($C_2O_4^{2-}$) species (Figure 3).

Another notable accomplishment this year has been the development of a reaction scheme to predict key intermediates in the reversible decomposition of $Mg(BH_4)_2$. The reaction scheme (Scheme 1) utilizes (i) a modification of the "BH condensation pathway," [1] to provide a rational reaction pathway for the clustering of the borane molecules,

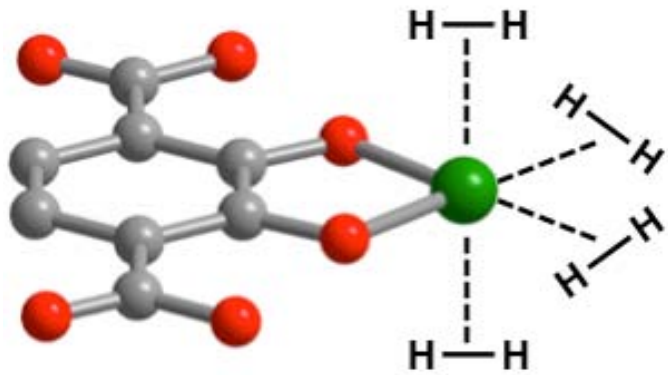

FIGURE 1. Illustration of an unsaturated metal center with multiple hydrogen molecules attached to the metal center

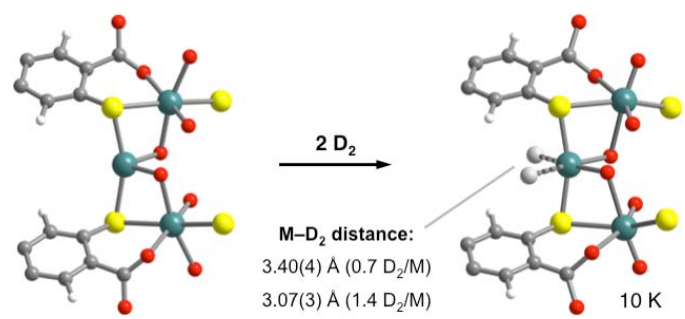

FIGURE 2. First demonstration of two H_2 molecules binding to a metal center in a metal organic framework. Mn_2(dsbdc)

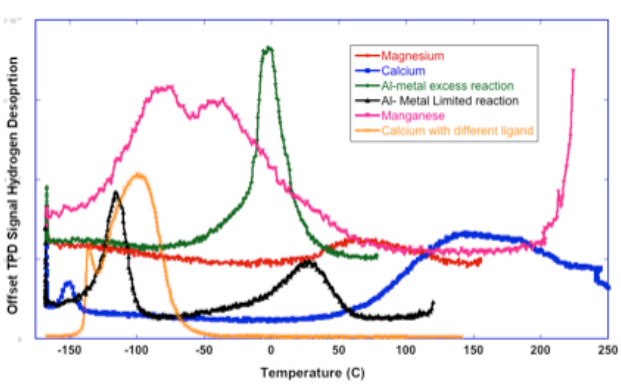

Metal/Ligand	Desorption Temperature (K)	Gravimetric capacity (1 bar) %w/w approximate
Be/mixed oxalate	150 K	<0.2%
Al/mixed oxalate	125 - 175 K (small pk 273K)	0.1 – 0.3%
Ca/mixed oxalate	150 – 225K	0.4 – 0.8%
Mg/croconate	340K	< 0.1%
Ca/Croconate	350 – 473 K	< 0.1%
Al/Croconate (a)	265 – 290 K	0.5 – 0.8%
Al/croconate (b)	140 – 170 K, 273 – 320K	0.1 – 0.3%
Mn/Croconate	200 K and 225 K (2 peaks)	0.2 – 0.4%

FIGURE 3. Left: Temperature programmed desorption (TPD) experiments for a series of M-croconate and metal-oxalate species. Samples were exposed to 1 bar hydrogen at 298 K for 10 min, quenched with liquid nitrogen, headspace evacuated to 10^{-8} torr and then heated at 10 K/min. Key observation: through experimental conditions (e.g., metal type, reagent concentrations), the hydrogen desorption temperatures were significantly affected. Right: table summarizing TPD results.

that can be formed under the reaction conditions (i.e., hydrides and H_2) and (ii) "Wades Rules" which provide a set of rules to define the connectivity of closo, nido, archno, and hypo borane clusters. Scheme 1 below shows an example of the reversible pathways linking BH_4^- to the closo-$B_{10}H_{10}$ dianion. This scheme provides a critical starting point that uses a rational explanation to predict key intermediates. This approach contrasts published literature where a great number of borane clusters have been proposed with little rationale of why they would form under the set of reaction conditions.

Another part of our effort was to model a series of metal-catecholate-based materials for the possible binding of multiple hydrogen molecules. The goal is part of our inverse design effort to determine the best unsaturated metal center for enhanced binding energies. A summary of the results is shown in Figure 4. From this effort, we are now pursing a

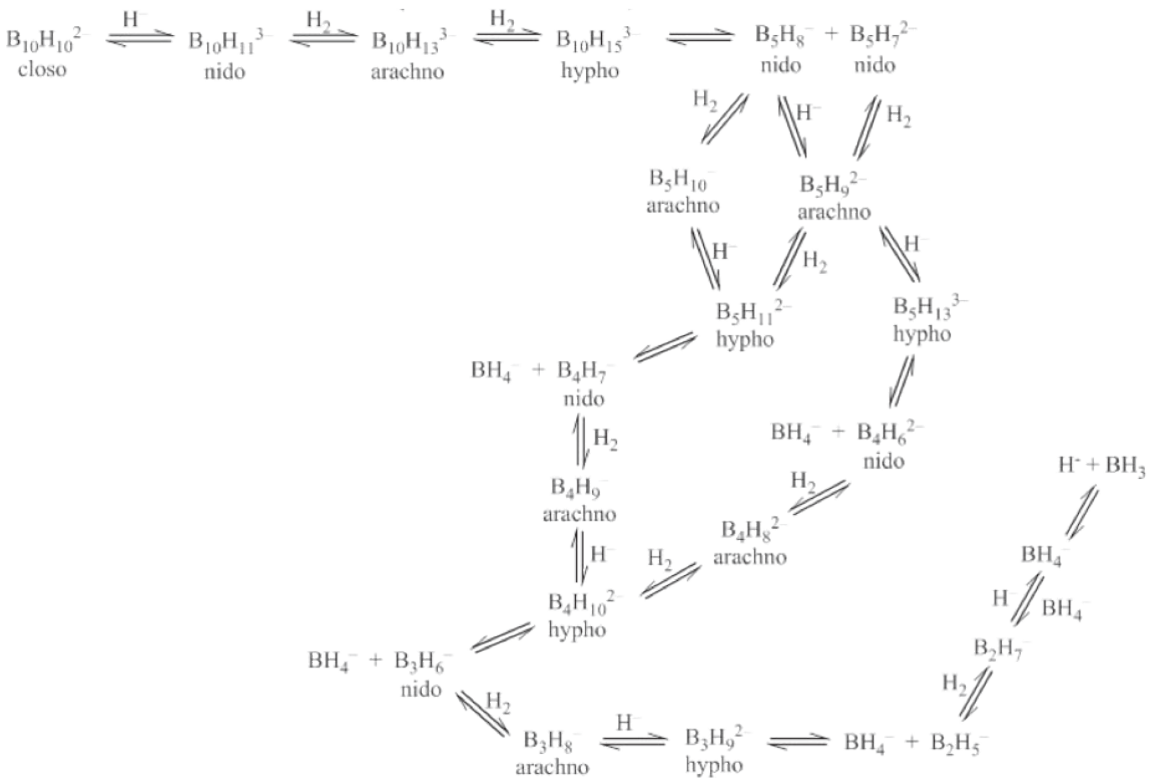

SCHEME 1. Proposed reversible reaction pathway for BH_4^- to $B_{10}H_{10}$

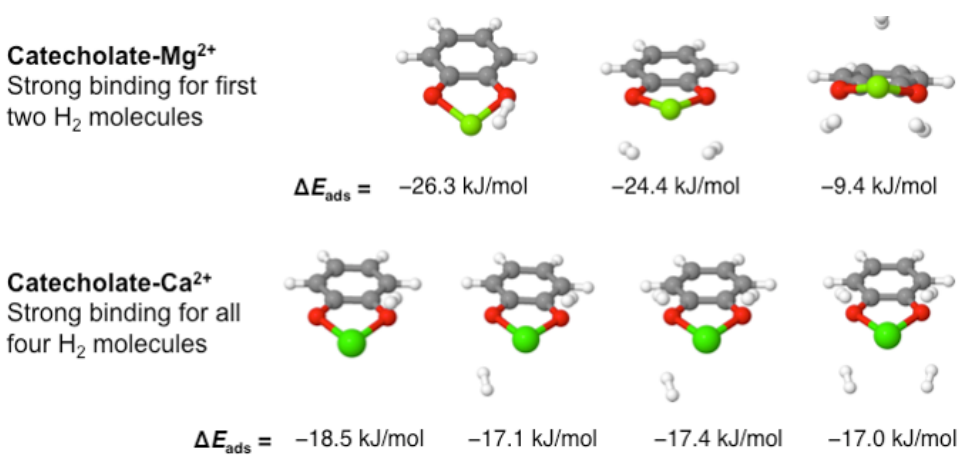

FIGURE 4. Calculated adsorption and binding energies for multiple hydrogen molecules bound to an unsaturated catecholate-M^{2+} species.

series of calcium-based framework and oxocarbon materials to test the model.

Characterization Techniques and Validation of Performance

In FY 2016 we designed and constructed a new advanced thermal conductivity apparatus capable of measuring the thermal conductivity of hydrogen storage materials under expected operating conditions. We have developed the instrument to enable measurements at temperatures from 50 to 380 K with up to 100 bar overpressure of gas. It is amenable to the evaluation of both pucks and powders. A picture of the apparatus is shown in Figure 5, and the validation of performance in Figure 6.

Another key objective in FY 2016 was to compare and contrast the results of a round-robin experiment to determine the gravimetric and volumetric capacities of two standard materials. A detailed protocol on how to degas the materials and prep them for measurement was included. A run sheet was included so all experimental conditions could be recorded and sent with the results. The round robin was initiated in December 2015, and while all the results are still not in, a sampling of the results is shown in Figure 7. We are working with all the participants and going over calculations and protocols, especially for those whose results seemed to have some systematic error. This hydrogen-storage characterization study assesses the accuracy of excess and total volumetric capacities measurements within the hydrogen storage community. Knowledge of the measurement accuracy enables meaningful comparison of the sorption capacities.

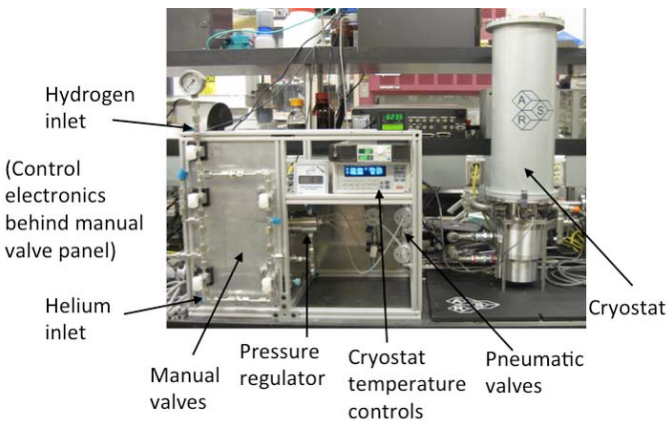

FIGURE 5. The assembled thermal conductivity apparatus for hydrogen storage materials

In FY 2016 we also have developed the engineering design for a new advanced diffuse reflectance infrared Fourier transform spectroscopy spectrometer that will be able to measure from 20–373 K with overpressures up to 100 bar. This instrument is expected to come online in FY 2017. Because of non-disclosure agreement limitations, the design and manufacturer cannot be disclosed at this time.

Finally in FY 2016 we developed a new utilization of advanced NMR spectroscopy techniques under a series of hydrogen overpressures at different temperatures and for different nuclei. One of most significant results was to be the first to measure the static solid state ^{1}H NMR spectra of H_2 physisorbed to Mg_2(*m*-dobdc) MOF. We are investigating approaches to extract T_1 relaxation data to gain insight into the binding energy of H_2 to a metal center in high surface area materials. In the next year we will develop dynamics models to fit experimental NMR data. NIST neutron (quasielastic neutron scattering and inelastic neutron scattering) and LBNL Fourier transform infrared will complement the NMR experiments. We have also calculated the Pake pattern of what should be observed for the ^{1}H

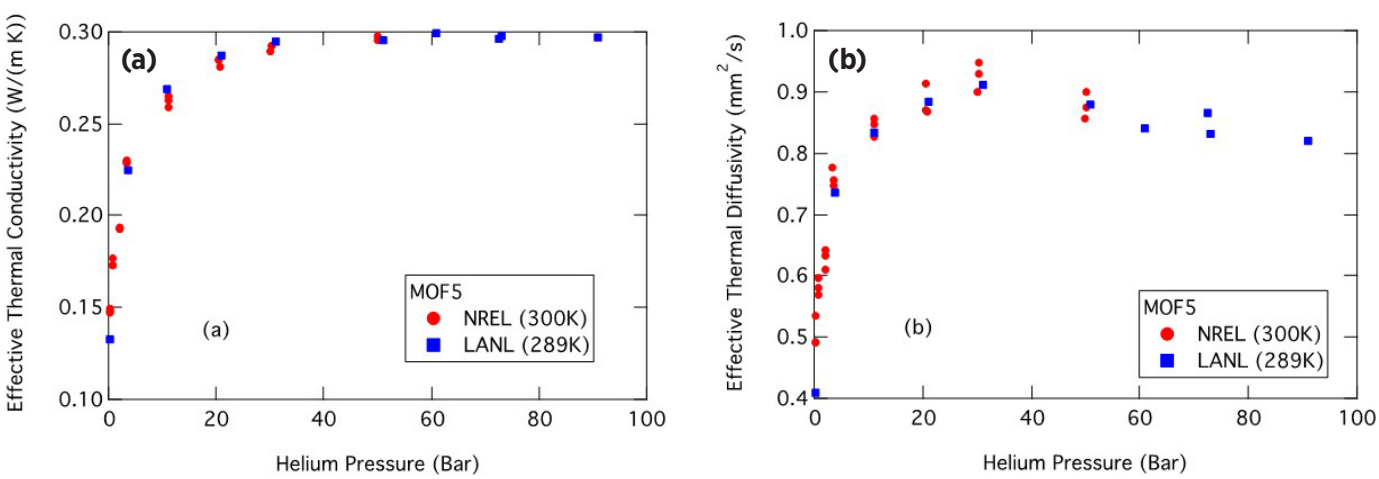

FIGURE 6. Measured thermal conductivity (a) and thermal diffusivity (b) of a MOF-5 sample in helium as a function of helium pressure. The performance was validated via a comparison to the fixed-temperature apparatus at LANL (Troy Semelsberger).

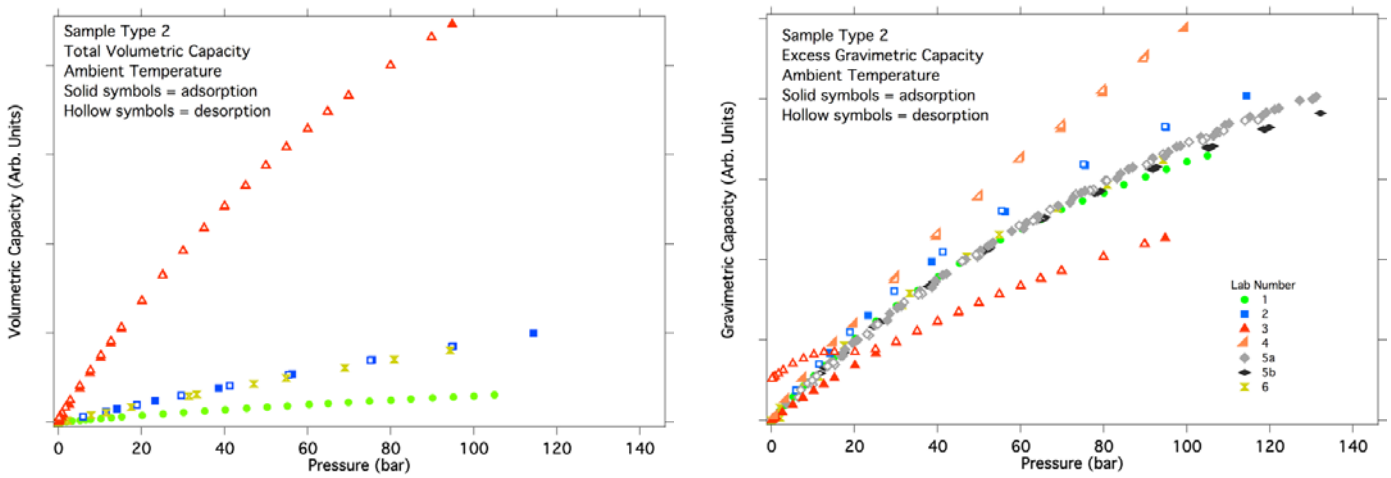

FIGURE 7. Sampling of results from the round robin. These results only represent those done at room temperature for Sample 2. We are also compiling 77 K data for both samples as well. Left: Range of the *total* volumetric capacities reported at room temperature, Right: Range of *excess* gravimetric capacity for Sample 2 at room temperature.

NMR spectra for two tightly bound hydrogen molecules per metal site.

CONCLUSIONS AND FUTURE DIRECTIONS

Our collaboration has provided us with the opportunity to validate several key aspects of hydrogen storage materials that were first reported in FY 2016. These include binding two hydrogen molecules to a metal center in a framework material (which was the Performance Evaluation and Measurement Plan milestone and go/no-go within FY 2016), controlling the binding energy by changing metal centers in model oxo-carbon species, increasing the binding energy in carbon sorbents by the introduction of catecholates and metal centers, improving the kinetics and elucidating the possible favorable pathways for the reversible hydrogenation of magnesium borohydride, validating several models or predictions of materials, developing advanced techniques that have already had a significant impact in the community, and establishing the effect of systematic error on the reported capacities of standard carbon materials. Taken together these results have established a multitude of possible solutions for advanced hydrogen storage materials, both sorbents and hydrides. Our future work will now work to continue our development of several new characterization tools in FY 2017 that will be essential to the DOE Fuel Cell Technologies Office hydrogen storage programs. We will also focus our efforts to continue to look at inverse designed materials as we strive to increase the capacity of the new genre of hydrogen sorbents and improve the reversibility kinetics of possible hydrides. Furthermore, we will also look at the validation of concepts associated with the claims that boron- and nitrogen-doped sorbents are possible materials for increased binding energies of physisorption; address the questions: (1) will the insertion of calcium into framework materials increase binding energy as predicted, and (2) is it possible to have the attachment of >2 hydrogen molecules; and finally, evaluate the application to heterolytic cleavage of hydrogen as a possible mechanism to reach the 2020 targets.

SPECIAL RECOGNITIONS & AWARDS/ PATENTS ISSUED

1. Jeff Long and Craig Brown received the DOE Fuel Cell Technologies Office Outstanding Achievement award at the June 2016 AMR meeting

FY 2016 PUBLICATIONS

1. "Hydrogen Storage in the Expanded Pore Metal-Organic Frameworks M_2(dobpdc) (M = Mg, Mn, Fe, Co, Ni, Zn)," Gygi, D.; Bloch, E.D.; Mason, J.A.; Hudson, M.R.; Gonzalez, M.I.; Siegelman, R.L.; Darwish, T.A.; Queen, W.L.; Brown, C.M.; Long, J.R. *Chem. Mater.* **2016**, *28*, 1128–1138.

2. "Adsorption of Two Gas Molecules at a Single Metal Site in a Metal-Organic Framework," Runčevski, T.; Kapelewski, M.T.; Torres-Gavosto, R.M.; Tarver, J.D.; Brown, C.M.; Long, J.R., *Chem. Commun.* **2016**, *52*, 8251–8254.

3. "Hydrogen Storage and Selective, Reversible O_2 Adsorption in a Metal-Organic Framework with Open Chromium(II) Sites," Bloch, E.D.; Queen, W.L.; Hudson, M.R.; Mason, J.A.; Xiao, D.J.; Murray, L.J.; Flacau, R.; Brown, C.M.; Long, J.R., Angew.Chem. Int.Ed. 2016, 55,8605 –8609.

4. "Olsalazine-Based Metal-Organic Frameworks as Biocompatible Platforms for H_2 Adsorption and Drug Delivery," Levine, D.J.; Runčevski, T.; Kapelewski, M.T.; Keitz, B.K.; Oktawiec, J.; Reed, D.A.; Mason, J.A.; Jiang, H.Z.H.; Colwell, K.A.; Legendre, C.; FitzGerald, S.A.; Long, J.R., *J. Am. Chem. Soc.,* 2016, 138 (32), pp 10143–10150

5. "An International Multi-Laboratory Investigation of Carbon-Based Hydrogen Sorbent Materials," Hurst, K.E.; Parilla, P.A.; O'Neill, K.J.; Gennett T. *Appl. Phys. A* **2016**, *122*, 42.

6. "Recommended Volumetric Capacity Definitions and Protocols for Accurate, Standardized and Unambiguous Metrics of Hydrogen Storage Materials," Parilla, P.A.; Gross, K.; Hurst, K.E.; Gennett, T. *Appl. Phys. A* **2016**, *122*, 201.

7. "Outlook and Challenges from Hydrogen Storage in Nanoporous Materials," Broom, D.P.; Webb, C.J.; Hurst, K.E.; Parilla, P.A.; Gennett, T.; Brown, C.M.; Zacharia, R.; Tylianakis, E.; Klontzas, E.; Froudakis, G.E.; Steriotis, Th.A.; Trikalitis, P.N.; Anton, D.L.; Hardy, B.; Tamburello, D.; Corgnale, C.; van Hassel, B.A.; Cossement, D.; Chahine, R.; Hirscher, M. *Appl. Phys. A* **2016**, *122*, 151.

8. "Dynamics of Pyramidal SiH_3 Ions in $ASiH_3$ (A = K and Rb) Investigated with Quasielastic Neutron Scattering," Österberg, C.; Fahlquist, H.; Häussermann, U.; Brown, C.M.; Udovic, T.J.; Karlsson, M. *J. Phys. Chem. C* **2016**, *120*, 6369–6376.

9. "Complex and Liquid Hydrides for Energy Storage," Callini, E.; Özlem, Z,; Atakli, K.; Hauback, B.C.; Orimo, S.; Jensen, C.; Dornheim, M.; Grant, D.; Cho, Y.W.; Chen, P.; Hjörvarsson, B.; deJongh, P.; Weidenthaler, C.; Baricco, M.; Paskevicius, M.; Jensen, T.R.; Bowden, M.E.; Autrey, T.S.; Züttel, A. *Appl. Phys. A* **2016**, *122*, 353.

10. "A Chemistry Perspective on Reversible Reaction Pathways Enabling Hydrogen Storage in Magnesium Borohydride," Edvenson, G.; Chong, M.; Autrey, T.; Jensen, C. Invited Feature Article in *Chem. Commun*.

11. "HyMARC-H_2 Core : Nanointerface-driven Reversible Hydrogen Storage in the Nanoconfined Li-N-H System," Wood, B.C.; Stavila, V.; Poonyayant, N.; Heo, T.W.; Ray, K.G.; Klebanoff, L.E.; Udovic, T.J.; Lee, J.R.I.; Angboonpong, N.; Pakawatpanurut, P, *Nature Mater.* response to reviewers submitted.

12. "Structure-Dependent Vibrational Dynamics in $Mg(BH_4)_2$ Polymorphs Probed with Neutron Vibrational Spectroscopy and First-Principles Calculations," Dimitrievska, M.; White, J.L.; Zhou, W.; Stavila, V.: Klebanoff, L.E.; Udovic, T.J. *Phys. Chem. Chem. Phys*, 2016,18, 25546-25552.

13. "Structural and Dynamical Trends in Alkali-Metal Silanides Characterized by Neutron Scattering Methods," Tang, W.S.; Dimitrievska, M.; Chotard, J.-N.; Zhou, W.; Janot, R.; Skripov, A.V.; Udovic, T.J.; *J. Phys. Chem. C, DOI: 10.1021/acs.jpcc.6b06591.*

14. "Vibrational Properties of β-$KSiH_3$ and β-$RbSiH_3$: A Combined Raman and INS Study," Mink, J.; Lin, Y-C; Karlsson, M.; Österberg, C.; Udovic, T.J. ; Fahlquist, H.; Häussermann, U.; *J. Raman Spectroscopy,* DOI 10.1002/jrs.5013.

FY 2016 PRESENTATIONS

1. *NREL Core Capabilities, a Review*, T. Gennett joint HyMARC meeting, 11/4/2015.

2. *Advances in Hydrogen Sorption: Sorbent and Hybrid Sorbent-Hydride, Characterization, and Validation*, P. Parilla, K. Hurst, M. Olsen, J. Blackburn, A. Dameron and T. Gennett at Pacific Chem. Honolulu, HI. 12/18/15

3. *Hydrogen Sorption Capacity Protocols*, K. Hurst, P. Parilla, K. Gross, and T. Gennett at the International Hydrogen and Energy Symposium Zao, Japan 2/21-16/2016.

4. *The Effect of Coordinated Metal Centers on Binding Energy in Non-Crystalline Materials*, K. Hurst, P. Parilla, M. Olsen, J. Blackburn, A. Dameron and T. Gennett at the IEA-HIA meeting, Sendai, Japan 2/27/2016.

5. *Research and Development of Advanced Hydrogen Storage Core Characterization Techniques and Materials*, Tom Gennett, Jeff Long, Craig Brown, Mark Bowden, Abhi Karkamkar, Tom Autrey at the International Hydrogen and Energy Symposium Zao, Japan 2/16-21, 2016.

6. *Hydrogen Storage Capacity Protocols K*.E. Hurst, P.A. Parilla, K. Gross, T. Gennett International Hydrogen and Energy Symposium Zao, Japan February 16–21, 2016.

7. *Variable-Pressure, Variable-Temperature Measurement of the Thermal Properties of Hydrogen Storage Materials,* Michele Olsen, Philip Parilla, Katherine Hurst, Thomas Gennett at MRS Spring Meeting, 4/1/2016.

8. *Hydrogen Storage Characterization Optimization and Research Effort, an Overview.* T. Gennett H_2ST^2 Tech Team review, 4/20/16.

9. *Hydrogen Storage Characterization and Research Optimization Effort: LBNL*, Jeff Long, Martin Head-Gordon H_2ST^2 Tech Team review, 4/20/16.

10. *Hydrogen Storage Characterization and Research Optimization Effort: PNNL*, Tom Autrey, Mark Bowden H_2ST^2 Tech Team review, 4/20/16.

11. *Hydrogen Storage Characterization and Validation Efforts*, T. Gennett, P. Parilla, J. Blackburn, A. Dameron, M. Olsen, K. Hurst, J. Tynan, S. Robbins, S. Ferrere, A. Dameron. H_2ST^2 Tech Team Review 4/20/16.

12. *Hydrogen Storage Characterization and Research Optimization Effort: NIST*, Craig Brown, Terry Udovic H_2ST^2 Tech Team Review 4/20/16.

13. *H_2 Storage Characterization and Optimization Research Effort,* Rory Andrykowski, Jeff Blackburn, Arrelaine Dameron, Mira Dimitrievska (NIST), Suzanne Ferrere, Katie Hurst, Michele Olsen, Phil Parilla, Steve Robbins, Jacob Tarver (NIST), Jerry Tynan, Tom Gennett (PI) DOE Hydrogen and Fuel Cells Program Annual Merit Review, 6/8/2016.

14. *Hydrogen Sorbent Measurement Qualification and Characterization,* Phil Parilla, Katherine Hurst, Michele Olsen, Steve Robbins, Jerry Tynan, Tom Gennett. DOE Hydrogen and Fuel Cells Program Annual Merit Review, 6/8/2016.

15. *H_2 Storage Characterization and Optimization Research Effort,* Craig Brown (NIST), Terrence Udovic (NIST), Jacob Tarver (NREL), Mirjana Dimitrievska (NREL) and Thomas Gennett (NREL). DOE Hydrogen and Fuel Cells Program Annual Merit Review, 6/8/2016.

16. *H_2 Storage Characterization and Optimization Research Effort,* Jeffrey Long, Martin Head-Gordon, DOE Hydrogen and Fuel Cells Program Annual Merit Review, 6/8/2016.

17. *H_2 Storage Characterization and Optimization Research Effort,* Tom Autrey, Mark Bowden, Abhi Karkamkar, Bojana Ginovska, Herman Cho, Marina Chong, Adrian Houghton, Gary Edvenson, DOE Hydrogen and Fuel Cells Program Annual Merit Review, 6/8/2016.

18. *Oxocarbon-Metal Microporous Channel Materials for Gas Sorption*, Thomas Gennett, Jacob Tarver, Katherine Hurst, Jeffrey R. Long, Tom Autrey, Mark Bowden and Craig Brown, 5th International Conference on Metal-Organic Frameworks and Open Framework Compounds 9/13/2016.

19. *PNNL Core NMR Capabilities and Application to Hydrogen Storage Materials Characteization,* T. Autrey, M. Bowden joint HyMARC meeting, 11/4/2015.

20. *Infrared Spectroscopy Applied to Hydrogen Storage in Metal-Organic Frameworks and Porous Polymers,* Matthew Kapelewski, Henry Jiang, Tomce Runcevski, Gokhan Barin, Mercedes Taylor, Ehud Tsivion, Martin Head-Gordon, Jeffrey Long joint HyMARC meeting, 11/4/2015.

21. *Structural and Dynamical Trends in Alkali-Metal Silanides Characterized by Neutron Scattering Methods*, Pacifichem 2015, Honolulu, HI, T.J. Udovic, December 18, 2015.

22. *NIST Center for Neutron Research an Overview of Capabilities*, C. Brown, T. Udovic joint HyMARC meeting, 11/4/2015.

23. *H_2 Storage on Open Metal Coordination Sites–Best Performance in Ni_2(m-dobdc) and Two H_2 Molecules on One Metal in Mn_2(dsbdc)***,** Matthew T. Kapelewski, Tomče Runčevski, Henry Z. Jiang, Katherine E. Hurst, Thomas Gennett, Stephen A. FitzGerald, Craig M. Brown, and Jeffrey R. Long. 5th International Conference on Metal-Organic Frameworks & Open Framework Compounds (MOF 2016). Long Beach, CA, 9/15/2016.

REFERENCES

1. E.L. Muetterties and W.H. Knoth, "Polyhedral Boranes," Marcel Dekker, Inc, New York, 1968. Chpt 5 Synthesis of polyhedral boranes.

IV.C.8 Design and Synthesis of Materials with High Capacities for Hydrogen Physisorption

Brent Fultz (Primary Contact), Channing Ahn, Ted Baumann*, R.C. Bowman, David Boyd, Hillary Smith, Nick Weadock
California Institute of Technology
1200 E. California Blvd.
Pasadena, CA 91125
Phone: (626) 395-2170
Email: btf@caltech.edu
*Lawrence Livermore National Laboratory
7000 East Ave.
Livermore, CA 94550

DOE Manager: Jesse Adams
Phone: (720) 356-1421
Email: Jesse.Adams@ee.doe.gov

Contract Number: DE-EE0007048

Project Start Date: August 1, 2015
Project End Date: July 31, 2018

Overall Objectives

- Develop a carbon-based, functionalized material prepared with new substrates (graphene) or old (exfoliated graphite) to maximize capacity for hydrogen physisorption at moderate temperatures.
- Understand how far hydrogen physisorption can extend beyond present capabilities with carbon materials.
- Demonstrate a near-constant isosteric heat of adsorption, excellent kinetics, and long cycle life.

Fiscal Year (FY) 2016 Objectives

- Develop Sieverts method for rapid screening of materials that is comparable to full isotherms at 77 K and 87 K for agreement to within 5%.
- Demonstrate functionalization of graphene with metal clusters <1 nm.
- Synthesize graphene and demonstrate retention of 80% of as-prepared surface area after compression to bulk density of 0.5 to 0.7 gm/cc.
- Meet or exceed present capabilities of carbon sorbents before functionalization.

Technical Barriers

This project addresses the following technical barriers from the Hydrogen Storage section of the Fuel Cell Technologies Office Multi-Year Research, Development, and Demonstration Plan:

(A) System Weight and Volume

(C) Efficiency

(O) Lack of Understanding of Hydrogen Physisorption and Chemisorption

Technical Targets

This project is developing functionalized graphene materials to maximize hydrogen uptake and increase temperatures of operation with the goal to meet the DOE hydrogen storage capacity targets.

- System gravimetric capacity: 1.8 kWh/kg
- System volumetric capacity: 1.3 kWh/L

FY 2016 Accomplishments

- Prepared graphene oxide, microwave exfoliated graphene oxide (meGO), and as-activated graphene at Caltech, achieving a Brunauer–Emmett–Teller (BET) specific surface area of 2,640 m^2/g, close to the theoretical value of 2,630 m^2/g for a single graphene sheet.
- Improved density of as-activated graphene from a tap density of <0.33 g/cc to 0.59 g/cc while retaining 80% of the initial surface area.
- Demonstrated functionalization of graphene with Au and Cu clusters <1 nm in diameter.
- Developed a rapid turnaround Sieverts method for screening materials without the need to collect full isotherms.

✧ ✧ ✧ ✧ ✧

INTRODUCTION

One of the advantages of adsorbents as a storage medium is that dihydrogen retains its molecular form throughout the adsorption/desorption cycle and the cycle requires minimal activation energy. The primary disadvantage of sorbents is that typical adsorption enthalpies are relatively weak, compared to bond formation with chemical hydrogen, or to interstitial atomic hydrogen in metal hydrides. Additionally, the van der Waals dimension of molecular hydrogen is large

in comparison to atomic hydrogen, putting limits on the overall volumetric density that systems based on dihydrogen can achieve.

Graphene-based materials offer an excellent starting platform for hydrogen sorption owing to their high surface area for dihydrogen adsorption. The key step is to optimize functional groups on the graphene for maximizing the volumetric density of dihydrogen sorption. Part of the effort at Caltech is directed toward this optimization. While prior work in the area of physisorbents has illustrated the importance of high surface area in achieving gravimetric uptakes of relevance to the program, volumetric densities have recently been recognized as a critical metric. Under many conditions, the nature of the adsorption process can still offer volumetric density advantages over the use of compressed gas storage, although not as high as intermetallic hydride densities. For dihydrogen that adsorbs onto a substrate, the London dispersion forces, regarded as transient dipoles in polarizable substances, are a major contributor to physisorption processes, and we are designing materials to optimize them.

Previous work at Caltech has shown that intercalated graphites, which have pore dimensions similar to the graphene geometries we seek, can result in constant isosteric enthalpies of adsorption. These specialized structures had the advantage of electron back donation from the alkali metal to the graphitic planes, but these observations motivate the addition of substituted metal atoms in the graphene or on graphene surfaces. These local centers could increase both the isosteric heat of adsorption, and increase the number of active sites for dihydrogen adsorption. We also note that for hydrogen on metal surfaces, adsorption and desorption typically occurs above room temperature.

APPROACH

The focus of this project is to functionalize newly developed graphene materials to maximize hydrogen uptake. Specific key goals are to attain a high volumetric density of hydrogen, a near-constant heat of adsorption, rapid kinetics for adsorption and desorption, and long cycle life. The materials will rely on physisorption of hydrogen onto surfaces, or into internal pores. Given that metal centers have proved successful for increasing the local hydrogen density in other materials such as coordination polymer structures, we plan to alter surfaces or incorporate chemical center substituents to increase the strength of the dispersion forces.

RESULTS

Efforts for the first phase of this project occurred in three primary areas: (1) synthesis of graphene and graphene oxide materials, (2) functionalization of graphene with metal nanoclusters, and (3) hydrogen adsorption measurements.

Synthesis efforts have yielded bulk quantities (>1 g) of high purity graphine oxide and meGO as characterized with scanning electron microscopy (SEM), transmission electron microscopy (TEM), Raman, and BET. An activation route employed to modify the meGO resulted in as-activated graphene with a BET specific surface area of 2,640 m^2/g. This surface area is within 5% of the theoretical surface for graphene of 2,630 m^2/g, and represents a 15X increase in surface area over meGO. The complex, three-dimensional framework of the as-activated graphene is seen in the SEM image in Figure 1. The vast improvement in the surface area as determined with nitrogen BET is shown in Figure 2 where the meGO (green curve) has a surface area of 167 m^2/g while the activated meGO (black curve) reaches 2,640 m^2/g. These results position us to achieve second phase milestones including scale-up of the synthetic process to 300 mg quantities and measure changes in specific surface area and hydrogen adsorption capacity resulting from plasma etching.

Maximization of volumetric density is now recognized as a key metric in gauging the merits of an adsorbent. Unlike

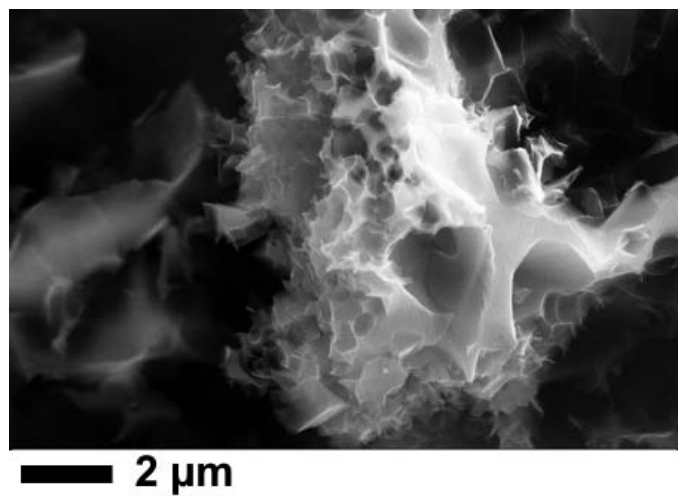

FIGURE 1. Morphology of the high surface area, as-activated graphene material imaged with SEM

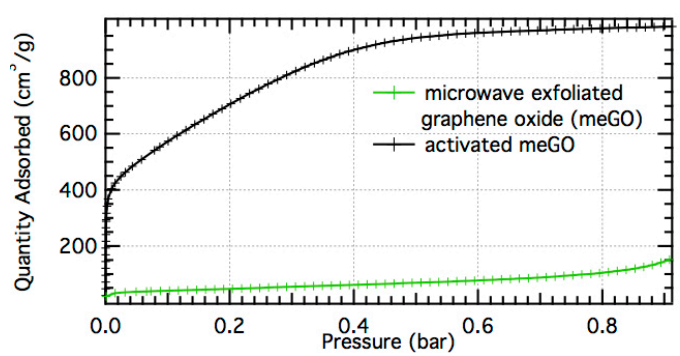

FIGURE 2. Comparison of the N_2 adsorption of the meGO and as-activated graphene shows a 15X increase in surface area

three-dimensional structures, two-dimensional graphene can withstand mechanical compression in a way that can preserve a substantial fraction of the surface area without loss due to the collapse of a "framework." We have successfully achieved our initial target to attain properties similar to that of a polyether ether ketone-based activated carbon. We have completed compression studies on as-activated graphene and MSC-30, compressing these materials to densities of 0.5 g/cc and 0.59 g/cc, respectively. As shown in Figure 3, the materials retained 85% and 80% of their BET specific surface areas, respectively. We note that 0.5–0.7 g/cc in an idealized structure would correspond to the removal of two or three planes of graphite in a graphitic structure and would provide the appropriate configuration to maximize the volumetric density of hydrogen consistent with retaining a practical gravimetric density. BET surface area analysis also revealed that in both materials, meso- and macro-pore surface areas were lost during compression, resulting in the overall loss of surface area, but micro-pore surfaces and micro-pore volume have increased from what were originally meso- and macro-pore volumes.

Our preliminary volumetric analyses, absent a full-scale engineering analysis that would include the storage tank and associated balance of plant components, indicates that we met our year one decision criteria. These criteria required meeting or exceeding present capabilities of carbons sorbents with 35 g/L total adsorption at 77 K and pressure <100 bar. Initial analysis of our as-activated graphene indicates we can achieve 35 g/L at 77 K and 84 bar. The assumptions made in this calculation are outlined in our 2016 go/no-go report to DOE.

Functionalization of the graphene and graphene-based carbons is at the core of our plan to reach DOE hydrogen storage targets for high volumetric density of hydrogen. We plan to incorporate metal substituents to increase the strength of the dispersion forces. In the first phase of the project, we demonstrated the deposition of Au and Cu metal nanoclusters <1 nm by both chemical and plasma deposition routes. Figure 4 shows a dark field TEM image of Cu nanoclusters on graphene. The chemical route used to deposit the Cu

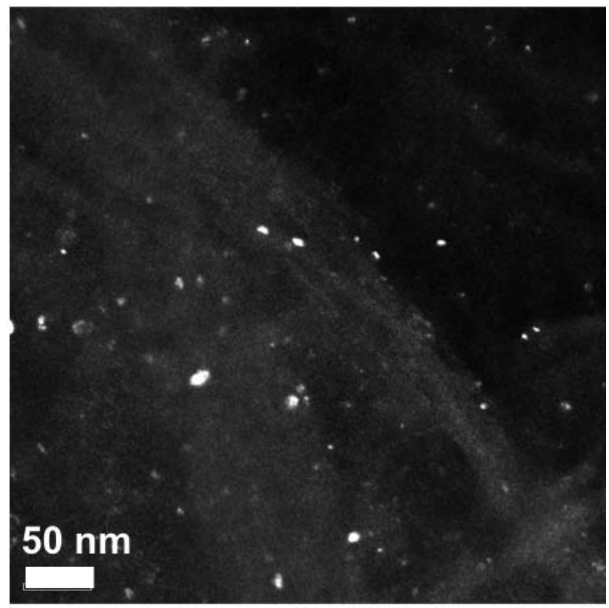

FIGURE 4. TEM dark field image of graphene functionalized with Cu nanoclusters (appearing in bright white regions)

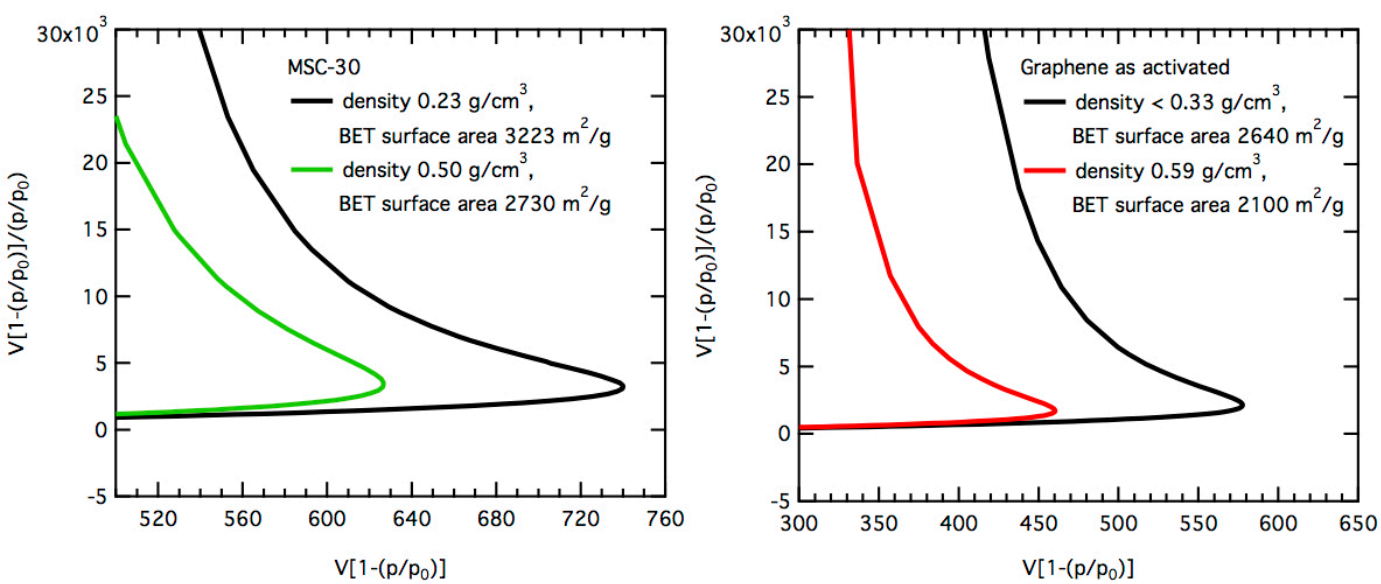

FIGURE 3. Compression tests on two materials demonstrate retention of >80% of initial BET surface area after densification

particles, which appear white in the image, produced some large clusters but a majority <1 nm, as evidenced from the small white dots. These results position us to achieve our second phase milestone of depositing sub-nanometer clusters of metal atoms onto carbon materials while reducing surface area by <10%, improving average isosteric heat, and achieving ≥1.3 wt% excess H_2 per 500 m^2/g of material.

Hydrogen adsorption measurements using the Sieverts method are critical to characterization of the materials we develop. The long turnaround time for collection of full isotherms was identified as a potential bottleneck in our development and assessment of new materials, and the first phase of the project included milestones to mitigate this problem. A second Sieverts apparatus on long-term loan from Jet Propulsion Laboratory was installed in new lab space and is now fully commissioned. A "Rapid Sieverts" screening method was developed to obtain key data in shorter times by measuring a single data point at 77 K and 20 bar. This decreases data acquisition time by a factor of three, and provides the means to quickly assess whether full isotherm data should be collected. We tested this approach by comparing the Rapid Sieverts method to full multipoint isotherm data on several samples and the agreement is excellent. Hydrogen adsorption measurements plays a key role in the second phase of the project, and these first phase achievements position us to achieve goals for characterization of materials developed in phase two.

CONCLUSIONS AND FUTURE DIRECTIONS

Although the project is still in early stages, several conclusions can be drawn.

- Graphene can be functionalized with small metal clusters with sizes below 1 nm, validating the proposed approach to measure hydrogen adsorption after introduction of these sites.
- High-surface area graphene-based materials have been synthesized and compressed to 0.59 g/cc, retaining >80% of original surface area and achieving an estimated 35 g/L at 77 K and 84 bar.
- Methods for rapid hydrogen adsorption analysis were developed to reduce the time required for a detailed work-up.

Goals for work in the second phase of the project are:

- Scale-up of synthetic processes to 300 mg quantities with gravimetric and volumetric capacities within 5% of the performance observed in small batch material.
- Use of oxygen plasma etching to induce 1–2 nm pores in graphene sheet structures and demonstrate >10% increase in BET surface area and to sorption properties.
- Deposition of sub-nanometer clusters of metal atoms onto carbon materials while reducing surface area by <10%.
- Improvement of average isosteric heat and ≥1.3 wt% excess H_2 per 500 m^2/g in material with >3,000 m^2/g surface area and 35 g/L total volumetric capacity at pressures less than 100 bar and 77 K.

IV.C.9 High-Capacity and Low-Cost Hydrogen-Storage Sorbents for Automotive Applications

Joe Zhou (Primary Contact), Di-Jia Liu, Zachary Perry
Texas A&M University
PO Box 30012
College Station, TX 77842
Phone: (979) 845-4034
Email: Zhou@chem.tamu.edu

DOE Manager: Jesse Adams
Phone: (720) 356-1421
Email: Jesse.Adams@ee.doe.gov

Subcontractor:
Argonne National Laboratory, Lemont, IL

Project Start Date: August 1, 2015
Project End Date: July 31, 2018

Overall Objectives

- Produce materials capable of meeting or exceeding DOE's 2020 performance target of gravimetric capacity of 0.055 kg H_2/kg$_{\text{—system}}$, volumetric capacity of 0.040 kg H_2/L$_{\text{—system}}$ at a cost of \$333/kg_$H_{2\ \text{stored}}$.
- Study the effects of post-synthetic addition of metals to induce higher hydrogen binding affinities.
- Show that such materials are stable under the conditions expected of hydrogen sorbents.
- Show that these materials have appropriate sorption kinetics to quickly load and deliver hydrogen.

Fiscal Year (FY) 2016 Objectives

- Reproduce preliminary results of porous coordination network (PCN)-250 excess uptake of 6.75 wt%.
- Year 1 Go/No-Go: demonstrate an sorbent material with at least a reversible 1.5 wt% excess hydrogen per 500 m^2/g (1.5X greater than Chahine's rule) with at least 2,000 m^2/g specific surface area and 60 g/L total volumetric capacity (assuming single crystal density) at pressures less than or equal to 100 bar and 77 K. In addition, demonstrate repeatable activation procedures which result in some quantitative, known level of desolvation and no metal-bound water generation as validated by an independent lab directed by DOE.
- Show through advanced X-ray characterization the desolvation of open metal sites.

Technical Barriers

This project addresses the following technical barriers from the Hydrogen Storage section of the Fuel Cell Technologies Office Multi-Year Research, Development, and Demonstration Plan.

(A) System Weight and Volume

(O) Lack of Understanding of Hydrogen Chemisorption and Physisorption

(J) Thermal Management

Technical Targets

Metal-Organic Frameworks with Enhanced Hydrogen Storage: This project is generating materials for the express purpose of storing hydrogen in vehicular systems. The materials are targeted toward the project's end reach values which would allow them to be incorporated into systems meeting the DOE system targets.

- Excess gravimetric H_2 uptake:
  - Project Target: 10 wt% excess material basis
  - DOE 2020 Target: 5.5 wt% system basis
- Volumetric H_2 uptake:
  - Project Target: 0.055 kg H_2/L of material (total)
  - DOE 2020: Target 0.040 kg H_2/L of system
- Cost per kg/H_2 stored DOE 2020 Target: \$333/kg_$H_{2\ \text{stored}}$
- Increase material capacity and heat of adsorption >10% via post-synthetic modification

FY 2016 Accomplishments

- Observed that Fe_3O cluster based materials show changes indicating desolvation and possible reduction at temperatures above 150°C.
- Several new metal organic frameworks (MOFs) generated which show potential for increased capacity.

✧ ✧ ✧ ✧ ✧

INTRODUCTION

Hydrogen storage technology is critical for next generation energy conversion devices such as proton exchange membrane fuel cells. Further interest in the direct

use of hydrogen as a fuel source is driving a significant amount of research to find more efficient ways of storing and transporting hydrogen for consumer use. To be practical for transportation applications, the storage system should reach gravimetric capacity of 0.055 kg H_2/kg$_{\text{system}}$, volumetric capacity of 0.040 kg H_2/L$_{\text{system}}$ at a cost of \$333/kg_H_2 stored according to the performance targets set by DOE for 2020. No current technology meets all of these goals. Compared with chemical or metal hydride based approaches, sorption based technology has the advantages of (a) low parasitic energy consumption for desorption, (b) fast kinetics for storage and delivery, and (c) light material for high gravimetric and reasonable volumetric storage capacity. The main challenge, however, is its limited capacity even under low temperature, high pressure conditions. In general, the H_2 uptake by sorbents at liquid N_2 temperature follows the so called Chahine's rule, i.e., the excess gravimetric capacity increases proportionally at the rate of 1 wt% for every 500 m^2/g Brunauer-Emmett-Teller (BET) specific surface area (SSA). This is calculated based on the surface area required for an arrangement of non-interacting hydrogen atoms on a flat surface. Excessive increase of SSA, however, leads to the reduction of sorbent's density therefore reducing the volumetric storage capacity. Studies show that the volumetric capacity peaks near the BET SSA of 3,000 m^2/g, suggesting a ceiling of 6 wt% gravimetric capacity if the sorbent follows Chahine's rule strictly. To achieve DOE's 2020 gravimetric and volumetric capacity goals simultaneously, the new adsorbent must exceed this limitation. To reach these goals metal-organic frameworks are being pursued as high surface area and low density sorbents.

APPROACH

This project is a collaborative effort between Texas A&M University and Argonne National Laboratory in developing low-cost and high-capacity hydrogen-storage sorbents with appropriate stability, sorption kinetics, and thermal conductivity. The objective of this three-year project is to produce hydrogen storage materials that meet or exceed DOE's 2020 performance target. The proposal adopts approaches of rational design, novel synthesis, and engineering development of new sorbents, supported by studies of storage capacity, kinetics, and H_2–sorbent interaction using advanced characterization techniques. The proposed activities focus on the preparation of sorbents with improved hydrogen binding and the uptake capacity that surpasses the conventional cryogenic storage limit. The focus of these studies involves generating materials with uncoordinated metal sites and geometric features which increase the ability for the materials to adsorb hydrogen. This involves both initial material design to include such uncoordinated metal sites as well as post synthetic modification through atomic layer deposition to achieve increased binding site density.

RESULTS

The initial goal of reproducing the previously reported hydrogen capacity of PCN-250 was the primary focus at the outset of the program. Initial difficulties resulted in the use of PCN-250(Fe) rather than PCN-250(Co) to ensure homogeneity within the samples. For the mixed metal species it is possible that all iron clusters could be present in the samples. However as shown in Figure 1, the validation test performed by National Renewable Energy Laboratory gave a value of 4.85 wt%, which was well below that previously measured for the Fe_2CoO based cluster [1]. The measured surface area of the material of 1,750 m^2/g predicts a value of 3.5 wt% excess based on Chahine's rule. Thus this material still exceeded the expected excess gravimetric capacity by 50%, indicating that there are still structural features in PCN-250 which provide advantageous hydrogen sorption. Several of these materials show gravimetric excess uptakes of >2 wt% at 1 bar and 77 K. These are undergoing synthesis for high-pressure measurements. However, by generating structures which retain pore shape and volume similar to PCN-250 while also increasing the pore size slightly, it is hypothesized that the overall capacity of these materials can be increased. MOFs with significantly larger pores yielded low hydrogen excess uptake values and would likely give exceedingly low volumetric values. A zirconium system, which at present has below the Quarter 3 target of 1,500 m^2/g with a BET SSA of 1,359 m^2/g, shows excess gravimetric uptake of ~2.2 wt% and volumetric uptake of 25.8 g/L at 77 K and 1 bar. At high pressure we expect it to exceed 2.7 wt% (based on Chahine's rule) and it may have a high volumetric uptake as well. The ligands shown in Figure 2 are of the most current interest (Figure 2a is the ligand for PCN-250, Figure 2b and Figure 2d are pyrazolate and triazolate ligands respectively, which provide a different connectivity giving us access to different pore profiles, and Figure 2c being the ligand for the new zirconium system).

In situ X-ray absorption spectroscopy experiments were conducted by the Argonne National Laboratory team for three MOF samples received from Texas A&M including: PCN-250-Fe_3, PCN-250-Fe_2Co and PCN-250-Fe_2Ni. For this experiment, we designed an in situ reactor consisting of a quartz tube flow reactor and a stainless steel sample holder. X-ray absorption near edge structure (XANES) and extended X-ray absorption fine structure spectroscopic data near Fe K-edge (7.1109 KeV) were taken continuously as the temperature increased to record the oxidation state and coordination structural changes. Figure 3a shows the change of iron XANES spectra of PCN-250-Fe_3 during the thermal activation. A common feature among all the spectra is the presence of dominant white line peak near 7,125 eV for the as-prepared samples which indicates a higher oxidation state induced by the binding of oxygenate functional group from solvent. With the increase of temperature, the white line peak in PCN-250-Fe_3 gradually reduces its intensity with

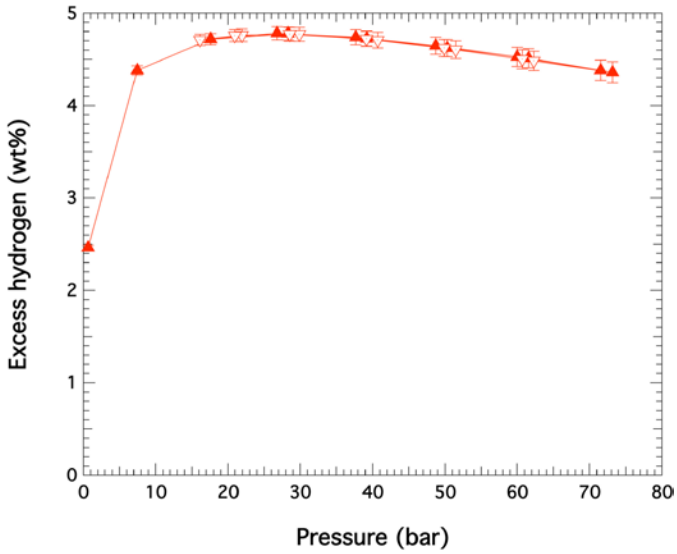

FIGURE 1. High-pressure H_2 isotherm at 77 K measured by National Renewable Energy Laboratory

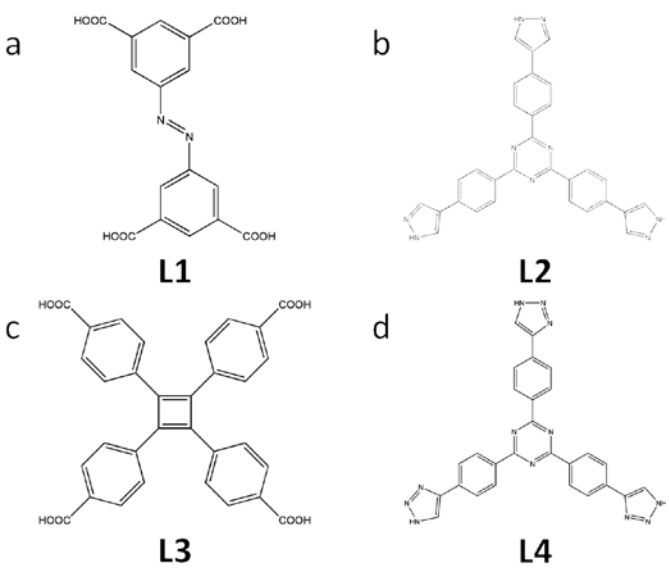

FIGURE 2. Ligands of high interest for increased H_2 sorption

the process accelerated between 150°C to 180°C. Figure 3b shows the radial distribution function derived from the extended X-ray absorption fine structure spectra taken at selected temperatures. Radial distribution function can be interpreted as the "shells" of atoms surrounding to the center Fe atom.

CONCLUSIONS AND FUTURE DIRECTIONS

Based on the uptake measurements for PCN-250, hydrogen adsorption saturates at ~28 bar meaning that no improvement in hydrogen capacity is achieved after this

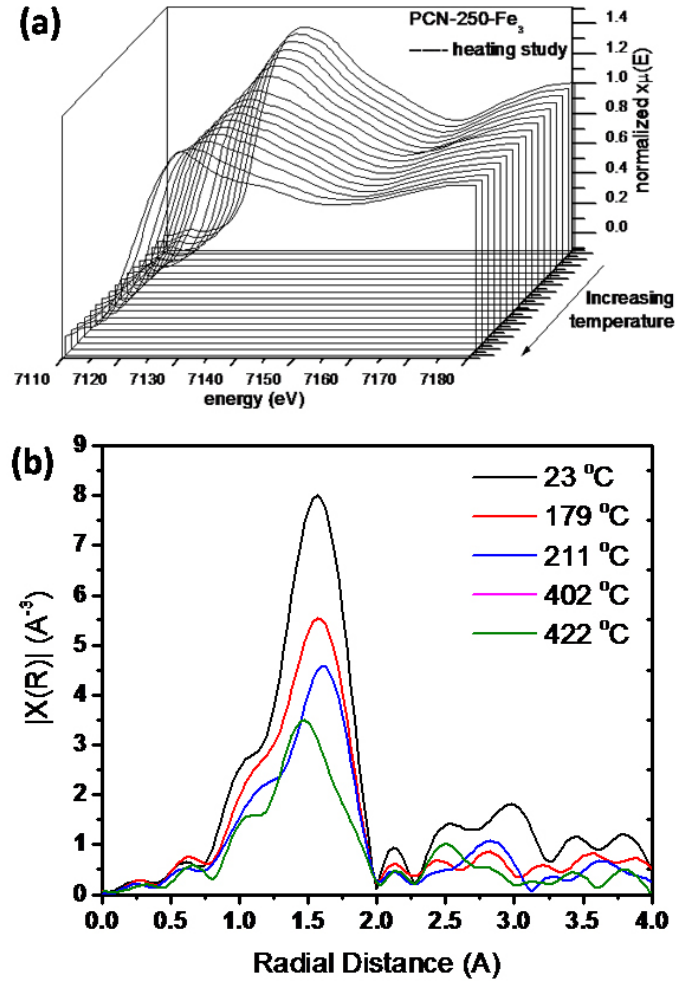

FIGURE 3. XANES progression during heating (a) and radial distribution function of Fe-O distances (b)

point. This indicates that the pore volume is likely filled meaning that a material with larger pores will be necessary to meet the DOE's goals. As a result of the lower than expected performance of PCN-250, new materials were tested at sub-ambient pressures. Further, based on the initial X-ray studies, the metal choice, solvent exchange, and desolvation criteria as observed for the M_3O cluster based materials must be carefully controlled to fully activate the materials and avoid decomposing them. The application of atomic layer deposition in Year 2 to increase the content of uncoordinated metal sites in the materials will be investigated as a way to compensate for the typical disadvantages of larger pores such as poor volumetric capacity by increasing the materials' affinity for hydrogen. The zirconium system shows promise and though it does not meet our current targets, it may provide a structural avenue towards creating MOFs with more favorable hydrogen affinities. If we can achieve a structural analogue using a first row transition metal, the performance should increase on a gravimetric basis and may meet the project goals.

REFERENCES

1. Feng, et al., "Kinetically tuned dimensional augmentation as a versatile synthetic route towards robust metal–organic frameworks," *Nature Communications* 5, 5723. 2014.

IV.C.10 Hydrogen Adsorbents with High Volumetric Density: New Materials and System Projections

Donald J. Siegel (Primary Contact, UM), Alauddin Ahmed (UM), Yiyang Liu (UM), Adam Matzger (UM), Justin Purewal (Ford), Anuska Shresth (UM), Mike Veenstra (Ford), and Antek Wong-Foy (UM)
University of Michigan (UM)
Ann Arbor, MI 48109
Phone: (734) 764-4808
Email: djsiege@umich.edu

DOE Manager: Jesse Adams
Phone: (720) 356-1421
Email: Jesse.Adams@ee.doe.gov

Contract Number: DE-EE0007046

Subcontractor:
Ford Motor Company, Dearborn, MI

Project Start Date: August 1, 2015
Project End Date: July 31, 2018

Overall Objectives

- Demonstrate metal-organic frameworks (MOFs) that exhibit high volumetric and gravimetric hydrogen densities simultaneously, and that exceed the performance of the benchmark adsorbent, MOF-5, at cryogenic conditions.
- Project the performance of most promising compounds to the system level by parameterizing models developed by the Hydrogen Storage Engineering Center of Excellence (HSECoE).

Fiscal Year (FY) 2016 Objectives

- Quantify the usable and total hydrogen capacity of the benchmark adsorbent, MOF-5.
- Drawing from established MOF crystal structure databases, predict the hydrogen capacity of several thousand candidate MOFs computationally.
- Demonstrate experimentally at least one MOF with >90% of the projected surface area, >3,000 m^2/g, and with a hydrogen capacity at least matching the MOF-5 baseline compound.

Technical Barriers

This project addresses the following technical barriers from the Hydrogen Storage section of the Fuel Cell Technologies Office Multi-Year Research, Development, and Demonstration Plan.

(A) System Weight and Volume

(B) System Cost

(C) Efficiency

Technical Targets

The outcomes of this project contribute to the optimization and assessment of hydrogen storage materials, and also provide input to models that project the performance of these materials at the system level. Insights gained from this study can be applied towards the development of materials that attempt to meet the DOE 2020 and ultimate hydrogen storage targets, which are summarized in Table 1. The ultimate success of this project rests upon developing MOFs that out-perform the baseline MOF-5 adsorbent. Therefore, Table 1 also summarizes the materials-level hydrogen capacity of single-crystal MOF-5 and compares against the best adsorbent identified by this project to-date, isoreticular metal organic framework (IRMOF)-20.

FY 2016 Accomplishments

- Characterized the hydrogen capacity of the benchmark adsorbent MOF-5 (on a usable and total basis) by performing air-free synthesis and hydrogen isotherm measurements.

TABLE 1. System-Level Technical Targets Compared to Materials-Level Performance of the Baseline MOF-5 Adsorbent and the Highest-Performing MOF Identified by this Project To-Date, IRMOF-20. Total capacities are reported at 77 K and 100 bar. Usable capacities are determined assuming an isothermal pressure swing at 77 K between 100 bar and 5 bar. All materials-level capacities are based on single-crystal densities.

Storage Parameter	Units	DOE 2020 Target (System Level, Usable)	DOE Ultimate Target (System Level, Usable)	MOF-5 Baseline (Materials Level, Total/Usable)	Project Status: IRMOF-20 (Materials Level, Total/Usable)
Gravimetric Capacity	wt%	5.5	7.5	8.0/4.5	9.3/5.7
Volumetric Capacity	$g{\cdot}H_2/L$	40	70	53/31	52/33

- Screened more than 2,000 known MOFs using Grand Canonical Monte Carlo and semi-empirical computational methods; identified several promising compounds.
- Synthesized and characterized seven candidate MOFs.
- Demonstrated IRMOF-20 as capable of surpassing the usable capacity of MOF-5.

INTRODUCTION

A high-capacity, low-cost method for storing hydrogen remains one of the primary barriers to the widespread commercialization of fuel cell vehicles. Although many storage technologies have been proposed, storage via adsorption remains one of the more promising approaches due to its fast kinetics, facile reversibility, and high gravimetric densities. Adsorbents struggle, however, in two key measures: volumetric density and operating temperature. For example, it is well known that high surface area adsorbents such as MOFs can achieve high gravimetric densities. Nevertheless, high volumetric densities are uncommon in these materials, and it has recently been suggested that total volumetric density and gravimetric density are inversely related beyond a threshold surface area [1]. In the case of operating temperatures, the relatively weak enthalpy of H_2 adsorption implies that high hydrogen densities are possible only at cryogenic temperatures.

Although an ideal adsorbent would overcome both of these shortcomings, it is important to recognize that volumetric density and operating temperature are controlled by different factors: the former depends upon the adsorbent's *structure*, whereas the latter depends on the *chemistry* of the H_2-adsorbent bond. Therefore, distinct approaches are needed to address these independent issues. While some effort has previously been devoted to increasing DH (e.g., MOFs with open metal sites), attempts to increase volumetric densities have received much less attention. This is unfortunate, as analysis by the HSECoE has indicated that vehicle range is highly sensitive to volumetric density. Consequently, the development of adsorbents that simultaneously achieve high volumetric and gravimetric hydrogen densities – while maintaining reversibility and fast kinetics – would constitute a significant advance. Moreover, these materials would serve as logical starting points for follow-on efforts aimed at increasing the operating temperature.

APPROACH

This project aims to circumvent the tradeoff between total volumetric and gravimetric hydrogen densities typical of most hydrogen adsorbents. This will be accomplished by combining computational screening for promising compounds with experimental synthesis and measurement of hydrogen storage densities within those compounds. The ultimate goal is to demonstrate materials having balanced gravimetric and volumetric performance that can surpass the storage density of the benchmark compound, MOF-5. The performance of the most promising compounds will be projected to the system level by parameterizing system models developed by the HSECoE.

RESULTS

As described above, a major milestone for this effort is to demonstrate MOFs whose hydrogen density surpasses that of MOF-5 in its optimal or "pristine" form (i.e., MOF-5 which has not been exposed to air, and from which all solvents and reactants have been removed). Synthesis efforts following the air-free procedure described by Kaye et al. [2] were performed to establish unambiguously the usable capacity of pristine MOF-5. Modifications to this protocol were also explored; nevertheless, the resulting materials performed identically. The surface area of the as-synthesized material, 3,512 m^2/g, was found to be in very good agreement with our calculated value, 3,563 m^2/g.

Figure 1 presents a comparison of the H_2 isotherms for as-synthesized MOF-5 and pre-commercial MOF-5 supplied by BASF. These measurements revealed that hydrogen uptake is essentially identical in both compounds. Table 2 tabulates the measured usable and total uptake in as-synthesized MOF-5 as a function of pressure. Assuming isothermal (T = 77 K) pressure swing operation between 100 bar and 5 bar, the usable capacity was measured to be 31.1 g H_2/L and 4.5 wt%.

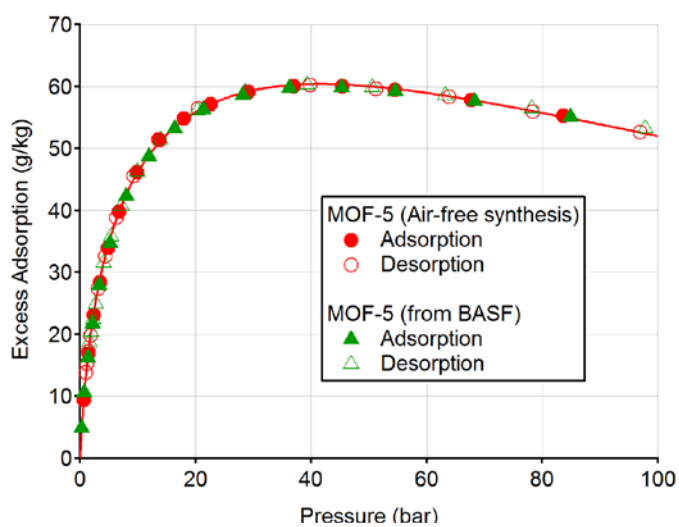

FIGURE 1. Measured excess H_2 isotherms in as-synthesized MOF-5 and in a pre-commerical version of MOF-5 supplied by BASF

TABLE 2. Total and usable hydrogen uptake in as-synthesized MOF-5 as a function of pressure

	Total		Usable (P-swing)	
P (bar)	Vol. (g/L)	Grav. (wt%)	Vol. (g/L)	Grav. (wt%)
5	22.2	3.5	-	-
35	44.4	6.8	22.2	3.3
50	47.8	7.3	25.6	3.8
100	53.3	8.0	31.1	4.5

Computational screening was performed to identify MOFs that could meet or exceed the performance of MOF-5. Figure 2 shows total and usable capacities for approximately 2,000 MOFs whose crystal structures were extracted from our own "Michigan MOF" database [1], from the CoRE database [3], and for MOFs suggested by chemical intuition. These predictions were based on Grand Canonical Monte Carlo calculations employing two different interatomic potentials: the so-called pseudo-FH model [4] and MGS model [5].

These calculations identified IRMOF-20 [6] as a promising, high-capacity compound. This compound was synthesized, and demonstrated a surface area of 4,073 m^2/g. This value is in very good agreement with (i.e., within 94% of) the calculated surface area, 4,324 m^2/g. Pressure-composition-temperature measurements were used to evaluate the gravimetric and volumetric capacity of IRMOF-20 at 77 K. Figure 3 illustrates the hydrogen isotherms for this compound, which are reported on a total basis and assuming single crystal density. To place this performance in context, isotherms for MOF-5 are also plotted.

The isotherms show that the total gravimetric capacity of IRMOF-20 exceeds that of MOF-5 for all pressures measured (up to 100 bar). On the other hand, total volumetric performance is slightly lower for IRMOF-20 up to approximately 100 bar.

The measured total hydrogen capacities were converted into usable capacities assuming operation via an isothermal pressure swing at 77 K. The minimum pressure ("empty vessel") was set to 5 bar, in accordance with the DOE targets. Three maximum "full vessel" pressures, P_{max}, were examined: 35 bar, 50 bar, and 100 bar. The usable capacity of IRMOF-20 was measured to match or exceed that of MOF-5 for all values of P_{max}. The HSECoE previously demonstrated MOF-5 based storage systems operating at P_{max} = 100 bar. Under these same conditions the usable, materials-only capacity of IRMOF-20 is 33.1 g H_2/L and 5.7 wt%. These values are, respectively, 6% and 27% larger than the corresponding values for MOF-5 (Table 2).

In addition to MOF-5 and IRMOF-20, six additional MOFs were synthesized and characterized with regard to their hydrogen capacity. Of these, the compounds with Cambridge Structure Database identifiers SUKYON, EPOTAF, and DIDDOK, exhibited surface areas far below the calculated values. This was attributed to pore collapse and/or incomplete activation. The other three compounds included UMCM-4 and two MOF-5 variants with modified linkers. Although these compounds did achieve reasonably

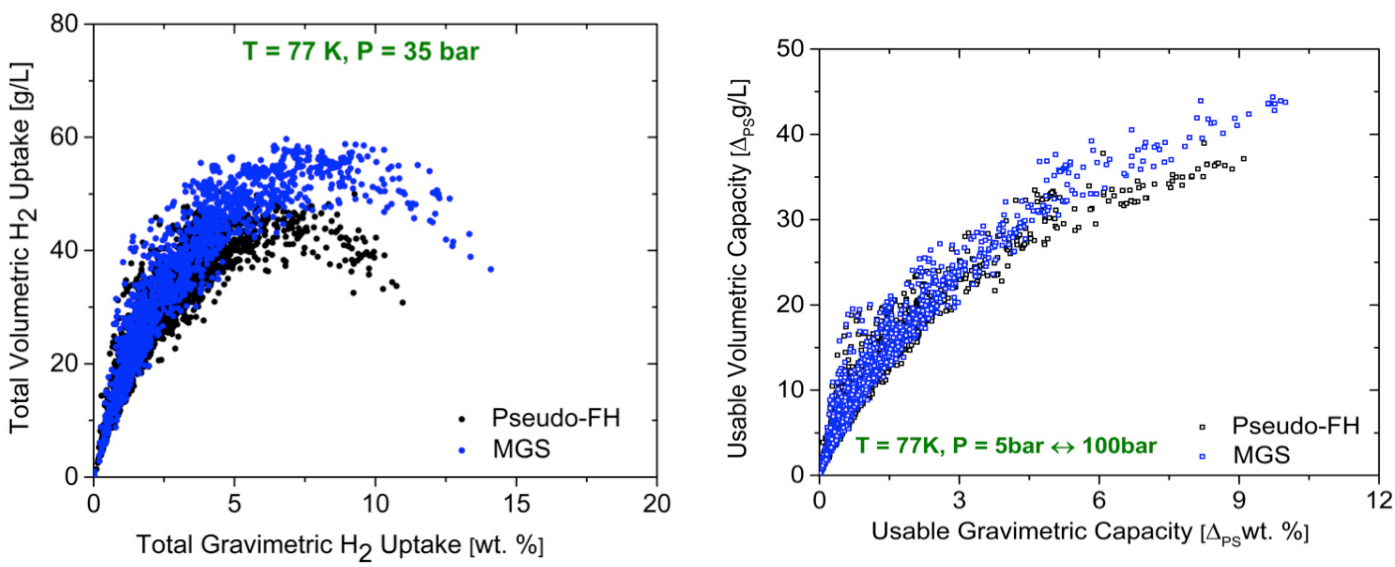

FIGURE 2. Total (left) and usable (right) capacities predicted by Grand Canonical Monte Carlo for approximately 2,000 MOFs. Crystal structures are primarily drawn from the UM and CoRE MOF databases; MOFs suggested by intuition are shown with red data points. Two forms of the H_2-MOF interatomic potential (Pseudo-FH and MGS) are examined. The performance of MOF-5 is depicted with a blue symbol. All calculations assume T = 77 K and single crystal MOF densities.

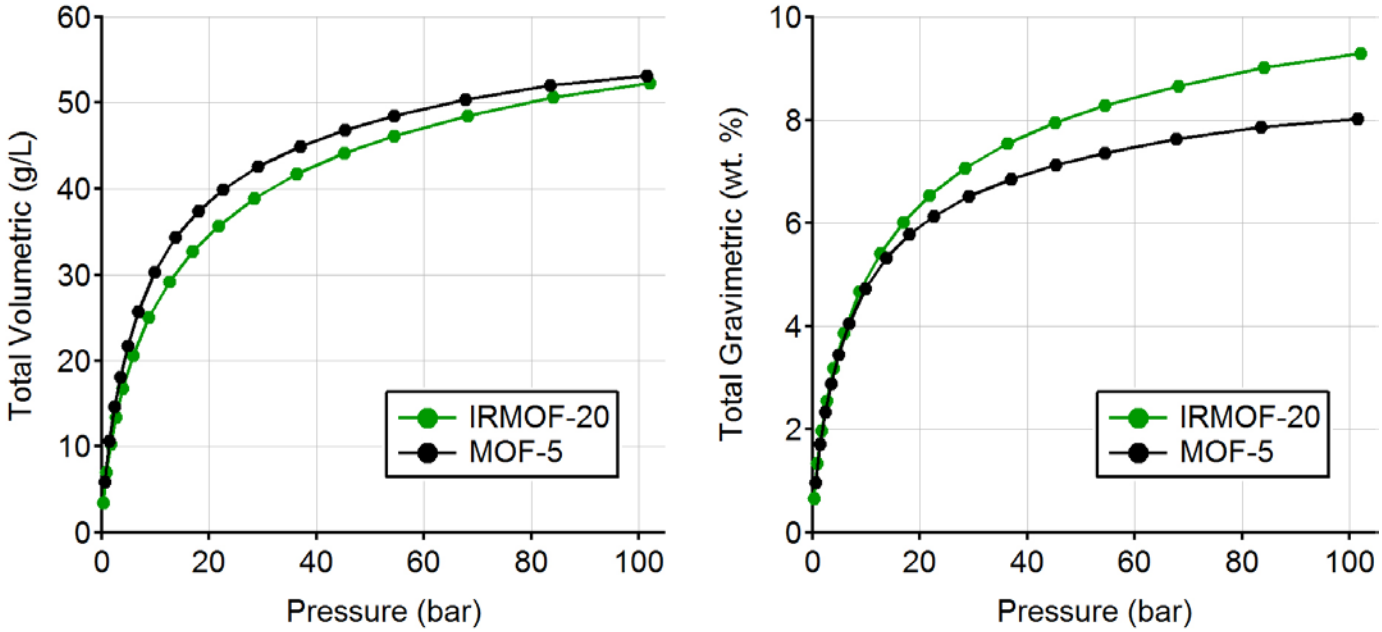

FIGURE 3. Total measured volumetric (left) and gravimetric (right) hydrogen capacity of IRMOF-20 compared to MOF-5

high surface areas, they did not surpass MOF-5 in both volumetric and gravimetric hydrogen uptake.

CONCLUSIONS AND FUTURE DIRECTIONS

Computational screening and experimental synthesis/characterization revealed IRMOF-20 as a hydrogen adsorbent which can surpass the usable capacity of the benchmark compound MOF-5 under cryogenic conditions. Future directions for this effort will focus on screening additional compounds with the goal of identifying MOFs that can surpass the performance of MOF-5 by 15%.

FY 2016 PUBLICATIONS/PRESENTATIONS

1. D.J. Siegel, "Hydrogen Adsorbents with High Volumetric Density: New Materials and System Projections," 2016 DOE Hydrogen and Fuel Cells Program Annual Merit Review Meeting, Washington, June 8, 2016.

REFERENCES

1. Goldsmith et al., Chem. Mater. **25**, 3373 (2013).

2. Kaye et al. J. Am. Chem. Soc. **192**, 14176 (2007).

3. Chung et al., *Chem. Mater.* **26**, 6185 (2014).

4. Fischer et al., *ChemPhysChem*, **10,** 2947 (2009).

5. Michels et al., *Physica*, **26,** 393, (1960).

6. Rowsell et al., *J. Am. Chem. Soc.***128**, 1304 (2006).

IV.C.11 Electrochemical Reversible Formation of α-Alane

Ragaiy Zidan (Primary Contact), Joe Teprovich, Patrick Ward, Scott Greenway
Savannah River National Laboratory (SRNL)
999-2W Room 121
Savannah River Site
Aiken, SC 29808
Phone: (803) 646-8876
Email: ragaiy.zidan@srnl.doe.gov

DOE Manager: Ned Stetson
Phone: (202) 586-999
Email: Ned.Stetson@ee.doe.gov

Project Start Date: October 1, 2011
Project End Date: Project continuation and direction determined annually by DOE

Objectives

- Develop methods of α-alane production and regeneration that lower the cost of α-alane production to less than $10/kg.
- Demonstrate and characterize alane production system that lowers the cost of α-alane production with the lowest possible capital and operating costs.
- Identify and quantify fundamental properties of α-alane production chemistry and physics that will lead to improved design and modeling of systems for α-alane production and use.

Technical Barriers

This project addresses the following technical barriers from the Hydrogen Storage section of the Hydrogen, Fuel Cells and Infrastructure Technologies Program Multi-Year Research, Development, and Demonstration Plan.

(A) System Weight and Volume

(B) System Cost

(C) Efficiency

(Q) Regeneration Processes

Technical Targets

In this project studies are being conducted to lower cost and improve efficiency of the electrochemical method to form α-AlH_3. This material has the potential to meet long-term and near-term target for portable power applications [1,2]. The research performed as part of this contract is equally applicable to both areas.

- By 2020, develop and verify a single-use hydrogen storage system for portable power applications achieving 1.3 kWh/kg system (4.0 wt% hydrogen) and 1.7 kWh/L system (0.050 kg H_2/L) at a cost of $0.03/Wh net ($1/g H_2 stored).

FY 2016 Accomplishments

- Demonstrated recovery and recycling of 99.9% of crystallization additives.
- Demonstrated transamination of alane-tetrahydrofurane (THF) adduct to alane-triethylamine adduct,
- Improved ambient pressure crystallization of α-alane to 88% yield without producing unwanted phases.

✧ ✧ ✧ ✧ ✧

INTRODUCTION

The U.S. Department of Energy (DOE) is supporting research to demonstrate viable materials for hydrogen storage. Aluminum hydride (alane [AlH_3]), having a gravimetric capacity of 10 wt% and volumetric capacity of 149 g H_2/L and a desorption temperature of ~60°C to 175°C (depending on particle size and the addition of catalysts) has the potential to meet the 2015 and 2020 DOE system-level targets for portable power applications. The main barrier for using alane as a hydrogen storage material is the high material cost and unfavorable thermodynamics towards (re)hydrogenation. Zidan et al. [3] were the first to show a reversible cycle utilizing electrochemistry and direct hydrogenation, where gram quantities of alane were produced, isolated and characterized. This regeneration method is based on a complete cycle that uses electrolysis and catalytic hydrogenation of spent Al(s). This cycle avoids the impractical high pressure needed to form α-AlH_3 and the chemical reaction route of α-AlH_3 that leads to the formation of alkali halide salts, such as LiCl or NaCl, which become a thermodynamic sink because of their stability.

During FY 2016, SRNL focused on advanced alane-etherate crystallization strategies that will allow efficient and low cost conversion to α-alane. The project focused on improving processes for alane synthesis and regeneration that have been developed by SRNL in prior years including: (1) electrochemical synthesis of alane from commercial Al and spent alane, and (2) solid state alane production. The goals the FY 2016 efforts were to exceed 85% yield

of α-alane through advanced crystallization. SRNL also continued to develop recovery and recycling methods to recover and reuse over 75% of the solvents and additives during the crystallization process.

APPROACH

The electrochemical generation of α-alane has been shown by Zidan et al. [3,4] to be capable of generating high purity material using methods that can be developed into a fueling cycle for hydrogen vehicles, portable power systems, or other applications. This research has demonstrated methods to enhance the practicality of utilizing the electrochemical method for the large scale production of alane etherate as well as the crystallization of the etherate to stable crystals of α-alane. The focus this year has been to refine the crystallization process to reduce costs and produce high quality material with only the alpha phase at a high yield. Additionally, focus has been placed on moving to the crystallization of the alane-THF adduct that has high ionic conductivity and will enable the electrochemical process. The crystallization has focused on ambient pressure crystallization of alane-etherate in toluene due to lower toxicity and lower required energy input compared to performing the crystallization at reduced pressure.

RESULTS

In collaboration with Ardica and SRI, SRNL identified that the use of $LiBH_4$ and $LiAlH_4$ as crystallizing aids was a significant additional cost for alane crystallization if the products were not recycled between batches. Although the recycling of these compounds has been assumed as a cost savings, the ability to isolate them in high yield from product rinses and show that they are not changed in the crystallization process had never been done. To demonstrate the recovery, SRNL collected the product ether rinses from batches of alane. The ether rinses were then evaporated to remove the solvent on a Schlenk line with heating. The dried product was weighed and X-ray diffraction (XRD) and thermogravimetric analysis (TGA) were performed on the product. The 99.9% recovery of the theoretical amount of $LiAlH_4$ and $LiBH_4$ in the washes was obtained. The XRD of the recovered product (Figure 1) only has peaks from $LiAlH_4$ and $LiBH_4$. The TGA of the recovered product (Figure 2) has weight loss peaks from $LiAlH_4$ and $LiBH_4$. These results demonstrate fulfillment of the first two milestones for the year and validate that recovery of $LiAlH_4$ and $LiBH_4$ crystallizing aids is very feasible.

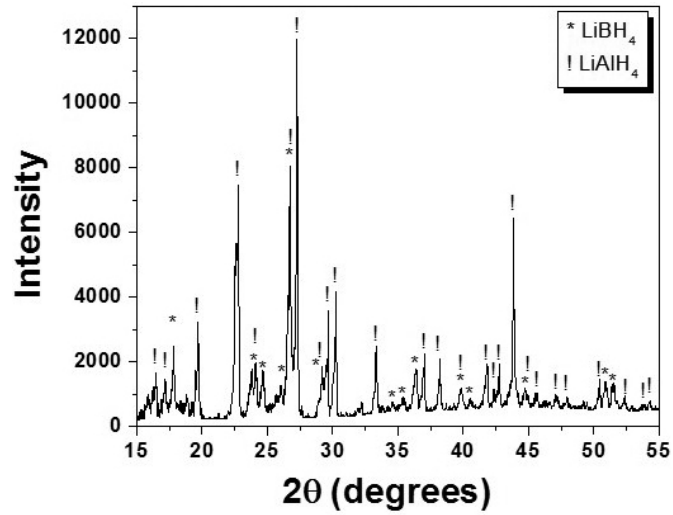

FIGURE 1. XRD showing $LiAlH_4$ and $LiBH_4$ recovered from the ether washes

The SRNL team was successful in reproducibly synthesizing α-alane with 9.8 wt% hydrogen content during synthesis runs at the 15 g scale as measured by TGA, but the yield during these runs was low due to difficulties with recovering the product from the glassware. Figure 3 shows a scanning electron micrograph of the alane produced on the 15 g scale and it can be seen that there are square crystallites. Figure 4 shows a TGA of the material produced at the 15 g scale with >9.8 wt% H_2. Crystallization at the 150 g scale

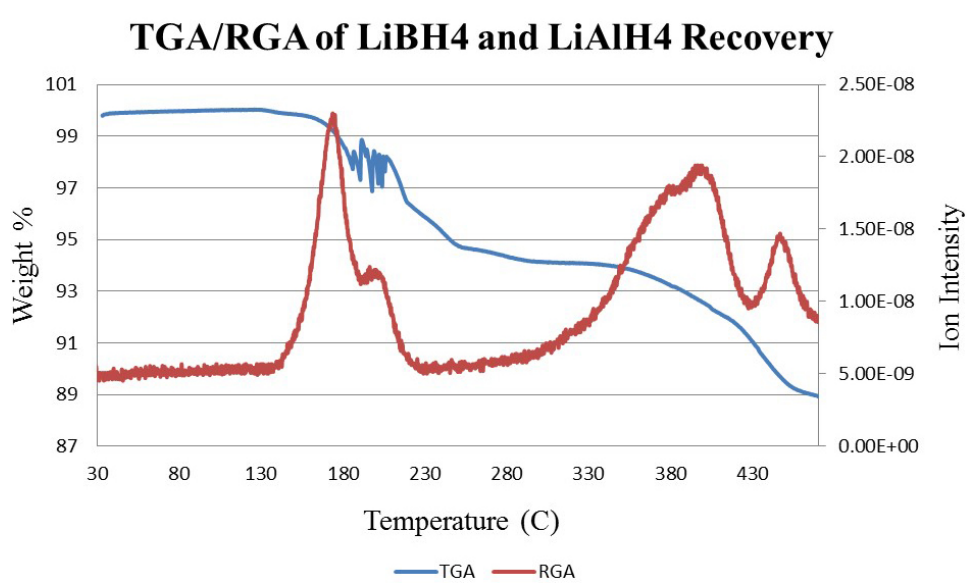

RGA – Residual gas analysis

FIGURE 2. TGA showing dehydrogenation of $LiBH_4$ and $LiAlH_4$ recovered from ether washes

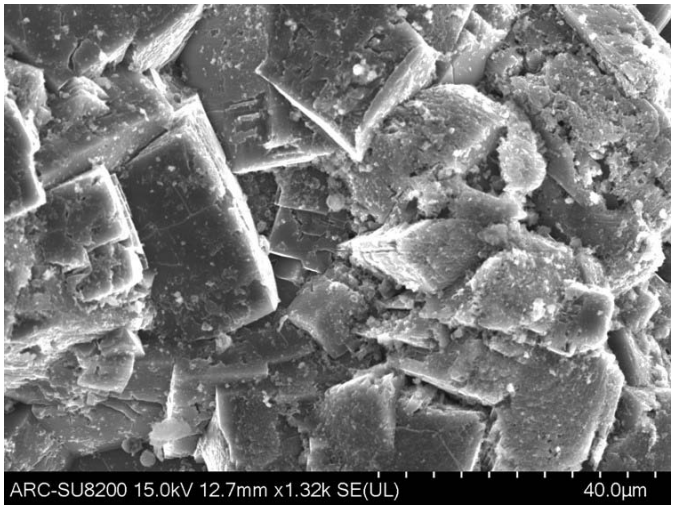

FIGURE 3. Scanning electron micrograph image of α-alane agglomerates synthesized at the 15 g scale

reproducibly yielded 88% α-alane with >9.8 wt% H_2. The yield was enhanced due to the lower surface area to volume ratio for the vessels. This demonstrated that large scale alane crystallization at ambient pressure with high yield is possible. The stability of the α-alane produced through this set-up is excellent and behaves exactly like former Soviet Union samples. The passivated α-alane is inert to direct exposure to oxygen, water, and impacts. This was confirmed by experiments at Ardica/SRI.

The SRNL team has demonstrated the crystallization of alternative adducts such as triethylamine -alane formed by transamination reactions with THF-alane adducts. Research is continuing to increase the yield of the adduct and to identify the optimal conditions for crystallization.

CONCLUSIONS AND FUTURE DIRECTIONS

- Increasing the current of the electrochemical cell is one of the last critical issues related to alane adduction production.
- Investigate alternative crystallization pathways which may be suitable for the use of higher ionic conductivity solvent.
- Investigate additives and other solvents that may increase the conductivity of the electrochemical cell for increase alane adduct production rates.

SPECIAL RECOGNITIONS & AWARDS/ PATENTS ISSUED

1. Ragaiy Zidan, Joseph A. Teprovich, Ted Motyka; Two step novel hydrogen system using additives to enhance hydrogen release from the hydrolysis of alane and activated aluminum, US9,199,844B2, December 2015.

2. Ragaiy Zidan; High energy density battery based on complex hydrides, US9,325,030B2, April 2016.

FY 2016 PUBLICATIONS/PRESENTATIONS

1. Patrick Ward, Joseph Teprovich, Scott Greenway, Ragaiy Zidan. "Current Progress in the Low-cost Production of Alane." PacifiChem. December 2015.

2. Ted Motyka. "Investigation of Metal and Chemical Hydrides for H_2 Storage in Fuel Cell Systems." 2016 ONR Undersea Energy and Propulsion Review. April 2016.

3. Ragaiy Zidan. "Reversible Formation of Alane." Department of Energy Annual Merit Review 2016.

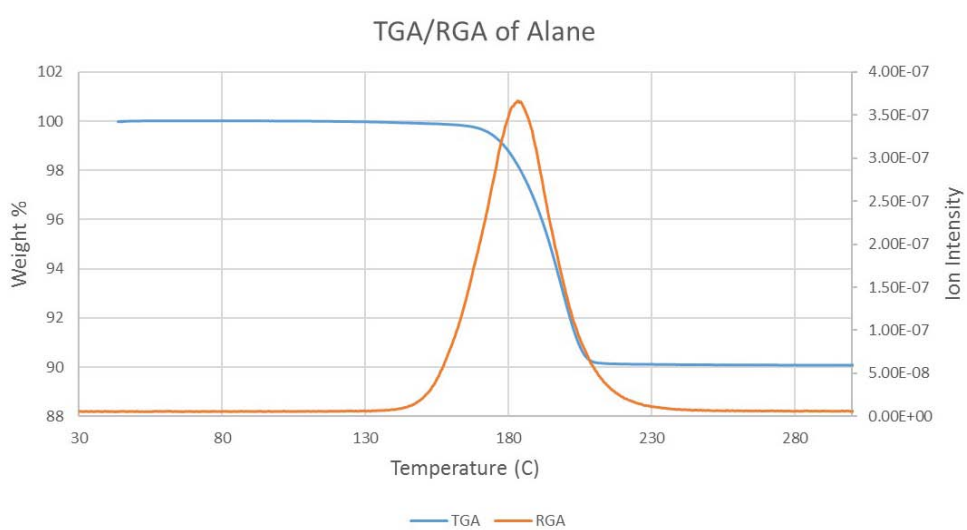

FIGURE 4. TGA and RGA data showing dehydrogenation of AlH_3 obtained from the 15 g batch that contains greater than 9.8 wt% H_2

4. Ragaiy Zidan, Patrick Ward, and Joseph Teprovich. "Current Progress in the Low-cost Production of Alane." MH Conference. August 2016.

REFERENCES

1. Teprovich, J.A., T. Motyka, and R. Zidan, International Journal of Hydrogen Energy, 2012. **37**(2): p. 1594–1603.

2. Graetz, J. and J.J. Reilly, J. Phys. Chem. B, 2005. **109**(47): p. 22181–22185.

3. Zidan, R., et al., Chemical Communications, 2009(25): p. 3717–3719.

4. Martinez-Rodriguez, M.J., et al., Appl. Phys. A-Mater. Sci. Process., 2012. **106**(3): p. 545–550.

IV.C.12 Low-Cost α-Alane for Hydrogen Storage

Richard Martin
Ardica Technologies, Inc.
2325 3rd Street, Suite 424
San Francisco, CA 94107
Phone: (412) 445-8612
Email: dmartin@ardica.com

DOE Manager: Katie Randolph
Phone: (240) 562-1759
Email: Katie.Randolph@ee.doe.gov

Technical Advisor: Mark Petrie
Phone: (650) 859-4574
Email: mark.petrie@sri.com

Contract Number: DE-EE0006629

Subcontractor:
SRI International, Menlo Park, CA

Project Start Date: July 15, 2014
Project End Date: July 14, 2017

Overall Objectives

- Reduce production cost of α-alane (AlH_3) to meet the DOE 2015 and 2020 hydrogen storage system cost targets for portable low- and medium-power applications. This will enable broader applications in consumer electronics (i.e., smart phones, tablets, laptops), back-up power, unmanned aerial vehicles, forklifts, and vehicles.

Fiscal Year (FY) 2016 Objectives

- Update process and economic models.
- Develop baseline performance of electrochemical process.
- Set up fluidized bed reactor and establish test operations.

Technical Barriers

This project addresses the following technical barriers from the Hydrogen Storage section of the Fuel Cell Technologies Office Multi-Year Research, Development, and Demonstration Plan.

(A) System Weight and Volume

(B) System Cost

(C) Efficiency

(J) Thermal Management

(K) System Life-Cycle Assessments

(Q) Regeneration Processes

Technical Targets

Table 1 shows the progress made towards the DOE technical targets.

TABLE 1. Progress towards Meeting Technical Targets for Hydrogen Storage
Note: Chemical and electrochemical route productions costs are for a 320 Mton/yr process

			Current Cost	Chemical Route (1,2)	Electrochemical Route		
					Baseline (1,3)	Cathode Recycle (1)	Increased Scale to 3,200 MT/yr
Storage System Costs			Pilot Plant	Commercial Scale	(80% AlH3 from R1)	(80% AlH3 from R1, 80% LiAlH4 regenerated)	(80% AlH3 from R1, 80% LiAlH4 regenerated)
Alane Fuel Costs		$/kg alane	3500	112	81	56	29
Cartridge Cost (4)		$/kg alane	79	53	53	53	44
Total		$/kg alane	3579	165	134	109	73
Storage System Cost		$/g H2	38.91	1.79	1.46	1.18	0.79
DOE Metrics		$/g H2		Target Met?			
Low Power	2015	3	N	Y	Y	Y	Y
	2020	1	N	N	N	N	Y
Medium Power	2015	6.7	N	Y	Y	Y	Y
	2020	3.3	N	Y	Y	Y	Y

1. Chemical and electrochemical route productions costs are for a 320 MT/yr process.
2. Commercial scale estimate provided by Albemarle.
3. Cost of alane entirely from reaction (R2) is $101, compared to $81 for 80% from reaction (R1).
4. New cartridge costs based on manufacturer estimates. $79/kg AlH_3 at small scale production, $53/kg AlH_3 at 4 M cartridges/year and $44//kg AlH_3 at 20 M cartridges/year. Further cost savings of 25-33% per cartridge can be realized through recycling, not shown.

Baseline (Anode Reactions)

(**R1-80%**) $3\ LiAlH_4 + Al_{metal} \rightarrow 4\ AlH_3 + 3\ Li^+ + 3\ e^-$

(**R2-20%**) $LiAlH_4 \rightarrow AlH_3 + 1/2H_2 + Li^+ + e^-$

FY 2016 Accomplishments

Accomplishments include:

- Updated the cost model.
- Designed a fluidized bed in collaboration with Prof. Jim Evans (University of California, Berkeley).
- Calculated minimal flow rates for fluidization of various particle sizes. Determined the optimal dimensions of the anode cell and size of the pump.
- Constructed the cell (Adams & Chittenden scientific glass) and the system that pumps the electrolyte through the bed of aluminum particles.
- Investigated the dependence of current versus distance between electrodes in the fluidized bed reactor system. Performed experiments that determined the amount of alane produced from the anode in the current fluidized bed cell configuration.
- Investigated the cathode products under various electrochemical reactor conditions.
- Performed initial experiments to isolate the N-ethylmorpholine alane adduct from $LiAlH_4$/$NaAlH_4$ tetrahydrofuran (THF)-based electrolytes and its conversion into α-alane.

✧ ✧ ✧ ✧ ✧

INTRODUCTION

This project is developing improvements to the Savannah River National Laboratory lab-scale electrochemical synthesis of alane and Ardica-SRI chemical downstream processes that are necessary to meet DOE cost metrics and transition alane synthesis to large scale production. These modifications are focused on critical cost-saving design improvements to the electrochemical cell.

The use of a fluidized bed reactor will replace the sheet aluminum electrodes of the current Savannah River National Laboratory process with a bed of conductive aluminum particles maintained in a stage of agitation by a flowing electrolyte and/or a fluidizing gas. Electrical contact with these particles is maintained through a sheet current collector, and the high surface area of these particles will ensure efficiency of reaction. In our approach, spent alane particles can be provided directly to the reactor. This avoids the costs required to convert spent alane into sheet or rod form for use in other electrochemical reactor designs or the need for costly disposal.

APPROACH

To develop synthesis technology to reduce the cost of α-alane to <$5/kg, the approach is to transition a bench-scale electrochemical route to alane to an electrochemical process that will be more conducive and economical for large-scale alane production. Specifically, we propose a process that uses spent fuel as a starting material in a continuous synthesis/regeneration of alane from less costly elemental aluminum and hydrogen. This technique could greatly reduce fuel costs and accelerate the commercial acceptance of alane-based fuel-cell technology. The cost of alane produced by the electrochemical route (Table 1) translates to a storage system cost of <$1/g H_2, achieving the DOE hydrogen storage system metrics for 2015 and 2020 for both low and medium portable power. The longer-term goal of the project is to reduce the cost of the initial alane charge to $4/kg and the recycling cost to $2/kg. This will result in hydrogen costs that are competitive with the cost of gasoline.

RESULTS

During Phase 2, updates were made to the process and economic models for the electrochemical route for the synthesis of α-alane. The costing included detailed estimates for material and utilities requirements and capitol and manufacturing costs. The updated cost table shows alane fuel costs associated with the chemical route (pilot plant and 320 MT/yr scale) and different developmental stages of the electrochemical process. The alane production cost is estimated to be <$81/kg alane at 320 MT/yr and an estimated storage system cost of <$1.46/g H_2 for worst-case scenario.

Cathode products were evaluated and analyzed under various electrochemical conditions and electrolytes. Gravimetric and X-ray diffraction analysis of the solid cathode products in lithium-based systems were also carried out. Figure 1 shows the dependencies of cathode mass on charge that was passed in pulsed and non-pulsed experiments

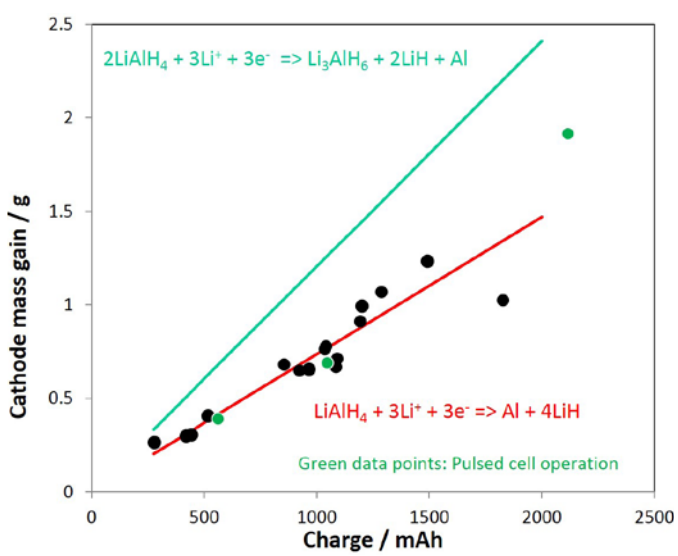

FIGURE 1. Cathode reaction products

(points) as compared with the expected dependencies for two putative cathode reactions (lines) using 1 M $LiAlH_4$ in THF as the electrolyte. In agreement with X-ray diffraction and elemental analysis data, the dominant cathode products include lithium hydride and aluminum which may be used to regenerate $LiAlH_4$ in a separate operation.

During Phase 2, a fluidized bed reactor shown in Figure 2 was designed and set up with recirculating electrolyte. Fluidization experiments were performed on <1 mm particles and a mixture consisting of particles that ranged from 106–150 µm. The critical point of fluidization was achieved at ~2.0 L/hr using the 106–150 µm-sized particles. Current densities of 10 mA/cm^2 to >100 mA/cm^2 were observed that meet and/or exceed the milestone current densities of M2.06 (10 mA/cm^2) and M2.08 (100 mA/cm^2).

As expected, reduction of the electrode spacing increases current dramatically. THF-based electrolytes provide strikingly higher conductivities compared to diethyl ether. (Figure 3)

The alane fuel storage system energy densities based on the hydrogen produced were:

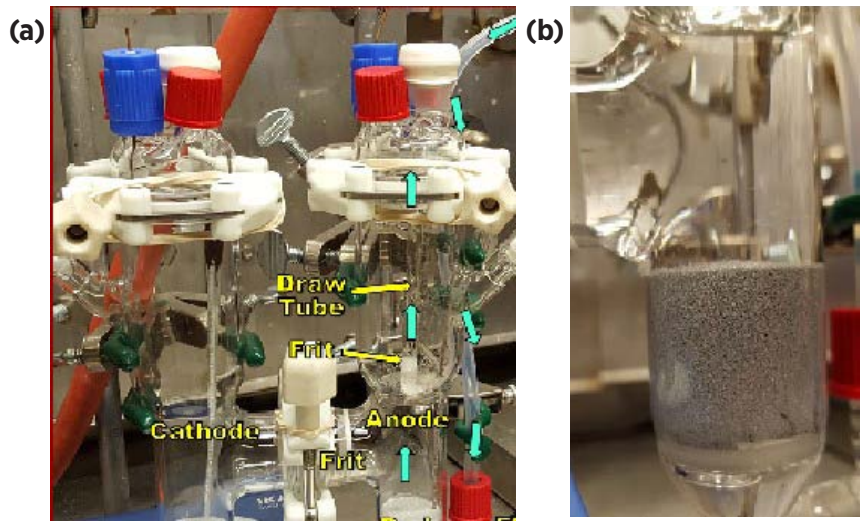

FIGURE 2. (a) Picture of the fluidized electrochemical cell system. (b) The fluidized anode compartment using aluminum particles with sizes that ranged from 106–150 µm.

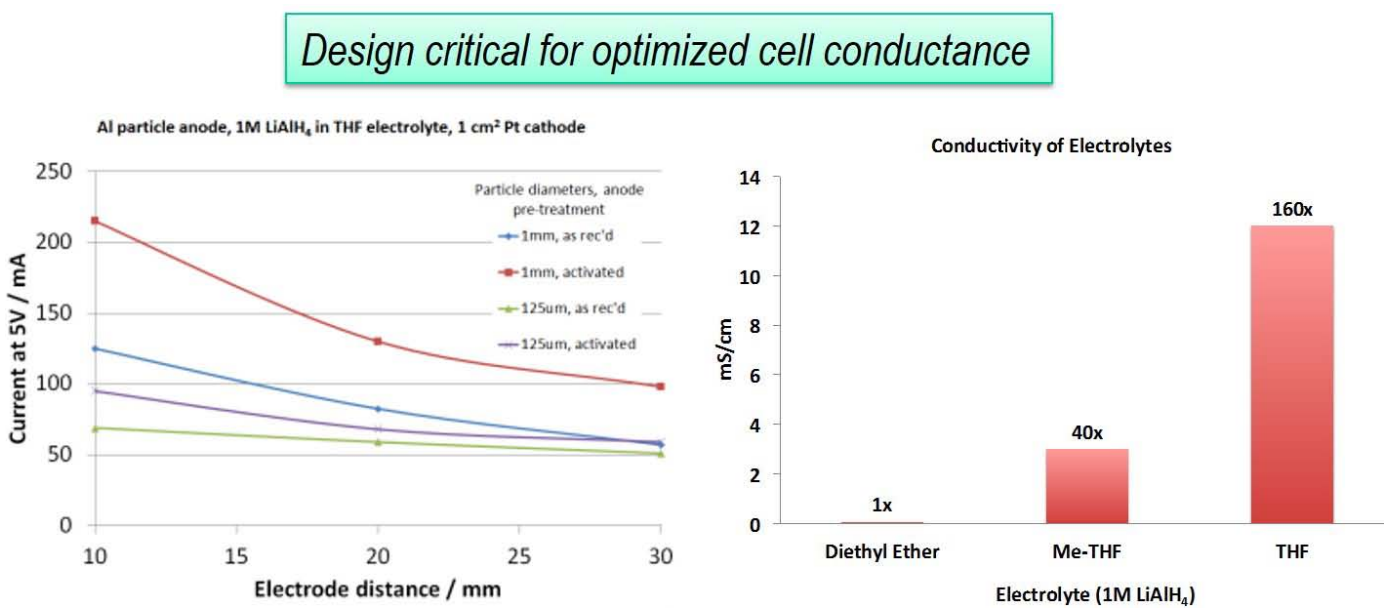

FIGURE 3. Current at constant voltage (5 V) vs. electrode separation

- 0.98 kWh/kg (target was 1.0 kWh/kg)
- 1.26 kWh/L (target was 1.3 kWh/kg)

CONCLUSIONS AND FUTURE DIRECTIONS

- Design, fabricate, and test a scalable electrochemical cell that builds on our experience with the H-cell that optimizes electrode kinetics, enables high-current, and hence high-throughput operation. Collaboration with Prof. Evans (University of California, Berkeley) is critical for this activity. (2016–2017)
- Deposition of cathode products at high activity and yield for further reaction and regeneration of lithium or sodium aluminum hydride ($MAlH_4$). Modify pulse methods and fluidization of cathodic bed aluminum particles for deposition/capture of these materials. Improve morphology and optimize conversion to $MAlH_4$. (2016–2017)
- Optimize solvent swap methods for complete separation of alane adduct from the concentrated $NaAlH_4$-based electrolyte. Optimize thermal conversion to α-alane from amine adducts using crystallization aides and heating profiles. (2016–2017)

SPECIAL RECOGNITIONS & AWARDS/ PATENTS ISSUED

The Ardica alane-fueled soldier Wearable Power System (WPS) participated in the Army Expeditionary Warrior Exercise at Ft. Benning, Georgia, in January–February 2016. The exercise uses realistic 72-hr missions to test new technology solutions in combat scenarios with aggressor forces. The WPS performed to specification and was highlighted in the senior leader wrap up briefing as reducing the battery weight carried by soldiers by 55%. DOE paid for developing the electrochemical processes to lower the cost of alane while the Army paid for the WPS development. The Army has concluded the following: the WPS has a significant weight advantage over the conformal wearable battery option for a centralized power source in the small unit power suite of equipment. The current cost of alane fuel makes the cost of the fuel cartridge prohibitively expensive. Implementation of large scale alane production and development of electrochemical routes to manufacture of alane are likely means of making the cartridges affordable for the army.

IV.D.1 Enhanced Materials and Design Parameters for Reducing the Cost of Hydrogen Storage Tanks

David W. Gotthold
Pacific Northwest National Laboratory
P.O. Box 999, MSIN
Richland, WA 99352
Phone: (509) 375-2073
Email: David.Gotthold@pnnl.gov

DOE Manager: Grace Ordaz
Phone: (202) 586-8350
Email: Grace.Ordaz@ee.doe.gov

Subcontractors:

- Hexagon Lincoln, Lincoln, NE
- Ford Motor Company, Dearborn, MI
- Toray Composites America, Decatur, AL
- AOC, LLC, Collierville, TN

Project Start Date: January 18, 2012
Project End Date: September 30, 2016

Overall Objectives

- Reduce carbon fiber (CF) usage and hydrogen tank cost through a series of combined material and design approaches for a cumulative 37% cost savings.
- Reduce tank cost by reducing composite mass through: (1) resin matrix modifications and alternatives, (2) CF surface properties that increase load translational efficiency, (3) alternate CF placement and materials, and (4) enhanced operating conditions to increase the energy density vs. pressure.
- Demonstrate the combined cost reductions through modeling, materials, and burst testing.

Fiscal Year (FY) 2016 Objectives

- Acquire and test physical insulations for cold gas storage.
- Complete low temperature materials compatibility testing.
- Complete impact and fatigue testing of vinyl ester resin tanks.
- Assess tank burst performance at cold gas operating temperatures.

Technical Barriers

This project addresses the following technical barriers from the Hydrogen Storage section of the Fuel Cell Technologies Office Multi-Year Research, Development, and Demonstration Plan.

(A) System Weight and Volume

(B) System Cost

(G) Materials of Construction

(J) Thermal Management

(L) Lack of Tank Performance Data and Understanding of Failure Mechanisms

Technical Targets

This project contributes to achieving the following DOE milestone from the Manufacturing R&D section of the Fuel Cell Technologies Office Multi-Year Research, Development and Demonstration Plan.

- By 2020, develop and verify onboard automotive hydrogen storage systems achieving 1.8 kWh/kg system (5.5 wt% H_2) and 1.3 kWh/L system (0.040 kg H_2/L) at a cost of $10/kWh ($333/kg $H_{2\ stored}$). The progress toward targets is shown in Table 1. The gravimetric and volumetric capacities decrease slightly, due to the required insulation weight and volume. The storage system cost decreases 22% from the 2012 cost, due to the reduced carbon fiber composite in the 500 bar tank vs. the 700 bar tank.

TABLE 1. Progress toward Meeting Technical Targets for Onboard Hydrogen Storage for Light-Duty Fuel Cell Vehicles

Storage Parameter	Units	2020 Targets	2012 Project Start, 700 bar, T = 293K	2016 PNNL Status, 500 bar, T = 200K
System Gravimetric Capacity	kg H_2/kg system	0.055	0.042	0.039
System Volumetric Capacity	kg H_2/L system	0.040	0.025	0.024
Storage System Cost	$/kWh net	10	17.00	13.30

T – Temperature; PNNL – Pacific Northwest National Laboratory

FY 2016 Accomplishments

- Eleven sets of six tanks were built and burst tested to evaluate previous theoretical design improvements with statistically significant sample sizes. This included testing of tanks with varying wind patterns, nanoparticle reinforced resins, and the alternate vinyl ester resin. The results of each is described below.
- Low cost resin alternative developed and tested with equivalent or better performance than existing epoxy resin that, based on analysis by Strategic Analysis, will reduce the storage system cost by $0.59/kWh compared to DOE's 2013 baseline of $16.8/kWh.
- Optimized nanoparticulate materials and processing selected and scaled to tens of gallons of modified resin to enable production of 70-L batches of modified resins. The modified resins did not show increases in burst pressure and caused increased manufacturing variations. Nanoparticles did not increase the strength or stiffness of the resin enough to significantly increase the composite lamina strength or stiffness. In addition, clumping of nanoparticles led to defects that may be connected to increased performance variation.
- Alternate winding patterns were tested. An improved failure model that accounts for high shear stresses more accurately explains the lower burst pressures observed in tank winding patterns with higher interlaminar shear stress. The trade-off between fiber tensile failure and interlaminar shear failure demonstrates that the existing winding pattern is near optimal for the selected tank dimensions and manufacturing processes.
- Advanced physical insulation materials (vacuum insulated panel [VIP] and aerogel batting) were procured and tested to estimate dormancy performance at cold gas operating conditions. The measured insulation R-values of VIP (R-25/in) and aerogel batting (R8.5/in) were about 12% and 4% as effective (respectively) as multi-layer vacuum insulation (approximately R-215 equivalent).
- Multiple nonmetallic component materials were evaluated at cold temperatures (-129°C to 23°C) to determine feasibility for cold gas operation expected to be at approximately -73°C.
- Cold gas burst tests were done on 250 bar standard test and evaluation bottle (STEB) poly(vinyl ester) (PVE) tanks precooled to 200 K. Average burst pressure was 714 bar, which exceeds the target room temperature burst of ~625 bar.

✧ ✧ ✧ ✧ ✧

INTRODUCTION

The goal of this research was to reduce the cost of compressed hydrogen storage vessels by at least 37% from the current high volume projections of $17/kWh to $11/kWh for commercialization in early-market and light-duty hydrogen fuel cell vehicles. The cost and performance baseline was the current 70 MPa Type IV pressure vessel (high-strength, standard modulus carbon fiber in an epoxy matrix filament wound on a high density polyethylene liner). The high-strength carbon fiber composite can account for nearly 70%–80% of the overall tank costs. Therefore, the team's research objective is to reduce carbon fiber usage and associated tank cost through a series of combined material and design improvements that were estimated to total nearly 37% of the project initial baseline tank cost. The project identified through modeling a series of material design optimizations and experiments that were expected to achieve the cost savings goal. It was initially estimated that these cost savings, combined with future reductions in CF cost, could lead to the 50% cost reduction toward the ultimate DOE target.

APPROACH

The project took a holistic approach to improve performance by lowering the required gas pressure at lower operating temperature, refining the tank composite design with local reinforcement and hybrid layups, plus increasing the composite translation efficiency with material modifications at the composite constituent level. The project team includes industry experts in each of the following focus areas of improvement: enhanced operating conditions to improve energy density/pressure ratios, load translational efficiency improvements by CF surface modification, resin matrix modifications and alternatives, and alternate fiber placement and materials. The team expects these savings approaches to be compatible and additive.

RESULTS

The key work for 2016 was to validate the performance of the improved resins and the ability to operate tanks with cold gas. This included measuring the impact and fatigue performance of full vinyl ester resin tanks, burst testing of the nano-particle reinforced resin tanks, plus low temperature testing of tank materials, insulations and full tanks. Additional work was done on updating the cost estimates for tank manufacturing both for ambient temperatures and enhanced operating conditions.

Improved and Modified Resins

Based on the FY 2015 work showing improved performance of the vinyl ester (VE) tanks, a series of additional impact and fatigue tests were performed on a second batch of VE tanks to understand the suitability for

transition to manufacturing. A series of 250 bar STEB tanks were made with both VE and epoxy resins. The tanks were then subjected to a calibrated impact and then burst tested after either 0, 5,000, or 10,000 cycles. The results are shown in Table 2. For the unimpacted tanks, the relative performace of the VE and epoxy resins was as expected based on the initial results. The initial burst was slightly improved and the fatigue testing was within expected variations. In the initial round of impact tests, one VE tank failed early in the pressure cycling (the one marked "Did Not Finish" in Table 2), with a clear damage pattern from the impact point shown in Figure 1. In a repeat of the testing, the VE tanks actually outperformed the epoxy tanks for all three test conditions. Note that while the vinyl ester tanks demonstrated equivalent or better structural performance, challenges remain with managing the styrene vapors (approximately 30% by weight) during the winding and curing processes. This is managed in the fiberglass industry with the use of industrial fume hoods and air handling design.

In FY 2016, testing was performed on tanks with carbon and silica nano-particle resins. Previous work had been on measuring mechanical performance of resin-only samples and scaling up the mixing process to enable full tank testing. Multiple tanks were built and burst tested with generally poor results. With the carbon nanoparticles, the best tank had a burst strength of only 98.7% of the reference tank. More importantly, the tank-to-tank variation was extremely high, with a variation of +/-14% which is well above the typical variation of less than 4% and unacceptable for production. The silica nano-particle tanks showed similar results, with the best tank at only 96.9% of the baseline burst pressure and a tank-to-tank variation +/-8.1%. With none of the tanks achieving improved performance, it was determined that at least within the materials scope of this program that the reinforced resins were not going to provide any potential improvement. To confirm this, the team did a brief study using a commercially available nano-particle reinforced epoxy resin. While the tank-to-tank variation was better, it was still higher than the standard process and there was no improvement in overall burst pressure. Impact and fatigue testing also showed no significant improvement. The nanoparticle additives did not increase the strength or stiffness of the resin enough to significantly increase the composite lamina strength or stiffness. In addition, the increased variation in burst pressure was attributed to the non-uniform distribution and clumping of particles, which was observed in composite samples from the ruptured tanks, as well as electron microscopy analysis.

TABLE 2. Summary of Measured Burst Results after Impact and Pressure Cycling

		Epoxy	Vinyl Ester
	Test Type	**Relative Burst**	**Relative Burst**
No Impact	Burst	105%	111%
	Cycle A	100%	103%
	Cycle B	99%	95%
Impact Test Round 1	Burst	57%	55%
	Cycle A	67%	Did Not Finish
	Cycle B	58%	63%
Impact Test Round 2	Burst	70%	82%
	Cycle A	55%	74%
	Cycle B	62%	67%

FIGURE 1. Image of burst tank made with vinyl ester resin after impact testing

Enhanced Operating Conditions

Burst Tests

Low temperature burst tests of full VE resin tanks were carried out to evaluate enhanced operating condition performance. Testing was performed by Cimarron

Composites using 250 bar STEB tanks precooled to 200 K. The average burst pressure was 714 bar with a 6% variation. The burst pressure exceeds the room temperature performance (target burst ~625 bar) and the variation, while slightly higher than room temperature, is still acceptable.

Materials Cold Performance Testing

In FY 2016, the team completed the cold material testing for the enhanced operating conditions. Testing was done in an MTS environmental chamber mounted on a 20 kip MTS mechanical testing frame. The chamber was cooled using a dewar of liquid nitrogen controlled by a solenoid valve to achieve the desired temperature. The temperature was verified with thermocouples inside the chamber to monitor the environment as well as a thermocouple on or near the sample to verify sample temperature.

Tensile tests were performed at seven temperatures ranging from room temperature (23°C) down to -129°C in 30°C increments. Tensile specimens were made from sheets of high-density polyethylene, low-density polyethylene, nylon, polytetrafluoroethylene, and ultra-high-molecular-weight polyethylene using the specimen dimensions from the ASTM D638 Standard Test Method for Tensile Properties of Plastics. Load and displacement data was gathered and used to calculate the ultimate tensile strength, yield strength, ultimate strain, and modulus of elasticity.

Flexural tests were performed according to ASTM Standard D6272 using a four-point bend fixture. The samples were approximately 1/8-in thick and 1-in wide so they were much better suited for flexural testing than tensile because of their brittle nature. Testing was performed with a support span of 2 in and a loading span of 1 in. Samples were cooled and tested at temperatures from room temperature to -129°C and data was collected to calculate the flexural strength, flexural strain, and modulus of elasticity.

Short beam strength testing (Figure 2) was performed according to ASTM D2344 Short Beam Strength of Polymer Matrix Composite Materials. Samples were made of two cured resins designated L047 and L046. L047 is the baseline epoxy resin material and L046 is VE resin. Samples chosen for testing were the most uniform samples available from the cured resin panels that were provided. This was done to minimize adverse effects of stress concentrations due to irregularities in the sample microstructure. Testing was performed using a short beam strength fixture conforming to ASTM standards and three tests were done at each of the standard temperatures that the other tests were performed at.

Data for the short beam shear as a function of temperature is shown in Figure 2. Here one can readily observe that while both the epoxy (L047) and the PVE (L046) generally increase in strength with decreasing temperature, it appears that the PVE peaks at 100°C. This may indicate that the sweet spot for the PVE resin is between -70°C and -100°C, which aligns well with the enhanced operating conditions expected.

Most of the materials tested, including the previously developed vinyl ester resin, were found to be suitable for use at the enhanced operating conditions. Nylon was found to be unsuitable for temperatures below approximately -40°C.

Physical Insulation Testing

Samples of VIP insulation were procured and tested at dry ice temperature to compare their measured insulating properties for cold gas operation with the available literature values. The results of the testing of three different VIP panels are shown in Table 3.

The insulation R-values achieved in the tests were estimated by comparing the measured temperature histories with the steady state and transient temperatures from a finite element model that varied the R-value. In each case, the

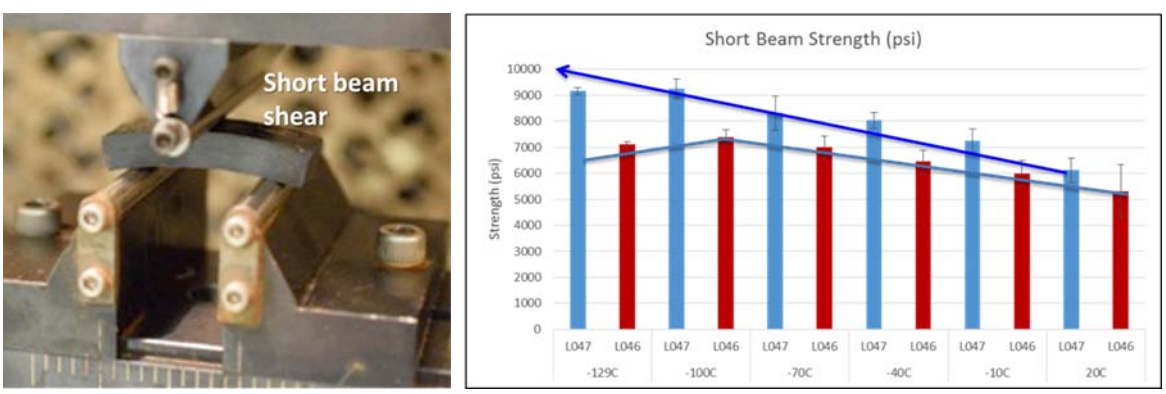

FIGURE 2. (left) Photograph of a short beam shear test of a portion of an ASTM ring made by Hexagon Lincoln. (right) The strength of both the epoxy (L047) and the PVE (L046) increases generally with decreasing temperature. Interestingly, the PVE strength appears to peak at approximately -100°C.

TABLE 3. Reported and Observed Insulation Values

Test Designation	Brand Name	Thickness (mm)	Reported Conductivity (W/mK)	Reported R/inch	Observed Conductivity (W/mK)	Observed R/inch
VIP 1	Kevothermal, VIP-AM	19	0.004 (website)	36 (website)	0.0053	27
VIP 2	Kevothermal, VIP	13	0.004 (website)	36 (website)	0.0044	33
VIP 3	Promat (SlimVac), VIP-AM	16	0.0042 (brochure)	34.3 (website)	0.0058	25

observed insulation values were similar but somewhat less than the reported values.

Dormancy tests were also conducted with a sub-scale composite tank capable of containing 1 kg of hydrogen at 50 MPa and 200 K. Unpressurized tests were performed by adding sand to replace the thermal mass of the hydrogen. Models that matched the measured temperature rise estimate that the VIP panels as configured provided about half the insulation value of the single panel tests. It is expected that the most significant factor in this reduced performance is heat loss through the joints between the panels used to construct the rectangular insulation boxes for the tests.

Finally, the transient thermal performance of tanks insulated with 1-in R30, 2-in R30, and multi-layer vacuum insulation was simulated to estimate when hydrogen venting would be required and how much hydrogen would be lost as the tank warmed to 300 K. The initial vent (62.5 MPa to 50 MPa) was estimated to occur at about 1.6, 3, and 12 days, and the second partial vent (62.5 MPa to 58.1 MPa) was estimated to occur at about 6.1, 11, and 36 days for the 1-in R30, 2-in R30, and multi-layer vacuum insulations, respectively. However, this study demonstrates that hydrogen loss from pressure relief could be eliminated if 10% of the tank capacity could be used efficiently (i.e., through driving, active cooling, battery charging, etc.) before the first vent time, followed by an additional 3.2% usage before the second vent time. Thus, usage cycles are significant in determining the required insulation for cold hydrogen storage options.

CONCLUSIONS AND FUTURE DIRECTIONS

Research completed in FY 2016 has demonstrated that the VE resin has performance and cost benefits that are encouraging for transition to manufacturing scales. However, this will require significant additional testing plus addressing the safety and environmental issues around the styrene content of the uncured resin. The materials compatibility testing for enhanced operating conditions reveals no critical issues. Testing of currently available physical insulations revealed that they are not yet capable of providing the long dormancy times targeted for cold gas storage.

FY 2016 Future Work

- Identify future development efforts around production, delivery, and storage of cold hydrogen.

FY 2016 PUBLICATIONS/PRESENTATIONS

1. D.W. Gotthold et al. 2015. "Enhanced Materials and Design Parameters for Reducing the Cost of Hydrogen Storage Tanks." Project ID# ST101. DOE Hydrogen and Fuel Cells Program Annual Merit Review, June 6–10, 2016, Washington, D.C., Pacific Northwest National Laboratory, Richland, WA.

IV.D.2 Thermomechanical Cycling of Thin Liner High Fiber Fraction Cryogenic Pressure Vessels Rapidly Refueled by Liquid Hydrogen Pump to 700 Bar

Salvador M. Aceves (Primary Contact),
Guillaume Petitpas
Lawrence Livermore National Laboratory (LLNL)
7000 East Avenue
Livermore, CA 94550
Phone: (925) 422-0864
Email: aceves6@llnl.gov

DOE Manager: Jesse Adams
Phone: (720) 356-1421
Email: jesse.adams@ee.doe.gov

Subcontractors:
Spencer Composites Corporation, Sacramento, CA
BMW, Munich, Germany
Linde LLC, Hayward, CA

Project Start Date: January 2014
Project End Date: January 2017

Overall Objectives

- Develop ultra-light cryogenic pressure vessels with a 12-in diameter up to 700 bar.
- Optimize metallic liner thickness, composite fiber fraction, and ultra-thin vacuum jacket.
- Quantify liquid hydrogen (LH_2) pump durability to 700 bar over 6,000 refuelings.
- Demonstrate full-scale system density of 50 g H_2/L_{system} and 9 wt% H_2, and a cycle life of at least 1,500 refills.

Fiscal Year (FY) 2016 Objectives

- Complete construction and commission LLNL's hydrogen test facility.
- Analyze, design, and fabricate full-scale (65 L) 700 bar cryogenic pressure vessel prototypes with long cycle life.
- Demonstrate minimum pressure vessel life of 1,500 thermomechanical (pressure and temperature) cycles at LLNL's hydrogen test facility,

Technical Barriers

This project addresses the following technical barriers from the Hydrogen Storage section (3.3.5) of the Fuel Cell Technologies Office Multi-Year Research, Development, and Demonstration Plan.

(A) System Weight and Volume

(D) Durability/Operability

(N) Hydrogen Venting

Contribution to Achievement of DOE Hydrogen Storage Milestones

This project will contribute to achievement of the following DOE milestones from the Hydrogen Storage section of the Fuel Cell Technologies Office Multi-Year Research, Development, and Demonstration Plan.

- Milestone 2.6: Transportation: Develop and verify onboard storage systems achieving capacity of 5.5% by weight and an energy density of 0.04 kg H_2/L. (4Q, 2020)

FY 2016 Accomplishments

- Built and commissioned hydrogen test facility.
- Built and hydraulically cycle tested six thin lined pressure vessels rated for 700 bar.
- Built a seventh thin lined vessel and cycle tested it with hydrogen.

✧ ✧ ✧ ✧ ✧

INTRODUCTION

Storing cryogenic hydrogen in a pressurized, insulated system has many benefits in terms of safety, volumetric and gravimetric densities, and ownership cost that have been studied and demonstrated by LLNL [1-3] and external parties [4-7]. High utilization (>1,500 kg H_2/d) commercial-scale fueling stations will likely require the use of LH_2 by means of a fast, energy efficient LH_2 pump. Until now, the development of cryogenic pressure vessels by LLNL has used off the shelf pressure vessels with an aluminum liner, a maximum operating pressure limited to 350 bar with large capacity (151 L, equivalent to 10.7 kg H_2) and large diameter (25 in). We believe that system densities (both volumetric and gravimetric), cycle life, and manufacturability could be improved by developing pressure vessels specifically tailored towards cryogenic utilization, even at a 5.6 kg H_2 scale, by exploring thin liner design (especially important for 12-in

diameter), non-Al liner materials, high fiber fraction for the composite overwrap, 700 bar operating pressure, and ultra-thin vacuum jacket designs.

APPROACH

Within this project, we are designing, manufacturing and cryogenically pressure testing full-scale (65 L) 700 bar pressure vessels with a thin (<2 mm), non-Al liner and high fiber fraction. Our primary goal is to assess the *cryogenic* strength of those prototype composite vessels after 1,500 thermomechanical hydrogen cycles, while other secondary objectives will be accomplished in parallel: (1) measure LH_2 pump performance at 700 bar after 6,000 refuelings (~24 tonnes of LH_2), (2) demonstrate lightweight vacuum jackets for cryogenic hydrogen pressure vessels, and (3) design and fabricate an experimental cryogenic hydrogen storage system with 5.6 kg H_2 capacity.

In order to achieve the thermomechanical cycling, the hydrogen test facility was constructed next to the existing 875 bar LH_2 pump, capable of rapidly cycling full-scale (65 L) non-certified cryogenic pressure vessels up to 700 bar and performing strength testing of those vessels up to 160 K and 1,300 bar. One to two vessels can be cycled at the same time in this single-manned, remotely operated facility that also includes a vent stack and will include a 40-kW heat exchanger.

RESULTS

Work in the reporting period focused on building and commissioning the hydrogen test facility, and on building and cycle testing thin-lined pressure vessels.

Hydrogen Test Facility

LLNL's hydrogen test facility, completed during the reporting period (Figure 1), offers a unique platform for testing hydrogen systems over a wide range of pressures, temperatures, volumes and flow rates.

The main component of LLNL's hydrogen facility is a liquid hydrogen pump. Manufactured by Linde, a leading supplier of cryogenic equipment, the pump takes liquid hydrogen from the station dewar at low pressure (2–3 bar) and very low temperature (23–25 K) and pressurizes it up to an 875 bar cryogenic fluid. The flow rate is very high (up to 120 kg of hydrogen per hour) enabling (future) 5-min refuels. The station dewar has 11,000-L capacity, sufficient to refuel ~150 vehicles. When empty, it is refilled by a liquid hydrogen truck.

Another key component of the facility is a containment vessel that enables testing of thin-lined experimental pressure vessel prototypes. These one-of-a-kind experimental vessels are not certified by current standards (American Society of Mechanical Engineers, International Organization for Standardization, Federal Motor Vehicle Safety Standards)

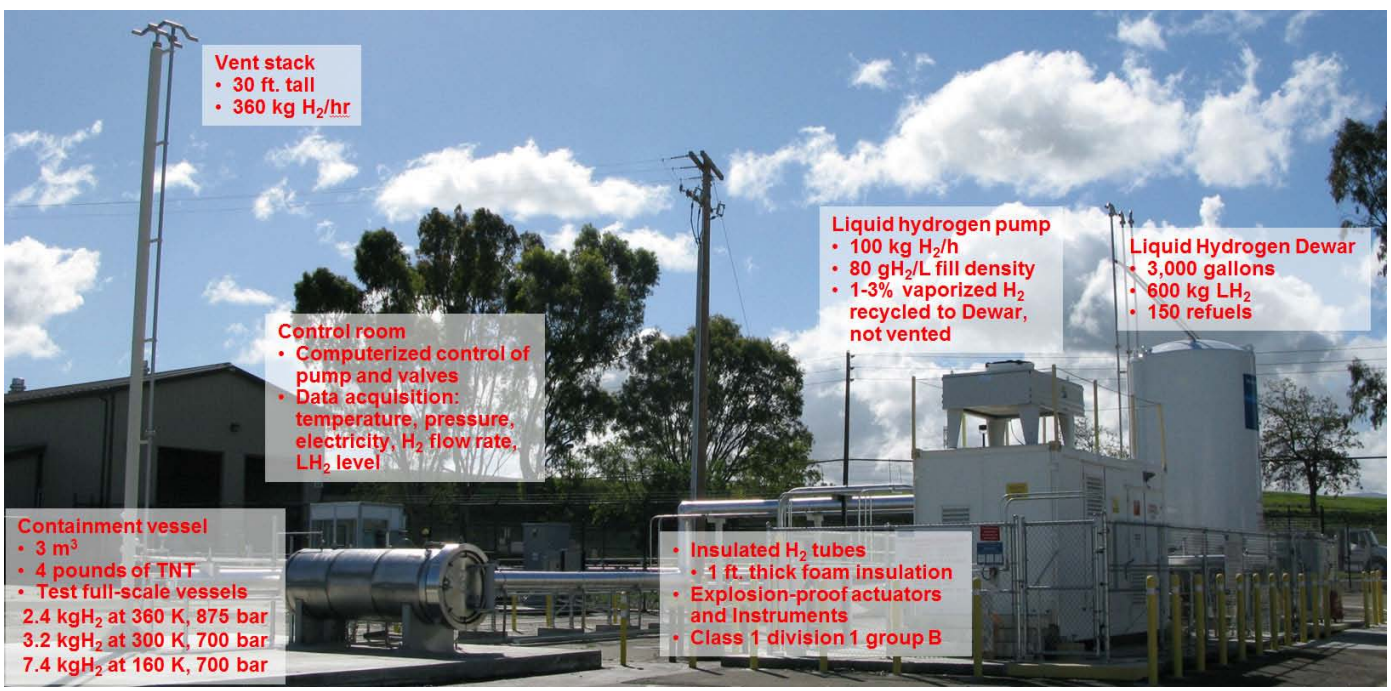

FIGURE 1. Hydrogen test facility at LLNL showing the main components and their performance metrics: liquid hydrogen pump, liquid hydrogen dewar, containment vessel, control room, insulated hydrogen tubes, and vent stack.

and are therefore unsafe to pressurize in manned areas. Made of 3.2-cm thick stainless steel 304 and weighing almost 5,000 kg, the containment vessel is rated for 65 bar maximum pressure and can contain the equivalent energy of 1.8 kg of trinitrotoluene, therefore enabling testing of full-scale vessels and hydrogen systems. The containment vessel can also hold high vacuum down to 0.1 Pa.

The test facility can be operated from a control room strategically located for maximum visibility and far enough from the dewar (23 m) to meet National Fire Protection Association (NFPA) standards. Full instrumentation is also available with sensors for temperature, pressure, flow, liquid hydrogen level, electricity, and vent rates. All sensors and system components are explosion-proof (Class 1 Division 1 Group B), as demanded by NFPA for systems that may be exposed to hydrogen.

A 9-m high vent stack completes the facility, enabling rapid venting of hydrogen subsequent to pressure testing. High altitude venting of hydrogen is demanded by NFPA for rapid dispersion away from personnel at ground level. Hydrogen, being so light and therefore buoyant, rapidly diffuses upward once it is released and warms up to ambient temperature.

In the next quarter (fall of 2016), a 40-kW electric heater and heat exchanger will be added in order to provide varying hydrogen outlet temperature, from cryogenic to room temperature, enabling cost effective, rapid thermomechanical testing at high pressure and low (60 K) to elevated (360 K) temperature.

Thin-Lined Pressure Vessels

Following last year's strength testing of a pressure vessel to 1,560 bar (2.23 safety factor for 700 bar operation), we dedicated this year to designing and producing a vessel that could be cryogenically cycled over 1,500 times. This demanded detailed finite element and fatigue analysis (Figure 2) to determine composite layer strength necessary to meet cyclability requirements. In collaboration with BMW, we also conducted linked thermo-fluid and stress analysis of the fill process to determine improved boss designs for

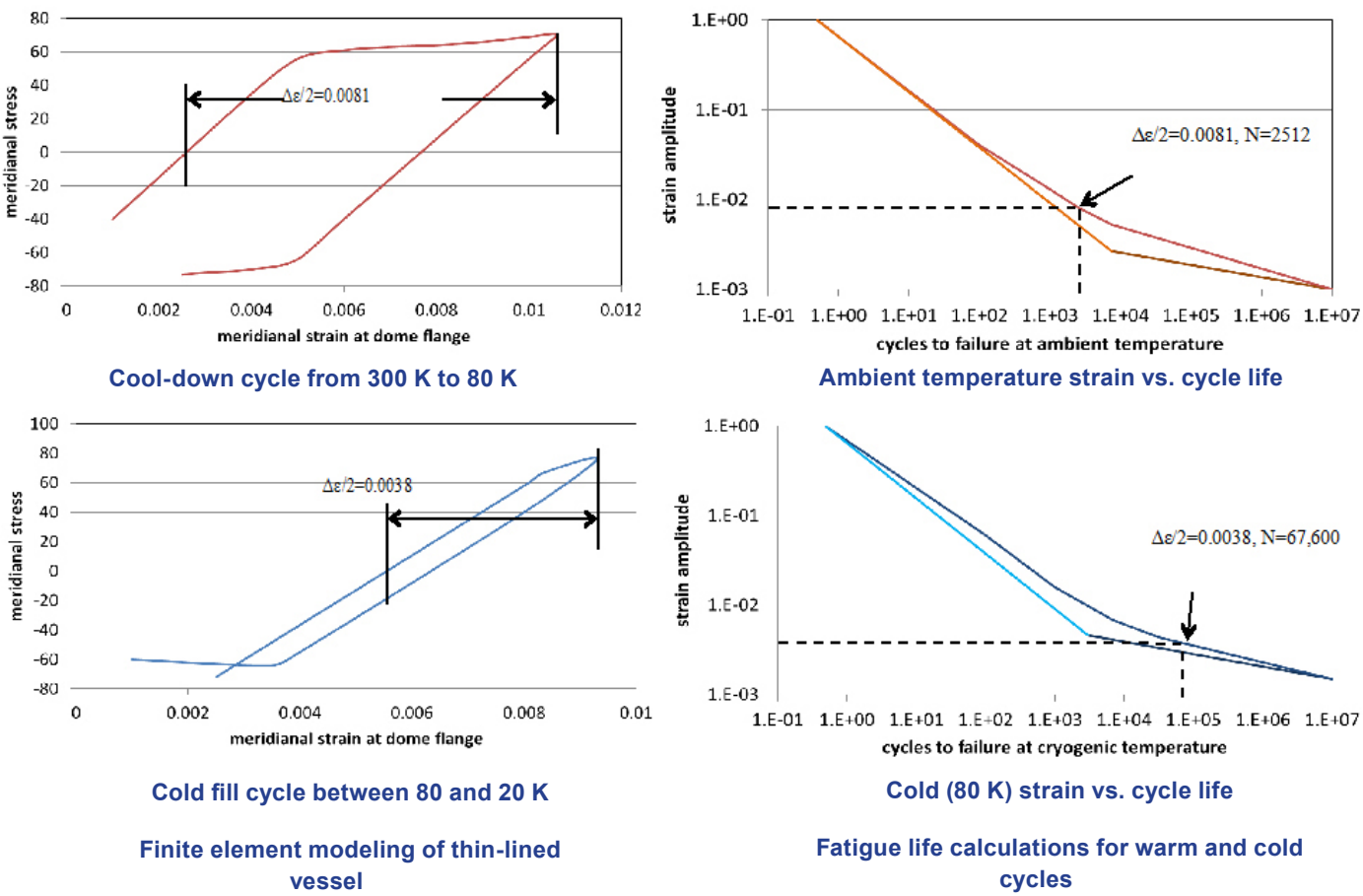

Finite element modeling of thin-lined vessel

Fatigue life calculations for warm and cold cycles

FIGURE 2. Finite element and fatigue analysis of thin-lined cryogenic pressure vessels. Left: finite element model results indicating stress vs. strain for the metal liner during a cool-down and pressurization cycle (above) and a cold pressurization cycle (below). Right: Calculation of fatigue analysis based on strain amplitude vs. number of cycles to failure for both cool-down (above) and cold (below) cycles.

surviving thermal gradients that may result while filling an initially warm vessel with cryogenic hydrogen (Figure 3).

In total, we manufactured and tested seven vessels during the year (Table 1). The first two vessels failed during autofrettage. Research into this failure mode indicated that lack of roundness of the liner weakened the structure and resulted in premature failure at low pressure. Process modifications finally led to vessels that survived autofrettage and an increased number of water pressure cycles to 700 bar (except for Vessel 6 that failed during autofrettage while researching alternate resins). After partial success with water cycling, a final vessel was tested with cryogenic hydrogen, reaching 456 cycles, well short of the 1,500 cycle target.

CONCLUSIONS AND FUTURE DIRECTIONS

Research into the cause of the failure indicates that liner welds area the likely culprit. Hand tungsten inert gas welds are irregular by nature and introduce flaws that may initiate crack propagation during vessel cycling. Future work in this topic will demand new liner manufacture techniques such as e-beam welding, pulsed laser welding, or spin forming. The potential still remains to manufacture thin-lined vessels with long cycle life to demonstrate the ultimate performance limits of cryogenic pressure vessels.

After careful review of the experimental results, DOE decided to reduce the scope of the project eliminating vessel

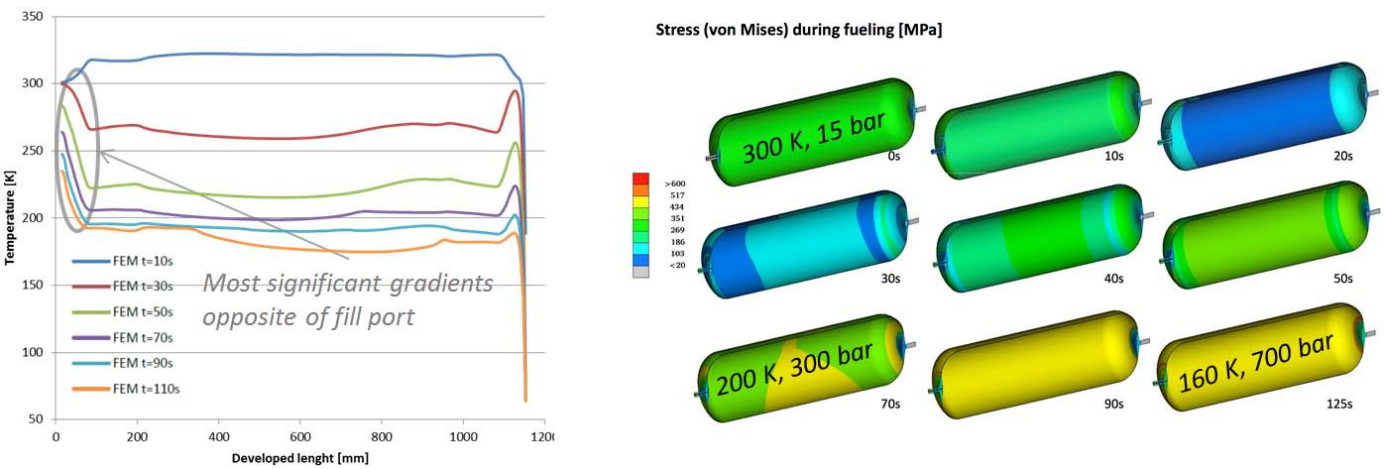

FIGURE 3. Linked thermo-fluid and stress analysis of the cryogenic fill process of an initially warm thin-lined pressure vessel indicating temperature distribution along vessel (left) and Von Mises stress distribution (right) as a function of time (from BMW).

TABLE 1. Experimental results from the testing of the seven thin-lined experimental pressure vessels built and tested for this project.

Date	#	Liner	Resin	Test result
Aug 15	1	1.3 mm Steel	High Fiber Fraction	Buckling then burst @ 8 ksi (during autofrettage)
Sep 15	2	1.5 mm Alternate	Epoxy	Buckling then burst @ 12 ksi (during autofrettage)
Oct 15	3	1.7 mm Alternate	Epoxy	Leak after **133** cycles, T-weld failure
Nov 15	4	1.5 mm Alternate	Epoxy	Leak after **247** cycles, root cause not found, NOT at T-weld
Jan 16	5	1.7 mm Steel	Epoxy	Leak after **468** cycles, longitudinal weld failure
Mar 16	6	1.7 mm Steel, annealed	High Fiber Fraction	Burst @ 10 ksi (during autofrettage)
May 16	7	1.7 mm steel	Epoxy	Leak after **456** cryogenic hydrogen cycles

development activities and instead testing pressure vessels supplied by BMW. This may initiate in the fall of 2016 once vessels are received, a test protocol is identified, and the electric heater (possibly necessary for vessel testing) is installed at LLNL's test facility.

REFERENCES

1. Aceves S.M., Espinosa-Loza F., Ledesma-Orozco E., Ross T.O., Weisberg A.H., Brunner T.C., et al. High-density automotive hydrogen storage with cryogenic capable pressure vessels. International Journal of Hydrogen Energy 2010;35:1219–26. doi:10.1016/j.ijhydene.2009.11.069.

2. Petitpas G., Aceves S.M. Modeling of Sudden Hydrogen Expansion from Cryogenic Pressure Vessel Failure. International Conference on Hydrogen Safety, San Francisco: 2011.

3. Aceves S.M., Petitpas G., Espinosa-Loza F., Matthews M.J., Ledesma-Orozco E. Safe, long range, inexpensive and rapidly refuelable hydrogen vehicles with cryogenic pressure vessels. International Journal of Hydrogen Energy 2013;38:2480–9. doi:10.1016/j.ijhydene.2012.11.123.

4. Kircher O., Greim G., Burtscher J., Brunner T. Validation of cryo-compressed hydrogen storage (cch2) – a probabilistic approach. Proceeding of the International Conference on Hydrogen Safety, San Francisco: 2011.

5. Paster M.D., Ahluwalia R.K., Berry G., Elgowainy A., Lasher S., McKenney K., et al. Hydrogen storage technology options for fuel cell vehicles: Well-to-wheel costs, energy efficiencies, and greenhouse gas emissions. International Journal of Hydrogen Energy 2011;36:14534–51. doi:10.1016/j.ijhydene.2011.07.056.

6. Ahluwalia R.K., Hua T.Q., Peng J.-K., Lasher .S, McKenney K., Sinha J., et al. Technical assessment of cryo-compressed hydrogen storage tank systems for automotive applications. International Journal of Hydrogen Energy 2010;35:4171–84. doi:10.1016/j.ijhydene.2010.02.074.

7. Ahluwalia R.K., Hua T.Q., Peng J.K., Roh H.S., Bailey J., Kumar R. System Level Analysis of Hydrogen Storage Options, DOE Annual Merit Review, Washington, DC: 2012.

IV.D.3 Conformable Hydrogen Storage Pressure Vessel Project

Erik Bigelow
Center for Transportation and the Environment (CTE)
730 Peachtree Street, Suite 760
Atlanta, GA 30308
Phone: (404) 376-5390
Email: erik@cte.tv

DOE Manager: Grace Ordaz
Phone: (202) 586-8350
Email: Grace.Ordaz@ee.doe.gov

Contract Number: DE-EE0006967

Subcontractors:
- High Energy Coil Reservoirs, LLC, (HECR) Fort Wayne, IN
- University of Texas at Austin, Center for Electromechanics, Austin, TX

Project Start Date: September 1, 2015
Project End Date: August 31, 2016

Overall Objectives

- To develop and demonstrate a conformable, lightweight, 700 bar gaseous hydrogen storage system with nominal capacity of approximately 1 kg.

Fiscal Year (FY) 2016 Objectives

- Order tooling to support a 700 bar capable pressure vessel.
- Demonstrate 2,170 bar burst pressure capability.
- Build test and data collection rig to safely test prototype hydrogen pressure vessels.
- Build pressure vessels using new tooling and test hydrogen permeability.

Technical Barriers

- Resin selection that offers low permeability, flexibility, durability, impact resistance and thermoplastic (extrusion) performance
- Over braiding design to reach 2,170 bar
- Safe testing of prototype hydrogen pressure vessels

This project addresses the following technical barriers from the Hydrogen Storage section of the Fuel Cell Technologies Office Multi-Year Research, Development, and Demonstration Plan.

(A) System Weight and Volume

(B) System Cost

Technical Targets

- The key material requirements to meet for resin selection:
  - Low hydrogen leakage (<0.05 g/hr/kg H_2 stored at 700 bar)
  - Operational temperature limit (-40°C ≤ T ≤ 85°C)
  - Corrugation process compatibility (i.e., needs to be process compatible, range of viscosity, melt temperature, and durometer)
- Burst pressure exceeding 2,170 bar

This project seeks to address the high cost of conventional gaseous 700 bar hydrogen storage, as well as the overall weight of the hydrogen storage system. Although this project will not improve the volumetric efficiency of gaseous storage, the pressure vessel design should allow a more flexible on-vehicle packaging than a conventional rigid cylinder. Possible tank layouts could optimize the use of areas in the same way that current gasoline tanks are molded to best use available space. Using HECR's pressure vessel technology for hydrogen storage promises to provide breakthroughs in commercially available pressure vessel costs, conformability, and weight.

At the time of this progress report, the project has not produced the prototype vessels, and the targets are the predictions based on the project proposal.

Table 1 shows how the proposed HPM Vessel technology compares to existing Type IV vessels and DOE's 2017 and ultimate targets for passenger vehicle hydrogen storage systems.

FY 2016 Accomplishments

- The tooling required to produce the resin liner was specified, ordered and delivered during FY 2016. This tooling fits into a commercial plastic corrugation and extrusion machine, and will produce the liners that will prevent the hydrogen permeating out of the vessel (Figure 1).
- Resin candidates selected include Hytrel 5556, Acetal, EVAL M100, and EVAL F101. Acetal and EVAL resins have an acceptable predicted thickness (<0.060 in) based on predicted hydrogen permeability and compatibility with the liner extrusion and corrugation process.
- Completed thermodynamic model of vessel filling.

TABLE 1. Performance Target Summary

	DOE Projections for Type IV 700 bar Storage at 500,000 units/yr	DOE 2017 Target	DOE Ultimate Target	Proposed HPM Vessel
Gravimetric **Capacity**	1.5 kWh/kg (4.5 wt% H_2)	1.8 kWh/kg (5.5 wt% H_2)	2.5 kWh/kg (7.5 wt% H_2)	3.7 kWh/kg (10.0 wt% H_2)
Volumetric Capacity	0.8 kWh/L (24 g H_2/L)	1.3 kWh/L (40 g H_2/L)	2.3 kWh/L (70 g H_2/L)	0.7 kWh/L (20 g H_2/L)
Cost	$17/kWh ($570/kg H_2 stored)	$12/kWh ($400/kg H_2 stored)	$8/kWh ($267/kg H_2 stored)	$8.40/kWh ($280/kg H_2 stored)

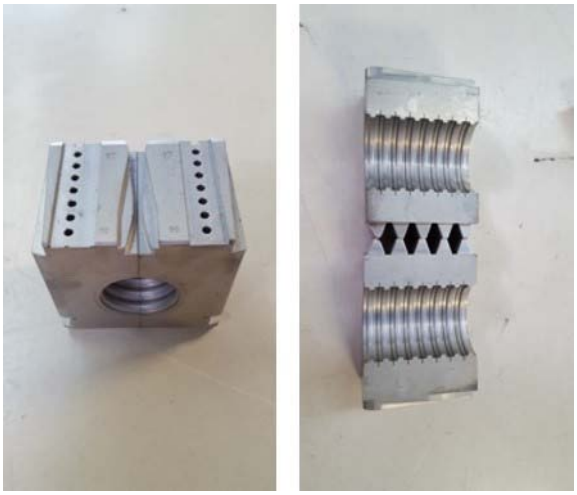

FIGURE 1. Example tooling to create resin liner

- Filling rate to meet J2601 fueling standard (11.5 MPa/min) does not seem restricted by smaller vessel connecting end sections.
- Temperature rise in end vessels is above 85°C in initial models.

- Completed fabrication of test safety containment vessel: designed to withstand 5,000 psi
- Completed initial testing with baseline compressed natural gas vessels to prove test system workability and data collection system, and measure baseline permeability performance for Hytrel resin. The measured permeability value is about half of the expected value. More detail is shown in Table 2.

INTRODUCTION

This project consists of three organizations, (1) Center for Transportation and the Environment, project prime recipient responsible for project management; (2) HECR, responsible for design and prototype development of the storage vessel; and (3) The University of Texas Center for Electromechanics, responsible for permeability testing and resin technical information.

The overall goal of this research and development project is to develop an approach for compressed hydrogen gas storage that will provide a cost-effective and conformable storage solution for hydrogen. The team will develop and demonstrate a conformable, lightweight 700 bar gaseous hydrogen storage system with a nominal capacity of approximately 1 kg. The nature of the HECR's technology allows for a higher capacity pressure vessel to be constructed simply by creating a longer vessel through the same process.

APPROACH

The hydrogen storage system development will occur over two budget periods beginning with an initial design, including candidate resin down selection and over-braid final development. The design includes overwrapping an extruded thermoplastic elastomeric resin liner with high performance Kevlar™. The team will then build test vessels and perform key testing to validate the suitability for hydrogen containment. This testing will include hydrostatic burst testing, hydrostatic pressure cyclic testing, and hydrogen permeability testing conducted on a number of resin liners.

RESULTS

Following an extensive decision matrix search, three resin candidates were identified which have appropriate characteristics to serve as low permeability liners for a conformable hydrogen storage vessel. Available data for CO_2, N_2, and He and H_2 permeability showed Acetal and EVAL resin to have superior permeability resistance. While the team did not find clearly linear and general relationships between permeability for any one gas and hydrogen, generally those resins with greater permeability resistance were better with hydrogen. As process compatibility is critical, candidates were selected to be similar to Hytrel 4275, the current resin used in pressure vessels for other applications.

Three candidate resins have a predicted permeability below the limit calculated to meet the proposed hydrogen leakage rate, with a liner thinner than 0.60 in. This is the upper end of the expected resin liner thickness than can be

TABLE 2. Selected Resin Characteristics

Resin / Polymer	Permeability (cm³ (cm)/ atm sec cm²)				Required thickness to meet 0.05 g/hr-kg H2 stored @ 700 bar	
	H_2	CO_2	He	N_2	(cm)	(in)
Hytrel 5556	na	1.80E-07	9.90E-08	1.40E-08	na	na
Acetal	1.50E-10	2.30E-09	na	na	0.0192	0.049 ★
EVALM100	1.62E-11	na	na	na	0.0021	0.005 ★
EVAL F101	1.30E-11	1.90E-12	3.70E-10	3.94E-14	0.0017	0.004 ★

reliably produced. The calculated liner thickness is shown on the right column of Table 2.

Resin candidates were narrowed down using a decision matrix. The decision matrix was based on density (>1.2 g/cm^3), melting temperature (190 +/-5°C), durometery (>55), and melt flow rate (<6 g/10 min), and viscosity (<250 Pa*s) characteristics. In the final selection round, hydrogen permeability was also added to the characteristics considered. Three candidate resins which have predicted hydrogen permeability to allow the vessel to be less than 0.060 in and otherwise meet the decision matrix criteria are Acetal, EVAL M100, and EVAL F100 (Table 3).

A conceptual design and fabrication of the hydrogen leak test cell was completed, and initial testing was conducted using HECR's existing 2-in diameter pressure vessels. The first testing was completed with nitrogen to validate the test rig. Results are shown in Table 4. The measured nitrogen permeability was about 50% lower than available data, and in the expected order of magnitude.

Leakage testing was then done using hydrogen at 1,000 psig and 1,800 psig to study the effects of pressure on leak rate (Table 5). An interesting observation from the leak tests was that the leak rate scaled with approximately

TABLE 3. Final Filtered Decision Matrix

Polymer Resin Evaluation		Durometer Scale Reading	Subtotal	Melting Temperature	Subtotal	Viscosity	Subtotal	Density	Subtotal	H2 Permeability	Subtotal	Grand Total
		2		2		1		1		4		
		Hard resin favored, Durometry values of ≥ 55 are preferred		Preferred Temperature 190 +/- 5 °C		High viscosity favored, values of < 6 (250) are preferred		High density favored, values > 1.2 are preferred				
#	Resin Properties	Hardness, Shore D		°C		g/10 min (Pa s)		g/cm3		cm3 (cm)/ atm sec cm2		
1	Acetal	77.0 A	4.00	190.0 A	4.00	2.4 A	4.00	1.42 A	4.00	1.5E-10 B	3.00	**356.5**
2	Polybutylene terephthalate (Crastin)	55.0 B	3.00	225.0 D	1.00	7.0 B	3.00	1.30 A	4.00	1.5E-08 D	1.00	**159.7**
3	EVAL M100	76.0 A	4.00	195.0 A	4.00	4.0 A	4.00	1.22 B	3.00	1.6E-11 A	4.00	**388.7**
4	EVAL F101	77.0 A	4.00	183.0 B	3.00	3.2 A	4.00	1.19 C	2.00	1.3E-11 A	4.00	**352.3**
5	PCTFE	90.0 A	4.00	212.0 C	2.00	1.8 A	4.00	2.10 A	4.00	4.2E-09 C	2.00	**263.9**
6	PTFE	55.0 B	3.00	164.0 D	1.00	200.0 A	4.00	2.20 A	4.00	7.4E-08 D	1.00	**164.4**

PCTFE - Polychlorotrifluoroethylene; PTFE - Poly-tetrafluoroethylene

TABLE 4. Permeability Data from Initial Nitrogen Testing with Hytrel

Measured PV N_2 dP	Measured TC N_2 dP	Mass N_2 leaked from PV	Resulting TC N_2 dP	Leak Rate N_2	Duration	Measured Permeability	Permeability in Literature	Permeability Difference	Permeability Difference
(psi)	(psi)	(g)	(psi)	(g/hr-kg N_2)	(hr)	(cm^3-cm/ atm-s-cm^2)	(cm^3-cm/ atm-s-cm^2)	(cm^3-cm/ atm-s-cm^2)	(%)
6	0.9	1.29	0.881	0.25542	24	5.51E-09	1.41E-08	-8.57E-09	-61%
13.4	2.2	2.87	1.968	0.28522	48	6.16E-09	1.41E-08	-7.92E-09	-56%
10	1.3	2.14	1.469	0.2838	36	6.13E-09	1.41E-08	-7.95E-09	-56%
13.212	1.09843	2.83	1.94	0.37496	25	7.07E-09	1.41E-08	-7.01E-09	-50%

TABLE 5. Permeability Data from Initial Hydrogen Testing

Measured PV H_2 dP	Measured TC N_2+H_2 dP	Mass H_2 leaked from PV	Resulting TC N_2+H_2 dP	Leak Rate H_2	Duration	Measured Permeability
(psi)	(psi)	(g)	(psi)	(g/hr-kg H_2)	(hr)	(cm^3-cm/ atm-s-cm^2)
Nominal Test Pressure 1,000 psig						
23.1	3.52	0.33	3.142	0.306	10.3	4.83×10^{-8}
122.7	19.43	1.76	16.755	0.264	63.3	4.18×10^{-8}
145.8	22.95	2.09	19.896	0.270	73.6	4.27×10^{-8}
Nominal Test Pressure 1,800 psig						
52	6.88	0.70	6.670	0.543	12.3	8.58×10^{-8}
31.7	4.78	0.43	4.092	0.458	8.9	7.24×10^{-8}
39.4	6.6	0.53	5.037	0.449	11.2	7.09×10^{-8}
123.1	17.66	1.66	15.799	0.487	32.4	7.70×10^{-8}

linearly with pressure as expected. The average permeability at 1,000 psi was 4.43, and at 1,800 psi was 7.65, in the above units. Linearly scaling the permeability rate for 1,000 psi up by 1.8X predicts a permeability of 7.97, which is approximately 5% off the expected value for a linear permeability variation with pressure.

Figure 2 shows the pressure and temperature variation between the high pressure vessel, and low pressure safety containment vessel over approximately 40 hr of testing. The temperature variation shows the building temperature changing over the course of the two-day test. The red line shows the fairly linear pressure loss of the high pressure vessel through permeation. The steep drop shown in the red curve at the beginning of the test is thought to be due to the initial relaxation of the pressure vessel following filling. The black line shows the increase of pressure in the containment vessel corresponding to the hydrogen permeated through the pressure vessel.

Modeling of a 10- and 20-vessel hydrogen storage system was done to observe the effects of a single chain of vessels in series versus a manifold system of vessels in parallel. There was a significant temperature variance in the vessels, which could also be the potential limiting issue for the conformable hydrogen storage concept and its fill rate. The results shown in Figure 3 include heat transfer between the internal hydrogen and, through the pressure vessel wall, to

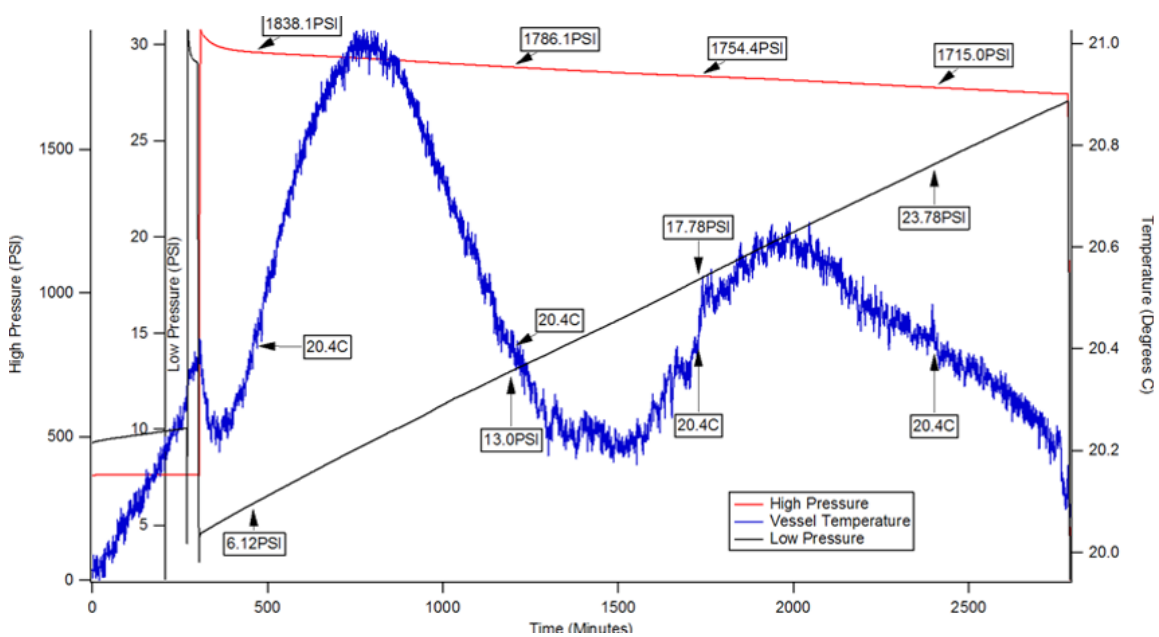

FIGURE 2. Captured pressure data from initial hydrogen testing

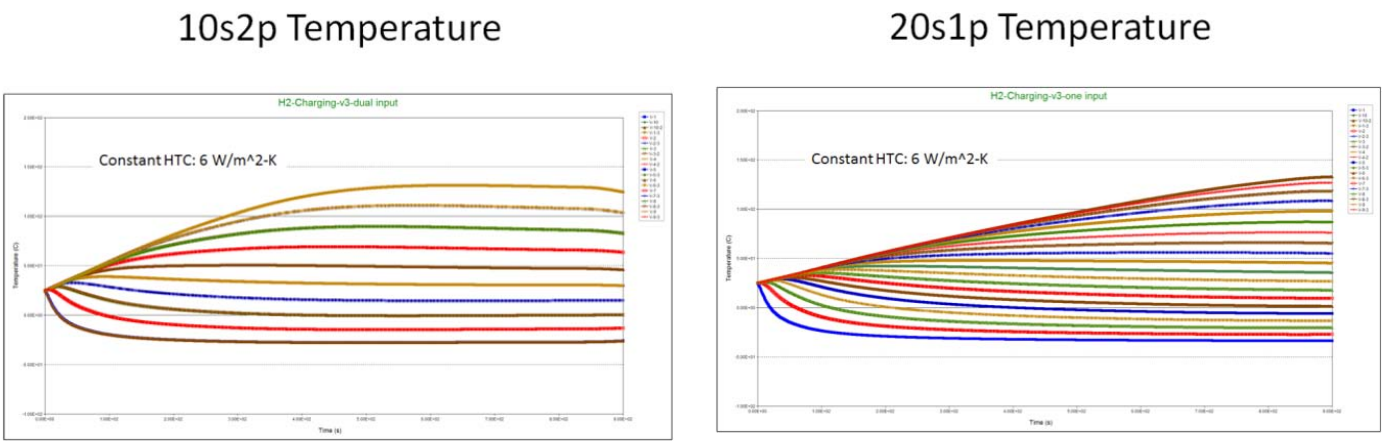

HTC – Heat transfer coefficient

FIGURE 3. Temperature results of hydrogen filling simulations

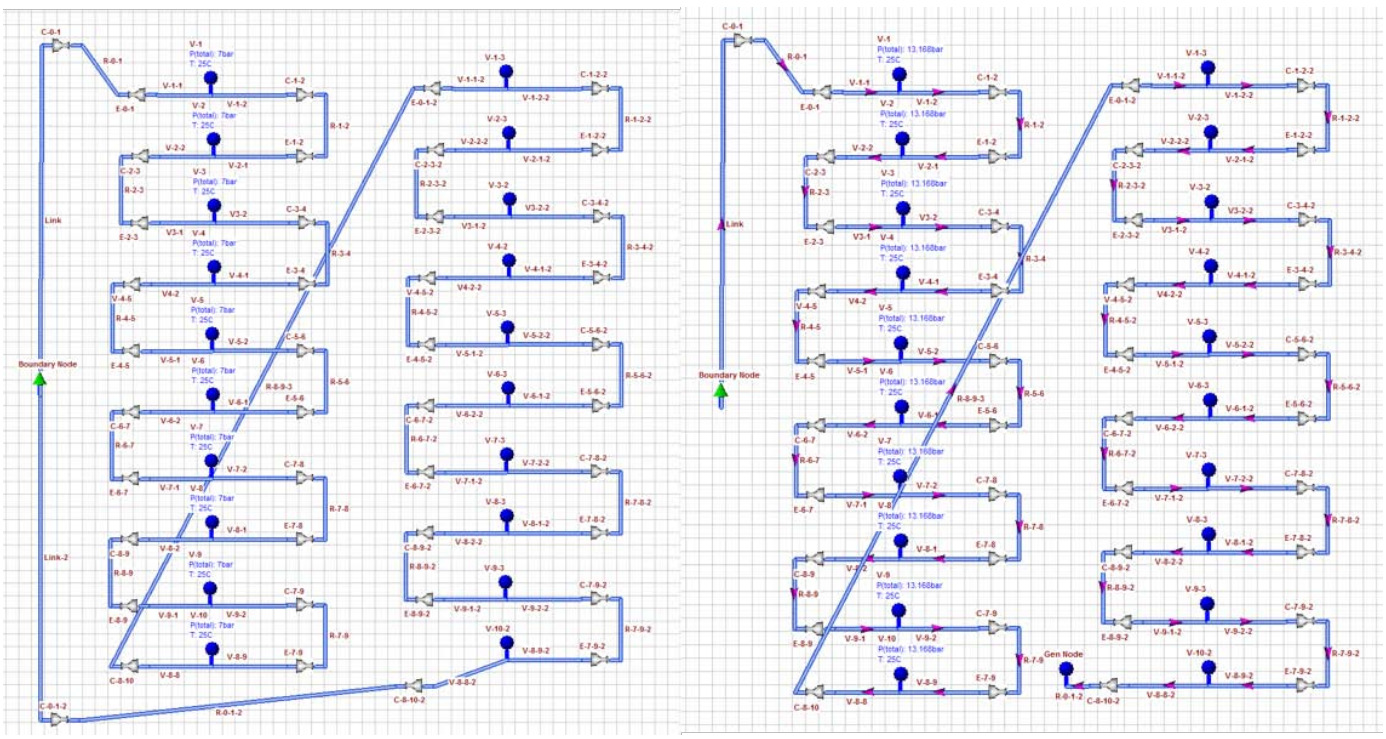

FIGURE 4. Macroflow network models of a 20-vessel conformable storage system. Left: 10 series, 2 parallel configuration. Right: 20 series configuration.

ambient air at 40°C with an effective heat transfer coefficient of 6 W/m^2-K. The vessels at the end of the chain experience a significant rise in temperature approaching 150°C. The first pressure vessels quickly approach the hydrogen filling temperature, which is modeled at -40°C. While this simulation is preliminary, it does suggest that close attention needs to be paid to thermal performance during filling, and system survivability from exposure to high temperature.

The series and parallel configurations are shown in Figure 4.

CONCLUSIONS AND FUTURE DIRECTIONS

Some conclusions that can be drawn at this point in the project are:

- Hydrogen filling in a long, conformable vessel at J2719 will likely see temperatures in excess of 85°C.
- Selecting a resin with all needed processing characteristics will still likely be difficult in advance of prototype production testing.

- The Center for Electromechanics test apparatus is capable of measuring pressure loss due to permeability through the pressure vessel and correlating this with a pressure rise in the containment vessel.

Future work for this project includes:

- Start prototype production of resin cores.
- Achieve 2,170 bar burst pressure.
- Measure permeability with baseline resin and new prototype resins.

FY 2016 PUBLICATIONS/PRESENTATIONS

1. 2016 DOE Hydrogen and Fuel Cells Program Annual Merit Review Presentation.

IV.D.4 Next Generation Hydrogen Storage Vessels Enabled by Carbon Fiber Infusion with a Low Viscosity, High Toughness System

Brian Edgecombe
Materia, Inc.
60 N. San Gabriel Blvd.
Pasadena, CA 91107
Phone: (626) 584-8400, Ext. 210
Email: bedgecombe@materia-inc.com

DOE Manager: Grace Ordaz
Phone: (202) 586-8350
Email: Grace.Ordaz@ee.doe.gov

Contract Number: DE-EE0006625

Subcontractors:
- Montana State University, Bozeman, MT
- Spencer Composites Corporation, Sacramento, CA

Project Start Date: August 5, 2014
Project End Date: August 30, 2017

Overall Objectives

The project is focused on supporting the key DOE metrics for a 700-bar, Type IV tank by meeting the following objectives:

- Reduce the carbon fiber (CF) composite volume by 35%.
- Demonstrate cost of composite materials of $6.5/kW-hr. This component cost is an important element of the DOE 2020 system cost target of $10/kW-hr.
- Demonstrate industry-standard performance (burst strength of 1,575 bar and 90,000 cycle life).

Fiscal Year (FY) 2016 Objectives

- Optimize infusion on full-scale tanks with aid of infusion models.
- Manufacture full-size tanks with CF reduction and test.
- Conduct key tests to confirm performance current standards.

Technical Barriers

This project addresses the following technical barriers from the Hydrogen Storage section of the Fuel Cell Technologies Office Multi-Year Research, Development, and Demonstration Plan.

(A) System Weight and Volume

(B) System Cost

(D) Durability/Operability

(G) Materials of Construction

Technical Targets

The project is focused on the technical targets highlighted in Table 1 related to the gravimetric and cost metrics of onboard automotive hydrogen storage systems. Since a significant portion of the cost is directly from the carbon-fiber composite overwrap, the project aims to reduce the amount of composite necessary to meet the tank specifications. During FY 2016, the project has met some key milestones to provide updated estimates on the progress towards the technical targets in Table 1.

TABLE 1. Progress towards Technical Targets for Onboard Automotive Hydrogen Storage System

Characteristic	Units	2020 Target	FY 2016 Status
Gravimetric	kW-hr/kg sys	1.8	1.6 to 1.8 Estimated*
System Cost	$/kW-hr at 500,000 units/yr	10	9 to 10.5 Estimated*

*Estimates based on assumptions of 30% and 15% CF reduction

FY 2016 Accomplishments

- Demonstrated improved vacuum processing with reduced fabrication time from 2.0 hours to 0.5 hours for high-quality 7.5-liter prototype vessels.
- Leveraged infusion modelling in order to optimize vacuum infusion processing by refining the infusion/vacuum port placement.
- Achieved equivalent burst strength in static testing of small prototype vessels (Type III, 7.5 L) for vacuum-infused version versus wet-wound epoxy (26,586 psi).
- Pursued process scale-up to full-size pressure vessel from 7.5 liters to 133 liters.

✧ ✧ ✧ ✧ ✧

INTRODUCTION

DOE Office of Energy Efficiency and Renewable Energy has established aggressive performance targets for Type IV

hydrogen storage vessels for Year 2020. Current designs and materials of construction for composite-overwrapped pressure vessels (COPVs) within the industry do not reach the performance targets, as shown by the base-case published by Ahluwalia et al. from Argonne National Laboratory. The specialty chemical producer, Materia, has developed a novel composite resin system, Proxima®, with ultra-low viscosity (5 cP to 10 cP) that enables vacuum infusion processing for thick CF composite components. The use of this process with Proxima circumvents some challenges inherent with traditional wet filament winding, such as the presence of voids and dry spots. The use of vacuum infusion processing, also known as VARTM (Vacuum-Assisted Resin Transfer Molding), for fiberglass composite parts is commonplace in several large-scale industries (marine, wind blades), but the feasibility of VARTM for compressed gas vessels is not clear. While the concept of infusing dry-filament wound structures has been mentioned in the open literature, the small inter-fiber gaps associated with high-performance CF composites potentially presents significant processing difficulties. Therefore, the commercial application of this approach appears to be limited—which may be related to traditional resin possessing viscosities >200 cP.

In addition to reducing void content, Proxima-based composites also have significantly improved fracture toughness (>3X higher interlaminar fracture toughness) and fatigue performance over currently employed composites for hydrogen storage tanks. The project seeks to leverage this combination of tough resin and new processing to produce CF composite overwrap with better performance, especially in fatigue and damage-tolerance testing. These high-performing composites will enable the reduction of the quantity of CF composite overwrap, which alone can account for over 75% of the storage tank system cost. The processing-related costs for this new approach are expected to be similar to current processing costs with wet-winding. By reducing the CF composite content in COPVs by 35%, the project aims to reduce the cost and weight of COPVs and contribute to meeting the DOE 2020 cost target of $10/kW-hr.

APPROACH

Since the project requires expertise in a variety of fields, the project team includes Spencer Composites Corporation to lead the specialized filament-winding effort. Montana State University-Bozeman will experimentally characterize composite materials and also use finite element analysis (FEA) models to anticipate problem areas in tanks designs. Materia is leveraging its experience in infusion process optimization with low-viscosity resin (<10 cP) to demonstrate a series of prototype parts, including tanks and model flat plates of filament wound composites. In order to manage the risks associated with a new resin and a new process for COPVs, the project activities have been divided into stages and the objectives (1) process optimization, (2) COPV design, (3) design optimization, and (4) scale-up of process for vessel testing.

RESULTS

During FY 2016, important progress was made to support the transition from smaller prototype vessels (Type III, 7.5 L) to full-scale pressure vessels (Type IV, 133 L). The smaller vessels were useful for optimization of the vacuum infusion process to confirm low void content and good burst strength compared to epoxy controls. For example, the team found a preferred port placement for resin infusion (shown in Figure 1) resulting in shorter infusion time (0.5 hr vs. 2.0 hr). In this new set-up, resin is first introduced at each dome to ensure complete infusion past the tangent region. Then a third resin inlet located at the bottom of the cylinder is opened to help complete the infusion more quickly.

In addition to process optimization, the team made progress in vessel performance by preparing and testing a small vessel based on a new winding pattern to eliminate a stress concentration in the shoulder region of the 7.5-liter vessel. The desired failure mode was obtained with the new winding pattern (hoop failure vs. dome failure). Accordingly, excellent values of burst pressure and demonstrated fiber strength were observed. In Table 2, the most recent results in the last row are compared to results obtained in the previous report period, FY 2015.

Moving forward from the small vessels, full-size prototypes were prepared for vacuum infusion studies at Spencer Composites. In Figure 2, the full-scale, dry-wound tank is shown just before resin infusion begins. Several infusion trials have been conducted with increasing degrees of success; however, a vessel ready for testing has not yet been achieved due to some vacuum leaks before curing. Necessary changes in the process have been identified to obtain a high-quality vessel and reduce the chance of a process upset, such as vacuum leaks. Lastly, the efforts have been sufficient to provide preliminary cost estimates for the full-scale COPV along with sensitivity analysis, as shown in Figure 3. As expected, the cost benefits of CF reductions can

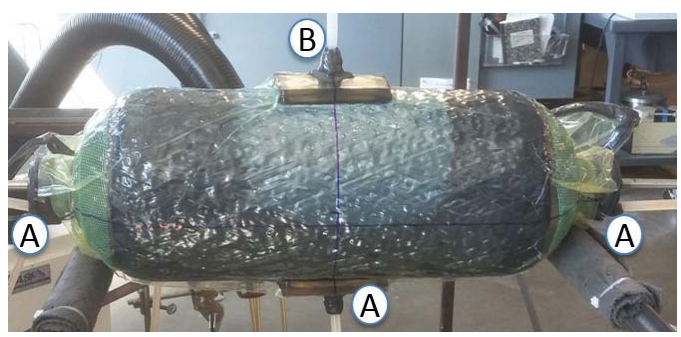

FIGURE 1. A 7.5-liter vessel during the optimized vacuum infusion process with "A" ports allowing introduction of resin and the "B" port providing the vacuum outlet

TABLE 2. Improvements in Small Prototype COPV (Type III, 7.5 L)

Fabrication Type	Resin	Winding	Burst Strength	Demon. Fiber Strength	% Deliv. Fiber Strength
Wet Wound	Anhydride-Cured Epoxy	Winding Pattern #1	1,834 bar (26,595 psi)	693 ksi	92
Dry Wound/ Resin Infused	Proxima ACR	Winding Pattern #1	1,001 bar (14,524 psi)	356 ksi	47
Dry Wound/ Resin Infused	Proxima ACR	Winding Pattern #1	1,694 bar (25,569 psi)	634 ksi	84
Dry Wound/ Resin Infused	**Proxima ACR**	**Winding Pattern #2 to minimize gaps**	**1,833 bar (26,586 psi)**	732 ksi	97

ACR – Area coverage ratio

FIGURE 2. Full-scale tank (133 L) prepared for vacuum infusion

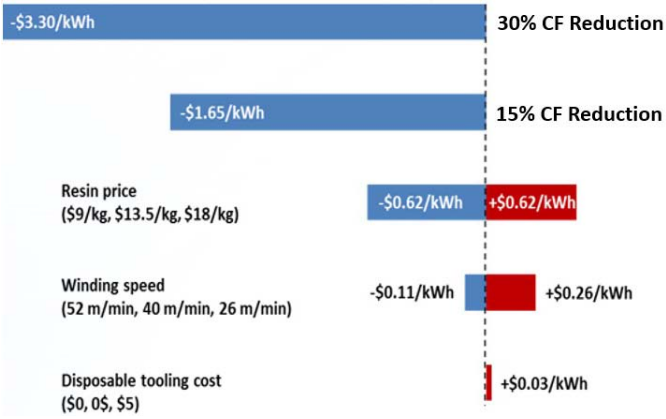

FIGURE 3. Sensitivy analysis of COPV cost based on preliminary processing and design estimates. The dotted line denotes a baseline cost of $12.03/kWh before any CF reductions. (Analysis performed by Strategic Analysis, Inc.)

counter-balance the extra processing time for the additional processing steps for vacuum infusion.

In order to compare the damage tolerance of composite laminates using different resins, epoxy-based and Proxima-based laminates were prepared using triaxial glass-fiber fabrics. While we are in the process of conducting similar studies with carbon fiber laminates, the initial study employed a readily obtainable triaxial glass fabric as a preliminary step. After cycling (tension-tension stress ratio, R = 0.1, for 90,000 cycles) at strain levels expected for the maximum operating pressure, as shown in Table 3, Proxima composite laminates showed excellent retention of static tensile strength (>95%). In a comparative test, a low-void laminate based on anhydride-cured epoxy was tested to have only 70% strength retention after 90,000 cycles. Initial strengths were equivalent for the two types of laminates. Panels with higher void content (3–5 vol%) were pursued but proved to be difficult to prepare in a reproducible manner.

TABLE 3. Comparison of Residual Strength of Composite Laminates after Cycling

Resin Type	Anhydride- Epoxy		Proxima ACR	
Void %	1.1		1.6	
Specimen Conditioning	Initial	90,000 Cycles	Initial	90,000 Cycles
Tensile Strength (MPa)	680	477	667	631
Strength Retention after Cycling		70%		95%

Epoxy = Dow DER 354 Epoxy/Lindride 36 V Anhydride Cure System, cured at 90°C

CONCLUSIONS AND FUTURE DIRECTIONS

From the current results of the project, the team has derived the following conclusions:

- Optimization of dry-fiber placement yielded measurable improvements in burst strength.
- Preparation of small COPV (Type III, 7.5 L) can achieve complete resin infusion within 30 min.
- Residual strength of composite plates after fatigue cycling is improved with tougher Proxima matrix resin.

The following activities will be the area of focus in the future:

- Optimize the process to produce full-scale vessels in a reliable and manufacturing-friendly manner.
- Update current cost model of tanks based on design and processes.
- Generate key performance data including drop-testing and pressure cycling for full-scale vessels with lower CF content.

IV.D.5 Optimizing the Cost and Performance of Composite Cylinders for H_2 Storage using a Graded Construction

Andrea E. Haight
Composite Technology Development, Inc. (CTD)
2600 Campus Drive, Suite D
Lafayette, CO 80026
Phone: (303) 664-0394
Email: andrea.haight@ctd-materials.com

DOE Manager: Ned Stetson
Phone: (202) 586-9995
Email: Ned.Stetson@ee.doe.gov

Contract Number: DE-SC0009449

Subcontractors:
Adherent Technologies, Inc., Albuquerque, NM
Oak Ridge National Laboratory, Oak Ridge, TN

Project Start Date: February 19, 2013
Project End Date: July 9, 2016

Overall Objectives

- Develop 700-bar Type IV graded structure pressure vessel design incorporating low cost carbon fiber.
- Optimize composite performance of low cost fibers.
- Demonstrate performance of graded structure pressure vessel.

Fiscal Year (FY) 2016 Objectives

- Demonstrate fatigue performance of composite fabricated with a combination of Toray T700 and commercial low cost carbon fibers.
- Fabricate and test Type IV graded structure pressure vessels.

Technical Barriers

This project addresses the following technical barriers from the Hydrogen Storage section of the Fuel Cell Technologies Office Multi-Year Research, Development, and Demonstration Plan.

(A) System Weight and Volume

(B) System Cost

Technical Targets

The overall goal of this program is to address the high cost of physical hydrogen storage in Type IV composite overwrapped pressure vessels (COPVs) with an overall cost reduction target of 25%. The cost of these COPVs is currently driven by the high cost of carbon fiber; this program aims to replace 40–60% of the high cost fiber with a low cost carbon fiber to achieve the cost reduction target.

A combination of finite element analysis driven composite design, experimental data, prototype construction, testing, and cost analysis will be used to demonstrate the approach.

FY 2016 Accomplishments

Accomplishments during the current project period include the following.

- Tensile strength retention of flat panels reinforced with a mixture of Toray T700 and Panex® 35 carbon fibers after 30,000 cycles to as high as 63% above the target operating pressure was in excess of 80%.
- A tank design was developed, using experimental data for Toray T700 and low cost Panex® 35 carbon fiber composites, allowing for 35–50% low cost carbon fiber.
- Type IV pressure vessels (Toray T700 control and graded structure) were fabricated and tested. One control tank burst at 21,925 psi, graded structure tanks did not burst, but leaked at the liner–boss interface after achieving pressures in excess of 13,000 psi. No visible damage to the composite was noted.

✧ ✧ ✧ ✧ ✧

INTRODUCTION

The challenges associated with bringing reasonably priced hydrogen fuel cell vehicles to market are numerous. One significant challenge is reducing the cost for onboard hydrogen storage tanks while continuing to provide a driving range of greater than 300 miles. COPVs have been designed and qualified for this application. However, as currently manufactured, these tanks are extremely expensive due in large part to the high strength carbon fibers (e.g., Toray's T700S) used; the cost of carbon fiber alone can constitute as much as 75% of the total cost of the vessel [1].

DOE's near-term goal is to reduce the cost of COPVs for high pressure hydrogen storage by 25%. CTD believes that this can be achieved by constructing the structural shell using a graded composite, in which a portion of the expensive, high-performance fiber is replaced with lower

cost carbon fibers based on common textile fibers. Since the projected cost for these newer fibers is significantly lower than that for carbon fibers produced from higher grade precursors, their utilization in a significant portion of the mass of the composite material in the vessel will translate to a corresponding reduction in the cost of the raw materials for the vessel, thereby meeting DOE's target for cost reduction.

APPROACH

In this effort, CTD is investigating the use of a graded composite tank structure, in which a portion of the high cost T700S carbon fiber is replaced by lower cost fibers, such as the low cost carbon fibers being developed at Oak Ridge National Laboratory with DOE funding. The reduced strain requirements for the composite through the thickness of the pressure vessel enables the use of lower cost, lower performing fibers for a substantial portion of the composite structure. A design has been developed based on experimentally derived low cost fiber properties that would allow for replacement of a large fraction of the costly T700S fiber with a less expensive option.

Work during FY 2016 focused primarily on design, construction, and testing of Type IV COPVs using either Toray T700 carbon fiber or a combination of Toray T700 fiber and Panex® 35 carbon fiber.

RESULTS

Work during this period focused on further demonstration of the graded structure concept for reducing cost of 700-bar hydrogen storage tanks. Demonstration of graded composite fatigue performance as well as fabrication and testing of graded structure tanks is discussed in the following paragraphs.

Fatigue Testing

CTD conducted fatigue testing of the baseline fibers and resin system per ASTM D3479. To determine the stress levels for fatigue testing, finite element models were used to predict the maximum stresses that would be experienced by the fibers when pressurized to the target burst pressure of 23,852 psi. The maximum stresses would be 310,179 psi and 252,482 psi for the Toray and Panex® 35 fibers, respectively. The ultimate strength values for T700 and Panex® 35 are 320,000 psi and 265,600 psi, respectively. Using these values, starting stress levels were then determined for the fatigue testing (Table 1). CTD set a maximum number of cycles of 30,000 for this fatigue testing; ~5000 cycles would resemble weekly refueling for 10 years.

All of the specimens survived 30,000 cycles at both stress levels. Tensile testing to failure after fatigue showed excellent retention of properties; all specimens failed at >80% of the ultimate tensile strength after cycling. This indicates that the change in fiber properties at the interface between the T700 and the low cost carbon fiber should not result in any performance issues for the tank relative to one made with a single type of carbon fiber.

Subscale Tank Fabrication and Testing

Using the experimentally derived composite properties shown in Table 2, our previously developed finite element model was used to determine the amount of Panex® 35 fiber that could be used for tank fabrication. This amount, between 35% and 50%, was determined to be large enough to offer significant cost savings in tank production.

TABLE 2. Material Properties of Toray T700S and Panex® 35 Fiber Composites

Property	T700S Composite	Panex 35 Composite
Bandwidth (in)	1.69	1.69
Hoop Thickness (in)	0.027	0.027
Helical Thickness (in)	0.0164	0.0164
Longitudinal Elastic Modulus, E_1 (Msi)	18.5	19.05
Transverse Elastic Modulus, E_2 (Msi)	1.3	1.01
Poisson Ratio, ν_{12}	.28	.28
Shear Modulus, G_{12} (Msi)	0.5	0.5
Failure Strain in Fiber Direction (%)	1.8	1.34

High density polyethylene liners were rotomolded by RMB Products (Fountain, Colorado) to specifications provided by CTD. Tanks were filament wound at CTD; liners were pressurized during the winding process to avoid

TABLE 1. Stress Levels for Fatigue Testing of Composite Panels

65% of Ultimate:		Resulting Tank Pressure is:		% above OP
Stress T700 =	208000 psi	T700 =	15995 psi	60%
Stress Panex =	172640 psi	Panex =	16309 psi	63%

Using 30% above OP:		Tank Pressure:	% of Ultimate	% above OP
Stress T700 =	169056 psi	**13,000 psi**	53%	**Using 30%**
Stress Panex =	137610 psi	**13,000 psi**	52%	**Using 30%**

OP – Operating pressure

collapsing the liner. A total of five tanks (two control with T700 fiber only and three graded structure) were produced. Two control (T700) and two graded structure tanks were then subjected to hydrostatic burst testing. Results were as follows:

- Control 1: 21,925 psi, burst (Figure 1)
- Control 2: 18,833 psi, leak at the composite/liner/boss interface
- Graded 1: 15,831 psi, leak at the composite/liner/boss interface
- Graded 2: 14,377 psi, leak at the composite/liner/boss interface (Figure 2)

Since there was no visible damage to the composite structure in cases where leaks occurred, liner failures were assumed.

FIGURE 1. Type IV pressure vessel with Toray T700 carbon fiber after burst

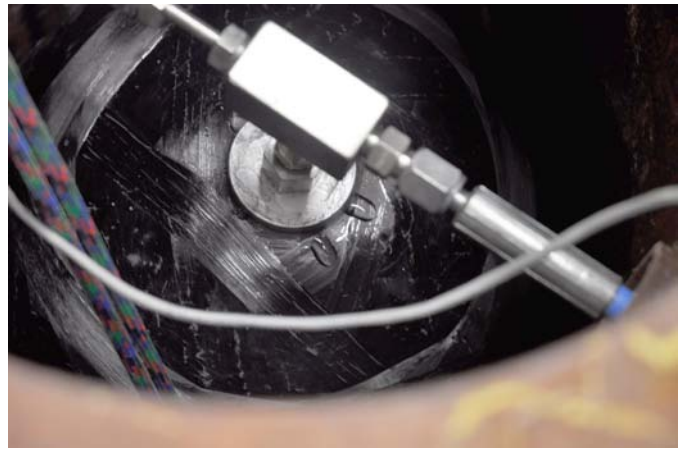

FIGURE 2. Graded Type IV pressure vessel (Toray T700/Panex® 35) showing leakage at composite/liner/boss interface

CONCLUSIONS AND FUTURE DIRECTIONS

This program has demonstrated the potential for using low cost carbon fibers in combination with Toray T700 for the production of thick wall, 700 bar pressure vessels. While burst of the graded structure tanks was not achieved, it appears that the graded structure has high potential to perform as well as a 100% T700 COPV in the absence of liner failure; pressurization in excess of the expected operating pressure was achieved in all cases. Further work will be required to unequivocally establish the performance in a situation where liner failure does not occur.

Whether or not cost savings can truly be achieved using low cost carbon fiber remains an open question. While fabrication using the Panex® 35 low cost fiber is possible, it is far from optimum. In contrast to the Toray T700, which unspooled and deposited onto the tank with no fuzzing, the Panex® fiber was extremely challenging with significant fuzzing occurring during the process. This resulted in frequent stoppages of the winder in order to clean deposited fiber from the rollers and resin bath. Significant improvement in handling of the Panex® fiber would be required in order for its use in production to be truly feasible. Impact of the added touch labor related to the fuzzing of the low cost fiber is currently being evaluated in the cost model.

REFERENCES

1. Fuel Cell Technologies Office Multi-Year Research, Development, and Demonstration Plan, Section 3.3 – Hydrogen Storage, updated May 2015.

IV.D.6 Achieving Hydrogen Storage Goals through High-Strength Fiber Glass

Hong Li (Primary Contact), Brian Kornish, Norman Newhouse, Kenneth Johnson
PPG Industries, Inc.
400 Guys Run Road
Cheswick, PA 15024
Phone: (412) 820-8132
Email: hli@ppg.com

DOE Manager: Grace Ordaz
Phone: (202) 586-8350
Email: Grace.Ordaz@ee.doe.gov

Contract Number: DE-EE0006626

Subcontractors:
- Hexagon Lincoln, Lincoln, NE
- Pacific Northwest National Laboratory, Richland, WA

Project Start Date: September 1, 2014
Project End Date: August 30, 2017

Overall Objectives

The objective is to demonstrate a Type IV composite overwrapped pressure vessel (COPV) reinforced exclusively with glass fiber. This will be achieved through the following steps:

- Develop a new glass fiber with strength exceeding Toray T-700 carbon fiber at less than half its cost.
- Demonstrate a novel glass fiber manufacturing process.
- Conduct composite validation laboratory tests to determine the safety factor for the tank made by using new high-strength glass fiber.
- Build cost models to demonstrate the new tank will reduce the composite contribution to system cost by nearly 50% with minimal impact on tank weight and capacity compared to tanks made with T-700 carbon fiber.

Fiscal Year (FY) 2016 Objectives

- Produce multi-end roving packages of two candidate high-strength glass fibers that offer tensile strength of fiber strands close to 5,000 MPa.
- Build high-strength fiber-reinforced vessels for mechanical evaluations and compare with performance of vessels made from T-700 carbon fibers. (See Table 3b for comparison of mass, burst pressure, and fiber translation efficiency of tanks wound on this project. See Table 5 for modeled cost, gravimetric, and volumetric performance of the DOE 5.6 kg hydrogen tank.)
- Perform stress rupture tests for high-strength fiber strands to provide a basis for determining any changes from the fiber glass safety factor (3.5) currently used for hydrogen tank design to 3.0.
- Demonstrate a new, high-throughput, high-temperature batch melting unit to produce high-strength fiber glass cullet from batch by 4X comparing with the existing melting unit.
- Project the commercial production cost of making high-strength fibers based on the current small-scale fiber-making platform.
- Perform preliminary tank cost calculations and performance projections and compare against the 2020 DOE cost, volumetric, and gravimetric targets (see Table 5).

Technical Barriers

This project addresses the following technical barriers from the Hydrogen Storage section of the Fuel Cell Technologies Office Multi-Year Research, Development, and Demonstration Plan.

(B) System Cost

Technical Targets

The project is to demonstrate the technical and commercial feasibility of using high-strength glass fibers to match the tensile strength of Toray T-700 carbon fibers, at about 50% of the cost. At the completion of the project, experimental results and modeling output will enable the team to benchmark with the key parameters shown in Tables 1 and 2. The actual targets for the project are detailed in the Introduction section of this report.

FY 2016 Accomplishments

During the first phase of the project under FY 2016, the team has successfully completed the following objectives:

- Completed high-strength fiber multi-end roving packages to cover glass fiber chemistry A with two binders and fiber chemistry B with one binder, plus reference E-glass packages with one binder.

TABLE 1. Technical System Targets: Onboard Hydrogen Storage for Light-Duty Fuel Cell Vehicles [1]

Storage Parameter	Units	2020	Ultimate	Project Towards Targets (2015)
System Gravimetric Capacity	kWh/kg	1.8	2.5	0.31 Well Below Target
System Volumetric Capacity	kWh/L	1.3	2.3	0.43 Well Below Target
Storage System Tank Cost	$/kWh net $/kg H_2 stored	10 333	8 266	34.1 Well Above Target 1,136 Well Above Target

TABLE 2. Projected Performance of Hydrogen Storage Systems [1] [a]

Hydrogen Storage System (Including Balance of Tank Cost)	Gravimetric (kWh/kg sys)	Volumetric (kWh/L sys)	Cost ($/kWh; Projected to 500,000 units/yr)	Project Towards Targets (2016)
700-bar Compressed Type IV[b] (Estimated Project Performance)	1.4 (0.31)	0.81 (0.43)	14.8 (34.1 + 3.64 = 37.74)	Gravimetric and Volumetric Below Targets. Cost well Above Target.

[a] Assumes a storage capacity of 5.6 kg of usable H_2.
[b] DOE Hydrogen and Fuel Cells Program Record # 15013, "Onboard Type IV Compressed Hydrogen Storage System–Cost and Performance Status 2015." September 30, 2015. This includes a balance of tank cost of $3.64/kWh.

- Successfully demonstrated 4X high-throughput, high-temperature melting unit run using high-strength fiber glass batch, making high-strength fiber glass cullet.
- Built 38 all glass fiber COPVs per the STEB02-250 design using reference E-glass and two types of high-strength fibers and confirmed no technical issues for using the existing commercial tank winding process.
- Completed mechanical evaluations for all COPVs, burst pressure, pressure cycle, and stress rupture at 80% burst pressure per Hexagon Lincoln procedures, NGV2-2012 (Hydrostatic Burst Test for Project 4548 REVB 150423 and Ambient Cycle Test for Project 4548 REVB 150423).
- Completed initial performance and translation assessment of high-strength fiber COPV, 81%, against 91% for Toray T-700 COPV. (cf. Table 3b).
- Completed preliminary stress rupture tests on one of the high-strength fiber strands with two types of sizing to compare with reference E-glass fiber and S-glass fiber as a basis for determining potential to change the currently required safety factor for fiber glass pressure vessels. Based on the results, current safety factor of 3.5 should be used unless better quality of high-strength glass fiber can be realized.
- Completed cost modeling for a high-strength glass fiber COPV based on the current high-strength fiber performance in comparison with a Toray T-700 carbon fiber COPV. In terms of composite cost contribution ($/kWh) and storage system tank cost ($/kWh net), the current high-strength glass fiber COPV are still too high by 5.2X and 2.8X, respectively (cf. Table 5). However, this result is solely driven by the lower than expected fiber strength which results in the high mass and cost of fiber required in the tank design.

✧ ✧ ✧ ✧ ✧

INTRODUCTION

This project addresses the Fuel Cell Technologies Office's intermediate 2017 goals for onboard hydrogen storage for light-duty fuel cell vehicles. Specifically, the team targets a fiber cost less than $6/lb, a composite contribution to system cost of less than $6/kWh, a volumetric capacity of 0.86 kWh/L (26 g/L), and a gravimetric capacity of 1.3 kWh/kg (4 wt%), while minimizing increased tank mass compared to T-700 carbon fiber vessels. The project tasks are organized to continually decrease project risk, moving from a technology readiness level of 4 to 6.

APPROACH

To begin, in Budget Period 1 (BP1), the team develops fibers at the bench and characterizes stress rupture at the fiber level. The team then develops a pilot version of the new glass manufacturing process to produce the high-strength fibers. BP1 ends with test data from prototype tanks built from up to four new fiber samples, i.e., fiber chemistry and sizing chemistry in combination.

In Budget Period 2 (BP2), the team optimizes the best performing fiber and the production process, characterizes stress rupture at the composite level, and investigates alternate tank designs. The project ends with a prototype tank built according to a design tailored to the properties of the new glass that can be tested against a wide range of industry testing standards.

RESULTS

The project under BP1 has made a total of 1,200 lb of multi-end roving packages (with nominal 450 yield or yd/lb) of high-strength fibers of A-I, A-II, and B-I types. A Type IV composite overwrapped pressure vessel design based upon reference E-glass fiber was completed. Based on the design, 38 all glass fiber COPVs, using A-I, A-II, and B-I packages, were built for mechanical testing. The two selected fiber sizings were compatible with the commercial epoxy resin used for building Toray T-700 carbon tanks; no processing issues were apparent during fabrication of the all glass fiber COPVs. The all glass fiber design is designated as STEB02-250, which is a 250 bar tank designed to a 3.5 factor of safety (875 bar). In comparison, STEB01-250 is an all carbon fiber (T-700) 250 bar design to 2.25 factor safety (563 bar). Figure 1 provides a schematic description of the processes from fiber drawing to vessel winding.

Mechanical properties and density of the high-strength fiber strands are summarized in Table 3a. Also included are properties of reference E-glass strands and T-700 carbon fiber strands for comparison. Due to various limitations of the current small-scale production platform, including fibers with high counts of hollow fibers, large yardage variations, or large fiber diameter variation, thermal inhomogeneity, etc., the final strands of assembled roving showed about 40% translation losses against the pristine fiber strength values reported in 2015 (cf. Table 3). Fiber products from typical commercial scale production furnaces generally exhibit about 15% translation losses as compared with their counterpart of single filament pristine strength. The observed differences point out that the current small scale and discontinuous fiber drawing platform is inadequate in making high quality fiber strand samples. Table 3b compares tank geometry and performance of vessels made from high-strength glass fiber (A-I) and T700 carbon fibers. Deficiency of high-strength glass fibers (cf. Table 3a) translates to poor performance of the vessels against the commercial vessels made from T700 carbon fibers. High-strength fiber reinforced vessels had average translation of 81% as compared with 91% of T700 carbon fiber reinforced vessels.

The vessels were grouped, typically three each, for mechanical testing to determine their burst pressure, pressure cycle, and stress rupture. The results are shown in Figure 2. Relative to the E-glass reference fibers, tanks made from all of the high strength fiber and sizing combinations exhibited improved performance. The A-I fiber tanks performed the best overall, passing both the burst and pressure cycle tests. They also had the longest time to stress rupture when held

FIGURE 1. Process flow of high-strength glass fiber production, multi-end roving package assembling, and tank winding processes

TABLE 3a. Mechanical Properties and Density of Glass Fiber Strands Compared with T-700 Carbon Fibers*

Composition Type	A	A	B	B	E (Reference)	T-700
Sizing Type	I	II	I	II	I	N/A
Tensile Strength (MPa)	3192 ± 79	3289 ± 96	3372 ± 45		2848 ± 138	4900
Tensile Modulus (GPa)	88.1 ± 1.1	89.8 ± 0.7	87.7 ± 0.7		82.8 ± 1.1	230
Elongation at Break (%)	5.5	5.6	5.8		5.5	2.1
Density (g/cm^3)	2.58	2.58	2.58	2.58	2.64	1.8

* Pristine tensile strength of single fiber: Composition A - 5357±71 MPa; Composition B - 5583±58 MPa; N/A - Not applicable

TABLE 3b. Vessel Parameters and Vessel Test Results and Comparison Between High-Strength Glass Fiber and T700 Carbon Fiber Reinforcement

Parameter and Property	STEB01-250 Bar T700 Carbon	STEB02-250 Bar A-I Glass Fiber	Difference relative to T700 (%)
Tank Length (in)	27.8	27.8	0.0%
Tank OD (in)	9.95	10.65	7.0%
Nominal Internal Volume (liter)	24.2	24.2	0.0%
Tank Weight (lbs)	17.0	40.3	137.1%
Liner Weight (lbs)	6.3	6.3	0.0%
Fiber Weight (lbs)	7.1	26.3	270.4%
Resin Weight (lbs)	3.6	7.7	113.9%
Safety Factor	2.25	3.50	55.6%
Burst Pressure (avg) (PSI)	10323	13062	26.5%
Actual Burst Relative to Service Pressure	2.85	3.60	26.5%
Avg. Translation	91%	81%	-11.0%
Stress Rupture at 80% Peak Load (min)	indefinite	661	-
Total Wind Time (min)	35	75	114.3%

OD - outside diameter

at 80% of the average burst pressure. However, significant variations were found in the stress rupture tests.

Stress rupture tests were also performed using fiber strands or rods of the reference E-glass and high-strength glass A-I, and A-II, which were impregnated with the epoxy resin used for T-700 carbon reinforced tanks. These tests were performed to investigate if there is a technical basis to consider revising the current safety factor of 3.5 for glass fiber reinforced tanks to a lower value for the team's high strength glass formulation. The current value of 3.5 is based on the slope of the applied tensile stress vs. time to failure from long-time fiber strand stress rupture tests. Figure 3 summarizes the stress rupture test data along with the S-glass strand data from the literature (used to establish the current 3.5 value) [2] and the reference E-glass stress rupture data from PPG's previous tests [3]. The slopes from the A-I, and the A-II high-strength strand tests are similar to the S-glass strands and the reference E-glass (2026-CR) fibers. The similar slopes suggest that a similar safety factor of 3.5 is warranted for the A-I and A-II fibers that were currently produced.

A model developed by Pacific Northwest National Laboratory (PNNL) was used to assess the cost, volumetric, and gravimetric performance of a DOE standard-sized compressed hydrogen tank (5.8 kg hydrogen, 700 bar, 147.3 L, inside length/diameter = 3.3 in, T-700 carbon fiber) using the achieved glass fiber strengths. As a benchmark, the PNNL model gives tank composite masses that are within 5% of the 2013 and 2015 DOE tank estimates (DOE Records 13010 and 15013). The model was also used to estimate the mass of the standard test evaluation bottles (STEBs) wound by Hexagon Lincoln using the glass fibers. Using the liner dimensions of the Hexagon Lincoln and the A-I average strand strength (3,192 MPa), Table 4 shows that the model predicts composite mass and outside tank dimensions that are very similar to the A-I fiber, 250 bar STEB.

Table 5 presents model results for the DOE standard size compressed hydrogen tank (5.8 kg stored/5.6 kg usable hydrogen, 700 bar, 147.3 L, inside length/diameter = 3.3 in). Seven different design cases are presented along with the 2020 DOE performance targets. Cases 1 through 4 are the reference cases presented in the original proposal. Cases 1 and 2 are tanks with T-700 carbon fiber and E-glass properties. Cases 3 and 4 were the projected BP1 and BP2 performance targets. Note that these numbers are slightly different from the original proposal, due to small adjustments in the fiber stress equations of the model. Case 5 estimates the mass and cost performance of a tank with the properties of 2026-CR E-glass measured during BP1. Cases 2 and 5 with common E-glass strengths estimate very large composite masses. With tank pressure of 700 bar and strand strengths around 3,000 MPa, the tank wall is so thick that the through-thickness composite compression makes it difficult to limit the inner layer stresses by adding more thickness. This is seen in Case 5 for the 2026-CR E-glass (2,848 MPa average strand strength) with estimated composite mass of 653 kg, compared to the Case 2 E-glass (3,000 MPa average strand strength) with estimated composite mass of 543 kg. Case 6 estimates the tank performance for the A-I glass fibers (3,192 MPa average strand strength) produced in BP1. The volumetric capacity is predicted to be 0.48 kWh/L compared to the BP1 goal of 0.81 kWh/L, gravimetric capacity of 0.38 kWh/kg compared to the BP1 goal of 1.1 kWh/kg, and the composite contribution to system cost is predicted to be $27.9/kWh compared to the BP1 goal of $8/kWh. A projected fiber production cost of $5.2/lb (4X standard E-glass at $1.3/lb) is used in the cost estimate. These trends result entirely from the large composite thickness required to support the pressure load with the lower-than-expected fiber strand strengths produced in BP1. The reasons for the low strengths are identified in previous sections of this report. An approach to increase the fiber strand strengths to meet the

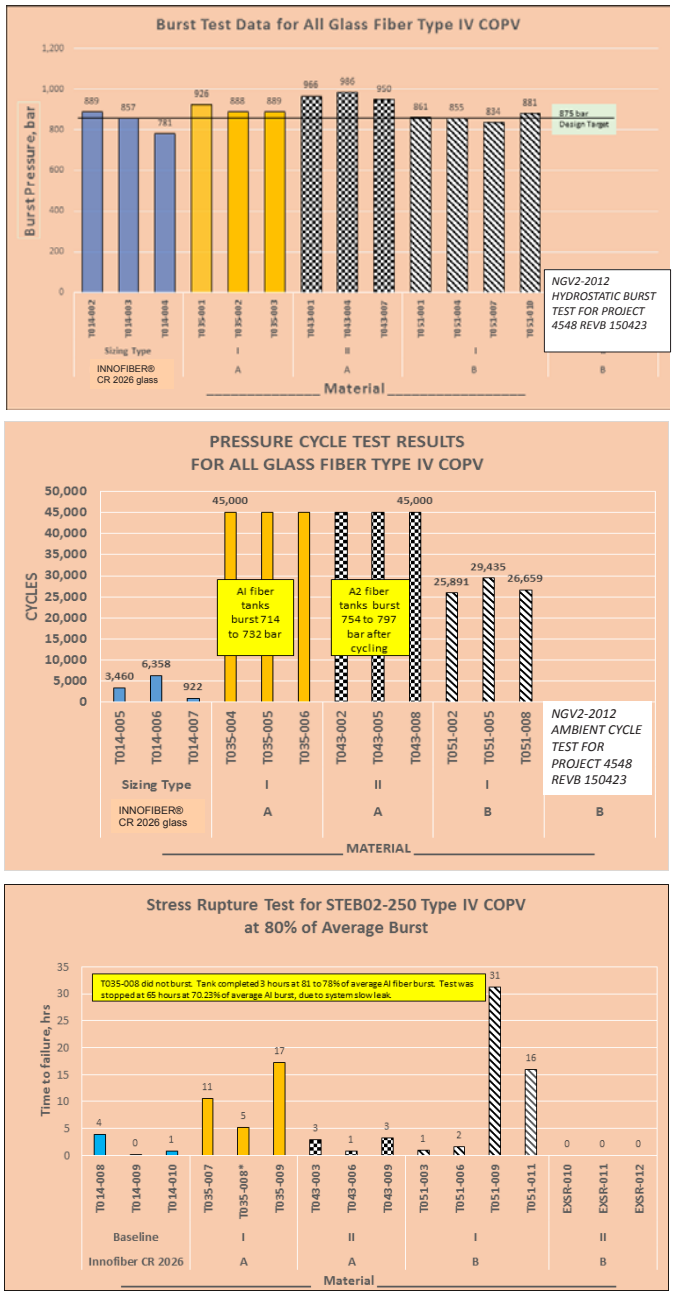

FIGURE 2. Tank mechanical evaluations: top – burst pressure, mid – pressure cycle, and bottom – stress rupture

project goals has been developed and recently discussed with DOE and evaluation of our paths is ongoing

Case 7 estimates the tank performance if an improved A-I glass can be produced with a higher average strand strength of 5,500 MPa. The 10% coefficient of variation results in a design strand strength of 4,950 MPa, 0.76 kWh/L volumetric capacity, 0.88 kWh/kg gravimetric capacity, and a composite contribution to system cost of $11.0/kWh.

Additional cases were simulated with average strand strengths ranging from 3,000 MPa to 7,000 MPa to show

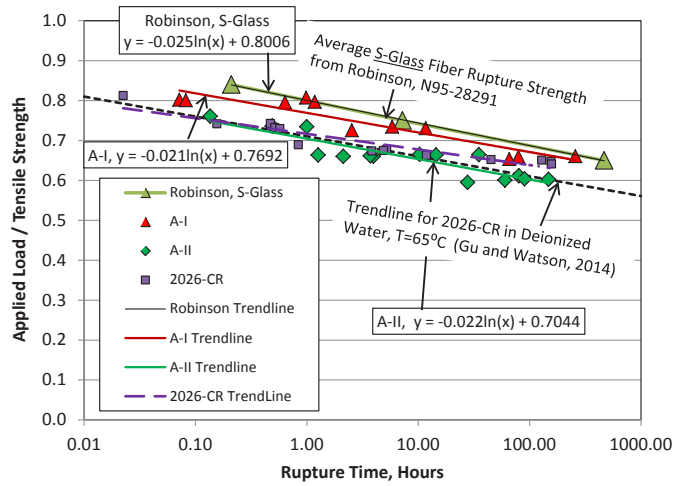

FIGURE 3. Stress rupture test data comparing reference E-glass (2026-CR), A-I, and A-II. The literature data for 2026-CR tested in water plus the S-glass stress rupture data reported in literature [2] are included for comparison. Each glass type has similar stress rupture characteristics in terms of the slope of the normalized load vs. time at rupture.

TABLE 4. Comparison of As-Wound Tank Mass and Dimensions with PNNL Model Predictions for the A-I Glass Fiber, 250 bar STEB Tank

Parameter and Property	STEB02-250 Bar A-I Glass Fiber	PNNL Model A-I Glass STEB
Tank Length (in)	27.8 With End Bosses	25.8 Without End Bosses
Tank OD (in)	10.65	10.70
Nom. Internal Volume (L)	24.2	24.3
Tank Weight (lb)	40.3	42.4
Liner Weight (lb)	6.3 With End Bosses	4.1 Without End Bosses
Fiber Weight (lb)	26.3	29.2
Resin Weight (lb)	7.7	9.1
Safety Factor	3.5	3.5
Design Burst Pressure (psi)	12690	12690
Avg. Translation	81%	79%

the sensitivity of the tank performance trends to strand strength. Figure 4 shows the trends in composite cost, volumetric capacity, and gravimetric capacity. It is estimated that an average strand strength of 6,111 MPa (design strand strength of 5,500 MPa) is required to meet the BP1 goal of 0.81 kWh/L with a gravimetric capacity of 1.0 kWh/kg, and composite cost of $9.6/kWh (based on $5.2/lb fiber cost). At average strand strength of 6,500 MPa (5,850 MPa design strand strength) the estimated volumetric capacity is 0.82 kWh/L with a gravimetric capacity of 1.07 kWh/kg, and a composite cost of $8.8/kWh. At 7,000 MPa (6,300 MPa design strand strength) the estimated volumetric capacity

TABLE 5. The estimated performance of glass fiber tanks compared with the BP1 and BP2 goals. Estimated performance of the carbon fiber reference tank is also listed. All calculations are for the DOE standard size pressurized hydrogen tank (5.8 kg stored/5.6 kg usable hydrogen, 700 bar, 147.3 L, inside length/diameter = 3.3 in).

Case #	1	2	3	4	5	6	7	
			BP1 Goal	BP2 Goal	BP1 Actual	BP1 Actual	Conceptual	
Summary Metrics	T-700 Carbon Fiber	E-Glass	High-Strength Glass Design-1	High-Strength Glass Design-2	2026-CR E-Glass	Glass A-I	Increased Strength Glass A-I	2020 DOE Targets
Fiber Cost ($/lb)	13	1.3	5.2	5.2	1.3	5.2	5.2	6
Average Fiber Strand Strength, S, MPa	4,900	3,000	6,111	6,111	2,848	3,192	5,500	
Coefficient of Variation, Cv	0.1	0.1	0.1	0.1	0.1	0.1	0.1	
Design Strand Strength, S*(1-Cv)	4,410	2,700	5,500	5,500	2,563	2,873	4,950	
Resin Density (g/cm^3)	1.25	1.20	1.20	1.00	1.20	1.20	1.20	
Safety Factor	2.25	3.50	3.50	3.00	3.50	3.50	3.50	
Storage System Tank Cost ($/kWh net)	14.2	13.0	9.7	7.8	15.6	28.1	11.3	10.0
Composite Cost Contribution ($/kWh)	12.2	12.8	9.4	7.5	15.4	27.9	11.0	6.5
Gravimetric Capacity (kWh/kg)	1.44	0.34	1.02	1.24	0.28	0.38	0.88	1.80
Volumetric Capacity (kWh/L)	0.85	0.45	0.79	0.85	0.40	0.48	0.76	1.30
Tank Mass without H_2 (kg)	123	543	178	145	653	487	205	
Tank Composite Mass (kg)	103	523	157	124	632	466	184	

is 0.84 kWh/L with a gravimetric capacity of 1.16 kWh/kg, and a composite cost of $8.1/kWh. It is important to note that these are only model trends (not actual glass fiber performance) which are useful to project glass composite performance at higher strand strengths.

The trends in Figure 4 suggest that high strength glass fibers must exceed T-700 tensile strength to reach the project goals. Gravimetric capacity is particularly challenging since glass fiber has a higher density than carbon fiber. It is estimated that the best expected performance of the team's current A or B fibers would be 5,500 MPa. In practice, the

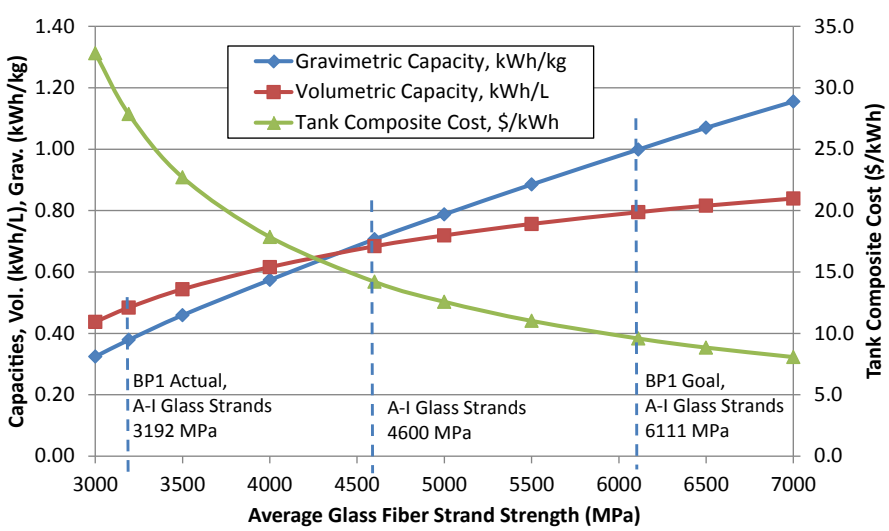

FIGURE 4. Sensitivity of cost, volumetric, and gravimetric performance to glass fiber strand strength

best achievable strand tensile strength would then be about 4,600 MPa (based on 15% loss). Therefore, at 4,600 MPa strand strength, Figure 4 would estimate tank performance to be about 0.68 kWh/L volumetric capacity, 0.71 kWh/kg gravimetric capacity, and about $14.2 kWh composite contribution in a 700 bar pressure vessel capable of storing 5.6 L of usable hydrogen at room temperature.

The assessment discussed above was performed using a safety factor of 3.5. BP2 relies on the new fibers exhibiting improved stress rupture characteristics, i.e., the rupture time would need to be less sensitive to the level of applied tensile stress than what was determined for the A-I fibers or S-fibers reported in literature [2]. If achieved, this improved performance could be used to justify the use of a lower safety factor for tank design, making it possible to close the gap reaching the target strand tensile of 5,500 MPa instead of 6,500 MPa by the projection discussed earlier (Figure 4).

CONCLUSIONS AND FUTURE DIRECTIONS

Progress during BP1 has not achieved the project goal demonstrating high-strength fiber strand with 5,500 MPa tensile strength. High single-fiber strengths were achieved, however 40% translation losses in the strand strength (relative to pristine fiber strength) were caused primarily by processing challenges in the small scale glass-melting and fiber-forming platform, plus the inability to make fiber packages on a continuous basis. The deficiencies can be resolved in BP2 by using a continuous, larger scale fiber production platform that is under consideration. The new platform can enable the team to produce larger, more consistent fiber forming packages for assembling to reduce translation losses as it has been commercially used. In turn, fibers and final assembly roving packages with better quality can translate to greater tank performance improvements.

FY 2015 PUBLICATIONS/PRESENTATIONS

1. H. Li, "Achieving Hydrogen Storage Goals through High-Strength Fiber Glass," at U.S. DRIVE Technical Meetings in Detroit, MI, on May 19, 2016.

2. H. Li, "Achieving Hydrogen Storage Goals through High-Strength Fiber Glass," at 2015 U.S. DOE Hydrogen and Fuel Cells Program and Vehicle Technologies Office Annual Merit Review and Peer Evaluation Meeting, Washington D.C., June 9, 2015.

REFERENCES

1. http://energy.gov/eere/fuelcells/downloads/fuel-cell-technologies-office-multi-year-research-development-and-22

2. Robinson, E.Y. 1991. "Design Prediction of Long-Term Stress Rupture Service of Composite Pressure Vessels." The Aerospace Corporation. El Segundo, CA.

3. Gu, P., Watson J., "Corrosion Resistance of E-Glass Fiber Reinforced Composites: Boron and Interface Factors," CAMX 2014 Conference Proceedings, Orlando, FL, USA, October 13–16, 2014. CAMX–The Composites and Advanced Materials Expo.

IV.D.7 Melt Processable PAN Precursor for High Strength, Low-Cost Carbon Fibers (Phase II)

Felix L. Paulauskas (Principal Investigator),
Bob Norris (Primary Contact), Ken Yarborough, and Fue Xiong
Oak Ridge National Laboratory (ORNL)
MS 6053
Oak Ridge, TN 37831-6053
Phone: (865) 576-1179
Email: norrisrejr@ornl.gov

DOE Manager: Grace Ordaz
Phone: (202) 586-8350
Email: Grace.Ordaz@ee.doe.gov

Subcontractors:
- Donald G. Baird, Judy Riffle, Jianhua Huang, Greg Miller Virginia Polytechnic Institute and State University (Virginia Tech), Blacksburg, VA

Project Start Date: October 2013
Project End Date: Project continuation and direction determined annually by DOE

Overall Objectives

- Demonstrate means to achieving cost reduction of ≥25% in the manufacturing of carbon fiber, which meets the properties of industry baseline carbon fiber utilized in the fabrication of composite pressure vessels for hydrogen storage.
- Develop and demonstrate new chemistry and spinning techniques, while assessing the capability for advanced conversion technologies to meet the needs of carbon fiber manufacturing costs reduction for meeting program performance goals.

Fiscal Year (FY) 2016 Objectives

- Completed the required modifications to the extruder necessary to produce and improve melt spun precursor samples that meet progressively greater properties as demonstrated by the testing of converted carbon fiber. Key precursor target is polyacrylonitrile co-polymerized with methyl acrylate (PAN-MA) fibers with greater than 100 filaments and continuous lengths >100 m by June 30 to facilitate production of carbon fiber achieving 22 Msi modulus and 250 ksi strength with 25–50 m tow by September 30.
- Down-select appropriate chemistry, PAN-MA. Constituent levels and molecular weight of this recipe will allow spinning precursor that can be fully processed through conversion, while not necessarily meeting ultimate project performance goals. Utilize an integrated effort of formulation and processing by team members. With baselines established, the optimum chemistry will be developed in iterations moving towards these ultimate objectives.
- Implement better and more precise stretching tools to facilitate low temperature drawing immediately after spinning and conversion trials with precursors. This is to minimize the time required in developing and demonstrating appropriate conversion protocol for producing carbon fiber.

Technical Barriers

High-strength carbon fibers account for approximately 65% of the cost of the high-pressure storage tanks. This project addresses the following technical barriers from the Hydrogen Storage section of the Fuel Cell Technologies Office Multi-Year Research, Development and Demonstration Plan.

(A) System Weight and Volume

(B) System Cost

(D) Durability/Operability

(G) Materials of Construction

High strength carbon fiber enables the manufacturing of durable, lightweight, compressed hydrogen storage vessels for use in high-pressure storage (i.e., 700 bar). Unfortunately, current high strength carbon fiber products are far too expensive to meet DOE goals for storage system costs.

Technical Targets

Working targets are approximate equivalence with Toray T-700 at substantially reduced production costs.

- 700 ksi ultimate tensile strength
- 33 Msi tensile modulus
- Production cost reduction of at least 25% versus baseline

Accomplishments

- Successfully completed a carbon fiber precursor production milestone: Based on results of continuing trials with polyacrylonitrile co-polymerized with vinyl acetate (PAN-VA) process development materials, the

team down-selected processing conditions and water–plasticizer formulations and demonstrate spinning of >100 filament tows of length >10 m.

- Improvements continue to be implemented in developing simplified processes for pelletizing the carbon fiber precursor material for near-term trials. At the time of this report, fiber has been produced with the modified spinning system, but the quality of this fiber in terms of length (~10 m), fiber count (~140 filaments) and fiber diameter (>40 microns) is not sufficient for proceeding with conversion trials.
- Initiated a series of spinning–extrusion trials utilizing twin screw extrusion equipment and expertise at Leistritz in late March as a parallel effort and backup approach to complement the spinning work with the single screw extruder at Virginia Tech. The team was able to extrude some short sections of polyacrylonitrile (PAN) plasticized with water and/or acetonitrile at up to a foot in length, but success was inconsistent.
- Processes for producing and characterizing specific formulations of PAN and MA have been established, along with the effectiveness of various plasticizer approaches in suppressing the melt temperature to acceptable processing temperatures in the range of 145°C–175°C which is significantly below the cross-linking temperatures. Significant data including melt temperatures and viscosity as a function of temperature as well as other characteristics on a wide variety of formulations has been produced to guide the program in establishing spinning baselines and then providing alternatives for improving properties towards program goals.
- A baseline PAN-MA blend at a specific molecular weight (~150,000) and PAN-MA (93:7) ratio have been selected. This was performed via collaboration among the chemistry, spinning, and conversion teams and procured via contract in quantities adequate to support several months of further formulation development and spinning trials.

✧ ✧ ✧ ✧ ✧

INTRODUCTION

High strength carbon fiber enables the manufacturing of durable, lightweight, compressed hydrogen storage vessels for use in high pressure storage. Unfortunately, current high strength carbon fiber products are too expensive to meet DOE goals for storage system costs [1]. Developing and demonstrating a melt spun PAN approach to producing precursor for carbon fiber will provide a more cost-effective route to achieving performance necessary for high pressure gas storage. Melt spinning removes significant costs in handling and recovering solvents involved in solution spinning, as well as eliminating a significant bottleneck in production rates required by the time, space, and energy utilized in the solvent recovery steps. Although somewhat similar processes have been demonstrated in the past, no PAN-based carbon fiber is produced currently utilizing this approach. This is due to specific materials employed in the previously demonstrated process and lack of investment from industry to revisit and revamp that process. It is anticipated that the melt spinning approach could save 25% of cost involved in producing carbon fiber for high pressure gas storage systems and that additional savings may be possible, in combination with ORNL advanced conversion approaches. It is also projected that the melt spinning process would be more attractive for PAN fiber production in the United States, possibly helping to revitalize some of the acrylic fiber business lost due to environmental concerns.

A major milestone was achieved during latter portions of Phase I with demonstration of carbon fiber properties exceeding the go/no-go point established at 15 Msi modulus and 150 ksi strength. Properties meeting follow-on milestone levels up to 25 Msi modulus and 250 ksi strength were also achieved. These properties were achieved with melt spun PAN produced at Virginia Tech and utilizing conversion protocol developed by ORNL in earlier work. Phase II is scaling the process up from very small batch quantities to continuous extrusion and improving properties towards the program targets.

APPROACH

This project is structured into tasks focused on precursor development and conversion process improvements. Development and demonstration of melt-spinnable PAN is the project's primary precursor option. If successful, melt spinning is projected to be significantly less costly than wet spinning with capability to produce high quality, relatively defect-free precursor. This requires concurrent activities in both development of melt-stable PAN copolymer and blends as well as the processes necessary to successfully spin the formulations into filamentary tows. Melt processing of PAN is a difficult issue, although Virginia Tech and others have made modest progress over the last decade [2–6]. One of the principal problems is that polyacrylonitrile degrades (cross-links) even without main chain scission or weight loss—this essentially precludes melt processing. Reactions of the side groups have been discussed in many reports [7–10]. These degradative reactions can take place both in an intra-molecular manner, but also via inter-molecular branching and gelation. This quickly alters the capacity for these materials to be melt fabricated. At 200–220°C, the material can quickly increase in viscosity, thus rendering an intractable material in a very short time. Ideally, one would like to maintain constant viscosity for a required period, and practical

considerations suggest that this should be at least 30 min or longer.

The following have been identified as key elements of the project approach:

- Melt-spun precursors are being formulated for evaluation, with the goal of developing a pelletized form for later melt spinning.
- Methods for handling, melting, and spinning the polymer are being developed to produce precursor fiber for the oxidative stabilization and carbonization conversion processes.
- Processing of the new polymer into finished carbon fiber will be necessary to demonstrate achievable properties, beginning with conventional processes.
- Processing of the new polymer into finished carbon fiber using the alternative manufacturing processes will be assessed.

RESULTS

The project team has made accomplishments during this period in advancing techniques required to produce adequate quality and quantities of precursor fiber necessary to establish stable and continuous conversion processes. To facilitate progress in spinning, the team utilized lower cost and somewhat easier to process samples of PAN-VA formulations. Note, making the full transition to PAN-MA formulations projected is necessary to achieve both economic and ultimate performance goals during this period. To establish spinning baselines, the team set molecular weight, molecular weight distribution, and acrylonitrile content ranges to focus on during this project period. All of these parameters, in conjunction with the plasticizer type, plasticizer and content, and spinning parameters will determine the spinnability of a particular composition. The current objectives are to provide trial materials with approximately 93–95 wt% acrylonitrile and 5–7 wt% methyl acrylate. The materials are being screened in the modified capillary rheometer spinning apparatus using plasticizers such as water and acetonitrile to determine the spinnability.

Formulation Development

The overall objective is to develop a melt spinning process for polyacrylonitrile copolymer fibers that can be converted to high strength carbon fibers. PAN is typically spun from solutions of dipolar aprotic solvents such as dimethylformamide (DMF), which is subsequently extracted in a downstream water bath. The solvent is necessary, because the copolymers have melting points that are far above the onset temperature of cyclization (i.e., accompanied by an increase in melt viscosity), and therefore they cannot be melt-processed without special conditions. Formulations containing plasticizers can reduce both glass transition temperature (T_g) and melting temperature (T_m) relative to the base copolymers alone. Thus, the team's approach includes determining thermal and rheological properties of polyacrylonitrile copolymers, and thermal and rheological effects of including "external" plasticizers in the copolymer formulations. The plasticizers tend to disrupt strong polar interactions among nitrile groups along the polymer chain, thus lowering the glass transition and melting temperatures of the polymer [11]. This is critical for melt processing because neat polyacrylonitrile copolymers melt at such high temperatures (~320°C) that decomposition and cyclization occur before the high melting point can be overcome. In addition to their propensity to lower the transition temperatures, the choice of additive is based on ease of removal from the spun fibers, any potential toxicity, boiling point, and flash point, all of which can contribute to the overall cost of fiber production as well as to the quality of the resulting fibers.

A compilation of potential plasticizers is provided in Table 1. All of the additives in Table 1 are synergistic with water in terms of lowering the melting points of the copolymer formulations. One consideration is how difficult it may be to quantitatively remove the additive(s) following spinning, and thus a high boiling point–low vapor pressure additive may cause challenges. N-methylpyrrolidone (NMP) acts similarly to DMF as a plasticizer in terms of reducing the polymer transitions, but NMP has a higher boiling point. It is reasoned that it may be more difficult to extract NMP from the fibers once they are spun. Isopropanol functions similarly to ethanol and likely could be substituted.

TABLE 1. Plasticizers and Their Properties Pertinent to Melt Spinnability

Plasticizer	Boiling point	Vapor pressure (20°C)	Flash point	Toxicity
DMF	152–154°C	516 Pa	58°C	Not a carcinogen. May cause birth defects.
Ethanol	78°C	5,950 Pa	~14°C	Non-toxic
Adiponitrile	295°C	0.3 Pa	93°C	Not a carcinogen. Skin exposure may cause skin irritation.
Acetonitrile	81°C	9,710 Pa	2°C	Not classified as a carcinogen. Modestly toxic in small doses.

Melt extrusion will require a temperature window of opportunity that lies above the melting point of the particular formulation and below the temperature–time upper limit, as characterized by the onset of cyclization. Additives that open up this window by depressing the melting points are thus of great interest. Thermograms illustrating depressions of transition temperatures of PAN-MA/water/second plasticizer formulations are depicted in Figures 1–4. These properties

were measured by differential scanning calorimetry (DSC) at a heating rate of 10°C/min in "high volume pans" to avoid any contamination of the instrumentation caused by any evolution of additives. All reported data are from second heating scans. The equilibrium maximum water uptake was measured at 25°C for both the PAN-MA copolymer and the PAN–vinyl acetate–vinyl alcohol copolymer. The PAN-MA copolymer absorbed ~6 wt% of water, whereas the PAN–vinyl acetate–vinyl alcohol copolymer absorbs significantly more water (16 wt%) under these conditions. Figure 4 shows glass transition temperatures of blends of the PAN-MA copolymer with varied amounts of water added. It should be noted that it is difficult to make such blends for DSC analysis with these low water contents and know exactly how much water is added to the DSC pan, since some of the blends are heterogeneous. The peak centered around 0°C corresponds to the melting endotherm of the water and the discontinuity in heat flow at the higher temperatures denote the T_gs of these blends. One observes a large depression in T_g from the PAN-MA alone (104°C) to the blends with very little water added (~75°C). However, with further increases in water, no additional depression is observed. This is likely related to the equilibrium water uptake being low. It is reasoned that excess water may be "free" water that does not interact effectively with the copolymer.

Melting endotherms for the PAN-MA–water–DMF and PAN-MA–water–acetonitrile are depicted in Figures 2 and 3, respectively. In all of these cases where melting points are depressed, water is synergistic with the second plasticizer. In Figure 2, the lower thermogram is of a blend of the PAN-MA with 30 wt% of DMF, and no melting point is observed within the needed temperature range for extrusion. The orange curve (second from bottom) is for a blend of PAN-MA containing 20 wt% of water and no DMF. From Figures 1 and 2, this blend has a T_g of 75°C and a T_m of 156°C. As varied amounts of DMF are added to the PAN-MA–20 wt% water blend, the melting point continues to decrease. This suggests a synergism between these two additives regarding melting point depression. Figure 3 shows a similar trend as acetonitrile is added, but the effect is even more substantial.

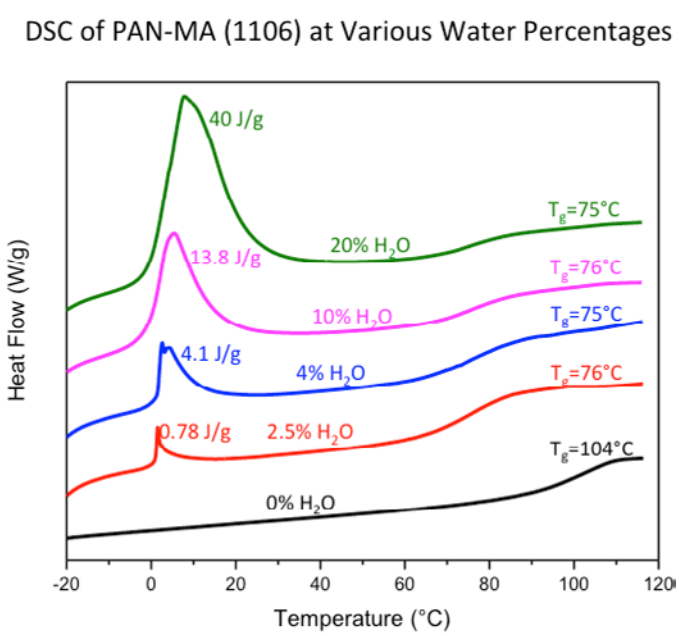

FIGURE 1. Glass transition temperatures of PAN-MA–water blends

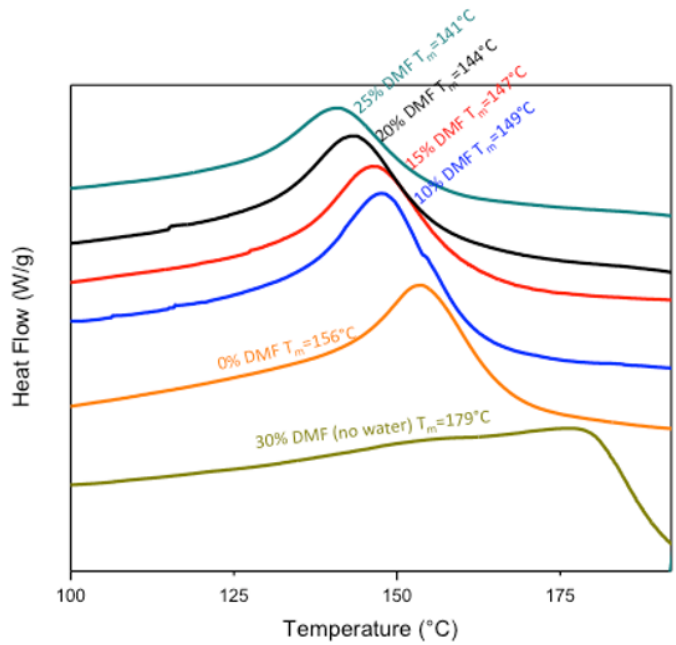

FIGURE 2. Melting endotherms of PAN-MA containing water and DMF

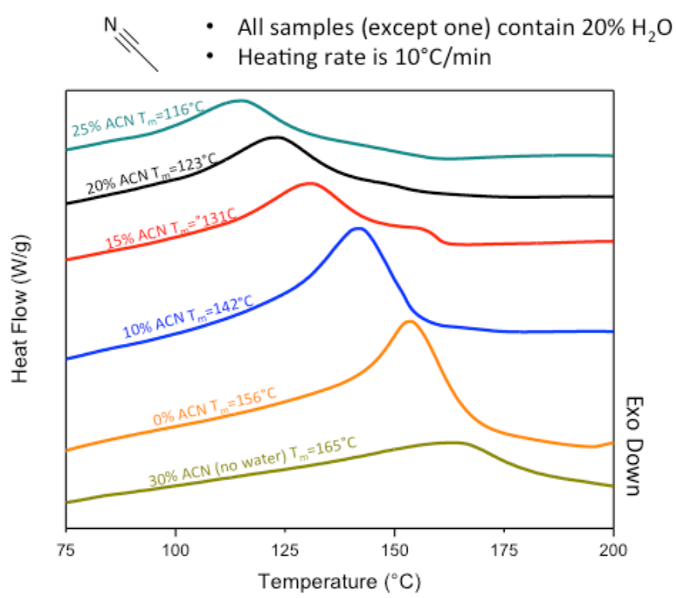

FIGURE 3. DSC thermograms showing melting endotherms of PAN-MA–water–acetonitrile formulations

With a formulation of 70% PAN-MA–20% water–10% acetonitrile, the melting point is depressed to 142°C, whereas a similar formulation with DMF shows a melting point at 149°C. Neither water alone nor do any of the other plasticizers alone depress the melting points as effectively as the combinations. A select compilation of melting points with PAN-MA–20 wt% water–second plasticizer is shown in Figure 4 and Table 2. DMF, NMP, and acetonitrile are good solvents for the copolymer, whereas water and ethanol are non-solvents. The mechanism by which the plasticizers depress the thermal transitions of the formulations are not yet understood. Figure 4 shows that the melting points with acetonitrile and adiponitrile (both containing nitriles) are the lowest, and that DMF and NMP (both dipolar aprotic solvents for the copolymer) are in the intermediate range.

Spinning Process Development

Rheological testing is being performed on formulations of interest to support spinning process development. Generally, both time-dependent viscosity measurements and shear rate-dependent viscosity measurements for polyacrylonitrile copolymers with various plasticizers were conducted. Some of the data is presented and analyzed.

Figures 5 and 6 show the time-dependent rheological data for PAN-VA–EtOH–H_2O and PAN-VA–H_2O. Generally, the viscosity increased when temperature was higher than 180°C. This suggests that the PAN-VA copolymer begins to cyclize under these conditions. However, there was no significant viscosity increase within 35 min even at 190°C. That suggests that the team may spin the PAN-VA fiber at such a temperature without significant cyclization with concomitant viscosity increase with a residence time of at least 30–35 min. However, because tails in the residence time distribution in the extruder can exceed 30 min, cyclization of the PAN-VA can occur at temperatures above 180°C.

Various purge materials have been evaluated as a means for initial sealing of the extruder to assist in maintaining the volatile plasticizers, while initiating spinning as well as cleaning the extruder when spinning is completed. Evaluated purge materials include those shown in Table 3, as well as other formulations. With the mixture of PAN-VA, ethylene carbonate, and water being used as the purge material, the team could start fiber spinning and obtain PAN-VA filaments wound on a bobbin successfully. However, there was a common problem observed in all spinning trials. That is, the pressure of the PAN melt dropped about 20 min after the fibers first exited from the spinneret. At the same time,

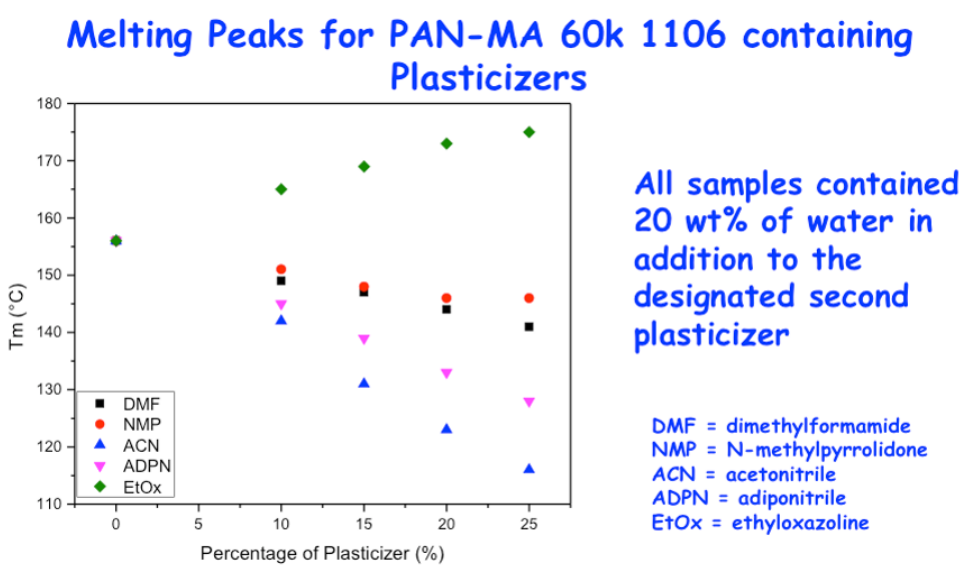

FIGURE 4. Melting points of PAN-MA¬20 wt% water–second plasticizer formulations

TABLE 2. Thermal Properties of PAN-MA Plus Plasticizer Compositions

70 wt% PAN-MA–20 wt% H_2O	+ 10 wt% DMF	+ 10 wt% Ethanol	+ 10 wt% Adiponitrile	+ 10 wt% Acetonitrile
T_m 156°C	T_m 149°C	T_m 148°C	T_m 145°C	T_m 142°C
60 wt% PAN-MA–20 wt% H_2O	+ 20 wt% DMF	+ 20 wt% Ethanol	+ 20 wt% Adiponitrile	+ 20 wt% Acetonitrile
T_m ~156°C	T_m 144°C	T_m 149°C	T_m 133°C	T_m 123°C

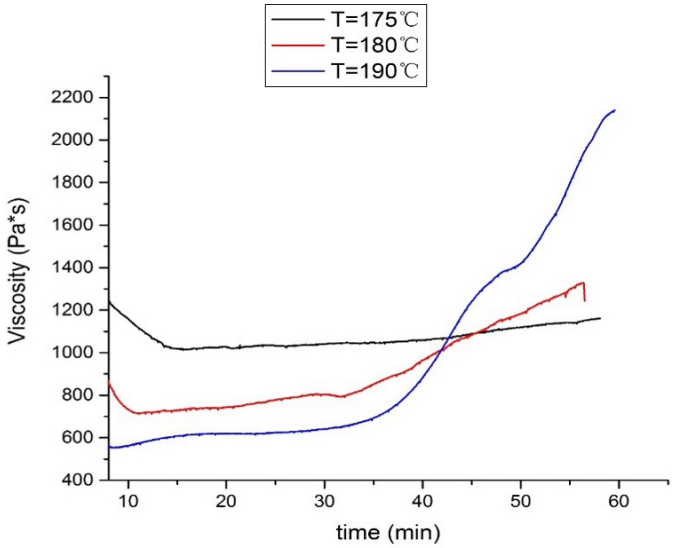

FIGURE 5. Time dependent apparent viscosity data for the PAN-VA copolymer plasticized with water–ethanol

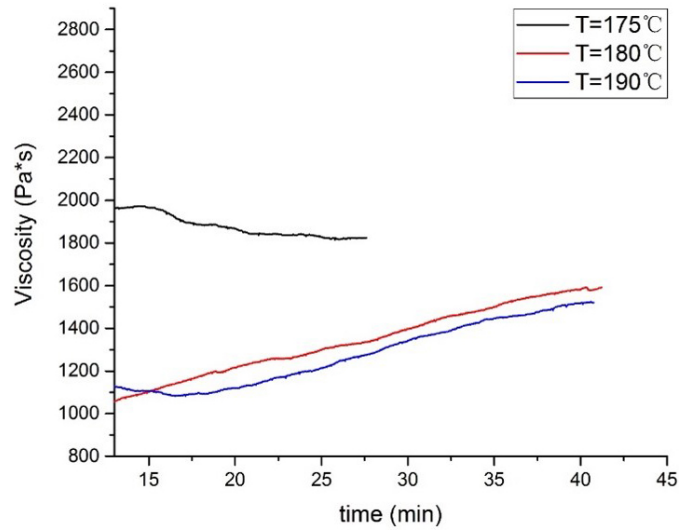

FIGURE 6. Time dependent apparent viscosity data for the PAN-VA plasticized with water only

TABLE 3. Summary of PAN-VA Fiber Spinning (Plasticized with 20 wt% of Water) Initiated with Purge Materials

Purge Materials (PM)	Form of PM	Temperature (°C)	PM passes spinneret?	Were PAN fibers obtained?	Observation/ Comments
Barex*	Pellet	190	No	No	190°C may be too low for the Barex
Polyethylene	Pellet	190	Yes	No	PAN degraded seriously inside the spin pack
PAN-VA + H_2O + Ethylene Carbonate	Powder	190	Yes	No	PAN degraded seriously inside the spin pack
PAN-VA + H_2O + Ethylene Carbonate	Powder	185	Yes	Yes	No serious PAN degradation

* Commercial name for 65AN/25MA/10Elastomer Copolymer.

the number of filaments decreased and the fiber diameter decreased.

A further study confirmed that the PAN-VA pellets had stopped feeding some 20 min after the spinning began. It is believed the reason for this is that some of the water in the hot zones may have evaporated and then condensed in the cold zone (feed section). It is believed that the pellets in the feed section may have absorbed the condensed water and become too wet to be fed continuously.

Several methods were investigated to solve this problem, including the use of an open hopper, increasing the hopper/extruder pressure, use of a nitrogen purge in the hopper and starved feeding of materials (PAN pellets). The starved feeding method was successful. For the device needed for this method, the team started with a valve to control the feeding speed manually, and then designed and constructed a motor-driven feeder to control the feed speed automatically. The feeder was mounted between the hopper and the feed section and was designed and outfitted to operate under pressure. Since the feeder was implemented, it was found easier to feed the PAN pellets continuously. The melt pressure was also more stable.

Figure 7 shows the PAN-VA fibers generated in March and April of 2016. The spinning was conducted at 185°C with water (20 wt%) as a plasticizer. The fiber tow generated in March (Figure 7A) had a length of 20 m and a filament number of 280, whereas another generated in April met the DOE milestone of December 31, 2015 which read as: "Down-select processing conditions and water/plasticizer formulations for PAN-VA and demonstrate spinning of >100 filament tows of length >10 m."

Experiments showed that it was difficult to feed the PAN powders mixed with water (as a plasticizer) through the extruder. Thus, PAN pellets were made first and then used in the fiber spinning process. Several methods have been developed and evaluated at varying levels of success; additional work is continuing in this area.

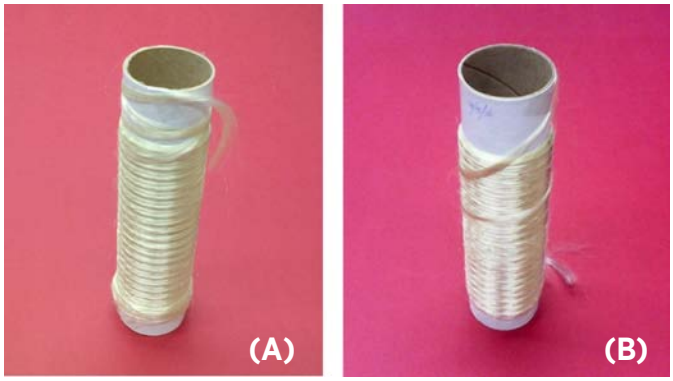

FIGURE 7. PAN-VA fiber tow with a filament number of 280 and length of 20 m generated on March 22, 2016 (A), and another with a filament number of 315 and length of 50 m generated on April 25, 2016 (B)

FIGURE 8. PAN-MA fibers generated on April 5, 2016

The focus of the team's spinning work has been moved from PAN-VA to PAN-MA, since a key milestone was achieved in March 2016 when PAN-VA fibers were successfully generated. The team was able obtain some fibers and wind them on a bobbin. One of the fiber tow samples had 140 filaments that were approximately 10 m long (see Figure 8). This is promising, but will require further investigations to improve the feeding process and also adjust the plasticizer and temperature parameters to lower the melt viscosities over the residence time needed for extrusion.

As a parallel effort and backup approach to complement the spinning work with the single screw extruder at Virginia Tech, a series of spinning/extrusion trials utilizing twin screw extrusion equipment and expertise was initiated at Leistritz to investigate potential benefits of a twin-screw approach. Specific capabilities of interest in their laboratories include (1) modular construction allows rapid change-out of screw types overall and sections of the screw along the length as well as adjustment of screw length and barrel as shown in Figure 9, (2) production rates are more tunable in optimizing conditions, and (3) Leistritz extruder modules have ports available for downstream injection of second and third phases – powder can be fed dry and the plasticizers then injected downstream. Early trials demonstrated capability to extrude some short sections of PAN plasticized with water and/or acetonitrile, but success was inconsistent. At the time of this report, potential for the twin screw extrusion approach is still inconclusive.

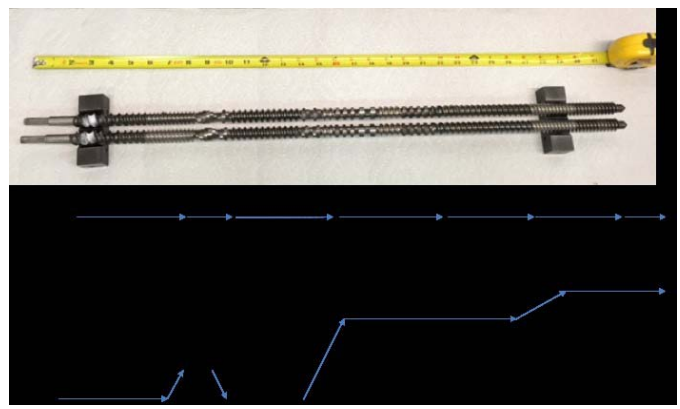

FIGURE 9. Example screw setup at Leistritz showing modularity and functions of various screw sections

CONCLUSIONS AND FUTURE DIRECTIONS

Continuing progress is being made in improving melt spinning processes towards producing precursor fiber in sufficient quality and minimum quantity to begin carbon fiber conversion investigations. Work on the precursor chemistry necessary to enhance baseline properties and move towards the ultimate goals of 33 Msi modulus and 700 ksi strength is making significant progress. Near-term objectives are for Virginia Tech to produce longer and more uniform tows that are then drawn in a secondary step. ORNL will characterize fiber and conduct more extensive conversion trials on precursor filaments generated using its precursor evaluation system. The filaments at various steps of the conversion process will be fully characterized and the data used to commence optimization of precursor chemistry and the filament generation process. In order to fully address application requirements, the team will also need to evaluate and implement appropriate post treatment operations including surface treatment and sizing for the fiber. Plans are also in place to evaluate whether advanced plasma-based conversion processes (oxidative stabilization and carbonization) under development at ORNL are appropriate for these fibers in reducing costs while meeting performance goals.

FY 2016 PUBLICATIONS/PRESENTATIONS

1. Felix L. Paulauskas and Bob Norris, "Melt Processable PAN Precursor for High Strength, Low-Cost Carbon Fibers," presentation at 2016 DOE Hydrogen and Fuel Cells Program and Vehicle Technologies Office Annual Merit Review and Peer Evaluation Meeting, June 8, 2016.

REFERENCES

1. Fuel Cell Technologies Office Multi-Year Research, Development, and Demonstration Plan Planned program activities for 2005-2015, October 2007 update.

2. Wiles, K.B., V.A. Bhanu, A.J. Pasquale, T.E. Long, and J.E. McGrath, Journal of Polymer Science: Part A: Polymer Chemistry, Vol. 42, 2994–3001 (2004).

3. Bhanu, V.A. P. Rangarajan, K. Wiles, M. Bortner, S. Sankarapandian, D. Godshall, T.E. Glass, A.K. Banthia, J. Yang, G. Wilkes, D. Baird, and J.E. McGrath, Polymer, 43, 4841–4850, (2002).

4. Godshall, D., P. Rangarajan, D.G. Baird, G.L. Wilkes, V.A. Bhanu, and J.E. McGrath, "Polymer 44 (2003), 4221–4228.

5. Rangarajan, P., V.A. Bhanu, D. Godshall, G.L. Wilkes, J.E. McGrath, and D.G. Baird, Polymer 43, 2699–2709 (2002).

6. Bortner, Michael J., Vinayak Bhanu, James E. McGrath, and Donald G. Baird, Journal of Applied Polymer Science, 93(6), 2856–2865 (2004).

7. Peng, Fred M., "Acrylonitrile Polymers," in Mark, Herman F.; Bikales, Norbert M.; Overberger, Charles G.; Menges, Georg; Editors. Encyclopedia of Polymer Science and Engineering, Vol. 1: A to Amorphous Polymers. (1986), 843 pp, pages 426–470, and references therein.

8. Back, Hartwig, C, and Knorr, Raymond S. "Acrylic Fibers," in Mark, Herman F.; Bikales, Norbert M.; Overberger, Charles G.; Menges, Georg; Editors. Encyclopedia of Polymer Science and Engineering, Vol. 1: A to Amorphous Polymers. (1986), 843 pp, pages 334–388, and references therein.

9. Capone, Gary J.; Masson, James C. Fibers, acrylic. Kirk-Othmer Encyclopedia of Chemical Technology (5th Edition) (2005), 11 188–224

10. Frushour, Bruce G.; Knorr, Raymond S. Acrylic fibers. International Fiber Science and Technology Series (2007), 16(Handbook of Fiber Chemistry (3rd Edition)), 811–973.

11. Min, B.G., Son, T.W., Kim, B.C., Lee, C.J., Jo, W.H., Plasticization Behavior of Polyacrylonitrile and Characterization of Acrylic Fiber Prepared from the Plasticized Melt. Polymer Journal 1992, 24 (9), 841–848.

IV.D.8 Innovative Development, Selection and Testing to Reduce Cost and Weight of Materials for BOP Components

Chris San Marchi (Primary Contact),
Jonathan Zimmerman
Sandia National Laboratories
7011 East Avenue – MS 9161
Livermore, CA 94550
Phone: (925) 294-4880
Email: cwsanma@sandia.gov

DOE Manager: Ned Stetson
Phone: (202) 586-9995
Email: Ned.Stetson@ee.doe.gov

Subcontractor:
Hy-Performance Materials Testing LLC, Bend, OR

Project Start Date: July 15, 2014
Project End Date: September 30, 2017

Overall Objectives

- Reduce weight of structural materials for balance of plant (BOP) components by 50%.
- Reduce cost of structural materials for BOP components by 35%.
- Expand the scope of materials of construction for BOP components.
- Identify simplified testing procedures to enable materials qualification.

Fiscal Year (FY) 2016 Objectives

- Quantify fatigue life of commercially available low-nickel alloy with/without internal hydrogen at near-room and sub-ambient temperatures.
- Establish correlations of stacking fault energy (SFE) with performance metrics (e.g., tensile strength, ductility) known from project experiments and literature.
- Estimate SFEs for Fe-Cr-Ni-based and stainless steel alloys of interest and validate estimates against experimental measurements and literature values.
- Quantify cost and weight savings based on maximum allowable stress in the presence of hydrogen.

Technical Barriers

This project addresses the following technical barriers from Hydrogen Storage section of the Fuel Cell Technologies Office Multi-Year Research, Development, and Demonstration Plan.

(A) System Weight and Volume

(B) System Cost

(H) Balance-of-Plant (BOP) Components

Technical Targets

No specific technical targets have been set. This project is a basic study of materials of construction for BOP with the goals of identifying lower-cost alternatives to the baseline of annealed Type 316L that can be implemented in lighter-weight designs (i.e., high strength materials). The project targets are:

- Reduce weight of structural materials for BOP components by 50%.
- Reduce cost of structural materials for BOP components by 35%.

FY 2016 Accomplishments

- Notched stresslife fatigue data have been collected for XM-11 (21Cr6Ni9Mn) austenitic stainless steel at room and low (50°C) temperature with and without internal hydrogen.
- Normalization of the maximum cyclic stresses by the yield strength collapses hydrogen-assisted fatigue life data to a master curve, enabling extrapolation of the effects of both precharging and temperature on intrinsic fatigue performance in high-pressure hydrogen.
- Analysis of the available scientific literature reveals a general trend between stacking fault energy and reduction of area (i.e., tensile ductility) for service in hydrogen. Data also shows that this correlation persists with Mn-stabilized steels.
- Developed an atomic-level approach to calculate SFE including contributions due to magnetic entropy, which are significant for Fe-Cr-Ni alloys. This approach predicts a value of 35.4 mJ/m^2 for an alloy of approximate composition $Fe_{66}Cr_{14}Ni_{20}$, in close agreement to available literature.
- Quantified SFE for 316L stainless steel to be ~60–100 mJ/m^2 (a range consistent with the scientific literature) using transmission electron microscopy. Predicted a lower limit of 63 mJ/m^2 for the SFE of a low-Ni, high-Mn stainless steel alloy.

- Developed computational approach for alloy exploration based on optimizing SFE.

✧ ✧ ✧ ✧ ✧

INTRODUCTION

The primary objective of this effort is to identify alloys to replace Type 316/316L in hydrogen service for balance of plant (BOP) applications onboard fuel cell electric vehicles. Type 316/316L austenitic stainless steels are used extensively in hydrogen systems for their resistance to hydrogen embrittlement, which is attributed to the relatively high nickel content of Type 316/316L alloys. Nickel content, however, drives the cost of austenitic stainless steels, thus Type 316/316L alloys impose a cost premium compared to similar alloys with lower nickel content. Since the cost of BOP components is a large fraction of the cost of hydrogen fuel systems (even dominating the cost at low production volumes [1]), alternative materials are desired. In addition, Type 316/316L alloys are relatively low strength, thus high-pressure components tend to be heavy to accommodate the stresses associated with the pressure loads. Higher-strength materials will reduce weight of the components (an added benefit for onboard components) and contribute to lower cost since less material is needed. However, engineering data to justify selection of lower cost and higher strength alloys for high-pressure hydrogen service are currently unavailable. Moreover, alloy design could enable low cost solutions to the specific needs of onboard hydrogen storage.

APPROACH

The objective of this project is addressed from two perspectives: (1) experimental evaluation of commercial alloys and (2) computational materials discovery of new alloys. In the first case, fatigue properties in hydrogen environments will be evaluated for low-cost, high-strength alloys and compared to the benchmark of annealed Type 316/316L. The test program seeks appropriate trade-offs between materials cost and performance, such that hydrogen embrittlement can be effectively managed in design. This performance includes low temperature performance associated with refueling protocols at -40°C; the effect of hydrogen on fatigue as a function of temperature has not been previously reported. An additional goal of the experimental activity is to demonstrate a straightforward, simplified methodology by which materials may be qualified for safe hydrogen service, including the use of internal hydrogen (saturation of the material with hydrogen by thermal precharging) as a robust substitute for testing in gaseous hydrogen.

The goal of the computational discovery activity, like the experimental activity, is to identify low-Ni content (and thus lower cost) stainless steel alloys to be used in BOP components that are compatible for hydrogen service. To achieve this goal from a computational perspective, a framework is being developed that combines sophisticated optimization and uncertainty quantification with ab initio calculations. Our objective is to use this framework to create a comprehensive database and materials design relations that identify stainless steel alloys that optimize stacking fault energy (indicative of hydrogen embrittlement resistance) with reduced Ni content. This effort represents a new initiative in the DOE Fuel Cell Technologies Office research portfolio to use computational materials science coupled with high-performance computing to identify and evaluate low-cost stainless steels that are tailored for hydrogen embrittlement resistance. This innovative approach will provide the DOE and U.S. industry with a framework and computational tools to efficiently and effectively explore the design space for next-generation materials used in fuel cell technologies.

RESULTS

Experimental Evaluation of Commercial Alloys

Using the method established during the first year of the project, fatigue life measurements were made for a low-Ni stainless steel alloy, XM-11 (21Cr6Ni9Mn). Overall, the observed life at a given stress level was observed to be the same or slightly better than annealed (the baseline material for this study) or strainhardened 316L. When tested at 20°C, this material demonstrates similar stress-life characteristics for both its as-received (AR) condition and H-precharged condition (PC). In contrast, the fatigue life when tested in 103 MPa external gaseous hydrogen was found to be noticeably less than the AR condition. Differences between the PC and external hydrogen testing could be attributed to the increase in yield strength observed to occur from the H-precharging process. Accounting for this increase aligns the results from PC specimens with those from testing in external hydrogen, with both data sets with hydrogen clearly occupying a single band below the average life of the AR condition, as shown in Figure 1. This suggests that H-precharging provides a method to efficiently probe the H-assisted fatigue performance of austenitic stainless steels.

Testing of XM-11 was also performed at a temperature of -50°C. Test results show a longer fatigue life at low temperature compared to room temperature for equivalent test conditions. As with the effect of H-precharging on fatigue at room temperature, normalization of the fatigue stress with yield strength collapses the fatigue life curves to a master curve for both temperatures with and without internal hydrogen, also shown in Figure 1.

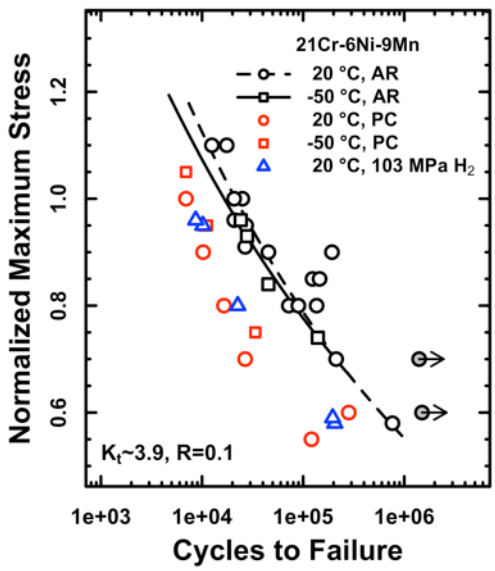

FIGURE 1. Tensiontension stresslife fatigue curves for notched specimens plotted as a function of the maximum imposed stress normalized by the yield strength for 21Cr6Ni9Mn austenitic stainless steel for the tested conditions. The lines on the plots represent fits to the AR data at room temperature (dashed) and at temperature of -50°C (solid). Shaded symbols with arrows represent test conditions that did not result in failure.

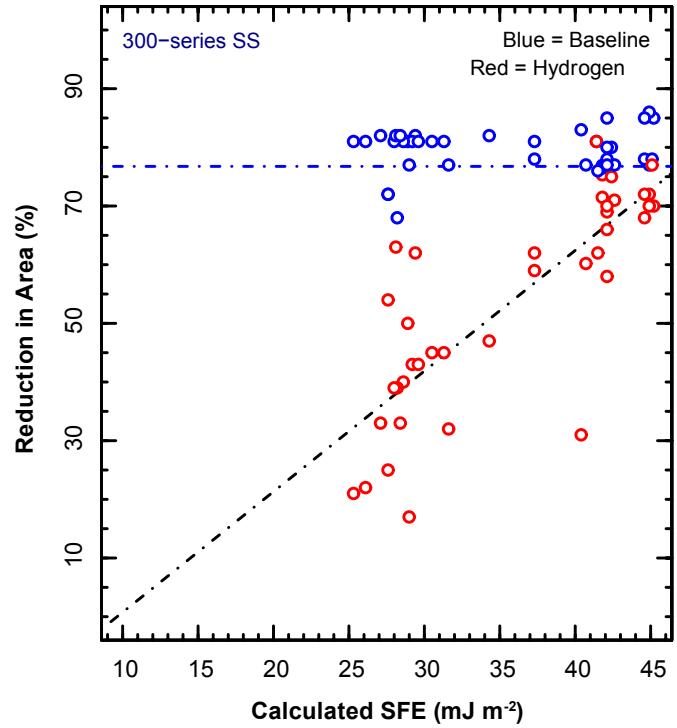

SS – Stainless steel

FIGURE 2. Reduction of area for various 300-series stainless steels from literature plotted as a function of calculated stacking fault energy for the alloy

Correlating Stacking Fault Energy to Hydrogen Degradation

To quantify the correspondence between stacking fault energy (SFE) and resistance to hydrogen degradation, we performed a systematic evaluation of the existing literature. Use of a thermodynamic model by Curtze et al. [2] that estimates SFE based on composition enabled consideration of a larger set of literature results than just those in which SFE was measured. Considering only 300-series stainless steels, several mechanical properties, including yield strength, were observed to have no correlation with SFE. However, the reduction of area in the presence of hydrogen shows a general decreasing trend with decreasing SFE value, as shown in Figure 2. The substantial decrease in reduction of area in hydrogen at low SFE with no corresponding variation in yield strength-based metrics suggests that hydrogen degradation in austenitic stainless steels is dependent on plastic strain generated during tensile testing. A similar trend has been established for Mnstabilized austenitic stainless steels, suggesting that Mn may be an effective replacement for Ni when considering alloys for hydrogen service.

Computational Materials Discovery

We calculate an alloy's SFE from a combination of cohesive energies for the face-centered cubic (fcc), hexagonal close-packed (hcp) and double hcp (dhcp) crystal structures. To include the effect of temperature, we assume the material to be in a paramagnetic state (i.e., net zero magnetic moment) and determine the average value of individual atomic magnetic moments based on statistical mechanics and the system's temperature. The computational expense associated with this approach is quite considerable as a total of 70,656 processors are used for approximately 8 hr to obtain the magnetic/spin contribution to the SFE. Figure 3 shows a distribution of average magnetic/spin moments determined for a $Fe_{66}Cr_{14}Ni_{20}$ alloy. Using this distribution, we estimate the magnetic/spin entropy to be 9.5 mJ/m^2 at 300 K, a value in close agreement with published results [3]. We combine this entropy contribution with the enthalpy corresponding to a configuration of very similar composition for a total SFE of 35.4 mJ/m^2. Unfortunately, upon examining other alloy compositions we determined that the initial electron spin configuration can significantly impact the enthalpy calculated for the system. It is unclear whether this issue can be addressed without drastically increasing the cost of these calculations.

We have developed a computational approach to enable automated exploration of the material composition space (1) to explore and understand tradeoffs with regard to composition effects on SFE and (2) to identify compositions that maximize SFE values. The software infrastructure consists of a combination of tools for model exploration, tools for data analysis and visualization, our own implementation

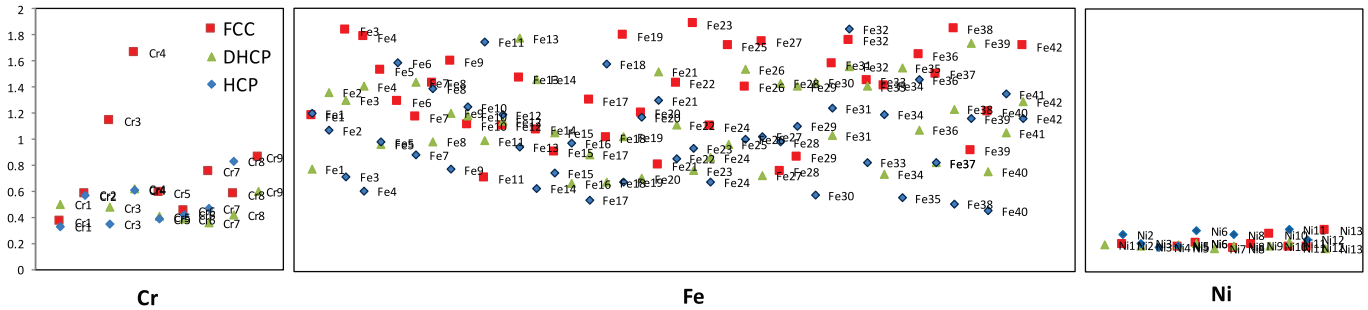

FIGURE 3. Comparison of average magnetic moments of all atoms within a 64-atom system between different structural phases, fcc, dhcp and hcp, at a temperature of 300 K

of the thermodynamic model, and code to enable interfacing between all of these pieces.

Transmission Electron Microscopy Measurements of Stacking Fault Energy

We have used transmission electron microscopy to investigate dislocation structures in stainless steel alloys, and to measure the SFE in order to validate the predictions of our modeling. By measuring the width associated with partial dislocation dissociation (shown in Figure 4), we determined that 316L has a SFE value in the range of 60–100 mJ/m^2, consistent with measurements of SFE = 78 mJ/m^2 reported in the literature [4]. We have also examined dislocations in a low-Ni, high-Mn stainless steel alloy and estimated a lower limit to the alloy's SFE of about 63 mJ/m^2.

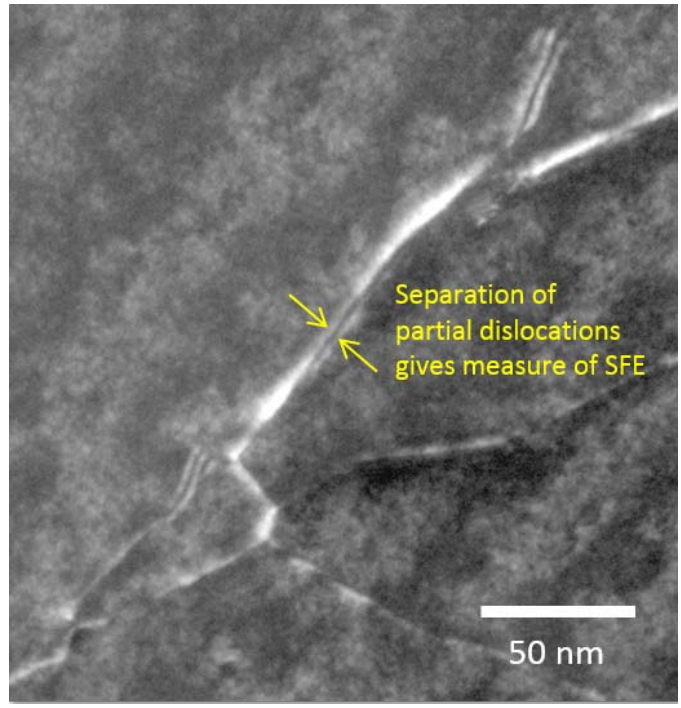

FIGURE 4. Transmission electron microscopy image of dislocation splitting in 316L stainless steel imaged using weak-beam dark-field. Measurement of the partial dislocation separation provides a measure of stacking fault energy.

CONCLUSIONS AND FUTURE DIRECTIONS

- Testing and analysis of strain-hardened 316L and XM-11 austenitic stainless steels reveals that normalization of stress values by yield strength collapses fatigue life data to a master curve, enabling extrapolation of the effects of hydrogen condition and temperature on performance.
- Analysis of literature shows that, for 300-series and Mn-stabilized stainless steels, stacking fault energy (SFE) appears to correlate with metrics for ductility for service in hydrogen.
- An atomic-level approach has been used to calculate SFE for Fe-Cr-Ni-based alloys, which produces predictions in close agreement with the available literature. A computational approach has been developed for alloy exploration based on optimizing SFE, and can be configured to use either thermodynamic models or ab initio calculations as an input/analysis tool.
- SFE has been measured for 316L stainless steel, and bounded for a low-Ni, high-Mn stainless steel alloy.
- In the final year of this project, commercial high-strength (i.e., strain-hardened) alloys will be evaluated to assess their potential for achieving the weight savings target. In addition, our computational framework will be more fully developed and used to explore a wide range of compositions within the Fe-Cr-Ni-Mn-Al system. Initial surveys will be performed using the available thermodynamic model, while avenues for improving the efficiency and consistency of ab initio calculations will be pursued.

FY 2016 PUBLICATIONS/PRESENTATIONS

1. C. San Marchi (presenter), "Fatigue testing methodologies in gaseous hydrogen," (SAND2015-9931C), presented at the

International Workshop on Hydrogen Embrittlement in Metal, Jeju, Korea, 13 November 2015.

2. P.J. Gibbs (presenter), "Hydrogen Influences on Notched Fatigue Life of Stainless Steels," (SAND2016-1544C), presented at the 2016 TMS Annual Meeting and Exhibition, Nashville, TN, 17 February 2016.

3. P.J. Gibbs, K.A Nibur, X. Tang, C. San Marchi, "Comparison of Internal and External Hydrogen on FatigueLife of Austenitic Stainless Steel," (PVP2016-63563), *Proceedings of the ASME 2016 Pressure Vessels and Piping Conference*, Vancouver, Canada, 17–21 July 2016.

4. P.J. Gibbs, K.A. Nibur, C. San Marchi, "Fatigue behavior of austenitic steels with hydrogen," (SAND2016-1283A), *Abstract for the 2016 International Hydrogen Conference*, Moran, WY, 11–14 September 2016.

REFERENCES

1. DOE Fuel Cell Technologies Office Record # 13010.

2. S. Curtze et al., "Thermodynamic modeling of the stacking fault energy of austenitic steels," *Acta Materialia* 59 (2011): 1068–1076.

3. L. Vitos et al., "Stacking fault energy and magnetism in austenitic stainless steels," *Physica Scripta* 77 (2008): 065703.

4. R.E. Schramm and R.P. Reed, "Stacking fault energies of seven commercial austenitic stainless steels," Metallurgical Transactions A 6A (1975): 1345–1351.

Sandia National Laboratories is a multi-program laboratory managed and operated by Sandia Corporation, a wholly owned subsidiary of Lockheed Martin Corporation, for the U.S. Department of Energy's National Nuclear Security Administration under contract DE-AC04-94AL85000.

V.0 Fuel Cells Program Overview

INTRODUCTION

The Fuel Cells program supports research, development, and demonstration of fuel cell technologies for transportation applications, as well as stationary and early market applications, with a primary focus on reducing cost and improving durability. Efforts predominantly concentrate on research and development (R&D) of fuel cell stack components, as opposed to system balance-of-plant components, subsystems, and system integration. The program seeks a balanced, comprehensive approach to fuel cells for near-, mid-, and longer-term applications. The development of fuel cells for transportation applications is a primary focus due to the nation's goal of significantly reducing its energy and petroleum needs and the benefits inherent in fuel cell electric vehicles (FCEVs) (e.g., high efficiency, long driving range, zero emissions). Stationary applications include the development of fuel cells for distributed power generation, including combined heat and power (CHP) for residential and commercial applications. Existing early markets and near-term markets generating market traction for adoption of FCEVs include backup power, auxiliary power units, and specialty applications such as material handling equipment. The program's R&D portfolio is primarily focused on polymer electrolyte membrane (PEM) fuel cells, but also includes longer-term technologies, such as alkaline fuel cells and higher-temperature fuel cells like molten carbonate fuel cells for stationary applications.

The program's fuel cell tasks in the Fuel Cell Technologies Office *Multi-Year Research, Development, and Demonstration Plan*, updated in Fiscal Year (FY) 2016, are organized around the development of components, stacks, subsystems, and systems; supporting analysis; and testing, technical assessment, and characterization activities.

GOAL

The program's goal is to advance fuel cell technologies for transportation, stationary, and early market applications.

OBJECTIVES[1]

The program's key objectives include:

- Developing a 65% peak-efficient, direct hydrogen fuel cell power system for transportation that can achieve 5,000-h durability (ultimate 8,000 h) and be mass produced at a cost of $40/kW by 2020 (ultimate $30/kW).
- Developing distributed generation and micro-CHP fuel cell systems (5 kW) operating on natural gas that achieve 45% electrical efficiency and 60,000-h durability at an equipment cost of $1,500/kW by 2020.
- Developing medium-scale CHP systems (100 kW–3 MW) by 2020 that achieve 50% electrical efficiency, 90% CHP efficiency and 80,000-h durability at a cost of $1,500/kW for operation on natural gas and $2,100/kW when configured for operation on biogas.

FY 2016 TECHNOLOGY STATUS AND ACCOMPLISHMENTS

Reducing cost and improving durability while maintaining performance continues to be the key challenge facing fuel cell technology R&D. For platinum group metal (PGM)-based catalysts, both a reduction in PGM loading and an increase in membrane electrode assembly (MEA) area power density are required to reduce material costs. Current state-of-the-art MEAs with very low cathode PGM loadings experience a higher-than-expected reduction in performance when operating at high power (e.g., near the rated power point), but FY 2016 saw continued progress towards addressing this performance loss. Commercial fuel cells are expected to use PGM-based catalysts in the near term; however, reaching cost competitiveness with conventional automobiles in the long term will require a transition from PGM-based catalysts to PGM-free catalysts. Advances in FY 2016 have brought PGM-free catalysts significantly closer to parity with conventional PGM-based catalysts. Major advances in FY 2016 were also made in development of durable, high-performance membranes that will allow fuel cells to operate for longer periods of time under harsh conditions.

[1] Note: Targets and milestones were recently revised; therefore, individual project progress reports may reference prior targets.

One of the most important metrics used to guide the program's R&D efforts is the projected high-volume manufacturing cost for automotive fuel cells, which is tracked on an annual basis. The program is targeting a cost reduction to $40/kW by 2020. Long-term competitiveness with alternative powertrains is expected to require further cost reduction to $30/kW, which represents the program's ultimate cost target. This year, the preliminary cost projection for an 80-kW_{net} automotive PEM fuel cell system based on next-generation laboratory technology and operating on direct hydrogen is $53/$kW_{net}$ when manufactured at a volume of 500,000 units/year and $59/ kW_{net} when manufactured at 100,000 units/year. For comparison, the expected cost of automotive PEM fuel cell systems that are based on current technology and planned for commercialization in the 2016 time frame is approximately $230/$kW_{net}$ when manufactured at a volume of 1,000 units/year.

The 2016 cost estimate was based again this year on Argonne National Laboratory's (ANL's) projected stack performance for a real de-alloyed $PtNi_3$ catalyst (d-PtNi) from Johnson Matthey. The main changes from last year's analysis that materially impacted the cost included an improved cathode catalyst with a reduced Pt loading and increased power density, the use of more expensive bipolar plate stamping processes and equipment upon re-evaluation, and the incorporation of thinner gas diffusion layers. Taken together and with others, the changes made in 2016 result in almost no net change in system cost from 2015. Also of note in 2016 was the addition of an acid washing step to the catalyst coated membrane (CCM) preparation during the MEA fabrication process, a step incorporated based on research done at ANL as a means to prevent performance loss at low humidity levels. The results of the current year's cost analysis are compared to those of previous years in Figure 1.

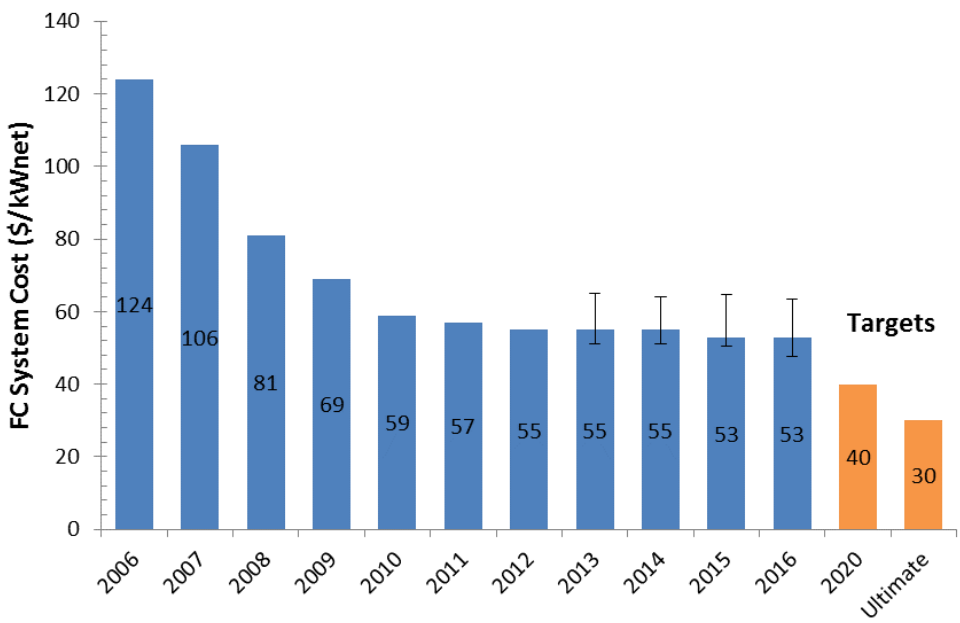

FIGURE 1. Modeled cost of an 80-kW_{net} PEM fuel cell (FC) system based on projection to high-volume manufacturing (500,000 units/year)

To enable vehicle commercialization, fuel cell systems must also meet the program's durability targets. These targets vary by application; for automotive systems, DOE has set a 2020 target of 5,000 h, and in 2016 increased its ultimate durability target to 8,000 h. This increase serves to more accurately represent the durability requirement in terms of miles driven (150,000 mi) for a larger range of drivers, specifically capturing requirements for people who drive at a lower average speed. Analysis in 2016 found that the current average lab-tested durability status is approximately 3,500 h.

Meanwhile, DOE independent validation of on-road FCEVs showed a more than four-fold increase in the maximum projected durability of fuel cell systems, increasing from 950 h in 2006 to over 4,100 h in 2016. Additionally, the maximum operating hours recorded for a single FCEV has remained at 5,600 h. For comparison, state-of-the-art maximum lab durability is projected to be over 12,000 h. The durability of fuel cell electric buses has

also been evaluated since 2000 in transit agency demonstrations and has continued to increase after having surpassed the 2016 interim 18,000 h target in 2015. The current bus maximum lifetime is over 23,000 h and was set by a bus that continues to operate.

Consortia

To simultaneously address performance and durability challenges, the program announced the creation of the Fuel Cell Performance and Durability (FC-PAD) Consortium in FY 2015. The consortium coordinates work under the thrust areas defined in Figure 2. There are three thrust areas related to components (electrocatalysts and supports; electrode layers; ionomers, gas diffusion layers, bipolar plates, interfaces) and three thrust areas that are cross-cutting in nature (modeling and validation; operando evaluation: benchmarking, accelerated stress tests, and contaminants; component characterization and diagnostics). This R&D consortium is led by a team of national laboratories and began operations in FY 2016. FC-PAD has met its FY 2016 milestones, including the development of new durability accelerated test protocols and the development of multiple electrode designs for optimizing high-current-density performance. The consortium is actively incorporating collaborators selected from the program's FY 2016 funding opportunity into its steering committee.

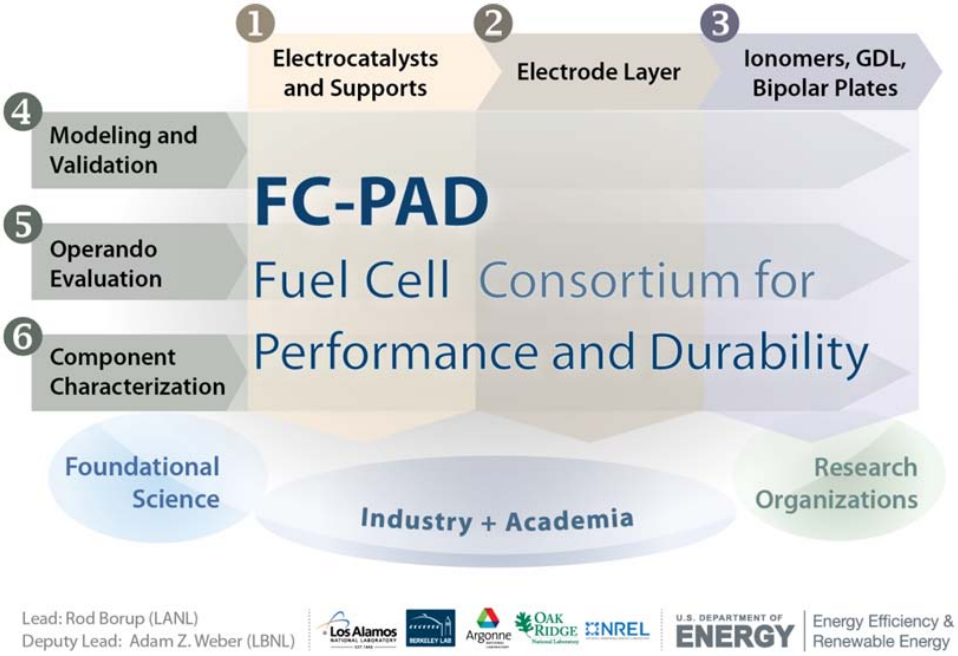

GDL – gas diffusion layer; LANL – Los Alamos National Laboratory; LBNL – Lawrence Berkeley National Laboratory

FIGURE 2. FC-PAD is structured across six components and cross-cutting thrusts

The program also established a second consortium in FY 2016, under the umbrella of DOE's Energy Materials Network, to address the materials problem of developing high-performance, low-cost, PGM-free catalysts for automotive fuel cells. Called ElectroCat (for Electrocatalysis consortium), the consortium aims to accelerate PGM-free catalyst and electrode development by coordinating relevant expertise and tools at the national labs to provide easy access to external researchers. Electrocat's capabilities consist of high-throughput combinatorial methodologies, computational tools, and PGM-free catalyst expertise. Several outreach events were carried out in FY 2016 to educate the broader research community about these capabilities and the general purpose of the consortium.

Examples of R&D advancements achieved in FY 2016 are described below, including major improvements in fuel cell catalysts, membranes, and MEAs.

Catalysts

Projects continued to make advances in low-PGM catalysts, and six new projects were initiated in FY 2016 on the topic of low-PGM catalysts and durable supports. Core-shell catalysts with platinum-monolayer shells have been established as alternatives to conventional platinum-alloy catalysts. In particular, researchers found that nitriding core components can facilitate the development of high-performance platinum-monolayer catalysts with low- or no-noble-metal cores. Nitriding NiPd alloy cores prior to depositing Pt monolayers to prepare PtPdNi/C core-shell catalysts results in a 50% reduction in Pd content as compared to previous Pt/Pd/C catalysts while enhancing overall stability and activity (Figure 3). This has the direct consequence of lowering the cost of these catalysts. At the same time, the formation of Ni nitride was found to stabilize Ni in the core. (Brookhaven National Laboratory)

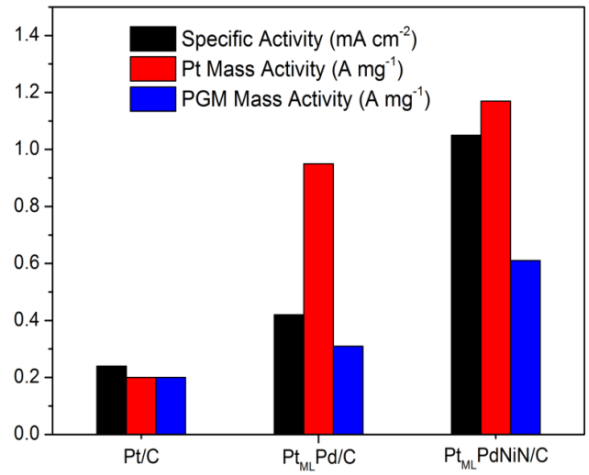

FIGURE 3. Specific activity, Pt mass activity, and PGM mass activity for commercial Pt/C, $Pt_{ML}Pd/C$, and $Pt_{ML}PdNiN/C$ catalysts measured at 0.9 V

Researchers have also developed a new in situ experimental technique including a rotating disk electrode (RDE) combined online with inductively coupled plasma mass spectrometry for the detection of ultra-low (parts per trillion) concentrations of metals including Pt, Au, Ni, Co, Fe, and others. This allows for detailed insight into foundational properties related to catalyst stability in an electrochemical environment. This setup has achieved extremely high sensitivity and was demonstrated in studying platinum dissolution from the extended single crystalline surfaces of Pt electrodes, as well as from commercially available carbon supported platinum. For Pt, the technique has allowed for the distinction between Pt dissolution and Pt particle detachment from the substrate. The technique can be used to study low-PGM and PGM-free catalyst durability and can serve as a valuable tool for researchers to use in optimizing catalyst structure and composition. (ANL)

A newly initiated project at General Motors focuses on the need to develop catalysts with high performance and durability at both low and high current densities. In order to develop low-PGM catalysts that meet these requirements, the effects of Pt surface area and local oxygen transport resistance on overall catalyst function were studied. Large performance losses at high current density were observed on low-Pt-content cathodes due to a higher flux of oxygen over a given Pt area, as seen in Figure 4 for PtCo alloys. The project highlights the importance of selection of a carbon support and electrolyte ionomer with favorable transport properties in the process of developing PtCo catalysts with improved dispersion and stability. As a starting point in demonstrating this, a 50 cm^2 General Motors MEA containing a PtCo alloy catalyst and a high-surface-area carbon support achieved a catalyst specific power of 6.9 kW/g_{PGM}. The MEA was tested at 150 kPa and at 94°C, meeting the Q/ΔT requirement imposed by DOE targets. When tested at a pressure of 250 kPa, the MEA achieved a specific power of 7.7 kW/g_{PGM}.

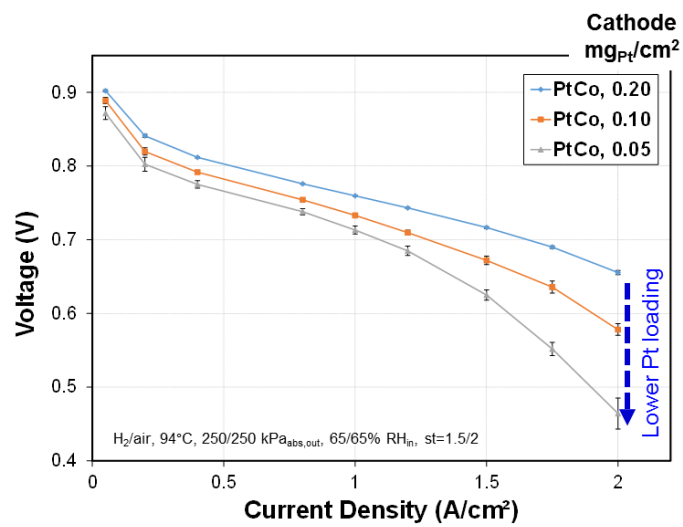

FIGURE 4. Fuel cell polarization curves of PtCo/C catalyst at different cathode Pt loadings showing large performance loss at high current density as Pt loading is reduced due to increasing flux of O_2 per a given Pt area

Electrolytes

Improved nanofiber-supported fuel cell membranes containing multi-acid side chain ionomers continued to progress in FY 2016. These membranes, which combine low equivalent weight (EW) perfluoro imide acid (PFIA) ionomers with new electrospun nanofiber supports and chemical stabilizing additives, meet DOE's area specific

proton resistance targets at 80°C for all humidities and at 120°C for the highest specified humidity. Additionally, the membranes meet all mechanical and chemical durability targets laid out for membranes. Figure 5 shows the cell voltage and resistance for two PFIA-based membranes and a 725 EW-based perfluorosulfonic acid (PFSA) control with similar fiber and additive loading. The potential and resistance values are not very different between samples at high relative humidity (RH), but as the RH decreases, the resistance of the PFIA-based membranes remains low and, as a result, its performance at 1.5 A/cm^2 is as much as 100 mV higher than the control at the lowest RH tested (20%).

Polarization curves for the PFIA-based membranes and control under dry conditions (95°C, 50% inlet RH) are shown in Figure 6. Membranes based on PFIA ionomer have lower cell resistance and higher performance at all current densities, with up to 50 mV higher performance at 1.5 A/cm^2. (3M)

An improved electrolyte matrix for molten carbonate fuel cells with increased porosity and improved pore size distribution compared to a baseline matrix also continued to advance in FY 2016. The baseline matrix has already demonstrated over five years of field service in many commercial units. The improved porous ceramic matrix formulation demonstrated an increase of over 25% in mechanical strength compared to the baseline. A stable pore size, high phase stability (less than 3% phase transformation), low particle growth (over 3.5x reduction in coarsening), and over 80% reduction in gas crossover were also demonstrated during accelerated stress test (AST) conditions (Figure 7). The matrix achieved 5,000-h AST durability, demonstrating a projected 80,000-h stack durability. Attaining a stack durability of 80,000 h will reduce the number of stack replacements needed over the 20-year lifetime of the fuel cell to one, significantly lowering the cost of the system. This reduced life cycle cost of the fuel cell system will enable larger-scale deployment of molten carbonate fuel cells for distributed generation of electricity and hydrogen, CHP applications, and carbon capture from the exhaust of fossil fuel power plants and chemical processes. (FuelCell Energy)

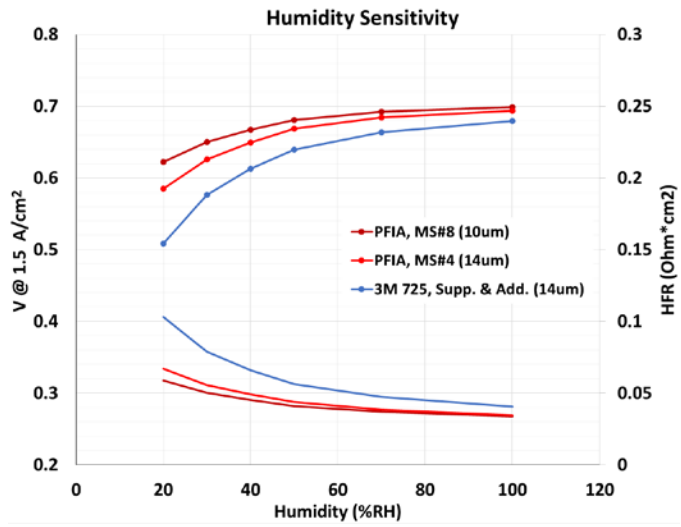

FIGURE 5. Voltage and high frequency resistance (HFR) for PFIA based membranes (red lines) and a PFSA control (blue lines), as a function of humidity at 1.5 A/cm^2

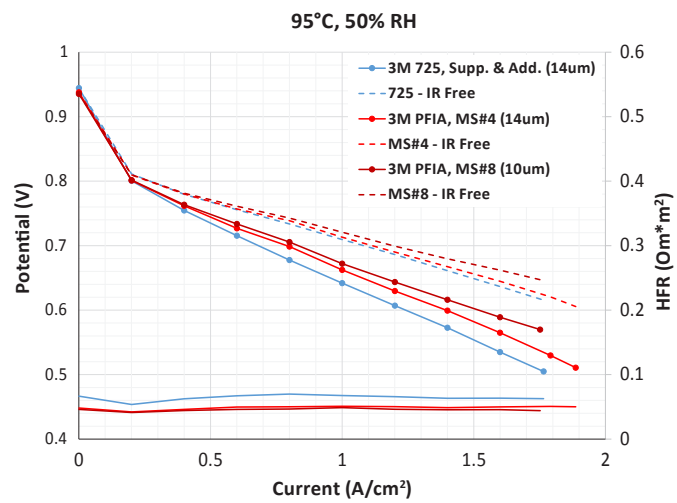

IR – internal resistance

FIGURE 6. Polarization curves at 95°C and 50% inlet humidity for PFIA-based membranes (red lines) and a PFSA control (blue lines). Voltage versus current density data are shown by lines with symbols, HFR is shown with solid lines, and HFR corrected data are shown with dashed lines.

Membrane Electrode Assembly Integration

Improved integration of fuel cell components based on nano-structured thin film (NSTF) catalysts into high-performance MEAs enabled a further increase in performance in FY 2016. High-performance, low-cost, and operationally robust MEAs were fabricated via continuous, scalable pilot processes and demonstrated a power output per gram of PGM at rated power of 6.8 kW/g_{PGM}. This is an increase from the 2.8 kW/g_{PGM} measured in FY 2008 and the 6.5 kW/g_{PGM} measured in FY 2015 and was observed under conditions that satisfy the DOE heat rejection (Q/ΔT) target (see Figure 8). The MEA included a platinum nanoparticle-based cathode interlayer to improve its robustness and tolerance to non-ideal operating conditions. The NSTF-based MEA developed in FY 2016 had an

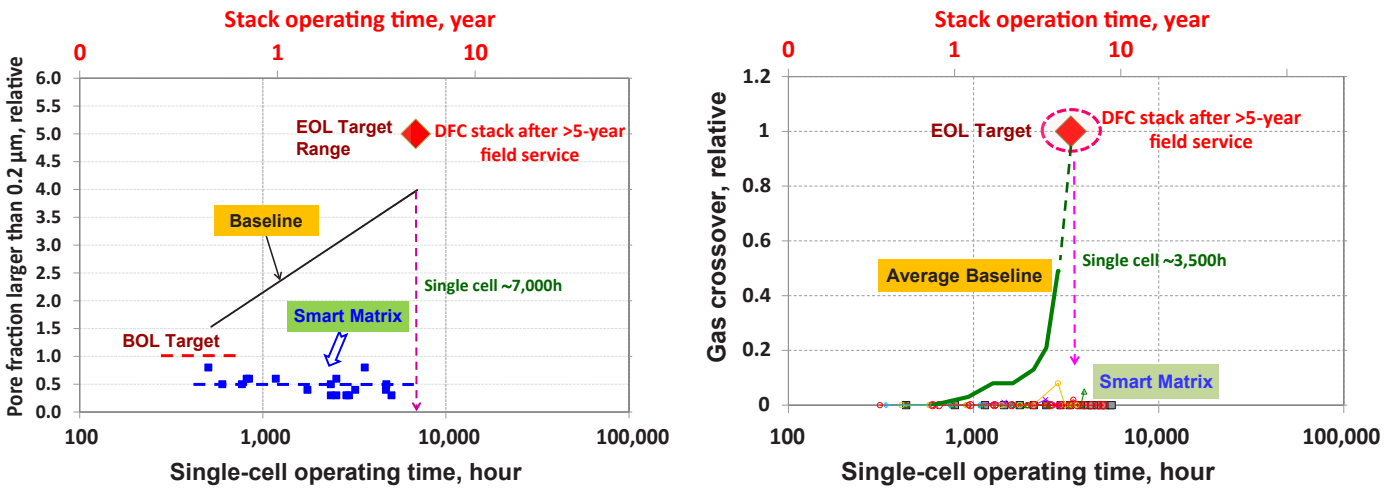

BOL – beginning of life; EOL – end of life; DFC – direct fuel cell.

FIGURE 7. Left: Pore fraction larger than 0.2 µm over a 5,000-h AST. Right: Gas crossover over a 5,000-h AST. Both metrics meet the end-of-life target, demonstrating a projected 80,000-h stack durability.

operational range similar to that of the FY 2015 Best Of Class (BOC) NSTF-based MEA but yielded higher cell performance at cell temperatures between 40°C and 80°C. Further work is still required to meet performance, durability, and robustness targets simultaneously. (3M)

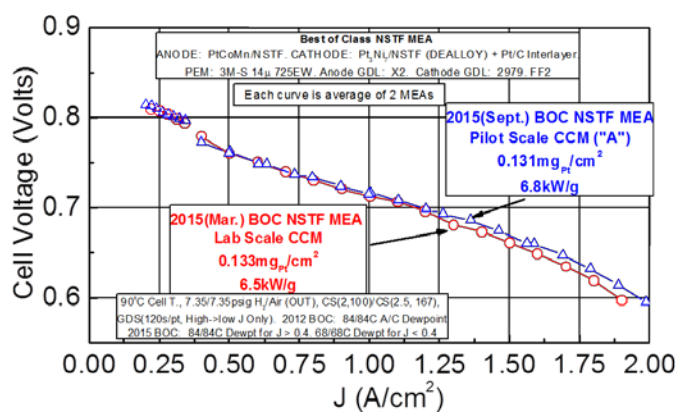

FIGURE 8. Improved MEAs produce 6.8 kW/g_{PGM} under conditions that satisfy DOE's Q/ΔT target

Investigations were carried out to find methods for realizing the oxygen reduction reaction (ORR) mass activity benefits of advanced Pt-based cathode electrocatalysts in both MEAs and stacks operating at high current densities, on air and at low PGM loading (≤0.1 mgPt/cm² on the cathode and <0.025 mgPt/cm² on the anode). These efforts resulted in improved MEA performance, as well as an increased understanding into the aspects of MEA preparation that affect the performance of de-alloyed PtNi catalysts at high current density, particularly at low RH. In FY 2016, the performance of dealloyed-$PtNi_3$ (d-PtNi) based catalysts was increased at high current density by (1) decreasing the initial Ni content of the d-PtNi/C catalyst; (2) using an organic solvent in the catalyst-ionomer ink; (3) increasing the ionomer-to-catalyst ratio from 0.8 to 1.0; (4) using an intermediate EW ionomer, 850 EW; and (5) acid-washing the catalyst-coated membrane after fabrication (see Figure 9). The d-PtNi MEAs achieved 1,259 mA/cm^2 at 0.675 V, with a total cell loading of 0.1107 mg_{Pt}/cm^2 and under differential conditions, and achieved 6.6 kW/g_{PGM} at rated power in a 50 cm^2 MEA tested under conditions meeting the Q/ΔT target (90°C, 40% RH, and 150 kPa). The d-PtNi catalysts exceed the mass activity and electrochemically active surface area durability targets after being subjected to the catalyst AST (<40% loss after 30,000 cycles between 0.6 V and 1.0 V at 50 mV/s) and the high current density durability target (<30 mV at 1.5 A/cm^2) when limiting the upper potential limit of the AST to 0.925 V. (ANL)

PEM fuel cell MEA integration studies will be further pursued in FY 2017 primarily under FC-PAD.

Alkaline Membrane Fuel Cells

An alkaline membrane fuel cell (AMFC) workshop was held in FY 2016 to assess the current status of and the R&D needs for AMFC technology. There have been substantial advances in AMFC technology since the previous workshop held in 2011. Alkaline membranes stabilized through cationic group and polymer backbone modifications

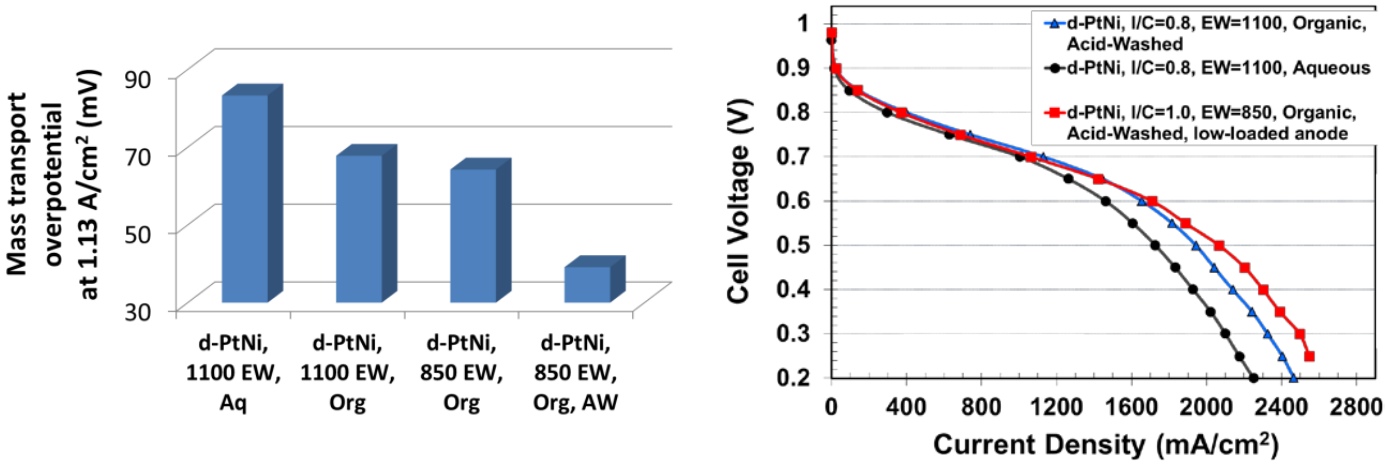

FIGURE 9. Left: MEA performance for d-PtNi MEAs with varying EW ionomer, catalyst-ionomer ink solvent, and post-fabrication procedures, showing the improvement in performance with intermediate EW ionomer, ionomer to catalyst ratio (I/C) = 1.0, organic solvent, and acid-washing of CCM. Right: Effect of organic versus aqueous solvent, lower EW ionomer, and acid-washing of CCM (AW) on polarization curve mass transport voltage losses at 1.13 A/cm^2 in d-PtNi MEAs.

have now been demonstrated. However, implementation of these membranes in MEAs and subsequent characterization of their stability and performance under realistic fuel cell operating conditions is still needed. Also, ionomers which are specific to the different operating environments of the anode and cathode need development. While improved PGM-free hydrogen oxidation reaction and ORR catalytic activity has been demonstrated, at least at the RDE level, performance in MEAs still needs significant improvement. Finally, additional efforts are required to address AMFC-specific water management issues as well as CO_2 tolerance and mitigation.

Standardized protocols and metrics for AMFCs were also discussed. Existing performance and durability protocols for PEM fuel cells may be used as a solid starting point for assessing alkaline fuel cells, but longer term ones specific to AMFCs may be required. The workshop report and presentations can be found on http://energy.gov/eere/fuelcells/downloads/2016-alkaline-membrane-fuel-cell-workshop.

Characterization and Analysis

In FY 2016, microstructural and microchemical studies continued to provide insight into materials comprising MEAs, offering valuable information on the stability and durability of specific components during operation. Studies were primarily focused on three-dimensional (3D) electron tomography of electrocatalysts, supports, and fully intact catalyst layers. A 3D reconstruction providing visualization of ionomer dispersions in "real" catalyst layers and correlation with porosity is shown in Figure 10. An additional advantage of 3D tomography, especially when utilized to analyze a fully intact catalyst layer, is that it provides more direct quantitative information regarding the size characteristics of the individual constituents than traditional two-dimensional images do. (Oak Ridge National Laboratory)

FIGURE 10. 3D imaging of ionomer dispersions in catalyst layers. Individual F maps were acquired from slices and stacked to create a 3D rendering of the ionomer distribution.

System material-derived contamination of the fuel cell has also been studied and has led to a public dataset of materials providing leaching indices, identities and quantities of contaminants, and recommended testing procedures to assess contamination. These materials include structural plastics, hoses, lubricants, adhesives, and seals (Figure 11). Researchers correlated a high "leaching index" to MEA degradation and lower material cost. Based on these findings, the project identified a cleaner polyphthalamide (PPA) structural material that resulted in no significant

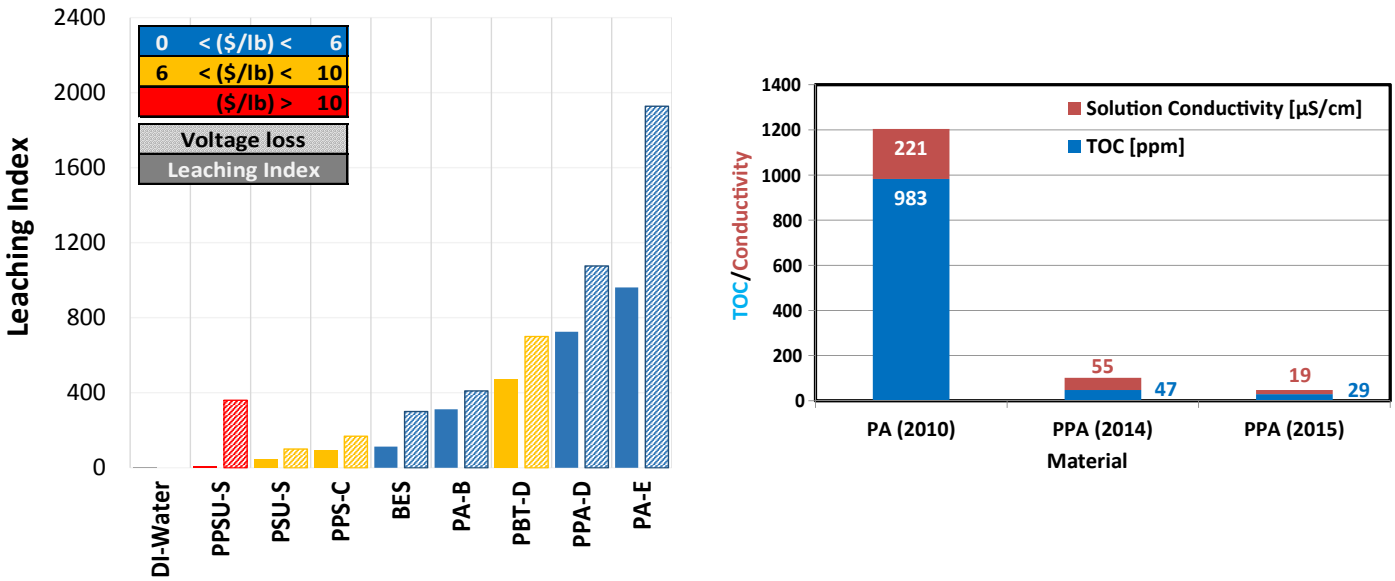

DI – deionized; PPSU – polyphenylsulphone; PSU – phenylsulphone; PPS – polyphenylene sulfide; BES – Bakelite epoxy-based structural material from Sumitomo; PA – polyamide; PBT – polybutylene terephthalate; BPS – bisphenol S.

FIGURE 11. Left: Leaching index for various materials increased with decreasing material cost. Right: 25x improvement in combined total organic carbon (TOC) and solution conductivity for a cleaner PPA (2015) material.

increase in material cost yet afforded higher performance. The publicly available balance-of-plant material screening data tool and extensive database have had approximately 1,400 site visits since May 2013 (see http://www.nrel.gov/hydrogen/system_contaminants_data/). (National Renewable Energy Laboratory, General Motors)

BUDGET

The President's FY 2017 budget request calls for $35 million for the Fuel Cells program, which is equal to the FY 2016 appropriation.

Figure 12 shows the budget breakdown by R&D area for the FY 2016 appropriation and the FY 2017 budget request. The program continues to focus on reducing costs and improving performance and durability with an emphasis on fuel cell stack components. New projects were initiated in FY 2016 for R&D on advanced catalysts and supports and on alkaline membrane fuel cells. Additionally, new industry/university-led projects targeting the advancement of fuel cell performance and durability were selected in FY 2016 and will be incorporated into FC-PAD. FY 2016 also saw the launch of ElectroCat as part of the Energy Materials Network to expedite the development

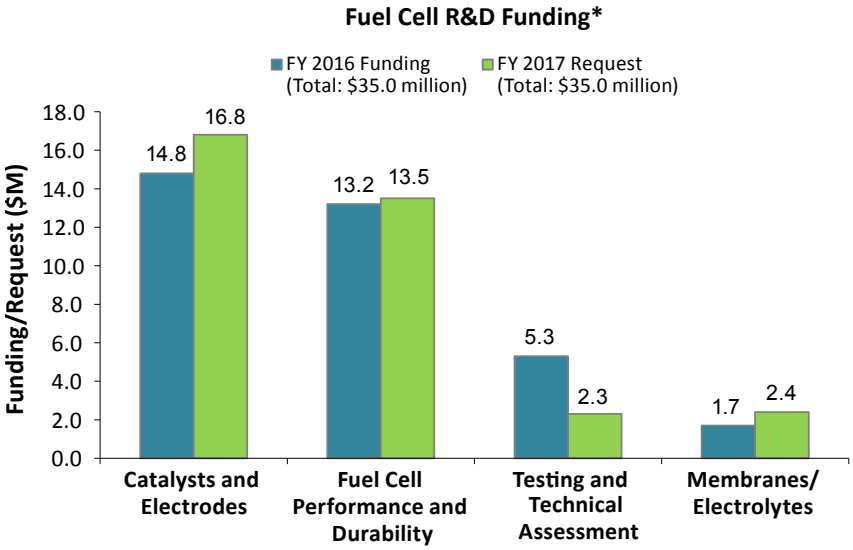

*Subject to appropriations, project go/no-go decisions, and competitive selections. Exact amounts will be determined based on research and development progress in each area and the relative merit and applicability of projects competitively selected through planned funding opportunity announcements.

FIGURE 12. Budget breakdown for FY 2016 through FY 2017

of PGM-free catalysts and electrodes. In FY 2017, the program plans to issue an ElectroCat funding opportunity announcement for awards to be selected and funded in FY 2017.

FY 2017 PLANS

As part of its Tech-to-Market activities in FY 2016, DOE's Fuel Cell Technologies Office developed an approach coined the L'Innovator (for "lab innovator") to accelerate the commercialization of innovative hydrogen and fuel cell technologies developed at national labs and enable a robust domestic industry and supply base in the emerging area of hydrogen and fuel cells. The approach involves bundling intellectual property from various labs to offer the most promising hydrogen/fuel cell technologies to prospective manufacturers with the ability to attract investors. In FY 2017, the Fuel Cells program will support an initial pilot intellectual property bundle: LANL's MEA technology will be optimized to integrate core-shell catalyst technology developed at Brookhaven National Laboratory. National Renewable Energy Laboratory will be involved in developing and applying roll-to-roll processing methods to demonstrate manufacturability.

In FY 2017, the Fuel Cells program will continue R&D efforts on fuel cells and fuel cell systems for diverse applications that employ a variety of technologies (including PEM and alkaline membrane fuel cells) and a range of fuels (including hydrogen, natural gas, and liquid fuels). Support will continue for R&D that addresses critical issues with membranes and electrolytes, catalysts, electrodes, and component integration at the cell level, with an emphasis on cost reduction and durability improvement. The program's consortia will continue accelerating innovation both within the national laboratories and in the greater research community. Ongoing support of modeling will guide component R&D, benchmarking complete systems before they are built and enabling exploration of alternate system components and configurations.

Dimitrios Papageorgopoulos
Fuel Cells Program Manager
Fuel Cell Technologies Office
Office of Energy Efficiency and Renewable Energy
U.S. Department of Energy
1000 Independence Ave., SW
Washington, DC 20585-0121
Phone: (202) 586-5463
Email: Dimitrios.Papageorgopoulos@ee.doe.gov

V.A.1 Non-Precious Metal Fuel Cell Cathodes: Catalyst Development and Electrode Structure Design

Piotr Zelenay (Primary Contact), H. Chung, U. Martinez, E. Holby, X. Yin, G. Purdy, L. Ling
Materials Physics and Applications Division
Los Alamos National Laboratory (LANL)
Los Alamos, NM 87545
Phone: (505) 667-0197
Email: zelenay@lanl.gov

DOE Manager: Nancy L. Garland
Phone: (202) 586-5673
Email: Nancy.Garland@ee.doe.gov

Subcontractors:
- J. Ziegelbauer (PI), General Motors, Warren, MI
- M. Odgaard (PI), J.H. Brewster, D. Schlueter, IRD Fuel Cells, Albuquerque, NM
- S. Litster (PI), S.K. Babu, Carnegie Mellon University, Pittsburgh, PA
- M. Neidig (PI), J. Kehl, J. Kneebone, University of Rochester, Rochester, NY
- Z. Chen (PI), P. Zamani, X. Fu, J.-Y. Choi, University of Waterloo, Waterloo, Canada
- K.L. More (PI), D. Cullen, Oak Ridge National Laboratory, Oak Ridge, TN

Project Start Date: April 1, 2013
Project End Date: March 31, 2016

Overall Objectives

Advance platinum group metal (PGM)-free cathode technology through the development of new materials and implementation of novel electrode concepts to assure:

- High oxygen reduction reaction (ORR) activity viable for automotive systems.
- Practical catalyst durability.
- High ionic/electronic conductivity within the cathode.
- Efficient oxygen transport and effective removal of the water product.

Fiscal Year (FY) 2016 Objectives

- Demonstrate improved ORR activity in fuel cell with advanced PGM-free catalyst.
- Determine corrosion and fluoride emission rates of PGM-free catalysts compared to Pt/C.
- Demonstrate enhancement of ORR activity of Fe-free catalysts.
- Complete electrode optimization study, including first-generation spray-coated membrane electrode assemblies (MEAs).
- Scale up MEA to at least 50 cm^2 with selected PGM-free catalyst.

Technical Barriers

This project addresses the following technical barriers from the Fuel Cells section of the Fuel Cell Technologies Office Multi-Year Research, Development, and Demonstration Plan [1].

(A) Durability (catalysts, electrode layers)

(B) Cost (catalyst, MEAs)

(C) Performance (catalysts, electrodes, MEAs)

Technical Targets

PGM-free fuel cell cathode catalyst research in this project focuses on the DOE technical targets outlined in Table 3.4.7 in Section 3.4.4 (Technical Challenges) of the Multi-Year Research, Development, and Demonstration Plan [1]. The ultimate technical targets of the project are as follows.

- Catalyst activity in H_2/O_2 MEA at 0.044 A cm^{-2} (80°C): ≥0.90 V (internal resistance [iR]-free)
- Four-electron selectivity (rotating ring disk electrode [RRDE]): ≥99% ($H_2O_2 \leq 1\%$)
- MEA maximum power density at 80°C: ≥1.0 W cm^{-2}
- Performance loss at 0.80 A cm^{-2} after 30,000 cycles in N_2: ≤30 mV

TABLE 1. Progress towards Meeting Technical Targets for PGM-free Electrocatalysts and MEAs for Transportation Applications

Characteristic	Units	2018 Target	2020 Target	2016 Status
Voltage at 0.044 A/cm^2 *	$V_{iR\text{-}free}$	0.88	0.90	0.87

* Test at 80°C H_2/O_2 in MEA; fully humidified with total outlet pressure of 150 kPa (abs); anode stoichiometry 2; cathode stoichiometry 9.5 [2].

FY 2016 Accomplishments

- Improvements to ORR PGM-free catalyst activity in FY 2016 resulted in a fuel cell voltage of 0.87 V at the reference current density of 0.044 A cm^{-2} (0.01 V below

the intermediate 2018 target of 0.88 V)—nearly fourfold increase in activity over the life of this three-year project.

- A patent license agreement was executed on February 1, 2016, between LANL and Pajarito Powder, LLC, for LANL-developed PGM-free ORR catalysts.
- In addition to improvements in ORR activity, catalyst synthesis pursued in FY 2016 has focused, like never before, on PGM-free catalyst durability. Approaches involved:
  - Three catalysts derived from polyaniline (PANI) with amine side chains for high active site density.
  - Catalysts with Zn-induced microporosity for high activity ($E_{½}$ 0.81 V) and potentially improved durability (thanks to the use of a higher heat-treatment temperature).
  - Homemade "Fe-MOF" (metal organic framework) catalyst with best durability to date (collaboration with University at Buffalo).
  - Fe-free catalysts with improved ORR activity ($E_{½}$ only 30 mV lower than for Fe-based catalysts, activity likely to improve further based on the modeling study).
- CO_2 and F^- emissions from PGM-free cathode (Fe-based catalyst) have been found to be very similar to those measured with Pt-based catalysts under the same test conditions.
- Nitrogen has been found to be associated with Fe-to-N ratio of 1:4 on the PGM-free catalyst surface. This is possibly the first ever direct observation of FeN_4 (often suggested as the most likely ORR active site).
- Parametric study of cathode performance has revealed active site activity and density values and properties of the electrode/ionomer required to meet practically viable power density targets.
- Pre-selected (cyanamide [CM]+PANI)-Fe-C catalyst with specified target performance has been delivered to IRD for 50-cm^2 MEA optimization and project deliverable.

✧ ✧ ✧ ✧ ✧

INTRODUCTION

Pt-based catalysts represent almost half of the entire polymer electrolyte fuel cell (PEFC) stack cost at high production rates and as much as 20% of the overall system cost [2]. Since Pt is a precious metal, its cost will not benefit from economies of scale and is subject to price fluctuations and monopolized global distributions. Reducing, or ideally replacing, expensive Pt and/or Pt-alloy catalysts in PEFC systems is highly desirable and has been a major focus of research and development efforts in fuel cell electrocatalysis. Owing to the inherently sluggish ORR occurring at the fuel cell cathode, higher Pt content is required at the cathode than at the anode. Successful development of PGM-free catalysts for ORR would provide the most significant economic advantage. However, hindering the successful elimination of Pt cathode catalysts from PEFCs is the lack of PGM-free catalysts that can provide sufficiently high ORR activity and, especially, high durability under the conditions of fuel cell cathode operation.

APPROACH

In this project, we have aimed to achieve major advancements in PGM-free cathode technology through the development and implementation of novel materials and concepts. The PGM-free catalyst development effort has focused on novel synthesis methods, including high-temperature catalyst synthesis using multiple nitrogen-containing precursors, advanced carbon supports, as well as transition metals alternative to iron. Comprehensive testing of materials, including initial performance screening by in situ electrochemical techniques and ex situ characterization to assess catalyst activity and durability, identify catalytic sites, and validate fuel cell performance of the most promising materials, represents a substantial fraction of the efforts.

The use of PGM-free ORR catalysts results in cathodes with increased thickness compared to that of Pt-based cathodes. Therefore, significant effort is required to address the resulting electrode design challenges. Key issues include oxygen mass transport, proton conductivity, and prevention of catalyst layer flooding. Our research has concentrated on the validation of an existing General Motors electrode model for PGM-free electrodes and parameter approximation using in situ microstructured electrode scaffold (MES) diagnostics. Electrode optimization is based on the insight obtained from the modeling, nanoscale X-ray computed tomography (XCT) imaging, and advanced microscopy analysis. In parallel to the catalyst and electrode development components of this project, MEA fabrication, optimization, and scale-up is being performed to obtain a 50-cm^2 (or larger, if needed) MEA with the best-performing materials for independent testing and evaluation at a DOE-approved facility.

RESULTS

- *Achieved fuel cell voltage of 0.87 V (iR-free) at 0.044 A cm^{-2} in H_2/O_2 fuel cell testing.*
  Fuel cell performance of advanced PGM-free (CM+PANI)-Fe-C catalyst was further improved through modifications to the catalyst synthesis as well as improvements in electrode design, enhancing O_2

transport within the catalyst layer and achieving fuel cell voltage of 0.87 V (*iR*-free) at 0.044 A cm^{-2} in H_2/O_2 MEA testing at 80°C (Figure 1a). Furthermore, new PGM-free catalyst development from unsupported homemade Fe-MOF precursor (collaboration with University at Buffalo) also achieved high activity in H_2-air (0.075 A/cm^2 at 0.80 V) and H_2-O_2 fuel cell (0.87 V at 0.044 A/cm^2, *iR*-free) (Figure 1b). High-temperature treated homemade Fe-MOF retained a unique cubic morphology and atomically dispersed Fe. The achieved fuel cell voltage of 0.87 V is only 0.01 V below the 2018 intermediate project activity target (see Table 1).

- *Achieved a half-wave potential of 0.77 V from alternative Fe-free catalysts.* PGM-free catalysts with alternative transition metals to Fe, namely Co, Mn, and Ni, have been synthesized via the high-temperature treatment of multiple nitrogen-containing precursors. Enhancement of ORR activity was obtained from alternative Co-based PGM-free catalysts achieving a half-wave potential of 0.77 V (Figure 2). Furthermore, durability cycling studies showed better stability than Fe-based PGM-free catalysts with only 10 and 11 mV drop in half-wave potential after 10,000 cycles for Co- and Mn-based materials, respectively.
- *Identified Fe-free target structures and durability descriptor using density functional theory (DFT)-based modeling.* DFT models including spontaneously formed *OH ligands explain experimentally observed trends in ORR activity with varied transition metal (Figure 3). An edge $MnCoN_5$ complex is calculated to have higher thermodynamic limiting potential (activity descriptor) than monometallic Me-N_4 edge structures (Me = Mn, Co, Ni). A first-principles molecular dynamics beam damage model was utilized to determine the knock-on displacement threshold energy for defected carbon structures. It is proposed that this figure of merit may be used as a durability descriptor for PGM-free catalyst structures, capturing the important kinetic contributions to atom removal during corrosion.
- *Made major progress in durability improvement of PGM-free catalysts at high fuel cell voltage.* Several new strategies were developed to improve durability of PGM-free catalysts: (i) active site templating *via* amine affinity to Fe^{3+}, (ii) Zn-induced microporosity with high-temperature treatments, and (iii) unsupported homemade Fe-MOF precursor with unique cubic morphology preserved after high-temperature treatment. Initial testing for the latter approach revealed for the first time promising durability performance of a PGM-free catalyst under viable fuel cell operating conditions: ambient air feed and high voltage (0.70 V).
- *Attained first direct imaging of Fe-N_x sites at the atomic level via high-resolution electron microscopy.* Advanced scanning electron microscopy was used to detect individual Fe atoms on the (CM+PANI)-Fe-C catalyst surface, providing an atomic-level insight of Fe-N_x sites for the first time. Probing of sites via high-resolution electron energy loss spectroscopy revealed nitrogen associated with iron at a ratio of 4:1. This observation is the first direct imaging of Fe-N_4 sites on the PGM-free catalyst surface (Figure 4).
- *Demonstrated synergistic collaboration modeling-characterization-testing to achieve PGM-free electrode structure optimization.* Microstructurally consistent cathode models with morphology and transport properties were obtained from nano-X-ray tomography imaging and analysis. These models highlighted the

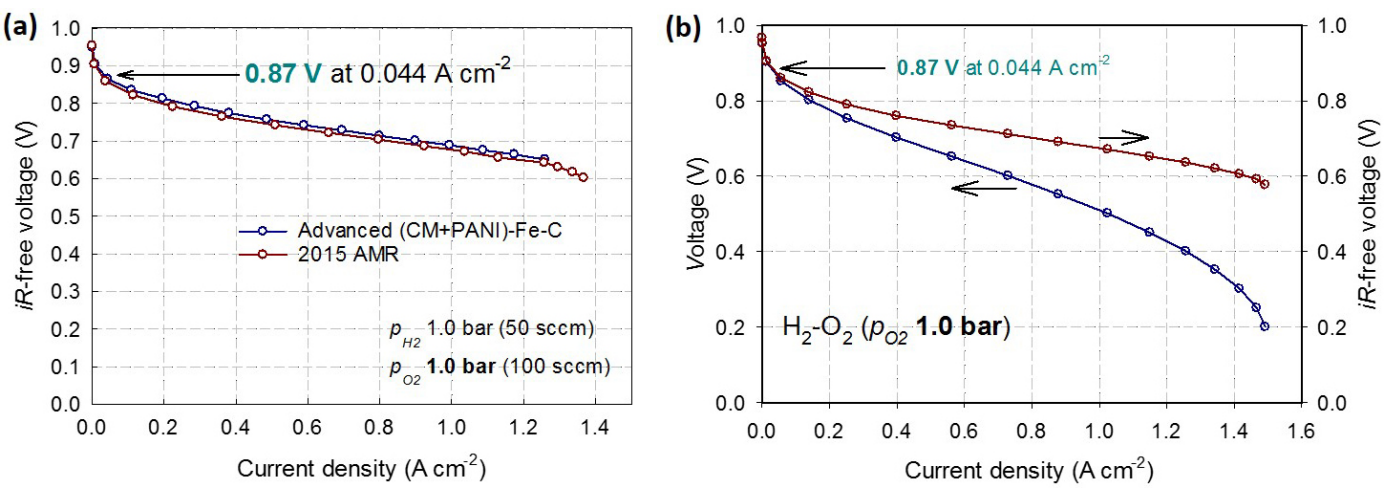

FIGURE 1. Fuel cell performance of two PGM-free catalysts demonstrating fuel cell voltage of 0.87 V (*iR*-free) at 0.044 A cm^{-2} in H_2-O_2. (a) Advanced (CM+PANI)-Fe-C catalyst and (b) PGM-free catalyst from homemade Fe-MOF precursor. Anode: 0.2 mg_{Pt} cm^{-2} Pt/C H_2, 50 sccm, 1.0 bar H_2 partial pressure, cathode: *ca.* 4.0 mg cm^{-2} air, 100 sccm, 1.0 bar air partial pressure, membrane: Nafion 117, cell size: 5 cm^2.

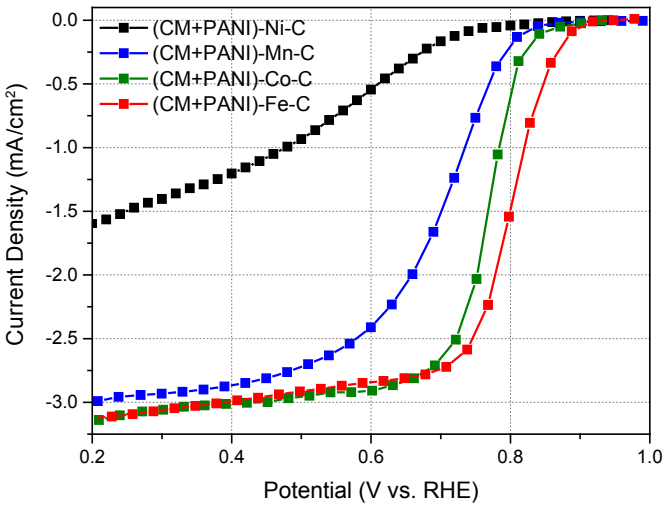

RHE - Reversible hydrogen electrode

FIGURE 2. Rotating disk electrode (RDE) results of Fe-free (CM+PANI)-Me-C catalysts (Me = Fe, Co, Mn, Ni) demonstrating $E_{½}$ of 0.77 V for (CM+PANI)-Co-C, only *ca.* 30 mV from (CM+PANI)-Fe-C. RDE: 0.5 M H_2SO_4, O_2-saturated, 900 rpm, 25ºC, Ag/AgCl (3.0 M KCl) reference electrode, graphite counter electrode, steady-state potential program: 30 mV steps, 30 s/step.

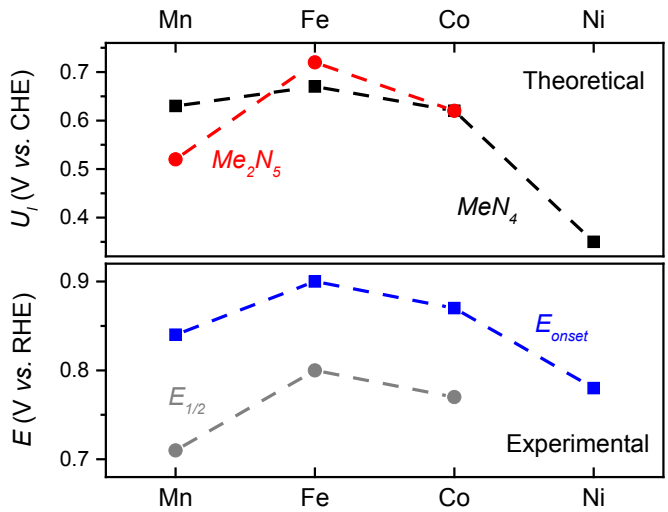

CHE - Computational hydrogen electrode

FIGURE 3. Calculated activity descriptors, U_l, for all (CM+PANI)-Me-C catalysts for mono- and bi-metallic edge structures compared to experimental E_{onset} and $E_{½}$ values

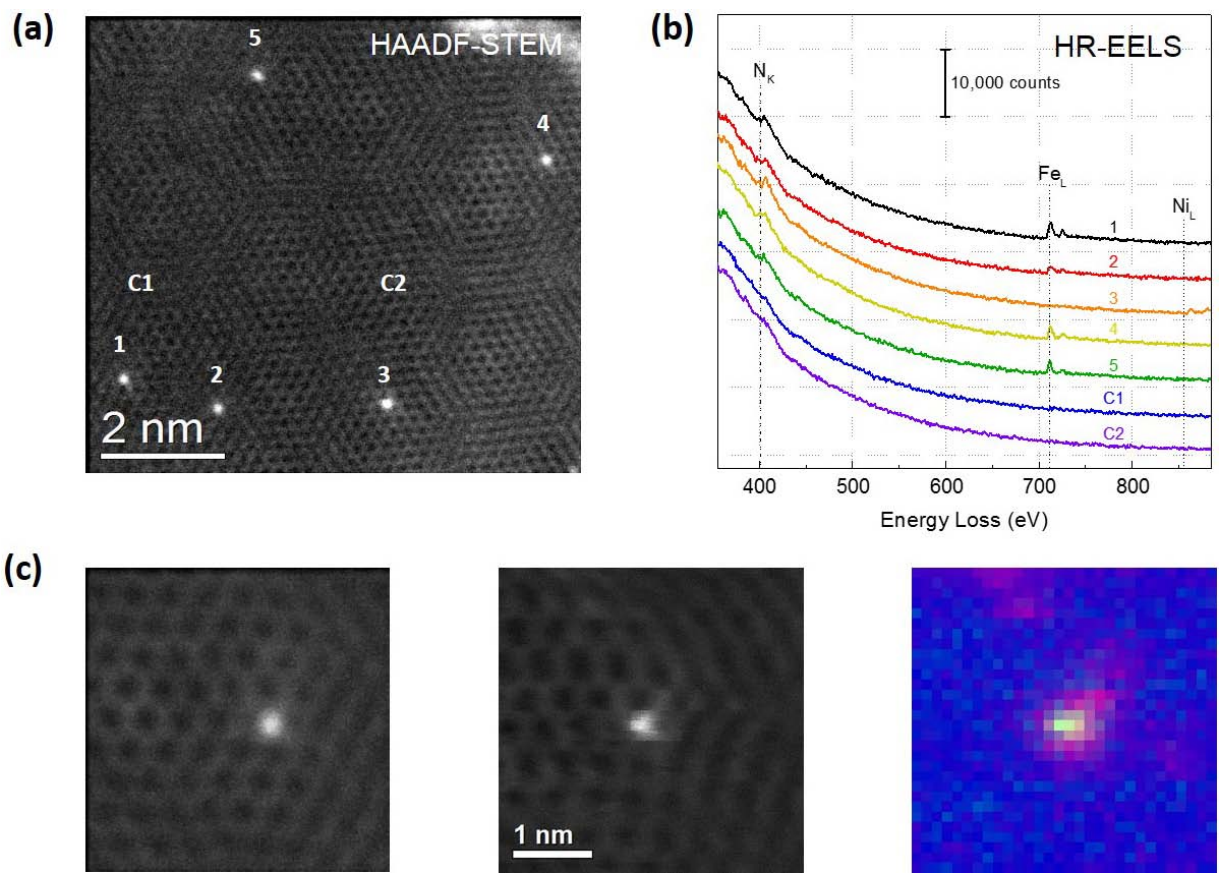

FIGURE 4. Atomic-level characterization of Fe-N_x sites on the surface of (CM+PANI)-Fe-C catalyst. (a, c) High-angle annular dark-field imaging – scanning transmission electron microscopy (HAADF-STEM) imaging of Fe-N_4 sites. (b) Elemental composition of various sites using high-resolution electron energy loss spectroscopy (HR-EELS), confirming the 1:4 ratio of Fe:N.

Fuel Cell Polarization Plots

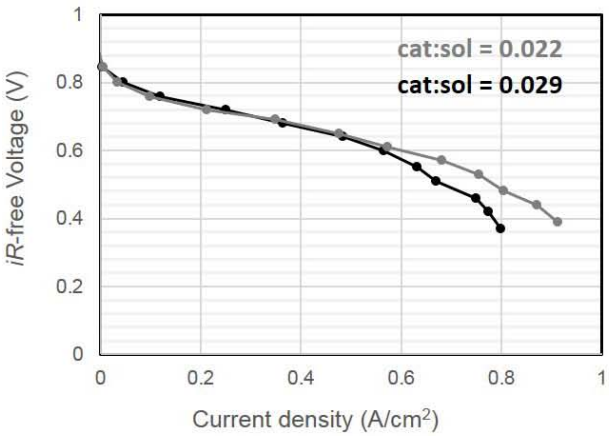

Ink particle-size distribution

cat:sol	$d_{(0.1)}$ (µm)	$d_{(0.5)}$ (µm)	$d_{(0.9)}$ (µm)	Average pore size from EM (µm)
0.029	0.70	2.73	4.77	0.16
0.022	0.69	1.91	3.41	0.37

Electron Microscopy Analysis

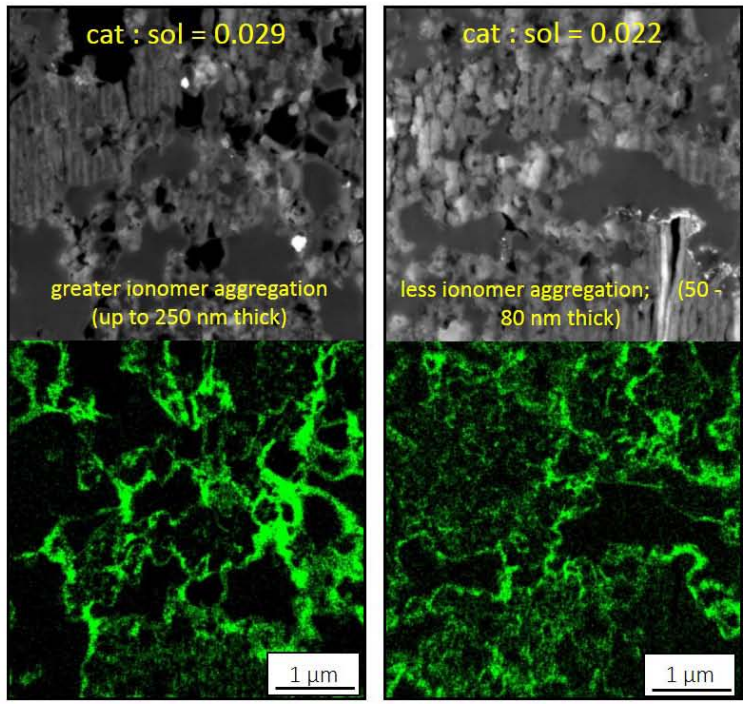

FIGURE 5. Improved fuel cell performance in the mass transport region resulting from better ionomer distribution as observed from the electron microscopy (EM) analysis. Anode: 0.15 mg_{Pt} cm^{-2} Pt/C H_2, 1.5 bar H_2 partial pressure, cathode: 3.0 mg cm^{-2} air, 1.5 bar air partial pressure, 100% relative humidity, cell size: 5 cm^2.

importance of electrode hydrophobicity (reducing flooding) and higher conductivity or lower tortuosity of the ionomer for electrode development. Application of these models to modify ink preparation and deposition techniques allowed for better ionomer distribution into smaller pores, resulting in improved performance in the mass transport region (Figure 5).

CONCLUSIONS

- Continued development of PGM-free catalysts with improved ORR activity resulted in two different catalysts developed in FY 2016 with a fuel cell voltage of 0.87 V at the reference current density of 0.044 A cm^{-2} (0.01 V below the intermediate 2018 target of 0.88 V)—nearly fourfold increase in activity over the life of this three-year project.
- Major progress in durability of PGM-free catalysts has been demonstrated with homemade Fe-MOF and Fe-free catalysts.
- CO_2 and F^- emissions from PGM-free cathode (Fe-based catalyst) have been found to be very similar to those measured with Pt-based catalysts under the same test conditions.
- The first ever direct observation of FeN_4 (often suggested as the most likely ORR active site) has been demonstrated.
- All project performance measures have been met; final electrode design is nearing completion with the help of microstructural analysis of factors determining electrode performance. Project deliverables remain on schedule.

FUTURE DIRECTIONS

Although the official end date of this project is listed as March 2016, continuing PGM-free catalyst development in future projects should target:

- Molecular-level dispersion of transition-metal ORR active sites (for activity enhancement) in highly graphitized carbon matrices (for durability enhancement).
- Rational design of PGM-free catalysts based on the knowledge of ORR active-site(s).
- Improvement in the activity of Fe-free catalysts, e.g., via inducing strain in bimetallic catalysts.

- Full utilization of national laboratory capabilities, in particular through the recently established Electrocatalysis Consortium (ElectroCat), part of the DOE Office of Energy Efficiency and Renewable Energy's Energy Materials Network.

SPECIAL RECOGNITIONS & AWARDS/ PATENTS ISSUED

1. H.T. Chung and P. Zelenay, "Non-precious Metal Catalysts Prepared from Precursor Comprising Cyanamide," U.S. Patent 9,169,140 issued on October 27, 2015.

FY 2016 PUBLICATIONS

1. "First-Principles Molecular Dynamics Study of Carbon Corrosion in PEFC Catalyst Materials," E.F. Holby, *Fuel Cells,* In Press.

2. "Linking Structure to Function: The Search for Active Sites in Non-Platinum Group Metal Oxygen Reduction Reaction Catalysts," E.F. Holby and P. Zelenay, *Nano Energy*, available online 24 May 2016, ISSN 2211–2855, http://dx.doi.org/10.1016/j.nanoen.2016.05.025.

3. "Highly active and porous graphene encapsulating carbon nanotubes as a non-precious oxygen reduction electrocatalyst for hydrogen-air fuel cells," P. Zamani, D.C. Higgins, F.M. Hassan, X. Fu, J.Y. Choi, M.A. Hoque, G. Jiang, Z. Chen, *Nano Energy*, **26**, 267–275, 2016.

4. "Heat-Treated Non-Precious Metal Catalysts for Oxygen Reduction," H. Chung, G. Wu, D. Higgins, P. Zamani, Z. Chen, and P. Zelenay, in *Electrochemistry of N4 Macrocyclic Metal Complexes*, Volume 1: Energy, F. Bedioui and J.H. Zagal (*eds.*), Springer, pp. 41–68.

5. "Critical Role of the Removal of Intercalated Water for Electrocatalytically Active Graphitic Systems," U. Martinez, G.M. Purdy, E.F. Holby, K. Artyushkova, J.H. Dumont, A. Singh, N.H. Mack, P. Atanassov, D.A. Cullen, K.L. More, M. Chhowalla, P. Zelenay, A.M. Dattelbaum, A.D. Mohite, and G. Gupta, *Sci. Adv.*, **2**, e1501178, 2016.

6. "Co-N Decorated Hierarchically Porous Graphene Aerogel for Efficient Oxygen Reduction Reaction in Acid," X. Fu, J.Y. Choi, P. Zamani, G. Jiang, M.D. Hoque, F.M. Hassan, Z.W. Chen, *ACS Appl. Mater. Interfaces*, 6488–6495, 2016.

7. "The application of graphene and its composites in oxygen reduction electrocatalysis: A perspective and review of recent progress," D. Higgins, P. Zamani, A. Yu, Z.W. Chen, *Energy Environ. Sci.*, **9**, 357–390, 2016.

8. "Experimental Observation of Redox-Induced Fe–N Switching Behavior as a Determinant Role for Oxygen Reduction Activity," Q. Jia, N. Ramaswamy, H. Hafiz, U. Tylus, K. Strickland, G. Wu, B. Barbiellini, A. Bansil, E.F. Holby, P. Zelenay, S. Mukerjee, *ACS Nano*, **9**, 12496–12505, 2015.

9. "In-Situ through-Plane Measurements of Ionic Potential Distributions in Non-Precious Metal Catalyst Electrode for PEFC," S. Komini Babu, H.T. Chung, P. Zelenay, and S. Litster, *ECS Trans.*, **69** (17) 23–33, 2015.

10. "Non-Precious Metal Fuel Cell Cathodes: Catalyst Development and Electrode Structure Design," P. Zelenay, H. Chung, U. Martinez, E. Holby, U. Tylus, G. Purdy, J. Ziegelbauer, M. Odgaard, D. Schlueter, S. Litster, S.K. Babu, M. Neidig, J. Kehl, J. Kneebone, Z. Chen, D. Higgins, G. Jiang, M.-H. Seo, K.L. More, and D. Cullen, U.S. Department of Energy, Hydrogen and Fuel Cells Program, 2015 Annual Progress Report, V-43–V-50.

11. https://www.hydrogen.energy.gov/pdfs/progress15/v_a_7_zelenay_2015.pdf

12. "Dynamic nature of active sites in iron-based catalysts during electrocatalysis," Q. Jia, N. Ramaswamy, H. Hafiz, U. Tylus, K. Strickland, G. Wu, B. Barbiellini, A. Bansil, E.F. Holby, P. Zelenay, and S. Mukerjee, *ACS Nano*, **9** (12), 12496–12505, 2015.

13. "A Simple Synthesis of Nitrogen-Doped Carbon Micro and Nanotubes," H.T. Chung and P. Zelenay, *Chem. Commun.*, **51**, 13546–13549, 2015.

14. "High-Activity PtRuPd/C Catalyst for Direct Dimethyl Ether Fuel Cell," Q. Li, X. Wen, G. Wu, H.T. Chung, and P. Zelenay, *Angew. Chem. Int. Ed.*, **54**, 1–6, 2015.

FY 2016 PRESENTATIONS

1. U.S. Department of Energy, Energy Efficiency and Renewable Energy, Fuel Cell Technologies Office, 2016 Merit Review and Peer Evaluation Meeting, Washington, D.C., June 6–10, 2016. Title: "Non-Precious Metal Fuel Cell Cathodes: Catalyst Development and Electrode Structure Design," P. Zelenay (*DOE invited lecture*). https://www.hydrogen.energy.gov/pdfs/review16/fc107_zelenay_2016_o.pdf

2. 229th Meeting of the Electrochemical Society, May 29–June 2, 2016, San Diego, California. "Non-PGM ORR Catalysts Based on Transition Metal Alternative to Iron," U. Martinez*, E.F. Holby, J.H. Dumont, H.T. Chung, P. Zelenay.

3. 2016 MRS Spring Meeting & Exhibit, Phoenix, Arizona, March 28–April 1, 2016. "Non-Precious Metal Electrocatalysts for Oxygen Reduction," P. Zelenay (*invited lecture*).

4. 18th Topical Meeting of the International Society of Electrochemistry, Gwangju, South Korea, March 11, 2016. Title: "Precious Metal-Free Electrocatalysts for Fuel Cell Applications: In Pursuit of Performance and Understanding," P. Zelenay*, E.F. Holby, H.T. Chung, U. Martinez, G.M. Purdy, X. Yin (*invited keynote lecture*).

5. Korea Institute for Energy Research & Korea Advanced Institute for Science and Technology, Daejeon, South Korea, March 7, 2016. Title: "Recent Progress in PGM-free Oxygen Reduction Reaction Electrocatalysis at Los Alamos," P. Zelenay (*invited lecture*).

6. Workshop on New Generation Energy Storage Technologies: Challenges and Opportunities, Taormina, Italy, December 2–3, 2015. Title: "New Research Directions for Fuel Cell Systems," P. Zelenay (*invited lecture*).

7. Department of Chemistry, University of Warsaw, Warsaw, Poland, November 26, 2015. Title: "Catalysis of Selected Electrode Processes in Polymer Electrolyte Fuel Cells," P. Zelenay (*invited lecture*).

8. 2015 MRS Fall Meeting & Exhibit, Boston, Massachusetts, USA, November 29–December 4, 2015. Title: "Analytical Characterization of non-PGM Catalysts for PEM Fuel Cells," D. Cullen*, B. Sneed, H. Meyer III, K. More, H. Chung, and P. Zelenay.

9. Fuel Cell Seminar & Energy Exposition, Los Angeles, California, USA, November 16–19, 2015. Title: "A Disruptive Fuel in the System: Electricity from a Carbon-Neutral Fuel," E.S. De Castro*, P. Zelenay, V. Gregoriou.

9. 228th Meeting of the Electrochemical Society, Phoenix, Arizona, USA, October 11–15, 2015. Title: "Water Management in PEM Fuel Cells with Non-Precious Metal Catalyst Electrodes," D. Spernjak*, H.T. Chung, R. Mukundan, R.L. Borup, D.S. Hussey, D.L. Jacobson, G. Wu, and P. Zelenay.

10. 228th Meeting of the Electrochemical Society, Phoenix, Arizona, USA, October 11–15, 2015. Title: "Graphite-Based Non Precious Metal Catalyst for Oxygen Reduction Reaction", J.H. Dumont*, U. Martinez, A. Mohite, G.M. Purdy, P. Atanassov, P. Zelenay, and G. Gupta.

11. 228th Meeting of the Electrochemical Society, Phoenix, Arizona, USA, October 11–15, 2015. Title: "High-Performance Direct Dimethyl Ether Fuel Cell Operating with an Advanced Activation Process," D.C. Ua Cearnaigh, J.H. Dumont*, H.T. Chung, and P. Zelenay.

12. 228th Meeting of the Electrochemical Society, Phoenix, Arizona, USA, October 11–15, 2015. Title: "In-Situ through-Plane Measurements of Ionic Potential Distributions in Non-Precious Metal Catalyst Electrode for PEFC," S. Komini Babu*, H.T. Chung, P. Zelenay, and S. Litster.

13. 228th Meeting of the Electrochemical Society, Phoenix, Arizona, USA, October 11–15, 2015. Title: "Non-PGM ORR Catalyst Active-Site Screening," E. Holby*, S. Choudhury, and P. Zelenay.

14. 228th Meeting of the Electrochemical Society, Phoenix, Arizona, USA, October 11–15, 2015. Title: "Solvent-Engineering of High-Performance Non-Precious Metal Catalysts," U. Martinez*, J. Dumont, G. Purdy, K. Artyushkova, H. Chung, P. Atanassov, A. Mohite, A. Dattelbaum, G. Gupta, and P. Zelenay.

15. 228th Meeting of the Electrochemical Society, Phoenix, Arizona, USA, October 11–15, 2015. Title: "Combining Nitrogen Precursors in Synthesis of Non-Precious Metal ORR Catalysts with Improved Fuel Cell Performance," H.T. Chung*, E.F. Holby, G.M. Purdy, S. Komini Babu, S. Litster, D. Cullen, K.L. More, and P. Zelenay.

16. 228th Meeting of the Electrochemical Society, Phoenix, Arizona, USA, October 11–15, 2015. Title: "Non-PGM ORR Catalyst Active-Site Screening," E. Holby*, S. Choudhury, and P. Zelenay.

17. 66th Annual Meeting of the International Society of Electrochemistry, Taipei, Taiwan, October 4–9, 2015. Title: "Non-Precious Metal Catalysts for Oxygen Reduction: Accomplishments and Challenges," P. Zelenay (*invited keynote lecture*).

18. New Devices for Energy Conversion and Storage, Hong Kong University of Science and Technology, Hong Kong, October 1–3, 2015. Title: "Oxygen Reduction on Non-Precious Metal Electrocatalysts," U. Tylus, U. Martinez, E.F. Holby, H.T. Chung, G. Purdy, and P. Zelenay* (*invited keynote lecture*).

19. CEA tech, Laboratoire d'innovation pour les technologies des énergies nouvelles et les nanomatérieux (Liten), Grenoble, France, September 18, 2015. Title: "Fuel Cell Electrocatalysis Research at Los Alamos National Laboratory," P. Zelenay (*invited lecture*).

20. EFCD2015 – Challenges towards Zero Pt for Oxygen Reduction, La Grande Motte, France, September 13–16, 2015. Title: "How much value there really is in non-precious metal ORR catalysts for fuel cells?" P. Zelenay (*invited plenary lecture*).

21. International Energy Agency, Annex 31 Meeting, Pfinztal, Germany, July 6–7, 2015. Title: "A Few Highlights from Recent Fuel Cell Electrocatalysis Research at Los Alamos National Laboratory," P. Zelenay.

22. 5th European PEFC and H2 Forum (EFCF2015), Lucerne, Switzerland, June 30–July 3, 2015. Title: "Electrocatalysis of Oxygen Reduction Reaction: Catalyst Development, Theory, and Model Systems," P. Zelenay (*invited keynote lecture*).

23. Turin Polytechnic, Turin, Italy, June 26, 2015. Title: "Non-Precious Metal Fuel Cell Cathodes: Catalyst Development and Electrode Structure Design," P. Zelenay (*invited lecture*).

24. U.S. Department of Energy, Energy Efficiency and Renewable Energy, Fuel Cell Technologies Office, 2015 Merit Review and Peer Evaluation Meeting, Arlington, Virginia, June 8–12, 2015. Title: "Non-Precious Metal Fuel Cell Cathodes: Catalyst Development and Electrode Structure Design," P. Zelenay (DOE invited lecture).

25. "Nano-scale X-ray computed tomography applied to fuel cell and battery electrode characterization and optimization," U. of Texas-Austin, Texas Materials Institute Seminar, Austin, TX, October 29, 2015, S. Litster (*invited lecture*).

26. "High Resolution Imaging, Modeling, and Characterization of Non-Precious Metal Fuel Cell Electrodes," Keynote - Society of Engineering Science 52nd Annual Technical Meeting, College Station, TX, October 28, 2015, S. Litster (*invited lecture*).

27. "Nano-scale X-ray computed tomography applied to fuel cell and battery electrode characterization and optimization," National Institute of Advanced Industrial Science and Technology (AIST) Kansai, Osaka, Japan, May 12, 2015, S. Litster (*invited lecture*).

28. "Nano-scale X-ray computed tomography applied to fuel cell and battery electrode characterization and optimization," Chemical Engineering, Kyoto University, Kyoto, Japan, May 11, 2015, S. Litster (*invited lecture*).

REFERENCES

1. *Multi-Year Research, Development, and Demonstration Plan: Section 3.4 Fuel Cells*, Fuel Cell Technologies Office, 2016. http://energy.gov/sites/prod/files/2016/06/f32/fcto_myrdd_fuel_cells_0.pdf

2. H. Gasteiger *et al.*, *Appl. Catal. B-Environ.*, **56**, 9–5, 2005.

V.A.2 Development of PGM-free Catalysts for Hydrogen Oxidation Reaction in Alkaline Media

Alexey Serov
Department of Chemical and Biological Engineering
University of New Mexico (UNM)
MSC01 1120 1 University of New Mexico
Albuquerque, NM 87131-0001
Phone: (505) 238-9837
Email: serov@unm.edu

DOE Manager: Nancy L. Garland
Phone: (202) 586-5673
Email: Nancy.Garland@ee.doe.gov

Contract Number: DE-EE0006962

Subcontractors:
- Los Alamos National Laboratory (LANL) Los Alamos, NM
- IRD Fuel Cells LLC, Albuquerque, NM
- Pajarito Powder LLC, Albuquerque, NM

Project Start Date: June 1, 2015
Project End Date: May 31, 2017

Overall Objectives

- Develop and scale up a platinum group metal (PGM)-free electrocatalyst for hydrogen oxidation in alkaline media.
- Develop novel alkaline exchange ionomer.
- Integrate PGM-free catalysts and novel ionomers into high performed alkaline exchange membrane fuel cell.

Fiscal Year (FY) 2016 Objectives

- Screen possible candidates for hydrogen electro-oxidation.
- Scale up best performing material.
- Down-select ionomers for integration of materials into a membrane electrode assembly (MEA).

Technical Barriers

This project addresses the following technical barriers from the Fuel Cells section of the Fuel Cell Technologies Office Multi-Year Research, Development, and Demonstration Plan.

(B) Cost
- (Task 1.B) Reduce/eliminate PGM loading of catalysts
- (Task 1.B) Design and demonstrate small-scale production of newly-developed and promising catalysts (minimum viable product)

(C) Performance
- (Task 2.C) Improve electrolyte conductivity, for both proton and alkaline systems, over the entire temperature and humidity operating range
- (Task 3.C) Integrate catalysts with membranes and GDLs (gas diffusion layers) into MEAs

Technical Targets

The goal of this project is an integration of PGM-free anodic electrocatalysts with novel anion exchange ionomer in highly perform MEA. The project is in earlier stage compared with well-established polymer electrolyte membrane fuel cell technology, however achieving the goals of project will allow to reach DOE fuel cell targets (Table 1).

- Cost: $14/kWh net
- Start-up/shutdown durability: >5,000 cycles
- Performance at 0.8 V: 300 mA/cm^2

FY 2016 Accomplishments

- Most active Ni-Mo-Cu catalysts were synthesized at UNM by sacrificial support method (SSM). Technology was transferred to Pajarito Powder and scaled up to 25 g per batch.

TABLE 1. Progress towards Meeting Technical Targets for Electrocatalysts and MEAs for Transportation Applications

Characteristic	Units	DOE 2020 Electrocatalyst and MEA Targets	Project Status (5 cm^2 cell, H_2/O_2)
PGM total loading	mg-PGM/cm$^2_{geo}$	≤0.125	0.1, cathode
PGM-free catalyst activity	A/cm^2 @ 900 mV$_{IR\text{-}free}$	0.044	0.005
MEA performance	mW/cm$^2_{geo}$ @ 675 mV	≥1,000	~10

- The LANL team screened several alkaline exchange ionomers with different cationic groups and studied their interaction with catalyst. Ionomer was supplied to UNM for integration of PGM-free catalysts.
- IRD Fuel Cells optimized the automatic ink deposition system in order to manufacture MEAs by catalyst coated membrane (CCM) and catalyst coated substrate (CCS) methods. Several MEAs with area of 5 cm^2 and 25 cm^2 were fabricated and tested.

✧ ✧ ✧ ✧ ✧

INTRODUCTION

Alkaline membrane fuel cells have been drawing attention because they have the potential to convert hydrogen fuel to electricity without using precious metal catalysts in the electrodes. Contrary to proton exchange membrane fuel cells that require substantial amounts of expensive Pt catalyst to catalyze the inherently sluggish oxygen reduction reaction, alkaline membrane fuel cells are able to operate using inexpensive and earth abundant PGM-free oxygen reduction reaction catalysts. One of the most significant reasons for the substitution of anode materials from Pt to other catalysts is much slower hydrogen oxygen reduction (HOR) kinetics of electrocatalyst under high pH conditions. Gasteiger et al. reported that the HOR of platinum electrocatalysts is several orders of magnitude slower in alkaline electrolytes compared to acidic electrolytes [1].

Our proposed project has an enabling impact on the DOE alkaline membrane fuel cell portfolio for two major reasons. First, this is the first project on PGM-free catalysts for electro-oxidation of hydrogen in alkaline media; second, this is a project that catalyst and ionomer developers are teamed up for industrial scale-up and MEA fabrications. Our project directly ties to the Fuel Cell Technologies Office mission, goals and targets, both through addressing the capital cost targets for fuel cells, as well as advancing materials applicable for electro-oxidation of different liquid fuels.

APPROACH

In general, the approach towards successful achievement of project goals can be described through the roles of team members. UNM focuses on the modification of SSM to create Ni-based materials with controlled properties as well as synthesis, characterization, and electrochemical performance of several Ni-based classes of materials. LANL prepares perfluorinated anion exchange ionomers having selected cationic groups and electrochemical characterization at the catalyst-ionomer interface. Pajarito Powder focuses on technology transfer of SSM approach for Ni-based materials and direct scale-up using identical equipment as UNM and using down-selected formulations, scale up of the SSM approach, and manufacture batches of best performing formulations developed by UNM. IRD Fuel Cells focuses on integration of the HOR catalyst and anion exchange ionomers to an MEA with a peak power density >50 mW cm^{-2} (first generation), development and manufacture of alkaline exchange MEAs based on scalable processes, and manufacture and proof of concept of MEAs based on the scaled up catalyst and ionomer (second generation).

RESULTS

The overall goals of first phase of the project were (1) down-selection of most active PGM-free electrocatalysts for HOR in alkaline media, (2) ranking and synthesis of novel anion exchange membrane ionomer, and (3) establishing of the MEA fabrication protocols.

From the point of materials synthesis more than 45 different Ni-based catalysts were synthesized, the variable parameters were co-catalytic elements to nickel, ratio between elements, and SSM parameters (temperature, duration, atmosphere, etc.). Among the studied systems, the Ni-Mo system was selected as most promising, and additional experiments were performed using nickel and molybdenum as a main catalytic matrix. An influence of the addition of a third element was studied by rotating disk electrode (RDE) method. It was shown that Ni-Mo-Re, Ni-Mo-Cu, and Ni-Mo-Co catalysts were most active. Taking into account that rhenium, even though not PGM, has a high price, the continuation of experiments was conducted with inexpensive Ni-Mo-Cu and Ni-Mo-Co systems.

After full optimization of SSM parameters and choice of metal precursors, the UNM team decided to use a Ni-Mo-Cu as the main material for the anode in the fuel cell. The main problem of ternary system was a phase separation of Ni and Mo as well as substantial formation of oxides. Oxides are not conductive and substantially decrease the overall performance. Further, this issue was solved via modification of SSM and addition of carbon support. As can be seen on Figure 1, phase pure $Ni_{87}Mo_{13}$/KB was prepared.

In order to obtain reliable and reproducible RDE data, the UNM team developed two methods: (a) based on ink drop-cast and (b) using a pressed gas diffusion electrode. Both methods allow the team to achieve performance milestones (Figure 2). Based on the results of RDE HOR experiments, the preparation method of Ni-rich unsupported and supported on carbon catalysts was transferred to scale-up subcontractor Pajarito Powder. The method was successfully adopted and scaled up to the level of 25 g of catalyst per single batch. The performance of scaled material was ±10% by limiting current compared to Ni-Mo-Cu synthesis at UNM. Using most active materials, the UNM team could achieve the current density at low potential (0.01 V) with the value of 0.095 mA cm^{-2}, which is higher than the go/no-go design point of 0.085 mA cm^{-2} (Figure 3).

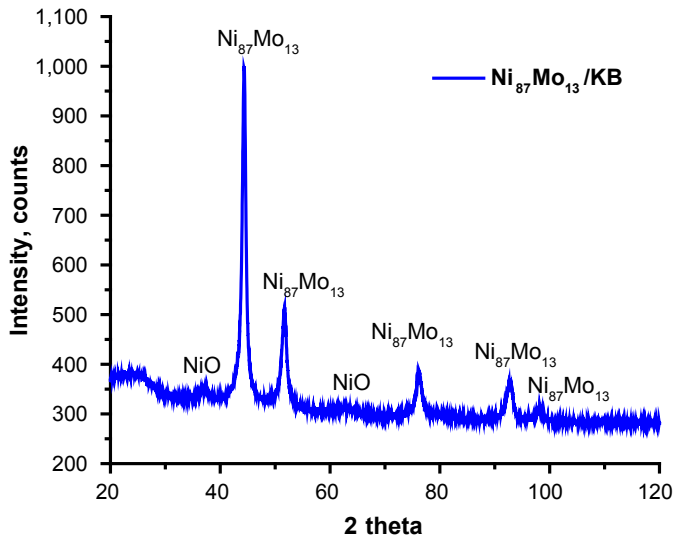

FIGURE 1. X-ray diffraction diffractogram of NiMo/KB electrocatalyst

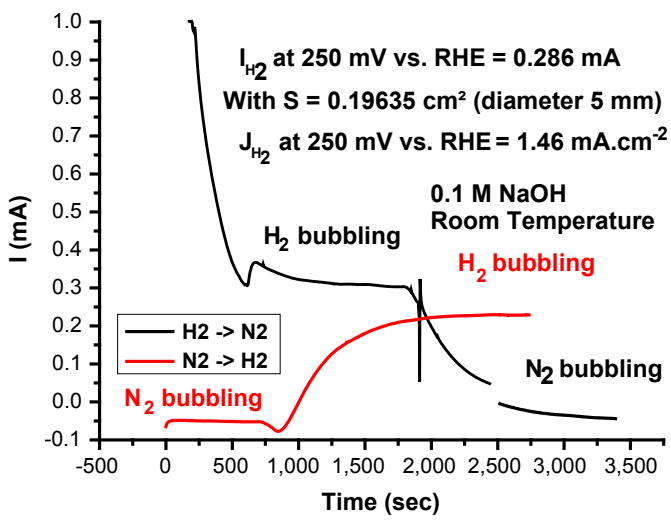

RHE – Reference hydrogen electrode; RPM – revolutions per minute

FIGURE 2. RDE data in NiMoCu materials in HOR. Conditions: 0.1 M NaOH, 1,600 RPM.

In the preparation to Phase II and namely integration of Ni-Mo catalyst with LANL ionomer into MEA, IRD Fuel Cells performed optimization of automatic ink deposition. The initial experiments were started with commercial Pt/C and ionomers from Tokuyama and FumaTech. IRD Fuel Cell successfully deposited catalysts on carbon paper (CCS) and on membrane (CCM). The results of MEA tests using two different ionomers and platinum catalysts are shown on Figure 4.

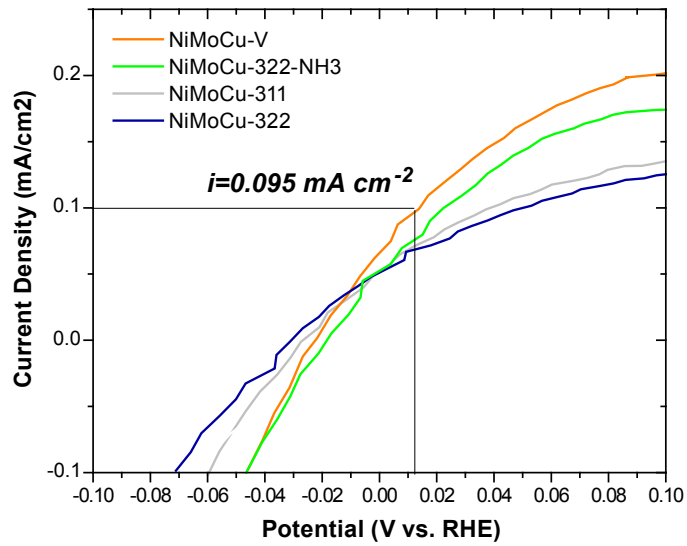

FIGURE 3. RDE data for best performing NiMoCu materials in HOR. Conditions: 0.1 M NaOH, 1,600 RPM.

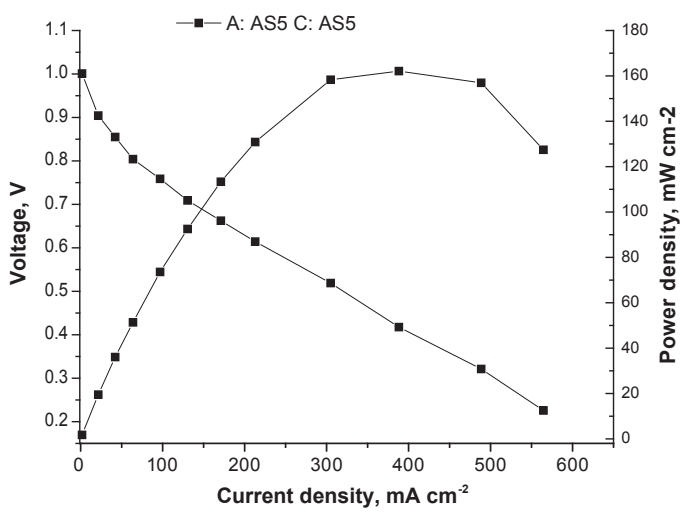

FIGURE 4. Fuel cell performance of MEA prepared by IRD Fuel Cells. Conditions: Pt/C (anode and cathode, 0.4 mg cm^{-2}), Tokuyama AS5 ionomer (anode and cathode), CCS, T_{cell} = 60°C, 100 relative humidity, 20 psi_g back pressure.

CONCLUSIONS AND FUTURE DIRECTIONS

The conclusions from the first year of the project can be summarized as:

- Materials were synthesized, and all milestones were met: particle size, phase purity, surface area. Two RDE protocols were developed. Milestones on performance were met.
- LANL developed ionomer was supplied to UNM for integration of PGM-free catalysts.

- IRD Fuel Cells optimized the automatic ink deposition system in order to manufacture MEAs by CCM and CCS methods. Several MEAs with area of 5 cm^2 and 25 cm^2 were fabricated and tested.
- First go/no-go design point was successfully passed.

The conclusions from the first year of the project can be summarized as:

- Integration of Ni-Mo catalysts with LANL ionomer.
- Manufacturing MEAs.
- Development of activation and testing protocols.

FY 2016 PUBLICATIONS/PRESENTATIONS

1. A. Serov, Y. S. Kim, M. Odgaard, B. Halevi, P. Atanassov "Electrocatalysts for H_2/Air(O_2) Anion Exchange Membrane Fuel Cells: Building a New non-PGM Materials Set", PACIFICHEM (2015).

REFERENCES

1. W. Sheng, H.A. Gasteiger, Y. Shao-Horn, J. Electrochem. Soc. 157, (2010), B1529–B1536.

V.A.3 Innovative Non-PGM Catalysts for High-Temperature PEMFCs

Sanjeev Mukerjee
Department of Chemistry and Chemical Biology
Northeastern University (NEU)
360 Huntington Ave., HT 102
Boston, MA 02115
Phone: (617) 373-2382
Email: s.mukerjee@neu.edu

DOE Manager: David Peterson
Phone: (240) 562-1747
Email: David.Peterson@ee.doe.gov

Contract Number: DE-EE0006965

Subcontractors:
- University of New Mexico (UNM), Albuquerque, NM (Plamen Atanassov)
- Fuel Cell Energy (FCE), Danbury, CT (Ludwig Lipp)
- Pajarito Powder, LLC, Albuquerque, NM (Barr Halevi)

Project Start Date: October 1, 2015
Project End Date: August 31, 2017

Overall Objectives

The objective of this project is to revolutionize high-temperature proton exchange membrane fuel cell (PEMFC) technology based on polymer membranes imbibed with phosphoric acid through development of stable, high-performance precious metal free (PGM-free) cathode catalysts. High-temperature PEMFCs operate in a range of 150–220°C, making them ideal candidates for combined heat and power (CHP) applications. This incubator effort is however, exclusively focused on catalyst development for H_3PO_4-imbibed PEMFCs.

Fiscal Year (FY) 2016 Objectives

The principle objectives of this effort are:

- Develop PGM-free catalysts based on a metal-organic framework (MOF) with unique iron-nitrogen-carbon active sites that are immune to anion poisoning. Elimination of Pt from the cathode would lower total Pt loading from the current state of the art of 3 mg/cm^2 to less than 1.5 mg/cm^2, thereby halving the cost of the catalyst in the membrane electrode assembly (MEA). These catalysts will be scaled up from the ~1 g laboratory level to 100 g batch size.
- Develop unique corrosion resistant support structures for enhanced corrosion resistance as compared to conventional carbon-based supports.
- Provide enhanced mass transport within the reaction layer and gas diffusion layer using a combination of modeling and experiments for obtaining mass transport parameters designed to enable systematic formulation of the gas diffusion and reaction layers.
- Prepare MEAs and perform fuel cell testing using test conditions designed to experimentally obtain mass transport parameters. Perform durability testing relevant to stationary fuel cells. This project aims to meet and exceed the current PGM-based high-temperature polymer electrolyte membrane MEA metrics of 200 mA/cm^2 in H_2/air at 0.65 V with 2.5 bar total pressure at 180°C.
- Perform economic analysis of the fuel cell system to determine market segments for deployment.

Technical Barriers

This project addresses the following technical barriers from the Fuel Cells section of the Fuel Cell Technologies Office Multi-Year Research, Development, and Demonstration Plan:

(A) Durability

(B) Cost

Cost is the primary barrier preventing membrane imbibed phosphoric acid (PA) fuel cells and similar systems from reaching commercial reality, with noble metal loading representing a significant cost component. Cost of noble metals in current state of the art membrane-based PA systems is approximately $800–$1,000/kW. Our goal is to bring this cost to below $500/kW. Durability limitations due to carbon corrosion also represent a major barrier to commercialization. This project will address both of these issues, thereby enabling commercialization of membrane imbibed PA fuel cells on an accelerated schedule.

Technical Targets

The technical targets for this project are listed in Table 1.

Status at end of the fourth quarter (Q4):

- First quarter (Q1) target, catalyst preparation and scale up, to batch size of 5 g. Test of both inter- and intra-batch reproducibility in terms of anion ($H_2PO_4^-$) tolerance tested in 0.1 M $HClO_4$ with varying amounts of H_3PO_4 (up to 100 mM) successfully met.

TABLE 1. Milestone Summary

Recipient Name		Northeastern University, Sanjeev Mukerjee (Principal Investigator)			
Project Title		Innovative Non-PGM Catalysts for CHP Relevant Proton Conducting Fuel Cells			
Task Number	Task or Subtask Title	Milestone Description (Go/No-go Decision Criteria)	Milestone Verification Process	Anticipated Quarter	
				Date	Quarter
1.1	Catalyst Preparation and Scale Up with MOF Chemistry	Develop scale up chemistry based on reactive ball milling for achieving 5 g batch of MOF-based PGM-free cathode catalyst material	Less than 5% inter- and intra-batch variation in RDE performance using 0.1 M $HClO_4$ with up to 100 mM H_3PO_4	3 mo	Q1
1.1	Catalyst Preparation and Scale Up with MOF Chemistry	Demonstrate initial MEA activity of PGM-free cathode catalyst with PA-imbibed membrane	Polarization measurements demonstrating 100 mA/cm^2 at 0.7 V using H_2/O_2 at 180°C 1.5 bar total pressure	6 mo	Q2
2.1	Improving Mass Transport Characteristics	MEA testing of SSM-templated PGM-free catalyst	MEA performance of 200 mA/cm^2 at 0.65 V, H_2/air, 180°C, 2.5 bar total pressure	9 mo	Q3
Go/No-Go Decision		Fuel cell measurements and validation	To meet/exceed 200 mA/cm^2 at 0.60 V with 2.5 bar total pressure, H_2/air, 180°C. Total PGM catalyst loading on the PA-imbibed membrane-based MEA to be lower than 1.5 mg/cm^2 Pt exclusive to the anode electrode with a PGM-free cathode	12 mo	End of Q4
2.3	Durability Studies	Corrosion testing of SSM-based materials	Open circuit test on SSM-based materials at 180°C, H_2/air	21 mo	Q6
3.2	Fuel Cell Test Validation	Fuel cell test validation at OEM partner facility with 100 cm^2 MEA using PA-imbibed membrane and PGM-free cathode catalyst	Achieving H_2/air performance target of 200 mA/cm^2 at 0.65 V, 180°C, 2.5 bar total pressure	24 mo	Q8

RDE – Rotating disk electrode; OEM – Original equipment manufacturer ; SSM - Sacrificial support method; Q6 - Sixth quarter; Q8 - Eighth quarter

- Second quarter (Q2) target, polarization measurements demonstrating 100 mA/cm^2 at 0.7 V using H_2/O_2 at 180°C 1.5 bar total pressure.
  - NEU MOF: tests conducted at NEU with a polybenzimidazole (PBI) membrane at 200°C in O_2 show performance at 100 mA/cm^2 of 690+ mV (within instrumentation error of 700 mV), therefore successfully meeting the stated target.
  - UNM IMID (blended catalyst from UNM): tests conducted by Brian Benicewicz at the University of South Carolina (USC) with PBI membrane at 180°C in O_2 show performance at 100 mA/cm^2 of 700 mV, therefore successfully meeting the stated target.
- Third quarter (Q3) target, polarization measurements demonstration of 200 mA/cm^2 at 0.6 V using H_2/air at 180°C 2.5 bar total pressure.
  - NEU MOF: tests conducted at NEU with PBI membrane at 200°C show performance at 200 mA/cm^2 of 545 mV, 55 mV shy of the stated target.
  - UNM IMID: tests conducted at USC with PBI membrane at 180°C show performance at 200 mA/cm^2 of 600 mV, therefore successfully meeting the stated target.
- Q4 target, demonstration of replication of stated air performance target from Q3.
  - Given that the required testing was done with different catalysts at different testing facilities, and that performance at each facility was at or near both performance testing, this can be taken as a sign of validation of the required testing systems.

✧ ✧ ✧ ✧ ✧

INTRODUCTION

Some initial testing examined hybrid catalysts which consisted of a combination of the PGM-free catalysts materials with a low loading of Pt. Testing switched to pure PGM-free cathodes in high-temperature a PEMFC. Early testing had been done in the absence of poly-tetrafluoroethylene (PTFE). However, durability was very poor due to flooding in the electrode. Therefore, introduction of PTFE to alleviate these issues was dealt with subsequently. Additionally, a full redesign of the electrode and MEA fabrication is underway, and the results have been very encouraging thus far.

APPROACH

For the data shown in this report there are two catalysts in question. First is the solid state reaction scale up MOF provided by Pajarito Powder (MOF Lot #104) , hereon referred to as the NEU MOF. Secondly, another blended catalyst from UNM (UNM IMID), was tested by Brian Benicewicz at USC.

In order to introduce an additional level of morphology control, the UNM team modified the SSM to utilize relatively large (~250 nm) monodispersed silica particles. The second modification in SSM was usage of two imidazole-based precursors, methyl imidazole and imidazolidinyl urea. The combination of two precursors results in an increase of the nitrogen content and graphitization level, which is crucial for durability of PGM-free catalysts. In general, materials were prepared as follows: 5 g methyl imidazole and 5 g imidazolidinyl urea mixed with 2 g of EH5 and 4 g of monodispersed silica. The mixture was dry ball-milled for 20 min and heat treated in N_2 atmosphere for 45 min at T = 925°C. The silica was removed by washing with 25 wt% of HF. The powder was then washed with deionized water until pH ~6 and dried. Dry powder was heat treated in NH_3 atmosphere for 30 min at T = 945°C. The materials are under evaluation by scanning electron microscopy, X-ray photon spectroscopy, and transmission electron microscopy methods. MEA performance was tested at USC using a PBI membrane at 180°C. This MEA is also slated tobe tested at NEU.

A new technique for electrode fabrication has been developed with help from Advent Technologies. An aqueous ink including catalyst, PTFE, as well as stabilization additives, was made and mixed using the Advent Technologies commercial protocol. Using Advent's draw-down method, the ink was deposited onto a commercial gas diffusion layer (GDL) (ELAT HT1200W). Unlike earlier preparatory methods, no heat treatment of the electrode was done following application of the catalyst. Traditionally, heat treatments are used to "activate" the PTFE, and create higher hydrophobicity. However, it was eventually determined that these heat treatments were in fact altering the chemistry of the catalyst, rendering them far less active.

RESULTS

BASF A1100W Pt electrodes (1 mg_{Pt}/cm^2) were used as standard anodes (provided by Advent Technologies), together with commercial PBI membranes. Cathode, anode, membrane, and the requisite sub-gaskets were hot pressed under conditions provided by Advent Technologies. MEAs using the PBI membrane were then placed in an oven at 160°C for 30 min before testing.

Testing of the NEU MOF was done at 200°C (for time purposes, no break-in procedure was done at 180°C as is customary with Advent MEAs). Performance was measured as a function of applied backpressure in both oxygen and air.

Figures 1 and 2 show the oxygen performance of the NEU MOF catalyst, acquired at NEU (Figure 1), as well as the oxygen performance of the UNM IMID catalyst, acquired at USC (Figure 2). Both catalysts met the required oxygen performance targets. Recent studies were done at NEU in order to optimize the PTFE content, the catalyst loading, and the operating temperature. Additionally, newer generation Pt anodes and thinner GDLs were introduced. These changes yielded large increases in performance in both oxygen in air, as will be evident later in this report.

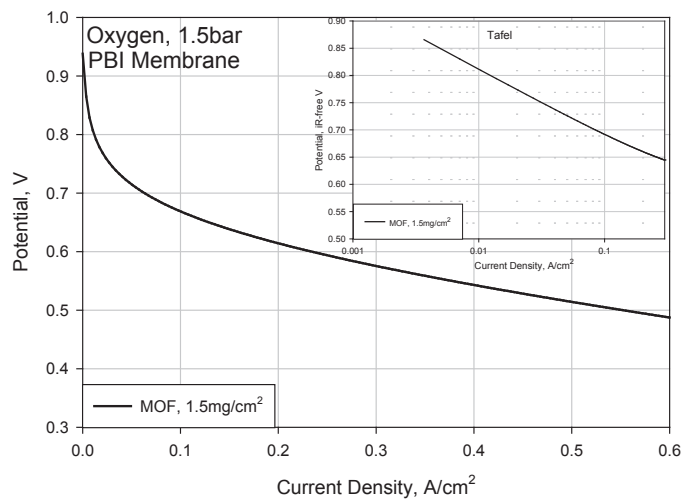

FIGURE 1. Performance in oxygen of the NEU MOF catalyst, tested at NEU. Inset: associated Tafel plot.

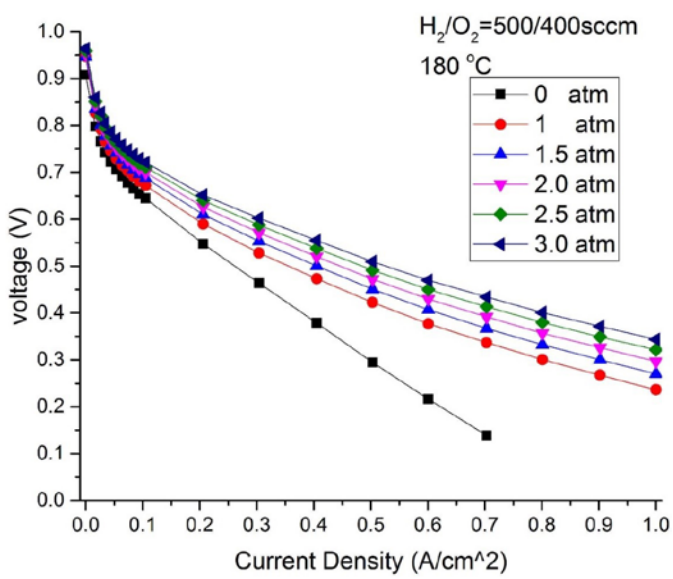

FIGURE 2. Performance in oxygen of the UNM IMID catalyst, tested at USC

The performance in air at NEU (Figure 3) and USC (Figure 4) is presented.

The aforementioned changes to the MEA and testing protocols allowed the NEU performance to get within 55 mV of the stated target, while the USC performance on the UNM IMID catalyst achieved the designated target. Figure 5 shows the rapid progress towards meeting these two performance targets over the recent months.

As is apparent, the changes made at NEU to the fabrication process of the MEAs over the past few months have yielded great progress in terms of performance, both in oxygen as well as in air. The oxygen performance has increased by 150 mV, while the air performance has increased by more than 250 mV (at 200 mA/cm^2, 2.5 bar total pressure). Given that the performance increase in air exceeded that of oxygen, it subsequently reduced the oxygen gain. This is evidence of improved gas transport throughout the catalyst layer. However, the oxygen gain is still nearly double that of a Pt cell, indicating that there is more optimization to be done on fabrication of the cathodes. Nevertheless, this upward trend in performance is very promising towards the development of high-performing, high-temperature PEMFCs using a pure non-PGM cathode catalyst.

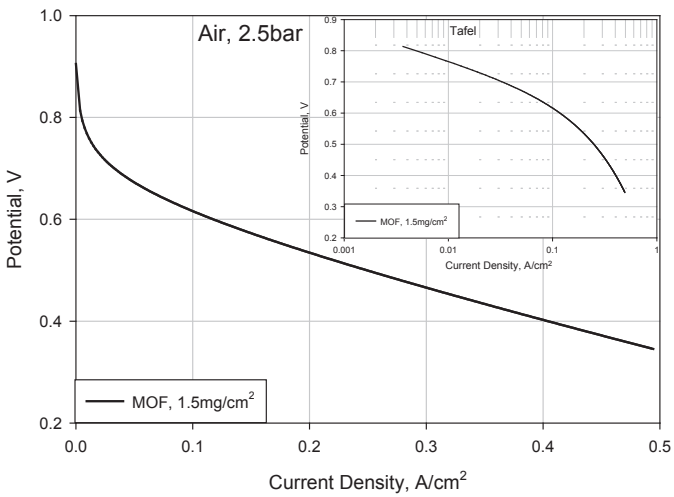

FIGURE 3. Performance in air of the NEU MOF catalyst, tested at NEU. Inset: associated Tafel Plot.

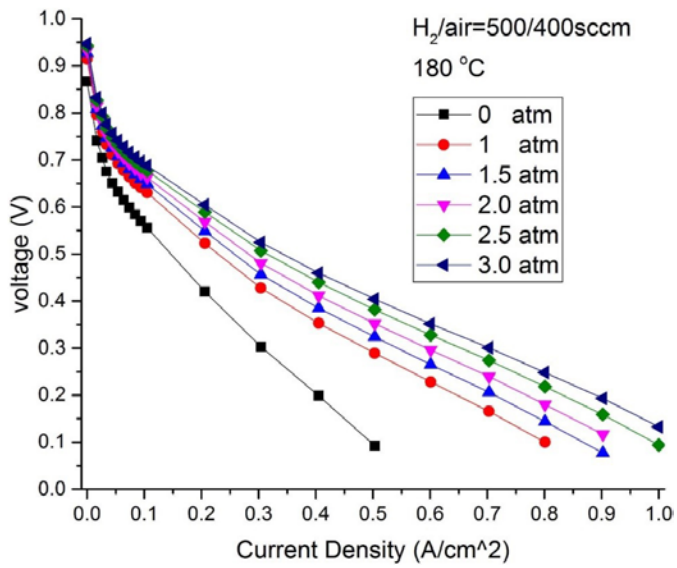

FIGURE 4. Performance in air of the UNM IMID catalyst, tested at USC.

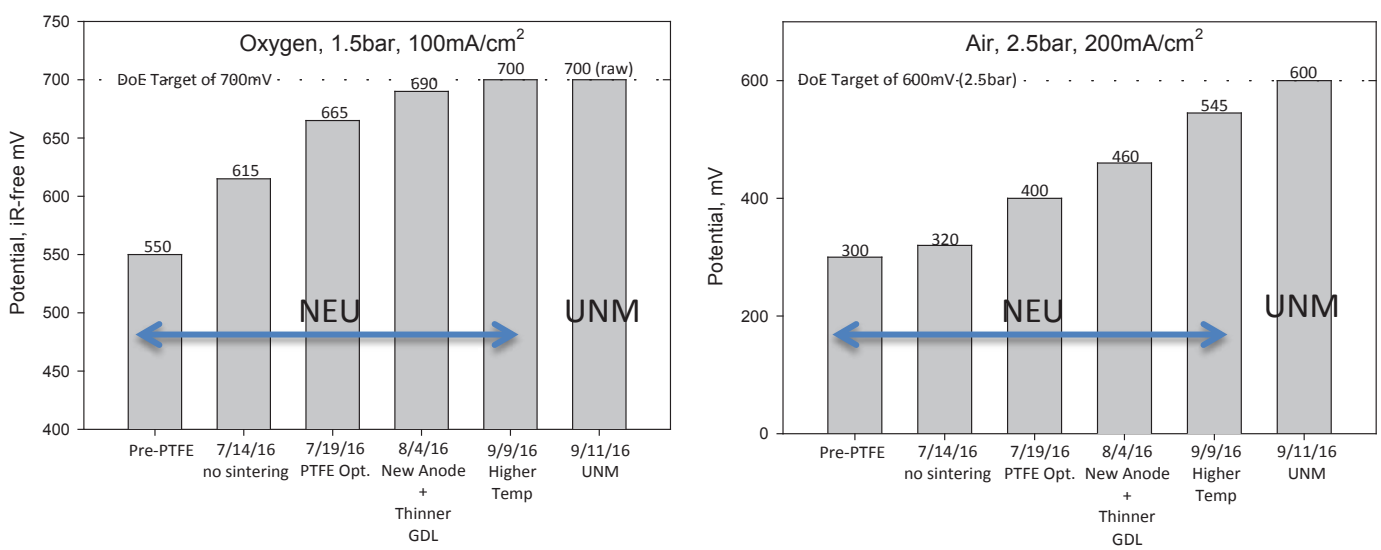

iR - Internal resistance

FIGURE 5. Increase in oxygen and air performance throughout the course of the MEA redesign undertaken at NEU.

CONCLUSIONS AND FUTURE DIRECTIONS

The most recent work was primarily invested in completing a full redesign of our electrode and MEA preparation techniques. The redesign was clearly a success given the performance increases in both oxygen and air.

While there are still more studies to be done to further increase the performance through technological advances in the electrode fabrication, the project will additionally switch gears in an effort to test additional materials beyond the two catalysts specifically referenced in this report. These catalysts will include variants of the MOF, synthesized both at NEU as well as at Pajarito Powder. Additionally, UNM will continue to synthesize new catalysts for testing.

As is directed in the statement of work, experiments will begin in an effort to study the durability of these fuel cells. This will be done through several methods, including chronoamperometric measurements, corrosion testing, and temperature cycling. These protocols should give increased information regarding any potential degradation mechanisms of these catalysts.

Finally, FCE will participate in an effort to scale up to larger MEAs that would be more indicative of commercial utilization, rather than the standard 5 cm^2 electrodes used for testing at NEU. Validation of the FCE testing facilities has already been completed using Pt MEAs fabricated at both Advent Technologies as well as at NEU. Once preliminary catalyst testing has been done at NEU, larger MEAs (45 cm^2 and up), will be manufactured at NEU and shipped to FCE for validation.

FY 2016 PRESENTATIONS

1. "Use of Hybrid Cathodes to Reduce Platinum Content in High Temperature PEMFCs," Ryan Pavlicek. Kara Strickland, Sanjeev Mukerjee, Presentation at the 229th Meeting of the Electrochemical Society, June 1, 2016; San Diego, CA.

V.A.4 Tailored High-Performance Low-PGM Alloy Cathode Catalysts

Vojislav R. Stamenkovic (Primary Contact) and Nenad M. Markovic
Argonne National Laboratory (ANL)
Argonne, IL 60439
Phone: (630) 252-8946
Email: vrstamenkovic@anl.gov

DOE Manager: Nancy L. Garland
Phone: (202) 586-5673
Email: Nancy.Garland@ee.doe.gov

Subcontractors:
- Karren More, Oak Ridge National Laboratory (ORNL) Oak Ridge, TN
- Peidong Yang, Lawrence Berkeley National Laboratory (LBNL), Berkeley, CA
- Rod Borup Los Alamos National Laboratory (LANL) Los Alamos, NM

Project Start Date: October 2015
Project End Date: September 2018

Overall Objectives

- Develop and deliver advanced low platinum group metal (PGM) cathode catalysts for use in polymer exchange membrane (PEM) fuel cells with increased mass activity at high electrode potentials, enhance performance at high current density.
- Improve durability while reducing the total loading of PGM and cost.
- Reduce PGM loading in the catalyst through alloying of Pt with other transition metals.
- The low-PGM materials will be in form of nanomaterials deployed on high surface area supports.
- Rational development and evaluation of durable high surface area supports for tailored nanomaterials.
- Development and implementation of scalable chemistry that would allow synthesis of tailored nanomaterials at the gram scale.
- Insight on the differences and similarities between the rotating disk electrode (RDE) and membrane electrode assembly (MEA) performance.
- Ionomer catalyst interaction and optimization of catalyst layers.
- The MEA will have a total PGM loading of <0.125 mg_{PGM}/cm^2 and 0.125 g_{PGM}/kW with mass activity higher than 0.44 A/mg_{PGM}.
- Total loss of electrochemically mass activity will be less than 40%.

Fiscal Year (FY) 2016 Objectives

- Development of active and durable catalysts for fuel cell cathodic reaction.
- Synthesis, structural and electrochemical evaluation of Pt-alloy nanoparticles with controlled physical parameters such as size, compositional profile and topmost surface.
- Development of scalable process to produce larger quantities of catalysts.
- Integration and evaluation of novel carbon supports with tailored Pt-alloy nanoparticles.
- Reproducibility of performance measured in MEA for tailored Pt-alloy catalysts with total PGM loading of <0.125 mg_{PGM}/cm^2 and mass activity over 0.44 A/mg_{PGM}.

Technical Barriers

This project addresses the following technical barriers from the Fuel Cells section 3.4.5 Technical Task Descriptions section of the Hydrogen, Fuel Cells and Infrastructure Technologies Program Multi-Year Research, Development, and Demonstration Plan.

(A) Durability: Develop improved catalysts
- Reduce precious metal loading of catalysts
- Increase the specific and mass activities of catalysts
- Increase the durability/stability of catalysts with cycling
- Test and characterize catalysts

Technical Targets

The project is aimed to develop nanoparticles with tailored architectures and composition based on Pt-alloys with transition metals PtM (M = Ni, Co, Cr, V, Ti, etc.), including alloys with Au, to improve performance for the fuel cell cathodic oxygen reduction reaction. The design principles will be focused to produce systems with low content of platinum group metals while exhibiting highly active and durable electrochemical properties evaluated in MEAs that will meet and/or exceed the DOE 2020 targets (Table 1).

TABLE 1. Progress Towards Meeting DOE 2020 Technical Targets for Electrocatalysts

	Unit	2015 DOE Targets	Project Status
PGM Total Loading	mg_{PGM}/cm^2	0.125	0.120
Mass Activity	A/mg_{Pt} @ 900 mV	0.44	0.60
Mass Activity Loss	%	<40	<20

FY 2016 Accomplishments

- Established three new labs at ANL as integral part of this project:
  - Development of an RDE coupled online with inductively coupled plasma mass spectrometry (ICP-MS) for detection of ultra-low concentration, part per trillion (ppt), of metals such as Pt, Au, Ni, Co, Fe, etc.
- Development of an MEA characterization test stand.
- Development of a laboratory for scaling the amounts of synthesized nanomaterials.
- Demonstrated capabilities of RDE ICP-MS setup by quantifying the amounts of dissolved Pt in a single potential cycle for different Pt surfaces, including Pt nanoparticles (NPs).
- Achieved detection limit of a micro monolayer of dissolved Pt.
- Evaluated benefits of subsurface Au in stabilization of Pt-based catalysts that completely diminished Pt dissolution.
- Developed highly active and durable multi-metallic system based on subsurface Au and PtNi over layer with Pt-skin surface.
- Evaluated transition from solid solution into intermetallic structure for Pt_3Co and PtCo by high-angle annular dark field (HAADF) and energy dispersive X-ray (EDX).
- Electrochemical characterization of PtCo catalysts with intermetallic structures.
- Identified Pt-skin surface in PtNi nanoframes as a descriptor for highly active and stable nanoframes by in situ extended X-ray absorption fine structure analysis (EXAFS).
- Synthesized novel nanoscale architectures in form of nanowires, nanoflowers, and highly porous Pt-alloy particles with promising catalytic properties.
- Established scalable chemistry to produce grams amount of PtNi catalyst with multilayered Pt-skin surfaces.
- Exceeded mass activity 2020 DOE Technical Targets for PtNi catalyst in MEA; mass activity = 0.6 A/mg_{Pt}.

✧ ✧ ✧ ✧ ✧

INTRODUCTION

The major obstacle for broad utilization of polymer electrolyte fuel cells (PEMFCs) in transportation is cost, performance, and durability of Pt catalysts that are employed in each individual cell of a fuel cell stack. Considering that Pt is the best known catalyst for both hydrogen oxidation reaction and oxygen reduction reaction (ORR), it is of paramount importance to develop a practical catalysts that will exhibit optimal performance through high specific activity (current per electrochemical surface area of catalyst), with minimal content of PGM that will ensure high mass activity (current per mass unit of PGM). Cathodes in PEMFCs suffer from substantial kinetic limitations and degradation of catalysts for ORR; and for that reason, the main focus in catalyst development is to create highly efficient, durable cathodes with low content of PGM. Therefore, this project will aim to develop and deliver advanced, low-PGM cathode catalysts for PEMFC that will increase mass activity at high electrode potentials, enhance performance at high current density, and improve durability while decreasing the cost. The decrease of the total loading of PGM in the fuel cell will be accomplished by improving activity and durability of Pt-based catalysts through alloying with other transition metals [1]. These PGMs in the form of nanomaterials will be deployed on high surface area supports in the cathode of MEA with total PGM loading less than the DOE 2020 target of 0.125 mg_{PGM}/cm^2 and 0.125 mg_{PGM}/kW with mass activity higher than 0.44 A/mg_{PGM}.

APPROACH

This is a multi-performer project led by ANL supported by inter-laboratory collaborations with LBNL, LANL, and ORNL. ANL will lead and coordinate this applied research effort with other national laboratories; will define project scope, topics, and milestones; and will be responsible for deliverables as well as quarterly and annual reports to Fuel Cell Technologies Office. LBNL will be involved in chemical synthesis of advanced nanoscale structures and development of scaling-up protocols of the most promising catalytic systems. LANL will execute fabrication and testing of the MEA and will provide alternative carbon based supports to conventional high surface area carbon. ORNL will perform electron microscopy characterization of synthesized materials and catalyst deployed in MEA before and after testing protocols. The approach of this project is based on the knowledge obtained from well-defined systems that will be used to tailor functional properties of corresponding nanoscale materials, with desired shape, size, structure and compositional profile. Integration of engineered nanomaterials in electrochemical systems requires integration of a broad range of scientific disciplines such as

solid state physics, surface science, physical chemistry, and electrochemistry. This effort also includes the combination of highly diverse experimental tools supported by state-of-the-art synthesis and characterization strategies, together with the fabrication and testing capabilities. The project is executed *simultaneously* in five tasks throughout duration of the project: Task 1 well-defined systems, Task 2 synthesis of nanoscale materials, Task 3 electrochemical and structural characterization of catalysts, Task 4 supporting materials for novel catalysts, and Task 5 scaling up of catalysts.

RESULTS

Insight into Pt Dissolution by RDE ICP-MS. In addition to development of novel catalytically active materials for fuel cells, it is of paramount importance to get detailed insight into fundamental properties related to their stability in an electrochemical environment. An analytical setup was developed for characterization of catalyst in the form of single crystals, thin films, and nanoparticles by coupling RDE with ICP-MS, see schematic illustration in Figure 1. This setup has achieved an ultimate sensitivity that was verified first on the extended single crystalline surfaces of Pt electrodes [2]. In these experiments it was possible to detect and measure the amount Pt dissolved in a single potential cycle. The range of dissolved Pt varies depending on crystallographic orientation and it was found to increase with the decrease of Pt coordination number. The most stable surface was Pt(111), while the least stable was Pt(110). The amounts of dissolved Pt ranged from 2–83 μML (mono atomic layer) in a single potential cycle for Pt(111) and Pt(110) respectively. For fuel cell applications, the most relevant finding was the amount of dissolved Pt in a single potential cycle from Pt/C catalyst, which was found to be around 103 μML per cycle in the case of Pt/C TKK particles with mean diameter of 3 nm, as shown in Figure 1a. It would also

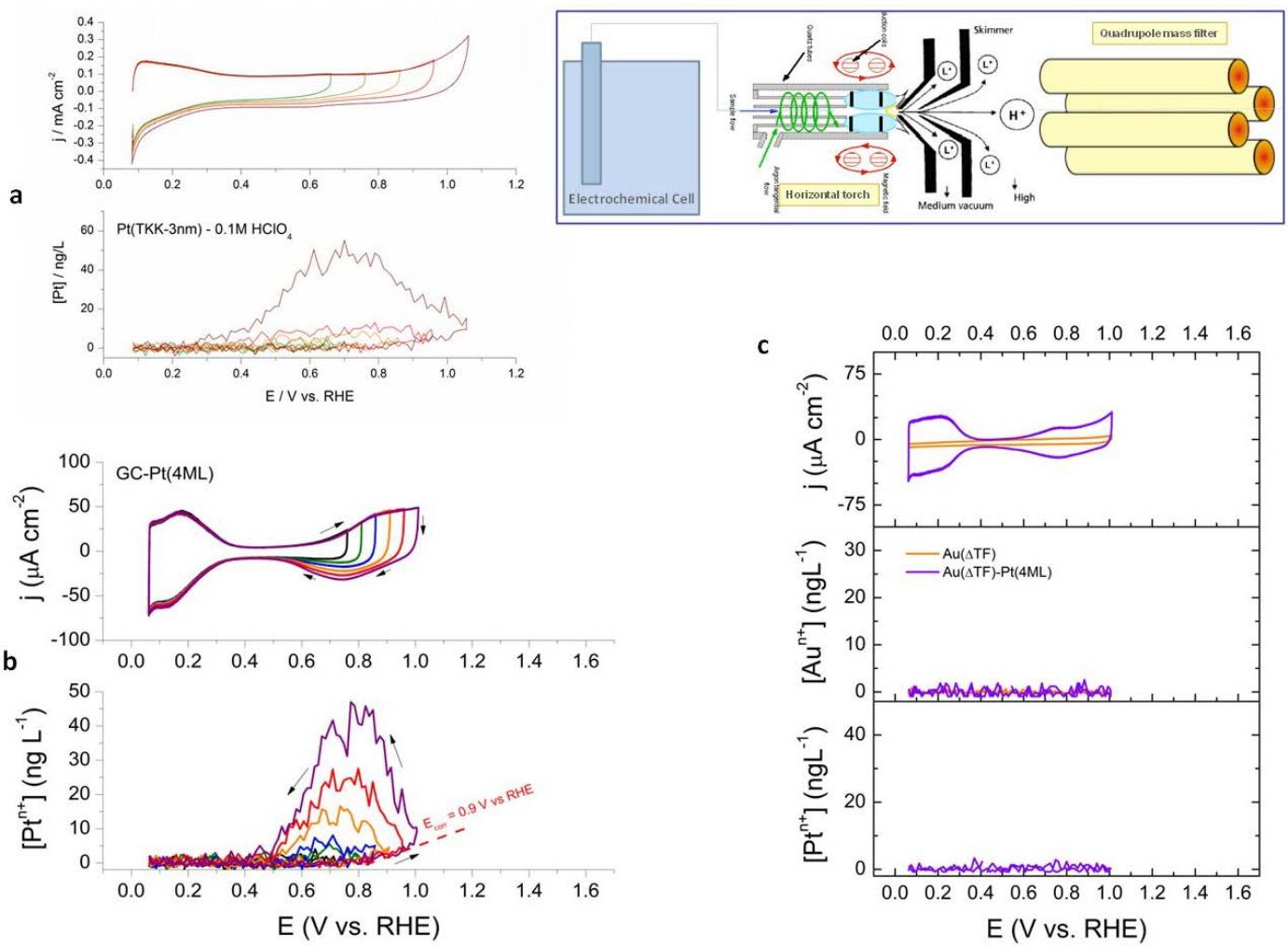

GC – Glassy carbon; RHE - Reference hydrogen electrode

FIGURE 1. Schematic illustration of RDE ICP-MS method and cyclic voltammetry with corresponding Pt dissolution curve in 0.1 M $HClO_4$. (a) Pt/C TKK-3 nm catalyst. (b) 4 atomic monolayer thick Pt thin film on glassy carbon electrode. (c) 4 atomic monolayer thick Pt thin film over Au subsurface deposited on glassy carbon electrode.

be important to mention, that RDE ICP-MS setup developed in our labs is capable to distinguish two events, dissolution of Pt vs. detachment of particle from the substrate. For that reason, the measured amount of dissolved Pt has not been assigned to detached Pt particles. Considering our previous reports on the beneficial role of subsurface Au [3,4] and the fact that these values are closely tied to Pt fundamental properties as well as, it was intriguing to evaluate Pt systems with Au substrate and check by RDE ICP-MS whether addition of the metal that is less oxophilic affects dissolution of Pt. For that purpose we have done a series of experiments with well-defined thin films' compositional profiles, with and without Au substrate. It has been found that addition of Au as a substrate can dramatically affect the amount of dissolved Pt. Figure 1b and 1c shows the results measured on a glassy carbon electrode covered only with 4 ML of Pt, and the same amount, 4 ML thick topmost Pt layer that was deposited over Au substrate in the form of thin film. While Pt dissolution from 4 ML Pt thin film is severe, glassy carbon electrode covered first with Au substrate does not exhibit any signal for dissolved Pt. This is rather strong proof that subsurface Au can play a major role in hindering Pt dissolution. This finding will serve as foundation for the follow up studies related to the optimization of parameters such as thickness of the Au substrate as well as Pt over layer, including associated annealing conditions. This approach is expected to evolve towards more complex systems which would allow identification of the most desirable composition in terms of minimal amount of precious metals and high catalytic activity for the ORR.

Atomic Structure of Pt_3Ni Nanoframe Electrocatalysts by In Situ X-ray Absorption Spectroscopy. The success rate in synthesis and quality of the nanoframe catalyst has been evaluated by in situ X-ray absorption near-edge spectroscopy (XANES) and EXAFS measurements to address the difference in performance among lab scale batches that were verified by both RDE and MEA [5]. The surface characteristics of the nanoframes were probed through electrochemical hydrogen underpotential deposition and carbon monoxide electro-oxidation, which showed that nanoframe surfaces with different structure exhibit varying levels of binding strength to adsorbate molecules. In our previous work we have shown that Pt-skin formation on Pt-Ni catalysts will enhance ORR activity by weakening the binding energy between the surface and adsorbates [6,7]. Ex situ and in situ XAS results reveal that nanoframes which bind adsorbates more strongly have a rougher Pt surface caused by insufficient segregation of Pt to the surface and consequent Ni dissolution. In contrast, nanoframes which exhibit rather high ORR activity simultaneously demonstrate more significant segregation of Pt over Ni-rich subsurface layers, allowing better formation of the critical Pt-skin. In situ XAS analyses performed with the working electrode that was cycled to condition the catalyst and then held at 0.9 V vs. RHE for in situ ORR, yields a clear picture of the differences in atomic distribution and structuring in $Pt_3Ni(1.0)$ and $Pt_3Ni(1.5)$, where 1.0 and 1.5 reflect the ratio between integrated charges obtained from the H_{upd} and CO stripping curves. From the XANES spectra in Figure 2a at the Ni *K*-edge and Pt L_3-edge, the decrease in white line intensity indicates surface NiO dissolution in the acidic electrolyte after potential cycling. It was also found that at both metal edges, the XANES spectra were identical, and therefore, the oxidation states of both metals in both samples were deemed identical (Figures 2a–2b). The near-edge region of X- ray absorption probes electronic transitions from a core level into local, unoccupied states just above the Fermi level energy. During in situ ORR, the Fermi levels of the Pt_3Ni metallic samples are controlled by the potentiostat at an identical potential relative to a reference electrode potential. Therefore, the probability of an X-ray absorption-induced transition into the unoccupied states is similar for these samples while under potential control, and their XANES spectra are identical. However, as can be seen from Figures 2c–2d, after removing the electrode from the electrolyte and rinsing and drying it, the XANES spectra are no longer identical between $Pt_3Ni(1.0)$ and $Pt_3Ni(1.5)$. The Ni in $Pt_3Ni(1.0)$ is more oxidized while the Pt is more reduced, indicating increased donation of electron density from Ni to Pt in $Pt_3Ni(1.0)$. The increased alloying in $Pt_3Ni(1.0)$ was further supported by the EXAFS analysis. Figure 2e shows a XANES difference spectrum at the Ni *K*-edge for $Pt_3Ni(1.0)$ and $Pt_3Ni(1.5)$ samples where the normalized absorption in situ is subtracted from the normalized absorption after ORR. After the catalyst is rinsed and dried under nitrogen, the nickel in $Pt_3Ni(1.0)$ is more easily oxidized as indicated by the more intense peak at the white line position, approximately 16–17 eV after the edge. The platinum shell is not protecting the nickel as thoroughly in $Pt_3Ni(1.0)$, suggesting the surface has more low coordination sites and a thinner platinum shell, as illustrated in Figure 2f. These conclusions were further substantiated by EXAFS data. The initial observation in the first shell fit is that the total coordination numbers N_{Pt} and N_{Ni} are similar for both samples, with N_{Pt} significantly smaller than N_{Ni}. As mentioned, this indicates that Pt atoms have segregated to the surface to form some variation of the desired Pt-skin structure because of the lower coordination number of surface atoms. It was also found that the heterometallic coordination of nickel to platinum is decreased in $Pt_3Ni(1.5)$, and correspondingly the homometallic coordination is increased. This depicts the nanoframe of $Pt_3Ni(1.5)$ as one with more segregation of Pt from Ni, which is also indicated by the smaller extent of alloying parameters for platinum, J_{Pt}, calculated for $Pt_3Ni(1.5)$ vs. $Pt_3Ni(1.0)$. In situ EXAFS demonstrated that $Pt_3Ni(1.0)$ had a larger extent of alloying while $Pt_3Ni(1.5)$ had more significant segregation of Pt to the surface of the nanoframe. It was concluded that $Pt_3Ni(1.0)$ has a thinner, rougher Pt surface caused by insufficient segregation of Pt to the surface. $Pt_3Ni(1.5)$ exhibits extremely high ORR activity due to its significant segregation of Pt

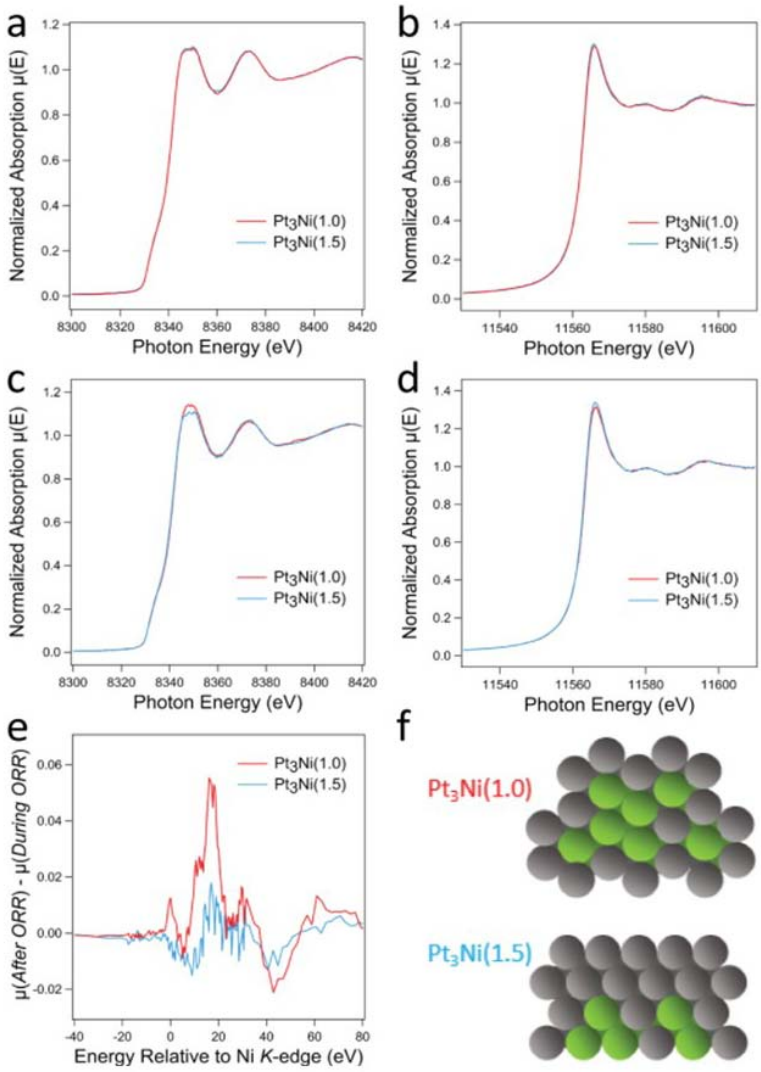

FIGURE 2. XANES of Pt_3Ni/C catalysts in situ and after electrochemistry. (a) Ni *K*-edge at 0.9 V. (b) Pt *L3*-edge at 0.9 V. (c) Ni *K*-edge after in situ. (d) Pt *L3*-edge after in situ. (e) Ni *K*-edge in situ XANES subtracted from after in situ XANES. (f) Model surfaces of Pt_3Ni(1.0) and Pt_3Ni(1.5), where gray atoms are Pt and green atoms are Ni. With permission from the American Chemical Society [5].

from Ni, allowing for better formation of a Pt-skin [5]. The activity of a given nanoframe sample was resolved to be primarily predetermined by the level of platinum enrichment at the edges of the rhombic dodecahedron, which altogether represents important guidelines for successful synthesis of highly active PtNi nanoframes.

Evolution of Surface Faceting and Elemental Diffusion at the Atomic-level for Pt_3Co Nanocatalysts. In situ high temperature annealing in an aberration-corrected scanning transmission electron microscope (STEM) was performed to discern the thermally driven structural and compositional evolution of individual Pt-Co alloy NPs [8]. It was found that Pt_3Co nanoparticles undergo five distinct stages of elemental surface rearrangement upon thermal annealing from room temperature (RT) to 800°C: (1) random elemental distribution; (2) surface skin-layer formation; (3) ordered domain nucleation; (4) ordered framework development; and (5) amorphization. A comprehensive interplay among phase evolution, surface faceting, and elemental inter-diffusion is revealed. No obvious faceting was observed on the initial NP surface at RT. Increasing the temperature to 350°C results in Pt segregation to the surface region, as evidenced by a slightly brighter contrast on the particle surface compared to that at RT (Figure 3a). Pt segregation can be clearly demonstrated from an image intensity profile taken across the diameter of the NP, where the intensity measurement of the contrast associated with the atomic columns shows an obvious increase in contrast at the surface region, which is consistent with segregation of Pt atoms to the surface. Similar Pt surface segregation behavior was observed for other Pt_3Co NPs on the same sample; this is consistent with results from some earlier studies of Pt_3Ni NPs [1,]. Furthermore, the surface facets appear to sharpen at 350°C compared to those observed at RT, where {1-10} and {110} facets are clearly observed (marked by arrow in Figure 3a). Surface faceting is likely a combined result of Pt segregation to the surface and the initiation of atomic surface reconstruction during the early stage of annealing, which is consistent with earlier studies. It is important to note that such Pt-enriched surfaces disappear once the annealing temperature is increased to 550°C. Hence, the results show that the formation of a Pt-segregated surface over as-synthesized Pt_3Co NPs is sensitive to the annealing temperature. Such sensitivity can be explained by the interplay between surface segregation and compositional disordering. The segregation process of Pt to the NP surface (with disordered Pt and Co elemental atoms) is mainly driven by the decrease in free energy owing to negative surface segregation enthalpy. Such segregation will lead to a decrease in configurational entropy of the system by inducing surface compositional ordering. While surface-segregation free energy eventually turns positive due to the increased entropic contribution, increasing annealing temperature, therefore, results in the observed disappearance of the Pt-segregated surface. Such surface diffusion of Pt was also confirmed by energy dispersive X-ray spectroscopy (EDS) chemical mapping in other particles at different annealing temperatures. The Pt_3Co nanoparticle originally attains a homogenous elemental distribution at RT. Pt enrichment could be seen when the particle was heated to 350°C, but it vanished when the temperature was increased

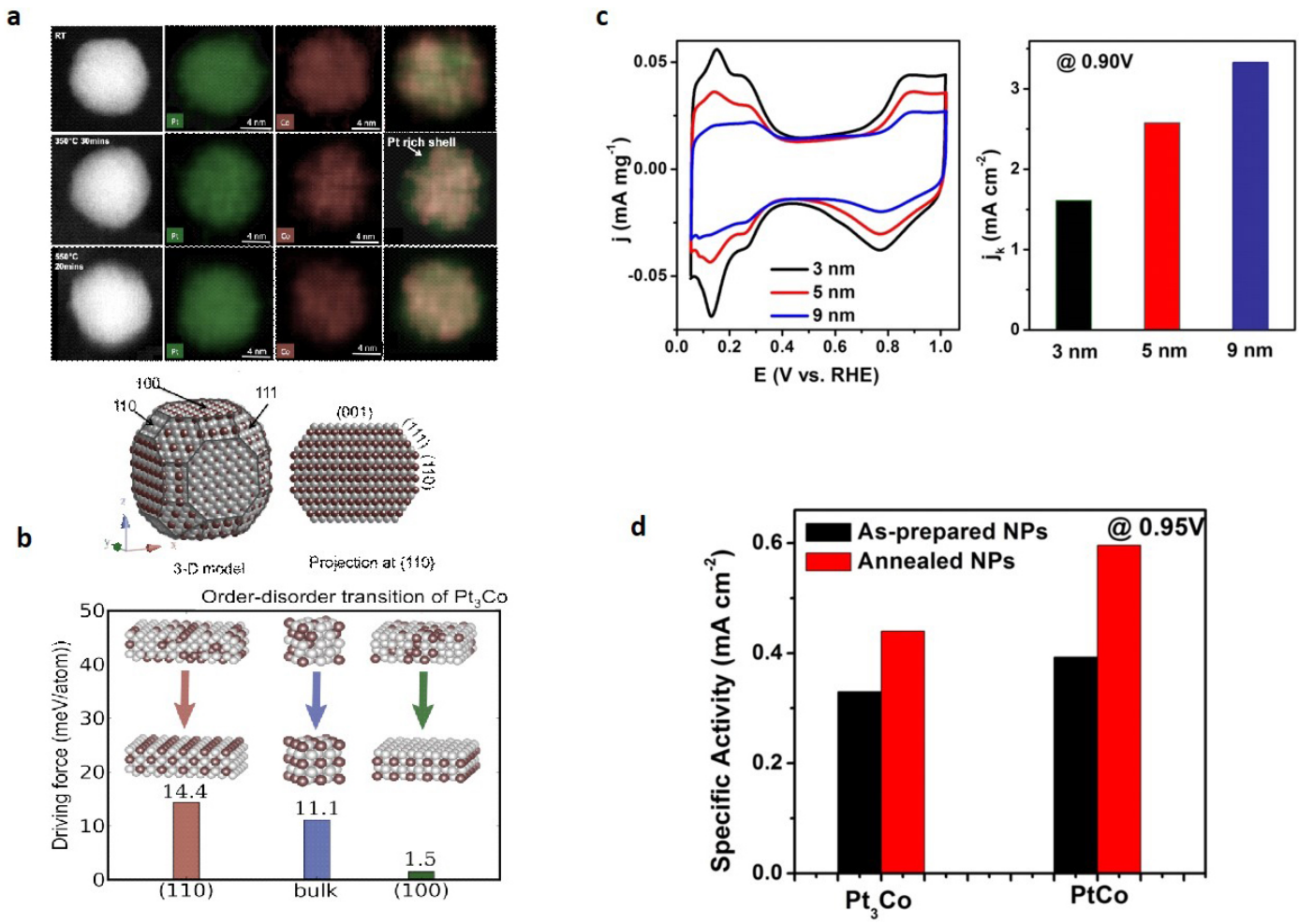

FIGURE 3. Evolution of surface faceting and elemental diffusion at the atomic-level for Pt_3Co nanoparticle during thermal annealing and corresponding electrochemical properties. (a) HAADF images and corresponding EDS elemental maps of a Pt_3Co nanoparticle which was annealed at different temperatures: RT, 350°C, and 550°C respectively. The overlapped maps of Co and Pt (shown in the last column) demonstrate that Pt segregates to the particle surface at 350°C and diminishes at the surface when it is annealed at 550°C. (b) Detailed geometry correspondence between the facets and the two dimensional projection down [110] and the driving forces to form ordered structure at different facets and bulk by using first-principles density functional theory, showing that [110] has the highest driving force to form ordered structure. (c, d) Cyclic voltammetry of intermetallic Pt_3Co NPs along with the ORR bar graphs that show particle size dependence and electrochemical performance at both 0.9 V and 0.95 V. With permission from the Nature publishing group [8].

further to 550°C. Our results suggest that careful selection of annealing temperature is indispensable in order to form Pt-segregated surface architecture for enhanced catalytic activity. Moreover, the ordered structures on the (1–10) surface propagated throughout the {001} planes to the [-110] planes with further annealing at 600°C (Figures 3a and 3b). When the particle was annealed at 600°C for a longer time, elemental inter-diffusion into the bulk increased as evidenced by the largely inhomogeneous intensity distribution. The ordering structure on two sides, i.e., those close to {001} surfaces, eventually formed with a further annealing at 600°C, resulting in a completely ordered structure. This phase transformation is consistently characterized by the distinct Pt_3Co NPs under these annealing conditions. Continued annealing at 600°C for 20 min does not change the ordering architecture but leads to further elemental inter-diffusion. No noticeable elemental diffusion or structure change was observed with further annealing at 700°C for 30 min, which suggests that the particle has reached a thermally stable state with an $L1_2$ structure. Our observation on the evolution of the ordering structure shows that the ordered framework was established first in the NPs followed by additional diffusion to a stable ordered structure. When the particle is further annealed at 800°C, the atomic columns in the HAADF image were blurred resulting from increased atomic vibration at the elevated temperature, although the ordering structure is still vaguely visible. Longer annealing times at 800°C activate the amorphization (i.e., pre-melting) of the nanoparticle and the morphology eventually takes on a rounded shape. Electrochemical characterization shown

in Figures 3c and 3d depicts noticeable improvement in catalytic properties of the ORR for both Pt_3Co and PtCo NPs. Influence of ordered phase in Pt-alloys on electrochemical durability will be explored in future.

MEA Evaluation of PtNi/C with Multilayered Pt-skin Surfaces. The NP evaluations were made in RDE and 5 cm^2 MEA at ANL. The MEAs were made by the decal method with the ionomer and membrane in the proton form and hot-pressing of the decals to the membrane at 130°C. The ionomer to carbon ratio was 0.8. The summary of the MEA test results is given in Figure 4. The MEAs were tested temperatures ranging from room temperature to 80°C, with 150 kPa(abs) humidified hydrogen on the anode at 1 L/min, and with 150 kPa(abs) humidified oxygen and/or air on the cathode, with a relative humidity of 100%. The mass activities are shown in the table of Figure 4c. High performance PtNi or multilayered Pt-skin NPs have been evaluated by MEA and it has been confirmed that high durability originates from the protective multilayered Pt-skin surface that encapsulates core that is Ni rich, as mentioned before. The multilayered Pt-skin catalyst was prepared from colloidal PtNi NPs (~5 nm) by following the recent report from our group (more details about synthesis will be given in the next section). In the previous quarter we have achieved DOE 2020 Technical Target, while in this quarter, mass

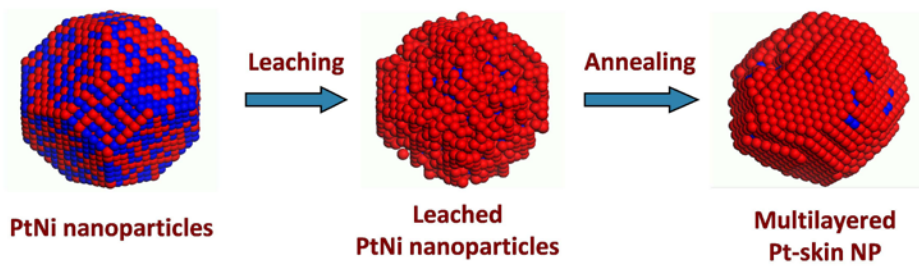

a

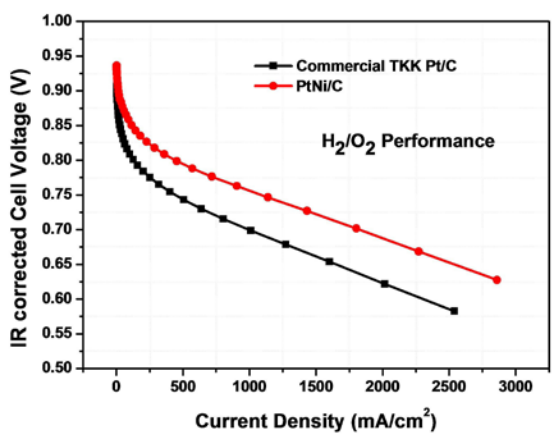

b

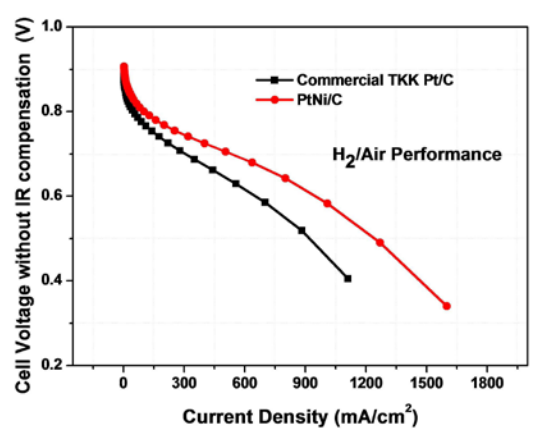

c

	Units	PtNi	TKK Pt
Pt loading	mg_{PGM}/cm^2_{geo}	0.045	0.045
Mass Activity (H2-O2)	A/mg_{PGM} @ 0.9 $V_{iR\text{-}free}$	0.60	0.27
Specific Activity (H2-O2)	mA/cm^2_{PGM} @ 0.9 $V_{iR\text{-}free}$	1.85	0.39
MEA performance (H2-Air)	mA/cm^2 @ 0.8 V	101	47
ECSA	m^2/g_{PGM}	35.10	52.5

ECSA – Electrochemically active surface area

FIGURE 4. Electrochemical evaluation of ~20 wt% PtNi/C with multilayered Pt-skin surfaces (red) and Pt/C TKK (black) obtained by 5 cm^2 MEA. (a) Hydrogen–oxygen polarization curves. (b) hydrogen–air polarization curves. The cathode Pt loading is 0.046 mg_{Pt}/cm^2, ionomer to catalyst = 1, 80°C, 150 kPa, 100% relative humidity. (c) Performance parameters of PtNi/C retrieved from MEA hydrogen–oxygen polarization curves.

activity over-achieved the DOE target even though the Pt loading on cathode was substantially decreased to the value of 0.045 mg_{PGM}/cm^2. Measured mass activity was found to be 0.60 A/mg_{PGM} at 0.9 V. Achieved mass activity combined with the catalyst loading indicates that the project milestone has been met.

CONCLUSIONS AND FUTURE DIRECTIONS

- Evaluation of activity, durability, and optimization of MEA protocols at ANL and LANL.
- Alternative approaches towards highly active and stable catalysts with low PGM content.
- Tailoring of the structure and composition that can optimize durability and performance in Pt-alloys.
- Synthesis of tailored low-PGM practical catalysts with alternative supports.
- Structural characterization (in situ XAS, high resolution transmission electron microscopy, X-ray diffraction).
- Resolving the surface chemistry in MEAs through electrochemical evaluation in RDE and MEA.
- In situ durability studies for novel catalyst-support structures (RDE ICP-MS).
- Scale-up of chemical processes to produce gram quantities of the most promising catalysts.

SPECIAL RECOGNITIONS & AWARDS/ PATENTS ISSUED

1. V.R. Stamenkovic, C. Wang, N.M. Markovic, *Bimetallic Alloy Electrocatalysts with Multilayered Platinum Skin Surfaces*, United States Patent; US 9,246,177 B2, Jan. 26, 2016.

2. C. Chen, Y. Kang, N.M. Markovic, G. Somorjai, Peidong Yang and V.R. Stamenkovic, Patent Pending *Highly Crystalline Pt_3Ni Nanoframes with Three-Dimensional Electrocatalytic Surfaces*.

FY 2016 PUBLICATIONS/PRESENTATIONS

1. H. Lv, D. Li, D. Strmcnik, A.P. Paulikas, N.M. Markovic, V.R. Stamenkovic, *The design of tailored nanomaterials for efficient oxygen reduction reaction,* DOI:10.1016/j.nanoen.2016.04.008, **Nano Energy (2016)**.

2. D. Li, H. Lv, Y. Kang, N.M. Markovic, and V.R. Stamenkovic, *Recent Advances in the Development of Oxygen Reduction Reaction Catalysts for Low Temperature Fuel Cells,* DOI: 10.1146/annurev-chembioeng-080615-034526, **Annual Review of Chemical and Biomolecular Engineering**, Vol. 7 (2016).

3. P.P. Lopes, D. Strmcnik, J. Connell, V.R. Stamenkovic and N.M. Markovic, *Relationships between Atomic Level Surface Structure and Stability/Activity of Platinum Surface Atoms in Aqueous Environments,* **ACS Catalysis**, 6 (4), 2536-2544, 2016.

4. D. Li, D. Strmcnik, N. Markovic and V. Stamenkovic*, (Invited Lecture)Progress in Material Design of Electrocatalysts for Fuel Cells,* **2016 Materials Research Society Spring Meeting**, 2016, Phoenix, AZ,

5. D. Li, Y. Kang, J. Snyder, D. Strmcnik, N. Markovic and V. Stamenkovic *(Invited Lecture) Electrocatalysts with Advanced Properties,* **2015 Materials Research Society Fall Meeting**, 2015, Boston, MA.

6. D. Li, D. Strmcnik, N.Markovic and V. Stamenkovic (*Key Note Lecture*) *Advanced Catalysts with Ultra-Low PGM Content for PEMFC Cathode,* **The 2015 Electrolysis and Fuel Cells Discussions**, 2015, La Grande Motte, France.

7. N. Becknell, Y. Kang, Chen Chen, J. Resasco, N. Kornienko, J. Guo, N.M. Markovic, G.A. Somorjai, V.R. Stamenkovic, P. Yang, *Atomic Structure of Pt_3Ni Nanoframe Electrocatalysts by in Situ X-ray Absorption Spectroscopy,* **Journal of American Chemical Society**, 137 (2015) 15817.

8. V. Stamenkovic, N. Markovic, D. Strmcnik, D. Li., Y. Kang, *(Plenary Lecture) From Well-Defined Interfaces to Functional Nanoscale Materials,* **The 7th International Fuel Cells Workshop**, 2015, Kofu, Japan.

9. M. Chi, C. Wang, Y. Lei, G. Wang, K.L. More, F. Allard, N.M. Markovic, and V.R. Stamenkovic, *Surface faceting and elemental diffusion behaviour at atomic scale for alloy nanoparticles during in situ annealing*, **Nature Communications**, 6 (2015) *No.* 8925.

REFERENCES

1. V. Stamenkovic, B. Fowler, B.S. Mun, G. Wang, P.N. Ross, C. Lucas, and N.M. Markovic, "Improved Oxygen Reduction Activity on $Pt_3Ni(111)$ via Increased Surface Site Availability," *Science.*, 315 (2007) 493–497.

2. P.P. Lopes, D. Strmcnik, J. Connell, V.R. Stamenkovic and N.M. Markovic, "Relationships between Atomic Level Surface Structure and Stability/Activity of Platinum Surface Atoms in Aqueous Environments," *ACS Catalysis*, 6 (4), 2536–2544, 2016.

3. C. Wang, D. van derVliet, K.L. More, N.J. Zaluzec, S. Peng, S. Sun, H. Daimon, G. Wang, J. Greeley, J. Pearson, A.P. Paulikas, G. Karapetrov, D. Strmcnik, N.M. Markovic, V.R. Stamenkovic, "Multimetallic Au/$FePt_3$ Nanoparticles as Highly Durable Electrocatalysts," *Nano Letters*, 11 (2011) 919–928.

4. Y. Kang, J. Snyder, D. Li, K. More, N.M. Markovic and V.R. Stamenkovic, "Multimetallic Core/Interlayer/Shell Nanostructures as Advanced Electrocatalysts," *Nano Letters*, 14 (2014) 6361–6367.

5. N. Becknell, Y. Kang, Chen Chen, J. Resasco, N. Kornienko, J. Guo, N.M. Markovic, G.A. Somorjai, V.R. Stamenkovic, P. Yang, "Atomic Structure of Pt_3Ni Nanoframe Electrocatalysts by in Situ X-ray Absorption Spectroscopy," *Journal of American Chemical Society*, 137 (2015) 15817.

6. C. Chen, Y. Kang, J. Snyder, M. Mavrikakis, Y. Li, N.M. Markovic, G. Somorjai, Peidong Yang, V.R. Stamenkovic, "*Highly Crystalline Multimetallic Nanoframes with Three-Dimensional Electrocatalytic Surfaces,"* Science, 343(2014)1339–1343.

7. C. Wang, M. Chi, D. Li, D. Strmcnik, D. van derVliet, G. Wang, V. Komanicky, K-C. Chang, A.P. Paulikas, D. Tripkovic, J. Pearson, K.L. More, N.M. Markovic and V.R. Stamenkovic, "Design and Synthesis of Bimetallic Electrocatalyst with Multilayered Pt-Skin Surfaces," *Journal of American Chemical Society*, **133** (2011)14396.

8. M. Chi, C. Wang, Y. Lei, G. Wang, K.L. More, F. Allard, N.M. Markovic, and V.R. Stamenkovic "Surface faceting and elemental diffusion behaviour at atomic scale for alloy nanoparticles during in situ annealing," *Nature Communications*, 6 (2015) *No.* 8925.

V.A.5 Platinum Monolayer Electrocatalysts

Radoslav Adzic (Primary Contact), Jia Wang, Miomir Vukmirovic, Kotaro Sasaki
Brookhaven National Laboratory, Bldg. 555
Upton, NY 11973-5000
Phone: (631) 344-4522
Email: adzic@bnl.gov

DOE Manager: Nancy L. Garland
Phone: (202) 586-5673
Email: Nancy.Garland@ee.doe.gov

Collaborator:
Piotr Zelenay, Los Alamos National Laboratory
Los Alamos, NM

Project Start Date: July 1, 2015
Project End Date: July 2018

Overall Objectives

- Synthesizing high performance Pt monolayer (ML) electrocatalysts for the oxygen reduction reaction (ORR) consisting of a Pt ML shell on stable, inexpensive metal, alloy, metal oxide, nitride or carbide nanoparticle cores.
- Increasing activity and stability of Pt ML shells and stability of supporting cores while reducing noble metal contents.

Fiscal Year (FY) 2016 Objectives

- Exploring synthesis of new non-noble metal cores.
- Modifying core components by nitriding, alloying, doping.
- Syntheses of specific structures using reactive spray deposition technique without oxidation of core components.
- Electrodeposition of rare earths and refractory metal alloys from ionic liquids and non-aqueous solvents.
- Improving catalysts response at high current densities.

Technical Barriers

This project addresses the following technical barriers from the Fuel Cells section of the Fuel Cell Technologies Program Multi-Year Research, Development, and Demonstration Plan.

(A) Durability

(B) Cost

(C) Performance

Technical Targets

We are focusing on simplifying the synthetic processes to obtain better catalyst activity, higher Pt utilization, lower content of platinum group metal (PGM), and simpler membrane electrode assembly (MEA) fabrication (See Table 1).

FY 2016 Accomplishments

- Developed nitrided refractory metal and non-noble metal cores for a Pt ML shell.
- Developed electrocatalysts based on cores modified by alloying with Mo.
- Developed a new class of core-shell catalysts with oxidized species segregated to edges and vertices of nanoparticles.
- Demonstrated the electrodeposition from ionic liquids and non-aqueous solvents of Y, Y alloys with Pt and Pd with high ORR activity.
- Achieved improved proton penetration into the catalyst layer by functionalizing carbon nanotubes.
- Improved gas diffusion electrodes as a method for fast screening of catalysts before MEA tests.

✧ ✧ ✧ ✧ ✧

INTRODUCTION

Further improvements of oxygen reduction electrocatalysts are necessary to overcome the remaining technological difficulties that hinder automotive applications of fuel cells. Our research was focused on reducing Pt or PGM contents in our electrocatalysts while increasing their stability and activity. Optimizing the properties of supporting cores by varying their composition, size and shape makes possible further improvements of the Pt ML catalysts.

APPROACH

Our approach to improving Pt ML catalysts is based on developing new synthetic methods to obtain novel cores including:

- Nitriding non-noble metal core components for increased stability.
- Modifying cores by alloying for a better support for a Pt ML.
- A new class of core-shell catalysts having oxide segregated to edges and vertices of nanoparticles.

TABLE 1. Progress toward Meeting DOE Fuel Cell Electrocatalysts Technical Targets

	DOE 2017 Targets	Pt_{ML}/Pd/Nb/ RDE	Pt_{ML}/Pd/Ni/N/GDL 80°C, H^2/Air, 300 kPa	PtAuTiOx	$Pt_{ML}/AuNi_{alloy}$ $Pt_{ML}/AuNi_{core\text{-}shell}$
Pt loading mg/cm^2		0.0009	0.1		
PGM total loading, mg_{PGM}/cm^2	<0.125	0.0059 at the cathode	0.2 at the cathode		
Loss in performance @ 0.8 A/cm^2 after 30,000 AST	<30 mV	No loss after 1,000 AST	7 mV after 34,000 AST	No loss after 10,000 AST	No loss 5,000 AST 25 mV
Mass activity @ 900 $mV_{iR\ free,}$ A/mg_{Pt}		4.2	1.2	3	
Mass activity @ 900 $mV_{iR\ free,}$ A/mg_{PGM}	>0.44	0.64	0.6	0.34 (Pt + Au)	1.52 1.18

RDE – Rotating disk electrode; AST – Accelerated stress test

- Electrodeposition from ionic liquids and non-aqueous solvents of metals inaccessible from aqueous solutions, and impractical by other methods.
- Achieve better proton penetration into the catalyst layer to increase the ORR kinetics.
- Gas diffusion electrodes improved as a method for fast screening of electrocatalysts.

RESULTS

We describe four results illustrating the new methods developed in FY 2016 for improving Pt ML catalysts for the ORR.

Nitride-Stabilized Pt-M Core-Shell Electrocatalysts in Acid Media

We further developed highly active and stable oxygen reduction catalysts by depositing Pt monolayers on a nitrided PdNi alloy core (Figure 1). Pd content is reduced by 50% in comparison with the Pt/Pd/C catalyst; RDE stability test with 50,000 potential cycles indicates a negligible change in activity.

MEA performance in H_2–air test shows a clear sensitivity to back pressures indicating mass transfer limitations with this catalyst. Further application of nitriding involved study of niobium nitride as a core. Commercial NbN nanoparticles had an initial size of 500 nm, which was reduced after ball milling to 50 nm. NbN has low resistance with resistivity of 150 μΩcm. Far from optimized, the Pt/NbN/C catalyst shows MA = 0.35 mA/mg_{Pt}, which is also the PGM activity and specific activity, SA = 0.49 mA/cm^2.

Nb and Nb Alloys as Cores

In addition to NbN as a core, we synthetized several catalysts with Nb without nitriding, but combined with other core constituents. A comparison of the activities of these

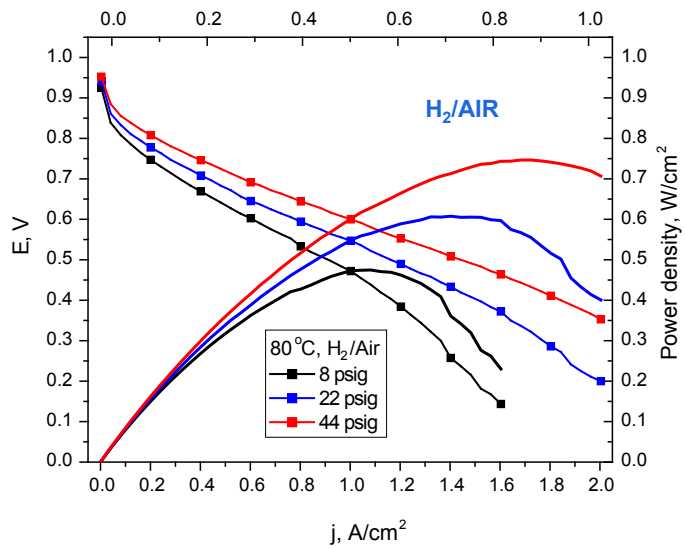

FIGURE 1. MEA polarization curve with H_2–air feed at three different back pressures in the cathode obtained: nitriding PdNi core. Anode Pt (TKK 46%), cathode PtPdNi/C, 17% Pt with loading of 0.1 mg/cm^2.

catalysts is given in Figure 2. Their PGM mass activities are high although the cores contained some noble metal. Optimization of Pt/Nb-containing catalysts is expected to produce further improvements.

Doping Cores with Mo

Along the same approach, modifications of cores were attempted by doping them by several metals. The effect of doping with Mo was quite pronounced. The Pt monolayer on Pd_3Mo has seven and eight times higher mass and specific activities than commercial catalysts, respectively. MEA tests showed the activity similar to the commercial Pt catalyst, which had about three times larger Pt loading than the Pt

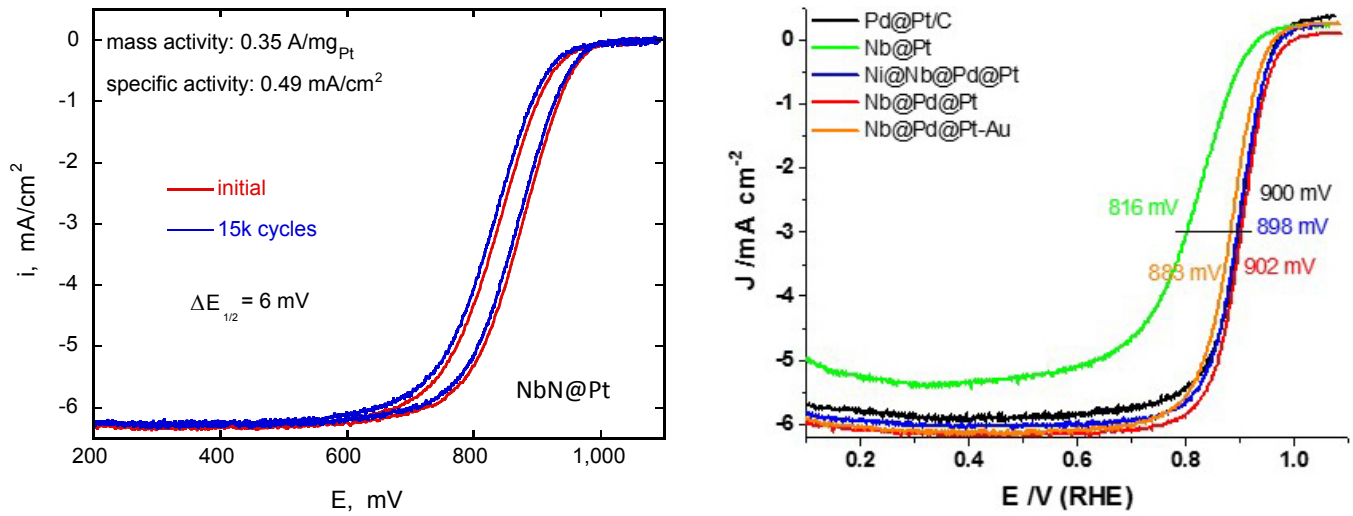

RHE – Reference hydrogen electrode

FIGURE 2. Polarization curves for a Pt nanocrystallites on NbN on a RDE (left panel). Polarization curves for several Nb-based nanoparticles on C with a Pt ML shell. Composition of the catalysts is indicated in the graph. 0.1 M $HClO_4$; 1,600 rpm; 10 mV/s.

monolayer catalyst. Further increase of PGM mass activity is possible.

Ordered Intermetallic $AuPt_4Co_5$/C

We have demonstrated that intermetallic compounds, and in particular, ordered intermetallics can be excellent core for a Pt monolayer shell and even catalysts on their own right. Here we show that a small addition of Au to PtCo alloy at appropriate temperature (800ºC) can make an ordered compound. Figure 3 (left panel) shows electron energy loss spectroscopy mapping for Pt and Co, indicating a uniform distribution of both components, (middle panel) shows atomic resolution scanning transmission electron microscopy image that identifies Pt and Co atoms, and (right panel) displays polarization curves. The catalyst has an excellent stability and high mass activity is 0.5 A/mg$_{PGM}$.

Core-shell Nanoparticle Catalysts Having Edges and Vertexes Covered by Refractory Metal Oxide

We developed a new class of core-shell nanoparticle catalysts having edges and vertexes covered by refractory metal oxide that preferentially segregates onto these catalyst sites. The monolayer shell is deposited on the oxide-free core atoms. The oxide on edges and vertexes induces high catalyst stability and activity. This is exemplified by fabrication of Au nanoparticles doped by Ti atoms that segregate as oxide onto low-coordination sites of edges and vertexes. Pt monolayer shell deposited on Au sites has the mass and specific

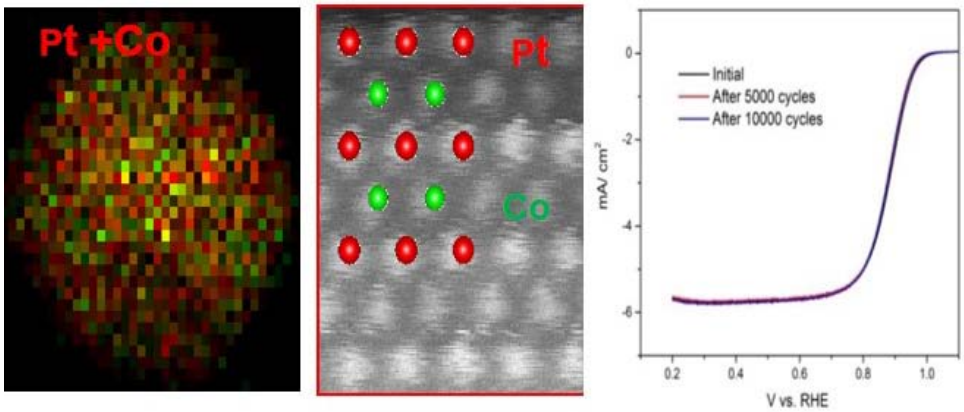

FIGURE 3. Two dimensional electron energy loss spectroscopy mapping of Pt and Co in Pt_4Co_5Au (left panel); High resolution scanning transmission electron microscopy-high angle annular dark field image showing intermetallic structure of PtCo with Pt atoms (red) and Co (blue) (middle panel) and the ORR polarization curves the AuPtCo/C before and after 5,000 and 10,000 potential cycles. 0.1 M $HClO_4$; 1,600 rpm; 10 mV/s. (right panel).

activities for the ORR about 13 and five times higher than those of commercial Pt/C catalysts (Figure 4). The durability tests show no activity loss after 10,000 potential cycles from 0.6 V to 1.0 V. The superior activity and durability of the Ti-Au@Pt catalyst originate from protective titanium oxide located at the most dissolution-prone edge and vertex sites and Au supported active and stable Pt shell.

New Insights in Behavior of Core-Shell Catalysts

We demonstrated a very strong effect of the structure of bimetallic AuNi cores on the activity of Pt shell. Considerably higher activity of AuNi alloy as the core was found compared to a core-shell nanoparticle support. Electronic effects of the alloy change the O_2 and H_2O interaction with the Pt shell and facilitate increased ORR kinetics. This finding will be very useful in designing new core-shell catalysts.

Electrodeposition of Y and Y-Pt Alloys from Ionic Liquids and Non-Aqueous Solvents

High activity of Pt-Y alloys for the ORR has been predicted using density functional theory calculations and shown using sputter deposition catalyst's components [1]. Electrodeposition from ionic liquids offers a promising possibility for nanoparticle synthesis from metals such as yttrium that cannot be deposited from aqueous solutions and is not suitable for other synthetic methods. PtY was electrodeposited from ionic liquid 1-ethyl-3-methylimidazolium tetrafluoroborate (EMI), acetonitrile (AN) and dimethylformamide (DMF). The highest activity found for PtY-EMI catalyst, larger than for PtY-AN, PtY-DMF, or commercial Pt/C.

CONCLUSIONS AND FUTURE DIRECTIONS

New results show the possibility of developing high-performance, low cost Pt ML catalysts with non-noble metal cores. Nitriding core components can help achieve that. Non-precious metal NbN core is very promising.

New class of core-shell catalysts include oxidized component segregated to edges and vortexes causing stability and improved activity. Complex synthesis may be an obstacle.

Ordered intermetallic compounds can be cores with excellent properties. Y-Pt alloy deposition from ionic liquid and AN produced catalysts with high activity. This deposition opens new synthesis possibilities unachievable by conventional methods.

Improvements of the gas diffusion electrode response at the high current densities (CDs) have been obtained using functionalized carbon nanotubes and reducing the Nafion content in the catalyst ink.

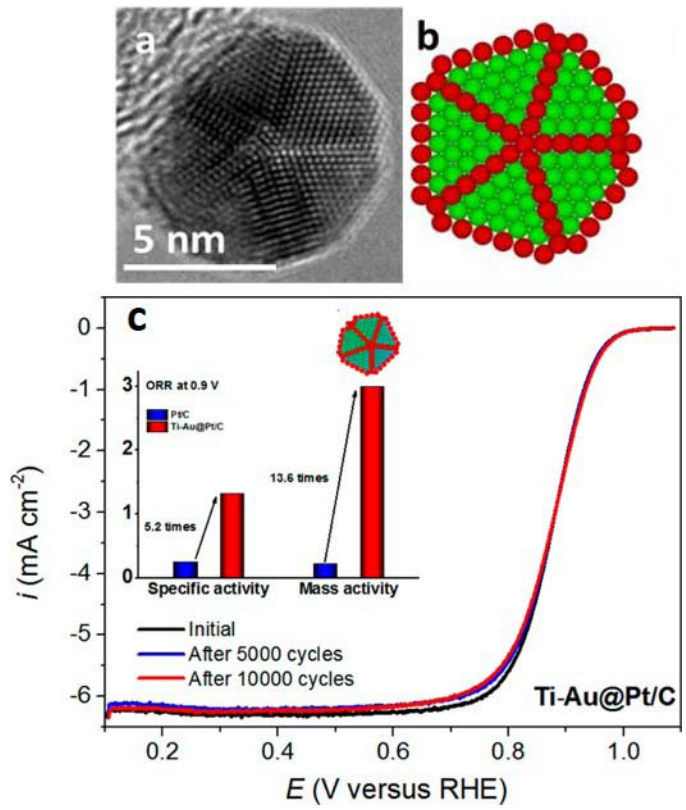

FIGURE 4. (a) High resolution transmission electron microscopy image of a Ti-Au nanoparticle viewed along five-fold axis ([110] direction in face-centered cubic lattice), showing five twins and truncated decahedral shape. (b) Schematic of a partially truncated decahedral Ti–Au multiply twinned nanoparticle with Au (green spheres) at core and Ti (red spheres) at the <110> edge of the facets. (c) ORR polarization curves (inset) of Ti-Au@Pt/C catalyst before and after 5,000 and 10,000 potential cycles between 0.6 V and 1.0 V. 1,600 rpm and a scan rate of 10 mV s^{-1}. Inset: Comparison of specific activities and mass activities at 0.9 V for Ti-Au@Pt/C and commercial Pt/C. Pt loadings for Ti-Au@Pt/C, Au@Pt/C and commercial Pt/C catalysts were 1.1 µg cm^{-2}, 1.3 µg cm^{-2}, and 9.7 µg cm^{-2} respectively.

Future work will focus on:

- Nb-based non-noble metal cores synthesized using thermal routes and reactive spray deposition technique of non-noble metal alloys without oxidation of components.
- New synthesis of hollow Pd cores with a simple scale up will be completed.
- High pressure nitridation performed in a new tube reactor at temperatures up to 1,100°C in an NH_3 gas at pressures up to 10 MPa to generate various types of nitride nanoparticles with refractory metals such as Ti, V, Nb, Ta, and W to enhance the stability and activity of Pt shells.

- Electrodeposition of refractory metal alloys and earth metals using ionic liquids and/or non-aqueous solvents will be continued. This method will help obtaining the onion-structured nanoparticles with new cores of multiple metal layers. The goal is to tune Pt monolayer properties and shifts E° closer to 1.23 V. Supporting density functional theory calculations have been completed. Electrodeposited Pt_{ML}/Pd/WNi will be improved for response at high CD. For these conditions, we will design nanoparticle cores to have porosity to provide a good response. Functionalized carbon nanotubes and reducing the Nafion content in the catalyst ink will be used to address that problem. Selected catalysts will be tested in MEAs and optimize for high CD response and durability.

SPECIAL RECOGNITIONS & AWARDS/ PATENTS ISSUED

1. Adzic, R.R. Harris A.; "Platinum-based electrocatalysts synthesized by depositing contiguous adlayers on carbon nanostructures," US 20150303488, October 22, 2015.

2. Adzic, Radoslav, Bliznakov, Stoyan, Vukmirovic, Miomir, "Electrochemical Synthesis of Elongated Noble Metal Nanoparticles, such as Nanowires and Nanorods, on High-Surface Area Carbon Supports," US 20160160376 June 9, 2016.

3. Adzic, Radoslav, Zhang, Junliang, Sasaki, Kotaro; (June 2016), "Method and Electrochemical Cell for Synthesis of Electrocatalysts by Growing Metal Monolayers, or Bilayers and Treatment of Metal, Carbon, Oxide and Core-Shell Nanoparticles."

FY 2016 PUBLICATIONS/PRESENTATIONS

1. J. Hu, L. Wu, K.A. Kuttiyiel, K.R. Goodman, C. Zhang, Y. Zhu, M.B. Vukmirovic, M.G. White, K. Sasaki, and R.R. Adzic, "Increasing Stability and Activity of Core−Shell Catalysts by Preferential Segregation of Oxide on Edges and Vertexes: Oxygen Reduction on Ti−Au@Pt/C," J. Am. Chem. Soc., DOI: 10.1021/jacs.6b04999.

2. D. Buceta, C. Tojo, M.B. Vukmirovic, F. Leonard Deepak, and M. Arturo López-Quintela, "Controlling Bimetallic Nanostructures by the Microemulsion Method with Subnanometer Resolution Using a Prediction Model," Langmuir 31 (2015) 7435–7439.

3. Megan E. Scofield, Christopher Koenigsmann, Dara Bobb-Semple, Jing Tao, Xiao Tong, Lei Wang, Crystal S. Lewis, Miomir B. Vukmirovic, Yimei Zhu, Radoslav R. Adzic, and Stanislaus S. Wong, "Correlating the chemical composition and size of various metal oxide substrates with the catalytic activity and stability of as-deposited Pt nanoparticles for the methanol oxidation reaction," Catal. Sci. Technol. 6 (2016), 2435–2450.

4. Megan E. Scofield, Yuchen Zhou, Shiyu Yue, Lei Wang, Dong Su, Xiao Tong, Miomir B. Vukmirovic, Radoslav R. Adzic, and Stanislaus S. Wong, "Role of Chemical Composition in the Enhanced Catalytic Activity of Pt-Based Alloyed Ultrathin Nanowires for the Hydrogen Oxidation Reaction under Alkaline Conditions," ACS Catal. 6 (2016), 3895–3908.

5. K.A. Kuttiyiel, Y.M. Choi, K. Sasaki, D. Su, S.-M. Hwang,S.-D. Yim, T.-H. Yang, G.-G. Park, R.R. Adzic, "Tuning Electrocatalytic Activity of Pt Monolayer Shell by Bimetallic Ir-M (M = Fe, Co, Ni or Cu) Cores for the Oxygen Reduction Reaction," Nano Energy, accepted.

6. K. Kuttiyiel, S. Kattel, S. Cheng, L. Wu, Y. Zhu, G. Park, P. Liu, K. Sasaki, J.G. Chen, R. Adzic, "Structure and activity of Au-doped stable platinum cobalt ordered intermetallic nanoparticle catalysts for the oxygen reduction reaction," Nat. Comm. accepted.

7. K. Kuttiyiel, K. Sasaki, G. Park, M. Vukmirovic, L. Wu, Y. Zhu, J.G. Chen, R. Adzic, "Janus structured Pt clusters on Fe-N-C nanoparticles as catalyst for the ORR." Manuscript Submitted.

8. M. Vukmirovic, K. Kuttiyiel, H. Meng, R. Adzic. "Controllable deposition of Pt layers on oxide surfaces for fuel cell catalyst syntheses," ChemElectroChem, Submitted.

9. K. Kuttiyiel, Y. Choi, K. Sasaki, D. Su, S. Hwang, S. Yim, T. Yang, G. Park, R. Adzic, "Tuning electrocatalytic activity of Pt monolayer shell by bimetallic Ir-M (M = Fe, Co, Ni or Cu) cores for the oxygen reduction reaction," Nano Energy, 2016, In Press.

10. G. Chen, K. Kuttiyiel, D. Su, M. Li, C. Wang, D. Buceta, C. Du, Y. Gao, G. Yin, K. Sasaki, M. Vukmirovic, R. Adzic, "Oxygen reduction kinetics on Pt monolayer shell highly affected by the structure of bimetallic AuNi cores," Chemistry of Materials, 2016, In Press.

11. G. Chen, M. Li, K. Kuttiyiel, K. Sasaki, F. Kong, C. Du, Y. Gao, G. Yin, R. Adzic, "Evaluation of oxygen reduction activity by the thin-film rotating disk electrode methodology: The Effects of Potentiodynamic parameters," Electrocatalysis, 2016, 7, 305–316.

12. S. Hwang, Y. Choi, M. Kim, Y. Sohn, T. Yang, S. Yim, K. Kuttiyiel, K. Sasaki, R. Adzic, G. Park, "Enhancement of oxygen reduction reaction activities by Pt nanoclusters decorated on ordered mesoporous porphyrinic carbons," Journal of Materials Chemistry A, 2016, 4, 5869–5876.

13. Miomir B. Vukmirovic, Kurian A. Kuttiyiel, Hui Meng, Radoslav R. Adzic, "Controllable deposition of Pt layers on oxide surfaces for fuel cell catalyst syntheses," ChemElectroChem, submitted.

Presentations

1. S.T. Bliznakov, M.B. Vukmirovic, J. Wegrzyn, and R.R. Adzic, "Semi-Automated System for Electrodeposition of Pt Monolayer Shell on Refractory Metal Core Fuel Cell Electrocatalysts Directly on Gas Diffusion Layer," 228th ECS Meeting, Phoenix, AZ, October 11–15, 2015.

2. Jue Hu, Lijun Wu, Kurian A. Kuttiyiel, Kenneth R. Goodman, Chengxu Zhang, Yimei Zhu, Miomir B. Vukmirovic, Michael G. White, Kotaro Sasaki, Radoslav R. Adzic, "Increasing Stability and Activity of Core-shell Catalysts by Preferential Segregation of Oxide on Edges and Vertexes: Oxygen Reduction on Ti-Au@Pt/C," 229th ECS Meeting, San Diego, CA, May 29–June 3, 2016.

3. K. Sasaki, K.A. Kuttiyiel, D. Su, L. Wu, Y. Zhu, R.R. Adzic, "Gold-promoted structurally ordered intermetallic palladium cobalt nanoparticles for the oxygen reduction reaction," the 66th Annual Meeting of the International Society of Electrochemistry, October 2015, Taipei, Taiwan.

Book Chapters

1. Stoyan Bliznakov, Miomir Vukmirovic, Radoslav Adzic, "Electrochemical Atomic-Level Controlled Syntheses of Electrocatalysts for the Oxygen Reduction Reaction," Atomically-Precise Methods for Synthesis of Solid Catalysts, Sophie Hermans and Thierry Visart de Bocarme (Eds.), RSC Catalysis Series No. 22, The Royal Society of Chemistry, 2015, 144–166.

2. K. Sasaki, N. Marinkovic, "X-ray Absorption Spectroscopic Characterization of Nanomaterial Catalysts in Electrochemistry and Fuel Cells," submitted to the 5th volume of SPRINGER book series on Characterization Tools for Nanoscience & Nanotechnology, submitted.

REFERENCES

1. J. Greeley, I. Stevens, A. Bondarenko, T.P. Johansson, H.A. Hansen, T. Jaramillo, J. Rossmeisl, I. Chrorkendorff, J.K. Nørskov, Nat. Chem., 2009,1, 552–556.

V.A.6 Extended Surface Electrocatalyst Development

Bryan Pivovar (Primary Contact), Shaun Alia, K.C. Neyerlin, Katie Hurst, Jason Zack, Scott Mauger, Frank Caravaglia, Guido Bender, Shyam Kocha
National Renewable Energy Laboratory
15013 Denver West Parkway
Golden, CO 80401
Phone: (303) 275-3809
Email: Bryan.Pivovar@nrel.gov

DOE Manager: David Peterson
Phone: (240) 562-1747
Email: David.Peterson@ee.doe.gov

Subcontractors:
- Yushan Yan (PI), Jarrid Wittkopf, University of Delaware, Newark, DE
- Svitlana Pylypenko, Sarah Shulda, Chilan Ngo, Colorado School of Mines, Golden, CO
- Al Weimer, Will Medlin, Wilson McNeary, University of Colorado, Boulder, CO
- Karen Buechler, Joe Spencer, ALD Nanosolutions, Broomfield, CO

Project Start Date: December 10, 2015
Project End Date: September 30, 2018

Overall Objectives

- Increase mass activity and durability of Pt-based electrocatalysts through the synthesis and implementation of high surface area extended surface electrocatalysts.
- Optimize fuel cell performance of extended surface electrocatalysts.
- Demonstrate DOE 2020 target performance and durability in fuel cell tests.

Fiscal Year (FY) 2016 Objectives

- Using extended surface catalysts prepared by atomic layer deposition (ALD), demonstrate initial mass activity in rotating disc electrode (RDE) >2,200 mA/mg Pt (900 mV internal resistance free) (5X DOE membrane electrode assembly [MEA] target).
- Demonstrate a mass activity of 880 mA mgPt–1 at 0.9 V (2 X DOE 2020 target) and less than a 5% loss after durability testing (30,000 cycles, mass activity) in RDE tests with a total transition metal dissolution of less than 1% of initial catalyst mass.
- Demonstrate a mass activity of >440 mA mgPt–1 at 0.9 V (DOE 2020 target) in fuel cell MEA tests (stretch goal) and demonstrate synthesis of Ni nanostructures with Ni (111) surface-faceted, extended surfaces with aspect ratios >50.

Technical Barriers

This project addresses the following technical barriers from the Fuel Cells section (3.4.4) of the Fuel Cell Technologies Office Multi-Year Research, Development, and Demonstration Plan.

(A) Durability (of catalysts and membrane electrode assemblies)

(B) Cost (of catalysts and membrane electrode assemblies)

(C) Performance (of catalysts and membrane electrode assemblies)

(D) Start-up and Shut-down Time and Energy/Transient Operation

Technical Targets

This project synthesizes novel extended thin film electrocatalyst structures (ETFECS) and incorporates these catalysts into electrodes with and without carbon blacks for further study. The project has targets outlined in the Multi-Year Research, Development, and Demonstration Plan for both electrocatalysts for transportation applications (Table 3.4.13) and MEAs (Table 3.4.14). The specific targets and status of highest relevance are presented in Table 1.

TABLE 1. Technical Targets for Electrocatalysts for Transportation Applications

Characteristic	Units	2017/2020 Targets	Status
Mass Activity (150,000 Pa H_2/O_2 80°C 100% RH)	A/mg-Pt @ 900 mV	0.44/0.44	0.15
Electro Catalyst Support Stability	% mass activity loss	<10/<10	TBD
Loss in Initial Catalytic Activity	% mass activity loss	<40/<40	TBD

TBD – To be determined; RH – Relative humidity

FY 2016 Accomplishments

- The project has demonstrated the ability to deposit both Pt and Ni by ALD onto extended surface nanostructures.
- Surface areas of 90 m^2/g Pt and specific activities of 8 mA/cm^2 Pt (0.9 V infrared free) have been reached

although not in the same sample, mass activity Pt of 2,400 mA/mg Pt has been demonstrated (in RDE).

- ETFECS materials have been incorporated into MEAs showing greatly improved performance with acid leaching.
- Diagnostic studies including limiting current and impedance have been applied to elucidate performance losses and optimized structures.

✧ ✧ ✧ ✧ ✧

INTRODUCTION

Conventional nanoparticle Pt/C electrocatalysts (2–5 nm) used in automotive fuel cells appear to have plateaued in terms of electrochemical area and catalytic activity. ETFECS offer the possibility of higher specific activities, comparable to that of bulk poly-Pt. ETFECS materials formed by galvanic displacement have shown promising performance and durability in RDE tests, but have shown limitations in compositional control, reproducibility and batch size (scale-up). We are focusing on Pt and Ni ALD in order to address the limitations found with galvanic displacement. The materials are then explored for optimum electrode structures through cell diagnostics that isolate and target mitigation strategies for loss mechanisms.

APPROACH

Our overall approach is towards developing extended surface Pt catalysts synthesized by ALD with high mass activity and durability and incorporating these structures into robust, high efficiency MEAs. This approach focuses on the synthesis of novel ETFECS formed by ALD, specifically with the co-deposition of Ni and Pt. We are targeting high surface areas as this has been a specific challenge for extended surface Pt catalysts (3M [1], others [2]). Our multi-tiered approach involves the synthesis of novel template nanostructures, the synthesis and characterization of ALD synthesized ETFECS, and the optimization of these materials in fuel cells.

RESULTS

In the area of novel template nanostructure development we have been delayed due to contracting issues, but the University of Delaware has demonstrated Ni nanoflowers and we have begun working with our Ni nanowire supplier to impact upstream processing, as we have found that the properties of the supplied nanowires have varied greatly over time as highlighted in Table 2 below.

TABLE 2. Ni Nanowire Properties

Ni Nanowire Batch Size and Date Received	Fe Content (at%)	Surface Area (m^2/g)	Maximum Pt ECA (m^2/g)
1 g (2014)	0.4	6.1	~90
50 g (2015)	0.8	2.0	~50
100 g (2016)	0.5	1.1	TBD

ECA – Electrochemical surface area

The application of Ni and Pt ALD onto nanostructures as a novel synthesis technique has been the primary focus of our efforts to date. We have demonstrated the ability to deposit both Pt and Ni onto samples using hydrogen chemistry based ALD. Figure 1 shows high resolution microscopy and elemental mapping of Pt and Ni deposited onto Ni nanowires. While ALD was targeted for ability to go to larger batch sizes, improve sample homogeneity, and independently control Pt and Ni deposition, ALD turned out to have greater heterogeneity compared to spontaneous galvanic displacement (SGD). Figure 2 shows the relative deviation between six digestions for Pt composition. This data shows that SGD is much more homogeneous relative to ALD (for both oxygen and hydrogen based ALD routes). Still, we were able to demonstrate exceptionally high site specific activity (is) above 8,000 $\mu A/cm^2$ Pt and a mass activity of

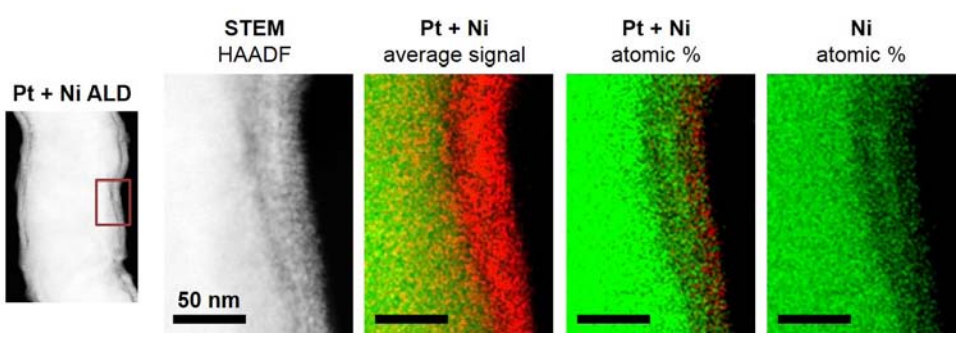

STEM – Scanning transmission electron microscopy; HAADF – High-angle annular dark-field

FIGURE 1. High resolution microscopy and elemental mapping of Ni nanowires following deposition of Pt and Ni by ALD

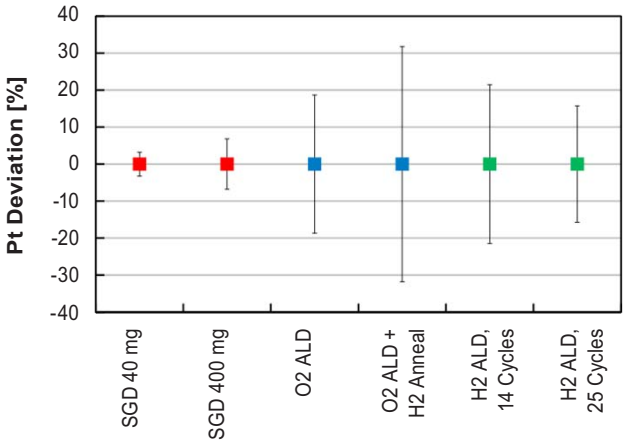

FIGURE 2. Standard deviation of six separate inductively coupled plasma mass spectrometry measurements of Pt composition for various synthesis routes of ETFECS including SGD, oxygen-based (O2) and hydrogen-based (H2) ALD

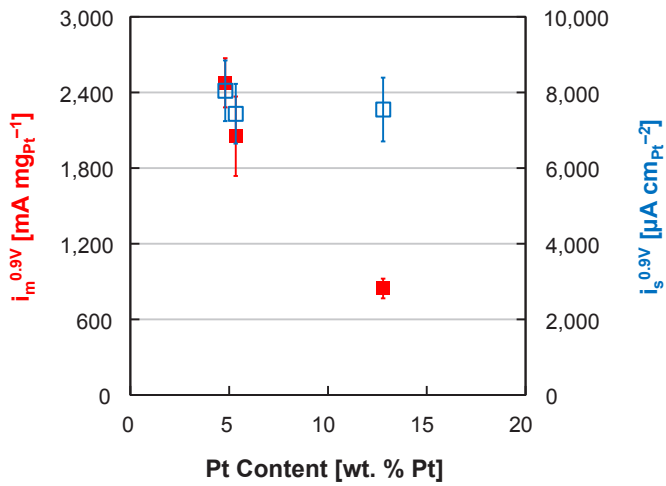

FIGURE 3. Site specific (i_s) and mass (i_m) activity for ALD synthesized PtNi nanowires as a function of Pt deposition

>2,400 mA/mg Pt (~5 X the DOE 2020 MEA target when characterized by RDE, as shown in Figure 3.)

We have also made significant efforts into incorporating the novel electrocatalysts synthesized within the project and optimizing performance in fuel cells. The high transition metal content of the as synthesized materials creates Ni dissolution concerns that we are investigating through acid pre-leaching. Fuel cell results with current materials are shown in Figure 4 as a function of acid washing. This data shows that Ni contamination is a critical limitation for unwashed MEAs with performance improving significantly with subsequent acid washing steps. We have also begun to perform advanced diagnostics on these MEAs to better understand optimized electrode structures.

Specifically, we have performed impedance measurements that have shown high proton conductivity is maintained in these systems at ionomer contents down to 10 wt%. Our impedance studies suggest that even at these low ionomer contents we still exhibit limitations in limiting current. These results suggest we should be targeting even lower ionomer contents than those investigated to date (10–30 wt%).

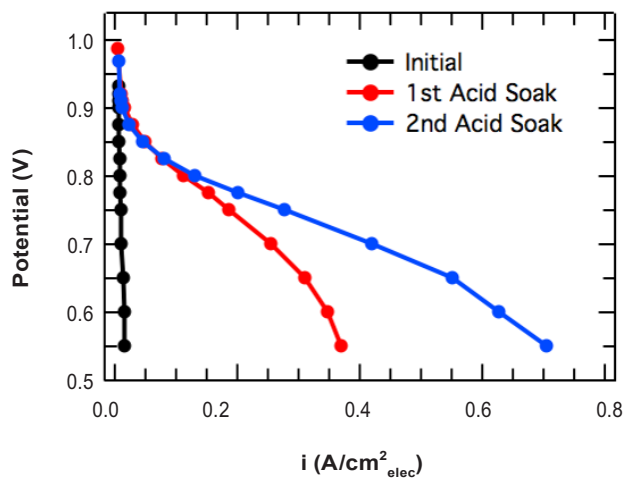

FIGURE 4. Fuel cell polarization curves of PtNiWs as a function of acid washing steps to remove Ni contamination from the MEA

CONCLUSIONS AND FUTURE DIRECTIONS

The project has demonstrated the ability to deposit both Pt and Ni by ALD onto extended surface nanostructures. Surface areas of 90 m^2/g Pt and specific activities of 8 mA/cm^2 Pt (0.9 V internal resistance free) have been reached although not in the same sample; mass activity of 2,400 mA/mg Pt has been demonstrated. ETFECS materials have been incorporated into MEAs showing greatly improved performance with acid leaching. Diagnostic studies including limiting current and impedance have been applied to elucidate performance losses and optimized structures. Future work includes:

- Nanotemplate synthesis:
  - Develop routes to novel Ni nanostructures and demonstrate at useful scale. Focus on clean, well shape controlled nanowires and nanoflowers.
- Electrocatalyst synthesis:
  - ALD-controlled co-deposition of Pt/Ni onto nanotemplates.
  - Post-processing optimization of resultant catalysts (annealing and acid leaching).
  - Characterization and optimization (electrochemical and structural studies).

- Electrode structure and fuel cell studies:
  - Optimization of electrode structure and performance (including electrospinning and spraying and incorporation of different geometry carbons).
  - Isolation and minimization of overpotential losses in MEA electrodes (separation of mass transfer, ohmic, and kinetic losses).
  - Durability studies to quantify and minimize performance losses.

FY 2016 PUBLICATIONS/PRESENTATIONS

1. Kazuma Shinozaki, Jason W. Zack, Svitlana Pylypenko, Bryan S. Pivovar, and Shyam S. Kocha, "Oxygen Reduction Reaction Measurements on Platinum Electrocatalysts Utilizing Rotating Disk Electrode Technique: II. Influence of Ink Formulation, Catalyst Layer Uniformity and Thickness Fuel Cells, Electrolyzers, and Energy Conversion," J. Electrochem. Soc. 2015 162(12): F1384–F1396. doi:10.1149/2.0551512jes.

2. Shaun M. Alia, Svitlana Pylypenko, K.C. Neyerlin, Shyam S. Kocha, and Bryan S. Pivovar, "Platinum Nickel Nanowires as Methanol Oxidation Electrocatalysts Fuel Cells, Electrolyzers, and Energy Conversion," J. Electrochem. Soc. 2015 162(12): F1299–F1304. doi:10.1149/2.0231512jes.

3. Shinozaki, K.; Zack, J.W.; Richards, R.; Pivovar, B.S.; Kocha, S.S.; "Oxygen Reduction Reaction Measurements on Platinum Electrocatalysts Utilizing Rotating Disk Electrode Technique," J. Electrochem. Soc., 162 (10), F1144–F1158, 2015. DOI: 10.1149/2.1071509jes.

4. Chlistunoff, J. and Pivovar, B., "Effects of Ionomer Morphology on Oxygen Reduction on Pt," J. Electrochem. Soc., 162(8), F890–900, 2015. DOI: 10.1149/2.0661508jes.

5. Shaun M. Alia, Svitlana Pylypenko, K.C. Neyerlin, Shyam S. Kocha, and Bryan S. Pivovar, "Nickel Nanowire Oxidation and Its Effect on Platinum Galvanic Displacement and Methanol Oxidation," ECS Trans. 2014 64(3): 89–95; doi:10.1149/06403.0089ecst.

6. Pivovar, B. (Feb, 2016). "An Overview of Fuel Cell R&D at the National Renewable Energy Lab (NREL)," Michigan State University, February 18, 2016.

REFERENCES

1. http://www.hydrogen.energy.gov/pdfs/review08/fc_1_debe.pdf.

2. Z. Chen, W. Li, M. Waje, Y.S. Yan, *Angew. Chem. Int. Ed.* 2007, 46:4060–4063.

V.A.7 Highly Active, Durable, and Ultra-low PGM NSTF Thin Film ORR Catalysts and Supports

Andrew Steinbach (Primary Contact), Amy Hester, Sean Luopa, Cemal Duru, Andrew Haug, John Abulu, Monika Kuznia, and Isaac Davy
3M Company, Energy Components Program
3M Center, Building 201-2N-19
St. Paul, MN 55144-1000
Phone: (651) 737-0103
Email: ajsteinbach2@mmm.com

DOE Manager: David Peterson
Phone: (240) 562-1747
Email: David.Peterson@ee.doe.gov

Technical Advisor: Thomas Benjamin
Phone: (630) 252-1632
Email: benjamin@anl.gov

Contract Number: DE-EE0007270

Subcontractors
- J. Erlebacher, Johns Hopkins University, Baltimore, MD
- J. Greeley, Purdue University, West LaFayette, IN
- D. Cullen, Oak Ridge National Laboratory Oak Ridge, TN
- D. Myers and J. Kropf, Argonne National Laboratory Lemont, IL

Project Start Date: January 1, 2016
Project End Date: March 31, 2019

Overall Objectives

The overall objective is development of improved thin film oxygen reduction reaction (ORR) catalysts on nanostructured thin film (NSTF) supports which achieve:

- Mass activity of 0.80 A/mg_{PGM} or higher
- Platinum group metal (PGM) total content (both electrodes) of ≤0.1 g/kW @ 0.70 V
- PGM total loading (both electrodes) <0.1 mg_{PGM}/cm^2
- Mass activity durability of <20% loss
- Loss of performance <20 mV @ 0.8 and 1.5 A/cm^2.

Fiscal Year (FY) 2016 Objectives

- Initiate project at 3M and partner organizations.
- Develop new ultra-thin film (UTF) and nanoporous thin film (NPTF) electrocatalysts, towards achievement of first year project targets.
- Employ advanced composition and structural analysis to guide electrocatalyst development, including transmission electron microscopy, energy dispersive X-ray spectroscopy (EDS), and X-ray adsorption spectroscopy (XAFS).
- Initiate density functional theory (DFT) and kinetic Monte Carlo (kMC) model refinement efforts, towards enabling predictive capability of novel electrocatalyst concepts.
- Develop and validate high throughput electrocatalyst fabrication and characterization methods, towards acceleration of project electrocatalyst development.

Technical Barriers

This project addresses the following technical barriers from the Fuel Cells section of the Fuel Cell Technologies Office Multi-Year Research, Development, and Demonstration Plan.

(A) Durability

(B) Cost

(C) Performance

Technical Targets

Table 1 summarizes 2016 project status against the relevant 2020 DOE targets and 2019 project targets. All reported status values are measurements made in membrane electrode assembly (MEA) format. PGM total content and PGM total loading are reported for two MEAs, the project baseline and an MEA with an improved durability "NPTF+M" cathode catalyst. The two MEAs, evaluated in Best of Class format (including a cathode interlayer for operational robustness), achieved 0.16 g/kW (at 0.70 V) with PGM total loading of 0.105 mg_{PGM}/cm^2 and 0.18 g/kW (at 0.70 V) with 0.127 mg_{PGM}/cm^2, respectively. Durability status is assessed with a NPTF PtNi+"M" cathode catalyst containing 0.109 mg_{PGM}/cm^2, which achieved 42% loss in mass activity after the DOE electrocatalyst accelerated stress test (AST) and performance at 0.8 A/cm^2 and 1.5 A/cm^2 increased by 8 mV and 68 mV, respectively. Beginning of life mass activity status is reported for three electrocatalysts, ranging from 0.28 A/mg_{PGM} for NPTF PtNi+M, 0.39 A/mg_{PGM} for UTF "A", and 0.47 A/mg_{PGM} for baseline NPTF PtNi.

FY 2016 Accomplishments

- Initiated development of first UTF electrocatalyst series ("A"), including composition and fabrication processing optimization. Best UTF "A" electrocatalyst mass

TABLE 1. Status Against Technical Targets

Characteristic	2020 Target and Units	Project Target	2016 Status
PGM total content (both electrodes)	0.125 g/kW	0.1 (0.70 V)	0.16[1] 0.18[2]
PGM total loading (both electrodes)	0.125 mg/cm^2	0.10	0.105[1] 0.127[2]
Loss in catalytic (mass) activity	40%	20	42[3]
Loss in performance at 0.8 A/cm^2	30 mV	20	-8[3]
Loss in performance at 1.5 A/cm^2	30 mV	20	-68[3]
Mass activity @ 900 mV$_{iR\text{-}free}$	0.44 A/mg (MEA)	0.80	0.28[3] (NPTF "M") 0.47[4] (NPTF) 0.39[5] (UTF)

[1]0.015 mg$_{Pt}$/cm^2 NSTF anode, 0.075 dealloyed PtNi/NSTF cathode, 0.015 mg$_{Pt}$/cm^2 cathode interlayer.
[2]0.02 mg$_{Pt}$/cm^2 NSTF anode, 0.091 mg$_{PGM}$/cm^2 NPTF "M" cathode, 0.016 mg$_{Pt}$/cm^2 cathode interlayer.
[3]NPTF "M" cathode, 0.109 mg$_{PGM}$/cm^2 after 30,000 electrocatalyst AST cycles.
[4]Annealed NPTF P4A Pt_3Ni_7/NSTF, 0.12 mg$_{Pt}$/cm^2; adjusted from 0.900 V$_{MEAS}$ (70 mV/dec)
[5]Best UTF "A", 0.027 mg$_{PGM}$/cm^2. Average of two MEAs.
"Best of Class" refers to the currently-determined optimal combination of components.

activity of 0.39 A/mg$_{PGM}$ approaches DOE 2020 target (0.44 A/mg) in MEA format, and is 3.9X higher than UTF baseline Pt/NSTF. Significant correlations were identified between electrocatalyst activity, composition, and structure.

- Optimized integration of durability additive "M" into NPTF PtNi/NSTF. Best to-date PtNi+"M" NPTF electrocatalyst loses 42% mass activity after 30,000 electrocatalyst AST cycles (vs. 40% target), and H_2/air performance at 0.8 A/cm^2 and 1.5 A/cm^2 improved by 8 mV and 68 mV, respectively (vs. 30 mV loss target). When integrated into best of class format, resultant MEA achieves 0.18 g/kW at 0.70 V.
- Initiated DFT and kMC model refinement with baseline project electrocatalysts. DFT has determined trends in electrocatalyst activity and surface structure stability induced by bulk and near-surface composition variations. kMC model refinement has focused on incorporation of relevant physics for dealloying via potential cycling, and preliminary predictions of composition evolution with dealloying agree in trend with experiment.
- Method development for high throughput (HT) electrocatalyst fabrication, physical characterization, and electrochemical characterization has been initiated. HT fabrication and physical characterization methods are reproducible and validated.

✧ ✧ ✧ ✧ ✧

INTRODUCTION

State-of-the-art proton exchange membrane fuel cell MEAs utilized in today's prototype automotive traction fuel cell systems continue to suffer from key technical and economical limitations of high cost, insufficient durability, and low robustness to off-nominal operating conditions. State-of-the-art MEAs based on conventional carbon-supported Pt nanoparticle catalysts currently incorporate precious metal loadings which are significantly above those needed to achieve MEA cost targets; performance, durability, and/or robustness decrease significantly as loadings are reduced.

This project focuses on development of novel thin-film electrocatalysts based on 3M's NSTF catalyst technology platform. NSTF electrocatalysts and electrodes are a unique approach towards addressing key technical commercialization challenges. The thin film electrocatalyst structure imparts substantially higher ORR specific and mass activities (4.7 mA/cm$^2_{Pt}$ and 0.8 A/mg$_{PGM}$ in rotating disk electrode, 2.5 mA/cm$^2_{Pt}$ and 0.47 A/mg$_{PGM}$ in MEA) [1] and high resistance to electrocatalyst dissolution and sintering induced by electrochemical cycling [2]. The NSTF support is based on an oriented, sub-micron scale crystalline organic pigment whisker, not carbon nanoparticles, which enables exceptional resistance to corrosion in fuel cell and water electrolysis applications [3]. NSTF electrodes, which are a single layer of NSTF electrocatalyst particles partially embedded into an ion-conducting membrane, are ultrathin (<1 µm) and do not require ionomer for proton conduction [4]. When integrated into state-of-the-art, operationally robust MEAs, this electrode structure enables high absolute and specific power densities (0.89 W/cm^2 and 6.8 kW/g at 0.692 V cell voltage) at ultra-low MEA PGM loadings (0.13 mg$_{PGM}$/cm^2 total) [5].

APPROACH

The project approach is to establish relationships between electrocatalyst functional response (activity,

durability), physical properties (bulk and surface structure and composition), and fabrication processes (deposition, annealing, dealloying) via systematic investigation. Electrocatalysts will be generated in one of two distinct morphologies, NPTF and UTF, each with distinct pathways towards achieving project targets. Additionally, this project utilizes high throughput material fabrication and characterization, electrocatalyst modeling, and advanced physical characterization to guide and accelerate development.

RESULTS

Since project initiation in January 2016, significant progress has been made towards development of new, improved electrocatalysts with target activity, durability, and cost. This work has included development of new electrocatalyst compositions, fabrication process optimization, electrochemical and physical characterization, and modeling.

UTF development has focused on optimization of a single Pt alloy system, termed UTF "A". Optimization work has included studies to evaluate the influence of composition and annealing. Figure 1 summarizes key initial findings relating mass and specific activities, measured in MEA, to electrocatalyst composition and structure. Unannealed and annealed electrocatalysts were initially evaluated in fuel cell for mass and specific activity in MEA, with areal PGM loadings of 28±2 $\mu g_{PGM}/cm^2$, substantially below the DOE 2020 target. Tested catalysts were then evaluated for atomic-scale structure by Z-contrast scanning transmission electron microscopy (STEM) imaging and bulk composition by EDS at Oak Ridge National Laboratory and for Pt-Pt bond lengths by XAFS at Argonne National Laboratory. Figure 1A shows that as the Pt mole fraction decreased, mass activity generally increased for both unannealed and annealed UTF "A". Annealing was especially beneficial for relatively lower Pt fractions, achieving 0.29 A/mg at the minimum Pt mole fraction evaluated.

Figure 1B and Figure 1C compares the influence of annealing on the resultant electrocatalyst structure after fuel cell testing at a single initial composition. The annealed, tested catalyst's structure (Figure 1C) is largely similar to the unannealed, tested catalyst (Figure 1B), but the annealed catalyst's surface appears moderately smoother, suggestive of larger surface facets. Figure 1D shows that the specific

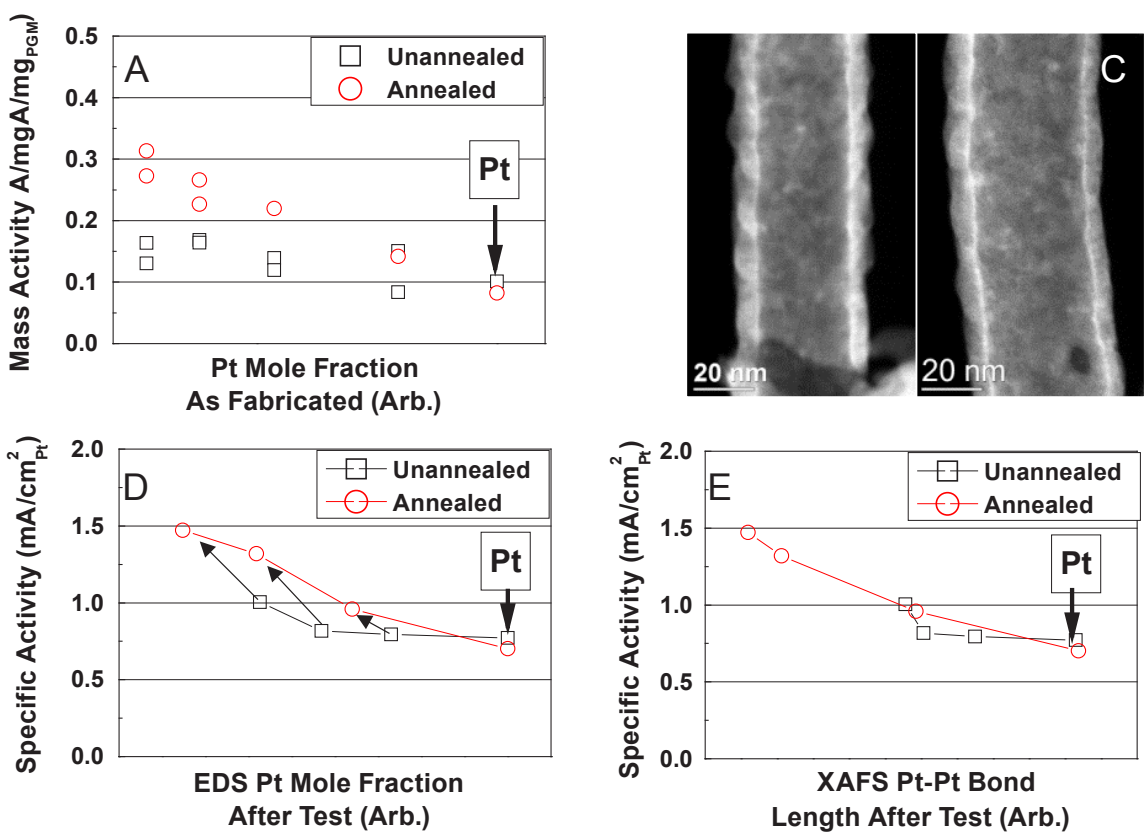

FIGURE 1. (A) Influence of composition and annealing on UTF "A" mass activity. (B, C) Z-contrast STEM of tested unannealed and annealed catalysts, respectively. (D, E) Specific activity dependencies on Pt mole fraction (EDS) and Pt-Pt bond distances (XAFS), determined after fuel cell testing.

activity increases monotonically as the EDS-determined Pt mole fraction in the tested electrocatalyst decreases, and annealed electrocatalysts have higher specific activity than unannealed at a given Pt mole fraction. Figure 1E suggests that the specific activity differences between annealed and unannealed catalysts with varying initial Pt mole fractions may be rationalized by the Pt-Pt bond distance in the catalyst after evaluation, as determined by XAFS.

One UTF "A" composition from the preceding series was annealed at a variety of conditions and evaluated for mass activity in MEA (Figure 2). All annealed UTF "A" catalysts achieved higher mass activity than unannealed, and mass activity decreased with increased annealing extent. The average mass activity of UTF "A" at the optimal annealing conditions was 0.39 A/mg, 3.9X higher than Pt. Further annealing optimization is in progress.

We have previously reported that one NPTF alloy system, PtNi, is insufficiently stable to achieve the DOE durability targets when evaluated under the electrocatalyst AST. [6] In pre-project work, we have identified that incorporation of durability additive "M" into the PtNi electrocatalyst greatly improved the durability, but MEA H_2/Air performance was suppressed as compared to the "M"-free catalyst. Initial NPTF development in this project has focused on optimization of "M" integration for improved durability and performance. To date, four different "M" integration methods have been evaluated for beginning of life mass activity and performance with dealloyed PtNi catalyst, with PGM contents ranging from ca. 0.09–0.11 mg_{PGM}/cm^2. For each integration method, several method-dependent integration variables have also been evaluated. Figure 3A and 3B show that beginning of life mass activity and H_2/air performance depend strongly on the integration method (A–D) and integration method variables (0–20). Methods "C" and "D" yielded the overall highest beginning of life mass activity, achieving as high as 0.30 A/mg_{PGM}, but

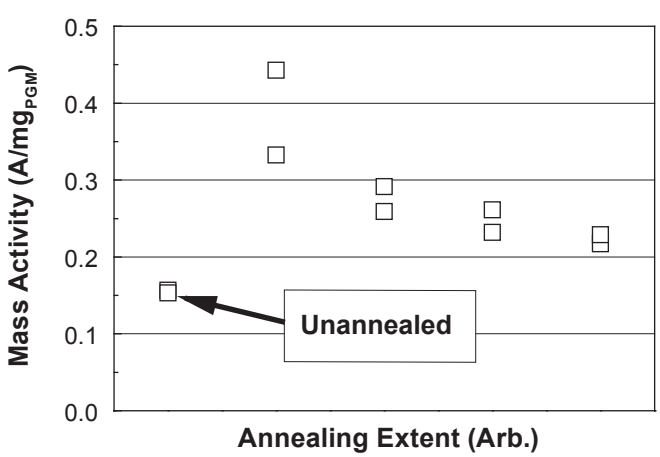

FIGURE 2. Mass activity sensitivity vs. annealing extent for single UTF "A" composition

Method "D" yielded appreciably higher H_2/air performance at 1 A/cm^2. Series "D" samples, with varying "M" content, were evaluated under the DOE electrocatalyst AST; changes in mass activity and H_2/air performance are summarized in Figure 3C. Without "M" (Level 0), mass activity loss was 70% and H_2/Air loss at 1 A/cm^2 was 44 mV after the AST. With level 5 "M" content, mass activity loss after the AST was reduced to 42% and H_2/air performance at 1 A/cm^2 increased by 7 mV. NPTF PtNi "M" catalysts can also generate high rated power performance when integrated with improved MEA components. Figure 3D summarizes H_2/air performance at 90°C cell temperature vs. reactant pressures for Series "A", Level 5 NPTF PtNi+"M" cathode catalyst, in best of class MEA format, including a cathode interlayer for operational robustness. [5] At 0.70 V, specific power values of 5.3 kW/g, 6.3 kW/g, and 7.0 kW/g are obtained at 1.5 atmA, 2.0 atmA, and 2.5 atmA reactant pressures.

As indicated in the preceding sections, ultimate electrocatalyst performance and durability depend strongly upon composition and fabrication parameters, including electrocatalyst deposition method, annealing method, and dealloying method. These parameters in combination represent a large, time-consuming variable space to simultaneously optimize, and HT electrocatalyst development can result in substantial acceleration. Method development for HT electrocatalyst fabrication, physical characterization, and electrochemical characterization by segmented fuel cell has been initiated. To date, HT electrocatalyst fabrication consists of physical vapor deposition of Pt and another alloying element where the other element deposition rate varies monotonically across the NSTF substrate. Figure 4 (left) summarizes loading and composition analysis of three replicate gradient binary alloy electrocatalysts fabricated with identical conditions. Composition analysis consisted of scanning X-ray fluorescence with 1 mm spatial resolution. The relative standard deviation for Pt loading vs. position was on average 3.4% (maximum 11%) and for Pt mole fraction was on average 2.6% (maximum 6.5%), both exceeding expectations and the project milestone. Figure 4 (right) summarizes HT electrocatalyst structural characterization by wide angle X-ray scattering (WAXS), conducted at Argonne National Laboratory. WAXS spectra were analyzed to determine the FCC lattice constant and (111) grain size. The WAXS-determined lattice constants agreed well with expectation, decreasing with decreasing Pt mole fraction and were generally similar to Vegard's law predictions. (111) grain sizes were constant with Pt mole fraction, also consistent with expectation.

A new kMC simulation package has been developed that incorporates oxidation and reduction cycles, surface diffusion, and electrochemical dealloying. The physical features incorporated into this code include (a) potential-dependent dissolution of a first base metal, (b) potential-dependent oxidation or reduction of all surface species, and

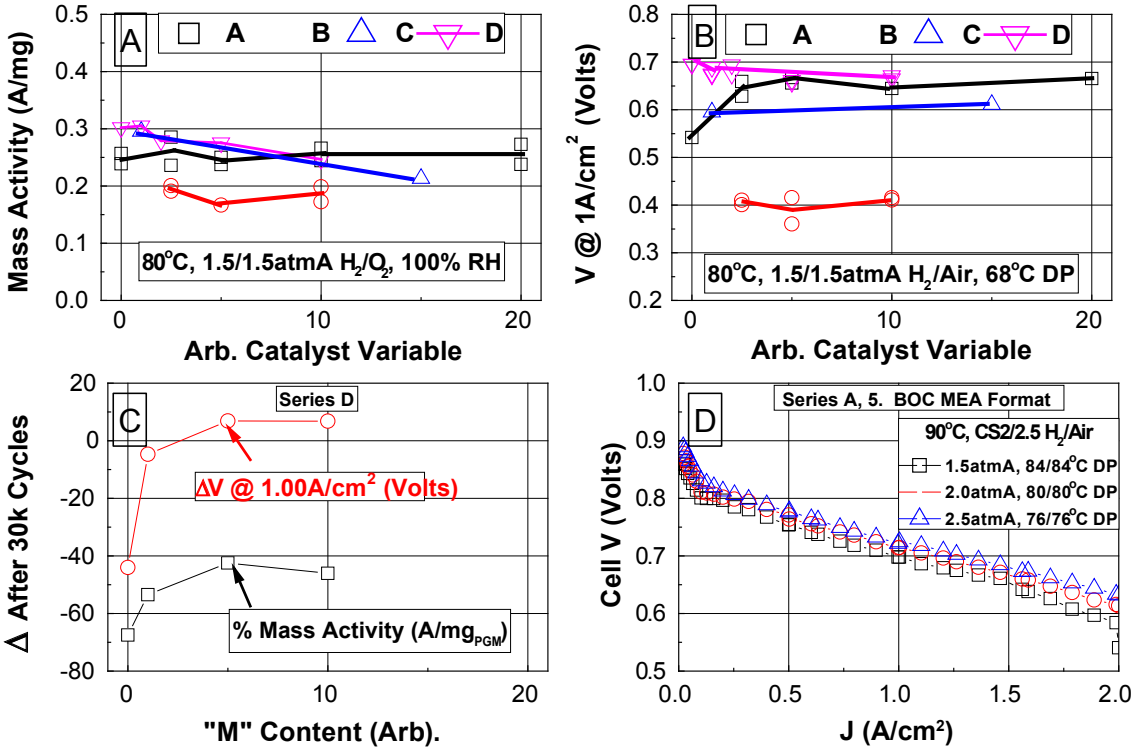

RH – Relative humidity

FIGURE 3. NPTF PtNi "M" integration. Top row: Beginning of life mass activity (A) and H_2/air performance (B) vs. "M" integration method (A–D) and integration variable (0–20). (C) Mass activity and H_2/air performance change after 30,000 DOE electrocatalyst AST cycles. (D) PtNi+M in best of class MEA format, with 0.13 mg_{PGM}/cm^2 total loading.

(c) surface diffusion of all surface species. The code is being optimized so that input parameters lead to behavior that is approximately similar to the behavior of real Pt alloys. Figure 5 compares compositional evolution of experimental NSTF catalyst to preliminary representative output of the package versus the number of oxidation/reduction cycles. Composition evolution with cycling is similarly sigmoidal for both the simulation and experiment data, and final average composition agrees reasonably. It is relevant, and perhaps surprising, that even after 100 cycles and the development of full porosity, there is still significant residual base metal on the surface of the simulated material.

To complement our efforts in experimental electrochemical reactivity measurements, characterization, and kMC modeling, we have begun a program of detailed DFT modeling to predict the atomic-scale structures, stability, and ORR reactivity of UTF "A" alloy surfaces under electrochemical conditions. The alloys are modeled with periodic boundary conditions, and smooth surfaces, which have been found to be most active for ORR, are considered (Figure 6). To estimate the stability of the surfaces with Pt skins, we calculate the average surface stress for different Pt mole fractions and for different thicknesses of platinum skins. Surfaces with low stress values are identified, and these surfaces are considered for additional analysis of ORR activity. The ORR rate estimates, in turn, are plotted as a function of the amount of strain in the surface platinum layers. Alloys with Pt skins thicknesses of approximately three layers are found to be very active for the ORR, while thicker or thinner skins show modestly reduced activity. These predictions are currently being calibrated against the experimental results on ultrathin films that we have recently measured and will provide a target for future synthesis efforts in our program. In addition, the structural models of the alloy surfaces will be refined using the results of detailed kMC simulations, which can provide dynamical information about catalyst structures under reaction conditions.

CONCLUSIONS AND FUTURE DIRECTIONS

New NSTF electrocatalysts have been developed which are approaching several DOE 2020 targets based on two electrocatalyst morphologies: ultra-thin film and nanoporous thin films. UTF "A" electrocatalysts have demonstrated mass activity as high as 0.39 A/mg, 3.9X higher than the pure Pt/NSTF baseline. Analysis of UTF "A" electrocatalysts by STEM+EDS and XAFS reveal dependencies of catalyst activity on compositional and structural parameters.

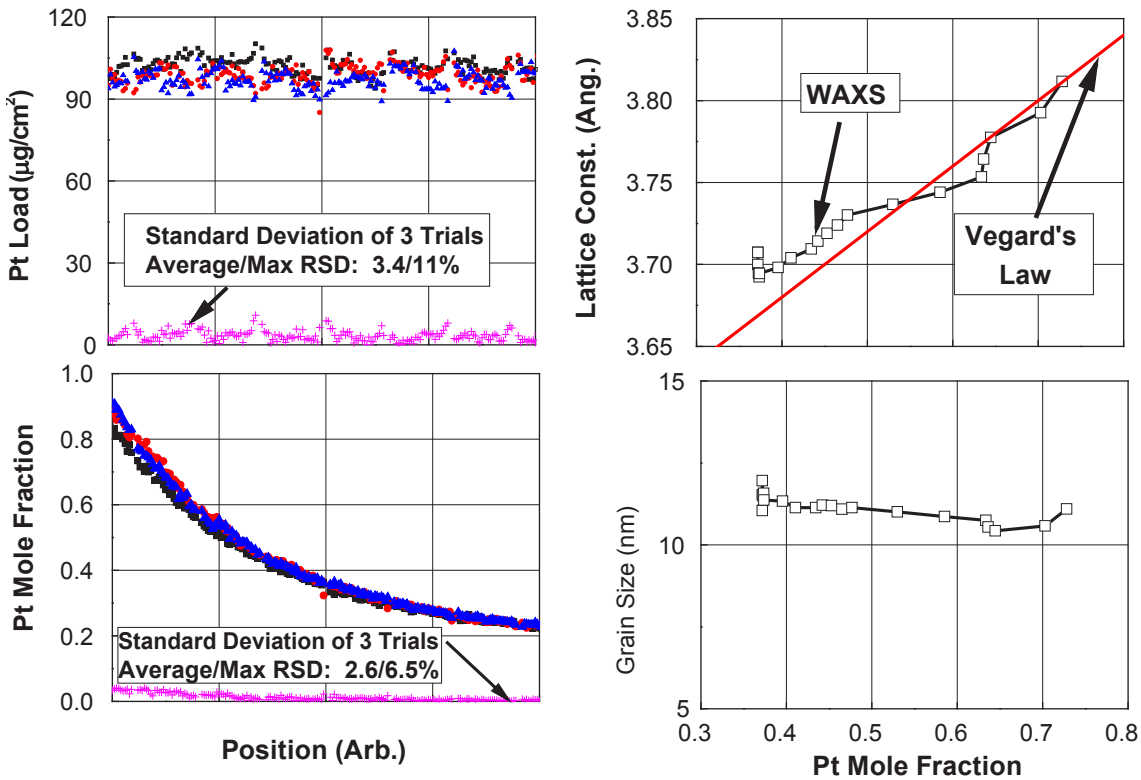

FIGURE 4. HT electrocatalyst composition (left) and WAXS structural characterization (right) for gradient composition electrocatalysts

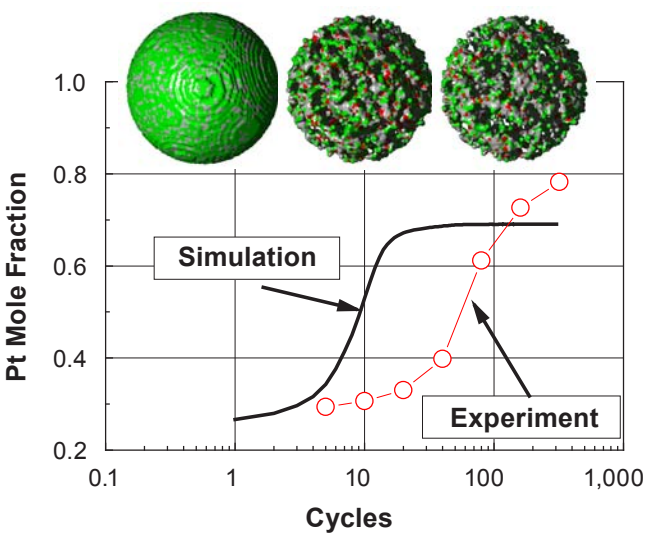

FIGURE 5. Comparison of composition evolution of experimental NSTF catalyst to simulated average composition of a ~20 nm Pt binary alloy sphere as a function of oxidation/reduction cycle number. (Silver) Pt; (red) oxidized Pt; (green) alloying element.

NPTF PtNi+"M" electrocatalyst optimization has resulted in improving mass activity and H_2/air performance, and durability has approached DOE 2020 targets. DFT modeling has provided insight into the influence of electrocatalyst subsurface composition and Pt skin thickness on electrocatalyst activity and stability of a first Pt alloy. kMC modeling of a first Pt binary alloy has predicted evolution of NPTF composition evolution during dealloying, with reasonable agreement with experimental results. Methods for HT electrocatalyst fabrication and composition and structure characterization have been validated.

In future work, the project will fabricate and characterize several new NPTF and UTF electrocatalysts to establish functional relationships between electrocatalyst composition, physical properties, fabrication process parameters, and functional response. HT electrocatalyst processing and electrochemical characterization methods will be developed, validated, and utilized when available to accelerate development. kMC and DFT models will be refined to capture experimentally-observed trends for baseline NPTF and UTF catalysts, which will enable predictive capability for new electrocatalyst concepts. Highly durable PtNi+"M" electrocatalysts will continue to be refined for further improved mass activity and H_2/air performance. Finally, project electrocatalysts will be incorporated into advanced NSTF electrodes and evaluated for performance, operational robustness, and durability.

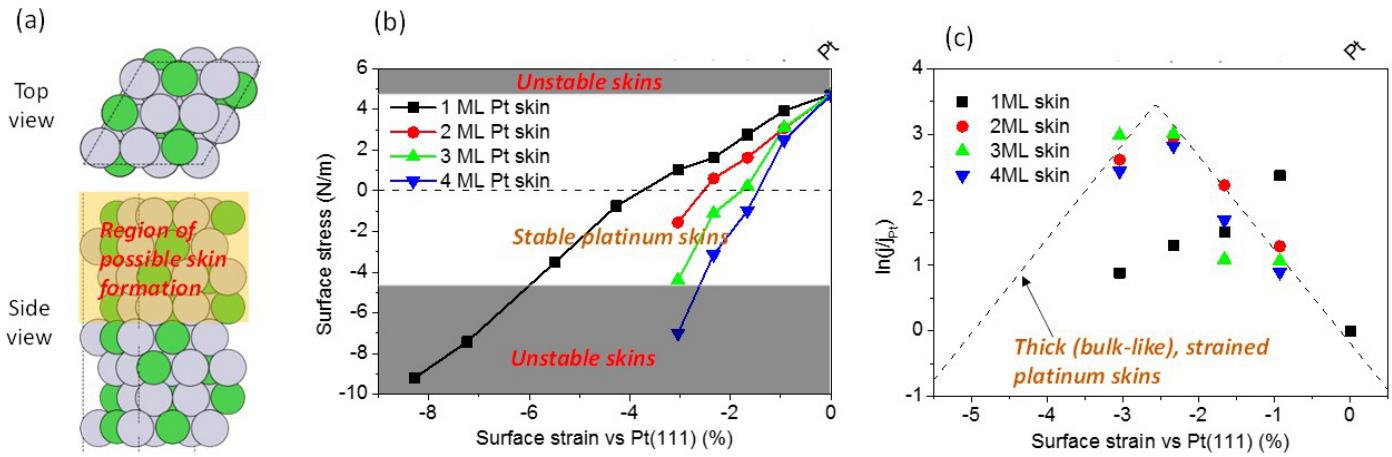

FIGURE 6. DFT predictions of stability and activity for platinum skins. (a) Schematic of Pt alloy structures, with highlighted region where formation of pure platinum skins is considered. (b) Stability map for pseudomorphic platinum skins on Pt alloy substrates. Skins with large positive or negative surface stresses are likely to be unstable. (c) Predicted oxygen reduction activities for platinum skins on Pt alloy substrates. Active skins are predicted to have approximately 3 ML of platinum. Predictions for very thick platinum skins are shown with the dashed line.

FY 2016 PUBLICATIONS/PRESENTATIONS

1. A.J. Steinbach, Presentation FC143, 2016 U.S. Department of Energy Hydrogen and Fuel Cells Program Annual Merit Review, June 2016, Washington, D.C.

2. A.J. Steinbach, "Highly Active, Durable, and Ultra-low PGM NSTF Thin Film ORR Catalysts and Supports," Presentation to DOE Catalyst Working Group, July 27, 2016.

3. A.J. Steinbach, "Highly Active, Durable, and Ultra-low PGM NSTF Thin Film ORR Catalysts and Supports," Presentation to USCAR Fuel Cell Tech Team, August 17, 2016.

REFERENCES

1. A.J. Steinbach et al., "Recent Progress in Nanostructured Thin Film (NSTF) ORR Electrocatalyst Development for PEM Fuel Cells," *ECS Trans.* **69**(17) 291–301 (2015).

2. M.K. Debe et al., "Stop-Start and High-Current Durability Testing of Nanostructured Thin Film Catalysts for PEM Fuel Cells," *ECS Trans.* **3**(1) 835–853 (2006).

3. M.K. Debe et al., "Initial Performance and Durability of Ultra-Low Loaded NSTF Electrodes for PEM Electrolyzers," *J. Electrochem. Soc.* **159**(6) K165–K176 (2012).

4. M.K. Debe, "Tutorial on the Fundamental Characteristics and Practical Properties of Nanostructured Thin Film (NSTF) Catalysts," *J. Electrochem. Soc.* **160**(6) F522–F534 (2013).

5. A.J. Steinbach, Presentation FC104, 2016 U.S. Department of Energy Hydrogen and Fuel Cells Program Annual Merit Review, June 2016, Washington, D.C.

6. D.A. Cullen et al., "Linking morphology with activity through the lifetime of pretreated PtNi nanostructured thin film catalysts," *J. Mater. Chem. A*, **3** 11660–11667 (2015).

V.A.8 Highly-Accessible Catalysts for Durable High-Power Performance

Anusorn Kongkanand
General Motors Company
850 Glenwood Ave.
Pontiac, MI 48340-2920
Phone: (585) 953-5538
Email: anusorn.kongkanand@gm.com

DOE Manager: Gregory Kleen
Phone: (240) 562-1672
Email: Gregory.Kleen@ee.doe.gov

Contract Number: DE-EE0007271

Subcontractors
- Andrew Haug, 3M Company, St. Paul, MN
- Joshua Snyder, Drexel University, Philadelphia, PA
- David Muller and Héctor Abruña, Cornell University, Ithaca, NY
- Shawn Litster, Carnegie Mellon University, Pittsburgh, PA
- K.C. Neyerlin, National Renewable Energy Lab, Golden, CO

Project Start Date: April 1, 2016
Project End Date: June 30, 2019

Overall Objectives

- Reduce overall stack cost by improving high-current-density (HCD) performance in H_2–air fuel cells adequate to meet DOE heat rejection and Pt-loading targets.
- Maintain high kinetic mass activities.
- Mitigate catalyst degradation by using supports with more corrosion resistance than the current high-surface-area carbon (HSC).

Fiscal Year (FY) 2016 Objectives

- Quantify performance loss terms observed on state-of-the-art cathode catalyst and membrane-electrode assembly (MEA).
- Identify pathways to improve the fuel cell performance toward DOE targets.
- Evaluate effects of carbon supports on fuel cell performance.

Technical Barriers

This project addresses the following technical barriers from the Fuel Cells section of the Fuel Cell Technologies Office Multi-Year Research, Development, and Demonstration Plan.

(B) Cost

(C) Performance

(A) Durability

Technical Targets

See Table 1.

FY 2016 Accomplishments

- Identified and quantified the primary source of HCD performance limitation on low-Pt loaded fuel cell, then

TABLE 1. Progress towards Meeting Technical Targets for Electrocatalysts and MEAs for Transportation Applications

Metric	Units	2016 Status	End of Project Target	DOE 2020 Target
Power per PGM content (150 kPa)	kW_{rated}/g_{PGM}	6.9	*[7.5]*	>8
Power per PGM content (250 kPa)	kW_{rated}/g_{PGM}	7.7	*8.8*	-
PGM total loading	mg/cm^2	0.125	<0.125	<0.125
Loss in catalytic mass activity	% loss	0–40%	<40%	<40%
Catalyst cycling (0.6–1.0 V, 30,000 cycles)	mV loss at 0.8 A/cm^2	30	<30	<30
Support cycling (1.0–1.5 V, 5,000 cycles)	mV loss at 1.5 A/cm^2	Not tested	<30	<30
Mass activity @ 900 $mV_{iR\text{-}free}$	A/mg_{PGM}	0.6–0.7	>0.6	>0.44
Performance at rated power (150 kPa)	W/cm^2	0.86	[0.94]	>1.0
Performance at rated power (250 kPa)	W/cm^2	1.01	*>1.1*	-

PGM – Precious group metal; iR – Internal resistance

generated a catalyst technology roadmap for future catalyst development.

- Developed test criteria for carbon support selection.

INTRODUCTION

The amount of expensive platinum used as the oxygen reduction catalyst in fuel cells must be reduced at least 4-fold to make proton exchange membrane fuel cells cost-competitive with other power sources. In our previous DOE-funded project, we have demonstrated that carbon-supported Pt-alloy catalysts (PtNi/HSC and PtCo/HSC) could show very high oxygen catalytic activity and impressive durability, exceeding the DOE targets [1]. However, their high-power performance fell short of the target.

As the Pt content is reduced in the cathode approaching <0.1 mg_{Pt}/cm^2, large amount of oxygen and proton must be delivered to the Pt surface, causing a performance loss due to a relatively high local transport resistance in the state-of-the-art electrode. In addition, the transition metal, such as Ni and Co in the catalyst, can dissolve and migrate into the ionomer phase replacing proton, consequently, reducing ionomer proton conductivity and causing hydrodynamic performance loss. As a result, although these newly developed Pt-alloy catalysts show excellent durable high activity at low power, the target performance at high power has not been realized.

APPROACH

The general approach for this project is to select a carbon support and an electrolyte that have favorable transport properties, then develop a high performance Pt-alloy electrode using these subcomponents. The efforts can be divided into four thrusts: (1) development of carbon support, (2) selection of electrolyte (ionomer or ionic liquid), (3) development of stable highly-dispersed Pt alloy, and (4) understanding of the effect of transition metal on performance.

RESULTS

As Pt loading and the available Pt area for oxygen reduction reaction (ORR) is reduced, higher oxygen and proton fluxes must be delivered to the Pt surface which leads to noticeable performance losses. The detailed analysis has shown that this performance loss was predominantly oxygen transport resistance, and the resistance showed a strong dependency ton available Pt area, also known as the Pt roughness factor [2]. This parameter is the product of Pt loading (mg_{Pt}/cm^2_{MEA}) and Pt-mass-specific electrochemical surface area (m^2_{Pt}/g_{Pt}). As a result, particularly on low-Pt electrode, Pt surface area becomes a very important factor in determining the performance at high power.

Here, we have performed an analysis to reflect the fuel cell requirement for transportation application. Figure 1 provides boundaries (constant voltage lines) for catalyst developers showing material-characteristic regions that meet vehicle power requirements at the end-of-life for a given Pt loading and rated current density. The catalyst ORR mass activity and Pt surface area must be higher than the corresponding dashed parabolic lines to meet the high-power performance requirement. Clearly, materials positioned toward the upper right part of the plot are most desirable and effective in reducing the stack area requirement and thus cost. The electrode reaches end-of-life due to power limitation once the values drop below the dashed line. In the figure, we also include the status (open symbols) and estimates of achievable targets (shaded areas) for some representative catalysts. This analysis will serve as a roadmap for future catalyst development.

The PtCo/HSC developed in the previous project shows a relatively high local oxygen resistance of 25 s/cm. According to the above analysis, we can achieve the DOE target if the resistance can be reduced to 10 s/cm. The project target hence is to search for a carbon support and ionomer that achieves such resistance. During the first year of the project, we have chosen to focus on investigating Pt/C system in order to avoid complication due to the dissolved Co. Figure 2 shows the ORR mass activity and local oxygen resistance of Pt on three types of carbon supports. Although HSC shows the highest

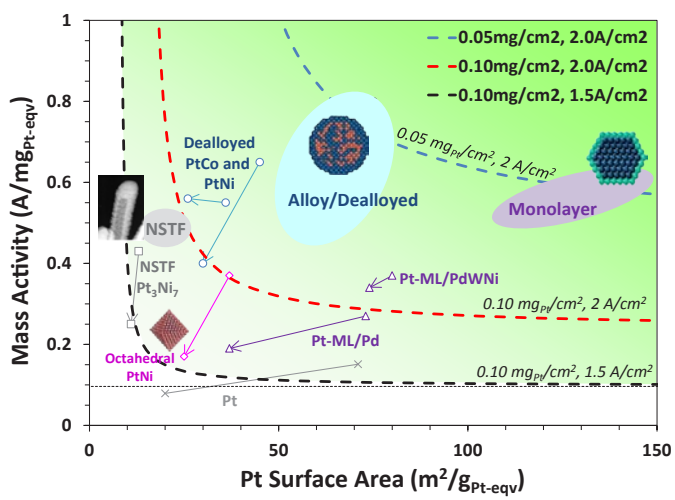

NSTF – Nanostructured thin film

FIGURE 1. ORR mass activity and Pt electrochemical surface area targets which enable the cathode to meet vehicle requirements (0.58 V) at the indicated current density and cathode catalyst loadings. Local resistance of 12 s/cm was used in the analysis. Dashed lines and dotted lines show the minimum values to meet the requirement with and without local resistance, respectively. Catalysts that are above and to the right of a given boundary are sufficient to meet or exceed the voltage requirement. Data points from MEAs at beginning of life (arrow start) and end of life (arrow end) are shown for various catalyst systems, and shaded areas indicate estimate of achievable targets.

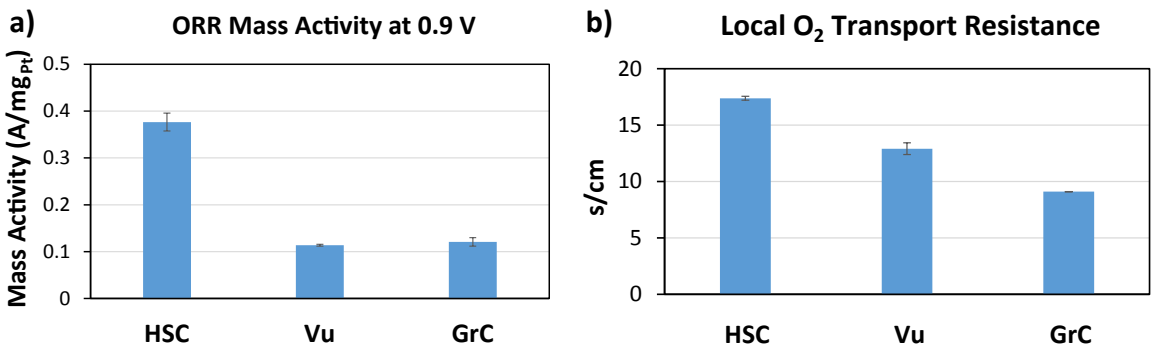

FIGURE 2. ORR mass activity at 0.9 V (a) and local-Pt O_2 transport resistance (b) of Pt catalysts on three different carbon supports

ORR activity, it also shows the largest oxygen resistance. On the other hand, some solid carbons, particularly GrC, show relatively low local oxygen resistance (~10 s/cm). Note that the target is expected to be met if high activity Pt alloy catalyst is successfully developed using this carbon.

Detailed tomographic analysis at Cornell was done to quantify the location of Pt in relation to the carbon for two types of carbon. As shown in Figure 3, porous carbon such as HSC contains a large number of Pt particles inside its carbon particles. These internal Pt may have restricted access to oxygen and proton, resulting in poor HCD performance. Solid carbon such as medium-surface-area carbon, on the other hand, contains mostly surface Pt. This transmission electron microscopy capability will be very powerful in developing new catalysts as well as understanding the structure-function correlation of the electrodes.

To understand the effects of leached transition metal on fuel cell performance, we intentionally introduced known amount of cobalt ions into the MEAs. Electrochemical diagnostic revealed that the local oxygen transport resistance increases with Co^{2+} concentration (Figure 4). This is concerning because it suggests that the HCD performance fall off will be more severe as the catalyst ages. More study is needed to understand how to mitigate these effects.

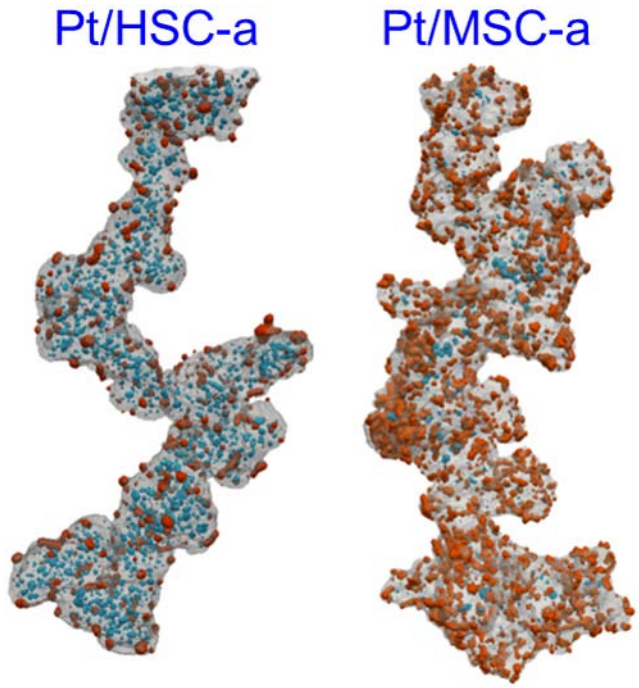

FIGURE 3. Scanning transmission electron microscopic tomographs of Pt/HSC and Pt/Vu showing Pt locating inside (blue dots) and on the surface (red dots) of carbon

CONCLUSIONS AND FUTURE DIRECTIONS

Although the project is still in an early stage, several conclusion can be drawn:

- In developing low-Pt fuel cell, Pt surface area and local oxygen transport resistance must be carefully considered.
- Solid carbon tends to show lower local oxygen transport resistance which may make it a preferred choice for a support.

Future work includes:

- Select preferred carbon support and ionomer and develop Pt catalyst with improved transport property.
- Develop PtCo catalyst with improved dispersion and stability.

FY 2016 PUBLICATIONS/PRESENTATIONS

1. "The Priority and Challenge of High-Power Performance of Low-Platinum Proton-Exchange Membrane Fuel Cells," Anusorn Kongkanand, Mark F. Mathias. *J. Phys. Chem. Lett.* (2016) 7, 1127 [Perspective].

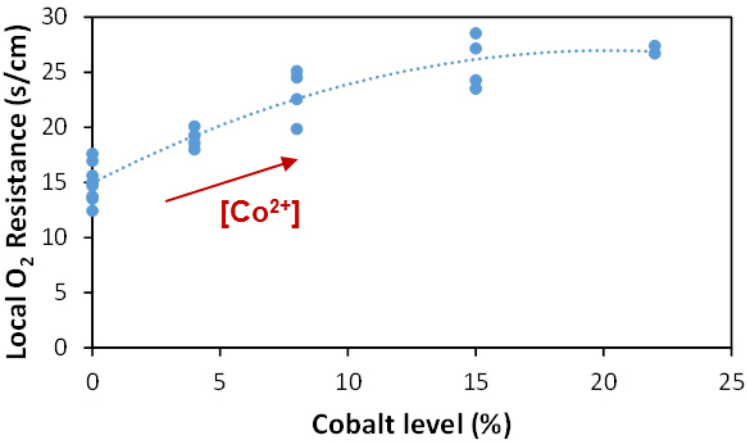

FIGURE 4. Local oxygen resistances measured by limiting current test of MEAs with different levels of Co^{2+} concentration

2. "Electrochemical Diagnostics and Modeling in Developing the PEMFC Cathode," Anusorn Kongkanand, Venkata Yarlagadda, Taylor Garrick, Thomas E. Moylan, Wenbin Gu. *ECS Trans.* (2016).

3. (Invited) "Characterizing the Pt-Electrolyte Interface in PEM Fuel Cells," The 14th International Conference on Electrified Interfaces, Changi, Singapore, July 3–8, 2016.

REFERENCES

1. B. Han, et al., *Record Activity and Stability of Dealloyed Bimetallic Catalysts for Proton Exchange Membrane Fuel Cells.* Energy Environ. Sci. 2015, 8(1): p. 258–266.

2. A. Kongkanand and M. Mathias, *The Priority and Challenge of High-Power Performance of Low-Platinum Proton-Exchange Membrane Fuel Cells*. J. Phys. Chem. Lett. 2016, 7: p. 1127–1137.

V.A.9 Corrosion-Resistant Non-Carbon Electrocatalyst Supports for PEFCs

Vijay K. Ramani
Illinois Institute of Technology (IIT)
10 W 33rd Street 127 PH
Chicago, IL 60616
Phone: (312) 567-3064
Email: ramani@iit.edu

DOE Manager: Gregory Kleen
Phone: (240) 562-1672
Email: Gregory.Kleen@ee.doe.gov

Contract Number: DE-EE-0007272

Subcontractors
- Nilesh Dale, Nissan Technical Center, North America, Farmington Hills, MI
- Plamen Atanasov, University of New Mexico (UNM), Albuquerque, NM

Project Start Date: March 1, 2016
Project End Date: February 28, 2019

Overall Objectives

- Design, develop and demonstrate high-surface-area (>70 m^2g^{-1}), high conductivity (>0.2 S/cm) and corrosion-resistant (as per funding opportunity announcement requirements), non-carbon supports based on doped metal oxides (that do not contain platinum group metals [PGMs]).
- Derivatize said supports to yield functional supported platinum (Pt) electrocatalysts that leverage strong metal support interactions (SMSI).
- Demonstrate stability, activity, and performance approaching the Department of Energy's 2020 targets using DOE-prescribed accelerated tests and protocols by optimizing the structure of the support and the structure of the electrode.
- Provide DOE with at least six 50 cm^2 membrane electrode assemblies (MEAs) prepared using the best down-selected formulations that (a) meet all the stability metrics and (b) provide a clear pathway to meeting DOE 2020 targets for Pt loading and mass activity metrics.

Fiscal Year (FY) 2016 Objectives

- Density functional theory (DFT) calculations to evaluate conductivity and SMSI of relevant doped metal oxides (MO)
- Synthesis and characterization of Tantalum (Ta)-doped-TiO_2 and other doped MO
- High surface area support synthesis by sacrificial support method (SSM)
- Characterization of the doped MOs and derived catalysts
- Electrochemical evaluation of support and Pt/MO stability
- Investigation of SMSI in Pt/doped-metal-oxide systems using X-ray photon spectroscopy
- Measurement of beginning of life, electrochemical active surface area, and oxygen reduction reaction activity of selected catalysts in rotating disk electrode

Technical Barriers

This project addresses the following technical barriers from the Fuel Cell section of the Fuel Cell Technologies Office Multi-Year Research, Development, and Demonstration Plan.

(A) Durability

(B) Cost

(C) Performance

Fuel cell catalyst and catalyst support durability need to be improved, in line with DOE 2020 targets.

Technical Targets

Table 1 shows current status (with Pt/C and with Pt/RTO developed in our prior project) and proposed targets. The preliminary data obtained with our proposed approach (see Table 1, Pt/TiO_2-Ta) was obtained without any optimization of the support, the catalyst deposition process, or the electrode preparation process. Clearly, there is much room for improvement in performance and baseline mass activity, which is precisely our goal in this project. These improvements, in conjunction with the enhancement in durability, will allow us to advance towards the DOE 2020 targets. The advantages of our approach over the incumbent technology and any alternate approach (and to even our prior success with RTO) are that we eliminate the noble metal in the support, ensure 100% tolerance towards start-stop cycling, and promote SMSI between the support and Pt, which provides us a clear pathway to enhance beginning of life mass activity and stability under load cycling. Hence, the proposed approach addresses remaining challenges or technical issues and provides a pathway to advance the state of the art and meet the DOE 2020 targets.

TABLE 1. Technical Targets

Metric	Units	SOA (Pt/C)	SOA (Pt/RTO)	Proposed Approach Status (Pt/TiO_2-Ta)	End Target	DOE 2020 Target
Total PGM Content	g kW^{-1}	0.55	0.55	Not Available	0.25	<0.125
Total PGM Loading	mg cm^{-2}	0.4	0.4	0.6	0.25	<0.125
Voltage at 1.5 A cm^{-2} (air)	mV	0.45	0.48	0.3	0.55	N/A
Loss in Mass Activity	% loss	32	33	<10%	<5%	<40
Voltage Loss at 0.8 A cm^{-2}	mV	81	9	<15	<10	30
Voltage Loss at 1.5 A cm^{-2}	mV	182	20	N/A; 20 mV at 1 Acm^{-2}	<20	30
Mass Activity @ 900 $mV_{iR\text{-}free}$	A mg^{-1}_{PGM}	0.07	0.07	ca. 0.05	0.3	0.44

SOA – State of the art; N/A – Not available

FY 2016 Accomplishments

- DFT calculations have been performed by UNM to examine the effect of doping (with Ta and Nb) of TiO_2 on the conductivity and stability of the resultant doped oxide. The results show that doping with Ta or Nb (at 4% levels) creates an n-type semiconductor with increased conductivity due to "metallization" of the oxide.
- Nb-doped TiO_2, Mo-doped TiO_2, Mo-doped NbO_2, W-doped TiO_2, Ta-doped TiO_2 were successfully synthesized at IIT using sol-gel and hydrothermal methods, their structures probed using X-ray diffraction (XRD), and their conductivities and surface areas measured.
- Nb-TiO_2 was evaluated to have an electron conductivity ≥0.2 S/cm (above the target) and a surface area of 25 m^2/g (marginally below target).
- Using the sacrificial support method at UNM, the surface area of Ta-TiO_2 was shown to be enhanced to 150 m^2/g. We anticipate a similar effect for Nb-TiO_2, which will put us over the target.

✧ ✧ ✧ ✧ ✧

INTRODUCTION

Carbon black is an exceptional catalyst support for polymer electrolyte fuel cell (PEFC) electrocatalysts due to its high surface area and high conductivity. However, under fuel cell operation conditions (start-stop), carbon corrodes easily [1]. To address this issue, it is necessary to explore non-carbon supports with high conductivity, high surface areas, and high corrosion resistance under fuel cell operating conditions. In this project we will design, develop, and evaluate electrochemically stable, high-surface-area, metal-oxide supports and supported electrocatalysts for PEFCs. The Pt/MO catalysts should meet the DOE 2020 targets for stability and approach DOE 2020 targets for the beginning of life mass activity and Pt loading.

APPROACH

In this study, as opposed to our prior work, we select the base oxide to be PGM-free oxides that are thermodynamically stable in the operative potential and pH window. Furthermore, we have refined the choice of the base oxide to prioritize those that allow for SMSI. To induce electron conductivity, we will tune the oxide structure by appropriate selection and introduction of a non-PGM dopant atom, selected from among transition metals of similar ionic size, but having an electronic structure designed to promote the n-type doping necessary to induce electronic conductivity and to induce electron donation from the support to the catalyst (SMSI). We view SMSI and support electronic properties as a route to enhance baseline mass activity and minimize platinum dissolution upon load cycling. The effect of composition (doping level) and processing parameters (annealing temperature) on surface area, porosity, electron conductivity, and SMSI with platinum will be evaluated, and tuned to achieve high oxygen reduction reaction activity and stability against Pt dissolution. DFT simulations will be performed to understand the electronic structure of the oxide upon doping, and to examine SMSI between Pt clusters and the support. The DFT results will guide dopant choice and doping level. Once suitable combinations are identified and evaluated, we will employ the sacrificial support method pioneered by UNM to prepare the supports with high surface area.

RESULTS

DFT calculations performed by UNM to examine the effect of doping (with Ta and Nb) of TiO_2 on the conductivity and stability of the resultant doped revealed that that doping with Ta or Nb (at 4% doping levels) creates an n-type semiconductor with increased conductivity due to metallization of the oxide (Figure 1). These results lend credence to our doping approach, though DFT studies are still ongoing.

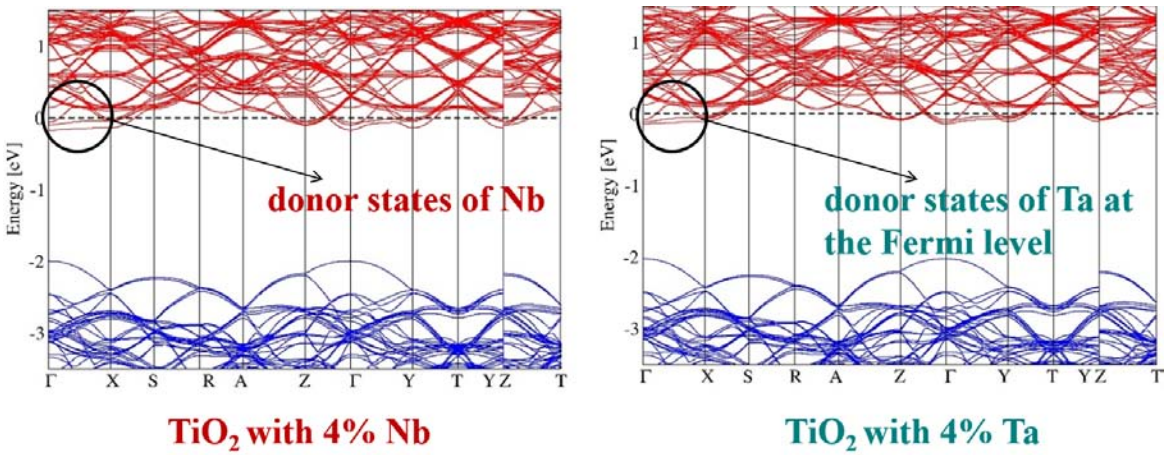

FIGURE 1. DFT modeling for Nb- and Ta- doped TiO_2 materials

We have synthesized Nb-doped-TiO_2, Mo-doped-TiO_2, Mo-doped-NbO_2, W-doped-TiO_2, and Ta-doped TiO_2 doped metal oxides and tested their electronic conductivity (Figure 2) and surface area (Figure 3). The structure of the doped MOs was confirmed through XRD. The dopant levels were set to 30% and 50% mol/mol. From the conductivity measurements we have found that $Nb_{0.3}Ti_{0.7}O_2$ and $Nb_{0.5}Ti_{0.5}O_2$ had conductivities of approximately 0.2 S/cm (commensurate with our target), after suitable processing and annealing. However, at this stage, the Nb-TiO_2 surface area (Figure 3) is still lower (25 m^2/g) than what would be required. Please note though that these were oxides made at IIT by the conventional hydrothermal and sol-gel methods, UNM has, in parallel, been performing syntheses with the sacrificial support method and have shown Ta-doped TiO_2 materials with Brunauer-Emmett-Teller surface areas approaching 150 m^2/g, well above the target. XRD peak analysis (Figure 4) of the SSM-derived supports showed (1) Ta and TiO_2 precursors mixed with silica are highly amorphous, (2) the structure goes from amorphous to crystalline following heat treatment, and (3) TiO_2 transitioned from anatase to rutile phase under annealing at 850°C. From our XRD analysis at IIT we have found that at annealing temperatures below 800°C, the material was composed partially of the anatase phase and that the electronic conductivity was much lower. For annealing temperatures above 800°C the phase transformation to the rutile structure was observed (observation replicated by UNM) and the electronic conductivity reached 0.2 S/cm. Based on these results, we can preliminarily conclude that the rutile phase is required to reach the electronic conductivity required for the milestones, especially for TiO_2-based supports.

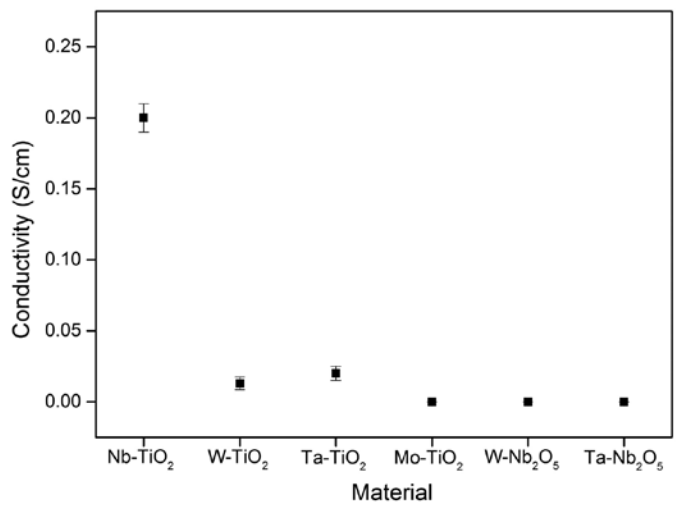

FIGURE 2. Electronic conductivity of different doped supports

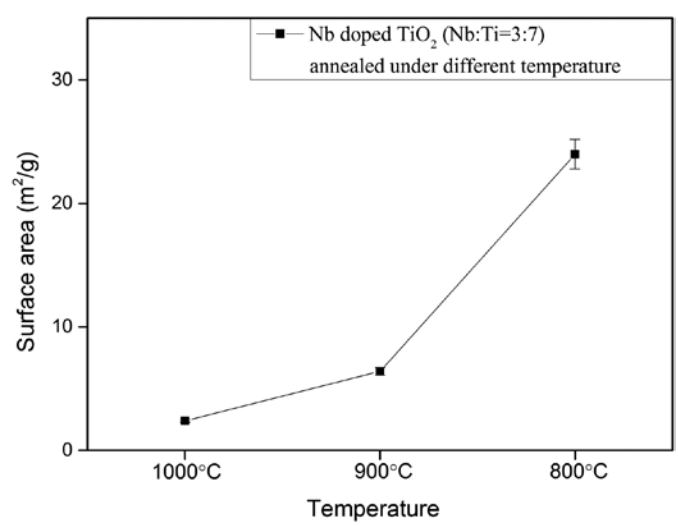

FIGURE 3. Surface area of Nb doped TiO_2 (Nb:Ti = 3:7) under different annealing temperatures

CONCLUSIONS AND FUTURE DIRECTIONS

We have found Nb-TiO_2 materials had conductivities close to or above 0.2 S/cm, and have potential to be conductive catalyst supports. We will continue to evaluate

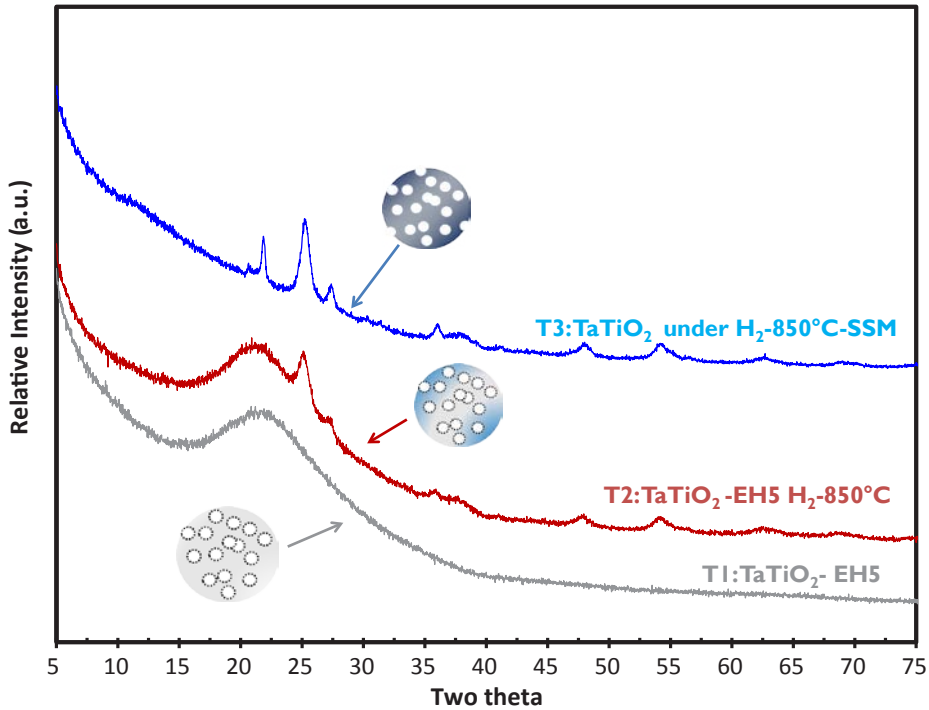

FIGURE 4. XRD patterns of Ta-doped TiO_2 prepared using SSM

these supports (for stability, SMSI, and to enhance surface area and conductivity) using both DFT and experimental methods over the rest of FY 2016.

REFERENCES

1. N. Takeuchi; T.F. Fuller, J. Electrochemical Society, 155 (2008) B770–B775.

V.B.1 Fuel Cell-Performance and Durability (FC-PAD) Consortium Overview

Rod Borup[1] (Primary Contact, Director), Adam Weber[2] (Deputy Director, Thrust 3 Coordinator), Deborah Myers[3] (Thrust 1 Coordinator), Shyam Kocha[4] (Thrust 2 Coordinator), Rajesh Ahluwalia[3] (Thrust 4 Coordinator), Rangachary Mukundan[1] (Thrust 5 Coordinator), Karren More[5] (Thrust 6 Coordinator)*

[1]Los Alamos National Laboratory
MS D429, P.O. Box 1663
Los Alamos, NM 87545
Phone: (505) 667-2823
Email: Borup@lanl.gov

DOE Managers:

Dimitrios Papageorgopoulos
Phone: (202) 586-5463
Email: Dimitrios.Papageorgopoulos@ee.doe.gov

Greg Kleen
Phone: (240) 562-1672
Email: Gregory.Kleen@ee.doe.gov

Subcontractors:

[2] Lawrence Berkeley National Laboratory, Berkeley, CA
[3] Argonne National Laboratory, Argonne, IL
[4] National Renewable Energy Laboratory, Golden, CO
[5] Oak Ridge National Laboratory, Oak Ridge, TN

* Only the director and thrust area coordinators are listed in the author list. Each laboratory has multiple scientists contributing to FC-PAD.

Project Start Date: October 1, 2015
Project End Date: September 30, 2020

Overall Objectives

- Advance performance and durability of polymer electrolyte membrane fuel cells (PEMFCs) primarily at a pre-competitive level.
- Develop the knowledge base and optimize structures for more durable and high-performance PEMFC components.
- Improve high current density performance at low Pt loadings.
  - Loading: 0.125 mg Pt/cm^2 total
  - Performance at 0.8 V: 300 mA/cm^2
  - Performance at rated power: 1,000 mW/cm^2
- Improve component durability (e.g., membrane stabilization, self-healing, electrode-layer stabilization).
- Provide support to industrial and academic developers.
- Development of new diagnostics, characterization tools, and models.
- Each thrust area has a sub-set of objectives which lead to the overall performance and durability objectives.

Fiscal Year (FY) 2016 FC-PAD Organizational Objectives

- Coordinate activities across the core national labs involved in FC-PAD, including in-person coordination meetings and regular conference calls.
- Develop data sharing approaches, including internal and external websites.
- Develop a structure to ease addition of industrial and academic partners, including streamlined multi-lab agreements.
- Conduct outreach to fuel cell developers and develop mutually beneficial collaborations.

Fiscal Year (FY) 2016 Technical Objectives

The technical objectives for FC-PAD are covered by the individual thrust areas, and are found in the separate annual reports for those thrust areas.

- Quantify gas-phase transport improvement of electrospun fibers in cathode electrode layer by electrochemical impedance spectroscopy.
- Compare the spatial distribution of reversible degradation during power cycling and constant power operation.
- Quantify cerium migration within the membrane in microns per second under both applied potential and applied current.
- Propose freeze/thaw protocol to DOE Fuel Cell Technology Team that simulates appropriate transportation shutdown/startup (SD/SU) conditions.
- Quantify by ex situ measurements the steady state concentration and dissolution rates of dissolved Pt and base metal from state-of-the-art Pt alloy catalysts.
- Develop and test protocol for characterizing performance and durability of state-of-the-art Pt alloy-based cathode catalyst layers.

- Measure structural and transport properties of reinforced perfluorosulfonic-acid membrane including impact of hygrothermal ageing.
- Measure critical ionomer thin-film properties including simultaneous water uptake and swelling, gas permeability, and surface conductivity.
- Propose relevant diagnostic techniques for the identification of local Pt transport resistance.
- Fabricate, integrate, and evaluate electrode layers with modulated properties (e.g., catalyst wt%, carbon type) that can affect local Pt resistance in low-loaded PEMFCs.
- Quantify changes in local Pt transport resistance before and after durability measurements of down-selected electrode materials.
- Establish critical measurement protocol via cross-sectional transmission electron microscopy and scanning transmission electron microscopy with energy dispersive spectrum for several Pt-alloy catalysts to understand alloy catalyst degradation (dissolution) during testing.
- Study ionomer structural changes in low Pt-loaded membrane electrode assemblies (MEAs) subjected to extensive fuel cell operation.
- Establish complete database of Pt-alloy, Ce/ceria, carbon corrosion effects, and ionomer distribution observations as input data for model development.

Technical Barriers

This project addresses the following technical barriers from the Fuel Cells section of the Fuel Cell Technologies Office Multi-Year Research, Development, and Demonstration Plan.

(A) Durability

(B) Cost

(C) Performance

A more detailed list of the Technical Barriers addressing A, B, and C above that this project addresses includes:

- The catalyst layer is not fully understood and <u>is key in lowering costs</u> by meeting rated power.
  - Mitigation of transport losses is required to improve performance.
  - Rated power at low Pt loadings reveals unexpected losses.
- The electrocatalyst remains a challenge for reducing the cost to meet system cost targets.
  - The catalyst, its interaction with other electrode components, the stability of alloying components, and the effect of this instability are not fully understood and are key to achieving performance, cost, and durability targets.
- The ionomer presents challenges in terms of performance and durability.
  - Unknown membrane durability additive movement
  - Local losses associated with ionomer thin films
- Water and thermal management is needed, especially at lower temperatures.
- Tolerance to impurities and chemical and mechanical integrity has not been established.
- Sufficient durability of fuel cell systems operating over automotive drive cycles has not been demonstrated and is not fully understood.
- Development and implementation of accelerated stress tests (ASTs) are needed to shorten the time required to address durability issues.

Technical Targets

This project develops MEAs that meet the following DOE MEA targets (Table 1).

TABLE 1. Technical Targets: Membrane Electrode Assemblies for Transportation Applications

Characteristic	Units	2020 Targets
Cost	$\$/kW_{net}$	14
Durability with cycling	hours	5,000
Start-up/shutdown durability	cycles	5,000
Performance @ 0.8 V	mA/cm^2	300
Performance @ rated power (150 kPa_{abs})	mW/cm^2	1,000
Robustness (cold operation)		0.7
Robustness (hot operation)		0.7
Robustness (cold transient)		0.7

Meeting these targets enables the overall fuel cell system target for cost of $40/kW.

FY 2016 Accomplishments

- FC-PAD consortium's core lab team operating with integrated thrusts.
  - Websites operational (internal and external)
  - Outreach activities, including >10 external presentation and site visits

  - Collaborations with academic and industrial partners include ~20 different entities at various levels of interaction
- Expanded previous work in examining performance and durability of Pt-alloy catalysts.
- Fabricated multiple variations of electrode designs to optimize high current density performance.
- Conducted experiments related to thin-film ionomer for catalyst layer optimization with modeling supporting the experimental measurements.
- New durability ASTs were developed and accepted by DOE U.S. DRIVE Fuel Cell Tech Team.
- Experimental measurement of recoverable degradation and developed methods relating to recovering the reversible performance losses.

✧ ✧ ✧ ✧ ✧

INTRODUCTION

Although fuel cells are being deployed in cars as part of demonstration fleets, they still fall short of the DOE targets for this technology, which are required for widespread consumer acceptance. The FC-PAD consortium was formed to advance performance and durability of polymer electrolyte membrane fuel cells (PEMFCs) at a pre-competitive level to further enable their commercialization. This consortium coordinates national laboratory activities related to fuel-cell performance and durability, provides technical expertise and harmonizes activities with industrial developers. The consortium serves as a resource that amplifies the Office of Energy Efficiency and Renewable Energy impact by leveraging the core capabilities of several labs.

The major challenge to be addressed by this consortium is to develop the knowledge base and optimize structures for more durable, high-performing PEMFC component technologies, while simultaneously reducing cost. Current research is focused on achieving high performance and durability in low Pt-loaded PEMFCs. The lower Pt-loading has already revealed several key performance and durability issues that need to be overcome for successful PEMFC commercialization. The low-Pt content and advanced alloys and structures used in the catalyst layer impose severe constraints on the optimization of MEAs. New transport and durability models and diagnostics that capture accurately the ionomer transport resistance in the MEA are required and being developed. Moreover, additives used in PEMFC components to increase durability can be mobile and further development is required to stabilize them. Finally, the interactions of the various low-cost components including metal bi-polar plates and gas diffusion layers with the MEA need to be optimized to meet all DOE targets simultaneously.

APPROACH

This consortium incorporates national laboratory investigators with proven experience (developed in prior projects) related to durability, transport, and performance, and combines them into one highly coordinated effort. The consortium formalizes already existing and effective collaborations amongst the national laboratories that have established leadership in PEMFC performance and durability research and development. The consortium coordinates work under the thrust areas defined in Figure 1. Three thrust areas are related to components (electrocatalysts and supports; electrode layers; ionomers, gas diffusion layers, bipolar plates, interfaces), and three thrust areas are cross-cutting in nature (modeling and validation; operando evaluation: benchmarking, ASTs, and contaminants; component characterization and diagnostics).

This project builds on existing capabilities at the five participating laboratories to improve the performance and durability of PEMFCs. Transport losses in advanced state-of-the-art MEAs will be identified and cell design will be optimized to maximize performance. Comprehensive multiphase transport models will be developed and then validated using novel diagnostic techniques. Degradation modes of individual material components will be identified and quantified providing detailed information to predict performance and durability. Interactions between the material components will be measured in terms of their effect on changing PEMFC performance. New ASTs will be designed to reflect accurately the degradation mechanisms observed during PEMFC operation. The research on degradation modes and performance will be used to define material requirements and enable future materials development.

RESULTS

FC-PAD is a newly developed consortium with a core team of U.S. national laboratories. The primary objective of this consortium is to implement improvements to PEMFCs and their components with respect to cost, durability, and performance. As a resource to DOE and industrial developers, the consortium will provide technical capabilities to future projects focusing on performance and durability of PEMFCs. This support will include providing relevant and validated testing protocols, critical information about material properties, advanced structures for performance improvements, and methods for mitigating performance losses due to degradation.

To coordinate effective collaborations, FC-PAD has been organized with a steering committee including Director (Rod Borup), Deputy Director (Adam Weber), and six thrust area coordinators: Deborah Myers, Shyam Kocha, Adam Weber, Rajesh Ahluwalia, Rangachary Mukundan, and Karren More. To speed the ability of FC-PAD to interact with outside organizations, a team of technology transfer specialists has

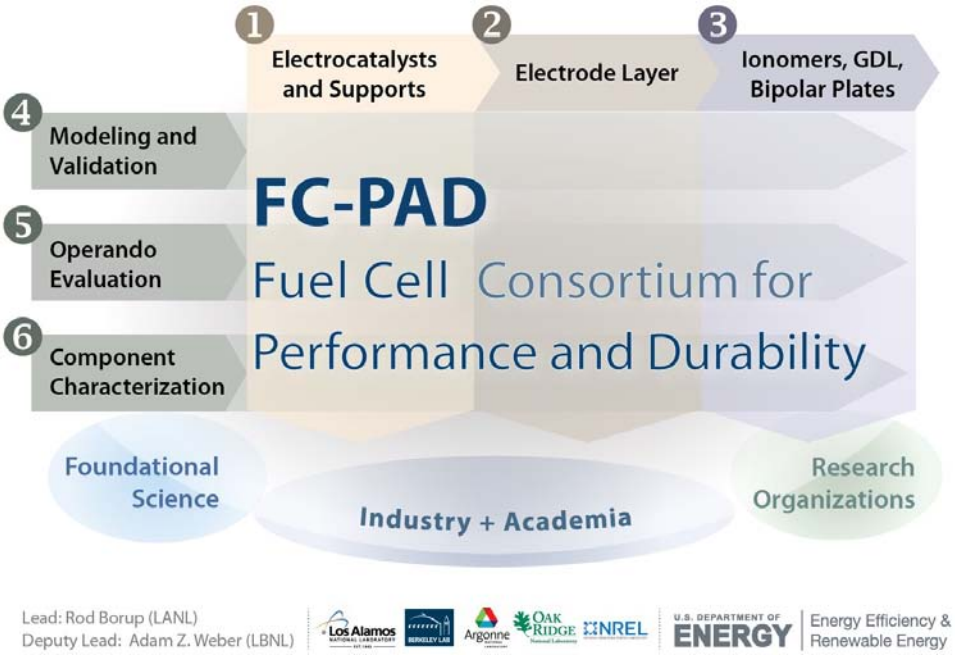

LANL – Los Alamos National Laboratory; LBNL – Lawrence Berkeley National Laboratory

FIGURE 1. FC-PAD Structure. Structure is divided into three component thrust areas (1, 2, 3) and three cross-cutting thrust areas (4, 5, 6).

been formed, and are developing a set of multi-laboratory agreements, such as a multi-lab non-disclosure-agreement, to ease legal interactions with outside entities. Similarly, a set of individuals from the consortium members have been identified to identify methods for data analysis and sharing. The organizational structure of FC-PAD is depicted in Figure 2. Future additions will include Associate Steering Committee members from newly awarded FC-PAD projects from DE-FOA-0001412.

Key to the FC-PAD consortium success is successful coordination of research between the technical thrust areas. An example of successful coordination between FC-PAD thrust areas is shown in Figure 3. In this example, an experimental matrix related to drive cycle induced catalyst carbon corrosion was developed between various researchers representing catalysts, operando evaluation, modeling and characterization. With this inclusive approach, data was produced with feedback that was beneficial to all four of those thrust areas, and was the most valuable in terms of understanding the causes and mitigations to carbon corrosion during drive cycle operation.

Dissemination and collaboration is key to the success of FC-PAD. FC-PAD researchers have an extensive publication and presentation record, and substantial outreach during FY 2016 was conducted. FC-PAD has successfully developed an external website to help with dissemination of results at www.fcpad.org.

This website is currently being populated with new technical results, the FC-PAD organization and ways to collaborate with FC-PAD. In terms of collaboration, there are multiple paths available for collaboration. These include utilizing the vast array of characterization techniques and equipment that exist in the national lab system to examine material properties and characteristics, and validation of performance plus modeling support. The consortia is especially interested in new SOA materials to validate performance models, understand different material properties related to performance and durability and understand degradation mechanisms. An example of some of the capabilities related to FC-PAD is shown in Figure 4. Interested collaborators should contact the FC-PAD Director about methods for collaboration.

For other key technical accomplishments related to FC-PAD, readers should refer to the other FC-PAD thrust area related reports.

CONCLUSIONS AND FUTURE DIRECTIONS

Additional technical details are found in the individual thrust area reports.

- Incorporate collaborators from DE-FOA-0001412 into FC-PAD.
  - Define mechanisms for collaboration.
    - Conduct lab and capability matching exercise.

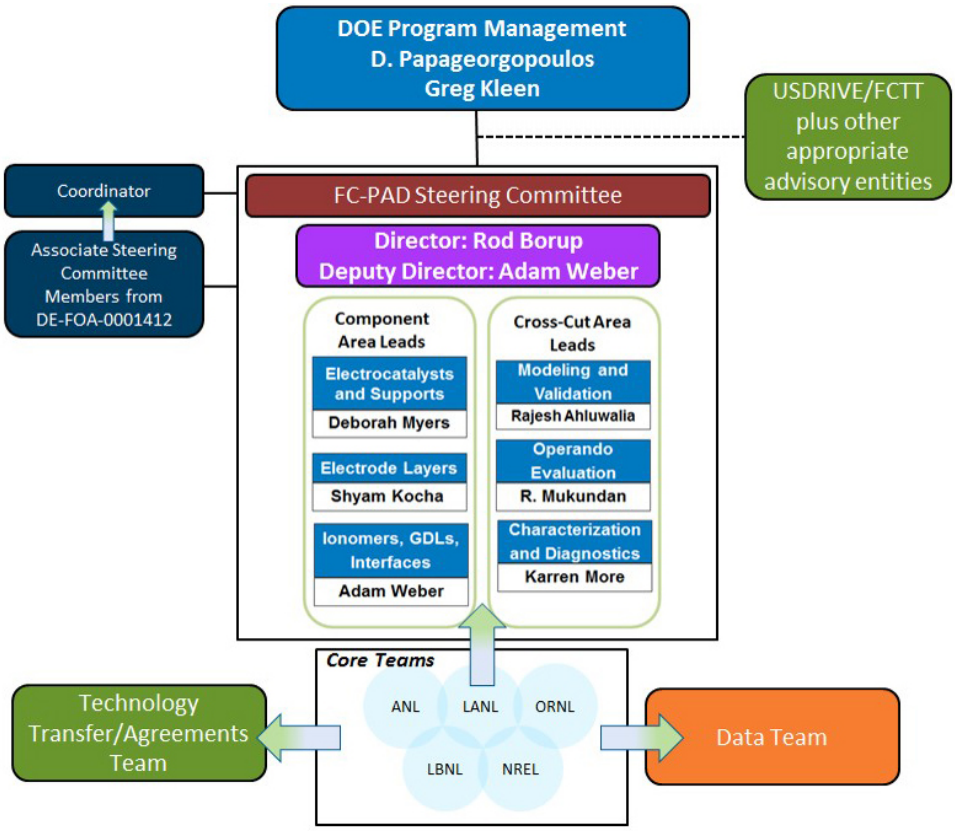

FCTT – Fuel Cell Tech Team; ANL – Argonne National Laboratory; ORNL – Oak Ridge National Laboratory; NREL – National Renewable Energy Laboratory; GDLs – Gas diffusion layers

FIGURE 2. FC-PAD organizational structure

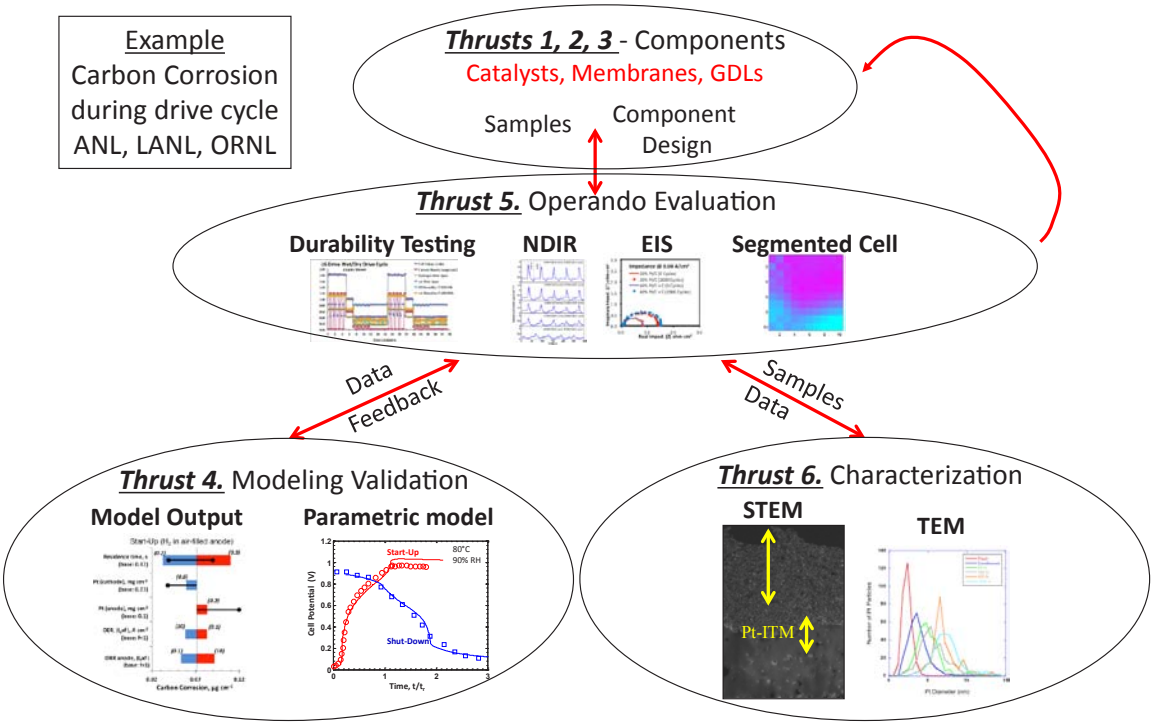

NDIR – Nondispersive infrared sensor; EIS – Electrochemical impedance spectroscopy; STEM – Scanning transmission electron microscopy; TEM – Transmission electron microscopy

FIGURE 3. Example of how FC-PAD coordinates between component and cross-cutting thrust areas

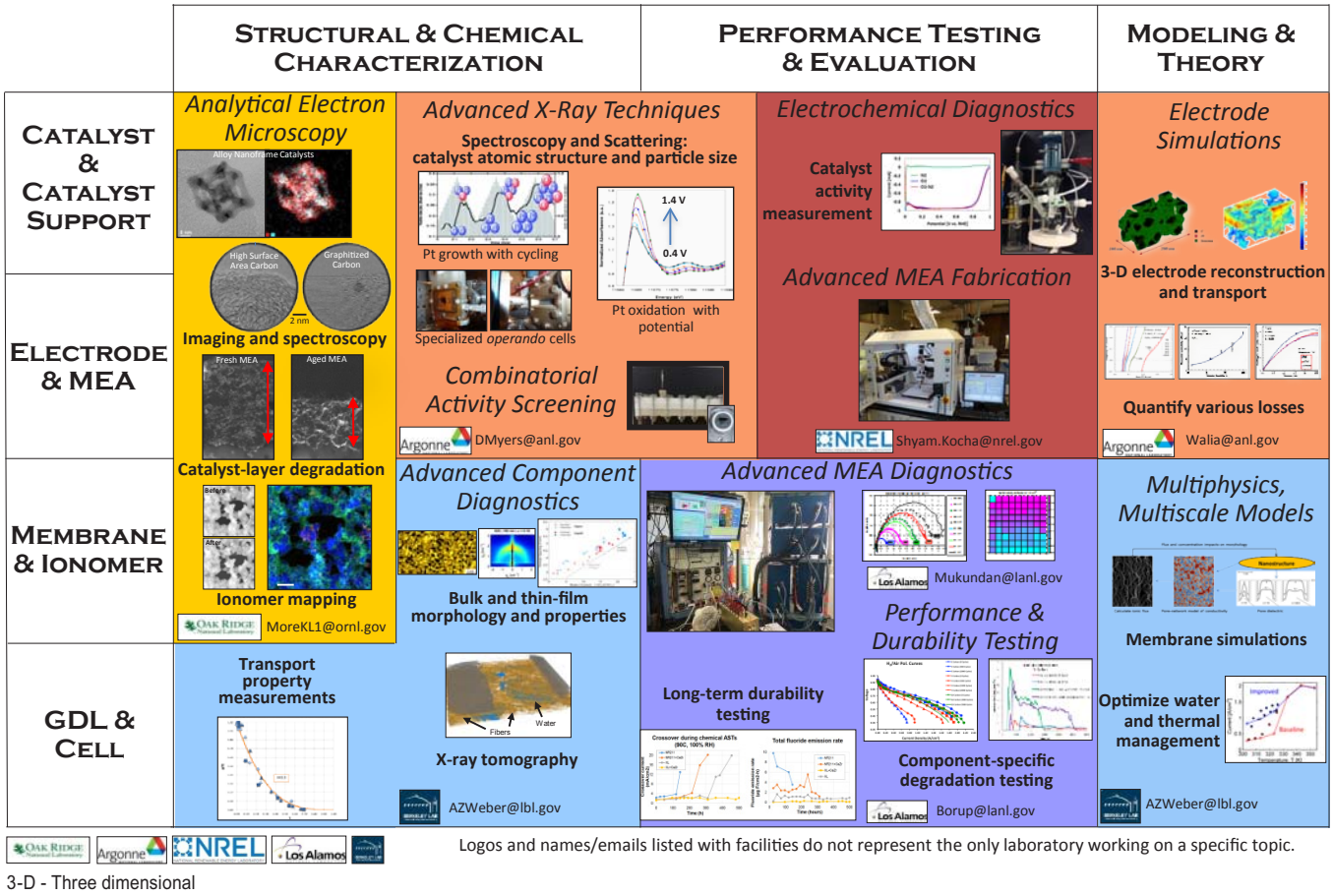

FIGURE 4. Capabilities related to FC-PAD at the consortium members. List is an example of capabilities and not meant to represent all capabilities.

  - Identify roles for the FC-PAD core national labs for supporting roles.
  - Develop milestones for the FC-PAD national labs related to newly awarded projects.
  - Integrate new collaborators (industrial/academic/national laboratories) with core national labs.
  - Continue outreach to develop new collaborators.
- Populate external FC-PAD website with relevant information.
- Thrust 1: Concentration on Pt-X alloys; developing understanding related to supports and durability.
- Thrust 2: Optimize catalyst layers with state-of-the-art catalysts; implement alternative designs for cathode catalyst layers.
- Thrust 3: Investigate side-chain chemistry effects; relationship between cerium migration and durability.
- Thrust 4: Thin-film structure and property modeling; modeling of catalyst layer/gas diffusion layer/channel interfaces.
- Thrust 5: Segmented cell evaluation of durability; adoption and development of differential cell protocols.
- Thrust 6: Characterization of catalyst layer structure; ionomer mapping and ionomer interactions with catalyst; provide characterization to collaborators.

SPECIAL RECOGNITIONS & AWARDS/ PATENTS ISSUED

1. Rod Borup received an award at 2016 DOE Hydrogen and Fuel Cells Program Annual Merit Review related to FC-PAD.

2. Andrew Baker won 1st place poster at the 2015 Fuel Cell Seminar. Poster Titled: *Cerium Migration during PEM Fuel Cell Operation.*

3. Andrew Baker won 2nd place for the Bernard Baker Award.

4. Peter Dudenas won 1st place poster for the PEFC 15 student poster competition at Electrochemical Society. Poster titled:

Heterogeneous Substrate Effects on Perfluorosulfonic-Acid Thin Films.

5. Rangachary (Mukund) Mukundan has been selected to receive the 2016 Sensor Division Outstanding Achievement Award from the Sensor Division of the Electrochemical Society (ECS).

FY 2016 PUBLICATIONS/PRESENTATIONS

Publications/Presentations Relevant to FC-PAD from Consortium Members:

1. Shouwen Shi, Thomas J. Dursch, Colin Blake, Rangachary Mukundan, Rodney L. Borup, Adam Z. Weber, and Ahmet Kusoglu, "Surface Anhydride Degradation-Induced Changes in Structure/Property Relationship of Perfluorosulfonic-acid (PFSA) membranes," *Journal of Polymer Science B: Polymer Physics*, (2016). doi: 10.1002/polb.23946.

2. Ahmet Kusoglu and Adam Z. Weber, "Electrochemical/Mechanical Coupling in Ion-Conducting Soft Matter," *The Journal of Physical Chemistry Letters*, 6, 4547–4552 (2015) doi: 10.1021/acs.jpclett.5b01639 (*perspective*).

3. Shouwen Shi, Thomas J. Dursch, Rod L. Borup, Adam Z. Weber, and Ahmet Kusoglu, "Effect of Hygrothermal Ageing on PFSA Ionomers' Structure/Property Relationship," *ECS Transactions,* 69 (17), 1017–1025 (2015). doi: 10.1149/06917.1017ecst.

4. Shouwen Shi, Colin Blake, Rodney L. Borup, Rangachary Mukundan, Adam Z. Weber, and Ahmet Kusoglu, "Effect of Hygrothermal Ageing on PFSA ionomers' Structure/Property Relationship," *ECS Meeting*, Phoenix, AZ, October 2015.

5. Ahmet Kusoglu and Adam Weber, "Characterization of Low EW Ionomers in Fuel Cells," *ECS Meeting*, Phoenix, AZ, October 2015.

6. Adam Weber, "Understanding Transport in Polymer-Electrolyte Fuel-Cell Ionomer," Colloquium, U. Kansas, 2015. (invited)

7. Ahmet Kusoglu, Peter Dudenas, Meron Tesfaye, and Adam Z. Weber, "Confinement Effects in PFSA Thin Films," *Pacific Polymer Conference 14*, Kuaui, December 2015.

8. Ahmet Kusoglu and Adam Weber, "Correlating transport and stability of ion-exchange polymers through nanostructure,'" *Pacifichem*, Honolulu, December 2015. (invited)

9. Iryna V. Zenyuk, Ezequiel Medici, Jeffrey Allen, and Adam Z. Weber, "Coupling continuum and pore-network models for polymer-electrolyte fuel cells," *International Journal of Hydrogen Energy*, 40, 16831–16845 (2015). doi: 10.1016/j.ijhydene.2015.08.009.

10. Iryna V. Zenyuk, Ezequiel Medici, Jeffrey Allen, and Adam Z. Weber, "Coupling Continuum and Pore-Network Models in Polymer-Electrolyte Fuel Cells," *European Fuel Cell Technology & Applications Conference - Piero Lunghi Conference*, Naples, 2015.

11. Iryna V. Zenyuk and Adam Z. Weber, "Understanding Liquid-Water Management in PEFCs using X-ray Computed Tomography and Modeling," *ECS Conference*, Phoenix, 2015. (invited)

12. James A. Gilbert, A. Jeremy Kropf, Nancy N. Kariuki, Stacy DeCrane, XiaopingWang, Somaye Rasouli, Kang Yu, Paulo J. Ferreira, Dane Morgan, and Deborah J. Myers, "In-Operando Anomalous Small-Angle X-Ray Scattering Investigation of Pt_3Co Catalyst Degradation in Aqueous and Fuel Cell Environments," *Journal of The Electrochemical Society*, 162 (14) (2015) F1487–F1497.

13. L. Xin, F. Yang, A. Uzunoglu, T. Rockward, R.L. Borup, L. Stanciu, and J. Xie, "Highly Stable Hierarchical Polybenzimidazole (PBI) Grafted Graphene/Nanographene Hybrids As Catalyst Supports for Polymer Electrolyte Membrane Fuel Cells," Submitted to the 230th Meeting of the Electrochemical Society.

14. L. Xin, Y. Kang, F. Yang, A. Uzunoglu, T. Rockward, P.J. Ferreira, R.L. Borup, J. Ilavsky, L. Stanciu, and J. Xie, "Novel Catalyst-Layer Structures with Rationally Designed Catalyst/Ionomer Interfaces and Pore Structures Aided By Catalyst Functionalization," Submitted to the 230th Meeting of the Electrochemical Society.

15. K.C. Neyerlin, J.W. Zack, N. Macauley, R. Mukundan, R.L. Borup, K.L. More and S.S. Kocha, "Investigation of the Performance of PtCo/C Cathode Catalyst Layers for ORR Activity and Rated Power for Automotive PEMFCs," Submitted to the 230th Meeting of the Electrochemical Society.

16. D. Spernjak, R.L. Borup, D.S. Hussey, P. Zelenay, and R. Mukundan, "Imaging Fuel Cell Components: From Flow Field Channels to Catalyst Layers," Submitted to the 230th Meeting of the Electrochemical Society.

17. J.S. Spendelow, L. Castanheira, G. Hinds, T. Rockward, D.A. Langlois, R. Mukundan, and R.L. Borup, "Measurement of Local Electrode Potentials in an Operating PEMFC Exposed to Contaminants," Submitted to the 230th Meeting of the Electrochemical Society.

18. Andrew M. Baker, Dusan Spernjak, Rangachary Mukundan, Rod L. Borup, Elizabeth J. Judge, Suresh G. Advani, and Ajay K. Prasad, "Cerium Migration during PEM Fuel Cell Operation," Submitted to JECS.

19. Iryna V. Zenyuk, Prodip K. Das, and Adam Z. Weber, "Understanding Impacts of Catalyst-Layer Thickness on Fuel-Cell Performance via Mathematical Modeling," *Journal of the Electrochemical Society*, 163, in press (2016). doi: 10.1149/2.1161607jes.

20. Ahmet Kusoglu, Thomas J. Dursch, and Adam Z. Weber, "Nanostructure/Swelling Relationships of Bulk and Thin-Film PFSA Ionomers," *Advanced Functional Materials*, in press (2016). doi: 10.1002/adfm.201600861.

21. Iryna V. Zenyuk, Adrien Lamibrac, Jens Eller, Felix N. Büchi, and Adam Z. Weber, "Understanding Evaporation in Fuel-Cell Gas-Diffusion Layers with X-ray Computed Tomography," *Interpore: 8th International Conference on Porous Media*, Cincinnati, OH, May 2016.

22. Ahmet Kusoglu and Adam Weber, "Exploring the Parameters Controlling the Crystallinity-Conductivity Correlation of PFSA Ionomers," *APS Meeting*, Baltimore, March 2016.

23. Ahmet Kusoglu and Adam Weber, 'Understanding Ionomer Thin-Films in Fuel Cells," *MRS Meeting*, Phoenix, AZ, March 2016. (*invited*)

24. Rodney L. Borup, Rangachary Mukundan, Dusan Spernjak, David Langlois, G. Maranzana, A. Lamibrac, J. Dillet, S. Didierjean, O. Lottin, L. Guetaz, D.D. Papadias, R. Ahluwalia and Karren More, "Material Degradation in PEM Fuel Cells," *MRS Meeting*, Phoenix, AZ, March 2016. (*invited*)

25. Deborah J. Myers, James Gilbert, Nancy N. Kariuki, Xiaoping Wang, A. Jeremy Kropf, Zhiwei Yang, Mallika Gummalla, Mike Perry, Sarah Ball, Jonathan Sharman, Brian Theobald, Alex Martinez, Dash Fongalland, Somaye Rasouli, Kang Yu, and Paulo J. Ferreira, "Mechanisms of PEMFC Cathode Catalyst Dissolution and Degradation X-ray scattering and absorption studies of polymer electrolyte fuel cell cathode electrocatalysts," 3rd International Workshop on Degradation Issues of Fuel Cells and Electrolysers, Santorini, Greece, September 30, 2015. (Invited)

26. F. Cetinbas, R. Ahluwalia, N. Kariuki (Argonne National Laboratory), K.L. More, D.A. Cullen, B. Sneed (Oak Ridge National Laboratory), R.P. Winarski, J. Ilavsky, V. De Andrade, and D.J. Myers (Argonne National Laboratory), "Structural Characterization and Transport Modeling of Pt and Pt alloy Polymer Electrolyte Fuel Cell Cathode Catalyst Layers."

V.B.2 FC-PAD Fuel Cell – Performance and Durability Electrocatalysts and Supports

Debbie Myers[1] (Primary Contact), Nancy Kariuki,[2] Xiaoping Wang,[2] Dennis Papadias,[2] Rajesh Ahluwalia,[2] Shyam Kocha,[3] KC Neyerlin,[3] Jason Christ,[3] Jason Zack,[3] Rangachary Mukundan,[4] Rod Borup,[4] Yu Seung Kim,[4] Karren More,[5] and David Cullen[5]

[1]Argonne National Laboratory
9700 S. Cass Avenue
Lemont, IL 60439
Phone: (630) 252-4261
Email: dmyers@anl.gov

Subcontractors:

[2] Argonne National Laboratory, Argonne, IL
[3] National Renewable Energy Laboratory, Golden, CO
[4] Los Alamos National Laboratory, Los Alamos, NM
[5] Oak Ridge National Laboratory, Oak Ridge, TN

DOE Managers:

Dimitrios Papageorgopoulos
Phone: (202) 586-5463
Email: Dimitrios.Papageorgopoulos@ee.doe.gov

Greg Kleen
Phone: (240) 562-1672
Email: Gregory.Kleen@ee.doe.gov

Project Start Date: October 1, 2015
Project End Date: September 30, 2020

Overall Objectives

- Achieve durable and high performance at both low and high current densities for membrane electrode assemblies based on low precious group metal cathode catalysts/supports with the following targets:
  - Loading: 0.125 mg Pt/cm^2 (cathode + anode)
  - Performance at 0.8 V: 300 mA/cm^2
  - Performance at rated power: 1,000 mW/cm^2
  - Durability: 5,000 hours by 2020, 8,000 hours ultimate
- Develop the knowledge base for more durable and high-performance cathode catalysts and supports, by studying:
  - Catalyst and catalyst support durability and degradation mechanisms
  - Catalyst/support interactions
  - Impact of catalyst degradation on the properties defining the performance of the cathode catalyst layer (e.g., oxygen and water transport)

Fiscal Year (FY) 2016 Objectives

The technical objectives for FC-PAD are covered by the individual thrust areas, and are found in the separate annual reports for those thrust areas.

- Quantify, by ex situ measurements, the steady state concentration and dissolution rates of dissolved Pt and base metal from state-of-the-art Pt alloy catalysts.
- Measure the impact of transition metal dissolution on oxygen permeability of ionomer.
- Determine the effects of carbon type (e.g., high, medium, and low surface area) on catalyst durability and degradation mechanisms.

Technical Barriers

This project addresses the following technical barriers from the Fuel Cells section (3.4) of the Fuel Cell Technologies Office Multi-Year Research, Development, and Demonstration Plan.

(A) Durability

(B) Cost

(C) Performance

Specifically, this FC-PAD thrust area addresses the following issues related to Technical Barriers A, B, and C:

- Lack of high performance at high current densities for cathodes utilizing low loadings of advanced Pt-based cathode electrocatalysts which have oxygen reduction reaction (ORR) mass activities exceeding the DOE target (>0.44 A/mg-Pt).
- Loss of electrochemically active surface area (ECA) and oxygen reduction reaction activity of the cathode electrocatalyst during fuel cell operation.
- Degradation in fuel cell performance due to instability of Pt and alloying components.

Technical Targets

This project develops membrane electrode assemblies that meet the following DOE membrane electrode assembly targets (Table 1).

TABLE 1. Technical Targets: Membrane Electrode Assemblies for Transportation Applications

Characteristic	Units	2020 Targets
Cost	$\$/kW_{net}$	14
Durability with cycling	Hours	5,000
Start-up/shutdown durability	Cycles	5,000
Performance @ 0.8 V	mA/cm^2	300
Performance @ rated power (150 kPa_{abs})	mW/cm^2	1,000
Robustness (cold operation)		0.7
Robustness (hot operation)		0.7
Robustness (cold transient)		0.7

FY 2016 Accomplishments

- Determined potential and potential cycling dependence of Pt and Co dissolution from several Pt_3Co alloys and Pt oxide formation kinetics and thermodynamics and developed a model based on these data for the thermodynamics and kinetics of Pt and Co loss from catalyst particles.
- Initiated solid-state cell measurements of oxygen permeability in ionomer thin films.
- Developed a model for the corrosion of the cathode catalyst carbon support during drive cycles.

✧ ✧ ✧ ✧ ✧

INTRODUCTION

The FC-PAD consortium's mission is to advance the performance and durability of polymer electrolyte membrane fuel cells (PEMFCs) at a pre-competitive level to further enable their commercialization. The performance of the cathode electrocatalyst, primarily at high current densities, and the durability of the electrocatalyst and support under load cycling and start-stop conditions are major challenges to the widespread and cost competitive commercialization of PEMFC systems. Current research is focused on achieving high performance and durability in low Pt-loaded PEMFCs utilizing advanced Pt alloy catalysts.

APPROACH

The Electrocatalyst and Support thrust area's approach is to provide foundational understanding of cathode electrocatalyst activity, performance, and durability by studying the following: (1) catalyst and catalyst support durability and degradation mechanisms, (2) catalyst/support interactions, and (3) the effects of catalyst instability on cathode-catalyst-layer properties. More specifically, the first area focuses on elucidating the degradation mechanisms of the catalyst and support as a function of catalyst/support physicochemical properties, and defining the impact of cell operating conditions and catalyst/support types on degradation rates and mechanisms utilizing ex situ and operando measurements. The second area focuses on understanding the interplay between the catalyst and support properties and their mutual interactions, determining the effects of carbon type (e.g., high, medium, and low surface area) and carbon dopants on the strength of the catalyst/support and ionomer/support interactions, and investigating the impact of these interactions on catalyst and support stability, durability, and performance. The third area focuses on quantifying the impact of catalyst degradation on the properties defining the performance of the cathode catalyst layer (e.g., impact of base metal leaching from Pt alloy catalyst on proton conductivity, oxygen permeability, and water uptake in ionomer). These three areas, especially areas (1) and (2), rely extensively on the capabilities of the cross-cutting thrust areas of FC-PAD.

RESULTS

Several state-of-the-art Pt alloy electrocatalysts were acquired from commercial sources for use by FC-PAD: 30.5 wt% 4.4 nm Pt_7Ni_3/C (Umicore); 55 wt% 6.0 nm PtCo/C (IRD); 46.5 wt% 5.7 nm Pt_3Co/C (Tanaka Kikinzoku Kogyo [TKK]); and 4.9 nm, 8.7 nm, and 14.3 nm 40 wt% Pt_3Co/C (Johnson Matthey). For comparison, two Pt/C catalysts were also acquired: 46 wt% 5.5 nm Pt/C (Umicore) and 47.5 wt% 2.5 nm Pt/C (TKK). The morphology of all the catalysts could be classified as "solid," with the exception of the IRD PtCo catalyst which had a "spongy" morphology (Figure 1). The ORR activity of these catalysts was screened using the thin-film rotating disk electrode (RDE) technique. The RDE-determined specific surface areas and ORR mass and specific activities of a selection of these catalysts are shown in Figure 1 along with representative transmission electron microscopy images for the alloy catalysts. All but one set of these data were taken utilizing perfluorosulfonic acid (PFSA) binder. The alloys were found to have higher ORR activities than the Umicore Pt/C baseline catalyst and to meet or exceed the DOE 2020 mass activity target of 0.44 A/mg-Pt. These data also illustrate the detrimental impact of PFSA ionomer on ORR activity; the ORR activity was suppressed by 40% in the presence of PFSA for the Umicore Pt_7Ni_3/C catalyst.

The Pt and Co dissolution behavior of the TKK Pt_3Co/C was determined as a function of potential, potential cycling, time, and number of cycles, utilizing an aqueous electrochemical cell and inductively-coupled plasma-mass spectrometry detection of dissolved Pt and Co concentrations, to determine the thermodynamics and kinetics of metal dissolution. The oxide formation kinetics and thermodynamics were also determined as a function of potential. These data and previously acquired data for the three Johnson Matthey Pt_3Co/C catalysts, shown in Figure 2,

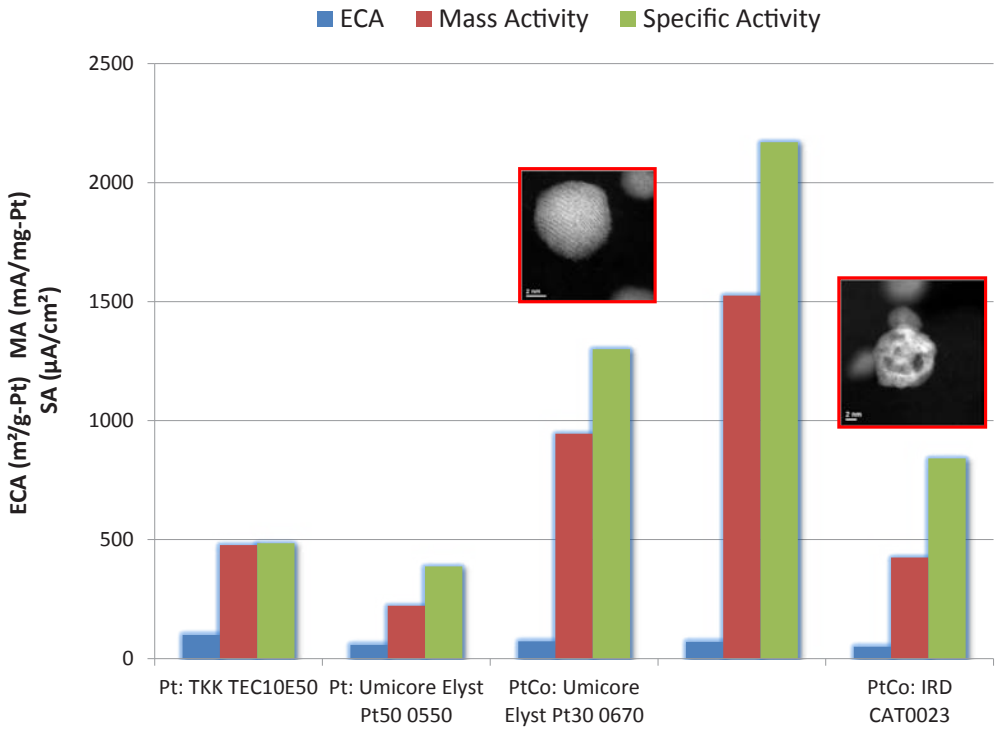

FIGURE 1. The RDE-determined specific surface areas and ORR mass and specific activities of a selection of catalysts being studied by FC-PAD and representative transmission electron microscopy images for the alloy catalysts. All except one set of these data, as indicated, were taken utilizing PFSA binder for the RDE catalyst thin film.

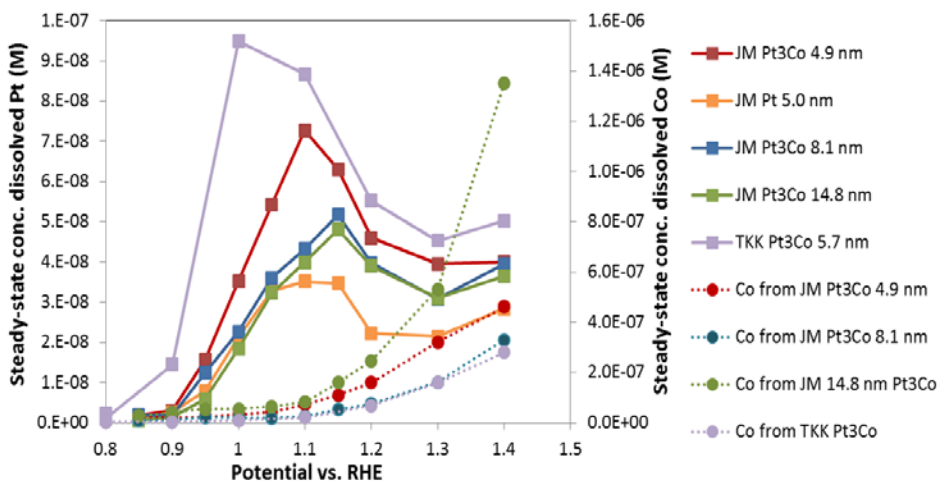

RHE – Reference hydrogen electrode; JM – Johnson Matthey

FIGURE 2. Dissolved concentrations of Pt and Co in room-temperature perchloric acid electrolyte after holding the potential on the catalysts indicated for 72 hr

were utilized to develop a model for the thermodynamics and kinetics of Pt and Co loss from catalyst particles. The rate constants for Pt dissolution were derived from the potentiostatic dissolution data as a function of time and were used to interpret the behavior observed in the potential cycling tests. Findings from the modeling of the dissolution data, correlation with the oxide formation and reduction kinetics, and comparison with similar studies of Pt catalysts are as follows.

- The standard potential (E^o) for Pt dissolution from Pt_3Co is higher than that from Pt which results in the Pt in

Pt_3Co being more stable at potentials <~1.0 V, but less stable at higher potentials due to higher extents of Pt oxide formation in the alloys (Figure 3).

- Under potential cycling conditions and with upper potential limits <1.1 V, Pt dissolves as Pt and PtOH and there is no significant re-deposition during the cathodic sweep of the potential cycle.
- Under potential cycling conditions and with upper potential limits >1.1 V, Pt dissolves as PtOH and Pt^{2+} re-deposits as Pt during the cathodic sweep (Figure 4).
- Surface Co is thermodynamically unstable ($E^o = 0.28$ V) and dissolves during pre-treatment to create a core-shell structure. Subsurface Co (SS-Co) is thermodynamically stable with a dissolution potential (E^o) of 1.158 V which increase with increasing Pt skin thickness.

Experiments were initiated to determine the impact of transition metal dissolution on the oxygen permeability using a solid state Pt microelectrode electrochemical cell. These initial measurements, taken at room temperature and at 100% relative humidity, showed a substantial decrease in

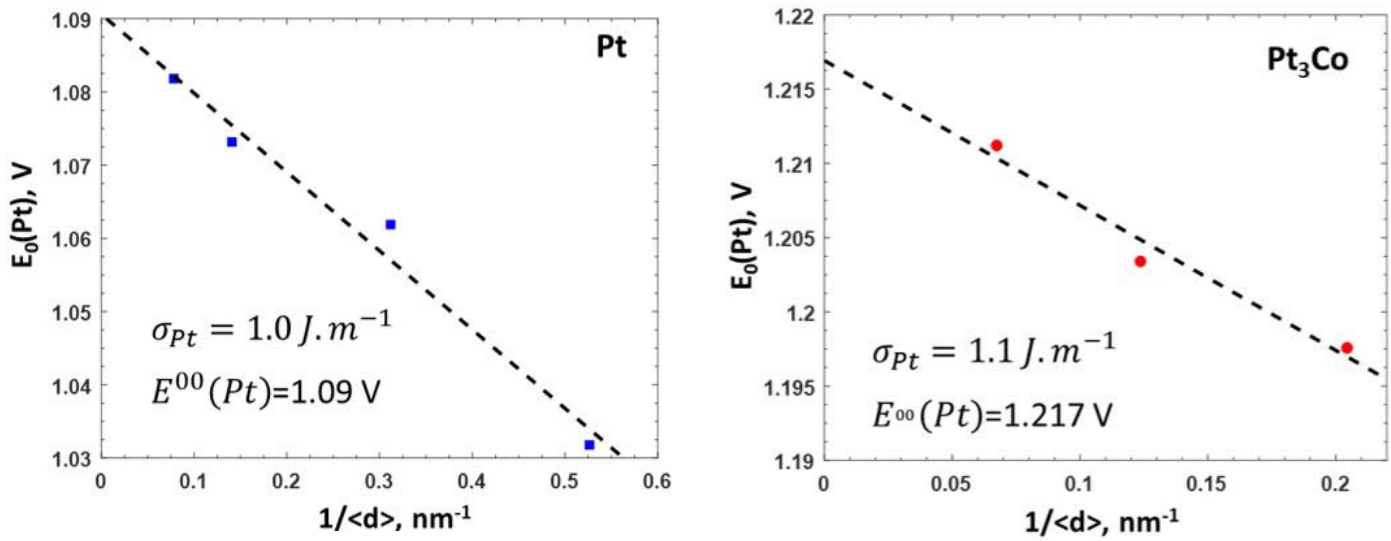

FIGURE 3. Standard potential (E^o) for Pt dissolution ($Pt = Pt^{2+} + 2e^-$) from Pt_3Co alloy and Pt nanoparticles and its dependence on particle diameter. Derived from Pt potentiostatic dissolution data at 0.85 V.

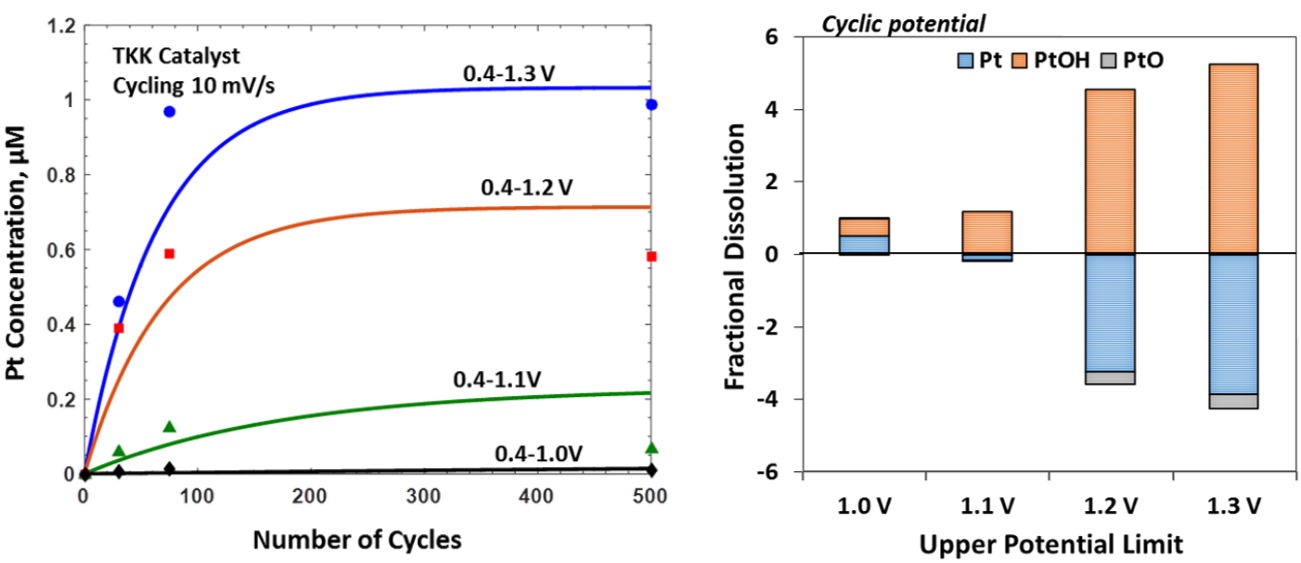

FIGURE 4. Dissolved Pt concentrations as a function of number of triangle potential cycles from 0.4 V to the potentials indicated at a scan rate of 10 mV/s for the TKK Pt_3Co catalyst. Identity of species dissolved as a fraction of the total Pt dissolved. Negative fractions indicate re-deposition.

both oxygen permeability (15%) and ORR kinetics with Ni^{2+} doping of an ionomer film over the Pt microelectrode. These results qualitatively agree with previous RDE measurements of oxygen permeability through an ionomer thin film [1].

A model for carbon corrosion was developed based on a series of in-cell CO_2 evolution measurements during voltage cycling using cells with TKK Pt catalysts cathode catalysts supported on either high surface area Ketjen carbon (E), graphitized low surface area carbon (EA), and intermediate surface area Vulcan (V) [2]. The experimental data were modeled using four potential-dependent processes: (1) formation of active ($C^{\#}OH$) and passive ($C^{\#}O_x$) carbon surface oxide species, (2) formation of OH and oxide surface species on Pt, (3) oxidation of active carbon surface species ($C^{\#}OH$) with OH spill-over from Pt at intermediate potentials, and (4) oxidation of active carbon surface species ($C^{\#}OH$) with H_2O at high potentials. The modeling effort showed that the extents of corrosion are linked to formation of carbon oxides and interaction of these oxides with Pt hydroxide and oxide and water. The corrosion mechanism during drive cycles and the corrosion rates for the three carbon types can be summarized as follows.

- Formation of surface oxides on carbon defect sites (C#)
  - Defect sites hydrolyze to form active oxides ($C^{\#}OH$) at cathode potentials >0.3 V.
  - $C^{\#}OH$ converts to passive oxides ($C^{\#}O_x$) at E > 0.8 V.
- Carbon corrosion is catalyzed by PtOH
  - PtOH begins to form at E > 0.6 V.
  - PtOH converts to PtO at E > 0.9 V.
- Steady-state corrosion mechanism
  - Corrosion rate peaks at ~0.6 V cathode potential, small at 0.95 V.
  - Corrosion is primarily due to oxidation of $C^{\#}OH$ by H_2O.
  - All three carbons (Ketjen [E-type], Vulcan [V-type], and graphitized Ketjen [EA-type]) show similar steady-state corrosion rates.
- Carbon corrosion under transient potentials can be much higher
  - Spikes in corrosion rates while transitioning from high (0.95 V) to low cell potentials (0.4 V) are due to formation of $C^{\#}OH$ and its reaction with PtOH.
  - Larger spikes in corrosion rates while transitioning from low (0.4 V) to high cell potentials (0.95 V) are due to accelerated oxidation of $C^{\#}OH$ by H_2O at elevated potentials.
- Transient corrosion rates: E-Type ~ V-Type >> EA-Type

CONCLUSIONS AND FUTURE DIRECTIONS

Conclusions

- For catalyst particles with solid morphology and over the particle size studied (5–14 nm), Pt_3Co alloy nanoparticles are more stable against Pt dissolution than Pt nanoparticles with potential holds at <1.0 V, but less stable at >1.0 V.
- Subsurface Co in PtCo nanoparticles with a core-shell morphology is stabilized against dissolution with a Co dissolution potential ~880 mV higher than the standard potential for Co dissolution.
- Dissolved Co^{2+} decreases the oxygen permeability of PFSA thin films.
  - Carbon corrosion is primarily due to oxidation of activated carbon oxides, formed on defect sites in the carbon, by H_2O and is catalyzed by PtOH.

Future Directions

This FC-PAD thrust area will continue to focus on the impact of catalyst and support type on performance and durability and the impact of the degradation of these components on the performance impacting properties of other electrode layer components through the following research activities:

- Experimentally determine and model the effects of alloy catalyst morphology on Pt and alloying element dissolution rates (i.e., IRD spongy PtCo and Umicore solid Pt_7Co_3).
- Provide additional data needed for to catalyst degradation model: measurements of Pt re-deposition rates as a function of potential.
- Application of catalyst corrosion model to cell data using transmission electron microscopy-energy dispersive X-ray and X-ray fluorescense quantification of Pt and Co in cell components.
- Correlate changes in Pt and alloying element coordination numbers, bond distances, and surface Pt strain with changes in ORR activity resulting from application of accelerated stress tests.
- Determine impact of Co^{2+} and Ni^{2+} on the oxygen permeability of PFSA thin films as a function of relative humidity and temperature using solid state microelectrode apparatus.
- Determine rates and mechanisms of carbon corrosion for Pt alloy catalysts vs. Pt catalysts of similar particle size distribution.
- Determine effects of carbon type on Pt dissolution rates.

FY 2016 PUBLICATIONS/PRESENTATIONS

Publications/Presentations Relevant to FC-PAD from Thrust Members

1. James A. Gilbert, A. Jeremy Kropf, Nancy N. Kariuki, Stacy DeCrane, XiaopingWang, Somaye Rasouli, Kang Yu, Paulo J. Ferreira, Dane Morgan, and Deborah J. Myers, "In-Operando Anomalous Small-Angle X-Ray Scattering Investigation of Pt_3Co Catalyst Degradation in Aqueous and Fuel Cell Environments," Journal of The Electrochemical Society, 162 (14) (2015) F1487–F1497.

2. Deborah J. Myers, James Gilbert, Nancy N. Kariuki, Xiaoping Wang, A. Jeremy Kropf, Zhiwei Yang, Mallika Gummalla, Mike Perry, Sarah Ball, Jonathan Sharman, Brian Theobald, Alex Martinez, Dash Fongalland, Somaye Rasouli, Kang Yu, and Paulo J. Ferreira, "Mechanisms of PEMFC Cathode Catalyst Dissolution and Degradation X-ray scattering and absorption studies of polymer electrolyte fuel cell cathode electrocatalysts," 3rd International Workshop on Degradation Issues of Fuel Cells and Electrolysers, Santorini, Greece, September 30, 2015. (Invited)

3. Rodney L. Borup, D.D. Papadias, Rangachary Mukundan, Dusan Spernjak, David Langlois, R. Ahluwalia, Karren More, and Steve Grot, "Carbon Corrosion in PEM Fuel Cells During Drive Cycle Operation," ECS Transactions, 69 (17) 1029–1038 (2015).

4. F. Cetinbas, R. Ahluwalia, N. Kariuki (Argonne National Laboratory), K.L. More, D.A. Cullen, B. Sneed (Oak Ridge National Laboratory), R.P. Winarski, J. Ilavsky, V. De Andrade, and D.J. Myers (Argonne National Laboratory), "Structural Characterization and Transport Modeling of Pt and Pt alloy Polymer Electrolyte Fuel Cell Cathode Catalyst Layers," Submitted to the 230th Meeting of the Electrochemical Society.

REFERENCES

1. D. Myers, "Rationally Designed Catalyst Layers for PEMFC Performance Optimization," U.S. Department of Energy, Fuel Cell Technologies Office, 2015 Annual Merit Review and Peer Evaluation. https://www.hydrogen.energy.gov/pdfs/review15/fc106_myers_2015_o.pdf.

2. R. Borup, "V.E.1. Durability Improvements through Degradation Mechanism Studies," U.S. Department of Energy, Fuel Cell Technologies Office, 2015 Annual Progress Report, https://www.hydrogen.energy.gov/pdfs/progress15/v_e_1_borup_2015.pdf.

V.B.3 FC-PAD: Electrode Layer Integration

Shyam S. Kocha (Primary Contact), Jason Christ, Jason Zack, KC Neyerlin (NREL)

Debbie Myers Nancy Kariuki, C. Firat Cetinbas, Rajesh Ahluwalia (Argonne National Laboratory)

Adam Weber, Kelsey Hatzell, Huai-Suen Shiau, Anna Freiburg, Tobias Schuler (Lawrence Berkeley National Laboratory)

Rod Borup, Mukund Rangachary, Natalia Macauley, Mahlon Wilson, Yu Seung Kim (Los Alamos National Laboratory)

Karren More, David Cullen (Oak Ridge National Laboratory)

National Renewable Energy Laboratory (NREL)
15013 Denver West Parkway
Golden, CO 80401
Phone: (303) 275-3284
Email: shyam.kocha@nrel.gov

DOE Managers:

Dimitrios Papageorgopoulos
Phone: (202) 586-5463
Email: Dimitrios.Papageorgopoulos@ee.doe.gov

Gregory Kleen
Phone: (240) 562-1672
Email: Gregory.Kleen@ee.doe.gov

Project Start Date: October 1, 2015
Project End Date: September 30, 2020

Overall Objectives

- Demonstrate improvements in component stability and durability.
- Demonstrate improvements in cell performance due to optimized transport.
- Develop new capabilities (such as advanced diagnostic tools or models) to aid developers, advance knowledge of component properties, and develop advanced structures, strategies, and methods to achieve these objectives.
- The consortium will provide technical capabilities to future projects focusing on performance and durability of polymer electrolyte membrane fuel cells as a resource to DOE and industrial developers.

Fiscal Year (FY) 2016 Objectives

- Identify sources for state-of-the-art (SOTA) electrocatalysts that meet or exceed the DOE mass activity targets of 440 mA/mgPt.
- Integrate SOTA electrocatalysts that meet or exceed the DOE mass activity targets of 440 mA/mgPt and optimize the catalyst layer to attain the DOE peak power density requirements of 1 W/cm^2 and 0.125 gPt/kW while simultaneously meeting durability targets.
- Identify the source(s) of the unanticipated substantial performance losses observed at loading below 0.1 mgPt/cm^2 using existing and novel diagnostic techniques.

Technical Barriers

This project addresses the following technical barriers from Fuel Cells section of the Fuel Cell Technologies Office Multi-Year Research, Development, and Demonstration Plan.

(C) Performance

(B) Cost

(A) Durability

Technical Targets

See Table 1.

TABLE 1. Progress towards Meeting Technical Targets for Electrocatalysts and Membrane Electrode Assemblies (MEAs) for Transportation Applications

Characteristic	Units	DOE 2020 Electrocatalyst and MEA Targets	Project Status (50 cm^2 cell, differential conditions)
Mass activity	A/mg$_{PGM}$ @ 0.9 mV$_{iR\text{-}free}$	≥0.44	≥0.44
PGM total loading	mg-PGM/cm$^2_{geo}$	≤0.125	0.1, cathode
MEA performance	mW/cm$^2_{geo}$ @ 600 mV	≥1,000	700–800

PGM – precious group metals; IR - Internal resistance

FY 2016 Accomplishments

- Three SOTA catalyst layers were identified.
- Catalyst layers evaluated have all met the DOE mass activity target of 440 mA/mgPt.
- Progress has been made on understanding transport through the layer using diagnostic tools and modeling using limiting current diagnostics and kinetic studies.

✧ ✧ ✧ ✧ ✧

INTRODUCTION

The primary objective of the FC-PAD consortium is to implement improvements to polymer electrolyte membrane fuel cells and their components with respect to cost, durability, and performance. Although catalysts that have met the DOE targets of oxygen reduction reaction (ORR) activity have been demonstrated in half-cells, implementing them in cathode catalyst layers at low loadings while maintaining low mass transport at high current densities has been elusive due to the presence of an additional transport resistance at the catalyst-ionomer interface.

The consortium will develop new capabilities (such as advanced diagnostic tools or models) to aid developers, advance knowledge of component properties, and develop advanced structures, strategies, and methods to achieve these objectives that may be summarized as:

- Improvements in component stability and durability
- Improvements in cell performance due to optimized transport
- Development of new diagnostics, characterization tools, and models

The expected outcome will be polymer electrolyte membrane fuel cell MEAs and components that demonstrate world-class performance and durability, meeting and exceeding the 2020 targets listed in the consortium-related target tables in the addendum. The major durability targets to be met include 5,000 h of operation under simulated vehicle power cycling and shut-down/start-up cycling with <10% loss in rated power. In terms of performance, the key targets are meeting efficiency, power, startup time and energy, and related metrics within the cost and durability constraints. In specific developing MEAs with SOTA catalysts that demonstrate performance >1 W/cm^2 with Pt loading <0.125 mg/cm^2.

APPROACH

Our approach involves identifying SOTA catalysts, optimizing them in catalyst layers, developing diagnostics to help resolve the high current density, low loading problem and mitigating the problem through the use of novel electrode design, novel components, novel diagnostics techniques all complemented with modeling. The research concentrates on improving the performance of low Pt loaded electrode layers at high current densities and limiting the degradation losses at the electrode layer level, including electrocatalyst and support composition and morphology changes and electrode-structure changes. Mass-transport issues are a performance limitation at high current densities and during operation under non-optimal conditions, such as with high water content (e.g., encountered at low temperature), with low surface area catalysts at low loadings, and with alloy catalysts, particularly at low relative humidity. In this project, the impact of different catalyst-layer compositions (including low equivalent-weight ionomer) will be explored to ascertain how transport phenomena change. Applying existing diagnostics using limiting current and developing new techniques, the transport limitations will be quantified and the resistance better defined. The formation of electrode layers is still a black art. In this work, various techniques including rheology, dynamic light scattering, etc., will be applied to ink formulations to determine the critical properties to ensure optimal layer structure and performance and durability. Changes including altering the ionomer-solvent-catalyst ink composition, solvent removal methods, and/or ionomer properties, such as equivalent weight, will be explored in coordination with related activities. In addition, to increase high-current-density performance, new electrode-layer structures will be explored including those involving two separate phases of ionomer in the catalyst layer (i.e., a very thin first layer coating the catalyst surfaces to provide local conductivity with a minimal transport barrier and a second phase of a solid network to provide bulk ionic conductivity and structural integrity) as well as extended PGM skins, both of which can be utilized with electrospun ionomer.

RESULTS

Sources and Benchmarking of Catalysts and MEAs

Sources of state-of-the-art (SOTA) and baseline catalysts were identified and obtained from (i) commercial vendors or suppliers of catalysts who can supply hundreds of grams of catalyst, and (ii) novel catalysts that have been developed under DOE programs by various national laboratories that may be available in gram quantities. Ideally, FC-PAD would prefer catalysts that can be analyzed thoroughly before and after performance and durability studies without any restrictions.

IRD, New Mexico, is one of the vendors that provided catalyst and catalyst layers for evaluation by the FC-PAD. Los Alamos National Laboratory obtained catalyst coated membranes (CCMs) from IRD and distributed it to the FC-PAD labs. Catalyst from Umicore, Germany, catalysts have been studied in rotating disk electrode at NREL and their PtCo/C has shown enhanced activity over Pt/C. Umicore has provided Pt/C and PtCo/C catalysts for the FC-PAD through NREL to the various labs for MEA preparation and performance evaluation. General Motors (GM) provided proprietary SOTA MEAs for evaluation. Prior to MEA fabrication and evaluation, screening of some of the catalysts and comparisons were made using Rotating disk electrode techniques [1-6].

Activity and Performance of Baseline and SOTA MEAs in Fuel Cells

The objective was to fabricate and optimize cathode catalysts layers have loadings approaching ~0.1 mg/cm^2 that have high performance and durability for conventional supported catalysts and to develop and apply novel diagnostics to understand issues at high current densities. As new fabrication technology and materials and diagnostics are developed, they will all be applied to obtain MEAs that perform to DOE targets but catalyst layers in this work were fabricated using spray-coating techniques.

The ORR activity of baseline Pt/C has not been updated and reported recently in the literature suing a clearly defined test protocol [7]. Prior to evaluating the SOTA MEAs, the baseline MEAs were evaluated and the results summarized in Figure 1. Baseline as well as SOTA catalysts and catalyst layers were imaged using transmission electron microscopy at Oak Ridge National Laboratory as shown in Figure 2. The ORR activity of PtCo/C SOTA MEAs were evaluated using the same hardware and test protocols as the baseline MEAs. The Tafel plots for the three SOTA MEAs as well as a table reporting the ORR activity and surface area are presented in Figure 3. All the SOTA MEAs met the DOE targets of ORR activity at beginning of life. These results corroborate studies in rotating disk electrode that demonstrated these PtCo/C catalysts as having higher activity compared to baseline Pt/C. The performance of these MEAs under wet hydrogen-air conditions are compared in Figure 4. At this time in the first iteration of fabricating these catalyst layers, the MEAs

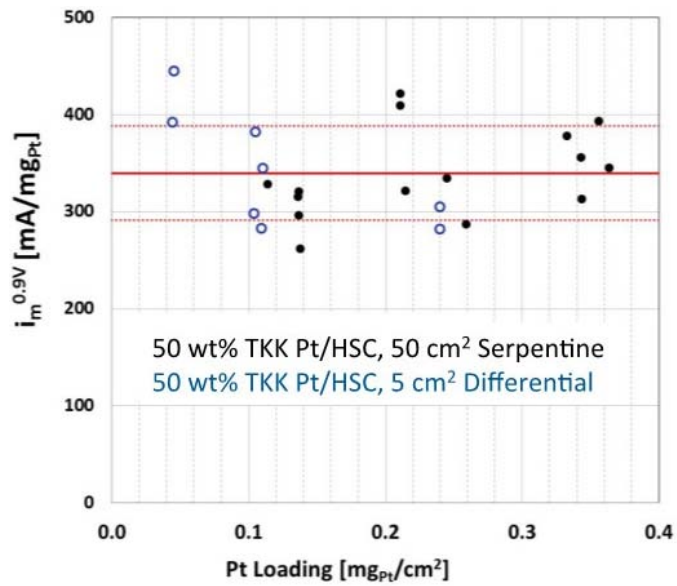

FIGURE 1. Mass activity vs. catalyst loading for 50 wt% baseline Pt/HSC MEAs fabricated at NREL using TKK TEC10E50E Pt/C at various loadings and operating conditions as well as hardware conducted using FC-PAD protocols

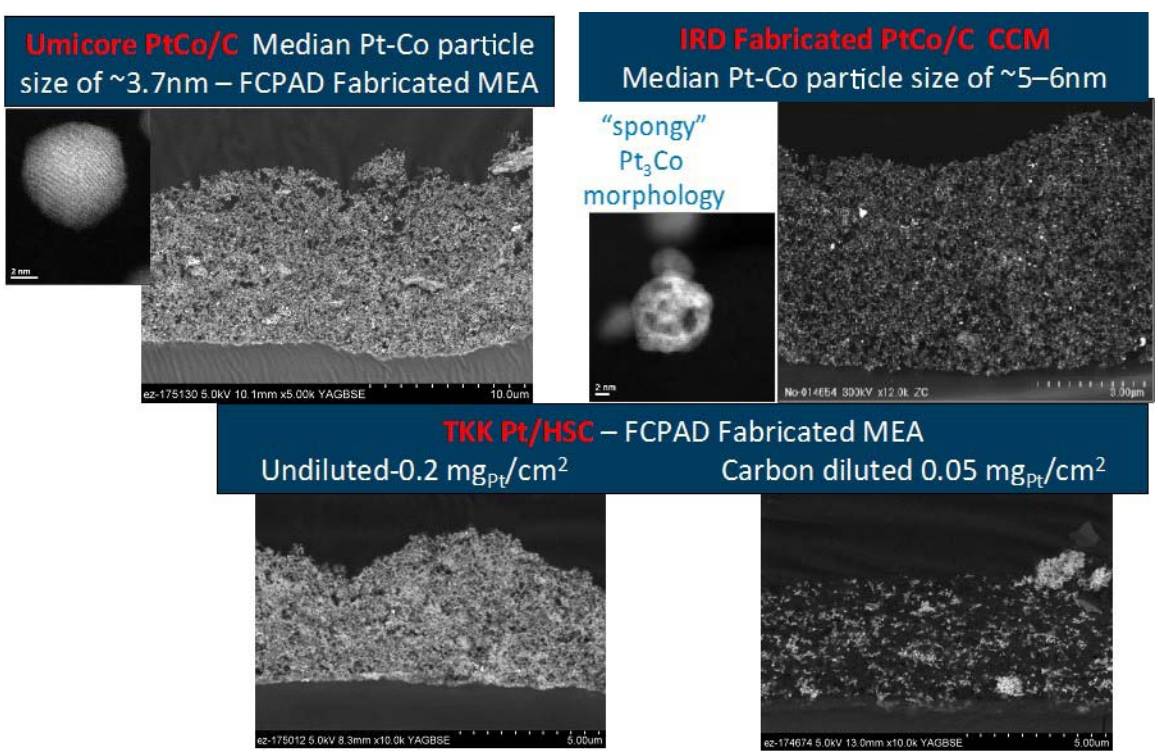

FIGURE 2. Transmission electron microscopy images of electrocatalysts and electrode layers based on SOTA catalysts and baseline Pt/C catalysts

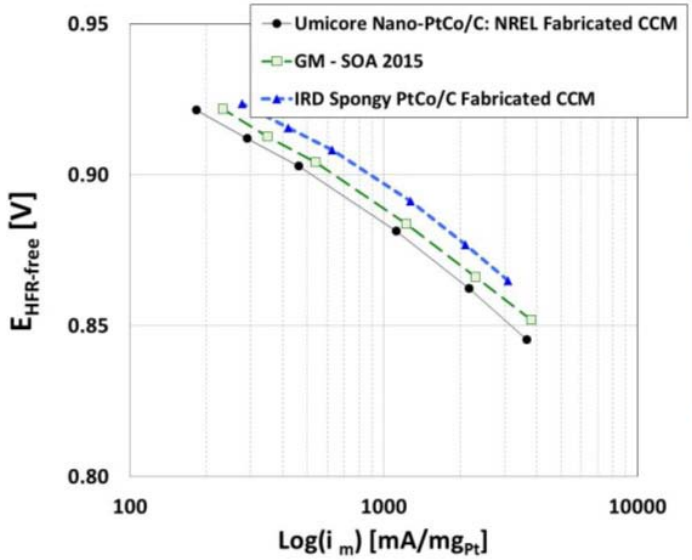

ORR Activity @ 0.90 V

	MA	SA	ECA
Umicore	514 ±40	1406 ±135	37 ±2
GM	620 ±60	1440 ±130	43 ±1
IRD	820 ±20	2000 ±6	41 ±1

MA = mA/mg$_{Pt}$; SA = μA/cm$^2_{Pt}$ ECA = m^2/g$_{Pt}$

SOA – State of the art; ECA – Electrochemical surface area; SA – specific amperage

FIGURE 3. ORR activity of three SOTA catalysts and tabulated activity values. Operating conditions for evaluation are: H_2, O_2 150 kPa, 80°C, 100% RH, S = 2/9.

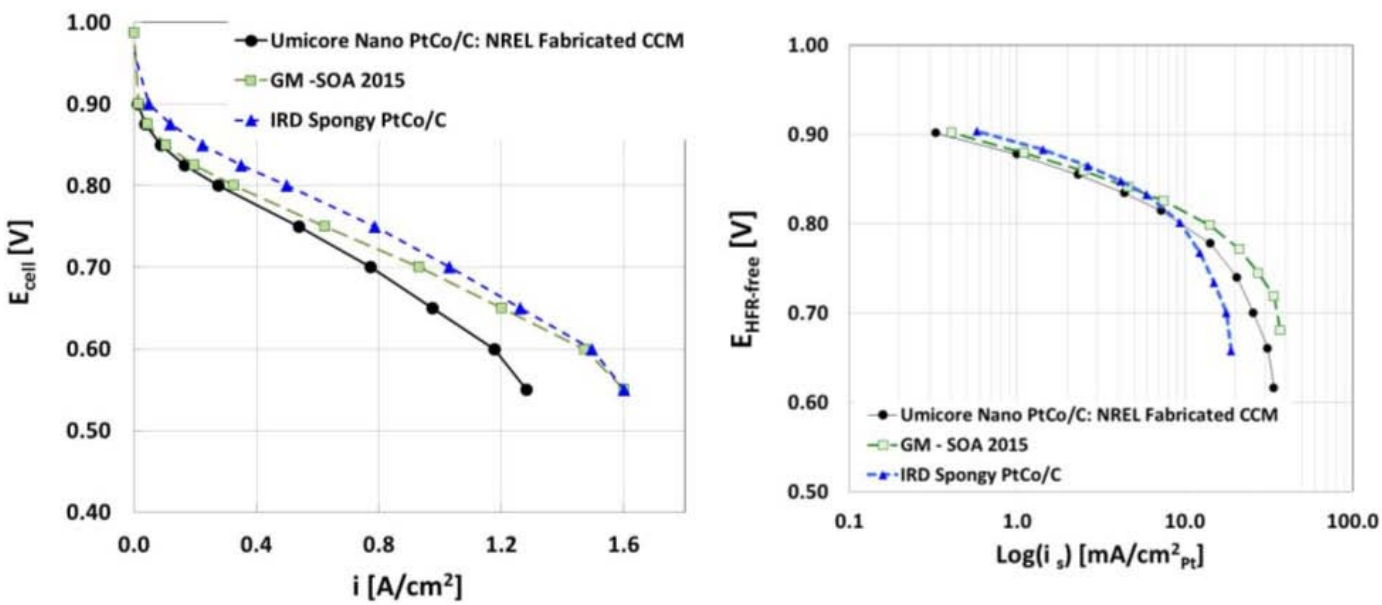

FIGURE 4. H_2-air performance of SOTA catalysts conducted under wet conditions, 80°C, 150 kPa, and 100% RH.

do not meet the high current density or peak power density DOE target. Optimization of these layers is likely to improve the high current density performance approaching limiting currents. Results and insights from parallel work being conducted to diagnose and mitigate the losses at high current density at low catalyst loadings will be applied to the catalyst layers to improve their performance in the future.

Mass Transport Diagnostics Development

In order to understand and resolve the complex issue of lower than expected performance at high current densities for low loaded cathode catalyst layers that have been observed by a majority of groups [8-15], development and refinement of diagnostic techniques is necessary to identify the source(s) of additional losses and find mitigation pathways. FC-PAD will study both existing diagnostics and establish and verify their

value at several labs as well as develop new techniques that may provide insight into the problem.

Several diagnostics have been recently established that involve limiting current studies as well as kinetic studies. Diluted oxygen as well as pure oxygen was employed to obtain limiting currents. The following limiting diagnostics were evaluated:

- Dilute oxygen in nitrogen limiting current data was acquired on Pt/Vu as a function of Pt loading, relative humidity (RH), and oxygen partial pressure.
- Pure oxygen limiting current measurements under vacuum conditions were performed on Pt/Vu as a function of Pt loading, RH, and oxygen partial pressure.
- CO limiting current data was acquired on Pt/Vu electrodes to assess the relevance of such measurements in the future towards the elucidation of local Pt transport resistance.

Since it is not known if the kinetics of ORR changes at low potentials and low oxide coverage, it is important to determine the kinetics accurately so that any additional losses can be identified and attributed to alternative sources that are relevant to high current density operation. This kinetic information is also crucial for inputting in models. Sub-ambient ORR kinetic measurements were conducted along with Pt oxide dependent kinetics on Pt/Vu electrodes using a vacuum panel system and a highly automated test stand. These measurements were coupled with the Pt oxide measurements to produce a Pt oxide dependent kinetic model. Analysis of the magnitude of local resistance at the catalyst-ionomer interface from limiting currents is elucidated in Figure 5.

Electrode-Layer Designs and Fabrication

The cathode catalyst layer structure is typically based of an ink of Pt/C, ionomer and solvents that are sonicated or mixed together to form a slurry. Advancement of the catalyst layer is possible through the separation of some of the functions and better pathways for protonic transport. Excessive ionomer mixed with an ink leads to catalyst layers that flood due to plugged pores. By providing a major low resistance highway for protons to move through the catalyst layer by means of fibers or a network and lowering the amount of ionomer that is applied directly to the catalyst surface, it may be possible to obtain a much higher performance electrode. Ionomer adsorption may also be reduced if less ionomer is in direct contact with the Pt. Using electro-spun fiber in the catalyst layer is one of the design pathways. Issues such as fiber integrity are being addressed by choice of solvent, use of TBA^+ blended with Na^+ and heat treatment. Temperature and TBA+ can be tailored to obtain preferred structures. Spray coating of the ink onto the membrane requires elimination of the hot pressing step and cryo-milling of the fibers. Insights from these studies will be input into obtaining high performance using commercial as well as laboratory synthesized scale state-of-the-art catalysts. Research was conducted at Los Alamos National Laboratory on improving the solubility resistance of electro-spun ionomer fibers to withstand MEA processing conditions by using the TBA+ ionomer form. For example, Na^+ form ionomer fibers heat treated at 200°C are substantially distorted and dissolved or recast by simple additions of methanol. Varying TBA+/Na+ ratios and heat treatments: by exchanging the Nafion in the electro-spinning solution into the tetrabutyl-ammonium cation (TBA+) form, the spun fibers become thermoplastic. Thus heat treatments substantially improve the durability of the spun fibers. However, the extremely thin fibers melt very easily and coalesce even at relatively modest temperatures if the ionomer is in the purely TBA^+ form. Thus, work progresses in identifying suitable TBA^+/Na^+ ratios and treatment temperatures. Even the low TBA^+ content results in appreciable fusion, but if carefully controlled the process can potentially yield highly advantageous fiber networks.

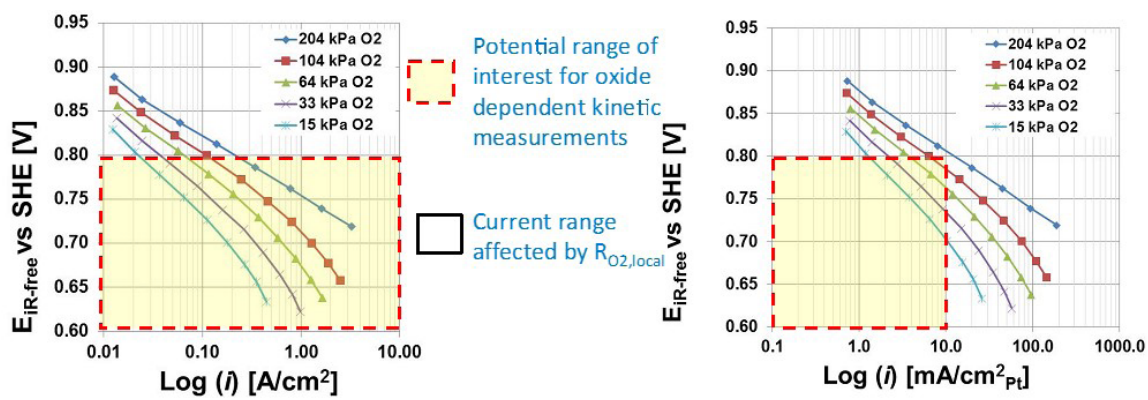

SHE – Standard hydrogen electrode

FIGURE 5. Oxide dependent Pt kinetics for Pt/Vu 0.05 mg_{Pt}/cm^2 conducted under H_2/O_2 80°C, 100% RH and 150 kPa

Optimization of the electrode components like ionomer morphology and content are being pursued to improve fuel cell performance at high current densities. Modeling results have indicated that controlled thickness and density variations in the catalyst layer can lead to improved water management and better fuel cell performance. To make controlled Pt layer stratifications, multiple approaches are being explored; the primary progress towards catalyst layer stratification was by developed designed catalyst layer structures via a spray coating technique. This technique is used to fabricate electrodes with stratified catalyst layers with alternating thick and thin layers providing a pathway for the liquid water to efficiently exit the catalyst layer efficiently, thus preventing flooding at high current densities.

CONCLUSIONS AND FUTURE DIRECTIONS

All three SOTA catalyst layers evaluated so far have met the DOE MA target of 440 mA/mg_{Pt} but do not meet the peak power requirements. Preliminary work has been conducted on developing modified electrode layer designs intended to reduce mass transport in the catalyst layer. Progress has been made on understanding transport through the layer using diagnostic tools and modeling.

Future work involves the following: (a) determine whether kinetics actually comes into play at high current densities; (b) identify and implement alternative ionomers in catalyst layers to examine effects on performance; (c) model performance diagnostics data at high current densities; and (d) identify alternative designs for cathode catalyst layer that enhance both performance and durability at high current densities.

REFERENCES

1. Shinozaki, Kazuma, Jason W. Zack, Ryan M. Richards, Bryan S. Pivovar, and Shyam S. Kocha. "Oxygen Reduction Reaction Measurements on Platinum Electrocatalysts Utilizing Rotating Disk Electrode Technique I. Impact of Impurities, Measurement Protocols and Applied Corrections." Journal of the Electrochemical Society 162, no. 10 (2015): F1144–F1158.

2. Shinozaki, Kazuma, Jason W. Zack, Svitlana Pylypenko, Bryan S. Pivovar, and Shyam S. Kocha. "Oxygen reduction reaction measurements on platinum electrocatalysts utilizing rotating disk electrode technique II. Influence of ink formulation, catalyst layer uniformity and thickness." Journal of the Electrochemical Society 162, no. 12 (2015): F1384–F1396.

3. Shinozaki, Kazuma, Jason W. Zack, Svitlana Pylypenko, Ryan M. Richards, Bryan S. Pivovar, and Shyam S. Kocha. "Benchmarking the oxygen reduction reaction activity of Pt-based catalysts using standardized rotating disk electrode methods." International Journal of Hydrogen Energy 40, no. 46 (2015): 16820–16830.

4. Shinozaki, Kazuma, Yu Morimoto, Bryan S. Pivovar, and Shyam S. Kocha. "Suppression of oxygen reduction reaction activity on Pt-based electrocatalysts from ionomer incorporation." Journal of Power Sources 325 (2016): 745–751.

5. Kocha, Shyam S., and Kazuma Shinozaki. "Suppression of Oxygen Reduction Reaction on Pt-Based Electrocatalysts from Ionomer Interaction." In Meeting Abstracts, no. 37, pp. 1432–1432. The Electrochemical Society, 2015.

6. Shinozaki, Kazuma, and Shyam S. Kocha. "Re-Examination of the Particle Size Effect on the ORR for Nafion-Free Ultrathin Uniform Pt/C Catalyst Layers." In Meeting Abstracts, no. 37, pp. 1327–1327. The Electrochemical Society, 2015.

7. Bender, Guido, and Shyam S. Kocha. (Invited) "Benchmarking and Protocol Development for Data Comparison Between Laboratories." In Meeting Abstracts, no. 24, pp. 1486–1486. The Electrochemical Society, 2015.

8. "Considerations of Oxide Species Coverage on the Kinetic Parameters of Pt-based Catalysts," Jason Christ, GM folks, Shyam S. Kocha and KC Neyerlin.

9. A. Kongkanand and M. F. Mathias, Journal of Physical Chemistry Letters, 7, 1127 (2016).

10. N. Subramanian, T. Greszler, J. Zhang, W. Gu and R. Makharia, Journal of The Electrochemical Society, 159, B531 (2012).

11. A. Kongkanand, J.E. Owejan, S. Moose, M. Dioguardi, M. Biradar, R. Makharia, Journal of The Electrochemical Society, 159, F676 (2012).

12. T.A. Greszler, D.A. Caulk, P. Sinha, Journal of the Electrochemical Society 159, F831 (2012).

13. K. Shinozaki, H. Yamada, Y. Morimoto K. Journal of the Electrochemical Society, 158, B467 (2011).

14. H. Iden, T. Mashio, A. Ohma, Journal of Electroanalytical Chemistry 708, 87 (2013).

15. T. Suzuki, K. Kudo, Y. Morimoto, Journal of Power Sources, 222, 379 (2013).

V.B.4 FC-PAD: Ionomer, GDLs, Interfaces

Adam Weber[1] (Primary Contact), Ahmet Kusoglu[1], Kelsey Hatzell[1], Lalit Pant[1], Shouwen Shi[1], Rangachary Mukundan[2], Yu Seung Kim[2], Andrew Baker[2], Rod Borup[2], Karren More[3], Huyen Dinh[4], K.C. Neyerlin[4], Debbie Myers[5], Nancy Karuiki[5], Rajesh Ahluwalia[5]

[1]Lawrence Berkeley National Laboratory (LBNL)
1 Cyclotron Rd., MS70-108B
Berkeley, CA 94720
Phone: (510) 486-6308
Email: AZWeber@lbl.gov

[2] Los Alamos National Laboratory (LANL), Los Alamos, NM
[3] Oak Ridge National Laboratory (ORNL), Oak Ridge, TN
[4] National Renewable Energy Laboratory (NREL), Golden, CO
[5] Argonne National Laboratory (ANL), Argonne, IL

Additional No-Cost Partners:

- Tufts University, Iryna Zenyuk
- Paul Scherrer Institute, Felix Buchi and Jens Eller
- 3M Company, Michael Yandrasits and Steve Hamrock
- University of Delaware, Mike Santare
- Colorado School of Mines, Andy Herring

DOE Managers:

Dimitrios Papageorgopoulos
Phone: (202) 586-5463
Email: Dimitrios.Papageorgopoulos@ee.doe.gov

Gregory Kleen
Phone: (240) 562-1672
Email: Gregory.Kleen@ee.doe.gov

Project Start Date: October 1, 2015
Project End Date: September 30, 2020

Overall Objectives

- Demonstrate improved performance and durability of fuel cells.
- Develop and implement characterization techniques for gas diffusion layers (GDLs), membranes, and ionomers.
- Characterize and understand the effects of interfaces and interfacial properties on fuel cell performance and durability.
- Elucidate and mitigate ionomer film resistances in the catalyst layer through model studies to better evaluate performance and durability of fuel cells.
- Explore and optimize transport phenomena related to liquid water.

Fiscal Year (FY) 2016 Objectives

- Characterize ionomer thin films to determine substrate interactions and impact of confinement.
- Initiate studies on ionomer thin film formation.
- Examine membrane durability strategies.
- Model impact of interfaces on transport phenomena and cell performance.
- Explore multiphase flow and interactions within the GDLs using advanced diagnostics and imaging.

Technical Barriers

This project addresses the following technical barriers from the Fuel Cells section of the Fuel Cell Technologies Office Multi-Year Research, Development, and Demonstration Plan.

(A) Durability

(B) Cost

(C) Performance

FY 2016 Accomplishments

- Initiated studies on ionomer formation from inks using X-ray and light scattering and compared the impact of different solvents on electrode morphology.
- Characterized ionomer thin-film structure and properties for different conditions as a function of equivalent weight and side-chain length.
- Characterized Nafion® XL to understand the transport and mechanical properties and how they vary compared to standard Nafion.
- Explored changes due to hygrothermal ageing of membranes in terms of mechanical and transport properties.
- Correlated cerium movement and washout from membranes with cell-level performance.
- Examined composite membranes and reinforcement.
- Modeled the impact of interface effects for water droplets at the GDL/channel interface and water flooding at the catalyst layer/microporous layer (MPL) interface.

- Measured the interfacial resistance of ionomers as a function of humidity, temperature, and side-chain length.
- Measured and visualized water evaporation from GDLs using X-ray tomography.

✧ ✧ ✧ ✧ ✧

INTRODUCTION

The FC-PAD consortium was formed to advance performance and durability of polymer electrolyte membrane fuel cells (PEMFCs) to meet DOE targets and further enable their commercialization. The major challenge to be addressed by this consortium is to develop the knowledge base and optimize structures for more durable, high-performing PEMFC component technologies, while simultaneously reducing cost. In this project, we will develop validated models and advanced in- and ex-situ characterization techniques to further improve the performance and durability of fuel cells. We will also evaluate PEMFC component issues from low to operating temperatures of interest, including the impact of liquid water. We will characterize and understand components from the membrane to the porous media and their interfaces, with a focus on the ionomer within the catalyst layers.

APPROACH

The FC-PAD consortium incorporates national laboratory investigators with proven experience (developed in prior projects) related to durability, transport, and performance, and combines them into one highly coordinated effort. The effort is sub-divided into six thrust areas, including three materials-related thrusts and three cross-cutting thrusts. This report summarizes some of the work performed in the three cross-cutting thrust areas: 1) Modeling and Validation; 2) Operando Evaluation: Benchmarking, Accelerated Stress Tests, and Contaminants; and 6) Component Characterization and Diagnostics. The thrust areas of the consortium are highly integrated, and the work performed related to the various specific components is presented in the reports of the three materials thrust areas. The project will also benchmark the performance and durability of state-of-the-art membrane electrode assemblies provided by original equipment manufacturers and materials suppliers. Finally, the project will apply in situ and ex situ characterization techniques to reveal the performance losses and related degradation mechanisms operating in fuel cells and propose strategies to improve performance and durability.

Thrust 3 focuses on the membrane, GDLs, MPLs, catalyst-layer ionomer, and the interfaces between these components. The overall approach is to elucidate the governing phenomena using advanced diagnostics and continuum-level modeling, and use that knowledge to optimize performance and durability by mitigating the identified critical bottlenecks.

RESULTS

It is well accepted that low-Pt-loaded electrodes suffer from a local resistance that is due in part to mass transport [1,2]. It is believed that such resistance could be due to the ionomer films covering the reaction site, and thus we have investigated different ionomers to determine their properties and behavior. Going towards lower equivalent weight (EW) could enable better transport; thus, we have characterized 3M as well as Nafion perfluorinated sulfonic acid (PFSA) ionomers across lengthscales. In particular, we investigated their morphology and swelling as bulk membrane (>10 µm) and dispersion-cast thin film (<100 nm) to identify the roles of EW and side-chain length in phase separation across lengthscales. For the first time, humidity-dependent structural changes as well as different PFSA chemistries were explored in the thin-film regime, allowing for the development of a thickness-EW phase diagram as shown in Figure 1. Such a finding can serve as a basis for those trying to understand, synthesize, and improve these materials. It was also found that the ratio of macroscopic (thickness) to nanoscopic (domain spacing) swelling during hydration is affine (1:1) in thin films, but increases as the thickness approaches bulk, revealing the existence of a mesoscale organization governing the multiscale swelling in PFSAs. Ionomer chemistry, in particular the EW, is found to play a key role in altering the confinement-driven structural changes, including anisotropy, in PFSA thin films, with

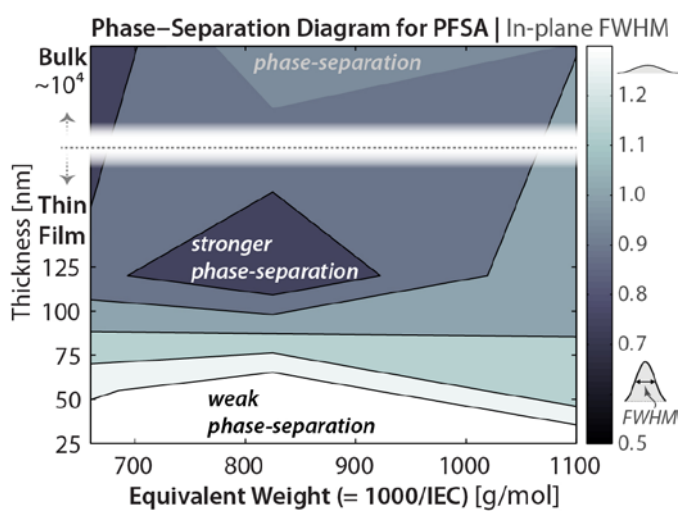

FIGURE 1. Phase-separation diagram generated from the full-width half max (FWHM) values of the ionomer peak determined from small angle X-ray scattering for bulk and thin-film PFSA ionomers

phase separation becoming weaker as the film thickness is reduced below 25 nm or as EW is increased. For the lower-EW 3M PFSA ionomers, confinement appears to induce even stronger phase separation accompanied by domain alignment parallel to the substrate. Finally, studies were initiated on the formation of these ionomer films in electrodes where detailed characterization of the inks and the resultant morphology were started. It was seen how the choice of casting solvent changes the colloid size and eventually the ionomer distribution in the electrode, where the LANL dispersion demonstrated the best Pt and ionomer distribution.

The ionomer thin films can also be related to suspected different interfacial morphology of bulk membranes. To analyze this interface, we developed a water-transport setup where the water flux is measured as a function of membrane thickness for differential humidity changes. This was accomplished with different EW and side-chain PFSAs. As shown in Figure 2, it is found that contrary to intuition, shorter side-chain ionomers demonstrate a larger interfacial resistance than Nafion. As membranes become thinner, such interfacial resistance can dominate the overall water response of the membrane and thus could limit transport. In addition, composite structures, including reinforced membranes, could exhibit multiple interfaces. On this last point, Nafion XL was studied to determine its various mechanical and transport properties, including anisotropic behavior, due to the reinforcement to establish structure/function/property relationships. It was also found that (pre)conditioning of the membrane by heating in water at different temperatures could have significant impacts on its structure/property relationship, in particular, the mechanical stability and conductivity, and its anisotropy.

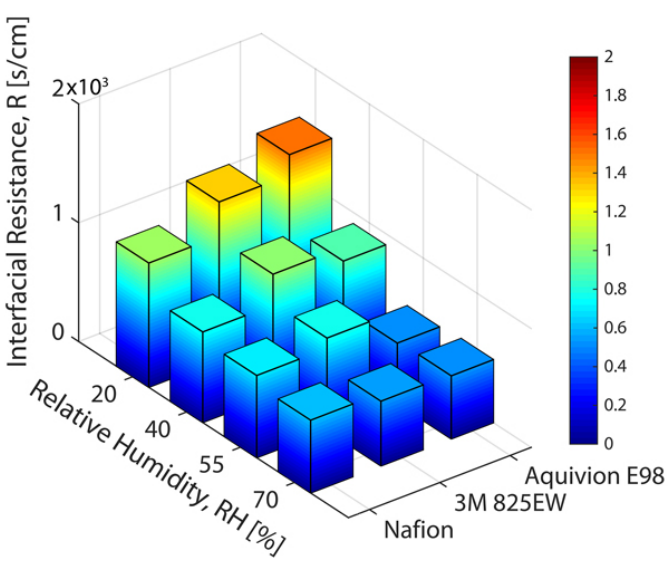

FIGURE 2. Membrane interfacial resistance for water transport as a function of humidity for three different PFSA ionomers

In terms of membrane durability, the impact of hygrothermal ageing on membrane properties was explored, where minor contamination resulted in the membrane becoming more brittle and having lower water uptake and conductivity. This was related to possible cross-linking between the ionic groups, and ageing at mid humidities provided the most severe effects. In terms of chemical durability, extensive work on the movement of Ce, a common radical scavenger, was conducted. It was determined that Ce moves quite rapidly through a membrane, especially when an ionic potential gradient is applied that effectively drives protons as well as water molecules through the membrane. The Ce content of membrane electrode assemblies was shown to migrate towards the gasket regions and the catalyst layers and was sustained there even after the applied potential was removed. In accelerated stress tests, it was shown how the fluoride emission rate was coupled to the Ce concentration (see Figure 3), thus implying that the Ce is removed to the liquid water once there are sufficient anions due to membrane fragmentation. Thus, there is a feedback where increased degradation results in more fluoride emission and hence less protection by Ce, leading to more degradation. As Figure 3 shows, this removal mechanism and degradation occur more rapidly for wet/dry cycling rather than different humidity holds, where saturated conditions provide the most stability for the membrane and Ce.

For exploring multiphase water interactions, both modeling and experimental studies were conducted. It was shown how poor contact between the MPL and catalyst layer can result in zones with a high propensity to flood, thus limiting performance, especially if they occur under the channels. Interestingly, constant-current simulations demonstrate a much larger performance decrease than constant-potential ones, thereby suggesting that cells in stacks (which are constant-current) may have different performance than single-cell tests (which are

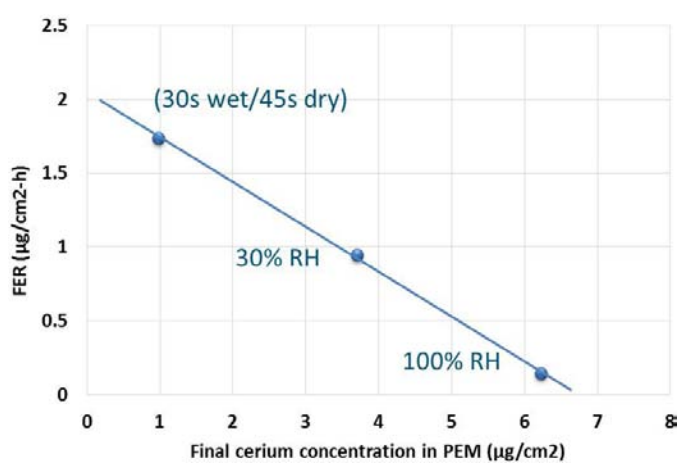

FIGURE 3. Fluoride emission rate after different cell testing—either cycling or hygrothermal ageing—as a function of final cerium concentration in the membrane (RH = relative humidity)

constant-potential). Also, the impact of water dynamics and droplet emergence from the GDL to the channel in terms of capillary pressure was explored, and a criterion for when time-averaging can be used for the boundary condition was developed. In terms of other interactions, an extensive study on evaporation kinetics and mechanisms was conducted for GDLs using a combination of theory and X-ray tomography imaging. Thus, the evaporation rate under different conditions was measured and correlated to the actual liquid/vapor interfacial area measured by the tomography (see Figure 4). The results demonstrate that once this area is considered, the evaporation rate is constant and not increasing as one would measure experimentally. In particular, the interfacial surface area is essentially linear with saturation or total water volume fraction. The concomitant modeling demonstrated that the evaporation was heat and mass-transfer limited and not kinetically limited; thus, the actual evaporation kinetics are rapid.

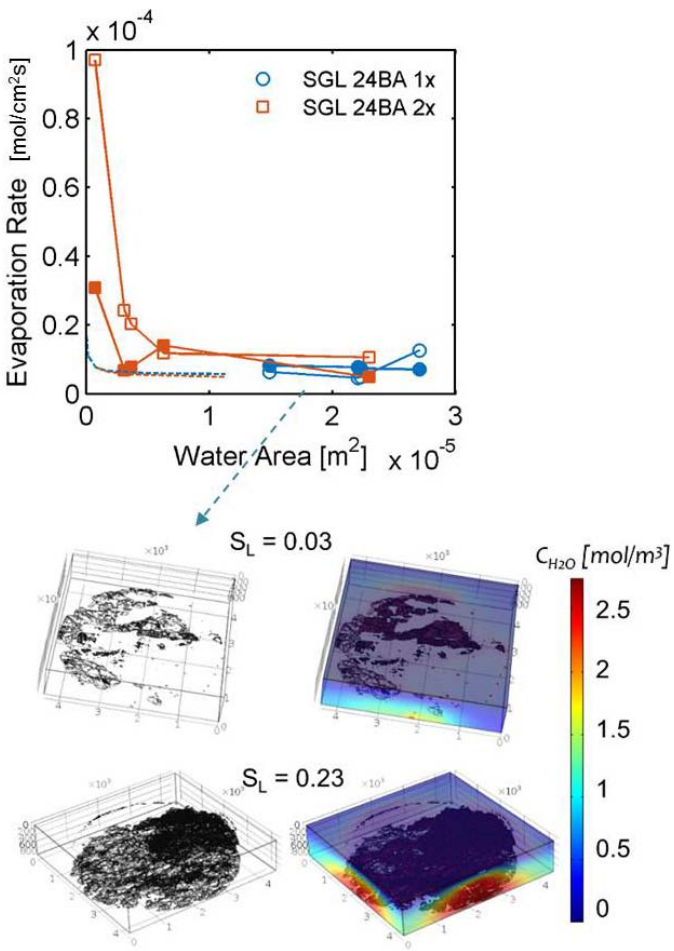

FIGURE 4. Measured evaporation rate as a function of measured water area for two different GDLs. The bottom shows the X-ray tomographs at two saturations and evaporation simulation results.

CONCLUSIONS AND FUTURE DIRECTIONS

To optimize performance and durability of fuel cell components, including ionomers, interfaces, and diffusion media, in this thrust of FC-PAD, we have enacted a synergistic combination of the crosscutting thrusts to explore component properties, behavior, and phenomena. Combined modeling and experiment to understand interfaces demonstrated the water-related issues, including blockage and droplet conditions, along with accurate measurements as to how interfacial area scales with saturation in GDLs. Newer shorter-side-chain and lower-EW ionomers demonstrate interfacial water-transport resistance as membranes and intriguing phase separation for thin films around the 50-nm range. For membrane durability, Nafion XL is promising, but there are concerns both with the mechanical reinforcement breaking as well as cerium migration to the electrodes and perhaps out the effluent water with membrane degradation products.

Going into the future work, the membrane focus on reinforcement and side chains will continue as well as further exploration of the relationship between cerium migration and durability, where the focus will be on understanding the relative influence of each migration mechanism and determining methods to stabilize cerium in the polymer electrolyte membrane and localize it to areas of highest radical generation. For the ionomer diagnostics, there is a continued need to understand thin films, develop a thin-film structure/property model, and explore the conditioning protocols for thin films relevant to catalyst-layer preparation. This last effort will be synergistic to understanding the impact of dispersions and casting on catalyst-layer performance, including direct observation of shear-induced transformation of dilute solutions and using model compounds to elucidate interactions during solvent evaporation with different solvents. Finally, for the various porous media, multiphase simulations with an emphasis on interfacial effects will be explored for both the membrane and GDL/channel.

FY 2016 PUBLICATIONS/PRESENTATIONS

1. Adam Weber, "Understanding Transport in Polymer-Electrolyte Fuel-Cell Ionomer," Colloquium, U. Kansas, 2015. (invited)

2. Iryna V. Zenyuk, Ezequiel Medici, Jeffrey Allen, and Adam Z. Weber, "Coupling continuum and pore-network models for polymer-electrolyte fuel cells," *International Journal of Hydrogen Energy*, 40, 16831–16845 (2015). doi: 10.1016/j.ijhydene.2015.08.009

3. Iryna V. Zenyuk and Adam Z. Weber, "Understanding Liquid-Water Management in PEFCs using X-ray Computed Tomography and Modeling," ECS Conference, Phoenix, 2015. (invited)

4. Ahmet Kusoglu, Thomas J. Dursch, and Adam Z. Weber, "Nanostructure/Swelling Relationships of Bulk and Thin-Film PFSA Ionomers," *Advanced Functional Materials*, 26, 4961–4975, (2016). doi: 10.1002/adfm.201600861

5. Ahmet Kusoglu and Adam Weber, "Exploring the Parameters Controlling the Crystallinity-Conductivity Correlation of PFSA Ionomers," APS Meeting, Baltimore, March 2016.

6. Ahmet Kusoglu and Adam Weber, "Understanding Ionomer Thin-Films in Fuel Cells," *MRS Meeting*, Phoenix, March 2016. (*invited*)

7. Iryna V. Zenyuk and Adam Z. Weber, "Understanding Liquid-Water Management in PEFCs Using X-Ray Computed Tomography and Modeling," *ECS Transactions*, **69** (17), 1253–1565 (2015). doi: 10.1149/06917.1253ecst.

8. Shouwen Shi, Thomas J. Dursch, Rod L. Borup, Adam Z. Weber, and Ahmet Kusoglu, "Effect of Hygrothermal Ageing on PFSA Ionomers' Structure/Property Relationship," *ECS Transactions,* **69** (17), 1017–1025 (2015). doi: 10.1149/06917.1017ecst.

9. Iryna V. Zenyuk, Prodip K. Das, and Adam Z. Weber, "Understanding Impacts of Catalyst-Layer Thickness on Fuel-Cell Performance via Mathematical Modeling," *Journal of the Electrochemical Society*, **163** (7), F691–F703 (2016). doi: 10.1149/2.1161607jes.

10. Shouwen Shi, Adam Z. Weber, and Ahmet Kusoglu, "Structure/property relationship of Nafion XL composite membranes," *Journal of Membrane Science*, **516**, 123–134 (2016). doi: 10.1016/j.memsci.2016.06.004

11. Ahmet Kusoglu and Adam Z. Weber, "Electrochemical/Mechanical Coupling in Ion-Conducting Soft Matter," *The Journal of Physical Chemistry Letters*, **6**, 4547–4552 (2015). doi: 10.1021/acs.jpclett.5b01639 (*perspective*)

12. Shouwen Shi, Thomas J. Dursch, Colin Blake, Rangachary Mukundan, Rodney L. Borup, Adam Z. Weber, and Ahmet Kusoglu, "Impact of Hygrothermal Ageing on Structure/Function Relationship of Perfluorosulfonic-acid membrane," *Journal of Polymer Science B: Polymer Physics*, **54** (5), 570–581 (2016). doi: 10.1002/polb.23946

13. Adam Weber, "Understanding Transport and Limitations in Fuel-Cell Catalyst Layers," FC Cubic, Tokyo, Japan, 2016.

14. A. Kusoglu and A.Z. Weber, "Understanding Ionomer Thin Films," MRS Meeting, Phoenix, 2016.

15. A.Z. Weber and A. Kusoglu, "Understanding Transport in Polymer-Electrolyte-Fuel-Cell Ionomer Thin Films," MRS Meeting, Phoenix, 2016.

16. A.Z. Weber, "Multiscale Modeling of Polymer-Electrolyte-Fuel-Cell Components," ECS meeting, San Diego, 2016. (keynote)

17. A.Z. Weber and R. Ahluwalia, "Modeling Performance and Durability in Polymer-Electrolyte Fuel Cells," CaRPE-FC, Vancouver, 2016.

18. Andrew M. Baker, Dusan Spernjak, Rangachary Mukundan, Rod L. Borup, Suresh G. Advani, and Ajay K. Prasad, "Cerium Migration during PEM Fuel Cell Accelerated Stress Testing," 228th ECS Meeting (2015).

19. Andrew M. Baker, Dusan Spernjak, Rangachary Mukundan, Rod L. Borup, Suresh G. Advani, and Ajay K. Prasad, "Cerium Migration during PEM Fuel Cell Operation," 2015 Fuel Cell Seminar and Energy Exposition (2015).

20. Iryna V. Zenyuk and Adam Z. Weber, "Understanding Liquid-Water Management in PEFCs using X-ray Computed Tomography and Modeling," 228th ECS Meeting (2015).

21. Ahmet Kusoglu and Adam Weber, "Correlating Transport And Stability Of Ion-Exchange Polymers Through Nanostructure," Pacifichem 2015 (2015).

22. Shouwen Shi, Colin Blake, Rodney L. Borup, Rangachary Mukundan, Adam Z. Weber, and Ahmet Kusoglu, "Effect of Hygrothermal Ageing on PFSA Ionomers' Structure/Property Relationship," 228th ECS Meeting (2015).

23. Iryna V. Zenyuk, Adrien Lamibrac, Jens Eller, Felix N. Büchi, and Adam Z. Weber, "Understanding Evaporation in Fuel-Cell Gas-Diffusion Layers with X-ray Computed Tomography," Interpore: 8th International Conference on Porous Media, Cincinnati, May 2016.

24. Rodney L. Borup, Rangachary Mukundan, Dusan Spernjak, David Langlois, G. Maranzana, A. Lamibrac, J. Dillet, S. Didierjean, O. Lottin, L. Guetaz, D.D. Papadias, R. Ahluwalia, and Karren More, "Material Degradation in PEM Fuel Cells," MRS Meeting, Phoenix, March 2016. (*invited*)

REFERENCES

1. A.Z. Weber, A. Kusoglu, J. Mat. Chem. A, 2014, 2, 17207.

2. A. Kongkanand, Mark F. Mathias, J. Phys. Chem. Lett., 2016, 7 (7), 1127–1137.

V.B.5 FC-PAD: Modeling, Evaluation, Characterization

Rangachary Mukundan[1] (Primary Contact), Rod Borup[2], David Langlois[2], Jacob Spendelow[2], Natalia Macauley[2], Karren More[3], David Cullen[3], Huyen Dinh[4], Guido Bender[4], K. C. Neyerlin[4], Shyam Kocha[4], Rajesh Ahluwalia[5], Adam Weber[6]

[1]Los Alamos National Laboratory
MS D429, P.O. Box 1663
Los Alamos, NM 87545
Phone: (505) 665-8523
Email: Mukundan@lanl.gov

[2]Los Alamos National Laboratory, Los Alamos, NM

[3]Oak Ridge National Laboratory, Oak Ridge, TN

[4]National Renewable Energy Laboratory, Golden, CO

[5]Argonne National Laboratory, Argonne, IL

[6]Lawrence Berkeley National Laboratory, Berkeley, CA

DOE Managers:

Dimitrios Papageorgopoulos
Phone: (202) 586-5463
Email: Dimitrios.Papageorgopoulos@ee.doe.gov

Gregory Kleen
Phone: (240) 562-1672
Email: Gregory.Kleen@ee.doe.gov

Project Start Date: October 1, 2015
Project End Date: September 30, 2020

Overall Objectives

- Demonstrate improved performance and durability of fuel cells.
- Develop and implement characterization techniques to better evaluate performance and durability of fuel cells.
- Develop and implement validated fuel cell models.
- Develop and optimize accelerated stress tests (ASTs) to rapidly evaluate durability of fuel cells.
- Quantify the effect of impurities on fuel cell performance and durability.

Fiscal Year (FY) 2016 Objectives

- Refine membrane and electrocatalyst ASTs.
- Evaluate the durability of state-of-the-art (SOA) alloy catalyst-based membrane electrode assemblies (MEAs).
- Quantify effect of sulfate poisoning on fuel cell performance.
- Develop models to address the mass transport limitation in low Pt loaded MEAs at high current densities.
- Develop new diagnostic capabilities including reference electrodes and segmented cells.

Technical Barriers

This project addresses the following technical barriers from the Fuel Cells section (3.4) of the Fuel Cell Technologies Office Multi-Year Research, Development, and Demonstration Plan.

(A) Durability

(B) Cost

(C) Performance

Technical Targets

See Table 1.

FY 2016 Accomplishments

- Developed a combined mechanical/chemical membrane AST and a more accelerated (5X) electrocatalyst AST.
- Discovered that alloy catalysts of ≥5.5 nm particle size do not show coarsening.

TABLE 1. Progress towards Meeting Technical Targets for Electrocatalysts and MEAs for Transportation Applications

Characteristic	Units	DOE 2020 Electrocatalyst and MEA Targets	Project Status (50 cm^2 cell, differential conditions)
Mass activity	A/mg_{PGM} @ 0.9 $mV_{iR\text{-}free}$	≥0.44	≥0.44
PGM total loading	mg-PGM/cm^2_{geo}	≤0.125	0.1, cathode
MEA performance	mW/cm^2_{geo} @ 600 mV	≥1,000	700–800
Electrocatalyst durability	% loss after 30,000 AST cycles (0.6 V to 0.95 V; 3 s square wave)	<40% loss in ECSA <40% loss in mass activity <30 mV loss @ 0.8 A/cm^2	<40% loss for electrocatalyst particle size ≥4.5 nm ≈50% loss in mass activity for $PtCo_x$ electrocatalyst >30 mV loss @ 0.8 A/cm^2

PGM – Platinum group metal; ECSA – Electrochemical surface area

- Quantified that $PtCo_x$ catalysts lose performance during catalyst potential cycling due to de-alloying, resulting in the loss of up to 70% of Co from the catalyst.
- Developed reference electrode hardware with assistance from National Physical Laboratory (United Kingdom).
- Developed three-dimensional fuel cell model to quantify mass transport losses in low loaded MEAs at high current densities.
- Quantified sulfate poisoning in low loaded MEAs.

✧ ✧ ✧ ✧ ✧

INTRODUCTION

The FC-PAD consortium was formed to advance performance and durability of polymer electrolyte membrane fuel cells (PEMFCs) to meet DOE targets and further enable their commercialization. The major challenge to be addressed by this consortium is to develop the knowledge base and optimize structures for more durable, high-performing PEMFC component technologies, while simultaneously reducing cost. In specific, we will develop validated models and advanced in situ and ex situ characterization techniques to further improve the performance and durability of fuel cells. We will also evaluate the performance and durability of SOA MEAs using both AST protocols and simulated durability drive cycle experiments. We will refine the AST protocols and adopt standardized hardware to accelerate the evaluation and incorporation of material advances.

APPROACH

The FC-PAD consortium incorporates national laboratory investigators with proven experience (developed in prior projects) related to durability, transport, and performance, and combines them into one highly coordinated effort. The effort is sub-divided into six thrust areas, including three materials related thrusts and three cross-cutting thrusts. This report summarizes some of the work performed in the three cross-cutting thrust areas of (1) Modeling and Validation, (2) Operando Evaluation: Benchmarking, ASTs, and Contaminants, and (3) Component Characterization and Diagnostics. The thrust areas of the consortium are highly integrated and the work performed related to the various specific components is presented in the reports of the three materials thrust areas.

The project will develop validated three-dimensional models that take into account the catalyst layer microstructure. The models will be validated using diagnostics from a standardized differential cell and advanced characterization techniques to resolve the oxygen transport resistance within the catalyst layer pores and ionomer thin films. The project will also benchmark the performance and durability of SOA MEAs provided by original equipment manufacturers and materials suppliers. Finally the project will apply in situ and ex situ characterization techniques to reveal the performance losses degradation mechanisms operational in fuel cells and propose strategies to improve performance and durability.

RESULTS

Two new ASTs were adopted by the DOE United States Driving Research and Innovation for Vehicle efficiency and Energy sustainability (U.S. DRIVE) Partnership's Fuel Cell Tech Team (FCTT) [1]. A combined mechanical/chemical degradation AST (relative humidity [RH] cycling under open circuit voltage at 90°C) and a square wave (0.6 V for 3 s and 0.95 V for 3 s) AST for catalyst durability. The combined chemical/mechanical AST provides an additional test that mimics the RH stress (as measured by the high frequency resistance) and the chemical stress (as measured by fluoride emission) of the existing two membrane ASTs in a single test. By combining these stressors in a single test, this AST is expected to closely resemble the conditions encountered in real world operations. Ex situ characterization of MEAs subjected to this AST revealed that the failure mechanism (extensive local thinning, some global thinning, and Pt band in the membrane) in this combined test is similar to that encountered in the FCTT durability protocol.

The durability of SOA PtCo/C alloy catalyst-based MEAs that meet the DOE mass activity target of 440 $mA/mg._{Pt}$ were evaluated using the square wave AST. The results from two different MEAs using a 4.4 nm PtCo/C catalyst and a 5.5 nm PtCo/C respectively are presented in Figure 1. While the 4.4 nm PtCo/C showed ≈40% ECSA loss, the 5.5 nm PtCo/C showed no loss in ECSA (Figure 1a). However both these MEAs exhibiting identical mass activity loss (Figure 1b) and increased kinetic resistance (Figure 1c) indicating a loss in performance of the catalyst irrespective of ECSA. Moreover the mass transport resistance at high current density (Figure 1d) of the 5.5 nm PtCo/C catalyst was unchanged while that of the 4.4 nm PtCo/C increased by ≈50%. It should be noted that the Pt-loading of the 5.5 nm PtCo/C was 0.21 mg/cm^2 while that of the 4.4 nm PtCo/C was only 0.1 mg/cm^2. These results are indicative that this mass transport loss is associated with transport losses observed in highly active catalysts at very low loadings at high current densities and this loss can be exacerbated by a further decrease in catalyst surface area.

Transmission electron microscopy characterization (Figure 2) of this MEA revealed that both these catalysts were 5.5 nm after the test. The catalyst particle size distribution (Figure 2a, b) illustrated that the 5.5 nm PtCo/C did not grow during this test while the 4.4 nm PtCo/C grew consistent with the ECSA measurements. The Pt/Co ratio of

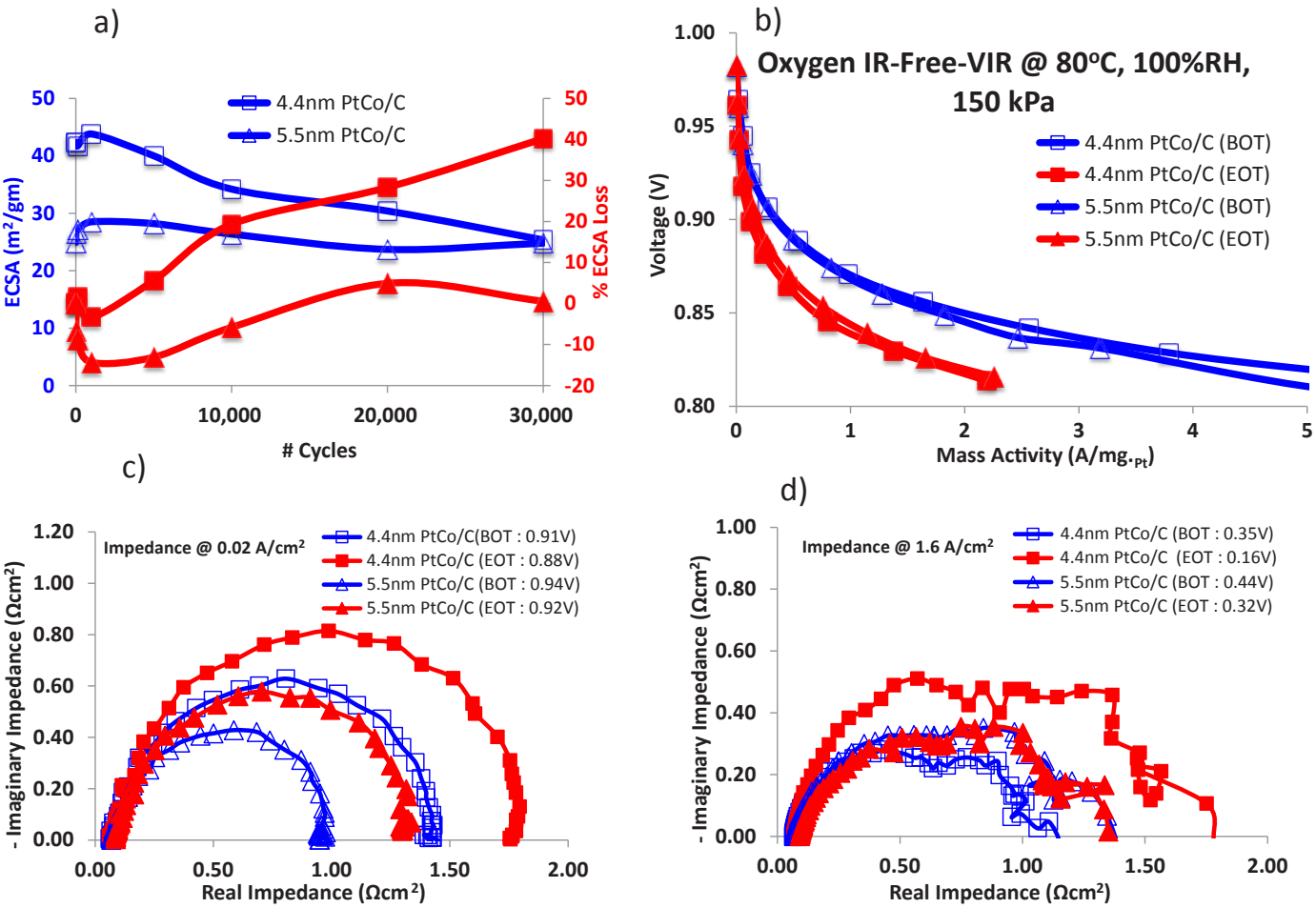

FIGURE 1. Evolution of (a) ECSA (measured at 80°C) and percent ECSA loss, (b) mass activity before (blue) and after (red) 30,000 cycles, (c) impedance at low current density (kinetic region) before (blue) and after (red) 30,000 cycles, and (d) impedance at high current density (mass transport region) of two PtCo/C catalyst-based MEAs during a 30,000 cycle square wave (3 s at 0.65 V and 3 s at 0.95 V) AST. Square = 4.4 nm PtCo catalyst at 0.1 mg_{Pt}/cm^2, and triangle = 5.5 nm PtCo catalyst at 0.21 mg_{Pt}/cm^2.

these two catalysts at various stages is illustrated in Figure 2c where both catalysts exhibited de-alloying and Co loss. This confirms that the ECSA loss is not the main degradation mechanism in these SOA alloy catalysts, which is controlled by mass activity loss due to de-alloying. The extent of Co loss was between 60–66% for the two MEAs and this Co was found primarily as Co ions throughout the membrane. Figure 2d illustrates this, where the Co was primarily concentrated in the catalyst layer in the fresh MEA whereas the Co was evenly distributed in the aged MEA. Further studies are underway to examine the effect of this Co in the membrane on performance and durability.

Full three-dimensional fuel cell models are being developed to quantify the various transport losses and these models are being validated using differential cell testing. A schematic of the three-dimensional cell used in the model is illustrated in Figure 3a where oxygen transport is by molecular diffusion in the gas diffusion layer, by Knudsen diffusion in the catalyst layer pores, and pressure independent in the ionomer film. When the channel RH is 100% and the ionomer is saturated with water and the catalyst layer contains liquid water, the gas transport resistance is primarily controlled by gas diffusion limitation in the pores of the catalyst layer and gas diffusion layer. The transport resistance contribution from the gas channels and the ionomer film are significantly lower. Figure 3b shows the transport losses in the catalyst layer (R_{cf}) separated into ionomer component (R_f) and pore component (R_c) where the pore resistance dominates. These results are consistent with HelOx data obtained in the lab showing marked improvement in performance when air is replaced with HelOx.

Reversible degradation due to adsorption of membrane degradation fragments on the catalyst has been identified by the FCTT as one of the durability issues of concern in low loaded MEAs. Several studies have examined reversible degradation and suggested recovery methods [2,3]. However, a detailed understanding of this degradation mechanism is lacking and has been initiated in this project. To isolate

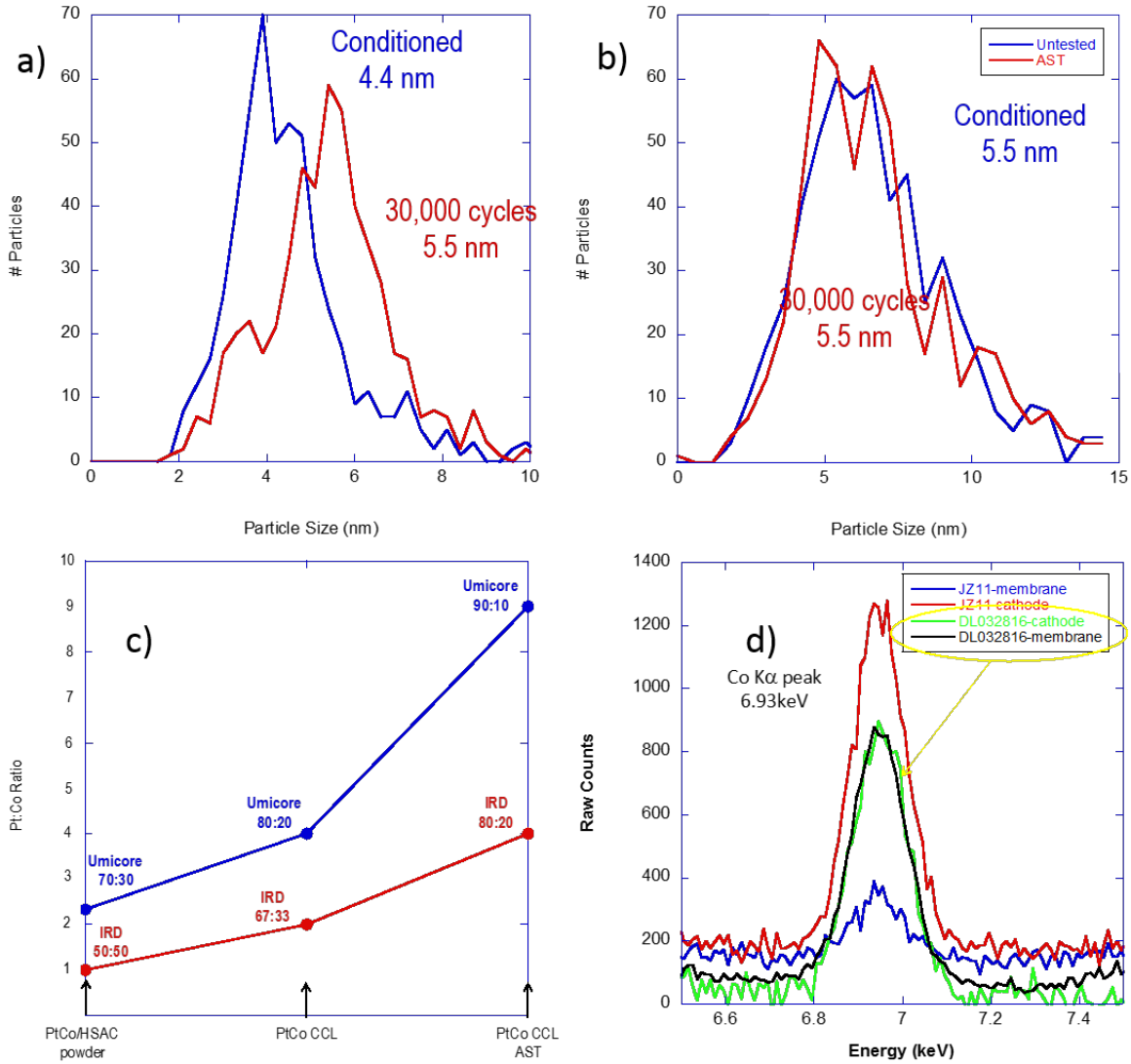

FIGURE 2. Comparison of transmission electron microscopy particle size distribution of two PtCo/C catalyst-based MEAs before (blue) and after (red) 30,000 cycles of a square wave potential cycle (3 s at 0.65 V and 3 s at 0.95 V) AST. (a) 4.4 nm PtCo catalyst at 0.1 mg_{Pt}/cm^2, and (b) 5.5 nm PtCo catalyst at 0.21 mg_{Pt}/cm^2. (c) Variation of the Pt/Co ratio of the 4.4 nm Pt/Co catalyst (blue) and the 5.5 nm Pt/Co catalyst (red) at various stages of testing. (d) Raw Co counts in beginning of test membrane (blue) and cathode catalyst (red) compared to the end of test membrane (black) and cathode catlalyst (green).

the effect of membrane degradation products, sulfate ions were deliberately introduced into the cathode gas stream by using dilute H_2SO_4 instead of water to humidify the cathode stream. At 10 mM concentration of H_2SO_4 infusion, no degradation was observed in high Pt-loaded catalysts (0.4 mg/cm^2) while significant voltage loss was observed at a cathode catalyst loading of 0.1 $mg_{\cdot Pt}/cm^2$ (Figure 4a). Moreover, this voltage did not recover when the infusion was stopped (Figure 4a) but was fully recoverable (Figure 4b blue curve) after several cyclic voltammetric scans down to <0.1 V, where sulfate desorption can be expected. Further experiments are underway to quantify sulfate loss from stabilized and unstabilized membranes to better quantify this degradation mechanism.

New diagnostic capability is being added within FC-PAD to better characterize the performance and durability of PEMFCs. One such technique is the use of multiple reference electrodes to accurately evaluate potential drops at the cathode and anode at various points in the flow-field. This technique was originally developed at National Physical Laboratory (United Kingdom) and researchers there have trained FC-PAD researchers in this technique and helped reproduce this experimental setup within FC-PAD. Preliminary results obtained at the National Physical Laboratory indicate that this technique can be a useful tool

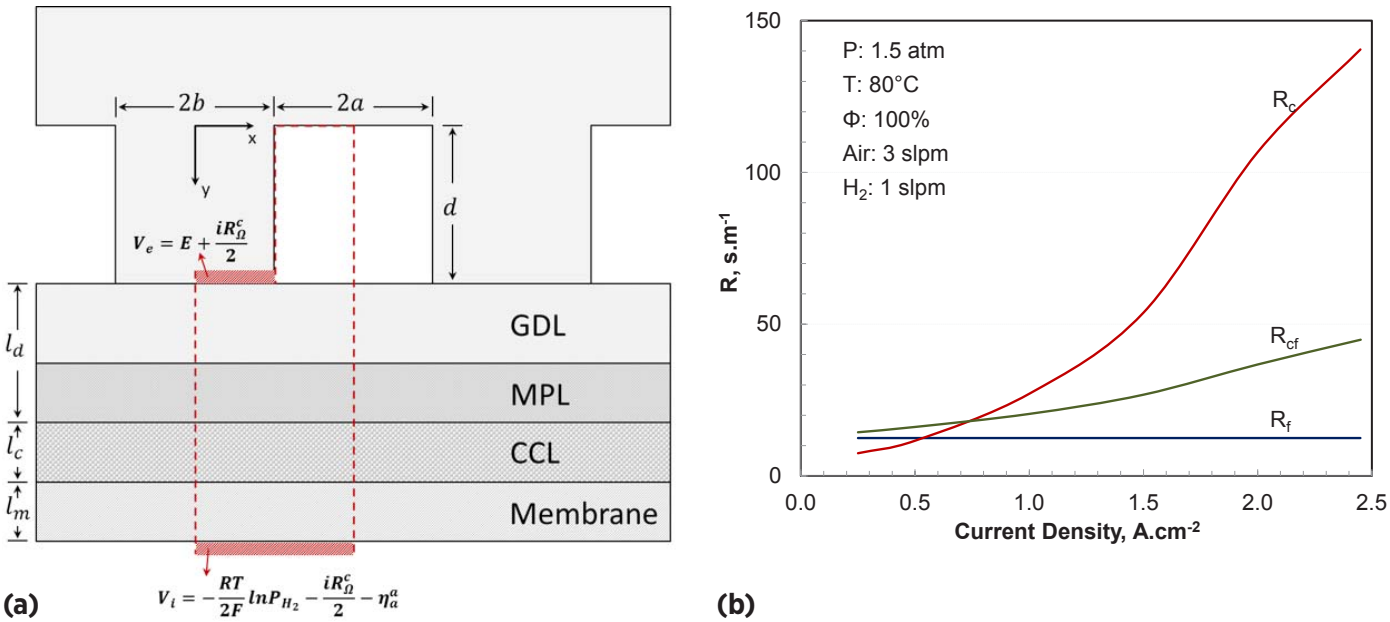

GDL – Gas diffusion layer; MPL – Micro-porous layer; CCL – Cathode catalyst layer

FIGURE 3. (a) Schematic illustrating the dimensions of three-dimensional cell used in the model. (b) Example of calculated catalyst layer transport resistance at different current densities separated into ionomer component (Ri) and pore component (Rf).

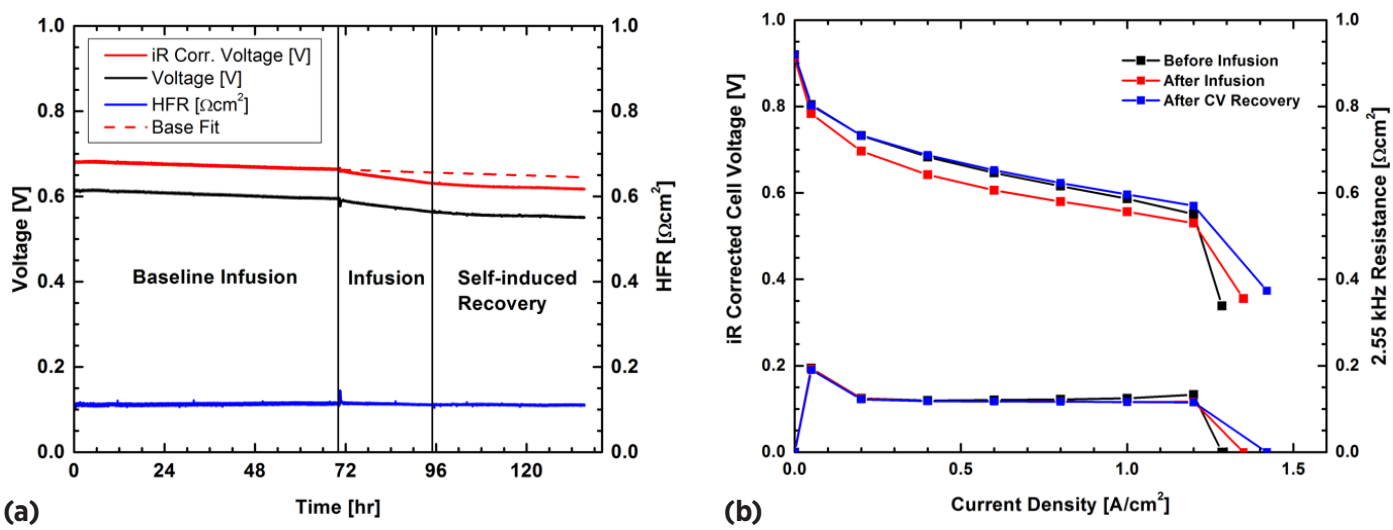

FIGURE 4. (a) Performance of a low loaded (0.1 mg/cm^2 cathode) Pt/C MEA at 0.6 A/cm^2 before during and after an infusion of 10 mM H_2SO_4. (b) Polarization curves before (black) and after (red) 10 mM sulfate infusion, and after a cyclic voltammetry (CV, between 0.05 and 1 V vs. reversible hydrogen electrode) recovery procedure (blue).

in the study of durability. Six different reference electrodes were embedded into the anode channel of a 50 cm^2 cell and their response was monitored when 50 ppm CO was introduced into the anode H_2 stream (Figure 5). When the CO is first introduced, the reference electrodes near the anode inlet immediately see a rise in potential corresponding to CO adsorption on the anode catalyst. Moreover the extent of anode poisoning decreases with increasing distance from the anode inlet and there is a lag time before the anode outlet gets poisoned. However, when the CO is released, the desorption rate seems to be uniform from the inlet to the outlet. This experimental set up will be completed and used to examine other durability issues in the future.

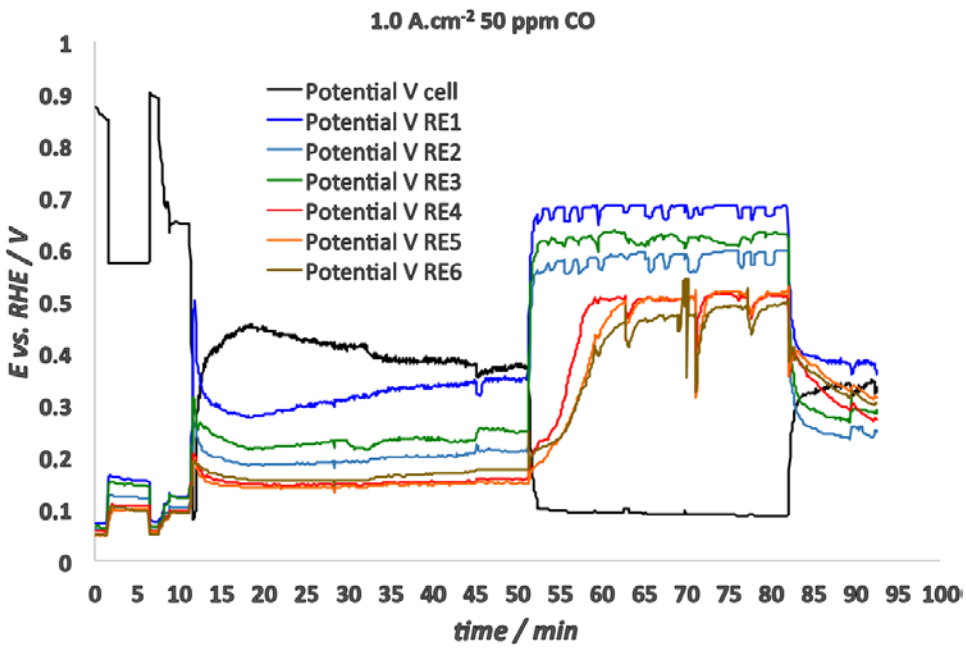

RHE – Reversible hydrogen electrode

FIGURE 5. Evolution of voltage at 1.0A/cm^2 at six different reference electrodes near the anode inlet (RE1, RE2, RE3) and anode outlet (RE4, RE5, RE6) of a 50 cm^2 fuel cell before (<10 min), during (≈10 min to ≈50 min) and after (>50 min) the injection of 50 ppm CO.

CONCLUSIONS AND FUTURE DIRECTIONS

New ASTs for membrane chemical/mechanical degradation and electrocatalysts were adopted by the U.S. DRIVE Partnership's FCTT. The main degradation mechanism in PtCo/C catalyst-based MEAs was the de-alloying of Co and the accompanying loss in mass activity. In low loaded MEAs using PtCo/C catalysts, additional increase in mass transport resistance due to decreased catalyst surface area was also observed. Models were developed to quantify the transport losses within GDLs, catalyst layers and ionomer films. A segmented cell and a reference electrode cell were developed for advanced diagnostics. The sulfate anion was also found to affect performance (reversible degradation) of low loaded MEAs.

The durability studies will be extended to MEAs utilizing de-alloyed PtNi/C catalyst and advanced carbons. The data from the electrocatalyst AST will be correlated to the data obtained from the durability protocol to confirm degradation mechanisms and quantify acceleration factors. The fuel cell models will be refined and validated utilizing data from a standardized differential cell. Extensive segmented cell evaluation of durability will be conducted and differential cell protocols will be proposed and adopted. Novel characterization of catalyst layer structures including ionomer mapping and ionomer interactions with catalyst will be developed.

FY 2016 PUBLICATIONS/PRESENTATIONS

1. Adam Weber, "Understanding Transport in Polymer-Electrolyte Fuel-Cell Ionomer," Colloquium, U. Kansas, 2015. (invited)

2. Iryna V. Zenyuk, Ezequiel Medici, Jeffrey Allen, and Adam Z. Weber, "Coupling continuum and pore-network models for polymer-electrolyte fuel cells," *International Journal of Hydrogen Energy*, 40, 16831–16845 (2015). doi: 10.1016/j.ijhydene.2015.08.009

3. Iryna V. Zenyuk, Ezequiel Medici, Jeffrey Allen, and Adam Z. Weber, "Coupling Continuum and Pore-Network Models in Polymer-Electrolyte Fuel Cells," *European Fuel Cell Technology & Applications Conference - Piero Lunghi Conference*, Naples, 2015.

4. Iryna V. Zenyuk and Adam Z. Weber, "Understanding Liquid-Water Management in PEFCs using X-ray Computed Tomography and Modeling," *ECS Conference*, Phoenix, 2015. (invited)

5. James A. Gilbert, A. Jeremy Kropf, Nancy N. Kariuki, Stacy DeCrane, XiaopingWang, Somaye Rasouli, Kang Yu, Paulo J. Ferreira, Dane Morgan,and Deborah J. Myers, "In-Operando Anomalous Small-Angle X-Ray Scattering Investigation of Pt_3Co Catalyst Degradation in Aqueous and Fuel Cell Environments," Journal of The Electrochemical Society, 162 (14) (2015) F1487-F1497.

6. D. Spernjak, R. L. Borup, D. S. Hussey, P. Zelenay, and R. Mukundan, "Imaging Fuel Cell Components: From Flow Field Channels to Catalyst Layers," Submitted to the 230th Meeting of the Electrochemical Society.

7. J.S. Spendelow, L. Castanheira, G. Hinds, T. Rockward, D.A. Langlois, R. Mukundan, and R.L. Borup, "Measurement of Local Electrode Potentials in an Operating PEMFC Exposed to Contaminants," Submitted to the 230th Meeting of the Electrochemical Society.

8. Iryna V. Zenyuk, Prodip K. Das, and Adam Z. Weber, "Understanding Impacts of Catalyst-Layer Thickness on Fuel-Cell Performance via Mathematical Modeling," *Journal of the Electrochemical Society*, 163, in press (2016). doi: 10.1149/2.1161607jes.

9. Iryna V. Zenyuk, Adrien Lamibrac, Jens Eller, Felix N. Büchi, and Adam Z. Weber, "Understanding Evaporation in Fuel-Cell Gas-Diffusion Layers with X-ray Computed Tomography," *Interpore: 8th International Conference on Porous Media*, Cincinnati, May 2016.

10. Rodney L. Borup, Rangachary Mukundan, Dusan Spernjak, David Langlois, G. Maranzana, A. Lamibrac, J. Dillet, S Didierjean, O. Lottin, L. Guetaz, D.D. Papadias, R. Ahluwalia and Karren More, "Material Degradation in PEM Fuel Cells," *MRS Meeting*, Phoenix, March 2016. (invited)

11. F. Cetinbas, R. Ahluwalia, N. Kariuki (Argonne National Laboratory), K.L. More, D.A. Cullen, B. Sneed (Oak Ridge National Laboratory), R.P. Winarski, J. Ilavsky, V. De Andrade, and D.J. Myers (Argonne National Laboratory), "Structural Characterization and Transport Modeling of Pt and Pt alloy Polymer Electrolyte Fuel Cell Cathode Catalyst Layers."

12. H. Dinh, G. Bender, J. Christ, J. Zack (National Renewable Energy Laboratory), L. McGovern, J. Przywara, C. Carey (University of South Carolina), "Effect of Sulfate Contaminant on ORR Activity and PEMFC Performance," Abstract Submitted to the 230th Meeting of the Electrochemical Society, Honolulu, HI, October 2016.

REFERENCES

1. FCTT Protocols as published in the Fuel Cell Technologies Office Multi-Year Research, Development, and Demonstration Plan, Section 3.4, Fuel Cells. http://energy.gov/eere/fuelcells/downloads/fuel-cell-technologies-office-multi-year-research-development-and-22

2. S.J.C. Cleghorn, et al, *J. Power Sources*, **158 (1)**, 446–454 (2006).

3. J. Zhang, B.A. Litteer, F.D. Coms, and R. Makharia, *J. Electrochem. Soc.,* ***159(7),*** F287-F293 (2012).

4. E. Brightman, G. Hinds, *J. Power Sources,* **267***,* 160-170 (2014).

V.B.6 Multiscale Modeling of Fuel Cell Membranes

Adam Weber (Primary Contact), Andrew Crothers
Lawrence Berkeley National Laboratory
1 Cyclotron Road, Mailstop 70R0108B
Berkeley, CA 94720
Phone: (510) 486-6308
Email: azweber@lbl.gov

DOE Manager: Donna Ho
Phone: (202) 586-8000
Email: Donna.Ho@ee.doe.gov

Project Start Date: September 2014
Project End Date: Project continuation and direction determined annually by DOE

Overall Objectives

- Develop multiscale model of ion and solvent transport through fuel-cell membranes.
- Propose material optimization strategies and explore design criteria for ion-conducting membranes across multiple length scales.

Fiscal Year (FY) 2016 Objectives

- Develop detailed nanoscale model of ion transport in the membrane.
- Develop upscaling methodology to predict macroscopic properties.
- Identify limiting aspects of membrane performance.

Technical Barriers

This project addresses the following technical barriers from the Fuel Cell section of the Fuel Cell Technologies Office Multi-Year Research, Development, and Demonstration Plan:

(C) Performance

Technical Targets

The aim of this project is modeling and validation of a model of transport in fuel cell membranes. Insights gained from these studies will be applied toward the design and synthesis of fuel cell membranes and membrane electrode assemblies that meet the following DOE hydrogen storage targets:

- Membrane electrode assembly performance: 300 mA/cm^2 at 0.8 V
- Membrane electrode assembly performance: 1,000 mW/cm^2 at rated power
- Membrane area specific proton resistance: 0.02 ohm cm^2 at maximum operating temperature and water partial pressures from 40–80 kPa

FY 2016 Accomplishments

- Modeled transport within the ionomer network using a resistor network approach.
- Developed an energy balance framework for the electrochemical potential of cations based on atomistic simulations.
- Validated the model using experimental measurements and atomistic simulations.
- Identified areas to improve membrane conductivity through material design.

✧ ✧ ✧ ✧ ✧

INTRODUCTION

Ionomer membranes are a critical component of fuel cell operation because they ensure efficient operation by separating hydrogen and oxygen reactants while allowing proton transport between the anode and cathode. To improve fuel cell performance by increasing proton conduction between the anode and cathode, DOE has identified a target for the reduction of the membrane specific area resistance to 0.02 ohm cm^2 at maximum operating temperature and water partial pressure from 40 kPa to 80 kPa. The membrane consists of a structural hydrophobic phase surrounding conducting nanoscale hydrophilic domains that are connected to form a conductive network across the membrane. Despite the broad use of ionomer membranes in fuel cells, there is not a clear and quantitative understanding of how the nano- and network-scales inherent in transport in ionomers affect macroscopic properties, such as ionic resistance. Moreover, transport at these multiple length scales in membranes have associated time scales, which impact dynamic operando behavior. The complexity of this multiscale problem presents a challenge for rational design of improved membranes. The goal of this project is to develop a model that can predict transport behavior across lengthscales and determine how each scale impacts macroscopic properties. This model will be used to identify limitations in current membranes and propose strategies for designing materials with improved performance. Under this work, a detailed and predictive nanoscale model for proton conductivity has been developed. The model was upscaled to predict membrane conductivity and identify sources of ion transport resistances.

APPROACH

The general approach of this project is to model each length scale relevant for transport in ionomers and connect these models through a generalized upscaling methodology. The nanoscale was modeled using a mean field physics model. The network-scale was modeled using a resistor network methodology. The results of the simulations are validated with molecular dynamics simulations at the nanoscale and experimental conductivity measurements at the macroscale. The material properties that are critical for membrane performance can be elucidated by analyzing the results of the model at each length scale.

RESULTS

The methodology was developed to model proton conductivity in ionomer membranes individually at both the nanoscale and network-scale, and communicate between these scales to predict macroscopic conductivity. This framework was then used to understand sources of resistance for proton conduction and identify potential avenues to improve performance.

The nanoscale model was developed and simulations were performed. The results at the nanoscale were upscaled to predict macroscopic properties by using a bundle of capillaries methodology. The model was shown to be predictive of experimental membrane conductivity for both lithium- and proton-form membranes, as shown in Figure 1.

The nanoscale model provides a fundamental understanding of molecular interactions that can be leveraged to elucidate potential avenues for improved material design. Protons in the ionomer are either solvated and mobile or bound to the ionomer and immobile. The fraction of the population in either of these states is the result of an interplay between solvation and electrostatic forces. By tuning the membrane properties (e.g., delocalizing the negative charges of the ionomer and making the membrane more acidic), more protons dissociate from the ionomer and participate in ion transport, thus increasing membrane conductivity, as shown in Figure 2.

The importance of the resistance at each length scale was investigated using the model. As shown in Figure 3, conductivity in the ideal limit actually decreases with increasing water content because the water dilutes the concentration of protons. However, as the membrane fills with water, a greater fraction of the nanodomains becomes conductive, which results in the observed increased conductivity with increasing water content. Moreover, as the water content increases, the protons at the nanoscale are mobilized, which further increases conductivity. Finally, as the water content of the membrane increases, there is increased connectivity across the network and its tortuosity decreases, thus facilitating increased conductivity. Figure 3 provides a quantitative framework for strategies to improve membrane conductivity to achieve the goal of a specific

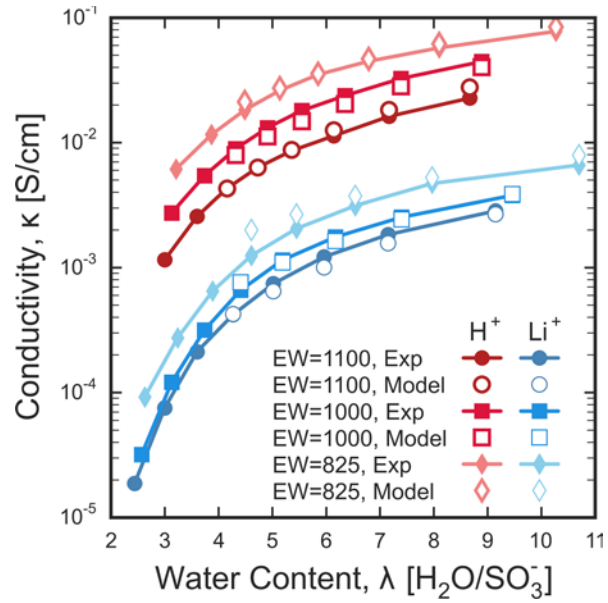

FIGURE 1. 3M membrane conductivity of lithium- and proton-form membranes as a function of water content as determined from the model (open) and experiments (filled, with red and blue lines to guide the eyes for proton- and lithium-form membranes, respectively) for different equivalent weights (EWs) of 1,100 (circles), 1,000 (squares), and 825 g/mol (SO_3^-) (diamonds).

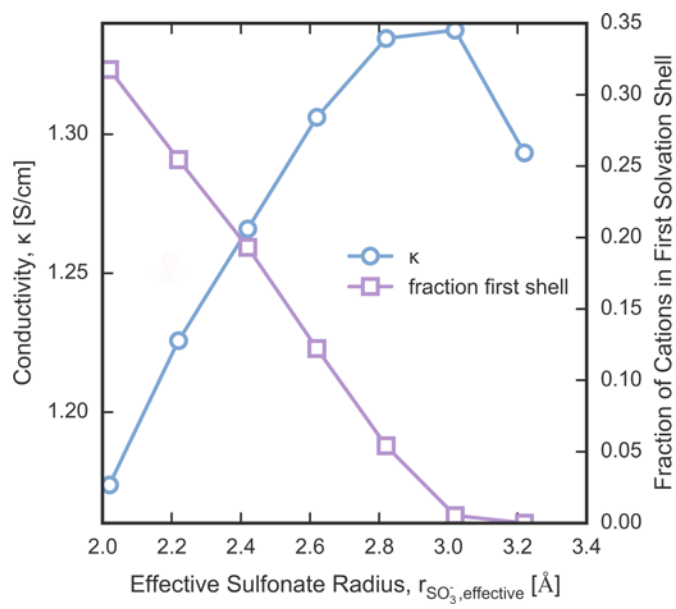

FIGURE 2. Proton conductivity (circle, left axis) and fraction probability of protons in the primary solvation shell of sulfonate groups (square, right axis) at λ = 9 [H_2O/SO_3^-] for a varying size of the effective volume of the negatively charge side-chain moiety. Lines are guides to the eyes only.

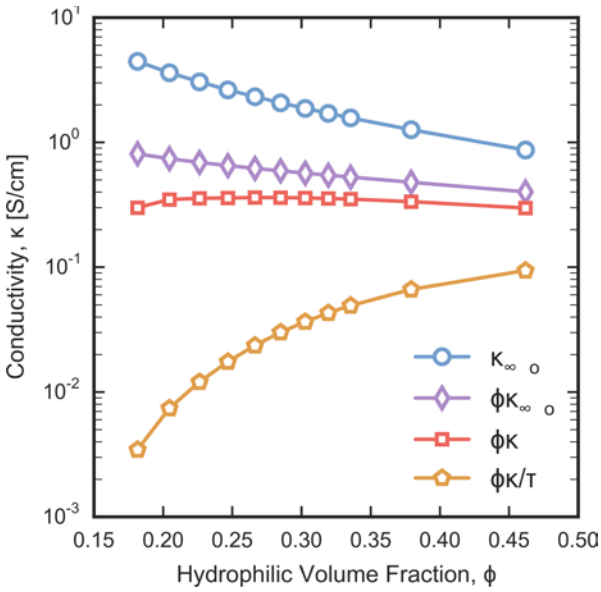

FIGURE 3. Breakdown of contributors to proton conductivity as a function of hydrophilic volume fraction. κ_∞ (circles) is the conductive ideal limit in a nanodomains (which changes due to nanodomains size), $\phi\kappa_\infty$ (diamonds) accounts for the presence of the volume fraction of the nanodomains, $\phi\kappa$ (squares) accounts for the local interactions as well, and $\phi\kappa/\tau$ (pentagons) also accounts for the network tortuosity. Lines are guides to the eyes only.

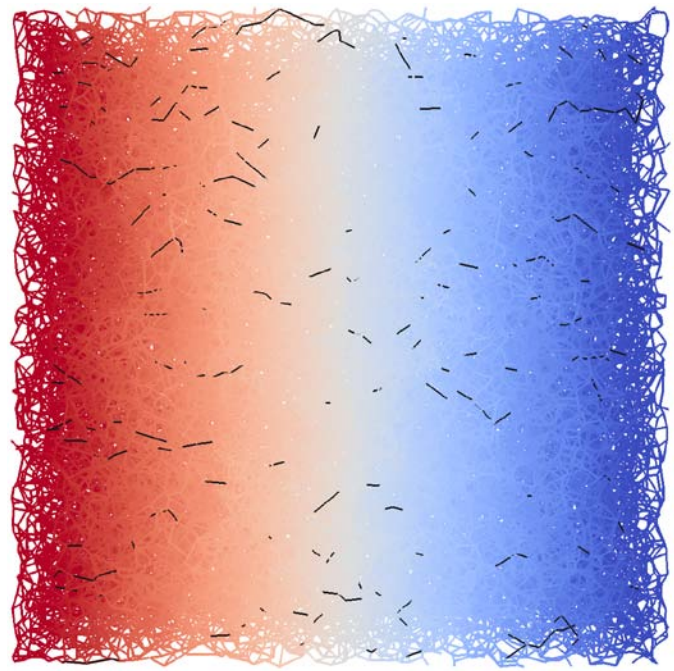

FIGURE 4. Proton transport in a two-dimensional slice of the Nafion™ network. The lines in the figure are segments of the network connecting nodes. Segments are colored to show potential drop from high potential (red) to low (blue). Segments colored black are those with a current flux one standard deviation above the average.

area resistance of 0.02 ohm cm^2. Namely, by increasing the hydrophilic fraction of the membrane, increasing the acidity of the ionomer, or decreasing the tortuosity of the conductive network the goal can be approached.

To understand why the tortuosity of the conductive network is an important factor of membrane conductivity, an experimentally consistent resistor-network model was developed to calculate the effective conductivity of the membrane. The resistor network was obtained by analyzing three-dimensional images from cryo-transmission electron microscopy of a hydrated ionomer and extracting the conductive pathways [1]. The results of the network simulation, as shown in Figure 4, show that the membrane is heterogeneous and some pathways dominate. If the membrane were treated as a homogeneous medium, isopotential lines would be straight, vertical lines. The medium is not homogeneous, but has small nonuniformities existing across the network making isopotential lines (lines following a constant color) circuitous. There are dominant pathways in the network, as indicated by segments colored black, but these pathways do not stretch across the entire network. There are also large regions through which little current passes. The conductivity of the membrane may be increased by designing ionomers that are more homogeneous at the mesoscale, and thus less tortuous.

CONCLUSIONS AND FUTURE DIRECTIONS

This project has resulted in several findings that provide a deeper understanding of proton conduction in fuel cell membranes and potential avenues for further improvement.

- Resistances to proton transport in the membrane are due to molecular-scale interactions, the fraction of the membrane that is nonconductive, and the tortuosity of the conductive network.
- Reducing the fraction of protons bound to the ionomer through novel materials, such as membranes with increased acidity, would reduce membrane resistance. Reducing the tortuosity of the conductive pathway in the membrane would also reduce membrane resistance.

While these strategies for decreasing membrane resistances are valuable, the overall performance of the membrane goes beyond simply the resistance, with durability and water uptake and transport playing important roles. Future work seeks to incorporate these aspects to make a holistic understanding of the interplay of factors influencing membrane performance. Specific activities include:

- Incorporate solvent uptake and transport into the membrane model.

- Model how the conductive pathways in the membrane change under different water contents and what the response is under dynamic, operando conditions.
- Understand how contaminates and additives move through the membrane.

SPECIAL RECOGNITIONS & AWARDS/ PATENTS ISSUED

1. Adam Weber, IAHE Sir William Grove Award.

FY 2016 PUBLICATIONS/PRESENTATIONS

1. Gostick, J.T. and A.Z. Weber, Resistor-Network Modeling of Ionic Conduction in Polymer Electrolytes. *Electrochimica Acta*, 2015. **179**: p. 137–145.

2. Crothers, A.R., C.J. Radke, and A.Z. Weber, Multiscale Model of Proton Transport in Perfluorosulfonic-Acid Membrane. *ECS Transactions*, 2015. **69**: p. 731–742.

3. Crothers, A.R., C.J. Radke, and A.Z. Weber, Multiscale Model of Proton Transport in Perfluorosulfonic-Acid Membrane. 228 ECS Meeting, 2015.

REFERENCES

1. Frances I. Allen, Luis R. Comolli, Ahmet Kusoglu, Miguel A. Modestino, Andrew M. Minor, and Adam Z. Weber, "Morphology of Hydrated As-Cast Nafion Revealed through Cryo Electron Tomography," *ACS Macro Letters*, **4**, 1–5 (2015).

V.B.7 The Effect of Airborne Contaminants on Fuel Cell Performance and Durability

Jean St-Pierre (Primary Contact),
Michael Angelo, Jing Qi, Tatyana Reshetenko,
Yunfeng Zhai, Trent Molter,[1] Leonard Bonville,[1]
Ugur Pasaogullari,[1] Charles Banas,[1]
Selvarani Ganesan,[1] Mehmet Ozdemir,[1]
Jaehyung Park,[1] Muhammad Uddin,[1]
William Collins,[2] Tommy Cheng[3]
Hawaii Natural Energy Institute
1680 East-West Road, POST 109
Honolulu, HI 96822
Phone: (808) 956-3909
Email: jsp7@hawaii.edu

DOE Managers:
Nancy L. Garland
Phone: 202-586-5673
Email: Nancy.Garland@ee.doe.gov

Gregory Kleen
Phone: (240) 562-1672
Email: Gregory.Kleen@ee.doe.gov

Contract Number: DE-EE0000467

Subcontractors:
[1] University of Connecticut, Storrs, CT
[2] WPCSOL, East Windsor, CT
[3] Ballard Power Systems, Burnaby, BC, Canada

Project Start Date: April 1, 2010
Project End Date: December 31, 2015

Overall Objectives

- Identify and mitigate the adverse effects of airborne contaminants on fuel cell system performance and durability.
- Provide contaminants and tolerance limits for filter specifications (preventive measure).
- Identify fuel cell stack's material, design, operation, or maintenance changes to remove contaminant species and recover performance (recovery measure).

Fiscal Year (FY) 2016 Objectives

- Demonstrate successful mitigation of the impact of the four most important airborne contaminants.

Technical Barriers

This project addresses the following technical barriers from the Fuel Cells section of the Fuel Cell Technologies Office Multi-Year Research, Development, and Demonstration Plan.

(A) Durability

(B) Cost

(C) Performance

Technical Targets

The following 2020 technical targets for 80-kW_e (net) integrated transportation fuel cell power systems operating on direct hydrogen, are considered.

- Durability: 5,000 h in automotive drive cycle
- Cost: \$40/kW_{net}
- Performance: 65% peak energy efficiency

The effects of specific airborne contaminants are studied, including a commercially relevant low cathode catalyst loading, and the resulting information will be used to impact both preventive measures and recovery procedures.

- Airborne contaminant tolerance limits to support the development of filtering system component specifications and ensure negligible fuel cell performance losses.
- Fuel cell stack's material, design, operation, or maintenance changes to recover performance losses derived from contamination mechanisms.

FY 2016 Accomplishments

- Developed mitigation strategies based on the contamination mechanism for bromomethane, the only organic contaminant that led to an incomplete recovery after contaminant injection was interrupted. The performance loss during constant cell voltage tests is recoverable (>90% current density recovery) by desorbing Br^- anions from the Pt catalyst surface at a low cathode potential and promoting the formation of liquid water for dissolution and entrainment of anions.
- Assessed the impact of a lower cathode catalyst loading (decrease from 0.4–0.1 mg Pt cm^{-2}) and a dilute contaminant mixture (0.5 ppm acetonitrile CH_3CN, 1 ppm bromomethane CH_3Br and 2 ppm propene C_3H_6) on cell performance. The loss was ~200 mV after 100 h (the almost linear decay did not reach a steady state) and

an incomplete recovery of ~100 mV was observed after interruption of the contaminant mixture injection.

- Evaluated the tolerance of a commercial PtCo cathode catalyst to SO_2. The performance loss after 20 h (134 ppb SO_2, 1.5 A cm^{-2}, 0.4 mg Pt cm^{-2} cathode loading) and irrecoverable losses after the contaminant injection was interrupted were similar for PtCo and Pt catalysts (respectively ~150 mV and ~70 mV).
- Determined the impact of four additional cleansers diluted by a factor of 20 or more on fuel cell performance.

✧ ✧ ✧ ✧ ✧

INTRODUCTION

The composition of atmospheric air cannot be controlled and typically includes other gases including many volatile organic compounds, as well as ions entrained in liquid water and encountered as droplets in the form of rain, mist, etc., especially near marine environments. Materials require cleansers to remove oils and dirt introduced by fuel cell manufacturing and assembly operations. Specific types of air contaminants and cleansers may cause deleterious effects which include decreased cell performance and durability [1,2] of proton exchange membrane fuel cells. Numerous air contaminants and cleansers have not yet been tested in fuel cells and consequently their effects as well as recovery methods are unknown [2,3]. Furthermore, prevention is difficult to achieve because tolerance limits are also missing in most cases [2]. This increases the risk of failure for fuel cell systems and thus jeopardizes their introduction into the market.

Airborne contaminants and foreign ions have previously been selected using a cost effective two tiered approach combining qualitative and quantitative criteria [3]. Automotive fuel cells are used under a wide range of operating conditions resulting from changes in power demands (drive cycle). Temperature and current density impact fuel cell contamination the most [4]. The effect of contaminant concentration is also particularly important. Contaminant threshold concentrations for predetermined fuel cell performance losses were determined [5] to facilitate the definition of air filtering system tolerances (prevention). Subsequently, contamination mechanisms were investigated for downselected contaminants (acetonitrile, acetylene, bromomethane, iso-propanol, methyl methacrylate, naphthalene, propene, Ca^{2+}) using a variety of ex situ and in situ characterization techniques [6] to facilitate the development of performance recovery procedures.

Only bromomethane and Ca^{2+} led to irrecoverable losses by interrupting contaminant injection (isopropanol only leads to irrecoverable losses if used in the more concentrated form of a cleanser). Ca^{2+} recovery procedures were reported [7]. Bromomethane recovery procedures were devised based on its contamination mechanism [8] and are summarized. Single contaminants were studied but do not readily occur in ambient air. Rather, air contains a mixture of contaminants. It was deemed important to obtain information about contaminant mixtures under realistic operating conditions, expose a commercially relevant low catalyst loading and reduce commercialization risks. This statement equally applies to the use of Pt alloys developed to minimize energy losses associated with the reduction of oxygen to water [9] because the overwhelming majority of contamination studies were devoted to Pt [2]. Finally, cleansers were selected for fuel cell screening tests because that contaminant class has not been previously explored. Screening results for four cleansers were reported [7]. Results for another four cleansers are summarized.

APPROACH

For bromomethane recovery tests, the performance loss was first established at a constant cell voltage of 0.63 V to facilitate data interpretation because catalyst surface processes are potential dependent. Subsequently, changes in operating conditions were used to desorb Br^- (N_2 or H_2 circulation in the cathode compartment). As a final step, the presence of liquid water was favored (high current density operation, liquid water injection in the cathode compartment, increase in air relative humidity from 50% to 100%, cell temperature decrease from 80°C to 55°C) to enable dissolution of the bromide ions and their entrainment toward the cell outlet port.

For the contaminant mixture test, only three species were used to minimize the injection system complexity. Acetonitrile, bromomethane and propene were selected because they were the only downselected organic species leading to ohmic losses, irrecoverable losses and small gains in performance after recovery, respectively. Contaminant concentrations were decreased from 20–0.5 ppm acetonitrile, 20–1 ppm bromomethane and 100–2 ppm propene. The larger concentrations were previously used for tests focusing on the determination of contamination mechanisms. The concentration decreases are insufficient to reach typical values in air for all mixture species (respectively 1.6 ppm, 0.0066 ppm, and 0.034 ppm annual maximum over a 24 h period for acetonitrile, bromomethane, and propene) but were deemed sufficiently large to anticipate a significant degradation within a reasonable amount of time. The cell was first operated with air to define a baseline. The contaminant mixture was subsequently introduced into the cell for a period of ~100 h. Contaminant injection was stopped after an ~100-h period because the cell voltage loss was already large and the decay was not slowing down. The cell was then operated until a steady state was reached and the recovery

was maximized. Diagnostics were regularly performed (impedance spectroscopy, polarization, cyclic voltammetry).

The impact of SO_2 was measured for both Pt and PtCo catalysts with a concentration of 134 ppb (near the 75 ppb daily maximum over a 1 h period). A temporary sulfur dioxide injection of 20 min was used and diagnostics were completed before and after the contaminant injection period (polarization, cyclic voltammetry).

Cleansers were selected on the basis of prior suggestions provided by industry. The fuel cell injection method is based on the cleanser boiling point. The cleanser is evaporated for a liquid with a boiling point below 20°C whereas it is injected as a mist above that temperature. The cleanser is diluted by a factor of 20 or more (a 5% cleanser–water mixture by volume) which is the leftover concentration estimated on the basis of two rinses (approximate high speed water entrainment or evaporation depending on vapor pressure). The cleanser is temporarily injected in the cathode compartment. Focus is given to the cell performance loss resulting from the cleanser injection for screening and selection purposes although diagnostics were completed (impedance spectroscopy, cyclic voltammetry).

RESULTS

Figure 1a illustrates the evolution of the current density at 0.63 V for a cell with a low cathode catalyst loading of 0.1 mg cm^{-2} contaminated by bromomethane. The cell current before the introduction of the contaminant is relatively stable (0–50 h). After the contaminant is introduced, the current density rapidly decreases to a value near 0 in approximately 50 h. A following period of operation in excess of 100 h without contaminant did not significantly recover the current density. A two-step recovery procedure was applied to the cell. First, the cathode potential was decreased by replacing air with N_2 (non-operating cell) to desorb the Br^- from the catalyst surface. These bromide ions are produced by hydrolysis of bromomethane [8]. This step was followed by successive cell operation periods at a progressively lower cell voltage (higher current density) to promote the presence of liquid water within the cell. Liquid water is necessary to dissolve the desorbed anions and entrain them along the flow field channel toward the cell outlet. Figure 1b shows polarization curves with air and oxygen obtained before contamination and after recovery which indicate that the two-step recovery procedure is effective and does not lead to any residual losses assigned to contamination for practical cell voltages above 0.6 V.

Figure 2 depicts cell voltage and high frequency resistance transients for a cell with a low cathode catalyst loading of 0.1 mg cm^{-2} contaminated with the ternary mixture. The cell voltage is constant before the contaminant mixture is injected. Upon injection, a short and rapid cell voltage drop is observed (~50 mV) which is followed by

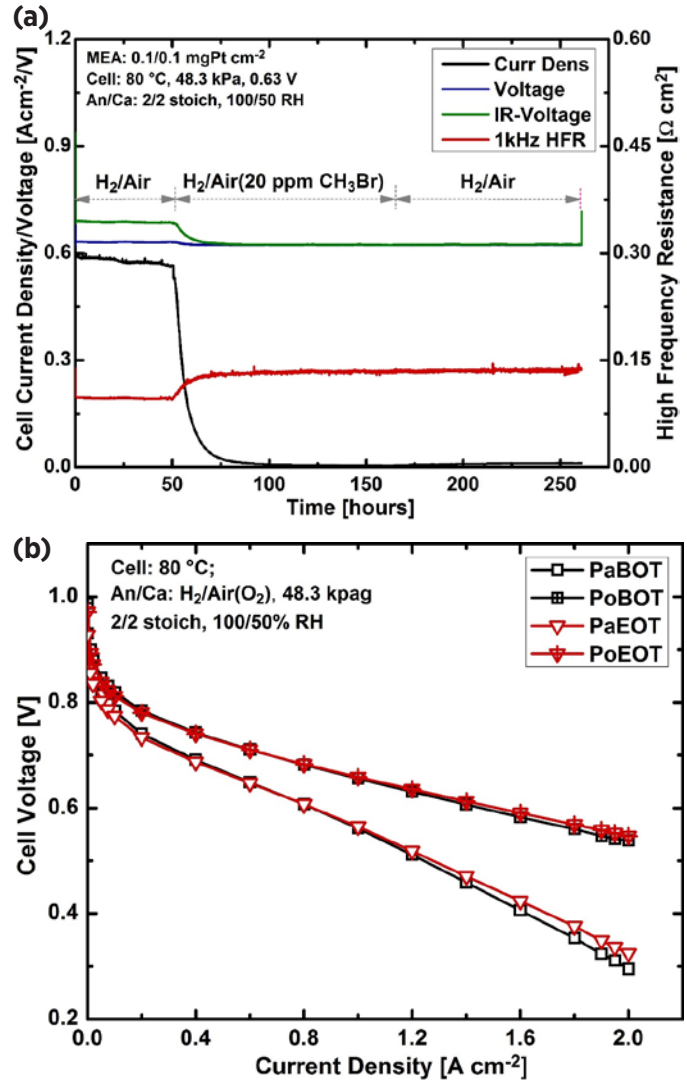

MEA – Membrane electrode assembly; RH – Relative humidity; IR – Current and resistance product; BOT – Beginning of test; EOT – End of test

FIGURE 1. (a) Cell voltage, ohmic loss compensated cell voltage, current density, and high frequency resistance at 1 kHz transients for a cell temporarily exposed to 20 ppm bromomethane. (b) Polarization curves obtained with air and oxygen before the cell was contaminated with bromomethane and after the cell was subjected to recovery procedures.

a large and approximately constant voltage decay rate (~1.5 mV h^{-1}). The total cell voltage loss at the end of the contamination period is ~200 mV. After the injection of the contaminant mixture is interrupted, the cell voltage recovers but reaches a value at steady state which is significantly lower than the original value by ~100 mV. The high frequency resistance slightly increases especially toward the end of the contamination period. The change in high frequency resistance is reversed at the end of the recovery period. Bromomethane is the only mixture contaminant leading to irrecoverable losses. Thus, irrecoverable voltage losses

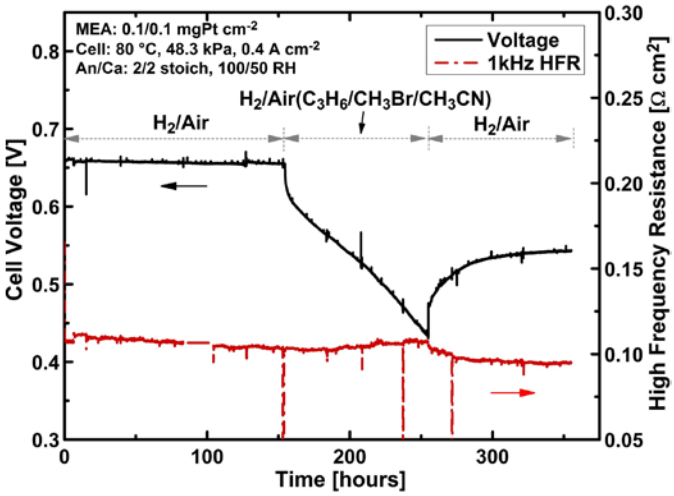

FIGURE 2. Cell voltage and high frequency resistance transients for a cell exposed to a temporary contaminant mixture of 0.5 ppm acetonitrile, 1 ppm bromomethane, and 2 ppm propene

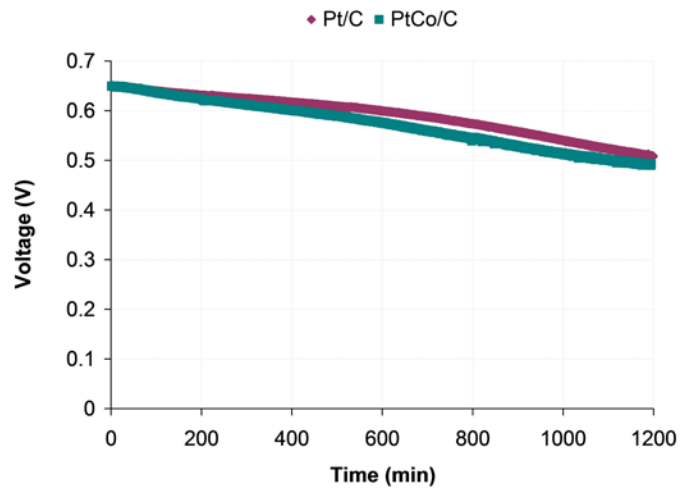

FIGURE 3. Cell voltage transients for cells temporarily exposed to 134 ppb sulfur dioxide. 0.4 mg Pt cm^{-2}/0.1 mg Pt cm^{-2} for the cathode/anode, 1.5 A cm^{-2}

are attributed to the formation of Br^- by bromomethane hydrolysis which cannot be desorbed from the catalyst surface at the operating cathode potential of ~0.49 V (~0.45 V + ~0.1 ohm cm^2 x 0.4 A cm^{-2}) [8]. Acetonitrile is the only mixture contaminant leading to ohmic losses. Therefore, the increase in high frequency resistance is ascribed to the formation of NH_4^+ by acetonitrile hydrolysis which are exchanged with ionomer and membrane protons H^+ [10]. Although signatures from the single contaminants are noted in Figure 2, data are insufficient to evaluate the presence of interactions between the three mixture species. This situation is in part due to the dual decrease in catalyst loading and contaminant concentration. For a larger catalyst loading of 0.4 mg Pt cm^{-2}, the decrease in acetonitrile and propene concentration to respectively 0.5–2 ppm was not expected to modify the cell voltage [11]. However, the cell voltage loss due to bromomethane was expected to be still significant at 1 ppm as it is weakly dependent on concentration (a 49% to 38% loss in cell voltage for a decrease from 20–2 ppm) [11]. For the relatively large and fixed contaminant concentrations employed for the determination of mechanisms, a decrease in Pt loading from 0.4–0.1 mg cm^{-2} promoted an increase in cell voltage loss of respectively 58%, –10%, and 224% for acetonitrile, bromomethane, and propene [12]. Data were not obtained for changes in both contaminant concentration and catalyst loading. Even if interactions between the three contaminants cannot be evaluated, the dilute ternary contaminant mixture creates a large cell voltage loss for a commercially relevant catalyst loading. Additional work should be pursued in this area to revise and predict contaminant tolerance limits for mixtures and commercially relevant cathode catalyst loadings.

Figure 3 summarizes the impact of a temporary exposure to SO_2 on Pt and PtCo catalysts. The cell voltage for both catalysts linearly decreases by ~150 mV without reaching a steady state. After the contaminant injection was interrupted, the cell voltage partly recovered leaving 70 mV in irrecoverable losses (not shown). Therefore, the alloy does not have an advantage in terms of contamination. This statement may not necessarily apply to other contaminants or PtCo alloys.

The results obtained by temporarily contaminating cells with four different cleansers were briefly reported [7]. Data for four additional cleansers were acquired during this reporting period. Data for all eight cleansers are summarized in Table 1. None of the cleansers are compatible with fuel cells either because the cell voltage was partially recoverable within a single vehicle fuel fill (~14 h), or the cell voltage fell below the power electronics low end operating point (0.45 V). Therefore, additional work is needed to identify a suitable cleanser, design an appropriate cleanser composition or develop cleaning alternatives for fuel cell components (such as cleanser removal).

CONCLUSIONS AND FUTURE DIRECTIONS

- An effective method was established to reverse irrecoverable cell voltage losses induced by bromomethane contamination.
- A dilute ternary contaminant mixture led to a large cell voltage loss and an irrecoverable loss for a commercially relevant 0.1 mg Pt cm^{-2} cathode catalyst loading, prompting additional work to revise and predict tolerance limits for such operating conditions.
- A commercial PtCo alloy cathode catalyst has a similar tolerance to SO_2 than a Pt catalyst.

TABLE 1. Summary of the Screened Fuel Cell Components' Cleansers, Experimental Parameters and Key Results

Sample	Class	Principal Component	Injection Method	Concentration (%)	Injection Rate (μL min^{-1})	Decay Rate[a] (mV h^{-1})	Recovery (%)[b]
A	cationic	2-butoxyethanol	nebulizer	5	130	~1.4	~0
B	amine	triethanolamine	nebulizer	5	130	~22	~46
C	cationic	sodium dodecylbenzenesulfonate	nebulizer	5	130	<1.4	<0[c]
D	citrate	citrus terpenes	nebulizer	5	130	~1,500	~96
				0.5	130	~2	~60
E	amine	sodium lauryl ether sulfate	nebulizer	5	130	<15	~25
F	amine	ethylenediaminetetraacetic acid	nebulizer	5	130	~3.3	<0[c]
G	organic	naphtha	nebulizer followed by vaporization	0.2	10	5[d]	~100
				1	50	100[d]	~100
				3	250	150[d]	~100
				3	250	240[d,e]	~100
H	organic	isopropanol	nebulizer followed by vaporization	0.2	10	70[d]	~90

[a]Baseline decay rate is ~0.2 mV h^{-1}. [b]After interruption of cleanser injection. [c]The cell voltage continues to drop during the recovery period. [d]Step change in mV. [e]100% relative humidity at the cathode.

- All eight cleansers for fuel cell components, readily available and common name brands, were unsuitable suggesting additional work to identify a suitable cleanser, design an appropriate cleanser composition or develop cleaning alternatives.
- Bromomethane contamination tests with metallic bipolar plates will be completed to assess the existence of interactions (bromine promotes corrosion).
- We will continue to analyze, summarize, and disseminate the large fuel cell contamination database.

SPECIAL RECOGNITIONS & AWARDS/ PATENTS ISSUED

1. J. St-Pierre, J. Ge, "Fuel Cell Catalyst Ink Active Surface Area Measurement," United States provisional patent 62/262,137, December 2, 2015 (inspired by the contamination mechanisms that were developed).

FY 2016 PUBLICATIONS/PRESENTATIONS

1. M.A. Uddin, J. Park, S. Ganesan, U. Pasaogullari, L. Bonville, "Cathode Catalyst Layer Thinning in Polymer Electrolyte Fuel Cell: A Cation Contamination Effect," *J. Electrochem. Soc.*, submitted.

2. C.J. Banas, U. Pasaogullari, "Statistical Analysis of Salt Deposition inside PEFC GDL from X-Ray Tomography," *J. Electrochem. Soc.*, submitted.

3. T.V. Reshetenko, J. St-Pierre, "Study of the Aromatic Hydrocarbons Poisoning of Platinum Cathodes on Proton Exchange Membrane Fuel Cell Spatial Performance Using a Segmented Cell System," *J. Power Sources*, submitted.

4. Y. Zhai, J. Ge, J. St-Pierre, *Electrochem. Commun.*, **66** (2016) 49.

5. Y. Zhai, O. Baturina, D. Ramaker, E. Farquhar, J. St-Pierre, K. Swider-Lyons, *Electrochim. Acta*, **213** (2016) 482.

6. J. St-Pierre, Y. Zhai, J. Ge, *J. Electrochem. Soc.*, **163** (2016) F247.

7. C.J. Banas, U. Pasaogullari, "Computational Modelling of Cationic Contamination in PEFCs: a Multiphase Mixture Approach," *Electrochem. Soc. Trans.*, accepted.

8. C.J. Banas, U. Pasaogullari, *Electrochem. Soc. Trans.*, **69**(17) (2015) 511.

9. C.J. Banas, U. Pasaogullari, 230th Electrochemical Society meeting oral presentation, abstract 2837.

10. T. Reshetenko, J. St-Pierre, 230th Electrochemical Society meeting poster presentation, abstract 2716.

11. T. Reshetenko, K. Artyushkova, J. St-Pierre, 230th Electrochemical Society meeting poster presentation, abstract 2701.

12. Y. Zhai, O. Baturina, D. Ramaker, J. St-Pierre, K. Swider-Lyons, 230th Electrochemical Society meeting oral presentation, abstract 2520.

13. J. St-Pierre, U.S. DRIVE Fuel Cell Tech Team meeting oral presentation, July 20, 2016.

14. W. Collins, SAE International meeting oral presentation, November 3, 2015.

15. J. St-Pierre, Y. Zhai, J. Ge, 228th Electrochemical Society meeting oral presentation, abstract 1528.

16. Y. Zhai, J. Ge, J. St-Pierre, 228th Electrochemical Society meeting oral presentation, abstract 1508.

17. C.J. Banas, U. Pasaogullari, 228th Electrochemical Society meeting oral presentation, abstract 1358.

18. Y. Zhai, J. Ge, J. Qi, K. More, J. St-Pierre, "Long Term Effects of an Airborne Contaminant on a Proton Exchange Membrane Fuel Cell," 3rd International Workshop on Degradation Issues of Fuel Cells and Electrolysers oral presentation.

19. Y. Zhai, J. Ge, J. St-Pierre, 15th International Symposium on Electroanalytical Chemistry oral presentation, abstract K-4.

REFERENCES

1. J. St-Pierre, "Air Impurities," in *Polymer Electrolyte Fuel Cell Durability*, Edited by F.N. Büchi, M. Inaba, T.J. Schmidt, Springer, 2009, p. 289.

2. J. St-Pierre, M. Angelo, K. Bethune, J. Ge, S. Higgins, T. Reshetenko, M. Virji, Y. Zhai, *Electrochem. Soc. Trans.*, **61**(23) (2014) 1.

3. J. St-Pierre, Y. Zhai, M.S. Angelo, *J. Electrochem. Soc.*, **161** (2014) F280 and **162** (2015) X7.

4. J. St-Pierre, Y. Zhai, M. Angelo, *Int. J. Hydrogen Energy*, **37** (2012) 6784.

5. J. St-Pierre, Y. Zhai, J. Ge, M. Angelo, T. Reshetenko, T. Molter, L. Bonville, U. Pasaogullari, W. Collins, S. Wessel, DOE Hydrogen and Fuel Cells Program, FY 2013 Annual Progress Report, p. V-3.

6. J. St-Pierre, United States Department of Energy 2015 Annual Merit Review meeting oral presentation, June 10, 2015.

7. J. St-Pierre, Y. Zhai, J. Ge, T. Reshetenko, M. Angelo, J. Qi, T. Molter, L. Bonville, U. Pasaogullari, O. Ozdemir, M.A. Uddin, J. Park, S. Ganesan, W. Collins, T. Cheng, DOE Hydrogen and Fuel Cells Program, FY 2015 Annual Progress Report, pp. V-121-V-122.

8. Y. Zhai, O. Baturina, D. Ramaker, E. Farquhar, J. St-Pierre, K. Swider-Lyons, *Electrochim. Acta*, **213** (2016) 482.

9. H.A. Gasteiger, S.S. Kocha, B. Sompalli, F.T. Wagner, *Appl. Catal. B*, **56** (2005) 9.

10. Y. Zhai, J. Ge, J. St-Pierre, *Electrochem. Commun.*, **66** (2016) 49.

11. J. St-Pierre, Y. Zhai, M. Angelo, T. Molter, L. Bonville, U. Pasaogullari, M. Aindow, W. Collins, S. Wessel, DOE Hydrogen and Fuel Cells Program, FY 2012 Annual Progress Report, p. V-66.

12. J. St-Pierre, Y. Zhai, J. Ge, T. Reshetenko, M. Angelo, T. Molter, L. Bonville, U. Pasaogullari, X. Wang, J. Qi, O. Ozdemir, A. Uddin, N. Khajeh-Hosseini-Dalasm, J. Park, S. Ganesan, W. Collins, S. Wessel, T. Cheng, DOE Hydrogen and Fuel Cells Program, FY 2014 Annual Progress Report, p. V-136.

V.C.1 New Fuel Cell Membranes with Improved Durability and Performance

Michael Yandrasits
3M Company
3M Center, Building 201-1W-28
St. Paul, MN 55144
Phone: (651) 736-5719
Email: mayandrasits@mmm.com

DOE Manager: Gregory Kleen
Phone: (240) 562-1672
Email: Gregory.Kleen@ee.doe.gov

Contract Number: DE-EE0006362

Subcontractors:
- Craig Gittleman, General Motors (GM) Fuel Cell Activities, Pontiac MI
- Peter Pintauro, Vanderbilt University, Nashville, TN

Project Start Date: October 1, 2013
Project End Date: December 31, 2016

Overall Objectives

- Meet all of the Department of Energy (DOE) Fuel Cell Technologies Office (FCTO) Multi-Year Research, Development, and Demonstration (MYRDD) Plan membrane performance, durability, and cost targets simultaneously with a single membrane.
- Membranes will be based on Multi-Acid Side Chain (MASC) ionomers.
- Electrospun nanofiber structures will be developed to reinforce membranes.
- Peroxide scavenging additives will be used to enhance chemical stability.
- New membranes will have improved mechanical properties, low area specific resistance and excellent chemical stability compared to current state of the art.
- Experimental membranes will be integrated into membrane electrode assemblies (MEAs) and evaluated in single fuel cells and finally fuel cell stacks.

Fiscal Year (FY) 2016 Objectives

- Produce enough perfluoroimide acid (PFIA) ionomer at pilot scale to fabricate membranes for Milestones 7 and 8.
- Optimize peroxide scavenging additive type and amount for PFIA-based membranes to maximize durability in the open circuit voltage (OCV) accelerated stress test.
- Produce membrane comprising a MASC ionomer, a nanofiber support, and a stabilizing additive which meets all of the 2020 membrane milestones in Table 3.4.12 (Technical Targets: Membranes for Transportation Applications) in the DOE FCTO MYRDD Plan, Section 3.4, update July 2013. This represents project go/no-go Milestone 8.
- Develop a process for producing the membrane described in Milestone Q8 in quantities large enough to produce membranes for use in Milestone Q10 (at least 20 linear meters)
- Manufacture for stack testing at least 30 MEAs with a minimum cell area of 250 cm^2. Evaluate in fuel cells and ex situ tests. Begin stack testing.

Technical Barriers

This project addresses the following technical barriers from the Fuel Cells section of the FCTO MYRDD Plan.

(A) Durability

(B) Cost

(C) Performance

Technical Targets

The DOE 2020 technical targets for the membrane are shown in Table 1 along with the data for the membrane developed in this program (Milestone 8). This membrane consists of ionomer and nanofiber developed in this project and optimized peroxide stabilizing additives.

FY 2016 Accomplishments

- Pilot scale quantities of PFIA ionomer were produced for membrane development.
- Peroxide scavenging additive levels were optimized for membranes developed in this project.
- Go/no-go project Milestone 8 was met for all DOE 2020 targets except area specific resistance (ASR) at 120°C and 40 kPa water vapor pressure.
- Suitable quantities of membrane have been fabricated for stack testing.
- Stack testing initiated at GM.

TABLE 1. Fuel Cell Membrane Targets from DOE FCTO MYRDD Plan and Results for Project Milestone 8 Membrane

Characteristic	Units	2017 & 2020 Targets	MS#8 PFIA-S (10 µm)
Maximum oxygen cross-over	mA/cm^2	2	0.6[a], 3.5 [b]
Maximum hydrogen cross-over	mA/cm^2	2	1.9[c]
Area specific proton resistance at:			
120°C, P_{H2O} 40 kPa	Ohm cm^2	0.02	0.054
120°C P_{H2O} 80 kPa	Ohm cm^2	0.02	0.019
80°C P_{H2O} 25 kPa	Ohm cm^2	0.02	0.020
80°C P_{H2O} 45 kPa	Ohm cm^2	0.02	0.008
30°C P_{H2O} up to 4 kPa	Ohm cm^2	0.03	0.018
-20°C	Ohm cm^2	0.2	0.2[d]
Minimum electrical resistance	Ohm cm^2	1,000	1,635[e]
Cost	$/$m^2$	20	Not available
Durability			
Mechanical	Cycles with <10 sccm crossover	20,000	>24,000
Chemical	Hrs	>500	614

a. O_2 crossover based on DOE Table 3.4.12 indicating measurement at 0.5 V
b. Calculated from GM O_2 permeability data at 80°C, 100% relative humidity (RH), 1 atm.
c. In cell measurements at 3M 70°C, 100% RH, 1 atm.
d. Calculated from in-plan data
e. Data provided by GM
sccm – standard cubic centimeters per minute; MS - Milestone

- Electrospinning nanofiber ionomer and support fibers has led to unique membrane constructions for evaluation.

✧ ✧ ✧ ✧ ✧

INTRODUCTION

Fuel cell membranes with low resistance are highly desirable in order to maximize system power and efficiency. This objective is especially difficult under low humidity conditions, where the proton resistance of the membrane is the highest. Increasing the number of charge carriers and decreasing the thickness can both be effective in reducing resistance, however, they can compromise the membrane durability if not designed properly. Proton conductivity can be increased by simply adding charge carriers, such as sulfonic acid groups, to a polymer backbone, however, it will ultimately become a water soluble polymer and not be effective as a membrane. Likewise, reducing the thickness of a membrane can result in poor durability in both accelerated testing and actual use conditions. Because of these reasons, a membrane is needed that has increased conductivity, is water insoluble, and is stable to chemical and mechanical degradation. This project aims to develop a new membrane based on a perfluorinated ion conducting polymer and nanofiber support that is able to meet the DOE targets for membrane performance, durability, and cost.

APPROACH

The approach for this project is to develop a new ionomer based on a perfluorinated polymer that contains MASC in order to provide improved conductivity at dry conditions. This strategy has the advantage of creating a polymer with a large number of charge carriers, high ion exchange capacity, while maintaining a polytetrafluoroethylene backbone that prevents the polymer from dissolving in water. Both perfluorosulfonic acid (PFSA) and perfluoro bis(sulfonyl) imides are strong acids and have excellent conductivity characteristics. The bis(sulfonyl)imide functionality also serves as a chain extender, allowing for multiple acid groups per side chain. When the side chain contains one imide and one sulfonic acid group it is designated a PFIA ionomer (Figure 1). In the case where multiple imides are used per side chain, the ionomer is considered perfluoro ionene chain extended (PFICE). In combination with the new ionomer, mechanical support will be provided by electrospun nanofibers. Work at both 3M and Vanderbilt University will determine an optimum architecture for the fiber supported membrane based on filling an existing nanofiber mat with ionomer (3M) or spinning both ionomer fibers and support fiber simultaneously followed by consolidating the ionomer fibers into a continuous matrix (Vanderbilt).

Membranes developed in this project are evaluated against the DOE 2020 targets using a variety methods with the ultimate program objective of demonstrating 2,000 h of durability in a small stack, tested at GM. Additional information regarding the failure modes and insight into improved durability will be obtained by post-mortem analysis at the end of this test.

RESULTS

This year we successfully passed the second project go/no-go milestone (#8) to meet all of the DOE 2020 targets for membrane performance, durability, and cost simultaneously with one membrane. The membrane designed for this

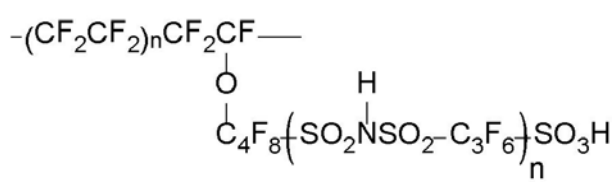

FIGURE 1. Ionomer with bis(sulfonyl)imide and sulfonic acid side chain. The ionomer is designated PFIA when n = 1 and PFICE when n > 1.

milestone was produced using a pilot scale PFIA ionomer with an equivalent weight of 650 g/mol and electrospun fluoropolymer (FC1) nanofiber support. The details of the Milestone 8 membrane construction are shown in Table 2 along with a PFSA-based control and Milestones 4 and 7 membranes for comparison. The specific results for the Milestone 8 membrane, for each target, are shown in Table 1. This membrane has met most of the DOE targets with the exception of area specific resistance at 120°C and low humidity and, depending on test conditions, the oxygen cross over target.

TABLE 2. Membrane Construction for Membranes Developed in this Project and Control

Milestone	Ionomer	Fiber Type	Additive	Fiber (vol%)	Thickness (µm)
Control	3M 725 EW	B1	Type A	20.6	14
#4	PFIA – Lab	FC1	Type A	17.2	14
#7	PFIA – Lot #1	FC1	Type A	17.3	14
#8	PFIA – Lot #1	FC1	Type A	18.0	10

EW – Equivalent weight

In order to assess the potential for the MASC approach to meet the most aggressive resistance target, we plotted both the through-plan and in-plane resistance for the Milestone 8 membrane versus relative humidity at 80°C and 120°C (Figure 2). Clearly the data falls within the DOE target range for the 80°C data but only at the highest humidity for the 120°C data. Analysis of this data suggests that, in order for a 10-micron membrane with typical levels of peroxide scavenging additives and supporting fiber content to meet the 120° resistance targets at all specified humidities, an ionomer with an equivalent weight of about 450 g/mol would be needed. This value is not achievable with the PFIA system and would require further development of the PFICE ionomers with between three and four acidic groups per side chain.

Despite the difficulty in meeting the most aggressive resistance target, the membrane developed in this project have demonstrated significant improvements in fuel cell performance, especially under low humidity conditions. Figure 3 shows typical performance for the Milestone 8 membrane when measured at 1.5 A/cm^2, as a function of inlet gas relative humidity. The cell voltage is over 100 mV higher at the lowest humidity when compared to the traditional PFSA-based membrane.

In addition to performance testing, durability is measured under the OCV accelerated stress test. The membranes developed under this program have routinely exceed the 500-hour target when fabricated with peroxide scavenging additives similar to those used in PFSA-based membranes. However, an unusual decrease in OCV has been observed in the first 200 h of testing for the PFIA-based membranes (Figure 4). Diagnostic testing has shown that this decrease is not due to hydrogen cross over or shorting, and the origin of this behavior is under investigation.

Larger quantities of the Milestone 8 and similar membranes were fabricated with different levels of peroxide scavenging additives. These membranes were assembled into MEAs for stack testing by GM.

Electrospinning developments at Vanderbilt University have shown that a variety of novel constructions are possible

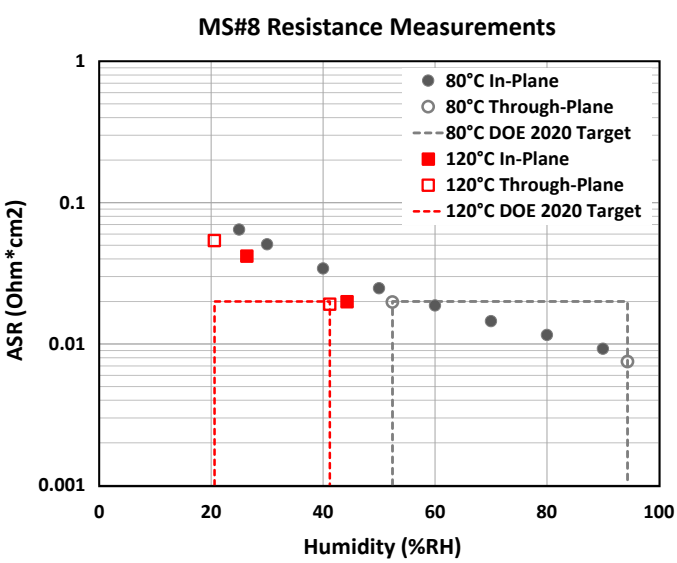

RH – Relative humidity

FIGURE 2. Area specific resistance vs. relative humidity measured through-plane (open symbols) or calculated from in-plane conductivity (filled symbols) for Milestone 8 membrane measured at 80°C and 120°C. DOE targets are shown in dashed lines.

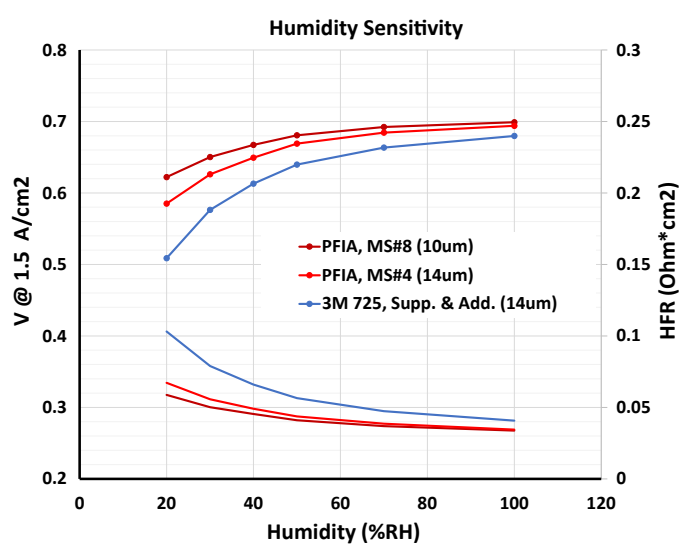

FIGURE 3. Voltage and high frequency resistance (HFR) for Milestone 4 and 8 membranes, as a function of humidity at 1.5 A/cm^2.

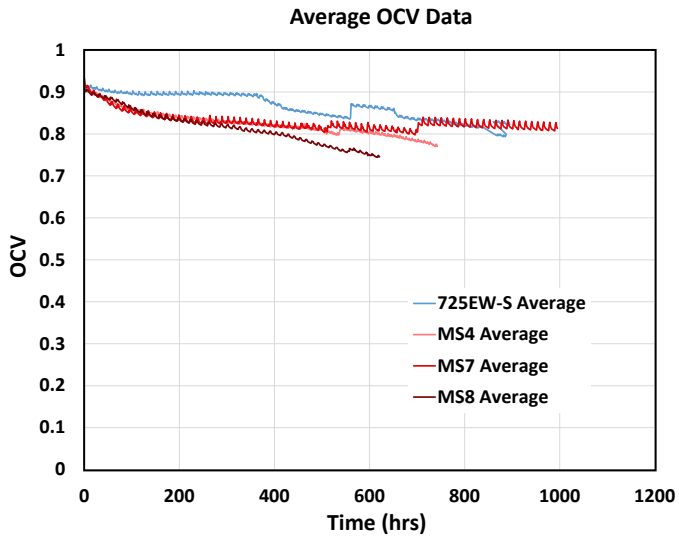

FIGURE 4. Average OCV vs. time for three PFIA-based membranes (MS4, MS7, and MS8) compared to a PFSA control (725 EW-S).

for distributing a mechanical support polymer within an ion conducting matrix.

CONCLUSIONS AND FUTURE DIRECTIONS

- Nearly all of the DOE 2020 targets for membrane performance and durability have been met with one membrane based on a pilot scale PFIA ionomer and electrospun nanofiber support.
- Peroxide scavenging additive levels were optimized for this membrane, based on the OCV accelerated stress test.
- Over 30 m of membrane were produced for use in stack testing at GM.
- Analysis of the resistance targets at 120°C and 40 kPa water vapor pressure suggests an ionomer with equivalent weight of 450 g/mol or less is necessary to meet this target with a 10-micron supported membrane.
- Accelerated OCV stress tests show a reduction in voltage within the first 200 h. The origin of this loss will be further investigated.
- Stack testing has been initiated at GM with a target run time of 2,000 h.
- Post mortem analysis is planned for MEAs run in the stack to better understand failure modes for membranes developed under this project.

FY 2016 PUBLICATIONS/PRESENTATIONS

1. FC109 at DOE's Annual Merit Review in Washington, D.C. on June 9, 2015.

2. USCAR Fuel Cell Tech Team Presentation; "New Fuel Cell Membranes with Improved Durability and Performance," October 7, 2015, Southfield, MI.

3. "V.C.1 New Fuel Cell Membranes with Improved Durability and Performance," 2015 DOE Hydrogen and Fuel Cells Annual Progress Report.

4. D.M. Peppin, M.A. Yandrasits, A.S. Fochs, "Resistance Measurements for Multilayer Supported Membranes," Fall ECS meeting Phoenix, AZ, October 2015.

5. D.M. Peppin, M.A. Yandrasits, A.S. Fochs, "Resistance Measurements for Multilayer Supported Membranes," ECS Transactions, 69 (17) 1105–1110 (2015).

6. Leslie Dos Santos, Jun Woo Park, Ryszard Wycisk, Peter N. Pintauro, Graeme Nawn, Keti Vezzù, Enrico Negro, Federico Bertasi, Vito Di Noto, "Membranes from Blended Ionomer/PVDF Nanofibers: 1. PFSA/PVDF and PFIA/PVDF Fiber Spinning and Membrane Fabrication," Fall ECS meeting Phoenix AZ, October 2015.

V.C.2 Advanced Hybrid Membranes for Next Generation PEMFC Automotive Applications

Andrew M. Herring (Primary Contact),
Mei-Chen Kuo, James L. Horan, and
Andrew R. Motz
Colorado School of Mines
1500 Illinois St.
Golden, CO 80401
Phone: (303) 384-2082
Email: aherring@mines.edu

DOE Manager: Gregory Kleen
Phone: (240) 562-1672
Email: Gregory.Kleen@ee.doe.gov

Technical Advisor: John Kopasz
Phone: (630) 252-7531
Email: Kopasz@anl.gov

Contract Number: DE-EE0006363TDD

Subcontractors:
- Bryan Pivovar, National Renewable Energy Laboratory, Golden, CO
- Nilesh Dale, Nissan Technical Center North America, Farmington Hills, MI
- Steven Hamrock and Michael Yandrasits, 3M Fuel Cell Components Group, St. Paul, MN

Project Start Date: October 1, 2013
Project End Date: July 31, 2017

Overall Objectives

- Fabricate a low-cost, high-performance proton exchange membrane to operate at the temperature of an automotive fuel cell stack, with excursions to 120°C and requiring no system inlet humidification.
- Optimize the membrane to meet durability, crossover, and electrical resistance targets.
- Incorporate the membrane into a 50-cm^2 membrane electrode assembly (MEA).

Fiscal Year (FY) 2016 Objectives

- Show that heteropoly acid (HPA)-containing films can be fabricated thin and have a low area specific resistance (ASR) at the temperature of an automotive fuel cell stack and at higher temperatures likely to be operational transients whilst also functioning as an electrical resistor.
- Increase HPA loading and organization for maximum proton conduction in a functionalized commercial fluoroelastomer manufactured by 3M.
- Begin the development of electrodes specifically for these membranes so that MEA testing can begin.

Technical Barriers

This project addresses the following technical barriers from the Fuel Cells section of the Fuel Cell Technologies Office Multi-Year Research, Development, and Demonstration Plan.

(A) Durability

(B) Cost

(C) Performance

Technical Targets

The technical targets are shown in Table 1.

TABLE 1. Progress towards Meeting Technical Targets for Membranes for Transportation Applications

DOE 2020 Target Conditions	2020 ASR Target Ω cm^2	ASR Result June 2016 Ω cm^2	Film Thickness µm	Measured Conditions
120°C and water partial pressures from 40–80 kPa	0.02	0.015	40	110°C and 95% RH
80°C and water partial pressures from 25–45 kPa	0.02	<0.01	10	80°C and 95% RH
	0.02	0.018	40	80°C and 50% RH
30°C and water partial pressures up to 4 kPa	0.03	<0.005	10	30°C and 95% RH

RH – relative humidity

FY 2016 Accomplishments

- Continued to redesign the synthesis of the FC-2178-HPA material to increase efficiency and yield, moving the polymer platform closer to the DOE cost target of <\$20 m^2.
- Showed that the FC-2178-HPA material could be fabricated into films with thickness <20 µm and ASR of <0.02 Ω cm^2 at a range of temperatures from 30°C to 110°C and RH from 50% to 95%.

- Began work on making large-area reinforced membranes for incorporation into MEAs and fuel cell testing.

✧ ✧ ✧ ✧ ✧

INTRODUCTION

The objective of this project is to fabricate a low-cost, high-performance hybrid inorganic/polymer membrane that has a proton ASR of <0.02 ohm cm^2 at the operating temperature of an automotive fuel cell stack (95–120°C) at water partial pressures from 40 kPa to 80 kPa with good mechanical and chemical durability. Additionally, the membrane will be optimized for low hydrogen and oxygen crossover with high electrical ASR at all temperatures and adequate proton ASR at lower temperatures. We also seek to gain valuable insights into rapid proton transport at the limit of proton hydration. Additional research will be performed to incorporate the membrane into a 50-cm^2 MEA.

The materials at the start of this project are at a technology readiness level of 2, as we have shown that they have proton conductivity under high and dry conditions, but we have not yet consistently shown that they will function in an operational fuel cell. At the project's end, the materials will be at a technology readiness level of 4 and will be integrated into an MEA, demonstrating that they can function with electrodes as a single fuel cell. This work will enable hydrogen-powered fuel cells as it will negate the need for costly and bulky external humidification unit operations in the fuel cell system. Additionally, excess water will not be an issue for freeze or fuel cell reactant supply. The project is addressing the 2020 DOE technical targets for membranes for transportation applications.

APPROACH

With past funding from DOE and the National Science Foundation (NSF), we have developed completely new ionomer systems based on incorporation of inorganic super acids into polymer systems. These ionomer systems demonstrate high proton conductivity under low-humidity conditions, as well as higher-temperature operation, high oxidative stability, and little swelling when wet. This project will perform the work to optimize the proton conductivity and mechanical properties in these materials to produce a robust thin film for proton exchange membrane fuel cells (PEMFCs) in automotive applications. The technical concept is to use functionalized inorganic super acids that utilize little water for high proton conductivity as the protogenic group covalently attached to a polymer backbone optimized for all other functions of the membrane.

Many composite inorganic/polymer films have been fabricated, but unless the particles have dimensions on the nano-scale, there is no advantage, as the improvement to film properties occurs at the particle polymer interface. The limit of this approach is to use molecules with high acidity as the highly activating functionalities, but to do this we must immobilize them, control the morphology of the proton-conducting channel, and fabricate an amorphous material. The two moieties that have received the most attention and appear to greatly enhance proton transport are HPAs and zirconyl phosphonates. In previous work, we demonstrated these materials as composite membranes [1–3], but the inorganic super acid in the membrane was not immobilized. Here we continue our work to fabricate true hybrid materials where the inorganic super acid is incorporated as a functionalized monomer [4–6]. At the beginning of the project, these materials were not yet fuel cell ready, as the syntheses were inefficient and there were no methods of processing the polymers into thin proton conductive films. In this project, we will overcome all of these disadvantages with an innovative approach to amorphous materials to produce high proton conductivity and all other properties desired of a proton exchange membrane.

RESULTS

We have now down-selected the materials under consideration to HPA functionalized flouroelastomers. In Figure 1 we show the current synthesis that has been optimized to increase yield and purity in each step, minimize the total number of steps, and decrease the use of solvents. This not only allows more rapid synthesis of the materials but also facilitates scale-up and should allow the DOE cost targets for the material to be achieved. The key to the synthesis is to first do the functionalization on a small molecule. In step 1, *para*-bromophenol is converted to the *para*-phenol phosphonic diethyl ester. The dirthylphosphonic acid is then reacted with the fluoroelastomer under basic conditions where the polymer dehydroflourinates and is functionalized by the small molecule. This step is a major improvement on the older procedure where the polymer was dehydrofluorinated in a separate step, which led to lack of control of where the phosphonic acid would attach to the polymer. In the third step, the ester is hydrolyzed to the phosphonic acid. Finally, the lacunary HPA ($SiW_{11}O_{39}^{8-}$) is added to form cross-linking bonds to the polymer. These last two steps can be performed in one pot. We experienced some difficulties in attachment of the lacunary HPA as we were drying the phosphonic acid functionalized membrane in a vacuum oven, which led to the formation of the unreactive phosphonic anhydride. Fortuitously, the anhydride was easily unzipped back to the phosphonic acid by simply boiling the polymer. The resultant film is a transparent brown film of 10–40 μm.

The proton conductivities of these materials at 95% RH and temperatures from ambient to 95°C remain some of the highest observed for polymer electrolytes; recently, values approaching 1 S cm^{-1} have been achieved under these

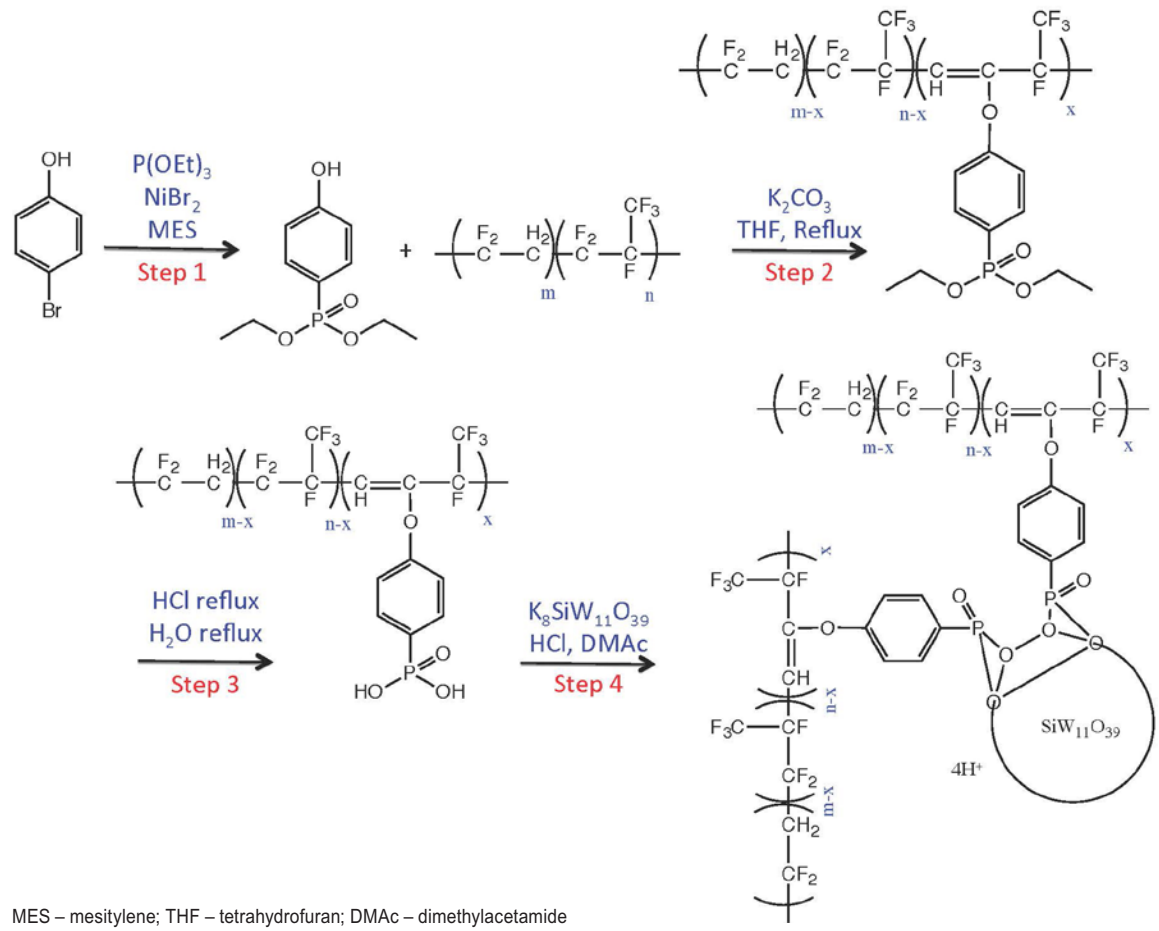

MES – mesitylene; THF – tetrahydrofuran; DMAc – dimethylacetamide

FIGURE 1. Improved synthetic route to produce the HPA hybrid materials

conditions at 95°C. The materials easily meet the DOE ASR targets at 30°C and 80°C, with ASRs at 95% RH <0.01 Ω cm^2 throughout this temperature range. The objective of this project is low ASRs at higher temperatures and low RHs enabling fuel cell operation at lower partial pressures of water than can currently be achieved. Our initial approach to meet these objectives was to simply increase the HPA loadings from 70 wt% to 80 wt%. At 70 wt% loading, we approached an ASR of 0.1 Ω cm^2 at 110°C and 50% RH; increasing the loading to 80 wt% achieved an ASR at best of 0.03 Ω cm^2, which was just shy of the DOE target at 120°C and low partial pressure of water. Our emphasis had been on casting 10-µm films; microscopic examination of the films at 10 µm revealed a series of cracks, which could be eliminated by casting 40-µm films (Figure 2). This had a dramatic effect on the ASR. The 10-µm films at 110°C and 50% RH typically had values from 0.03 Ω cm^2 to 0.1 Ω cm^2, but the 40-µm films all had ASRs lower than 0.02 Ω cm^2 (Figure 3), which satisfied the project's year two go/no-go decision point.

To improve film properties, we have initiated a film processing study. Moderate heat treatment of the material leads to a film that swells only *ca.* 40 wt%, whereas the unprocessed films typically swell *ca.* 100 wt%. We believe that the improvements to the film are due to the formation of additional crosslinks in the material as more of the lacunary HPA are bound in a bifunctional manner. Boiling films with 70 wt% loadings of HPA still lose 10 wt% of their mass. Our working hypothesis is that dually bound HPA should be stable to boiling water, so it is obvious from theses studies that we still have not perfected the crosslinking process. Nevertheless, boiled films of this chemistry still have exceedingly high ionic conductivities. The final optimized films are expected to be brittle, so we have begun studies to support the material in 10-µm expanded polytetrafluoroethylene. Initial attempts have produced transparent, strong films.

CONCLUSIONS AND FUTURE DIRECTIONS

- A completely overhauled synthetic scheme has been implemented and now allows the HPA-containing material to be synthesized in scaled-up batches quickly and efficiently.

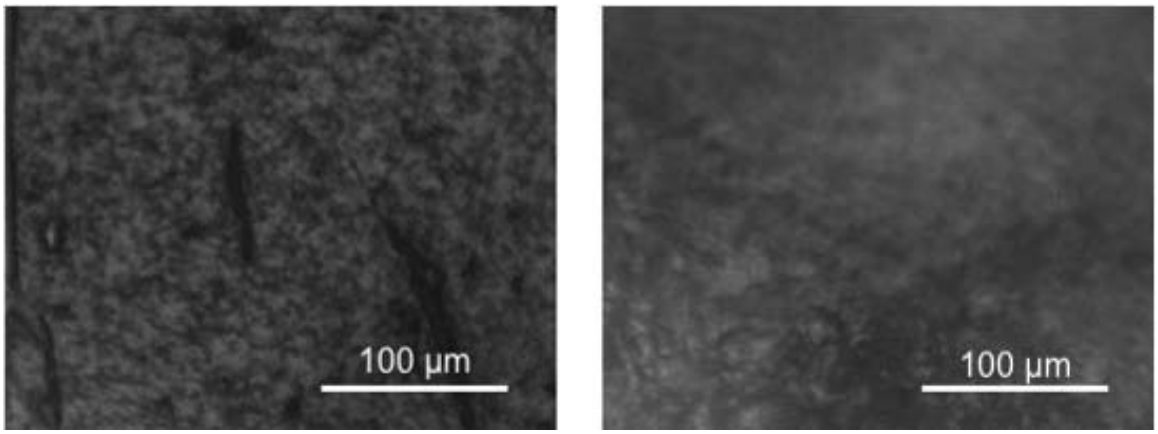

FIGURE 2. Scanning electron microscope images of 80 wt% HPA films: (left) 10 µm and (right) 40 µm

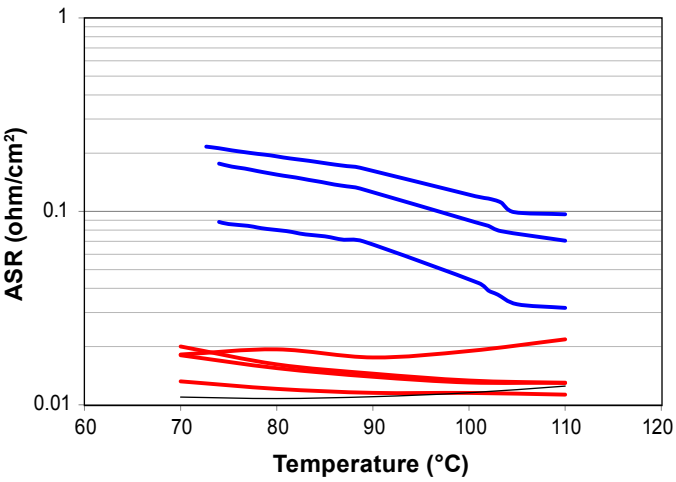

FIGURE 3. ASRs for 80 wt% HPA films: 10 µm (blue) and 40 µm (red)

- Materials can be boiled with minimal HPA loss, and they give ASRs <0.02 Ω cm^2 under a variety of conditions.
- Further improvements in film processing should yield fully cross-linked and water-stable materials with low ASRs that will meet DOE targets under all conditions.
- In the final year of this project, the material will be integrated into MEAs for testing, and all remaining barriers for membranes for automotive applications will be overcome.

FY 2016 PUBLICATIONS/PRESENTATIONS

1. "Water Uptake in Novel, Water-Stable, Heteropoly Acid Films." A.R. Motz, J.L. Horan, M.C. Kuo, and A.M. Herring, oral presentation, presented at the 228th ECS Meeting, Phoenix, AZ, October 2015.

REFERENCES

1. Haugen, G.; Meng, F.; Aieta, N.; Horan, J.; Kuo, M.; Frey, M.; Hamrock, S.; Herring, A. *Electrochemical and Solid State Letters* **2007**, *10*, B51.

2. Malers, J.; Sweikart, M.; Horan, J.; Turner, J.; Herring, A. *Journal of Power Sources* **2007**, *172*, 83.

3. Meng, F.; Aieta, N.; Dec, S.; Horan, J.; Williamson, D.; Frey, M.; Pham, P.; Turner, J.; Yandrasits, M.; Hamrock, S.; Herring, A. *Electrochimica Acta* **2007**, *53*, 1372.

4. Horan, J.; Genupur, A.; Ren, H.; Sikora, B.; Kuo, M.; Meng, F.; Dec, S.; Haugen, G.; Yandrasits, M.; Hamrock, S.; Frey, M.; Herring, A. *ChemSusChem* **2009**, *2*, 226.

5. Schlichting, G.J.; Horan, J.L.; Jessop, J.D.; Nelson, S.E.; Seifert, S.; Yang, Y.; Herring, A.M. *Macromolecules* **2012**, *45*, 3874.

6. Horan, J.L.; Lingutla, A.; Ren, H.; Kuo, M.-C.; Sachdeva, S.; Yang, Y.; Seifert, S.; Greenlee, L.F.; Yandrasits, M.A.; Hamrock, S.J.; Frey, M.H.; Herring, A.M. *The Journal of Physical Chemistry C* **2014**, *118*, 135.

V.C.3 Smart Matrix Development for Direct Carbonate Fuel Cell

Chao-Yi Yuh (Primary Contact), Abdelkader Hilmi, Arun Surendranath
FuelCell Energy (FCE), Inc.
3 Great Pasture Road
Danbury, CT 06813
Phone: (203) 825-6112
Email: cyuh@fce.com

DOE Manager: David Peterson
Phone: (240) 562-1747
Email: David.Peterson@ee.doe.gov

Contract Number: DE-EE0006606

Subcontractors:
- University of Connecticut, Storrs, CT
- Illinois Institute of Technology, Chicago, IL

Project Start Date: September 22, 2014
Project End Date: October 31, 2017

Overall Objectives

Develop an innovative durable DFC® (Direct Fuel Cell) electrolyte matrix (smart matrix) to enable >420 kW rated stack power and 10-year (80,000-h) stack service life (current generation: 350 kW rated stack power and 5-year stack service life).

- Increase market penetration for stationary fuel cells.
- Enable domestic clean-energy job growth.
- Enable technology for hydrogen infrastructure and CO_2 capture.

Fiscal Year (FY) 2016 Objectives

- Develop matrix degradation mechanistic understanding.
- Achieve by projection end of life (EOL) targets of matrix mechanical strength, sealing efficiency, and phase-stable fine-pore microstructure.
- Scale-up manufacture and initiate 30 kW technology stack evaluation.

Technical Barriers

This project addresses the following technical barriers from the Fuel Cells section of the Fuel Cell Technologies Office Multi-Year Research, Development, and Demonstration Plan [1].

(A) Durability: incomplete understanding of degradation mechanism and lack of clear long-term degradation mitigation schemes

(B) Cost: cost-effective matrix degradation-mitigation schemes

Technical Targets

This project aims to develop an innovative smart matrix to enable combined heat and power (CHP) distributed generation fuel cell systems to meet DOE 2020 research, development, and demonstration technical targets [1] (Table 1).

TABLE 1. FCE Progress towards Meeting DOE research, development, and demonstration Technical Targets for 100 kW–3 MW CHP Distributed Generation Fuel Cell Systems Operating on Natural Gas

Characteristic	Units	2020 Targets	DFC Baseline
Electrical Efficiency at Rated Power	%	>50	47
CHP Energy Efficiency	%	90	90
Operating Lifetime	Hours	80,000	>44,000

Specific technical targets for the smart matrix are established based on multi-year DFC field operation experience:

- >25% beginning of life (BOL) mechanical strength increase, >20% porosity increase, and improved fine-pore microstructure (>30% reduction of pores larger than 0.2 μm) compared to the baseline.
- Stable fine-pore microstructure (<50% pores larger than 0.2 μm at EOL) for enhanced capillary electrolyte retention, projected from >5,000 h accelerated cell and technology stack tests.
- Understand matrix material degradation mechanism.
- Scale-up production of smart matrix for 1 m^2 full-area 30 kW technology stack validation.

FY 2016 Accomplishments

- Verified selected smart matrix meeting (by projection) EOL targets in ~3,000–5,000 h accelerated single-cell tests.
- Delivered a topic report on matrix degradation mechanistic understanding.
- Successfully fabricated ~1 m^2 full-size high-porosity smart matrix meeting BOL targets for 30 kW technology stack evaluation.

✧ ✧ ✧ ✧ ✧

INTRODUCTION

FCE's DFC products based on high-temperature internal-reforming carbonate fuel cell technology are striving to meet growing worldwide demand for high-efficiency, ultra-clean power generation. DFC has already advanced to a single stack capable of 350 kW net alternating current power and 5-year service life. Stack power and service life increases will further enhance DFC's commercial competitiveness. The electrolyte matrix holds a very important key to higher power density operation, longer service life, and lower cost. The matrix, a porous microstructure consisting mainly of ultra-fine sub-micron α-$LiAlO_2$ powders sandwiched between two electrodes, immobilizes the liquid electrolyte, isolates fuel from oxidant and facilitates ionic transport. However, $LiAlO_2$ slowly coarsens, lowering capillary force leading to matrix drying and electrolyte redistribution, contributing to gas crossover and performance loss. This program aims to develop a high-yield production-ready smart matrix with robust and stable fine-pore microstructure to enable DFC meeting DOE 2020 targets for CHP distributed generation fuel cell systems.

APPROACH

The approaches to achieve the technical targets are listed below in Table 2. The technical targets will be validated in long-term >5,000 h accelerated cell and full-area 30 kW technology stack tests. Full-scale production trials will be conducted to fabricate full-size smart matrices for the technology stack tests and to assure the manufacturing process ready for product implementation.

TABLE 2. Approaches to Achieve Smart Matrix Technical Targets

Technical Targets	Approaches
BOL: >25% mechanical strength increase, >20% porosity increase, and improved fine-pore microstructure (>30% reduction of pores larger than 0.2 μm) compared to baseline	Nano-pore former for increased porosity Reinforcement additives to increase mechanical strength
	Optimize slurry formulation and processing for improved particle-size distribution, particle packing and production yield
EOL: Stable fine-pore microstructure for maintaining capillary electrolyte retention (<50% pores larger than 0.2 μm)	Stabilized $LiAlO_2$ or additives to slow down coarsening to maintain capillary electrolyte retention
Coarsening mechanistic understanding	Investigate effects of temperature, gas atmosphere, and electrolyte composition on matrix microstructure evolution, $LiAlO_2$ stability, wettability and solubility in single cells/stacks and controlled out-of-cell tests

RESULTS

Multi-year operation of DFC revealed gradual α-$LiAlO_2$ coarsening, more pronounced at the reducing anode side and accelerated by temperature. Literature reported that α-$LiAlO_2$ solubility increased with increasing temperature, lower CO_2 partial pressure, and in strong basic melts, whereas $\alpha \rightarrow \gamma$ phase transformation also occurred at higher temperatures (≥700°C) [2,3]. Literature also reported that the coarsening rate increased with finer particles. All these pointed to dissolution-precipitation Ostwald ripening as the leading coarsening mechanism. However, the detailed fundamentals of the faster reducing anode-side coarsening had not yet been established.

X-ray photon spectroscopy and X-ray diffraction analyses revealed substantial surface Li deficiency and cationic disorder of the as-made baseline powders. Thermal stability tests in the absence of electrolyte at 700°C for 50 h under a reducing environment (4% H_2-N_2) led to powder darkening and enhancements of the nonstoichiometry and surface aluminum metallic characteristics (regardless of the presence of moisture) without apparent phase transformation. These phenomena were not observed upon exposure to the oxidizing atmospheres (air, O_2-CO_2-N_2). Re-oxidation of the pre-reduced darkened powders at 700°C in air restored the original powder characteristics. These results attest that the reducing environment amplifies surface disorder, likely promoting phase nucleation and coarsening. Some metastable hydrated impurities were also observed transforming to less stable γ-$LiAlO_2$ in the reducing atmosphere. Powders synthesized with a more stoichiometric structure and without metastable hydrated phases showed minimal changes in powder characteristics upon the exposure to the same reducing atmosphere.

Electrolyte immersion tests of the baseline powder under various gas environments (such as 4% H_2-H_2O-N_2, 4% H_2-1% CO_2-N_2, N_2, and 5% O_2-N_2) at 700°C showed that the CO_2-free more basic environment (reducing as well as oxidizing) caused significant coarsening (>95% surface-area decay) and >90% $\alpha \rightarrow \gamma$ transformation, whereas coarsening was significantly suppressed by CO_2 addition (by only ~1%). These results point to a strong relationship between the phase transformation and coarsening.

It was originally postulated that in the absence of CO_2, the concentration of $[O^{2-}]$ in the electrolyte increases sharply, leading to a very high $LiAlO_2$ solubility and accelerated Ostwald ripening. However, the rate of coarsening and phase transformation could not be correlated well with the measured solubility difference at 650°C under the CO_2-containing oxidizing (air-30% CO_2) and CO_2-free reducing atmospheres (4% H_2-3% H_2O-N_2). It instead points to the formation of surface non-stoichiometry or disorder under reducing environment as the predominant factor. Based on the above fundamental understanding, more stable

powders with higher crystallinity, less surface disorder and less metastable impurities, in conjunction with innovative approaches, are being developed in this program to mitigate the coarsening.

In order to evaluate the impact of coarsening on matrix wetting properties, specially designed high-temperature, contact-angle tests under reducing atmosphere on different baseline matrix samples operated for up to ~40,000 h (single cells as well as stacks) showed rapid complete wetting and fast electrolyte absorption (indicating ~0° contact angle), suggesting little effect of coarsening on the inherent contact angle. Therefore, capillary electrolyte retention is mainly controlled by pore size distribution and a stable fine-pore matrix structure is expected to be capable of maintaining electrolyte retention.

The consistency and reproducibility of the developed smart matrix slurry formulation and process were verified in >200 lab-scale batches (~500 cc). ~250 cm^2 bench-scale accelerated single cells operated for up to ~3,500 h demonstrated essentially no gas cross-over (leakage) and >20-mΩcm^2 resistance reduction. Numerous single cells operated for up to 5,000 hours showed excellent smart matrix phase and pore-structure stability (Figure 1). In order to accurately project the durability of the developed smart matrix capable of meeting the 10-year life EOL target, an accelerated single-cell test protocol to promote matrix coarsening and electrolyte loss (higher temperature, steam content, and fuel utilization than in typical DFC) has been established. The post-test information from accelerated single-cell and product baseline matrices operated for up to five years forms the basis of the protocol. The developed smart matrix showed essentially no increase in pores larger than 0.2 µm and stable cross-over (~0%) in accelerated single cells, projecting the capability of meeting the 10-year life EOL target (Figures 2 and 3).

Scale-up manufacturing development of the selected smart matrix, from ~500 cc lab-scale size to pilot scale (~1 gal) and production-scale full size (~90 gal slurry), has been initiated to optimize manufacturing process parameters such as mixing, milling, casting, drying, and lamination. Full-size (~1 m^2) smart matrices with desired fine-pore structure were successfully fabricated for technology stack evaluation (Figure 4). It also met the BOL pore-structure target, confirming the process robustness and consistency (Figure 1). The physical and mechanical properties were consistent with the lab-scale matrices. These full-size matrices also duplicated same improved gas-sealing efficiency and cell resistance reduction in short-term single cells.

CONCLUSIONS AND FUTURE DIRECTIONS

Lab-scale smart matrix has successfully met all BOL and EOL targets based on accelerated single-cell tests operated for up to ~5,000 h. It was successfully scaled up to full-size ~1 m^2 for 30 kW technology stack evaluation.

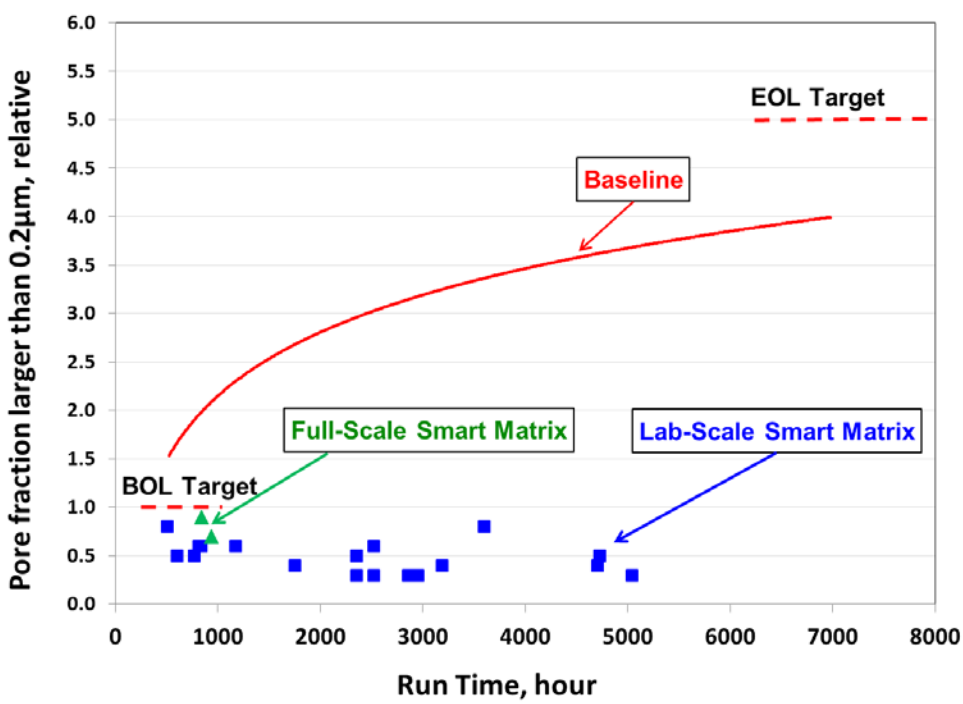

FIGURE 1. Both lab-scale and full-size smart matrices achieved excellent pore-structure stability

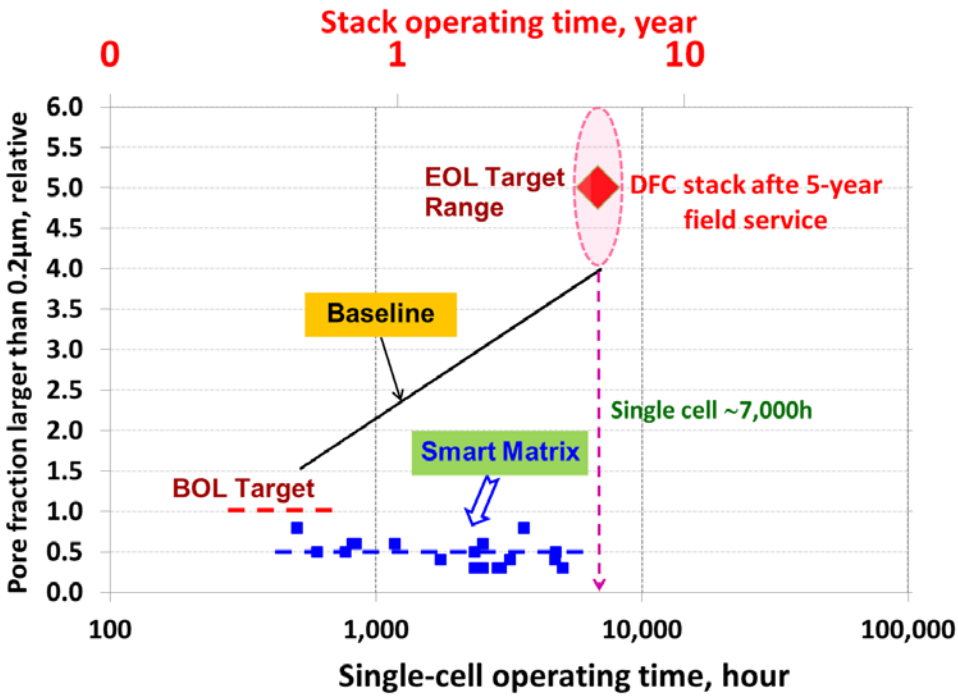

FIGURE 2. Smart matrix is projected capable of achieving EOL 10-year life pore-structure target from long-term accelerated single-cell tests

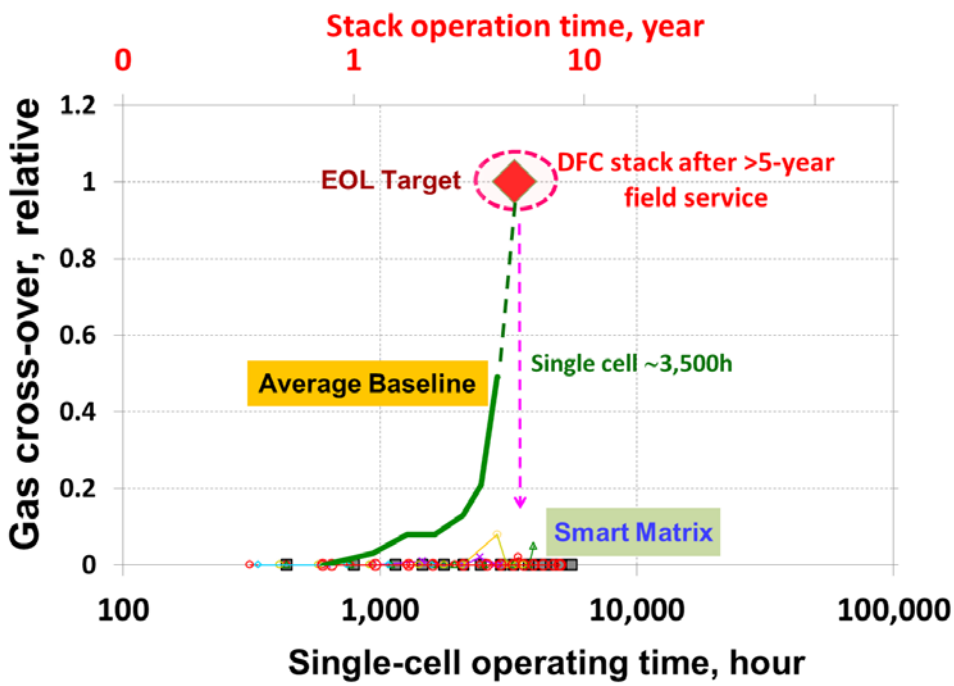

FIGURE 3. Smart matrix showed excellent sealing efficiency in accelerated single cells, projecting capable of 10-year service life

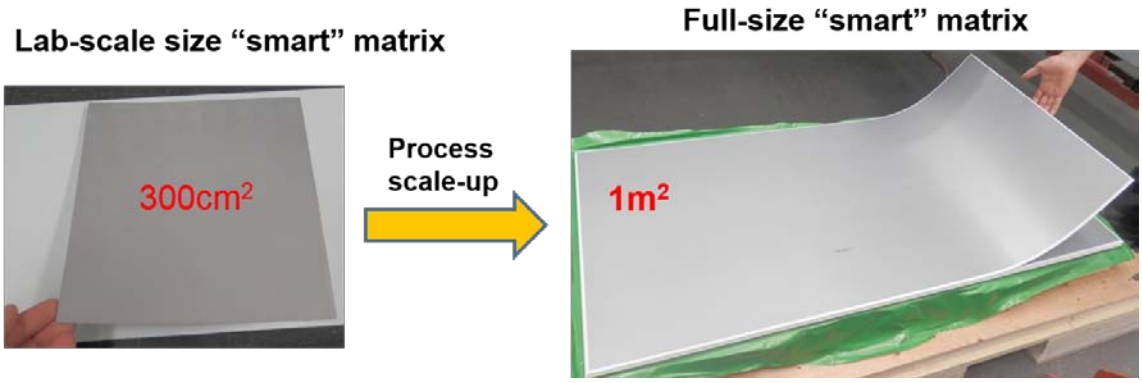

FIGURE 4. Full-size 1 m^2 high-porosity smart matrix was successfully manufactured

The remainder of the project will focus on further refining mechanistic understanding, optimizing smart matrix formulation, scale-up manufacturing, and validation in long-term technology stacks.

FY 2016 PUBLICATIONS/PRESENTATIONS

1. Program Go/No Go decision presentation to DOE EERE, November 12, 2015.

2. Program quarterly review presentation to DOE EERE, February 16, 2016.

3. "Stability of Lithium Aluminate in Reducing and Oxidizing Atmospheres at 700ºC," manuscript accepted for publication in International Journal of Hydrogen Energy, 2016.

4. A. Hilmi, A. Surendranath, and C. Yuh, "The Next Generation Carbonate Fuel Cell Matrix," Abstract# 76, 229th ECS Meeting, San Diego, CA, May 29–June 2, 2016.

5. C. Yuh and A. Hilmi, "Smart Matrix Development for Direct Carbonate Fuel Cell," 2016 DOE Hydrogen and Fuel Cells Program and Vehicle Technologies Office Annual Merit Review and Peer Evaluation Meeting, Arlington, Virginia, June 8, 2016.

REFERENCES

1. DOE Office of Energy Efficiency and Renewable Energy Fuel Cell Technologies Office's Multi-Year Research, Development, and Demonstration (MYRDD) Plan, Section 3.4 "Fuel Cells," Updated June 2016, http://energy.gov/sites/prod/files/2016/06/f32/fcto_myrdd_fuel_cells_0.pdf

2. C. Yuh, M. Farooque, and H. Maru, "Advances in Carbonate Fuel Cell Matrix and Electrolyte," in *Proc. Symp. Carbonate Fuel Cell Technology V*, The Electrochemical Society, **PV99-20**, 1999: 189–201.

3. C. Yuh and M. Farooque, "Materials and Life Considerations," in *Fuel Cells-Molten Carbonate Fuel Cells, Encyclopedia of Electrochemical Power Sources,* 497–507, Elsevier Science, 2009.

V.C.4 Ionomer Dispersion Impact on Fuel Cell and Electrolyzer Performance and Durability

Hui Xu (Primary Contact), Brian Rasimick, Zachary Green, Tom McCallum
Giner, Inc.
89 Rumford Ave.
Newton, MA 02466
Phone: (781) 529-0573
Email: hxu@ginerinc.com

DOE Manager: Donna Ho
Phone: (202) 586-8000
Email: Donna.Ho@ee.doe.gov

Contract Number: DE-SC0011307 (Small Business Innovation Research)

Subcontractor:
Yu-Seung Kim, Los Alamos National Laboratory (LANL)
Los Alamos, NM

Project Start Date: July 28, 2015
Project End Date: July 27, 2017

Overall Objectives

- Further develop and commercialize LANL's non-aqueous solvent-based ionomer dispersion technology.
- Scale up ionomer and dimensionally stable membrane (DSM™) production to allow for continuous roll-to-roll production of low-platinum-group-metal membrane electrode assemblies (MEAs) for fuel cells and electrolyzers.
- Demonstrate the durability of proton exchange membrane (PEM) fuel cell and electrolyzer MEAs at more extensive cycling and operating conditions.

Fiscal Year (FY) 2016 Objectives

- Prepare ionomer dispersions on a large scale to produce 1–2 kg.
- Fabricate DSM using ionomer dispersions from LANL in a more scalable continuous roll-to-roll process.
- Fabricate scaled-up, low-platinum-group-metal-loading MEAs for fuel cells (overall PGM loading less than 0.25 mg/cm^2) and electrolyzers (PGM loading less than 0.4 mg/cm^2 for anode plus cathode).

Technical Barriers

This project addresses the following technical barriers from the Fuel Cells section of the Multi-Year Research, Development, and Demonstration Plan of the DOE Fuel Cell Technologies Office.

(A) Durability

(B) Cost

Technical Targets

The target of this project is to apply ionomer dispersion technology to make durable fuel cell and electrolyzer MEAs. DOE targets for PEM fuel cells are listed in Table 1.

TABLE 1. Progress towards Meeting Technical Targets for MEA Durability Targets

Characteristic	Units	DOE 2020 Target
Platinum group metal (PGM) total content (both electrodes)	g/kW	<0.125
PGM total loading (both electrodes)	mg-PGM/cm$^2_{geo}$	<0.125
Loss in catalytic (mass) activity	% Loss	<40
Loss in performance at 0.8 A/cm^2	mV	<30
Loss in performance at 1.5 A/cm^2	mV	<30
Mass activity @ 900 mV$_{iR\text{-}free}$	A/mg$_{PGM}$	0.44

For PGM electrolyzers, DOE has not set a target. Giner's targets are as follows:

- Low-PGM-loading electrolyzer MEAs demonstrate less than 20 mV loss (at 1.5 mA/cm^2) after 50,000 cycles from 1.4 V to 1.9 V.
- Low-PGM-loading electrolyzer MEAs demonstrate less than 20 mV performance loss after 1,000-hour test at 1.5 A/cm^2.

FY 2016 Accomplishments

- Various ionomer dispersions were produced in batch sizes up to over 1 kg. More than 40 non-aqueous solvents were evaluated.
- Significant progress was made to transition manufacturing to a roll-to-roll process. Electrode layer manufacturing was changed from batch spraying to an ink-casting process. DSM-based MEAs were fabricated from selected ionomer dispersions.

- MEAs produced by the new process were evaluated as fuel cells and electrolyzers. Short-term durability was evaluated.

✧ ✧ ✧ ✧ ✧

INTRODUCTION

LANL has developed a revolutionary method of building an MEA for PEM fuel cells that can significantly reduce manufacturing costs and extend MEA lifetimes. This method incorporates unique polymer dispersions in non-aqueous liquids to produce superior electrode performance, stability, and durability during harsh fuel cell operating conditions [1–6]. The LANL-produced MEA has been evaluated and certified using an accelerated stress test developed by DOE in conjunction with car manufacturers; the voltage loss of LANL's MEA remained below 30 mV even after 70,000 cycles.

The ionomer dispersion work at LANL has a great potential to significantly improve the lifetime of PEM fuel cells [2–4]. However, the ionomer dispersion used was Nafion® 1,100 equivalent weight (EW); there has been a strong push in the industry towards membranes with lower EW that can increase proton conductivity. Low-EW ionomers are less dimensionally stable and could benefit more from Giner's well-established DSM™ technology. Also, the work at LANL has been done with dispersions of ionomer in the salt form, rather than in the proton form. This requires additional processing after membrane production to put the membrane in the acid form. Using dispersions from LANL in the acid form and utilizing Giner's DSM technology, this Phase II project will validate these technologies towards viable commercial applications in advanced fuel cell and electrolyzer systems.

APPROACH

The approach used for this project is shown in Figure 1. First, the ionomer dispersion technology invented by LANL was applied in the platforms of the DSM™ developed at Giner; the impregnation of the novel low-EW ionomer dispersion into porous DSM supports has created more durable membranes with excellent proton conductivity for PEM fuel cells. Second, Giner will extend the ionomer dispersion studies to state-of-the-art PEM fuel cell catalysts. Most experiments performed at LANL were based on ETEK 20 wt% Pt supported on VULCAN 72 (20% Pt/C). Giner will examine the ionomer dispersion technology paired with more advanced catalysts (e.g., Tanaka catalyst). Finally, the project will also investigate the impact of ionomer dispersion on PEM electrolyzer MEAs that generally use unsupported iridium (Ir) catalysts. Giner will perform MEA durability tests following the DOE accelerated stress test protocols.

RESULTS

Giner and LANL have formed a wide range of ionomer dispersions starting from either Nafion 1100 EW or 3M's 825 EW perfluorosulfonic acid (PFSA). More than 40 non-aqueous solvents were investigated. The selected ionomer dispersions were used to fabricate membranes, DSM-reinforced membranes, and catalyst layers.

Membranes were made using 3M low-EW PFSA solutions and evaluated according to the following performance criteria: ionic conductivity, mechanical strength, and dimensional change on hydration. The materials were evaluated at 80°C when immersed in liquid water or equilibrated at various humidity levels. The ionic conductivity of the materials is shown in Figure 2a. Ionic conductivity was typically measured using a four-

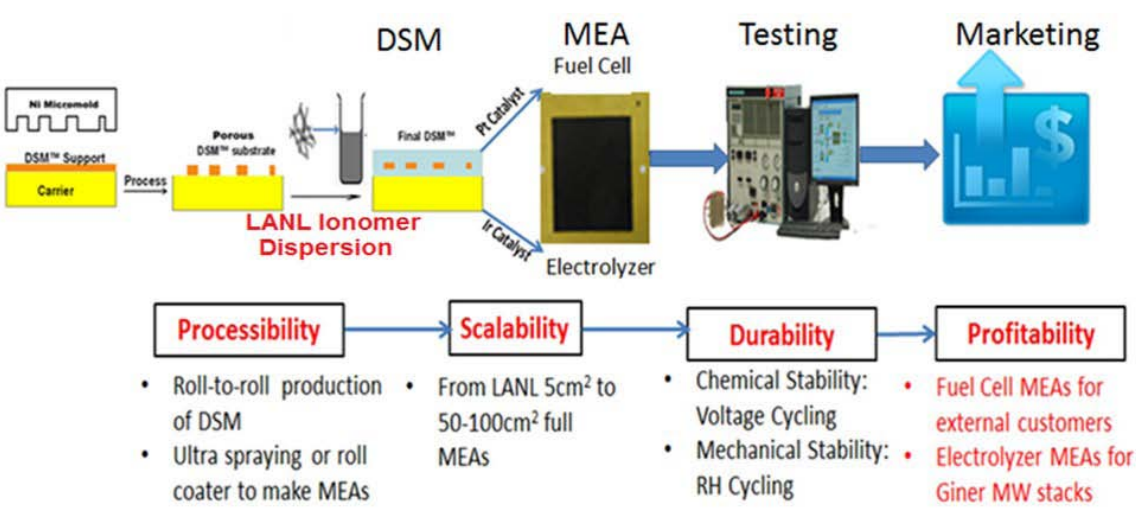

RH - Relative humidity

FIGURE 1. Technical approaches for PEM fuel cell and electrolyzer durability tests based on LANL's ionomer dispersion

point probe with platinum wires attached to a sine wave generator at 1 kHz. When immersed in liquid water, the ionic conductivity of all materials was on the same order of magnitude. Many of the solvent-cast materials had conductivity higher than that of Nafion; this is expected as the 3M PFSA has a lower EW than Nafion and is known to be more conductive. Certain solvent-cast membranes, namely dimethylacetamide (DMAc) and N-methylpyrrolidone (NMP), showed lower-than-normal conductivity when immersed in water and extremely low conductivity when only exposed to humid air. It is possible that DMAc or NMP were hydrolyzing during fabrication and form amines that might poison the membrane by ion exchange. If poisoning were occurring, one would expect a strong reduction in conductivity under humid conditions but a much weaker reduction when immersed in water, which allows contaminants to diffuse away. The results of dynamic mechanical testing upon the membranes are shown in Figure 2b. The solvent-cast materials had a lower stress at 10% strain (roughly equivalent to modulus) compared to Nafion. All materials other than methyl ethyl ketone (MEK) had a strain at break of greater than 150%.

We prepared cathodes with catalysts having different Pt loading on the carbon. At a fixed Pt loading, as the Pt weight percent decreases, the electrode thickness increases since the density of the carbon is more than 20 times lower than the density of the platinum. Figure 3a shows the polarization curves of 5-cm^2 standard MEAs having different Pt weight percent in the cathode. The Pt loading was fixed to ~0.05 mg/cm^2 for these MEAs. As expected, the fuel cell performance is improved as Pt weight percent decreases. No notable high frequency resolution (HFR) difference between the MEAs was observed. Currently LANL is investigating the durability of low Pt/C cathodes during potential cycling from 0.6 to 1.0 V. The performance and durability data will be used as the baseline for our further study using LANL ionomer dispersions.

The effect of the dispersing agents of low-Pt-loading cathodes on initial fuel cell performance was investigated. In this experiment, five LANL dispersing agents were used and compared with water/isopropyl alcohol (IPA) dispersing agents. All MEAs had a Pt loading of ~0.05 mg_{Pt}/cm^2. The initial fuel cell performance is shown in Figure 3b. All cathodes prepared from LANL dispersing agents showed at least comparable performance to the water/IPA dispersing agent processed cathode. There was a slight difference between cathodes using different dispersing agents. The cathodes processed from NMP, DMAc, and ethanol showed relatively better kinetic performance than the cathodes processed from pentanediol, glycerol, and water/IPA. The cathodes processed from NMP and DMAc showed relatively better mass transfer performance than the other cathodes. The improved mass transport performance using NMP and DMAc is in good agreement with higher-Pt-loading cathodes, i.e., 0.2–0.5 mg/cm^2.

The 3M PFSA ionomer solutions were evaluated for use in casting electrolyzer anode decals via a blade-casting method. The three most promising decals were tested in electrolyzer cells. The resulting performance after 100 hours of operation at 2 A/cm^2 is given in Figure 4a. The blade-cast decals performed just as well as Giner's standard spray-cast decal method. Tafel slope analysis indicated that the blade-cast decals displayed some curvature at high current densities. Based on prior experience, this indicates that the ionomer content in the anode decal layer may be too high, and decreasing it could lead to performance gains. Cells were also built to evaluate durability via accelerated stress testing. Figure 4b shows the performance change for a cell built using an anode cast from a dimethylformamide (DMF)-based solution on Nafion 1110 membrane. Little to

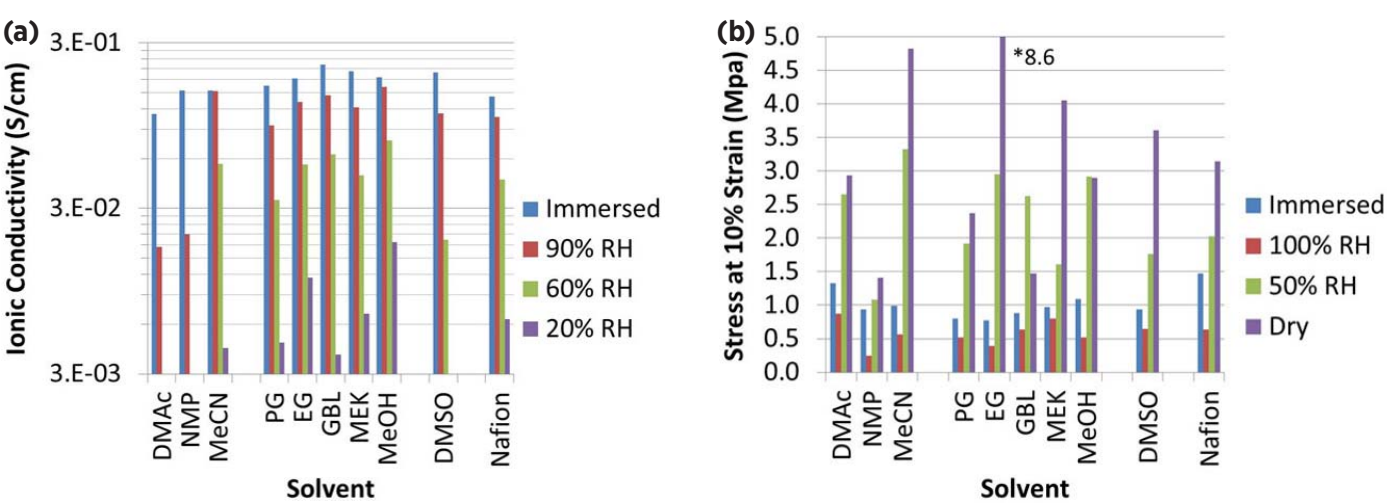

MeCN – Acetonitrile; PG – Propylene glycol; EG – Ethylene glycol; GBL – γ-butyrolactone; MeOH – Methanol; DMSO – Dimethyl sulfoxide

FIGURE 2. Selected properties of membranes cast from various solvent dispersions: ionic conductivity (a) and stress at 10% strain (b)

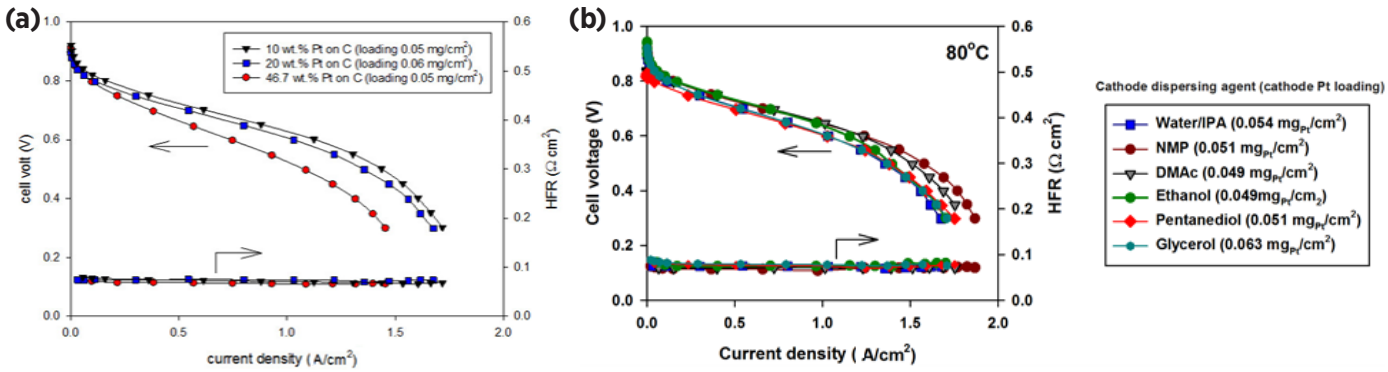

FIGURE 3. H_2/air fuel cell performance: 80°C, 100% relative humidity, 30 psi back pressure, stoic number: H_2:3, air:2: (a) effect of cathode Pt wt% in the catalyst; (b) effect of the solvent for the ionomer dispersion

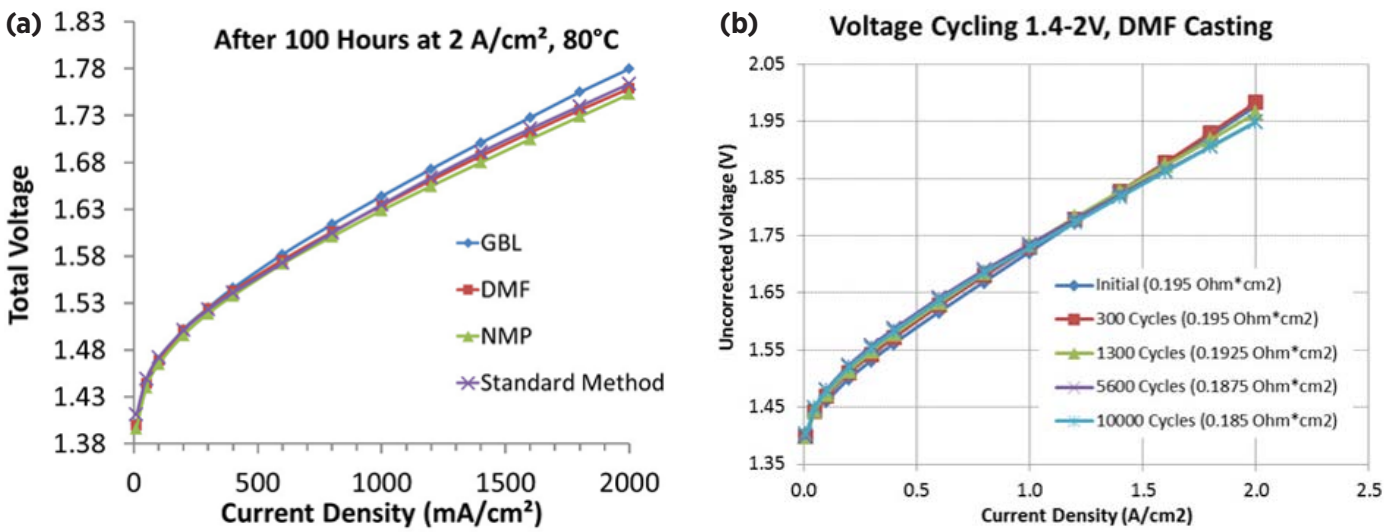

FIGURE 4. Electrolyzer cell performance at 80°C using the blade-cast electrodes: constant current operation (a) and accelerated stress testing via voltage cycling (b)

no signs of degradation were observed. In fact, performance below 1.2 A/cm^2 improved as the result of decreasing high-frequency resistance. The other solvent systems produced similar results.

CONCLUSIONS

- A variety of non-aqueous ionomer dispersions were evaluated in terms of ionomer concentration, conductivity, dimensional expansion, and mechanical properties of cast membranes.
- Selected solvents include DMSO, GBL, and MeOH.
- Low-Pt-loading fuel cell electrodes using non-aqueous ionomer dispersions were developed; glycerol-based electrodes demonstrated a good trade-off between performance and durability.
- Water electrolyzer electrodes using non-aqueous ionomer dispersions were investigated. GBL-, NMP-, and DMF-based ionomer dispersions led to uniform electrodes with good performance and durability.

FUTURE DIRECTIONS

- Further investigate the transport properties of fuel cell electrodes using low-Pt-loading and non-aqueous ionomer dispersions.
- Use non-aqueous ionomer dispersions to develop fully scalable and processible electrode and MEA manufacturing platforms for Giner's water electrolyzer.

FY 2016 PUBLICATIONS/PRESENTATIONS

1. Xu, H., "Ionomer Dispersion Impact on Advanced PEM Fuel Cell Performance and Durability," Oral Presentation. DOE Hydrogen and Fuel Cell Annual Merit Review Meeting, Washington, DC. June 2016.

REFERENCES

1. Brosha, E.; Garzon, F.; Johnston, C.; Labourieau, A.; Kim, Y.S.; Lee, K.-S.; Orler, B.; Pivovar, B.; Torraco, D.; Welch, C.; and Xu, H., "Studies Towards Optimizing Fuel Cell Electrode Structure and Composition," Canada to USA Fuel Cell and Hydrogen Cluster Connection Workshop, Vancouver, BC, Canada, February 16–17, 2009.

2. Kim, Y.S.; Lee, K.S.; Rockward T. U.S. Patent 7981319 B2, 2011.

3. Kim, Y.S.; Lee, K.S.; Rockward T. U.S. Patent 8236207 B2, 2012.

4. Kim, Y.S.; Labouriau, A.; Welch, A; Hjelm, R.; and Mack, N., "Solvation and Gelation Process of Nafon," presented in the 216th Meeting of the Electrochemical Society, San Francisco, October 2013.

5. Mittelsteadt, C.; Argun, A.; Laicer, C.; and Willey, J., U.S. Patent 20140342271A.

6. Welch, C.; Labouriau, A.; Hjelm, R.; Orler, B.; Johnston, C.; and Kim, Y.S., "Nafon in Dilute Solvent Systems: Dispersion or Solution?" *ACS Macro Lett.*, 1, 1403–1407 (2012).

V.C.5 Highly Stable Anion-Exchange Membranes for High-Voltage Redox-Flow Batteries

Yushan Yan (Primary Contact), Shuang Gu, Bingjun Xu
University of Delaware
150 Academy Street
Newark, DE 19716
Phone: (302) 831-2552
Email: yanys@udel.edu

DOE Manager: Donna Ho
Phone: (202) 368-6830
Email: Donna.Ho@ee.doe.gov

Contract Number: DE-EE0006964

Subcontractor:
Bryan Pivovar, National Renewable Energy Laboratory
Golden, CO

Project Start Date: June 1, 2015
Project End Date: August 31, 2017

Overall Objectives

- Develop a new class of anion exchange membranes (AEMs) with very high oxidation resistance for high-voltage cerium redox flow batteries (RFBs), and other alkaline membrane-based electrochemical devices such as fuel cells and electrolyzers.

Fiscal Year (FY) 2016 Objectives

- Demonstrate $9MeTTP^+$–cation functionalized polymers with oxidation stability in 0.5 M $Ce(IV)(ClO_4)_4$ at 40°C for 1,000 hours or its equivalent.

Technical Barriers

This project addresses the following technical barriers from the Fuel Cells section of the Fuel Cell Technologies Office Multi-Year Research, Development, and Demonstration Plan:

(A) Durability

(B) Cost

(C) Performance

Technical Targets

This project aims to develop new AEMs with high oxidation stability. These AEMs are targeted for applications in high-voltage cerium RFBs, and other alkaline membrane-based electrochemical devices such as fuel cells and electrolyzers.

FY 2016 Accomplishments

- Screened multiple polymers for oxidation resistance.
- Explored multiple chemistries for tethering $9MeTTP^+$ to selected polymer backbones.
- Developed a new synthesis strategy through brominated $9MeTTP^+$ cation, and obtained the desired $9MeTTP^+$-functionalized polysulfone (PSf) and hexafluoro polybenzimidazole (6FPBI).
- Demonstrated excellent oxidation stability of $9MeTTP^+$-functionalized hexafluoro polybenzimidazole (9MeTTP-PBI) that met the go/no-go milestone.

✧ ✧ ✧ ✧ ✧

INTRODUCTION

As a reversible fuel cell, RFBs are one of the most promising electrochemical technologies with the great scalability and durability (e.g., 15–20 years) required for intermittent renewable energy storage. In particular, cerium redox pair [Ce(IV)/Ce(III)]-based RFBs are appealing because of their unprecedented high cell voltages (up to 3.08 V) in an aqueous system. High cell voltage is a key factor in achieving high energy and power densities, which lead to low storage cost. An AEM is needed as a key component in cerium RFBs to achieve stable cell voltage and high columbic efficiency. However, existing commercial ammonium cation-based AEMs have very limited stability when working with Ce(IV) electrolytes (e.g., less than 200 h of durability). The lack of stable AEMs causes cerium RFBs to suffer from either high self-discharge rate or low coulombic efficiency. The development of highly stable and conductive AEMs has become one of the most urgent challenges for cerium RFBs to become a viable electricity storage solution. We recently developed an oxidation-resistant phosphonium cation (i.e., tris(2,4,6-trimethylphenyl) phosphonium, or $9MeTTP^+$), with the oxidative stability a factor of 1,500+ better than the conventional trimethyl ammonium cation and a factor of 25+ better than our previous-generation phosphonium cation (i.e., tris(2,4,6-trimethoxyphenyl) phosphonium, or $9MeOTTP^+$). The excellent oxidation resistance of $9MeTTP^+$ cation is attributed to protection from substantially improved steric hindrance. Herein we propose to develop highly stable AEMs functionalized with the $9MeTTP^+$ cation.

APPROACH

Our approach is to examine a number of common polymers that are likely to meet the oxidation resistance requirement and then explore multiple pathways and chemistries for connecting $9MeTTP^+$ to the selected polymers.

RESULTS

We have screened a number of polymers and found that PSf, Polyether ether ketone (PEEK) and 6FPBI are stable (Table 1).

TABLE 1. Stability Test of Polymer Backbone at 40°C for 1,000 h in 0.5 M $Ce(IV)(ClO_4)_4$

	Weight loss (%) at 500 h	Weight loss (%) at 1,000 h	Morphography change
PS	0 [a]	5	No
PPO	10	30	Cloudy and Brittle
PSf	0 [a]	0 [a]	No
PEEK	0 [a]	0 [a]	No
6FPBI	0 [a]	0 [a]	No

[a] 0 means that the polymer has less than 1% weight loss
PS - Polystyrene; PPO - Poly(p-phenylene oxide)

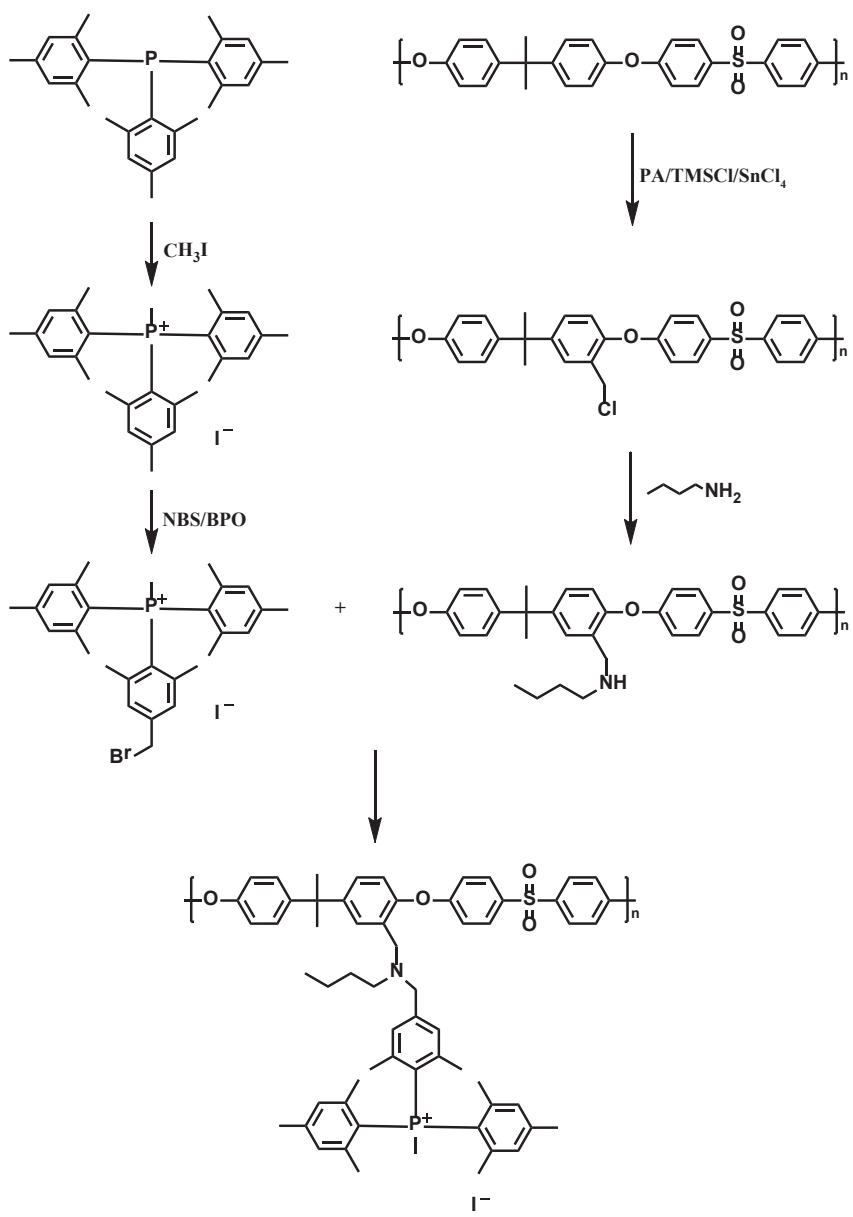

FIGURE 1. Synthesis route for 9MeTTP-PSf

As for tethering of the 9MeTTP$^+$ to the polymer backbone, direct attachment through the central phosphorus atom proved infeasible due to the high steric hindrance of the 9MeTTP molecule. We then devised a new synthesis strategy through the brominated 9MeTTP$^+$ cation, and obtained the desired 9MeTTP$^+$-functionalized PSf and 6FPBI. Synthesis routes for 9MeTTP-PSf and 9MeTTP-PBI are shown in Figure 1 and Figure 2 respectively. The functionalized PSf was not stable enough due to the presence of cations on the tether, which activate the backbone degradation. Therefore, we chose to work on 9MeTTP$^+$-functionalized 6FPBI.

9MeTTP-PBI has shown excellent oxidation stability. In an accelerated ageing test in 0.5M Ce(IV) ClO_4 at 55°C, the 9MeTTP-PBI lost only 0.59% of its ion exchange capacity after 100 hours (equivalent to 1,000 hours at 40°C based on the activation energy of decay of the 9MeTTP+ cation) and met the Year 1 go/no-go milestone (Table 2).

TABLE 2. 9MeTTP$^+$-Functionalized Polymer Ion Exchange Capacity (IEC) Test at 40°C for 1,000 h in 0.5 M Ce(IV)$(ClO_4)_4$

Time (h)	0	500	1,000
9MeTTP-PSf IEC	0.5660	0.3023 (46.59% loss)	
9MeTTP-PBI IEC [a]	0.5591		0.5558 (0.59% loss)

[a] 9MeTTP-PBI polymer was tested via accelerated test at 55°C for 100 h in 0.5 M Ce(IV)$(ClO_4)_4$ (this condition is equivalent as 40°C for 1,000 h in 0.5 M Ce(IV)$(ClO_4)_4$)

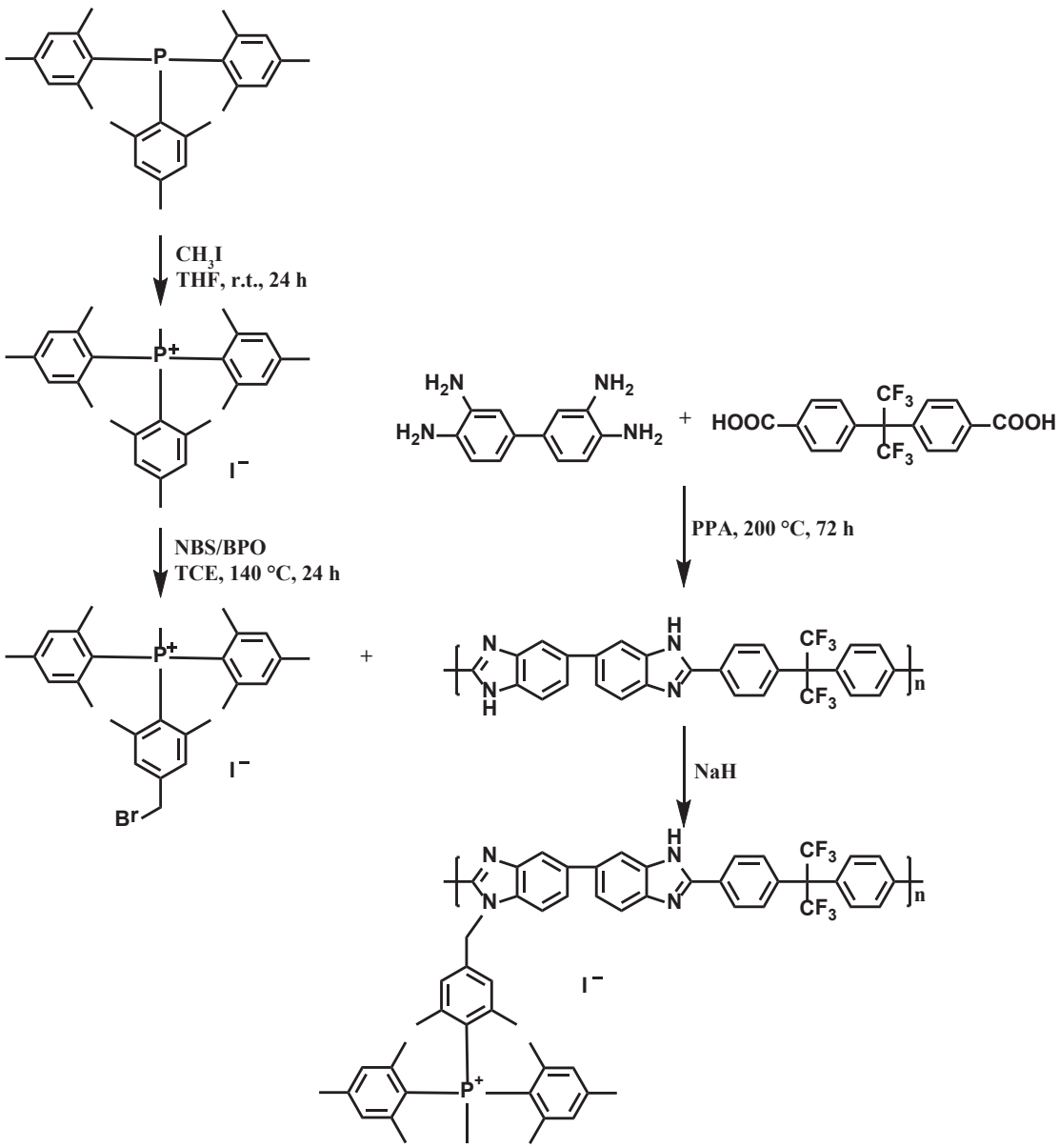

FIGURE 2. Synthesis route for 9MeTTP-PBI

CONCLUSIONS AND FUTURE DIRECTIONS

Although the project is still ongoing, several conclusions can be drawn.

- The direct quaternization method through the central phosphorus atom proved infeasible due to the high steric hindrance of the 9MeTTP molecule.
- The new bromination method proved feasible and led to a 9MeTTP-PBI polymer that met the year one durability target.

Future work includes:

- Development of a membrane preparation method for 9MeTTP+-functionalized polymers.
- Development of alternative P^+-functionalized polymers that have higher yield.
- Testing the stability of $9MeTTP^+$-based polymer membranes against Ce(IV) ions.
- Testing of the membrane in both RFB and fuel cell.

V.C.6 Advanced Materials for Fully-Integrated MEAs in AEMFCs

Yu Seung Kim (Primary Contact), Kwan-Soo Lee
Los Alamos National Laboratory
MPA-11: Materials Synthesis and Integrated Devices
Los Alamos, NM 87545
Phone: (505) 667-5782
Email: yskim@lanl.gov

DOE Manager: David Peterson
Phone: (240) 562-1747
Email: David.Peterson@ee.doe.gov

Subcontractors:
- Cy Fujimoto, Michael Hibbs, Sandia National Laboratory, Albuquerque, NM
- Vojislave Stamenkovic, Argonne National Laboratory, Lemont, IL
- Chulsung Bae, Woo Hyung Lee, Rensselaer Polytechnic University, Troy, NY

Project Start Date: November 2, 2015
Project End Date: November 1, 2018

Overall Objectives

- Synthesize highly conductive and stable hydrocarbon based anion exchange membranes (AEMs).
- Prepare ionomeric electrode binders for the fabrication of fuel cell electrodes.
- Integrate non-precious or low Pt metal loading electrocatalysts into membrane electrode assemblies (MEAs) for alkaline anion exchange membrane fuel cells (AEMFCs).
- Demonstrate high performance of alkaline AEMFCs.
- Demonstrate long-term alkaline AEMFC stability under steady and accelerated stress conditions.

Fiscal Year (FY) 2016 Objectives

- Down-select highly conductive and alkaline stable AEMs.
- Establish design aspects on ionomeric binding materials for hydrogen oxidation reaction (HOR).
- Prepare and characterize hydrocarbon-based ionomeric binders.

Technical Barriers

This project addresses the following technical barriers from the Fuel Cells section (3.4) of the Fuel Cell Technologies Office Multi-Year Research, Development, and Demonstration Plan.

(A) Durability (polymer electrolytes)

(B) Cost (non-precious metal catalysts)

(C) Performance (alkaline AEMFCs)

Technical Targets

This project is investigating technical aspects of AEMFCs for practical use in intermediate (10–50 kW) power applications. Insights gained from this project will be applied towards the next stage of advanced AEMFC systems. The technical targets for AEMFCs in the Multi-Year Research, Development, and Demonstration Plan [1] are listed below.

- Develop AEMs with an area specific resistance $\leq 0.1\ \Omega\ cm^2$, maintained for 500 hours during testing at 600 mA/cm^2 at T > 60°C. (Q2, 2017)
- Demonstrate AEMFC peak power performance >600 mW/cm^2 on H_2/O_2 (maximum pressure of 1.5 atm abs) in MEA with a total loading of $\leq 0.125\ mg_{PGM}/cm^2$. (Q4, 2017)

FY 2016 Accomplishments

- Down-selected most promising AEMs through aryl ether-free polymer backbone approach. The selected AEMs were prepared from acid-catalyzed Friedel-Crafts polycondensation without using expensive metal catalysts. The selected AEMs with ion exchange capacity (IEC) of 1.9 meq/g has desired properties that exceed the DOE technical milestone from standalone AEM property measurement.
  - Alkaline stability: no structural change after 720 h in 0.5 M NaOH at 80°C.
  - Areal resistance: 0.07 $\Omega\ cm^2$ at 80°C.
  - Tensile elongation at 50°C and 50% relative humidity: >90%.
- Prepared hexamethyl trimethyl ammonium functionalized Diels-Alder poly(phenylene) (DAPP) cathode binders. The prepared cathode binders showed improved AEMFC performance. The cathode binder developed in FY 2016 has properties such as:
  - Ion exchange capacity: 1.8–2.2 meq/g.
  - Alkaline stability: no IEC change and <5% conductivity change.
  - Found a major HOR inhibition mechanism. Rotating disk electrode and surface Fourier transform infrared spectroscopy (FTIR) elucidated that

co-adsorbed layer of organic cation, hydroxide, and water adversely impact the HOR of Pt electrodes.

- Prepared phenylguanidinium functionalized DAPP anode binders. The guanidinium functionalized anode binders showed exceptional stability through total resonance structure of phenylguanidinium (no structural change after 1,000 h, 0.5 M NaOH treatment at 80°C).

✧ ✧ ✧ ✧ ✧

INTRODUCTION

Developing high-performing alkaline AEMFCs may effectively reduce fuel cell cost through the use of non-precious metal group electrocatalysts. The purpose of this project is to develop improved AEMs and ionomeric binders in order to integrate into MEAs for advanced alkaline AEMFCs. Over the last decade, significant progress on improving chemical stability of AEMs has been made. In addition, other technical issues such as carbonation, low hydroxide conductivity, low oxygen reduction activity of non-platinum group metal catalysts have been investigated. However, current alkaline AEMFC performance and durability are still inferior to those of the state of the art proton exchange membrane fuel cells. The Los Alamos National Laboratory team has involved AEMFC component development since 2008 and has made an effort to improve material properties associated with the key technical issues of alkaline AEMFCs. In this newly awarded project, we are trying to develop advanced materials for fully integrated AEMFCs.

In the previous research (2008–2013), we identified that aryl-ether linkage of the polymer backbone is not chemically stable under high pH conditions [2,3]. Based on this result, we have developed several aryl-ether free AEMs over the last two years [4–6]. In FY 2016, we further evaluated the AEM properties and down-selected the most promising AEMs for MEA integration. We also started to develop advanced hydrocarbon ionomeric binding materials for AEMFC electrodes. Electrochemical and spectroscopic analyses elucidated a major HOR inhibition mechanism, which helps to design advanced ionomeric binders for AEMFC anode.

APPROACH

Our general approach to prepare stable and highly conductive AEMs is to synthesize cationic group functionalized aryl-ether-free polymers. In addition, strategy to change most popular benzyl trimethyl ammonium group to more stable alkylammonium. There are several viable synthetic pathways to accomplish synthesizing such polymer structure. First, alkyl ammonium functionalized poly(phenylene)s can be prepared using DAPP precursor developed by Fujimoto et al. [7] or acid-catalyzed Friedel-Crafts polycondensations [4]. Second, alkyl ammonium functionalized poly(styrene-ethylene-butylene-styrene) block copolymers can be prepared via transition metal-catalyzed C-H borylation and Suzuki coupling reaction.

Our approach to prepare advanced ionomeric binders for AEMFCs is to develop different cationic groups for anode and cathode catalyst layers. For this, we evaluated the catalytic activities of Pt using various electrolytes and screened the candidate functional groups. Then the candidate functional groups have been employed into a polymeric structure and further structural optimization was made. For anode, methyl ammonium should be avoided as the cation adsorption adversely impact the HOR activity of the electrocatalysts. Candidate cationic functional groups for the anode electrolyte include alkyl ammonium, guanidinium, and alkyl phosphonium [8]. For the cathode, methyl ammonium works better than other bulky cationic group.

RESULTS

Anion exchange membranes: The most promising AEM was down-selected from several candidate materials (Table 1). For the AEM, hexamethyl ammonium functionalized poly(biphenyl alkylene) (PBPA) (No. 5 in Table 1) was selected for further study.

While traditional polyaromatic AEMs are synthesized via nucleophilic aromatic substitution in a basic medium, the PBPA polymers were prepared from an acid catalyzed Friedel-Crafts polycondensation (Figure 1a). The chemical structures of the ionic polymers were analyzed by nuclear magnetic resonance (NMR) spectroscopies, which confirmed that the ratio of the two quaternized and unquaternized repeating units of the polymers matched well with the monomer feed ratio. We prepared three PBPAs with different IECs (2.70 meq/g, 1.94 meq/g, and 1.46 meq/g). The alkaline stability of PBPAs was quantitatively evaluated by measuring the change in IEC after certain periods of time. The ^{1}H NMR spectral data suggest that the three AEMs maintained their IECs even after immersion in 1 M NaOH solution at 80°C for 720 h; the NMR-based IEC values were 2.65 meq/g, 1.92 meq/g, and 1.48 meq/g, which were close to the initial values (2.60 meq/g, 1.93 meq/g, and 1.46 meq/g, respectively) (Figure 1b). Hydroxide conductivity was also only negligibly different after the same alkaline test, indicating that these membranes exceed the 2017 DOE AEM stability milestone, ca. >500 h stability at T > 60°C. The hydroxide conductivity of PBPAs was evaluated with an *in-plane* four-point probe method and *through-plane* MEA method. The hydroxide conductivity increased as IEC and temperature as expected. For example, the AEM with the highest IEC of 2.61 meq/g had the highest conductivity (62 mS/cm), a value almost four times that of the AEM with

TABLE 1. Property Comparison of Anion Exchange Polymer Electrolytes

No.	Polymer		Stability	Conductivity	Mechanical property	Processibility	Cost
	Backbone	Cationic group					
1	Poly(phenylene)	BTMA	○	○	○	○	○
2		Alkyl ammonium	●	○	●	△	○
3		Guanidinium	●	○	△	△	○
4	Poly(phenyl alkylene)	Alkyl ammonium[a]	●	○	○	●	○
5		Alkyl ammonium[b]	●	●	●	●	△
6	Styrene-ethylene-butylene-styrene	BTMA	●	●	●	X	Not available
7	Perfluorinated	Guanidinium	△	△	△	△	●
8	Polystyrene	Ethyl ammonium	Not available	△	△	●	○

[a] DAPP based; [b] Acid catalyzed; ●: excellent, ○: good, △: intermediate, **X**: poor
BTMA – Benzyltrimethyl ammonium

the IEC of 1.45 meq/g at 30°C. The areal resistance of the MEA using 18 µm thick AEM (IEC = 1.9 meq/g) was 0.07 Ωcm^2, which met the 2017 DOE milestone, ca. <0.1 Ωcm^2 at 60°C. The PBPAs showed excellent mechanical properties compared to the other poly(phenylene) copolymers. For example, the tensile elongation of the AEM with IEC = 1.9 meq/g is over 90% vs. ~20% for quaternized DAPP at 50°C and 50% relative humidity.

Anion exchange ionomers: Oxygen reduction reaction (ORR) voltammograms of Pt in 0.1 M NaOH, tetramethyl ammonium hydroxide (TMAOH), BTMAOH and TBPOH indicated that the ORR activity of Pt in NaOH and TMAOH were better than the activity in BTMAOH and TBPOH (Figure 2). Based on this result, we decided to synthesize DAPP with hexamethyltrimethyl ammonium functional group (No. 2 in Table 1) for the cathode binder. In order to synthesize the alkyl ammonium functionalized DAPP, bromo-alkylated poly(phenylene) was first synthesized from the reaction of DAPP precursor with 6-bromohexanoyl chloride in the presence of aluminum chloride. To a bromo-alkylated poly(phenylene) solution in 1,2-dichloroethan, trifluoroacetic acid and triethylsilane were added to reduce the carbonyl groups [9]. The poly(phenylene) ionomer has excellent alkaline stability under high pH conditions. For example, the IEC of the polymer did not change after 14 days in 4 M KOH at 90°C. The ionomer

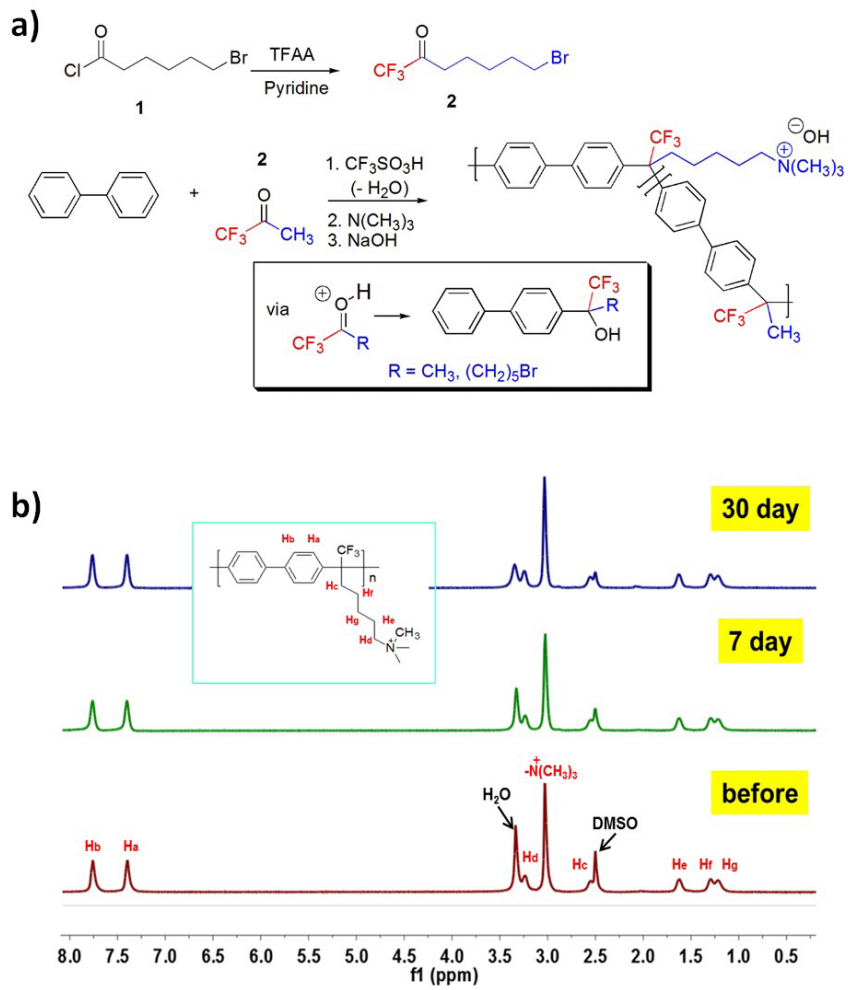

DMSO - Dimethyl sulfoxide

FIGURE 1. (a) Synthetic scheme of PAPB; (b) ^1H NMR spectra during alkaline stability test; testing condition: immersion in 1M NaOH at 80°C.

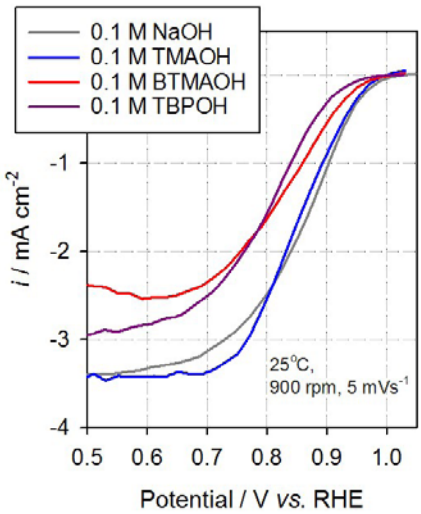

RHE – Reference hydrogen electrode

FIGURE 2. ORR voltammogram of Pt/C rotating disk electrode in 0.1 M NaOH, TMAOH, BTMAOH, and TBPOH

dispersion using ethylene glycol was prepared to evaluate the ionomer performance [10].

A major achievement for alkaline ionomer development during FY 2016 is the identification of the HOR inhibition mechanism by cation-hydroxide-water co-adsorption. We have performed HOR voltammograms of Pt in various organic cation solutions. The experiments reveal that the HOR activity of Pt substantially decreased in alkaline electrolytes. Surface FTIR elucidated that such HOR activity loss is related with co-adsorption of organic cation, hydroxide and water on Pt surface. Electrochemical impedance analysis further indicates that the hydrogen diffusion through the co-adsorbed layer is significantly reduced. The HOR inhibition is strongly dependent on the type of cations. HOR voltammograms of Pt/C in 0.1 M TMAOH, tetrabuthylammonium hydroxide and TBPOH indicates that the HOR activity loss of Pt increased with TMAOH cations. Further study indicates that phenylguanidinium allowed less cation adsorption compared to BTMAOH and imidazolium. Based on these results, we attempted to synthesize phenyl guanidinium functionalized DAPP ionomer (No. 3 in Table 1) for AEMFC anode binder (Figure 3a). The guanidinium functionalized polymer was synthesized by active fluorine-amine reaction we developed in 2011 [11]. The synthesized ionomer has IEC of 1.88 meq/g and hydroxide conductivity of 14 mS/cm at 30°C. The alkaline stability of the ionomer was excellent; no structural and conductivity change after 1,000-h life test at 0.5 M NaOH at 80°C (Figure 3b).

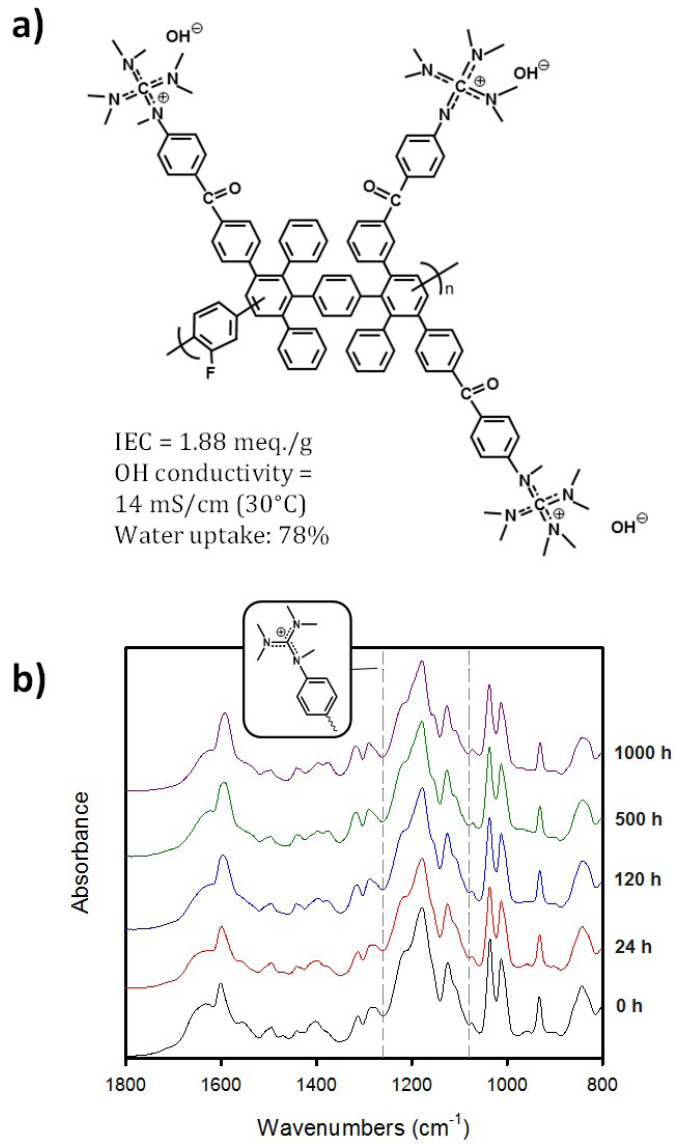

FIGURE 3. (a) Chemical structure of guanidinium functionalized poly(phenylene)ionomer; (b) FTIR change of the ionomer during 0.5 M NaOH at 80°C treatment

CONCLUSIONS AND FUTURE DIRECTIONS

- A series of aryl-ether-free AEMs were prepared from various synthetic routes. Acid catalyzed PBPA was down selected for AEMs. The selected AEMs met the DOE 2017 conductivity milestone when measured with either standalone or MEA configuration. The alkaline stability of the PBPA AEM was excellent and met the DOE 2017 stability milestone but needs further evaluation in MEA configuration.
- The ORR activity of Pt in BTMAOH was low. Instead of BTMAOH, hexamethyltrimethyl ammonium cationic group was incorporated into DAPP to improve ORR activities of AEMFCs. The hexamethyltrimethyl ammonium functionalized poly(phenylene) was successfully synthesized from multi-step synthetic process. Preliminary data indicated that the hexamethyltrimethyl functionalized poly(phenylene) outperformed to the previous BTMAOH functionalized

poly(phenylene). Further performance evaluation will be made during FY 2017.

- The HOR activity of Pt was greatly affected by the cationic group. Unlike the cathode ionomer, tetramethyl ammonium cationic group easily adsorbed onto the Pt surface and lowered the HOR activity. Based on this result, we successfully synthesized guanidinium functionalized DAPP via activated fluorine-amine reaction. Further performance evaluation for this polymer will be made during FY 2017. In addition, alternative ionomeric binding materials will be developed for further performance improvement.

SPECIAL RECOGNITIONS & AWARDS/ PATENTS ISSUED

1. Cy Fujimoto and Yu Seung Kim, 2016 DOE Hydrogen and Fuel Cells Program R&D Award.

2. Polyol-based Compositions Comprising Cationic Group-Functionalized Polyphenylene Polymers, Yu Seung Kim, US Patent Application No. 15/204,523, (2016).

3. Poly(phenylene) Based Anion Exchange Polymers and Method Thereof, Cy Fujimoto, Kwan-Soo Lee and Yu Seung Kim, US Patent Application No. 62/274592, (2016).

4. Novel Polymers and Methods for Their Manufacture, Chulsung Bae, PCT/US2015/061036 (2015).

FY 2016 PUBLICATIONS/PRESENTATIONS

1. Angela D. Mohanty, Chang Y. Ryu, Yu Seung Kim, Chulsung Bae, "Stable Elastomeric Anion Exchange Membranes Based on Quaternary Ammonium-Tethered Polystyrene-b-poly (ethylene-co-butylene)-b-polystyrene Triblock Copolymers," *Macromolecules* 48 (2015): 7085.

2. Woo-Hyung Lee, Yu Seung Kim, Chulsung Bae, "Robust Hydroxide Ion Conducting Poly (biphenyl alkylene) s for Alkaline Fuel Cell Membranes," *ACS Macro Letters*, 4 (2015): 814.

3. Hoon T. Chung, Ulises Martinez, Jerzy Chlistunoff, Yu Seung Kim, Yoong-Kee Choe, Ivana Matanovic, "Impact of Organic Cation Adsorption on the Hydrogen Oxidation Reaction of Pt in Alkaline Fuel Cells," (paper presented at the 218th ECS Meeting, Phoenix, AZ, October 11–15, 2015).

REFERENCES

1. Fuel Cell Technologies Office Multi-Year Research, Development, and Demonstration Plan 2014. http://energy.gov/sites/prod/files/2014/12/f19/fcto_myrdd_fuel_cells.pdf.

2. Cy Fujimoto, Dae-Sik Kim, Michael Hibbs, Debra Wrobleski, Yu Seung Kim, "Backbone Stability of Quaternized Polyaromatics for Alkaline Membrane Fuel Cells," *J. Memb. Sci.* 423–424 (2012): 438.

3. Yoong-Kee Choe, Cy Fujimoto, Kwan-Soo Lee, Luke T. Dalton, Kathy Ayers, Neil J. Henson, Yu Seung Kim, "Alkaline Stability of Benzyl Trimethyl Ammonium Functionalized Polyaromatics: A Computational and Experimental Study," *Chem. Mater.* 26 (2014): 5675.

4. Woo-Hyung Lee, Yu Seung Kim, Chulsung Bae, "Robust Hydroxide Ion Conducting Poly(biphenyl alkylene)s for Alkaline Fuel Cell Membranes," *ACS Macro Letters* 4 (2015): 814.

5. Angela D. Mohanty, Chang Y. Ryu, Yu Seung Kim, Chulsung Bae, "Stable Elastomeric Anion Exchange Membranes Based on Quaternary Ammonium-Tethered Polystyrene-b-poly (ethylene-co-butylene)-b-polystyrene Triblock Copolymers," *Macromolecules* 48 (2015): 7085.

6. Woo-Hyung Lee, Angela D. Mohanty, Chulsung Bae, "Fluorene-Based Hydroxide Ion Conducting Polymers for Chemically Stable Anion Exchange Membrane Fuel Cells," *ACS Macro Lett*. 4 (2015) 453.

7. Cy Fujimoto, Michel Hickner, Christopher Cornelius, Douglas Loy, "Ionomeric Poly(phenylene) prepared by Diels-Alder Polymerization: Synthesis and Physical Properties of a Novel Polyelectrolyte," *Macromolecules* 38 (2005): 5010.

8. Hoon T. Chung, Ulises Martinez, Jerzy Chlistunoff, Yu Seung Kim, Yoong-Kee Choe, Ivana Matanovic, "Impact of Organic Cation Adsorption on the Hydrogen Oxidation Reaction of Pt in Alkaline Fuel Cells," (paper presented at the 218th ECS Meeting, Phoenix, AZ, October 11–15, 2015).

9. M.R. Hibbs, "Alkaline Stability of Poly(phenylene)-based Anion Exchange Membranes with Various Cations," *Journal of Polymer Science, Part B: Polymer Physics* 51 (2013): 1736.

10. Polyol-based Compositions Comprising Cationic Group-Functionalized Polyphenylene Polymers, Yu Seung Kim, US Patent Application No. 15/204,523, (2016).

11. Dae Sik Kim, Andrea Labouriau, Micahel Guiver, Yu Seung Kim, "Guanidinium-functionalized Anion Exchange polymer Electrolytes via Activated Fluorophenyl-Amine Reaction," *Chem. Mater.* 23 (2011): 3795.

V.C.7 Advanced Ionomers and MEAs for Alkaline Membrane Fuel Cells

Bryan Pivovar (Primary Contact), Andrew Park, Matt Sturgeon, Ami Neyerlin, K.C. Neyerlin, Shaun Alia, Logan Garner, Hai Long, Zbyslaw Owczarczyk
National Renewable Energy Laboratory (NREL)
15013 Denver West Parkway
Golden, CO 80401
Phone: (303) 275-3809
Email: Bryan.Pivovar@nrel.gov

DOE Manager: David Peterson
Phone: (240) 562-1747
Email: David.Peterson@ee.doe.gov

Subcontractors:
- Adam Weber, Huai-Suen Shiau, Lawrence Berkeley National Laboratory, Berkeley, CA
- Tom Zawodzinski, Ramez Elgammel, Zhijiang Tang, Oak Ridge National Laboratory/University of Tennessee, Oak Ridge, TN
- Andy Herring, Ashutosh Divekar, Colorado School of Mines, Golden, CO
- Mike Yandrasits, Krzysztof Lewinski, 3M, St. Paul, MN

Project Start Date: October 1, 2015
Project End Date: September 30, 2018

Overall Objectives

- Improve novel perfluoro (PF) anion exchange membrane (AEM) properties and stability.
- Employ high performance PF AEM materials in electrodes and as membranes in alkaline membrane fuel cells (AMFCs).
- Apply models and diagnostics to AMFCs to determine and minimize losses (water management, electrocatalysis, and carbonate related).

Technical Barriers

This project addresses the following technical barriers from the Fuel Cells section (3.4.4) of the Fuel Cell Technologies Office Multi-Year Research, Development, and Demonstration Plan.

(A) Durability (of membranes and membrane electrode assemblies)

(B) Cost (of membranes and membrane electrode assemblies)

(C) Performance (of membranes and membrane electrode assemblies)

Technical Targets

This project will synthesize novel PF AEMs and ionomers and incorporate these membrane electrode assemblies (MEAs) for fuel cell testing. The project generally supports targets outlined in the Multi-Year Research, Development, and Demonstration Plan in application specific areas (portable, stationary, transportation). However, as alkaline membrane fuel cells are at an earlier stage of development, specific target tables have not yet been developed. Instead, there are four milestones, given below, that are included in the Multi-Year Research, Development, and Demonstration Plan.

	Milestones
Q2, 2017	Develop anion-exchange membranes with an area specific resistance ≤0.1 ohm cm^2, maintained for 500 h during testing at 600 mA/cm^2 at T > 60°C.
Q4, 2017	Demonstrate alkaline membrane fuel cell peak power performance >600 mW/cm^2 on H_2/O_2 (maximum pressure of 1.5 atm_a) in MEA with a total loading of ≤0.125 mg PGM/cm^2.
Q2, 2019	Demonstrate alkaline membrane fuel cell initial performance of 0.6 V at 600 mA/cm^2 on H_2/air (maximum pressure of 1.5 atm_a) in MEA a total loading of <0.1 mg PGM/cm^2 , and less than 10% voltage degradation over 2,000 h hold test at 600 mA/cm^2 at T > 60°C. Cell may be reconditioned during test to remove recoverable performance losses.
Q2, 2020	Develop non-PGM catalysts demonstrating alkaline membrane fuel cell peak power performance >600 mW/cm^2 under hydrogen/air (maximum pressure of 1.5 atm_a) in PGM-free MEA.

PGM – Platinum group metals

FY 2016 Accomplishments

- The project has successfully synthesized PF AEM sulfonamide-linked chemistries for two generations of polymer chemistry.
- Extensive characterization has been performed on synthesized PF AEMs that has demonstrated conductivity >50 mS/cm, reasonable water uptakes, and high water diffusion coefficients.
- Implementing PF AEMs into devices yielded reasonable AMFC power densities (up to 450 mW/cm^2 at 60°C, 121 kPa) that surpass those for commercial AEMs.
- Modeling and diagnostic techniques are being performed to advance/optimize AMFC architecture, performance, and durability.

✧ ✧ ✧ ✧ ✧

INTRODUCTION

AMFCs are of interest primarily because they enable the use of non-Pt catalysts, the main cost and supply limitation of proton exchange membrane fuel cells. AMFCs, therefore, offer the potential of greatly decreased polymer electrolyte fuel cell cost. Operating AMFCs under ambient conditions where carbon dioxide is present remains a challenge due to carbonate formation. An approach that has shown promise for carbon dioxide tolerance is increased operating temperature. Unfortunately, the stability of the cation side chains on the membrane polymer and water management within the membrane both become more difficult as temperature rises.

The use of perfluorinated ionomers, similar to those used in proton exchange membrane systems, with tethered cation head groups that allow hydroxide conduction should help improve water transport properties and offer exceptional chemical durability of the backbone. The significant advances demonstrated in AMFC systems have been accomplished primarily through improving water management and the bonding between membrane and electrode. Both issues can be tackled much more effectively when employing PF AEMs and ionomers. The project consists of three sub-tasks: synthesis of novel perfluorinated alkaline ionomers (NREL); characterization of PF AEMs (NREL, Oak Ridge National Laboratory/Univeristy of Tennessee, Colorado School of Mines); and fuel cell performance and modeling optimization (NREL, Lawrence Berkeley National Laboratory).

APPROACH

The team has focused on achieving higher-temperature, higher-power-density AMFC operation through implementation of novel alkaline PF membranes and ionomeric dispersions. The PF materials proposed are expected to enhance water transport capabilities and electrode performance and durability significantly, thereby enabling higher temperature and power density operation. The combination of high current density and operating temperature will improve the ability of these devices to tolerate ambient CO_2 and potentially enabling tolerance to these conditions. Starting with the sulfonyl fluoride form of current perfluoro ionomers we have identified, and in several cases verified, the ability to convert commercially available precursors into anion exchange polymers and membranes. The synthesized PF ionomers have been cast into membranes, made into polymeric dispersions, and characterized in fuel cell tests. Modeling efforts have been made in parallel to better understand cell performance, loss mechanisms, and mitigation approaches.

RESULTS

While PF chemistry improves PF sulfonic acid acidity, the strongly electron withdrawing PF backbone creates challenges for anion exchange membranes. From the readily available perfluoro sulfonyl fluoride precursor, different strategies can be employed to tether cations to the polymer backbone. We have focused on an amide linkage as shown in Figure 1 for our Generations (Gen) 1 and 2 PF AEMs. We have improved our processing of Gen 1 PF AEM and have demonstrated the ability to fully methylate the sulfonamide linkage resulting in non-zwitterionic polymers with conductivity as high as 55 mS/cm (liquid equilibrated at room temperature). These materials have demonstrated reasonable water uptakes and conductivity as a function of relative humidity. They have also demonstrated high water self-diffusion coefficients (7.2×10^{-6} cm^2/s). Unfortunately, our Gen 1 materials have shown greater than 90% loss of ion exchange capacity after two days in 2 M KOH at 80°C. We have recently demonstrated greatly (~30 X) improved stability using Gen 2 polymer, and future work is focusing on this material.

While Gen 1 PF AEM showed durability concerns, we were able to test this material as both membranes and electrode binder in fuel cell tests. Figure 2 shows the results of our Gen 1 PF AEM when used as an electrode binder compared to that of AS-4 a commercially available ionomer from Tokuyama. The PF AEM-based electrode shows slightly decreased performance relative the AS-4 in our tests. This result was surprising, as PF ionomers generally outperform hydrocarbon ionomers in proton exchange membrane systems. The Gen 1 PF AEM had limited processibility and was limited to electrode fabrication using dimethyl acetamide. Our future efforts are exploring other solvent systems that may result in improved electrode performance. When PF AEMs have been investigated as membranes in fuel cells using AS-4-based electrodes, Figure 3, performance has been slightly higher than that of commercial A201

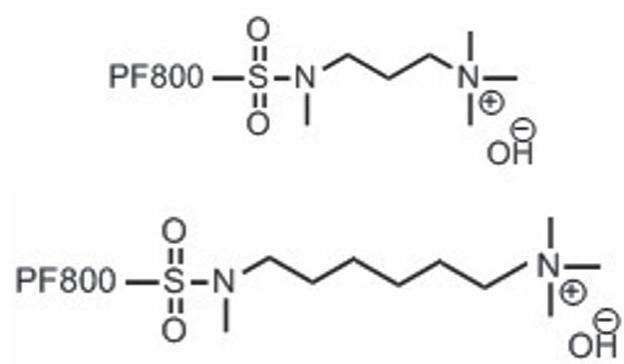

FIGURE 1. Chemical structures of Generation 1 and Generation 2 PF AEMs

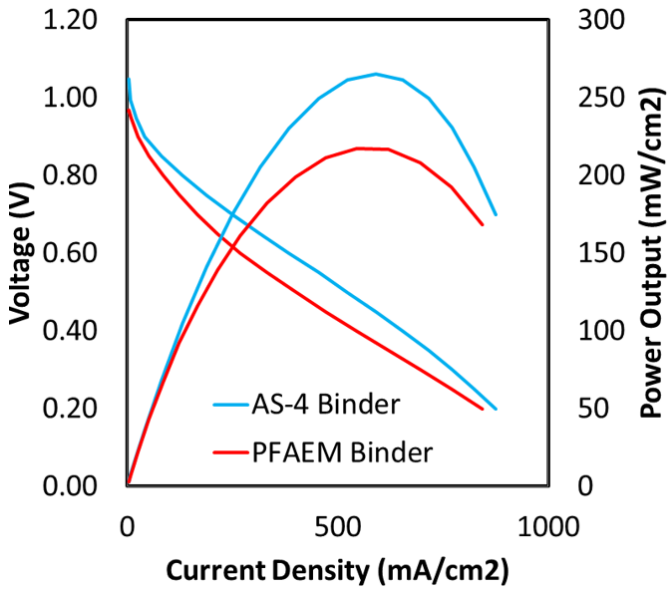

FIGURE 2. Fuel cell performance of PF AEM-based electrodes compared to AS-4-based electrodes

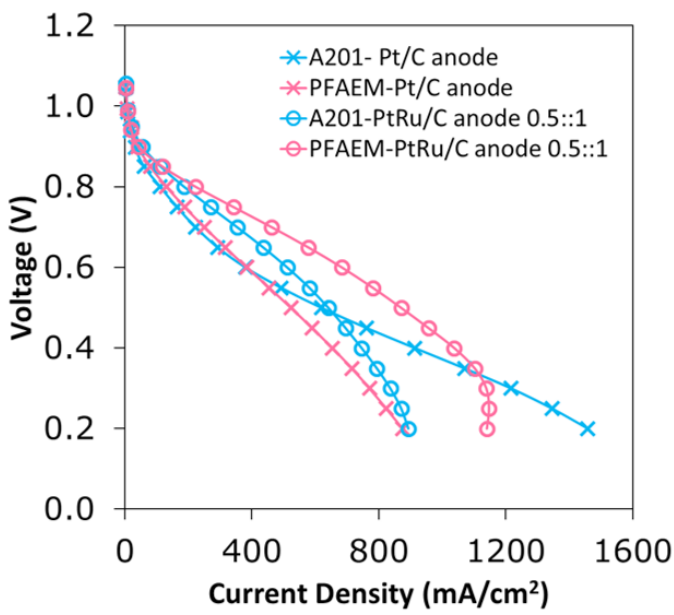

FIGURE 3. AMFC performance of PF AEM membrane compared to A201, 60°C, 121 kPa

from Tokuyama, perhaps due to improved water transport characteristics.

The areas of modeling and advanced diagnostics have both been lacking in the AMFC area, and we have been addressing them in this project. We have modeled the impact of relative humidity on performance as well as the impact of membrane thickness and water diffusivity. We have also applied CO stripping for surface area determination and

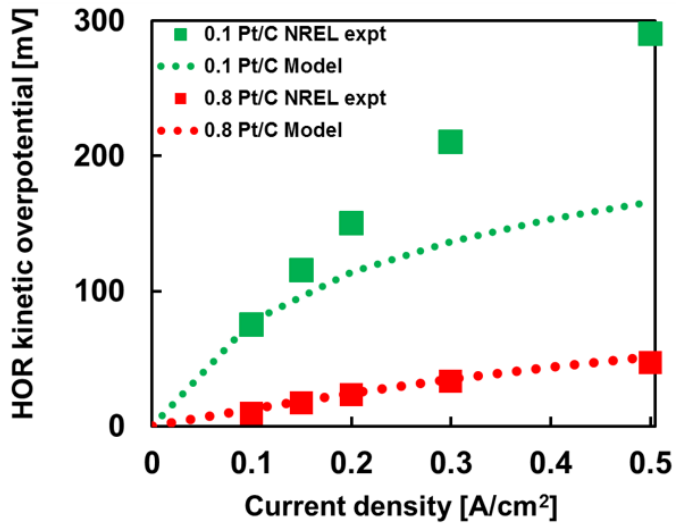

FIGURE 4. Modeling and experimental comparison of PF AEM hydrogen pump system

hydrogen pump tests to quantify anode overpotential losses. Figure 4 highlights the leveraged activities of modeling and advanced diagnostics of the project, where experimental hydrogen pump data is compared to modelling results. At high loading, the model results fit well with experimentally observed data. At lower loading, the model deviates substantially from experimentally observed performance suggesting loss mechanisms not currently captured by the model. These studies help quantify and establish mitigation approaches for performance loss.

CONCLUSIONS AND FUTURE DIRECTIONS

The project has successfully synthesized PF AEM sulfonamide-linked chemistries for highly OH- conductive AEMs. Extensive characterization has been performed on the polymer. Implementing this polymer into devices yields reasonable AMFC power densities that surpass those for commercial AEMs. Modeling and diagnostic techniques are being performed to advance/optimize AMFC architecture. Future work focuses on:

- Membrane Synthesis
  - Gen 3 polymer development (avoiding sulfonamide linkage)
  - Gen 2 polymer scale-up
- Characterization
  - Conductivity, stability, water transport, carbonate formation, and resulting effects
- Modeling
  - Parametric studies exploring operating conditions (temperature, relative humidity, current density, CO_2 concentration)

  - Coupling oxygen reduction reaction kinetics to water transport and elucidation of water transport within the cell
- Fuel Cell Testing
  - Improved performance and durability through optimization of individual component performance

FY 2016 PUBLICATIONS/PRESENTATIONS

1. Matthew R. Sturgeon, Hai Long, Andrew Park, Bryan S. Pivovar, "Advancements in Anion Exchange Membranes," 228th ECS Meeting, Polymer Electrolyte Fuel Cells, October 14, 2015, Phoenix, AZ.

2. Andrew Park, Matt Sturgeon, Ami Neyerlin, Zbyslaw Owczarczyk, Bryan Pivovar "Advances in Perfluorinated Anion Exchange Membrane Fuel Cells," Spring 2016 MRS, March 30, 2016, Phoenix, AZ.

3. Bryan Pivovar, "AMFC Workshop Overview," 2016 AMFC Workshop, April 1, 2016, Phoenix, AZ.

V.C.8 Dimensionally Stable High Performance Membranes

Cortney Mittelsteadt (Primary Contact),
Jason Willey
Giner, Inc.
89 Rumford Avenue
Newton, MA 02466
Phone: (781) 529-0529
Email: cmittelsteadt@ginerinc.com

DOE Manager: Donna Ho
Phone: (202) 586-8000
Email: Donna.Ho@ee.doe.gov

Contract Number: DE-SC0015165 (Small Business Innovation Research)

Subcontractor:
Chulsung Bae, Rensselaer Polytechnic Institute (RPI)
Troy, NY

Project Start Date: February 22, 2016
Project End Date: November 21, 2016

Overall Objectives

- Develop novel hydrocarbon membranes with high performance at low relative humidity (RH) and high temperature for use in transportation fuel cells.
- Quantitatively characterize these membranes at various RH and temperatures for the following.
  - Gas permeability
  - Water uptake
  - Proton conductivity
  - Mechanical stability

Fiscal Year (FY) 2016 Objectives

- Initialize development and characterization of the above membranes.

Technical Barriers

This project addresses the following technical barriers from the Fuel Cells section of the Fuel Cell Technologies Office Multi-Year Research, Development, and Demonstration Plan.

(A) Durability

(B) Cost

(C) Performance (cell issues)

Technical Targets

The main objective of this Phase I project is to fully characterize the fundamental properties of truly novel hydrocarbon membranes for use in fuel cell membrane electrode assemblies. Future projects will assess actual performance and lifetimes in a fuel cell environment with the goal of meeting the following DOE fuel cell targets.

- Area specific proton resistance at maximum operating temperature and water partial pressures from 40–80 kPa: 0.02 ohm cm²
- Area specific proton resistance at 80°C and water partial pressures from 25–45 kPa: 0.02 ohm cm²
- Area specific proton resistance at 30°C and water partial pressures up to 4 kPa: 0.03 ohm cm²
- Cost: $20/m²
- Durability: 20,000 cycles until >15 mA/cm² crossover or >20% loss in open circuit voltage

FY 2016 Accomplishments

- Synthesized two polysulfone ionomers with fluoroalkylsulfonic acid side chains for testing.
- Designed the synthesis of a graft copolymer based on poly(biphenyl alkylene).

✧ ✧ ✧ ✧ ✧

INTRODUCTION

The development of perfluorosulfonic acid membranes, such as Nafion®, has greatly contributed to fuel cell technologies and these materials are still widely used as the benchmark membrane in fuel cells. Due to its perfluorinated structure and superacidic pendant side chain, Nafion® possesses high proton conductivity as well as good chemical stability. Although higher charge density and proton conductivity could be achieved by shortening the length of side chains bearing the sulfonic acid group (i.e., lowering equivalent weight), such as Hyflon Ion® of Solvay and 3M ionomer, their improvements have been incremental. Thus, perfluorosulfonic acids are still not an ideal fuel cell membrane material and their drawbacks (e.g., high cost and low mechanical strength at high temperature) require development of alternative polymer electrolyte membranes (PEMs) for successful adoption of fuel cells as reliable and inexpensive energy conversion devices. Using novel hydrocarbon-perfluorinated hybrid ionomers with high hydrophilic–hydrophobic phase separation, Rensselaer Polytechnic Institute will develop an improved

fuel cell membrane with high conductivity at low RH and high temperature. Giner will use its dimensionally stable membrane technology to improve the strength and dimensional stability of these membranes, as well as their world class membrane characterization facility to screen the PEMs. The goal of this proposed project is the development of ionomeric membranes with high conductivity and mechanical strength for use in low RH, high temperature transportation fuel cell applications.

APPROACH

Over the past decades, extensive efforts have been devoted to the development of hydrocarbon-based PEMs, and many aryl and alkyl sulfonated polymers have been described. In general, these sulfonated aromatic polymer PEMs with high ion exchange capacity and high conductivity swell excessively under high hydration conditions and give much lower proton conductivity than Nafion when RH or water content of the membrane is reduced. To achieve highly conductive materials under low hydration conditions, creation of well-connected hydrophilic channels within the membrane through architectural controls of polymer morphology has been pursued over the past decade. The low proton conductivity of these aromatic PEMs under reduced RH conditions is generally believed to be due to (i) the lack of a nanostructured domain morphology with sufficient domain size and connectivity through which protons and water molecules can transport rapidly, and (ii) the less acidic pendant side chain compared to that of Nafion. Concerns about ionic domain size and connectivity have prompted research efforts focused on PEM morphology. Morphology control can be manipulated by many factors, such as concentration and length of sulfonic acid group, structures of polymer backbones, and pendant chains and their distribution sequences. The general consensus is that ionic nanostructure achieved by phase separation of hydrophilic ionic groups and hydrophobic polymer backbone is critical for enhanced proton transport at low RH. Accordingly, multiblock copolymer PEMs with well defined ionic domains have been prepared by polycondensation of sulfonated hydrophilic oligomers and non-sulfonated hydrophobic oligomers and they achieved more enhanced proton conductivities than the corresponding randomly sulfonated counterparts. The goal of this program will be to take these findings and generate a polymer with large segregated domains, with the highest possible localized charge density using acid functionalities of the highest possible strength. The general structure of these polymers is shown in Figure 1.

RESULTS

Two sulfonated poly(arylene ether sulfone) (PSU) ionomers with fluoroalkylsulfonic acid (200-PSU(22K)-S1 and 200-PSU(60K)-S1) were synthesized for this project at RPI and sent to Giner for characterization. These samples are similar in structure to Figure 2, but with different molecular weights (22 and 60 kg/mol). Previous work by the RPI group [1] has shown that these superacid-functionalized membranes have large segregated domains with high localized charge density.

Unfortunately, these ionomers formed very brittle films that could not withstand testing. Different solvent structures and casting methods were tried, but the poor mechanical properties persisted.

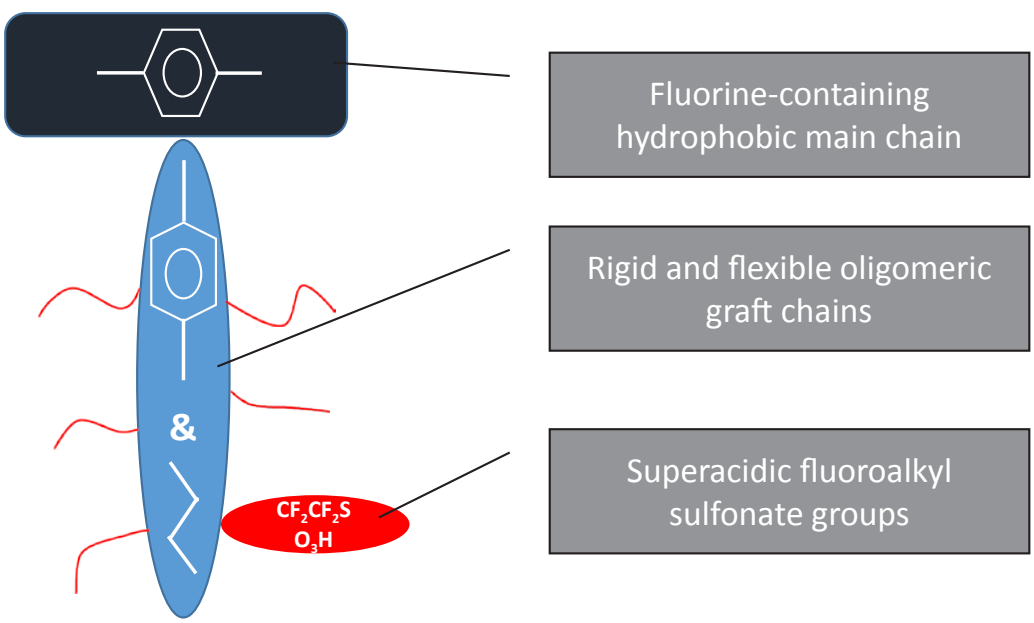

FIGURE 1. The general structure of the target ionomeric polymers for this project

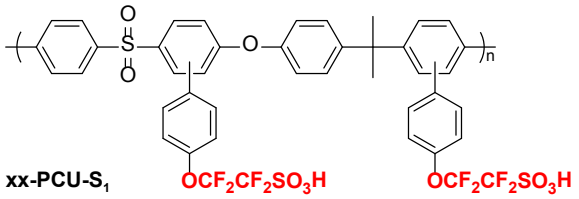

FIGURE 2. The molecular structure of sulfonated PSU ionomers

Currently, the RPI group is working on the synthesis of graft copolymers based on poly(biphenyl alkylene), shown in Figure 3. The main polymer backbone was prepared using acid-catalyzed polycondensation method, which affords high molecular weight, aryl-ether free, chemically and mechanically stable backbone. The copolymer composed of the hydrophobic main chain and the graft chain with pendant perfluoroalkylsulfonic acid group is expected to show the formation of ionic aggregates thus larger segregated ionic domains. The unexpected leaving of a post doc at RPI has pushed back the timing of this synthesis, but Giner should be receiving samples soon.

FUTURE DIRECTIONS

- Optimize casting procedure for polysulfone with fluoroalkylsulfonic acid to improve mechanical properties.
- Synthesize the graft copolymers based on poly(biphenyl alkylene).
- Optimize casting for the graft copolymers.
- Incorporate the dimensionally stable membrane substrate with the ionomers to increase mechanical strength.
- Characterize the membranes at various RH and temperatures with respect to the following.
  - Proton conductivity
  - Water uptake
  - Gas permeability
  - Mechanical strength

REFERENCES

1. *Polym. Chem.* **2013**, *3*, 272–281.

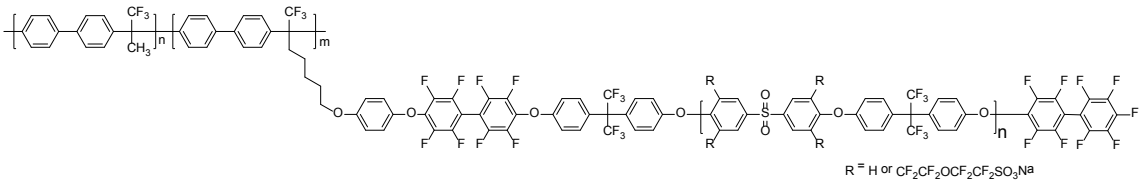

FIGURE 3. The molecular structure of perfluoroalkylsulfonated graft copolymers

V.C.9 Low-Cost Proton Conducting Membranes for PEM Fuel Cells

Hongxing Hu (Primary Contact),
Ayyasamy Aruchamy
Amsen Technologies LLC
1684 S Research Loop, Suite 518
Tucson, AZ 85710
Phone: (520) 546-6944
Email: hhu1@mindspring.com

DOE Manager: Donna Ho
Phone: (202) 586-8000
Email: Donna.Ho@ee.doe.gov

Contract Number: DE-SC0015203 (Small Business Innovation Research)

Project Start Date: February 22, 2016
Project End Date: November 21, 2016

Overall Objectives

- Develop a low-cost, high-performance proton conducting membrane for polymer electrolyte membrane (PEM) fuel cells. Determine the best material system for the new PEM.
- Establish a suitable process for fabrication of the new PEM.
- Characterize the new PEM in terms of physical and chemical properties.
- Test the new PEM under fuel cell conditions.
- Evaluate economical significance of the new PEM.

Fiscal Year (FY) 2016 Objectives

- Develop a low-cost, high-performance proton conducting membrane for PEM fuel cells. Determine the best material system for the new PEM.
- Establish a suitable process for fabrication of the new PEM.
- Characterize the new PEM in terms of physical and chemical properties.
- Test the new PEM under fuel cell conditions.
- Evaluate economical significance of the new PEM.

Technical Barriers

This project addresses the following technical barriers from the Fuel Cells section of the Fuel Cell Technologies Office Multi-Year Research, Development, and Demonstration Plan.

(A) Durability: Membrane and membrane electrode assembly durability

(B) Cost: PEM that is much cheaper than Nafion membranes

(C) Performance: High membrane electrode assembly performance at low relative humidity and high temperatures

Technical Targets

Table 1 lists DOE's technical targets with regard to fuel cell membranes for transportation applications.

TABLE 1. DOE Technical Targets: Fuel Cell Membranes for Transportation Applications

Characteristics	Units	2020 Target
Maximum operating temperature	°C	120
Area specific proton resistance at:		
Maximum operating temperature and water partial pressures from 40 kPa to 80 kPa	Ohm cm^2	≤0.02
80°C and water partial pressure from 25–45 kPa	Ohm cm^2	≤0.02
30°C and water partial pressure up to 4 kPa	Ohm cm^2	≤0.03
-20°C	Ohm cm^2	≤0.2
Maximum oxygen cross-over	mA/cm^2	2
Maximum hydrogen cross-over	mA/cm^2	2
Minimum electrical resistance	Ohm cm^2	1,000
Cost	$\$/m^2$	≤20
Durability:		
Mechanical	Cycles with <2 mA/cm^2 crossover	≤20,000
Chemical	Hours	≥500

This project is developing a new type of proton conducting membrane to meet the DOE targets in all facets. It will present not only high proton conductivity and fuel cell performance over a wide range of temperature and humidity conditions, along with high chemical stability and mechanical durability, but also low cost to meet the targets in the membrane cost (≤$20/m^2). As the new membrane will be very thin, the DOE targets of low area specific proton resistance, as shown in Table 1, can also be easily met.

FY 2016 Accomplishments

New PEM samples of 15–20 μm have been prepared. The new PEM shows high mechanical durability and chemical

stability, high proton conductivity, and low area specific proton resistance, promising to meet the DOE targets.

✧ ✧ ✧ ✧ ✧

INTRODUCTION

Polymer electrolyte membrane fuel cells represent a promising power source for a variety of applications. They are a leading candidate to power zero emission vehicles, with several major automakers already in the early stages of commercializing fuel cell powered vehicles. Fuel cells are also of interest for stationary power applications, including primary power, backup power, and combined heat and power. While many breakthroughs have been made over the last few years in the development of fuel cells, technical and economic barriers for their wide spread commercialization still exist. Key areas where improvements are still needed are in expanding the temperature range and lowering the humidification requirements of the stack. For transportation applications, requirements of system size, efficiency, performance, start-up and cooling mean that fuel cells must be able to run robustly and exhibit adequate durability under a wide variety of operating temperatures, including temperatures up to 120°C. They must also be able to do this with little or no external gas humidification (i.e., "dry"), and during start-up, shut-down, or periods of lower stack temperatures, they must run in the presence of, and be stable to, some liquid water in the gas channels. The polymer electrolyte membrane, typically being PEM, is the key component in PEM fuel cells that critically determines the system performance and its economic viability. Presently, the state-of-the-art PEMs, such as Nafion® membranes, are based on perfluorosulfonic acid (PFSA) ionomers. But these ionomer materials are expensive, particularly at the low volumes that will be needed for initial commercialization. Besides, they are not suitable for fuel cells operated beyond 100°C, because of the limitations connected to the humidification requirement of such membrane materials, limiting the maximum operating temperature to about 90°C. Non-PFSA polymer electrolyte membranes, including those based on hydrocarbon membranes, represent a lower-cost alternative, but relatively low performance and durability has limited applications of these alternative membranes to date. Therefore, DOE is seeking new approaches in the development of novel non-PFSA ionomers and PEMs for fuel cells.

Amsen Technologies LLC chooses to address the DOE call with a novel reinforced PEM approach based on new, non-PFSA proton conducting ionomers developed from our previous DOE Small Business Innovation Research projects. The reinforcement scheme will make the membrane highly durable yet very thin (15–20 µm). As such, the new proton conducting membrane to be developed is expected to meet the DOE targets in all facets.

APPROACH

Amsen Technologies LLC will develop a novel reinforced PEM based on new, non-PFSA proton conducting ionomers developed from our previous DOE Small Business Innovation Research projects. Specifically, Amsen has developed a low-cost, non-PFSA proton exchange membrane from cheap commodity polymers for redox flow battery applications. Several new proton conducting ionomers have been synthesized for the first time based on copolymers of a ternary system with a poly(vinylidene fluoride) (PVDF) backbone. Unlike some widely-reported hydrocarbon-based ionomers, such as sulfonated poly(ether ether ketone) and sulfonated polysulfone, which are single polymers and have a serious stability problem, our new ionomers are all copolymer in nature, and are highly stable even in the highly acidic and oxidizing vanadium redox flow battery electrolyte. These new ionomers showed higher ion-exchange capacity (IEC) and proton conductivity than Nafion. PEMs made from these ionomers have shown significant potential of not only lower cost than the Nafion membranes, but also superior properties to the Nafion membranes in some aspects, including higher proton conductivity (0.0786 S/cm at room temperature (20°C) and full hydration state, in contrast with 0.0611 S/cm for Nafion 117, measured under the same conditions, showing an increase of 28%), and better performance in vanadium redox flow batteries.

Our effort in development of the new PEM has been distinctly differentiated from many other researchers who have been working in the development of PVDF-based PEMs, in that our new PEM was formed as a whole from ionomer resins that were independently developed and synthesized in our company, while many other researchers produced the PVDF-based PEM by merely surface modification of existing PVDF films. For instance, a PVDF-based PEM was reportedly made by grafting the surface of a commercial available PVDF film with styrene and dimethylaminoethyl methacrylate using γ-irradiation techniques, followed by sulfonation and protonation processes [1]. Most of the reported efforts on PVDF-based PEMS use similar approaches as the referenced one. Apparently, such surface-modification approach has limited potential of producing fundamentally new PEM, because it does not produce new ionomer resins. In contrast, our products are new ionomer resins, from which new PEMs are formed.

However, there are still two major challenges in using our new ionomers to fabricate the new fuel cell PEM meeting the DOE targets: increased durability and significantly reduced thickness. According to the DOE targets, the fuel cell membrane should mechanically withstand ≤20,000 humidity cycles with <2 mA/cm^2 crossover of gases, and chemically withstand >500 h in the fuel cell environment. In the meantime, in order to meet the DOE targets for the low area specific resistance (≤0.02 ohm–cm^2) and the low cost (≤20 \$/m^2), the membrane should be very thin (preferably

10–20 μm). Therefore, our current thrust in the present effort is to make the new PEM highly durable yet very thin (≤20 μm). Our approach is to reinforce the membrane with ultra-thin microporous polyolefin meshes. This would result in ultra-thin membranes with significantly enhanced durability, which would likely meet all of the technical and cost targets set by DOE.

The prepared PEM membranes will be systematically characterized in terms of relevant physical and chemical properties to demonstrate feasibility of meeting the DOE targets.

RESULTS

In the present project, the new ionomer developed by Amsen has been further optimized. Sample membranes of the new PEM have been successfully prepared by immobilizing the ionomer matrix on the microporous polyolefin reinforcement support. Figure 1 shows a typical sample membrane of the new PEM prepared at Amsen. The critical variables in fabricating the new PEM include the pre-treatment of the microporous polyolefin mesh support, the solvent used to dissolve the ionomer resin into a solution, and the heat-treatment schedule to cure the membrane. With appropriate selections of these variables, the process for integration of the ionomer matrix with the reinforcement support is simply pulling the microporous polyolefin mesh support through the ionomer solution, by which the microporous mesh support is impregnated with the ionomer solution. Then the formed PEM membrane is laid on glass plate and cured at elevated temperatures up to 160°C by a designated heat-treatment schedule.

The pre-treatment of the polyolefin meshes is a significant step of the processing, bringing in two merits to the reinforcement support: First, the originally hydrophobic meshes are modified to be hydrophilic, so as to facilitate the impregnation of the ionomer solution. Second, the originally inert polyolefin surfaces are activated with reactive moieties so as to ensure chemical bonding between the reinforcement support and the ionomer matrix immobilized on it. Therefore, the microporous polyolefin mesh support not only provides mechanical reinforcement to the membrane, but also leads to significant enhancement in chemical stability of the membrane.

The heat-treatment in curing the formed membrane is another significant step of the processing, in that optimized heat-treatment schedule needs to be determined to attain high crosslinking within the ionomer matrix as well as maximum chemical bonding between the reinforcement support and the ionomer matrix.

The resultant membranes are very thin and highly flexible, with thicknesses typically ranging from 15–20 μm. Yet they are quite tough and strong, with tensile strengths measured at about 1,500 kgf/cm^2, increased by more than one order of magnitude relative to the non-reinforced membranes made from the same ionomer.

Proton conductivity measured from the new PEM is as high as 0.1–0.12 s/cm at room temperature and full hydration state, which is nearly twice of that for Nafion membranes. However, to be conservative we have used the lowest values measured to plot the Arrehenius plots of proton conductivity of the new membrane at 100% relative humidity, as shown in Figure 2. Even with the lowest values as shown, proton conductivity of the new membrane exceeds that of Nafion membranes by over 25%. With the high proton conductivity and the low membrane thickness, it is expected that the DOE

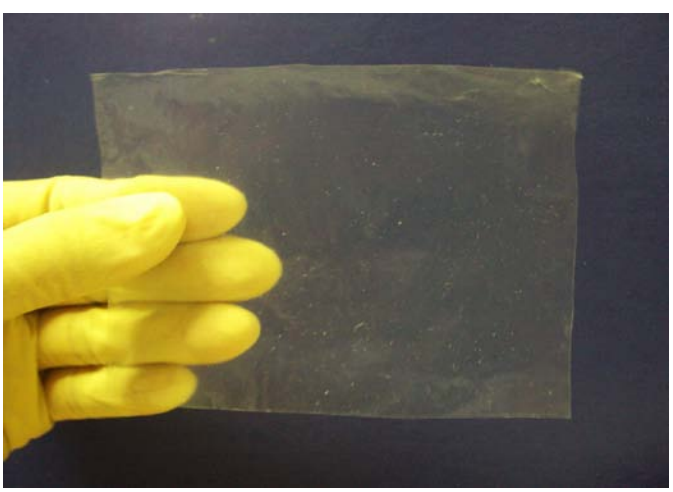

FIGURE 1. A sample membrane of the new PEM prepared at Amsen

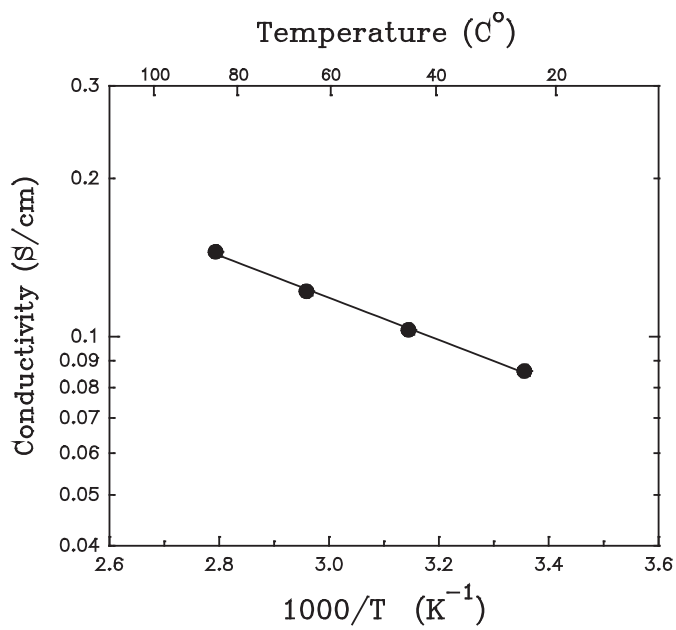

FIGURE 2. Arrehenius plots of proton conductivity of the new membrane at 100% relative humidity

targets of low area specific proton resistance, as shown in Table 1, can be easily met.

Tests conducted so far revealed that these membranes are quite chemically stable and mechanically durable. First, we have exposed the membranes to different environments (1 M hydrogen peroxide at 75°C for overnight; 1 M H_2SO_4 at 90°C for overnight; and water at 90°C for overnight), and have not observed any conductivity loss after such exposures. Furthermore, we have used hydration-dehydration cycling as one of the stability tests. No conductivity loss was observed after more than 10 times of such cycling. Still another method we have used in evaluating stability of the membrane is keeping the membrane sample in water, and periodically measuring its conductivity over a period of time. The results of this test also suggest high stability of the membrane, as no change in conductivity was observed over three weeks.

As the ionomer matrix is strongly confined by the reinforcement support, the new PEM attains high dimensional stability. The dimension change along x-y plane upon hydration is minimum (less 3%, almost no expansion along x-y plane at full hydration), while the expansion along z-axis is 20–25% at full hydration.

Some samples of the new PEM have been sent to Los Alamos National Laboratory for independent testing, while we keep working on further development and evaluation of the new membrane for the remaining three months of the present project.

CONCLUSIONS AND FUTURE DIRECTIONS

New PEM samples of 15–20 μm have been prepared. The new PEM shows high mechanical durability and chemical stability, high proton conductivity, and low area specific proton resistance, promising to meet the DOE targets. In the remaining three months, we will keep working on the project to complete the Phase I work as planned, including:

- Determine the best material system for the new PEM.
- Establish a suitable process for fabrication of the new PEM.
- Characterize the new PEM in terms of structural and microstructural features.
- Characterize the new PEM in terms of physical and chemical properties including maximum operating temperature, proton conductivity and area specific proton resistance in a range of temperature and humidity conditions, oxygen crossover, hydrogen crossover, resistance to electronic conduction, and mechanical and chemical durabilities.
- Test the new PEM under fuel cell conditions.

FY 2016 PUBLICATIONS/PRESENTATIONS

1. H. Hu, "Low-Cost Proton Conducting Membranes for PEM Fuel Cells," Poster presentation at 2016 Hydrogen and Fuel Cells Program Annual Merit Review meeting, Washington D.C., June 2016.

REFERENCES

1. Qiu J, Zhang J, Chen J, et al. "Amphoteric ion exchange membrane synthesized by radiation-induced graft copolymerization of styrene and dimethylaminoethyl methacrylate into PVDF film for vanadium redox flow battery applications," Journal of Membrane Science, 334, 9-15 (2009).

V.C.10 Novel Hydrocarbon Ionomers for Durable Proton Exchange Membranes

William L. Harrison, Ph.D.
NanoSonic, Inc.
158 Wheatland Dr.
Pembroke, VA 24136
Phone: (540) 626-6266
Email: Wharrison@nanosonic.com

DOE Manager: Bahman Habibzadeh
Phone: (202) 287-1657
Email: Bahman.Habibzadeh@ee.doe.gov

Contract Number: DE-SC0015215 (Small Business Innovation Research)

Project Start Date: February 22, 2016
Project End Date: November 21, 2016

Overall Objectives

- Develop hydrocarbon-based polymer electrolyte membrane (PEM) composites capable of operating at 120°C for automotive applications.
- Optimize chemical and mechanical properties of developed PEM doped composites.
- Demonstrate operation of low cost PEMs in fuel cells with high proton conductivity over a range of temperatures and humidity conditions.

Fiscal Year (FY) 2016 Objectives

- Synthesis a series of non-perfluorinated sulfonic acid materials of polymer electrolytes via known synthetic routes stable to automotive fuel cell conditions.
- Optimize proton conductivity, film-forming properties, and acid-doping levels.
- Demonstrate preliminary operation of acid-doped polymer composites at low humidity levels and high (120°C) temperatures.

Technical Barriers

This project seeks to address the following technical barriers from the Fuel Cell 3.4.1 section of the Fuel Cell Technologies Office Multi-Year Research, Development, and Demonstration Plan.

(A) Durability

(B) Cost

(C) Performance

Develop a 65% peak-efficient, direct hydrogen fuel cell power system for transportation that can achieve 5,000-hour durability and be mass produced at a cost of $40/kW by 2020 (ultimate $30/kW).

More specifically, this research effort shall progress to develop new polymer electrolyte membranes displaying:

- High proton conductivity over a range of temperature and humidity conditions.
- Good film forming properties enabling formation of thin membranes.
- Durable membranes (chemical durability of hours >500[1])

Technical Targets

Progress has been made in achieving the DOE targets listed in the Multi-Year Research, Development, and Demonstration Plan. The table excerpt (see Table 1) are some of DOE technical targets specific to PEMs.

TABLE 1. DOE 2020 Technical Targets for Polymer Electrolyte Membranes Per the Multi-Year Research, Development, and Demonstration Plan

Membranes/Electrolytes
• Develop and identify electrolytes and membranes or matrices (for low and high-temperature proton exchange, alkaline membrane, molten carbonate) with improved conductivity over the entire temperature and humidity range of a fuel cell and increased mechanical, chemical, and thermal stability, with reduced or eliminated fuel cross-over
• Fabricate membranes from ionomers with scalable fabrication processes, increased mechanical, chemical, and thermal stability, and reduced cost
• Perform membrane testing and characterization to improve durability

The goal of this project is to develop durable hydrocarbon-based polymer electrolyte membrane composites. The hydrocarbon composites shall improve upon the current capabilities of expensive perfluorinated sulfonic acid-based membranes. The developed PEM composites will be manufactured by easily scaled, solution casting fabrication techniques on a reasonable scale to ensure appropriate market suitability and cost.

[1] Based on Fuel Cell Technologies Office Fuel Cell RD&D plan, table 3.4.6, http://energy.gov/sites/prod/files/2016/06/f32/fcto_myrdd_fuel_cells_0.pdf

FY 2016 Accomplishments

- Synthesized several high molecular weight polymer structures as a novel backbone for tough, ductile polymeric films.
- Designed and demonstrated a straightforward procedure to reproducibly functionalize polymers as PEM precursors.
- Developed a procedure to successfully prepare up to 8 in x 8 in films via solution casting as stable intermediate prior to composite activation. This procedure will allow for successful scale up and significant cost saving in manufacturing.

✧ ✧ ✧ ✧ ✧

INTRODUCTION

The widespread use of fossil fuels and continuous demand for energy over the past several decades has resulted in environmental concerns and an accelerated need for alternative energy and related technologies. Fuel cells are electrochemical energy conversion devices that convert chemical energy in fuels directly into electrical energy without combustion. The concept and principle of environmentally friendly fuel cells offer a unique collection of advantages in design, system management and flexibility, energy density, and fuel sources over other alternative energy systems. DOE has recognized the need for low cost, alternative PEMs to current state-of-the-art perfluorinated polymer membranes which have limited service range and no applicability at temperatures above 80°C. PEMs capable of operating at 120°C afford more efficient operation, potential for lower catalyst loadings or even non-platinum catalyst usage.

Indeed, all PEM systems require a medium for proton conductivity. Liquid water is the natural selection, however, water is not applicable at 120°C for fuel cell operation. The objective of this DOE Small Business Innovation Research project is to develop acid-doped PEMs with maximum protonic conductivity and good mechanical strengths to provide hundreds of hours of duty cycles. The appropriate acid doping levels will be a function of several factors but is expected to be lower that classic phosphoric acid fuel cells, hence avoiding corrosive side reactions.

APPROACH

The general approach for this project is to synthesis tough, mechanically stable polymeric film with select backbone functionality. Those films showing good mechanical stability will be tested for protonic conductivity and durability. The down-selected membrane candidates will undergo preliminary fuel cell testing (Table 2).

TABLE 2. Comparison between Nafion® and the Proposed Ionomer Composites

	Nafion®	Functionalized Hydrocarbon Ionomers
Proton Conductivity	✓	✓
Chemical Stability	✓	✓
Cost	$$$	$
Operating Temperature	↓	↑
Low RH Operation	✗	✓
Tolerance to Impurities	✗	✓
Improved Catalyst Activity	✗	✓
Additional Catalysts Viable	✗	✓
Straightforward Thermal Management	✗	✓
Low Methanol Crossover	✗	✓

RH – Relative humidity

RESULTS

The overall goal of the first phase of this project is the synthesis hydrocarbon-based polymer electrolyte membrane composites for automotive fuel cell applications capable of operating at 120°C. The PEM composites must be durable for a greater service lifetime and lower cost than perfluorinated sulfonic acid-based PEM systems.

To date, 10 different polymers have been synthesized as candidate polymeric backbones. These polymers differ in polarities and also stiffness. Variations in polarities are of interest with regard to the acid-doping step and the stability of the composites. Backbones with different stiffness are important when evaluating toughness and durability. The ideal polymer backbone will have the right balance of polarity and stiffness. Polymers that are too stiff may be brittle, also polymers with very high polarity may swell too great to be an effective barrier to the fuels (i.e., hydrogen gas, methanol, and air). Characterizations, which include chemical, thermal, and mechanical testing and thermomechanical analysis, are ongoing on these polymeric systems. Figure 1 shows the influence of functionalization on the polymer thermos-oxidative stability. The level of functionalization is also confirmed from this type analysis. This representative thermogram displays the exceptional stability of the control, un-functionalized polymer (green)

and the polymer backbones modified with two different levels of polar side groups (red, blue).

Characterization of the polymer backbones and their corresponding functionalized membranes will be presented in detail elsewhere. Below is a collection of some of the data for the various systems:

Glass Transition (Tg):	130–220°C
Melting Temperature:	160–250°C
Modulus (GPa):	2.2–3.4
Percent Elongation (%):	5–25

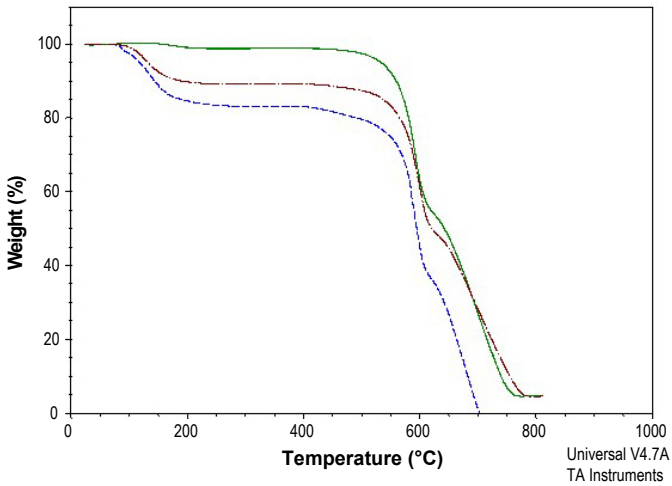

FIGURE 1. Thermogravimetric analysis of one series of functionalized hydrocarbon polymers

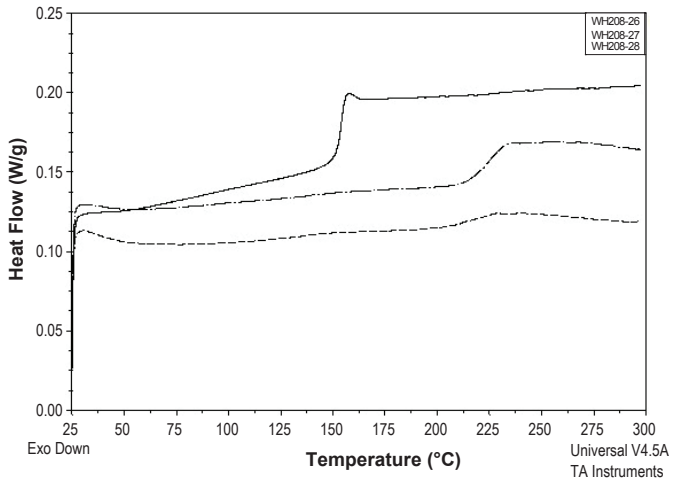

FIGURE 2. Differential scanning calorimetry of select candidate polymer systems displays high glass transition temperatures, greater than the 120°C target use temperature

CONCLUSIONS AND FUTURE DIRECTIONS

Although early in the project, several novel polymer backbones have been synthesized. These materials have undergone preliminary characterization and demonstrate exceptional thermal stability and mechanical strength. Select polymer backbones have successfully been functionalized with polar moieties. The polar moieties are expected to have significant influence the properties of the acid-doped membranes and stability of the composites fuel cell performance. Tough, ductile films have been fabricated via simple solution casting procedure.

Ongoing characterizations will guide further polymer development. Future works include:

- Film preparation and durability evaluations
- Acid composite fabrication
- Composite(s) proton conductivity measurements
- Initial fuel cell performance testing

V.C.11 Novel Nanocomposite Polymer Electrolyte Membranes for Fuel Cells

Runqing Ou (Primary Contact), Ganesh Skandan
NEI Corporation
400 Apgar Drive Suite E
Somerset, NJ 08873
Phone: (732) 868-3141
Email: rou@neicorporation.com

DOE Manager: Bahman Habibzadeh
Phone: (202) 287-1657
Email: Bahman.Habibzadeh@ee.doe.gov

Contract Number: DE-SC0015096 (Small Business Innovation Research)

Subcontractor:
ElectroChem, Inc., Woburn, MA

Project Start Date: February 22, 2016
Project End Date: November 21, 2016

Overall Objectives

- Develop a composite polymer electrolyte membrane (PEM) with high proton conductivity, low gas permeability and lower cost than perfluorinated sulphonic acid (PFSA)-based membrane.
- Demonstrate feasibility of a novel concept for PEM that has not been explored before.

Fiscal Year (FY) 2016 Objectives

- Construct 4 in x 4 in composite PEM
- Optimize membrane architecture
- Measure proton conductivity and gas permeability
- Demonstrate advantages over state of the art

Technical Barriers

This project addresses the following technical barriers from Fuel Cells section of the Fuel Cell Technologies Office Multi-Year Research, Development, and Demonstration Plan.

(B) Cost

(C) Performance (cell issues)

Technical Targets

This project is developing a novel composite PEM and demonstrating its benefits. We have demonstrated higher proton conductivity than state-of-the-art PFSA based membrane measured at 65°C and 76% and 23% relative humidity (RH) conditions. Further developments will bring us closer to the following DOE membranes for transportation applications targets for 2020.

- Maximum oxygen crossover: 2 mA/cm^2
- Maximum hydrogen crossover: 2 mA/cm^2
- Area specific proton resistance at maximum operating temperature and water partial pressures from 40–80 kPa: 0.02 ohm cm^2
- Maximum operating temperature: 120°C
- Cost: \$20/m^2

FY 2016 Accomplishments

- Designed a composite membrane which can be used to incorporate highly proton conducting heteropolyacid (HPA) in a 3-D network.
- Composite design optimization has resulted in higher proton conductivity than PFSA based membrane measured at 65°C and different humidity conditions.

✧ ✧ ✧ ✧ ✧

INTRODUCTION

The state-of-the-art PEM for fuel cells is based on PFSA ionomers. Besides the high cost, PFSA materials face challenges such as decreased proton conductivity at higher temperatures, water management issues and CO poisoning. Although efforts have been made to find low cost alternatives, to date non-PFSA membranes have not stood up against PFSA membranes in terms of performance and durability.

The proposed Phase I program aims to develop a novel non-PFSA polymer electrolyte membrane, utilizing highly proton conducting HPAs in an organic matrix in a way that has not been explored before. The novel HPA–polymer membrane has a unique structure that ensures that the active proton conducting species (HPA) are contained in a continuous interconnected channel. The overall objective of the Phase I program is to demonstrate the feasibility of a robust PEM that has high proton conductivity, low H_2 and O_2 cross-over and is highly durable for extended use in a fuel cell.

APPROACH

In this demonstration project, we develop a polymer–HPA composite membrane in ways that have not been explored before. The uniqueness of our approach is that HPA is stored in microvascular channels, which provide continuous proton pathway for improved conductivity. HPA is a water soluble proton conductor which suffers from the problem of leaching out in conventionally mixed polymer–HPA composite. In our composite membrane, HPA is shielded to prevent from leaching. The polymer matrix provides mechanical strength and gas barrier property to the composite membrane. Finally, all our processes use standard industrial practices which can greatly help commercialization of this technology.

RESULTS

Figure 1 illustrates a polymer–HPA composite membrane that is fabricated. The center area, which is greater than 4 in x 4 in, is the area where HPA are stored in microvascular channels. The composite membrane is fabricated using standard industrial processes.

Table 1 lists the proton conductivity of our initial membrane measured at room temperature after the membrane has been stored in a container with saturated water vapor. The conductivity of the initial sample approaches that of Nafion® membrane.

FIGURE 1. Composite polymer–HPA membrane

TABLE 1. In-Plane Proton Conductivity Measured at Room Temperature

In-Plane	Length, cm	Width, cm	Thickness, cm	Resistance, ohm	Conductivity, S/cm
NEI-4	0.457	0.318	0.025	976.5	0.06
Nafion® 115	0.457	0.318	0.013	143.5	0.79

With improved processing and optimization, the newer membranes demonstrated higher proton conductivity. Table 2 lists the proton conductivity measured at 65°C at different humidity conditions.

TABLE 2. In-Plane Proton Conductivity Measured at 65°C at Different Relative Humidity Conditions

Sample\Conductivity	Conductivity (S/cm) (RH = 76%)	Conductivity (S/cm) (RH = 23%)
NEI-29	0.25	0.22
Nafion®115	0.19	0.17

CONCLUSIONS AND FUTURE DIRECTIONS

Although the project is still in its early stages of development, some conclusions can be drawn:

- Novel polymer–HPA membrane has been designed to maximize the benefits of highly proton conducting HPA while locking them in microvascular channels.
- Polymer–HPA membrane samples have demonstrated higher proton conductivity than PFSA based membrane.

Future work includes:

- Conduct further architecture optimization to improve proton conductivity and gas barrier properties.
- Measure gas permeability in a quantitative manner.
- Assemble membrane in a membrane electrode assembly and evaluate performance.

FY 2016 PUBLICATIONS/PRESENTATIONS

1. "Novel Nanocomposite Polymer Electrolyte Membranes for Fuel Cells," presentation made at 2016 Hydrogen and Fuel Cells Program Annual Merit Review meeting.

V.D.1 High Performance, Durable, Low Cost Membrane Electrode Assemblies for Transportation Applications

Andrew Steinbach (Primary Contact), Amy Hester, Cemal Duru, Andrei Komlev, Darren Miller, Mike Yandrasits, Andrew Haug, John Abulu, and Matthew Pejsa
3M Company, Fuel Cell Components Program
3M Center, Building 201-2N-19
St. Paul, MN 55144-1000
Phone: (651) 737-0103
Email: ajsteinbach2@mmm.com

DOE Managers:
Dimitrios Papageorgopoulos
Phone: (202) 586-5463
Email: Dimitrios.Papageorgopoulos@ee.doe.gov

Greg Kleen
Phone: (240) 562-1672
Email: Gregory.Kleen@ee.doe.gov

Contract Number: DE-EE0005667

Subcontractors:
- Johns Hopkins University, Baltimore, MD
- Michigan Technological University, Houghton, MI
- Lawrence Berkeley National Laboratory, Berkeley, CA
- General Motors (GM) Co., Pontiac, MI
- Argonne National Laboratory, Argonne, IL (collaborator)
- Los Alamos National Laboratory, Los Alamos, NM

Project Start Date: September 1, 2012
Project End Date: August 31, 2016

Overall Objectives

- Demonstrate a durable, low-cost, and high performance membrane electrode assembly (MEA) for transportation applications, characterized by:
  - Total platinum (Pt) group metal (PGM) loadings of ≤0.125 mg/cm^2 of MEA area.
  - Performance at rated power of ≥1,000 mW/cm^2.
  - Performance at ¼ power (0.8 V) of ≥0.3 A/cm^2.
  - Durability of ≥5,000 hours under cycling conditions.
  - Q/ΔT of ≤1.45 kW/°C.
  - Cost of $5/kW-$9/kW, projected at high volume.
- Improve operational robustness to allow achievement of transient response, cold-startup, and freeze-startup system targets.

Fiscal Year (FY) 2016 Objectives

- Fabricate project Best of Class (BOC) MEAs and constituent components via pilot-scale production processes.
- Validate performance and operational robustness of pilot scale BOC MEAs in single cell and short stack formats.
- Evaluate BOC MEA performance under wide range of operating conditions to generate data to support performance and cost modeling at Argonne National Laboratory and Strategic Analysis, Inc.

Technical Barriers

This project addresses the following technical barriers from the Fuel Cells section of the Fuel Cell Technologies Office Multi-Year Research, Development, and Demonstration Plan.

(A) Durability

(B) Cost

(C) Performance

Technical Targets

This project is focused on development of a durable, high performance, low cost, and robust MEA for transportation applications. Table 1 lists current project status against the DOE Technical Targets for Membrane Electrode Assemblies (Table 3.4.14) and a subset of Electrocatalyst Targets (Table 3.4.13) from the 2012 Multi-Year Research, Development, and Demonstration Plan. The project status values are provided by results from the 2015 (September) Best of Class MEA, described at the bottom of Table 1. This MEA has met the DOE 2020 Q/ΔT and performance @ 0.8 V characteristics, is within 11% of the performance at rated power characteristic, and is within 5% of the PGM total loading characteristic. Status of durability with cycling to 10% voltage loss is estimated to be between 656–1,864 h at 0.8 A/cm^2, based on a single 3M durability test at 80°C, significantly less than the 5,000-hour target.

FY 2016 Accomplishments

- Generated all final project BOC components on pilot scale equipment. Resultant BOC MEA, evaluated in single cell at 3M, yielded improved ultimate performance (5% improved specific power [kW/g]) and operational robustness (33% improved current density at 40°C cell temperature) over last year's status.

TABLE 1. Status against Technical Targets

Characteristic	Units	2020 Targets	3M 2016 Status*
Q/ΔT	kW/°C	1.45	1.45
Cost	$/kW	7	8.62**
Durability with Cycling	hours	5,000	656–1,864
Performance @ 0.8 V	mA/cm^2	300	310
Performance @ Rated Power	mW/cm^2	1,000	891
Platinum Group Metal Total Content (Both Electrodes)	g/kW (rated)	0.125	0.147
Platinum Group Metal Total Loading	mg PGM/cm^2 Electrode Area	0.125	0.131

*3M Status with 2015 (September) Best of Class MEA: 0.019 mg_{PGM}/cm^2 PtCoMn/NSTF anode electrode, 0.096 mg_{PGM}/cm^2 Pt_3Ni_7 (TREATED)/NSTF + 0.016 mg_{PGM}/cm^2 Pt/C interlayer cathode electrode, 14 µm 725 EW 3M supported PEM, 3M "X3"/2979 Anode/Cathode GDLs, "FF2" Flow Fields. Performance assessed at 90°C, 150 kPa H_2/air (outlet), 2.0/2.5 H_2/air Stoichiometry, 84°C Dewpoints (J > 0.4 A/cm^2), 68°C Dewpoints (J < 0.4 A/cm^2); rated power defined at 0.692 V, which achieves Q/ΔT = 1.45 kW/°C.

"Best of Class" refers to the currently-determined optimal combination of components. Durability with cycling evaluated in single 50cm^2 cell under 3M 80°C load/RH cycle and assessed at 0.8A/cm^2, 1.5 atmA H_2/air.

**MEA cost estimated by Strategic Analysis, Inc. at 500,000 systems/year volume [1].

PEM – Polymer electrolyte membrane; GDL – Gas diffusion layer; RH – Relative humidity; NSTF – Nanostructured thin film; EW – Equivalent weight

- Conducted extensive evaluation (>200 tests) of BOC MEAs to support generation of performance and cost models at Argonne National Laboratory and Strategic Analysis, Inc. Resultant models predicted 25% higher stack power density and 16.8% lower stack cost as compared to 2015 status.
- Conducted 80°C load/RH cycle durability evaluation of BOC MEAs in 50 cm^2 single cell format. Single cell has operated for >3,000 hours with 10 µV/h and 15 µV/h degradation rates at open circuit voltage (OCV) and 0.2 A/cm^2, respectively, but time to 10% voltage loss at 0.8 A/cm^2 is estimated between 656–1,864 h.
- BOC MEAs were integrated into two 3-cell and one 28-cell rainbow short stacks at General Motors. Resultant performance and operational robustness was substantially below single cell results obtained at 3M and GM. Diagnostic experiments indicated issue was largely due to anode hydrogen oxidation reaction deactivation, and a new anode activation method was developed which is believed to be stack-compatible.

✧ ✧ ✧ ✧ ✧

INTRODUCTION

While significant progress has been made, state-of-the-art proton exchange membrane fuel cell MEAs utilized in today's prototype automotive traction fuel cell systems continue to suffer from significant limitations due to high cost, insufficient durability, and low robustness to off-nominal operating conditions. State-of-the-art MEAs based on conventional carbon-supported Pt nanoparticle catalysts currently incorporate precious metal loadings which are significantly above those needed to achieve MEA cost targets; performance, durability, and/or robustness decrease significantly as loadings are reduced. This project focuses on integration of 3M's state-of-the-art nanostructured thin film (NSTF) anode and cathode catalysts with 3M's state-of-the-art polymer electrolyte membranes (PEM), advanced and low-cost GDLs, and robustness-enhancing interfacial layers. At significantly lower precious metal content, the NSTF catalyst technology platform has several significant demonstrated benefits in performance, durability, and cost over conventional catalysts.

APPROACH

Optimize integration of advanced anode and cathode catalysts with next generation perfluosulfonic acid (PFSA) PEMs, gas diffusion media, and flow fields for best overall MEA performance, durability, robustness, and cost by using a combined experimental and modeling approach.

RESULTS

This year, a first focus area was generation of project BOC MEAs on pilot-scale fabrication processes, of sufficient quality and quantity to enable evaluation in short stacks. This included fabrication of catalyst coated membrane (CCM) comprising NSTF anode catalyst, dealloyed PtNi/NSTF cathode catalyst, and 3M 725 EW supported membrane, 3M "X3" anode GDL, and 3M "2979" cathode GDL with type "B" interlayer. More than 30 m of each was produced and validated with multiple lab-scale fuel cell tests. Figure 1 compares the performance and operational robustness of the final project 2015 (September) BOC MEA to the previous 2015 (March) BOC MEA, and Table 2 summarizes the MEA construction and key performance metrics. The September BOC MEA yielded modestly higher performance than the March BOC MEA. Specific power at 0.692 V (which meets the DOE Q/ΔT target of 1.45 kW/°C) increased from 6.5 kW/g to 6.8 kW/g, and performance at 0.80 V increased from 0.304 A/cm^2 to 0.310 A/cm^2. Figure 1B summarizes performance under a load transient test conducted at several cell temperatures, a measure of operational robustness. The 2015 (September) BOC MEA had similar operational range as the 2015 (March) BOC MEA, but yielded higher cell performance between 40–80°C cell temperature.

Figure 2 summarizes specific power progression over the course of the project at 150, 200, and 250 kPaA H_2/air reactant pressures. As compared to the 2012 (March) pre-project baseline MEA, specific power of the final 2015 (September) BOC MEA increased 57% at 150 kPaA, and

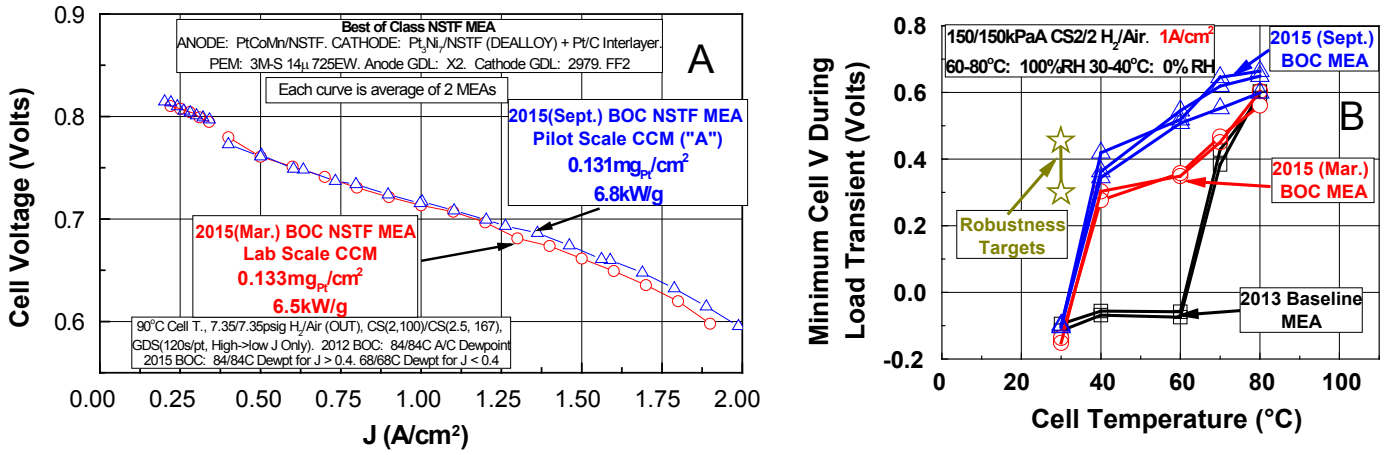

FIGURE 1. 2015 (September) Best of Class MEA performance (A) and operational robustness (B)

TABLE 2. Best of Class MEA Construction and Performance (90°C, 1.5 atmA H_2/air)

MEA	Anode Catalyst	PEM	Cathode Catalyst	Anode GDL / Cathode GDL+IL	PGM Total Loading (mg/cm^2)	Spec. Power @ 0.692 V (kW/g)	Performance @ 0.80 V (A/cm^2)
2015 (Mar.)	PtCoMn/ NSTF 15 μg/cm^2	3M-S 725EW 14 μm w/add.	Dealloyed PtNi/NSTF, 0.103 mg/cm^2	"X2"/ 2979 + "A" (15 μg/cm^2)	0.133	6.5	0.304
2015 (Sept.)	PtCoMn/ NSTF 19 μg/cm^2		Dealloyed PtNi/NSTF, 0.096 mg/cm^2	"X3"/ 2979 + "B" (16 μg/cm^2)	0.131	6.8	0.310

IL – Ionic liquid; w/ – With

the DOE target of 8 kW/g was exceeded when operated with 200 kPaA reactant pressures or higher.

The 2015 (September) BOC MEA was evaluated for performance sensitivity to a wide range of operating conditions to generate datasets to be used for performance and cost modeling. Tests were conducted on an MEA with a 5 cm^2 active area in a 50 cm^2 test cell with relatively high reactant flows, allowing operation in "differential" mode. Figure 3 summarizes polarization curve performance as a function of cathode oxygen concentration, reactant total pressure, cell temperature, and reactant relative humidity. Performance sensitivity to the above operational variables were largely as expected, and the limiting current density at 80°C, 1.5 atmA H_2/air approached 3 A/cm^2. The resultant dataset was provided to Argonne National Laboratory and Strategic Analysis, Inc. for performance and cost modeling. The model analysis indicated that as compared to 2015 status, the power density increased 25% and stack cost was decreased by $4.32/kW, a decrease of 16.8% [2].

2015 (September) BOC MEAs were evaluated for durability under a 3M load/RH cycle test conducted at 80°C cell temperature and 1.5 atmA H_2/air reactant pressures. Three 50-cm^2 MEAs were evaluated. Two MEAs completed <200 h prior to unanticipated or uncontrolled shutdowns due to facility issues, after which performance was irreversibly

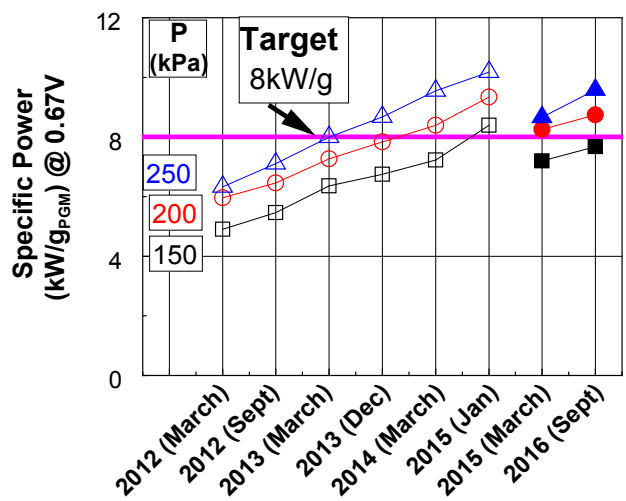

FIGURE 2. Best of Class MEA specific power progression over project

changed and testing was halted. The remaining MEA completed over 3,000 h of testing. Figure 4 summarizes the H_2/air performance and cathode F^- emission rates of the remaining MEA, and the timing of all shutdowns (controlled and uncontrolled). Performance change over time is due

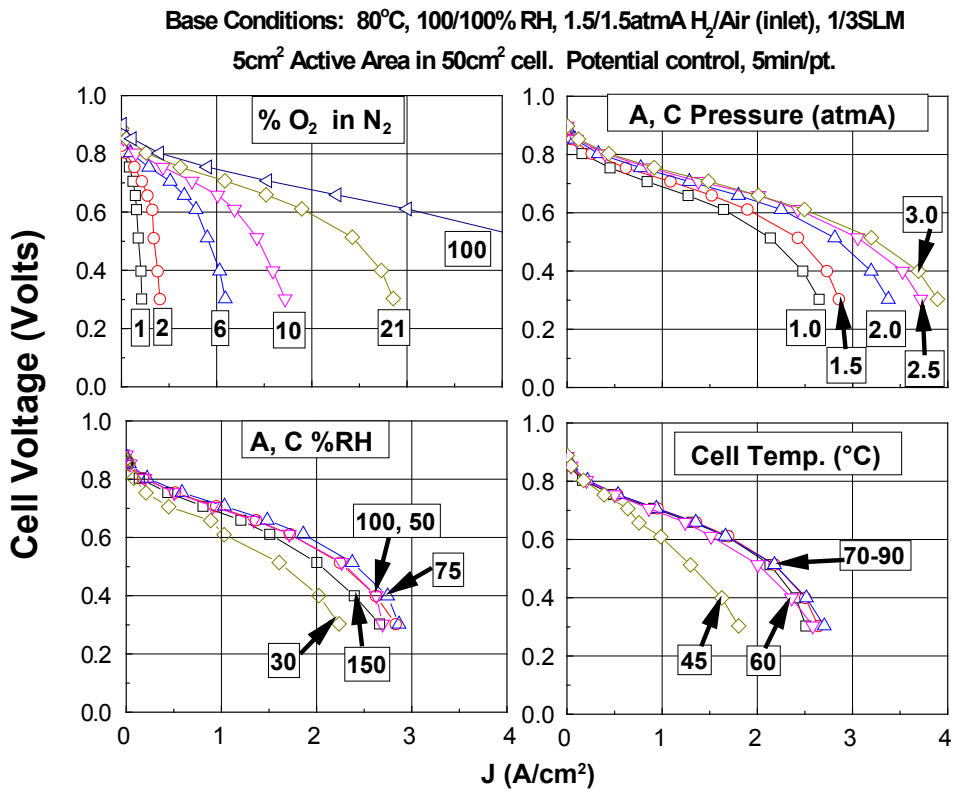

FIGURE 3. 2015 (September) Best of Class MEA performance sensitivity testing in 5 cm^2 differential cell format

to both reversible and irreversible loss factors and due to partial recoveries consistent with shutdowns. The cell voltage at OCV and 0.2 A/cm^2 was relatively steady with decay rates of -9.7 ± 0.4 µV/h and -15.2 ± 0.4 µV/h, respectively, estimated by linear regression fits. Performance at 0.8 A/cm^2 decreased at a higher rate than at lower current densities. After a shutdown at 656 h of operation, performance decreased 53 mV as compared to beginning of life (-81 µV/h average) and after a shutdown at 1,864 h of operation, total performance loss was 88 mV (-47 µV/h average). 10% voltage loss at 0.8 A/cm^2 (70 mV) was estimated to occur between 656 h and 1,864 h, or 13–37% of the 5,000-hour DOE 2020 target.

Based on previous project work, two key performance degradation modes with BOC NSTF MEAs are expected. The first performance degradation mode is further dealloying of the PtNi/NSTF cathode catalyst, leading to reduced mass activity and rated power loss due to Ni^{2+} contamination of the PFSA PEM. A second primary degradation mode is deactivation of the cathode catalyst due to PFSA decomposition, which correlates to F^- emission rate and rated power loss [2]. Analysis of the first degradation mode may occur once testing is complete, while the second degradation mode is assessable by cathode F^- emission. Figure 4 shows that cathode F^- emission was low and relatively constant over the period of measurement, averaging 7.3 ± 1.8 $ng/cm^2/h$

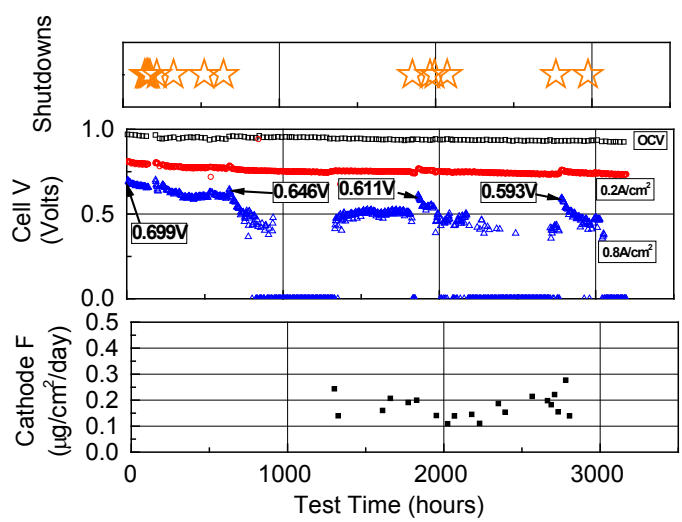

FIGURE 4. 2015 (September) Best of Class MEA performance during 3M load/RH cycling testing, conducted at 80°C cell temperature and 1.5/1.5 atmA H_2/air

which was largely within expected values and consistent with the observed performance decay.

Pilot scale baseline and project BOC MEAs were provided to GM for evaluation for performance and

operational robustness in automotive short stacks. Integration work consisted of numerous 50 cm^2 single cells, two 3-cell stacks, and one 28-cell rainbow stack. Figure 5A summarizes performance of a 3M baseline MEA and 3M BOC MEAs, relative to a GM baseline MEA. Performance of the 3M MEAs was substantially below expectation, based on single cell results. Figure 5B summarizes performance of the MEAs under load transient testing, a measure of operational robustness. The BOC MEAs failed under this testing, as indicated by a negative cell voltage at 1 A/cm^2, whereas all other MEAs passed, including GM baseline MEAs and other NSTF MEAs.

During this work, it was determined that in single cells, the 2015 (September) BOC MEAs require extensive hours of conditioning (>100 h) to achieve expected performance and robustness, and the conditioning method used in single cells is difficult to implement at stack level. Figure 6 shows that H_2/air performance between 30–90°C cell temperature is substantially improved after activation of the MEA anode in single cell. A substantial fraction of the relatively low BOC MEA performance and operational robustness in short stack was attributed to insufficient anode conditioning, caused by incompatibility of the single cell method with short stack operation. This strong requirement for substantial anode activation is likely a consequence of contamination

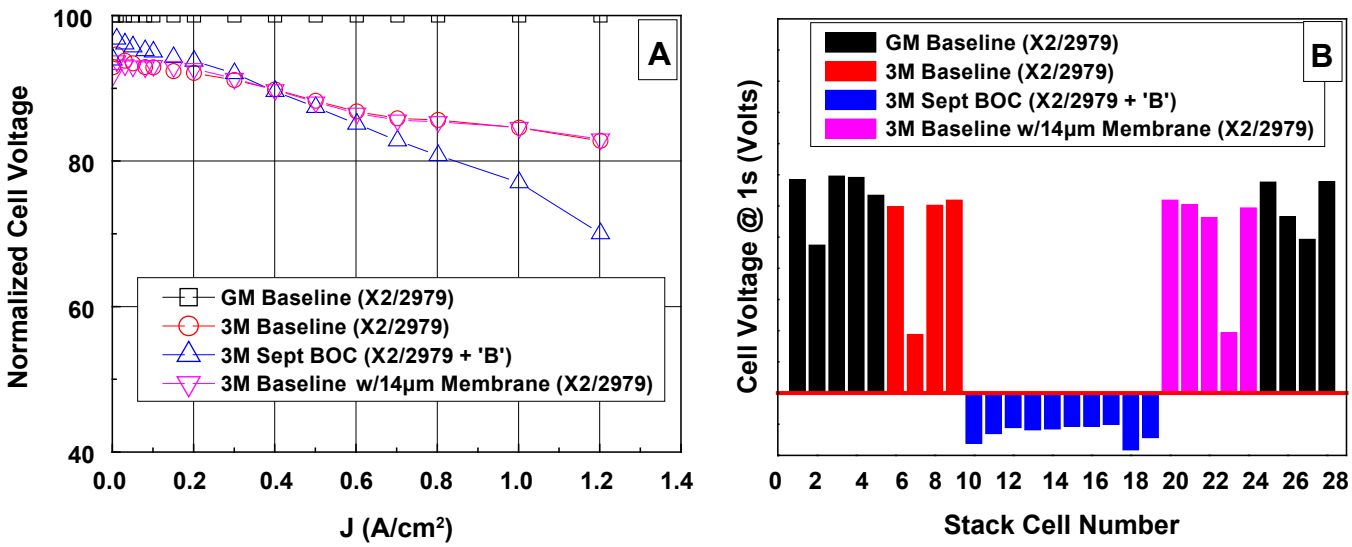

FIGURE 5. Relative performance and operational robustness of 2015 (September) BOC MEAs, 3M baseline MEA, and GM baseline MEA in 28-cell rainbow short stack

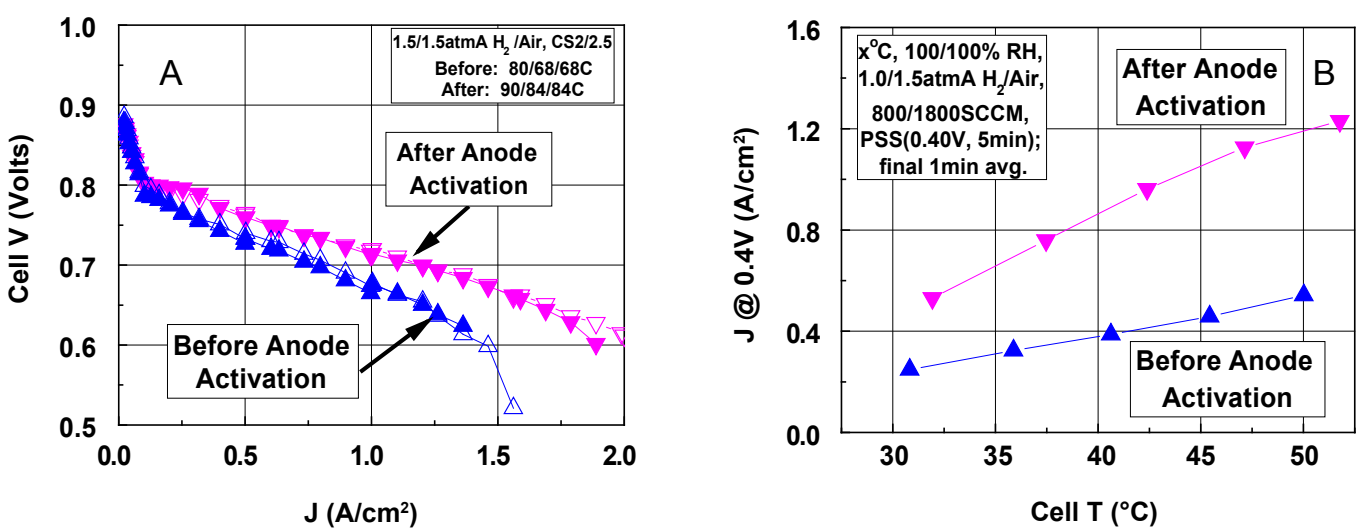

FIGURE 6. Impact of anode electrode conditioning on H_2/air rated power performance (A) and operational robustness (B)

of the low-loading (0.02 mg_{Pt}/cm^2), low specific area (<20 m^2/g) electrode. Work to develop a robust, stack-friendly conditioning method has been conducted at both 3M and GM and is planned to be implemented in short stack testing to occur over the remainder of the project.

CONCLUSIONS AND FUTURE DIRECTIONS

Significant progress has been made towards improvement of NSTF MEA performance, cost and operational robustness, and all but one relevant DOE 2020 targets have been reached or substantially approached. High performance, low cost, operationally robust MEAs have been fabricated via continuous, scalable pilot processes, indicative of feasibility of several project approaches. Key future work within this project is implementation of improved BOC MEA activation methods at short stack scale and to allow demonstration of anticipated performance and operational robustness.

Development of NSTF MEAs with improved rated power durability and activation will continue beyond the end of this project. Durability of rated power performance remains a primary challenge, but factors which cause this degradation mode are now reasonably understood and will require new material development to first partially, then fully mitigate. A second primary concern is the long and complex activation required for activation of ultra-low loading electrodes to achieve full performance and robustness. While some factors are understood, significant future work is needed to implement improved operational and material solutions.

FY 2016 PUBLICATIONS/PRESENTATIONS

1. A.J. Steinbach, "Challenges and Opportunities with 3M Nanostructured Thin Film (NSTF) Ultra-low PGM ORR Electrocatalysts," Challenges towards zero platinum for oxygen reduction, September 15, 2015, Le Grande Motte, France; *invited*.

2. A.J. Steinbach, D.F. van der Vliet, A.E. Hester, J. Erlebacher, C. Duru, I. Davy, M. Kuznia, and D.A. Cullen, "Recent Progress in Nanostructured Thin Film (NSTF) ORR Electrocatalyst Development for PEM Fuel Cells," 228th Meeting of the Electrochemical Society, October 13, 2015, Phoenix, AZ USA; *invited*.

3. A.J. Steinbach, D.F. van der Vliet, A.E. Hester, J. Erlebacher, C. Duru, I. Davy, M. Kuznia, and D. A. Cullen, "Recent Progress in Nanostructured Thin Film (NSTF) ORR Electrocatalyst Development for PEM Fuel Cells," *ECS Trans.* 2015 **69**(17): 291–301.

4. I.V. Zenyuk, E.F. Médici, J.S. Allen, and A.Z. Weber, "Coupling Continuum and Pore- Network Models in Polymer-Electrolyte Fuel Cells," European Fuel Cell 2015 – Piero Lunghi Conference, Naples, December 16–18, 2015.

5. A.J. Steinbach, "High Performance, Durable, Low Cost Membrane Electrode Assemblies for Transportation Applications," Presentation to USCAR Fuel Cell Tech Team, February 17, 2016.

6. R.K. Ahluwalia, X. Wang, and A.J. Steinbach, "Performance of Advanced Automotive Fuel Cell Systems with Heat Rejection Constraint," *J. Power Sources* **309** 178–191 (2016).

7. E. Medici, I.V. Zenyuk, D.Y. Parkinson, A.Z. Weber, J. Allen "Understanding Water Transport in Polymer-Electrolyte Fuel Cells Using Coupled Continuum and Pore-Network Models," *Fuel Cells* (2016). DOI 10.1002/fuce.201500213.

8. E.F. Medici and J.S. Allen, "A Quantitative Technique to Compare Experimental Observations and Numerical Simulations of Percolation in Thin Porous Materials," *Transport in Porous Media* (2016). DOI 10.1007/s11242-016-0672-4.

REFERENCES

1. B. James, Presentation FC018, 2016 U.S. Department of Energy Hydrogen and Fuel Cells Annual Merit Review, June 2016, Washington, D.C.

2. R.K. Ahluwalia, Presentation FC017, 2016 U.S. Department of Energy Hydrogen and Fuel Cells Annual Merit Review, June 2016, Washington, D.C.

V.D.2 Novel Structured Metal Bipolar Plates for Low Cost Manufacturing

Conghua "CH" Wang
TreadStone Technologies, Inc.
201 Washington Road
Princeton, NJ 08543
Phone: (609) 734-3071
Email: cwang@TreadStone-Technologies.com

DOE Manager: Bahman Habibzadeh
Phone: (202) 287-1657
Email: Bahman.Habibzadeh@ee.doe.gov

Contract Number: DE-SC0009215 (Small Business Innovation Research)

Subcontractor:
University of Hawaii, Honolulu, HI

Project Start Date: July 1, 2014
Project End Date: September 30, 2016

Overall Objectives

The technical objective of the Phase II project is to optimize the electrically conductive doped titanium oxide (doped TiO_x) coating technology that has been developed in the Phase I project, and to demonstrate its performance in an automobile short stack. The objective is to optimize the technology for the full size, high volume production using industrial available physical vapor deposition (PVD) systems. It will include the titanium alloy targets optimization, PVD process development for the uniform coating, and if it is necessary, a post deposition reactive ion etching process to obtain the desired surface composition and microstructure.

Fiscal Year (FY) 2016 Objectives

The objective of the project in 2016 is to further develop the PVD process for the doped TiO_x coating deposition and demonstrate the long-term stability of the doped TiO_x coated stainless steel bipolar plates by an in situ durability test in a short automobile stack. The coating process will be focused on the post stamping coating in this phase of the project. In addition, formability of the coated stainless steel foil will be evaluated for the future pre-stamping coating.

Technical Targets

The targets of the technology development include:

1. Low electrical contact resistance with gas diffusion layer (<5 mΩ cm)
2. Low corrosion resistance: <1 $\mu A/cm^2$
3. Low cost: <$3/kW by 2020
4. Low cost coolant side coating for low contact resistance (<2 mΩ cm) of cathode and anode plates
5. Capable of roll to roll coating and postcoating stamping

FY 2016 Accomplishments

- Optimized the PVD process for the large amount plate processing with consistent quality.
- Coated full size automobile fuel cell plates, assembled the short stack with the support from Ford. The long-term durability testing is on-going at University of Hawaii.
- Finished the formability tests of the coated stainless steel foil.

✧ ✧ ✧ ✧ ✧

INTRODUCTION

The thrust of the proposed work is to use the nanostructured, electrically conductive titanium oxide layer grown on the titanium alloy surface to protect stainless steel metal plates from corrosion. This technology will go beyond TreadStone's current gold-dot technical solution to meet the latest metal plate technical requirements, which are aimed at cost reduction and performance improvements to guarantee lifetime performance of fuel cell vehicles.

APPROACH

The scope of the Phase II project is focused on the titanium alloy target material development, PVD process development for the titanium alloy surface coating layer deposition. The electrically conductive titanium oxide coating will be grown by thermal oxidization under controlled conditions. The surface layer composition and microstructure will be determined. The coated stainless steel plates will be tested by ex situ evaluation and in situ tests using small (16 cm^2) single cells (Task 1 and 2), and full size, short (10 cells) stack (Task 3) under automobile dynamic driving conditions.

RESULTS

In TreadStone's doped TiO_x coating technology, PVD method is used for the titanium alloy deposition. In the project we have compared the impacts of the titanium alloy target composition and PVD process parameters to the performance of the coated stainless steel plates.

In total, four different Ti-Nb alloy targets are compared. The niobium concentration in titanium alloy targets are 2%, 3%, 5%, and 7% (noted as Ti-2Nb, Ti-3Nb, Ti-5Nb, and Ti-7Nb, respectively). It was found that the through plate resistance (TPR) of the as-coated plate is related with the target composition. As shown in Figure 1, Ti-2Nb and Ti-3Nb coated plates have much lower TPR than that of Ti-5Nb and Ti-7Nb. The hypothesis is that the high niobium content titanium alloy will form high niobium content β-phase that lead to the high TPR.

The difference between Ti-2Nb and Ti-3Nb is shown in the ex situ corrosion test of the coated stainless steel plates. Figure 2 and 3 show the TPR comparison of coated stainless steel before and after corrosion tests. The Ti-3Nb coated plates have small TPR increase after the corrosion tests for 100 h at 0.8 V_{NHE} in pH3 H_2SO_4 + 0.1 ppm hydrofluoric acid solutions at 80°C. On the other hand, there is no TPR increase of Ti-2Nb coated stainless steel plate after the same and more aggressive (at 1.6 V_{NHE} and 2.0 V_{NHE} 20 h) corrosion tests. It is possible that there are still small amount of niobium rich β-phase in the Ti-3Nb coating, which will grow the more resistant niobium oxide during corrosion test. Ti-2Nb coating could be in pure α-phase that surface oxide layer keeps the semi-conductive doped TiO_x phase through the corrosion tests.

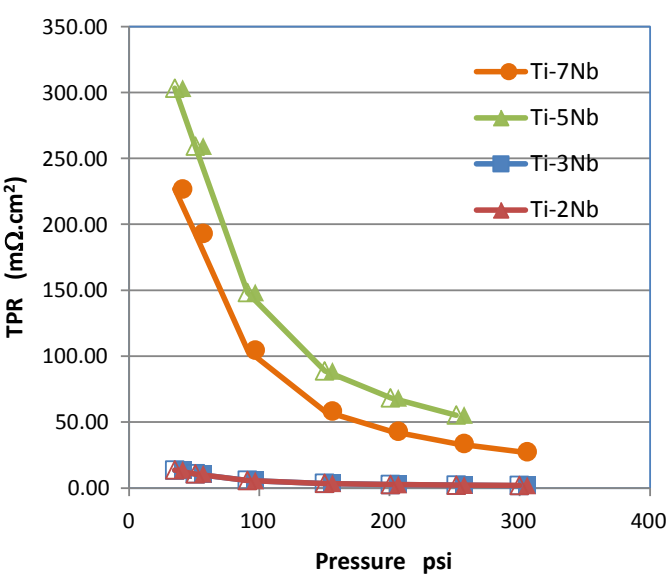

FIGURE 1. TPR comparison of coated stainless steel plate using different Ti-Nb target

Therefore, the project is focused on the coating using Ti-2Nb target to prepare full size bipolar plates for automobile short stack tests. Twenty plates were prepared in the project and were sent to Ford for the stack assembly. Ford used 11 plates to assemble a 10-cell stack in their facility. After the initial testing at Ford, the stack was delivered to University of Hawaii for the durability test. The stack has finished ~600 h test under automobile dynamic testing conditions. One bipolar plate was taken out of the stack after 524 h for middle of life inspection. There was not visible corrosion marks on the plate after the 524 h test. The TPR of the plate has small increase comparing with the original plate (beginning of the life), as shown in Figure 4. But the TPR still meets DOE's technical target (<20 mΩ.cm^2). The project is planned to finish the 2,000 h of this stack.

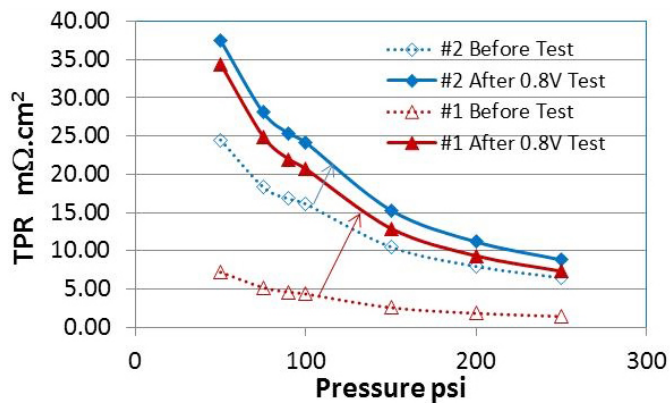

FIGURE 2. TPR comparison of stainless steel plates coated with Ti-3Nb alloy processed at different conditions (#1 and #2) before and after the corrosion tests at 0.8 V_{NHE} in pH3 H_2SO_4 + 0.1 ppm hydrofluoric acid solutions at 80°C

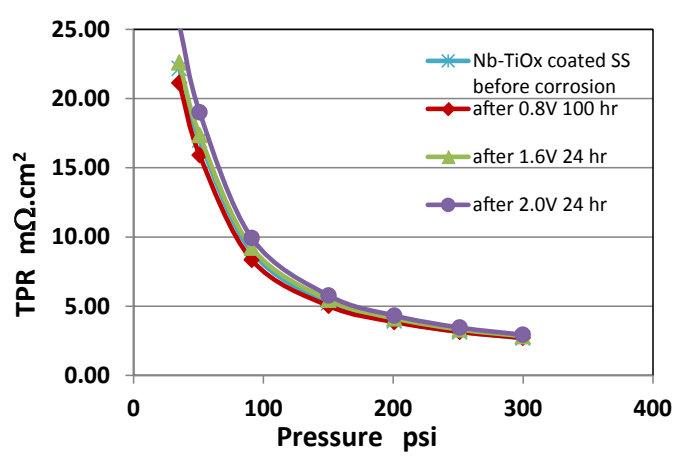

FIGURE 3. TPR comparison of stainless steel (SS) plates coated with Ti-2Nb alloy before and after corrosion tests in pH3 H_2SO_4 + 0.1 ppm hydrofluoric acid solutions at 80°C

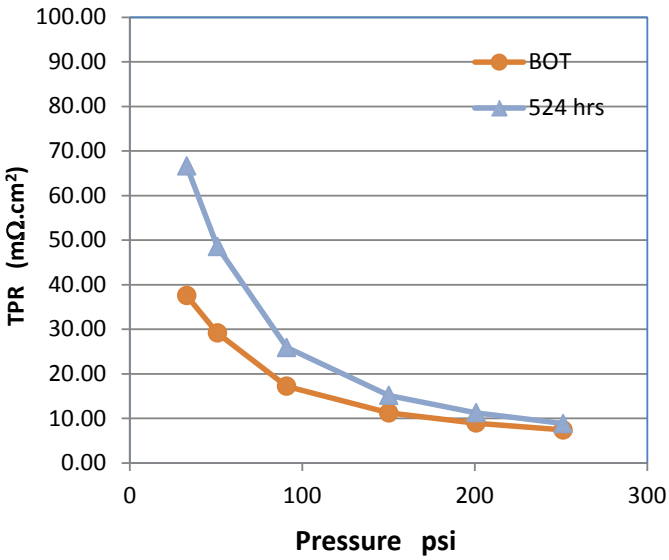

BOT – Beginning of test

FIGURE 4. TPR comparison of the bipolar plate before and after 524 h stack test

The formability of the titanium alloy coated stainless plates is evaluated in this phase of the project. It was found that coating thickness has major impacts on the plate formability. It was found that a thick Ti-Nb alloy coating layer will crack after stamping. After comparing stainless steel foil with different thickness Ti-Nb alloy coating, it is concluded that the titanium alloy coating thickness has to be less than 0.2 µm to avoid the coating layer crack during stamping. On the other hand, the stainless steel substrate may have some micro-cracking or micro-tearing during stamping. The substrate micro-cracking behavior is highly related with the flow field and forming-die designs. For the pre-stamping coating process, it is desired to have proper stamping process to avoid the substrate micro-cracking. With this condition, it is feasible to develop the pre-stamping coating of the doped TiO_x coating with a thin (<0.2 µm) Ti alloy coating.

CONCLUSIONS AND FUTURE DIRECTIONS

TreadStone demonstrated the low electrical contact resistance and superior corrosion resistance of the semi-conductive Nb doped TiO_x grown on Ti-2Nb alloy sub-layer coated on 316L stainless steel plates. The experimental results of this precious metal free coating technology indicates the potential of this technology for polymer electrolyte membrane fuel cell applications. Additionally, it was found in the project that the coating performance depends on the processing conditions. Some critical questions have to be answered before the development of the large volume production for automobile applications.

Further technology development should be focused to provide answers to these questions.

- ***PVD process optimization:*** The Ti alloy sub-layer deposition process has to be optimized for high volume production. It is desired to eliminate the hydrofluoric acid etching process used in Phase II project for low cost manufacturing, and fabrication cost of the coating technology need to be analyzed.
- ***Doped TiO_x surface layer growth mechanism:*** It was found in Phase II project that the properties of doped TiO_x surface layer grown on Ti alloy sub-layer is highly related with the titanium alloy composition and the processing conditions. It is necessary to understand the mechanism of the doped TiOx layer growth on the titanium alloy sublayer surface. This understanding is critical for quality control of the bipolar plate production process.

V.D.3 Rationally Designed Catalyst Layers for PEMFC Performance Optimization

Deborah J. Myers (Primary Contact),
Nancy N. Kariuki, Rajesh Ahluwalia,
Xiaohua Wang, Jui-Kun Peng, and C. Firat Cetinbas
Argonne National Laboratory
9700 S. Cass Avenue
Lemont, IL 60439
Phone: (630) 252-4261
Email: dmyers@anl.gov

DOE Manager: Nancy L. Garland
Phone: (202) 586-5673
Email: Nancy.Garland@ee.doe.gov

Subcontractors:
- Jonathan Sharman, Alex Martinez, Dash Fongalland, Brian Theobald, L. Smith, D. Ozkaya, M. Gutierrez, and Graham Hards, Johnson Matthey Fuel Cells, Sonning Common, United Kingdom
- Zhiwei Yang and Michael Perry, United Technologies Research Center, East Hartford, CT
- Paulo Ferreira, Kang Yu, Somaye Rasouli, Andres Godoy, and Daniel Groom, University of Texas at Austin, Austin, TX
- Jian Xie, Le Xin, Zhefei Li, Yadong Liu, Yuan Zhou, and Fan Yang, Indiana University Purdue University Indianapolis, Indianapolis, IN

Project Start Date: May 1, 2013
Project End Date: April 30, 2016

Overall Objectives

- Realize the oxygen reduction reaction (ORR) mass activity benefits of advanced Pt-based cathode electrocatalysts in membrane electrode assemblies (MEAs) and stacks operating at high current densities and on air and at low precious group metal (PGM) loading (≤0.1 mgPt/cm² on cathode).
- Determine the source(s) of performance limitations of de-alloyed PtNi (d-PtNi)-containing MEAs at high current densities (>1,000 mA/cm^2) when operating on air.
- Design and develop an electrode layer composition and/or structure, based on in-cell diagnostics, advanced characterization, and performance modeling to exceed the technical targets for MEAs for transportation applications.

Fiscal Year (FY) 2016 Objectives

- Determine effect of the equivalent weight (EW) of the ionomer in the cathode catalyst layer (CCL) on cell performance and performance durability.
- Diagnose source of performance loss with Ni^{2+} contamination in CCL utilizing X-ray scattering, water uptake measurements, and doping Ni^{2+} into Pt-based CCLs.
- Diagnose source(s) of activity losses of d-PtNi with functionalized support.
- Calculate porosities and diffusivities of Pt/C and d-PtNi/C electrodes utilizing X-ray tomography and transmission electron microscopy images, image analysis, and image reconstructions.
- Achieve a hydrogen-air current density of 1,250 mA/cm^2 at 0.675 V, under differential cell conditions (high stoichiometries), using cells with 0.125 mg-Pt/cm^2 fabricated using the best compositions and preparation procedures developed throughout the project.
- Determine the durability of cells with d-PtNi cathode catalysts and total cell Pt loadings of <0.125 mg-Pt/cm^2 using DOE-recommended protocols and alternative protocols. Performance and durability goals are 6.5 kW/g-Pt at peak power and <10% drop in power after application of the U.S. DRIVE Fuel Cell Tech Team Cell (FCTT) component accelerated stress tests (ASTs).

Technical Barriers

This project addresses the following technical barriers from the Fuel Cell section of the Fuel Cell Technologies Program Multi-Year Research, Development and Demonstration Plan.

(C) Performance

(B) Cost

(A) Durability

Technical Targets

The technical targets for this project are listed in Table 1.

FY 2016 Accomplishments

- Achieved a hydrogen-air current density of 1,259 mA/cm^2 at 0.675 V with cathode loading of 0.112 mg-Pt/cm^2 and under differential conditions. Achieved 1,060 mA/cm^2 at 0.675 V with a total cell

TABLE 1. Progress towards Meeting Technical Targets for Electrocatalysts and MEAs for Transportation Applications

Metric/Units	DOE 2020 Target	Project Status with High Anode Loading	Project Status with Low Anode Loading
Mass activity (A/mg_{PGM} @ $0.9mV_{iR\text{-}free}$)	≥0.44	0.59	0.6
Specific activity ($\mu A/cm^2_{PGM}$ @ $0.9\ mV_{iR\text{-}free}$)	≥720	1,151	1,015
PGM total loading ($mg\text{-}PGM/cm^2_{geo}$)	≤0.125	0.112 cath.	0.1159 cath. 0.018 anode
MEA performance (mA/cm^2_{geo} @ 800 mV) FCTT Pol Curve	≥300	347 n/d	371 200
MEA performance (mW/cm^2_{geo} @ 675 mV) FCTT Pol Curve	≥1,000	878 n/d	850 672
MEA performance (mW/cm^2_{geo} @ 600 mV) FCTT Pol Curve	≥1,000	999 n/d	1,025 750

n/d – not determined

loading of 0.1107 mg-Pt/cm^2 when using a modified FCTT protocol with higher cell operating temperature, allowing cell to meet Q/ΔT targets. (Achieved 890 mA/cm^2 at 0.675V using standard FCTT protocol).

- MEA with d-PtNi/C cathode at a loading of 0.1159 mg-Pt/cm^2 and a Pt/C anode at a loading of 0.018 mg-Pt/cm^2 achieved 7.7 kW/g-Pt at peak power under differential conditions and 6.2 kW/g-Pt under standard DOE FCTT-recommended polarization curve protocol.
- Achieved a 7% loss in peak power after 30,000 triangle cycles (0.6–0.925 V, 50 mV/s) and 22% loss in peak power after 30,000 trapezoid cycles (0.6–0.95 V, 700 mV/s, 6 s/cycle).

✧ ✧ ✧ ✧ ✧

INTRODUCTION

One of the major contributors to the cost of PEMFC systems for automotive and stationary power applications is the PGM cathode electrocatalyst [1]. The high cost of the cathode electrocatalyst results from the high loadings of catalyst necessary to overcome the limitations of low ORR activity, low utilization of PGM, and loss of activity with operating time. Alloying platinum with base metals (e.g., cobalt, iron, and nickel) is well known to improve its intrinsic ORR activity [2]. While ORR mass activities exceeding the DOE 2020 targets (>0.44 A/mg PGM and 720 µA/cm² at 900 mV) have been demonstrated for numerous Pt alloy and core-shell nanoparticle catalysts [3], the full high current density performance of CCLs based on low loadings of these promising catalysts has yet to be achieved in MEAs. There are several possible reasons the full potentials of these advanced catalysts have not been realized in MEAs, such as inadequate transport of protons and oxygen to the catalytic sites arising from less than optimum spatial distribution of ionomer, catalyst, and pores. The goal of this project is to optimize the composition, structure, and materials properties of cathodes based on an advanced cathode catalyst to translate the catalyst's intrinsically high ORR mass activity into high performance at peak power. The advanced catalyst chosen for this project is dealloyed PtNi (d-PtNi) developed by Johnson Matthey Fuel Cells within a DOE-supported General Motors project [3].

APPROACH

The overall approach of the project is to:

- Determine the properties of advanced alloy-based catalysts and/or cathode catalyst layers that limit the high current density/air performance using:
  - *In-cell* diagnostics of d-PtNi/C versus high surface area Pt/C and Pt/C of comparable electrochemically active surface area.
  - A suite of in situ and ex situ techniques, such as transmission electron microscopy, cryogenic transmission electron microscopy, dynamic light scattering, ultra-small angle X-ray scattering, X-ray absorption spectroscopy, X-ray tomography, and porosimetry.
- Design the catalyst layer composition and structure and support functionality to mitigate the performance limitations, guided by computational modeling, by:
  - Studying the dispersion of d-PtNi/C catalyst aggregates and the ionomer particles in liquid media and in electrodes and compare them to Pt/C-based inks and electrodes.
  - Developing an ink composition and/or ink processing (e.g., solvent removal process) that result in optimum agglomerate structure in d-PtNi/C-based electrodes.

- Developing the catalyst support surface functionality to increase the performance of the catalyst and cathode – to decouple proton conductivity from ionomer content.

The d-PtNi catalysts were synthesized by Johnson Matthey Fuel Cells using a catalyst precursor comprised of 5.4 nm mean diameter $PtNi_3$ alloy particles deposited on Ketjen black carbon, via a commercially-scalable method, followed by annealing to drive alloy formation. The resulting catalyst precursor is dealloyed via an acid treatment step to leach Ni to form a catalyst with an approximate composition of Pt_3Ni_2 and a Pt loading on the carbon support of approximately 30 wt%. As shown in Table 1, the ORR mass activity of this catalyst in an MEA far exceeds the DOE 2020 target.

RESULTS

The effects of ionomer EW on the agglomerate structure in catalyst-ionomer-solvent inks, agglomerate structure in electrodes, and CCL performance and performance durability under a variety of oxygen partial pressures and relative humidities (RHs) were determined for the d-PtNi/C catalyst and, for comparison, for a Pt/C catalyst with a particle size distribution comparable to that of the d-PtNi/C (An-Pt/C). The following summarizes the results of these characterization and performance studies.

- Lower EW ionomer in inks:
  - In general causes greater break-up of agglomerate structure than the standard 1100 EW ionomer, effect is dependent on I/C (Figure 1)
  - Best overall cell performance under high and low RHs observed for lowest EW ionomer and intermediate I/C (1.0) (Figure 2)
- Functionalization of carbon support with $–SO_3H$ groups improves low RH performance, but decreases catalyst mass activity.
  - Lower mass activity due to adsorption of sulfur species on Pt surface and to loss of both Pt and Ni from catalyst during functionalization
- Performance Status (cells with ~0.1 mg-Pt/cm^2 anode loading):
  - Differential conditions, organic ink, I/C = 0.8, acid-washed CCM: 1,300 mA/cm^2 at 0.675 V
- Performance Status (cells with ~0.025 mg-Pt/cm^2 anode loading):
  - Differential conditions, organic ink, I/C = 1.0, 850 EW, acid-washed CCM: 1,259 mA/cm^2 at 0.675 V

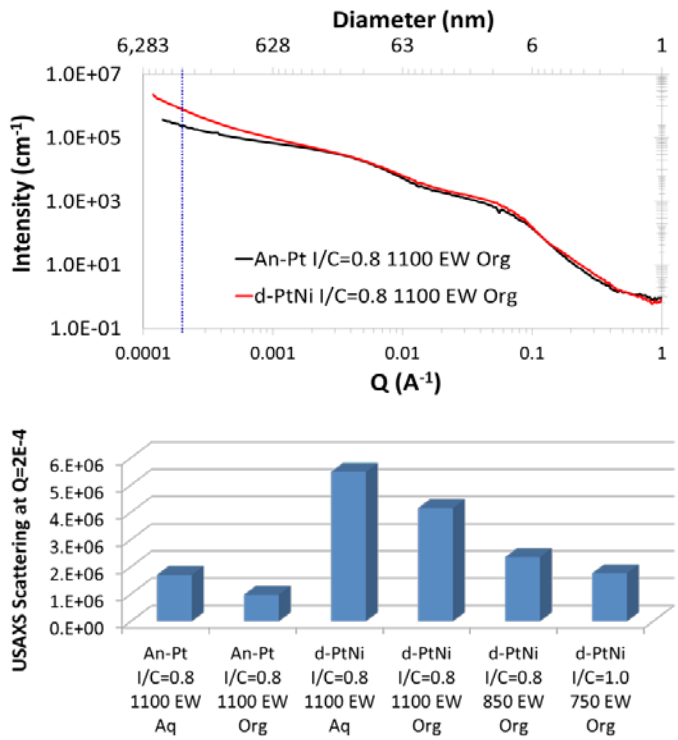

USAXS – Ultra-small angle X-ray scattering

FIGURE 1. (Top) Ultra-small angle X-ray scattering curves of d-PtNi/C and An-Pt/C electrode layers. Vertical line shows the scattering angle for ~3 µm diameter agglomerates. The scattering intensity at this angle is plotted in the (Bottom). (Bottom) Effect of catalyst type, catalyst ink solvent, and ionomer EW on the prevalence of large agglomerates (>~3 µm equivalent diameter) in the electrode structures.

  - FCTT polarization curve:
    - 1,060 mA/cm^2 at 0.675 V with a total cell loading of 0.1107 mg-Pt/cm^2 at 90°C
    - 890 mA/cm^2 at 0.675 V under standard FCTT conditions (80°C)
- Durability status after 30,000 AST cycles (cells with ~0.025 mg-Pt/cm^2 anode loading) (Figure 3)
  - Mass activity loss: 34%; electrochemical surface area (ECA) loss: 49%, (0.6–1.0 V, 50 mV/s, triangle, limited diagnostics)
  - Mass activity loss: 26%; ECA loss: 26%; Voltage decrease at 1.5 A/cm^2: 33 mV (0.6–0.925 V, 50 mV/s, triangle, limited diagnostics)
  - Mass activity loss: 46%; ECA loss: 51%; Voltage decrease at 1.5 A/cm^2: 121 mV (0.6–0.95 V, 700 mV/s trapezoid, extensive diagnostics)

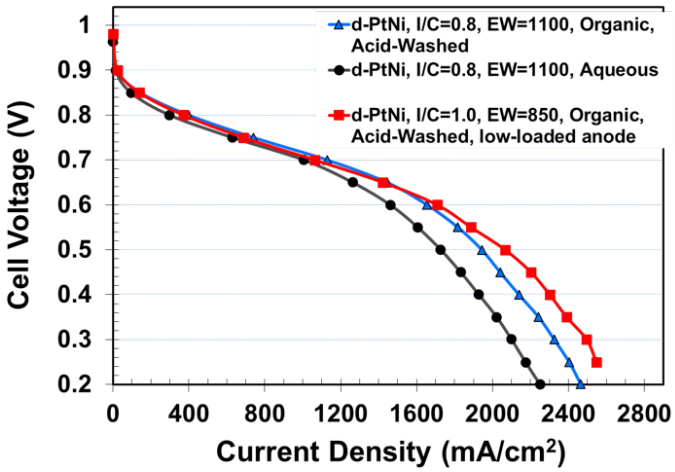

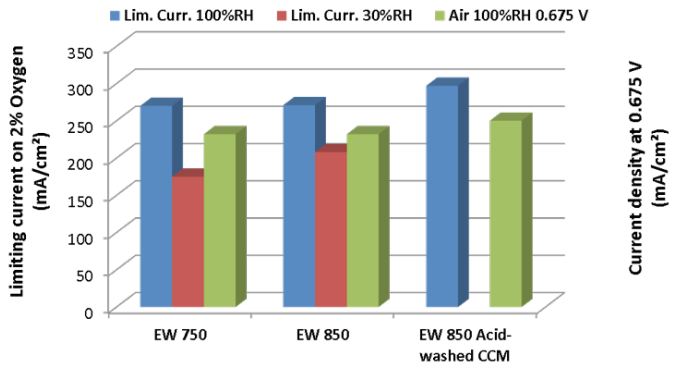

FIGURE 2. (Top) Hydrogen-air polarization curves with 0.1 mg-Pt/cm^2 d-PtNi/C cathode and either 0.1 mg-Pt/cm^2 or <0.02 mg-Pt/cm^2 Pt/C anode, 80°C, 150 kPa (abs.), high and fixed flow for differential conditions (3 slpm air). (Bottom) Limiting current on 2% oxygen at 80°C at 100% RH and 30% RH and current density on air at 0.675 V. Conditions: 150 kPa, 80°C, perfluorosulfonic acid ionomer to carbon ratio (I/C) = 1.0 in cathode, organic solvent used in cathode catalyst ink.

CONCLUSIONS AND FUTURE DIRECTIONS

Issues with the d-PtNi/C catalyst-based electrodes are drop-off in performance at >1,000 mA/cm^2 (i.e., not maintaining mass activity benefit relative to high-surface area Pt/C) under high and intermediate humidity conditions and a severe drop-off at low RHs. The sources of these issues and potential solutions to the issues are:

- Mass transport to low loadings of large particles.
  - Can be mitigated with smaller particles that are >~4 nm to insure stability against dissolution-related ECA loss.
- Sensitivity to low humidity conditions is unique to d-PtNi/C and can be partially mitigated with increased ionomer content, organic solvents, and lower EW ionomer which improve dispersion of d-PtNi/C particles, and can be greatly improved with acid treatment of CCM.

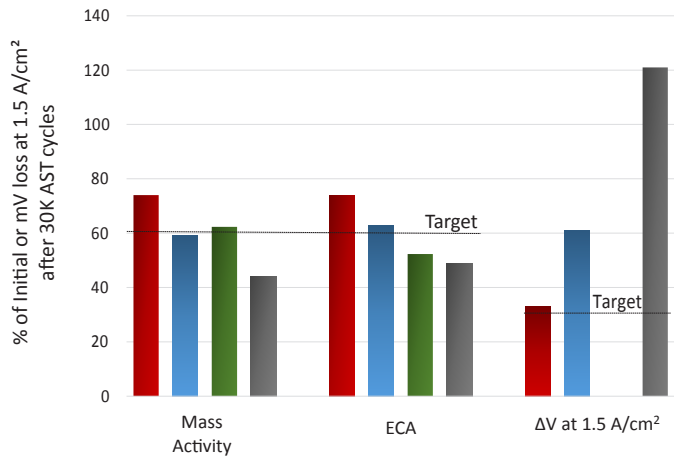

FIGURE 3. Durability results for MEAs with ~0.1 mg-Pt/cm^2 d-PtNi/C cathode catalyst and ~0.02 mg-Pt/cm^2 Pt/C anode. Organic solvent and 850 EW ionomer with I/C = 1.0 used in cathode catalyst ink. CCMs were acid-washed after fabrication.
Red: 0.6–0.925 V triangle, 50 mV/s; limited intra-cycle diagnostics
Blue: 0.6–0.925 V triangle, 50 mV/s; extensive intra-cycle diagnostics
Green: 0.6–1.0 V triangle, 50 mV/s; limited intra-cycle diagnostics
Grey: 0.6–0.95 trapezoid, 700 mV/s; extensive intra-cycle diagnostics

- Results indicate that Ni^{2+} in ionomer, leached during ink and CCM fabrication is altering the structure of the ionomer, which alters the agglomerate structure of cathode catalyst layer, decreasing mass transport, especially at low RH.
  - More aggressive leaching of Ni^{2+} prior to ink synthesis and CCM fabrication can improve d-PtNi/C cathode performance, especially under dry conditions.
- Leaching of Ni from particles continues during ASTs, especially when upper potential of the AST is 1.0 V
  - Mitigate through control of highest voltage encountered by cathode.
  - Continue development of catalyst particles with more uniform morphology, intra-particle composition distribution, more uniform Pt shell.
- d-PtNi/C shows higher ECA, mass activity, and high current density performance loss than An-Pt/C when subjected to catalyst ASTs.
- Acid-washing d-PtNi/C-containing CCMs does not adversely affect ECA and mass activity decay with AST cycling and decreases low and high current density performance decay.
- The decay rates with AST cycling were comparable for d-PtNi/C-containing electrodes containing either 850 or 1100 EW ionomer.

- Intra-AST-cycling diagnostics, such as CO stripping for ECA measurement, dramatically increases ECA, mass activity, and high and low current density performance loss of the d-PtNi/C-based CCL (Figure 3).
- New trapezoid AST causes more degradation of ECA, mass activity, and air performance than DOE 0.6–1.0 V, 50 mV/s triangle AST and General Motors-suggested 0.6–0.925 V triangle AST (Figure 3).
- d-PtNi/C can meet ECA and mass activity durability targets and approaches high current density performance loss durability target (30 mV) when limiting upper potential of triangle AST to 0.925 V (Figure 3).

FY 2016 PUBLICATIONS/PRESENTATIONS

1. N.N. Kariuki, D.J. Myers, D. Fongalland, A. Martinez, and J. Sharman, "Microstructure Analysis of Polymer Electrolyte Membrane Fuel Cell Catalyst-Ionomer Inks and Cathode Catalyst Layers by Ultra Small Angle X-ray Scattering," 229th Electrochemical Society Meeting, San Diego, CA, May 29–June 2, 2016.

2. Le Xin, Fan Yang, Zhe-Fei Li, Somaye Rasouli, Paulo J. Ferreira, Cheng-Jun Sun, Yu-Zi Liu, and Jian Xie, "Understanding of Pt nanoparticle anchoring on graphene supports through surface functionalization," ACS Catalysis, 2016, 6 (4), 2642–2653.

3. S. Rasouli, Z. Yang, M. Gummalla, S.C. Ball, D. Myers, and P.J. Ferreira, "Surface Area Loss Mechanisms of Pt_3Co Nanocatalysts in PEM Fuel Cells: A Parametric Study" (submitted).

4. James A. Gilbert, A. Jeremy Kropf, Nancy N. Kariuki, Stacy DeCrane, Xiaoping Wang, Somaye Rasouli, Kang Yu, Paulo J. Ferreira, Dane Morgan, Deborah J. Myers, "In-Operando Anomalous Small-Angle X-Ray Scattering Investigation of Pt_3Co Catalyst Degradation in Aqueous and Fuel Cell Environments," Journal of The Electrochemical Society, 162, 2015, F1487–F1497.

5. Mallika Gummalla, Sarah C. Ball, David A. Condit, Somaye Rasouli, Kang Yu, Paulo J. Ferreira, Deborah J. Myers, Zhiwei Yang, "Effect of Particle Size and Operating Conditions on Pt_3Co PEMFC Cathode Catalyst Durability," Catalysts, 5, 2015, 926–948.

6. Zhe-Fei Li, Le Xin, Fan Yang, Yadong Liu, Yuzi Liu, Hangyu Zhang, Lia Stanciu, and Jian Xie, "Hierarchical Polybenzimidazole-grafted Graphene/Carbon Hybrids as Supports for Pt Nanoparticle Catalysts with Excellent PEMFC Performance," NanoEnergy, 16, 2015, 281.

7. Paulo Ferreira, "NanoSpain 2016," Logrono, Spain, March 2016.

8. Paulo Ferreira, "Nano Monterrey 2015," Monterrey, Mexico, October 22–23, 2015.

9. Paulo Ferreira, "Seeing small: Enabling new discoveries in energy materials through advanced transmission electron microscopy," AGH University of Science and Technology, Krakow, Poland, December 2015.

10. Somaye Rasouli, Best Poster Award, 15th Frontiers of Electron Microscopy in Materials Science, (FEMMS), 2015.

REFERENCES

1. Brian D. James, "Fuel Cell Vehicle and Bus Cost Analysis," 2015 DOE Hydrogen and Fuel Cells Program Review, Arlington, VA, June 8–12, 2015.

2. H.A. Gasteiger, S.S. Kocha, B. Sompalli, F.T. Wagner, "Activity benchmarks and requirements for Pt, Pt-alloy, and non-Pt oxygen reduction catalysts for PEMFCs." Appl. Catal B-Environ., 2005, 56 (1-2), 9–35.

3. A. Kongkanand, "High-Activity Dealloyed Catalysts," 2014 DOE Hydrogen and Fuel Cells Program Review, Washington, D.C., June 16–20, 2014.

V.D.4 Affordable, High Performance, Intermediate Temperature Solid Oxide Fuel Cells

Bryan Blackburn (Primary Contact),
Thomas Langdo, Dong Ding, Lei Wang,
Luis Correa, and Colin Gore
Redox Power Systems
4467 Technology Drive
Suite 2107, Bldg. 387
College Park, MD 20742
Phone: (301) 314-1959
Email: bryan@redoxenergy.com

DOE Manager: David Peterson
Phone: (240) 562-1747
Email: David.Peterson@ee.doe.gov

Contract Number: DE-EE0006735

Subcontractor:
University of Maryland, College Park, MD

Project Start Date: October 1, 2014
Project End Date: March 31, 2016 (No Cost Extension until September 30, 2016)

Overall Objectives

Redox Power Systems' overall objectives in this project are to improve the performance and durability of Redox solid oxide fuel cell (SOFC) technology through the:

- Development of an optimized bilayer electrolyte with increased open circuit potential (OCP) and thus greater fuel efficiency for natural gas fueled, intermediate temperature (IT) operation of ~600°C.
- Optimization of compositions and microstructures for the cathode to increase power density and the anode to improve carbon- and sulfur-tolerance in hydrocarbon fuels for IT operation.
- Use of a custom multiphysics model and advanced materials to optimize the performance of bilayer stack designs for IT operation.
- Creation of bilayer cell performance maps and demonstration of a ~1 kW_e stack for IT operation under combined heat and power (CHP) conditions with natural gas and minimal external reforming.

Fiscal Year (FY) 2016 Objectives

- Demonstration of bilayer electrolyte cell with OCP performance of ≥0.9 V at both button cell and larger 10 cm x 10 cm size for operation at ≤600°C.
- Demonstration of 10 cm x 10 cm cell operating at ≤600°C with a cell area specific resistance ≤0.2 Ωcm^2 and power density ≥1 W/cm^2.
- Demonstration of 10 cm x 10 cm bilayer cell stack in CHP conditions with natural gas.

Technical Barriers

This project addresses the following technical barriers from the Fuel Cells section of the Fuel Cell Technologies Office Multi-Year Research, Development, and Demonstration Plan.

(A) Durability

(B) Cost

(C) Performance

Technical Targets

This project's goals are focused on stack improvements with increased power density for operation at intermediate temperatures (≤600°C), which supports DOE technical targets. The results of this project can be applied to the design of advanced natural gas fueled power systems in the low and intermediate power range (1–100 kWe). Lower operating temperature SOFCs can result in simpler, more compact and lightweight systems with longer lifetimes. Furthermore, higher power densities at lower temperatures result in reduced system and operating costs, while IT operation still maintains sufficient exhaust temperatures for efficient CHP applications. Such systems have the potential to meet or exceed the following 2020 DOE stationary fuel cell technical targets.

- Equipment Cost: $\$1,700/kW_{avg}$
- Transient Response (10–90% rated power): 2 min
- Degradation with Cycling: 0.3%/1,000 h
- Electrical Efficiency: >45%
- CHP Efficiency: 90%

FY 2016 Accomplishments

Accomplishments during the current project period include:

- Demonstration of a 10 cm x 10 cm bilayer cell with an OCP of 0.91 V at ~600°C.
- Successful scale-up of a porous anode-supported cell architecture to the 10 cm x 10 cm size as a step toward matching the 1.25 W/cm^2 seen at the button cell level at 600°C.

INTRODUCTION

We have previously demonstrated a high power density SOFC technology using advanced materials in a novel bilayer electrolyte design with graded electrode structures at the button cell level. Redox has also been able to scale our base (single layer gadolinia doped ceria [GDC] electrolyte) cells to a larger 10 cm x 10 cm production size and achieve similar performance as button cells. Furthermore, we have scaled up production of the erbia-stabilized bismuth oxide (ESB) material which together with GDC comprises the bilayer electrolyte. However in addition to integrating the ESB–GDC bilayer into the larger format cells, significant improvements in cell performance and efficiency can still be achieved to make systems based on our technology more commercially viable with lower costs, higher efficiency, and superior durability. Moreover, integrated development of the anode for operation on readily available hydrocarbon fuels with a maximum degree of internal reforming are necessary to take full advantage of SOFC fuel flexibility. Achieving these advancements while maintaining high power density at intermediate temperatures (~600°C) will help us deploy this technology for distributed generation and CHP.

APPROACH

Redox's approach involves the synergistic use of two electrolyte materials in a bilayer structure to result in superior performance (i.e., higher conductivity) at lower temperatures [1]. The first material is cerium oxide-based such as GDC, which has more than five times the ionic conductivity of conventional yttrium stabilized zirconia at 600°C, but due to the electronic leakage that occurs in reducing environments (i.e., fuel conditions), can result in decreased cell efficiency. The second material is bismuth oxide-based such as ESB, which has 60 times the conductivity of yttrium stabilized zirconia at 600°C but is unstable in reducing environments. The bilayer electrolyte combines the cerium oxide and bismuth oxide layers (i.e., GDC–ESB) with the latter being situated on the cathode air side of the cell. In this case, the GDC protects the ESB from decomposing while the ESB blocks the electronic leakage in the GDC, thus boosting cell power and efficiency at lower operating temperatures. We have also developed new, bilayer-compatible cathode materials (e.g., composite lanthanum strontium manganate [LSM]–ESB) with exceptionally low area specific resistance and are leveraging past work on infiltration of electrodes that can enhance the performance of the cathode and anode. For the anode, catalyst infiltration can significantly increase power density and stability in the presence of hydrocarbon fuels such as natural gas even in the presence of sulfur compounds like H_2S [2]. To assist in the development of cells and stacks for operation at ~600°C, an advanced, custom multi-physics model, which takes into account the unique thermochemical and physical properties of the Redox materials, is used. This is critical due to variations in conductivity and chemical activity of GDC as a function of temperature and effective oxygen partial pressure PO_2, which varies significantly down the channel in SOFC anodes with increasing fuel utilization [3].

RESULTS

During FY 2016, Redox worked to scale up our results from the button cell level to a cell size of 10 cm x 10 cm for a porous anode-supported bilayer electrolyte SOFC with high OCP and high power density at 600°C. In FY 2015, we adjusted the relative and total GDC–ESB bilayer thickness to improve the cell OCP. Figure 1A shows the typical

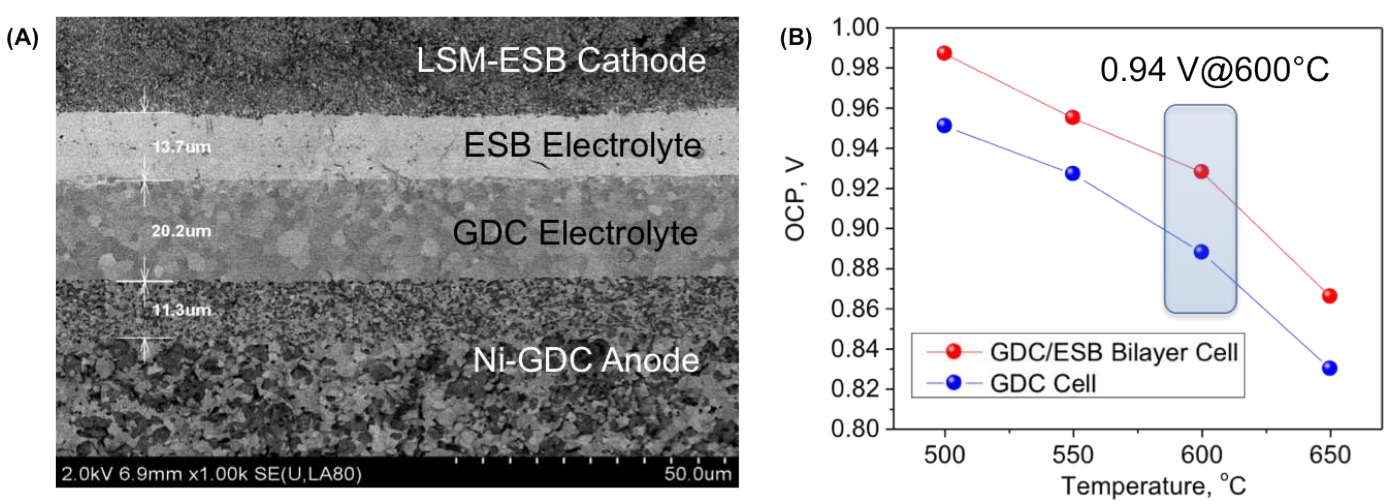

FIGURE 1. Button cell bilayer electrolyte cell results with (A) a scanning electron microscopy cross-section displaying the typical microstructure, and (B) OCP results for a bilayer electrolyte cell versus a GDC-only electrolyte cell from 500°C to 650°C

microstructure for a bilayer cell. As previously reported the GDC thickness was varied between ~12 µm and ~40 µm, while the ESB thickness was kept between 4 µm and 20 µm. The cells were tested in a standard button cell reactor using humidified hydrogen and air. Figure 1B shows the OCP at different temperatures (500–650°C) for a bilayer electrolyte cell and a GDC-only electrolyte cell. In these cases the GDC layer was ~20 µm for both cells, while the bilayer cell additionally had an ESB layer that was ~4 µm thick. There was a ~40 mV increase in OCP at each temperature, which can translate to a gain in cell efficiency for operating temperatures ≤600°C.

As the scale-up efforts on the porous anode support progressed during FY 2016, we used standard Redox production cells to scale up the bilayer electrolyte configuration to the 10 cm x 10 cm size. As shown in Figure 2, we demonstrated a 10 cm x 10 cm ESB–GDC bilayer electrolyte cell exhibiting an OCP of 0.91 V at ~600°C. This demonstration was achieved by the integration and scaling of earlier project efforts and deliverables. The cell was a standard Redox production cell with a ~20 µm GDC layer, a ~12 µm ESB layer, and a ~20 µm LSM–ESB cathode. While this was higher than the target OCP (≥0.9 V), the value was lower than what was achieved for the button cells. Our multi-physics model predicted that this was due in part to an undesirable porosity in the ESB layer for the 10 cm x 10 cm cell, which could have caused a decreased conductivity and/or reduced triple phase boundary, which, due to the mixed electronic and ionic conductivity in the GDC layer, can result in a lower OCP. Figure 3A shows the microstructure of the ESB layer for the button cell which was sintered at temperature T1. Figure 3B and 3C show the microstructure for a 10 cm x 10 cm cell sintered at T1 and T2, respectively, where T1 > T2. Due to furnace temperature gradients, the 10 cm x 10 cm cell whose results are shown in Figure 2 was actually fired at T2 even though the furnace setpoint was the same as in the button cell fabrication. When the furnace was adjusted so the actual temperature was T1, the larger size cell still was denser but still more porous than the button cell. Additional optimization of the ESB layer is needed to match the density achieved for the button cells.

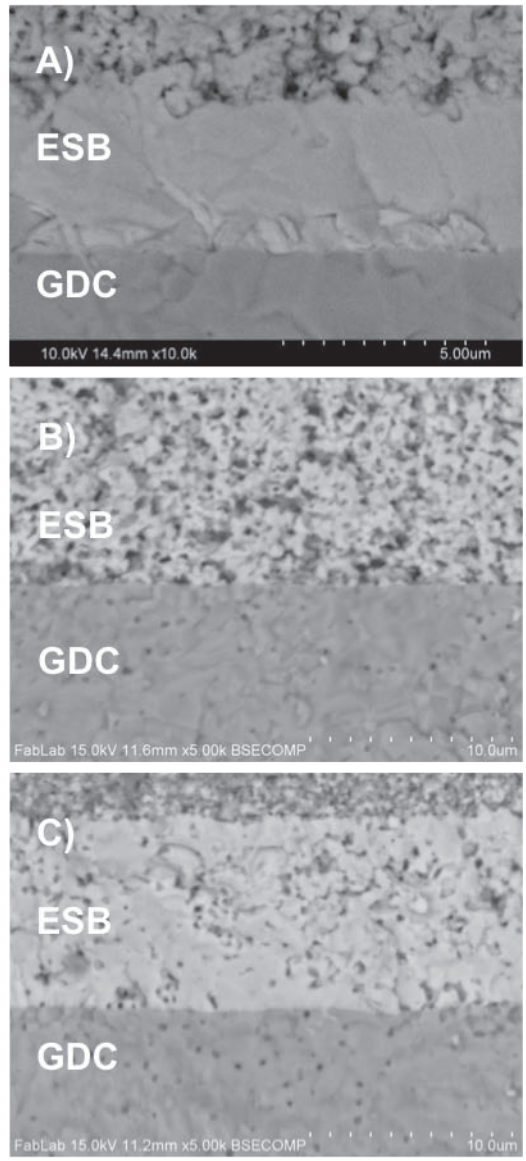

FIGURE 3. Scanning electron microscopy cross-sections comparing ESB microstructure for (A) a button cell sintered at T1, (B) a 10 cm x 10 cm cell fired at T2 < T1, and (C) a 10 cm x 10 cm cell fired at T1

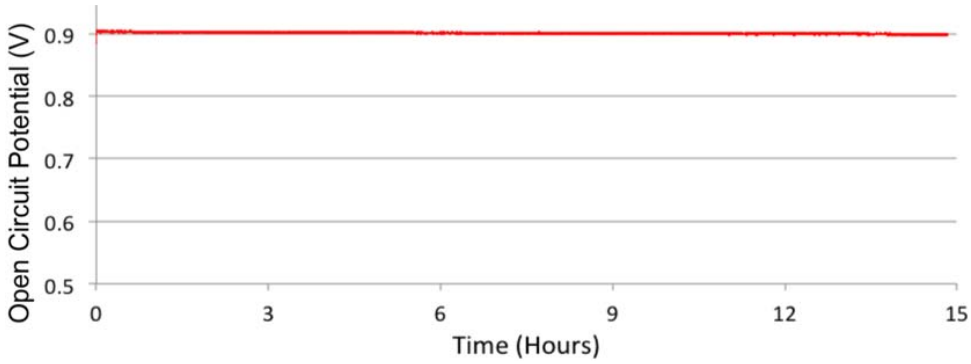

FIGURE 2. OCP for Redox 10 cm x 10 cm production cell tested at ~600°C in hydrogen

As reported previously, in FY 2015, we achieved more than 1.25 W/cm^2 at ≤600°C (cell area specific resistance <0.180 Ωcm^2) using a porous anode-supported, bilayer cell and various electrode catalyst infiltrants. Figure 4 compares results of a first attempt at a scaled up porous anode-supported 10 cm x 10 cm cell and the optimized version. The half cells utilized production tape cast layers. As seen in Figure 4A, the initial cells had a great deal of closed porosity in the anode support layer (ASL) and a dense anode functional layer (AFL). In order to gain a more interconnected pore network we used a broader particle size distribution for the pore former. We also made a porous AFL, which together with the optimized ASL resulted in a microstructure that was very similar to those of the porous anode-supported button cells used to achieve >1.25 W/cm^2 at ≤600°C.

CONCLUSIONS AND FUTURE DIRECTIONS

Conclusions from the FY 2016 work include the following:

- The bilayer electrolyte configuration was shown to have increased the OCP in excess of the target of 0.90 V using a 10 cm x 10 cm cell at ~600°C.
- The porous anode-supported cell has been successfully scaled up to the 10 cm x 10 cm size, and has similar microstructure as the button cells that displayed >1.25 W/cm^2.

Future work will include the following:

- Optimization of the ESB microstructure to further boost OCP for a 10 cm x 10 cm cell.
- Implementation and demonstration of a 10 cm x 10 cm, porous anode-supported bilayer cell with a power density ≥1 W/cm^2 at ≤600°C.
- Demonstration of a 10 cm x 10 cm bilayer cell stack in CHP conditions with natural gas.

FY 2016 PUBLICATIONS/PRESENTATIONS

1. Bryan Blackburn, "Affordable, High Performance, Intermediate Temperature Solid Oxide Fuel Cells," 2016 U.S. Department of Energy Hydrogen and Fuel Cells Program Annual Merit Review and Peer Evaluation Meeting, Washington, D.C., June 9, 2016.

REFERENCES

1. Eric D. Wachsman and Kang Taek Lee, *Science*, **334**, 935-939 (2011).

2. Zhangbo Liu, Beibei Liu, Dong Ding, Mingfei Liu, Fanglin Chen, and Changrong Xia, "Fabrication and Modification of Solid Oxide Fuel Cell Anodes Via Wet Impregnation/ Infiltration Technique," *Journal of Power Sources*, 237, 243-259 (2013).

3. Lei Wang, Greg S. Jackson, and Bryan M. Blackburn, *ECS Transactions*, 57(1), 2583 (2013).

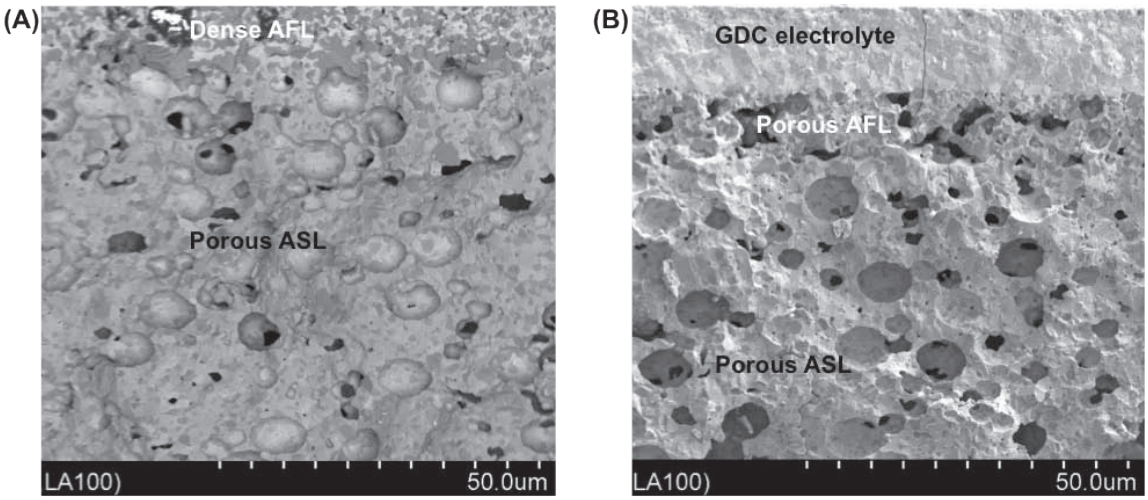

FIGURE 4. Scanning electron microscopy cross-sections comparing microstructure of a production manufactured, porous anode-supported cells using (A) original and (B) optimized scaled-up tape materials

V.D.5 Facilitated Direct Liquid Fuel Cells with High Temperature Membrane Electrode Assemblies

Emory S. De Castro
Advent Technologies, Inc.
One Mifflin Place, Suite 400
Cambridge, MA 02138
Phone: (857) 264-7035
Email: EmoryDeCastro@Advent-Energy.com

DOE Manager: Gregory Kleen
Phone: (240) 562-1672
Email: Gregory.Kleen@ee.doe.gov

Contract Number: DE-EE0006959

Subcontractors:
Piotr Zelenay (PI), Hoon T. Chung, Gerie Purdy, Xi Yin,
Los Alamos National Laboratory (LANL), Los Alamos, NM

Project Start Date: October 1, 2015
Project End Date: September 30, 2017

Overall Objectives

- Demonstrate direct dimethyl ether (DME) oxidation at high temperature membrane electrode assembly (MEA) significantly better than direct methanol fuel cells (DMFC).
- Leverage a highly active ternary catalyst for high temperature DME fuel cells.

Fiscal Year (FY) 2016 Objectives

- Establish equivalent test results between Advent Technologies Inc. and LANL.
- Construct test apparatus that controls DME/water ratio in a fuel stream.
- Evaluate benchmark binary PtRu/C catalysts for high temperature DME fuel cells.

Technical Barriers

This project addresses the following technical barriers from the Fuel Cell section of the Fuel Cell Technologies Program Multi-Year Research, Development and Demonstration Plan [1], using DMFC systems as a reference fuel cell system.

(A) Durability (catalyst, membrane)

(B) Cost (catalyst, system)

(C) Performance (catalyst, electrodes, MEAs)

Technical Targets

This program falls under DOE's incubator initiative, which explores high impact research in new areas. Thus, the technical targets for this program were created relative to the state-of-the-art DMFC system, the only other viable direct fuel oxidation system at this time (see Table 1).

FY 2016 Accomplishments

- Confirmed equivalent performance using standard commercial materials at the two different test sites: successful down-scaling of test setup from 50 cm^2 to 5 cm^2.
- Successful design and construction of a test apparatus that allows precise control of DME to water ratios, critical for optimizing reaction conditions.
- Early results with a binary benchmark catalyst demonstrates nearly 50% decrease in platinum group metal (PGM), leading to nearly double the specific power (W/g_{PGM}) when comparing the same catalyst at low temperature to high temperature operation (80°C vs. 180°C).

✧ ✧ ✧ ✧ ✧

TABLE 1. Progress towards Meeting Technical Targets for Direct DME Oxidation

Key Performance Indicator	Current DMFC	Target	Program Status (after six months)
Maximum power (>)	0.180 W/cm^2	0.270 W/cm^2	0.062 W/cm^2
Total precious metal loading	5 mg_{PGM}/cm^2	3 mg_{PGM}/cm^2	2.7 mg_{PGM}/cm^2
Degradation rate	19 μV/h at a 0.2 A/cm^2	10 μV/h at a 0.2 A/cm^2	Not applicable this phase
Loss in start/stop cycling	1.5 mV/cycle; cycle	0.75 mV/cycle; cycle	Not applicable this phase
Anode mass-specific activity	50 A/g at 0.5 V	75 A/g at 0.5 V	25 A/g at 0.5 V

INTRODUCTION

In searching for an exemplary carbon-neutral fuel, DME may be one of the most appealing. This simplest of the ethers can be readily produced from renewably sourced hydrogen and CO_2, making it essentially a hydrogen carrier. Both nontoxic and easy to liquefy under moderate pressure, DME closely matches diesel and has been run in trucks. Recently, LANL demonstrated the potential for direct oxidation of DME in a fuel cell [2]. Thus, one fuel could bridge both internal combustion and fuel cell technologies, while remaining carbon neutral with low or no ancillary emissions.

LANL has identified a highly active catalyst for direct oxidation of DME that already in the early phase of development allows for matching performance of the DMFC when using typical low-temperature perflurosulfonic acid membranes. However, the output is not sufficient to approach commercial acceptance targets for higher power applications or precious metal cost. More importantly, the LANL work has noted an acute sensitivity of the DME oxidation rate to temperature increase. High-temperature MEAs, based on phosphoric-acid-imbibed membranes, operate at 160°C to 180°C without additional water and are highly tolerant to carbon monoxide – an intermediate of DME oxidation. This work is to exploit a novel ternary LANL anode catalyst with the features of high-temperature operation to produce high-power, low-cost direct DME MEAs. We envision the use of such systems as auxiliary electrical power for transport applications.

APPROACH

The project consists of three phases. In the first phase, we will demonstrate direct oxidation of DME at a small-scale (5 cm^2) MEA without the advanced catalyst. The second phase will focus on the development of a small-scale gas diffusion electrode matched for the advanced LANL catalyst; however, we will first use a binary catalyst that has good activity for DME oxidation. In the last phase, we will scale up MEA to a 50 cm^2 size and optimize the gas diffusion electrode structure for the use in practical devices. We initially employ two kinds of high temperature membranes. One is polybenzimidazole (PBI) and is characterized as a high-acid, low-solids material. The other is referred to by a generic Advent trademark TPS®, and, relative to PBI, is low-acid, high-solids material based on pyridine and polysulfone. Throughout the three experimental phases, key performance indicators, such as power output, amount of precious metal employed, and durability, will be compared to the state of the art and incorporated as project milestones.

RESULTS

- *Verified baseline testing at Advent and LANL.* Due to the novelty of this system and the nuances of operating MEAs at temperatures higher than 160°C, the first task in this program is to verify that test systems perform as expected. Since the purpose of this program is to demonstrate proof of concept, we need to keep the test scale small but relevant, thus, 5 cm^2 MEAs were tested in H_2-air fuel cells. The results verified that both TPS and PBI 5 cm^2 MEAs tested at LANL showed performance within the variation of commercial materials (45 cm^2), tested at Advent.
- *Achieved precise control of the DME-to-H_2O molar ratio in fuel stream.* For every mole of DME oxidized, three moles of water are needed to support the reaction. This stoichiometry is critical, and early attempts to control water content in the DME vapor via flowing the fuel through humidification bottles was not precise enough to obtain relevant data. During this project, by designing a steam generator/mixer in together with a precision water pump, we were able to control the molar ratio of DME to H_2O and study the impact of this ratio on power from the test cell. Figure 1 shows the polarization curve of PtRu/C PBI MEA at 180°C at different DME-to-H_2O molar ratios, with the best performance achieved with the DME-to-H_2O ratio of 1:3.
- *Demonstrated higher direct DME fuel cell performance with increased operation temperature.* PBI and TPS MEAs with both Pt/C and PtRu/C anode catalysts were tested at various temperatures. Direct DME fuel cell performance was improved with the increase in cell temperature. A monotonic increase of the DME oxidation current in PtRu/C PBI MEA was observed with the increase of temperature from 150°C to 180°C

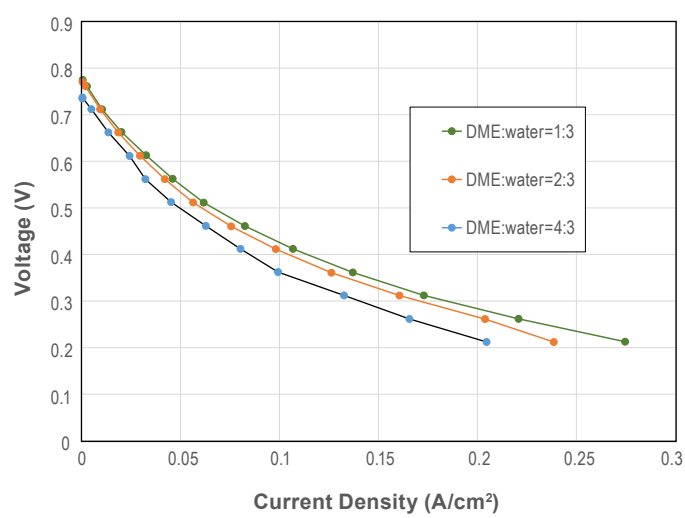

FIGURE 1. DME fuel cell performance of PBI-based MEA with different DME-to-H_2O molar ratios. Cell temperature 180°C. Anode: PtRu/C, HiSPEC® 12100 PtRu/C, 4.5 mg/cm^2; DME 500 sccm, backpressure 3.5 psig. Cathode: Pt-alloy/C 1.0 mg/cm^2; air 500 sccm, backpressure 3.5 psig.

(Figure 2). At 0.5 V, the current density increased from 0.024 A/cm^2 to 0.053 A/cm^2 when temperature increased from 150°C to 180°C.

- Lowered PGM content. A more relevant comparison than polarization curves is calculating the power of current normalized to the amount of PGMs employed in the assembly (Figure 3). The reference data of Nafion® membrane PtRu/C catalyst at lower temperature (80°C) is still better than the PBI membrane Pt/C catalyst at high temperature (180°C). However, the PBI membrane PtRu/C catalyst at high temperature (180°C) exhibits higher specific current than the reference Nafion® membrane PtRu/C catalyst at lower temperature (80°C). While our final target is to show mass-specific current density higher than 50 A/g_{PGM} at 0.5 V, the state-of-the-art DMFC specific current, even in this early stage we are at 25 A/g_{PGM} at 0.5 V. A specific power comparison is listed in Table 2, where the maximum power is measured at 0.2 V and normalized to PGM loading. The highest specific power is obtained with the PBI membrane PtRu/C catalyst at 180°C.

TABLE 2. Specific Power at 0.2 V for Direct DME Oxidation

MEA	Specific power W/gPGM
Nafion® PtRu (80°C)	14
PBI Pt (180°C)	13
PBI PtRu (180°C)	23

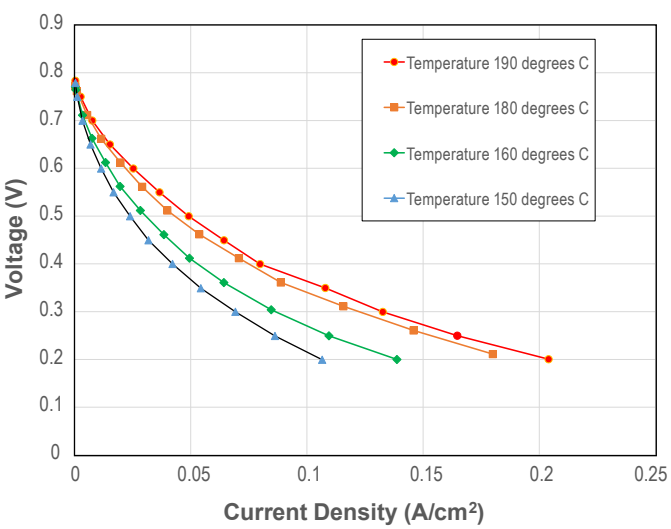

FIGURE 2. DME fuel cell performance of PBI-based MEA at various temperatures. Anode: PtRu/C, HiSPEC® 12100 PtRu/C, 4.5 mg/cm^2; DME 500 sccm, DME-to-H_2O molar ratio 1:3, backpressure 3.5 psig. Cathode: Pt-alloy/C 1.0 mg/cm^2; air 500 sccm, backpressure 3.5 psig.

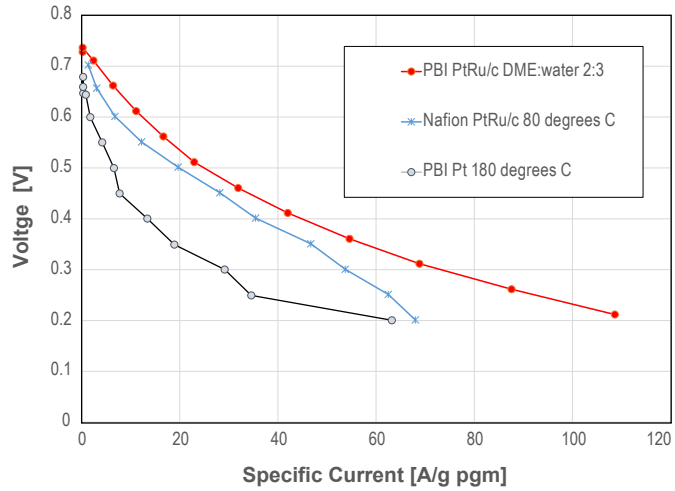

FIGURE 3. Specific current density (A/g_{PGM}) for Nafion® membrane HiSPEC® 12100 PtRu/C 4.0 mg_{metal}/cm^2 anode at 80°C (DME 40 sccm, backpressure 26 psig), PBI membrane Pt/C 1.0 mg/cm^2 anode at 180°C (DME 500 sccm, backpressure 30 psig), and PBI membrane HiSPEC® 12100 PtRu/C 1.9 mg/cm^2 anode at 180°C (DME 500 sccm, backpressure 20 psig).

CONCLUSIONS AND FUTURE DIRECTIONS

Although early in the program, these results support our basic concept that DME can be directly oxidized through the use of tuned catalysts and operation at higher temperatures. It is important to note that the data of the Figures 1 and 2 are derived from MEA assembly conditions optimized for fuels such as reformate (a mix of hydrogen, carbon monoxide, and carbon dioxide). There is no reason to suspect these conditions are best for direct DME oxidation, and the bulk of our efforts in this next period is to understand and fabricate MEAs that facilitate this reaction. Variables that we will investigate include phosphoric acid loading in the catalyst layer, hydrophobicity and porosity gradients, and compression during lamination of the MEA. We anticipate demonstrating direct DME oxidation key performance indicators that exceed that for the state of the art DMFC.

FY 2016 PUBLICATIONS/PRESENTATIONS

1. De Castro, E.S., Zelenay, P. and Gregoriou, V., "A Disruptive Fuel in the System: Electricity from a Carbon-Neutral Fuel," A paper presented at the Fuel Cell Seminar and Energy Exposition, Los Angeles, CA, USA, November 16–19, 2015; Abstract 104.

REFERENCES

1. Multi-Year Research, Development and Demonstration Plan: Section 3.4 Fuel Cells, Fuel Cell Technologies Office, 2016, http://energy.gov/sites/prod/files/2016/06/f32/fcto_myrdd_fuel_cells_0.pdf.

2. Li, Q., Wen, X., Wu, G., Chung, H.T., and Zelenay, P., "High-Activity PtRuPd/C Catalyst for Direct Dimethyl Ether Fuel Cell," *Angew. Chem. Int. Ed., 54, 1–6, 2015.*

V.D.6 Advanced Catalysts and Membrane Electrode Assemblies (MEAs) for Reversible Alkaline Membrane Fuel Cells

Hui Xu (Primary Contact), Shuai Zhao, Brian Rasimick
Giner, Inc.
89 Rumford Ave.
Newton, MA 02466
Phone: (781) 529-0573
Email: hxu@ginerinc.com

DOE Manager: David Peterson
Phone: (720) 356-1747
Email: David.Peterson@ee.doe.gov

Contract Number: DE-EE0006960

Subcontractors:
- Gang Wu, University at Buffalo-SUNY, Buffalo, NY
- Bryan Pivovar, National Renewable Energy Laboratory, Golden, CO

Project Start Date: June 1, 2015
Project End Date: May 31, 2017

Overall Objectives

- Develop highly efficient bifunctional platinum group metal free electrocatalysts and optimize them to meet the rotating disk electrode (RDE) activity targets for the oxygen reduction reaction (ORR) and oxygen evolution reaction (OER).
- Supply perfluorinated anion exchange membranes (AEM) and ionomers with an aim to improve the performance of alkaline membrane fuel cell (AMFC) relative to commercial membranes (Tokuyama).
- Fabricate regenerative fuel cell membrane electrode assemblies (MEAs) using as developed bifunctional catalysts and perfluorinated AEMs (after their optimization).
- Test the fabricated MEAs in a regenerative fuel cell system under both fuel cell and electrolyzer modes to demonstrate its performance and to meet the reversible fuel cell targets.

Fiscal Year (FY) 2016 Objectives

- Develop highly efficient bifunctional electrocatalysts related to platinum group metal free perovskite, spinel oxides, and heteroatom doped carbon nanotubes.
- Optimize these bifunctional catalysts to meet the RDE activity targets for ORR–OER as set by DOE.
- Develop perfluorinated AEM and ionomers with an aim to improve the performance of AMFCs relative to commercial membranes (Tokuyama).

Technical Barriers

This project addresses the following technical barriers from the Fuel Cells section of the Fuel Cell Technologies Office Multi-Year Research, Development, and Demonstration Plan [1].

(A) Durability (catalysts, electrode layers)

(B) Cost (catalyst, MEAs)

(C) Performance (catalysts, electrodes, MEAs)

Technical Targets

This project will develop novel bifunctional ORR and OER catalysts and MEAs for reversible alkaline fuel cells. The new materials will achieve the following targets at the end of the project for viable applications.

- In RDE, demonstrate ORR activity >1 mA/mg at 0.9 V (internal resistance [IR]-free); and OER activity >15 mA/mg at 1.6 V (IR-free).
- Achieve reversible current density of 600 mA/cm^2 at 0.55 V for fuel cell mode operation and 1.6 V for electrolyzer mode operation.
- Achieve fuel cell and electrolyzer life of 500 hr with less than 10% performance decay.

FY 2016 Accomplishments

- Identified that multi-walled carbon nanotubes (CNTs) are much more stable during potential cycling (0.0–1.9 V), when compared to amorphous carbon black and graphene (reduced graphene oxide).
- Synthesized spinel oxide (e.g., Co_3O_4) supported on N-doped advanced carbon materials via three routes. The activity of Co_3O_4 supported on carbon nanotubes (Co_3O_4/CNTs) met the first year no/no-go milestone of ORR activity >1 mA/mg oxide at 0.9 V (IR-free); and OER activity >15 mA/mg oxide at 1.6 V (IR-free) in RDE testing.
- Discovered that the activity and stability of the spinel on CNT catalysts are largely impacted by the size, oxidation state, and functional groups attached to the CNTs.

- Developed a low cost and scalable synthesis approach to preparing novel graphene tubes. Integrating $CoNiO_x$ with active graphene tubes led to enhanced ORR and OER activity exceeding Pt and Ir, respectively. OER and ORR activity determined by RDE has met the first year's go/no-go milestone.
- Synthesized core-shell Pt-Ni nanowires as bi-functional hydrogen oxidation reaction (HOR) and hydrogen evolution reaction (HER) catalysts. The high catalytic activity was achieved by lowering the Pt content to 10 wt% and via hydrogen annealing at >250°C.

INTRODUCTION

The primary goal of this project is to design advanced bifunctional platinum group metal free catalyst MEAs for a reversible electrochemical energy storage and conversion device. The single device can either operate in one direction as an electrolyzer to generate H_2 and O_2 from water, or operate in reverse by utilizing H_2 and O_2 as an AMFC to produce electricity. The performance of the innovative reversible AMFC technology greatly relies on a bifunctional oxygen electrode capable of high activity for the ORR and OER. Our overall approach is to prepare transition metal-based oxide nanocomposites and heteroatom doped graphene tube catalysts with optimal chemical formulation, surface defects, and morphology in order to maximize the ORR–OER activity and stability. The best performing catalyst will then be integrated with selected anion-exchange ionomers and membranes. The constructed MEAs will be operated as reversible AMFCs for stationary energy storage. In the first year, we will primarily focus on the synthesis of novel nanocomposite catalysts capable of catalyzing both the ORR and OER in alkaline media.

The development of highly efficient bifunctional cathode catalysts derived from earth-abundant elements faces two grand challenges. The first is that the optimal active sites for the ORR differ from those for the OER. The second is stability during the high potential/voltage (>1.6 V) of the OER. As a result, most of the studied traditional carbon catalysts likely suffer from significant performance loss during ORR–OER dual-operation modes. This incubator project addresses these catalyst challenges by developing non-platinum group metal catalysts coupled with novel AEMs and ionomers. Therefore, special emphasis is given to exploring highly stable oxides and graphitized nanocarbons under appropriate accelerated stress tests.

APPROACH

Our overall approach is to prepare transition metal-based oxide nanocomposites and heteroatom doped graphene tube catalysts with optimal chemical formulation, surface defects, and morphology in order to maximize the ORR–OER activity and stability. One of the grand challenges in developing bifunctional ORR–OER catalysts is likely due to different active sites for corresponding ORR and OER. By tuning the electronic structures of oxide catalysts, an enhancement of ORR activity is often accompanied with a reduction of OER activity. We explored robust nanocarbon components that maintain stability over the wide potential range spanning from 0–1.9 V vs. reference hydrogen electrode (RHE). Such a material could be the ORR component and integrated with OER active oxide catalysts to form a bifunctional nanocomposite.

As shown in Figure 1a, our overall approach is to integrate active transition metal-based oxides with highly active and stable graphitized nanocarbons to maximize the

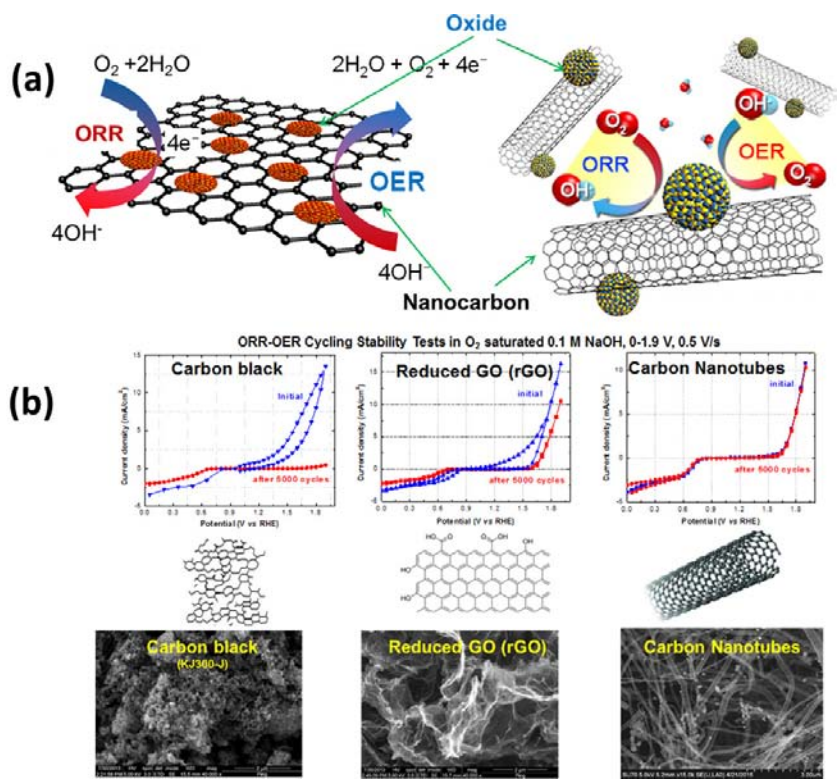

FIGURE 1. (a) Proposed schemes of ORR–OER bifunctional cathode catalysts consisting of active oxide nanocrystals onto highly stable graphene (left) and carbon tubes (right). (b) Identification of nanocarbons in terms of their potential cycling stabilities in 0.1 M NaOH electrolyte (0–1.9 V vs. RHE, 500 mV/s at room temperature).

ORR–OER activity and stability in alkaline media. The best performing catalyst will be integrated with selected anion-exchange ionomers and membranes to construct a MEA that helps to revive reversible AMFCs in stationary energy storage. As shown in Figure 1b, we identified that multi-walled CNTs are much more stable during potential cycling (0–1.9 V), thanamorphous carbon black and graphene (reduced graphene oxide). This interesting finding suggests the stability of carbon materials is greatly dependent on their nanostructure and morphology. The remarkable stability enhancement is likely due to the closed-tube morphology.

RESULTS

Commercially available nitrogen-doped carbon nanotubes (N-CNT) were integrated with metal oxides to design bifunctional catalysts at Giner due to the good stability of the N-CNTs. The cobalt oxide (Co_3O_4) was supported on oxidized CNTs (oCNTs), forming a Co_3O_4/oCNT hybrid structure as shown Figure 2a. X-ray diffraction patterns for Co_3O_4/oCNT before and after NH_3 treatment are shown in Figure 2b. The five major characteristic peaks of the well-defined face-centered cubic Co_3O_4 (red pattern) corresponded to the (220), (311), (400), (511) and (440) reflections (JCPDS 43-1003, red triangles), respectively. Two peaks appeared at 26.2° and 43.2° corresponding to the (002) and (100) planes of the multi-walled CNTs, respectively. After NH_3 treatment (blue pattern), the Co_3O_4 character decreased, indicated by the disappearance of the (511) and (440) peaks. Among all of the studied samples, the best performing NH_3-treated cobalt oxide Co_3O_4/oCNT was compared with Pt/C (50 wt%) and Ir in terms of their ORR and OER activities, respectively. (Figure 2c and 2d). Both the ORR onset and half-wave potentials of Co_3O_4/oCNT were about 0.1 V less than those of the commercial Pt/C. The OER onset potential for Co_3O_4/oCNT was only 0.05 V higher than that of Ir black. Both the ORR and OER activity of Co_3O_4/oCNT were much enhanced relative to oxide-free N-CNT as shown in Figure 2e, and they both approach or exceed the first year's go/no-go milestone. Moreover, the durability test of NH_3 treated Co_3O_4/oCNT was conducted in O_2-saturated 0.1 M KOH electrolyte for 2,000 cycles (0–1.9 V) at a scan rate of 500 mV/s. Intermediate polarization curves were collected at 1,600 rpm, 20 mV/s (Figure 2f), demonstrating insignificant changes for both ORR and OER activities even after 2,000 cycles in this harsh oxidizing environment.

In the project, University at Buffalo-SUNY has developed an approach to prepare a new type of large sized and few-layered nitrogen-doped graphene nanotube (N-GT). The synthesis (Figure 3a) is low-cost and easily scalable via a simple one step thermal treatment using inexpensive carbon and nitrogen precursors (i.e., dicyanadiamide, ~$2/kg). During the catalyst development, we discovered the type of transition metal used is able to tune the chemical and physical properties of the resulting graphene tubes. This allows us to engineer the doping, tube morphology and structure to yield maximum performance for bifunctional applications. The best performing N-GT(FeCoNi) achieved an outstanding

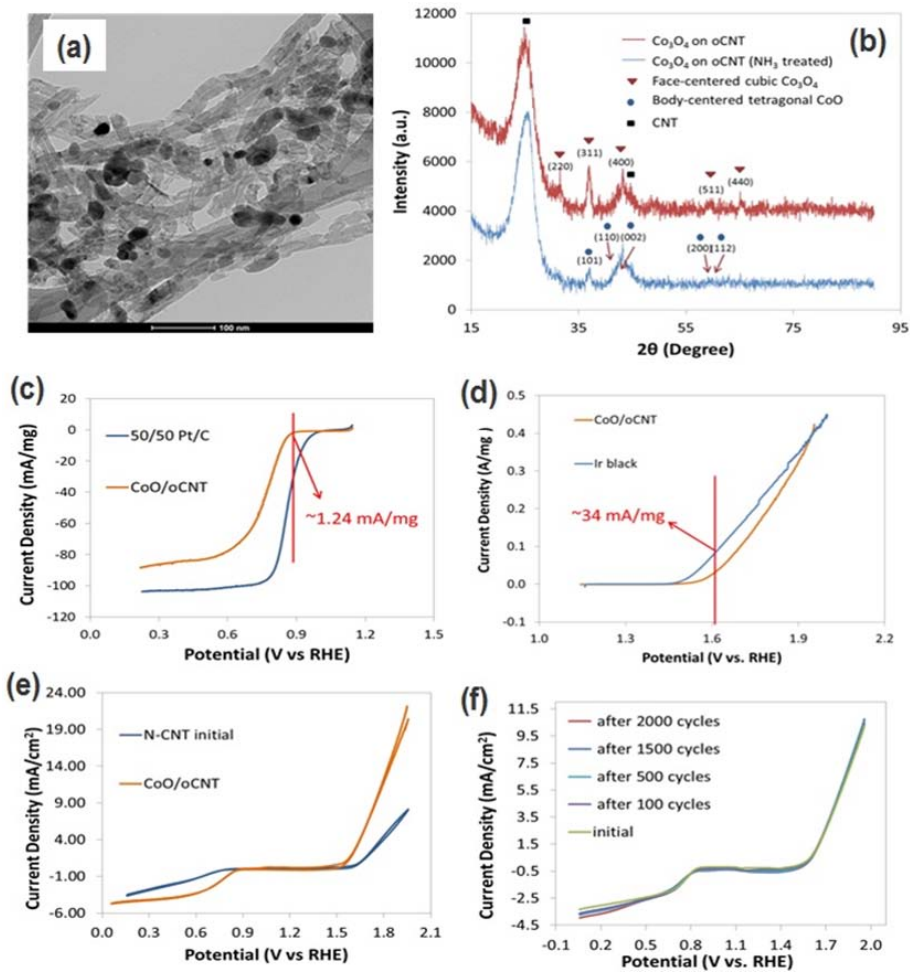

FIGURE 2. (a) Transmission electron microscopy image of the best performing Co_3O_4/oCNT after NH_3 treatment with Co $(C_2H_3O_2)$•$4H_2O$ to oCNT weight ratio of 5:3. (b) X-ray diffraction patterns of Co_3O_4/oCNT (red) and NH_3 treated Co_3O_4/oCNT (blue). (c) ORR and (d) OER activity of NH_3 treated Co_3O_4/oCNT compared to Pt/C and Ir black, respectively. (e) OER–ORR activity comparsion between the NH_3 treated Co_3O_4/oCNT sample and as received N-CNT. (f) durability test of NH_3 treated Co_3O_4/oCNT for 2,000 cycles.

current density of 29.6 mA/cm^2 (28 mA/mg catalyst) at 1.6 V during the OER (Figure 3b). This result is around four times higher than that obtained for commercial Ir catalyst and has exceeded the first year go/no-go decision milestone (15 mA/mg catalyst). With respect to the ORR, the onset potential for the N-GT(FeCoNi) catalyst is 1.05 V vs. RHE, which is similar to that of Pt (1.10 vs. RHE), suggesting the nature of active sites on the N-GT catalysts is intrinsically active for the ORR in alkaline media. Half wave potential, which corresponds to the total number of active sites, is as high as 0.89 V vs. RHE at a catalyst loading of 0.60 mg/cm^2. This value is only 10 mV lower than that of Pt/C catalyst at a loading 60 μg_{Pt}/cm^2. In addition, its diffusion limiting current density was greater than that for platinum, suggesting higher mass transport of O_2 through its pores as a result of its exceptionally high electrochemically active surface area. Importantly, the current density generated at 0.9 V is 1.31 mA/mg catalyst and successfully met the first year go/no-go decision point (Figure 3c).

Apart from excellent bifunctional performance of N-GT(FeCoNi), extensive electrochemical durability tests were also performed to evaluate durability of the catalysts in 0.1 M NaOH in a potential window covering both

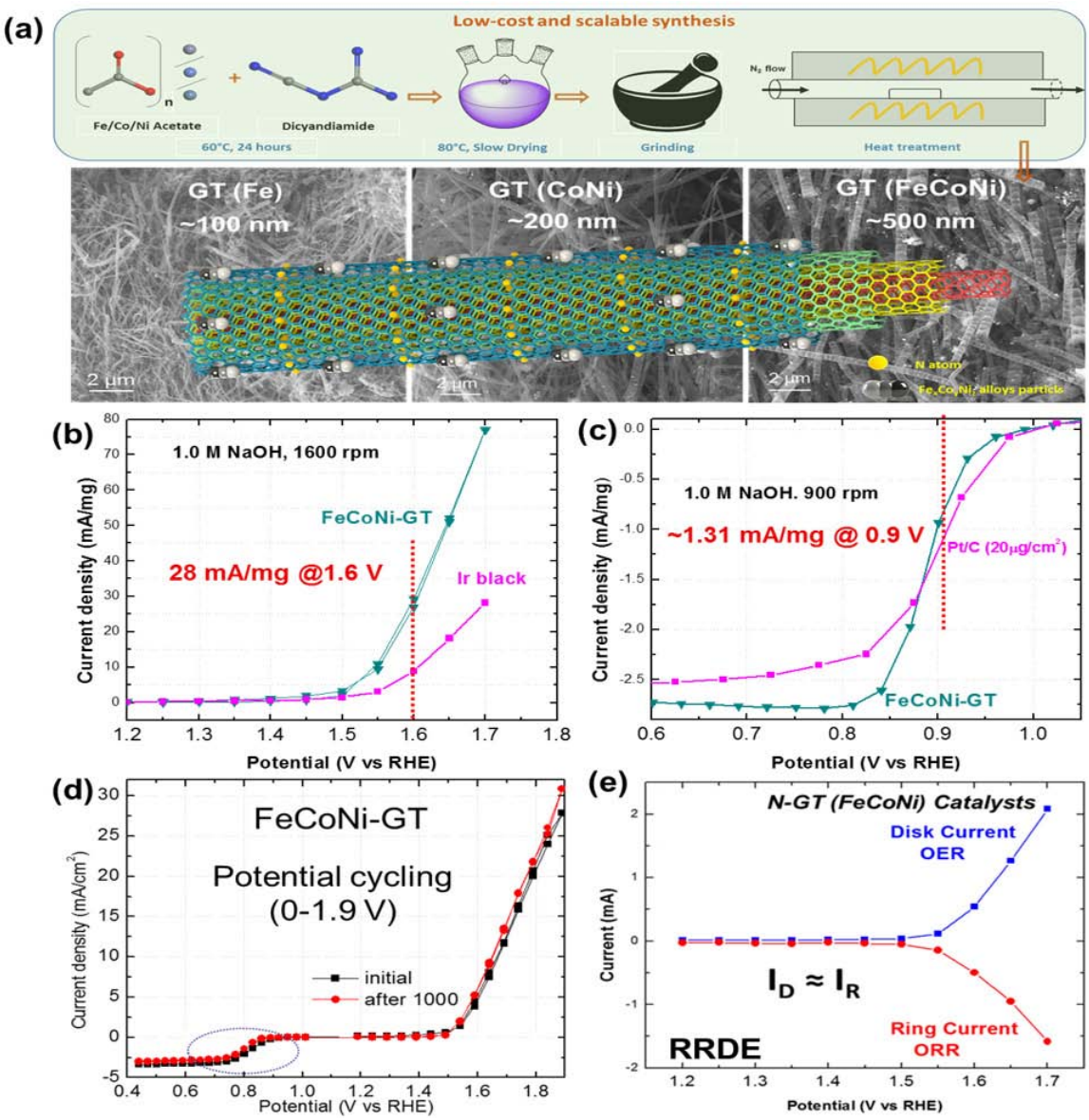

RRDE – Rotating ring disk electrode

FIGURE 3. Graphene tube catalysts: (a) low-cost and scalable synthesis; (b) OER activity; (c) ORR activity; (d) potential cycling stability; and (e) rotating ring disk electrode tests to verify O_2 evolution rather than carbon oxidation during the OER.

ORR and OER reactions (0.0–1.9 V). After 1,000 cycles, N-GT(FeCoNi) exhibited exceptional durability during the harsh potential cycling tests, showing only 17 mV decay in ORR half-wave potential, along with 30.7% enhancement in the current density measured at 1.6 V during the OER (Figure 3d). Combined with the rotating ring disk electrode test in Figure 3e, these results provide strong evidence that the active sites for ORR and OER on N-GT(FeCoNi) are highly stable. Generation of a mixed metal catalyst, i.e., FeCoNi during the graphitization process is the key factor to yield improved activity and durability.

National Renewable Energy Laboratory has worked on the development of platinum (Pt) catalysts in the HOR and HER for reversible AMFCs. Although this work involves the use of precious metal catalysts, the work seeks to reduce the amount of Pt in the catalyst layer to reduce cost and to improve upon slower HOR–HER kinetics in the AEM environment. Pt/Ni nanowires (Figures 4a and 4b) were formed by the spontaneous galvanic displacement of Ni nanowires with Pt. Lower levels of displacement appeared to thin the Pt layer and improve Pt utilization, leading to higher catalytic activity (Figure 4c). Post-synthesis annealing of the nanowires in hydrogen served to integrate the previously segregated Pt and Ni zones, compressing the Pt lattice and improving the site-specific exchange current densities (Figure 4d). Annealed Pt-Ni nanowires exceeded the HOR–HER mass exchange current density of Pt/HSC by 10 times in a 0.1 M potassium hydroxide electrolyte.

CONCLUSIONS

- Integration of active transition metal-based oxides with highly active and stable graphitized nanocarbons leads to bifunctional ORR–OER catalysts in alkaline media.
- NH_3 treated Co_3O_4 spinel type catalysts on CNTs demonstrated superior ORR– OER activity; activity and stability of the spinel on CNTs catalysts are largely impacted by the size, oxidation state, and functional groups attached to the CNTs.
- FeCoNi-derived N-GT catalysts also demonstrated high ORR activity (28 mA/mg catalyst @ at 1.6 V IR-free), and OER activity (1.31 mA/mg catalyst ORR activity at 0.9V IR-free) in the same catalyst, comparable to the baseline catalyst Pt and Ir, respectively.

FUTURE DIRECTIONS

- Explore MEA fabrication for bifunctional catalysts and optimize test conditions for both fuel cell and electrolyzer mode.

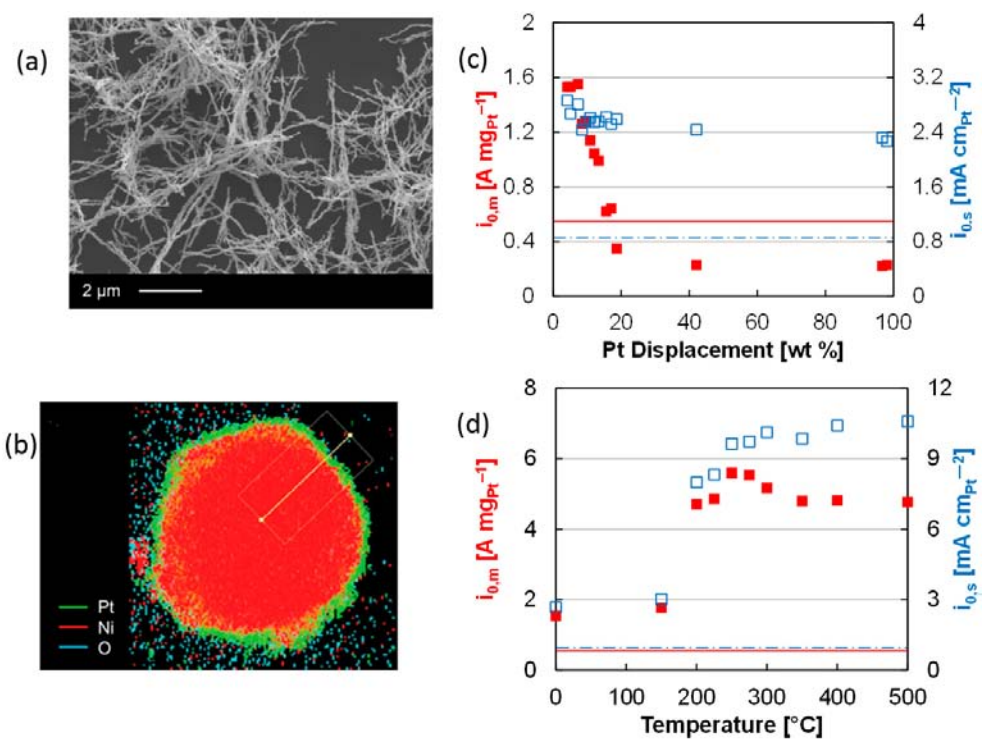

FIGURE 4. (a) Synthesized core-shell Pt-Ni nanowires as bi-functional HOR–HER catalysts and (b) morphology and structure of the Pt-Ni nanowire catalyst. (c) Effect of Pt loading on the catalyst activity. (d) Effect of H_2 annealing temperature on the catalyst activity.

- Modify fuel cell configuration and test station to operate fuel cell (discharge) and electrolyzer (charge) intermittently.

SPECIAL RECOGNITIONS & AWARDS/ PATENTS ISSUED

1. Prof. Gang Wu was appointed as an Associate Editor for *RSC Advances*, published by Royal Society of Chemistry in the United Kingdom, and was selected as one of the Editorial Board Members for *ChemistrySelect* (Wiley-VCH, Germany) and *Scientific Reports* (Nature Publishing Group).

FY 2016 PUBLICATIONS/PRESENTATIONS

Peer-Reviewed Publications

1. Gupta, S.; Kellogg, W.; Xu, H.; Liu, X.; Cho, J.; Wu, G.; "Bifunctional perovskite oxide catalysts for oxygen reduction and evolution in alkaline media," *Chemistry–An Asian Journal,* **11**(1), 10–21, 2016.

2. Wu, G.; Santandreu, A.; Kellogg, W.; Gupta, S.; Ogok, O.; Zhang, H.; Wang, H.-L.; Dai, L., "Carbon nanocomposite catalysts for oxygen reduction and evolution reactions: from nitrogen doping to transition-metal addition," *Nano Energy,* doi:10.1016/j.nanoen.2015.12.032, 2016.

3. Osgood, H.; Devaguptapu, S.V.; Xu, H.; Wu, G., "Transition metal (Fe, Co, Ni, and Mn) oxides for oxygen reduction and evolution bifunctional catalysts in alkaline media," *Nano Today*, *minor revision*, 2016.

4. Gupta, S.; Qiao, L.; Zhao, S.; Devaguptapu, S.V.; Xu, H.; Swihart, M.T.; Wu, G., "Highly active and stable graphene tubes decorated with FeCoNi alloy nanoparticles via a template-free graphitization for bifunctional oxygen reduction and evolution," *Advanced Energy Materials*, accepted, 2016.

Presentations at International Conferences

1. Zhao, S.; Rasimick, B.; Mustain, W.E.; Xu, H., Metal oxides supported on carbon nanotubes as bifunctional eectrocatalysts for reversible alkaline membrane fuel cells, 229th ECS meeting, San Diego, CA, May 29, 2016.

2. Wu, G., Bifuncational nanocomposite catalysts for reversible electrochemical energy applications, 229th ECS meeting, San Diego, CA, May 29, 2016.

3. Gupta, S.; Wang, X.; Wu, G., Large-size and few walled graphene tube catalyst for electrochemical energy storage and conversion, 2016 International Carbon Conference, State College, PA, July 10–15, 2016.

REFERENCES

1. *Multi-Year Research, Development, and Demonstration Plan: Section 3.4 Fuel Cells*, Fuel Cell Technologies Office, 2011. http://www1.eere.energy.gov/hydrogenandfuelcells/mypp/pdfs/fuel_cells.pdf

V.E.1 Regenerative Fuel Cell System

Paul Matter (Primary Contact), Minette Ocampo, Michael Beachy, and Chris Holt
pH Matter, LLC
1275 Kinnear Rd.
Columbus, OH 43212
Phone: (614) 484-5038
Email: info@phmatter.com

DOE Manager: Donna Ho
Phone: (202) 586-8000
Email: Donna.Ho@ee.doe.gov

Contract Number: DE-SC0013111

Subcontractors:
- Giner, Inc., Newton, MA
- National Renewable Energy Laboratory (NREL), Golden, CO

Project Start Date: April 12, 2016
Project End Date: April 11, 2018

Overall Objectives

- Demonstrate a reversible 25 cm^2 anion exchange membrane fuel cell (AEMFC) for 1,000 cycles (42% round-trip efficiency; >250 mA/cm^2 power generation; >50 mA/cm^2 energy storage).
- Incorporate membrane electrode assemblies (MEAs) into a regenerative stack.
- Perform economic analysis on reversible AEMFC system following established DOE guidelines for candidate grid load leveling technologies.

Fiscal Year (FY) 2016 Objectives

- Prepare and characterize a matrix of precious group metal (PGM) free catalysts and incorporate them into MEAs for use in reversible AEMFC systems.
- Demonstrate a bi-functional gas diffusion electrode (GDE) that is consistent with DOE AEMFC performance targets with <10% degradation over hundreds of cycles.
- Perform economic analysis on a reversible AEMFC system following established DOE guidelines for candidate grid load leveling technologies.

Technical Barriers

This project addresses the following technical barriers from the Fuel Cell section of the Fuel Cell Technologies Office Multi-Year Research, Development, and Demonstration Plan, with respect to AEMFCs for energy storage:

(A) Durability: increase the durability/stability of catalysts

(B) Cost: development of low-cost PGM-free catalysts for reversible anion-exchange membrane fuel cells

(C) Performance: integrate catalysts with membranes and gas diffusion layers into MEAs that operate at high power and efficiency

Technical Targets

This Phase II Small Business Innovation Research project is developing new catalyst materials and MEAs for a regenerative AEMFC stack. The materials being developed address the following technical targets for energy storage applications:

- 1,000 cycles above target operating efficiency and current density
- 42% efficiency; >250 mA/cm^2 power generation; >50 mA/cm^2 energy storage

FY 2016 Accomplishments

Since the previous reporting period, the following work related to the technical objectives has been accomplished on this Small Business Innovation Research Phase I and Phase II project:

- In half-cell testing, demonstrated GDE for 200 cycles between projected oxygen reduction reaction (ORR) and oxygen evolution reaction (OER) voltages at 50°C, and ORR current density of 200 mA/cm^2.
- Built an economic model as a basis for the technical targets in the Phase II project. The model indicated that if the performance targets are achieved at the system level, then the reversible AEMFC could deliver electricity at <$0.18/kWh using the assumptions developed by Steward et al. [1].
- Established baseline MEA performance in AEMFC single cell testing.
- Began evaluation of PGM-free hydrogen electrode materials.

✧ ✧ ✧ ✧ ✧

INTRODUCTION

Low temperature fuel cells, such as proton exchange membrane (PEM) and AEMFCs, offer an efficient and clean means of energy conversion of hydrogen to electricity. However, PEM fuel cells typically require platinum in the cathode to operate at high power density and high efficiency, which hurts the economics for this technology. Platinum is used as an electro-catalyst for the ORR, the cathode side half reaction is shown below for acidic and alkaline electrolytes, respectively:

(1) ORR (acid) $O_2 + 4\ H^+ + 4\ e^- \rightarrow 2\ H_2O$

(2) ORR (alkaline) $O_2 + 2\ H_2O + 4\ e^- \rightarrow 4\ OH^-$

The slow kinetics in the cathode is one of the largest sources of inefficiency in fuel cells, thus high platinum catalyst loadings are needed to prevent even more voltage losses (or overpotential). At commercial scale, precious metals in the cathodes of PEM fuel cells would comprise a significant portion of the entire stack cost [1,2]. Additionally, Pt-based ORR catalysts can degrade quickly under fuel cell operating conditions, such as frequent load cycling.

More recently, there has been renewed interest in AEMFCs for stationary applications. Development of commercial anion exchange membranes is helping to alleviate system-level problems with alkaline fuel cells, such as pressure balance. Further, recent published results at Los Alamos National Laboratory have shown that alkaline fuel cells could potentially operate at high efficiency with non-platinum ORR catalysts [3]. AEMFCs are of particular interest for energy storage applications that do not have size or volume limitations, such as grid load leveling. In an alkaline fuel cell oxygen is reduced by reaction (2) above, and hydrogen is oxidized by reaction (3) below.

(3) Hydrogen Oxidation Reaction (HOR) (alkaline)

$H_2 + 2\ OH^- \rightarrow 2\ H_2O + 2\ e^-$

AEMFCs could potentially be operated in a reversible manner, allowing renewable energy to be stored in the form of hydrogen. This would be particularly valuable when coupled with renewable energy generation (wind or solar) to provide energy storage and load leveling. However, when operating in regeneration mode, cathode degradation is even more pronounced for conventional ORR catalysts because of the high voltages required for the OER, the reverse of Reaction 2 above. Consequently, in existing reversible systems, separate cell stacks for fuel cell and electrolysis operation are used, adding to the already high system cost. If a low-cost regenerative stack could be developed, it would be a key breakthrough in the commercial viability of energy storage systems [4]. In this project, pH Matter, LLC is partnering with Giner, Inc., and NREL to develop and demonstrate a low-cost regenerative AEMFC system.

APPROACH

The overall objective of the proposed project is to develop and demonstrate a regenerative fuel cell stack technology that is economically viable in stationary energy storage. In the project, researchers at pH Matter will synthesize a matrix of PGM-free HOR/hydrogen evolution reaction (HER) catalysts, and GDEs based on these materials. Researchers at NREL will synthesize a matrix of low-PGM hydrogen electrode materials. The HOR/HER materials and GDEs will be fully characterized and tested under cycling conditions to determine performance and stability. Additionally, pH Matter will further optimize nitrogen- and phosphorus-doped carbon electrodes ORR/OER electrodes developed in Phase I for improved performance and durability at higher temperatures and pressures. The hydrogen and oxygen electrodes will then be demonstrated in 25 cm^2 single cells for over 1,000 cycles. Cells that degrade during cycling will be characterized by pH Matter and NREL to determine degradation mechanisms. This information will be used to iteratively prepare more optimized cells. Engineers at Giner will test cells in conjunction with Giner's water-management membrane technology. Down-selected cells will then be incorporated into a regenerative fuel cell stack and demonstrated in simulated application testing at Giner. The project will establish a foundation for future work, where the technology will be incorporated into a prototype regenerative fuel cell system. Additionally, a design and economic model of the regenerative fuel cell system will be built to verify advantages of the approach compared to available energy storage technologies. The successful result of the proposed Phase II work will demonstrate the feasibility of a regenerative fuel cell system with economic advantages compared to existing technologies.

RESULTS

In previous Phase I work on this project a matrix of novel PGM-free catalysts for ORR and OER were synthesized and tested in a rotating disk electrode set-up. GDEs were made using a screen-printing method using down-selected catalysts. Various catalyst formulations, catalyst loadings, ionomers and/or binders, ink compositions, and electrode substrates were examined. Testing was conducted with commercial AEMs in an in-house constructed stainless steel half-cell set-up. For the grid load-leveling application, it is expected that current density will be highest (by a factor of 5–6) during periodic cell discharges (ORR operation) compared to OER operation. Half-cell GDE testing examined cycling between ORR and OER conditions. For these tests at 45°C, cycles were conducted at 40 mA/cm^2 for OER, and 200 mA/cm^2 for ORR with the direction of the current being reversed every 2 min (1 min of current, 1 min of rest). Some GDE configurations showed excellent stability for ORR and OER cycling during these tests in up to 200 cycles. Figure 1

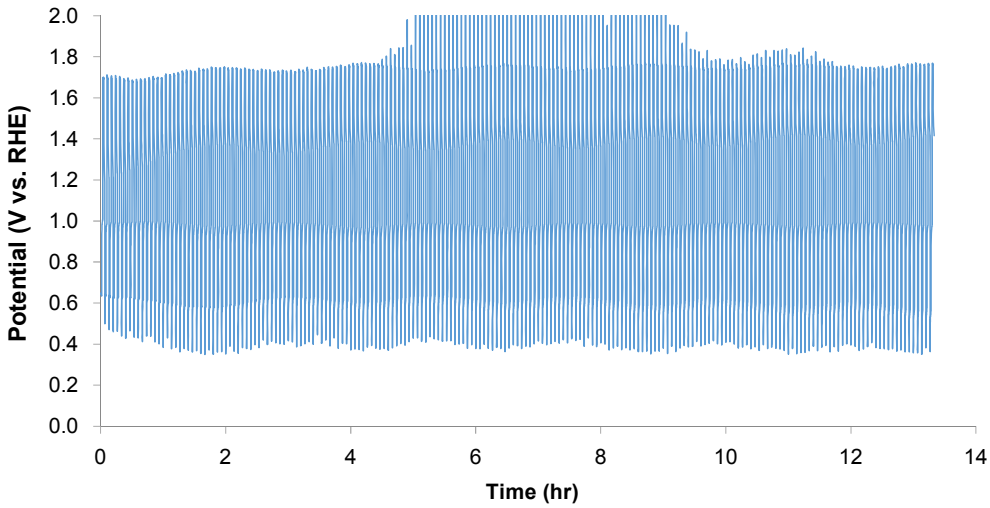

FIGURE 1. ORR–OER cycle testing for 200 cycles obtained in half-cell GDE at 50°C for non-precious metal catalyst in humidified oxygen; aqueous 5 M KOH fed to the counter electrode chamber; 200 mA/cm^2 ORR, 50 mA/cm^2 OER

shows the half-cell cycle test for pH Matter's non-PGM GDE compressed to a commercial AEM, and operating in pure oxygen. The results demonstrate the ability of this class of catalysts to undergo a number of cycles without rapid degradation.

Testing also examined long-term durability of electrodes at steady-state for OER or ORR. In testing on parallel projects, the stability of the non-PGM catalysts were found to be excellent over 100 h at 70°C during steady-state ORR operation at 350 mA/cm^2 in pure oxygen at 1 atm (data not shown). No degradation could be measured, as performance improved slightly over a 100-hour test. Stability was also excellent for steady-state OER testing over 100 h, as shown in Figure 2. For operation of the non-PGM GDE, the electrode was pressed to a commercial AEM and flooded with 5 M KOH at 45°C and run at 40 mA/cm^2. The OER stability was excellent over the 100-hour test.

At the end of the Phase I Small Business Innovation Research, an economic model was updated to project electricity costs for energy stored with a reversible AEMFC system based on test results. The guidelines for the model and assumptions generally followed those used by Steward et al. [1], but assumed a reversible AEMFC stack that could operate at Phase II targets. The model demonstrated that if technical targets can be achieved at the stack scale, then a reversible AEMFC would be cost-competitive with compressed air energy storage and pumped hydro energy storage approaches. However, unlike these approaches, a fuel cell system is not subject to geologic restrictions. The projected delivered electricity would cost less than $0.18/kWh. The model was also used to determine sensitivity of the electricity cost to a number of factors, particularly those that have yet to be demonstrated. The sensitivity analysis found

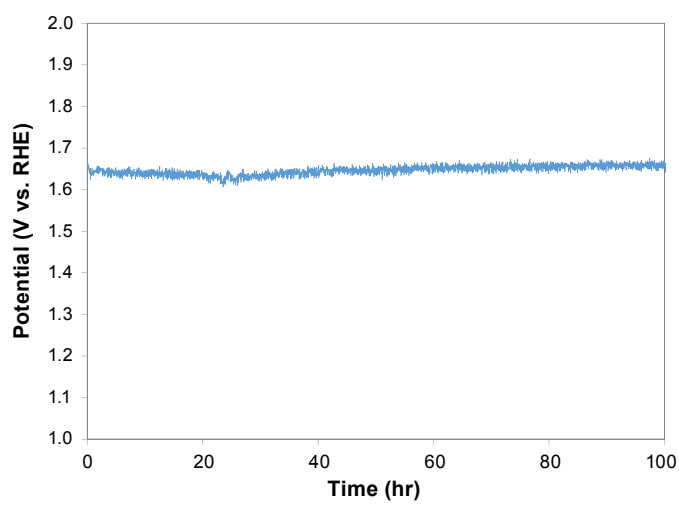

FIGURE 2. Steady-state OER testing over 100 h at 45°C for non-precious metal catalyst in 5 M KOH operating at 40 mA/cm^2 OER

that competitive economic performance will be dependent on achieving a stack life-time of greater than four years.

In the first quarter of the Phase II project, work has begun on development of non-PGM hydrogen electrode catalysts for the HOR and HER. Testing has focused on obtaining baseline performance and stability for platinum–ruthenium catalysts, and comparison to non-PGM catalysts. The durability during cycling for the hydrogen electrode appears to be less challenging than the oxygen electrode, as all materials tested have shown excellent durability. However, further performance improvements are required to match the PGM standard. Further optimization has also begun on the non-PGM ORR/OER electrodes. Future work will target

cycling and performance demonstration in single cells with the non-PGM electrodes.

CONCLUSIONS AND FUTURE DIRECTIONS

The following conclusions can be drawn from work completed to this point:

- The novel ORR/OER PGM-free catalysts being developed in this project show performance in alkaline conditions comparable to that of precious metal ORR/OER catalysts, and good stability during cycling from ORR to OER voltages.
- ORR/OER cycling stability for 200 cycles has been demonstrated with GDEs, and degradation during steady-state operation is less of a concern.
- Economic modeling suggests that the reversible AEM fuel cell concept would be an excellent energy storage option for grid load leveling if performance targets can be achieved at the system level.

Future work in the remainder of the Phase II project will include:

- Further hydrogen electrode materials development and incorporation of the materials into cells and stacks.
- Optimization of the electrode-membrane interface.
- Demonstration of low-cost 25 cm^2 reversible cells.
- Characterization of the electrodes before and after cycling to better understand any degradation mechanisms.
- Demonstration of single cell durability over 1,000 cycles.
- Demonstration of a regenerative stack.
- Design of a prototype energy storage system that incorporates the stack.
- Economic analysis of a reversible AEMFC system for a specific energy storage application.

FY 2016 PUBLICATIONS/PRESENTATIONS

1. Matter, Paul H., Minette Ocampo, Michael Beachy, and Chris Holt, "Regenerative Fuel Cell System," *DOE Hydrogen and Fuel Cells Program Annual Merit Review and Peer Evaluation* (2016), June 8, 2016, Washington, D.C.

REFERENCES

1. Steward, D., G. Saur, M. Penev, and T. Ramsden, "Lifecycle Cost Analysis of Hydrogen Versus Other Technologies for Electrical Energy Storage." NREL Report NREL/TP-560-46719 (2009). Accessed July 23, 2015. http://www.nrel.gov/docs/fy10osti/46719.pdf

2. James, Brian D., Jennie M. Moton, and Whitney G. Colella, "Mass Production Cost Estimation of Direct H_2 PEM Fuel Cell Systems for Transportation Applications: 2013 Update." Accessed July 23, 2015. http://energy.gov/sites/prod/files/2014/11/f19/fcto_sa_2013_pemfc_transportation_cost_analysis.pdf

3. Chung, H.T., J.H. Won, and P. Zelenay, "Active and stable carbon nanotube/nanoparticle composite electrocatalyst for oxygen reduction." *Nature Communications* 4 (2013). Accessed July 23, 2015. doi: 10.1038/ncomms2944.

4. Remick, R.J., and D. Wheeler, "Reversible Fuel Cells Workshop Summary Report." Accessed July 23, 2015. http://www1.eere.energy.gov/hydrogenandfuelcells/pdfs/rev_fc_wkshp_report.pdf

V.F.1 New Fuel Cell Materials: Characterization and Method Development

Karren L. More (Primary Contact)
Oak Ridge National Laboratory (ORNL)
1 Bethel Valley Road
Oak Ridge, TN 37831-6064
Phone: (865) 574-7788
Email: morekl1@ornl.gov

DOE Manager: Donna Ho
Phone: (202) 586-8000
Email: Donna.Ho@ee.doe.gov

Project Start Date: October 1, 2015
Project End Date: Project continuation and direction determined annually by DOE

Overall Objectives

- Identify and/or develop novel high-resolution imaging and compositional/chemical analysis techniques, and unique specimen preparation methodologies, for the µm- to sub-Å scale characterization of material constituents comprising fuel cell (FC) catalyst layers (electrocatalysts, catalyst supports, ionomer films).
- Optimize imaging and spectroscopy methodologies towards characterizing specific fuel cell materials; electrocatalyst atomic-scale structure and chemistry, ionomer mapping in catalyst layers, and three-dimensional (3D) electron tomography.
- Integrate microstructural characterization within other DOE projects and establish collaborations with industrial partners.
- Make capabilities and expertise available to broad fuel cell research community.

Fiscal Year (FY) 2016 Objectives

- Establish microscopy expertise for conducting high-resolution 3D electron tomography and apply to electrocatalyst, support, and ionomer studies.
- Use structural and spectroscopy data derived from extensive microscopy analyses to optimize materials through iterative synthesis/fabrication and characterization. Correlate materials structure and chemistry with durability, stability, and performance measurements when applicable.
- A goal of this new project is to establish new collaborations with industry and university partners via a Fuel Cell Technologies Office (FCTO) opportunity to support collaborative projects with a 50% cost share through a streamlined, short-form cooperative research and development agreement (CRADA). ORNL staff scientists can collaborate directly with partners on DOE FCTO mission-aligned projects.

Technical Barriers

This project addresses the following technical barriers from the Fuel Cells section of the FCTO Multi-Year Research, Development, and Demonstration Plan.

(A) Durability

(C) Performance

Technical Targets

This project is focused on conducting fundamental characterization studies on individual material constituents comprising FCs, with an emphasis on new materials including electrocatalysts, supports, and ionomer before and after incorporation into membrane electrode assemblies (MEAs), and identification and optimization of methods directed specifically towards characterization of FC materials and MEAs. Insights gained through extensive microstructural studies will be applied toward the design and manufacture of catalysts and catalyst supports that meet the DOE 2017 and 2020 targets for integrated polymer electrolyte membrane fuel cell (PEMFC) power systems and FC stacks operating on direct hydrogen for transportation applications (listed in Table 1).

FY 2016 Accomplishments

- Imaged ionomer dispersions in catalyst layers in 3D for the first time using novel ultramicrotomy method combined with high-resolution compositional mapping via electron microscopy. The 3D renderings were used not only to visualize the ionomer, but allowed for quantification of ionomer dispersions in real catalyst layers (CLs) and to develop a correlation with porosity.
- Initiated a significant effort in performing 3D electron tomography of a variety of catalyst nanostructures and supports, including Pt and Pt-alloy catalysts, and PGM-free catalysts, and developed methodology for conducting 3D electron tomography of intact CLs. These data allowed the quantification of differences between catalyst loadings, catalyst dispersions, and catalyst agglomeration and nearest neighbor distances.

TABLE 1. Technical Targets: Electrocatalysts for Transportation Applications

Characteristic	Units	2011 Status	2017 Target	2020 Target
PGM total content (both electrodes)	g/kW (rated)	0.19	0.125	0.125
PGM total loading	mg PGM/cm^2 electrode area	0.15	0.125	0.125
Loss in initial catalytic activity	% mass activity loss	48	<40	<40
Electrocatalyst support stability	% mass activity loss	<10	<10	<10
Mass activity	A/mg Pt @ 900 mV	0.24	0.44	0.44
Non-Pt catalyst activity per volume of supported catalyst	A/cm^2 @ 800 mV	60 (at 0.8 V) 165 (extrapolated from > 0.85 V)	300	300

PGM – Platinum (Pt) group metal

- Further optimized the use of low-voltage, sub-Å-scale imaging and spectroscopy of PGM-free catalysts.
- Established new industrial collaboration through streamlined CRADA process, with several additional industrial partnerships being considered and/or negotiated.

✧ ✧ ✧ ✧ ✧

INTRODUCTION

PEMFCs are being developed for future use as efficient, zero-emission power sources. However, the performance of PEMFCs degrades with time during electrochemical aging in automotive and stationary applications. Performance degradation can be directly attributed to the durability of individual material constituents comprising the MEA, including the electrocatalyst, catalyst support, recast ionomer, and polymer membrane. In order to enhance the stability of PEMFCs, the structural and chemical characteristics of the materials used must be understood and optimized. The "New Fuel Cell Materials: Characterization and Method Development" project at ORNL is focused on several primary objectives: (i) characterizing the microstructural and microchemical nature of new materials developed for PEMFCs using state-of-the-art imaging and spectroscopy techniques, (ii) identifying, developing, and/or optimizing methodologies specifically aimed at materials for FCs, and (iii) forming collaborative relationships with industrial PEMFC developers/manufacturers, universities, and national laboratories, to apply ORNL's advanced electron microscopy techniques and expertise (available through ORNL's Materials Characterization Center via a streamlined CRADA process) to conduct relevant studies towards understanding materials stability and durability issues and to develop materials-based strategies required for optimizing PEMFC durability and performance.

APPROACH

ORNL's microstructural characterization and method development project utilizes advanced electron microscopy analysis techniques to characterize the individual material components comprising PEMFCs, before and after incorporation into an MEA, and after electrochemical aging. Our approach is focused on identifying and optimizing novel high-resolution imaging and compositional/chemical analysis techniques, and developing unique specimen preparation methodologies, for the µm-to-sub-Å-scale characterization of the material constituents of fuel cells (electrocatalysts, catalyst supports, recast ionomer films, membranes, etc.). ORNL applies these advanced analytical and imaging techniques for the evaluation of the microstructural and microchemical characteristics of each material constituent and correlates these observations with FC performance. Most importantly, ORNL is making the techniques and expertise available to FC researchers outside of ORNL via several mechanisms: (1) strategic partnership projects for proprietary research, (2) a new streamlined short-form CRADA process whereby DOE's FCTO provides a 50% cost share to collaborate with ORNL's Materials Characterization Center on DOE FCTO mission-aligned projects, and (3) access via ORNL user facilities (e.g., Center for Nanophase Materials Sciences).

RESULTS

Electron tomography research was initiated in collaboration with Laure Guatez at CEA-Grenoble, France several years ago to study the morphological changes in PtNi nanostructured thin film catalysts during aging [3]. Electron tomography was a concerted effort at ORNL during FY 2016, which was specifically aimed at optimizing the technique towards conducting "four-dimensional (4D) electron tomography" studies on fully intact MEAs to combine high-resolution scanning transmission electron microscopy (STEM) imaging and chemical/compositional spectroscopy such that materials inter-relationships within CLs can be further understood at the nm-scale. Recent improvements

in the application of advanced/enhanced energy dispersive spectroscopy techniques to quantify ionomer layer/film dispersions within catalyst layers complement existing capabilities to image the carbon support and nanoparticle catalyst structures; these datasets can be combined to produce 3D renderings towards fully interrogating the various material components and interfaces comprising the CLs, and to understand the role of constituent dispersions and interfaces within the architectures of catalyst inks and electrodes.

STEM-based tomography was performed on a 200 kV FEI Talos F200X using a Gatan high-tilt tomography holder. Bright field and high-angle annular dark field STEM images were acquired in 2° increments over a 140° tilt range (±70° for a total of 71 image pairs). Tilt series alignment and tilt-axis corrections were performed manually for each image in the sequence using Gatan software and adjusted iteratively prior to reconstruction to ensure convergence. 3D reconstructions were performed using a model-based iterative reconstruction algorithm [1,2]. Visualizations were rendered using FEI Aviso and Fiji/ImageJ software. High- and low-pass filter thresholding was applied to the reconstructed volumes for 3D segmenting and rendering of both Pt and C, with statistics computed using Aviso.

To demonstrate STEM tomography, Pt/C catalysts were compared with different Pt loadings (5%, 20%, 50%) and three different carbon supports (Vulcan XC-72 [V], high surface area carbon [HSAC], and low surface area graphitized carbon black [LSAC]) for a total of six Pt/C samples. These samples were chosen to compare the differences associated with Pt nanoparticle dispersion as a function of carbon support structure and Pt loading. A comparison of 3D tomography results for the lowest Pt loading (5%) on HSAC, V, and LSAC supports are shown in Figure 1. For the same carbon support area, there are significantly more Pt nanoparticles on HSAC compared with Vulcan and LSAC, and the average diameter of the Pt nanoparticles on HSAC (2.0 nm) and Vulcan (~2.75 nm) were much smaller than Pt deposited on LSAC (4.25 nm).

To visualize ionomer distributions within CLs, a different sample preparation was employed. MEAs (in this example, a 40% Pt/V CL was used) were embedded using standard procedures for ultramicrotomy after a Au fiducial layer/marker was sputter coated on the catalyst layer surface (used to locate same area for imaging and elemental mapping). The Leica ultramicrotome was used to carefully slice individual MEA cross-sections, one slice at a time, to "depth-profile" through the catalyst layer cross-section. Each catalyst layer slice was approximately 100 nm thick and we were able to cut 17 sections to use for reconstruction of the catalyst layer. 3D reconstructions were performed using FEI's Aviso software package.

A 3D reconstruction of the stacked images from the 17 microtome slices showing the ionomer distribution

FIGURE 1. STEM electron tomography reconstructions demonstrating the location and size differences of Pt nanoparticles (loading of 5%) supported on HSAC (top image), V (middle image), and LSAC (bottom image)

(green fluorine energy dispersive spectroscopy maps acquired for each microtome slice reconstructed into the volumetric rendering) within a volume of the catalyst layer (7 µm X 7 µm X 1.5 µm) is shown in Figure 2. In addition to visualization of ionomer features within a specific volume, the strength of acquiring electron tomography data, especially within a fully intact CL, is the ability to quantify size characteristics of the individual constituents as opposed to extracting data from traditional two-dimensional (2D)

images. This becomes especially relevant for quantifying the ionomer dispersions and porosity, where the sizes of specific features are larger than the thickness of the microtomed cross-section (50–100 nm). Figure 3 shows the results of quantifying the ionomer aggregate size and porosity size distributions for the 3D tomography data shown in Figure 2. The color-coding shown in both the 3D rendering and size distribution plots are directly correlated with specific feature size ranges. For this particular CL, the average ionomer aggregate size is ~164 nm and the pore size is ~254 nm. The ionomer aggregate size is much larger than expected, and indicates severe ionomer aggregation associated with regions of the electrode with no ionomer; the aggregates are characterized as having an aspect ratio of 2:1, as shown in Figure 4, and are associated directly with "filling in" asperities in the large scale secondary pores as well as filling smaller pores within the CL.

FIGURE 2. 3D electron tomography reconstruction of the ionomer dispersion within a 40% Pt/V CL containing ~30 vol% Nafion®. Green represents fluorine signal (energy dispersive spectroscopy) from each slice reconstructed into 3D volume

CONCLUSIONS AND FUTURE DIRECTIONS

Microstructural and microchemical studies continue to provide insight regarding the structural and compositional characteristics of PEMFC constituents that ultimately dictate the specific material's stability and durability during operation. In FY 2016, studies were primarily focused on 3D electron tomography of electrocatalysts, supports, and fully intact CLs. We will continue to support these studies in FY 2017 through collaborations with industrial and academic partners, which will be a significant focus of the project, while emphasizing studies focused on new materials for PEMFCs and using the knowledge gained towards materials optimization and improving electrocatalyst and ionomer interactions and dispersions.

- Continue to establish new collaborations with FC manufacturers and researchers to identify and

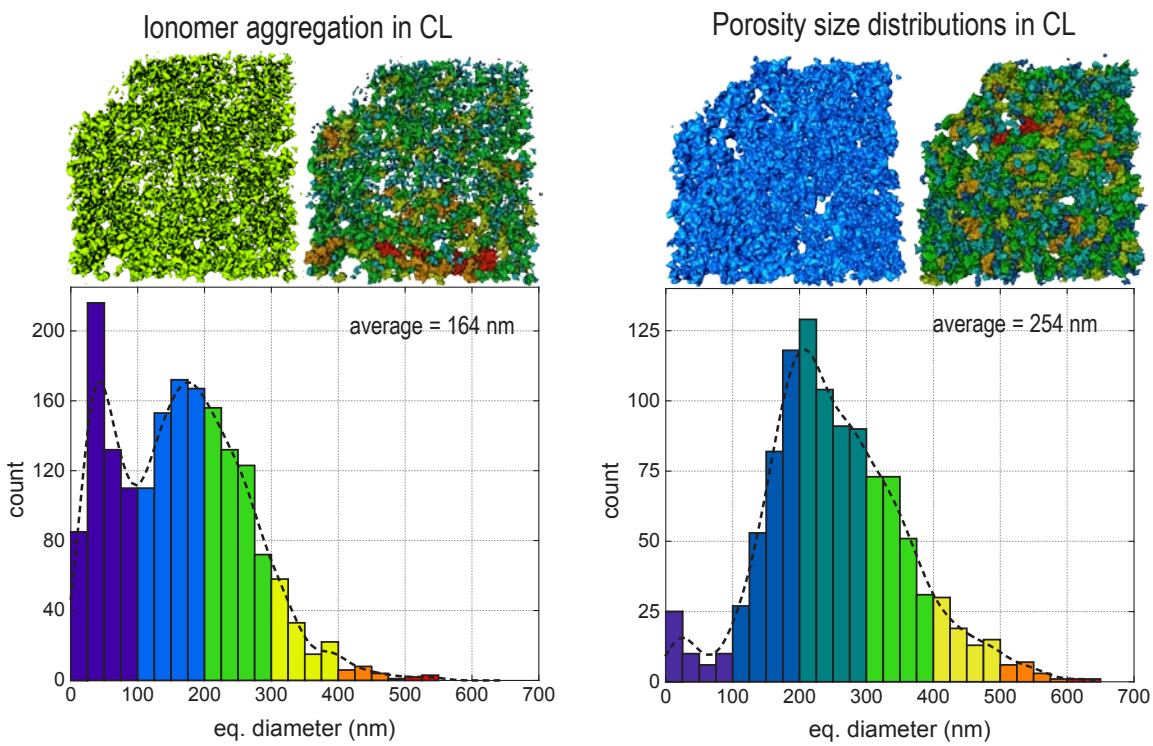

FIGURE 3. Ionomer aggregate size distribution and associated 3D renderings of ionomer (left) and pore size distribution and associated 3D renderings of pores (right) acquired from the same CL shown in Figure 2

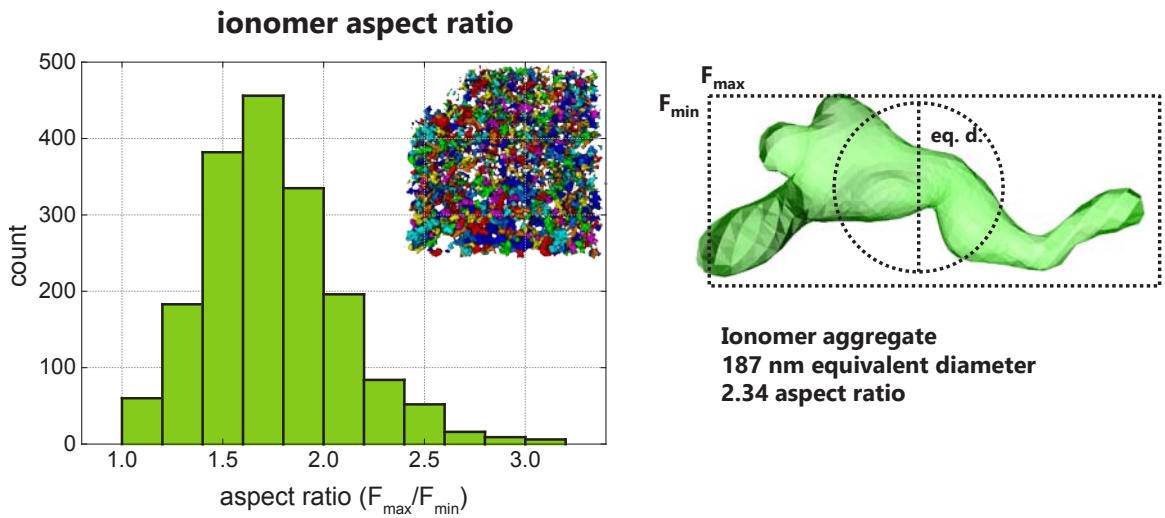

FIGURE 4. Plot of ionomer aspect ratios determined for 3D ionomer map (left) and rendering of a typical ionomer aggregate (right) extracted from ionomer map shown in Figure 2

characterize new FC materials to improve stability and durability. Input from the Fuel Cell Tech Team, reviewer comments from the Annual Merit Review, and establishing new collaborations are key to the success of this Characterization and Method Development project and to identify relevant and critical research directions.

- Refine 3D electron tomography methods to correlate and quantify interactions between ionomer layers, Pt-based catalysts and their distributions within CLs, and new/novel catalyst supports. Establish relationships between ionomer-Pt-support resulting from ink preparation methods.
- Continue to characterize ionomer distributions in "real" CLs through the use of high-resolution 3D electron tomography studies (combine structural and compositional tomography).

FY 2016 PUBLICATIONS/PRESENTATIONS

1. U. Martinez, J.H. Dumont, E.F. Holby, K. Artyushkova, G.M. Purdy, A. Singh, N.H. Mack, P. Atanassov, D.A. Cullen, K.L. More, M. Chhowalla, P. Zelenay, A.M. Dattelbaum, A.D. Mohite, and G. Gupta, "Critical Role of Intercalated Water for Electrocatalytically Active Nitrogen-doped Graphitic Systems," *Science Advances* **2**[3] e1501178 (2016).

2. D. Raciti, J. Kubal, C. Ma, M. Barclay, M. Gonzalez, M. Chi, J. Greeley, K.L. More, and C. Wang, "Pt_3Re Alloy Nanoparticles as Electrocatalysts for the Oxygen Reduction Reaction," *Nano Energy* **20** 202–211 (2016).

3. F.H. Garzon, M.S. Wilson, D. Banham, S.Y. Ye, and K.L. More, "Carbonaceous Nanowire Supports for Polymer Electrolyte Membrane Fuel Cells," *Journal of the Electrochemical Society* **163**[2] F115–F121 (2016).

4. M. Chi, C. Wang, Y.K. Lei, G.F. Wang, D.G. Li, K.L. More, A. Lupini, L.F. Allard, N.M. Markovic, and V.R. Stamenkovic, "Surface Faceting and Elemental Diffusion Behavior at Atomic Scale for Alloy Nanoparticles During *in situ* Annealing," *Nature Communications* **6** Article 8925 (2015).

5. L. Elbaz, J. Phillips, K. Artyushkova, K.L. More, and E.L. Brosha, "Evidence of High Electrocatalytic Activity of Molybdenum Carbide Supported Platinum Nanorafts," *Journal of The Electrochemical Society* **162**[9] H681–H685 (2015).

6. Invited Presentation: K.L. More, D.A. Cullen, B. Sneed, and K.S. Reeves, "Materials/Interfacial Homogeneity within PEM Fuel Cell Electrode Structures: The Interplay between Electrocatalyst, Catalyst-Support, and Ionomer Films and Effect on Durability and Performance," 3rd International Workshop on Degradation Issues of Fuel Cells and Electrolyzers, Santorini, Greece, September 29–October 1, 2015.

7. Contributed Presentation: K.L. More, "Assessment of Nanofiber Electrode MEA Durability through Advanced Microscopy," 228th Electrochemical Society Fall Meeting, Phoenix, AZ, October 12–16, 2015.

8. Contributed Presentation: B.T. Sneed, D.A. Cullen, and K.L. More, "Characterization of Catalytic Materials for PEM Fuel Cells by STEM Tomography," MRS Fall Meeting, Boston, MA, November 29–December 3, 2015.

9. Contributed Presentation: D.A. Cullen, K.L. More, H.M. Meyer III, H.T. Chung, and P. Zelenay, "Analytical Characterization of Non-PGM Catalysts for PEM Fuel Cells," MRS Fall Meeting, Boston, MA, November 29–December 3, 2015.

10. Invited Presentation: K.L. More, D.A. Cullen, and B.T. Sneed, "New Fuel Cell Materials: Characterization and Technique Development," USCAR Fuel Cell Tech Team, Detroit, MI, February 17, 2016.

11. Contributed Presentation: K.L. More, D.A. Cullen, and B.T. Sneed, "Understanding Ionomer Dispersions in PEM Fuel Cell

Catalyst Layers," MRS Spring Meeting, Phoenix, AZ, March 28–April 1, 2016.

12. Contributed Presentation: B.T. Sneed, D.A. Cullen, and K.L. More, "Towards 4D STEM Imaging of PEM Fuel Cell Catalyst Dispersions," MRS Spring Meeting, Phoenix, AZ, March 28–April 1, 2016.

13. Invited Presentation: D.A. Cullen, "Advancing Fuel Cell Materials through Electron Microscopy," Tech Connect, Washington DC, May 14–17, 2016.

14. Contributed Presentation: D.A. Cullen, B.T. Sneed, and K.L. More, "Impact of Evolving Electrode Morphology on Fuel Cell Performance: From the Nano to Mesoscale," 229th Electrochemical Society Meeting, San Diego, CA, May 29–June 3, 2016.

15. Contributed Presentation: K.L. More, B.T. Sneed, and D.A. Cullen, "Understanding Electrocatalyst Morphology, Dispersion, and Stability in Catalyst Layers of PEM Fuel Cells Via 3D Electron Tomography," 229th Electrochemical Society Meeting, San Diego, CA, May 29–June 3, 2016.

16. Invited Presentation: D.A. Cullen, B.T. Sneed, and K.L. More, "Fuel Cell Electrode Optimization through Multi-scale Analytical Microscopy," Microscopy & Microanalysis 2016, Columbus, OH, July 24–28, 2016.

REFERENCES

1. S.V. Venkatakrishnan, L.F. Drummy, M.A. Jackson, M. DeGraef, J. Simmons, and C.A. Bouman, "A Model-based Iterative Reconstruction Algorithm for HAADF-STEM Tomography," Image Processing, IEEE Transactions 22[11] 4532–4544 (2013).

2. S.V. Venkatakrishnan, L.F. Drummy, M. DeGraef, J.P. Simmons, and C.A. Bouman, "Model-based Iterative Reconstruction for BF Electron Tomography," Computational Imaging, IEEE Transactions 1[1] 1–15 (2014).

3. D.A. Cullen, M. Lopez-Haro, P. Bayle-Guillemaud, L. Guetaz, M.K. Debe, and A.J. Steinbach, "Linking Morphology with Activity through the Lifetime of Pretreated PtNi Nanostructure Thin Film Catalysts," *Journal of Materials Chemistry A* **3**[21] 11660-11667 (2015).

V.F.2 Neutron Imaging Study of the Water Transport in Operating Fuel Cells

Muhammad Arif (Primary Contact),
David L. Jacobson, Daniel S. Hussey,
Jacob LaManna, Elias Baltic
National Institute of Standards and Technology (NIST)
100 Bureau Drive
Gaithersburg, MD 20899
Phone: (301) 975-6303
Email: arif@nist.gov

DOE Manager: Nancy L. Garland
Phone: (202) 586-5673
Email: Nancy.Garland@ee.doe.gov

Contract Number: DE-AI-01-01EE50660

Project Start Date: Fiscal Year (FY) 2001
Project End Date: Project continuation and direction determined annually by DOE

Overall Objectives

- Provide state-of-the-art research and testing infrastructure to enable the fuel cell industry to design, test, and optimize prototype to commercial grade fuel cells using in situ neutron imaging techniques.
- Provide a secure facility for proprietary research by industry. Provide beam time at no cost to non-proprietary research through a competitive proposal process. Make open research data available for beneficial use by the general fuel cell community.
- Continually improve and develop methods and technology to accommodate rapidly changing industry and academia needs.

Fiscal Year (FY) 2016 Objectives

- Collaborate and support groups from the DOE Hydrogen and Fuel Cells Program performing water transport measurements with neutron imaging at NIST.
- Deploy new cold neutron fuel cell imaging facility for high resolution imaging of fuel cells.
- Install fuel cell and support infrastructure at the new cold imaging facility.
- Explore and develop high resolution neutron imaging methods to enable water transport studies of catalyst and membrane electrode assemblies (MEAs).
- Employ a high resolution imaging method to achieve resolution approaching 1 µm to resolve water concentration in fuel cell electrodes.
- Deploy and develop in situ X-ray imaging for fuel cells at the neutron imaging facility.

Technical Barriers

This project addresses the following technical barriers from the Fuel Cells section of the Fuel Cell Technologies Program Multi-Year Research, Development, and Demonstration Plan.

(A) Durability

(B) Cost

(C) Performance

Technical Targets

This project is conducting fundamental studies of water transport in the fuel cell. Insights gained from these studies will be applied toward the design of components and operation strategies of proton exchange membrane fuel cells that meet the following 2020 DOE fuel cell targets.

- Durability with cycling at operating temperature of ≤80°C: 5,000 h
- System energy density: 650 W/L
- System specific power: 850 W/kg
- Energy efficiency: 60% at 25% rated power
- Cost: $40/kW$_e$
- Start-up time to 50% power: 30 s from -20°C, 5 s from 20°C
- Assisted start from low temperatures: -40°C

FY 2016 Accomplishments

- First 4 µm resolution fuel cell images using slits
- Installation of a new, second neutron imaging instrument
- Installation of micro-focus X-ray source for simultaneous neutron/X-ray imaging
- Components for new high resolution imaging detector systems acquired

✧ ✧ ✧ ✧ ✧

INTRODUCTION

At NIST, we maintain the premier fuel cell neutron imaging facility in the world and continually seek to improve its capabilities to meet the changing needs of the fuel cell community. This facility provides researchers with a powerful and effective tool to visualize and quantify water transport inside operating fuel cells. Imaging the water dynamics of a fuel cell is carried out in real time with the required spatial resolution needed for fuel cells that are being developed today. From these images, with freely available NIST-developed image analysis routines, fuel cell industry personnel and researchers can obtain in situ, non-destructive, quantitative measurements of the water content of an operating fuel cell. Neutron imaging is the only in situ method for visualizing the water distribution in a "real-world" fuel cell. Unlike X-rays, whose interaction with materials increases with the number density of electrons, neutrons interact via the nuclear force, which varies somewhat randomly across the periodic table, and is isotopically sensitive. For instance, a neutron's interaction with hydrogen is approximately 100 times greater than that with aluminum, and 10 times greater than that with deuterium. It is this sensitivity to hydrogen (and insensitivity to many other materials) that is exploited in neutron imaging studies of water transport in operating fuel cells.

APPROACH

The typical length scales of interest in a fuel cell are: channels approximately 1 mm wide and 1 mm deep, the diffusion media (DM) are 0.1 mm to 0.3 mm thick, the membrane is 0.01 mm to 0.02 mm thick, and the active area of test sections can range from 2 cm^2 to 500 cm^2. Though the study of water transport within these length scales is technically very challenging, the unique capabilities of neutron imaging have already successfully addressed many questions. However, as fuel cell research matures, the water transport questions become increasingly more demanding, requiring for instance resolving the water content in catalyst layers. To meet these demands, based on fuel cell community feedback and need, we continue to develop new facilities and improve existing capabilities for obtaining higher spatial and temporal resolution neutron images. These improvements will enable users to perform even more detailed, nondestructive, and in situ studies of the water and hydrogen transport in fuel cells to meet DOE goals. In addition, employing mathematical models of neutron scattering, we will develop a software suite that enables users to obtain reliable, accurate, quantitative measurements of the water content in an operating fuel cell. Due to the complexity of fuel cells and the large number of remaining open questions regarding water transport, we will develop partnerships with industry, academia, national laboratories, and the DOE Fuel Cell program consortia to train them in the use of the facility, seek their feedback, and collaborate with them on research projects, to seek measurement breakthroughs that will facilitate the rapid, efficient, and robust development of fuel cells.

RESULTS

The NIST Neutron Imaging Facility provides year-to-year support for DOE Hydrogen and Fuel Cell Program projects through beam time and by collaboration with users on a variety of related neutron imaging projects that support the DOE mission. For FY 2016 General Motors, Los Alamos National Laboratory, University of California, Merced, University of Toronto, South African Nuclear Energy Corporation, and University of Tennessee, Knoxville have received project support for experiments at the facility. The results published during FY 2016 from these experiments are reflected in the publication list attached to this report.

Researchers from the Thermal and Electrochemical Energy Laboratory, at the University of California, Merced performed a study of two different diffusion media looking at the onset liquid water condensation using a fuel cell based on the Los Alamos National Laboratory high resolution cell. Two cells were built: the first labeled here as Cell 4, with a Nafion® XL (~30 µm) membrane, and Toray (~178 µm) DM and the second labeled Cell 5, with Nafion XL (~30 µm) membrane and Freudenberg (~203 µm) DM. The test conditions were: 50°C, 77% relative humidity; 0.3V; 300 kPa abs, high flow conditions (stoichiometry ratios > 30/30 anode/cathode), 100% hydrogen concentration with 2%, 8%, and 16% oxygen concentration. Starting under dry conditions (2% O_2), the water saturation in the DM of both cells is similar (see Figure 1). Under wet condition (8% O_2), liquid water is saturated throughout the diffusion media thickness for Toray DM. In contrast, liquid water is only saturated away from the MEA near the land for Freudenberg DM.

The same trend is observed for DM under the channel area. It can be clearly observed that Freudenberg DM provides much more open path for oxygen diffusion compared to Toray DM.

In consultation with the fuel cell community, one of the leading issues this project has been asked to address is fuel cell flooding and degradation due to liquid water in the catalyst layers. To study commercial grade platinum based catalysts requires at least a factor of 10 improvement in spatial resolution over current state-of-the-art (about 15 µm). The limiting factor in spatial resolution for current detector systems stems from the range of charged particles (3.5 µm to 150 µm) that are used to detect neutrons. To overcome this limit, we are exploring several methods. The first method uses nanofabricated neutron absorbing gratings with an opening of ~2 µm or less in width to define the neutron illuminated area of the fuel cell with high spatial resolution in one dimension. By translating the grating across

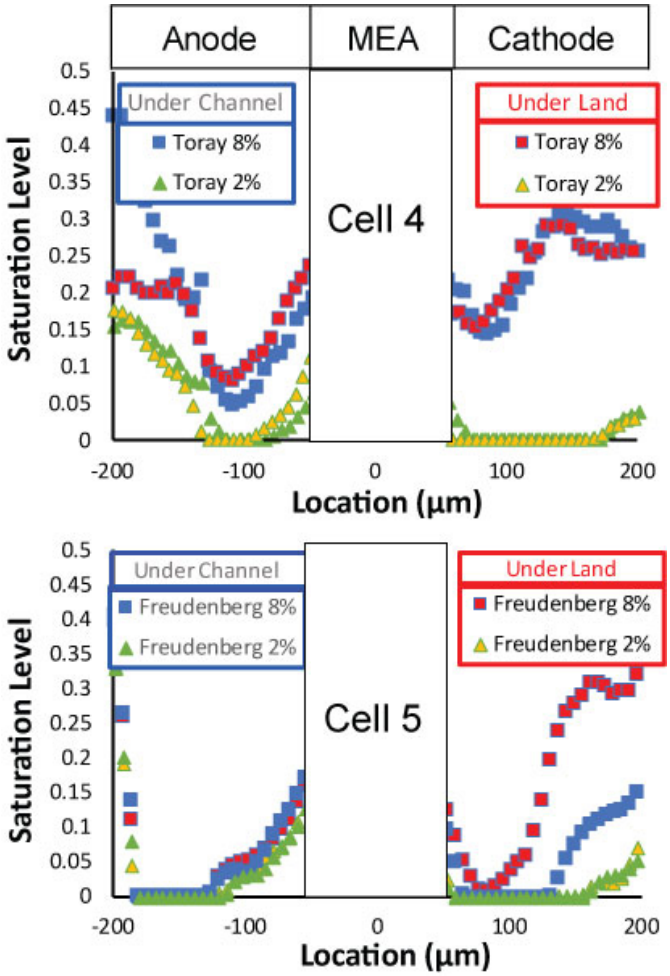

FIGURE 1. Measurements as the onset of liquid water saturation measured with neutrons for both Toray and Freudenburg DM. Under (8% O_2) liquid water saturation, the Freudenburg DM shows less liquid water saturation allowing for greater pathways of O_2 diffusion than Toray DM.

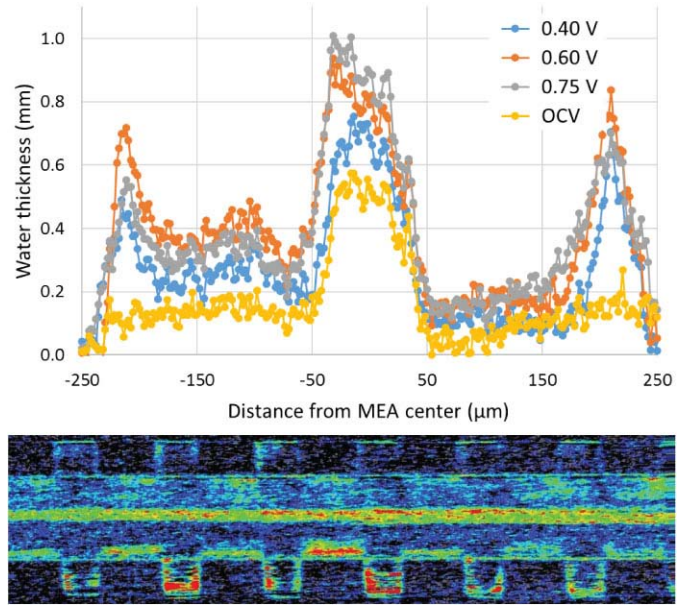

FIGURE 2. Resolution of 4 µm was achieved to measure through-plane water saturations of a fuel cell running at several different current densities. The images were taken using 2 µm gratings translated across the fuel cell during a 17 h acquisition.

the through-plane direction of the fuel cell, one obtains a high resolution image of the water content from anode to cathode, overcoming the resolution limit of the detector. New silicon gratings with thicker deposits of neutron absorbing gadolinium oxysulfide particles were developed by collaborators from Pusan University, Korea, and a new image intensifier required to improve the detector signal-to-noise ratio was finally accepted in January. This allowed for the first time to image a fuel cell with 4 µm spatial resolution (double the sampling resolution as required by the Shannon-Nyquist theorem) (see Figure 2).

With the new intensified camera, it was also possible to test a centroiding method with the gadolinium oxysulfide scintillators. By capturing images quickly (0.005 s exposures), it was possible to see individual neutron events in the camera and find the center of mass of each event. This method has shown improved spatial resolution of about 5 µm and may be able to be used to further improve spatial resolution with other methods. As this first test involved saving many images and post processing them, future work will look toward a hardware based real time centroiding method.

Ultimately resolution of 1 µm is expected to be efficiently and practically achieved using a neutron magnifying lens. By using a neutron lens, it could be possible to increase the neutron intensity by 50 to 100 times than currently available. Previously, practical lenses for neutrons have not been available due to the low neutron refractive power of all materials. However, a new X-ray telescope lens technology using thin nickel foil mirrors developed by NASA has shown great promise to provide a practical lens for neutron imaging. By nesting several mirrors, the flux can be increased up to a factor of 100 over that achievable at BT2. An engineering demonstration of the new lens with 20 µm spatial resolution was performed in July 2016 and has shown good results that are currently being analyzed. A picture of the test lens is shown in Figure 3. If successful, a complete optic with 10 nested shells will be produced in 2017 for 20 µm resolution imaging, and in 2018 a magnifying optic to reach ~1 µm resolution. Such "Wolter optics" will be installed at the new cold neutron imaging instrument that was commissioned August of 2015 and is shown in Figure 3. The cold neutron imaging instrument will also serve as a test bed for new high spatial resolution detector systems and methods and with the lower energy neutron spectrum enable discrimination of ice and water in the fuel cell during freeze operation.

FIGURE 3. Top showing the inside the new cold neutron imaging instrument that was commissioned in August of 2015. Bottom showing the engineering test optic mounted on the beam line to test the NASA fabrication methods. Based on the analysis of the results a final 1:1 optic will be delivered to NIST for the user program in 2017.

CONCLUSIONS AND FUTURE DIRECTIONS

- NIST Neutron Imaging Facility continues to maintain a robust fuel cell user program.
- New cold imaging facility will allow more rapid development of high resolution methods to measure MEA water content.
- Good progress has been made towards developing the method to measure liquid saturation values in the catalyst and membrane.
  - Slit scanning
    - 4 µm spatial resolution was demonstrated.
    - Acquisition time is 17 h, but could be improved to less than 8 h with a smaller grating period.
  - Centroiding has shown that 5 µm is possible
    - Method needs further refinement.
    - Future: develop hardware based centroiding to allow high throughput.
    - Future: method could be combined with the lens to improve resolution beyond the targets of this project.
  - Wolter optics
    - Flagship method to achieve spatial resolution of 1 µm
    - Validation of NASA fabrication techniques during July 2016
    - Future 2017: high speed 20 µm optics, 2018: 1 µm optics
- User program
  - New cold imaging facility is currently being upgraded to include full support.
  - Including electrochemical impedance spectroscopy into the scripting of the test stand would be a great benefit to the users.
  - It was observed from fuel cell testing that Freudenberg DM shows improved performance under wet and cold operating condition due to improved oxygen diffusion over Toray DM.

FY 2016 PUBLICATIONS/PRESENTATIONS

1. Hussey, D.S.; Brocker, C.; Cook, J.C.; Jacobson, D.L.; Gentile, T.R.; Chen, W.C.; Baltic, E.; Baxter, D.V.; Doskow, J.; Arif, M.; "A New Cold Neutron Imaging Instrument at NIST," Physics Procedia 69 (2015), p. 48–54.

2. Anthony D. Santamaria, Maxwell K. Becton, Nathanial J. Cooper, Adam Z. Weber, Jae Wan Park, "Effect of cross-flow on PEFC liquid-water distribution: An in-situ high-resolution neutron radiography study," Journal of Power Sources, 293, (2015), Pages 162–169.

3. F. Nandjou, J.-P. Poirot-Couvezier, M. Chandesris, S. Rosini, D.S. Hussey, D.L. Jacobson, J.M. LaManna, A. Morin, Y. Bultel, "A pseudo-3D model to investigate heat and water transport in large area PEM fuel cells – Part 2: Application on an automotive driving cycle," submitted to Int. J. Hydrogen Energy.

4. Jacob LaManna, Matthew Mench, "Channel-land configuration control of temperature driven water transport in polymer electrolyte fuel cells," in preparation (2016).

5. Jacob LaManna, Jon Owejan, Matthew Mench, "Anode water content control using high tortuosity anode diffusion media," in preparation (2016).

6. Jacob LaManna, Alan Pezeshki, Gabriel Veith, Matthew Mench, "Changes to water balance and material properties with operational age in polymer electrolyte fuel cells," in preparation (2016).

7. Jacob LaManna, Matthew Mench, "Thermally driven water transport in PEFCs: A parametric design guide," in preparation (2016).

8. N. Macauley, R.W. Lujan, D.S. Hussey, D.L. Jacobson, K. More, D. Spernjak, R.L. Borup, and R. Mukundan, "Durability of Polymer Electrolyte Membrane Fuel Cells Operated at Subfreezing Temperatures," in preparation (2016).

9. D.S. Hussey, K.J. Coakley, E. Baltic, D.L. Jacobson, "Quantitative neutron radiography with scattering samples," in preparation (2016).

10. Spernjak, D., G. Wu, J. Fairweather, D. Hussey, R. Mukundan, R. Borup & P. Zelenay, "In situ measurement of flooding in thick Pt and PANI-derived catalyst layers in PEM fuel cells," Journal of the Electrochemical Society, In preparation (2016).

11. Hussey, Daniel S; Jacobson, David L; (Invited) "Accurate Measurement of the Water Content of Proton-Exchange Membrane Fuel Cells Using Neutron Radiography," The Electrochemical Society Meeting Abstracts 28 (2015) 1654–1654.

12. Hussey, Daniel S; LaManna, Jacob M; Baltic, Elias; Jacobson, David L; "New Neutron Imaging Detectors for PEMFC through-Plane Water Content Measurement," The Electrochemical Society Meeting Abstracts 37 (2015) 1354–1354.

13. Clement, Jason T; Aaron, Douglas; Hussey, Daniel S; Jacobson, David L; Mench, Matthew M; "Neutron Radiography Applied to All-Vanadium Redox Flow Batteries for Side Reaction Detection," The Electrochemical Society Meeting Abstracts 1 (2015) 95–95.

14. LaManna, Jacob M; Hussey, Daniel S; Jacobson, David L; Mench, Matthew M; "Influence of Thermal Conductivity and 2-D Temperature Distribution of Liquid Water Saturation," The Electrochemical Society Meeting Abstracts 37 (2015) 1539–1539.

15. Spernjak, Dusan; Chung, Hoon T; Mukundan, Rangachary; Borup, Rod L; Hussey, Daniel S; Jacobson, David L; Wu, Gang; Zelenay, Piotr; "Water Management in PEM Fuel Cells with Non-Precious Metal Catalyst Electrodes," The Electrochemical Society Meeting Abstracts 37 (2015) 1540–1540.

V.F.3 Technical Assistance to Developers

Tommy Rockward (Primary Contact) and
Rod Borup, LANL Fuel Cell Team
Los Alamos National Laboratory (LANL)
P.O. Box 1663
Los Alamos, NM 87545
Phone: (505) 667-9587
Email: trock@lanl.gov

DOE Manager: Nancy L. Garland
Phone: (202) 586-5673
Email: Nancy.Garland@ee.doe.gov

Project Start Date: October 2006
Project End Date: Project continuation and direction determined annually by DOE

Overall Objectives

This task supports LANL technical assistance to fuel cell component and system developers as directed by the DOE. This task includes:

- Testing and validation of materials and components.
- Participating in the further development and validation of single cell test protocols.
- Partaking in Durability Working Groups, the U.S. Council for Automotive Research (USCAR) and the USCAR U.S. Driving Research and Innovation for Vehicle efficiency and Energy sustainability (U.S. DRIVE) Fuel Cell Technology Team (FCTT) meetings and activities.
- Providing assistance includes making technical experts available to DOE and FCTT as questions arise.

Fiscal Year (FY) 2016 Objectives

- Perform fuel cell tests on different non-Pt anode catalyst materials provided by an outside developer; measure and verify performance and durability.
- Perform fuel cell tests on Pt/polybenzimidazole (PBI)-graphene, Pt-amine, Pt-SO_3-H, and a family of PtNi catalysts verifying performance and durability provided by an outside developer.
- Investigate the integrity and stability of the structure of novel membrane electrode assemblies (MEAs) using high resolution imaging (1–2 μ).
- Assist with ceramic coating of metal bipolar fuel cell components.
- Assist with novel supports for catalyst development by physical vapor deposition of noble metals on developer provide supports.
- Perform test on precious group metal (PGM)-free materials, testing for performance and durability using DOE accelerated stress tests (ASTs).
- Investigate high potential redox active species present in select PGM-free fuel cell electrocatalysts for the oxygen reduction reaction in acidic medium.
- Evaluate two-cell stack for hydrogen/air application. Provide feedback regarding any needed improvements that can be implemented to assist in its commercial development.
- Support DOE FCTT and working groups.

Technical Barriers

This project addresses the following technical barriers from the Technology Validation section of the Fuel Cell Technologies Office Multi-Year Research, Development, and Demonstration Plan.

(A) Durability

(B) Cost

(C) Performance (Electrode)

FY 2016 Accomplishments

- Indiana University–Purdue University Indianapolis (IUPUI):
  - Performed fuel cell tests on the impact of spacers on nanographene vs. graphene.
    - Nanographene effectively shortens the length of pore and channels within typical graphene structures which inherently leads to improved mass transport.
  - Tested Pt/PBI-nanographene with and without spacers.
    - The addition of spacers between the graphene sheets shows significant improvements at the larger current densities, particularly in the mass transport region. Results performed at LANL were improved over IUPUI results.
    - AST results show larger losses in the mass transport region of the polarization as the number of voltage cycles increase.
    - Comparison of graphene vs. XC-72 carbon black supports proved graphene as a more durable support when subjected to AST.

  - Co-authored papers (two abstracts submitted and accepted to the Electrochemical Society).
- Nissan:
  - Characterized nanofiber MEAs to compare fresh vs. aged electrode using X-ray micro-tomography.
  - Provided high resolution images and movie of the samples.
  - Results revealed only minimal changes in the electrode structure after 1,000 voltage cycles.
- Ford Motor Company: Catalyst Support Development and Bipolar Plate Coatings
  - Built and tested sample tower for heating.
  - Added residual gas analyzer mass spectrometer for measuring surface contaminants.
  - Performed ~eight depositions and characterized each; sent Ford three samples. (X-ray diffraction, scanning electron microscopy, and energy dispersive X-ray analysis) for catalyst support development.
  - Performed over 100 depositions and delivered 42 samples with protective coatings for metal bipolar plates.
- Pajarito Powder, LLC:
  - Performed ASTs on three PGM-free samples.
  - Evaluated the samples' performance and durability as a function of pressure after ASTs.
  - Reported results to customer.
- DOE FCTT:
  - Provided a permanent member to the DOE U.S. DRIVE FCTT.
  - Provided input on new AST protocols.
  - Provided input on refined Fuel Cell targets and Multi-Year Research, Development, and Demonstration Plan.

✧ ✧ ✧ ✧ ✧

INTRODUCTION

This task provides technical support to fuel cell component and system developers, free of cost to the developer, by experts within the LANL fuel cell team. In addition, it also includes participation in the further development and validation of single cell test protocols; interacting with Durability Working Groups, USCAR, and the U.S. DRIVE FCTT; and making technical experts available to DOE and FCTT.

The work performed this fiscal year, approved by the DOE, included customers and collaborators from industry, national laboratories, and various universities. In FY 2016, technical assistance included requests from Ford Motor Company, Pajarito Powders, LLC (Albuquerque, NM), IUPUI, ElectroChem Inc., Nissan, Savannah River National Laboratory (SRNL), and Amalyst.

APPROACH

LANL experts provide support to a broad customer base using available in-house equipment such as Scanning electron microscopy, energy dispersive X-ray analysis, X-ray fluorescence spectroscopy, differential scanning calorimetry, Fourier transform infrared spectroscopy, tapered element oscillating microbalance, thermogravimetric analysis, simultaneous thermogravimetric analysis and differential scanning calorimetry, differential thermal analysis, solid-phase and liquid-phase nuclear magnetic resonance, gas chromatography, mass spectroscopy, X-ray diffraction, solid-state diffuse reflectance infrared Fourier transform spectroscopy, Raman spectrometer, electron beam evaporation, radio frequency magnetron sputtering, alternating current impedance spectroscopy, and Brunauer-Emmett-Teller surface area measurements. LANL also has 38 test stands equipped with automated data acquisition and computer-controlling features that is available for this project. In FY 2016, requests included, but weren't limited to, perform fuel cell comparison tests on different non-Pt anode catalyst materials, PGM-free materials and Pt/PBI-graphene, Pt-amine, Pt-SO_3-H, and a family of PtNi catalysts by verifying performance and durability. In addition to using X-ray tomography to investigate the integrity and stability of a nanofiber electrode structure using high resolution imaging (1–2 μ), and deposition techniques to assist with ceramic coating of fuel cell components and catalyst development. Requests also included evaluation of high potential redox active species present in select PGM-free fuel cell electrocatalysts for the oxygen reduction reaction in acidic medium and a two-cell fuel cell stack for hydrogen–air application and provide feedback to assist in its commercialization.

RESULTS

We provided completed results and findings to our customers as detailed in the *FY 2016 Accomplishments* section of the 2016 DOE Hydrogen and Fuel Cells Program Annual Merit Review presentation. Due to the length constraint of this report, we will only discuss results from some of the objectives mentioned above.

For example, we worked closely with IUPUI to evaluate the performance and durability of their MEAs made with graphene-type supports. Several challenges exist when graphene is used as a support for Pt catalysts in fuel cell

type applications. Because graphene is hydrophobic, it is often difficult to create a uniform dispersion of Pt on the substrate and hard to establish a bond between the two materials. Also, graphene substrates form layering sheets that can inhibit gas access to the catalyst which can reduce the electrochemical surface area and typically there are defects at the edges which can facilitate carbon corrosion due to its poor stability. By overcoming these challenges, the expectations are improvements in fuel cell performance and durability. IUPUI scientists functionalized the graphene to reduce hydrophobicity, introduced spacers to prevent layering of graphene sheets, and seal their edges to eliminate defects. Tests were conducted on these materials using, 5 cm^2 MEAs, made with Nafion® 212 membranes and 0.1 mg/cm^2 Pt at each electrode. The performance was measured using both H_2–air and H_2/O_2 at 80°C, 100% relative humidity, and 300 kPa of back pressure. Figure 1 shows the impact of adding spacers. The results show the significant improvements at the larger current densities, particularly in the mass transport region for the samples prepared with spacers. This may be due to the spacers producing a more open-type structure with pores and channels formed to allow better mass transport. We also tested their MEAs made with spacers using nanographene versus graphene as the support under the same operating conditions aforementioned as well as using the DOE AST protocol for supports (Triangle sweep: 500 mV/s from 1.0–1.5 V, H_2/N_2, 80°C, ambient pressure, and 100% relative humidity). The MEA made with nanographene and spacers performed much better at the beginning of life but suffered from larger losses in mass activity and electrochemical surface area after the 10,000 cycles using the AST (results not shown here).

In the analysis of samples provided by Nissan, LANL used high resolution imaging (X-ray tomography) to investigate the integrity and stability of their nanofiber structure used for MEAs. The MEA was aged using the above mentioned DOE AST protocol for 1,000 cycles. High resolution images comparing a "fresh" vs. "aged" MEA, showed only minimal changes in the electrode structure. This is captured in Figure 2.

The LANL-Ford cooperation began in FY 2015 and is ongoing. LANL is using a novel system for multi-layer deposition of materials to treat surfaces in order to

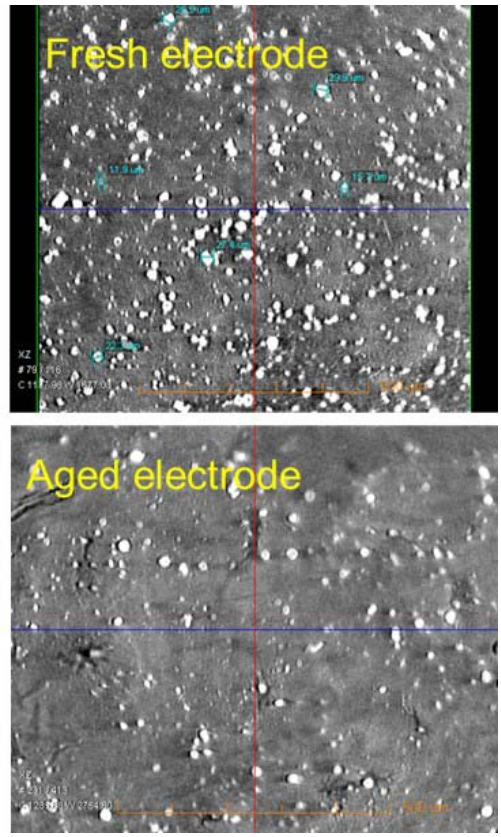

FIGURE 2. X-ray tomography results of nanofiber MEAs: fresh vs. aged

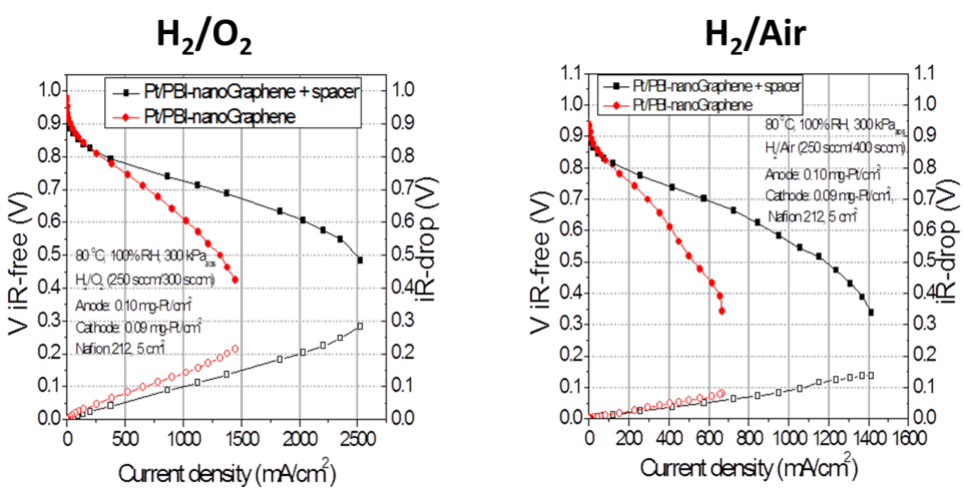

FIGURE 1. The impact of spacers on Pt/PBI-nanographene: H_2–air and H_2/O_2

prevent corrosion. LANL performed eight depositions and characterized each using X-ray diffraction, scanning electron microscopy, and energy dispersive X-ray analysis related to catalyst support materials, and over 100 depositions with 42 samples delivered for metal-ceramic coatings for bipolar plate materials.

In this fiscal year, LANL and SRNL started complementary work to investigate high potential redox active species present in select non-PGM fuel cell electrocatalysts for the oxygen reduction reaction in acidic medium. SRNL is currently conducting a study to investigate the electrochemistry of a catalyst prepared by SRNL from a metallic organic framework that displays high oxygen reduction reaction activity and a high potential redox couple measured during potential cycling. LANL will perform an electrochemical characterization similar to SRNL's study using catalysts synthesized from different materials and methodologies. Results produced will be compared to LANL's high activity catalysts.

FUTURE WORK

A large portion of work in this project is still ongoing and expected to continue into FY 2017. Below we list the collaborators along with the details of the anticipated work.

- Ford Motor Company:
  - Complete the test matrix of bi-polar plate multi-layer passivation samples.
  - Optimize coating catalyst supports with metals deposited using LANL acoustic agitation approach developed in FY 2015 and tested in FY 2016.
- Amalyst:
  - Non-Pt Anode catalyst (verify performance, durability)
- IUPUI:
  - Investigate novel catalyst–MEA architecture.
  - Continue testing PtNi MEAs.
- SRNL:
  - PGM-free testing of metal organic framework catalyst
- ElectroChem, Inc.:
  - Stack testing and validation
- Pajarito Powder, LLC:
  - Continue testing MEA samples with DOE ASTs.
- Participate on the DOE USCAR U.S. DRIVE Fuel Cell Tech Team.
- Continue to support DOE working groups.
  - Durability Working Group
  - Mass Transport Working Group
- Provide technical assistance to developers as requested by DOE and report on the results to DOE and the U.S. DRIVE Fuel Cell Tech Team.

FY 2016 PUBLICATIONS/PRESENTATIONS

A significant portion of this effort often goes unpublished at the customer's request.

1. *Polybenzimidazole (PBI) functionalized nanographene as highly stable catalyst support for polymer electrolyte membrane fuel cells (PEMFCs)*, Le Xin, Fan Yang, Yang Qiu, Aytekin Uzunoglu, Tommy Rockward, Rodney L. Borup, Lia A. Stanciu, Wenzhen Li and Jian Xie (submitted to Journal of the Electrochemical Society).

2. *Novel Catalyst-Layer Structures with Rationally Designed Catalyst/Ionomer Interfaces and Pore Structures Aided by Catalyst Functionalization,* Le Xin[1], Kang Yu[2], Fan Yang[1], Aytekin Uzunoglu[3], Tommy Rockward[5], Paulo Ferreira[2], Rod L. Borup[5], Jan Ilavsky[6], Lia A. Stanciu[3,4], Jian Xie[1*]

V.F.4 Fuel Cell Technology Status: Degradation

Jennifer Kurtz (Primary Contact), Huyen Dinh, and Genevieve Saur
National Renewable Energy Laboratory
15013 Denver West Parkway
Golden, CO 80401-3305
Phone: (303) 275-4061
Email: jennifer.kurtz@nrel.gov

DOE Manager: David Peterson
Phone: (720) 356-1747
Email: David.Peterson@ee.doe.gov

Project Start Date: July 1, 2009
Project End Date: Project continuation and direction determined annually by DOE

Overall Objectives

- Conduct an independent assessment to benchmark current fuel cell system cost and price in a non-proprietary method.
- Leverage National Fuel Cell Technology Evaluation Center (NFCTEC) activities.
- Collaborate with key fuel cell developers on the voluntary data share and NFCTEC analysis.

Fiscal Year (FY) 2016 Objectives

- Receive and analyze new laboratory durability data.
- Publish aggregated, current fuel cell voltage durability status.
- Include electrolysis data.

Technical Barriers

This project addresses the following technical barriers from the Fuel Cells section of the Fuel Cell Technologies Office Multi-Year Research, Development, and Demonstration Plan.

(A) Durability (Lack of data for current fuel cell durability status per targets)

(B) Cost (Lack of data for current fuel cell costs and status per targets)

Technical Targets

This project is conducting an independent assessment of the current fuel cell durability test data from leading fuel cell developers. All results are aggregated to protect proprietary information and are reported by the system application. Table 1 shows the durability targets.

TABLE 1. Fuel Cell Durability Target and Status Table

Application	2020 Durability Target	Lab Status – Ave. Hours to 10% Voltage Degradation
Light-Duty Automotive	5,000 h	3,500
Public Transit	25,000 h	6,200
Forklift	20,000 h Target Under Review	13,200
Backup	10,000 h Target Under Review	2,600
Stationary 1–10 kW	0.3%/1,000 h	8,600
Stationary 100 kW–3 MW	80,000 h	

Per the Fuel Cells section of the Fuel Cell Technologies Office Multi-Year Research, Development, and Demonstration Plan, the cost targets are as follows:

- The 2017 transportation fuel cell system cost target is $30/kW.
- The 2020 micro-combined heat and power (5 kW) fuel cell system cost target is $1,500/kW.
- The 2020 medium combined heat and power (100 kW–3 MW) fuel cell system cost target is $1,000/kW for natural gas and $1,400/kW for biogas.

FY 2016 Accomplishments

- Collected new fuel cell voltage degradation data sets from fuel cell developers (including data on proton exchange membrane, direct methanol, and solid oxide fuel cell of full active area short stacks and full stacks with systems).
- Analyzed, aggregated, and published current status of electrolysis voltage degradation.
- Analyzed, aggregated, and published current status of fuel cell voltage degradation versus DOE targets.
- Published 17 composite data products (CDPs) [1] with data from 23 domestic and international fuel cell and electrolysis developers.

✧ ✧ ✧ ✧ ✧

INTRODUCTION

DOE has funded significant research and development activity with universities, national laboratories, and the fuel

cell industry to improve the market competitiveness of fuel cells. Most of the validation tests to confirm improved fuel cell stack performance and durability (indicators of market competitiveness) are completed by the research organizations themselves. Although this allows the tests to be conducted by the developers most familiar with their specific technology, it also presents a number of challenges in sharing progress publicly because test conditions and data analysis take many forms and data collected during testing are often considered proprietary.

The National Renewable Energy Laboratory (NREL) is benchmarking the state-of-the-art fuel cell performance, specifically focusing on durability, through independent assessment of current laboratory data sets. NREL's data processing, analysis, and reporting capitalize on capabilities developed in DOE's Fuel Cell Electric Vehicle Learning Demonstration. Fuel cell stack durability status is reported annually and includes a breakdown of status for different applications. A key component of this project is the collaborative effort with key fuel cell developers to understand what is being tested in the laboratory, study analysis results, and expand the included data sets.

APPROACH

The project involves voluntary submission of data from relevant fuel cell developers. NREL is contacting fuel cell developers for fuel cell voltage degradation and cost and price data for multiple fuel cell types to either continue or begin a data sharing collaboration. A continuing effort is to include more data sets, types of fuel cells, quantity of units sold, and developers. The fuel cell voltage degradation data are sent from fuel cell developer testing and studied over time against DOE's voltage degradation targets.

Raw and processed data are stored in NREL's NFCTEC. The NFCTEC is an off-network room with access provided to a small set of approved users. Processing capabilities are developed or modified for new data sets and then included in the analytical processing of NREL's Fleet Analysis Toolkit, an internally developed tool for data processing and analysis structured for flexibility, growth, and simple addition of new applications. Analyses are created for general performance studies as well as application- or technology-specific studies. The incoming raw data may be new or a continuation of data that have already been supplied to NREL. An internal analysis of all available data is completed annually and a set of technical CDPs is published every year. Publications are uploaded to NREL's technology validation website [1] and presented at industry-relevant conferences. The CDPs present aggregated data across multiple systems, sites, and teams to protect proprietary data and summarize the performance of hundreds of fuel cell systems and thousands of data records. A review cycle is completed before the CDPs are published. This review cycle includes providing detailed data products of individual system- and site-performance results to the specific data provider. Detailed data products also identify the individual contribution to the CDPs.

RESULTS

Results published in May 2016 were the sixth update for this analysis effort. The annual voltage degradation analysis of state-of-the-art laboratory durability was completed in advance of the milestone to provide an update that could be presented at DOE's Annual Merit Review and Peer Evaluation Meeting. In the current published data set, seven applications were covered and 23 fuel cell and electrolyzer developers supplied data (more than one data set in many cases). The data sets covered proton exchange membrane, direct methanol, and solid oxide fuel cell stack testing as well as electrolyzer testing. A total of 174 data sets have been analyzed. Note that a data set represents a short stack, full stack, or system test data. Of the total data sets, 90% have been retired, meaning the system or stack is not accumulating any new operation hours either because of test completion, technology upgrades, or failures. The published data results include 17 CDPs. The power capability illustrates the range of fuel cell power for the data sets by application from less than 2 kW to more than 50 kW. Most of the analyzed data sets are laboratory systems at less than 14 kW power.

The analyzed data sets are from laboratory testing of full active area short stacks (e.g., stacks with fewer cells than the expected full power stack) and test systems with full power stacks. The data sets also vary from one to the other in how the stack or system was tested. Data were generated between 2004 and late 2015 from different testing methods that included constant load, transient load, and accelerated testing. The variability in test conditions and test setups created a group of data that can be difficult to compare.

Fuel cell durability is studied at a design-specific current point and measured against a target of 10% voltage drop from beginning of life. The 10% voltage drop metric is used for assessing voltage degradation with a common measurement, but the metric may not be the same as end-of-life criteria and does not address catastrophic failure modes. Figure 1 is an aggregated set of results separated by application. For each application, the average, maximum, and 25th and 75th percentile values are identified for the operation hours and the projected hours to 10% voltage drop. Current density variation (Figure 2) is dependent on developer-selected test protocols and objectives. A future comparison could be the study of voltage degradation at one chosen current density for all data sets within a category or type. The current density points used for the aggregated durability results are based on individual designs, and data may not be available at multiple current densities. The most variety in current density is seen in the prime and automotive categories.

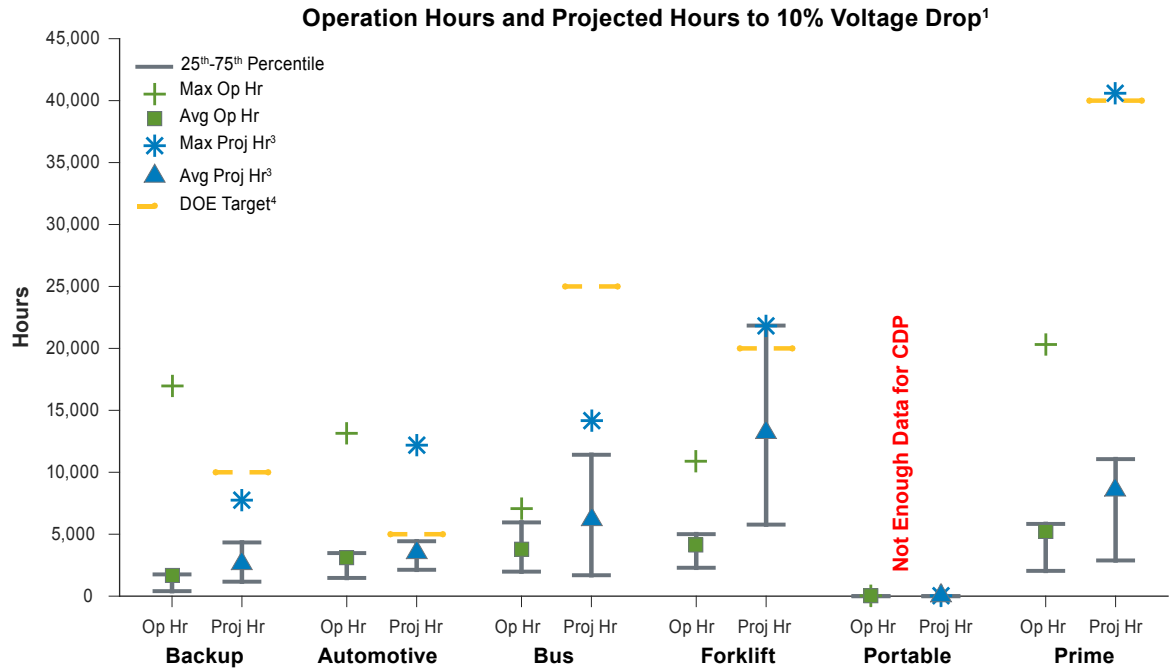

FIGURE 1. Voltage degradation results by application

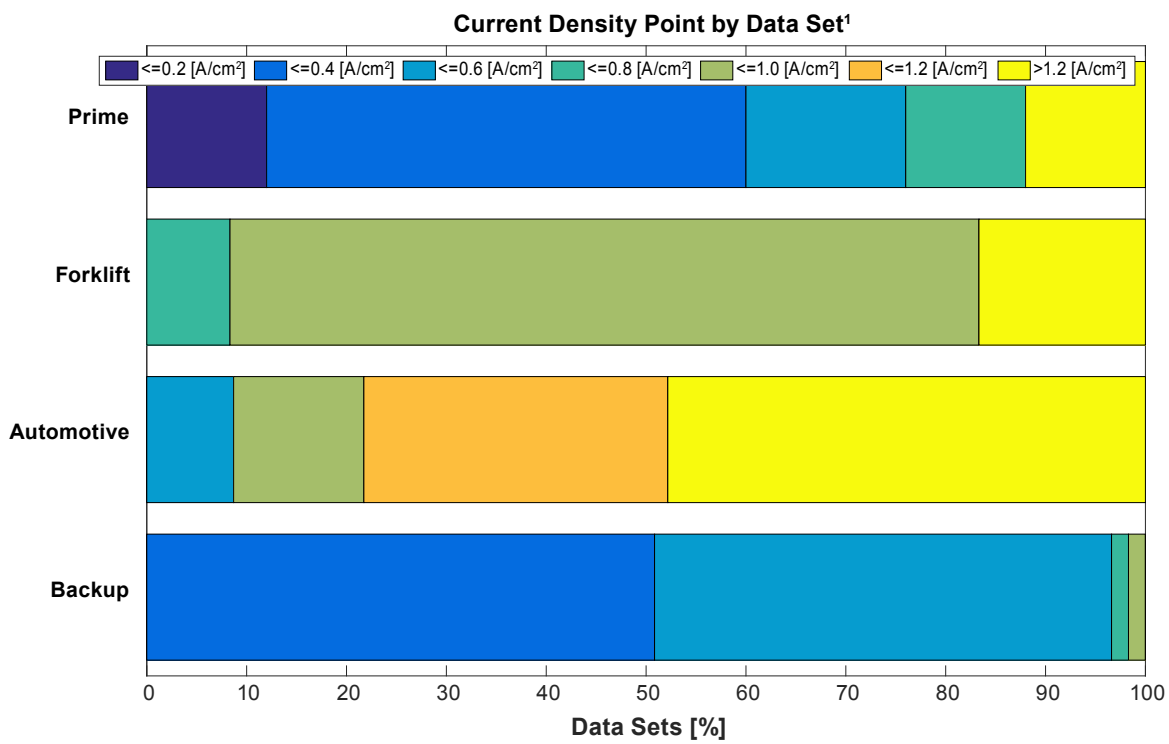

FIGURE 2. Current density variation between data

The 10% voltage drop level is not necessarily a measurement for end of life or even a significant reduction in performance. Many data sets have not passed (or did not pass) the metric of 10% voltage degradation. The reason data sets operated beyond 10% voltage degradation could be because end-of-life criteria may be greater than 10% voltage degradation or because the test was designed to operate until a failure occurred. The stack configuration and test

conditions can have a significant impact on the projected time to 10% voltage degradation within an application. In general, the average projection decreases with more aggressive test conditions and full systems. Not all applications have data sets in each configuration or test condition group. The test condition groups include:

- Steady—little or no change to load profile
- Duty Cycle—load profile mimics real-world operating conditions
- Accelerated—test profile is more aggressive than real-world operating conditions.

In the automotive category, voltage durability projections are relatively stable over the years of analysis (Figure 3). A possible reason for this is a shift in focus from durability to cost reduction while maintaining an acceptable degradation rate. Another reason is the inclusion of legacy data with current results. There is symbiosis between cost and durability, and, depending on the economics, durability may not be the driving technical parameter at this time.

This fiscal year the capability to study electrolyzer voltage degradation was added and results were published (Figure 4). The method is similar to the process for the fuel cell data sets, except voltage is increasing over time. Mechanisms (e.g., operating temperature) impacting durability can be added to the analysis. No targets currently exist for electrolyzer voltage degradation.

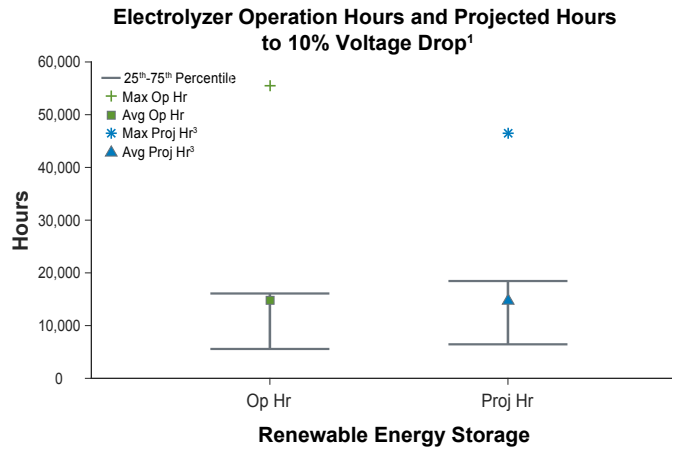

FIGURE 4. Voltage degradation for electrolyzers

CONCLUSIONS AND FUTURE DIRECTIONS

This project has leveraged other technology validation projects and existing industry relationships to steadily increase the quantity and depth of reporting on the state-of-the-art fuel cell durability status with a relatively low investment from DOE. U.S. and international developers have voluntarily supplied at least one data set, and it is an ongoing effort to include new data sets, update data sets already included (if applicable), and include new fuel cell developers, applications, and types. The voluntary participation of

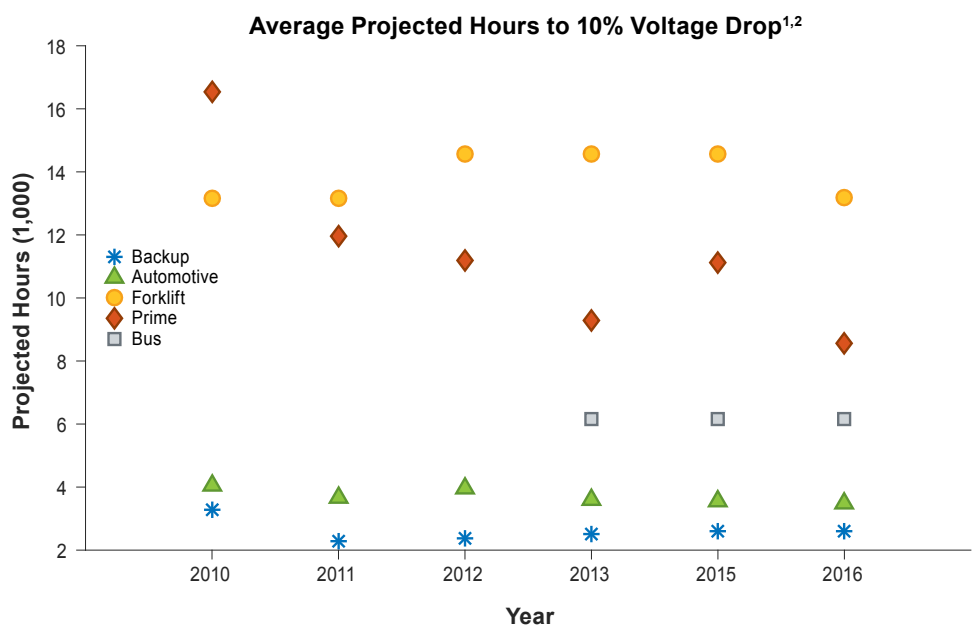

FIGURE 3. Voltage degradation trend over time by application

leading fuel cell and electrolyzer developers provides an overall technology benchmark (with the published aggregated data) and an individual developer benchmark (with the detailed data products). Additional breakdown of the data sets is an important aspect of future work and is dependent on the accumulation of more data sets to not reveal an individual data supplier's contribution to the results or proprietary data. Future work, following the path of degradation and cost and price status updates every other year, includes the following:

- Continue cultivating existing collaborations and developing new collaborations with fuel cell and electrolyzer developers.
- Gather, process, and report on current fuel cell product cost and/or price.
- Add data set specifications (e.g., platinum content range) and accelerated testing comparisons, and address legacy data.

FY 2016 PUBLICATIONS/PRESENTATIONS

1. Jennifer Kurtz, Huyen Dinh, Genevieve Saur, and Chris Ainscough, "Fuel Cell Technology Status – Degradation," presented at the 2016 DOE Annual Merit Review and Peer Evaluation Meeting, Washington, D.C., June 2016.

2. "Transportation Big Data: Unbiased Analysis and Tools to Inform Sustainable Transportation Decisions," NREL/BR-5400-66285, Golden, CO: National Renewable Energy Laboratory, June 2016.

3. Jennifer Kurtz, Huyen Dinh, Genevieve Saur, and Chris Ainscough, "Fuel Cell Technology Status – Degradation: FC Tech Team," presented to the Fuel Cell Tech Team, May 2016.

4. Jennifer Kurtz, Huyen Dinh, Chris Ainscough, and Genevieve Saur, "State-of-the-Art Fuel Cell Voltage Durability Status: 2016 Composite Data Products," NREL/PR-5400-66581, Golden, CO: National Renewable Energy Laboratory, May 2016.

5. Jennifer Kurtz, Huyen Dinh, Chris Ainscough, and Genevieve Saur, "Fuel Cell Technology Status – Degradation," excerpt from the 2015 DOE Hydrogen and Fuel Cells Program Annual Progress Report, December 2015.

6. "Fuel Cell Technology Status Analysis Project: Partnership Opportunities," NREL/FS-5400-65090, Golden, CO: National Renewable Energy Laboratory, September 2015.

REFERENCES

1. "Fuel Cell Technology Status Analysis," National Renewable Energy Laboratory, http://www.nrel.gov/hydrogen/proj_fc_analysis.html.

V.F.5 Performance and Durability of Advanced Automotive Fuel Cell Stacks and Systems with Nanostructured Thin Film Catalyst Based Membrane Electrode Assemblies

Rajesh K. Ahluwalia (Primary Contact),
Xiaohua Wang, and J-K Peng
Argonne National Laboratory
9700 South Cass Avenue
Argonne, IL 60439
Phone: (630) 252-5979
Email: walia@anl.gov

DOE Manager: Nancy L. Garland
Phone: (202) 586-5673
Email: Nancy.Garland@ee.doe.gov

Project Start Date: October 1, 2003
Project End Date: Project continuation and direction determined annually by DOE

Overall Objectives

- Develop a validated model for automotive fuel cell systems, and use it to assess the status of the technology.
- Conduct studies to improve performance and packaging, to reduce cost, and to identify key R&D issues.
- Compare and assess alternative configurations and systems for transportation and stationary applications.
- Support DOE U.S. DRIVE automotive fuel cell development efforts.

Fiscal Year (FY) 2016 Objectives

- Quantify the impact of thinner membranes, lower anode Pt loadings, and high-activity de-alloyed nanostructure thin film (NSTF) Pt_3Ni_7 cathode on the performance of automotive stacks and fuel cell systems.
- Understand the durability of NSTF electrode under long potentiostatic holds.
- Extend system analysis to alternate non-NSTF membrane electrode assemblies (MEAs) with conventional Pt/C and advanced Pt alloy/C cathode catalysts.
- Incorporate durability considerations in system analysis.
- Provide modeling support to Eaton's development of Roots air supply system.

Technical Barriers

This project addresses the following technical barriers from the Fuel Cells section of the Hydrogen, Fuel Cells, and Infrastructure Technologies Program Multi-Year Research, Development, and Demonstration Plan:

(A) Durability

(B) Cost

(C) Performance

Technical Targets

This project is conducting system level analyses to address the following DOE 2020 technical targets for automotive fuel cell power systems operating on direct hydrogen.

- Energy efficiency: 60% at 25% of rated power
- Q/DT: 1.45 kW/°C
- Power density: 850 W/L for system, 2,500 W/L for stack
- Specific power: 850 W/kg for system, 2,000 W/kg for stack
- Transient response: 1 s from 10% to 90% of maximum flow
- Start-up time: 30 s from –20°C and 5 s from +20°C ambient temperature
- Precious metal content: 0.125 g/kW_e rated gross power

Accomplishments

- Quantified the sources of 14–20% decrease in power density and \$2.20/kW_e increase in cost due to the heat rejection (Q/DT) constraint.
- Identified the dominant NSTF catalyst degradation mode and determined that the cumulative fluoride release (CFR) must be limited to 0.7 $mg.cm^{-2}$ for 10% performance degradation over 5,000 h.
- Projected 25% increase in power density and 16.8% reduction in stack cost by reducing anode Pt loading to 0.02 mg/cm^2, and replacing $Pt_{68}(CoMn)_{32}$/NSTF with Pt_3Ni_7/NSTF cathode catalyst and 20-mm 835 equivalent weight (EW) membrane with supported 14-mm 725 EW membrane.
- Demonstrated that, compared to a baseline unit, the V250 module (without expander) reduces parasitic

power by 6.4% at full flow (92 g/s) and by 35% at quarter flow (25 g/s).

✧ ✧ ✧ ✧ ✧

INTRODUCTION

While different developers are addressing improvements in individual components and subsystems in automotive fuel cell propulsion systems (i.e., cells, stacks, balance-of-plant components), we are using modeling and analysis to address issues of thermal and water management, design-point and part-load operation, and component-, system-, and vehicle-level efficiencies and fuel economies. Such analyses are essential for effective system integration.

APPROACH

Two sets of models are being developed. The GCtool software is a stand-alone code with capabilities for design, off-design, steady state, transient, and constrained optimization analyses of fuel cell systems (FCS). A companion code, GCtool-ENG, has an alternative set of models with a built-in procedure for translation to the MATLAB Simulink platform commonly used in vehicle simulation codes, such as Autonomie.

RESULTS

We collaborated with 3M in designing tests on 5-cm^2 active-area differential cells and analyzing the data to model the performance of full-area (>250 cm^2) cells with 3M's state-of-the-art binary dealloyed NSTF catalyst with Pt/C cathode interlayer [1]. The following are the details of the MEA selected for this study.

- Ternary Anode: $Pt_{68}(CoMn)_{32}$, 0.019 mg_{Pt}/cm^2
- Binary Cathode: Pt_3Ni_7/NSTF, dealloyed (Johns Hopkins University chemistry), 0.096 mg_{Pt}/cm^2
- Membrane: 3M-S (supported) 725 EW) perfluorosulfonic acid stabilized with chemical additive, 14 mm
- Anode Gas Diffusion Layer (GDL): 3M "X3" (experimental backing, 3M hydrophobization)
- Cathode GDL: 3M 2979
- Cathode Interlayer: 3M Type "B", 0.016 mg_{Pt}/cm^2

For reproducibility of data, the test campaign included three thermal conditioning cycles (TCs) in normal and reverse flow before each test series and 1 TC before each polarization curve. Test series were designed to obtain performance data over a wide range of pressure (P: 1–3 bar), temperature (T: 45–90°C), O_2 mole fraction ($X(O_2)$: 1–21%, 100%;), anode relative humidity (RH(a): 30–100%) and cathode relative humidity (RH(c): 30–150%), all at constant hydrogen ($Q(H_2)$: 1 slpm) and air (Q(air): 3 slpm) flow rates. Changes in high frequency resistance, H_2 crossover, mass activity, electrochemical surface area (ECSA), and short resistance were monitored. Over ~735 h actual test time, the ECSA decreased by ~25% from 22.9 to 17.2 m^2/g. Figure 1a shows the variability in polarization curve at the reference conditions that were visited multiple times during the course of the campaign. We did not observe any significant systematic degradation and have classified the polarization curves in two groups, high performance (HIP) and representative performance (REP).

We estimated the oxygen reduction reaction (ORR) kinetic parameters from internal resistance and crossover corrected cell voltages at low current densities in H_2/O_2 and H_2/air (see Figures 1b, 1c, and 1d). The modeled mass activity of binary Pt_3Ni_7/NSTF with cathode interlayer was compared with the data for two other NSTF catalysts analyzed in earlier works [2,3]. In general, the modeled mass activities of all three catalyst systems are consistent with the data obtained using the 3M standard protocol. Compared to the baseline ternary $Pt_{68}(CoMn)_{32}$/NSTF catalyst, the mass activity of binary d-Pt_3Ni_7/NSTF catalyst with cathode interlayer is 78–144% higher.

We determined the limiting current density (i_L) and correlated mass transfer overpotential (h_m) with reduced the current density (i/i_L). For convenience, we defined i_L as the current density at which h_m = 300 mV. In our terminology, h_m includes any internal resistance drop in the electrode. We also determined relationships between h_m (and i_L) and all operating variables: P, T, $X(O_2)$, RH(a), RH(c), i/i_L. Figures 1e and 1f are illustrative examples of this relationship for one variable, i.e., pressure.

Work is underway to calibrate the performance model developed using differential cell data with 50-cm^2 cell data for finite cathode/anode stoichiometries and operating temperatures needed to satisfy the Q/DT constraint. The preliminary results indicate that 3M's best-of-class (BOC) 50-cm^2 cell data are closer to the modeled results without mass transfer overpotentials. There is a parallel ongoing effort to replicate 3M's BOC performance with identical cells and conditioning procedures. In the future, we also hope to validate our model with data from full-area short stack being built.

We integrated the cell model in our FCS analysis code and conducted a study to project the beginning of life performance of FCS with d-Pt_3Ni_7/NSTF catalyst and cathode interlayer, subject to Q/DT constraint [3], The MEAs in this study have 0.131 mg/cm^2 total Pt loading and 725 EW, 14 mm 3M-S membrane. At optimal conditions, the optimal power density is determined by high frequency resistance and ORR activity rather than mass transfer overpotentials. The projected cost ($1,500/tr-oz Pt price) and Pt content are

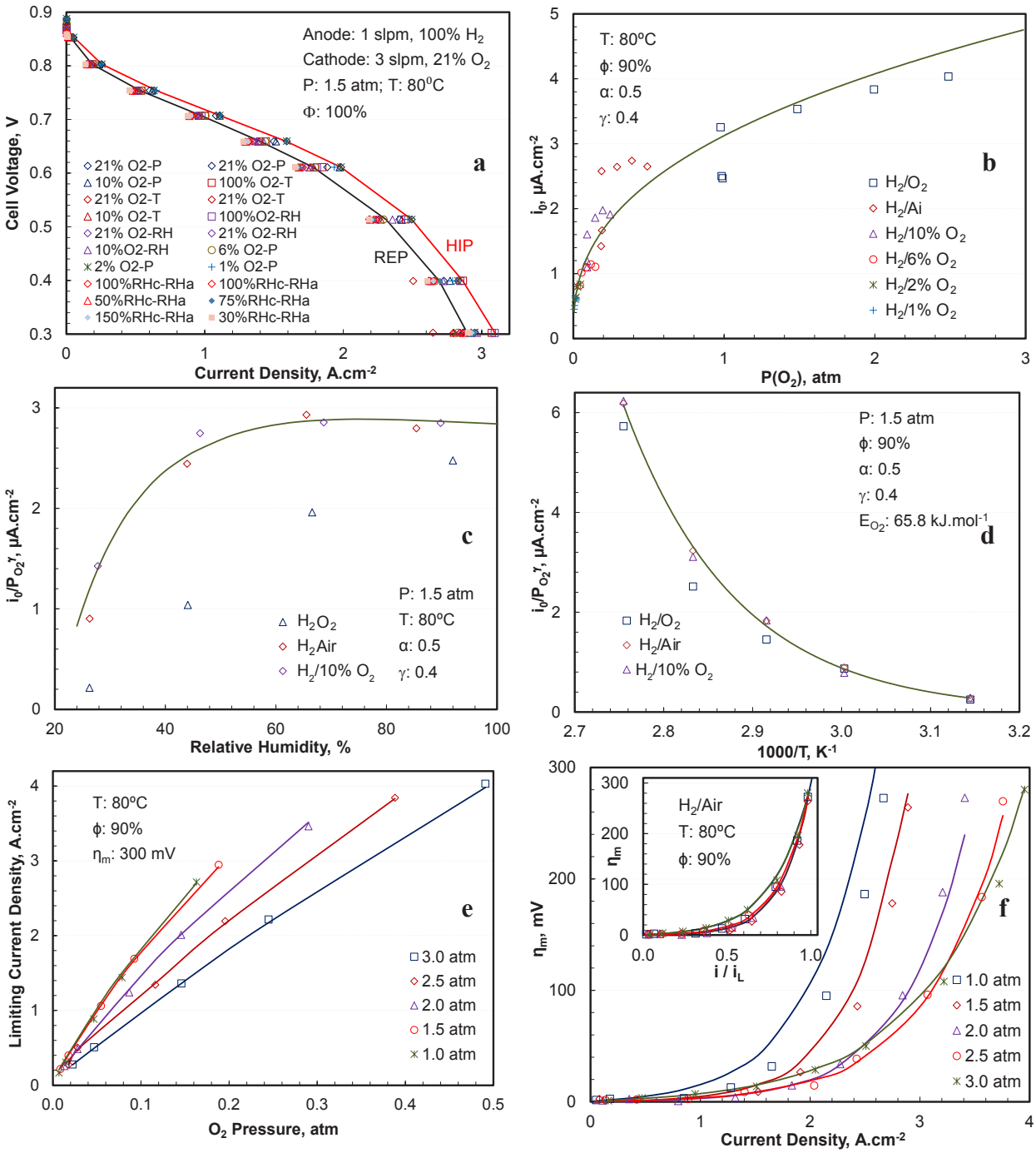

FIGURE 1. Development of performance model using differential cell data for MEA with d-Pt_3Ni_7 NSTF catalyst with cathode interlayer. Equation for ORR kinetics: $i + i_x = i_{0r} P_{O2}^{\gamma} \phi^{\beta} e^{\frac{E_{O2}}{R}\left(\frac{1}{T}-\frac{1}{T_r}\right)} e^{\frac{\alpha n F}{RT}\eta}$. Reproducibility of test data for standard conditions; (b) ORR kinetics: $P(O_2)$ dependence; (c) ORR kinetics: RH dependence; (d) ORR kinetics: T dependence; (e) Limiting current density correlation; (f) Mass transfer overpotential correlation. Solid lines are model results.

\$48.4–48.7/kW_e at 2.2–2.5 atm, and 0.152–0.155 g-Pt/kW_e at 2.5–3.0 atm stack inlet pressure, see Figures 2a and 2b.

Figures 2c, 2d, and Table 1 compare the cost and performance of fuel cell systems with different NSTF catalysts and membranes. The 2015 reference FCS includes ternary catalyst MEA and 20 mm, 835 EW membrane without mechanical reinforcement [4]. The 2016 reference FCS includes binary NSTF catalyst with Pt/C cathode

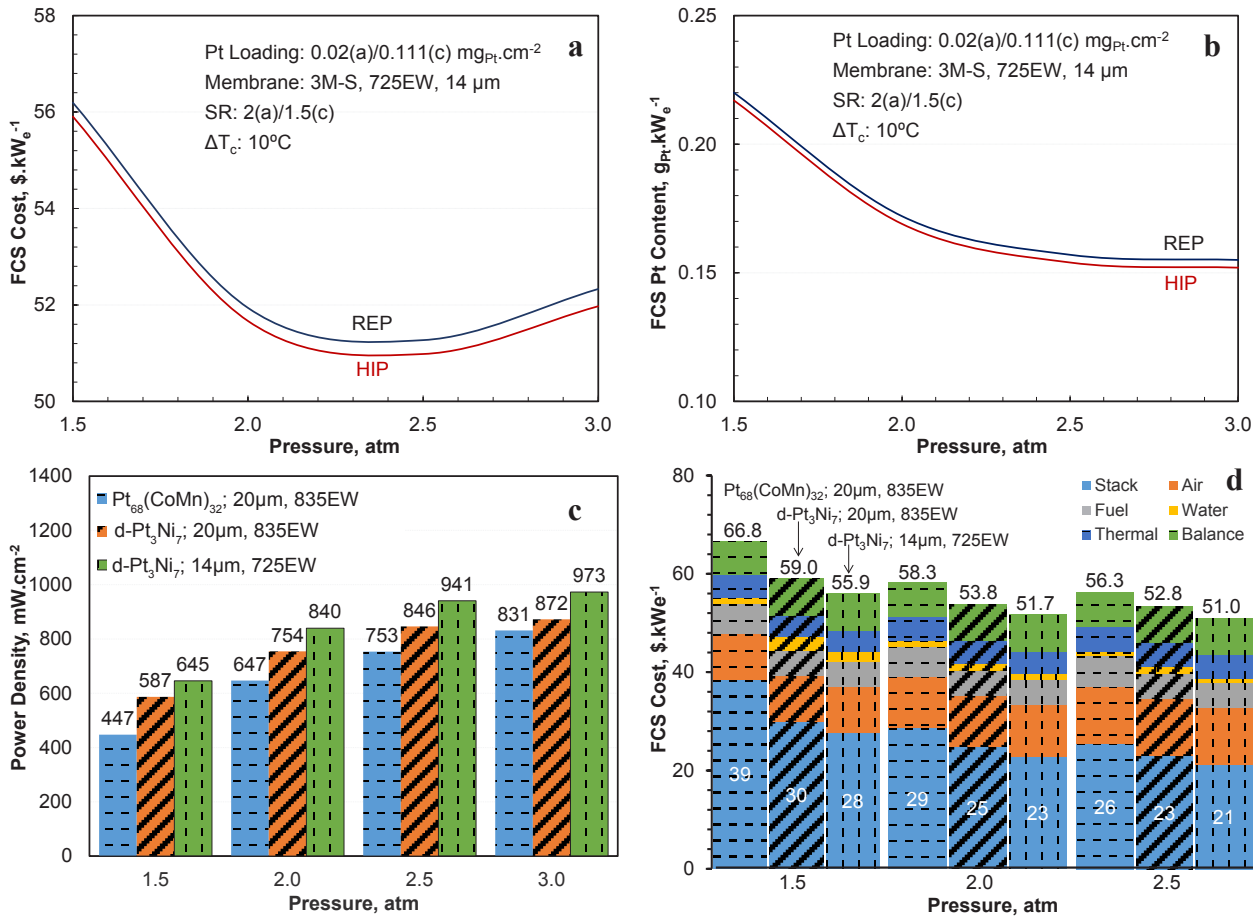

SR - Stoichiometric ratio

FIGURE 2. Projected performance and cost of automotive fuel cell systems with NSTF catalyst based MEAs. (a) Minimum FCS cost at different stack inlet pressures; (b) FCS Pt content at optimum conditions; (c) Stack power density for different NSTF MEAs; (d) FCS cost for different NSTF MEAs

TABLE 1. Summary Performance of Stacks with Different NSTF Catalysts and Membranes

Cathode / Anode Catalyst	Membrane	Cathode / Anode Pt Loading	Power Density (2.5 atm)	Stack Cost (2.5 atm)
C: $Pt_{68}(CoMn)_{32}$ A: $Pt_{68}(CoMn)_{32}$	20 µm, 835 EW	0.1 mg/cm^2 0.05 mg/cm^2	753 mW/cm^2	25.69 $/kW$_e$
C: d-Pt_3Ni_7 + Cathode Interlayer A: $Pt_{68}(CoMn)_{32}$	20 µm, 835 EW	0.095 + 0.016 (CI) mg/cm^2 0.02 mg/cm^2	+12.3%	-10.0%
C: d-Pt_3Ni_7 + Cathode Interlayer A: $Pt_{68}(CoMn)_{32}$	14 µm (S), 725 EW	0.095 + 0.016 (CI) mg/cm^2 0.02 mg/cm^2	+25.0%	-16.8%

interlayer and mechanically reinforced 14 mm, 725 EW membrane. For better understanding of results, we included an FCS with binary NSTF catalyst and Pt/C cathode interlayer but 20 mm, 835 EW membrane as in 2015 FCS. Compared to the 2015 reference FCS, the 2016 FCS has 25% higher stack power density: 12.3% due to higher ORR activity and 12.7% due to thinner membrane. It also has 16.8% lower stack cost: 10% due to higher ORR activity and 6.8% due to thinner membrane. The projected performance and cost of 2016 FCS are 973 mW/cm^2 stack power density,

0.152 g/kW$_e$ Pt content, and 48.40 \$/kW$_e$ system cost at high volume manufacturing.

Durability of MEAs with NSTF Catalysts

We have been collaborating with 3M to develop a test protocol for determining the stability of the baseline ternary NSTF catalyst under potentiostatic conditions [5]. The protocol consists of repeatedly degrading the cell for 10 h at constant potential with periodic F^- collection and partial reconditioning with 1 TC cycle. Every 20 h of degradation, polarization curves are taken in H_2/air. Every 40–80 h of degradation, the cell is reconditioned more fully with 3 TC cycles and data are obtained to measure the cathode ORR activity, cathode ECSA, H_2 crossover, shorting resistance, and cell polarization in H_2/air. The tests were run on 50-cm^2 cells with quad serpentine flow fields and ternary catalysts with 0.05 mg/cm^2 Pt loading on anode and 0.15 mg/cm^2 Pt loading on cathode. The cells used 3M, 825 EW, membrane that was 20 mm thick. The membrane was chemically stabilized with an anti-oxidant additive but was not mechanically supported.

Figures 3a and 3b present voltage degradation determined from the polarization curves for three current densities representing near open-circuit condition (0.032 A/cm^2), kinetic region (0.32 A/cm^2), and the region where the mass transfer overpotentials may become important (1 A/cm^2). The voltage degradation rates are comparable at 0.032 A/cm^2 and 0.32 A/cm^2 indicating that the underlying mechanism may be related to the slowdown of ORR kinetics at low current densities. The voltage degradation rates are much larger at 1 A/cm^2 suggesting that mass transfer in the MEA is also impeded with exposure time. The data quantitatively confirms that the voltage degradation rates are accelerated at lower hold potentials and higher exposure temperatures.

Figures 3c and 3d present the fluoride emission rate (FER) measured by ion chromatography of the collected water samples. F^- concentrations in the water samples were

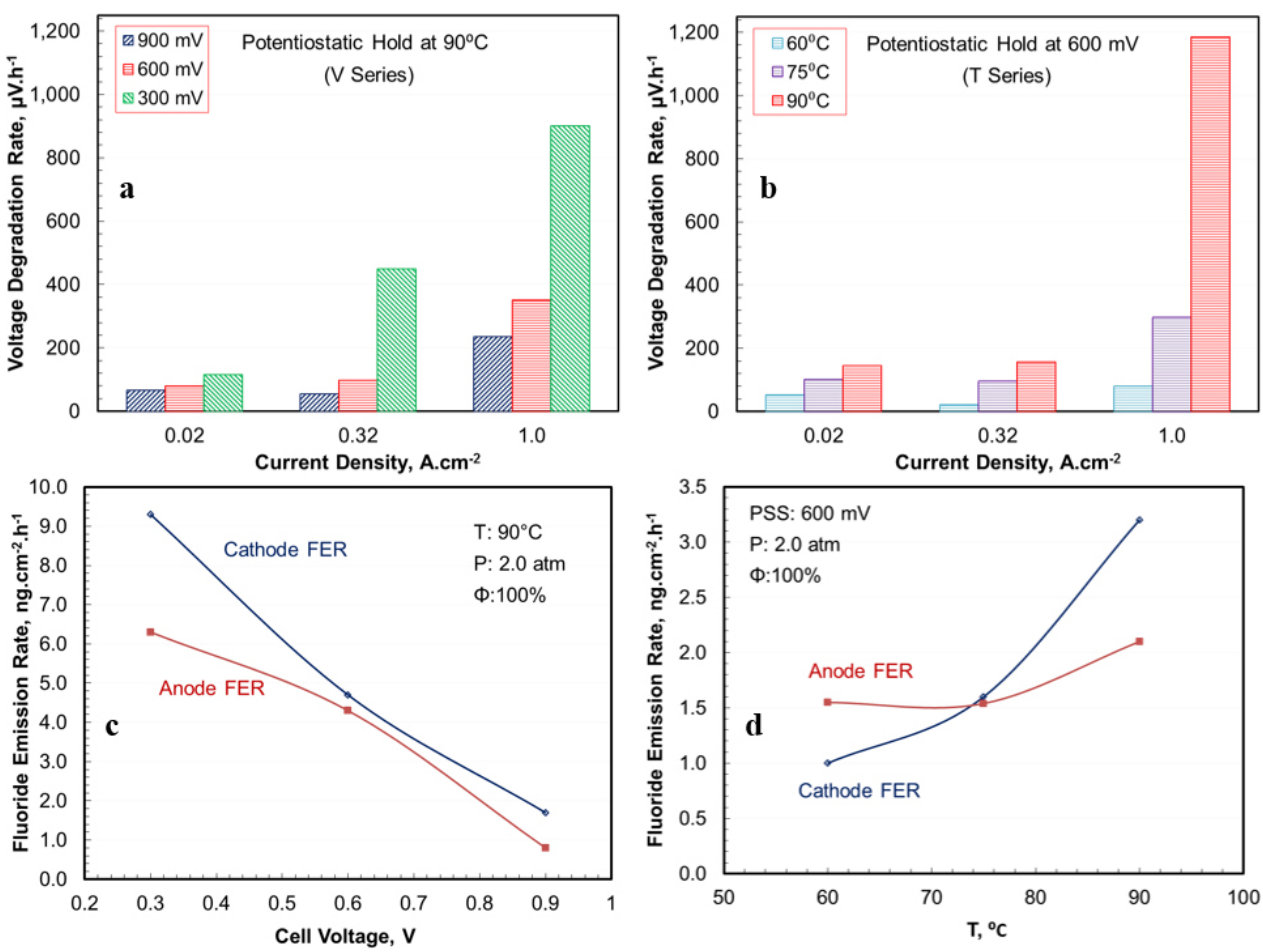

PSS – Potentiostatic scan

FIGURE 3. Durability of NSTF catalyst and MEA under long potentiostatic holds at 0.3–0.9 V. (a) Voltage degradation at different hold potentials; (b) Voltage degradation at different temperatures; (c) FER at different hold potentials; (d) FER at different temperatures.

very low, 20 ppb or less. Although the concentrations were similar, F^- generation rate increases with decreasing hold potential (i.e., increasing current density) due to higher effluent water flow rate (production + supplied). The measured FERs are similar but higher on cathode than on anode for all hold potentials, suggesting that FER measured in cathode effluent was produced locally in cathode. The trend of measured cathode FER increasing with decreasing cell voltage is consistent with the observed dependence of H_2O_2 production on potential in rotating ring disk electrode tests [6]. The measured anode FER correlates with the cell voltage rather than the anode potential. Rotating ring disk electrode experiments in a hydrogen environment have shown that H_2O_2 generation decreases as the anode potential is raised. For these reasons, it is unlikely that the measured F^- in anode effluent water was due to H_2O_2 produced locally in the anode by the reaction of O_2 crossing over from the cathode ($2H^+ + O_2 + 2e^- = H_2O_2$). Further work is needed to determine whether FER on cathode and anode are related and if F^- detected in anode water was actually produced in the cathode and permeated through the membrane.

We used the data for F^- concentration in effluent cathode water samples obtained during V-series and T-series to develop the following empirical correlation for cathode FER (N_F, mg/cm^2.h) as a function of cell potential (E, V) and exposure temperature (T, K).

Figure 4a presents the measured loss in surface enhancement factor (SEF, cm^2-Pt/cm^2-planar), that is the product of the ECSA (cm^2-Pt/mg-Pt) and the Pt loading (L_{Pt}, mg-Pt/cm^2). It indicates that the higher the exposure temperature the greater is the rate of loss of SEF at 600 mV hold potential, but the maximum loss is limited to about 30% to 40% at 60 A/cm^2 90°C. SEF loss appears to be self-limiting and ceases when the whiskerettes dissolve and disappear. Previous studies showed similar SEF loss when the NSTF catalyst was subjected to 30,000 triangle potential cycles in H_2/N_2 (cyclic voltammetry) and H_2/air

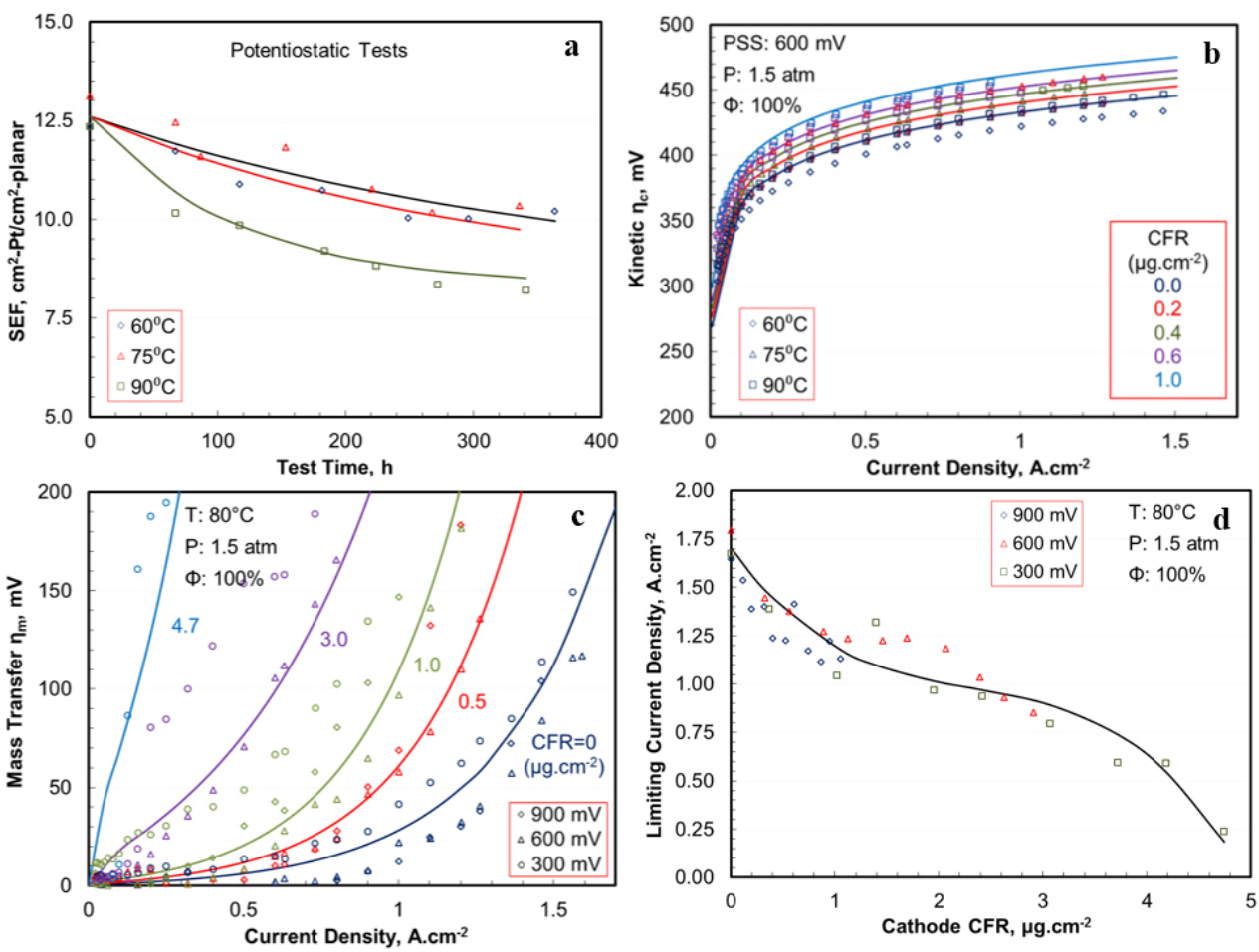

FIGURE 4. Development of NSTF MEA durability model using measured degradation in ECSA, ORR kinetics, limiting current density and O_2 mass transfer. (a) Loss in electrochemical surface area; (b) Increase in ORR kinetic loss; (c) Increase in mass transfer overpotential; (d) Reduction in limiting current density. Solid lines are model results.

(dynamic load cycles) with 0.6 V lower potential limit, 0.9 to 1.0 V upper potential limit, and 50 mV scan rate at 80°C and 100% RH [7]. These results may be compared with 60–80% SEF loss from 3–5 nm diameter or smaller nano-Pt particles dispersed on high-surface area carbon support (>60–80 m^2/g-Pt ECSA), when subjected to cyclic potentials. The NSTF ternary catalyst is supported on 27±7 nm x 55±12 nm rectangular lath-like 0.6–2µm length organic whiskers, has much smaller initial ECSA (A^0_{Pt}), <10 m^2/g-Pt, but its ECSA is more stable. Whereas, the dispersed nano-Pt/C catalysts lose ECSA as Pt dissolves and the particles coarsen due to the Ostwald ripening mechanism and coalescence and sintering, the NSTF catalyst loses ECSA because of the dissolution of Pt whiskerettes and the resulting reduction in surface roughness.

We determined the kinetic parameters from the measured polarization curves at low current densities where the mass transfer overpotentials are negligible. Figure 4b presents the estimated kinetic overpotentials as a function of current density and CFR for the six tests. The solid linear lines in Figure 4b, representing the least-square fit of the data, are nearly parallel, implying that there are only small changes in the Tafel slope with ageing at potentiostatic hold and the symmetry factor has remained constant. The linear offset in parallel lines is a measure of the changes in the exchange current density and ECSA. We have used these data to estimate the changes in the exchange current density, (µA/cm^2-Pt), with ageing, and found a strong and explicit correlation between and CFR, the cumulative fluoride release (N_F, mg/cm^2). The dependence of on hold potential and exposure temperature, however, is implicit since and, therefore, N_F is a function of E and T.

We determined the mass transfer overpotentials (η_m) from the measured polarization curves and the derived ORR kinetic parameters. As defined, η_m includes any Ohmic drops (iR^c_Ω) in the electrode layer, which may be small since the electrode is extremely thin, <0.5 mm. Figure 4c quantifies the increase in mass transfer overpotentials with ageing; this increaseis larger at lower hold potentials and higher exposure temperatures. The effect of ageing on is related to the diminished O_2 diffusion through the MEA. We suggest that the observed increase in after long potentiostatic hold is due to the degradation of the catalyst layer rather than due to changes in the GDL or the gas flow field.

We developed a correlation for the limiting current density, defined for convenience as the reference current density (i_L) at which the mass transfer overpotential (h_m) equals 200 mV. Figure 4d shows that is strongly correlated with N_F, and decreases as more fluoride is released at the cathode. Since the absolute amount of F^- release is small, the decrease in is likely related to contamination of the NSTF catalyst (~15 cm^2-Pt/cm^2 planar area) with membrane decomposition products rather than degradation of GDL (>30 cm^2/cm^2 surface area) or the gas channel. One plausible mechanism by which contaminants in small quantities can affect O_2 mass transport in NSTF catalysts is by modifying its wetting characteristic. Compared to the dispersed Pt/C catalysts, the NSTF catalysts are known to be more susceptible to poisoning by external impurities because of their smaller surface area. We developed a correlation for mass transfer overpotential (h_m in mV) assuming that it is only a function of . Implicitly, h_m is also a function of the hold potential and the exposure temperature since and N_F depend on these variables.

The current automotive targets specify 5,000 h lifetime with an allowance for 10% voltage degradation at rated power. Assuming 0.66–0.7 V cell voltage and 1–1.5 A/cm^2 at rated power, these specifications translate to 66–70 mV allowable voltage loss at rated power over lifetime, or 13–14 mV/h average degradation rate. As a comparison, the measured voltage degradation rate corresponding to 1 A/cm^2 varies for the experimental MEA varies between 200–900 mV/h at 300–900 mV hold potential (90°C exposure temperature) and 80–1,200 mV/h at 60 A/cm^2 90°C exposure temperature (600 mV hold potential). The actual degradation rate depends on the duty cycle and can be evaluated using the data and correlations presented in this work. However, the necessity to operate at temperatures below 60°C while avoiding extended excursions at temperatures above 90°C is quite apparent.

Independent of the duty cycle, we can make some observations about the requisite membrane stability. Since our data showed only small changes in the high frequency resistance, hydrogen crossover and shorting resistance, we conclude that the voltage loss with ageing is mostly due to degradation in ORR kinetics and O_2 mass transport. The allowable N_F corresponding to $Dh_c + Dh_m$ = 70 mV leads to an estimate of N_F = 0.7 mg/cm^2 which is slightly less stringent than the allowable N_F (0.5 mg/cm^2) for Dh_m = 35 mV.

CONCLUSIONS AND FUTURE DIRECTIONS

We determined the ORR kinetic parameters from IR and crossover corrected cell voltages at low current densities in H_2/O_2 and H_2/air. Compared to the baseline ternary $Pt_{68}(CoMn)_{32}$/NSTF catalyst, the mass activity of binary d-Pt_3Ni_7/NSTF catalyst with cathode interlayer is 78–144% higher.

We determined the performance and cost of a reference 2016 automotive FCS that includes a stack with binary NSTF catalyst with Pt/C cathode interlayer and mechanically reinforced 14 mm, 725 EW, reinforced membrane. Compared to the 2015 reference FCS that includes a ternary catalyst and 20 mm, 835 EW, unsupported membrane, the 2016 FCS has 25% higher stack power density: 12.3% due to higher ORR activity and 12.7% due to thinner membrane. It also has 16.8% lower stack cost: 10% due to higher ORR activity and 6.8% due to thinner membrane. The projected performance

and cost of 2016 FCS are 973 mW/cm^2 stack power density, 0.152 g/kW$_e$ Pt content, and \$48.40/kW$_e$ system cost at high volume manufacturing.

We have conducted tests (3M collaboration) and developed a model for NSTF catalyst durability under long potentiostatic hold. The model and data show the mechanisms of degradation of ECSA, kinetic activity and O_2 mass transfer and their relationship with fluoride release from membrane. We project that the target of less than 10% lifetime performance degradation can be achieved by restricting CFR to 0.7 mg/cm^2.

FY 2016 PUBLICATIONS/PRESENTATIONS

1. R.K. Ahluwalia, X. Wang, W.B. Johnson, F. Berg, and D. Kadylak, "Performance of a Cross-Flow Humidifier with a High Flux Water Vapor Transport Membrane," Journal of Power Sources, Vol. 291, pp. 225–238, 2015.

2. R.K. Ahluwalia, X. Wang, and A.J. Steinbach, "Performance of Advanced Automotive Fuel Cell Systems with Heat Rejection Constraint," Journal of Power Sources, Vol. 309, pp. 178–191, 2016.

3. R.K. Ahluwalia, X. Wang, and J-K Peng "Fuel Cells Systems Analysis," U.S. DRIVE Fuel Cell Tech Team Meeting, Southfield, MI, July 15, 2015.

4. R.L. Borup, R. Mukundan, Dusan Spernjak, D. Langlois, R. Ahluwalia, D.D. Papadias, Karren More, and Steve Grot, "Carbon Corrosion in PEM Fuel Cells During Drive Cycle Operation," 228th ECS Meeting, Phoenix, AZ, Oct. 11–15, 2015.

5. R.K. Ahluwalia, D.D. Papadias, R.L. Borup, R. Mukundan, and D. Spernjak, "Mechanism and Kinetics of Carbon Corrosion in Polymer Electrolyte Fuel Cells during Drive Cycles," 228th ECS Meeting, Phoenix, AZ, Oct. 11–15, 2015.

6. R.K. Ahluwalia, and N. Garland, "Report from the Annexes: Annex 34," IEA AFC ExCo 51st Meeting, Phoenix, AZ, Oct. 15–16, 2015.

7. Rajesh Ahluwalia and Sunita Satyapal, "U.S. Department of Energy Hydrogen and Fuel Cells Program," Eco-Mobility 2025Plus, Vienna, Austria, November 9–10, 2015.

8. R.K. Ahluwalia, D.D. Papadias, J.K. Thompson, H.M. Meyer III, M.P. Brady H. Wang, J.A. Turner, R. Mukundan, and R. Borup, "Performance Requirements of Bipolar Plates for Automotive Fuel Cells," IEA Annex 34 Meeting, Vienna, Austria, Nov. 11, 2015.

REFERENCES

1. A.J. Steinbach, "High Performance, Durable, Low Cost Membrane Electrode Assemblies for Transportation Applications," DOE Hydrogen and Fuel Cells Program, FY 2015 Annual Progress Report (2015) V-73 – V-79.

2. R.K. Ahluwalia, X. Wang, A. Lajunen, A.J. Steinbach, S.M. Hendricks, M.J. Kurkowski, and M.K. Debe, "Kinetics of Oxygen Reduction Reaction on Nanostructured Thin-Film Platinum Alloy Catalyst," J. Power Sources 215 (2012) 7788.

3. R.K. Ahluwalia, X. Wang, and A.J. Steinbach, "Performance of Advanced Automotive Fuel Cell Systems with Heat Rejection Constraint," J. Power Sources 309 (2016) 178–191.

4. R.K. Ahluwalia, X. Wang, and J-K Peng, "Performance and Durability of Advanced Automotive Fuel Cell Stacks and Systems," DOE Hydrogen and Fuel Cells Program, FY 2015 Annual Progress Report (2015) V-133 – V-140.

5. A. Kongkanand, J. Zhang, Z. Liu, Y-H Lai, P. Sinha, E.L. Thompson, and R. Makharia, "Degradation of PEMFC observed on NSTF electrodes," J. Electrochem. Soc. 161 (2013) F291–F304.

6. V.A. Sethuraman, J.W. Weidner, A.T. Haug, S. Motupally, and L.V. Protsailo, "Hydrogen Peroxide Formation Rates in a PEMFC Anode and Cathode: Effect of Humidity and Temperature," J. Electrochem Soc., 155 (1) (2008) B50–B57.

7. M.K. Debe, "Tutorial on the Fundamental Characteristics and Practical Properties of Nanostructured Thin Film (NSTF) Catalysts," J. Electrochem. Soc. 160 (6) (2013) F522–F534.

V.F.6 Fuel Cell Vehicle and Bus Cost Analysis

Brian D. James (Primary Contact),
Jennie M. Huya-Kouadio, Cassidy Houchins,
Daniel A. DeSantis
Strategic Analysis, Inc.
4075 Wilson Blvd., Suite 200
Arlington, VA 22203
Phone: (703) 778-1114
Email: bjames@sainc.com

DOE Manager: Jason Marcinkoski
Phone: (202) 586-7466
Email: Jason.Marcinkoski@ee.doe.gov

Contract Number: DE-EE0005236

Project Start Date: September 30, 2011
Project End Date: September 30, 2016

Overall Objectives

- Define low temperature proton exchange membrane (PEM) fuel cell power system operational and physical characteristics that reflect the current status of system performance and fabrication technologies.
- Estimate the production cost of the fuel cell systems (FCSs) for automotive and bus applications at multiple rates of annual production.
- Identify key cost drivers of these systems and pathways to further cost reduction.

Fiscal Year (FY) 2016 Objectives

- Update 2015 automotive and bus fuel cell power system cost projections to reflect latest performance data and system design information.
- Benchmark automotive FCS cost estimate against commercial fuel cell vehicle.
- Re-evaluate multiple fuel cell stack components: bipolar plates (BPPs), laser welding of coolant gasket, and gas diffusion layer (GDL).
- Investigate lifecycle cost (LCC) of two fuel cell bus system designs incorporating fuel usage for multiple drive cycles.

Technical Barriers

This project addresses the following technical barriers from the Fuel Cells section of the Fuel Cell Technologies Office Multi-Year Research, Development, and Demonstration Plan.

(B) Cost

Technical Targets

This project conducts cost modeling to attain realistic, process-based system cost estimates for integrated transportation fuel cell power systems operating on direct hydrogen. These values can help inform future technical targets as seen in Table 1.

TABLE 1. DOE Technical Targets for 80-kW_{net} Integrated Transportation Fuel Cell Power Systems Operating on Direct Hydrogen

Characteristic	Units	DOE 2020 Targets	DOE Ultimate Targets
Cost of Transportation Fuel Cell Power Systems	$/$kW_{net}$	40	30
Cost of Transportation Fuel Cell Stacks	$/$kW_{net}$	20	15
Cost of Bipolar Plates	$/$kW_{net}$	3	NA

NA – Not applicable

FY 2016 Accomplishments

- Projected the fuel cell power system cost for an 80 kW_{net} light-duty vehicle application using a Design for Manufacturing and Assembly (DFMA®) methodology at annual production rates of 1,000 to 500,000 FCSs per year.
- Projected the fuel cell power system cost of a 160 kW_{net} fuel cell power system for a bus at annual production rates of 200 to 1,000 systems per year.
- Analyzed improvement in performance of de-alloyed platinum nickel on carbon (PtNi/C) catalyst cells to show cost reduction compared to ternary platinum cobalt manganese (PtCoMn) nano-structured thin film (NSTF) catalyst.
- Investigated BPP forming, coating, and laser welding process to enhance model details and refine cost to align with original equipment manufacturer reported values (between $7–$100/kW_{net}).
- Analyzed cost of 91 kW_{net} (114 kW_{gross}) Toyota Mirai FCS design, estimating $233/$kW_{net}$ for materials and manufacturing cost at 1,000 systems per year.
- Conducted fuel cell bus LCC analysis, projecting a range of $2.40/mi to $3.50/mi for two different real-world drive cycles.

✧ ✧ ✧ ✧ ✧

INTRODUCTION

This project assesses the cost and performance impact of research advancements on fuel cells for transportation applications using a DFMA®-style [1] cost analysis methodology. Results from this analysis provides insight into the cost and performance impact for the Fuel Cell Technologies Office, which is useful in assessing the impact of current project portfolios and in identifying areas where R&D is still needed to address shortfalls in meeting cost targets. Low temperature (LT) PEM FCSs operating on hydrogen with peak electrical capacities of 80 kW_{net} for light-duty vehicle (automobile) applications and 160 kW_{net} for 40 ft transit bus applications are analyzed. Onboard compressed hydrogen storage, battery energy storage, or traction drive motor subsystems are not included in this cost assessment. The impact of annual production rates on the cost of the automotive and bus systems is examined to assess the difference between a nascent and a mature product manufacturing base. The annual production rates analyzed are 1,000, 10,000, 30,000, 80,000, 100,000, and 500,000 FCSs per year for automotive systems and 200, 400, 800, and 1,000 systems per year for the bus systems.

This work focuses primarily on updating the existing automobile FCS DFMA® cost model as well as efforts to design and model the manufacturing cost of bus FCSs. Stack and balance of plant (BOP) designs and performance parameters are discussed, and the methods of modeling each are explained. New technologies, materials data, and optimization modeling are incorporated to provide updated system cost. Cost trends are evaluated in terms of the capital costs per unit of installed electrical capacity ($/$kW_{net}$) and system annual production rate.

APPROACH

A DFMA®-style analysis is conducted to estimate the manufacturing cost of PEM FCSs for automobiles and buses at various manufacturing production rates. The optimum stack operating conditions and operating point are selected in collaboration with Argonne National Laboratory (ANL) and the Fuel Cell Tech Team. ANL first principles models of fuel cell stack operating conditions [2] and Strategic Analysis (SA) DFMA® cost models are used to identify cost and performance optimized conditions, which are vetted by the Fuel Cell Tech Team. Output from the ANL model provides insight into cell voltage, stack pressure, cathode catalyst loading, air stoichiometry, and stack outlet coolant temperature while the DFMA® cost model provides insight into cost and performance tradeoffs. The FCS is sized to provide 80 kW_{net} based on rated power operating parameters. System performance is based on performance estimates of individual components, built up into an overall system energy budget.

DFMA® process-based cost estimation techniques are applied to the major system components (and other specialty components) such as the fuel cell stack, membrane humidifier, air compressor/expander/motor unit, and hydrogen recirculation ejectors. For each of these, a manufacturing process train details the specific manufacturing and assembly machinery, and processing conditions are identified and used to assess component cost. For 2016, the full DFMA® analysis was extended to the Toyota Mirai system based on publicly available sources.

RESULTS

As in previous years, the 2016 high volume manufacturing cost will be reported separately in a DOE data record when available later this year. A blend of the final 2015 cost results (reported for the first time) and 2016 component results are described in this report.

2015 Automotive and Bus System Cost

The operating conditions and assumptions used to calculate costs for the 2015 auto and bus systems are summarized in Table 2. The 2015 automotive system cost at 500,000 systems per year is $52.84/$kW_{net}$ compared to the 2014 projected cost of $54.84/$kW_{net}$. The major changes in 2015 result from switching from ternary PtCoMn NSTF catalyst to a dispersed de-alloyed PtNi/C catalyst. Although the 2015 system with de-alloyed PtNi/C catalyst has lower power density (834 mW/cm^2 to 746 mW/cm^2), the overall Pt group metal total content increased (0.0189 g/kW_{gross} to 0.204 g/kW_{gross}) and the air stoichiometry was lowered (2 to 1.5), leading to an overall lower system cost (-$1.04/$kW_{net}$) in 2015. Additional changes include improved parasitic load calculations for coolant pump and fans and air pressure drop between system components (-$0.92/$kW_{net}$). Further, hydrogen sensor costs were updated to reflect current market pricing (-$0.23/$kW_{net}$) and a re-evaluation of the active to total cell area ratio (to better reflect current designs) from 0.8 to 0.625 increased the fuel cell stack cost (+0.87/kW_{net}). Other minor changes to the stack and BOP components resulted in a reduction in system cost (-0.68/kW_{net}).

The projected bus FCS cost decreased from $278.62/$kW_{net}$ to $261.97/$kW_{net}$ at 1,000 systems per year production between 2014 and 2015. Similar changes that were made for the automotive system were also applied to the bus system. The catalyst changed from PtCoMn NSTF to dispersed Pt on carbon, and parasitic load calculations, hydrogen sensor costs (single largest cost reduction of -$15.84/$kW_{net}$), and active to total cell area ratio were updated.

TABLE 2. PEM Fuel Cell (FC) Auto and Bus System Operating Conditions and Assumptions

	2015 Auto System	2015 Bus System
System Gross Power (kW_{net})	88.22	194.7
System Net Power (kW_{net})	80	160
Power Density (mW/cm^2)	746	739
Cell Voltage (mV)	661	659
Stack Temp (Coolant Exit Temp) (°C)	94	72
Pressure (atm)	2.5	1.9
Platinum Group Metal Total Content (g/ kW_{gross})	0.204	0.721
Air Stoichiometry	1.5	1.8
Catalyst System	Anode: Dispersed Pt/C Cathode: Dispersed d-PtNi/C	Anode and Cathode: Dispersed Platinum on Carbon
Cells per System	378	758

2016 Automotive Fuel Cell Stack Component Investigation

In an effort to obtain current manufacturing costs for automotive fuel cell components, vendors were asked to provide feedback on SA's manufacturing process assumptions. The feedback from these vendors led to changes in cost estimates for BPP forming, laser welding the coolant gasket, and GDLs.

In the auto baseline analysis, BPP forming is modeled as progressive stamping of coiled stainless steel sheets (3 mil). Hydroforming has also been investigated, but will likely not be used at high production volumes (>150 million plates per year). The intricacy of BPP flow fields has become quite detailed, at nine channels per centimeter. The force required for stamping these intricate designs can be greater than 1,500 tons in a progressive stamping machine. At these stamping forces, stamping speeds start to decline to approximately 20 strokes per minute. The capital costs can also range between $1.5–2M depending on the stamping force. Previously modeled high volume BPP stamping costs were approximately$7/$kW_{net}$ based on <200 tons stamping force at 60 strokes/min. Updated projections at high volume are $8.50/$kW_{net}$ based on an 1,800 ton press at 20 strokes/min, inclusive of materials, forming, and anti-corrosion coating.

Previously modeled BPPs were welded together along their perimeter to form cooling cells. To reflect recent input from vendors, the model was updated to include additional welding over the active area of the BPPs to ensure excellent electrical contact between the plates. The length of laser welding increased from 1.5 m in 2015 to 4.2 m in 2016, increasing total plate welding time from 6 s per weldment to ~33 s per weldment. However, additional high volume production manufacturing changes were postulated to increase the number of laser welding heads and the number of progressive welding stations. This reduced the effective cycle time per welded bipolar plate assembly to ≤6 s. The combined increase in laser welding length and reduction in effective cycle time resulted in an increase in total laser welding cost from $0.38/$kW_{net}$ in 2015 to $0.50/$kW_{net}$ in 2016.

A wide range in cost quotes for GDL material from distributors prompted a more thorough investigation. A preliminary DFMA® analysis was completed in 2016 to compare with quotations and to gain better insight on the current process and its cost. The GDL with microporous layer is based on the Ballard Material Products process flow [3]. The projected GDL cost is ~$6/$m^2$ at 500,000 systems per year for a 150 µm thick uncompressed (inclusive of MPL) material.

Benchmarking Against Toyota Mirai FCS

The unveiling of the Toyota Mirai system provides a unique opportunity for SA to compare the baseline system to a mass produced automotive FCS. While Toyota has not released many of its operating conditions, SA was able to make educated guesses for various aspects of the Mirai system using Toyota news releases and publications [4], discussions with original equipment manufacturers and the DOE Fuel Cell Tech Team, and the patent literature [5,6]. Given reported sizing and operating techniques such as internal cell humidification and power output, SA was able to make educated guesses for operating conditions that were deemed reasonable by the DOE Fuel Cell Tech Team. External stack humidification is one of the key differences between SA's baseline system and the Toyota Mirai system. In order to humidify the membrane within the stack, a thin membrane is used to facilitate water transport across the membrane and into the hydrogen flow. A hydrogen recirculation blower is then used to circulate humidified hydrogen from the anode exhaust back to the anode inlet where it can humidify the membrane.

The power density estimate (1.3 W/cm^2) is derived from the estimated total active area (9 m^2/stack) and Toyota reported gross power (114 kW) [4]. The calculation for the active area is based on Toyota's documented stack sizing (37 L, at 1.34 mm thickness per cell) and number of cells (370 cells/stack) [4], SA's estimate for ratio of active cell height to active cell width (0.5:1), SA's estimate for the housing thickness (1 cm), and SA's estimate of the cell active to total area ratio (0.4:1). The net power of the stack is not specified by Toyota; however with air compressor sizing and other ancillary loads from the system, net power is estimated to be 91 kW. Ancillary loads include 20 kW for the air compressor, 1 kW for the hydrogen recirculation blower, and 1 kW for the coolant loop pumps and fans.

The estimated cost for the Toyota Mirai FCS is \$233/kW$_{net}$ at 1,000 systems per year production and is approximately 18% higher than the \$197/kW$_{net}$ projected cost of SA's baseline automotive system (scaled to 91 kW$_{net}$, also at 1,000 systems per year). Figure 1 is a bar chart comparing the component and sub-system costs for the two systems and illustrates the few obvious components that make up the difference. For example the titanium BPPs used in the Mirai have high material cost (compared to the stainless steel used in the baseline) for very thin sheets (estimated to be 3–4 mils thick). The Pt loading estimated for the Mirai stack is likely much higher than the baseline assumption to ensure durability (estimated at 0.3 mgPt/cm^2 compared to 0.142 mgPt/cm^2 for the baseline). The balance of stack for the Mirai is much higher than the SA baseline balance of stack due to extra components in the Mirai stack, including a manifold for gas feed connections. The baseline system uses a combination of low and high flow ejectors for hydrogen recirculation while the Mirai system incorporates a hydrogen recirculation pump. Due to internal humidification, the Mirai does not require an external humidifier like the one used within the baseline system. This trade-off in BOP components makes the systems surprisingly close in BOP cost, making it quite clear that variation in the stack components is the primary source of the cost variation.

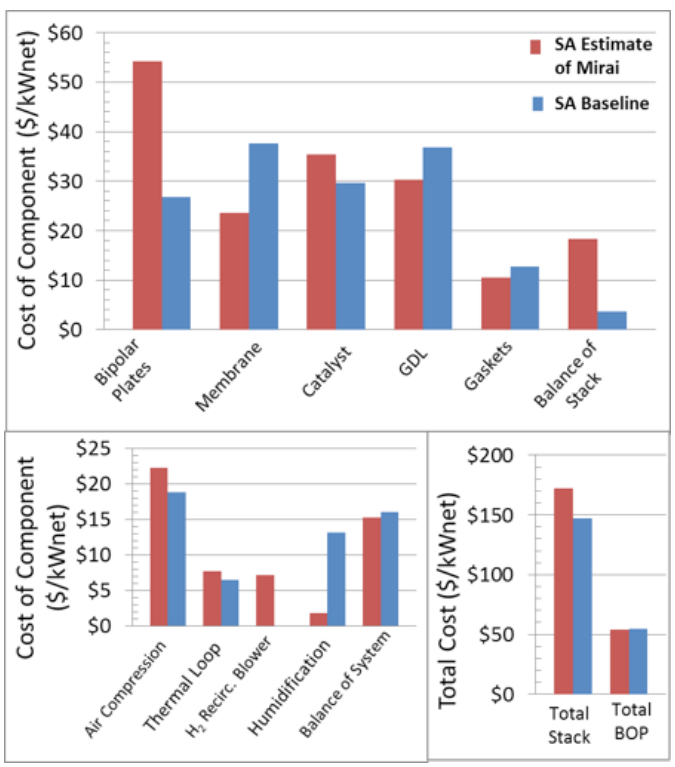

FIGURE 1. Comparison of SA's DFMA® baseline system scaled to 91 kW$_{net}$ (\$197/kW$_{net}$ at 1,000 systems per year) to SA's estimate of the Toyota Mirai FCS (\$233/kW$_{net}$ at 1,000 systems per year)

Fuel Cell Bus LCC Analysis

In collaboration with ANL and Aalto University, SA conducted a bus LCC analysis using performance modeling data (built from experimental results) to determine fuel consumption over a drive cycle. Fuel consumption was provided to SA by ANL/Aalto and used to construct the LCC model. Aalto University has conducted a similar study of bus LCC with the same bus routes, but with different parameter assumptions and capital cost [7] than the present study. ANL modeled bus system performance for two types of air compressor designs for this study: (1) roots air compressor-only and (2) roots air compressor/expander/motor. Aalto University used the FCS operating conditions within the Autonomie vehicle simulation software[1] to obtain the energy requirements for each system at various drive cycles. The modeling results for the roots compressor-only had the lowest fuel consumption (kg H_2/100 km) and highest efficiency

[1] Autonomie is a Matlab©- based vehicle simulation software used for automotive control-systems analysis. http://www.autonomie.net/expertise/Autonomie.html

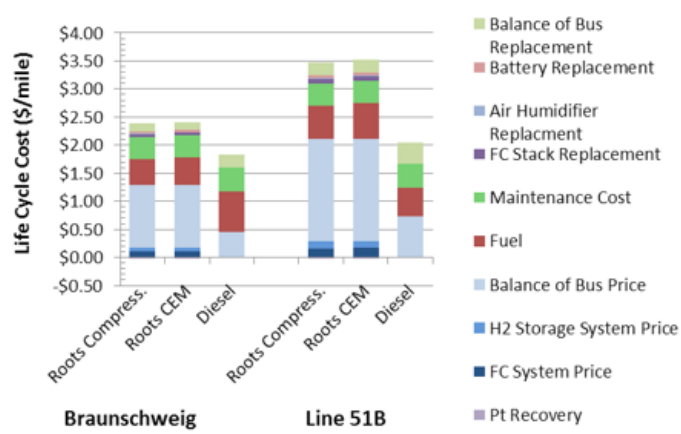

CEM – compressor/expander/motor

FIGURE 2. Lifecycle cost results for two fuel cell system types for two different bus routes: Braunschweig and Line 51B Berkeley compared to a diesel bus

for all types of drive cycles. The roots air compressor-only system was used in the 2015 bus final DFMA® analysis.

Results from the bus LCC model do not show an appreciable difference between air compressor types, but there is a large impact based on the type of drive cycle and the annual distance driven. As seen in Figure 2, the LCC ranges from $2.40/mi to $3.50/mi depending on the drive cycle. In comparison to diesel bus LCCs for the same bus route, the FC bus LCC is 50% higher due to balance of bus cost (made up of power electronics, electric motor, and bus chassis and body).

CONCLUSIONS AND FUTURE DIRECTIONS

- The 2015 final auto and bus system cost results decreased since 2014, due to a series of specific analysis and assumption improvements. The 2016 final system cost analyses for the automotive and bus systems are to be reported in the 2016 DOE Cost Record.
- The automotive FCS cost for 2015 ($52.84/$kW_{net}$) reduced exactly $2/$kW_{net}$ from the 2014 analysis ($54.84/$kW_{net}$). The reduction in cost comes primarily from switching to a dispersed de-alloyed PtNi/C catalyst with a lower required air stoichiometric ratio.
- The 160 kW_{net} LT PEM FC bus system cost reduced from $279–$262/kW_{net} in 2015 due to the combination of updated sensor costs and increased power density (from 601–739 mW/cm^2).
- Feedback from the FC community prompted a re-evaluation of 2016 FC stack manufacturing process parameters for BPP forming, coolant gasket laser welding, and GDLs.
- To benchmark against a mass produced FC vehicle, the SA baseline DFMA® cost model was scaled to 91 kW_{net} and compared to SA's estimate of the Toyota Mirai system showing a cost of $197/$kW_{net}$ (baseline) compared to $233/$kW_{net}$ (Mirai).
- An LCC model was added for the 2016 analysis by incorporating ANL performance models for three types of systems for multiple bus drive cycles. The LCC for the Braunschweig bus route was ~$2.40/mi while the Line 51B Berkeley bus route was ~$3.50/mi. Two FC LCC projections are 50% to almost 100% higher than those of diesel buses under similar routes (~$1.60–$1.80/mi).

FY 2016 PUBLICATIONS/PRESENTATIONS

1. Moton, J.M., James, B.D., Houchins, C., DeSantis, D.A., "Re-evaluation of Cost and Identification of Risk for Low Volume Manufacturing Techniques Applied to Automotive Fuel Cell Systems," Presentation given at the 2015 Fuel Cell Seminar, Los Angeles, CA, November 17, 2015.

2. Houchins, C., Moton, J.M., DeSantis, D.A., James, B.D., "Assessment of Polymer Electrolyte Fuel Cell Catalyst Cost, Performance and Manufacturability," Presentation given at the 2015 Fuel Cell Seminar, Los Angeles, CA, November 17, 2015.

3. "Mass Production Cost Estimation of Direct H_2 PEM Fuel Cell Systems for Transportation Applications: 2015 Update," Strategic Analysis Report prepared by Brian D. James, Jennie M. Huya-Kouadio, and Cassidy Houchins, December 2015.

4. James, B.D., Houchins, C., Huya-Kouadio, J.M., "Transportation Fuel Cells Cost Analysis Update Automotive Cost Analysis," Presented to the Fuel Cell Technical Team, Southfield, MI, May 18, 2016.

5. James, B.D., Huya-Kouadio, J.M., Houchins, C., DeSantis, D.A., "2016 DOE Hydrogen and Fuel Cells Program Review: Fuel Cell Vehicle and Bus Cost Analysis," Presented at the 2016 DOE Hydrogen and Fuel Cells Program Annual Merit Review Meeting, Washington, D.C., June 9, 2016.

REFERENCES

1. Boothroyd, Geoffrey, Peter Dewhurst, and Winston A. Knight. *Product Design for Manufacture and Assembly, Third Edition*. CRC Press, 2010.

2. Ahluwalia, Rajesh. "Fuel Cell Systems Analysis." presented at the DOE Fuel Cell Tech Team, Southfield, MI, July 15, 2016.

3. Morgan, Jason, Donald Connors, and Michael Hickner. "Reduction in Fabrication Costs of Gas Diffusion Layers." Ballard Material Products, July 10, 2012.

4. Konno, Norishige, Seiji Mizuno, Hiroya Nakaji, and Yuji Ishikawa. "Development of Compact and High-Performance Fuel Cell Stack." SAE International Journal of Alternative Powertrains 4, no. 2015-01–1175 (2015): 123–129.

5. Tabata, Toshiharu, Tomoaki Terada, Takahiro Nagata, Susumu Enomoto, Yosuke Horiuchi, Hiroaki Takahashi, Tetsuo Kawamura, and Hideyasu Kawai. Conductive Carbon Carrier for Fuel Cell, Electrode Catalyst for Fuel Cell and Solid Polymer Fuel Cell Comprising Same. US8372562 (B2), issued February 12, 2013.

6. Fujii, Toshiro, and Yoshiyuki Nakane. Electric pump. US7980830 (B2), issued July 19, 2011.

7. Lajunen, Antti, and Timothy Lipman. "Lifecycle Cost Assessment and Carbon Dioxide Emissions of Diesel, Natural Gas, Hybrid Electric, Fuel Cell Hybrid and Electric Transit Buses." *Energy* 106 (2016): 329–342.

V.F.7 Stationary and Emerging Market Fuel Cell System Cost Analysis–Primary Power and Combined Heat and Power Applications

Vince Contini (Primary Contact), Fritz Eubanks, Mike Heinrichs, Mike Jansen, Paul George and Mahan Mansouri
Battelle
505 King Avenue
Columbus, OH 43201
Phone: (614) 424-7249
Email: continiv@battelle.org

DOE Manager: Donna Ho
Phone: (202) 586-8000
Email: Donna.Ho@ee.doe.gov

Contract Number: DE-EE0005250/001

Project Start Date: September 30, 2011
Project End Date: January 31, 2017

Overall Objectives

The objective of this project is to assist the U.S. Department of Energy in developing fuel cell system technologies for stationary and emerging markets by developing independent cost models for manufacture and ownership. In particular:

- Identify the fundamental drivers of system cost and the sensitivity of the cost to system parameters.
- Help DOE prioritize investments in research and development of components (e.g., metal bipolar plates versus composite graphite plates in polymer electrolyte membrane [PEM] fuel cells for low volume markets) to reduce the costs of fuel cell systems while considering systems optimization.
- Identify manufacturing processes that must be developed to commercialize fuel cells.
- Provide insights into the optimization needed for use of off-the-shelf components in fuel cell systems.

Fiscal Year (FY) 2016 Objectives

- Finalize cost estimates of 100-kW and 250-kW PEM and solid oxide fuel cell (SOFC) systems for primary power and combined heat and power (CHP) applications at annual production volumes of 100, 1,000, 10,000, and 50,000 units.
- Finalize cost estimates of 5-kW and 10-kW PEM fuel cell systems for backup power applications at annual production volumes of 100, 1,000, and 10,000 units.
- Revisit all applications in previous four budget periods and update reports.

Technical Barriers

This project addresses the following technical barriers from the Fuel Cell section of the Fuel Cell Technologies Program Multi-Year Research, Development, and Demonstration Plan.

(B) Cost

Technical Targets

To widely deploy fuel cells, significant strides must be made in lowering the cost of components and overall systems without compromising reliability and durability. Through estimating system costs at varying production volumes this analysis will:

- Identify the fundamental drivers of component and system cost and the sensitivity of the cost to various component and system parameters.
- Provide the DOE information on the impact of production volumes on lowering costs of fuel cells and the types of high volume manufacturing processes that must be developed to enable the widespread commercialization.
- Provide insights into the optimization needed for use of off-the-shelf components in fuel cell systems to drive down system costs.
- Analyze the lifecycle costs of owning and operating a fuel cell to estimate primary costs drivers for the end user in applicable markets.

FY 2016 Accomplishments

- Completed detailed manufacturing cost analysis of 100-kW and 250-kW PEM and SOFC systems for primary power and CHP applications.
- Completed detailed manufacturing cost analysis of 5-kW and 10-kW PEM fuel cell systems for backup power applications.

✧ ✧ ✧ ✧ ✧

INTRODUCTION

Fuel cell power systems may be beneficially used to offset all or a portion of grid-purchased electrical power and supplement onsite heating requirements. For this application the fuel of choice will usually be pipeline natural gas or onsite propane storage. These fuel sources generally have much higher reliability than utility electric power, being less subject to damage related outages, and can therefore provide for some continued operation in the event of grid outage – performing both primary power and back-up power functions. Battelle evaluated low temperature PEM and SOFC systems for use as a continuous power supplement (primary power) and to provide auxiliary heating in CHP configurations. The power levels considered this year were 100 kW and 250 kW. A primary-power or CHP commercial market has not yet developed in this size range; however, our analysis suggests an attractive business opportunity under the right conditions.

APPROACH

Battelle will apply the established methodology used successfully in previous fuel cell cost analysis studies performed for the DOE [1-3]. This technical approach consists of four steps: market assessment, system design, cost modeling, and sensitivity analysis (Figure 1). The first step characterizes the potential market and defines the requirements for system design. The second step involves developing a viable system design and the associated manufacturing process vetted by industry. The third step involves building the cost models and gathering inputs to estimate manufacturing costs. Manufacturing costs will be derived using the Boothroyd-Dewhurst Design for Manufacture Assembly Software (DFMA®). Custom manufacturing process models will be defined where necessary and parametrically modeled based on knowledge of the machine, energy, and labor requirements for individual steps that comprise the custom process. The fourth step will evaluate the sensitivity of stack and system costs to various design parameters. In addition to the sensitivity analysis, we will conduct a lifecycle cost analysis to estimate total cost of ownership for the target application and markets.

RESULTS

To provide insight into the cost drivers that may be unique to primary power and combined heat and power, the final system cost was broken into three categories associated with different aspects of operation and production: total stack manufacturing cost, the expense of balance of plant (BOP) hardware, and the final cost of complete system assembly and testing. BOP was further broken out into four subsets of:

- Fuel, water, and air supply components
- Fuel processor components
- Heat recovery components
- System assembly

A sales markup of 50% was integrated at the end and is called out separately in Tables 1–4. At high production volumes, the final ticket prices are estimated to be $2,437 and $1,697 per kW, respectively, for 100-kW and 250-kW CHP PEM fuel cell systems and $1,443 and $1,181 per kW for the 100-kW and 250-kW CHP SOFC systems. This work provides a detailed cost breakdown that helps identify key

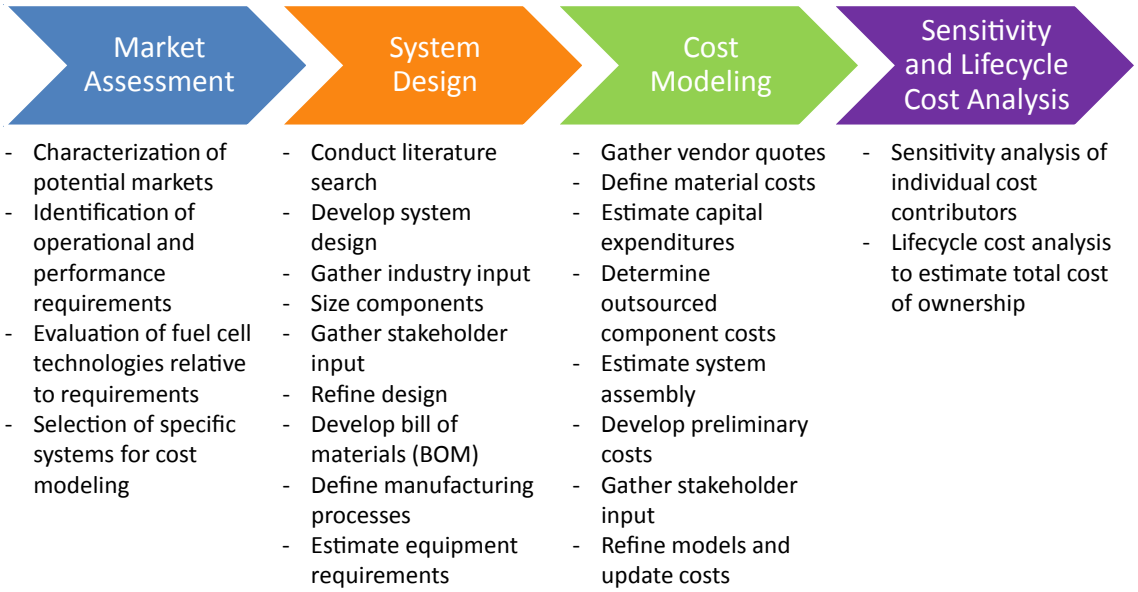

FIGURE 1. Battelle's Cost Analysis Methodology

TABLE 1. 100-kW CHP PEM Fuel Cell System Cost Summary

Description	100 Units	1,000 Units	10,000 Units	50,000 Units
Total Stack Manufacturing	$73,522	$34,480	$23,303	$20,390
Fuel, Water, and Air Supply Components	$25,832	$22,857	$20,894	$19,622
Fuel Processor Components	$55,616	$48,005	$43,629	$41,395
Heat Recovery Components	$37,440	$33,994	$30,868	$29,466
Power Electronic, Control, and Instrumentation	$52,536	$43,221	$35,258	$29,859
Assembly Components	$29,500	$26,790	$24,080	$21,705
Total system cost, pre-markup	$274,446	$209,348	$178,032	$162,438
System cost per kW_{net}, pre-markup	$2,744	$2,093	$1,780	$1,624
Sales markup	50%	50%	50%	50%
Total system cost, with markup	$411,670	$314,021	$267,048	$243,657
System cost per kW_{net}, with markup	$4,117	$3,140	$2,670	$2,437

TABLE 2. 250-kW CHP PEM Fuel Cell System Cost Summary

Description	100 Units	1,000 Units	10,000 Units	50,000 Units
Total Stack Manufacturing	$126,587	$71,151	$53,494	$48,737
Fuel, Water, and Air Supply Components	$35,472	$31,447	$28,662	$26,881
Fuel Processor Components	$94,462	$79,221	$70,458	$66,491
Heat Recovery Components	$56,215	$51,218	$46,680	$44,665
Power Electronic, Control, and Instrumentation	$117,058	$94,238	$74,725	$61,509
Assembly Components	$46,840	$42,590	$38,340	$34,500
Total system cost, pre-markup	$476,635	$369,865	$312,359	$282,782
System cost per kW_{net}, pre-markup	$1,906	$1,479	$1,249	$1,131
Sales markup	50%	50%	50%	50%
Total system cost, with markup	$714,952	$554,797	$468,538	$424,174
System cost per kW_{net}, with markup	$2,860	$2,219	$1,874	$1,697

TABLE 3. 100-kW CHP SOFC System Cost Summary

Description	100 Units	1,000 Units	10,000 Units	50,000 Units
Total Stack Manufacturing	$48,191	$32,005	$28,537	$28,273
Fuel and Air Supply Components	$10,108	$8,306	$7,465	$6,956
Fuel Processor Components	$8,245	$5,693	$5,247	$4,962
Heat Recovery Components	$21,057	$19,698	$18,430	$17,621
Power Electronic, Control, and Instrumentation	$52,988	$43,627	$35,622	$30,213
Assembly Components	$11,105	$10,080	$9,055	$8,175
Total system cost, pre-markup	$151,694	$119,410	$104,354	$96,200
System cost per kW_{net}, pre-markup	$1,517	$1,194	$1,044	$962
Sales markup	50%	50%	50%	50%
Total system cost, with markup	$227,541	$179,115	$156,532	$144,300
System cost per kW_{net}, with markup	$2,275	$1,791	$1,565	$1,443

TABLE 4. 250-kW CHP SOFC System Cost Summary

Description	100 Units	1,000 Units	10,000 Units	50,000 Units
Total Stack Manufacturing	$94,814	$73,566	$70,452	$70,113
Fuel and Air Supply Components	$18,298	$15,700	$14,309	$13,556
Fuel Processor Components	$14,347	$9,797	$8,604	$8,253
Heat Recovery Components	$33,857	$31,718	$29,718	$28,470
Power Electronic, Control, and Instrumentation	$117,962	$95,050	$75,453	$62,217
Assembly Components	$19,110	$17,410	$15,710	$14,180
Total system cost, pre-markup	$298,389	$243,241	$214,244	$196,789
System cost per kW_{net}, pre-markup	$1,194	$973	$857	$787
Sales markup	50%	50%	50%	50%
Total system cost, with markup	$447,583	$364,861	$321,367	$295,184
System cost per kW_{net}, with markup	$1,790	$1,459	$1,285	$1,181

cost drivers and offers insight at various value propositions through the lifecycle cost analyses.

CONCLUSIONS AND FUTURE DIRECTIONS

The following lists some of the conclusions drawn from this analysis:

- BOP costs dominate system cost.
- Within BOP costs
  - Power electronics is a major contributor for both technologies.
  - Heat recovery and fuel processing contribute significantly for PEM systems.
  - An attractive value proposition exists under specific utility rate conditions (high spark-spread) and is improved if able to utilize waste heat.
- Manufacturing readiness level for many BOP components not ready for mass production—significant cost driver.

By the end of FY 2016 Battelle will have completed full cost assessments of 5-kW and 10-kW PEM fuel cell systems for backup power applications.

FY 2016 PUBLICATIONS/PRESENTATIONS

1. V. Contini, F. Eubanks, M. Heinrichs, M. Jansen, P. George and Mahan Mansouri, November 2015. "Manufacturing Cost Analysis–Primary Power and Combined Heat and Power Applications." Fuel Cell Seminar, Los Angeles, CA.

2. V. Contini, F. Eubanks, M. Heinrichs, M. Jansen, P. George and Mahan Mansouri, June 2016. "Stationary and Emerging Market Fuel Cell System Cost Analysis – Primary Power and Combined Heat and Power Applications." DOE Annual Peer Review. Washington D.C.

REFERENCES

1. Battelle. 2011. "The High Volume Manufacture Cost Analysis of 5 kW Direct Hydrogen Polymer Electrolyte Membrane (PEM) Fuel Cell for Backup Power Applications." Contract No. DE-FC36GO13110.

2. K. Mahadevan, K. Judd, H. Stone, J. Zewatsky, A. Thomas, H. Mahy, and D. Paul. 2007. "Identification and characterization of near-term direct hydrogen proton exchange membrane fuel cell markets." Contract No. DE-FC36GO13110.

3. H. Stone, K. Mahadevan, K. Judd, H. Stein, V. Contini, J. Myers, J. Sanford, J. Amaya, J. Upton, and D. Paul 2006. "Economics of Stationary Proton Exchange Membrane Fuel Cells." Contract No. DE-FC36-03GO13110.

V.F.8 A Total Cost of Ownership Model for Design and Manufacturing Optimization of Fuel Cells in Stationary and Emerging Market Applications

Max Wei (Primary Contact), Roberto Scataglini, Hanna Breunig
Lawrence Berkeley National Laboratory (LBNL)
1 Cyclotron Road, MS 90R-4000
Berkeley, CA 94706
Phone: (510) 486-5220
Email: mwei@lbl.gov

DOE Manager: Donna Ho
Phone: (202) 586-8000
Email: Donna.Ho@ee.doe.gov

Subcontractors:
University of California, Berkeley, CA
Strategic Analysis, Arlington, VA

Project Start Date: October 1, 2011
Project End Date: September 30, 2016

Overall Objectives

- Develop total-cost-of-ownership (TCO) modeling tool for design and manufacturing of fuel cell systems in emerging markets (e.g., co-generation and back-up power systems) for low temperature (LT) polymer electrolyte membrane (PEM), high temperature (HT) PEM, and solid oxide fuel cell (SOFC) technologies.
- Expand cost modeling framework to include life-cycle analysis and possible ancillary financial benefits, including carbon credits, health and environmental externalities, end-of-life recycling, and reduced costs for building operation.
- Perform sensitivity analysis to key cost assumptions, externality valuation, and policy incentive structures.

Fiscal Year (FY) 2016 Objectives

- Update direct manufacturing cost model for SOFC fuel cell systems in combined heat and power and stationary power applications
- Revise total cost of ownership model for LT PEM combined heat and power (CHP) systems.

Technical Barriers

This project addresses the following technical barriers from the Fuel Cells section (3.4) and the Manufacturing R&D section (3.5) of the Fuel Cell Technologies Office Multi-Year Research, Development, and Demonstration Plan.

Fuel Cells

(B) Cost: Expansion of cost envelope to total cost of ownership including full life cycle costs and externalities

Manufacturing R&D

(A) Lack of High-Volume Membrane Electrode Assembly Processes

(B) Lack of High-Speed Bipolar Plate Manufacturing Processes

Technical Targets

This project is conducting cost of ownership studies of LT PEM, HT PEM, and SOFC fuel cell systems in non-automotive applications. Insights gained from these studies can be applied toward the development of lower-cost, higher-volume manufacturing processes that can meet the DOE combined heat and power system equipment cost targets (Table 1).

- PEM: For reference, the LT PEM and HT PEM costs from earlier work are shown.

TABLE 1. DOE Combined Heat and Power System Equipment Cost Targets

System	Units/yr (Annual Volume in MW)	2015 DOE equipment cost target with markup	2020 DOE equipment cost target with markup	This Work		
				LT PEM equipment cost with 50% markup	HT PEM equipment cost with 50% markup	SOFC direct equipment cost with 50% markup
10 kW CHP System	50,000 (500 MW)	$1,900/kW	$1,700/kW	$2,585/kW	$2,925/kW	$1,650/kW
100 kW CHP System	1,000 (100 MW)	$2,300/kW	$1,000/kW	$1,800/kW	$2,235/kW	$1,140/kW

- SOFC: Updated estimated costs are shown for SOFC CHP system direct equipment cost with a 50% markup in price. At the annual production volumes shown, the SOFC cost per unit kW is estimated to be about 35% lower than LT PEM systems.
- The 10-kW SOFC CHP system cost of $1,650/kW at an annual production volume of 50,000 units per year meets the 2020 DOE target under the assumptions made in this work, e.g., automated stack production processes and high process yields at high production volumes.
- The 100-kW SOFC CHP system cost of $1,140/kW at an annual production volume of 1,000 units per year exceeds the 2020 DOE equipment cost target by 14% under the assumptions made in this work, e.g., automated stack production processes and high process yields at high production volumes.

FY 2016 Accomplishments

- Updated direct manufacturing cost model for SOFC CHP applications.
- Revised total cost of ownership model for LT PEM CHP systems.

✧ ✧ ✧ ✧ ✧

INTRODUCTION

The DOE has supported cost analysis studies for fuel cell systems for both automotive [1,2] and non-automotive [3,4] systems over the last decade. These studies have primarily focused on the manufacturing costs associated with fuel cell system production. This project expands the scope and modeling capability from existing direct manufacturing cost modeling in order to quantify more fully the benefits of fuel cell systems by taking into account life cycle assessment, air pollutant impacts and policy incentives. TCO modeling becomes important in a carbon-constrained economy and in a context where health and environmental impacts are increasingly valued. TCO is also critical as an input to industry and governments decisions on funding research, development and deployment as well as an input to organizations and individuals who make long-term investment decisions.

Three components of the TCO model are (1) direct manufacturing costs, (2) life-cycle or use- phase costs, such as cost of operations and fuel, and (3) life-cycle impact assessment (LCIA) costs, such as health and environmental impacts. FY 2016 has been focused on updating the direct manufacturing cost model for SOFC systems for application in CHP and stationary power and updating the LCIA model for LT PEM CHP systems.

APPROACH

Data for system designs and component costing is derived from (1) existing cost studies where applicable, (2) literature and patent sources, and (3) industry and national laboratory advisors. Vertically integrated manufacturing is assumed for stack components with high-speed roll-to-roll processes for gas diffusion layer, gas diffusion electrode, and catalyst coated membrane components and largely purchased components for balance of plant. Life cycle or use-phase costing utilizes existing LBNL tools [5], a National Renewable Energy Laboratory database of commercial building electricity and heating demand profiles by building type and geographical region [6], and earlier CHP modeling work by one of the authors [7].

LCIA is focused on use-phase impacts from energy use, carbon emissions, and pollutant emissions [8], specifically on particulate matter emissions since particulate matter is the dominant contributor to life-cycle impacts [9]. The health impact from particulate matter is disaggregated by geographical region using existing LBNL health impact models [10] and an estimation of the amount of displaced grid-based electricity and heating fuel for a fuel cell CHP system in that building type and geographical region.

RESULTS

Direct cost modeling of SOFC stack has been revised to more accurately model labor requirements, factory costs, and the electrode/electrolyte assembly (EEA) sintering process, based on review of our assumptions with several manufacturing equipment vendors. Updated system costs are shown in Figures 1 and 2. Direct costs for SOFC CHP 10-kW systems are found to be $2,650/kW at annual production volumes of 100 systems per year and $1,100/kW at 50,000 systems per year (Figure 1). Balance of plant costs make up 60–80% of overall direct costs while Figure 2 shows

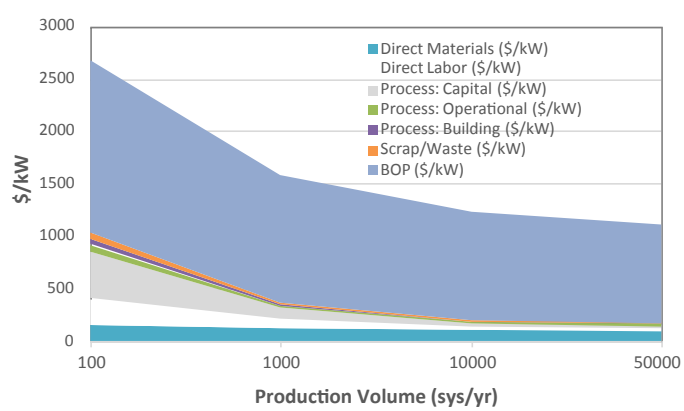

BOP - Balance of plant

FIGURE 1. 10 kW SOFC CHP direct costs vs. production volume

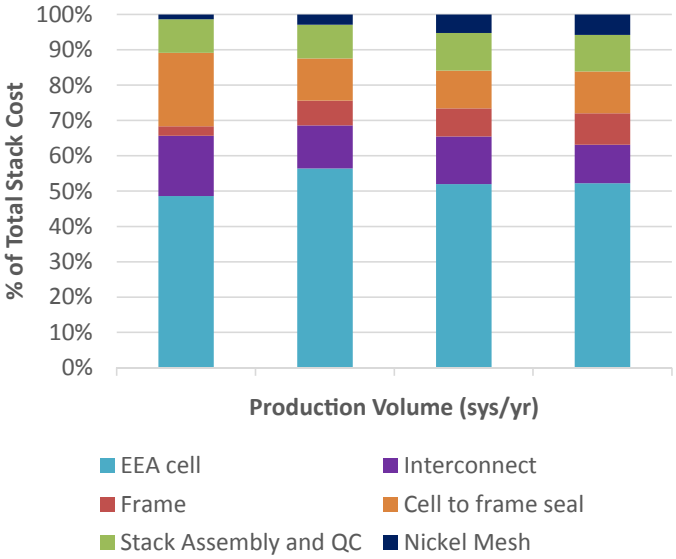

QC – Quality control

FIGURE 2. Break-down of total stack cost by module for 10 kW SOFC CHP system as a function of annual manufacturing volume

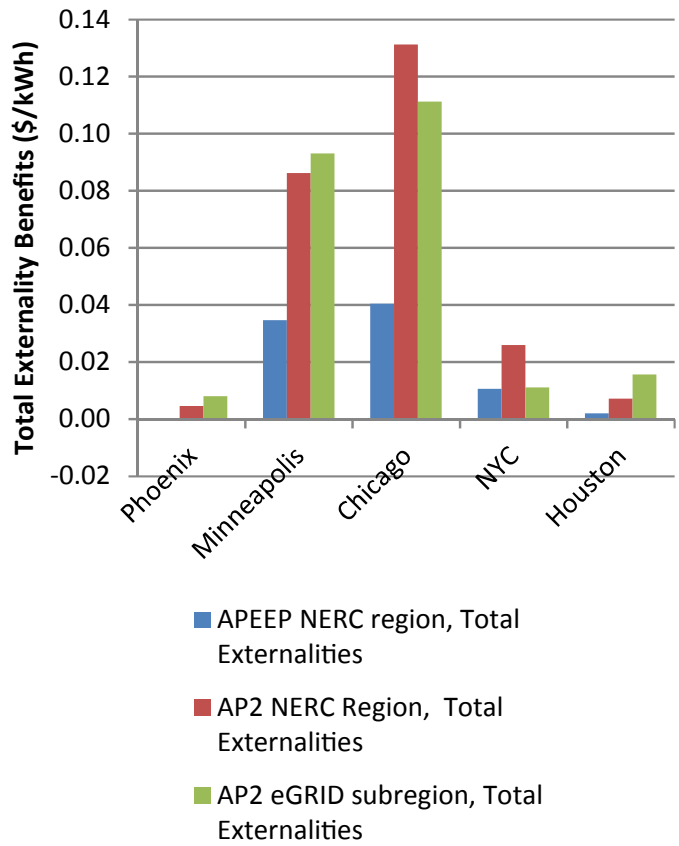

FIGURE 3. Updated externality savings per unit of displaced grid electricity for a 50 kW LT PEM CHP system in small hotels. The first bar for each city represents values used in the project's earlier modeling while the third bar represents values incorporating (1) updated AP2 externality valuation factors and (2) updated eGRID emission factors by subregion.

that stack costs are dominated by the EEA cell across all production volumes.

Detailed revisions were made to the LCIA (or externality valuation) models for LT PEM CHP systems and are summarized in Figure 3. First, monetary benefit estimates for displaced criteria pollutants (e.g., SO_2 and NO_x) in dollars per ton of emissions were updated from the Air Pollution Emission Experiments and Policy (APEEP) analysis model to revised values from AP2 [11]. These displaced criteria pollutant monetary benefits effectively increase the benefits by a factor three to five times over values from APEEP, but bring benefit estimates to the same range as estimates quoted by the Environmental Protection Agency in the Clean Power Plan (CPP) Regulatory Impact Assessment from October 2015 [12]. Second, marginal emission factors were revised from large-area North American Electric Reliability Corporation (NERC) regions from Siler-Evans et al. (2012) [13] to sub-regional emission factors from the Emissions & Generation Resource Integrated Database (eGRID) [14]. This provides greater regional specificity of pollutant emission factors (tons/kWh). The net of these changes is that total externality benefits (CO_2, health, environmental) are up to 5X greater than previously reported values. We find values for displaced grid-electricity emissions that are comparable to earlier reported data by Siler-Evans et al. (2013) [15], i.e., up to $0.10/kWh in the Midwest and upper Midwest.

The second extension to the LCIA model is that we have explored the reduction in externality benefits for fuel cell CHP from 2016–2030 assuming that the CPP is implemented as proposed. The CPP would reduce average CO_2 emissions by an estimated 13% from current levels and SO_2 and NO_x would be reduced an average of 80% and 50%, respectively across all NERC regions. Thus, the expected benefits of fuel cell CHP from displaced CO_2, NO_x, and SO_2, and other criteria pollutants would be reduced over time. Even with this clean-up of the electricity system, we find that the installation of LT PEM fuel cell CHP still has net positive societal benefits from 2016–2030 in regions which currently have high grid-electricity emissions (e.g., the upper Midwest). A notional or "societal" cash flow from 2016–2030 for a 50 kW LT PEM CHP system including total cost of ownership savings for a small hotel in Chicago is shown in Figure 4.

CONCLUSIONS AND FUTURE DIRECTIONS

- Direct costs for SOFC CHP 10-kW systems are found to be $2,650/kW at annual production volumes of 100 systems per year and $1,100/kW at 50,000 systems per year (Figure 3). Adding a 50% markup gives a direct equipment cost of $3,975/kW at 100 systems per year and $1,650/kW at 50,000 systems per year.

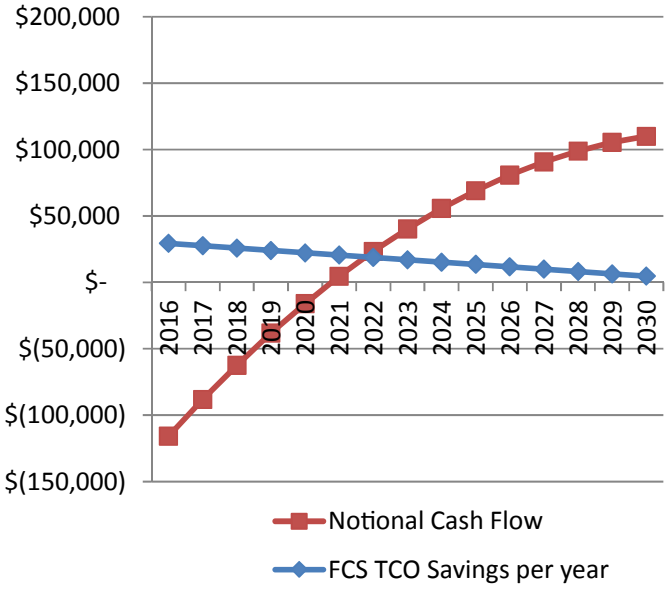

FCS – Fuel cell systems

FIGURE 4. Notional cash flow for a 50 kW LT PEM CHP system in small hotel in Chicago from 2016–2030 including total cost of ownership savings. Reductions in grid emissions factors for CO_2 and NO_x/SO_2 to 2030 are estimated from the CPP.

- Non-stack costs (balance of plant and fuel processor) are generally found to be the largest component of CHP system costs for LT PEM, HT PEM systems, and SOFC systems. For example, the BOP is estimated to be 60% of system cost at low volumes (100 systems per year) and 80% at high volumes (50,000 systems per year) for 10-kW SOFC CHP systems.
- Scenario modeling has been done for fuel cell system lifetime costs vs. the no-fuel cell case of grid electricity and conventional heating as a function of fuel and electricity costs, and the carbon intensity of grid electricity using goals from the CPP. Even with the CPP's proposed clean-up of the electricity system, we find that the installation of fuel cell CHP still has net positive societal benefits from 2016–2030 in regions which currently have high grid-electricity emissions (e.g., the upper Midwest).
- The research team plans to release an updated LT PEM total cost of ownership report in the final quarter of FY 2016.

FY 2016 PUBLICATIONS/PRESENTATIONS

1. Max Wei, Tim Lipman, Roberto Scataglini, Ahmad Mayyas, Shuk-Han Chan, Hanna Breunig, Tom McKone. "Total Cost of Ownership Model for SOFC CHP systems," Fuel Cell Seminar Conference, Los Angeles, CA. November 2015.

2. Roberto Scataglini, Ahmad Mayyas, Max Wei, Shuk Han Chan, Timothy Lipman, David Gosselin, Anna D'Alessio, Hanna Breunig, Whitney G. Colella, and Brian D. James. "A Total Cost of Ownership Model for Solid Oxide Fuel Cells in Combined Heat and Power and Power-Only Applications." Lawrence Berkeley Lab Report LBNL-1005725. December 2015.

REFERENCES

1. James, Brian, Kalinoski, J., and K. Baum. Mass-Production Cost Estimation for Automotive Fuel Cell Systems. 2010 Annual Merit Review Proceedings, Department of Energy, Hydrogen and Fuel Cells Program. Washington, D.C., June 2010.

2. Sinha, Jayanti and Y. Yang. *Direct Hydrogen PEMFC Manufacturing Cost Estimation* for Automotive Applications. 2010 Annual Merit Review Proceedings, Department of Energy, Hydrogen and Fuel Cells Program. Washington, D.C., June 2010.

3. Mahadevan, Kathya , V. Contini, M. Goshe, J. Price, F. Eubanks, and F. Griesemer. Economic Analysis of Stationary PEM Fuel Cell Systems. 2010 Annual Merit Review Proceedings, Department of Energy, Hydrogen and Fuel Cells Program. Washington, D.C., June 2010.

4. James, B., Spisak, A., Colella, W. *Manufacturing Cost Analysis of Stationary Fuel Cell Systems*, Strategic Analysis Inc. Arlington VA, September 2012.

5. Stadler, Michael, Marnay, C., Gonçalo Cardoso, G. et al. *The Carbon Dioxide Abatement Potential of California's Mid-Sized Commercial Buildings*. California Energy Commission, PIER Program. CEC-500-2010-050 (2011).

6. Deru, M., Field, K., Studer, D., Benne, K., Griffith, B., Torcellini, P., Liu, B., Halverson, M., Winiarski, D., Rosenberg, M., Yazdanian, M., Huang, J., Crawley, D. (2011). *Reference Building Models of the National Building Stock*. NREL Technical Report NREL/TP-5500-46861.

7. Lipman, Timothy E., Jennifer L. Edwards, and Daniel M. Kammen, *Fuel Cell System Economics: Comparing the Costs of Generating Power with Stationary and Motor Vehicle PEM Fuel Cell Systems*, Energy Policy 32(1): 101–125 (2004).

8. Van Rooijen, Jaap. *A Life Cycle Assessment of the PureCell™ Stationary Fuel Cell System: Providing a Guide for Environmental Improvement, Center for Sustainable Systems*, Report No. CSS06-09 University of Michigan, Ann Arbor, MI, June 30, 2006.

9. National Research Council. *Hidden Costs of Energy: Unpriced Consequences of Energy Production and Use*. The National Academies Press: Washington, D.C., 2010.

10. Muller, N.Z., and R.O. Mendelsohn, *The Air Pollution Emission Experiments and Policy Analysis Model (APEEP)*: Technical Appendix [online]. Yale University, New Haven, CT. December 2006. Available at: https://segueuserles.middlebury.edu/nmuller/APEEP_Tech_Appendix.pdf

11. AP2 Model, https://sites.google.com/site/nickmullershomepage/home/ap2-apeep-model-2, Accessed February 15, 2016.

12. Environmental Protection Agency 2015. *Regulatory Impact Analysis for the Clean Power Plan Final Rule*. October 23, 2015. Available at https://www.epa.gov/sites/production/files/2015-08/documents/cpp-final-rule-ria.pdf

13. Siler-Evans, K.; Lima Azevedo, I.; Morgan, M.G. *Marginal Emissions Factors for the U.S. Electricity System*. Environ. Sci. Technol. 2012. *46*, 4742–4748.

14. Environmental Protection Agency 2015. eGRID database, https://www.epa.gov/energy/egrid, Accessed February 15, 2016.

15. Kyle Siler-Evans, Inês Lima Azevedo, M. Granger Morgan, and Jay Apt, *Regional variations in the health, environmental, and climate benefits of wind and solar generation*, PNAS 2013 110 (29) 11768–11773.

V.G.1 Structure and Function in Electrocatalysis of Reactions for Direct Energy Conversion

Radoslav Adzic (Primary Contact), Jia X. Wang, Miomir B. Vukmirovic, and Kotaro Sasaki
Brookhaven National Laboratory
P.O. Box 5000
Upton, NY 11973
Phone: (631) 344-4522
Email: adzic@bnl.gov

DOE Program Manager: Raul Miranda
Phone: (240) 252-8306
Email: Raul.Miranda@science.doe.gov

Program Scope

We conduct studies of Pt monolayer electrocatalysts, and related core-shell catalysts for reactions of direct energy conversion including the O_2 reduction and O_2 evolution reactions, oxidation of ethanol and methanol, H_2 oxidation and evolution and CO_2 reduction. We aim at increasing our understanding of their kinetics and synthesizing ultimately low Pt content electrocatalysts with high activity and good stability. The results of some of our recent studies are highlighted below.

FY 2016 Highlights

Oxygen Evolution Reaction Mechanism and Enhanced Activity of the RuO_2@IrO_2 Core-Shell Nanocatalysts

Iridium dioxide is the gold standard for oxygen evolution reaction (OER) in proton exchange membrane water electrolyzers (PEMWE). However, iridium's low abundance restricts the application of PEMWE in carbon-free hydrogen production using solar- and wind-generated electricity. To maximize the performance of IrO_2-based catalysts we developed a facile synthesis method to prepare RuO_2@IrO_2 core-shell nanocatalysts, which has the specific activity RuO_2@IrO_2 for the OER is three-fold that of IrO_2. To further enhance activity, we studied the OER mechanism. There are controversial views on the reaction pathway and rate-determining-step, making rational design of advanced OER catalysts difficult. While it is generally agreed that the dominant pathway for hydrogen evolution involves the Tafel reaction that combines two adsorbed H in forming H_2, the OER pathways with the O-O bond formed from two adsorbed oxygen species are challenged by the density functional theory (DFT) studies suggesting that the activation barrier is lower with addition of a second O to an adsorbed one via sequential water dissociative adsorption on the O-adsorbed site. We resolved the controversy by fitting measured polarization curves for the RuO_2, RuO_2@IrO_2, and IrO_2 catalysts using a two-step kinetic equation for sequential water dissociation with adsorbed O as the major OER intermediate. Differing from the previous DFT predictions, we found the major role of free energy of O adsorption in determining the OER activity, and concluded that the rate-determining step on IrO_2 is the formation of O adsorbed phase, while the OOH formation limits the reaction rate on RuO_2. The new insight suggests that a more suitable oxide core should slightly strengthening the O-adsorption on the IrO_2 shell's for enhancing the OER activity, which will guide our future studies in developing highly active and low cost OER catalysts.

Elucidating Hydrogen Oxidation/Evolution Kinetics in Alkaline and Acid Solutions

Hydrogen oxidation and evolution reactions on Pt in acid are facile processes, while in alkaline electrolytes they are two orders of magnitude slower. This behavior is not understood. Thus, increasing the understanding of different kinetics and developing catalysts that are more active than Pt for these two reactions is important for advancing the performance of anion-exchange-membrane fuel cells and water electrolyzers. We found a four-fold enhancement in Pt mass activity for single crystalline Ru@Pt core-shell nanoparticles with two-monolayer-thick Pt shells, which doubles the activity on Pt-Ru alloy nanocatalysts. For Pt specific activity, the 2- and 1-monolayer-thick Pt shells, respectively, exhibited an enhancement factor of 3.1 and 2.3 compared to the Pt nanocatalysts in base, differing considerably from the values of 1 and 0.4 in acid. To explain such behavior and the orders-of-magnitude difference in activity in acid and base, we performed kinetic analyses of polarization curves over a wide range of potential, from -250 mV to 250 mV using the dual-pathway kinetic equation. From acid to base, the activation free energies increase the most for the Volmer reaction, resulting in a switch of the rate-determining step from the Tafel- to the Volmer-reaction, and a shift to a weaker optimal hydrogen-binding energy. The much higher activation barrier for the Volmer reaction in base than in acid is ascribed to one or both of the two catalyst-insensitive factors, slower transport of OH^- than H^+, and a stronger O-H bond in water molecules (HO-H) than in hydrated protons (H_2O-H^+).

Enhancing Oxidation Kinetics of Methanol and the C-C Bond Splitting in Ethanol on Pt Monolayer Under Tensile Strain

We demonstrated that the Pt monolayer under tensile strain on Au substrates has a highly enhanced activity for methanol and ethanol oxidation. In methanol oxidation formation of CO is precluded, while in oxidation of ethanol the C-C bond splitting facilitate enhanced activity [1]. The activity of Pt_{ML}/Au can be further improved by incorporating active co-catalysts, and the Ru/Pt_{ML}/Au/C and $RhSnO_2$/Pt_{ML}/Au/C electrocatalysts were designed and synthesized for practical application in a direct alcohol fuel cell. In situ infrared spectroscopy studies with single-crystal- and nanoparticle-based catalysts showed no adsorbed CO band (~2,090 cm^{-1}) in methanol oxidation, which proceeded to CO_2. This observation was in agreement with theoretical prediction by DFT calculation. Moreover, the addition of Ru co-catalyst in Ru/Pt_{ML}/Au/C successfully moved onset of CO_2 band (~2,343 cm^{-1}) to around 0.3 V vs. reference hydrogen electrode. During ethanol oxidation on Pt_{ML}/Au(111), the absence of both the CO_{ads} and CO_2 bands suggested that ethanol dissociative adsorption did not occur and that the reaction followed partial oxidation pathway without cleavage of the C−C bond. However, the splitting of C-C bond was observed on nanoparticles Pt_{ML}/Au/C and $RhSO_2$/Pt_{ML}/Au/C catalysts, as evidenced by the CO_2 band. Future work is needed to explain the difference and to further optimize these catalysts.

References

1. Li, M.; Liu, P.; Adzic, R.R., J. Phys. Chem. Lett. 3, 3480−3485. 2012.

V.G.2 Catalysis and Electrocatalysis for Fuel Synthesis: Hydrogen Production and the Water-Gas Shift

Jose A Rodriguez (Primary Contact), Ping Liu, Sanjaya Senanayake, Dario Stacchiola, Mike G. White
Brookhaven National Laboratory
Chemistry Department
PO Box 5000
Upton, NY 11973
Phone: (631) 344-2246
Email: rodrigez @bnl.gov

DOE Manager: Raul Miranda
Phone: (301) 903-1411
Email: Raul.Miranda@science.doe.gov

Program Scope

The water-gas shift reaction (WGS: $CO + H_2O$ à $H_2 + CO_2$) is a critical process in providing pure hydrogen for fuel cells and other applications. Improved air-tolerant, cost-effective WGS catalysts for lower temperature processing are needed. Ceria-, titania- and molybdena-based catalysts are expected to be the next generation of WGS catalysts for industrial applications. The design and optimization of these WGS catalysts depends on a better understanding of their structures and functions. This project involves a coordinated research program to understand the active sites and reaction mechanism for the WGS on these promising metal/oxide catalysts. Our goal is to develop the ability to predict, and ultimately design, improved cost-effective WGS low temperature catalysts. Our approach exploits a uniquely powerful combination of synthetic and characterization methods for both model systems and industrially relevant powder catalysts. It utilizes unique capabilities for in situ studies using time-resolved X-ray diffraction (XRD), X-ray absorption spectroscopy, photoemission, infrared spectroscopy, and transmission electron microscopy (TEM). Most experiments are closely coupled to theoretical studies on the chemisorption of the reactants, the stability of possible intermediates, and activation barriers for elementary reaction steps, providing critical guidance in developing a complete picture of the links between catalyst structure and reaction mechanism in this important process for the production of pure hydrogen.

FY 2016 Highlights

(1) A new type of metal-support interaction that can be quite useful for the rational design of highly active water-gas shift catalysts was discovered and is under study.

(2) Studies carried out using inverse oxide/metal catalysts showed the important role played by the oxide phase in the WGS reaction. This led to a shift of paradigm for the design of WGS catalysts. The optimization of the properties of the oxide phase is as important as the optimization of the metal phase.

(3) Highly active powder catalysts that combine Au or Pt and CeO_2 nanoparticles on a titania substrate were prepared and fully characterized.

(4) New tools were developed for the in situ characterization of WGS catalysts. A new instrument will combine X-ray absorption fine structure (XAFS) with infrared or Raman spectroscopy. This new instrumentation will allow us to perform unique mechanistic studies.

A series of model catalysts [CeOx/Cu(111), CeOx/Au(111), Pt/CeO_2(111), Ni/CeO_2(111), Pt/TiO_2(110), Pt/CeOx/TiO_2(110)] was used to study fundamental aspects of the water-gas shift reaction. These studies studies revealed that the oxide component of the catalyst can affect the reaction process in two different ways. First, the presence of O vacancies in the oxide greatly facilitates the dissociation of water. Second, the electronic properties of the metal can be affected by interactions with the oxide producing special chemical properties. This is the case in the Ni/CeO_2(111), Pt/ CeO_2(111) and Pt/CeO_x/TiO_2(110) systems. In Figure 1, small coverages of Ni on CeO_2(111) are highly active for the WSG reaction and do no produce

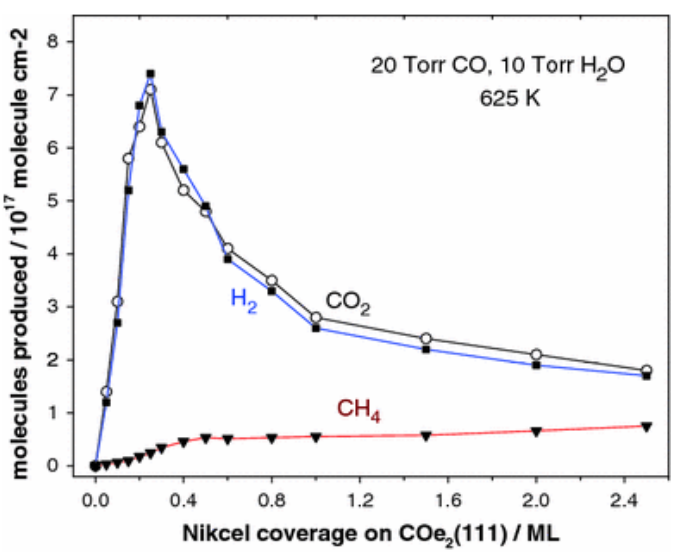

FIGURE 1. Water-gas shift activity of Ni/CeO_2(111) as a function of Ni coverage.

methane, although bulk Ni is a very good catalyst for the methanation of CO. The electronic properties of Ni and Pt nanoparticles deposited on CeO_2(111) and CeO_x/TiO_2(110) have been examined using core and valence photoemission. The results of valence photoemission point to a new type of metal-support interaction which produces large electronic perturbations for small Ni and Pt particles in contact with ceria. The Ni/CeO_2(111) Pt/CeO_2(111) and Pt/CeO_x/TiO_2(110) systems exhibited a density of metal d states near the Fermi level that was much smaller than that expected for bulk metallic Ni or Pt. The electronic perturbations induced by ceria on Ni made this metal a very poor catalyst for CO methanation, but transformed Ni into an excellent catalyst for the production of hydrogen through the water-gas shift (Figure 2) and the steam reforming of ethanol. Furthermore, the large electronic perturbations seen for small Pt particles in contact with ceria significantly enhanced the ability of the admetal to adsorb and dissociate water made it a highly active catalyst for the WGS (Figure 2). The behavior seen for Ni/CeO_2(111), Pt/CeO_2(111) and Pt/CeO_x/TiO_2(110) systems illustrates the positive effects derived from electronic metal-support interactions and points to a promising approach for improving or optimizing the performance of metal/oxide catalysts.

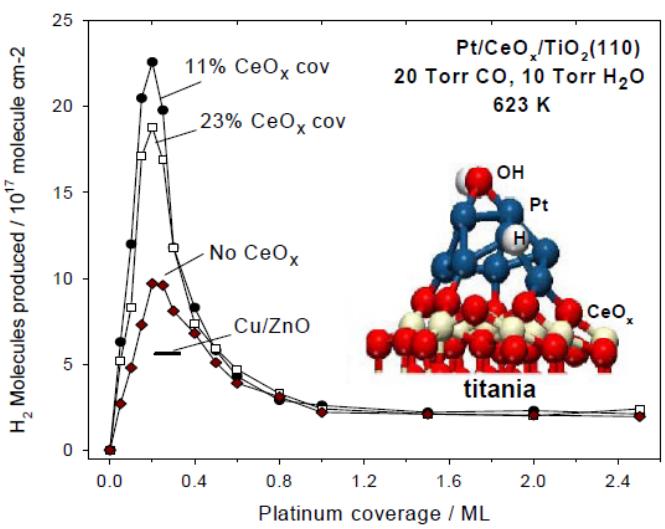

FIGURE 2. Water-gas shift activity of Pt/TiO_2(110) and Pt/CeO_x/TiO_2(111) as a function of Pt coverage.

The active phase of a series of metal/oxide powder catalysts (Pt/CeO_2, Pt-Ru/CeO_2, Pt/CeOx/TiO_2, Au/CeO_x/TiO_2, $Ce_{1-x}Ni_xO_{2-y}$, CeO_x/CuO) was investigated using a combination of in situ time-resolved XRD, Pair-distribution function (PDF) analysis, XAFS, and environmental TEM. Under reaction conditions most of these WGS catalysts underwent chemical transformations that drastically modified their composition with respect to that obtained during the synthesis process. The active phase of catalysts which combine Cu, Ni, Au or Pt with oxides such as CeO_2, TiO_2 and CeO_x/TiO_2 essentially involved nanoparticles of the reduced metals. The oxide support underwent partial reduction and was not a simple spectator, facilitating the dissociation of water and in some cases modifying the chemical properties of the supported metal. Therefore, to optimize the performance of these catalysts one must take into consideration the properties of the metal and oxide phases. Figures 3 shows a TEM image and PDF data for an inverse CeOx/CuO powder catalysts. In the TEM image, taken for the as-prepared catalysts, one can see crystallites that in many cases exhibit a (111) surface termination. The PDF results to water-gas shift reaction conditions and show a simultaneous disappearance of the Cu-O vector of CuO with the appearance of a Cu-Cu vector for metallic copper. These data, and in situ results obtained for other catalysts in our group, indicate that a WGS metal/oxide catalyst is a dynamic entity that changes with reaction conditions.

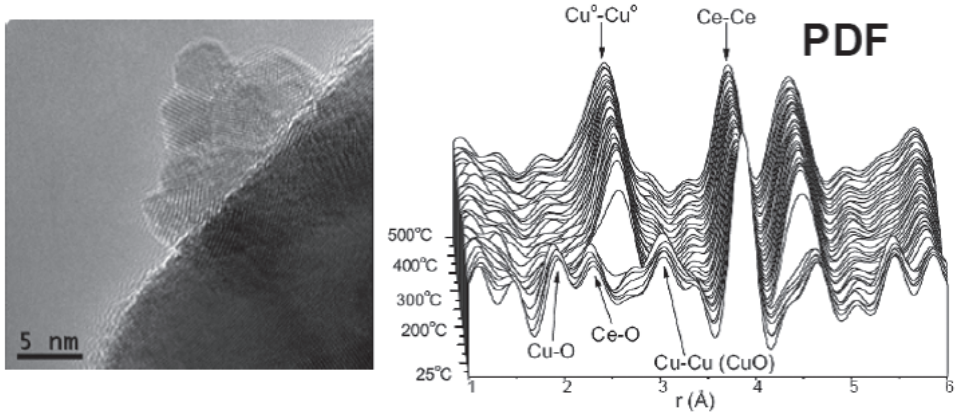

FIGURE 3. Left: TEM image of an inverse CeO_x/CuO catalyst. Right: in situ time-resolved PDF data for a CeO_2/CuO catalyst during the WGS.

V.G.3 Control of Reactivity in Nanoporous Metal/Ionic Liquid Composite Catalysts

Jonah Erlebacher (Primary Contact), Ellen Benn, Bernard Gaskey
Johns Hopkins University
3400 N. Charles St.
206 MD Hall
Baltimore, MD 21218
Phone: (410) 516-6077
Email: Jonah.Erlebacher@jhu.edu

DOE Manager: Raul Miranda
Phone: (301) 903-8014
Email: Raul.Miranda@science.doe.gov

Program Scope

In this program, we have been exploring a new concept in nanostructured heterogeneous catalysis design: the use of a nanoporous metal, either alone or impregnated with an ionic liquid (IL) to form a composite catalyst [3,4]. The idea behind this concept is to tailor the chemical environment within and near the pores of a metallic electrocatalyst in order to enhance the aggregate composite activity and selectivity. Most recent electrocatalyst design focuses upon lowering the activation barrier for a particular synthesis reaction. While we also try to minimize this quantity, one should also recognize that significant catalytic enhancements can be made by biasing the reaction to completion via control of the environment in which the reaction occurs. Specific ideas we are exploring in this program include (a) bias of mass transport of reactants to the surface and products away from it and (b) corralling of reactants and products to spatially separate them and reduce side reactions.

Fiscal Year (FY) 2016 Highlights

A more specific aim of this program is to develop electrocatalysts for the electroreduction of small molecules such as oxygen, carbon dioxide, or ultimately nitrogen. The oxygen reduction reaction (ORR), for its relevance to the fuel cathode reaction, has been a first choice of study. In recent studies, by ourselves and others [1,2], it was found that impregnating dealloyed nanoporous nickel-platinum (np-NiPt) with hydrophobic and oxophilic ionic liquids increases the aggregate activity of the electrocatalyst. Multiple mechanisms are potentially operative here, in particular, (a) higher oxygen solubility near the catalyst surface adds a diffusive driving force to draw oxygen in from the aqueous environment, (b) hydrophobicity expels products from the catalyst surface, and (c) IL properties such as proticity or viscosity are affecting reaction conditions. Figure 1 shows results of oxygen reduction activity over np-NiPt for a survey of ionic liquids exhibiting a range of properties, each of which to some extent improves the ORR activity by shifting the half-wave to higher potentials. This study concluded that the primary determinants of ORR improvement are simultaneous high oxygen solubility and high hydrophobicity [3].

An ancillary goal of this study was to see if aprotic ionic liquids in the nanoporous metal could stymie proton

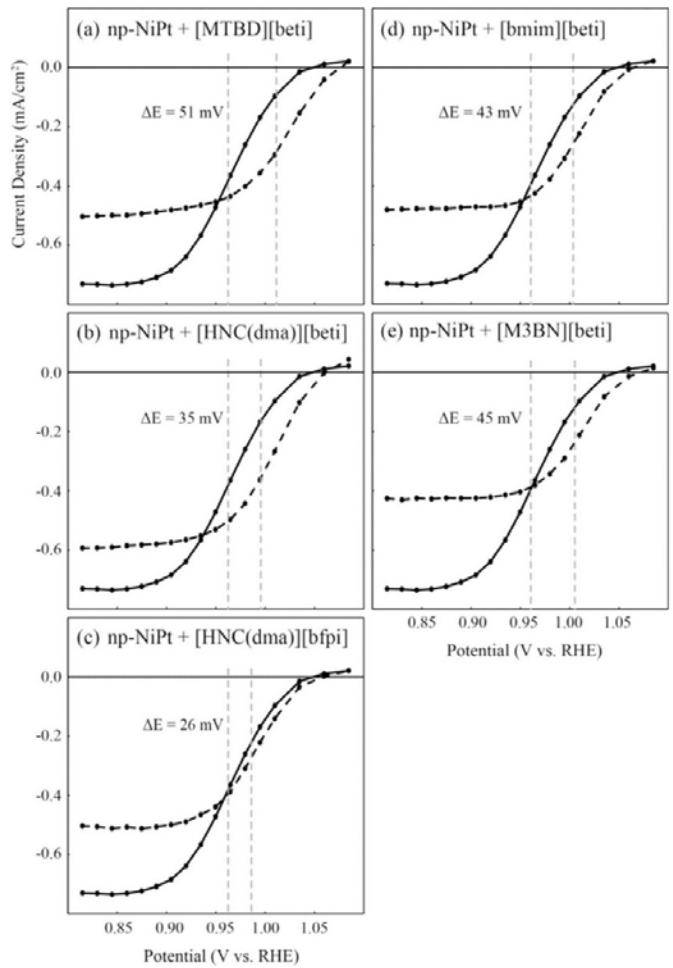

FIGURE 1. Potentiostatic ORR current density versus potential for np-NiPt (solid line) filled with a variety of different ionic liquids (a) np-NiPt+[MTBD][beti] (high oxygen solubility), (b) np-NiPt+[HNC(dma)][beti] (high proton conductivity and low viscosity), (c) np-NiPt+[HNC(dma)][bfpi] (relatively high hydrophobicity), (d) np-NiPt+[bmim][beti] (aprotic and high viscosity), and (e) np-NiPt+[M3BN][beti] (aprotic and low viscosity) [3]

transport to the electrocatalyst surface. If this were possible, then reduction of other small molecules from an essentially aqueous solution could occur even at highly reducing potentials, in particular at potentials at which hydrogen evolution occurs, below 0.0 V vs. reference hydrogen electrode (RHE). This remains a viable new strategy for CO_2 or N_2 reduction, but requires design and synthesis of ionic liquids with essentially no water solubility. In our above-mentioned survey, we found that even "very hydrophobic" ionic liquids had water solubilities of order 1 M.

However, the result also suggested a second strategy to stymie hydrogen evolution via control of reaction kinetics in aqueous solution. Our hypothesis was that if the oxygen flux to the surface can be maintained higher than a proton flux to the surface, then adsorbed oxygen will block hydrogen evolution. Such a scenario is easily satisfied without an IL in O_2-saturated electrolytes above ~ pH 3, because O_2 solubility is of order 1 mM. Figure 2 shows a key result, that at pH 4, oxygen evolution under proton-diffusion limited conditions in a rotating disk electrode setup can be maintained to potentials nearly 400 mV below 0.0 V vs. RHE, to potentials negative enough to reduce water directly. Most interestingly, this effect is only possible using a nanoporous electrode which is transiently conditioned to introduce a pH gradient within the porosity itself. Having established a viable reaction scenario in which hydrogen evolution is kinetically suppressed, we are exploring this strategy for CO_2 reduction, and will be extending this strategy to non-aqueous electrolytes to reach extreme reducing potentials without reducing water.

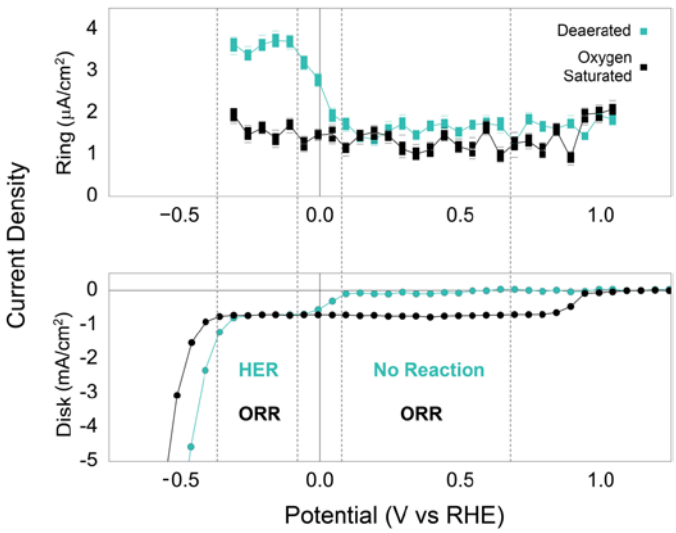

FIGURE 2. Potentiostatic rotating ring disk electrode measurements of current density vs. potential at pH 4 in oxygen-saturated vs. deaerated solutions. Here, both hydrogen evolution reaction (HER) and ORR is expected to occur under proton diffusion limited conditions. Hydrogen evolved in deaerated solutions below 0.0 V vs. RHE is detected via hydrogen oxidation at the ring. In oxygen-saturated solutions, HER is suppressed in favor of oxygen reduction, due to a combination of a higher flux of oxygen to the electrode than protons, and a pH gradient within the pores [4].

References

1. C. Chen, et al., "Highly Crystalline Multimetallic Nanoframes with Three-Dimensional Electrocatalytic Surfaces," Science, 343 (2014), 1339-1343.

2. J. Snyder, K. Livi, J. Erlebacher, "Oxygen Reduction Reaction Performance of [MTBD][beti]-Encapsulated Nanoporous NiPt Alloy Nanoparticles," Adv. Func. Mat., 23 (2013), 5494-5501.

3. E. Benn, H. Uvegi, J. Erlebacher, "Characterization of Nanoporous Metal-Ionic Liquid Composites for the Electrochemical Oxygen Reduction Reaction," J. Electrochem. Soc., 162 (2015), H759-H766.

4. E. Benn, J. Erlebacher, "Oxygen Reduction Suppresses Hydrogen Evolution Under Proton Diffusion Limited Kinetics," in preparation for submission to Nature Chemistry.

V.G.4 Multifunctional Catalysis to Synthesize and Utilize Energy Carriers

Tom Autrey (Primary Contact), Abhi Karkamkar, Bojana Ginovska, Don Camaioni, Greg Schenter, Adrian Houghton
Pacific Northwest National Laboratory
P.O. Box 999
902 Battelle Blvd.
Richland, WA 99352
Phone: (506) 375-3792
Email: tom.autrey@pnnl.gov

DOE Manager: Viviane Schwartz
Phone: (301) 903-0448
Email: Viviane.Schwartz@science.doe.gov

Program Scope

The goal of the Institute for Integrated Catalysis (structure shown in Figure 1) is the development of the fundamental science basis for a significant step forward in the way we catalytically transform common carbon resources, such as bio-derived molecules and CO_2, and how we access and activate H_2 at lower temperatures and with higher rates than practiced today. We are convinced that gaining fundamental understanding of the basic steps of the individual reactions involved will enable us to achieve the knowledge-based development of catalysts essential to realize these transformations. The strategy is to focus on a few chemical transformations and to explore, in depth, the molecular and atomistic pathways of these selected reactions on catalysts spanning from single-crystal surfaces to molecular complexes.

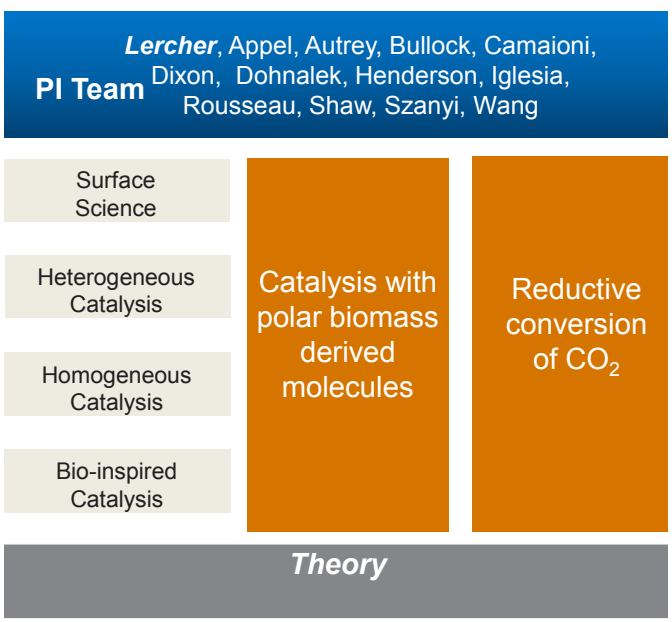

FIGURE 1. The goal structure of the Institute for Integrated Catalysis.

FY 2016 Highlights

Activation of Small Molecules with Bifunctional Ambiphilic Catalyst Complexes: Catalytic activation of molecular hydrogen is critical for the efficient upgrading of energy carriers ranging from conventional hydrocarbons to renewables such as biomass. Metals are often used to activate H_2, however, a number of research groups have shown that frustrated Lewis pairs (FLPs) can be used to mimic the chemistry of transition metals and provide an alternate pathway for the catalytic reduction of polar and polarizable substrates. FLPs are of interest as they provide an approach to heterolytically activate H_2 catalytically, at moderate pressures and temperatures. The heterolytic activation of H_2, i.e., H+/H-, using a combination of a spatially oriented Lewis acid, A, and Lewis base, B, will provide a route that favors the reduction of polar and polarizable substrates H_2 + X=Y à HX-YH.

Our research interests are focused on the development of tools and approaches that use a combination of theory and experiment to understanding how molecular hydrogen is activated heterolytically without using metals in frustrated Lewis pairs. We have developed novel approaches to using reaction calorimetry to measure both kinetic and thermodynamics of H_2 activation and transfer to a series of polar substrates to gain a quantitative measure of both activation barriers and enthalpic driving force under catalytic

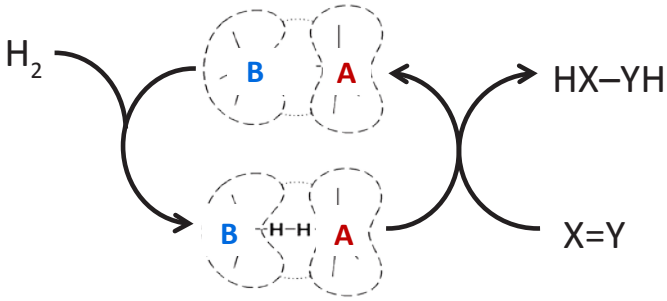

SCHEME 1. Illustration of a catalytic cycle for the reduction of polar substrate X=Y using a bifunctional Lewis acid Lewis base pair. Optimal spatial alignment prevents quenching of Lewis acid and Lewis base resulting in novel reactivity that mimics transition metals.

reaction conditions. This approach has provided the first experimental measure of the activation barrier for the heterolysis of H_2 by FLPs. Surprisingly these results show that the barrier for heterolysis is quite small, 15–20 kJ/mol for a reaction with a moderate driving force.

Inspired by this insight we began to investigate the reactivity of crystal FLPs over the past year. We hypothesized that the crystalline molecular complex, 1-{2-[bis(pentafluorophenyl)boryl]phenyl}-2,2,6,6-tetramethylpiperidine, abbreviated KCAT, could react with gaseous H_2 for the corresponding ion pair, KCATH2. Our theory calculations suggest the driving force is greater in the crystalline state than in solution. Figure 2 shows the crystallographic overlay of KCAT and KCATH2. Note the minute change in structure suggesting the possibility of a single crystal–single crystal transformation.

Optical microscopy was used to follow the transformation of the colored KCAT crystals to form the colorless KCATH2 in the presence of H_2 gas at room temperature. The results show that some regions of the crystal react faster than other regions, but the boundaries between these regions are diffuse, showing there is not a clear preference for reactivity at surface or interior sites.

Inelastic neutron scattering spectroscopy (INS) provides a unique approach to study both the energetics and dynamics of hydrogen interactions in condensed phase materials. Using the VISION spectrometer at the Spallation Neutron Source we were able to investigate the single crystal–single crystal transformation of solid KCAT, to the corresponding ion pair, KCATH2, quantitatively upon exposure to gaseous H_2. The reaction does not occur until temperatures exceeded 200 K. Ab initio molecular dynamics approaches used to calculate the INS spectra are in excellent agreement with the experimentally measured spectra.

The chemical transformation of a crystalline FLP to the corresponding crystalline ion pair provides the first example of a non-metal activation of H_2 in the solid state. Insight from these studies will permit the development of new approaches to *heterogenize* Lewis acid Lewis base pairs on conventional catalyst supports, e.g., metal oxides, metal organic frameworks, or high surface area carbons. The reactivity of these novel complexes is currently under investigation.

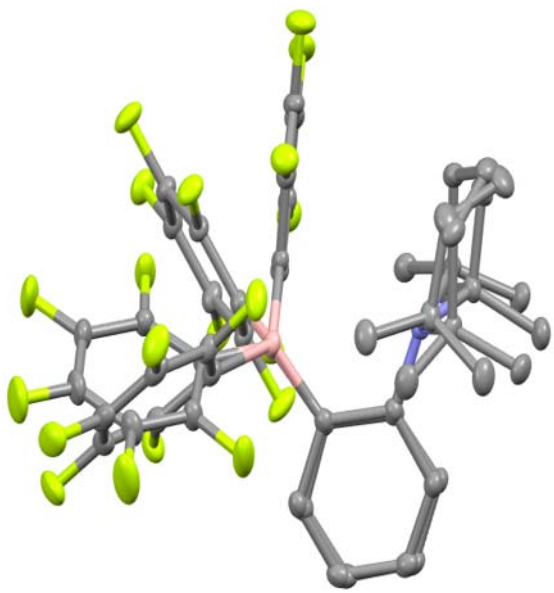

FIGURE 2. Crystallographic overlay of KCAT and KCATH2.

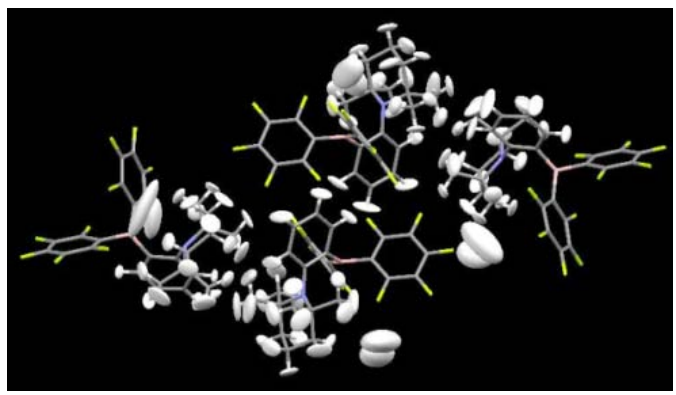

FIGURE 4. Thermal ellipsoids predicted from harmonic calculations of H_2 interacting with KCAT.

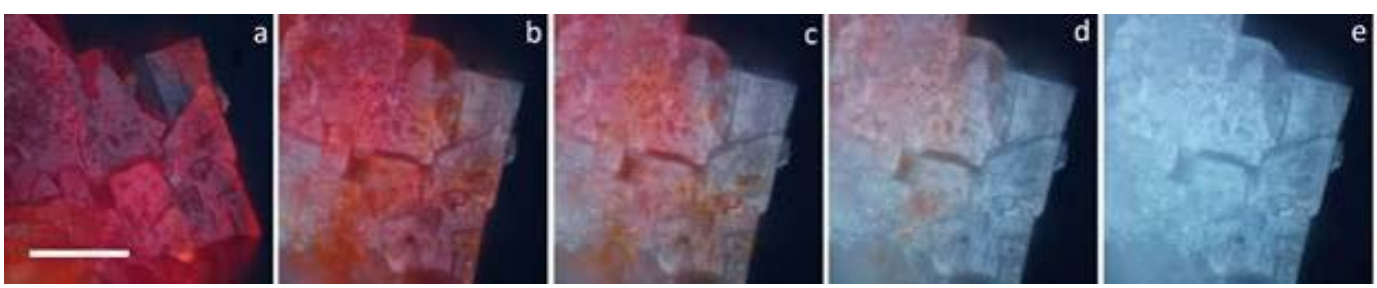

FIGURE 3. Optical micrographs of KCAT crystals exposed to H_2 gas for (a) 0 min, (b) 55 min, (c) 85 min, (d) 112 min, (e) 150 min. Scale bar = 100 µm.

V.G.5 Modeling Catalyzed Growth of Single Walled Carbon Nanotubes

Perla B. Balbuena (Primary Contact),
Jose L. Gomez-Ballesteros, Behnaz Rahmani Didar
Department of Chemical Engineering
Texas A&M University
College Station, TX 77843
Phone: 979-845-3375
Email: balbuena@tamu.edu

DOE Manager: Raul Miranda
Phone: (301) 903-8014
Email: Raul.Miranda@science.doe.gov

Program Scope

Understanding and controlling synthesis processes are key scientific challenges which are needed to achieve significant advances in the field of nanomaterials. Single-walled carbon nanotubes (SWCNTs) have unusual physical-chemical properties that make them promising materials for a large number of innovative applications in electronics, biomedicine, micro and nano separations among others. Their structure, diameter, and degree of helicity (also known as chirality) are responsible for their specific physical-chemical behavior. SWCNTs may be synthesized by catalytic decomposition of a carbon containing species over metallic nanoparticles using chemical vapor deposition methods. Many advances have been achieved in the last decade tuning this synthesis process aiming toward products with specific properties, and there is nowadays a consensus regarding the role of the catalyst on the associated growth of specific carbon structures on its surface. In previous work we (and others) have demonstrated the existence of structural correlations between the nanocatalyst and the nascent nanotube at different growth stages. Such correlations can be dominated by either the nanotube (inverse template effect) or the nanoparticle (template effect). We have shown that achieving chirality control depends on determining synthesis conditions where crucial structural features of the nanoparticles are maintained during growth (i.e., favoring a template effect). Thus, we have advanced in understanding the factors that influence specific growth behaviors and the next challenge must be oriented toward controlling these factors via smart synthesis procedures.

In our current studies we focus on the overall catalytic system that includes catalyst and support. We aim to elucidate the role of the support material on the nanocatalyst structure and composition, and therefore, on the growth of specific chiral carbon nanotubes. These studies will allow a systematic search of nanotube growth conditions where the nanoparticle stability can be optimized thus allowing template effect and selective growth. Moreover, our systematic fundamental study of catalyst–support interactions will be useful for other catalytic processes and is a first step to elucidating nanocatalyst synthesis.

FY 2016 Highlights

Changes in Nanocatalyst Shape and Composition during Nucleation of SWCNTs

This work was done in collaboration with the group of Dr. Renu Sharma at the National Institute of Standards and Technology, who has experimental capabilities of obtaining real-time atomic-resolution videos taken in an environmental transmission electron microscope during SWCNT growth. Thus, the dynamic evolution of supported Co carbide nanoparticles (Co_2C/MgO) during the nucleation stage of single-walled carbon nanotube growth was explored using reactive- and ab initio-molecular dynamics simulations coupled with in situ environmental transmission electron microscopy imaging. Changes in the nanocatalyst shape and composition were examined throughout the nucleation process beginning with carbon dissolution, diffusion and formation of carbon chains on the surface until a cap is fully formed and the nanotube structure defined (Figure 1). The amount of carbon dissolved in the carbide-like nanoparticle decreases as C atoms precipitate at the surface. Once nucleation of the surface C atoms begins, a steady state global C concentration is reached. Changes in the nanoparticle shape occur linked with changes in the dynamics of C atoms according to experiments and RMD simulations: a decrease of the nanoparticle height and spreading over the substrate is observed while the C composition is stabilized, no changes occur as the cap is being formed, and subsequent elongation and shape recovery take place due to interactions with the cap as it lifts off. The main two factors influencing nanoparticle shape and C distribution can thus be summarized as: interactions with the substrate and interactions with the nascent nanotube. The nanoparticle evolution in relation to its interaction with the substrate from AIMD studies reveals that the nanoparticle–substrate interface is dominated by interactions between Co atoms located atop O atoms in the substrate. Strong nanoparticle–substrate interactions were characterized by electron transfer and re-arrangement of Co atoms at the interface stemming from a given Co_2C surface termination, i.e., (020) and (210). The interactions of the nanocatalyst with the cap are responsible for the C gradient observed along the direction perpendicular to the substrate in both simulations

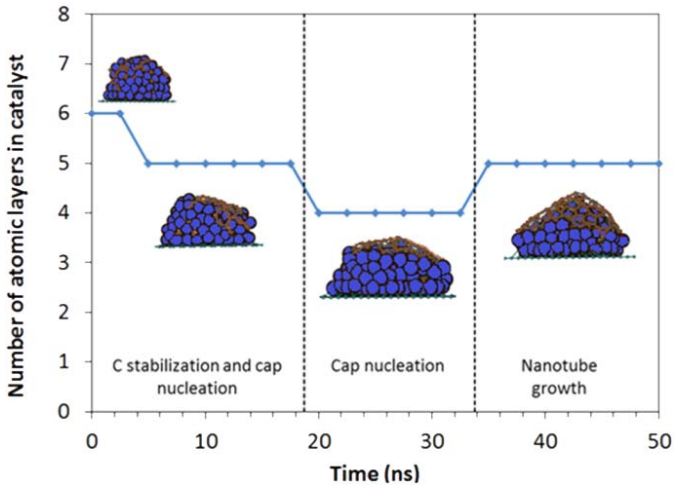

FIGURE 1. Shape evolution of the catalyst nanoparticle during nucleation and growth stages. Reactive MD simulations illustrate that during carbon stabilization, the metal layer in contact with the substrate tends to wet the substrate. Carbon nucleation starts before carbon stabilization is reached and leads to further reduction in the number of layers of the nanocatalyst particle. The slight vertical elongation of the nanocatalyst particle coincides with the beginning of the growth stage.

and experiments. This suggests that the catalyst topmost layer is a primary source of C atoms for the formation of the nanotube cap. Overall, the combination of atomistic simulations and in situ observation of SWCNT growth provides insights into the fundamental phenomena driving the observed changes in the nanoparticle and allows the identification of key aspects for the formulation of models and mechanisms to better understand and control the catalytic process.

V.G.6 Room Temperature Electrochemical Upgrading of Methane to Oxygenate Fuels

William E. Mustain
Department of Chemical & Biomolecular Engineering
University of Connecticut
191 Auditorium Rd., Unit 3222
Storrs, CT 06269-3222
Phone: (860) 486-2756
Email: mustain@engr.uconn.edu

DOE Program Manager: Raul Miranda
Phone: (301) 903-8014
Email: Raul.Miranda@science.doe.gov

Program Scope

This program supports the Office of Basic Energy Sciences mission to control energy-relevant molecular transformations. Specifically, this program focuses on the design and understanding of the reaction pathways involved in the near room temperature electrochemical activation of methane and synthesis of small molecule organic molecules such as methanol. Aqueous, low temperature (25°C–220°C) methane electrochemistry has been studied extensively since the 1960s. Acid reactions typically result in the either no reaction or complete oxidation to CO_2, and alkaline transformations have been ineffective because OH- anions tend to oxidize species by accepting protons rather than donating oxygen – giving OH^- anions a limited ability to attack methane. The lack of an efficient alkaline oxygen donor has severely handicapped the low temperature electrochemical conversion of methane to syngas.

Unlike previous low temperature electrochemical cells, this program leverages our group's recent discovery that carbonate (CO_3^{2-}) anions can act as an efficient oxygen donor at room temperature. The fact that carbonate oxidizes incoming species by oxygen donation is very important and provides an opportunity to form new C-O bonds through oxygen insertion and not C-H bond breakage, which is a key reason why this project has succeeded where previous attempts have failed. The early work done during this program shows that near room temperature, carbonate-enabled natural gas, and biogas conversion has significant promise, but there is considerable fundamental work remaining.

One of the most important aspects of this program is to better understand the electrochemistry and electrocatalysis behind the formation and reaction of carbonate anions, uncovering the key catalytic properties to allow for the rational design of high efficiency, room temperature methane electrocatalysts.

FY 2016 Highlights

- Elucidated the dynamics of CO_3^{2-}, HCO_3^- and OH^- formation, transport and consumption in the presence of various oxygen acceptors.
- Investigated (bi)carbonate decomposition and the possibility of using this chemistry for electrochemical CO_2 separation from flue gas effluent and utilization.
- Investigated methane activation dynamics using OH^- anions coupled with transition metal hydroxide-oxyhydroxide transformations.
- Developed electrode structures and processes to increase turnover number and improved spectroscopic sensitivity to products.
- Explored reaction pathways on multi-functional oxide-oxide and metal alloy nanocage catalysts.

V.G.7 Nanostructured, Targeted Layered Metal Oxides as Active and Selective Heterogeneous Electrocatalysts for Oxygen Evolution

Eranda Nikolla (Primary Contact), Anirban Das, and Xiangkui Gu
Wayne State University
Department of Chemical Engineering and Material Sciences
5050 Anthony Wayne Dr.
Detroit, MI 48202
Phone: (313) 577-4159
Email: Erandan@wayne.edu

DOE Program Manager: Viviane Schwartz
Phone: (301) 903-0448
Email: Viviane.Schwartz@science.doe.gov

Program Scope

The oxygen evolution reaction (OER) is an important chemical transformation that governs the performance of technologically relevant energy conversion and storage processes, such as electrochemical water splitting in electrolyzers and metal-air batteries. This reaction involves the evolution of oxygen gas from (i) oxygen ions formed from water splitting at high temperatures, (ii) oxygen containing species (i.e., OH^-, OOH^-) formed from water splitting at low temperatures, and (iii) metal-oxide discharge products (M_xO_2) in metal-air batteries. The main challenges to overcome in energy conversion via OER are expense (when catalyzed by noble metal-based electrocatalysts at low temperatures) and inadequate efficiency (when catalyzed by metal oxide based electrocatalysts at high temperatures). It has been shown that non-noble metal oxide electrocatalysts with layered structures, known as nickelate oxides, ($A_2MO_{4+\delta}$), that belong to the Ruddlesden-Popper first (R-P-1) series and comprise of alternating perovskite-like and rocksalt-like layers, exhibit promising OER activity [1,2]. We have recently demonstrated, the potential success of a bottom-up approach to design and synthesize lanthanum nickelate oxide (LNO) catalysts with optimal surface structure and surface oxygen exchange activity (process of exchanging lattice oxygen with gas-phase oxygen, which plays an important role in oxygen reduction and evolution on these materials) [3]. Inspired by the ability to control the nanostructure of nickelate oxide materials and their high oxygen exchange properties, we proposed to explore the potential of nanostructured nickelate oxides as highly active electrocatalysts for oxygen evolution. Our objective is to combine quantum chemical density functional theory (DFT) calculations with well-controlled synthesis techniques and kinetic studies to develop structure–performance relationships that would enable the design of optimal nickelate oxide electrocatalysts for OER.

FY 2016 Highlights

We have employed DFT calculations, combined with experimental studies, to investigate the energetics associated with the surface oxygen exchange process on B-site modified LNO with well-defined nanostructures. Spin-polarized DFT calculations were performed using Vienna ab initio Simulation Package (VASP). A series of LNO materials with varying B-site compositions were studied, including La_2MnO_4, La_2FeO_4, $La_2Ni_{0.5}Fe_{0.5}O_4$, La_2CoO_4, $La_2Co_{0.5}Ni_{0.5}O_4$ and La_2NiO_4. We found that the surface chemistry of La_2NiO_4 can be tuned via substitution of the B (Ni) site. Our results showed that the binding energies of O on the transition metal site and O_2 on the surface O vacancy became gradually weaker as the B-site metal was varied from Mn to Fe, Co, and Ni. A volcano-type relationship between the calculated oxygen exchange rates and the binding energies for O_2 was found, suggesting that the binding energy of O_2 might be a good descriptor for identifying nickelate oxide materials with optimal activity. Furthermore, our calculations predicted that Co-doped LNO would lead to the highest activity for surface oxygen exchange when compared to the other nickelate oxides considered.

To support the computational predictions, a series of nanostructured B-site modified LNO ($La_2Ni_{0.868}Co_{0.132}O_{4+\delta}$, $La_2Ni_{0.838}Cu_{0.162}O_{4+\delta}$, $La_2Ni_{0.911}Fe_{0.089}O_{4+\delta}$) were synthesized using a reverse micro-emulsion method previously reported by our group for the synthesis of unmodified LNO nanorods selectively surface terminated predominantly by (001) NiO [3]. This synthesis method allows for control over the shape, morphology, and surface termination of nickelate oxides, which can be challenging to achieve using conventional solid state and citrate nitrate methods. Briefly, two separate quaternary reverse micro-emulsions each containing the surfactant cetyltrimethylammonium bromide (CTAB), water, hexane and n-Butanol were prepared. In the first reverse micro-emulsion an appropriate amount of precipitating agent KOH was added, while in the second one the appropriate metal salts (La, Ni and dopant B site metal) were added. The two separate micro-emulsions were then mixed and stirred. The resulting gel was separated by centrifugation, washed, dried and calcined to yield the desired catalyst. We found that the ratio of water to the surfactant CTAB in the final mixed micro-emulsion played a critical role in obtaining the rod-shaped nanostructures.

Steady state kinetic isotopic exchange studies were utilized to determine the high temperature oxygen exchange

kinetics on the nanostructured nickelate oxide catalysts with different compositions. Our experimental results showed that the trends were consistent with the theoretical predictions. For example, out of the catalysts tested, Co-doped LNO displayed the best performance for the surface oxygen exchange process. An approximate decrease of 25 kJ/mol in the activation energy for surface oxygen exchange was obtained on $La_2Ni_{0.868}Co_{0.132}O_{4+\delta}$ as compared to $La_2NiO_{4+\delta}$ [3]. The kinetics of surface oxygen exchange on Fe and Cu doped LNO were also consistent with the DFT calculations. We are currently working on developing a microkinetic model for the oxygen exchange kinetics on these nickelate oxides to obtain additional insights into the reaction mechanism. Our future plan also involves determining the kinetics of low-temperature oxygen evolution on these nanostructured nickelate oxides in alkaline media using well-controlled rotating ring disk electrode studies. We anticipate that these studies will lead to structure–performance relationships that can be used to design optimal nickelate oxide catalyst for low and high-temperature OER.

References

1. Chen, D.J.; Chen, C.; Baiyee, Z.M.; Shao, Z.P.; Ciucci, F. Nonstoichiometric Oxides as Low-Cost and Highly-Efficient Oxygen Reduction/Evolution Catalysts for Low-Temperature Electrochemical Devices. *Chem Rev* 2015, *115* (18), 9869–9921.

2. Das, A.; Xhafa, E.; Nikolla, E. Electro- and Thermal-Catalysis by Layered, First Series Ruddlesden – Popper Oxides. *Catal. Today* 2016, Re-submitted after minor revision.

3. Ma, X.; Carneiro, J.S.A.; Gu, X.-K.; Qin, H.; Xin, H.; Sun, K.; Nikolla, E. Engineering Complex, Layered Metal Oxides: High-Performance Nickelate Oxide Nanostructures for Oxygen Exchange and Reduction. *ACS Catal.* 2015, *5* (7), 4013–4019.

V.G.8 Analysis of the Mechanisms of Electrochemical Oxygen Reduction and Development of Ag-alloy and Pt-alloy Electrocatalysis for Low Temperature Fuel Cells

Suljo Linic
University of Michigan
500 S. State Street
Ann Arbor, MI 48109
Phone: (734) 647-7984
Email: linic@umich.edu

DOE Manager: Viviane Schwartz
Phone: (301) 903-0448
Email: Viviane.Schwartz@science.doe.gov

Subcontractors:
- Adam Holewinski, University of Colorado Boulder, Boulder, CO
- Hongliang Xin, Tim Van Cleve, Saman Moniri, Virginia Polytechnic Institute and State University, Blacksburg, VA

Program Scope

Electrochemical oxygen reduction reaction (ORR) is the major source of overpotential loss in low-temperature fuel cells. Expensive, Pt-based materials have been found to be the most effective catalysts. Exploration of alternatives has been hampered by stability constraints at the typical operating conditions of low pH and high potential.

I will discuss our studies of elementary mechanism of ORR on various metal electrodes using kinetic analysis of reaction pathways and quantum chemical calculations. These studies allowed us to identify the elementary steps and molecular descriptors that govern the rate of ORR. Using these performance descriptors we have been able to identify families of Pt and Ag-based alloys that exhibit superior ORR performance is acid and base respectively.

We have synthesized these alloys to demonstrate the superior ORR activity with rotating disk electrode experiments. We have also performed thorough structural characterization of the bulk and surface properties with a combination of cyclic voltammetry, X-ray diffraction, and electron microscopy with spatially resolved energy-dispersive X-ray spectroscopy and electron energy loss spectroscopy

Objectives: The broad objective of our research efforts is to employ combined experimental–theoretical approaches to study the impact of small perturbations in the structure of solid catalysts (for example, promotion by alkali promoters, poisoning, or alloying) on the outcome of chemical and catalytic surface reactions. Ultimately, we are interested in developing predictive theories that would guide us in the design of new or improved solid catalysts and electrocatalysts [1,2].

FY 2016 Highlights

Accomplishments: So far we have focused on four central themes, (a) development of a general, physically transparent framework designed to shed light on underlying mechanisms associated with the impact of the perturbation of a metal surface on the chemical transformation on the surface, (b) the analysis of the impact of alkali promoters on chemical transformation on metals and, (c) the study of the effect of the perturbation in the chemical composition of active metal sites by formation of an alloy on the chemical activity of the site, and (d) applying the predictive models to identify promising alloy catalysts in a number of probe reactions, including electrochemical ORR. Concrete accomplishments include the following.

- We have developed a general and physically transparent model, based on density functional theory (DFT) methodology, which allows us to identify underlying physical mechanisms that govern the changes in the chemical activity of a metal surface site as the local chemical environment of the site is perturbed. This framework allows us to de-convolute and quantify various mechanisms by which the perturbation of a metal surface changes its chemical activity. These mechanisms induce (i) local electronic effect, (ii) electrostatic, and (iii) polarization effect. This framework can be used to study various perturbations, including chemical promotion, poisoning and alloying. The work has been accepted for publication in The Journal of Chemical Physics [3].
- This model was utilized in a case study of the effect of Cs adsorbates (promoters) on the O_2 dissociation reaction on Ag(111). These studies revealed that the main mode by which Cs affects the dissociation of O_2 on Ag(111) is a long-range electrostatic/polarization interaction between Cs and relevant reaction intermediates. These interactions stabilize the transition state involved in the dissociation of O_2, therefore lowering the activation barrier. We demonstrated that these findings are fairly universal for metal surfaces promoted with alkali promoters [3].
- We have also studied how a working state of an alkali promoter changes as a function of external conditions, i.e., pressure and temperature of reactants. In this

context, we have examined possible formation of Cs-oxide complexes as a function of the chemical potential of gas-phase O_2 (pressure and temperature). We employed ab initio statistical mechanics to account for the effect of finite temperature and pressure of reactants. We have investigated whether and how the underlying mechanism of promotion depends on the nature of the alkali complex.

- We have also employed the model, referenced in the first bullet, to analyze mechanisms associated with the changes in the chemical activity of metal surfaces in response to the formation of alloys. In this context, we developed a predictive framework that can relate the geometric structure of an active center in a metal alloy material to its chemical activity [3-5]. The model allows us to relate readily accessible physical properties of the metals that form the active site in the alloy (electronegativity and the geometric extend of d-orbitals) to various descriptors of catalytic activity (e.g., the adsorption energy of critical adsorbates). We performed a number of experimental studies verifying and validating the predictive capacity of the proposed framework [3-5].
- We have used this predictive model to screen through large libraries of alloy materials identifying the most optimal active sites for electrochemical ORR in acid and base [1,5,6].
- The screening process has led us to the discovery of a number of Ag-based alloys for ORR in base that could meet techno-economic targets [7]. We have synthesized and tested one of these alloys in the form of Ag-Co nanoparticles. Rigorous measurements demonstrated the superior activity and stability of this material in electrochemical ORR compared to pure Ag nanoparticles of equal size. In base, this material reaches approximately 50 % the rate of commercial Pt electro-catalysts which meets the techno-economic target [7,8].
- More recently, we have expanded our studies to the development of a new family of Pt-based ORR electro-catalysts for ORR in acid. This has led to the development of novel Pt-alloy compositions which include layered structures of Au-Co core, covered by layers of Au and one layer of Pt. Testing of these alloy materials showed that the materials are approximately four times more active that the commercial Pt standards for this reaction [9].

References

1. Holewinski, A.; Xin, H.; Nikolla, E.; Linic, S. "Identifying Optimal Active Sites for Heterogeneous Catalysis by Metal Alloys Based on Molecular Descriptors and Electronic Structure Engineering." *Curr. Opin. Chem. Eng.* **2013**, *2* (3), 312–319.

2. Linic, S.; Christopher, P.; Xin, H.; Marimuthu, A. "Catalytic and Photocatalytic Transformations on Metal Nanoparticles with Targeted Geometric and Plasmonic Properties." *Acc. Chem. Res.* **2013**, *46* (8), 1890–1899.

3. Xin, H.; Linic, S. "Analyzing Relationships between Surface Perturbations and Local Chemical Reactivity of Metal Sites: Alkali Promotion of O_2 Dissociation on Ag(111)." *J. Chem. Phys. Accepted for publicaton*.

4. Xin, H.; Holewinski, A.; Schweitzer, N.; Nikolla, E.; Linic, S. "Electronic Structure Engineering in Heterogeneous Catalysis: Identifying Novel Alloy Catalysts Based on Rapid Screening for Materials with Desired Electronic Properties." *Top. Catal.* **2012**, *55* (5-6), 376–390.

5. Xin, H.; Holewinski, A.; Linic, S. "Predictive Structure–Reactivity Models for Rapid Screening of Pt-Based Multimetallic Electrocatalysts for the Oxygen Reduction Reaction." *ACS Catal.* **2012**, *2* (1), 12–16.

6. Holewinski, A.; Xin, H.; Nikolla, E.; Linic, S. "Identifying Optimal Active Sites for Heterogeneous Catalysis by Metal Alloys Based on Molecular Descriptors and Electronic Structure Engineering." *Curr. Opin. Chem. Eng.* **2013**.

7. Holewinski, A.; Idrobo, J.-C.; Linic, S. "High-Performance Ag–Co Alloy Catalysts for Electrochemical Oxygen Reduction." *Nat. Chem.* **2014**, *6* (9), 828–834.

8. Van Cleve, T.; Gibara, E.; Linic, S. "Electrochemical Oxygen Reduction Reaction on Ag Nanoparticles of Different Shapes." *ChemCatChem* **2016**, *8* (1), 256–261.

9. Van Cleve, T.; Moniri, S.; Linic, S. "Atomistic Engineering of Efficient Oxygen Reduction Electro-Catalysts by Tailoring Local Chemical Environment of Pt Surface Sites." *Rev.*

V.G.9 Computational Design of Graphene-Nanoparticle Catalysts

Ashwin Ramasubramaniam
Department of Mechanical and Industrial Engineering
University of Massachusetts Amherst
160 Governors Drive
Amherst, MA 01035
Phone: (413) 545-4866
Email: ashwin@umass.edu

DOE Manager: Viviane Schwartz
Phone: (301) 903-0448
Email: Viviane.Schwartz@science.doe.gov

Program Scope

This program supports the mission of the Office of Basic Energy Sciences Catalysis Science Program through the development of a systematic computational approach for the rational design of nanoscale transition-metal catalysts supported on graphene, a two-dimensional sheet of carbon atoms arranged in a honeycomb lattice. The use of graphene, as compared to traditional carbon supports, has been experimentally shown to enhance significantly the catalytic activity of metal nanoclusters in fuel cell electrodes. However, there is no clear mechanistic understanding of the role played by graphene supports in improving catalyst performance. This program is concerned with development and implementation of computational models to understand and predict electronic interactions between transition-metal nanoclusters and graphene supports, taking into account practical complexities that arise from statistical variations in cluster size and morphology, quantum size effects at the nanoscale, and the presence of physical and chemical defects in graphene. Model transition metal/graphene catalysts are employed for statistical sampling of selected reactions pathways, in particular, the technologically important methanol decomposition reaction, to probe the influence of substrate–cluster interactions on reaction thermodynamics and kinetics. The fundamental understanding gained from these studies seeks to guide the rational design of superior, graphene-supported, transition-metal nanocatalysts with potential applications in energy conversion pathways for alternative fuels.

FY 2016 Highlights

Theoretical studies by our group have pursued advances along two interrelated fronts, namely (1) the implementation and application of Genetic Algorithms to predict ground-state morphologies and electronic structures of graphene-supported Pt nanoclusters and (2) studies of reaction thermodynamics of the methanol decomposition reaction on graphene-supported Pt nanoclusters.

Genetic Algorithms for Structural Optimization of Supported Nanoclusters

Graphene-supported Pt nanoclusters were recently found to be promising electrocatalysts for fuel-cell applications due to their enhanced activity and tolerance to CO poisoning, as well as their long-term stability toward sintering. However, structure–function relationships that underpin the improved performance of these catalysts are still not well understood. We developed a combined approach that uses empirical potential simulations and density functional theory (DFT) calculations to investigate structure–function relationships of small Pt_N (N=2-80) clusters on model graphene supports. A bond-order empirical potential was employed within a Genetic Algorithm to go beyond local optimizations for obtaining minimum energy structures of Pt_N clusters on pristine as well as defective graphene supports. Point defects in graphene were found to strongly anchor Pt clusters and also appreciably affect the morphologies of small clusters, which were characterized via various structural metrics such as the radius of gyration, average bond length, and average coordination number. A key finding from the structural analysis is that the fraction of potentially active surface sites in supported clusters is maximized for stable Pt clusters in the size range of 20–30 atoms, which provides a useful design criterion for optimal utilization of the precious metal. Through selected ab initio studies, we found a consistent trend for charge transfer from small Pt clusters to defective graphene supports resulting in the lowering of the cluster *d*-band center, which has implications for the overall activity and poisoning of the catalyst. The combination of a robust empirical potential-based Genetic Algorithm for structural optimization with ab initio calculations opens up avenues for systematic studies of supported catalyst clusters at much larger system sizes than are accessible to purely ab initio approaches. Our ongoing work aims at extending this computational framework to alloy clusters, notably, the Pt-Ru system, which is among the most efficient catalysts for direct methanol fuel cells.

Thermodynamics of Methanol Decomposition on Graphene-Supported Pt_{13} Nanoclusters

Defective graphene has been shown experimentally to be an excellent support for transition-metal electrocatalysts in direct methanol fuel cells. Computational modeling reveals that the improved catalytic activity of graphene-supported metal clusters is in part due to increased resistance to catalyst sintering and to CO poisoning, but the increased reaction rate for the methanol decomposition reaction (MDR) is not yet fully explained. Using DFT, we investigated the adsorption and reaction thermodynamics of MDR intermediates on defective graphene-supported Pt_{13} nanoclusters with realistic, low-symmetry morphologies. We found that the support-

induced shifts in catalyst electronic structure correlate well with an overall change in adsorption behavior of MDR intermediates and that the reaction thermodynamics are modified in a way that suggests the potential of greater catalytic activity. We also found that adsorption energy predictors established for traditional heterogeneous catalysis studies of MDR on macroscopic crystalline facets are equally valid on catalyst nanoclusters (supported or otherwise) with irregular, low-symmetry surface morphologies. Our studies provide theoretical insights into experimental observations of enhanced catalytic activity of graphene-supported Pt nanoclusters for MDR and suggest promising avenues for further tuning of catalytic activity through engineering of catalyst–support interactions. Ongoing research pursues ab initio calculation of reaction barriers with the aim of establishing robust predictors for the MDR kinetics and applying these in microkinetic models.

V.G.10 Atomic-Scale Design of Metal and Alloy Catalysts: A Combined Theoretical and Experimental Approach

Manos Mavrikakis (Primary Contact),
James A. Dumesic
University of Wisconsin-Madison
Department of Chemical & Biological Engineering
1415 Engineering Dr.
Madison, WI 53706
Phone: (608) 262-9053
Email: emavrikakis@wisc.edu

DOE Manager: Raul Miranda
Phone: (301) 903-8014
Email: Raul.Miranda@science.doe.gov

Subcontractor:
Younan Xia, Georgia Institute of Technology, Atlanta, GA

Program Scope

This program combines theory, inorganic synthesis, and catalytic reaction kinetics experiments in an integrated approach towards identifying metal and alloy catalysts with high activity and selectivity for high-impact reactions. Theoretical calculations identify the most promising catalyst structures and compositions for novel controlled synthesis, while reaction kinetics experiments evaluate the as-synthesized catalysts for their activity and stability. Potential applications involve low-temperature fuel cells, hydrogen production and purification, and liquid fuels production, which all strongly support the DOE's mission.

FY 2016 Highlights

Shape-Selected Alloy Nanocatalysts for the Oxygen Reduction Reaction (ORR) [1-4]

Depositing ultrathin Pt layers onto a Pd template of controlled shape is an attractive approach to reducing the content of precious Pt while improving its activity for the ORR, which is limited by strong binding of adsorbed O and OH intermediates. We have deposited a controlled number of Pt layers onto nanostructured Pd cubes, octahedra, and icosahedra, and the measured ORR activities surpassed those of a commercial Pt catalyst by two, three and four times, respectively, on the basis of Pt-mass. Density functional theory (DFT) calculations reliably predicted the experimentally-observed activity trends as a function of number of Pt overlayers deposited on the Pd template. The calculations attributed the enhanced activity to the compressive strain imposed on the Pt overlayers by the Pd substrate, which weakened the binding of O and OH. We also identified a unique atomic arrangement of the Pt overlayers in the icosahedral catalysts, in which tensile strain on the underlying Pd lattice facilitated the incorporation of extra Pt atoms in the overlayers relative to the Pd template and therefore led to a net beneficial compressive strain on the Pt overlayers.

Additionally, we have shown that the Pd templates can be selectively etched to yield hollow Pt nanocage structures, which exhibited more than double the activity of their Pd@Pt core@shell counterparts. DFT calculations on novel "membrane" models attributed the enhanced activity to a further shortened Pt-Pt interatomic distance relative to the already-compressed core@shell structure.

Formation Mechanism of Hollow Nanocage Structures [4]

In addition to predicting catalyst activity toward ORR, DFT calculations also elucidate the mechanisms by which the hollow nanostructures form. Rigorous DFT calculations demonstrate that Pd can only be etched through vacancies in the Pt shell. We show that these vacancies can be readily formed by removal of Pd atoms dispersed in the Pt shell during the core@shell formation process. As shown in Figure 1, it is energetically more favorable for Pt adatoms (deposited from solution) to substitute into the Pd template, thus yielding a mixed surface composition as Pt is continually deposited in a layer-by-layer fashion. It is therefore possible for contiguous Pd channels to form; these enable the etching of the core to yield the hollow structure. We further identified an optimal Pt shell thickness of four to six layers. Thinner than this would allow for too many channels to form, which jeopardizes the mechanical stability of the hollow structure. On the contrary, thicker layers would inhibit the formation of contiguous Pd channels. This optimal shell thickness was confirmed by experimental observations that hollow structures could only be successfully formed from Pt-Pd core@shell catalysts with four to six overlayers of Pt.

Reaction Mechanism for Electro-Oxidation of Ammonia [5]

We have constructed a free energy diagram (see Figure 2) for two mechanisms for NH_3 electro-oxidation on Pt(111). The two mechanisms differ in the extent of dehydrogenation needed before making an N-N bond, with the N+N mechanism requiring full dehydrogenation to atomic N before N-N bond formation, while the *Gerischer-Mauerer* mechanism allows for this bond to form between

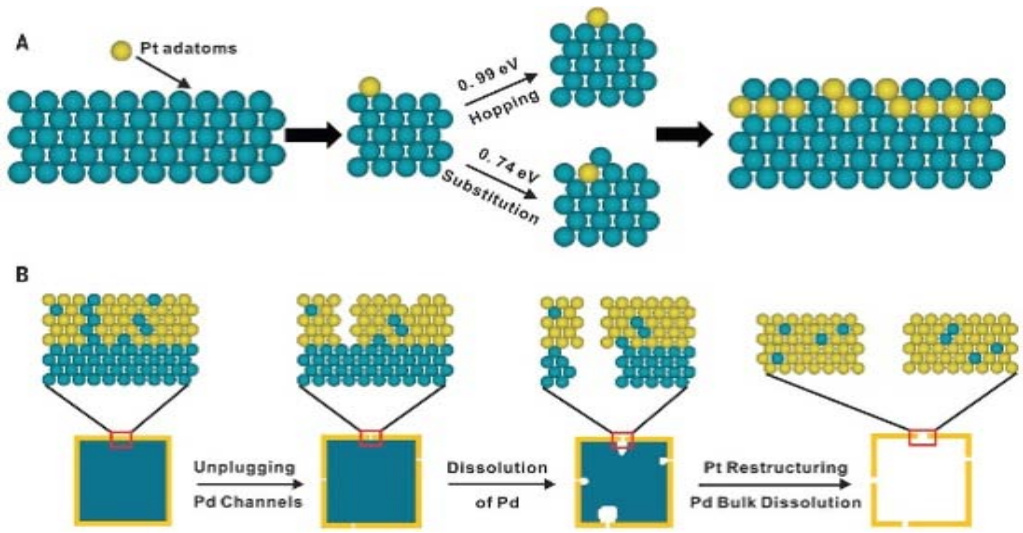

FIGURE 1. Mechanistic details involved in the deposition and etching processes. (A) Pt atoms deposited on the Pd surface may "hop" across the surface or substitute into the surface (activation barriers are shown), leading to a mixed outer-layer catalyst composition. (B) Schematic of the major steps involved in the continuous dissolution of Pd atoms from a Pd@Pt4L nanocube to generate a Pt cubic nanocage.

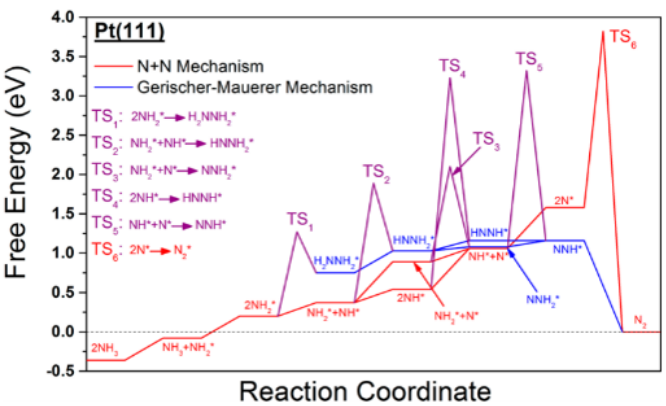

FIGURE 2. Free energy diagram for two mechanisms of N_2 formation on Pt(111) at 0 V_{RHE}. Stoichiometry is implicitly balanced by H^+, OH^-, H_2O, and e^-.

hydrogenated NH_x species. Our calculations explain the experimentally-observed narrow active operating window of potentials for Pt(111), which starts with activating the *Gerischer-Mauerer* mechanism, and ends with poisoning the surface with N adatoms at the onset of the N+N mechanism. Similar studies were performed on 11 other close-packed monometallic surfaces, and reinforced the need to avoid the N+N mechanism for avoiding N poisoning. A simple Sabatier analysis shows Pt to be most active, followed by Ir and Cu. Hence, improved catalysts should bind atomic N weaker than Pt, but stronger than Cu.

References

1. J. Park, L. Zhang, S. Choi, L.T. Roling, N. Lu, J.A. Herron, S. Xie, J. Wang, M. J. Kim, M. Mavrikakis and Y. Xia, *ACS Nano* **9**, 2635 (2015).

2. X. Wang, S. Choi, L.T. Roling, M. Luo, C. Ma, L. Zhang, M. Chi, J. Liu, Z. Xie, J.A. Herron, M. Mavrikakis, and Y. Xia, *Nature Communications* **6**, 7594 (2015).

3. S. Xie, S.-I. Choi, N. Lu, L.T. Roling, J.A. Herron, L. Zhang, J. Park, J. Wang, M.J. Kim, Z. Xie, M. Mavrikakis, Y. Xia**,** *Nano Letters* **14**, 3570 (2014).

4. L. Zhang, L.T. Roling, X. Wang, M. Vara, M. Chi, J. Liu, S. Choi, J. Park, J.A. Herron, Z. Xie, M. Mavrikakis, and Y. Xia**,** *Science* **349**, 412 (2015).

5. J.A. Herron, P. Ferrin, and M. Mavrikakis**,** *Journal of Physical Chemistry C* **119**, 14692 (2015).

V.G.11 Dual Site Requirements for Hydrodeoxygenation of Model Biomass Compounds

Lars Christian Grabow (Primary Contact),
Byeongjin Baek, Sashank Kasiraju,
Juan Manuel Arce Ramos
University of Houston
4726 Calhoun Rd.
Houston, TX 77204
Phone: (713) 743-4326
Email: grabow@uh.edu

DOE Manager: Viviane Schwartz
Phone: (301) 903-0448
Email: Viviane.Schwartz@science.doe.gov

Program Scope

This program supports the Office of Basic Energy Sciences mission through the development of unifying principles in hydrotreating catalysis. This goal will be achieved through detailed theoretical investigations using density functional theory (DFT) and kinetic modeling performed on high performance computing clusters, which will be interpreted along with available experimental data. This major goal is pursued by accomplishing two specific aims, (a) identification of the active site and mechanism of known hydrodeoxygenation catalysts using model bio-oil compounds, and (b) juxtaposition of the active site and reaction pathways of oxides and their corresponding sulfides, to develop universal design principles for hydrotreating catalysts.

FY 2016 Highlights

Fast pyrolysis of biomass is a promising low-cost technology that produces bio-oil suitable for the production of chemicals and use as transportation fuel after an appropriate upgrade step. The upgrade is necessary to increase the heating value, lower the viscosity and improve the long-term stability, and can be achieved by reducing the oxygen content through hydrotreatment over heterogeneous catalysts [1]. However, the complexity of bio-oils and the fact that this technology has only recently gained interest are both responsible for the lack of fundamental knowledge in this field. In the recent literature there is a growing number of bifunctional catalyst combinations that show good activity and selectivity for hydrodeoxygenation (HDO) [2-4]. These catalysts have in common that they have two types of sites: one with metallic character and one with acidic character. In this study we use DFT to generate fundamental insight into the role of each type of site and propose a dual site structure-performance relationship for efficient HDO catalysts.

Our study combining theory and experiments provides evidence for the direct deoxygenation of phenol and *m*-cresol on Ru/TiO_2 catalysts to occur at perimeter sites at the interface between the Ru metal and the TiO_2 support. A key step in producing this active perimeter site is heterolytic H_2 cleavage across the interface. Electron density difference and Bader charge analysis suggests that this step forms a support site with Brønsted acid character and a metal-hydride on the metallic Ru cluster. The following direct C-O scission in phenol or *m*-cresol is then assisted by the support proton, which results in a substantial reduction of the activation barrier. We propose that the key property of the support is its amphoteric character, i.e., its ability to accept protons during H_2 activation and to donate protons during C-O scission. Another example of an amphoteric support suitable for HDO is ZrO_2 [5], especially when combined with Pd as metal.

We find that this dual site requirement extends to other catalysts systems as well. Of particular interest are Mo-oxycarbides, which have acidic sites similar to those of Mo-oxide, whereas Mo-carbide sites have metallic character. We have compared the potential energy diagram for HDO of furan on Mo-oxide and Mo-carbide with the equivalent reaction of thiophene hydrodesulfurization (HDS) on MoS_2. Our results show that H_2 activation for both HDO and HDS requires metallic sites, which are present on the brim sites of MoS_2 or are provided by Mo-carbide-like phases in Mo-oxycarbide. Once H_2 dissociates, the acid site for C-O scission can readily form.

In conclusion, we have obtained DFT results for HDO of phenolics and furan on Ru/TiO_2, Pd/ZrO_2, and MoO_3/Mo_2C, which support the hypothesis that a good HDO catalyst requires both metal and acid sites. However, the acid sites should not be too strong such that reprotonation is hindered. Amphotheric materials that are readily protonated/deprotonated appear most suitable. Ultimately, our work suggests that the right balance between metal and acid character is necessary for the design of an optimal HDO catalyst.

References

1. G.W. Huber, A. Corma, Angew. Chemie Int. Ed. 46 (2007) 7184.

2. R.C. Nelson, B. Baek, P. Ruiz, B. Goundie, A. Brooks, M.C. Wheeler, B.G. Frederick, L.C. Grabow, R.N. Austin, ACS Catal. 5 (2015) 6509.

3. F. Anaya, L. Zhang, Q. Tan, D.E. Resasco, J. Catal. 328 (2015) 173.

4. P.M. Mortensen, H.W.P. de Carvalho, J. Grunwaldt, P.A. Jensen, A.D. Jensen, J. Catal. 328 (2015) 208.

5. J.-M. Arce-Ramos, L.C. Grabow, B.E. Handy, M.-G. Cárdenas-Galindo, J. Phys. Chem. C 119 (2015) 15150.

V.G.12 Fundamentals of Catalysis and Chemical Transformations

Steven. H. Overbury (Primary Contact),
Ariana Beste, Sheng Dai, Michelle Kidder,
Danny Lutterman, David R. Mullins, Aditya Savara,
Zili Wu
Oak Ridge National Laboratory (ORNL)
Chemical Sciences Division
1 Bethel Valley Rd.
Oak Ridge, TN 37831
Phone: (865) 574 5040
Email: overburysh@ornl.gov

DOE Manager: Viviane Schwartz
Phone: (301) 903-0448
Email: Viviane.Schwartz@science.doe.gov

Program Scope

The overarching goal of this project is to understand how to control reaction selectivity through tuning cooperativity in multi-functional catalysts. The vision of our research is that by fundamentally understanding the catalytic sites and mechanistic pathways, we will be enabled to precisely assemble closely interacting components into a catalyst to achieve the desired level of selectivity and activity. Specifically, we aim to elucidate the role of site geometry, surface and bulk composition, acid-base and redox sites, confinement, and metal support interactions in controlling selectivity in reactions catalyzed by oxides surfaces and supported metal particles. Our approach has been based on model catalysts with increasing complexity and model reactions with rich pathways. The model catalysts range from thin films and single crystal in ultra-high vacuum (UHV) surface science study to oxide nanocrystals with controlled surface facets and compositions, and supported metals with defined architectures. This allows us to bridge the materials and pressure gaps between UHV and reactor based methods. The reactions are the transformation of model oxygenates and hydrocarbons with controlled reactivity and selectivity. The surface chemistry, reaction kinetics and catalytic properties are studied by a collection of state-of-the-art operando and in situ methods including the neutron scattering methods at ORNL. The experimental work combines computational methods to aid interpretation of the experimental measurements and to create detailed models of reaction pathways.

FY 2016 Highlights

Surface Structural Effect of Oxide Catalysts

We have observed many cases where molecules react differently on $CeO_2(111)$ and $CeO_2(100)$. In general, the $CeO_2(100)$ surface has been more reactive than $CeO_2(111)$ as indicated by a stronger adsorption energy for molecules such as water, CO_2, alcohols and aldehydes. However, the reactions on $CeO_2(100)$ are generally less selective and organic molecules tend to fully decompose in CO, CO_2, H_2 and H_2O.

SO_2 Adsorption: CeO_2 has been shown to have a high affinity for the adsorption of SO_2. This can be detrimental as in the poisoning of automotive exhaust catalysts but could also possibly be exploited by utilizing ceria to traps SO_2 in effluent streams. Previous studies have shown that SO_2 adsorbs on fully oxidized $CeO_2(111)$ as sulfite, SO_3^{2-}. This species is non-reactive and eventually desorbs as SO_2 at elevated temperatures. On partially reduced $CeO_{2-X}(111)$ the SO_2 adsorbs as sulfite at low temperatures but decomposes into O^{2-} and S^{2-} creating a sulfide and re-oxidizing Ce^{3+} to Ce^{4+}.

We hypothesized that the increased reactivity of $CeO_2(100)$ might result in sulfate (SO_4^{2-}) following SO_2 exposure and possibly different decomposition paths with S^0 as a product. Surprisingly, considering the differences observed for other molecules on $CeO_2(111)$ and $CeO_2(100)$, the adsorption of SO_2 on these two surfaces was virtually identical in terms of the species formed on the surfaces and their stabilities. SO_3^{2-} was the only species observed on the fully oxidized surfaces. The sulfite decomposed into sulfide on the reduced surfaces.

Density Functional Theory (DFT) of Ethanol Reaction: In addition to our experimental efforts, we used computational methods to gain insights into chemical conversion on ceria surfaces at the atomic level. Specifically, we employed DFT, where the surfaces were modeled as semi-infinite, two-dimensional slabs applying periodic boundary conditions. We studied ethanol reactions on the (111) and (100) ceria surfaces starting from ethoxy, the experimentally determined dominant surface species. Ethylene and acetaldehyde can be produced in a single step through simultaneous β-scission and oxygen-carbon bond cleavage and α-scission, respectively. Alternatively, ethylene and acetaldehyde can be formed through a common radical intermediate that is product of a β-scission reaction. The kinetically and thermodynamically preferred pathway on both surfaces, however, is the single step acetaldehyde formation via α-scission. We observed that intermediate and transition state structures are stabilized on the (100) surface compared to the (111) surface. To assess pathway

contributions, we computed transition state rate constants and carried out kinetic analysis. Our results are consistent with temperature programmed surface reaction and steady-state experiments, where acetaldehyde was found as the main product and evidence was presented that ethylene formation at higher temperature originates from changes in adsorbate and surface structure.

Surface Composition Effect of Oxide Catalysts

Adsorption and reaction of oxygenates and hydrocarbon can be controlled not only by the surface structure of oxides such as CeO_2 with different facets (mentioned above), but also by the surface composition of oxides such as binary oxides including perovskites and mixed oxides.

Alcohol Reactions over Perovskite Particles: The wide tunability of the A and B cations in ABO_3 perovskites provides an opportunity in tuning not only the redox property but also the acid-base property. We aim to understand how the coupling of the acid-base and redox properties of perovskite oxides is controlling the reactivity and selectivity in alcohol conversion. In an on-going effort, we tested ABO_3 where A = Ba, Sr, Zn and B = Ti and Zr for isopropanol conversion because they differ in reducibility and acid-base property. The dehydration vs. dehydrogenation of isopropanol was used as a model reaction to understand the acid-base catalysis by these perovskites. In situ infrared and microcalorimetry were used to characterize both qualitatively and quantitatively the surface acid-base and redox sites. The type, strength and amount of acid-base sites were found to vary with the A and B cations in the perovskites. Reactivity test of isopropanol is currently underway to correlate the acid-base property to the reaction activity and selectivity.

Ambient Pressure X-Ray Photoelectron Spectroscopy of Alcohol on Perovskite Thin Film: Methanol and ethanol oxidation on doped $La_{0.7}Sr_{0.3}MnO_3(001)$ thin film have been studied using ambient pressure X-ray photoelectron spectroscopy $La_{0.7}Sr_{0.3}MnO_3(001)$ was grown on single crystal Nb-doped $SrTiO_3(001)$ by pulse laser deposition. In order to investigate the so-called "pressure gap" that may occur between reactions studied under vacuum conditions and at pressure approaching atmospheric pressure, experiments were conducted at nominally 10^{-5} torr and at 0.1 torr between 250°C and 350°C. Results using methanol or ethanol as the reactant are generally the same, i.e., only methoxy/ethoxy on the surface at lower pressures, a mixture of methoxy/ethoxy and formate/acetate at higher pressure in the absence of O_2, and exclusively formate/acetate on the surface when O_2 was present. The only significant difference between methanol and ethanol was a greater tendency for ethanol to form the carboxylate in the absence of O_2. At the higher pressure the Mn 2p spectra indicated that the alcohol partially reduced Mn^{3+} to Mn^{2+} and there was also an indication in the O 1s spectra that O was removed from the surface. These observations indicated that methanol was being oxidized through reaction with the surface.

Hydrocarbon Oxidation over Mixed Oxides: Catalytic synergism often occurs when two oxides are intimately mixed such as in solid solution mode. We synthesized a $Mn_{0.5}Ce_{0.5}O_x$ solid solution that shows exceptional catalytic performance in the low temperature, heterogeneous oxidation of cyclohexane (100°C, conversion: 17.7%, selectivity for KA oils [K: cyclohexanone, A: cyclohexanol]: 81%) with molecular oxygen as the oxidant. It is significantly superior to the results of current technology (140–160°C, conversion: 3–5%). Detailed investigation indicates several unique characteristics of the $Mn_{0.5}Ce_{0.5}O_x$ solid solution: (1) A high proportion (44.1%) of active oxygen species on the surface to promote O–O/C–H bond activation; (2) the introduction of 50 mol% Mn4þ ions into ceria matrix for the formation of maximum solid solution phases that can lower the energy for oxygen vacancy formation and benefit the rapid migration of oxygen vacancies from the bulk to the surface, thus continuing the activation of gas oxygen molecules; (3) a mesoporous structure for fast mass transfer/diffusion, and rich porosity to expose any more active sites ready for interaction with cyclohexane/O_2. We expect that the $Mn_{0.5}Ce_{0.5}O_x$ solid solution will provide a strategy for oxidation of cyclohexane and other hydrocarbons under mild conditions.

Supported Metal Nanoparticles

Catalysis of oxides can be drastically tuned or changed when metal nanoparticles are attached on the surface. More complication is the introduced metal–support interaction where the perimeter sites between metal and oxide seem to be important for catalysis. We have explored ways how to tune the interface structure to tune the catalysis of supported metal nanoparticles.

Interface Engineering via Surface Structure of Oxide: The strong support effect is known for metal catalysis, especially known for gold catalysis. Instead of the changing the composition of the support, we investigated how the surface structure of an oxide (CeO_2) can affect the catalysis of gold nanoparticles. The different CeO_2 nanostructures can impact the size, morphology, and interface structures of Au catalysts through the metal-support interaction. Yet a detailed and atomistic view of the interface in Au-CeO_2 catalytic system is still missing. Recently we have performed aberration-corrected high angle annular dark field scanning transmission electron microscopy imaging on Au-CeO_2 nanostructures with well-defined shapes. With atoms clearly resolved, the size, morphology, and atomic interface structures of the Au-CeO_2 catalysts before and after the water-gas shift (WGS) reaction were systematically analyzed. It was found that the oxidation state of the ceria substrate plays a major role for both Au-CeO_2 systems, with larger adhesion for Au under oxidative condition.

Under oxidative condition, Au particles with SK layers are present on the Au-CeO_2 nanocubes. The SK layers vanish and there is a morphological change of the Au particles after the WGS reaction, which is attributed to reduction of the Au-CeO_2 (100) interface. In contrast, the Au-CeO_2 nanorods contain regular Au particles and some rafts under oxidative conditions. After the WGS reaction, the Au atoms in the rafts migrate to the particles. The Au particles on the CeO_2 nanorods are almost uncharged before and after the WGS reaction. The loss of strong adhesion of Au to the support CeO_2 (the SK layer and the rafts) is partly responsible for the decrease of the activities in the WGS reaction.

Construction of Hierarchical Interfaces: Decreasing the size of metal nanoparticles is a general approach to enhance the catalytic activity. But it comes with the price of instability of small metal particles. One-dimensional (1D) metal nanowires, small in diameter and expose high percentage of active sites, are more stable than the nanoparticle counterparts. Further increase of their activity can involve the engineering of the interfaces. We demonstrated in constructing catalytic active hierarchical interfaces in 1D nanostructure as exemplified by the synthesis of TiO_2-supported PtFe−FeOx nanowires (NWs). The hierarchical interface, constituting atomic level interactions between PtFe and FeOx within each NW and the interactions between NWs and support (TiO_2), enables CO oxidation with 100% conversion at room temperature. We identify the role of the two interfaces by probing the CO oxidation reaction with isotopic labeling experiments. Both the oxygen atoms (Os) in FeO_x and TiO_2 participate in the initial CO oxidation, facilitating the reaction through a redox pathway. Moreover, the intact 1D structure leads to the high stability of the catalyst. After 30 h in the reaction stream, the PtFe−FeOx/TiO_2 catalyst exhibits no activity decay. Our results provide a general approach and new insights into the construction of hierarchical interfaces for advanced catalysis.

Publications

1. Poutsma, M.L., Extension of Structure-Reactivity Correlations for the Hydrogen Abstraction Reaction by Bromine Atom and Comparison to Chlorine Atom and Hydroxyl Radical. *J. Phys. Chem. A* 2016, 120, 183-190.

2. Mullins, D.R., SO2 Adsorption on CeO2(100) and CeO2(111). *Top. Catal.* 2016, in press.

3. Mullins, D.R., The Interaction of Carbon Monoxide with Rhodium On Potassium-Modified CeO2(111) *Surface Science* 2016, DOI: 10.1016/j.susc.2016.01.024.

4. Moon, J.; Phelps, T.J.; Fitzgerald, C.L.; Lind, R.F.; Elkins, J.G.; Jang, G.G.; Joshi, P.C.; Kidder, M.K.; Armstrong, B.L.; Watkins, T.R.; Graham, D.E., Manufacturing demonstration of microbially mediated zinc sulfide nanoparticles in pilot-plant scale reactors. *Applied Microbiology and Biotechnology* 2016, in press.

5. Beste, A.; Overbury, S.H., Dehydrogenation of Methanol to Formaldehyde Catalyzed by Pristine and Defective Ceria Surfaces. *PCCP* 2016, 18, 9990.

V.G.13 Sub Nanometer Sized Clusters for Heterogeneous Catalysis

Abhaya Datye (Primary Contact),
Andrew DeLaRiva, Eric Peterson, Christopher Riley
Department of Chemical and Nuclear Engineering
University of New Mexico
Albuquerque, NM 87131
Phone: (505) 277-0477
Email: datye@unm.edu

DOE Manager: Raul Miranda
Phone: (301) 903 8014
Email: Raul.Miranda@science.doe.gov

Subcontractors:
Yong Wang, Jianghao Zhang,
Xavier Isidro Pereira Hernandez,
Voiland School of Chemical Engineering and
Bioengineering, Washington State University
Pullman, WA

Program Scope

Providing sustainable sources of energy, chemicals, and materials is one of the most important long-term issues facing society. Catalysis plays a central role in creating sustainable sources of energy through efficient transformations of hydrocarbon resources. Our quality of life depends on myriad products that involve a catalytic step at some point in their manufacture. It is widely accepted that chemical catalysis is a major economic driver in both the U.S. and world economies, with estimates as high as ~35% of the world's gross domestic product arising via catalytic processes. Due to this significant commercial impact, there is a heavy demand for rare and expensive transition metals whose pricing and availability is at risk due to increasing geopolitical pressures. As our resource base shifts to alternate energy sources such as natural gas or biomass, there will be a need to develop new catalysts for converting these materials. Our project focuses on sub-nanometer (nm) clusters, of size <30 atoms, which provide unusual reactivity and selectivity for catalytic reactions. The objective of our project is to improve methods to tailor surfaces of high surface area supports to anchor platinum group metals (PGM). Heterogeneous catalysis using nanoparticles of PGMs is highly developed, but the science of using ionic forms of these metals as heterogeneous catalysts is still in its infancy. New methods only recently available allow us to study these atomically dispersed metals. Catalysis using single isolated atoms provides the highest atom efficiency for conducting catalytic reactions. As we learn how to obtain desired catalytic properties in these tailored catalysts, we will develop a fundamental understanding of how catalyst activity and selectivity can be improved. This understanding will allow us to create more selective and energy efficient processes for catalytic transformations. The atomically dispersed catalysts developed here will be ideally suited for reactions of interest to the DOE as described in the "Basic Research Needs: Catalysis for Energy" report. Atomically dispersed PGMs tend to coarsen and form sub-nm clusters. Stabilizing these structures under industrial operating conditions is a challenge. The proposed research will help advance the science of anchoring single metal atoms and sub-nm clusters on high surface area supports.

FY 2016 Highlights

Our FY 2016 accomplishment includes the fundamental understanding of the roles of tin (Sn) in stabilizing and re-dispersing Pt and elucidation of the roles of sub-nm sized palladium (Pd) in the promotion of activity and stability of iron (Fe)-based catalysts.

Alumina-supported Pt is one of the major industrial catalysts for light alkane dehydrogenation. This catalyst loses activity during reaction, with coke formation often considered as the reason for deactivation. As we recently demonstrated, the amount and nature of carbon deposits do not directly correlate with the loss of activity. Rather, it is the transformation of sub-nm Pt species into larger Pt nanoparticles that appears to be responsible for the loss of catalytic activity. Surprisingly, a portion of the Sn remains atomically dispersed on the alumina surface in the spent catalyst and helps in the redispersion of the Pt. In the absence of Sn on the alumina support, the larger Pt nanoparticles formed during the reaction are not redispersed during oxidative regeneration. It is known that Sn is added as a promoter in the industrial catalyst to help in achieving high propene selectivity and to minimize coke formation. We have shown that an important role of Sn is to help in the regeneration of Pt, by providing nucleation sites on the alumina surface. Aberration-corrected scanning transmission electron microscopy helps to provide unique insights into the operating characteristics of an industrially important catalyst by demonstrating the role of promoter elements, such as Sn, in the oxidative regeneration of Pt on γ-Al_2O_3.

Hydrodeoxygenation (HDO) of phenolic compounds is an important model reaction in understanding the fundamental and application of catalysis in lignin-based biofuel production. Recently, Fe has emerged as a promising catalyst for HDO of phenolics, due to its low cost and high selectivity in C-O bond cleavage. However, Fe's low HDO activity and poor stability under HDO conditions has limited its application. We have recently developed an efficient approach to promote Fe's activity and stability without altering its unique selectivity in HDO of phenolics, by doping noble metals such as Pd onto the Fe catalyst surface.

A series of noble metal doped Fe catalysts were tested in HDO of m-cresol. Noble metals remarkably promoted Fe's activity and stability, while maintaining Fe's high C-O bond cleavage selectivity. The Pd-on-Fe nanostructure with sub-nm Pd clusters on a reduced Fe surface in a Pd-Fe catalyst was evidenced by high resolution scanning transmission electron microscopy and pseudo in situ X-ray photoelectron spectroscopy (XPS). A direct C-O bond cleavage mechanism, in which m-cresol decomposes on Fe surface into C_7H_7* and OH* species and the formed species further reacts with H atoms to form toluene and water, respectively, was proposed based on density function theory calculation and kinetic modeling. Kinetic modeling and in situ ambient pressure XPS results suggested that the Fe catalyst surface is dominated by OH* species, which ultimately lead to a deactivation of the Fe catalyst. Addition of Pd to Fe significantly changes its kinetics by creating new sites for H_2 activation and new reaction pathways via reaction between H activated on Pd sites and C_7H_7* and OH* on Fe sites, as suggested by kinetic modeling. As a result, the surface of Pd-Fe is no longer dominated by OH*, and catalyst deactivation by water-induced oxidation is thus avoided.

V.G.14 Element Specific Atomic Arrangement of Binary and Ternary Alloy Nanosized Catalysts in As-Prepared and Active State

Valeri Petkov (Primary Contact),
Chuan-Jian Zhong (State University of New York)
Central Michigan University
1200 S. Franklin St.
Mount Pleasant, MI 48859
Phone: (989) 774-3395
Email: petko1vg@cmich.edu

DOE Manager: Lane Wilson
Phone: (301) 903-5877
Email: Lane.Wilson@science.doe.gov

Program Scope

This program supports the Office of Basic Energy Sciences (X-ray scattering) mission through the application and further advancement of cutting-edge X-ray scattering techniques for determining the atomic-level structure of nanosized catalysts vital for the development of fuel cell and battery technologies, production of alternative fuels, removal of pollutants, and others. Our work focuses on chemically ordered and disordered nanoalloys, core-shell, onion-like, metal-metal oxide composites and other unconventional multi-metallic nanosystems. Structure determination is done by high-energy synchrotron X-ray diffraction (HE-XRD) coupled to atomic pair distribution function (PDF) analysis and three-dimensional (3D) computer simulations. The resulting full-scale models of nanocatalysts are used to establish the relationship between their atomic structure and performance. The relationship is then used to improve the latter through fine tuning the former. HE-XRD experiments include ex situ studies on as-synthesized and used catalysts, in situ studies on catalysts under gas-phase reaction conditions and in operando studies on catalysts as they function inside fuel cells, in particular proton exchange membrane fuel cells (PEMFCs). Resonant HE-XRD studies providing information particular about the arrangement of atomic species deemed important to the performance of metallic nanocatalysts are carried out as well. Special attention is paid to revealing the arrangement of atoms at the surface of nanocatalysts whereat chemical reactions indeed take place. Near future studies include in situ gas phase reaction HE-XRD experiments combined with diffuse reflectance infrared Fourier transform spectroscopy (DRIFTS), in operando PEMFC experiments combined with energy dispersive X-ray spectroscopy (EDX) and grazing incidence HE-XRD & PDF analysis on very thin layers of catalyst nanoparticles (NPs).

FY 2016 Highlights

In Operando PEMFC Studies on Noble Metal-Transition Metal (NM-TM) Nanoalloys

A key challenge to the viability of fuel cell technology is the development of efficient catalysts for speeding up the sluggish chemical reactions driving cells' operation, such as the oxygen reduction reaction (ORR). Indeed a number of excellent metallic nanocatalysts for ORR were developed over the last decade. Unfortunately, their superb ORR activity would decay during cells' operation, thereby limiting the cells' performance. Good knowledge of the impact of the environment inside fuel cells on the ORR activity of metallic NPs is needed to solve this problem. Recently, we studied the evolution of the atomic structure and ORR activity of Pd-Ni and Pt-Ni-Co nanoalloy catalysts as they function at the cathode of an operating PEMFC (shown in Figure 1). Studies showed that under actual operating conditions, NM-TM nanocatalysts can undergo structural changes that differ significantly in both length-scale and dynamics and so can suffer ORR activity losses that differ significantly in both character and magnitude. In particular, we found that highly dynamic (see Figure 2) structural fluctuations occurring at the Ångstrom length-scale and irreversible large scale structural changes such as a gradual growth in the order of a few nm, can indeed be equally responsible for the losses in the ORR activity of metallic nanocatalysts during cells' operation. Hence, we argue that, to be fully successful, efforts to reduce these losses should strive to achieve control

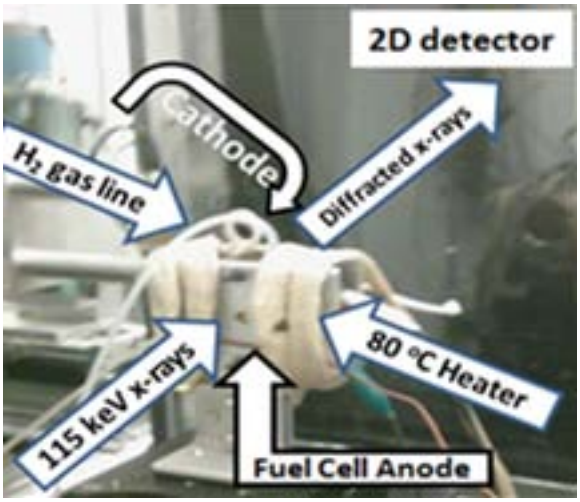

FIGURE 1. Custom-made PEMFC as used at the beamline 11-ID-C, APS.

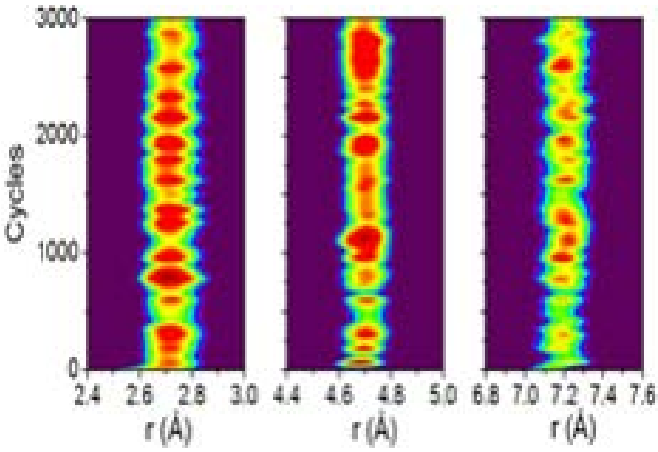

FIGURE 2. Color maps of the low-r peaks in the in operando PDFs for Pd-Ni nanocatalyst obtained in interval of 3 min while the nanocatalyst is undergoing 3,000 voltage cycles (0.6 V–1.2 V) inside the PEMFC. The maps emphasize the presence of local structural fluctuations in the nanocatalyst during the voltage cycling.

not only over the irreversible but also over the rapidly fluctuating structural changes that metallic nanocatalysts indeed undergo inside operating fuel cells (PEMFCs).

3D Atomic Arrangement at Functional Interfaces Inside Nanocatalysts by Resonant HE-XRD

Using Ru core-Pt shell NPs as an example, we demonstrated that precise atomic-level knowledge of functional interfaces inside metallic nanocatalysts can be obtained by resonant HE-XRD (K edge of Pt at 78,400 keV) coupled to element-specific PDF analysis. Moreover, using the unique structure knowledge obtained, we scrutinized the still debatable influence of hcp(Ru)\fcc(Pt) interface on the catalytic activity of Ru core-Pt shell NPs for CO oxidation, "reformate" hydrogen oxidation (HOR) at the PEMFC anode and ethanol/methanol electro-oxidation. In particular, we evaluated the importance of so called ligand and strain effects induced by the interface and, based on the experimental data for the evolution of surface Pt-Pt distances (see Figure 3) with the thickness of Pt shell, concluded that strained metal-to-metal bond lengths (~ 2 %) and not heterometallic (Ru-Pt) interactions at the interface are the likely reason for the superb catalytic activity of Ru core-Pt shell NPs for the foregoing reactions.

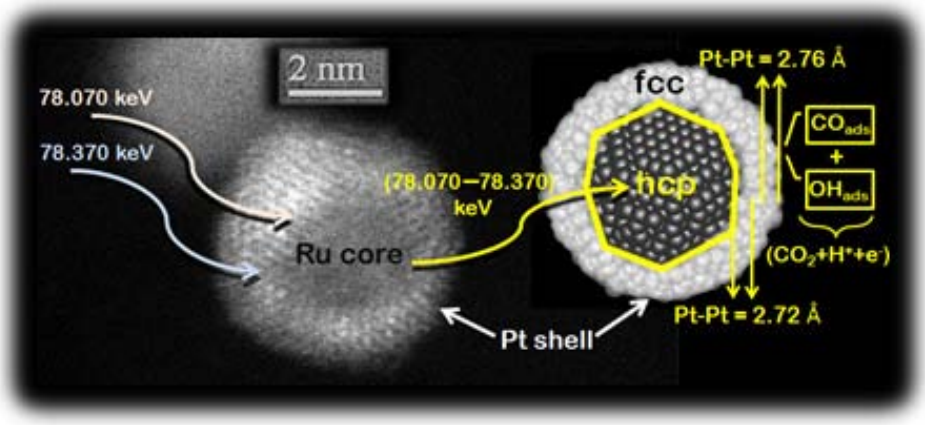

FIGURE 3. Influence of the hcp\fcc interface inside Ru core-Pt shell NPs on their catalytic properties as deciphered by resonant HE-XRD coupled to element specific atomic PDF analysis.

V.G.15 Thermodynamic, Kinetic and Electrochemical Studies on Mixed Proton, Oxygen Ion and Electron (Hole) Conductors

Anil V. Virkar
Department of Materials Science and Engineering
University of Utah
122 S. Central Campus Drive
Salt Lake City, UT 84112
Phone: (801) 581-5396
Email: anil.virkar@utah.edu

DOE Program Manager: Refik Kortan
Phone: (301) 903-3308
Email: Refik.Kortan@science.doe.gov

Program Scope

The principal objective of the work is to conduct thermodynamic, kinetic and electrochemical studies on mixed proton, oxygen ion and electron (hole) conductors. Transport processes are analyzed using linear non-equilibrium thermodynamics. Onsager coefficients including cross terms in coupled transport are determined. Transport processes in fuel cells, electrolyzers, reversible cells, and lithium batteries are examined using linear non-equilibrium thermodynamics. The role of low level electronic transport on chemical potentials of electrically neutral species is assessed. Relative directions of ionic and electronic flows determine whether or not chemical potentials within the electrolyte are bounded by the electrode values. The relative directions of ionic and electronic currents determine the sign of the Onsager non-diagonal terms (L_{ij} where $i \neq j$). That is, in mixed proton–oxygen ion–electron/hole conductors through which H^+ and O^{2-} ions transport and effectively hydrogen (H_2) and oxygen (O_2) are transported, the sign of $L_{H_2O_2}$ is dictated by the relative directions of ionic and electronic currents. If the ionic and the electronic currents are *anti-parallel*, the $L_{H_2O_2}$ is positive. If the ionic and the electronic currents are *parallel*, the $L_{H_2O_2}$ is negative. It is shown that if the ionic (e.g., H^+, O^{2-}, Li^+) and the electronic currents are *parallel*, the chemical potentials of the corresponding neutral species (H_2, O_2, lithium(Li)) in the electrolyte can exceed electrode values. This can lead to either electrolyte reduction or precipitation (and pressurization) of neutral species (H_2, O_2, Li) and failure of the electrochemical devices. Thermodynamic stability of electrochemical devices such as fuel cells, electrolyzers, lithium ion batteries is examined.

The experimental part involves the use of alternating current and direct current techniques to investigate transport properties (Onsager transport coefficients, ionic and electronic conductivites) and a study of local thermodynamics by embedded probes. Using these techniques, spatial distributions of chemical potentials of electrically neutral species (H_2, O_2, Li) inside an electrolyte are calculated and measured. The role of coupled transport is also examined in the stability of proton exchange membrane fuel cell (PEMFC) cathodes. The thermodynamics of catalyst–support interaction are examined both theoretically and experimentally. This examination includes a study of electrochemical Ostwald ripening of platinum-based nanocatalysts and the role of the catalyst support. Ostwald ripening of PEMFC catalysts thus involves transport of two charged species (Pt^{2+} ions and electrons), through two different phases.

Many transport processes can be formulated within the linear non-equilibrium thermodynamic framework (Onsager equations), in which the departure from thermodynamic equilibrium is assumed to be small. However, if the assumption of small departure from equilibrium is not valid, then the description of local thermodynamics requires the use of nonlinear non-equilibrium thermodynamics. If a system is sufficiently far away from thermodynamic equilibrium, oscillatory behavior may be observed. Determination of whether oscillatory behavior can be observed in all solid state systems is of particular interest.

FY 2016 Highlights

- A parametric equation describing polarization in solid oxide fuel cells (SOFCs) in terms of experimentally measurable parameters was developed. The equation explicitly describes activation and concentration polarizations at the two electrodes and the ohmic loss as functions of current density. Using known values of parameters measured on cell materials and components, various polarizations are estimated as functions of current density and the possible performance characteristics are assessed. The calculated performance curves using measurements made on cell materials and components are in good agreement with actual fuel cell tests. Using the model, prospects for ultra-high power density SOFC at intermediate temperatures (<800°C) are examined. The results show that even in thin electrolyte film anode-supported cells, the ohmic contribution can be substantial, not all of it being attributable to electrolyte and electrode materials. The results also show that the electrode particle size has a substantial effect on the activation polarization. A manuscript based on this work was published in the *Journal of Power Sources* (2015).

- A new oxygen permeation (transient) technique was developed to measure the electronic conductivity of yttria-stabilized zirconia (YSZ). The permeation cell is a YSZ disc with an embedded Pt probe and a cavity at the center. Two porous platinum (Pt) electrodes are applied on the disc surfaces. By applying a small DC bias across one surface electrode and the embedded probe, oxygen is pumped into the disc and stored in the cavity. In steady state, a stable Nernst potential is developed between the cavity and the outer surfaces. When the DC bias is removed, oxygen permeates out of the cavity leading to a decay of the Nernst potential. Electronic conductivity of YSZ corresponding to the ambient oxygen pressure is determined by analyzing the decay of the Nernst potential. The measured electronic conductivity is in good agreement with literature values. A manuscript based on this work was published in the *Journal of Power Sources* (2016).
- A YSZ tube with Pt electrodes was used for the measurement of potential with one electrode exposed to air and the other to H_2-H_2O gas mixtures. Measurements were conducted over a temperature range from 30°C to 475°C using two different meters, one with an input impedance of 10 GW and the other with an input impedance >200 TW. With the high impedance meter, a voltage of 0.93 V was measured at 30°C, while it was much lower with the low impedance meter. From the measurements, the actual cell voltage and the net cell resistance including all polarization resistances were estimated. Above 275°C, the measured voltage was in agreement with the expected Nernst voltage. At lower temperatures, the voltage even with the electrometer was lower than the calculated Nernst voltage indicating that H_2-H_2O gas phase mixture did not reach equilibrium. Electrochemical impedance spectra (EIS) were obtained. From the EIS spectra, the ohmic resistance was obtained. Above 75°C much of the cell resistance is attributed to electrode polarization. A manuscript based on this work was published in the *Journal of The Electrochemical Society* (2016).
- Disc-shaped samples of 8 mol% YSZ with two embedded Pt + YSZ circular electrodes and contacting Pt wires were made by sintering in air at 1500°C. In one sample, four Pt probes were embedded for local electric potential measurements. Porous surface Pt electrodes were applied on the two exposed surfaces. The samples were heated in air over a temperature range from 800°C to 900°C. A DC voltage between 1 V and 1.7 V was applied across the surface electrodes and the embedded electrodes, with the positive connected to the surface electrodes. This resulted in the formation of black zirconia between the two embedded electrodes by electrochemical pumping out oxygen. In the sample with embedded Pt probes, the local potential was measured as a function of time. A manuscript based on this work has been published in the *Journal of the Electrochemical Society* (2016).

V.G.16 Computer Simulation of Proton Transport in Fuel Cell Membranes

Gregory Voth
Department of Chemistry and The James Franck Institute
University of Chicago
5735 S. Ellis Ave., SCL 231
Chicago, IL 60637
Phone: (773) 702-9092
Email: gavoth@uchicago.edu

DOE Manager: Philip Wilk
Phone: (301) 903-4537
Email: Philip.Wilk@science.doe.gov

Program Scope

Understanding the proton transport mechanism is essential for designing next generation proton exchange membranes (PEMs). Our research focuses on the development and application of computational models that can accurately treat proton transport. Grotthuss shuttling, i.e., proton transfer involving the rearrangement of covalent and hydrogen bonds, is a primary mechanism for proton transport in aqueous systems. We have therefore developed a highly accurate reactive molecular dynamics (RMD) approach, which explicitly treats bond breaking and formation, to study proton transport in water and PEM systems. With such a tool, we are able to investigate the influence of morphology, hydration level, and temperature on proton transport in PEMs.

FY 2016 Highlights

In order to capture the proton transfer mechanism most accurately, we have updated our model used to simulate the process [1]. The new model is fit to MP2 and additive-increase/multiplicative decrease data, and shows an improved (higher) proton diffusion constant. The primary difference with the updated model is the inclusion of a presolvation water in the hydronium solvation structure, which allows the hydronium to be transiently 4-fold coordinated (see Figure 1a). Because water is typically 4-fold coordinated, when the hydronium molecule undergoes transfer and forms water, the solvation structure is more stable, thus allowing for more efficient proton hopping and enhancing the overall proton diffusion constant.

We have also continued our study of proton transport in perfluorosulfonic acid (PFSA) membranes, in particular investigating the effect of morphology [2]. Several experimental groups have proposed ordered straight-chain morphologies for PFSA membranes: lamellar structures with alternating slabs of hydrophobic and hydrophilic domains; and bundles, in which the polymer chains form nanorods surrounded by hydrophilic regions. To better understand the role of morphology in proton transport, we built structures according to two experimental proposals and calculated diffusion properties as a function of hydration level (see Figure 1b). Simulating morphologies with straight chain polymers of equivalent weights and length scales relevant to experiment required that we increase the size of our simulations by a factor of three over previous work, which demanded a major programming effort to improve the parallelization algorithm for our RMD work.

Our simulations yielded several interesting results. First, we found that proton transport is fastest in systems with lamellar morphologies. This speed is the result of several key features. Water diffusion is also fastest in the lamellar morphology (which effects proton transport) and is in fact faster than experimental water diffusion. The lamellar morphology also has the smallest surface area at the hydrophobic-hydrophilic interface, and because all of the charged sulfonate groups reside at this interface, a smaller surface area forces these groups to be closer together. Our previous work on PFSA materials of varying side chain length has shown that the primary mechanism of proton transport in PEM systems involves the excess hydrated proton getting "passed" between adjacent sulfonate groups. Our current work also shows that this mechanism can be enhanced through morphology by minimizing the surface area of the interface.

We also propose that the bundle morphology is most representative of experiment. While the proton diffusion constant is understated for the system, the water diffusion very closely reflects experimental values. We use the Simple Point Charge/flexible water model in our RMD simulations, which has been shown to give a very accurate diffusion constant. As stated above, the water diffusion constant is too high in the lamellar morphology, and given the accuracy for the bundle morphology with respect to experiment (and the accuracy of bulk water with respect to experiment), we suggest the bundle morphology is the more realistic of the straight-chain morphologies.

We have also started simulations of PFSA thin film membranes, which involve a three-phase interface with air and a catalyst layer (see Figure 1c). Thin film membranes have been shown to have very different transport properties from bulk membranes, so we set out to determine the morphological, hydration, and temperature effects on proton transport in such systems. Consistent with experiment, we find that the proton diffusion constant of thin films is greatly

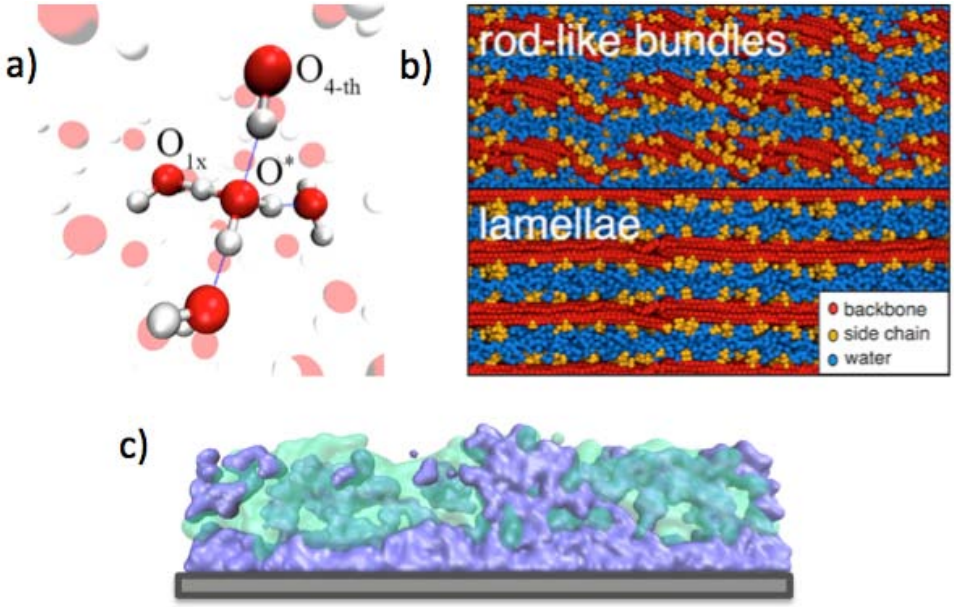

FIGURE 1. (a) Solvated hydronium molecule with transient presolvation water shown. (b) Snapshots of bundle and lamellar morphologies showing phase separation between hydrophobic backbone and water regions, with sulfonated side chains extended into aqueous region. (c) Thin film morphology with the aqueous layer rendered blue, the polymer layer rendered green, and the catalyst shown in black

reduced in comparison to bulk membranes. In addition, we have modulated the hydrophobicity of the catalyst layer, and found a substantial effect on the morphology. As hydrophilicity of the catalyst surface increases, water, hydronium, and sulfonate side chains aggregate at the catalyst layer, and push the polymer backbone to the air interface.

References

1. R. Biswas, Y.-L.S. Tse, A. Tokmakoff, and G.A. Voth, "Role of Presolvation and Anharmonicity in Aqueous Phase Hydrated Proton Solvation and Transport," J. Phys. Chem. B **120**, 1793–1804 (2016).

2. J. Savage and G.A. Voth, "Proton Solvation and Transport in Realistic Proton Exchange Membrane Morphologies," J. Phys. Chem. C **120**, 3176–3186 (2016).

V.G.17 Hydroxide Conductors for Energy Conversion Devices

Brian Pivovar (Primary Contact), Logan Garner, Zbyslaw Owczarczyk, Andrew Park, Matthew Sturgeon, Hai Long
Chemistry and Nanoscience Center
National Renewable Energy Laboratory
Golden, CO 80401
Phone: (303) 275-3809
Email: bryan.pivovar@nrel.gov

DOE Manager: Michael Sennett
Phone: (301) 903-6051
Email: Michael.Sennett@science.doe.gov

Program Scope

The present lack of stable, high performance, hydroxide conducting anion exchange membranes (AEMs) is a key limitation for several extremely promising energy conversion and storage systems and development of such materials is critical if the true potential of these technologies is to be realized. The main goal of this project is to evaluate and understand the factors that govern the stability of quaternary ammonium cationic group, linkage, and tether components of polymer electrolyte anion exchange membranes towards development of novel AEM materials with improved stability. Degradation routes and stability of quaternary ammonium cationic groups bound to perfluorinated polymer backbones are of particular interest. Our previous work within this space focused on evaluating the stability of benzyltrimethylammonium and imidazolium cationic groups as well as establishment of an applied and novel method to evaluate and quantify cation stability under conditions representative of those experienced by AEM materials during device operation. We have since expanded our focus to include not only the stability of cationic groups themselves but also their linkage and tether structure. The stability of AEM materials depends on several factors including the structure of cationic groups as well as tethers and covalent linkages. Using a combined experimental and computational approach we have been developing structure-function-property relationships that have resulted in notable increases in stability and development of improved AEM materials. More specifically, by preparing a series of model ammonium cations with varying linkage, tether, and cationic group structure and evaluating their stability using our established method, we have identified key degradation routes and problematic structures as well as key structural features that perturb degradation and improve stability. Computational modeling focused on our library of model cations has afforded further understanding of relevant degradation methods. Overall, our work represents a systematic progression of identification of optimized covalent linkage, tether, and cationic group structure for improved stability.

FY 2016 Highlights

- Synthesis and evaluation of several model cationic compounds in terms of their stability towards hydroxide has resulted in notable improvements in stability.
- We have developed structure-function-property relationships relevant to AEM stability by preparing series of model cationic compounds with varying covalent linkages, tether lengths, and cationic groups and evaluating the hydroxide stability of these compounds using our established method. Modulation of covalent linkage, tether length and structure, and cationic functional groups followed by analysis of degradation routes and breakdown products has resulted in emergence of trends that are currently being applied to develop AEM materials with improved stability.
- We have demonstrated a strong correlation between acidity of hydrogen in b position to quaternary ammonium cation and the rate of the cation degradation (Hoffman elimination).
- We have established that b-hydrogen acidity is strongly influenced by the length of the aliphatic tether and properties of alkyl group (aliphatic vs. perfluoroalkyl) detached to sulfonamide functionality.
- For a particular series of model compounds representing AEM materials with perfluorinated polymer backbones containing cationic functionality bound via sulfonamide linkages, we have demonstrated significant increases in stability (~30x). By varying tether length/structure we have perturbed certain key degradation methods and identified tethers optimized for maximum stability.
- We have identified optimal tether structure and length for elimination of unfavorable interactions between polymer backbone/covalent linkage that result in degradation.
- By applying trends and information obtained from our series of degradation studies we identified new model cation targets that have been designed to perturb key degradation methods.
- We have extended our previous computational modeling research to investigate the stability of substituted phosphonium cations and cyclic quaternary ammonium cations, and then compared our calculation results with the experimental measurements from our collaborators.

- For the substituted phosphonium, the major degradation pathways are the nucleophilic addition pathway and the S_N2 pathway. Our calculation results have good correlation with the experimental data for both pathways.
- For the cyclic quaternary ammonium cations, major degradation pathways are the S_N2 pathway and *E2* pathway. Our computational results show some correlation with the experimental data for the S_N2 pathway but underestimate the reaction barriers for the *E2* pathway. Our current computational works are aimed to understand why the density functional theory calculation resulted in underestimated *E2* reaction barriers.

VI.0 Manufacturing R&D Program Overview

INTRODUCTION

The Manufacturing Research and Development (R&D) program supports activities needed to reduce the cost of manufacturing hydrogen and fuel cell systems and components. Manufacturing R&D will enable the mass production of components in parallel with technology development and will foster a strong domestic supplier base. The program's R&D activities address the challenges of moving today's technologies from the laboratory to high-volume, pre-commercial manufacturing to drive down the cost of hydrogen and fuel cell systems. The program focuses on the manufacturing of components and systems that will be needed in the early stages of commercialization. Research investments are focused on reducing the cost of components currently used or planned for use, as well as reducing overall processing times. Progress toward targets is measured in terms of reductions in the cost of producing fuel cells, increased manufacturing processing rates, and growth of manufacturing capacity.

In Fiscal Year (FY) 2016, manufacturing projects continued progress in the following areas: use of rolled goods quality control to detect defects in membrane electrode assembly materials and modeling of the effect of defects on fuel cell material performance. We ramped up new efforts to assess the global supply chain. In addition, we launched HFCNexus.com, the U.S. Hydrogen and Fuel Cell Directory, showcasing commercial hydrogen and fuel cell products.

GOAL

Reduce the cost of manufacturing hydrogen production, delivery, storage, and fuel cell component systems through research, development, and demonstration.

OBJECTIVES[1]

Key objectives for Manufacturing R&D include the following:

- Develop manufacturing techniques to reduce the cost of automotive fuel cell stacks at high volume (500,000 units/year) from the 2008 value[2] of $38/kW to $20/kW by 2020.
- Develop fabrication and assembly processes to produce compressed hydrogen pressure vessels to enable a total onboard storage system cost of $10/kWh for widespread commercialization of hydrogen fuel cell vehicles across most light-duty platforms by 2020, with an ultimate target of $8/kWh.
- Support efforts to reduce the cost of manufacturing components and systems to produce hydrogen at <$4/gge (2007 dollars, untaxed, delivered, and dispensed) by 2020. Current cost estimates for producing, delivering, and dispensing hydrogen in the near-term market are between $13/kg and $16/kg (untaxed) without incentives.[3]

FY 2016 TECHNOLOGY STATUS

Presently, fuel cell systems are fabricated in small quantities. The cost of a 10-kW, low-temperature polymer electrolyte membrane (PEM) fuel cell system for combined heat and power (CHP) is projected to be ~$1,720/kW at a volume of 50,000 systems/year.[4] For automotive applications, the cost of an 80-kW PEM fuel cell system is projected to be $53/kW for high-volume manufacturing (500,000 systems/year).[2] Projected costs include labor, materials, and related expenditures, but do not account for manufacturing R&D investment.

FY 2016 KEY ACCOMPLISHMENTS

Advancements in the manufacture of fuel cells and hydrogen storage systems in FY 2016 include the following:

[1] Note: Targets and milestones were recently revised; therefore, individual project progress reports may reference prior targets.

[2] http://www1.eere.energy.gov/hydrogenandfuelcells/pdfs/mass_production_cost_estimation_report.pdf

[3] https://www.hydrogen.energy.gov/pdfs/15011_low_volume_production_delivery_cost.pdf

[4] http://www1.eere.energy.gov/hydrogenandfuelcells/pdfs/mass_production_cost_estimation_report.pdf

- Establishment of four regional Technical Exchange Centers to collect and categorize hydrogen and fuel cell information that will be included in a national web-centered database to facilitate purchases of hydrogen and fuel cell components and systems. (Ohio Fuel Cell Coalition)
- Launch of www.hfcnexus.com website (Figure 1) to provide a database of supplier information for hydrogen and fuel cell technologies as well as matchmaking capabilities to introduce suppliers and integrators. (Virginia Clean Cities)
- Development of a detailed questionnaire with current DOE cost target and process assumptions; input was gathered at four vehicle volumes (1,000, 10,000, 100,000, and 500,000 units/year). Seven original equipment manufacturers were interviewed and three visited. (GLWN)
- Generation of drawings and specifications for five key components (bipolar plate, membrane, gas diffusion layer, catalyst, and hydrogen storage vessel). The drawings were sent out to suppliers to obtain price quotations at four vehicle volume levels (1,000, 10,000, 100,000, and 500,000 units/year). (GLWN)

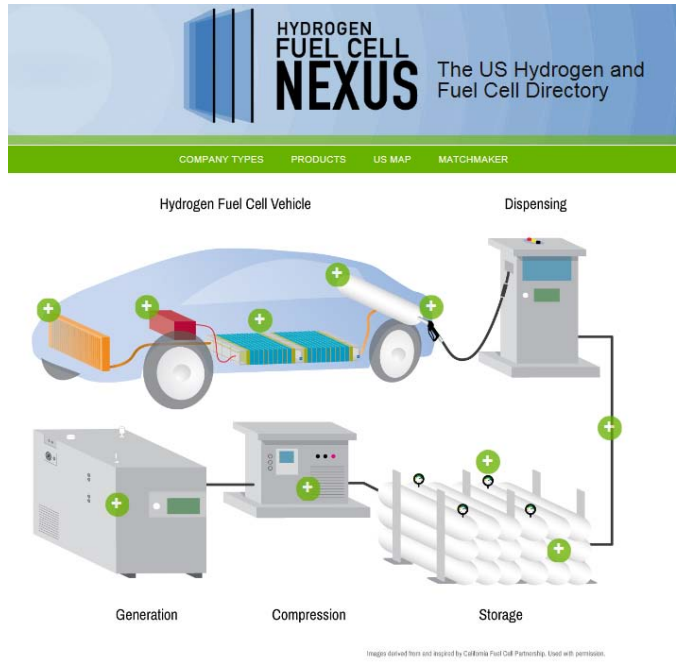

FIGURE 1. www.HFCnexus.com homepage

- Development of an innovative polymer composite hydrogen pipeline coupler. (Automated Dynamics)
  - Refined and developed the design specification with no metal parts to eliminate the possibility of hydrogen embrittlement. The design included mechanical loading, environmental effects, and leak rates.
  - Designed, manufactured, and tested electrofusion coupons with continuous fiber composite and established baseline bond strength expectations for adjacent coupler components.
  - Designed, manufactured, and tested the wire placement process for use on the design of an innovative coupler.
- Quality control of fuel cell materials following roll-to-roll processing. (National Renewable Energy Laboratory [NREL])
  - Identified the following defects in Nafion membranes (Figure 2): a 25-µm-diameter pinhole (smallest size tested), a 10-µm-wide scratch, and a 100-µm-wide fold. (NREL)

FIGURE 2. Membrane samples illustrating each of the main defect types, including pinholes, scratches, and folds taken edge-lit with a compact camera

- Demonstration of an optical system that detected forty out of forty 100-µm pinhole defects in real time on NREL's continuous roll-to-roll web line with Nafion211 membrane material at speeds of up to 30 ft/min. With post processing, all defects were successfully identified at web line speeds up to 100 ft/min. (Mainstream)

BUDGET

The FY 2017 budget request for the Manufacturing R&D program is $3 million. The FY 2016 appropriation for Manufacturing R&D was $3 million, as shown in Figure 3.

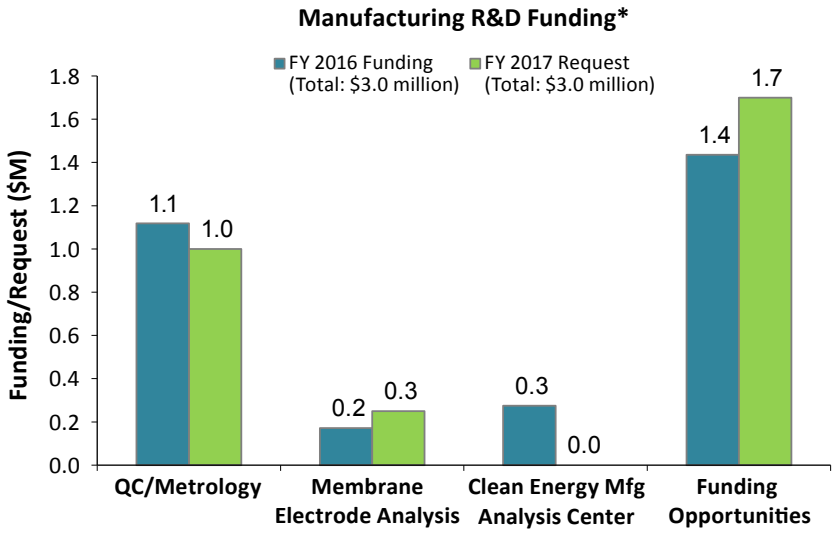

*Subject to appropriations, project go/no-go decisions, and competitive selections. Exact amounts will be determined based on research and development progress in each area and the relative merit and applicability of projects competitively selected through planned funding opportunity announcements.

QC – quality control; Mfg – manufacturing

FIGURE 3. FY 2016 appropriations and FY 2017 budget request for the Manufacturing R&D program

FY 2017 PLANS

In FY 2017, the Manufacturing R&D program will:

- Complete projects on supply chain development (Ohio Fuel Cell Coalition and Virginia Clean Cities at James Madison University) and global manufacturing competitiveness analysis (GLWN – Westside Industrial Retention & Expansion Network) in collaboration with DOE's Clean Energy Manufacturing Initiative and NREL's Clean Energy Manufacturing Analysis Center.
- Engage a four-laboratory consortium to explore and improve manufacturing processes to produce roll-to-roll goods materials for fuel cells in collaboration with and leveraging investment by the Advanced Manufacturing Office.
- Continue a project to manufacture reliable joints (with very low leak rates) that connect fiber-reinforced pipeline for hydrogen delivery at 100 bar.
- Correlate size of defects generated during membrane and/or membrane electrode assembly fabrication to loss of fuel cell performance.
- Continue to use predictive modeling and single and segmented cell test methods to assist diagnostic development.
- Develop novel defect detection via infrared detection of the thermal response of material.

- Expand implementation of defect diagnostic techniques on industry production lines to original equipment manufacturers.

The FY 2017 funding opportunity announcement will include topics on hydrogen manufacturing R&D, with awards subject to appropriation and announced later in the fiscal year. The Office will continue to coordinate with other agencies (including the National Institute of Standards and Technology and the U.S. Department of Defense) and with other technology offices within the Office of Energy Efficiency and Renewable Energy to identify synergies and leverage efforts.

Nancy Garland
Manufacturing R&D Team Lead
Fuel Cell Technologies Office
Office of Energy Efficiency and Renewable Energy
U.S. Department of Energy
1000 Independence Ave., SW
Washington, DC 20585-0121
Phone: (202) 586-5673
Email: Nancy.Garland@ee.doe.gov

VI.1 Fuel Cell Membrane Electrode Assembly Manufacturing R&D

Michael Ulsh (Primary Contact), Guido Bender, Peter Rupnowski
National Renewable Energy Laboratory (NREL)
15013 Denver West Parkway
Golden, CO 80401
Phone: (303) 275-3842; Fax: (303) 275-3840
Email: michael.ulsh@nrel.gov

DOE Manager: Nancy L. Garland
Phone: (202) 586-5673
Email: Nancy.Garland@ee.doe.gov

Partners:
- Lawrence Berkeley National Laboratory (LBNL), Berkeley, CA
- Colorado School of Mines, Golden, CO
- Georgia Institute of Technology, Atlanta, GA
- General Motors, Pontiac, MI
- 3M Company, St. Paul, MN
- Mainstream Engineering, Rockledge, FL

Project Start Date: July 16, 2007
Project End Date: Project continuation and direction determined annually by DOE

Overall Objectives

- Evaluate and develop in-line diagnostics for cell and component quality control and validate diagnostics in-line.
- Investigate the effects of membrane electrode assembly (MEA) component manufacturing variations on MEA performance and lifetime to understand the required performance of diagnostic systems and contribute to the basis of knowledge available to functionally determine manufacturing tolerances for these materials.
- Use established models to predict the effects of local variations in MEA component properties, and integrate modeling of the operational and design characteristics of diagnostic techniques into the design and configuration of in-line measurement systems.
- These objectives have strong support from the industry. Specifically, the outcomes of the 2011 NREL/DOE Hydrogen and Fuel Cell Manufacturing R&D Workshop, the Office of Naval Research-funded Manufacturing Fuel Cell Manhattan Project, and the 2013 DOE Energy Efficiency and Renewable Energy Office Quality Control Workshop confirmed the importance of continued development of in-line quality control techniques for cell manufacturing. Our specific development activities have been and will continue to be fully informed by direct input from industry. As new technologies emerge and as the needs of the industry change, the directions of this project will be adjusted.

Fiscal Year (FY) 2016 Objectives

- Complete evaluation of new prototype segmented cell hardware to improve our capabilities to study the effects of defects.
- Complete experiments for single-point membrane thickness measurement by optical reflectance.
- Use our segmented cell test system to perform total cell and spatially resolved performance (polarization) measurements of MEAs with anode and cathode defects at least as small as 0.5 cm^2.
- Based on LBNL predictive modeling, demonstrate an improvement to the infrared/reactive impinging flow (RIF) technique that will decrease noise and/or increase sensitivity, e.g., using a gas knife with an improved jet array design or using a backing configuration to reduce reactive gas loss.

Technical Barriers

This project addresses the following technical barriers from the Manufacturing R&D section (3.5) of the Fuel Cell Technologies Office Multi-Year Research, Development, and Demonstration Plan.

(E) Lack of Improved Methods of Final Inspection of MEAs

(H) Low Levels of Quality Control

Contribution to Achievement of DOE Manufacturing R&D Milestones

This project contributes to the achievement of the following DOE milestones from the Manufacturing R&D section (3.5) of the Fuel Cell Technologies Office Multi-Year Research, Development, and Demonstration Plan.

- Milestone 5.1: Establish models to predict the effect of manufacturing variations on MEA performance. (1Q, 2016)
- Milestone 5.2: Demonstrate improved sensitivity, resolution, and/or detection rate for MEA inspection methods. (4Q, 2016)
- Milestone 5.4: Design and commercialize an in-line QC device for PEMFC MEA materials based on NREL's optical reflectance technology. (4Q, 2017)

Accomplishments

NREL accomplished the following in FY 2016:

- Performed in situ studies of performance effects in cells with as-manufactured and/or created electrode defects.
- Initiated new collaboration with Georgia Tech, leveraging their membrane casting expertise, to fabricate and study the effects of as-manufactured membrane defects.
- Completed an evaluation of a new segmented cell hardware prototype.
- Established methods and initiated in situ failure onset studies of defected MEAs.
- Demonstrated the detection of membrane pinholes at least as small as 25-µm diameter in MEAs and membrane-containing subassemblies using the through-plane reactive excitation (TPRE) technique.
- Developed multi-physics modeling to predict detection limits and potential pathways for in-line implementation of TPRE.
- Demonstrated single-point membrane thickness measurement by reflectance spectroscopy.
- Assisted Mainstream Engineering in demonstrating their optical quality control (QC) prototype.
- Studied the applicability of the RIF technique to non-Pt-only catalysts.
- Expanded multi-physics modeling of RIF technique to further explore potential process improvements.
- Continued collaboration with our industry partners in accordance with our project charter.

✧ ✧ ✧ ✧ ✧

INTRODUCTION

Defects in MEA components differ in type and extent depending on the fabrication process used. The effects of these defects also differ, depending on size, location in the cell relative to the reactant flow-field, cell operating conditions, and the type of component that contains the defect. Understanding the effects of these different kinds of defects is necessary to specify and/or develop diagnostic systems with the accuracy and data acquisition/processing rates required for the speed and size scales of high-volume continuous manufacturing methods. Furthermore, predictive capabilities for manufacturers are critical to assist in the development of tolerances and to enable assessment of the effects of material and process changes.

APPROACH

NREL and its partners are addressing the DOE manufacturing milestones listed above by evaluating, developing, and validating (in-line) diagnostics that will support the use of high-volume manufacturing processes for the production of MEAs and MEA component materials. Prioritization of this work is based on inputs from our industry partners on their critical manufacturing quality control needs. We are focusing on diagnostic capabilities not addressed by commercially available in-line systems; in particular we are evaluating methods to make areal rather than point measurements such that discrete defects can be identified. We are also developing test methodologies to study the effects of the size and/or extent of each important type of variability or defect. These results will assist our industry partners in validating manufacturing tolerances for these materials, ultimately reducing scrap rates and cost, and improving supply chain efficiency. Finally, predictive models are being used at LBNL to understand the operational and design characteristics of diagnostic techniques by simulating the behavior of MEA components in different excitation modes. These results are being fed back to our design effort in configuring the diagnostics for in-line implementation. MEA models are also being utilized to understand the in situ behavior of defected MEAs to guide and further elucidate experiments.

RESULTS

Our major milestone for the past year was addressing a go/no-go decision on further development of the TPRE technique. The criteria for the decision were detection of a pinhole of less than 150 µm at an exposure time to the reactive gas of less than 5 s. These criteria were met, as shown in Figure 1, where a membrane with a 90-µm diameter pinhole was detected in a half-cell configuration. Using a 0.5 slpm flow of hydrogen and a 5 s pulse duration, a temperature rise of 1°C was observed after only 2 s of exposure. In additional studies, pinholes as small as 25 µm were detected. LBNL utilized a hybrid version of their RIF and TPRE multi-physics models to provide an initial analysis of possible pathways to in-line implementation of TPRE. The new model in fact predicted that an impinging-flow version of TPRE could potentially detect small pinholes at small exposure times using hydrogen concentrations in the reactive gas of less than the lower flammability limit in air (4%).

We continued to have a major focus on in situ testing to understand the effects of manufacturing variations in electrodes. A broad range of electrode variations were studied using our segmented cell system, including cathode centered bare spots, defects on the anode vs. the cathode, defects at the inlet vs. center vs. outlet of the cell, defect shape and total catalyst layer volume reduction, thick spots vs. thin spots, comparison of defects as a function

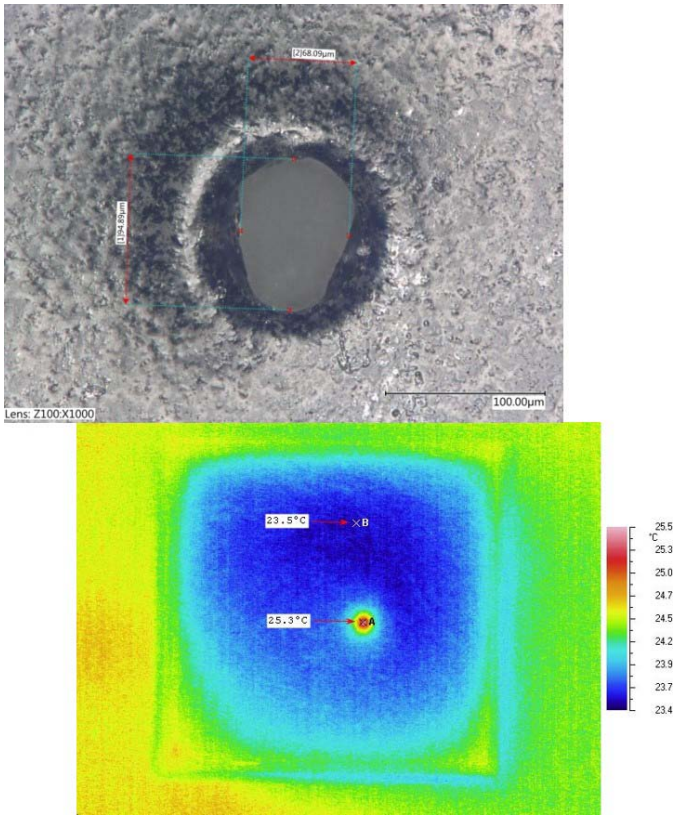

FIGURE 1. TPRE demonstration data, showing optical microscopy of an 18-µm thick membrane sample with a 90-µm diameter pinhole, and the thermal response of a half-cell including this membrane and a gas diffusion electrode with a catalyst loading of 0.2 mg Pt/cm^2. The excitation conditions were a 5 s pulse of hydrogen at 0.5 slpm. A detectable temperature rise of 1°C was observed after 2 s of exposure.

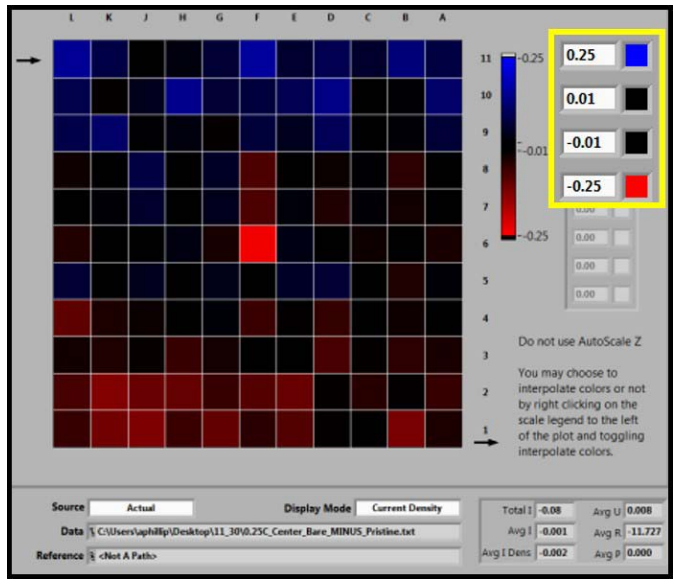

FIGURE 2. Segmented cell data showing the spatially resolved performance effect of a 0.25 cm^2 bare spot in the cathode at a total cell current density of 1.2 A/cm^2. The color scale shows the difference in local current density between the defected cell and a pristine cell. The cell uses a NRE 212 (50 µm Nafion®) membrane and has a nominal loading of 0.2 mg Pt/cm^2 on both anode and cathode, and is operated at anode/cathode conditions of 32/32 % relative humidity (RH), 150/150 kPa, 1.5/2.0 stoich, H_2/air, and a cell temperature of 80°C.

of membrane thickness and nominal catalyst loading, and comparison of defects in catalyst-coated membrane-based MEAs vs. gas diffusion electrode-based MEAs. As an example of these studies, Figure 2 shows the local performance effect of a 0.25 cm^2 bare spot in the center of the cathode. The difference in current density between the defected cell and an associated pristine cell in each of the 121 segments is shown. Red contours indicate poorer performance in the defected cell, while blue contours indicate increased performance. The local effect of the defect in the center segment is clearly seen; however, it is also seen that normal along-the-flowfield variations in cell performance are close to the same magnitude as the effect of the defect. In addition, we performed further development of an accelerated stress test, in coordination with Los Alamos National Laboratory, which would enable us to detect and spatially resolve the onset of failure in a cell. In Figure 3, we show example data from failure testing of a pristine MEA using this testing protocol. Decrease of open circuit voltage and increase in hydrogen crossover current density are used as in situ indicators of failure. Upon indication of failure, we use our novel cell hardware and an infrared camera with a hydrogen crossover test to image the location and extent of the failure.

In a key study that sets the path toward real-time imaging of membrane thickness, we confirmed that optical reflectance spectroscopy could be used with the well-known film interference fringe method to measure single-point thickness of membranes. This was an expected result. However, we also demonstrated that the technique could be used to measure membrane thickness (a) while the membrane was still laminated to one or two casting or protective films, and (b) of membranes with reinforcing layers. These were critical findings given the widespread use of reinforced membranes and the understanding that, until final assembly into an MEA, polymer electrolyte membranes are rarely handled in a stand-alone fashion. We tested different PEMFCs, including several with reinforcing layers, over a range of thickness from 6 to 50 µm. Figure 4 provides visible and infrared spectroscopy of an 18-µm thick membrane, both of which show measurable interference fringes. The inset shows the peak resulting from a Fourier transform of the infrared spectrum, which indicates thickness.

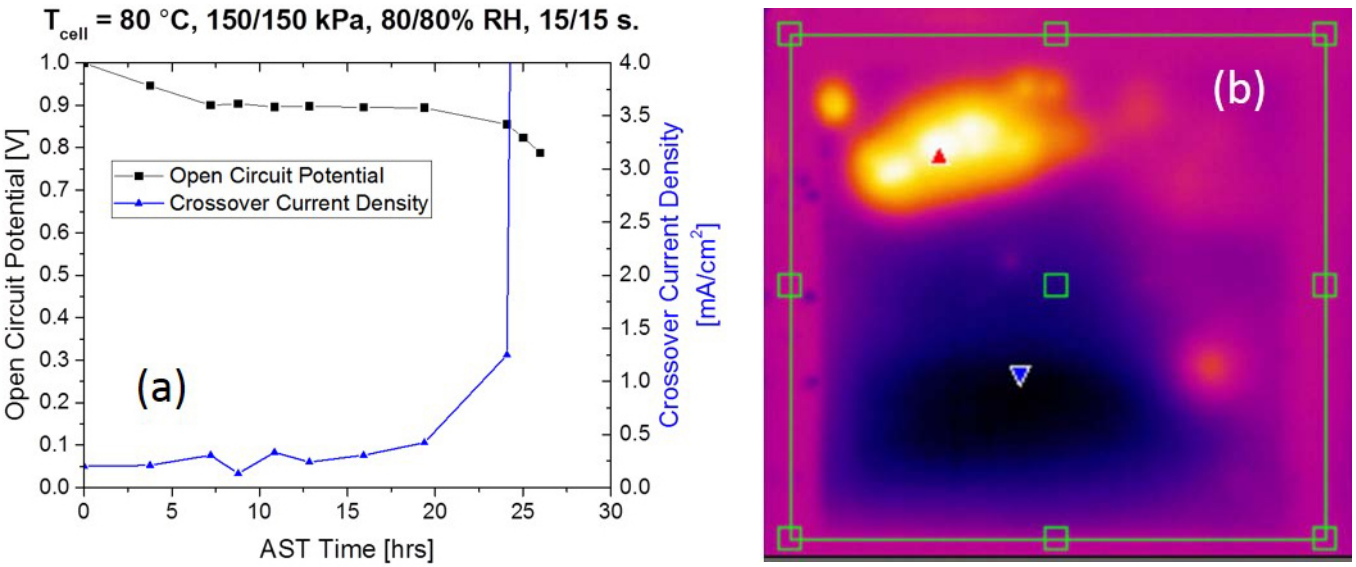

FIGURE 3. Failure study data for a pristine cell having a NRE 212 (50 µm Nafion) membrane and a nominal loading of 0.2 mg Pt/cm^2 on both anode and cathode, operated at accelerated stress test (AST) conditions of 150 kPa, H_2/air, and cell temperature of 80°C, cycling from 0 to 80% RH in 15 s intervals; (a) open circuit voltage and hydrogen crossover current density data showing the onset of the failure, and (b) infrared thermography during hydrogen crossover test showing the location and extent of failure.

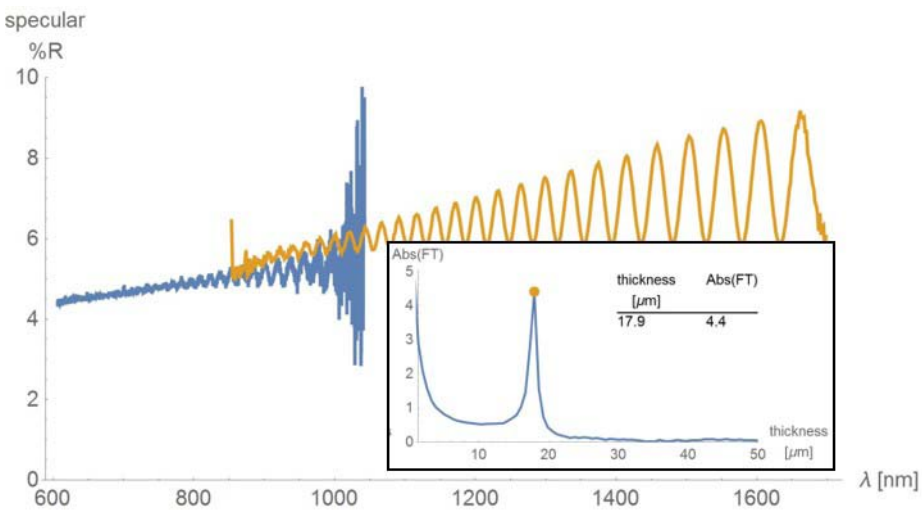

FIGURE 4. Visible wavelength (blue) and infrared wavelength (orange) optical reflectance spectroscopy data for an 18-µm thick membrane showing measurable interference fringes. The inset shows the thickness peak resulting from a Fourier transform of the infrared spectrum.

FUTURE DIRECTIONS

- Demonstrate improvement in RIF detectability based on LBNL modeling.
- Develop a concept, using modeling and experimentation, for in-line TPRE.
- Demonstrate a prototype system for in-line membrane thickness imaging.
- Continue to use predictive modeling and single and segmented cell test methods to study the effects of as-manufactured defects on MEA performance and lifetime using standard or accelerated stress tests.
- Continue to work toward the implementation of more of our techniques on industry production lines.

SPECIAL RECOGNITIONS & AWARDS/ PATENTS ISSUED

1. Issued US Patent #9,234,843, "On-line continuous monitoring in solar cell and fuel cell manufacturing using spectral reflectance imaging."

FY 2016 PUBLICATIONS/PRESENTATIONS

1. P. Rupnowski, M. Ulsh, B. Sopori, "High Throughput and High Resolution In-line Monitoring of PEMFC Materials by Means of Visible Light Diffuse Reflectance Imaging and Computer Vision," PowerEnergy2015-49212, and presented at the ASME 2015 Power and Energy Conversion Conference, San Diego, CA; July 1, 2015.

2. M. Ulsh, J.M. Porter, D.C. Bittinat, G. Bender, "Defect Detection in Fuel Cell Gas Diffusion Electrodes Using Infrared Thermography," Fuel Cells Journal, DOI: 10.1002/fuce.201500137, 2016.

3. M. Ulsh, P. Rupnowski, B. Sopori, I. Zenyuk, A. Weber, G. Bender, "In-line Quality Control for Fuel Cell and Electrolysis Materials," MRS Spring Meeting, Symposium EE9 invited lecture, Phoenix, AZ; March 29, 2016.

VI.2 Clean Energy Supply Chain and Manufacturing Competitiveness Analysis for Hydrogen and Fuel Cell Technologies

Patrick Valente
Ohio Fuel Cell Coalition (OFCC)
151 Innovation Drive, Suite 240D
Elyria, OH 44035
Phone: (614) 542-7308
Email: pat.valente@fuelcellcorridor.com

DOE Managers:
Nancy L. Garland
Phone: (202) 586-5673
Email: Nancy.Garland@ee.doe.gov
Greg Kleen
Phone: (240) 562-1672
Email: Greg.Kleen@ee.doe.gov

Contract Number: DE-EE0006931

Subcontractors:
- Connecticut Center for Advanced Technology, East Hartford, CT
- DJW Technology, Inc., Dublin, OH
- National Renewable Energy Laboratory, Golden, CO
- National Fuel Cell Research Center, Irvine, CA

Project Start Date: September 1, 2015
Project End Date: August 30, 2018

Overall Objectives

- Establish regional Technical Exchange Centers to increase communication between original equipment manufacturers (OEMs) and hydrogen and fuel cell component and subsystem suppliers.
- Establish a readily web-accessible database containing inputs from suppliers and OEMs along with a supplier contact lists.
- Standardize component and subsystem component specifications.
- Develop strategies for lowering cost, increasing performance, and improving durability of components and subsystem components.

Fiscal Year (FY) 2016 Objectives

- Create four regional Technical Exchange Centers and operate supply chain exchanges to facilitate one-to-one communication between suppliers and OEMs.
- Identify participants and initiate supplier working group; select component for standardization.
- Develop projections of cost reduction based on working group activities.
- Input information from suppliers and OEMs into a web-accessible database and increase the number of suppliers registered and providing data to centers.

Technical Barriers

This project addresses the following technical barriers from the Fuel Cells section of the Fuel Cell Technologies Office Multi-Year Research, Development, and Demonstration Plan.

(A) Durability

(B) Cost

(C) Performance

This project also addresses the following technical barrier from the Manufacturing R&D section of the Fuel Cell Technologies Office Multi-Year Research, Development, and Demonstration Plan.

(I) Lack of Standardized Balance-of-Plant Components

FY 2016 Accomplishments

- Four regional Technical Exchange Centers were established to collect and categorize hydrogen and fuel cell information that will be included in a national web-centered database.
- Two subcontractors (Connecticut Center for Advanced Technology and National Fuel Cell Research Center) held successful supply chain exchanges in Massachusetts and California. These exchanges were partnered with larger, relevant events for additional exposure.
- Increased collaboration with partner organizations, such as the Colorado Cleantech Industries Association, Great Lakes Wind Network, and Fuel Cell and Hydrogen Energy Association. A broader cross-section of organizations was contacted to enable us to extend our reach in information for the centers.
- The OFCC database verification and updating continues, with approximately 500 entries to be added to the national database.
- Supply chain mapping in Connecticut and the Northeast has been completed.
- The OFCC participated in the DOE Clean Transportation Summit in Berkeley, California (May 2016).

- Initial key suppliers and OEMs have been contacted to participate in a working group, focusing on standardization of components and subsystems with the focus on cost reduction without loss of functionality.

✧ ✧ ✧ ✧ ✧

INTRODUCTION

The project goal is to facilitate the development of a robust supply chain for fuel cell and hydrogen systems that will accelerate mass production, reduce cost, and improve performance and durability of these systems. The project will accentuate the identification of critical opportunities in the hydrogen and fuel cell supply chain where the United States can achieve or maintain a competitive advantage.

This project builds on existing manufacturing infrastructure to help reverse the decline in and/or create new manufacturing jobs, as well as acts as economic lever for additional technology development. This will accelerate mass production, reduce cost, and improve performance and durability of fuel cell systems, which will facilitate commercialization of hydrogen and fuel cell technologies, and promote energy efficiency and renewable energy.

APPROACH

Regional Technical Exchange Centers will be established to increase communication between OEMs and hydrogen and fuel cell component and subsystem suppliers. These centers will collect and catalog nonproprietary company and product information from their regional suppliers and OEMs. This information will be combined and added to a national web-centered database.

Supply Chain Exchange events will be held to promote communication between suppliers and OEMs. A supplier working group will facilitate and assess pathways to standardization of fuel cell components and subsystem components with the focus on cost reduction without loss of functionality. The project focus is two-way technology transfer between OEMs and suppliers.

RESULTS

The establishment of the four regional Technical Exchange Centers will enable the OFCC and its subcontractors to outreach and catalog those stakeholders relevant to the hydrogen and fuel cell industry, and to eliminate any duplication in contacts or regions. Assessment of the OFCC database fields was done to determine compatibility with the Virginia Clean Cities/James Madison University database, which is where the national web-centered database will be housed. The information gained through this collaboration will contribute to the national database, expand our domestic supply chain, as well as promote economic enhancement and communication within the industry.

Supply Chain Exchange events were a more personal, one-on-one way to facilitate communication between suppliers and OEMs. At the events, suppliers were able to meet with each OEM face-to-face to present their company's capabilities and value proposition, to determine if further communication between the two is warranted. "Matchmaking" of OEMs and suppliers helps bridge the communication gap between the two. Approximately 160 suppliers, integrators, and other stakeholders were invited and participated. These exchanges increase connections between the OEMs and suppliers to make introductions and match needs with availability. The information gathered is used in the regional Technical Exchange Centers database, and eventually become part of the national database.

Supply chain mapping in the Northeast gave us a view of where the supply chain is strongest and where gaps occur in the following areas: Maine, New Hampshire, Vermont, New York, New Jersey, Connecticut, Rhode Island, and Massachusetts. In Connecticut alone, over 400 stakeholders have been identified in the hydrogen and fuel cell industry. In New Jersey, 246 companies were identified that could be included in the Northeast supply chain database.

All of the above project work and results contribute to the United States working towards and maintaining a competitive advantage in the hydrogen and fuel cell industry. This work is the building block for developing a robust supply chain, increasing manufacturing, providing the necessary resources to advance the industry, and working to fulfill the objectives of this project.

CONCLUSIONS AND FUTURE DIRECTIONS

We have found stakeholders, as a whole, are eager to focus and continue to strengthen the industry. We have seen how valuable our partnerships and collaborations are in working towards that goal. We were able to identify what regions are strongest with respect to the supply chain, where the gaps are that will need to be addressed, and where we can promote diversity within the manufacturing industry through our national database and standardization of components. Our next steps will be taking this information to the next level. We anticipate expansion of the number of suppliers providing data to the centers. We will be holding several additional supply chain exchanges, and focus on locations where the suppliers are concentrated. We will be examining standardization of component specifications in an effort to become more cost efficient and improve durability and performance of the components and subsystems.

FY 2016 PUBLICATIONS/PRESENTATIONS

1. Presentation at the Hydrogen and Fuel Cell Technical Advisory Committee meeting in Washington, D.C., October 27–28, 2015.

2. Presentation at the DOE Annual Merit Review in Washington, D.C., on June 8, 2016.

VI.3 Fuel Cell and Hydrogen Opportunity Center, www.hfcnexus.com

Alleyn Harned
James Madison University (Virginia Clean Cities [VCC])
800 South Main Street
Harrisonburg, VA 22807
Phone: (540) 568-8896
Email: aharned@vacleancities.org

DOE Managers:
Nancy L. Garland
Phone: (202) 586-5673
Email: Nancy.Garland@ee.doe.gov

Greg Kleen
Phone: (240) 562-1672
Email: Greg.Kleen@ee.doe.gov

Contract Number: DE-EE0006932

Subcontractors:
- Birch Studio, Charlottesville, VA
- Breakthrough Technologies Institute, Washington, D.C.

Project Start Date: July 1, 2015
Project End Date: May 31, 2018

Overall Objectives

- To expand the domestic supply chain of hydrogen components and systems.
- Scale-up of the fuel cell and hydrogen supply chain by building and populating a comprehensive communications database.
- Drive U.S. companies to the free website via an engaging outreach campaign.
- Advance hydrogen fuel cell suppliers in the transportation, utility, industrial, commercial, and residential sectors, with a focus on the transportation sector in fuel and infrastructure supply chain systems.
- Reduce greenhouse gas emissions, and air pollution and contribute to a more diverse and efficient energy balance by facilitating the widespread commercialization of hydrogen and fuel cell technologies.

Fiscal Year (FY) 2016 Objectives

- Input and feedback will be collected from DOE and laboratories on the visually accessible public interface to ensure critical parties' interests are addressed. The survey was created and administered at the 2015 Fuel Cell Seminar; survey data were able to provide an initial baseline of categories and contacts. A second collaborative data gathering process was used to gain feedback from National Renewable Energy Laboratory, DOE, and project partners on a website project name.
- The list of fuel cell system components to be initially included in the database is completed.
- The opportunity center will be up and running within six months of sub agreement completion and be populated with the information collected to date.
- The web portal will be developed to house the opportunity center for industry to gather and input information.
- Input and feedback from project partners on technical specifications of the opportunity center including user experience and functionality is obtained.
- An interface will be developed to allow fuel cell companies and hydrogen companies to partner based off of similar needs.
  - Status: Ongoing
- The project team will update the database continuously and technical specification will be monitored and updated quarterly.
  - Status: Ongoing
- The project team will identify the fuel cell system gaps and cater the opportunity center to narrow the gaps identified.
  - Status: Ongoing

Technical Barriers

This project addresses the crosscutting technical barriers of supply chain transparency and business and product information of the manufacturing R&D section. The project also addresses the following specific barrier from the Education and Outreach section of the Fuel Cell Technologies Office Multi-Year Research, Development, and Demonstration Plan.

(A) Lack of Readily Available, Objective, and Technically Accurate Information

Contribution to Achievement of DOE Milestones

This project will directly contribute to achievement of DOE milestones from the Education and Outreach section of the Fuel Cell Technologies Office Multi-Year Research, Development, and Demonstration Plan. The project is a

cross-cutting effort to publish available supply chain business content and connect industry partners. As such, milestones associated with development and demonstration in the Manufacturing R&D section are supported, and this project takes those milestones to deployment.

FY 2016 Accomplishments

- Focus groups initiated with Department of Energy and hydrogen fuel cell industry. Comments collected and reviewed.
- First and second gap analyses initiated with Breakthrough Technologies Institute.
- Birch Studio developed and continues to refine the website's user interface and user account controls.
- Permanent server space engaged at James Madison University.
- A baseline of 220 company entries verified and entered into the database.
- Review of companies for accuracy. Several have been removed, all have been updated.
- Soft launch of website on June 1, 2016. Live launch on July 11, 2016.
- Staff attended the Fuel Cell Seminar in Los Angeles, California, and the ACT Expo in Long Beach, California and co-located hydrogen business connection events and seminars to beta-test the project and network with hydrogen and fuel cell companies.

✧ ✧ ✧ ✧ ✧

INTRODUCTION

The Fuel Cell and Hydrogen Opportunity Center, renamed the Hydrogen Fuel Cell Nexus (and live at www.hfcnexus.com and www.hfcnexus.org, Figure 1) will expand the domestic supply chain of components and systems necessary for the manufacture and distribution of the hydrogen and fuel cell equipment. The supply chain will benefit through the development of a comprehensive online database. This effort will advance hydrogen fuel cell suppliers in the transportation, utility, industrial, commercial, and residential sectors, with a focus on the transportation sector in fuel and infrastructure supply chain systems.

APPROACH

VCC and project partners addressed the main objective of the Fuel Cell and Hydrogen Opportunity Center project by collaboratively identifying gaps and developing elements of interest for a comprehensive supplier tool, gathering national supplier information to fill the database, identifying and encouraging new suppliers to become engaged in the hydrogen industry, and releasing and maintaining a public directory tool for interaction with the data. Birch Studio developed the user interface for the website. Virginia Clean Cities populated the database with U.S. companies from the FuelCells2000 directory. After the website was launched, VCC began an aggressive outreach campaign using trade association outreach, webinars, social media, and personal contact to drive companies to this resource.

RESULTS

The FY 2016 efforts of the Fuel Cell and Hydrogen Opportunity Center project team culminated in the release of a live and interactive website directory on July 11, 2016. The website directory has an initial population of 220 companies (Figure 2). These companies were verified that they are active in the hydrogen or fuel cell industries. Phone numbers, email addresses, and mailing information for employees at each company was uploaded for each company to provide a method for website users to contact the company (Figure 4).

CONCLUSIONS AND FUTURE DIRECTIONS

During the third quarter of 2016, the project team will be active in several areas of the project related to improving the website and adding companies. The project team will continue verifying data and company information and revising as needed. The website will go live on July 11, 2016 at which time the project team will begin direct marketing and outreach to hydrogen and fuel cell companies. During this period VCC will develop and disseminate marketing and outreach materials that describe the website and how

FIGURE 1. www.HFCnexus.com homepage

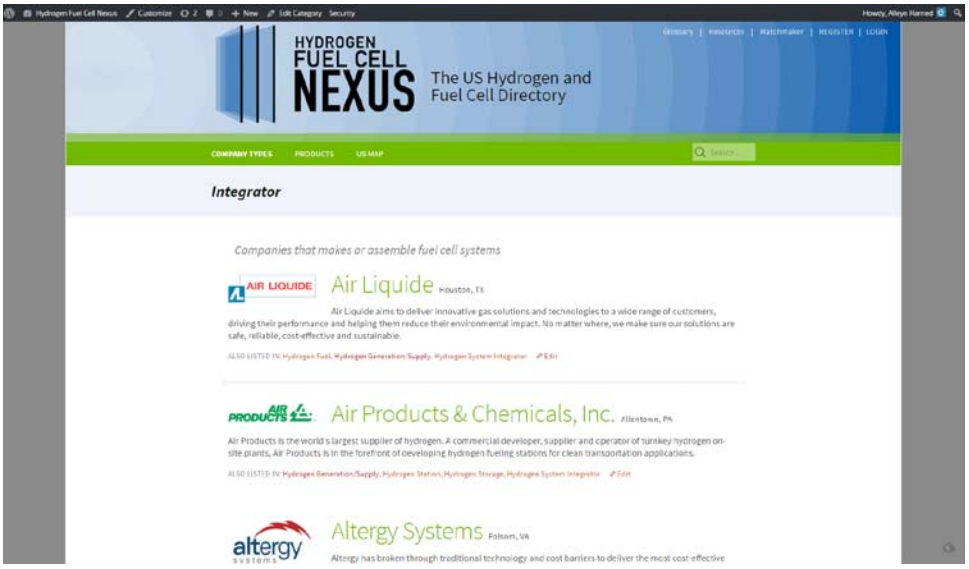

FIGURE 2. Example of a company's directory page

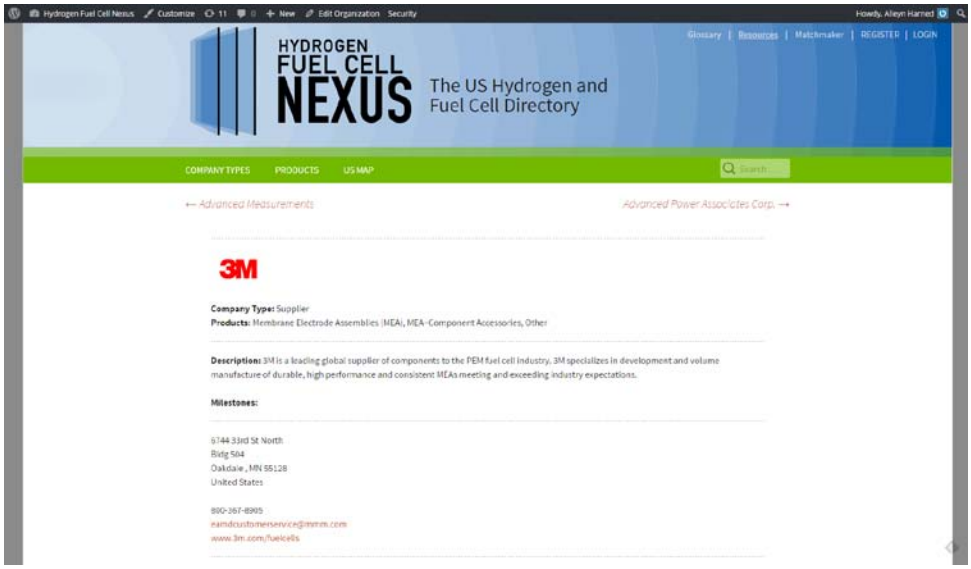

FIGURES 3. Examples of company category page

to utilize it. Birch Studio will develop the Matchmaker Interface for companies to connect to one another. Birch Studio will being a maintenance and iteration phase to continue improving the website interface. VCC staff will continue promoting the database at events and collecting data on hydrogen and fuel cell companies to include in the database. Project staff will develop website branding with DOE guidance.

Throughout the rest of the year and moving through to June 30, 2017, the project team will enter a supply chain growth phase. Throughout the second budget year the team will engage in an outreach campaign to drive appropriate suppliers to the site, by initiating friendly partnerships with business-to-business marketing associations and other business associations in areas of critical need.

The database and website tools will have three main areas for public access, supplier secure access, and system administrator's access. The content will be accessible 24/7.

FY 2016 PUBLICATIONS/PRESENTATIONS

1. *Virginia Clean Cities at James Madison University*
VCC's Deputy Director Matthew Wade attended the Fuel Cell Seminar in Los Angeles to present an update on the Hydrogen

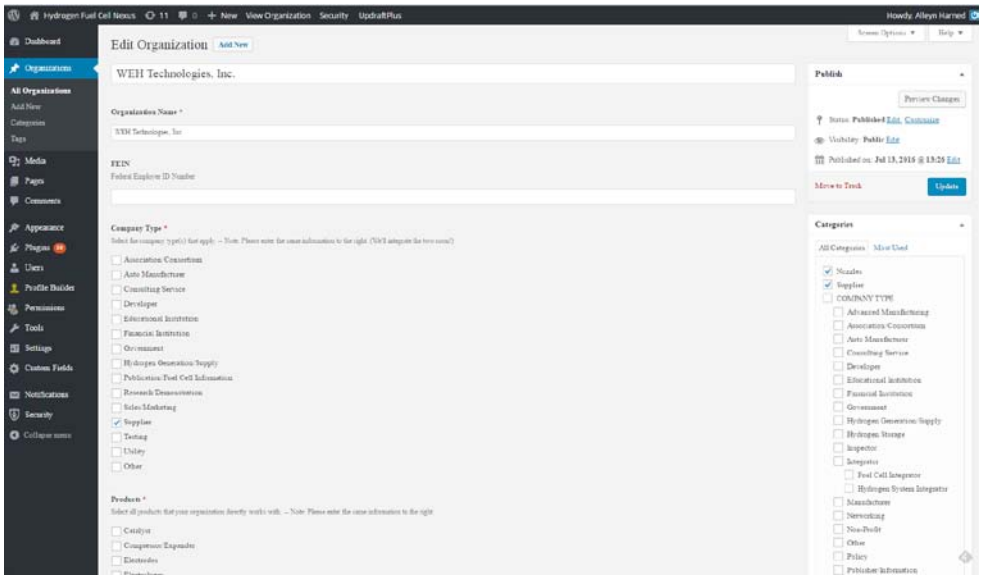

FIGURE 4. Example of company information page

Opportunity Center on November 18, 2015. Principal Investigator Alleyn Harned presented at the Annual Merit Review, Washington, D.C. June 8, 2016. Alleyn Harned presented an early release mobile version of the website to individuals at two hydrogen summits at ACT Expo from May 2 to May 6, 2016.

2. *Birch Studio*
David Robinson presented an early release mobile version of the website to individuals at two hydrogen summits at ACT Expo from May 2–May 6, 2016.

3. *Breakthrough Technologies Incorporated*
Robert Rose made a presentation to the Hydrogen and Fuel Cell Technical Advisory Committee in October 2016.

VI.4 U.S. Clean Energy Hydrogen and Fuel Cell Technologies: A Competiveness Analysis

Patrick Fullenkamp
GLWN, Westside Industrial Retention & Expansion Network
4855 West 130th Street, Suite 1
Cleveland, OH 44135-5137
Phone: (216) 920-1956
Email: pfullenkamp@glwn.org

DOE Managers:
Nancy L. Garland
Phone: (202) 586-5673
Email: Nancy.Garland@ee.doe.gov

Jesse Adams
Phone: (240) 562-1421
Jesse.Adams@ee.doe.gov

Contract Number: DE-0006935

Subcontractors:
- Strategic Analysis, Inc, Arlington, VA
- DJW Technology, LLC, Dublin, OH
- E4tech, Lausanne, Switzerland
- Bowen Liu, Newmarket, Ontario, Canada
- Brent Fourman, New Paris, OH

Project Start Date: June 1, 2015
Project End Date: May 31, 2019

Overall Objectives

- Global competitiveness analysis of hydrogen and fuel cell systems and components manufactured including 700 bar compressed hydrogen storage system in the United States, Europe, and Asia to determine the global cost leaders, the best current manufacturing processes, the key factors determining competitiveness, and the potential means of cost reductions.
- Analysis to assess the status of global hydrogen and fuel cell markets for four years, 2014 to 2017. The analysis of units, megawatts by country and by application, will focus on polymer electrolyte membrane fuel cell (PEMFC) systems (automotive and stationary).

Fiscal Year (FY) 2016 Objectives

- Map automotive fuel cell system supply chain evolution.
- Develop detailed questionnaire with current DOE cost targets and process assumptions baseline shared and conduct 30 interviews.
- Update the current DOE cost model as provided by Strategic Analysis.
- Generate drawings and specifications for five key components and send out to suppliers to get actual price quotations at four vehicle volume levels: 1,000, 10,000, 100,000, and 500,000 units/year
- Complete cost breakdown analysis and value stream mapping based upon quotations.
- Gather and deliver fuel cell systems shipment data for 2015.

Technical Barriers

This project addresses the following technical barriers from the Manufacturing R&D section of the Fuel Cell Technologies Office Multi-Year Research, Development, and Demonstration Plan.

(A) Lack of High-Volume MEA Processes (includes catalyst, membrane, gas diffusion layer)

(B) Lack of High-Speed Bipolar Plate Manufacturing Processes

(I) Lack of Standardized Balance-of-Plant Components

(K) Lack of Low-Cost Fabrication Techniques for Storage Tanks

Contribution to Achievement of DOE Manufacturing R&D Milestones

This project will contribute to achievement of the following DOE milestones from the Manufacturing R&D section of the Fuel Cell Technologies Office Multi-Year Research, Development, and Demonstration Plan.

- Milestone 1.6: Develop fabrication and assembly processes for PEMFC MEA components leading to an automotive fuel cell stack that costs $20/kW. (4Q, 2020)
- Milestone 2.1: Develop manufacturing processes for PEMFC bipolar plates that cost <$3/kW while meeting all other technical targets. (1Q, 2017)
- Milestone 3.3: Develop fabrication and assembly processes for automotive PEMFC stacks that meet the cost of $20/kW. (4Q, 2020)
- Milestone 6.1: Develop fabrication and assembly processes for high-pressure hydrogen storage technologies that cost $12/kW for Type IV, 700 bar tanks. (4Q, 2017)

FY 2016 Accomplishments

- Mapped automotive fuel cell system supply chain evolution.
- Detailed questionnaire developed with current DOE cost target and process assumptions with baseline shared and input gathered at four vehicle volume levels of 1,000, 10,000, 100,000, and 500,000 units/year: seven original equipment manufacturers (OEMs) interviewed, three OEMs visited, 21 suppliers interviewed, 19 suppliers visited.
- Updated the current DOE cost model as provided by Strategic Analysis from interview input.
- Generated drawings and specifications for five key components (bipolar plate, membrane, gas diffusion layer, catalyst, hydrogen storage vessel) and sent out to suppliers to get actual price quotations at four vehicle volume levels: 1,000, 10,000, 100,000, and 500,000 units/year.
- Completed cost breakdown analysis and value stream mapping of five key components in three global regions with request for quotations in process.
- Gathered and delivered fuel cell systems shipment data for 2015.

✧ ✧ ✧ ✧ ✧

INTRODUCTION

A healthy component supply chain is needed to support global OEMs as they launch hydrogen fuel cell vehicles into the market. OEMs need suppliers that can meet performance quality and cost targets. This project will provide a global analysis of the current supply chain technology and manufacturing readiness levels and cost levels through updated cost modeling and actual quotations and recommendations. This will aid the DOE Clean Energy Manufacturing Initiative in identifying strategic research and development (R&D) investments. This study will also provide a four-year analysis of units, megawatts by country and by application of PEMFC systems (automotive, portable, and stationary)

APPROACH

A questionnaire was developed for OEMs and suppliers which reflected the DOE cost model of five key components at four production levels to serve as the baseline for discussion. Feedback was requested on the cost breakdown, process assumptions, technology and manufacturing readiness, R&D projects and investment needed to support cost reductions. Interviews were conducted by phone and/or plant visits. Generic drawings and specifications were developed to get actual quotations. The quotations will be compared to the current DOE cost models and adjustments made.

Supplier relationships will be identified and mapped with annual shipment data of automotive and stationary PEMFCs. Data will be gathered on government funding, capital available, and technology focus.

RESULTS

A comprehensive questionnaire was developed to gather key industry information in an information sharing manner that enabled OEMs and suppliers to provide directional and discrete information on the DOE cost model, technical and manufacturing readiness, current and future manufacturing process assumptions, and future development to meet the high volume needs of this industry at >100,000 vehicles per year. A large quantity of data has been gathered from the questionnaire interview with seven OEMs and 21 suppliers with actual visits at three OEMs and 19 suppliers. The following are the findings and themes to date:

- Global OEMs have a focus on performance and cost through design and manufacturing process development to build a positive business case for hydrogen fuel cell vehicles with a targeted sales price of $50,000. The leading OEMs are reporting 30–40% incremental cost reduction as they introduce next generation models. OEMs are in the initial phases of growing the supply chain. Most have a lead supplier for each of the key components, with a goal of at least two per component in maturity.
- Suppliers have a focus on component design and process development with no OEM or supplier capable of producing 100,000 vehicle units/year. Most are comfortable with 1,000 to 5,000 units per year. Suppliers are very cautious about investing in new manufacturing facilities with the limited book of business and the concern for potential major designs which could obsolete the current manufacturing process.
- Bipolar plate suppliers have current capability up to 10,000 vehicle units/year with further substantial investment needed for 100,000 units/year. R&D projects would be stamping in line process or roll-to-roll continuous production, elimination of plate coatings, sealing solutions, and electrical conductivity.
- Membrane suppliers have current capability up to 10,000 vehicle units/year with further substantial investment needed for 100,000 units/year. R&D projects to improve output would be: defined tolerance, improved inspection and quality metrics, high volume roll to roll processing, and improved performance at lower Pt loading targets.

- Pressure vessel suppliers have current capability up to 50,000 units/year with further substantial investment needed for 100,000 units/year. R&D projects would be design and manufacturing alternatives to carbon fiber winding, and lower carbon fiber strength/higher quality resin.
- Table 1 shows the range of the OEM cost projections for the fuel cell stack components studied with Strategic Analysis DOE cost. OEMs are in closer agreement at the 100,000 and 500,000 volumes.
- Figure 1 is the cost breakdown analysis preliminary example of quoted supplier data. The actual data is just beginning to be gathered on all five key components.
- Figure 2 is a value stream map of the bipolar plate manufacturing process flows. Maps will be made of all five key components.
- Figure 3 is the E4tech 2015 market data.
- In Japan, national support for markets (e.g. fueling infrastructure) has built a level of tentative certainty in the market which has enabled suppliers to develop manufacturing knowledge and capability. Serial production of fuel cell systems is being demonstrated by Toyota (Mirai) and Honda (Clarity) and a nascent supply chain exists.
- In China, support in the form of subsidies for consumers at the national and provincial level is focused on applications relevant to China's national goals of reducing greenhouse gas emissions and air pollution starting with buses. We are in the process of acquiring a copy of China's policy statement. One supplier has reported that the use of the China government funded and constructed research facility is being turned over to the company at no cost and 60% of the equipment is covered by the government. The company will only have to pay for 40% of the cost of the equipment.

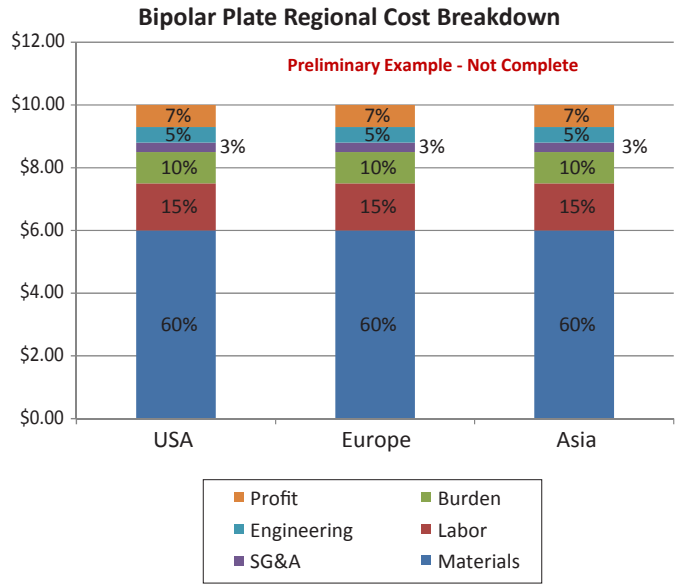

USA – United States of America; SG&A – selling, general and administrative

FIGURE 1. Preliminary example Cost breakdown analysis. The $10.00 price is only a placeholder along with the % of the major cost categories. This graph will be adjusted once we get actual quotes.

CONCLUSIONS AND FUTURE DIRECTIONS

The fuel cell supply chain is in the development/introduction stage with further design and manufacturing readiness development and substantial investment needed to get to the growth/maturity stage. OEMs are still developing the Tier 1 supply chain with most having one lead supplier per component with the target of two. Tier 1s state they need to invest in automated fabrication lines but are very cautious with high potential for major design changes. Five more months of work is required to complete the competiveness analysis portion of the project which includes the following: finish request for quotes; identify three

TABLE 1. Strategic Analysis Projected Cost versus OEM Forecast for Fuel Cell Stack Components (i.e., example: For bipolar plates at 1,000 vehicle units the OEMs average cost is 14 times higher than the SA cost numbers. For bipolar plates at 500,000 vehicle units the OEMs average cost is the same as SA cost numbers)

	Annual System Production Rate			
	1,000	10,000	100,000	500,000
Catalyst Ink & Application	9x	5x	3x	1.5x
Bipolar Plates	14x	18x	10x	1x
Membranes	2x	2x	2x	2x
GDLs	1.4x	4x	3x	1.3x

GDLs – gas diffusion layers

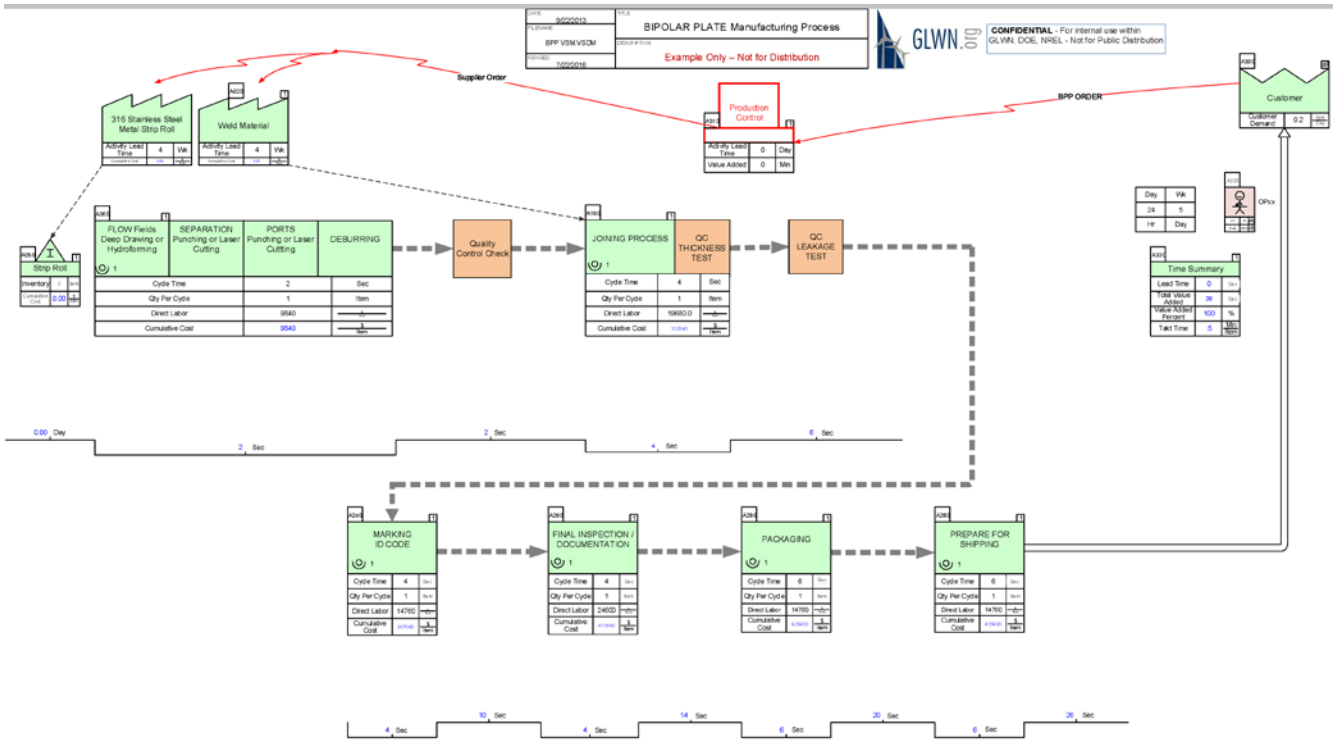

QC – quality control

FIGURE 2. Value stream map of the bipolar plate manufacturing process flow

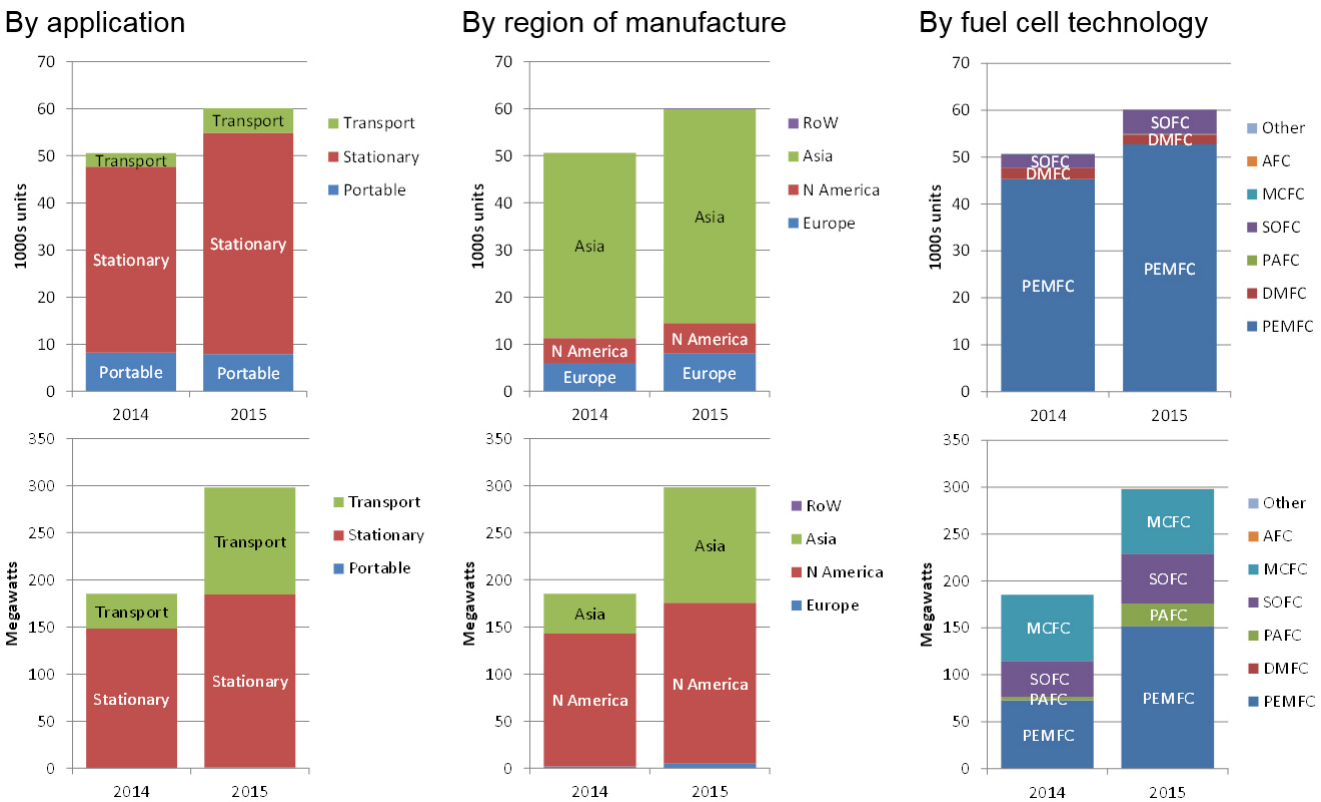

SOFC – solid oxide fuel cell; DMFC – direct methanol fuel cell; MCFC – molten carbonate fuel cell; PAFC – phosphoric acid fuel cell; AFC – alkaline fuel cell

FIGURE 3. E4tech 2015 market data of fuel cell systems shipped by MW and number of units.

manufacturing opportunities, three tipping points, three high value opportunities, three strengths for United States manufacturers; complete assessment of trade flows, supply and demand, global suppliers, government funding, capital available, country's development technology, and the United States' manufacturing advantage.

FY 2016 PUBLICATIONS/PRESENTATIONS

1. Patrick Fullenkamp, "U.S. Clean Energy Hydrogen and Fuel Cell Technologies: A Competitiveness Analysis" Presentation at HTAC, April 22, 2015.

2. Patrick Fullenkamp, "U.S. Clean Energy Hydrogen and Fuel Cell Technologies: A Competitiveness Analysis" Presentation at AMR, June 11, 2015.

3. Patrick Fullenkamp, "U.S. Clean Energy Hydrogen and Fuel Cell Technologies: A Competitiveness Analysis" Presentation at HFC Seminar, Los Angeles, November 17, 2015.

4. Patrick Fullenkamp, "U.S. Clean Energy Hydrogen and Fuel Cell Technologies: A Competitiveness Analysis" Presentation at WIRE-Net Board of Directors, December 2015.

REFERENCES

1. Pike Research Report, executive summary at http://www.navigantresearch.com/wp-content/uploads/2012/02/FCSC-12-Executive-Summary.pdf

VI.5 Continuous Fiber Composite Electrofusion Coupler

Brett Kimball
Automated Dynamics
2 Commerce Park Dr.
Niskayuna, NY 12211
Phone: (518) 377-6471 x239
Email: bkimball@automateddynamics.com

DOE Manager:
Nancy L. Garland
Phone: (202) 586-5673
Email: Nancy.Garland@ee.doe.gov

Contract Number: DE-EE0007274

Subcontractors:
- NOV Fiberglass Systems, Houston, TX
- Savanah River National Laboratory, Aiken, SC

Project Start Date: December 1, 2015
Project End Date: November 30, 2018

Overall Objectives

- Quantify
  - Various mechanical characteristics of coupler: burst strength, axial strength, leak rates, and fatigue characteristics.
  - Manufacturing costs of coupler.
- Optimize
  - Mechanical design of composite coupler: maximize strength characteristics while constraining costs.
- Demonstrate
  - Coupler without mechanical components, which would be subject to hydrogen embrittlement.
  - Manufacturability of a coupler that reduces cost and complexity of hydrogen pipeline installation.
  - Advanced electrofusion coupler meets mechanical requirements for pipeline designed to transport hydrogen at 225 bar.

Fiscal Year (FY) 2016 Objectives

- Quantify
  - Initial mechanical properties of coupler: burst strength, axial strength, and leak rates.
  - Heat and electrical requirements to electrofuse the coupler.
  - Design lengths for coupler based on mechanical requirements.
  - Manufacturing costs for the coupler.
- Optimize
  - Design of mechanical fit between various layers in the coupler, and the dimensions of the modified pipe ends. Decreasing tolerances bring potentially better design but also increased costs and reduced ease of manufacturing. This must be optimized.
- Demonstrate
  - Manufacturability of coupler with particular focus on fiber placing wire to form an electrofusion bond.

Technical Barriers

This project addresses the following technical barrier from the Hydrogen Delivery section of the Fuel Cell Technologies Office Multi-Year Research, Development, and Demonstration Plan.

(D) High As-Installed Cost of Pipelines

Contribution to Achievement of DOE Hydrogen Delivery Milestones

This project will contribute to achievement of the following DOE milestones from the Hydrogen Delivery section of the Fuel Cell Technologies Office Multi-Year Research, Development, and Demonstration Plan.

- Milestone 1.5: Coordinating with the H_2 Production and Storage sub-programs, identify optimized delivery pathways that meet a H_2 delivery and dispensing cost of <$2/gge for use in consumer vehicles. (4Q, 2020)
- Milestone 6.3: By 2020, reduce the cost of hydrogen delivery from the point of production to the point of use in consumer vehicles to <$2/gge of hydrogen for the gaseous delivery pathway. (4Q, 2020)

FY 2016 Accomplishments

- Refined and developed the design specification for the coupler including mechanical loading, environmental effects, and leak rates.
- Designed, manufactured, and tested electrofusion coupons with continuous fiber composite, establishing baseline bond strength expectations for adjacent coupler components.

- Designed, manufactured, and tested the wire placement process for use on this particular design of coupler. This is a baseline for future work.
- Completed an evaluation of appropriate adhesives for use in the coupler. Down-selected to top adhesive and short list of backup options.

✧ ✧ ✧ ✧ ✧

INTRODUCTION

Past pipe couplers employed steel components in sealing mechanisms that were subject to hydrogen embrittlement. This coupler will focus on nonmetallic solutions by way of electrofusion (heat via electrical current) of two adjacent cylindrical plastic surfaces. A backup solution is present, which uses mechanical couplings; however the steel would not be exposed to hydrogen. This will enable low maintenance costs of composite pipelines to hit hydrogen delivery price targets set in milestones above.

APPROACH

This research draws from existing electrofusion pipe coupling technology, but extends to be suitable for use on a variety of materials available for composite pipelines. Automated Dynamics' technology is well-suited to couple thermoplastic bonded pipes (where each of the pipe's radial adjacent layers are bonded to each other), by our fiber placement technology that bonds continuous media (fiber reinforced composite, plastic coated wire) on the fly without need for post-curing. Coupler designed in this project shall be available for such pipes, and for nonbonded pipes. Existing electrofusion couplers do not allow continuous fiber composite reinforcement necessary to achieve high pressures sought by the DOE. Our coupler will employ this continuous fiber thermoplastic composite as the structural layer for high pressures and high induced axial loads.

RESULTS

Results to date have centered on design of the coupler and preliminary lab-scale tests. Lab-scale tests have established electrofusion processes to be used on the coupler prototypes. Prototypes are being manufactured presently and will be tested in the third quarter of 2016.

CONCLUSIONS AND FUTURE DIRECTIONS

Initial results year to date (July 2016) indicate the technology is suitable to meet the goals of the DOE program and specific milestones above. The coupler requires a high degree of precision and the automated manufacturing processes established and refined over 30 years at Automated Dynamics have yielded such precise components. For example, the wire embedded in the coupler used for electrofusion must be manufactured at a very consistent and precise diameter to fit with adjacent components. Similarly, repeatability is achieved through automated fiber placement which allows the reliability required for the demanding specifications of a hydrogen delivery pipeline.

VI.6 In-line Quality Control of PEM Materials

Paul Yelvington (Primary Contact), Andrew Wagner, Philip Cox
Mainstream Engineering
200 Yellow Place
Rockledge, FL 32955
Phone: (321) 631-3550
Email: pyelvington@mainstream-engr.com

DOE Manager: Nancy L. Garland
Phone: (202) 586-5673
Email: Nancy.Garland@ee.doe.gov

Contract Number: DE-SC0013774

Subcontractor:
National Renewable Energy Laboratory (NREL), Golden, CO (Phase II)

Project Start Date: Phase I – June 8, 2015, Phase II – August 1, 2016
Project End Date: Phase I – March 7, 2016, Phase II – July 31, 2018

Overall Objectives

- Identify membrane defect size that leads to cell failure.
- Create a fully packaged prototype (TRL 7) automated vision system to perform quality control and demonstrate it on a full-speed membrane web line.
- Detect defects down to 4 µm at 100 ft/min.
- Determine membrane thickness to 0.5 µm resolution.
- Achieve a 5σ false-positive and false-negative rate.

Fiscal Year (FY) 2016 Objectives

- Develop membrane rejection criteria, standard samples, and image evaluation methods.
- Develop software and processing algorithms to automate membrane thickness and defect image analysis and identification.
- Fabricate and test a prototype system at roll-to-roll membrane coating line conditions up to 60 ft/min.
- Apply real time processing methods to an array of membranes types and thicknesses to determine the breadth of applicability of the analysis methodology.

Technical Barriers

This project addresses the following technical barriers from the Manufacturing R&D section of the Fuel Cell Technologies Office Multi-Year Research, Development, and Demonstration Plan.

(E) Lack of Improved Methods of Final Inspection of MEAs

(H) Low Levels of Quality Control

Contribution to Achievement of DOE Manufacturing R&D Milestones

This project will contribute to achievement of the following DOE milestones from the Manufacturing R&D section of the Fuel Cell Technologies Office Multi-Year Research, Development, and Demonstration Plan.

- Milestone 1.3: Develop continuous MEA manufacturing processes that increase throughput and efficiency and decrease complexity and waste. (4Q, 2017)
- Milestone 1.6: Develop fabrication and assembly processes for PEMFC MEA components leading to an automotive fuel cell stack that costs $20/kW. (4Q, 2020)
- Milestone 5.2: Demonstrate improved sensitivity, resolution, and/or detection rate for MEA inspection methods. (4Q, 2016)
- Milestone 5.4: Design and commercialize an in-line QC device for PEMFC MEA materials based on NREL's optical reflectance technology. (4Q, 2017)
- Milestone 5.6: Demonstrate methods to inspect full MEAs and cells for defects prior to assembly into stacks in a production environment. (4Q, 2018)
- Milestone 5.8: Implement demonstrated in-line QC techniques on pilot or production lines at PEMFC MEA material manufacturers. (4Q, 2020)

FY 2016 Accomplishments

- Mainstream's lab prototype optical system successfully identified the following defects in Nafion® membranes: a 25-µm diameter pinhole (smallest tested), a 10-µm wide scratch, and a 100-µm wide fold.
- The system was successfully demonstrated on NREL's continuous roll-to-roll web line with Nafion-211 detecting 40 out of 40 100 µm pinhole defects in real time up to 30 ft/min. With post processing, all defects were successfully identified at web line speeds up to 100 ft/min.

- Nafion membrane thickness was measured autonomously in real time to ±1 µm.
- Successfully combined an encoder that measured roll speed/position and a printer that marked defects at the locations identified with the real-time optical analysis.
- Demonstrated broad applicability of our approach to eleven unique membranes for a range of applications, including polymer electrolyte membrane fuel cells (PEMFCs), reverse osmosis, electrolysis, anion exchange membranes, and hydrocarbon membranes.

INTRODUCTION

Fuel cells stand on the cusp of commercialization for large scale applications such as zero pollution automotive systems. They are held back by high manufacturing costs and expensive catalysts. The membrane alone accounts for as much as 45% of the total material cost of a commercial fuel cell system at low volume [1]. Moreover, manufacturing defects in the membrane not only lead to wasted expensive materials, they also cause cell failures that can cascade into complete stack failure. This requires additional labor reworking the stack as well as the loss of expensive catalyst and gas diffusion electrode materials. Current inspection methods look for defects after batch production of the membrane leading to delayed correction of issues with the membrane and membrane electrode fabrication process. Reaching the quality targets for fuel cell system manufacturing requires a new, high efficiency real-time quality control system. Mainstream Engineering is developing a real-time optical quality control system that provides significant benefits with increased resolution, improved accuracy, and increased detection speeds for the examination of fuel cell and other membranes.

APPROACH

Mainstream's overall approach was to rigorously prove out the optical technique with a wide-range of commercially available membranes and select optimized hardware for Nafion, the primary initial target membrane. Ultraviolet–visible spectroscopy was used to demonstrate thickness measurement by absorbance and select the most applicable light source wavelengths and configuration. A wide range of typical defects were induced and examined in the Nafion membranes and characterized with Mainstream's sensor. Pinholes, scratches, and folds were selected for in-depth analysis in Phase I, and the limits of the hardware used to find these defects were identified. Software to perform automated image analysis for both defects and thickness was created and initially tested on a group of static membrane samples to validate the detection accuracy of the hardware and processing scheme. The prototype system was combined with a printer and encoder and demonstrated on NREL's web line at speeds up to 100 ft/min to validate the ability to identify and mark defects in a continuous process in real time.

RESULTS

Membrane Defect Types Evaluated by Mainstream's Prototype Quality Control System

The Phase I Small Business Innovation Research project evaluated three initial target defect types including pinholes, scratches, and folds (creases) that were identified as feasible from baseline ultraviolet–visible spectroscopy. A pinhole is defined as a small hole that penetrates completely through the membrane and is less than 1 mm in size, as shown in Figure 1. Pinholes commonly occur from mechanical damage to the membrane, the presence of bubbles in the coating that have subsequently burst, dirt or fibers that have been subsequently removed in the processing leaving a void, or dewetting spots in the membrane coating process. A scratch is a surface defect where part of the membrane has been eroded or removed, as shown in Figure 1. Scratches commonly occur due to mechanical damage in the coating line from the presence of dirt particles or rough surfaces on the rollers. A fold is a defect where the membrane has been creased or overlapped on itself causing surface as well as thickness abnormalities, as shown in Figure 1. Folds commonly occur due to issues in handling. Additional defects are possible in the membrane including bubbles, dirt or undissolved polymer particles and gels. These are easily detectable using our approach but were not present in significant and controlled numbers in the commercially available membrane samples used for validation of the process on the web line. In Phase II, Mainstream will obtain samples with controlled sizes of these defects for additional validation and optimization of our inspection equipment.

Demonstration on a Moving Roll-to-Roll Web Line

The Phase I prototype system was tested on NREL's 14-in wide web line with Nafion-211, the primary commercially

FIGURE 1. Membrane samples illustrating each of the main defect types including pinholes, scratches, and folds taken edge-lit with a compact camera

available membrane investigated (Figure 2). Forty 500 µm pinholes and forty 100 µm pinholes were induced randomly in the Nafion-211 membrane at a variety of locations across and down the membrane roll. The web line was run at speeds of 10, 30, 60, and 100 ft/min while the detector analyzed the membrane for the 80 induced defects. Figure 3 shows a time series of captured processed images taken during this experiment. The roll direction was to the left, while time progressed to the right. The defects were shown in white in the black analysis area and were outlined in red by the image processing software. Additionally, in the figure, a large colored circle was placed around the defect to further highlight the location. The time series continued through the next four images where the defects were moving with the roll to the left. The defects were highlighted before they entered the area of analysis and after they left to help track the passage of time through the images. They were detected in real time by the system as they passed through the black analysis area. The detector was able to find all the defects in real time up to 30 ft/min. At higher speeds, the computer processing speed and camera data transfer rate became an issue. When the video recorded by the detector was analyzed with post-processing, all defects could be detected up to the maximum speed of 100 ft/min. In the Phase II, the algorithm, processing speed, and camera hardware will be upgraded to allow the analysis in real time.

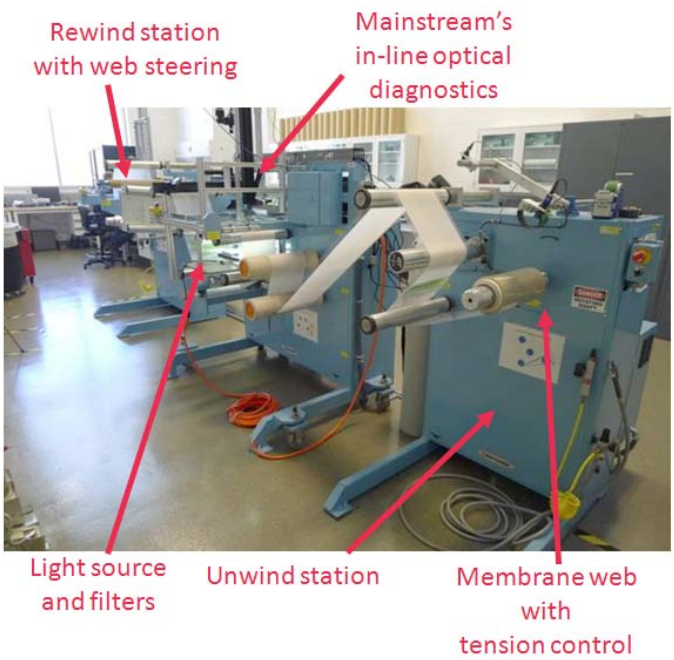

FIGURE 2. Mainstream's in-line quality control diagnostic system installed in the middle web transport zone of NREL's web line

Membrane Thickness Measurement

Membrane thickness was demonstrated with a sample of Nafion-115 processed to create areas of variable thickness as shown in Figure 4. The sample was nominally 132 µm and was processed to produce sample areas from 130 to 140-µm thickness across the sample surface. The thicknesses were mapped with a precision micrometer. The membrane was imaged with the sensor system, and the thickness was calculated from the optical image data. There was excellent agreement between Mainstream's optical method and the micrometer mapping with an error of ±1 µm, which is comparable to the micrometer error. Mainstream will perform additional optimization and automation of this method in Phase II, allowing the detection of membrane thin spots as well as membrane thickness with a variable membrane composition.

CONCLUSIONS AND FUTURE DIRECTIONS

Mainstream Engineering developed a low-cost real time optical detector for quality control using continuous analysis of membranes for PEMFC membrane electrode assemblies (MEAs). The inspection system samples, logs, and marks every location on the roll of material such that defects in MEA materials can be removed prior to assembly into complete cells. A prototype system was built and integrated into NREL's 14-in wide web line and successfully ran autonomously with real-time defect analysis. Mainstream's system was tested on NREL's web line with Nafion-211 and

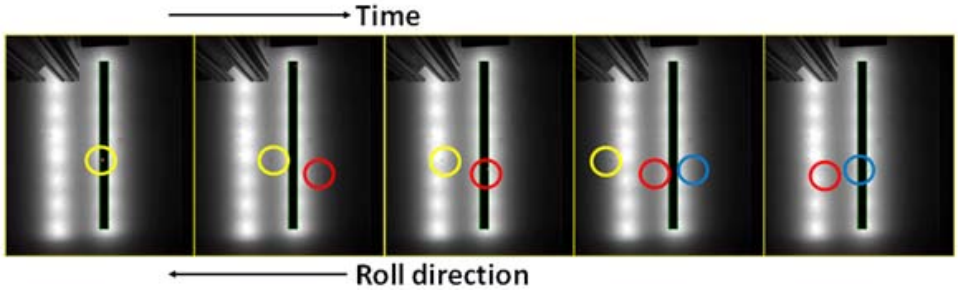

FIGURE 3. Stop frame time-series of images showing roll-to-roll defect detection in Nafion-211 where defects are detected as they pass through the central black band and colored circles indicate the defects as the roll progresses by the detector

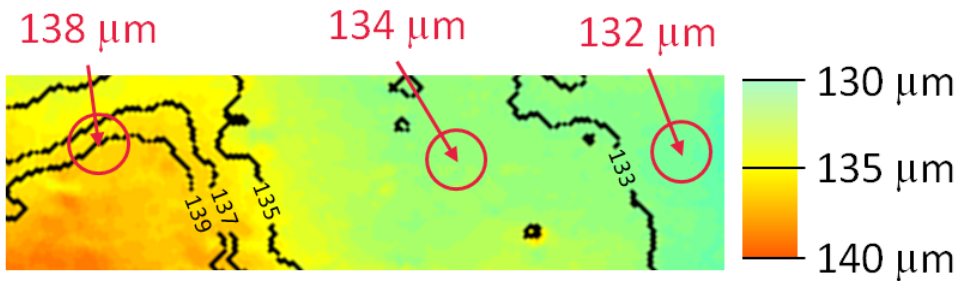

FIGURE 4. Colorized image of a Nafion-115 sample initially 132 µm that that has been processed to different thicknesses and measured by micrometer (highlighted in red on the image) as well as optically quantified (color scale on the right and contour lines on image)

able to find 40 out of 40 100 µm pinhole defects in real-time up to 30 ft/min. An encoder to independently measure roll-speed and printer to mark defects were successfully paired to the optical analysis system to mark defective membrane in real-time at speeds up to 30 ft/min.

The overall goal of the Phase II project is to research, develop, and commercialize an in-line quality control machine for roll-to-roll membrane manufacturing. The device will identify and mark defects as well as monitor membrane thickness in real-time to improve line efficiency and to reduce waste. For FY 2017, the main goals will be to produce defective membranes for use in determining defect size that leads to cell failure, design a prototype system for 24-in wide membrane, and assemble and test new components for enhanced resolution, including upgraded hardware and software.

SPECIAL RECOGNITIONS & AWARDS/ PATENTS ISSUED

1. Yelvington, P.E., and Wagner, A. 2016. "Apparatus and Method for Cross-polarized, Optical Detection of Polymer Film Thickness and Defects." U.S. Patent Application Serial No. 15/170,360.

FY 2016 PUBLICATIONS/PRESENTATIONS

1. Wagner, A., Cox, P., Yelvington, P.E., "In-line Quality Control of PEM Materials," poster, DOE 2016 Annual Merit Review, Washington, D.C., June 2016.

REFERENCES

1. Kleen, G.J., "Membrane Development in the U.S. DOE Fuel Cell Technologies Program," Fuel Cell Seminar and Exhibition, Orlando, FL, 2011.

VI.7 Manufacturing Competitiveness Analysis for Hydrogen Refueling Stations

Ahmad Mayyas (Primary Contact), Margaret Mann
National Renewable Energy Laboratory
15013 Denver West Parkway
Golden, CO 80401
Phone: (303) 384-7446
Email: Ahmad.Mayyas@nrel.gov

DOE Manager: Nancy L. Garland
Phone: (202) 586-5673
Email: Nancy.Garland@ee.doe.gov

Project Start Date: April, 6, 2015
Project End Date: December, 31, 2016

Overall Objectives

- Develop manufacturing cost models for major components in hydrogen refueling stations including compressors, storage system, dispenser, chiller and heat exchanger.
- Identify cost drivers associated with manufacturing hydrogen station parts and systems and highlight potential cost reduction opportunities through economies of scale and standardization.

Fiscal Year (FY) 2016 Objectives

- Develop analytical models to estimate capital costs for hydrogen refueling stations.
- Provide a platform for a manufacturing cost analysis for major hydrogen refueling station (HRS) systems and components.
- Identify cost drivers of hydrogen compressors which constitute approximately 40%–60% of the total HRS capital cost.
- Identify cost drivers of various storage tank technologies and configurations.
- Investigate the effect of learning experience on the chiller, heat exchanger, and dispenser costs.

Technical Barriers

This project addresses the following technical barriers from the Hydrogen Delivery section of the Fuel Cell Technologies Office Multi-Year Research, Development, and Demonstration Plan.

(A) Lack of Hydrogen/Carrier and Infrastructure Options Analysis

(B) Reliability and Costs of Gaseous Hydrogen Compression

(E) Gaseous Hydrogen Storage and Tube Trailer Delivery Costs

Contribution to Achievement of DOE Hydrogen Delivery Milestones

This project will contribute to achievement of the following DOE milestones from the Hydrogen Delivery section of the Fuel Cell Technologies Office Multi-Year Research, Development, and Demonstration Plan.

- Milestone 6.1: Define potential research, development, and demonstration activities for other long-term market fueling/terminal needs. (4Q 2015)
- Milestone 6.3: By 2020, reduce the cost of hydrogen delivery from the point of production to the point of use in consumer vehicles to less than $2/gge of hydrogen for the gaseous delivery pathway. (4Q 2020).

FY 2016 Accomplishments

In FY 2016 we have:

- Developed a regression analysis to estimate capital and installation costs for hydrogen stations in different regions in North America, Europe, and Asia.
- Developed manufacturing cost models for hydrogen piston compressors with different compression capacities.
- Developed manufacturing cost models for Type I hydrogen pressure vessels, dispensers, heat exchangers, and chillers.
- Developed a set of supply chain and international trade flows for installed hydrogen stations in the past 11 years (2005–2016).

✧ ✧ ✧ ✧ ✧

INTRODUCTION

This study has two main goals: (1) develop manufacturing competiveness analysis for hydrogen stations by evaluating manufacturing cost of principal components in the hydrogen stations in some countries in North America, Europe, and Asia; and (2) develop supply chain and

international trade flow maps to help decision makers visualize the primary trade flows in the international markets and to spot the main markets for hydrogen station components.

APPROACH

This study includes three major analyses: manufacturing competiveness, supply chain analysis, and an assessment of the effect of qualitative factors on selection of the factory locations for manufacturing hydrogen compressors and other parts in the hydrogen refueling stations.

Manufacturing competiveness analysis is used to evaluate relative manufacturing cost in selected countries in North America, Europe, and Asia, for the principal components in the hydrogen stations including compressors, storage vessels, chillers, heat exchangers, and dispensers. Supply chain analysis was conducted with the aid of trade flow maps which show main trade flows between international markets from country of production to the installation locations. This study also seeks to address major factors that play a role in selecting manufacturing locations in the United States and other countries and considers how these factors can act as measures of competitiveness in these countries. Examples of these qualitative factors include manufacturing experience, product quality, skilled labor requirements and availability, tax policy, and currency fluctuations.

RESULTS

Hydrogen Refueling Station Capital Cost

Knowing that the United States, Germany, Japan, and South Korea are the leading countries in terms of fuel cell vehicles and required hydrogen refueling infrastructure, we collected data to evaluate relative capital cost in these countries and to investigate the effect of governmental and safety regulations on the overall hydrogen station equipment and installation costs (Figure 1). We found that hydrogen station cost is increasing with the capacity of the station (expressed in dispensed kg H_2 per day) in all countries. In Japan, the relative cost of hydrogen stations doubled as a result of safety and standard regulations enacted due to seismic activity and recent earthquakes (Figure 1c).

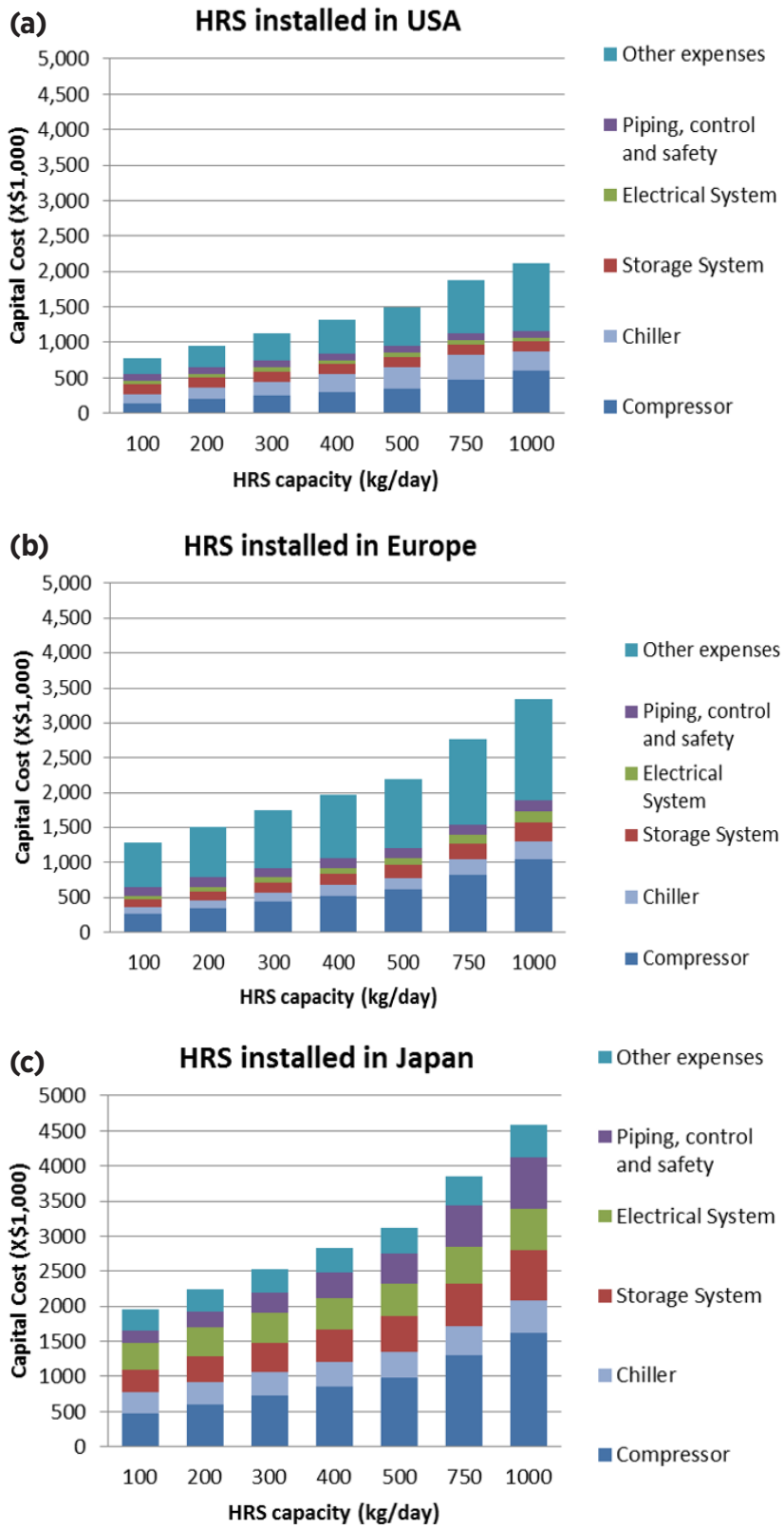

FIGURE 1. Capital and installation costs for HRS installed in: (a) United States; (b) Europe; and (c) Japan

Manufacturing Competitiveness Analysis

This analysis dives deeper into cost drivers associated with manufacturing of some systems and major parts in the hydrogen stations such as hydrogen compressors, Type I storage tanks, dispensers, chillers, and heat exchangers. Taking an example for piston compressors, manufacturing cost analysis starts with a process flow diagram, which shows a series of individual casting and hot forging steps, followed by cleaning and machining steps for individual components, and then assembly of these components into one structural unit to form the compressor housing and its internal parts (Figure 2a). After that, other components that make the balance of system such as the motor, control unit, valves, and sensors, can be added to get the final product. Once we get the direct manufacturing cost (Figure 2b) and balance of system cost with the required assembly cost, we can add a profit margin and shipping cost to estimate the minimum sustainable price (MSP) which is defined as the minimum price that sustains a manufacturer's business (Figure 2c). The MSP curve indicates potential cost reductions from producing more units in a manufacturing facility as direct results of better resource utilizations.

A comparative cost analysis using minimum sustainable prices was performed for piston compressors in some countries (Figure 3a). Figure 3b shows a comparison between Chinese- and United States-based manufacturing facilities. Both figures show that Chinese- and Mexican-based manufacturers have advantages of lower labor cost, lower building cost, lower materials cost, and lower energy cost (China only).

Supply Chain and Trade Flow Maps

This analysis is used as a qualitative measure to assess manufacturing competiveness in selected countries and investigate level of specialization in manufacturing certain components used in HRS.

CONCLUSIONS AND FUTURE DIRECTIONS

This project provides a set of manufacturing competitiveness and supply chain analyses that can help in understanding cost associated with manufacturing major components used in hydrogen stations. Bottom up cost analysis using design for manufacturing and assembly

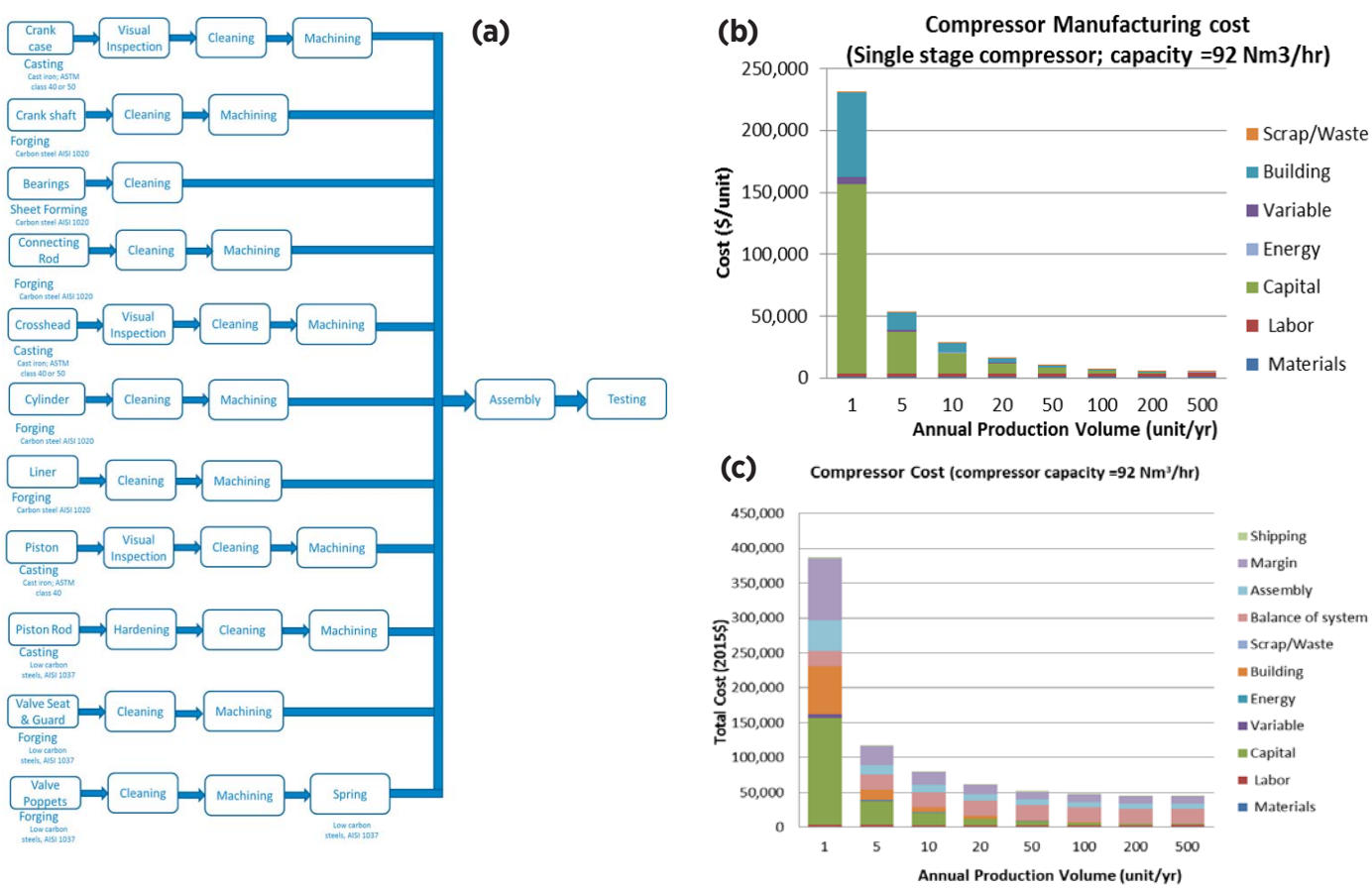

FIGURE 2. (a) Process flow diagram for making piston compressors; (b) direct manufacturing cost for compressor housing and internal parts as function of annual production rate (units/yr); (c) minimum sustainable price for piston compressors as function of annual production rate (units/yr)

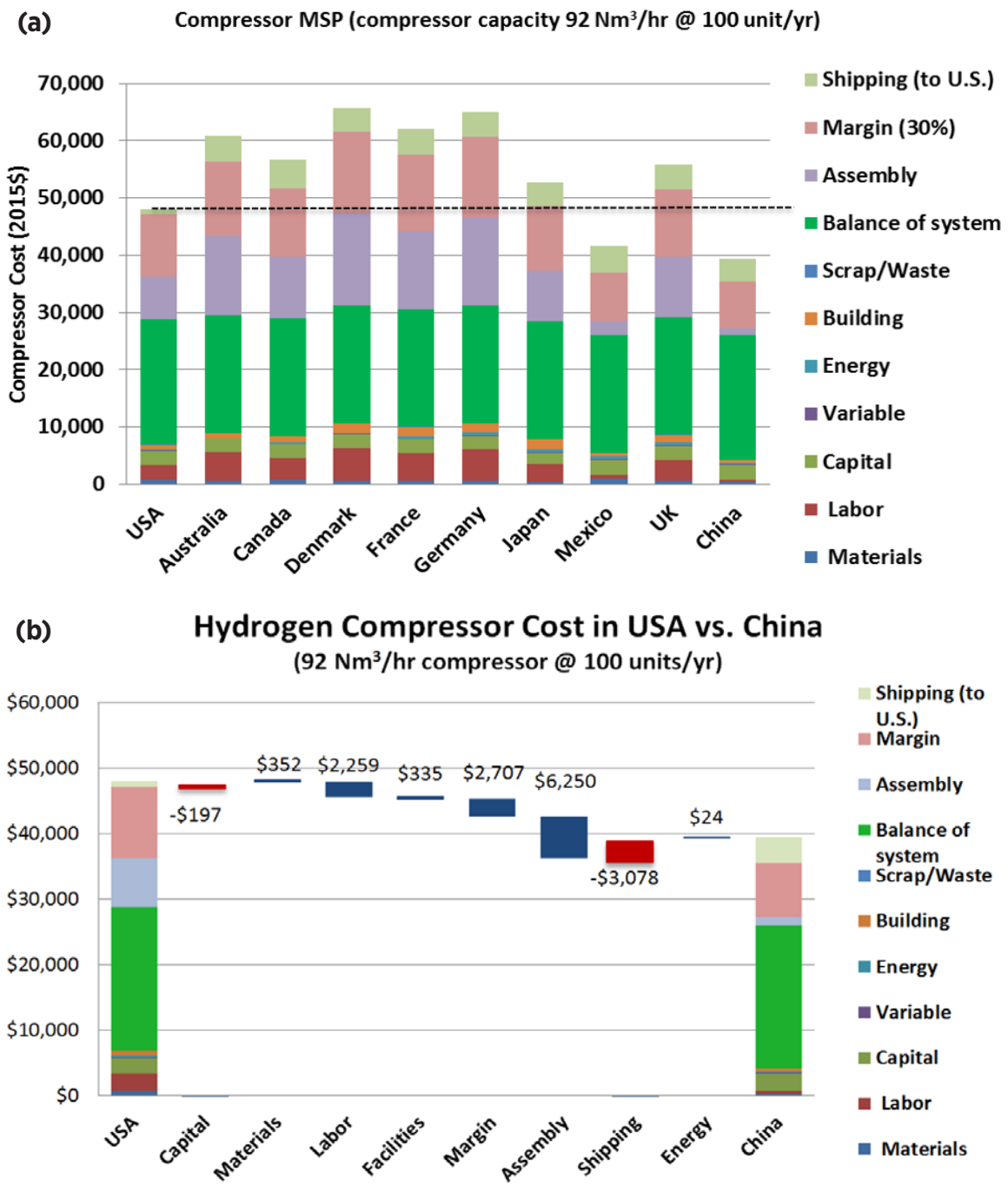

FIGURE 3. (a) Minimum sustainable prices for hydrogen piston compressors in some countries; (b) comparative cost analysis using MSP between United States- and Chinese-based manufacturers

methodology was used to develop a manufacturing cost model and was added to the balance of system and assembly costs to get equipment cost. This cost then was added to the profit margin and shipping cost to estimate MSP for several systems in the hydrogen station such as compressors, dispensers, storage vessels, chillers, and heat exchangers. Cost curves using MSP values for piston compressors indicate that cost reductions of 50% or more can be achieved if 100 units/yr are manufactured, relative to costs at production levels of 10 units/yr.

Based on international trade flow maps shown in Figure 4, we can say that that the United States and Germany, followed by Canada and Japan, are the leading countries in the number of manufactured hydrogen stations and number of installations.

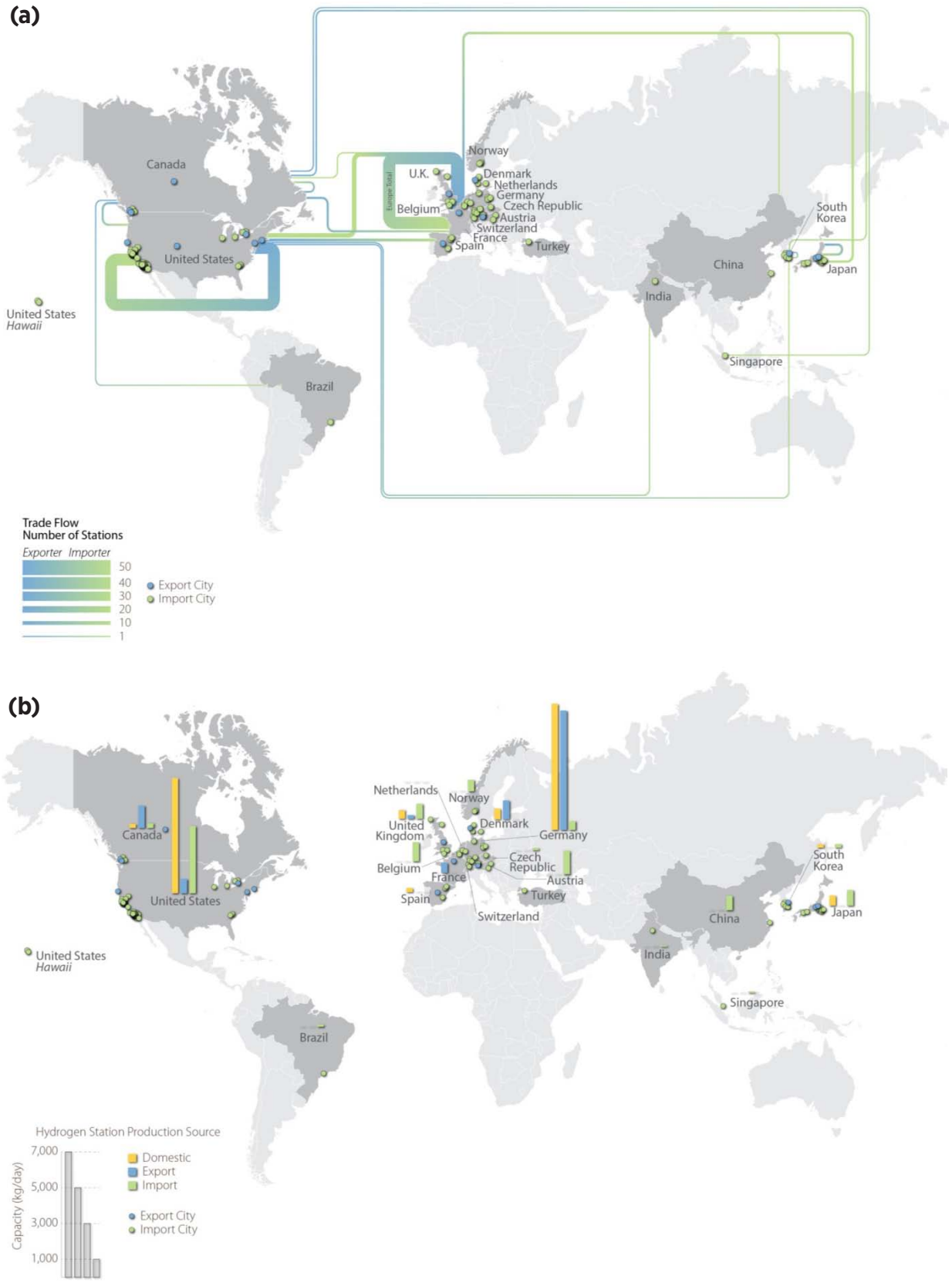

FIGURE 4. (a) International trade flows for hydrogen refueling stations; and (b) hydrogen refueling stations classified by countries of production and countries of installations

For FY 2017, manufacturing cost models and minimum sustainable price curves will be developed for other systems in hydrogen stations such as Type I storage tanks, dispensers, heat exchangers, and chillers. Then, the estimated MSP values will be summed to estimate the capital cost of HRS in different regions, followed by an analysis of the effect of cost reductions on hydrogen prices.

FY 2016 PUBLICATIONS/PRESENTATIONS

1. Ahmad Mayyas, "Clean Energy Manufacturing Analysis Center: A Case Study of the Fuel Cell Manufacturing Supply Chain Analysis." Fuel Cell Seminar and Energy Exposition. November 19, 2015, Los Angeles, CA.

2. Ahmad Mayyas, "Manufacturing Competitiveness Analysis for Hydrogen Refueling Stations." Presentation at the Annual Merit Review, June 8, 2016. Washington, DC.

3. Ahmad Mayyas, "Analysis of Current and Future Technologies for Hydrogen Refueling Stations From Manufacturing Competitiveness and Supply Chain Perspectives." Advanced Automotive Batteries Conference, June 17, 2016. Detroit, MI.

VII.0 Technology Validation Program Overview

INTRODUCTION

The Technology Validation program demonstrates, tests, and validates hydrogen and fuel cell technologies and uses the results to provide feedback to the Fuel Cell Technologies Office's research and development (R&D) activities. Continuing efforts include real-world evaluation and data collection associated with fuel cells operating in transportation applications (e.g., light-duty vehicles, medium- and heavy-duty trucks, and buses) and with hydrogen stations. The program is also implementing projects that support the advancement of hydrogen infrastructure by developing and validating a prototype device to measure hydrogen dispenser performance; validating infrastructure components; implementing and validating advanced hydrogen storage, delivery, and dispensing technologies; and creating tools to enhance access to hydrogen station status information. Activities of the program have expanded into examining hydrogen-based energy storage, where electrolyzers may be used as a controllable electrical load that can provide real-time grid services.

GOAL

The goal of the Technology Validation program is to validate the state-of-the-art of fuel cell systems in transportation and stationary applications, as well as hydrogen production, delivery, and storage systems, and assess technology status and progress to determine when technologies should be moved to the market transformation phase.

OBJECTIVES

The objectives of the Technology Validation program are to:

- Validate a hydrogen fueling station capable of producing and dispensing 200 kg hydrogen/day (at 5 kg/3 min; 700 bar) to fuel cell electric vehicles (FCEVs) by 2019.
- Validate large-scale systems for grid energy storage that integrate renewable hydrogen generation and storage by operating for more than 10,000 hours with an electrolysis system efficiency of 60% lower heating value by 2021.
- Validate hydrogen FCEVs with 65% lower heating value fuel cell system efficiency and 5,000 hours fuel cell durability by 2023.

FISCAL YEAR (FY) 2016 TECHNOLOGY STATUS AND ACCOMPLISHMENTS

Vehicles

Fuel Cell Electric Vehicle Evaluation

Over the last 10 years, National Renewable Energy Laboratory (NREL) has completed analysis of more than 220 on-road vehicles, which have accumulated more than 6.4 million miles. The current data analyzed come from 55 vehicles and six original equipment manufacturers, with model years spanning 2006 to 2012. Fuel cell durability has steadily and significantly improved over the last decade, and on-road fuel economy and actual driving range between fills have also increased over the last 10 years. Current analyses performed include driving behavior, fueling behavior, fuel economy, emissions, range, and reliability. While the 55 vehicles analyzed do not represent all FCEVs on the road today, it is a statistically significant set of data for evaluation with 3,052,000 total miles traveled and 101,400 total fuel cell operation hours from on-road trips analyzed since 2014. The maximum vehicle miles traveled is 190,300 miles (approximately 10% of vehicles have passed 100,000 miles), and the maximum fuel cell operation hours is 5,605. NREL also assessed the carbon dioxide (CO_2) and greenhouse gas emissions of FCEVs versus two baseline vehicles (passenger car and light-duty truck) and found that, on average, FCEV greenhouse gas emissions are 23% lower than that of a baseline gasoline passenger vehicle when using gaseous hydrogen produced from natural gas at a central steam methane reforming plant (without carbon sequestration), and 95% lower when using a 100% renewable hydrogen production pathway. (NREL)

Fuel Cell Electric Bus (FCEB) Evaluation

Fuel cell propulsion systems in buses have continued to show progress in increasing the durability and reliability of FCEBs and the primary components, and current technology meets the ultimate reliability target for road call frequency of both the overall bus and fuel cell system (Table 1). During FY 2016, NREL collected and analyzed data on 17 FCEB demonstrations at two transit agencies in the United States and Canada. Eleven fuel cell power plants with operation hours in excess of 12,000 hours were documented, and one of these systems has logged more than 22,600 hours in service, while three additional systems have surpassed 16,000 hours each. Based on in-service fuel economy of 6.8 miles per diesel gallon equivalent, the hybrid FCEBs currently in service can achieve a range of approximately 270 miles per fill. Moreover, the fuel economy of FCEBs was found to be 1.6 to 2.1 times higher than that of diesel and compressed natural gas buses (operating under the same conditions), respectively. Reliability has shown a marked increase over time, reaching the ultimate targets for both bus miles between road call and fuel cell system miles between road call, and fuel cell-related issues made up only 15% of the road calls during the period. (NREL)

TABLE 1. Progress in Meeting FCEB Targets

	Fleet Min	Fleet Max	Fleet Average	2016 Target	Ultimate Target	Target Met
Bus lifetime (years)	0.7	5.4	3.9	12	12	
Bus lifetime (miles)	8,351	131,203	91,381	500,000	500,000	
Powerplant lifetime[1] (hours)	2,013	22,203	11,462	18,000	25,000	2016
Bus availability (%)	40	92	73	85	90	
Roadcall frequency[2] (bus)	4,374	4,513	4,492	3,500	4,000	Ultimate
Roadcall frequency (fuel cell system)	19,085	23,261	22,532	15,000	20,000	Ultimate
Maintenance cost ($/mi)	0.53	2.06	1.61	0.75	0.40	
Fuel economy (mpDGE)	5.81	7.48	6.85	8	8	
Range (miles)[3]	221	345	271	300	300	

mpDGE – miles per diesel gallon equivalent
[1] Fuel cell hours accumulated to date from newest fuel cell power plant to oldest fuel cell power plant. Does not indicate end of life.
[2] Miles between road call: average for current designs.
[3] Estimated range based on fuel economy and 95% tank capacity. Transit agencies report lower real-world range.

Fuel Cell Electric Truck Component Sizing

This study examined the suitability of converting a representative sample of medium- and heavy-duty diesel trucks into fuel cell electric trucks, while ensuring similar truck performance in terms of range, payload, acceleration, speed, gradeability, and energy consumption. Models for 12 medium- and heavy-duty vehicles from various classes and vocations were developed. The component power requirement for fuel cell, battery, and electric machine to be used in these applications, and the onboard hydrogen storage requirement, were estimated. While cost will be addressed in the future, the analysis demonstrated that there are no major technological hurdles to meeting the performance and range requirements for trucks with hydrogen and fuel cell systems. (Argonne National Laboratory)

Fuel Cell Hybrid Electric Delivery Van Development and Deployment

This project developed and demonstrated a hydrogen fuel cell hybrid electric van that provides fleet operators with a zero-emission vehicle capable of meeting route range requirements while matching the performance characteristics of existing fleet vehicles. The vehicle will be validated through in-service deployment in a California United Parcel Service (UPS) fleet. Modeling activity and a component trade study performed during Phase 1 of the project showed that a 32 kW fuel cell module, 49 kWh battery energy storage, and 10–15 kg of hydrogen are required to meet the 125-mile driving range objective on actual UPS delivery routes. The proposed propulsion system configuration will allow the van to outperform existing battery–electric vans in UPS's fleet, with double the battery–electric mile range. (Center for Transportation and the Environment)

Hydrogen Fueling Stations

Hydrogen Station Data Collection and Analysis

In this evaluation period, data from state-of-the-art hydrogen fueling facilities that receive funding through DOE awards, California Energy Commission awards, and other sources were collected and analyzed by NREL. Working with codes and standards stakeholders and fueling facility owners–operators, NREL benchmarked performance of the fueling events relative to current SAE procedures. For fills greater than 1 kg with pre-cooling at -40°C, the average fueling rate was 0.87 kg/min, time to fill was 3.7 min, and the average amount dispensed was 2.8 kg. Hydrogen compressors were found to be the primary items needing maintenance both in terms of number of events and in terms of hours. Dispenser maintenance, entire system inspections, safety items (e.g., false alarms and sensors), and storage were found to have the next highest number of maintenance events for hydrogen stations. (NREL)

Performance Evaluation of Delivered Hydrogen Fueling Stations

This project aimed to integrate data collection systems at five 100 kg/d delivered liquid hydrogen fueling stations located in California for a 24-month performance period and to provide useful data to accurately benchmark and characterize station capacity, utilization, maintenance, and safety. Data on monthly dispensed hydrogen, energy used in compression and precooling of the hydrogen, maintenance and safety logs, and hydrogen quality control results were collected from operational sites (San Juan Capistrano and West Sacramento stations). A root cause failure analysis was completed, and a permanent solution was found for a data logger error that was caused by network issues. The solution has allowed for continuous data collection. All of the equipment required for data collection was ordered and assembled for installation at a third station, Bishop Ranch, which began construction on June 20, 2016. (Gas Technology Institute and Linde)

Brentwood (Washington, D.C.) Hydrogen Station Case Study

A modular hydrogen fueling advanced technology demonstration station was successfully sited, constructed, installed, and permitted in Washington, D.C., at the National Park Service Brentwood facility (Figure 1). This enabled the world's first commercially available fuel cell vehicles to become part of the DOE and National Park Service fleets (through no-cost loans). The goal of this project was to capture the lessons learned from the siting, construction, installation, and permitting process of a hydrogen station and to publish a report to document those findings, which can inform future station implementation. Some major takeaways include the following: conduct an initial environmental audit, improve coordination between multiple authorities having jurisdiction, and investigate the site for previous safety issues or limited documentation. Overall, the study provided valuable lessons learned that can be used to improve the process for creating hydrogen fueling stations. Hydrogen station data will also be collected as part of this effort. (NREL)

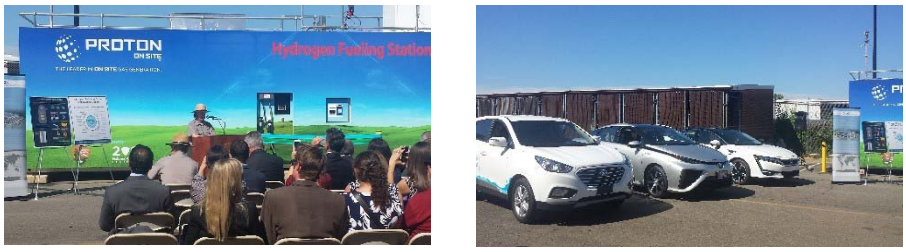

FIGURE 1. Brentwood hydrogen station opening (July 11, 2016)

Hydrogen Infrastructure Support

Hydrogen Component Validation

The goal of this project is to address the challenges associated with fuel contamination, reliability, and energy consumption related to major station components. Sample kits were provided to nine hydrogen stations to collect contaminants from failed parts. Results showed shards of metal and elastomer material likely from tubing and failed seals, along with the buildup of lubricant. Through data collected at both the NREL test facility and nine stations in

industry, this project showed that the hydrogen compressors and dispensers are large contributors to downtime and system maintenance. Future work will utilize detailed maintenance and performance logs to investigate the power and energy consumption of different station components from NREL's hydrogen station, the Hydrogen Infrastructure Testing and Research Facility. (NREL)

Hydrogen Station Equipment Performance (HyStEP) Device

Currently, each automotive manufacture independently tests the performance of a hydrogen station for use with their vehicles, and this leads to a long commissioning process before opening the station for business. The HyStEP device (Figure 2) was developed to accelerate commercial hydrogen station acceptance and commissioning by measuring hydrogen dispenser performance against SAE J2601 protocols. The device has been used at three stations including at NREL, California State University, Los Angeles, and South Coast Air Quality Management District, along with a training session at the Santa Barbara fueling station. It provided consistent, reliable performance tests for over 45 fills, including leak checks, sensor and instrument checks, Infrared Data Association communications checks, and original equipment manufacturer test fills. The California Air Resources Board is leading the deployment of the HyStEP device for commissioning hydrogen stations in California. (Sandia National Laboratories)

FIGURE 2. HyStEP device

Advanced Hydrogen Tube Trailers

In order to reduce the compression needs at hydrogen fueling stations, this project aims to design, procure, construct, and demonstrate a U.S. Department of Transportation approved composite tube trailer capable of 8,500 psi delivery pressure. The project is still in the early stages, but a cost model has been developed, and the team has begun work. Experience is being leveraged from existing 7,500 psi trailers that are in operation in California and Europe for the distribution of hydrogen. (Air Products)

Cryogenic Vessels and High-Pressure Liquid Hydrogen Pump

Larger quantities of hydrogen are often transported as a liquid because of its high density. The density of liquid hydrogen has advantages during bulk transport and when storing hydrogen at the forecourt station when there is enough demand at the hydrogen station to mitigate the cost of liquefaction and avoid boil-off. If liquid hydrogen becomes available at the stations, then high-density liquid hydrogen can also be leveraged in vehicles. The objectives of this project are to demonstrate high volumetric and gravimetric (50 g hydrogen/L and 9% hydrogen weight fraction) hydrogen storage performance of cryogenic pressure vessels while achieving durability of 1,500 cycles. The performance of the liquid hydrogen pump will be measured after reaching 6,000 fueling events. In FY 2016, the cryogenic hydrogen test facility was built and commissioned, and seven total pressure vessel designs were tested for durability. After falling short on the durability tests for developed pressure vessels, the project is focusing on testing tanks provided by BMW in conjunction with hydrogen pump performance testing. The Technology Validation program is coordinating with the Hydrogen Delivery and Hydrogen Storage programs on this project. (Lawrence Livermore National Laboratory)

Hydrogen Meter Benchmark Testing

Accurate measurement of dispensed fuel is necessary for commercial sale of hydrogen to ensure fair transactions between the fuel provider and customer. At NREL, three different commercial meters are being tested to determine the performance accuracy according to the gravimetric flow standard. A test stand was constructed to allow for testing of J2601 protocols for two Coriolis and one turbine flow meter. The test results will show whether the commercially available meters are able to meet the ±1.5% accuracy required during dispensing according to National Institute of Standards and Technology standards. (NREL)

Station Operational Status System (SOSS)

In the initial stages of station deployment, limitations in geographical coverage, station reliability, and station capacity, as well as station and component supply chain and technical support, can lead to customers arriving at a station which is unavailable for fueling. To mitigate this early-stage problem, the SOSS is designed to consistently and reliably report the status of current hydrogen fueling stations to customers through a client app for their phone or vehicle dashboard electronics. Customers can see which stations are operational, and they can be directed to the closest available hydrogen fueling station to ensure they can refuel with convenience. During FY 2016, sorting capabilities were added, and more information about the stations is now available to users. Another 20 open retail stations have been added to the existing seven for a total of 27 stations that are currently participating in SOSS. The team will continue to add new stations as they come online and improve the functionality for users. (California Fuel Cell Partnership)

Hydrogen Energy Storage/Grid Integration

As renewable energy sources penetrate the electric grid at a larger scale, the variability in the supply of this power has a greater impact on the stability of the overall power supplied to the grid. Electrolyzers can quickly ramp up and ramp down their demand to help balance the grid while utilizing extra hydrogen energy storage to ensure hydrogen energy demand is met for vehicles and other applications. This project aims to validate the benefits of hydrogen electrolyzers to the electricity grid and characterize the potential and highest economic value that they can provide. Utilizing real-time digital simulators at Idaho National Laboratory and a 120 kW electrolyzer stack as power hardware in the loop at NREL, 200 hours of operation were demonstrated and provided valuable performance data. A utility-scale network based on the Pacific Gas and Electric distribution network has been created in real-time digital simulators in order to accommodate future hydrogen refueling stations in the Bay Area. Future work will study the potential deployment of fueling stations and establish the multiple value streams for the stations. (Idaho National Laboratory)

BUDGET

The Technology Validation program's funding portfolio (Figure 3) will enable it to continue to collect and analyze data from fuel cells operating in transportation applications (e.g., light-duty vehicles, medium- and heavy-duty trucks, and buses), hydrogen infrastructure activities (e.g., fueling stations, components, and tools), and grid integration/hydrogen energy storage activities. The FY 2016 appropriation was $7 million. The FY 2017 request of $7 million is subject to congressional appropriations.

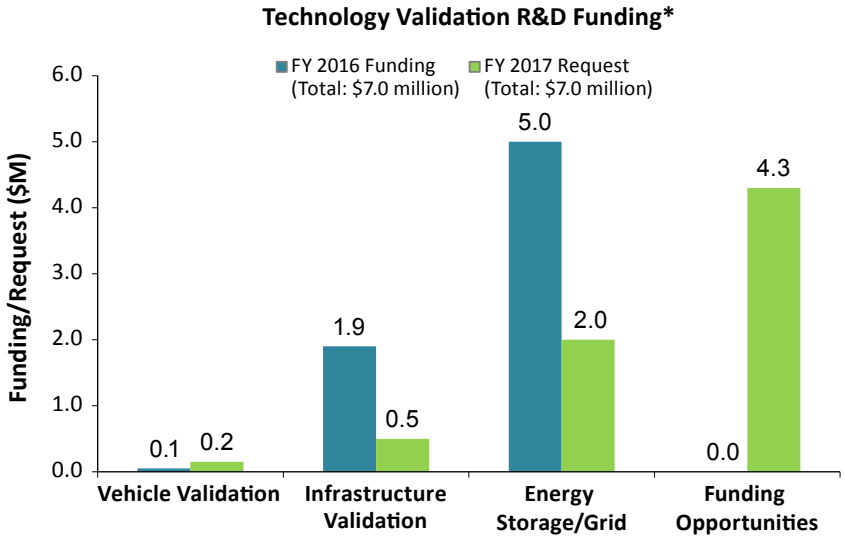

*Subject to appropriations, project go/no-go decisions, and competitive selections. Exact amounts will be determined based on research and development progress in each area and the relative merit and applicability of projects competitively selected through planned funding opportunity announcements.

FIGURE 3. FY 2016 appropriations and FY 2017 budget request for the Technology Validation program

FY 2017 PLANS

In FY 2017, the Technology Validation program will continue its detailed evaluations of FCEVs, FCEBs, hydrogen fueling stations, advanced hydrogen refueling components, and infrastructure support activities. Potential future funding opportunities may emphasize hydrogen refueling station and components validation, subject to appropriations. The fuel cell hybrid electric delivery van being developed by Center for Transportation and the Environment will be fully built and validated in real-world conditions through demonstration in the UPS fleet, and its performance data will be collected and evaluated. A stakeholder workshop is planned to help develop targets for medium- and heavy-duty fuel cell trucks.

In coordination with the U.S. Department of Energy's Office of Energy Efficiency and Renewable Energy and Office of Electricity, a key focus in FY 2017 will be hydrogen-based energy storage and grid integration activities. A related workshop is planned to gain industry feedback. Support will also continue for four projects within the Grid Modernization cross-cutting effort. Two of these projects are foundational—Lawrence Berkeley National Laboratory is developing a siting and optimization tool for distributed energy resources, while Idaho National Laboratory is implementing smart technology solutions to enhance the reliability of the Idaho Falls Power distribution network. The other two projects relate more specifically to the Fuel Cell Technologies Office— Lawrence Berkeley National Laboratory is developing a tool to quantify and optimize interactions between hydrogen stations, vehicles, and the grid; NREL is developing optimal dispatch and control strategies to improve the management of fuel cell-integrated building systems.

Another area of coordination will be the Hydrogen at Scale effort, which seeks to enable deep decarbonization of industrial, transportation, and power generation sectors through wide-scale deployment of hydrogen. The Technology Validation program will coordinate with several other programs in this effort, including Hydrogen Delivery, Systems Analysis, and Market Transformation.

Jason Marcinkoski
Technology Validation Team Lead
Fuel Cell Technologies Office
Office of Energy Efficiency and Renewable Energy
U.S. Department of Energy
1000 Independence Ave., SW
Washington, DC 20585-0121
Phone: (202) 586-7466
Email: Jason.Marcinkoski@ee.doe.gov

VII.A.1 Fuel Cell Electric Vehicle Evaluation

Jennifer Kurtz (Primary Contact), Sam Sprik, Chris Ainscough, and Genevieve Saur
National Renewable Energy Laboratory (NREL)
15013 Denver West Parkway
Golden, CO 80401-3305
Phone: (303) 275-4061
Email: Jennifer.Kurtz@nrel.gov

DOE Manager: Jason Marcinkoski
Phone: (202) 586-7466
Email: Jason.Marcinkoski@ee.doe.gov

Project Start Date: October 1, 2012
Project End Date: Project continuation and direction determined annually by DOE

Overall Objectives

- Validate hydrogen fuel cell electric vehicles (FCEVs) in a real-world setting.
- Identify current status and evolution of the technology.

Fiscal Year (FY) 2016 Objectives

- Provide a status of FCEV durability compared with the DOE 2020 durability target.
- Analyze real-world fuel economy and range.
- Make results available through online publications, highlights, and presentations.
- Complete two publication cycles (Fall 2015 and Spring 2016).

Technical Barriers

This project addresses the following technical barriers from the Technology Validation section of the Fuel Cell Technologies Office Multi-Year Research, Development, and Demonstration Plan.

(A) Lack of Fuel Cell Electric Vehicle and Fuel Cell Bus Performance and Durability Data

Contribution to Achievement of DOE Technology Validation Milestones

This project contributes to the achievement of the following DOE milestone from the Technology Validation section of the Fuel Cell Technologies Office Multi-Year Research, Development, and Demonstration Plan.

- Milestone 2.3: Validate fuel cell electric vehicles achieving 5,000-hour durability (service life of vehicle) and a driving range of 300 miles between fuelings. (4Q, 2019)

FY 2016 Accomplishments

- Completed two publication cycles of real-world FCEV operation data. The data analyzed have come from 55 vehicles, with model years spanning 2006 to 2012.
- Published new analyses for driving behavior, fueling behavior, fuel economy, emissions, range, and reliability.
- While the 55 vehicles analyzed do not represent all FCEVs on the road today, it is a statistically significant set of data for evaluation with 3,052,000 total miles traveled and 101,400 total fuel cell operation hours. The maximum vehicle odometer is 190,300 miles (approximately 10% of vehicles have passed 100,000 miles), and the maximum hours of fuel cell operation is 5,605.
- Compared current FCEV performance with past data from the Learning Demonstration (LD) phases. The comparisons to the LD project have provided insight into the steady progress made over the last eight years, specifically in fuel cell voltage durability, fuel economy, range, and driving trends. The current values are summarized in Table 1.

✧ ✧ ✧ ✧ ✧

INTRODUCTION

Under FOA-625, the U.S. DOE has funded projects for the collection and delivery of FCEV data to NREL for analysis, aggregation, and reporting. Multiple real-world sites and customers are included in this FCEV demonstration project. This activity addresses the lack of on-road FCEV data and seeks to validate improved performance and longer durability from comprehensive sets of early FCEVs, including first-production vehicles. NREL's objective in this project is to support DOE in the technical validation of hydrogen FCEVs under real-world conditions. This is accomplished through evaluating and analyzing data from the FCEVs to identify the current status of the technology, comparing that status to DOE program targets, and assisting in evaluating progress between multiple generations of technology, some of which will include commercial FCEVs for the first time.

TABLE 1. Current Status against DOE 2020 Targets

Vehicle Performance Metrics	DOE Target (Year 2020)[a]	LD3[b]	LD2+[c]	LD2[c]	LD1[c]
Durability					
Max fuel cell durability projection (hours)	5,000	4,130	—	2,521	1,807
Average fuel cell durability projection (hours)		2,149	1,748	1,062	821
Max fuel cell operation (hours)		5,605	1,582	1,261	2,375
Efficiency					
Adjusted dyno range (miles) (window sticker)		200–320	—	196–254	103–190
Median on-road distance between fuelings (miles)		123 miles	98	81	56
Fuel economy (mi/kg) (window sticker)		51 (median)	—	43–58	42–57
Fuel cell efficiency at ¼ power	60%	57% (average)	—	53%–59% (max)	51%–58%
Fuel cell efficiency at full power		43% (average)	—	42%–53%	30%–54%
Specs					
Specific power (W/kg)	650	240–563	—	306–406	183–323
Power density (W/L)	850	278–619	—	300–400	300–400
Storage					
System gravimetric capacity (kg H_2/kg system)	5.5%	2.5%–3.7%	—	—	2.5%–4.4%
System volumetric capacity (kg H_2/L system)	0.04	0.018–0.054	—	—	0.017–0.025

[a] Fuel Cell Technologies Office Multi-Year Research, Development, and Demonstration Plan [1]
[b] Current results are available online [3] (updated May 2016)
[c] National Fuel Cell Vehicle Learning Demonstration Final Report [2]

The project includes six original equipment manufacturers (OEMs): General Motors, Mercedes-Benz, Hyundai, Nissan, Toyota, and Honda. The latter three OEMs were part of one DOE project with Electricore. Up to 90 vehicles are expected to supply data over potentially two phases, with particular attention on fuel cell stack durability and efficiency, vehicle range and fuel economy, driving behavior, maintenance, on-board storage, refueling, and safety. Previous technology validation work on FCEVs and hydrogen infrastructure was performed through the FCEV LD [2], also known as the Controlled Hydrogen Fleet and Infrastructure Demonstration and Validation Project. Some of the current partners were also part of the LD. Those vehicles and technologies are not necessarily the same as the vehicles currently under evaluation even though some of the platforms are the same. Except where referenced or labeled, all of the data reported here are for the current project.

APPROACH

The project's data collection plan builds on other technology validation activities. Operation, maintenance, and safety data for fuel cell system(s) and accompanying infrastructure are collected on site by project partners. NREL receives the data quarterly and stores, processes, and analyzes the data in NREL's National Fuel Cell Technology Evaluation Center (NFCTEC). The NFCTEC is an off-network room with access provided to a small set of approved users. An internal analysis of all available data is completed quarterly and a set of technical composite data products (CDPs) is published every six months. Publications are uploaded to NREL's technology validation website [3] and presented at industry-relevant conferences. The CDPs present aggregated data across multiple systems, sites, and teams in order to protect proprietary data and summarize the performance of hundreds of fuel cell systems and thousands of data records. A review cycle is completed before the CDPs are published. This review cycle includes providing detailed data products of individual system- and site-performance results to the specific data provider. Detailed data products also identify the individual contribution to the CDPs. The NREL Fleet Analysis Toolkit is an internally developed tool for data processing and analysis structured for flexibility, growth, and simple addition of new applications. Analyses are created for general performance studies as well as application- or technology-specific studies.

RESULTS

The current FCEV evaluation analyses include the following categories: durability, deployment (e.g., number of vehicles included), system specifications, range, fuel economy, efficiency, fill performance, reliability, drive and fill behaviors, power and energy management, fuel cell transients (e.g., frequency of rapid increases or decreases in fuel cell power), emissions, and benchmarking against

technical targets and typical gasoline vehicle operation. All of the public results are available on NREL's technology validation website [3].

The current evaluation includes 55 vehicles with more than three million miles traveled and more than 101,000 fuel cell operation hours. As of December 2015, 24 vehicles were retired. Many of the OEMs are retiring legacy vehicles because commercial product vehicles are on the road or are soon to be on the road. The durability target for fuel cell systems is 5,000 hours (equivalent to 150,000 miles), which is on par with light-duty vehicle customer expectations and conventional technologies. Two parameters used in this evaluation project to track and validate system durability are projected operation time to 10% voltage degradation and actual operation hours. Fuel cell durability results were initially published in 2006 (the first generation of the LD project). The voltage durability trend from four unique reporting periods is shown in Figure 1. FCEVs in a fleet and a reporting period are of the same generation and design. The operation time to 10% voltage degradation for each stack in a fleet is averaged to determine the fleet voltage degradation value. The average of the fleets' average operation time to 10% voltage degradation in a reporting period is shown in light green and has increased 162% since the first LD period. The maximum of the fleets' average operation time to 10% voltage degradation, 4,130 hours, has increased 129% since the first reporting period in 2006–2007. More than 60% of analyzed stacks have not yet operated beyond the 10% voltage degradation metric.

In a newly released CDP, NFCTEC has evaluated the carbon dioxide (CO_2) and greenhouse gas (GHG [includes CO_2 and the CO_2-equivalent global warming potential of methane, nitrous oxide, volatile organic carbon VOC, carbon monoxide, nitrogen oxides, black carbon, and organic carbon]) emissions of FCEVs versus two baseline vehicles (passenger car and light-duty truck) using the GREET Fuel Cycle Model [4]. Five hydrogen production pathways are evaluated using validated FCEV fuel economy ratings to illustrate the well-to-wheels emissions effects of different pathways and how they compare to baseline gasoline vehicles. The scenarios for hydrogen refueling stations are as follows: (A) central steam methane reforming (SMR) of natural gas for liquid hydrogen delivery, (B) central SMR for gaseous hydrogen delivery, (C) onsite renewable electrolysis, (D) onsite electrolysis with 33% renewable electricity, and (E) onsite electrolysis using California grid mix electricity. These scenarios are evaluated with the min, max, and median FCEV fuel economies reported [5] in the project—40.9 mi/kg, 57.5 mi/kg, and 52.9 mi/kg, respectively—to show a range of emissions for each scenario (note: 1 kg of hydrogen has the same energy content as 1 gallon [3.2 kg] of gasoline). The FCEV scenarios are compared to the emissions of a passenger vehicle and light duty truck using California mix gasoline and the GREET baseline fuel economy values for model year 2015, which

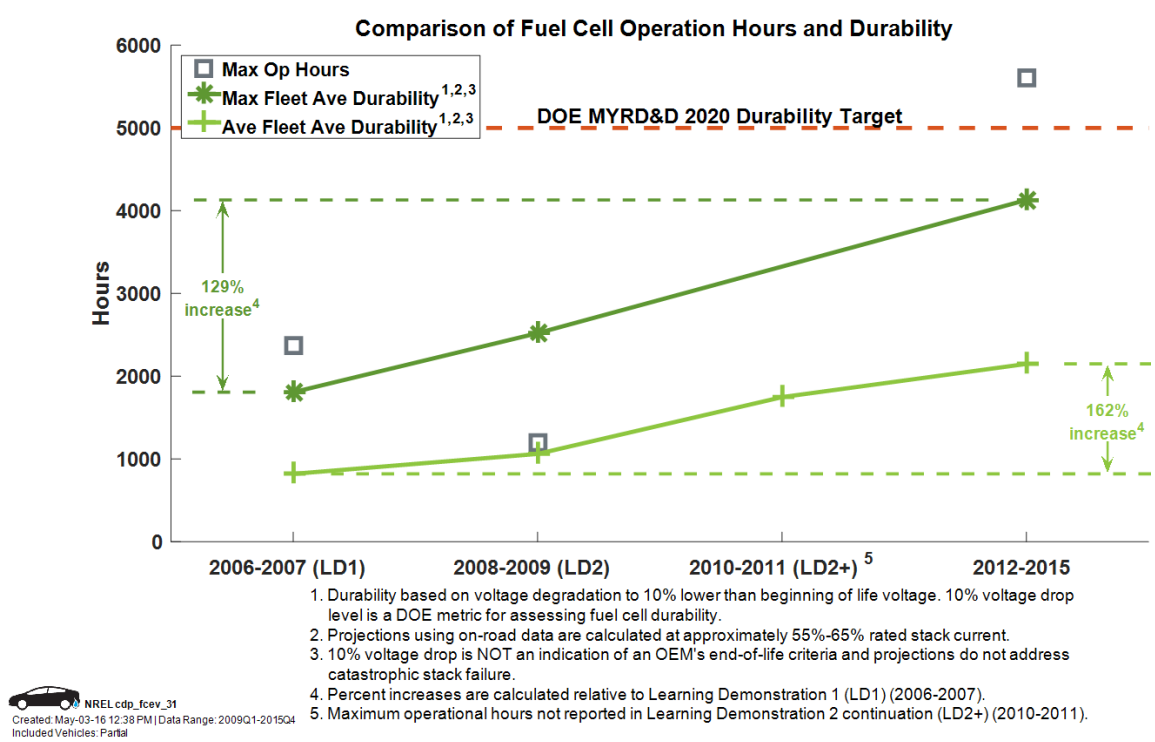

Op – Operation

FIGURE 1. FCEV durability trend and comparison

are 28.8 mpg for a gasoline passenger car and 26.8 mpg for a gasoline light-duty truck (gross weight <6,000 lb). Two baseline gasoline vehicles were chosen to represent the range of body types in the evaluated FCEVs.

CDP FCEV 69 (Figure 2) shows that, on average, FCEV GHG emissions are 23% lower than that of a baseline gasoline passenger vehicle for the most common hydrogen production and delivery pathway, Scenario B—gaseous hydrogen produced from natural gas at a central SMR plant—and 95% lower for the 100% renewable hydrogen production pathway, Scenario C—onsite electrolysis using 100% renewable electricity. Even partially renewable onsite electrolysis can provide emissions benefits as seen in Scenario D using California's requirements [6] for hydrogen produced from 33% renewables. In this scenario, FCEV GHG emissions are 21% lower than that of FCEVs using hydrogen from average central SMR (Scenario B) and 39% lower than that of the baseline gasoline passenger vehicle.

Figure 3 is a graphic depiction of a study looking at the temperature and pressure limits of 35 MPa and 70 MPa hydrogen fills. More than 16,000 fills were analyzed. The highest concentration of fills were in the preferred (that is, fastest fills within acceptable safety limits) region (shown in green), and the pressure and temperature limits were not exceeded. The temperature and pressure measurements were all taken from the vehicles' on-board storage systems.

Maintenance analysis (Figure 4) shows that three subsystems account for approximately 75% of all maintenance events analyzed; nearly 75% of all maintenance events are filter replacements and coolant top offs. The maintenance events analyzed include maintenance to early model versions that were not specifically designed for commercial-grade maintenance expectations. However, the majority of these maintenance events were relatively simple and only 3.5% of failures occurred on the road. The average maintenance event count and labor time per vehicle both have been decreasing over the last couple of years.

CONCLUSIONS AND FUTURE DIRECTIONS

Over the last 10 years, NFCTEC has completed analysis of 222 on-road vehicles that have accumulated more than 6.3 million miles. The current data analyzed come from 55 vehicles and six OEMs, with model years spanning 2006 to 2012. Fuel cell durability has steadily and significantly improved over the last decade, and on-road fuel economy and actual driving range between fills have also increased over the last 10 years.

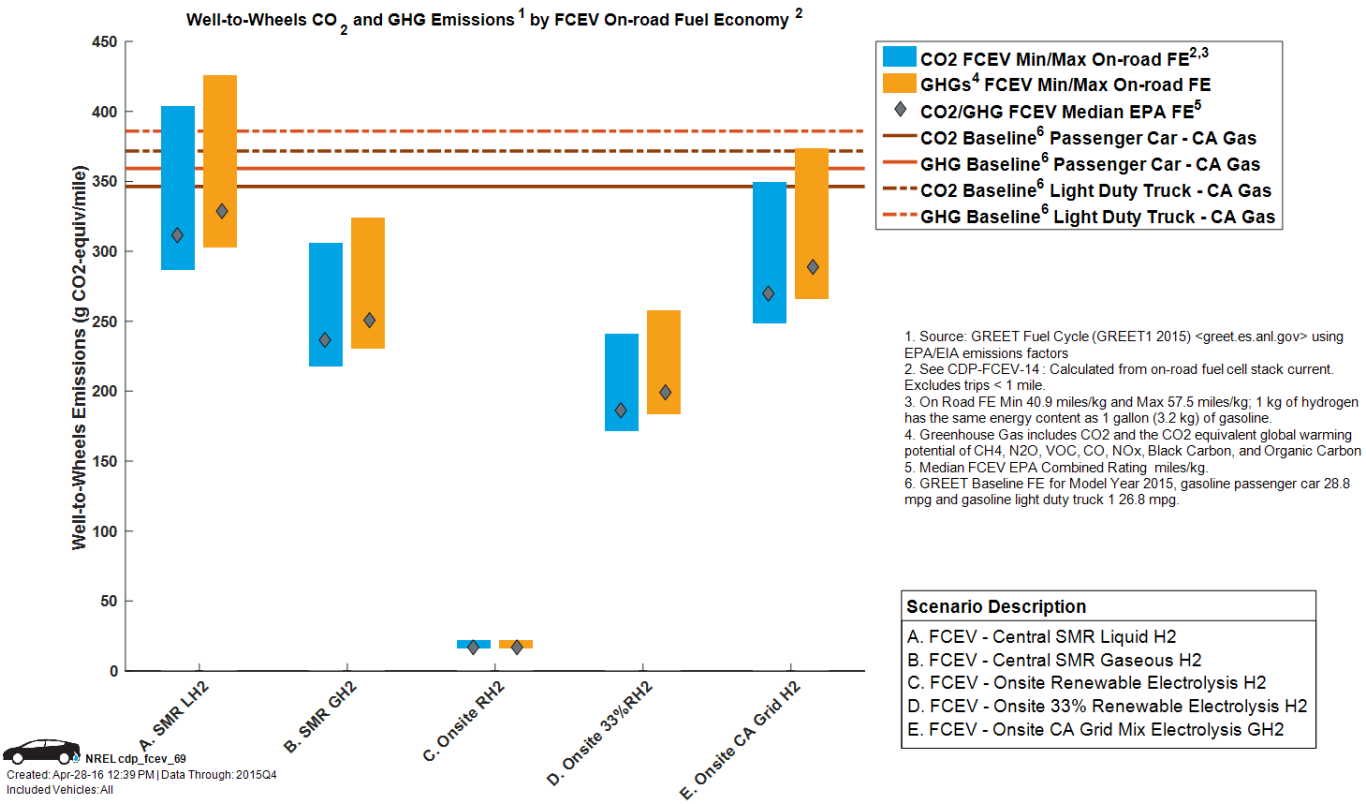

EPA – Environmental Protection Agency; FE – Fuel economy; CA – California; VOC – Volatile organic compound

FIGURE 2. GHG emissions comparisons

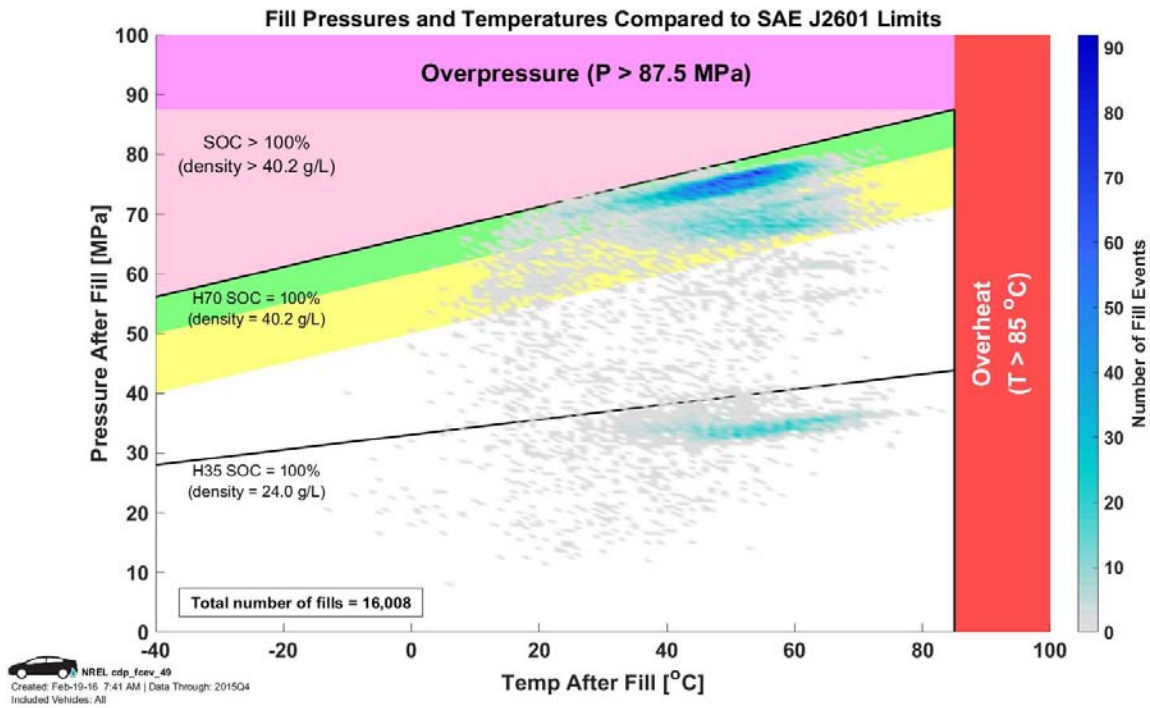

SOC – State of charge

FIGURE 3. FCEV fill comparison to SAE J2601 temperature and pressure limits

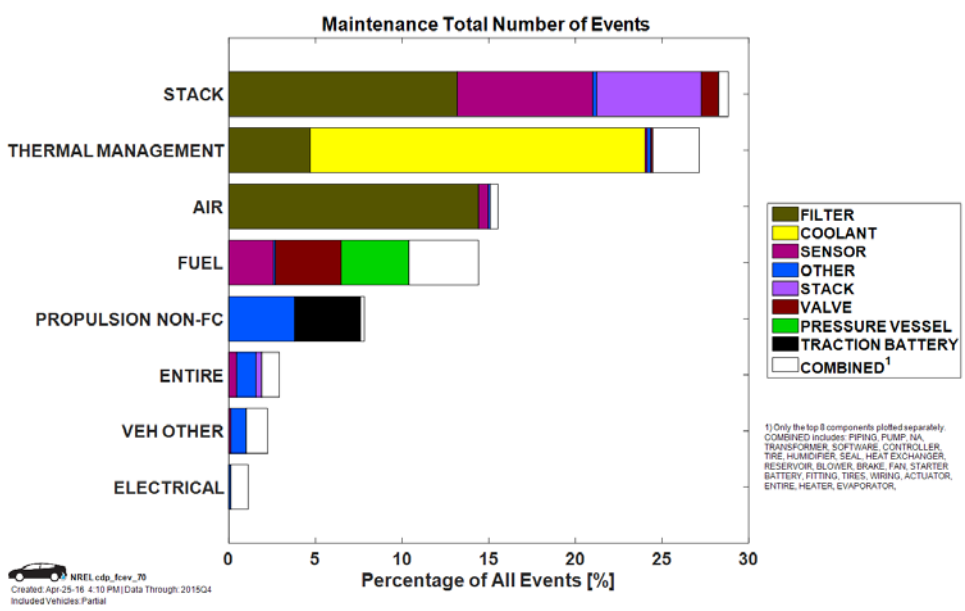

FIGURE 4. FCEV maintenance by system and category

While the 55 vehicles in the current analysis do not represent all FCEVs on the road today, it is a statistically significant set of data for evaluation with more than three million miles traveled, 101,000 total fuel cell operation hours, and 15% of vehicles passing 100,000 miles. The future work includes the following:

- Study the interdependence between FCEV and hydrogen station performance.
- Quantify FCEV benefits based on real-world data.
- Complete a drive cycle analysis to categorize the different FCEV drive cycles for comparison with

standard drive cycles and supply data to the research and development community for fuel cell testing.

FY 2016 PUBLICATIONS/PRESENTATIONS

1. J. Kurtz, S. Sprik, C. Ainscough, G. Saur, and M. Jeffers, "Fuel Cell Electric Vehicle Evaluation," presented at the Advanced Automotive Battery Conference, Detroit, Michigan, June 2016.

2. J. Kurtz, S. Sprik, C. Ainscough, G. Saur, and M. Jeffers, "Fuel Cell Electric Vehicle Evaluation: 2016 Annual Merit Review," presented at the 2016 DOE Annual Merit Review and Peer Evaluation Meeting, Washington, D.C., June 2016.

3. "Transportation Big Data: Unbiased Analysis and Tools to Inform Sustainable Transportation Decisions," NREL/BR-5400-66285, Golden, CO: National Renewable Energy Laboratory, June 2016.

4. J. Kurtz, S. Sprik, C. Ainscough, G. Saur, and M. Jeffers, "Spring 2016 FCEV Evaluation Results," Golden, CO: National Renewable Energy Laboratory, May 2016.

5. J. Kurtz, S. Sprik, C. Ainscough, G. Saur, and M. Jeffers, "Fuel Cell Electric Vehicle Evaluation," presented via webinar at the Interagency Working Group Meeting, Washington, D.C., December 2015.

6. J. Kurtz, S. Sprik, C. Ainscough, and G. Saur, "Fuel Cell Electric Vehicle Evaluation," excerpt from the 2015 DOE Hydrogen and Fuel Cells Program Annual Progress Report, December 2015.

7. S. Sprik and J. Kurtz, "Technology Validation of Fuel Cell Vehicles and Infrastructure," presented at the Fuel Cell Seminar 2015, Los Angeles, California, November 2015.

8. J. Kurtz and S. Sprik, "Fall 2015 FCEV Evaluation Results," Golden, CO: National Renewable Energy Laboratory, November 2015.

REFERENCES

1. *Fuel Cell Technologies Office Multi-Year Research, Development, and Demonstration Plan*, Fuel Cells chapter, Table 3.4.3 Technical targets for automotive application, Washington, D.C.: U.S. Department of Energy, 2012, accessed October 13, 2014, http://energy.gov/eere/fuelcells/downloads/fuel-cell-technologies-office-multi-year-research-development-and-22.

2. K. Wipke, S. Sprik, J. Kurtz, T. Ramsden, C. Ainscough, and G. Saur, *National Fuel Cell Electric Vehicle Learning Demonstration Final Report*, NREL/TP-5600-54860. Golden, CO: National Renewable Energy Laboratory, July 2012, http://www.nrel.gov/hydrogen/pdfs/54860.pdf.

3. "Fuel Cell and Hydrogen Technology Validation," National Renewable Energy Laboratory, http://www.nrel.gov/hydrogen/proj_tech_validation.html.

4. "The Greenhouse Gases, Regulated Emissions, and Energy Use in Transportation (GREET) Model," GREET Fuel Cycle (GREET 1) 2015 using EPA/EIA emissions factors, Argonne National Laboratory, https://greet.es.anl.gov.

5. "Fuel Cell Electric Vehicle Evaluations: Composite Data Products," CDP FCEV 14: Average Vehicle Fuel Economy, National Renewable Energy Laboratory, http://www.nrel.gov/hydrogen/proj_fc_vehicle_evaluation.html.

6. California Senate Bill 1505, September 2006, http://www.leginfo.ca.gov/pub/05-06/bill/sen/sb_1501-1550/sb_1505_bill_20060930_chaptered.pdf.

VII.A.2 Technology Validation: Fuel Cell Bus Evaluations

Leslie Eudy (Primary Contact), Matthew Post, Matthew Jeffers
National Renewable Energy Laboratory (NREL)
15013 Denver West Parkway
Golden, CO 80401
Phone: (303) 275-4412
Email: Leslie.Eudy@nrel.gov

DOE Manager: Jason Marcinkoski
Phone: (202) 586-7466
Email: Jason.Marcinkoski@ee.doe.gov

Project Start Date: March 2001
Project End Date: Project continuation and direction determined annually by DOE

Overall Objectives

- Validate fuel cell electric bus (FCEB) performance and cost compared to DOE and U.S. Department of Transportation targets and conventional technologies.
- Coordinate with the U.S. Department of Transportation Federal Transit Administration (FTA) on the data collection for the National Fuel Cell Bus Program and with international work groups to harmonize data collection methods and enable the comparison of a wider set of vehicles.

Fiscal Year (FY) 2016 Objectives

- Document performance results from each current FCEB demonstration site.
- Complete an annual status report comparing results from the different demonstrations.

Technical Barriers

This project addresses the following technical barriers from the Technology Validation section of the Fuel Cell Technologies Office Multi-Year Research, Development, and Demonstration Plan.

(A) Lack of Fuel Cell Electric Vehicle and Fuel Cell Bus Performance and Durability Data

(D) Lack of Hydrogen Refueling Infrastructure Performance and Availability Data

Contribution to Achievement of DOE Technology Validation Milestones

This project has contributed to achievement of the following DOE milestone from the Technology Validation section of the Fuel Cell Technologies Office Multi-Year Research, Development, and Demonstration Plan.

- Milestone 2.3: Validate fuel cell electric vehicles achieving 5,000-hour durability (service life of vehicle) and a driving range of 300 miles between fuelings. (4Q, 2019)

FY 2016 Accomplishments

Through FY 2016, NREL collected data on 17 FCEBs.

- Documented 11 fuel cell power plants (FCPPs) with operation hours in excess of 12,000 hours. One of these systems has logged more than 22,600 hours in service, and three additional systems have surpassed 16,000 hours.
- Bus fuel economy is dependent on duty cycle. Based on in-service fuel economy of 6.8 mi/kg, the hybrid FCEBs currently in service can achieve a range of approximately 270 miles per fill.
- Published reports on performance and operational data covering 17 full-size FCEBs in revenue service in the United States.

✧ ✧ ✧ ✧ ✧

INTRODUCTION

Transit agencies continue to aid the FCEB industry in developing and optimizing fuel cells for buses. These in-service demonstration programs are vital to validate the performance of fuel cell systems in buses and to determine issues that require resolution. Using fuel cells in a transit application can help accelerate the learning curve for the technology because of the high mileage accumulated in short periods of time. During the last year, the project teams have made progress in improving fuel cell durability, availability, and reliability. More work is still needed to meet the performance needs of transit, lower capital and operating costs, and transition the maintenance to transit staff.

APPROACH

NREL uses a standard evaluation protocol to provide:

- Comprehensive, unbiased evaluation results of advanced technology vehicle development and operations.

- Evaluations of hydrogen infrastructure development and operation.
- Descriptions of facility modifications required for the safe operation of FCEBs.
- Detailed FCEB performance and durability results to validate status against technical targets, educate key stakeholders, and further DOE goals.

The evaluation protocol includes collecting operation and maintenance data on the bus and infrastructure. The analysis, which consists of economic, technical, and safety factors, focuses on performance and use, including progress over time and experience with vehicle systems and supporting infrastructure. The data are compared to DOE and FTA technical targets and to conventional baseline buses in similar service.

RESULTS

During FY 2016, NREL collected and analyzed data on the following FCEB demonstrations at two transit agencies in the United States:

- Zero Emission Bay Area (ZEBA) Demonstration—Five Bay Area transit agencies led by AC Transit (Oakland, California) are demonstrating thirteen 40-foot Van Hool buses with US Hybrid fuel cells in a Siemens hybrid system. The hybrid system was integrated by Van Hool and uses lithium ion batteries from EnerDel.
- American Fuel Cell Bus (AFCB) Project—In December 2012 SunLine began operating an ElDorado National 40-foot bus with a BAE Systems hybrid propulsion system using Ballard Power Systems fuel cells and lithium batteries. This project is part of FTA's National Fuel Cell Bus Program. SunLine added two more AFCBs in 2014 and a third in 2015. NREL collected data on all four buses.

These projects involve fuel-cell-dominant hybrid buses. NREL's evaluations of these projects were funded by DOE. A summary of selected results is included in this report. NREL completed reports on operational and performance data from the FCEBs and from conventional baseline buses at each agency. The results are also compared to technical targets for FCEB performance established by DOE and FTA and published in a Fuel Cell Technologies Program Record in September 2012 [1]. Tables 1 and 2 provide a summary of the reported results from the operation at each agency, including data from the baseline buses.

One performance target set by DOE and FTA is for an FCPP durability of 4–6 years (or 25,000 hours), which would be approximately half the life of the bus. The FCPP would be rebuilt or replaced at that time, similar to what transit agencies typically do for diesel engines. Over the last year, NREL collected data on 17 FCPPs. Figure 1 shows the total hours accumulated on individual FCPPs for the current projects tracked by NREL. The average of 12,217 h is shown on the graph as a dashed line. The 2016 and ultimate targets are included on the graph. As of May 2016, the highest-hour

TABLE 1. 2016 Summary Data Results for ZEBA FCEBs

Vehicle data	FCEB	Diesel
Number of buses	13	10
Data period (month, year)	Sep 2011 – Mar 2016	Jul 2013 – Mar 2016
Number of months	47	33
Total fleet miles	1,320,920	1,534,138
Average miles per month	2,334	4,649
Total FC hours	153,853	–
Fuel economy (mi/kg)	6.03	–
Fuel economy (mi/diesel gal equivalent)	6.82	3.91
Average speed (mph)	8.8	–
Availability (%)	74	88

FC – Fuel cell

TABLE 2. 2016 Summary Data Results for SunLine FCEBs

Vehicle data	AFCB	CNG
Number of buses	4	5
Data period (month, year)	Mar 2012 – Apr 2016	Mar 2012 – Apr 2016
Number of months	50	50
Total fleet miles	258,370	1,157,589
Average miles per month	2,514	5,008
Total FC hours	18,107	–
Fuel economy (mi/kg)	5.84	–
Fuel economy (mi/diesel gal equivalent)	6.34	2.94
Average speed (mph)	14.3	16.3
Availability (%)	74	86

CNG – Compressed natural gas

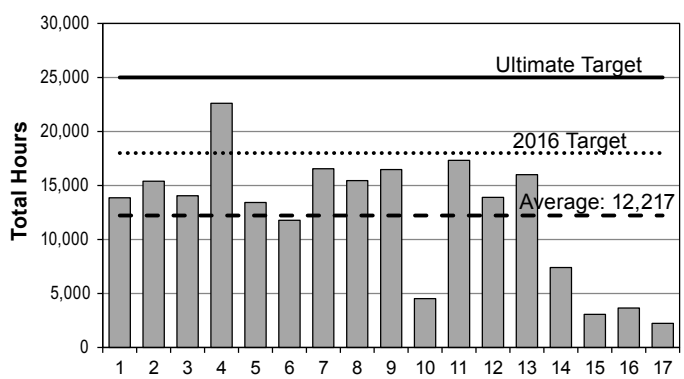

FIGURE 1. Total fuel cell hours accumulated on each FCPP

FCPP had reached 22,600 h, surpassing the 2016 target of 18,000 hours. Of the 17 total FCPPs included in the graph, 61% (11) have surpassed 13,000 h of operation. (The FCPPs with the lowest hours accumulated are newer buses.) This shows significant improvement in durability toward meeting the 25,000-hour target.

The transit industry measures reliability as mean distance between failures, also known as miles between road call (MBRC). Figure 2 tracks the MBRC over time for the ZEBA and SunLine FCEB demonstrations and includes the MBRC for the bus as a whole and MBRC for the fuel cell system. The targets for each category are included on the chart. Table 3 provides the MBRC by year since 2012. Reliability has shown a marked increase over time, reaching the ultimate targets for both bus MBRC and fuel cell system MBRC. Road calls due to bus-related issues—such as problems with doors and air conditioning—made up 40% of the total failures. Fuel cell-related issues made up approximately 15% of the road calls during the period.

CONCLUSIONS AND FUTURE DIRECTION

Fuel cell propulsion systems in buses have continued to show progress in increasing the durability and reliability of FCEBs and the primary components. The current technology meets the ultimate reliability target for road call frequency of both the overall bus and fuel cell system. The fuel cell system on one bus has surpassed the 2016 target for power plant lifetime. Table 4 summarizes the current status compared to the DOE and FTA performance targets. There are still challenges to overcome before fuel cell buses can match the current performance standard of diesel buses. These include:

- Continuing operation to validate durability and reliability of the fuel cell systems and other components to match transit needs.
- Completing the transfer of all maintenance work to transit personnel.
- Lowering the costs of purchasing, operating, and maintaining buses and infrastructure.
- Scaling up the introduction and operation of larger numbers of FCEBs.

Future work by NREL includes:

- Continuing data collection, analysis, and reporting on performance data for FCEBs in service at the following sites.
  - ZEBA FCEB demonstration led by AC Transit
  - SunLine
  - University of California, Irvine
  - Massachusetts Bay Transportation Authority, Boston
  - Additional sites as funding allows
- Investigating reliability, durability, and life cycle of FCEBs as a part of ongoing evaluations.
- Coordinating with FTA to collect data on the demonstrations funded under the National Fuel Cell Bus Program.
- Coordinating with national and international FCEB demonstration sites.

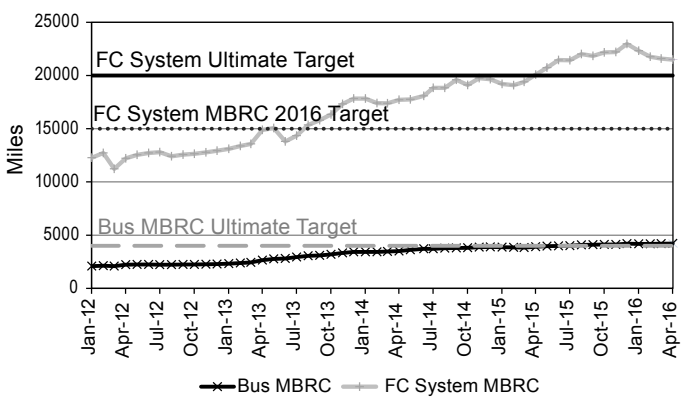

FIGURE 2. Miles between road call

TABLE 3. MBRC by Year through May 2016

	Bus MBRC	FC System MBRC
April 2012	2,230	12,215
April 2013	2,644	14,884
April 2014	3,510	17,714
April 2015	3,910	20,082
April 2016	4,210	21,482
% improvement from 2012 to 2016	89	76

FY 2016 PUBLICATIONS/PRESENTATIONS

1. L. Eudy, M. Post, *Zero Emission Bay Area (ZEBA) Fuel Cell Bus Demonstration Results: Fifth Report*, National Renewable Energy Laboratory, Golden, CO, NREL/TP-5400-66039, June 2016.

2. L. Eudy, *Technology Validation: Fuel Cell Bus Evaluations*, Presentation at the DOE Hydrogen and Fuel Cells Program Annual Merit Review, Washington, D.C., June 2016.

3. L. Eudy, *U.S. Zero Emission Bus Evaluation Results and Status*, Presentation at the American Public Transit Association Annual Bus and Paratransit Conference, May 2016.

4. L. Eudy, *U.S. Zero Emission Bus Evaluation Results and Status*, Presentation at the California Air Resources Board Advanced Clean Transit Technology Symposium, February 2016.

TABLE 4. 2016 Summary of Progress Toward Meeting DOE and FTA Targets

	Units	2016 Status	2016 Target	Ultimate Target
Bus lifetime	Years/miles	5.6/150,000[a]	12/500,000	12/500,000
Power plant lifetime	Hours	2,200–22,200[a]	18,000	25,000
Bus availability	%	74	85	90
Road call frequency (Bus/fuel cell system)	Miles between road call	4,300/ 21,500	3,500/15,000	4,000/20,000
Operation time	Hours per day/days per week	19/7	20/7	20/7
Maintenance cost	$/mile	0.50–2.11	0.75	0.40
Fuel economy	Miles per diesel gallon equivalent	5.5–7.4	8	8
Range	Miles	230–300	300	300

[a] Accumulation of miles and hours to date—not end of life.

5. L. Eudy, *Technology Validation: FCEB Evaluations*, Presentation for the California Fuel Cell Partnership Bus Team meeting, December 2015.

6. L. Eudy, M. Post, C. Gikakis, *Fuel Cell Buses in U.S. Transit Fleets: Current Status 2015*, National Renewable Energy Laboratory, Golden, CO, NREL/TP-5400-64974, December 2015.

7. L. Eudy, M. Post, *American Fuel Cell Bus Project Evaluation: Second Report*, National Renewable Energy Laboratory, Golden, CO, NREL/TP-5400-64344, December 2015.

8. L. Eudy, *U.S. Fuel Cell Electric Bus Evaluation Results*, Presentation at the 2015 Fuel Cell Seminar, November 2015.

REFERENCES

1. Fuel Cell Technologies Program Record #12012, September 2012, www.hydrogen.energy.gov/pdfs/12012_fuel_cell_bus_targets.pdf.

VII.A.3 Fuel Cell Electric Truck (FCET) Component Sizing

Ram Vijayagopal
Argonne National Laboratory
9700 S. Cass Avenue
Argonne, IL 60439
Phone: (630) 252-6960
Email: rvijayagopal@anl.gov

DOE Manager: Jason Marcinkoski
Phone: (202) 586-7466
Email: Jason.Marcinkoski@ee.doe.gov

Project Start Date: June 15, 2015
Project End Date: March 28, 2016

Overall Objectives

- Understand the range and performance capabilities of FCETs.
- Develop design concepts that are functionally equivalent to conventional internal combustion engine powered trucks, for multiple classes and vocations.
- Analysis aims to reveal:
  - Fuel cell and battery power required for trucks.
  - Stored hydrogen weight and total weight of the fuel cell system.
  - Fuel economy and range expected from FCETs.
  - Whether the concept designs meet real-world requirements.

Fiscal Year (FY) 2016 Objectives

- Develop component sizing logic for FCETs.
- Demonstrate the design feasibility of fuel cell-dominant trucks.

Technical Barriers

This project addresses the following technical barriers from the Technology Validation section of the Fuel Cell Technologies Office Multi-Year Research, Development, and Demonstration Plan.

(A) Lack of Fuel Cell Electric Vehicle and Fuel Cell Bus Performance and Durability Data

(C) Hydrogen Storage

Contribution to Achievement of DOE Technology Validation Milestones

This project will contribute to achievement of the following DOE milestones from the Technology Validation section of the Fuel Cell Technologies Office Multi-Year Research, Development, and Demonstration Plan.

- Validate fuel cell electric vehicles achieving 5,000-hour durability (service life of vehicle) and a driving range of 300 miles between fuelings. (4Q, 2019)

FY 2016 Accomplishments

- Developed a generic powertrain sizing logic for FCETs, aimed to meet performance targets derived from comparable conventional trucks.
- Developed models for 12 medium- and heavy-duty vehicles from various classes and vocations. This will serve as a reference for multiple DOE-funded activities.
- Estimated the component power requirement for fuel cell, battery, and electric machine to be used in medium- and heavy-duty applications.
- Estimated the onboard hydrogen storage requirement.

✧ ✧ ✧ ✧ ✧

INTRODUCTION

This study examines the suitability of converting a representative sample of medium- and heavy-duty diesel trucks into FCETs, while ensuring similar truck performance, in terms of range, payload, acceleration, speed, gradeability, and energy consumption. The large number of truck body types, weight classes, and vocational uses results in a large potential design space. Each class and vocation has unique functional requirements that determine specific design choices.

To capture the medium-duty and heavy-duty markets, candidate truck classes and vocations were identified by their recent market size using the Vehicle Inventory and Use Survey [1]. The list spans nearly all classes and many vocations, and is shown in Table 1. Baseline trucks were selected for each candidate class and vocation based on their market share. Some of these choices span multiple weight classes and are popular in multiple vocations. Truck manufacturers design these trucks with requirements arising from a variety of use cases. When such trucks are converted

to FCETs, it is important to ensure that functional capabilities are not sacrificed.

TABLE 1. Overview of the Weight Classes and Vocations Considered in this Study

Vehicle Class	Weight	Vocation/Description
Class 2b	6,000–10,000 lb	Small van
Class 3	10,001–14,000 lb	Enclosed van
Class 3	10,001–14,000 lb	School bus
Class 3	10,001–14,000 lb	Service, utility truck
Class 4	14,001–16,000 lb	Walk-in, multi-stop, step van
Class 5	16,001–19,500 lb	Utility, tow truck
Class 6	19,501–26,000 lb	Construction, dump truck
Class 7	26,001–33,000 lb	School bus
Class 8	33,001 lb or heavier	Construction, dump truck
Class 8	33,001 lb or heavier	Line haul
Class 8	33,001 lb or heavier	Refuse, garbage pickup, cab over type
Class 8	33,001 lb or heavier	Tractor trailer

APPROACH

The baseline truck models were developed based on data available from manufacturers and third parties [2]. Autonomie was used to perform the vehicle simulations because of its existing validated models. To demonstrate the design and simulation process, this report focuses on a Class 4 delivery van as an example. It is possible to calculate important vehicle performance characteristics that are directly related to the powertrain's capabilities. This is done by benchmarking the baseline vehicle model. The parameters characterizing vehicle performance for this process are shown in Table 2. The goal of the FCET sizing process is to ensure that the fuel cell powered vehicle can match or better these performance results.

TABLE 2. Benchmark Values for the Class 4 Delivery Van

Performance Criteria	Baseline
Cargo Mass (lb)	5,280
Cruising Speed (mph)	70
Grade Speed (mph)	50
0–30 mph acceleration time (s)	7.2
0–60 mph acceleration time (s)	29.8

RESULTS

The FCET considered in this study is a hybrid vehicle that uses a fuel cell as its primary source of energy. The battery is sized to assist the fuel cell during high-power transient operations and is also used for regenerative braking. The major components that are being sized in this study include the electric machine, battery, fuel cell, and overall gear ratio. This sizing logic is used to estimate the power required for each of the performance tests. This example shows the sizing results for a Class 4 pickup and delivery vehicle.

TABLE 3. Results of the Motor Power and Final Drive Sweep Test

Selected Component	Size
Motor Continuous Power (kW)	151
Motor Rated Power (kW)	260
Fuel Cell Power (kW)	164
Battery Power (kW)	54
Battery Total Energy (Wh)	1,426
Battery Volume (L)	53.4
Motor Speed Ratio	8.9

The FCET component specification that was sized using the methodology described in this study met all the vehicle requirements within the desired tolerance of 2%. The designed vehicle can carry the same cargo, meet the grade and cruise performance of the baseline vehicle, and significantly exceed the acceleration performance requirements. These vehicles, which were tested on real world drive cycles from the National Renewable Energy Laboratory's FleetDNA database, met most real world driving requirements for all vocations other than line-haul applications. The driving range requirement for line-haul is currently fixed at 400 mi, but real world driving shows that many vehicles drive more than that distance in a trip. It is not clear from the driving data whether they have refueling stops. Other than this specific case, we find that the FCETs can match the real world daily driving requirements for other classes and vocations.

Similar analysis on other vehicle classes yielded the fuel cell and onboard hydrogen storage requirement shown in Figure 1. This shows that a 180-kW fuel cell and approximately 15 kg of onboard hydrogen storage could satisfy the need of many medium- and heavy-duty vocations. This could serve as a component target for future development work.

CONCLUSIONS AND FUTURE DIRECTIONS

This study puts forth a preliminary process to estimate the component sizes of a fuel cell powered electric truck that would be necessary to meet the functional requirements of a reference baseline vehicle. It accounts for the weight difference due to component changes, and the feasibility of finding the necessary volume for the hydrogen tanks. This report used Class 4 trucks as an example, but similar analysis

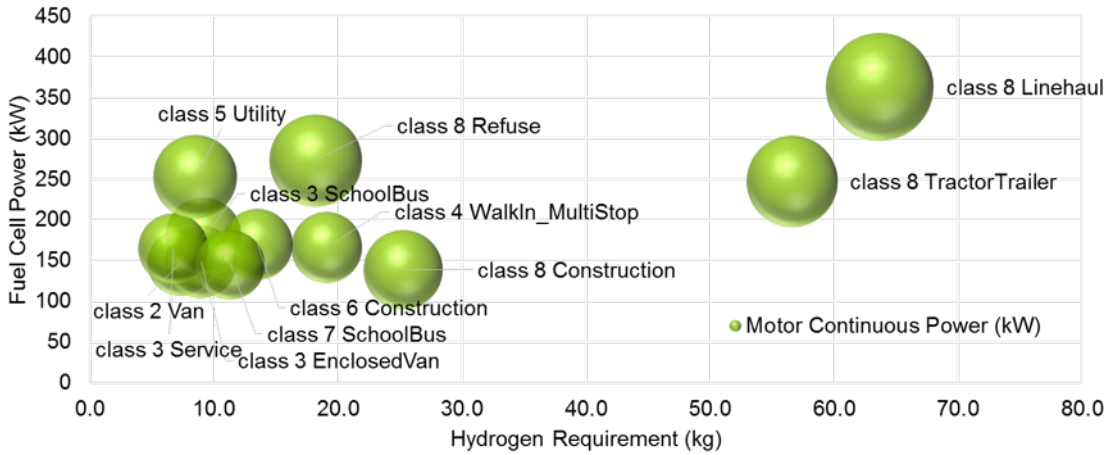

FIGURE 1. Fuel Cell and Hydrogen Tank Sizing Result for FCETs

was performed for additional classes and vocations. The analysis demonstrated that there are no major technological hurdles to meeting the performance requirements for trucks with hydrogen and fuel cell systems.

Cost and durability have not been considered, but they may present challenges until markets are established and economies of scale reduce the cost of producing fuel cell systems. The vehicle use cases were compared against national surveys and against data collected from major fleet operators. The next step will be to add the ownership cost component into this study to examine the economic feasibility of these vehicles. This would also look at the impact of component sizing on energy consumption, and the tradeoff between initial cost and ownership costs.

FY 2016 PUBLICATIONS/PRESENTATIONS

1. Marcincoski, J., Vijayagopal, R., Kast, J., Duran, A., 2016. "Driving an Industry: Medium and Heavy Duty Fuel Cell Electric Truck Component Sizing." Paper presented at Electric Vehicle Symposium, Montreal, Canada, June 2016.

2. Kast J., Vijayagopal, R., Gangloff,J., Marcincoski, J. 2016. "Clean Commercial Transportation: Medium and Heavy Duty Fuel Cell Electric Truck Targets." Paper presented at World Hydrogen Energy Conference, Zaragoza, Spain, June 2016.

REFERENCES

1. U.S. Census Bureau. 2002. "Vehicle Inventory and Use Survey." Accessed June 24, 2015 http://www.census.gov/svsd/www/vius/2002.html.

2. "2014 Truck Index," Truck Index, Inc., Santa Ana.

VII.A.4 Fuel Cell Hybrid Electric Delivery Van Project

Jason Hanlin
Center for Transportation and the Environment
730 Peachtree Street, Suite 760
Atlanta, GA 30308-1209
Phone: (404) 808-6489
Email: Jason@cte.tv

DOE Manager: Jason Marcinkoski
Phone: (202) 586-7466
Email: Jason.Marcinkoski@ee.doe.gov

Contract Number: DE-EE0006523/0002

Subcontractors:
- Hydrogenics USA, San Diego, CA
- United Parcel Service (UPS), Sandy Springs, GA
- Unique Electric Solutions (UES), Stony Brook, NY
- University of Texas at Austin Center for Electromechanics, Austin, TX
- Valence Technology, Austin, TX

Project Start Date: July 15, 2014
Project End Date: November 30, 2020

Overall Objectives

- Increase the zero-emission driving range and commercial viability of medium-duty electric drive trucks.
- Phase 1: Develop a fuel cell hybrid electric delivery van and validate its design and construction through in-service operation.
- Phase 2: Build the Phase 1 delivery van at precommercial volume (up to 16 vehicles) and perform at least 5,000 operation hours of in-service demonstration.
- Develop an Economic/Market Opportunity Assessment for medium-duty fuel cell hybrid electric trucks.

Fiscal Year (FY) 2016 Objectives

- Complete vehicle design.
- Complete subcontractor change.
- Secure complete project funding.
- Coordinate hydrogen fueling infrastructure at demonstration sites and investigate fueling issues associated with medium-duty vehicles.

Technical Barriers

This project addresses the following technical barriers from the following sections of the Fuel Cell Technologies Office Multi-Year Research, Development, and Demonstration Plan.

Technology Validation

(A) Lack of Fuel Cell Electric Vehicle and Fuel Cell Bus Performance and Durability Data

Market Transformation

(D) Market uncertainty around the need for hydrogen infrastructure versus timeframe and volume of commercial fuel cell applications

(F) Inadequate user experience for many hydrogen and fuel cell applications

Technical Targets

This project directly addresses Market Transformation Section 3.9.4 Sub-Program Targets. This project lays out a very specific and rational pathway for the introduction of fuel cell technologies into the medium-duty vehicle market. The project has a technology validation phase and a follow-on deployment of precommercial volumes of the vehicles. The project is built upon the initial structure that DOE prescribed in the Funding Opportunity Announcement and is augmented by the active participation and guidance of a major commercial fleet operator, UPS. UPS operates 46,000 medium-duty vehicles worldwide. Further, the vehicles will be deployed in California to take advantage of that state's focused growth of fueling infrastructure and desire to deploy zero-emission vehicles. The Center for Transportation and the Environment has coordinated with station providers early in the project in order to identify and overcome fueling station barriers for this emerging application of fuel cell technologies, such as the limitation of J2601 fueling protocol described below. This project further leverages the resources and support of the State of California. The project team has also focused on upfront design to ensure that (1) selection of the fuel cell size will take advantage of volume growth from other applications and markets, and (2) the design will meet the needs of our commercial fleet operator by matching the performance of incumbent technologies, while meeting the range requirements for over 97% of delivery van duty cycles.

FY 2016 Accomplishments

- Resolved outstanding administrative issues and executed a contract modification with DOE, which enables the

project team to resume technical activity after being "on-hold" for much of FY 2016.

- Secured $980,000 in additional project cost share, which makes the Phase 1 budget whole and enables the team to perform the nonrecurring engineering, project management, design, and build work required to deploy six vehicles in Phase 2.
- Updated vehicle performance models and repeated simulation activity to capture most recent mass estimates and the impact of utilizing a switch-reluctance motor. A trade study of component sizes and specifications was performed. The team ensured that components meet technical requirements and align with commercialization strategy (e.g., utilize off-the-shelf systems and minimize custom solutions).
- Evaluated thermal management strategy and estimated battery thermal characteristics under simulated loads.
- Continued vehicle solid modeling and component layout and packaging activities. Involved the fleet operator (UPS) during the design phase to ensure the van aligns with the end user's expectations and to help promote commercial acceptance of final product.

✧ ✧ ✧ ✧ ✧

INTRODUCTION

Parcel delivery van fleets are currently dominated by diesel and compressed natural gas powered Class 3–6 trucks. In recent years, some parcel delivery services have integrated battery–electric trucks into their fleet; however, these battery–electric vehicles have been unable to match the performance of existing delivery vans and their limited range significantly impacts deployment strategy. The intent of this project is to develop a hydrogen fuel cell hybrid electric van that provides fleet operators with a zero-emission vehicle capable of meeting route range requirements while matching the performance characteristics of its existing fleet vehicles. According to Fleet DNA Project Data compiled by the National Renewable Energy Laboratory, a vehicle with a 125-mi range will meet 97% of Class 3–6 daily delivery driving distances [1]. Meeting this 125-mi range threshold will increase the attractiveness of zero-emission trucks to fleet operators and increase their commercial viability.

APPROACH

This project aims to develop and demonstrate a hydrogen fuel cell hybrid electric van with a 125-mi operational range and validate the vehicle through in-service deployment in a California UPS fleet. This project has two phases:

- Develop a fuel cell hybrid electric delivery van and validate its design and construction through in-service operation.
- Build the Phase 1 delivery van at precommercial volume (up to 16 vehicles) and perform at least 5,000 operation hours of in-service demonstration.

During Phase 1, real-world delivery van route data is collected to define the expected duty cycle requirements. All potential fuel cell hybrid electric van powertrain configurations are then modeled and simulated on the duty cycles to assess vehicle performance and aid final design. Trade studies (including cost and projected costs at high volumes) are accomplished and vehicle components are then down-selected and the physical layout is completed. The first delivery van can then be built and validated through in-service operation. If the delivery van meets Phase 1 performance requirements, the project team will build and deploy up to 16 additional vans in Phase 2. All of the vans will be demonstrated in California. Vehicle performance data during the demonstration periods will be collected and provided to the National Renewable Energy Laboratory's National Fuel Cell Technology Evaluation Center for analysis.

The project team benefits from having members with extensive hydrogen fuel cell experience, including the Center for Electromechanics and Hydrogenics, and one of the largest medium-duty truck fleet operations in the world, UPS. UPS has deployment experience with delivery vans powered by various fuels, including gasoline, diesel, compressed natural gas, and battery–electric. This experience gives them a unique perspective on the commercial viability of alternative-fueled vehicles and their project contributions are invaluable. Project funding is provided by the DOE, the California Energy Commission, and the South Coast Air Quality Management District. UPS is providing cost share during the demonstration periods by supplying operation, maintenance, and fueling costs.

RESULTS

The team's modeling activity and component trade study showed that a 32-kW fuel cell module, 49-kWh battery energy storage, and 10–15 kg of hydrogen are required to meet the 125-mi driving range objective on actual UPS delivery routes. The team also simulated the van's performance on the Hybrid Truck User's Forum Parcel Delivery drive cycles. In all simulation scenarios, the team found that drive cycles created from real-world data were more strenuous than available industry-standard drive cycles.

Thermal response of the battery pack varies with pack size and configuration. The 49-kWh battery pack has more favorable thermal response characteristics than a 33-kWh system, which was also being considered. Onboard hydrogen

storage should be maximized, but is limited by physical packaging and off-the-shelf tank options. The team has performed the design and layout work required to fit 350 bar hydrogen tank cylinders with 10-kg capacity on the van, but the project team learned that 700 bar tank cylinders suitable for integration with medium-duty vehicles are not currently commercially viable. Development of Type 4 700 bar tanks, which would allow 15 kg of hydrogen to be stored onboard, will be reevaluated for vehicles in Phase 2 of the project.

The proposed propulsion system configuration will allow the van to outperform existing battery-electric vans in UPS' fleet, as shown in the example simulation results in Figure 1. With 15 kg of hydrogen on board, the simulated fuel cell van operates for the full Napa route and drives 125 mi. The battery–electric van cannot reach 400 min of operation and only travels 70 mi.

After repeating the modeling activity, the team updated the vehicle specifications, which includes the following:

Physical Specifications:	Battery System:
Vehicle Chassis – Navistar International 1652SC 4X2	Chemistry – LiFeMgPO4
Maximum Speed – 65 mph	49 kWh
Maximum Range – 125 mi	Configuration – 16s3p
Acceleration (0 to 60 mph) – 26 s at 19,500 lb	1,500 cycles / 5 yr
GVW – Class 6 (23,000 lb)	Fuel Cell:
Wheel Base – 176 in	Rated Power – 32 kW continuous
Capacity – 970 ft^3	Peak Efficiency – 55%
	Hydrogen Storage:
	Capacity – 9.78 kg
	Pressure – 350 bar

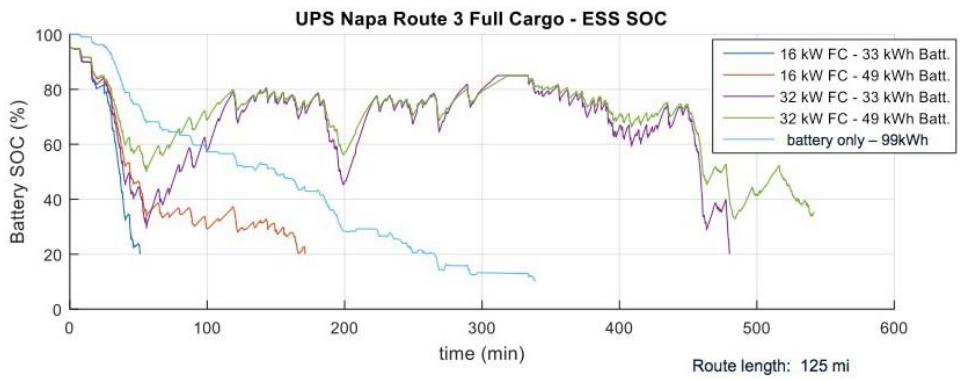

SOC – State of charge; FC – Fuel cell; Batt. – Battery

FIGURE 1. Simulated performance of fuel cell and battery–electric vans on UPS delivery route

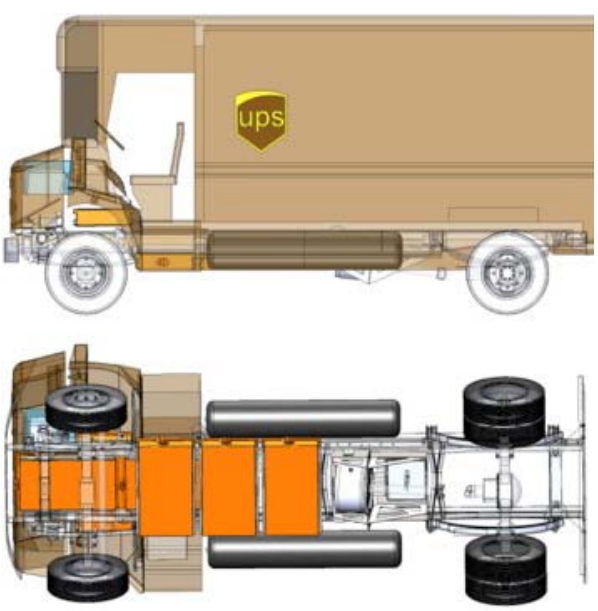

FIGURE 2. Physical layout and component packaging with van body

Initial solid models of the van's physical layout and component packaging are shown in Figure 2.

CONCLUSIONS AND FUTURE DIRECTIONS

The Fuel Cell Hybrid Electric Delivery Van project is utilizing team member experience with hydrogen fuel cell technologies, alternate fuel vehicle fleet familiarity, and stakeholder feedback to develop commercially viable zero-emission medium-duty trucks. The team has developed:

- Vehicle and component specifications to promote commercial acceptance.
- Component selection to ensure performance on real-world delivery duty cycles.
- Solid models of major components within the vehicle body.
- Strategy to ease UPS fleet acceptance and fueling procedures.

Future work includes:

- Completing safety hazard analysis with support from the Hydrogen Safety Panel.
- Coordinating fueling availability and continue coordinating the development of medium-duty hydrogen fueling protocol.
- Completing final design for the vehicle.
- Building and commissioning initial van design.
- Validating prototype van through in-service operation.
- Building final van design at precommercial volume (up to 16 vehicles).
- Training and educating end user fleet operations personnel.
- Deploying and supporting vans in UPS California fleets.
- Collecting and evaluating in-service data during demonstration period.
- Developing an Economic/Market Opportunity Assessment for the vehicles.

FY 2016 PUBLICATIONS/PRESENTATIONS

1. J. Hanlin, "Fuel Cell Hybrid Electric Delivery Van Project," presented at the DOE Annual Merit Review, Washington, DC, June 6–10, 2016.

REFERENCES

1. Walkowicz, K.; Kelly, K.; Duran, A.; Burton, E. (2014). *Fleet DNA Project Data*. National Renewable Energy Laboratory. http://www.nrel.gov/fleetdna

VII.B.1 Hydrogen Station Data Collection and Analysis

Sam Sprik (Primary Contact), Jennifer Kurtz, Chris Ainscough, Genevieve Saur, Matt Jeffers, and Mike Peters
National Renewable Energy Laboratory (NREL)
15013 Denver West Parkway
Golden, CO 80401-3305
Phone: (303) 275-4431
Email: Sam.Sprik@nrel.gov

DOE Manager: Jason Marcinkoski
Phone: (202) 586-7466
Email: Jason.Marcinkoski@ee.doe.gov

Project Start Date: October 1, 2011
Project End Date: Project continuation and direction determined annually by DOE

Overall Objectives

- Analyze current, state-of-the-art hydrogen infrastructure using several metrics including efficiency, performance, cost, and reliability of station components and systems.
- Perform an independent assessment of technology in real-world operating conditions, focusing on hydrogen infrastructure for on-road vehicles.
- Leverage the data processing and analysis capabilities at the National Fuel Cell Technology Evaluation Center (NFCTEC), originally developed under the Fuel Cell Vehicle Learning Demonstration, as well as from forklift, backup power, and bus projects.

Fiscal Year (FY) 2016 Objectives

- Obtain and collect data from state-of-the-art hydrogen fueling facilities that receive funding through DOE Funding Opportunity Announcement (FOA) 626 awards, California Energy Commission (CEC) awards, and others, to enrich the analyses and the set of publicly available composite data products (CDPs) on hydrogen fueling infrastructure.
- Work with codes and standards activities and fueling facility owners-operators to benchmark performance of the fueling events relative to current Society of Automotive Engineers procedures.
- Perform analysis and provide feedback on sensitive data from hydrogen infrastructure for industry and DOE. Aggregate these results for publication.
- Participate in technical review meetings and site visits with industry partners to discuss results from NREL's analysis.
- Transition national database of location and status of hydrogen stations to the Alternative Fuels Data Center (AFDC) station locator and work with California and AFDC to keep the database up to date. Also work on adding fields and online status of the stations together with AFDC and the California Fuel Cell Partnership.

Technical Barriers

This project addresses the following technical barrier from the Technology Validation section of the Fuel Cell Technologies Office Multi-Year Research, Development, and Demonstration Plan.

(D) Lack of Hydrogen Refueling Infrastructure Performance and Availability Data

Contribution to Achievement of DOE Technology Validation Milestones

This project contributes to achievement of the following DOE milestone from the Technology Validation section of the Fuel Cell Technologies Office Multi-Year Research, Development, and Demonstration Plan.

- Milestone 4.4: Complete evaluation of 700-bar fast fill fueling stations and compare to SAE J2601 specifications and DOE fueling targets. (3Q, 2016)

FY 2016 Accomplishments

- Internally processed and analyzed quarterly infrastructure data in the NFCTEC for inclusion in CDPs every six months and created new Fall 2015 and Spring 2016 CDPs.
- Transitioned NREL's internal database of stations and their locations to AFDC. Worked with Pacific Northwest National Laboratory and California Fuel Cell Partnership to consolidate information and continue to work with California and AFDC to keep the list updated to the latest information.
- Updated the infrastructure data collection templates for the latest CEC grant funding opportunity.
- Analyzed data and provided updates on stations under DOE FOA 626-funded projects.
- Updated NREL Fleet Analysis Toolkit code to accept and analyze data in multiple formats from stations.
- Participated in the California Fuel Cell Partnership working group meetings and the H2USA hydrogen fueling station working group.

✧ ✧ ✧ ✧ ✧

INTRODUCTION

In the past, approximately 60 hydrogen fueling stations supported a few hundred fuel cell electric vehicles (FCEVs) in the United States. Of these stations, 25 supported the 183 DOE Learning Demonstration vehicles. As we move out of a learning demonstration environment and into a commercialization environment, manufacturers are ramping up FCEV production alongside an infrastructure effort to build out a network of consumer-friendly stations in a retail environment, upgrade existing stations to increase fueling output, and cluster stations to cover areas where vehicles are introduced.

California has been a leader in supporting hydrogen infrastructure with a goal of 100 stations within a carefully planned network. Early efforts in California focus on clusters of stations near population centers in the Los Angeles and San Francisco Bay areas. Through past funding efforts, eight non-private stations are in place in California with 18 more in near-term development. The most recent awards from the CEC through PON-13-607, which were announced in May of 2014, are resulting in multiple stations opening in 2016. That effort is funding the building of 28 new stations and a mobile fueler with $46 million of state money through the CEC's Alternative and Renewable Fuel and Vehicle Technology Program. These stations will be included in subsequent evaluations and would bring the California public station count to 54. Besides California, there are efforts in other states, including the northeastern states, which will establish hydrogen infrastructure for the upcoming FCEVs.

Keys to success for improving hydrogen fueling availability are selecting the fueling location, ensuring customer-friendly public access, and providing adequate and reliable output to support the vehicles. Hydrogen output from existing and upcoming facilities varies from 50 kg/d to 350 kg/d, with most new fueling facilities being more than 100 kg/d. Although it is currently most economical to make hydrogen from natural gas, there are efforts and requirements to make hydrogen from renewable sources. Using available hydrogen energy from landfills and wastewater treatment plants is one way to make use of a renewable feedstock and to lower greenhouse gas emissions. Another renewable pathway is to make hydrogen through electrolysis with the electrical energy coming from a renewable source such as wind or solar. As more vehicles come online, all fueling facilities will need to be accessible to anyone with a hydrogen vehicle. As these fueling facilities are developed, there is a need to continue data collection and analysis to track the progress and determine future technology development needs.

APPROACH

The emphasis of this project is documenting the innovations in hydrogen fueling and how well they meet customer needs. This includes analysis that captures the technology capability (such as back-to-back filling capability, impact of pre-cooling temperature, and radio-frequency identification of vehicles to allow unique fueling profiles) as well as the customer perspective (such as fueling times and rates, safety, and availability). Individual components, such as compressors, are evaluated with the available data to establish current status and research needs. Station locations are evaluated within the context of both available vehicles and future vehicles and their fueling patterns. NREL also uses the analysis results to support DOE in identifying trends from the data that will help guide DOE's R&D activities.

Data analysis is performed on sensitive industry hydrogen fueling data in the NFCTEC and recommendations are provided to DOE on opportunities to refocus or supplement R&D activities. Aggregation of the analyzed data allows for creation of composite results for public dissemination and presentation. Some existing CDPs from the previous learning demonstration are updated with new data, as appropriate. All this involves working with industry partners to create and publish CDPs that show the current technology status, without revealing proprietary data. Feedback to industry takes form in detailed data products (protected results) and provides direct benefit to them from the NREL analysis performed on their data. NREL will continue exercising the fueling analysis functionality of the NREL Fleet Analysis Toolkit to preserve and archive a snapshot of the analysis results from each quarter. This allows a deeper level of results to be stored in an easy-to-access form within the NFCTEC.

Using unique analysis capabilities and tools developed at NREL, researchers are providing valuable technical recommendations to DOE based on real-world experiences with the technology. NREL will continue to provide multiple outputs in the form of CDPs and presentations and papers at technical conferences.

RESULTS

As stations are built or retired, the AFDC station database is updated for public viewing. Currently, there are 29 public stations in the United States with 29 more planned in the near future. The newer stations are being built to be accessible to the public and most are located in California. Using the data reported to NREL by 11 of these stations, 61 CDPs were created by analyzing and aggregating the station data, and results were published on NREL's website.

Although the primary goal of the early stations is geographic coverage for FCEV customers to prevent range anxiety, the current analysis includes how these stations are being used. The amount of dispensed hydrogen per day of the week (Figure 1) shows more filling is happening

Monday through Friday than on Saturday and Sunday. The highest-use station shows an average of 35 kg/d on Wednesdays. A new CDP shows the historical failure rate

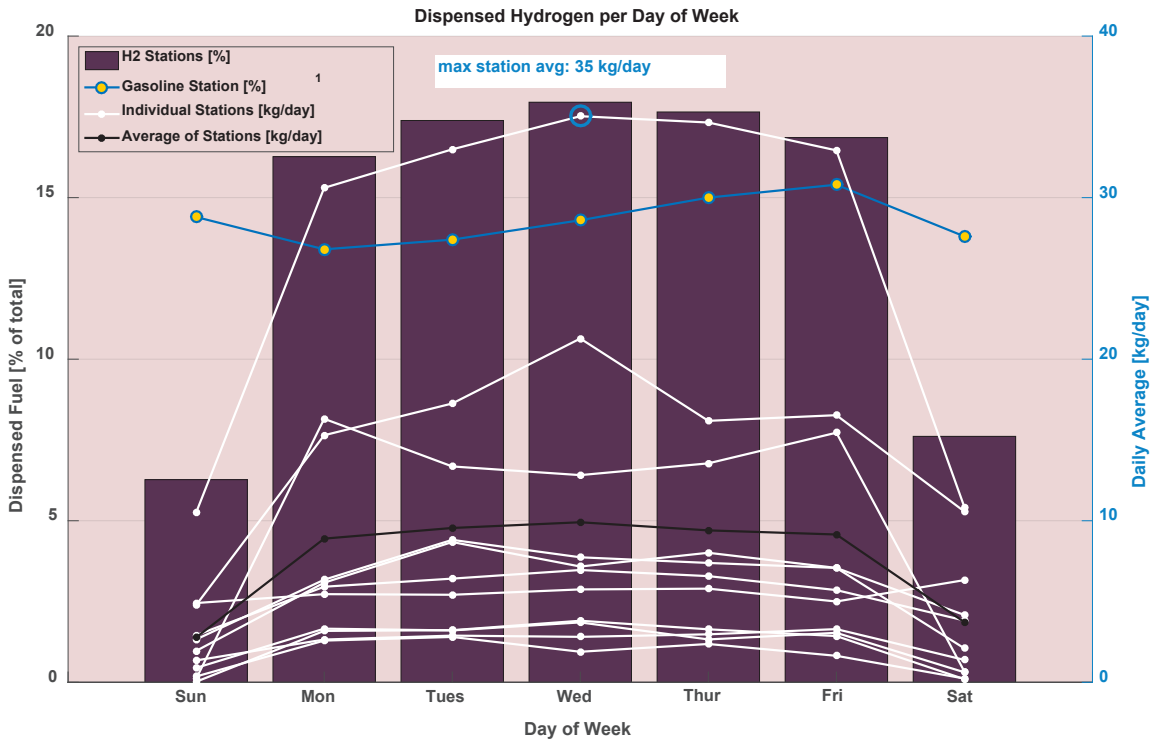

FIGURE 1. Dispensed hydrogen per day of week

by the amount dispensed (Figure 2) and shows the left and mid part of a typical "bathtub" curve where the right side, if projected out, would be expected to go back up as failures due to aging equipment ramp up. The average fueling rates, times and amounts for new stations (Figure 3) is for fills greater than 1 kg with precooling at -40°C. For these fills the average rate is 0.87 kg/min, time to fill is 3.7 min, and the average amount is 2.8 kg. A look at maintenance by equipment type (Figure 4) shows that hydrogen compressors are the primary items needing maintenance both in terms

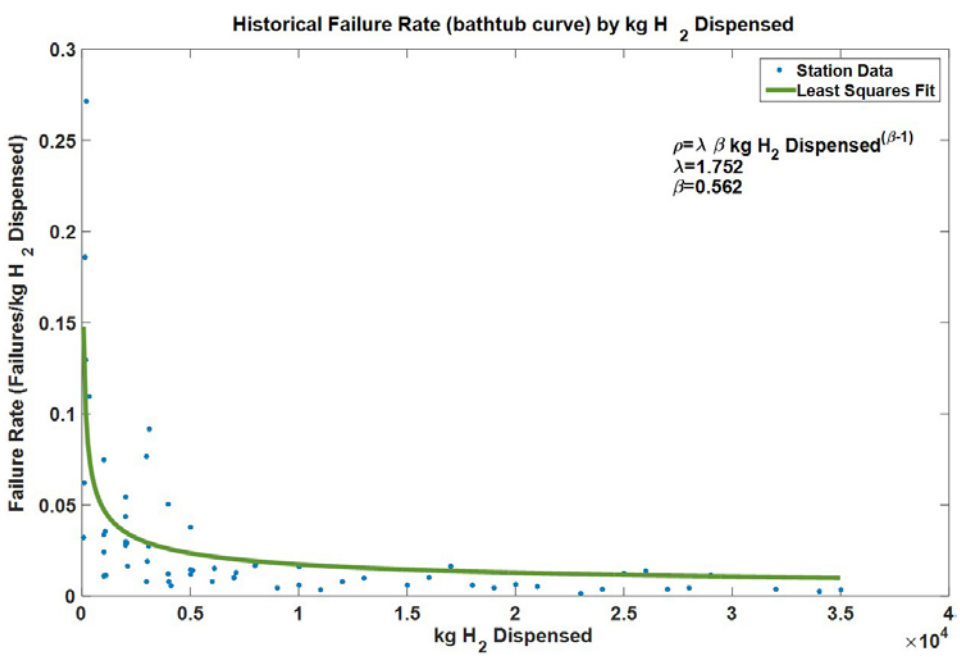

FIGURE 2. Historical failure rate by kilogram hydrogen dispensed

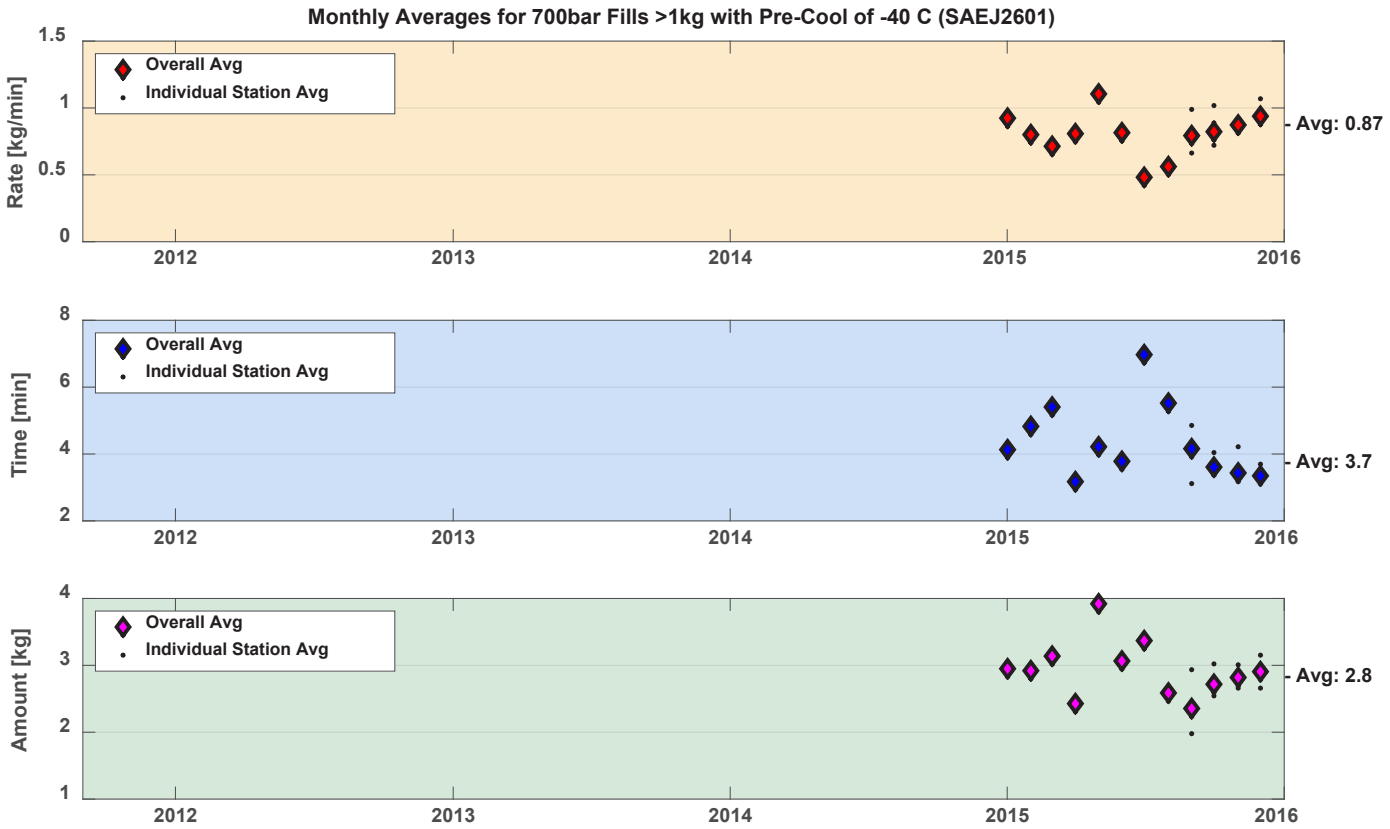

FIGURE 3. Monthly fueling rates, times, and amounts for new stations

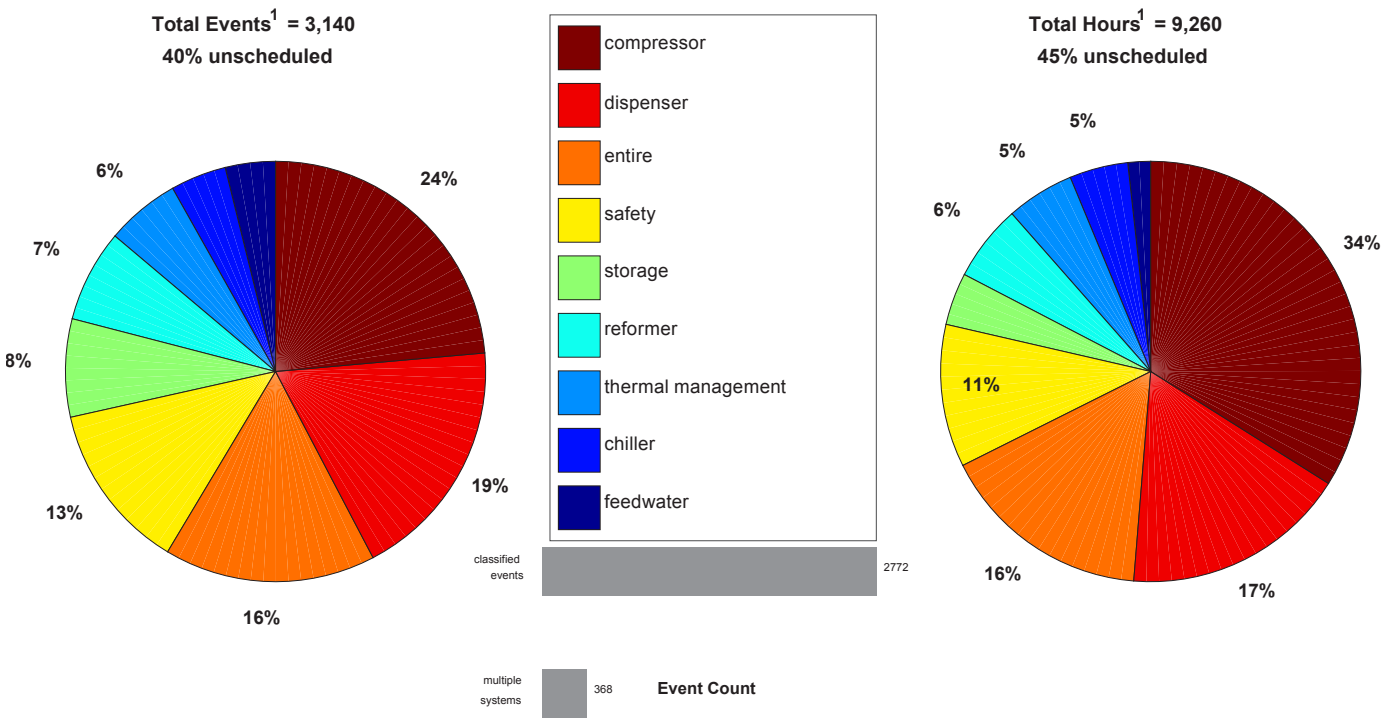

FIGURE 4. Maintenance by equipment type

of number of events and in hours. Dispenser maintenance, entire system inspections, safety items (e.g., false alarms and sensors), and storage are the next highest items in terms of number of maintenance events. These results and all the other CDPs are published on NREL's website.

CONCLUSIONS AND FUTURE DIRECTIONS

As new stations come online or are updated, their performance and availability will affect how successfully they support the current and upcoming fleet of fuel cell vehicles. Continual data collection, analysis, and feedback will provide DOE and the hydrogen and fuel cell community with awareness of the technology readiness and identify areas for improvement that could be research topics. Many new stations are coming online and will be included in the data set as they report data. Their data will be aggregated and published in CDPs without revealing individual station identity and will help identify general trends for the latest stations. As more data become available from newer stations and as more FCEVs enter the market, there will be an increase in data analysis possibilities to validate the technology for hydrogen infrastructure, including focusing on trends over time for usage, reliability, and performance of the stations.

FY 2016 PUBLICATIONS/PRESENTATIONS

1. Sam Sprik, Jennifer Kurtz, Chris Ainscough, Matt Jeffers, Genevieve Saur, and Mike Peters, "TV017: Hydrogen Station Data Collection and Analysis," presented at the 2016 DOE Annual Merit Review and Peer Evaluation Meeting, Washington, D.C., June 2016.

2. Sam Sprik, Jennifer Kurtz, Chris Ainscough, Mike Peters, Matt Jeffers, and Genevieve Saur, "Performance Status of Hydrogen Stations and Fuel Cell Vehicles," presented at 2015 Fuel Cell Seminar IND32-3, Los Angeles, CA, November 2015.

3. "Hydrogen Fueling Infrastructure Analysis: Composite Data Products," National Renewable Energy Laboratory, http://www.nrel.gov/hydrogen/proj_infrastructure_analysis.html.

VII.B.2 Performance Evaluation of Delivered Hydrogen Fueling Stations

Ted Barnes (Primary Contact) and Devin Halliday
Gas Technology Institute (GTI)
1700 S Mt. Prospect Rd.
Des Plaines, IL 60018
Phone: (847) 544-3405
Email: ted.barnes@gastechnology.org

DOE Manager: Jason Marcinkoski
Phone: (202) 586-7466
Email: Jason.Marcinkoski@ee.doe.gov

Contract Number: DE-EE0005886

Subcontractor:
Linde Gas, LLC, Heyward, CA

Project Start Date: March 1, 2013
Project End Date: April 30, 2018

Overall Objectives

- Integrate non-intrusive data collection systems at five 100 kg/d delivered liquid hydrogen fueling stations located in California for a 24-month performance period.
- Submit complete sets of the National Renewable Energy Laboratory (NREL) Hydrogen Station Data Templates to the National Fuel Cell Technology Evaluation Center (NFCTEC).
- Provide useful data to accurately benchmark and characterize station capacity, utilization, maintenance, and safety.

Fiscal Year (FY) 2016 Objectives

- Installation and commissioning of the second system at San Juan Capistrano, CA site location.
- Produce the complete sets of data for the first two project sites at the end of each quarter after startup and commissioning is completed.
- Obtain approval to continue project efforts into Budget Period 2.
- Monitor progress on other three planned hydrogen fueling stations to ensure data acquisition systems are prepared for installation.

Technical Barriers

This project addresses the following technical barriers from the Technology Validation section of the Fuel Cell Technologies Office Multi-Year Research, Development and Demonstration Plan.

(A) Lack of Fuel Cell Electric Vehicle and Fuel Cell Bus Performance and Durability Data

(D) Lack of Hydrogen Refueling Infrastructure Performance and Availability Data

Contribution to Achievement of DOE Technology Validation Milestones

This project will contribute to the achievement of the following DOE milestones from the Technology Validation section of the Fuel Cell Technologies Program Multi-Year Research, Development and Demonstration Plan.

- Milestone 3.2: Validate novel hydrogen compression technologies or systems capable of >200 kg/day that could lead to more cost-effective and scalable (up to 500 kg/day) fueling station solutions for motive applications. (4Q, 2014)
  - The stations currently being constructed will incorporate Linde's patented ionic fluid compressor. This technology utilizes a liquid piston to compress gas rather than a diaphragm or metal piston used in conventional compressor technologies. Linde is optimistic that this technology can be cost effectively scaled to larger capacity stations in the future.
- Milestone 3.4: Validate station compression technology provided by the delivery team. (4Q, 2018)
  - See Milestone 3.2.
- Milestone 3.8: Validate reduction of cost of transporting hydrogen from central production to refueling sites to <$0.90/gge. (4Q, 2019)
  - This project will yield data directly aiding to develop baseline benchmarking and measure improved cost of delivery of liquid hydrogen to fueling stations in California.
- Milestone 4.4: Complete evaluation of 700-bar fast fill fueling stations and compare to SAE J2601 specifications and DOE fueling targets. (3Q, 2016)
  - This project will supply data to the NFCTEC that aid the program in the characterization of the stations' storage and delivery capacities, compression

performance, fueling transactional data, operational cost, maintenance, and safety. Data supplied will provide points of direct comparison to SAE fueling standards and DOE fueling targets.

FY 2016 Accomplishments

- Completed installation of the GTI-designed data acquisition system at San Juan Capistrano and data submitted to NREL.
- Data submitted to NREL each quarter for West Sacramento station.
- Tasks under Budget Period 1 were completed and approval to move to Budget Period 2 was received.
- A root cause failure analysis was completed and a permanent solution was found for a data logger error that was caused by network issues. Solution has allowed for continuous data collection.
- All equipment ordered and assembled for installation at third station, Bishop Ranch. The Bishop Ranch station began construction June 20, 2016.

✧ ✧ ✧ ✧ ✧

INTRODUCTION

The objective of this project is to collect, organize, and report on operational, transactional, safety, and reliability data for five hydrogen fueling stations located in California. Goals of the project are as follows. (1) The data collected will be statistically meaningful and the stations will have sufficient throughput and vehicle fueling frequency to minimize data aberrations. (2) The data collected will be accurate. (3) The data collected will be comprehensive and timely.

This project will directly assist DOE in assessing the readiness level of current infrastructure and state of the art technologies utilized to support planned fuel cell vehicle deployment within the next five years. The data and observations collected during the performance period of this project will provide NREL with information detailing the operational costs, efficiencies, and reliability of the delivered hydrogen fueling station design. Furthermore, the Linde design utilizes the patented IC90 ionic fluid compressor package; through this project GTI will provide the performance data which will enable DOE and original equipment manufacturers to evaluate real-world efficiencies further gauging the technology's adequacy in this application. This system is a first of its kind utilized for hydrogen fueling applications in the United States.

APPROACH

Hydrogen station data will be submitted quarterly to the NFCTEC at NREL using the appropriate Hydrogen Station Data Templates. GTI's project partner, Linde, is currently developing delivered hydrogen fueling stations under programs sponsored by the California Energy Commission. The sites will be accessible to the public for fueling consumer fuel cell vehicles, commercial vehicles, or government-owned vehicles. All five of the sites will be developed at existing or at new sites along with, conventional gasoline stations operated by major, branded fuel providers. This provides the project with vehicle fueling data from a broad, cross-section of real-world vehicle applications. The station sites were selected to provide convenient, consumer-friendly vehicle fueling for drivers of fuel cell vehicles. Development of each of these stations has the support of vehicle original equipment manufacturers and each site has passed stringent location selection requirements of the California Energy Commission to ensure the stations will be utilized by a high volume of fuel cell vehicle operators.

The data collection system will utilize a variety of methods in order to provide the entire data requirements set forth by NREL. This system will utilize the existing control architecture of the compressor and dispenser equipment as well as monitor and record signals from a set of installed instrumentation that will supplement information required that is not already captured inherently by the stations' operating system. There are multiple descriptive (opposed to measured data) deliverables that will be taken manually and submitted to GTI for processing and formatting prior to delivery to NREL. Manually collected data templates include:

- NREL Site Log: recording safety drills, training, or public meetings
- Storage and Delivery: compiling liquid hydrogen supplies delivery quantities and cost
- Fuel Log: transferring transactional data from monthly reports emanating from fuel management system
- Maintenance: station maintenance and operations reporting
- Hydrogen Cost: collection of utility bills
- Safety: station environmental, health, and safety reporting
- Hydrogen Quality: SAE quality analysis completed annually and submitted

GTI will collaborate with Linde and create a reporting/submittal process to collect this type of data required to populate the NREL templates.

RESULTS

The past year has shown substantial progress including installing the data acquisition system and retrieving data from the two hydrogen stations and making progress toward installing the system at the third station. Figures 1 and 2 show the monthly dispensed hydrogen data collected from the operational sites. This is just a small subset of the large amount of data that is being reported to NREL each quarter. Other data collected includes the energy used in compression and precooling of the hydrogen, maintenance and safety logs, and hydrogen control quality results.

The West Sacramento station was completed and commissioned in December 2014. The data collection portion of this project has continued and six quarters of data have been collected from the site and submitted to NREL. The San Juan Capistrano station was completed and commissioned in September 2015. The data collection portion of this project has continued and three quarters of data have been collected from the site and submitted to NREL. The Bishop Ranch station began construction June 20, 2016. Installation of the GTI panel will likely occur in September or October of this year. The GTI-supplied hydrogen gas flow meter for the system (longest lead item) has been delivered to the Linde

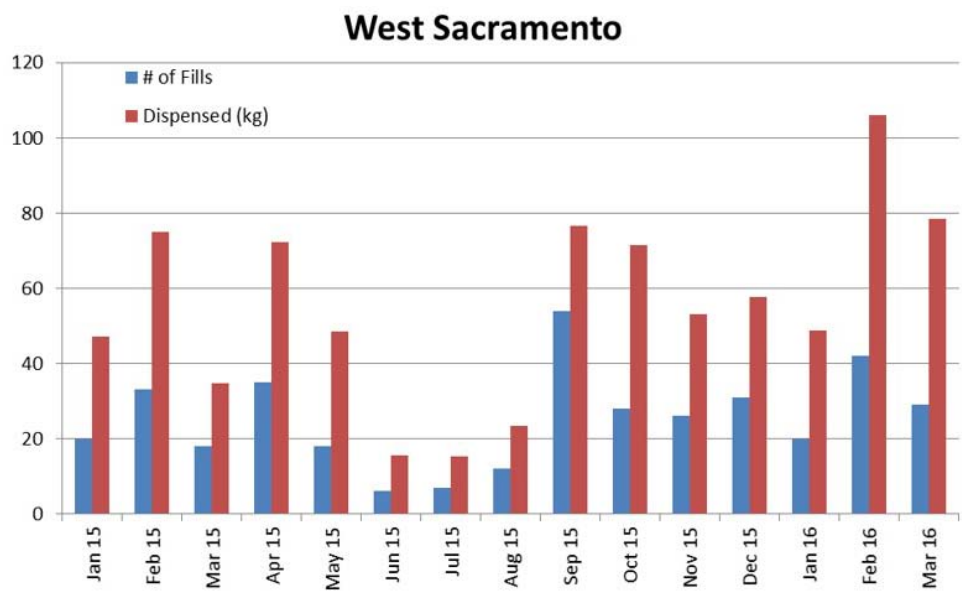

FIGURE 1. West Sacramento usage data

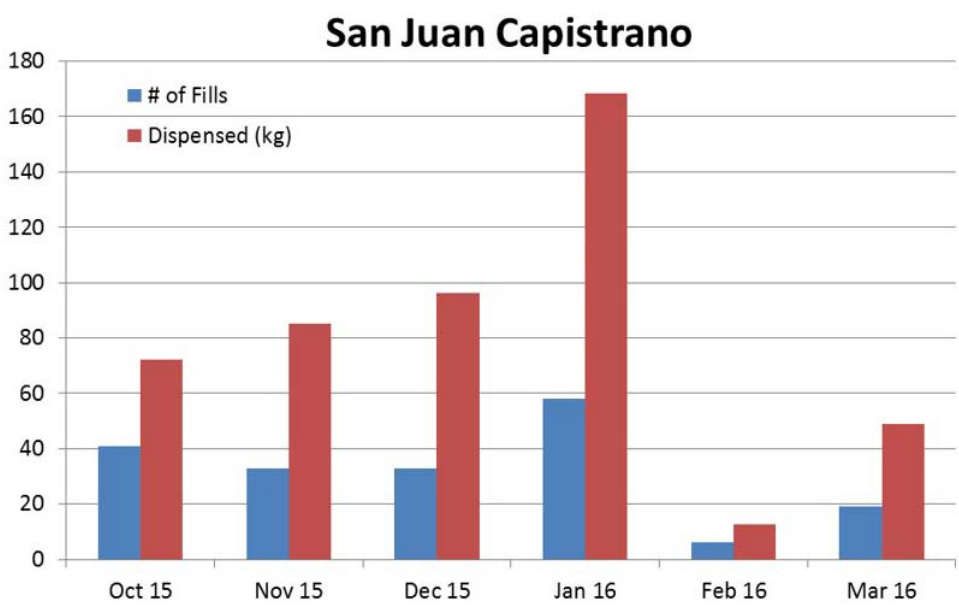

FIGURE 2. San Juan Capistrano usage data

staging area for integration into the compressor skid prior to the skid being installed at the site. The GTI data logger panel was assembled in early 2016 and is ready for installation whenever site construction progress allows. Lastly, progress continues to be made on the installation of the remaining two stations though these installations have progressed slowly due to permitting issues. Sites have all been identified and early engineering has been initiated. These sites are each in various stages of city planning discussions with the local authorities. The major equipment for each site has already been built and is awaiting installation.

CONCLUSIONS AND FUTURE DIRECTIONS

- Complete construction panel installation at Bishop Ranch.
- Produce the complete sets of data for three project sites at the end of each quarter after startup and commissioning is completed.
- Continue progress on remaining two sites.

FY 2016 PUBLICATIONS/PRESENTATIONS

1. "tv025_barnes_2016_p.pptx" – Poster Presentation 2016 AMR.

VII.B.3 Validation of an Advanced High Pressure PEM Electrolyzer and Composite Hydrogen Storage, with Data Reporting, for SunHydro Stations

Larry Moulthrop (Primary Contact), Joe Sieverman
Proton Energy Systems d/b/a Proton OnSite
10 Technology Drive
Wallingford, CT 06492
Phone: (203) 678-2188
Email: lmoulthrop@protononsite.com

DOE Manager: Jason Marcinkoski
Phone: (202) 586-7466
Email: Jason.Marcinkoski@ee.doe.gov

Contract Number: DE-EE0005887

Subcontractors:
- SunHydro LLC, Wallingford, CT
- Air Products and Chemicals, Inc. (APCI), Allentown, PA

Project Start Date: December 1, 2012
Project End Date: June 30, 2017

Overall Objectives

- Validate energy savings of up to 11 kWh/kg H_2 through system and stack advancements.
- Double usable hydrogen storage per unit volume by increasing pressure cycling range.
- Provide advanced packaging design to reduce station footprint.
- Collect and report station performance for up to 24 months.

Fiscal Year (FY) 2016 Objectives

- Validate advanced packaging arrangement.
- Conduct reporting of station performance.

Technical Barriers

This project addresses the following technical barriers from the Technology Validation section of the Fuel Cell Technologies Program Multi-Year Research, Development and Demonstration Plan.

(C) Hydrogen Storage

(D) Lack of Hydrogen Refueling Infrastructure Performance and Availability Data

(E) Codes and Standards

Technical Targets

Advanced Electrolysis-Based Fueling Systems

There isn't a target table in the Technology Validation section of the Multi-Year Research, Development, and Demonstration Plan specific to hydrogen refueling infrastructure. This project is conducting technology validation of improved cell stack, system, and storage components for an electrolysis-based hydrogen refueling station. These improvements will support the following targets.

- Reduce station energy use by up to 11 kWh/kg.
- Reduce the storage volume by 50% per kg of hydrogen dispensed.
- Package a station based on proton exchange membrane (PEM) electrolysis within a 12-m International Organization for Standardization (ISO) container.

FY 2016 Accomplishments

- Installed Sun Hydro 2 compact station at a National Park Service (NPS) maintenance facility in Washington, D.C.
- Validated compact station installation footprint and code-directed clearances.
- Reported SunHydro 1 hydrogen energy usage data to fuel cell electric vehicle (FCEV) Infrastructure Composite Data Product (CDP) database.

✧ ✧ ✧ ✧ ✧

INTRODUCTION

This multi-year, two-phase project primarily leverages Proton's SunHydro 1 station in Wallingford, Connecticut, with access to over 100 kg/d in generation capacity, and a new containerized SunHydro 2 station in Washington, D.C., for technology validation of improved components for hydrogen fueling stations (Figure 1). Our compact, containerized SunHydro™ station design embodied by SunHydro 2 can address initial demand for small, manufactured hydrogen fueling infrastructure in a manner that affords rapid, scalable deployment. The SunHydro station product "skid," integrating hydrogen generation, compression, storage, and dispensing in an intermodal transport ISO container, mitigates significant site permitting

issues by virtue of its small 40 ft × 8 ft footprint and an innovative application of hydrogen code that drastically reduces required clearances.

Proton and SunHydro LLC are continuing down this pathway to demonstrate advanced generation, compression, and storage component technologies, including: (1) higher pressure hydrogen generation with electrochemical compression; (2) higher efficiency generation with lower resistance electrolyte and advanced catalyst; (3) higher addressable capacity composite storage; and (4) advanced packaging concepts for reduced footprint.

APPROACH

These hydrogen fueling improvements have been accomplished based on the following approaches. For higher pressure, higher efficiency PEM cell stacks, Proton has qualified a 30% reduction in PEM thickness for 15 bar and 30 bar hydrogen generator product lines. Furthermore, Proton has been developing advanced catalyst materials and processes that simultaneously reduce the cost of the product and improve the electrochemical performance. A 55 bar militarized cell stack design was built using the thinner material and advanced catalyst deposition to show the performance improvement at full-scale compared to previous technology stacks. We upgraded a commercial 30 bar C Series electrolyzer to operate at 55 bar by strengthening the gas drying components. An increase in hydrogen generation pressure from 30 bar to 55 bar can improve hydrogen fueling system efficiency in two areas – hydrogen gas drying and dried hydrogen compression into station storage. The dryer purge losses can be expected to decrease substantially since the water vapor concentration at 55 bar will be about 55% of the concentration at 30 bar. Higher dry hydrogen pressure into the station mechanical compressor results in better combined compression energy and higher throughput capability.

For higher addressable capacity storage and reduced station footprint, Proton has installed and validated new compact Type II composite storage tubes and applied fresh interpretations of the hydrogen safety code to design a complete fueling station within the compact footprint of an ISO container. Proton applied these new rules to the design of the SunHydro 2 station. The impact of all performance improvements was reported through instrumentation of the station before and after the design changes. The impact of new compact station arrangements was reported in site approval time and in station operability data.

FIGURE 1. SunHydro 1 and SunHydro 2 stations

RESULTS

Task 1.0: Validate full-scale 57 bar higher efficiency PEM cell stack. Work on this task was concluded during the last reporting period. The project goal was to implement advanced membranes and electrodes in a full-scale 57 bar PEM electrolyzer stack to show energy savings approaching 8 kWh/kg H_2 over the 30 bar commercial version. The full-scale 55 bar PEM cell stack was successfully installed into the 57 bar capable C Series and was operated at 55 bar over 900 h through the second and third quarter of 2014. This stack continues to operate stably at 30 bar and remains capable of 55 bar operating pressures through the current reporting period. Most recent demonstrated operating voltages of 2.03 VDC/cell, a performance improvement of 120 mV over baseline, is routinely achieved on Proton's 0.73 ft^2 active area commercial cell stacks. Based on this 120 mV per cell improvement, we have demonstrated energy savings of 3.2 kWh/kg H_2.

Task 2.0: Validate full-scale 57 bar, 65 kg/d hydrogen generator. Work on this task was concluded during the last

reporting period. The build of the Proton C Series hydrogen generator that is the test bed for the advanced cell stack was completed in late 2012 and supplies the hydrogen used by the SunHydro 1 station at Proton. Specific energy data from the upgraded 55 bar C Series electrolyzer and the fueling station compressor were gathered in kWh/kg H_2 over a period of approximately 30 days in the second and third quarter of 2014. The resulting values were compared to the specific energy data produced under 30 bar operation within a similar time frame. By increasing the PEM water electrolyzer generation pressure from 30 bar to 55 bar, Proton achieved an electrolyzer energy reduction of 1.5 kWh/kg H_2 and a compressor energy reduction of 0.3 kWh/kg H_2 for a total savings of 1.8 kWh/kg H_2, halfway toward the statement of project objectives goal of 3.6 kWh/kg H_2.

Task 3.0: Validate higher addressable capacity composite hydrogen storage tubes. Storage tube validation continues as the SunHydro 1 station continues to service vehicles and as SunHydro 2 comes on line in 2016. The newer Type II SunHydro 1 tubes serve as the primary bank as they are used first to fill; the other three banks of previous generation Type II tubes serve to top up. On average the new tubes are pressure cycled three days per week from 89 MPa to less than 46 MPa based on the demands of an average fleet size of 10 fuel cell vehicles. A second set of storage tubes has entered into validation testing with the deployment of SunHydro 2 station in 2016.

Task 4.0: Validate compressor increased throughput capacity with 57 bar input. Work on this task was concluded during the last reporting period. With the successful completion of Task 2 and 3, validation of the anticipated increased throughput capacity of the compressor is completed. By increasing the PEM water electrolyzer generation pressure from 30 bar to 55 bar, Proton achieved an electrolyzer energy reduction of 1.5 kWh/kg H_2 and a compressor energy reduction of 0.3 kWh/kg H_2 for a total savings of 1.8 kWh/kg H_2, halfway toward the statement of project objectives goal of 3.6 kWh/kg H_2.

Task 5.0: Hydrogen station safety operation procedure and EX (potential hazardous area) zone review. In prior reporting periods, results of Chapters 6, 7, and 13 of the National Fire Protection Agency (NFPA) 2 "Hydrogen Technologies Code" [1] were used to determine hazardous equipment zones and methods to mitigate code-directed separation distances to develop the novel compact component layout and model in Task 6 with respect to classified and non-classified areas. As previously reported, this compact hydrogen station arrangement and a corresponding site general arrangement permitted was granted by Braintree, Massachusetts, authorities in October 2014.

The station hardware was subsequently redirected to provide demonstration of a compact hydrogen station infrastructure in Washington, D.C. In this reporting period, this compact hydrogen station was successfully installed at the NPS Brentwood Maintenance Facility in Washington, D.C., after a siting review that addressed tight clearance requirements of the NPS installation site. A safety operating and emergency response procedure was approved, then used to train more than 200 Washington, D.C., firefighters and first responders.

Proton is an industry member of the NFPA 2 Hydrogen Technologies Code technical committee, and has a representative on the Hydrogen Safety Panel. The technical committee is now preparing the 2018 update to the original 2016 edition of NFPA 2. Improvements to Chapter 7 concerning hydrogen equipment in enclosures, specific code that addresses hydrogen processing equipment and storage in prefabricated intermodal enclosures, will help code officials with permitting compact containerized hydrogen fueling stations.

Task 6.0: Validate novel compact and non-EX rated component arrangements. The compact SunHydro hydrogen fueling station was formally opened in July 2016 at the NPS Brentwood Maintenance Facility in Washington, D.C., a validation of the 8 ft × 40 ft compact station footprint goal. Component general arrangement is shown in Figure 2, and separation distances to site exposures are shown in Figure 3. Proton's analysis of compact hydrogen station component arrangements under this work shows an advantage to using the non-classified area immediately around our PEM hydrogen generator to house almost all electrical power and control equipment. Installation effort is confined to pouring three concrete footings, construction of a concrete vehicle fueling pad, and supply of electrical and water utilities. NFPA 2 hydrogen code permits reduction of separation distances to near-zero values when a 2-h rated firewall is interposed. Our arrangement shows significant space saving advantages in placing this firewall in between the non-classified electrolyzer generator container space and the classified container space that houses compression, storage, and a built-in dispenser. This approach enabled SunHydro 2 station installation within the tight confines of the NPS Brentwood site.

Task 7.0: Hydrogen station data acquisition system & Task 8.0 Quarterly Operation data reporting. The data acquisition system is installed in SunHydro 1 and has provided operating data for quarterly reports to the FCEV Infrastructure CDP. Identical data acquisition equipment is installed in SunHydro 2 and is now active ready to acquire data as the station starts to be used. Four reports of SunHydro 1 station data were prepared for the FCEV Infrastructure CDP during the previous fiscal year, 11 in total since the start of our contract.

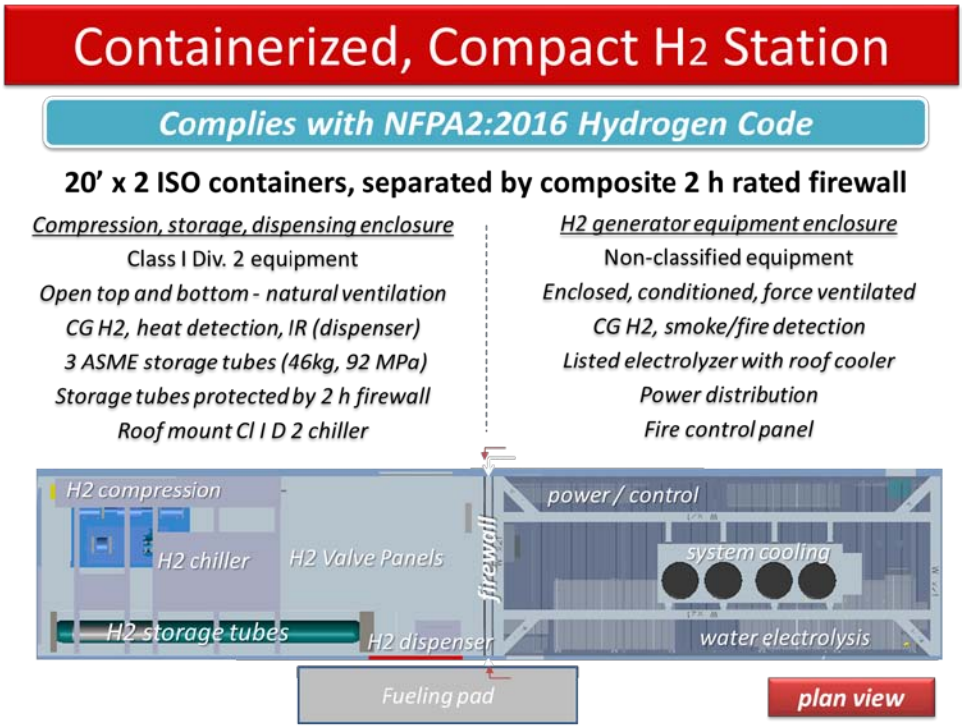

CG – Combustible gas sensor

Figure 2. Arrangement, hydrogen generator container, SunHydro concept, combined containers

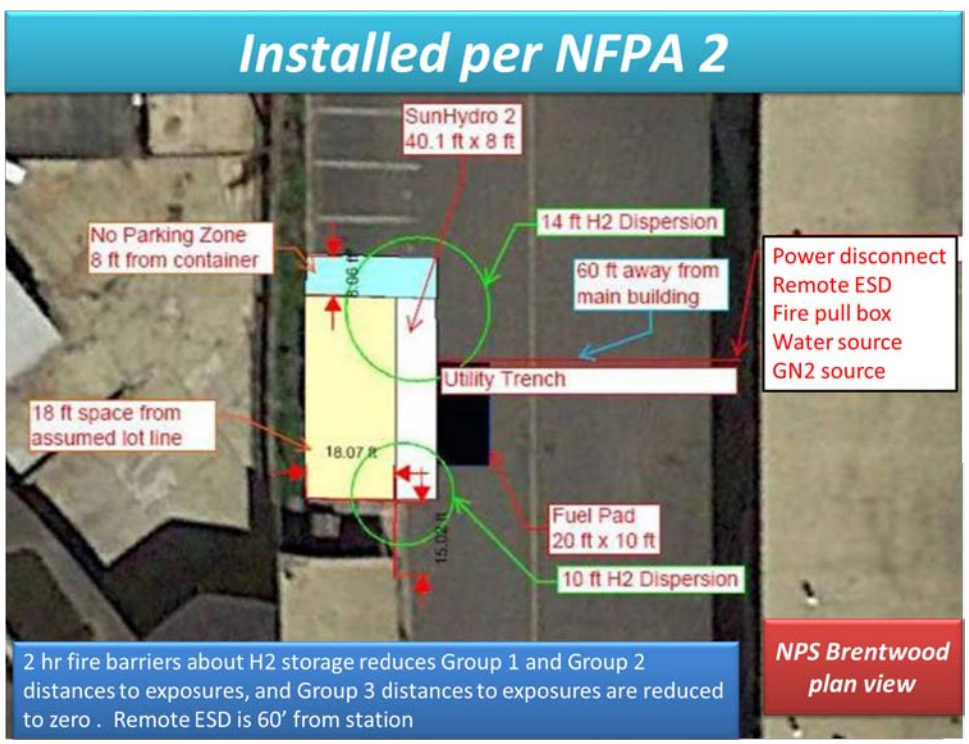

ESD – Emergency shutdown device; GN2 – Nitrogen, gaseous

FIGURE 3. General arrangement and distances to exposures, SunHydro 2 station

CONCLUSIONS AND FUTURE DIRECTIONS

Conclusions

- Compact station arrangements using non-EX rated components can be approved for installation using NFPA 2 code.
- 55 bar generation and compression yields efficiency gains over the 30 bar baseline.

Future Directions

- Initiate SunHydro 2 data acquisition CDP operational data reporting.
- Continue reporting SunHydro 1 CDP operational data reporting.

FY 2016 PUBLICATIONS/PRESENTATIONS

1. AMR 2016 moulthrop TV-012.

REFERENCES

1. NFPA 2 Hydrogen Technologies Code, NFPA, 1 Batterymarch, Quincy, MA.

VII.B.4 CSULA Hydrogen Refueling Facility Performance Evaluation and Optimization

David Blekhman
California State University, Los Angeles (CSULA)
Los Angeles, CA 90032
Phone: (323) 343-4569
Email: blekhman@calstatela.edu

DOE Manager: Jason Marcinkoski
Phone: (202) 586-7466
Email: Jason.Marcinkoski@ee.doe.gov

Contract Number: DE-EE0005890

Subcontractor:
Hydrogenics, Mississauga, ON, Canada

Project Start Date: October 1, 2012
Project End Date: June 30, 2017

Overall Objectives

Technical Objectives

- Test, collect data, and validate hydrogen refueling architecture deployed at CSULA and its individual components in a real-world operating environment.
- Provide the performance evaluations data to the Hydrogen Secure Data Center at the National Renewable Energy Laboratory (NREL).
- Contribute to the development of new industry standards.
- Develop and implement fueling station system performance optimization.

Educational Objectives

- Conduct outreach and training activities promoting the project and hydrogen and fuel cell technologies.
- Provide a living-lab environment for engineering and technology students pursuing interests in hydrogen and fuel cell technologies.

Fiscal Year (FY) 2016 Objectives

- Perform regular collection of station performance data and submit quarterly reports to NREL.
- Conduct outreach and training activities for public and government and engage students in station related activities.
- Review station performance based on data collected, identify potential areas for optimization, and implement if within budget.

Technical Barriers

This project addresses the following technical barriers from the Fuel Cell Technologies Program Multi-Year Research, Development, and Demonstration Plan:

Hydrogen Production

(L) Operations and Maintenance

(M) Control and Safety

Technology Validation

(D) Lack of Hydrogen Refueling Infrastructure Performance and Availability Data

Contribution to Achievement of DOE Hydrogen Production and Technology Validation Milestones

This project will contribute to achievement of the following DOE milestones from the Hydrogen Production and Technology Validation section of the Fuel Cell Technologies Program Multi-Year Research, Development, and Demonstration Plan:

Hydrogen Production

- Milestone 2.6: Verify the total capital investment for a distributed electrolysis system against the 2015 targets using H2A. (Q2, 2016)
- Milestone 2.7: Verify 2015 distributed hydrogen production levelized cost target through pilot scale testing coupled with H2A analysis to project economies of scale cost reduction. (Q3, 2017)

Technology Validation

- Milestone 3.4: Validate station compression technology provided by delivery team. (4Q, 2018)

FY 2016 Accomplishments

- The station continues to collect and regularly submit performance data to NREL.
- CSULA recertified its state approval for commercial sale of hydrogen on a per kilogram basis.
- The station has collaborated with Sandia National Laboratories, NREL, and California Air Resources

Board to test the performance of DOE sponsored HyStEP device after its arrival to California.

- CSULA has performed physical and programming upgrades toward improving safety, meeting fueling standards and per NREL data collection.
- The station has had a steady flow of visitors learning about hydrogen. In addition, several engineering students are interning at the station. Former interns have secured jobs in the hydrogen field.

✧ ✧ ✧ ✧ ✧

INTRODUCTION

The CSULA hydrogen station deploys the latest technologies with the capacity to produce and dispense 60 kg/d, sufficient to fuel 15–20 vehicles. The station utilizes a Hydrogenics electrolyzer, first and second stage compressors enabling 350 bar and 700 bar fueling and 60 kg of hydrogen storage. The station is grid-tied with certified 100% renewable power.

In addition to collecting data per NREL specifications, the comprehensive data collection enhances research opportunities in evaluating and optimizing performance of the hydrogen fueling facility. The facility is actively engaged in research projects and demonstrations to speed up the development of hydrogen infrastructure. As an educational institution, CSULA actively promotes the technology to various audiences and prepares students with a background in fuel cell and hydrogen applications.

APPROACH

To enable effective data collection on the station performance, a significant number of sensors and meters had been installed on the station equipment. A custom designed software package is utilized for data collection and reporting to NREL.

As data is collected and analyzed, the station hardware and software is gradually upgraded for performance optimization and other technical/safety enhancements.

RESULTS

Over the past year, CSULA has regularly submitted NREL quarterly reports on the station performance and hydrogen purity according to the contract with DOE. The reports have been generated automatically using power, temperature, pressure, and mass flow meters. Based on NREL feedback, supplementary reporting on the daily stored amount of hydrogen has been implemented. Based on the observed performance and industry feedback, the station hardware and programming has been updated to improve station safety and compliance with fueling standards. In particular, up to three safety leak tests were added, fueling pressure corridors were implemented to meet 2014 SAE J2601, and the hydrogen chiller was adjusted from -24°C down to -32°C. The station availability has been improved by addressing valve leaking in the dispenser. The main flow valve was upgraded by its manufacturer, TESCOM, based on the station staff feedback and the weeping holes from this and another valve were routed externally to the dispenser.

In 2015, CSULA became the first station in the United Stated to receive a seal of approval for commercial sales of hydrogen on a per kilogram basis. In January 2016, the station passed annual recertification. During testing the flow meter was recalibrated to meet the accuracy requirements. A point of sale credit card reader has been installed in the control room enabling commercial sales in addition to original equipment manufacturer contracts.

The station has been supporting outreach and collaborative research efforts. In September 2015 CSULA hosted a training workshop and a shake-down testing of the HyStEP device designed by NREL and Sandia National Laboratories, Figure 1. Sponsored by DOE, HyStEP is designed to test new stations to comply with 2014 fueling protocols. CSULA has used this opportunity to identify potential areas for improvement.

FIGURE 1. HyStEP workshop attendees at the CSULA hydrogen station

About 1,500 visitors have toured the facility in the past year with about 85% of them being students of all ages. To enhance student learning, an educational poster has been developed and installed on a unit in the fueling island and another in the station touring area, Figure 2. Additionally, CSULA has hosted a number of professional meetings, first-responder training, etc. Several students have been interning at the station and some have secured jobs in the hydrogen infrastructure field. The campus has acquired three Hyundai fuel cell vehicles, which are deployed in public safety and commuter roles, Figure 3.

FIGURE 2. Hydrogen station operation educational poster in the station touring area

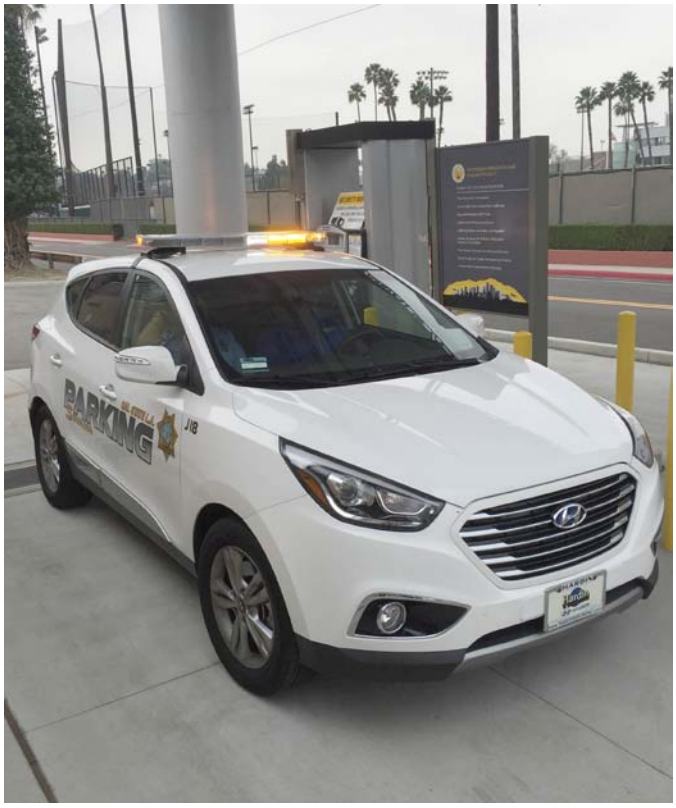

FIGURE 3. CSULA hydrogen public safety vehicle

CONCLUSIONS AND FUTURE DIRECTIONS

The project has completed Phases I and II, and has transitioned in to Phase III. The station provides a reliable fueling experience and generates data that is furnished to NREL. In collaboration with its partners, CSULA has received funding from the California Energy Commission to secure two fuel cell shuttles to operate on campus.

VII.B.5 Brentwood Case Study

Carl Rivkin (Primary Contact), Melanie Caton, and Christopher Ainscough
National Renewable Energy Laboratory (NREL)
15301 Denver Parkway West
Golden, CO 80401
Phone: (303) 275-3839
Email: Carl.Rivkin@nrel.gov

DOE Manager: Jason Marcinkoski
Phone: (202) 586-7466
Email: Jason.Marcinkoski@ee.doe.gov

Subcontractors:
- Proton Onsite, Wallingford, CT
- Werken, Washington, DC
- Anderson Burton, Colorado Springs, CO

Project Start Date: May 15, 2015
Project End Date: Project continuation and direction determined annually by DOE

Overall Objectives

This project will document lessons from the permitting and construction of a hydrogen fueling station to further reduce the time and costs associated with deploying hydrogen-fueling technology. This work will address key barriers defined in the Multi-Year Research, Development, and Demonstration Plan, including:

- Lack of knowledge regarding project siting.
- Inadequate installation expertise.
- High permitting costs.

Fiscal Year (FY) 2016 Objectives

- Document lessons learned for future hydrogen infrastructure projects.
- Publish NREL technical report of lessons learned.

Technical Barriers

This project addresses the following technical barriers from the Fuel Cell Technologies Office Multi-Year Research, Development, and Demonstration Plan.

Market Transformation

(A) Inadequate Standards and Complex and Expensive Permitting Procedures

(G) Lack of Knowledge Regarding the Use of Hydrogen Inhibits Siting (e.g., Indoor Refueling)

(L) Inadequate Installation Expertise

Technology Validation

(A) Lack of Data on Stationary Fuel Cells in Real-World Operation

Contribution to Achievement of DOE Technology Validation Milestones

This project will contribute to achievement of the following DOE milestones from the Fuel Cell Technologies Office Multi-Year Research, Development, and Demonstration Plan.

- Milestone 3.5: Validate distributed production of hydrogen from renewable liquids at a projected cost of $5/gge and from electrolysis at a projected cost of $3.70 with an added delivery cost of <$4/gge. (4Q, 2018)

FY 2016 Accomplishments

- The fueling station permitting has been completed.
- The report documenting the lessons learned is drafted as an NREL technical report and will be published shortly.

✧ ✧ ✧ ✧ ✧

INTRODUCTION

Deploying hydrogen fueling stations (HFSs) is a critical step in the overall process of hydrogen technologies deployment. The placement of high-pressure hydrogen fueling dispensers in the retail environment represents a significant change in retail fueling technology. The purpose of this project is to better understand the obstacles to HFS deployment. This project will document lessons form the permitting and construction of a hydrogen fueling station (shown in Figure 1) to further reduce the time and costs associated with deploying hydrogen fueling technology.

APPROACH

NREL leveraged the strengths and knowledge of the project partners to derive the best understanding of the issues with siting and building hydrogen fueling stations.

RESULTS

The lessons learned analysis produced the following key lessons.

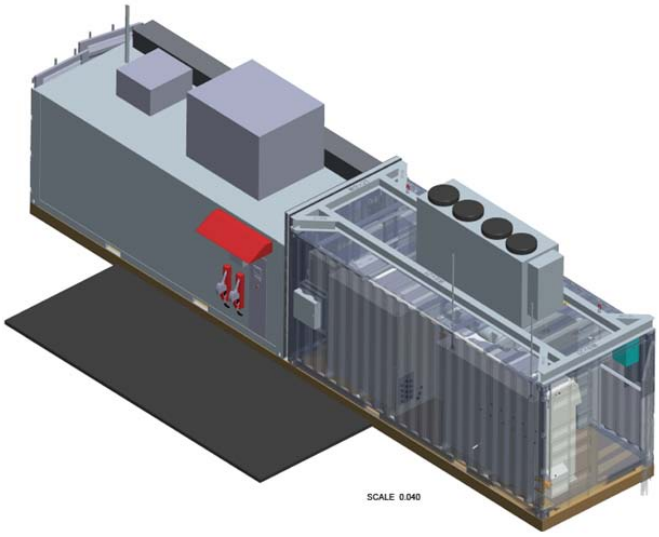

FIGURE 1. Modular hydrogen fueling station

- A Phase I environmental audit would be very valuable for project developers to evaluate the potential for siting a hydrogen fueling station.
- Coordination of the multiple authorities having jurisdiction involved in any project can save time and money and will likely only be accomplished effectively by a single advocate.
- An existing site may have serious safety problems that a new project such as a hydrogen fueling station uncovers and must be resolved before the station project can proceed.
- Integrating a new project into an existing site, particularly an older site that may have limited documentation, will present challenges that must be weighed against the prospects of employing a new site.

CONCLUSIONS AND FUTURE DIRECTIONS

This study produced valuable lessons learned that could aid project developers for hydrogen fueling stations that would be located at both commercial and government sites. The station can also be used as learning tool to explain both safety issues and the elements of hydrogen technologies for a variety of stakeholders, including project developers, the safety community, and the general public.

FY 2016 PUBLICATIONS/PRESENTATIONS

1. Brentwood Lessons Learned Draft NREL Technical Report August 2016.

VII.C.1 Hydrogen Component Validation

Danny Terlip
National Renewable Energy Laboratory (NREL)
15013 Denver West Parkway
Golden, CO 80401
Phone: (303) 275-4180
Email: danny.terlip@nrel.gov

DOE Manager: Jason Marcinkoski
Phone: (202) 586-7466
Email: Jason.Marcinkoski@ee.doe.gov

Subcontractor:
Spectrum Automation, Arvada, CO

Project Start Date: October 2012
Project End Date: Project continuation and direction determined annually by DOE

Overall Objectives

- Reduce fuel contamination introduced by forecourt station components.
- Improve station reliability and uptime.
- Increase the publicly available energy and performance data of major station components.

Fiscal Year (FY) 2016 Objectives

- Develop a contaminant library through H2Tools.org.
- Improve maintenance and reliability data collection and analysis at NREL Hydrogen Infrastructure Testing and Research Facility (HITRF).
- Collect and analyze power and energy consumption data for major hydrogen station components.

Technical Barriers

This project addresses the following technical barrier from the Technology Validation section of the Fuel Cell Technologies Office Multi-Year Research, Development, and Demonstration Plan.

(D) Lack of Hydrogen Refueling Infrastructure Performance and Availability Data

FY 2016 Accomplishments

- Nine forecourt hydrogen stations are participating in a contaminant collection program.
- Began discussions with H2Tools.org for a section on the contaminant library.
- Installed three power and energy meters on major station equipment at HITRF and automated the data collection; analyzed data used by other DOE researchers for station energy and cost analysis.
- Discussions with compressor manufacturers resulted in changing the lubricant used for components in hydrogen service from a substance harmful to fuel cells to a known safe substance.
- Installed and commissioned a 900 bar, 140 SCFM linear piston compressor at HITRF.
- Generated first maintenance graphic for comparison to composite data product (CDP) INFR 21 showing the contribution of HITRF station components to overall maintenance events.

✧ ✧ ✧ ✧ ✧

INTRODUCTION

The Hydrogen Component Validation task is focused on addressing three challenges currently facing forecourt hydrogen stations today that were prioritized from an H2USA Fueling Stations Working Group brainstorming session: fuel contamination introduced by forecourt station components; station reliability and uptime; and lack of publicly available energy and performance data of major station components. Improvement in each one of these topic areas is critical for successful station operation, positive fuel cell driver experience, and a robust hydrogen economy.

APPROACH

NREL is working to better understand particulate contamination in the hydrogen process stream by distributing contaminant collection packets to forecourt station operators. When a maintenance event occurs, the participating station operators will collect any particulate matter found in the hydrogen tubing or components and send the samples to NREL, where they will be analyzed, anonymized, and published to the Hydrogen Station Contaminant Research Library for the larger community to reference for root cause analysis of contamination events.

Station reliability and uptime are being studied in depth at the HITRF station, where detailed logs of planned and unplanned maintenance events are kept. The process media, component materials of construction, failure mechanism, and station downtime are all recorded. Data are aggregated monthly and compared with data collected by National Fuel Cell Technology Evaluation Center on forecourt hydrogen stations. The major contributors to downtime are identified and studied.

NREL installed power meters on two hydrogen compressors and the hydrogen pre-cooling system at HITRF. The HITRF Supervisory Control and Data Acquisition (SCADA) system is collecting power and energy data as each of these components operates to support the HITRF. NREL engineers are analyzing the data and collaborating with other DOE researchers to better understand operating costs of forecourt hydrogen stations and possible precursors to equipment failures that can be used to indicate the need for preemptive maintenance.

RESULTS

NREL has provided sample kits including swabs, vials, baggies, and an information form to nine forecourt hydrogen stations. Multiple samples have been collected, typically from failed parts. Contaminants found range from metal shards—likely from tubing cutting—to elastomer material —likely from failed seals. Figure 1 shows two examples of particulate contaminants that were collected. The image on the left shows metal shards embedded in a valve seat. The image on the right shows elastomer material collected in a filter just upstream of the dispenser.

It is clear from other samples collected that lubricant, normally used on elastomer seals, is collecting at certain areas in the process stream. This reinforces the need for lubricants that do not adversely affect fuel cell operation, such as Krytox. Often the lubricant acts as an aggregator for particulates and is commonly found discolored. NREL has advised three major compressor manufacturers on the composition and application of appropriate lubricant on process stream components.

NREL has collected maintenance data on the HITRF since it began operating in February 2015. This data includes component failures and routine maintenance on all major system components. NREL compiles the maintenance data collected at HITRF in a similar manner to data collected from CDPs to promote a direct comparison, as shown in Figure 2. Like at retail stations, the dispenser and compressor are large contributors to downtime and system maintenance.

There are some notable differences in maintenance events for the HITRF station and aggregated industry data. The reason for these differences is that the HITRF data was collected during the commissioning and initial phases of station operation. Additionally, the HITRF is a research station that, while similar to a retail station, is not operated in the same manner. For instance, the electrolyzer system at HITRF is a bespoke system designed by NREL engineers and has multiple research projects associated with it. This results in maintenance events that would not normally occur with retail hydrogen stations. Despite these differences, the data collected is still informative for deep dive failure analysis and improving station uptime.

NREL engineers installed power meters on two hydrogen compressors and the pre-cooling system. The HITRF SCADA system is collecting data on the amount of power and energy consumed by each component at one-second intervals. NREL engineers perform detailed analysis on the data, resulting in quantitative performance information.

For instance, the 400 bar compressor, with a constant suction pressure (6.89 bar), was found to consume 3.53 kWh/kg[1] at a flow rate of 2.78 kg/hr. The 20 hp motor consumed a peak power of 11.5 kW when compressing from 350 bar to 400 bar. This type of data is important when budgeting for the operation of a hydrogen station. For example, a 100 kg/d station would require a station operator

[1] Compressor motor consumption only. Balance-of-plant components, such as jacketed cooling and control system, have been found to consume 1.5 kW to 2 kW.

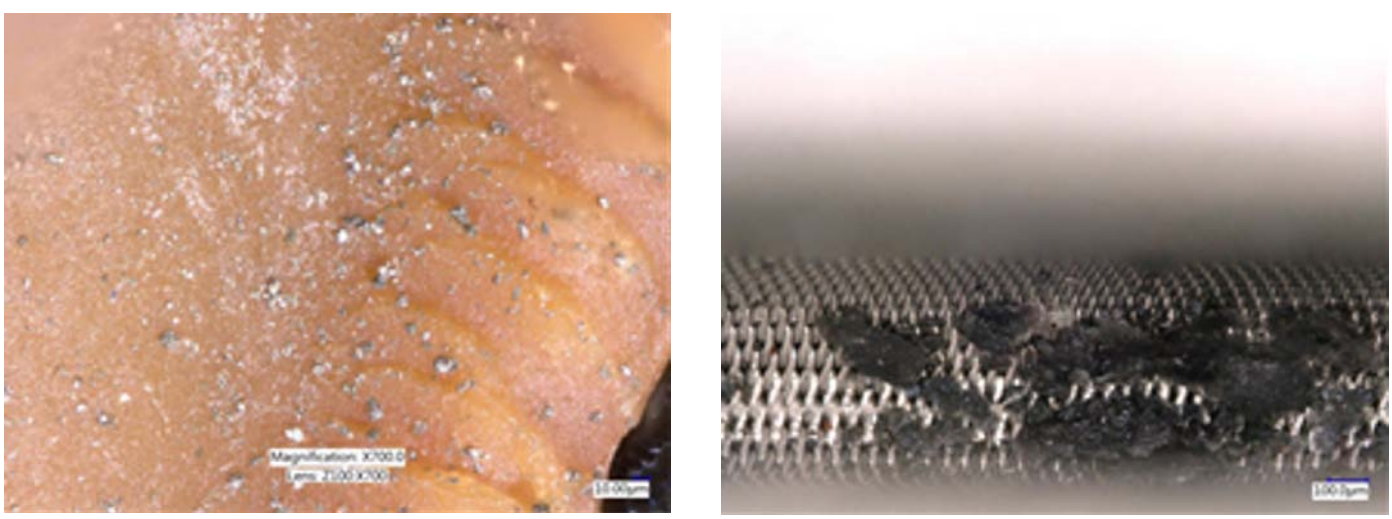

FIGURE 1. Two contaminant samples collected as part of the Hydrogen Station Contaminant Research Library task

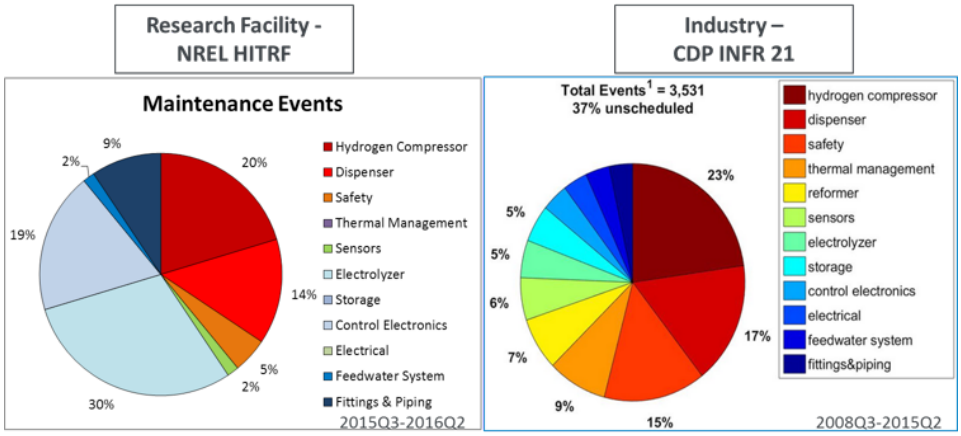

FIGURE 2. NREL HITRF (left) and aggregated industry (right) maintenance events for hydrogen stations

to purchase 353 kWh of electricity to compress 7 bar gas to 400 bar.

The energy and power requirements for recovery of the pre-cooling system after a vehicle fill is another example of impactful performance analysis. As a fuel cell electric vehicle is filled, heat from the hydrogen flowing from the station is added to the heat exchanger. The chiller then needs to run a compressor to cool the block back down. Figure 3 shows one-second data collected from the power meter on the chiller and other sensors in the heat exchanger.

Analysis from this data capture shows that full cooling block recovery takes 6 kWh and 58.9 min. Reaching the allowable fill temperature only takes 3.7 kWh and 35.4 min. This information is critical to a hydrogen station operator that will likely have more than one customer every 35.4 min and thus will consider sizing of the pre-cooling system. In addition to the energy cost of recovering from a fill, the station operator must consider the energy cost to maintain the block temperature during non-filling periods, which is data that NREL collects.

CONCLUSIONS AND FUTURE DIRECTIONS

The Hydrogen Component Validation project addresses three major challenges facing forecourt hydrogen stations today: fuel contamination, reliability, and energy consumption related to major station components. The Hydrogen Station Contaminant Research Library was developed to collect field samples of particulate matter, determine the origin, and publish the results to identify major issues impacting a high percentage of stations. Currently nine stations are participating, and NREL is reaching out to more as stations become operational.

NREL has implemented a detailed maintenance log at the HITRF station in Golden, Colorado. This database allows NREL to not only document failures on station components,

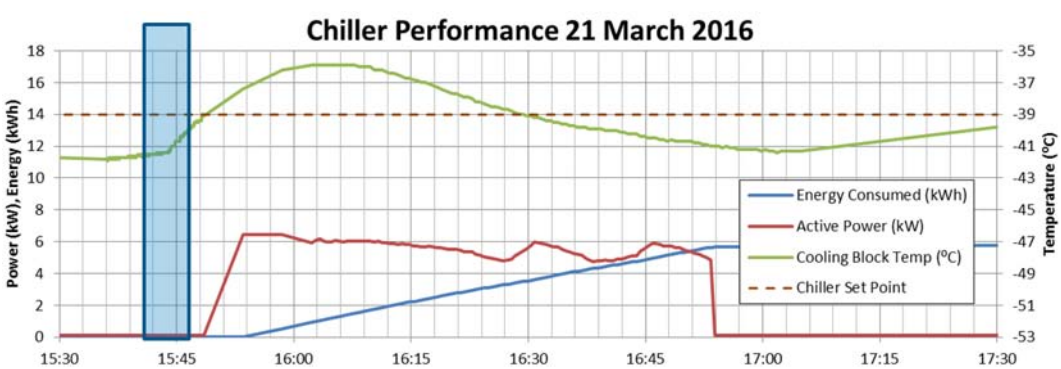

FIGURE 3. Chiller performance data showing the power (red line) and energy (blue line) requirements to recover the heat exchanger block temperature (green line) from a fill (indicated by the blue shaded rectangle). The system is unable to perform a fill when the cooling block temperature is above the set point (orange dotted line).

but also perform analysis on the causes of the failures. The data collected is compared to retail hydrogen stations to help identify the most common failures at forecourt hydrogen stations that impact station uptime and their causes. The HITRF will continue to be a test bed for new components and designs for hydrogen service as they are made available.

Power and energy consumption of major station components impacts operating costs at hydrogen stations. NREL has installed power meters on two hydrogen compressors and the hydrogen pre-cooling system. The HITRF SCADA system continually records data during operation, and NREL engineers analyze the data. The analysis is used to inform modeling efforts of hydrogen stations. Future work will involve analyzing the data for possible precursors to failure and impacts for reducing operating costs at hydrogen stations.

FY 2016 PUBLICATIONS/PRESENTATIONS

1. "Hydrogen Component Validation," Terlip, Danny. U.S. Department of Energy Hydrogen and Fuel Cells Program Annual Merit Review 2016. Washington D.C., 7 June 2016.

VII.C.2 Development of the Hydrogen Station Equipment Performance (HyStEP) Device

Terry Johnson (Primary Contact),
Danny Terlip (NREL), Chris Ainscough (NREL)
Sandia National Laboratories
7011 East Avenue
Livermore, CA 94551-0969
Phone: (925) 294-2512
Email: tajohns@sandia.gov

DOE Manager: Jason Marcinkoski
Phone: (202) 586-7466
Email: Jason.Marcinkoski@ee.doe.gov

Subcontractor:
Powertech Labs Inc., Surrey, B.C., Canada

Project Start Date: September 2014
Project End Date: March 2016

Overall Objectives

- Accelerate commercial hydrogen station acceptance by developing and validating a prototype device to measure hydrogen dispenser performance.
- Develop a device capable of testing to the Canadian Standards Association (CSA) Hydrogen Gas Vehicle (HGV) 4.3 test method to test dispensers for compliance with the table-based fueling protocol defined by SAE J2601-2014.
- Make the device available for use by the state of California to commission existing and new hydrogen stations in the 2016–2017 timeframe.

Fiscal Year (FY) 2016 Objectives

- Publication of the device design to a publicly accessible website to enable third party development of such devices.
- Validation of the HyStEP device performance at National Renewable Energy Laboratory's (NREL's) Energy Systems Integration Facility (ESIF).
- Training of the HyStEP operators from the California Air Resources Board (CARB) and California Department of Food and Agriculture Division of Measurement Standards.
- Validation of the device performance at two hydrogen stations in California.
- Development of a contract to loan the device to CARB for deployment in California.
- Successful performance validation and handoff to CARB for deployment such that station providers and vehicle manufacturers accept the device for station commissioning.

Technical Barriers

This project addresses the following technical barriers from the Technology Validation section of the Fuel Cell Technologies Office Multi-Year Research, Development, and Demonstration Plan.

(D) Lack of Hydrogen Refueling Infrastructure Performance and Availability Data

(E) Codes and Standards

Contribution to Achievement of DOE Technology Validation Milestones

This project contributes to achievement of the following DOE milestone from the Technology Validation section of the Fuel Cell Technologies Office Multi-Year Research, Development, and Demonstration Plan.

- Milestone 4.4: Complete evaluation of 700-bar fast fill fueling stations and compare to SAE J2601 specifications and DOE fueling targets. (3Q, 2016)

FY 2016 Accomplishments

- Posted all design documents to the Pacific Northwest National Laboratory-managed H2Tools website: https://h2tools.org/h2first/HyStEP.
- Successfully validated the performance of the device at NREL's ESIF by completing a comprehensive test matrix over a five-week period.
- Trained the California HyStEP operators during a week-long training session lead by Powertech, NREL, and Sandia at NREL's ESIF.
- Validated the HyStEP performance through three days of testing at the Hydrogen Research/Fueling Facility at California State University, Los Angeles (CSULA).
- Further validated the HyStEP performance through four days of testing at the Diamond Bar hydrogen station at South Coast Air Quality Management District (SCAQMD) headquarters, including side-by-side comparisons with Honda and Toyota fuel cell electric vehicles.

- Documented the successful validation testing in a series of three reports to the Fuel Cell Technologies Office.
- Completed a final training test with the HyStEP operators at the Santa Barbara hydrogen station which included side-by-side testing with Mercedes-Benz and Hyundai.
- Coordinated the deployment of the HyStEP device in California with CARB including execution of a contract between Sandia and CARB for the loan of the device.

✧ ✧ ✧ ✧ ✧

INTRODUCTION

It is generally agreed that policies and technology solutions need to be developed and implemented to help reduce the time to commission a hydrogen station. The current practice of hydrogen station acceptance, which burdens vehicle original equipment manufacturers (OEMs) with serial testing of stations because each OEM conducts its own testing and evaluation, can take months. This process is not practical or sufficient to support the timely development of a hydrogen fueling station network. This is especially true in the state of California where new stations are coming online currently and as many as 35 new stations are scheduled to be commissioned in 2016. Ultimately, a hydrogen station test device that can be used to verify station fueling protocol, average daily and peak fueling capacity, and fuel quality would be desirable to commission new stations. In the near-term, a test device designed specifically to test station fueling protocol that is technically effective, safe, robust, and user friendly will accelerate the commissioning of hydrogen stations. This device must be safe and effective to be useful, but also simple enough to design, fabricate, assemble, and implement quickly to meet the timetable of current station deployment in California. This project was carried out to develop such a device.

To meet this goal, the project team, along with contractor Powertech Labs, has developed the HyStEP device. The device includes three Type IV 70 MPa tanks capable of storing a total of 9 kilograms of hydrogen and instrumented with pressure and temperature sensors. The tanks are connected to a 70 MPa receptacle equipped with pressure and temperature sensors as well as Infrared Data Association (IrDA) communications integrated with a data acquisition, analysis, and control system. A valve near the receptacle attached to a vent manifold can be used to both simulate a leak for fault detection tests and for controlled defueling. A nitrogen purge system is also included. Additional temperature sensors will record ambient temperature near the receptacle and various external system temperatures. The HyStEP device is capable of performing the station validation tests defined in CSA HGV 4.3. These include IrDA communication tests, fault detection tests, and communication and non-communication fills.

APPROACH

The project team selected the device supplier through a competitive bid process and collaborated with the supplier on the design and acceptance testing of the HyStEP device. In order to prepare the device for real-world deployment, the device underwent extensive validation testing at NREL's ESIF. This testing included using the device to carry out many, if not all, of the tests defined in CSA HGV 4.3 to ensure safe and reliable operation. The method for data reporting was also refined during testing and proved out for a real-time report of the results that would be available at a commercial station. Following validation testing at NREL, the device was shipped to California for pre-deployment testing at two commercial hydrogen stations. The device was then put into service by the state through a contract between Sandia National Laboratories and CARB.

The device supplier provided the project team with a comprehensive set of documentation covering device design, operation, maintenance, and safety. The required documents were published by Sandia to a publicly accessible website.

RESULTS

Prior to shipping the device to NREL, validation testing of the HyStEP device at Powertech included leak and pressure tests, IrDA communication confirmation, alarm matrix validation, fueling tests, defueling, and purging. Several leak and pressure tests were completed at Powertech. A leak check to 87.5 MPa was carried out for the entire hydrogen fueling system except for the tanks. This test was completed just before the device was shipped to NREL with no leaks. The hydrogen fueling system, including the three tanks, thermocouple probes, and thermally-activated pressure relief devices, was then leak checked in increments of 10 MPa to 100% state-of-charge (~77 MPa and 42°C). The tanks remained at 100% state-of-charge for three days indicating zero leaks.

IrDA communications were verified using a benchtop system as well as using the Powertech hydrogen dispenser. In addition, halt and abort tests were successfully carried out using the dispenser. The alarm matrix was validated at Powertech through a series of tests. The system responses were checked and verified prior to shipping the device to NREL.

A number of fueling tests were carried out using the Powertech hydrogen dispenser at 35 MPa and 70 MPa as shown in Figure 1. Both communications and non-communication fuelings were carried out. Several of these tests were SAE J2601 compliant fills to target pressure or state-of-charge. Defueling procedures were carried out

FIGURE 1. HyStEP device sited at the Powertech hydrogen dispenser

and verified at Powertech as part of the fueling tests. This included defueling with the remote vent stack to verify operation. Finally, the hydrogen tanks were purged with nitrogen using the purge system prior to shipping the device to NREL.

Validation testing of the HyStEP device at NREL included six test sequences: (1) checkout and device training; (2) general instrument tests; (3) communication capability tests; (4) safety system tests; (5) dispenser communication tests; and (6) table-based fueling tests, defueling tests, and purge tests.

A Powertech engineer traveled to NREL for the checkout and training test sequence which took place over the first full week that the HyStEP device was on site. Initial checkout included an electrical inspection which the system passed with one minor modification. Training was provided by Powertech on the device setup, controls, fueling, defueling, and purging.

Instrument operation and sensor accuracy were checked then rechecked. Pressure transducer and gauge agreement was acceptable. Data collected from the pressure transducers on HyStEP was within +/-1% of the NREL pressure transducer in the dispenser. Hose temperature, as measured by the NREL dispenser, and receptacle temperature, as measured by HyStEP, were in good agreement. Thermocouples on HyStEP tubing were in good agreement with HyStEP tank inlet temperatures. HyStEP in-tank thermocouples were compared with externally placed NREL thermocouples. While general trends in the readings were similar, a large offset was observed as expected due to the thermocouple locations.

Safety system tests included tests of the hydrogen detectors as well as a select list of other alarms. Many of these tests involved confirming the safety system response to a valve failing to close. In addition, the electrostatic discharge button, nitrogen pressure monitor, and trailer door monitor were checked. All alarm conditions were confirmed as programmed.

To begin the communications test sequence, operators confirmed that protocol identifier (ID), software version number (VN), tank volume (TV), receptacle type (RT), fueling command (FC), commands sent from the HyStEP device were appropriately communicated to the dispenser. Then, during fills, three repeats each of the abort, halt, data loss then resume, data loss then abort and cyclic redundancy check fault tests were performed. In each test, the HyStEP performed as expected.

The team performed general fault detection tests by overriding volume, temperature, and pressure values during a fill.

The objective of the fueling, defueling, and purging tests was to exercise the device as it would be used in the field for these operations. To this end, NREL and Powertech performed both communications and non-communications fills. In conjunction with these fills, the team also tested the full tank refusal and exercised the defuel and purging systems.

A week-long operator training session was then carried out by Powertech, NREL, and Sandia at ESIF. Figure 2 shows the operators from CARB and Division of Measurement Standards next to the device sited at the NREL dispenser during the training. Operators were walked through the *Operations and Maintenance Manual* along with key design and safety documentation and then performed a series of hands-on tests using the device.

The HyStEP device was then shipped from Colorado directly to the Hydrogen Research/Fueling Facility at CSULA. The device was offloaded from the flatbed truck on

FIGURE 2. NREL's Hydrogen Infrastructure Testing and Research Facility

Friday, December 11, and setup at the dispenser as shown in Figure 3. Most of the CSA HGV 4.3 test matrix was carried out over a three day period the following week (December 14–16). Overall, the device worked according to expectations and the HyStEP operators were able to test most of its functionality, within the limitation of the station. While the station did not pass all of the tests, HyStEP was able to carry them out as expected and prescribed except as noted below. These tests included five complete tank fills with various combinations of the three HyStEP tanks.

Tests Completed

- Fault Detection Tests: All except for the ambient temperature and minimum fuel delivery temperature were tested. This was due to the limitation of the station. Operators were unable to modify the temperature signals on the dispenser.
- Communication Tests: All communication tests were carried out except for a couple of the invalid data value tests. We found that the HyStEP software was not compatible with these tests as defined in HGV 4.3. Powertech was notified of this discrepancy and modified the infrared hardware and software to resolve this issue.
- Fueling Protocol Tests: The CSULA station was originally designed to the SAE J2601 technical information report, not the new 2014 standard. However, it performs fills that meet the 2014 H70-T20 requirement. So, fills were performed with this protocol. Five fills were completed.
  - Single tank (76 L, 3 kg) non-communication X 2
  - Single tank (76 L, 3 kg) communication
  - Two tank (152 L, 6 kg) communication
  - Three tank (228 L, 9 kg) communication

FIGURE 3. Hydrogen Research/Fueling Facility at CSULA

HyStEP device testing at SCAQMD was successfully completed on Friday, January 22, after four days of testing (see Figure 4). As at CSULA, the device worked as expected, and the operators were able to carry out nearly all of the CSA HGV 4.3 test matrix over the four day period (Tuesday–Friday). While the station did not pass all of the tests, HyStEP was able to carry them out as expected and prescribed, with two exceptions. The tests included more than a dozen complete tank fills with various combinations of the three HyStEP tanks. These also include fills in comparison to two Toyota test vehicles and two Honda test vehicles.

Tests Completed

- Fault Detection Tests: All except for the ambient temperature and minimum fuel delivery temperature tests were completed. This was due to the limitation of the station. The ambient temperature sensor and the hose temperature sensor could not be modified as per the requirements of the test procedure.
- Communication Tests: As at CSULA, all communication tests were carried out except for a couple of the invalid data value tests.
- Fueling Protocol Tests: The SCAQMD station follows SAE J2601-2014 and includes an H70 and H35 nozzle. So, fills were performed with both nozzles, although most were H70 fills. Twenty-one fueling protocol tests were completed:
  - Six communication fills with various initial conditions and tank sizes.
  - Five non-communication fills (H35 and H70) with various initial conditions and tank sizes.
  - Ten additional tests per HGV 4.3.

FIGURE 4. Diamond Bar station at SCAQMD headquarters

FIGURE 5. First Element station in Santa Barbara

The final DOE-funded station test was carried out at the First Element hydrogen station in Santa Barbara as shown in Figure 5. This series of tests was primarily focused on operator training and OEM vehicle comparisons. Mercedes-Benz and Hyundai brought test vehicles to the site during the three day testing period for side-by-side comparisons. A similar test matrix was carried out as at SCAQMD.

CONCLUSIONS AND FUTURE DIRECTIONS

Validation testing of the HyStEP device was carried out at three hydrogen fueling stations (NREL Hydrogen Infrastructure Testing and Research Facility, CSULA, and SCAQMD), and a final training session at the Santa Barbara hydrogen fueling station. Overall, the HyStEP device provided consistent, reliable performance over all of the testing that included over 45 fills. The tests carried out at these stations included leak checks, sensor and instrument checks, IrDA communication checks, and tests that were carried out per the latest draft of CSA HGV 4.3. In addition, at the SCAQMD and Santa Barbara stations, OEM test vehicle fills were carried out along with HyStEP fills for comparison. The device was able to successfully carry out all tests per the HGV 4.3 procedures with the exception of two of the general fault detection tests and two table based communications tests. The two general fault detection tests both require modification of station temperature sensors that could not be performed at any of the stations. The communication tests were not performed correctly due to a limitation of the HyStEP IrDA hardware and software which was subsequently corrected by Powertech.

While no DOE-funded work has been carried out since March, CARB is now leading the deployment of the HyStEP device for commissioning hydrogen stations in California. Following pre-deployment testing, CARB, in conjunction with Division of Measurement Standards has operated the HyStEP device under a loan agreement with Sandia National Laboratories that may continue for a period of up to two years. To prepare for and carry out the deployment, CARB leads a California HyStEP Task Force that is responsible for determining a test schedule, station test matrices, and test data evaluation criteria. The task force consists of CARB and other state agency participants along with fuel cell vehicle manufacturers, hydrogen station providers, and H2FIRST members.

SPECIAL RECOGNITIONS & AWARDS/ PATENTS ISSUED

1. DOE Hydrogen and Fuel Cells Program Distinguished Achievement Award.

FY 2016 PUBLICATIONS/PRESENTATIONS

1. Johnson, T.A. and Kashuba, M., Presentation at the CaFCP Station Providers group meeting, "Overview of the HyStEP Device," CSULA campus, December 2015.

2. Johnson, T.A. and Kashuba, M., Presentation at the CaFCP Vehicle OEM group meeting, "Overview of the HyStEP Device," Diamond Bar, CA, January 2016.

3. Johnson, T.A., Ainscough, C., Terlip, D., Meadows, G., et al., "Development of the HyStEP Device," SAE Technical Paper 2016-01-1190, 2016, doi:10.4271/2016-01-1190.

4. Johnson, T.A., "Development of the HyStEP Device," Presentation at the SAE 2016 World Congress, Detroit, MI, April 14, 2016.

5. Johnson, T. "Development of the Hydrogen Station Equipment Performance (HyStEP) Device," 2016 DOE Hydrogen and Fuel Cells Program and Vehicle Technologies Office Annual Merit Review and Peer Evaluation Meeting, June 2016.

6. Terlip, D. and Ainscough, C., "HyStEP Validation Test Report," submitted to DOE on October 30, 2015, in fulfillment of NREL/ Sandia National Laboratories Annual Operating Plan Milestone D13.

7. Terlip, D. and Ainscough, C., "HyStEP Validation Test Report," submitted to DOE on November 30, 2015, in fulfillment of NREL/ Sandia National Laboratories Annual Operating Plan Milestone 17.1.

8. Johnson, T.A., "HyStEP Final Validation Report," submitted to DOE on February 2016 in fulfillment of NREL/Sandia National Laboratories Annual Operating Plan Milestone M20.1 Task 2.20.

VII.C.3 Advanced Hydrogen Fueling Station Supply: Tube Trailers

Brian Bonner (Primary Contact), John Aliquo, Greg Daub
Air Products and Chemicals, Inc.
7201 Hamilton Blvd.
Allentown, PA 18195-1501
Phone: (610) 481-5222
Email: bonnerbb@airproducts.com

DOE Manager: Jason Marcinkoski
Phone: (202) 586-7466
Email: Jason.Marcinkoski@ee.doe.gov

Contract Number: DE-EE0006524

Subcontractor:
Worthington Cylinder Corporation, Pomona, CA

Project Start Date: September 1, 2014
Project End Date: September 30, 2018

Overall Objectives

- Design, procure, construct, and demonstrate a U.S. Department of Transportation-approved composite tube trailer capable of 8,500 psi (586 bar) or higher delivery pressure. Increasing hydrogen delivery pressure to 8,500 psi or higher will increase the capacity of hydrogen deliveries, reduce the need for compression at hydrogen fueling stations, and reduce the overall hydrogen delivery cost.

Fiscal Year (FY) 2016 Objectives

- Develop a preliminary design for storage vessels with an operating pressure of 8,500 psi (586 bar) or higher.
- Conduct a feasibility analysis on the new storage vessel and tube trailer design.
- Pending the feasibility analysis, initiate the manufacture of prototype vessels and conduct performance testing to validate the engineering design.

Technical Barriers

This project addresses the following technical barriers from the Fuel Cell Technologies Office Multi-Year Research, Development, and Demonstration Plan.

Hydrogen Delivery

(A) Lack of Hydrogen/Carrier and Infrastructure Options Analysis

(E) Gaseous Hydrogen Storage and Tube Trailer Delivery Costs

(I) Other Fueling Site/Terminal Operations

(K) Safety, Codes and Standards, Permitting

Technology Validation

(D) Lack of Hydrogen Refueling Infrastructure Performance and Availability Data

Contribution to Achievement of DOE Hydrogen Delivery and Technology Validation Milestones

This project will contribute to achievement of the following DOE milestones from the Fuel Cell Technologies Office Multi-Year Research, Development, and Demonstration Plan.

Hydrogen Delivery

- Milestone 1.5: Coordinating with the H_2 Production and Storage programs, identify optimized delivery pathways that meet a H_2 delivery and dispensing cost of <$2/gge for use in consumer vehicles. (4Q, 2020)
- Milestones 2.1 and 6.2: By 2015, reduce the cost of hydrogen delivery from the point of production to the point of use for emerging regional consumer and fleet vehicle markets to <$4/gge. (4Q, 2015)
- Milestone 2.3: Verify 2020 targeted cost and performance for H_2 pressurization and/or containment technologies that minimize delivery pathway cost for long-term markets. (2Q, 2018)
- Milestones 2.4 and 6.3: By 2020, reduce the cost of hydrogen delivery from the point of production to the point of use in consumer vehicles to <$2/gge. (4Q, 2020)

Technology Validation

- Milestone 3.8: Validate reduction of cost of transporting hydrogen from central production to refueling sites to <$0.90/gge. (4Q, 2019)

FY 2016 Accomplishments

- Air Products established a tube trailer cost model to support conceptual vessel design(s) and trailer configuration(s).
- Work has begun with Worthington Cylinders in support of the project objective of increasing hydrogen delivery pressure to 8,500 psi (586 bar) or higher.

- Air Products is leveraging work outside of this project through commercialization of hydrogen distribution trailers with 7,500 psi (520 bar) operating pressure at hydrogen stations in California and Europe. This "Learning by Doing" serves as an important building block in further advancing lightweight composite tube trailers to the next level in this project.

✧ ✧ ✧ ✧ ✧

INTRODUCTION

Hydrogen delivery is a critical component to the cost, energy consumption, and environmental emissions associated with the market development of hydrogen infrastructure. Air Products and Chemicals, Inc. (Air Products) and Worthington Cylinder Corporation will develop and introduce a new composite over-wrapped pressure vessel that is safe, cost-effective, efficient, reliable, free of contaminants, and capable of being utilized for gaseous hydrogen tube trailer applications. High-pressure storage applied to hydrogen distribution can offer many advantages in serving the key hydrogen energy markets and lower hydrogen infrastructure costs. Supply systems can be deployed to provide a superior match of product supply to customer demand and growth, provide a higher level of reliability, reduce maintenance costs, and provide other business benefits.

APPROACH

To properly assess the benefits of the Advanced Hydrogen Fueling Station Supply, a preliminary techno-economics analysis of new tube trailer designs will first be conducted. The analysis will benchmark the new tube trailer design to current high-pressure hydrogen tube trailers with design criteria and constraints (Figure 1) in the areas of (1) capacity, (2) size, (3) weight, (4) pressure, (5) temperature, and (6) costs. The techno-economic analysis must prove the technical and cost viability of ≥8,500 psi (586 bar) hydrogen storage tubes with the appropriate frame and chassis to proceed with detailed vessel design under the project.

Further development of a vessel suitable for hydrogen storage at pressure of 8,500 psi (586 bar) or higher will involve initial prototype vessel development and optimization of vessel design prior to manufacturing vessels for U.S. Department of Transportation certification and testing. Testing of the high-pressure vessels will be in accordance with International Organization for Standardization (ISO) 1119-2 criteria for hydrogen storage vessels. Test data will support the submission of a Special Permit application to the U.S. Department of Transportation, and after receipt of a U.S. Department of Transportation Special Permit, a new delivery trailer will be designed, fabricated, and tested. The delivery trailer unit will be deployed to supply hydrogen to hydrogen fueling stations. Also, trailer performance data will be collected and reported to the National Fuel Cell Technology Center at the National Renewable Energy Laboratory for independent review and analysis.

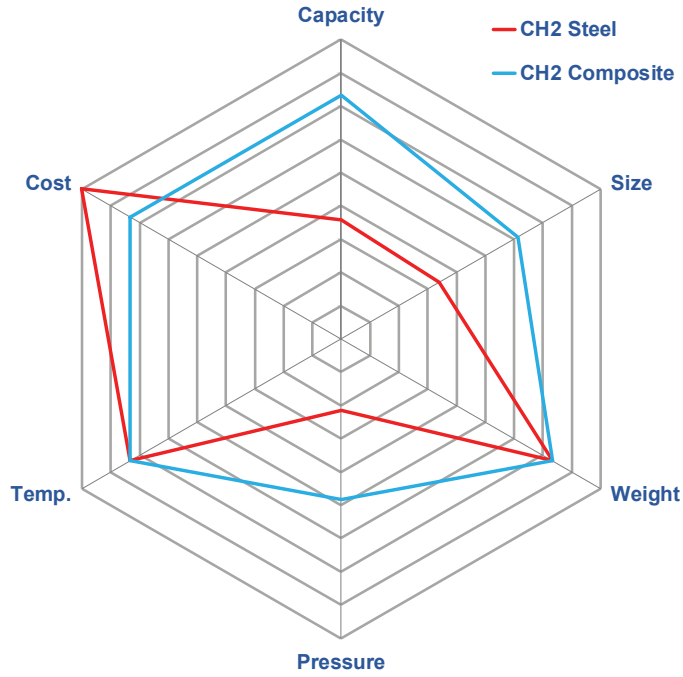

CH2 – compressed hydrogen

FIGURE 1. Tube trailer design constraints

RESULTS

- This is a new project with expected official start in the third quarter of FY 2016.
- A significant amount of preliminary work and learning has been accomplished by the project team prior to official project kick-off. Air Products established a tube trailer cost model to support conceptual vessel design(s) and trailer configurations(s). Work has begun with Worthington Cylinders in support of the project objective of increasing hydrogen delivery pressure to 8,500 psi (586 bar) or higher.
- Air Products is also leveraging work outside of this project through commercialization of hydrogen distribution trailers with 7,500 psi (520 bar) operating pressure at hydrogen stations in California and Europe. The work serves as an important building block in further advancing lightweight composite tube trailers to the next level in the hydrogen energy market. The "Learning by Doing" experience helped identify and address technical challenges related to high-pressure trailer design, components, and construction, along with high-pressure trailer filling, trailer operability, and hydrogen fueling station interface. This project will benefit from the experience gained at 7,500 psi (520 bar).

CONCLUSIONS AND FUTURE DIRECTIONS

The advancement of tube trailer distribution to higher pressure under this project enables "compressionless" fueling at fill pressures greater than 5,000 psi (350 bar).

The preliminary techno-economic analysis will be performed to confirm the acceptability of the higher-pressure units as a viable storage solution. After the analysis is complete and the vessel units have been confirmed as acceptable, the design for a new ≥8,500 psi (586 bar) vessel will be completed by Worthington Cylinder Corporation. Test vessels will be prepared, and the necessary testing will be performed on the vessels for U.S. Department of Transportation certification. An application will be submitted to the U.S. Department of Transportation to obtain a special permit. Upon receipt of this permit, Air Products will design the complete trailer unit for delivery of hydrogen to fueling stations.

FY 2016 PUBLICATIONS/PRESENTATIONS

1. John Aliquo, "Advanced Hydrogen Fueling Station Supply: Tube Trailers." Poster at the DOE Hydrogen and Fuel Cells Program Annual Merit Review.

VII.C.4 Performance and Durability Testing of Volumetrically Efficient Cryogenic Vessels and High Pressure Liquid Hydrogen Pump

Salvador M. Aceves (Primary Contact),
Guillaume Petitpas
Lawrence Livermore National Laboratory (LLNL)
7000 East Avenue
Livermore, CA 94550
Phone: (925) 422-0864
Email: aceves6@llnl.gov

DOE Manager: Jason Marcinkoski
Phone: (202) 586-7466
Email: Jason.Marcinkoski@ee.doe.gov

Subcontractors:
- Spencer Composites Corporation, Sacramento, CA
- Linde LLC, Hayward, CA

Project Start Date: January 2014
Project End Date: January 2017

Overall Objectives

- Demonstrate small (63.5-L internal volume), high aspect ratio (34 cm outer diameter and 100 cm length) cryogenic pressure vessels with high volumetric and gravimetric hydrogen storage performance (50 gH_2/L and 9% H_2 weight fraction).
- Demonstrate durability (1,500 thermomechanical cycles) of thin-lined high fiber fraction pressure vessels.
- Measure liquid hydrogen pump performance after 6,000 refuelings (24 tonnes of liquid hydrogen).

Fiscal Year (FY) 2016 Objectives

- Complete construction and commission LLNL's hydrogen test facility.
- Analyze, design, and fabricate full-scale (65 L) 700 bar pressure vessel prototypes with thin metal liner (<2 mm).
- Demonstrate long life of thin-lined vessels by conducting 1,500 thermomechanical cycles with cryogenic hydrogen at LLNL's test facility.

Technical Barriers

This project addresses the following technical barriers from the Technology Validation section of the Fuel Cell Technologies Office Multi-Year Research, Development, and Demonstration Plan.

(C) Hydrogen Storage

(D) Lack of Hydrogen Refueling Infrastructure Performance and Availability Data

Contribution to Achievement of DOE Technology Validation Milestones

This project will contribute to achievement of the following DOE milestones from the Technology Validation section of the Fuel Cell Technologies Office Multi-Year Research, Development, and Demonstration Plan.

- Milestone 3.4: Validate station compression technology provided by delivery team. (4Q, 2018)

FY 2016 Accomplishments

- Built and commissioned LLNL's hydrogen test facility.
- Built and cycle tested—with water—six thin-lined pressure vessels rated for 700 bar.
- Built a seventh thin lined vessel and cycle tested it with hydrogen.

✧ ✧ ✧ ✧ ✧

INTRODUCTION

Cryogenic pressure vessels have demonstrated high performance for automotive hydrogen storage, with density (43 gH_2/L), weight fraction (7.3%), cost ($12/kWh), and safety advantages (~8X lower expansion energy than compressed gas and secondary protection from vacuum jacket) [1-3]. This project explores the potential for reaching high volumetric (50 g H_2/L target) and gravimetric (9% H_2 weight fraction target) storage performance within a small (63.5-L internal volume), high aspect ratio (34 cm outer diameter and 100 cm length) cryogenic pressure vessel with long durability (1,500 thermomechanical cycles) refueled by a liquid hydrogen pump to be tested for degradation after delivery of 24 tonnes of liquid hydrogen.

APPROACH

Reaching the very challenging weight and volume targets set for this project demands innovative cryogenic pressure vessel design. Spencer Composites Corporation, in collaboration with LLNL, is developing thin-lined, high fiber fraction cryogenic pressure vessels. At a target liner thickness of 1.5 mm and 80% fiber fraction, these thin-walled vessels may be able to reach the weight and volume targets

when installed within a thin vacuum gap and refueled at high density (up to 80 gH_2/L) with the liquid hydrogen pump.

RESULTS

Work in the reporting period focused on building and commissioning the hydrogen test facility, and on building and cycle testing thin-lined pressure vessels.

Hydrogen Test Facility

LLNL's hydrogen test facility, completed during the reporting period (Figure 1), offers a unique platform for testing hydrogen systems over a wide range of pressures, temperatures, volumes and flow rates.

The main component of LLNL's hydrogen test facility is a liquid hydrogen pump. Manufactured by Linde, a leading supplier of cryogenic equipment, the pump takes liquid hydrogen from the station dewar at low pressure (2–3 bar) and very low temperature (23–25 K) and pressurizes it up to an 875 bar cryogenic fluid. Flow rate is very high (up to 120 kg of hydrogen per hour), enabling (future) 5 minute refuels. The station dewar has an 11,000-L capacity, sufficient to refuel ~150 vehicles. When empty, it is refilled by a liquid hydrogen truck.

Another key component of the hydrogen test facility is a containment vessel (Figure 2) that enables testing thin-lined pressure vessels manufactured for this project. These one-of-a-kind experimental vessels are not certified by current standards (American Society of Mechanical Engineers, International Organization for Standardization, Federal Motor Vehicle Safety Standards) and are therefore unsafe to pressurize in manned areas. Made of 3.2 cm thick stainless steel 304 and weighing almost 5,000 kg, the containment vessel is rated for 65 bar maximum pressure and can contain the equivalent energy of 1.8 kg of trinitrotoluene, therefore enabling testing of full-scale vessels and hydrogen systems. The containment vessel can also hold high vacuum down to 0.1 Pa.

The Hydrogen Test Facility can be operated from a control room strategically located for maximum visibility and far enough from the dewar (23 m) to meet National Fire Protection Association (NFPA) standards. Full instrumentation is also available with sensors for temperature, pressure, flow, liquid hydrogen level, electricity, and vent rates. All sensors and system components are explosion-proof (Class 1 Division 1 Group B), as demanded by NFPA for systems that may be exposed to hydrogen.

A 9-m high vent stack completes the facility, enabling rapid venting of hydrogen subsequent to pressure testing. High altitude venting of hydrogen is demanded by NFPA for rapid dispersion away from personnel at ground level. Hydrogen, being so light and therefore buoyant, rapidly diffuses upward once it is released and warms up to ambient temperature.

In the next quarter, a 40-kW electric heater and heat exchanger will be added in order to provide varying hydrogen outlet temperature, from cryogenic to room temperature, enabling cost effective, rapid thermomechanical testing at high pressure and low (60 K) to elevated (360 K) temperature.

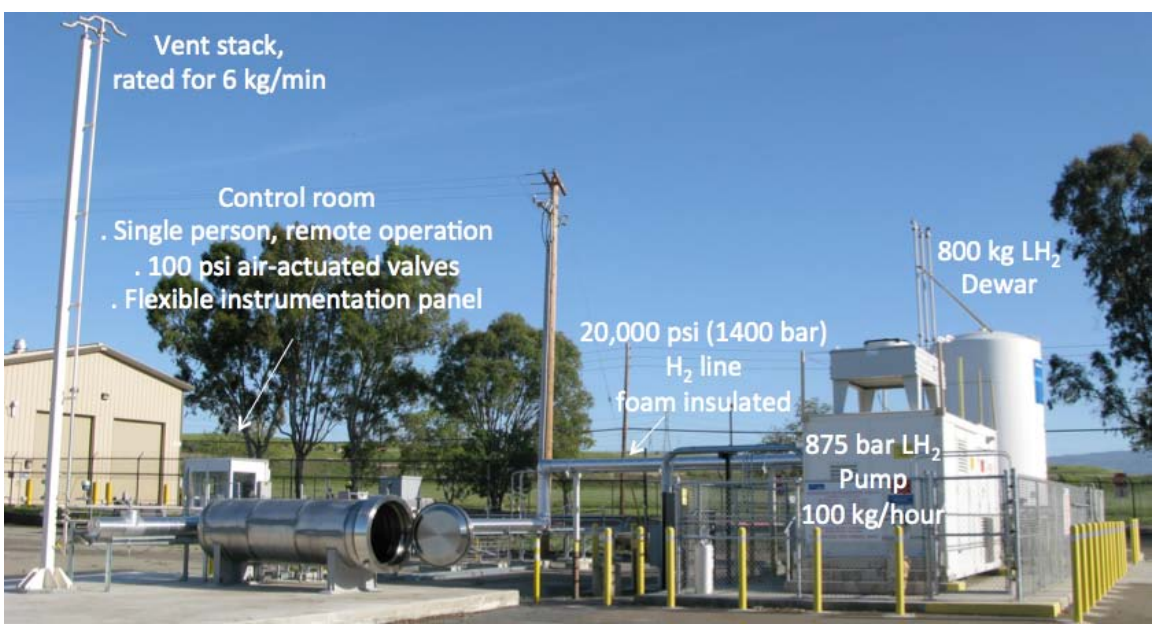

FIGURE 1. LLNL's hydrogen test facility showing the main components and their performance metrics: liquid hydrogen pump, liquid hydrogen dewar, containment vessel, control room, insulated hydrogen tubes, and vent stack

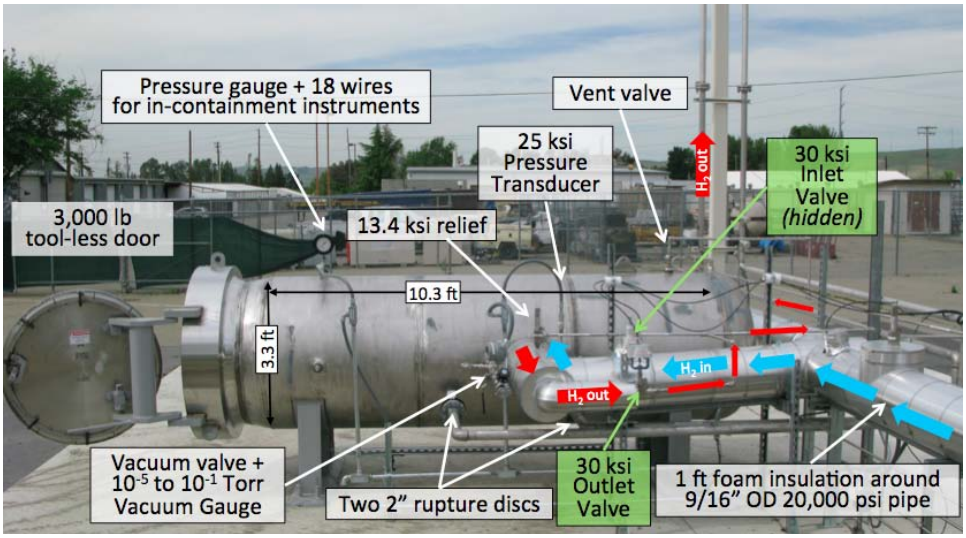

OD – Outside diameter

FIGURE 2. Containment vessel for testing pressure vessels and systems with cryogenic and ambient temperature hydrogen

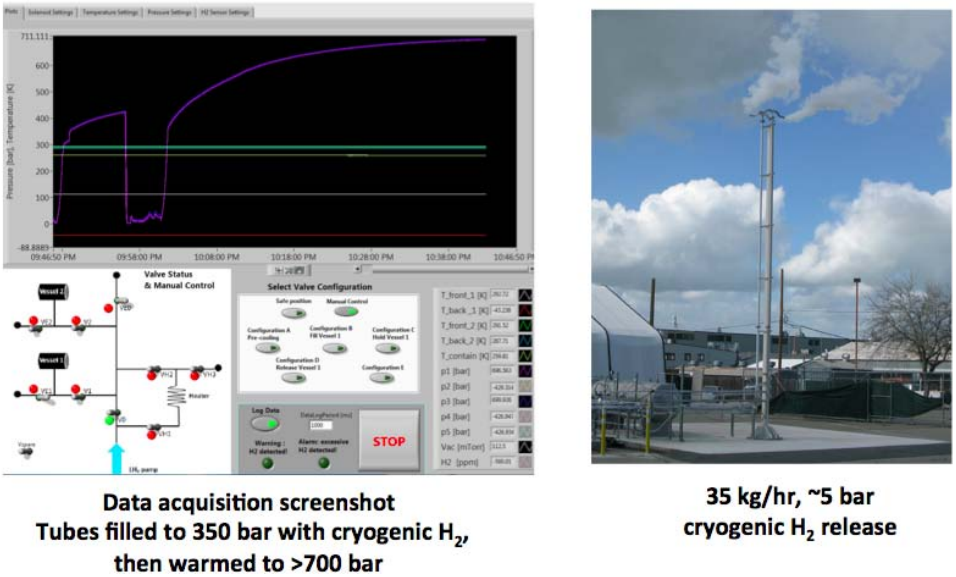

FIGURE 3. Commissioning of hydrogen test facility showing a data acquisition system screen shot (left) and 35 kg/h hydrogen vent (right)

The hydrogen test facility was commissioned in February of 2016 (Figure 3), on time for cycle testing the new generation of thin-lined pressure vessels.

Thin-lined Pressure Vessels

Following last year's strength testing of a pressure vessel to 1,560 bar (2.23 safety factor for 700 bar operation), we dedicated this year to designing and producing a vessel that could be cryogenically cycled over 1,500 times. This demanded detailed finite element and fatigue analysis to determine composite layer strength to meet cyclability requirements. In collaboration with BMW, we conducted linked thermo-fluid and stress analysis of the fill process to determine improved boss designs for surviving thermal gradients that may result while filling an initially warm vessel with cryogenic hydrogen.

In total, we manufactured and tested seven vessels during the year (Table 1). The first two vessels failed during autofrettage. Research into this failure mode indicated that lack of roundness weakened the structure and resulted in

TABLE 1. Experimental Results from the Testing of Seven Pressure Vessels

Date	#	Liner	Resin	Test result
Aug 15	1	1.3 mm Steel	High Fiber Fraction	Buckling then burst @ 8 ksi (during autofrettage)
Sep 15	2	1.5 mm Alternate	Epoxy	Buckling then burst @ 12 ksi (during autofrettage)
Oct 15	3	1.7 mm Alternate	Epoxy	Leak after **133** water cycles, T-weld failure
Nov 15	4	1.5 mm Alternate	Epoxy	Leak after **247** water cycles, root cause not found, NOT at T-weld
Jan 16	5	1.7 mm Steel	Epoxy	Leak after **468** water cycles, longitudinal weld failure
Mar 16	6	1.7 mm Steel, annealed	High Fiber Fraction	Burst @ 10 ksi (during autofrettage)
May 16	7	1.7 mm Steel	Epoxy	Leak after **456** hydrogen cycles

premature failure at low pressure. Process modifications led to vessels that survived autofrettage and an increased number of water pressure cycles to 700 bar (except for Vessel 6 that failed during autofrettage while researching alternate resins). After partial success with water cycling, a final vessel was tested with cryogenic hydrogen, reaching 456 cycles, well short of the 1,500 cycle target.

CONCLUSIONS AND FUTURE DIRECTIONS

Research into the cause of failure points to liner welds as the likely culprit. Tungsten inert gas welds done by hand are irregular by nature and introduce flaws that may initiate crack propagation during vessel cycling. Future work in this topic will demand alternative liner manufacture techniques such as e-beam welding, pulsed laser welding, or spin forming. The potential still remains to manufacture thin-lined vessels with long cycle life to demonstrate the ultimate performance limits of cryogenic pressure vessels. In addition to this, future experiments remain to be done to determine pump performance parameters (fill density, flow rate, energy consumption, venting losses) when filling vessels to 700 bar.

After careful review of the experimental results, DOE decided to reduce the scope of the project, eliminating vessel development activities and instead testing pressure vessels supplied by BMW. This may be initiated in Fall 2016 after vessels are received, a test protocol is identified, and the 40 kW electric heater (possibly necessary for vessel testing) is installed at LLNL's test facility.

REFERENCES

1. Aceves, S.M., Espinosa-Loza, F., Ledesma-Orozco, E., Ross, T.O., Weisberg A.H., Brunner T.C., et al. High-density automotive hydrogen storage with cryogenic capable pressure vessels. International Journal of Hydrogen Energy 2010;35:1219–26. doi:10.1016/j.ijhydene.2009.11.069.

2. Aceves, S.M., Petitpas, G., Espinosa-Loza, F., Matthews, M.J., Ledesma-Orozco, E. Safe, long range, inexpensive and rapidly refuelable hydrogen vehicles with cryogenic pressure vessels. International Journal of Hydrogen Energy 2013;38:2480–9. doi:10.1016/j.ijhydene.2012.11.123.

3. Kircher, O., Greim, G., Burtscher, J., Brunner T. Validation of cryo-compressed hydrogen storage (cch2) – a probabilistic approach. Proceeding of the International Conference on Hydrogen Safety, San Francisco: 2011.

VII.C.5 Hydrogen Meter Benchmark Testing

Michael Peters (Primary Contact), Robert Burgess, Matt Post, Josh Martin, Jeff Tomerlin, Chris Ainscough
National Renewable Energy Laboratory (NREL)
15013 Denver West Parkway
Golden, CO 80401-3305
Phone: (303) 275-3712
Email: Michael.Peters@nrel.gov

DOE Manager: Jason Marcinkoski
Phone: (202) 586-7466
Email: Jason.Marcinkoski@ee.doe.gov

Subcontractor:
Spectrum Automation Controls, Arvada, CO

Project Start Date: September 1, 2015
Project End Date: September 30, 2016

Overall Objectives

- Design and build a laboratory-grade gravimetric standard for measurement of hydrogen flow. The gravimetric standard will be capable of verifying compliance with National Institute of Standards and Technology (NIST) Handbook 44 requirements for ±1.5% accuracy for the dispensing of motor vehicle fuel (gravimetric standard capability of 1/3 the required level or ±0.5%).
- Measure flow meter performance of three commercially available meters using the gravimetric standard. Testing will be conducted with high-pressure hydrogen under flow conditions simulating the range of dispenser operation.
- Disseminate results through communications and reporting to provide data on current flow meter performance, identifying the shortfalls to meeting regulations.

Fiscal Year (FY) 2016 Objectives

This project is scheduled to be completed by the end of FY 2016. The overall objectives of designing, building, and conducting flow meter performance testing will be completed.

Technical Barriers

This project addresses the following technical barriers from the Technology Validation and Hydrogen Safety, Codes and Standards sections of the Fuel Cell Technologies Office Multi-Year Research, Development, and Demonstration Plan.

Technology Validation Barriers

(D) Lack of Hydrogen Refueling Infrastructure Performance and Availability Data

Hydrogen Safety, Codes and Standards Barriers

(F) Enabling National and International Markets Requires Consistent RCS

(G) Insufficient Technical Data to Revise Standards

(J) Limited Participation of Business in the Code Development Process

Contribution to Achievement of DOE Milestones

This project contributes to achievement of the following DOE milestones from the Technology Validation and Hydrogen Safety, Codes and Standards sections of the Fuel Cell Technologies Office Multi-Year Research, Development, and Demonstration Plan.

- Technology Validation Milestone 4.5: Based on field validation data, publish assessment of remaining fuel cell technology gaps requiring additional RD&D to satisfy residential/commercial fuel cell CHP markets. (4Q, 2016)
- Hydrogen Safety, Codes and Standards Milestone 3.1: Develop, validate, and harmonize test measurement protocols. (4Q, 2014)

FY 2016 Accomplishments

- Finalized the design and build of a gravimetric flow standard. The design includes two composite overwrapped Type III cylinders mounted on a common scale.
- Completed market survey of existing flow meter technologies. Results presented to DOE and at the stakeholder project review to down-select three meters for testing. Final selection includes two coriolis meters and one turbine meter.
- Conducted gravimetric standard design review with NIST Fluid Metrology Group in Gaithersburg, Maryland. This review provided feedback from the NIST experts in fluid metrology on important aspect of the gravimetric standard design and operation.
- Performed project review with industry stakeholder group to ensure that the project plan meets the needs of the fuel cell vehicle market. Data from this project will be utilized to address the gap in meter performance

relative the motor vehicle fueling requirements in NIST Handbook 44.

- Verified system performance by conducting pre-test system level testing. This testing includes system integrity leak checking, structural interaction measurements, dynamic flow effects testing and quantification of PVT (pressure, volume, and temperature) system corrections.

✧ ✧ ✧ ✧ ✧

INTRODUCTION

The hydrogen meter benchmarking project is being supported under the DOE Technology Validation program and is part of the DOE/NREL/Sandia H2FIRST (Hydrogen Fueling Infrastructure Research and Station Technology) project. The H2FIRST objective is to ensure that fuel cell electric vehicle customers have a positive fueling experience similar to conventional gasoline and diesel stations as vehicles are introduced (2015–2017) and transition to advanced fueling technology beyond 2017. The H2FIRST activities are expected to positively impact the cost, reliability, safety, and consumer experience of fuel cell electric vehicle stations.

APPROACH

Background: The hydrogen flow meter benchmarking study will provide data for state weights and measures groups that are working toward station certification. All 50 state agencies have adopted NIST Handbook 44 in whole or in part for their state motor vehicle fuel metrology requirements. As a result, flow meter manufacturers are working toward developing a product capable of meeting NIST Handbook 44 requirements as specified in section 3.39 Hydrogen Gas-Measuring Devices. The acceptance criterion for flow measurement accuracy is defined as ±1.5% acceptance tolerance and ±2.0% maintenance tolerance. California Code of Regulation has adopted amendments to the Handbook 44 requirements, adding accuracy classes of 3%, 5%, and 10% as a temporary allowance for hydrogen dispensers. This action is a result of known limitations in flow meter accuracy for high-pressure hydrogen.

Experience: NREL's experience with hydrogen metrology includes a project with the California Department of Food and Agriculture Division of Measurement Standards. NREL was contracted to design and build the Hydrogen Field Test Standard employing gravimetric, volumetric, and master meter capability. The gravimetric method was shown to be capable of ±0.5% accuracy, or three times the accuracy requirement in NIST Handbook 44. This accuracy level is required for use as a standard for certification of motor vehicle fuel dispensing and was used as a basis for the gravimetric design of the meter benchmarking apparatus.

Technical Description: Flow meter testing was conducted to quantify meter accuracy over a range of environmental conditions (input variables: flow, pressure, temperature, and transient time). Testing was conducted on representative meters that are production models or are prototype models with potential for near-term production. Test priority was given to commercially available devices. The hydrogen metering benchmarking apparatus consists of a stationary hydrogen flow loop capable of controlling input variables of temperature, pressure and flow as it passes through a flow measuring device. The minimum and maximum input conditions were per the SAE J2601 fueling protocol. The flow loop is able to measure the flow rate by gravimetric methods. A future work task being considered is the addition of a critical flow venturi as a secondary master meter concept. Both these methods will incorporate traceability to NIST standards.

Gravimetric Method: The NREL-designed apparatus incorporates two Type III composite overwrapped pressure vessels (COPVs) mounted on a NIST traceable scale to measure the mass of dispensed hydrogen vs. time. The COPVs are lightweight cylinders that minimize scale tare weight. A high accuracy stationary Sartorius scale was used for the gravimetric measurement.

RESULTS

Flow Meter Survey and Selection: Coriolis meters are typically used for compressed natural gas dispensing where the dispensed pressure is much lower than 70 MPa. When designing for high-pressure hydrogen, thicker walls are needed for pressure containment. The thicker wall reduces the deflections required for coriolis meter operation. Thicker walls are also a challenge for an ultrasonic meter, reducing the signal to noise ratio. Material selection is also dependent on the effects of hydrogen mechanical properties. Project scope for this effort included testing of three commercially available meters.

The final selection process included two coriolis meters and one turbine meter. The two coriolis meters are being used in 70 MPa stations. Data provides a benchmark for future development. The turbine meter is a product that is used extensively in industry but is new for 70 MPa hydrogen applications. The turbine meter drawback is that it is a volumetric device so the output will require conversion to gravimetric units. This data provides valuable information on the applicability of a turbine meter and also shows the incremental inaccuracies of a gravimetric conversion.

Gravimetric Standard Design/Build: The test hardware shown in the isometric view was mounted on an 80/20 frame with protection from wind. The location of the two COPV cylinders can be seen in Figure 1. The inner frame is positioned on the Sartorius scale. The entire inner frame can be lifted off the scale for scale maintenance and calibration.

FIGURE 1. Flow meter test apparatus

The device under test is mounted upstream of the tank/scale, employing a gravimetric method for validation of flow measurements. The apparatus was designed with the following design considerations.

- Wind protection
- Removable scale
- Device leveling
- Two 40-L COPVs
- Program logic controls
- 80/20 aluminum

System Design Meter Location: Three potential meter locations are depicted in Figure 2. Stations in operation today have the meter upstream of the hydrogen chiller due to the meter being a heat sink if placed downstream of the chiller (compromising the ability to meet SAE J2601 cool down times). As a result, during this testing, meter performance was explored under conditions simulating positions 1 and 2.

System Pretesting: System pretesting is required to quantify both static and dynamic effects that would otherwise adversely affect the accuracy of the gravimetric measurement. Interactions between the gas lines and the scale were quantified by conducting four system level pretests.

- Inner and outer structure interaction – Confirmation tests were conducted to verify separation between the outer and inner structure by pressurizing lines up to isolation valve separating inner and outer structure and confirming zero readout on the scale when pressurized.

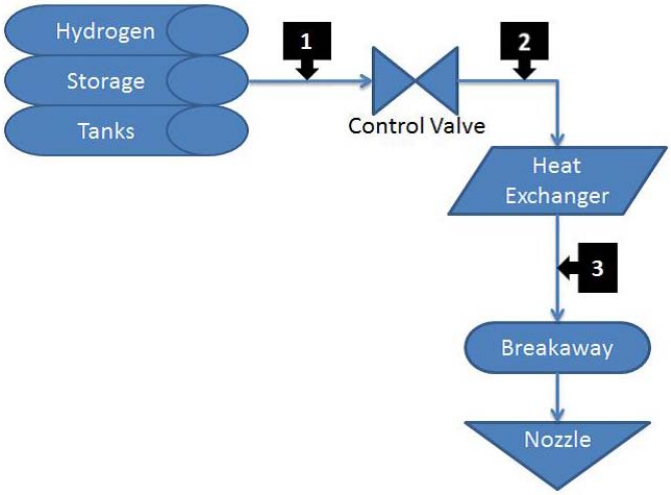

FIGURE 2. Meter location determination

- Slow and fast step up of hydrogen – This test was performed by stepping up the pressure in hydrogen lines connected to the vessels and comparing static scale reading to PVT estimates. These data were used to establish a correlation between PVT calculations and scale readings under static conditions.
- Flow momentum effects – Dynamic effects caused by the momentum of turning flow can offset scale readings. This test was conducted by flowing nitrogen (for safety) through the lines with the vessel isolation valve closed. A correlation was determined between flow and scale reading.
- Pressure step down effects – Scale reaction to fill line depressurization was quantified and if greater than zero a correlation was used for scale correction.

CONCLUSIONS AND FUTURE DIRECTIONS

The DOE funded Hydrogen Meter Benchmarking project is scheduled to be completed by the end of FY 2016. The data generated characterize three high-pressure hydrogen flow meters and will be used to support further development of flow meters. The sale of dispensed hydrogen is governed by state regulations that reference NIST Handbook 44 requirements. Currently NIST Handbook 44 requires ±1.5% accuracy when dispensing motor vehicle fuels; however these requirements are being reviewed by NIST based on the experience with California Code of Regulation and the reduced accuracy classes that have been instituted for early market adoption of fuel cell vehicles.

Results from this project will be compiled into a composite data product that will show the current capability of the flow meter market without identifying performance of specific meters. NREL will work closely with meter manufacturers, station providers, and other key stakeholders

to disseminate results of the benchmarking study. These test results are aimed at enabling the development of commercially available hydrogen flow meters for 70 MPa dispensing stations.

FY 2016 PUBLICATIONS/PRESENTATIONS

1. "Meter Benchmarking Stakeholder Project Review," Burgess, R., Peters, M., Post, M., National Renewable Energy Laboratory, January 19, 2016. (presentation)

2. "Hydrogen Meter Benchmarking Interim Report," Burgess, R., Peters, M., Post, M., Ainscough, C., National Renewable Energy Laboratory, January 2016. (report)

3. "Meter Benchmarking Project Review," Joint Tech Team Meetings, Sandia National Laboratories, Livermore, CA, April 5, 2016. (presentation)

4. "Hydrogen Meter Benchmark Testing," 2016 DOE Hydrogen and Fuel Cells Program, Annual Merit Review, June 9, 2016. (presentation)

VII.C.6 Station Operational Status System (SOSS) 3.0 Implementation, SOSS 3.1 Upgrade, and Station Map Upgrade Project

Ben Xiong (Primary Contact), Nico Bouwkamp
California Fuel Cell Partnership (CaFCP)
3300 Industrial Blvd., Suite 1000
West Sacramento, CA 95691
Phone: (916) 371-2870
Email: bxiong@cafcp.org

DOE Manager: Jason Marcinkoski
Phone: (202) 586-7466
Email: Jason.Marcinkoski@ee.doe.gov

Project Start Date: October 1, 2015
Project End Date: September 30, 2016

Overall Objectives

- Consistently and reliably report hydrogen station operational status information to fuel cell electric vehicle (FCEV) customers to increase customer satisfaction and station demand.

Fiscal Year (FY) 2016 Objectives

- Improve user interface and data quality.
- Increase data transmission interval from stations (once every 15 minutes at minimum) and data sharing capabilities.

Technical Barriers

This project addresses the following technical barrier from the Technology Validation section of the Fuel Cell Technologies Office Multi-Year Research, Development, and Demonstration Plan.

(D) Lack of Hydrogen Refueling Infrastructure Performance and Availability Data

Contribution to Achievement of DOE Technology Validation Milestones

This project will contribute to achievement of the following DOE milestone from the Technology Validation section of the Fuel Cell Technologies Office Multi-Year Research, Development, and Demonstration Plan.

- Milestone 2.3: Validate fuel cell electric vehicles achieving 5,000-hour durability (service life of vehicle) and a driving range of 300 miles between fuelings. (4Q, 2019)

FY 2016 Accomplishments

- Improved SOSS interface by adding sorting capabilities and additional information for users.
- Twenty-seven total (open-retail and other non-retail) stations in California participating in SOSS and reporting data:
  - Completed integrating SOSS at 20 new open-retail hydrogen stations.
  - Continued to maintain the existing seven non-retail stations on SOSS.
- Disaster Recovery Plan (DRP) development and implementation in progress.
- Station Map upgrade complete. Transfer to a standalone site is in progress.

✧ ✧ ✧ ✧ ✧

INTRODUCTION

Argonne National Laboratory and DOE are continuing partners in the California Fuel Cell Partnership. Funds are used to accomplish the goals of the Partnership and to provide critical information and data necessary for DOE to determine the status and prospects for commercialization of fuel cell technology. The Partnership supports SOSS, a mobile web application that provides status information about each of the available hydrogen stations in California

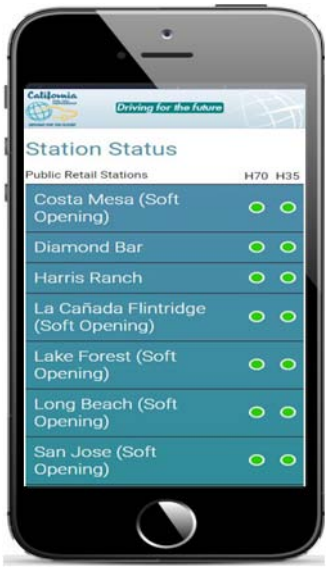

FIGURE 1. SOSS home page

(Figure 1). At specific intervals, each station sends a message to CaFCP's server to report the station status (online, limited, or offline), available fuel (Figure 2), and available pressures. It also provides the station address, contact number, and GPS coordinates. CaFCP will include all new stations under development and construction on SOSS. As automakers are currently launching FCEVs into the commercial market and use SOSS as the primary source of station status information, SOSS needs to operate with minimal downtime to ensure customer confidence.

APPROACH

A primary goal is to increase FCEV customer satisfaction—and thereby station demand—by consistently providing relevant station status information for end users to better assess hydrogen station availability. This is accomplished through an upgrade of SOSS, improving the SOSS user interface by enabling users to sort stations based on their preference (Figure 3) and to receive additional information. Additional information includes an "Unknown" status to alert customers when the data connection has been lost between the station and the SOSS server; "Capacity" is also available for customers to view through a settings toggle.

A DRP is being put in place so the server, database, and files can be quickly restored in the case of an event leading to the outage of the system. The DRP also consists of communication strategies to reach out to stakeholders and customers to notify of outages and resolution steps.

The CaFCP Station Map (Figure 4) is being upgraded to allow for a more customer-focused and friendly interface and is also being moved to its own website to allow for additional information that stakeholders need, but which is not essential for the customer audience.

Newly built hydrogen stations will be solicited to participate in SOSS.

RESULTS

Implementation to update the SOSS interface has been completed to allow for an "Unknown" status, as well as a display of the current available capacity. Implementation of the DRP and Station Map upgrades are in progress and on track to be completed as planned.

Twenty-seven total hydrogen stations in California are participating on SOSS with 20 new open-retail stations and seven existing non-retail stations (as of 7/22/2016).

Status of SOSS implementation at new open-retail stations:

- First Element Fuel has completed implementation of SOSS at 13 new open-retail stations in California.
  - Campbell (First Element Fuel)
  - Costa Mesa (First Element Fuel)
  - Harris Ranch (First Element Fuel)
  - Hayward (First Element Fuel)
  - La Canada Flintridge (First Element Fuel)

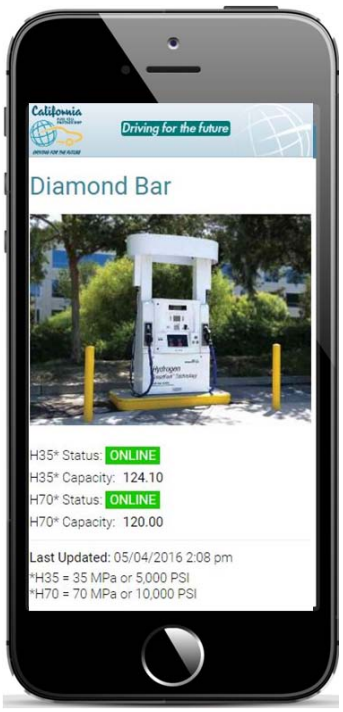

FIGURE 2. SOSS capacity view

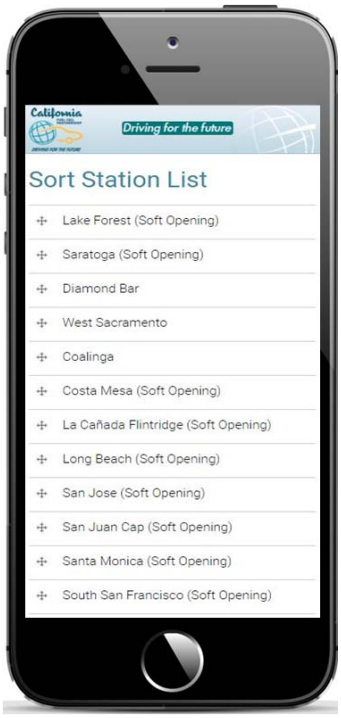

FIGURE 3. SOSS sort view

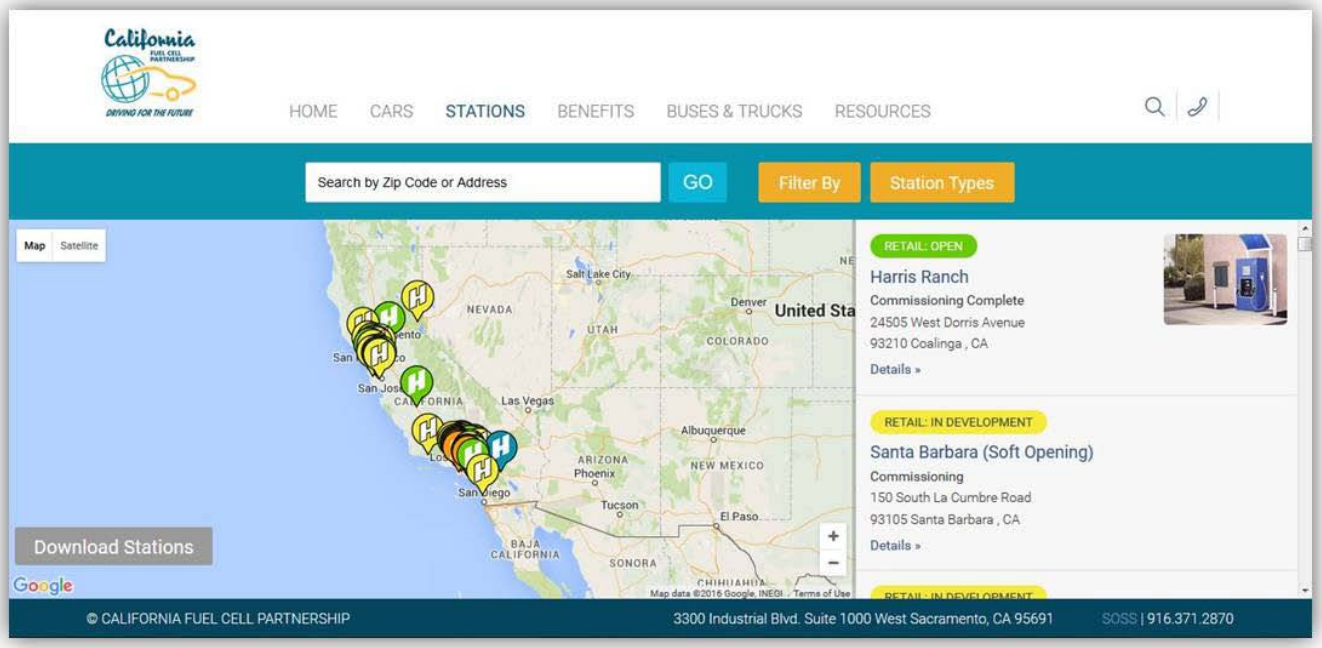

FIGURE 4. Station Map

- Lake Forest (First Element Fuel)
- Long Beach (First Element Fuel)
- Mill Valley (First Element Fuel)
- San Jose (First Element Fuel)
- Santa Barbara (First Element Fuel)
- Saratoga (First Element Fuel)
- South San Francisco (First Element Fuel)
- Truckee (First Element Fuel)

- Linde has completed implementation of SOSS at two new open-retail stations in California.
  - San Juan Capistrano (Linde)
  - West Sacramento (Linde)
- Air Products has completed implementation of SOSS at five new open-retail stations in California.
  - Diamond Bar (Air Products)
  - Fairfax-LA (Air Products)
  - Santa Monica (Air Products)
  - University of California, Irvine (Air Products)
  - West LA (Air Products)
- ITM Power and Powertech have completed implementation of SOSS at the Riverside station. Testing of SOSS connectivity is complete. Waiting on finalization of commissioning to set the station live.
- California State University, Los Angeles completed implementation of SOSS and connectivity testing. The station is still undergoing commissioning before being listed on SOSS.

CONCLUSIONS AND FUTURE DIRECTIONS

SOSS is increasingly serving the customer need for station availability data, leading to more satisfied and informed FCEV customers, per direct reports from vehicle original equipment manufacturers. Delays in station implementation and rollout continues to be a limiting factor for the increase of the number of new stations participating on SOSS. Despite these delays, station operators, developers, automakers, and other stakeholders agree that SOSS continues to be critical for the early market launch of fuel cell vehicles and customer satisfaction. An initial proposal of future improvements to SOSS includes the following:

- Solicit new hydrogen stations to participate on SOSS.
- Implement user interaction and feedback system.
- Research mobile native app capabilities and implement if economically feasible.
- Implement real-time reporting.
- Implement a mobile map interface.
- Expand data collection opportunities.
- Develop reporting capabilities.

VII.D.1 Stationary Fuel Cell Evaluation

Genevieve Saur (Primary Contact), Jennifer Kurtz, Sam Sprik, Chris Ainscough, and Matt Post
National Renewable Energy Laboratory (NREL)
15013 Denver West Parkway
Golden, CO 80401-3305
Phone: (303) 275-3783
Email: genevieve.saur@nrel.gov

DOE Manager: Jason Marcinkoski
Phone: (202) 586-7466
Email: Jason.Marcinkoski@ee.doe.gov

Project Start Date: October 1, 2011
Project End Date: Project continuation and direction determined annually by DOE

Overall Objectives

- Independently assess, validate, and report operation targets and performance of stationary fuel cell (FC) systems in real-world operating conditions.

Fiscal Year (FY) 2016 Objectives

- Develop more voluntary data partners, especially for operations data.
- Conduct stationary fuel cell efficiency analysis at varying operating conditions.
- Publish 39 technical stationary fuel cell composite data products (CDPs) biannually.
- Update a public website for dissemination of CDPs.

Technical Barriers

This project addresses the following technical barrier from the Technology Validation section of the Fuel Cell Technologies Office Multi-Year Research, Development, and Demonstration Plan.

(B) Lack of Data on Stationary Fuel Cells in Real-World Operation

Contribution to Achievement of DOE Technology Validation Milestones

This project contributes to the achievement of the following DOE milestone from the Technology Validation section of the Fuel Cell Technologies Office Multi-Year Research, Development, and Demonstration Plan.

- Milestone 1.2: Complete validation of commercial fuel cell CHP systems that demonstrate 45% efficiency and 50,000 hour durability. (4Q, 2017)

FY 2016 Accomplishments

- Operations Data (power, fuel flow, temperature, etc.); Units >100 kW
  - The mean fuel cell electrical efficiency is 45% lower heating value (LHV), exceeding the DOE target of 43% LHV.
  - Mean capacity factor of base load units was 89.2% of the rated capacity.
  - Capacity factor of load-following units was between 40% and 100% of rated capacity.
    - Capacity factor is dependent on the size of the fuel cell relative to the building load profile.
  - Mean availability of both the base load and load-following units exceeds the DOE Technology Validation target for 2015 and 2020 for commercial power availability of 97% and 98%, respectively.
- California's Self-Generation Incentive Program (SGIP)
  - Mean cost per unit capacity was $(2010) 10,709/kW without incentives and $(2010) 7,616/kW with incentives.
  - SGIP costs may include additional costs not included in a 2020 DOE target of $1,500/kW or 2015 DOE target of $3,000/kW installed cost for commercial fuel cells running on natural gas.

✧ ✧ ✧ ✧ ✧

INTRODUCTION

This project aims to provide status on stationary fuel cell systems to inform DOE, the public, fuel cell manufacturers, and other stakeholders. This is the only technology validation project working directly on Technical Barrier (B): Lack of Data on Stationary Fuel Cells in Real-World Operation.

APPROACH

The project's data collection plan builds on other technology validation activities. Data (operation, maintenance, and safety) are collected on site by the project partners for the fuel cell system(s) and infrastructure. NREL receives the data quarterly and stores, processes, and analyzes the data in NREL's National Fuel Cell

Technology Evaluation Center (NFCTEC). The NFCTEC is an off-network room with access provided to a small set of approved users. An internal analysis of all available data is completed quarterly, and a set of technical CDPs is published every six months. Publications are uploaded to NREL's technology validation website and presented at industry-relevant conferences. The CDPs present aggregated data across multiple systems, sites, and teams in order to protect proprietary data and summarize the performance of hundreds of fuel cell systems and thousands of data records. A review cycle is completed before the CDPs are published. This review cycle includes providing detailed data products of individual system- and site-performance results to the specific data provider. Detailed data products also identify the individual contribution to the CDPs.

RESULTS

In April 2015, a set of 39 CDPs was published, which included updates to 33 CDPs and 6 new CDPs. The set includes efficiency, operation hours, capacity factors, and availability. The operations CDPs have now been segmented into fuel cells that are less than 100 kW and greater than 100 kW. New load profile CDPs for fuel cell units greater than 100 kW show the frequency of operation time at different load fractions and the ratio of electrical output per rated capacity of the fuel cell unit, separately, for both base load and load-following units. The load profiles show that base load units operate mostly in the 90–100% load fraction range as expected, load-following units have operation time at a wider range, and some units spend time above 100% rated capacity.

The electrical efficiency for fuel cells greater than 100 kW has also been validated, and shown to exceed the 2015 DOE Technology Validation target of 43% based on the lower heating value of hydrogen (39% higher heating value, HHV, of hydrogen). The mean fuel cell electrical efficiency is 45% LHV (Figure 1).

A new analysis was completed to study the stationary fuel cell system availability, where availability is the percentage of unscheduled downtime over total time period. Downtime in this analysis may include scheduled maintenance decreasing calculated availability. The mean availability for fuel cells >100 kW exceeds the DOE Technology Validation target for 2015 and 2020 for commercial power availability at 97% and 98%, respectively. The mean availability for units operating as base load is 98.3% (Figure 2). The mean availability for units operating as load-following is 99.4%.

The size of the fuel cell relative to the building profile affects the capacity factor greatly, where capacity factor is defined as the ratio of the electrical energy produced by a generating unit for the period of time considered to the electrical energy that could have been produced at continuous full power operation during the same period. Base load units operated at 89.2% of the rated capacity and load-following units operated between 40% and 100% of rated capacity with a mean of 72.9% (Figure 3).

California's SGIP has helped deploy 460 fuel cell systems, for a total of 178 MW, since 2001. The fuel cell deployment increased approximately 16% in 2015. These fuel cell deployments have shown that fuel cells may be applied with a wide variety of fuels, including renewable

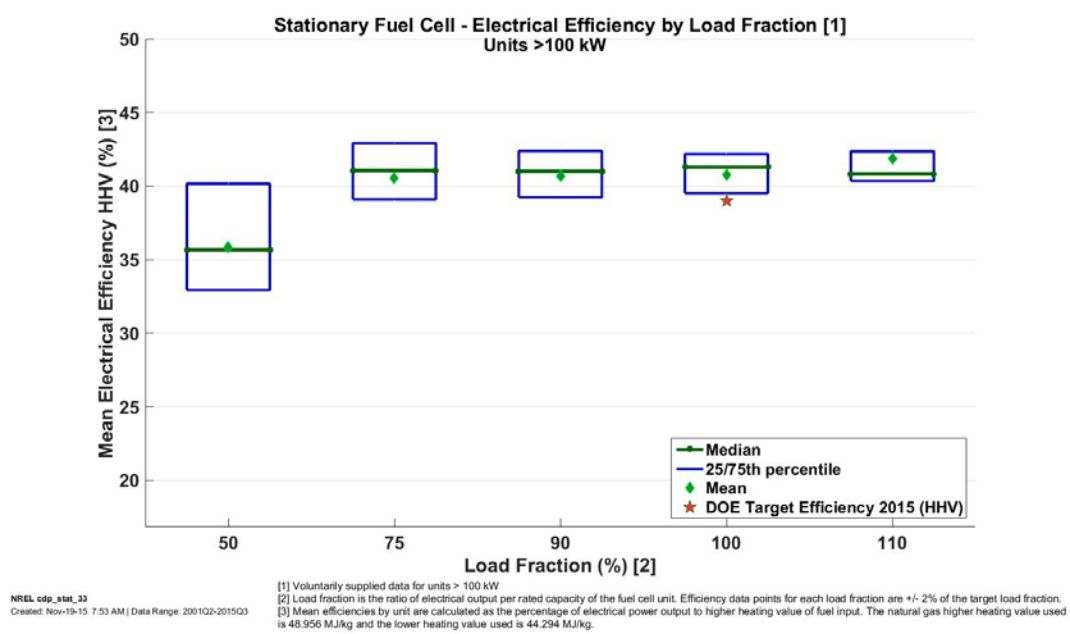

FIGURE 1. Electrical efficiency by load fraction for stationary fuel cells >100 kW

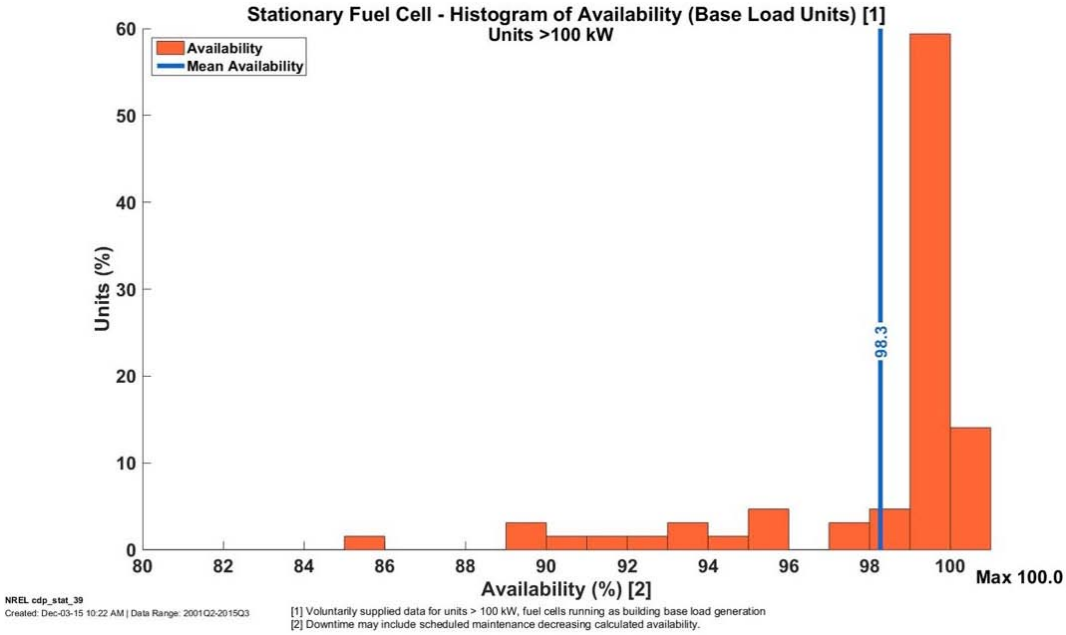

FIGURE 2. Availability of base load units >100 kW

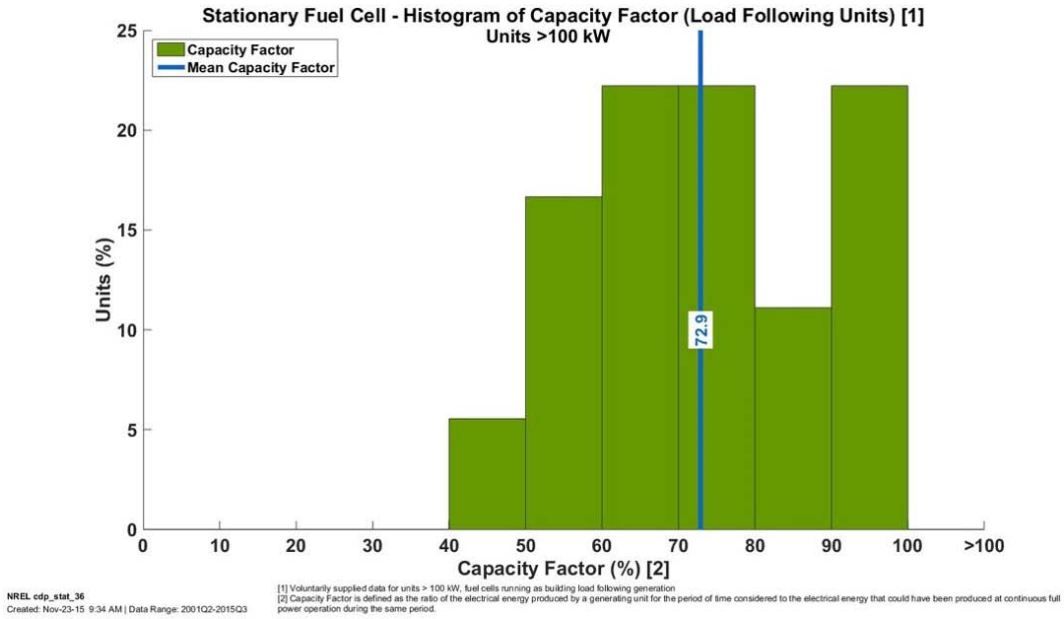

FIGURE 3. Capacity factor for load-following units

biogas from landfill, biomass, and digester sources. Natural gas is the dominant fuel type, accounting for 82% of projects and 73% of the capacity. Since 2011, electric-only fuel cell projects have been increasing at a rate (number and capacity) greater than other competing technologies, which include gas turbines, internal combustion turbines, microturbines, and pressure reduction turbines. Deployment numbers have increased even in a climate of declining incentives. Also, in 2014, fuel cell combined heat and power systems neared the cost per kilowatt of gas turbines, and beat the cost when incentives were applied.

The average unit costs in the SGIP are significantly higher than the DOE target of $1,500/kW; however, SGIP costs may include additional costs that are not included in the DOE target. Generally, larger projects (those with larger capacities) have lower unit costs and also receive more incentives. Mean cost per unit capacity was $(2010)

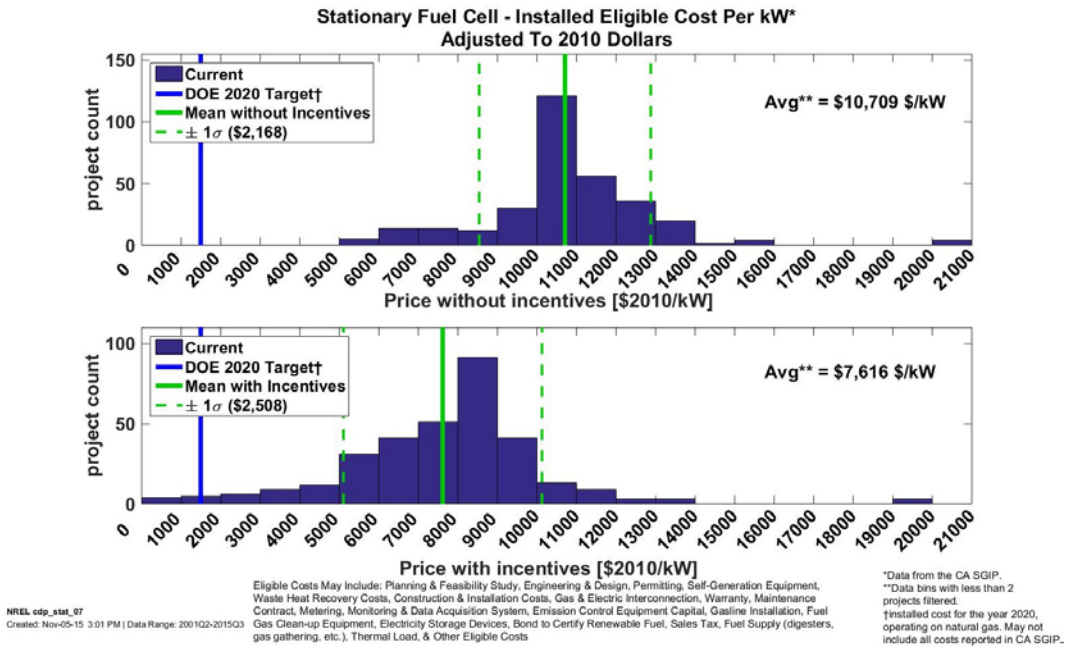

FIGURE 4. California SGIP installed costs with and without incentives

10,709/kW without incentives and $(2010) 7,616/kW with incentives (Figure 4). SGIP costs may include additional costs not included in a 2020 DOE target of $1,500/kW or 2015 DOE target of $3,000/kW installed cost for commercial fuel cells running on natural gas. SGIP eligible costs may include planning and feasibility study, engineering and design, permitting, self-generation equipment, waste heat recovery costs, construction and installation costs, gas and electric interconnection, warranty, maintenance contract, metering, monitoring and data acquisition system, emission control equipment capital, gasline installation, fuel gas clean-up equipment, electricity storage devices, bond to certify renewable fuel, sales tax, fuel supply (digesters, gas gathering, etc.), thermal load, and other eligible costs.

CONCLUSIONS AND FUTURE DIRECTIONS

- Stationary fuel cell deployments in California have increased steadily with the support of the SGIP, and the deployment numbers have increased even in a climate of declining incentives.
- Stationary fuel cell systems >100 kW have surpassed the DOE targets for electrical efficiency and availability.
- Voluntarily supplied operation data has been difficult to obtain and has limited the quantity and breadth of operation/performance CDPs.
- The project will complete a final report summarizing current benchmark and progress documented.

FY 2016 PUBLICATIONS/PRESENTATIONS

1. Saur, G., Kurtz, J., Ainscough, C., Sprik, S., Post, M. "Stationary Fuel Cell System Composite Data Products: Data through Quarter 3 of 2015," Golden, CO: National Renewable Energy Laboratory, published December 2015. (report)

2. Saur, G., Kurtz, J., Ainscough, C., Sprik, S. "Stationary Fuel Cell Evaluation: 2015 Annual Merit Review," DOE Annual Merit Review meeting, June 2015. (presentation)

3. "Stationary Fuel Cell Systems Analysis Project: Partnership Opportunities" Fact sheet describing opportunities for fuel cell developers and end users to participate in an analysis of stationary fuel cell systems to benchmark the current state of the technology. (June 2015)

VII.D.2 Material Handling Equipment Data Collection and Analysis

Chris Ainscough (Primary Contact), Jennifer Kurtz
National Renewable Energy Laboratory (NREL)
15013 Denver West Parkway
Golden, CO 80401-3305
Phone: (720)-431-7296
Email: Chris.Ainscough@nrel.gov

DOE Manager: Jason Marcinkoski
Phone: (202) 586-7466
Email: Jason.Marcinkoski@ee.doe.gov

Project Start Date: October, 2012
Project End Date: Project continuation and direction determined annually by DOE

Overall Objectives

- Perform independent technology assessment in real-world operation conditions.
- Focus on fuel cell system performance and operation.
- Leverage data processing and analysis capabilities developed under the fuel cell vehicle learning demonstration project.
- Evaluate material handling equipment (MHE).
- Support market growth.
- Provide analyses and results relevant to the markets' value proposition.
- Report on technology status to fuel cell and hydrogen communities and other key stakeholders like end users.

Fiscal Year (FY) 2016 Objectives

- Leverage existing data and results developed under the American Reinvestment and Recovery Act (ARRA) to continue the collection of MHE data on new systems, on a voluntary basis.
- Validate the status of the MHE market, which continues to expand and evolve.
- Develop at least 20 updated Composite and Detailed Data Products (CDPs and DDPs) on fuel cell MHE on durability, operation, and infrastructure performance.

Technical Barriers

This project addresses the following technical barriers from the Technology Validation section of the Fuel Cell Technologies Office Multi-Year Research, Development, and Demonstration Plan.

(A) Lack of Fuel Cell Electric Vehicle and Fuel Cell Bus Performance and Durability Data

(D) Lack of Hydrogen Refueling Infrastructure Performance and Availability Data

Contribution to Achievement of DOE Technology Validation Milestones

This project contributes to achievement of the following DOE milestones from the Technology Validation section of the Fuel Cell Technologies Office Multi-Year Research, Development, and Demonstration Plan.

- Milestone 4.2: Updated composite data products for material handling and backup power published. (3Q, 2012)
- Milestone 4.3: Report safety event data and information from ARRA projects. (3Q, 2013)

FY 2016 Accomplishments

- Published the tenth set of technical CDPs on performance and operation for MHE, with 12 updated (and one new) results.[1]
- Negotiated access to the largest single set of technology validation data in the program's history for the second year in a row, including approximately 2,000 new-generation vehicles in different MHE classes, from private commercial sites receiving no direct government funding.
- Documented over 450,000 hydrogen fills.
- Validated mean fueling time of 2.2 min, which is key to the fuel cell MHE value proposition. This is a 13% decrease since last year.
- Validated average daily site hydrogen usage of 230 kg/d. Newer sites use much more than older sites, indicative of the penetration of fuel cells into distribution center operations.
- Validated mean vehicle operating times between fueling of 4.5 h, up from 3.7 h last year, a 22% increase.

✧ ✧ ✧ ✧ ✧

[1] All results and publications are available on NREL's technology validation website, at http://www.nrel.gov/hydrogen/proj_fc_market_demo.html#cdp

INTRODUCTION

The U.S. Department of Energy designated more than $40 million in ARRA funds for the deployment of up to 1,000 fuel cell systems. This investment is enabling fuel cell market transformation through development of fuel cell technology, manufacturing, and operation in strategic markets where fuel cells can compete with conventional technologies. The strategic markets include MHE, backup power, stationary power, and portable power, and the majority of the deployed systems are in the MHE and backup power markets. NREL continues to analyze operational data from the MHE sector, because it is the market segment with the most rapid growth and technological evolution. MHE data are currently provided voluntarily by industry. The data collection has ended for backup power and stationary systems.

The project includes both end users and system developers: Air Products, FedEx, GENCO, Nuvera Fuel Cells, Plug Power, and Sysco Houston. The evaluation focused on fuel cell stack durability, reliability, refueling, safety, and value proposition. The deployment partners provided approximately $53 million in industry cost share [1]. In addition to the ARRA co-funded fuel cell backup power demonstrations, DOE supported additional demonstration projects with other federal agencies through interagency agreements. The Department of Defense and the Federal Aviation Administration are two agencies with fuel cell backup power demonstrations that also submitted operational and deployment data to NREL. All results covered in this report will include ARRA and private commercial sites that received no direct government funding. The degradation result, Figure 1, also includes interagency agreement data.

APPROACH

The project's data collection plan builds on other technology validation activities. Project partners collect operation, maintenance, and safety data for fuel cell system(s) and accompanying infrastructure. Then they send data to NREL in a manner consistent with security procedures. NREL receives the data quarterly, then stores, processes, and analyzes the data in NREL's National Fuel Cell Technology Evaluation Center (NFCTEC). The NFCTEC is a controlled-access, off-network analysis facility. An internal analysis of all available data is completed quarterly, and a set of technical CDPs is generally published every six months. Publications are uploaded to NREL's technology validation website [2] and presented at industry-relevant meetings. The CDPs present aggregated data across multiple systems, sites, and teams in order to protect proprietary data and summarize the performance of hundreds of fuel cell systems and thousands of data records. A review cycle is completed before the CDPs are published. This review cycle includes providing DDPs of individual system and site performance results to the specific data provider. DDPs also identify the individual contribution to the CDPs. The NREL Fleet Analysis Toolkit is an internally developed tool for data processing and analysis structured for flexibility, growth, and simple addition of new applications. Analyses are created for general performance as well as application- or technology-specific studies.

RESULTS

The initial ARRA funding for MHE kicked off rapid growth of the fuel cell MHE industry. This growth is reflected directly in the large amount of additional data NREL was able to secure from private commercial sites receiving no direct government funding.

The new data set represents an increase in vehicles represented by approximately 2,000. This new data set dwarfs all other ARRA data combined. Yet, these data represent only a piece of the MHE fleet deployed in United States logistics warehouses. MHE are broken down into classes based on the capabilities of the vehicle. These data represent Class I (sit-down counterbalance), II (stand-up, high reach, narrow aisle), and III (powered pallet jacks and tow tractors) trucks.

The new fleet data represent newer systems, which are newer-generation technologies being deployed in ever-greater numbers. This can be seen in Figure 1, showing the average daily hydrogen usage at ARRA sites as a cluster well less than 100 kg/d. Newer sites cluster around 180 kg/d.

As reported earlier in this project [1], refueling time (i.e., fast fueling) is critical to the value proposition for MHE. Without fast fueling, the productivity improvements upon which distribution centers rely become much more difficult to achieve, with a corresponding increase in the difficulty of justifying fuel cells. Over the past year, fueling times have decreased 13% to an average of 2.18 minutes, down from 2.5 minutes (see Figure 2). This was achieved with an average fill amount of 0.61 kg.

Operation times have increased 22% from last year to an average of 4.5 h (see Figure 3). This does not necessarily represent the vehicle autonomy, as there are other human factors that dictate when fueling is convenient (e.g. breaks, shift changes, or proximity to a fuel dispenser).

One-third of fueling events take place within 5 min of one another, and 19% within 20 min (see Figure 4). This usage pattern has important implications for station design with respect to back-to-back fills, something that light duty vehicle stations currently struggle with. The shift from 250 bar fueling is complete, with 250 bar fueling only represented in the ARRA data.

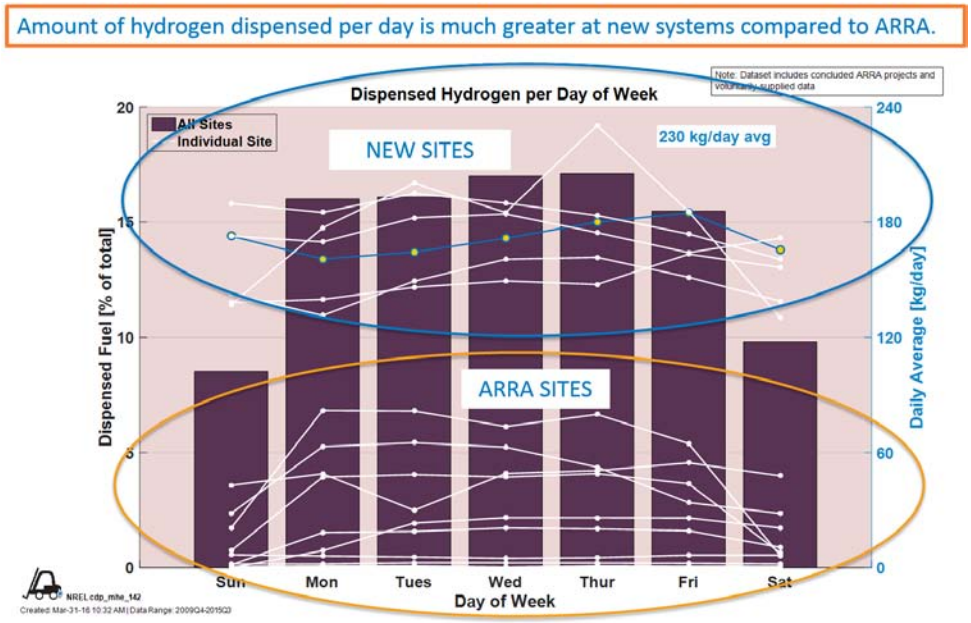

avg – Average

FIGURE 1. Dispensed hydrogen by day of week showing ARRA and newer sites (cdp_mhe_142)

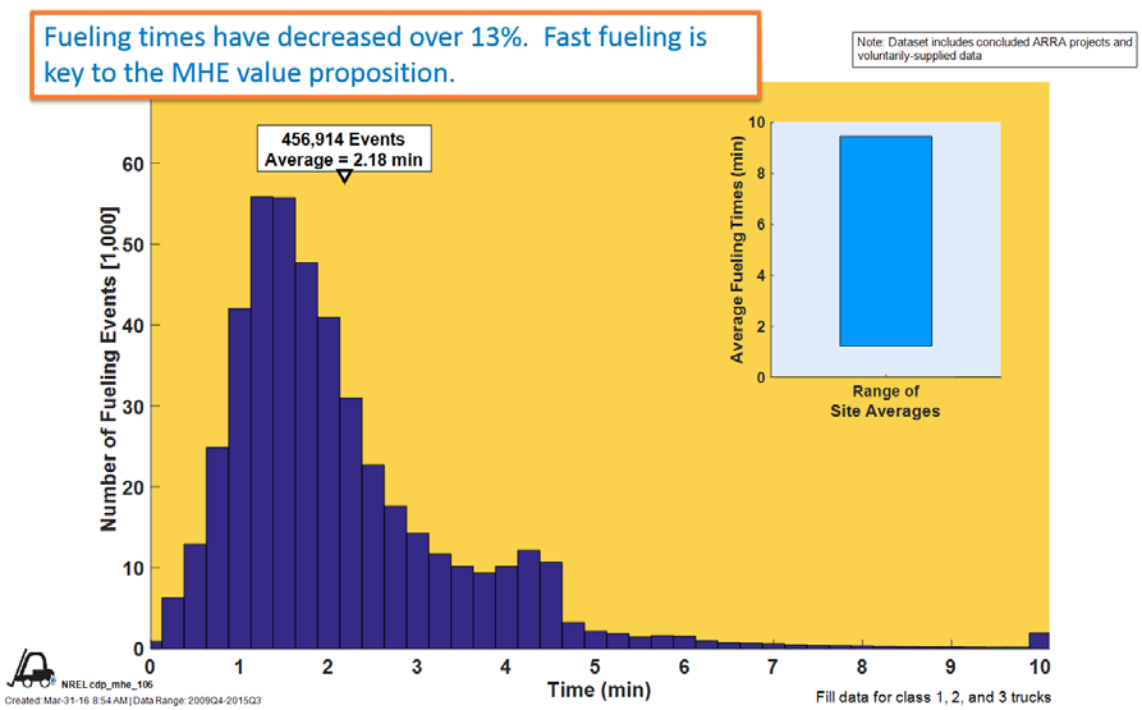

FIGURE 2. Histogram of fueling times, combined fleet (cdp_mhe_106)

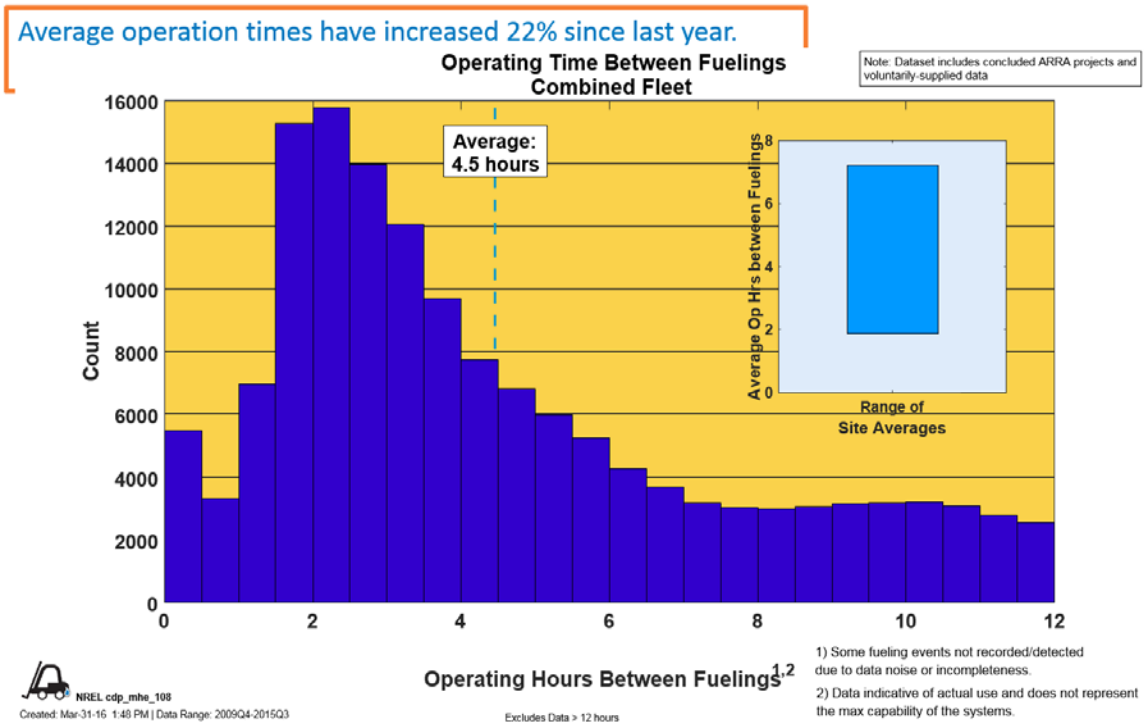

FIGURE 3. Operating time between fuelings, combined fleet (cdp_mhe_108).

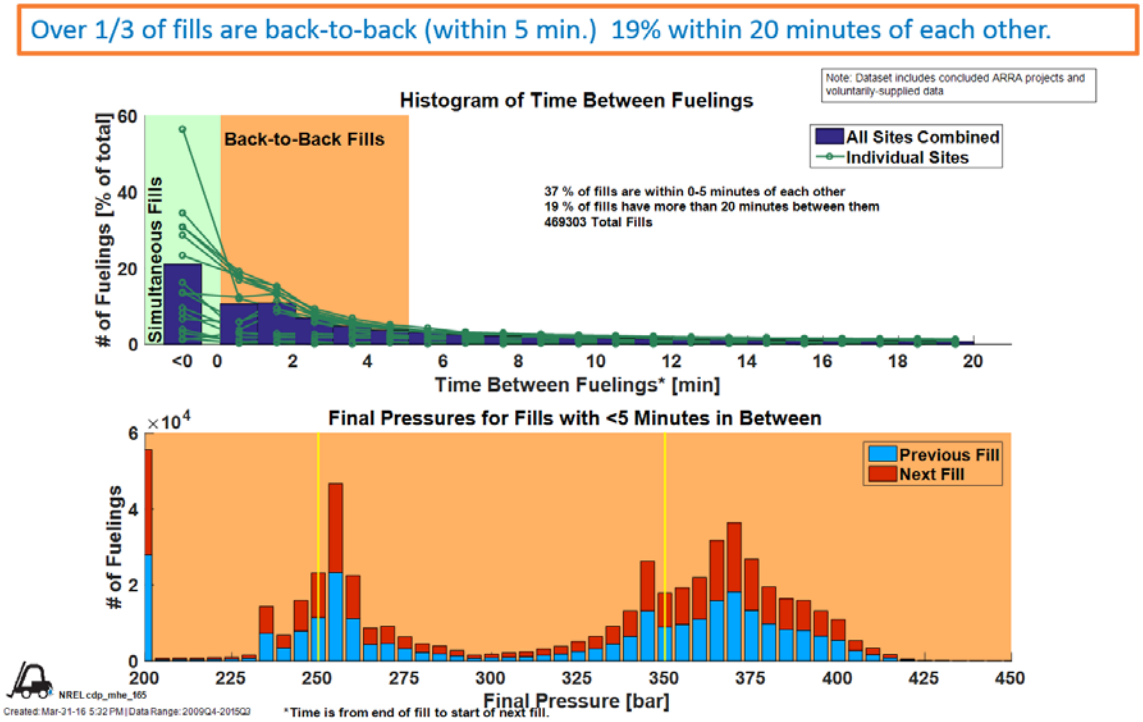

FIGURE 4. Histogram of time between fuelings, relative to the dispensers (cdp_mhe_165).

CONCLUSIONS AND FUTURE DIRECTIONS

The project is concluded.

FY 2016 PUBLICATIONS/PRESENTATIONS

1. Ainscough, C., Kurtz, J., *ARRA Material Handling Equipment Composite Data Products: Data through Quarter 2 of 2015*, Golden, CO: The National Renewable Energy Laboratory, 2016.

2. Ainscough, C., *Material Handling Equipment Data Collection and Analysis,* Washington, DC: U.S. Department of Energy, 2016.

REFERENCES

1. Ramsden, T., *An Evaluation of the Total Cost of Ownership of Fuel Cell-Powered Material Handling Equipment*. Golden, CO: National Renewable Energy Laboratory, April 2013.

VII.D.3 Dynamic Modeling and Validation of Electrolyzers in Real-Time Grid Simulation

Rob Hovsapian
Idaho National Laboratory
750 University Blvd.
Idaho Falls, ID 83406
Phone: (208) 526-8217
Email: rob.hovsapian@inl.gov

DOE Manager: Jason Marcinkoski
Phone: (202) 586-7466
Email: Jason.Marcinkoski@ee.doe.gov

Subcontractors:
- Humboldt State University, Arcata, CA
- Florida State University, Tallahassee, FL

Project Start Date: June 1, 2015
Project End Date: September 30, 2017

Overall Objectives

- Validate the benefits of hydrogen electrolyzers through grid services and hydrogen sale to fuel cell vehicles for full-scale deployment.
- Characterize the potential and highest economic value based on the needs of multiple stakeholders for specific grid regions.
- Demonstrate reliable, fast-reacting performance of hydrogen-producing electrolyzers for at-scale energy storage devices.
- Develop and verify the communications and controls needed for successful participation in electricity markets and demand response (DR) programs.

Fiscal Year (FY) 2016 Objectives

- Perform power hardware-in-the-loop (PHIL) at the National Renewable Energy Laboratory (NREL) using Digital Real-Time Simulator (DRTS) coupled with electrolyzers to verify the operational system and to characterize and validate the existing electrolyzer model.
- Create a distribution network that contains current hydrogen refueling stations, based on Pacific Gas and Electric (PG&E) infrastructure and feeder data in real-time environment used for PHIL testing. This platform will be used to assess the value of electrolyzers under existing DR programs and any other grid services using historical energy and ancillary service prices.
- Define the requirements and implement the front end controller (FEC) that will interpret the utility signals and coordinate multiple hydrogen refueling stations. The FEC will generate the necessary control signals for the lower level controller to respond to different utility signals and hence participate in DR and ancillary service programs.

Technical Barriers

This project addresses the following technical barriers from Technology Validation section of the Fuel Cell Technologies Office Multi-Year Research, Development, and Demonstration Plan.

(B) Lack of Data on Stationary Fuel Cells in Real-World Operation

(G) Hydrogen from Renewable Resources

(H) Hydrogen and Electricity Co-Production

Contribution to Achievement of DOE Technology Validation Milestones

This project will contribute to achievement of the following DOE milestones from the Technology Validation section of the Fuel Cell Technologies Office Multi-Year Research, Development, and Demonstration Plan.

- Milestone 3.9: Validate large-scale system for grid energy storage that integrates renewable hydrogen generation and storage with fuel cell power generation by operating for more than 10,000 hours with a round-trip efficiency of 40%. (4Q, 2020)

FY 2016 Accomplishments

- Completed design specification document for the FEC for electrolyzer application that enables response of electrolyzers to grid signals.
- Completed development of reduced-order PG&E California Bay Area sub-network in DRTS for testing current and future electrolyzer deployments and related technical aspects.

✧ ✧ ✧ ✧ ✧

INTRODUCTION

The project aims to quantify the value of fuel cells and electrolyzers from a grid integration perspective. This work uses a novel approach of distributed real-time PHIL

simulations to use an electrolyzer hardware at NREL working in conjunction with power system simulations at Idaho National Laboratory (INL). The proposed project strives to leverage existing work at both the national labs related to fuel cells, electrolyzers, and grid integration. INL and NREL have performed PHIL simulation using a 120 kW electrolyzer in distributed real time environment. Part of the research resources are focused on developing the FEC for integration with the electrolyzer. The proposed FEC can communicate with supervisory control and data acquisition systems to effectively process the commands from grid management systems. It will also optimize the operation of connected electrolyzers to meet objectives of the power grid, as well as those of electrolyzer owners. Thus, a carefully designed, flexible FEC integrated with a distribution management system will enable an electrolyzer to operate as a revenue generating resource, while extending benefits to the grid.

APPROACH

In FY 2016, INL and NREL performed 200 hours of PHIL simulation using the 120 kW electrolyzer in distributed real-time simulations. Techniques to counter impact of latency on PHIL simulations were also created and tested. Based on the lessons learned during the testing and subsequent data analysis, it was deemed by the DOE leadership, INL, and NREL researchers that 300-hour testing with the electrolyzer would be redundant. The affirmative results obtained from electrolyzer PHIL testing using DRTS in the second quarter of FY 2016 were used for further research and development to enhance the interaction of electrolyzers with the power markets. Thus, in the third quarter of FY 2016 research resources were focused on developing the FEC for integration with the electrolyzer. It is possible to operate the designed FEC in several "modes" to meet varying priorities (ranging from utility-friendly, environment-friendly, and self-preservation).

For the design of the FEC, several review meetings took place between INL and NREL researchers during the development phase. From the discussions, a specifications document that describes in detail the rationale for choosing electrolyzers as a grid service device, technical specifications for parsing utility signals, methods for integration of FEC to distribution management systems, and modes of operation was developed. The design specifications in this document will be followed to create a real-time FEC for enabling grid services from electrolyzers in particular, but can be generalized as necessary. The team also successfully completed the development of a reduced-order PG&E sub-network of California's Bay Area in the DRTS environment for studying practical cases.

RESULTS

Distributed real-time simulations were performed to demonstrate the real-time PHIL for 200 hours between INL and NREL. These are important from the perspective of understanding the response capabilities of an electrolyzer as a controllable load and the potential to provide services. Data were used to validate the electrolyzer model by operating at an average of 60% (lower heating value) stack efficiency. Typical values of stack efficiency were greater than 90% at times. Scenario 1 (Figure 1) is load step-change and it provides a measure of both response time and accuracy

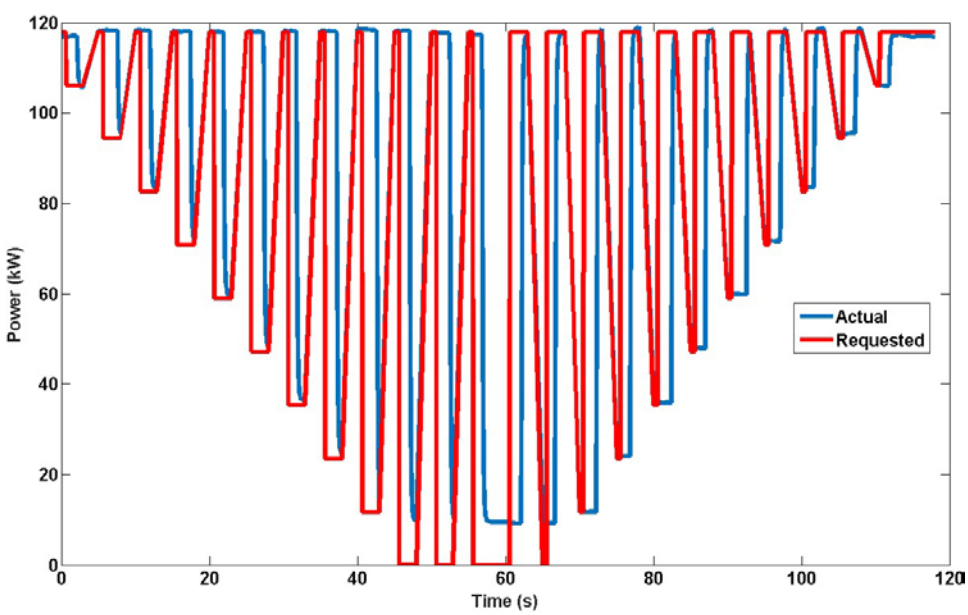

FIGURE 1. Electrolyzer response registered for the reference signal from Scenario 1

when changing load levels of operation of the electrolyzer. Scenario 2 (Figure 2) is the optimal operation for "time-of-use" utility rate by optimizing the operation of an electrolyzer using the PG&E E-20 utility rate. To counter the impact of data latency (15 ms shown in Figure 3) on distributed real-time simulations between INL and NREL, a linear prediction technique was developed. The mechanism to implement automated response of the electrolyzers to grid signals is envisioned to be the FEC as shown in Figure 4. Distributed PHIL and latency mitigation technique (200 hours) contributed to Objectives 1 and 2 whereas FEC development contributed to Objectives 2 and 3.

CONCLUSIONS AND FUTURE DIRECTIONS

Capabilities of an electrolyzer as a controllable load and in providing grid services was realized to be significant. Additionally, the resistive attribute of the electrolyzer imparts a certain level of damping of oscillations in distribution networks. A 200-hour test of distributed PHIL performed in the second quarter of 2016 was a significant accomplishment as it was a one of a kind real-time simulation that yielded accurate results and leveraged laboratory assets. Hardware-based testing in real-time was used to infer and augment the understanding of the role electrolyzers can play in markets for additional revenue. An FEC that will enable

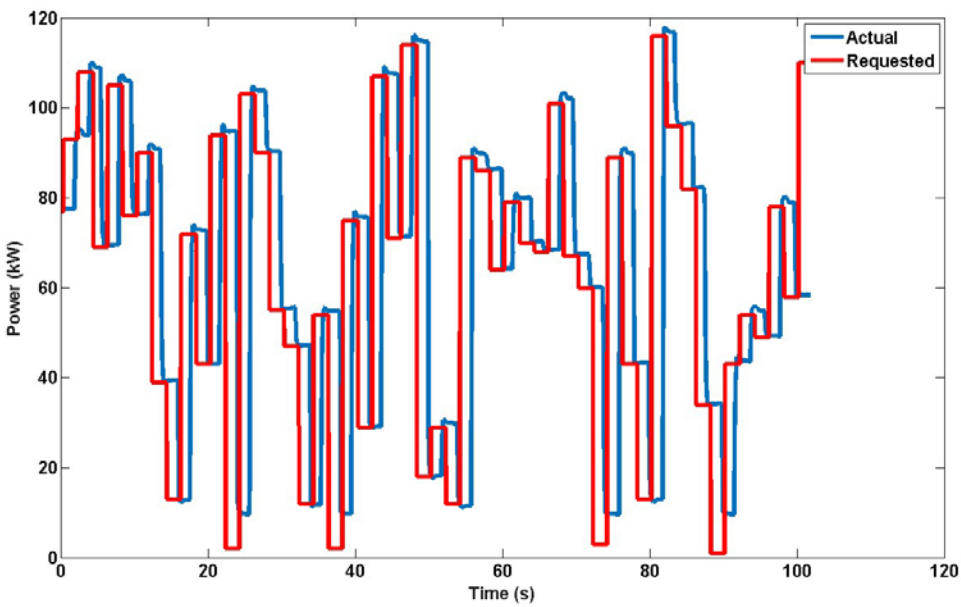

FIGURE 2. Electrolyzer response to PG&E E-20 signals from Scenario 2

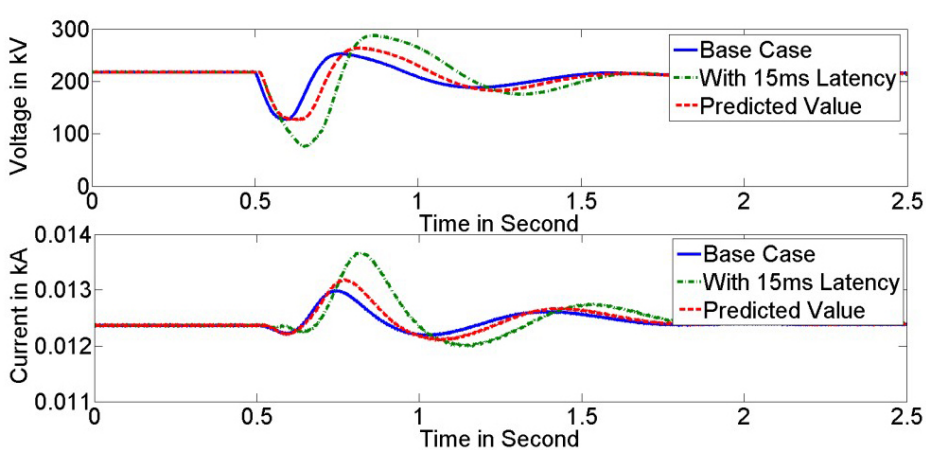

FIGURE 3. Linear prediction technique to counter impacts of latency on distributed PHIL

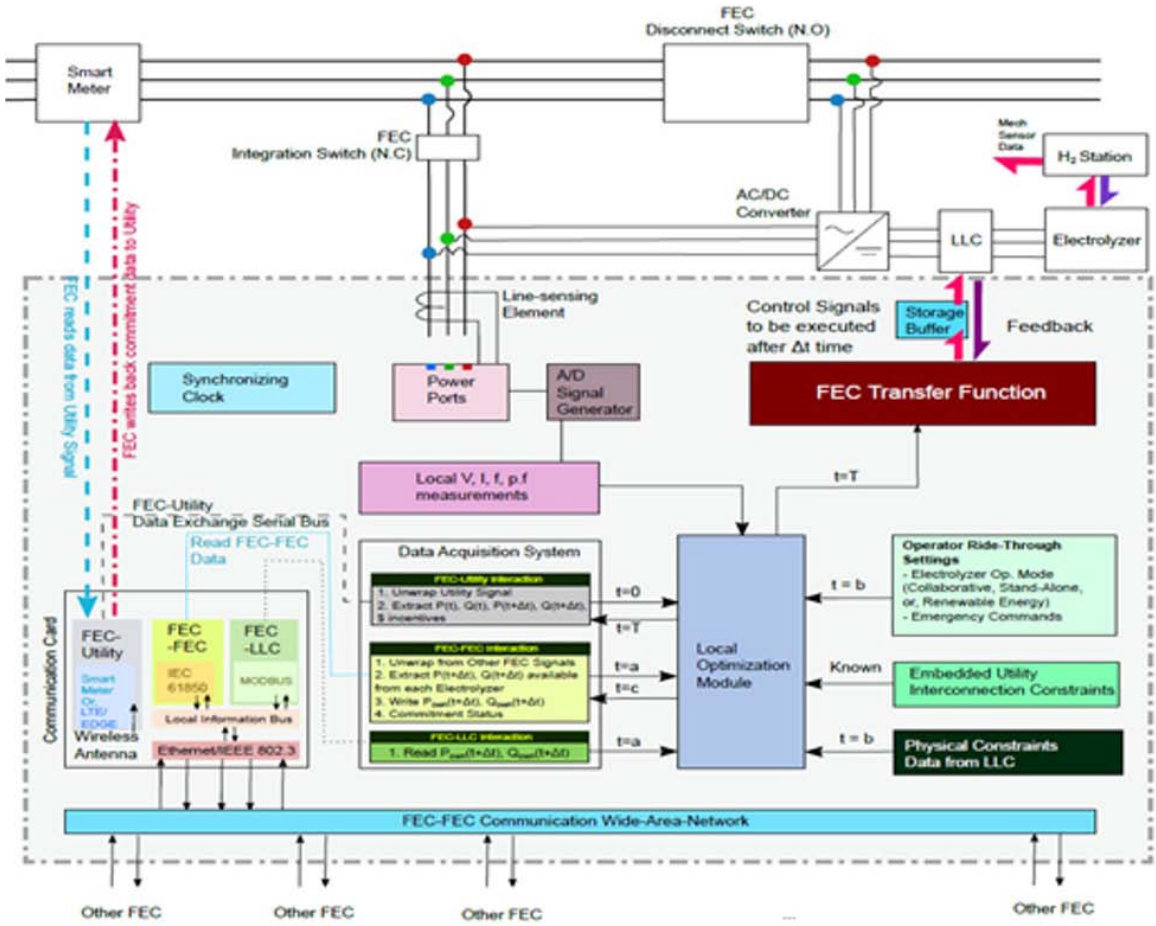

FIGURE 4. FEC schematic representation enabling electrolyzers to provide grid services

automated participation in markets was developed and will be implemented in the DRTS environment to respond to grid signals. Integration of the FEC with the electrolyzer model, and eventually hardware that interprets utility signals to provide reference signals for the lower level controller, are planned. A utility-scale network (PG&E distribution network) was modeled in DRTS in order to accommodate the future refueling stations as planned in the San Francisco Bay Area served by PG&E. This will enable studying the deployment of hydrogen refueling stations in the Bay Area and assessing the technical and economic impacts. Distributed real-time simulation for the expanded distribution networks with future refueling stations under novel DR programs will also be performed. In the future, establishment of multiple value streams for hydrogen refueling stations is anticipated as a result of learnings from this study.

FY 2016 PUBLICATIONS/PRESENTATIONS

1. M. Mohanpurkar, M. Panwar, S. Chanda, M. Stevic, R. Hovsapian, V. Gevorgian, S. Suryanarayanan, A. Monti, "Distributed Real-time Simulations for Power Systems Engineering," Cyber-Physical-Social Systems and Constructs in Electric Power Engineering, October 2016, pp. 35.

2. R. Liu, M. Mohanpurkar, M. Panwar, R. Hovsapian, A. Srivastava, S. Suryanarayanan, "Geographically distributed real-time digital simulations using linear prediction," International Journal of Electrical Power & Energy Systems, Volume 84, 01/2017, pp. 309–317.

VIII.0 Safety, Codes & Standards Program Overview

INTRODUCTION

The Safety, Codes and Standards program identifies research and development (R&D) needs and performs high-priority R&D to provide an experimentally validated fundamental understanding of the relevant physics, critical data, and safety information needed to define the requirements for technically sound and defensible codes and standards. This information is used to facilitate and enable the widespread deployment and commercialization of hydrogen and fuel cell technologies. In Fiscal Year (FY) 2016, the program continued to identify and evaluate safety and risk management measures that can be used to define the requirements and close the gaps in codes and standards in a timely manner.

The program promotes collaboration among government, industry, codes and standards development organizations (CDOs and SDOs), universities, and national laboratories in an effort to harmonize regulations, codes, and standards (RCS) both internationally and domestically. Communication and collaboration among codes and standards stakeholders, the Federal government, industry, national labs, and trade associations is emphasized in order to maximize the impact of the program's efforts and activities in international RCS development.

The program has achieved accomplishments in R&D for codes and standards support. In FY 2016, the Hydrogen Risk Assessment Model (HyRAM) version 1.0 was released for public use and is available to download online[1]. In addition, a new cryogenic hydrogen release laboratory was constructed, and planned releases will help inform separation distances for liquid hydrogen. The program continues to advance its materials work by conducting fatigue testing in Cr-Mo steels, populating a database with materials-in-hydrogen properties, and initiating a new project on hydrogen compatibility of non-metallic materials. Furthermore, in the area of fuel quality assurance, a prototype in-line fuel quality analyzer was developed. These R&D accomplishments feed into the program's Continuous Codes and Standards Improvement process, which submitted revised bulk gaseous hydrogen separation distances for consideration to National Fire Protection Association (NFPA) 2/55.

The program continues to utilize the expertise of the Hydrogen Safety Panel to disseminate relevant information and implement safe practices pertaining to the operation, handling, and use of hydrogen and fuel cell technologies in program-funded projects. The program also continues to share current safety information and knowledge with the community through the continued development of resources for H2Tools.org. The program continues to place emphasis on ensuring the continual availability of safety knowledge tools, to reach the largest number of safety personnel possible. During FY 2016, the program's training for code officials and first responders has reached more than 36,000 individuals through on-line and classroom training.

GOAL

The program's key goals are to provide the validated scientific and technical basis required for the development of codes and standards, to promulgate safety practices and procedures to allow for the safe deployment of hydrogen and fuel cell technologies, and to ensure that best safety practices are followed in Hydrogen and Fuel Cells Program activities.

OBJECTIVES

The program's key objectives are to:

- Support and facilitate development and promulgation of essential codes and standards to enable widespread deployment and market entry of hydrogen and fuel cell technologies and completion of all essential domestic and international RCS.
- Conduct R&D to provide critical data and information needed to define requirements in developing codes and standards.
- Ensure that best safety practices underlie research, technology development, and market deployment activities supported through DOE-funded projects.

[1] http://energy.sandia.gov/transportation-energy/hydrogen/quantitative-risk-assessment/hydrogen-risk-assessment-model-hyram/

- Develop and enable widespread sharing of safety-related information resources and lessons learned with first responders, authorities having jurisdiction, and other key stakeholders.

FY 2016 STATUS AND ACCOMPLISHMENTS

The program continues to support R&D to provide the scientific basis for codes and standards development, with projects in fuel specification, separation distances, materials and components compatibility, and hydrogen sensor technologies. Utilizing the results from these R&D activities, the program continues to actively participate in discussions with SDOs such as the NFPA, the International Code Council, SAE International, the CSA Group, and the International Organization for Standardization (ISO) to promote domestic and international collaboration and harmonization of RCS.

The H2Tools website (http://h2tools.org/) provides additional, up-to-date information relevant to the status of the program's activities. Resources available on the H2Tools.org site include the Technical Reference for Hydrogen Compatibility of Materials, the Hydrogen Lessons Learned Database, the Hydrogen Bibliographic Database, the Hydrogen Safety Best Practices Manual, the National Hydrogen and Fuel Cell Emergency Response Training Resource, Hydrogen Safety Training for Researchers, the Introduction to Hydrogen for Code Officials, Hydrogen Safety for First Responders, and Codes and Standards – Permitting Tools, including the National Permitting Guide. This year, the National Hydrogen and Fuel Cell Emergency Response Training Resource was also translated into Japanese. The H2Tools website continues to see increasing traffic, with ~10,000 visits as of May 2016, many of which are international visits.

The Program continued to make progress in several key areas, including the following:

- Hydrogen Behavior, Risk Assessment (Sandia National Laboratories):
  - Completed design, construction, and commissioning of the cryogenic liquid hydrogen release laboratory to enable advanced diagnostic studies of cryogenic hydrogen releases.
  - Publicly released a free version of Hydrogen Risk Assessment Models (HyRAM) V1.0 software for risk analysis of hydrogen infrastructure systems, including modules for simulating gas plume dispersion, overpressure, and layering behavior from user-defined releases, as well as engineering tools such as simple hydrogen safety calculations (e.g., thermodynamic conversions and mass flow rate calculations).
  - Calculated revised bulk gaseous separation distances using modified risk criteria for adoption by the NFPA 2/55 technical committees, which will enable more sites to readily accept hydrogen infrastructure. These changes demonstrated the potential for up to an additional 50% reduction in gaseous hydrogen separation distances over previous code requirements.
- Materials Compatibility (Sandia National Laboratories, Pacific Northwest National Laboratory, Oak Ridge National Laboratory):
  - Completed fatigue initiation testing of Cr–Mo steel specimens provided by the Fuel Cell Hydrogen Joint Undertaking's MATHRYCE project at two hydrogen gas pressures (30 and 100 MPa). Results show that the number of cycles for crack initiation decreases as hydrogen pressure increases from 30 to 100 MPa, confirming that fatigue testing at 30 MPa is non-conservative relative to a service pressure of 100 MPa.
  - Compiled input from over 50 hydrogen infrastructure stakeholders on polymers of interest, current utilized test methods, operating conditions, and applications to identify knowledge gaps for hydrogen compatibility with polymeric materials. Stakeholders included hydrogen system designers, component manufacturers, polymer producers, code committee members, and hydrogen suppliers. Initiated testing of selected materials.
- Hydrogen Quality (Los Alamos National Laboratory):
  - Developed a prototype in-line hydrogen fuel quality analyzer with a hydration scheme that allows for constant baseline measurements.
  - Measured the fuel cell response to 50 ppm CO (limited only by the lag time of the system) in hydrogen after switching from neat hydrogen. To date, this was the fastest response time (<< 1 min) obtained, although the CO concentration was much higher than the SAE/ISO limit.

- Coordination of Codes and Standards Development, Domestic and International, and Codes and Standards Outreach (Sandia National Laboratories, National Renewable Energy Laboratory, Oak Ridge National Laboratory):
  - Managed the development of numerous draft public inputs to NFPA 2, NFPA 55, and the International Fire Code, with the aim of addressing key industry needs, including for fuel cell electric vehicle repair booths and harmonized requirements for defueling, and of addressing inconsistencies or lack of clarity between model codes.
  - Developed a training video titled "Permitting Hydrogen Fueling Stations" in collaboration with an authority having jurisdiction in the Los Angeles metropolitan area and the Orange County Fire Authority, where several hydrogen fueling stations will be located. This video should reduce the time and cost of both preparing and processing hydrogen fueling station permit applications by quickly orienting people to both the basics of the fueling technology and the code requirements.
- Hydrogen Safety Panel, Databases, Props, and First Responders (Pacific Northwest National Laboratory):
  - Led a team of four first responders from the United States to participate in the European Hydrogen Emergency Response Training Program for First Responders (HyResponse), held at L'École Nationale Supérieure des Officiers de Sapeurs-Pompiers (ENSOSP) (The French Academy for Fire, Rescue, and Civil Protection Officers) in Aix en Provence, France, May 9–13, 2016.
  - Added additional resource tools for codes and standards permitting, Hydrogen Fueling Infrastructure Research and Station Technology (H2FIRST), and the Hydrogen Station Equipment Performance (HyStEP) device to the Hydrogen Tools Portal (http://h2tools.org).
- Hydrogen Sensors (National Renewable Energy Laboratory & Los Alamos National Laboratory):
  - Quantified the impact of potential chemical poisons, as identified in ISO 26140, on the major hydrogen sensor platform types in collaboration with the Joint Research Centre Institute for Energy and Transport.
  - Formed a group among the National Renewable Energy Laboratory and the Joint Research Centre sensor experts with computation fluid dynamics modelers and risk assessment experts to provide guidelines on hydrogen sensor placement for various facilities (e.g., maintenance repair) that will contain hydrogen.

BUDGET

The program received an appropriation of $7 million in FY 2016 (Figure 1). FY 2016 funding has allowed for continued support of codes-and-standards-related R&D and of the domestic and international collaboration and harmonization efforts for codes and standards that are needed to support the commercialization of hydrogen and fuel cell technologies. The FY 2017 request of $10 million will allow the program to broaden its existing R&D efforts and expand its focus to include infrastructure-related activities. The "Research and Development" category includes such activities as hydrogen behavior, risk assessment and mitigation, materials compatibility, hydrogen fuel quality, metering, sensors, and component testing. The "Safety Management and Resources" category includes the Hydrogen Safety Panel, databases, training, and props. The "Outreach" category includes codes and standards, permitting, continuous codes and standards improvement, and resource dissemination.

FY 2017 PLANS

The Safety, Codes and Standards program will continue to work with CDOs and SDOs to develop technical information and performance data to enhance hydrogen-specific codes and standards. To address these needs, the program will continue to support a rigorous technical R&D program—including assessment of materials compatibility for component designs and high-pressure tank cycle testing—and continue to promote a performance-based quantitative risk assessment approach to assess risks and establish protocols to identify and mitigate risk. A major focus will be R&D to inform appropriate revised separation distance requirements for liquid hydrogen installations. Future work will also focus on facilitating the permitting of hydrogen fueling stations and early market applications and testing, measurement, and verification of hydrogen fuel specifications.

The program will also continue to promote the domestic and international harmonization of test protocols for qualification and certification, as well as the harmonization of RCS for hydrogen fuel quality and other key

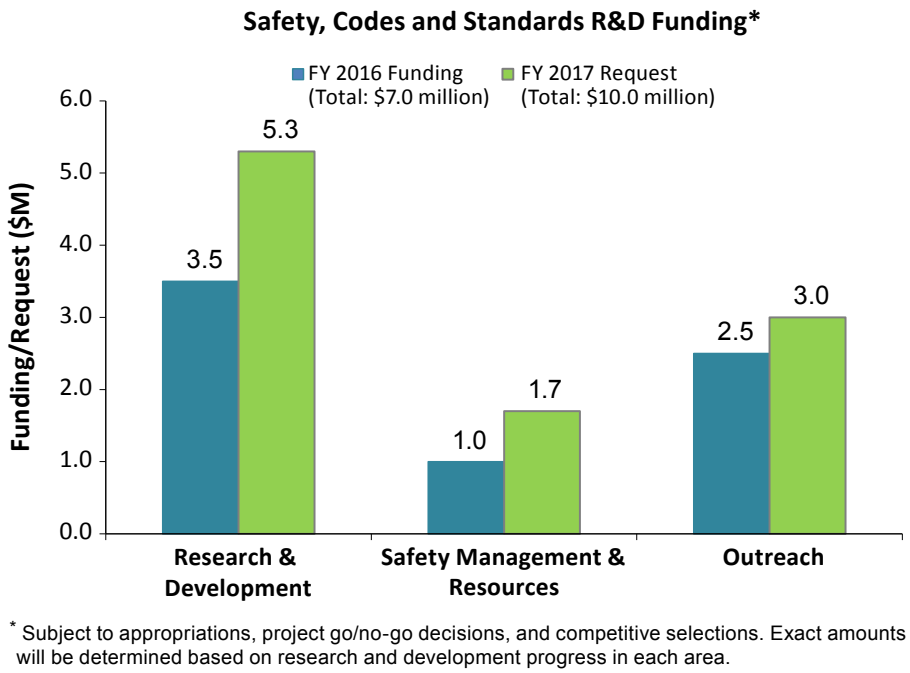

FIGURE 1. FY 2016 appropriations and FY 2017 budget request for the Safety, Codes and Standards program

international standards. These efforts will be enabled by working with the appropriate domestic and international organizations such as the NFPA, International Code Council, SAE International, the CSA Group, and the ISO. For the first time, the Safety, Codes and Standards program is collaborating with the Federal Energy Management Program to develop hydrogen safety training materials utilizing existing training resources. The program will also continue to participate in the International Partnership for Hydrogen and Fuel Cells in the Economy's RCS Working Group and the International Energy Agency's Hydrogen Implementing Agreement, both of which are engaged in hydrogen safety work.

Charles James
Safety, Codes & Standards Program Manager
Fuel Cell Technologies Office
Office of Energy Efficiency and Renewable Energy
U.S. Department of Energy
1000 Independence Ave., SW
Washington, DC 20585-0121
Phone: (202) 287-6223
Email: Charles.James@ee.doe.gov

VIII.1 Fuel Cell Technologies National Codes and Standards Development and Outreach

Carl Rivkin (Primary Contact), Robert Burgess, and William Buttner
National Renewable Energy Laboratory (NREL)
15013 Denver West Parkway
Golden, CO 80401
Phone: (303) 275-3839
Email: Carl.Rivkin@nrel.gov

DOE Manager: Will James
Phone: (202) 287-6223
Email: Charles.James@ee.doe.gov

Subcontractors:
- Branded by Media, Orange, CA
- A.V. Tchouvelev & Associates, Mississauga, ON, Canada

Project Start Date: October 1, 2002
Project End Date: Project continuation and direction determined annually by DOE

Overall Objectives

- Support the deployment of hydrogen technologies for hydrogen fuel cell vehicles, industrial trucks, and stationary fuel cell applications.
- Make critical safety information readily available through webinars, training sessions, safety reports, online training, and technical presentations.
- Inform key stakeholders of the safety, codes, and standards requirements for the safe use of hydrogen technologies.
- Work with potential infrastructure developers to accelerate the deployment of hydrogen fueling stations and other key infrastructure.
- Identify and resolve safety issues associated with hydrogen technologies infrastructure.
- Support the continuous improvement of codes and standards through incorporating research and field data into the code development process.

Fiscal Year (FY) 2016 Objectives

- Publish a paper on the application of the Continuous Codes and Standards Improvement (CCSI) process in developing new risk-based requirements for bulk hydrogen storage.
- Support the deployment efforts through participation in the H2USA's Market Support and Acceleration Working Group.
- Support the development of the next edition of the National Fire Protection Association (NFPA) 2 Hydrogen Technologies Code by chairing the Technical Committee on Hydrogen Technology, leading the NFPA Hydrogen Storage Task Group, and acting as principal committee member of the NFPA Technical Committee on Industrial and Medical Gases.
- Develop outreach products for permitting hydrogen technologies, including an updated National Permitting Guide for Hydrogen Refueling Stations.
- Implement CCSI process by evaluating field data to determine codes and standards development priorities.
- Provide codes and standards information to critical stakeholders such as code officials through in-person training, updated on-line training, and development of relevant videos.
- Support the coordination of international and domestic hydrogen standards by participating in International Organization for Standardization/Technical Committee 197 hydrogen technology projects, hydrogen component development working groups, and domestic standards organizations such as the CSA Group.

Technical Barriers

This project addresses the following technical barriers from the Hydrogen Safety, Codes and Standards section of the Fuel Cell Technologies Office Multi-Year Research, Development, and Demonstration Plan:

(A) Safety Data and Information: Limited Access and Availability

(D) Lack of Hydrogen Knowledge by AHJs

(F) Enabling National and International Markets Requires Consistent RCS

(G) Insufficient Technical Data to Revise Standards

(H) Insufficient Synchronization of National Codes and Standards

(I) Lack of Consistency in Training of Officials

(K) No Consistent Codification Plan and Process for Synchronization of R&D and Code Development

(L) Usage and Access Restrictions

Contribution to Achievement of DOE Safety, Codes & Standards Milestones

This project will contribute to achievement of the following DOE milestones from the Hydrogen Safety, Codes and Standards section of the Fuel Cell Technologies Office Multi-Year Research, Development, and Demonstration Plan:

- Milestone 4.6: Completion of standards for critical infrastructure components and systems. (4Q, 2014)
- Milestone 4.7: Complete risk mitigation analysis for advanced transportation infrastructure systems. (1Q, 2015)
- Milestone 4.8: Revision of NFPA 2 to incorporate advanced fueling and storage systems and specific requirements for infrastructure elements such as garages and vehicle maintenance facilities. (3Q, 2016)
- Milestone 4.9: Completion of GTR Phase 2. (1Q, 2017)

FY 2016 Accomplishments

- NREL provided broad coordination of codes and standards development by:
  - Supporting the Codes and Standards Tech Team; gave three presentations on sensors and codes and standards development activities.
  - Implementing the CCSI through several projects including:
    - Supporting the Hydrogen Code Improvement Team through Fuel Cell & Hydrogen Energy Association codes and standards development activities including support of the H2USA codes and standards development efforts.
    - Leading the NFPA Hydrogen Storage Task Group to develop technical basis for setback distances and safety mitigation measures in NFPA 55 and NFPA 2 and submitting the revised setback distances to the Technical Committee on Industrial and Medical Gases.
- Developed new permitting and codes and standards training modules for hydrogen technologies deployment that includes lessons learned and brings in information from current deployment activities.
- Developed a training video titled "Permitting Hydrogen Fueling Stations" in collaboration with an authority having jurisdiction in the Los Angeles metropolitan area, the Orange County Fire Authority, where several hydrogen fueling stations will be located. This video should reduce the time and cost of both preparing and processing hydrogen fueling station permit applications by quickly orienting people to both the basics of the fueling technology and the code requirements.
- Collaborated effectively with other DOE laboratories, including Sandia National Laboratories and Pacific Northwest National Laboratory, to develop training materials that are available through H2 Tools.

✧ ✧ ✧ ✧ ✧

INTRODUCTION

The fundamental purpose of this work is to support the safe deployment of hydrogen technologies. To achieve this objective, codes and standards must be in place to protect public safety and any significant safety issues must be resolved before deployment proceeds.

The work under this project has helped develop a national set of codes and standards to safely deploy hydrogen technologies. Additionally, key safety issues have been identified and are in the process of being resolved. Safety, codes, and standards information has been distributed to interested parties using a variety of techniques including webinars, NREL technical reports, workshops, in-person presentations, videos, online training tools, and web-based products.

APPROACH

The project approach involves as many key stakeholders as possible in codes and standards development and coordination and outreach activities to achieve maximum impact. These stakeholders include industry partners, standards development organizations, research organizations including other national laboratories, authorities having jurisdiction, local government in locations where projects will be deployed, and trade organizations involved in technology development and deployment.

RESULTS

NREL, at the direction of DOE, has helped develop a baseline set of codes and standards for the deployment of hydrogen technologies. This accomplishment helps meet several DOE milestones, including 4.4 and 4.8.

The next step in this codes and standards development process after the promulgation of the baseline set of codes and standards is monitoring the field performance of these documents, determining where modifications are required (including the research required to support these modifications), and supporting the implementation of those modifications. Examples of these modifications include the revised setback distances for bulk gaseous hydrogen storage and the development of requirements of fuel cell

electric vehicles in repair garages. This helps DOE meet Milestone 4.5.

This modification process is illustrated in Figure 1. The process consists of evaluating field deployment of hydrogen technologies through use of NREL data and site visits, determining whether there are issues with codes and standards based on this information, and developing modified codes and standards requirements to resolve these issues. This process also integrates NREL laboratory research activities involving hydrogen technologies safety by using this research to address codes and standards issues.

The CCSI process has already begun to produce results in the following areas:

- The NFPA Hydrogen Storage Task Group has revisited the assessment made for bulk gaseous hydrogen setback distances and has developed a plan for revising these distances in the 2019 edition of NFPA 55/2. This plan produced proposals to NFPA 55/2 that were submitted in June 2016.
- The Hydrogen Code Improvement Team has produced proposals to the Uniform Fire Code to coordinate NFPA 2 and the Uniform Fire Code. Proposals were submitted to coordinate requirements for repair garages in the International Fire Code and NFPA 2.
- The NFPA Enclosures Task Group has developed an extensive set of proposals to the 2019 edition of NFPA 2 to address modular hydrogen fueling stations.

NREL completed codes and standards and permitting training tools such as the "Permitting Hydrogen Fueling Stations" video done in collaboration with the Orange County Fire Authority.

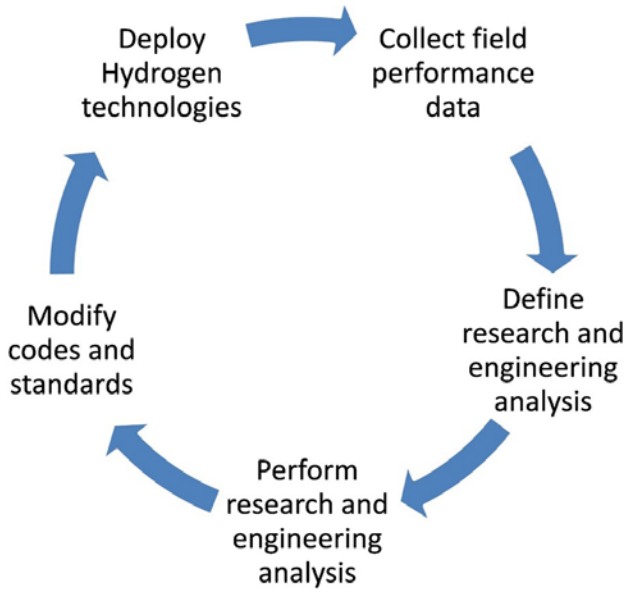

FIGURE 1. CCSI process

NREL supported the work of H2USA by participating as a member of the Market Support and Acceleration Working Group. This participation included presenting information on hydrogen fueling station codes and standards at the 2016 National Association of State Fire Marshals meeting.

NREL supported testing required to develop Federal Motor Vehicle Safety Standards required to implement Global Technical Regulation in the United States. This supports DOE Milestone 4.9.

NREL has acted as Task Group Leader for the NFPA Hydrogen Storage Task Group that will develop new requirements for bulk gaseous and liquefied hydrogen and associated safety mitigation measures for the next edition of NFPA 55/2. This supports DOE Milestone 4.9.

CONCLUSIONS AND FUTURE DIRECTIONS

Conclusions

- Codes and standards
  - Codes and standards development support will continue through direct support of standards development organizations by NREL staff participation on or operation of technical committees.
  - Ongoing coordination of the fire and building codes and key hydrogen codes and standards is a priority.
  - Field deployment information will help set codes and standards development priorities and improve the quality and relevance of codes as this information is incorporated through the American National Standards Institute-proscribed revision process.
- Outreach
  - Deployment support will be focused on infrastructure at locations with project activity and concrete deployment plans, for example jurisdictions in California and the Northeast.
  - These goals can only be accomplished through collaborations with key stakeholders at all levels.
  - NREL will continue to support deployment of hydrogen and fuel cell technologies through programs such as technical reports, webinars, safety reviews, and the web-based information compendium. NREL will develop permitting tools that address the different needs of stakeholders and are readily accessible through the internet.

  - NREL will work with H2USA to support the efforts of key organizations involved in infrastructure deployment.

Future Directions

- Continue work to coordinate codes and standards with special focus on taking information from deployment projects back to code development committees.
- Resolve infrastructure codes and standards issues such as hydrogen setback distances in NFPA codes.
- Continue coordination between National Fire Codes and International Code Council codes, as well as International Organization for Standardization hydrogen component standards and domestic hydrogen component standards.
- Support efforts to adopt NFPA 2 Hydrogen Technologies Codes (and other key codes), such as the work done by the California's Office of the State Fire Marshal to adopt NFPA 2 earlier than adoption of the International Fire Code would dictate.
- Continue to incorporate research into the codes through the CCSI process.

Outreach

- Continue to publish NREL technical reports, deliver webinars, and provide web-based information on key safety issues required to support hydrogen technologies deployment.
- Assist code officials, project developers, and other interested parties in use of new codes and standards and safety information through outreach activities, with special focus on key jurisdictions such as California and the Northeast.
- Utilize NREL hydrogen fueling station for training purposes such as videos on hydrogen fueling operations and maintenance.
- Work with interested parties to provide information to assist in infrastructure deployment.
- Provide in-person codes and standards training in key locations such as California and other zero-emission vehicle states.
- Work with H2USA to support infrastructure development such as fuel cell electric vehicles using tunnels.

FY 2016 PUBLICATIONS/PRESENTATIONS

1. Rivkin, C., R. Burgess, and W. Buttner. 2016. *Guide to Permitting Hydrogen Motor Fuel Dispensing Facilities*. NREL Report No. TP-5400-64042. Golden, CO: National Renewable Energy Laboratory.

2. Rivkin, C., R. Burgess, and W. Buttner. 2016. "Continuous Codes and Standards Improvement (CCSI)." International Conference on Hydrogen Safety.

3. Rivkin, C., C. San Marchi, and M. Rangachary. 2015. "History of Regulations, Codes and Standards." Presented at 2015 International Conference on Hydrogen Safety, Yokohama, Japan, October 19–21.

4. *Guide for Compliance with Regulations, Codes and Standards for the Deployment of Stationary Fuel Cells*. 2016. Telecommunications Industry Association. (Manuscript under review.)

5. Rivkin, C., C. LaFleur, and M. Gresho. "Siting Bulk Hydrogen Storage Systems: Advances in Risk-Informed Siting Procedures in NFPA Codes." 2016. Presented at AIChE Loss Prevention Symposium, Houston, Texas, April 11–13.

VIII.2 R&D for Safety, Codes and Standards: Materials and Components Compatibility

Chris San Marchi (Primary Contact),
Brian Somerday
Sandia National Laboratories
7011 East Ave.
Livermore, CA 94550
Phone: (925) 294-4880
Email: cwsanma@sandia.gov

DOE Manager: Will James
Phone: (202) 287-6223
Email: Charles.James@ee.doe.gov

Project Start Date: October 1, 2003
Project End Date: Project continuation and direction determined annually by DOE

Overall Objectives

- Optimize the reliability and efficiency of test methods for structural materials and components in hydrogen gas.
- Generate critical hydrogen compatibility data for structural materials to enable technology deployment.
- Create and maintain information resources such as the "Technical Reference for Hydrogen Compatibility of Materials."
- Demonstrate leadership in the international harmonization of standards for qualifying materials and components for high-pressure hydrogen service.

Fiscal Year (FY) 2016 Objectives

- Evaluate relevant high hardenability (Ni–Cr–Mo) steels for advanced high-pressure storage.
- Develop material property database for hydrogen effects on materials.
- Establish coordinated fatigue life testing activities and data sharing with international stakeholders.
- Demonstrate low-temperature fatigue life method for austenitic stainless steels.

Technical Barriers

This project addresses the following technical barriers from the Hydrogen Safety, Codes and Standards section of the Fuel Cell Technologies Office Multi-Year Research, Development, and Demonstration Plan:

(A) Safety Data and Information: Limited Access and Availability

(F) Enabling National and International Markets Requires Consistent RCS

(G) Insufficient Technical Data to Revise Standards

Contribution to Achievement of DOE Safety, Codes & Standards Milestones

This project will contribute to achievement of the following DOE milestones from the Hydrogen Safety, Codes and Standards section of the Fuel Cell Technologies Office Multi-Year Research, Development, and Demonstration Plan:

- Milestone 2.9: Publish technical basis for optimized design methodologies of hydrogen containment vessels to account appropriately for hydrogen attack. (4Q, 2014)
- Milestone 2.16: Demonstrate the use of new high-performance materials for hydrogen applications that are cost-competitive with aluminum alloys. (4Q, 2017)
- Milestone 2.18: Implement validated mechanism-based models for hydrogen attack in materials. (4Q, 2018)
- Milestone 3.3: Reduce the time required to qualify materials, components, and systems by 50% relative to 2011 with optimized test method development. (1Q, 2017)
- Milestone 3.4: Develop hydrogen material qualification guidelines including composite materials. (Q4, 2017)
- Milestone 4.9: Completion of the GTR Phase 2. (1Q, 2017)
- Milestone 5.2: Update materials compatibility technical reference. (4Q, 2011 – 2020)
- Milestone 5.4: Develop and publish database for properties of structural materials in hydrogen gas. (2Q, 2013)

FY 2016 Accomplishments

- Completed fatigue initiation testing of Cr–Mo steel specimens provided by the MATHRYCE project at two hydrogen gas pressures (30 and 100 MPa). Results show that the number of cycles for crack initiation decreases as hydrogen pressure increases from 30 to 100 MPa, confirming that fatigue testing at 30 MPa is nonconservative relative to the service pressure of 100 MPa.

- Initiated testing campaign on high hardenability (Ni–Cr–Mo) pressure vessels steels. This activity includes partnership with pressure vessel manufacturers from the United States, Europe, and Asia. Preliminary results show consistency with Cr–Mo pressure vessels steels, suggesting that Ni–Cr–Mo can be used for thicker wall hydrogen pressure vessels.
- Demonstrated public trial of Uniform Resource Locator-based GRANTA MI™ database of materials properties in hydrogen environments.

✧ ✧ ✧ ✧ ✧

INTRODUCTION

A principal challenge to the widespread adoption of hydrogen infrastructure is the lack of quantifiable data on its safety envelope and concerns about additional risk from hydrogen. To convince regulatory officials, local fire marshals, fuel suppliers, and the public at large that hydrogen refueling is safe for consumer use, the risk to personnel and bystanders must be quantified and minimized to an acceptable level. Such a task requires strong confidence in the safety performance of high-pressure hydrogen systems. Developing meaningful materials characterization and qualification methodologies in addition to enhancing understanding of performance of materials is critical to eliminating barriers to the development of safe, low-cost, high-performance, high-pressure hydrogen systems for the consumer environment.

APPROACH

The Materials and Components Compatibility project leverages decades of experience in high-pressure hydrogen systems, well-developed industry partnerships, and a core capability in hydrogen–materials interactions anchored by the Hydrogen Effects on Materials Laboratory to focus on three critical activities: (1) optimize materials characterization methodologies, (2) generate critical hydrogen compatibility data for materials to enable technology deployment, and (3) provide international leadership by assembling and maintaining a technical reference that is populated with vetted data and includes a technical assessment of the data and its application.

RESULTS

Crack Initiation of Cr–Mo Steels

Sandia collaborated with the European Union-supported MATHRYCE project (www.mathryce.eu) to perform fatigue testing on notched specimens in high-pressure hydrogen gas. The tested materials were Cr–Mo steel, representative of pressure boundary materials in stationary hydrogen pressure vessels. The MATHRYCE project performed fatigue crack initiation and growth testing on these steels in lower-pressure hydrogen gas (less than 30 MPa) for the purpose of evaluating methods to inform fatigue life assessments of stationary pressure vessels. Since the testing systems operated by the MATHRYCE partners are limited to the lower pressure range, Sandia performed analogous fatigue testing on the Cr–Mo steel specimens at 100 MPa pressure in the Hydrogen Effects on Materials Laboratory. Sandia completed testing on the four instrumented specimens provided by the MATHRYCE project. Three of the specimens were tested in 100 MPa hydrogen gas (the upper limit expected for pressure vessels at refueling stations) with two different mechanical loading waveforms, i.e. sinusoidal and triangular. The fourth specimen was tested at 30 MPa to confirm the measurement by MATHRYCE. The results are summarized in Table 1.

TABLE 1. Summary of fatigue testing on notched Cr–Mo steel specimens

H_2 Pressure (MPa)	Waveform	Cycles for Crack Initiation
100	sinusoidal	763
100	sinusoidal	860
100	triangular	1017
30	triangular	2589
30	triangular	2764†
10	triangular	7136†
2	triangular	18292†

†measurements made by MATHRYCE program

The results in Table 1 demonstrate that increasing hydrogen pressure from 30 MPa to 100 MPa reduces the number of load cycles to initiate cracking at the notch, confirming that testing at 30 MPa cannot represent the service condition at 100 MPa. In addition, the number of cycles for crack initiation at 30 MPa as measured at Sandia is consistent with the result measured by MATHRYCE, validating the consistency of testing in the two laboratories (Sandia and MATHRYCE). These results represent the first attempt at quantification of crack initiation in gaseous hydrogen at high pressure (>70 MPa). These results suggest that the number of cycles to initiate a crack can be relatively low. A robust methodology for extrapolating crack initiation studies to design has not yet been achieved.

High-Hardenability Pressure Vessel Steels

The partnership for testing high-hardenability (Ni–Cr–Mo) pressure vessel steels includes Fiba Technologies (United States), Tenaris-Dalmine (Europe/Italy), and Japan Steel Works (Asia/Japan). All of the partners are provided steel panels for extracting specimens or actual specimens. Testing has begun with steel panels (SA-372 Grade L) provided as part of previous work with the American Society

of Mechanical Engineers (ASME) Project Team on Hydrogen Tanks. Sandia has two panels, one that satisfies the SA-372 Grade L strength specification (very high yield strength for hydrogen service, >1,000 MPa) and the other with an experimental heat treatment to achieve lower strength consistent with Grade J (yield strength of ~750 MPa). The fatigue crack growth rates for the low strength Ni–Cr–Mo pressure vessel steel is compared in Figure 1 with fatigue crack growth rates for several varieties of Cr–Mo pressure vessels steels. The Cr–Mo steels were tested in gaseous hydrogen at pressure of 45 MPa, while the Ni–Cr–Mo steel was tested at pressure of 106 MPa. The test frequency was either 1 Hz (4130X, Grade L) or 10 Hz (Grade J, 34CrMo4), while an R ratio of 0.1 was used for all tests. The different test configurations likely account for the modest differences in the observed fatigue crack growth rates, but in general, for high ΔK (>12 MPa $m^{1/2}$) the fatigue crack rates are consistent for these materials and test conditions. The steels from the partners will be consistent with SA-723, an ASME standard for Ni–Cr–Mo pressure vessel steels that includes yield strength criteria of around 700 MPa (Class 1). This relatively low strength is consistent with the Grade J steels from SA-372 and appropriate for hydrogen pressure vessels. The higher classes represent higher yield strength criteria (>825 MPa) and are unlikely to show sufficient fracture resistance in hydrogen environments to meet design requirements, such as those in ASME Boiler and Pressure Vessel Code VIII.3 [1]. Steels from the partners are expected in August 2016.

Information Resources

Granta agreed to a public trial of the Technical Database for Hydrogen Compatibility of Materials (https://granta-mi.sandia.gov). The initial effort to expand the content of the database includes the data from the technical reference, with the restriction of only including results measured in gaseous hydrogen environments. Recent publications on pipeline steels and pressure vessels steels will also be included in the database. This focus, we believe, serves the interests in a materials database of hydrogen effects previously expressed by ASME committee members (Project Team on Hydrogen Tanks and representatives from the ASME Pressure Piping Code [2]). The database will enable comparison of data from different sources, verification of materials and testing pedigrees, as well as potentially development of design data.

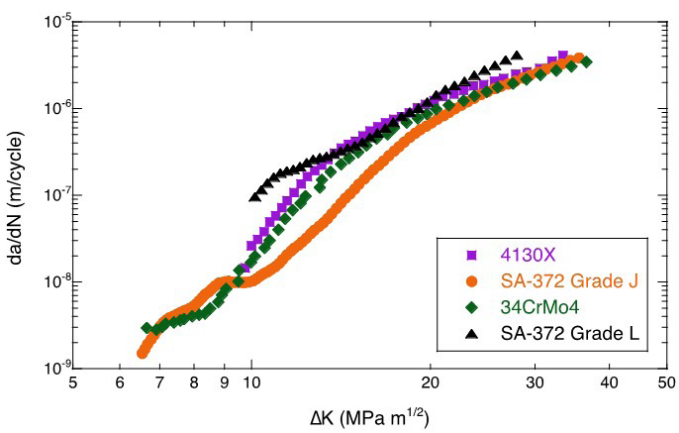

FIGURE 1. Fatigue crack growth rates comparing Ni–Cr–Mo pressure vessel steel (SA-372 Grade L) to Cr–Mo pressure vessel steels (4130X, SA-372 Grade J and 34CrMo4). The test pressure was 45 MPa, with the exception of the Grade L, where the test pressure was 106 MPa. Testing of the Grade L and 4130X was conducted at frequency of 1 Hz, while the other tests were conducted at frequency of 10 Hz. All tests were conducted with an R ratio of 0.1.

Low-Temperature Testing Apparatus

Low-temperature evaluation of materials is critical to expansion of the alloys that can be used in vehicle applications (due, in part, to precooling requirements during refueling). This is the motivation for construction of a high-pressure testing system with the capability of controlling temperature as low approximately 200 K. Delivery of the low-temperature testing apparatus has been delayed several times by the vendor. The current estimate for receiving the autoclave for low-temperature testing is end of summer 2016. Other major hardware components have been purchased and integrated (to the extent possible). The initial focus of testing is anticipated to be austenitic stainless steels in coordination with international partners at MPA Stuttgart and Kyushu University. Preliminary data from other projects suggest that fatigue performance may not be limited by low temperature, but this hypothesis needs verification.

CONCLUSIONS AND FUTURE DIRECTIONS

- The qualification of high-hardenability steels (Ni–Cr–Mo) will be an important advance for storage as pressure vessels with thicker walls are needed to support high-pressure hydrogen storage for refueling. Evaluation of Ni–Cr–Mo steels in comparison to qualified Cr–Mo steels will be the focus of high-pressure fatigue and fracture testing the coming months.
- The Technical Database for Hydrogen Compatibility of Materials will show significant expansion before the end of FY 2016. The public trial will end and a longer-term solution must be negotiated with Granta. At the very least, the database will be distributed for free and GRANTA MI users will have access to the data.
- Completion of the system for low-temperature testing is critical to validation of low-temperature performance. Austenitic stainless steels will be the focus of international coordination of testing at low temperature once the low-temperature testing system is operational near the end of FY 2016.

SPECIAL RECOGNITIONS & AWARDS/ PATENTS ISSUED

1. 2015 ASME PVP Heki Shibata Outstanding International Technical Session (awarded at the PVP 2016 conference): "Effects of Gaseous Hydrogen on Pressure Vessel Steels."

FY 2016 PUBLICATIONS/PRESENTATIONS

1. T. Michler, C. San Marchi, K. Berreth, J. Naumann, R.K. Misha, R.C. Kubic: "Microstructure, deformation mechanisms and influence of hydrogen on tensile properties of the Co based super alloy DIN 2.4711/UNS N30003." Mater Sci Eng A662 (2016) 36–45.

2. C. San Marchi, E.S. Hecht, I.W. Ekoto, K.M. Groth, C. LaFleur, B.P. Somerday, R. Mukundan, T. Rockward: "Overview of the DOE Hydrogen Safety, Codes and Standards Program, Part 3: Advances in research and development to enhance the scientific basis for hydrogen regulations, codes and standards." Intern J Hydrogen Energy (accepted; DOI: 10.1016/j.ijhydene.2016.07.014).

3. L. Zhang, B. An, T. Iijima, C. San Marchi: "Effect of gaseous hydrogen charging on nanohardness of austenitic stainless steels" (PVP2016-63390). Proceedings of the 2016 ASME Pressure Vessels & Piping Conference, 17–21 July 2016, Vancouver, BC, Canada.

4. B.P. Somerday, J.A. Campbell, K.L. Lee, J.A. Ronevich, C. San Marchi: "Enhancing safety of hydrogen containment components through materials testing under in-service conditions." 6th International Conference on Hydrogen Safety (ICHS), 19–21 October 2015, Yokohama, Japan.

5. C. San Marchi, E.S. Hecht, I.W. Ekoto, K.M. Groth, C. LaFleur, B.P. Somerday, R. Mukundan, T. Rockward: "Advances in research and development to enhance the scientific basis for hydrogen regulations, codes and standards." 6th International Conference on Hydrogen Safety (ICHS), 19–21 October 2015, Yokohama, Japan.

6. C. San Marchi: "Fatigue testing methodologies in gaseous hydrogen." International Workshop on Hydrogen Embrittlement in Metal, at the Korean Society of Mechanical Engineers Annual Fall Conference, 13 November 2015, Jeju, Korea.

7. C. San Marchi: "Pressure cycling of all steel pressure vessels with gaseous hydrogen." Joint HYDROGENIUS and I2CNER International Workshop on Hydrogen-Materials Interactions 2016, 4 February 2016, Kyushu, Japan.

REFERENCES

1. American Society of Mechanical Engineers (ASME), Boiler and Pressure Vessel Code (BPVC), Section VIII, Division 3, Article KD-10.

2. American Society of Mechanical Engineers (ASME), Hydrogen Piping and Pipelines, B31.12, ASME Code for Pressure Piping.

VIII.3 Hydrogen Fuel Quality

Tommy Rockward (Primary Contact), Jacob Valdez, Chris Romero, Stefan Williams, Eric Brosha, Mahlon Wilson, and Rangachary Mukundan
Los Alamos National Laboratory (LANL)
P.O. Box 1663
Los Alamos, NM 87545
Phone: (505) 667-9587
Email: trock@lanl.gov

DOE Manager: Will James
Phone: (202) 287-6223
Email: Charles.James@ee.doe.gov

Collaborators/Partners

- Japan Automotive Research Institute
- National Hydrogen and Fuel Cell Codes and Standards Coordinating Committee
- ASTM International
- SAE International
- Smart Chemistry
- Commissariat à l'énergie atomique et aux énergies alternatives (CEA), Liten, France
- VTT, Helsinki, Finland
- International Electrotechnical Commission Technical Committee 105 Working Group 11 (IEC/TC 105/WG 11)

Project Start Date: October 2006
Project End Date: Project continuation and direction determined annually by DOE

Overall Objectives

To support the Hydrogen Safety, Codes and Standards sub-program through:

- Participation in working groups.
- Providing leadership to hydrogen fuel quality efforts.
- Performing the R&D needed to develop science-based codes and standards.
- Developing tools that can remove safety and hydrogen fuel quality barriers to the commercialization of fuel cells.

Fiscal Year 2016 Objectives

- Evaluate fuel quality impacts on membrane electrode assemblies (MEAs) with DOE 2015 loadings and disseminate data to inform the revision of fuel quality standards.
- Build a prototype fuel quality analyzer based on the proof of concept demonstrated in FY 2015.
- Collaborate with international institutions to harmonize testing protocols to aid istandards development.
- Serve as subcommittee chair for ASTM D03.14: Gaseous Fuels and participate in ASTM interlaboratory studies.
- Provide technical support to IEC/TC 105/WG 11.

Technical Barriers

This project addresses the following technical barriers from the Hydrogen Safety, Codes, and Standards section of the Fuel Technologies Program Multi-Year Research, Development, and Demonstration Plan.

(F) Enabling National and International Markets Requires Consistent RCS (regulations, codes and standards)

(G) Insufficient Technical Data to Revise Standards

(H) Insufficient Synchronization of National Codes and Standards

(K) No Consistent Codification Plan and Process for Synchronization of R&D and Code Development

FY 2016 Accomplishments

- Demonstrated hydration scheme that allows for constant baseline measurements in the prototype fuel quality analyzer, which subsequently allowed for a provisional patent application to be initiated with LANL Richard P. Feynman Center for Innovation.
- Obtained a response to 50 ppm CO (limited only be the lag time of the system) in hydrogen after switching from neat hydrogen. To date, this was the fastest response time ($t < 1$ min) obtained even though the CO concentration was much higher than the SAE International Organization for Standardization (ISO) limit.
- Several ASTM test methods have been published. "Standard Test Method for Determination of Trace Carbon Dioxide, Argon, Nitrogen, Oxygen, and Water in Hydrogen Fuel by Jet Pulse Injection and Gas Chromatography/Mass Spectrometer Analysis (D7649)," "Standard Test Method for Sampling of Particulate Matter in High Pressure Hydrogen used as a Gaseous Fuel with an In Stream Filter (D7650)," and "Standard Test Method for Gravimetric Measurement of Particulate Concentration of Hydrogen Fuel (D7651)" were reviewed (five years after initial publication), approved by ballot, and resubmitted.

- Chaired two semi-annual ASTM meetings whose outcome led to the development of a database which helped identify interested test-sites with existing capabilities for conducting interlaboratory studies according to ASTM guidelines. These meetings were held in Austin, Texas, in December 2015, and Bellevue, Washington, in June 2016.
- Fuel quality work performed with several international partners (CEA, VTT, Joint Research Centre)
- LANL and Japan Automotive Research Institute baseline tests demonstrated fuel cell performance to be within 5% of each other, using either institutions protocol, hardware, and facilities.
- Hydrogen impurity testing is ongoing and will continue (collaboration with Hydrogen Contaminant Risk Assessment [HyCoRA] project that was extended). LANL initiated a parametric study to determine CO tolerance with lower loaded MEAs varying the relative humidity (RH) and pressure. Their test matrix probes three different RHs and three pressures, along with various CO concentrations. To date, we have completed testing at two different RHs and two different pressures.
- Extensive impurity testing performed using a fuel re-circulation system (VTT collaboration). These tests allow comparisons between single-pass mode and recirculation of CO, H_2S and CO/H_2S fuel mixtures. We have completed 100 hours of fuel cell testing with CO and H_2S, at the SAE limits, as single impurities in hydrogen.

✧ ✧ ✧ ✧ ✧

INTRODUCTION

LANL scientists' interactions with the fuel cell community through the DOE's Safety, Codes and Standards program continues to provide expertise in the area of hydrogen fuel quality testing in support of developing international fuel quality standards, guidance and leadership for ASTM standards development, as well as the development of an in-line fuel quality analyzer.

In the hydrogen fuel quality efforts, LANL has continued its investigation on the impact of fuel impurities at the levels listed in the "Hydrogen Fuel Quality for Fuel Cell Vehicles" SAE J2719 [1], and ISO 14687-2:2012 [2]. This ongoing effort has continued to focus on the "critical constituents: carbon monoxide, hydrogen sulfide, and ammonia" as fuel contaminants for fuel cells operated with low platinum loaded electrodes (anode: 0.05 mg/cm^2 and cathode: 0.1 mg/cm^2).

LANL has also made advances in the development of a prototype in-line fuel quality analyzer. Previous years' work has progressed to finalizing the design and testing of a novel hydration scheme. The most recent results of the analyzer indicate that the prototype is getting closer to field testing. Our goal is to accomplish this in FY 2017.

APPROACH

R&D for Fuel Quality Standards

LANL carried out parametric studies to help determine the tolerance to fuel impurities as a function of fuel cell operating conditions. Also, the newly installed re-circulating system was used to compare the impact of CO and H_2S in single pass mode versus recirculating the fuel. LANL continues to interact with several International collaborations to harmonize impurity testing. Finally, LANL scientists will host IEC/TC 105/WG 11 to finalize the development of an international document entitled, "Single Cell Test Methods for Polymer Electrolyte Fuel Cell (PEFC)."

In-line Fuel Quality Analyzer

LANL built and tested their new prototype design and hydration scheme for the fuel quality analyzer in FY 2016. A series of tests were conducted to determine the best conditions for maintaining membrane hydration. LANL scientists determined the various operating parameters that optimize sensitivity, response time, and stability.

RESULTS AND DISCUSSIONS

R&D for Fuel Quality Standards

In previous studies, LANL scientists determined CO tolerance using a common MEA tested at fixed fuel cell conditions, i.e., 1 A/cm^2, 100% RH, 83% fuel utilization, 25 psig. The tests used a constant dosage of CO. The voltage loss versus CO concentration was measured and the CO tolerance value was extrapolated to determine CO tolerance level. Our approach has expanded to include a similar parametric study to determine CO tolerance with lower loaded MEAs varying the relative humidity and pressures. Our test matrix probes three different RHs and three pressures. To date, we have completed testing at two different RHs and two different pressures. These preliminary fuel cell results indicate as the RH increases, the losses due to CO are enhanced, while the losses decreased as the pressure was increased.

In FY 2015, fuel cell performance in single-pass operation versus hydrogen recirculation with 200 ppb CO/H_2 was compared at 80°C in constant current mode at 1 A/cm^2 with 80°C with the back pressure set to 150 kPa. After 100 h of operation, the single-pass results showed a 38 mV voltage loss, while the recirculation system loss 50 mV. Similar studies were conducted with H_2S in FY 2016, and the

findings also show an increase in voltage loss when the fuel is recirculated. This result also was anticipated considering the interactions between CO and platinum surfaces are similar to that of sulfur, which has an even stronger interaction. In preparation for additional comparison tests, LANL has completed single-mode tests with ammonia, carbon monoxide, and hydrogen sulfide present simultaneously at the SAE J2719 levels. The tests conditions used were identical to when individual CO and H_2S contaminants were used. We included a subsequent test varying the RH from 100% to 50%. The results showed (Figure 1) an increase in voltage loss when the RH was lowered. At 100% RH, the voltage loss was 60 mV and it increased to 67 mV when the RH was reduced to 50%.

In-line Analyzer

LANL scientists have systematically studied materials for electrodes that are best suited for a hydrogen fuel quality analyzer and have strategically incorporated them into a newly developed prototype. Maintaining membrane hydration is essential in order to ensure the analyzer's viability. This particular task was challenging considering the hydrogen gas being monitored will be dry and that water is considered an impurity and will not be available. Using a unique water-wicking scheme, LANL tested the stability of the analyzer at various flow rates with two different membrane thicknesses, 2 mil (N112) and 7 mil (N117). High frequency resistance measurements of the membranes indicated that the thicker membranes maintained hydration longer at identical flow rates. The membrane resistance was measured and it was concluded that flow rates play an important role in the operation of the analyzer. Tests of the prototype analyzer with the thicker membrane and specially designed flow fields and gas diffusion layers resulted in a stable high frequency resistance and stable analyzer baseline in dry hydrogen. Figure 2 shows a stable current from the analyzer operated at 1.15 mA for up to 2 h before the introductions of CO. Figure 2 also illustrates the sensitivity of the analyzer to CO. Further studies are underway to optimize this analyzer for improved sensitivity to the SAE J2719 levels and response time to within 5 min. Finally, the analyzer was exposed to neat hydrogen to obtain a baseline response followed by exposure to 50 ppm CO in hydrogen and we observed an instant response. Figure 2 highlights the response.

Hydrogen Fuel Quality: International Collaborations

LANL scientists have completed their efforts within IEC/TC 105/WG 11 to advance the "Single Cell Test Methods–PEFC" document. In FY 2016, LANL and DOE

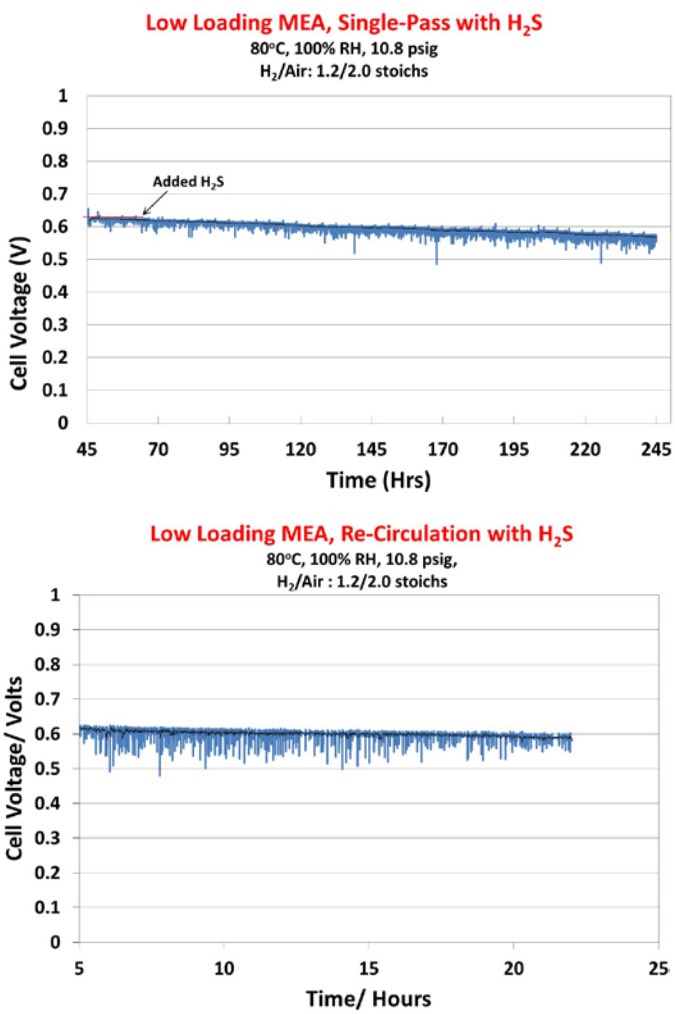

FIGURE 1. Comparison of fuel cell results using single-pass vs. recirculated fuel: 200 ppb H_2S

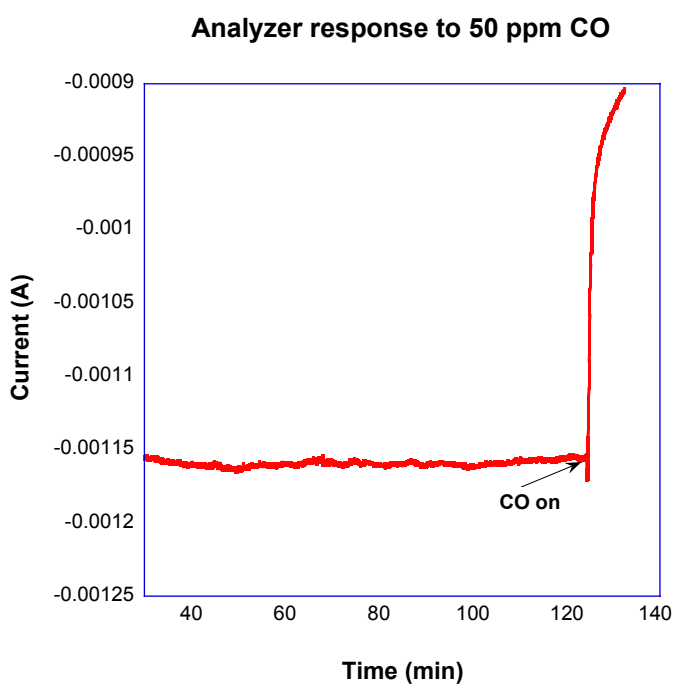

FIGURE 2. Analyzer results: 50 ppm CO response

hosted the members of WG 11 in Washington, D.C., where the document was finalized for submission. LANL has also continued fuel quality testing initiatives with CEA and VTT-Finland. LANL completed fuel cell tests with 25 cm^2 MEAs using LANL hardware at CEA's testing facility. These results (Figure 3) measured by LANL scientists investigated the impact of CO after pre-dosing the fuel cell with H_2S. The rationale behind this approach was to probe the fuel cell performance in the presence of CO in the hydrogen fuel stream after unexpected exposure to H_2S. Two days of fuel cell experiments were completed at the CEA fuel cell testing facility. The tests were carried out at 80°C and 50% RH. We used 20 ppm H_2S as the unexpected exposure concentration in the fuel stream. Afterward, we injected CO to investigate its impact on a partially poisoned fuel cell. During the first day of testing, the fuel cell was exposed to 20 ppm H_2S for 1 h and subsequently exposed to 1 ppm CO for another hour. The results of CO, for the given exposure time, showed minimal voltage losses (i.e., voltage loss < 10 mV). The next day we exposed the fuel cell to the same dosage of hydrogen sulfide and varied the CO concentration during the 1 h of exposure. We perform this test sequence three times and recorded the voltage response. Unlike the experiments results from Day 1, after subsequent exposures to CO, we observed a gradual decay in the cell voltage that became more pronounced over time.

In our collaboration with VTT-Finland, we probed the impact of internal air bleeding on CO by assessing the carbon balance using an operating fuel cell. We tested this impact using 25 cm^2 hardware with a low loading MEA, describe above. The fuel cell was run on neat hydrogen for 2.5 h before introducing 1.86 ppm CO into the anode stream with the current fixed at 0.4 A/cm^2. Using gas chromatography connected before and after the anode feed, the carbon monoxide and carbon dioxide concentrations were measured before, during and after CO exposure in the fuel cell. At the onset, the gas chromatography did not show any evidence of CO, however it did show high CO_2 concentrations that eventually reduced to a fixed amount. Afterwards, during the CO poisoning, we observed the CO_2 concentration increased. This CO_2 was due to the oxidation of CO to CO_2 from the internal air bleed of oxygen crossing the membrane. The window of opportunity for the CO_2 measurement existed only at the introduction of CO as its concentration returned to the same value as before CO poisoning. The source of the pre-existing CO_2 was from either the fuel or oxidant. The amount of pre-existing CO_2 was overwhelmingly large and made it challenging to obtain an accurate carbon balance.

Contributions to ASTM Standards Development

The ASTM hydrogen and fuel cells committee (D03.14) held its two semi-annual meetings in FY 2016, which LANL chaired. The first meeting was held in June in Austin, Texas, and the subsequent meeting in December in Bellevue, Washington. A highlight of this year was the addition of an excel spreadsheet that helped identify test sites and test facilities with capabilities and interests in participating in interlaboratory studies. While momentum was gained with the development of this database of test facilities, the committee also unveiled the lack of funding for testing labs as a critical barrier.

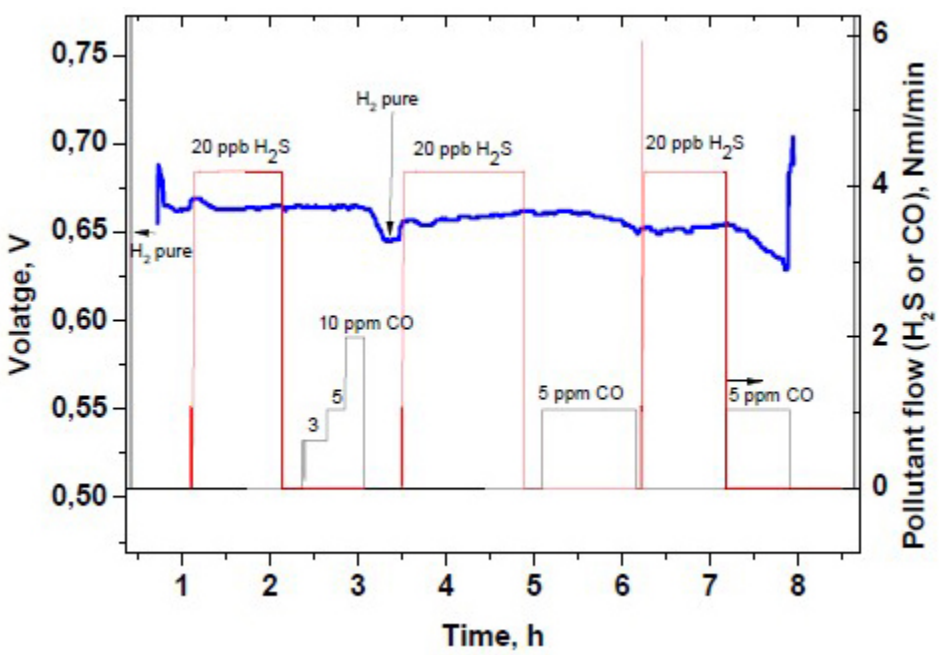

FIGURE 3. CEA-LANL pre-dosing experiments

CONCLUSIONS AND FUTURE DIRECTIONS

In FY 2016, LANL's hydrogen fuel quality efforts continued to investigate CO tolerance in order to assess the concentrations in existing fuel specifications. A test matrix was developed to compile findings into a format that will be made available to the fuel cell community. Also, using the fuel recirculation system, comparisons between recirculation vs. single-pass mode were completed using CO and H_2S.

The international collaborations with CEA and VTT through HyCoRA expanded to include impurity testing with CO and H_2S and these interactions should continue into FY 2017. Some of the work expected includes the completion of an international round robin and impurity testing using fuel cell stack systems. The work with IEC/TC 105/WG 11 concluded with the development and submission of the final draft technical specification for a polymer electrolyte membrane fuel cell testing protocol document.

In FY 2017, LANL will transition from their leadership in ASTM to focus more on the fuel quality, international collaborations, and the deployment of an in-line fuel quality analyzer.

REFERENCES

1. SAE J2719: Hydrogen Fuel Quality for Fuel Cell Vehicles, www.sae.org

2. Organization, I.S., *Hydrogen fuel — Product specification — Part 2: Proton exchange membrane (PEM) fuel cell applications for road vehicles*, in *ISO TC 197*2012, ISO copyright office: Case postale 56 • CH-1211 Geneva 20.

VIII.4 R&D for Safety, Codes and Standards: Hydrogen Behavior

Ethan S. Hecht (Primary Contact), Pratikash Panda
Sandia National Laboratories
7011 East Ave.
Livermore, CA 94550
Phone: (925) 294-3741
Email: ehecht@sandia.gov

DOE Manager: Will James
Phone: (202) 287-6223
Email: Charles.James@ee.doe.gov

Project Start Date: October 1, 2003
Project End Date: Project continuation and direction determined annually by DOE

Overall Objectives

- Develop a science and engineering basis for the release, ignition, and combustion behavior of hydrogen across its range of use (including high pressure and cryogenic).
- Facilitate the assessment of the safety (risk) of hydrogen systems and enable use of that information for revising regulations, codes, and standards, and permitting hydrogen fueling stations.

Fiscal Year (FY) 2016 Objectives

- Complete construction and commissioning of the cryogenic hydrogen release laboratory.
- Perform initial experimental campaign on cryogenic hydrogen and analyze data such that it can be used for validation of the cold plume model.
- Include additional physics models (e.g., a plume model with an energy balance, improved boundary conditions to the plume model) along with appropriate documentation in the Hydrogen Risk Assessment Models (HyRAM) toolkit.
- Experimentally measure the concentration to velocity spreading ratio for hydrogen.

Technical Barriers

This project addresses the following technical barriers from the Hydrogen Safety, Codes and Standards section of the Fuel Cell Technologies Office Multi-Year Research, Development, and Demonstration Plan.

(A) Safety Data and Information: Limited Access and Availability

(G) Insufficient Technical Data to Revise Standards

Contribution to Achievement of DOE Safety, Codes & Standards Milestones

This project will contribute to achievement of the following DOE milestones from the Hydrogen Safety, Codes and Standards section of the Fuel Cell Technologies Office Multi-Year Research, Development, and Demonstration Plan.

- Milestone 2.13: Develop and validate simplified predictive engineering models of hydrogen dispersion and ignition. (4Q 2015)
- Milestone 4.8: Revision of NFPA 2 to incorporate advanced fueling and storage systems and specific requirements for infrastructure elements such as garages and vehicle maintenance facilities. (3Q, 2016)
- Milestone 2.19: Validate inherently safe design for hydrogen fueling infrastructure. (4Q, 2019)

FY 2016 Accomplishments

- Completed design, construction, and commissioning of the cryogenic hydrogen release laboratory, enabling advanced diagnostic studies of cryogenic hydrogen releases in a unique facility worldwide.
- Released ultra-cold (37 K) hydrogen in the laboratory and studied the laser-spark ignition properties of cold hydrogen.
- Characterized the radiative heat flux emissions of flames from cryogenic hydrogen sources.

✧ ✧ ✧ ✧ ✧

INTRODUCTION

Fire codes govern the required distances between hydrogen sources (e.g., a hydrogen fueling station) and hazards (e.g., ignition sources). Revisions to the fire code distances require justification, which is facilitated by models. These models must be validated with carefully controlled experiments, under relevant conditions, which can include high pressures (10,000 psi) or cryogenic temperatures (20 K). Over the course of this project, experiments have been designed and run to provide validation data for models. Models have been developed and exercised to inform the fire codes. This work has enabled quantitative risk assessments of hydrogen systems, and subsequent reduction of setback distances from high pressure hydrogen sources. Currently, we are focusing on developing a scientific basis for modeling dispersion and flames from cryogenic hydrogen sources. This will provide a technical basis for the revision of fire codes related to liquid hydrogen.

APPROACH

The goals of this work are to develop and validate scientific models to accurately predict hazards and consequences from unintentional hydrogen releases. In this project, we develop one-dimensional and engineering models of hydrogen dispersion and flames that can run quickly on a personal computer. While these models are one-dimensional, they include enough physics (e.g., the effect of buoyancy) to be accurate under a wide range of scenarios. These models are able to characterize the hazards from hydrogen releases and flames and are fast enough that they can be run multiple times and incorporated into a quantitative risk assessment framework. To develop and validate these models, we run carefully controlled experiments. Advanced optical and laser diagnostics are used, along with more conventional diagnostics (e.g., thermocouples) to characterize the dispersion and flame properties of releases, at a lab scale. The temperature, pressure, and orifice of the unignited releases and flames is controlled while characteristics are measured (e.g., concentration, flame temperature, radiative heat flux).

RESULTS

Construction and commissioning of the cryogenic hydrogen release laboratory was realized this fiscal year. This laboratory, shown in Figure 1, enables the study of cryogenic hydrogen releases and flames. Compressed hydrogen is metered and its pressure is controlled within the laboratory, before it flows through a three-stage heat exchanger outside the laboratory. Within the heat exchanger, hydrogen is first cooled by flowing through a coil immersed in liquid nitrogen. A counterflow tube-in-tube heat exchanger, with cold helium vapor, further cools the hydrogen in Stage 2. Finally, in Stage 3, a coil immersed in liquid helium condenses the hydrogen to a liquid, with the helium boil-off acting as the coolant in Stage 2. A single vacuum jacketed line penetrating into the lab facilitates laboratory releases while minimizing the volume of hazardous fluid. A temperature sensor and pressure transducer near an interchangeable nozzle enables careful measurement and control of the boundary conditions for the experiments, which are either unignited, or ignited releases of cryogenic hydrogen. The nozzle is mounted on a three-dimensional translation stage, allowing the release point to move while maintaining diagnostics in a fixed position. The cryogenic hydrogen system can cool hydrogen to a liquid (20–30 K, depending on the pressure), and operate at up to 10 bar, which are characteristic of liquid hydrogen storage tank operating conditions. The nozzles used in the laboratory are small (on the order of 1 mm), and typical cryogenic hydrogen flow rates are on the order of 1 g/s.

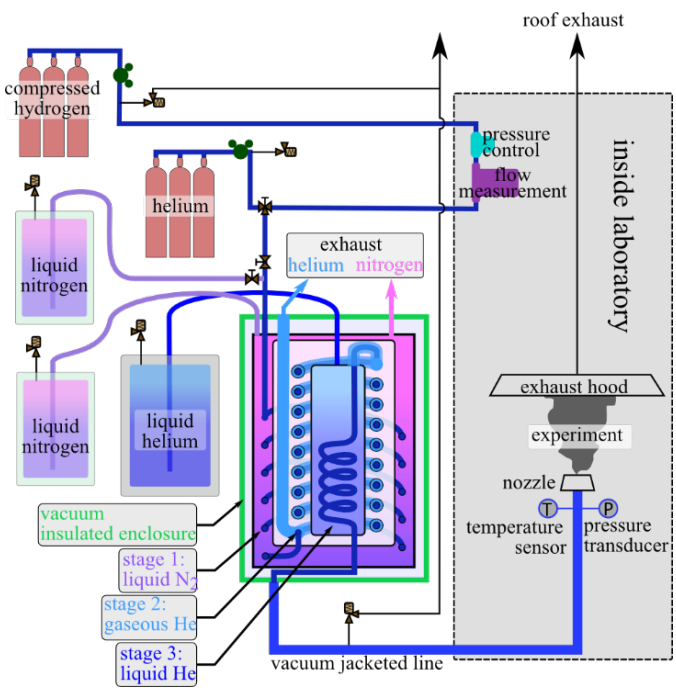

FIGURE 1. Sketch of the cryogenic hydrogen release experiment at the Turbulent Combustion Laboratory, Sandia National Laboratories

The cryogenic hydrogen release laboratory has been used to perform a study on the ignition and radiative properties of jet flames of cryogenic hydrogen. An 8-mm beam from a neodymium-doped yttrium aluminum garnet laser (9-ns pulse duration, 100-mJ/pulse, 532-nm wavelength) was focused, causing a plasma channel, roughly 1 mm in diameter and 4-mm long, to form along the centerline of vertical hydrogen releases. The release point, which began far from the laser-spark, was moved closer to the laser-spark until a sustained jet flame was formed. The cold hydrogen was discovered to ignite further from the release point than warm hydrogen, at a fixed mass flow rate. However, even for cryogenic hydrogen, the ignition distance (the distance between the laser-spark and the nozzle where a jet flame forms), was found to scale with the effective diameter, a relationship that is shown in Figure 2. The effective diameter is the diameter through which the jet mass flow rate, would pass at atmospheric pressure and temperature, to give the same momentum flux as the under-expanded jet at the nozzle exit. This relationship, which has been demonstrated for atmospheric temperature hydrogen releases, was shown to hold true, for cryogenic hydrogen, for the first time in this work.

Radiometers were placed around jet flames of cryogenic hydrogen, to study the heat flux, which is important for determining the hazard to humans and structures, from hydrogen flames. Previous studies [6] have shown that the radiant fraction, which is the fraction of energy released by combustion that is emitted as radiation, scales as a function of the residence time of the flame. We determined this relationship to also be valid for cryogenic hydrogen, as shown in Figure 3. This relationship can be used in a jet flame model, to calculate the radiative heat flux from flames

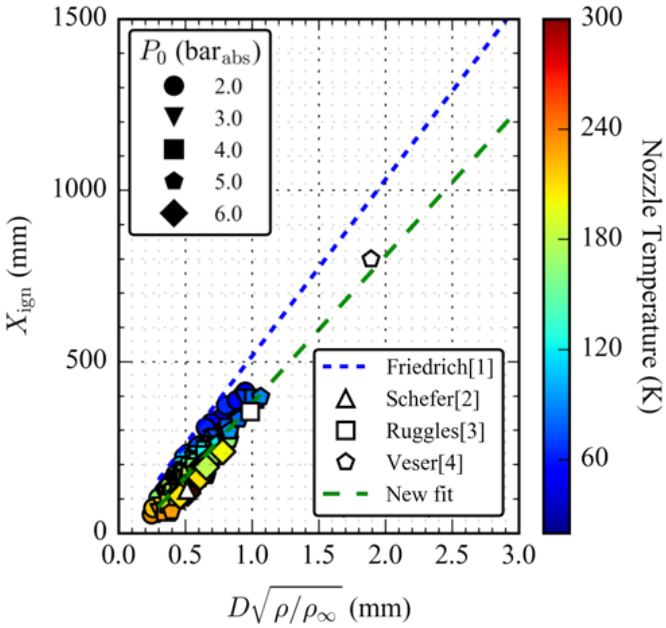

FIGURE 2. Maximum ignition distance as a function of effective diameter, for the cryogenic hydrogen releases in the current study and data from the literature. Blue dashed line shows a correlation from Friedrich et al. [1].

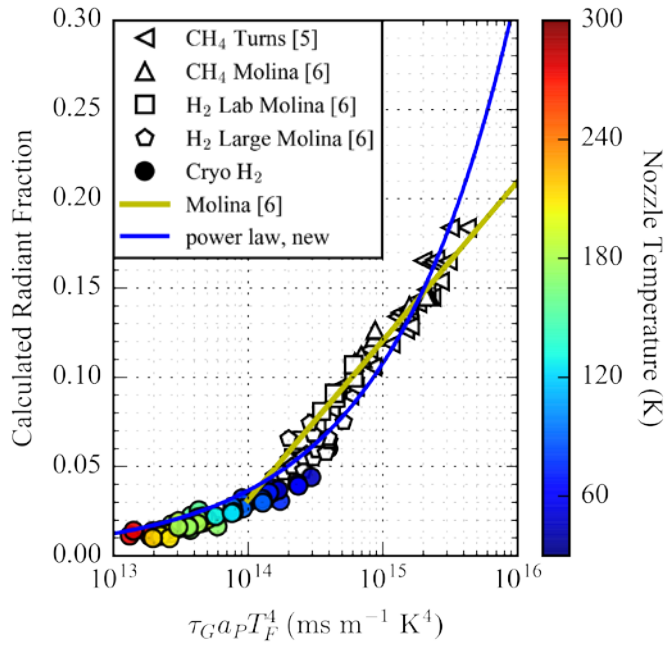

FIGURE 3. Radiant fraction from cryogenic hydrogen jet flames and literate data of flames from atmospheric temperature source gases

of hydrogen from cryogenic or atmospheric temperature sources. The flame length and width were also measured, for cryogenic hydrogen jet flames, using a visible and an infrared camera. As shown by other researchers [8], the flame width was found to be 0.17 times the flame length, for cryogenic and atmospheric temperature flames. The flame length (normalized by the release diameter), shown in Figure 4, was found to scale with the square root of the nozzle exit Reynolds number. This correlation, which was previously shown to be valid for room temperature hydrogen [12], was also shown to hold true for cryogenic hydrogen.

The initial measurements on cryogenic hydrogen ignition, flame radiation, and flame size, using the cryogenic hydrogen release laboratory, have shown that several correlations known to be valid for room temperature hydrogen are also valid for cryogenic hydrogen. These correlations have important modeling and safety, codes, and standards implications. The ignition distance from cryogenic hydrogen sources can now be calculated, which can be used to determine the distance ignition sources should be kept from potential leak points of cryogenic hydrogen systems. The radiative heat flux measurements will help to calculate the human harm distance, and structural damage distance from cryogenic hydrogen jet flames. Additional data from experiments in the cryogenic hydrogen release laboratory and models developed from this data will enable the DOE Milestone 2.19: Validate inherently safe design for hydrogen fueling infrastructure, to be met by its target date of the fourth quarter of 2019.

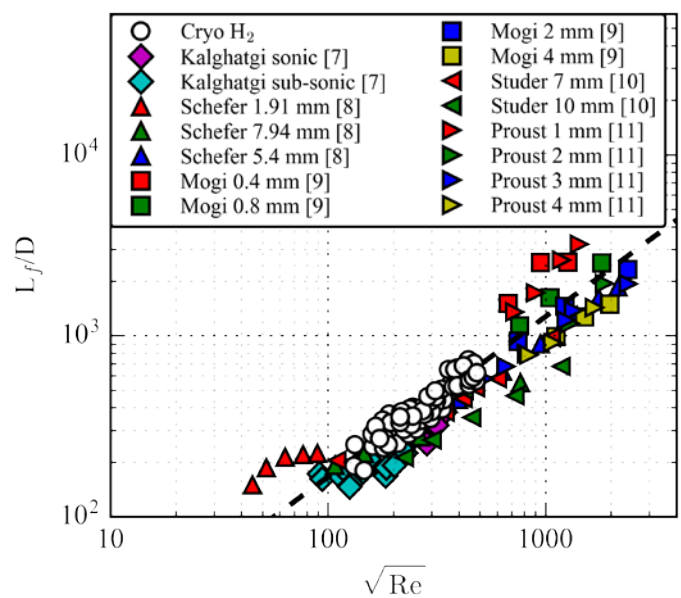

FIGURE 4. Variation of flame length as a function of Reynolds number (Re), for the cryogenic hydrogen releases from the current study, along with data from the literature

CONCLUSIONS AND FUTURE DIRECTIONS

In FY 2016, the cryogenic hydrogen release laboratory was constructed and commissioned. The laboratory was then utilized to measure the distance ignition sources should be kept from cryogenic hydrogen releases, by using

a laser-spark to ignite underexpanded hydrogen jets from varied temperature, pressure, and nozzle diameter sources. The properties of flames of cryogenic hydrogen were also studied this fiscal year, including the flame length, width, and radiative heat flux. This data will be used in models of cryogenic hydrogen flames, for example, to calculate the radiative heat flux from cryogenic hydrogen jet flames. This data, and models developed from this data, will be used to inform codes and standards that govern the separation distances for liquid hydrogen.

In the near term, we will be using the cryogenic hydrogen release laboratory to measure the concentration of unignited cryogenic hydrogen releases. To accomplish this, we will be measuring filtered planar laser Rayleigh light scattering. We are currently repairing our laser, so that we can utilize this diagnostic. Concentration data will be used to validate and guide development of a model of cryogenic hydrogen releases. This model will be tied into our quantitative risk assessment toolkit, HyRAM (discussed in the Hydrogen Quantitative Risk Assessment annual progress report), so that it can be used by codes and standards committees and other stakeholders.

In the long term, we plan on designing new experiments to study other phenomena that occur when cryogenic hydrogen is released. These include interactions between liquid hydrogen and the ground (i.e. pooling and evaporation), the effect of the ambient gas (e.g., crosswinds, humidity levels), and the condensation of air and moisture in cryogenic hydrogen. We anticipate that this work will lead to defensible, science-informed separation distances for liquid hydrogen being included in the fire protection safety codes (e.g., National Fire Protection Association 2).

SPECIAL RECOGNITIONS & AWARDS/ PATENTS ISSUED

1. *Robert Schefer Memorial Best Paper Award.* Presented to Katrina Groth and Ethan Hecht at the International Conference on Hydrogen Safety (ICHS) for "HyRAM: A methodology and toolkit for QRA of hydrogen systems." Tokyo, Japan, October 2015.

2. Copyright: HyRAM (Hydrogen Risk Assessment Models) v. 1.0. Feburary 17, 2016.

FY 2016 PUBLICATIONS/PRESENTATIONS

1. K.M. Groth and E.S. Hecht. "HyRAM: A methodology and toolkit for Quantitative Risk Assessment of Hydrogen Systems." In Proceedings of the International Conference on Hydrogen Safety (ICHS 2015), Yokohama, Japan, October 19–21, 2015.

2. C. San Marchi, E.S. Hecht, I.W. Ekoto, K.M. Groth, C. LaFleur, B.P. Somerday, R. Mukundan and T. Rockward. "Advances in research and development to enhance the scientific basis for hydrogen regulations, codes, and standards." In Proceedings of the International Conference on Hydrogen Safety (ICHS 2015), Yokohama, Japan, October 19–21, 2015.

3. Katrina M. Groth, Ethan S. Hecht and John T. Reynolds. Methodology for assessing the safety of Hydrogen Systems: HyRAM 1.0 technical reference manual. SAND2015-10216, Sandia National Laboratories, Albuquerque, NM, November 2015.

4. Li, Xuefang, Ethan S. Hecht, and David M. Christopher. "Validation of a reduced-order jet model for subsonic and underexpanded hydrogen jets." International Journal of Hydrogen Energy (2015). doi:10.1016/j.ijhydene.2015.10.071.

5. Hecht, Ethan S., Xuefang Li, and Isaac Ekoto (presentation made by X. Li) "Validated equivalent source model for an underexpanded hydrogen jet." Presented at the International Conference on Hydrogen Safety (ICHS 2015), Yokohama, Japan, October 21, 2015. SAND2015-8994 C.

6. Hecht, Ethan S. and Pratikash Panda (presentation). "Validation data for releases from cryogenic hydrogen sources." Presented to the H2 Codes & Standards Tech Team, November 11, 2015 and to the Hydrogen Safety Panel, December 11, 2015. SAND2015-9782 PE.

7. Jay Keller, Laura Hill, Kristian Kiuru, Katrina Groth, Ethan Hecht, Will James, & Thomas Jordan. HySafe research priorities workshop report. Sandia National Laboratories, Albuquerque, NM, SAND2016-2644. Sandia National Laboratories, March 2016.

8. Hydrogen Risk Assessment Model (HyRAM) website. http://hyram.sandia.gov First published January 2016.

9. E.S. Hecht, P. Panda. Liq.uid Hydrogen Behavior Studies. SAND2016-3269 PE. Presented to the Project Technical Panel Kick-off Meeting for 'Spatial Separation Distances for Liquid Hydrogen Storage.' April 2016.

10. E.S. Hecht, P. Panda (presentation). "R&D for Safety, Codes and Standards: Hydrogen Behavior" at DOE FCTO Hydrogen Program Annual Merit Review, Washington, D.C., June 7, 2016.

11. E.S. Hecht, P. Panda (presentation). Liquid Hydrogen Behavior Studies. SAND2016-6149 PE. Presented to the Project Technical Panel Meeting for 'Spatial Separation Distances for Liquid Hydrogen Storage.' June 27, 2016.

12. C. San Marchi, E.S. Hecht, I.W. Ekoto, K.M. Groth, C. LaFleur, B.P. Somerday, R. Mukundan, T. Rockward, J. Keller, L. & C.W. James. "Overview of the DOE hydrogen safety, codes and standards program, part 3: Advances in Research and Development to Enhance the Scientific Basis for Hydrogen regulations, Codes and Standards." Accepted for publication in International Journal of Hydrogen Energy, (Accepted July 2016).

13. Katrina M. Groth & Ethan S. Hecht. "HyRAM: A methodology and toolkit for Quantitative Risk Assessment of hydrogen systems." Accepted for publication in International Journal of Hydrogen Energy (Accepted July 2016).

14. P.P. Panda and E.S. Hecht. "Ignition and Flame Characteristics of Under-Expanded Cryogenic Hydrogen Releases." Submitted for publication in International Journal of Hydrogen Energy (Submitted July 2016).

REFERENCES

1. Friedrich, A., Breitung, W., Stern, G., Veser, A., Kuznetsov, M., Fast, G., Oechsler, B., Kotchourko, N., Jordan, T., Travis, J.R.,

Xiao, J. Ignition and heat radiation of cryogenic hydrogen jets. International Journal of Hydrogen Energy. 2012; 37(22):17589–98.

2. Schefer, R.W., Evans, G.H., Zhang, J., Ruggles, A.J., Greif, R. Ignitability limits for combustion of unintended hydrogen releases: Experimental and theoretical results. International Journal of Hydrogen Energy. 2011; 36(3):2426–35.

3. Ruggles, A.J., Ekoto, I.W. Ignitability and mixing of underexpanded hydrogen jets. International Journal of Hydrogen Energy. 2012; 37(22):17549–60.

4. Veser, A., Kuznetsov, M., Fast, G., Friedrich, A., Kotchourko, N., Stern, G., Schwall, M., Breitung, W. The structure and flame propagation regimes in turbulent hydrogen jets. International Journal of Hydrogen Energy. 2011; 36(3):2351–9.

5. Turns, S.R., Myhr, F.H. Oxides of nitrogen emissions from turbulent jet flames: Part I—Fuel effects and flame radiation. Combustion and Flame. 1991; 87(3):319–35.

6. Molina, A., Schefer, R.W., Houf, W.G. Radiative fraction and optical thickness in large-scale hydrogen-jet fires. Proceedings of the Combustion Institute. 2007; 31(2):2565–72.

7. Kalghatgi, G.T. Lift-off heights and visible lengths of vertical turbulent jet diffusion flames in still air. Combustion Science and Technology. 1984; 41(1-2):17.

8. Schefer, R.W., Houf, W.G., Bourne, B., Colton, J. Spatial and radiative properties of an open-flame hydrogen plume. International Journal of Hydrogen Energy. 2006; 31(10):1332–40.

9. Mogi, T., Nishida, H., Horiguchi, S. Flame Characteristics of high-pressure hydrogen gas jet. In: Proceedings of the 1st International Conference on Hydrogen Safety, Pisa; 2005.

10. Studer, E., Jamois, D., Jallais, S., Leroy, G., Hebrard, J., Blanchetie`re V. Properties of large-scale methane/hydrogen jet fires. International Journal of Hydrogen Energy 2009; 34: 9611.

11. Proust, C., Jamois, D., Studer, E.. High pressure hydrogen fires. Proceedings of the Third International Conference on Hydrogen Safety, 16–18 September 2009, Ajaccio, France, Paper 214; 2009.

12. Molkov, V., Saffers, J.B. Hydrogen jet flames. International Journal of Hydrogen Energy. 2013; 38(19):8141–58.

VIII.5 Hydrogen Quantitative Risk Assessment

Katrina Groth (Primary Contact), Ethan Hecht, John Reynolds (SAIC), Myra Blaylock, Alice Muna, Chris LaFleur
Sandia National Laboratories
P.O. Box 5800 MS 0748
Albuquerque, NM 87185
Phone: (505) 844-6766
Email: kgroth@sandia.gov

DOE Manager: Will James
Phone: (202) 287-6223
Email: Charles.James@ee.doe.gov

Project Start Date: October 1, 2003
Project End Date: Project continuation and direction determined annually by DOE

Overall Objectives

- Develop algorithms, models, and data to enable industry-led codes and standards revisions to be based on a strong, traceable science and engineering basis.
- Develop hydrogen-specific quantitative risk assessment (QRA) and consequence models and methods to support regulations, codes, and standards decisions and to enable alternate means of code compliance, such as performance-based design.
- Develop the Hydrogen Risk Assessment Model (HyRAM) toolkit to provide a rigorous, documented basis for analyzing hydrogen infrastructure safety with QRA and consequence modeling.

Fiscal Year (FY) 2016 Objectives

- Extend HyRAM modules for simulating gas plume, overpressure, and laying behavior to enable their use in safety assessment for hydrogen fueling infrastructure.
- Make an unsupported research version of HyRAM available for free download by national and international stakeholders.
- Facilitate use of HyRAM by publishing documentation, engaging with stakeholders.

Technical Barriers

This project addresses the following technical barriers from the Hydrogen Safety, Codes and Standards section of the Fuel Cell Technologies Office Multi-Year Research, Development, and Demonstration Plan.

(A) Safety Data and Information: Limited Access and Availability

(F) Enabling National and International Markets Requires Consistent RCS

(G) Insufficient Technical Data to Revise Standards

(L) Usage and Access Restrictions

Contribution to Achievement of DOE Safety, Codes & Standards Milestones

This project will contribute to achievement of the following DOE milestones from the Hydrogen Safety, Codes and Standards section of the Fuel Cell Technologies Office Multi-Year Research, Development, and Demonstration Plan.

- Milestone 2.4: Publish a methodology for estimating accident likelihood. (2Q, 2013)
- Milestone 2.8: Publish risk mitigation strategies. (2Q, 2014)
- Milestone 2.11: Publish a draft protocol for identifying potential failure modes and risk mitigation. (4Q, 2014)
- Milestone 2.13: Develop and validate simplified predictive engineering models of hydrogen dispersion and ignition. (4Q, 2015)
- Milestone 2.19: Validate inherently safe design for hydrogen fueling infrastructure. (4Q, 2019)
- Milestone 4.7: Complete risk mitigation analysis for advanced transportation infrastructure systems. (1Q, 2015)
- Milestone 4.8: Revision of NFPA 2 to incorporate advanced fueling storage systems and specific requirements for infrastructure elements such as garages and vehicle maintenance facilities. (3Q, 2016)

FY 2016 Accomplishments

- Publicly released a free version of HyRAM V1.0 software for risk analysis of hydrogen infrastructure systems.
- Expanded HyRAM capabilities to include modules for simulating gas plume dispersion, overpressure, and layering behavior from user-defined releases. Added an Engineering Toolkit to facilitate simple hydrogen safety calculations, including thermodynamic conversions and mass flow rate calculations.
- Published a technical reference manual documenting the methodology and models used in HyRAM V1.0. Published a user guide for the HyRAM V1.0 software.

✧ ✧ ✧ ✧ ✧

INTRODUCTION

DOE has identified consistent safety, codes, and standards as a critical need for the deployment of hydrogen technologies, with key barriers related to the availability and implementation of technical information in the development of regulations, codes, and standards. Advances in codes and standards have been enabled by risk-informed approaches to create and implement revisions to codes, such as National Fire Protection Association (NFPA) 2, NFPA 55, and International Organization for Standardization (ISO) Technical Specification TS-19880-1. This project provides the technical basis for these revisions, enabling the assessment of the safety of hydrogen fuel cell systems and infrastructure using QRA and physics-based models of hydrogen behavior. The risk and behavior tools that are developed in this project are motivated by, shared directly with, and used by the committees revising relevant codes and standards, thus forming the scientific basis to ensure that code requirements are consistent, logical, and defensible.

APPROACH

This work leverages Sandia's unique experimental and modeling capabilities and combines these efforts with stakeholder engagement and international leadership. Sandia develops the algorithms and methods for performing QRA, including scenario development, likelihood and consequence analysis, and risk quantification. Sandia's Turbulent Combustion Laboratory develops and validates predictive engineering models for flame initiation, flame sustainment, radiative heat flux, and overpressures. The resulting QRA and hydrogen behavior models are integrated into the HyRAM toolkit to enable consistent, traceable, and rigorous risk and consequence assessment. HyRAM's hydrogen behavior and QRA models are then applied to relevant technologies and systems to provide insight into the risk level and risk mitigation strategies with the aim of enabling the deployment of fuel cell technologies through revision of hydrogen safety, codes, and standards.

RESULTS

Code committees and industry are both interested in using QRA and behavior modeling to enable code development and code compliance for hydrogen systems. Gaps and limited availability of data, models and tools relevant to hydrogen infrastructure systems form a barrier to this goal. This core research activity addresses this gap by developing and releasing HyRAM, an innovative software tool that integrates QRA and physical models of hydrogen behavior and consequences. HyRAM reduces industry burden and allows hydrogen safety experts to focus on obtaining safety insights rather than creating, validating, and documenting risk assessment algorithms and physical models.

The HyRAM package will enable installation designers and code and standards development organizations to conduct consequence modeling and QRA with state-of-the-art, validated science and engineering models (see Figure 1). HyRAM formalizes the tools and methods which have been developed by Sandia through multiple Fuel Cell Technologies Office projects. HyRAM development began in FY 2014. In FY 2015 we issued a prototype HyRAM (V1.0alpha) to selected stakeholders with limitations on its use.

During FY 2016 we significantly increased the functionality of HyRAM and we also revised the HyRAM copyright to make HyRAM available for use by anyone. HyRAM is available for free download at http://hyram.sandia.gov; the current version is 1.0.1. HyRAM now has click-to-accept license terms, which relax the usage restrictions from prior releases and requires users to acknowledge the limitations of this research software.

A new key feature is a model and user interface for hydrogen gas plume dispersion; sample results are shown in Figure 2. The new gas plume model is based on the experimental work completed in 2015 in Sandia's Turbulent Combustion Laboratory. We also completed a module which allows users to calculate two behaviors of hydrogen within an enclosure: overpressure (for ignited hydrogen release) and layering/accumulation behavior (for unignited hydrogen releases). HyRAM now uses the stable overpressure model from the fourth quarter of FY 2015, which resolved discrepancies with expected results. This HyRAM module allows the user to visualize the time-dependent hydrogen accumulation and to calculate and plot peak overpressure given different ignition times (Figure 3). We also added an Engineering Toolkit, which allows users to perform additional calculations relevant to hydrogen systems. Currently the Engineering Toolkit includes tank volume-to-mass conversion, calculation of a release rate (steady-state or blowdown), and density, temperature, and pressure conversion.

A major thrust for the year included working with external stakeholders to obtain feedback about usability and functionality. We created 29 HyRAM versions (23 internal test versions, four alpha releases, and two public releases). We partnered with eight external stakeholders who provided feedback on HyRAM V1.0alpha. We presented HyRAM in numerous national and international forums (see presentations list). We used this stakeholder feedback to focus our software improvements, including the new features and streamlined input and output windows.

We also completed important HyRAM documentation, including the technical reference manual and multiple reports and papers documenting for HyRAM V1.0 (see list of

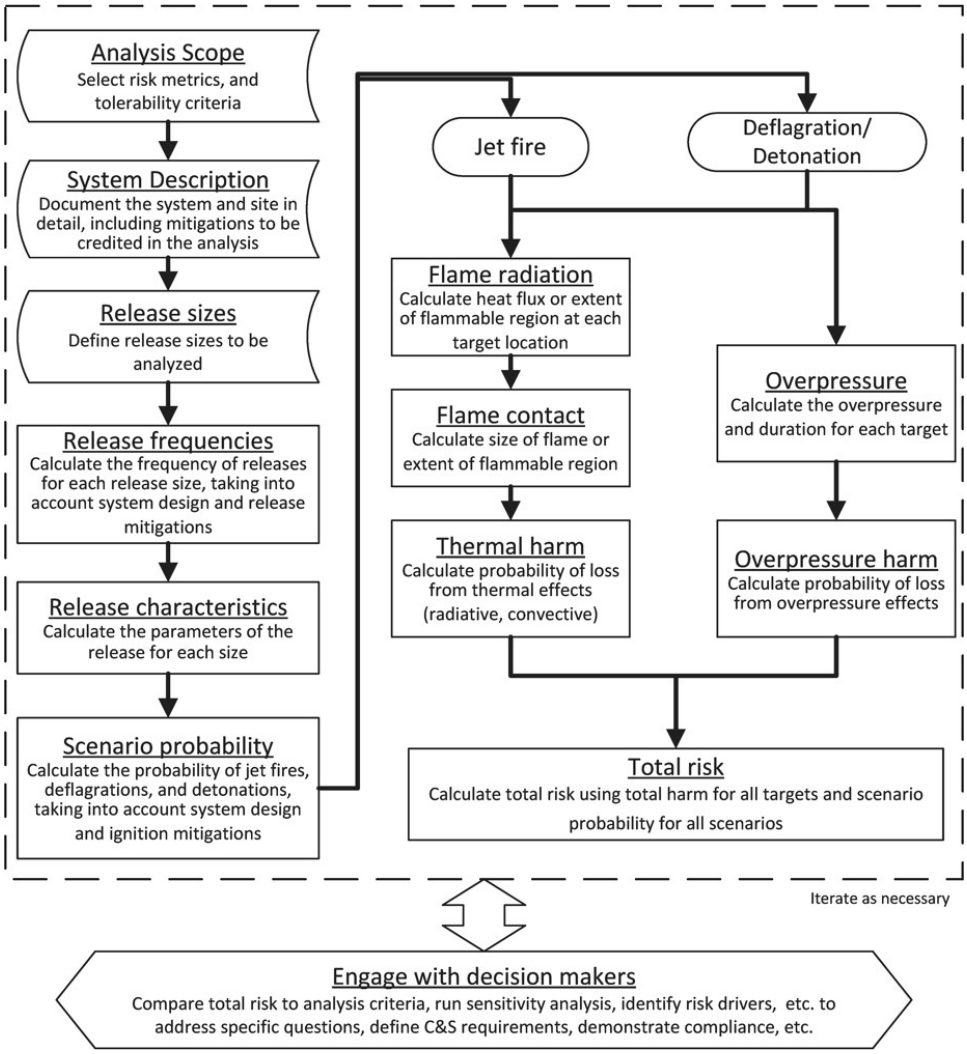

C&S – Codes and standards

FIGURE 1. Summary of QRA methodology implemented in HyRAM

publications). This documentation provides traceability and enables verification and validation of the HyRAM algorithm, models, approach, assumptions, and information sources.

HyRAM is actively being used for codes and standards development by the NFPA 2 and ISO Technical Specification TS-19880-1, both for risk-informed code development and for risk-informed code compliance (e.g., performance-based design). During FY 2016, HyRAM was used extensively by ISO Technical Committee (TC) 197 WG24 in the development of ISO TS-19880-1. The safety assessment methodology in TS-19980-1, which is based on the HyRAM methodology, allows countries to follow a common methodology for performing safety assessment with county- or region-specific assumptions and modeling choices. HyRAM was used to support the development of regional examples contained in Annex A. HyRAM provides a means for rapidly evaluating different examples, which helped the committee overcome significant barriers to an international consensus.

During FY 2016 HyRAM was used to support performance-based designs for hydrogen fueling stations within NFPA 2. HyRAM was used to calculate baseline risk metrics for a generic station and to provide a platform for industry to compare specific design proposals to that baseline (see [1] on publication list). HyRAM is also being used to explore liquid separation distances for NFPA 2.

HyRAM could be used to support the establishment of safety distances and other mitigation credits, and furthermore can be used to enable a performance-based compliance option within these codes and standards. Longer-term, HyRAM is anticipated to support development of safety cases and design decisions for user-defined hydrogen installations, and can also be used to demonstrate improvements in facility safety.

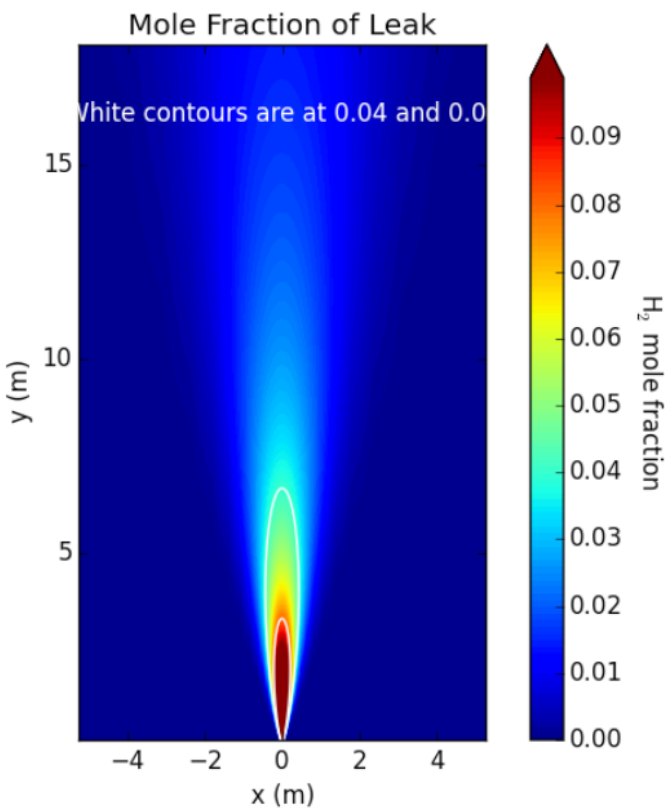

FIGURE 2. Output from new HyRAM feature to calculate the mole fraction of release from a user-defined leak. The white contours outline the edges of user-specified concentrations (in this image, the 4% and 8% contours are displayed).

CONCLUSIONS AND FUTURE DIRECTIONS

The HyRAM toolkit provides a platform with state-of-the-art hydrogen models for assessing the risk of hydrogen systems and the consequences of hydrogen releases and fires, to enable industry-led analyses. During FY 2016 we used HyRAM to revise important requirements in both NFPA 2 and ISO TS-19880-1, thereby reducing barriers to hydrogen infrastructure deployment. However, additional challenges remain within both codes, including the development of defensible separation distances for liquid hydrogen stations and need for additional data for QRA.

HyRAM development activities are focused on adding capabilities necessary to inform near-term regulations, codes, and standards needs, including those from NFPA 2 and ISO TS-19880-1. There are several important scientific gaps that must be addressed including: a need for validated models of liquid hydrogen behavior and an ongoing need for data about hydrogen system failures, hydrogen component reliability (and failures), and mitigation effectiveness. There is also a need to extend HyRAM to address a wider variety of hydrogen infrastructure systems, including containerized systems and new types of infrastructure.

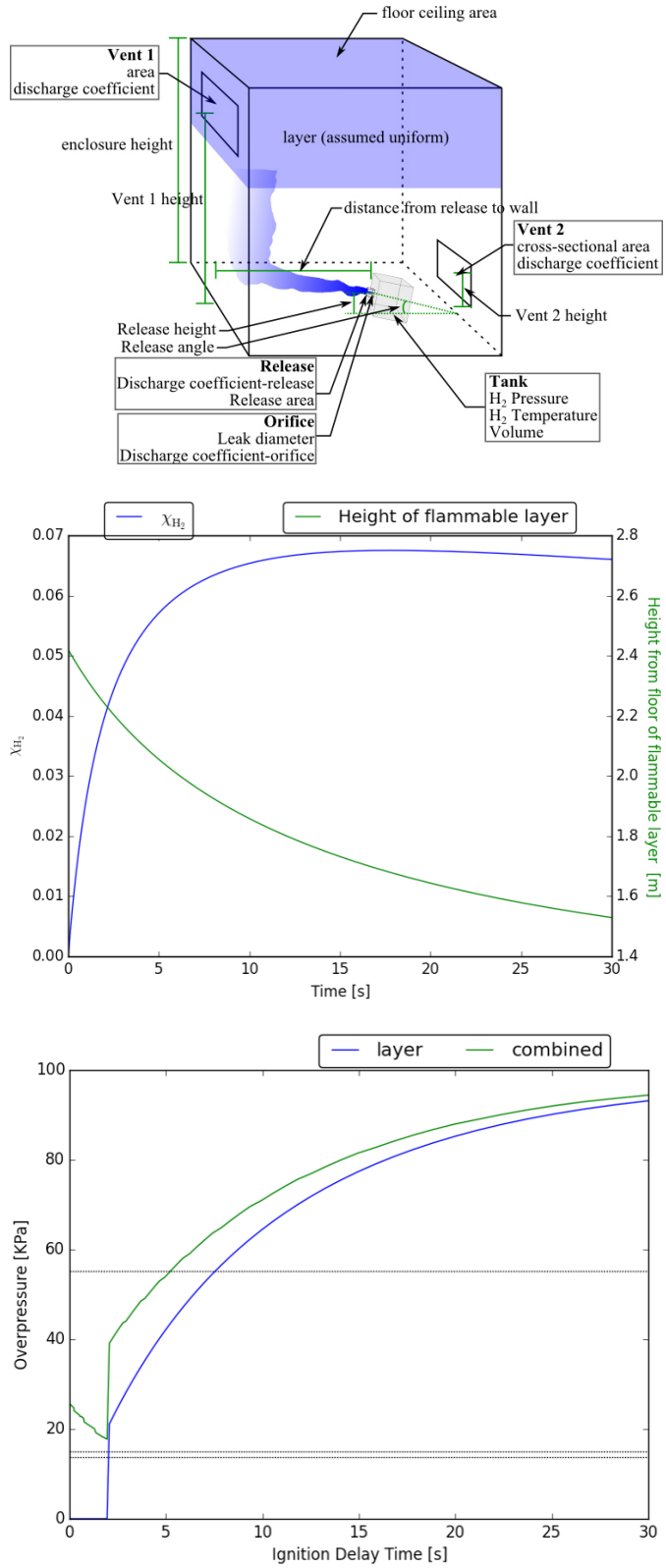

FIGURE 3. New HyRAM overpressure module, including illustrate of required used input (top), and output graphs of peak overpressure at different ignition times (bottom) and height of the flammable hydrogen layer within the enclosure (center)

The flexible architecture of the HyRAM framework enables the incorporation of additional features including both physical models and QRA capabilities. We plan to add modules for consequence modeling, including the ability to calculate the physical effects of liquid hydrogen releases, cold plumes, and subsequent ignitions. We will also add new physics-based modules for calculating hydrogen ignition probability. Existing HyRAM models (e.g. the gas plume model) will be kept current as scientific consensus changes. We will expand the capabilities of the QRA algorithm to support modeling of additional scenarios as well as features to enable more detailed insight into system reliability.

We will design a set of HyRAM example cases which will facilitate testing and verification of the modules by users. HyRAM will continue to be a research prototype; external partners are needed to support formal software development activities.

SPECIAL RECOGNITIONS & AWARDS/ PATENTS ISSUED

1. *Robert Schefer Memorial Best Paper Award.* Presented to Katrina Groth and Ethan Hecht at the International Conference on Hydrogen Safety (ICHS) for "HyRAM: A methodology and toolkit for QRA of hydrogen systems." Tokyo, Japan, October 2015.

2. *2016 DOE Hydrogen and Fuel Cells Program R&D Award* (Safety, Codes, and Standards program). Presented to Katrina Groth for "outstanding leadership and technical contribution to hydrogen safety and risk assessment." Washington, DC, June 2016.

3. Copyright: HyRAM (Hydrogen Risk Assessment Models) v. 1.0. February 17, 2016.

FY 2016 PUBLICATIONS/PRESENTATIONS

1. A.C. LaFleur, A.B. Muna, and K.M. Groth. *Fire Protection Engineering Design Brief Template: Hydrogen Refueling Station*, SAND2015-4500, Sandia National Laboratories, June 2015.

2. Hannah R. Zumwalt and Katrina M. Groth. *HyRAM V1.0 User's Manual.* SAND2015-7380 R, Sandia National Laboratories, Albuquerque, NM, August 2015.

3. K.M. Groth and E.S. Hecht. "HyRAM: A methodology and toolkit for Quantitative Risk Assessment of Hydrogen Systems." *In Proceedings of the International Conference on Hydrogen Safety (ICHS 2015),* Yokohama, Japan, October 19–21, 2015.

4. A.C. LaFleur, A.B. Muna and K.M. Groth. "Application of Quantitative Risk Assessment for Performance-Based Permitting of Hydrogen Fueling Stations." *In Proceedings of the International Conference on Hydrogen Safety (ICHS 2015)*, Yokohama, Japan, October 19–21, 2015.

5. T. Skjold, D. Siccama, H. Hisken, A. Brambilla, P. Middha, K.M. Groth and A.C. LaFleur. "3D Risk management for hydrogen installations (Hy3DRM)." *In Proceedings of the International Conference on Hydrogen Safety (ICHS 2015),* Yokohama, Japan, October 19–21, 2015.

6. J. Schneider, G. Dang-Nhu, N. Hart and K. Groth. "ISO 19880-1, Hydrogen Fueling Station and Vehicle Interface Safety Guideline." *In Proceedings of the International Conference on Hydrogen Safety (ICHS 2015),* Yokohama, Japan, October 19–21, 2015.

7. C. San Marchi, E.S. Hecht, I.W. Ekoto, K.M. Groth, C. LaFleur, B.P. Somerday, R. Mukundan, and T. Rockward. Advances in research and development to enhance the scientific basis for hydrogen regulations, codes, and standards. In Proceedings of the International Conference on Hydrogen Safety (ICHS 2015), Yokohama, Japan, October 19–21, 2015.

8. K.M. Groth. "HyRAM: A methodology and toolkit for QRA of hydrogen systems." Presented at the International Conference on Hydrogen Safety (ICHS 2015), Yokohama, Japan, October 21, 2015.

9. K.M. Groth. "Application of quantitative risk assessment for performance-based permitting of hydrogen fueling stations." Presented at the International Conference on Hydrogen Safety (ICHS 2015), Yokohama, Japan, October 21, 2015.

10. K.M. Groth. "H2 safety integration toolkits: HyRAM Version 1.0." Presented at the IEA HIA Hydrogen Safety Task 37 Meeting, Tokyo, Japan, October 23, 2015.

1.1 K.M. Groth. "A brief intro to Human Reliability Analysis." Presented at the IEA HIA Hydrogen Safety Task 37 Meeting, Tokyo, Japan, October 23, 2015.

12. K. Groth. "Safety assessment & mitigation sub-team update." Presented at ISO TC197 WG24 meeting, Tokyo, Japan, October 27, 2015.

13. Katrina M. Groth, Ethan S. Hecht and John T. Reynolds. *Methodology for assessing the safety of Hydrogen Systems: HyRAM 1.0 technical reference manual*. SAND2015-10216, Sandia National Laboratories, Albuquerque, NM, November, 2015.

14. Katrina M. Groth. "HyRAM: A methodology and toolkit for hydrogen QRA & behavior modeling." Presentation to US DRIVE - H2 Codes & Standards Tech Team, November 12, 2015.

15. Hydrogen Risk Assessment Model (HyRAM) website. http://hyram.sandia.gov First published January 2016.

16. C. San Marchi, E.S. Hecht, I.W. Ekoto, K.M. Groth, C. LaFleur, B.P. Somerday, R. Mukundan, T. Rockward, J. Keller & C.W. James. "Overview of the DOE hydrogen safety, codes and standards program, part 3: Advances in Research and Development to Enhance the Scientific Basis for Hydrogen regulations, Codes and Standards." *Submitted for publication in International Journal of Hydrogen Energy,* (Submitted Feb 2016).

17. Katrina M. Groth, Hannah R. Zumwalt, Andrew Clark. *HyRAM V1.0 User Guide*. Sandia National Laboratories, Albuquerque, NM, March 2016.

18. Jay Keller, Laura Hill, Kristian Kiuru, Katrina Groth, Ethan Hecht, Will James, and Thomas Jordan. HySafe research priorities workshop report. Sandia National Laboratories, Albuquerque, NM, SAND2016-2644, 2016.

19. Katrina M. Groth (presentation). "Overview of HyRAM (Hydrogen Risk Assessment Models) Software for Science-Based Safety, Codes, and Standards." U.S. Department of Energy Fuel Cell Technologies Office webinar series, April

26, 2016. Archived version available at http://energy.gov/eere/fuelcells/2016-webinar-archives.

20. K. Groth. "SCS011: Hydrogen Quantitative Risk Assessment." Presented at DOE FCTO Hydrogen Program Annual Merit Review, Washington, DC, June 7, 2016.

21. K. Groth. "Safety assessment & mitigation sub-team update." Presented at ISO TC197 WG24, Munich, Germany, 22 June 2016.

22. Katrina M. Groth & Ethan S. Hecht. "HyRAM: A methodology and toolkit for Quantitative Risk Assessment of hydrogen systems." Accepted for publication in International Journal of Hydrogen Energy (Accepted July 2016).

VIII.6 Hydrogen Safety Panel, Safety Knowledge Tools and First Responder Training Resources

Nick Barilo
Pacific Northwest National Laboratory (PNNL)
P.O. Box 999
Richland, WA 99352
Phone: (509) 371-7894
Email: nick.barilo@pnnl.gov

DOE Manager: Will James
Phone: (202) 287-6223
Email: Charles.James@ee.doe.gov

Subcontractors:
- David J. Farese, Air Products and Chemicals, Inc., Allentown, PA
- William C. Fort, Shell Global Solutions (ret), Fairfax, VA
- Larry Fluer, Fluer, Inc., Paso Robles, CA
- Don Frikken, Becht Engineering, St. Louis, MO
- Livio Gambone, CSA Group, Langley, B.C., Canada
- Jennifer Hamilton, BKi, West Sacramento, CA
- Aaron Harris, Air Liquide, Houston, TX
- Richard A. Kallman, City of Santa Fe Springs, CA
- Larry Moulthrop, Proton OnSite, Wallingford, CT
- Glenn W. Scheffler, GWS Solutions of Tolland, LLC, Tolland, CT
- Steven C. Weiner, Excelsior Design, Inc., Richland, WA
- Tom Witte, Witte Engineered Gases, Seminole, FL
- Robert G. Zalosh, Firexplo, Wellesley, MA

Project Start Date: 2004
Project End Date: Project continuation and direction determined annually by DOE

Overall Objectives

- Provide expertise and recommendations to DOE and help identify safety-related technical data gaps, best practices, and lessons learned.
- Help DOE integrate safety planning into funded projects to ensure that all projects address and incorporate hydrogen and related safety practices.
- Collect information and share lessons learned from hydrogen incidents and near misses to help prevent similar safety events in the future.
- Capture vast and growing knowledge base of hydrogen experience and make it publicly available to the "hydrogen community" and stakeholders.
- Support implementation of hydrogen and fuel cell technologies by providing technically accurate hydrogen safety and emergency response information to first responders.

Fiscal Year (FY) 2016 Objectives

- Provide updated content for first responder web-based and operations-level courses and the national training template.
- Participate in outreach events on hydrogen safety aimed at a variety of stakeholder groups to emphasize available tools and resources.
- Complete a third-party hydrogen certification guide to facilitate timely project permitting and approval by code officials.
- Incorporate additional enhancements for the Hydrogen Tools Portal, including workspace customization, mobile device display improvements, search engine optimization, and site performance.

Technical Barriers

This project addresses the following technical barriers from the DOE Fuel Cell Technologies (FCT) Office Multi-Year Research, Development, and Demonstration Plan [1].

Hydrogen Safety, Codes and Standards

(A) Safety Data and Information: Limited Access and Availability

(B) Availability and Affordability of Insurance

(C) Safety is Not always Treated as a Continuous Process

(D) Lack of Hydrogen Knowledge by Authorities Having Jurisdiction

(E) Lack of Hydrogen Training Materials and Facilities for Emergency Responders

(F) Insufficient Technical Data to Revise Standards

Education and Outreach

(A) Lack of Readily Available, Objective and Technically Accurate Information

(D) Lack of Educated Trainers and Training Opportunities

Contribution to Achievement of DOE Milestones

This project contributes to achievement of the following DOE tasks and milestones from the FCT Office Multi-Year Research, Development, and Demonstration Plan.

Hydrogen Safety, Codes and Standards

- Task 1: Address Safety of DOE Research and Development (R&D) Projects (ongoing)
- Task 5: Dissemination of Data, Safety Knowledge, and Information (ongoing)
- Milestone 5.1: Update Safety Bibliography and Incidents Databases (4Q, 2011-2020)

Education and Outreach

- Task 1: Educate Safety and Code Officials (ongoing)
- Milestone 1.1: Update "Introduction to Hydrogen Safety for First Responders" Course for First Responders (biannually)

FY 2016 Accomplishments

The 22nd Hydrogen Safety Panel (HSP) meeting was held in Torrance, California, December 8–10, 2015, enabling consideration of timely and relevant safety issues and the engagement of key hydrogen infrastructure stakeholders.

- The HSP conducted 23 reviews (including safety plans and project designs) since July 1, 2015, for projects within the FCT Office.
- Revised the National Hydrogen and Fuel Cells Emergency Response Training resource in December 2015 to include up-to-date pictures, text, and speaker notes.
- Released a draft Hydrogen Equipment Certification Guide for stakeholder review in December 2015, and feedback is currently being incorporated.
- Provided support to the DOE H2 Refuel competition by developing safety criteria, evaluating safety plans, and providing guidance and recommendations.
- PNNL led a team of team of four first responders from the United States to participate in the European Hydrogen Emergency Response Training Program for First Responders (HyResponse), held at L'École Nationale Supérieure des Officiers de Sapeurs-Pompiers (The French Academy for Fire, Rescue, and Civil Protection Officers) in Aix en Provence, France, May 9–13, 2016.
- Added additional resource tools for codes and standards permitting, the Hydrogen Fueling Infrastructure Research and Station Technology project, and the Hydrogen Station Equipment Performance (HyStEP) device to the Hydrogen Tools Portal (http://h2tools.org).
- Provided outreach and educational sessions for a variety of audiences, including the International Code Council (ICC), International Association of Fire Chiefs, Sacramento fire prevention officers, and stakeholders and code officials in New York and Massachusetts.

✧ ✧ ✧ ✧ ✧

INTRODUCTION

Safety is essential for realizing the "hydrogen economy"—safe operation in all of its aspects from hydrogen production through storage, distribution, and use; from research, development, and demonstration; to deployment and commercialization. As such, safety is given paramount importance in all facets of the research, development, demonstration, and deployment work of the DOE FCT Office. This annual report summarizes activities associated with three project tasks: the HSP, Safety Knowledge Tools, and First Responder Training Resources.

Recognizing the nature of the DOE FCT program and the importance of safety planning, the HSP was formed in December 2003 to assemble a broad cross-section of expertise from the industrial, government, and academic sectors to help ensure the success of the program as a whole. The panel's experience resides in industrial hydrogen production and supply, hydrogen R&D and applications, process safety and engineering, materials technology, risk analysis, accident investigation, and fire protection. The panel provides expertise and recommendations on safety-related issues and technical data gaps, reviews individual projects and their safety plans, and explores ways to develop and disseminate best practices and lessons learned, all broadly benefiting the FCT program. The panel currently has 16 members with a total of over 400 years of industry and related experience (see Table 1 for FY 2016 panel membership).

Widespread availability and communication of safety-related information are crucial to ensuring the safe operation of future hydrogen and fuel cell technology systems. The entire hydrogen community benefits if hydrogen safety-related knowledge is openly and broadly shared. To that end, PNNL continues to improve the safety knowledge software tools and develop new techniques for disseminating this information. This report covers the Hydrogen Tools Portal (http://h2tools.org), the Hydrogen Lessons Learned database (http://h2tools.org/lessons/), and the Hydrogen Safety Best Practices online manual (https://h2tools.org/bestpractices). These resources are key to reaching, educating, and informing stakeholders whose contributions will help enable the deployment of new hydrogen and fuel cell technologies.

A suitably trained emergency response force is essential to a viable infrastructure. The FCT Office has placed a high priority on training emergency response personnel, not only because these personnel need to understand how to respond to a hydrogen incident, but also because firefighters and other emergency responders are influential

TABLE 1. Current Hydrogen Safety Panel Membership

Nick Barilo, Program Manager	PNNL
Richard Kallman, Chair	City of Santa Fe Springs, CA
David Farese	Air Products and Chemicals
Larry Fluer	Fluer, Inc.
Bill Fort	Shell Global Solutions (ret)
Don Frikken	Becht Engineering
Livio Gambone*	CSA Group
Aaron Harris	Sandia National Laboratories
Chris LaFleur	Sandia National Laboratories
Miguel Maes	NASA White Sands Test Facility
Steve Mathison	Honda Motor Company
Larry Moulthrop	Proton OnSite
Glenn Scheffler	GWS Solutions of Tolland, LLC
Steven Weiner	Excelsior Design, Inc.
Tom Witte*	Witte Engineered Gases
Robert Zalosh	Firexplo

* New panel members

in their communities and can be a positive force in the introduction of hydrogen and fuel cells into local markets. This report covers hazardous materials emergency response training to provide a tiered hydrogen safety education program for emergency responders. The effort started with development and distribution of the awareness-level online course in FY 2006–2007. An operations-level classroom curriculum was developed in FY 2008–2009, including design, construction, and operation of a fuel cell vehicle prop for hands-on training. PNNL and the California Fuel Cell Partnership collaborated to develop a national hydrogen safety training resource for emergency responders, which was made publicly available in September 2014.

APPROACH

The HSP strives to raise safety consciousness most directly at the project level through organizational policies and procedures, safety culture, and priorities. Project safety plans and design documents are reviewed to encourage thorough and continuous attention to safety aspects of the specific work being conducted. Panel safety reviews focus on engagement, learning, knowledge sharing, and active discussion of safety practices and lessons learned, rather than audits or regulatory exercises. Through this approach, the HSP is trying to achieve safe operation, handling and use of hydrogen and hydrogen systems for all projects.

The approach for disseminating safety knowledge in FY 2016 focused on adding resources to the existing Hydrogen Tools Portal and participating in impactful outreach activities. The portal brings together and enhances the utility of a variety of tools and web-based content on the safety aspects of hydrogen and fuel cell technologies. It's intended to help inform those tasked with designing, approving, or using systems and facilities, as well as those responding to incidents. Additional discussion is provided in the Results section of this report.

PNNL collaborates with subject matter experts in hydrogen safety and first responder training to develop, review, and revise training materials as needed. The PNNL project team works with DOE to inform stakeholder groups of training opportunities and to provide "live" training when appropriate. The online awareness-level course provides the student with a basic understanding of hydrogen properties, uses and appropriate emergency response actions. The operations-level classroom/hands-on prop-based course has been presented at the Volpentest Hazardous Material Management and Materials Response Federal Training Center in Richland, Washington, and at several fire-training centers in California and Hawaii to reach larger audiences in areas where hydrogen and fuel cell technologies are being deployed. The National Hydrogen and Fuel Cell Emergency Response Training Resource provides a consistent source of accurate information and current knowledge to ensure that training organizations have the information needed to develop or supplement their own courses. As part of this resource, a training template has been developed to guide the delivery of a variety of training regimens to various audiences.

RESULTS

The 22nd HSP meeting was held in Torrance, California, December 8-10, 2015. The meeting provided opportunities to consider timely and relevant safety issues and provide direct input to the FCT Office. The topics discussed and outcomes achieved at the meeting are detailed in the meeting minutes [2]. Two panel task groups were formed at the meeting to (1) evaluate recent HSP reviews for new and unique applications (e.g., mobile auxiliary power units, mobile fuelers, refrigeration units, etc.) to determine if safety or code gaps exist and (2) capture unique learnings from projects and make the information available to future projects through a document or online resource.

During the past year, the HSP has provided safety reviews and support to projects identified in Table 2. Since 2004, the panel has participated in 441 project reviews (including safety plans, site visit reviews, follow-up phone interviews, and design review work). In addition to reviewing safety plans, the HSP provided crucial support to the DOE H2 Refuel competition by developing safety criteria, leading a safety webinar, and providing recommendations to both the judges and applicants. FY 2016 also marked the start of the HSP providing support for non-DOE projects. This included a review for the California Air Resources Board and support for the California general funding opportunity for

TABLE 2. HSP Project Safety Work since July 1, 2015

Work	Project Title	Contractor
Safety Plan Review	Biohydrogen production and bench-scale hydrogen-producing reactors	Oregon State University
Site Visit	Brentwood Hydrogen Fueling Station	National Renewable Energy Laboratory (NREL)
Design Review	NREL H_2 Station Reconfiguration	NREL
Document Review	HyStEP Procedures Review (two reviews)	California Air Resources Board
Safety Plan Review	Conformable Hydrogen Storage Coil Reservoir	Center for Transportation and the Environment
Safety Plan Review	Tandem Particle-slurry Batch Reactors for Solar Water Splitting (two reviews)	University of California, Irvine
Safety Plan Review	High Performance Platinum Group Metal Free Membrane Electrode Assemblies Through Control of Interfacial Processes	Proton OnSite
Safety Plan Review	Hydrogen Adsorbents with High Volumetric Density: New Materials and System Projections	University of Michigan
Safety Plan Review	H-Prize - Ion Submittal	Ion Power, Inc.
Safety Plan Review	H-Prize - Katsu Submittal	Katsu Technologies, Inc.
Safety Plan Review	H-Prize - Millennium Submittal (two reviews)	Millennnium Reign Energy
Safety Plan Review	H-Prize - Reactwell Submittal	ReactWell, LLC
Safety Plan Review	H-Prize - Simple.Fuel. Submittal	Simple.Fuel.
Safety Plan Review	H-Prize - WSU Submittal	Washington State University
Safety Plan Review	Design and Synthesis of Materials with High Capacities for Hydrogen Physisorption (two reviews)	Caltech
Safety Plan Review	Advanced Catalysts and Membrane Electrode Assemblies (MEAs) for Reversible Alkaline Membrane Fuel Cells (two reviews)	Giner, Inc.
Design Review	Mobile Fuel Cell Generator	California Air Resources Board
Document Review	Fire Protection Engineering Design Brief Template: Hydrogen Refueling Station	Sandia National Laboratories

fueling stations through a safety-planning webinar and safety consultation for applicants.

A significant HSP accomplishment during FY 2016 was the public release of the draft Hydrogen Equipment Certification Guide. The purpose of the guide is to enable designers, users, and code officials to better apply the requirements in cases where the use of listed, labeled, certified, or approved equipment or methods is required and to increase awareness and understanding of what the equipment is expected to do. The challenge with equipment certification is that the listing process for rapidly changing products, consistent with developing technologies, tends to be cost-prohibitive for equipment providers (each change to the equipment requires recertification). The circumstance of new technologies under development and low demand for early market applications results in few components and systems being currently listed. The scarcity of listed equipment places an extraordinary burden on code officials to ensure (and approve) that products include the appropriate inherent or automatic safety measures. The guide identified listing requirements in the ICC codes and National Fire Protection Association 2 (Hydrogen Technologies Code) for hydrogen equipment, and suggests criteria for approval when listed equipment is not available. Stakeholder comments were received and the guide is being revised for a fall 2016 release.

Panel members also helped the Hydrogen Technical Advisory Committee draft a safety communications plan. The plan assesses the status of resources and practices that support a comprehensive, consistent, and coordinated response to hydrogen safety-related events. The goal is to enable the hydrogen stakeholder community to understand event causes, address issues, share lessons learned, communicate status effectively with multiple stakeholders (including media), and maintain focus on advancing commercialization of hydrogen fuel.

International collaboration is important to PNNL's hydrogen safety work. PNNL led a team of four first responders to participate in the European Hydrogen Emergency Response Training Program for First Responders (HyResponse), held at L'École Nationale Supérieure des Officiers de Sapeurs-Pompiers in Aix en Provence, France, May 9–13, 2016 (additional discussion provided below). PNNL also offered highlights of accomplishments of the HSP and other international collaborations through two presentations at the 2015 International Conference on Hydrogen Safety in Yokohama, Japan [3,4]:

- "Overview of the DOE Hydrogen Safety, Codes and Standards Program Part 2: Hydrogen and Fuel Cells - Emphasizing Safety to Enable Commercialization"

- "First Responder Training: Supporting Commercialization of Hydrogen and Fuel Cell Technologies."

The Hydrogen Tools Portal was made publicly available in June 2015. The portal saw mostly steady growth in its use as a resource during FY 2016 (see Figure 1). Additional resources added to the portal included information from NREL on codes and standards permitting; the Hydrogen Fueling Infrastructure Research and Station Technology project; and information from Sandia National Laboratories on the HyStEP device, including specifications and design documents to enable others to replicate the equipment.

Disseminating safety information continues to be an important aspect of this project. A significant outreach effort during this reporting period focused on membership associated with the ICC Annual Business Meeting and conference. ICC membership includes building, fire, plumbing, mechanical, and energy officials representing state, county, municipal, and federal government agencies. Ensuring that this group is informed on hydrogen safety-related issues and resources can help facilitate a safe and timely transition to fuel cell technologies. The outreach event for the ICC's annual business meeting was a collaboration between PNNL, H2USA, and the California Fuel Cell Partnership. The event included a ride-and-drive event, a Toyota Mirai booth display, an educational session, and tours of a fueling station and fuel cell vehicle repair garage. Other hydrogen safety outreach activities during this reporting period are listed below:

- Boston area fire chiefs and code officials (August 2015)
- Sacramento Fire Prevention Officers (August 2015)
- International Association of Fire Chiefs (September 2015)
- The ICC Colorado Code Official Institute (March 2016)
- A joint Toyota, Air Liquide, NREL and PNNL outreach to code officials and stakeholders in New York and Massachusetts (April 2016)
- The Washington State Alternative Vehicles Working Group (July 2016)

To facilitate a more strategic approach for outreach activities, PNNL will lead a collaboration with NREL and Sandia National Laboratories to develop a DOE Safety, Codes and Standards long-term outreach plan. The goal of the plan is to reach all stakeholders that can impact the development, deployment and/or continued safe use of technologies that use hydrogen as a fuel. The plan is expected to be completed in early FY 2017.

FY 2016 activities directed toward the first responder training task included updating content for the National Hydrogen and Fuel Cell Emergency Response Training Resource (https://h2tools.org/fr/nt); development work for updating the Introduction to Hydrogen Safety for First Responders (http://hydrogen.pnl.gov/FirstResponders/) online course; organizing a team of four U.S. first responders to participate in HyResponse training; and planning classroom training activities for the Northeast in FY 2017.

PNNL organized a team of four U.S. first responders from Los Angeles County Fire Department, San Jose Fire Department, Littleton Massachusetts Fire Department and New York City Fire Department, for participation in the European Hydrogen Emergency Response Training Program for First Responders (HyResponse), held at L'École Nationale Supérieure des Officiers de Sapeurs-Pompiers in Aix en Provence, France, May 9-13, 2016. The HyResponse training included lectures focused on the fundamentals of hydrogen safety and tactics for responding to a variety of events, hands-on training exercises with well-developed props, and virtual reality interactive sessions. The four U.S. first responders participated directly in all activities, and staff from PNNL observed. Participation in this training afforded a number of positive benefits:

- Provided first responders with the needed experience and knowledge to train others in their region and support additional United States-based training outreach.
- Gained valuable first responder feedback on the training strategies implemented by the HyResponse project in

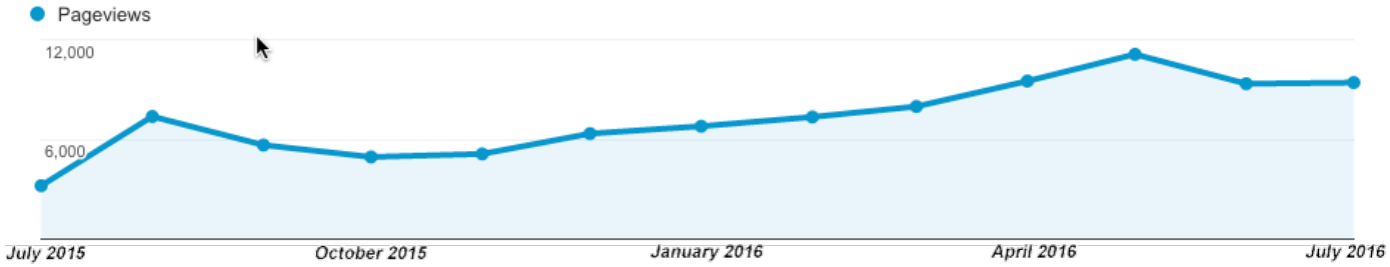

FIGURE 1. Hydrogen Tools Portal pageviews (source: Google Analytics)

order to consider improvements to PNNL/DOE first responder training activities.

- Discussed opportunities for future collaborations with HyResponse organizations (including participating in a proposed Spring 2017 Northeast United States training event).

CONCLUSIONS AND FUTURE DIRECTIONS

The HSP will continue to focus on how safety knowledge, best practices, and lessons learned can promote the safe conduct of project work and the deployment of hydrogen technologies and systems in applications of interest and priority in the DOE FCT Office. The HSP can also be used more broadly as an asset for safe commercialization by reaching out to new stakeholders and users involved in early deployment.

HSP initiatives over the next year will include the following:

- Support the rollout of California's hydrogen fueling stations by reviewing safety plans for applicants to the Energy Commission's general funding opportunity.
- Engage non-DOE entities to identify opportunities to use the panel to review hydrogen and fuel cell initiatives and promote safety.
- Release the Hydrogen Equipment Certification Guide to the public in the fall of 2016.
- Continue to evaluate the panel membership to maintain its leadership role in hydrogen safety through an appropriate mix of safety expertise and perspective to perform safety reviews and address relevant issues.

Hydrogen safety knowledge tools help remove barriers to the deployment and commercialization of hydrogen and fuel cell technologies. The introduction of the Hydrogen Tools Portal opens new opportunities for sharing safety information and reaching broader audiences. In FY 2017, opportunities to collaborate with other national laboratories, state organizations, and industry partners will continue to be explored to identify and integrate new resources into this valuable website. It is also anticipated that PNNL will participate in a number of strategic outreach efforts similar to FY 2016.

The project's First Responder Training Resources address a key H2USA barrier, ensure a safe transition to fuel cell vehicles and a hydrogen infrastructure, and pave the way for broader public acceptance. Potential activities for FY 2017 will include deployment of the updated online training, and onsite training activities in New York, Massachusetts, Connecticut, and Rhode Island. It is anticipated that this training will take place in November 2016 and the spring of 2017. The latter date will likely include classroom training and prop demonstrations, and could also include virtual reality training exercises through collaboration with participants in the HyResponse project.

REFERENCES

1. U.S. Department of Energy, "Fuel Cell Technologies Office Multi-Year Research, Development, and Demonstration Plan," http://energy.gov/eere/fuelcells/downloads/fuel-cell-technologies-office-multi-year-research-development-and-22.

2. Barilo, N.F. to Farese, D. et al., "Minutes from the 22nd Hydrogen Safety Panel Meeting," February 8, 2016.

3. Barilo, N.F., and S.C. Weiner, "Overview of the DOE Hydrogen Safety, Codes and Standards Program Part 2: Hydrogen and Fuel Cells - Emphasizing Safety to Enable Commercialization," International Conference on Hydrogen Safety, Yokohama, Japan, October 20, 2015.

4. Barilo, N.F., J.J. Hamilton, and S.C. Weiner, "First Responder Training: Supporting Commercialization of Hydrogen and Fuel Cell Technologies," 2015 International Conference on Hydrogen Safety, Yokohama, Japan, October 19, 2015.

FY 2016 PUBLICATIONS/PRESENTATIONS

1. Barilo, N.F., "Hydrogen Equipment Certification Guide Listing, Labeling and Approval Considerations," PNNL-25053, Richland, WA, December 2015.

2. Barilo, N.F., "Safety Planning for Hydrogen and Fuel Cell Projects," PNNL-25279, Richland, WA, March 2016.

3. Barilo, N.F., Weiner, S.C., and James, C.W., "Overview of the DOE Hydrogen Safety, Codes and Standards Program Part 2: Hydrogen and Fuel Cells: Emphasizing Safety to Enable Commercialization," International Journal of Hydrogen Energy, June 2016.

4. Barilo, N.F., Hamilton, J.J., and Weiner, S.C., "First Responder Training: Supporting Commercialization of Hydrogen and Fuel Cell Technologies," International Journal of Hydrogen Energy, July 2016.

5. Barilo, N.F., "Safety Considerations for Hydrogen and Fuel Cell Applications," presented at the ICC Annual Business Meeting, Long Beach, CA, September 29, 2015.

6. Barilo, N.F., and Frikken, D., "Safety Planning for the H-Prize Competition," presented at the "Safety First" webinar for the H2 Refuel competition online webinar on August 6, 2015.

7. Barilo, N.F., "Hydrogen and Fuel Cells Are Coming...Are You Ready?" presented at the United States Fire Administration and International Association of Fire Chiefs online webinar on September 15, 2015.

8. Barilo, N.F., Hamilton, J.J., and Weiner, S.C., "First Responder Training: Supporting Commercialization of Hydrogen and Fuel Cell Technologies," presented at the International Conference on Hydrogen Safety, Yokohama, Japan on October 19, 2015.

9. Barilo, N.F., and Weiner, S.C., "Overview of the DOE Hydrogen Safety, Codes and Standards Program Part 2: Hydrogen and

Fuel Cells - Emphasizing Safety to Enable Commercialization," presented at the International Conference on Hydrogen Safety, Yokohama, Japan on October 20, 2015.

10. Barilo, N.F., "Hydrogen and Fuel Cell Applications," presented at the Colorado Chapter Educational Institute (ICC), Denver, CO on March 3, 2016.

11. Barilo, N.F., "Hydrogen Safety Panel, Safety Knowledge Tools and First Responder Training Resources," presented at the 2016 DOE Hydrogen Program Annual Merit Review and Peer Evaluation Meeting, Washington, DC, on June 7, 2016.

12. Barilo, N.F., "Hydrogen Fueling Stations," presented at outreach events in New York and Massachusetts in April 2016.

13. Barilo, N.F., "Hydrogen Safety Information Resources," presented at outreach events in New York and Massachusetts in April 2016.

14. Barilo, N.F., "Safety Planning for Hydrogen and Fuel Cell Projects," presented at outreach events in New York and Massachusetts in April 2016.

15. Barilo, N.F., Markwort, J.M., and Jo, I.D., "Hydrogen Tools Information Video," PNNL-SA-113244, Richland, WA, September 2015.

VIII.7 NREL Hydrogen Sensor Testing Laboratory

William Buttner (Primary Contact), Robert Burgess, Carl Rivkin
National Renewable Energy Laboratory (NREL)
15013 Denver West Parkway
Golden, CO 80401-3305
Phone: (303) 275-3903
Email: William.Buttner@nrel.gov

DOE Manager: Will James
Phone: (202) 287-6223
Email: Charles.James@ee.doe.gov

Subcontractors:
- Element One, Boulder, CO
- Bloomfield Automation, Denver, CO

Project Start Date: October 1, 2010
Project End Date: Project continuation and direction determined annually by DOE

Overall Objectives

- Quantify performance of commercial hydrogen sensors relative to DOE metrics.
- Support development and assess performance of advanced sensor technologies.
- Support development and updating of hydrogen sensor codes and standards.
- Support infrastructure and vehicle deployment by providing expert guidance on the use of hydrogen sensors and analyzers.
- Educate the hydrogen community on the proper use of hydrogen sensors.

Fiscal Year (FY) 2016 Objectives

- Support Department of Transportation (DOT)/ National Highway Traffic Safety Administration on the development of the Federal Motor Vehicle Safety Standard (FMVSS) for hydrogen fuel cell vehicles (FCEVs), especially with regards to hydrogen detection requirements identified in the Global Technical Regulation (GTR) 13 [1].
- Quantify performance metrics of developmental sensor technologies from both the private sector and government laboratories.
- Support infrastructure deployment by providing sensor testing capability and guidance to stakeholders in the hydrogen energy field.
- Qualify hydrogen safety sensors for specific infrastructure and vehicle applications.
- Facilitate safe deployment of FCEVs by participation on the SAE Fuel Cell Vehicle Crash Testing Safety Guidelines Task Force and the Fuel Cell Safety Task Force. As part of the Fuel Cell Task Force, the NREL Sensor Laboratory is leading the development of SAE Technical Information Report J3089, "Characterization of On-board Vehicular Hydrogen Sensors," which is to provide guidance for qualifying on-board hydrogen sensors.
- Support NREL component testing and facility upgrades with sensors and expertise for both safety and quantitation of hydrogen releases.
- Support hydrogen safety code and standard development by performing prenormative research on intended and unintended hydrogen releases.
- Support the deployment and implementation of hydrogen sensors for safety and fuel quality.

Technical Barriers

This project addresses the following technical barriers identified in the Hydrogen Safety, Codes and Standards section of the Fuel Cell Technologies Office Multi-Year Research, Development, and Demonstration Plan.

(A) Safety Data and Information: Limited Access and Availability

(C) Safety is Not Always Treated as a Continuous Process

(D) Lack of Hydrogen Knowledge by AHJs

(F) Enabling National and International Markets Requires Consistent RCS

(G) Insufficient Technical Data to Revise Standards

(H) Insufficient Synchronization of National Codes and Standards

(K) No Consistent Codification Plan and Process for Synchronization of R&D and Code Development

Contribution to Achievement of DOE Safety, Codes & Standards Milestones

This project will contribute to the achievement of the following DOE milestones from the Hydrogen Safety, Codes and Standards section of the Fuel Cell Technologies Office Multi-Year Research, Development, and Demonstration Plan.

- Milestone 2.15: Develop holistic design strategies. (4Q, 2017)

- Milestone 2.19: Validate inherently safe design for hydrogen fueling infrastructure. (4Q, 2019)
- Milestone 3.1: Develop, validate, and harmonize test measurement protocols. (4Q, 2014)
- Milestone 4.9: Completion of GTR Phase 2. (1Q, 2017)
- Milestone 5.1: Update safety bibliography and incidents databases. (4Q, 2011 – 2020)

FY 2016 Accomplishments

- Implemented or maintained multiple formal agreements with industrial partners on the use of sensors in support of infrastructure deployment, for on-board vehicle applications, and in support of new advanced sensor technology development.
- Provided technical support to DOT/National Highway Traffic Safety Administration pertaining to FCEV hydrogen detection requirements as specified in the GTR, including requirements for both FCEV crash test and allowable tailpipe emissions. A prototype tailpipe analyzer has been demonstrated in the laboratory and will be configured for field deployment. This activity supports the development of the FMVSS (Milestone 4.9).
- In collaboration with the Joint Research Centre (JRC), Institute for Energy and Transport (IET), completed a study quantifying the impact of potential chemical poisons as identified in International Organization for Standardization (ISO) 26140 [2] on the major hydrogen sensor platform types (Milestone 3.1).
- Supported the development of the first draft of SAE Technical Information Report J3089, "Characterization of On-board Vehicular Hydrogen Sensors," under the auspices of SAE Fuel Cell Standards Committee.
- Formed an experts group among the NREL and the JRC sensor experts with computational fluid dynamics modelers and risk assessment experts to provide guidelines on hydrogen sensor placement.
- Developed a prototype analyzer for the in situ deployment in cold hydrogen releases to characterize plume dispersion in support of dispersion models and code development.
- Co-authored a book on hydrogen sensors (published January 2016): "Sensors for Safety and Process Control in Hydrogen Technology," Thomas Hűbert, Lois Boon-Brett, and William J. Buttner, CRC Press, Taylor and Francis Group, Boca Raton, ISBN 13-978-1-4665-9654-2 (2016).

✧ ✧ ✧ ✧ ✧

INTRODUCTION

Safety is a major concern for the emerging hydrogen infrastructure. A reliable safety system is comprised of various elements that can include intrinsic design features (e.g., pressure control systems), engineering controls (e.g., sample size minimization), and the use of hydrogen sensors to monitor for releases. Both the International Fire Code 2009 and National Fire Protection Association (NFPA) 2 require hydrogen sensors for numerous applications, and accordingly sensors will be mandatory in all jurisdictions that adopt either the International Fire Code or NFPA 2. To assure the availability of reliable safety sensors, DOE established the NREL Safety Sensor Testing Laboratory. The NREL sensor test facility provides stakeholders (e.g., sensor developers and manufacturers, end users, and code officials) a resource for an independent, unbiased evaluation of hydrogen sensor technologies. Test protocols are guided by the requirements in national and international sensor standards, as well as sensor performance targets established by DOE [3] or by the requirements of the application. In addition to laboratory assessment of sensor performance, a critical mission of the NREL Safety Sensor Testing Laboratory is to educate end users on the proper use of hydrogen sensors. This is achieved, in part, through topical studies designed to illustrate fundamental properties and limitations of various hydrogen sensor technologies, and through outreach activity such as participation on standards development organizations committees, workshops, conferences, and webinars. The NREL sensor laboratory also facilitates deployment by partnering with end-users to assist in the design and implementation of their sensor system.

APPROACH

Evaluation of hydrogen safety sensors is an on-going activity at NREL. This activity supports sensor developers and end-users, as well as code developers and permitting official. The goal of the sensor laboratory is to assure that stakeholders in the hydrogen community have the sensor technology they need. Sensor performance evaluation is performed using custom-built NREL sensor test apparatus, which were designed with advanced capabilities, including parallel testing of multiple hydrogen sensors, sub-ambient to elevated temperature, sub-ambient to elevated pressure, active humidity control and accurate control of gas parameters with multiple precision digital mass flow meters operating in parallel. The test apparatus are fully automated for control and monitoring of test parameters and for data acquisition with around-the-clock operation capability. Selected sensors are subjected to an array of tests to quantify the impact of variation of environmental parameters and chemical matrix on performance. Although standard test protocols have been developed [4], these can be adapted for specialized requirements. Results are

reported back to the developer or manufacturer to support their future development work.[1] NREL sensor testing also supports end users by qualifying sensor technology for their application and by educating the hydrogen community on the proper use of hydrogen sensors. The NREL sensor laboratory maximizes its impact by working directly with stakeholders in the hydrogen community; this is achieved in part through numerous formal agreements with industrial partners. Strategic partnerships have also been maintained with other government organizations, most notably with the Sensor Testing Facility at the JRC–IET, under which we collaborate on hydrogen sensor research projects of common interests. The NREL–JRC collaboration provides a platform for the international distribution of the sensor research and development.

In addition to sensor performance characterization, the scope of the NREL Safety Sensor Testing Laboratory has expanded its active participation on a variety of national and international codes and standards development organizations, including NFPA 2, ISO Technical Committee (TC) 197, ISO TC 158, SAE, UL, ASTM International, and the GTR. Various levels of support is provided by the NREL Safety Sensor Testing Laboratory for codes and standards development:

- Prenormative research to support code and standard development
- Document development
- Development and deployment of verification technology
- Expert support/guidance/recommendations
- Dissemination of results is through a variety of venues, including participation on international hydrogen safety panels, including the International Association for Hydrogen Safety [5] and International Energy Agency, Hydrogen Implementing Agreement, Task 37 (Safety) [6], presentations at international conferences and workshops, publications in the open literature, and direct outreach to the hydrogen community.

RESULTS

To support hydrogen deployment, the NREL sensor test facility strives to assure the availability of hydrogen sensors to meet stakeholder needs. This is achieved in part by providing an unbiased assessment of sensor performance to developers and manufacturers as well as end-users. NREL has also performed numerous topical studies aimed at educating the hydrogen community on the proper use of hydrogen sensors. The sensor laboratory also supports the implementation of codes and standards by providing tools for normative research (see below: *Hydrogen Cold Plume Release Analysis*) and verification technology (see below: S*upport of the GTR 13 and the United States FMVSS*. Results reported here summarize major studies or critical steps in on-going activity completed in FY 2016 on the characterization and use of hydrogen sensors.

Sensor Testing and Evaluation—Support of Deployment: Sensor testing and evaluation remains a core activity within the NREL sensor laboratory. The NREL sensor laboratory continues to provide the resources necessary to quantify sensor performance for specific applications; clients include sensor developers and manufacturers, as well as end-users, including both infrastructure and vehicular applications. NREL has numerous agreements with industrial partners to facilitate these collaborations. The NREL sensor laboratory activity includes topical studies, such as evaluating the impact of environmental stress on chemical sensor performance [7].

Support of the GTR 13 and the United States FMVSS: GTR 13, which is the defining document regulating hydrogen vehicle safety requirements, has been formally implemented. Accordingly, national authorities overseeing development and enforcement of vehicle regulations shall endeavor to harmonize their national regulations with the GTR. Within the United States, the national authority for vehicle safety is the DOT and the prevailing regulatory code is the FMVSS. Included within the GTR are safety requirements on allowable hydrogen emission levels in vehicle enclosures during in-use and post-crash test conditions, and on the allowable hydrogen content in vehicle exhaust during certain modes of normal operation. However, methods to verify compliance must exist in order for specific requirements to be incorporated into regulations. The NREL Safety Sensor Testing Laboratory, in cooperation with DOT, has been developing an analytical apparatus and methods for compliance verification of the various hydrogen emission requirements specified in the GTR. The NREL sensor laboratory had successfully qualified a commercial hydrogen sensor for use in an FCEV crash test [8]. These results have been shared with the SAE Hydrogen Fuel Cell Vehicle Crash Testing Safety Guidelines Task Force. In cooperation with the DOT, Transport Canada is preparing for an FCEV crash test as part of their mission to verify compliance to vehicle safety regulation. This FCEV crash test is tentatively scheduled for the fourth quarter of 2016. NREL will assist by instrumenting the crash test vehicle with hydrogen sensors, including sensors that have been previously qualified for this application along with models from other manufacturers; the qualified sensor product line has been discontinued by the manufacturer. In a second application, GTR 13 also specifies allowable hydrogen levels in tailpipe emission—specifically the exhaust gas shall not exceed 4 vol% H_2 during any moving three-second time interval but with a maximum short-term hydrogen level remaining below 8 vol%. The NREL Safety Sensor Testing Laboratory is developing an off-

[1] It is the policy of the NREL sensor laboratory to treat test results as proprietary, and thus results pertaining to specific clients will not be disclosed without permission.

vehicle analyzer for use by regulatory agencies such as DOT to verify compliance to this GTR specification. A laboratory bench top prototype analyzer has been demonstrated [9] (Figure 1 shows an early probe design), which is currently being configured by NREL for in-field use by DOT and Transport Canada. Several vehicle manufacturers have also expressed interest in this technology, and agreements are in place to facilitate this testing.

Hydrogen Cold Plume Release Analysis: Liquid hydrogen is routinely delivered to a facility using road transport vehicles and transferred on-site to a stationary storage tank. Following transfer, up to 60 kg of cold hydrogen, which may include liquid hydrogen droplets, is vented from the transport vessel. A liquid hydrogen dispersion model is under development, but there is little data for verification. The NFPA 2 Hydrogen Storage Task Group has been tasked with developing a scientific basis for liquid hydrogen set back distances, which will support permitting of hydrogen stations with on-site liquid hydrogen storage. Liquid hydrogen storage at commercial fueling stations will increase as the number of hydrogen FCEVs grows. The task group specifically identified a need to characterize the plume generated during a liquid hydrogen release from the vent stack. Empirical profiling of the plume is needed to

- Better understand the behavior of cold plume releases.
- Determine if the plume can drop below the release point based on interactions with the atmosphere such as the liquefaction of the atmosphere that plume is being released in to.
- Further validate computer model.

The NFPA 2 Hydrogen Storage Task Group formed a sub-group to address the need to characterize the plume profile. The sub-group includes representatives from a hydrogen producer (the Linde Group), risk assessment and computational fluid dynamics experts (Sandia National Laboratories), and hydrogen safety, codes, and standards (NREL). The sub-group approached the NREL sensor laboratory to assist in the design, construction, demonstration, and deployment of an analyzer for the temporal, in situ profiling of the cold hydrogen plume formed during the liquid hydrogen venting. A prototype Cold Hydrogen Plume Analyzer design has been developed by the NREL Safety Sensor Testing Laboratory. The analyzer consists of a support structure for in situ deployment in the plume, a sample collection system with multiple sampling points, and a remote analyzer box consisting of multiple chemical (hydrogen and oxygen) and physical sensors (temperature and humidity) to provide quantitative information of the plume gas. The analyzer box also includes a pump and a multi-port valve to allow multiplexing of sample collection points for analysis by a single array of chemical and physical sensors. Figure 2 shows the analyzer box. Presently, all sub-systems have been demonstrated, including the support structure, the sample collection system, chemical and physical sensors, and implementation of a computer data acquisition system for control of experimental parameters and data acquisition. System integration is nearly complete and the first field deployment is expected sometime in the third quarter of 2016.

Assessment of a Colorimetric Hydrogen Leak Detection (DetecTape®): A highly selective colorimetric indicator for the detection of leaks from hydrogen pneumatic systems was recently developed by Element One, Inc. The colorimetric indicator was integrated into a pliable, self-adhesive tape that can readily wrap around pneumatic fittings, and is marketed under the tradename DetecTape. In its native state, the indicator pigment is a pale gray color, but becomes black upon exposure to hydrogen. The colorimetric change can be readily observed by the naked eye without the need for supplemental electronics or other hardware. Figure 3 shows the commercial version of DetecTape along with an indicator sample in its native state and one that had been exposed to hydrogen. Under the auspices of a Memorandum of Understanding with Element One, Inc. [10] and with support from the NREL Commercialization Assistance Program [11], the effectiveness of DetecTape as a hydrogen leak detector was evaluated. The deployment study lasted nearly eight months, and included both indoor and outdoor hydrogen operations, as well as supplemental laboratory assessments. During the course of the deployment study, several small but unexpected leaks were identified, thereby guiding appropriate

FIGURE 1. Prototype hydrogen probe for FCEV tailpipe exhaust. A ruggedized probe for field use is under development.

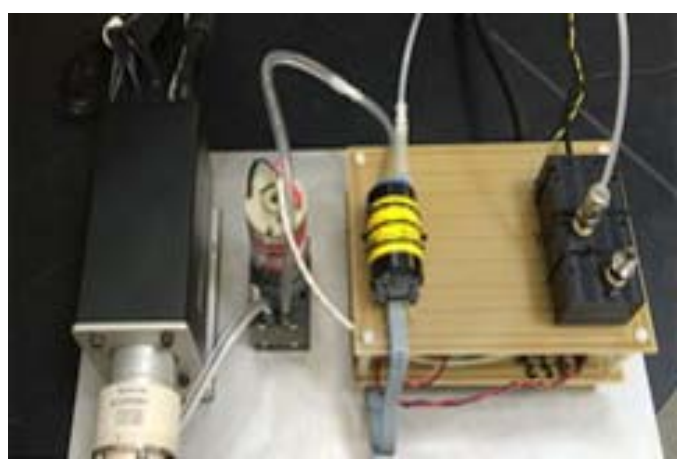

FIGURE 2. Analyzer box (bench top configuration) for the Cold Hydrogen Plume Analyzer

FIGURE 3. Colorimetric hydrogen leak detection (DetecTape). Exposure to hydrogen transforms the indicator from a pale gray color to black.

corrective measures. Furthermore, it was found that the indicator remained active (e.g., sensitive to hydrogen) for the eight-month deployment, demonstrating a robustness against normal outdoor environmental conditions. Details on the deployment study have been reported [12].

International Collaborations (NREL and JRC Sensor Laboratories Collaboration): Recognizing the importance of hydrogen sensors, the European JRC independently established hydrogen sensor testing facilities at the Institute for Energy and Transport. The NREL and JRC sensor laboratories have been collaborating since 2008 in support of the international utilization of hydrogen as an energy carrier. This collaboration has been formalized under the auspices of different agreements, including a Memorandum of Agreement [13] and through a common call between DOE and the European Fuel Cell and Hydrogen Joint Undertaking, however each laboratory maintains independent research programs and directives. The NREL–JRC sensor laboratory arrangement synergizes the effort of each facility and leverages the respective impact of their output by minimizing duplicated research efforts to save resources and maximize throughput, increasing international exposure and visibility of results, and facilitating implementation of the hydrogen infrastructure via an expanding international collaboration among stakeholders. The scope and productivity of this collaboration is demonstrated in the FY 2016 Publications/Presentations section, which list the NREL and JRC sensor laboratories joint publications, including four papers at the World Hydrogen Energy Conference (Zaragoza, Spain, June 13–16), one paper at the International Conference on Hydrogen Safety (Yokohama, Japan, October 19–21, 2015), plus collaborative talks at the International Energy Agency Hydrogen Implementing Agreement Task 37 Experts meetings. In addition, the NREL and JRC sensor laboratories co-authored one journal article and collaborated on a book on hydrogen sensors [14]. Current collaborative activity between NREL and the JRC include

- Hydrogen sensors for power to gas.
- Response time measurements on commercial and developing sensor.
- Development and comparison of sensor performance evaluation test methods for consistency of results.
- Experts team to develop Sensor Placement Guidance Document.

DOE Small Business Voucher Award Recipient: The DOE's Office of Energy Efficiency and Renewable Energy Small Business Voucher (SBV) program was implemented to foster collaborations between United States small businesses and the national laboratories [15]. While not a funding source for the small business, the SBV provides a venue to utilize the resources of the national laboratories. The SBV program is characterized by a simple application process and minimal administrative paperwork. The NREL sensor laboratory was a recipient of one SBV award and is supporting Los Alamos National Laboratory on a second award.

Publication of a Book on Hydrogen Sensors: In 2016, a book on hydrogen sensors was published by the CRC Press [14] — *Sensors for Safety and Process Control in Hydrogen Technology*. The authors included sensor experts from the Bundesanstalt für Materialforschung und –prüfung (Thomas Hűbert), the JRC (Lois Boon-Brett), and NREL (William J. Buttner).

CONCLUSIONS AND FUTURE DIRECTIONS

In the next year and beyond, the NREL sensor laboratory will build off its current accomplishment and capabilities through via two main themes—continued evaluation of hydrogen sensors in support of deployment, and support of hydrogen codes and standards development. Hydrogen sensor evaluations will continue to be guided through direct collaboration with stakeholders in the hydrogen community, including sensor developers and manufacturers as well as end-users, which includes infrastructure and vehicular applications.

Sensor Performance Assessment and Guidance

- End user support to support deployment
  - Guidance on the use of hydrogen sensors in infrastructure deployments, including repair facilities and fueling facilities.
  - Sensor performance testing protocol standards for vehicles.
  - Qualification support for use of sensors in infrastructure and vehicles.
  - Barriers to sensor certification and the impact.
- Manufacturer/developer support
  - Commercial and developmental sensor technology performance validation.

  - Assessment of wide area monitoring and distributed sensor technology.
  - Sensors and analytical methods for the detection of contaminants in hydrogen fuel.

Support of Codes and Standards

- Prenormative data
  - Hydrogen Cold Plume Release Analysis: Continued testing over a range of conditions. Results will be use to validate cold plume models and to assist in verifying appropriate set back distances.
    - Sensor Placement Guidance: An expert group consisting of sensor experts from NREL and JRC and computational fluid dynamics experts. The initial system will be ISO containers.
- Verification technology
  - Verification of FCEV crash test requirements (GTR and FMVSS).
  - Verification of FCEV tailpipe emissions requirements (GTR and FMVSS).
- Document development
  - SAE Technical Information Report J3089 "Characterization of On-board Vehicular Hydrogen Sensors:" The first draft is completed, but revisions are on-going and additional annexes are being considered.
  - ISO TC197/WG 28 (fuel quality verification): The document does not yet include requirements for on-site measurements.
- Expert input and guidance
  - SAE Fuel Cell Vehicle Crash Testing Safety Guidelines Task Force
  - SAE Fuel Cell Safety Task Force
  - ISO TC/158 WG 7: Fuel quality analytical methods
  - ISO TC/197 WG 27: FCEV fuel quality requirements
  - ISO TC/197 WG 28: Fuel quality verification

Strategic Partnerships and Collaborations

- DOT/Transport Canada to support FCEV crash test and tailpipe emission verification, in support of the GTR and FMVSS.
- Industrial partners to qualify sensor and validate sensor-based analytical methods.
- IET–JRC Sensor laboratory collaboration.
- Hydrogen Safety Committees including International Energy Agency Hydrogen Implementing Agreement and the International Association for Hydrogen Safety.

SPECIAL RECOGNITIONS & AWARDS/ PATENTS ISSUED

1. NREL ROI-15-119: **"**In-Situ, Low-Cost, Low-Pressure Interface to a Fuel Contaminant Analyzer within a High Pressure Hydrogen Dispenser" (W. Buttner and K. Harrison). (undergoing NREL internal review)

FY 2016 PUBLICATIONS/PRESENTATIONS

Presentations

1. "Overview of the U.S. DOE Hydrogen Safety, Codes and Standards Program--Part 4: Hydrogen Sensors," W.J. Buttner, C. Rivkin, R. Burgess, Eric Brosha, Rangachary Mukundan, C. Will James, and Jay Keller, Sixth International Conference on Hydrogen Safety (October 19–21) Yokohama, Japan.

2. "Hydrogen Monitoring Requirements in the Global Technical Regulation on Hydrogen and Fuel Cell Vehicles," W. Buttner, C. Rivkin, R. Burgess, K. Hartmann, I. Bloomfield, M. Bubar, M. Post, L. Boon-Brett, E. Weidner, and P. Moretto, Sixth International Conference on Hydrogen Safety (October 19–21) Yokohama, Japan.

3. (Invited Talk) Hydrogen Sensor--Overview of the Sensor Laboratory; Bill Buttner, Carl Rivkin, Robert Burgess, Japanese Automotive Research Institute (JARI) (October 23, 2015), Tokyo, Japan.

4. "Sensor Testing Lab Overview," Bill Buttner, Carl Rivkin, Robert Burgess, K. Hartmann, Ian Bloomfield, M. Bubar, K. Schmidt, H. Wright, DOE Hydrogen Codes and Standards Tech Team (May 12, 2016), Telecom Meeting.

5. "NREL Hydrogen Sensor Testing Laboratory," William Buttner, C. Rivkin, R. Burgess, M. Bubar, K. Hartmann, K. Schmidt, H. Wright, U.S. Department of Energy Hydrogen and Fuel Cell Program Annual Merit Review and Peer Evaluation (June 6–10, 2015) Washington, D.C.

6. "Analyzer for FCEV Tailpipe Hydrogen Emissions as Specified in the Global Technical Regulation Number 13," William Buttner, C. Rivkin, R. Burgess, M. Bubar, K. Hartmann, and Eveline Weidner, 21st World Hydrogen Energy Conference (June 13–26, 2016) Zaragoza, Spain.

7. "Impact of Environmental Parameters on H_2 Sensor Performance," William Buttner, C. Rivkin, R. Burgess, K. Hartmann, M. Bubar, and E. Weidner, 21st World Hydrogen Energy Conference (June 13–26, 2016) Zaragoza, Spain.

8. "Sensor for hydrogen concentration in Natural Gas," E. Weidner, R. Ortiz Cebolla, C. Bonato, L. Wooninck, and W. Buttner, 21st World Hydrogen Energy Conference (June 13–26, 2016) Zaragoza, Spain.

9. "The NREL and JRC Sensor Test Laboratories Instrumentation and Methods for Hydrogen Sensor Performance Verification,"

W. Buttner, M. Post, L. Brett-Boon, G. Black, V. Palmisano, C. Rivkin, R. Burgess, E. Weidner, and R. Ortiz-Cebolla, 21st World Hydrogen Energy Conference (June 13–16, 2016) Zaragoza, Spain.

10. "NREL and JRC Sensor Test Laboratories Activity in Support of Codes, Standards, and Regulations," W. Buttner, C. Rivkin, R. Burgess, E. Weidner, and Pietro Moretto, Experts Meeting of the International Energy Agency, Hydrogen Implementation Agreement Task 37 (Safety) (June 17) San Sebastian, Spain.

11. (Invited Talk) Part I: NREL and NREL's Fuel Cell & Hydrogen Program; Part II: DOE SCS/NREL Hydrogen Sensor Technology Program, Bill Buttner, Carl Rivkin, Robert Burgess, (Matt Post), Hannah Wright, Kara Schmidt, Kevin Hartmann, Max Bubar, Ian Bloomfield, Joint Research Centre, Institute for Energy and Transport, Clean Air Divison, (June 24, 2016), Petten, the Netherlands.

12. "Hydrogen Detection in FCEV Crash Tests," William Buttner, Kara Schmidt, Matt Post, Telecom meeting of the SAE Hydrogen Fuel Cell Vehicle Crash Testing Safety Guidelines Task Force, August 17, 2016.

Journal Articles and Meeting Papers

1. "Overview of the U.S. DOE Hydrogen Safety, Codes and Standards Program--Part 4: Hydrogen Sensors," W.J. Buttner, C. Rivkin, R. Burgess, Eric Brosha, Rangachary Mukundan, C. Will James, and Jay Keller, Proceedings of the Sixth International Conference on Hydrogen Safety (October 19–21) Yokohama, Japan.

2. "Hydrogen Monitoring Requirements in the Global Technical Regulation on Hydrogen and Fuel Cell Vehicles," W. Buttner, C. Rivkin, R. Burgess, K. Hartmann, I. Bloomfield, M. Bubar, M. Post, L. Boon-Brett, E. Weidner, and P. Moretto, Sixth International Conference on Hydrogen Safety (October 19–21), Yokohama, Japan.

3. "Analyzer for FCEV Tailpipe Hydrogen Emissions as Specified in the Global Technical Regulation Number 13," William Buttner, C. Rivkin, and R. Burgess, M. Bubar, K. Hartmann, and Eveline Weidner, International Journal of Hydrogen Energy (2016) in press.

4. "Analyzer for FCEV Tailpipe Hydrogen Emissions as Specified in the Global Technical Regulation Number 13," William Buttner, C. Rivkin, R. Burgess, M. Bubar, K. Hartmann, and Eveline Weidner, Extended Abstract, 21st World Hydrogen Energy Conference (June 13–26, 2016), Zaragoza, Spain.

5. "Impact of Environmental Parameters on H_2 Sensor Performance," William Buttner, C. Rivkin, R. Burgess, K. Hartmann, M. Bubar, and E. Weidner, Extended Abstract, 21st World Hydrogen Energy Conference (June 13–26, 2016), Zaragoza, Spain.

6. "Sensor for Hydrogen Concentration in Natural Gas" E. Weidner, R. Ortiz Cebolla, C. Bonato, L. Wooninck, and W. Buttner, Extended Abstract, 21st World Hydrogen Energy Conference (June 13–26, 2016), Zaragoza, Spain.

7. The NREL and JRC Sensor Test Laboratories Instrumentation and Methods for Hydrogen Sensor Performance Verification," W. Buttner, M. Post, L. Brett-Boon, G. Black, V. Palmisano, C. Rivkin, R. Burgess, E. Weidner, and R. Ortiz-Cebolla, Extended Abstract, 21st World Hydrogen Energy Conference (June 13–26, 2016), Zaragoza, Spain.

Technical Reports

1. "Passive Leak Detection Using Commercial Hydrogen Colorimetric Indicator," Kevin Hartmann, William Buttner, Robert Burgess, and Carl Rivkin, NREL Technical Report (2016).

Book

1. "Sensors for Safety and Process Control in Hydrogen Technology," Thomas Hűbert, Lois Boon-Brett, and William J. Buttner, CRC Press, Taylor and Francis Group, Boca Raton, ISBN 13-978-1-4665-9654-2 (2016).

REFERENCES

1. Addendum 13: Global technical regulation No. 13 Global technical regulation on hydrogen and fuel cell vehicles ECE/TRANS/180/Add.13, July 19, 2013). (see http://www.unece.org/fileadmin/DAM/trans/main/wp29/wp29wgs/wp29gen/wp29registry/ECE-TRANS-180a13e.pdf, accessed July 22, 2015)

2. "ISO 26142 Hydrogen Detector for Stationary Apparatus"

3. Hydrogen, Fuel Cells & Infrastructure Technologies Program Multi-Year Research, Development and Demonstration Plan, Planned program activities for 2005–2015, U.S. DOE Office of Renewable Energy and Efficiency (EERE), 2005. http://www.nrel.gov/docs/fy08osti/39146.pdf

4. "Standard Hydrogen Test Protocols for the NREL Sensor Testing Laboratory," NREL Brochure (see http://www.nrel.gov/hydrogen/pdfs/53079.pdf, accessed July 22, 2016).

5. The International Association for Hydrogen Safety (see http://www.hysafe.org/IAHySafe, accessed July 22, 2016).

6. International Energy Association, Hydrogen Implementing Agreement, Task 37 (see http://ieahia.org/Activities/Task-37-Hydrogen-Safety-Task.aspx, accessed July 22, 2016).

7. "Impact of Environmental Parameters on H_2 Sensor Performance," William Buttner, C. Rivkin, R. Burgess, K. Hartmann, M. Bubar, and E. Weidner, Extended Abstract, 21st World Hydrogen Energy Conference (June 13–26, 2016) Zaragoza, Spain.

8. Onboard Hydrogen/Helium Sensors in Support of the Global Technical Regulation: An Assessment of Performance in Fuel Cell Electric Vehicle Crash Tests, Matthew B. Post, Robert Burgess, Carl Rivkin, William Buttner, Kathleen O'Malley, and Antonio Ruiz, Technical Report NREL/TP-5600-56177 (September 2012).

9. "Analyzer for FCEV Tailpipe Hydrogen Emissions as Specified in the Global Technical Regulation Number 13," William Buttner, C. Rivkin, R. Burgess, M. Bubar, K. Hartmann, and Eveline Weidner, International Journal of Hydrogen Energy (2016) in press.

10. Memorandum of Understanding, Alliance for Sustainable Energy, LLC (National Renewable Energy Laboratory) with Element One, Inc., MOU Number MOU-14-334 (February 28, 2014).

11. "Performance of a Hydrogen Colorimetric Indicator, NREL Commercialization Assistance Program, NCAP Project Number: NCAP16-00085.

12. "Passive Leak Detection Using Commercial Hydrogen Colorimetric Indicator," Kevin Hartmann, William Buttner, Robert Burgess, and Carl Rivkin, NREL Technical Report, in press (2016).

13. Buttner, W., et al., *Steering Committee Progress Report on Hydrogen Sensor Performance Testing and Evaluation under the Memorandum of Agreement between NREL, U.S. DOE and JRC-IET, EC,* NREL Technical Report: NREL/TP-5600-57207 (2012).

14. "Sensors for Safety and Process Control in Hydrogen Technology," Thomas Hűbert, Lois Boon-Brett, and William J. Buttner, CRC Press, Taylor and Francis Group, Boca Raton, ISBN 13-978-1-4665-9654-2 (2016). (see https://www.crcpress.com/Sensors-for-Safety-and-Process-Control-in-Hydrogen-Technologies/Hubert-Boon-Brett-Buttner/p/book/9781466596542, accessed July 22)

15. DOE EERE Small Business Voucher Award. (see https://www.sbv.org; accessed July 22, 2016)

VIII.8 Fuel Cell & Hydrogen Energy Association Codes and Standards Support

Karen Quackenbush (Primary Contact),
Morry Markowitz, Connor Dolan
Fuel Cell and Hydrogen Energy Association (FCHEA)
1211 Connecticut Ave. NW, Suite 650
Washington, DC 20036
Phone: (202) 261-1331
Email: khall@fchea.org

DOE Manager: Will James
Phone: (202) 287-6223
Email: Charles.James@ee.doe.gov

Project Start Date: November 16, 2011
Project End Date: October 31, 2016 - Project continuation and direction determined annually by DOE

Overall Objectives

Enhance and sustain industry participation to enable:

- Timely development of regulations, codes, and standards (RCS) deemed critical by industry for the commercial deployment of hydrogen and fuel cell technologies and the infrastructure needed to support them.
- Timely and coordinated industry participation in key forums for safety and RCS development for hydrogen energy and fuel cell technologies.
- Efficient, productive, and timely information exchange between the hydrogen and fuel cell industry, regulatory officials, codes and standards development organizations, and other interested parties by providing a common, current, and factual information base.

Fiscal Year (FY) 2016 Objectives

- Optimize technical consistency in national and international codes, standards, and regulations. The 2016 focus is on United States model codes and national and international standards on hydrogen fueling stations and components.
- Optimize industry participation in developing technical requirements.
- Develop and promulgate safety-related information resources and lessons learned with first responders, authorities having jurisdiction, and other key stakeholders.

Technical Barriers

This project addresses the following barriers identified in the DOE Fuel Cell Technologies Office Multi-Year Research, Development, and Demonstration (MYRDD) Plan, Section 3.7: Hydrogen Safety, Codes and Standards. This plan can be accessed at http://energy.gov/eere/fuelcells/downloads/fuel-cell-technologies-office-multi-year-research-development-and-22.

(F) Enabling National and International Markets Requires Consistent RCS

(H) Insufficient Synchronization of National Codes and Standards

(J) Limited Participation of Business in the Code Development Process

Contribution to Achievement of DOE Safety, Codes & Standards Milestones

This project will contribute to achievement of the following DOE milestones from the Hydrogen Safety, Codes and Standards section of the Fuel Cell Technologies Office MYRDD Plan.

- Milestone 2.17: Publication of updated international fuel quality standard to reflect fuel cell technology advancement. (3Q, 2018)
- Milestone 2.19: Validate inherently safe design for hydrogen fueling infrastructure. (4Q, 2019)
- Milestone 4.6: Completion of standards for critical infrastructure components and systems. (4Q, 2014)
- Milestone 4.8: Revision of NFPA 2 to incorporate advanced fueling and storage systems and specific requirements for infrastructure elements such as garages and vehicle maintenance facilities. (3Q, 2016)

FY 2016 Accomplishments

- Identified, raised awareness of, and began developing national and international support to fill in technical gaps for micro fuel cell power systems to facilitate national and international harmonization of shipping regulations.
- Managed the development of over 300 draft public inputs to National Fire Protection Association (NFPA) 2, NFPA 55, and the International Fire Code to address key industry needs for fuel cell electric vehicle repair booths and harmonized requirements for defueling, and

addressing inconsistencies or lack of clarity between model codes.

- Managed the development of industry comments to draft international standards for hydrogen fueling components to support harmonization of national and international requirements, and supported these comments in the U.S. Technical Advisory Group and International Organization for Standardization Working Group meetings.

✧ ✧ ✧ ✧ ✧

INTRODUCTION

As the premiere trade association for the fuel cell and hydrogen energy industry, FCHEA utilizes a working group structure to facilitate focused effort in each of the three following applications: portable power, stationary power, and transportation, which includes vehicles and the infrastructure to support them.

FCHEA's project contributes directly to achievement of four of the seven objectives outlined in the Fuel Cell Technologies Office MYRDD Plan, Chapter 3.7, Hydrogen Safety, Codes and Standards by engaging industry to develop consistent technical requirements and harmonized national and international safety, codes, and standards.

APPROACH

FCHEA working groups and monthly facilitation of the National Hydrogen and Fuels Cells Codes & Standards Coordinating Committee provide regular opportunities to engage industry in developing RCS through discussion of priorities, opportunities to participate in technical committees and working groups directly, and opportunities to comment on draft standards. Industry priorities in codes and standards development are captured and tracked in FCHEA's regulatory matrix, which is updated regularly and published quarterly (see Figure 1).

Our bimonthly Hydrogen and Fuel Cell Safety Report, available online at www.hydrogenandfuelcellsafety.info (Figure 2), provides timely information on the progress of developing codes, standards, and regulations to stakeholders including authorities having jurisdiction, emergency responders, industry, researchers, and other interested parties.

RESULTS

Our Portable Power Working Group provided input during the Pipeline and Hazardous Materials Safety Administration Office of Hazardous Materials Safety R&D Forum on interest in classification for novel micro fuel cell systems and testing of modern cartridge designs. This effort supports the following barrier from the MYRDD Plan - *Enabling National and International Markets Requires Consistent RCS*, by ensuring national and international standards for micro fuel cell applications are harmonized, then adopted by international regulations.

Our Transportation Working Group Hydrogen Codes Task Group developed harmonized public inputs for the next development cycles of key model codes. The public inputs

Significance to Commercialization
⇦ More Critical
Moderate Effort

A. Essential To or Enables Commercialization	B. Important to Commercialization	C. Supports Commercialization	
Cargo Shipping regulations of Fuel Cells, Fuel Cell Cartridges, Fuel Cell Engines and Fuel Cell Vehicles: in force now, revised periodically ICAO Dangerous Goods Panel IMO Dangerous Goods Code ADR/ADN Joint Meeting US DOT Transport Canada PHMSA Office of Hazardous Materials Safety held R&D Forum March 23/24. Video and slides to be made available soon.	~~US DOT Harmonization NPRM – HM215L~~ ~~**Proposed rule on Hazardous Materials Harmonization with International Standards** – FCHEA submitted comments supporting harmonization and reiterating comments on HM215K. Both HM215L and the response to the final rule and the response to the appeal on HM215K were published in January 2013. Harmonization with IEC 62282-6-100 for both carry-on and checked baggage, however DOT continues to not be harmonized with inclusion of division 2.1 and 6.3 fuel cartridges for checked baggage. (micro fuel cell applications)~~ ~~Recent publication of DOT rulemaking 49 CFR Part 175~~ ~~[Docket No. PHMSA-2009-0126, Notice No. 15-3]~~ ~~Hazardous Materials; Spare Fuel Cell Cartridges Containing Flammable Gas Transported by Aircraft in Passenger and Crew Member Checked Baggage~~ ~~available at~~ ~~http://www.gpo.gov/fdsys/pkg/FR-2015-03-30/pdf/2015-07328.pdf~~		TRANSPORTATION
Global Technical Regulations (GTRs) for Vehicles: GTR for H2 and FC vehicles was approved in June 2013; will be proposed for adoption into the U.S. FMVSS (could take up to 2 years). Phase II underway. **SAE J2579- H2 Storage Systems (design & performance):** revision published 3/2013. Minor	**ISO 19881 - Gaseous Hydrogen - Land Vehicle Fuel Tanks:** ~~CD is out for vote and comment.~~ Comments from CD have been resolved and document is in DIS phase. **ISO 19882: Thermally-activated Pressure Relief Devices (TPRDs)** ~~Voting underway to approve CD for DIS ballot and provide~~	**SAE J2990-1: Hydrogen and Fuel Cell Vehicle First and Second Responder – Recommended Practice.** Crosswalk/coordination with J2990 and ISO. This document passed ballot and comments received during ballot are being addressed. Required changes are straight-forward and a 14-day affirmation	VEHICLES

FIGURE 1. Sample page from FCHEA's Regulatory Matrix, showing progress in developing codes, standards, and regulations during the first half of 2016

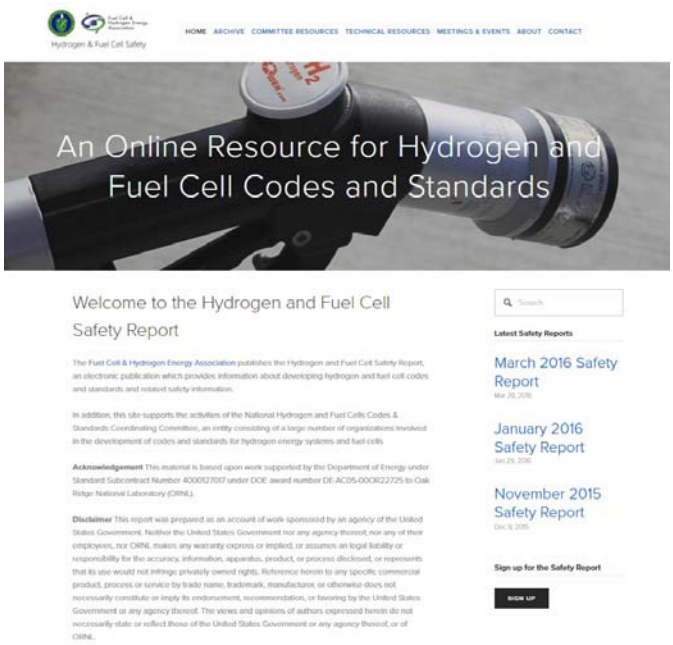

FIGURE 2. Typical Hydrogen and Fuel Cell Safety Report

were solicited from business and experts with operational experience, and focus on harmonizing requirements with other industry-accepted standards and codes. This effort supports the following objective from the MYRDD Plan – *Provides consistent RCS and synchronization of national codes and standards*.

Our Stationary Power Working Group completed a two-year effort to support a fuel cell focus group created by the Telecommunications Industry Association. The working group provided support and fuel cell experts, and assisted in populating a new draft guideline with relevant information from existing codes, standards, and guides. This effort supports the following objective from the MYRDD Plan – *Develop and enable widespread sharing of safety-related information resources and lessons learned with first responders, authorities having jurisdiction, and other key stakeholders*. Working closely with related industries provides consistency in requirements and reduces duplication of effort.

Publication of our Regulatory Matrix and the Hydrogen and Fuel Cell Safety Report keep stakeholders informed of the progress and issues encountered in the development of RCS. It has introduced industry to the many new working groups in the International Organization for Standardization Technical Committee 197 and the call for participation in United States standards committees. The integrated calendar of events aids in scheduling meetings. Facilitation of the monthly web-based meetings of the National Hydrogen and Fuel Cells Codes and Standards Coordinating Committee provides a regular forum to coordinate and align efforts in standards activities and harmonize requirements. This effort contributes to the DOE goal to *develop and enable widespread sharing of safety-related information resources and lessons learned with first responders, authorities having jurisdiction, and other key stakeholders*. These activities also increase participation of stakeholders in development of harmonized RCS.

CONCLUSIONS AND FUTURE DIRECTIONS

FCHEA's Portable Power Working Group will continue to develop international standards through International Techno-Electrical Commission/Technical Committee 105, and work through International Civil Aviation Organization and Department of Transportation to ensure harmonization with international standards for fuel cells as carry on and checked baggage. The Department of Transportation continues to not be harmonized with inclusion of Division 2.1 and 4.3 fuel cartridges for checked baggage (micro fuel cell applications). FCHEA is pursuing inquiry within the Department of Transportation Pipeline and Hazardous Materials Safety Administration to determine options to have these regulations harmonized.

FCHEA's Transportation Working Group will support public inputs in line with industry priorities through the next round of code revisions, and begin to predict potential future needs. FCHEA will continue dialog with component manufacturers to resolve issues in advance of infrastructure roll-out.

FCHEA's Stationary Power Working Group will continue to review international standards and in the United States as well as state regulations to ensure consistency with accepted United States requirements and best practices.

FCHEA will continue to administer the National Hydrogen & Fuel Cells Codes & Standards Coordinating Committee – identify key issues, and document discussions and outcomes. FCHEA will provide industry feedback to the Department of Energy Safety and Codes and Standards Subprogram on RCS development needs and priorities; outreach needs and priorities; and R&D needs and priorities to support RCS development activities.

FCHEA will continue to produce the Hydrogen and Fuel Cell Safety Report to report on the developing RCS to increase awareness of published and developing requirements, improve coordination of activities, and improve information transfer.

FY 2016 PUBLICATIONS/PRESENTATIONS

1. Markowitz, Quackenbush, and Dolan; "Fuel Cell & Hydrogen Energy Association Codes and Standards Support;" (project presented at the DOE Annual Merit Review; June 6–9, 2016, Washington, DC).

VIII.9 Compatibility of Polymeric Materials Used in the Hydrogen Infrastructure

Kriston Brooks (Primary Contact),
Kyle Alvine (PNNL), Edward Duranty (PNNL),
Nalini Menon (Sandia National Laboratories),
Barton Smith (ORNL), Amit Naskar (ORNL),
Mike Veenstra (Ford)

Pacific Northwest National Laboratory (PNNL)
P.O. Box 999
Richland, WA 99352
Phone: (509) 372-4343
Email: kriston.brooks@pnnl.gov

DOE Manager: Will James
Phone: (202) 287-6223
Email: Charles.James@ee.doe.gov

Subcontractor:
Ford Motor Company, Detroit, MI

Project Start Date: October 1, 2015
Project End Date: September 30, 2018

Overall Objectives

- Provide scientific and technical basis to enable full deployment of hydrogen and fuel cell technologies by filling the critical knowledge gap for polymer performance in hydrogen environments.
- Identify applications, conditions, and materials of interest to the hydrogen infrastructure community by interfacing with stakeholders.
- Develop experimental test methodologies for evaluating polymer hydrogen compatibility that are relevant to the stakeholder's needs.
- Evaluate relevant polymeric materials with these test methodologies and disseminate the results through literature, databases, or codes and standards organizations to support the deployment of the hydrogen infrastructure.

Fiscal Year (FY) 2016 Objectives

- Gather and evaluate stakeholder input with regards to challenges, materials, and conditions of interest for hydrogen polymeric compatibility.
- Develop standard test methods for evaluating polymer compatibility with high pressure hydrogen; specifically for: (1) pressure cycling tests, (2) in situ tribology tests, and (3) neutron scattering.
- Develop an approach to disseminate these test methods and compatibility data to stakeholders and support the deployment of hydrogen infrastructure.

Technical Barriers

This project addresses the following technical barriers from the Hydrogen Safety, Codes and Standards section of the Fuel Cell Technologies Office Multi-Year Research, Development, and Demonstration Plan.

(A) Safety Data and Information: Limited Access and Availability

(G) Insufficient Technical Data to Revise Standards

(J) Limited Participation of Business in the Code Development Process

(K) No Consistent Codification Plan and Process for Synchronization of R&D and Code Development

Contribution to Achievement of DOE Safety, Codes & Standards Milestones

This project will contribute to achieving the following DOE milestones from Hydrogen Safety, Codes and Standards section of the Fuel Cell Technologies Office Multi-Year Research, Development, and Demonstration Plan.

- Milestone 5.2: Update materials compatibility technical reference. (4Q, 2011 – 2020)

FY 2016 Accomplishments

- Solicited input from over 50 hydrogen infrastructure stakeholders on polymers of interest, test methods currently employed, and challenging operating conditions and applications to identify knowledge gaps for hydrogen compatibility with polymeric materials. Stakeholders included hydrogen system designers, component manufacturers, polymer producers, code committee members, and hydrogen suppliers.
- Based on infrastructure applications such as compressors, valves, hoses, and piping, we have selected an initial set of materials to evaluate with tribology and pressure cycle aging. These include the elastomers Buna-N and Viton®, PTFE as a low temperature appropriate thermoplastic, polyoxymethylene (Delrin®) as a hose material and a HDPE as a piping liner material. These materials offer a good span of the polymers used in infrastructure and will enable sound test methodologies. Further down-select or materials for

consideration will be revisited during the course of the project.

- Developed an in situ hydrogen tribometer at PNNL with the capability of operating under hydrogen pressures up to 345 bar and 99.995% purity. Carried out initial comparative tests on Buna-N material at 345 bar hydrogen and observed increased friction and wear in the hydrogen environment.
- Performed at Sandia National Laboratories a static, isobaric (1,000 bar) soak of target polymer materials: Buna-N, Viton, HDPE, and PTFE. These materials were then evaluated using dynamic mechanical thermal analysis, compression set (elastomers only), polymer volume change, thermal gravimetric analysis/differential scanning calorimetry, tensile strength (thermoplastics only), and micro-computed tomography (micro-CT) analysis before and after high pressure hydrogen exposure.
- Performed small angle neutron scattering, wide angle X-ray diffraction, and small angle X-ray scattering on HDPE samples exposed to a high pressure hydrogen soak.
- Initiated the evaluation of relevant American Society of Mechanical Engineers, ASTM International, and other standards and test methodologies that could be adapted to evaluate hydrogen compatibility with polymers. Also initiated conversations with CSA Group (Canadian Standards Association) on relevant input to "Test Methods for Evaluating Material Compatibility in Compressed Hydrogen Applications—Non-Metals" (CHMC 2) for hydrogen interactions with non-metallics. Ford subcontractor Mike Veenstra was selected as its interim chair.

✧ ✧ ✧ ✧ ✧

INTRODUCTION

Polymers are critical to hydrogen infrastructure applications to reduce cost and mitigate potential design constraints of metallic components. However, unlike metals that have been studied extensively in high pressure hydrogen, there is a significant knowledge gap in the understanding of polymer performance under these conditions. Also, standardized qualification methods and databases of acceptable conditions and polymers are not currently available to the hydrogen design community to guide material selection. The overall goal of this project is to address these knowledge gaps and support stakeholders in the safe selection of polymers for use in the wide range of required applications and conditions for infrastructure needs.

This will be accomplished by developing a technical foundation to understand the effects of high pressure hydrogen environments and pressure cycling on polymers and composites to enable the development of appropriate test protocols for evaluating these materials for hydrogen service. The information generated from tests of target polymeric materials will be disseminated to interested stakeholders and standards and code development organizations.

APPROACH

The project consists of four main tasks: (1) gather information from stakeholders, (2) develop test methodologies, (3) characterize polymers for hydrogen compatibility, and (4) disseminate the information generated. The information gathered from stakeholders will be used to ensure that the materials being evaluated, the range of conditions of study, and the testing protocols being developed as part of this project will benefit stakeholders from polymer, component, and system manufacturers. The aim of the test methodologies being developed is to generate a set of appropriate experimental guidelines to evaluate hydrogen compatibility. As a by-product of this test methodology development, the project will also develop a partial database of the hydrogen effects on certain polymers used to generate these tests. Because properties differ widely for a single polymeric material based on its additives and processing approach, testing results would be meaningless unless key polymer characteristics are understood. The project will fully characterize the baseline properties of the polymers to allow others to compare their materials to those that were tested. The information generated will be disseminated through material databases, standards organizations, and peer-reviewed journals.

RESULTS

Approximately 20 stakeholders have provided feedback (to date) to the questionnaire requesting information about the knowledge gaps for compatibility of hydrogen with polymers. The challenges with hydrogen compatibility most often cited in the questionnaire results were rapid pressure transients, wear and abrasion of valves, and long-term impacts of pressure cycling. Based on these results, it appears that the pressure cycling tests planned at Sandia National Laboratories and the tribology tests at PNNL do represent concerns of high importance within the hydrogen infrastructure stakeholder community. The questionnaire results suggested a wide range of polymers of interest for testing including thermoplastics, elastomers, and thermosets. These results helped direct the identification of the following polymers for initial test methodology development: (1) Viton and Buna-N as representatives of elastomeric materials; (2) PTFE for its use in low temperature seals; (3) HDPE as a typical pipe liner material; and (4) Delrin as a delivery hose material. Conditions of interest were pressures between atmospheric and 880 bar and temperatures between -40 and

+85°C. This questionnaire result has prompted future plans to expand the range of testing temperatures for the tribology and pressure cycling in future years. We are continuing to reach out to additional stakeholders as they are brought to our attention as the project progresses.

PNNL is developing test methodologies for in situ high pressure hydrogen tribology as tied into application for infrastructure valves and seals. The new PNNL system is a linear reciprocating pin configuration as shown in Figure 1. Frictional load and wear track depth are measured in situ both in air and with 99.995% pure hydrogen up to 345 bar. The current system was developed for room temperature operation but future upgrade plans include sample heating and cooling. Preliminary testing has been performed with Viton and Buna-N in an effort to begin the development of test methodologies, and quantify the impact of the hydrogen environment on the material friction and wear performance. During an initial shake down and debugging phase, researchers have mitigated the lateral wobble of the sample during reciprocation to improve the reproducibility of the system. Preliminary results suggest that for Buna-N, friction and wear may be elevated in hydrogen as compared with identical load conditions in ambient pressure air (Figure 2). Furthermore, a post mortem analysis of the wear tracks with optical profilometry indicates increased damage in the high pressure hydrogen environment as compared to ambient air. Further testing is being carried out to confirm and better understand these preliminary findings.

Sandia National Laboratories performed preliminary experiments to investigate the testing parameters of a high pressure hydrogen system for a select group of two elastomers (Buna-N and Viton) and two thermoplastics (HDPE and PTFE). These polymers were exposed to static conditions of 100 MPa hydrogen at ambient temperature for one week. Both non molded and molded parts made from these polymers were examined to differentiate the effect of residual thermal stresses that can be present in molded specimens and potentially influence performance in a real-life hydrogen application. Characterization of the materials before and after exposure included dynamic mechanical thermal analysis, compression set (elastomers only), polymer volume change, thermal gravimetric analysis/differential scanning calorimetry), tensile strength (thermoplastics only), and micro-CT.

As expected, the elastomeric materials experience significantly more swelling than the thermoplastics as a result of the hydrogen soak. Viton showed a higher change in volume and hydrogen retention than Buna-N. In both materials swelling subsided after the material was removed from the hydrogen, with most of the recovery occurring within the first 48 h. However, some residual swelling remained indefinitely. Viton's higher capacity to hold hydrogen may be due to the greater amount of free volume in the Viton polymer microstructure compared to Buna-N and agrees with the fact that its solubility coefficient is higher than Buna-N. Furthermore, micro-CT demonstrated that hydrogen produced voids that can be seen around the filler particles in the Viton but were not seen with Buna-N. The elastomers also experienced an increase in compression set with hydrogen exposure as seen in Figure 3. Unexposed Buna-N has a higher compression set than Viton, but Viton showed the larger increase with hydrogen exposure. The dynamic mechanical thermal analysis showed a decrease in

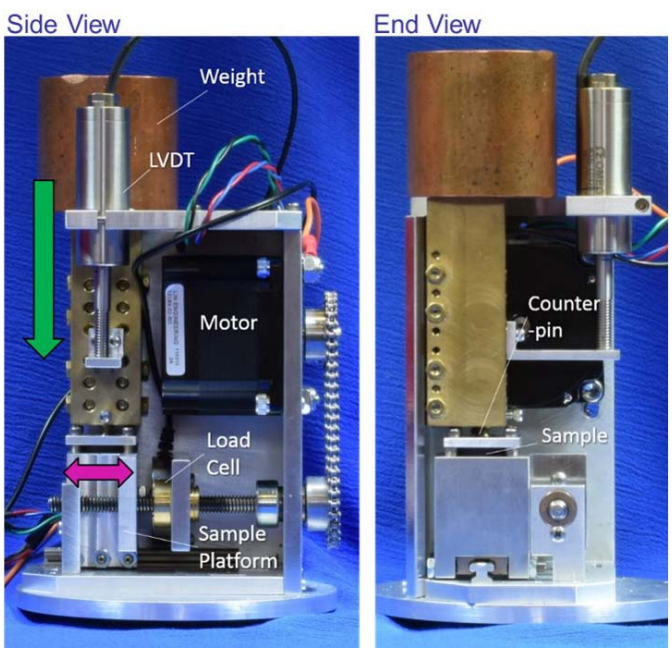

LVDT – Linear variable differential transformer

FIGURE 1. Photograph of the tribometer being developed to operate at hydrogen pressures up to 345 bar

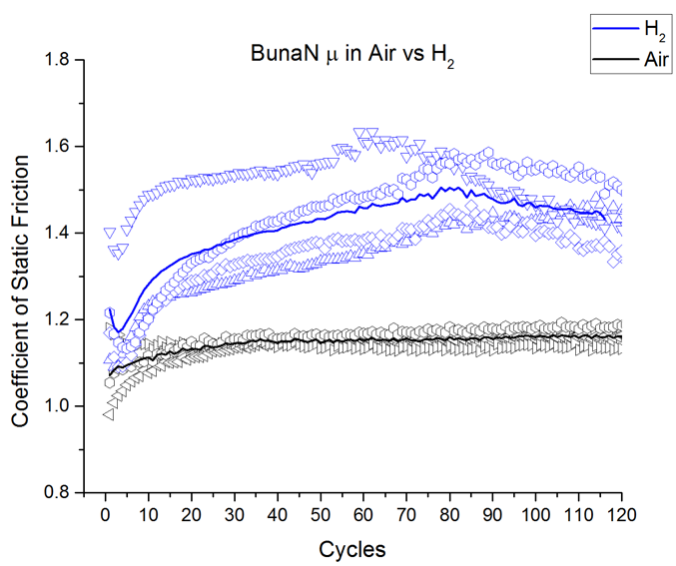

FIGURE 2. Comparison of coefficient of friction for Buna-N in air and 275 bar hydrogen

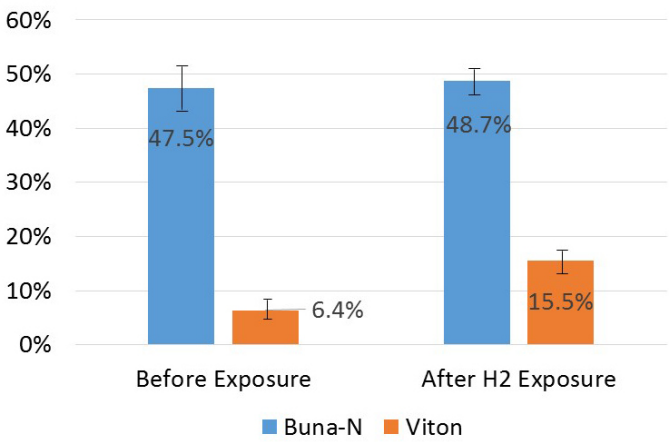

FIGURE 3. Comparison of compression set for Viton and Buna-N both before and after exposure to 1,000 bar hydrogen for 7 days

the storage modulus of the polymers after hydrogen exposure as compared to those before exposure as shown in Table 1. The glass transition temperature was only marginally affected.

In contrast to elastomers, the thermoplastic materials did not exhibit significant changes with hydrogen exposure. There was very little change in density, strength, and glass transition temperature between the samples exposed to hydrogen and those that were not. Unlike the elastomers, these thermoplastics showed a slight increase in the storage modulus with hydrogen exposure rather than a decrease.

Although the stress strain results for the thermoplastics showed a small increase in tensile strength before and after hydrogen exposure, there was a significant increase in the Young's modulus after exposure as shown in Table 2. It was 35% higher for PTFE and 15% higher for HDPE. It is possible that there was a crystalline phase change that results in a stiffening of the material due to the hydrogen exposure.

To address the changes found in the thermoplastic samples from Sandia National Laboratories, the samples exposed to hydrogen were provided to Oak Ridge National Laboratory (ORNL) for X-ray and neutron scattering studies. Both wide angle X-ray diffraction and small angle X-ray scattering were performed with the samples. Of particular interested was the impact of the hydrogen soak on the HDPE which showed a discoloration after hydrogen exposure and rapid decompression. Wide angle X-ray diffraction was performed on the pre- and post-exposure HDPE samples and the change in the patterns demonstrate different intensity ratios of orthorhombic (110) and (200) diffraction peaks. This change suggests that applied high pressure hydrogen induced lamellar rotation along the in-plane direction (see Figure 4). Evaluation with small angle X-ray scattering also showed a change in intensity (q) as a function of hydrogen exposure. The scattering upturn at low-q indicates the formation of micro voids while the peak shift to higher q values indicates that the inter-lamellar distance was compressed from 26.9 to 25.4 nm with hydrogen exposure. These changes in material

TABLE 1. Dynamic Mechanical Thermal Analysis Results Before and After Hydrogen Exposure

	Before Hydrogen Exposure		After Hydrogen Exposure	
Polymer Properties	T_g (°C)	Storage Modulus (MPa)	T_g (°C)	Storage Modulus (MPa)
Buna-N	-32	34.0 ± 2	-31	19.9 ± 3.7
Viton	-2	10.7 ± 0.5	-3	5.4 ± 1.4
HDPE	-110	848 ± 7	-111	913 ± 25
PTFE	34, 137*	431 ± 12	36, 137*	441 ± 14

*PTFE shows two T_g because of possible separation of components

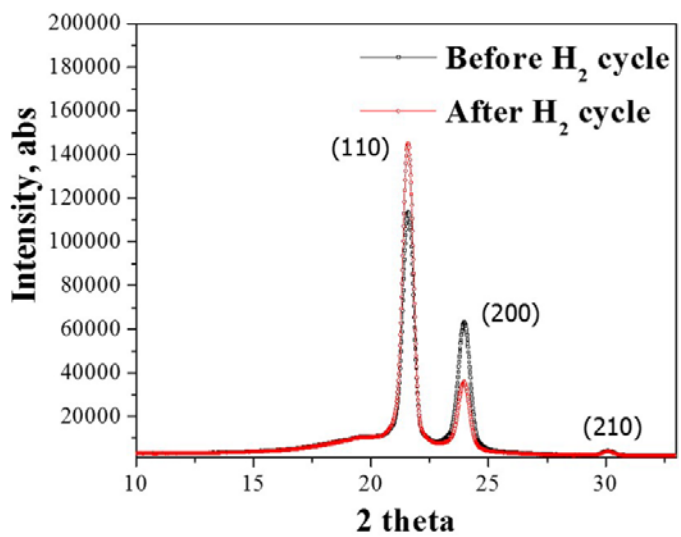

FIGURE 4. Wide angle X-ray diffraction patterns of HDPE both before and after exposure to 1,000 bar hydrogen for 7 days

TABLE 2. Stress–Strain Properties of the Thermoplastic Materials Before and After Hydrogen Exposure

	Before Hydrogen Exposure			After Hydrogen Exposure		
Polymer Properties	Young's Modulus (MPa)	Yield Stress (MPa)	Strength (MPa)	Young's Modulus (MPa)	Yield Stress (MPa)	Strength (MPa)
HDPE	863	20.3	24.0	990	22.3	25.8
PTFE	493	8.8	24.4	667	9.1	25.4

properties will help us better understand the fundamental polymer changes that drive their compatibility with hydrogen.

CONCLUSIONS AND FUTURE DIRECTIONS

Work has begun to address the knowledge gaps that exist in regards to the performance and degradation of polymers in hydrogen environments. Stakeholder feedback has been elicited to assist the project in identifying the applications of concern, polymers to be tested, and temperature and pressure conditions. An in situ tribology system has been developed and tested with elastomers. Preliminary results indicate high pressure hydrogen can impact the frictional properties of the materials. Preliminary high pressure hydrogen soak tests were performed with the initial materials. Significant differences in the response to physical tests were observed for the thermoplastic and elastomeric materials evaluated after hydrogen exposure. Analysis with X-ray scattering identified polymer microstructural changes as well. A high pressure cycling manifold for pressure cycle aging has been designed and is in the initial stages of assembly for further polymer testing.

Future work will continue to develop test procedures and conditions for tribological tests and high pressure cycling tests. Although the initial scoping studies are being performed with non-pedigreed materials, as the test procedure and conditions are refined, characterized materials will be used to ensure statistically meaningful results can be produced and compiled into a database. As the samples are produced during the scoping studies, we will evaluate hydrogen effects on the microstructure of the polymers using neutron scattering and X-ray diffraction to provide a fundamental understanding of the microstructural changes in the polymer upon hydrogen exposure. Work has begun to reach out to codes and standards committees such as the Canadian Standards Association to contribute to the next generation documents such as CHMC 2 or SAE 2579. We will continue to be involved in this effort, and these standards documents will be developed in synergy with our technical accomplishments.

FY 2016 PUBLICATIONS/PRESENTATIONS

1. Alvine, K., K. Brooks, et al, "Hydrogen Compatibility of Polymers for Infrastructure Applications," presentation accepted for the 2016 International Hydrogen Conference, Moran, WY, September 2016.

2. Alvine, Brooks, et al., "Hydrogen Compatibility with Polymers: Tribology and Cycle Aging," presentation accepted for ASME 2016 Pressure Vessels and Piping Conference, July 17–21, 2016, Vancouver, British Columbia, Canada, July 2016.

3. Menon, N., A. Kruizenga, A. Nissen, C. San Marchi, K. Alvine, K. Brooks, "Behavior of Polymers in High Pressure Environments as Applicable to the Hydrogen Infrastructure," PVP2016-63713, Proceedings of the ASME 2016 Pressure Vessels and Piping Conference, July 17–21, 2016, Vancouver, British Columbia, Canada, July 2016.

VIII.10 Enabling Hydrogen Infrastructure Through Science-Based Codes and Standards

Chris LaFleur (Primary Contact), Alice Muna, Katrina Groth, Ethan Hecht
Sandia National Laboratories
PO Box 5800 MS 0748
Albuquerque, NM 87185
Phone: (505) 844-5425
Email: aclafle@sandia.gov

DOE Manager: Will James
Phone: (202) 287-6223
Email: Charles.James@ee.doe.gov

Project Start Date: October 1, 2003
Project End Date: Project continuation and direction determined annually by DOE

Overall Objectives

- Enable the growth of hydrogen infrastructure through science and engineering-based codes and standards.
- Enable industry-led codes and standards revision and safety analyses by providing a strong science and engineering basis code improvements.
- Eliminate barriers to deployment of hydrogen fuel cell technologies through scientific leadership in codes and standards development efforts.

Fiscal Year (FY) 2016 Objectives

- Optimize cost and time for station permitting by demonstration of alternative approaches to code compliance.
- Revise/update codes and standards that address critical limitations to station implementation.

Technical Barriers

This project addresses the following technical barriers from the Hydrogen Safety, Codes and Standards section of the Fuel Cell Technologies Office Multi-Year Research, Development, and Demonstration Plan.

(G) Insufficient Technical Data to Revise Standards

(H) Insufficient Synchronization of National Codes and Standards

(K) No Consistent Codification Plan and Process for Synchronization of R&D and Code Development

Contribution to Achievement of DOE Safety, Codes & Standards Milestones

This project will contribute to achievement of the following DOE milestones from the Hydrogen Safety, Codes and Standards section of the Fuel Cell Technologies Office Multi-Year Research, Development, and Demonstration Plan.

- Milestone 2.19: Validate inherently safe design for hydrogen fueling infrastructure. (4Q, 2019)
- Milestone 4.7: Complete risk mitigation analysis for advanced transportation infrastructure systems. (1Q, 2015)
- Milestone 4.8: Revision of NFPA 2 to incorporate advanced fueling storage systems and specific requirements for infrastructure elements such as garages and vehicle maintenance facilities. (3Q, 2016)

FY 2016 Accomplishments

- Developed a benchmark risk value for a Hydrogen Fueling Infrastructure Research and Station Technology (H2FIRST) gaseous hydrogen reference refueling station which demonstrates the use of quantitative risk assessment (QRA) methods, promotes safety through the use of performance criteria rather than explicit prescriptive requirements, and enables a risk-informed compliance option.
- Calculated revised bulk gaseous separation distances using revised risk criteria for adoption by the National Fire Protection Association (NFPA) 2/55 technical committees which will enable more sites to readily accept hydrogen infrastructure.
- Incorporated QRA into the International Organization for Standardization Technical Report 19880-1 Gaseous Hydrogen-Fueling Stations and provided leadership and support for integrating safety assessments into the standard.

✧ ✧ ✧ ✧ ✧

INTRODUCTION

DOE Fuel Cell Technologies Office has identified safety, codes, and standards as a critical barrier to the deployment of hydrogen, with key barriers related to the availability and implementation of technical information in the development of regulations, codes and standards. This project provides the technical basis for assessing the safety of hydrogen fuel cell

systems and infrastructure using QRA and physics-based models of hydrogen behavior. The risk and behavior tools are used to support both alternate methods of code compliant hydrogen infrastructure as well as direct support of code committees in support of science-based revisions that address critical limitations to refueling station implementation. This project provides the scientific basis to ensure that code requirements are consistent, logical, and defensible.

APPROACH

State-of-the-art integrated hydrogen behavior and QRA models are applied to relevant technologies and systems to provide insight into the risk level and risk mitigation strategies with the aim of enabling the deployment of fuel cell technologies through revision of hydrogen safety, codes, and standards. In the short term focus of providing alternative methods for code compliance, a benchmark risk value for an H2FIRST system design utilizing the previously developed template is calculated in order to provide hydrogen information and risk analysis methods to authorities having jurisdiction. This effort will enable hydrogen refueling stations that are unable to explicitly meet prescription code requirements to utilize alternate means allowed by the current code. Implementing the template at a real world hydrogen station planned in California will provide precedence for a performance-based design and will allow the cost and schedule for developing this type of station design to be optimized.

Towards the longer term goal of achieving science-based revisions of codes and standards, a review and revision of the risk-informed code requirements for bulk gaseous hydrogen storage will enable behavior models and technology not available during the 2009 revision to be incorporated in to the risk criteria used to determine these requirements. The bulk liquid hydrogen storage code requirements will also be revised following a similar process once the cold plume release model is validated.

RESULTS

Calculate Benchmark Risk Value

NFPA 2, Hydrogen Technologies Code, allows for the use of alternate means of code compliance, including performance-based design, for hydrogen facilities as a means of complying with the code without strict adherence to the prescriptive code requirements. While the Hydrogen Risk Assessment Model (HyRAM) can be used as a means of evaluating the risk of alternate designs, it can also be used to quantitatively evaluate risks associated with alternate means of code compliance. The establishment and demonstration of alternate means will directly increase the availability of locations for hydrogen fueling stations, reduce the effort required by industry to use alternate approaches and lay the groundwork for similar QRA-backed design processes for other alternative fuels.

The HyRAM software was used to calculate risks of an outdoor, gaseous hydrogen fueling station that is fully compliant with NFPA 2 requirements and is accessible to the public in order to establish benchmark risk values for these metrics for a specific station configuration. Two methods for analyzing a hydrogen fueling station were demonstrated: QRA and consequence-only analysis. The two methods were implemented to provide detailed insight into different aspects of station risk. The benchmark report provided a single example of each approach, applied to the H2FIRST reference station design for a gaseous hydrogen fueling station with a 300 kg/d capacity [1]. The benchmark values calculated are presented in Table 1.

TABLE 1. Summary of Risk Calculations for Prescribed Distances

Cases	Safety Calculation	Baseline Result
Lot Line Separation Distance	Perform **QRA** on H2FIRST reference station to determine potential loss of life metric at 60 ft	The potential loss of life for this scenario is equal to **2.18 x 10^{-5}** fatalities/ system-year.
Parked Vehicle Separation Distance	Perform **consequence** calculation to determine jet flame temperature at 30 ft	The temperature at 30 ft is close to **ambient temperature**.

Update Science Basis of Bulk Hydrogen Separation Distances

The bulk separation distances in NFPA 2/55 are categorized into three groups depending on the hazard scenario and harm criteria used to determine the separation distances. A task group was formed for the purposes of revising the risk-informed distances in the tables. The harm criteria for the bulk gaseous hydrogen analysis performed in 2009 were revisited and revised by the task group. In order to determine the impact of these changes on the distance requirements, we calculated the revised distances for bulk gaseous storage. The resulting reductions in the separations distances are shown in Table 2 which will be proposed for adoption in the 2019 revision to NFPA 2/55.

The task group also worked to apply the risk-informed process to the bulk liquefied hydrogen storage separation distances using the same process as the gaseous storage. We performed a risk prioritization on a published representative liquefied hydrogen system described in the Risk Management Plan Guidance Document for Bulk Liquid Hydrogen Systems 2009 (CGA P-28) utilizing the hazard and operability study in that document. The resulting high risk release scenarios include those that occur during liquid hydrogen transfer operations from a tanker truck to the bulk liquid hydrogen storage tank as well as during normal system operations. These scenarios will be modeled with Sandia's hydrogen

TABLE 2. Draft Updated Values to 2016 NFPA 2 and NFPA 55 Tables with 1.5 Safety Factor

Exposures		Separation Distance			
		>0.10 to 1.7 MPa (>15 to 250 psig)	>1.7 to 20.7 MPa (>250 to 3,000 psig)	>20.7 to 51.7 MPa (>3,000 to 7,500 psig)	51.7 to 103.4 MPa (7,500 to 15,000 psig)
Group 1	Existing	12 m (40 ft)	14 m (46 ft)	9 m (29 ft)	10 m (34 ft)
	Proposed New	**5 m (16 ft)**	**6 m (20 ft)**	**4 m (13 ft)**	**5 m (16 ft)**
Group 2	Existing	6 m (20 ft)	7 m (24 ft)	4 m (13 ft)	5 m (16 ft)
	Proposed New	**5 m (16 ft)**	**6 m (20 ft)**	**3 m (10 ft)**	**4 m (13 ft)**
Group 3	Existing	5 m (17 ft)	6 m (19 ft)	4 m (12 ft)	4 m (14 ft)
	Proposed New	4 m (13 ft)	5 m (16 ft)	3 m (10 ft)	4 m (13 ft)

release model to help revise the distances in the next code cycle so that they are risk-informed and based on sound science and physics for the behavior of release hydrogen.

Codes and Standards Participation

- CSA Hydrogen Gas Vehicle 4.9 and 4.3 – Hydrogen fueling station guidelines have been reviewed by industry and comments received. The CSA standards were both issued after all were resolved and dispositioned.
- Hydrogen Safety Panel – Sandia participated in several hydrogen safety plan reviews for innovative industrial hydrogen implementations.
- International Organization for Standardization Technical Report 19880-1 – Sandia led the incorporation of QRA and safety assessment methodologies into the standard. The safety assessment methodology in TS-19980-1, which is based on the HyRAM methodology, allows countries to follow a common methodology for performing safety assessment with county- or region-specific assumptions and modeling choices. HyRAM was used to support the development of regional examples contained in Annex A.
- NFPA 2 – Sandia is providing ongoing technical leadership in the Bulk Hydrogen Storage Task Group of NFPA 2 Hydrogen Technologies Code. The task group began work on revision and update of the prescriptive requirements for both liquefied and gaseous hydrogen separation distances for the next revision cycle of the code.

CONCLUSIONS AND FUTURE DIRECTIONS

- The template for implementing the performance-based approach will be used to demonstrate a credible alternate means of code compliance as part of the permitting process to demonstrate acceptance of the approach by an authority having jurisdiction in a real-world station.
  - Extend performance-based design template to other hydrogen application where an alternative solution is needed (future).
- The prioritized liquid hydrogen release scenarios will be analyzed with the validated cold plume release model to characterize the unintended release of liquid–vapor mixed-phase hydrogen releases to revise bulk hydrogen storage code requirements.
  - Identify research gaps in evaluating and prioritizing mitigation features in hydrogen systems (future).
  - Incorporate recent research and technological advancements into further revisions to the bulk gaseous storage requirements (future).

FY 2016 PUBLICATIONS/PRESENTATIONS

1. A.C. LaFleur, A.B. Muna, and K.M. Groth. *Fire Protection Engineering Design Brief Template: Hydrogen Refueling Station*, SAND2015-4500, Sandia National Laboratories, June 2015.

2. LaFleur, A.C., "Enabling Hydrogen Infrastructure Through Science-based Codes and Standards." Presented at the 2015 DOE Hydrogen and Fuel Cells Program and Vehicle Technologies Office Annual Merit Review and Peer Evaluation Meeting, June 2015.

3. A.C. LaFleur, A.B. Muna and K.M. Groth. "Application of Quantitative Risk Assessment for Performance-Based Permitting of Hydrogen Fueling Stations." In Proceedings of the International Conference on Hydrogen Safety (ICHS 2015), Yokohama, Japan, October 19–21, 2015.

4. T. Skjold, D. Siccama, H. Hisken, A. Brambilla, P. Middha, K.M. Groth and A.C. LaFleur. "3D Risk management for hydrogen installations (Hy3DRM)." In Proceedings of the International Conference on Hydrogen Safety (ICHS 2015), Yokohama, Japan, October 19–21, 2015.

5. J. Schneider, G. Dang-Nhu, N. Hart, and K. Groth. "ISO 19880-1, Hydrogen Fueling Station and Vehicle Interface Safety Guideline." In Proceedings of the International Conference on Hydrogen Safety (ICHS 2015), Yokohama, Japan, October 19–21, 2015.

6. C. San Marchi, E.S. Hecht, I.W. Ekoto, K.M. Groth, C. LaFleur, B.P. Somerday, R. Mukundan, and T. Rockward. "Advances

in research and development to enhance the scientific basis for hydrogen regulations, codes, and standards." In Proceedings of the International Conference on Hydrogen Safety (ICHS 2015), Yokohama, Japan, October 19–21, 2015.

7. K.M. Groth. "Application of quantitative risk assessment for performance-based permitting of hydrogen fueling stations." Presented at the International Conference on Hydrogen Safety (ICHS 2015), Yokohama, Japan, October 21, 2015.

8. K. Groth. "Safety assessment & mitigation sub-team update." Presented at ISO TC197 WG24 meeting, Tokyo, Japan, October 27, 2015.

9. C. San Marchi, E.S. Hecht, I.W. Ekoto, K.M. Groth, C. LaFleur, B.P. Somerday, R. Mukundan, T. Rockward, J. Keller & C.W. James. "Overview of the DOE hydrogen safety, codes and standards program, part 3: Advances in Research and Development to Enhance the Scientific Basis for Hydrogen regulations, Codes and Standards." Submitted for publication in International Journal of Hydrogen Energy, (Submitted February 2016).

10. K. Groth. "Safety assessment & mitigation sub-team update," Presented at ISO TC197 WG24, Munich, Germany, 22 June 2016.

11. C. LaFleur, A.B. Muna and K.M. Groth. "Application of Quantitative Risk Assessment for Performance-Based Permitting of Hydrogen Fueling Stations." Accepted for publication in International Journal of Hydrogen Energy (Accepted July 2016).

12. A. Muna, C. LaFleur, M. Gresho, C. Rivkin, "*Siting Bulk Hydrogen Storage Systems: Advances in Risk-Informed Siting Procedures in NFPA Codes,*".American Institute of Chemical Engineers, 12th Global Congress on Process Safety, paper submitted to be published in the proceedings of the April 2016 meeting.

REFERENCES

1. Pratt, J., Terlip, D., Ainscough, C., H2FIRST– Reference Station Design Project Deliverable 2-2, SAND2015-2660, Sandia National Laboratories and National Renewable Energy Laboratory, 2014.

IX.0 Systems Analysis Program Overview

INTRODUCTION

The Systems Analysis program supports the decision-making of the Fuel Cell Technologies Office (FCTO) by providing a greater understanding of technology gaps, options, and risks. The Systems Analysis team analyzes the contribution of individual technology components and systems to overall pathways. For example, the team will provide technoeconomic analysis of fuel production to utilization on a lifecycle basis. Analysis is also conducted to assess cross-cutting issues, such as integration of hydrogen and fuel cells with the electric grid for energy storage and hydrogen infrastructure development.

The Systems Analysis program made several significant contributions to the Hydrogen and Fuel Cells Program in Fiscal Year (FY) 2016. The hydrogen financial analysis scenario tool (H2FAST) was expanded to provide in-depth financial and stochastic analysis of hydrogen refueling stations. The impact of improving the fuel cell efficiency on the costs of the fuel cell and storage systems and fuel cell electric vehicle (FCEV) performance was studied. The Greenhouse gases, Regulated Emissions, and Energy use in Transportation (GREET) model continues to be enhanced for the analysis of greenhouse gas (GHG) emissions, petroleum use, and water consumption for emerging renewable hydrogen pathways on a lifecycle basis.

GOAL

The goal of the Systems Analysis program is to provide system-level analysis to support hydrogen and fuel cell technology development and technology readiness by evaluating technologies and pathways, including resource and infrastructure issues, to guide the selection of research, development, and demonstration projects, and to estimate the potential value of specific research, development, and demonstration efforts.

OBJECTIVES

- By 2017, complete assessment of potential employment impacts and establish linkages with U.S. veteran community for growing hydrogen and fuel cell industries.
- By 2017, complete sustainability analysis and develop framework for incorporating metrics (such as greenhouse gas emissions, ecological footprint, economic/societal impact, etc.) into hydrogen production and infrastructure assessments.
- By 2017, complete analysis of program performance, cost status, and potential for use of fuel cells for a portfolio of commercial applications.
- By 2017, complete a preliminary resource analysis supporting the H2@Scale initiative and identify excess hydrogen generation capacity available for hydrogen fueling or other applications.
- By 2019, complete analysis of the potential for hydrogen, stationary fuel cells, fuel cell vehicles, and other fuel cell applications such as grid services. The analysis will address necessary resources, hydrogen production, transportation infrastructure, performance of stationary fuel cells and vehicles, and the system effects resulting from the growth of fuel cell market shares in the various sectors of the economy.
- Provide milestone-based analysis, including risk analysis, independent reviews, financial evaluations, and environmental analysis, to support the fuel cell technologies' needs prior to technology readiness.
- Periodically update the lifecycle energy, petroleum use, and greenhouse gas and criteria emissions analysis for technologies and pathways for fuel cell technologies to include technological advances or changes.

FY 2016 STATUS

The Systems Analysis program focuses on examining the economics, benefits, opportunities, and impacts of fuel cells and renewable fuels with a consistent, comprehensive analytical framework. Analysis conducted in FY 2016 included assessment of socio-economic impacts such as employment impacts from the penetration of hydrogen and FCEVs, enhancement of the financial analysis tool (H2FAST), quantification of the reduction in fuel cell and

storage system costs resulting from improved fuel cell efficiency, development of an interim hydrogen cost target for early markets, and analysis of lifecycle water use for multiple hydrogen and conventional fuel/vehicle pathways. The Systems Analysis program leverages the key models shown in Figure 1. These models have been developed in prior years for critical program analyses, as evidenced by the completed and ongoing analysis activities in the Accomplishments section that follows.

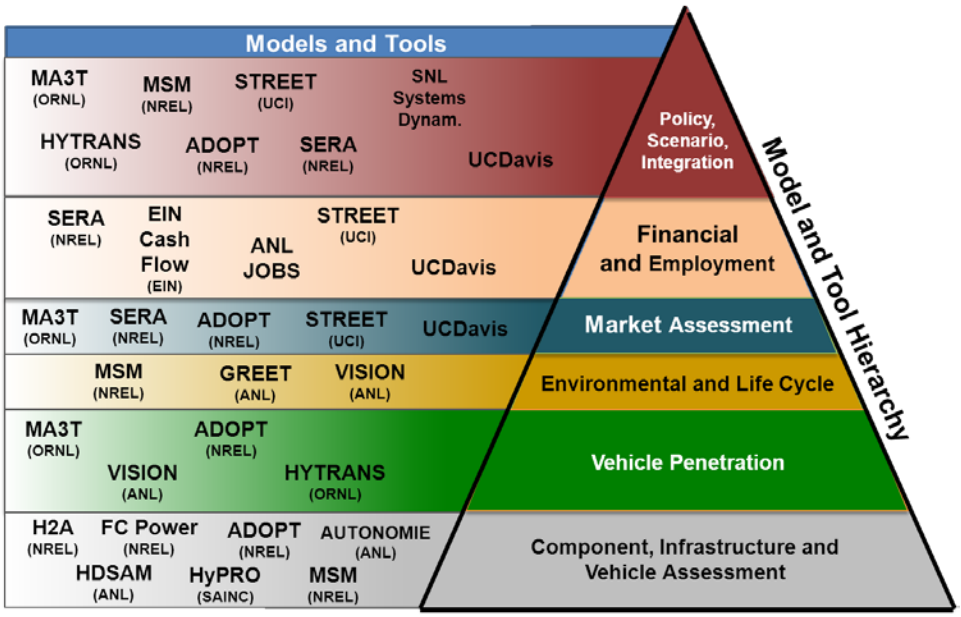

Source: Argonne National Laboratory

FIGURE 1. Systems Analysis models and tools (see Section XII: Acronyms, Abbreviations, and Definitions, for full model and organization names)

FY 2016 ACCOMPLISHMENTS

Models and Systems Integration

Lifecycle Analysis of Emerging Hydrogen Production Technologies

The GREET model has been used by DOE to evaluate the environmental footprint of fuel production, vehicle production, and vehicle operation. In this preliminary study, three emerging hydrogen production technologies, including dark fermentation of lignocellulosic biomass (DF), high temperature electrolysis with a solid oxide electrolyzer cell (SOEC), and reforming of biomass-derived liquid (BDL), have been incorporated into the GREET model. Figure 2 shows the lifecycle GHG emissions from the three hydrogen production pathways evaluated; the major GHG emission sources are identified and compared to conventional hydrogen production technologies such as steam methane reforming (SMR) and electrolysis. The analysis showed that hydrogen produced from DF, SOEC, and BDL can reduce well-to-wheels GHG emissions by 26%, 82%, and 43%, respectively, when compared to hydrogen produced from SMR. The corresponding GHG emission reductions are 58%, 90%, and 68%, respectively, when compared to a gasoline internal combustion engine vehicle on a per-mile-driven basis. The GREET model will continue to be expanded to include other emerging hydrogen production technologies such as solar thermochemical, photobiological, and photoelectrochemical. (Argonne National Laboratory [ANL])

The Hydrogen Financial Analysis Scenario Tool (H2FAST)

The H2FAST tool has been enhanced to provide quick and convenient in-depth financial analysis for hydrogen fueling stations. H2FAST is available in two formats: an interactive online tool and a downloadable Excel spreadsheet. The spreadsheet version of H2FAST offers basic and advanced user interface modes for modeling individual stations or groups of up to 300 stations. It provides users with detailed annual finance projections in the form of income

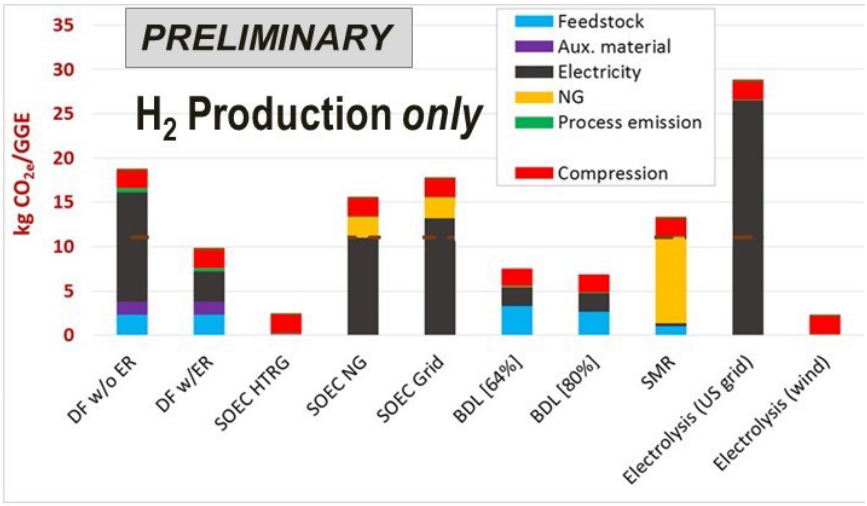

Source: ANL GREET Model

Legend

DF – Dark Fermentation
SMR– Steam Methane Reforming
SOEC – Solid Oxide Electrolysis
HTRG – Hi Temp Gas-Cooled Reactor
BDL – Biological Derived Liquids
ER – Energy Recovery
NG – Natural Gas

FIGURE 2. Lifecycle GHG emissions of hydrogen production pathways

statements, cash flow statements, and balance sheets. It also provides graphical presentation of financial performance parameters for 65 common metrics; lifecycle cost breakdown for each analysis scenario; and common ratio analysis results such as debt/equity position, return on equity, and debt service coverage ratio. The expanded version includes risk analysis for input parameters, assessment of incentives and policies, take or pay contract implications, and additional feedstocks for hydrogen production. It also increases the numbers of stations. (National Renewable Energy Laboratory)

Future developments will include capability to assess investments for multiple stations or components across different timeframes, linkages between supply chain components, and incorporation of externality costs such as water impacts or the social cost of carbon. The tool was thoroughly peer reviewed and issued to the public through the following URL: http://www.nrel.gov/hydrogen/h2fast/.

Environmental Analysis

Lifecycle Analysis

The GREET model was used to compare the GHG emissions associated with current gasoline, hybrid electric, battery electric, and fuel cell vehicles versus future versions of gasoline and alternative fuel vehicles based on expected technology advancements. As shown in Figure 3, the lifecycle GHG emissions of the current alternative vehicles are 20–50% less than the current gasoline internal combustion engine vehicle. The GHG emissions of the future versions of these vehicles are 20–50% lower than the current versions.

Programmatic Analysis

Impact of Fuel Cell System Peak Efficiency on Fuel Consumption and Cost

The impact of different fuel cell targets on vehicle energy consumption and cost was studied using the Autonomie model and compared to conventional gasoline internal combustion powertrains. This study shows that if the 2030 technology targets for fuel cell technologies are achieved, then FCEVs could be economically feasible with present-day vehicle technologies. The current technology targets for 2030 are sufficient to overcome any uncertainties associated with other vehicle technologies. Fuel cell system improvement has the greatest impact on FCEV fuel consumption.

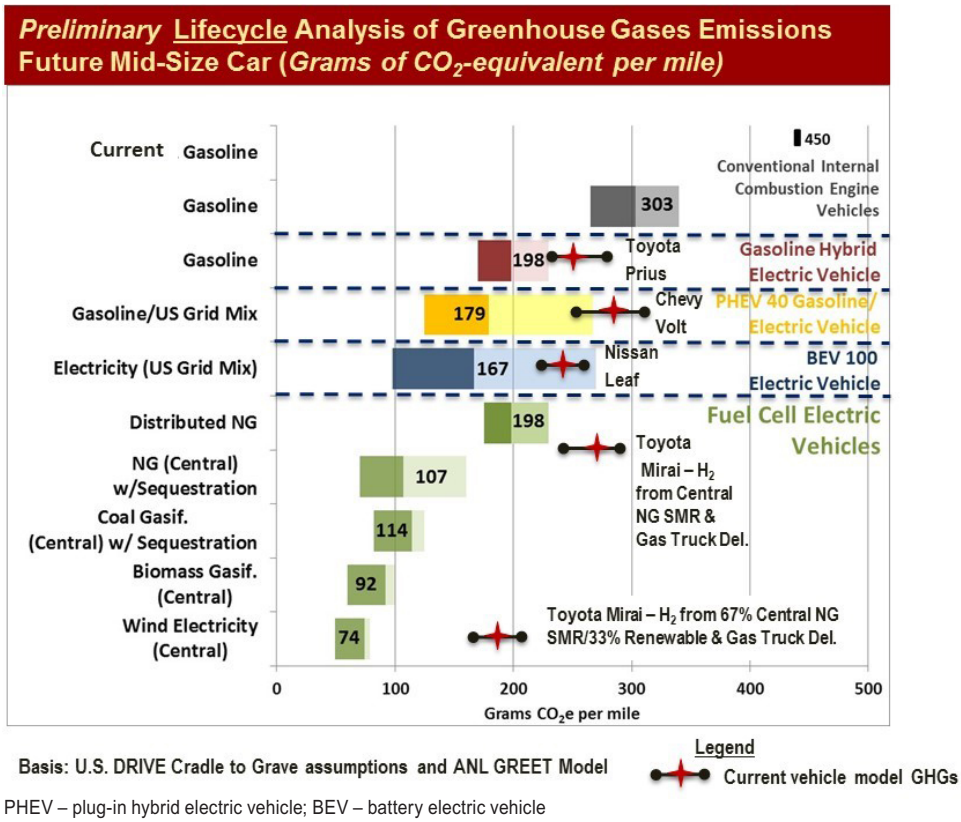

PHEV – plug-in hybrid electric vehicle; BEV – battery electric vehicle

FIGURE 3. Well-to-wheels GHG emissions of H_2 FCEV pathways compared to gasoline internal combustion engine vehicle pathways

Manufacturing costs will decrease mostly due to the decrease in both fuel cell system and hydrogen tank costs. Future work will be focused on examining the marginal benefits of improved fuel cell efficiency and onboard storage versus the marginal cost. (ANL)

Analysis of Current Hydrogen Cost and Targets

The current hydrogen delivered cost was assessed relative to the early market cost target, which was developed to guide and prioritize research and development (R&D) for the Hydrogen and Fuel Cells Program. Figure 4 shows that the current delivered cost of hydrogen is $13/gge–$16/gge compared to the 2020 early market hydrogen cost estimate of $7/gge, untaxed and dispensed at the pump, and the ultimate target of <$4/gge. This current hydrogen cost was documented in DOE Record #15012, which was peer reviewed by a panel that included industrial gas suppliers. URL: https://www.hydrogen.energy.gov/pdfs/15012_hydrogen_early_market_cost_target_2015_update.pdf

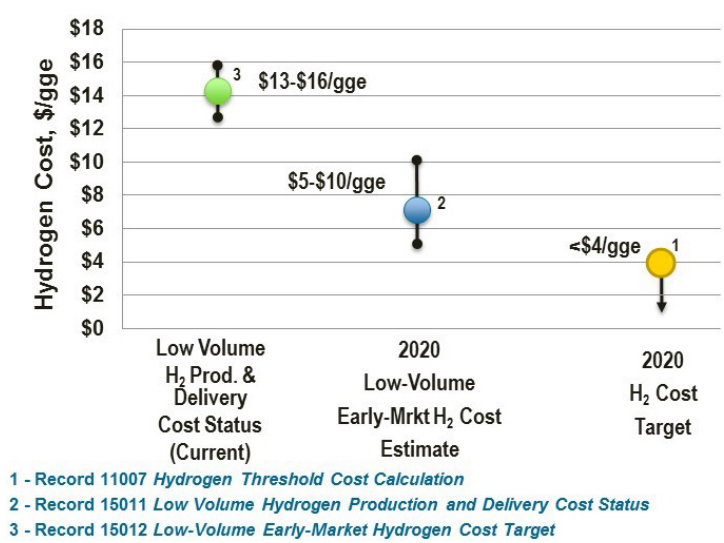

FIGURE 4. Hydrogen cost status and targets

Program Benefits

The implementation of fuel cell technologies R&D has resulted in a cumulative GHG emissions reduction of over 1 million metric tons of CO_2.

Figure 5 shows that the largest GHG reduction has resulted from the stationary fuel cell penetration in the power market. Other fuel cell applications in the transportation sector have resulted in lower GHG reductions due to the lower market penetration in these applications. The ANL GREET model was used to perform this analysis.

Commercial Products and Patents Resulting from DOE-Sponsored R&D

The commercial impact of FCTO funding continues to be analyzed by tracking the commercial products entering the market and patents resulting from FCTO R&D projects. The benefits of FCTO-funded projects continue to grow, as illustrated in Figures 6 and 7. Over 589 patents were awarded and 46 products were commercialized by 2015 as a result of research funded by FCTO in the areas of storage, production, delivery, and fuel cells, which will be highlighted in the FY 2015 Pathways to Commercial Success Report. (Pacific Northwest National Laboratory)

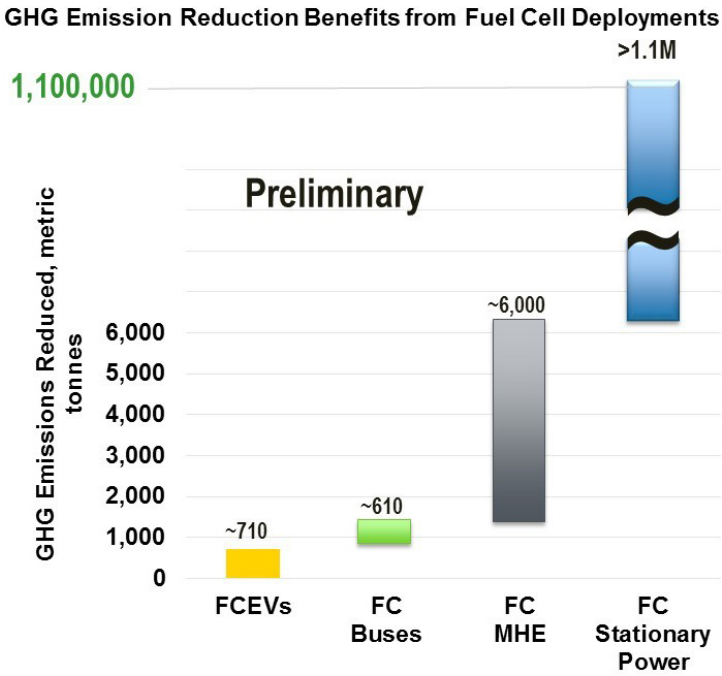

FC – fuel cell; MHE – material handling equipment

FIGURE 5. Cumulative GHG emissions reductions from fuel cell deployments

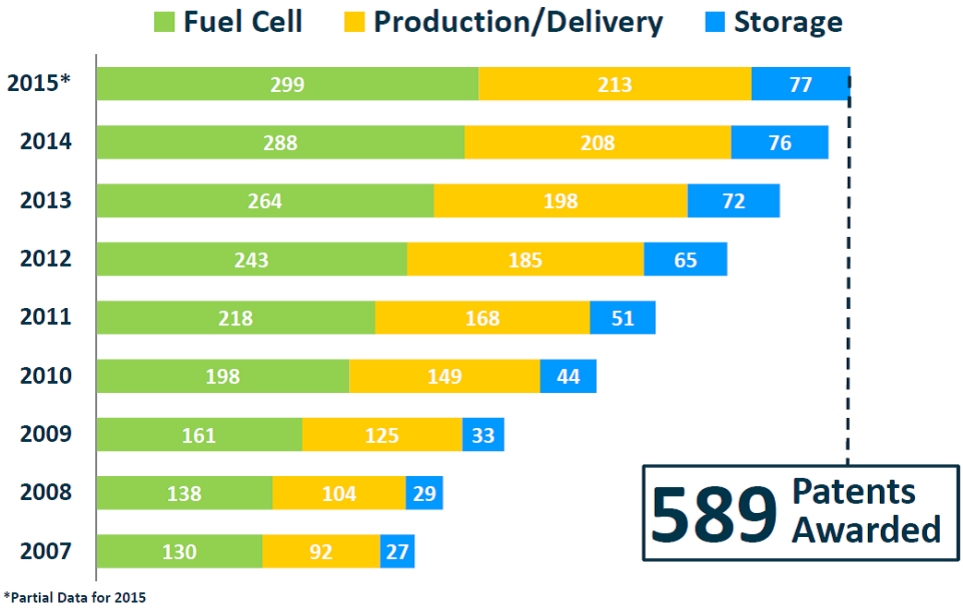

FIGURE 6. Cumulative number of patents awarded

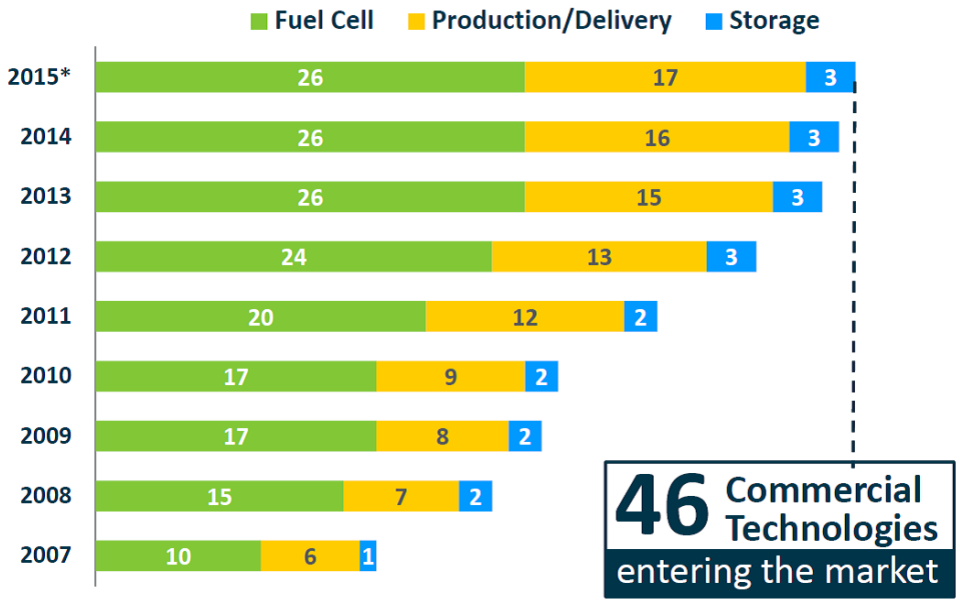

FIGURE 7. Cumulative number of commercial products entering the market

BUDGET

The FY 2016 appropriation for the Systems Analysis program was $3 million (Figure 8). Funding continues to focus on conducting analysis using the models developed by the program. In particular, analysis projects are concentrated on the following:

- Early market adoption of fuel cells
- Lifecycle analysis of water use for advanced hydrogen production technology pathways
- Determining the levelized cost of hydrogen from emerging hydrogen production pathways

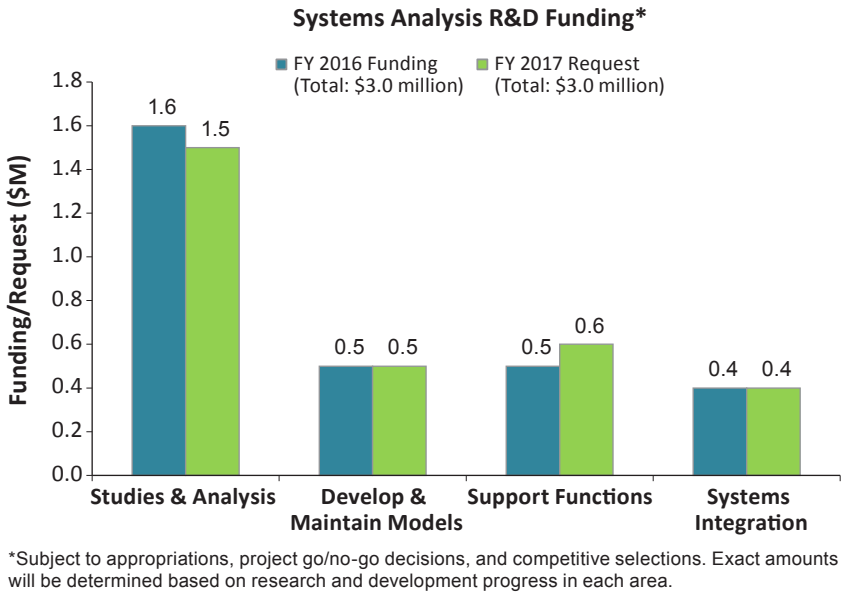

FIGURE 8. FY 2016 appropriations and FY 2017 budget request for the Systems Analysis program

- Quantifying employment impacts of hydrogen and fuel cell technologies
- Calculating the cost of onboard hydrogen storage options
- Estimating the reduction in GHG emissions and petroleum use based on various hydrogen pathways
- Performing hydrogen fueling station business assessments
- Analysis of the use of hydrogen as an energy carrier with applications across sectors (e.g., industrial, grid services, in addition to vehicles) supporting the H2@Scale initiative

The FY 2017 request level of $3 million, subject to congressional appropriation, provides greater emphasis in several areas. Analysis in FY 2017 will focus on the large-scale deployment and utilization of hydrogen through the H2@Scale concept as well as the employment impacts of hydrogen and fuel cell technologies. Analysis of pathway sustainability will be expanded to include regional variability. Additional hydrogen fueling station business assessments such as a mobile refueling scenario will be analyzed, and GREET will be expanded to include lifecycle analysis of GHG emissions and petroleum use for future hydrogen production technology pathways including solar thermochemical, photobiological, and photoelectrochemical. A study is also planned to look at hydrogen production capacity at the national and regional levels. Finally, activities included in the Vehicle Technologies Office's Smart Mobility Decision Science pillar will be leveraged to look at the impacts of consumer behavior.

Fred Joseck
Systems Analyst
Fuel Cell Technologies Office
Office of Energy Efficiency and Renewable Energy
U.S. Department of Energy
1000 Independence Ave., SW
Washington, DC 20585-0121
Office: (202) 586-7932
Email: Fred.Joseck@ee.doe.gov

IX.1 Employment Impacts of Hydrogen and Fuel Cell Technologies

Marianne Mintz
Argonne National Laboratory
9700 S. Cass Ave.
Argonne, IL 60439
Phone: (630) 252-5627
Email: mmintz@anl.gov

DOE Manager: Fred Joseck
Phone: (202) 586-7932
Email: Fred.Joseck@ee.doe.gov

Subcontractors:
- RCF Economic and Financial Consulting, Inc., Chicago, IL
- Energetics, Inc., Colombia, MD

Project Start Date: October 1, 2015
Project End Date: September 30, 2018

Overall Objectives

- Update 2008 DOE Report to Congress, *Effects of a Transition to a Hydrogen Economy on Employment in the United* States.
- Expand the 2008 report by adding materials handling, backup power and other early market applications of fuel cells, and modeling the effects of market development between industries and regions.
- Estimate net impacts of hydrogen and fuel cell (FC) deployment on national and regional employment, earnings, and economic output under alternative scenarios.
- Identify implications of scenario results on work force development.

Fiscal Year (FY) 2016 Objectives

- Select most appropriate methodology and acquire model to be used for analysis.
- Identify industries likely to be impacted by hydrogen and FC deployment. Examine occupational composition of affected industries.
- Develop reference scenario and industry cost vectors.
- Initiate outreach to stakeholders.

Technical Barriers

This project addresses the following technical barriers from the Systems Analysis section of the Fuel Cell Technologies Office (FCTO) Multi-Year Research, Development, and Demonstration Plan.

(A) Future Market Behavior

(B) Stove-piped/Siloed Analytical Capability

(C) Inconsistent Data, Assumptions and Guidelines

(D) Insufficient Suite of Models and Tools

Contribution to Achievement of DOE Systems Analysis Milestones

This project will contribute to achieving the following milestones for the Systems Analysis section of the FCTO Multi-Year Research, Development, and Demonstration Plan.

- Milestones 1.7, 1.10, and 1.14: Perform Studies and Analysis
- Milestones 2.3–2.6: Develop and Maintain Models and Tools

FY 2016 Accomplishments

- Identified and procured the Regional Economic Models, Inc. (REMI) Policy Insight model in a configuration to permit detailed analysis for five regions.
- Summarized baseline trends in regional employment and wages for relevant industries and occupations within REMI.
- Held a web-enabled facilitated workshop ("webshop") with stakeholders to review project plans and obtain input for development of reference and alternative scenarios.
- Compared existing forecasts of market growth and hydrogen and FC penetration in select applications. Assembled input data for construction of reference scenario within REMI.

✧ ✧ ✧ ✧ ✧

INTRODUCTION

The project is analyzing long and short-term economic impacts associated with the deployment of FCs and associated hydrogen infrastructure. Insights from this work will assist FCTO and its stakeholders in estimating employment and other economic benefits from DOE

technology development and in identifying FC markets and regions that are most likely to see growth in jobs and economic activity from the deployment of these technologies. In earlier work, Argonne National Laboratory and RCF Economic and Financial Consulting analyzed economic impacts associated with a large-scale transition to hydrogen and fuel cells. That work formed the basis for a 2008 DOE Report to Congress [1] which is being updated and expanded in this effort.

APPROACH

FCs are being developed for a range of demands and duty cycles, from small portable devices to megawatt-scale, from steady-state to variable power output, and from continuous to quick-start backup operation. Each of these applications represents a unique market with different packaging and integration, installation, and operation and maintenance needs. Not only do these markets differ in size and anticipated growth, they also displace incumbent technologies with different production locations and supply chains. Thus, modeling the net effects of hydrogen and FC deployment requires an understanding of likely applications and their anticipated growth; the penetration of FCs into those markets and their associated hydrogen fueling needs; the cost of FCs, hydrogen, and the existing technologies currently serving those markets; and supply chains for hydrogen and FCs as well as incumbent technologies. Since economic impacts include induced as well as direct and indirect effects, modeling also requires a platform that can capture second-order impacts from the respending of dollars in the economy.

RESULTS

As the initial year of a three-year project, FY 2016 efforts focused on model selection and acquisition, and data collection and evaluation to assist in scenario selection and to provide the context for the overall study.

Model Selection

Following a review of alternative options, the REMI Policy Insight model was selected for this analysis. REMI is a robust, integrated model incorporating elements of (a) input-output analysis which captures transactions between industries; (b) general equilibrium theory which balances supply and demand in response to long-run changes in prices, production, consumption, etc.; (c) econometric analysis; and (d) economic geography which captures effects of industry clustering and labor market access on interregional trade, productivity, and competitiveness. Figure 1 shows the five regions into which the model has been configured for this analysis. Unlike other models, U.S. results are the summation of regional results.

Scenario Development

Reference scenario parameters from the 2008 study were summarized and potential sources for updated estimates were reviewed with DOE and stakeholders at a web-enabled

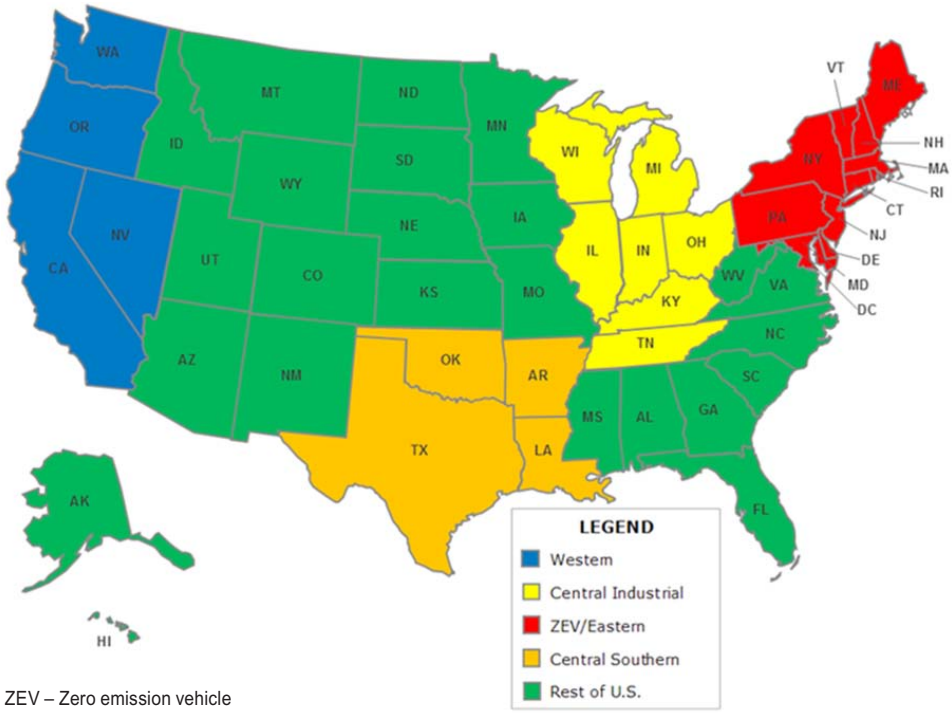

ZEV – Zero emission vehicle

FIGURE 1. Economic analysis regions

webshop and in follow-up communications. Based on those discussions it was agreed that this study's reference scenario should be based on the DOE Energy Information Administration *2016 Annual Energy Outlook*, utilizing existing FCTO-supported tools for any necessary expansion and regionalization.

REMI estimates of initial or baseline employment and wages for each region were summarized by broad industrial and occupational categories to provide a picture of how jobs are expected to evolve in the absence of a concerted effort to deploy hydrogen and FCs. The resulting categories were constructed from the 160 industries and 95 occupational groups contained in REMI. Figure 2 shows annual estimates of employment (in millions of jobs) from 2015 through 2025 for seven occupational categories and two regions. The seven occupational categories represent the occupations likely to see the greatest impact from hydrogen and FC deployment and account for approximately 25% of total employment in these two regions. As shown in Figure 2, the largest occupational category (assemblers, fabricators) is expected to see a decline in jobs over the next decade while the construction category (e.g., pipefitters, carpenters, electricians) is expected to see the most rapid growth.

CONCLUSIONS AND FUTURE DIRECTIONS

FY 2016 work focused on identifying and acquiring the most suitable model for this effort, defining a reference case and beginning work on the largest hydrogen and FC application that will be considered in this analysis, namely light-duty vehicles. Estimation of industry cost vectors for the light-duty vehicle supply chain began in FY 2016 and will conclude by the end of the calendar year. A similar effort to estimate industry cost vectors for other applications (including material handling equipment, backup power, and prime power) will begin in FY 2017.

FY 2016 PUBLICATIONS/PRESENTATIONS

1. Jones, D., 2016. *Summary of 2008 DOE Report to Congress*, Economic Impact of Hydrogen and Fuel Cell Deployment Webshop, Argonne National Laboratory, April 28.

2. Mintz, M., 2016. *Study Rationale*, Economic Impact of Hydrogen and Fuel Cell Deployment Webshop, Argonne National Laboratory, April 28, 2016.

3. Mertes, C., 2016. *Modeling Economic Impacts*, Economic Impact of Hydrogen and Fuel Cell Deployment Webshop, Argonne National Laboratory, April 28.

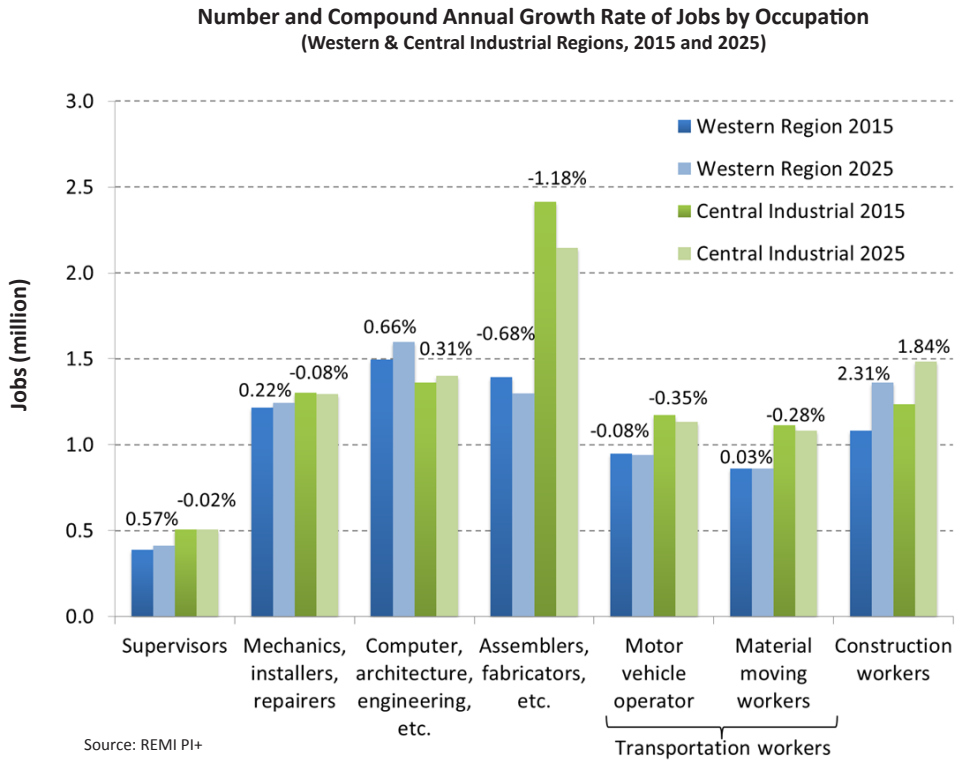

FIGURE 2. Jobs by occupation, western, and central industrial regions, 2015–2025

4. Mertes, C., 2016. *Modeling Economic Impacts of Hydrogen and Fuel Cell Deployment with REMI-PI+*, Regional Economic Models, Inc. Conference, Chicago, June 3.

REFERENCES

1. U.S. Department of Energy, 2008. *Effects of a Transition to a Hydrogen Economy on Employment in the United States: Report to Congress*, July.

IX.2 Life-Cycle Analysis of Water Consumption for Hydrogen Production

Amgad Elgowainy (Primary Contact),
Jeongwoo Han, Uisung Lee, Jeff Li, Jennifer Dunn, and Michael Wang
Argonne National Laboratory
9700 South Cass Avenue
Argonne, IL 60439
Phone: (630) 252-3074
Email: aelgowainy@anl.gov

DOE Manager:Fred Joseck
Phone: (202) 586-7932
Email: Fred.Joseck@ee.doe.gov

Project Start Date: April 2013
Project End Date: Project continuation and direction determined annually by DOE

Overall Objectives

- Incorporate water consumption associated with hydrogen as a transportation fuel for use in fuel cell electric vehicles (FCEVs).
- Compare water consumption of hydrogen for use in FCEVs with other fuel or vehicle systems on a life cycle basis.
- Identify major contributors in upstream supply chain to water consumption.

Fiscal Year (FY) 2016 Objectives

- Review and update water consumption for baseline petroleum fuels and hydrogen production technologies, such as natural gas steam methane reforming (SMR), electrolysis and biomass gasification.
- Examine the impact of various cooling technologies (e.g., single loop vs. recirculating and tower vs. pond) and cooling water source (e.g., freshwater, saline, brackish water and wastewater) in thermoelectricity generation.
- Address outstanding water consumption issues for hydrogen production
  - System boundary
  - Fate of discharged water from a process

Technical Barriers

This project directly addresses Technical Barriers B, C and D in the System Analysis section of the Fuel Cell Technologies Office Multi-Year Research, Development, and Demonstration Plan. These barriers are as follows.

(B) Stove-piped/Siloed Analytical Capability

(C) Inconsistent Data, Assumptions and Guidelines

(D) Insufficient Suite of Models and Tools

Contribution to Achievement of DOE Systems Analysis Milestones

This project contributes to achievement of the following DOE milestone from the Systems Analysis section of the Fuel Cell Technologies Office Multi-Year Research, Development, and Demonstration Plan.

- Task 1.13: Complete environmental analysis of the technology environmental impacts for hydrogen and fuel cell scenarios and technology readiness. (4Q, 2015)
- Task 2.2: Annual model update and validation. (4Q, 2011 through 4Q, 2020)

FY 2016 Accomplishments

- Updated water consumption for petroleum products.
- Evaluated impact of various cooling technologies and cooling water source in thermoelectricity generation.
- Examined wastewater treatment plants (WWTPs) to evaluate impact of discharged water in water consumption factor (WCF) calculations.
- Revised WCFs for hydrogen production via biomass gasification, SMR and electrolysis.
- Expanded the GREET model to include updated and new WCFs.
- Compared water consumption on per mile basis for various fuel and vehicle combinations and showed that FCEVs fueled by H_2 from SMR and biomass gasification consume 37% and 24% less water compared to baseline gasoline internal combustion engine vehicles (ICEVs), respectively.

✧ ✧ ✧ ✧ ✧

INTRODUCTION

Providing a consistent accounting of energy use and emissions associated with the production of transportation fuels, lifecycle analysis has played an important role in decision-making at various places. Recently, Argonne have expanded the lifecycle analysis boundary into water consumption in order to estimate water consumption along the supply chain of different transportation fuels since water consumption is an important sustainability metric. The focus of this study is on hydrogen production pathways since hydrogen is a zero-carbon energy carrier with potential for significant reduction in greenhouse gas and air pollutant emissions. Moreover, hydrogen is essential for processing and upgrading of crude oil and the production of biofuels, such as the processing of heavy crude in refineries and the hydroprocessing of bio-oils.

APPROACH

Water withdrawal is the water uptake from a source by any given process, while water consumption is the net of the withdrawal amount minus the amount returned to the same withdrawal source. Argonne developed WCFs by identifying major contributors in the supply chain to fuel production and developing WCFs for fuel production stages from various data sources. For example, Argonne updated WCFs for petroleum products using a detailed refinery water analysis model developed by Jacobs Consultancy. The WCFs for thermoelectric generation by cooling technology and by cooling water source were developed from Energy Information Administration's database. Also, WCFs for hydrogen production via biomass gasification, SMR and electrolysis were revised from open literature data as well as data provided by industrial sources. Moreover, Argonne examined WWTPs to evaluate impact of discharged water in WCF calculation using open literature data and Environmental Protection Agency's database.

RESULTS

Figure 1 shows the updated WCFs for petroleum products. Since WCFs vary by refinery configuration and refinery cooling technology, three refinery configuration models, each with three water consumption scenarios were examined. The three refinery configuration models included cracking, light coking, and heavy coking refineries. The three water consumption scenarios included base water consumption case as well as low and high water consumption cases, denoted by lower and upper error bars in Figure 1, respectively. As shown in Figure 1, gasoline and liquefied petroleum gas consume more water than the other products because their production involves water-intensive processes, such as alkylation and reformation. Also, more complex refineries (i.e., the heavy coking refinery) are more water-intensive in general than less complex refineries (i.e., the cracking refinery). Note that water consumption in refineries correlates well with energy consumption since cooling is a major water consumption source.

Figure 2 shows the overall and fresh WCFs of thermoelectric generation by North American Electric Reliability Corporation region. The overall WCFs include the consumption of fresh, saline, brackish water or treated wastewater. The national average of overall and fresh WCFs for thermoelectric generation are 0.36 gal/kWh and 0.29 gal/kWh, respectively. Thermoelectric power plants in the Southwest Power Pool are the most water-intensive at 0.47 gal/kWh while those in Northeast Power Coordinating Council (NPCC) are the least water intensive at 0.08 gal/kWh. The map in Figure 2 shows the location and generation of thermoelectric power plants using non-freshwater for cooling, most of which are located near the coastal areas. As a result, the fresh WCFs in Florida Reliability Coordinating Council (FRCC), Western Electricity Coordinating Council (WECC) and NPCC are significantly lower than the overall WCFs in each of these regions (0.07 gal/kWh vs. 0.24 gal/kWh in FRCC, 0.25 gal/kWh vs. 0.39 gal/kWh in WECC, and 0.03 gal/kWh vs. 0.08 gal/kWh in NPCC).

Figure 3 presents the updated WCF for hydrogen production via biomass gasification using two data sources: Spath et al. (2005) and Choi et al. (2009) [1,2]. The resulting WCFs of hydrogen from biomass gasification from these two independent sources are quite similar (3.3 gal/kg H_2 and 3.7 gal/kg H_2) when excluding the discharged water that goes into WWTPs. The process water consumption is in the range of 1.4–1.7 gal/kg H_2, while the cooling water consumption is 1.9–2 gal/kg H_2.

Approximately, 0.7–1 gal of WCF shown in Figure 3 represents discharged water that goes to WWTPs. Thus, the fate of wastewater and the energy, and the water consumption

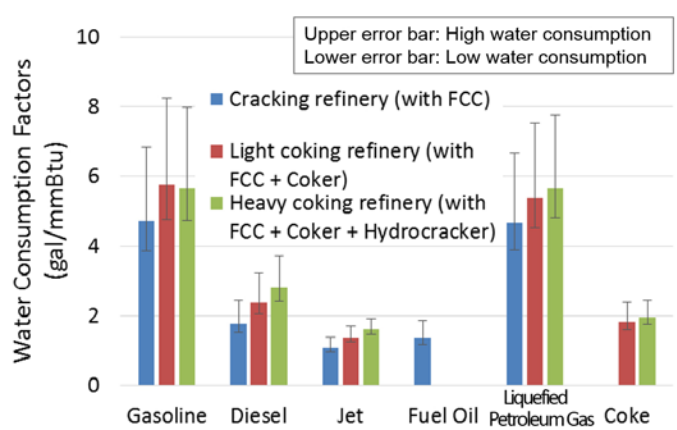

FCC – Fluid catalytic cracking

FIGURE 1. Water consumption factors for petroleum products

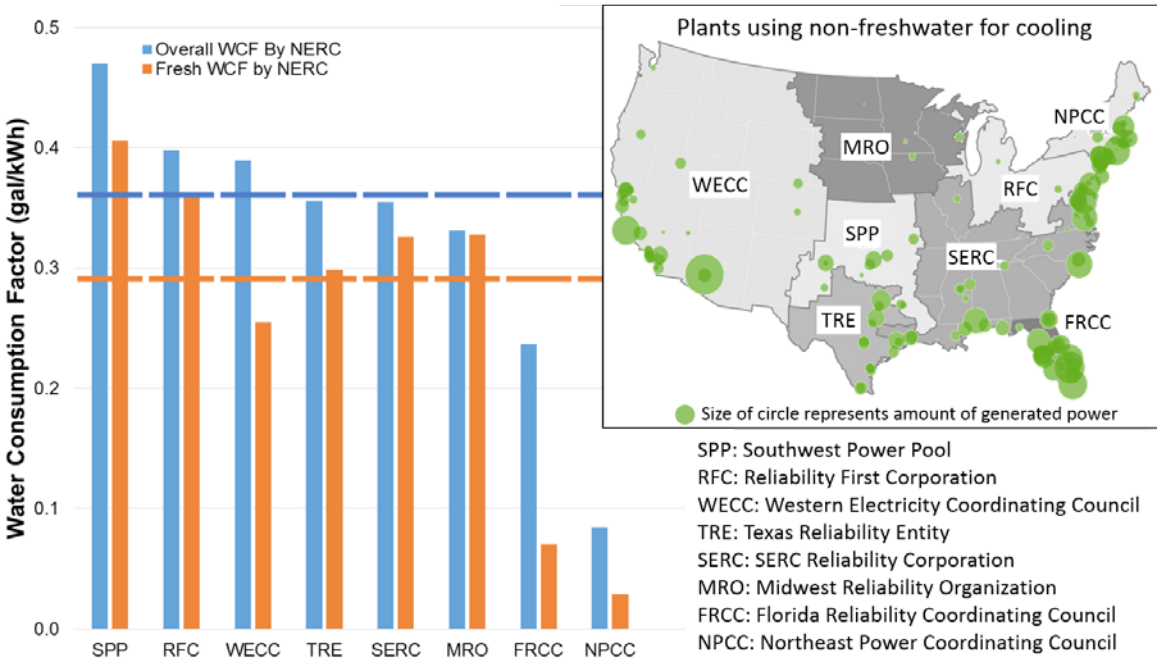

FIGURE 2. Overall and fresh water consumption factors of thermoelectric generation by region

associated with WWTPs were also investigated. In a WWTP, there are two sources of water consumption: the water consumed in the upstream of electricity generation, and the water consumption by solid disposal. The water consumption associated with wastewater treatment use of electricity were estimated at 0.0028 gal/gal of treated water (or 0.28%) without internal generation of electricity from biogas. With internal generation of electricity, the WCF for WWTP decreases to 0.03–0.15%. On the other hand, digestate is a key water outlet by solid disposal. From the digestate's typical solid content (17–33%), the water consumption by solid disposal is estimated at only 0.1–0.2%. Moreover, water consumption via evaporation is negligible since water in WWTPs continuously flows. Conclusively, WCF of wastewater treatment is very small and is considered negligible.

Table 1 shows the updated WCFs for hydrogen production via SMR and electrolysis in central production

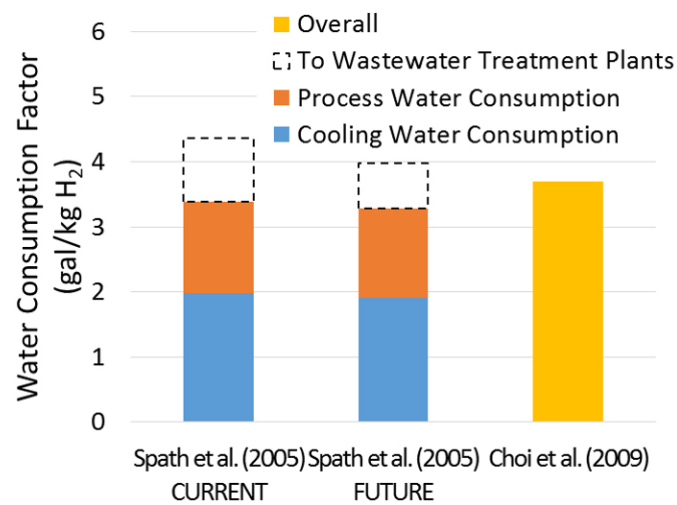

FIGURE 3. Water consumption factors for hydrogen production via biomass gasification

TABLE 1. WCFs for Central and Distributed SMR and Electrolysis Hydrogen Production (gal/kg H_2)

	SMR			Electrolysis	
Process	**Central w/o Carbon Capture**	**Central w/ Carbon Capture**	**Distributed**	**Central**	**Distributed**
Production Process	1.7	1.7	2.5	2.9	2.9
Cooling Loss	0.65	1.15	0	1.2	0
Total	2.4	2.9	2.5	4.1	2.9

w/o – Without; w/ – With

and distributed locations based on information acquired from industry data. One key revision made to these WCFs compared to previous estimates is that the water discharge amount (0.7–3.9 gal/kg H_2) is excluded from the WCF calculations, assuming negligible water consumption by WWTPs. Thus, the updated WCFs for SMR and electrolysis are lower from our previous estimates by 0.7–3.9 gal/kg H_2.

Figure 4 shows the life cycle water consumption per 100 miles for various fuel and vehicle systems of the midsize vehicle class with the fuel economies shown at the bottom of the figure. Figure 4 shows the significant impact of irrigation for corn ethanol on the baseline gasoline ICEV pathway (due to the 10% ethanol blending). The figure also shows the significant impact of water embedded in the U.S. electricity grid mix on the electrolysis and battery electric vehicle pathways. Except for the FCEVs fueled by H_2 from electrolysis, the FCEV pathways consume less water than baseline gasoline ICEV on a life cycle basis. For example, FCEVs fueled by H_2 from SMR and biomass gasification consume 37% and 24% less water compared to baseline gasoline ICEVs, respectively.

CONCLUSIONS AND FUTURE DIRECTIONS

The water consumption factors for hydrogen production via biomass gasification, SMR and electrolysis vary by feedstock source and conversion processes. While hydrogen production from SMR, wind electrolysis and biomass gasification consume less water on a well-to-wheels basis compared to gasoline (E10) ICEV and BEV (using U.S. average generation mix), water consumption for hydrogen production via electrolysis using U.S. average generation mix is higher compared to other hydrogen pathways, BEV and gasoline ICEV. The fate of discharged water in WWTPs shows negligible loss of water during water treatment for its reuse, thus the discharged water is now excluded from our calculations of WCF associated with all fuel production processes. Our future modeling and analysis will address emerging hydrogen production pathways and the variability of water consumption by region for various fuel production pathways.

FY 2016 PUBLICATIONS/PRESENTATIONS

1. Lampert, David J., Hao Cai, and Amgad Elgowainy. 2016. "Well to Wheels: Water Consumption for Transportation Fuels in the United States." *Energy & Environmental Science* 9 (3): 787–802.

REFERENCES

1. Spath, Pamela L, Andy Aden, T. Eggeman, Matthew Ringer, B. Wallace, and J. Jechura. 2005. "Biomass to Hydrogen Production Detailed Design and Economics Utilizing the Battelle Columbus Laboratory Indirectly-Heated Gasifier." NREL/TP-510-37408. Golden, CO: National Renewable Energy Laboratory.

2. Choi, DongWon, David C. Chipman, Scott C. Bents, and Robert C. Brown. 2009. "A Techno-Economic Analysis of Polyhydroxyalkanoate and Hydrogen Production from Syngas Fermentation of Gasified Biomass." *Applied Biochemistry and Biotechnology* 160 (4): 1032–46.

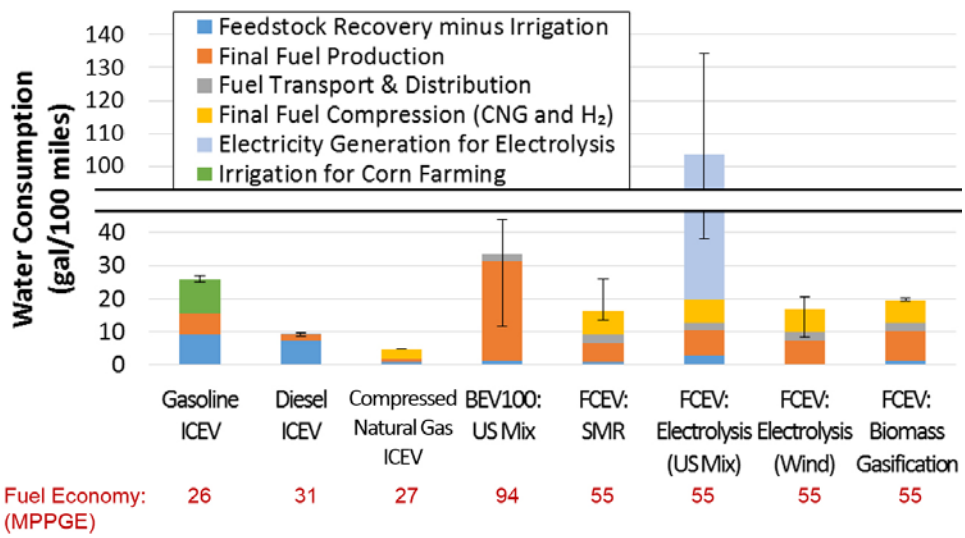

CNG – Compressed natural gas; BEV – Battery electric vehicle

FIGURE 4. Life cycle water consumption for alternative fuel/vehicle systems

IX.3 Impact of Fuel Cell and H_2 Storage Improvements on FCEVs

Aymeric Rousseau
Argonne National Laboratory
9700 S. Cass Avenue
Argonne, IL 60439
Phone: (630) 252-7261
Email: arousseau@anl.gov

DOE Manager: Fred Joseck
Phone: (202) 586-7932
Email: Fred.Joseck@ee.doe.gov

Project Start Date: September 1, 2015
Project End Date: August 31, 2016

Overall Objectives

- Quantify the impact of system improvements on energy consumption and economic viability of fuel cell electric vehicles (FCEVs).

Fiscal Year (FY) 2016 Objectives

- Quantify the impact of fuel cell stack improvement on the cost of driving FCEVs.
- Quantify the impact of hydrogen storage improvement on the cost of driving FCEVs.
- Quantify the impact of fuel cell system improvement on the cost of driving FCEVs.
- Verify whether the current fuel cell and storage technology targets are sufficient to make FCEVs viable, even with the present day vehicle technologies.

Technical Barriers

This project addresses the following technical barriers from the System Analysis section of the Fuel Cell Technologies Office Multi-Year Research, Development and Demonstration Plan.

(A) Future Market Behavior

(C) Inconsistent Data, Assumptions and Guidelines

(D) Insufficient Suite of Models and Tools

(E) Unplanned Studies and Analysis

Contribution to Achievement of DOE Systems Analysis Milestones

This project will contribute to achievement of the following DOE milestones from the Fuel Cells section of the Fuel Cell Technologies Program Multi-Year Research, Development and Demonstration Plan.

- Milestone 1.1: Complete an analysis of the hydrogen infrastructure and technical target progress for hydrogen fuel and vehicles. (2Q, 2011)
- Milestone 1.11: Complete analysis of the impact of hydrogen quality on the hydrogen production cost and the fuel cell performance for the long range technologies and technology readiness. (2Q, 2015)
- Milestone 1.12: Complete an analysis of the hydrogen infrastructure and technical target progress for technology readiness. (4Q, 2015)
- Milestone 1.16: Complete analysis of program performance, cost status, and potential use of fuel cells for a portfolio of commercial applications. (4Q, 2018)
- Milestone 1.17: Complete analysis of program technology performance and cost status, and potential to enable use of fuel cells for a portfolio of commercial applications. (4Q, 2018)
- Milestone 2.2: Annual model update and validation. (4Q, 2011 through 4Q, 2020)

FY 2016 Accomplishments

- A process was developed to quantify the individual and collective impact of improvements made in the following systems.
  - Fuel cell stack improvements
  - H_2 storage
- The impact on the following parameters was quantified.
  - FCEV weight
  - Fuel cell power requirement
  - Onboard hydrogen mass requirement
  - Fuel cell system cost
  - Hydrogen storage cost
  - FCEV fuel economy, cost, and lifecycle cost

✧ ✧ ✧ ✧ ✧

INTRODUCTION

FCEVs are one of the technology choices considered in the baseline and scenario (BaSce) analysis [1]. It is understood that when combined with various vehicle technology improvements, FCEVs can become economically

feasible by 2025. Improvements made in light-weighting, aerodynamics, batteries, and motors help to lower the power requirement and onboard hydrogen storage that FCEVs need. In this study, we examine a scenario in which FCEV-specific technologies meet their development goals, while other vehicle technologies stagnate. This analysis will reveal the technology targets that should be met, to make FCEVs feasible with existing vehicle technologies.

Table 1 shows the technology targets assumed for this study. For each year, there are target values that could be assumed with a "low," "medium," and "high" level of technology progress. These three assumptions are shown below each year (2020, 2025, 2030, and 2045).

APPROACH

The baseline vehicle chosen for this study is the 2015 FCEV used in the BaSce analysis. This vehicle has specifications similar to vehicles currently in the market. Autonomie enables us to evaluate the fuel economy, and initial and operating costs for such a vehicle. With that information, the cost of ownership is computed. The FCEV is considered to be a feasible choice if it has the same or lower lifecycle cost ($/mile) as a conventional vehicle.

For each target year, the expected improvements in FCEV-specific technologies are added to this baseline vehicle model. Simulation results provide the improvement observed in vehicle mass, power, onboard hydrogen storage, and cost. Three scenarios are evaluated for each year.

- Fuel Cell (FC) System Impact: Fuel cell system improves over time.
- Hydrogen Storage (H_2) System Impact: Hydrogen storage system improves over time.
- Combined (H_2 FC) Impact: Both fuel cell and hydrogen systems improve over time.

This reveals the relative importance of each FCEV-specific technology, as well as their combined contribution in making FCEVs technically and economically viable.

RESULTS

Higher power and energy density for the fuel cell stack and hydrogen storage systems results in lower vehicle mass, as shown in Figure 1.

A lighter vehicle requires less power from the prime mover and less onboard energy storage. This allows us to use smaller fuel cell stacks and smaller hydrogen tanks, which will help to reduce the cost of the FCEV in the future (Figure 2).Such a vehicle will also have better fuel economy. Simulations predict about a 20% improvement in FCEV fuel economy by 2045. This will result in a reduction in operating costs. Figure 3 shows the overall lifecycle cost, expressed as the cost of driving a mile.

Present-day conventional vehicles have a lifecycle cost of 43¢/mile [1]. FCEVs are expected to match that by 2030, if the fuel cell technology targets are met. If all vehicle technologies develop as expected, then the combined improvements in batteries, motors, and vehicle light-weighting could make fuel cells competitive by 2025.

TABLE 1. Technology Assumptions

Parameter	Unit	2015	2020			2025			2030			2045		
			low	med	high	low	med	high	low	med	high	low	med	high
Peak Fuel Cell System Efficiency	%	59	63	65	66	64	66	67	65	67	68	68	69	70
Platinum Price	$/Troy oz	$1,500	$1,500			$1,500			$1,500			$1,500		
Specific Power FC System	W/kg	659	659	670	680	659	665	710	659	680	740	670	760	870
Power Density	W/L	640	640	720	850	640	730	890	640	740	970	690	880	1,150
Storage System Gravimetric Capacity	Useable kWh/kg	1.5	1.5	1.6	1.8	1.6	1.7	2	1.6	1.8	2.3	1.7	2	2.5
	Weight % of H_2	4.5	4.5	4.8	5.4	4.8	5.1	6	4.8	5.4	6.9	5.1	6	7.5
Storage System Cost	$/kg H_2 Useable	576	450	391	335	430	375	310	391	317	274	380	311	267
	$/kWh Stored	17.3	13.5	11.7	10.1	12.9	11.3	9.3	11.7	9.5	8.2	11.4	9.3	8
% H_2 Used in Tank	%	96	96	96	96	96	96	97	96	97	97	96	97	97

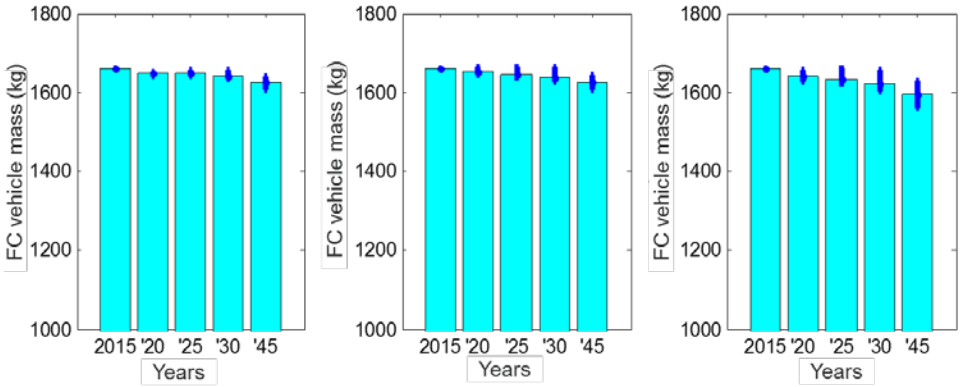

FIGURE 1. Impact of FC and H_2 technologies on FCEV mass

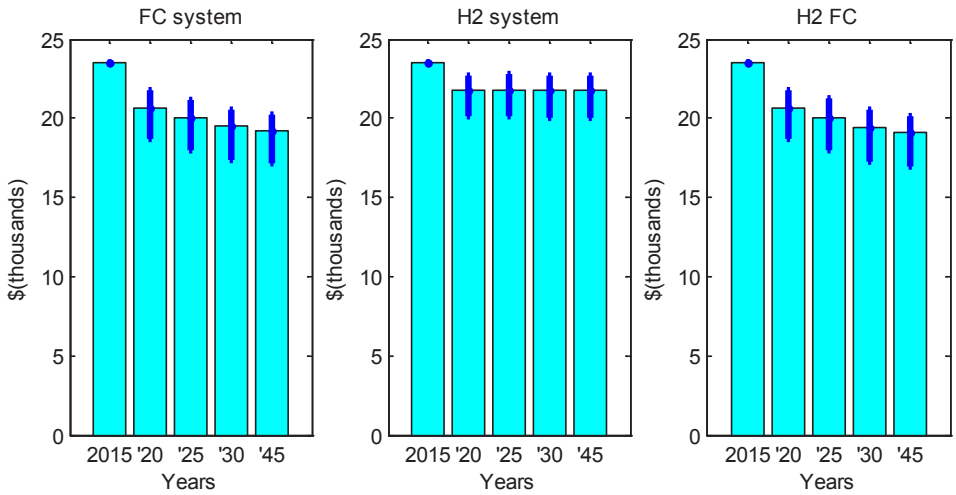

FIGURE 2. Impact of FC and H_2 technologies on FCEV cost

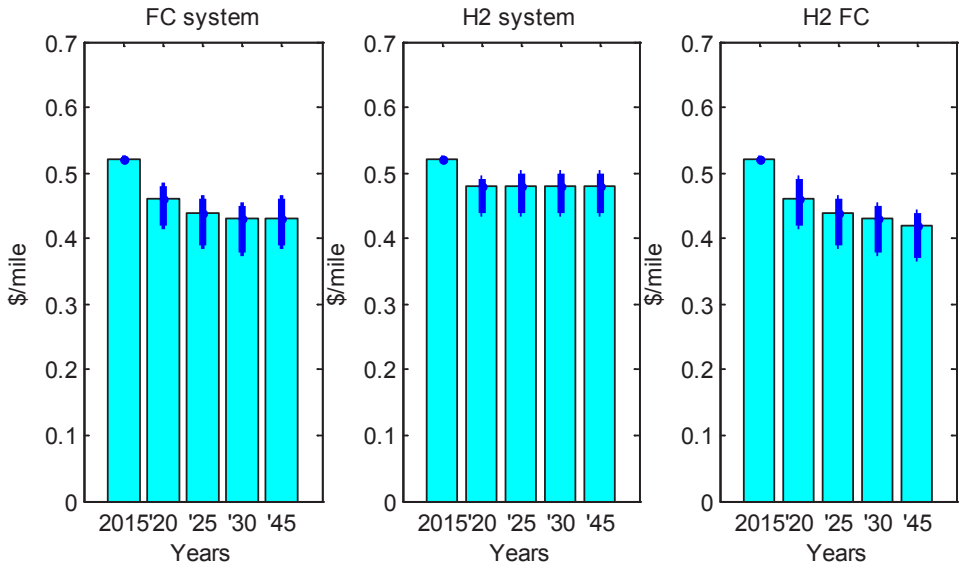

FIGURE 3. Impact of FC and H_2 technologies on lifecycle cost of FCEVs

CONCLUSIONS AND FUTURE DIRECTIONS

This study shows that if the 2030 technology targets for fuel cell technologies are achieved, then FCEVs can be economically feasible with present-day vehicle technologies. The current technology targets for 2030 are sufficient to overcome any uncertainties associated with other vehicle technologies. Fuel cell system improvement is the main factor that reduces FCEV fuel consumption. Manufacturing costs will decrease mostly due to the decrease in both fuel cell system and hydrogen tank costs.

REFERENCES

1. BaSce Analysis, 2015, *Report: Assessment of Vehicle Sizing, Energy Consumption and Cost through Large Scale Simulation of Advanced Vehicle Technologies*. Available at http://www.autonomie.net/publications/fuel_economy_report.html. Accessed May 4, 2016.

IX.4 Hydrogen Analysis with the Sandia ParaChoice Model

Rebecca S. Levinson (Primary Contact) and
Todd H. West
Sandia National Laboratories
P.O. Box 969
Livermore, CA 94551
Phone: (925) 294-2402
Email: rslevin@sandia.gov

DOE Manager: Fred Joseck
Phone: (202) 586-7932
Email: Fred.Joseck@ee.doe.gov

Project Start Date: October 1, 2014
Project End Date: Project continuation and direction determined annually by DOE

Overall Objectives

- Model the evolving market penetration potential of fuel cell electric vehicles (FCEVs) and hydrogen fuel.
- Assess the factors that influence the competition between FCEVs, conventional vehicles, and other alternative vehicle technologies such as battery electric vehicles.
- Assess impacts of FCEV market penetration and hydrogen production pathways on greenhouse gas (GHG) emissions and petroleum consumption.
- Provide context for the role of policy, technology development, infrastructure, and consumer behavior on the vehicle and fuel mix.

Fiscal Year (FY) 2016 Objectives

- Conduct scenario analyses to understand and provide context for the market penetration potential of FCEVs, hydrogen demand, costs, and production pathways.
- Conduct parametric analyses to understand sensitivities and tipping points driving FCEV sales, emissions, and hydrogen consumption and production.
- Examine market penetration of FCEVs and competition between FCEVs and alternate powertrains in different market segments.

Technical Barriers

This project addresses the following technical barriers from the Systems Analysis section of the Fuel Cell Technologies Office (FCTO) Multi-Year Research, Development, and Demonstration Plan.

(A) Future Market Behavior

(C) Inconsistent Data, Assumptions and Guidelines

(D) Insufficient Suite of Models and Tools

Contribution to Achievement of DOE Systems Analysis Milestones

This project will contribute to achievement of the following DOE milestones from the System's Analysis section of the FCTO Multi-Year Research, Development, and Demonstration Plan.

- Milestone 1.1: Complete an analysis of the hydrogen infrastructure and technical target progress for hydrogen fuel and vehicles. (2Q, 2011)
- Milestone 1.12: Complete an analysis of the hydrogen infrastructure and technical target progress for technology readiness. (4Q, 2015)
- Milestone 1.13: Complete environmental analysis of the technology environmental impacts for hydrogen and fuel cell scenarios and technology readiness. (4Q, 2015)
- Milestone 1.19: Complete analysis of the potential for hydrogen, stationary fuel cells, fuel cell vehicles, and other fuel cell applications such as material handling equipment including resources, infrastructure and system effects resulting from the growth in hydrogen market shares in various economic sectors. (4Q, 2020)
- Milestone 2.2: Annual model update and validation. (4Q, 2011 through 4Q, 2020)

FY 2016 Accomplishments

- Submitted "Fuel Cell Electric Vehicles: Drivers and Impacts of Adoption" for publication in *Energy Policy*. Following analyses conducted therein, where impact on vehicle sales or future petroleum or emissions were assessed as appropriate:
  - Baseline/business as usual scenario analysis
  - Low cost electrolysis scenario analysis
  - Carbon tax scenario analysis
  - Future oil price and natural gas price trade space analysis
  - Future battery price and fuel cell price trade space analysis
  - FCEV vehicle cost and clean electrolysis cost trade space analysis

  - FCEV purchasing incentive parametric and scenario analyses
  - Global sensitivity correlation coefficient analysis
  - FCEV utopia scenario analysis
- Assessed impact of FCEVs on GHG emissions on scenarios with and without compressed natural gas vehicles.
- Added modeling capability for parametric efficiency analysis of FCEVs isolated from efficiency analyses of other electric vehicle powertrains.
- Parametric assessment of impact of increased efficiency for FCEVs on FCEV sales and GHG emissions.
- Assessment of market driven infrastructure growth rates on FCEV sales.
- Beginning assessment of segment specific market competition for FCEVs.

✧ ✧ ✧ ✧ ✧

INTRODUCTION

In the coming decades, light-duty vehicle options and their supporting infrastructure must undergo significant transformations to achieve aggressive national targets for reducing petroleum consumption and lowering greenhouse gas emissions. FCEVs, battery and hybrid electric vehicles, and biofuels are among the promising advanced technology options. In addition, natural gas vehicles, fueled with domestically produced natural gas, have significant potential to displace petroleum use in the light-duty vehicle mix. This project examines the market penetration of FCEVs in a range of market segments, and in different energy, technology, and policy futures. Analyses are conducted in the context of varying hydrogen production and distribution pathways, as well as public infrastructure availability, fuel (gasoline, natural gas, hydrogen) and electricity costs, vehicle costs and fuel economies to better understand under what conditions, and for which market segments, FCEVs can best compete with battery electric and other alternative fuel vehicles.

APPROACH

The ParaChoice model simulates the dynamic interaction and evolution of the light duty vehicle stock, fuel production, and energy supplies through 2050. At its core, ParaChoice is very simple, taking inputs for current vehicle price and vehicle price projections, fuel prices, etc., and asking a set of modeled consumers at each time step which powertrain vehicles are the least expensive options given their driving habits and the cost of inconvenience for finding alternative fueling stations or being stuck with a very short range vehicle. The choice model structure is similar to [1] and [2]. In implementation, we model the fuel sector internally capturing the feedback between fuel production pathways, refueling infrastructure, and the vehicle market. Additionally, the market is segmented by state, vehicle size, population density, driver intensity, and dwelling type to capture consumer and fuel production and price market niches

In order to explore uncertainty, sensitivities to inputs, and trade spaces, we run the core model thousands of times with varying inputs. The model is designed to vary parameters of uncertain variables easily to facilitate these analyses. These parametric analyses provide insights that are not as easily accessible to individual scenario-focused studies.

RESULTS

Our primary result and accomplishment in the last year was the formal write up and analysis of the drivers and impacts of FCEV market adoption using the ParaChoice model. This formal manuscript was reviewed and iterated upon internally by experts at Sandia, by DOE stakeholders, and then submitted to *Energy Policy* under the title "Fuel Cell Electric Vehicles: Drivers and Impacts of Adoption." The analyses conducted for this work and written in this work support the FCTO objectives and work towards FCTO milestones. In particular, the manuscript addresses the potential market competition and drivers for FCEVs, the potential GHG emissions impacts, the interplay between the vehicle market and the fuel production pathways, and potential impacts of policy and technology. We leverage our parametric capabilities to address market uncertainties and to identify tipping points and trade spaces. The following analyses are detailed in the work:

- Baseline/business as usual scenario analysis
- Low cost electrolysis scenario analysis
- Carbon tax scenario analysis
- Future oil price and natural gas price trade space analysis
- Future battery price and fuel cell price trade space analysis
- FCEV vehicle cost and clean electrolysis cost trade space analysis
- FCEV purchasing incentive parametric and scenario analyses
- Global sensitivity correlation coefficient analysis
- FCEV utopia scenario analysis

One interesting finding from our study shows that future FCEV sales are much more sensitive to FCEV vehicle costs than to the cost of clean hydrogen. Figure 1, shows the

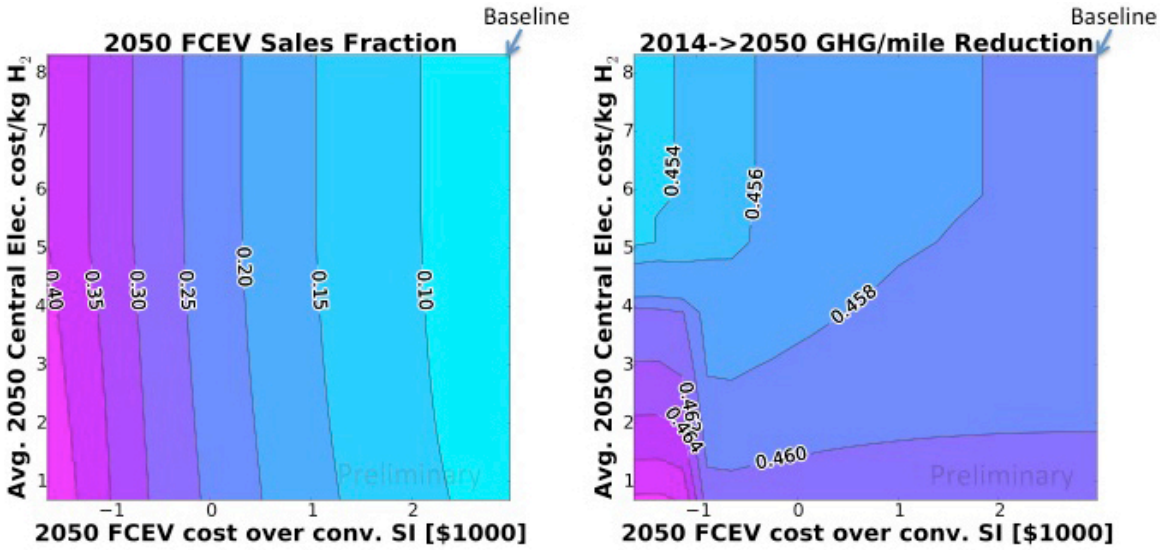

FIGURE 1. Impact of fuel cell vehicle price and hydrogen price on (a) fuel cell electric vehicle sales and (b) fleet wide emissions, showing the sensitivity of sales to vehicle price and relative insensitivity to fuel price

sensitivity of 2050 FCEV sales (left) and fleet wide emissions (right) to FCEV costs as compared to conventional vehicle costs (horizontal axes) and the pump fuel cost of hydrogen generated with dedicated wind power (vertical axes). 2050 FCEV sales fractions increase much more substantially with decreasing vehicle price than with decreasing fuel price. However, GHG emissions increase with increasing FCEV sales unless the renewable hydrogen is inexpensive. This is because natural gas reformation is a more commercially viable hydrogen production pathway than electrolysis in the baseline case. Therefore, while FCEVs are less carbon intensive than conventional, non-hybrid vehicles, they are only comparably carbon intensive to non-plug-in gasoline hybrids and compressed natural gas vehicles, and more carbon intensive than low and mid-range plug-in hybrids and full battery electric vehicles.

Additionally in this last year, we have added new capabilities to the ParaChoice model and conducted additional analyses in support of the FCTO Systems Analysis program goals. In particular, we conducted an assessment of FCEV market competition with the other alternative vehicle powertrains, finding more competition with compressed natural gas vehicles than others. We also performed an assessment of FCEV impact in a scenario without compressed natural gas vehicles. We have added modeling capability to allow parametric efficiency analysis of FCEVs and found (preliminary) that efficiency increases in FCEV powertrains can lead to both increased sales and decreased fleet wide emissions, even in cases where vehicle cost must increase to accommodate the efficiency boost. Results are shown in Figure 2. We have also examined the impact of renewable mandates (preliminary), finding that a renewable mandate for hydrogen production is an effective tool for driving down fleet wide GHG emissions. Results are shown in Figure 3.

CONCLUSIONS AND FUTURE DIRECTIONS

Fuel cell electric vehicles play a role in the future light duty vehicle mix, diversifying the fuel source and options to consumers. With improved FCEV efficiency, technology improvements in renewable hydrogen production, or renewable mandates for hydrogen production, FCEVs can contribute to a lower carbon future as well.

Future work includes a publication showing pathways to lower GHG emission futures through FCEVs. Additional future work includes ParaChoice modeling refinements for hydrogen pricing at low demand, and the inclusion of at home hydrogen refueling and analysis of potential benefits of the same.

FY 2016 PUBLICATIONS/PRESENTATIONS

1. Rebecca S. Levinson and Todd H. West, "Hydrogen Analysis with the Sandia ParaChoice Model." Presentation at the Annual Merit Review.

REFERENCES

1. Lin, Zhenhong and Greene, David L. "A Plug-In Hybrid Consumer Choice Model with Detailed Market Segmentation." Transportation Research Board 10-1698, 2010.

2. Struben, Jeroen and Sterman, John D. "Transition challenges for alternative fuel vehicle and transportation systems." Environment and Planning B: Planning and Design, 35:1070–1097, 2008.

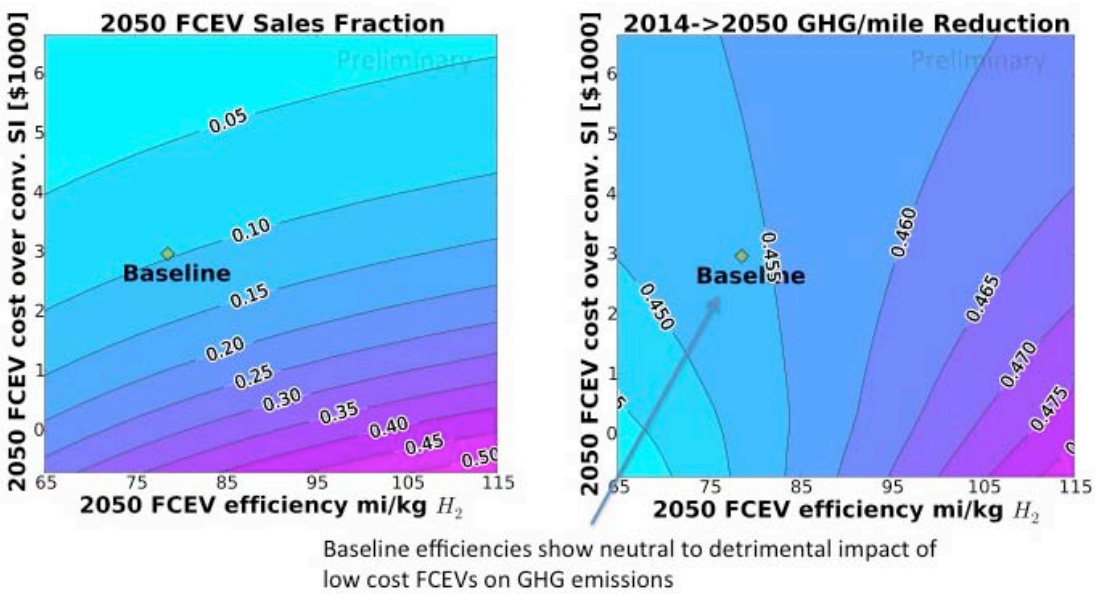

FIGURE 2. Impact of fuel cell vehicle price and efficiency on (a) fuel cell electric vehicle sales and (b) fleet wide emissions, showing the positive impact of efficiency on both sales and emissions, even if efficiency improvements necessitate a slight vehicle price increase

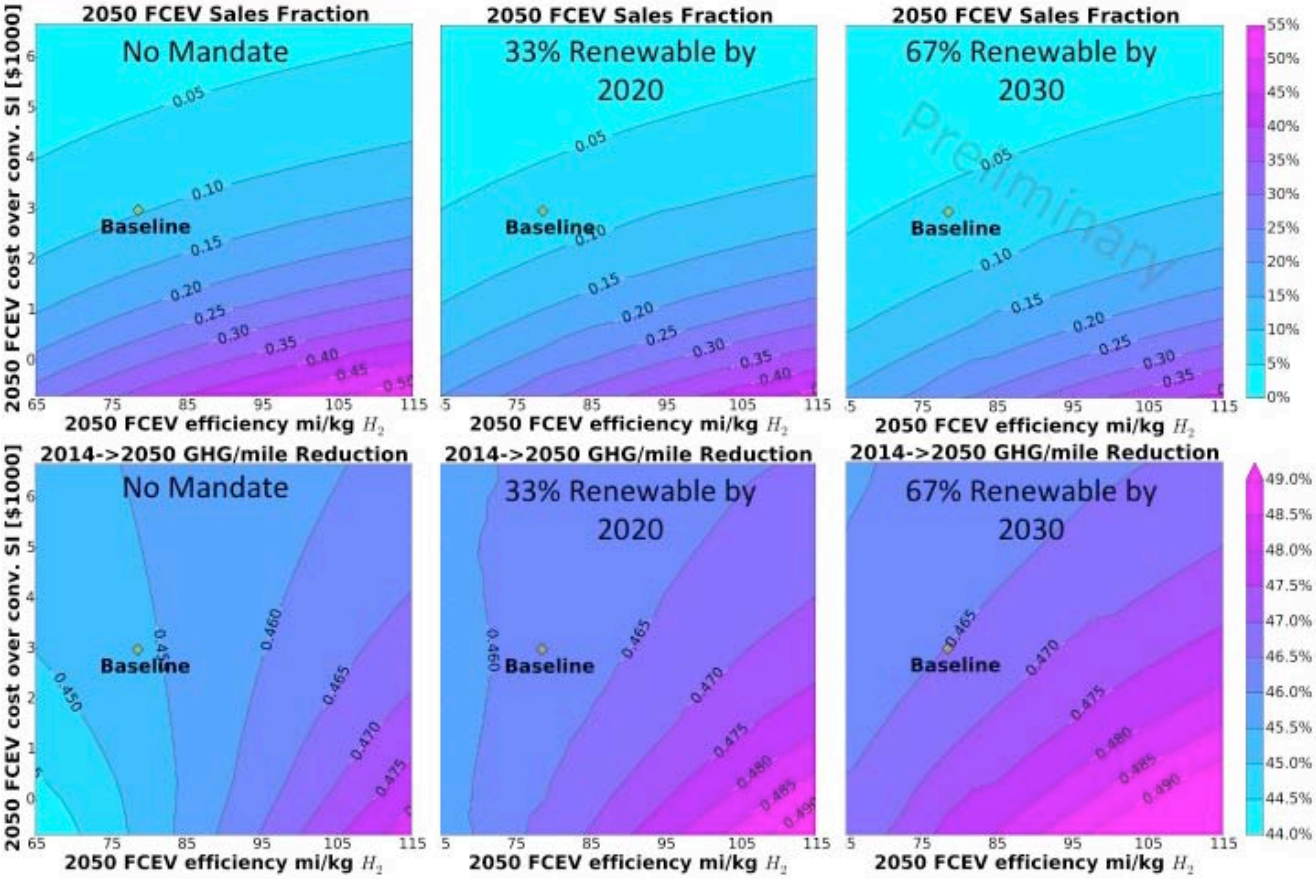

FIGURE 3. Impact of renewable fuel mandate on fuel cell vehicle price and efficiency trade space, showing the positive impact of a renewable mandate on fleet wide emissions, even at the detriment of fuel cell electric vehicle sales

IX.5 Life Cycle Analysis of Emerging Hydrogen Production Technologies

Amgad Elgowainy (Primary Contact), Qiang Dai, Jeongwoo Han, Michael Wang
Argonne National Laboratory
9700 South Cass Avenue, Building 362
Lemont, IL 60439
Phone: (630) 252-3074
Email: aelgowainy@anl.gov

DOE Manager: Fred Joseck
Phone: (202) 586-7932
Email: Fred.Joseck@ee.doe.gov

Project Start Date: October 1, 2015
Project End Date: Project continuation and direction determined annually by DOE

Overall Objectives

- Quantify environmental impacts associated with emerging hydrogen production pathways.
- Identify greenhouse gas (GHG) reduction potential of various hydrogen production technologies and pathways compared to natural gas steam methane reforming (SMR).
- Support existing DOE-sponsored tools for hydrogen production.

Fiscal Year (FY) 2016 Objectives

- Conduct life cycle analysis of emerging hydrogen production pathways, including dark fermentation of lignocellulosic biomass, high temperature electrolysis (HTE) with a solid oxide electrolysis cell (SOEC), and reforming of biomass-derived liquids (BDL).
- Quantify GHG emissions along the supply chains of investigated hydrogen production pathways.
- Identify sensitivity of life cycle GHG emissions to system performance parameters and GHG reduction potentials.

Technical Barriers

This project addresses the following technical barriers from the System Analysis section of the Fuel Cell Technologies Office (FCTO) Multi-Year Research, Development, and Demonstration Plan.

(B) Stove-piped/Siloed Analytical Capability

(C) Inconsistent Data, Assumptions and Guidelines

(D) Insufficient Suite of Models and Tools

Contribution to Achievement of DOE Systems Analysis Milestones

This project will contribute to achievement of the following DOE milestones from the System Analysis section of the FCTO Multi-Year Research, Development, and Demonstration Plan.

- Milestone 1.13: Complete environmental analysis of the technology environmental impacts for hydrogen and fuel cell scenarios and technology readiness. (4Q, 2015)
- Milestone 1.15: Complete analysis of program milestones and technology readiness goals – including risk analysis, independent reviews, financial evaluations, and environmental analysis – to identify technology and risk mitigation strategies. (4Q, 2015)
- Milestone 2.2: Annual model update and validation. (4Q, 2011 through 4Q, 2020)
- Milestone 3.1: Annual update of Analysis Portfolio. (4Q, 2011 through 4Q, 2020)

FY 2016 Accomplishments

- Completed life cycle analysis of hydrogen production from dark fermentation of corn stover, HTE with SOEC, and steam reforming of BDL.
- Produced estimates of the GHG emissions and GHG reduction potentials of alternative hydrogen production pathways, and compared them to conventional hydrogen production technologies, such as SMR and electrolysis.
- Demonstrated that, compared with hydrogen from SMR, hydrogen from dark fermentation, HTE and BDL can reduce well-to-wheels (WTW) GHG by 26%, 82%, and 43%, respectively, when used in a fuel cell electric vehicle (FCEV). The corresponding GHG reductions are 58%, 90%, and 68% when compared to a gasoline internal combustion engine vehicle (ICEV) on a per mile driven basis.
- Expanded the Greenhouse gases, Emissions, and Energy use in Transportation (GREET®) model's capabilities to evaluate the environmental impacts of new and emerging hydrogen production pathways.

✧ ✧ ✧ ✧ ✧

INTRODUCTION

Argonne National Laboratory's GREET model has been used by DOE to evaluate environmental footprints of fuel production, vehicle production and vehicle operation [1]. In this study, three emerging hydrogen production technologies of interest to FCTO, including dark fermentation of lignocellulosic biomass, HTE with SOEC, and reforming of BDL, have been incorporated into the GREET model. Life cycle GHG emissions from the three hydrogen production pathways are evaluated, with major GHG emission sources identified. Together with existing techno-economic analysis of emerging hydrogen production pathways, this study enables FCTO to conduct a comprehensive evaluation of risks and benefits of different hydrogen production technologies, and to guide FCTO research, development, and demonstration planning.

APPROACH

Material and energy flows pertaining to the three hydrogen production pathways have been compiled based on engineering modeling and experimental measurements by partner labs, and incorporated in the GREET model. With GREET, GHG emissions along the supply chain of each hydrogen production pathway are calculated and compared with those of conventional hydrogen production technologies (SMR and water electrolysis). Since system performance dictates material and energy flows of the system, sensitivity analyses of WTW GHG to different assumptions of major system performance metrics have also been conducted. To fully illustrate the environmental benefits of the emerging hydrogen production technologies, the WTW per mile GHG emissions for a FCEV fueled by hydrogen produced from aforementioned technologies have been compared with that for an ICEV fueled by gasoline.

RESULTS

Hydrogen from Dark Fermentation of Lignocellulosic Biomass

Process flow of the dark fermentation pathway is depicted in Figure 1. WTW GHG emissions is 9.8 kg CO_{2e}/kg of hydrogen produced via dark fermentation of corn stover, compared to 13 kg CO_{2e}/kg of hydrogen produced from SMR, and 29 kg CO_{2e}/kg hydrogen produced via electrolysis with electricity from U.S. average grid mix. Energy recovered through combustion of lignin, biogas from wastewater treatment, and purged hydrogen from the gas cleaning unit completely satisfies the steam requirement of the biomass pretreatment process, and partially offset the electricity requirement of the entire system. Without energy recovery (ER), the WTW GHG emissions associated with 1 kg

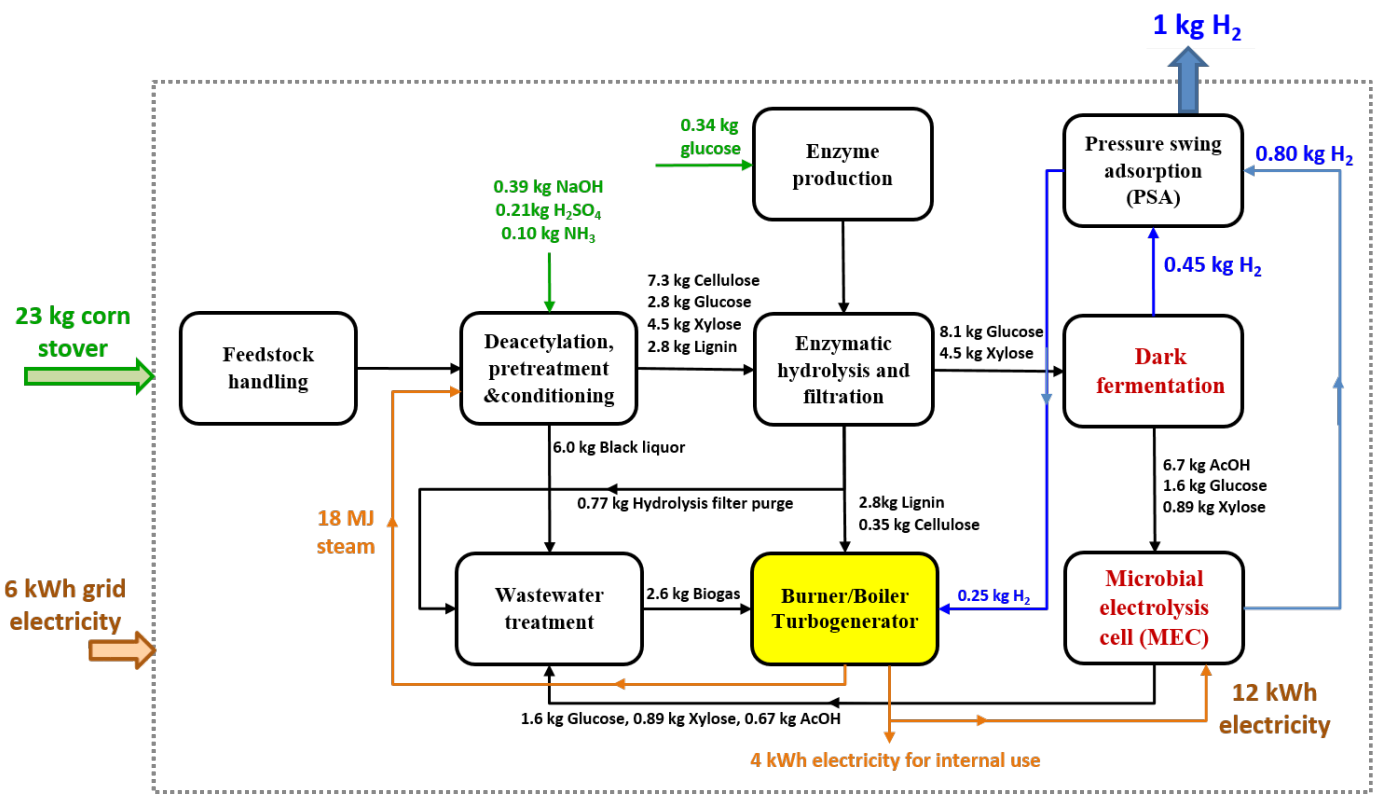

FIGURE 1. Hydrogen production process from dark fermentation of corn stover

hydrogen produced from the dark fermentation pathway increases to 19 kg CO_{2e}/kg. Therefore, ER offers the greatest potential of GHG reduction for hydrogen production from dark fermentation but likely at increased capital investment. In addition, electricity requirement by the production process is identified as a major contributor to the WTW GHG emissions of hydrogen produced from dark fermentation. Increasing hydrogen yield of the fermenter and the microbial electrolysis cell, and improving system energy efficiency are also viable means to achieve further GHG emissions reduction.

Hydrogen from HTE with SOEC

Process flow of the HTE pathway is depicted in Figure 2. Electricity consumed by the SOEC and heat required to produce the high temperature steam (at 900°C) are the major energy inputs for this process. When integrated with a high temperature gas-cooled nuclear reactor (HTGR) such that both heat and electricity are derived from non-fossil nuclear source (U_{235}), the system produces hydrogen with a WTW GHG emissions of 2.5 kg CO_{2e}/kg, which is 78% lower compared to hydrogen produced from SMR. In contrast, if both electricity and heat are generated using natural gas, hydrogen produced from HTE pathway produces WTW GHG emissions of 20 kg CO_{2e}/kg. Utilizing a non-fossil energy source is therefore key to GHG emissions reduction for hydrogen produced from HTE. Electrolysis with high temperature steam produces oxygen in addition to hydrogen. If the co-produced oxygen is collected and sold as a commodity, heat and electricity input to the production process can be allocated based on the economic values of produced hydrogen and oxygen. After economic allocation, the WTW GHG emissions are estimated at 2.4 kg CO_{2e}/kg hydrogen produced from the HTGR-integrated system, and 16 kg CO_{2e}/kg hydrogen produced from the natural gas-fueled system.

Hydrogen from Steam Reforming of BDL

Process flow of the BDL pathway is depicted in Figure 3. WTW GHG emissions are estimated at 7.5 kg CO_{2e}/kg hydrogen produced via reforming of BDL, which is 43% lower compared to hydrogen production from SMR. Pyrolysis oil, which is the feedstock for this production process, and electricity input are the major GHG emissions contributors, accounting for 44% and 29% of the WTW GHG emissions, respectively. Recycling unreacted pyrolysis oil can increase the pyrolysis oil-to-hydrogen conversion rate from 64% to 80%, with the potential to further reduce the WTW GHG emissions to 6.8 kg CO_{2e}/kg hydrogen for the BDL pathway.

WTW GHG Emissions Comparison

WTW GHG emissions comparison of hydrogen from various hydrogen production pathways compared to gasoline ICEV are summarized in Figure 4. To account for the higher fuel economy of FCEVs relative to gasoline ICEVs (ratio of 2.1), a per-mile gallon of gasoline equivalent (GGE) is used as a functional unit to compare WTW GHG emissions of various vehicle–fuel pathways on a consistent basis. Compared with hydrogen from SMR, hydrogen from dark fermentation, HTE and BDL can reduce WTW GHG emissions by 26%, 82%, and 43% respectively. On a per

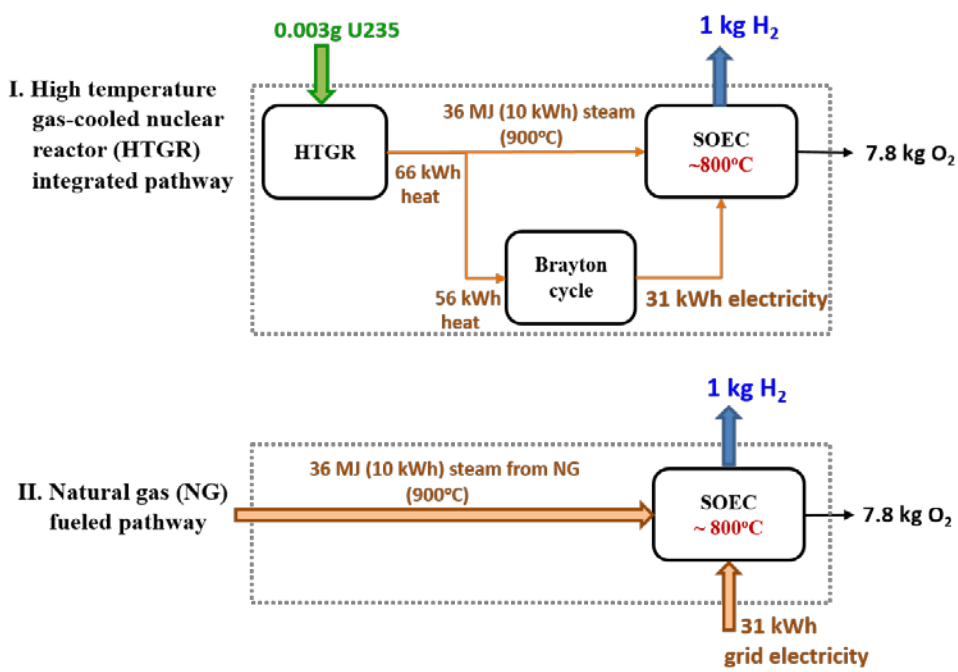

FIGURE 2. Hydrogen production process via high-temperature electrolysis using SOEC

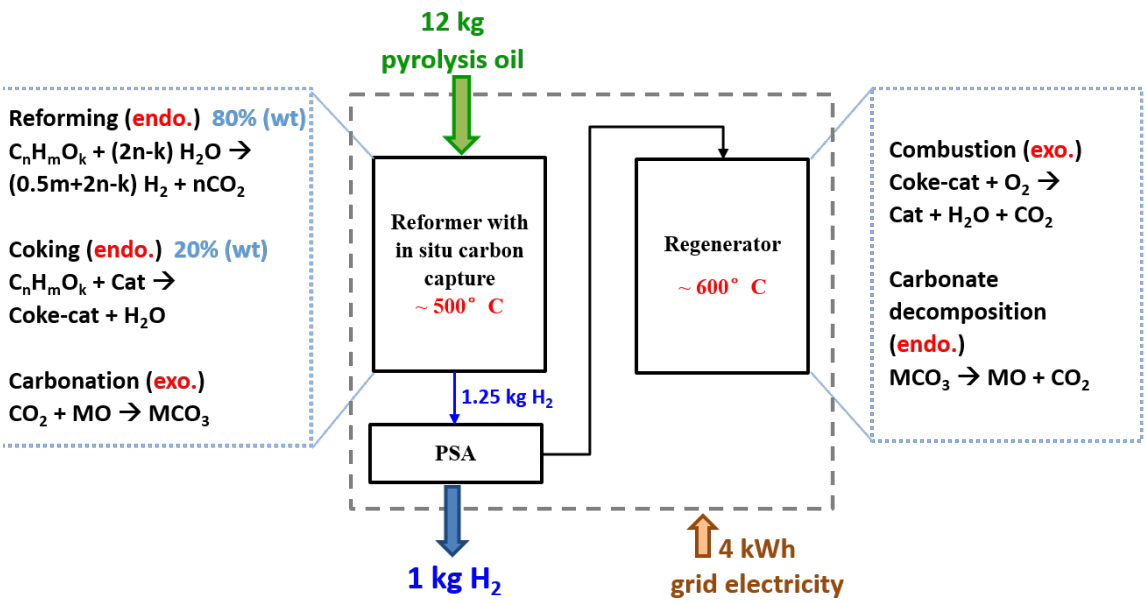

PSA – Pressure swing absorption

FIGURE 3. Hydrogen production process via reforming of pyrolysis oil

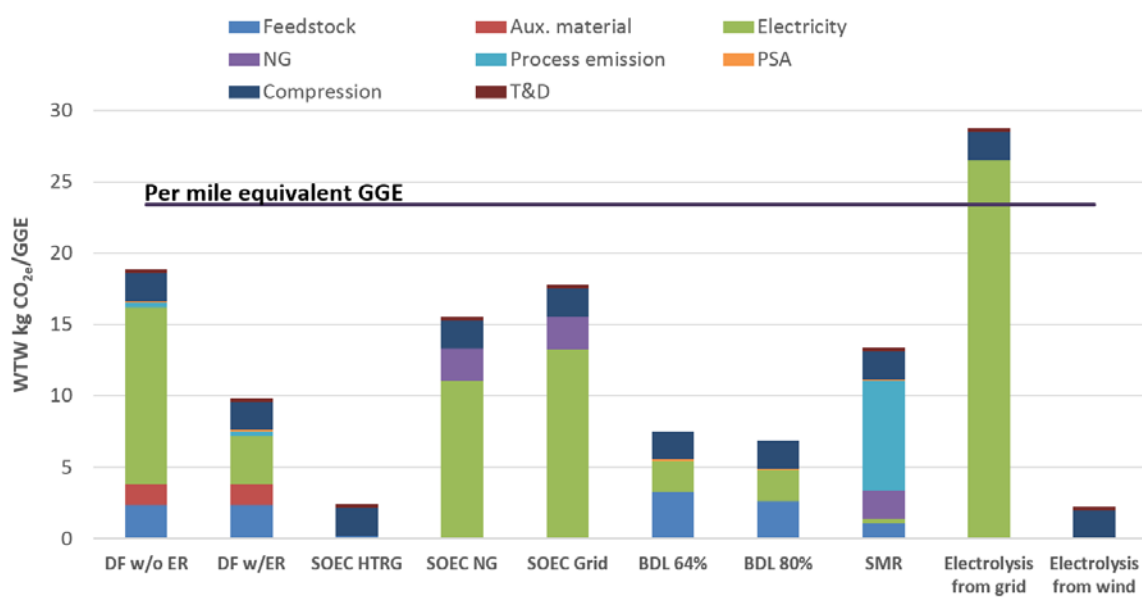

GGE – Gallon of gasoline equivalent; NG – natural gas; T&D – Transportation and distribution; DF – Dark fermentation

FIGURE 4. WTW GHG emissions comparison of hydrogen from the various hydrogen production pathways compared to gasoline ICEV

mile basis, FCEVs using hydrogen produced from dark fermentation, nuclear HTE and BDL provide WTW GHG emissions reductions of 58%, 90%, and 68% compared to gasoline ICEV.

CONCLUSIONS AND FUTURE DIRECTIONS

- In general, hydrogen produced from non-fossil energy sources outperforms hydrogen produced from fossil sources (e.g., SMR and grid electrolysis) in terms of life cycle GHG emissions.
- Increasing hydrogen yield and improving process efficiency of the investigated pathways offer GHG emissions reduction opportunities for all hydrogen production pathways.
- Energy recovery from lignin, biogas, and purged hydrogen is critical to materialize large reduction in GHG emissions for the dark fermentation pathway,

whereas the recycling of unreacted pyrolysis oil is important for GHG emissions reduction for the BDL pathway.

In the future, we will continue the development and implementation of other emerging hydrogen production technologies in GREET. In addition to GHG emissions, other environmental impact metrics, such as water consumption and criteria air pollutants emissions will be evaluated. To facilitate better understanding of the uncertainty of system performance parameters and their impact on life cycle GHG emissions, we will also develop probability distribution functions for key system parameters and conduct stochastic analyses on the various production pathways.

REFERENCES

1. "Argonne GREET Model," Argonne National Laboratory, accessed July 20, 2016, https://greet.es.anl.gov/

IX.6 Policies to Promote Alternative Fuel Vehicles

David L. Greene
Howard H. Baker, Jr. Center for Public Policy
The University of Tennessee
1640 Cumberland Avenue
Knoxville, TN 37996-3340
Phone: (865) 974-3839
Email: dlgreene@utk.edu

DOE Manager: Fred Joseck
Phone: (202) 586-7932
Email: Fred.Joseck@ee.doe.gov

Project Start Date: October 1, 2013
Project End Date: September 30, 2016

Overall Objectives

- By means of quantitative analysis, research, and synthesis of the literature, advance the understanding of how policies have and could affect the market success of hydrogen and fuel cell technologies.
- Assist in the development and use of models and analytical tools that are useful for predicting the effects of policies on the deployment of hydrogen infrastructure and consumers' purchases of fuel cell vehicles.
- Assist DOE and Argonne National Laboratory with planning and analysis of the transition to hydrogen fuel cell vehicles in the United States.

Fiscal Year (FY) 2016 Objectives

- Conduct a thorough review of the past 15 years of peer-reviewed literature addressing policies to promote alternative fuel vehicles and summarize lessons learned in a published report.
- Develop a level playing field analysis of the refueling infrastructure costs of alternative fuels, with special focus on battery electric and hydrogen fuel cell electric vehicles.
- Provide analytical support to DOE's participation in H2USA, as requested by DOE.

Technical Barriers

This project addresses the following technical barriers from the Systems Analysis section of the Fuel Cell Technologies Office Multi-Year Research, Development, and Demonstration Plan:

(A) Future Market Behavior

(C) Inconsistent Data Assumptions and Guidelines

(D) Insufficient Suite of Models and Tools

(E) Unplanned Studies and Analysis

Contribution to Achievement of DOE Systems Analysis Milestones

This project will contribute to achievement of the following DOE milestones from the Systems Analysis section of the Fuel Cell Technologies Office Multi-Year Research, Development, and Demonstration Plan:

- Milestone 1.16: Complete analysis of program performance, cost status, and potential use of fuel cells for a portfolio of commercial applications. (4Q, 2018)
- Milestone 1.19: Complete analysis of the potential for hydrogen, stationary fuel cells, fuel cell vehicles, and other fuel cell applications such as material handling equipment including resources, infrastructure and system effects resulting from the growth in hydrogen market shares in various economic sectors. (4Q, 2020)

FY 2016 Accomplishments

- Completed a critical review of the past 15 years of peer-reviewed and gray literature that sheds light on the effectiveness of policies to promote alternative fuel vehicles. The review has been published as a Baker Center report and is available on the website of the Howard H. Baker, Jr. Center for Public Policy [1].
- Presented results of the literature review to DOE's Hydrogen and Fuel Cells Technical Advisory Committee, Hydrogen and Fuel Cells Program Annual Merit Review, and other venues.
- Completed a level playing field analysis of the costs of alternative fuel refueling infrastructure using the best available current information on costs and technology status.

✧ ✧ ✧ ✧ ✧

INTRODUCTION

Since the energy crises of the 1970s, the United States has tried to substitute alternative energy sources for petroleum use by motor vehicles. Achieving reductions in light-duty vehicle greenhouse gas emissions of 50% to 100% by 2050 would likely require that a majority of new vehicles sold in 2050 are battery electric or hydrogen fuel cell electric

vehicles [3,6]. Accomplishing such a large-scale energy transition for the public good poses new challenges for public policy [2].

More than a decade ago, McNutt and Rodgers [4] published a seminal assessment of alternative fuels policies from the enactment of the Alternative Motor Fuels Act of 1988 until 2003. This report updates and expands on their analysis.

APPROACH

More than 90 recent studies covering a wide range of policies to promote alternative fuels and vehicles were analyzed to glean insights about the effectiveness of policies addressing the natural barriers faced by alternative fuel vehicles (AFVs).

- Lack of scale economies in the vehicle and fuel supply chains
- The need for further technological progress and learning by doing
- Consumers' lack of familiarity with and aversion to the risk of novel products
- Lack of diversity of AFV choices in vehicle markets (e.g., make, model, vehicle class)
- Lack of refueling infrastructure
- Lack of a market for alternative fuel
- Inappropriate administrative and regulatory infrastructure (e.g., codes, standards, ordinances)

Policies were grouped into six areas and findings were summarized.

- Reducing the cost of AFVs to consumers
- Increasing consumer awareness and reducing perceived risk
- Increasing the availability of alternative fuel refueling infrastructure
- Reducing the cost of alternative fuels
- Establishing supportive institutional and regulatory infrastructure
- Advantages of a systemic policy strategy

Cost estimates from 25 recent studies were analyzed to estimate current refueling infrastructure costs per mile and cost per gallon of gasoline equivalent (GGE) for light-duty vehicles. A spreadsheet was created to document all calculations. The estimates account for the energy content of fuels and relative efficiencies based on current vehicle technology. Various sizes of refueling stations were considered.

RESULTS

The importance of providing substantial and sustained financial incentives to reduce the costs of AFVs to consumers is the most consistent finding in the literature. Financial incentives given at the time of purchase have two to ten times the impact of income tax credits or deductions and subsidies should be large relative to the incremental cost of an alternative fuel vehicle to insure salience in consumers' vehicle choice decisions. Financial incentives should be designed to be readily understandable by consumers and their availability should be well publicized. California's zero emission vehicle mandates have played a critical role in early market transformation by inducing manufacturers not only to research, design and offer zero emission vehicles, but also to subsidize their sale and the deployment of supporting recharging and refueling infrastructure.

Lack of awareness, unfamiliarity, and the perceived risk of purchasing a novel technology appear to be the most important non-financial barriers to AFV adoption. Most consumers' knowledge of AFVs is minimal and often inaccurate and many are waiting to see large numbers of AFVs on the road before they will consider purchasing one. Early adopters therefore play a critical role in the diffusion process. Maximizing the opportunities for consumers to experience an AFV first hand can accelerate early market development. Individuals concerned about climate change and energy security are far more likely to be early adopters than others, yet don't expect to pay more for vehicles that help achieve the same societal goals. Non-financial policies such as high occupancy vehicle lane access, free parking, and free plug-in electric vehicle (PEV) charging have value in their own right when local circumstances are favorable and serve as positive reinforcement for early adopters.

Findings about the importance of recharging and refueling infrastructure to AFV sales come chiefly from stated preference surveys and model simulations. Statistical analyses of PEV sales generally indicate that charging infrastructure promotes PEV sales. While public recharging infrastructure is beneficial to adoption of battery electric vehicles, it is not absolutely critical and is somewhat less important to potential plug-in hybrid electric vehicle than battery electric vehicle customers. For hydrogen fuel cell vehicles, refueling infrastructure is essential. The literature has not yet satisfactorily measured the importance of policies to increase fuel availability at low levels of availability. Underutilization of infrastructure in the early transition appears to be inevitable, yet excess infrastructure is almost certainly necessary to encourage the growth of the stock of AFVs. How much infrastructure should be provided, of what kind, where, and when continues to be a conundrum.

Reducing the price of alternative fuels is also critically important. Consumers expect alternative fuels to be competitive with the price of gasoline. Insuring competitive

pricing is challenging because the early stages of transition require excess investment in refueling infrastructure and therefore low utilization rates for AFV refueling stations. Direct public subsidies, investment tax credits, and public–private partnerships (driven by regulatory mandates) have all been tried with some degree of success.

Policy makers at local levels emphasize the importance of developing appropriate regulatory and institutional infrastructure for alternative fuels and increasing public awareness (e.g., through public information but also standardized signage), issues that are taken for granted with conventional fuels but that are critically important during the early stages of transition.

Because of the complexity and variety of market barriers to a transition to alternative fuels, comprehensive policy strategies that systemically address all barriers are more likely to be effective and economically efficient. Cross-national and regional analyses tend to support this conclusion, as well.

Graphs of refueling infrastructure costs per GGE and per vehicle mile were developed, based on current vehicle and refueling technologies. Figures 1 and 2 summarize the results.

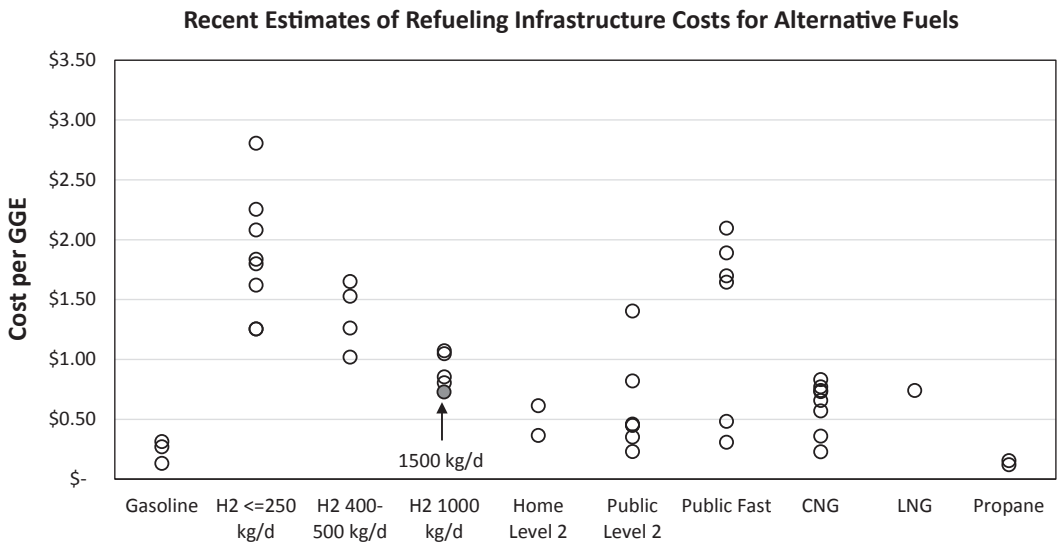

CNG – Compressed natural gas; LNG – Liquefied natural gas

FIGURE 1. Estimates of refueling infrastructure costs per gallon of gasoline equivalent

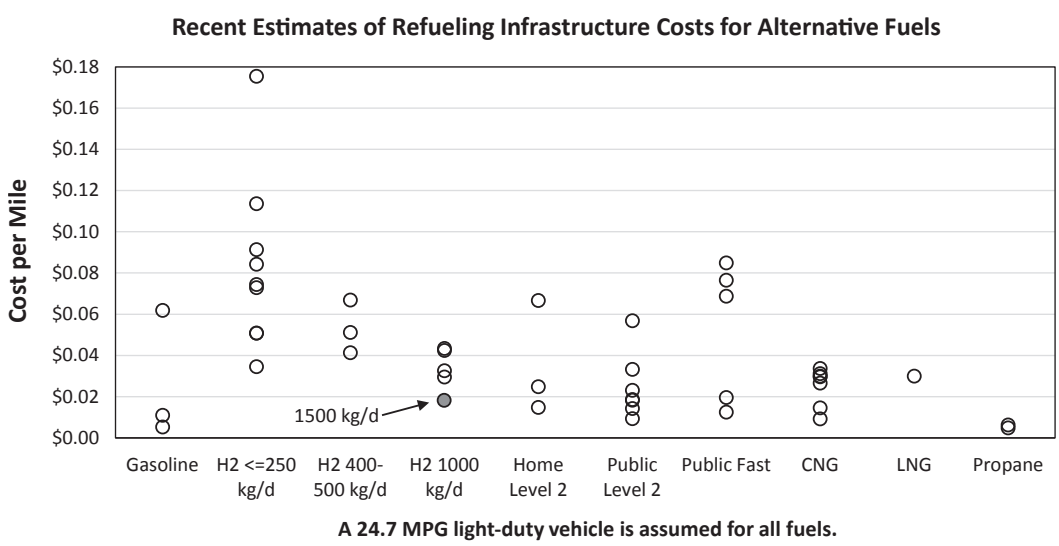

MPG – Miles per gallon

FIGURE 2. Recent estimates of refueling infrastructure costs per mile for alternative fuels

CONCLUSIONS AND FUTURE DIRECTIONS

Transitioning to low-greenhouse gas energy for motor vehicles will take several decades and the success of any one alternative is uncertain. Because of this, public policy must be persistent and flexible [5].

Accomplishing a large-scale energy transition for the public good is a new challenge for public policy. As more experience is gained from the ongoing market transformation process, future research will provide additional insights that will enable policy makers to refine and improve policies to promote the transition to sustainable energy for motor vehicles.

Future research should address accurately quantifying the interdependence of fuel availability and alternative fuel vehicle choice and developing effective means of modeling the coevolution of alternative vehicles and fuels. Further analysis of the benefits and costs of systemic policy strategies is needed.

FY 2016 PUBLICATIONS/PRESENTATIONS

1. Greene, D.L. and S. Ji, 2016. "Policies for Promoting Low-Emission Vehicles and Fuels: Lessons from Recent Analyses," Baker Center Report 4:16, Howard H. Baker, Jr. Center for Public Policy, The University of Tennessee, Knoxville, available at: http://bakercenter.utk.edu/policies-promoting-low-emission-vehicles-fuels-report-released.

2. Greene, D.L., 2016. "Analysis of Incentives and Policy Impacts on the Market for Alternative Fuels and Vehicles," presentation SA058, DOE Annual Merit Review and Peer Evaluation Meeting, Washington, D.C., June 8.

3. Greene, D.L., 2016. "PEV Charging Infrastructure: What can we learn from the literature?" STEPS Workshop, Critical Barriers and Opportunities for PEV Commercialization in California, University of California, Davis, CA, April 26.

4. Greene, D.L., 2016. "Policies to Promote Alternative Fuel Vehicles: What can we learn from the literature?" Hydrogen and Fuel Cell Technical Advisory Committee, Livermore, California, April 6.

5. Greene, D.L., 2016. "Why Hydrogen Fuel Cell Vehicles?" Pollution Probe Pathways Initiative Workshop, Toronto, Ontario, Canada, March 22.

6. Greene, D.L., 2016. "Accelerating Change: Towards Low Carbon Transportation," Center for Climate and Energy Solutions Webinar, February 18.

REFERENCES

1. Greene, D.L. and S. Ji, 2016. "Policies for Promoting Low-Emission Vehicles and Fuels: Lessons from Recent Analyses," Baker Center Report 4:16, Howard H. Baker, Jr. Center for Public Policy, The University of Tennessee, Knoxville, available at: http://bakercenter.utk.edu/policies-promoting-low-emission-vehicles-fuels-report-released.

2. Greene, D.L., S. Park and C. Liu, 2014b. "Public policy and the transition to electric drive vehicles in the U.S.: The role of the zero emission vehicles mandates," *Energy Strategy Reviews*, vol. 5, pp. 66–77.

3. McCollum, D. and C. Yang, 2009. "Achieving deep reductions in US transport greenhouse gas emissions: Scenario analysis and policy implications," *Energy Policy*, vol. 37, pp. 5580–5596.

4. McNutt, B.D. and D. Rodgers, 2004. "Lessons Learned from 15 Years of Alternative Fuels Experience – 1988 to 2003", in D. Sperling and J.S. Cannon, eds., *The Hydrogen Energy Transition*, Elsevier Academic Press, San Diego, CA.

5. Melton, N., J. Axsen and D. Sperling, 2016. "Moving beyond alternative fuel hype to decarbonize transportation," *Nature energy*, article no. 16013, 2/22/2016, www.nature.com/natureenergy .

6. National Research Council (NRC), 2013a. *Transitions to Alternative Vehicles and Fuels*, National Academies Press, Washington, D.C.

IX.7 Sustainability Analysis of Hydrogen Supply and Stationary Fuel Cell Systems Using the Hydrogen Regional Sustainability (HyReS) Framework

Marc Melaina (Primary Contact), Brian Bush, Michael Penev, Joshua Sperling
National Renewable Energy Laboratory
15013 Denver West Parkway
Golden, CO 80401
Phone: (303) 275-3836
Email: marc.melaina@nrel.gov

DOE Manager: Fred Joseck
Phone: (202) 586-7932
Email: Fred.Joseck@ee.doe.gov

Project Start Date: October 1, 2015
Project End Date: September 30, 2018

Overall Objectives

- Develop a regional hydrogen sustainability analysis assessment framework (HyReS) that can be applied to hydrogen supply and fuel cell systems and is consistent with a broad range of existing sustainability assessment tools used by relevant stakeholders.
- Apply the framework as an enhancement to the existing suite of hydrogen systems analysis models developed for the Fuel Cell Technology Office (FCTO).
- Refine the framework to incorporate the latest developments in the field of sustainable development assessment, including recent data and analytic approaches, and to capture current issues relevant to key stakeholders.
- Implement the framework through a user interface that is accessible to target audiences, including private sector sustainability managers, industry stakeholders, government and non-government agencies, and potential investors.

Fiscal Year (FY) 2016 Objectives

- Review existing sustainable development frameworks and tools to identify the most relevant and applicable metrics and approaches for hydrogen supply and fuel cell systems.
- Engage with leaders in the field of sustainable development assessment through a Project Advisory Committee.
- Develop an expanded systems analysis assessment framework to account for a broader range of sustainability metrics, focusing on environmental criteria.

Technical Barriers

This project addresses the following technical barriers from the Systems Analysis section of the FCTO Multi-Year Research, Development, and Demonstration Plan.

(A) Future Market Behavior

(B) Stove-piped/Siloed Analytical Capability

(D) Insufficient Suite of Models and Tools

Contribution to Achievement of DOE Systems Analysis Milestones

This project will contribute to achievement of the following DOE milestones from the Systems Analysis section of the FCTO Multi-Year Research, Development, and Demonstration Plan.

- Milestone 1.19: Complete analysis of the potential for hydrogen, stationary fuel cells, fuel cell vehicles, and other fuel cell applications such as material handling equipment including resources, infrastructure and system effects resulting from the growth in hydrogen market shares in various economic sectors. (4Q, 2020)
- Milestone 2.2: Annual model update and validation. (4Q, 2011 through 4Q, 2020)

FY 2016 Accomplishments

- Planned and executed an expert roundtable event, held on April 12–13, 2016, on the National Renewable Energy Laboratory campus in Golden, Colorado, to brainstorm and discuss framework scope and prioritize action items and areas of focus.
- Collected and prioritized stakeholder feedback on key questions related to future framework users, use characteristics, framework outputs and inputs, and framework maintenance and evolution considerations.
- Developed and proposed an indicator classification system for regional supply systems, which includes integrating spatial sustainability data with the Scenario Evaluation and Regionalization Analysis model.

- Identified existing frameworks to use as a reference for HyReS development, including ENVISION and metrics from the Natural Capital Coalition.

✧ ✧ ✧ ✧ ✧

INTRODUCTION

Analytic methods for hydrogen systems developed to date include a broad range of relevant metrics, including technical specifications, costs, finances, and lifecycle greenhouse gas emissions. This project will enhance the existing set of FCTO analysis tools to include additional regional sustainability metrics across three pillars: environmental, economics and equity. The resulting HyReS framework will serve as an information warehouse, providing information of use to existing sustainability assessment frameworks.

APPROACH

The HyReS project is a three-year project with distinct tasks in each year. The first year involves a review of the literature on sustainability assessment methods, establishment of a project steering team, and development of a general framework structure with a select number of case study applications. Year 2 involves additional expansions to the framework, application of the framework to a broader set of regional hydrogen pathways, alignment of the framework with corporate-level sustainability assessment tools, and release of a beta version of the tool. Year 3 involves refinement of the tool in response to feedback on the beta tool and implementation of the final HyReS framework.

The key target audiences for the HyReS framework include the general public and consumer advocacy groups, engineering firms and funding agencies assessing specific projects, and impact investor or green fund managers. Case study pathways proposed for application of the framework in year one include central steam methane reforming with gaseous truck delivery and remote wind production with pipeline delivery.

RESULTS

Definitions of sustainability vary significantly depending upon context and subject area. A general and widely quoted definition from the Brundtland Report is "…development that meets the needs of the present without compromising the ability of future generations to meet their own needs" [1]. More recent developments emphasize the importance of transitions and transformations across complex interactions of social, ecological, and infrastructural systems [5]. Of particular interest for regional hydrogen supply systems is the ability to design resilient civil infrastructure systems through an adaptive management approach to account for future shifts away from business-as-usual conditions, such as increased prevalence of droughts, floods, or other systems stresses [2,6]. Resilience, a complementary concept to sustainability, is highly relevant to both the design and social value of future regional hydrogen infrastructures, and has been defined in terms of adaptive capacities that support system functionality in times of crisis or stress [4].

The HyReS framework goals, as presented to attendees at the roundtable event on April 12–13, 2016, include the following:

- R&D Needs: Inform hydrogen fuel cell production goals and priorities.
- Sector Assessment: Support market transformation efforts by multiple stakeholders within formal and informal public-private partnership consortiums.
- Public Outreach: Engage with and contribute to public dialogue on progress and options towards achieving sustainable development goals.

The categorization of sustainability indicators that follows from these goals is presented in Figure 1, and involves three overlapping spheres across two dimensions: (1) scope of sustainability audience and (2) commercialization progress. R&D needs fall within the first sphere of technology indicators, relevant to pre- or early-commercial status technologies and of interest to a relatively limited audience. Sector-wide assessments are addressed through supply chain indicators, and broader

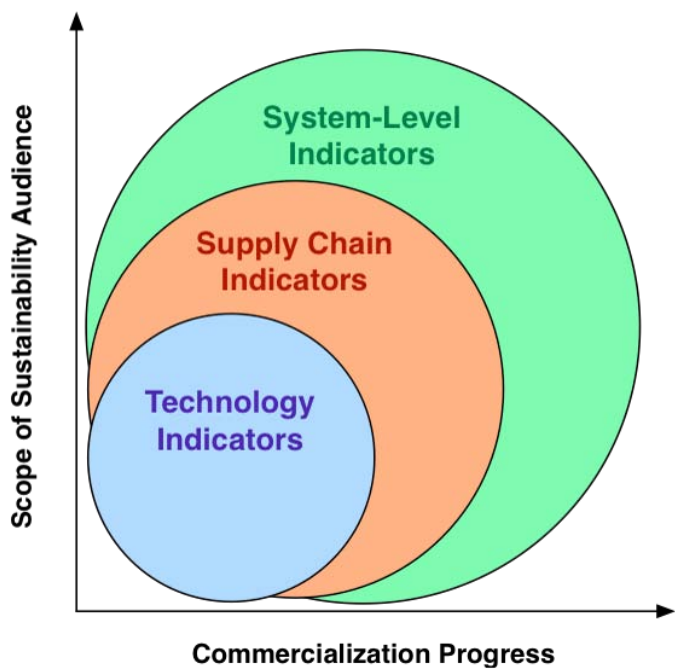

FIGURE 1. Categorization of HyReS indicators

general audiences concerned with full commercialization of regional hydrogen systems are addressed through system-level indicators. For example, improvements in electrolysis efficiency would fall under technology indicators, while total greenhouse gas emissions from hydrogen produced from future wind farms would fall under system-level indicators.

One of the key challenges of the HyReS project will be integration of multiple levels and types of sustainability data into a consistent geographic framework that both extends into the future and is relevant to project-specific assessments. The geographically detailed Scenario Evaluation and Regionalization Analysis model will serve as as the means of reconciling any data inconsistencies, and can also be used as an optimization tool or for multi-criteria assessment comparisons. One of the proposed analytic approaches to achieving consistency with quantitative assessment methods used in the broader corporate sustainability community is alignment with the framework and valuation assumptions contained within the Protocol developed through the Natural Capital Coalition [3]. Some additional high-priority items resulting from the expert roundtable include the following:

- Design HyReS with government agencies, policy makers, investors and original equipment manufacturers (autos and fuel equipment) as key framework users.
- The framework should enable comparisons of various technologies and policies with regard to sustainability outcomes, provide flexibility to serve different types of users, and identify gaps to improve assessment results.
- Key HyReS outputs should include carbon intensity, investments metrics (e.g., return on investment), ecological inputs, regional results, water impacts, and monetized natural capital value per vehicle-mile driven.
- Key HyReS inputs should include data from regulatory programs and agencies, feedback from industry users, future climate data, and regulations and incentives.
- Maintenance and evolution considerations include use of measurable outputs, focusing on subject matter experts first and then other stakeholders, establishment of a formal feedback and revision process, ability for users to tailor results, and creation of a self-sustaining business model to support for the framework over the long term.

CONCLUSIONS AND FUTURE DIRECTIONS

This three-year project began in FY 2016 with initial scoping and development of a preliminary framework structure, which was presented along with key framework development questions at an expert roundtable event held April 12–13, at National Renewable Energy Laboratory in Golden, Colorado. Next steps and key attributes for the HyReS framework were prioritized by roundtable attendees. Proceedings from the roundtable will be published as a technical report, as well as a select number of case studies applying the framework to specific regional hydrogen pathways.

FY 2016 PUBLICATIONS/PRESENTATIONS

1. Marc Melaina, Brian Bush, Michael Penev, Dana Stright, Darlene Steward, Joshua Sperling, "Sustainability Analysis: Sustainability analysis of hydrogen supply and stationary fuel cell systems using the Hydrogen Regional Sustainability (HyReS) framework." Presented at the DOE Hydrogen and Fuel Cells Program Annual Merit Review and Peer Evaluation Meeting, Washington, D.C., June 6–10, 2016.

REFERENCES

1. Brundtland, G.H. 1987. Our common future: Report of the 1987 World Commission on Environment and Development. United Nations.

2. Lee, E.E., J.E. Mitchell, and W.A. Wallace, 2007. "Restoration of Services in Interdependent Infrastructure Systems: A Network Flows Approach," IEEE Transactions on Systems, Man, and Cybernetics, Part C (Applications and Reviews), 37(6): 1303–1317.

3. NCC, 2016. Natural Capital Protocol, Natural Capital Coalition, available online: http://naturalcapitalcoalition.org/protocol/

4. Norris, F.H., S.P. Stevens, B. Pfefferbaum, K.F. Wyche, and R.L. Pfefferbaum, "Community Resilience as a Metaphor, Theory, Set of Capacities, and Strategy for Disaster Readiness," American Journal of Community Psychology, vol. 41, no. 1, pp. 127–150, March 2008.

5. Ramaswami, A., C. Weible, D. Main, T. Heikkila, S. Siddiki, A. Duvall, A. Pattison, and M. Bernard, 2012. "A Social-Ecological-Infrastructural Systems Framework for Interdisciplinary Study of Sustainable City Systems," Journal of Industrial Ecology, 16(6): 801–813.

6. White, J.W.C., R.B. Alley, D.E. Archer, A.D. Barnosky, E. Dunlea, J. Foley, R. Fu, M.M. Holland, M.S. Lozier, J. Schmitt, L.C. Smith, G. Sugihara, D.W.J. Thompson, A.J. Weaver, and S.C. Wofsy, 2014. "Abrupt Impacts of Climate Change: Anticipating Surprises," EGU General Assembly Conference Abstracts, vol. 16, May.

IX.8 Evaluation of Technology Status Compared to Program Targets

Marc Melaina (Primary Contact), Yuche Chen, Aaron Brooker
National Renewable Energy Laboratory
15013 Denver West Parkway
Golden, CO 80401
Phone: (303) 275-3000
Email: Marc.Melaina@nrel.gov

DOE Manager: Fred Joseck
Phone: (202) 586-7932
Email: Fred.Joseck@ee.doe.gov

Project Start Date: October 1, 2014
Project End Date: September 30, 2016

Overall Objectives

- Quantify the potential impact of fuel cell electric vehicle (FCEV) research and development under the U.S. Department of Energy's (DOE's) Fuel Cell Technologies Office technology program.
- Estimate how competitive FCEVs could become in the future.
- Identify the most influential parameters for FCEV success.

Fiscal Year (FY) 2016 Objectives

- Estimate how competitive FCEVs could become in the future using two approaches:
  - Comparing the cost of equivalent vehicles using different powertrains.
  - Evaluating the market adoption of FCEVs introduced among all currently existing vehicle options.
- Understand the influence of meeting, exceeding, or falling short of DOE Fuel Cell Technologies Office program goals on future market adoption of FCEVs.

Technical Barriers

This project addresses the following technical barriers from the Systems Analysis section of the Fuel Cell Technologies Office Multi-Year Research, Development, and Demonstration Plan.

(A) Future Market Behavior

(B) Stove-piped/Siloed Analytical Capability

(D) Insufficient Suite of Models and Tools

Contribution to Achievement of DOE Systems Analysis Milestones

This project contributes to achievement of the following DOE milestones from the Systems Analysis section of the Fuel Cell Technologies Office Multi-Year Research, Development, and Demonstration Plan.

- Milestone 1.15: Complete analysis of program milestones and technology readiness goals - including risk analysis, independent reviews, financial evaluations, and environmental analysis - to identify technology and risk mitigation strategies. (4Q, 2015)
- Milestone 1.17: Complete analysis of program technology performance and cost status, and potential to enable use of fuel cells for a portfolio of commercial applications. (4Q, 2018)

FY 2016 Accomplishments

- In all scenarios that assume similar vehicles using different powertrains, the combined energy and component costs of future FCEVs were found to be lower than those of conventional vehicles and comparable to those of hybrid electric vehicles (HEVs).
- The market share analysis was completed and shows FCEVs could gain as much as one-third of new vehicle sales by 2050. The market analysis improved on past approaches by expanding on the scenarios reviewed and using a model that includes all existing vehicles rather than model-created representations, evolves the vehicle powertrains based on market conditions, and validates with historical sales.
- For some scenarios, HEVs and plug-in hybrid electric vehicles (PHEVs) had greater market share than FCEVs because they can combine their engine and battery power to the wheels for better acceleration, whereas fuel cell and battery power is delivered through a larger and more expensive electric motor.
- Some scenarios found significant FCEV sales, assuming only FCEV technical targets are met, oil prices are high, and either the accelerated FCEV targets are met in 2025 or the FCEV incentives are extended to two million vehicles per manufacturer.

✧ ✧ ✧ ✧ ✧

INTRODUCTION

The DOE's Fuel Cell Technologies Office technology program focuses on research and development to overcome technical barriers related to hydrogen production, delivery, and storage technologies as well as fuel cell technologies for transportation, distributed stationary power, and portable power applications. These research and development activities could result in significant benefits as more hydrogen and fuel cell technologies are deployed. The main goal of this project is to show the effects on FCEV market adoption of meeting, exceeding, or falling short of Fuel Cell Technologies Office program goals. In this study, both techno-economics and consumer choice analyses were conducted to assess the competitiveness of FCEVs in the future.

APPROACH

To achieve the objective of the study, a novel analytic approach is adopted that integrates vehicle simulation (techno-economics) with market adoption potential (consumer choice). In addition, distinct technology trends (based on trends from the Government Performance and Results Act, National Research Council, and other sources) were developed to explore a wide range of potential vehicle technology progress outcomes.

For techno-economic analysis, conventional vehicles (CVs), HEVs, and FCEVs with the same acceleration, range, and battery-to-total-power ratio were simulated and compared in a powertrain simulation model, Future Automotive Systems Technology Simulator (FASTSim). FASTSim is a user-friendly powertrain simulation model, validated against hundreds of existing vehicles. The FASTSim model takes vehicle component parameters as input and simulates efficiency, performance, and cost of vehicles on standard time-versus-speed drive cycles.

The market adoption analysis expanded on the techno-economic analysis perspective of FASTSim using the vehicle choice model, Automotive Deployment Option Projection Tool (ADOPT). It replaced the representative vehicles in the techno-economic approach with all of the existing vehicle options to capture how FCEVs will compete given a realistic variety of vehicle acceleration rates, sizes, and efficiencies. Additionally, through ADOPT's vehicle evolution process, it captured how FCEVs compete when all of the powertrains are optimized to take advantage of their unique characteristics and market conditions.

RESULTS

Techno-Economic Analysis: The total vehicle costs in a 2035 showroom of a CV, HEV, and FCEV with the same acceleration performance, range, and battery-to-total-power ratio are compared under Low, Base, and Accelerated scenarios (Figure 1). The total vehicle cost to the consumer equals the manufacturing cost multiplied by a retail markup factor (1.5) plus net present value of lifetime fuel cost. The gasoline price is assumed to be $3.53 per gallon, and the hydrogen price is assumed to be $4.40 per gallon gasoline equivalent. A discounting factor of 4.1% is used to calculate net present values, based on the 20-year median real annual return of the S&P 500 [1]. The results show that under any of the technology development scenarios, total costs of FCEVs are lower than those of CVs, but comparable to those of HEVs. A detailed look at reductions in normalized total FCEV cost attributed to technology improvements is shown in Figure 2. It shows that the largest reductions in normalized total FCEV cost come from vehicle mass reduction (5.7%) and fuel cell system cost (2.2%). It is also worth noting that the third largest reduction is attributed to the combination effect, which is achieved when all technology improvements are combined.

The market share analysis shows that HEVs and PHEVs can be more marketable than FCEVs when each powertrain is optimized for its unique strengths. Specifically, HEVs and PHEVs could provide very fast acceleration and low fuel cost at a relatively low price because their fuel converters and motors can provide power to the wheels in parallel. The FCEV requires a larger, more expensive electric motor to achieve the same acceleration because the fuel cell cannot directly power the wheels. The improved HEVs and PHEVs prevent significant FCEV market share in the base and accelerated scenarios. However, significant FCEV sales can be achieved by modifying the scenarios, assuming only FCEV technical targets are met, oil prices are high, and either the accelerated FCEV targets are met in 2025 or the

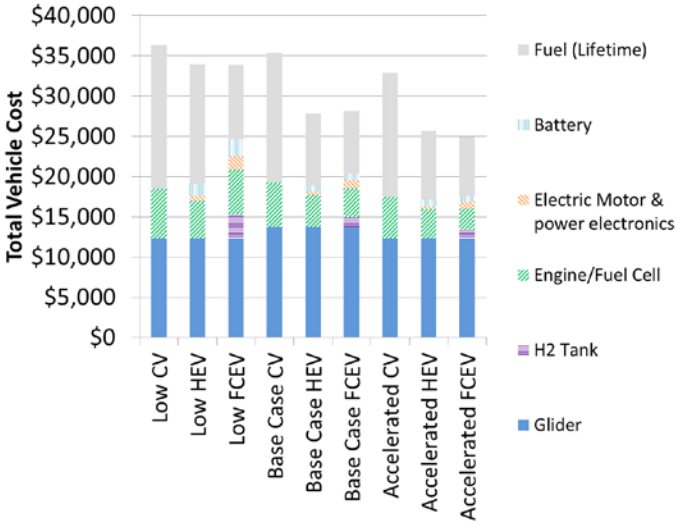

FIGURE 1. Component costs comparison of CVs, HEVs, and FCEVs in 2035 showroom under different scenarios

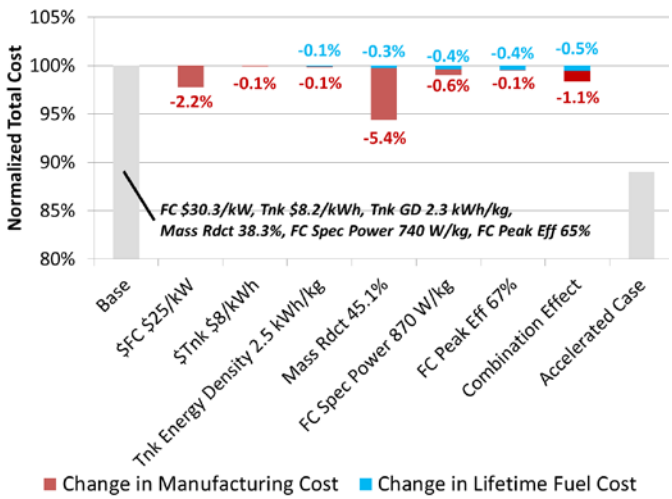

FC – Fuel cell, Tnk – Tank, Rdct – Reduction, Spec – Specific, Eff – Efficiency

FIGURE 2. Reductions in normalized total FCEV cost attributed to technology improvements

FCEV incentives are extended from 200,000 to two million vehicles per manufacturer (Figure 3 and Figure 4).

CONCLUSIONS AND FUTURE DIRECTIONS

This study investigates the impacts of technological improvements on vehicle features, efficiency, performance, manufacturing cost, and operating cost in 2035 in the U.S. In addition, it simulates the market penetration of FCEVs and other vehicle types under various scenarios. Key observations from the analysis include the following:

- In all scenarios, the FCEV's manufacturing cost is higher than the CV's and HEV's. However, when combining the manufacturing cost and lifetime fuel cost, the CV is the worst economic choice, and the HEV and FCEV costs are comparable.
- In the base scenario, the FCEV's consumer-perceived price (manufacturer's suggested retail price plus first four years of fuel costs) is lower than the CV's but higher than the HEV's. This suggests that this level of technological advancement alone cannot guarantee FCEV success and that additional policies would be needed to promote FCEV consumer acceptance.
- Fuel cell stack cost, hydrogen tank cost, and mass-reduction targets have major impacts on FCEV manufacturing cost and price to consumers. Fuel cell engine peak efficiency influences fuel cost but not component costs. The combined effects of technological improvements play an important role in reducing FCEV costs and consumer prices.
- Assuming battery prices drop significantly, market share analysis shows that HEVs and PHEVs can be more marketable than FCEVs when each powertrain is optimized for its unique strengths. The improved HEVs and PHEVs prevent significant FCEV market share in the base and accelerated scenarios. However, significant FCEV sales can be achieved by modifying the scenarios: assuming only FCEV technical targets are met, oil prices are high, and either the accelerated FCEV targets are met in 2025 or the FCEV incentives are extended to two million vehicles per manufacturer.

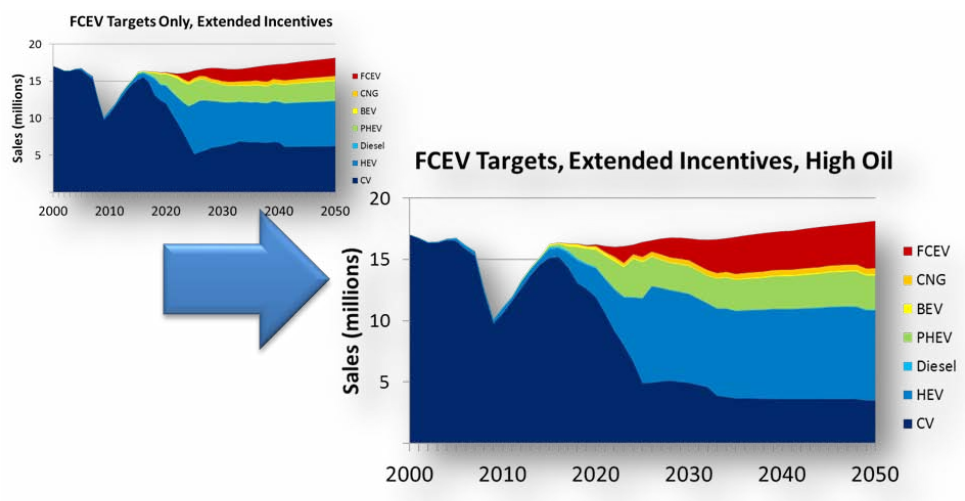

BEV - Battery-electric vehicle, CNG - Compressed natural gas vehicle

FIGURE 3. Market share due to achieving only FCEV-related targets, extending FCEV incentives to two million vehicles per manufacturer, and assuming high oil prices

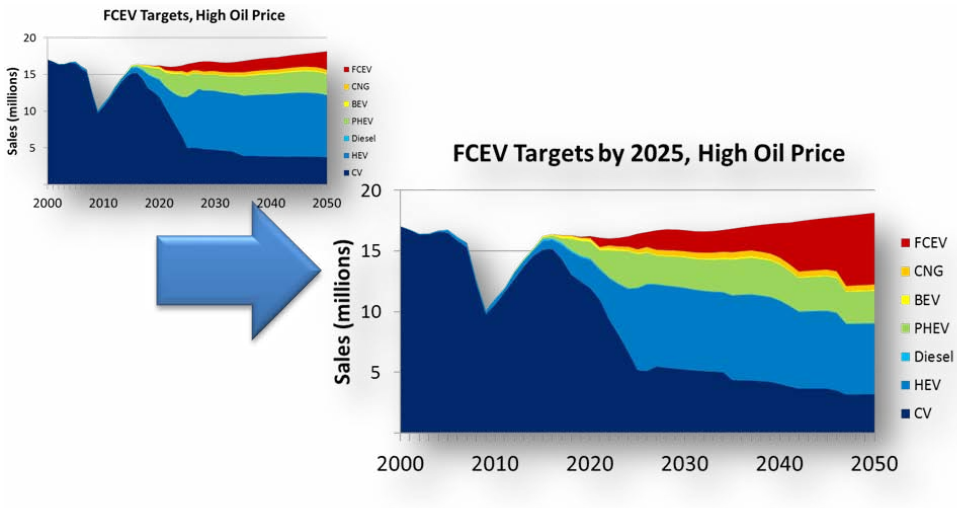

FIGURE 4. Market share due to achieving only FCEV-related targets by 2025 and assuming high oil prices

Suggested future research based on this study includes the following:

- Develop improved mass reduction cost curve to better represent tradeoffs in component sizes and acceleration.
- Incorporate zero-emission vehicle mandate influence by simulating credit system.
- Consider the learning-curve effect in relation to FCEV technology. In the present analysis, FCEV costs decline as U.S. FCEV sales increase. However, because automakers manufacture and sell vehicles globally, the impact of global FCEV sales could be considered in the analysis.

FY 2016 PUBLICATIONS/PRESENTATIONS

1. Melaina, M., Y. Chen, and A. Brooker. "Evaluation of Technology Status Compared to Program Targets." Presented at the DOE Hydrogen and Fuel Cells Program 2016 Annual Merit Review and Peer Evaluation Meeting, Washington, D.C., June 8, 2016.

REFERENCES

1. New York Times. 2011. "In Investing, It's When You Start and When You Finish." New York Times, 2011. http://www.nytimes.com/interactive/2011/01/02/business/20110102-metrics-graphic.html?_r=1&.

IX.9 Expanded Capabilities for the Hydrogen Financial Analysis Scenario Tool

Michael Penev (Primary Contact), Marc Melaina, Brian Bush
National Renewable Energy Laboratory
15013 Denver West Pkwy
Golden, CO 80401
Phone: (303) 275-3880
Email: mike.penev@nrel.gov

DOE Manager: Fred Joseck
Phone: (202) 586-7932
Email: Fred.Joseck@ee.doe.gov

Project Start Date: September 2014
Project End Date: Project continuation and direction determined annually by DOE

Overall Objectives

- Provide convenient detailed hydrogen infrastructure financial analysis to facilitate investments in hydrogen refueling stations and improve policy-design decisions to support early hydrogen station and fuel cell electric vehicle market development.
- Inform multiple stakeholders: policy and government decision makers, station operators, equity investors, strategic investors, lenders.
- Enable transparent incentive analysis.
- Provide embedded investment risk analysis.

Fiscal Year (FY) 2016 Objectives

- Complete additional refinements to the Hydrogen Financial Analysis Scenario Tool (H2FAST), such as the following examples of potential revisions or additions:
  - Sensitivity analysis capability (Monte Carlo/risk analysis)
  - Capability to analyze additional stations
  - More supply chain component titles (e.g., pipeline, gasifier) and feedstocks (e.g., woody biomass)
  - Salvage value (or net expense at end of life), including capital gains considerations
  - Cumulative column on pareto chart, profitability index, $/kg incentives
  - Add custom station types (e.g., half electrolysis, half delivered)

Technical Barriers

This project addresses the following technical barriers from the Systems Analysis section of the Fuel Cell Technologies Office Multi-Year Research, Development, and Demonstration Plan:

- Section 4.2 Technical Approach: Infrastructure Analysis
- Section 4.5 A. Future Market Behavior: Scenarios to understand vehicle-fuel interactions
- Section 4.5 E. Unplanned Studies and Analysis: Response to H2USA public-private partnership and infrastructure deployment goals

Contribution to Achievement of DOE Systems Analysis Milestones

This project will contribute to achievement of the following DOE milestones from the Systems Analysis section of the Fuel Cell Technologies Office Multi-Year Research, Development, and Demonstration Plan:

- Milestone 1.12: Complete an analysis of the hydrogen infrastructure and technical target progress for technology readiness. (4Q, 2015)
- Milestone 1.15: Complete analysis of program milestones and technology readiness goals - including risk analysis, independent reviews, financial evaluations, and environmental analysis - to identify technology and risk mitigation strategies. (4Q, 2015)
- Milestone 1.16: Complete analysis of program performance, cost status, and potential use of fuel cells for a portfolio of commercial applications. (4Q, 2018)
- Milestone 1.17: Complete analysis of program technology performance and cost status, and potential to enable use of fuel cells for a portfolio of commercial applications. (4Q, 2018)
- Milestone 1.19: Complete analysis of the potential for hydrogen, stationary fuel cells, fuel cell vehicles, and other fuel cell applications such as material handling equipment including resources, infrastructure and system effects resulting from the growth in hydrogen market shares in various economic sectors. (4Q, 2020)
- Milestone 2.2: Annual model update and validation. (4Q, 2011 through 4Q, 2020)

FY 2016 Accomplishments

- Added risk analysis with triangular distribution for any input parameter (lowest, most likely, highest values).
- Added quick visualization for any input or output stochastic distribution.
- Enabled reporting of 5th, 50th, and 95th percentile for each input or output parameter
- Added ability to specify fixed hydrogen price or fixed internal rate of return (IRR)
- Added profitability index, a robust financial performance metric (unlike IRR, which sometimes does not yield a value)
- Added consideration of byproducts such as grid service, waste heat, user-defined co-products (enabling combined heat, hydrogen, and power [CHHP] and other non-conventional system analysis)
- Added per-kilogram ($/kg) revenue for modeling: Low Carbon Fuel Standard, Renewable Identification Number credits, others
- Incorporated take-or-pay contract specifications
- Added more feedstocks, allowing custom station modeling (e.g., half delivered, half produced hydrogen; H2A case implementation)
- Added linear depreciation, enabling International Financial Reporting Standard analysis
- Added consideration of non-depreciable assets (e.g., land)
- Added salvage value and capital gains considerations (allowing land sale and equipment salvage considerations)
- Expanded case count to 300 for larger portfolio analysis
- Increased maximum project life to 100 yr (allowing pipeline analysis)

✧ ✧ ✧ ✧ ✧

INTRODUCTION

In this project, DOE is distilling investor-grade analysis capability for evaluating hydrogen infrastructure. The DOE is sponsoring numerous technology developments which coalesce in hydrogen infrastructure's ability to enter mainstream markets. A financial modeling framework is necessary to determine the financial performance potential for these emerging technologies. The DOE has a large suite of models which provide similar analysis but none of them is designed with detailed investor-grade financial analysis capability.

APPROACH

Model design follows U.S. financial reporting standards known as Generally Accepted Accounting Principles[1]. This analytic framework is applied in an Excel-based model, which can be readily shared and used among stakeholders, as well as through a web-based calculator [1]. To assure model articulation relevance and usefulness, the team has worked closely with H2USA Investment and Finance Working Group members. Direct input into model design and functionality has been provided by financial experts from the banking and venture capital sectors.

RESULTS

Some of the key new functions of the model are described in this section. Multi-product, multi-feedstock analysis capability enables users to analyze complex systems such as CHHP, as shown in Figure 1. In addition, H2FAST

[1] The model has capability to analyze financial performance in line with International Financial Reporting Standards.

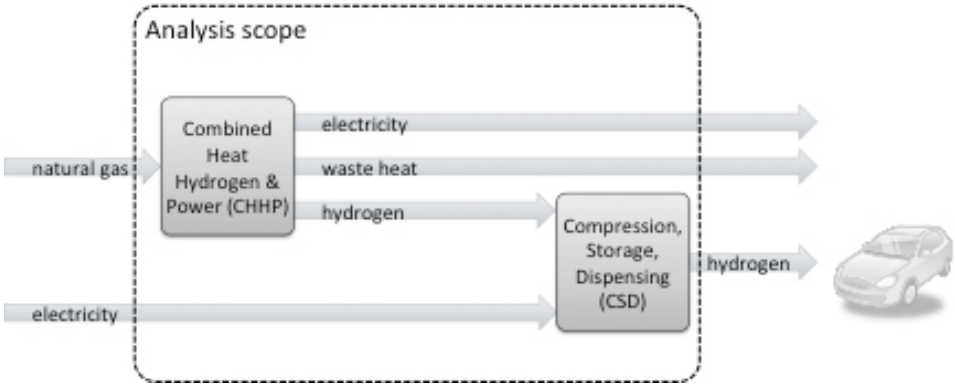

FIGURE 1. Analysis scope capability has been improved to allow analysis of multiple feedstock and products streams as well as breakdown of capital between subsystem components

can be used to analyze sub-system performance and overall system financial performance for scenarios where multiple stakeholders own and operate components. For example, if one entity owns a stationary fuel cell and another owns retail hydrogen equipment. The model can be quickly utilized to determine each stakeholder's financial position.

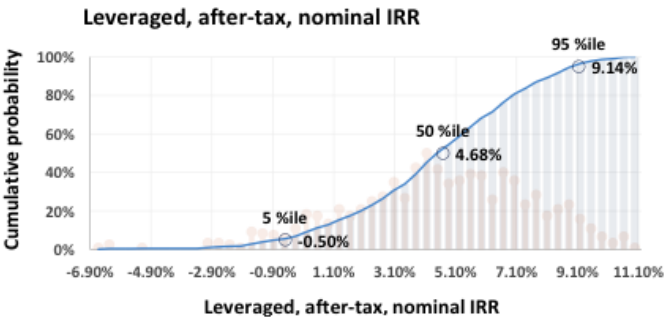

FIGURE 2. Model capability has been expanded to allow uncertainty analysis and articulation of ranges of financial outcomes

Risk analysis has been implemented and allows users to specify uncertainty ranges around most input parameters, as shown in Figure 2. The model performs statistical analysis and yields ranges for possible financial outcomes. Detailed cash flow attribution is expressed in a simple Pareto chart, which allows users to determine financial performance drivers, as shown in Figure 3. Additional incentive analysis capability and take-or-pay contract modelling has been implemented in the model to allow performance estimation on complex financial scenarios.

CONCLUSIONS AND FUTURE DIRECTIONS

The H2FAST model provides a platform for hydrogen infrastructure financial performance analysis. The model is being actively used for many efforts, and as a new tool in the DOE's portfolio, developers are receiving constructive feedback from multiple users. Expanded capabilities and model refinements in FY 2016 have been made in response to a wide range of end user suggestions and interactions. As hydrogen infrastructure components become commercialized, and engagement with the

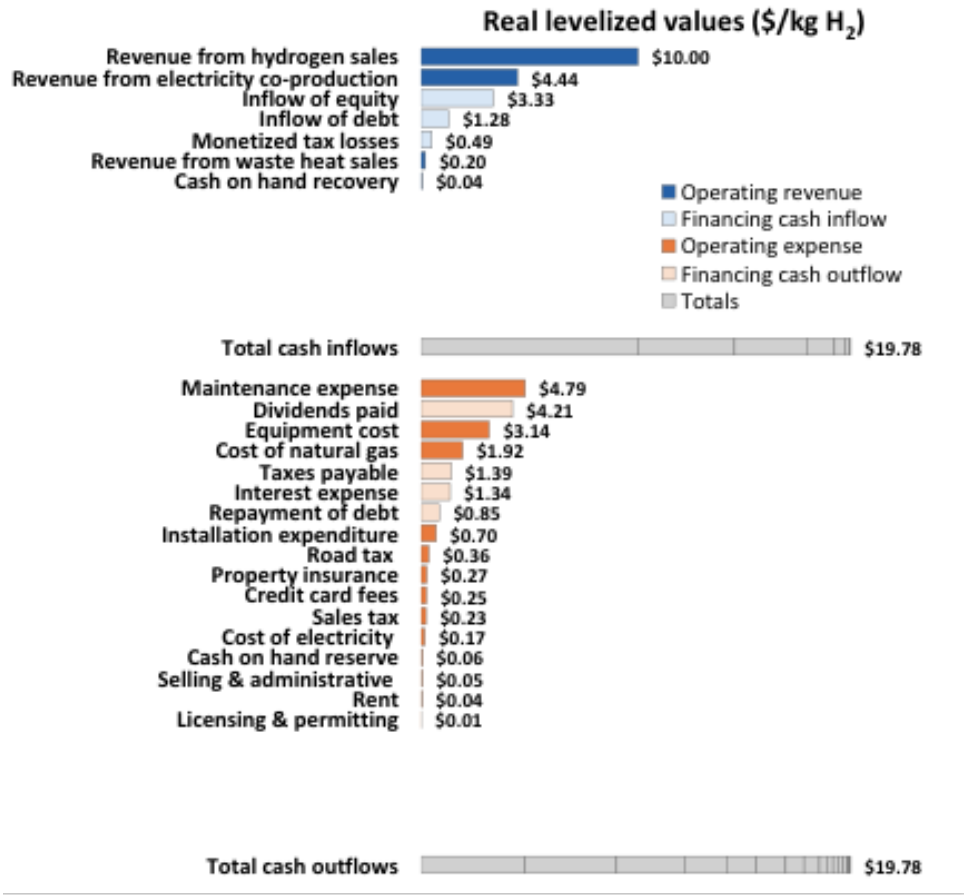

FIGURE 3. Pareto chart is generated for each analysis, which highlights cash flow contributions on a normalized basis to help communicate relative cash flow magnitudes

investment community increases, it is prudent to provide a clear articulation of financial scenarios and metrics, and to respond to and incorporate ongoing improvement requests from users. Future developments will include capability to assess investments for multiple stations or components across different timeframes, linkages between supply chain components, and incorporation of externality costs such as water impacts or the social cost of carbon.

FY 2016 PUBLICATIONS/PRESENTATIONS

1. Michael Penev, Brian Bush, Marc Melaina, "Expanded Capabilities for the Hydrogen Financial Analysis Scenario Tool (H2FAST)," Presented at the DOE Hydrogen and Fuel Cells Program Annual Merit Review and Peer Evaluation Meeting, Washington, D.C., June 6–10, 2016.

REFERENCES

1. H2FAST, Hydrogen Financial Analysis Scenario Tool, 2016, Available online: http://www.nrel.gov/hydrogen/h2fast/

IX.10 The Business Case for Hydrogen-powered Passenger Cars: Competition and Solving the Infrastructure Puzzle

Robert Rosner (Primary Contact), Carlo Graziani, and Robert Topel
The University of Chicago
Eckhardt Research Center 509
Chicago, IL 60615
Phone: (773) 702-0560
Email: rrosner@uchicago.edu

DOE Manager: Fred Joseck
Phone: (202) 586-7932
Email: Fred.Joseck@ee.doe.gov

Project Start Date: March 1, 2016
Project End Date: September 30, 2016

Overall Objectives

- Establish the competitive posture of hydrogen fueled private vehicles in the current market place.

Fiscal Year (FY) 2016 Objectives

- Establish the conditions under which a business case can be made for private unsubsidized investment in hydrogen fueling capability, at the time of the 101st station in California.

Technical Barriers

This project addresses the following technical challenges from the Systems Analysis section of the Fuel Cell Technologies Office Multi-Year Research, Development, and Demonstration Plan:

(A) Future Market Behavior: for example, (a) the number of hydrogen-powered cars sold in target markets and (b) the competition posed by battery-powered electric vehicles (BEVs)

(A) Future Market Behavior: for example, technological developments for high throughput cryo pumps at reasonable costs are uncertain, resulting in uncertainties in the business case for liquid hydrogen fueling stations

(C) Inconsistent Data, Assumptions and Guidelines: for example, large variations in existing literature, for both hydrogen filling station construction and operating costs

(E) Unplanned Studies and Analysis: Lack of existing market experience for hydrogen-powered passenger vehicles – and the as-yet unanswered question of market acceptability for hydrogen-fueled passenger vehicles.

Contribution to Achievement of DOE Systems Analysis Milestones

A key question for the success of hydrogen-fueled vehicles is whether a plausible business case can be made for building out the hydrogen filling station network, once the initial subsidies phase out. This kind of analysis will be needed in order to have venture capitalists consider investing in this market without counting on subsidies. This is a key economic milestone for the DOE Hydrogen and Fuel Cells Program.

FY 2016 Accomplishments

- Given the lack of extensive experience on the economics of hydrogen fueling stations, we examined the economics of E85 filling capability at existing gasoline stations. This was done in order to establish the conditions under which unsubsidized private investment would move forward in add a green fueling capability to an existing gasoline station.
- We confirmed that, by and large, the retail operation of the fuel vending side of a gasoline station is "junior partner" to the retail operation of the on-site convenience store, with the fuel filling operation largely serving to bring in the customer base for the high-margin convenience store.
- Applying this insight to possible addition of hydrogen fueling capability to an existing gasoline station, we established the tipping point in the construction cost of such an additional capability, which we estimate to be of order $2,100,000 (2009 dollars).

✧ ✧ ✧ ✧ ✧

INTRODUCTION

We consider the economics governing the installation of a hydrogen fueling station at an already existing gasoline filling station. Our aim is to establish whether a private investment in such an operation that is *not* partnered with governmental subsidy would make business sense.

APPROACH

In order to establish the conditions that would lead to private, unsubsidized, investment, we did the following.

- We examined the financial issues surrounding investments in E85 fueling capability at existing filling stations. E85 is also viewed as a relatively green fuel, and therefore shares with hydrogen some of the patina of promoting an environmentally benign transport sector. Our assumption is thus that the economics governing the installation of E85 fueling capability is very likely to be similar to that governing the addition of hydrogen fueling capability.
- We used existing literature [2–4] in order to identify the least expensive technical route to a retail hydrogen fueling capability of 300 kg/d, which we viewed as appropriate for the 101st station. This station design uses gaseous hydrogen, delivered on site using tube trailers, and uses a cascade-based fueling design.
- We used the National Renewable Energy Laboratory (NREL) Hydrogen Financial Analysis Scenario Tool (H2FAST) to establish the tipping point at which private investment in the absence of subsidy no longer makes sense. The key point of our analysis is the recognition that, assuming that the fueling operation of a filling station is not the primary contributor to the operating margin of a station, the break-even point of a hydrogen fueling operation may only require a very modest return on investment.

RESULTS

Our preliminary analysis showed the following.

- Examination of the fueling station literature confirmed that the dominant contributor to the operating margin of a filling station is the associated convenience store; the filling operations, independent of the nature of the fuel being dispensed, tends to be a very low-margin business activity [1]. This implies that any kind of filling operation, including a hydrogen fueling station, that does not include a retail convenience store is very unlikely to be an attractive target for venture capitalist investments, especially in the absence of governmental subsidies.
- By conducting a bounding financial analysis of a hydrogen fueling capability, using NREL H2FAST modeling, we established:
  - Adding a hydrogen fueling capability to an existing gasoline station has a substantial advantage over creating a "green field" site. Advantages include sharply reduced frictions involved with site preparation and licensing, lowered tensions with potential site neighbors, reduced impacts of real estate costs (such as rents, taxes, and fees), and lowered staff costs. Thus, it does not make sense for the 101st hydrogen station to be built at a green field site.
  - Because the key determinant of the financial success of a fueling station is the retail operation of the on-site convenience store, the key financial contribution of a new fuel filling capability (e.g., E85 or hydrogen fueling) to an existing station is the additional traffic brought on site, traffic that would contribute to the convenience store operations. Thus, the retail margin of the "green fuel" operation is not only likely to be always small, but is likely to be small enough that it does not really contribute in a significant way to the business case of the station taken as a whole (meaning, fueling and convenience store operations considered together). Certainly, one would not want to be losing money on the sale of the fuel, but this does imply that the threshold for the return on investment required in order to make an investment plausible can be much lower than would be expected if one were to operate a fueling operation in the absence of an onsite convenience store.
  - Using H2FAST, we then determined the tipping point in construction costs at which the retail hydrogen fueling operation would no longer make sense in the absence of subsidies. The input data assumed the afore-mentioned station filling design and capacity, and took into account the cost reductions in both construction and operation that flow from using an existing filling station as the hydrogen fueling site. We currently estimate that tipping point in construction costs to be $2,100,000 (2009 dollars).

CONCLUSIONS AND FUTURE DIRECTIONS

The key missing elements of our study are:

- A detailed analysis of the progress made in selling hydrogen fuel cell vehicles in the California marketplace over the next two years.
- An analysis of the cost reductions in hydrogen fueling stations, again over the next two years.
- An analysis of the changes in retail conditions at California gasoline stations that feature a commercial hydrogen fueling island.

These elements are essential to validating the fundamentals of our study, namely the assertions that a hydrogen fueling operation only needs to break even in its economics in order to be attractive to private investment, as long as it successfully serves as part of a rebranding strategy for the filling station, serving to increase its customer base for its convenience store operation.

FY 2016 PUBLICATIONS/PRESENTATIONS

1. Presentation at the 2016 U.S. Department of Energy Hydrogen and Fuel Cells Program Annual Merit Review (sa052_rosner_2016_o.ppt).

REFERENCES

1. Johnson, C., & Melendez, M. (2007). *E85 retail business case: When and why to sell E85*. NREL/TP-540-41590. Golden, CO: National Renewable Energy Laboratory.

2. Melaina, M., & Penev, M. (2013), *Hydrogen Station Cost Estimates: Comparing Hydrogen Station Cost Calculator Results with other Recent Estimates*, NREL Technical Report NREL/TP-5400-56412.

3. Parks, G., Boyd, R., Cornish, J., & Remick, R. (2014), *Hydrogen Station Compression, Storage, and Dispensing: Technical Status and Costs*, NREL Technical Report NREL/BK-6A10-58564.

4. Pratt, J., Terlip, D., Ainscough, C., Kurtz, J., and Elgowainy, A. (2015), Technical Report *NREL/PP-5400-64107* (April 2015).

IX.11 National FCEV and Hydrogen Refueling Station Scenarios

Marc Melaina (Primary Contact), Brian Bush
National Renewable Energy Laboratory
15013 Denver West Parkway
Golden, CO 80401
Phone: (303) 275-3836
Email: marc.melaina@nrel.gov

DOE Manager: Fred Joseck
Phone: (202) 586-7932
Email: Fred.Joseck@ee.doe.gov

Subcontractor:
Lexidyne, LLC, Colorado Springs, CO

Project Start Date: October 1, 2014
Project End Date: September 30, 2016

Overall Objectives

- Develop and analyze self-consistent national scenarios of fuel cell electric vehicle (FCEV) market growth and hydrogen refueling station (HRS) deployment.
- Work with industry and other stakeholders.
- Accurately represent early market trends.
- Explore long-term possibilities for FCEV adoption.

Fiscal Year (FY) 2016 Objectives

- Develop and analyze national FCEV scenarios with respect to financing and station locations.
- Work with industry and other stakeholders to develop financial metrics for HRSs.
- Accurately represent early market trends for specific regions.
- Explore long-term possibilities for HRS financing with respect to assumed FCEV market adoption trends.

Technical Barriers

This project addresses the following technical barriers from the Systems Analysis section of the Fuel Cell Technologies Office Multi-Year Research, Development, and Demonstration Plan.

(A) Future Market Behavior

(C) Inconsistent Data, Assumptions and Guidelines

(E) Unplanned Studies and Analysis

Contribution to Achievement of DOE Systems Analysis Milestones

This project will contribute to achievement of the following DOE milestones from the Systems Analysis section of the Fuel Cell Technologies Office Multi-Year Research, Development, and Demonstration Plan.

- Milestone 1.19: Complete analysis of the potential for hydrogen, stationary fuel cells, fuel cell vehicles, and other fuel cell applications such as material handling equipment including resources, infrastructure and system effects resulting from the growth in hydrogen market shares in various economic sectors. (4Q, 2020)
- Milestone 2.2: Annual model update and validation. (4Q, 2011 through 4Q, 2020)

FY 2016 Accomplishments

- Developed and analyzed three distinct scenarios with detailed geographic, temporal, and financial information for vehicles, stations, and networks.
- Completed sensitivity analysis of the aforementioned scenarios.
- Delivered an interactive scenario design and browsing tool to stakeholders and demonstrated the tool in workshops.
- Prototyped the Business Case Scenario tool for exploring the full range of scenario outputs geographically over time.

✧ ✧ ✧ ✧ ✧

INTRODUCTION

Integrated scenario analysis assesses interactions among FCEV adoption, infrastructure requirements, and investment. This project examines market and financial implications of strategies to support vehicle and infrastructure expansion nationally.

APPROACH

The scenarios developed in this project embody high levels of self-consistency and quantify key variabilities in the evolution of FCEV adoption. They match published regional early market plans and forecasts and coordinate changes in number of vehicles, number of stations, and station finances. The staging of states with and without zero-emission vehicle mandates (ZEV and non-ZEV states), the market penetration

for FCEVs, the station utilization, and the financial metrics vary among the scenarios. The scenarios' inputs and algorithms capture historical experience and near-term regional plans.

In particular, the three scenarios frame emphases and time periods relevant to different stakeholder audiences. The near-term (2015–2025) period emphasizes early adopter markets and a California ramp-up period along with coordination, planning, and coverage in other ZEV states. The mid-term (2025–2035) period focuses on early adopter markets beyond California and provides significant national coverage, based on broad state coalitions where the ZEV mandate is a major influence. The long-term (2035+) period extends beyond early markets so that many states are onboard and the transition is complete in some markets.

RESULTS

In the *Urban Green Tech* scenario, national FCEV adoption rates are relatively modest, and growth is restricted to the most promising urban markets with high concentrations of early adopters. Early adopters are consumers willing to pay a premium for green vehicles or high-tech vehicles. These consumers tend to be concentrated in large urban areas along the West Coast and East Coast and in a select number of additional urban markets. The clustering effects are strong in this scenario, and the development of station networks in response to early adopter demand results in an increase in local market share across other consumer segments, including fast followers and mainstream consumers. The result is relatively deep pockets of FCEV adoption in major urban areas, with station coverage along highway corridors linking clusters of cities.

In the *State Success* scenario, strong national market growth is achieved due to the influence of state policies such as vehicle rebates and ZEV mandates. Early station networks tend to be limited to urban areas in these states, and they only expand to other states after FCEVs have become a mainstream consumer product. Early adopters are still important in this scenario, but less so than in the Urban Green Tech scenario, and the neighbor effect has a modest influence on the expansion of markets geographically.

In the *National Expansion* scenario, California continues to be a key early market for FCEVs, but additional growth is distributed across a broad range of markets due to both the successful market adoption of FCEVs and aggressive investments in hydrogen station networks. Concentrations of early adopters help guide the placement of early-coverage stations but otherwise have little influence on larger market growth trends. Barriers to hydrogen infrastructure development are removed and overcome quickly, and rapid adoption of FCEVs occurs due to removal of information barriers in general rather than due to the neighbor effect. FCEV technology and cost improves quickly, and consumers purchase FCEVs as replacements for conventional vehicles with little concern over availability of stations, due to rapid network expansion.

The early market portion of the *State Success* scenario matches published forecasts for California and ZEV states. The three scenarios achieve different overall FCEV market shares, but all three scenarios show substantial FCEV

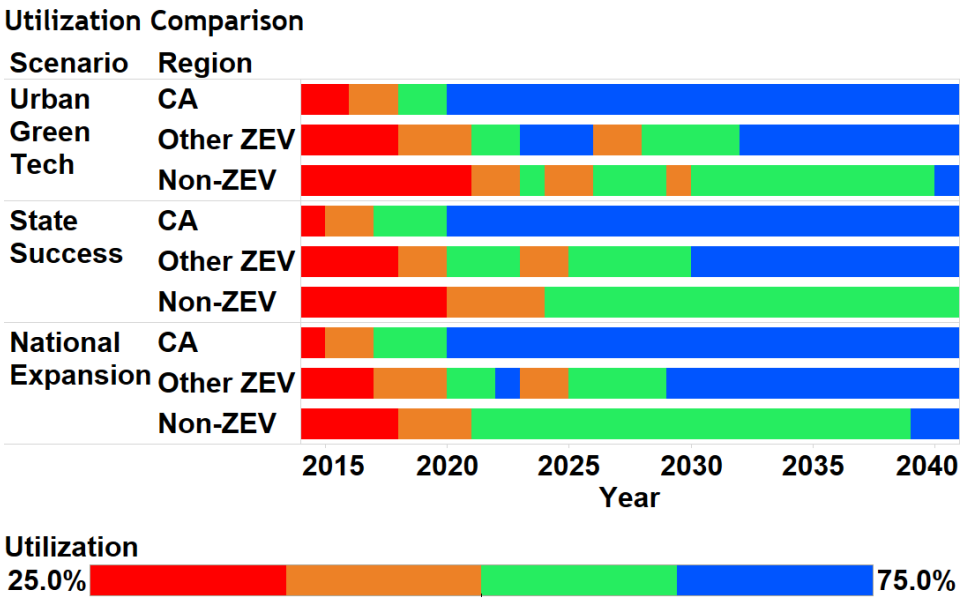

FIGURE 1. Overall average station utilization becomes favorable in stages over time and geographically, varying by scenario

market growth by 2035. The more aggressive scenarios have substantially greater numbers of hydrogen refueling stations, and all scenarios embody different geographic emphases on sales of FCEVs (see Figure 1).

An interactive scenario design and browsing tool has been delivered to stakeholders and demonstrated in workshops (see Figure 2). Furthermore, the prototype Business Case Scenario tool explores the full range of scenario outputs geographically over time. Financial metrics for different stakeholders (funding organizations, investors, lenders, consumers) summarize the business case for hydrogen refueling stations in each of the scenarios.

CONCLUSIONS AND FUTURE DIRECTIONS

In FY 2016, this project developed and analyzed three self-consistent national FCEV scenarios that accurately represent early market trends but also explore long-term possibilities for FCEV adoption. It directly addresses DOE objectives for stakeholder-engaged scenario development and analysis. The three scenarios are grounded in empirical data, early market plans, and technical analysis. Results indicate how many hydrogen refueling stations are required, and where and when they would be installed, in response to variations in the scale and regional distribution of market demand for FCEVs.

The project will continue to provide direct support for H2USA working group activities, engaging with stakeholders to improve analyses; update scenarios to adjust to updated input data and market trends; and disseminate results to H2USA members and the general public. Future work will integrate the national scenarios with explicit representations of finance strategies, incentives, and hydrogen prices. The scenario results will be published as a report and an interactive website.

FY 2016 PUBLICATIONS/PRESENTATIONS

1. Brian Bush and Marc Melaina, "National FCEV and Hydrogen Fueling Station Scenarios." Presented at the DOE Hydrogen and Fuel Cells Program Annual Merit Review and Peer Evaluation Meeting, Washington, D.C., June 6–10, 2016.

2. Marc Melaina, Brian Bush, Michael Penev, Dana Stright, Jarett Zuboy, "National Hydrogen Scenarios for the United States: How many Stations, Where and When?" Presented at the 21st World Hydrogen Energy Conference, Zaragoza, Spain, June 13–16, 2016.

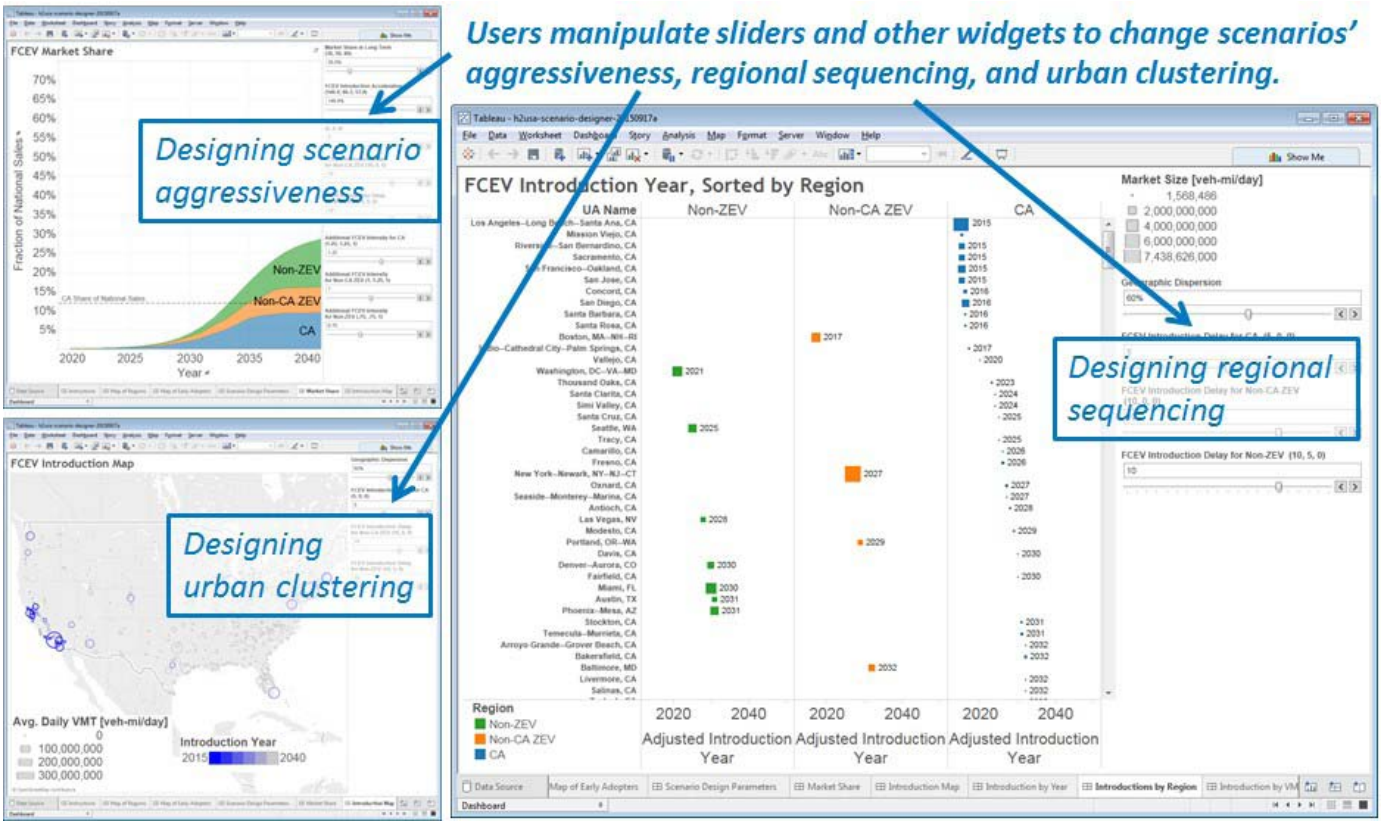

FIGURE 2. Screen captures from the interactive scenario design and browsing tool that has been delivered to stakeholders and demonstrated in workshops

X.0 Market Transformation Program Overview

INTRODUCTION

The purpose of the Market Transformation program is to spur market growth for domestically produced hydrogen and fuel cell systems. The Market Transformation program is conducting activities to help promote and implement commercial and pre-commercial hydrogen and fuel cell systems in real-world operating environments and to provide feedback to research programs, U.S. industry manufacturers, and potential technology users. By supporting increased technology operations testing and use in key early applications, this program helps to identify and overcome non-technical barriers to commercial deployment and to reduce the life cycle costs of fuel cell power by helping to achieve manufacturing economies of scale. These early market deployments will also address other market acceptance factors, resulting in further expansion of technology opportunities.

The Market Transformation program aims to replicate past successes in material handling equipment (MHE) (e.g., lift trucks) and emergency backup power applications that were part of The American Recovery and Reinvestment Act of 2009 (Recovery Act). For example, Market Transformation has projects in applications like fuel cell powered airport ground support baggage tractors and fuel cell electric medium-duty hybrid trucks for parcel delivery applications. These projects are highly leveraged, with an average of more than half of the projects' funds being provided by DOE's partners. Partners providing resources and financial investment to these projects show their high level of interest in continuing to explore these applications and markets, and this level of industry interest is very promising for the potential growth of the domestic fuel cell industry. Market Transformation also partners with other federal agencies and various stakeholders to deploy new applications, such as auxiliary power for ships in port and on board ocean-going vessels in collaboration with the U.S. Department of Transportation's Maritime Administration.

GOAL

Market Transformation activities provide financial and technical assistance for the use of hydrogen and fuel cell systems in early market applications, with the key goals of achieving sales volumes that will enable cost reductions through economies of scale, supporting the development of a domestic industry, and providing feedback to testing programs, manufacturers, and potential technology users.

OBJECTIVES

The objectives of the Market Transformation program are to:

- Evaluate status against target performance metrics for commercially available emergency backup, MHE, and other systems and provide feedback to component suppliers regarding cost reduction opportunities.
- Test emerging approaches to grid management using renewable hydrogen.
- Advance the knowledge and expertise of waste-to-energy fuel cells, shipboard and truck auxiliary power units (APUs), fuel cell electric truck parcel delivery, and aviation ground support applications through targeted testing and evaluation efforts in coordination with the Technology Validation program and in partnership with the U.S. Navy, the U.S. Marine Corps, and civilian agencies such as the U.S. Department of Transportation's Maritime and Federal Aviation Administrations.
- Identify lessons learned from promulgated policies and regulations and promote the development of the most effective and applicable incentives for hydrogen and fuel cell technologies.
- Conduct market transformation deployment projects to enable life cycle cost and performance of early market applications such as fuel cell powered lift trucks and emergency backup power systems to be on par with conventional technologies.

FISCAL YEAR (FY) 2016 TECHNOLOGY STATUS AND ACCOMPLISHMENTS

Fuel cells have been enjoying growing success in key early markets, particularly in MHE and backup power applications. The program's early market deployment efforts—including Market Transformation funding and Recovery Act funding—have successfully catalyzed a significant level of market activity in these areas, which has

been accompanied by substantial reductions in the price of fuel cells. For example, material handling and backup power orders are up 32% and 24% respectively this year (see DOE Records 16012 and 16013) from the cumulative total orders in 2009 through 2014. Ongoing activities and additional areas of interest include the following.

- **Hydrogen Energy Storage Project:** This project is supporting the demonstration of a hydrogen energy storage system as a grid management tool. While hydrogen produced from the system could be used in a variety of value-added applications, the initial phase of the project will use the hydrogen in fuel cell buses operated by the County of Hawaii Mass Transportation Agency and the National Park Service. This year construction began, and initial operation is expected to begin in Spring 2017. (Naval Research Laboratory and the State of Hawaii)
- **Airport Ground Support Vehicles:** This project has a high potential to meet program goals and enable demonstration for a wide breadth of additional airport applications such as lift trucks and shuttle buses. The design has been completed, and the 15 units were assembled with the cargo tractor and tested in field operations. Failures in the stacks occurred, including leaking seals and crossover through the membranes. Analysis revealed that the stacks were not robust enough for the air cargo duty cycle. The stacks are now being replaced with a new design, and initial testing shows satisfactory operations. The next step is to complete stack replacements for all units and begin Phase 2 testing in field operations. (Plug Power)
- **Maritime Fuel Cell Generator Project:** Testing of a first-of-its-kind hydrogen fuel cell power generator for maritime applications was completed. The system was designed to replace pier side diesel generators for refrigerated containers on board ocean vessels. Initial operations testing at a pier-side site was completed with results showing energy efficiency improvements. However, many balance-of-plant components need to be redesigned and replaced. A Phase 2 project scope is now being prepared. (Sandia National Laboratories)
- **Fuel Cell Hybrid Electric Delivery Van Project:** In this project, a design is being developed for a battery electric powertrain system hybridized with fuel cell power to improve drive performance and range on a medium-duty cargo truck. The project has been awarded, and a prototype design effort is underway. A prototype vehicle will be tested on a dynamometer in the next year. (Federal Express Corporation)
- **Fuel Cell Auxiliary Power Unit Project:** This activity now includes a second awarded project that will design and develop a multi-temperature transportation refrigeration unit power system. The first awarded project to demonstrate a single-temperature power system will assemble the subsystems and test an integrated prototype next year. (Pacific Northwest National Laboratory)
- **Fuel Cell–Battery Electric Hybrid for Utility of Bucket Trucks Project:** This Small Business Innovation Research project's Phase 1 design concept found that bucket trucks can be economically viable when using fuel cell power for the bucket's boom motor and not as prime motive power. This was due to the long non-use time associated with the prime power system when the boom is in use at a work site. Other application user values identified include low noise and zero harmful air emissions when in use. (US Hybrid)
- **Light-Duty Utility Van Range Extender:** This project will design, build, test, and operate a fleet of fuel cell range extended plug-in hybrid light-duty utility vehicles. By adding a fuel cell and a few kilograms of hydrogen to a battery electric powertrain, the zero-emission driving range of the vehicles will be extended from ~100 mi up to as much as 250 mi before the batteries need to be recharged, greatly increasing the commercial potential of these all-electric utility vehicles. Upon the successful validation of one initial prototype vehicle, US Hybrid will deploy a fleet of 19 additional vehicles for use by National Grid, a leading utility fleet owner and operator in the northeastern United States. The project scope also includes collection and validation of performance data and a complete economic assessment of the value proposition. (US Hybrid)
- **Commercial Acceleration Training and Analysis:** Efforts this past year focused on enabling the commercialization process for various industries and organizations, including forums for investors and infrastructure developers; training of state and municipal staff on technology operations; and developing novel hydrogen and fuel cell business cases. In collaboration with H2USA, the Investor Forum was conducted in New York City, bringing together private hydrogen refueling developers and potential investors. Five developing organizations presented individually their business plans to potential investors. Based on positive private sector feedback, a second investor forum was held in Los Angeles, California, this past fall in collaboration with H2USA. To help the launch of fuel cell electric vehicles and hydrogen fueling infrastructure in the Northeast, training sessions were conducted to educate state and city officials and municipal authorities in New Jersey, New York, Connecticut, and Massachusetts on safe and effective business practices. Hundreds of building and fire code officials, first responders, and state and municipal agency staff attended these sessions. To help to accelerate the

commercialization of various fuel cell technologies and overcome technology cost barriers, the program supported various focused business case studies, such as car sharing and renewable hydrogen refueling scenarios.

BUDGET

The FY 2016 appropriation for the Market Transformation program was $3 million, and $3 million was requested in FY 2017 (Figure 1).

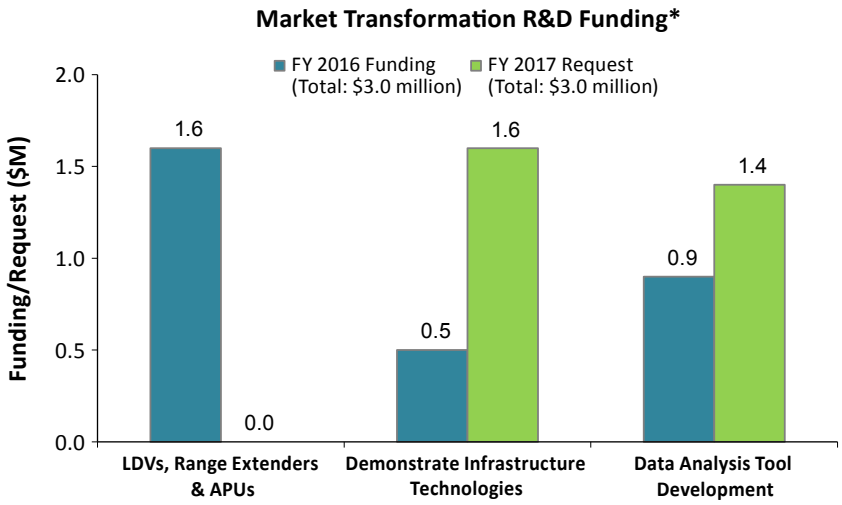

*Subject to appropriations, project go/no-go decisions, and competitive selections. Exact amounts will be determined based on research and development progress in each area.

FIGURE 1. FY 2016 appropriation and FY 2017 budget request for the Market Transformation program

FY 2017 PLANS

In FY 2017, the program will continue to collect and analyze early market project data that can be used to assess the performance of integrated hydrogen and fuel cell systems and to determine the economic viability of these applications. A new project will begin for the design and deployment of hybrid fuel cell–battery powered light-duty vehicles in dispatch utility applications. Strategies for road vehicle market entry and refueling station development, including risk management with respect to safety, environmental, and siting requirements, will continue to be a priority. Data will be made publicly available so that potential customers can become aware of the benefits of integrated hydrogen and fuel cell systems. In addition, collaboration with other federal agencies will continue in accordance with existing interagency cooperative agreements such as the DOE–U.S. Department of Defense memorandum of understanding. This effort aims to increase the use of fuel cells in market-ready applications and the awareness of the benefits of these deployments across the federal government. A potential new activity that could be initiated, subject to Congressional appropriations, is the development and deployment of novel renewable hydrogen refueling technologies to support the commercialization of fuel cell battery powered vehicles in various part of the country.

Pete Devlin
Market Transformation and Interagency Coordination Manager
Fuel Cell Technologies Office
Office of Energy Efficiency and Renewable Energy
U.S. Department of Energy
1000 Independence Ave., SW
Washington, DC 20585-0121
Phone: (202) 586-4905
Email: Peter.Devlin@ee.doe.gov

X.1 Hydrogen Energy Systems as a Grid Management Tool

Richard (Rick) E. Rocheleau (Principal Investigator),
Mitch Ewan (Primary Contact)
Hawaii Natural Energy Institute (HNEI)
University of Hawaii at Manoa
1680 East-West Road, POST 109
Honolulu, HI 96822
Phone: (808) 956-2337; (808) 956-8346
Email: ewan@hawaii.edu; rochelea@hawaii.edu

DOE Manager: Peter Devlin
Phone: (202) 586-4905
Email: Peter.Devlin@ee.doe.gov

Technical Advisor: Karen Swider-Lyons
Naval Research Laboratory
Phone: (202) 404-3314
Email: karen.lyons@nrl.navy.mil

Contract Number: DE-EE0002811

Project Start Date: September 30, 2010
Project End Date: September 29, 2015

Overall Objectives

- Demonstrate the use of electrolyzers to mitigate the impacts of intermittent renewable energy by regulating grid frequency.
- Characterize performance/durability of commercially available electrolyzers under dynamic load conditions.
- Supply hydrogen to fuel cell shuttle buses operated by County of Hawaii Mass Transit Agency and Hawaii Volcanoes National Park (HAVO).
- Conduct performance and cost analysis to identify benefits of an integrated system including grid ancillary services and off-grid revenue streams.
- Evaluate effect on reducing overall hydrogen costs offset by value-added revenue streams.

Fiscal Year (FY) 2016 Objectives

- Conduct a hydrogen site safety review utilizing an independent third-party consultant.
- Install site improvements and utilities at Natural Energy Laboratory Hawaii Authority (NELHA) to support the operation of the hydrogen system.
- Install, commission, and operate the hydrogen system at NELHA.
- Install a 350-bar hydrogen fuel dispenser at NELHA to fuel the Mass Transit Agency fuel cell electric shuttle bus.
- Characterize performance and durability of the electrolyzer system under dynamic load conditions at Powertech Labs facilities in Vancouver, Canada, prior to shipping equipment to Hawaii.
- Conduct performance and cost analysis to identify benefits of integrated systems including grid services and off-grid revenue streams.

Technical Barriers

This project addresses the following technical barriers from the Market Transformation section of the Fuel Cell Technologies Office Multi-Year Research, Development, and Demonstration Plan.

(A) Inadequate standards and complex and expensive permitting procedures

(B) High hydrogen fuel infrastructure capital costs for Polymer Electrolyte Membrane (PEM) fuel cell applications

(C) Inadequate private sector resources available for infrastructure development

(F) Inadequate user experience for many hydrogen and fuel cell applications

(G) Lack of knowledge regarding the use of hydrogen inhibits siting (e.g., indoor refueling)

(H) Utility and other key industry stakeholders lack awareness of potential renewable hydrogen storage application

Technical Targets

No specific technical targets have been set.

FY 2016 Accomplishments

- Conducted workshop utilizing Boyd Hydrogen for County of Hawaii planning, permitting, and fire department leadership on National Fire Protection Association (NFPA)-2 hydrogen codes and standards in order to facilitate permitting.
- Awarded contract for the installation of site improvements and utilities at NELHA to support the operation of the hydrogen system.
- Secured additional funding from the State of Hawaii to support site improvements.

- Conducted second factory acceptance trial at Powertech Labs.
- Modified electrolyzer control system to improve response time.
- Conducted three months of testing and analysis at Powertech Labs supervised by onsite HNEI staff.

INTRODUCTION

While solar and wind resources offer a major opportunity for supplying energy for electrical grid electricity production and delivery systems, their variability and intermittency can raise challenges for the cost-effective and high-reliability integration of these renewable sources on electrical grids. In Hawaii, the curtailment and grid management related challenges experienced by these renewable sources are a challenge at today's level of generation capacity, and these costs will hinder the substantive additional penetration of electricity generation supplied by these renewable resources. Hydrogen production through electrolysis may provide an opportunity to mitigate curtailment and grid management costs by serving as a controllable load allowing real-time control in response to changes in electricity production. The renewable hydrogen product can also create new and incremental revenue streams to the power producers through the sale of hydrogen products to customers outside of the electricity delivery system. Accordingly, hydrogen energy production at a utility scale offers the potential for increasing the levels of variable renewable energy that can be harnessed by the power producers or systems operators.

APPROACH

This project evaluates the value proposition of using utility-scale electrolyzers to both regulate the grid and use the product hydrogen for transportation applications. An electrolyzer system is being installed at NELHA on the Big Island. The electrolyzer will be ramped up and down to provide frequency regulation. Data will be collected to analyze the optimum electrolyzer ramp rates and determine its durability and performance under dynamic operating conditions over time. The hydrogen produced by the system will be used to fuel three hydrogen-fueled buses. It is planned to deliver hydrogen to HAVO as per the original plan to support two HAVO buses. The third bus will be operated in Kailua-Kona. A schematic of the project concept is shown in Figure 1.

FIGURE 1. Hydrogen production and delivery system

RESULTS

A revised infrastructure design was developed and reviewed by a third-party hydrogen safety consultant (Boyd Hydrogen). A site improvement bid package was prepared and issued for public tender, and a contract was awarded in June 2016. In parallel to the site work, HNEI ran cycling tests on the electrolyzer system utilizing test protocols based on operational data collected from a 1 MW battery energy storage system (BESS) installed on the Hawaii Electric Light Company grid for frequency regulation. An HNEI-designed programmable logic controller and power monitoring system was used for control of the electrolyzer system to facilitate implementation of the electrolyzer testing protocols and support data collection. A second factory acceptance trial was conducted at Powertech Labs facilities in Vancouver, Canada, in February 2016 to validate technical modifications that were made by Powertech to address technical issues identified during the commissioning phase. HNEI staff modified and tested the electrolyzer control system. The control system modifications improved the reaction time of the electrolyzer by a factor of ten and demonstrated the potential of the electrolyzer to provide grid frequency support.

CONCLUSIONS AND FUTURE DIRECTIONS

This project has coordinated the efforts of a diverse group of stakeholders to provide a technology solution to facilitate integration of intermittent renewable energy

sources on an electrical grid while producing hydrogen for transportation. The project has identified and provided valuable solutions to the many non-technical barriers associated with introducing hydrogen technology into a community for the first time. Lessons learned from this project will make the way easier for projects that follow.

It is concluded that a hydrogen energy system is a valuable grid frequency management tool capable of controlling intermittent renewable sources of energy for grid frequency management applications. While the hydrogen energy system is not as fast as the BESS, the performance measured with the modified control system under different load demands is much closer to the BESS performance. However, our current thinking is that replicating the exact operational response time as the BESS cannot be achieved with an electrolyzer. The data show that the electrolyzer can only be used for slower acting changes (1 Hz to 0.5 Hz). A potential solution is to design an electrolyzer–BESS hybrid system and develop a modeling program to find the optimum mix of battery and electrolyzer to provide the maximum grid regulation services at minimum cost. Additional work is required to develop a control scheme that can manage power distribution between the electrolyzer and BESS.

While DOE participation in the project formally ended on September 30, 2015, the project will continue using other funding. Future work involves the following:

- Completing installation, and operating hydrogen production systems and dispensing infrastructure at the NELHA site.
- Operating the 26-passenger fuel cell electric bus based at the NELHA site.
- Transporting hydrogen in hydrogen transport trailers from the NELHA production site to the HAVO dispenser to support the two park service fuel cell electric buses.
- Collecting and analyzing hydrogen system and fuel cell electric bus performance data.
- Preparing performance reports and sharing them with project sponsors and industry.
- Conducting outreach activities with the public to inform them about hydrogen technologies.

FY 2016 PUBLICATIONS/PRESENTATIONS

1. Ewan, M., Rocheleau, R., Oral presentation at U.S. Department of Energy Hydrogen and Fuel Cells Program Annual Merit Review, "Hydrogen Energy Systems as a Grid Management Tool," Washington, D.C., June 9, 2016.

X.2 Ground Support Equipment Demonstration

Jim Petrecky
Plug Power
968 Albany-Shaker Road
Latham, NY 12110
Phone: (518) 817-9124
Email: James_Petrecky@plugpower.com

DOE Manager: James Alkire
Phone: (720) 356-1426
Email: James.Alkire@ee.doe.gov

Contract Number: DE-EE0006093

Project Start Date: January 2013
Project End Date: December 2017

Overall Objectives

- To create a hydrogen fuel cell-based solution for cargo tow tractors (airport vehicle) that is cost-competitive and more energy-efficient as compared to incumbent internal combustion engine-powered alternatives (Table 1).
- To enable airport end users to accomplish daily tasks with a hydrogen fuel cell solution while reducing consumption of gasoline and diesel fuels, reducing U.S. demand for petroleum.
- To demonstrate lower carbon emissions with fuel cells.
- To demonstrate a value proposition that shows decreased energy expenditures when compared to diesel-powered airport vehicles.

Fiscal Year (FY) 2016 Objectives

- Complete first year of demonstration.
- Summarize learning from first year.
- Incorporate improvements to design and service.
- Begin second year of demonstration.
- Greater integration into service operations.

Technical Barriers

- Market Transformation Barrier B, High hydrogen fuel infrastructure capital costs for Polymer Electrolyte Membrane (PEM) fuel cell applications [1]
- Market Transformation Barrier F, Inadequate user experience for many hydrogen and fuel cell applications [1]
- Adapt GenDrive architecture to tractor voltage/power requirements
- Weatherproof for outdoor application

Technical Targets

- Power: Capable of 5,000 lb drawbar capacity
- Availability: >80%
- Run Time: >1 shift
- Reliability Mean Time Between Failures (MTBF): >100 h
- Speed Rating: 10 mph
- Outdoor Operation: no non-recoverable issues
- Hydrogen Fills: 350 bar

FY 2016 Accomplishments

- Completed first year of demonstration.
- Decision to move away from third party stack (16 stack failures averaging 61 h life) and build a new design

TABLE 1. Program Objectives

DOE Project Objectives	Plug Power-FedEx Project Expectations
Reduce petroleum consumption	Each tractor uses ~2 gal/hr. Total tractor run time of 15 tractors over 2 years will be upwards of 175,200 gallons of diesel fuel reduced.
Reduce emissions at airports	AT 9.8 kg CO2 per gal of diesel, there will be upwards of 1717 metric tonnes of CO2 eliminated at airports.
Operate 10 hrs/day & 5,000+ hours	Tractor operation occurs during two shifts: day (10 AM-2 PM) and night (10 PM-2 AM). The total clock day is 10AM-2PM (16 hours). Actual tractor activity is 8 hours per day. Total run time of 15 tractors over 2 years will be upwards of 87,600 fleet hours.
Drawbar capacity 3,000 to 6,000 lbs.	The tractor will be able to tow 4 FedEx containers each weighing 40,000 lbs. The corresponding drawbar capacity of the fuel cell-powered tractor is 5,000 lbs.
Accelerated development of FC-powered GSE	Fleet of 15 80V fuel cell systems in real world application gaining significant field experience while allowing a premier tractor end user to evaluate for larger deployments.

GSE – Ground support equipment; FC – Fuel cell

with Plug Power stacks for the second year of the demonstration.

  - Note: stack issues included hard failures requiring refurbishment, inability to start, and excessive purging.

- Incorporated design improvements into the new design to optimize serviceability.
- Summarized learning from Year 1:
  - The tractor handles application of load.
  - Operating outdoors 24/7 is not a problem.
  - The weatherproofing strategy works well—no water ingress.
  - Air filtration protects the system from airport hydrocarbon emissions.
  - The tractor can operate the worst route for a full shift without needing to refuel.
  - A handful of components had a drastic effect on reliability.
- First year evaluation:
  - Power: Capable of 5,000 lb drawbar capacity YES
  - Availability: >80% NO (Initially 70% but dropped due to accelerating stack failures)
  - Run Time: >1 shift YES
  - Reliability MTBF: >100 h NO (98 h)
  - Speed Rating: 10 mph YES
  - Outdoor Operation: no non-recoverable issues YES
  - Hydrogen Fills: 350 bar YES
- Redesigned system with Plug Power stacks (Figure 1).
- Redesigned system completed and tested.

✧ ✧ ✧ ✧ ✧

INTRODUCTION

This project deploys 15 fuel cell-powered units for two years at FedEx's busiest airport. The project is planned for two phases. The first is a one-year development phase where Plug Power develops, builds and tests the 80 VDC (20 kW) fuel cell system for the baggage tow tractor (BTT) application. The second is a two-year demonstration where a fleet of BTTs are integrated into Charlatte CT5E electric tow tractors and deployed at the FedEx locations under real world conditions. The fuel cell fleet is fueled by a GenFuel hydrogen compression, storage, and dispensing solution.

APPROACH

Plug Power designs an 80 VDC fuel cell system as a drop-in-place replacement of an electric Charlatte tractor (Figure 2).

Hydrogen is supplied to the tractors via GenFuel hydrogen infrastructure, which provides onsite hydrogen at 350 bar dispensed directly to the fuel cell in the tractor (Figure 3).

- Definition of Requirements – complete
- Alpha Prototype – complete
- BTT Beta Builds – complete
- BTT Testing and Certification – complete
- Site Preparation – complete

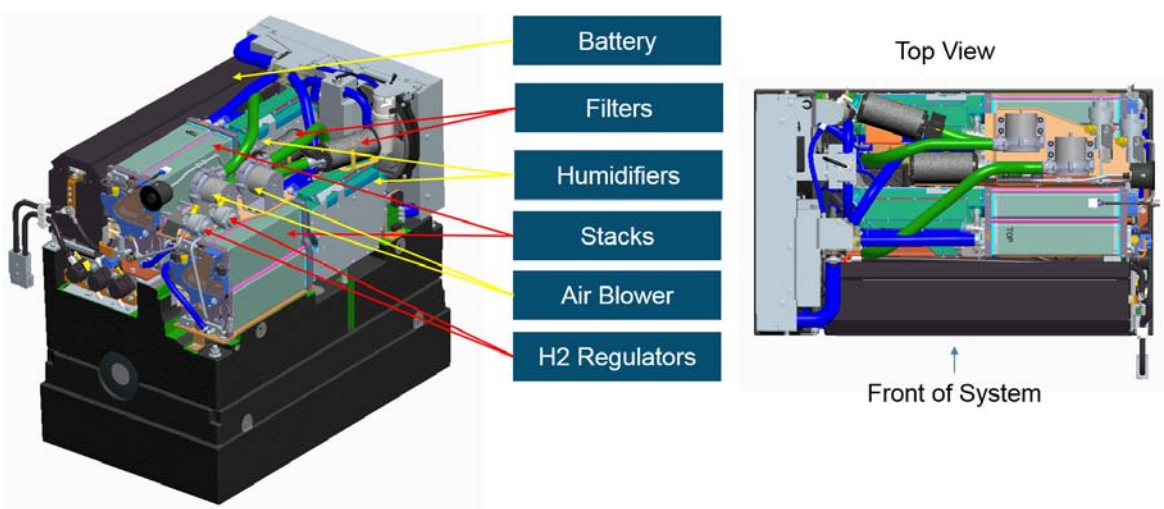

FIGURE 1. System redesign with Plug Power stacks

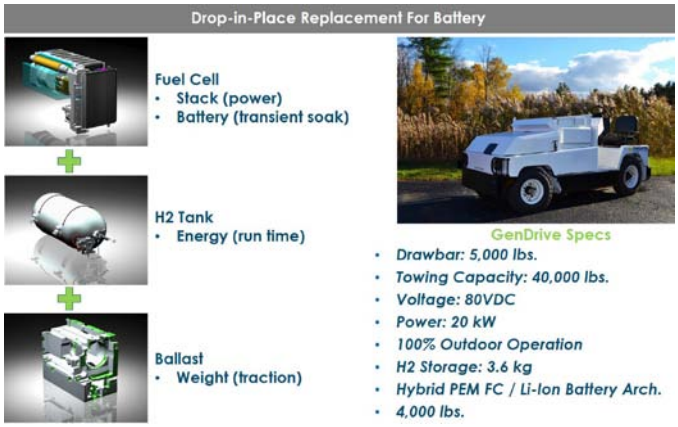

PEM-FC – Polymer electrolyte membrane fuel cell

FIGURE 2. Fuel cell system as drop-in-place replacement of battery

- Commissioning – complete
- First Year of Demonstration – complete
- Assessment after Year 1 – complete
- Second Year of Demonstration – Third quarter 2016 to Fourth quarter 2017
- Assessment after Year 2 –Fourth quarter 2017

RESULTS

The program delivered a tractor that meets the application requirements in terms of towing the required weight in an outdoor airport application, even in the face of elevated hydrocarbon emissions. Stack lifetime has not been sufficient. The program has recovered with a system redesign using Plug Power stacks. The demonstration continues with design and service improvements in order to validate the changes made as a result of the learning in the first year.

FIGURE 3. Liquid hydrogen station on airport ramp

CONCLUSION AND FUTURE DIRECTION

The first year showed that fuel cells are technically viable for ground support equipment operations. The fuel cell stack is critical to demonstrate lifetime and economic viability. Future direction is to deploy the redesigned fuel cell solution in the tractor fleet. Focus of the second year of demonstration is on system lifetime and economic evaluation.

FY 2016 PUBLICATIONS/PRESENTATIONS

1. J. Petrecky, "MT011 Ground Support Equipment Demonstration," presented at the DOE Hydrogen and Fuel Cells Program Annual Merit Review, Washington, D.C., June 9, 2016.

REFERENCES

1. Fuel Cell Technologies Office Multi-Year Research, Development, and Demonstration Plan, Section 3.9 Market Transformation, http://energy.gov/eere/fuelcells/downloads/fuel-cell-technologies-office-multi-year-research-development-and-22.

X.3 Maritime Fuel Cell Generator Project

Joe Pratt (Primary Contact)
Sandia National Laboratories
PO Box 969, MS-9051
Livermore, CA 94551
Phone: (925) 294-2133
Email: jwpratt@sandia.gov

DOE Manager: Peter Devlin
Phone: (202) 586-4905
Email: Peter.Devlin@ee.doe.gov

Subcontractor:
Hydrogenics, Mississauga, Ontario, Canada

Project Start Date: September 15, 2013
Project End Date: Project continuation and direction determined annually by DOE

Overall Objectives

- Lower the technology risk of future port fuel cell deployments by providing performance data of hydrogen proton exchange membrane (PEM) fuel cell technology in the marine environment.
- Lower the investment risk by providing a validated business case assessment for this and future potential projects.
- Enable easier permitting and acceptance of hydrogen fuel cell technology in maritime applications by assisting U.S. Coast Guard and the American Bureau of Shipping develop hydrogen and fuel cell codes and standards.
- Act as a stepping stone for more widespread shipboard fuel cell auxiliary power unit deployments.
- Reduce port emissions with this and future deployments.

Fiscal Year (FY) 2016 Objectives

- Enable new maritime-specific regulations for hydrogen and fuel cells.
- Enable new user experiences.
- Lower technology and business risk.
- Maintain hydrogen infrastructure capability on Oahu in support of this and future strategic projects.

Technical Barriers

This project addresses the following technical barriers from the Market Transformation section of the Fuel Cell Technologies Office Multi-Year Research, Development, and Demonstration Plan.

(A) Inadequate standards and complex and expensive permitting procedures

(E) A lack of flexible, simple, and proven financing mechanisms

(F) Inadequate user experience for many hydrogen and fuel cell applications

Technical Targets

No specific technical targets have been set.

FY 2016 Accomplishments

- Performed on-site commissioning of the generator at Young Brothers (YB) and completed operational turnover to YB personnel.
- Performed eight refuelings for a total of ~400 kg of dispensed hydrogen at the Hickam Air Force Base station.
- Ran for 55 d and ~250 h, displacing 6,660 kWh of diesel generator fuel and emissions, powering 130 refrigerated containers.
- Concluded the YB deployment.

✧ ✧ ✧ ✧ ✧

INTRODUCTION

Fuel costs and emissions in maritime ports are an opportunity for transportation energy efficiency and emissions reduction efforts. For example, a 2004 study showed the Port of Los Angeles had average daily emissions exceeding that of 500,000 vehicles [1]. Diesel fuel costs continue to rise as low-sulfur limits are imposed, making power generation more expensive for fleets. Hydrogen fuel cells have the potential to meet the electrical demands of vessels in the port as well as supply power for other port uses such as yard trucks, forklifts and other material handling specialty equipment. Validation of the commercial value proposition of both the application and the hydrogen supply infrastructure is the next step towards widespread use of hydrogen fuel cells in the maritime environment, and is determined by meeting necessary equipment and operating costs and customer expectations such as reliability, form, and function.

Sandia National Laboratories' recent report, "Vessel Cold-Ironing Using a Barge Mounted PEM Fuel Cell: Project Scoping and Feasibility," identified several opportunities

for demonstrating technical and commercial viability of a fuel cell in the maritime environment [2]. One identified opportunity is in Honolulu Harbor at the Young Brothers Ltd. wharf. YB provides barge transport of goods between Oahu and the Hawaiian neighbor islands and is an ideal demonstration location because of their high fuel costs and corporate interest in low emission, low environmental impact solutions. YB uses refrigerated containers ("reefers"), which keep perishable goods cold while on the dock and on the barge by using dedicated diesel generators mounted inside mobile 20-ft containers. Sandia's report concluded that it is technically feasible to build a containerized hydrogen fuel cell generator to replace the diesel generator in YB operations.

APPROACH

This project developed and demonstrated a nominally 100 kW, integrated fuel cell prototype for marine applications. This project brought together industry partners in this prototype development as a first step towards eventual commercialization of the technology. To be successful, the project incorporated interested industry and regulatory stakeholders: an end user, technology supplier and product integrator, and land- and maritime-based safety and code authorities. Project costs were shared by the primary stakeholders in the form of funds, in-kind contribution, and material/equipment either loaned or donated to the project. Funding provided by the Department of Transportation Maritime Administration (MARAD) was used to provide assistance with the integrated system and packaging designs, data collection and assistance during the demonstration period, and technical assistance and project management throughout the project. In addition some MARAD funds were used to purchase specialized equipment needed to construct the prototype. DOE funds were used to provide overall project management, technical design assistance, and deployment facilitation, and used via subcontract to the prototype manufacturer for the design, build, and testing of the final product.

The project had four phases:

1. Establishment and specification (September 2013–December 2013)
2. Detailed design and engineering (January 2014–March 2015)
3. Prototype fabrication and site construction (October 2014–June 2015)
4. Deployment (onsite demonstration at YB) and analysis (August 2015–September 2016)

RESULTS

The generator was commissioned on-site in the fourth quarter of FY 2015 over 12 d and placed into service in the YB fleet (Figure 1). Commissioning included first fill at the Hickam station, which was performed with no issues. During this period 20–30 YB staff were given hands-on training and experience with the generator (Figure 2).

FIGURE 1. The Maritime Fuel Cell Generator (blue container, middle left) contains 75 kg of compressed hydrogen storage and produces over 100 kW net electricity, packaged in a 20-ft shipping container. Here it powers refrigerated containers at Young Brothers, Ltd. in Honolulu Harbor.

FIGURE 2. Nader Zaag (left) from Hydrogenics provides hands-on training to Young Brothers operators. Over 100 YB personnel were given hydrogen familiarity and/or operational training through this project.

Following that, a "ribbon-cutting" ceremony organized by Sandia and hosted by YB welcomed 55 people, mainly in the energy industry, military/government sectors, and project partners (Figure 3). It included speeches by Senator Brian Schatz (Hawaii), Mark Glick (Administrator, Hawaii State Energy Office), Pete Devlin (DOE–Office of Energy Efficiency and Renewable Energy–Fuel Cell Technology Office), John Quinn (Associate Administrator for Environment and Compliance, MARAD), Ryan Sookhoo (Director of New Initiatives, Hydrogenics), Glenn Hong, (President of Young Brothers) and Marianne Walck (Vice President of Energy and Climate, Sandia).

Concurrent with the ribbon cutting the project's outreach team issued a press release announcing the event and the start of the on-site deployment. An accompanying video described the technology and the project's objectives. The press release was reprinted in 36 unique locations on the web with approximately 10.5 million page views since its issuance.

Throughout the subsequent deployment usage data was compiled and tracked by Sandia. This included detailed and summary technical information whenever the generator is used, maintenance logs, and refuelings. This was done in a format compatible with the existing data collection activities at the National Renewable Energy Laboratory for other projects (primarily material handling equipment). The Sandia team has devised a method for determining the actual mass of hydrogen dispensed into the unit during fills from Hickam despite the fact there are no flow measuring devices at that station that are active when fueling the generator. The Sandia team has also been working to calculate fuel burn rates for different usage scenarios, which is desired by the YB operators, and gross and net efficiency curves, made difficult because of no direct measurements of net power.

The overall generator usage during the deployment fell short of expectations. Both technical and administrative/personnel factors were the reasons for the low usage. Technical issues were primarily due to the inverter, which had nine issues over the course of the deployment resulting in over 90 cumulative days of downtime. Inverter issues ranged from controls/software to isolated circuit board failures. Battery issues were second in frequency and resulting downtime, with seven issues and more than 60 days resulting downtime. Battery issues were primarily an inability to provide sufficient voltage to start the system, sometime compounded due to long times between runs and battery depletion during off periods. The battery was replaced in third quarter of FY 2016. Detailed descriptions of these and other technical issues affecting downtime will be detailed in the project's final report.

The most common administrative/personnel factor related to labor and manpower availability. Staff obligations to daily operational tasks resulted in additional days of downtime. For a perfectly operating generator the availability of personnel would be a minor issue. However, at this first generation deployment stage, technical issues with the generator required additional attention and the lack of availability of hands-on support for troubleshooting and maintenance compounded downtime. YB operators have recommended that a dedicated operator be assigned to the generator on subsequent deployments to deal with unexpected issues that commonly arise with new technology. An additional administrative factor was establishment of a

FIGURE 3. Project team members with the generator at the ribbon cutting outreach event.

formal agreement between Sandia and YB. This caused an operational delay of 35 days while both parties worked to reach mutually agreeable liability terms.

Fueling at Hickam Air Force Base was always smooth and uneventful. The generator was filled eight times over the course of the deployment, taking an average of ~60 kg each time, filling to 350 bar, and lasting an average of 27 min per fill (over 2 kg/min). The Hickam station is managed by Hawaii Center for Advanced Transportation Technologies and operated under a contract to U.S. Hybrid (Figure 4). Data exchange between the project team members helps all parties to understand the unique aspects of quickly fueling large quantities at one time and will help to enable fueling of other equipment and large vehicles in the future.

Overall, the generator ran for 55 d and ~250 h in YB custody, displacing 6,660 kWh of diesel generator fuel and emissions, and powered 130 refrigerated containers. Technical and business case analyses will be presented in the project's final report.

CONCLUSIONS AND FUTURE DIRECTIONS

The Maritime Fuel Cell Project is a wholly collaborative effort with early and continuous stakeholders feedback that facilitated removal of nontechnical barriers to hydrogen and fuel cell use.

The DOE/MARAD/Sandia project leads are currently working to arrange a follow-on deployment at a different partner following upgrade/refurbishment of generator features by the manufacturer. It is expected that this generator will continue to be deployed by various partners in the future, displacing additional diesel generator emissions and breaking down market barriers to widespread hydrogen fuel cell technology deployment at each stop.

SPECIAL RECOGNITIONS & AWARDS

1. DOE Hydrogen and Fuel Cells Program R&D Award, "For outstanding dedication to the advancement of hydrogen and fuel cell technologies in the early market, including the world's first pier-side maritime fuel cell power system," awarded to Joseph Pratt, June 2016.

FY 2016 PUBLICATIONS/PRESENTATIONS

1. Pratt, J., "Deployment of a Mobile Hydrogen Fuel Cell Generator for Ports and on Marine Vessels," Fuel Cell Seminar, November 17, 2015, SAND2016-1192 C.

2. Pratt, J., "Zero Emission Fuel Cell Power and Propulsion for Marine Applications," Ship Operations Cooperative Program, April 7, 2016, SAND2016-2848 PE.

3. Pratt, J., "Maritime Fuel Cell Generator Project," DOE Annual Merit Review, June 9, 2016, SAND2016-3746 PE.

FIGURE 4. The generator was fueled at the Hickam Hydrogen Station (managed by Hawaii Center for Advanced Transportation Technologies and operated by U.S. Hybrid). Here is it being refueled to 350 bar with 49 kg of hydrogen in 18 min.

REFERENCES

1. D. Bailey, T. Plenys, G. M. Solomon, T.R. Campbell, G.R. Feuer, J. Masters, and B. Tonkonogy, "Harboring Pollution - Strategies to Clean Up U.S. Ports," National Resources Defense Council, NY, August, 2004.

2. J.W. Pratt and A.P. Harris, "Vessel Cold Ironing Using a Barge Mounted PEM Fuel Cell: Project Scoping and Feasibility," Sandia National Laboratories, Report SAND2013-0501, available at http://energy.gov/eere/fuelcells/downloads/vessel-cold-ironing-using-barge-mounted-pem-fuel-cell-project-scoping-and.

X.4 Demonstration of Fuel Cell Auxiliary Power Units (APUs) to Power Transport Refrigeration Units (TRUs) in Refrigerated Trucks

Kriston Brooks
Pacific Northwest National Laboratory
P.O. Box 999
Richland, WA 99352
Phone: (509) 372-4343
Email: kriston.brooks@pnnl.gov

DOE Manager: Peter Devlin
Phone: (202) 586-4905
Email: Peter.Devlin@ee.doe.gov

Subcontractors:
Nuvera Fuel Cells, Billerica, MA
Ballard Power Systems, Burnaby, BC, Canada

Project Start Date: June 1, 2012
Project End Date: December 31, 2017

Overall Objectives

- Demonstrate the viability of fuel cell-based transport refrigeration units (TRUs) for refrigerated Class 8 trailers.
- Assess the performance of the fuel cell-based TRUs by demonstrating these systems with 800–1,000 hours of commercial deliveries. During the demonstration, the system performance will be independently evaluated.
- Use the demonstration data and market assessment to develop a business case that will determine if lifecycle cost parity can be achieved with incumbent technologies.

Fiscal Year (FY) 2016 Objectives

- Manage the subcontract team led by Nuvera Fuel Cells as they develop a fuel cell-based TRU for refrigerated Class 8 trailers.
- Compete and place subcontract for second fuel cell-based auxiliary power unit (APU) for a commercial TRU.

Technical Barriers

This project addresses the following technical barriers from the Market Transformation section of the Fuel Cell Technologies Office Multi-Year Research, Development, and Demonstration Plan.

(C) Inadequate private sector resources available for infrastructure development

(E) A lack of flexible, simple, and proven financing mechanisms

(F) Inadequate user experience for many hydrogen fuel cell applications

Technical Targets

This project directly addresses the Market Transformation subprogram targets described in Section 3.9.4 of the Fuel Cell Technologies Office Multi-Year Research, Development, and Demonstration Plan by developing a pathway for the introduction of fuel cell technologies into the transport refrigeration unit market. The project involves the two primary United States TRU manufactures, ThermoKing and Carrier Transicold. They will be actively involved in overcoming the logistical and other nontechnical challenges associated with implementing this new technology, resulting in a smoother adoption into the marketplace. The deployments by large potential customers who already have used or are using fuel cell-based lift trucks will provide valuable data on the performance of the technology in real-world operations and can be used to benchmark the benefits of the technologies. The TRU manufacturers and demonstrators will provide input into the business case to create a clear picture of the value proposition of this new technology. Furthermore, this particular niche market will significantly increase hydrogen usage, reduce hydrogen cost, and further establish the hydrogen infrastructure at food distribution centers.

FY 2016 Accomplishments

- Developed a preliminary value proposition analysis to determine the tipping point between positive, marginal, and negative net present values. This value proposition will help determine the conditions when lifecycle cost parity can be achieved with incumbent technologies.
- Performed laboratory demonstrations integrating the fuel cell stack, prototypic balance of plant, power electronics, and TRU in preparation for the real-world demonstration that will benchmark the benefits of the technology.
- Competed and awarded subcontract to Ballard Power Systems for a second fuel cell-based TRU demonstration to allow a second pathway for the introduction of fuel cell technologies into the transport refrigeration unit market.

INTRODUCTION

A TRU is a high-powered air conditioning system used in cooling cold goods during on-road transport. It is generally powered by a separate diesel engine. Replacing this diesel engine with a fuel cell will address recent state and federal environmental mandates to reduce emissions, address noise restrictions found in many urban areas, reduce system maintenance, and improve the overall energy efficiency of the system. The initial market for this application would be food distributions centers where vehicles return to a central facility for refueling and where fuel cell lift trucks have already been established. This market will further expand the hydrogen usage at these sites and increase fuel cell market penetration.

The purpose of this project is to perform two demonstrations of fuel cell-based TRUs using two separate fuel cell teams as shown in Table 1. These demonstrations will provide user experience for over-the-road fuel cell applications that will mitigate commercial risk in developing this new technology.

TABLE 1. Fuel Cell-Based Transport Refrigeration Unit Demonstration Teams

Project Role	Nuvera Team	Ballard Team
Fuel Cell Supplier, System Integrator	Nuvera	Ballard
Transport Refrigeration Unit Supplier	ThermoKing	Carrier Transicold
Demonstration Partner	H-E-B	Walmart

APPROACH

Each of the two demonstrations will be performed by a team consisting of a fuel cell system supplier and integrator, TRU system supplier, and demonstration site. Each demonstration will be 800 to 1,000 hours in duration and will consist of actual deliveries of cold goods. During the demonstration, data will be collected from the hydrogen refueling station, fuel cell system, TRU, and the delivery truck to allow an independent techno-economic analysis and a system evaluation relative to available DOE targets. These results will be used to develop a business case and commercialization plan that can be implemented at the conclusion of the demonstration.

In preparation for these demonstrations, a preliminary business case will be developed and safety and regulatory issues addressed. The system development will include appropriately sizing the fuel cell stack to be comparable with the incumbent technology. The system must be designed and tested to ensure road-worthiness. These demonstration may also require the installation of the on-site hydrogen infrastructure for refueling.

RESULTS

The Nuvera and Ballard team's progress with the fuel cell-based TRU demonstration projects are described below.

ThermoKing Business Case Development. A critical piece of the development of a fuel cell-based TRU is the value proposition analysis. Although the Nuvera/ThermoKing commercial system has not been developed, a preliminary evaluation was performed to determine the impact of hydrogen and diesel costs on the net present values of the system as shown in Table 2. The study included an estimate for the incremental cost increase for a fuel cell TRU with assumptions regarding the operational duration, maintenance, and tax credit benefits from using a fuel cell. The results of the analysis indicate that if the $4.00/kg DOE target for hydrogen price can be achieved, a positive net present value is possible with modest diesel price increase over current values.

TABLE 2. Nuvera/ThermoKing Example Value Proposition Analysis

With Investment Tax Credit				
Hydrogen	TRU Incremental Cost	Diesel $4.00	Diesel $6.00	Diesel $8.00
Hydrogen $2.50	$21,000	$ 21,888	$ 57,399	$ 92,980
Hydrogen $4.00	$21,000	$ 9,297	$ 44,878	$ 80,459
Hydrogen $6.00	$21,000	$ (21,990)	$ 13,592	$ 49,173
Hydrogen $8.00	$21,000	$ (53,276)	$ (17,695)	$ 17,887
Hydrogen $10.00	$21,000	$ (84,563)	$ (48,981)	$ (13,400)
Hydrogen $12.00	$21,000	$ (115,849)	$ (80,268)	$ (44,686)

Assumptions: (1) 20 kW fuel cell with twice the efficiency improvement over diesel, (2) 12-year trade cycle, (3) 2,000 operating hours per year, (4) Diesel internal combustion engine maintenance cost delta $3,400, (5) federal tax credit of 30% of fuel cell system cost, up to $3,000/kW.

In addition to the value proposition analysis, the business case performed a "voice of the customer" activity where interviews were made with fuel service distribution and grocery companies representing the functions of warehousing, fleet operations and maintenance, engineering, and senior management. As expected, the biggest driver was found to be the return on investment. Use of a fuel cell-based TRU must make economic sense. However, companies meeting their sustainability goals was also important to those interviewed. A part of this sustainability is driven to ensure recently mandated regulatory requirements are met. Additional customer needs included the need to reduce noise pollution, reduce fuel cost uncertainty, and ensure food product integrity. A key customer need is that of reducing the risk of new technologies. While companies are willing to be technology leaders by employing new technologies such as fuel cells, a proven "track record" of the technology is very important before it is implemented. The demonstrations being performed for this project will provide the beginnings of this much-needed "track record."

Nuvera Fuel Cell System Development. In addition to the development of a business case, the Nuvera team has designed the packaging of the fuel cell system. It will be undermounted on a Class 8 trailer using the frame of an existing ThermoKing SGSM 3000 diesel genset. The original components will be removed and replaced with the fuel cell stack, balance of plant, and power electronics as shown in Figure 1. The ThermoKing TRU selected for the demonstration is the Precedent C-600. This particular TRU is a plug-in hybrid system that allows the use of either the diesel generated power or 480 VAC three-phase shore power during operations. As a result, the demonstration of this system requires that the fuel cell direct current (DC) power be converted to alternating current (AC) power to supply the TRU.

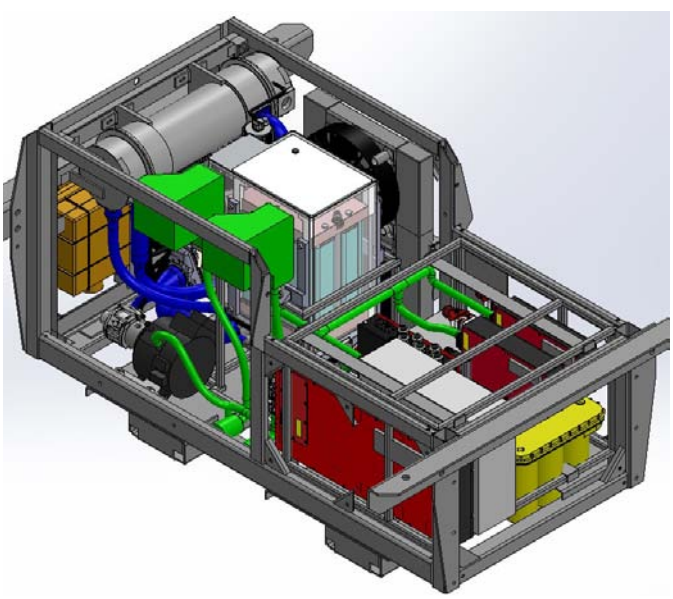

FIGURE 1. Preliminary design of the Nuvera team fuel cell system for the TRU APU

The four subsystems in the fuel cell-based TRU system being developed by Nuvera are the prototypic balance of plant, fuel cell stack, power electronics, and the TRU itself. The goal of the laboratory acceptance test before the demonstration was to test all of subsystems together as an integrated system. Although this full integration was not completed before Nuvera went into an 18-month project pause, they did test several subsystems together as shown with the circles in Figure 2.

The first demonstration was performed with the fuel cell and prototypic balance of plant. The balance of plant components used in this demonstration were assembled to fit within the trailer under-mounted generator frame. The testing was performed for three hours and successfully demonstrated a maximum of 28 kWe DC power in both a modulated and sentry cycle mode. One of these two operational modes will be down-selected before the commercial demonstration. Modulated mode varies the power as required by the TRU while the sentry cycle is a simple on/off configuration.

The second demonstration evaluated the fuel cell with the power electronics subsystem. Non-prototypical balance of plant components were used. In this 2.5 h test, the system successfully demonstrated 21 kWe of three-phase 480 VAC power. Power generated was dissipated with an induction motor and brake load. The final demonstration coupled the fuel cell stack and power electronics with a SLXe-300 TRU. Once again non-prototypical balance of plant components were used in this demonstration. This European TRU operates at 9 kWe maximum and a single power level as compared to the Precedent that operates at 17 kWe and two power levels. The test lasted for four hours and demonstrated that the fuel cell system can be successfully integrated with a TRU (see Figure 3).

Selection of the Ballard Team. During FY 2016 a second team was selected to develop and demonstrate a fuel cell-based TRU. The process of development of a request for proposal, performance of an open competition, technical and cost evaluation of the proposals, and negotiation with the selected offeror were performed. The results of this process yielded the Ballard team as the second demonstration team.

CONCLUSIONS AND FUTURE DIRECTIONS

The development and demonstration of a fuel cell auxiliary power system for Class 8 refrigerated trailers is a first step in expanding fuel cell use to TRUs. This demonstration will increase fuel cell market penetration and further break down technical and nontechnical barriers to hydrogen and fuel cell use.

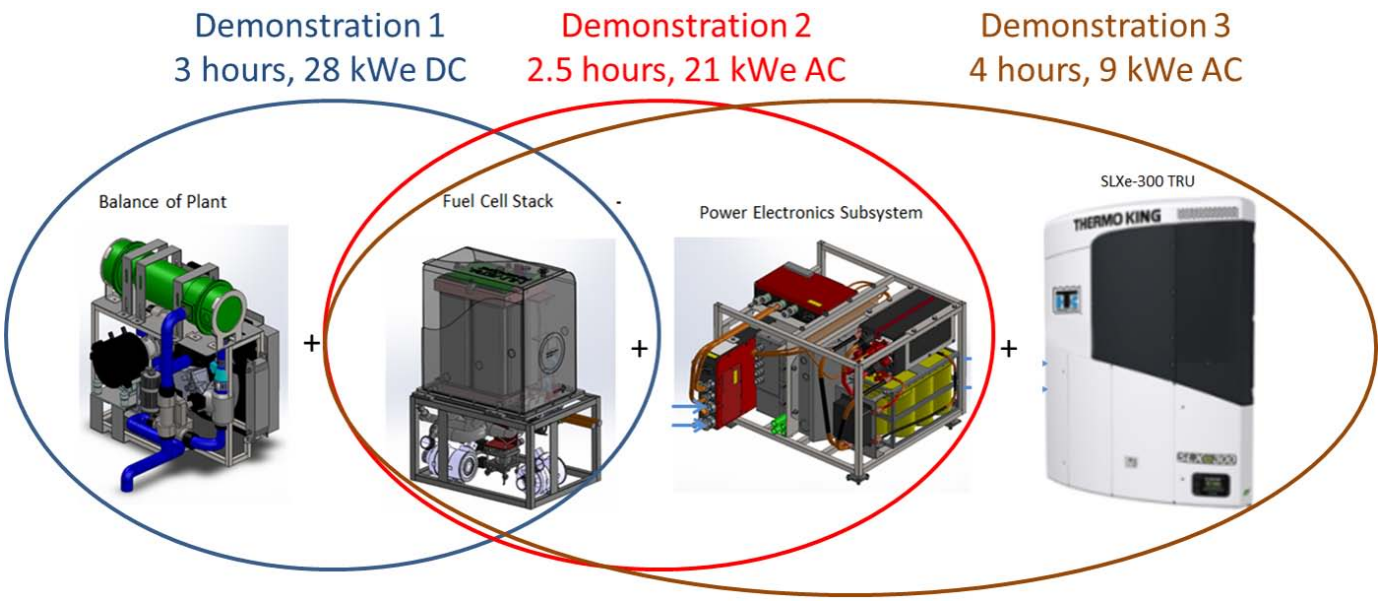

FIGURE 2. Laboratory integration demonstration performed with the Nuvera team fuel cell system

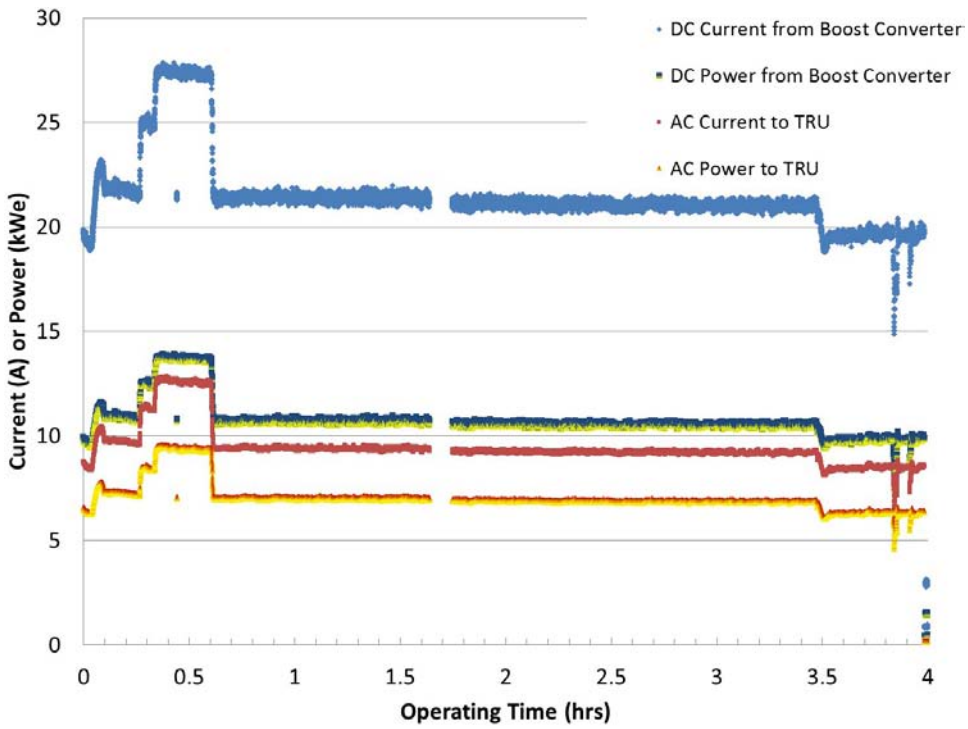

FIGURE 3. Results of the Nuvera team fuel cell system integration with a SLXe-300 TRU

Work performed to this point includes the development of a business case and assembly of a fuel cell system for the Nuvera team. It also includes the selection of the Ballard team to begin their development and demonstration.

Future Nuvera work in FY 2017 includes the completion of the fuel cell/TRU integration for on-road demonstration. Two 400 h demonstrations will be performed with actual deliveries of refrigerated and frozen goods from the H-E-B grocery distribution center in San Antonio, Texas. Fuel cell and TRU data will be collected and analyzed for system technical and economic performance.

The Ballard team future work will develop a preliminary business case, design the system and complete safety documentation as part of Phase I to be completed early in FY17. If they pass the DOE go/no-go decision, they continue into Phase II where they will develop the appropriately sized system and package it for on-road operation.

FY 2016 PUBLICATIONS/PRESENTATIONS

1. Brooks, K., G. Block, T. Lutkauskas, 2016, "Demonstration of Fuel Cell Auxiliary Power Unit (APU) to Power Truck Refrigeration Units (TRUs) in Refrigerated Trucks," 2015 Fuel Cell Seminar & Energy Exposition, November 18, 2015, Los Angeles, CA.

2. Brooks, K., G. Block, T. Lutkauskas, 2016, "Development and Demonstration of Fuel Cell-Powered Transport Refrigeration Units for Refrigerated Trucks," Advanced Automotive Battery Conference, June 17, 2016, Detroit, MI.

X.5 FedEx Express Hydrogen Fuel Cell Extended-Range Battery Electric Vehicles

Imran Ahmed
Federal Express Corporation
3690 Hacks Cross Rd.
Memphis, TN 38125
Phone: (901) 434-5725
Email: Imran.ahmed@fedex.com

DOE Manager: James Alkire
Phone: (720) 356-1426
Email: James.Alkire@ee.doe.gov

Contract Number: DE-EE0006522

Subcontractors:
- Workhorse Technologies Inc., Loveland, OH
- Plug Power Inc., Latham, NY

Project Start Date: October 15, 2015
Project End Date: October 10, 2019

Overall Objectives

- Convert an existing electric parcel delivery unit (PUD) into an extended range electric vehicle by utilizing hydrogen fuel cell.
- Demonstrate and deploy hydrogen fuel cell technologies in a real world environment.

Fiscal Year (FY) 2016 Objectives

- As part of the first budget period, optimize, test, and complete the integration between the fuel cell and the electric vehicle (EV).
- Identify and analyze the proper route and location for the assets placement.
- Determine the optimal hydrogen storage quantity and location.

Technical Barriers

This project addresses the following technical barriers from the Market Transformation section of the Fuel Cell Technologies Office Multi-Year Research, Development, and Demonstration Plan [1].

(B) High hydrogen fuel infrastructure capital costs for polymer electrolyte membrane (PEM) fuel cell applications

(D) Market uncertainty around the need for hydrogen infrastructure versus timeframe and volume of commercial fuel cell applications

(F) Inadequate user experience for many hydrogen and fuel cell applications

(J) Insufficient numbers of trained and experienced servicing personnel

(L) Lack of qualified technicians for maintenance

(M) Lack of certified service providing organizations for installation and maintenance

Technical Targets

The target is to achieve a driving range of 150 miles. No additional targets have been set.

FY 2016 Accomplishments

- Identified replacement EV original equipment manufacturer.
- New EV sub-recipient has experience with range extension.
- Technical kick-off meeting held among program partners at a manufacturing facility to discuss component requirements and placement.
- Program kick-off meeting held among program partners at Memphis headquarters.
- Site and product review visit to Workhorse.
- Analyzed the 150-mile drive cycle with up to 60-mile stem length at beginning and end.
- Planning in process for dyno testing.
  - Variable payloads
  - Temperature effects
  - Parasitic loads
- Integration activity kick off.
- Integration hardware identified and tested.
- Upcoming testing planned and finalized.
- PUD placement location identified.
- Fueling challenges discussed and mitigated.
- Hydrogen tank location and storage finalized.
- Design integration between the partners was launched (Figure 1).

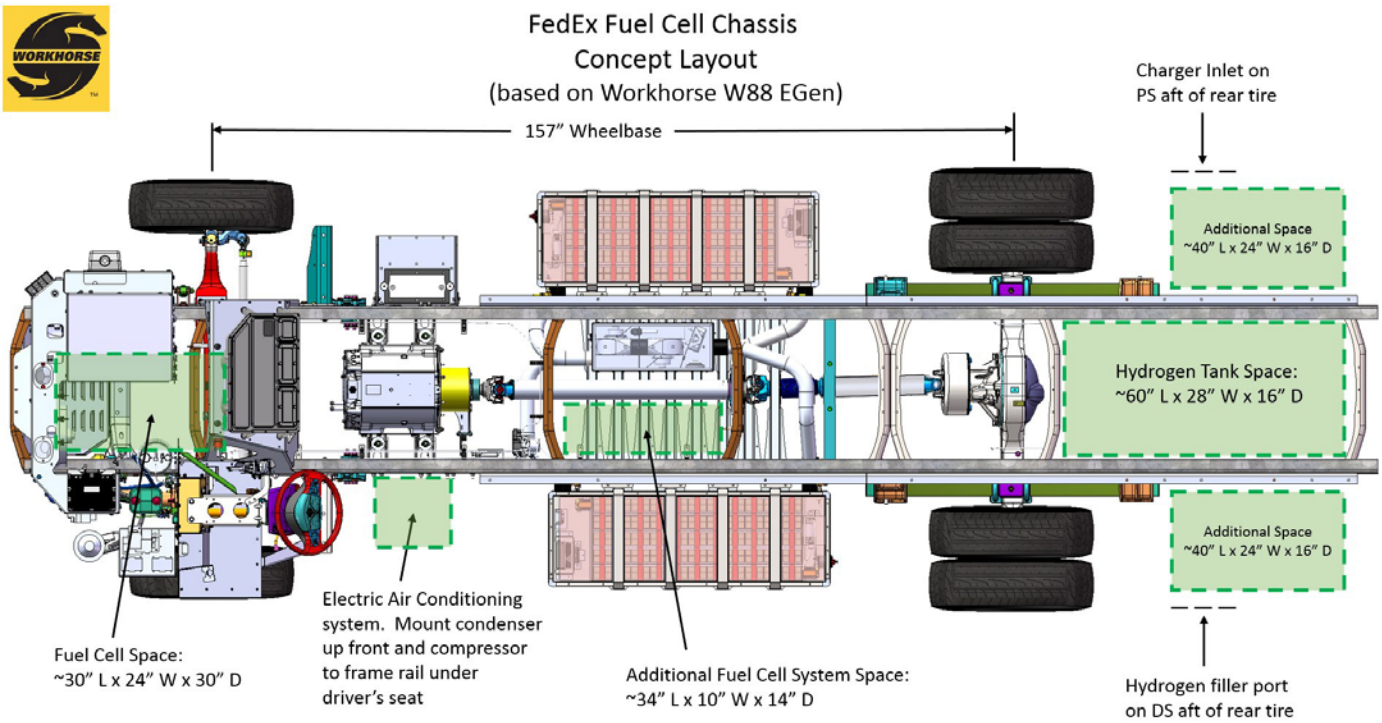

FIGURE 1. Usage profile baseline electric vehicle

INTRODUCTION

The ability to reduce fuel consumption and emissions while delivering packages is an immense challenge, particularly with the existing technology. This is further complicated by the diversity of the different duty cycles utilized by the PUDs at FedEx. The possibilities and opportunities for an electric PUD that can have its range extended without producing any emissions are enormous. This is exactly what this project aims to achieve.

As a part of this project we will be converting 20 existing electric vehicles into hydrogen fuel cell powered extended range electric vehicles (eREV), in two different budget periods (BP). We will be able to demonstrate the deployment and successful utilization of fuel cell technologies in real world environments. Lessons learned can be applied to additional duty cycles eventually reducing costs because of economies of scale, while providing safe, secure, and affordable energy.

APPROACH

The first step was to find industry partners that had the experience, capabilities and the knowledge to collaborate with us in embarking on this project. As a result, we are collaborating with Workhorse, the EV manufacturer, and Plug Power, the fuel cell manufacturer; in addition, Morgan Olson is providing us the body for the asset. The project is split into two separate budget periods (BP1 and BP2). The first period concentrates on the conversion of just one asset. This will enable the project team to analyze and measure the performance. The second period is launched if the first phase is considered successful, and we will convert an additional 19 EVs into fuel cell eREV PUDs.

In BP1, we found the optimum route so an accurate performance and charge strategy could be established. Next, we will integrate the fuel cell system into the EV system. At the same time, the optimal hydrogen tank size, packaging, and compartmentation was finalized with body builder. Based on the tank sizes and locations, the interior of the body will be modified. Next, the eREV will be taken through a series of factory, dyno, and durability tests before it is placed in active service.

RESULTS

Since this is an ongoing project, the desired results have not been achieved, but our analysis of the drive cycle has enabled us to simulate the best performance and charge strategy (Figure 2). The size and capacity of the hydrogen tanks have been determined and the main components for the integration between the two systems are well underway.

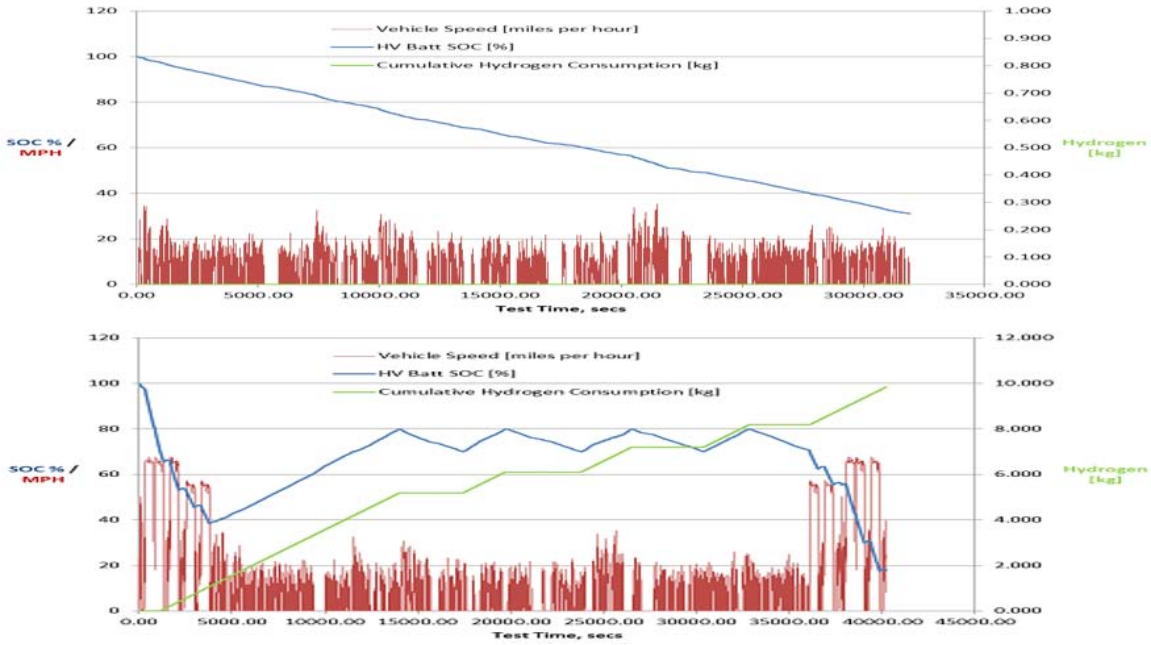

FIGURE 2. Simulated fuel cell eREV

CONCLUSIONS AND FUTURE DIRECTIONS

Based on the initial results, the fuel cell eREV PUD is proving to be a viable option when looking at the overall emission reduction requirements. This will be further clarified as the first unit is put into service and actual data from real life utilization is collected and evaluated.

Since the project is split into two separate BPs, the future direction is divided accordingly.

Budget Period 1

- Fuel system design
- Safety planning
- Design requirements
- Verify optimization analysis
- Communications and control strategies
- Leak detection and fuel isolation
- Integration of fuel cell into first truck
- Performance testing
- Shock and vibration testing
- Commissioning
- Place into revenue service
- Validation
- Prepare for BP2

FY 2016 PUBLICATIONS/PRESENTATIONS

1. Thomas Griffin, "Medium Duty Parcel Delivery Truck," presented at the DOE Hydrogen and Fuel Cells and Vehicle Technologies Program Annual Merit Review and Peer Evaluation Meeting, Washington, D.C., June 6–10, 2016.

REFERENCES

1. Fuel Cell Technologies Office Multi-Year Research, Development, and Demonstration Plan, Section 3.9 Market Transformation (n.d.). Retrieved September 13, 2016, from http://energy.gov/eere/fuelcells/downloads/fuel-cell-technologies-office-multi-year-research-development-and-22.

XI.0 Small Business Innovation Research (SBIR) Fuel Cell Technologies Office New Projects Awarded in FY 2016

The Small Business Innovation Research (SBIR) program provides small businesses with opportunities to participate in DOE research activities by exploring new and innovative approaches to achieve research and development (R&D) objectives. The funds set aside for SBIR projects are used to support an annual competition for Phase I awards of up to $225,000 each for about nine months to explore the feasibility of innovative concepts. Phase II R&D efforts further demonstrate the technologies to move them into the marketplace, and these awards are up to $1,500,000 over a two-year period. Small Business Technology Transfer (STTR) projects include substantial (at least 30%) cooperative research collaboration between the small business and a non-profit research institution.

Tables 1 and 2 list the SBIR Phase I and Phase II projects awarded in Fiscal Year (FY) 2016 related to the Hydrogen and Fuel Cells Program, respectively, followed by brief descriptions of each project.

TABLE 1. FY 2016 SBIR Phase I Projects Related to the Hydrogen and Fuel Cells Program

	Title	Company	City, State
XI.1	Development of Low Cost Magnetocaloric Nanomaterials for Sub 80 K Refrigeration Applications[1]	General Engineering & Research, LLC	San Diego, CA
XI.2	Development of Next-Generation Magnetocaloric Materials	Nanohmics, Inc.	Austin, TX
XI.3	High Charge Density Hydrocarbon-Based PEMs[2]	Giner, Inc.	Newton, MA
XI.4	Novel Hydrocarbon Ionomers for Durable Proton Exchange Membranes[2]	NanoSonic, Inc.	Pembroke, VA
XI.5	Novel Nanocomposite Polymer Electrolyte Membranes for Fuel Cells[2]	NEI Corporation	Somerset, NJ
XI.6	Low-Cost Proton Conducting Membranes for PEM Fuel Cells[2]	Amsen Technologies LLC	Tucson, AZ

TABLE 2. FY 2016 SBIR Phase II Projects Related to the Hydrogen and Fuel Cells Program

	Title	Company	City, State
XI.7	Cross-Polarized Near-UV/Vis Detector for In-line Quality Control of PEM Materials[3]	Mainstream Engineering Corporation	Rockledge, FL
XI.8	Hydrogen Contamination Detection[3]	Sustainable Innovations, LLC	Hartford, CT
XI.9	Regenerative Fuel Cell System[2]	PH Matter, LLC	Columbus, OH
XI.10	Economical Production of Hydrogen Through Development of Novel, High Efficiency Electrocatalysts for Alkaline Membrane Electrolysis[2]	Proton Energy Systems	Wallingford, CT
XI.11	Diode Laser Sensor for Contaminants in Hydrogen Fuel[2]	Southwest Sciences, Inc.	Santa Fe, NM

[1] STTR Projects
[2] Funded under the Basic Energy Sciences (BES) Office
[3] Technology Transfer Opportunity (TTO) Projects

PHASE I PROJECTS

XI.1 Development of Low Cost Magnetocaloric Nanomaterials for Sub 80 K Refrigeration Applications

General Engineering & Research, LLC
10459 Roselle Street, Suite A
San Diego, CA 92121

The energy consumption of liquefaction is a major contributor to the cost of hydrogen fuel. This project aims to develop a low cost magnetocaloric material for sub 80 K refrigeration applications. Most magnetocaloric materials in use today are high in cost because they use rare earth metals, such as gadolinium. This project will synthesize and characterize novel materials that avoid rare earth metals and have demonstrated potential in previous research.

XI.2 Development of Next-Generation Magnetocaloric Materials

Nanohmics, Inc.
6201 E Oltorf Street, Suite 400
Austin, TX 78741

This project will design next-generation technologies to cool hydrogen from room temperature by leveraging both the magnetocaloric and magnetoelastic effects in known magnetocaloric materials. The team will leverage their capabilities in nanofabrication to develop and demonstrate materials with geometries that maximize these effects.

XI.3 High Charge Density Hydrocarbon-Based PEMs

Giner, Inc.
89 Rumford Avenue
Newton, MA 02466

This project will develop novel hydrocarbon-based ionomeric membranes with high conductivity and mechanical strength for use in low relative humidity, high temperature fuel cell applications. Giner's proven Dimensionally Stable Membrane technology will be used to further increase the strength of the membranes and increase resistance to creep at high temperatures. The end product of this project will be a less expensive, viable alternative to perfluorosulfonic acid for use in automotive fuel cells and other applications.

XI.4 Novel Hydrocarbon Ionomers for Durable Proton Exchange Membranes

NanoSonic, Inc.
158 Wheatland Drive
Pembroke, VA 24136-3645

The objective of this program is to develop and demonstrate high temperature hydrocarbon-based membranes that possess the chemical, thermal, and mechanical properties necessary to qualify for the demanding environments within a fuel cell vehicle. The approach involves the synthesis of novel, high molecular weight, aromatic hydrocarbon membranes with polar moieties along the polymer backbone and pendant quaternary ammonium groups.

XI.5 Novel Nanocomposite Polymer Electrolyte Membranes for Fuel Cells

NEI Corporation
400 Apgar Drive, Suite E
Somerset, NJ 08873

This project will develop a novel non-perfluorosulfonic acid polymer electrolyte membrane (PEM), utilizing highly proton conducting heteropolyacids (HPAs) in an organic matrix in a way that has not been explored before. The novel HPA/polymer membrane has a unique structure that ensures that the active proton conducting species (HPA) are contained in a continuous interconnected channel. The overall objective of the Phase I project is to demonstrate the feasibility of a robust PEM that has high proton conductivity, low H_2 and O_2 cross-over, and is highly durable for extended use in a fuel cell. NEI has partnered with a well-established fuel cell company to test membrane properties in a fuel cell assembly. The combined effort will advance the state of the art of PEM for fuel cells.

XI.6 Low-Cost Proton Conducting Membranes for PEM Fuel Cells

Amsen Technologies LLC
1684 S Research Loop, Suite 518
Tucson, AZ 85710

This project aims to develop a new, low-cost, proton-conducting membrane for intermediate-temperature fuel cells based on a novel composite approach, which encompasses both the development of new, highly proton-conducting ionomers and the integration of an intriguing membrane support. The use of cheap materials will result in a low-cost membrane and meeting the DOE cost targets.

PHASE II PROJECTS

XI.7 Cross-Polarized Near-UV/Vis Detector for In-line Quality Control of PEM Materials

Mainstream Engineering
200 Yellow Place
Rockledge, FL 32955-5327

This project is developing a real-time, in-line optical detector for the simultaneous determination of membrane thickness and detection of defects. This quality control device will help drive down the costs of fuel cells by reducing waste and improving the efficiency of roll-to-roll manufacturing of fuel cell polymer electrolyte membranes and other specialized membranes.

XI.8 Hydrogen Contamination Detection

Sustainable Innovations, LLC
111 Roberts Street, Suite J
East Hartford, CT 06108

This project is developing a low-cost hydrogen contaminant sensor that is critically important in expanding markets for hydrogen used in industrial and fueling applications. Sustainable Innovations has teamed with the University of

Connecticut to develop an innovative multi-channel hydrogen fuel quality monitor to detect multiple impurities at low levels in hydrogen.

XI.9 Regenerative Fuel Cell System

PH Matter, LLC
1275 Kinnear Road
Columbus, OH 43212

This project will demonstrate a low-cost fuel cell technology. The components developed on this project will improve the efficiency and lower the cost of fuel cell systems. The technology will be used for stationary energy storage applications.

XI.10 Economical Production of Hydrogen Through Development of Novel, High Efficiency Electrocatalysts for Alkaline Membrane Electrolysis

Proton Energy Systems
10 Technology Drive
Wallingford, CT 06492

This project aims to reduce the cost required to manufacture water electrolyzers through development and commercialization of an alkaline exchange membrane (AEM)-based system, enabling the use of non-noble metal and lowering the cost of materials of construction. A prototype laboratory hydrogen gas generator product will be developed to serve as an opportunity for introducing these materials to market at a lower risk entry point and gaining field experience on the pathway to eventually applying AEM technology for larger, energy-related applications, including integrating with renewable energy sources to generate hydrogen fuel while producing minimal carbon emissions.

XI.11 Diode Laser Sensor for Contaminants in Hydrogen Fuel

Southwest Sciences, Inc.
1570 Pacheco Street
Santa Fe, NM 87505

A contaminant detector for hydrogen fuel is needed to prevent fouling of hydrogen fuel cell vehicle engines. This project will develop a laser instrument for the detection of hydrogen contaminants at fuel stations.

XII. Acronyms, Abbreviations, and Definitions

~	Approximately
@	At
°C	Degrees Celsius
°F	Degrees Fahrenheit
Δ	Change, delta
ΔH	Enthalpy of reaction, Enthalpy of hydrogenation
$\Delta H°_{des}$	Desorption enthalpy
ΔK	Stress intensity factor
ΔP	Pressure drop, pressure change
≈	Equals approximately
>	Greater than
≥	Greater than or equal to
<	Less than
≤	Less than or equal to
µm	Micrometer(s), micron(s)
#	Number
Ω	Ohm(s)
Ω/cm^2	Ohm(s) per square centimeter
$\Omega\text{-}cm^2$	Ohm-square centimeter
ρ	Average fiber density
%	Percent
®	Registered trademark
$	United States dollars
1-D, 1D	One-dimensional
1Q	First quarter of the fiscal year
2-D, 2D	Two-dimensional
2Q	Second quarter of the fiscal year
III-V	three-five (semiconductor materials)
3-D, 3D	Three-dimensional
3Q	Third quarter of the fiscal year
4D	Four dimensional
4Q	Fourth quarter of the fiscal year
6PGDH	6-phosphogluconate dehydrogenase
A	Ampere, amps
A	Alkali
Å	Angstrom
Abs	absolute
AC	Activated carbon
AC	Alternating current
A/C	Anode/cathode
A/cm^2	Amps per square centimeter
ACR	Area coverage ratio
AD	Adsorption
ADOPT	Automotive Deployment Options Projection Tool
AE	Acceptability envelope; Acoustic emissions
Ae	Alkaline earth
AEM	Anion exchange membrane; Analytical electron microscopy
AEMFC	Anion exchange membrane fuel cell
AEO	Annual Energy Outlook
AFC	Alkaline fuel cell
AFCB	American Fuel Cell Bus Project
AFDC	Alternative Fuels Data Center
AFL	Anode functional layer
AFV	Alternative fuel vehicle
Ag	Silver
A-h	Amp-hour
AHJ	Authorities having jurisdiction
AIMD	Ab initio molecular dynamics
Al	Aluminum
Al_2O_3	Aluminum oxide
ALD	Atomic layer deposition
AlH_3	Aluminum hydride; Alane
ALS	Advanced Light Source at Lawrence Berkeley National Laboratory
A/m^3	Amps per cubic meter
AMFC	Anion exchange membrane fuel cell; Alkaline membrane fuel cell
AMR	U.S. Department of Energy Hydrogen and Fuel Cells Annual Merit Review
AMR	Active magnetic regenerator
AN	Acrylonitrile
ANL	Argonne National Laboratory
ANSI	American National Standards Institute
APEEP	Air Pollution Emission Experiments and Policy model
APRR	Average pressure ramp rates
APU	Auxiliary power unit
Ar	Argon
AR	As received
ARRA	American Recovery and Reinvestment Act
As	Arsenic
ASL	Anode support layer
ASME	American Society of Mechanical Engineers

ASPEN	Modeling software, computer code for process
ASR	Area-specific resistance; areal surface resistance
AST	Accelerated stress test
ASTM	ASTM International, originally known as the American Society for Testing and Materials
at%	Atomic percent
atm	Atmosphere
atmA	Atmospheres pressure, absolute
a.u.	Arbitrary units
Au	Gold
Autonomie	Plug-and-Play Powertrain and Vehicle Model Architecture and Development Environment software model by Argonne National Laboratory to support the rapid evaluation of new powertrain/propulsion technologies for improving fuel economy through virtual design and analysis in a math-based simulation environment
Avg	Average
B	Boron
B2B	Back-to-back
Ba	Barium
bara	Bar absolute
BaSce	Baseline and Scenario Analysis
BBNO	Barium bismuth niobium oxide
BDL	Biomass derived liquid
Be	Beryllium
BES	Basic Energy Sciences office within the DOE Office of Science
BESS	Battery energy storage system
BET	Brunauer-Emmett-Teller surface area analysis method
BEV	Battery electric vehicle
BF	Bright field
Bi	Bismuth
BNL	Brookhaven National Laboratory
BOC	Best of class
BOL	Beginning of life
BOM	Bill of materials
BOP, BoP	Balance of plant
BOT	Beginning of test
BP	Budget Period; Bisphenol; Biphenyl
BP1	Budget Period 1
BP2	Budget Period 2
BPP	Bipolar plate
BPV	Boiler and pressure vessel
BPVC	Boiler and Pressure Vessel Code
Br	Bromine
BTMA	Benzyltrimethyl ammonium hydroxide
BTT	Baggage tow tractor; Benzene tris-tetrazole
BTU, Btu	British thermal unit(s)
BV	Benzyl viologen
BVPC	Boiler and pressure vessel code (ASME)
C	Carbon
C	Couloumb
C_2H_4	Ethylene
C_2H_6	Ethane
C_3H_8	Propane
ca.	About, approximately
Ca	Calcium
CaFCP	California Fuel Cell Partnership
cal	Calorie(s)
CARB	California Air Resources Board
CaS	Calcium sulfide
cc	Cubic centimeter(s)
CCL	Cathode catalyst layer
CCM	Catalyst-coated membrane; Coordinate measuring machine
Cc/min, ccm	Cubic centimeters per minute
ccp	Cubic close-packing
CCP	Combined cooling and power
CCS	Carbon capture and sequestration; catalyst coated substrate
Cd	Cadmium
CD	Current density; Compact disk; Charge depleting; Cathode dewpoint
CDP	Constant dew point
CDP	Composite data product
Ce	Cerium
CEA	Commissariat à l'Energie Atomique
CEC	California Energy Commission
CEM	Compressor/expander/motor
CF	Carbon fiber
CFD	Computational fluid dynamics
cfm	Cubic feet per minute
CFR	Cumulative fluoride release
CG	Combustible gas sensor
CH	Chemical hydride
cH_2	Compressed hydrogen gas
CH_4	Methane

CHES	Corral Hollow Experimental Station
CHEX	Cold heat exchanger
CHG	Compressed hydrogen gas
CHHP	Combined heat, hydrogen, and power
CHMC	Compressed Hydrogen Materials Compatibility
CHP	Combined heat and power
Cl	Chlorine
CL	Catalyst layer
cm	Centimeter
CM	Controls module
CM	Cyanamide
cm^2	Square centimeter
CNG	Compressed natural gas
CNGV	Compressed natural gas vehicle
CNII	Cold neutron imaging instrument
CNT	Carbon nanotube
Co	Cobalt
CO	Carbon monoxide
CO_2	Carbon dioxide
CoE	Center of Excellence
COMSOL	Multiphysics modeling and engineering simulation software
COP	cooefficient of performance
COPV	Composite overwrapped pressure vessel
COV	Coefficient of variation
cP	Centipoise
CPP	Clean Power Plant
CPR2	Cascading pressure receiver reactor
CPU	Computer processing unit
CPV	Composite pressure vessel
Cr	Chromium
CR	Compression ratio
CRADA	Cooperative Research and Development Agreement
Cs	Cesium
CSA	Canadian Standards Association
CSD	Compression, storage, and delivery
CSM	Colorado School of Mines
CSULA	California State University, Los Angeles
CTD	Composite Technology Development, Inc.
CTE	Coefficient of thermal expansion
CTE	Center for Transportation and the Environment
Cu	Copper
CU	University of Colorado
CV	Conventional vehicle; Cyclic voltammatry; Cyclic voltammogram
CVD	Chemical vapor deposition
CY	Calendar year
d	Day(s)
D-A	Dubinin-Astakhov
da/dN	Fatigue crack growth rate
DAPP	Diels-Alder poly(phenylene)
DARPA	Defense Advanced Research Projects Agency
DC	Direct current
DCDA	Dicyanadiamide
DDP	Detailed data product
ΔG	Gibbs free energy of reaction
ΔH	Enthalpy of reaction; Enthalpy of hydrogenation
ΔK	Stress intensity factor
ΔP	Pressure drop; Pressure change
DF	Dark fermentation
DFC®	Direct fuel cell
DFM	Design for manufacturing
DFMA®	Design for Manufacturing and Assembly
DFT	Density functional theory
dhcp	Double hexagonal close-packing
DI	Deionized; De-ionized water
DM	Diffusion media
DMA	Dynamic mechanical analysis
DMAc	Dimethyl acetamide
DME	Dimethyl ether
DMF	n, n-di-methyl formamide
DMFC	Direct methanol fuel cell
DMS	Division of Measurement Standards
DMSO	Dimethyl slfoxide
DNA	Deoxyribonucleic acid
dobdc	2,5-dioxido-1,4-benzenedicarboxylate
DOD	Department of Defense
DOE	Department of Energy
DOT	Department of Transportation
d-PtNi, d-PtNi/C	Dealloyed platinum-nickel alloy cathode electrocatalyst supported on high surface area carbon
DR	Demand response
DRIFTs	Diffuse reflectance infrared Fourier transform spectroscopy
DRP	Disaster Recovery Plan
DRTS	Digital real-time simulator

DSC	Differential scanning calorimetry
dsbdc	2,5-disulfido-benzene-1,4-dicarboxylate
DSM™	Dimensionally stable membrane
$E_{1/2}$	Half-wave potential
E85	85%-15% blend of ethanol with gasoline
ECA	Electrochemical surface area
ECS	Electrochemical Society
ECSA	Electrochemically active surface area; Electrochemical surface area
EDAX	Manufacturer of energy dispersive X-ray hardware and software
EDS	Energy dispersive X-ray spectroscopy; Energy dispersive spectrum
EDX	Energy dispersive X-ray
EEA	Energy & Environmental Analysis, Inc.
EEA	Electrode/electrode assembly
EELS	Electron energy loss spectroscopy
EENW	Emerald Energy NW, LLC
EERE	U.S. DOE Office of Energy Efficiency and Renewable Energy
e.g.	*Exempli gratia*: for example
EG	Ethylene glycol
EGR	Exhaust gas recirculation
eGRID	Emissions & Generation Resource Integrated Database
EHC	Electrochemical hydrogen compressor; Ethylperhydrocarbazole
EHS	Environmental Health and Safety
EIA	Energy Information Administration of the U.S. Department of Energy
EIN	Energy Independence Now
EIS	Electrochemical impedance spectroscopy
EM	Electron mediator
EOL	End of life
EOT	End of test
EPA	Environmental Protection Agency
ER	Emergency responder
ER	Energy recovery
eREV	Extended range electric vehicles
ES	Energy storage
ESA	Electrochemical surface area
ESB	Erbium-stabilized bismuth oxide
ESD	Electro-static discharge; emergency shutdown device
ESIF	Energy Systems Integration Facility
ESLL	Extruded shell with loose head liner
ESOL	Extruded shell with overlaid head liner
et al.	*Et Alii:* and others
etc.	*Et cetera*: and so on
ETFECS	Extended thin-film electrocatalyst structures
eV	Electron volt
EW	Equivalent weight
EX	Hazardous area due to possible flammable gas concentration
EXAFS	Extended X-ray absorption fine structure analysis
F	Fluorine
F	Faraday constant, the amount of electric charge in one mole of electrons (96,485.3383 coulomb/mole)
f	Frequency
F^-	Fluorine ion
FASTSim	Fugure Automotive Systems Technology Simulator
FC	Fuel cell
FCB	Fuel cell bus
FCC	Face-centered cubic; Fuel Cell Catalyst; Fluid catalytic cracking
FCE	FuelCell Energy
FCEB	Fuel cell electric bus
F-Cell	Daimler Fuel Cell vehicle
FCET	Fuel cell electric truck
FCEV	Fuel cell electric vehicle
FCGR	Fatigue crack growth rate
FCHEA	Fuel Cell Hydrogen Energy Association
FCH JU	Joint Fuel Cell and Hydrogen Energy
FC-PAD	Fuel Cell Performance and Durability
FCS	Fuel cell system
FCT	Fuel Cell Technologies
FCTO	Fuel Cell Technologies Office
FCTT	Fuel Cell Technical Team
FCV	Fuel cell vehicle
Fe	Iron
FEA	Finite element analysis
FEC	Front end controller
FEM	Finite element model
FER	Fluoride emission rate
FLUENT	Computer code for computational fluid dynamics
FMEA	Failure modes and effects analysis
F-MEC	Fermentation and microbial electrolysis cell
FOA	Funding opportunity announcement

FOM	Figure of merit
fpm	Feet per minute
FPR	Falling particle receiver
FRCC	Florida Reliability Coordinating Council
FSLL	Formed shell with loose head liner
FSOL	Formed shellw ith overlaid head liner
F-SPEEK	Fluorosulfonic acid of polyetheretherketone
ft	Feet
ft^2	Square feet
ft^3	Cubic feet
FTIR	Fourier transform infrared
FTO	Fluorine-doped tin oxide
FY	Fiscal year
FZ	fusion zone
g	Gram; acceleration of gravity
G	Graphite
G6P	Glucose 6-phosphate
G6PDH	Glucose 6-phosphate dehydrogenase
Ga	Gallium
GAAP	Generally accepted accounting principles
gal	Gallon
GaP	Gallium phosphide
GB	Gigabyte
GBL	γ-Butyrolactone
GC	Gas chromatograph; General computational
GC	Glassy, or vitreous carbon; a pure carbon that is amorphous (non-crystalline)
g/cc	Grams per cubic centimeter
GCLP	Grand-canonical linear programming
GCMC	Grand Canonical Monte Carlo
GCNT	Graphitized carbon nanotubes
GCtool	Software package developed at ANL for analysis of fuel cells and other power systems
Gd	Gadolinium
GDC	Gadolinium-doped ceria
GDE	Gas diffusion electrode
GDL	Gas diffusion layer
GDM	Gas diffusion media
Ge	Germanium
Gen	Generation
GEN I	First generation
GEN II	Second generation
GEN III	Third generation
GGE, gge	Gasoline gallon equivalent
GH_2	Gaseous hydrogen
GHG	Greenhouse gas
GIS	Geographic information system
GJ	Gigajoule(s)
GKB	Grapitized Ketjenblack®
g/kW	Gram(s) per kilowatt
GLWN	Westside Industrial Retention & Expansion Network
gm	Gram(s)
GM	General Motors
gm/day	Gram(s) per day
g/min	Gram(s) per minute
GN2	Gaseous nitrogen
GNR	Graphene nanoribbon
GO	Graphene oxide
GPa	Gigapascal(s)
GREET	Greenhouse gases, Regulated Emissions and Energy use in Transportation model
g/s	Grams per second
G-S	Gas-solid
GTI	Gas Technology Institute
GUI	Graphical user interface
GWe, GW_e	Gigawatt(s) electric
h	Hour(s)
H	Hydrogen
H+	Proton
H^-	Hydride
H_2	Diatomic hydrogen
H2A	Hydrogen Analysis project sponsored by DOE
H2FAST	Hydrogen Financial Analysis Scenario Tool
H2I	Hawaii Hydrogen Initiative
H_2O	Water
H_2O_2	Hydrogen peroxide
H_2S	Hydrogen sulfide
H_2SO_4	Sulfuric acid
H2USA	Hydrogen Technology Learning Centers (for CA, FL, and NY)
HAADF	High-angle annular dark field
HAADF-STEM	High angle annular dark field scanning transmission electron microscopy
HA-FCG	Hydrogen accelerated fatigue crack growth
HAVO	Hawaii Volcanoes National Park
HAZ	Heat-affected zone
HC	Hydrocarbon
HCD	Hydrogen contaminant detector
HCER	High Energy Coil Reservoir, LLC

HCl	Hydrochloric acid
$HClO_4$	Perchloric acid
hcp	Hexagonal close-packing
HDPE	High-density polyethylene
HDSAM	Hydrogen Delivery Scenario Analysis Model
He	Helium
HE	Hydrogen embrittlement
H-E-B	H-E-B Grocery Company, Inc.
HER	Hydrogen evolution reaction
HEV	Hybrid electric vehicle
HEX	Heat exchanger
Hf	Hafnium
HFCTF	Hawaii Fuel Cell Test Facility
HFCV	Hydrogen fuel cell vehicle
HFR	High-frequency resistance
HGV	Hydrogen gaseous vehicle
HHV	Higher heating value
HIP	High performance
HiPoD	High power density
HITRF	Hydrogen Infrastructure Testing and Research Facility
HNEI	Hawaii Natural Energy Institute
HOR	Hydrogen oxidation reaction
HOV	High occupancy vehicle
hp	Horsepower
HPA	Heteropoly acid
HPTB	High powered test bay at NREL
hr	Hour(s)
HRS	Hydrogen refueling station
HRSAM	Hydrogen refueling station analysis model
HR-STEM	High resolution scanning transmission electron microscopy
HRT	Hydraulic retention time
HR-TEM	High resolution transmission electron microscopy
HSA	High surface area
HSAC	High surface area carbon
HSC	Database name derived from the letters for enthalpy, entropy and heat capacity
HSE	High surface area electrode
HSECoE	Hydrogen Storage Engineering Center of Excellence
HSP	Hydrogen Safety Panel
HT	High throughput; High temperature
HTAC	Hydrogen and Fuel Cell Technical Advisory Committee
HTC	High temperature coolant
HTE	High-temperature electrolysis
HTF	Heat transfer fluid
HTGR	High-temperature gas-cooled reactor
HTP	High throughput
HTPEM	High-temperature polymer electrolyte membrane
HX	Heat exchanger
HyCoRA	Hydrogen Contaminant Risk Assessment
HyMARC	Hydrogen Storage Materials Advanced Research Consortium
HyRAM	Hydrogen Risk Assessment Models
HyRes	Hydrogen Regional Sustainability framework
HyS	Hybrid sulfur
HyStEP	Hydrogen Station Equipment Performance
HYSYS®	Process simulation software by Aspentech, computer code for flowsheet analysis
HyTRANS	Hydrogen Transition Model
Hz	Hertz
i	Current density (mA/cm^2)
I	Current
I2CNER	International Institute for Carbon-Neutral Energy Research
I/C	Ionomer to catalyst
ICC	International Code Council
ICE	Internal combustion engine
ICEV	Internal combustion engine vehicle
iCVD	Initiated chemical vapor deposition
ID	Inside diameter
i.e.	*id est*: that is
IEC	International Electrotechnical Commission
IEC	Ion exchange capacity, milliequivalents of acid groups per gram of material
IFRS	International financial reporting standards
IFWG	Investment and Finance Working Group
IL	Illinois
IL	Ionic liquid
ILS	Inter-laboratory studies
IMM	Inverted metamorphic multijunction
In	Indium
In., in	Inch
in^2	Square inch
INL	Idaho National Laboratory
I-O	Input-output
IR, iR	Internal resistance
Ir	Iridium

IRDA	Infrared data acquisition
IrDA	Infrared Data Association
IRMOF	Isoreticular metal organic framework
IRR	Internal rate of return
ISO	International Organization for Standardization
IT	Intermediate temperature
IUPUI	Indiana University–Purdue University Indianapolis
IV	Current-voltage
J	Current
J	Joule(s)
JARI	Japan Automobile Research Institute
JM	Johnson Matthey
JMFC	Johnson-Matthey Fuel Cells, Inc.
JRC	Joint Research Centre
J-T	Joule-Thompson
K	Kelvin, absolute temperature
K	Potassium
kA/m^2	Kilo-ampere(s) per square meter
kcal	Kilocalorie(s)
kcal/mol	Kilocalorie(s) per mole
KeV	Kilo electron volt(s)
kg	Kilogram(s)
kg/d	Kilogram(s) per day
kg/hr	Kilogram(s) per hour
kg/m^3	Kilogram(s) per cubic meter
kHz	Kilohertz
kJ	Kilojoule(s)
KJ300	Ketjen Black EC 300J; a high surface-area carbon support
kJ/mol	Kilojoule(s) per mole
km	Kilometer(s)
KMC, kMC	Kinetic Monte Carlo; Kilauea Military Camp; Kia Motors Corporation
kPa	Kilopascal(s)
kph	Kilometer(s) per hour
ksi	1,000 pound-force per square inch
kVA	Kilovolt-amp (units of apparent power)
kW	Kilowatt(s)
kWe, kW_e	Kilowatt(s) electric
kWh	Kilowatt-hour(s)
kWh/kg	Kilowatt-hour(s) per kilogram
kWh/L	Kilowatt-hour(s) per liter
kW/kg	Kilowatt(s) per kilogram
kWt	Kilowatt(s) thermal
L, l	Liter(s)
La	Lanthanum
LA	Los Angeles
λ	Lambda, hydration number
LANL	Los Alamos National Laboratory
LAX	Los Angeles International Airport
lb	Pound(s)
LBL	Lawrence Berkeley National Laboratory
lbmol	Pound-mole(s)
LBNL	Lawrence Berkeley National Laboratory
LC	Levelized cost;Liquid carrier; Low concentration
LCA	Life cycle assessment; Life-cycle analysis
LCC	Life cycle cost
LCIA	Life-cycle impact assessment
LDH	Lactate dehydrogenase
LDV	Light-duty vehicle
LEIS	Low-energy ion scattering
LFL	Lower flammability limit
L/h, l/h	Liter(s) per hour
LH2, LH_2	Liquid hydrogen
LHSV	Liquid hourly space velocity, h^{-1}
LHV	Lower heating value
Li	Lithium
LLC	Limited Liability Company
LLNL	Lawrence Livermore National Laboratory
L/min, l/min	Liter(s) per minute
LMRC	Linear motor reciprocating compressor
LN_2	Liquid nitrogen
LNG	Liquefied natural gas
LP	Lattice parameter; low pressure
LSAC	Low surface area carbon
LSM	Lanthanum strontium manganate
LT	Low-temperature
LTPEM	Low temperature polymer exchange membrane
m	Meter(s)
M	Mole, molar
M	Million
m^2	Square meter(s)
m^2/g	Square meter(s) per gram
m^2/s	Square meter(s) per second
m^3	Cubic meter(s)
μA	Micro ampere(s)
mA	MilliAmps (s)

MA	Mass activity
$\mu A/cm^2$	Micro ampere(s) per square centimeter
mA/cm^2	Milliamp(s) per square centimeter
MASC	Multi-acid side-chain
MA3T	Market Acceptance of Advanced Automotive Technologies Model
MATI	Modular Adsorption Tank Insert
MAWP	Maximum allowable working pressure
MB	Megabyte
MBRC	Miles between roadcall
MC	Monte Carlo
MC	Microchannel
MCC	Materials Characterization Center
MCF	Mesostructured cellular foam
MCFC	Molten carbonate fuel cell
MCHL	Magnetocaloric hydrogen liquefier
µCHP	Micro-combined heat and power
mCHP	Micro-combined heat and power
µCHX	Microscale combustor/heat exchanger
MEA	Membrane electrode assembly
MEC	Microbial electrolysis cell
MeCN	Acetonitrile
meGo	Microwave exfoliated graphene oxide
MeOH	Methanol
meq	Milliequivalents
meq/g	Milliequivalents/gram
MES	Microstructered electrode scaffold
MeV	Mega electron volt
MFC	Microbial fuel cell, Mass flow controller
Mg	Megagram(s)
µg	Microgram(s)
mg	Milligram(s)
MGCLP	Multi-gas canonical linear programing
mg/cm^2	Milligram(s) per square centimeter
MgO	Magnesium oxide
$mgPt/cm^2$	Milligram (s) of platinum per square centimeter
MH	Metal hydride
MHE	Material handling equipment
MHz	Megahertz
mi	Mile(s)
mi/kg	Mile(s) per kilogram
min	Minute(s), minimum
MJ	Megajoule(s)
mL, ml	Milliliter(s)
ML	Monolayer; mono atomic layer
µm	Micrometer(s); micron(s)
µM	Micromolar
mM	Millimolar
mm	Millimeter(s)
MMOF	Microporous metal-organic framework
mmol	Millimole(s)
µmol	Micromole(s)
Mn	Manganese
mΩ	Milli-ohm(s)
MΩ	Mega-ohm(s)
$m\Omega/cm^2$	Milli-ohm(s) per square centimeter
$\mu\Omega\text{-}cm^2$	Micro-ohm(s) - square centimeter
Mo	Molybdenum
MO	metal oxide
MOF	Metal-organic framework
mol	Mole(s)
MOL	Middle of life
mol%	Mole percent
mol/min	Mole(s) per minute
MOPS	3-morpholinoproprane-1-sulfonic acid
MPa	Megapascal (s)
MPG, mpg	Mile(s) per gallon
MPGGE	Miles per gasoline gallon equivalent
mph	Mile(s) per hour
MPL	Microporous layer; monoporous layer
MRCAT	Materials Research Collaborative Access Team
MREC	Microbial reverse-electrodialysis electrolysis cell
MRL	Manufacturing readiness level
ms	Millisecond(s)
mS/cm	Milli-Siemen(s) per centimeter
MSM	Macro-System Model
MSU	Montana State University
mtorr	Millitorr
MTPD	Metric tonne per day
µV	Microvolt(s)
mV	Millivolt(s)
mW	Milliwatt(s)
MW	Megawatt(s)
MW	Molecular weight
MWAP	Maximum allowable workable pressure
mW/cm^2	Milliwatt(s) per square centimeter
MWCNT	Multiple-wall carbon nanotube

MWe	Megawatt(s) electric
MWh	Megawatt-hour(s)
MWNT	Multi-wall carbon nanotube
MYPP	Multi-Year Program Plan (the Fuel Cell Technologies Program's Multi-Year Research, Development, and Demonstration Plan)
MYRDD	Multi-Year Research, Development, and Demonstration
N	Nitrogen atom
N	Newton (unit of force)
N112	Nafion® 1100 equivalent weight, 2 millimeter thick membrane
N_2	Diatomic nitrogen
N_2O	Nitrous oxide
Na	Sodium
NA	North American
Na_2S	Sodium sulfide
NAD	Nicotinamide adenine dinucleotide
NADP	Nicotinamide adenine dinucleotide phosphate
NADPH	Nicotinamide adeninine dinucleotide phosphate
Nafion®	Registered Trademark of E.I. DuPont de Nemours
NASA	National Aeronautics and Space Administration
Nb	Niobium
N-C	Nitrogen doped porous carbon
N/cm^2	Newton(s) per square centimeter
NCNT; N-CNT	Nitrogen doped carbon nanotube
NEC	National Electrical Code
NECSA	South African Nuclear Energy Corporation
NELHA	Natural Energy Laboratory Hawaii Authority
NERC	North American Electric Reliability Corporation
NEU	Northeastern University
NFCTEC	National Fuel Cell Technology Evaluation Center, at NREL
NFPA	National Fire Protection Association
ng	Nanogram
NG	Natural gas
N-GT	Nitrogen doped graphene nanotube
NGV	Natural gas vehicle
NH_3	Ammonia
NHE	Normal hydrogen electrode
NHTSA	National Highway Traffic Safety Administration of the U.S. Department of Transportation
Ni	Nickel
NiMH	Nickel metal hydride
NIST	National Institute of Standards and Technology
nm	Nanometer(s)
NMN	Nicotinamide mononucleotide
nmol	Nanomole(s)
NMP	N-methylpyrrolidone
NMR	Nuclear magnetic resonance
NO_2	Nitric oxide
NOx, NO_x	Oxides of nitrogen
Non-PGM	Non-precious metal group
NP	Nanoparticle
NPCC	Northeast Power Coordinating Council
NPS	National Park Service
NPTF	Nanoporous thin film
NR	Nicotinamide riboside
NR211	Nafion® 211 membrane
NR212	Nafion® 212 membrane
NREL	National Renewable Energy Laboratory
NROR	NADPH rubredoxin oxidoreductase
NSF	National Science Foundation
NSTF	Nanostructured thin film
NT	Nanotube
NUWC	Naval Underwater Warfare Center
NW	Nanowire
NYSERDA	New York State Energy Research and Development Authority
Ω	Ohm(s)
Ωcm^2	Ohm(s) - square centimeter
O	Oxygen
O_2	Diatomic oxygen
O/C	Oxygen-to-carbon ratio
OCP	Open circuit potential
OCV	Open-circuit voltage
o.d.,OD	Outer diameter
OEM	Original equipment manufacturer
OER	Oxygen evolution reaction
O&M	Operation and maintenance
ORNL	Oak Ridge National Laboratory
ORR	Oxygen reduction reaction
OSU	Ohio State University

OSU	Oregon State University (Microproducts Breakthrough Institute)
P	Phosphorus
P	Pressure
Pa	Pascal(s)
PA	Phosphoric acid, Phenylacetylene; Polyamide
P&D	Production and delivery
PAFC	Phosphoric acid fuel cell
PAN	Polyacrylonitrile
P&ID	Piping and instrumentation diagram
PANI	Polyaniline
PAN-MA	Polyacrylonitrile with methyl acrylate
PAN-VA	Polyacrylonitrile with vinyl acetate
Pb	Lead
PB	Polyborazylene
PbA	Lead acid
PBCTF	Pressurized button cell test facility
PBI	Polybenzimidazole
PBPA	Hexamethyl ammonium functionalized poly(biphenyl alkylene)
PBS	Phosphate buffer solution
PCN	Porous coordination network
PCR	Polymerase chain reaction
PCT	Pressure-composition-temperature
PCTFE	Polychlorotrifluoroethylene
Pd	Palladium
PEC	Photoelectrochemical; Photoelectrocatalyst; Photoelectrochemical cell
PECVD	Plasma-enhanced chemical vapor deposition
PEEK	Polyether ether ether ketone
PEFC	Polymer electrolyte fuel cell
PEGS	Prototype electrostatic ground state
PEM	Proton exchange membrane; Polymer electrolyte membrane
PEMFC	Polymer electrolyte membrane fuel cell
PEMFC	Proton exchange membrane fuel cell
PEV	Plug-in electruc vehicle
PF	Perfluoro; Phenolic
PFAEM	Perfluorinated anion exchange membranes
PFD	Process flow diagram
PFIA	Perfluoroimide acid
PFICE	Perfluoro ionene chain extended
PFL	Pyruvate formate lyase
PFSA	Perfluorinated sulfonic acid, perfluorosulfonic acid, poly(fluorosulfonic acid)
PF-SFP	perfluoro sulfonyl fluoride precursor
PFSI	Perfluorosulfonate ionomer
PG	Propylene glycol
PG&E	Pacific Gas and Electric Company
PGM	Precious group metal; Platinum-group metal
pH	Power of the hydronium ion
PHEV	Plug-in hybrid electric vehicle
PHIL	Power hardware in the loop
PI	Principal investigator
P&ID	Piping and instrumentation diagram; Process and instrumentation diagram
PID	Proportional, integral, derivative; Process identifier number
PM	Particulate matter; permanent magnet
PNNL	Pacific Northwest National Laboratory
POC	Point of contact; Proof of concept
POM	Polyoxometallate
ppb	Part(s) per billion
ppbv	Part(s) per billion by volume
PPC	Pajarito Powder
PPI	Plug Power, Inc.
ppm, PPM	Part(s) per million
ppmv	Part(s) per million by volume
ppmw	Part(s) per million by weight
PPO	Phenyl phosphine oxide
ppt	Parts per trillion
PREP	Plasma rotating electrode process
PS	Polysiloxane; polystyrene
PSA	Pressure swing adsorption, adsorber
PSf	Poly(arylene ether sulfone)
psi, PSI	Pound(s) per square inch
psia	Pound(s) per square inch absolute
psid	Pound(s) per square inch differential
psig, PSIG	Pound(s) per square inch gauge
PSS	Potentiostatic scan
PSU	Polysulfone
PSU	Pennsylvania State University
PSV	Pressure safety valve
Pt	Platinum
Pt/C	Platinum/carbon
PTFE	Teflon® – poly-tetrafluoroethylene
PtO	Platinum oxide
PV	Photovoltaic; Present value
PVD	Physical vapor deposition
PVP	Pressure vessel and piping
PVT, P-V-T	Pressure-Volume-Temperature

Q1, Q2, Q3, Q4	Quarters of the fiscal year
QC	Quality control
QENS	Quasielastic neutron scattering
QMC	Quantum Monte Carlo
R	Universal or ideal gas constant, $8.314472\ J \cdot K^{-1} \cdot mol^{-1}$
RAMAN	A spectroscopic technique
RCF	RCF Economic & Financial Consulting, Inc.
RCS	Regulations codes and standards
R&D	Research and development
RD&D, R,D&D	Research, development & demonstration
RDE	Rotating disk electrode
Re	Rhenium
RE	Rare earth metal
Ref	Reference
REMI	Regional Enconomic Models, Inc.
REP	Reformer-Electrolyzer-Purifier; Representative performance
RFB	Redox flow battery
RFC	Regenerative fuel cell
RFDT	Reactive spray deposition technique
rGO	Reduced graphene oxide
Rh	Rhodium
RH	Relative humidity
RHE	Reference hydrogen electrode; Reversible hydrogen electrode
RIE	Reactive ion etching
ROI	Return on investment
RPI	Rensselaer Polytechnic Institute
rpm	Revolution(s) per minute
RRDE	Rotating ring disc electrode
RT	Room temperature
RTO	Titanium dioxide-ruthenium dioxide
Ru	Ruthenium
s	Second(s)
S	Siemen(s)
S	Sulfur
SA	Strategic Analysis, Inc.
SA	Specific amperage
SAE	SAE International, originally known as the Society of Automotive Engineers
SAINC	Strategic Analysis, Inc.
SBA	Santa Barbara Amorphous
SBIR	Small Business Innovation Research
S/C	Steam to carbon ratio
SCADA	Supervisory Control and Data Acquisition system
SCAQMD	South Coast Air Quality Management District
sccm, SCCM	Standard cubic centimeter(s) per minute
SCCV	Steel/concrete composite vessel
SCF, scf	Standard cubic feet; Supercritical fluid
scfd	Standard cubic feet per day
SCFM	Standard cubic feet per minute
S/cm	Siemen(s) per centimeter
SDE	SO_2-depolarized electrolyzer
SD/SU	Shut-down/start-up
Se	Selenium
sec	Second(s)
SECA	Solid State Energy Conversion Alliance
SEF	Surface enhancement factor
SEHP	Sorption Enhanced Hydrogen Production
SEM	Scanning electron microscopy; Scanning electron microscope
SERA	Scenario Evaluation, Regionalization and Analysis
SFE	Stacking fault energy
SFR	Stagnation flow reactor
SG&A	Sales, general, and administration
SGD	Spontaneous galvanic displacement; System gravimetric density
SH1	Soluble [FeNi]-hydrogenase 1
SHE	Standard hydrogen electrode
Si	Silicon
S-I	Sulfur-iodine
slpm, slm, sL/min	Standard liter(s) per minute
SLMA	Sr- and Mn-doped $LaAlO_3$
SMR	Steam methane reformer; Steam methane reforming
SMSI	Strong metal support interaction
SMYS	Specified minimum yield strength
Sn	Tin
SNL	Sandia National Laboratories
SLPH	Standard liter(s) per hour
SLPM	Standars liter(s) per minute
SnO	Tin oxide
SnO_2	Tin oxide
SO_2	Sulfur dioxide
SO_3	Sulfur trioxide
SOA	State of the art

SOC	State-of-charge
SOEC	Solid oxide electrolyzer cell
SOFC	Solid oxide fuel cell
SOFEC	Solid oxide fuel-assisted electrolysis cell
SOSS	Station Operational Status System
SOTA	State of the art
SOW	Statement of work
S-PEEK	Sulfonated poly(ether ether ketone)
SPP	Southwest Power Pool; strategic partnership project
S-PSU	Sulfonated polysulfone
sq. in.	Square inch(es)
Sr	Strontium
SR	Steam reformer; Steam reforming; Stoichometric ratio
SRNL	Savannah River National Laboratory
SrO	Strontium oxide
SS	Stainless steel
SSA	Specific surface area
SSFF	Stainless steel fiber felt
SSM	Sacrificial support method; Stainless steel mesh; Stress strain microprobe
SSNMR	Solid-state nuclear magnetic resonance
SSW	Stainless steel wool
STEB	Standard test evaluation bottles
STEM	Scanning transmission electron microscopy
STEM	Science, technology, engineering, and mathematics
STH	Solar-to-hydrogen
STREET	Spatially and Temporally Resolved Energy and Environment Tool STTRSmall Business Technology Transfer
STWS	Solar thermal water splitting
SUNY	State University of New York
SU/SD	Start up and shut down
SwRI®	Southwest Research Institute®
T	Temperature
T, t	Ton, tonne
T	Tesla (unit of magnetic induction)
t	Time
Ta	Tantalum
TAMU	Texas A&M University
TBD	To be determined
TC	Thermocouple
TC	Technical committee; Thermal conditioning
TCO	Transparent conductive oxide; Total cost of ownership
Te	Tellurium
TEM	Transmission electron microscopy
tf	Thin film
TF-RDE	Thin film rotating disk electrode
TGA	Thermal gravimetric analysis; Thermogravimetric analysis; Thermogravimetric analyzer
THF	Tetrahydrofuran
Ti	Titanium
TIR	Technical information report
TKK	Tanaka Kikinzoku Kogyo K. K.
TMAOH	Tetramethyl ammonium hydroxide
TPB	Triple phase boundary
TPD	Tonne(s) per day
TPR	Through plate resistance;
TPRD	Thermally-activated pressure relief device
TR	Thermal reduction chamber
TRL	Technology readiness level
TRU	Trailer refrigeration unit
UAV	Unmanned aerial vehicle
UC	University of California
UCB	University of California, Berkeley
UCDavis	University of California, Davis
UCI	University of California, Irvine
UCLA	University of California, Los Angeles
UCONN	University of Connecticut
UGA	University of Georgia, Athens
UH	University of Hawaii
UM	University of Michigan
UNLV	University of Nevada, Las Vegas
UNM	University of New Mexico
UPS	United Parcel Service
UQTR	Université du Québec à Trois-Rivières
U.S.	United States
USA	United States of America
USAXS	Ultra-small angle X-ray scattering
USC	University of South Carolina
USC	University of Southern California
USCAR	United States Council for Automotive Research, U.S. Cooperative Automotive Research
U.S. DRIVE	United States Driving Research and Innovation for Vehicle efficiency and Energy sustainability

UT	Utah
UT	University of Tennessee
UTF	Ultrathin film
UTRC	United Technologies Research Center
UTS	Ultimate tensile strength
UUV	Unmanned underwater vehicle
UW	University of Washington
V	Vanadium
V	Volt; Vulcan
VAC	Volts alternating current
VACD	Variable area control device
VC	Venture capitalist; Vulcan carbon
VCC	Virginia Clean Cities at James Madison University
VDC	Volts direct current
vdW	van der Waals
V-I, V/I	Voltage – current
VOC	Voltage open circuit
Vol., vol.	Volume
vol%	Volume percent
W	Tungsten
W	Watt(s)
WAXS	Wide angle X-ray scattering
WCF	Water consumption factor
W/cm^2	Watt(s) per square centimeter
We, W_e	Watt(s) electric
WECC	Western Electric Coordinating Council
WG	Working group
Wh	Watt-hour(s)
W-h/kg	Watt-hour(s) per kilogram
W-h/L, Wh/L	Watt-hour(s) per liter
W/kg	Watt(s) per kilogram
W/L, W/l	Watt(s) per liter
W/m-K, W/mK	Watt(s) per meter-Kelvin (unit of thermal conductivity)
Wppm	Weight part(s) per million
WPS	Wearable power system
WS	Water splitting
WSU	Washington State University
wt	Weight
Wt	Watt(s) thermal
wt%, wt.%	Weight percent (percent by weight)
WTW	Well-to-wheels
w/v	Weight by volume
WWTP	Waste water treatment plant
XAFS	X-ray absorption fine structure
XANES	X-ray absorption near-edge spectroscopy
XAS	X-ray absorption spectroscopy
XCT	X-ray computed tomography
XES	X-ray emission spectroscopy
XPS	X-ray photoelectron spectroscopy, X-ray photon spectroscopy, XRDX-ray diffraction
XRF	X-ray fluorescence
XRT	X-ray tomography
Y	Yttrium
yr, YR	Year
YSZ	Yttria-stablized zirconia
ZEV	Zero emission vehicle
Zn	Zinc
ZnO	Zinc oxide
Zr	Zirconium

XIII. Primary Contacts Index

A

Aceves, Salvador. IV.D.2, VII.C.4
Adzic, Radoslav V.A.5, V.G.1
Ahluwalia, Rajesh. IV.A.1, V.F.5
Ahmed, Imran X.5
Ainscough, Christopher III.9, III.14, VII.D.2
Allendorf, Mark IV.C.1, IV.C.2
Anton, Donald. IV.B.1
Ardo, Shane II.D.3
Arif, Muhammad V.F.2
Autrey, Tom V.G.4
Ayers, Katherine II.B.3, II.B.6

B

Balbuena, Perla V.G.5
Barilo, Nick. VIII.6
Barnes, Ted VII.B.2
Bigelow, Erik IV.D.3
Blackburn, Bryan V.D.4
Blekhman, David VII.B.4
Bonner, Brian VII.C.3
Borup, Rod V.B.1
Broerman, Eugene III.4
Brooks, Kriston. VIII.9, X.4
Buttner, Bill VIII.7

C

Contini, Vincent V.F.7

D

Datye, Abhaya V.G.13
DeCastro, Emory V.D.5
Deutsch, Todd II.D.1

E

Edgecombe, Brian IV.D.4
Elgowainy, Amgad III.1, III.13, IX.2, IX.5
Erlebacher, Jonah V.G.3
Eudy, Leslie VII.A.2
Ewan, Mitch X.1

F

Feng, Zhili. III.3, III.5
Fullenkamp, Patrick VI.4
Fultz, Brent IV.C.8

G

Gaillard, Nicolas II.D.2
Gennett, Thomas IV.C.7
Gotthold, David IV.D.1
Grabow, Lars V.G.11
Greene, David. IX.6
Groth, Katrina. VIII.5

H

Haight, Andrea IV.D.5
Hanlin, Jason VII.D.4
Harned, Alleyn VI.3
Harrison, Kevin III.11
Harrison, William. V.C.10
Hecht, Ethan VIII.4
Herring, Andrew. V.C.2
Holladay, Jamie. III.10
Hovsapian, Robert VII.D.3
Hu, Hongxing V.C.9

J

Jahnke, Fred II.F.2
James, Brian II.A.1, IV.A.2, V.F.6
Johnson, Terry VII.C.2

K

Kim, Yu Seung V.C.6
Kimball, Brett VI.5
Kocha, Shyam. V.B.3
Kongkanand, Anusorn V.A.8
Kriha, Kenneth III.7
Kurtz, Jennifer V.F.4, VII.A.1

L

LaFleur, Chris. VIII.10
Lalli, Jennifer III.12
Levinson, Rebecca IX.4
Li, Hong IV.D.6
Linic, Suljo V.G.8
Liu, Hong II.E.3

M

Maness, Pin-Ching II.E.1
Martin, Richard IV.C.12
Matter, Paul. V.E.1

Mavrikakis, Manos V.G.10
Mayyas, Ahmad VI.7
McDaniel, Anthony II.C.1
Melaina, Marc IX.7, IX.8, IX.11
Mintz, Marianne IX.1
Mittelsteadt, Cortney II.B.4, V.C.8
More, Karren V.F.1
Motyka, Theodore IV.B.3
Moulthrop, Larry VII.B.3
Mukerjee, Sanjeev V.A.3
Mukundan, Rangachary V.B.5
Musgrave, Charles II.C.4
Mustain, Bill V.G.6
Myers, Deborah V.B.2, V.D.3

N

Nikolla, Eranda V.G.7
Norris, Robert IV.D.7

O

O'Shaughnessy, Shannan III.8
Ou, Runquing V.C.11
Overbury, Steve V.G.12

P

Pecharsky, Vitalij IV.C.6
Penev, Michael IX.9
Peters, Michael II.B.1, VII.C.5
Petkov, Valeri V.G.14
Petrecky, Jim X.2
Petri, Randy II.B.5
Pivovar, Bryan V.A.6, V.C.7, V.G.17
Prakash, Amit III.6
Pratt, Joe X.3

Q

Quackenbush, Karen VIII.8

R

Ramani, Vijay V.A.9
Ramasubramaniam, Ashwin V.G.9
Rappe, Kenneth II.F.1
Rivkin, Carl VII.B.5, VIII.1
Rockward, Tommy V.F.3, VIII.3
Rodriguez, Jose V.G.2
Ronevich, Joseph III.2
Rosner, Robert IX.10
Rousseau, Aymeric IX.3

S

San Marchi, Chris IV.D.8, VIII.2
Saur, Genevieve VII.D.1
Serov, Alexey V.A.2
Siegel, Donald IV.C.10
Simon, A.J. III.15
Sprik, Sam VII.B.1
Stamenkovic, Vojislav V.A.4
Steinbach, Andrew V.A.7, V.D.1
St-Pierre, Jean V.B.7
Summers, William II.C.3

T

Terlip, Daniel VII.C.1
Thornton, Matthew IV.B.2

U

Ulsh, Michael VI.1
Urban, Jeffrey IV.C.4

V

Valente, Patrick VI.2
Vijayagopal, Ram VII.A.3
Virkar, Anil V.G.15
Voth, Greg V.G.16

W

Wagener, Earl II.B.7
Wang, Conghua "CH" V.D.2
Weber, Adam V.B.4, V.B.6
Wei, Max V.F.8
Weimer, Alan II.C.2
Wood, Brandon IV.C.3, IV.C.5

X

Xiong, Ben VII.C.6
Xu, Hui II.B.2, V.C.4, V.D.6

Y

Yan, Yushan V.C.5
Yandrasits, Michael V.C.1
Yelvington, Paul VI.6
Yuh, Chao-Yi V.C.3

Z

Zelenay, Piotr V.A.1
Zhang, Y-H Percival II.E.2
Zhou, Joe IV.C.9
Zidan, Ragaiy IV.C.11

XIV. Hydrogen and Fuel Cells Program Contacts

Sunita Satyapal
Director
Fuel Cell Technologies Office
Office of Energy Efficiency and Renewable Energy
U.S. Department of Energy
Phone: (202) 586-2336
Email: Sunita.Satyapal@ee.doe.gov

Rick Farmer
Operations Supervisor
Fuel Cell Technologies Office
Office of Energy Efficiency and Renewable Energy
U.S. Department of Energy
Phone: (202) 586-1623
Email: Richard.Farmer@ee.doe.gov

John Vetrano
Materials Sciences and Engineering Division
Basic Energy Sciences Program
Office of Science
U.S. Department of Energy
Phone: (301) 903-5976
Email: John.Vetrano@science.doe.gov

Jai-Woh Kim
Advanced Combustion & Fuel Cells Program Manager
Office of Fossil Energy
U.S. Department of Energy
Phone: (301) 903-9448
Email: Jay-Woh.Kim@hq.doe.gov

Carl Sink
Office of Advanced Reactor Deployment
Office of Nuclear Energy
U.S. Department of Energy
Phone: (301) 903-5131
Email: Carl.Sink@nuclear.energy.gov

HYDROGEN PRODUCTION AND DELIVERY

Eric Miller
Hydrogen Production and Delivery Program Manager
Fuel Cell Technologies Office
Office of Energy Efficiency and Renewable Energy
U.S. Department of Energy
Phone: (202) 287-5829
Email: Eric.Miller@ee.doe.gov

HYDROGEN STORAGE

Ned Stetson
Hydrogen Storage Program Manager
Fuel Cell Technologies Office
Office of Energy Efficiency and Renewable Energy
U.S. Department of Energy
Phone: (202) 586-9995
Email: Ned.Stetson@ee.doe.gov

FUEL CELLS

Dimitrios Papageorgopoulos
Fuel Cells Program Manager
Fuel Cell Technologies Office
Office of Energy Efficiency and Renewable Energy
U.S. Department of Energy
Phone: (202) 586-5463
Email: Dimitrios.Papageorgopoulos@ee.doe.gov

MANUFACTURING R&D

Nancy Garland
Manufacturing R&D Team Lead
Fuel Cell Technologies Office
Office of Energy Efficiency and Renewable Energy
U.S. Department of Energy
Phone: (202) 586-5673
Email: Nancy.Garland@ee.doe.gov

TECHNOLOGY VALIDATION

Jason Marcinkoski
Technology Validation Team Lead
Fuel Cell Technologies Office
Office of Energy Efficiency and Renewable Energy
U.S. Department of Energy
Phone: (202) 586-7466
Email: Jason.Marcinkoski@ee.doe.gov

SAFETY, CODES & STANDARDS

Charles James, Jr.
Safety, Codes & Standards Program Manager
Fuel Cell Technologies Office
Office of Energy Efficiency and Renewable Energy
U.S. Department of Energy
Phone: (202) 287-6223
Email: Charles.James@ee.doe.gov

EDUCATION

Gregory J. Kleen
Education Project Manager
Fuel Cell Technologies Office
Golden Field Office
U.S. Department of Energy
Phone: (720) 356-1672
Email: Gregory.Kleen@ee.doe.gov

MARKET TRANSFORMATION

Pete Devlin
Market Transformation and Interagency Coordination Manager
Fuel Cell Technologies Office
Office of Energy Efficiency and Renewable Energy
U.S. Department of Energy
Phone: (202) 586-4905
Email: Peter.Devlin@ee.doe.gov

SYSTEMS ANALYSIS

Fred Joseck
Systems Analyst
Fuel Cell Technologies Office
Office of Energy Efficiency and Renewable Energy
U.S. Department of Energy
Phone: (202) 586-7932
Email: Fred.Joseck@ee.doe.gov

AMERICAN RECOVERY AND REINVESTMENT ACT (ARRA) ACTIVITIES

Jim Alkire
Project Manager and Recovery Act Activities Lead
Fuel Cell Technologies Office
Office of Energy Efficiency and Renewable Energy
U.S. Department of Energy
Phone: (720) 356-1426
Email: James.Alkire@ee.doe.gov

XV. Project Listings by State

Alabama

IV.D.1 Toray Composites America: Enhanced Materials and Design Parameters for Reducing the Cost of Hydrogen Storage Tanks

Arizona

II.C.1 Arizona State University: High Efficiency Solar Thermochemical Reactor for Hydrogen Production

V.C.9 Amsen Technologies LLC: Low-Cost Proton Conducting Membranes for PEM Fuel Cells

Arkansas

III.6 Ashok Saxena, Consultant: Low Cost Hydrogen Storage at 875 Bar Using Steel Liner and Steel Wire Wrap

California

II.C.1 Sandia National Laboratories: High Efficiency Solar Thermochemical Reactor for Hydrogen Production

II.C.1 Stanford University: High Efficiency Solar Thermochemical Reactor for Hydrogen Production

II.D.2 Lawrence Livermore National Laboratory: Wide Bandgap Chalcopyrite Photoelectrodes for Direct Solar Water Splitting

II.D.2 Stanford University: Wide Bandgap Chalcopyrite Photoelectrodes for Direct Solar Water Splitting

II.D.3 University of California, Irvine: Tandem Particle-Slurry Batch Reactors for Solar Water Splitting

II.D.3 California Institute of Technology: Tandem Particle-Slurry Batch Reactors for Solar Water Splitting

II.D.3 Lawrence Berkeley National Laboratory: Tandem Particle-Slurry Batch Reactors for Solar Water Splitting

II.E.1 Lawrence Berkeley National Laboratory: Biomass to Hydrogen

II.F.2 University of California, Irvine: Reformer-Electrolyzer-Purifier (REP) for Production of Hydrogen [CO_2 Pump]

III.2 Sandia National Laboratories: Fatigue Performance of High-Strength Pipeline Steels and Their Welds in Hydrogen Gas Service

III.3 Ben C. Gerwick, Inc.: Vessel Design and Fabrication Technology for Stationary High-Pressure Hydrogen Storage

III.5 Bevilacqua Knight Inc.: Steel Concrete Composite Vessel for 875 bar Stationary Hydrogen Storage

III.5 LightSail: Steel Concrete Composite Vessel for 875 bar Stationary Hydrogen Storage

III.6 Structural Integrity Associates, Inc.: Low Cost Hydrogen Storage at 875 Bar Using Steel Liner and Steel Wire Wrap

III.15 Lawrence Livermore National Laboratory: Cryo-Compressed Pathway Analysis (2016)

IV.B.1 California Institute of Technology: Hydrogen Storage Engineering Center of Excellence

IV.B.1 Jet Propulsion Laboratory: Hydrogen Storage Engineering Center of Excellence

IV.C.1 Sandia National Laboratories: HyMARC: A Consortium for Advancing Solid-State Hydrogen Storage Materials

IV.C.2 Sandia National Laboratories: Hydrogen Storage Materials Advanced Research Consortium: Sandia Effort

IV.C.3 Lawrence Livermore National Laboratory: HyMARC: Hydrogen Storage Materials Advanced Research Consortium (LLNL Effort)

IV.C.4 Lawrence Berkeley National Laboratory: HyMARC: A Consortium for Advancing Solid-State Hydrogen Storage Materials

IV.C.4 Lawrence Livermore National Laboratory: HyMARC: A Consortium for Advancing Solid-State Hydrogen Storage Materials

IV.C.4 Sandia National Laboratories: HyMARC: A Consortium for Advancing Solid-State Hydrogen Storage Materials

IV.C.5 Lawrence Livermore National Laboratory: Improving the Kinetics and Thermodynamics of $Mg(BH_4)_2$ for Hydrogen Storage

IV.C.5 Sandia National Laboratories: Improving the Kinetics and Thermodynamics of $Mg(BH_4)_2$ for Hydrogen Storage

IV.C.7 Lawrence Berkeley National Laboratory: H_2 Storage Characterization and Optimization Research Efforts

California (Continued)

IV.C.8 California Institute of Technology: Design and Synthesis of Materials with High Capacities for Hydrogen Physisorption

IV.C.8 Lawrence Livermore National Laboratory: Design and Synthesis of Materials with High Capacities for Hydrogen Physisorption

IV.C.12 Ardica Technologies, Inc.: Low-Cost α-Alane for Hydrogen Storage

IV.C.12 SRI International: Low-Cost α-Alane for Hydrogen Storage

IV.D.2 Lawrence Livermore National Laboratory: Thermomechanical Cycling of Thin Liner High Fiber Fraction Cryogenic Pressure Vessels Rapidly Refueled by Liquid Hydrogen Pump to 700 Bar

IV.D.2 Linde LLC: Thermomechanical Cycling of Thin Liner High Fiber Fraction Cryogenic Pressure Vessels Rapidly Refueled by Liquid Hydrogen Pump to 700 Bar

IV.D.2 Spencer Composites Corporation: Thermomechanical Cycling of Thin Liner High Fiber Fraction Cryogenic Pressure Vessels Rapidly Refueled by Liquid Hydrogen Pump to 700 Bar

IV.D.4 Materia, Inc.: Next Generation Hydrogen Storage Vessels Enabled by Carbon Fiber Infusion with a Low Viscosity, High Toughness System

IV.D.4 Spencer Composites Corporation: Next Generation Hydrogen Storage Vessels Enabled by Carbon Fiber Infusion with a Low Viscosity, High Toughness System

IV.D.8 Sandia National Laboratories: Innovative Development, Selection and Testing to Reduce Cost and Weight of Materials for BOP Components

V.A.4 Lawrence Berkeley National Laboratory: Tailored High Performance Low-PGM Alloy Cathode Catalysts

V.B.1 Lawrence Berkeley National Laboratory: Fuel Cell-Performance and Durability (FC-PAD) Consortium Overview

V.B.3 Lawrence Berkeley National Laboratory: FC-PAD: Electrode Layer Integration

V.B.4 Lawrence Berkeley National Laboratory: FC-PAD: Ionomer, GDLs, Interfaces

V.B.5 Lawrence Berkeley National Laboratory: FC-PAD: Modeling, Evaluation, Characterization

V.B.6 Lawrence Berkeley National Laboratory: Multiscale Modeling of Fuel Cell Membranes

V.C.7 Lawrence Berkeley National Laboratory: Advanced Ionomers and MEAs for Alkaline Membrane Fuel Cells

V.D.1 Lawrence Berkeley National Laboratory: High Performance, Durable, Low Cost Membrane Electrode Assemblies for Transportation Applications

V.F.8 Lawrence Berkeley National Laboratory: A Total Cost of Ownership Model for Design and Manufacturing Optimization of Fuel Cells in Stationary and Emerging Market Applications

V.F.8 University of California, Berkeley: A Total Cost of Ownership Model for Design and Manufacturing Optimization of Fuel Cells in Stationary and Emerging Market Applications

VI.1 Lawrence Berkeley National Laboratory: Fuel Cell MEA Manufacturing R&D

VI.2 National Fuel Cell Research Center: Clean Energy Supply Chain and Manufacturing Competitiveness Analysis for Hydrogen and Fuel Cell Technologies

VII.A.4 Hydrogenics USA: Fuel Cell Hybrid Electric Delivery Van Project

VII.B.2 Linde Gas, LLC: Performance Evaluation of Delivered Hydrogen Fueling Stations

VII.B.4 California State University, Los Angeles: CSULA Hydrogen Refueling Facility Performance Evaluation and Optimization

VII.C.2 Sandia National Laboratories: Development of the Hydrogen Station Equipment Performance (HyStEP) Device

VII.C.3 Worthington Cylinder Corporation: Advanced Hydrogen Fueling Station Supply: Tube Trailers

VII.C.4 Lawrence Livermore National Laboratory: Performance and Durability Testing of Volumetrically Efficient Cryogenic Vessels and High Pressure Liquid Hydrogen Pump

VII.C.4 Linde LLC: Performance and Durability Testing of Volumetrically Efficient Cryogenic Vessels and High Pressure Liquid Hydrogen Pump

VII.C.4 Spencer Composites Corporation: Performance and Durability Testing of Volumetrically Efficient Cryogenic Vessels and High Pressure Liquid Hydrogen Pump

California (Continued)

VII.C.6 California Fuel Cell Partnership: Station Operational Status System (SOSS) 3.0 Implementation, SOSS 3.1 Upgrade, and Station Map Upgrade Project

VII.D.3 Humboldt State University: Dynamic Modeling and Validation of Electrolyzers in Real Time Grid Simulation

VIII.1 Branded by Media: National Codes and Standards Deployment and Outreach

VIII.2 Sandia National Laboratories: R&D for Safety, Codes and Standards: Materials and Components Compatibility

VIII.3 Smart Chemistry: Hydrogen Fuel Quality

VIII.5 Sandia National Laboratory: Hydrogen Quantitative Risk Assessment

VIII.6 Bki: Hydrogen Safety Panel, Safety Knowledge Tools and First Responder Training Resources

VIII.6 City of Santa Fe Springs: Hydrogen Safety Panel, Safety Knowledge Tools and First Responder Training Resources

VIII.6 Fluer, Inc.: Hydrogen Safety Panel, Safety Knowledge Tools and First Responder Training Resources

VIII.10 Sandia National Laboratory: Enabling Hydrogen Infrastructure Through Science-Based Codes and Standards

IX.4 Sandia National Laboratories: Hydrogen Analysis with the Sandia ParaChoice Model

X.3 Sandia National Laboratories: Maritime Fuel Cell Generator Project

Colorado

II.B.1 National Renewable Energy Laboratory: Renewable Electrolysis Integrated System Development and Testing

II.B.1 Spectrum Automation Controls: Renewable Electrolysis Integrated System Development and Testing

II.B.2 National Renewable Energy Laboratory: High-Performance, Long-Lifetime Catalysts for Proton Exchange Membrane Electrolysis

II.C.1 Colorado School of Mines: High Efficiency Solar Thermochemical Reactor for Hydrogen Production

II.C.2 University of Colorado Boulder: Flowing Particle Bed Solarthermal RedOx Process to Split Water

II.C.2 National Renewable Energy Laboratory: Flowing Particle Bed Solarthermal RedOx Process to Split Water

II.C.4 University of Colorado Boulder: NSF/DOE Solar Hydrogen Fuel: Accelerated Discovery of Advanced RedOx Materials for Solar Thermal Water Splitting to Produce Renewable Hydrogen

II.D.1 National Renewable Energy Laboratory: High-Efficiency Tandem Absorbers for Economical Solar Hydrogen Production

II.D.2 National Renewable Energy Laboratory: Wide Bandgap Chalcopyrite Photoelectrodes for Direct Solar Water Splitting

II.E.1 National Renewable Energy Laboratory: Biomass to Hydrogen

III.2 Colorado School of Mines: Fatigue Performance of High-Strength Pipeline Steels and Their Welds in Hydrogen Gas Service

III.9 National Renewable Energy Laboratory: Improved Hydrogen Liquefaction through Heisenberg Vortex Separation of Para- and Orthohydrogen

III.11 National Renewable Energy Laboratory: 700 bar Hydrogen Dispenser Hose Reliability Improvement

III.11 Spectrum Automation Controls: 700 bar Hydrogen Dispenser Hose Reliability Improvement

III.12 National Renewable Energy Laboratory: Cryogenically Flexible, Low Permeability H_2 Delivery Hose

III.14 National Renewable Energy Laboratory: H2FIRST--Consolidation

IV.B.1 National Renewable Energy Laboratory: Hydrogen Storage Engineering Center of Excellence

IV.B.2 National Renewable Energy Laboratory: Hydrogen Storage System Modeling: Public Access, Maintenance, and Enhancements

IV.C.7 National Renewable Energy Laboratory: H_2 Storage Characterization and Optimization Research Efforts

IV.D.5 Composite Technology Development, Inc.: Optimizing the Cost and Performance of Composite Cylinders for H_2 Storage using a Graded Construction

V.A.6 National Renewable Energy Laboratory: Extended Surface Electrocatalyst Development

V.A.6 ALD Nanosolutions: Extended Surface Electrocatalyst Development

Colorado (Continued)

V.A.6 Colorado School of Mines: Extended Surface Electrocatalyst Development

V.A.6 University of Colorado Boulder: Extended Surface Electrocatalyst Development

V.A.8 National Renewable Energy Laboratory: Highly-Accessible Catalysts for Durable High-Power Performance

V.B.1 National Renewable Energy Laboratory: Fuel Cell-Performance and Durability (FC-PAD) Consortium Overview

V.B.2 National Renewable Energy Laboratory: FC-PAD Fuel Cell-Performance and Durability Electrocatalysts and Supports

V.B.3 National Renewable Energy Laboratory: FC-PAD: Electrode Layer Integration

V.B.4 Colorado School of Mines: FC-PAD: Ionomer, GDLs, Interfaces

V.B.4 National Renewable Energy Laboratory: FC-PAD: Ionomer, GDLs, Interfaces

V.B.5 National Renewable Energy Laboratory: FC-PAD: Modeling, Evaluation, Characterization

V.C.2 Colorado School of Mines: Advanced Hybrid Membranes for Next Generation PEMFC Automotive Applications

V.C.2 National Renewable Energy Laboratory: Advanced Hybrid Membranes for Next Generation PEMFC Automotive Applications

V.C.5 National Renewable Energy Laboratory: Highly Stable Anion-Exchange Membranes for High-Voltage Redox-Flow Batteries

V.C.7 National Renewable Energy Laboratory: Advanced Ionomers and MEAs for Alkaline Membrane Fuel Cells

V.C.7 Colorado School of Mines: Advanced Ionomers and MEAs for Alkaline Membrane Fuel Cells

V.D.6 National Renewable Energy Laboratory: Advanced Catalysts and Membrane Electrode Assemblies (MEAs) for Reversible Alkaline Membrane Fuel Cells

V.E.1 National Renewable Energy Laboratory: Regenerative Fuel Cell System

V.F.4 National Renewable Energy Laboratory: Fuel Cell Technology Status: Degradation

V.G.8 University of Colorado Boulder: Analysis of the Mechanisms of Electrochemical Oxygen Reduction and Development of Ag-alloy and Pt-alloy Electrocatalysis for Low Temperature Fuel Cells

V.G.17 National Renewable Energy Laboratory: Hydroxide Conductors for Energy Conversion Devices

VI.1 National Renewable Energy Laboratory: Fuel Cell Membrane Electrode Assembly Manufacturing R&D

VI.1 Colorado School of Mines: Fuel Cell Membrane Electrode Assembly Manufacturing R&D

VI.2 National Renewable Energy Laboratory: Clean Energy Supply Chain and Manufacturing Competitiveness Analysis for Hydrogen and Fuel Cell Technologies

VI.6 National Renewable Energy Laboratory: In-line Quality Control of PEM Materials

VI.7 National Renewable Energy Laboratory: Manufacturing Competitiveness Analysis for Hydrogen Refueling Stations

VII.A.1 National Renewable Energy Laboratory: Fuel Cell Electric Vehicle Evaluation

VII.A.2 National Renewable Energy Laboratory: Technology Validation: Fuel Cell Bus Evaluations

VII.B.1 National Renewable Energy Laboratory: Hydrogen Station Data Collection and Analysis

VII.B.5 National Renewable Energy Laboratory: Brentwood Case Study

VII.B.5 Anderson Burton: Brentwood Case Study

VII.C.1 National Renewable Energy Laboratory: Hydrogen Component Validation

VII.C.1 Spectrum Automation Controls: Hydrogen Component Validation

VII.C.5 National Renewable Energy Laboratory: Hydrogen Meter Benchmark Testing

VII.C.5 Spectrum Automation Controls: Hydrogen Meter Benchmark Testing

VII.D.1 National Renewable Energy Laboratory: Stationary Fuel Cell Evaluation

VII.D.2 National Renewable Energy Laboratory: Material Handling Equipment Data Collection and Analysis

VIII.1 National Renewable Energy Laboratory: National Codes and Standards Deployment and Outreach

VIII.4 Sandia National Laboratories: R&D for Safety, Codes and Standards: Hydrogen Behavior

VIII.7 National Renewable Energy Laboratory: NREL Hydrogen Sensor Testing Laboratory

Colorado (Continued)

VIII.7 Bloomfield Automation: NREL Hydrogen Sensor Testing Laboratory

VIII.7 Element One: NREL Hydrogen Sensor Testing Laboratory

IX.7 National Renewable Energy Laboratory: Sustainability Analysis of Hydrogen Supply and Stationary Fuel Cell Systems Using the Hydrogen Regional Sustainability (HyReS) Framework

IX.8 National Renewable Energy Laboratory: Evaluation of Technology Status Compared to Program Targets

IX.9 National Renewable Energy Laboratory: Expanded Capabilities for the Hydrogen Financial Analysis Scenario Tool

IX.11 National Renewable Energy Laboratory: National FCEV and Hydrogen Refueling Station Scenarios

IX.11 Lexidyne, LLC: National FCEV and Hydrogen Refueling Station Scenarios

Connecticut

II.B.3 Proton OnSite: High Performance Platinum Group Metal Free Membrane Electrode Assemblies Through Control of Interfacial Processes

II.B.5 FuelCell Energy: Solid Oxide Based Electrolysis and Stack Technology with Ultra-High Electrolysis Current Density (>3 A/cm^2) and Efficiency

II.B.6 Proton OnSite: Economical Production of Hydrogen Through Development of Novel, High Efficiency Electrocatalysts for Alkaline Membrane Electrolysis

II.B.7 Proton OnSite: New Approaches to Improved PEM Electrolyzer Ion Exchange Membranes

II.F.2 FuelCell Energy: Reformer-Electrolyzer-Purifier (REP) for Production of Hydrogen [CO_2 Pump]

IV.B.1 United Technologies Research Center: Hydrogen Storage Engineering Center of Excellence

V.A.3 FuelCell Energy: Innovative Non-PGM Catalysts for High-Temperature PEMFCs

V.B.7 University of Connecticut: The Effect of Airborne Contaminants on Fuel Cell Performance and Durability

V.B.7 WPCSOL: The Effect of Airborne Contaminants on Fuel Cell Performance and Durability

V.C.3 FuelCell Energy: Smart Matrix Development for Direct Carbonate Fuel Cell

V.C.3 University of Connecticut: Smart Matrix Development for Direct Carbonate Fuel Cell

V.D.3 United Technologies Research Center: Rationally Designed Catalyst Layers for PEMFC Performance Optimization

V.G.6 University of Connecticut: Room Temperature Electrochemical Upgrading of Methane to Oxygenate Fuels

VI.2 Connecticut Center for Advanced Technology: Clean Energy Supply Chain and Manufacturing Competitiveness Analysis for Hydrogen and Fuel Cell Technologies

VII.B.3 Proton OnSite: Validation of an Advanced High Pressure PEM Electrolyzer and Composite Hydrogen Storage, with Data Reporting, for SunHydro Stations

VII.B.3 SunHydro LLC: Validation of an Advanced High Pressure PEM Electrolyzer and Composite Hydrogen Storage, with Data Reporting, for SunHydro Stations

VII.B.5 Proton OnSite: Brentwood Case Study

VIII.6 GWS Solutions of Tolland, LLC: Hydrogen Safety Panel, Safety Knowledge Tools and First Responder Training Resources

VIII.6 Proton OnSite: Hydrogen Safety Panel, Safety Knowledge Tools and First Responder Training Resources

Delaware

V.A.6 University of Delaware: Extended Surface Electrocatalyst Development

V.B.4 University of Delaware: FC-PAD: Ionomer, GDLs, Interfaces

V.C.5 University of Delaware: Highly Stable Anion-Exchange Membranes for High-Voltage Redox-Flow Batteries

Florida

VI.1 Mainstream Engineering: Fuel Cell Membrane Electrode Assembly Manufacturing R&D

VI.6 Mainstream Engineering: In-line Quality Control of PEM Materials

Florida (Continued)

VII.D.3 Florida State University: Dynamic Modeling and Validation of Electrolyzers in Real Time Grid Simulation

VIII.6 Witte Engineered Gases: Hydrogen Safety Panel, Safety Knowledge Tools and First Responder Training Resources

Georgia

II.B.6 Georgia Institute of Technology: Economical Production of Hydrogen Through Development of Novel, High Efficiency Electrocatalysts for Alkaline Membrane Electrolysis

II.E.2 University of Georgia: Sweet Hydrogen: High-Yield Production of Hydrogen from Biomass Sugars Catalyzed by in vitro Synthetic Biosystems

IV.D.3 Center for Transportation and the Environment: Conformable Hydrogen Storage Pressure Vessel Project

V.G.10 Georgia Institute of Technology: Atomic-Scale Design of Metal and Alloy Catalysts: A Combined Theoretical and Experimental Approach

VI.1 Georgia Institute of Technology: Fuel Cell Membrane Electrode Assembly Manufacturing R&D

VII.A.4 Center for Transportation and the Environment: Fuel Cell Hybrid Electric Delivery Van Project

VII.A.4 United Parcel Services: Fuel Cell Hybrid Electric Delivery Van Project

Hawaii

II.D.1 University of Hawaii: High-Efficiency Tandem Absorbers for Economical Solar Hydrogen Production

II.D.2 University of Hawaii: Wide Bandgap Chalcopyrite Photoelectrodes for Direct Solar Water Splitting

IV.C.7 University of Hawaii: H_2 Storage Characterization and Optimization Research Efforts

V.B.7 Hawaii Natural Energy Institute: The Effect of Airborne Contaminants on Fuel Cell Performance and Durability

V.D.2 University of Hawaii: Novel Structured Metal Bipolar Plates for Low Cost Manufacturing

X.1 Hawaii Natural Energy Institute: Hydrogen Energy Systems as a Grid Management Tool

Idaho

VII.D.3 Idaho National Laboratory: Dynamic Modeling and Validation of Electrolyzers in Real Time Grid Simulation

Illinois

II.C.1 Northwestern University: High Efficiency Solar Thermochemical Reactor for Hydrogen Production

III.1 Argonne National Laboratory: Hydrogen Delivery Infrastructure Analysis

III.7 Gas Technology Institute: Compressor-Less Hydrogen Refueling Station Using Thermal Compression

III.13 Argonne National Laboratory: Hydrogen Fueling Station Precooling Analysis

IV.A.1 Argonne National Laboratory: System Analysis of Physical and Materials-Based Hydrogen Storage

IV.C.9 Argonne National Laboratory: High-Capacity and Low-Cost Hydrogen-Storage Sorbents for Automotive Applications

V.A.4 Argonne National Laboratory: Tailored High Performance Low-PGM Alloy Cathode Catalysts

V.A.7 Argonne National Laboratory: Highly Active, Durable, and Ultra-low PGM NSTF Thin Film ORR Catalysts and Supports

V.A.9 Illinois Institute of Technology: Corrosion-Resistant Non-Carbon Electrocatalyst Supports for PEFCs

V.B.1 Argonne National Laboratory: Fuel Cell-Performance and Durability (FC-PAD) Consortium Overview

V.B.2 Argonne National Laboratory: FC-PAD Fuel Cell-Performance and Durability Electrocatalysts and Supports

V.B.3 Argonne National Laboratory: FC-PAD: Electrode Layer Integration

V.B.4 Argonne National Laboratory: FC-PAD: Ionomer, GDLs, Interfaces

V.B.5 Argonne National Laboratory: FC-PAD: Modeling, Evaluation, Characterization

V.C.3 Illinois Institute of Technology: Smart Matrix Development for Direct Carbonate Fuel Cell

V.C.6 Argonne National Laboratory: Advanced Materials for Fully-Integrated MEAs in AEMFCs

Illinois (Continued)

V.D.1 Argonne National Laboratory: High Performance, Durable, Low Cost Membrane Electrode Assemblies for Transportation Applications

V.D.3 Argonne National Laboratory: Rationally Designed Catalyst Layers for PEMFC Performance Optimization

V.F.5 Argonne National Laboratory: Performance and Durability of Advanced Automotive Fuel Cell Stacks and Systems with Nanostructured Thin Film Catalyst Based Membrane Electrode Assemblies

V.G.16 University of Chicago: Computer Simulation of Proton Transport in Fuel Cell Membranes

VII.A.3 Argonne National Laboratory: Fuel Cell Electric Truck (FCET) Component Sizing

VII.B.2 Gas Technology Institute: Performance Evaluation of Delivered Hydrogen Fueling Stations

IX.1 Argonne National Laboratory: Employment Impacts of Hydrogen and Fuel Cell Technologies

IX.1 RCF Economic and Financial Consulting, Inc.: Employment Impacts of Hydrogen and Fuel Cell Technologies

IX.2 Argonne National Laboratory: Life-Cycle Analysis of Water Consumption for Hydrogen Production

IX.3 Argonne National Laboratory: Impact of Fuel Cell and H_2 Storage Improvements on FCEVs

IX.5 Argonne National Laboratory: Life Cycle Analysis of Emerging Hydrogen Production Technologies

IX.10 University of Chicago: The Business Case for Hydrogen-powered Passenger Cars: Competition and Solving the Infrastructure Puzzle

Indiana

III.5 AccerlorMittal: Steel Concrete Composite Vessel for 875 bar Stationary Hydrogen Storage

IV.D.3 High Energy Coil Reservoirs, LLC: Conformable Hydrogen Storage Pressure Vessel Project

V.A.7 Purdue University: Highly Active, Durable, and Ultra-low PGM NSTF Thin Film ORR Catalysts and Supports

V.D.3 Indiana University Purdue University: Rationally Designed Catalyst Layers for PEMFC Performance Optimization

Iowa

IV.C.6 Ames Laboratory: High-capacity Hydrogen Storage Systems via Mechanochemistry

Kentucky

III.5 Adaptive Intelligent Systems LLC: Steel Concrete Composite Vessel for 875 bar Stationary Hydrogen Storage

Maryland

III.2 National Institute of Standards and Technology: Fatigue Performance of High-Strength Pipeline Steels and Their Welds in Hydrogen Gas Service

IV.C.7 National Institute of Standards and Technology: H_2 Storage Characterization and Optimization Research Efforts

V.A.7 John Hopkins University: Highly Active, Durable, and Ultra-low PGM NSTF Thin Film ORR Catalysts and Supports

V.D.1 John Hopkins University: High Performance, Durable, Low Cost Membrane Electrode Assemblies for Transportation Applications

V.D.4 Redox Power Systems: Affordable, High Performance, Intermediate Temperature Solid Oxide Fuel Cells

V.D.4 University of Maryland: Affordable, High Performance, Intermediate Temperature Solid Oxide Fuel Cells

V.F.2 National Institute of Standards and Technology: Neutron Imaging Study of the Water Transport in Operating Fuel Cells

V.G.3 John Hopkins University: Control of Reactivity in Nanoporous Metal/Ionic Liquid Composite Catalysts

IX.1 Energetics, Inc.: Employment Impacts of Hydrogen and Fuel Cell Technologies

Massachusetts

II.B.2 Giner, Inc.: High-Performance, Long-Lifetime Catalysts for Proton Exchange Membrane Electrolysis

II.B.3 Northeastern University: High Performance Platinum Group Metal Free Membrane Electrode Assemblies through Control of Interfacial Processes

Massachusetts (Continued)

- II.B.4 Giner, Inc.: High Temperature, High Pressure Electrolysis
- III.8 GVD Corporation: Advanced Barrier Coatings for Harsh Environments
- V.A.3 Northeastern University: Innovative Non-PGM Catalysts for High-Temperature PEMFCs
- V.B.4 Tufts University: FC-PAD: Ionomer, GDLs, Interfaces
- V.C.4 Giner, Inc.: Ionomer Dispersion Impact on Fuel Cell and Electrolyzer Performance and Durability
- V.C.8 Giner, Inc.: Dimensionally Stable High Performance Membranes
- V.C.11 ElectroChem, Inc.: Novel Nanocomposite Polymer Electrolyte Membranes for Fuel Cells
- V.D.5 Advent Technologies Inc.: Facilitated Direct Liquid Fuel Cells with High Temperature Membrane Electrode Assemblies
- V.D.6 Giner, Inc.: Advanced Catalysts and Membrane Electrode Assemblies (MEAs) for Reversible Alkaline Membrane Fuel Cells
- V.E.1 Giner, Inc.: Regenerative Fuel Cell System
- V.G.9 University of Massachusetts Amherst: Computational Design of Graphene-Nanoparticle Catalysts
- VIII.6 Firexplo: Hydrogen Safety Panel, Safety Knowledge Tools and First Responder Training Resources
- X.4 Nuvera Fuel Cells: Demonstration of Fuel Cell Auxiliary Power Units (APUs) to Power Transport Refrigeration Units (TRUs) in Refrigerated Trucks

Michigan

- IV.B.1 Ford Motor Company: Hydrogen Storage Engineering Center of Excellence
- IV.B.1 General Motors Company: Hydrogen Storage Engineering Center of Excellence
- IV.B.1 University of Michigan: Hydrogen Storage Engineering Center of Excellence
- IV.C.5 University of Michigan: Improving the Kinetics and Thermodynamics of $Mg(BH_4)_2$ for Hydrogen Storage
- IV.C.10 University of Michigan: Hydrogen Adsorbents with High Volumetric Density: New Materials and System Projections
- IV.C.10 Ford Motor Company: Hydrogen Adsorbents with High Volumetric Density: New Materials and System Projections
- IV.D.1 Ford Motor Company: Enhanced Materials and Design Parameters for Reducing the Cost of Hydrogen Storage Tanks
- V.A.1 General Motors Company: Non-Precious Metal Fuel Cell Cathodes: Catalyst Development and Electrode Structure Design
- V.A.8 General Motors Company: Highly-Accessible Catalysts for Durable High-Power Performance
- V.A.9 Nissan Technical Center, North America: Corrosion-Resistant Non-Carbon Electrocatalyst Supports for PEFCs
- V.C.1 General Motors Company: New Fuel Cell Membranes with Improved Durability and Performance
- V.C.2 Nissan Technical Center, North America: Advanced Hybrid Membranes for Next Generation PEMFC Automotive Applications
- V.D.1 General Motors Company: High Performance, Durable, Low Cost Membrane Electrode Assemblies for Transportation Applications
- V.D.1 Michigan Technological University: High Performance, Durable, Low Cost Membrane Electrode Assemblies for Transportation Applications
- V.G.7 Wayne State University: Nanostructured, Targeted Layered Metal Oxides as Active and Selective Heterogeneous Electrocatalysts for Oxygen Evolution
- V.G.8 University of Michigan: Analysis of the Mechanisms of Electrochemical Oxygen Reduction and Development of Ag-alloy and Pt-alloy Electrocatalysis for Low Temperature Fuel Cells
- V.G.14 Central Michigan University: Element Specific Atomic Arrangement of Binary and Ternary Alloy Nanosized Catalysts in As-Prepared and Active State
- VI.1 General Motors Company: Fuel Cell Membrane Electrode Assembly Manufacturing R&D
- VIII.9 Ford Motor Company: Compatibility of Polymeric Materials Used in the Hydrogen Infrastructure

Minnesota

V.A.7 3M Company: Highly Active, Durable, and Ultra-low PGM NSTF Thin Film ORR Catalysts and Supports

V.A.8 3M Company: Highly-Accessible Catalysts for Durable High-Power Performance

V.B.4 3M Company: FC-PAD: Ionomer, GDLs, Interfaces

V.C.1 3M Company: New Fuel Cell Membranes with Improved Durability and Performance

V.C.2 3M Company: Advanced Hybrid Membranes for Next Generation PEMFC Automotive Applications

V.C.7 3M Company: Advanced Ionomers and MEAs for Alkaline Membrane Fuel Cells

V.D.1 3M Company: High Performance, Durable, Low Cost Membrane Electrode Assemblies for Transportation Applications

VI.1 3M Company: Fuel Cell Membrane Electrode Assembly Manufacturing R&D

Missouri

II.B.6 Washington University: Economical Production of Hydrogen Through Development of Novel, High Efficiency Electrocatalysts for Alkaline Membrane Electrolysis

IV.C.6 University of Missouri: High-capacity Hydrogen Storage Systems via Mechanochemistry

VIII.6 Becht Engineering: Hydrogen Safety Panel, Safety Knowledge Tools and First Responder Training Resources

Montana

IV.D.4 Montana State University: Next Generation Hydrogen Storage Vessels Enabled by Carbon Fiber Infusion with a Low Viscosity, High Toughness System

Nebraska

IV.B.1 Hexagon Lincoln: Hydrogen Storage Engineering Center of Excellence

IV.D.1 Hexagon Lincoln: Enhanced Materials and Design Parameters for Reducing the Cost of Hydrogen Storage Tanks

IV.D.6 Hexagon Lincoln: Achieving Hydrogen Storage Goals through High-Strength Fiber Glass

Nevada

II.D.1 University of Nevada: High-Efficiency Tandem Absorbers for Economical Solar Hydrogen Production

II.D.2 University of Nevada: Wide Bandgap Chalcopyrite Photoelectrodes for Direct Solar Water Splitting

New Hampshire

III.5 Sustain X: Steel Concrete Composite Vessel for 875 bar Stationary Hydrogen Storage

III.12 New England Wire Technologies, Inc.: Cryogenically Flexible, Low Permeability H_2 Delivery Hose

New Jersey

V.C.11 NEI Corporation: Novel Nanocomposite Polymer Electrolyte Membranes for Fuel Cells

V.D.2 TreadStone Technologies, Inc.: Novel Structured Metal Bipolar Plates for Low Cost Manufacturing

New Mexico

II.B.3 University of New Mexico: High Performance Platinum Group Metal Free Membrane Electrode Assemblies through Control of Interfacial Processes

II.B.6 Pajarito Powder: Economical Production of Hydrogen Through Development of Novel, High Efficiency Electrocatalysts for Alkaline Membrane Electrolysis

II.E.1 Sandia National Laboratories: Biomass to Hydrogen

IV.B.1 Los Alamos National Laboratory: Hydrogen Storage Engineering Center of Excellence

IV.D.5 Adherent Technologies, Inc.: Optimizing the Cost and Performance of Composite Cylinders for H_2 Storage using a Graded Construction

V.A.1 Los Alamos National Laboratory: Non-Precious Metal Fuel Cell Cathodes: Catalyst Development & Electrode Structure Design

New Mexico (Continued)

V.A.1 IRD Fuel Cells: Non-Precious Metal Fuel Cell Cathodes: Catalyst Development & Electrode Structure Design

V.A.2 University of New Mexico: Development of PGM-free Catalysts for Hydrogen Oxidation Reaction in Alkaline Media

V.A.2 IRD Fuel Cells: Development of PGM-free Catalysts for Hydrogen Oxidation Reaction in Alkaline Media

V.A.2 Los Alamos National Laboratory: Development of PGM-free Catalysts for Hydrogen Oxidation Reaction in Alkaline Media

V.A.2 Pajarito Powder: Development of PGM-free Catalysts for Hydrogen Oxidation Reaction in Alkaline Media

V.A.3 Pajarito Powder: Innovative Non-PGM Catalysts for High-Temperature PEMFCs

V.A.3 University of New Mexico: Innovative Non-PGM Catalysts for High-Temperature PEMFCs

V.A.4 Los Alamos National Laboratory: Tailored High Performance Low-PGM Alloy Cathode Catalysts

V.A.5 Los Alamos National Laboratory: Platinum Monolayer Electrocatalysts

V.A.9 University of New Mexico: Corrosion-Resistant Non-Carbon Electrocatalyst Supports for PEFCs

V.B.1 Los Alamos National Laboratory: Fuel Cell-Performance and Durability (FC-PAD) Consortium Overview

V.B.2 Los Alamos National Laboratory: FC-PAD Fuel Cell-Performance and Durability Electrocatalysts and Supports

V.B.3 Los Alamos National Laboratory: FC-PAD: Electrode Layer Integration

V.B.4 Los Alamos National Laboratory: FC-PAD: Ionomer, GDLs, Interfaces

V.B.5 Los Alamos National Laboratory: FC-PAD: Modeling, Evaluation, Characterization

V.C.4 Los Alamos National Laboratory: Ionomer Dispersion Impact on Fuel Cell and Electrolyzer Performance and Durability

V.C.6 Los Alamos National Laboratory: Advanced Materials for Fully-Integrated MEAs in AEMFCs

V.C.6 Sandia National Laboratories: Advanced Materials for Fully-Integrated MEAs in AEMFCs

V.D.1 Los Alamos National Laboratory: High Performance, Durable, Low Cost Membrane Electrode Assemblies for Transportation Applications

V.D.5 Los Alamos National Laboratory: Facilitated Direct Liquid Fuel Cells with High Temperature Membrane Electrode Assemblies

V.F.3 Los Alamos National Laboratory: Technical Assistance to Developers

V.G.13 University of New Mexico: Sub Nanometer Sized Clusters for Heterogeneous Catalysis

VIII.3 Los Alamos National Laboratory: Hydrogen Fuel Quality

VIII.5 Sandia National Laboratories: Hydrogen Quantitative Risk Assessment

VIII.10 Sandia National Laboratories: Enabling Hydrogen Infrastructure Through Science-Based Codes and Standards

New York

V.A.1 University of Rochester: Non-Precious Metal Fuel Cell Cathodes: Catalyst Development and Electrode Structure Design

V.A.5 Brookhaven National Laboratory: Platinum Monolayer Electrocatalysts

V.A.8 Cornell University: Highly-Accessible Catalysts for Durable High-Power Performance

V.C.6 Rensselaer Polytechnic University: Advanced Materials for Fully-Integrated MEAs in AEMFCs

V.C.8 Rensselaer Polytechnic University: Dimensionally Stable High Performance Membranes

V.D.6 University at Buffalo-SUNY: Advanced Catalysts and Membrane Electrode Assemblies (MEAs) for Reversible Alkaline Membrane Fuel Cells

V.G.1 Brookhaven National Laboratory: Structure and Function in Electrocatalysis of Reactions for Direct Energy Conversion

V.G.2 Brookhaven National Laboratory: Catalysis and Electrocatalysis for Advanced Fuel Synthesis: Hydrogen Production and the Water-Gas Shift

VI.5 Automated Dynamics: Continuous Fiber Composite Electrofusion Coupler

VII.A.4 Unique Electric Solutions: Fuel Cell Hybrid Electric Delivery Van Project

New York (Continued)

X.2 Plug Power: Ground Support Equipment Demonstration

X.5 Plug Power: FedEx Express Hydrogen Fuel Cell Extended-Range Battery Electric Vehicles

Ohio

III.4 ACI Services: Hydrogen Compression Application of the Linear Motor Reciprocating Compressor (LMRC)

III.6 N&R Engineering: Low Cost Hydrogen Storage at 875 Bar Using Steel Liner and Steel Wire Wrap

III.12 Swagelok: Cryogenically Flexible, Low Permeability H_2 Delivery Hose

V.E.1 pH Matter, LLC: Regenerative Fuel Cell System

V.F.7 Battelle: Stationary and Emerging Market Fuel Cell System Cost Analysis—Primary Power and Combined Heat and Power Applications

VI.2 Ohio Fuel Cell Coalition: Clean Energy Supply Chain and Manufacturing Competitiveness Analysis for Hydrogen and Fuel Cell Technologies

VI.2 DJW Technology, LLC: Clean Energy Supply Chain and Manufacturing Competitiveness Analysis for Hydrogen and Fuel Cell Technologies

VI.4 GLWN, Westside Industrial Retention & Expansion Network: U.S. Clean Energy Hydrogen and Fuel Cell Technologies: A Competiveness Analysis

VI.4 DJW Technology, LLC: U.S. Clean Energy Hydrogen and Fuel Cell Technologies: A Competiveness Analysis

X.5 Workhorse Technologies Inc.: FedEx Express Hydrogen Fuel Cell Extended-Range Battery Electric Vehicles

Oregon

II.E.3 Oregon State University: Novel Hybrid Microbial Electrochemical System for Efficient Hydrogen Generation from Biomass

III.3 Harris Thermal Transfer Products: Vessel Design and Fabrication Technology for Stationary High-Pressure Hydrogen Storage

III.6 Hy-Performance Materials Testing, LLC: Low Cost Hydrogen Storage at 875 Bar Using Steel Liner and Steel Wire Wrap

IV.B.1 Oregon State University: Hydrogen Storage Engineering Center of Excellence

IV.D.8 Hy-Performance Materials Testing, LLC: Innovative Development, Selection and Testing to Reduce Cost and Weight of Materials for BOP Components

Pennsylvania

II.B.3 Pennsylvania State University: High Performance Platinum Group Metal Free Membrane Electrode Assemblies through Control of Interfacial Processes

II.C.1 Bucknell University: High Efficiency Solar Thermochemical Reactor for Hydrogen Production

II.E.1 Pennsylvania State University: Biomass to Hydrogen

III.3 Temple University: Vessel Design and Fabrication Technology for Stationary High-Pressure Hydrogen Storage

III.5 Temple University: Steel Concrete Composite Vessel for 875 bar Stationary Hydrogen Storage

III.6 CP Industries: Low Cost Hydrogen Storage at 875 Bar Using Steel Liner and Steel Wire Wrap

III.14 PDC Machines: H2FIRST—Consolidation

IV.D.6 PPG Industries: Achieving Hydrogen Storage Goals through High-Strength Fiber Glass

V.A.1 Carnegie Mellon University: Non-Precious Metal Fuel Cell Cathodes: Catalyst Development and Electrode Structure Design

V.A.8 Carnegie Mellon University: Highly-Accessible Catalysts for Durable High-Power Performance

V.A.8 Drexel University: Highly-Accessible Catalysts for Durable High-Power Performance

VII.B.3 Air Products and Chemicals, Inc.: Validation of an Advanced High Pressure PEM Electrolyzer and Composite Hydrogen Storage, with Data Reporting, for SunHydro Stations

VII.C.3 Air Products and Chemicals, Inc.: Advanced Hydrogen Fueling Station Supply: Tube Trailers

Pensylvania (Continued)

VIII.3 ASTM International: Hydrogen Fuel Quality

VIII.3 SAE International: Hydrogen Fuel Quality

VIII.6 Air Products and Chemicals, Inc.: Hydrogen Safety Panel, Safety Knowledge Tools and First Responder Training Resources

South Carolina

II.B.7 Tetramer Technologies, LLC: New Approaches to Improved PEM Electrolyzer Ion Exchange Membranes

II.C.3 Savannah River National Laboratory: Electrolyzer Component Development for the HyS Thermochemical Cycle

II.C.3 Savannah River Consulting LLC: Electrolyzer Component Development for the HyS Thermochemical Cycle

IV.B.1 Savannah River National Laboratory: Hydrogen Storage Engineering Center of Excellence

IV.B.2 Savannah River National Laboratory: Hydrogen Storage System Modeling: Public Access, Maintenance, and Enhancements

IV.B.3 Savannah River National Laboratory: Investigation of Metal and Chemical Hydrides for Hydrogen Storage in Novel Fuel Cell Systems

IV.B.3 Savannah River Consulting LLC: Investigation of Metal and Chemical Hydrides for Hydrogen Storage in Novel Fuel Cell Systems

IV.C.11 Savannah River National Laboratory: Electrochemical Reversible Formation of Alane

VI.5 Savannah River National Laboratory: Continuous Fiber Composite Electrofusion Coupler

Tennessee

III.2 Oak Ridge National Laboratory: Fatigue Performance of High-Strength Pipeline Steels and Their Welds in Hydrogen Gas Service

III.3 Oak Ridge National Laboratory: Vessel Design and Fabrication Technology for Stationary High-Pressure Hydrogen Storage

III.5 Oak Ridge National Laboratory: Steel Concrete Composite Vessel for 875 bar Stationary Hydrogen Storage

III.6 Oak Ridge National Laboratory: Low Cost Hydrogen Storage at 875 Bar Using Steel Liner and Steel Wire Wrap

IV.D.1 AOC, LLC: Enhanced Materials and Design Parameters for Reducing the Cost of Hydrogen Storage Tanks

IV.D.5 Oak Ridge National Laboratory: Optimizing the Cost and Performance of Composite Cylinders for H2 Storage using a Graded Construction

IV.D.7 Oak Ridge National Laboratory: Melt Processable PAN Precursor for High Strength, Low-Cost Carbon Fibers (Phase II)

V.A.1 Oak Ridge National Laboratory: Non-Precious Metal Fuel Cell Cathodes: Catalyst Development and Electrode Structure Design

V.A.4 Oak Ridge National Laboratory: Tailored High Performance Low-PGM Alloy Cathode Catalysts

V.A.7 Oak Ridge National Laboratory: Highly Active, Durable, and Ultra-low PGM NSTF Thin Film ORR Catalysts and Supports

V.B.1 Oak Ridge National Laboratory: Fuel Cell-Performance and Durability (FC-PAD) Consortium Overview

V.B.2 Oak Ridge National Laboratory: FC-PAD Fuel Cell-Performance and Durability Electrocatalysts and Supports

V.B.3 Oak Ridge National Laboratory: FC-PAD: Electrode Layer Integration

V.B.4 Oak Ridge National Laboratory: FC-PAD: Ionomer, GDLs, Interfaces

V.B.5 Oak Ridge National Laboratory: FC-PAD: Modeling, Evaluation, Characterization

V.C.1 Vanderbilt University: New Fuel Cell Membranes with Improved Durability and Performance

V.C.7 Oak Ridge National Laboratory: Advanced Ionomers & MEAs for Alkaline Membrane Fuel Cells

V.F.1 Oak Ridge National Laboratory: New Fuel Cell Materials: Characterization and Method Development

V.G.12 Oak Ridge National Laboratory: Fundamentals of Catalysis and Chemical Transformations

IX.6 University of Tennessee: Policies to Promote Alternative Fuel Vehicles

X.5 Federal Express Corporation: FedEx Express Hydrogen Fuel Cell Extended-Range Battery Electric Vehicles

Texas

III.3 Hanson Pressure Pipe: Vessel Design and Fabrication Technology for Stationary High-Pressure Hydrogen Storage

III.4 Southwest Research Institute®: Hydrogen Compression Application of the Linear Motor Reciprocating Compressor (LMRC)

III.5 Air Liquide: Steel Concrete Composite Vessel for 875 bar Stationary Hydrogen Storage

III.5 Forterra Water Pipe: Steel Concrete Composite Vessel for 875 bar Stationary Hydrogen Storage

IV.C.9 Texas A&M University: High-Capacity and Low-Cost Hydrogen-Storage Sorbents for Automotive Applications

IV.D.3 University of Texas at Austin: Conformable Hydrogen Storage Pressure Vessel Project

V.D.3 University of Texas at Austin: Rationally Designed Catalyst Layers for PEMFC Performance Optimization

V.G.5 Texas A&M University: Modeling Catalyzed Growth of Single Walled Carbon Nanotubes

V.G.11 University of Houston: Dual Site Requirements for Hydrogenoxygenation of Model Biomass Compounds

VI.5 NOV Fiberglass Systems: Continuous Fiber Composite Electrofusion Coupler

VII.A.4 University of Texas at Austin: Fuel Cell Hybrid Electric Delivery Van Project

VII.A.4 Valence Technology: Fuel Cell Hybrid Electric Delivery Van Project

VIII.6 Air Liquide: Hydrogen Safety Panel, Safety Knowledge Tools and First Responder Training Resources

Utah

III.3 MegaStir Technologies LLC: Vessel Design and Fabrication Technology for Stationary High-Pressure Hydrogen Storage

III.5 MegaStir Technologies LLC: Steel Concrete Composite Vessel for 875 bar Stationary Hydrogen Storage

V.G.15 University of Utah: Thermodynamic, Kinetic and Electrochemical Studies on Mixed Proton, Oxygen Ion and Electron (Hole) Conductors

Virginia

II.A.1 Strategic Analysis, Inc.: Hydrogen Pathways Analysis for H_2 Production via a Monolithic Piston Reforming Reactor and Reformer-Electrolyzer-Purifier Technology

II.B.4 Virginia Polytechnic Institute and State University: High Temperature, High Pressure Electrolysis

II.E.2 Virginia Polytechnic Institute and State University: Sweet Hydrogen: High-Yield Production of Hydrogen from Biomass Sugars Catalyzed by in vitro Synthetic Biosystems

III.5 Wiretough Cylinders: Steel Concrete Composite Vessel for 875 bar Stationary Hydrogen Storage

III.6 Wiretough Cylinders: Low Cost Hydrogen Storage at 875 Bar Using Steel Liner and Steel Wire Wrap

III.12 NanoSonic, Inc.: Cryogenically Flexible, Low Permeability H_2 Delivery Hose

IV.A.2 Strategic Analysis, Inc.: Hydrogen Storage Cost Analysis

IV.D.7 Virginia Polytechnic Institute and State University: Melt Processable PAN Precursor for High Strength, Low-Cost Carbon Fibers (Phase II)

V.C.10 NanoSonic, Inc.: Novel Hydrocarbon Ionomers for Durable Proton Exchange Membranes

V.F.6 Strategic Analysis, Inc.: Fuel Cell Vehicle and Bus Cost Analysis

V.F.8 Strategic Analysis, Inc.: A Total Cost of Ownership Model for Design and Manufacturing Optimization of Fuel Cells in Stationary and Emerging Market Applications

V.G.8 Virginia Polytechnic Institute and State University: Analysis of the Mechanisms of Electrochemical Oxygen Reduction and Development of Ag-alloy and Pt-alloy Electrocatalysis for Low Temperature Fuel Cells

VI.3 Virginia Clean Cities at James Madison University: Fuel Cell and Hydrogen Opportunity Center, www.hfcnexus.com

VI.3 Birch Studio: Fuel Cell and Hydrogen Opportunity Center, www.hfcnexus.com

VI.4 Strategic Analysis, Inc.: U.S. Clean Energy Hydrogen and Fuel Cell Technologies: A Competiveness Analysis

VIII.6 Consultant: Hydrogen Safety Panel, Safety Knowledge Tools and First Responder Training Resources

Washington

II.E.3 Pacific Northwest National Laboratory: Novel Hybrid Microbial Electrochemical System for Efficient Hydrogen Generation from Biomass

II.F.1 Pacific Northwest National Laboratory: Monolithic Piston-Type Reactor for Hydrogen Production through Rapid Swing of Reforming/Combustion Reactions

II.F.1 Dason Technology: Monolithic Piston-Type Reactor for Hydrogen Production through Rapid Swing of Reforming/Combustion Reactions

II.F.1 Washington State University: Monolithic Piston-Type Reactor for Hydrogen Production through Rapid Swing of Reforming/Combustion Reactions

III.3 Global Engineering and Technology, LLC: Vessel Design and Fabrication Technology for Stationary High-Pressure Hydrogen Storage

III.5 Global Engineering and Technology, LLC: Steel Concrete Composite Vessel for 875 bar Stationary Hydrogen Storage

III.9 Washington State University: Improved Hydrogen Liquefaction through Heisenberg Vortex Separation of Para- and Orthohydrogen

III.10 Pacific Northwest National Laboratory: Magnetocaloric Hydrogen Liquefaction

III.10 Emerald Energy NW LLC: Magnetocaloric Hydrogen Liquefaction

IV.B.1 Pacific Northwest National Laboratory: Hydrogen Storage Engineering Center of Excellence

IV.B.2 Pacific Northwest National Laboratory: Hydrogen Storage System Modeling: Public Access, Maintenance, and Enhancements

IV.C.7 Pacific Northwest National Laboratory: H_2 Storage Characterization and Optimization Research Efforts

IV.D.1 Pacific Northwest National Laboratory: Enhanced Materials and Design Parameters for Reducing the Cost of Hydrogen Storage Tanks

IV.D.6 Pacific Northwest National Laboratory: Achieving Hydrogen Storage Goals through High-Strength Fiber Glass

V.G.4 Pacific Northwest National Laboratory: Multifunctional Catalysis to Synthesize and Utilize Energy Carriers

V.G.13 Washington State University: Sub Nanometer Sized Clusters for Heterogeneous Catalysis

VIII.6 Pacific Northwest National Laboratory: Hydrogen Safety Panel, Safety Knowledge Tools and First Responder Training Resources

VIII.6 Excelsior Design, Inc.: Hydrogen Safety Panel, Safety Knowledge Tools and First Responder Training Resources

VIII.9 Pacific Northwest National Laboratory: Compatibility of Polymeric Materials Used in the Hydrogen Infrastructure

X.4 Pacific Northwest National Laboratory: Demonstration of Fuel Cell Auxiliary Power Units (APUs) to Power Transport Refrigeration Units (TRUs) in Refrigerated Trucks

Washington, D.C.

VI.3 Breakthrough Technologies Institute: Fuel Cell and Hydrogen Opportunity Center, www.hfcnexus.com

VII.B.5 Werken: Brentwood Case Study

VIII.8 Fuel Cell & Hydrogen Energy Association: Fuel Cell & Hydrogen Energy Association Codes and Standards Support

Wisconsin

V.G.10 University of Wisconsin-Madison: Atomic-Scale Design of Metal and Alloy Catalysts: A Combined Theoretical and Experimental Approach

Foreign Countries

Canada

II.B.5 Versa Power Systems, Ltd.: Solid Oxide Based Electrolysis and Stack Technology with Ultra-High Electrolysis Current Density (>3 A/cm^2) and Efficiency

Canada (Continued)

IV.B.1 Universite du Quebec a Trios-Rivieres: Hydrogen Storage Engineering Center of Excellence

V.A.1 University of Waterloo: Non-Precious Metal Fuel Cell Cathodes: Catalyst Development and Electrode Structure Design

V.B.7 Ballard Power Systems: The Effect of Airborne Contaminants on Fuel Cell Performance and Durability

VI.4 Bowen Liu: U.S. Clean Energy Hydrogen and Fuel Cell Technologies: A Competiveness Analysis

VII.B.4 Hydrogenics: CSULA Hydrogen Refueling Facility Performance Evaluation and Optimization

VII.C.2 Powertech: Development of the Hydrogen Station Equipment Performance (HyStEP) Device

VIII.1 A.V. Tchouvelev & Associates: National Codes and Standards Deployment and Outreach

VIII.6 CSA Group: Hydrogen Safety Panel, Safety Knowledge Tools and First Responder Training Resources

X.3 Hydrogenics: Maritime Fuel Cell Generator Project

X.4 Ballard Power Systems: Demonstration of Fuel Cell Auxiliary Power Units (APUs) to Power Transport Refrigeration Units (TRUs) in Refrigerated Trucks

Finland

VIII.3 VTT: Hydrogen Fuel Quality

France

VIII.3 Commissariat a l'energie atomique et aux energies alternatives: Hydrogen Fuel Quality

Germany

IV.D.2 BMW: Thermomechanical Cycling of Thin Liner High Fiber Fraction Cryogenic Pressure Vessels Rapidly Refueled by Liquid Hydrogen Pump to 700 Bar

Japan

III.3 Kobe Steel, LTD.: Vessel Design and Fabrication Technology for Stationary High-Pressure Hydrogen Storage

VIII.3 Japan Automotive Research Institute: Hydrogen Fuel Quality

South Korea

III.5 POSCO: Steel Concrete Composite Vessel for 875 bar Stationary Hydrogen Storage

Switzerland

V.B.4 Paul Scherrer Institute: FC-PAD: Ionomer, GDLs, Interfaces

VI.4 e4tech: U.S. Clean Energy Hydrogen and Fuel Cell Technologies: A Competiveness Analysis

United Kingdom

V.D.3 Johnson Matthey Fuel Cells: Rationally Designed Catalyst Layers for PEMFC Performance Optimization

XVI. Project Listings by Organization

3M Company

V.A.7 Highly Active, Durable, and Ultra-low PGM NSTF Thin Film ORR Catalysts and Supports
V.A.8 Highly-Accessible Catalysts for Durable High-Power Performance
V.B.4 FC-PAD: Ionomer, GDLs, Interfaces
V.C.1 New Fuel Cell Membranes with Improved Durability and Performance
V.C.2 Advanced Hybrid Membranes for Next Generation PEMFC Automotive Applications
V.C.7 Advanced Ionomers and MEAs for Alkaline Membrane Fuel Cells
V.D.1 High Performance, Durable, Low Cost Membrane Electrode Assemblies for Transportation Applications
VI.1 Fuel Cell Membrane Electrode Assembly Manufacturing R&D

AccerlorMittal

III.5 Steel Concrete Composite Vessel for 875 bar Stationary Hydrogen Storage

ACI Services

III.4 Hydrogen Compression Application of the Linear Motor Reciprocating Compressor (LMRC)

Adaptive Intelligent Systems LLC

III.5 Steel Concrete Composite Vessel for 875 bar Stationary Hydrogen Storage

Adherent Technologies, Inc.

IV.D.5 Optimizing the Cost and Performance of Composite Cylinders for H_2 Storage using a Graded Construction

Advent Technologies Inc.

V.D.5 Facilitated Direct Liquid Fuel Cells with High Temperature Membrane Electrode Assemblies

Air Liquide

III.5 Steel Concrete Composite Vessel for 875 bar Stationary Hydrogen Storage
VIII.6 Hydrogen Safety Panel, Safety Knowledge Tools and First Responder Training Resources

Air Products and Chemicals, Inc.

VII.B.3 Validation of an Advanced High Pressure PEM Electrolyzer and Composite Hydrogen Storage, with Data Reporting, for SunHydro Stations
VII.C.3 Advanced Hydrogen Fueling Station Supply: Tube Trailers
VIII.6 Hydrogen Safety Panel, Safety Knowledge Tools and First Responder Training Resources

ALD Nanosolutions

V.A.6 Extended Surface Electrocatalyst Development

Ames Laboratory

IV.C.6 High-capacity Hydrogen Storage Systems via Mechanochemistry

Amsen Technologies LLC

V.C.9 Low-Cost Proton Conducting Membranes for PEM Fuel Cells

Anderson Burton

VII.B.5 Brentwood Case Study

AOC, LLC

IV.D.1 Enhanced Materials and Design Parameters for Reducing the Cost of Hydrogen Storage Tanks

Ardica Technologies, Inc.

IV.C.12 Low-Cost α-Alane for Hydrogen Storage

Argonne National Laboratory

III.1 Hydrogen Delivery Infrastructure Analysis
III.13 Hydrogen Fueling Station Precooling Analysis
IV.A.1 System Analysis of Physical and Materials-Based Hydrogen Storage
IV.C.9 High-Capacity and Low-Cost Hydrogen-Storage Sorbents for Automotive Applications
V.A.4 Tailored High Performance Low-PGM Alloy Cathode Catalysts
V.A.7 Highly Active, Durable, and Ultra-low PGM NSTF Thin Film ORR Catalysts and Supports
V.B.1 Fuel Cell-Performance and Durability (FC-PAD) Consortium Overview
V.B.2 FC-PAD Fuel Cell-Performance and Durability Electrocatalysts and Supports
V.B.3 FC-PAD: Electrode Layer Integration
V.B.4 FC-PAD: Ionomer, GDLs, Interfaces
V.B.5 FC-PAD: Modeling, Evaluation, Characterization
V.C.6 Advanced Materials for Fully-Integrated MEAs in AEMFCs
V.D.1 High Performance, Durable, Low Cost Membrane Electrode Assemblies for Transportation Applications
V.D.3 Rationally Designed Catalyst Layers for PEMFC Performance Optimization
V.F.5 Performance and Durability of Advanced Automotive Fuel Cell Stacks and Systems with Nanostructured Thin Film Catalyst Based Membrane Electrode Assemblies
VII.A.3 Fuel Cell Electric Truck (FCET) Component Sizing
IX.1 Employment Impacts of Hydrogen and Fuel Cell Technologies
IX.2 Life-Cycle Analysis of Water Consumption for Hydrogen Production
IX.3 Impact of Fuel Cell and H_2 Storage Improvements on FCEVs
IX.5 Life Cycle Analysis of Emerging Hydrogen Production Technologies

Arizona State University

II.C.1 High Efficiency Solar Thermochemical Reactor for Hydrogen Production

ASTM International

VIII.3 Hydrogen Fuel Quality

Automated Dynamics

VI.5 Continuous Fiber Composite Electrofusion Coupler

A.V. Tchouvelev & Associates

VIII.1 National Codes and Standards Deployment and Outreach

Ballard Power Systems

V.B.7 The Effect of Airborne Contaminants on Fuel Cell Performance and Durability
X.4 Demonstration of Fuel Cell Auxiliary Power Units (APUs) to Power Transport Refrigeration Units (TRUs) in Refrigerated Trucks

Battelle

V.F.7 Stationary and Emerging Market Fuel Cell System Cost Analysis—Primary Power and Combined Heat and Power Applications

Becht Engineering

VIII.6 Hydrogen Safety Panel, Safety Knowledge Tools and First Responder Training Resources

Ben C. Gerwick, Inc.

III.3 Vessel Design and Fabrication Technology for Stationary High-Pressure Hydrogen Storage

Bevilacqua Knight Inc.

III.5 Steel Concrete Composite Vessel for 875 bar Stationary Hydrogen Storage

Birch Studio

VI.3 Fuel Cell and Hydrogen Opportunity Center, www.hfcnexus.com

Bki

VIII.6 Hydrogen Safety Panel, Safety Knowledge Tools and First Responder Training Resources

Bloomfield Automation

VIII.7 NREL Hydrogen Sensor Testing Laboratory

BMW

IV.D.2 Thermomechanical Cycling of Thin Liner High Fiber Fraction Cryogenic Pressure Vessels Rapidly Refueled by Liquid Hydrogen Pump to 700 bar

Bowen Liu

VI.4 U.S. Clean Energy Hydrogen and Fuel Cell Technologies: A Competiveness Analysis

Branded by Media

VIII.1 National Codes and Standards Deployment and Outreach

Breakthrough Technologies Institute

VI.3 Fuel Cell and Hydrogen Opportunity Center, www.hfcnexus.com

Brookhaven National Laboratory

V.A.5 Platinum Monolayer Electrocatalysts

V.G.1 Structure and Function in Electrocatalysis of Reactions for Direct Energy Conversion

V.G.2 Catalysis and Electrocatalysis for Advanced Fuel Synthesis: Hydrogen Production and the Water-Gas Shift

Bucknell University

II.C.1 High Efficiency Solar Thermochemical Reactor for Hydrogen Production

California Fuel Cell Partnership

VII.C.6 Station Operational Status System (SOSS) 3.0 Implementation, SOSS 3.1 Upgrade, and Station Map Upgrade Project

California Institute of Technology

II.D.3 Tandem Particle-Slurry Batch Reactors for Solar Water Splitting

IV.B.1 Hydrogen Storage Engineering Center of Excellence

IV.C.8 Design and Synthesis of Materials with High Capacities for Hydrogen Physisorption

California State University, Los Angeles

VII.B.4 CSULA Hydrogen Refueling Facility Performance Evaluation and Optimization

Carnegie Mellon University

V.A.1 Non-Precious Metal Fuel Cell Cathodes: Catalyst Development and Electrode Structure Design

V.A.8 Highly-Accessible Catalysts for Durable High-Power Performance

Center for Transportation and the Environment

IV.D.3 Conformable Hydrogen Storage Pressure Vessel Project

VII.A.4 Fuel Cell Hybrid Electric Delivery Van Project

Central Michigan University

V.G.14 Element Specific Atomic Arrangement of Binary and Ternary Alloy Nanosized Catalysts in As-Prepared and Active State

City of Santa Fe Springs

VIII.6 Hydrogen Safety Panel, Safety Knowledge Tools and First Responder Training Resources

Colorado School of Mines

II.C.1 High Efficiency Solar Thermochemical Reactor for Hydrogen Production

III.2 Fatigue Performance of High-Strength Pipeline Steels and Their Welds in Hydrogen Gas Service

V.A.6 Extended Surface Electrocatalyst Development

V.B.4 FC-PAD: Ionomer, GDLs, Interfaces

V.C.2 Advanced Hybrid Membranes for Next Generation PEMFC Automotive Applications

V.C.7 Advanced Ionomers and MEAs for Alkaline Membrane Fuel Cells

VI.1 Fuel Cell Membrane Electrode Assembly Manufacturing R&D

Commissariat a l'energie atomique et aux energies alternatives

VIII.3 Hydrogen Fuel Quality

Composite Technology Development, Inc.

IV.D.5 Optimizing the Cost and Performance of Composite Cylinders for H_2 Storage using a Graded Construction

Connecticut Center for Advanced Technology

VI.2 Clean Energy Supply Chain and Manufacturing Competitiveness Analysis for Hydrogen and Fuel Cell Technologies

Cornell University

V.A.8 Highly-Accessible Catalysts for Durable High-Power Performance

CP Industries

III.6 Low Cost Hydrogen Storage at 875 bar Using Steel Liner and Steel Wire Wrap

CSA Group

VIII.6 Hydrogen Safety Panel, Safety Knowledge Tools and First Responder Training Resources

Dason Technology

II.F.1 Monolithic Piston-Type Reactor for Hydrogen Production through Rapid Swing of Reforming/Combustion Reactions

DJW Technology, LLC

VI.2 Clean Energy Supply Chain and Manufacturing Competitiveness Analysis for Hydrogen and Fuel Cell Technologies

VI.4 U.S. Clean Energy Hydrogen and Fuel Cell Technologies: A Competiveness Analysis

Drexel University

V.A.8 Highly-Accessible Catalysts for Durable High-Power Performance

e4tech

VI.4 U.S. Clean Energy Hydrogen and Fuel Cell Technologies: A Competiveness Analysis

ElectroChem, Inc.

V.C.11 Novel Nanocomposite Polymer Electrolyte Membranes for Fuel Cells

Element One

VIII.7 NREL Hydrogen Sensor Testing Laboratory

Emerald Energy NW LLC

III.10 Magnetocaloric Hydrogen Liquefaction

Energetics, Inc.

IX.1 Employment Impacts of Hydrogen and Fuel Cell Technologies

Excelsior Design, Inc.

VIII.6 Hydrogen Safety Panel, Safety Knowledge Tools and First Responder Training Resources

Federal Express Corporation

X.5 FedEx Express Hydrogen Fuel Cell Extended-Range Battery Electric Vehicles

Firexplo

VIII.6 Hydrogen Safety Panel, Safety Knowledge Tools and First Responder Training Resources

Florida State University

VII.D.3 Dynamic Modeling and Validation of Electrolyzers in Real Time Grid Simulation

Fluer, Inc.

VIII.6 Hydrogen Safety Panel, Safety Knowledge Tools and First Responder Training Resources

Ford Motor Company

IV.B.1 Hydrogen Storage Engineering Center of Excellence

IV.C.10 Hydrogen Adsorbents with High Volumetric Density: New Materials and System Projections

IV.D.1 Enhanced Materials and Design Parameters for Reducing the Cost of Hydrogen Storage Tanks

VIII.9 Compatibility of Polymeric Materials Used in the Hydrogen Infrastructure

Forterra Water Pipe

III.5 Steel Concrete Composite Vessel for 875 bar Stationary Hydrogen Storage

Fuel Cell & Hydrogen Energy Association

VIII.8 Fuel Cell & Hydrogen Energy Association Codes and Standards Support

FuelCell Energy

II.B.5 Solid Oxide Based Electrolysis and Stack Technology with Ultra-High Electrolysis Current Density (>3 A/cm^2) and Efficiency

II.F.2 Reformer-Electrolyzer-Purifier (REP) for Production of Hydrogen [CO_2 Pump]

V.A.3 Innovative Non-PGM Catalysts for High-Temperature PEMFCs

V.C.3 Smart Matrix Development for Direct Carbonate Fuel Cell

Gas Technology Institute

III.7 Compressor-Less Hydrogen Refueling Station Using Thermal Compression

VII.B.2 Performance Evaluation of Delivered Hydrogen Fueling Stations

General Motors Company

IV.B.1 Hydrogen Storage Engineering Center of Excellence

V.A.1 Non-Precious Metal Fuel Cell Cathodes: Catalyst Development and Electrode Structure Design

V.A.8 Highly-Accessible Catalysts for Durable High-Power Performance

V.C.1 New Fuel Cell Membranes with Improved Durability and Performance

V.D.1 High Performance, Durable, Low Cost Membrane Electrode Assemblies for Transportation Applications

VI.1 Fuel Cell Membrane Electrode Assembly Manufacturing R&D

Georgia Institute of Technology

II.B.6 Economical Production of Hydrogen Through Development of Novel, High Efficiency Electrocatalysts for Alkaline Membrane Electrolysis

V.G.10 Atomic-Scale Design of Metal and Alloy Catalysts: A Combined Theoretical and Experimental Approach

VI.1 Fuel Cell Membrane Electrode Assembly Manufacturing R&D

Giner, Inc.

II.B.2 High-Performance, Long-Lifetime Catalysts for Proton Exchange Membrane Electrolysis

II.B.4 High Temperature, High Pressure Electrolysis

V.C.4 Ionomer Dispersion Impact on Fuel Cell and Electrolyzer Performance and Durability

V.C.8 Dimensionally Stable High Performance Membranes

V.D.6 Advanced Catalysts and Membrane Electrode Assemblies (MEAs) for Reversible Alkaline Membrane Fuel Cells

V.E.1 Regenerative Fuel Cell System

Global Engineering and Technology, LLC

III.3 Vessel Design and Fabrication Technology for Stationary High-Pressure Hydrogen Storage

III.5 Steel Concrete Composite Vessel for 875 bar Stationary Hydrogen Storage

GLWN, Westside Industrial Retention & Expansion Network

VI.4 U.S. Clean Energy Hydrogen and Fuel Cell Technologies: A Competiveness Analysis

GVD Corporation

III.8 Advanced Barrier Coatings for Harsh Environments

GWS Solutions of Tolland, LLC

VIII.6 Hydrogen Safety Panel, Safety Knowledge Tools and First Responder Training Resources

Hanson Pressure Pipe

III.3 Vessel Design and Fabrication Technology for Stationary High-Pressure Hydrogen Storage

Harris Thermal Transfer Products

III.3 Vessel Design and Fabrication Technology for Stationary High-Pressure Hydrogen Storage

Hawaii Natural Energy Institute

V.B.7 The Effect of Airborne Contaminants on Fuel Cell Performance and Durability

X.1 Hydrogen Energy Systems as a Grid Management Tool

Hexagon Lincoln

IV.B.1 Hydrogen Storage Engineering Center of Excellence
IV.D.1 Enhanced Materials and Design Parameters for Reducing the Cost of Hydrogen Storage Tanks
IV.D.6 Achieving Hydrogen Storage Goals through High-Strength Fiber Glass

High Energy Coil Reservoirs, LLC

IV.D.3 Conformable Hydrogen Storage Pressure Vessel Project

Humboldt State University

VII.D.3 Dynamic Modeling and Validation of Electrolyzers in Real Time Grid Simulation

Hydrogenics

VII.A.4 Fuel Cell Hybrid Electric Delivery Van Project
VII.B.4 CSULA Hydrogen Refueling Facility Performance Evaluation and Optimization
X.3 Maritime Fuel Cell Generator Project

Hy-Performance Materials Testing, LLC

III.6 Low Cost Hydrogen Storage at 875 bar Using Steel Liner and Steel Wire Wrap
IV.D.8 Innovative Development, Selection and Testing to Reduce Cost and Weight of Materials for BOP Components

Idaho National Laboratory

VII.D.3 Dynamic Modeling and Validation of Electrolyzers in Real Time Grid Simulation

Illinois Institute of Technology

V.A.9 Corrosion-Resistant Non-Carbon Electrocatalyst Supports for PEFCs
V.C.3 Smart Matrix Development for Direct Carbonate Fuel Cell

Indiana University-Purdue University Indianapolis

V.D.3 Rationally Designed Catalyst Layers for PEMFC Performance Optimization

IRD Fuel Cells

V.A.1 Non-Precious Metal Fuel Cell Cathodes: Catalyst Development and Electrode Structure Design
V.A.2 Development of PGM-free Catalysts for Hydrogen Oxidation Reaction in Alkaline Media

Japan Automotive Research Institute

VIII.3 Hydrogen Fuel Quality

Jet Propulsion Laboratory

IV.B.1 Hydrogen Storage Engineering Center of Excellence

Johns Hopkins University

V.A.7 Highly Active, Durable, and Ultra-low PGM NSTF Thin Film ORR Catalysts and Supports
V.D.1 High Performance, Durable, Low Cost Membrane Electrode Assemblies for Transportation Applications
V.G.3 Control of Reactivity in Nanoporous Metal/Ionic Liquid Composite Catalysts

Johnson Matthey Fuel Cells

V.D.3 Rationally Designed Catalyst Layers for PEMFC Performance Optimization

Kobe Steel, LTD.

III.3 Vessel Design and Fabrication Technology for Stationary High-Pressure Hydrogen Storage

Lawrence Berkeley National Laboratory

- II.D.3 Tandem Particle-Slurry Batch Reactors for Solar Water Splitting
- II.E.1 Biomass to Hydrogen
- IV.C.4 HyMARC: A Consortium for Advancing Solid-State Hydrogen Storage Materials
- IV.C.7 H_2 Storage Characterization and Optimization Research Efforts
- V.A.4 Tailored High Performance Low-PGM Alloy Cathode Catalysts
- V.B.1 Fuel Cell-Performance and Durability (FC-PAD) Consortium Overview
- V.B.3 FC-PAD: Electrode Layer Integration
- V.B.4 FC-PAD: Ionomer, GDLs, Interfaces
- V.B.5 FC-PAD: Modeling, Evaluation, Characterization
- V.B.6 Multiscale Modeling of Fuel Cell Membranes
- V.C.7 Advanced Ionomers and MEAs for Alkaline Membrane Fuel Cells
- V.D.1 High Performance, Durable, Low Cost Membrane Electrode Assemblies for Transportation Applications
- V.F.8 A Total Cost of Ownership Model for Design and Manufacturing Optimization of Fuel Cells in Stationary and Emerging Market Applications
- VI.1 Fuel Cell Membrane Electrode Assembly Manufacturing R&D

Lawrence Livermore National Laboratory

- II.D.2 Wide Bandgap Chalcopyrite Photoelectrodes for Direct Solar Water Splitting
- III.15 Cryo-Compressed Pathway Analysis (2016)
- IV.C.3 HyMARC: Hydrogen Storage Materials Advanced Research Consortium (LLNL Effort)
- IV.C.4 HyMARC: A Consortium for Advancing Solid-State Hydrogen Storage Materials
- IV.C.5 Improving the Kinetics and Thermodynamics of $Mg(BH_4)_2$ for Hydrogen Storage
- IV.C.8 Design and Synthesis of Materials with High Capacities for Hydrogen Physisorption
- IV.D.2 Thermomechanical Cycling of Thin Liner High Fiber Fraction Cryogenic Pressure Vessels Rapidly Refueled by Liquid Hydrogen Pump to 700 bar
- VII.C.4 Performance and Durability Testing of Volumetrically Efficient Cryogenic Vessels and High Pressure Liquid Hydrogen Pump

Lexidyne, LLC

- IX.11 National FCEV and Hydrogen Refueling Station Scenarios

LightSail

- III.5 Steel Concrete Composite Vessel for 875 bar Stationary Hydrogen Storage

Linde LLC

- IV.D.2 Thermomechanical Cycling of Thin Liner High Fiber Fraction Cryogenic Pressure Vessels Rapidly Refueled by LH_2 Pump to 700 bar
- VII.B.2 Performance Evaluation of Delivered Hydrogen Fueling Stations
- VII.C.4 Performance and Durability Testing of Volumetrically Efficient Cryogenic Vessels and High Pressure Liquid Hydrogen Pump

Los Alamos National Laboratory

- IV.B.1 Hydrogen Storage Engineering Center of Excellence
- V.A.1 Non-Precious Metal Fuel Cell Cathodes: Catalyst Development and Electrode Structure Design
- V.A.2 Development of PGM-free Catalysts for Hydrogen Oxidation Reaction in Alkaline Media
- V.A.4 Tailored High Performance Low-PGM Alloy Cathode Catalysts

Los Alamos National Laboratory (Continued)

V.A.5 Platinum Monolayer Electrocatalysts
V.B.1 Fuel Cell-Performance and Durability (FC-PAD) Consortium Overview
V.B.2 FC-PAD Fuel Cell-Performance and Durability Electrocatalysts and Supports
V.B.3 FC-PAD: Electrode Layer Integration
V.B.4 FC-PAD: Ionomer, GDLs, Interfaces
V.B.5 FC-PAD: Modeling, Evaluation, Characterization
V.C.4 Ionomer Dispersion Impact on Fuel Cell and Electrolyzer Performance and Durability
V.C.6 Advanced Materials for Fully-Integrated MEAs in AEMFCs
V.D.1 High Performance, Durable, Low Cost Membrane Electrode Assemblies for Transportation Applications
V.D.5 Facilitated Direct Liquid Fuel Cells with High Temperature Membrane Electrode Assemblies
V.F.3 Technical Assistance to Developers
VIII.3 Hydrogen Fuel Quality

Mainstream Engineering

VI.1 Fuel Cell Membrane Electrode Assembly Manufacturing R&D
VI.6 In-line Quality Control of PEM Materials

Materia, Inc.

IV.D.4 Next Generation Hydrogen Storage Vessels Enabled by Carbon Fiber Infusion with a Low Viscosity, High Toughness System

MegaStir Technologies LLC

III.3 Vessel Design and Fabrication Technology for Stationary High-Pressure Hydrogen Storage
III.5 Steel Concrete Composite Vessel for 875 bar Stationary Hydrogen Storage

Michigan Technological University

V.D.1 High Performance, Durable, Low Cost Membrane Electrode Assemblies for Transportation Applications

Montana State University

IV.D.4 Next Generation Hydrogen Storage Vessels Enabled by Carbon Fiber Infusion with a Low Viscosity, High Toughness System

N&R Engineering

III.6 Low Cost Hydrogen Storage at 875 bar Using Steel Liner and Steel Wire Wrap

NanoSonic, Inc.

III.12 Cryogenically Flexible, Low Permeability H_2 Delivery Hose
V.C.10 Novel Hydrocarbon Ionomers for Durable Proton Exchange Membranes

National Fuel Cell Research Center

VI.2 Clean Energy Supply Chain and Manufacturing Competitiveness Analysis for Hydrogen and Fuel Cell Technologies

National Institute of Standards and Technology

III.2 Fatigue Performance of High-Strength Pipeline Steels and Their Welds in Hydrogen Gas Service
IV.C.7 H_2 Storage Characterization and Optimization Research Efforts
V.F.2 Neutron Imaging Study of the Water Transport in Operating Fuel Cells

National Renewable Energy Laboratory

II.B.1	Renewable Electrolysis Integrated System Development and Testing
II.B.2	High-Performance, Long-Lifetime Catalysts for Proton Exchange Membrane Electrolysis
II.C.2	Flowing Particle Bed Solarthermal RedOx Process to Split Water
II.D.1	High-Efficiency Tandem Absorbers for Economical Solar Hydrogen Production
II.D.2	Wide Bandgap Chalcopyrite Photoelectrodes for Direct Solar Water Splitting
II.E.1	Biomass to Hydrogen
III.9	Improved Hydrogen Liquefaction through Heisenberg Vortex Separation of Para- and Orthohydrogen
III.11	700 bar Hydrogen Dispenser Hose Reliability Improvement
III.12	Cryogenically Flexible, Low Permeability H_2 Delivery Hose
III.14	H2FIRST—Consolidation
IV.B.1	Hydrogen Storage Engineering Center of Excellence
IV.B.2	Hydrogen Storage System Modeling: Public Access, Maintenance, and Enhancements
IV.C.7	H_2 Storage Characterization and Optimization Research Efforts
V.A.6	Extended Surface Electrocatalyst Development
V.A.8	Highly-Accessible Catalysts for Durable High-Power Performance
V.B.1	Fuel Cell-Performance and Durability (FC-PAD) Consortium Overview
V.B.2	FC-PAD Fuel Cell-Performance and Durability Electrocatalysts and Supports
V.B.3	FC-PAD: Electrode Layer Integration
V.B.4	FC-PAD: Ionomer, GDLs, Interfaces
V.B.5	FC-PAD: Modeling, Evaluation, Characterization
V.C.2	Advanced Hybrid Membranes for Next Generation PEMFC Automotive Applications
V.C.5	Highly Stable Anion-Exchange Membranes for High-Voltage Redox-Flow Batteries
V.C.7	Advanced Ionomers and MEAs for Alkaline Membrane Fuel Cells
V.D.6	Advanced Catalysts and Membrane Electrode Assemblies (MEAs) for Reversible Alkaline Membrane Fuel Cells
V.E.1	Regenerative Fuel Cell System
V.F.4	Fuel Cell Technology Status: Degradation
V.G.17	Hydroxide Conductors for Energy Conversion Devices
VI.1	Fuel Cell Membrane Electrode Assembly Manufacturing R&D
VI.2	Clean Energy Supply Chain and Manufacturing Competitiveness Analysis for Hydrogen and Fuel Cell Technologies
VI.6	In-line Quality Control of PEM Materials
VI.7	Manufacturing Competitiveness Analysis for Hydrogen Refueling Stations
VII.A.1	Fuel Cell Electric Vehicle Evaluation
VII.A.2	Technology Validation: Fuel Cell Bus Evaluations
VII.B.1	Hydrogen Station Data Collection and Analysis
VII.B.5	Brentwood Case Study
VII.C.1	Hydrogen Component Validation
VII.C.5	Hydrogen Meter Benchmark Testing
VII.D.1	Stationary Fuel Cell Evaluation
VII.D.2	Material Handling Equipment Data Collection and Analysis
VIII.1	National Codes and Standards Deployment and Outreach
VIII.7	NREL Hydrogen Sensor Testing Laboratory
IX.7	Sustainability Analysis of Hydrogen Supply and Stationary Fuel Cell Systems Using the Hydrogen Regional Sustainability (HyReS) Framework

National Renewable Energy Laboratory (Continued)

IX.8 Evaluation of Technology Status Compared to Program Targets
IX.9 Expanded Capabilities for the Hydrogen Financial Analysis Scenario Tool
IX.11 National FCEV and Hydrogen Refueling Station Scenarios

NEI Corporation

V.C.11 Novel Nanocomposite Polymer Electrolyte Membranes for Fuel Cells

New England Wire Technologies, Inc.

III.12 Cryogenically Flexible, Low Permeability H_2 Delivery Hose

Nissan Technical Center, North America

V.A.9 Corrosion-Resistant Non-Carbon Electrocatalyst Supports for PEFCs
V.C.2 Advanced Hybrid Membranes for Next Generation PEMFC Automotive Applications

Northeastern University

II.B.3 High Performance Platinum Group Metal Free Membrane Electrode Assemblies through Control of Interfacial Processes
V.A.3 Innovative Non-PGM Catalysts for High-Temperature PEMFCs

Northwestern University

II.C.1 High Efficiency Solar Thermochemical Reactor for Hydrogen Production

NOV Fiberglass Systems

VI.5 Continuous Fiber Composite Electrofusion Coupler

Nuvera Fuel Cells

X.4 Demonstration of Fuel Cell Auxiliary Power Units (APUs) to Power Transport Refrigeration Units (TRUs) in Refrigerated Trucks

Oak Ridge National Laboratory

III.2 Fatigue Performance of High-Strength Pipeline Steels and Their Welds in Hydrogen Gas Service
III.3 Vessel Design and Fabrication Technology for Stationary High-Pressure Hydrogen Storage
III.5 Steel Concrete Composite Vessel for 875 bar Stationary Hydrogen Storage
III.6 Low Cost Hydrogen Storage at 875 bar Using Steel Liner and Steel Wire Wrap
IV.D.5 Optimizing the Cost and Performance of Composite Cylinders for H_2 Storage using a Graded Construction
IV.D.7 Melt Processable PAN Precursor for High Strength, Low-Cost Carbon Fibers (Phase II)
V.A.1 Non-Precious Metal Fuel Cell Cathodes: Catalyst Development and Electrode Structure Design
V.A.4 Tailored High Performance Low-PGM Alloy Cathode Catalysts
V.A.7 Highly Active, Durable, and Ultra-low PGM NSTF Thin Film ORR Catalysts and Supports
V.B.1 Fuel Cell-Performance and Durability (FC-PAD) Consortium Overview
V.B.2 FC-PAD Fuel Cell-Performance and Durability Electrocatalysts and Supports
V.B.3 FC-PAD: Electrode Layer Integration
V.B.4 FC-PAD: Ionomer, GDLs, Interfaces
V.B.5 FC-PAD: Modeling, Evaluation, Characterization
V.C.7 Advanced Ionomers and MEAs for Alkaline Membrane Fuel Cells
V.F.1 New Fuel Cell Materials: Characterization and Method Development
V.G.12 Fundamentals of Catalysis and Chemical Transformations

Ohio Fuel Cell Coalition

VI.2 Clean Energy Supply Chain and Manufacturing Competitiveness Analysis for Hydrogen and Fuel Cell Technologies

Oregon State University

II.E.3 Novel Hybrid Microbial Electrochemical System for Efficient Hydrogen Generation from Biomass

IV.B.1 Hydrogen Storage Engineering Center of Excellence

Pacific Northwest National Laboratory

II.E.3 Novel Hybrid Microbial Electrochemical System for Efficient Hydrogen Generation from Biomass

II.F.1 Monolithic Piston-Type Reactor for Hydrogen Production through Rapid Swing of Reforming/Combustion Reactions

III.10 Magnetocaloric Hydrogen Liquefaction

IV.B.1 Hydrogen Storage Engineering Center of Excellence

IV.B.2 Hydrogen Storage System Modeling: Public Access, Maintenance, and Enhancements

IV.C.7 H_2 Storage Characterization and Optimization Research Efforts

IV.D.1 Enhanced Materials and Design Parameters for Reducing the Cost of Hydrogen Storage Tanks

IV.D.6 Achieving Hydrogen Storage Goals through High-Strength Fiber Glass

V.G.4 Multifunctional Catalysis to Synthesize and Utilize Energy Carriers

VIII.6 Hydrogen Safety Panel, Safety Knowledge Tools and First Responder Training Resources

VIII.9 Compatibility of Polymeric Materials Used in the Hydrogen Infrastructure

X.4 Demonstration of Fuel Cell Auxiliary Power Units (APUs) to Power Transport Refrigeration Units (TRUs) in Refrigerated Trucks

Pajarito Powder

II.B.6 Economical Production of Hydrogen through Development of Novel, High Efficiency Electrocatalysts for Alkaline Membrane Electrolysis

V.A.2 Development of PGM-free Catalysts for Hydrogen Oxidation Reaction in Alkaline Media

V.A.3 Innovative Non-PGM Catalysts for High-Temperature PEMFCs

Paul Scherrer Institute

V.B.4 FC-PAD: Ionomer, GDLs, Interfaces

PDC Machines

III.14 H2FIRST—Consolidation

The Pennsylvania State University

II.B.3 High Performance Platinum Group Metal Free Membrane Electrode Assemblies through Control of Interfacial Processes

II.E.1 Biomass to Hydrogen

pH Matter, LLC

V.E.1 Regenerative Fuel Cell System

Plug Power

X.2 Ground Support Equipment Demonstration

X.5 FedEx Express Hydrogen Fuel Cell Extended-Range Battery Electric Vehicles

POSCO

III.5 Steel Concrete Composite Vessel for 875 bar Stationary Hydrogen Storage

Powertech

VII.C.2 Development of the Hydrogen Station Equipment Performance (HyStEP) Device

PPG Industries

IV.D.6 Achieving Hydrogen Storage Goals through High-Strength Fiber Glass

Proton OnSite

II.B.3 High Performance Platinum Group Metal Free Membrane Electrode Assemblies through Control of Interfacial Processes

II.B.6 Economical Production of Hydrogen through Development of Novel, High Efficiency Electrocatalysts for Alkaline Membrane Electrolysis

II.B.7 New Approaches to Improved PEM Electrolyzer Ion Exchange Membranes

VII.B.3 Validation of an Advanced High Pressure PEM Electrolyzer and Composite Hydrogen Storage, with Data Reporting, for SunHydro Stations

VII.B.5 Brentwood Case Study

VIII.6 Hydrogen Safety Panel, Safety Knowledge Tools and First Responder Training Resources

Purdue University

V.A.7 Highly Active, Durable, and Ultra-low PGM NSTF Thin Film ORR Catalysts and Supports

RCF Economic and Financial Consulting, Inc.

IX.1 Employment Impacts of Hydrogen and Fuel Cell Technologies

Redox Power Systems

V.D.4 Affordable, High Performance, Intermediate Temperature Solid Oxide Fuel Cells

Rensselaer Polytechnic University

V.C.6 Advanced Materials for Fully-Integrated MEAs in AEMFCs

V.C.8 Dimensionally Stable High Performance Membranes

SAE International

VIII.3 Hydrogen Fuel Quality

Sandia National Laboratories

II.C.1 High Efficiency Solar Thermochemical Reactor for Hydrogen Production

II.E.1 Biomass to Hydrogen

III.2 Fatigue Performance of High-Strength Pipeline Steels and Their Welds in Hydrogen Gas Service

IV.C.1 HyMARC: A Consortium for Advancing Solid-State Hydrogen Storage Materials

IV.C.2 Hydrogen Storage Materials Advanced Research Consortium: Sandia Effort

IV.C.4 HyMARC: A Consortium for Advancing Solid-State Hydrogen Storage Materials

IV.C.5 Improving the Kinetics and Thermodynamics of $Mg(BH_4)_2$ for Hydrogen Storage

IV.D.8 Innovative Development, Selection and Testing to Reduce Cost and Weight of Materials for BOP Components

V.C.6 Advanced Materials for Fully-Integrated MEAs in AEMFCs

VII.C.2 Development of the Hydrogen Station Equipment Performance (HyStEP) Device

VIII.2 R&D for Safety, Codes and Standards: Materials and Components Compatibility

VIII.4 R&D for Safety, Codes and Standards: Hydrogen Behavior

VIII.5 Hydrogen Quantitative Risk Assessment

VIII.10 Enabling Hydrogen Infrastructure Through Science-Based Codes and Standards

IX.4 Hydrogen Analysis with the Sandia ParaChoice Model

X.3 Maritime Fuel Cell Generator Project

Savannah River Consulting LLC

II.C.3 Electrolyzer Component Development for the HyS Thermochemical Cycle

IV.B.3 Investigation of Metal and Chemical Hydrides for Hydrogen Storage in Novel Fuel Cell Systems

Savannah River National Laboratory

II.C.3 Electrolyzer Component Development for the HyS Thermochemical Cycle

IV.B.1 Hydrogen Storage Engineering Center of Excellence

IV.B.2 Hydrogen Storage System Modeling: Public Access, Maintenance, and Enhancements

IV.B.3 Investigation of Metal and Chemical Hydrides for Hydrogen Storage in Novel Fuel Cell Systems

IV.C.11 Electrochemical Reversible Formation of Alane

VI.5 Continuous Fiber Composite Electrofusion Coupler

Smart Chemistry

VIII.3 Hydrogen Fuel Quality

Southwest Research Institute®

III.4 Hydrogen Compression Application of the Linear Motor Reciprocating Compressor (LMRC)

Spectrum Automation Controls

II.B.1 Renewable Electrolysis Integrated System Development and Testing

III.11 700 bar Hydrogen Dispenser Hose Reliability Improvement

VII.C.1 Hydrogen Component Validation

VII.C.5 Hydrogen Meter Benchmark Testing

Spencer Composites Corporation

IV.D.2 Thermomechanical Cycling of Thin Liner High Fiber Fraction Cryogenic Pressure Vessels Rapidly Refueled by Liquid Hydrogen Pump to 700 bar

IV.D.4 Next Generation Hydrogen Storage Vessels Enabled by Carbon Fiber Infusion with a Low Viscosity, High Toughness System

VII.C.4 Performance and Durability Testing of Volumetrically Efficient Cryogenic Vessels and High Pressure Liquid Hydrogen Pump

SRI International

IV.C.12 Low-Cost α-Alane for Hydrogen Storage

Stanford University

II.C.1 High Efficiency Solar Thermochemical Reactor for Hydrogen Production

II.D.2 Wide Bandgap Chalcopyrite Photoelectrodes for Direct Solar Water Splitting

Strategic Analysis, Inc.

II.A.1 Hydrogen Pathways Analysis for Hydrogen Production via a Monolithic Piston Reforming Reactor and Reformer-Electrolyzer-Purifier Technology

IV.A.2 Hydrogen Storage Cost Analysis

V.F.6 Fuel Cell Vehicle and Bus Cost Analysis

V.F.8 A Total Cost of Ownership Model for Design and Manufacturing Optimization of Fuel Cells in Stationary and Emerging Market Applications

VI.4 U.S. Clean Energy Hydrogen and Fuel Cell Technologies: A Competiveness Analysis

Structural Integrity Associates, Inc.

III.6 Low Cost Hydrogen Storage at 875 bar Using Steel Liner and Steel Wire Wrap

SunHydro LLC

VII.B.3 Validation of an Advanced High Pressure PEM Electrolyzer and Composite Hydrogen Storage, with Data Reporting, for SunHydro Stations

Sustain X

III.5 Steel Concrete Composite Vessel for 875 bar Stationary Hydrogen Storage

Swagelok

III.12 Cryogenically Flexible, Low Permeability H_2 Delivery Hose

Temple University

III.3 Vessel Design and Fabrication Technology for Stationary High-Pressure Hydrogen Storage

III.5 Steel Concrete Composite Vessel for 875 bar Stationary Hydrogen Storage

Tetramer Technologies, LLC

II.B.7 New Approaches to Improved PEM Electrolyzer Ion Exchange Membranes

Texas A&M University

IV.C.9 High-Capacity and Low-Cost Hydrogen-Storage Sorbents for Automotive Applications

V.G.5 Modeling Catalyzed Growth of Single Walled Carbon Nanotubes

Toray Composites America

IV.D.1 Enhanced Materials and Design Parameters for Reducing the Cost of Hydrogen Storage Tanks

TreadStone Technologies, Inc.

V.D.2 Novel Structured Metal Bipolar Plates for Low Cost Manufacturing

Tufts University

V.B.4 FC-PAD: Ionomer, GDLs, Interfaces

Unique Electric Solutions

VII.A.4 Fuel Cell Hybrid Electric Delivery Van Project

United Parcel Services

VII.A.4 Fuel Cell Hybrid Electric Delivery Van Project

United Technologies Research Center

IV.B.1 Hydrogen Storage Engineering Center of Excellence

V.D.3 Rationally Designed Catalyst Layers for PEMFC Performance Optimization

Université du Québec à Trois-Rivières

IV.B.1 Hydrogen Storage Engineering Center of Excellence

University at Buffalo-SUNY

V.D.6 Advanced Catalysts and Membrane Electrode Assemblies (MEAs) for Reversible Alkaline Membrane Fuel Cells

University of California, Berkeley

V.F.8 A Total Cost of Ownership Model for Design and Manufacturing Optimization of Fuel Cells in Stationary and Emerging Market Applications

University of California, Irvine

II.D.3 Tandem Particle-Slurry Batch Reactors for Solar Water Splitting

II.F.2 Reformer-Electrolyzer-Purifier (REP) for Production of Hydrogen [CO_2 Pump]

University of Chicago

V.G.16 Computer Simulation of Proton Transport in Fuel Cell Membranes

IX.10 The Business Case for Hydrogen-powered Passenger Cars: Competition and Solving the Infrastructure Puzzle

University of Colorado Boulder

II.C.2 Flowing Particle Bed Solarthermal RedOx Process to Split Water

II.C.4 NSF/DOE Solar Hydrogen Fuel: Accelerated Discovery of Advanced RedOx Materials for Solar Thermal Water Splitting to Produce Renewable Hydrogen

V.A.6 Extended Surface Electrocatalyst Development

V.G.8 Analysis of the Mechanisms of Electrochemical Oxygen Reduction and Development of Ag-alloy and Pt-alloy Electrocatalysis for Low Temperature Fuel Cells

University of Connecticut

V.B.7 The Effect of Airborne Contaminants on Fuel Cell Performance and Durability

V.C.3 Smart Matrix Development for Direct Carbonate Fuel Cell

V.G.6 Room Temperature Electrochemical Upgrading of Methane to Oxygenate Fuels

University of Delaware

V.A.6 Extended Surface Electrocatalyst Development

V.B.4 FC-PAD: Ionomer, GDLs, Interfaces

V.C.5 Highly Stable Anion-Exchange Membranes for High-Voltage Redox-Flow Batteries

University of Georgia

II.E.2 Sweet Hydrogen: High-Yield Production of Hydrogen from Biomass Sugars Catalyzed by in vitro Synthetic Biosystems

University of Hawaii

II.D.1 High-Efficiency Tandem Absorbers for Economical Solar Hydrogen Production

II.D.2 Wide Bandgap Chalcopyrite Photoelectrodes for Direct Solar Water Splitting

IV.C.7 H_2 Storage Characterization and Optimization Research Efforts

V.D.2 Novel Structured Metal Bipolar Plates for Low Cost Manufacturing

University of Houston

V.G.11 Dual Site Requirements for Hydrogenoxygenation of Model Biomass Compounds

University of Maryland

V.D.4 Affordable, High Performance, Intermediate Temperature Solid Oxide Fuel Cells

University of Massachusetts Amherst

V.G.9 Computational Design of Graphene-Nanoparticle Catalysts

University of Michigan

IV.B.1 Hydrogen Storage Engineering Center of Excellence

IV.C.5 Improving the Kinetics and Thermodynamics of $Mg(BH_4)_2$ for Hydrogen Storage

IV.C.10 Hydrogen Adsorbents with High Volumetric Density: New Materials and System Projections

University of Michigan (Continued)

V.G.8 Analysis of the Mechanisms of Electrochemical Oxygen Reduction and Development of Ag-alloy and Pt-alloy Electrocatalysis for Low Temperature Fuel Cells

University of Missouri

IV.C.6 High-capacity Hydrogen Storage Systems via Mechanochemistry

University of Nevada

II.D.1 High-Efficiency Tandem Absorbers for Economical Solar Hydrogen Production

II.D.2 Wide Bandgap Chalcopyrite Photoelectrodes for Direct Solar Water Splitting

University of New Mexico

II.B.3 High Performance Platinum Group Metal Free Membrane Electrode Assemblies through Control of Interfacial Processes

V.A.2 Development of PGM-free Catalysts for Hydrogen Oxidation Reaction in Alkaline Media

V.A.3 Innovative Non-PGM Catalysts for High-Temperature PEMFCs

V.A.9 Corrosion-Resistant Non-Carbon Electrocatalyst Supports for PEFCs

V.G.13 Sub Nanometer Sized Clusters for Heterogeneous Catalysis

University of Rochester

V.A.1 Non-Precious Metal Fuel Cell Cathodes: Catalyst Development and Electrode Structure Design

University of Tennessee

IX.6 Policies to Promote Alternative Fuel Vehicles

University of Texas at Austin

IV.D.3 Conformable Hydrogen Storage Pressure Vessel Project

V.D.3 Rationally Designed Catalyst Layers for PEMFC Performance Optimization

VII.A.4 Fuel Cell Hybrid Electric Delivery Van Project

University of Utah

V.G.15 Thermodynamic, Kinetic and Electrochemical Studies on Mixed Proton, Oxygen Ion and Electron (Hole) Conductors

University of Waterloo

V.A.1 Non-Precious Metal Fuel Cell Cathodes: Catalyst Development and Electrode Structure Design

University of Wisconsin-Madison

V.G.10 Atomic-Scale Design of Metal and Alloy Catalysts: A Combined Theoretical and Experimental Approach

Valence Technology

VII.A.4 Fuel Cell Hybrid Electric Delivery Van Project

Vanderbilt University

V.C.1 New Fuel Cell Membranes with Improved Durability and Performance

Versa Power Systems, Ltd.

II.B.5 Solid Oxide Based Electrolysis and Stack Technology with Ultra-High Electrolysis Current Density (>3 A/cm^2) and Efficiency

Virginia Clean Cities at James Madison University

VI.3 Fuel Cell and Hydrogen Opportunity Center, www.hfcnexus.com

Virginia Polytechnic Institute and State University

II.B.4 High Temperature, High Pressure Electrolysis

II.E.2 Sweet Hydrogen: High-Yield Production of Hydrogen from Biomass Sugars Catalyzed by in vitro Synthetic Biosystems

IV.D.7 Melt Processable PAN Precursor for High Strength, Low-Cost Carbon Fibers (Phase II)

V.G.8 Analysis of the Mechanisms of Electrochemical Oxygen Reduction and Development of Ag-alloy and Pt-alloy Electrocatalysis for Low Temperature Fuel Cells

VTT

VIII.3 Hydrogen Fuel Quality

Washington State University

II.F.1 Monolithic Piston-Type Reactor for Hydrogen Production through Rapid Swing of Reforming/Combustion Reactions

III.9 Improved Hydrogen Liquefaction through Heisenberg Vortex Separation of Para- and Orthohydrogen

V.G.13 Sub Nanometer Sized Clusters for Heterogeneous Catalysis

Washington University

II.B.6 Economical Production of Hydrogen through Development of Novel, High Efficiency Electrocatalysts for Alkaline Membrane Electrolysis

Wayne State University

V.G.7 Nanostructured, Targeted Layered Metal Oxides as Active and Selective Heterogeneous Electrocatalysts for Oxygen Evolution

Werken

VII.B.5 Brentwood Case Study

Wiretough Cylinders

III.5 Steel Concrete Composite Vessel for 875 bar Stationary Hydrogen Storage

III.6 Low Cost Hydrogen Storage at 875 bar Using Steel Liner and Steel Wire Wrap

Witte Engineered Gases

VIII.6 Hydrogen Safety Panel, Safety Knowledge Tools and First Responder Training Resources

Workhorse Technologies Inc.

X.5 FedEx Express Hydrogen Fuel Cell Extended-Range Battery Electric Vehicles

Worthington Cylinder Corporation

VII.C.3 Advanced Hydrogen Fueling Station Supply: Tube Trailers

WPCSOL

V.B.7 The Effect of Airborne Contaminants on Fuel Cell Performance and Durability

U.S. DEPARTMENT OF
ENERGY

www.hydrogen.energy.gov